McDOWELL RACKNER GIBSON PC
419 SW 11th Ave, Suite 400 | Portland, OR 97205

ALISHA TILL
Direct (503) 290-3628
alisha@mrg-law.com

February 22, 2023

VIA ELECTRONIC FILING

Public Utility Commission of Oregon
Filing Center
P.O. Box 1088
201 High Street S.E., Suite 100
Salem, OR 97308-1088

Re: Docket No. PCN 5 – In the Matter of Idaho Power Company's Petition for Certificate of Public Convenience and Necessity.

Attention Filing Center:

Attached for filing in the above-referenced docket is Idaho Power Company's Reply Testimony and Exhibits of Dr. Jeffrey M. Ellenbogen (Idaho Power/1200-1220).

Please note that, because the only confidential information contained in Dr. Ellenbogen's testimony and exhibits is confidential medical information, there are only two versions of the testimony and exhibits—the public version, which contains redactions, and the confidential version. The confidential version is being sent via encrypted zip file only to the Filing Center and Mr. Greg Larkin pursuant to Administrative Law Judge Mellgren's February 17, 2023 Ruling.

Please contact this office with any questions.

Thank you,

Alisha Till

Alisha Till
Paralegal

Attachments

DOCKET PCN 5 - CERTIFICATE OF SERVICE

I hereby certify that on February 22, 2023 the redacted version of Idaho Power Company's Reply Testimony and Exhibits of Dr. Jeffrey M. Ellenbogen (Idaho Power/1200-1220) was served by USPS First Class Mail and Copy Center to said person(s) at his or her last-known address(es) as indicated below:

By: USPS First Class Mail and Copy Center:

John C. Williams
PO Box 1384
La Grande, OR 97850

Copies Plus
1904 Adams Ave,
La Grande, OR 97850
(541) 663-0725
copiespluslg@yahoo.com

DATED: February 22, 2023

/s/ Alisha Till
Alisha Till
Paralegal

**BEFORE THE PUBLIC UTILITY COMMISSION
OF OREGON**

DOCKET PCN 5

In the Matter of	)
	)
IDAHO POWER COMPANY'S	)
	)
PETITION FOR A CERTIFICATE OF PUBLIC CONVENIENCE AND NECESSITY.	)
	)
	)
	)

IDAHO POWER COMPANY

REPLY TESTIMONY

OF

DR. JEFFREY M. ELLENBOGEN

REDACTED

FEBRUARY 22, 2023

Table of Contents

Exhibit List

- Exhibit 1201 - Curriculum Vitae of Dr. Jeffrey Ellenbogen
- Exhibit 1202 - Buxton, O. M. et al., Sleep Disruption Due to Hospital Noises: A Prospective Evaluation (2012)
- Exhibit 1203 - McKinney, S. et al., Covert Waking Brain Activity Reveals Instantaneous Sleep Depth (2011)
- Exhibit 1204 - Dang-Vu, T. T. et al., Spontaneous Brain Rhythms Predict Sleep Stability in the Face of Noise (2010)
- Exhibit 1205 - Ellenbogen, J. M. et al., Wind Turbine Health Impact Study: Report of Independent Expert Panel (2012)
- Exhibit 1206 - Vér, I. L. & Beranek, L. L., Noise and Vibration Control Engineering: Principles and Applications (2006)
- Exhibit 1207 - Michaud, D. S. et al., Self-Reported and Measured Stress Related Responses Associated with Exposure to Wind Turbine Noise (2016)
- Exhibit 1208 - Michaud, D. S. et al., Exposure to Wind Turbine Noise: Perceptual Responses and Reported Health Effects (2016)
- Exhibit 1209 - Michaud, D. S. et al., Effects of Wind Turbine Noise on Self-Reported and Objective Measures of Sleep (2016)
- Exhibit 1210 - U.S. Army Public Health Command, Readiness Through Hearing Loss Prevention (July 2014)
- Exhibit 1211 - Riemann, D. et al., Insomnia Disorder: State of the Science and Challenges for the Future (2022)
- Exhibit 1212 - Bauer, C. A., Tinnitus (2018)
- Exhibit 1213 - Dinces, E. A., Etiology and Diagnosis of Tinnitus (2023)
- Exhibit 1214 - WHO, Environmental Noise Guidelines for the European Region (2018)
- Exhibit 1215 - Walkup, J. T. et al., Cognitive Behavioral Therapy, Sertraline, or a Combination in Childhood Anxiety (2008)
- Exhibit 1216 **(Confidential)** - Greg Larkin's Response to Idaho Power Company's First Set of Data Requests (Feb. 8, 2023)
- Exhibit 1217 **(Confidential)** - [redacted]

- Exhibit 1218 **(Confidential)** - [redacted]

- Exhibit 1219 - WHO, Night Noise Guidelines for Europe (2009)

- Exhibit 1220 - WHO, Guidelines for Community Noise (1999)

I. INTRODUCTION

Q. Please state your name, your place of employment, and your position.

A. My name is Dr. Jeffrey M. Ellenbogen and I am a physician, scientist and teacher in the state of Maryland. I am the Director of The Sound Sleep Project and President of Ellenbogen Scientific, LLC.

Q. Please describe your educational experience.

A. I received a Bachelor of Arts ("BA") from the University of Michigan, a Master of Medical Sciences degree ("MMSc") from Harvard Medical School, and a Medical Doctor degree ("MD") from Tufts University. After completing medical school, I went to the University of Pennsylvania where I completed an internship in medicine, residency in neurology, and fellowship in clinical electrophysiology. I then completed a two-year post-doctoral fellowship in Sleep, Circadian, and Respiratory Neurobiology at Harvard Medical School. A comprehensive list of my training, experience, and education is included in my resume, which is attached as an exhibit to this testimony.[1]

Q. Please describe your clinical, academic, and leadership experience as a physician.

A. I am a licensed and practicing physician and have been for more than 20 years. My clinical work experience includes practice as a neurologist and sleep-medicine specialist at the following hospitals: Massachusetts General Hospital ("MGH"), Johns Hopkins Hospital, and Walter Reed National Military Medical Center ("WRNMMC"). I was Division Chief and Lab Director of Sleep Medicine at MGH. I was an Assistant Professor of Neurology at Harvard Medical School and at Johns Hopkins University. Then, I was an Associate Professor of Neurology and of Military & Emergency Medicine, and Vice Chair of Neurology at the Uniformed Services University. At WRNMMC, I saw inpatients with neurological emergencies, and outpatients in three areas: Neurology Department;

[1] Idaho Power/1201 (Curriculum Vitae of Dr. Jeffrey Ellenbogen).

Otolaryngology Department (i.e., ENT: ear, nose, and throat); and the National Intrepid Center of Excellence ("NICoE"), which included work on traumatic brain injury, other neurological diseases, and on sleep medicine.

Q. Please discuss your specific background and expertise regarding noise impacts on health.

A. When I was Director of the Sleep Division at Harvard's MGH, I ran a sleep-research acoustical laboratory. The purpose of this lab was to help people suffering from noise-induced sleep loss.[2] I also spent several years working with the acoustics engineering firm, Bose Corporation.

Q. One of the parties in this matter has raised concerns regarding the impact of noise on his insomnia and tinnitus. Do you have specific education, training, or experience to address these topics as a subject-matter expert?

A. Yes. Regarding insomnia, I am a fellowship-trained, board-certified specialist in sleep medicine, and have been recognized as a Fellow of the American Academy of Sleep Medicine. Regarding tinnitus, I have worked directly with patients with tinnitus, mostly active-duty members of the military returning from combat. I have also seen patients with problems of the inner ear (including tinnitus and vertigo) as an outpatient doctor. Both of these experiences were at the WRNMMC.

As a neurologist and sleep-medicine specialist for the past 15 years, I frequently treat insomnia. Most recently, at the NICoE (in Bethesda, Maryland), it was my responsibility to join a multi-disciplinary team whose goal was to provide medical and related services to active-duty service members returning to the United States from combat. Most of these service members had tinnitus and insomnia. I participated in the

---

[2] *See* Idaho Power/1202 (Buxton, O. M. et al., Sleep Disruption Due to Hospital Noises: A Prospective Evaluation (2012)); Idaho Power/1203 (McKinney, S. et al., Covert Waking Brain Activity Reveals Instantaneous Sleep Depth (2011)); Idaho Power/1204 (Dang-Vu, T. T. et al., Spontaneous Brain Rhythms Predict Sleep Stability in the Face of Noise (2010)).

care of both. During this time, I also saw outpatients at the WRNMMC. This included outpatients in the Otolaryngology Clinic who came for treatment from our multidisciplinary team dealing with inner-ear problems that included vertigo, dizziness, tinnitus, and hearing loss.

Q. Do you have any industry experience related to noise and human health?

A. Yes. I worked as a scientific consultant for the consumer-related, acoustical, electrical-engineering company, Bose Corporation, for approximately three years. I have also provided expert testimony concerning topics such as noise-induced sleep loss, including for the wind energy company Invenergy.

Q. Do you have experience with municipal organizations related to noise and human health?

A. Yes. In 2011, the Department of Public Health and Department of Environmental Protection of the Commonwealth of Massachusetts appointed me to a panel of professionals (the "Panel") to perform an independent evaluation of the scientific and medical literature regarding wind turbines (including noise generated by them), and their potential impact on human health, as well as to solicit information from the public to hear about any potential issues not already reflected in the literature. The Panel's findings and conclusions were published in 2012.[3]

Q. Do you have experience with architectural acoustics and/or noise mitigation?

A. Yes. I helped develop two sleep laboratories for the purpose of studying sleep and noise. My role included insights concerning how to minimize noise intrusion for the purpose of optimizing sleep. One laboratory was at MGH, and the other at Walter Reed Army Institute of Research.

[3] Idaho Power/1205 (Ellenbogen, J. M. et al., Wind Turbine Health Impact Study: Report of Independent Expert Panel (2012)).

Q. In developing your testimony, have you relied on the testimony of any other Idaho Power witness in this case?

A. Yes. I relied on the noise modeling and weather data included in the Reply Testimony of Mark Bastasch.[4]

Q. What is the purpose of your testimony?

A. I was retained by representatives of Idaho Power to evaluate the testimony of Greg Larkin regarding potential health-related consequences of living near the Boardman to Hemingway Transmission Line Project ("B2H" or the "Project"), and to evaluate and to provide an expert opinion concerning Mr. Larkin's specific concerns regarding the impact of corona noise from B2H on his health.

II. GENERAL BACKGROUND ON NOISE AND HUMAN HEALTH

Q. What are the topics you will be addressing in this section of your testimony?

A. First, I will address noise characteristics and how they may be perceived by the hearer, otherwise referred to in this testimony as the "receiver" or "receptor." Second, I will discuss the levels and types of noises that can have impacts on health. Third, I will discuss noise mitigation strategies. And fourth, given that Mr. Larkin has raised his own insomnia and tinnitus as concerns, I will discuss how these conditions might be impacted by corona noise.

A. Noise Characteristics and Perception

Q. Please provide a general discussion regarding noise characteristics and human perception.

A. When considering how a particular sound might be perceived by a receptor, three variables are among the ones most important to note: steady-state vs. impulse; broadband vs. narrow band; and high amplitude vs. low amplitude.

[4] *See generally* Idaho Power/1100 (Feb. 21, 2023).

- ***Steady-state vs. impulse noise.*** Noise is generally characterized as steady-state (i.e., continuous) or impulse (i.e., comes and goes, abruptly). An example of a source of steady-state noise is a bedroom fan. An example of a source of impulse noise is the discharging of a firearm.

  Our brains are primarily change detectors. So steady-state noises are less likely to be detected than impulse noise, particularly when they contain a wide range of frequencies (i.e., broadband, see below). In fact, steady-state noises are often introduced into quiet spaces to help people not to notice annoying or unwanted noises, including impulse noises around or below the energy of the introduced noise. This is referred to as "masking" in my testimony below.

  Neither the crackling nor the hum-like features of corona noise are considered impulse noises.

- ***Broadband vs. narrow band noise.*** The frequency composition of a noise can be broadband (i.e., including many pitches) or narrow band (e.g., as narrow as a single pitch). Frequencies are reported in cycles per second, called Hertz ("Hz"). Our brains tend to find single pitches or narrow bands (i.e., just a few pitches) to be more noticeable than broadband. Examples of broadband include "white" or "brown" noise. It is also important to note that the human ear is not infinitely capable of hearing all the pitches in the physical universe. In fact, just like our eyes cannot see infrared or ultraviolet light, our ears have great difficulty hearing frequencies lower than about 20 Hz or higher than about 20,000 Hz.

  The crackling feature of corona noise is not considered a narrowband noise. While the hum is not technically tonal, it can have a narrow spectrum.

- ***High amplitude vs. low amplitude noise.*** For any given noise, it can be high or low energy, what we casually refer to as volume, which is the experience by a person of a noise's sound pressure level ("SPL").[5] This measure is often reported in some form of decibel ("dB"), typically A-weighted decibel ("dBA"), to account for the specifics of human hearing ranges. If you play a single piano key softly, the sound from the piano has a low SPL. Play the exact same key harder and the noise from the piano will have more energy—a higher SPL. That is, if you are playing a single piano key harder, the noise from the piano has the same frequency as the sound from the piano when you play the same key softly, but the noise has a higher energy or SPL. The less energetic a noise is (i.e., a lower SPL), the less likely a person will perceive that noise. In fact, there are known minimum thresholds beyond which our ear cannot hear at all. Furthermore, people with hearing loss require a higher energy or high SPL sound in order to perceive the sound.

The crackling and hum-like features of corona noise are of low amplitude in fair weather and rise to higher levels in foul weather. With respect to the noise sensitive receptors ("NSRs") in this case, and the data presented in Mr. Bastasch's testimony, under foul weather conditions, for the average person, the noise might be audible depending on the ambient background from the environment (i.e., the higher the ambient background sound level, for example from foul weather conditions, the less likely an individual will hear the corona noise) and also depending on whether the individual is indoors or outdoors (i.e., if an individual is indoors rather than outdoors, the individual is less likely to hear corona noise).

B. Noise and Human Health

Q. Are you aware of any studies on the health impacts of noise, and in particular of the impacts of corona noise?

[5] *See generally* Idaho Power/1206 (Vér, I. L. & Beranek, L. L., Noise and Vibration Control Engineering: Principles and Applications (2006)) (provides precise definitions of acoustical-engineering terms and concepts, including power, pressure, intensity, tonality, etc., as referenced in my testimony).

A. I am unaware of any health studies that have focused specifically on corona noise. However, of particular relevance to this case is a study that was published by Health Canada—the department of the Government of Canada responsible for national health policy—regarding wind turbine noise. This study provides the largest, and most rigorous and objective set of scientific data on the general issue of wind turbine noise (hereinafter, referred to in this testimony as the "Health Canada Study"). Data analysis and findings from the Health Canada Study became publicly available in several publications in 2016, all in well-regarded, peer-reviewed, clinically minded, scientific journals.[6]

While corona noise and wind turbine noise are not identical, they are similar enough that the findings of the Health Canada Study are worth considering here.

The purpose of the Health Canada Study was to rigorously examine a large population of people living near wind turbines in order to establish whether human exposure to noise from wind turbines leads to negative health-related consequences. Topics addressed in the Health Canada Study included sleep, stress, cardiovascular disease, and a number of other health-related issues, including headaches and tinnitus. The 2013 Health Canada Study took place among people living in either Prince Edward Island or southwestern Ontario.[7] These locations were chosen because of their relative similarities among people, similarities of the topography, and the wind turbines which were present and operating.[8]

This large, cross-sectional, epidemiological study examined well over 1,200

[6] *See* Idaho Power/1207 (Michaud, D. S. et al., Self-Reported and Measured Stress Related Responses Associated with Exposure to Wind Turbine Noise (2016)); Idaho Power/1208 (Michaud, D. S. et al., Exposure to Wind Turbine Noise: Perceptual Responses and Reported Health Effects (2016)); Idaho Power/1209 (Michaud, D. S. et al., Effects of Wind Turbine Noise on Self-Reported and Objective Measures of Sleep (2016)).

[7] *See, e.g.*, Idaho Power/1208, Ellenbogen/3 (Michaud, D. S. et al., Exposure to Wind Turbine Noise: Perceptual Responses and Reported Health Effects (2016)).

[8] *See, e.g.*, Idaho Power/1208, Ellenbogen/3 (Michaud, D. S. et al., Exposure to Wind Turbine Noise: Perceptual Responses and Reported Health Effects (2016)).

people living near wind turbines.[9] Participants were asked a range of health-related questions (subjective measures) and were physically examined for a range of health-related metrics (objective measures).[10] Specifically, the Health Canada Study was an "exposure-response" design.[11] Pursuant to this design method, examiners look to see if any health problems had more of a causal relationship to sound levels from wind turbines than others. Health problems are a part of life and will be discovered in any large population. The objective of the Health Canada Study was to see if any health problems resulted from or were associated with wind turbine noise. The Health Canada Study assumed that there was a dose-response relationship between wind turbine noise and the health condition.[12] Simply put, the Health Canada Study assumed that if wind turbine noise caused a health problem, that health problem should be more and more severe as the level of the noise got higher and higher.

The participants in the Health Canada Study were exposed to a range of noise from wind turbines, from less than 25 dBA up to 46 dBA.[13] A control group of persons being exposed to less than 25 dBA having similar demographics to the remaining participants in the study was utilized. Sound levels were calculated based on the location of the dwelling.[14] Health Canada's Scientific Advisory Board reviewed the design of the study, as did experts from the World Health Organization ("WHO"). The study design was also subjected to a 60-day public consultation, and review by the Research Ethics Board.

---

[9] *See, e.g.*, Idaho Power/1209, Ellenbogen/2 (Michaud, D. S. et al., Effects of Wind Turbine Noise on Self-Reported and Objective Measures of Sleep (2016)).

[10] *See, e.g.*, Idaho Power/1209, Ellenbogen/3-4 (Michaud, D. S. et al., Effects of Wind Turbine Noise on Self-Reported and Objective Measures of Sleep (2016)).

[11] *See, e.g.*, Idaho Power/1209, Ellenbogen/7 (Michaud, D. S. et al., Effects of Wind Turbine Noise on Self-Reported and Objective Measures of Sleep (2016)).

[12] *See, e.g.*, Idaho Power/1209, Ellenbogen/7 (Michaud, D. S. et al., Effects of Wind Turbine Noise on Self-Reported and Objective Measures of Sleep (2016)).

[13] *See, e.g.*, Idaho Power/1209, Ellenbogen/5-6 (Michaud, D. S. et al., Effects of Wind Turbine Noise on Self-Reported and Objective Measures of Sleep (2016)).

[14] *See, e.g.*, Idaho Power/1209, Ellenbogen/2-3 (Michaud, D. S. et al., Effects of Wind Turbine Noise on Self-Reported and Objective Measures of Sleep (2016)).

The subjective measures considered in the Health Canada Study included questions about a wide range of conditions, including migraines, tinnitus, dizziness, sleep disturbance, sleep disorders, quality of life, and perceived stress.[15] The objective measures examined in the Health Canada Study included stress (via hair cortisol measures); cardiovascular outcomes (heart rate, blood pressure); and sleep.[16]

None of the subjective measures nor objective measures of human health were found to be related to noise levels from wind turbines, demonstrating no relationship between noise from wind turbines and any adverse health impacts.[17] With respect to Mr. Larkin's concerns, it is important to point out that wind turbine noises up to 46 dBA did not impact any health conditions, including tinnitus, stress (objectively measured or subjectively reported), blood pressure (objectively measured), and sleep (objectively measured or subjectively reported). The highest modeled noise level at Mr. Larkin's property during foul weather conditions is 43 dBA and this assumes a conservative late-night ambient background of 31 dBA—a background ambient value that was calculated for periods of low winds (less than 10 mph) and without foul weather conditions.[18]

Q. In his testimony, Mr. Larkin has raised a concern that corona noise from B2H could cause hearing loss.[19] Are there known thresholds for noise induced hearing loss?

---

[15] *See, e.g.*, Idaho Power/1207, Ellenbogen/7 (Michaud, D. S. et al., Self-Reported and Measured Stress Related Responses Associated with Exposure to Wind Turbine Noise (2016)).

[16] *See, e.g.*, Idaho Power/1207, Ellenbogen/7 (Michaud, D. S. et al., Self-Reported and Measured Stress Related Responses Associated with Exposure to Wind Turbine Noise (2016)).

[17] *See, e.g.*, Idaho Power/1207, Ellenbogen/11-12 (Michaud, D. S. et al., Self-Reported and Measured Stress Related Responses Associated with Exposure to Wind Turbine Noise (2016)).

[18] Mr. Larkin's property is NSR 125. Idaho Power's Supplement to Petition for CPCN, Attachment 1 (Final Order, Attachment X-4, Revised Tabulated Summary of Acoustic Modeling Results by Receptor Location) at 10557 of 10603 (Oct. 7, 2022) [hereinafter, "Final Order, Attachment X-4"].

[19] Greg Larkin's Amended Opening Testimony and Exhibits (Greg Larkin/100, Larkin/20) (Feb. 1, 2023) ("On Page 28 of this document it indicates that there are three broad categories of health effects from exposure to noise. a. Subjective effects such as annoyance which can mean a significant degradation in the quality of life; b. Sleep, communication and concentration impacts; c. physiological effects such as anxiety, hearing loss and tinnitus. For individuals who already have underlying health issues, the addition of the corona noise will clearly exacerbate existing hearing, tinnitus, sleep and anxiety issues.").

A. Yes, depending on the level of the noise, and whether or not it is steady-state or impulse, noise can cause hearing loss. In fact, noise-related hearing loss is the most common health-related consequence of noise exposure. With respect to noise levels, the United States Department of Labor, Occupational Safety and Health Administration ("OSHA") has longstanding guidelines that allow up to eight hours of steady-state noise exposure at 90 dBA (see Table 1 below).

Table 1. Permissible Noise Exposure[20]

Duration Per Day (Hours)	Sound Level Slow Response (dBA)
8	90
6	92
4	95
3	97
2	100
1½	102
1	105
½	110
¼ or less	115

When daily noise exposure is composed of two or more periods of noise exposure of different levels, their combined effect should be considered, rather than the individual effect of each. If the sum of the following fractions: *C1/T1* + *C2/T2Cn/Tn* exceeds unity, then, the mixed exposure should be considered to exceed the limit value. *Cn* indicates the total time of exposure at a specified noise level, and *Tn* indicates the total time of exposure permitted at that level.

Exposure to impulsive or impact noise should not exceed 140 dB peak sound pressure level.

It is further well understood that impulse noises of very high energy (i.e., higher than 140 dB peak sound pressure or "dBP") can lead to hearing loss as well (see Table 1 above and Figure 1 below).

[20] 29 CFR 1910.95(b) (Table G-16 – Permissible Noise Exposure).

1 **Figure 1. Comparison of Continuous Noise and Impulse Noise**[21]

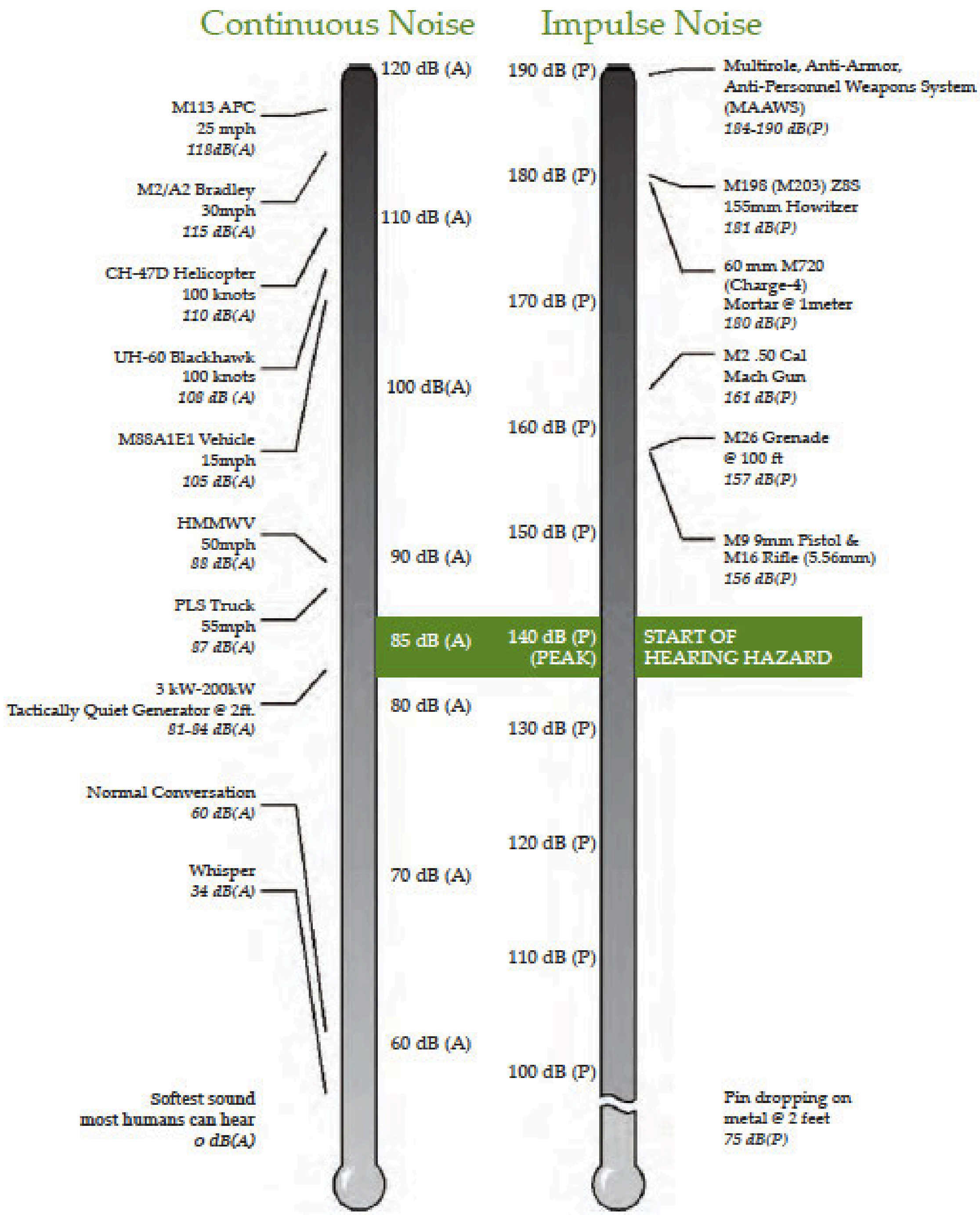

[21] Idaho Power/1210, Ellenbogen/3 (U.S. Army Public Health Command, Readiness Through Hearing Loss Prevention (July 2014)).

It should be noted that, based on the sound monitoring performed by Idaho Power's expert acoustical engineers as described in the Reply Testimony of Mr. Bastasch, the B2H transmission line noise as it relates to the NSRs in this case is nowhere near the threshold of noise necessary to cause or worsen hearing loss.[22]

C. Mitigation for Noise Impacts

Q. What about sound mitigation—is there anything to do to make the impact of corona noise less of a problem for nearby residents?

A. Yes. There are many things that can be done to reduce the impact of a noise on a person. Doing so is often referred to as "noise mitigation."

Generally speaking, noise mitigation leverages psychological and physical principles under a couple of different disciplines within acoustics, including psychoacoustics (i.e., the discipline addressing how people perceive sound) and architectural acoustics (i.e., the discipline addressing how sound is handled in and around spaces, including everything from concert halls to bedrooms).

The item that makes noise is often referred to as the "noise source." And the item that hears the noise is referred to as the noise "receiver" or "receptor." A source of noise can be plucking the string of a guitar or revving the engine of a car. The receptor can be many things, including a studio microphone or a human ear. For the purpose of this discussion, a receiver will be a person in their bedroom.

Broadly speaking, there are three categories of how one might mitigate noise. These categories address: (1) the noise source (i.e., the item that makes the noise); (2) the path the noise takes through the atmosphere; and (3) the receiver (e.g., the listener in a home). Manipulating any of these variables, sometimes a combination of these variables, can reduce the impact of noise on human health, safety, and welfare. Moreover,

[22] Final Order, Attachment X-4 at 10553-58 of 10603.

perception of a noise might be masked by similar or higher ambient background sound levels.

- ***Source.*** It is often optimal to deal with a noise by resolving it at the source. Providing lubrication to a squeaking wheel, for example, might help reduce the friction that causes a noise. In other words, addressing the source of the noise might make the noise reduced or even eliminated.
- ***Path.*** For noise to travel from the source to the receiver, the vibration energy needs to be transmitted from the source to the receiver. This is achieved by energy that sequentially vibrates molecules in the atmosphere along that pathway. Because there are no molecules in space, this is why noise does not travel in space. Conversely, because liquid water is more densely packed with molecules compared to the air in our atmosphere, noise travels faster in water than in air. But there is a catch to this movement of vibration energy. It is imperfectly efficient. More specifically, along the way of the path, there are energy losses due to friction as each molecule passes its energy to the next. The further the noise has to travel, the more and more friction it encounters, making its energy less and less along the way. We have all intuitively experienced this phenomenon. The further we are from a noise, the less we hear it.

As a result of this loss of energy due to friction (and other physical principles), setting the noise source further away from the receiver will reduce the level of the sound at the receiver. Also, placing barriers between the noise source and the receiver can not only cause a great deal of friction and energy loss, but can also cause the energy to be reflected and travel in a different direction than the receiver. The result of a barrier—which can be trees, a wall, or a window—is that the SPL of the noise is reduced by the time it reaches the receiver, if it reaches the receiver at all. And if the noise reaches the receiver at a similar SPL to the ambient background sound level or less, then the receiver's perception of the noise will likely be reduced, or the receiver might not notice the noise at all.

Earplugs are another example of attempting to obstruct the path of a noise getting to the receiver's eardrum from the noise source.

- ***Receiver or receptor.*** Once a noise has been produced and has traveled all the way to a human ear, whatever frequency and energy that remains will cause the eardrum to transmit that energy through the acoustic nerve and to the auditory portion of the brain where it is then brought to the attention of the person via attention mechanisms in the brain. That is, if the noise is made of a frequency too high or too low for human perception (below 20 Hz or above 20,000 Hz), or if the noise is of such a low level that it is whisper-quiet, the noise does not generate a signal from the ear to the brain such that it is perceivable.
- ***Masking.*** Even if a noise is able to generate a signal that is transmitted to the brain, there are a number of different conditions and mitigation measures that would reduce the receiver's perception of the noise, or even allow the noise to go unnoticed by the receiver. First, as discussed above, if the noise reaches the receiver at a similar SPL to the ambient background sound level or less, then the receiver's perception of the noise will likely be reduced, or the receiver might not notice the noise at all. For example, if a broadband sound is of modest SPL (like a breeze through trees or rain at night), that broadband ambient background sound makes it difficult to hear a novel noise of similar or lesser level. When one deliberately introduces a background sound, with the goal of not hearing unwanted noise, that process is referred to as "sound masking." Sound masking can be done with a wearable device, like a programmable hearing aid or earbuds with a feed of music or noises. Sound masking can also be achieved without contact to the body, such as turning on a fan in a bedroom. A fan running in the bedroom at a modest SPL would produce a steady-

state, broadband noise and a mild energy state that will make it difficult to perceive other noises at or below the SPL of the fan.

- ***Other.*** If a novel noise is not reduced or eliminated at the noise source or path, and the noise reaches and is perceived by the receiver, then another important variable to consider beyond sound masking is to reduce the receiver's attention to the noise and vigilance of it. Any noise that produces a fear response, for instance, will be attended to with vigilance. A fear response to a novel noise is adaptive and helpful if the noise source is threatening. Conversely, a fear response is maladaptive if the noise source is not threatening. Importantly, in his testimony, Mr. Larkin has raised the concern that noise can impact anxiety.[23] Disorders such as anxiety [redacted] might lead to distortions of significance and threat level, triggering the receiver's fear response and resulting in maladaptive hyper-attention to a non-threatening noise. Therefore, it is important to treat disorders that may trigger a maladaptive fear response and cause unnecessary stress to the receiver. To prevent or reduce a maladaptive fear response, it is equally important for the receiver to be adequately informed of what noise constitutes a threat, and what does not. This information might come in the form of a broader cognitive-behavioral therapy ("CBT") strategy, which can be therapeutic for people with anxiety [redacted].

[23] Greg Larkin/100, Larkin/20 (Feb. 1, 2023) ("For individuals who already have underlying health issues, the addition of the corona noise will clearly exacerbate existing hearing, tinnitus, sleep and anxiety issues.").

D. Insomnia and Tinnitus

Q. What is insomnia, and how might it relate to noise?

A. Insomnia is the inability to fall asleep or stay asleep, or both, and an overall concern regarding insomnia is the sleep disorder's impact on daily life. In this response, I will first address the topic of insomnia, in general, including terminology and diagnosis. I will then relate insomnia to noise.

To the general public, the term insomnia is sometimes used with a relaxed definition to mean anything that impairs good sleep. To a medical provider, however, the term "insomnia" does not merely mean the inability to sleep. Instead, the field of sleep medicine has criteria that forge the definition of chronic insomnia as a disorder. The six criteria below defining insomnia are from the International Classification of Sleep Disorders, ICSD-3,[24] and similar criteria have been adapted by the psychiatry field in the Diagnostic and Statistical Manual of Mental Disorders, DSM-5-TR.[25]

A. The patient reports one or more of the following:

1. Difficulty initiating sleep.

2. Difficulty maintaining sleep.

3. Waking up earlier than desired.

4. Resistance to going to bed on appropriate schedule.

5. Difficulty sleeping without parent or caregiver intervention.

B. The patient reports one or more of the following related to the night-time sleep difficulty:

1. Fatigue/malaise.

2. Attention, concentration or memory impairment.

[24] American Academy of Sleep Medicine, International Classification of Sleep Disorders (3d ed. 2014)).

[25] American Psychiatric Association Publishing, Diagnostic and Statistical Manual of Mental Disorders: DSM-5-TR (5th ed. 2022).

3. Impaired social, family, occupational or academic performance.

4. Mood disturbance/irritability.

5. Daytime sleepiness.

6. Behavioral problems (e.g. hyperactivity, impulsivity, aggression).

7. Reduced motivation/energy/initiative.

8. Proneness for errors/accidents.

9. Concerns about or dissatisfaction with sleep.

C. The reported sleep/wake complaints cannot be explained purely by inadequate opportunity (i.e. enough time is allotted for sleep) or inadequate circumstances (i.e. the environment is safe, dark, quiet and comfortable) for sleep.

D. The sleep disturbance and associated daytime symptoms occur at least three times per week.

E. The sleep disturbance and associated daytime symptoms have been present for at least 3 months.

F. The sleep/wake difficulty is not better explained by another sleep disorder.

For purposes of our discussion—in considering whether the noise from the transmission line causes or worsens insomnia—it is important to highlight two components of this clinical definition of insomnia. First is Criterion C, which requires adequate opportunity and circumstances, such as quiet environments to sleep. In other words, if I were unable to fall asleep at night due to a very loud noise from a neighbor, I would not have a diagnosis of insomnia; rather, I would have inadequate circumstances conducive for sleep. Such circumstances still result in lost sleep and are still a problem, but do not constitute insomnia. The diagnosis of insomnia requires difficulty initiating or maintaining sleep under reasonable circumstances, such as quiet environments. This distinction is important when discussing an individual's concerns regarding their inability to sleep, as inability to initiate or maintain sleep might be due to either the circumstance (e.g., noise) or the disorder (i.e., insomnia)—knowing which is the real cause of the patient's inability to sleep will optimize problem solving.

The second component of this clinical definition of insomnia that is worth noting is Criterion F, which requires that the patient's inability to initiate or maintain sleep is not best explained by another factor, such as a different medical condition. For example, when a person has [redacted] pain, that individual can have difficulty initiating or maintaining sleep. The signal of pain to the brain is an alerting signal, like a flashing light or loud noise. While this person can be said to lack adequate sleep due to pain, they would not be given the separate diagnosis of insomnia as well. Efforts to treat the pain would be more suitable than efforts to generically treat insomnia. A particularly problematic treatment plan would be to exclusively address the alleged insomnia without consideration of a patient's pain. [redacted]

Separately, when a person has insomnia, they have, by definition, difficulty initiating or maintaining sleep, or both. In those situations, people will often become frustrated or anxious while awake. A patient is more likely to become frustrated or anxious under such circumstances if they already have a disorder, such as anxiety [redacted]. Furthermore, while lying in bed awake, an individual with insomnia might attribute their inability to initiate or maintain sleep to subtle sensory experiences. For example, a subtle sound at night like a dripping faucet. To a person with insomnia, this is often a mistaken attribution. The individual's insomnia is keeping them awake, not the noise from the dripping faucet. At least, that is the case initially. But then the patient with insomnia unintentionally conditions themselves to find the signal (dripping faucet, in this example) to be the cause of their insomnia. Hearing the faint dripping sound—a noise that might not disturb the average person—can create an anxious and awakening response in the patient with insomnia. In fact, this phenomenon is particularly robust when the person ***feels*** the signal is dangerous. And the interesting thing is that the signal does not need to be dangerous in reality; the signal just needs to be considered dangerous in the mind of the person having trouble sleeping. Threat responses of the mind are alerting and prevent sleep.

This concept of conditioning can perpetuate the symptoms of insomnia, and even make them worse. And while fixing the dripping faucet might help, the real problem is the patient's underlying insomnia and anxiety, and those disorders should be the primary focus of treatment. If the underlying insomnia and anxiety are not the primary focus of treatment, then even when the faucet is fixed, the person with insomnia will condition themselves to another stimulus they mistakenly attribute as the cause of their inability to sleep.

This approach to insomnia is commonly referred to as the "3P" model of insomnia: predisposing, precipitating, and perpetuating of insomnia symptoms.[26] Factors that predispose a patient to insomnia include, among other inherent health conditions, genetics. Precipitating factors, such as life events, initiate insomnia symptoms. Precipitating factors might specifically include a traumatic event, or an onset of a disorder, such as anxiety [redacted]. Perpetuating factors are conditions that maintain the

[26] *See, e.g.*, Idaho Power/1211, Ellenbogen/5-7 (Riemann, D. et al., Insomnia Disorder: State of the Science and Challenges for the Future (2022)).

patient's insomnia. For example, these factors can include fixed and false beliefs that produce anxiety, or an alerting response. If, as stated by Mr. Larkin in his testimony,[27] an individual believes that the very faint sound of a transmission line will render their house uninhabitable by causing a serious health condition, such as high blood pressure, then the faint sound of a transmission line might impair sleep, even if it would not do so for the average person.

To be sure, noise can and does awaken people from sleep—particularly people who are "light sleepers," meaning they tend to have difficulty achieving deep stages of sleep that prevent sensory awareness. This can become a problem if noises are of high amplitude and significantly above ambient background sound levels, and if these noises have certain characteristics such as sudden rise and fall (i.e., impulse noise), tonality (i.e., narrow bandwidth), or other alerting acoustical properties.

In some circumstances, noise can be a major contributor to a person's inability to sleep. Noise-induced sleep loss can be an aggravating and important problem. This is rarely the case unless the noise has the features discussed above, namely, that it has an energy level well above ambient background sound levels, and has alerting features to it, such as impulse and narrow bandwidth. A smoke-detector siren, for example, has such features.

With respect to treatment of insomnia, one of the most effective forms of treatment available today is cognitive behavioral therapy for insomnia, CBT-I. This therapy has been demonstrated to be as or more effective than many current medications for insomnia, and so CBT-I is felt by many sleep doctors to be a first-line treatment for most people with insomnia.[28]

[27] Greg Larkin/100, Larkin/18-19 (Feb. 1, 2023).
[28] Idaho Power/1211, Ellenbogen/7-10 (Riemann, D. et al., Insomnia Disorder: State of the Science and Challenges for the Future (2022)).

Treatment of insomnia must include approaches to sleep that are healthful. These approaches include regular nighttime routines such as a disciplined sleep schedule; reduced electronics in bed; and other strategies collectively referred to as “sleep hygiene.” [redacted]

Q. What is tinnitus and how might it relate to noise?

A. Tinnitus is the perception of sound that has no external source.[29] There are many causes to tinnitus, but the most common-known cause is noise-induced hearing loss. It is no surprise, then, that the highest associated cause of tinnitus is occupational noise exposure at a very high SPL since such exposure is also one of the most common causes of noise-induced hearing loss. Tinnitus and hearing loss can result from impulse noise like the discharging of a firearm, or from sustained noise like large engines at close range for long periods of time. Other considerations besides noise exposure that cause tinnitus, however, include neurological diseases, infection, and medications that can either cause tinnitus or make it worse.[30]

While tinnitus affects approximately 50 million people in the United States, “the majority of people with tinnitus are minimally bothered by the sensation.”[31] [redacted]

[29] *See generally* Idaho Power/1212 (Bauer, C. A., Tinnitus (2018)).
[30] Idaho Power/1213, Ellenbogen/20-23 (Dinces, E. A., Etiology and Diagnosis of Tinnitus (2023)).
[31] Idaho Power/1212, Ellenbogen/3 (Bauer, C. A., Tinnitus (2018)).

[redacted] anxiety are among the two key variables that can make the experience of tinnitus worse. The mechanism of this worsening is unclear. One model points to these [redacted] disorders leading to inappropriate attention to the sensation, and excessive worry about its impact on health and well-being.

The medical management of tinnitus includes numerous treatment strategies, none of which are cures. The first is acoustic stimulation. By exposing the patient to noises below the threshold for causing noise-induced hearing loss, their ambient background sound levels are increased, and thus they are less apt to notice the tinnitus sensation. This can be as simple as turning on broadband masking noise, such as turning on a quiet fan in the room. Or, as discussed above, sound masking can be achieved through hearing devices in the ear, such as hearing aids that can be programmed to generate sound or more simply just amplify existing sounds in the room. Finally, mental health is essential in dealing with tinnitus. Accordingly, if the patient presents with [redacted] anxiety, then therapy for these disorders is necessary. Additionally, people with tinnitus often benefit from CBT [redacted].

III. B2H AND HEALTH IMPACTS

Q. Are you familiar with the Reply Testimony of Mark Bastasch—specifically those portions of his testimony where he describes corona noise and the results of Idaho Power's sound monitoring studies?

A. Yes, I am familiar with the Reply Testimony of Mr. Bastasch concerning the Project in which he discusses: (1) the characteristics of corona noise; (2) how corona noise is produced, and what conditions trigger corona noise; (3) how often corona noise occurs during foul weather events, both regionally and across the entire analysis area for the Project; (4) what the modeled noise levels in terms of dBA are at NSRs during fair and foul weather; and (5) what level of increases from ambient sound levels are expected at NSRs during foul weather.

Q. Please summarize the aspects of Mr. Bastasch's testimony that are salient to your opinions as to the potential of corona noise from B2H to impact the people who live near B2H.

A. There are many details in Mr. Bastasch's Reply Testimony that are worth consideration. With respect to health, there are a few notable things to consider.

The average ambient sound levels in the regions B2H crosses are remarkably low, which is reflected in the representative ambient sound levels used for many of the NSRs. From a non-medical perspective, I can appreciate the desire to maintain that low ambient background. In normal operations, during fair weather conditions, the corona noise from B2H is similarly of low sound-pressure levels for all NSRs. I understand that B2H's normal operations (i.e., operating at a voltage less than 550-kV) and fair-weather conditions to be occurring the majority of the time. During these fair-weather conditions and normal operations, I doubt corona noise will be heard at residences in the vicinity of this Project, and even if perceived faintly, corona noise from the Project does not pose any health effect.

During foul weather, the corona noise will be elevated and possibly be heard at NSRs. In these instances, the highest sound-pressure level that is expected to occur along the route when corona noise occurs (during foul weather conditions) is reported to be 46 dBA.[32] Despite this level of corona noise being potentially audible, this is a fairly quiet noise level and does not pose a health risk, as discussed elsewhere in my testimony.

As reported in Mr. Bastasch's testimony, foul weather events—which correlate to a potential for exceedance—are expected to occur 1.3 percent of the hours in a year

[32] This NSR is NSR-115. Final Order, Attachment X-4 at 10557 of 10603.

averaged across the entire Project area.[33] If looking at specific regions, foul weather events in the La Grande region are anticipated to occur 2.7 percent of the hours in the year, and this frequency is the highest out of all four regions.[34] If one then considers Idaho Power's sensitivity analysis focusing on late-night data when exceedances are most likely to occur because of the lower ambient background sound levels, the frequency of calendar days with one hour or more of foul weather during the late night is four percent for the entire Project area and seven percent for LaGrande (with the regional frequencies ranging between two and seven percent).[35] I have no specific medical opinion regarding the methods for predicting whether Oregon's ambient antidegradation standard is met or not. But it struck me that Idaho Power may be overestimating NSR exceedances of the ambient antidegradation standard based on the Company's overly conservative assumptions and inputs.[36] It is reasonable to expect that the volume of corona noise would increase during foul weather events. But I would also expect that the ambient background sound level would also increase during foul weather, and Idaho Power did not appear to account for elevated ambient background sound levels when considering whether an NSR is in exceedance or not.

Specifically, if I understood correctly, the ambient background sound levels were measured or calculated during quiet, calm, good-weather situations (i.e., optimal conditions).[37] However, I would not expect these ambient background sound levels to maintain those low numbers in foul-weather conditions. Wind, rain, and other natural features would be expected to reduce the gap between the actual ambient background sound level and modeled corona noise during foul weather. Such conditions, however,

[33] Idaho Power/1100, Bastasch/16-17 (Feb. 21, 2023).
[34] Idaho Power/1100, Bastasch/16-17 (Feb. 21, 2023).
[35] Idaho Power/1100, Bastasch/17-18 (Feb. 21, 2023).
[36] Idaho Power/1100, Bastasch/18-20 (Feb. 21, 2023).
[37] Idaho Power/1100, Bastasch/19 (Feb. 21, 2023).

might not be enough to create a masking sound sufficient to narrow the gap between ambient background sound level and modeled corona noise during foul weather, such that the difference would fall below the exceedance threshold for the ambient antidegradation standard. As such, corona noise might still be audible for some receptors.

Further still, on foul-weather nights when corona noise is expected to occur at its worst, I would anticipate residents to be indoors, with windows partly or fully closed. This process would substantially reduce noise-pressure levels of corona noise indoors, independent of the ambient background sound level outdoors. Specifically, in their 2018 report, the World Health Organization or WHO explained that “the differences between indoor and outdoor levels are usually estimated at around 10 dB for open, 15 dB for tilted or half-open and about 25 dB for closed windows.”[38]

Taken together—during most hours of the year, corona noise is faint and likely inaudible. During foul-weather conditions, the noise might be audible, and might exceed the ambient antidegradation standard, but even in these circumstances, corona noise for the Project is not at a level posing a health risk, even among the 41 NSRs that exceed the ambient antidegradation standard. While my opinion here is not linked to any specific amount of time of the year that the predicted exceedances take place, it is worth noting that the exceedances themselves are infrequent.

Q. In general, how can the corona noise from B2H be expected to impact someone with or without underlying conditions?

A. Given the predicted corona noise levels from B2H, the overly conservative ambient background sound levels, the assumption that people close their windows during foul weather (i.e., when corona noise is predicted to be at its worst), and that Idaho Power will mitigate noise impacts at NSRs with predicted exceedances, I expect that corona noise

[38] Idaho Power/1214, Ellenbogen/29 (WHO, Environmental Noise Guidelines for the European Region (2018)).

from the transmission line will have no impact on human health, even among those with underlying conditions. It might be possible for a person to hear the transmission line, in foul weather conditions, particularly those landowners anticipated to experience corona noise levels well above the ambient background sound levels. But with mitigation measures in place, even this perception can be substantially reduced.

Q. In general, how would corona noise be expected to impact someone with tinnitus? Please discuss the expected impact both indoors and outdoors.

A. I would not expect that corona noise would impact someone's tinnitus, neither favorably nor unfavorably. At the noise levels produced by B2H, even in worst-case scenario conditions, there is no reasonable concern that corona noise will provoke or worsen an individual's tinnitus.

Q. In general, how would corona noise be expected to impact someone with insomnia?

A. The expected noise from B2H in normal-operating, fair-weather conditions is well below the conservative ambient background sound levels for the NSRs.[39] As such, I expect that B2H will not be perceived at all during these conditions. Accordingly, it is my opinion that during fair weather, corona noise would not have any impact on sleep, even among those who are light sleepers.

Even in foul weather, it is still unlikely that corona noise would have any impact on sleep, even among those who are light sleepers, because predicted corona noise levels are not high. This is particularly true given that Idaho Power is required to provide mitigation in those cases where an exceedance of the ambient antidegradation standard is predicted.

However, for those individuals with insomnia, anxiety, [redacted] it is possible for a resident to learn or develop the false belief that corona noise is dangerous for their

[39] Final Order, Attachment X-4 at 10557-58 of 10603.

health, resulting in the potential worsening of their sleep, mood, or anxiety. In addition to mitigation strategies, there are a number of considerations here that I discuss below.

Q. How would you expect that corona noise would impact someone with [redacted] stress, or anxiety?

A. As a general rule, the impact of noise on people with stress, anxiety, [redacted] is highly specific to the person and to the underlying cause of the stress, anxiety, [redacted] As with insomnia, discussed above, people who have anxiety can condition themselves to a non-threatening stimulus, believing it is, in fact, threatening.

The very nature of anxiety as a disorder is that a person with anxiety is prone to have exaggerated responses, even to items that pose no threat whatsoever. As such, it is possible for someone with anxiety to become more anxious, merely at the perception of corona noise, even if the noise is faint as a whisper—or, even if not perceived at all. The mere thought of a threat to personal safety—however inaccurate—is enough to provoke a worsening anxious response.

As a general rule, there are several, non-exclusive approaches to a person with anxiety who is having anxious thoughts, anxious feelings, or anxious responses to a stimulus that is not actually a threat, such as corona noise from the B2H transmission line. In all situations, the starting point of treatment is for the provider to have compassion for the anxious person. This person inhabits a world even more threatening than is warranted, and that is challenging for their daily living. This distinguishes anxious thoughts we all have, particularly from threatening stimuli. For someone with an anxiety disorder, the response is exaggerated, sometimes irrational.

Beyond compassion, the next most common step for a provider is to take effort to educate the patient about the non-threat. In short, a provider should educate the individual such that they are able to become aware of their automatic thoughts, unrealistic concerns, or unsubstantiated worries. A provider should further provide the patient with a mental process that helps them to overcome these anxious responses to non-threatening stimuli. Collectively, this and related processes are referred to as CBT.

CBT has been demonstrated to be effective for the treatment of anxiety, as have some anxiolytic medications, and the combination of the two (CBT plus medication) appears to be most potent.[40] The decision concerning which of these treatments—or combination of treatments—is most effective for any individual should be tailored to the patient. If a patient were to focus on pharmacological therapy for anxiety, it is important that they work with a healthcare provider who is familiar with which medications are effective for anxiety, at what dose, and how to deal with potential side effects.

It is essential that the patient work with a mental-health care provider to resolve these matters of anxiety. It might seem to an outsider that the person is having an anxious feeling about a particular stimulus; and that may be true. But while anxiety may manifest with something particular in the moment, removing the stimulus causing the anxiety will likely lead to the anxious person finding a new stimulus to be anxious about. Exceptions may exist when an anxious person has a particular phobia, like snakes. Therefore, generally speaking, it is most important to focus on treatment of the underlying anxiety disorder rather than exclusively focusing on the non-threatening stimulus.

IV. NOISE MITIGATION PLANS FOR B2H

Q. Have you reviewed the mitigation strategies that Idaho Power is required to undertake to reduce the impact of corona noise on persons living near B2H? How would you expect these strategies to affect the impact of corona noise on people living near the transmission line?

A. Yes, I have reviewed the mitigation strategies that Idaho Power is required to undertake to reduce the impact of corona noise on persons living near B2H. There are numerous

[40] *See generally* Idaho Power/1215 (Walkup, J. T. et al., Cognitive Behavioral Therapy, Sertraline, or a Combination in Childhood Anxiety (2008)).

mitigation strategies that are capable of addressing the corona noise produced by B2H such that there should be limited or no perception of the noise, and no risk to health or safety.

First, it should be re-emphasized that none of the residents (NSR property owners) are exposed to noise in excess of the Oregon Department of Environmental Quality's ("ODEQ") fixed Table 8 noise level standards of 55 dBA (L_{50}) daytime or 50 dBA (L_{50}) at night. The exceedances we are discussing that would require mitigation are exceedances of ODEQ's ambient antidegradation standard in which a generated noise may not be more than 10 dBA above ambient background sound levels. Idaho Power's predicted exceedances at certain NSRs are due to the ambient background sound levels for many of these NSRs being exceedingly quiet, making it more likely that a resident might hear a faint sound of the B2H transmission line even if it is under 50 dBA. In these situations, there appears to be a robust mitigation requirement of Idaho Power.

As I noted above, exceedances of ODEQ's ambient antidegradation standard will be infrequent. Moreover, the corona noise levels, as experienced in residents' homes, will be low. And, in all cases where exceedances are expected, Idaho Power is required to offer robust mitigation measures. The full mitigation process contained in Noise Control Conditions 1 and 2 can be read in detail in Idaho Power's site certificate for B2H.[41] I will briefly note a few key elements of the mitigation conditions that I found to be impressive, and that give me confidence that the mitigation process will lead to resolution of any nearby resident's concerns regarding health, safety, or welfare.

1. ***Idaho Power is required to be proactive in notifying landowners.*** Idaho Power will send notices to all landowners that might be at risk for an exceedance of the

[41] Idaho Power's Supplement to Petition for CPCN, Attachment 1 (Final Order, Attachment 1, Site Certificate) at 785-89 of 10603 (Oct. 7, 2022) (Noise Control Conditions 1 and 2) [hereinafter, "Final Order, Attachment 1"].

ambient antidegradation standard at their property (Attachment X-7). In other words, the process will not require the NSR property owner to reach out to Idaho Power. Rather, Idaho Power is required to initiate contact and inform residents of the potential noise exceedances.

2. ***Mitigation measures are robust.*** The requirements for noise mitigation include a primary intervention, alternative options, requirement of mutual agreement among the parties, and allowances for specific instances and circumstances of individual landowner preferences and relevant health conditions.

3. ***Mitigation measures are required to be in place prior to operation.*** Site-specific noise mitigation plans are required to be in effect prior to operation. So there is no window of time in which corona noise from B2H would be anticipated to impact the health, safety, or wellness of nearby residents without mitigation.

4. ***A system is in place to receive and respond to complaints if they arise.*** If a situation were to arise in which a landowner experiences a noise exceedance after B2H begins operating (which is not contemplated by the exception to and variance from ODEQ's ambient antidegradation standard under Noise Control Conditions 4 and 5),[42] or the landowner was not initially identified as an NSR with an exceedance, it is important that they have a means to voice that complaint, an expectation that their complaint will be responded to in a timely fashion, and that there is objective, agency oversight of the complaint process—especially if a disagreement should occur between the complainant and Idaho Power. Idaho Power is required to have this process in place, and to notify potentially impacted landowners within one mile of the Project's site boundary (Attachment X-7) of the

[42] Final Order, Attachment 1 at 812 of 10603 (Noise Control Conditions 4 and 5).

site certificate conditions prescribing this complaint process in a plain language summary.

V. RESPONSE TO MR. GREG LARKIN'S CONCERNS ABOUT HIS OWN HEALTH

Q. Mr. Greg Larkin has provided testimony regarding his concerns that corona noise generated by B2H would exacerbate his pre-existing health conditions and has provided medical records attesting to his health conditions. Are you familiar with Mr. Larkin's testimony and his medical records that he provided?

A. Yes. I have reviewed the medical records of Mr. Larkin that were made available to me through representatives of Idaho Power.[43] I also reviewed the portion of Mr. Larkin's testimony in which he raised general concerns and specific concerns that B2H may affect his health, and his related claims concerning the habitability of his home resulting from these potential health effects.[44]

Q. [redacted]

A. [redacted]

[43] [redacted]

[44] Greg Larkin/100, Larkin/16-21 (Feb. 1, 2023); Greg Larkin's Opening Testimony (Greg Larkin/100, Larkin/11-14) (Jan. 17, 2023).

[redacted]

Q. In Mr. Larkin's testimony, did he raise specific concerns about his health that might be affected by corona noise from B2H?

A. Yes. In Mr. Larkin's testimony, he raises concerns that both his insomnia and his tinnitus would be affected by noise from B2H: "My medical records document that my current medical conditions make me particularly sensitive to noise."[46]

[redacted]

[45] [redacted]

[46] Greg Larkin/100, Larkin/19 (Feb. 1, 2023).

[47] [redacted]

[48] [redacted]

Mr. Larkin continues in his testimony: "A lack of sleep can make my tinnitus worse, and I am to be 'cautious about additional exposure to loud noise, as additional damage to the inner ear may aggravate my tinnitus.'"[49]

I agree that additional damage to Mr. Larkin's inner ear might aggravate his tinnitus further. However, as I discussed above, the corona noise from the B2H transmission line at Mr. Larkin's home—or any of the 41 NSRs expected to experience an exceedance of the ambient antidegradation standard—are noises of orders of magnitude below any concern for noise-induced hearing loss.

As pointed out in Table 1 of this testimony, hearing loss is felt to be of potential concern with continuous exposures at or above 90 dBA (or 140 dBP).[50] None of the receptors for this project are predicted to be exposed to sound levels from corona noise above 46 dBA. Note that dB is not an arithmetic scale where it only takes twice as much noise to reach levels of concern in this example. Since dB is a logarithmic scale, the acoustical energy doubles every 3 dB. So, in this example, to reach 90 dBA from 46 dBA, that would require several thousand of these transmission lines to approach 90 dBA in order to be concerned regarding causes or contributions to noise-induced hearing damage to the inner ear.

Similar criteria to OSHA's guidelines have been implemented by the Environmental Protection Agency, National Institute of Occupational Safety and Health, and the United States Department of Defense branches.[51]

[redacted]

---

[49] Greg Larkin/100, Larkin/19 (Feb. 1, 2023).

[50] 29 CFR 1910.95(b) (Table G-16 – Permissible Noise Exposure); *see also* Idaho Power/1210, Ellenbogen/3 (U.S. Army Public Health Command, Readiness Through Hearing Loss Prevention (July 2014)).

[51] *See* Idaho Power/1206, Ellenbogen/444-60 (Vér, I. L. & Beranek, L. L., Noise and Vibration Control Engineering: Principles and Applications (2006)).

[redacted]

Q. Would you expect the corona noise from B2H to disrupt Mr. Larkin's sleep or worsen insomnia?

A. There are not absolute thresholds of noise by which one would certainly be awakened or not. However, there are certain key principles that I touched on above that are worth examining here in the case of B2H.

First, the character of a noise is most alerting when it is impulse noise, has frequency composition optimized for human hearing, and has substantial amplitude modulation. These characteristics can be found in emergency responder sirens, for example.

Second, it depends on the depth of the sleep, with increasing depth of sleep being more resistant to disruption.

Third, it is worth noting that even healthy sleepers awaken briefly numerous times during the night. If during these brief moments, a noise is perceived, and that noise is felt to be a threat to one's health, safety, or welfare, then the person is more likely to be alerted by the noise and therefore less likely to return to sleep. They may feel the noise awaken them, but in this scenario, it is their feeling about the noise that prevents them from

---

52 [redacted]

returning to sleep. This is adaptive when the noise is an actual threat, but maladaptive when the noise is not, [redacted]

In Mr. Larkin's circumstance, [redacted]

[53] [redacted]

[54] Greg Larkin/100, Larkin/19 (Feb. 1, 2023).

[55] Greg Larkin/100, Larkin/19-20 (Feb. 1, 2023) ("I also developed high blood pressure due to the stress that has occurred over the years with the threat of losing my home.").

[56] [redacted]

[redacted]

Mr. Larkin's [redacted] stress can be best appreciated by the following two statements from his testimony:

- "I also developed high blood pressure due to the stress that has occurred over the years with the threat of losing my home. I developed heart issues which necessitated me wearing a heart monitor for a period of time during the [Energy Facility Siting Council ("EFSC")] Contested Case Process."[59]
- "The corona noise predicted to occur at my home will make my residence uninhabitable for me."[60]

Mr. Larkin's concerns deserve compassion. Part of that compassion includes empathy, and another includes providing him accurate information—that the corona noise is not a risk to his health [redacted]

Q. [redacted]

[57] [redacted]

[58] [redacted]

[59] Greg Larkin/100, Larkin/19 (Feb. 1, 2023).

[60] Greg Larkin/100, Larkin/18 (Feb. 1, 2023).

A. [redacted]

Q. Would you expect that the corona noise levels from B2H would worsen Mr. Larkin's [redacted] tinnitus?

A. No. [redacted] The noise from B2H will be library-room quiet, and well away from any level of concern for [redacted] provoking or worsening tinnitus, as noted above. Corona noise from B2H will not worsen Mr. Larkin's tinnitus.

Q. [redacted]

A. [redacted]

---

[61] [redacted]

[62] [redacted]

[63] Greg Larkin/100, Larkin/18 (Feb. 1, 2023) ("I suffer from tinnitus resulting from my previous employment with the railroad.").

[64] [redacted]

[65] [redacted]

Q. [redacted]

A. [redacted]

[redacted]

[redacted]

[redacted]

66 [redacted]

67 [redacted]

68 [redacted]

[redacted]

---

69 [redacted]

70 [redacted]

71 [redacted]

72 [redacted]

73 [redacted]

74 [redacted]

[redacted]

Q. Please address Mr. Larkin's statement in his testimony that he is to be "cautious about additional exposure to loud noise, as additional damage to the inner ear may aggravate my tinnitus."[80] Is the corona noise expected at Mr. Larkin's home of the volume that could cause inner ear damage?

A. [redacted]

---

[75] [redacted]

[76] [redacted]

[77] [redacted]

[78] [redacted]

[79] [redacted]

[80] Greg Larkin/100, Larkin/19 (Feb. 1, 2023)

[redacted]

Q. Please specifically address Mr. Larkin's statement that he has developed high blood pressure due to the stress that has occurred over the years with the threat of losing his home.[83]

A. [redacted]

Q. Please specifically address Mr. Larkin's claim that once B2H is constructed, his home will become "uninhabitable."[84] [redacted] **How would you recommend that this** [redacted] **stress be addressed?**

A. Once B2H is constructed, it is possible that on occasion (i.e., during foul weather conditions) an average healthy person living in Mr. Larkin's home would faintly hear the corona noise generated by B2H. An individual's perception of the corona noise will be further reduced, however, by noise-mitigation required of Idaho Power. In short, the

[81] 29 CFR 1910.95(b) (Table G-16 – Permissible Noise Exposure).
[82] [redacted]
[83] Greg Larkin/100, Larkin/19 (Feb. 1, 2023).
[84] Greg Larkin/100, Larkin/18 (Feb. 1, 2023).

average healthy person might hear the faint sound of B2H. [redacted]

Q. Have you reviewed the report that Mr. Larkin references in his testimony, the Oregon Health Authority report entitled "Strategic Health Impact Assessment on Wind Energy Development in Oregon"? Does that report support Mr. Larkin's view that his health will be significantly impacted by corona noise from B2H? If not, are there more updated scientific studies to consider?

A. I am familiar with the report referenced by Mr. Larkin, "Strategic Health Impact Assessment of Wind Energy Development in Oregon," published in 2013.[86] The report

[85] [redacted]

[86] Greg Larkin/119 (Public Health Division of the Oregon Health Authority, Strategic Health Impact Assessment of Wind Energy Development in Oregon (Mar. 2013)).

does not support Mr. Larkin's view that his health will be significantly impacted by corona noise from B2H. Mr. Larkin makes the following statement in his testimony:

> It is well documented that elevated noise levels can create a variety of health concerns for individuals including exacerbating tinnitus (Strategic Health Impact Assessment on Wind Energy Development in Oregon, March 2013, Public Health Division, Oregon Health Authority, March 2013, Prepared by the Public Health Division, Oregon Health Authority includes Section B on Noise. Exhibit 119) This section provides general information regarding the impacts of noise. It states, "This section begins with an overview of sound and noise, the impacts of noise on human health, and methods to measure and assess community noise." On Page 25 it states that noise from a lineal object (such as a transmission line) appear to have lower rates of decrease (attenuation) because of the contribution of sound from multiple sources. On Page 28 of this document it indicates that there are three broad categories of health effects from exposure to noise. a. Subjective effects such as annoyance which can mean a significant degradation in the quality of life; b. Sleep, communication and concentration impacts; c. physiological effects."[87]

Since the publication of this review and recommendation, written by the Public Health Division of the Oregon Health Authority, there have been significant developments with respect to the science of wind energy, noise, and its potential for impacting health. The Health Canada Study I discuss above is one such example.

Q. Mr. Larkin also cites a 2009 report by the WHO that recommends nighttime noise levels below 40 decibels.[88] Can you place that report in context?

A. Yes. There are many organizations that have attempted to evaluate and create guidelines concerning the potential for noise to impact human health. None are perfectly suited for comparison to corona noise from the B2H transmission line.

Institutions like the WHO have attempted to broadly address concerns from a variety of noises, and their impact on human health. In its most recent and updated guidelines, published in 2018, the WHO addresses a range of noises and potential health implications. Noises evaluated include road-traffic noise, railway noise, airplane noise,

---

[87] Greg Larkin/100, Larkin/19-20 (Feb. 1, 2023).
[88] Greg Larkin/100, Larkin/21 (Feb. 1, 2023).

noise from wind turbines, and leisure noises. Health implications evaluated included sleep loss, ischemic heart disease, hypertension, cognitive impairment, hearing impairment, tinnitus, metabolic outcomes, mental health, etc.

This report produced by the WHO in 2018 was not merely a supplement to their prior reports on noise. The WHO published community noise guidelines and night noise guidelines for Europe in 1999 and 2009, respectively.[89] Since then, significant new evidence has accumulated on the health effects of environmental noise. As a result, the WHO's 2018 report was meant to be the more comprehensive and more updated version of the institution's policy recommendations for noises, including at night in which this new report proposed "an updated set of public health recommendations on exposure to environmental noise."[90] Based on the defined scope and key questions, the WHO's guidelines reviewed the pertinent literature in order to incorporate significant research undertaken in the area of environmental noise and health since the community noise guidelines and night noise guidelines for Europe were issued.[91]

In addition, it is essential to understand that the WHO's recommended levels are ***yearly averages***. Corona noise levels are well below WHO-recommended levels most of the time. Therefore, the yearly average for corona noise from B2H will be below the thresholds of concern raised by WHO for other noise sources—notably air, rail, road, wind or leisure noise.[92] This applies to health concerns raised by the WHO as possible outcomes of noise, including ischemic heart disease, hypertension, sleep loss, etc.

---

[89] Idaho Power/1214, Ellenbogen/21 (WHO, Environmental Noise Guidelines for the European Region (2018)); *see also* Idaho Power/1219, (WHO, Night Noise Guidelines for Europe (2009)); Idaho Power/1220 (WHO, Guidelines for Community Noise (1999)).

[90] Idaho Power/1214, Ellenbogen/21 (WHO, Environmental Noise Guidelines for the European Region (2018))

[91] Idaho Power/1214, Ellenbogen/17 (WHO, Environmental Noise Guidelines for the European Region (2018))

[92] Idaho Power/1214, Ellenbogen/19-20 (WHO, Environmental Noise Guidelines for the European Region (2018))

Finally, the WHO's recommendations are not only highly restrictive, but at times their conservative restrictions are outdated and unreliable. For instance, when it comes to wind turbine noise, the WHO recommends a 45 L_{den} yearly maximum.[93] Yet the largest, most rigorous, and most objective study on the potential health impacts of wind-turbine noise—i.e., the Health Canada Study—demonstrated that at 46 dBA there were no known health outcomes of concern.[94] Since 46 dBA is the equivalent of about 52 L_{den}, that new information should place an updated average noise exposure recommendation at 52 L_{den}. In either case, these numbers are equal to or exceed modeled corona noise produced by the B2H transmission line at NSRs.

Q. Mr. Larkin has suggested that prior to mitigation discussions, the Company should have evaluated the owners of all NSRs for health conditions that may be exacerbated by noise.[95] Do you believe that approach is superior to the approach required by EFSC's site certificate conditions?

A. It appears to me that the requirements of EFSC's site certificate conditions are robust and sufficient. Among other things, Noise Control Condition 1 requires that Idaho Power proactively approach landowners who may be impacted by exceedances of the ambient antidegradation standard and develop together site-specific noise mitigation plans tailored to the landowners' specific health issues and/or individual preferences. In other words, the site certificate conditions do not require the landowner to initiate the negotiation process, and specifically take into account a landowner's preexisting health conditions in

---

[93] Idaho Power/1214, Ellenbogen/19 (WHO, Environmental Noise Guidelines for the European Region (2018))

[94] *See* Idaho Power/1207 (Michaud, D. S. et al., Self-Reported and Measured Stress Related Responses Associated with Exposure to Wind Turbine Noise (2016)); Idaho Power/1208 (Michaud, D. S. et al., Exposure to Wind Turbine Noise: Perceptual Responses and Reported Health Effects (2016)); Idaho Power/1209 (Michaud, D. S. et al., Effects of Wind Turbine Noise on Self-Reported and Objective Measures of Sleep (2016)).

[95] Greg Larkin/100, Larkin/18 (Feb. 1, 2023) (stating that the Public Utility Commission of Oregon must decide whether or not "Idaho Power is obligated to determine the health and safety impacts the transmission line will have on all citizens who will be exposed to corona noise as a result of their development.").

developing more robust and alternative mitigation measures. In my opinion, it is not reasonable or appropriate or necessary for Idaho Power to proactively evaluate the health issues of individual landowners.

Q. Does this conclude your Reply Testimony?

A. Yes.

BEFORE THE PUBLIC UTILITY COMMISSION
OF OREGON

Docket PCN 5

In the Matter of

IDAHO POWER COMPANY'S
PETITION FOR CERTIFICATE OF PUBLIC CONVENIENCE
AND NECESSITY

Curriculum Vitae of Dr. Jeffrey Ellenbogen

February 22, 2023

CURRICULUM VITAE

Jeffrey M. Ellenbogen, MMSc, MD, FAASM 19 JANUARY 2023

CURRENT ACTIVITIES

Jun 2009 – present
Director, The Sound Sleep Project

Feb 2017 – present
President, Ellenbogen Scientific, LLC

2016 – present
Firefighter (Volunteer)
Baltimore County Fire Department (BCoFD)

2021 – present
Associate Medical Director ("Fire Surgeon," Volunteer)
Baltimore County Fire Department (BCoFD)

NATIONAL BOARD CERTIFICATION

1. Neurology (active)
2. Sleep & Circadian Medicine (active)

OTHER CERTIFICATIONS OR CERTIFICATES

1. **DiMM** – Diploma in Mountain Medicine
2. **ATLS** (instructor) – advanced trauma life support
3. **AWLS** – advanced wilderness life support
4. **Avalanche:** Level 1 and Avalanche Rescue
5. **SCUBA**: Rescue Diver; Advanced Open Water; Nitrox
6. **Firefighting**: Fire 1; Rescue Ops; Vehicle Extrication; Hazmat;
7. **TCCC** – tactical combat casualty care

EDUCATION & TRAINING

Undergraduate

1994 University of Michigan, Ann Arbor, MI
B.A. (with High Distinction)

Doctoral/graduate

2000 Tufts University School of Medicine, Boston, MA
M.D. (Doctor of Medicine)

2007 Harvard Medical School, Boston, MA
M.M.Sc. (Masters in Medical Science)

Postdoctoral

1 JUL 2000 - 30 JUN 2001
University of Pennsylvania, Philadelphia, PA
Intern, Internal Medicine

1 JUL 2001 - 30 JUN 2004
University of Pennsylvania, Philadelphia, PA
Resident, Neurology

1 JUL 2004 - 30 JUN 2005
University of Pennsylvania, Philadelphia, PA
Fellow, Clinical Electrophysiology

1 JUL 2005 - 30 JUN 2007
Harvard Medical School, Boston, MA
Fellow in Sleep, Circadian and Respiratory Neurobiology

PROFESSIONAL EXPERIENCE

1 JUL 2007 - 2012
Massachusetts General Hospital
-Chief, Sleep Division
-Director, Sleep Laboratory
-Physician: Neurologist and Sleep/Circadian Doctor

1 JAN 2009- 30 JUN 2013
Harvard Medical School
-Assistant Professor, Neurology and Sleep Medicine

1 JUL 2013 30 JUN 2018:
Johns Hopkins University
-Assistant Professor, Neurology
-Physician: Neurologist and Sleep-Medicine Doctor, Johns Hopkins Hospital

2017 - 2020:
Bose Corporation
-Subject-matter expert on interface of sound and sleep

JUL 2019 – AUG 2022
United States Department of Defense
-Associate Professor of Neurology and of Military & Emergency Medicine

Uniformed Services University (USU)
-<u>Vice Chair</u>, Neurology
Uniformed Services University (USU)
-<u>Neurologist and Sleep/Circadian Physician</u>
Walter Reed National Military Medical Center (WRNMMC)
1. Outpatient Clinic, Neurology Department
2. Vestibular Clinic, Otolaryngology Department
3. National Intrepid Center of Excellence (NICoE)

PUBLICATIONS

1. Soutter AD, **Ellenbogen J**, Folkman J. Splenosis is regulated by a circulating factor. *Journal of Pediatric Surgery.* 1994;29:1076-9.

2. Wolfe J, Grier HE, Klar N, Levin SB, **Ellenbogen JM**, Salem-Schatz S, Emanuel EJ, Weeks JC. Symptoms and suffering at the end of life in children with cancer. *New England Journal of Medicine.* 2000;342:326-33.

3. Aguirre GK, **Ellenbogen JM**, Pollard J, Stolzenberg ED, Galetta SL. Amyloid angiopathy. *Neurology.* 2002;59:1656.

4. Kolb SJ, Costello F, Lee AG, White M, Wong S, Schwartz ED, Messe SR, **Ellenbogen J**, Kasner SE, Galetta SL. Distinguishing ischemic stroke from the stroke-like lesions of MELAS using apparent diffusion coefficient mapping. *Journal of Neurological Sciences.* 2003;216:11-15.

5. Ances BM, **Ellenbogen JM**, Herman ST, Jacobs D, Liebeskind DS, Chatterjee A, Galetta SL. Balint's syndrome due to Creutzfeldt-Jakob disease. *Neurology.* 2004;63:395.

6. **Ellenbogen JM**. Cognitive benefits of sleep, and their loss due to sleep deprivation. *Neurology*. 2005;64:E25-7.

7. Roy S, **Ellenbogen JM**. Pathologic quiz case: seizures, frontal lobe mass and remote history of periodontal abscess. *Archives of Pathology & Laboratory Medicine.* 2005;129:805-6.

8. **Ellenbogen JM**, Hurford MO, Liebeskind DS, Neimark GB, Weiss D. Ventromedial frontal lobe trauma. *Neurology* 2005;64:757.

9. **Ellenbogen JM**, Hulbert JC, Stickgold R, Dinges DF, Stickgold R, Thompson-Schill SL. Interfering with theories of sleep and memory: Sleep, declarative memory and associative interference. *Current Biology*. 2006;16:1290-1294

10. **Ellenbogen JM**, Payne JD, Stickgold R. The role of sleep in declarative memory consolidation: passive, permissive or active or none? *Current Opinion in Neurobiology*. 2006;16:716-22.

11. **Ellenbogen JM**, Hu PT, Payne JD, Titone D, Walker MP. Human relational memory requires time and sleep. *Proceedings of the National Academy of Science, U S A (PNAS).* 2007;104:7723-8.

12. **Ellenbogen JM**. The interaction of sleep and memory. In: Chebykin OY, Bedny GB, Karwowski W, eds.

Ergonomics and Psychology: Developments in Theory and Practice. Taylor and Francis Group; 2008.

13. **Ellenbogen JM**, Hulbert JC, Jiang Y, Stickgold R. The Sleeping Brain's Influence on Verbal Memory: Boosting Resistance to Interference. *PLoS One*. 2009;4:e4117.

14. Dang-Vu TT, McKinney SM, Buxton OM, Solet JM, **Ellenbogen JM**. Spontaneous brain rhythms predict sleep stability in the face of noise. *Current Biology*. 2010;20:R626-R627.

15. **Ellenbogen JM**. Sleep-Specific Atrioventricular Block. *Neurology*. 2010;74:90

16. Dang-Vu TT, Foulkes D, Cartwright RD, **Ellenbogen JM**. Sleep. *Encyclopaedia Britannica*. 2010.

17. McKinney SM, Dang-Vu TT, Buxton OM, Solet JM, **Ellenbogen JM**. Covert waking brain activity reveals instantaneous sleep depth. *PLoS One*. 2011;6:e17351.

18. Babadi B*, McKinney SM*, Tarokh V, **Ellenbogen JM**. Data-Driven Bayesian Algorithm for Sleep Spindle Detection (DiBa). *IEEE Transactions in Biomedical Engineering*. 2012;59(2):483-93.

19. Payne JD Payne JD, Tucker MA, **Ellenbogen JM**, Wamsley EJ, Walker MP, Schacter DL, Stickgold R. Memory for Semantically Related and Unrelated Declarative Information: The Benefit of Sleep, the Cost of Wake. *PLoS One.* 2012;7:e33079

20. Buxton OM*, **Ellenbogen JM*** (co-first author), Wang W, Carballeira A, O'Connor S, Cooper D, Gordhandas AJ, McKinney SM, Solet JM. Sleep Disruption Due to Hospital Noises: A Prospective Evaluation. *Annals of Internal Medicine.* 2012; 157:170-179.

21. Shaw ND, Butler JP, McKinney SM, Nelson SA, **Ellenbogen JM**, Hall JE. Insights into Puberty: The Relationship Between Sleep Stages and Pulsatile LH Secretion. *The Journal of Clinical Endocrinology and Metabolism.* 2012;97:E2055-62.

22. Fellin T, **Ellenbogen JM**, De Pitta M, Ben-Jacob E, Halassa M. Astrocyte Regulation of Sleep Circuits: Experimental and Modeling Perspectives. *Frontiers in Computational Neuroscience.* 2012;6:65.

23. Eiseman NA, Westover MB, **Ellenbogen JM**, Bianchi MT. The impact of body posture and sleep stages on sleep apnea severity in adults. *Journal of Clinical Sleep Medicine*. 2012;8:655-6.

24. **Ellenbogen JM.** Pace-Schott EF. Drug-induced sleep: Theoretical and practical considerations. *Pflugers Archiv – European Journal of Physiology*. 2012;463(1):177-186.

25. Bianchi MT, Thomas RJ, **Ellenbogen JM**. Hypnotics and Mortality Risk. *The Journal of Clinical Sleep Medicine.* 2012;8(4):351-352

26. Bianchi MT, Williams KL, McKinney SM, **Ellenbogen JM**. The subjective-objective mismatch (SOM) in sleep perception among those with insomnia and sleep apnea. *The Journal of Sleep Research.* 2013;22(5):557-568.

27. **Ellenbogen JM**. Noise-induced sleep deprivation: Toward sleeping soundly on noisy nights. In: Bianchi MT. *Sleep Deprivation: Effects on Mind, Body, and Disease.* Springer New York Heidelberg Dordrecht

London; 2013.

28. **Ellenbogen JM.** Noise-induced sleep disruption among hospitalized patients: Brain-based approaches toward sleeping soundly on noisy nights. *Noise-Con*. 2013.

29. Marino, M, Li Y, Rueschman MD, Winkelman JW, **Ellenbogen JM**, Solet JM, Dulin H, Berkman LF, Buxton OM. Measuring Sleep: Accuracy, Sensitivity, and Specificity of Wrist Actigraphy Compared to Polysomnography. *Sleep.* 2013;36(11):1147-1155.

30. Pace-Schott EF, Tracy LE, Rubin Z, Mollica AM, **Ellenbogen JM**, Bianchi MT, Milad MR, Pitman RK, Orr SP. Interactions of time of day and sleep with between-session habituation and extinction memory in young adult males. *Experimental Brain Research*. 2014.

31. Geyer MB, **Ellenbogen JM**. Insomnia and Sleep Disorders. In: Kiefer MM, Chong CR, eds. Pocket Primary Care: A Massachusetts General Hospital Handbook. Philadelphia: Lippincott Williams & Wilkins; 2014.

32. Prerau MJ, Hartnack KE, Obregon-Henao G, Sampson A, Merlino M, Gannon K, Bianchi MT, **Ellenbogen JM**, Purdon PL. Tracking the Sleep Onset Process: An Empirical Model of Behavioral and Physiological Dynamics. *PLOS Computational Biology*. 2014.

33. Alameddine Y, **Ellenbogen JM**, Bianchi MT. Sleep-Wake Time Perception Varies by Direct or Indirect Query. *Journal of Clinical Sleep Medicine*. 2015.

34. **Ellenbogen JM**. Sleepiness. *Seminars in Neurology*. 2016.

35. Prerau MJ, Bianchi MT, Brown RE, **Ellenbogen JM**, Patrick PL. Sleep neurophysiologic dynamics through the lens of multitaper spectral analysis. *Physiology*. 2017.

36. Akeju O, Hobbs LE, Gao L, Burns SM, Pavone KJ, Plummer GS, Walsh GS, Houle TT, Kim SE, Bianchi MT, **Ellenbogen JM**, Brown EN. Dexmedetomidine promotes biomimetic non-rapid eye movement stage 3 sleep in humans: A pilot study. *Clinical Neurophysiology*. 2017.

37. **Ellenbogen JM, Guay, Christian.** Emergency Sleep Medicine. *Seminars in Neurology*. 2017.

38. Gottlieb DJ, **Ellenbogen JM**, Bianchi MT, Czeisler CA. Sleep deficiency and motor vehicle crash risk in the general population: a prospective cohort study. *BMC Medicine*. 2018.

39. Fogarty AE, Guay, CS, Simoneau G, Colorado BS, Segal GR, Werner JK, **Ellenbogen JM**. Head Motion Predicts Transient Loss of Consciousness in Human Head Trauma a Case-Control Study of Mixed Martial Artists. American Journal of Physical Medicine and Rehabilitation. 2019.

40. Goldstein JN, **Ellenbogen JM**. Emergency Neurology. *Seminars in Neurology*. 2019.

41. Schneider L, **Ellenbogen J**. Images: Facial cataplexy with demonstration of persistent eye movements. Journal of Clinical Sleep Medicine. 2020.

42. **Ellenbogen JM**. Wind turbine noise and sleep. *Sleep.* 2022.

LICENSURE and MEMBERSHIPS

Medical licenses:

2004 - 2008	Pennsylvania # 424784 (inactive)
2005 - 2014	Massachusetts # 226436 (inactive)
2013 - present	Maryland # D0075375 (active)

Boards Memberships:

2005 - present	Neurology (American Board of Psychiatry and Neurology);
2009 - present	Sleep Medicine (American Board of Psychiatry and Neurology)

AWARDS and HONORS

1991	Branstrom Prize for Academic Excellence, University of Michigan
2006 - 2011	Certificate of Distinction in Teaching, Harvard University
2011 - present	Fellow, American Academy of Sleep Medicine
2011	John E. Dowling Teaching Award in Neurobiology, Harvard University
2012	Wayne A. Hening Sleep Medicine Investigator Award, American Academy of Neurology
2017	Firefighter training award, (station 29), Baltimore County Fire Department

LEADERSHIP TRAINING

1 JAN 2009 – 31 DEC 2010

Physician Leadership Development Program, MGH/Harvard

BEFORE THE PUBLIC UTILITY COMMISSION
OF OREGON

Docket PCN 5

In the Matter of

IDAHO POWER COMPANY'S
PETITION FOR CERTIFICATE OF PUBLIC CONVENIENCE
AND NECESSITY

Buxton, O. M. et al., Sleep Disruption Due to Hospital Noises:
A Prospective Evaluation (2012)

February 22, 2023

ORIGINAL RESEARCH | Annals of Internal Medicine

Sleep Disruption due to Hospital Noises

A Prospective Evaluation

Orfeu M. Buxton, PhD*; Jeffrey M. Ellenbogen, MD*; Wei Wang, PhD; Andy Carballeira, BM; Shawn O'Connor, BS; Dan Cooper, BS; Ankit J. Gordhandas, SB; Scott M. McKinney, BA; and Jo M. Solet, PhD

Background: Sleep plays a critical role in maintaining health and well-being; however, patients who are hospitalized are frequently exposed to noise that can disrupt sleep. Efforts to attenuate hospital noise have been limited by incomplete information on the interaction between sounds and sleep physiology.

Objective: To determine profiles of acoustic disruption of sleep by examining the cortical (encephalographic) arousal responses during sleep to typical hospital noises by sound level and type and sleep stage.

Design: 3-day polysomnographic study.

Setting: Sound-attenuated sleep laboratory.

Participants: Volunteer sample of 12 healthy participants.

Intervention: Baseline (sham) night followed by 2 intervention nights with controlled presentation of 14 sounds that are common in hospitals (for example, voice, intravenous alarm, phone, ice machine, outside traffic, and helicopter). The sounds were administered at calibrated, increasing decibel levels (40 to 70 dBA [decibels, adjusted for the range of normal hearing]) during specific sleep stages.

Measurements: Encephalographic arousals, by using established criteria, during rapid eye movement (REM) sleep and non-REM (NREM) sleep stages 2 and 3.

Results: Sound presentations yielded arousal response curves that varied because of sound level and type and sleep stage. Electronic sounds were more arousing than other sounds, including human voices, and there were large differences in responses by sound type. As expected, sounds in NREM stage 3 were less likely to cause arousals than sounds in NREM stage 2; unexpectedly, the probability of arousal to sounds presented in REM sleep varied less by sound type than when presented in NREM sleep and caused a greater and more sustained elevation of instantaneous heart rate.

Limitations: The study included only 12 participants. Results for these healthy persons may underestimate the effects of noise on sleep in patients who are hospitalized.

Conclusion: Sounds during sleep influence both cortical brain activity and cardiovascular function. This study systematically quantifies the disruptive capacity of a range of hospital sounds on sleep, providing evidence that is essential to improving the acoustic environments of new and existing health care facilities to enable the highest quality of care.

Primary Funding Source: Academy of Architecture for Health, Facilities Guidelines Institute, and The Center for Health Design.

Ann Intern Med. 2012;157:170-179. www.annals.org
For author affiliations, see end of text.
* Drs. Buxton and Ellenbogen contributed equally to the manuscript.
This article was published at www.annals.org on 12 June 2012.

Sleep is essential for the restoration of health and well-being (1). However, in hospitals, where healing is paramount, noise frequently disrupts patients' sleep. In a recent national survey, patients identified the noise levels in and around rooms at night as the quality-of-care factor with the most need for improvement (2). Acoustic measurements from a major urban hospital document a crescendo of nighttime hospital noise over the past 45 years from an average level of 42 dBA (decibels, adjusted for the range of normal hearing) to more than 55 dBA in 2005 (3). Hospitals are exposed to external noise sources known to disrupt sleep, such as traffic and airplane sounds (4), with documented dose-related consequences for next-day cognitive performance (5). Patient care also produces noise specific to treatment and protection, such as intravenous and cardiac monitor alarm signals (6). Improving acoustics in environments of care to protect sleep and enhance outcomes for the more than 37 million patients who are hospitalized annually in the United States (7) has become a transdisciplinary priority (8–11).

See also:

Print
Summary for Patients. I-32

Web-Only
Samples of acoustic stimuli

The goal of this study was to provide essential information about the effect of sound on sleep to guide architectural, technological, and programmatic advances to facilitate sleep and improve clinical outcomes for patients who are hospitalized. We hypothesized that the capacity for sleep disruption varies by the type of sound and increases for each type as the sound level increases. We further hypothesized that the stages of sleep, characterized by diverse cortical activity patterns, are differentially vulnerable to disruption by noise. Sleep stages cycle through the night and vary in their relative proportions with age (12), medications (13), and certain medical and psychiatric disorders (14), among other factors. Therefore, a useful exploration of the responses of sleep to noises must include sleep stage during noise exposure.

Sleep stages include 2 brain state categories: rapid eye movement (REM) sleep and non-REM (NREM) sleep stages. The range of NREM sleep stages includes progressively deepening levels from drowsiness to deep sleep, termed *N1*, *N2*, and *N3* (15): N1 is the brief transition between wakefulness and sleep, N2 is typically the most abundant stage of sleep in adults, and N3 (or slow-wave sleep) is the deepest level. These REM and NREM brain states seem to be driven by different nuclei and neurotransmitters (16). They can be readily discerned through distinct patterns appearing on electroencephalograms (EEGs) (15) and neuroimaging (17). In addition, behavioral evidence demonstrates that the sleeping brain responds to auditory stimuli differently during REM than during NREM sleep (18). We sought to elaborate on this evidence by examining differential responses to hospital noise exposures between REM and NREM states and exploring variability in sleep disruption within the deepening stages of NREM.

We designed a protocol to examine the influence of graded noise exposures during all stages of sleep, through polysomnographic (PSG) assessments (combined EEG, electrooculogram, and electromyogram), a standard (19, 20) and sensitive (21, 22) system to measure sleep strongly correlated with awakenings (21). Because elevations in heart rate are known to occur during full EEG-documented awakenings from sleep (23), we used the electrocardiogram to detect the presence of clinically relevant heart rate responses to noise-induced arousals. We predicted heart rate elevations during these EEG-documented sleep arousals in participants who were exposed to common hospital sounds.

Methods

Design Overview

All study procedures were approved by the human research committees of the involved institutions. The design was a 3-day PSG study, beginning with a baseline (sham) quiet night followed by 2 noise exposure intervention nights, during which EEG arousals and electrocardiogram heart rate accelerations were documented.

Participants and Setting

Participants were recruited through flyers, Web site postings, and word of mouth and then screened by questionnaire, physical examination, and laboratory testing. Participants who reported medical or psychiatric conditions or use of substances or medications that potentially affect sleep were excluded from the study. Criteria for exclusion included history of drug or alcohol abuse; depression; anxiety; posttraumatic stress and obsessive compulsive disorders; neurologic or sleep disorders; infectious diseases; diseases of the cardiovascular system; or treatment with antidepressants, neuroleptics, or major tranquilizers. Urinalysis confirmed the absence of caffeine, nicotine, and alcohol. Standard audiometric screening confirmed normal hearing (that is, exceeding 20 dBA in both ears). The first 12 eligible and available participants were enrolled (**Figure 1**).

Participants slept at home on a regular schedule for at least 4 days before participation in the study. They reported sleeping a mean of 7.72 hours (SD, 0.27) over a mean of 6.5 days (SD, 1.1) through a time-stamped phone-answering system that was confirmed through wrist actigraphy (AW-64, Philips Respironics, Murrysville, Pennsylvania), which demonstrated a mean of 7.16 hours (SD, 0.29) of sleep over a mean of 6.7 monitored days (SD, 0.9).

Participants stayed at the Massachusetts General Hospital Sleep Laboratory for 3 days. Each night, participants were given an 8.5-hour sleep opportunity, which began at their normal bedtimes. Continuous video observation and wrist actigraphy confirmed that participants did not nap during the day. Light levels were maintained at less than 1 lux (darkness) during sleep periods and approximately 90 lux (ordinary daylight in room) during waking periods. Because of continuous air exchange (required in health care facilities), background ambient sound levels averaged between 34 and 35 dBA ($LA_{EQ,\ 10\text{-}s}$ [equivalent continuous A-weighted scale {adjusted for the range of normal human hearing} sound pressure level, averaged over the 10-second stimulus duration]). On the first night, participants slept undisturbed to allow adaptation to the PSG equipment and laboratory environment, confirm absence of sleep disorders (including sleep apnea), and establish baseline sleep recordings. On the second and third nights, recorded hospital sounds were presented to participants throughout sleep.

Intervention: Acoustic Stimuli

Recordings of hospital sounds were captured on a medical unit of Somerville Hospital, Cambridge Health Alliance, Somerville, Massachusetts. Each sound stimulus fit within 1 or more of the categories identified as salient in the American Institute of Architects Guideline on Sound and Vibration in Healthcare Facilities: external to building,

Context

The negative effects of hospital noise on sleep are among the most common concerns of inpatients and their families.

Contribution

During sleep laboratory studies of healthy volunteers, investigators found that the disruptive effect of recorded hospital noises varied by the type and level of sound emitted and by the volunteer's stage of sleep. Electronic sounds designed to be alerting were most disruptive, as were staff conversations and voice paging.

Caution

Volunteers were young and healthy. Sounds were not administered together.

Implication

Reduction of hospital noise through policies, procedures, and building design may lead to improved patient sleep.

—The Editors

Figure 1. **Study flow diagram.**

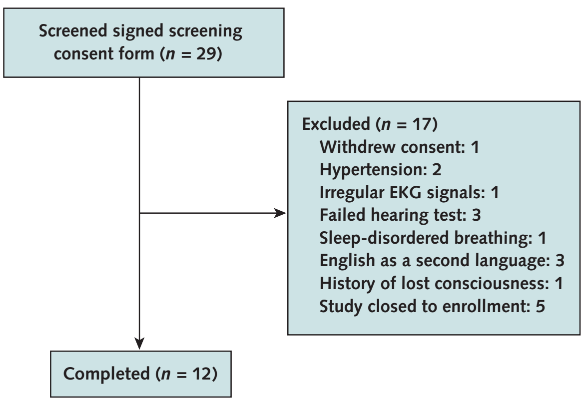

EKG = electrocardiogram.

within hospital, and within or outside patient rooms (8). Fourteen noise stimuli were selected: "good" conversation, which was defined as 1 male and 1 female voice discussing a positive patient outcome; "bad" conversation, which was defined as the same voices discussing a negative patient outcome; male voice from an overhead paging system calling a physician by name; door opening or closing; telephone ringing; toilet flushing; ice machine disgorging; IV alarm sounding; laundry cart rolling; automatic paper towel machine dispensing; helicopter takeoff; jet engine flyover; and outside traffic flow. Samples of acoustic stimuli are available at www.annals.org. To control for differences in duration across stimuli, sounds were normalized to 10 seconds (**Appendix Table 1**, available at www.annals.org).

Hospital noises were presented as stimuli with 2-dimensional verisimilitude (for example, airplane sounds moved across space) through use of 4 studio monitor loudspeakers (PS6, Event Electronics, Silverwater, Australia) arrayed about the head of the sleeping participants (a modified pattern from the ITU-R BS 775-1 Recommendation, omitting the center loudspeaker). Sound levels in the participants' room were logged in 1-second increments by using an environmental sound monitor (NL-31, with type 1 microphone [Rion, Tokyo, Japan]) installed roughly 10 inches above the head of the sleeping participants and programmed to output a direct current voltage proportional to the A-weighted fast-response sound level.

Once a steady sleep stage of at least 90 seconds was recorded, as assessed in real time by a technician, stimuli were systematically presented once per 30-second sleep epoch, starting at an exposure level ($LA_{EQ,\ 10\text{-}s}$) of 40 dBA in increasing steps of 5 dBA (**Figure 2**, *top*) until either sleep was disrupted by an arousal (**Figure 2**, *bottom*), sleep stage changed, or the 70-dBA maximum exposure level was reached. Because both the equivalent sound level and the duration of the noise stimuli were held constant, all stimuli were normalized to deliver an equal "noise dose," an integration of sound intensity over time (24). All stimuli were presented in a computer-generated random order within each sleep stage on both exposure nights for every participant.

Outcomes

Standard PSG recordings (Comet XL, Grass Technologies, West Warwick, Rhode Island) were collected on all 3 nights through skin surface electrodes. Sleep stages and arousals were identified by using current criteria (15). **Figure 2** (*bottom*) depicts a standard arousal, as defined by an

Figure 2. **Schematic diagram of study protocol.**

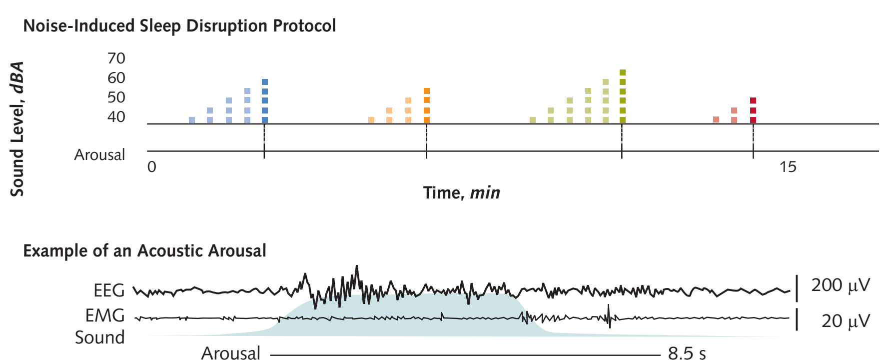

dBA = decibels, adjusted for the range of normal hearing; EEG = electroencephalogram; EMG = electromyogram; N2 = non-REM sleep stage 2; REM = rapid eye movement. **Top.** The solid vertical lines along the *x*-axis indicate stimuli evoking EEG arousals, and a sample of 4 noises is shown. Each color represents a different sound type. Ten-second noises were evaluated for their probability to induce a cortical arousal at increasing sound levels in varying stages of sleep and presented once per 30-second sleep epoch (while sleep stage was stable) until an arousal occurred, sleep stage changed, or the 70-dBA maximum was reached. **Bottom.** A typical sound-induced arousal from stage N2 sleep, as measured by polysomnography. Arousals are defined by their appearance on the EEG (the right frontal lead F3 shown here), characterized by an abrupt shift of frequency that lasts at least 3 seconds. Arousals during REM sleep require a concurrent increase in submental EMG activity. This transient arousal lasted for approximately 8.5 seconds before sleep resumed.

abrupt shift of EEG frequency lasting at least 3 seconds. Arousals during REM sleep also require a concurrent increase in submental electromyogram activity (**Figure 2**). Body position was scored from infrared video to allow for statistical adjustment based on whether either ear was occluded, potentially attenuating arousal responses. Body position (supine or not) was assessed continuously by a sleep technician viewing the infrared video on the same screen as the EEG signals they were using to score sleep stages in real time at the initiation of each acoustic stimulus.

Experimental tasks were coordinated by 2 researchers; a sleep technician maintained PSG signal quality classification of sleep stages and identification of cortical arousals indicating sleep disruption (25), along with documentation of body position. A second technician or investigator maintained the acoustic equipment and initiated the programmed, semiautomatic presentation of escalating noise stimuli. Discrepancies with the real-time scoring were resolved by a board-certified sleep physician.

Statistical Analysis

The probability of arousal by stimulus sound level and type and sleep stage was examined descriptively (graphically). Generalized linear mixed models were applied to evaluate the effects of hospital noises on the binary outcome (arousal from sleep) with a logit link, by using PROC GLIMMIX in SAS software, version 9.2 (SAS Institute, Cary, North Carolina), for determining differences by sleep stage, with factors of study night and body position. Because of large interperson differences, the participant was treated as a random effect, incorporating participant-specific intercepts into the model. We assume that, between 2 adjacent presented stimuli levels (for example, 50 and 55 dBA), the arousal probability increases linearly for the intervening stimuli levels (for example, 51 to 54 dBA). Because an ear against the pillow could attenuate the administered sound level, body position served as a covariate in the model where supine position (reference category) corresponded to having both ears exposed. This model was used to estimate the probability of arousal while accounting for stimulus, sound level, sleep stage, and body position. We separately estimate the additional effect of the night of study (see the Results section).

To assess the effects of noise on heart rate during sleep by sleep stage, we calculated the profile of instantaneous heart rate during each arousal relative to the average heart rate during the 10 seconds preceding each corresponding sound onset. To quantify the temporal dynamics of the heart rate response, we calculated the median durations from the sound onset to the time of peak heart rate during each arousal and to the time of arousal onset.

Role of Funding Source

Nonprofit entities, the Academy of Architecture for Health, Facilities Guidelines Institute, and The Center for Health Design, contributed resources to this investigator-initiated study. They did not play a role in the study design, conduct, reporting, or the decision to submit a manuscript.

Results

Twelve healthy, white participants (8 women; mean age, 27 years [SD, 7]; mean body mass index, 21.8 kg/m^2 [SD, 3.7]) successfully completed this study.

As expected, louder sounds were more apt to cause sleep disruption (**Figure 3**). Effects varied by the type of sound stimulus (for example, IV alarm vs. voices) and by the stage of sleep during which the sound stimulus was presented (for example, REM vs. N3).

We saw an effect of sleep stage on sound stimulus–evoked arousal probability (**Figure 3**, *top panels*); N2 differed from N3 and REM (both $P < 0.001$, Bonferroni-adjusted), but N3 and REM did not differ overall, using model-based probability estimates. The pattern of arousal probabilities from stages N2 to N3 were relatively consistent in terms of sound stimulus order from most to least arousing, but shifted to overall lower arousal rates during N3 compared with N2 (**Figure 3**, *middle panels*). In marked contrast, arousals from REM sleep revealed a more homogeneous and monotonic pattern across sounds presented than NREM stages (**Figure 3**, *middle panels*) not readily apparent from the mean curves alone (**Figure 3**, *top panels*). Arousals occurred at lower sound levels on the third study night compared with the second study night ($P < 0.001$). Testing for the stage–by–study-night interaction only showed a slight difference across nights among sleep stages ($P = 0.020$, adjusted for sound levels [**Appendix Table 2**, available at www.annals.org]; body position was not significant and was not included in the final interaction model). The significant interaction suggests that the arousal probability was lower on the third night for all sleep stages, but the magnitude of the difference varied across stages and may reflect some degree of sensitization of arousals to sound presentation. Depiction of arousal probabilities for individual sound stimuli by stage and sound level revealed considerable heterogeneity in the responses to the various stimuli (**Figure 4**).

We studied the change in heart rate during stimulus-induced arousals by subtracting the instantaneous heart rate from the average heart rate of the 10 seconds preceding the sound onset. The stage in which the arousal occurred substantially predicts the magnitude of the heart rate increase ($P < 0.001$); the greatest responses occurred during REM, followed by N3 and N2 (**Figure 3**, *bottom panels*). All pairwise comparisons are significant at an α level of $0.05/3 = 0.017$. Baseline (prearousal) heart rate does not predict the magnitude of the response ($P = 0.94$). Study night is not significant ($P = 0.83$), reflecting a lack of habituation of the electrocardiogram heart rate response.

Heart rate responses are aligned by their peaks in **Figure 3** (*bottom panels*). The stage in which the arousal occurred significantly predicts the duration of time from the

Figure 3. **Sleep disruption due to noise stimuli presented during sleep, by stage of sleep.**

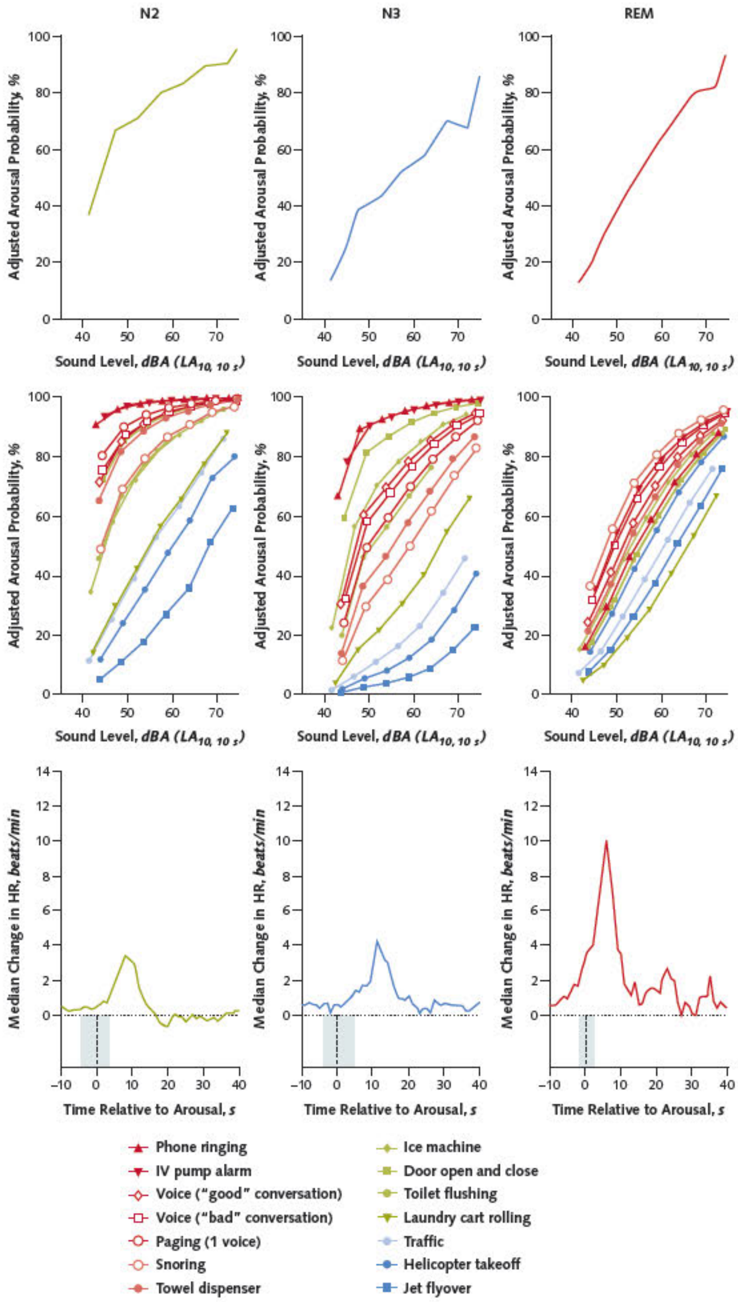

Arousal probability of sound stimuli presented in sleep stages N2, N3, and REM. Ten-second noises were introduced during sleep stages N2, N3, and REM to evaluate their propensity to disturb sleep. Once a stable stage of at least 90 seconds was reached, noises were initiated at sound levels of 40 dBA (equivalent continuous A-weighted [adjusted for the range of normal human hearing] sound pressure level, averaged over the 10-second stimulus duration) and presented every 30 seconds in 5-dBA increments until an arousal occurred or the 70-dBA exposure level was reached. dBA = decibels, adjusted for the range of normal hearing; HR = heart rate; IV = intravenous; $LA_{10,\ 10\text{-}s}$ = sound pressure level, averaged over the 10-second stimulus duration, exceeded 10% of the time; N2 = non-REM sleep stage 2; N3 = non-REM sleep stage 3; REM = rapid eye movement. **Top.** Mean arousal probabilities for stimuli presented during sleep stages N2, N3, and REM versus presented sound level and adjusted for stimulus and body position (see Methods section). **Middle.** Mean arousal probabilities for individual noise stimuli by sleep stage, adjusted for body position. **Bottom.** Changes in the median HR during nonspontaneous, noise-induced arousals are aligned by the time of the peak HR response and expressed relative to the average HR in the 10 seconds preceding the arousals in sleep stages N2, N3, and REM. The vertical lines represent the median times of arousal onset (with CIs) before that peak.

start of the arousal to the peak of the heart rate increase ($P < 0.001$); the fastest response times to peak were found during REM, then during N2 and N3. The median time from the start of the arousal to peak heart rate in REM is significantly shorter than N2 and N3; N3 is not significantly different from N2 adjusted for several comparisons at an α level of 0.017. No differences were seen in baseline heart rate across sleep stages ($P = 0.53$).

Discussion

This study systematically quantifies the disruptive capacity of hospital-recorded sounds on sleep. Sound presentations during sleep yielded arousal response curves that varied due to sound type and level and sleep stage. As predicted, for each stimulus higher sound levels led to a greater probability of sleep disruption. Electronic sounds, such as an IV alarm designed to alert medical staff, were consistently more arousing than other sounds at the same noise dose. Overall, the effect of sound level and type were modified by sleep stage physiology, producing unique arousal probability profiles for each sleep stage. We further demonstrate that the arousal effects of noise on sleep include heart rate elevations, even when disruptions are brief and frequent. Heart rate effects may be particularly relevant to critical care settings, in which monitor alarms are very frequent (6). These arousal probability profiles have the potential to drive needed innovation in design, construction, engineering, building materials, monitoring and communication equipment, and care-giving protocols to preserve sleep and enhance environments for healing. Improved acoustic environments consistent with current guidelines in the United States (8) and European Union (26) could deliver several clinical benefits, including reduced sedation and shorter hospital stays (4, 9, 10, 21, 27–29).

Disrupted sleep is known to be associated with hypertension (30), incidence of cardiovascular and coronary heart disease (31), impaired immune function (32), elevated stress hormone responses (33), attention and memory deficits (34), and depressed mood (35). Preservation of patients' sleep should be a priority for contributing to improved clinical outcomes for patients who are hospitalized (36). Spontaneous arousals are known to accelerate heart rate (36–39). Full awakenings evoked by noise lead to heart rate elevations of approximately 10 beats/min (36). We demonstrate that evoked arousals elicit heart rate acceleration from all stages of sleep, but a greater magnitude (10 beats/min) and faster onset of heart rate accelerations from REM, with lesser magnitude and less rapid accelerations in stages N2 and N3. Our data demonstrate that the effect of noise on sleep includes heart rate elevations, even when the disruption is brief and frequent, as might be seen in an intensive care unit setting. A recent synthesis of hospital soundscape surveillance data described a pattern of intensive care unit noise exceeding a "peak" of 60 dBA more than 50% of the time at night (40) and, thus, the frequency of sleep disruptions may be high in typical intensive care or other inpatient units, as described by patient self-reports (2), and in other units, such as the neonatal intensive care unit (41). A study of patients in the cardiac intensive care unit demonstrated that adverse acoustic environments are associated with higher pulse amplitude at night and elevated use of β-blockers. The patient group exposed to the unimproved acoustic environment also demonstrated higher rates of rehospitalization and poorer ratings of quality of care (29).

More broadly across the hospital, patients who are hospitalized frequently have delirium with immediate and long-term consequences, including an association with increased mortality rates. Sleep disruption has been proposed as a modifiable target for delirium interventions (42). A prospective and multifaceted delirium intervention study of older patients on a general medical ward—a study that included a sleep component and noise reduction—successfully reduced delirium symptoms and the rate of sleep medication use (43). Sleep is a cyclic orchestration of stages that alters with aging and can vary from person to person with specific medical, psychiatric, and situational differences (44). Older persons tend to have less N3 sleep (12, 45), and various medications can influence stage distributions (for example, antidepressants suppress REM sleep) (46). Our data provide a framework for implementing targeted strategies to mitigate noise-induced sleep disruption, which potentially contributes to delirium among patients who are hospitalized.

Approaches to mitigating noise for sleeping patients include eliminating or controlling the source of sound or blocking its path. The first approach, controlling sound at the source, includes public-policy restrictions on acceptable night noise, such as aircraft flyovers (9); substitution with quieter technologies, such as personal digital assistants in place of overhead paging; and telemetry from nurses' stations to limit intrusive oversight (11, 47). The night care intervention study at 1 hospital established a "quiet time" period, altered intrusive medication routines, and reduced sound level exposures from staff voices. This protocol resulted in a 25% reduction of unit-wide sedative medication use and improved patient satisfaction ratings (10). The second approach to mitigation focuses on "blocking" or attenuating sound along the transmission path, including hospital unit design configurations; application of advanced construction materials, such as acoustic surfaces (48); closing doors; and even supplying earplugs to patients.

As expected, the most potent sleep disruptors were electronic sounds intentionally designed to be alerting (49, 50). The arousal probability curves in **Figure 4** corresponding to these sounds (that is, phone ringing and IV alarm) reveal that these devices may not be suitably attenuated to spare sleep, even at their quietest settings: within the lowest tested ranges in this study, these sounds produced sleep disruption more than 50% of the time. Alarm signals have

Figure 4. **Electroencephalogram arousal probabilities for noise stimuli presented, adjusted for body position.**

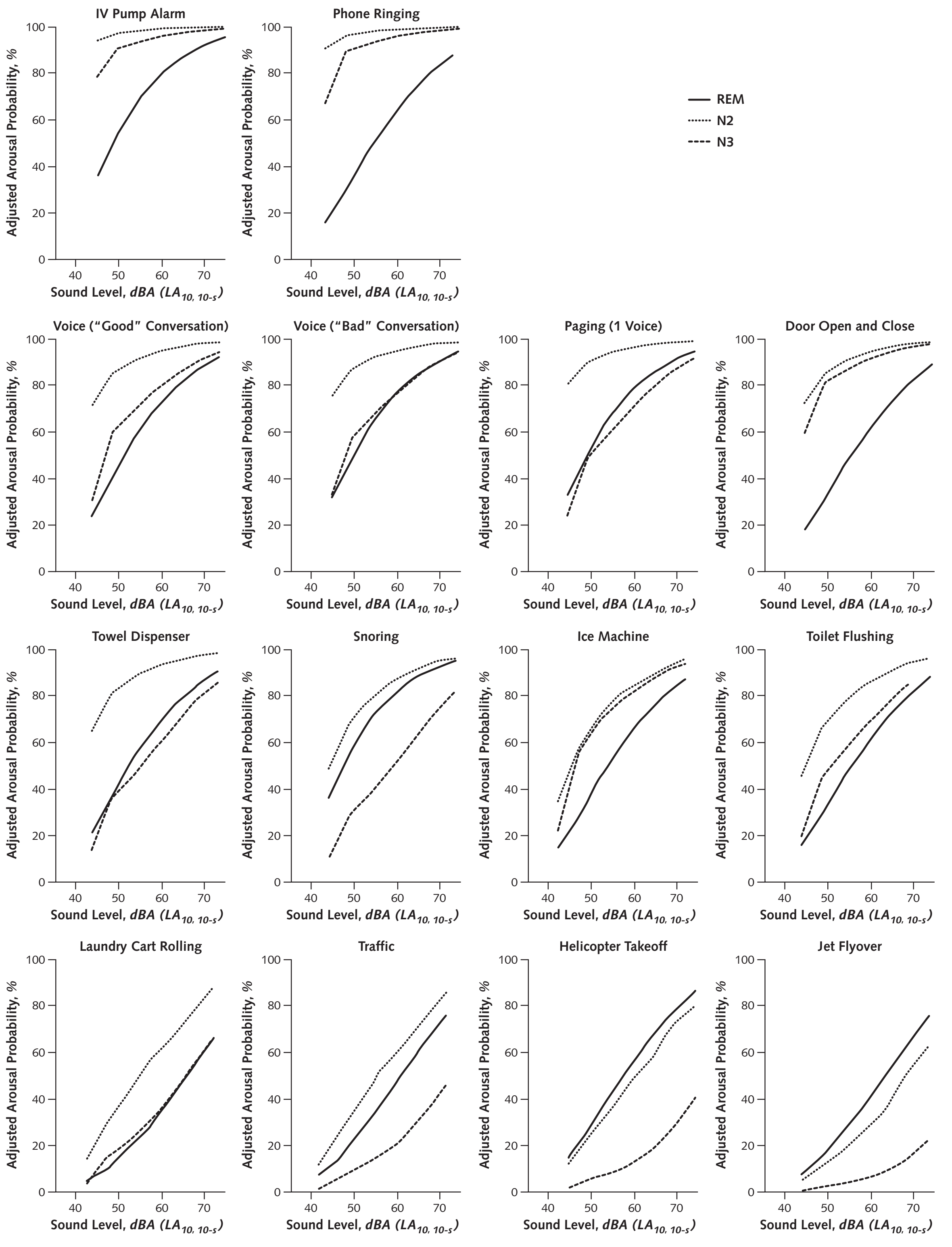

See Methods section. dBA = decibels, adjusted for the range of normal hearing; IV = intravenous; $LA_{10,\ 10\text{-}s}$ = sound pressure level, averaged over the 10-second stimulus duration, exceeded 10% of the time; N2 = non-REM sleep stage 2; N3 = non-REM sleep stage 3; REM = rapid eye movement.

proliferated in health care settings. Monitor alarms could be better managed through enhanced algorithms, more careful patient assignment and clinically relevant configuration standards, and targeting intended responders with technologies using nonauditory channels (6).

Staff conversations and voice paging were also found to be highly alerting, producing a 50% chance of arousal at 50 dBA ($LA_{10,\ 10\text{-}s}$, sound level exceeded 10% of the time) in N2 and REM sleep. Voice transmission can be modified behaviorally (10) and diminished through design and construction solutions. Simple strategies include planning for and directing conversation to designated consulting spaces. In many health care settings, policy still includes keeping patient doors open to allow for visual monitoring and easy accessibility by caregivers, which exposes patients to excess noise from the nurses' station and other sources. Centralized patient-monitoring technology may help minimize the need for this policy—at least at night—while still addressing patient-safety concerns. Proper door hardware and gasketing could decrease the sounds generated by door closing and limit sound transmission from halls.

Other tested hospital sounds (for example, ice machines, laundry carts, and overhead paging) that emanate from sources external to patient rooms (51–53) were, as a group, arousing at relatively low sound levels. Ice machines should be architecturally isolated from patient areas or reengineered. Modifying procedures and equipment, such as selection and maintenance of carts and organizing the schedule of use and routing, is a low-tech, low-cost contribution to reducing noise. Exterior-to-building noises (for example, jet, helicopter, traffic) were the least arousing among our group of stimuli, and our findings were consistent with other studies of sleep and airplane flyovers (21). The previous work determined that statistical description of average sound level (LA_{EQ}) over 24 hours is an inadequate measure for describing the sleep-disruptive effects from noise. Examining disruption at different sound levels is the more appropriate exposure metric (9), especially for sounds with broad ranges that peak. It is, therefore, not surprising that we determined that continuous stimuli (for example, traffic noise) are less arousing than intermittent stimuli (for example, phone ringing or IV alarm). At the same adjusted noise dose, higher transient sound levels and faster rise times are more likely to induce cortical arousals. In light of our findings, broad sleep-preserving steps should include changes in the design of health care facilities, construction materials chosen for acoustic properties, improved monitoring and alerting technology, sleep-protective night care routines, and education and retraining of health care personnel on the effect of noise on patient arousal and cardiac responses to such sleep disruptions (4, 9, 10, 21, 27–29).

During REM sleep, we saw a narrower range of cortical arousals, relative to NREM stages of sleep, and across the wide range of sounds administered in this experiment. This may demonstrate that the brain, during REM sleep, has less capacity to differentiate among sounds compared with NREM sleep. This finding is unexpected because REM sleep has an abundance of cerebral activity relative to stage N3 sleep, including in auditory areas of the brain (17). Auditory-evoked potentials elicited by saying a participant's name during REM sleep also seem similar in morphology to those seen during wakefulness (18), implying that there is some higher-order processing in REM sleep. This supports the broader notion that, in REM sleep, cerebral resources are dedicated to internal processing, such as dream content, rather than to differentiating external sound sources.

Although ecologically valid in many aspects, this experiment has some limitations that may cause an underestimation of the effects of noise on sleep. We presented noises individually for up to 10 seconds and halted if arousal occurred. This procedure minimized full awakenings and increased sleep time available for more stimulus presentations. In a hospital setting, sounds often last longer than 10 seconds and several sounds occur simultaneously. We do not account for relative proportion or intermittency of stimuli in a hospital setting; our data are intended to provide a framework by which a hospital unit could assess the sleep-disrupting effects of a specific hospital environment. We studied only 12 young, healthy adults. The typical patient who is hospitalized is older, with generally less of the most protected deep sleep, N3 (54). Medical and psychiatric conditions, as well as pain and medication use, compromise sleep in patients who are hospitalized, presumably rendering deep sleep, N3, more difficult to achieve. Noise can be expected to interact with these other sleep-disrupting stressors associated with hospitalization (55). Therefore, we judge our arousal probability profiles for N2 sleep to be most relevant for predicting acoustic disruption of sleep in inpatient populations. Future studies should assess the effect of noise on sleep disruption and heart rate changes in older participants to confirm generalizability and document effects on sleep stage proportions and architecture. Together, these limitations may cause our data to underestimate the effects of noise on sleep for patients who are hospitalized. Our data should be viewed as providing reference points that demonstrate sleep disruption caused by these common hospital noises, across a range of sound levels, and should be used to set a minimum for noise-attenuating standards.

In summary, protecting sleep from acoustic assault in hospital settings is a key goal in advancing the quality of care for inpatient medicine. We characterized the vulnerability of sleep to commonly encountered hospital sounds by deriving unique arousal probability profiles to enable customized target thresholds and interventions to limit noise-induced sleep disruption. This research has already informed the first acoustic standards in the Guidelines for the Design and Construction of Health Care Facilities (8). With the leading edge of baby boomers turning 66 this year and an aging health care infrastructure, billions of dollars in health care facility renovation and new construction are anticipated in the coming decade (7). Improving the acoustics in health care facilities will be critical to ensuring that these environments enable the highest quality care and the best clinical outcomes.

From Harvard Medical School, Brigham and Women's Hospital, Massachusetts General Hospital, and Berklee College of Music, Boston; Cambridge Health Alliance, Cambridge; and Cavanaugh Tocci Associates, Sudbury, Massachusetts.

Acknowledgment: The authors thank Jenny Lai Olsen, Margaret Merlino, Karen Gannon, Leah Rondon, Vanessa Castro, Carolina Smales, Deirdre McLaren, and James Porter for technical assistance; Peg Toro, audiologist, for consultation on screening for normal hearing; and Drs. Dean M. Hashimoto, John W. Cronin, and Matt Travis Bianchi for helpful comments on the manuscript.

Grant Support: This study was funded by investigator-initiated grants (Dr. Solet) from the Academy of Architecture for Health, the Facilities Guidelines Institute, and The Center for Health Design. Sleep laboratory work was completed through the generosity of Massachusetts General Hospital and with acoustic consultation by Cavanaugh Tocci Associates.

Potential Conflicts of Interest: Disclosures can be viewed at www.acponline.org/authors/icmje/ConflictOfInterestForms.do?msNum=M11-1159.

Reproducible Research Statement: *Study protocol, data set, and statistical code:* Available from Dr. Buxton (e-mail, orfeu_buxton@hms.harvard.edu). Execution of a materials transfer agreement is required for the transfer of data.

Requests for Single Reprints: Orfeu M. Buxton, PhD, 221 Longwood Avenue, BLI438-K, Boston, MA 02115; e-mail, orfeu_buxton@hms.harvard.edu.

Current author addresses and author contributions are available at www.annals.org.

References

1. **Colten HR, Altevogt BM, eds; Committee on Sleep Medicine and Research.** Sleep Disorders and Sleep Deprivation: An Unmet Public Health Problem. Washington, DC: National Academies Pr; 2006.
2. **Jha AK, Orav EJ, Zheng J, Epstein AM.** Patients' perception of hospital care in the United States. N Engl J Med. 2008;359:1921-31. [PMID: 18971493]
3. **Busch-Vishniac IJ, West JE, Barnhill C, Hunter T, Orellana D, Chivukula R.** Noise levels in Johns Hopkins Hospital. J Acoust Soc Am. 2005;118:3629-45. [PMID: 16419808]
4. **Griefahn B, Bröde P, Marks A, Basner M.** Autonomic arousals related to traffic noise during sleep. Sleep. 2008;31:569-77. [PMID: 18457245]
5. **Elmenhorst EM, Elmenhorst D, Wenzel J, Quehl J, Mueller U, Maass H, et al.** Effects of nocturnal aircraft noise on cognitive performance in the following morning: dose-response relationships in laboratory and field. Int Arch Occup Environ Health. 2010;83:743-51. [PMID: 20143082]
6. **Solet JM, Barach P.** Managing alarm fatigue in cardiac care. Prog Pediatr Cardiol. 2012;33:85-90.
7. **Carpenter D, Hoppszallern S.** Proceed with caution. Lean year expected for hospital construction. Health Facil Manage. 2010;23:11-8. [PMID: 21638945]
8. **Facilities Guidelines Institute.** Guidelines for Design and Construction of Health Care Facilities. Chicago: American Society for Healthcare Engineering of the American Hospital Association; 2010.
9. **Basner M, Samel A, Isermann U.** Aircraft noise effects on sleep: application of the results of a large polysomnographic field study. J Acoust Soc Am. 2006;119:2772-84. [PMID: 16708935]
10. **Bartick MC, Thai X, Schmidt T, Altaye A, Solet JM.** Decrease in as-needed sedative use by limiting nighttime sleep disruptions from hospital staff. J Hosp Med. 2010;5:E20-4. [PMID: 19768797]
11. **Montague KN, Blietz CM, Kachur M.** Ensuring quieter hospital environments. Am J Nurs. 2009;109:65-7. [PMID: 19704239]
12. **Ohayon MM, Carskadon MA, Guilleminault C, Vitiello MV.** Meta-analysis of quantitative sleep parameters from childhood to old age in healthy individuals: developing normative sleep values across the human lifespan. Sleep. 2004;27:1255-73. [PMID: 15586779]
13. **Schweitzer PK.** Drugs that disturb sleep and wakefulness. In: Kryger MH, Roth T, Dement WC, eds. Principles and Practice of Sleep Medicine, 5th ed. St. Louis: Elsevier Saunders; 2010:542-60.
14. **Witmans M.** Systematic review of the efficacy and safety of drug treatments and combination treatments in the management of chronic insomnia in adults. J Clin Sleep Med. 2005;1:e488-95.
15. **Iber C, Ancoli-Israel S, Chesson A, Quan SF.** The AASM Manual for the Scoring of Sleep and Associated Events: Rules, Terminology and Technical Specifications. Darien, IL: American Academy of Sleep Medicine; 2007.
16. **Siegel JM.** REM sleep. In: Kryger MH, Roth T, Dement WC, eds. Principles and Practice of Sleep Medicine. 5th ed. St. Louis: Elsevier Saunders; 2010:92-111.
17. **Braun AR, Balkin TJ, Wesenten NJ, Carson RE, Varga M, Baldwin P, et al.** Regional cerebral blood flow throughout the sleep-wake cycle. An H2(15)O PET study. Brain. 1997;120 (Pt 7):1173-97. [PMID: 9236630]
18. **Perrin F, García-Larrea L, Mauguière F, Bastuji H.** A differential brain response to the subject's own name persists during sleep. Clin Neurophysiol. 1999;110:2153-64. [PMID: 10616121]
19. **Bonnet MH, Arand DL.** EEG arousal norms by age. J Clin Sleep Med. 2007;3:271-4. [PMID: 17561594]
20. **Basner M.** Arousal threshold determination in 1862: Kohlschütter's measurements on the firmness of sleep. Sleep Med. 2010;11:417-22. [PMID: 20223705]
21. **Basner M, Glatz C, Griefahn B, Penzel T, Samel A.** Aircraft noise: effects on macro- and microstructure of sleep. Sleep Med. 2008;9:382-7. [PMID: 17870661]
22. **Halász P, Terzano M, Parrino L, Bódizs R.** The nature of arousal in sleep. J Sleep Res. 2004;13:1-23. [PMID: 14996030]
23. **Basner M, Griefahn B, Berg M.** Aircraft noise effects on sleep: mechanisms, mitigation and research needs. Noise Health. 2010;12:95-109. [PMID: 20472955]
24. **De Gennaro L, Casagrande M, Violani C, Di Giovanni M, Herman J, Bertini M.** The complementary relationship between waking and REM sleep in the oculomotor system: an increase of rightward saccades during waking causes a decrease of rightward eye movements during REM sleep. Electroencephalogr Clin Neurophysiol. 1995;95:252-6. [PMID: 8529555]
25. **Bonnet MH, Doghramji K, Roehrs T, Stepanski EJ, Sheldon SH, Walters AS, et al.** The scoring of arousal in sleep: reliability, validity, and alternatives. J Clin Sleep Med. 2007;3:133-45. [PMID: 17557423]
26. World Health Organization Regional Office for Europe. Night Noise Guidelines for Europe. Copenhagen, Denmark: World Health Organization; 2010.
27. **Cmiel CA, Karr DM, Gasser DM, Oliphant LM, Neveau AJ.** Noise control: a nursing team's approach to sleep promotion. Am J Nurs. 2004;104:40-8. [PMID: 14767379]
28. **Johnson AN.** Adapting the neonatal intensive care environment to decrease noise. J Perinat Neonatal Nurs. 2003;17:280-8. [PMID: 14655788]
29. **Hagerman I, Rasmanis G, Blomkvist V, Ulrich R, Eriksen CA, Theorell T.** Influence of intensive coronary care acoustics on the quality of care and physiological state of patients. Int J Cardiol. 2005;98:267-70. [PMID: 15686777]
30. **Cappuccio FP, Stranges S, Kandala NB, Miller MA, Taggart FM, Kumari M, et al.** Gender-specific associations of short sleep duration with prevalent and incident hypertension: the Whitehall II Study. Hypertension. 2007;50:693-700. [PMID: 17785629]
31. **Hoevenaar-Blom MP, Spijkerman AM, Kromhout D, van den Berg JF, Verschuren WM.** Sleep duration and sleep quality in relation to 12-year cardiovascular disease incidence: the MORGEN study. Sleep. 2011;34:1487-92. [PMID: 22043119]
32. **Cohen S, Doyle WJ, Alper CM, Janicki-Deverts D, Turner RB.** Sleep habits and susceptibility to the common cold. Arch Intern Med. 2009;169:62-7. [PMID: 19139325]

33. **Buxton OM, Pavlova M, Reid EW, Wang W, Simonson DC, Adler GK.** Sleep restriction for 1 week reduces insulin sensitivity in healthy men. Diabetes. 2010;59:2126-33. [PMID: 20585000]

34. **Drummond SP, Brown GG.** The effects of total sleep deprivation on cerebral responses to cognitive performance. Neuropsychopharmacology. 2001;25:S68-73. [PMID: 11682277]

35. **Ancoli-Israel S, Cooke JR.** Prevalence and comorbidity of insomnia and effect on functioning in elderly populations. J Am Geriatr Soc. 2005;53:S264-71. [PMID: 15982375]

36. **Basner M, Griefahn B, Müller U, Plath G, Samel A.** An ECG-based algorithm for the automatic identification of autonomic activations associated with cortical arousal. Sleep. 2007;30:1349-61. [PMID: 17969469]

37. **Catcheside PG, Chiong SC, Mercer J, Saunders NA, McEvoy RD.** Noninvasive cardiovascular markers of acoustically induced arousal from non-rapid-eye-movement sleep. Sleep. 2002;25:797-804. [PMID: 12405616]

38. **Sforza E, Chapotot F, Lavoie S, Roche F, Pigeau R, Buguet A.** Heart rate activation during spontaneous arousals from sleep: effect of sleep deprivation. Clin Neurophysiol. 2004;115:2442-51. [PMID: 15465431]

39. **Sforza E, Jouny C, Ibanez V.** Cardiac activation during arousal in humans: further evidence for hierarchy in the arousal response. Clin Neurophysiol. 2000;111:1611-9. [PMID: 10964073]

40. **Ryherd EE, Waye KP, Ljungkvist L.** Characterizing noise and perceived work environment in a neurological intensive care unit. J Acoust Soc Am. 2008;123:747-56. [PMID: 18247879]

41. **Williams AL, van Drongelen W, Lasky RE.** Noise in contemporary neonatal intensive care. J Acoust Soc Am. 2007;121:2681-90. [PMID: 17550168]

42. **Weinhouse GL, Schwab RJ, Watson PL, Patil N, Vaccaro B, Pandharipande P, et al.** Bench-to-bedside review: delirium in ICU patients–importance of sleep deprivation. Crit Care. 2009;13:234. [PMID: 20053301]

43. **Inouye SK, Bogardus ST Jr, Charpentier PA, Leo-Summers L, Acampora D, Holford TR, et al.** A multicomponent intervention to prevent delirium in hospitalized older patients. N Engl J Med. 1999;340:669-76. [PMID: 10053175]

44. **Dang-Vu TT, McKinney SM, Buxton OM, Solet JM, Ellenbogen JM.** Spontaneous brain rhythms predict sleep stability in the face of noise. Curr Biol. 2010;20:R626-7. [PMID: 20692606]

45. **Landolt HP, Dijk DJ, Achermann P, Borbély AA.** Effect of age on the sleep EEG: slow-wave activity and spindle frequency activity in young and middle-aged men. Brain Res. 1996;738:205-12. [PMID: 8955514]

46. **Mayers AG, Baldwin DS.** Antidepressants and their effect on sleep. Hum Psychopharmacol. 2005;20:533-59. [PMID: 16229049]

47. **Kahn DM, Cook TE, Carlisle CC, Nelson DL, Kramer NR, Millman RP.** Identification and modification of environmental noise in an ICU setting. Chest. 1998;114:535-40. [PMID: 9726742]

48. **Berg S.** Impact of reduced reverberation time on sound-induced arousals during sleep. Sleep. 2001;24:289-92. [PMID: 11322711]

49. **Bruck D, Ball M, Thomas I, Rouillard V.** How does the pitch and pattern of a signal affect auditory arousal thresholds? J Sleep Res. 2009;18:196-203. [PMID: 19302343]

50. **McNeer RR, Bohórquez J, Ozdamar O, Varon AJ, Barach P.** A new paradigm for the design of audible alarms that convey urgency information. J Clin Monit Comput. 2007;21:353-63. [PMID: 17973195]

51. **Yinnon AM, Ilan Y, Tadmor B, Altarescu G, Hershko C.** Quality of sleep in the medical department. Br J Clin Pract. 1992;46:88-91. [PMID: 1457316]

52. **Topf M, Bookman M, Arand D.** Effects of critical care unit noise on the subjective quality of sleep. J Adv Nurs. 1996;24:545-51. [PMID: 8876415]

53. **Southwell MT, Wistow G.** Sleep in hospitals at night: are patients' needs being met? J Adv Nurs. 1995;21:1101-9. [PMID: 7665774]

54. **Dijk DJ, Duffy JF, Czeisler CA.** Age-related increase in awakenings: impaired consolidation of nonREM sleep at all circadian phases. Sleep. 2001;24:565-77. [PMID: 11480654]

55. **Topf M, Thompson S.** Interactive relationships between hospital patients' noise-induced stress and other stress with sleep. Heart Lung. 2001;30:237-43. [PMID: 11449209]

Annals of Internal Medicine

Current Author Addresses: Dr. Buxton: 221 Longwood Avenue, BLI438-K, Boston, MA 02115.
Dr. Ellenbogen: Wang ACC 720, Massachusetts General Hospital, 55 Fruit Street, Boston, MA 02114.
Dr. Wang: 221 Longwood Avenue, BLI438-M, Boston, MA 02115.
Mr. Carballeira: 10 Upton Street, Cambridge, MA 02139.
Mr. O'Connor: 3535 Market Street, Room 1514, Philadelphia, PA 19104.
Mr. Cooper: 221 Longwood Avenue, BLI2-230, Boston, MA 02115.
Mr. Gordhandas: 15 Parkman Street, WACC 7, Boston, MA 02114.
Mr. McKinney: ICME, Suite 053B, Huang Engineering Center, 475 Via Ortega, Stanford, CA 94305.
Dr. Solet: 15 Berkeley Street, Cambridge, MA 02138.

Author Contributions: Conception and design: O.M. Buxton, A. Carballeira, J.M. Solet.
Analysis and interpretation of the data: O.M. Buxton, J.M. Ellenbogen, W. Wang, A. Carballeira, A. Gordhandas, S.M. McKinney, J.M. Solet.
Drafting of the article: O.M. Buxton, J.M. Ellenbogen, S. O'Connor, D. Cooper, S.M. McKinney, J.M. Solet.
Critical revision of the article for important intellectual content: O.M. Buxton, J.M. Ellenbogen, A. Carballeira, S. O'Connor, D. Cooper, J.M. Solet.
Final approval of the article: O.M. Buxton, A. Carballeira, S. O'Connor, D. Cooper, A. Gordhandas, J.M. Solet.
Provision of study materials or patients: O.M. Buxton, J.M. Ellenbogen, D. Cooper, J.M. Solet.
Statistical expertise: W. Wang.
Obtaining of funding: O.M. Buxton, J.M. Ellenbogen, J.M. Solet.
Administrative, technical, or logistical support: O.M. Buxton, J.M. Ellenbogen, A. Carballeira, S. O'Connor, J.M. Solet.
Collection and assembly of data: O.M. Buxton, J.M. Ellenbogen, A. Carballeira, S. O'Connor, D. Cooper, J.M. Solet.

Appendix Table 1. **Acoustic Descriptors of Sound Stimuli***

Acoustic Descriptor	Voice ("Bad" Conversation)	Voice ("Good" Conversation)	Door Open and Close	Helicopter Takeoff	Ice Machine	IV Pump Alarm	Jet Flyover	Laundry Cart Rolling	Overhead Paging (1 Voice)	Phone Ringing	Snoring	Toilet Flushing	Towel Dispenser	Traffic
L_{01}	76	78	78	76	73	76	74	73	77	73	74	75	74	72
L_{10}	74	74	74	74	72	75	74	72	74	73	74	74	73	71
L_{50}	67	68	67	69	70	66	69	71	67	71	68	69	67	70
L_{90}	52	56	55	54	69	47	52	60	46	35	35	45	45	57
L_{99}	50	41	36	36	46	42	36	36	35	35	35	35	37	35
L_{max}	76	78	79	76	73	76	74	74	78	73	74	76	74	72
L_{min}	35	35	35	35	35	35	35	35	35	35	35	35	35	35
L_{EQ}	70	70	70	70	70	70	70	70	70	70	70	70	70	70
L_{10}–L_{EQ}	4	4	4	4	2	5	4	2	4	3	4	4	3	1
L_{max}–L_{EQ}	6	8	9	6	3	6	4	4	8	3	4	6	4	2
L_{01}–L_{EQ}	6	8	8	6	3	6	4	3	7	3	4	5	4	2
L_{10}–L_{90}	22	17	20	20	3	28	22	13	28	38	39	28	29	14
L_{01}–L_{99}	26	37	42	40	26	34	38	37	42	38	39	40	37	37

IV = intravenous; L_{01} = sound level exceeded 1% of the time; L_{10} = sound level exceeded 10% of the time; L_{50} = sound level exceeded 50% of the time; L_{90} = sound level exceeded 90% of the time; L_{99} = sound level exceeded 99% of the time; L_{max} = maximum A-weighted root-mean square sound level; L_{min} = minimum A-weighted root-mean square sound level; L_{EQ} = equivalent continuous sound level.
* Sound stimuli = 70 dBA (adjusted for the range of normal human hearing).

Appendix Table 2. **Time Spent in Stages of Sleep and Wakefulness During 8.5-Hour Sleep Periods**

Variable	Night 1	Night 2	Night 3
Mean sleep stage (SD), *min*			
N1	58.0 (16.7)	63.6 (16.9)	59.3 (22.3)
N2	232.3 (26.3)	247.3 (36.3)	238.4 (28.7)
N3	90.5 (37.2)	69.2 (30.9)	80.5 (33.6)
REM	99.1 (23.6)	104.6 (19.2)	101.0 (18.7)
Mean wakefulness (SD), *min*	28.2 (14.9)	23.5 (18.9)	30.8 (14.9)

N1 = non-REM sleep stage 1; N2 = non-REM sleep stage 2; N3 = non-REM sleep stage 3; REM = rapid eye movement.

Idaho Power/1203
Witness: Dr. Jeffrey Ellenbogen

BEFORE THE PUBLIC UTILITY COMMISSION
OF OREGON

Docket PCN 5

In the Matter of

IDAHO POWER COMPANY'S
PETITION FOR CERTIFICATE OF PUBLIC CONVENIENCE
AND NECESSITY

McKinney, S. et al., Covert Waking Brain Activity
Reveals Instantaneous Sleep Depth (2011)

February 22, 2023

OPEN ACCESS Freely available online

PLoS one

Covert Waking Brain Activity Reveals Instantaneous Sleep Depth

Scott M. McKinney[1], Thien Thanh Dang-Vu[1,2,3], Orfeu M. Buxton[2,4], Jo M. Solet[2,5], Jeffrey M. Ellenbogen[1,2]*

1 Department of Neurology, Massachusetts General Hospital, Boston, Massachusetts, United States of America, 2 Division of Sleep Medicine, Harvard Medical School, Boston, Massachusetts, United States of America, 3 Cyclotron Research Centre, University of Liege, Liege, Belgium, 4 Department of Medicine, Brigham and Women's Hospital, Boston, Massachusetts, United States of America, 5 Department of Medicine, Cambridge Health Alliance, Cambridge, Massachusetts, United States of America

Abstract

The neural correlates of the wake-sleep continuum remain incompletely understood, limiting the development of adaptive drug delivery systems for promoting sleep maintenance. The most useful measure for resolving early positions along this continuum is the alpha oscillation, an 8–13 Hz electroencephalographic rhythm prominent over posterior scalp locations. The brain activation signature of wakefulness, alpha expression discloses immediate levels of alertness and dissipates in concert with fading awareness as sleep begins. This brain activity pattern, however, is largely ignored once sleep begins. Here we show that the intensity of spectral power in the alpha band actually continues to disclose instantaneous responsiveness to noise—a measure of sleep depth—throughout a night of sleep. By systematically challenging sleep with realistic and varied acoustic disruption, we found that sleepers exhibited markedly greater sensitivity to sounds during moments of elevated alpha expression. This result demonstrates that alpha power is not a binary marker of the transition between sleep and wakefulness, but carries rich information about immediate sleep stability. Further, it shows that an empirical and ecologically relevant form of sleep depth is revealed in real-time by EEG spectral content in the alpha band, a measure that affords prediction on the order of minutes. This signal, which transcends the boundaries of classical sleep stages, could potentially be used for real-time feedback to novel, adaptive drug delivery systems for inducing sleep.

Citation: McKinney SM, Dang-Vu TT, Buxton OM, Solet JM, Ellenbogen JM (2011) Covert Waking Brain Activity Reveals Instantaneous Sleep Depth. PLoS ONE 6(3): e17351. doi:10.1371/journal.pone.0017351

Editor: Naomi Rogers, Central Queensland University, Australia

Received September 30, 2010; **Accepted** January 29, 2011; **Published** March 3, 2011

Funding: This study was funded by the Academy of Architecture for Health, the Facilities Guidelines Institute, the Center for Health Design, and the Massachusetts General Hospital. The funders had no role in study design, data collection and analysis, decision to publish, or preparation of the manuscript.

Competing Interests: The authors have declared that no competing interests exist.

* E-mail: jeffrey_ellenbogen@hms.harvard.edu

Introduction

Sleep is not uniform, and certain moments are sounder than others. Indeed, resistance to acoustic disturbance—a measure of sleep depth—displays considerable variability throughout a night of sleep, even within sleep stage [1]. The factors that influence sleep's vulnerability to sensory insult have not been fully illuminated.

The very transition from wake to sleep involves a dissociation from the external world and a crescendo of internal brain rhythms. Heralding this transition is attenuation of the alpha rhythm, an 8–13 Hz electroencephalographic (EEG) oscillation prominent over posterior brain regions, and the signature of relaxed wakefulness [2]. Diminishing during the descent into sleep, alpha amplitude shadows the decline in external awareness that accompanies sleep onset [3,4]. And while it appears to vanish as sleep begins, quantitative analysis reveals that power in the alpha band actually fluctuates dynamically throughout the night (Fig. 1A) [5].

Given alpha activity's association with wakefulness and sensory intake, we hypothesized that covert levels of alpha activity would reveal a sleeper's instantaneous sensitivity to the environment. That is, inconspicuous fluctuations in wake-like background brain activity might correspond to changes in sleep depth, even beyond sleep stage designation.

To study this question in a realistic setting, we used ecological noises to probe environmental sensitivity throughout sleep, simultaneously monitoring subjects' brain activity with EEG. The sound intensity required to disturb subjects provided an empirical measure of their instantaneous sleep depth. In this paradigm, *sleep stability* denotes resistance to disruption, while *sleep fragility* denotes vulnerability to disruption. We sought to evaluate whether these qualities could be predicted using the covert level of waking brain activity just before each stimulus.

Results

We systematically challenged sleep with auditory stimulation in thirteen healthy subjects throughout two nights of sleep. Brain activity was monitored on each night using EEG. Ten-second, ecological noises (e.g., road and air traffic, a telephone ringing) were presented during bouts of stable sleep (Fig. 2). Each sound was initiated at 40 decibels (dB) and replayed every thirty seconds in 5 dB increments until the EEG signal was perturbed according to standard guidelines (i.e., an arousal was observed [6]).

We interrogated the relationship between alpha activity and sleep fragility using Cox regression, a tool from survival analysis (see Materials and Methods). The output of Cox regression is the hazard ratio (HR): this number represents the relative hazard of

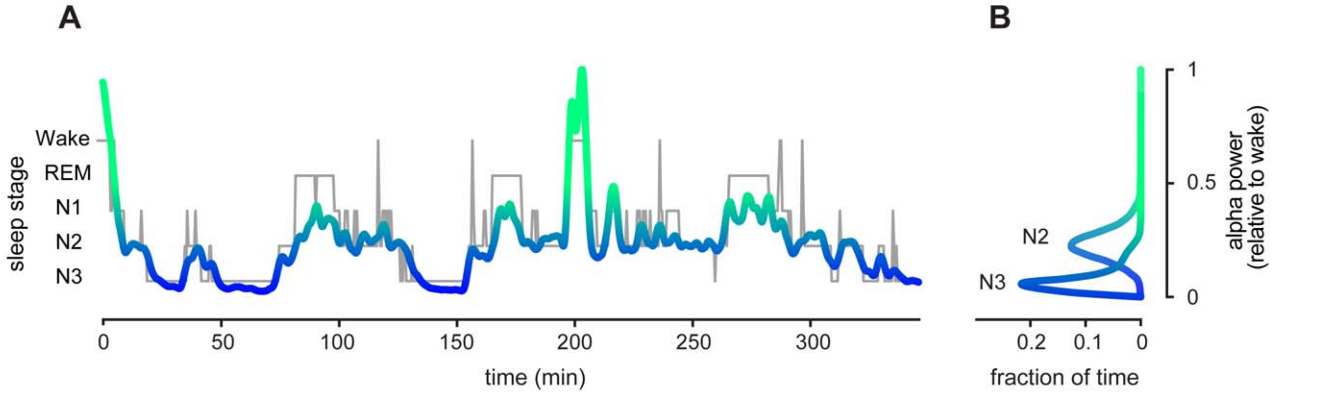

Figure 1. Alpha power fluctuates dynamically throughout the night. A. The trajectory of relative alpha power throughout a quiet night of sleep is shown from one representative subject. Simultaneous sleep stage designations run beneath the time course of alpha power. Diminishing as sleep begins, alpha power fluctuates throughout the night, in tandem with sleep depth. For display, the alpha power time-series was approximated using local linear regression in 4 minute windows, corresponding to the approximate length of each stimulation series (see Materials and Methods). This procedure removes noise and emphasizes slower fluctuations with fewer distortions than those imposed by simple low-pass filtering [42]. B. These histograms show the distribution of alpha power during NREM sleep, revealing that a range of values can be observed within each of stages N2 and N3. Power was computed in non-overlapping 10-second bins; epochs containing arousals, which may represent transient departures from stable sleep, were discarded.
doi:10.1371/journal.pone.0017351.g001

disruption in one condition compared to another. For continuous covariates, the HR represents the relative hazard of disruption incurred by a one-unit increase of the covariate. Hazard ratios greater than 1 imply that the covariate is associated with sleep fragility (vulnerability to disruption), while those less than 1 denote covariates accompanying sleep stability (resistance to disruption).

We focused our analysis on factors contributing to sleep fragility during non-rapid-eye-movement (NREM) sleep (stages N2 and N3, accounting for the majority of sleep [7]), as several difficulties arise when considering alpha activity during rapid-eye-movement (REM) sleep (see Discussion). The regression model contained two covariates, one indicating the visually scored sleep stage designation [6], the other indicating the spectral content preceding each stimulus (see Materials and Methods).

When comparing noise sensitivity across sleep stage, Cox regression yielded a HR of 0.54 ($P<0.0001$) associated with stage N3, so-called slow-wave sleep, relative to N2. In line with previous reports [1,8], this value indicates a suppressed hazard of disruption in N3 compared with N2 (the probability of tolerating noise at any loudness in N3 being roughly the square root of that in N2).

We next addressed the influence of occipital alpha activity on sleep fragility. Figure 1A shows that, on an undisturbed night of sleep, relative alpha power shadows the trajectory of qualitatively assessed sleep depth. Like the probability of disruption, alpha power is generally suppressed in N3 relative to N2 (Fig. 1B).

Although relative alpha power correlates well with sleep stage, a wide spectrum of variation still exists within each category. We therefore sought to determine whether fluctuations in this quantity—even within sleep stage—correspond to concurrent variations in sleep fragility.

To address this question, we included in the statistical model a measure of the alpha content during the ten seconds immediately preceding each sound (Fig. 2, light gray windows). Even controlling for stage, we observed a highly significant relationship between alpha power and sleep fragility ($HR = 5.74$, $P<0.001$). This suggests that, well beyond sleep stage designation, latent alpha content betrays heightened sensitivity to impending sounds.

To investigate the timescale over which alpha power predicts sleep fragility, we further characterized each sound series by a single spectral measure derived from a reference window of stable sleep preceding the sound series (Fig. 2, dark gray windows). This interval anticipated the eventual disruption by a variable latency of up to four minutes, as arousal may have occurred as late as 70 dB. Still, alpha power during this ninety-second baseline period predicted the probability of disruption in the moments that followed ($HR = 7.33$, $P<0.001$), suggesting that the brain state disclosed by alpha activity persists for several minutes (see also Results S1 and Figure S1).

Figure 3 illustrates a summary of our results, rendering the probability of sleep disruption in the face of noise as a function of

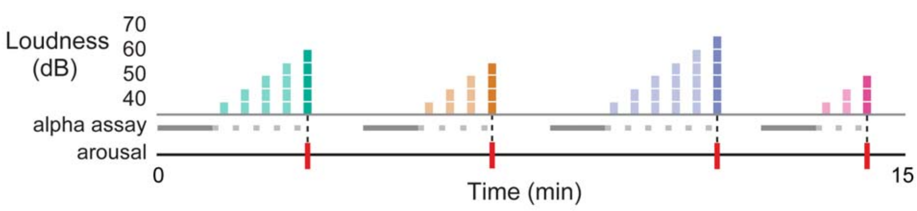

Figure 2. Sleep depth was probed with auditory stimulation. We systematically probed sleep depth with auditory stimulation during bouts of N2, N3 and REM sleep. Ten-second noises were initiated at 40 decibels (dB) and presented every thirty seconds in 5 dB increments until the EEG signal was perturbed (arousal, vertical bars on the bottom line). Each color represents a different sound type; a sample of four is shown here. The sound intensity required to disturb subjects provided an experimental measure of their immediate sleep depth. The gray windows beneath the sound level delineate periods during which alpha power was measured to predict sleep fragility.
doi:10.1371/journal.pone.0017351.g002

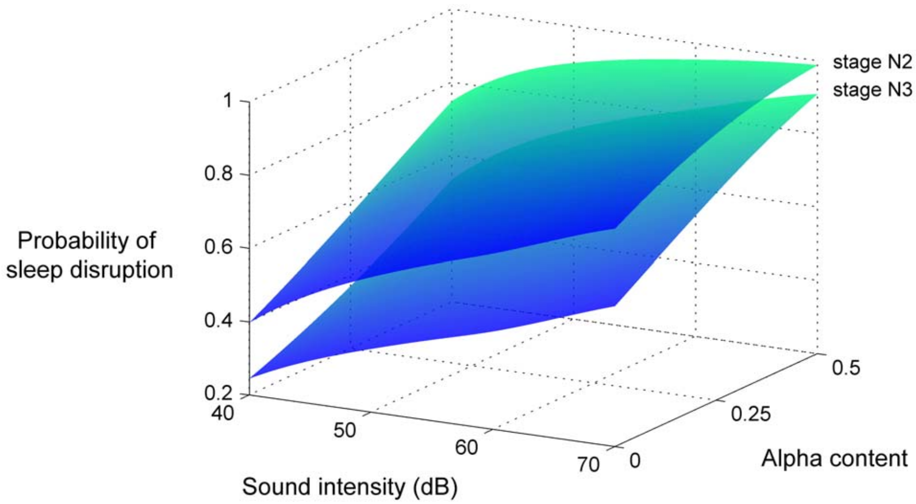

Figure 3. Alpha content reveals immediate sleep fragility. Using Cox regression, we found that alpha activity disclosed noise sensitivity during NREM sleep, even when controlling for stage. Here we reconstruct probability surfaces for sleep stages N2 and N3, rendering sleep fragility as a function of both stimulus intensity and EEG alpha content.
doi:10.1371/journal.pone.0017351.g003

both stimulus intensity and EEG alpha content. Here we depict a distinct surface for each NREM sleep stage, in which separate mechanisms may also regulate sensory perception [9,10]. Just as the probability of disruption increases monotonically with loudness, so too is sleep's vulnerability modulated by coincident alpha content.

We next explored the relationship between immediate sleep fragility and the broader EEG power spectrum. Toward this end, we estimated the power at frequencies between 0.5 and 25 Hz (in 0.5 Hz intervals) expressed over occipital electrodes during the ten seconds immediately preceding each stimulus (Fig. 2, light gray windows). To facilitate a meaningful comparison across frequencies, power values were standardized based on their waking levels and their dynamic ranges observed during NREM sleep (see Materials and Methods). The power at each frequency was then analyzed independently using Cox regression.

The resulting spectral portrait shows how power at each frequency, beyond stage designation, covaries with sleep fragility (Fig. 4). (For comparison across the entire EEG spectrum, estimates of the Cox regression coefficients reflect a change of one standard deviation in the log-power at each frequency.) The large, sustained contribution throughout the alpha band suggests that this region of the spectrum indeed contains a meaningful signal. We moreover observed strong tendencies toward sleep stability in conjunction with low-frequency power (including slow-wave, delta, and theta activity) and toward fragility in conjunction with high-frequency power (beta activity). Nonetheless, the only power value that achieved significance after a liberal correction for multiple comparisons (Holm-Bonferroni method) was that at 10.5 Hz ($P = 0.025$), centrally located within the alpha band.

As the approach just described manages to isolate the power at different frequencies, we took the opportunity to once more study

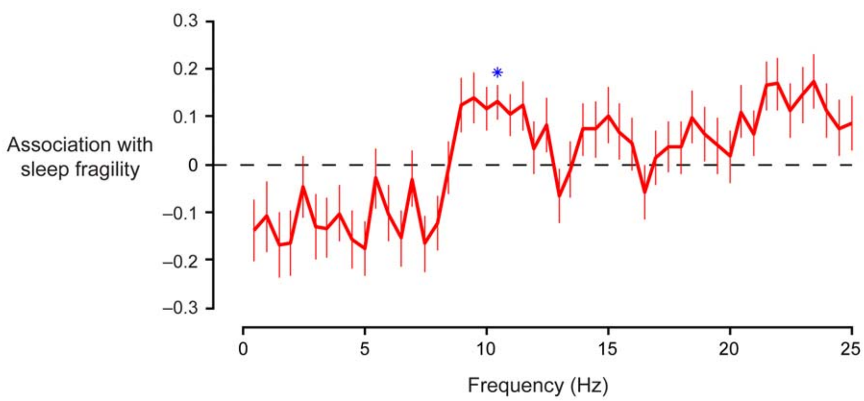

Figure 4. Alpha band power is a specific marker of sleep depth. We examined the broader relationship between EEG spectral content (beyond sleep stage designation) and NREM sleep depth. The power expressed over occipital electrodes immediately preceding each stimulus was standardized using a baseline waking spectrum and the dynamic range observed during sleep at each frequency. The relationship between spectral power values and sleep fragility was then assessed independently with Cox regression; the resulting regression coefficients (±SE) are shown for each frequency in 0.5 Hz bins. Coefficients less than zero imply an association with sleep stability (resistance to disruption), whereas coefficients greater than zero imply an association with sleep fragility (vulnerability to disruption). We observed a strong relationship between heightened sound sensitivity and spectral power throughout the alpha band. Trends toward sleep stability emerged in conjunction with low frequency (<8 Hz) power and toward fragility in conjunction with high frequency (>13 Hz) power. *$P<0.05$ after correction for multiple comparisons.
doi:10.1371/journal.pone.0017351.g004

the relationship between alpha activity and sleep fragility, this time including in our statistical model, in place of sleep stage designation, a measure of low-frequency oscillatory EEG activity (0.5–4 Hz), which may more faithfully track changes in sleep depth at the neuronal level [11]. This moreover teases apart the effects of alpha and delta activity, which may interact in the relative measure of alpha content employed earlier. In this context, slow-wave activity was associated with sleep stability (HR = 0.73; $P<10^{-11}$), and alpha activity again demonstrated a significant relationship with sleep fragility (HR = 1.13; $P = 0.002$).

Discussion

The present results show that the soundness of sleep, defined empirically and with ecological relevance, is revealed in real-time by EEG spectral content: greater vulnerability to noise-induced sleep disruption accompanies elevated alpha activity. Such spectral interrogation of sleep fragility has predictive power on the order of minutes. Furthermore, this effect transcended traditional sleep staging, imparting a greater sense of fluidity to what is typically seen as a rigid process.

From a behavioral perspective, alpha activity has been shown to resolve fine gradations in the sleep-wake continuum. On visual and auditory vigilance tasks, reduced alpha activity is associated with sluggish reaction times and an elevated probability of lapse [12,13,14,15,16]. Even during wakefulness, immediate levels of alertness are revealed by ongoing alpha activity: moments of higher parietal alpha amplitude have been associated with receptiveness to tactile stimuli and heightened attention [17]. These observations concerning alpha's relationship to sensory intake, in conjunction with several others, have emboldened some investigators to include the alpha oscillation among the neural correlates of consciousness [18]. Here we extend alpha activity's association with environmental awareness beyond wakefulness and drowsiness, and into NREM sleep.

Though the alpha oscillation was one of the first brain rhythms to be described in the human EEG [19], little is currently understood about its underlying generators or functional significance. The thalamus, which has been found to influence cortical alpha synchronization [20], might be the critical link between alpha activity and the brain's vulnerability to acoustic disruption. As the thalamus is involved in relaying sensory information to the cortex, alpha activity could be a reflection of this region's propensity for conveying external stimuli to cortical processing centers where it is capable of interrupting sleep. Intriguingly, it was recently shown that global expression of alpha power (and, to a weaker extent, beta power) is positively correlated with activity in a "tonic-alertness network," comprised of the dorsal anterior cingulate cortex, anterior insula, and thalamus [21]. The constituents of this network, with access to sensory information and broad projections throughout the cortex [22], are well positioned to support alerting functions and a "general readiness for perception and action" [21,23]. At least during wakefulness, then, elevated alpha activity seems to reflect the engagement of regions supporting sensory intake and alertness. Future studies should address the existence of a similar intrinsic connectivity network during sleep, and its connection with EEG alpha content.

The specificity of alpha power as a maker of NREM sleep depth

When we broadened the scope of our analysis to include the rest of the EEG power spectrum during NREM sleep, only an alpha frequency (10.5 Hz) remained significant after correction for multiple comparisons. Rather than suggesting that this lone frequency contains information regarding sleep fragility, we suspect that inter-individual variability in peak alpha rhythm frequency [24] undermined the effect when small slivers of the band were considered alone.

Although large scale associations between EEG power and sleep depth might be expected based on inherent correlations across frequencies in the power spectrum of the sleeping brain [5], we nonetheless observed several trends outside the alpha band that warrant attention. In particular, we noted a tendency toward sleep stability in conjunction with increased power in the frequencies below 8 Hz. This accords well with the view that low-frequency oscillatory activity (including slow-wave and delta activity) intensifies with increasing depth of NREM sleep [11]. It should be noted, however, that our analysis controlled for NREM sleep stage, so the overall relationship between sleep stability and low-frequency power, which is enhanced in stage N3 relative to N2, was necessarily blunted in this context. The association between reduced sound sensitivity and EEG spectral power in the low frequencies appeared to extend even to the theta band (4–7 Hz). In light of this observation, it is interesting to note that during vigilance tasks, theta-rich EEG has been found to be associated with reduced arousal [25] and deteriorated stimulus detection [12,26].

We further observed a tendency for increased vulnerability to disruption in conjunction with greater EEG power in higher frequencies, including the beta band (15–25 Hz). As with alpha activity, previous work has also shown a connection between variation in beta activity and fluctuations in cortical arousal and vigilance behavior [27,28]. A similar observation was made in sleep, with enhanced beta activity now thought to signify heightened arousal in patients with insomnia [29].

As might be expected, the association between alpha power and sleep fragility did not yield significance when REM sleep was considered alone ($P = 0.45$). During REM, the relative alpha power is more erratic and this activity may stem from heterogeneous brain sources. Alpha activity during REM occurs in at least two forms, conspicuous alpha bursts and background alpha activity, which are thought to be electrophysiologically distinct from one another and from that evident during wakefulness. Further, alpha amplitude may be modulated by visual imagery in the context of dreaming [2]. While the function of alpha activity during REM remains hypothetical, the present results suggest that it does not accompany heightened sensitivity to one's environment.

Future directions and applications

Previous electrophysiological studies have demonstrated that ongoing network activity profoundly influences evoked cortical responses and explains their dramatic variability [30]. Here we further emphasize the role of the immediate brain state in modulating perception by showing that beyond sleep stage [8] and the overt rhythms of sleep [31], inconspicuous background activity also varies with the soundness of sleep. In this light, alpha activity provides a potent window onto the instantaneous responsiveness of the sleeping brain. Future research should investigate the extent to which other features of EEG dynamics, such as spectral coherence [32,33], cross-frequency phase synchrony [34,35], or nested oscillations [36,37] offer useful information about empirical measures of sleep depth.

Given that real-time fluctuations in EEG parameters provide immediate information about sleep's depth and its vulnerability to disruption, it is enticing to speculate that this kind of information could be employed by adaptive hypnotic agents guided by direct feedback from neural activity. Such technology might be capable of combating the disruptive effects of environmental noise on sleep and next-day cognitive performance [38,39], while optimally preserving natural sleep physiology. At present, sleep medications are a blunt instrument. Administered before bed, conventional hypnotics last for a rigid duration fixed by their pharmacokinetic properties. These drugs dominate consciousness, inducing sleep-like sedation of unclear authenticity [40,41]. A system that allows for dynamic drug delivery based on instantaneous feedback (using a metric derived from alpha activity or the broader EEG power spectrum) could momentarily protect or facilitate sleep when vulnerable, otherwise letting natural brain rhythms run their course. Further, such an arrangement might allow for emergency interruptions or scheduled wake-times; such specificity is prohibited by the crude sleep medications used today. Besides using smaller doses, then, this system would afford enhanced precision and flexibility. The present study establishes a conceptual framework for such research, showing that sleep can be monitored in real-time and characterized along a rich continuum of depth.

Materials and Methods

The findings described here stem from an experiment conducted to study the disruptive salience of different sounds in sleep. Biomarkers for individual noise tolerance (i.e., traits) were presented in [10], whereas the current analysis seeks to elucidate moment-to-moment variations in sleep's vulnerability to disruption (i.e., states).

Ethics statement

Study procedures were approved by the Human Research Committees of the Brigham and Women's Hospital, the Massachusetts General Hospital (MGH), and the Cambridge Health Alliance. Written informed consent was obtained for all participants.

Participants

Thirteen healthy volunteers (9 females and 4 males, age 24.9±7.3; mean ± SD) were determined to be free from medical or psychiatric conditions on the basis of clinical history and a physical examination. Participants were also screened for drug, alcohol, or caffeine dependency. Subjects reported taking no medications that affect sleep or circadian rhythms. All participants demonstrated normal hearing on the basis of audiometric screening of each ear (minimum hearing level of 25 decibels [dB] at 500, 1000, 2000 and 4000 Hz).

Study conditions

Participants slept on a consistent schedule for at least 4 days prior to the study, as confirmed by wrist actigraphy (AW-64, Minimitter, Bend, OR). During the study, subjects stayed at the MGH Sleep Laboratory for 3 consecutive nights. Each night, subjects were given the opportunity to sleep for 8.5 hours at their normal bedtime. Research staff monitored the subjects 24 hours a day to ensure that they did not nap. Light levels were maintained at approximately 90 lux during waking periods, and <1 lux during sleep periods. The first night was used for adaptation; subjects adjusted to the laboratory environment and were screened for any sleep disorders visible on the polysomnogram. Acoustic stimulation was applied only on the second and third nights.

Sleep recordings

Polysomnographic recordings were collected using a Comet XL system (Grass-Telefactor, West Warwick, RI, USA). Skin surface electrodes (Beckman Instrument Company, Schiller Park, IL) captured EEG from frontal (F3 and F4), central (C3 and C4) and occipital (O1 and O2) positions; electrooculogram (EOG); submental electromyogram (EMG); and electrocardiogram (ECG). Data were conditioned by analogue filters (high-pass: 0.3 Hz; low-pass: 70 Hz), and digitally sampled at 200 Hz.

Experimental paradigm

On the second and third nights of the experiment, acoustic stimulation was applied systematically throughout stages N2, N3 and REM sleep. Once stable sleep was achieved (at least 90 consecutive seconds of the same stage scored in real time), sounds were initiated at 40 dB and replayed every thirty seconds in 5 dB increments until an arousal was observed or 70 dB was reached (Fig. 2). A 70 dB limit was imposed to minimize full awakenings from sleep and prevent significant disruption of sleep architecture. Each time an arousal was elicited, sound was withheld until stable sleep resumed, at which time a new sound was chosen.

Acoustic stimuli were each ten seconds in duration, and drawn from diverse sources. Noises included a telephone ringing, a toilet flushing, an IV alarm, a hospital intercom, a door creaking and slamming, a laundry machine, an ice machine, a towel dispenser, road traffic, snoring, a jet engine, a helicopter, and two conversations of positive and negative emotional valence. All sounds except the jet and helicopter were recorded on site in a medical unit of Somerville Hospital, Somerville, MA. Stimuli, which were repeated through each graduated sound series, were selected at random for each participant on each night.

Sound levels were measured using dBA-$L_{eq\text{-}10\ s}$, consistent with standard methods used to evaluate the clinical effects of noise. "A" refers to the weighting of sounds in ranges audible to humans, while "$L_{eq\text{-}10\ s}$" denotes an average intensity derived from the 10 seconds of the sound's duration. The sound level in the patient room was logged with an environmental sound monitor (Rion Type NL-31, with Type 1 microphone) located 10 inches above the subject's head. Stimuli were presented on a measured average background of 34–35 dB due to continuous ventilation in the room.

Stimuli were delivered in surround sound using an array of four studio-monitor loudspeakers (Event, model PS6) placed at the circumference of a circle centered around the subject's head. This arrangement enabled sounds with moving sources (e.g., the airplane) to be reproduced with apparent motion through space.

Sleep scoring

Sleep stages (in 30-second epochs) and arousals were identified in adherence with the recommendations of the American Academy of Sleep Medicine [6]. According to these criteria, an arousal consists of an abrupt increase in EEG frequency lasting at least 3 seconds, excluding that caused by a spindle, and preceded by at least 10 seconds of stable sleep. Sleep scoring was conducted by a registered polysomnographic technician under the supervision of the medical director of the MGH Sleep Laboratory.

Spectral estimation

The period preceding sound presentation was used to assay the electroencephalographic sleep depth associated with each sound. Power spectra were estimated using the multitaper method [42]. Spectra were derived from occipital electrodes (average of O1 and O2), as waking alpha tends to predominate over these posterior regions [43].

For each segment of analysis, alpha activity was computed as the integral of the power spectrum in the alpha band (8–13 Hz) divided by the total power generated in that interval. As utilized elsewhere [4,44,45,46], this metric seeks to eliminate variance resulting from non-brain-based factors (e.g., degradation of electrode contact) that occur during all-night EEG recordings. Moreover, this process facilitates an aggregate analysis across two experimental nights in each of thirteen subjects. To control for the degree to which alpha power signifies wakefulness in each individual (i.e., the subject's native alpha generation [47]), this measure was normalized to the corresponding value derived from a baseline period of eyes-closed wakefulness on the same night.

When a broader range of EEG oscillatory activity was considered (Fig. 4), the power at frequencies of 0.5 Hz to 25 Hz (in steps of 0.5 Hz) was estimated using Bartlett's method (2-second segments) and the Goertzel algorithm [48]. The quantities derived from occipital electrodes O1 and O2 were averaged for subsequent analysis. As before, the power spectral density was normalized to a baseline waking spectrum. To facilitate meaningful comparison across frequencies, which have different dynamic ranges, power values were log-transformed [42] and divided by the standard deviation of the log-spectrum observed during quiet NREM sleep (absent sound presentation) on the same night. When the power in the slow/delta band (0.5–4 Hz) and alpha band (8–13 Hz) were considered as absolute, as opposed to relative, measures, the Bartlett spectra were integrated in the corresponding ranges and the resulting power values were standardized in the manner just described.

Statistical analysis

The influence of EEG spectral content on sleep fragility was interrogated using survival analysis [49]. Each sound series defined a distinct risk period (a "lifetime") during which sleep could be disrupted—maintenance of sleep constitutes survival, disruption of sleep, a failure.

Only sound series that were preceded by three contiguous 30-second epochs of the same sleep stage and terminated in a sound-induced arousal were used for analysis. (An arousal was judged to be evoked from stimulation if the arousal occurred during the sound or within 5 seconds from its conclusion.) Among these sound series, 109 out of 724 in NREM and 45 out of 267 in REM were right-censored, meaning that sound presentation ended before arousal occurred.

In this paradigm, sleep stability, a function of loudness, describes the probability of tolerating sounds of any given intensity. Sleep fragility, the stability curve's complement, describes the probability of *disruption* due to sounds of any given intensity.

The effect of EEG spectral features on sleep fragility was evaluated with a Cox proportional hazards regression model. The model was stratified across subjects in order to account for individual differences in noise tolerance. Since our loudness scale grew in discrete, 5 dB increments, we employ the exact-partial likelihood method to handle multiple arousals at each sound intensity [50]. A categorical "stage" covariate was also included to control for the conventional measures available to characterize sleep depth.

When the power at distinct frequencies through 25 Hz were tested independently, *p*-values for each frequency were adjusted using the Holm-Bonferroni method for multiple comparisons [51].

Supporting Information

Figure S1 Alpha power is stable for minutes. This plot shows an unbiased estimate of the autocorrelation function of relative spectral content in the alpha band (8–13 Hz) measured in 10-second intervals (depicted smoothed in Figure 1A). The autocorrelogram portrays the correlation of alpha content with its subsequent values for a range of lags. The trajectory used for this figure transcended multiple sleep stages, thus portraying the global stability of alpha content that might be observed at an arbitrary time of night.
(PDF)

Results S1 Supplementary Results.
(PDF)

Acknowledgments

We thank B. Healy, M. Bianchi, and S. Cash for advice; A. Carballeira, M. Merlino, K. Gannon, D. Cooper, S. O'Connor, V. Castro, and C. Smales for assistance.

Author Contributions

Conceived and designed the experiments: JME OMB JMS. Performed the experiments: JME OMB. Analyzed the data: SMM TTD-V JME. Wrote the paper: SMM TTD-V JME.

References

1. Bonnet MH, Johnson LC, Webb WB (1978) The reliability of arousal threshold during sleep. Psychophysiology 15: 412–416.
2. Cantero JL, Atienza M, Salas RM (2002) Human alpha oscillations in wakefulness, drowsiness period, and REM sleep: different electroencephalographic phenomena within the alpha band. Neurophysiol Clin 32: 54–71.
3. Ogilvie RD (2001) The process of falling asleep. Sleep Med Rev 5: 247–270.
4. Magosso E, Ursino M, Provini F, Montagna P (2007) Wavelet analysis of electroencephalographic and electro-oculographic changes during the sleep onset period. Conf Proc IEEE Eng Med Biol Soc 2007: 4006–4010.
5. Aeschbach D, Borbely AA (1993) All-night dynamics of the human sleep EEG. J Sleep Res 2: 70–81.
6. Iber C, Ancoli-Israel S, Chesson AL, Quan SF (2007) The AASM Manual for the Scoring of Sleep and Associated Events. Westchester: American Academy of Sleep Medicine.
7. Ohayon MM, Carskadon MA, Guilleminault C, Vitiello MV (2004) Meta-analysis of quantitative sleep parameters from childhood to old age in healthy individuals: developing normative sleep values across the human lifespan. Sleep 27: 1255–1273.
8. Busby KA, Mercier L, Pivik RT (1994) Ontogenetic variations in auditory arousal threshold during sleep. Psychophysiology 31: 182–188.
9. Massimini M, Rosanova M, Mariotti M (2003) EEG slow (approximately 1 Hz) waves are associated with nonstationarity of thalamo-cortical sensory processing in the sleeping human. J Neurophysiol 89: 1205–1213.
10. Dang-Vu TT, McKinney SM, Buxton OM, Solet JM, Ellenbogen JM (2010) Spontaneous brain rhythms predict sleep stability in the face of noise. Curr Biol 20: R626–627.
11. Steriade M (2003) The corticothalamic system in sleep. Front Biosci 8: d878–899.
12. Morrell LK (1966) EEG frequency and reaction time-a sequential analysis. Neuropsychologia 4: 41–48.
13. Hori T, Hayashi M, Kato K (1991) Changes of EEG patterns and reaction time during hypnagogic state. Sleep Research 20: 20.
14. Makeig S, Inlow M (1993) Lapses in alertness: coherence of fluctuations in performance and EEG spectrum. Electroencephalogr Clin Neurophysiol 86: 23–35.
15. Gath I, Lehmann D, Bar-On E (1983) Fuzzy clustering of EEG signal and vigilance performance. Int J Neurosci 20: 303–312.
16. Lockley SW, Evans EE, Scheer FA, Brainard GC, Czeisler CA, Aeschbach D (2006) Short-wavelength sensitivity for the direct effects of light on alertness, vigilance, and the waking electroencephalogram in humans. Sleep 29: 161–168.
17. Linkenkaer-Hansen K, Nikulin VV, Palva S, Ilmoniemi RJ, Palva JM (2004) Prestimulus oscillations enhance psychophysical performance in humans. J Neurosci 24: 10186–10190.
18. Palva S, Palva JM (2007) New vistas for alpha-frequency band oscillations. Trends Neurosci 30: 150–158.
19. Berger H (1929) Über das Elektroenkephalogramm des Menschen. Archiv für Psychiatrie und Nervenkrankheiten 87: 527–570.
20. Lopes da Silva FH, Vos JE, Mooibroek J, Van Rotterdam A (1980) Relative contributions of intracortical and thalamo-cortical processes in the generation of alpha rhythms, revealed by partial coherence analysis. Electroencephalogr Clin Neurophysiol 50: 449–456.
21. Sadaghiani S, Scheeringa R, Lehongre K, Morillon B, Giraud AL, Kleinschmidt A (2010) Intrinsic connectivity networks, alpha oscillations, and tonic alertness: a simultaneous electroencephalography/functional magnetic resonance imaging study. J Neurosci 30: 10243–10250.

22. Scheibel ME, Scheibel AB (1967) Structural organization of nonspecific thalamic nuclei and their projection toward cortex. Brain Res 6: 60–94.
23. Sadaghiani S, Hesselmann G, Kleinschmidt A (2009) Distributed and antagonistic contributions of ongoing activity fluctuations to auditory stimulus detection. J Neurosci 29: 13410–13417.
24. Smit CM, Wright MJ, Hansell NK, Geffen GM, Martin NG (2006) Genetic variation of individual alpha frequency (IAF) and alpha power in a large adolescent twin sample. Int J Psychophysiol 61: 235–243.
25. Mackworth JF (1970) Vigilance and attention: a signal detection approach. Harmondsworth: Penguin. 189 p.
26. Beatty J, Greenberg A, Deibler WP, O'Hanlon JF (1974) Operant control of occipital theta rhythm affects performance in a radar monitoring task. Science 183: 871–873.
27. Townsend RE, Johnson LC (1979) Relation of frequency-analyzed EEG to monitoring behavior. Electroencephalogr Clin Neurophysiol 47: 272–279.
28. Belyavin A, Wright NA (1987) Changes in electrical activity of the brain with vigilance. Electroencephalogr Clin Neurophysiol 66: 137–144.
29. Perlis ML, Merica H, Smith MT, Giles DE (2001) Beta EEG activity and insomnia. Sleep Med Rev 5: 363–374.
30. Arieli A, Sterkin A, Grinvald A, Aertsen A (1996) Dynamics of ongoing activity: explanation of the large variability in evoked cortical responses. Science 273: 1868–1871.
31. Steriade M (1991) Alertness, quiet sleep, and dreaming. In: Peters A, Jones EJ, eds. Normal and Altered States of Function. New York: Plenum Press. pp 279–357.
32. Achermann P, Borbely AA (1998) Temporal evolution of coherence and power in the human sleep electroencephalogram. J Sleep Res 7 Suppl 1: 36–41.
33. Cantero JL, Atienza M, Salas RM, Gomez CM (1999) Alpha EEG coherence in different brain states: an electrophysiological index of the arousal level in human subjects. Neurosci Lett 271: 167–170.
34. Palva JM, Palva S, Kaila K (2005) Phase synchrony among neuronal oscillations in the human cortex. J Neurosci 25: 3962–3972.
35. Nikulin VV, Brismar T (2006) Phase synchronization between alpha and beta oscillations in the human electroencephalogram. Neuroscience 137: 647–657.
36. Vanhatalo S, Palva JM, Holmes MD, Miller JW, Voipio J, Kaila K (2004) Infraslow oscillations modulate excitability and interictal epileptic activity in the human cortex during sleep. Proc Natl Acad Sci U S A 101: 5053–5057.
37. Monto S, Palva S, Voipio J, Palva JM (2008) Very slow EEG fluctuations predict the dynamics of stimulus detection and oscillation amplitudes in humans. J Neurosci 28: 8268–8272.
38. Wilkinson RT, Campbell KB (1984) Effects of traffic noise on quality of sleep: assessment by EEG, subjective report, or performance the next day. J Acoust Soc Am 75: 468–475.
39. Muzet A (2007) Environmental noise, sleep and health. Sleep Med Rev 11: 135–142.
40. Borbely AA, Mattmann P, Loepfe M, Strauch I, Lehmann D (1985) Effect of benzodiazepine hypnotics on all-night sleep EEG spectra. Hum Neurobiol 4: 189–194.
41. Brunner DP, Dijk DJ, Munch M, Borbely AA (1991) Effect of zolpidem on sleep and sleep EEG spectra in healthy young men. Psychopharmacology (Berl) 104: 1–5.
42. Mitra P, Bokil H (2008) Observed Brain Dynamics. New York: Oxford University Press.
43. Cantero JL, Atienza M, Gomez CM, Salas RM (1999) Spectral structure and brain mapping of human alpha activities in different arousal states. Neuropsychobiology 39: 110–116.
44. Perlis ML, Smith MT, Andrews PJ, Orff H, Giles DE (2001) Beta/Gamma EEG activity in patients with primary and secondary insomnia and good sleeper controls. Sleep 24: 110–117.
45. Asyali MH, Berry RB, Khoo MC, Altinok A (2007) Determining a continuous marker for sleep depth. Comput Biol Med 37: 1600–1609.
46. Huber R, Ghilardi MF, Massimini M, Ferrarelli F, Riedner BA, Peterson MJ, Tononi G (2006) Arm immobilization causes cortical plastic changes and locally decreases sleep slow wave activity. Nat Neurosci 9: 1169–1176.
47. Smit DJ, Posthuma D, Boomsma DI, Geus EJ (2005) Heritability of background EEG across the power spectrum. Psychophysiology 42: 691–697.
48. Proakis JG, Manolakis DG (1996) Digital signal processing : principles, algorithms, and applications. Upper Saddle RiverN.J.: Prentice Hall.
49. Neckelmann D, Ursin R (1993) Sleep stages and EEG power spectrum in relation to acoustical stimulus arousal threshold in the rat. Sleep 16: 467–477.
50. Klein JP, Moeschberger ML (2003) Survival analysis : techniques for censored and truncated data. New York: Springer.
51. Holm S (1979) A Simple Sequentially Rejective Multiple Test Procedure. Scandinavian Journal of Statistics 6: 65–70.

Covert Waking Brain Activity Reveals Instantaneous Sleep Depth

Scott M. McKinney, Thien Thanh Dang-Vu, Orfeu M. Buxton, Jo M. Solet,
and Jeffrey M. Ellenbogen*

SUPPLEMENTARY RESULTS

To shed further light on the timescale over which alpha power might be capable of predicting sleep fragility, we studied the natural trajectory of alpha power during an entire night of sleep from one representative subject, as shown in Figure 1A. Here we used data from the quiet night of sleep, free of sound presentation.

The representation of Figure 1B conveys the magnitude of relative alpha power variability over the course of the night. To address the stability of such a measure from one moment to the next, we employed autocorrelation. The autocorrelation function shows the correlation of a time series with its future values at any given latency. Figure S1 shows an unbiased estimate of the autocorrelation function for the relative alpha power trajectory shown in Figure 1A, for lags up to 25 minutes long. This plot portrays the persistence, or inertia, of EEG alpha content from one observation to the next, understanding that stage transitions or awakenings occur many times throughout the night. Although our protocol involving frequent sound stimulation only permitted examination of latencies up to four minutes long, this information from the baseline night suggests that prediction of sleep fragility based on alpha power is not likely valid over time horizons greater than five minutes.

* To whom correspondence should be addressed. E-mail: jeffrey_ellenbogen@hms.harvard.edu

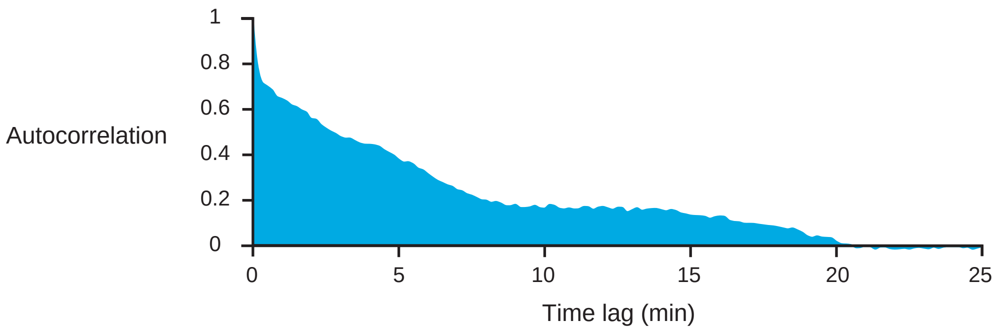

Figure S1

Idaho Power/1204
Witness: Dr. Jeffrey Ellenbogen

BEFORE THE PUBLIC UTILITY COMMISSION
OF OREGON

Docket PCN 5

In the Matter of

IDAHO POWER COMPANY'S
PETITION FOR CERTIFICATE OF PUBLIC CONVENIENCE
AND NECESSITY

Dang-Vu, T. T. et al., Spontaneous Brain Rhythms
Predict Sleep Stability in the Face of Noise (2010)

February 22, 2023

Correspondence

Spontaneous brain rhythms predict sleep stability in the face of noise

Thien Thanh Dang-Vu[1–3], Scott M. McKinney[2], Orfeu M. Buxton[1,4], Jo M. Solet[1,5] and Jeffrey M. Ellenbogen[1,2]

Quality sleep is an essential part of health and well-being. Yet fractured sleep is disturbingly prevalent in our society, partly due to insults from a variety of noises [1]. Common experience suggests that this fragility of sleep is highly variable between people, but it is unclear what mechanisms drive these differences. Here we show that it is possible to predict an individual's ability to maintain sleep in the face of sound using spontaneous brain rhythms from electroencephalography (EEG). The sleep spindle is a thalamocortical rhythm manifested on the EEG as a brief 11–15 Hz oscillation and is thought to be capable of modulating the influence of external stimuli [2]. Its rate of occurrence, while variable across people, is stable across nights [3]. We found that individuals who generated more sleep spindles during a quiet night of sleep went on to exhibit higher tolerance for noise during a subsequent, noisy night of sleep. This result shows that the sleeping brain's spontaneous activity heralds individual resilience to disruptive stimuli. Our finding sets the stage for future studies that attempt to augment spindle production to enhance sleep continuity when confronted with noise.

The brain's response to sensory input is modulated by ongoing, spontaneous neuronal activity [4]. Indeed, during sleep, the thalamus spontaneously engages with the cortex. This interaction can produce transient fluctuations of the brain's electric field visible on the EEG as rhythmic spindles (Figure 1A). As the thalamus relays sensory information to perceptual cortices, it has been proposed that brain processes involved in spindle production gate sensory input during sleep [2]. If spindles hinder the transmission of external stimuli from the thalamus to the cortex, a higher rate of spindle production throughout the night would be expected to preserve sleep stability in the face of noise. We hypothesized that individuals who generate more spindles would require sounds of higher intensity to disrupt their naturally occurring sleep.

Twelve healthy human volunteers (age 26.3 ± 7.5, mean ± SD) were studied in the sleep laboratory for three consecutive nights. The first night was quiet, while the second and third were noisy. Brain activity was monitored each night with EEG. We detected spindles on central channels (C3, C4) during the quiet night using an automatic algorithm (Figure 1A, and Figure S1A in the on-line Supplemental Information), defining each subject's spindle rate as the number of detected events per minute during stage N2 and N3 (stages 2 and 3 of non-REM sleep). On the noisy nights we presented frequently encountered sounds — for example road and air traffic, a telephone ringing, or hospital-based mechanical sounds — during stages N2, N3 and R (REM sleep). These ten-second noises were initiated at 40 decibels (dB) and presented every thirty seconds in 5 dB increments until the EEG signal was perturbed according to standard guidelines (that is, an arousal was observed) [5] (Figure 1B). In the present analysis, sleep

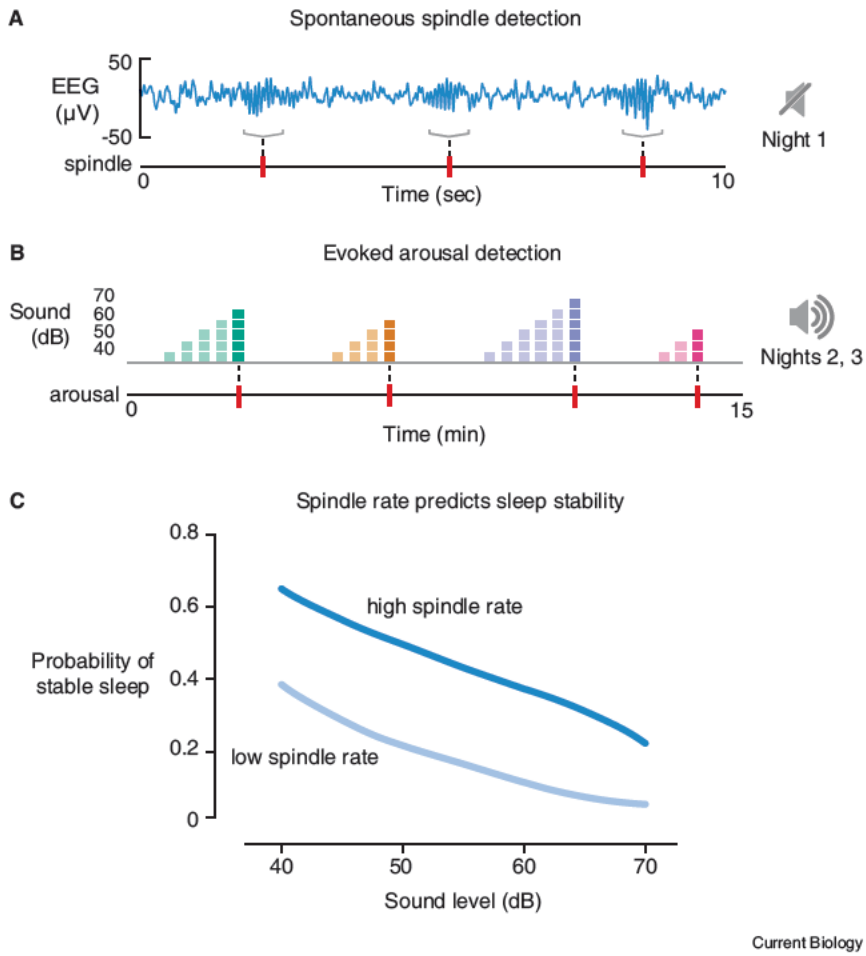

Figure 1. Spindle rate predicts sleep stability.

(A) Sleep spindles were automatically detected on central EEG channels during a quiet night of sleep. The number of detected events (vertical bars on the bottom line) per minute defined each subject's spindle rate. (B) On two subsequent nights we introduced ten-second noises, initiated at 40 decibels (dB) and presented every thirty seconds in 5 dB increments until the EEG signal was perturbed (arousal, vertical bars on the bottom line). Each colour represents a different sound type; a sample of four is shown here. (C) Observations were pooled among subjects in the lower and upper halves of the spindle rate distribution (ranges 4.57–5.44 and 5.48–6.14 spindles/min, respectively) based on EEG lead C3 during stage N2. Corresponding sleep survival curves were derived from each pool in stage N2 using the Kaplan-Meier (product-limit) method.

Current Biology Vol 20 No 15
R2

stability is defined as the maintenance of sleep without arousal.

We first considered the relationship between spindles and sleep stability during stage N2, when spindles predominate. Using Cox regression, we found that those with higher spindle rates on the quiet night exhibited greater sleep stability during the noisy nights: spindle rate carried a sleep disruption hazard ratio (HR) of 0.39 from C3 ($p = 0.001$) and 0.51 from C4 ($p = 0.002$) (see Figure 1C).

As spindles are also present in stage N3, we performed the same analysis considering stages N2 and N3 together. We again found a significant relationship between spindle rate and sleep stability (HR = 0.55, $p = 0.003$ for C3; HR = 0.64, $p = 0.018$ for C4).

This result shows that it is possible to predict an individual's ability to maintain sleep in the face of external sound: those with more abundant spindles are more resistant to sounds during sleep. It remains to be seen whether this relationship emerges from the cumulative effects of spindle and sound collision, as we suspect, or whether it is due to a yet undetermined biological process.

In line with previous reports [3], we observed consistent spindle rates from night to night (Figure S1B). We thus regard spindle rate as a stable trait, suitable for predicting sleep continuity under noisy conditions.

The extent to which the relationship between spindle rate and noise tolerance bears on different populations awaits exploration. Noise tolerance during sleep [6], like spindle rate [7], diminishes with age. On the other hand, despite reporting poor sleep, people with insomnia possess arousal thresholds similar to those of normal sleepers [8]. They likewise produce spindles at normal rates [9]. It is tempting to link these pairs of observations based on our result.

Our finding also suggests a tantalizing explanation for associations uncovered between spindle rate and learning potential (see for instance [10]): in addition to perhaps actively contributing to memory consolidation, spindles may shield sleep from disruption, allowing consolidating processes to operate unhindered.

Our data raise important questions about whether augmenting spindle rate through behaviour, drug or device might protect sleep by harnessing the spindle's ability to deflect incoming stimuli. While we await intervention-based exploration, this study provides evidence that sleep spindle rate — readily quantified from EEG — serves as a biomarker for vulnerability to sound during sleep.

Supplemental Information

Supplemental Information is available at doi:10.1016/j.cub.2010.06.032

Acknowledgements

This study was funded by the Academy of Architecture for Health, the Facilities Guidelines Institute, the Centre for Health Design, and the Mass. General Hospital. T.T. Dang-Vu is supported by the Belgian Fonds National de la Recherche Scientifique, the Belgian American Educational Foundation, Fonds Léon Frédéricq, Horlait-Dapsens Medical Foundation and Wallonie-Bruxelles International. We thank P. Maquet, M. Bedny, and B. Healy for insights and M. Merlino, P. Sorenson, K. Gannon, A. Carballeira, D. Cooper, S. O'Connor, V. Castro, C. Smales, and J. Comins and for technical expertise.

References

1. Muzet, A. (2007). Environmental noise, sleep and health. Sleep Med. Rev. *11*, 135–142.
2. Steriade, M. (1991). Alertness, quiet sleep, dreaming. In Cerebral Cortex, Volume 9: Normal and altered states of function, A. Peters and E.J. Jones, eds. (New York: Plenum Press), pp. 279–357.
3. Azumi, K., and Shirakawa, S. (1982). Characteristics of spindle activity and their use in evaluation of hypnotics. Sleep *5*, 95–105.
4. Arieli, A., Sterkin, A., Grinvald, A., and Aertsen, A. (1996). Dynamics of ongoing activity: explanation of the large variability in evoked cortical responses. Science *273*, 1868–1871.
5. Iber, C., Ancoli-Israel, S., Chesson, A.L., and Quan, S.F. (2007). The AASM Manual for the Scoring of Sleep and Associated Events, (Westchester: American Academy of Sleep Medicine).
6. Busby, K.A., Mercier, L., and Pivik, R.T. (1994). Ontogenetic variations in auditory arousal threshold during sleep. Psychophysiology *31*, 182–188.
7. De Gennaro, L., and Ferrara, M. (2003). Sleep spindles: an overview. Sleep Med. Rev. *7*, 423–440.
8. Mendelson, W.B., James, S.P., Garnett, D., Sack, D.A., and Rosenthal, N.E. (1986). A psychophysiological study of insomnia. Psychiatry Res. *19*, 267–284.
9. Bastien, C.H., St-Jean, G., Turcotte, I., Morin, C.M., Lavallee, M., and Carrier, J. (2009). Sleep spindles in chronic psychophysiological insomnia. J. Psychosom. Res. *66*, 59–65.
10. Fogel, S.M., Nader, R., Cote, K.A., and Smith, C.T. (2007). Sleep spindles and learning potential. Behav. Neurosci. *121*, 1–10.

[1]Division of Sleep Medicine, Harvard Medical School, Boston, MA 02115, USA. [2]Department of Neurology, Massachusetts General Hospital, Boston, MA 02114, USA. [3]Cyclotron Research Centre, University of Liege, Belgium. [4]Department of Medicine, Brigham and Women's Hospital, Boston, MA 02115, USA. [5]Department of Psychiatry, Cambridge Health Alliance, Cambridge, MA 02139, USA.
E-mail: jeffrey_ellenbogen@hms.harvard.edu

Supplemental Data: Spontaneous brain rhythms predict sleep stability in the face of noise

Thien Thanh Dang-Vu, Scott M. McKinney, Orfeu M. Buxton, Jo M. Solet, and Jeffrey M. Ellenbogen

Supplemental Experimental Procedures

Institutional review

Study procedures were approved by the Human Research Committees of the Brigham and Women's Hospital, Massachusetts General Hospital (MGH) and the Cambridge Health Alliance. Informed consent was obtained for all subjects.

Subjects

Twelve healthy volunteers (8 females and 4 males, age 26.3±7.5 [mean±SD]) were screened to be free from any acute or chronic medical or psychiatric conditions, established on the basis of clinical history and a physical examination obtained by a physician. History of illicit drug, alcohol, or caffeine dependency was also ruled out by clinical history and confirmed by toxicological urinalysis. Participants were taking no medications (prescription or over the counter) that affect circadian rhythms or sleep. Absence of sleep pathologies, including sleep-disordered breathing and periodic limb movements, was confirmed by standard polysomnographic sleep recording (see Sleep recordings). Volunteers with hearing impairment were excluded based on audiometric screening of each ear (hearing level threshold of 25 decibels [dB] at 500, 1000, 2000 and 4000Hz).

Study conditions

Prior to the study, subjects slept at home on a consistent schedule for at least 4 days, as assessed by wrist actigraphy (AW-64, Minimitter, Bend OR). Participants were admitted to the MGH Sleep Laboratory in the early evening and stayed for 3 days. Subjects were given the opportunity to sleep for 8.5 hours at their normal bedtime. Research staff was present 24 hours a day to monitor the subject via audio and video, as well as to check vital signs, deliver meals, and ensure that subjects did not nap. Light levels were maintained at approximately 90 lux during waking periods, and <1 lux during sleep periods in order to maintain normal circadian alignment.

Sleep recordings

Polysomnographic (PSG) recordings were collected using a Comet XL system (Grass-Telefactor West Warwick, RI, USA). On all three nights, skin surface electrodes (Beckman Instrument Company, Schiller Park, IL) captured EEG from frontal (F3 and F4), central (C3 and C4) and occipital (O1 and O2) positions, electrooculogram (EOG), submental electromyogram (EMG), and electrocardiogram (ECG). Data were captured at a sampling rate of 200 Hz and conditioned by analog filters (high pass 0.3 Hz, low pass 70 Hz).

Acoustic stimuli

Fourteen sounds were recorded in a medical unit of Somerville Hospital, Somerville, Massachusetts. Sounds were drawn from a broad range of sources: an IV alarm, a phone ringing, a toilet flush, a physician's pager sounding, a door creaking and slamming, a laundry machine, an ice machine, a towel dispenser, traffic noises, snoring, a jet engine, a helicopter, and two conversations of different emotional valence (positive and negative). All sounds were 10 seconds in duration.

Sounds were presented during sleep on the second and third nights of the study. The first night was quiet, containing merely "sham" acoustic stimulation: the audio equipment was positioned as it would be on subsequent (noisy) nights, but sleep was not disturbed for the entire 8.5 hr sleep opportunity. Subjects were not informed that they would have an initial quiet night, but were rather told that sounds would be delivered during all nights.

On the noisy nights, acoustic stimuli were presented in surround sound using an array of four studio-monitor loudspeakers (Event, model PS6) placed at the circumference of a virtual circle around the subject's head (i.e., modified ITU-R BS775-1 pattern). All sounds were veridical with respect to the soundscape. If a sound in real life had motion, such as a plane or car, then it was played as having motion in space during the study. The mean (± SE) number of presented sounds per subject was 193.1 (19.6) for the second night and 242.5 (34) for the third night. Stimuli were presented on a measured average background of 34-35 dB that was due to continuous ventilation in the room.

Sound levels were measured using dBA-$L_{eq\text{-}10sec}$, consistent with standard methods used to evaluate the clinical effects of noise: 'A' refers to the weighting of sounds in ranges audible to humans; $L_{eq\text{-}10sec}$ refers to the equivalent continuous sound level, i.e., averaging of sound pressure level across the 10 sec of sound presentation.

The sound level in the patient room was logged with an environmental sound monitor (Rion Type NL-31, with Type 1 microphone) installed on a tripod roughly 10 inches above the head of the sleeping subject, and programmed to output a DC voltage proportional to the A-weighted fast response sound level. This signal was integrated by the sleep recording software and calibrated using a 1 kHz sine wave.

Once stable sleep was achieved (at least 90 seconds of the same stage was scored in real time), sounds were initiated at 40 dB and presented every thirty seconds in 5 dB increments until an arousal was observed or until 70 dB was reached. A 70 dB limit was set in order to minimize full awakenings from sleep and thus prevent significant disruption of sleep architecture (Supplemental Results). Stimuli were presented in randomized order for each participant and night. Each time a sound elicited an arousal, no further sound was presented until stable sleep resumed.

Sleep analysis

Sleep stages, spindles and arousals were identified in adherence with the recommendations of the American Academy of Sleep Medicine [5]. According to these criteria, an arousal is defined as an abrupt increase in EEG frequency that lasts at least 3 seconds, excluding that caused by a spindle, preceded by at least 10 seconds of stable sleep. Scoring of sleep was conducted by a registered polysomnographic technician under the supervision of the medical director of the MGH sleep laboratory.

Arousal threshold

Acoustic arousal threshold was defined as the sound intensity observed to evoke an EEG arousal. The mean (± SE) number of sound-evoked arousals per subject was 42.7 (± 2.8) for the second night, and 44.6 (± 4.2) for the third night. Because our hypothesis focused on spindles, arousal thresholds were first examined in epochs of stage N2 sleep, the stage during which spindles predominate [5]. As spindles are also present during stage N3, sounds and corresponding arousal thresholds were also examined during stages N2 and N3 considered together. Sounds were delivered during two nights in order to increase the sample of presented sounds [S1].

For the computation of the linear regression (see Statistical analysis section), arousal thresholds were averaged across sound types within subject.

Spindle rate

Spindle rate was quantified on EEG channels C3 and C4 (referenced to the contralateral mastoid), since they are most pronounced in these locations [7]. To this end, an automatic spindle detection algorithm was adapted from Molle et al. and others [S2-S3] (Figure S1A). According to this method, the raw EEG signal was digitally bandpass filtered in the spindle frequency range (11-15 Hz) using a linear phase finite impulse response filters (-6 dB at 11 and 15 Hz). The average root mean square (rms) power of the filtered signal was calculated in time windows of 0.25 sec with 5 msec resolution. Sleep spindles were identified during those times in which the rms power of the filtered signal achieved a value above its 87th percentile. The presence of a spindle was validated by determining whether the spindle's peak-to-peak amplitude lay between 10 and 100 μV, and its duration was at least 0.5 sec. Spindle rate was calculated as the ratio of the number of detected spindles during stages N2 and N3 to the duration (in min.) of these stages in each subject.

Because of arguments suggesting the existence of two types of spindles (fast and slow) [S3], we also tested whether there was an effect of spindle type on sleep stability in the face of noise (Supplemental Results). Detected spindles were thus classified as either fast or slow according to the peak frequency of the filtered EEG signal during each detected spindle (slow = 11-13 Hz; fast = 13-15 Hz).

In order to test whether other properties of spindles, in addition to their rate, modulate sleep stability in the face of noise, we computed the average amplitude and duration of spindles characteristic to each subject. As described above, the beginning and end of a spindle were defined as two successive threshold-crossings of the power of the filtered signal, at least 0.5 sec apart. The amplitude was computed as the maximal peak-to-peak amplitude of the filtered EEG signal during a detected spindle. We also tested a joint measure of amplitude and duration by computing the total spectral power of the filtered signal (11-15 Hz) during detected spindles (Supplemental Results). Power spectra were estimated using the multitaper method [S4].

We confirmed that spindle rate is consistent across nights, as shown previously [S5], by measuring spindle rates during the second and third (noisy) nights in addition to the first (quiet) night. To achieve this, we applied the spindle detection algorithm to EEG collected from the second and third nights, after excluding all epochs during which sounds were presented, as well as those immediately afterward. This exclusion was performed because sounds are known to influence spindle production [S6]. (See Supplemental Results below, and Figure S1B.)

Statistical analysis

Sleep stability was defined as the maintenance of sleep in the absence of arousal. Sleep stability was interrogated using survival analysis, where maintenance of sleep constitutes survival, and arousal from sleep a failure. Each sound series defined a distinct risk period during which sleep could be disrupted by a sound-induced arousal.

Empirical descriptions of the cumulative distribution of arousal thresholds, called survivor functions, were estimated using the Kaplan-Meier product-limit method for censored data. The survivor function of loudness describes the probability of tolerating sound intensities at least that loud. Across all 565 observations, 138 were right-censored, meaning that sound presentation at the highest dB level was terminated before an arousal occurred.

The effect of spindle rates from EEG channels C3 and C4 on sleep stability (i.e., absence of arousal) was evaluated using a Cox proportional hazards regression model, accounting for shared frailty among sleep periods belonging to the same subject.

The hazard ratio (similar to a measure of relative risk) represents the proportional change in hazard due to a one-unit increase in spindle rate. In the current analysis, more spindles per minute resulted in a significantly lower hazard of sleep disruption due to noise. The same method was used to test the effects of spindle amplitude, duration and power on stage N2 sleep stability.

As an alternative presentation of these data, we also tested whether spindle rates were significantly correlated to each individual's mean arousal threshold using a linear regression. In this case, right-censored events were considered as arousal thresholds of 75 dB for the calculation of the mean. (Figure S1C and Supplemental Results, below.) This further substantiates our finding.

Supplemental Results

Sleep stages

Table S1 shows the composition of total sleep time (TST) averaged across subjects, during each of the three nights in this study. These values did not differ significantly across nights ($F = 0.00016$; $p = 0.99$), showing that, aside from very brief arousals, traditionally-defined sleep architecture was not affected by sound presentation. In agreement with previous reports [S7], amounts of stages N1, N2, N3 and REM sleep (either absolute time or % of TST) and TST were not significantly correlated with arousal thresholds during stage N2.

We also compared the same parameters from the quiet night (amounts of stages N1, N2, N3 and REM, TST) among subjects in the upper and lower halves of the spindle rate distribution, as depicted in figure 1C, and found no significant difference (two-sample t-tests). This suggests that the effects observed with spindle rate are not confounded by sleep stages and total sleep time.

Spindle rate

Spindle rates on C3 were not significantly different from spindle rates on C4 (paired t-test). Spindle rates were not significantly different between females and males, either on C3 or C4 (two-sample t-test).

In order to establish that spindle rate was consistent night to night for a given subject, we compared spindle rate on the quiet night to spindle rate on the quiet portions of the noisy nights. Thus, spindle rates on nights 2 and 3 were calculated after exclusion of 30-sec epochs with sounds, as well as the subsequent epoch after sound presentation. In order to compensate for the fewer number of quiet epochs in nights 2 and 3 compared to night 1, spindle rates in nights 2 and 3 were considered together. Spindles rates were not significantly different across nights (ANOVA), either for C3 ($p = 0.15$), or C4 ($p = 0.43$). Spindle rates on night 1 were also positively correlated with those on nights 2 and 3 ($r = 0.63$, $p = 0.028$ for C4; $r = 0.68$, $p = 0.01$ for C3) (Figure S1B). This stands in agreement with previous reports, showing a consistency of spindle rate across nights within subjects [S5]. In addition, using spindle rates from nights 2 and 3 (instead of the first, quiet, night) still predicted sleep stability in the face of noise during the same nights (Cox regression: $p < 0.001$ for C3, $p = 0.028$ for C4).

The average amplitude, duration or power of spindles during the quiet night did not have a significant effect on sleep stability during noisy nights. The spindle rate weighted by either the mean amplitude or mean spectral power of spindles likewise did not predict sleep stability. Only the spindle rate weighted by duration achieved significance with sleep stability ($p = 0.013$ and $p = 0.012$, for C3 and C4, respectively). However, we found that spindle rate weighted by the spindles' average duration was strongly correlated with spindle rate alone ($R^2 = 0.845$), demonstrating that this effect was likely driven by spindle rate alone with no effect of duration itself. This was due to the relative consistency in spindle duration across subjects (mean duration = 0.84 sec; SD = 0.035 sec). When spindles were classified into fast and slow spindles, the corresponding slow and fast spindle rates had no significant effect on sleep stability from noise. Altogether, these additional analyses suggest that the number (rate) rather than the properties (amplitude, duration, power or frequency) of spindles modulates sleep stability in the face of noise.

Figure S1C shows the correlation during stage N2 between spindle rate and mean arousal threshold as assessed by linear regression. We found that spindle rate on a quiet night was positively correlated with arousal threshold during noisy nights ($r = 0.77$; $p = 0.003$ for C3; $r = 0.71$; $p = 0.01$ for C4).

Supplemental References

S1. Bonnet, M.H., Johnson, L.C., and Webb, W.B. (1978). The reliability of arousal threshold during sleep. Psychophysiology 15, 412-416.

S2. Molle, M., Marshall, L., Gais, S., and Born, J. (2002). Grouping of spindle activity during slow oscillations in human non-rapid eye movement sleep. J Neurosci 22, 10941-10947.

S3. Schabus, M., Dang-Vu, T.T., Albouy, G., Balteau, E., Boly, M., Carrier, J., Darsaud, A., Degueldre, C., Desseilles, M., Gais, S., et al. (2007). Hemodynamic cerebral correlates of sleep spindles during human non-rapid eye movement sleep. Proc Natl Acad Sci U S A 104, 13164-13169.

S4. Mitra, P., and Bokil, H. (2008). Observed Brain Dynamics, (New York: Oxford University Press).

S5. Gaillard, J.M., and Blois, R. (1981). Spindle density in sleep of normal subjects. Sleep 4, 385-391.

S6. Sato, Y., Fukuoka, Y., Minamitani, H., and Honda, K. (2007). Sensory stimulation triggers spindles during sleep stage 2. Sleep 30, 511-518.

S7. Bonnet, M.H., and Johnson, L.C. (1978). Relationship of arousal threshold to sleep stage distribution and subjective estimates of depth and quality of sleep. Sleep 1, 161-168.

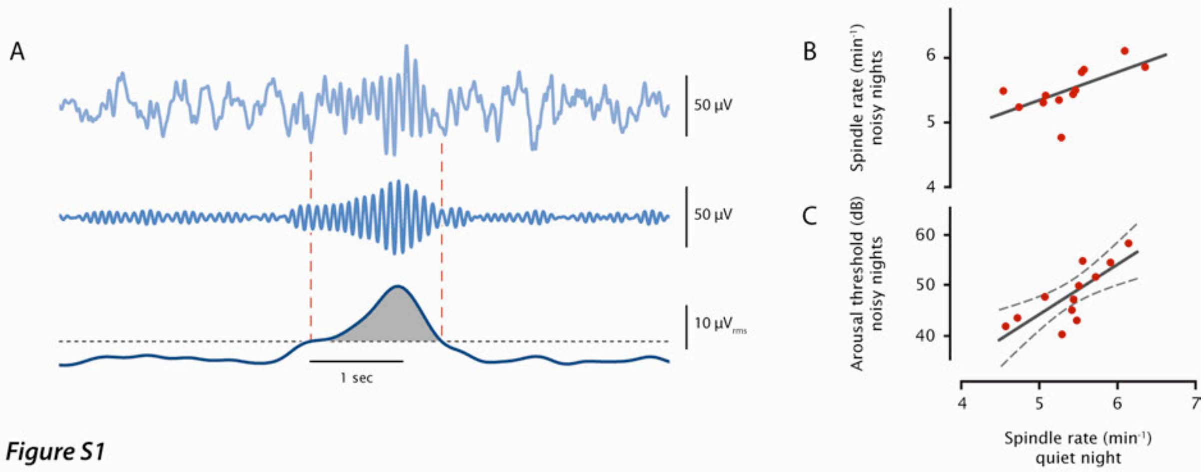

Figure S1

A. ***Spindle detection method***

(Upper trace) Electroencephalogram (EEG) depicting a typical spindle. This raw trace was derived from lead C3, referenced to the contralateral mastoid.

(Middle trace) For spindle detection, the raw signal (shown in upper trace) was first filtered in the spindle frequency band (11-15 Hz).

(Lower trace) Sleep spindles were then identified during those times when the average root mean square (rms) power of the filtered signal (shown in middle trace) achieved a value above its 87th percentile (horizontal dashed line). Additional criteria (not shown) included peak-to-peak amplitude between 10 and 100 µV, and duration longer than 0.5 sec. The vertical dashed lines delineate the detected spindle.

B. *Spindle rate is consistent across nights*

Spindle rate during the first (quiet) night positively correlated with spindle rate averaged over the second and third (noisy) nights ($r = 0.63$; $p = 0.028$), after exclusion of 30 sec-epochs during which sounds were presented as well as the epoch immediately following. Spindles rates are from EEG lead C4 and in stage N2 sleep. Each dot represents one subject. The solid line is the regression.

C. *Spindle rate predicts mean arousal threshold*

Spindle rate during the quiet night positively correlated with mean arousal threshold during noisy nights ($r = 0.77$; $p = 0.003$; the spindle rates represented here are calculated from EEG lead C3) during stage N2 sleep. Each dot represents one subject. The solid line is the regression. The dashed lines represent the 95% confidence interval.

Table S1. *Sleep composition across nights*

Sleep stage	**night 1 (quiet)**	**night 2 (noisy)**	**night 3 (noisy)**
Wake	28±4	26±6	31±5
Stage N1	52±6	53±6	54±9
Stage N2	239±9	254±10	237±9
Stage N3	92±10	68±8	89±11
REM	97±6	107±5	99±6
Latency to N2	13±2	12±2	16±3
Latency to N3	26±3	24±2	26±4
Latency to REM	94±11	79±8	74±6
Total Sleep	481±4	482±6	479±5

Mean time (± SE; min.) spent in different stages of sleep, and their corresponding latencies, across the 3 experimental nights.

Idaho Power/1205
Witness: Dr. Jeffrey Ellenbogen

BEFORE THE PUBLIC UTILITY COMMISSION
OF OREGON

Docket PCN 5

In the Matter of

IDAHO POWER COMPANY'S
PETITION FOR CERTIFICATE OF PUBLIC CONVENIENCE
AND NECESSITY

Ellenbogen, J. M. et al., Wind Turbine Health Impact Study:
Report of Independent Expert Panel (2012)

February 22, 2023

Wind Turbine Health Impact Study:

Report of Independent Expert Panel

January 2012

Prepared for:

Massachusetts Department of Environmental Protection

Massachusetts Department of Public Health

Expert Independent Panel Members:

Jeffrey M. Ellenbogen, MD; MMSc
Assistant Professor of Neurology, Harvard Medical School
Division Chief, Sleep Medicine, Massachusetts General Hospital

Sheryl Grace, PhD; MS Aerospace & Mechanical Engineering
Associate Professor of Mechanical Engineering, Boston University

Wendy J Heiger-Bernays, PhD
Associate Professor of Environmental Health, Department of Environmental Health,
Boston University School of Public Health
Chair, Lexington Board of Health

James F. Manwell, PhD Mechanical Engineering;
MS Electrical & Computer Engineering; BA Biophysics
Professor and Director of the Wind Energy Center, Department of Mechanical & Industrial
Engineering University of Massachusetts, Amherst

Dora Anne Mills, MD, MPH, FAAP
State Health Officer, Maine 1996–2011
Vice President for Clinical Affairs, University of New England

Kimberly A. Sullivan, PhD
Research Assistant Professor of Environmental Health, Department of Environmental Health,
Boston University School of Public Health

Marc G. Weisskopf, ScD Epidemiology; PhD Neuroscience
Associate Professor of Environmental Health and Epidemiology
Department of Environmental Health & Epidemiology, Harvard School of Public Health

Facilitative Support provided by Susan L. Santos, PhD, FOCUS GROUP Risk
Communication and Environmental Management Consultants

Table of Contents

List of Tables

The Panel Charge

The Expert Panel was given the following charge by the Massachusetts Department of Environmental Protection (MassDEP) and Massachusetts Department of Public Health (MDPH):

1. Identify and characterize attributes of concern (e.g., noise, infrasound, vibration, and light flicker) and identify any scientifically documented or potential connection between health impacts associated with wind energy turbines located on land or coastal tidelands that can impact land-based human receptors.
2. Evaluate and discuss information from peer-reviewed scientific studies, other reports, popular media, and public comments received by the MassDEP and/or in response to the *Environmental Monitor Notice* and/or by the MDPH on the nature and type of health complaints commonly reported by individuals who reside near existing wind farms.
3. Assess the magnitude and frequency of any potential impacts and risks to human health associated with the design and operation of wind energy turbines based on existing data.
4. For the attributes of concern, identify documented best practices that could reduce potential human health impacts. Include examples of such best practices (design, operation, maintenance, and management from published articles). The best practices could be used to inform public policy decisions by state, local, or regional governments concerning the siting of turbines.
5. Issue a report within 3 months of the evaluation, summarizing its findings.

To meet its charge, the Panel conducted a literature review and met as a group a total of three times. In addition, calls were also held with Panel members to further clarify points of discussion.

Executive Summary

The Massachusetts Department of Environmental Protection (MassDEP) in collaboration with the Massachusetts Department of Public Health (MDPH) convened a panel of independent experts to identify any documented or potential health impacts of risks that may be associated with exposure to wind turbines, and, specifically, to facilitate discussion of wind turbines and public health based on scientific findings.

While the Commonwealth of Massachusetts has goals for increasing the use of wind energy from the current 40 MW to 2000 MW by the year 2020, MassDEP recognizes there are questions and concerns arising from harnessing wind energy. The scope of the Panel's effort was focused on health impacts of wind turbines *per se*. The panel was *not* charged with considering any possible benefits of avoiding adverse effects of other energy sources such as coal, oil, and natural gas as a result of switching to energy from wind turbines.

Currently, "regulation" of wind turbines is done at the local level through local boards of health and zoning boards. Some members of the public have raised concerns that wind turbines may have health impacts related to noise, infrasound, vibrations, or shadow flickering generated by the turbines. The goal of the Panel's evaluation and report is to provide a review of the science that explores these concerns and provides useful information to MassDEP and MDPH and to local agencies that are often asked to respond to such concerns. The Panel consists of seven individuals with backgrounds in public health, epidemiology, toxicology, neurology and sleep medicine, neuroscience, and mechanical engineering. All of the Panel members are considered independent experts from academic institutions.

In conducting their evaluation, the Panel conducted an extensive literature review of the scientific literature as well as other reports, popular media, and the public comments received by the MassDEP.

ES 1. Panel Charge

1. Identify and characterize attributes of concern (e.g., noise, infrasound, vibration, and light flicker) and identify any scientifically documented or potential connection between health impacts associated with wind turbines located on land or coastal tidelands that can impact land-based human receptors.
2. Evaluate and discuss information from peer reviewed scientific studies, other reports, popular media, and public comments received by the MassDEP and/or in response to the *Environmental Monitor Notice* and/or by the MDPH on the nature and type of health complaints commonly reported by individuals who reside near existing wind farms.
3. Assess the magnitude and frequency of any potential impacts and risks to human health associated with the design and operation of wind energy turbines based on existing data.
4. For the attributes of concern, identify documented best practices that could reduce potential human health impacts. Include examples of such best practices (design, operation, maintenance, and management from published articles). The best practices could be used to inform public policy decisions by state, local, or regional governments concerning the siting of turbines.
5. Issue a report within 3 months of the evaluation, summarizing its findings.

ES 2. Process

To meet its charge, the Panel conducted an extensive literature review and met as a group a total of three times. In addition, calls were also held with Panel members to further clarify points of discussion. An independent facilitator supported the Panel's deliberations. Each Panel member provided written text based on the literature reviews and analyses. Draft versions of the report were reviewed by each Panel member and the Panel reached consensus for the final text and its findings.

ES 3. Report Introduction and Description

Many countries have turned to wind power as a clean energy source because it relies on the wind, which is indefinitely renewable; it is generated "locally," thereby providing a measure of energy independence; and it produces no carbon dioxide emissions when operating. There is interest in pursuing wind energy both on-land and offshore. For this report, however, the focus is on land-based installations and all comments are focused on this technology. Land-based wind turbines currently range from 100 kW to 3 MW (3000 kW). In Massachusetts, the largest turbine is currently 1.8 MW.

The development of modern wind turbines has been an evolutionary design process, applying optimization at many levels. An overview of the characteristics of wind turbines, noise, and vibration is presented in Chapter 2 of the report. Acoustic and seismic measurements of noise and vibration from wind turbines provide a context for comparing measurements from epidemiological studies and for claims purported to be due to emissions from wind turbines. Appendices provide detailed descriptions and equations that allow a more in-depth understanding of wind energy, the structure of the turbines, wind turbine aerodynamics, installation, energy production, shadow flicker, ice throws, wind turbine noise, noise propagation, infrasound, and stall vs. pitch controlled turbines.

Extensive literature searches and reviews were conducted to identify studies that specifically evaluate human population responses to turbines, as well as population and individual responses to the three primary characteristics or attributes of wind turbine operation: noise, vibration, and flicker. An emphasis of the Panel's efforts was to examine the biological plausibility or basis for health effects of turbines (noise, vibration, and flicker). Beyond traditional forms of scientific publications, the Panel also took great care to review other non-peer reviewed materials regarding the potential for health effects including information related to "Wind Turbine Syndrome" and provides a rigorous analysis as to whether there is scientific basis for it. Since the most commonly reported complaint by people living near turbines is sleep disruption, the Panel provides a robust review of the relationship between noise, vibration, and annoyance as well as sleep disturbance from noises and the potential impacts of the resulting sleep deprivation.

In assessing the state of the evidence for health effects of wind turbines, the Panel followed accepted scientific principles and relied on several different types of studies. It considered human studies of the most important or primary value. These were either human epidemiological studies specifically relating to exposure to wind turbines or, where specific exposures resulting from wind turbines could be defined, the panel also considered human experimental data. Animal studies are critical to exploring biological plausibility and understanding potential biological mechanisms of different exposures, and for providing information about possible health effects when experimental research in humans is not ethically or practically possible. As such, this literature was also reviewed with respect to wind turbine exposures. The non-peer reviewed material was considered part of the weight of evidence. In all cases, data quality was considered; at times, some studies were rejected because of lack of rigor or the interpretations were inconsistent with the scientific evidence.

ES 4. Findings

The findings in Chapter 4 are repeated here.

Based on the detailed review of the scientific literature and other available reports and consideration of the strength of scientific evidence, the Panel presents findings relative to three factors associated with the operation of wind turbines: noise and vibration, shadow flicker, and ice throw. The findings that follow address specifics in each of these three areas.

ES 4.1 Noise

ES 4.1.a Production of Noise and Vibration by Wind Turbines

1. Wind turbines can produce unwanted sound (referred to as noise) during operation. The nature of the sound depends on the design of the wind turbine. Propagation of the sound is primarily a function of distance, but it can also be affected by the placement of the turbine, surrounding terrain, and atmospheric conditions.
    a. Upwind and downwind turbines have different sound characteristics, primarily due to the interaction of the blades with the zone of reduced wind speed behind the tower in the case of downwind turbines.
    b. Stall regulated and pitch controlled turbines exhibit differences in their dependence of noise generation on the wind speed
    c. Propagation of sound is affected by refraction of sound due to temperature gradients, reflection from hillsides, and atmospheric absorption. Propagation effects have been shown to lead to different experiences of noise by neighbors.
    d. The audible, amplitude-modulated noise from wind turbines ("whooshing") is perceived to increase in intensity at night (and sometimes becomes more of a "thumping") due to multiple effects: i) a stable atmosphere will have larger wind gradients, ii) a stable atmosphere may refract the sound downwards instead of upwards, iii) the ambient noise near the ground is lower both because of the stable atmosphere and because human generated noise is often lower at night.

2. The sound power level of a typical modern utility scale wind turbine is on the order of 103 dB(A), but can be somewhat higher or lower depending on the details of the design and the rated power of the turbine. The perceived sound decreases rapidly with the distance from the wind turbines. Typically, at distances larger than 400 m, sound pressure levels for modern wind turbines are less than 40 dB(A), which is below the level associated with annoyance in the epidemiological studies reviewed.
3. Infrasound refers to vibrations with frequencies below 20 Hz. Infrasound at amplitudes over 100–110 dB can be heard and felt. Research has shown that vibrations below these amplitudes are not felt. The highest infrasound levels that have been measured near turbines and reported in the literature near turbines are under 90 dB at 5 Hz and lower at higher frequencies for locations as close as 100 m.
4. Infrasound from wind turbines is not related to nor does it cause a "continuous whooshing."
5. Pressure waves at any frequency (audible or infrasonic) can cause vibration in another structure or substance. In order for vibration to occur, the amplitude (height) of the wave has to be high enough, and only structures or substances that have the ability to receive the wave (resonant frequency) will vibrate.

ES 4.1.b Health Impacts of Noise and Vibration

1. Most epidemiologic literature on human response to wind turbines relates to self-reported "annoyance," and this response appears to be a function of some combination of the sound itself, the sight of the turbine, and attitude towards the wind turbine project.
   a. There is limited epidemiologic evidence suggesting an association between exposure to wind turbines and annoyance.
   b. There is insufficient epidemiologic evidence to determine whether there is an association between noise from wind turbines and annoyance independent from the effects of seeing a wind turbine and vice versa.

2. There is limited evidence from epidemiologic studies suggesting an association between noise from wind turbines and sleep disruption. In other words, it is possible that noise from some wind turbines can cause sleep disruption.
3. A very loud wind turbine could cause disrupted sleep, particularly in vulnerable populations, at a certain distance, while a very quiet wind turbine would not likely disrupt even the lightest of sleepers at that same distance. But there is not enough evidence to provide particular sound-pressure thresholds at which wind turbines cause sleep disruption. Further study would provide these levels.
4. Whether annoyance from wind turbines leads to sleep issues or stress has not been sufficiently quantified. While not based on evidence of wind turbines, there is evidence that sleep disruption can adversely affect mood, cognitive functioning, and overall sense of health and well-being.
5. There is insufficient evidence that the noise from wind turbines is *directly (i.e., independent from an effect on annoyance or sleep)* causing health problems or disease.
6. Claims that infrasound from wind turbines directly impacts the vestibular system have not been demonstrated scientifically. Available evidence shows that the infrasound levels near wind turbines cannot impact the vestibular system.
   a. The measured levels of infrasound produced by modern upwind wind turbines at distances as close as 68 m are well below that required for non-auditory perception (feeling of vibration in parts of the body, pressure in the chest, etc.).
   b. If infrasound couples into structures, then people inside the structure could feel a vibration. Such structural vibrations have been shown in other applications to lead to feelings of uneasiness and general annoyance. The measurements have shown no evidence of such coupling from modern upwind turbines.
   c. Seismic (ground-carried) measurements recorded near wind turbines and wind turbine farms are unlikely to couple into structures.
   d. A possible coupling mechanism between infrasound and the vestibular system (via the Outer Hair Cells (OHC) in the inner ear) has been proposed but is not yet fully understood or sufficiently explained. Levels of infrasound near wind turbines have been shown to be high enough to be sensed by the OHC. However, evidence does not

exist to demonstrate the influence of wind turbine-generated infrasound on vestibular-mediated effects in the brain.

e. Limited evidence from rodent (rat) laboratory studies identifies short-lived biochemical alterations in cardiac and brain cells in response to short exposures to emissions at 16 Hz and 130 dB. These levels exceed measured infrasound levels from modern turbines by over 35 dB.

7. There is no evidence for a set of health effects, from exposure to wind turbines that could be characterized as a "Wind Turbine Syndrome."
8. The strongest epidemiological study suggests that there is not an association between noise from wind turbines and measures of psychological distress or mental health problems. There were two smaller, weaker, studies: one did note an association, one did not. Therefore, we conclude the weight of the evidence suggests no association between noise from wind turbines and measures of psychological distress or mental health problems.
9. None of the limited epidemiological evidence reviewed suggests an association between noise from wind turbines and pain and stiffness, diabetes, high blood pressure, tinnitus, hearing impairment, cardiovascular disease, and headache/migraine.

ES 4.2 Shadow Flicker

ES 4.2.a Production of Shadow Flicker

Shadow flicker results from the passage of the blades of a rotating wind turbine between the sun and the observer.

1. The occurrence of shadow flicker depends on the location of the observer relative to the turbine and the time of day and year.
2. Frequencies of shadow flicker elicited from turbines is proportional to the rotational speed of the rotor times the number of blades and is generally between 0.5 and 1.1 Hz for typical larger turbines.
3. Shadow flicker is only present at distances of less than 1400 m from the turbine.

ES 4.2.b Health Impacts of Shadow Flicker

1. Scientific evidence suggests that shadow flicker does not pose a risk for eliciting seizures as a result of photic stimulation.

2. There is limited scientific evidence of an association between annoyance from prolonged shadow flicker (exceeding 30 minutes per day) and potential transitory cognitive and physical health effects.

ES 4.3 Ice Throw

ES 4.3.a Production of Ice Throw

Ice can fall or be thrown from a wind turbine during or after an event when ice forms or accumulates on the blades.

1. The distance that a piece of ice may travel from the turbine is a function of the wind speed, the operating conditions, and the shape of the ice.
2. In most cases, ice falls within a distance from the turbine equal to the tower height, and in any case, very seldom does the distance exceed twice the total height of the turbine (tower height plus blade length).

ES 4.3.b Health Impacts of Ice Throw

1. There is sufficient evidence that falling ice is physically harmful and measures should be taken to ensure that the public is not likely to encounter such ice.

ES 4.4 Other Considerations

In addition to the specific findings stated above for noise and vibration, shadow flicker and ice throw, the Panel concludes the following:

1. Effective public participation in and direct benefits from wind energy projects (such as receiving electricity from the neighboring wind turbines) have been shown to result in less annoyance in general and better public acceptance overall.

ES 5. Best Practices Regarding Human Health Effects of Wind Turbines

The best practices presented in Chapter 5 are repeated here.

Broadly speaking, the term “best practice” refers to policies, guidelines, or recommendations that have been developed for a specific situation. Implicit in the term is that the practice is based on the best information available at the time of its institution. A best practice may be refined as more information and studies become available. The panel recognizes that in countries which are dependent on wind energy and are protective of public health, best practices have been developed and adopted.

In some cases, the weight of evidence for a specific practice is stronger than it is in other cases. Accordingly, best practice* may be categorized in terms of the evidence available, as follows:

Descriptions of Three Best Practice Categories

Category	**Name**	**Description**
1	Research Validated Best Practice	A program, activity, or strategy that has the highest degree of proven effectiveness supported by objective and comprehensive research and evaluation.
2	Field Tested Best Practice	A program, activity, or strategy that has been shown to work effectively and produce successful outcomes and is supported to some degree by subjective and objective data sources.
3	Promising Practice	A program, activity, or strategy that has worked within one organization and shows promise during its early stages for becoming a best practice with long-term sustainable impact. A promising practice must have some objective basis for claiming effectiveness and must have the potential for replication among other organizations.

**These categories are based on those suggested in "Identifying and Promoting Promising Practices." Federal Register, Vol. 68. No 131. 131. July 2003.*
www.acf.hhs.gov/programs/ccf/about_ccf/gbk_pdf/pp_gbk.pdf

ES 5.1 Noise

Evidence regarding wind turbine noise and human health is limited. There is limited evidence of an association between wind turbine noise and both annoyance and sleep disruption, depending on the sound pressure level at the location of concern. However, there are no research-based sound pressure levels that correspond to human responses to noise. A number of countries that have more experience with wind energy and are protective of public health have developed guidelines to minimize the possible adverse effects of noise. These guidelines consider time of day, land use, and ambient wind speed. The table below summarizes the guidelines of Germany (in the categories of industrial, commercial and villages) and Denmark (in the categories of sparsely populated and residential). The sound levels shown in the table are for nighttime and are assumed to be taken immediately outside of the residence or building of concern. In addition, the World Health Organization recommends a maximum nighttime sound pressure level of 40 dB(A) in residential areas. Recommended setbacks corresponding to these values may be calculated by software such as WindPro or similar software. Such calculations are normally to be done as part of feasibility studies. The Panel considers the guidelines shown below to be Promising Practices (Category 3) but to embody some aspects of Field Tested Best Practices (Category 2) as well.

Promising Practices for Nighttime Sound Pressure Levels by Land Use Type

Land Use	**Sound Pressure Level, dB(A) Nighttime Limits**
Industrial	70
Commercial	50
Villages, mixed usage	45
Sparsely populated areas, 8 m/s wind*	44
Sparsely populated areas, 6 m/s wind*	42
Residential areas, 8 m/s wind*	39
Residential areas, 6 m/s wind*	37

**measured at 10 m above ground, outside of residence or location of concern*

The time period over which these noise limits are measured or calculated also makes a difference. For instance, the often-cited World Health Organization recommended nighttime noise cap of 40 dB(A) is averaged over one year (and does not refer specifically to wind turbine noise). Denmark's noise limits in the table above are calculated over a 10-minute period. These limits are in line with the noise levels that the epidemiological studies connect with insignificant reports of annoyance.

The Panel recommends that noise limits such as those presented in the table above be included as part of a statewide policy regarding new wind turbine installations. In addition, suitable ranges and procedures for cases when the noise levels may be greater than those values should also be considered. The considerations should take into account trade-offs between environmental and health impacts of different energy sources, national and state goals for energy independence, potential extent of impacts, etc.

The Panel also recommends that those involved in a wind turbine purchase become familiar with the noise specifications for the turbine and factors that affect noise production and noise control. Stall and pitch regulated turbines have different noise characteristics, especially in high winds. For certain turbines, it is possible to decrease noise at night through suitable control measures (e.g., reducing the rotational speed of the rotor). If noise control measures are to be considered, the wind turbine manufacturer must be able to demonstrate that such control is possible.

The Panel recommends an ongoing program of monitoring and evaluating the sound produced by wind turbines that are installed in the Commonwealth. IEC 61400-11 provides the standard for making noise measurements of wind turbines (International Electrotechnical Commission, 2002). In general, more comprehensive assessment of wind turbine noise in populated areas is recommended. These assessments should be done with reference to the broader ongoing research in wind turbine noise production and its effects, which is taking place internationally. Such assessments would be useful for refining siting guidelines and for developing best practices of a higher category. Closer investigation near homes where outdoor measurements show A and C weighting differences of greater than 15 dB is recommended.

ES 5.2 Shadow Flicker

Based on the scientific evidence and field experience related to shadow flicker, Germany has adopted guidelines that specify the following:

1. Shadow flicker should be calculated based on the astronomical maximum values (i.e., not considering the effect of cloud cover, etc.).
2. Commercial software such as WindPro or similar software may be used for these calculations. Such calculations should be done as part of feasibility studies for new wind turbines.
3. Shadow flicker should not occur more than 30 minutes per day and not more than 30 hours per year at the point of concern (e.g., residences).
4. Shadow flicker can be kept to acceptable levels either by setback or by control of the wind turbine. In the latter case, the wind turbine manufacturer must be able to demonstrate that such control is possible.

The guidelines summarized above may be considered to be a Field Tested Best Practice (Category 2). Additional studies could be performed, specifically regarding the number of hours per year that shadow flicker should be allowed, that would allow them to be placed in Research Validated (Category 1) Best Practices.

ES 5.3 Ice Throw

Ice falling from a wind turbine could pose a danger to human health. It is also clear that the danger is limited to those times when icing occurs and is limited to relatively close proximity to the wind turbine. Accordingly, the following should be considered Category 1 Best Practices.

1. In areas where icing events are possible, warnings should be posted so that no one passes underneath a wind turbine during an icing event and until the ice has been shed.
2. Activities in the vicinity of a wind turbine should be restricted during and immediately after icing events in consideration of the following two limits (in meters).

For a turbine that may not have ice control measures, it may be assumed that ice could fall within the following limit:

$$x_{\max,\, throw} = 1.5\left(2R + H\right)$$

Where: R = rotor radius (m), H = hub height (m)

For ice falling from a stationary turbine, the following limit should be used:

$$x_{\max,\, fall} = U\left(R + H\right)/15$$

Where: U = maximum likely wind speed (m/s)

The choice of maximum likely wind speed should be the expected one-year return maximum, found in accordance to the International Electrotechnical Commission's design standard for wind turbines, IEC 61400-1.

Danger from falling ice may also be limited by ice control measures. If ice control measures are to be considered, the wind turbine manufacturer must be able to demonstrate that such control is possible.

ES 5.4 Public Participation/Annoyance

There is some evidence of an association between participation, economic or otherwise, in a wind turbine project and the annoyance (or lack thereof) that affected individuals may express. Accordingly, measures taken to directly involve residents who live in close proximity to a wind turbine project may also serve to reduce the level of annoyance. Such measures may be considered to be a Promising Practice (Category 3).

ES 5.5 Regulations/Incentives/Public Education

The evidence indicates that in those parts of the world where there are a significant number of wind turbines in relatively close proximity to where people live, there is a close coupling between the development of guidelines, provision of incentives, and educating the public. The Panel suggests that the public be engaged through such strategies as education, incentives for community-owned wind developments, compensations to those experiencing documented loss of property values, comprehensive setback guidelines, and public education related to renewable energy. These multi-faceted approaches may be considered to be a Promising Practice (Category 3).

Chapter 1

Introduction to the Study

The Massachusetts Department of Environmental Protection (MassDEP), in collaboration with the Massachusetts Department of Public Health (MDPH), convened a panel of independent experts to identify any documented or potential health impacts or risks that may be associated with exposure to wind turbines, and, specifically, to facilitate discussion of wind turbines and public health based on sound science. While the Commonwealth of Massachusetts has goals for increasing the use of wind energy from the current 40 MW to 2000 MW by the year 2020, MassDEP recognizes there are questions and concerns arising from harnessing wind energy. Although fossil fuel non-renewable sources have negative environmental and health impacts, it should be noted that the scope of the Panel's effort was focused on wind turbines and is not meant to be a comparative analysis of the relative merits of wind energy vs. nonrenewable fossil fuel sources such as coal, oil, and natural gas. Currently, "regulation" of wind turbines is done at the local level through local boards of health and zoning boards. Some members of the public have raised concerns that wind turbines may have health impacts related to noise, infrasound, vibrations, or shadow flickering generated by the turbines. The goal of the Panel's evaluation and report is to provide a review of the science that explores these concerns and provides useful information to MassDEP and MDPH and to local agencies who are often asked to respond to such concerns.

The overall context for this study is that the use of wind turbines results in positive effects on public health and environmental health. For example, wind turbines operating in Massachusetts produce electricity in the amount of approximately 2,100–2,900 MWh annually per rated MW, depending on the design of the turbine and the average wind speed at the installation site. Furthermore, the use of wind turbines for electricity production in the New England electrical grid will result in a significant decrease in the consumption of conventional fuels and a corresponding decrease in the production of CO_2 and oxides of nitrogen and sulfur (see Appendix A for details). Reductions in the production of these pollutants will have demonstrable and positive benefits on human and environmental health. However, local impacts of wind turbines, whether anticipated or demonstrated, have resulted in fewer turbines being installed than might otherwise have been expected. To the extent that these impacts can be ameliorated, it should be possible to take advantage of the indigenous wind energy resource more effectively.

The Panel consists of seven individuals with backgrounds in public health, epidemiology, toxicology, neurology and sleep medicine, neuroscience, and mechanical engineering. With the exception of two individuals (Drs. Manwell and Mills), Panel members did not have any direct experience with wind turbines. The Panel did an extensive literature review of the scientific literature (see bibliography) as well as other reports, popular media, and the public comments received by the MassDEP.

Chapter 2

Introduction to Wind Turbines

This chapter provides an introduction to wind turbines so as to provide a context for the discussion that follows. More information on wind turbines may be found in the appendices, particularly in Appendix A.

2.1 Wind Turbine Anatomy and Operation

Wind turbines utilize the wind, which originates from sunlight due to the differential heating of various parts of the earth. This differential heating produces zones of high and low pressure, resulting in air movement. The motion of the air is also affected by the earth's rotation. Many countries have turned to wind power as a clean energy source because it relies on the wind, which is indefinitely renewable; it is generated "locally," thereby providing a measure of energy independence; and it produces no carbon dioxide emissions when operating. There is interest in pursuing wind energy both on-land and offshore. For this report, however, the focus is on land-based installations, and all comments will focus on this technology.

The development of modern wind turbines has been an evolutionary design process, applying optimization at many levels. This section gives a brief overview of the characteristics of wind turbines with some mention of the optimization parameters of interest. Appendix A provides a detailed explanation of wind energy.

The main features of modern wind turbines one notices are the very tall towers, which are no longer a lattice structure but a single cylindrical-like structure and the three upwind, very long, highly contoured turbine blades. The tower design has evolved partly because of biological impact factors as well as for other practical reasons. The early lattice towers were attractive nesting sites for birds. This led to an unnecessary impact of wind turbines on bird populations. The lattice structures also had to be climbed externally by turbine technicians. The tubular towers, which are now more common, are climbed internally. This reduces the health risks for maintenance crews.

The power in the wind available to a wind turbine is related to the cube of the wind speed and the square of the radius of the rotor. Not all the available power in the wind can be captured by a wind turbine, however. Betz (van Kuik, 2007) showed that the maximum power that can be extracted is 16/27 times the available power (see Appendix A). In an attempt to extract the maximum power from the wind, modern turbines have very large rotors and the towers are quite high. In this way the dependence on the radius is "optimized," and the dependence on the wind speed is "optimized." The wind speed is higher away from the ground due to boundary layer effects, and as such, the towers are made higher in order to capture the higher speed winds (more information about the wind profiles and variability is found in Appendix A). It is noted here that the rotor radius may increase again in the future, but currently the largest rotors used on land are around 100 m in diameter. This upper limit is currently a function of the radius of curvature of the roads on which the trucks that deliver the turbine blades must drive to the installation sites. Clearance under bridges is also a factor.

The efficiency with which the wind's power is captured by a particular wind turbine (i.e., how close it comes to the Betz limit) is a function of the blade design, the gearbox, the electrical generator, and the control system. The aerodynamic forces on the rotor blade play a major role. The best design maximizes lift and minimizes drag at every blade section from hub to tip. The twisted and tapered shapes of modern blades attempt to meet this optimal condition. Other factors also must be taken into consideration such as structural strength, ease of manufacturing and transport, type of materials, cost, etc.

Beyond these visual features, the number of blades and speed of the tips play a role in the optimization of the performance through what is called solidity. When setting tip speeds based on number of blades, however, trade-offs exist because of the influence of these parameters on weight, cost, and noise. For instance, higher tip speeds often results in more noise.

The dominance of the 3-bladed upwind systems is both historic and evolutionary. The European manufacturers moved to 3-bladed systems and installed numerous turbines, both in Europe and abroad. Upwind systems are preferable to downwind systems for on-land installations because they are quieter. The downwind configuration has certain useful features but it suffers from the interaction noise created when the blades pass through the wake that forms behind the tower.

The conversion of the kinetic energy of the wind into electrical energy is handled by the rotor nacelle assembly (RNA), which consists of the rotor, the drive train, and various ancillary components. The rotor grouping includes the blades, the hub, and the pitch control components. The drive train includes the shafts, bearings, gearbox (not necessary for direct drive generators), couplings, mechanical brake, and generator. A schematic of the RNA, together with more detail concerning the operation of the various parts, is in Appendix A.

The rotors are controlled so as to generate electricity most effectively and as such must withstand continuously fluctuating forces during normal operation and extreme loads during storms. Accordingly, in general a wind turbine rotor does not operate at its own maximum power coefficient at all wind speeds. Because of this, the power output of a wind turbine is generally described by a relationship, known as a power curve. A typical power curve is shown in the appendix. Below the cut-in speed no power is produced. Between cut-in and rated wind speed the power increases significantly with wind speed. Above the rated speed, the power produced is constant, regardless of the wind speed, and above the cut-out speed the turbine is shut down often with use of the mechanical brake.

Two main types of rotor control systems exist: pitch and stall. Stall controlled turbines have fixed blades and operate at a fixed speed. The aerodynamic design of the blades is such that the power is self-limiting, as long as the generator is connected to the electrical grid. Pitch regulated turbines have blades that can be rotated about their long axis. Such an arrangement allows more precise control. Pitch controlled turbines are also generally quieter than stall controlled turbines, especially at higher wind speeds. Until recently, many turbines used stall control. At present, most large turbines use pitch control. Appendices A and F provide more details on pitch and stall.

The energy production of a wind turbine is usually considered annually. Estimates are usually obtained by calculating the expected energy that will be produced every hour of a representative year (by considering the turbine's power curve and the estimated wind resource) and then summing the energy from all the hours. Sometimes a normalized term known as the capacity factor (CF) is used to characterize the performance. This is the actual energy produced (or estimated to be produced) divided by the amount of energy that would be produced if the turbine were running at its rated output for the entire year. Appendix A gives more detail on these computations.

2.2 Noise from Turbines

Because of the concerns about the noise generated from wind turbines, a short summary of the sources of noise is provided here. A thorough description of the various noise sources from a wind turbine is given in the text by Wagner et al. (1996).

A turbine produces noise mechanically and aerodynamically. Mechanical noise sources include the gearbox, generator, yaw drives, cooling fans, and auxiliary equipment such as hydraulics. Because the emitted sound is associated with the rotation of mechanical and electrical equipment, it is often tonal. For instance, it was found that noise associated with a 1500 kW turbine with a generator running at speeds between 1100 and 1800 rpm contained a tone between 20 and 30 Hz (Betke et al., 2004). The yaw system on the other hand might produce more of a grinding type of noise but only when the yaw mechanism is engaged. The transmission of mechanical noise can be either airborne or structure-borne as the associated vibrations can be transmitted into the hub and tower and then radiated into the surrounding space.

Advances in gearboxes and yaw systems have decreased these noise sources over the years. Direct drive systems will improve this even more. In addition, utility scale wind turbines are usually insulated to prevent mechanical noise from proliferating outside the nacelle or tower (Alberts, 2006)

Aerodynamic sound is generated due to complex fluid-structure interactions occurring on the blades. Wagner et al. (1996) break down the sources of aerodynamic sound as follows in Table 1.

Table 1

Sources of Aerodynamic Sound from a Wind Turbine (Wagner et al., 1996*)*.

Noise Type	**Mechanism**	**Characteristic**
Trailing-edge noise	Interaction of boundary layer turbulence with blade trailing edge	Broadband, main source of high frequency noise (770 Hz < f < 2 kHz)
Tip noise	Interaction of tip turbulence with blade tip surface	Broadband
Stall, separation noise	Interaction of turbulence with blade surface	Broadband
Laminar boundary layer noise	Non-linear boundary layer instabilities interacting with the blade surface	Tonal
Blunt trailing edge noise	Vortex shedding at blunt trailing edge	Tonal
Noise from flow over holes, slits, and intrusions	Unsteady shear flows over holes and slits, vortex shedding from intrusions	Tonal
Inflow turbulence noise	Interaction of blade with atmospheric turbulence	Broadband
Steady thickness noise, steady loading noise	Rotation of blades or rotation of lifting surface	Low frequency related to blade passing frequency (outside of audible range)
Unsteady loading noise	Passage of blades through varying velocities, due to pitch change or blade altitude change as it rotates* For downwind turbines passage through tower shadow	Whooshing or beating, amplitude modulation of audible broadband noise. For downwind turbines, impulsive noise at blade passing frequency

**van den Berg 2004.*

Of these mechanisms, the most persistent and often strongest source of aerodynamic sound from modern wind turbines is the trailing edge noise. It is also the amplitude modulation of this noise source due to the presence of atmospheric effects and directional propagation effects that result in the whooshing or beating sound often reported (van den Berg, 2004). As a turbine blade rotates through a changing wind stream, the aerodynamics change, leading to differences in the boundary layer and thus to differences in the trailing edge noise (Oerlemans, 2009). Also, the direction in which the blade is pointing changes as it rotates, leading to differences in the directivity of the noise from the trailing edge. This noise source leads to what some people call the “whooshing” sound.

Most modern turbines use pitch control for a variety of reasons. One of the reasons is that at higher wind speeds, when the control system has the greatest impact, the pitch controlled turbine is quieter than a comparable stall regulated turbine would be. Appendix E shows the difference in the noise from two such systems.

When discussing noise from turbines, it is important to also consider propagation effects and multiple turbine effects. One propagation effect of interest is due to the dependence of the speed of sound on temperature. When there is a large temperature gradient (which may occur during the day due to surface warming or due to topography such as hills and valleys) the path a sound wave travels will be refracted. Normally this means that during a typical day sound is “turned” away from the earth’s surface. However, at night the sound propagates at a constant height or even be “turned” down toward the earth’s surface, making it more noticeable than it otherwise might be.

The absorption of sound by vegetation and reflection of sound from hillsides are other propagation effects of interest. Several of these effects were shown to be influencing the sound field near a few homes in North Carolina that were impacted by a wind turbine installation (Kelley et al., 1985). A downwind 2-bladed, 2 MW turbine was installed on a mountaintop in North Carolina. It created high amplitude impulsive noise due to the interaction of the blades and the tower wakes. Some homes (10 in 1000) were adversely affected by this high amplitude impulsive noise. It is shown in the report by Kelley et al. (1985) that echoes and focusing due to refraction occurred at the location of the affected homes.

In flat terrain, noise in the audible range will propagate along a flat terrain in a manner such that its amplitude will decay exactly as distance from the source (1/distance). Appendix E provides formulae for approximating the overall sound level at a given distance from a source. In the inaudible range, it has been noted that often the sound behaves as if the propagation was governed by a $1/(\text{distance})^{1/2}$ (Shepherd & Hubbard, 1991).

When one considers the noise from a wind farm in which multiple turbines are located close to each other, an estimate for the overall noise from the farm can be obtained. Appendix E describes the method for obtaining the estimate. All these estimates rely on information regarding the sound power generated by the turbine at the hub height. The power level for several modern turbines is given in Appendix D.

2.2.a Measurement and Reporting of Noise

Turbines produce multiple types of sound as indicated previously, and the sound is characterized in several ways: tonal or broadband, constant amplitude or amplitude modulated, and audible or infrasonic. The first two characterization pairs have been mentioned previously. Audible refers to sound with frequencies from 20 Hz to 20 kHz. The waves in the infrasonic range, less than 20 Hz, may actually be audible if the amplitude of the sound is high enough. Appendix D provides a brief primer on acoustics and the hearing threshold associated with the entire frequency spectrum.

Sound is simply pressure fluctuations and as such, this is what a microphone measures. However, the amplitude of the fluctuations is reported not in units of pressure (such as Pascals) but on a decibel scale. The sound pressure level (SPL) is defined by

$$SPL = 10 \log_{10} [p^2/p^2_{ref}] = 20 \log_{10}(p/p_{ref})$$

the resulting number having the units of decibels (dB). The reference pressure p_{ref} for airborne sound is 20×10^{-6} Pa (i.e., 20 μPa or 20 micro Pascals). Some implications of the decibel scale are noted in Appendix D.

When sound is broadband (contains multiple frequencies), it is useful to use averages that measure approximately the amplitude of the sound and its frequency content. Standard averaging methods such as octave and 1/3-octave band are described in Appendix D. In essence, the entire frequency range is broken into chunks, and the amplitude of the sound at frequencies in each chunk is averaged. An overall sound pressure value can be obtained by averaging all of the bands.

When presenting the sound pressure it is common to also use a filter or weighting. The A-weighting is commonly used in wind turbine measurements. This filter takes into account the threshold of human hearing and gives the same decibel reading at different frequencies that would equate to equal loudness. This means that at low frequencies (where amplitudes have to be incredibly high for the sound to be heard by people) a large negative weight would be applied. C-weighting only filters the levels at frequencies below about 30 Hz and above 4 kHz and filters them only slightly between 0 and 30 Hz. The weight values for both the A and C weightings filters are shown in Appendix D, and an example with actual wind turbine data is presented.

There are many other weighting methods. For instance, the day-night level filter penalizes nighttime noise between the hours of 10 p.m. and 7 a.m. by adding an additional 10 dB to sound produced during these hours.

When analyzing wind turbine and other anthropogenic sound there is a question as to what averaging period should be used. The World Health Organization uses a yearly average. Others argue though that especially for wind turbines, which respond to seasonal variations as well as diurnal variations, much shorter averages should be considered.

2.2.b Infrasound and Low-frequency Noise (IFLN)

The term *infrasound* refers to pressure waves with frequencies less than 20 Hz. In the infrasonic range, the amplitude of the sound must be very high for it to be audible to humans. For instance, the hearing threshold below 20 Hz requires that the amplitude be above 80 dB for it to be heard and at 5 Hz it has to be above 103 dB (O’Neal, 2011; Watanabe & Moeller, 1990). This gives little room between the audible and the pain values for the infrasound range: 165 dB at 2 Hz and 145 dB at 20 Hz cause pain (Leventhal, 2006).

The *low frequency* range is usually characterized as 20–200 Hz (Leventhal, 2006; O’Neal, 2011). This is within the audible range but again the threshold of hearing indicates that fairly high amplitude is required in this frequency range as well. The A-weighting of sound is based upon the threshold of human hearing such that it reports the measured values adjusted by -50 dB at 20 Hz, -10 dB at 200 Hz, and + 1 dB at 1000 Hz. The A-weighting curve is shown in Appendix D.

It is known that low frequency waves propagate with less attenuation than high-frequency waves. Measurements have shown that the amplitude for the airborne infrasonic waves can be cylindrical in nature, decaying at a rate inversely proportional to the square root of the distance from the source. Normally the decay of the amplitude of an acoustic wave is inversely proportional to the distance (Shepherd & Hubbard, 1991).

It is difficult to find reliable and comparable infrasound and low frequency noise (ILFN) measurement data in the peer-reviewed literature. Table 2 provides some examples of such measurements from wind turbines. For each case, the reliability of the infrasonic data is not known (the infrasonic measurement technique is not described in each report), although it is assumed that the low frequency noise was captured accurately. The method for obtaining the sound pressure level is not described for each reported data set, and some may come from averages over many day/time/wind conditions while others may be just from a single day's measurement campaign.

Table 2
Literature-based Measurements of Wind Turbines; dB alone refers to unweighted values

Turbine Rating (kW)	Distance (m)	Frequency	Sound Pressure Level	Reference
500	200	5 20	55 dB(G)[2] 35 dB(G)[2]	Jakobsen, 2005[3]
3200	68	4 20	72 dB(G)[2] 50 dB(G)[2]	Jakobsen, 2005[3]
1500	65	5 20 100	>70 dB(A) 60 dB(A) 35 dB(A)	Leventhal, 2006
2000 (2)	100	5 20 200	95 dB 65 dB 55 dB	van den Berg, 2004[3]
1500	98	1 10 20 100 200	90 dB 70 dB 68 dB 68 dB 60 dB	Jung, 2008[3]
-	450	10 100 200	75 dB 55 dB 40 dB	Palmer, 2010
2300	305	5 20 100	73 dB(A) 55 dB(A) - 95 50 dB(A) - 70	O'Neal, 2011[3]

[1]dB alone refers to un-weighted values.
[2]G weighting reflects human response to infrasound. The curve is defined to have a gain of zero dB at 10 Hz. Between 1 Hz and 20 Hz the slope is approximately 12 dB per octave. The cut-off below 1 Hz has a slope of 24 dB per octave, and above 20 Hz the slope is -24 dB per octave. Humans can hear 95 dB(G).
[3]Indicates peer-reviewed article.

When these recorded levels are taken at face value, one might conclude that the infrasonic regime levels are well below the audible threshold. In contrast, the low frequency regime becomes audible around 30 Hz. Such data have led many researchers to conclude that the infrasound and low frequency noise from wind turbines is not an issue (Leventhal, 2009; O'Neal, 2011; Bowdler, 2009). Others who have sought explanations for complaints from those living near wind turbines have pointed to ILFN as a problem (Pierpont, 2009; Branco & Alves-

Pereira, 2004). Some have declared the low frequency range to be of greatest concern (Kamperman et al., 2008; Jung, 2008).

It is important to make the clear distinction between amplitude-modulated noise from wind turbines and the ILFN from turbines. Amplitude modulation in wind turbines noise has been discussed at length by Oerlemans (2009) and van den Berg (2004). Amplitude modulation is what causes the whooshing sound referred to as swish-swish by van den Berg (that sometimes becomes a thumping sound). The whooshing noise created by modern wind turbines occurs because of variations in the trailing edge noise produced by a rotor blade as it sweeps through its path and the directionality of the noise because of the perceived pitch of the blade at different locations along its 360° rotation. The sound is produced in the audible range, and it is modulated so that it is quiet and then loud and then quiet again at a rate related to the blade passing frequency (rate blades pass the tower) which is often around 1 Hz. Van den Berg (2004) noted that the level of amplitude modulation is often greater at night because the difference between the wind speed at the top and bottom of the rotor disc can be much larger at night when there is a stable atmosphere than during the day when the wind profile is less severe. It is further argued that in a stable atmosphere there is little wind near the ground so wind noise does not mask the turbine noise for a listener near the ground. Finally, atmospheric effects can change the propagation of the sound refracting the noise towards the ground rather than away from the ground. The whooshing that is heard is NOT infrasound and much of its content is not at low frequency. Most of the sound is at higher frequency and as such it will be subject to higher atmospheric attenuation than the low frequency sound. An anecdotal finding that the whooshing sound carries farther when the atmosphere is stable does not imply that it is infrasound or heavy in low frequency content, it simply implies that the refraction of the sound is also different when the atmosphere is stable. It is important to note then that when a complaint is tied to the thumping or whooshing that is being heard, the complaint may not be about ILFN at all even if the complaint mentions low frequency noise. Kamperman et al. (2008) state that, "It is not clear to us whether the complaints about "low frequency" noise are about the audible low frequency part of the "swoosh-boom" sound, the once-per-second amplitude modulation … of the "swoosh-boom" sound, or some combination of the two."

Chapter 3

Health Effects

3.1 Introduction

Chapter 3 reviews the evidence for human health effects of wind turbines. Extensive literature searches and reviews were conducted to identify studies that specifically evaluate population responses to turbines, as well as population and individual responses to noise, vibration, and flicker. The biological plausibility or basis for health effects of turbines (noise, vibration, and flicker) was examined. Beyond traditional forms of scientific publications, the Panel also reviewed other non-peer reviewed materials including information related to "Wind Turbine Syndrome" and provides a rigorous analysis of its scientific basis. Since the most commonly reported complaint by people living near turbines is sleep disruption, the Panel provides a robust review of the relationship between noise, vibration, annoyance as well as sleep disturbance from noises and the potential impacts of the resulting sleep deprivation.

In assessing the state of the evidence for health effects of wind turbines, the Panel relied on several different types of studies. It considered human studies of primary value. These were either human epidemiological studies specifically relating to exposure to wind turbines or, where specific exposures resulting from wind turbines could be defined, the Panel also considered human experimental data. Animal studies are critical to exploring biological plausibility and understanding potential biological mechanisms of different exposures, and for providing information about possible health effects when experimental research in humans is not ethically or practically possible (National Research Council (NRC), 1991). As such, this literature was also reviewed with respect to wind turbine exposures. In all cases, data quality is considered. At times some studies were rejected because of lack of rigor or the interpretations were inconsistent with the scientific evidence. These are identified in the discussion below.

In the specific case of the possibility of ice being thrown from wind turbine blades, the Panel discusses the physics of such ice throw in order to provide the basis of the extent of the potential for injury from thrown ice (see Chapter 2).

3.2 Human Exposures to Wind Turbines

Epidemiologic study designs differ in their ability to provide evidence of an association (Ellwood, 1998). Typical study designs include randomized trials, cohort studies, and case-control studies and can include elements of prospective follow-up, retrospective assessments, or cross-sectional analysis where exposure and outcome data are essentially concurrent. Each of these designs has strengths and weaknesses and thus can provide varying levels of strength of evidence for causal associations between exposures and outcomes, which can also be affected by analytic choices. Thus, this literature needs to be examined in detail, regardless of study type, to determine strength of evidence for causality.

Review of this literature began with a PubMed search for "wind turbine" or "wind turbines" to identify peer-reviewed literature pertaining to health effects of wind turbines. Titles and abstracts of identified papers were then read to make a first pass determination of whether the paper was a study on health effects of exposure to wind turbines or might possibly contain relevant references to such studies. Because the peer-reviewed literature so identified was relatively limited, we also examined several non-peer reviewed papers, reports, and books that discussed health effects of wind turbines. All of this literature was examined for additional relevant references, but for the purposes of determining strength of evidence, we only considered such publications if they described studies of some sort in sufficient detail to assess the validity of the findings. This process identified four studies that generated peer-reviewed papers on health effects of wind turbines. A few other non-peer reviewed documents described data of sufficient relevance to merit consideration and are discussed below as well.

3.3 Epidemiological Studies of Exposure to Wind Turbines

The four studies that generated peer-reviewed papers on health effects of wind turbines included two from Sweden (E. Pedersen et al., 2007; E. Pedersen & Waye, 2004), one from the Netherlands (E. Pedersen et al., 2009), and one from New Zealand (Shepherd at al., 2011). The primary outcome assessed in the first three of these studies is annoyance. Annoyance *per se* is not a biological disease, but has been defined in different ways. For example, as "a feeling of resentment, displeasure, discomfort, dissatisfaction, or offence which occurs when noise interferes with someone's thoughts, feelings or daily activities" (Passchier-Vermeer, 1993); or "a mental state characterized by distress and aversion, which if maintained, can lead to a deterioration of health and well-being" (Shepherd et al., 2010). Annoyance is usually assessed with questionnaires, and this is the case for the three studies mentioned above. There is consistent evidence for annoyance in populations exposed for more than one year to sound levels of 37 dB(A), and severe annoyance at about 42 dB(A) (Concha-Barrientos et al., 2004). In each of those studies annoyance was assessed by questionnaire, and the respondent was asked to indicate annoyance to a number of items (including wind turbines) on a five-point scale (do not notice, notice but not annoyed, slightly annoyed, rather annoyed, very annoyed). While annoyance as such is certainly not to be dismissed, in assessing global burden of disease the World Health Organization (WHO) has taken the approach of excluding annoyance as an outcome because it is not a formally defined health outcome *per se* (Concha-Barrientos et al., 2004). Rather, to the extent annoyance may cause other health outcomes, those other outcomes could be considered directly. Nonetheless, because of a paucity of literature on the association between wind turbines and other health outcomes, we consider here the literature on wind turbines and annoyance.

3.3.a Swedish Studies

Both Swedish studies were cross sectional and involved mailed questionnaires to potential participants. For the first Swedish study, 627 households were identified in one of five areas of Sweden chosen to have enough dwellings at varying distances from wind turbines and of comparable geographical, cultural, and topographical structure (E. Pedersen & Waye, 2004). There were 16 wind turbines in the study area and of these, 14 had a power of 600–650 kW, and the other 2 turbines had 500 kW and 150 kW. The towers were between 47 and 50 m in height. Of the turbines, 13 were WindWorld machines, 2 were Enercon, and 1 was a Vestas turbine. Questionnaires were to be filled out by one person per household who was between the ages of 18 and 75. If there was more than one such person, the one whose birthday was closest to May 20th was chosen. It is not clear how the specific 627 households were chosen, and of the 627, only 513 potential participants were identified, although it is not clear why the other households did not have potential participants. Of the 513 potential participants, 351 (68.4%) responded.

The purpose of the questionnaire was masked by querying the participant about living conditions in general, some questions on which were related to wind turbines. However, a later section of the questionnaire focused more specifically on wind turbines, and so the degree to which the respondent was unaware about the focus on wind turbines is unclear. A-weighted sound levels were determined at each respondent's dwelling, and these levels were grouped into

6 categories (in dB(A): <30, 30–32.5, 32.5–35, 35–37.5, 37.5–40, and >40). Ninety-three percent of respondents could see a wind turbine from their dwelling.

The main results of this study were that there was a significant association between noise level and annoyance. This association was attenuated when adjusted for the respondent's attitude towards the visual impact of the turbines, which itself was a strong predictor of annoyance levels, but the association with noise still persisted. Further adjustment for noise sensitivity and attitude towards wind turbines in general did not change the results. The authors indicated that the reporting of sleep disturbances went up with higher noise categories, but did not report on the significance of this association. Nor did the authors report on associations with other health-related questions that were apparently on the questionnaire (such as headache, undue tiredness, pain and stiffness in the back, neck or shoulders, or feeling tensed/stressed, or irritable).

The 68% response rate in this study is reasonably good, but it is somewhat disconcerting that the response rate appeared to be higher in the two highest noise level categories (76% and 78% vs. 60–69%). It is not implausible that those who were annoyed by the turbines were more inclined to return the questionnaire. In the lowest two sound categories (<32.5 dB(A)) nobody reported being more than slightly annoyed, whereas in the highest two categories 28% (37.5–40 dB(A)) and 44% (>40 dB(A)) reported being more than slightly annoyed (unadjusted percentages). Assuming annoyance would drive returning the questionnaires, this would suggest that the percentages in the highest categories may be somewhat inflated. The limited description of the selection process in this study is a limitation as well, as is the cross sectional nature of the study. Cross-sectional studies lack the ability to determine the temporality of cause and effect; in the case of these kinds of studies, we cannot know whether the annoyance level was present before the wind turbines were operational from a cross sectional study design. Furthermore, despite efforts to blind the respondent to the emphasis on wind turbines, it is not clear to what degree this was successful.

The second Swedish study (E. Pedersen & Persson Waye, 2007) took a similar approach to the first, but in this study the selection procedures were explained in more detail and were clearly rigorous. Specific details on the wind turbines in the area were not provided, but it was noted that areas were sought with wind turbines that had a nominal power of more than 500 kW, although some of the areas also contained turbines with lower power. A later publication by these authors (Pedersen et al., 2009) indicates that the turbines in this study were up to 1.5 MW and up to 65 m high. In the areas chosen, either all households were recruited or a random sample was used. In this study 1,309 questionnaires were sent out and 754 (57.6%) were returned. The response rate by noise category level, however, was not reported. There was a clear association between noise level and hearing turbine noise, with the percentage of those hearing turbine noise steadily increasing across the noise level categories. However, despite a significant unadjusted association between noise levels and annoyance (dichotomized as more than slightly annoyed or not), and after adjusting for attitude towards wind turbines or visual aspects of the turbines (e.g., visual angle on the horizon, an indicator of how prominent the turbines are in the field of view), each of which was strongly associated with annoyance, the association with noise level category was lost. The model from which this conclusion was drawn, however, imposed a linear relation on the association between noise level category and annoyance. But in the crude percentages of people annoyed across noise level categories, it appeared that the relation might not be linear, but rather most prevalent in the highest noise. The percentage of those in the highest noise level category (>40 dB(A)) reporting annoyance (~15%) appeared to be higher than among people in the lower noise categories (<5%).

Given the more rigorous description of the selection process in this study, it has to be considered stronger than the first Swedish study. While 58% is pretty good for a questionnaire response rate, the non-response levels still leave room for bias. The authors do not report the response rate by noise level categories, but if the pattern is similar to the first Swedish study, it could suggest that the percentage annoyed in the highest noise category could be inflated. The cross sectional nature of the study is also a limitation and complicates interpretation of the effects on the noise-annoyance association of adjustment for the other factors. Regarding the loss of the association after adjustment for attitude, if one assumes that the noise levels caused a negative attitude towards wind turbines, then the loss of association between noise and annoyance after adjusting for attitude does not argue against annoyance being caused by increasing turbine noise, but rather that that is the path by which noise causes annoyance (louder noise→negative attitude→annoyance). If, on the other hand, the attitude towards turbines was not caused by the noise, then the results would suggest that noise levels did not cause the annoyance. Visual angle, however, clearly does not cause the noise level; thus, the lack of association between noise and annoyance in analyses adjusted for visual angle more strongly suggest that the turbine noise level is not causing the annoyance, but perhaps the visual intrusion instead. This is similar to the conclusion of an earlier Danish report (T. H. Pedersen & Nielsen, 1994). Either way, however, the data still suggest that there may be an association between turbine noise and annoyance when the noise levels are >40 dB(A).

A more intricate statistical model of the association between turbine noise levels and annoyance that used the data from both Swedish studies was reported separately (Pedersen & Larsman, 2008). The authors used structural equation models (SEMs) to simultaneously account for several aspects of visual attitude towards the turbines and general attitude towards the turbines. These analyses suggested a significant association between noise levels and annoyance even after considering other factors.

3.3.b Dutch Study

The Dutch study aimed to recruit households that reflected general wind turbine exposure conditions over a range of background sound levels. All areas within the Netherlands that were characterized by one of three clearly defined land-use types—built-up area, rural area with a main road, and rural area without a main road—and that had at least two wind turbines of at least 500 kW within 500 meters of each other were selected for the study. Sites dominated by industry or business were excluded. All addresses within these areas were obtained and classified into one of five wind turbine noise categories (<30, 30–35, 35–40, 40–45, and >45 dB(A)) based on characteristics of nearby wind turbines, measurements of sound from those turbines, and the International Standards Organization (ISO) standard model of wind turbine noise propagation. Individual households were randomly selected for recruitment within noise/land type categories, except for the highest noise level for which all households were selected because of the small number exposed at the wind turbine noise levels of the highest category.

As with the Swedish studies, the Dutch study was cross sectional and involved a mailed questionnaire modeled on the one used in the Swedish studies. Of 1,948 mailed surveys, 725 (37%) were returned. There was only minor variation in response rate by turbine noise category, although unlike the Swedish studies, the response rate was slightly lower in the higher noise categories. A random sample of 200 non-responders was sent an abbreviated questionnaire asking only two questions about annoyance from wind turbine noise. There was no difference in the distribution of answers to these questions among these non-responders and those who responded to the full questionnaire.

One of the more dramatic findings of this study was that among people who benefited economically from the turbines (n=100; 14%)—who were much more commonly in the higher noise categories—there was virtually no annoyance (3%) despite the same pattern of noticing the noise as those who did not benefit economically. It is possible that this is because attitude towards turbines drives annoyance, but it was also suggested that those who benefit economically are able to turn off the turbines when they become annoying. However, it is not clear how many of those who benefited economically actually had that level of control over the turbines.

Similarly, there was very little annoyance among people who could not see a wind turbine from their residence even when those people were in higher noise categories (although none were in the highest category). In models that adjusted for visibility of wind turbines and economic benefit, sound level was still a significant predictor of annoyance. However, because of the way in which sound and visibility were modeled in this analysis, the association between higher noise levels and higher annoyance could have been driven entirely by those who could see a wind turbine, while there could still have been no association between wind turbine noise level and annoyance among those who could not see a wind turbine. Thus, this study has to be considered inconclusive with respect to an association between wind turbine sound level and annoyance *independent of* the effect of seeing a wind turbine (and vice versa).

The Dutch study has the limitation of being cross sectional as were the Swedish studies, and the non-response in the Dutch study was much larger than in the Swedish studies. The results of the limited assessment of a subset of non-responders mitigate somewhat against the concerns raised by the low response rate, but not completely.

3.3.c New Zealand Study

The New Zealand study recruited participants from what the authors refer to as two demographically matched neighborhoods (an exposed group living near wind turbines and a control group living far from turbines), although supporting data for this are not presented. The area with the turbines is described as being characterized by hilly terrain, with long ridges running 250–450 m above sea level, on which 66 125 m high wind turbines are positioned. The power of the turbines is not provided. For the exposed group, participants were drawn from those 18 years and older living in 56 houses located within 2 km of a wind turbine, and for the control group participants were drawn from those 18 years and older living in 250 houses located at least 8 km from the wind turbines. It is unclear how many participants per household were recruited, but the final study sample included 39 people in the exposed group and 158 in the control group. Response rates of 34% for the exposed group and 32% for the control group are given. The outcome assessed was response to the abbreviated version of the WHO's quality of life (QOL)-BREF (WHOQOL-BREF)—a health-related QOL questionnaire. These questions were embedded within a larger questionnaire with various facets designed to mask the focus on wind turbines. Although there were no statistically significant demographic differences between the two groups, 43.6% of those in the exposed group had a university education while only 34.2% in the control group did.

The exposed group was found to have significantly worse physical QOL (in particular the sleep and energy level items of this scale) and worse environmental QOL (in particular ratings of how healthy the environment is and satisfaction with the conditions of their living space). The groups did not differ in scores on the social or psychological scales. The mean ratings for an overall QOL item was significantly lower in the exposed group. All of these analyses were adjusted for length of residence, but for no other variables.

As with the other studies discussed, this study has the limitation of being cross sectional. As with the Dutch study, the response rate in the present study is rather low, and unfortunately, there are no data in the New Zealand study on non-participants. This raises concern that self-selection into the study could differ by important factors in some way between the two groups. The difference seen in education level between the groups exacerbates this concern. It is also unclear whether appropriate statistical analysis methods were used given that there may have been multiple respondents from the same household, which is not stated but would have needed to have been accounted for in the analysis. The lack of control for other variables that may be related to reporting of QOL is also a limitation. In this regard it is important to note that a lack of a statistically significant difference in factors between groups does not rule out the possibility of those factors potentially accounting for some of the difference in outcome scores between groups, particularly when the sample size is small like in this study. Whether participants could see wind turbines was not assessed, but it is likely that most if not all in the exposed group could and most if not all in the control group could not, given their locations. Given the findings in the

Swedish and Dutch studies, this means that even if the difference in QOL scores seen are due to wind turbines, it is possible that it is driven by seeing the turbines rather than sound from the turbines. Overall, the level of evidence from this study for a causal association between wind turbines and reported QOL is limited.

3.3.d Additional Non-Peer Reviewed Documents

Papers that appear in the peer-reviewed literature have by definition undergone a level of review external to the study team by not only the editors of the journal, but also two to three (usually) scientists familiar with the field of the study and the methodology used. These hurdles provide an opportunity to identify problems with the paper—from methodology to interpretation of the results—and either provide the opportunity to address problems or reject the paper if the problems are considered fatal to the interpretation of the results. Non-peer reviewed literature is not subject to this external review scrutiny. This does not mean that all peer-reviewed literature is of high quality nor that non-peered reviewed literature is necessarily inferior to peer-reviewed literature, but it does mean that non-peered reviewed literature does not need to undergo any review process to appear. Indeed, at times studies appear in non-peer reviewed outlets precisely because they did not meet the bar of quality necessary to appear in the peer-reviewed literature. Thus, non-peer reviewed literature needs to be scrutinized with this in mind. Four such non-peer-reviewed reports are described below. In addition to those four, a few early reports of annoyance from wind turbines generally found a weak relationship between annoyance and the equivalent A-weighted SPL, although those studies were mainly based on studies of smaller turbines of less than 500 kW (T. H. Pedersen & Nielsen, 1994; Rand & Clarke, 1990; Wolsink et al., 1993).

<u>Project WINDFARMperception: Visual and acoustic impact of wind turbine farms on residents (van den Berg et al., 2008).</u> This report describes the study upon which the Dutch paper summarized above (E. Pedersen et al., 2009) is based. The characteristics of the wind turbines are thus as described above. In addition to the data that appeared in the peer-reviewed literature, this report describes analyses of additional data that was collected. These additional data relate to health effects and turbine noise exposure. The questionnaire assessed stress levels with the General Health Questionnaire (GHQ), a validated scale that has been widely used in such studies and which assesses symptoms felt over the past several weeks. In models adjusted for age, economic benefit from the turbines, and sex, there was no association between sound

levels and stress. In contrast, there was a significant association between sound levels and interrupted sleep (at least once a month), even when further adjusting for background noise levels. This was most obvious at turbine noise levels >45 dB(A), but there appeared to be an increasing trend in occurrence of interrupted sleep with increasing noise categories even across the lower noise categories. This study also asked participants about chronic health conditions including diabetes, high blood pressure, tinnitus, hearing impairment, cardiovascular disease, and migraine. Although no associations were seen between wind turbine noise and these outcomes in adjusted analyses, the chronic nature of these outcomes and the lack of data on timing of onset with respect to when the wind turbines were introduced make interpreting these negative findings difficult.

Report to the commission related to Moturimu wind farm, New Zealand (Phipps, 2007). This report to a commission in New Zealand related to the Moturimu wind farm describes a survey conducted by Robyn Phipps to investigate the visual and acoustical effects experienced by residents living at least 2 km from existing wind farms in the Manawatu and Tararua regions of New Zealand. Most respondents were within 3 km, although a few lived further away, as far as 15 km. The characteristics and number of wind turbines was not provided. Although this work does not appear to have come out in the peer-reviewed literature, reasonable details about the methodology are provided.

Roughly 1,100 surveys were delivered to postal addresses and 614 (56%) were returned. Participants were asked to rate on a scale of 1–5 their agreement with different statements related to their perceptions of the wind turbines. When these questions dealt with visual issues, they were framed both positively and negatively (e.g., “I think the turbines spoil the view,” and “I think the turbines are quite attractive”). This apparently was not the case with other questions (e.g., “Watching the turbines can create an unpleasant physical sensation in my body”).

Overall, 9% of respondents endorsed being “affected” by the flicker of the wind turbines; 15% were sufficiently bothered by the visual and noise effects of the turbines to consider complaining, and 10% actually had complained. While 56% is a relatively good response rate for a mailed survey, the reasons for non-response of nearly half of potential participants must be considered. It is possible that non-respondents did not care enough about the effects of the wind turbines to bother responding, which presumably would lower the overall percentages that were “affected” by the turbines. On the other hand, it is not clear how long the turbines were in operation prior to the survey, and it is conceivable that some more affected people may have moved out of the area before the time of the survey.

A further drawback to the reported survey was that there was not a determination of how the percentage of "affected" respondents related to distance from the turbines, the ability to see the turbines, or noise levels experienced from the turbines. The report cites a lot of literature on noise and health effects, and while such effects have been reported in the literature, they are almost uniformly at sound levels above what is usually found for people living near turbines (and most certainly higher than those usually reported for people living more than 2 km from a turbine). A WHO report provides a good review of this literature (WHO, 2009). The lowest threshold levels for seeing any effect are about 35 dB(A) (maximum per event or L_{Amax}) for some physiological sleep responses (e.g., EEG, or duration of sleep stages), but these thresholds are for levels inside the house near the sleeper, which will be much lower than what is experienced outside the house. The lowest threshold level for complaints of well-being were estimated at 35 dB(A) as a yearly average outside the house at night ($L_{night,\ outside}$). But for health outcomes the thresholds for any effect are much higher, for example 50 dB(A) ($L_{night,\ outside}$) for hypertension or myocardial infarction.

<u>"Wind Turbine Syndrome" (Pierpont, 2009)</u>: This book describes several people who suffer health symptoms that they attribute to wind turbines. Such descriptions can be informative in describing phenomena and raising suggestions for possible follow-up with more rigorous study designs, but generally are not considered evidence for causality. In this particular case, though, there are elements that go beyond the most basic symptom descriptions and so warrant consideration as a study. But limitations to the design employed make it impossible for this work to contribute any evidence to the question of whether there is a causal association between wind turbine exposure and health effects. Given this, the very term "Wind Turbine Syndrome" is misleading as it implies a causal role for wind turbines in the described health symptoms.

The book describes health symptoms experienced among 38 people from 10 different families who lived near wind turbines and subsequently either moved away from the turbines or spent significant periods of time away. The participants ranged in age from less than 1 to 75 years old, with 13 (34%) younger than 16 years and 17 (45%) younger than 22. The participants were queried about their health symptoms before exposure to turbines (presumably before the turbines were operational), during exposure to turbines, and after moving away. There is an impressive detailed description of the extent and severity of health symptoms experienced by this group, with a core group of symptoms centered around vibratory responses and termed Visceral Vibratory Vestibular Disturbance (VVVD) by Pierpont. While these symptoms for the most part are attributed to exposure to the wind turbines by the participants—either because they appeared once the turbines were operational or because they seemed to diminish after going away from the turbines—the way in which these participants were recruited makes it impossible to draw any conclusions about attributing causality to the turbines.

The most critical problem with respect to inferring causality from Pierpont's findings lies in how the families were identified for participation. To be included in the study, among other criteria, at least one family member had to have severe symptoms *and* reside near a recently erected wind turbine. In epidemiological terms this is selecting participants based on both exposure and outcome, which guarantees a biased (non-causal) association between wind turbines and symptoms. While it could be argued that other family members may not have had severe symptoms—and so would not be selected based on outcome—it is hard to consider other family members as truly independent observations, as their reporting of symptoms, or indeed their experiencing of symptoms, could be influenced by the more severely affected family member. This is particularly so when the symptoms are in the realm of anxiety, sleep disturbance, memory, and concentration; and the severely affected family members are reporting increased irritability, anger, and shouting.

Although not always, several of the participants reported an improvement of symptoms after moving away from the wind turbines. While this is suggestive and should not be discounted as something to explore further, the highly selective nature of the interviewed group as a whole makes the evidence for causality from these data *per se* weak. There are also many factors that change when moving, making it difficult to attribute changes to any specific difference with certainty. Additional factors that contribute to the inability to infer causality from these data include the small sample size, lack of detail on the larger population that could have been considered for inclusion in the study, and lack of detail on precisely how the actual participants were recruited. In addition, while the clinical history was extensive, the symptom data were all self-reported. Another complication is that there are no precise data on distance to turbines, and noise levels or infrasound vibration levels at the participants' homes.

"Adverse health effects of industrial wind turbines: a preliminary report" (Nissenbaum et al., 2011): This report describes a study involving questionnaire assessment of mental and physical health (SF-36), sleep disturbance (Pittsburgh Sleep Quality Index), and sleepiness (Epworth Sleepiness Scale) among residents near one of two wind farms in Maine (Vinalhaven & Mars Hill). The Mars Hill site is a linear arrangement of 28 General Electric 1.5 MW turbines, sited on a ridgeline. The Vinalhaven site is a cluster of three similar turbines, sited on a flat, tree-covered island. All residents within 1.5 km of one of the turbines were identified, and all those older than 18 years and non-demented were considered eligible for the study. A set of households from an area of similar socioeconomic makeup but 3–7 km from wind turbines were also recruited. The recruitment process involved house-to-house visits up to three times to recruit participants. Among those within at most 1.5 km from the nearest turbine, 65 adults were identified and 38 (58%; 22 male, 16 female) participated from 23 unique households. Among those 3-7 km from the nearest turbine, houses were visited until a similar number of participants were recruited. This process successfully recruited 41 adults (18 male, 23 female) from 33 unique households. No information was given on the number of homes or people approached so the participation rate cannot be determined.

Analyses adjusted for age, sex, and site (the two different wind farms) found that those living within 1.5 km of a wind turbine had worse sleep quality and mental health scores and higher ratings of sleepiness than those living 3–7 km from a turbine. Physical health scores did not differ between the groups. Similar associations were found when distance to the nearest turbine was analyzed as a continuous variable.

This study is somewhat limited by its size—much smaller than the Swedish or Dutch studies described above—but nonetheless suggests relevant potential health impacts of living near wind turbines. There are, however, critical details left out of the report that make it difficult to fully assess the strength of this evidence. In particular, critical details of the group living 3–7 km from wind turbines is left out. It is stated that the area is of similar socioeconomic makeup, and while this may be the case, no data to back this up are presented—either on an area level or on an individual participant level. In addition, while the selection process for these participants is described as random, the process of recruiting these participants by going home to home until a certain number of participants are reached is not random. Given this, details of how homes were identified, how many homes/people were approached, and differences between those who did and did not participate are important to know. Without this, attributing any of the observed associations to the wind turbines (either noise from them or the sight of them) is premature.

3.3.e Summary of Epidemiological Data

There is only a limited literature of epidemiological studies on health effects of wind turbines. Furthermore, existing studies are limited by their cross sectional design, self-reported symptoms, limited ability to control for other factors, and to varying degrees of non-response rates. The study that accounted most extensively for other factors that could affect reported symptoms had a very low response rate (E. Pedersen et al., 2009; van den Berg, et al., 2008).

All four peer-reviewed papers discussed above suggested an association between increasing sound levels from wind turbines and increasing annoyance. Such an association was also suggested by two of the non-peer reviewed reports that met at least basic criteria to be considered studies. The only two papers to consider the influence of seeing a wind turbine (each one of the peer-reviewed papers) both found a strong association between seeing a turbine and annoyance. Furthermore, in the studies with available data, the influence of either sound from a turbine or seeing a turbine was reduced—if not eliminated, as was the case for sound in one study—when both of these factors were considered together. However, this precise relation cannot be disentangled from the existing literature because the published analyses do not properly account for both seeing and hearing wind turbines given the relation between these two that the data seem to suggest. Specifically, the possibility that there may be an association between either of those factors and annoyance, but possibly only for those who both see and hear sound from a turbine, and not for those who either do not hear sound from or do not see a turbine. Furthermore, in the one study to consider whether individuals benefit economically from the turbines in question, there appeared to be virtually no annoyance regardless of whether those people could see or hear a turbine. Even if one considers the data just for those who could see a wind turbine and did not benefit economically from the turbines, defining at what noise levels the percentage of those annoyed becomes more dramatic is difficult. Higher percentages of annoyance did appear to be more consistent above 40 dB(A). Roughly 27% were annoyed (at least 4 on a 1–5 point scale of annoyance; 5 being the worst), while roughly 18% were very annoyed (5 on a 1–5 scale). The equivalent levels of annoyed and very annoyed for 35–40 dB(A) were roughly 15% and 6%, respectively. These percentages, however, should be considered upper bounds for a specific relation with noise levels because, with respect to estimating direct effects of noise, they are likely inflated as a result of both selective participation in the studies and the fact that the percentages do not take into account the effect of seeing a turbine.

Thus, in considering simply exposure to wind turbines in general, while all seem to suggest an association with annoyance, because even the peer-reviewed papers have weaknesses, including the cross sectional designs and sometimes quite low response rates, **the Panel concludes that there is limited evidence suggesting an association between exposure to wind turbines and annoyance**. However, only two of the studies considered both seeing and hearing wind turbines, and even in these the possible contributions of seeing and hearing a wind turbine were not properly disentangled. Therefore, **the Panel concludes that there is insufficient evidence to determine whether there is an association between noise from wind turbines and annoyance independent from the effects of seeing a wind turbine and vice versa**. Even these conclusions must be considered in light of the possibility suggested from one of the peer-reviewed studies that there is extremely low annoyance—regardless of seeing or hearing sound from a wind turbine—among people who benefit economically from the turbines.

There was also the suggestion that poorer sleep was related to wind turbine noise levels. While it intuitively makes sense that more noise would lead to more sleep disruption, there is limited data to inform whether this is occurring at the noise levels produced from wind turbines. An association was indicated in the New Zealand study, suggested without presenting details in one of the Swedish studies, and found in two non-peer-reviewed studies. Therefore, **the Panel concludes that there is limited evidence suggesting an association between noise from wind turbines and sleep disruption and that further study would quantify precise sound levels from wind turbines that disrupt sleep**.

The strongest epidemiological study to examine the association between noise and psychological health suggests there is not an association between noise from wind turbines and measures of psychological distress or mental health problems. There were two smaller, weaker, studies: one did note an association, one did not. Therefore, **the Panel concludes the weight of the evidence suggests no association between noise from wind turbines and measures of psychological distress or mental health problems.**

One Swedish study apparently collected data on headache, undue tiredness, pain and stiffness in the back, neck, or shoulders, or feeling tensed/stressed and irritable, but did not report on analyses of these data. The Dutch study found no association between noise from wind turbines and diabetes, high blood pressure, tinnitus, hearing impairment, cardiovascular disease, and migraine, although this was not reported in the peer-reviewed literature. Therefore, **the Panel concludes that none of the limited epidemiological evidence reviewed suggests an association between noise from wind turbines and pain and stiffness, diabetes, high blood pressure, tinnitus, hearing impairment, cardiovascular disease, and headache/migraine.**

These conclusions align with those presented in the peer-reviewed article by Knopper and Ollson (2011). They write "Conclusions of the peer reviewed literature differ in some ways from those in the popular literature. In peer reviewed studies, wind turbine annoyance has been statistically associated with wind turbine noise, but found to be more strongly related to visual impact, attitude to wind turbines and sensitivity to noise. … it is acknowledged that noise from wind turbines can be annoying to some and associated with some reported health effects (e.g., sleep disturbance), especially when found at sound pressure levels greater than 40 db(A)."

3.4 Exposures from Wind Turbines: Noise, Vibration, Shadow Flicker, and Ice Throw

In addition to the human epidemiologic study literature on exposure to wind turbines and health effects described in the section above, the Panel assessed literature that could shed light on specific exposures resulting from wind turbines and possible health effects. The exposures covered here include noise and vibration, shadow flicker, and ice throw. Each of these exposures is addressed separately in light of their documented and potential health effects. When health effects are described in the popular media, these claims are discussed.

3.4.a Potential Health Effects Associated with Noise and Vibration

The epidemiologic studies discussed above point to noise from wind turbines as a source of annoyance. The studies also noted that some respondents note sleep disruption due to the turbine noise. In this section, the characteristics of audible and inaudible noise from turbines are discussed in light of our understanding of their impacts on human health.

It is clear that when sound levels get too high, the sound can cause hearing loss (Concha-Barrientos et al., 2004). These sound levels, however, are outside the range of what one would experience from a wind turbine. There is evidence that levels of audible noise below levels that cause hearing loss can have a variety of health effects or indicators. Detail about the evidence for such health effects have been well summarized in a WHO report that came to several relevant conclusions (WHO, 2009). First, there is sufficient evidence for biological effects of noise during sleep: increase in heart rate, arousals, sleep stage changes and awakening; second, there is limited evidence that noise at night causes hormone level changes and clinical conditions such as cardiovascular illness, depression, and other mental illness. What the WHO report also details is observable noise threshold levels for these potential effects. For such health effects, where data are sufficient to estimate a threshold level, that level is never below 40 dB(A)—as a yearly average—for noise outside (ambient noise) at night—and these estimates take into account sleeping with windows slightly open.

One difficulty with the WHO threshold estimate is that a yearly average can mask the particular quality of turbine noise that leads survey respondents to note annoyance or sleep disruption. For instance, the pulsatile nature of wind turbine noise has been shown to lead to respondents claiming annoyance at a lower averaged sound level than for road noise (E. Pederson, 2004). Yearly averaging of sound eliminates (or smooths) the fluctuations in the sound and ignores differences between day and night levels. Regulations may or may not take this into account.

Health conditions caused by intense vibration are documented in the literature. These are the types of exposures that result from jackhammers, vibrating hand tools, pneumatic tools, etc. In these cases, the vibration is called arm-body or whole-body vibration. Vibration can cause changes in tendons, muscles, bones and joints, and can affect the nervous system. Collectively, these effects are known as Hand-Arm Vibration Syndrome (HAVS). Guidelines and interventions are intended to protect workers from these vibration-induced effects (reviewed by European Agency for Safety and Health at Work, 2008; (NIOSH 1989). OSHA does not have standards concerning vibration exposure. The American Conference of Governmental Industrial Hygienists (ACGIH) has developed Threshold Limit Values (TLVs) for vibration exposure to hand-held tools. The exposure limits are given as frequency-weighted acceleration (NIOSH, 1989).

3.4.a.i Impact of Noise from Wind Turbines on Sleep

The epidemiological studies indicate that noise and/or vibration from wind turbines has been noted as causing sleep disruption. In this section sleep and sleep disruption are discussed. In addition, suggestions are provided for more definitively evaluating the impact of wind turbines on sleep.

All sounds have the potential to disrupt sleep. Since wind turbines produce sounds, they might cause sleep disruption. A very loud wind turbine at close distance would likely disrupt sleep, particularly in vulnerable populations (such as those with insomnia or mood disorders, aging populations, or "light sleepers"), while a relatively quiet wind turbine would not be expected to disrupt even the lightest of sleepers, particularly if it were placed at considerable distance.

There is insufficient evidence to provide very specific information about how likely particular sound-pressure thresholds of wind turbines are at disrupting sleep. Physiologic studies of noises from wind turbines introduced to sleeping people would provide these specific levels. Borrowing existing data (e.g., Basner, 2011) and guidelines (e.g., WHO) about noises at night, beyond wind turbines, might help provide reasonable judgment about noise limits at night. But it would be optimal to have specific data about the particular influence that wind turbines have on sleep.

In this section we introduce broad concepts about sleep, the interaction of sleep and noises, and the potential for wind turbines to cause that disruption.

Sleep

Sleep is a naturally occurring state of altered consciousness and reduced physical activity that interacts with all aspects of our physiology and contributes daily to our health and well-being.

Measurements of sleep in people are typically performed with recordings that include electroencephalography (EEG). This can be performed in a laboratory or home, and for clinical or experimental purposes. Other physiological parameters are also commonly measured, including muscle movements, lung, and heart function.

While the precise amount of sleep that a person requires is not known, and likely varies across different people and different ages, there are numerous consequences of reduced sleep (i.e., sleep deprivation).

Deficiencies of sleep can take numerous forms, including the inability to initiate sleep; the inability to maintain sleep; abnormal composition of sleep itself, such as too little deep sleep (sometimes called slow-wave sleep, or stage N3); or frequent brief disruptions of sleep, called arousals. Sources of sleep deprivation can be voluntary (desirable or undesirable) or involuntary. Voluntary sources include staying awake late at night or awakening early. These can be for work or school, or while engaging in some personal activities during normal sleep times. Sleep deprivation can also be caused by myriad involuntary and undesired problems (including those internal to the body such as pain, anxiety, mood disorders) and frequent need to urinate, or by numerous sleep disorders (including insomnia, sleep apnea, circadian disorders, parasomnias, sleep-related movement disorders, etc), or simply by the lightening of sleep depth in normal aging. Finally, sleep deprivation can be caused by numerous external factors, such as noises or other sensory information in the sleeper's environment.

Sleep is conventionally categorized into rapid eye movement (REM) and non-REM sleep. Within the non-REM sleep are several stages of sleep ranging from light sleep to deep sleep. Beyond these traditional sleep categories, the EEG signal can be analyzed in a more detailed and sophisticated way, including looking at the frequency composition of the signals. This is important in sleep, as we now know that certain signatures in the brain waves (i.e., EEG) disclose information about who is vulnerable to noise-induced sleep disruption, and what moments within sleep are most vulnerable (Dang-Vu et al., 2010; McKinney et al., 2011).

Insomnia can be characterized by a person having difficulty falling asleep or staying asleep that is not better explained by another condition (such as pain or another sleep disorder) (see ICSD, 2nd Edition for details of the diagnostic criteria for insomnia). Approximately 25% of the general population experience occasional sleep deprivation or insomnia. Sleep deprivation is defined by reduced quantity or quality of sleep, and it can result in excessive daytime sleepiness as well as problems including those associated with mood and cognitive function (Roth et al., 2001; Rogers, 2007; Walker, 2008). As might be expected, the severity of the sleep deprivation has an impact on the level of cognitive functioning, and real-life consequences can include driving accidents, impulsive behaviors, errors in attention, and mood problems (Rogers, 2007; Killgore, 2010). Loss of sleep appears to be cumulative, meaning it adds up night after night. This can result in subtle impairments in reaction times, decision-making ability, attentional vigilance, and integration of information that is sometimes only apparent to the sleep-deprived individual after an accident or error occurs, and sometimes not perceived by the sleep-deprived person at all (Rogers, 2007; van Dongen 2003).

Sleep and Wind Turbines

Given the effects of sleep deprivation on health and well-being, including problems with mood and cognition, it is possible that cognitive and mood complaints and other medical or psychological issues associated with sleep loss can stem from living in immediate proximity to wind turbines, if the turbines disrupt sleep. Existing data, however, on the relationship between wind turbines and sleep are inadequate. Numerous factors determine whether a sound disrupts sleep. Broadly speaking, they are derived from factors about the sleeper and factors about the sound.

Case reports of subjective complaints about sleep, particularly those not critically and objectively appraised in the normal scientific manner, are the lowest level of evidence, not simply because they lack any objective measurements, but also because they lack the level of scrutiny considered satisfactory for making even crude claims about cause and effect. For instance, consider the case of a person who sleeps poorly at home (near a wind turbine), and sleeps better when on vacation (away from a wind turbine). One might conclude from this case that wind turbines cause sleep disruption for this person, and even generalize that information to other people. But there are numerous factors that might make it more likely that a person can sleep well on vacation, having nothing to do with the wind turbine. Furthermore, given the enormous prevalence of sleep disorders, such as insomnia, and the potentially larger prevalence of disorders that impinge on sleep, such as depression, it is crucial that these factors be taken into consideration when weighing the evidence pointing to a causal effect of wind turbines on sleep disruption for the general population. It is also important to obtain objective measurements of sleep, in addition to subjective complaints.

Subjective reports of sleeping well or sleeping poorly can be misleading or even inaccurate. People can underestimate or overestimate the quality of their sleep. Future studies should examine the acoustic properties of wind turbines when assessing the elements that might disrupt sleep. There are unique properties of the noises wind turbines make, and there are some acoustic properties in common with other noises (such as trucks or trains or airplanes). It is important to make these distinctions when assessing the effects of wind turbines on noise, by using data from other noises. Without this physiologic, objective information, the effects of wind turbines on sleep might be over- or underestimated.

It should be noted that not all sounds impair the ability to fall asleep or maintain sleep. To the contrary, people commonly use sound-masking techniques by introducing sounds in the environment that hinder the perception of undesirable noises. Colloquially, this is sometimes called “white noise,” and there are certain key acoustic properties to these kinds of sounds that make them more effective than other sounds. Different noises can affect people differently. The emotional valence that is ascribed by an individual to a particular sound can have a major influence on the ability to initiate or maintain sleep. Certain aspects of sounds are particularly alerting and therefore would be more likely to disrupt sleep at lower sound pressure levels. But among those that are not, there is a wide range of responses to these sounds, depending partly on the emotional valence ascribed to them. A noise, for instance, that is associated with a distressing object, is more likely to impede sleep onset.

Finally, characteristics of sleep physiology change across a given night of sleep—and across the life cycle of a person—and are different for different people, including the effects of noise on sleep (e.g., Dang-Vu et al., 2010; McKinney et al., 2011). And some people might initially have difficulty with noises at night, but habituate to them with repeated exposure (Basner, 2011).

In summary, **sleep is a complex biological state, important for health and well-being across a wide range of physiologic functions. To date, no study has adequately examined the influence of wind turbines on sleep.**

Future directions: The precise effects of noise-induced sleep disruption from wind turbines may benefit from further study that examines sound-pressure levels near the sleeper, while simultaneously measuring sleep physiology to determine responses of sleep to a variety of levels of noise produced by wind turbines. The purpose would be to understand the precise sound-pressure levels that are least likely to disturb sleep. It would also be helpful to examine whether sleepers might habituate to these noises, making the impact of a given sound less and less over time. Finally, it would be helpful to study these effects in susceptible populations, including those with insomnia or mood disorders or in aging populations, in addition to the general population.

Summary of Sleep Data

In summary, sleep is a complex biological state, important for health and well-being across a wide range of physiologic functions. **To date, no study has adequately examined the influence of wind turbines and their effects on sleep.**

3.4.b Shadow Flicker Considerations and Potential Health Effects

Shadow flicker is caused when changes in light intensity occur from rotating wind turbine blades that cast shadows (see Appendix B for more details on the physics of the phenomenon.) These shadows move on the ground and on buildings and structures and vary in terms of frequency rate and intensity. Shadow flicker is reported to be less of a problem in the United States than in Northern Europe due to higher latitudes and lower sun angles in Europe. Nonetheless, it can still be a considerable nuisance to individuals exposed to shadow flicker for considerable amounts of time per day or year in the United States as well. Shadow flicker can vary significantly by wind speed and duration, geographic location of the sunlight, and the distance from the turbine blades to any relevant structures or buildings. In general, shadow flicker branches out from the wind turbine in a declining butterfly wing characteristic geographic area with higher amounts of flicker being closer to the turbine and less flicker in the outer parts of the geographic area (New England Wind Energy Education Project (NEWEEP), 2011; Smedley et al., 2010). Shadow flicker is present up until approximately 1400 m, but the strongest flicker is up to 400 m from the turbine when it occurs (NEWEEP, 2011). In addition, shadow flicker usually occurs in the morning and evening close to sunrise and sunset when shadows are the longest. Furthermore, shadow flicker can fluctuate in different seasons of the year depending on the geographic location of the turbine such that some sites will only report flicker during the winter months while others will report it during summer months. Other factors that determine shadow flicker rates and intensity include objects in the landscape (i.e., trees and other existing shadows) and weather patterns. For instance, there is no shadow flicker on cloudy days without sun as compared with sunny days. Also, shadow flicker speed (shadows passing per second) increases with the rotor speed (NRC, 2007). In addition, when several turbines are located relatively close to one another there can be combined flicker from the different blades of the different turbines and conversely, if situated on different geographic areas around structures, shadow flicker can occur at different times of the day at the same site from the different turbines so pre-planning of siting location is very important (Harding et al., 2008). General consensus in Germany resulted in the guidance of 30 hours per year and 30 minutes per day (based on astronomical, clear sky calculations) as acceptable limits for shadow flicker from wind turbines (NRC, 2007). This is similar to the Denmark guidance of 10 hours per year based on actual conditions.

3.4.b.i Potential Health Effects of Flicker

Because some individuals are predisposed to have seizures when exposed to certain types of flashing lights, there has been concern that wind turbines had the potential to cause seizures in these vulnerable individuals. In fact, seizures caused by visual or photic stimuli are typically observed in people with certain types of epilepsy (Guerrini & Genton, 2004), particularly generalized epilepsy. While it is not precisely known how many people have photosensitivity that causes seizures, it appears to be approximately 5% of people with epilepsy, amounting to about 100,000 people in the United States. And many of these people will already be treated with antiepileptic medications thus reducing this risk further.

Fortunately, not all flashing light will elicit a seizure, even in untreated people with known photosensitivity. There are several key factors that likely need to simultaneously occur in order for the stimulus to induce a seizure, even among the fraction of people with photosensitive seizures. The frequency of the stimulus is important as is the stimulus area and pattern (See below) (http://www.epilepsyfoundation.org/aboutepilepsy/seizures/photosensitivity/gerba.cfm).

Frequencies above 10 Hz are more likely to cause epileptic seizures in vulnerable individuals, and seizures caused by photic stimulation are generally produced at frequencies ranging from greater than 5 Hz. However, shadow flicker frequencies from wind turbines are related to the rotor frequency and this usually results in 0.3–1.0 Hz, which is outside of the range of seizure thresholds according to the National Resource Council and the Epilepsy Foundation (NRC, 2007). In fact, studies performed by Harding et al. (2008) initially concluded that because light flicker can affect the entire retina, and even if the eyes are closed that intermittent light can get in the retina, suggested that 4 km would be a safe distance to avoid seizure risk based on shadow flicker (Harding et al., 2008). However, a follow-up analysis considering different meteorological conditions and shadow flicker rates concluded that there appeared to be no risk for seizures unless a vulnerable individual was closer than 1.2 times the total turbine height on land and 2.8 times the total turbine height in the water, which could potentially result in frequencies of greater than 5 Hz (Smedley et al., 2010).

Although some individuals have complained of additional health complaints including migraines, nausea, dizziness, or disorientation from shadow flicker, only one government-sponsored study from Germany (Pohl et al., 1999) was identified for review. This German study was performed by the Institute of Psychology, Christian-Albrechts-University Kiel on behalf of the Federal Ministry of Economics and Technology (BMWi) and supported by the Office of Biology, Energy, and Environment of the Federal Ministry for Education and Research (BMBF), and on behalf of the State Environmental Agency of Schleswig. The purpose of this government-sponsored study was to determine whether periodic shadow with a duration of more than 30 minutes created significant stress-related health effects. The shadows were created by a projection system, which simulated the flicker from actual wind turbines.

Two groups of different aged individuals were studied. The first group consisted of 32 students (average age 23 years). The second group included 25 professionals (average age 47 years). Both men and women were included. The subjects were each randomly assigned to one of two experimental groups, so there was a control group and an experimental group. The experimental group was exposed to 60 minutes of simulated flicker. For the control group lighting conditions were the same as in the experimental group, but without periodic shadow. The main part of the study consisted of a series of six test and measurement phases, two before the light was turned on, three each at intervals of 20 minutes while the simulated shadow flickering was taking place, and one more after the flicker light was turned off. Among the variables measured were general performance indicators of stress (arithmetic, visual search tasks) and those of mental and physical well-being, cognitive processing, and stress in the autonomic nervous system (heart rate, blood pressure, skin conductance, and finger temperature). Systematic effects due to the simulated flicker could be detected in comparable ways in both exposure groups studied. Both physical and cognitive effects were found in this exposure scenario for shadow flicker.

It appears clear that shadow flicker can be a significant annoyance or nuisance to some individuals, particularly if they are wind project non-participants (people who do not benefit economically or receive electricity from the turbine) whose land abuts the property where the turbine is located. In addition, flashing (a phenomenon closely related to shadow flicker, but due to the reflection of sunlight – see Appendix B) can be a problem if turbines are sited too close to highways or other roadways. This could cause dangerous conditions for drivers. Accordingly, turbine siting near highways should be planned so as to reduce flashing as much as possible to protect drivers. However, use of low reflective turbine blades is commonly employed to reduce this potential flashing problem. Provisions to avoid many of these potential health and annoyance problems appear to be employed as current practice in many pre-planning sites with the use of computer programs such as WindPro. These programs can accurately determine shadow flicker rates based on input of accurate analysis area, planned turbine location, the turbine design (height, length, hub height, rotor diameter, and blade width), and residence or roadway locations. Many of these computer programs can then create maps indicating the location and incidence of shadow flicker. Such programs may also provide estimates of daily minutes and hours per year of expected shadow flicker that can then be used for wind turbine planning and siting or for mitigation efforts. Several states require these analyses to be performed before any new turbine projects can be implemented.

3.4.b.ii Summary of Impacts of Flicker

Collectively, although shadow flicker can be a considerable nuisance particularly to wind turbine project non-participants, the evidence suggests that there is no risk of seizure from shadow flicker caused by wind turbines. In addition, there is limited evidence primarily from a German government-sponsored study (Pohl et al., 1999) that prolonged shadow flicker (more than 30 minutes) can result in transient stress-related effects on cognition (concentration, attention) and autonomic nervous system functioning (heart rate, blood pressure). There was insufficient documentation to evaluate other than anecdotal reports of additional health effects including migraines or nausea, dizziness or disorientation. There are documented mitigation methods for addressing shadow flicker from wind turbines and these methods are presented in Appendix B.

3.4.c Ice Throw and its Potential Health Effects

Under certain weather conditions ice may form on the surface of wind turbine blades. Normally, wind turbines intended for use in locations where ice may form are designed to shut down when there is a significant amount of ice on the blades. The means to prevent operation when ice is present may include ice sensor and vibration sensors. Ice sensors are used on most wind turbines in cold climates. Vibration sensors are used on nearly all wind turbines. They would cause the turbine to shut down, for example, if ice buildup on the blades resulted in an imbalance of the rotor and hence detectable vibrations in the structure.

Ice built up on blades normally falls off while the turbine is stationary. If that occurs during high winds, the ice could be blown by the wind some distance from the tower. In addition, it is conceivable that ice could be thrown from a moving wind turbine blade under some circumstances, although that would most likely occur only during startup (while the rotational speed is still relatively low) or as a result of the failure of the control system. It is therefore worth considering the maximum plausible distance that a piece of ice could land from the turbine under two “worst case” circumstances: 1) ice falls from a stopped turbine during very high winds, and 2) ice is suddenly released from a blade when the rotor is rotating at its normal operating speed.

Ice is a physical hazard, that depending on the mass, velocity, and the angle of throw can result in a wide range of effects to humans: alarm and surprise to abrasions, organ damage, concussions, and perhaps death. Avoidance of ice throw is critical. More detail on ice throw and options for mitigation are presented in Appendix C.

3.5 Effects of Noise and Vibration in Animal Models

Domestic animals such as cats and dogs can serve as sentinels of problematic environmental conditions. The Panel searched for literature that might point to non-laboratory animal studies or well-documented cases of animals impacted by wind turbines. Anecdotal reports in the press of goat deaths (UK), premature births and adverse effects in cows (Japan, US) provide circumstantial evidence, but lack specifics regarding background rates of illness or extent of impact.

Laboratory-based animal models are often used to predict and to develop mechanistic explanations of the causes of disease by external factors, such as noise or chemicals in humans. In the absence of robust epidemiological data, animal models can provide clues to complex biological responses. However, the limitations of relying on animal models are well documented, particularly for endpoints that involve the brain. The benefits of using an animal model include ease of experimental manipulation such as multiple exposures, typically well-controlled experimental conditions, and genetically identical groups of animals.

Evaluation of biological plausibility for the multitude of reported health effects of wind turbines requires a suitable animal model documented with data that demonstrate cause and effect. Review of this literature began with a PubMed and ToxNet search for “wind turbine” or “wind turbines”; or “infrasound” or “low frequency noise”; and “animal” or “mammal” to identify peer-reviewed studies in which laboratory animals were exposed to noise or vibration intended to mimic that of wind turbines. Titles and abstracts of identified papers were read to make a first pass determination of whether the paper was a study on effects in mammals or might contain relevant references to other relevant studies. The searches yielded several studies, many of which were not peer-reviewed, were not whole-animal mammalian or were not experimental, but were reviews in which animal studies were mentioned or experiments conducted in dissected cochlea. The literature review yielded eight peer-reviewed studies, all relying on the laboratory rat as the model. The studies fall into two groups—those conducted in the 1970's and early 1980's and those conducted in 2007–2010. The most recent studies are conducted in China and are funded by the National Natural Science Foundation of China. Table AG.1 (in Appendix G) provides a summary of the studies.

There is no general agreement about the specific biological activity of infrasound on rodents, although at high doses it appears to negatively affect the cardiovascular, brain, and respiratory systems (Sienkiewicz, 2007). Early studies lacked the ability to document the doses of infrasound given the rats, did not report general pathologies associated with the exposures and lacked suitable controls. Since then, researchers have focused on the brain and cardiac systems as sensitive targets of infrasound. Experimental conditions in these studies lack a documented rationale for the selection and the use of infrasound of 5-15 Hz at 130 dB. While this appears to be standard practice, the relevance of these frequencies and pressures is unclear—both to the rat and more importantly to the human. The exposures are acute—short-term, high dose. Researchers do not document rat behaviors (including startle responses), pathologies, frank toxicities, and outcomes due to these exposures. Therefore, interpretation of all of the animal model data for infrasound outcomes must be with the lens of any high-dose, short-term exposure in toxicology, specifically questioning whether the observations are readily translatable to low-dose, chronic exposures.

Pei et al., (2007 and 2009) examine changes in cardiac ultrastructure and function in adult male Sprague-Dawley rats exposed to 5 Hz at 130 dB for 2 hours for 1, 7, or 14 successive days. Cardiomyocytes were enzymatically isolated from the adult left ventricular hearts after sacrifice. Whole cell patch-clamp techniques were employed to measure whole cell L-Type Ca^{2+} currents. The objective of these studies was to determine whether there was a cumulative effect of insult as measured by influx of calcium into cardiomyocytes. After infrasound exposure, rats in the 7– and 14–day exposure groups demonstrated statistically significant changes in intracellular Ca^{2+} homeostasis in cardiomyocytes as demonstrated by electrochemical stimulation of the cells, molecular identification of specific heart-protein levels, and calcium transport measurements.

Several studies examine the effects of infrasound on behavioral performance in rats. The first of these studies was conducted under primitive acoustic conditions compared with those of today (Petounis et al., 1977). In this study the researchers examined the behavior of adult female rats (undisclosed strain) exposed to increasing infrasound (2 Hz, 104 dB; 7 Hz, 122 dB; and 16

Hz, 124 dB) for increasing time (5-minute increments for up to 120 minutes). Decreased activity levels (sleeping more) and exploratory behavior were documented as dose and duration of exposure increased. The authors fail to mention that frank toxicity including pain is associated with these behaviors, raising the question of relevance of high dose exposures. In response to this and similar studies that identify increase in sleep, increase in avoidance behaviors and suppression of locomotor activity, Spyraki et al., (1977) hypothesized that these responses are mediated by norepinephrine levels in the brain and as such, exposed adult male Wistar rats to increasing doses of infrasound for one hour. Using homogenized brain tissue, norepinephrine concentrations were measured using fluorometric methods. Researchers demonstrated a dose-dependent decrease in norepinephrine levels in brain tissue from infrasound-treated rats, beginning at a dose of 7 Hz and 122 dB for one hour. No observations of frank toxicity were recorded. Liu et al., (2010) hypothesized that since infrasound could affect the brain, it potentially could increase cell proliferation (neurogenesis) in the dentate gyrus of the rat hippocampus, specifically a region that continues to generate new neurons in the adult male Sprague-Dawley rat. Using a slightly longer exposure period of 2 hours/day for 7 days at 16 Hz and 130 dB, the data suggest that infrasound exposure inhibits cell proliferation in the dentate gyrus, yet has no affect on early migration and differentiation. This study lacks suitable positive and negative controls that allow these conclusions to be drawn.

Several unpublished or non-peer reviewed studies reported behavioral responses as relevant endpoints of infrasound exposure. These data are not discussed, yet are the basis for several recent studies. In one more recent peer-reviewed behavioral rat study, adult male Wistar rats were classified as “superior endurance” and those as “inferior endurance” using the Rota-rod Treadmill (Yamamura et al., 1990). A range of frequencies and pressures were used to expose the rats for 60—150 minutes. Comparison of the pre-exposure endurance time on the Rota-Rod Treadmill with endurance after exposure to infrasound showed that the endurance time of the superior group after exposure to 16 Hz, 105 dB was not reduced. The endurance of the inferior group was reduced by exposure to 16 Hz, 105 dB after 10 minutes, to 16 Hz, 95 dB after 70 minutes, and to 16 Hz, 85 dB after 150 minutes. Of most relevance is the identification of a subset of rats that may be more responsive to infrasound due to their genetic makeup. There has been no follow-up regarding intra-strain susceptibility since this study.

More recent studies have focused on the mechanisms by which infrasound may disrupt normal brain function. As stated above, the infrasound exposures are acute—short-term, high dose. At the very least, researchers should document rat behaviors, pathologies, frank toxicities, and outcomes due to these high dose exposures in addition to measuring specific subcellular effects.

Some of the biological stress literature suggests that microglial activation can occur with heightened stress, but it appears to be short-lived and transitory affecting the autonomic nervous system and neuroendocrine system, resulting in multiple reported effects. To investigate the effect of infrasound on hippocampus-dependent learning and memory, Yuan et al. (2009) measure cognitive abilities and activation of molecular signaling pathways in order to determine the role of the neuronal signaling transduction pathway, BDNF-TRkB, in infrasound-induced impairment of memory and learning in the rat. Adult male Sprague-Dawley rats were exposed to infrasound of 16 Hz and 130 dB for 2 hours daily for 14 days. The acoustic conditions appeared to be well monitored and documented. The Morris water maze was used to determine spatial learning and retention, and molecular techniques were used to measure cell proliferation and concentrations of signaling pathway proteins. Using these semi-quantitative methods, rats exposed to infrasound demonstrated impaired hippocampal-dependent spatial learning acquisition and retention performance in the maze scheme compared with unexposed control rats, demonstrable downregulation of the BDNF-TRkB pathway, and decreased BrdU-labeled cell proliferation in the dentatel gyrus.

In another study, Du et al. (2010) hypothesize that microglial cells may be responsible for infrasound-induced stress. To test this hypothesis, 60 adult male Sprague-Dawley rats were exposed in an infrasonic chamber to 16 Hz at 130 dB for 2 hours. Brains were removed and sectioned and the hypothalamic paraventricular nucleus (PVN) examined. Primary microglial cells were isolated from whole brains of neonatal rats and grown in culture before they were exposed to infrasound under the same conditions as the whole animals. Molecular methods were used to identify the presence and levels of proteins indicative of biological stress (corticotrophin-releasing hormone (CRH) and corticotrophin-releasing hormone receptor (CRH type 1 receptor) in areas of the brain that control the stress response. Specifically, studies were done to determine whether microglial cells are involved in infrasound-response, changes in microglial activation, and CRH-R1 expression in vivo in the PVN and in vitro at time points after the two-hour infrasound exposure. The data show that the exposures resulted in microglial activation, beginning at 0.5 hours post exposure, and up-regulation of CRH-R1 expression. The magnitude of the response increased significantly from the control to 6 hours post exposure, returning to control levels, generally by 24 hours post-exposure. This study is well controlled, and while it does rely on a specific antagonist for dissecting the relative involvement of the neurons and the microglial cells, the data suggest that infrasound as administered in this study to rats can activate microglial cells, suggesting a possible mechanism for infrasound-induced ”stress” or nuisance at a physical level (i.e., proinflammatory cytokines causing sickness response behaviors).

In summary, there are no studies in which laboratory animals are subjected to exposures that mimic wind turbines. There is insufficient evidence from laboratory animal studies of effects of low frequency noise on the respiratory system. There is limited evidence that rats are a robust model for human infrasound exposure and effects. The reader is referred to Appendix G for specific study conditions. In any case, the infrasound levels and exposure conditions to which the rodents are exposed are adequate to cause pain to the rodents. When exposed to these levels of infrasound, there is some evidence of reversible molecular effects including short-lived biochemical alterations in cardiac and brain cells, suggesting a possible mechanism for high-dose, infrasound-induced effects in rats.

3.6 Health Impact Claims Associated with Noise and Vibration Exposure

The popular media contain a large number of articles that claim the noise and vibration from wind turbines adversely affect human health. In this section the Panel examines the physical and biological basis for these assertions. Additionally, the scientific articles from which these assertions are made are examined in light of the methods used and their limitations.

Pierpont (2009) has been cited as offering evidence of the physical effects of ILFN, referring to “Wind Turbine Syndrome” and its impact on the vestibular system—by disturbed sensory input to eyes, inner ears, and stretch and pressure receptors in a variety of body locations. The basis for the syndrome relies on data from research carried out for reasons (e.g., space missions) other than assessment of wind turbines on health. Such research can be valuable to understanding new conditions, however, when the presentation of data is incomplete, it can lead to inaccurate conclusions. A few such cases are mentioned here:

Pierpont (2009) notes that von Dirke and Parker (1994) show that the abdominal area resonates between 4 and 6 Hz and that wind turbines can produce infrasound within this range (due to the blade rotation rate). However, the von Dirke paper states that our bodies have evolved to be tolerant of the 4–6 Hz abdominal motion range: this range coincides with jogging and running. The paper also reveals that motion sickness (which was the focus of the study) only occurred when the vibrations to which people were subjected were between 0.01 and 0.5 Hz. The study exposed people to vibration from positive to negative 1 G forces. Subjects were also rotated around various axes to achieve the vibration levels and frequencies of interest in the study. Interpretation of these data may allow one to conclude that while the abdominal area has a resonance in a region at which there is infrasound being emitted by wind turbines, there will be no impact. Further, the infrasound emitted by wind turbines in the range of frequencies at which subjects did note motion sickness is orders of magnitude less than the level that induced motion sickness (see Table 2). So while a connection is made, the evidence at this point is not sufficient to draw a conclusion that a person's abdominal area or stretch point can be excited by turbine infrasound. If it were, this might lead to symptoms of motion sickness.

Pierpont (2009) points to a study by Todd et al. (2008) as potential proof that the inner ear may be playing a role in creating the symptoms of "Wind Turbine Syndrome." Todd et al. (2008) show that the vestibular system shows a best frequency response around 100 Hz. This is a fact, but again it is unclear how it relates to low frequency noise from wind turbines. The best frequency response was assessed by moving subjects' heads (knocking the side of the head) in a very specific direction because the portion of the inner ear that is being discussed acts as a gravitational sensor or an accelerometer; therefore, it responds to motion. A physical mechanism by which the audible sound produced by a wind turbine at 100 Hz would couple to the human body in a way to create the necessary motion to which this portion of the inner ear would respond is unknown.

More recently, Salt and Hullar (2010) have looked for something physical about the ear that could be responding to infrasonic frequencies. They describe how the outer (OHC) and inner (IHC) hair cells of the cochlea respond to different types of stimuli: the IHC responding to velocity and OHC responding to displacement. They discuss how the OHC respond to lower frequencies than the IHC, and how the OHC acts as an amplifier for the IHC. They state that it is known that low frequencies present in a sound signal can mask the higher frequencies—presumably because the OHC is not amplifying the higher frequency correctly when the OHC is responding to low frequency disturbances. However, they emphatically state that "although vestibular hair cells are maximally sensitive to low frequencies they typically do not respond to airborne infrasound. Rather, they normally respond to mechanical inputs resulting from head movements and positional changes with their output controlling muscle reflexes to maintain posture and eye position." It is completely unknown how the very few neural paths from the OHC to the brain respond, if they do at all (95% of the connections are between the IHC and the brain). So at this moment, inner ear experts have not found a method for airborne infrasound to impact the inner ear. The potential exists such that the OHC respond to infrasound, but that the functional role of the connection between the OHC and the brain remains unknown. Further, the modulation of the sound received at the IHC itself has not been shown to cause nausea, headaches, or dizziness.

In the discussion of amplitude-modulated noise, it was already noted that wind turbines produce audible sound in the low frequency regime (20–200Hz). It has been shown that the sound levels in this range from some turbines are above the levels for which subjects in a Korean study have complained of psychological effects (Jung & Cheung, 2008). O'Neal (2011) also shows that the sound pressure level for frequencies between 30 and 200 Hz from two modern wind turbines at roughly 310 m are above the threshold of hearing but below the criterion for creating window rattle or other perceptible vibrations. The issue of vibration is discussed more in the next section. It is noted that the amplitude-modulated noise is most likely at the heart of annoyance complaints. In addition, amplitude-modulated noise may be a source of sleep disturbance noted by survey respondents. However, direct health impacts have not been demonstrated.

3.6.a Vibration

Vibroacoustics disease (VAD) has been identified as a potential health impact of wind turbines in the Pierpont book. Most of the literature around VAD is attributed to Branco and Alves-Pereira. Related citations attributed to Takahashi (2001), Hedge and Rasmussen (1982) though are also provided. These studies all required very clear coupling to large vibration sources such as jackhammers and heavy equipment. The latter references focus on high levels of low frequency vibrations and noise. In particular, Rasmussen studied the response of people to vibrating floors and chairs. The vibration displacements in the study were on the order of 0.01 cm (or 1000 times larger than the motion found 100 m from a wind farm in a seismic study (Styles et al., 2005). Takahashi used loud speakers placed 2 m from subjects' bodies, only testing audible frequencies 20–50 Hz, using pressure levels on the order of 100–110 dB (roughly 30 dB higher than any sound measured from a wind turbine in this frequency range) to induce vibrations at various points on the body. The Hedge source is not a study but a bulleted list of points that seem to go along with a lecture in an ergonomics class for which no citations are provided. Branco's work is slightly different in that she considered very long-term exposures to moderately intense vibration inputs. While there may be possible connection to wind turbines, at present, the connection is not substantiated given the very low levels of vibration and airborne ILFN that have been measured from wind turbines.

While vibroacoustic disease may not be substantiated, vibration levels that lead to annoyance or feelings of uneasiness may be more plausible. Evidence for these responses is discussed below.

Pierpont refers to a paper by Findeis and Peters (2004). This reference describes a situation in Germany where complaints of disturbing sound and vibration were investigated through the measurement of the vibration and acoustics within the dwelling, noting that people complained about vibrations that were not audible. The one figure provided in the text shows that people were disturbed by what was determined to be structure-borne sound that was radiated by walls and floors at levels equivalent to 65 dB at 10 Hz and 40 dB at 100 Hz. The 10 Hz level is just below audible. The level reported at 100 Hz, however, is just above the hearing threshold. The authors concluded that the disturbances were due to a component of the HVAC system that coupled directly to the building.

The Findeis and Peters (2004), report is reminiscent of papers related to investigations of "haunted" spaces (Tandy, 1998, 1999). In these studies room frequencies around 18 Hz were found. The studies hypothesized that apparitions were the result of eye vibrations (the eye is sensitive to 18 Hz) induced by the room vibration field. In one of these studies, a ceiling fan was found to be the source of the vibration. In the other, the source was not identified.

When the source was identified in the previously mentioned studies, there appears to be an obvious physical coupling mechanism. In other situations it has been estimated that airborne disturbances have influenced structures. A NASA report from 1982 gives a figure that estimates the necessary sound pressure level at various frequencies to force vibrations in windows, walls, and floors of typical buildings (Stephens, 1982). The figure on page 14 of that report shows infrasound levels of 70–80 dB can induce wall and floor vibrations. On page 39 the report also shows some floor vibration levels that were associated with a wind turbine. On the graph these were the lowest levels of vibration when compared to vibrations from aircraft noise and sonic booms. Another figure on page 43 shows vibrations and perception across the infrasonic frequency range. Again, wind turbine data are shown, and they are below the perception line.

A second technical report (Kelley, 1985) from that timeframe describes disturbances from the MOD-1 wind turbine in Boone, North Carolina. This was a downwind turbine mounted on a truss tower. Out of 1000 homes within about 2 km, 10 homes experienced room vibrations under certain wind conditions. A careful measurement campaign showed that indeed these few homes had room vibrations related to the impulsive noise unique to downwind turbines. The report contains several findings including the following: 1) the disturbances inside the homes were linked to the impulsive sound generated by the turbine (due to tower wake/blade interaction) and not seismic waves, 2) the impulsive signal was feeding energy into the vibrational modes of the rooms, floors, and walls where the floor/wall modes were the only modes in the infrasonic range, 3) people felt the disturbance more than they heard it, 4) peak vibration values were measured in the frequency range 10–20 Hz (floor/wall resonances) and it was deduced that the wall facing the turbine was being excited, 5) the fact that only 10 homes out of 1000 (scattered in various directions around the turbine) were affected was shown to be related to complicated sound propagation paths, and 6) while the shape of the impulse itself was given much attention and was shown to be a driving force in the coupling to the structural vibrations, comments were made in the report to the effect that nonimpulsive signals with energy at the right frequency could couple into the structure. The report describes a situation in Oregon where resonances in the flow through an exhaust stack of a gas-run turbine plant had an associated slow modulation of the sound leading to annoyance near the plant. Again it was found that structural modes in nearby homes were being excited but this time by an acoustic field that was not impulsive in nature. This is an important point because modern wind turbines do not create impulsive noise with strong content around 20 Hz like the downwind turbine in North Carolina. Instead, they generate amplitude-modulated sound around 1 kHz as well as broadband infrasound (van den Berg, 2004). The broadband infrasound that also existed for the North Carolina turbine was not shown to be responsible for the disturbances. As well, the amplitude-modulated noise that existed was not shown to be responsible for the disturbances. So, while there are comparisons made to the gas turbine power plant and to the HVAC system component where the impulsiveness of the sound was not the same, direct comment on the effect of modern turbines on the vibration of homes is not possible.

A recent paper by Bolin et al. (2011), surveys much of the low frequency literature pertinent to modern wind turbines and notes that all measurements of indoor and outdoor levels of sound simultaneously do not show the same amplification and ringing of frequencies associated with structural resonances similar to what was found in North Carolina. Instead the sound inside is normally less than the sound outside the structure. Bolin et al. (2011) note that measurements indicate that the indoor ILFN from wind turbines typically comply with national guidelines (such as the Danish guideline for 44 dB(A) outside a dwelling). However, this does not preclude a situation where levels would be found to be higher than the standards. They propose that further investigations of an individual dwelling should be conducted if the measured difference between C-weighted and A-weighted sound pressure level of outdoor exposure is greater than 15 dB. A similar criterion is noted in the non-peer reviewed report by Kamperman et al. (2008).

Related to room vibration is window rattle. This topic is described in the NASA reports, discussed above (Stephens, 1982) and discussed in the articles by Jung and Cheung (2008) and O’Neal (2011). In these articles it has been noted that window rattle is often induced by vibrations between 5 and 9 Hz, and measurements from wind turbines show that there can be enough energy in this range to induce window rattle. Whether the window rattle then generates its own sound field inside a room at an amplitude great enough to disturb the human body is unknown.

Seismic transmission of vibration at the North Carolina site was considered. In that study the seismic waves were ruled out as too low of amplitude to induce the room vibrations that were generated. Related are two sets of measurements that were taken near wind farms to assess the potential impact of seismic activity on extremely sensitive seismic measurement stations (Styles, 2005, Schofield, 2010). One study considered both waves traveling in the ground and the coupling of airborne infrasound to the ground, showing that the dominant source of seismic motion is the Rayleigh waves in the ground transmitted directly by the tower, and that the airborne infrasound is not playing a role in creating measurable seismic motion. The two reports indicate that at 100 meters from a wind turbine farm (>6 turbines) the maximum motion that is induced is 120 nanometers (at about 1 Hz). A nanometer is 10^{-9} m. So this is 1.2×10^{-7} m of ground displacement. Extremely sensitive measuring devices have been used to detect this slight motion. To put the motion in perspective, the diameter of a human hair is on the order of 10^{-6} m. These findings indicate that seismic motion induced from one or two turbines is so small that it would be difficult to induce any physical or structural response.

Hessler and Hessler, (2010) reviewed various state noise limits and discussed them in connection with wind turbines. The article contains a few comments related to low frequency noise. It is stated that, “a link between health complaints and turbine noise has only been asserted based on what is essentially anecdotal evidence without any valid epidemiological studies or scientific proof of any kind.” The article states that if a metric for low frequency noise is needed, then a limit of 65 dB(C) could be used. This proposed criterion is not flexible for use in different environments such as rural vs. city. In this sense, Bolin et als’ suggestion of checking for a difference between C-weighted and A-weighted sound pressure level of outdoor exposure greater than 15 dB is more appropriate. This value of 15 dB, was based on past complaints associated with combustion turbines. The Bolin article, however, also cautions that obtaining accurate low frequency measurements for wind turbines is difficult because of the presence of wind. Even sophisticated windscreens cannot eliminate the ambient low frequency wind noise.

Leventhal (2006) notes that when hearing and deaf subjects are tested simultaneously, the subjects’ chests would resonate with sounds in the range of 50–80 Hz. However, the amplitude of the sound had to be 40–50 dB higher than the human hearing threshold for the deaf subjects to report the chest vibration. This leads one to conclude that chest resonance in isolation should not be associated with inaudible sound. If a room is vibrating due to a structural resonance, such levels may be obtained. Again, this effect has never been measured associated with a modern wind turbine.

The stimulation of house resonances and self-reported ill-effects due to a modern wind turbine appear in a report by independent consultants that describes pressure measurements taken inside and outside of a home in Falmouth Massachusetts in the spring of 2011 (Ambrose & Rand, 2011). The measurements were taken at roughly 500 meters from a single 1.65 MW stall-regulated turbine when the wind speeds were relatively high: 20-30 m/s at hub height. The authors noted feeling ill when the dB(A) levels indoors were between 18 and 24 (with a corresponding dB(G) level of 51-64). They report that they felt effects both inside and outside but preferred to be outside where the dB(A) levels ranged from 41-46 (with corresponding dB(G) levels from 54-65.) This is curious because weighted measurements account for human response and the weighted values were higher outside. However, the actual dB(L) levels were higher inside.

The authors present some data indicating that the G-weighted value of the pressure signal is often greater than 60 dB(G), the averaged threshold value proposed by Salt and Hullar (2011) for OHC activation. However, the method used to obtain the data is not presented, and the time scale over which the data are presented (< 0.015 seconds or 66 Hz) is too short to properly capture the low frequency content.

The data analysis differed from the common standard of practice in an attempt to highlight weaknesses in the standard measurement approach associated with the capture of amplitude modulation and ILFN. This departure from the standard is a useful step in defining a measurement technique such as that called for in a report by HGC Engineering (HGC, 2010), that notes policy making entities should "consider adopting or endorsing a proven measurement procedure that could be used to quantify noise at infrasonic frequencies."

The measurements by Ambrose and Rand (2011) show a difference in A and C weighted outdoor sound levels of around 15 dB at the high wind speeds (which is Bolin et. al.'s recommended value for triggering further interior investigations). The simultaneous indoor and outdoor measurements indicate that at very low frequencies (2-6 Hz) the indoor pressure levels are greater than those outdoors. It is useful to note that the structural forcing at the blade-passage-frequency, the time delay and the subsequent ringing that was present in the Boone homes (Kelley, 1985) is not demonstrated by Ambrose and Rand (2011). This indicates that the structural coupling is not forced by the amplitude modulation and is due to a much subtler process. Importantly, while there is an amplification at these lower frequencies, the indoor levels (unweighted) are still far lower than any levels that have ever been shown to cause a physical response (including the activation of the OHC) in humans.

The measurements did reveal a 22.9 Hz tone that was amplitude modulated at approximately the blade passage frequency. The source of the tone was not identified, and no indication as to whether the tone varied with wind speed was provided, a useful step to help determine whether the tone is aerodynamically generated. The level of this tone is shown to be higher than the OHC activation threshold. The 22.9 Hz tone did not couple to the structure and showed the normal attenuation from outside to inside the structure. In order to determine if the results that show potential tonal activation of the OHC are generalizable, it is necessary to identify the source of this tone which could be unique to stall-regulated turbines or even unique to this specific brand of turbine.

Finally, the measurements shown in the report are atypical within the wind turbine measurement literature and the data analysis is not fully described. Also, the report offers no plausible coupling mechanism of the sound waves to the body beyond that proposed by Salt and Hullar (2011). Because of this, the results are suggestive but require corroboration of the measurements and scientifically based mechanisms for human health impact.

3.6.b Summary of Claimed Health Impacts

In this section, the potential health impacts due to noise and vibration from wind turbines was discussed. Both the infrasonic and low frequency noise ranges were considered. Assertions that infrasound and low frequency noise from turbines affect the vestibular system either through airborne coupling to humans are not empirically supported. In the multitude of citations given in the popular media as to methods in which the vestibular system is influenced, all refer to situations in which there is direct vibration coupling to the body or when the wave amplitudes are orders of magnitudes greater than those produced by wind turbines. Recent research has found one potential path in the auditory system, the OHC, in which infrasound might be sensed. There is no evidence, however, that when the OHC sense infrasound, it then leads to any of the symptoms reported by complainants. That the infrasound and low frequency noise couple to humans through the forcing of structural vibration is plausible but has not been demonstrated for modern wind turbines. In addition, should it be shown that such a coupling occurs, research indicates that the coupling would be transient and highly dependent on wind conditions and localized to very few homes surrounding a turbine.

Seismic activity near a turbine due to vibrations transmitted down the tower has been measured, and the levels are too low to produce vibrations in humans.

The audible noise from wind turbines, in particular the amplitude modulated trailing edge noise, does exist, changes level based on atmospheric conditions, can change character from swish to thump-based on atmospheric effects, and can be perceived from home to home differently based on propagation effects. This audible sound has been noted by complainants as a source of annoyance and a cause for sleep disruption. Some authors have proposed nighttime noise regulations and regulations based on shorter time averages (vs. annual averages) as a means to reduce annoyance from this noise source. Some have conjectured that the low frequency content of the amplitude-modulated noise is responsible for the annoyance. They have proposed that the difference between the measured outdoor A- and C- weighted sound pressure levels could be used to identify situations in which the low frequency content is playing a larger role. Further, they note that this difference might be used as part of a regulation as a means to reduce annoyance.

Chapter 4

Findings

Based on the detailed review of the scientific literature and other available reports and consideration of the strength of scientific evidence, the Panel presents findings relative to three factors associated with the operation of wind turbines: noise and vibration, shadow flicker, and ice throw. The findings that follow address specifics in each of these three areas.

4.1 Noise

4.1.a Production of Noise and Vibration by Wind Turbines

1. Wind turbines can produce unwanted sound (referred to as noise) during operation. The nature of the sound depends on the design of the wind turbine. Propagation of the sound is primarily a function of distance, but it can also be affected by the placement of the turbine, surrounding terrain, and atmospheric conditions.
    a. Upwind and downwind turbines have different sound characteristics, primarily due to the interaction of the blades with the zone of reduced wind speed behind the tower in the case of downwind turbines.
    b. Stall regulated and pitch controlled turbines exhibit differences in their dependence of noise generation on the wind speed
    c. Propagation of sound is affected by refraction of sound due to temperature gradients, reflection from hillsides, and atmospheric absorption. Propagation effects have been shown to lead to different experiences of noise by neighbors.
    d. The audible, amplitude-modulated noise from wind turbines ("whooshing") is perceived to increase in intensity at night (and sometimes becomes more of a "thumping") due to multiple effects: i) a stable atmosphere will have larger wind gradients, ii) a stable atmosphere may refract the sound downwards instead of upwards, iii) the ambient noise near the ground is lower both because of the stable atmosphere and because human generated noise is often lower at night.
2. The sound power level of a typical modern utility scale wind turbine is on the order of 103 dB(A), but can be somewhat higher or lower depending on the details of the design and the rated power of the turbine. The perceived sound decreases rapidly with the distance from the wind turbines. Typically, at distances larger than 400 m, sound

pressure levels for modern wind turbines are less than 40 dB(A), which is below the level associated with annoyance in the epidemiological studies reviewed.

3. Infrasound refers to vibrations with frequencies below 20 Hz. Infrasound at amplitudes over 100–110 dB can be heard and felt. Research has shown that vibrations below these amplitudes are not felt. The highest infrasound levels that have been measured near turbines and reported in the literature near turbines are under 90 dB at 5 Hz and lower at higher frequencies for locations as close as 100 m.
4. Infrasound from wind turbines is not related to nor does it cause a "continuous whooshing."
5. Pressure waves at any frequency (audible or infrasonic) can cause vibration in another structure or substance. In order for vibration to occur, the amplitude (height) of the wave has to be high enough, and only structures or substances that have the ability to receive the wave (resonant frequency) will vibrate.

4.1.b Health Impacts of Noise and Vibration

1. Most epidemiologic literature on human response to wind turbines relates to self-reported "annoyance," and this response appears to be a function of some combination of the sound itself, the sight of the turbine, and attitude towards the wind turbine project.
   a. There is limited epidemiologic evidence suggesting an association between exposure to wind turbines and annoyance.
   b. There is insufficient epidemiologic evidence to determine whether there is an association between noise from wind turbines and annoyance independent from the effects of seeing a wind turbine and vice versa.
2. There is limited evidence from epidemiologic studies suggesting an association between noise from wind turbines and sleep disruption. In other words, it is possible that noise from some wind turbines can cause sleep disruption.
3. A very loud wind turbine could cause disrupted sleep, particularly in vulnerable populations, at a certain distance, while a very quiet wind turbine would not likely disrupt even the lightest of sleepers at that same distance. But there is not enough evidence to

provide particular sound-pressure thresholds at which wind turbines cause sleep disruption. Further study would provide these levels.

4. Whether annoyance from wind turbines leads to sleep issues or stress has not been sufficiently quantified. While not based on evidence of wind turbines, there is evidence that sleep disruption can adversely affect mood, cognitive functioning, and overall sense of health and well-being.
5. There is insufficient evidence that the noise from wind turbines is *directly (i.e., independent from an effect on annoyance or sleep)* causing health problems or disease.
6. Claims that infrasound from wind turbines directly impacts the vestibular system have not been demonstrated scientifically. Available evidence shows that the infrasound levels near wind turbines cannot impact the vestibular system.
    a. The measured levels of infrasound produced by modern upwind wind turbines at distances as close as 68 m are well below that required for non-auditory perception (feeling of vibration in parts of the body, pressure in the chest, etc.).
    b. If infrasound couples into structures, then people inside the structure could feel a vibration. Such structural vibrations have been shown in other applications to lead to feelings of uneasiness and general annoyance. The measurements have shown no evidence of such coupling from modern upwind turbines.
    c. Seismic (ground-carried) measurements recorded near wind turbines and wind turbine farms are unlikely to couple into structures.
    d. A possible coupling mechanism between infrasound and the vestibular system (via the Outer Hair Cells (OHC) in the inner ear) has been proposed but is not yet fully understood or sufficiently explained. Levels of infrasound near wind turbines have been shown to be high enough to be sensed by the OHC. However, evidence does not exist to demonstrate the influence of wind turbine-generated infrasound on vestibular-mediated effects in the brain.
    e. Limited evidence from rodent (rat) laboratory studies identifies short-lived biochemical alterations in cardiac and brain cells in response to short exposures to emissions at 16 Hz and 130 dB. These levels exceed measured infrasound levels from modern turbines by over 35 dB.

7. There is no evidence for a set of health effects, from exposure to wind turbines, that could be characterized as a "Wind Turbine Syndrome."
8. The strongest epidemiological study suggests that there is not an association between noise from wind turbines and measures of psychological distress or mental health problems. There were two smaller, weaker, studies: one did note an association, one did not. Therefore, we conclude the weight of the evidence suggests no association between noise from wind turbines and measures of psychological distress or mental health problems.
9. None of the limited epidemiological evidence reviewed suggests an association between noise from wind turbines and pain and stiffness, diabetes, high blood pressure, tinnitus, hearing impairment, cardiovascular disease, and headache/migraine.

4.2 Shadow Flicker

4.2.a Production of Shadow Flicker

Shadow flicker results from the passage of the blades of a rotating wind turbine between the sun and the observer.

1. The occurrence of shadow flicker depends on the location of the observer relative to the turbine and the time of day and year.
2. Frequencies of shadow flicker elicited from turbines is proportional to the rotational speed of the rotor times the number of blades and is generally between 0.5 and 1.1 Hz for typical larger turbines.
3. Shadow flicker is only present at distances of less than 1400 m from the turbine.

4.2.b Health Impacts of Shadow Flicker

1. Scientific evidence suggests that shadow flicker does not pose a risk for eliciting seizures as a result of photic stimulation.
2. There is limited scientific evidence of an association between annoyance from prolonged shadow flicker (exceeding 30 minutes per day) and potential transitory cognitive and physical health effects.

4.3 Ice Throw

4.3.a Production of Ice Throw

Ice can fall or be thrown from a wind turbine during or after an event when ice forms or accumulates on the blades.

1. The distance that a piece of ice may travel from the turbine is a function of the wind speed, the operating conditions, and the shape of the ice.
2. In most cases, ice falls within a distance from the turbine equal to the tower height, and in any case, very seldom does the distance exceed twice the total height of the turbine (tower height plus blade length).

4.3.b Health Impacts of Ice Throw

1. There is sufficient evidence that falling ice is physically harmful and measures should be taken to ensure that the public is not likely to encounter such ice.

4.4 Other Considerations

In addition to the specific findings stated above for noise and vibration, shadow flicker and ice throw, the Panel concludes the following:

1. Effective public participation in and direct benefits from wind energy projects (such as receiving electricity from the neighboring wind turbines) have been shown to result in less annoyance in general and better public acceptance overall.

Chapter 5

Best Practices Regarding Human Health Effects Of Wind Turbines

Broadly speaking, the term "best practice" refers to policies, guidelines, or recommendations that have been developed for a specific situation. Implicit in the term is that the practice is based on the best information available at the time of its institution. A best practice may be refined as more information and studies become available. The panel recognizes that in countries which are dependent on wind energy and are protective of public health, best practices have been developed and adopted.

In some cases, the weight of evidence for a specific practice is stronger than it is in other cases. Accordingly, best practice* may be categorized in terms of the evidence available, as shown in Table 3:

Table 3

Descriptions of Three Best Practice Categories

Category	Name	Description
1	Research Validated Best Practice	A program, activity, or strategy that has the highest degree of proven effectiveness supported by objective and comprehensive research and evaluation.
2	Field Tested Best Practice	A program, activity, or strategy that has been shown to work effectively and produce successful outcomes and is supported to some degree by subjective and objective data sources.
3	Promising Practice	A program, activity, or strategy that has worked within one organization and shows promise during its early stages for becoming a best practice with long-term sustainable impact. A promising practice must have some objective basis for claiming effectiveness and must have the potential for replication among other organizations.

**These categories are based on those suggested in "Identifying and Promoting Promising Practices." Federal Register, Vol. 68. No 131. 131. July 2003.*
www.acf.hhs.gov/programs/ccf/about_ccf/gbk_pdf/pp_gbk.pdf

5.1 Noise

Evidence regarding wind turbine noise and human health is limited. There is limited evidence of an association between wind turbine noise and both annoyance and sleep disruption, depending on the sound pressure level at the location of concern. However, there are no research-based sound pressure levels that correspond to human responses to noise. A number of countries that have more experience with wind energy and are protective of public health have developed guidelines to minimize the possible adverse effects of noise. These guidelines consider time of day, land use, and ambient wind speed. Table 4 summarizes the guidelines of Germany (in the categories of industrial, commercial and villages) and Denmark (in the categories of sparsely populated and residential). The sound levels shown in the table are for nighttime and are assumed to be taken immediately outside of the residence or building of concern. In addition, the World Health Organization recommends a maximum nighttime sound pressure level of 40 dB(A) in residential areas. Recommended setbacks corresponding to these values may be calculated by software such as WindPro or similar software. Such calculations are normally to be done as part of feasibility studies. The Panel considers the guidelines shown below to be Promising Practices (Category 3) but to embody some aspects of Field Tested Best Practices (Category 2) as well.

Table 4

Promising Practices for Nighttime Sound Pressure Levels by Land Use Type

Land Use	**Sound Pressure Level, dB(A) Nighttime Limits**
Industrial	70
Commercial	50
Villages, mixed usage	45
Sparsely populated areas, 8 m/s wind*	44
Sparsely populated areas, 6 m/s wind*	42
Residential areas, 8 m/s wind*	39
Residential areas, 6 m/s wind*	37

**measured at 10 m above ground, outside of residence or location of concern*

The time period over which these noise limits are measured or calculated also makes a difference. For instance, the often-cited World Health Organization recommended nighttime noise cap of 40 dB(A) is averaged over one year (and does not refer specifically to wind turbine noise). Denmark's noise limits in the table above are calculated over a 10-minute period. These limits are in line with the noise levels that the epidemiological studies connect with insignificant reports of annoyance.

The Panel recommends that noise limits such as those presented in the table above be included as part of a statewide policy regarding new wind turbine installations. In addition, suitable ranges and procedures for cases when the noise levels may be greater than those values should also be considered. The considerations should take into account trade-offs between environmental and health impacts of different energy sources, national and state goals for energy independence, potential extent of impacts, etc.

The Panel also recommends that those involved in a wind turbine purchase become familiar with the noise specifications for the turbine and factors that affect noise production and noise control. Stall and pitch regulated turbines have different noise characteristics, especially in high winds. For certain turbines, it is possible to decrease noise at night through suitable control measures (e.g., reducing the rotational speed of the rotor). If noise control measures are to be considered, the wind turbine manufacturer must be able to demonstrate that such control is possible.

The Panel recommends an ongoing program of monitoring and evaluating the sound produced by wind turbines that are installed in the Commonwealth. IEC 61400-11 provides the standard for making noise measurements of wind turbines (International Electrotechnical Commission, 2002). In general, more comprehensive assessment of wind turbine noise in populated areas is recommended. These assessments should be done with reference to the broader ongoing research in wind turbine noise production and its effects, which is taking place internationally. Such assessments would be useful for refining siting guidelines and for developing best practices of a higher category. Closer investigation near homes where outdoor measurements show A and C weighting differences of greater than 15 dB is recommended.

5.2 Shadow Flicker

Based on the scientific evidence and field experience related to shadow flicker, Germany has adopted guidelines that specify the following:

1. Shadow flicker should be calculated based on the astronomical maximum values (i.e., not considering the effect of cloud cover, etc.).
2. Commercial software such as WindPro or similar software may be used for these calculations. Such calculations should be done as part of feasibility studies for new wind turbines.
3. Shadow flicker should not occur more than 30 minutes per day and not more than 30 hours per year at the point of concern (e.g., residences).
4. Shadow flicker can be kept to acceptable levels either by setback or by control of the wind turbine. In the latter case, the wind turbine manufacturer must be able to demonstrate that such control is possible.

The guidelines summarized above may be considered to be a Field Tested Best Practice (Category 2). Additional studies could be performed, specifically regarding the number of hours per year that shadow flicker should be allowed, that would allow them to be placed in Research Validated (Category 1) Best Practices.

5.3 Ice Throw

Ice falling from a wind turbine could pose a danger to human health. It is also clear that the danger is limited to those times when icing occurs and is limited to relatively close proximity to the wind turbine. Accordingly, the following should be considered Category 1 Best Practices.

1. In areas where icing events are possible, warnings should be posted so that no one passes underneath a wind turbine during an icing event and until the ice has been shed.
2. Activities in the vicinity of a wind turbine should be restricted during and immediately after icing events in consideration of the following two limits (in meters).

For a turbine that may not have ice control measures, it may be assumed that ice could fall within the following limit:

$$x_{\max,\, throw} = 1.5\left(2R + H\right)$$

Where: R = rotor radius (m), H = hub height (m)

For ice falling from a stationary turbine, the following limit should be used:

$$x_{\max,\, fall} = U\left(R + H\right)/15$$

Where: U = maximum likely wind speed (m/s)

The choice of maximum likely wind speed should be the expected one-year return maximum, found in accordance to the International Electrotechnical Commission's design standard for wind turbines, IEC 61400-1.

Danger from falling ice may also be limited by ice control measures. If ice control measures are to be considered, the wind turbine manufacturer must be able to demonstrate that such control is possible.

5.4 Public Participation/Annoyance

There is some evidence of an association between participation, economic or otherwise, in a wind turbine project and the annoyance (or lack thereof) that affected individuals may express. Accordingly, measures taken to directly involve residents who live in close proximity to a wind turbine project may also serve to reduce the level of annoyance. Such measures may be considered to be a Promising Practice (Category 3).

5.5 Regulations/Incentives/Public Education

The evidence indicates that in those parts of the world where there are a significant number of wind turbines in relatively close proximity to where people live, there is a close coupling between the development of guidelines, provision of incentives, and educating the public. The Panel suggests that the public be engaged through such strategies as education, incentives for community-owned wind developments, compensations to those experiencing documented loss of property values, comprehensive setback guidelines, and public education related to renewable energy. These multi-faceted approaches may be considered to be a Promising Practice (Category 3).

Appendix A:

Wind Turbines - Introduction to Wind Energy

Although wind energy for bulk supply of electricity is a relatively new technology, the historical precedents for it go back a long way. They are descendents of mechanical windmills that first appeared in Persia as early as the 7^{th} century (Vowles, 1932) and then re-appeared in northern Europe in the Middle Ages. They were considerably developed during the 18^{th} and 19^{th} centuries, and then formed the basis for the first electricity generating wind turbine in the late 19^{th} century. Development continued sporadically through the mid 20^{th} century, with modern turbines beginning to emerge in the 1970's. It was the introduction of other technologies, such as electronics, computers, control theory, composite materials, and computer-based simulation capability that led to the successful development of the large scale, autonomously operating wind turbines that have become so widely deployed over the past twenty years.

The wind is the most important external factor in wind energy. It can be thought of as the "fuel" of the wind turbine, even though it is not consumed in the process. The wind determines the amount of energy that is produced, and is therefore referred to as the resource. The wind resource can vary significantly, depending on the location and the nature of the surface. In the United States, the Great Plains have a relatively energetic wind resource. In Massachusetts, winds tend to be relatively low inland, except for mountaintops and ridges. The winds tend to be higher close to the coast and then increase offshore. Average offshore wind speeds generally increase with distance from shore as well. The wind resource of Massachusetts is illustrated in

Figure AA.1: Map of the Massachusetts Wind Resource (From National Renewable Energy Laboratory, http://www.windpoweringamerica.gov/images/windmaps/ma_50m_800.jpg)

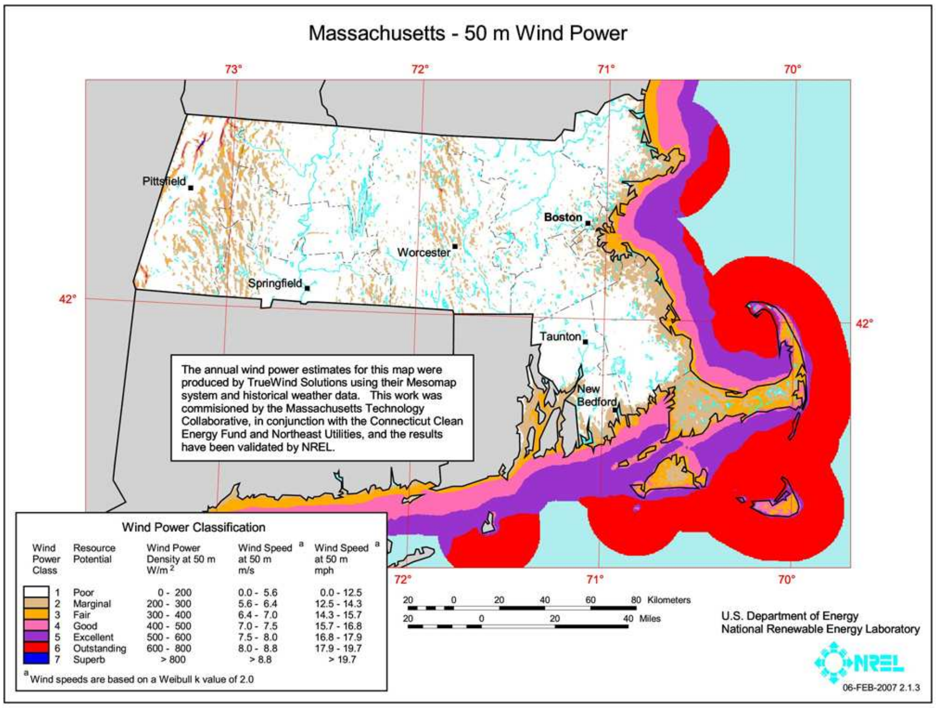

This section summarizes the basic characteristics of the wind in so far as they relate to wind turbine power production. Much more detail on this topic is provided in (Manwell et al., 2009). The wind will also affect the design of the wind turbines, and for this purpose it is referred to as an "external design condition." This aspect of the wind is discussed in more detail in a later section.

AA.1 Origin of the Wind

The wind originates from sunlight due to the differential heating of various parts of the earth. This differential heating produces zones of high and low pressure, resulting in air movement. The motion of the air is also affected by earth's rotation. Considerations regarding the wind insofar as it relates to wind turbine operation include the following: (i) the winds aloft (geostrophic wind), (ii) atmospheric boundary layer meteorology, (iii) the variation of wind speed with height, (iv) surface roughness, and (v) turbulence.

The geostrophic wind is the wind in the upper atmosphere, which results from the combined effects of the pressure gradient and the earth's rotation (via the Coriolis force). The gradient wind can be thought of as an extension of the geostrophic wind, the difference in this case being that centrifugal effects are included. These result from curved isobars (lines of constant pressure) in the atmosphere. It is these upper atmosphere winds that are the source of most of the energy that eventually impinges on wind turbines. The energy in the upper atmosphere is transferred down closer to the surface via a variety of mechanisms, most notably turbulence, which is generated mechanically (via surface roughness) and thermally (via the rising of warm air and falling of cooler air).

Although driven by higher altitude winds, the wind near the surface is affected by the surrounding topography (such as mountains and ridges) and surface conditions (such as tree cover or presence of buildings).

AA.2 Variability of the Wind

One of the singular characteristics of the wind is its variability, both temporal and spatial. The temporal variability includes: (i) short term (gusts and turbulence), (ii) moderately short term (e.g., hr to hr means), (iii) diurnal (variations over a day), (iv) seasonal, and (v) inter-annual (year to year). The wind may vary spatially as well, both from one location to another or with height above ground.

Figure AA.2 illustrates the variability of the hourly average wind speeds for one year at one location.

Figure AA.2: Typical hourly wind speeds over a year

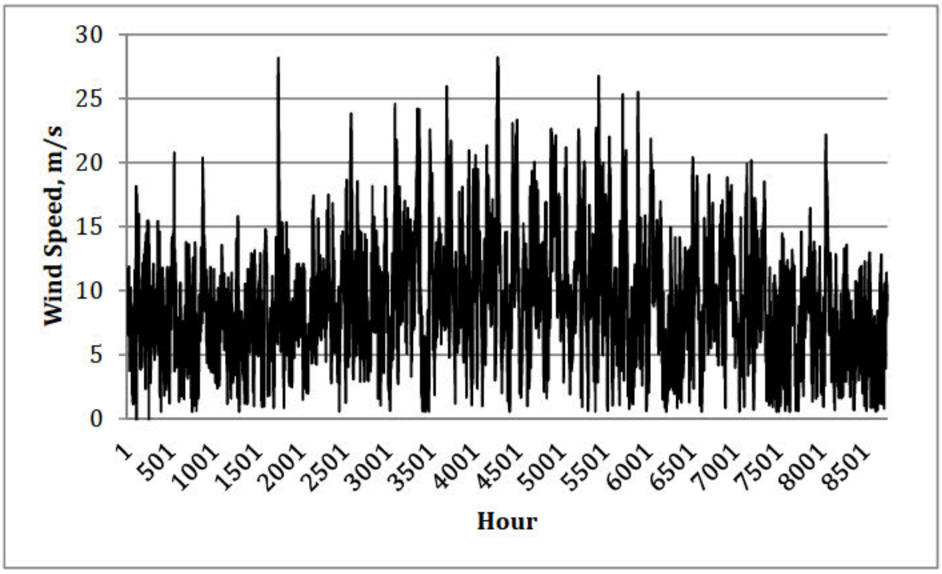

As can be seen, the hourly average wind speed in this example varies significantly over the year, ranging from zero to nearly 30 m/s.

Figure AA.3 illustrates wind speed at another location recorded twice per second over a 23-hour period. There is significant variability here as well. Much of this variability in this figure is associated with short-term fluctuations, or turbulence. Turbulence has some effect on power generation, but it has a more significant effect on the design of wind turbines, due to the material fatigue that it tends to engender. Turbulence is discussed in more detail in a later section.

Figure AA.3: Typical wind data, sampled at 2 Hz for a 23-hr period

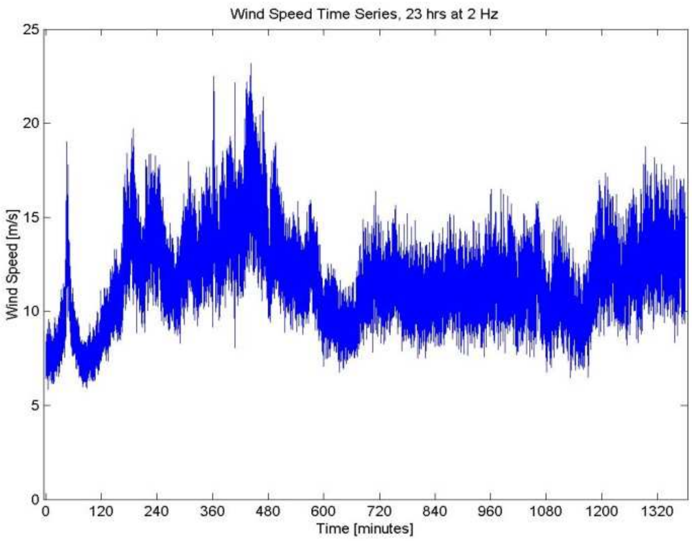

In spite of the variability in the wind time series, summary characteristics have much less variability. For example, the annual mean wind speed at a given location is generally within +/- 10% of the long-term mean at that site. Furthermore, the distribution of wind speeds, that is to say the frequency of occurrence of winds in various wind speed ranges, also tends to be similar from year. The general shape of such distributions is also similar from one location to another, even if the means are different. In fact, statistical models such as the Weibull distribution can be used to model the occurrences of various wind speeds in most locations on the earth. For example, the number of occurrences of wind speed in various ranges from the data set illustrated in Figure AA.2 are shown in Figure AA.4, together with the those occurrences as modeled by the Weibull distribution.

Figure AA.4: Typical frequency of occurrence of wind speeds, based on data and statistical model

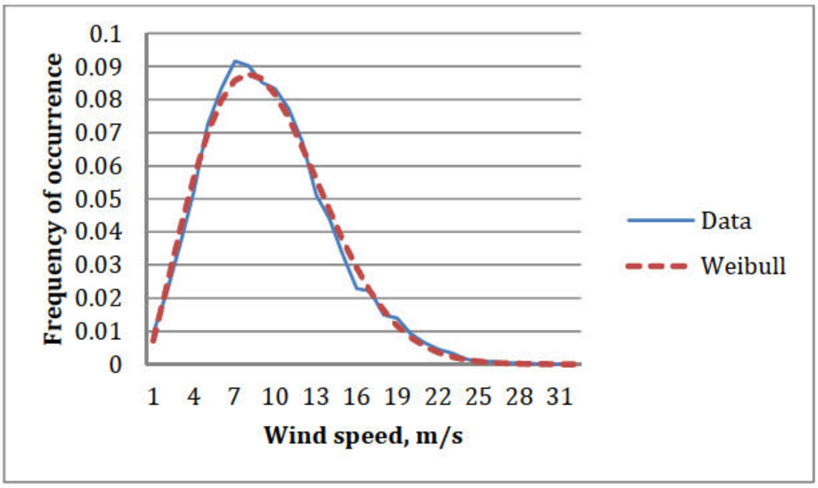

The Weibull distribution's probability density function is given by:

$$p(U) = \left(\frac{k}{c}\right)\left(\frac{U}{c}\right)^{k-1} \exp\left[-\left(\frac{U}{c}\right)^{k}\right] \tag{1}$$

Where c = Weibull scale factor (m/s) and k = Weibull shape factor (dimensionless)

For the purposes of modeling the occurrences of wind speeds, the scale and shape factors may be approximated as follows:

$$k \approx \left(\frac{\sigma_U}{\overline{U}}\right)^{-1.086} \tag{2}$$

$$c \approx \overline{U}\left(0.568 + 0.433 / k\right)^{-(1/k)} \tag{3}$$

Where $\overline{U}$ is the long-term mean wind speed (m/s, based on 10 min or hourly averages) and σ_U is the standard deviation of the wind speed, based on the same 10 min or hourly averages.

AA.3 Power in the Wind

The power available in the wind can be predicted from the fundamental principles of fluid mechanics. First of all, the energy per unit mass of a particle of air is given simply by ½ times the square of the velocity, U (m/s). The mass flow rate of the air (kg/s) through a given area A (m^2) perpendicular to the direction of the wind is $\dot{m} = \rho AU$, where ρ is the density of the air (kg/m^3). The power in the wind per unit area, P/A, (W/m^2) is then:

$$P / A = (\dot{m} / A)\frac{1}{2}U^2 = \frac{1}{2}\rho U^3 \qquad (4)$$

AA.4 Wind Shear

Wind shear is the variation of wind speed with height. Wind shear has relevance to power generation, to turbine design, and to noise generation. The variation of wind speed with height is typically modeled with a power law as follows:

$$U_2 = U_1 [h_2 / h_1]^{\alpha} \qquad (5)$$

Where U_1 = speed at reference height h_1, U_2 is the wind speed to be estimated at height h_2 and α is the power law exponent. Values of the exponent typically range from a 0.1 for smooth surfaces to 0.4 for very rough surfaces (such as forests or built-up areas.)

Wind shear can also be affected by the stability of the atmosphere. Equations have been developed that allow the incorporation of stability parameters in the analysis, but these too are outside the scope of this overview.

AA.5 Wind and Wind Turbine Structural Issues

As discussed previously, the wind is of particular interest in wind turbine applications, since it is the source of the energy. It is also the source of significant structural loads that the turbine must be able to withstand. Some of these loads occur when the turbine is operating; others occur when it is stopped. Extreme winds, for example, are likely to affect a turbine when it is stopped. High winds with sudden directional change during operation can also induce high loads. Turbulence during normal operation results in fatigue. The following is a summary of the key aspects of the wind that affect the design of wind turbines. More details may be found in (Manwell et al., 2009).

AA.5.a Turbulence

Turbulence in the wind can have significant effect on the structure of a wind turbine as well as its operation, and so it must be considered in the design process. The term “turbulence” refers to the short-term variations in the speed and direction of the wind. It manifests itself as apparently random fluctuations superimposed upon a relatively steady mean flow. Turbulence is not actually random, however. It has some very distinct characteristics, at least in a statistical sense.

Turbulence is characterized by a number of measures. These include: (i) turbulence intensity, (ii) turbulence probability density functions (pdf), (iii) autocorrelations, (iv) integral time scales and length scales, and (v) power spectral density functions. Discussion of the physics of turbulence is outside the scope of this overview.

AA.5.b Gusts

A gust is discrete increase and then decrease in wind speed, possibly associated with a change in wind direction, which can be of significance to the design of a wind turbine. Gusts are typically associated with turbulence.

AA.5.c Extreme Winds

Extreme winds need to be considered for the design of a wind turbine. Extreme winds are normally associated with storms. They occur relatively rarely, but often enough that the possibility of their occurring cannot be ignored. Statistical models, such as the Gumbel distribution (Gumbel, 1958), are used to predict the likelihood of such winds occurring at least once every 50 or 100 years. Such intervals are called return periods.

AA.5.d Soils

Soils are also important for the design and installation of a wind turbine. In particular, the nature of the soil will affect the design of the wind turbine foundations. Discussion of soils is outside the scope of this overview.

AA.6 Wind Turbine Aerodynamics

The heart of the wind turbine is the rotor. This is a device that extracts the kinetic energy from the wind and converts it into a mechanical form. Below is a summary of wind turbine rotor aerodynamics. More details may be found in (Manwell et al., 2009).

A wind turbine rotor is comprised of blades that are attached to a hub. The hub is in turn attached to a shaft (the main shaft) which transfers the energy through the remainder of the drive train to the generator where is it converted to electricity. The maximum power that a rotor can extract from the wind is first of all limited by the power in the wind, which passes through an area defined by the passage of the rotor. At the present time, most wind turbines utilize a rotor with a horizontal axis. That is, the axis of rotation is (nominally) parallel to the earth's surface. Accordingly, the area that is swept out by the rotor is circular. Assuming a rotor radius of *R* (m), the maximum power *P* (W) available in the wind is:

$$P = \frac{1}{2}\rho\pi R^2 U^3 \tag{6}$$

Early in the 20th century, it was shown by Betz (among others, see [4]) that the maximum power that could be extracted was less than the power in the wind; in fact, it was 16/27 times that value. Betz' work led to the definition of a power coefficient, C_p, which expresses the ratio of the actual power extracted by a rotor to the power in the wind. When considering efficiencies of other components in the drive train, as expressed by the η, the total power out a wind turbine, P_{WT}, would be given by:

$$P_{WT} = C_p \eta \frac{1}{2}\rho\pi R^2 U^3 \tag{7}$$

The maximum value of the power coefficient, known as the Betz limit, is thus 16/27.

Betz' original analysis was based on the fundamental principles of fluid mechanics including linear momentum theory. It also included the following assumptions: (i) homogenous, incompressible, steady state fluid flow; (ii) no frictional drag; (iii) a rotor with an infinite number of (very small) blades; (iv) uniform thrust over the rotor area; (v) a non-rotating wake; and (vi) the static pressure far upstream and far downstream of the rotor that is equal to the undisturbed ambient static pressure.

A real rotor operating on a horizontal axis will result in a rotating wake. Some of the energy in the wind will go into that rotation and will not be available for conversion into mechanical power. The result is that the maximum power coefficient will actually be less than the Betz limit. The derivation of the maximum power coefficient for the rotating wake case use a number of terms: (i) the rotational speed of turbine rotor, Ω, in radians/sec; (ii) tip speed ratio, $\lambda = \Omega R/U$; (iii) local speed ratio, $\lambda_r = \lambda\, r/R$; (iv) rotational speed of wake, ω; (v) an axial induction factor, *a*, which relates the free stream wind speed to the wind speed at the rotor and the wind speed in the far wake ($U_{rotor} = (1-a)U_{free\ stream}$ and $U_{wake} = (1-2a)U_{free\ stream}$); and (vi) an angular induction factor, $a' = \omega/2\,\Omega$. According to this analysis, the maximum possible power coefficient is given by:

$$C_{P,\max} = \frac{8}{\lambda^2}\int_0^{\lambda} a'(1-a)\lambda_r^3\,d\lambda_r \qquad (8)$$

The maximum power coefficient for a rotor with a rotating wake and the Betz limit are illustrated in Figure AA.5.

Figure AA.5: Maximum theoretical power coefficients for rotating and non-rotating wakes

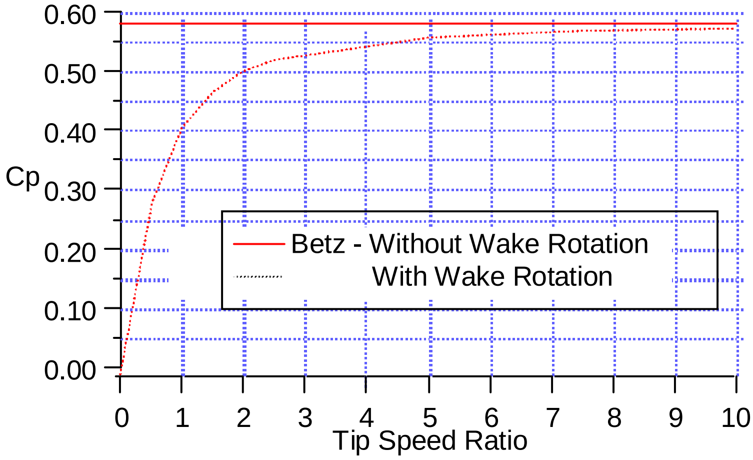

Neither of the analyses summarized above gives any indication as to what the blades of the rotor actually look like. For this purpose, a method called blade element momentum (BEM) theory was developed. This approach assumes that the blades incorporate an airfoil cross section. Figure AA.6 shows a typical airfoil, including some of the nomenclature.

Figure AA.6: Airfoil nomenclature

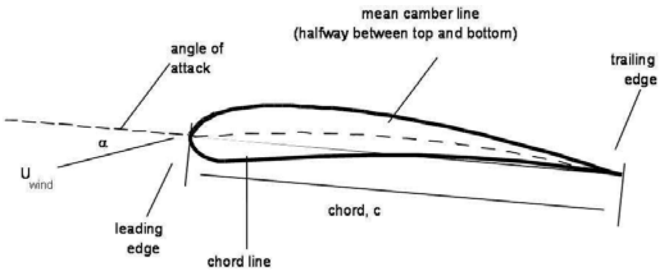

The BEM method equates the forces on the blades associated with air flowing over the airfoil with forces associated with the change in momentum of the air passing through the rotor. The starting point for this analysis is the assessment of the lift force on an airfoil. Lift is a force perpendicular to the flow. It is given by

$$\tilde{F}_L = C_L \frac{1}{2} \rho c U^2 \tag{9}$$

Where:

$\tilde{F}_L$ = force per unit length, N/m

C_L = lift coefficient, -

c = chord length (distance from leading edge to trailing edge of airfoil, m)

Thin airfoil theory predicts that for a very thin, ideal airfoil the lift coefficient is given by

$$C_L = 2\pi \sin\alpha \tag{11}$$

where α is the angle of attack, which is the angle between the flow and the chord line of the airfoil.

The lift coefficient for real airfoils typically includes a constant term but the slope, at least for low angles of attack, is similar to that for an ideal airfoil. For greater angles of attack (above 10–15 degrees) the lift coefficient begins to decrease, eventually approaching zero. This is known as stall. A typical lift coefficient vs. angle of attack curve is illustrated in Figure AA.7.

Figure AA.7: Typical airfoil lift vs. angle of attack

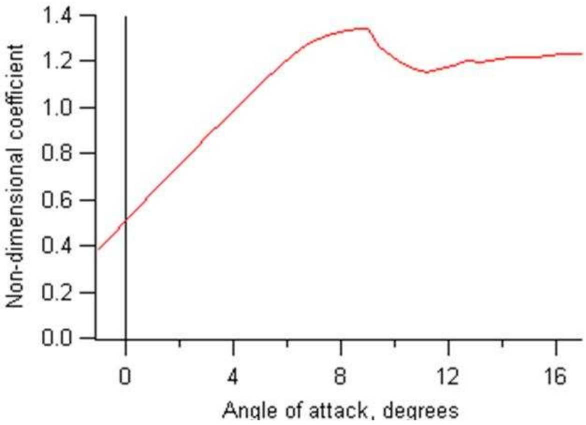

There is always some drag force associated with fluid flow. This is a force is in line with the flow. Drag force (per unit length) is given by:

$$\tilde{F}_D = C_D \frac{1}{2} \rho c U^2 \qquad (12)$$

Where C_D = drag coefficient

When designing blades for a wind turbine, it is generally desired to minimize the drag to lift ratio at the design point. This generally results in a lift coefficient in the vicinity of 1.0 and a drag coefficient of approximately 0.006, although these values can differ depending on the airfoil.

Blade element momentum theory, as noted above, relates the blade shape to its performance. The following approach is used. The blade is divided into elements and the rotor is divided into annuli. Two simultaneous equations are developed: one expresses the lift and drag coefficient (and thus forces) on the blade elements as a function of airfoil data and the wind's angle of attack. The other expresses forces on the annuli as a function of the wind through the rotor, rotor characteristics, and changes in momentum. Some of the key assumptions are: (i) the forces on blade elements are determined solely by lift/drag characteristics of the airfoil, (ii) there is no flow along the blade, (iii) lift and drag force are perpendicular and parallel respectively to a “relative wind,” and (iv) forces are resolved into components perpendicular to the rotor (“thrust”) and tangential to it (“torque”).

Using BEM theory, it may be shown for an ideal rotor that the angle of relative wind, φ, as a function of tip speed ratio and radial position on the blade is given by:

$$\varphi = \left(\tfrac{2}{3}\right)\tan^{-1}\left(1/\lambda_r\right) \qquad (13)$$

Similarly, the chord length is given by:

$$c = \frac{8\pi r}{BC_L}\left(1-\cos\varphi\right) \qquad (14)$$

Where B = the number of blades

There are some useful observations to be drawn out of the above equations. First of all, in the ideal case the blade will be twisted. In fact, the twist angle will differ from the angle of relative wind by the angle of attack and a reference pitch angle θ_p as follows:

$$\theta_T = \varphi - \alpha - \theta_p \qquad (15)$$

It may also be noted that the twist angle will at first increase slowly when moving from the tip inward and then increase more rapidly. Second, the chord of the blade will also increase upon moving from the tip inward, at first slowly and then more rapidly. In the ideal case then, a wind turbine blade is both significantly twisted and tapered. Real blades, however, are designed with a less than optimal shape for a variety of practical reasons.

Another important observation has to do with the total area of the blades in comparison to the swept area. The ratio of the projected blade area is known as the solidity, σ. For a given angle of attack, the solidity will decrease with increasing tip speed ratio. For example, assuming a lift coefficient C_L of 1.0, the solidity of an optimum rotor designed to operate at a tip speed ratio of 2.0 is 0.43 whereas an optimum rotor designed to operate at a tip speed ratio of 6.0 would have a solidity of 0.088. It is therefore apparent that in order to keep blade material (and thus cost) to a minimum, it is desirable to design for a tip speed ratio as high as possible.

There are other considerations in selecting a design tip speed ratio for a turbine other than the solidity, however. On the one hand, higher tip speed ratios will result in gearboxes with a lower speed up ratio for a given turbine. On the other hand, the effect of drag and surface roughness of the blade surface may become more significant for a higher tip speed ratio rotor. This effect could result in decreased performance. Another concern is material strength. The total forces on the rotor are nearly the same on the rotor regardless of the solidity. Thus the stresses would be higher. A final consideration is noise. Higher tip speed ratios generally result in more noise produced by the blades.

There are numerous other considerations regarding the design of a wind turbine rotor, including tip losses, type of airfoil to be used, ease of manufacturing and transport, type of control used, selection of materials, etc. These are all outside the scope of this overview, however.

Real wind turbine rotors are designed taking into account many factors, including but not only their aerodynamic performance. In addition, the rotor must be controlled so as to generate electricity most effectively and so as to withstand continuously fluctuating forces during normal operation and extreme loads during storms. Accordingly, a wind turbine rotor does not in general operate at its own maximum power coefficient at all wind speeds. Because of this, the power output of a wind turbine is generally described by curve, known as a power curve, rather than an equation such as the one for P_{WT} which given earlier. Figure AA.8 illustrates a typical power curve. As shown there, below the cut-in speed (3 m/s in the example) no power is produced. Between cut-in and rated wind speed (14.5 m/s in this example), the power increases significantly with wind speed. Above the rated speed, the power produced is constant, regardless of the wind speed, and above the cut-out speed (25 m/s in the example), the turbine is shut down.

Figure AA.8: Typical wind turbine power curve

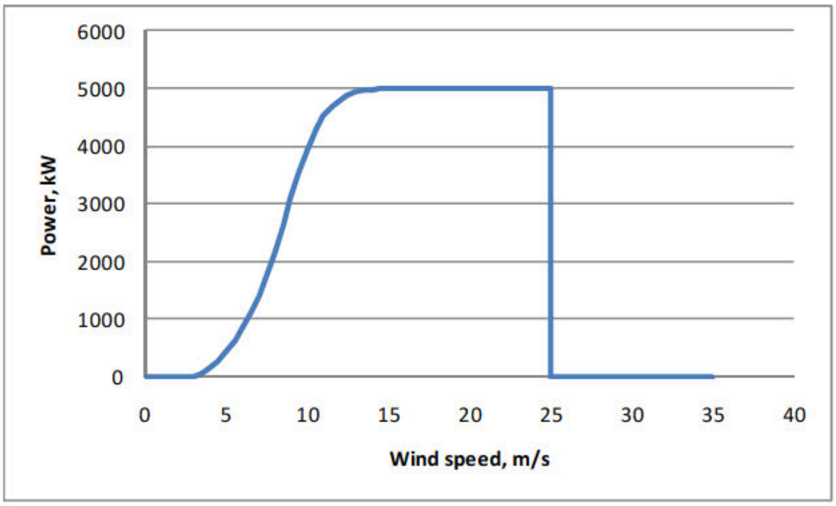

AA.7 Wind Turbine Mechanics and Dynamics

Earlier we discussed the aerodynamic aspects of a wind turbine, and how that related to its design, performance, and appearance. The next major consideration has to do with the turbine's survivability. This topic includes its ability to withstand the forces to which the turbine will be subjected, deflections of various components, and vibrations that may result during operations.

Issues that need to be considered include: (i) ultimate strength, (ii) relative motion of components, (iii) vibrations, (iv) loads, (v) responses, (vi) stresses, (vii) unsteady motion, resulting in fatigue, and (viii) material properties.

The types of loads that a turbine may be subjected to are as follows: static (non-rotating), steady (rotating), cyclic, transient, impulsive, stochastic, or resonance-induced. Sources of loads may include aerodynamics, gravity, dynamic interactions, or mechanical control. To understand the various loads that a wind turbine may experience, the reader may wish to review the fundamentals of statics (no motion), dynamics (motion), Newton's second law, the various rotational relations (kinematics), strength of materials (including Hooke's law and finding stresses from moments and geometry), gyroscopic forces/moments, and vibrations. Among other topics, the cantilevered beam is particularly important, since rotor blades as well as towers have similar characteristics.

Wind turbines are frequently both the source of and are subject to vibrations. Although the topic can become quite complicated, it is worthwhile to recall that the natural frequency of simple oscillating mass, *m*, and spring, with spring constant, *k*, and is given by:

$$\omega = \sqrt{k/m} \tag{16}$$

Similarly, rotational natural frequency about an axis of rotation is given by:

$$\omega = \sqrt{k_\theta / J} \tag{17}$$

Where k_θ is the rotational spring constant and J is the mass moment of inertia

A continuous body, such as a wind turbine blade, will actually have an infinite number of natural frequencies (although only the first few are important), and associated with each natural frequency will be a mode shape that characterizes it deflection. The vibration of a uniform cantilevered beam can be described relatively simply through the use of Euler's equation (see Manwell et al., 2009). Non-uniform elements require more complex methods for their analysis.

AA.7.a Rotor Motions

There is a variety of motions that occur in the rotor that can be significant to the design or operation of the turbine. These include those in the flapwise, edgewise, and torsional directions.

Flapwise motions are those that are perpendicular to plane of the rotor, and are considered positive in the direction of the thrust. Flapwise forces are the source of the highest aerodynamic bending moments, and accordingly the most significant stresses.

Lead-lag, or edgewise, motions are in plane of rotor and are considered positive when in the direction of the torque. Fluctuating motions in this direction are reflected in the power.

Torsion refers to the twisting of blade about its long axis. Torsional moments in the blades must be accounted for in the design of pitch control mechanisms.

The most important rotor load is the thrust. This is the total force on the rotor in the direction of the wind (flapwise). It is associated with the conversion of the kinetic energy of the wind to mechanical energy. The thrust, T, (N) is given by:

$$T = C_T \frac{1}{2} \rho \pi R^2 U^2 \tag{18}$$

Where C_T is the thrust coefficient. For the ideal rotor in which the axial induction factor, a, is equal to 1/3 (corresponding to the Betz limit), it is easy to show that the thrust coefficient is equal to 8/9. For the same rotor, the thrust coefficient may be as high as 1.0, but this would not occur at $C_p = C_{p,Betz}$.

This thrust gives rise to flapwise bending moments at the root of the blade. For example, for the ideal rotor when a = 1/3, and assuming a very small hub, it may be shown that the flapwise bending moment M_β at the root of the blade would be given by:

$$M_\beta = \frac{T}{B} \frac{2}{3} R \tag{19}$$

Where B = number of blades

From the bending moment, it is straightforward to find the maximum bending stress in the blade. For example, suppose that a blade is $2t$ m thick at the root, has a symmetrical airfoil, and that the thrust force is perpendicular to the chord line. Then the bending stress would be:

$$\sigma_{\beta,\max} = \frac{M_\beta t}{I_b} \tag{20}$$

(Note that for a real blade, the asymmetry and the angles would complicate the calculation, but the principle is the same.)

Another important load is torque, Q (Nm). Torque is given by:

$$Q = C_Q \frac{1}{2} \rho \pi R^2 U^2 \qquad (21)$$

Where C_Q = the torque coefficient, which also equal to C_p/λ.

Note that torque is also given by:

$$Q = P / \Omega \qquad (22)$$

Where P = power (W)

The dynamics of a wind turbine rotor are quite complicated and do not lend themselves to simple illustrations. There is one approach, however, due to Stoddard (Eggleston and Stoddard, 1987) and summarized by (Manwell et al., 2009) which is relatively tractable, but will not be discussed here. In general, the dynamic response of wind turbine rotors must be simulated by numerical models, such as the FAST code (Jonkman, 2005) developed by the National Renewable Energy Laboratory.

AA.7.b Fatigue

Fatigue is an important phenomenon in all wind turbines. The term refers to the degradation of materials due to fluctuating stresses. Such stresses occur constantly in wind turbines due to the inherent variability of the wind, the rotation of the rotor and the yawing of the rotor nacelle assembly (RNA) to follow the wind as its direction changes. Fatigue results in shortened life of many materials and must be accounted for in the design. Figure AA.9 illustrates a typical time history of bending moment that would give rise to fluctuating stresses of similar appearance.

Figure AA.9: Typical wind turbine blade bending moment

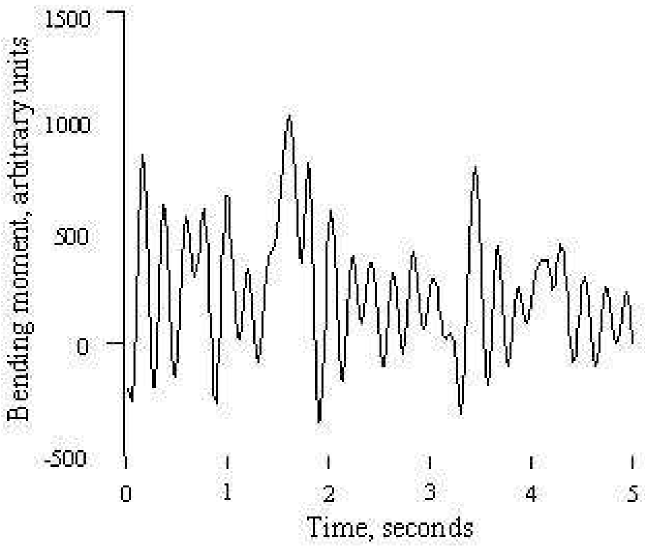

The ability of a material to withstand stress fluctuations of various magnitudes is typically illustrated in an S-N curve. In such curves the stress level is shown on the *y* axis and is plotted against the number of cycles to failure. As is apparent from the figure above, stress fluctuations of a variety of magnitudes are likely. The effect of a number of cycles of different ranges is accounted for by the damage due to each cycle using “Miner’s Rule.” In this case, an amount of damage, *d*, due to *n* cycles, where the stress is such that *N* cycles will result in damage is found as follows:

$$d = n / N \tag{23}$$

Miner’s Rule states that the sum of all the damage, *D*, from cycles of all magnitudes must be less than 1.0, or failure is to be expected imminently:

$$D = \sum n_i / N_i \leq 1 \tag{24}$$

Miner’s Rule works best when the cycling is relatively simple. When cycles of varying amplitude follow each other, an algorithm called "rainflow" cycle counting” (Downing and Socie, 1982) is used.

AA.8 Components of Wind Turbines

Wind turbines consist of two main subsystems, the rotor nacelle assembly and the support structure, and each of these is comprised of many components. The following provides some more description of these subsystems. More details, particularly on the rotor nacelle assembly may be found in (Manwell et al., 2009).

AA.8.a Rotor Nacelle Assembly

The rotor nacelle assembly (RNA) includes the majority of the components associated with the conversion of the kinetic energy of the wind into electrical energy. There are two major component groupings in the RNA as well as a number of ancillary components. The main groupings are the rotor and the drive train. The rotor includes the blades, the hub, and pitch control components. The drive train includes shafts, bearings, gearbox (if any), couplings, mechanical brake, and generator. Other components include the bedplate, yaw bearing and yaw drive, oil cooling system, climate control, other electrical components, and parts of the control system. An example of a typical rotor nacelle assembly is illustrated in Figure AA.10.

Figure AA.10: Typical Rotor Nacelle Assembly

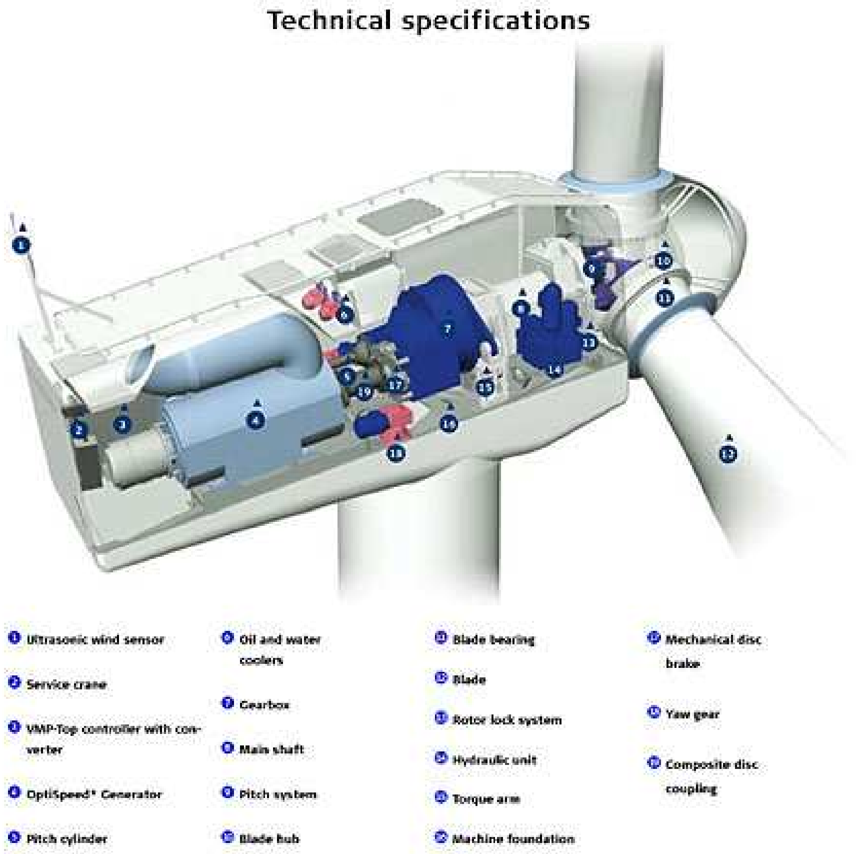

(From Vestas http://re.emsd.gov.hk/english/wind/large/large_to.html)

AA.8.b Rotor

The primary components of the rotor are the blades. At the present time, most wind turbines have three blades, and they are oriented so as to operate upwind of the tower. It is to be expected that in the future some wind turbines, particularly those intended for use offshore, will have two blades and will be oriented downwind of the tower, however. For a variety of reasons (including that downwind turbines tend to be noisier) it is less likely that they will be used on land, particularly in populated areas.

The general shape of the blades is chosen in accordance with the principles discussed previously. The other major factor is the required strength of the blades. For this reason, it is often the case that thicker airfoils are used nearer the root than are used closer to the tip. Blades for most modern wind turbines are constructed of composites. The laminates are primarily fiberglass with some carbon fiber for additional strength. The binders are polyester or epoxy.

At the root of the blades the composite material is attached to a steel root, which can then be subsequently bolted to the hub. Most utility scale wind turbines at present include blade pitch control, so there is a mechanism present at the interface of the hub and the blades that will both secure the blades and facilitate their rotation about their long axis.

The hub of the wind turbine rotor is constructed from steel. It is designed so as to attach to the main shaft of the drive train as well as to connect with the blades.

AA.8.c Drive train

The drive train consists of a number of components, including shafts, couplings, a gearbox (usually), a generator, and a brake.

AA.8.d Shafts

The main shaft of the drive train is designed to transmit the torque from the rotor to the gearbox (if there is one) or directly to the generator if there is no gearbox. This shaft may also be required to carry some or all of the weight of the rotor. The applied torque will vary with the amount of power being produced, but in general it is given by the power divided by the rotational speed. As discussed previously, a primary consideration in the aerodynamic design of a wind turbine rotor is the tip speed ratio. A typical design tip speed ratio is 7. Consider a wind turbine with a diameter of 80 m, designed for most efficient operation at a wind speed 12 m/s. The rotational speed of the rotor and thus the main shaft under these conditions would be 20 rpm.

AA.8.e Gearbox

Wind turbines are intended to generate electricity, but most conventional generators are designed to turn at higher speeds than do wind turbine rotors (see below). Therefore, a gearbox is commonly used to increase the speed of the shaft that drives the generator relative to that of the main shaft. Gearboxes consist of a housing, gears, bearings, multiple shafts, seals, and lubricants. Gearboxes for wind turbines are typically either of the parallel shaft or planetary type. Frequently a gearbox incorporates multiple stages, since the maximum allowed ratio per stage is usually well under 10:1. There are trade-offs in the selection of gearbox. Parallel shaft gearboxes are generally less expensive than planetary ones but they are also heavier. Gearboxes are generally quite efficient. Thus the power out is very nearly equal to the power in. The torque in the shafts is then equal to the power divided by the speed of the shaft.

AA.8.f Brake

Nearly all wind turbines incorporate a mechanical brake somewhere on the drive train. This brake is normally designed to stop the rotor under all foreseeable conditions, although in some cases it might only serve as a parking brake for the rotor. Mechanical brakes on utility scale wind turbines are mostly of the caliper/disc type although other types are possible. Brakes may be placed on either the low speed or the high speed side of the gearbox. The advantage of placing it on the high speed side is that less braking torque is required to stop the rotor. On the other hand, the braking torque must then pass through the gearbox, possibly leading to premature failure of the gearbox. In either case, the brake must be designed to absorb all of the rotational energy in the rotor, which is converted into heat as the rotor stops.

AA.8.g Generator

Electrical generators operate via the rotation of a coil of wire in a magnetic field. The magnetic field is created by one or more pairs of magnetic poles situated opposite each other across the axis of rotation. The magnetic field may be created either by electromagnets (as in conventional synchronous generators), by induction in the rotor (as in induction generators,) or with permanent magnets. In alternating current systems the number of pairs of poles and the grid frequency determine the nominal operating speed of the generator. For example, in a 60 Hz AC system, such as the United States, a generator with two pairs of poles would have a nominal operating speed of 1800 rpm. In most AC generators, the field rotates and while the current is generated in a stationary armature (the stator).

The majority of utility scale wind turbines today use wound rotor induction generators (WRIG). This type of generator can function over a relatively wide range of speeds (on the order of 2:1). Wound rotor induction generators are employed together with a power electronic converter in the rotor circuit. In such an arrangement approximately 2/3 of the power is produced on the stator in the usual way. The other third of the power is produced on the rotor and converted to AC of the correct frequency by the power electronic converter. In this configuration the WRIG is often referred to as a doubly fed induction generator (DFIG).

A number of wind turbines use permanent magnet generators. Such generators often have multiple pole pairs as well. This can allow the generator to have the same nominal speed as the wind turbine rotor so the main shaft can be connected directly to the generator without the use of a gearbox. Most permanent magnet generators are designed to operate together with power electronic converters. These converters facilitate variable speed operation of the turbine, while ensuring that the electricity that is produced is of constant frequency and compatible with the electrical grid to which the turbine is connected.

AA.8.h Bedplate

The bedplate is a steel frame to which components of the drive train and other components of the RNA are attached. It ensures that all the components are properly aligned.

AA.8.i Yaw System

Most wind turbines today include a yaw system. This system facilitates orienting the RNA into the wind as the wind direction changes. First of all, there is a slewing bearing that connects the top of the tower to the RNA, allowing the latter to rotate with respect to the former. Also attached to the top of the tower, and often to the outside perimeter of the slewing bearing, is a large diameter bull gear. A yaw motor connected to a smaller gear is attached to the bedplate. When the yaw motor is energized, the small gear engages the bull gear, causing the RNA to move relative to the tower. A yaw controller ensures that the motion is in the proper direction and that it continues until the RNA is aligned with the wind. A yaw brake holds the RNA fixed in position until the yaw controller commands a new orientation.

AA.8.j Control System

A wind turbine will have a control system that ensures the proper operation of the turbine at all times. The control system has two main functions: supervisory control and dynamic control. The supervisory control continuously monitors the external conditions and the operating parameters of the turbine, and starts it up or shuts it down as necessary. The dynamic control system ensures smooth operation of various controllable components, such the pitch of the blades or the electrical torque of the generator. The control system may also be integrated with or at least be in communication with a condition monitoring system that watches over the condition of various key components.

AA.8.k Support Structure

The support structure of a wind turbine is any part of the turbine that is below the main bearing. The support structure for land-based wind turbines may be conceptually divided into two main parts: the tower and the foundation. The tower of a wind turbine is normally constructed of tapered steel tubes. The tubes are bolted together on site to form a single structure of the desired height. The foundation of a wind turbine is the part of the support structure, which is in contact with the ground. Foundations are typically constructed of reinforced concrete. When turbines are installed on rock, the foundations may be attached to the rock with rods, which are grouted into predrilled holes.

AA.8.l Materials for Wind Turbines

The primary types of materials used in the various components of wind turbines are steel, copper, composites, and concrete.

AA.9 Installation

Installation of wind turbines may be a significant undertaking. It involves the following:

- Complete assessment of site conditions
- Detailed preparing for the installation
- Constructing the foundation
- Delivering the components to the site
- Assembling the components into sub-assemblies
- Lifting the sub-assemblies into place with a crane
- Installing the electrical equipment
- Final testing

More details may be found in (Manwell et al., 2009).

AA.10 Energy Production

The purpose of wind turbines is to produce energy. Energy production is usually considered annually. The amount of energy that a wind turbine will produce in a year, E_y, is a function of the wind resource at the site where it is installed and the power curve of the wind turbine. Estimates are usually done by calculating the expected energy that will be produced every hour of a representative year and then summing the energy from all of those hours as shown below:

$$E_y = \sum_{i=1}^{8760} P_{WT}(U_i)\Delta t \qquad (25)$$

Where U_i is the wind speed in the i^{th} hour of the year, $P_{WT}(U_i)$ is the average power (based on the power curve) during the i^{th} hour and Δt is the length of the time period of interest (here, one hr). The units of energy are Wh, but the amount of energy production is frequently expressed in either kWh or MWh for the sake of convenience.

It is sometimes cumbersome to characterize the performance of a wind turbine by its actual energy production. Accordingly, a normalized term known as the capacity factor, *CF*, is used. This is the given by the actual energy that is produced (or estimated to be produced) divided by the amount of energy that would be produced if the turbine were running at is rated output, P_R, for the entire year. It is found from the following equation:

$$CF = \frac{E_y}{8760 P_R} \qquad (26)$$

AA.11 Unsteady Aspects of Wind Turbine Operation

There are a number of unsteady aspects of wind turbine operation that are significant to the discussion of public reaction to wind turbines. These in particular include the variations in the wind field that can change the nature of the sound emitted from the rotor during operation. These unsteady effects include the following:

1. Wind shear – Wind shear refers to the variation of wind speed across some spatial dimension. Wind shear is most commonly thought of as a vertical phenomenon, that is to say, the increase of wind speed with height. Wind shear can also occur laterally across the rotor under some circumstances. Vertical wind shear is often modeled by a power law as discussed earlier. There are some situations, however, in which such a model is not applicable. One example has to with highly stable atmosphere, such that the wind near the ground is relatively light, but at the height of the rotor the wind is high enough that turbine may be operating. Under such conditions there may be sound emanating from the rotor, but relatively little wind induced sound near the ground to mask that from the rotor. Wind shear may also result in a cyclically varying aspect to the sound produced by the blades as they rotate. This occurs due to the changing magnitude and direction of the relative wind as the blades pass through zones of different wind speed.
2. Tower shadow or blockage – The wind flow near the tower is inevitably somewhat different from where there is no tower. The effect is much more pronounced on wind turbines with downwind rotors, but it still occurs with up-wind rotors. This tower effect can result in a distinct change in sound once per revolution of each blade.

3. Turbulence – Turbulence refers to changes in magnitude and direction of the wind at varying time scales and length scales. The presence of turbulence can affect the nature of the sound.
4. Changes in wind direction – Wind turbines are designed to yaw in response to changes in wind direction. The yawing process takes a finite amount of time and during that time the wind impinging on the rotor will do so at a different direction than it will when the yawing process is complete. Sound produced during the yawing process may have a somewhat different character than after it is complete.
5. Stall – Under some conditions part or all of the airfoils on the blades may be in stall. That is, the angle of relative wind is high enough that the airfoil begins to lose lift. Additional turbulence may also be generated. Again, the nature of the sound produced by the rotor may be different than during an unstalled state. It may also be noted that some turbines intentionally take advantage of stall to limit power in high winds. Under such conditions there may also be a change in sound in comparison to normal operation.

AA.11.a Periodicity of Unsteady Aspects of Wind Turbine Operation

Due to the rotation of the rotor and the nature of the wind, there tend to be certain features of the turbine's operation that are periodic in nature. The most dominant of these have frequencies associated with the rotational speed of the rotor and the blade passage frequency, which is simply the rotational speed times the number of blades. For example, the dominant frequencies in a 3-blade wind turbine rotating at 20 rpm would be 0.33 Hz and 1 Hz. Other significant frequencies may be the first few harmonics of the rotational frequency and blade passage frequency.

AA.12 Wind Turbines and Avoided Pollutants

Wind turbines have a positive impact on human health via avoiding emission of pollutants that would result if the electricity that they generate were produced instead by other generators. While the average emissions of various pollutants per MWh produced from conventional generators is relatively easy to estimate, it is harder to estimate the actual impact of wind turbine generation. This is because the electricity distributed by the electrical grid is produced by different types of generators, and the operation of these generators will be affected differently as a result of the supply of part of the total electrical demand by the wind turbines.

In general, electricity in any large utility network comes from three types of generators: base load, intermediate load, and peaking plants. The fuel or energy source supplying these generators is likely to be coal, fuel oil, natural gas, uranium (nuclear plants), or water (hydroelectric plants). Base load plants are typically coal fired or nuclear plants. Intermediate load plants often use fuel oil or natural gas. Peaking plants are normally natural gas or hydroelectric. There are a considerable number of plants that may be operating at any given time. Which plants are actually operating is determined by the system operator in accordance with what the near term forecasted load is expected to be and the estimated (bid) cost per MWh from all the plant operators in the system. For thermal plants the bid cost is close to that projected fuel cost/MWh. This in turn is found from heat rate of the fuel (kg/MWh) for the plant in question times the unit cost of the fuel ($/kg). Less efficient plants or those with higher unit fuel costs tend to have relatively high bid costs. (Note on the other hand, that wind turbines would have bid costs of zero, since they do not use fuel.)

If a large number of wind turbines are operating such that they are contributing a significant amount of electricity to the total load, the mix of generators may well be different than it would be if the turbines were not present. If only a small number of wind turbines are present, then the mix of generators may not change. However, certain of the plants would be curtailed so as to produce less energy and thus consume less fuel. The emissions of pollutants from all the operating plants could be calculated and so could the projected emissions that would have resulted if the wind turbines were not present. The difference in amount of pollutants produced could then be assigned to the wind turbine as the avoided emissions.

To do such an analysis properly involves estimating the actual impact of wind turbine generation on the mix of generators and the operating level of those generators for every hour of the year. This is a non-trivial exercise, but it has been done for an offshore wind farm that was proposed for the town of Hull, MA. That project was to have included four 3.6 MW turbines, for a total capacity of 14.4 MW. The pollutants considered in the study were CO_2, $NO_{X,}$ and SO_X. The results of that study are described in detail in (Rached, 2008). The results of that study are summarized in Table AA.1. The results in the table are normalized for a 1 MW (rated) wind turbine and use the medium estimated wind speed for the site. (Note under the assumptions of Rached's study, a one MW (rated) wind turbine in the medium wind speed scenario at the site would generate 2,580 MWh/yr).

Table AA.1:

Avoided emissions of pollutants for 14.4 MW wind project (based on Rached, 2008)

CO_2 (kg/MWyr)	SO_X (kg/MWyr)	NO_X (kg/MWyr)
1,970,000	3,480	1,490

A simpler but less accurate way to estimate the avoided emissions is to use the marginal rates for pollutants as specified by the Massachusetts Greenhouse Gas policy (MEPA, 2007). Applying this method Rached calculated avoided emissions per MW (rated) for the three pollutants for one year of 1,320,000 kg CO_2, 2,080 kg of SO_2, and 701 kg of NO_x.

In the analysis summarized above the majority of the avoidance of pollutant production would be due to reduced consumption of natural gas. If a larger fraction of Massachusetts' energy were to be produced by wind energy, there could be significant reductions of the consumption of fuel oil and coal as well. This should result in larger amounts of avoided pollution per unit of wind turbine production

Appendix B

Wind Turbines – Shadow Flicker

AB.1 Shadow Flicker and Flashing

Shadow flicker occurs when the moving blades of a wind turbine rotor cast moving shadows that cause a flickering effect. This flicker could annoy people living close to the turbine. Similarly, it is possible for sunlight to be reflected from gloss-surfaced turbine blades and cause a "flashing" effect. This phenomenon will occur during a limited amount of time in a year, depending on the altitude of the sun, α_s; the height of the turbine, H, the radius of the rotor, R, and the height, direction and distance to the viewing point. At any given time the maximum distance from a turbine that a flickering shadow will extend is given by:

$$x_{shadow,\max} = \left(H + R - h_{view}\right) / \tan\left(\alpha_s\right) \qquad (27)$$

Where h_{view} is the height of the viewing point.

The solar altitude depends on the latitude, the day of the year, and the time as given in the following equations (Duffie and Beckman, 2006)

$$\alpha_s = 90° - \cos^{-1}\left[\cos(\delta)\cos(\phi)\cos(\omega) + \sin(\delta)\sin(\phi)\right] \qquad (28)$$

Where δ = declination of the earth's axis, ø = latitude and ω = the hour angle

The declination is found from the following equation:

$$\delta = 23.45\sin(360(284 + n)/365) \qquad (29)$$

Where n = day of the year

The hour angle is found from the hours from noon (solar time, negative before noon, positive after noon), divided by 15 to convert to degrees.

Another relevant angle is the solar azimuth. This indicates the angle of the sun with respect to certain reference direction (usually north) at a particular time. For example, the sun is always in the south at solar noon, so its azimuth is 180° at that time. The solar azimuth is important since it determines the angle of the wind turbine's shadow with respect to the tower. See Duffie and Beckman (2006) for details on calculating the solar azimuth.

F r examp e consider a location that as a atitude of 4 °. Assum that the day is March 1 (day 60) and the time s 3:0 in the afternoon Also as me that h turbine has a tower height of 80 m an ra i s of 0 m and that the viewing height s 2 m. T e de lination is -8.3°, the solar altitude is 24.4°, and the solar zimuth is 5 .2° W of S. h ma imum extent of the shadow is 38 m from t e turbine. The angle of the shadow is 50.2° E of N.

S tes are typically characterized by charts such t e on ill st t i Figure AB.1 for a location in Den ark (WEA, 2004). T e chart gives the number of ho rs per year of flicker shadow as a function o direction a d distanc (me sured in un ts of hub height). In the example shown, two viewing points re consider d. One o them (A) s directly t the north of turbine at a distance of 6 times the hub height. The other (B) is l cated to the sou h east at a distance of 7 times the hub height. The figure shows th t the fir t viewing point ill e perience shadow flicker from the turbine for 5 ho rs per year. The second p i t will experien flicker for about 12 hours per year.

Figure AB 1: Diagram f shadow flic er ca cu ation WEA, 2004)

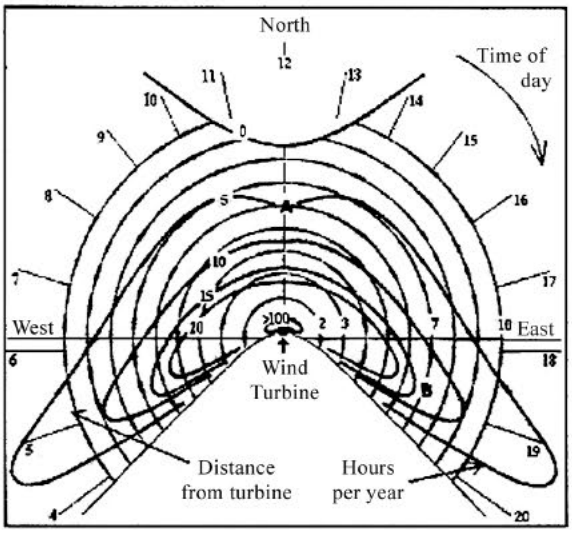

A, B are viewing points
Note tha t e equations above assume a cl r sk an the absence of rain, c ouds, etc.

AB.2 itigation Possibilit es

M st modern wind turbines allow for real-t me contr l f turb n peration by computer in order to shut down uring high shadow flicker times, if necessary. In addition, computer programs can allow for pre-plan ing of sitin lo ati n ahe d of ime to know what a project specific impac will be in t r s of shado fli ker when pla ning a wind turbine project (as discussed in the previous paragraph). This planning can be site-specific in order to avoid potential problems with specific sites based on geographical location or weather patterns.

In terms of safe distances to reduce shadow flicker, these are often project-specific because it depends on whether there are residences or roadways present and what the geographic layout is. This could be particularly important in areas with more forestry and existing shadow, which could reduce nuisance from turbine produced shadow flicker or whether it is an otherwise open land area such as farmland that would be more susceptible to the annoyance of shadow flicker. A general estimate for modeling a shadow flicker risk zone includes 10 times the rotor diameter such that a 90-meter diameter would be equivalent to a 900-meter impact area. However, only certain portions of this zone are actually likely to experience shadow flicker for a significant amount of time. Other modeling considerations include when at least 20% of the sun is covered by the blade and whether to include the blade width in estimates as well. In terms of distance, 2,000 meters is the WindPro computer program default distance (NEWEEP, 2011) for calculations of wind turbine produced shadow flicker. Finally, due to atmospheric effects, 1400 m is the maximum distance from a turbine within which shadow flicker is likely to be significant.

In terms of existing regulations regarding shadow flicker rates, there are no current shadow flicker regulations in Massachusetts (or many other New England states, but there are statewide and local guidelines that have been implemented. These guidelines were provided by the Department of Energy Resources in March 2009 and state that, “wind turbines shall be sited in a manner that minimizes shadowing or flicker impacts” and, “the applicant has the burden of proving that this effect does not have significant adverse impact on neighboring or adjacent uses.” Local Massachusetts regulations include the Worcester, MA zoning ordinance, which requires, “The facility owner and operator shall make reasonable efforts to minimize shadow flicker to any occupied building on a non-participating landowner’s property.” Also, a shadow flicker assessment report is required as is a plan showing the “area of estimated wind turbine shadow flicker.” Similarly, the Newburyport, MA regulations require that wind turbines do not result in significant shadow or flicker impacts and an analysis is required for planned projects (NEWEEP, 2011).

The Maine model wind energy facility ordinance states that wind turbines should, “avoid unreasonable adverse shadow flicker effect at any occupied building located on a non-participating landowner's property." They do not state any specific limit to shadow flicker other than these guidelines. However, the New Hampshire Model Small Wind Energy Systems Ordinance states that wind turbines, "shall be sited in a manner that does not result in significant shadow flicker impacts…significant shadow flicker is defined as more than 30 hours per year on abutting occupied buildings." Similar to Maine, several states in the US have adopted the German model of 30 hours per year of allowed shadow flicker that was primarily based on the government-sponsored study summarized above. However, other states or localities including Hutchinson, Minnesota have enacted stricter guidelines including no shadow flicker to be allowed at an existing residential structure, and up to 30 hours per year of shadow flicker allowed on roadways or residentially zoned properties and a computer analysis is required for project approval (NEWEEP, 2011).

In addition, computer programs such as WindPro are also recommended by most states and localities for use in all new planned installations to reduce this potential nuisance of shadow flicker on residential properties or potential health hazards to drivers on busy highways or roadways.

Appendix C

Wind Turbines – Ice Throw

AC.1 Ice Falling or Thrown from Wind Turbines

Under certain weather conditions ice may form on the surface of wind turbine blades. Normally, wind turbines intended for use in locations where ice may form are designed to shut down when there is a significant amount of ice on the blades. The means to prevent operation when ice is present may include ice sensor and vibration sensors. Ice sensors are used on most wind turbines in cold climates. Vibration sensors are used on nearly all wind turbines. They would cause the turbine to shut down, for example, if ice buildup on the blades resulted in an imbalance of the rotor and hence detectable vibrations in the structure.

Ice built up on blades normally falls off while the turbine is stationary. If that occurs during high winds, the ice could be blown by the wind some distance from the tower. In addition, it is conceivable that ice could be thrown from a moving wind turbine blade under some circumstances, although that would most likely occur only during startup (while the rotational speed is still relatively low) or as a result of the failure of the control system. It is therefore worth considering what the maximum plausible distance that a piece of ice could land from the turbine under two "worst case" circumstances: 1) ice falls from a stopped turbine during very high winds, and 2) ice is suddenly released from a blade when the rotor is rotating at its normal operating speed.

In both cases, the distance that the ice may travel is governed by Newton's laws and the principles of fluid mechanics. Calculations are quite simple when the effect of the air (and the wind) is ignored. For example, in that case if a piece of ice falls from a turbine, it will land directly below where it is released. The situation is a little more complex, but still readily solvable if the piece of ice is moving when it is released. For example, suppose that the ice is initially on the tip of a blade, and the blade is pointing vertically upward. Once the ice is released it will continue moving horizontally at the speed it had when it was still attached to the blade. But it will also begin to fall towards the ground, so the piece of ice will have two components of velocity until the ice hits the ground. The time t_g (s) it takes for the ice to reach the ground (assuming a horizontal surface) is $t_g = \sqrt{2h/g}$ where h = height (m) at which the ice is released and g = acceleration of gravity (9.81 m/s^2). The distance x (m) that the ice would travel is $x = t_g \Omega R$ where Ω is the rotational speed of the rotor (rad/s) and R is the length of the blade (m).

Such an analysis is overly simplified, however. It would underestimate the distance that the ice would travel if it fell from a stationary turbine in a high wind, and it would overestimate the distance that the ice would travel if it were suddenly released from a moving blade. It is necessary to consider the effect of the air and the force that it will impart upon the falling ice. For motion in the vertical (z) direction the equation of motion is the following:

$$F_z = ma_z \tag{30}$$

where F_z is the net force (N), m is the mass (kg), and a_z is the acceleration (m/s^2). The force includes two main components. One is the weight, W (N). It is due to gravity and acts in the negative z direction. The other one is due to the drag of the air and it acts opposite to the direction of the velocity. It is found from:

$$F_D = \frac{1}{2} C_D \rho A V_z^2 \tag{31}$$

where ρ is the density of air (1.225 kg/m^2 under standard conditions), A is the projected area (m^2) of the piece of ice, C_D is the drag coefficient of the ice and V_z is the velocity of the ice (m/s) in the z direction.

Acceleration is the derivative of the velocity, so we can rewrite the equation of motion for the vertical direction as follows:

$$\frac{dV_z}{dt} = \left(-W - sign(V_z) \frac{1}{2} C_D \rho A V_z^2 \right) / m \tag{32}$$

Where *sign* (…) indicates the direction of motion along the z axis. For the general case, the piece of ice may leave the blade with initial speed ΩR at an arbitrary angle θ with respect to the horizontal. Accordingly, there will be two components of the velocity, one in the z direction (as before) V_z, the other in the x direction, V_x. This assumes that the x axis is horizontal, is also in the plane of the rotor, and is positive in the direction of the tip of the blade at its apogee.

These velocities are initially:

$$V_{z,0} = \Omega R \sin(\theta) \tag{33}$$

$$V_{x,0} = \Omega R \cos(\theta) \tag{34}$$

The equation of motion for the *x* direction is:

$$\frac{dV_x}{dt} = \left(-sign(V_z)\frac{1}{2} C_D \rho A V_x^2 \right) / m \tag{35}$$

The above equations are a bit difficult to solve analytically, but they can be solved numerically fairly easily. Similar equations may also be developed for the case of a particle of ice falling from a stationary turbine.

Some data from actual ice throw has been compiled by Seifert et al. (2003). Figure AC.1, taken from that report is shown below.

Figure AC.1: Observed throwing distance of ice (from Seifert et al., 2003)

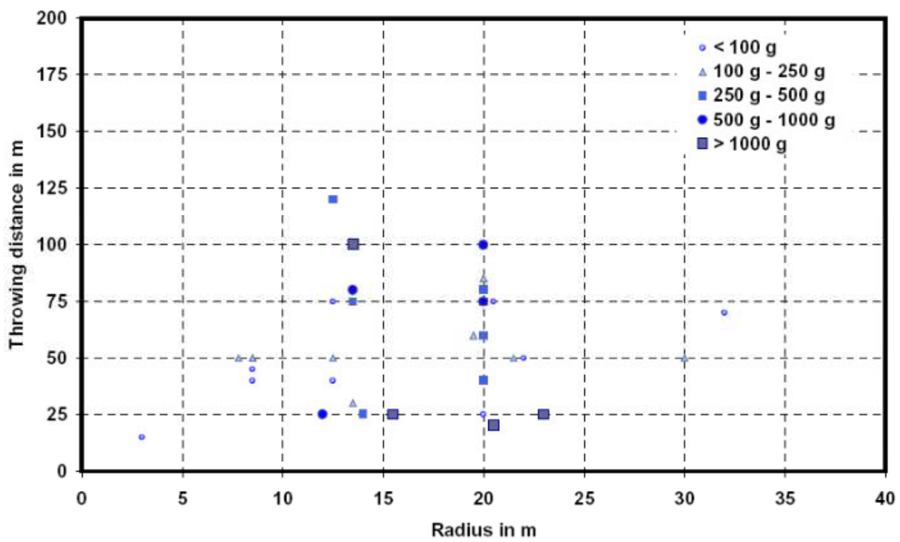

As may be seen in the figure, the maximum distance that ice was observed to fall from a turbine with a diameter of 20 m during operation was approximately 100 m. Based on the observed data, Seifert et al. suggest the following simplified formula for the maximum throwing distance:

$$x_{\max,throw} = 1.5\left(2R + H\right) \tag{36}$$

Where $x_{max,throw}$ = maximum throwing distance (m), R = rotor diameter (m) and H = hub height (m).

By way of illustration, Equation 36 was used to predict the maximum throwing distance of a piece of ice from a turbine with a rotor radius of 20 m installed on a tower 50 m high. That distance was 135 m. The theoretical equations given previously were also used to calculate throwing distance. The following assumptions were made: spherically shaped piece of ice, drag coefficient of 1.2, air density of 1.225 kg/m^3, ice density of 700 kg/m^3, rotor speed of 40 rpm (corresponding to a tip speed ratio of 7 at a wind speed of 12 m/s), angle of release of 45°, and instantaneous release of the ice. The equations predict a maximum throwing distance of 226 m or somewhat less than twice that predicted from the empirical equation. The difference is deemed to be reasonable, especially considering the idealized shape of the particle. Real pieces of ice would actually be highly non-spherical in shape and experience considerably more drag. It may also be noted that it was reported in Cattin et al. (2007) that ice did not fall as far from a wind turbine in the Swiss Alps as would be predicted from Equation 36. In that case the maximum observed distance from a turbine with radius of 20 m and a tower height of 50 m was 92 m. As noted above, Equation 36 predicts 135 m.

Seifert et al. also considered data regarding ice thrown from stationary turbines. Based on the available data they proposed a simple equation for predicted ice fall. That equation is

$$x_{\max,\,fall} = U\left(R + H\right)/15 \tag{37}$$

Where U = wind speed at hub height in m/s, $x_{max,fall}$ = maximum falling distance (m), R = rotor radius (m), H = hub height (m).

Using Equation 37, the predicted maximum distance for a turbine with a radius of 20 m, a tower height of 50 m, and a wind speed of 20 m/s is 120 m. By way of comparison, the fall distance was predicted from the theoretical equations given above for the same situation. The results are highly dependent on the size of the piece of ice and hence the surface to volume ratio. To take one example, a piece of ice that was assumed to be spherical and to have a weight of 10 g would land 110 m from the tower. In the examples discussed by Seifert et al., all the pieces of ice landed less than 100 m from the tower.

AC.2 Summary of Ice Throw Discussion

As noted above, there are two plausible scenarios in which ice may fall from a wind turbine and may land at some distance from the tower. In the first scenario, ice that falls from a stationary turbine is blown some distance from the tower. In the second scenario, ice is thrown from the blade of an operating turbine during a failure of the control system. In the first case, ice may land 100 m or more from the tower in high winds, depending on the wind speed, the height from which the ice falls, and the dimensions of the ice. In the second case, the ice could land even further from the turbine. Just how far would depend on the actual speed of the rotor when the ice was shed, the height of the tower, the length of the blade, the angular position of the blade when the ice was released, and the size and shape of the ice. In general, it appears that ice is unlikely to land farther from the turbine than its maximum vertical extent (tower height plus the radius.)

Appendix D

Wind Turbine – Noise Introduction

Noise is defined simply as unwanted sound. Sound is defined as the sensation produced by stimulation of the organs of hearing by vibrations transmitted through the air or other medium. In air, the transmission is due to a repeating cycle of compressed and expanded air. The frequency of the sound is the number of times per second, Hertz (Hz), that the cycle repeats. Sound at a single frequency is called a tone while sound that is a combination of many frequencies is called broadband.

The human ear is capable of responding over a frequency range from approximately 20 Hz to 20 kHz (Hz: Hertz = 1 cycle/second; Middle C on a piano is a frequency of 262 Hz).

AD.1 Sound Pressure Level

Sound is characterized by both its frequency and its amplitude. Sound pressure is measured in micro Pascals (μPa). Because sound pressure can vary over a wide range of magnitudes a logarithmic scale is used to convert micro Pascals to decibels. Thus sound pressure level (SPL) is defined by SPL = $10 \log_{10} [p^2/p^2_{ref}] = 20 \log_{10}(p/p_{ref})$ with the resulting number having the units of decibels (dB). The reference pressure p_{ref} for airborne sound is 20×10^{-6} Pa (i.e., 20μPa or 20 micro Pascals). This means that SPL of 0 dB corresponds to a sound wave with amplitude 20μPa. 140 dB is considered the threshold of pain and corresponds to 20,000,000 μPa. Doubling the amplitude of the sound wave increases the SPL by 6 dB.

Therefore, a 40μPa amplitude sound wave would have an SPL of about 6 dB.

When it is stated that there is a large frequency range over which humans can hear, it is also noted that the ear does not hear each frequency similarly. In fact, there is a frequency-dependent threshold of hearing (lower limit) and threshold of pain (higher limit). Experiments have been performed to determine these thresholds. The threshold of hearing curves show that one can hear a tone at 3 kHz (3000 Hz) with an SPL < 0 dB while at 100 Hz one does not hear the tone until its SPL is about 30 dB. Curves showing the thresholds can be easily found in textbooks and online (one online example is at

http://www.santafevisions.com/csf/html/lectures/007_hearing_II.htm). Experiments have also been conducted to determine equal loudness level contours. These contours indicate when two tones of dissimilar frequencies appear to be equally loud.

Some characteristics of human response to sound include:

- Changes in sound level <1 dB cannot be perceived
- Doubling the magnitude of the acoustic pressure leads to a 6 dB increase in SPL
- A 5 dB SPL change will result in a noticeable community response
- A 10 dB SPL change is subjectively heard as an approximate doubling in loudness

AD.2 Frequency Bands

Most sounds in our environment contain multiple frequencies and are variable in that successive identical experiments cannot result in the exact same plot or tabulation of pressure vs. time. Therefore, it is common to use averages that measure approximately the amplitude of the sound and its frequency content. Common averaging methods rely on the principle of octaves, such as 1/10, 1/3, and single octave bands. This means that the entire frequency range is broken into chunks such that the relation between the starting and ending frequencies of each chunk, f_1 and f_2 respectfully, are related by $f_2 = 2^{1/N}f_1$ where N = 1 for a single octave band and 3 for a 1/3 octave band. Because the bands can be constructed based on any starting frequency, a standardized set of bands have been specified. They are usually described by the center frequency of each band. The standard octave-bands are given in Table AD.1 (measured in Hz):

Table AD.1:

Octave bands. Values given in Hz.

Center Frequency	Lower Band limit	Upper Band Limit
16	11	22
31.5	22	44
63	44	88
125	88	177
250	177	355
500	355	710
1000	710	1420
2000	1420	2840
4000	2840	5680
8000	5680	11360
16000	11360	22720

A similar set of bands can be written for the 1/3 octaves. For each octave band there are 3-1/3 octave bands. Many text and online resources specify the 1/3 octave bands such as (http://www.engineeringtoolbox.com/octave-bands-frequency-limits-d_1602.html). The 1/10 octave band is a narrow-band filter and is used when the sound contains important tones.

AD.3 Weightings

Noise data are often presented as 1/3 octave band measurements. Again, this means that the sound in each frequency band has been averaged over that frequency range. Noise levels are also often reported as weighted values. The most common weighting is A weighting. It was originally intended to be such that sounds of different frequencies giving the same decibel reading with A weighting would be equally loud. The weighting of the octave band centered at 31.5 Hz requires one to subtract 39.4 dB from the actual SPL. The octave bands with centers from 1000 to 8000 where human hearing is most sensitive are corrected by only about +/- 1 dB. When considered together with the threshold of hearing, it is clear that the A-weighting is most applicable for sounds of small amplitude. C-weighting on the other hand subtracts only a few dB from the very highest and very lowest frequency bands. It is therefore more applicable for higher levels of sound. The figure below shows these two weightings. When weighted, the sound pressure level is reported as dBA or dBC respectively.

Figure AD.1: Weighting values for reporting sound pressure levels

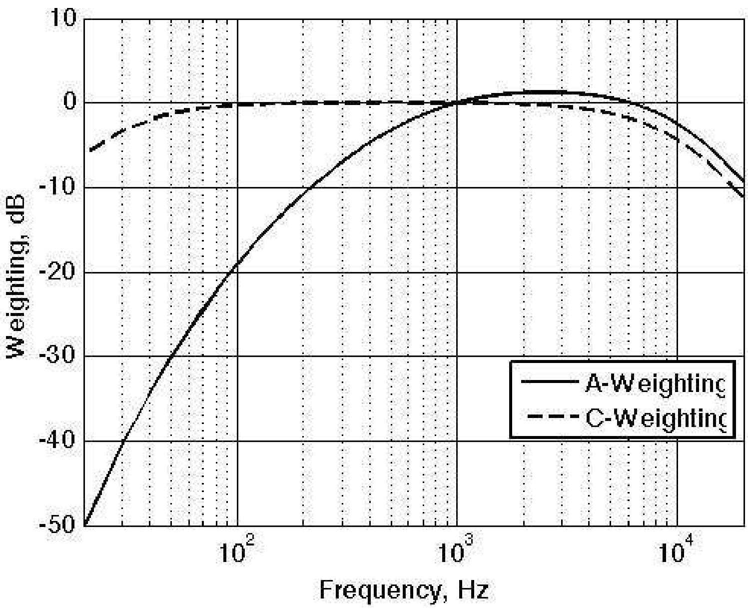

.

Noise levels change several times per day. To account for these differences other environmental noise measures are often used as shown in Table AD1.

Table AD 2:

A set of visual examples for these measures can be found at (*http://www.epd.gov.hk/epd/noise_education/web/ENG_EPD_HTML/m2/types_3.html*)

Indicator	**Meaning**
L_{max}	The maximum A-weighted sound level measured
L_{10}, L_{50}, L_{90}	The A-weighted sound level that is exceeded n%, of the time, where n is 10, 50, and 90 respectively. During the measurement period L_{90} is generally taken as the background sound level.
L_{eq}	Equivalent sound level. The average A-weighted sound pressure level, which gives the same total energy as the varying sound level during the measurement period of time.
Ldn	Day-night level. The average A-weighted sound level during a 24-hour day after addition of 10 dB to levels measured in the night between 10 p.m. and 7 a.m.

AD.4 Sound Power

Sound intensity and sound power are also often reported. Sound intensity is a measure of the energy transported per unit area and time in a certain direction. It can be shown that the intensity (I) perpendicular to the direction of sound propagation is related to the amplitude of the pressure wave squared, the density of the air (ρ), and the speed of sound (c), $I \sim p^2/\rho c$. The sound power, P, is the total intensity passing through a surface around a sound source. Intensity has units of Watts per square meter (W/m^2) and Power is measured in Watts (W). Both of these quantities are normally reported in dB where the intensity level is calculated as $L_I = 10 \log_{10}(|I|/I_{ref})$ and the power level is calculated as $L_W = 10 \log_{10}(P/P_{ref})$. The reference intensity level is related to the threshold of hearing at 1000 Hz such that $I_{ref} = 10^{-12}$ W/m^2. The reference power value is $P_{ref} = 10^{-12}$ W (1 picowatt). Here a doubling of the power leads to a 3 dB increase in the sound power level (PWL).

AD.5 Example Data Analysis

This is an example of the type of analysis done on sound measurements from a wind turbine. First, the actual signal might look something like what is shown in Figure AD.2.

Figure AD.2: Pressure signal from a wind turbine

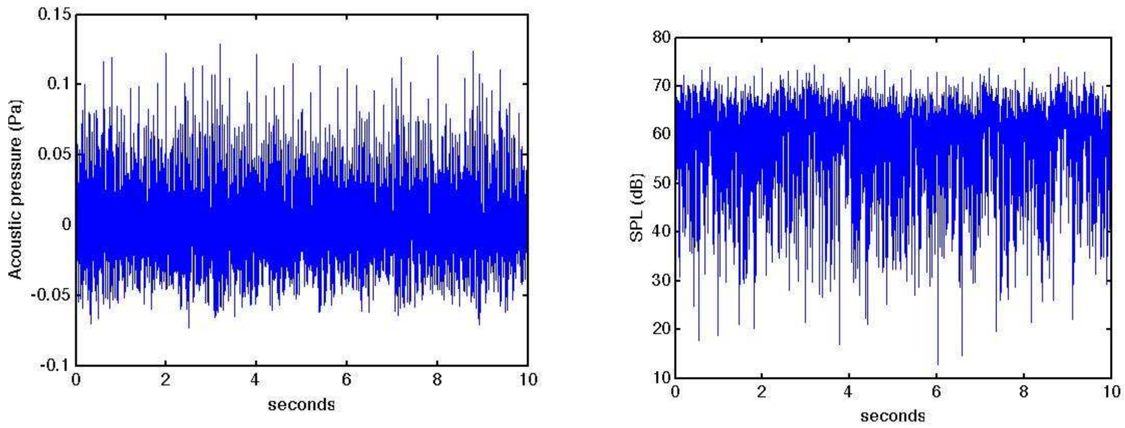

. *(From(van den Berg, 2011), related to Rheine wind turbine farm). Left in Pascals, right as SPL in dB.*

In Figure AD.2, just the acoustic pressure is shown, which means that atmospheric pressure, which is about 103,000 Pa, has been subtracted and the fluctuations then appear around 0 Pa. These data can easily be presented as SPL by transforming the pressure from Pa to dB. In order to analyze the pressure signal for low frequency content, a much longer time signal must be obtained. The frequency content of a long time signal is analyzed by performing a Fourier Transform. A typical transform of data from a wind turbine is shown in Figure AD.3.

Figu e AD.3: Frequency cont nt of typical wind tu b ne measu e e t. (fr m lmer ASA paper.)

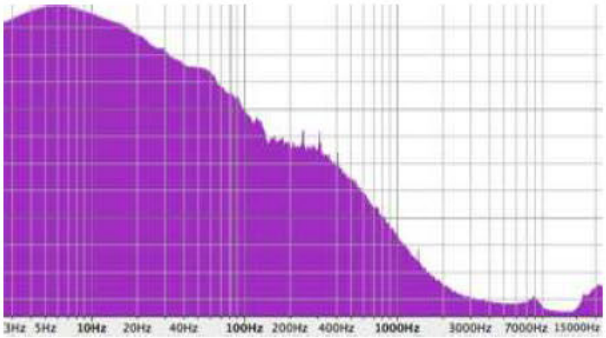

(This figure does n t corresp nd to the Rheine data for w i h the w iter is not ble to produce the full frequency domain plot.)

In ord r to better assess the bro dba d natu e of wind turbin und, the results are presented in 1/3-oc ave ban form. The averages that a e tak n i e ch 1 3-octave band can be done on fast or slow time i tervals. F r in ta ce, the ata i i ure 3 co ld be averaged on 1/3-oc ave bands to come up wit the overall SPL in the ban s. Or, as a measurement is being taken, the instrumentation can provide 1/3-oc ave ban verages on shor time s ales. For the Rheine data a fast average n 0.05 seconds was recorded. A few of the 1/3-oc a e band results are shown in Figure AD.4.

Figure AD.4: Fast averages for 1/3-octave band an ly is.

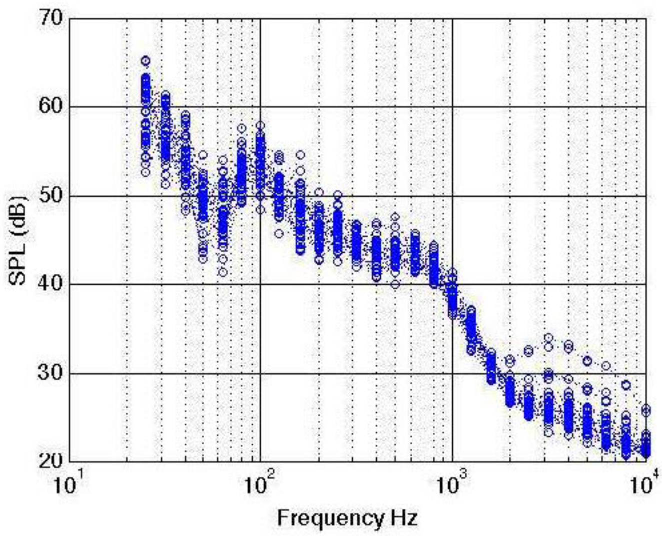

Shown results for 0–0.05, 5–0.05, 10–10.05, ..., 200– 00.05 seconds.

From hese a in l overall spectrum emerges. If t ese were presented as A-weighted spectrum, then Figure AD.5 is what is presented.

Figure AD.5: Fast averages for 1/3-octave band A-weighted analysis.

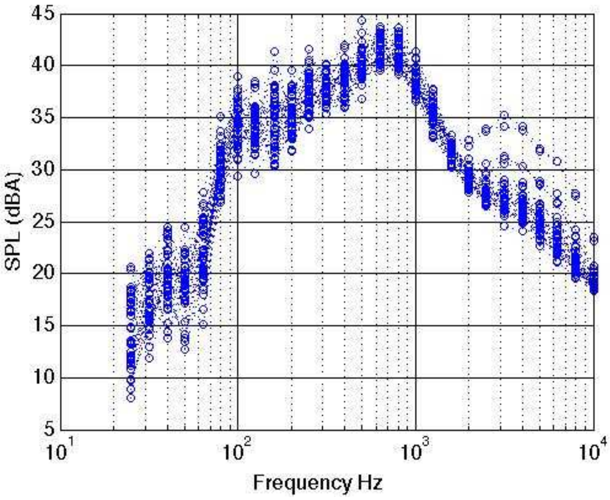

Shown results for 0–0.05, 5–0.05, 10–10.05, …, 200–200.05 seconds.

AD.6 Wind Turbine Noise from Some Turbines

What is known about aerodynamically generated noise from wind turbines is that it nominally increases with increasing wind speed until the max power is obtained, and it increases with increasing rotor tip speed. A report out of the Netherlands by (van den Berg et al., 2008) reports a vast amount of noise data related to wind turbines. The tables in Appendices B and C from the report clearly show these trends. Some of the data are reproduced here. Only measurements that were made by third parties (not specified by the wind turbine company) are reproduced here.

Table AD.3:

Sound power level in dB(A) from various wind turbines. (van den Berg et al., 2008).

Manufacturer Make and model	**Power kW**	**Hub Height m**	**Diameter m**	**rpm**	**4 m/s**	**5m/s**	**7m/s**	**8m/s**	**10m/s**
Enron TW1.5s	1500	80	70	11	100	100	100	100	
Enron TW1.5s	1500	81	70	22		102	102	103	104
NegMicon NM52	900	70	52	15	93	93			
NegMicon NM52	900	70	52	22		98	100	101	103
NegMicon NM54	950	46	54	15		95.6			
NegMicon NM54	950	46	54	22		101.6			
Vesta V66	1650	70	66	15	97	97	98	98	
Vesta V66	1650	70	66	19		101	101	102	102

It must be noted here that what has been reported are the sound power levels, which represents the total sound energy that propagates away from the wind turbine (i.e., the sound energy at the center of the blades, which propagates outward at the height of the hub). The sound level measured at a single position at the base of the turbine can easily be 50 dB lower (Lawrence rep.).

AD.7 Definition of Infrasound

Discussion of the aerodynamic source of sound known as thickness noise or self-noise requires one to define low frequency sound and infrasound. By definition, infrasound is a pressure wave that is not audible. Nominally this means waves with frequency less than 20 Hz. It is noted though that waves with high enough amplitude below 20 Hz may still be audible. Low frequency sound is characterized as having a frequency between 20 and 200 Hz. As mentioned earlier, some mechanical noise sources contribute to the low frequency range, and clearly some of the aerodynamic sources of broadband sound will contribute to noise in the low frequency range. Thickness noise, if present, would have an associated frequency equal to the blade passing frequency. Hence, a turbine with 3-bladed rotor turning at 20 rpm might generate thickness noise at a frequency of 1 Hz, which is clearly in the infrasonic range. Downwind rotors produce slightly stronger infrasound at the blade passing frequency because the blades interact directly with the wake behind the tower. The levels of the thickness noise generated by modern upwind turbines are not perceptible by the human auditory system. Any impulsive noise that is audible, which seems to have a frequency equivalent to the blade passing frequency, is actually the broadband noise generated by the other mechanisms being modified by differences in the flow that occur on a once-per-rev basis as discussed above. The frequencies of this pulsating sound are all in the audible range, and thus this sound is not infrasound.

Appendix E

Wind Turbine – Sound Power Level Estimates and Noise Propagation

AE.1 Approximate Wind Turbine Sound Power Level Prediction Models

The following are some approximate equations that are sometimes used to estimate the A-weighted sound power level, L_{WA}, from a typical wind turbine. The first equation gives the estimate in terms of the rated power of the turbine, P_{WT} (W). The second gives the estimate in terms of the diameter, D (m). The third gives it in terms of both the tip speed, V_{Tip} (m/s), and diameter. These equations should only be used when test data is not available.

$$L_{WA} = 10(\log_{10} P_{WT}) + 50 \quad (38)$$

$$L_{WA} = 22(\log_{10} D) + 72 \quad (39)$$

$$L_{WA} = 50(\log_{10} V_{Tip}) + 10(\log_{10} D) - 4 \quad (40)$$

AE.2 Sound Power Levels due to Multiple Wind Turbines

When multiple wind turbines are located close to each other, the total sound power can be estimated by applying logarithmic relations. For example, for two turbines with sound power levels L_{W1} and L_{W2}, the total sound power is:

$$L_{total} = 10 \log_{10} (10^{L_1/10} + 10^{L_2/10}) \quad (41)$$

For N turbines, the corresponding relation is:

$$L_{total} = 10 \log_{10} \sum_{i=1}^{N} 10^{L_i/10} \quad (42)$$

where L_{wi} is the sound power level of the i^{th} turbine. For turbines that are some distance away from each other the mathematics is more complicated, and the relations of interest (actually the sound pressure level) take into account the relative position of the turbines and the location of the observer as described below.

AE.3 Noise Propagation from Wind Turbines

The sound pressure level will decrease with distance from a turbine. For estimation purposes, a simple model based on hemispherical noise propagation over a reflective surface, including air absorption, is given as:

$$L_p = L_W - 10 \log_{10}(2\pi R^2) - \alpha R \tag{43}$$

where L_p is the sound pressure level (dB) a distance R from a noise source radiating at a power level L_W (dB) and α is the frequency-dependent sound absorption coefficient. For broadband estimates the absorption coefficient is often approximated by a constant value of 0.005 dB(A)/m.

Figure AE.1 (from Materialien 63) indicates the sound pressure level as a function of distance from a single wind turbine with a sound power level of 103 dB(A).

Figure AE.1: Typical sound pressure level vs. distance from a single wind turbine (From Materialien 63)

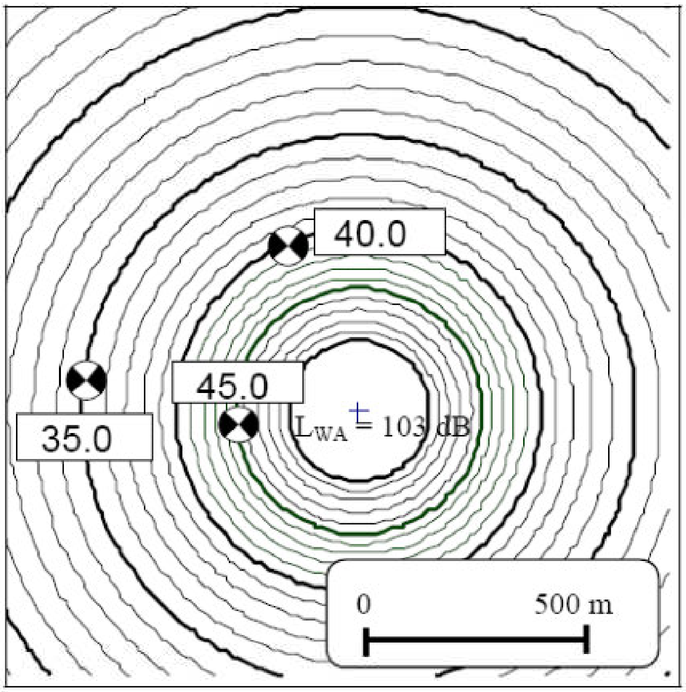

The results are summarized in Table AE-1.

Table AE-1

Sound pressure level vs. distance

Sound Pressure, dB(A)	**Distance, m**
45	280
40	410
35	620

It may be seen that Equation 43, using the broadband absorption coefficient, predicts results close to those in the table (270 m, 435 m, and 675 m respectively).

AE.4 Noise Propagation from Multiple Wind Turbines

The sound perceived at a distance from multiple wind turbines is a function of the sound power level from each wind turbine and the distance to that turbine. The perceived value can be approximated by the following equation:

$$L_p = 10\log_{10}\left[\sum_{i=1}^{N} \frac{10^{\left(L_{W,i}/10 - \alpha R_i/10\right)}}{2\pi R_i^2}\right] \qquad (44)$$

Where R_i is the distance to the ith turbine.

Figure AE-2 illustrates the sound pressure level at various distances and directions from a line of seven wind turbines, each of which is operating at a sound power level of 103 dB(A).

Figure AE.2: Sound pressure level due to a line of seven wind turbines, each operating at a sound power level of 103 dB(A) (from Materialien 63

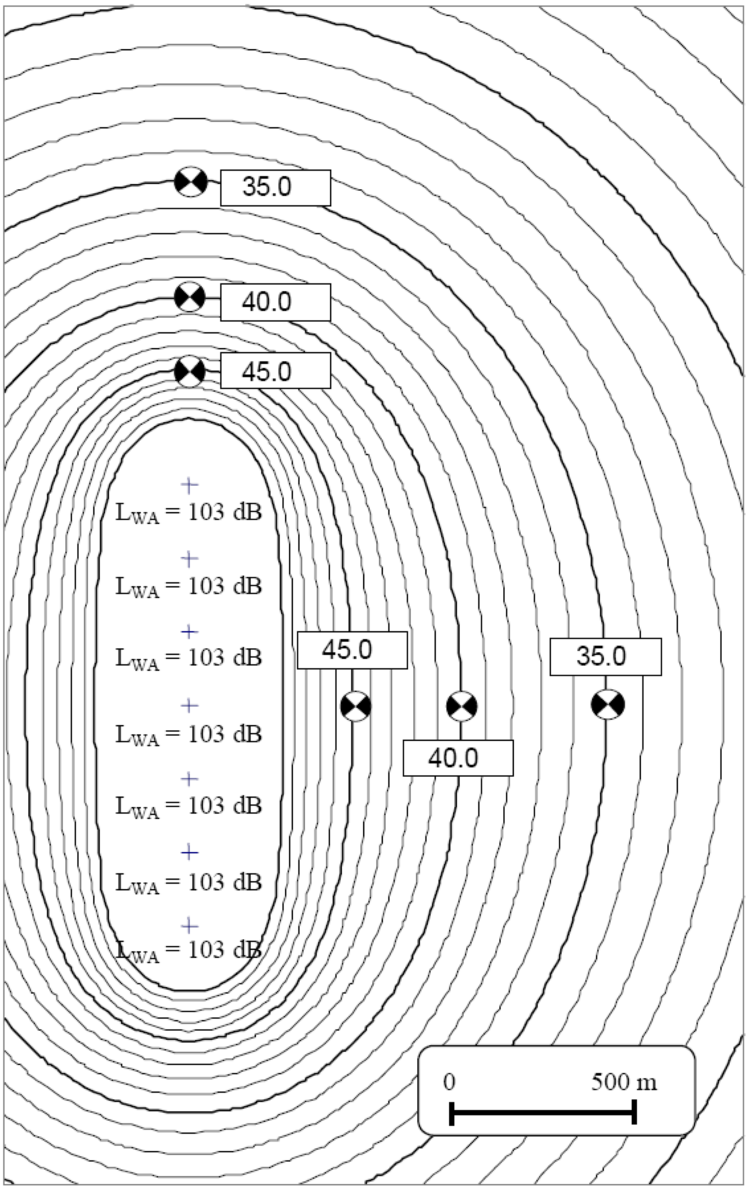

The results are summarized in the Table AE-2.

Table AE 2:

The distances shown are in the direction perpendicular to the line of the turbines

Sound Pressure, dB(A)	**Distance**
45	440
40	740
35	1100

.

Appendix F

Wind Turbine – Stall vs. Pitch Control Noise Issues

As noted in Appendix A, pitch regulated turbines are quieter than those with stall control. This is particularly the case at higher wind speeds. This appendix illustrates the difference, based on one source.

AF.1 Typical Noise from Pitch Regulated Wind Turbine

The figure below illustrates sound pressure level as a function of wind speed from a pitch regulated wind turbine (The data was taken at an unspecified distance from the turbine).

As can be seen, the noise level increases with wind speed up to a certain wind speed, here 9 m/s. After that wind speed is reached the blade pitch regulates the power and the noise level remains constant.

Figure AF.1: Sound pressure vs. wind speed from a pitch regulated wind turbine (from Materialien 63)

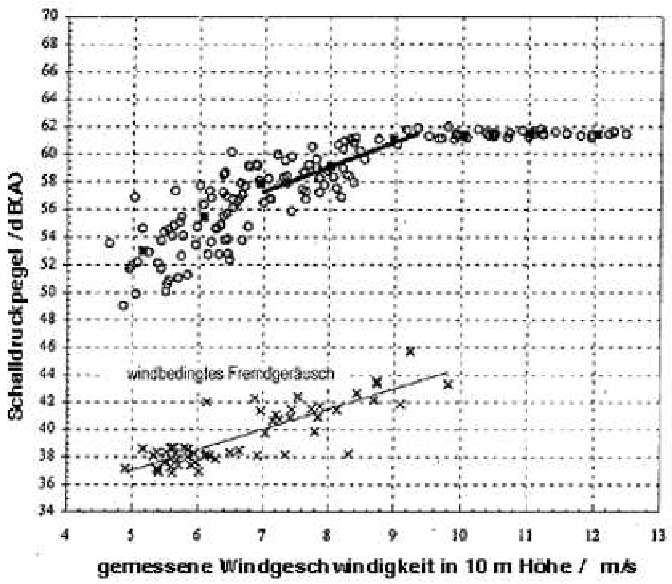

y-axis: sound pressure level, dB(A)

x- axis measured wind speed at 10 m height, m/s

lower line: wind-induced background noise

AF.2 Noise from a Stall Regulated Wind Turbine

The figure below illustrates sound pressure level as a function of wind speed from a stall controlled wind turbine (The data was taken at an unspecified distance from the turbine).

Figure AF.2: from Materialien 63

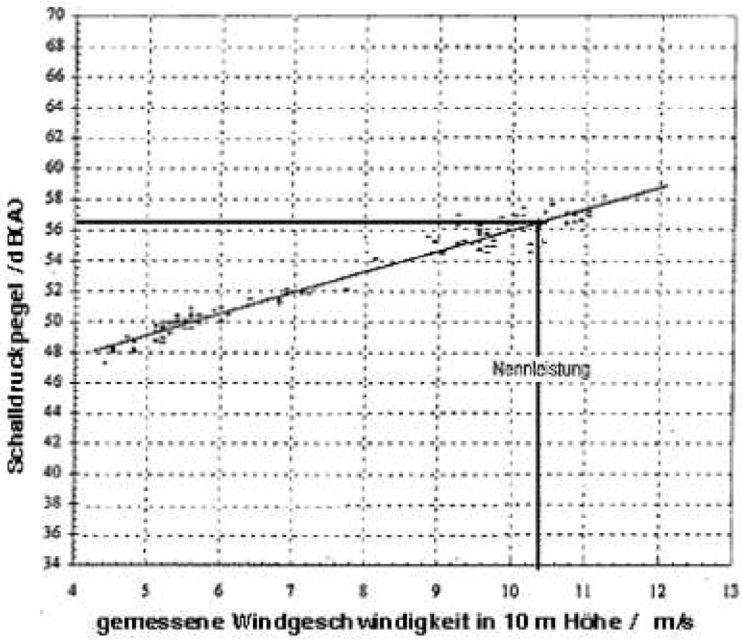

y-axis: sound pressure level, dB(A)

x- axis measured wind speed at 10 m height, m/s

The rated wind speed of this turbine is 10.4 m/s

As can be seen, the noise level increases approximately linearly with wind speed and does not level off.

Appendix G

Summary of Lab Animal Infrasound and Low Frequency Noise (IFLN) Studies

Table AG.1

Summary of Lab Animal Infrasound and Low Frequency Noise (IFLN) Studies

Study #	Animal Model	Endpoint	"Dose"	Timing	Measured Effects	Notes	Citation
1	Male Sprague-Dawley rats; 32 rat, 10 wks	Cardiac: ultrastructure observations, Ca2+, SERCA2 expression	5 Hz at 130 dB	2 hrs - 1 day	inc in [Ca2+]*l*; sig inc. SERCA2	No noted observation of frank toxicity. Responses increased across groups; heart rates increased in 1 day group, not in others; left ventricular pressures increased with dose chamber; Animal dose is at or slightly below 5 Hz/130 dB; Pentobarb anesthesia	Pei et al., 2007
			5 Hz at 130 dB	2 hrs - 7 days	inc in [Ca2+]*l*; Sig decr. In SERCA2 compared with control & 1 day		
			5 Hz at 130 dB	2 hrs - 14 days	inc in [Ca2+]*l*; Sig decin SERCA2 compared with control and 7 day group		
2	Male Adult Sprague-Dawley rats	Cardiac: whole-cell L-type Ca2+ currents (WLCC) in rat ventricular myocytes	5 Hz at 130 dB	2 hrs - 1 day; examined 1, 7 or 14 days post-exposure	Inc in [Ca2+](I) levels, LCC & SERCA2	No noted observation of frank toxicity. [Ca2+](I) levels as well as expression of LCC and SERCA2 may contribute to the infrasound exposure-elicited cardiac response; cannot concur with micrograph data	Pei et al., 2009
3	Male Sprague-Dawley rats	Neuronal release of stress-induced hormones	16 Hz at 130 dB	2 hrs - single exposure	activation of microglial cells and upregulation of Corticotrophin releasing hormone receptor (CRH R1); also upregulation expression is blocked by antalarmin	No noted observation of frank toxicity. .Measured in the hypothalamic paraventricular neurons. Antalarmin is a non-peptide drug that blocks the CRF-1 receptor, and, as a consequence, reduces the release of ACTH in response to chronic stress	Du et al., 2010
4	Male Sprague-Dawley rats	Neurogenesis	16 Hz at 130 dB	2 hrs/day - 7 days (sacrificed at 3, 6, 10, 14 & 18 days post-exposure)	Measured early migration and differentiation in newly generated progenitor cells by examining BUdR uptake in cells in the hippocampus (dentate gyrus)	No noted observation of frank toxicity. Authors conclude infrasound inhibits cell proliferation and that effects on proliferation appear to be reversible in the 18 days post exposure groupbackground - 40 dB; authors report reversibility, but the data don't support this - also, comparisons are with the "normal" group (in chamber, but no infrasound) but no comparison with control.	Liu et al., 2010
5	Male Albino Wistar Rats	Neural: Behavioral Performance - vestibular function	16 Hz at 72-105 dB		Rota-rod Treadmill evaluation	No noted observation of frank toxicity. Rats selected for superior performance were unaffected, but inferior rats were less able to perform for as long at same exposures.	Yamamura & Kishi, 1980
6	Male Wistar rats	Neurological - biochemical	2 Hz at 105 dB	1 hr & then sac'd	Measured brain neurepinephrine levels	No noted observation of frank toxicity. No control to determine whether Norepi levels were due to experimental design - not well controlled.	Spyraki et al., 1978
			7 Hz at 122 dB	1 hr & then sac'd	Measured brain neurepinephrine levels		
			26 Hz at 124 dB	1 hr & then sac'd	Measured brain neurepinephrine levels		
7	Female rats - no strain given	Neural	2 Hz at 105 dB 7 Hz at 122 dB 16 Hz at 124 dB		Observations made about rats' activity	Decreased time to sleep and decreased activity. Chamber and set-up is somewhat archaic and confirmatory measures are not made.	Spyraki et al., 1978
8	adult male Sprague-Dawley rats	Neural: hippocampus - dependent spatial learning and memory	16 Hz at 130 dB	14 days	Observations made using Morris water maze, measured expression and protein levels of brain-derived neurotrophic factor-tyrosine kinase receptor B.	No noted observation of frank toxicity. Calibration of sound chamber not discussed.	Yuan et al., 2009

References

Ambrose, S. E. & Rand R. W., (2011, December). The Bruce McPherson Infrasound and Low Frequency Noise Study: Adverse Health Effects Produced By Large Industrial Wind Turbines Confirmed. Retrieved from: http://www.wind-watch.org/-documents/bruce-mcpherson-infrasound-and-low-frequency-noise-study/

Alberts, D. (2006). Primer for Addressing Wind Turbine Noise. Retrieved from: http://www.maine.gov/doc/mfs/windpower/pubs/pdf/AddressingWindTurbineNoise.pdf. Lawerence Tech. University.

Balombin, J. R. (1980, April). An exploratory survey of noise levels associated with a 100 KW wind turbine. Proceedings from the 99th Meeting of the Acoustical Society of America. Atlanta, Georgia.

Betke K, von Glahn, M. S., Matuschek, R. (2004). Underwater noise emissions from offshore wind turbines. CFA-DAGA. Reviewed from: http://www.itap.de/daga04owea.pdf).

Betke, K., Remmer H. (1998). Messung und Bewertung von tieffrequentem Schall. Proc. DAGA.

Bolin, K., Bluhm, G., Eriksson, G., Nilsson, K. (2011). Infrasound and Low Frequency Noise from Wind Turbines: Exposure and Health Effects. Environ. Res. Lett. 6, 035103 (6pp)

Bowdler, D.; Bullmore, A.; Davis, B.; Hayes, M.; Jiggins, M.; Leventhall, G.; McKenzie, A. (March-April 2009). Prediction and assessment of wind turbine noise. *Acoustics Bulletin*, v 34, n 2, p 35-7.

Branco N, Santos J, Monteiro E, Silva A, & Ferreira J, Pereira M. (2004). The lung parenchyma in low frequency noise exposed. *Wistarrats.Rev Port Pneumol, Jan-Feb;10* (1),77–85.

Castelo, Branco NA. (1999, March). The Clinical Stages of Vibroacoustic Disease. 70 (3 Pt 2):A32-9. Aviat Space Environ Med.

Castello Branco NAA, Alves-Pereira M. (2004). Vibroacoustic Disease. *Noise Health* 6(23): 3–20.

Cattin, R., Kunz, S., Heimo, A., Russi, G., Russi, M., & Tiefgrabe, M. (2004). Wind turbine ice throw studies in the Swiss Alps. Proceedings of the European Wind Energy Conference. Milan, 2007.

Colby, David, M.D., Dobie, Robert, MD., Leventhall, Geoff, PhD., Lipscomb, David M. PhD., McCunney, Robert J., M.D., Seilo, Michael T., PhD., Sondergaard, Bo, M.Sc.. (2009, December). Wind Turbine Sound and Health Effects – An Expert Panel Review.

Concha-Barrientos, M., Campbell-Lendrum, D., & K. Steenland. (2004). Occupational noise: assessing the burden of disease from work-related hearing impairment at national and local levels (WHO Environmental Burden of Disease Series, No. 9). Geneva: World Health Organization.

Downing, S. D. & Socie, D. F. (1982). Simple rainflow counting algorithms. *International Journal of Fatigue, 4* (1), 31–40.

Du F, Yin L., Shi, M., Cheng, H., Xu, X., Liu, Z., Zhang, G., Wu, Z., Feng, G., & Zhao, G., (2010). Involvement of microglial cells in infrasonic noise-induced stress via upregulated expression of corticotrophin releasing hormone type 1 receptor.

Duffie, J. A. & Beckman, W. A., (2006) Solar Engineering of Thermal Processes, 3rd edition, John Wiley and Sons .

Eggleston, D. M. & Stoddard, F.S. (1987). Wind turbine engineering design. New York: Van Nostrand Reinhold.

Ellwood, J. M. (1998). Critical appraisal of epidemiological studies and clinical trials (Vol. 2d ed.). Oxford University Press: Oxford.

European Agency for Safety and Health at Work. (2008). Workplace exposure to vibration in Europe: an expert review. Luxembourg: Office for Official Publications of the European Communities, ISBN 978-92-9191-221-6. osha.europa.eu/en/publications/reports/8108322_vibration_exposure

EWEA (2004). Wind Energy, The Facts, Vols. 1-5. European Wind Energy Association, Brussels.

Federal Register. (2003, July). Identifying and Promoting Promising Practices. *Federal Register*, 68, No. 131. Retrieved from www.acf.hhs.gov/programs/ccf/about_ccf/gbk_pdf/pp_gbk.pdf.

Findeis, H., Peters, E. (2004). Disturbing Effects of Low Frequency Sound Immissions and Vibrations in Residential Buildings. *Noise and Health Year*. 6(23), pp. 29-35. Brandenburg State Environmental Agency, Germany.

Guerrini, R., & Genton, P. (2004). Epileptic syndromes and visually induced seizures. *Epilepsia, 45* (suppl. 1), 14-18.

Gumbel, E. J. (1958). Statistics of Extremes. New York: Columbia University Press.

Harding, G., Harding, P., & Wilkins, A. (2008). Wind turbines, flicker and photosensitive epilepsy: characterizing the flashing that may precipitate seizures and optimizing guidelines to prevent them. *Epilepsia*. *49* (6), 1095–1098.

Hinweise zur Ermittlung und Beurteilung der optischen Immissionen von Windenergieanlagen Länderausschuss. (2002). http://www.schleswigholstein.de/cae/servlet/contentblob/-613182/publicationFile/LAI_Hinweise_Schattenwurf_pdf.pdf (Advice on ascertaining and assessing the optical emissions ("shadow flicker") from wind turbines.) http://www.mst.dk/Virksomhed_og_myndighed/Stoej/Vindmoeller/Stoj_fra_vindmoller/.

Hubbard, H.H. & Shepherd, K.P. (1990) Wind Turbine Acoustics, NASA Technical Paper 3057, 1990 (microfiche in 1991).

International Electrotechnical Commission. (2002, Geneva). International Standard IEC 61400-11 Ed.2. *Wind turbine generator systems – Part 11: Acoustic noise measurement technique.*

Jakobsen, J. (2006). Infrasound emission from wind turbines. *Journal of Low Frequency Noise, Vibration and Active Control*, v 24, n 3, p 145-55.

Jonkman, J. (2005). *FAST User's Guide*, (NREL/EL-500-38230). National Renewable Energy Laboratory. Golden CO.

Jung, Cheung, J. (2008). Experimental Identification of Acoustic Emission: Characteristics of Large Wind Turbines with Empahsis on Infrasound and Low-Frequency Noise. *Korean Physical Soc*. 53, NO.4, 1897-1905.

Kawasaki, T. National Institute of Industrial Health, 6–21–1, Nagao, 214–8585, Japan.

Kelley, N. D., McKenna, H. E., Hemphill, R. R., Etter, C. L., Garrelts, R. L., & Linn, N. C. (1985). Acoustic noise associated with the MOD-1 wind turbine: its source, impact, and control. (SERI/TR-635-1166, UC Category: 60, DE85002947). Solar Energy Research Institute. Prepared for the U.S. Department of Energy, Contract No. DE-AC02-83CH-10093.

Knopper, L. D. & Ollson, C. A., Health effects and wind turbines: A review of the literature. *Environmental Health* 2011, 10:78 doi:10.1186/1476-069X-10-78.

Leventhall, G. (2006, June). Infrasound from wind turbines - fact, fiction or deception. *Canadian Acoustics*, v 34, n 2, p 29-36.

Leventhal, B (2009). Low Frequency Noise. What we know, what we do not know and what we would like to know. *Journal of Low Frequency Noise, Vibration and Active Control*, 28(2). 79-104.

Liu, J., Lin, T., Yan, X., Jiang, W., Shi, M., Ye, R., Rao, Z., & Zhao, G. (2010). Effects of infrasound on cell proliferation in the dentate gyrus of adult rats. *Neuroreport, Jun 2;21* (8), 585–9.

Manwell, J. F., McGowan, J. G., & Rogers, A. L. (2009). Wind Energy Explained: Theory, Design and Application 2nd Ed . Chichester, UK: John Wiley and Sons.

Materialien Nr. 63 Windenergieanlagen und Immissionsschutz, Landesumweltamt Nordrhein-Westfalen, Wallneyer Straße 6, 45133 Essen, Germany, 2002 (Protection from emissions from wind turbines).

Massachusetts Environmental Protection Agency (MEPA). (2007). Greenhouse Gas Emissions Policy and Protocol. Retrieved from http://www.env.state.ma.us/mepa/ghg.aspx

National Research Council (NRC). (1991). Animals as sentinels of environmental health hazards. Washington, DC: National Academy Press.

Neuroscience (2010). *May 19;167* (3), 909–19.

New England Wind Energy Project (NEWEEP). (2011, September 2). Understanding the Current Science, Regulation, Mitigation of Shadow Flicker. Webinar retrieved from http://www.windpoweringamerica.gov/filter_detail.asp?itemid=2967.

Nissenbaum, M., Aramini, J., & Hanning, C. (2011). Adverse health effects of industrial wind turbines: a preliminary report. Paper presented at the 10th International Congress on Noise as a Public Health Problem (ICBEN) London, UK.

O'Neal, R.D, Hellweg, R.D., Jr., Lampeter, R.M. (2011, March). Low frequency noise and infrasound from wind turbines. *Noise Control Engineering Journal*, v 59, n 2, p 135-57.

Palmer, W. (2011). Wind Turbine Noise - Clues to the Mystery of Why People are Hurting. *ASA 161st meeting. Paper 3aNSa2*.

Palmer, W. (2011, July). Collecting Data on Wind Turbine Sound to Identify Causes of Identified Concerns. POMA Volume 12, pp 040003; (21 pages).

Passchier-Vermeer, W. (1993). *Noise and health*. The Hague: Health Council of the Netherlands.

Pedersen, E., & Persson Waye, K. (2007). Wind turbine noise, annoyance and self-reported health and well-being in different living environments. *Occup Environ Med, 64*(7), 480–486.

Pedersen, E., van den Berg, F., Bakker, R., & Bouma, J. (2009). Response to noise from modern wind farms in The Netherlands. *Journal of the Acoustical Society of America, 126*(2), 634–643.

Pedersen, E. & Waye, K.P. (2004). Perception and annoyance due to wind turbine noise—a dose-response relationship. *Journal of the Acoustical Society of America, 116* (6), 3460–3470.

Pedersen, T. H., & Nielsen, K. S. (1994). Genvirkning af støj fra vindmøller (Annoyance by noise from wind turbines). Copenhagen: Lydtekniske Institut.

Pedersen, E., & Larsman, P. (2008). The impact of visual factors on noise annoyance among people living in the vicinity of wind turbines. *Journal of Environmental Psychology, 28*, 379–389.

Pei, Z., Sang, H., Li, R., Xiao, P., He, J., Zhuang, Z., Zhu, M., Chen, J., & Ma, H. (2007) Infrasound-induced hemodynamics, ultrastructure, and molecular changes in the rat myocardium. *Environ Toxicol*, *Apr; 22* (2), 169–75.

Pei, Z., Zhuang, Z., Xiao, P., Chen, J., Sang, H., Ren, J., Wu, Z., & Yan, G. (2009). Influence of infrasound exposure on the whole L-type calcium currents in rat ventricular myocytes. *Cardiovasc Toxicol,* Jun; *9* (2), 70–7.

Pederson, Moller. (2011) Low-Frequency Noise from Large Wind Turbines. JASA 129(6), 3727-3744.

Pederson, (2011). Health Aspects Associated with Wind Turbine Noise: Results from Three Field Studies, *Noise Control Engineering*. J. 59(1), 47-53.

Pedersen, Waye. (2004). Perception and Annoyance Due to Wind Turbine Noise – A Dose – Response Relationship, JASA 116 (6) 3460-3470.

Petounis ,A., Spyrakis, C., & Varonos, D. (1977). Effects of infrasound on activity levels of rats. *Physiol Behav,* Jan; *18* (1), 153–5.

Phipps, R. (2007). In the matter of Moturimu Wind Farm Application. Evidence to Joint Commissioners. Palmerston, North.

Pierpont, N. (2009). Wind turbine syndrome. A report on a natural experiment. Santa Fe, NM: K-selected books.

Pohl, J., Faul, F., & Mausfeld, R. (1999) Belästigung durch periodischen Schattenwurf von Windenergieanlagen - Laborpilotstudie (mit Anhang) and Feldstudie (mit Anhang), Staatliches Umweltamt Schleswig, Germany, (Annoyance due to shadow flicker from wind turbines- laboratory pilot study (with appendix) and field study (with appendix)).

Rached, T. (2008), Communicating complexity and informing decision-makers: challenges in the data and computation of environmental benefits of renewable energy. (M.Sc. Thesis in Technology and Policy), Massachusetts Institute of Technology.

Rand, M., & Clarke, A. (1990). The environmental and community impacts of wind energy in the UK. *Wind Eng, 14*, 319–330.

Rasmussen, (1983). Human Body Vibration Exposure and Its Measurement, *JASA* 73(6) 2229 (abstract), also a BandK Tech. Paper. 1982.

Rogers, A., Patient Safety and Quality: An Evidence Based Handbook for Nurses: Vol 2. Chapter 40, The effects of fatigue and sleepiness on nurse performance and patient safety. pp 2-509-2-254.

Salt, Hullar. (2010). Responses of the ear to low frequency sounds, infrasound and wind turbines . *Hearing Research* 268 12-21.

Schofield, R. Ph.D. (2010). Seismic Measurements at the Stateline Wind Project And A Prediction of the Seismic Signal that the Proposed Maiden Wind Project Would Produce at LIGO. University of Oregon. LIGO-T020104-00-Z.

Sefan Oerlemans, S. (2009). Detection of Aeroacoustic Sound Sources on Aircraft and Wind Turbines. *Thesis*, University of Twente, Enschede. ISBN 978-90-806343-9-8.

Shepherd, D., McBride, D., Welch, D., Dirks, K. N., & Hill, E. M. (2011). Evaluating the impact of wind turbine noise on health-related quality of life. *Noise Health, 13* (54), 333–339.

Shepherd, D., Welch, D., Dirks, K. N., & Mathews, R. (2010). Exploring the relationship between noise sensitivity, annoyance and health-related quality of life in a sample of adults exposed to environmental noise. *Int J Environ Res Public Health, 7* (10), 3579–3594.

Shepherd, K. P. & Hubbard, H.H. (1981, July). Sound Measurements and Observations of the MOD-OA Wind Turbine Generator NASA-CR165752. Hampton, VA : NASA Langley Research Center, 1982.

Seifert, H., Westerhellweg, A., & Kröning, J. (2003). Risk analysis of ice throw from wind turbines. Proceedings of Boreas VI, Pyhätunturi, Finland.

Sienkiewicz Z, (2007). Prog Biophys Mol Biol. *Jan-Apr; 93* (1-3), 414–20.Rapporteur report: roundup, discussion and recommendations.

Smedley, ARD., Webb, A.R. & Wilkins, A.J. (2010). Potential of wind turbines to elicit seizures under various meteorological conditions. *Epilepsia, 51* (7), 1146–1151.

Spyraki, C., Papadopoulou-Daïfoti, Z., & Petounis A. (1978). Norepinephrine levels in rat brain after infrasound exposure. *Physiol Behav.*, Sep; *21* (3), 447–8.

Stephens, D. G., Shepherd, K. P., Hubbard, H. H. & Grosveld, F. W. (2008). Guide to the evaluation of human exposure to the noise from large wind turbines. *NASA Technical Memorandum 83288*, March, 1982, Retrieved from http://ntrs.nasa.gov/archive/nasa/casi.ntrs.nasa.gov/19820016175_1982016175.pdf.

Styles, P., Stimpson, I., Dr., Toon, S., England, R., Wright, M. (2005). Microseismic and Infrasound Monitoring of low frequency noise and vibrations from windfarms – Eskdalemuir Schotland. *Keele University Report.*

Sugimoto, T., Koyama, K., Kurihara Y., Watanabe K. (2008, August). Measurement of Infrasound Generated by Wind Turbine Generator. Takanao, 20-22, University Electro-Communications. SICE Annual Conference, August 20-22, 2008. Japan.

Swinbanks, M. (2010). Wind Turbines: Low-Frequency Noise and Infrasound Revisited.. Retrieved from: http://www.knowwind.org/-webdoc/assets_library_documents_Malcolm_Swinbanks.pdf

Tandy, V., Lawrence, T., (1998, April). The Ghost in the Machine. Journal of the Society of Psychial Research, Vol 62 No 851.

Tandy, V. Something in the Cellar. *Journal of the society for Psychical Research*. Vol 64.3 No 860.

Takahashi Y., Kanada K., Yonekawa, Y. (2009). Some Characteristics of Human Body Surface Vibration Induced by Low Frequency Noise. *Journal of Low Frequency Noise, Vibration and Active Control*. National Institute of Industrial Health, 6-21-1, Nagao, Tama-ku, Kawasaki 214-8585, Japan. Pages 9 – 20.

Takahashi Y., Kanada K., Yonekawa, Y. (2001). A New Approach to Assess Low Frequency Noise in the Working Environment. *Industrial Health*, 39, 281–286.

Todd et al. (2008). Tuning and sensitivity of the human vestibular system to low-frequency vibration. *Neuroscience Letters* 444, 36-41.

van den Berg, G.P. (2004). Effects of the Wind Profile at Night on Wind Turbine Sound. *Journal of Sound and Vibration*, *277*, 955–970.

van den Berg, G.P., (2011) Private communication and transfer of data obtained near the Rheine wind farm.

van den Berg, G. P., Pedersen, E., Bouma, J., & Bakker, R. (2008). *Project* WINDFARMperception. Visual and acoustic impact of wind turbine farms on residents: *FP6-2005-Science-and-Society-20*. Specific Support Action Project no. 044628. Final report. . Retrieved from http://www.rug.nl/wewi/deWetenschapswinkels/-natuurkunde/publicaties/WFp-final-1.pdf related link: http://www.rug.nl/wewi/-deWetenschapswinkels/natuurkunde/onderzoek/WINDFARMperceptionproject/linksEerderOnderzoek?lang=en

Van Dongen et al. The Cumulative Cost of Additional Wakefulness: Dose-Response Effects on Neurobehavioral Functions and Sleep Physiology from Chronic Sleep Restriction and Total Sleep Deprivation. *Sleep* (2003) vol. 26 (2) pp. 117-26.

van Kuik, G. A. M. (2007). The Lanchester–Betz–Joukowsky Limit. *Wind Energy*, *10*, 289–291.

Vestas. Retrieved from http://re.emsd.gov.hk/english/wind/large/large_to.html.

Vindkraftsstatistik. (2010). (Wind Energy, 2010). www.energimyndigheten.se

Von Dirke, H.E., Parker, D.E. (1994, August). Differences in Otolith and Abdominal Viscera Gaviceptor Dynamics: Implications for Motion Sickness and Perceived Body Position. *Space and Environmental Medicine.* (maybe related to NASA CR-93 207267).

Von Hunerbein, S. , Kin, A., Hargreaves, J, Moorehouse, A, & Plack, C. (2010, October). Perception of noise from large wind turbines (EFP-06 Project). University of Salford, Reviewed from: http://www.windpower.org/download/942/-Perception_low_frequincy_noise.PDF

Vowles, H. P. (1932).Early Evolution of Power Engineering, *Isis*, *17* (2), 412–420.

Wagner, S., Bareib, R. & Guidati, G. (1996). *Wind Turbine Noise*. Springer, Berlin.

Watanabe T., Moeller, H. (1990). Low Frequency Hearing Thresholds in Pressure Field and in Free Field. *Low Frequency Noise Vibration and Active Control* Vol 9 number 3 106-115.

World Health Organization (WHO). (2009). *Night noise guidelines for Europe.*

Wolsink, M., Sprengers, M., Keuper, A., Pedersen, T. H., & Westra, C. A. (1993). Annoyance from wind turbine noise on sixteen sites in three countries. Paper presented at the European Community Wind Energy Conference, 8–12 March, Lübeck, Travemünde, Germany.

Yuan, H., Long, H., Liu, J., Qu,' L., Chen'' J., & Mou, X. (2009). Effects of infrasound on hippocampus-dependent learning and memory in rats and some underlying mechanisms. *Environ Tox and Pharm*, *28*, 243–247.

Yamamura, K & Kishi, R. (1980). Effects of infrasound on the rota-rod treadmill performance of rats. *Eur J Appl Physiol Occup Physiol.*, *45* (1), 81-6.

Bibliography

Alves-Pereira, M., et al. Legislation Hinders Research Into Low Frequency Noise.

Alves-Pereira, M. B., N.A.A.C. (2007). "Vibroacoustic disease: Biological effects of infrasound and low-frequency noise explained by mechanotransduction cellular signaling." Progress in Biophysics and Molecular Biology 93: 256-279.

A Bold Effort in Vermont: The 1941 Smith-Putnam wind turbine. Retrieved 9/5/11 from http://www.ieee.org/organizations/pes/public/2009/nov/peshistory.html

Bolinger, Mark (2011, January). Community Wind: Once Again Pushing the Envelope of Project Finance. Retrieved 9/10/11 from Environmental Energy Technologies Division. http://eetd.lbl.gov/EA/EMP/re-pubs.html

Bowdler, D. (2008). "Amplitude Modulation of Wind Turbine Noise: A Review of Evidence." Institute of Acoustics Bulletin 33(4): 31-41.

Bruck, D., Ball, M. Thomas, I, & Rouillard, V. (2009). "How does the pitch and pattern of a signal affect auditory arousal thresholds?" Journal of Sleep Research 18: 196-203.

Castello Branco, N.A.A.A.-P.M. (2004). "Vibroacoustic Disease." Noise and Health 6(23): 3-20.

Certificate of Public Good Issued Pursuant to 30 VSA Section 248, August 8, 2007, from Vermont Public Service Board to UPC Vermont Wind, LLC for Sheffield, VT Wind Project. Retrieved 9/4/11 from http://psb.vermont.gov/docketsandprojects/electric/-7156/ordersandmemos

Chapman, S. (2011) "Wind turbine sickness prevented by money drug." The Drum Opinion 2011. http://www.abc.net.au/unleashed/45730.html.

Chief Medical Officer of Health (CMOH) Report, O. (2010). The Potential Health Impact of Wind Turbines.

CLF Ventures, I. (2011). Land-based Wind Energy: A Guide to Understanding the Issues and Making Informed Decisions. http://www.clfventures.org/docs/wind_guide.pdf.

Colby, W. D., et al. (2009). Wind Turbine Sound and Health Effects - An Expert Panel Review.

Consulting, S. A. (2010). White Rock Wind Farm Environmental Noise Assessment, for Epuron Pty Ltd.

Council, A. N. H. a. M. R. (2010). Wind Turbines and Health - A Rapid Review of Evidence. https://majorprojects.affinitylive.com/public/985165fa5563af254cb13656534a9f8e/17Appendix%202%20-%20Noise%20Assessment%20Page%2037-48.pdf.

Council, A. N. H. a. M. R. (2010). Wind Turbines and Health Public Statement. A. N. H. a. M. R. Council.

Council, K. E. (2005). Wind Energy Siting Handbook: Guideline Options for Kansas Cities and Counties.

Council, N. R. (2007). Environmental Impacts of Wind-Energy Projects. http://www.nap.edu/catalog.php?record_id=11935.

Cummings, J. (2011). Wind Farm Noise 2011 - Science and Policy Overview.

Curthoys, I. S., Kim, J., McPhedran, S.K., & Camp, A.J. (2006). "Bone conducted vibration selectively activates irregular primary otolithic vestibular neurons in the guinea pig." Experimental Brain Research **175**(2): 256-267.

Danish Government, The (2011, February). Energy Strategy 2050: from coal, oil, and gas to green energy. Page 5. Retrieved 9/11/11 from http://ens.netboghandel.dk/publikationer/publikationsdetaljer.-aspx?PId=2cde3fff-a1f2-4539-b945-9e896fffc670

Danish Energy Agency. Retrieved 8/29/11 from http://www.ens.dk/en-US/supply/Renewableenergy/WindPower/Sider-/Forside.aspx.

Danish Energy Agency (2009). Wind Turbines in Denmark. Retrieved 8/28/11 from http://www.ens.dk/en-US/-supply/Renewable-energy/WindPower/Sider/Forside.aspx.

Danish Ministry of Interior and Health. Retrieved 8/29/11 from http://www.sum.dk/English.aspx.

Danish Ministry of the Environment. Retrieved 8/29/11 from http://www.mst.dk

Danish Ministry of the Environment, Environmental Protection Agency. Retrieved 8/29/11 from http://www.mst.dk/English/Focus_areas/FAQ_low_frequency_noise_from_wind_turbines.htm

de Quervain, D. J. F., Roosendaal, B., & McGaugh, J.L. (1998). "Stress and glucocorticoids impair retrieval of long-term spatial memory." Nature **394**: 787-790.

Donald, M. (2011). Presentation to the Falmouth Board of Selectmen - Falmouth Wind Turbine Shadow Flicker and Safety.

Energy, U. S. D. o. (2008). Workshop Report: Research Needs for Wind Resource Characterization.

Energy in Sweden. Facts and Figures 2010, Page 7. Retrieved 8/30/11 from http://www.energimyndigheten.se/en/Press/News/New-publication-Energy-in-Sweden-2010/

Environment, C. f. H. t. G. (2011). Mining Coal, Mounting Costs: the life cycle consequences of coal, Harvard Medical School - Center of Health and the Global Environment.

Environmentally Hazardous Activities and Public Health. (1998) Ordinance. 40.1 – 40.6, updated 2002

Feldmann, J. P., F. (2004). "Effects of low frequency noise on man - a case study." Noise and Health **7**(25): 23-24.

Fisk, Andy. Former Maine DEP Bureau Director. Fall of 2010. Personal email communication.

Fox Islands Wind Project Background. Retrieved 9/10/11 from http://www.foxislandswind.com/background.html

Fox Islands Wind Neighbors website. Retrieved 9/10/11 from http://fiwn.wordpress.com/category/vinalhaven/

Global Wind Energy Council. Retrieved 8/30/11 from http://www.gwec.net/index.php?id=121

Haggerty, F. D., J. (n.d.). "Commercial Land Wind Turbine Siting in Southeastern Massachusetts." from http://www.mass.gov/Eoeea/docs/doer/renewables/-wind/Public%20Comments_Wind%20On%20State%20Owned%20Lands_Listening%20Session%201_Frank%20Haggerty%20%20Joe%20DeLeo.pdf.

Halmstad University, Halmstad, Sweden. Retrieved 9/11/11 from http://www.ncbi.nlm.nih.gov/pubmed?term=pedersen%20wind%20turbines&itool=QuerySuggestion

Hanning Dr., Christopher (2009, June). "Sleep disturbance and wind turbine noise: on behalf of Stop Swinford Wind Farm Action Group.

Harding, G., Harding, P. & Wilkins, A. (2008). "Wind turbines, flicker, and photosensitive epilepsy: Characterizing the flashing that may precipitate seizures and optimizing guidelines to prevent them." Epilepsia **49**(6): 1095-1098.

Harrison, J. (2010). "The Global Wind Industry and Adverse Health Effects: Loss of Social Justice?" International Symposium on Adverse Health Effects from Wind Turbines, Picton, Ontario, Canada.

HGC Engineering. (2010, December). "Low Frequency Noise and Infrasound Associated with Wind Turbine Generator Systems". Ontario Ministry of the Environment, RFP No. OSS-078696

Hiskes, J. (2009) "One doctor's quest to sound the alarm on wind turbine syndrome." Grist. http://www.grist.org/article/2009-11-16-nina-pierpont-quest-to-sound-the-alarm-on-wind-turbine-syndrome.

Ising, H., W Babisch, B. Kruppa (1999). "Noise induced Endocrine Effects and Cardiovascular Risks". Federal Environmental Agency, Inst. Of Water, Soil and Air Hygiene, Berlin. Noise Health 1 (4): 37 – 48.

Ising H., Braun, C. (2000). "Acute and chronic endocrine effects of noise": Review of the research conducted at the Inst. For Water, Soil and Air Hygiene. Noise Health 2(7) 7 – 24.

Jakobsen, J. (2005). "Infrasound Emission from Wind Turbines." Journal of Low Frequency Noise, Vibration and Active Control 24(3): 145-155. http://www.amherstislandwindinfo.com/jakobsen-low-frequency-noise.pdf.

Jakobsen , J., Chief Advisor, Danish Ministry of the Environment. Personal email communication.

Kansas, E. C. (2005). Wind Energy Siting Handbook: Guideline Options for Kansas Cities and Counties.

Kartor over riksintresseomraden (Map over national interests). Retrieved from 9/4/11 http://www.energimyndigheten.se/sv/Om-oss/Var-verksamhet/Framjande-av-vindkraft1/Riksintresse-vindbruk-/Kartor-over-riksintresseomraden/ Translated through Google Translate

Keith, S. E., D. S. Michaud, & S. H. P. Bly. (2008). "A proposal for evaluating the potential health effects of wind turbine noise for projects under the Canadian Environmental Assessment Act.." Journal of Low Frequency Noise, Vibration and Active Control 27 (4):253-265.

Kjellberg, A., Tesarz, M., Holmberg, K., & Landstrom U. (1997). "Evaluation of Frequency-Weighted Sound Level Measurements for Prediction of Low-Frequency Noise Annoyance." Environment International **23**(4): 519-527.

Kollman, J. (2010). Potential Health Impacts of Wind Turbines.

Leventhall, G., Pelmear, P., & Benton, S. (2003). A Review of Published Research on Low Frequency Noise and its Effects:Report for DEFRA.

Leventhall, G. (2004). "Low Frequency Noise and Annoyance." Noise and Health **6**(23): 59-72.

Leventhall, G., Benton, S, & Robertson, D. (2005). Coping Strategies for Low Frequency Noise, Department for Environment, Food and Rural Affairs, U.K.

Leventhall, G. (2006). "Infrasound from Wind Turbines - Fact, Fiction, or Deception." Canadian Acoustics **34**(2): 29-36.

Leventhall, G. (2009). "Low Frequency Noise. What we know, what do not know, and what we would like to know". Journal of Low Frequency Noise, Vibration and Active Control 28(2): 79-104.

Lundberg, U. (1999). "Coping with stress; Neuroendocrine Reactions and Implications for Health". Department of Psychology, Stockholm. Noise Health 1 (4); 67 – 74

Maine Board of Environmental Protection (2011, July 7) hearing AR-69, Testimony of Steve Bennett. Retrieved 9/10/11 from http://www.maine.gov/dep/ftp/bep/ch375citizen_petition/pre-hearing/

Maine DEP Mars Hill Mountain Wind Turbine Farm Webpage. Retrieved 9/10/11 from http://www.maine.gov/dep/blwq/docstand/sitelaw/Selected%20developments/-Mars_Hill/index.htm

MRSA (Maine Revised Statute Annotated), Title 35-A, Chapter 34, Section 3401 – 3458. Retrieved 9/10/11 from http://www.mainelegislature.org/legis/statutes/35-A/title35-Asec3401.html

MRSA, Title 38, Chapter 3-A, Section 577. Retrieved 9/10/11 from http://www.mainelegislature.org/legis/statutes/38/title38sec577.html

Massachusetts, R. E. R. L.-U. o. Wind Power in Mattapoisett, Marion and Rochester: Siting Considerations for a Met Tower and Fatal Flaws Analysis for a Wind Turbine.

Massachusetts Department of Environmental Protection, Energy and the Evironment, Public Comment Received and Information Submitted: http://www.mass.gov/dep/energy/wind/comments.htm

Melamed, S., & Bruhis, S. (1996). "The Effects of Chronic Industrial Noise Exposure on Urinary Cortisol, fatigue, and irritability: A controlled Field Experiment." Journal of Occupational and Environmental Medicine 38(3): 252-256.

Michaud , D.; S.H.P. Bly, & S.E. Keith. (2008). "Using a change in percentage highly annoyed with noise as a potential health effect measure for projects under the Canadian Environmental Assessment Act." Canadian Acoustics 36(2): 13-28.

Minnesota, D. o. H.-E. H. D. (2009). Public Health Impacts of Wind Turbines.

Moller, H. P., C.S. (2011). "Low-frequency noise from large wind turbines." Acoustical Society of America **129**(6): 3727-3744. http://www.macvspc.info/M%C3%B8ller_Pedersen_2011.pdf.

Moorhouse, A., Waddington, D. & Adams, M. (2005). Procedure for the assessment of low frequency noise complaints, Acoustic Research Centre, Salford University.

O'Donnell, D., Silva, E., Munch, M., Ronda, J.M., Wang, W., & Duffy, J.F. (2009). "Comparison of subjective and objective assessments of sleep in health older subjects without sleep complaints." Journal of Sleep Research **18**: 254-263.

OLR Research Report for the State of Connecticut (2011 February). Standards in Other States for Siting Wind Projects, Retrieved 9/4/11 from http://www.cga.ct.gov/2011/rpt/2011-R-0023.htm

Ontario, M. o. t. E. (2009). Development of Noise Setbacks for Wind Farms - Requirements for Compliance with MOE Noise Limits.

Otolaryngology Department, W. U. o. S. L. (n.d.). "Wind Turbine Sound Measurements." Retrieved June 28, 2011, from http://oto2.wustl.edu/cochlea/wt4.html.

Pedersen, E. W., K.P. (2004). "Perceptions and annoyance due to wind turbine noise - a dose-response relationship." Journal of the Acoustical Society of America 116(6): 3460-3470.

Pedersen E, Larsman P. (2008) “The impact of visual factors on noise annoyance among people living in the vicinity of wind turbines.” Journal of Environmental Psychology 28(4):379-389.

Pedersen E (2007) “Human response to wind turbine noise.” The Sahlgrenska Academy, Goteborg Univ, Goteborg. Retrieved from https://guoa.ub.gu.se/dspace/bitstream/2077/4431/1/Pedersen_avhandling.pdf

Persson R. M. Albin, J.Ardö, J. Björk, & K. Jakobsson. (2007). ” Trait anxiety and modeled exposure determinants of self reported annoyance to sound, air pollution and other environmental factors in the home.” International Archives of Occupational and Environmental Health 18: 179-19

Phillips, C. V. (2010). Analysis of the Epidemiology and Related Evidence on the Health Effects of Wind Turbines on Local Residents, Windaction.org. http://www.windaction.org/documents/28175?theme=print.

Phillips, C. V. (2011). "Properly Interpreting the Epidemiologic Evidence about the Health Effects of Industrial Wind Turbines on Nearby Residents." *Bulletin of Science, Technology, and Society* **31**(4): 303-315.

Punch, J., James, R. & Pabst, D. (2010). Wind Turbine Noise: What Audiologists Should Know, Audiology Today. Jul/Aug. 2010. http://www.windturbinesyndrome.com/img/WindTurbineNoise.pdf.

Roberts, M., & Roberts, J. (2009). Evaluation of the Scientific Literature on the Health Effects Associated with Wind Turbines and Low Frequency Sound.

Salt, A. N. (2010). Infrasound: Your Ears "Hear" it but They Don't Tell Your Brain. Symposium on Adverse Health Effects of Industrial Wind Turbines.

Salt, A. N., & Hullar, T.E. (2010). "Responses of the ear to low frequency sounds, infrasound and wind turbines." *Hearing Research* 268: 12-21.

Salt, A. N. K., J.A. (2011). "Infrasound From Wind Turbines Could Affect Humans." *Bulletin of Science, Technology, and Society* 31(4): 296-302.

Schienle, A., Stark, R. & Vaitl, D. (1998). "Biological Effects of Very Low Frequency (VLF) Atmospherics in Humans: A Review." *Journal of Scientific Exploration* 12(3): 455-468.

Sciences, N. A. o. (2007). Environmental Impacts of Wind-Energy Projects. http://www.nap.edu/catalog.php?record_id=11935.

Shaw, W. J., Lundquist, J.K., & Schreck, S.J. (2009). Research Needs for Wind Resource Characterization. American Meteorology Society.

Slutrapport MPD Samordningsproj uppdaterad 0911031. (2009, April). Page 73. Retrieved 8/30/11 from http://www.vindlov.se/sv/. Translated through Google Translate

Spreng, M. (2000). "Possible health effects of noise induced cortisol increase". Department of Physiology, University Erlangen, Germany. *Noise Health* 2(7); 59 – 64

State of Maine. Governor's Office of Energy Independence and Security. Comprehensive State Energy Plan 2008 – 2009. Page 2 – 3. Retrieved 9/11/11 from http://www.maine.gov/oeis/

State of Maine. Governor's Task Force on Wind Power. Retrieved 9/4/11 from http://www.maine.gov/doc/mfs/windpower/

Stelling, K. (2009). Summary of Recent Research on Adverse Health Effects of Wind Turbines.

Swedish Energy Agency. (2009). The Electricity Certificate System. Retrieved 8/30/11 from http://www.energimyndigheten.se/en/International/Instruments/The-electricity-certificate-system/

Swedish Environmental Protection Agency. (1999). The Environmental Code. Retrieved 8/30/11 from http://www.naturvardsverket.se/en/In-English/Start/Legislation-and-other-policy-instruments/The-Environmental-Code/

Swedish Ministry of the Environment and Ministry of Enterprise, Energy, and Communication. (2009, July). An eco-efficient future: an overview of Swedish climate and energy policy. Retrieved 9/11/11 from http://www.sweden.gov.se/sb/d/574/a/129935

Swedish Wind Power Permitting (Vindlov Allt Om Tillstand) Retrieved from 8/30/11 http://www.vindlov.se/sv/ Translated through Google translate

Takahashi, Y., et al. (2005). "A Study of the Relationship between Subjective Unpleasantness and Body Surface Vibrations Induced by High-level Low-frequency Pure Tones." *Industrial Health* 43: 580-587.

Todd, N. P. M., Rosengren, S.M., & Colebatch, J.G. (2008). "Tuning and Sensitivity of the human vestibular system to low-frequency vibration." *Neuroscience Letters* 444: 36-41.

Town of Bethany, N. Y. (2005). "Report from the Bethany Wind Turbine Study Committee." from http://docs.wind-watch.org/bethany-windturbinestudycommittteereport.pdf.

Van den Berg, G. P. (2004). Do Wind Turbines Produce Significant Low Frequency Sound Levels? Low Frequency Noise and Vibration and its Control. Maastricht Netherlands. 11th International Meeting.

Van den Berg, G. P. (2005). "The Beat is Getting Stronger: The Effect of Atmospheric Stability on Low Frequency Modulated Sound of Wind Turbines." *Journal of Low Frequency Noise*, Vibration and Active Control 24(1): 1-24. http://www.stephanion.gr/aiolika/The_effect_of_atmospheric_stabilty.pdf.

Vermont Comprehensive Energy Plan, (2009). Page III-61. Retrieved 9/4/11 from http://publicservice.vermont.gov/pub/state-plans.html

Vermont Comprehensive Energy Plan Website. Retrieved 9/11/11 from http://www.vtenergyplan.vermont.gov/

Vermont Comprehensive Energy Plan,Draft 2011. Page III 52 – 53. Retrieved 9/4/11 from http://www.vtenergyplan.vermont.gov/

Vermont Department of Health. (2010, October 15) Potential Impact on the Public's Health from Sound Associated with Wind Turbine Facilities. Page 2.

Vermont Small-Scale Wind Energy Program. Retrieved 9/5/11 from. http://www.vtwindprogram.org/

Vermont Statute Title 30, Section 248. Powers and Duties of Vermont Public Service. Retrieved 9/4/11 from http://www.leg.state.vt.us/statutes/fullsection.cfm?Title=30&-Chapter=005&Section=00248

Vermont Wind Project Orders and Memoranda. Retrieved 9/4/11 from http://psb.vermont.gov/docketsandprojects/electric/7156/ordersandmemos.

Vindkraftsstatistik 2010. (Wind Energy, 2010). Page 15. Retrieved 9/4/11 from www.energimyndigheten.se Translated through Google Translate.

Vindkraftsstatistik 2010. (Wind Energy, 2010). Page 7. Retrieved 9/4/11 from www.energimyndigheten.se Translated through Google Translate.

Waye, K. P., et al. (2002). "Low Frequency Noise Enhances Cortisol Among Noise Sensitive Subjects During Work Performance." *Life Sciences* 70: 745-758.

Waye, K. P., & Ohrstrom, E. (2002). "Psycho-acoustic characters of relevance for annoyance of wind turbine noise." *Journal of Sound and Vibration* 250(1): 65-73.

Waye KP, Clow A, Edwards S, Hucklebridge F, Rylander R. (2003) "Effects of nighttime low frequency noise on the cortisol response to awakening and subjective sleep quality." *Life Sciences* _72(8):863-75.

Windfarms, C. (2011). "Wind Turbine Accidents." Retrieved July 25, 2011, from http://www.caithnesswindfarms.co.uk/fullaccidents.pdf.

wind-watch.org. (2009). "European Setbacks (minimum distance between wind turbines and habitations)." Retrieved July 1, 2011, from http://www.wind-watch.org/documents/european-setbacks-minimum-distance-between-wind-turbines-and-habitations/

Wind Power Projects in Maine. Retrieved 9/10/11 from http://www.nrcm.org/maine_wind_projects.asp.

The Panel would like to thank The UMass Donahue Institute for their logistical support.

The views and opinions expressed in this report are solely those of the original authors, the expert panelists whose research focused on the topic of the potential health impacts associated with wind turbines. These views and opinions do not necessarily represent the views and opinions of the University of Massachusetts or the UMass Donahue Institute.

Idaho Power/1206
Witness: Dr. Jeffrey Ellenbogen

BEFORE THE PUBLIC UTILITY COMMISSION
OF OREGON

Docket PCN 5

In the Matter of

IDAHO POWER COMPANY'S
PETITION FOR CERTIFICATE OF PUBLIC CONVENIENCE
AND NECESSITY

Vér, I. L. & Beranek, L. L., Noise and Vibration Control Engineering:
Principles and Applications (2006)

February 22, 2023

NOISE AND VIBRATION CONTROL ENGINEERING

PRINCIPLES AND APPLICATIONS

SECOND EDITION

ISTVÁN L. VÉR
LEO L. BERANEK

Idaho Power/1206
Ellenbogen/2

NOISE AND VIBRATION CONTROL ENGINEERING

PRINCIPLES AND APPLICATIONS

SECOND EDITION

Edited by

István L. Vér
and
Leo L. Beranek

WILEY
JOHN WILEY & SONS, INC.

This book is printed on acid-free paper. ♾

Published by John Wiley & Sons, Inc., Hoboken, New Jersey.
Published simultaneously in Canada.

Library of Congress Cataloging-in-Publication Data:

Noise and vibration control engineering : principles and applications / edited by Istvan L. Ver.—2nd ed.
p. cm.
Includes bibliographical references and index.
ISBN-13 978-0-471-44942-3
ISBN-10 0-471-44942-3
1. Noise control. 2. Vibration. 3. Soundproofing. I. Vér, I. L. (István L.), 1934–
TD892.N6512 2005
620.2′3—dc22

2005001372

Printed in the United States of America.

10 9 8 7 6 5 4 3 2 1

CONTENTS

PREFACE

The aim of this edition continues to be the presentation of the latest information on the most frequently encountered noise and vibration problems. We have endeavored to introduce new chapters and to update those chapters where the field has advanced. New or fully rewritten chapters are Sound Generation, Noise Control in Heating, Ventilating, and Air Conditioning Systems, Active Control of Noise and Vibration, Sound-Absorbing Materials and Sound Absorbers, Outdoor Sound Propagation, Criteria for Noise in Buildings and Communities, and Acoustical Standards for Noise and Vibration Control. Substantial new information has been added to Passive Silencers. All other chapters have been reviewed for timeliness.

Worldwide, there has been increased interest in noise and vibration control. Much of this interest has been generated by the expanding activities in the countries of the European Union and the Far East. Workshops on the latest developments in global noise policy are being held annually—the latest in Prague (Czech Republic) in 2004 and in Rio de Janeiro (Brazil) in 2005. There are signs of expanded interest in noise policy in the United States. Consumers are demanding quiet to a greater degree, the best example being the improved quiet interiors of automobiles. Other consumer products with greater noise control are already following or are likely to follow. Manufacturers must be alert to the increased competitiveness of imported products.

We are particularly indebted to John Bradley, Richard D. Godfrey, Colin H. Hanson, William W. Lang, George C. Mailing, Jr., Howie Noble, Robert Preuss, and Paul Schomer, who rendered help and criticism during the preparation of this book, and to the many individuals and organizations who gave us permission to use copyrighted technical information. We are also indebted to Acentech, Inc., BBN Technologies, Inc., Mueller-BBM Corporation and Harris Miller, Miller & Hanson, Inc., for encouraging members of their senior technical staff to contribute chapters and for assistance in many ways. It gives us special pleasure to acknowledge the help of Kathy Coleman and Jane Schultz, who assisted in the preparation of many chapters, and to Robert L. Argentieri, Fred Bernardi, and Robert H. Hilbert our editors at John Wiley & Sons, for their effective help and guidance in the production of this book.

István L. Vér
Leo L. Beranek

January 2005

CONTRIBUTORS

Grant S. Anderson, Harris Miller, Miller & Hanson Inc. Burlington, Massachusetts

Keith Attenborough, University of Hull, Hull, United Kingdom

James D. Barnes, Acentech, Inc., Cambridge, Massachusetts

H. D. Baumann, Consultant, Rye, New Hampshire

Leo L. Beranek, Consultant, Cambridge, Massachusetts

John Bradley, National Research Council of Canada, Ottawa, Canada

Angelo Campanella, Consultant, Columbus, Ohio

Ronald Coleman, BBN Systems and Technologies Corporation Cambridge, Massachusetts

W. B. Coney, BBN Systems and Technologies Corporation Cambridge, Massachusetts

Alan T. Fry, Consultant, Colchester, Essex, United Kingdom

Anthony G. Galaitsis, BBN Systems and Technologies Corporation, Cambridge, Massachusetts

Murray Hodgson, University of British Columbia, Vancouver, Canada

Ulrich J. Kurze, Mueller-BBM GmbH, Planegg near Munich, Germany

William W. Lang, Consultant, Poughkeepsie, New York

George C. Maling Jr., Consultant, Harpswell, Maine

M. L. Munjal, Indian Institute of Science, Bangalore, India

Donald J. Nefske, Vehicle Research Laboratory, General Motors R&D Center, Warren, Michigan

Charlers W. Nixon, Consultant, Kettering, Ohio, USA

Matthew A. Nobile, Consultant, IBM Hudson Valley Acoustics Laboratory, Poughkeepsie, New York

Allan G. Piersol, Piersol Engineering Company, Woodland Hills, California

Paul J. Remington, BBN Technologies Corporation, Cambridge, Massachusetts

Paul Schomer, Consultant, Champaign, Illinois

Shung H. Sung, Vehicle Development Research Laboratory, General Motors R&D Center, Warren, Michigan

Susanne D. Smith, Air Force Research Laboratory, Wright-Patterson Air Force Base, Ohio

Douglas H. Sturz, Acentech, Inc., Cambridge, Massachusetts

Jiry Tichy, The Pennsylvania State University, University Park, Pennsylvania

Eric E. Ungar, Acentech, Inc., Cambridge Massachusetts

István L. Vér, Consultant in Acoustics, Noise, and Vibration Control, Stow, Massachusetts

Henning E. von Gierke, Consultant, Yellow Spring, Ohio

Laura Ann Wilber, Consultant, Wilmette, Illinois

Eric W. Wood, Acentech, Inc., Cambridge, Massachusetts

Jeffrey A. Zapfe, Acentech, Inc., Cambridge, Massachusetts

CHAPTER 1

Basic Acoustical Quantities: Levels and Decibels

LEO L. BERANEK

Consultant
Cambridge, Massachusetts

1.1 BASIC QUANTITIES OF SOUND WAVES

Sound Waves and Noise

In the broadest sense, a *sound wave* is any disturbance that is propagated in an elastic medium, which may be a gas, a liquid, or a solid. Ultrasonic, sonic, and infrasonic waves are included in this definition. Most of this text deals with sonic waves, those sound waves that can be perceived by the hearing sense of a human being. *Noise* is defined as any perceived sound that is objectionable to a human being. The concepts basic to this chapter can be found in references 1–7. Portions are further expanded in Chapter 2.

Sound Pressure

A person who is not deaf perceives as sound any vibration of the eardrum in the audible frequency range that results from an incremental variation in air pressure at the ear. A variation in pressure above and below atmospheric pressure is called *sound pressure*, in units of pascals (Pa).* A young person with normal hearing can perceive sound in the frequency range of roughly 15 Hz (hertz) to 16,000 Hz, defined as the normal audible frequency range.

Because the hearing mechanism responds to sound pressure, it is one of two quantities that is usually measured in engineering acoustics. The normal ear is most sensitive at frequencies between 3000 and 6000 Hz, and a young person can detect pressures as low as about 20 μPa, which, when compared to the normal atmospheric pressure (101.3×10^3 Pa) around which it varies, is a fractional variation of 2×10^{-10}.

*One pascal (Pa) = 1 newton/meter squared (N/m^2) = 10 dynes/cm^2

Pure Tone

A pure tone is a sound wave that can be represented by the equation,

$$p(t) = p_0 \sin(2\pi f)t \tag{1.1}$$

where $p(t)$ is the instantaneous, incremental, sound pressure (above and below atmospheric pressure), p_0 is the maximum amplitude of the instantaneous sound pressure, and f is the frequency, that is, the number of cycles per second, expressed in hertz. The time t is in seconds.

Period

A full cycle occurs when t varies from zero to $1/f$. The $1/f$ quantity is known as the period T. For example, the period T of a 500-Hz wave is 0.002 sec.

Root-Mean-Square Amplitude

If we wish to determine the mean value of a full cycle of the sine wave of Eq. (1.1.) (or any number of full cycles), it will be zero because the positive part equals the negative part. Thus, the mean value is not a useful measure. We must look for a measure that permits the effects of the rarefactions to be added to (rather than subtracted from) the effects of the compressions.

One such measure is the root-mean-square (rms) sound pressure p_{rms}. It is obtained, first, by squaring the value of the sound pressure disturbance $p(t)$ at each instant of time. Next the squared values are added and averaged over one or more periods. The rms sound pressure is the square root of this time average. The rms value is also called the *effective value*. Thus

$$p_{\text{rms}}^2 = \tfrac{1}{2} p_0^2 \tag{1.2}$$

or

$$p_{\text{rms}} = 0.707 p_0 \tag{1.3}$$

In the case of nonperiodic sound pressures, the integration interval should be long enough to make the rms value obtained essentially independent of small changes in the length of the interval.

Sound Spectra

A sound wave may be comprised of a pure tone (single frequency, e.g., 1000 Hz), a combination of single frequencies harmonically related, or a combination of single frequencies not harmonically related, either finite or infinite in number. A combination of a finite number of tones is said to have a *line spectrum.* A combination of an infinite (large) number of tones has a *continuous spectrum.* A continuous-spectrum noise for which the amplitudes versus time occur with a

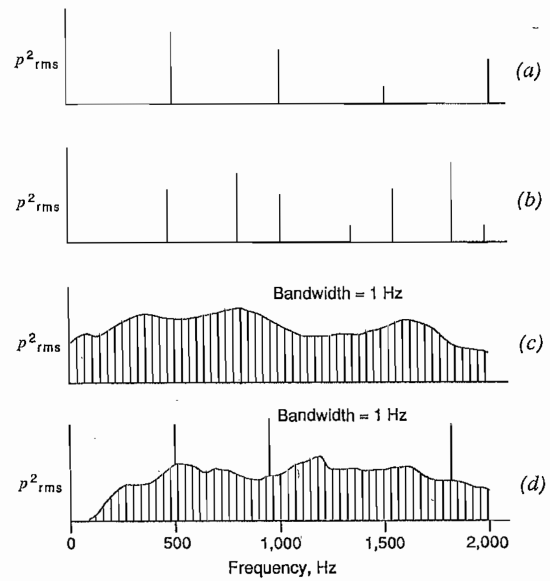

FIGURE 1.1 Mean-square sound pressure spectra: (*a*) harmonically related line spectrum; (*b*) inharmonically related line spectrum; (*c*) continuous power spectral density spectrum; (*d*) combination line and continuous power spectral density spectrum (complex spectrum).

normal (Gaussian) distribution is called *random noise*. Three of these types of noise are shown by the frequency spectra in Figs. 1.1*a–c*. A combination of a line and a continuous spectrum, called a complex spectrum, is shown in Fig. 1.1*d*.

Regardless of which type of sound wave is considered, when propagating at normal sound pressure amplitudes (to avoid nonlinearity) in air over reasonably short distances (so that sound attenuation in the air itself, which becomes significant at frequencies above 1000 Hz, can be neglected), the waveform is unchanged. Thus, a violin heard at a distance of 30 m sounds the same as at 5 m, although it is less loud.

Sound Intensity

The second quantity commonly measured in engineering acoustics is *sound intensity*, defined as the continuous flow of power carried by a sound wave through an incrementally small area at a point in space. The units are watts per square meter (W/m^2). This quantity is important for two reasons. First, at a point in free space, it is related to the total power radiated into the air by a sound source and, second, it bears at that point a fixed relation to the sound pressure.

Sound intensity at a point is directional (a vector) in the sense that the position of the plane of the incrementally small area can vary from being perpendicular to the direction in which the wave is traveling to being parallel to that direction. It has its maximum value, I_{max}, when its plane is perpendicular to the direction of travel. When parallel, the sound intensity is zero. In between, the component of I_{max} varies as the cosine of the angle formed by the direction of travel and a line perpendicular to the incremental area.

Another equation, which we shall develop in the next chapter, relates sound pressure to sound intensity. In an environment in which there are no reflecting surfaces, the sound pressure *at any point in any type of freely traveling* (plane, cylindrical, spherical, etc.) wave is related to the maximum intensity I_{max} by

$$p_{rms}^2 = I_{max} \cdot \rho c \quad \text{Pa}^2 \tag{1.4}$$

where p_{rms} = rms sound pressure, Pa (N/m^2)
ρ = density of air, kg/m^3
c = speed of sound in air, m/s [see Eq. (1.7)]
N = force, N

Sound Power

A sound source radiates a measurable amount of power into the surrounding air, called *sound power*, in watts. If the source is nondirectional, it is said to be a *spherical sound source* (see Fig. 1.2). For such a sound source the measured (maximum) sound intensities at all points on an imaginary spherical surface centered on the acoustic center of the source are equal. Mathematically,

$$W_s = (4\pi r^2) I_s(r) \quad \text{W} \tag{1.5}$$

where $I_s(r)$ = maximum sound intensity at radius r at surface of an imaginary sphere surrounding source, W/m^2
W_s = total sound power radiated by source in watts, W (N · m/s)
r = distance from acoustical center of source to surface of imaginary sphere, m

A similar statement can be made about a line source; that is, the maximum sound intensities at all points on an imaginary cylindrical surface around a *cylindrical sound source*, $I_c(r)$, are equal:

$$W_c = (2\pi r l) I_c(r) \quad \text{W} \tag{1.6}$$

where W_c = total sound power radiated by cylinder of length l, W
r = distance from acoustical centerline of cylindrical source to imaginary cylindrical surface surrounding source

Inverse Square Law

With a spherical source, the radiated sound wave is spherical and the total power radiated in all directions is W. The sound intensity $I(r)$ must decrease with

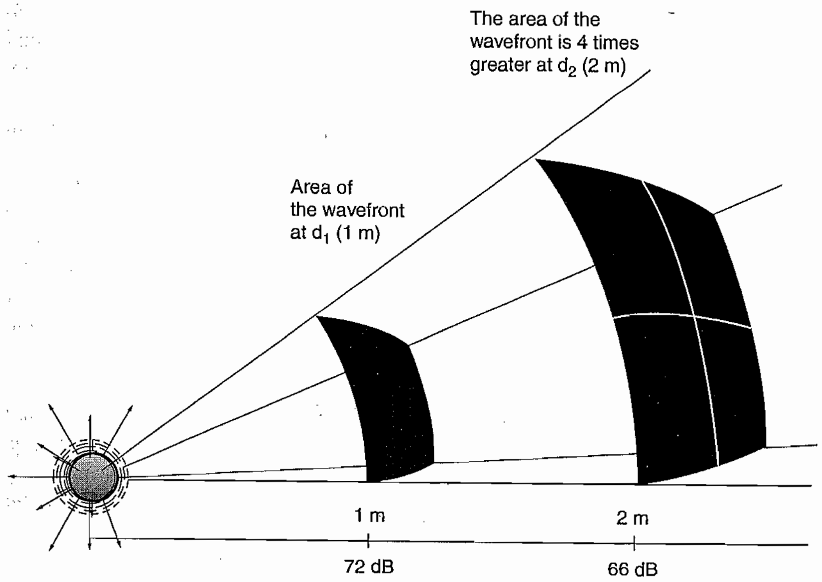

FIGURE 1.2 Generation of a one-dimensional spherical wave. A balloonlike surface pulsates uniformly about some equilibrium position and produces a sound wave that propagates radially away from the balloon at the speed of sound. (Courtesy of Ref. 8.)

distance in proportion to the sound pressure squared, that is $W/4\pi r^2$ [Eq. (1.5)]. Hence the name inverse square law. This is illustrated by the diagram in Fig. 1.2, where at a distance of 1 m the area of the wave front shown is a square meters and at 2 m it becomes $4a$ square meters. To preserve sound energy, the same amount of power flows through the larger area; thus Fig. 1.2 diagrammatically shows the intensity decreasing by a factor of 4, or, as shown later, 6 dB, from 72 to 66 dB.

Particle Velocity

Consider that the surface of the spherical source of Fig. 1.2 is expanding and contracting sinusoidally. During the first half of its sinusoidal motion, it pushes the air particles near its surface outward. Because air is elastic and compresses, the pressure near the surface will increase. This increased pressure overcomes the inertia of the air particles a short distance away and they move outward. That outward movement causes the pressure to build up at this new distance and, in turn, pushes more removed particles outward. This outward movement of the disturbance takes place at the speed of sound.

In the next half of the sinusoid, the sinusoidally vibrating spherical source reverses direction, creating a drop of pressure near its surface that pulls nearby air particles toward it. This reverse disturbance also propagates outward with the speed of sound. Thus, at any one point in space, there will be sinusoidal to-and-fro movement of the particles, called the *particle velocity*. Also at any point, there will be sinusoidal rise and fall of sound pressure.

From the basic equations governing the propagation of sound, as is shown in the next chapter, we can say the following:

1. In a *plane wave* (approximated at a large distance from a point source) propagated in free space (no reflecting surfaces) the sound pressure and the particle velocity reach their maximum and minimum values at the same instant and are said to be in phase.
2. In such a wave the particles move back and forth along the line in which the wave is traveling. In reference to the spherical radiation discussed above, this means that the particle velocity is always perpendicular to the imaginary spherical surface (the wave front) in space. This type of wave is called a longitudinal, or compressional, wave. By contrast, a transverse wave is illustrated by a surface wave in water where the particle velocity is perpendicular to the water surface while the wave propagates in a direction parallel to the surface.

Speed of Sound

A sound wave travels outward at a rate dependent on the elasticity and density of the air. Mathematically, the *speed of sound* in air is calculated as

$$c = \sqrt{\frac{1.4P_s}{\rho}} \quad \text{m/s} \tag{1.7}$$

where P_s = atmospheric (ambient) pressure, Pa
ρ = density of air, kg/m^3

For all practical purposes, the speed of sound is dependent only on the absolute temperature of the air. The equations for the speed of sound are

$$c = 20.05\sqrt{T} \quad \text{m/s} \tag{1.8}$$

$$c = 49.03\sqrt{R} \quad \text{ft/s} \tag{1.9}$$

where T = absolute temperature of air in degrees Kelvin, equal to 273.2 plus the temperature in degrees Celsius
R = absolute temperature in degrees Rankine, equal to 459.7 plus the temperature in degrees Fahrenheit

For temperatures near 20°C (68°F), the speed of sound is

$$c = 331.5 + 0.58^\circ\text{C} \quad \text{m/s} \tag{1.10}$$

$$c = 1054 + 1.07^\circ\text{F} \quad \text{ft/s} \tag{1.11}$$

Wavelength

Wavelength is defined as the distance the pure-tone wave travels during a full period. It is denoted by the Greek letter λ and is equal to the speed of sound divided by the frequency of the pure tone:

$$\lambda = cT = \frac{c}{f} \quad \text{m} \tag{1.12}$$

Sound Energy Density

In standing-wave situations, such as sound waves in closed, rigid-wall tubes, rooms containing little sound-absorbing material, or reverberation chambers, the quantity desired is not sound intensity, but rather the *sound energy density*, namely, the energy (kinetic and potential) stored in a small volume of air in the room owing to the presence of the standing-wave field. The relation between the *space-averaged sound energy density D* and the *space-averaged squared sound pressure* is

$$D = \frac{p_{\text{av}}^2}{\rho c^2} = \frac{p_{\text{av}}^2}{1.4P_s} \quad \text{W} \cdot \text{s/m}^3 \text{ (J/m}^3 \text{ or simply N/m}^2) \tag{1.13}$$

where p_{av}^2 = space average of mean-square sound pressure in a space, determined from data obtained by moving a microphone along a tube or around a room or from samples at various points, Pa^2
P_s = atmospheric pressure, Pa; under normal atmospheric conditions, at sea level, $P_s = 1.013 \times 10^5$ Pa

1.2 SOUND SPECTRA

In the previous section we described sound waves with line and continuous spectra. Here we shall discuss how to quantify such spectra.

Continuous Spectra

As stated before, a continuous spectrum can be represented by a large number of pure tones between two frequency limits, whether those limits are apart 1 Hz or thousands of hertz (see Fig. 1.3). Because the hearing system extends over a large frequency range and is not equally sensitive to all frequencies, it is customary to measure a continuous-spectrum sound in a series of contiguous frequency bands using a sound analyzer.

Customary bandwidths are one-third octave and one octave (see Fig. 1.4 and Table 1.1). The rms value of such a filtered sound pressure is called the one-third-octave-band or the octave-band sound pressure, respectively. If the filter bandwidth is 1 Hz, a plot of the filtered *mean-square* pressure of a *continuous-spectrum*

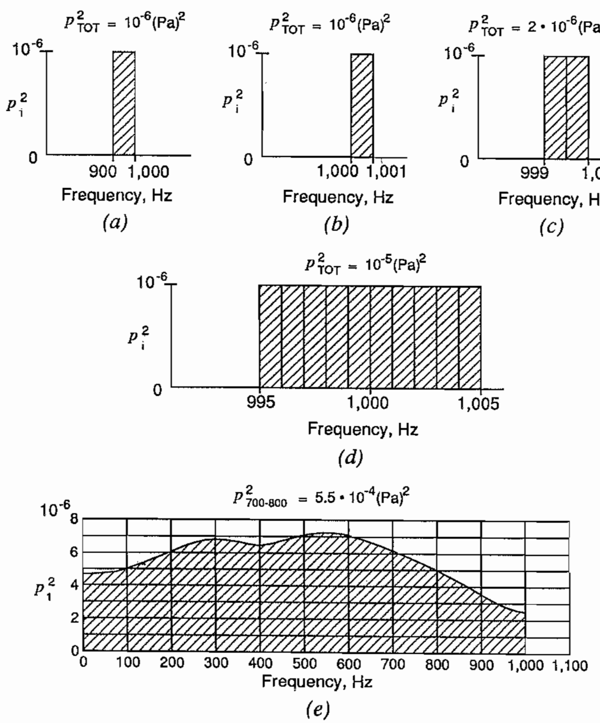

FIGURE 1.3 Power spectral density spectra showing the linear growth of total mean-square sound pressure when the bandwidth of noise is increased. In each case, p_1^2 is the mean-square sound pressure in a band 1 Hz wide.

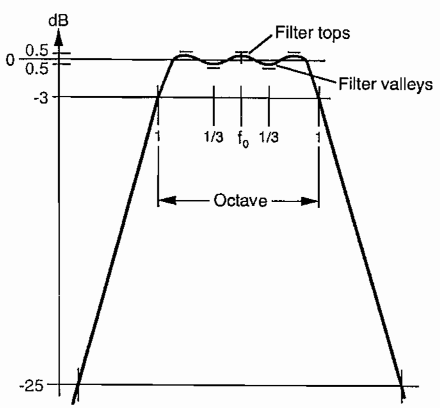

FIGURE 1.4 Frequency response of one manufacturer's octave-band filter. The 3-dB down points for the octave band and for a one-third-octave-band filter are indicated.

TABLE 1.1 Center and Approximate Cutoff Frequencies (Hz) for Standard Set of Contiguous-Octave and One-Third-Octave Bands Covering Audio Frequency Range[a]

	Octave			One-Third Octave		
Band	Lower Band Limit	Center	Upper Band Limit	Lower Band Limit	Center	Upper Band Limit
12	11	16	22	14.1	16	17.8
13				17.8	20	22.4
14				22.4	25	28.2
15	22	31.5	44	28.2	31.5	35.5
16				35.5	40	44.7
17				44.7	50	56.2
18	44	63	88	56.2	63	70.8
19				70.8	80	89.1
20				89.1	100	112
21	88	125	177	112	125	141
22				141	160	178
23				178	200	224
24	177	250	355	224	250	282
25				282	315	355
26				355	400	447
27	355	500	710	447	500	562
28				562	630	708
29				708	800	891
30	710	1,000	1,420	891	1,000	1,122
31				1,122	1,250	1,413
32				1,413	1,600	1,778
33	1,420	2,000	2,840	1,778	2,000	2,239
34				2,239	2,500	2,818
35				2,818	3,150	3,548
36	2,840	4,000	5,680	3,548	4,000	4,467
37				4,467	5,000	5,623
38				5,623	6,300	7,079
39	5,680	8,000	11,360	7,079	8,000	8,913
40				8,913	10,000	11,220
41				11,220	12,500	14,130
42	11,360	16,000	22,720	14,130	16,000	17,780
43				17,780	20,000	22,390

[a]From Ref. 6.

sound versus frequency is called the *power spectral (or spectrum) density spectrum.* Narrow bandwidths are commonly used in analyses of machinery noise and vibration, but the term "spectral density" has no meaning in cases where pure tones are being measured.

The mean-square (or rms) sound pressure can be determined for each of the contiguous frequency bands and the result plotted as a function of frequency (Fig. 1.3*e*).

Bandwidth Conversion. It is frequently necessary to convert sounds measured with one set of bandwidths to a different set of bandwidths or to reduce both sets of measurements to a third set of bandwidths. Let us imagine that we have a machine that at a point in space produces a mean-square sound pressure of $p_1^2 = 10^{-6}$ Pa^2 in a 1-Hz bandwidth between 999 and 1000 Hz (Fig. 1.3*a*). Now imagine that we have a second machine the same distance away that radiates the same power but is confined to a bandwidth between 1000 and 1001 Hz (Fig. 1.3*b*). The total spectrum now becomes that shown in Fig. 1.3*c* and the total mean-square pressure is twice that in either band. Similarly, 10 machines would produce 10 times the mean-square sound pressure of any one (Fig. 1.3*d*).

In other words, if the power spectral density spectrum in a frequency band of width Δf is flat (the mean-square sound pressures in all the 1-Hz-wide bands, p_1^2, within the band are equal), the total mean-square sound pressure for the band is given by

$$p_{\text{tot}}^2 = p_1^2 \frac{\Delta f}{\Delta f_0} \quad \text{Pa}^2 \tag{1.14}$$

where $\Delta f_0 = 1$ Hz.

As an example, assume that we wish to convert the power spectral density spectrum of Fig. 1.3*e*, which is a plot of $p_1^2(f)$, the mean-square sound pressure in 1-Hz bands, to a spectrum for which the mean-square sound pressure in 100-Hz bands, p_{tot}^2, is plotted versus frequency. Let us consider only the 700–800-Hz band. Because $p_1^2(f)$ is not equal throughout this band, we could painstakingly determine and add together the actual p_1^2's or, as is more usual, simply take the average value for the p_1^2's in that band and multiply by the bandwidth. Thus, for each 100-Hz band, the total mean-square sound pressure is given by Eq. (1.14), where p_1^2 is the average 1-Hz band quantity throughout the band. For the 700–800-Hz band, the average p_1^2 is 5.5×10^{-6} and the total is $5.5 \times 10^{-6} \times 100$ Hz $= 5.5 \times 10^{-4}$ Pa^2.

If mean-square sound pressure levels have been measured in a specific set of bandwidths such as one-third-octave bands, it is possible to present accurately the data in a set of wider bandwidths such as octave bands by simply adding together the mean-square sound pressures for the component bands. Obviously, it is not possible to reconstruct a narrower bandwidth spectrum accurately (e.g., one-third-octave bands) from a wider bandwidth spectrum (e.g., octave bands.) However, it is sometimes necessary to make such a conversion in order to compare sets of data measured differently. Then the implicit assumption has to be made that the narrower band spectrum is continuous and monotonic within the larger band. In either direction, the conversion factor for each band is

$$p_B^2 = p_A^2 \frac{\Delta f_B}{\Delta f_A} \tag{1.15}$$

where p_A^2 is the measured mean-square sound pressure in a bandwidth Δf_A and p_B^2 is the desired mean-square sound pressure in the desired bandwidth Δf_B.

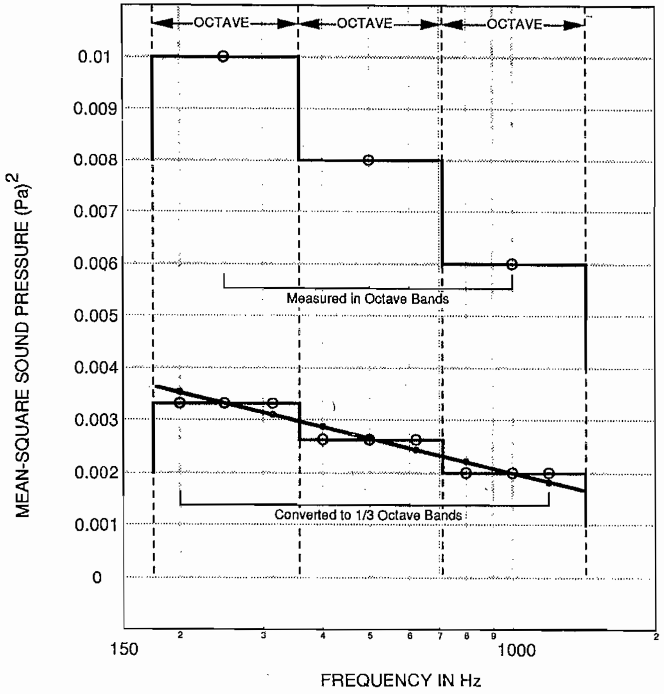

FIGURE 1.5 Conversion of octave-band mean-square sound pressures into third-octave-band mean-square sound pressures. Such conversion should be made only where necessary under the assumption that the third-octave-band mean-square pressure levels decrease monotonically with band midfrequency. The sloping solid curve is the assumed-correct converted spectrum.

As an example, assume that we have measured a sound with a continuous spectrum using a one-octave-band filterset and have plotted the intensity for the contiguous bands versus the midfrequency of each band (see the upper three circles in Fig. 1.5). Assume that we wish to convert to an approximate one-third-octave-band spectrum to make comparisons with other data possible. Not knowing how the mean-square sound pressure varies throughout each octave band, we assume it to be continuous and monotonic and apply Eq. (1.15). In this example, approximately, $\Delta f_B = \frac{1}{3}\Delta f_A$ for all the bands (see Table 1.1), and the mean-square sound pressure in each one-third-octave band with the same midfrequency will be one-third that in the corresponding one-octave band. The data would be plotted versus the midfrequency of each one-third-octave band (see Table 1.1 and Fig. 1.5). Then the straight, sloping line is added under the assumption that the true one-third-octave spectrum is monotonic.

Complex Spectra

The mean-square sound pressure resulting from the combination of two or more pure tones of different amplitudes p_1, p_2, p_3 and *different frequencies* f_1, f_2, f_3 is given by

$$p_{\mathrm{rms}}^2(\text{total}) = p_1^2 + p_2^2 + p_3^2 + \cdots \tag{1.16}$$

The mean-square sound pressure of two pure tones of the *same frequency* but different amplitudes and phases is found from

$$p_{\mathrm{rms}}^2(\text{total}) = p_1^2 + p_2^2 + 2p_1p_2 \cos(\theta_1 - \theta_2) \tag{1.17}$$

where the phase angle of each wave is represented by θ_1 or θ_2.

Comparison of Eqs. (1.16) and (1.17) reveals the importance of phase when combining two sine waves of the same frequency. If the phase difference $\theta_1 - \theta_2$ is zero, the two waves are in phase and the combination is at its maximum value. If $\theta_1 - \theta_2 = 180°$, the third term becomes $-2p_1p_2$ and the sum is at its minimum value. If the two waves are equal in amplitude, the minimum value is zero.

If one wishes to find the mean-square sound pressure of a number of waves all of which have different frequencies except, say, two, these two are added together according to Eq. (1.17) to obtain a mean-square pressure for them. Then this mean-square pressure and the mean-square pressures of the remainder of the components are summed according to Eq. (1.16).

1.3 LEVELS[6]

Because of the wide range of sound pressures to which the ear responds (a ratio of 10^5 or more for a normal person), sound pressure is an inconvenient quantity to use in graphs and tables. This is also true for the other acoustical quantities listed above. Early in the history of the telephone it was decided to adopt logarithmic scales for representing acoustical quantities and the voltages encountered in associated electrical equipment.

As a result of that decision, sound powers, intensities, pressures, velocities, energy densities, and voltages from electroacoustic transducers are commonly stated in terms of the logarithm of the ratio of the measured quantity to an appropriate reference quantity: Because the sound pressure at the threshold of hearing at 1000 Hz is about 20 μPa, this was chosen as the fundamental reference quantity around which the other acoustical references have been chosen.

Whenever the magnitude of an acoustical quantity is given in this logarithmic form, it is said to be a *level* in *decibels* (dB) *above* or *below* a zero *reference level* that is determined by a *reference quantity*. The argument of the logarithm is always a ratio and, hence, is dimensionless. The level for a very large ratio, for example the power produced by a very powerful sound source, might be given with the unit *bel*, which equals 10 dB.

Power and Intensity Levels

Sound Power Level. Sound power level is defined as

$$L_W = 10 \log_{10} \frac{W}{W_0} \quad \text{dB re } W_0 \tag{1.18}$$

and conversely

$$W = W_0 \operatorname{antilog}_{10} \frac{L_W}{10} = W_0 \times 10^{L_W/10} \quad \mathrm{W} \tag{1.19}$$

where W = sound power, W (watts)
W_0 = reference sound power, standardized at 10^{-12} W

As seen in Table 1.2, a *ratio* of 10 in the power W corresponds to a *level difference* of 10 dB regardless of the reference power W_0. Similarly, a ratio of 100 corresponds to a level difference of 20 dB. Power ratios of less than 1 are allowable: They simply lead to negative levels. For example (see Table 1.2), a power ratio of 0.1 corresponds to a level difference of −10 dB.

Column 4 of Table 1.2 gives sound power levels relative to the standard reference power level $W_0 = 10^{-12}$ W in watts.

Some sound power ratios and the corresponding sound-power-level differences are given in Table 1.3. We note from the last line that the sound power level for the *product of two ratios* is equal to the *sum of the levels* for the two ratios. For example, determine L_W for the quantity 2 × 4. From Table 1.3,

TABLE 1.2 Sound Powers and Sound Power Levels

Radiated Sound Power W, watts		Sound Power Level L_W, dB	
Usual Notation	Equivalent Exponential Notation	Relative to 1 W	Relative to 10^{-12} W (standard)
100,000	10^5	50	170
10,000	10^4	40	160
1,000	10^3	30	150
100	10^2	20	140
10	10^1	10	130
1	1	0	120
0.1	10^{-1}	−10	110
0.01	10^{-2}	−20	100
0.001	10^{-3}	−30	90
0.000,1	10^{-4}	−40	80
0.000,01	10^{-5}	−50	70
0.000,001	10^{-6}	−60	60
0.000,000,1	10^{-7}	−70	50
0.000,000,01	10^{-8}	−80	40
0.000,000,001	10^{-9}	−90	30

TABLE 1.3 Selected Sound Power Ratios and Corresponding Power-Level Differences

Sound Power Ratio W/W_0, R	Sound-Power-Level Difference[a] $10 \log W/W_0$, L_W (dB)
1000	30
100	20
10	10
9	9.5
8	9.0
7	8.5
6	7.8
5	7.0
4	6.0
3	4.8
2	3.0
1	0.0
0.9	−0.5
0.8	−1.0
0.7	−1.5
0.6	−2.2
0.5	−3.0
0.4	−4.0
0.3	−5.2
0.2	−7.0
0.1	−10
0.01	−20
0.001	−30
$R_1 \times R_2$	$L_{W_1} + L_{W_2}$

[a]To the nearest 0.1 dB.

$L_W = 3.0 + 6.0 = 9.0$ dB, which is the sound power level for the ratio 8. Similarly, L_W for a ratio of 8000 equals the sum of the levels for 8 and 1000, that is, $L_W = 9 + 30 = 39$ dB.

Sound Intensity Level. Sound intensity level, in decibels, is defined as

$$\text{Intensity level} = L_I = 10 \log \frac{I}{I_{\text{ref}}} \quad \text{dB re } I_{\text{ref}} \tag{1.20}$$

where I = sound intensity whose level is being specified, W/m^2
I_{ref} = reference intensity standardized as 10^{-12} W/m^2

Sound power levels should not be confused with intensity levels (or with sound pressure levels, which are defined next), which also are expressed in decibels. Sound power is a measure of the *total* acoustical power radiated by a source in watts. Sound intensity and sound pressure specify the acoustical "disturbance"

produced at a point removed from the source. For example, their levels depend on the distance from the source, losses in the intervening air path, and room effects (if indoors). A helpful analogy is to imagine that sound power level is related to the total rate of heat production of a furnace, while either of the other two levels is analogous to the temperature produced at a given point in a dwelling.

Sound Pressure Level

Almost all microphones used today respond to sound pressure, and in the public mind, the word *decibel* is commonly associated with sound pressure level or A-weighted sound pressure level (see Table 1.4). Strictly speaking, sound pressure level is analogous to intensity level, because, in calculating it, pressure is first squared, which makes it proportional to intensity (power per unit area):

$$\begin{aligned}\text{Sound pressure level} = L_p &= 10 \log \left[\frac{p(t)}{p_{\text{ref}}}\right]^2 \\ &= 20 \log \frac{p(t)}{p_{\text{ref}}} \quad \text{dB re } p_{\text{ref}}\end{aligned} \tag{1.21}$$

where p_{ref} = reference sound pressure, standardized at 2×10^{-5} N/m^2 (20 μPa) for airborne sound; for other media, references may be 0.1 N/m^2 (1 dyn/cm^2) or 1 μN/m^2 (1 μPa)
$p(t)$ = instantaneous sound pressure, Pa

Note that L_p re 20 μPa is 94 dB greater than L_p re 1 Pa.

As we shall show shortly, $p(t)^2$ is only proportional to sound intensity if its mean-square value is taken. Thus, in Eq. (1.21), $p(t)$ would be replaced by p_{rms}.

The relations among sound pressure levels (re 20 μPa) for pressures in the meter-kilogram-second (mks), centimeter-gram-second (cgs), and English systems of units are shown by the four nomograms of Fig. 1.6.

1.4 DEFINITIONS OF OTHER COMMONLY USED LEVELS AND QUANTITIES IN ACOUSTICS

Analogous to sound pressure level given in Eq. (1.21), *A-weighted sound pressure level* L_A is given by

$$L_A = 10 \log \left[\frac{p_A(t)}{p_{\text{ref}}}\right]^2 \quad \text{dB} \tag{1.22}$$

where $p_A(t)$ is the instantaneous sound pressure measured using the standard frequency-weighting A (see Table 1.4).

TABLE 1.4 A and C Electrical Weighting Networks for Sound-Level Meter[a]

Frequency, Hz	A-Weighting Relative Response, dB	C-Weighting Relative Response, dB
10	−70.4	−14.3
12.5	−63.4	−11.2
16	−56.7	−8.5
20	−50.5	−6.2
25	−44.7	−4.4
31.5	−39.4	−3.0
40	−34.6	−2.0
50	−30.2	−1.3
63	−26.2	−0.8
80	−22.5	−0.5
100	−19.1	−0.3
125	−16.1	−0.2
160	−13.4	−0.1
200	−10.9	0
250	−8.6	0
315	−6.6	0
400	−4.8	0
500	−3.2	0
630	−1.9	0
800	−0.8	0
1,000	0	0
1,250	+0.6	0
1,600	+1.0	−0.1
2,000	+1.2	−0.2
2,500	+1.3	−0.3
3,150	+1.2	−0.5
4,000	+1.0	−0.8
5,000	+0.5	−1.3
6,300	−0.1	−2.0
8,000	−1.1	−3.0
10,000	−2.5	−4.4
12,500	−4.3	−6.2
16,000	−6.6	−8.5
20,000	−9.3	−11.2

[a]These numbers assume a flat, diffuse-field (random-incidence) response for the sound-level meter and microphone.

Average sound level $L_{\mathrm{av},T}$ is given by

$$L_{\mathrm{av},T} = 10 \log \frac{(1/T)\int_0^T p^2(t)\,dt}{p_{\mathrm{ref}}^2} \quad \mathrm{dB} \tag{1.23}$$

where T is the (long) time over which the averaging takes place.

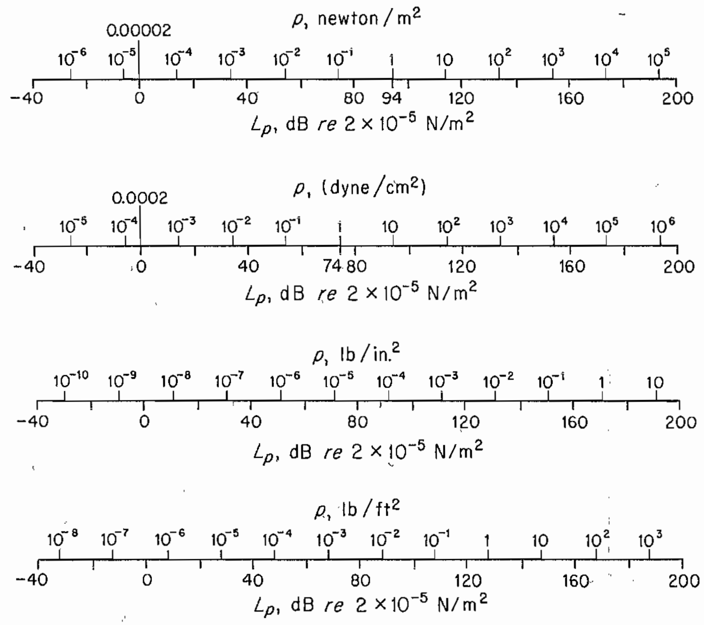

FIGURE 1.6 Charts relating L_p (dB re 20 μPa) to p in N/m²(Pa), dyn/cm², lb/in.², and lb/ft². For example, 1.0 Pa = 94 dB re 20 μPa.

Average A-weighted sound level $L_{A,T}$ (also called L_{eq}, *equivalent continuous A-weighted noise level*) is given by

$$L_{A,T} = L_{\mathrm{eq}} = 10 \log \frac{(1/T)\int_0^T p_A^2(t)\,dt}{p_{\mathrm{ref}}^2} \quad \mathrm{dB} \tag{1.24}$$

The time T must be specified. In noise evaluations, its length is usually one to several hours, or 8 h (working day), or 24 h (full day).

Day–night sound (noise) level L_{dn} is given by

$$L_{\mathrm{dn}} = 10 \log \frac{1}{24}\left[\frac{\int_{07:00}^{22:00} p_A^2(t)\,dt}{p_{\mathrm{ref}}^2} + \frac{\int_{22:00}^{07:00} 10\, p_A^2(t)\,dt}{p_{\mathrm{ref}}^2}\right] \quad \mathrm{dB} \tag{1.25}$$

where the first term covers the "daytime" hours from 07:00 to 22:00 and the second term covers the nighttime hours from 22:00 to 07:00. Here, the nighttime noise levels are considered to be 10 dB greater than they actually measure. The A-weighted sound pressure p_A is sampled frequently during measurement.

A-weighted sound exposure $E_{A,T}$ is given by

$$E_{A,T} = \int_{t_1}^{t_2} p_A^2(t)\,dt \quad \mathrm{Pa}^2 \cdot \mathrm{s} \tag{1.26}$$

This equation is not a level. The term $E_{A,T}$ is proportional to the energy flow (intensity times time) in a sound wave in the time period T. The period T starts and stops at t_1 and t_2, respectively.

A-weighted noise exposure level $L_{EA,T}$ is given by

$$L_{EA,T} = 10 \log \left(\frac{E_{A,T}}{E_0}\right) \quad \mathrm{dB} \tag{1.27}$$

where E_0 is a reference quantity, standardized at $(20\ \mu\mathrm{Pa})^2 \cdot \mathrm{s} = (4 \times 10^{-10}\ \mathrm{Pa})^2 \cdot \mathrm{s}$. However, the International Organization for Standardization standard ISO 1999: 1990-01-5, on occupational noise level, uses $E_0 = (1.15 \times 10^{-5}\ \mathrm{Pa})^2 \cdot \mathrm{s}$, because, for an 8-h day, $L_{EA,T}$, with that reference, equals the average A-weighted sound pressure level $L_{A,T}$. The two reference quantities yield levels that differ by 44.6 dB. For a single impulse, the time period T is of no consequence provided T is longer than the impulse length and the background noise is low.

Hearing threshold for setting "zero" at each frequency on a pure-tone audiometer is the standardized, average, pure-tone threshold of hearing for a population of young persons with no otological irregularities. The standardized threshold sound pressure levels at the frequencies 250, 500, 1000, 2000, 3000, 4000, 6000, and 8000 Hz are, respectively, 24.5, 11.0, 6.5, 8.5, 7.5, 9.0, 8.0, and 9.5 dB measured under an earphone. An audiometer is used to determine the difference at these frequencies between the threshold values of a person (the lowest sound pressure level of a pure tone the person can detect consistently) and the standardized threshold values. Measurements are sometimes also made at 125 and 1500 Hz.[7]

Hearing impairment (hearing loss) is the number of decibels that the permanent hearing threshold of an individual at each measured frequency is above the zero setting on an audiometer, in other words, a change for the worse of the person's threshold of hearing compared to the normal for young persons.

Hearing threshold levels associated with age are the standardized pure-tone thresholds of hearing associated solely with age. They were determined from tests made on the hearing of persons in a certain age group in a population with no otological irregularities and no appreciable exposure to noise during their lives.

Hearing threshold levels associated with age and noise are the standardized pure-tone thresholds determined from tests made on the hearing of individuals who had histories of higher than normal noise exposure during their lives. The average noise levels and years of exposure were determined by questioning and measurement of the exposure levels.

Noise-induced permanent threshold shift (NIPTS) is the shift in the hearing threshold level caused solely by exposure to noise.

1.5 REFERENCE QUANTITIES USED IN NOISE AND VIBRATION

American National Standard

The American National Standards Institute has issued a standard (ANSI S1.8-1989, Reaffirmed 2001) on "Reference Quantities for Acoustical Levels." This standard is a revision of ANSI S1.8-1969. The authors of this book have been surveyed for their opinions on preferred reference quantities. Table 1.5 is a combination of the standard references and of references preferred by the authors. The two references are clearly distinguished. All quantities are stated in terms of the International System of units (SI) and in British units.

Relations among Sound Power Levels, Intensity Levels, and Sound Pressure Levels

As a practical matter, the reference quantities for sound power, intensity, and sound pressure (in air) have been chosen so that their corresponding levels are interrelated in a convenient way under certain circumstances.

The threshold of hearing at 1000 Hz for a young listener with acute hearing, measured under laboratory conditions, was determined some years ago as a sound pressure of 2×10^{-5} Pa. This value was then selected as the reference pressure for sound pressure level.

Intensity at a point is related to sound pressure at that point in a free field by Eq. (1.14). A combination of Eqs. (1.4), (1.20), and (1.21) yields the sound intensity level

$$\begin{aligned} L_I &= 10 \log \frac{I}{I_{\mathrm{ref}}} = 10 \log \frac{p^2}{\rho c I_{\mathrm{ref}}} \\ &= 10 \log \frac{p^2}{p_{\mathrm{ref}}^2} + 10 \log \frac{p_{\mathrm{ref}}^2}{\rho c I_{\mathrm{ref}}} \\ L_I &= L_p - 10 \log K \quad \mathrm{dB\ re\ } 10^{-12}\ \mathrm{W/m^2} \end{aligned} \tag{1.28}$$

where K = const = $I_{\mathrm{ref}} \rho c / p_{\mathrm{ref}}^2$, which is dependent upon ambient pressure and temperature; quantity $10 \log K$ may be found from Fig. 1.7, or, $K = \rho c/400$

The quantity $10 \log K$ will equal zero, that is, $K = 1$, when

$$\rho c = \frac{p_{\mathrm{ref}}^2}{I_{\mathrm{ref}}} = \frac{4 \times 10^{-10}}{10^{-12}} = 400 \text{ mks rayls} \tag{1.29}$$

We may also rearrange Eq. (1.28) to give the sound pressure level

$$L_p = L_I + 10 \log K \quad \mathrm{dB\ re\ } 2 \times 10^{-5}\ \mathrm{Pa} \tag{1.30}$$

TABLE 1.5 Reference Quantities for Acoustical Levels from American National Standard ANSI S1.8-1989 (Reaffirmed 2001) and As Preferred by Authors

Name	Definition	Preferred Reference Quantities: SI	Preferred Reference Quantities: British
Sound pressure level (gases)	$L_p = 20 \log_{10}(p/p_0)$ dB	$p_0 = 20\ \mu\text{Pa} = 2 \times 10^{-5}\ \text{N/m}^2$	2.90×10^{-9} lb/in.^{2}
Sound pressure level (other than gases)	$L_p = 20 \log_{10}(p/p_0)$ dB	$p_0 = 1\ \mu\text{Pa} = 10^{-6}\ \text{N/m}^2$	1.45×10^{-10} lb/in.^{2}
Sound power level	$L_W = 10 \log_{10}(W/W_0)$ dB	$W_0 = 1\ \text{pW} = 10^{-12}\ \text{N}\cdot\text{m/s}$	8.85×10^{-12} in. · lb/s
	$L_W = \log_{10}(W/W_0)$ bel	$W_0 = 1\ \text{pW} = 10^{-12}\ \text{N}\cdot\text{m/s}$	8.85×10^{-12} in. · lb/s
Sound intensity level	$L_I = 10 \log_{10}(I/I_0)$ dB	$I_0 = 1\ \text{pW/m}^2 = 10^{-12}\ \text{N/m}\cdot\text{s}$	5.71×10^{-15} lb/in. · s
Vibratory force level	$L_{F0} = 20 \log_{10}(F/F_0)$ dB	$F_0 = 1\ \mu\text{N} = 10^{-6}\ \text{N}$	2.25×10^{-7} lb
Frequency level	$N = \log_{10}(f/f_0)$ dB	$f_0 = 1$ Hz	1.00 Hz
Sound exposure level	$L_E = 10 \log_{10}(E/E_0)$ dB	$E_0 = (20\ \mu\text{Pa})^2 \cdot \text{s} = (2 \times 10^{-5}\ \text{Pa})^2 \cdot \text{s}$	8.41×10^{-18} lb^2/in.^{4}
The quantities listed below are not officially part of ANSI S1.8. They either are listed there for information or are included here as the authors' choice.			
Sound energy level given in ISO 1683:1983	$L_e = 10 \log_{10}(e/e_0)$ dB	$e_0 = 1\ \text{pJ} = 10^{-12}\ \text{N}\cdot\text{m}$	8.85×10^{-12} lb · in.
Sound energy density level given in ISO 1683:1983	$L_D = 10 \log_{10}(D/D_0)$ dB	$D_0 = 1\ \text{pJ/m}^3 = 10^{-12}\ \text{N/m}^2$	1.45×10^{-16} lb/in.^{2}
Vibration acceleration level	$L_a = 20 \log_{10}(a/a_0)$ dB	$a_0 = 10\ \mu\text{m/s}^2 = 10^{-5}\ \text{m/s}^2$	3.94×10^{-4} in./s^2
Vibration acceleration level in ISO 16831983	$L_a = 20 \log_{10}(a/a_0)$ dB	$a_0 = 1\ \mu\text{m/s}^2 = 10^{-6}\ \text{m/s}^2$	3.94×10^{-5} in./s^2
Vibration velocity level	$L_v = 20 \log_{10}(v/v_0)$ dB	$v_0 = 10\ \text{nm/s} = 10^{-8}\ \text{m/s}$	3.94×10^{-7} in./s
Vibration velocity level in ISO 1683:1983	$L_v = 20 \log_{10}(v/v_0)$ dB	$v_0 = 1\ \text{nm/s} = 10^{-9}\ \text{m/s}$	3.94×10^{-8} in./s
Vibration displacement level	$L_d = 20 \log_{10}(d/d_0)$ dB	$d_0 = 10\ \text{pm} = 10^{-11}\ \text{m}$	3.94×10^{-10} in.

Notes: Decimal multiples and submultiples of SI units are formed as follows: 10^{-1} = deci (d), 10^{-2} = centi (c), 10^{-3} = milli (m), 10^{-6} = micro (μ), 10^{-9} = nano (n), and 10^{-12} = pico (p). Also J = joule = W · s(N · m), N = newton, and Pa = pascal = 1 N/m^2. Note that 1 lb = 4.448 N.
Although some international standards differ, in this text, to avoid confusion between power and pressure, we have chosen to use W instead of P for power; and to avoid confusion between energy density and voltage, we have chosen D instead of E for energy density. The symbol lb means pound force.
In recent international standardization $\log_{10}$ is written lg and $20 \log_{10}(a/b) = 10 \lg (a^2/b^2)$, i.e., "20" is never used.

Idaho Power/1206
Ellenbogen/16

TABLE 1.6 Ambient Pressures and Temperatures for Which ρc(Air) = 400 mks rayls

Ambient Pressure			Ambient Temperature T	
p_s, Pa	m of Hg, 0°C	in. of Hg, 0°C	°C	°F
0.7×10^5	0.525	20.68	−124.3	−192
0.8×10^5	0.600	23.63	−78.7	−110
0.9×10^5	0.675	26.58	−27.0	−17
1.0×10^5	0.750	29.54	+30.7	+87
1.013×10^5	0.760	29.9	38.9	102
1.1×10^5	0.825	32.5	94.5	202
1.2×10^5	0.900	35.4	164.4	328
1.3×10^5	0.975	38.4	240.4	465
1.4×10^5	1.050	41.3	322.4	613

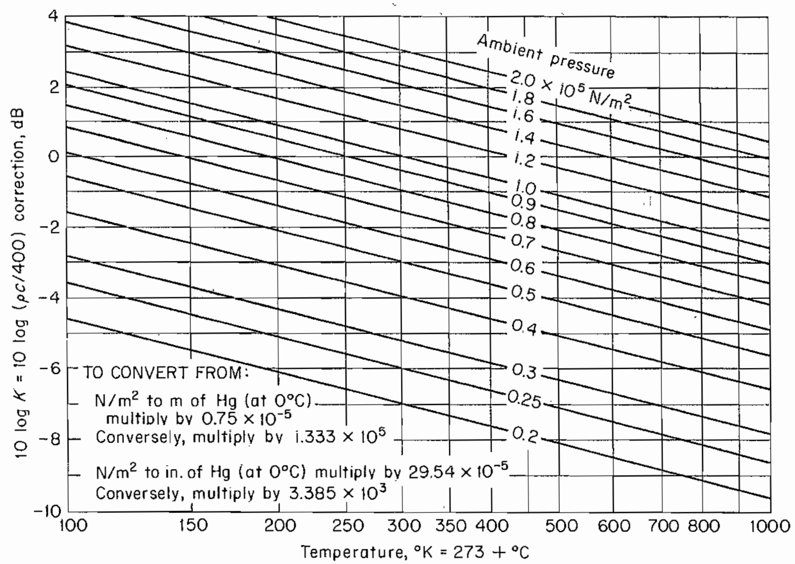

FIGURE 1.7 Chart determining the value of $10 \log(\rho c/400) = 10 \log K$ as a function of ambient temperature and ambient pressure. Values for which $\rho c = 400$ are also given in Table 1.6.

In Table 1.6, we show a range of ambient pressures and temperatures for which $\rho c = 400$ mks rayls. We see that for average atmospheric pressure, namely, 1.013×10^5 Pa, the temperature must equal 38.9°C (102°F) for $\rho c = 400$ mks rayls. However, if $T = 22$°C and $p_s = 1.013 \times 10^5$ Pa^2, $\rho c \approx 412$. This yields a value of $10 \log(\rho c/400) = 10 \log 1.03 = 0.13$ dB, an amount that is usually not significant in acoustics.

Thus, for most noise measurements, we neglect $10 \log K$ and in a free progressive wave let

$$L_p \approx L_I \tag{1.31}$$

Otherwise, the value of $10 \log K$ is determined from Fig. 1.7 and used in Eq. (1.28) or (1.30).

Under the condition that the *intensity is uniform over an area S*, the sound power and the intensity are related by $W = IS$. Hence, the sound power level is related to the intensity level as follows:

$$10 \log \frac{W}{10^{-12}} = 10 \log \frac{I}{10^{-12}} + 10 \log \frac{S}{S_0}$$

$$L_W = L_I + 10 \log S \quad \text{dB re } 10^{-12} \text{ W} \tag{1.32}$$

where S = area of surface, m^2
$S_0 = 1$ m^2

Obviously, only if the area $S = 1.0$ m^2 will $L_W = L_I$. Also, observe that the relation of Eq. (1.32) is not dependent on temperature or pressure.

1.6 DETERMINATION OF OVERALL LEVELS FROM BAND LEVELS

It is necessary often to convert sound pressure levels measured in a series of contiguous bands into a single-band level encompassing the same frequency range. The level in the all-inclusive band is called the *overall level* L(OA) given by

$$L_p(\text{OA}) = 20 \log \sum_{i=1}^{n} 10^{L_{pi}/20} \quad \text{dB} \tag{1.33}$$

$$L_p(\text{OA}) = 10 \log \sum_{i=1}^{n} 10^{L_{Ii}/10} \quad \text{dB} \tag{1.34}$$

The conversion can also be accomplished with the aid of Fig. 1.8. Assume that the contiguous band levels are given by the eight numbers across the top of Fig. 1.9. The frequency limits of the bands are not important to the method of calculation as long as the bands are contiguous and cover the frequency range of the overall band. To combine these eight levels into an overall level, start with any two, say, the seventh and eighth bands. From Fig. 1.8 we see that whenever the difference between two band levels, $L_1 - L_2$, is zero, the combined level is 3 dB higher. If the difference is 2 dB (the sixth band level minus the new level of 73 dB), the sum is 2.1 dB greater than the larger (75 + 2.1 dB). This procedure is followed until the overall band level is obtained, here, 102.1 dB.

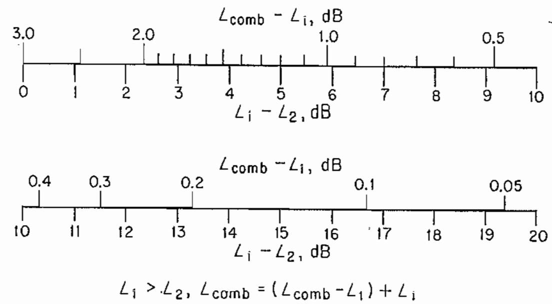

FIGURE 1.8 Nanogram for combining two sound levels L_1 and L_2 (dB). Levels may be power levels, sound pressure levels, or intensity levels. Example: $L_1 = 88$ dB, $L_2 = 85$ dB, $L_1 - L_2 = 3$ dB. Solution: $L_{comb} = 88 + 1.8 = 89.8$ dB.

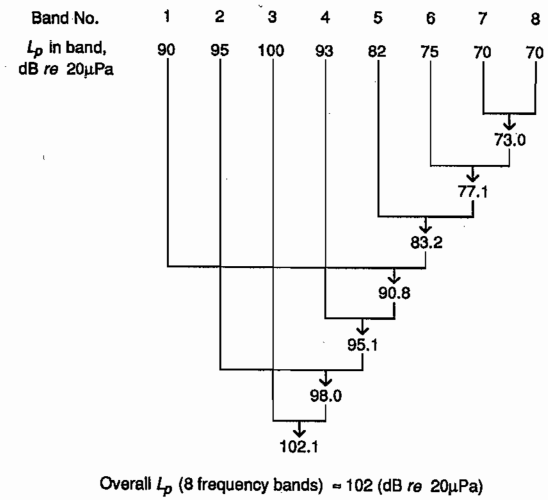

FIGURE 1.9 Determination of an overall sound pressure level from levels in frequency bands (see also Fig. 1.10).

If we set $L_{comb} - L_1 = A$, then A is the number to be added to L_1 (the larger) to get L_{comb}.

It is instructive to combine the bands in a different way, as is shown in Fig. 1.10. The first four bands are combined first; then the second four bands are combined. The levels of the two wider band levels are then combined. It is seen that the overall level is determined by the first four bands alone. This example points up the fact that characterization of a noise by its overall level may be completely inadequate for some noise control purposes because it may ignore a large

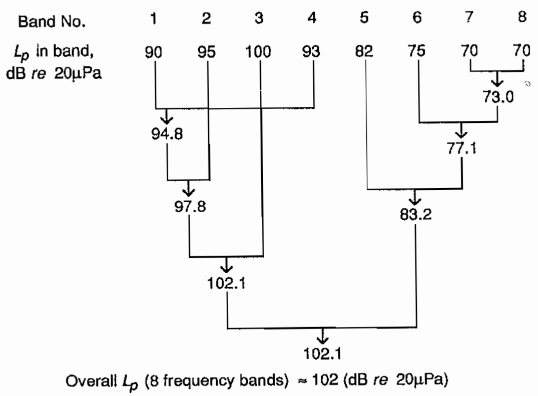

FIGURE 1.10 Alternate determination of an overall sound pressure level from levels in frequency bands (see also Fig. 1.9).

portion of the frequency spectrum. If the data of Fig. 1.10 represented a genuine noise control situation, the 102.1 overall level might be meaningless for some applications. For example, the sound pressure levels in the four highest bands might be the cause of annoyance or interference with speech communication, as is discussed in Chapter 19.

Finally, it should be remembered that in almost all noise control problems, it makes no sense to deal with small fractions of decibels. Rarely does one need a precision of 0.2 dB in measurements, and quite often it is adequate to quote levels to the nearest decibel.

REFERENCES

1. L. L. Beranek, *Acoustics*, Acoustical Society of America, Melville, NY, 1986.
2. M. Moeser, *Engineering Acoustics*, Springer, New York, 2004.
3. D. A. Bies and C. H. Hansen, *Engineering Noise Control*, 2nd ed., E&FN Spon, New York, 2002.
4. P. M. Morse and K. U. Ingard, *Theoretical Acoustics*, Princeton University Press, Princeton, NJ, 1987.
5. L. E. Kinsler, A. R. Frey, A. B. Coppens, J. B. Sanders, and L. Kinsler, *Fundamentals of Acoustics*, 4th ed., Wiley, New York, 1999.
6. L. L. Beranek, *Noise and Vibration Control*, rev. ed., Institute of Noise Control Engineering, Poughkeepsie, NY, 1988.
7. L. L. Beranek, *Acoustical Measurements*, rev. ed., Acoustical Society of America, Melville, NY, 1988.
8. Charles M. Salter Associates, *Acoustics*, William Stout, San Francisco, 1998.

CHAPTER 2

Waves and Impedances

LEO L. BERANEK

Consultant
Cambridge, Massachusetts

2.1 THE WAVE EQUATION[1]

Sound waves must obey the laws of physics. For gases these include Newton's second law of motion, the gas law, and the law of conservation of mass. Combined, these equations produce the wave equation that governs the behavior of sound waves regardless of the surroundings in which they occur.

Equation of Motion

The equation of motion (also called the force equation) is obtained by the application of Newton's second law to a small volume of gas in a homogeneous medium. Imagine the small volume of gas to be enclosed in a packet with weightless flexible sides and assume that there is negligible drag (friction) between particles inside and outside the packet. Suppose that this small volume exists in a part of the medium where the sound pressure p [actually $p(t)$] increases at the space rate of

$$\mathbf{grad}\ p = \mathbf{i}\frac{\partial p}{\partial x} + \mathbf{j}\frac{\partial p}{\partial y} + \mathbf{k}\frac{\partial p}{\partial z} \tag{2.1}$$

where $\mathbf{i}$, $\mathbf{j}$, and $\mathbf{k}$ are unit vectors in the x, y, and z directions, respectively. Obviously, **grad** p is a vector quantity.

The difference between the forces acting on the sides of the packet is a force $\mathbf{f}$ equal to the rate at which the force changes with distance times the incremental dimensions of the box:

$$\mathbf{f} = -\left[\mathbf{i}\left(\frac{\partial p}{\partial x}\Delta x\right)\Delta y\ \Delta z + \mathbf{j}\left(\frac{\partial p}{\partial y}\Delta y\right)\Delta x\ \Delta z + \mathbf{k}\left(\frac{\partial p}{\partial z}\Delta z\right)\Delta x\ \Delta y\right] \tag{2.2}$$

Note that a positive gradient causes the packet to accelerate in the negative direction.

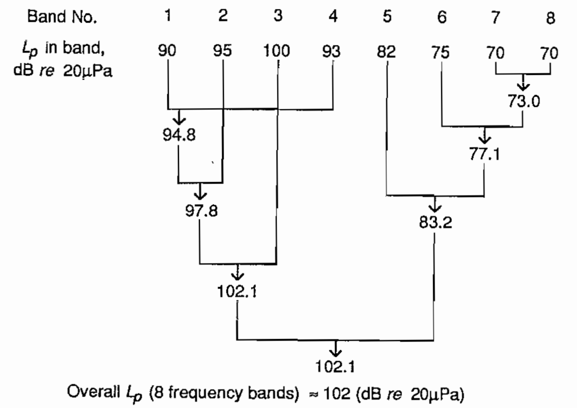

FIGURE 1.10 Alternate determination of an overall sound pressure level from levels in frequency bands (see also Fig. 1.9).

portion of the frequency spectrum. If the data of Fig. 1.10 represented a genuine noise control situation, the 102.1 overall level might be meaningless for some applications. For example, the sound pressure levels in the four highest bands might be the cause of annoyance or interference with speech communication, as is discussed in Chapter 19.

Finally, it should be remembered that in almost all noise control problems, it makes no sense to deal with small fractions of decibels. Rarely does one need a precision of 0.2 dB in measurements, and quite often it is adequate to quote levels to the nearest decibel.

REFERENCES

1. L. L. Beranek, *Acoustics*, Acoustical Society of America, Melville, NY, 1986.
2. M. Moeser, *Engineering Acoustics*, Springer, New York, 2004.
3. D. A. Bies and C. H. Hansen, *Engineering Noise Control*, 2nd ed., E&FN Spon, New York, 2002.
4. P. M. Morse and K. U. Ingard, *Theoretical Acoustics*, Princeton University Press, Princeton, NJ, 1987.
5. L. E. Kinsler, A. R. Frey, A. B. Coppens, J. B. Sanders, and L. Kinsler, *Fundamentals of Acoustics*, 4th ed., Wiley, New York, 1999.
6. L. L. Beranek, *Noise and Vibration Control*, rev. ed., Institute of Noise Control Engineering, Poughkeepsie, NY, 1988.
7. L. L. Beranek, *Acoustical Measurements*, rev. ed., Acoustical Society of America, Melville, NY, 1988.
8. Charles M. Salter Associates, *Acoustics*, William Stout, San Francisco, 1998.

CHAPTER 2

Waves and Impedances

LEO L. BERANEK

Consultant
Cambridge, Massachusetts

2.1 THE WAVE EQUATION[1]

Sound waves must obey the laws of physics. For gases these include Newton's second law of motion, the gas law, and the law of conservation of mass. Combined, these equations produce the wave equation that governs the behavior of sound waves regardless of the surroundings in which they occur.

Equation of Motion

The equation of motion (also called the force equation) is obtained by the application of Newton's second law to a small volume of gas in a homogeneous medium. Imagine the small volume of gas to be enclosed in a packet with weightless flexible sides and assume that there is negligible drag (friction) between particles inside and outside the packet. Suppose that this small volume exists in a part of the medium where the sound pressure p [actually $p(t)$] increases at the space rate of

$$\mathbf{grad}\ p = \mathbf{i}\frac{\partial p}{\partial x} + \mathbf{j}\frac{\partial p}{\partial y} + \mathbf{k}\frac{\partial p}{\partial z} \tag{2.1}$$

where $\mathbf{i}$, $\mathbf{j}$, and $\mathbf{k}$ are unit vectors in the x, y, and z directions, respectively. Obviously, **grad** p is a vector quantity.

The difference between the forces acting on the sides of the packet is a force $\mathbf{f}$ equal to the rate at which the force changes with distance times the incremental dimensions of the box:

$$\mathbf{f} = -\left[\mathbf{i}\left(\frac{\partial p}{\partial x}\Delta x\right)\Delta y\ \Delta z + \mathbf{j}\left(\frac{\partial p}{\partial y}\Delta y\right)\Delta x\ \Delta z + \mathbf{k}\left(\frac{\partial p}{\partial z}\Delta z\right)\Delta x\ \Delta y\right] \tag{2.2}$$

Note that a positive gradient causes the packet to accelerate in the negative direction.

Division of both sides of the equation by $\Delta x\ \Delta y\ \Delta z = V$ gives the force per unit volume acting to accelerate the box,

$$\frac{\mathbf{f}}{V} = -\mathbf{grad}\ p \tag{2.3}$$

By Newton's law, the force per unit volume of Eq. (2.3) equals the time derivative of the momentum per unit volume of the box. Because the box is a deformable packet, the mass inside is constant. Hence,

$$\frac{\mathbf{f}}{V} = -\mathbf{grad}\ p = \frac{M}{V}\frac{D\mathbf{q}}{Dt} = \rho'\frac{D\mathbf{q}}{Dt} \tag{2.4}$$

where $\mathbf{q}$ is the average vector velocity of the gas in the packet, ρ' is the average density of the gas in the packet, and $M = \rho' V$ is the total mass of the gas in the packet.

The partial derivative D/Dt is not a simple one but represents the total rate of the change of velocity of the particular bit of gas in the packet regardless of its position that is, because its position changes when a sound wave hits it:

$$\frac{D\mathbf{q}}{Dt} = \frac{\partial \mathbf{q}}{\partial t} + q_x\frac{\partial \mathbf{q}}{\partial x} + q_y\frac{\partial \mathbf{q}}{\partial y} + q_z\frac{\partial \mathbf{q}}{\partial z} \tag{2.5}$$

where q_x, q_y, and q_z are the components of the vector particle velocity $\mathbf{q}$.

If $\mathbf{q}$ is small enough, the rate of change of momentum of the particles in the box can be approximated by the rate of change of momentum at a fixed point $Dq/Dt \doteq \partial\mathbf{q}/\partial t$, and the instantaneous density ρ' can be approximated by the average density ρ. Then

$$-\mathbf{grad}\ p = \rho\frac{\partial \mathbf{q}}{\partial t} \tag{2.6}$$

Gas Law

At audible frequencies, the wavelength of a sound wave is long compared to the spacing between air molecules, so that expansions and contractions at two different parts of the medium occur so rapidly that there is no time for heat exchange between points of differing instantaneous pressures. Hence, the compressions and expansions are adiabatic. From elementary thermodynamics,

$$PV^{\gamma} = \text{const} \tag{2.7}$$

where γ for air, hydrogen, oxygen, and nitrogen equals 1.4. If we let $P = P_s + p$ and $V = V_s + \tau$, where P_s and V_s are the undisturbed pressure and volume of the packet, we get, for small values of incremental pressure p and incremental volume τ,

$$\frac{p}{P_s} = \frac{\gamma\tau}{V_s} \tag{2.8}$$

The time derivative of Eq. (2.8) yields

$$\frac{1}{P_s}\frac{\partial p}{\partial t} = -\frac{\gamma}{V_s}\frac{\partial \tau}{\partial t} \tag{2.9}$$

Continuity Equation

The continuity equation is a statement that the mass of the gas in the deformable packet is constant. Thus the change in the incremental volume τ depends only on the divergence of the vector displacement ξ:

$$\tau = V_s \text{ div } \xi \tag{2.10}$$

or

$$\frac{\partial \tau}{\partial t} = V_s \text{ div } \mathbf{q} \tag{2.11}$$

where $\mathbf{q}$ is the instantaneous (vector) particle velocity.

Wave Equation in Rectangular Coordinates

The three-dimensional wave equation is given by combining Eqs. (2.6), (2.9), and (2.11) and setting

$$c^2 = \frac{\gamma P_s}{\rho} \tag{2.12}$$

which yields

$$\nabla^2 p = \frac{1}{c^2}\frac{\partial^2 p}{\partial t^2} \tag{2.13}$$

where

$$\nabla^2 p = \frac{\partial^2 p}{\partial x^2} + \frac{\partial^2 p}{\partial y^2} + \frac{\partial^2 p}{\partial z^2} \tag{2.14}$$

The one-dimensional wave equation is simply

$$\frac{\partial^2 p}{\partial x^2} = \frac{1}{c^2}\frac{\partial^2 p}{\partial t^2} \tag{2.15}$$

We could also have eliminated p in the combination of the three equations and retained $\mathbf{q}$, in which case we would have had

$$\nabla^2 \mathbf{q} = \frac{1}{c^2}\frac{\partial^2 \mathbf{q}}{\partial t^2} \tag{2.16}$$

2.2 SOLUTIONS TO THE ONE-DIMENSIONAL WAVE EQUATION

General Solution

The general solution to Eq. (2.15) is the sum of two terms,

$$p(x,t) = f_1\left(t - \frac{x}{c}\right) + f_2\left(t + \frac{x}{c}\right) \quad \text{Pa} \tag{2.17}$$

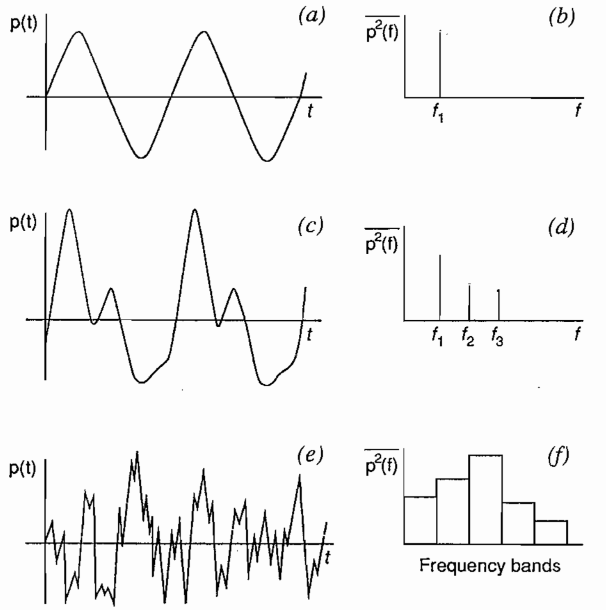

FIGURE 2.1 (*a, c, e*) Forms of time function f_1 or f_2 of Eq. (2.17). Corresponding spectra are shown on the right. (*b, d*) Line spectra. (*f*) Complex spectrum (very large number of tones in each band).

where f_1 and f_2 are arbitrary functions. As we shall illustrate shortly, the first term represents an outgoing wave and the second term a backward-traveling wave. The functions f_1 and f_2 represent the shapes of the two sound waves being propagated. Examples of typical time histories and spectra of $p(t)$ at a fixed location are given in Fig. 2.1. We also recognize c as the speed of sound in air.

Outwardly Traveling Plane Wave

An apparatus for producing an outward-traveling plane wave is shown in Fig. 2.2. A piston at the left moving sinusoidally generates a sound wave that travels outward in the positive x direction and becomes absorbed in the anechoic termination so that no reflected wave exists. Equation (2.17) becomes

$$p(x,t) = f_1\left(t - \frac{x}{c}\right) = P_R \cos k(x - ct) \quad \text{Pa} \tag{2.18}$$

where P_R is the peak amplitude of the sound pressure.

Let us choose the space and the time origins, as shown by the left-hand sine wave in Fig. 2.2, so that P_R has its maximum value at $x = 0$ and $t = 0$. After a time t_1, the wave will have traveled a distance $x_1 = ct_1$. Similarly for $x_2 = 2x_1 = 2ct_1$.

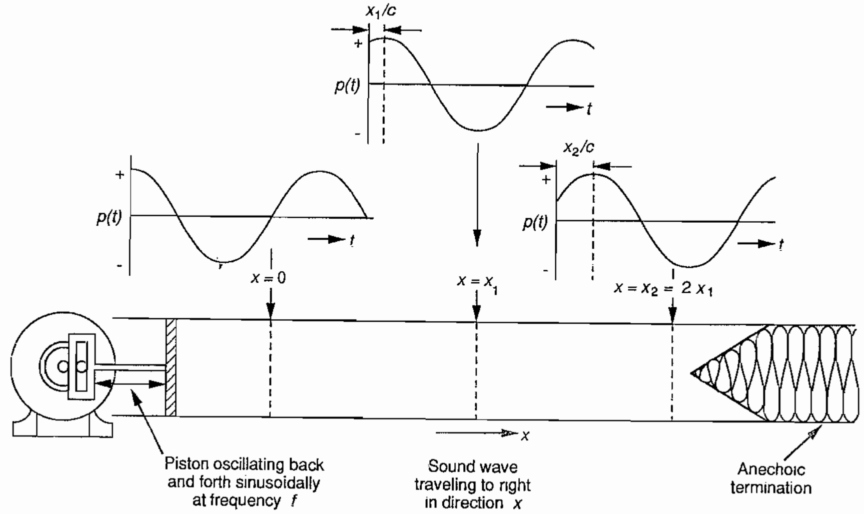

FIGURE 2.2 Apparatus for producing a plane forward-traveling sound wave. A plane wave generated by the piston at the left travels to the right and is absorbed by the anechoic termination. The three waves at the top give the variation in sound pressure with time at the three points indicated, $x = 0$, $x = x_1$, and $x = x_2 = 2x_1$.

Figure 2.3 shows a set of four spatial timeshots taken at $t = 0, \frac{1}{4}T, \frac{1}{2}T, \frac{3}{4}T$, where T is the time period of the piston machine. Each shows the sound pressure over a spatial extent of one wavelength, $\lambda = c/f = cT$. The 20 vertical lines along each snapshot enable one to observe the spatial variation of sound pressure at a given point at the four different times.

Snapshot (*a*) represents the pressure-versus-distance relation for times $t = 0, T, 2T, 3T, \ldots, nT$. The maximum value $+P_R$ exists at $x = 0$. Because the wave is periodic in space, the maximum value must also occur at $x = \lambda, 2\lambda, 3\lambda, \ldots$.

Snapshot (*b*) shows the sound pressure a quarter of a period, $\frac{1}{4}T$, later, that is, the wave in (*a*) has moved to the right a distance equal to $\frac{1}{4}\lambda$ to become the wave in (*b*). Similarly for (*c*) and (*d*). To convince yourself that the wave is traveling to the right, allow your eyes to jump successively from (*a*) to (*b*) to (*c*) to (*d*) and note that the peak, $+P_R$, moves successively to the right.

Wavenumber. The cosine function of Eq. (2.18) repeats its value every time the argument increases 2π radians (360°). From the definition of wavelength, $\lambda = c/f = cT$, we can write this periodicity condition as

$$\cos[k(x + \lambda - ct)] = \cos[k(x - ct) + 2\pi] \tag{2.19}$$

so that $k\lambda = 2\pi$ and $k = 2\pi/\lambda$ radians per meter. We see that the meaning of the parameter k, called the *wavenumber*, is a kind of "spatial frequency."

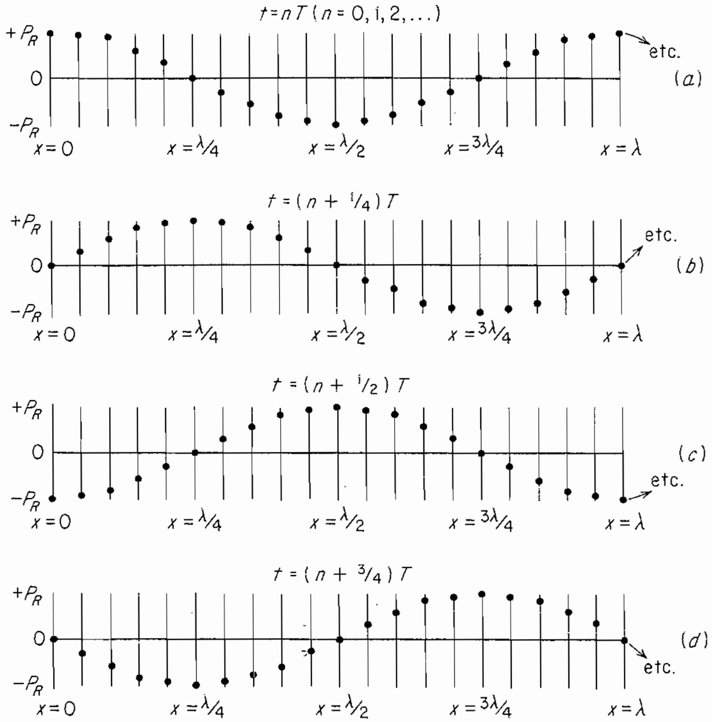

FIGURE 2.3 Graphs showing sound pressure in a plane free-progressive wave traveling from left to right at 20 equally spaced axial locations at four instants of time t. The wave is produced by a source at the left and travels to the right with the speed c. The length of time it takes a wave to travel a distance equal to a wavelength is called the period T. Forward-traveling wave: $p(x,t) = P_R \cos k(x - ct)$; $k = 2\pi/\lambda = 2\pi/(cT) = 2\pi f/c = \omega/c$.

The argument of the cosine in Eq. (2.18) may be written in any one of the following ways:

$$k(x - ct) = \frac{2\pi}{\lambda}(x - ct) = 2\pi f\left(\frac{x}{c} - t\right) = 2\pi\left(\frac{x}{\lambda} - \frac{t}{T}\right)$$
$$= \frac{2\pi x}{\lambda} - 2\pi f t = kx - \omega t$$

From Eq. (2.19) we can write the equations for the snapshots of Fig. 2.3 as

(a) $\quad t = nT \qquad p = P_R \cos \dfrac{2\pi x}{\lambda}$

(b) $\quad t = \left(n + \frac{1}{4}\right) T \qquad p = P_R \cos\left(\dfrac{2\pi x}{\lambda} - \dfrac{\pi}{2}\right)$

(c) $\quad t = \left(n + \frac{1}{2}\right) T \qquad p = P_R \cos\left(\dfrac{2\pi x}{\lambda} - \pi\right)$

(d) $\quad t = \left(n + \frac{3}{4}\right) T \qquad p = P_R \cos\left(\dfrac{2\pi x}{\lambda} - \dfrac{3\pi}{2}\right)$

where $n = 0, 1, 2, 3, \ldots$.

Root-Mean-Square Sound Pressure

As discussed in Chapter 1, a measure of the strength of a sound wave is needed that avoids the problem of directly averaging over a cycle. Such an average is zero. The measure that has been standardized is the rms sound pressure p_{rms}. Its magnitude is 0.707 times the peak value P_R [Eq. (2.18)]. The rms value is also called the *effective value*.

Particle Velocity

From Eq. (2.6) we may derive a relation between sound pressure p and particle velocity u, where u is the component of $\mathbf{q}$ in the x direction. In one dimension,

$$-\frac{\partial p}{\partial x} = \rho \frac{\partial u}{\partial t} \tag{2.20}$$

Substitution of Eq. (2.18) into Eq. (2.20) gives

$$-u = \frac{1}{\rho}\int \frac{\partial p}{\partial x}\,dt = \frac{-P_R}{\rho c}\cos\, k(x - ct) \tag{2.20a}$$

or

$$u = \frac{p}{\rho c} \tag{2.21}$$

where ρ = time-averaged density of air, = 1.18 kg/m^3 for normal room temperature $T = 22°\text{C}$ (71.6°F) and atmospheric pressure $P_s = 0.751$ m (29.6 in.) Hg

c = speed of sound [see Eqs. (1.5)–(1.8)], which at normal temperatures of 22°C equals 344 m/s (1129 ft/s)

ρc = 406 mks rayls (N · s/m^3) at normal room temperature and pressure; at other T's and P_s's, ρc is found from Fig. 1.7

Intensity

A freely traveling progressive sound wave transmits energy. We define this energy transfer as the *intensity* **I**, the energy that flows through a unit area in unit time. The units are watts per square meter (N/m · s). It has its maximum value, $I_{\max}$, when the plane of the unit area is perpendicular to the direction in which the wave is traveling. Intensity, analogous to electrical power, equals the time average of the product of sound pressure and particle velocity,

$$I_{\max} = \overline{p \cdot u} \quad \text{W/m}^2 \ (\text{N/m} \cdot \text{s}) \tag{2.22}$$

For the wave of Figs. 2.2 and 2.3,

$$I_{\max} = \lim_{T \to \infty} \frac{1}{T} \int_0^T \frac{P_R^2}{\rho c} \cos^2 k(x - ct)\, dt \tag{2.23}$$

where $I(\theta) = I_{\max} \cos\theta$, θ being the angle between the direction of travel of the wave and a line perpendicular to the plane of the unit area through which the flow of sound power is being determined.

Let $T = \infty$ be a time long enough that $I_{\max}$ has reached its asymptotic value within experimental error.

Because the time average of the cosine is zero,

$$I_{\max} = \frac{P_R^2}{2\rho c} = \frac{p_{\text{rms}}^2}{\rho c} \quad \text{W/m}^2 \tag{2.24}$$

where p_{rms} is the square root of the mean (time) square value of $p(t)$, as can be demonstrated by finding $I\rho c$ from Eq. (2.24) and W is watts.

Backward-Traveling Plane Wave

A backward-traveling plane wave may be produced by interchanging the source and termination of Fig. 2.2. The wave now travels in the $-x$ direction and is described by

$$p(x, t) = P_L \cos k(x + ct) \quad \text{Pa} \tag{2.25}$$

Comparison of Eqs. (2.18) and (2.25) show that, if the two variables x and ct are separated by a negative sign, the wave travels in the positive direction, and if the two variables are separated by a positive sign, the direction reverses.

The four "snapshots" of Fig. 2.4 illustrate the backward-traveling wave. Allowing your eyes to jump from (*a*) to (*b*) to (*c*) to (*d*) and following the movement of $+P_L$ from right to left convinces one that this is true.

One-Dimensional Spherical Wave

Sound Pressure. The equation for the sound pressure associated with a free-progressive, spherically traveling sound wave, produced as shown in Fig. 1.2 in Chapter 1, is

$$p(r, t) = \frac{A}{r} \cos k(r - ct) \quad \text{Pa} \tag{2.26}$$

where A is an amplitude factor with dimension newtons per meter. Because the sign between r and ct is negative, the wave is traveling outward in the positive

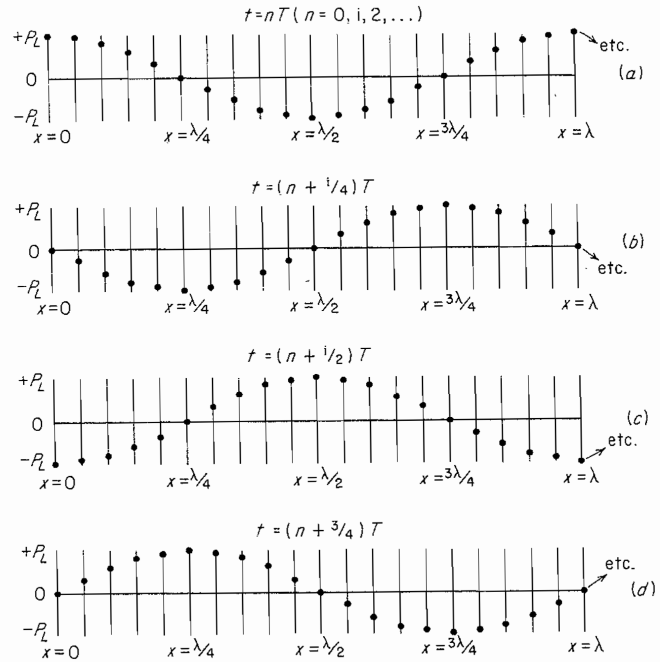

FIGURE 2.4 Graphs showing sound pressure in a plane free-progressive wave traveling from right to left at 20 equally spaced axial locations at four instants of time t. The wave is produced by a source at the right (or by being reflected from a boundary at the right) and travels to the left with a speed c. The period T is defined as for Fig. 2.3. Backward-traveling wave: $p(x, t) = P_L \cos[k(x+ct)]$; $k = 2\pi/\lambda = 2\pi/(cT) = 2\pi f/c = \omega/c$.

r direction. In a spherical wave, the pressure amplitude is inversely proportional to the radial distance r.

Particle Velocity. The particle velocity for a spherical wave, using Eq. (2.20a) with r substituted for x, is

$$u(r, t) = -\frac{1}{\rho} \int \left[\frac{A}{r} k \sin k(r - ct) + \frac{A}{r^2} \cos k(r - ct) \right] dt$$

$$= -\frac{1}{\rho} \left[\frac{-kA}{kcr} \cos k(r - ct) - \frac{A}{r^2 kc} \sin k(r - ct) \right]$$

or

$$u(r, t) = \frac{A}{\rho c r} \cos k(r - ct) \left[1 + \frac{1}{kr} \tan k(r - ct) \right] \tag{2.27}$$

For large values of kr,

$$u(r, t) \doteq \frac{p(r, t)}{\rho c} \qquad k^2 r^2 \gg 1 \tag{2.28}$$

For very small values of kr, $k^2r^2 \ll 1$,

$$u(r,t) \doteq \frac{A}{k\rho c r^2} \sin k(r-ct)$$

$$\doteq \frac{p(r,t)}{\rho c k r} \angle 90^\circ \text{ re phase of } p(r,t) \tag{2.29}$$

Equations (2.27) and (2.29) show that as one approaches the center of a spherical source, the sound pressure and particle velocity become progressively more out of phase, approaching 90° in the limit.

Intensity. For a freely traveling spherical wave, Eq. (2.26) states that for *all values of* r, the sound pressure varies as $1/r$. Because $u = p/\rho c$ [Eq. (2.28)] for the case $k^2r^2 \gg 1$, we can write for all values of r that

$$I_{\max} \text{ at radius } r = \overline{p \cdot u} = \frac{p^2_{\text{rms}} \text{at } r}{\rho c} \quad \text{W/m}^2 \tag{2.30}$$

2.3 SOUND POWER OUTPUT OF ELEMENTARY RADIATORS

Monopole (Radiating Sphere)

The total power W_M radiated from a simple source, a pulsating sphere, called a monopole, is given in Table 2.1, where

where $\hat{Q}_s$ = source strength, $= 4\pi a^2 \hat{v}_r$, m³/s
$\hat{v}_r$ = peak value of velocity of sinusoidally pulsating surface, m/s
a = radius of pulsating sphere, m
$k = 2\pi f/c$, m^{-1}
ρc = characteristic impedance of gas, 406 mks rayls (N · s/m³) for air at normal room temperature and atmospheric pressure

Dipole (Two Closely Spaced Monopoles)[2]

By definition, two monopoles constitute a dipole when $(kd)^2 \ll 1$ and when they vibrate 180° out of phase. A dipole has a figure-eight radiation pattern, with minimum radiation in the direction perpendicular to a line connecting the two monopoles. The total sound power, W_D, radiated is given in the second row of Table 2.1, where $\hat{Q}_s$, $\hat{v}_r$, a, k, and ρc are as given above and

where d = separation between monopoles, m

Oscillating Sphere[3,4]

An oscillating sphere is defined as a rigid sphere moving axially, back and forth, around its rest position. The total power, W_{OS}, radiated is given in the third row of Table 2.1, ρc and k are as defined for a monopole, and

where $\hat{v}_x$ = peak back-and-forth velocity, m/s
a = radius of oscillating sphere, m

TABLE 2.1 Sound Power Output of Elementary Radiators

Source Type	Source Behavior 180° Phase Difference	Sound Power Output, W	Auxiliary Expressions
Monopole	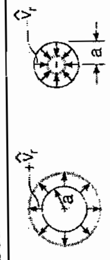	$W_M = \frac{\rho c k^2}{8\pi(1+k^2a^2)}\hat{Q}_s^2$	$\hat{Q}_s = 4\pi a^2 \hat{v}_r$
Dipole	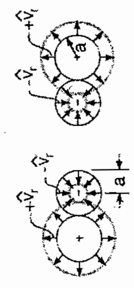	$W_D = \frac{\rho c k^4 d^2}{12\pi}\hat{Q}_s^2$	d = distance between monopoles
Oscillating sphere		$W_{OS} = \frac{2\pi\rho c k^4 a^6}{3(4+k^4a^4)}\hat{v}_x^2$	$\hat{v}_x$ = peak sinusoidal vibration velocity
Baffled piston	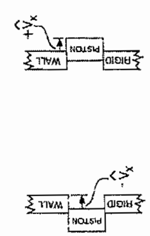	$W_{BP} = \frac{\rho c k^2}{4\pi}\hat{Q}^2 \quad ka \ll 1$ $W_{BP} = \frac{\rho c}{2\pi a^2}\hat{Q}^2 \quad ka \gg 1$	$\hat{Q} = \pi a^2 \hat{v}_x$ where $\hat{v}_x$ is as above

Baffled Piston[5]

An axially vibrating diaphragm in an infinite plate is called a baffled piston. The total power radiated to one side of the rigid wall, W_{BP}, is given in the fourth row of Table 2.1, both for the case of a piston whose radius is small compared to a wavelength, $ka \ll 1$, and vice versa, $ka \gg 1$, where

where $\hat{v}_x$ = peak axial velocity of piston, m/s
a = radius of piston, m

The other quantities are as defined above.

2.4 INTERFERENCE AND RESONANCE

The sound pressure and incremental density in a sound wave are generally very small in comparison with the equilibrium values on which they are superposed. This is certainly true for speech and music waves. As a result, it is possible in such acoustical situations to determine the effect of two sound waves in the same space by simple linear addition of the effects of each sound wave separately. This is a statement of the principle of *superposition*.

In the previous section we presented a series of spatial snapshots for plane sound waves traveling to the right (Fig. 2.3) and to the left (Fig. 2.4). According to the principle of superposition, the effect of the sum of these two waves will be the sum of their effects, which we can see graphically by adding Figs. 2.3 and 2.4. The result is shown in Fig. 2.5, where we have set the amplitude of the forward-traveling wave P_R equal to the amplitude of the backward-traveling wave P_L.

The interference of the two waves has produced a surprising change. No longer does the sound pressure at one place occur to the right or to the left of that place at the next instant. The wave no longer travels; it is a standing wave. We see that at each point in space the sound pressure varies sinusoidally with time, except at the points $x = \frac{1}{4}\lambda$ and $\frac{3}{4}\lambda$, where the pressure is always zero. The maximum value of the pressure variation at different points is different, being greatest at $x = 0$, $x = \frac{1}{2}\lambda$, and $x = \lambda$. The sound pressures at the points between the points $x = \frac{1}{4}\lambda$ and $x = \frac{3}{4}\lambda$ always vary together, that is, increase or decrease in phase. At the same times the sound pressures for the points to the left of $x = \frac{1}{4}\lambda$ and to the right of $x = \frac{3}{4}\lambda$ decrease or increase together (in phase). Thus all pressures are in time phase in the standing wave, but there is a space difference of phase of 180° between the sound pressures at the points at $x = 0$ and $x = \frac{1}{2}\lambda$.

Remembering that $P_R = P_L = P$, that is, that the amplitude of the wave traveling to the right is equal to the amplitude of the wave traveling to the left, we find that the sum of the two waves is

$$\begin{aligned} p(x,t) &= P\cos[k(x-ct)] + P\cos[k(x+ct)] \\ &= 2P(\cos kx)(\cos 2\pi ft) \quad \text{Pa} \end{aligned} \tag{2.31}$$

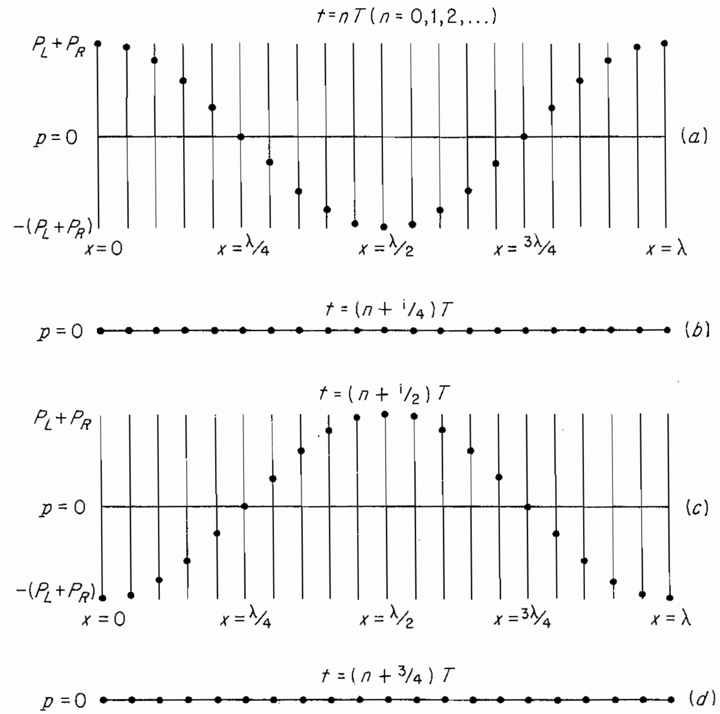

FIGURE 2.5 Graphs giving sound pressure in a plane standing wave at 20 places in space at four instants of time t. The wave is produced by two sources equal in strength at the right and left of the graphs (or the right source is a perfectly reflecting boundary that sends back a wave of equal amplitude to that produced by the source on the left). Standing wave: $p(x,t) = 2P(\cos kx)(\cos 2\pi ft)$, where k is the wavenumber.

From Eqs. (2.18), (2.20), and (2.31) we see very clearly the differences between a standing and a traveling wave. In a traveling wave distance x and time t occur as a sum or difference in the argument of the cosine. Hence, for the traveling wave, by adjusting both time and distance (according to the speed of sound) in the argument of the cosine, we can always keep the argument and thus the magnitude of the cosine the same. In Eq. (2.31) distance and time no longer appear together in the argument of a single cosine. So the same sound pressure cannot occur at an adjacent point in the space at a later time.

Standing waves will exist in any regular enclosure. In a rectangular room, for example, three classes of standing waves may exist (see Chapter 6). One class includes all waves that are perpendicular to one pair of opposing walls, that is, that travel at grazing incidence to two pairs of walls, the (n_x, 0, 0), (0, n_y, 0), (0, 0, n_z) modes of vibration. A second class travels at grazing incidence to only one pair of walls, the (n_x, n_y, 0), (n_x, 0, n_z), (0, n_y, n_z) modes of vibration. A third class involves all walls at oblique angles of incidence, the (n_x, n_y, n_z) modes of vibration. Each free-standing wave in an acoustical space is called a normal mode of vibration, or simply a resonance. The frequencies at which resonant standing waves can exist are related to the separation between the reflecting surfaces. For example, the lowest frequency for a resonant standing wave in a one-dimensional system consisting of two rigid parallel walls is given by

$$f = \frac{c}{2d} \quad \text{Hz} \tag{2.32}$$

where f = lowest frequency for resonant standing wave, Hz
c = speed of sound, m/s
d = distance separating two reflecting surfaces, m

Resonant standing waves can also exist at every integral multiple of this frequency. That is to say,

$$f = \frac{nc}{2d} \quad \text{Hz} \tag{2.33}$$

where n is an integer $1, 2, 3, \ldots$.

2.5 IMPEDANCE AND ADMITTANCE

Reference to Eqs. (2.18) and (2.21) reveals that the magnitudes of sound pressure and particle velocity are directly proportional to each other. Also, in the special case of plane-wave sound propagation, the time dependence of sound pressure is exactly the same as the time dependence of particle velocity, and at any point in the wave there is no phase difference between the two quantities. Thus, in a plane sound wave the ratio of sound pressure to particle velocity at all instants of time is a constant equal to ρc.

In general, however, for linear (small-signal) acoustical phenomena in the steady state, there is a difference in the time functions of sound pressure and particle velocity, leading to a phase difference of one relative to the other. Thus, at any point the particle velocity may lead or lag the sound pressure. In many situations, both the ratio of the magnitudes and the relative phase may be functions of frequency.

In several of the chapters that follow, it is convenient in acoustical design to avoid separate consideration of steady-state sound pressure and steady-state particle velocity (or other quantities that may be derived from them, such as force and volume velocity) and instead to deal with either one and with their complex ratio, as defined below.

Complex Notation

The foundations for the designation of steady-state signals with the same frequency but different phases by complex notation are expressed in the identities

$$|A| \cos(\omega t + \theta_1) \equiv \text{Re}\ \overline{A} e^{j\omega t} \tag{2.34}$$

where $|A| \equiv$ amplitude of cosine function
$\theta_1 \equiv$ phase shift at time $t = 0$
Re $\equiv$ "real part of"
$j \equiv \sqrt{-1}$

and

$$\overline{A} \equiv A_{\text{Re}} + jA_{\text{Im}} = |A|\ e^{j\theta_1} \tag{2.35}$$

$$|A| \equiv \sqrt{A_{\text{Re}}^2 + A_{\text{Im}}^2} \tag{2.36}$$

$$\theta_1 \equiv \tan^{-1}\left(\frac{A_{\text{Im}}}{A_{\text{Re}}}\right) \tag{2.37}$$

We note also that

$$e^{j\theta} \equiv \cos\theta + j \sin\theta \tag{2.38}$$

so that

$$A_{\text{Re}} \equiv |A| \cos\theta \tag{2.39}$$

$$A_{\text{Im}} \equiv |A| \sin\theta \tag{2.40}$$

These equations say that a cosinusoidal time-varying function, given by the left-hand side of Eq. (2.34), can be represented by the real-axis projection of a vector of magnitude $|A|$ given by Eq. (2.36), rotating at a rate ω radians per second. The angle θ_1 is the angle of the vector (in radians) relative to the positive real axis at the instant of time $t = 0$.

We might therefore express a time-varying steady-state sound pressure or force by

$$\overline{A} e^{j\omega t} = |A|\ e^{j\omega t} e^{j\theta_1} \tag{2.41}$$

Also, a time-varying steady-state velocity or volume velocity might be expressed by

$$\overline{B} e^{j\omega t} = |B|\ e^{j\omega t} e^{j\theta_2} \tag{2.42}$$

Definitions of Complex Impedance

Complex Impedance Z. In general, complex impedance is defined as

$$\overline{Z} \equiv \frac{\overline{A}}{\overline{B}} = \frac{|A|\ e^{j(\omega t + \theta_1)}}{|B|\ e^{j(\omega t + \theta_2)}} = \frac{|A|\ e^{j\theta_1}}{|B|\ e^{j\theta_2}} = |Z|\ e^{j\theta} \tag{2.43}$$

and

$$\overline{Z} \equiv R + jX = \sqrt{R^2 + X^2}\ e^{j\theta} = |Z|\ e^{j\theta} \tag{2.44}$$

where $\overline{Z}$ = *complex impedance as given above*
A = steady-state pressure or force

B = steady-state velocity or volume velocity
$|Z|$ = magnitude of complex impedance
θ = phase angle between the time functions A and B, $= \theta_1 - \theta_2$
R, X = real and imaginary parts, respectively, of complex impedance $\overline{Z}$
R = resistance, Re Z
X = reactance, Im $\overline{Z}$

Often $|A|$ and $|B|$ are taken to be the rms values of the phenomena they represent, although, if so taken, a factor of $\sqrt{2}$ must be added to both sides of Eq. (2.34) to make them correct in a physical sense. Whether amplitudes or rms values are used makes no difference in the impedance ratio.

Complex impedances are of several types, according to the quantities involved in the ratios. Types common in acoustics are given below.

Acoustical Impedance Z_A. The acoustical impedance at a given surface S is defined as the complex ratio of (a) sound pressure averaged over the surface to (b) volume velocity through it. The volume velocity $U = uS$. The surface may be either a hypothetical surface in an acoustical medium or the moving surface of a mechanical device. The unit is N · s/m^5, also called the mks acoustical ohm. That is,

$$Z_A = \frac{p}{U} \quad \text{N} \cdot \text{s/m}^5 \text{ (mks acoustical ohms)} \tag{2.45}$$

Specific Acoustical Impedance Z_s. The specific acoustical impedance is the complex ratio of the sound pressure at a point of an acoustical medium or mechanical device to the particle velocity at that point. The unit is N · s/m^3, also called the mks rayl. That is,

$$Z_s = \frac{p}{u} \quad \text{N} \cdot \text{s/m}^3 \text{ (mks rayls)} \tag{2.46}$$

Mechanical Impedance Z_M. The mechanical impedance is the complex ratio of the force acting on a specific area of an acoustical medium or mechanical device to the resulting linear velocity through or of that area, respectively. The unit is the N · s/m, also called the mks mechanical ohm. That is,

$$Z_M = \frac{f}{u} \quad \text{N} \cdot \text{s/m (mks mechanical ohms)} \tag{2.47}$$

Characteristic Resistance ρc. The characteristic resistance is the ratio of the sound pressure at a given point to the particle velocity at that point in a free, plane, progressive sound wave. It is equal to the product of the density of the medium and the speed of sound in the medium (ρc). It is analogous to the characteristic impedance of an infinitely long, dissipationless transmission line. The unit is the N · s/m^3, also called the mks rayl. In the solution of problems in this book we shall assume for air that $\rho c = 406$ mks rayls, which is valid for a temperature of 22°C (71.6°F) and a barometric pressure of 0.751 m (29.6 in.) Hg.

Idaho Power/1206
Ellenbogen/27

Normal Specific Acoustical Impedance Z_{sn}. At the boundary between air and a denser medium (such as a porous acoustical material) we find a further definition necessary, as follows: When an alternating sound pressure p is produced at the surface of an acoustical material, an alternating velocity u of the air particles is produced through the surface. The to-and-fro motions of the air particles may be at any angle relative to the surface. The angle depends both on the angle of incidence of the sound wave and on the nature of the acoustical material. For example, if the material is porous and has very low density, the particle velocity at the surface is nearly in the same direction as that in which the wave is propagating. By contrast, if the surface were a large number of small-diameter tubes packed side by side and oriented perpendicular to the surface, the particle velocity would necessarily be only perpendicular to the surface. In general, the direction of the particle velocity at the surface has both a normal (perpendicular) component and a tangential component.

The normal specific acoustical impedance (sometimes called the unit-area acoustical impedance) is defined as the complex ratio of the sound pressure p to the *normal component* of the particle velocity u_n at a plane, in this example at the surface of the acoustical material. Thus

$$Z_{sn} = \frac{p}{u_n} \quad \text{N} \cdot \text{s/m}^3 \text{ (mks rayls)} \tag{2.48}$$

Definition of Complex Admittance

Complex admittance is the reciprocal of complex impedance. In all ways, it is handled by the same set of rules as given by Eqs. (2.34)–(2.44). Thus, the complex admittance corresponding to the complex impedance of Eq. (2.43) is

$$\overline{Y} \equiv \frac{\overline{B}}{\overline{A}} = \frac{|B|\, e^{j\theta_2}}{|A|\, e^{j\theta_1}} = |Y|\, e^{j\phi} \tag{2.49}$$

where $|Y| = 1/|Z|$
$\phi = -\theta$

The choice between impedance and admittance is sometimes made according to whether $|A|$ or $|B|$ is held constant during a measurement. Thus, if $|B|$ is held constant, $|Z|$ is directly proportional to $|A|$ and is used. If $|A|$ is held constant, $|Y|$ is directly proportional to $|B|$ and is used.

REFERENCES

1. W. J. Cunningham, "Application of Vector Analysis to the Wave Equation," *J. Acoust. Soc. Am.*, **22**, 61 (1950); R. V. L. Hartley, "Note on 'Application of Vector Analysis to the Wave Equation,' " *J. Acoust. Soc. Am.*, **22**, 511 (1950).
2. H. Kuttruff, *Room Acoustics*, Halstead, New York, 2000.

3. M. Moeser, *Engineering Acoustics*, Springer-Verlag, New York, 2004.
4. L. Cremer, *Vorlesungen uber Technische Akustik*, Springer-Verlag, New York, 1971, Section 2.5.2.
5. L. L. Beranek, *Acoustics*, Acoustical Society of America, Melville, NY, 1986, Sections 4.3 and 7.5.

CHAPTER 3

Data Analysis

ALLAN G. PIERSOL

Piersol Engineering Company
Woodland Hills, California

For studies related to noise and vibration control engineering, the analysis of measured acoustical noise and/or vibration data may be accomplished with a number of goals in mind. The most important of these goals can be divided into four broad categories: (a) an assessment of the severity of an environment, (b) the identification of system response properties, (c) the identification of sources, and (d) the identification of transmission paths. The first goal is commonly accomplished using one-third-octave-band-level calculations, or perhaps frequency-weighted overall level measurements, as described in Chapter 1. The other goals often require more advanced data analysis procedures. Following a brief discussion of the general types of acoustical and vibration data of common interest, the most important data analysis procedures for accomplishing goals (b)–(d) are outlined, and important applications of the results from such analyses are summarized. Because of the broad and intricate nature of the subject, heavy use of references is employed to cover details.

3.1 TYPES OF DATA SIGNALS

Acoustical and vibration data are commonly acquired in the form of analog time history signals produced by appropriate transducers (details of acoustical and vibration transducers and signal conditioning equipment are available from the data acquisition documents listed in the Bibliography and the literature published by acoustical and vibration measurement system manufacturers). The signals are generally produced with the units of volts but can be calibrated into appropriate engineering units (g, m/s, Pa, etc.) as required. From a data analysis viewpoint, it is convenient to divide these time history signals into two broad categories, each with two subcategories, as follows:

1. Deterministic data signals: (a) steady-state signals; (b) transient signals.
2. Random data signals: (a) stationary signals; (b) nonstationary signals.

3. M. Moeser, *Engineering Acoustics*, Springer-Verlag, New York, 2004.
4. L. Cremer, *Vorlesungen uber Technische Akustik*, Springer-Verlag, New York, 1971, Section 2.5.2.
5. L. L. Beranek, *Acoustics*, Acoustical Society of America, Melville, NY, 1986, Sections 4.3 and 7.5.

CHAPTER 3

Data Analysis

ALLAN G. PIERSOL

Piersol Engineering Company
Woodland Hills, California

For studies related to noise and vibration control engineering, the analysis of measured acoustical noise and/or vibration data may be accomplished with a number of goals in mind. The most important of these goals can be divided into four broad categories: (a) an assessment of the severity of an environment, (b) the identification of system response properties, (c) the identification of sources, and (d) the identification of transmission paths. The first goal is commonly accomplished using one-third-octave-band-level calculations, or perhaps frequency-weighted overall level measurements, as described in Chapter 1. The other goals often require more advanced data analysis procedures. Following a brief discussion of the general types of acoustical and vibration data of common interest, the most important data analysis procedures for accomplishing goals (b)–(d) are outlined, and important applications of the results from such analyses are summarized. Because of the broad and intricate nature of the subject, heavy use of references is employed to cover details.

3.1 TYPES OF DATA SIGNALS

Acoustical and vibration data are commonly acquired in the form of analog time history signals produced by appropriate transducers (details of acoustical and vibration transducers and signal conditioning equipment are available from the data acquisition documents listed in the Bibliography and the literature published by acoustical and vibration measurement system manufacturers). The signals are generally produced with the units of volts but can be calibrated into appropriate engineering units (g, m/s, Pa, etc.) as required. From a data analysis viewpoint, it is convenient to divide these time history signals into two broad categories, each with two subcategories, as follows:

1. Deterministic data signals: (a) steady-state signals; (b) transient signals.
2. Random data signals: (a) stationary signals; (b) nonstationary signals.

Deterministic Data

Deterministic data signals are those for which it is theoretically feasible to determine a mathematical equation that would predict future time history values of the signal (within reasonable experimental error), based upon a knowledge of the applicable physics or past observations of the signal. The most common type of deterministic signal, called a periodic signal, has a time history $x(t)$ that exactly repeats itself after a constant time interval T_p, called the period of the signal; that is,

$$x(t) = x(t \pm T_p) \tag{3.1}$$

The most common sources of periodic acoustical and vibration signals are constant-speed rotating machines, including propellers and fans. Ideally, such signals would have only one dominant frequency, allowing them to be represented by a simple sine wave. However, it is more likely that the periodic source will produce a complex signal that must be described, using a Fourier series representation,[1] by a collection of harmonically related sine waves, as illustrated in Fig. 3.1. In any case, periodic signals are called steady state because their average properties (mean value, mean-square value, and spectrum) do not vary with time.

There are steady-state acoustical and vibration signals that are not rigorously periodic, for example, the data produced by a collection of independent (unsynchronized) periodic sources, such as the propellers on a multiengine propeller airplane. Such nonperiodic steady-state signals are referred to as almost periodic. Most nonperiodic deterministic signals, however, are also not steady state; that is, their average properties change with time. An important type of time-varying

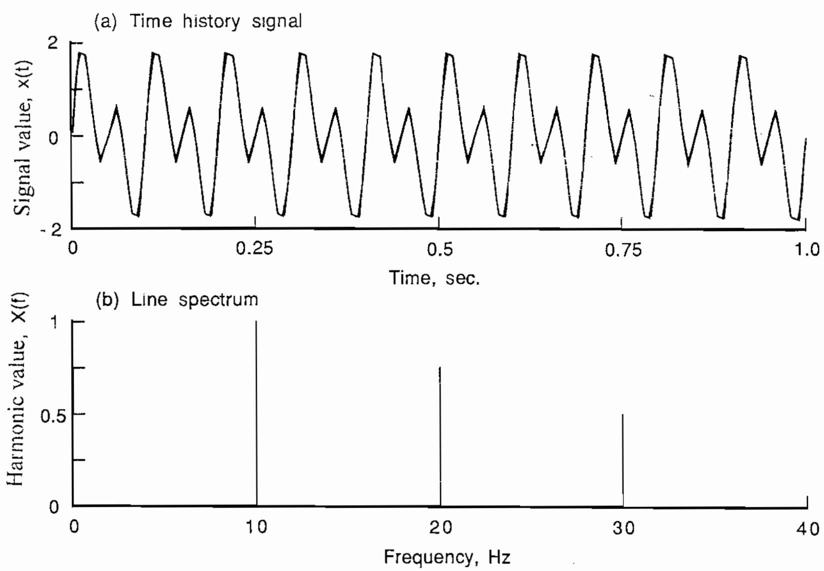

FIGURE 3.1 Time history and line spectrum for periodic signal.

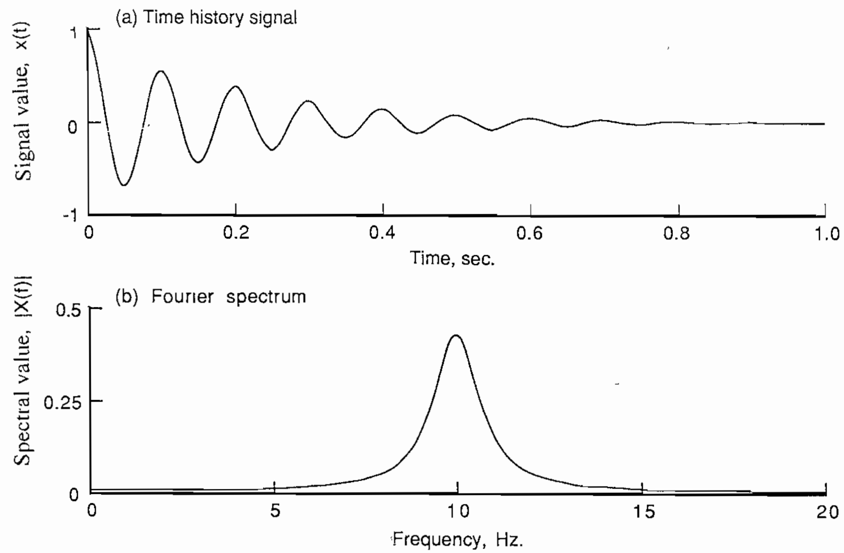

FIGURE 3.2 Time history and Fourier spectrum for deterministic transient signal.

signal is one that begins and ends within a reasonable measurement time interval. Such signals are called transient signals. Examples of deterministic transient signals include well-controlled impacts, sonic booms, and aircraft landing loads. Such data can be described, using a Fourier integral representation,[1] by a continuous spectrum, as illustrated for an exponentially decaying oscillation in Fig. 3.2.

Random Data

Random acoustical and vibration data signals may be broadly defined as all signals that are not deterministic, that is, where it is not theoretically feasible to predict future time history values based upon a knowledge of the applicable physics or past observations. In some cases, the border between deterministic and random signals may be blurred. For example, the pressure field produced by a high-speed fan at its blade passage rate with a uniform inflow would be deterministic, but turbulence in the inflow would introduce a random property to the pressure signal. In other cases, the data will be more fully random in character (sometimes called "strongly mixed"). Examples include the pressure fields generated by fluid dynamic boundary layers (flow noise), the loads produced by atmospheric turbulence, and the acoustical noise caused by the exhaust gas mixing from an air blower. These sources of acoustical and vibration signals cover a wide frequency range and have totally haphazard time histories, as illustrated in Fig. 3.3.

When the mechanisms producing random acoustical or vibration data are time invariant, the average properties of the resulting signals will also be time invariant. Such random data are said to be stationary. Unlike steady-state deterministic data, stationary random data must be described by a continuous spectrum.

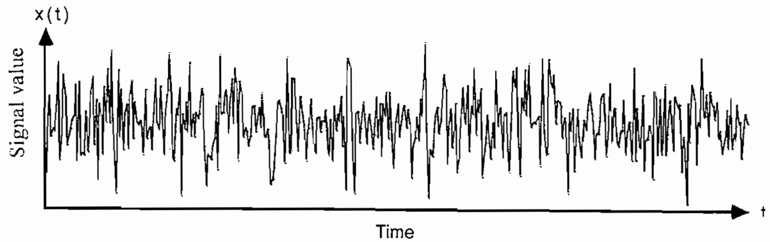

FIGURE 3.3 Time history for stationary random signal.

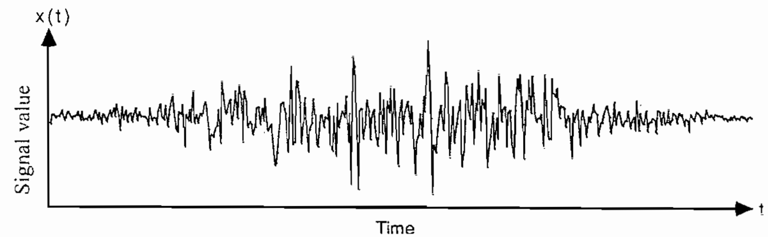

FIGURE 3.4 Time history for nonstationary random signal.

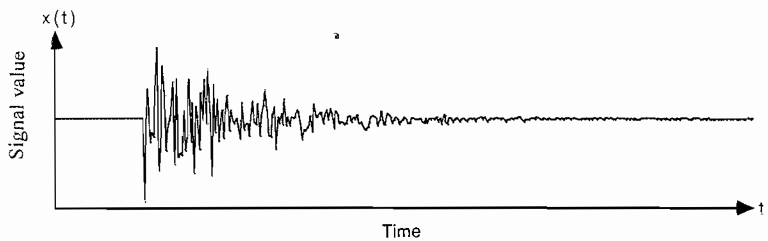

FIGURE 3.5 Time history for stochastic transient signal.

Furthermore, because of the probabilistic character of the data, the measurement of the spectrum and all other signal properties of interest will involve statistical sampling errors that do not occur in the analysis of deterministic signals. These statistical errors will be summarized later.

If the average properties of random signals vary with translations in time, the signals are said to be nonstationary. An illustration of nonstationary data is shown in Fig. 3.4. Although there is a well-developed theoretical methodology for the analysis of arbitrary nonstationary signals,[1] the analysis procedures often require more data than are commonly available and further involve extensive and complex computer calculations. An exception is a special class of nonstationary signals, called stochastic transients, that begin and end within a reasonable measurement time interval. Common sources of stochastic transients are hard impact loads and pyrotechnic devices. An illustration of a stochastic transient signal is shown in Fig. 3.5. Such data can be analyzed by procedures similar to those used to describe deterministic transients discussed earlier, except now there will be a statistical sampling error problem that must be addressed.

3.2 MEAN AND MEAN-SQUARE VALUES

The most rudimentary measures of any steady-state or stationary data signal are the mean value and the mean-square (ms) value (or variance), which provide single-valued descriptions of the central tendency and dispersion of the signal. Mean and ms values of signals can be measured using either digital computations[1] or analog instruments.[2] Hence, appropriate algorithms are presented for both digital and analog analysis procedures.

Mean Values

For acoustical and vibration signals, the mean value is commonly zero, simply because most transducers used for acoustical pressure and vibration acceleration measurements do not sense static values. However, if a transducer is used that senses static values and the central tendency of the signal is of interest, the mean value for a time history measurement, $x(t)$, of duration T_r is computed by

$$m_x = \frac{1}{T_r}\int_0^{T_r} x(t)\,dt \qquad (3.2a)$$

For digital data with a sampling interval of Δt, $x(t) = x(n\,\Delta t)$, $n = 1, 2, \ldots, N$, and the mean value is computed by

$$m_x = \frac{1}{N}\sum_{n=1}^{N} x(n\,\Delta t) \qquad (3.2b)$$

The mean value m_x in Eq. (3.2) has units of volts and is essentially the quantity computed by a direct current (DC) voltmeter. If the data signal is periodic, the calculation in Eq. (3.2) will be accurate as long as T_r (or $N\,\Delta t$) is an integer multiple of the period T_p. For random data, the calculation will involve a statistical sampling error that is a function of T_r (or N) and the spectral characteristics of the signal,[1] to be discussed later.

Mean-Square Values

The ms value of a steady-state or stationary acoustical or vibration signal $x(t)$ [or a digitized signal $x(n\,\Delta t)$] is defined by

$$w_x = \frac{1}{T_r}\int_0^{T_r} x^2(t)\,dt = \frac{1}{N}\sum_{n=1}^{N} x^2(n\,\Delta t) \qquad (3.3)$$

The ms value w_x in Eq. (3.3) has the units of volts squared, which is proportional to power or power per unit area, and hence w_x is often referred to as the overall "power" or "intensity" of the acoustical or vibration signal. If the mean value of the signal is zero, the ms value in Eq. (3.3) is equal to the variance of $x(t)$, defined as

$$s_x^2 = \frac{1}{T_r}\int_0^{T_r}[x(t) - \mu_x]^2\,dt = \frac{1}{N}\sum_{n=1}^{N}[x(n\ \Delta t) - \mu_x]^2 \tag{3.4}$$

where μ_x is the true mean value of the signal (m_x as $T_r \to \infty$). The positive square roots of the quantities defined in Eqs. (3.3) and (3.4), $w_x^{1/2}$ and s_x, are called the rms value and the standard deviation, respectively, of the signal $x(t)$. Again, $w_x^{1/2} = s_x$ if the mean value of the signal is zero, as will be assumed henceforth. The value s_x in Eq. (3.4), or $w_x^{1/2}$ in Eq. (3.3) when $\mu_x = 0$, is essentially the quantity measured by a true rms voltmeter (not to be confused with an alternating current (AC) voltmeter that employs a linear rectifier calibrated to measure the correct rms value for a sine wave and reads about 1 dB low when measuring random noise). As for mean-value calculations, the ms value calculation in Eq. (3.3) will be precise for periodic data if T_r is an integer multiple of the period T_p. For random data, however, there will be a statistical sampling error that is a function of T_r (or N) and the spectral characteristics of the signal,[1] to be discussed later.

Weighted Averages

The averaging operation indicated in Eqs. (3.2)–(3.4) is a simple linear sum of prior values over a specific time interval. This type of average, referred to as an unweighted or linear average, is the natural way one would average any set of discrete data values and is the simplest way for a digital computer to calculate an average value. However, some acoustical and vibration data analyses are still performed using analog instruments, where a relatively expensive operational amplifier is required to accomplish an unweighted average. Hence, the averaging operation in analog instruments is commonly weighted so that it can be accomplished using inexpensive passive circuit elements.[2] The most common averaging circuit used by analog instruments is a simple low-pass filter consisting of a series resistor and shunt capacitor (commonly called an RC filter) that produces an exponentially weighted average. For a ms value estimate (assuming the mean value is zero), the exponentially weighted average estimate is given by

$$w_x(t) = \frac{1}{K}\int_0^t x^2(\tau)\exp\left(-\frac{t-\tau}{K}\right)d\tau \tag{3.5}$$

where $K = RC$ is the product of the numerical values of the resistance in ohms and capacitance in farads used in the averaging circuit. The term K has units of time (seconds) and is referred to as the *time constant* of the averaging circuit. An exponentially weighted averaging circuit provides a continuous average value estimate versus time, which is based on all past values of the signal. It follows that after starting the average calculation, a period of time must elapse before the indicated average value is accurate. As a rule of thumb, when averaging a steady-state or stationary signal, at least four time constants ($t > 4K$) must elapse to obtain an average value estimate with an error of less than 2%. The error in question is a bias error. For the analysis of random data signals, there will also be a statistical sampling error, to be discussed later.

Running Averages

When the acoustical or vibration data of interest have average properties that are time varying (nonstationary data), "running" time averages are often used to describe the data. For the case of a ms value estimate, this could be accomplished by executing Eq. (3.3) repeatedly over short, contiguous time segments of duration $T \ll T_r$. Exponentially weighted averaging is particularly convenient for the computation of running averages because it produces a continuous average value estimate versus time. However, a near-continuous estimate can also be generated using an unweighted average (as is more desirable for digital data analysis) by simply recomputing an average value every data-sampling interval Δt rather than only at the end of the averaging time T. An illustration of a running average for the rms value of typical nonstationary acoustical data measured near an airport during an aircraft flyover is shown in Fig. 3.6 (the measurement in this illustration is a frequency-weighted rms value called *perceived noise level*).

The basic requirement in the computation of a running average is to select an averaging time T (or averaging time constant K) that is short enough not to smooth out the time variations of the data property being measured but long enough to suppress statistical sampling errors in the average value estimate at any time (assuming the data are at least partially random in character). Analytical procedures for selecting the averaging time T that provides an optimum compromise between the smoothing and statistical sampling errors have been formulated,[1] but trial-and-error procedures coupled with experience will usually provide adequate results. Also, many of the simpler acoustical and vibration

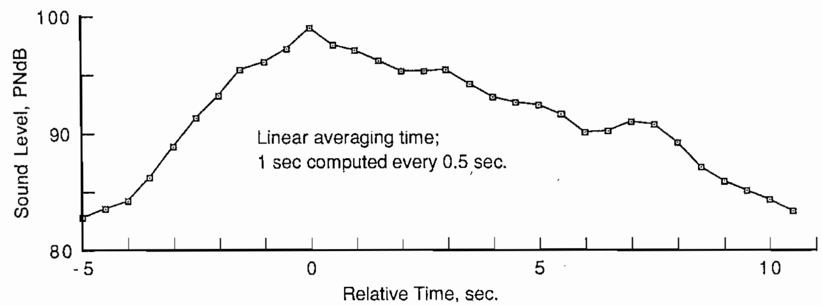

FIGURE 3.6 Running average for weighted rms value of aircraft flyover noise. (Courtesy of Acoustic Analysis Associates, Inc., Canoga, Park, CA.)

measurement instruments used in the field have fixed averaging times ("fast" and "slow" averaging circuits) built into the instrument.[2]

Statistical Sampling Errors

As mentioned earlier, there are no fundamental errors (other than instrument and calibration errors) associated with the calculation of mean and ms values of periodic data signals, assuming the averaging time is an integer multiple of the period of the signal. For random data signals, however, there will be a statistical sampling error due to the fact that the record duration and averaging time can never be long enough to cover all unique signal values. It is convenient to describe this statistical sampling error in terms of a normalized standard deviation of the resulting estimate, called the normalized random error (also called the coefficient of variation). The normalized random error of an estimate, $\hat{\theta}$, for a signal property θ is defined as

$$\epsilon_r[\hat{\theta}] = \frac{\sigma[\hat{\theta}]}{\theta} \tag{3.6}$$

where $\sigma[\cdot]$ denotes the standard deviation as defined in Eq. (3.4) with $T_r \to \infty$ and the hat denotes an estimate. The interpretation of the normalized random error is as follows. If a signal property θ is repeatedly estimated with a normalized random error of, say, 0.1, then about two-thirds of the estimates, $\hat{\theta}$, will be within $\pm 10\%$ of the true value of θ.

The normalized random errors of the mean, ms, and rms value estimates are summarized in Table 3.1.[1] In these error equations, B_s is a measure of the spectral bandwidth of the data signal, defined as[1]

$$B_s = \frac{w^2}{\int_0^\infty G^2(f)\,df} \tag{3.7}$$

where w is the ms value and $G(f)$ is the auto (power) spectrum of the data signal, to be addressed later. The error formulas in Table 3.1 are approximations that are valid for $\epsilon_r \leq 0.20$. Note in Table 3.1 that the random error for mean-value estimates is dependent on the true mean (μ_x) and standard deviation (σ_x) of the signal as well as the bandwidth (B_s) and averaging time (T or K). However, the

TABLE 3.1 Normalized Random Errors for Mean, ms, and rms Value Estimates

	Normalized Random Error, ϵ_r	
Signal Property	Linear Averaging with Averaging Time T	*RC* Weighted Averaging with Time Constant K
Mean value, m_x	$\sigma_x/[\mu_x(2B_sT)^{1/2}]$	$\sigma_x/[\mu_x(4B_sK)^{1/2}]$
ms value, w_x	$1/(B_sT)^{1/2}$	$1/(2B_sK)^{1/2}$
rms value, $w_x^{1/2}$	$1/(4B_sT)^{1/2}$	$1/(8B_sK)^{1/2}$

random error for ms and rms value estimates is a function only of the bandwidth and averaging time.

Synchronous Averaging

Periodic vibration and acoustical data signals produced by rotating machinery (including propellers and fans) are sometimes contaminated by additive, extraneous noise such that the measured signal is $x(t) = p(t) + n(t)$, where $p(t)$ is the periodic signal of interest and $n(t)$ is the noise. In such cases, the signal-to-noise ratio of the periodic signal can be strongly enhanced by the procedure of synchronous averaging,[3] where the data record is divided into a collection of segments $x_i(t)$, $i = 1, 2, \ldots, q$, each starting at exactly the same phase angle during a period of $p(t)$. The collection of segments can then be ensemble averaged to extract $p(t)$ from the extraneous noise as well as other periodic components that are not harmonically related to $p(t)$ as follows:

$$p(t) \approx \frac{1}{q} \sum_{i=1}^{q} x_i(t) \tag{3.8}$$

Synchronous averaging is illustrated in Fig. 3.7 for the pressure field generated in the plane of the propeller on the sidewall of a propeller airplane powered by a reciprocating engine. With 1000 ensemble averages (accomplished in less than 2 min), the procedure extracts the propeller pressure signal cleanly from the engine and boundary layer turbulence noise.

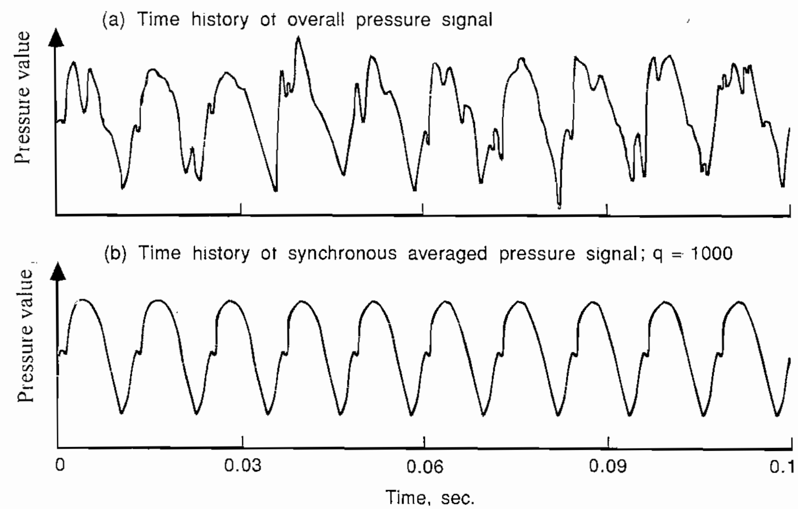

FIGURE 3.7 Original and synchronous averaged time histories for pressure measurement on sidewall of propeller airplane.

The primary requirement for synchronous averaging is the ability to initiate new records at a desired instant during a period of $p(t)$. This is most effectively accomplished using a trigger signal that is a noise-free indicator of the phase during each period of $p(t)$. For rotating machines, a noise-free trigger signal is commonly obtained using either an optical detector or a magnetic pulse generator on the rotating element of the machine. The time base accuracy of the trigger signal determines the accuracy of the magnitude of the resulting synchronous averaged signal; that is, time base errors in the trigger signal cause a reduction in the indicated signal amplitude with increasing frequency. The signal-to-noise ratio enhancement for the synchronous averaged signal is given in decibels by $10 \log_{10} q$, where q is the number of segments used in the ensemble-averaging operation[3].

3.3 SPECTRAL FUNCTIONS

The ms value of a digital signal constitutes an overall measure of the "power" or "intensity" represented by the measured quantity, but much more useful information is provided by a frequency decomposition of the signal values. As noted in Chapter 1, the computation of rms values in one-third-octave bands is widely used for the frequency analysis of acoustical data and sometimes for vibration data as well. However, the more advanced signal-processing techniques needed for system, source, and path identification problems require the computation of frequency spectra with a much finer resolution than one-third-octave bands. Furthermore, if the data are random in character, a frequency analysis in terms of power quantities per unit frequency (hertz) greatly facilitates the desired evaluations of the data signals.

Prior to 1965, most analysis of acoustical and vibration data signals, including the calculation of frequency spectra, was accomplished by analog instruments. Highly resolved frequency spectra were generally computed using narrow-band width analog filters, often employing mechanical elements such as resonant crystals or magnetostrictive devices.[2] Of course, narrow-bandwidth frequency spectra could also be computed, even at that time, on a digital computer using Fourier transform software, but the computations were time consuming and expensive because of the large number of data values needed to represent wide-bandwidth acoustical and vibration signals. In 1965, this situation changed dramatically with the introduction of an algorithm for the fast computation of Fourier series coefficients[4] that reduced the required computer calculations by several orders of magnitude. Various versions of this algorithm have since come into wide use and are generally referred to as fast Fourier transform (FFT) algorithms. The vast majority of all current narrow-bandwidth spectral analysis of acoustical and vibration data signals are performed using FFT algorithms.

The FFT Algorithm

Using lowercase letters for functions of time and uppercase letters for functions of frequency, the Fourier transform of a time history signal, $x(t)$, which is measured

over the time interval $0 \le t \le T$, is defined for all frequencies (both positive and negative) by

$$X(f, T) = \int_0^T x(t) e^{-j2\pi ft}\, dt \tag{3.9a}$$

In terms of a digital time series of N data values where $x(t) = x(n\ \Delta t)$, $n = 0, 1, \ldots, N-1$ (starting the indexing at $n = 0$ is helpful in maintaining consistent relationships between time and frequency functions), the Fourier transform may be written as

$$X(f, T) = X(k\ \Delta f, N) = \Delta t \sum_{n=0}^{N-1} x(n\ \Delta t)\ \exp(-j2\pi fn\ \Delta t) \tag{3.9b}$$

where the spectral components are generally complex valued and are defined only at N discrete frequencies given by

$$f_k = k\ \Delta f = \frac{k}{N\ \Delta t} \qquad k = 0, 1, 2, \ldots, N-1 \tag{3.9c}$$

The finite Fourier transform defined in Eq. (3.9), when divided by T (or $N\ \Delta t$), essentially yields the conventional Fourier series coefficients for a periodic function under the assumption that the time history record $x(t)$ is one period (or an integer multiple of one period) of the periodic function being analyzed. The Fourier components are unique only out to $k = \frac{1}{2}N$, that is, out to the frequency $f_k = 1/(2\ \Delta t)$, commonly called the Nyquist frequency, f_N, of the digitized signal. The Nyquist frequency is that frequency for which there are only two sample values per cycle and, hence, aliasing will initiate.[1] Comparing the digital result in Eq. (3.9b) with the analog formulation in Eq. (3.9a), the first $\frac{1}{2}N + 1$ Fourier coefficients, from $k = 0$ to $k = \frac{1}{2}N$, define the spectral components at nonnegative frequencies, while the last $\frac{1}{2}N - 1$ Fourier coefficients, from $k = \frac{1}{2}N + 1$ to $k = N - 1$, essentially define the spectral components at negative frequencies.

The details of the various FFT algorithms are fully documented in the literature (see refs. 1 and 4 and the signal analysis documents listed in the Bibliography). It is necessary here only to note a few basic characteristics of the most common algorithm used for acoustical and vibration work, which is commonly referred to as the *Cooley–Tukey algorithm* in recognition of the authors of the 1965 paper[4] that initiated the wide use of such algorithms:

1. It is convenient to restrict the number of data values for each FFT to a power of 2, that is, $N = 2^p$, where values of $p = 8$ to $p = 12$ are commonly used.
2. The fundamental frequency resolution of the Fourier components will be $\Delta f = 1/(N\ \Delta t)$.
3. The Nyquist frequency where aliasing will initiate, denoted by f_N, occurs at the $k = \frac{1}{2}N$ Fourier component, that is, $f_N = 1/(2\ \Delta t)$.

4. The first $\frac{1}{2}N+1$ Fourier components up to the Nyquist frequency are related to the last $\frac{1}{2}N-1$ components above the Nyquist frequency by $X(k)=X^*(N-k)$, $k=0,1,2,\ldots,N-1$, where the asterisk denotes complex conjugate.
5. The Fourier components defined only for positive frequencies (called a one-sided spectrum) are given by $X(0)$, $X(N/2)$, and $2X(k)$; $k=1,2,\ldots,N/2-1$.

Line and Fourier Spectral Functions

For deterministic signals that are periodic, a frequency decomposition or spectrum of the signal is directly obtained by computing the Fourier series coefficients of the signal over at least one period of the signal using an FFT algorithm. Assuming the mean value equals zero, the one-sided spectra of Fourier components for a periodic signal, $p(t)$, are given by

$$P(f)=\frac{2X(f,T)}{T} \qquad f>0 \text{ or } k=1,2,\ldots,\frac{N}{2}-1 \tag{3.10}$$

where $X(f,T)$ is as defined in Eq. (3.9). The Fourier component magnitudes, $|P(f)|$, are usually plotted versus frequency in the form of a discrete-frequency spectrum (often called a *line spectrum*), as illustrated earlier in Fig. 3.1*b*. Of course, each Fourier component is a complex number that defines a phase as well as a magnitude (the phases for the Fourier components in Fig. 3.1 are all zero). However, the phase information is generally retained only in those applications where there may be a need to reconstruct the signal time history or determine peak values.

Aliasing. Because of the aliasing problem inherent in digital spectral analysis,[1] it is important to assure there are no spectral components in the data signal being analyzed above the Nyquist frequency $[f_N=1/(2\,\Delta t)]$ for the analysis. This can be guaranteed only when the analog signal is low-pass filtered prior to the digitization to remove any spectral components that may exist in the signal above f_N. The low-pass filters employed to accomplish this task are commonly referred to as *antialiasing* filters and should always be used for all spectral analysis.

Leakage Errors and Tapering. Ideally, in the anaysis of periodic data, the spectral computations should be performed over an exact integer multiple of one period to avoid truncation errors in the Fourier series calculation. In practice, however, the computations are often terminated at a time that is convenient for the FFT algorithm and not related to the exact period of the data. The resulting truncation error leads to a phenomenon called side-lobe leakage[1,5] that can severely distort the desired results. To suppress this leakage, it is common to taper the measured time history signal in a manner that forces the values at the start and finish of the measurement to be zero, so as to eliminate the discontinuity between the beginning and ending data values. Numerous tapering functions (often called "windows") have been proposed over the years,[5] but one of the earliest and still most widely used is the *cosine-squared* taper (commonly called the *Hanning* window) given by

$$u_h(t)=1-\cos^2\frac{\pi t}{T} \qquad 0\le t\le T \tag{3.11}$$

The FFT is then performed on the signal, $y(t)=x(t)u_h(t)$, rather than directly on the original measured signal, $x(t)$. Leakage suppression can also be accomplished by equivalent operations in the frequency domain.

For deterministic signals that are not periodic and further have a well-defined beginning and end (transients), a spectrum of the signal is directly obtained by computing the Fourier transform of the signal over the entire duration of the signal, again using an FFT algorithm (to obtain a one-sided spectrum, the actual computation is $2X(k\,\Delta f)$, $k=1,2,\ldots,N/2-1$. The Fourier spectrum magnitude is plotted as a continuous function of frequency, as illustrated previously in Fig. 3.2*b*. Similar to the spectra for periodic signals, there is also a phase function associated with Fourier spectra, but it is generally retained only if the signal time history is to be reconstructed or peak values are of interest. As long as the FFT computation is performed over a measurement duration that covers the entire duration of the transient event, there is no side-lobe leakage problem in the analysis.

As a final point on transient signal analysis, it should be mentioned that transient data signals, particularly those produced by short-duration mechanical shocks, are often analyzed by a technique called the *shock response spectrum*,[6] which essentially defines the peak response of a hypothetical collection of single-degree-of-freedom mechanical systems to the transient input. The shock response spectrum can be a valuable tool for assessing the damaging potential of mechanical shock loads on equipment but is not particularly useful for noise and vibration reduction applications.

Auto (Power) Spectral Density Functions

The autospectral density function (also called the "power" spectral density function) provides a convenient and consistent measure of the frequency composition of random data signals. The autospectrum, denoted by $G_{xx}(f)$, is most easily visualized as the ms value of the signal passed through a narrow-bandpass filter divided by the filter bandwidth, as illustrated in Fig. 3.8. In equation form,

$$\hat{G}_{xx}(f)=\frac{1}{T\,\Delta f}\int_0^T x^2(f,\Delta f,t)\,dt \tag{3.12}$$

where $x(f,\Delta f,t)$ denotes the signal passed by the narrow-bandpass filter with a center frequency f and a bandwidth Δf. To obtain the exact autospectral density function, the operations in Fig. 3.8 would theoretically be carried out in the limit as $T\to\infty$ and $\Delta f\to 0$ such that $T\,\Delta f\to\infty$. It is clear from Fig. 3.8 and

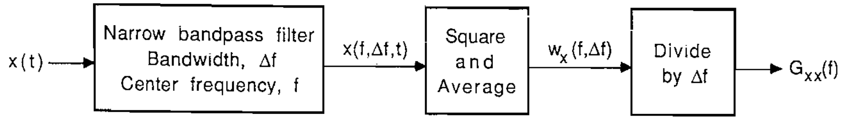

FIGURE 3.8 Autospectral density function measurement by analog filtering operations.

Eq. (3.12) that the units of the autospectral density function are volts squared per hertz.

The operations shown in Fig. 3.8 represent the way autospectra were computed by analog instruments[2] prior to the introduction of FFT algorithms and the transition to digital data analysis procedures. Today, with the ready availability of FFT hardware and software, the autospectral density function (at positive frequencies only) is estimated directly by[1]

$$G_{xx}(f) = \frac{2}{n_d T}\sum_{i=1}^{n_d} |X_i(f,\ T)|^2 \qquad f > 0 \tag{3.13}$$

where $X_i(f, T)$ is the FFT of $x(t)$ computed over the ith data segment of duration T, as defined in Eq. (3.9), and n_d is the number of disjoint (statistically independent) data segments used in the calculation. To obtain the exact autospectral density function, the operations in Eq. (3.13) would theoretically be carried out in the limit as $T \to \infty$ and $n_d \to \infty$. As will be seen later, the number of averages n_d determines the random error in the estimate, while the segment duration T for each FFT computation determines the resolution and, hence, a potential bias error in the estimate. The collection of disjoint data segments needed to estimate a statistically reliable autospectrum is usually created by dividing the total available measurement duration T_r into a sequence of contiguous segments of duration T, as illustrated in Fig. 3.9. It follows that $n_d = T_r/T = \Delta f\ T_r$, often referred to as the *BT product* of the estimate. It can be shown[1] that Eq. (3.13) is equal to the result in Eq. (3.12) when the appropriate limits are imposed, that is, when $T \to \infty$ and $\Delta f \to 0$ in Eq. (3.12) and $T \to \infty$ and $n_d \to \infty$ in Eq. (3.13). Note that the autospectral density function is always a real number (there is no phase information associated with autospectra).

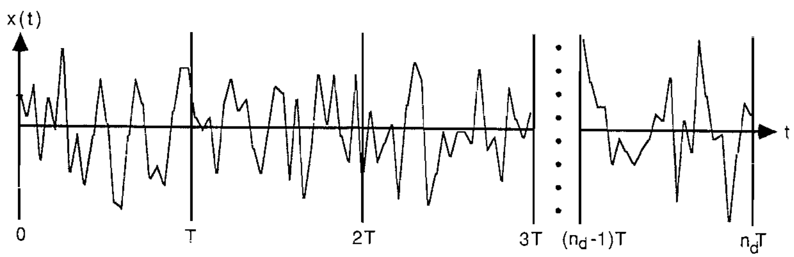

FIGURE 3.9 Subdivision of measured time history into n_d contiguous segments.

A number of grooming operations are commonly employed to enhance the quality of autospectral density estimates. A few of the more important ones are as follows (see the noted references for details).

Antialiasing Filters. As for periodic data analysis, to avoid aliasing, it is important that the random signal being analyzed have no spectral values above the Nyquist frequency, $f_N = 1/(2\ \Delta t)$. Hence, the analog signal must always be low-pass filtered prior to digitization to suppress any spectral content that may exist above f_N.[1]

Tapering Windows. Since random data signals essentially have an infinite period, there will always be a truncation error associated with the selected segment duration T. Hence, tapering operations (windows) are commonly used in random signal analysis to suppress the side-lobe leakage problem. Of the numerous available tapering functions,[5] the cosine-squared (Hanning) window defined in Eq. (3.11) is the most widely used.

Overlapped Processing. Although tapering operations on segments of the measured signal are desirable to suppress leakage, they also increase the bandwidth of the effective spectral window associated with the analysis.[5] If it is desired to maintain the same spectral window bandwidth with tapering that would have been achieved without tapering, the segment duration T for the analysis must be increased. However, assuming the total duration of the measurement T_r is fixed, this will reduce the number of disjoint averages n_d and increase the random error of the spectral estimates. This increase in random error can be counteracted by computing the spectrum with overlapped segments, rather than contiguous segments.[7,8] A 50% overlap is commonly used in such cases.

Zoom Transforms. As discussed earlier, FFT algorithms are usually implemented with a fixed number of data points. Hence once a desired upper frequency limit for an analysis (the Nyquist frequency f_N) has been chosen, the resolution of the analysis, Δf, as defined in Eq. (3.9c), is also fixed. Situations often arise when the desired upper frequency limit and frequency resolution are not compatible with the number of data points used by the FFT computation. In these cases, a finer resolution for a given value of f_N can be achieved using computation techniques referred to as *zoom transform* procedures.[1] The most common zoom transform techniques employ a complex demodulation calculation that essentially segments the frequency range of the signal into contiguous bands that are then analyzed separately.

Cross-Spectral Density Functions. The solution of acoustical and vibration control problems involving random processes is often facilitated by the identification of a linear dependence (correlation) between two measurements at different locations. The basic parameter that defines the linear dependence between two measured random signals, $x(t)$ and $y(t)$, as a function of frequency is the cross-spectral density function, which is estimated (at positive frequencies only) by[1]

$$G_{xy}(f) = \frac{2}{n_d T} \sum_{i=1}^{n_d} X_i^*(f, T) Y_i(f, T) \qquad f > 0 \tag{3.14a}$$

where $X_i(f, T)$ and $Y_i(f, T)$ are the FFTs of $x(t)$ and $y(t)$, respectively, computed over the ith simultaneous data segments of duration T, n_d is the number of disjoint records used in the calculation, and the asterisk denotes complex conjugate. As for autospectra, the exact cross-spectral density function would be obtained in the limit as $T \to \infty$ and $n_d \to \infty$. All of the computational considerations and grooming procedures discussed for autospectra apply to cross-spectra as well. Unlike the autospectrum, however, the cross-spectrum is generally a complex number that includes both magnitude and phase information and, hence, may be denoted in complex polar notation as

$$G_{xy}(f) = |G_{xy}(f)| e^{j\theta_{xy}(f)} \tag{3.14b}$$

Coherence Functions

For many applications, it is more convenient to work with a normalized version of the cross-spectral density function, called the coherence function (sometimes called coherency squared), which is defined as[1]

$$\gamma_{xy}^2(f) = \frac{|G_{xy}(f)|^2}{G_{xx}(f) G_{yy}(f)} \tag{3.15}$$

The coherence function is a real-valued quantity bounded by zero and unity, that is,

$$0 \le \gamma_{xy}^2(f) \le 1 \tag{3.16}$$

where a value of zero means there is no linear dependence and a value of unity means there is a perfect linear dependence between the signals $x(t)$ and $y(t)$ at the frequency f. A coherence value that is less than unity at one or more frequencies is usually indicative of one of the following situations[9]:

1. Extraneous noise is present in the measurements.
2. The frequency resolution of the spectral estimates is too wide.
3. The system relating $y(t)$ to $x(t)$ has time-dependent parameters.
4. The system relating $y(t)$ to $x(t)$ is not linear.
5. The output $y(t)$ is due to other inputs besides $x(t)$.

By carefully designing an experiment to minimize the first four possible reasons for a low coherence, the fifth reason provides the basis for a powerful procedure to identify acoustical noise and/or vibration sources. Specifically, if it is known that a constant-parameter linear system exists between a source and a receiver location, the source signal is measured with an adequate signal-to-noise ratio, and the spectra of the source and receiver signals are estimated with an adequate frequency resolution, then the coherence function defines the fractional portion of the receiver signal autospectral density that is due to the measured source signal. This is the basis for the coherent output power relationship, which is discussed and illustrated in Section 3.5.

Statistical Sampling Errors

There are no statistical sampling errors associated with the calculation of spectra for periodic signals, assuming the averaging time is an integer multiple of the period of the signal. The same is true of the calculation of Fourier spectra for deterministic transient signals, assuming the averaging time is longer than the transient. The calculation of spectral density quantities for random signals, however, will involve a random sampling error, as discussed previously in Section 3.2. First-order approximations for these random errors in autospectra, cross-spectra, and coherence function estimates are summarized in Table 3.2.[1] The random errors are presented in terms of the normalized random error (coefficient of variation) defined in Eq. (3.6), except for estimates of the cross-spectrum phase where the random error is given in terms of the standard deviation of the estimated phase angle in radians.

Beyond the random errors, there is also a bias error problem in the estimation of spectral density functions that occurs at peaks and valleys in the estimates. This bias error is caused by the finite-resolution bandwidth used for the calculations. For auto- and cross-spectral density magnitude estimates, the bias error is approximated in normalized terms by[1,9]

$$\epsilon_b[\hat{G}(f)] = \frac{b[\hat{G}(f)]}{G(f)} = -\frac{1}{3}\left(\frac{\Delta f}{B_r}\right)^2 \tag{3.17}$$

where $b[\cdot]$ denotes the bias error incurred by estimating $G(f)$ by its biased value $\hat{G}(f)$, Δf is the frequency resolution of the analysis, and B_r is the half-power-point bandwidth of a spectral peak in either $G_{xx}(f)$ or $|G_{xy}(f)|$ at that frequency. There is no general bias error equation for coherence function estimates, but error relationships have been formulated for special cases.[10]

TABLE 3.2 Normalized Random Errors for Autospectra, Cross-Spectra, and Coherence Function Estimates

Signal Property	Normalized Random Error ϵ_r or Standard Deviation σ_r
Autospectral density function, $G_{xx}(f)$	$\epsilon_r = 1/n_d^{1/2}$
Cross-spectral density magnitude, $\lvert G_{xy}(f)\rvert$	$\epsilon_r = 1/[n_d \gamma_{xy}^2(f)]^{1/2}$
Cross-spectral density phase, $\theta_{xy}(f)$	$\sigma_r = [1-\gamma_{xy}^2(f)]^{1/2}/[2n_d\gamma_{xy}^2(f)]^{1/2}$
Coherence function, $\gamma_{xy}^2(f)$	$\epsilon_r = [1-\gamma_{xy}^2(f)]/[0.5 n_d \gamma_{xy}^2(f)]^{1/2}$

3.4 CORRELATION FUNCTIONS

Certain noise and vibration control problems that involve relatively wide bandwidth random data signals are beast addressed using time domain signal-processing procedures, as opposed to the frequency domain spectral analysis techniques discussed in the previous section. The basic calculation of interest is the correlation function between two random data signals, $x(t)$ and $y(t)$, which is estimated by

$$R_{xy}(\tau) = \frac{1}{T-\tau}\int_0^{T-\tau} x(t)y(t+\tau)\,dt \tag{3.18a}$$

where τ is a time delay. In digital notation,

$$R_{xy}(r\ \Delta t) = \frac{1}{N-r}\sum_{n=1}^{N-r} x[n\ \Delta t]y[(n+r)\ \Delta t] \tag{3.18b}$$

where r is a lag number corresponding to a time delay of $r\ \Delta t$. The general quantity estimated in Eq. (3.18) is called the cross-correlation function between the signals $x(t)$ and $y(t)$. For the special case where $x(t) = y(t)$,

$$R_{xx}(\tau) = \frac{1}{T-\tau}\int_0^{T-\tau} x(t)x(t+\tau)\,dt \tag{3.19}$$

is called the autocorrelation function of $x(t)$. Note that for $\tau = 0$, the autocorrelation function is simply w_x, the ms value of the signal. In both Eqs. (3.18) and (3.19), the estimated quantities will become exact in the limit as the averaging time $T \to \infty$. For finite values of T, there will be a random sampling error in the estimates, to be discussed later.

The correlation function is related to the spectral density function through a Fourier transform,[1]

$$G_{xy}(f) = 2\int_{-\infty}^{\infty} R_{xy}(\tau)e^{-j2\pi f\tau}\,d\tau \tag{3.20}$$

Equation (3.20), often called the *Wiener–Khinchine relationship*, is the basis for computing correlation functions in practice. Specifically, the spectral density function is first computed by the FFT procedures outlined in Section 3.3. An inverse Fourier transform of the spectral density function is then computed to obtain the correlation function. Due to the remarkable efficiency of the FFT algorithm, this approach requires substantially fewer calculations than that needed to compute Eq. (3.18b) directly. However, due to the *circular effects* associated with the FFT algorithm, a number of special operations are needed to obtain correct results, as detailed in reference 1.

Correlation Coefficient Function

For many applications, it is more convenient to work with the normalized cross-correlation function between $x(t)$ and $y(t)$, called the correlation coefficient

function, which is given by (assuming the mean value is zero)

$$\rho^2(\tau) = \frac{R_{xy}^2(\tau)}{R_{xx}(0)R_{yy}(0)} = \frac{R_{xy}^2(\tau)}{w_x w_y} \tag{3.21}$$

The correlation coefficient function (sometimes called the squared correlation coefficient function) is similar to the coherence function, defined in Section 3.3, in that it is a real-valued quantity bounded by zero and unity, that is,

$$0 \le \rho_{xy}^2(\tau) \le 1 \tag{3.22}$$

where a value of zero means there is no linear dependence and a value of unity means there is a perfect linear dependence[1] between $x(t)$ and $y(t)$ at the time displacement τ. Hence, the correlation coefficient function is interpreted much like the frequency domain coherence function discussed in Section 3.3, except the correlation coefficient function applies to the entire frequency range of the two signals while the coherence function applies to specific frequencies. Also, from Eq. (3.14b), time delay information in the correlation coefficient function is related to the phase information in the cross-spectral density function by

$$\theta(f) = 2\pi f\tau \tag{3.23}$$

Hence, the phase of the cross-spectrum can be valuable for extracting time delay information when the time delay is a function of frequency.[11]

Statistical Sampling Errors

When applied to random data signals, the computation of correlation functions will involve a statistical sampling error. In terms of a normalized random error defined in Eq. (3.6), the error in a cross-correlation estimate can be approximated by[1]

$$\epsilon_r[\hat{R}_{xy}(\tau)] = \left(\frac{1 + 1/\rho_{xy}^2(\tau)}{2B_sT_r}\right)^{1/2} \tag{3.24}$$

where $\hat{R}_{xx}(\tau)$ is an estimate of $R_{xx}(\tau)$, T_r is the total measurement duration over which the computations are performed, and B_s is the smallest statistical bandwidth for the two data signals, as defined in Eq. (3.7).

3.5 DATA ANALYSIS APPLICATIONS

The applications for signal analysis in noise and vibration studies are extensive and can become quite elaborate.[9] However, as mentioned in the introduction to this chapter, there are three specific application areas of special interest for noise and vibration control problems: (a) the identification of system response properties, (b) the identification of excitation sources, and (c) the identification of transmission paths.

Identification of System Response Properties

The control of noise and vibration is often facilitated by the determination of gain factors between excitation sources and receiver location responses. The fundamental measurement of interest here is the frequency response function (sometimes called the transfer function) between the two points of interest. Given an excitation source signal $x(t)$ and a simultaneously measured response signal $y(t)$, the frequency response function between the source and receiver signal is given by[1]

$$H_{xy}(f) = \frac{G_{xy}(f)}{G_{xx}(f)} \tag{3.25a}$$

where the auto- and cross-spectral density functions are as defined in Eqs. (3.13) and (3.14), respectively. The frequency response function is generally a complex-valued quantity that is more conveniently expressed in complex polar notation as

$$H_{xy}(f) = |H_{xy}(f)|\ e^{i\phi_{xy}(f)} \tag{3.25b}$$

where the magnitude function $|H_{xy}(f)|$ is the gain factor and the argument $\phi_{xy}(f)$ is the phase factor between $x(t)$ and $y(t)$. In the more advanced applications, such as normal-mode analysis,[12] both the gain and phase factor are needed. In many elementary applications, however, only the gain factor may be of interest.

The normalized random error in frequency response magnitude (gain factor) estimates is approximated by[1]

$$\epsilon_r[|\hat{H}_{xy}(f)|] \approx \frac{[1-\gamma_{xy}^2(f)]^{1/2}}{[2n_d\gamma_{xy}^2(f)]^{1/2}} \tag{3.26}$$

where $\hat{H}_{xy}(f)$ is an estimate of $H_{xy}(f)$, $\gamma_{xy}^2(f)$ is the coherence function between the source and receiver signals, and n_d is the number of disjoint averages used to compute the autospectra and cross-spectra from which the gain factor is calculated. The random error in frequency response phase estimates is the same as given for the phase of cross-spectral density estimates in Table 3.2.

Like coherence function estimates, the random error in a gain factor estimate approaches zero as the coherence function approaches unity, even for a small number of averages in the spectral density estimates. Hence, if the coherence function is large, the gain factor can be estimated with greater accuracy than the spectral density estimates used in its computation.

There are several sources of bias errors in gain factor estimates,[1,9] but the most significant is due to the frequency resolution bias error in the spectral density functions used to compute the gain factor, as given by Eq. (3.17). As a rule of thumb, if there are at least four spectral components between the half-power points of peaks in the spectral data, that is, if $\epsilon_b[G(f)] < 0.02$ in Eq. (3.17), then the bias error in the gain factor estimate should be negligible.

As an illustration of the application of gain factor estimates, consider the experiment illustrated in Fig. 3.10, involving two vibration measurements made on a

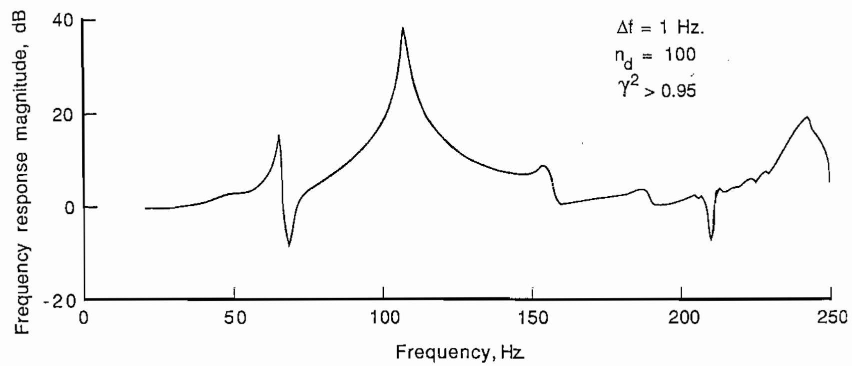

FIGURE 3.10 Gain factor estimate for component in space vehicle payload.

simulated spacecraft payload during a vibration test. One of the measurements is near the mounting point of the payload, and the other is on a critical payload element where vibration may adversely affect the payload performance. The gain factor clearly reveals a frequency region (around 110 Hz) where vibration at the mounting point is greatly magnified at the critical element of concern, due to a strong normal-mode response (resonance) of the payload at this frequency. It follows that efforts to reduce the vibration should be concentrated in this frequency region.

Identification of Periodic Excitation Sources

The identification of periodic acoustical and vibration excitations can usually be accomplished by a straightforward narrow-bandwidth spectral analysis plus a knowledge of the rpm of all rotating machinery producing the acoustical noise and/or vibration. This is illustrated in Fig. 3.11, which shows the spectrum for the vibration on the floor of a microelectronics manufacturing facility with extensive

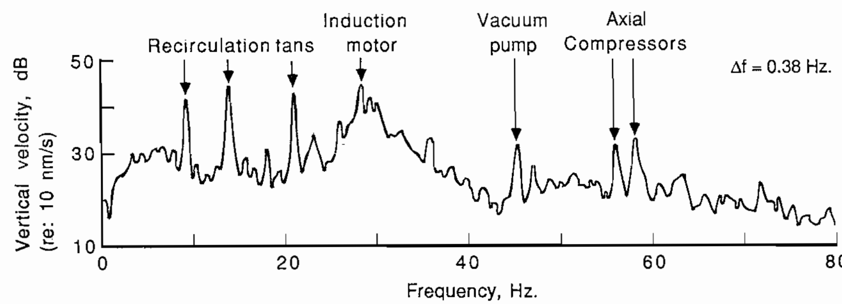

FIGURE 3.11 Fourier spectrum of floor vibration in microelectronics facility. (Courtesy of BBN Laboratories, Inc., Canoga Park, CA.)

air conditioning equipment. It is seen that the more intense spectral peaks in the vibration data can be directly identified with specific rotating machines simply through a knowledge of the rotational frequencies. Of course, this approach cannot separate the vibration contributions of two rotating machines that operate at exactly the same frequency. However, as long as there is some difference in the rotational speed between two machines, say, Δg hertz, the contributions of the machines can theoretically be separated by a spectral analysis with a frequency resolution Δf that is less than Δg. In practice, it is desirable to have

$$\Delta f = \frac{1}{T} < \frac{\Delta g}{3} \tag{3.27}$$

where T is the segment duration for the spectral computation. Since the signals are periodic or almost periodic, there is no random error associated with the resulting spectral estimates.

Identification of Random Excitation Sources

When two or more sources of an acoustical and/or vibration environment are random in character and further cover essentially the same frequency range, the identification of the contributions of the individual sources is more difficult. If possible, the contribution of each source of excitation should be identified by turning off all but one of the sources so that the effects of each source can be measured individually. If this is not possible, then the principle of coherent output power might be applied. Specifically, measure the acoustical or vibration signal produced at the source location for each of a collection of q suspected sources, denoted by $x_i(t)$, $i = 1, 2, \ldots, q$. For each individual source signal, simultaneously measure the receiver signal $y(t)$ and compute the coherence function between the ith source and receiver signals using Eq. (3.15). Under proper conditions, the autospectrum of the receiver signal due solely to the contribution of the ith source signal is given by

$$G_{y:i}(f) = \gamma_{iy}^2(f) G_{yy}(f) \tag{3.28}$$

where $G_{y:i}(f)$ reads "the portion of the autospectrum of the receiver signal that is due only to the source signal $x_i(t)$." Equation (3.28) is called the coherent output power relationship. If used properly, it can be a powerful tool for separating the contributions of various possible sources of random excitation in acoustical noise and vibration problems. The primary requirements for the proper application of the coherent output power relationship are as follows[9]:

1. The candidate sources of excitation (or the responses in the immediate vicinity of the sources) must be measured accurately and with negligible measurement noise. However, since the coherence function is dimensionless, any type of transducer (pressure, velocity, acceleration, or displacement) can be used for the source measurements as long as it generates a signal that has a linear relationship with the excitation phenomenon.

2. The candidate sources must be statistically independent, and there must be no interference (crosstalk) in the measurement of any one source due to energy propagating from the other sources; that is, the coherence functions among the measured source signals must all be zero.
3. There must be no significant feedback or nonlinear effects between the candidate source and receiver signals.

The normalized random error for coherent output power measurements is approximated by[1]

$$\epsilon_r[\hat{G}_{y:i}(f)] \approx \frac{[2 - \gamma_{iy}^2(f)]^{1/2}}{[n_d \gamma_{iy}^2(f)]^{1/2}} \tag{3.29}$$

where $\hat{G}_{y:i}(f)$ is an estimate of $G_{y:i}(f)$, $\gamma_{iy}^2(f)$ is the coherence function between the ith source signal and the receiver signal, and n_d is the number of disjoint averages used to compute the autospectra and cross-spectra from which the coherent output is calculated. It is clear from Eq. (3.29) that the number of disjoint records (and hence the total measurement duration, $T_r = n_d T$) required for an accurate coherent output power calculation will be substantial when $\gamma_{iy}^2(f) \ll 1$, as will commonly occur if there are numerous independent sources contributing to $y(t)$.

A serious bias error can occur in coherent output power calculations due to time delays between the source and receiver signals that may arise when there is a substantial distance between the source and receiver measurement positions[1,9,10,13] or the measurements are made in a reverberant environment[9,14] Since the two measurements are usually recorded and analyzed on a common time base, time delays between the source and receiver signals will cause a portion of the received signal to be uncorrelated with the source signal. These time-delay-induced bias errors can be suppressed by the use of precomputation delays or the selection of an appropriately long block duration T in the data analysis, as detailed in references 9, 13, and 14.

To illustrate the coherent output power calculation, consider the experiment outlined in Fig. 3.12, where a panel section excited by a broadband random vibration source radiates acoustical noise to a receiver microphone. The autospectrum of the radiated noise, $y(t)$, as seen by the receiver microphone with no other

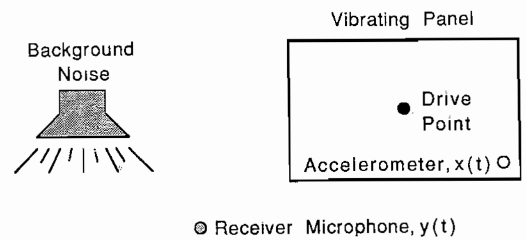

FIGURE 3.12 Acoustical source identification experiment with radiating panel in background noise.

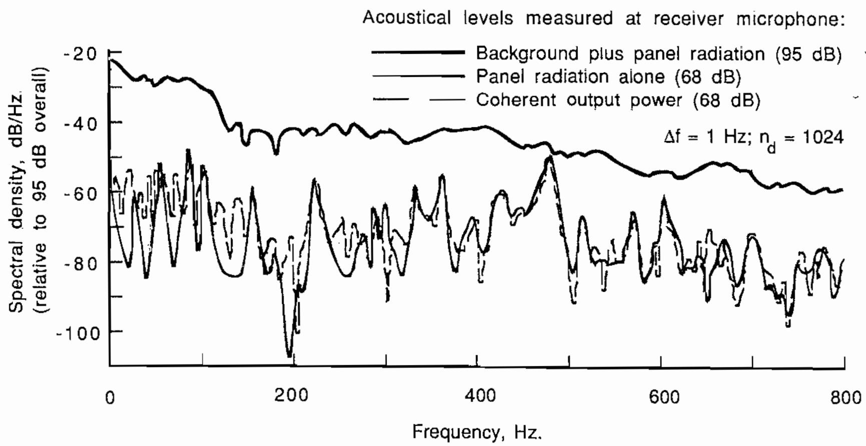

FIGURE 3.13 Overall and coherent output power spectra for radiating panel in background noise. (From Ref. 9 with the permission of the authors.)

noise sources present, is shown by the thin solid line in Fig. 3.13. Statistically independent background noise is now introduced by a speaker to produce acoustical energy with an overall value that is about 500 times more intense (27 dB higher) than the panel-radiated noise. The autospectrum of the total received microphone signal due to both the panel radiation plus the background noise is also shown in Fig. 3.13, by the heavy solid line. Finally, the coherent output power between the microphone and an accelerometer mounted on the panel is computed with the background noise present. This result is shown by the dashed line in Fig. 3.13. It is seen that the coherent output power calculation extracts the autospectrum of the radiated panel noise, as measured by an accelerometer, from the intense background noise with reasonable accuracy at most frequencies. The reason the procedure works in this example is that the radiated noise from the panel has a linear relationship with the panel motion measured by the accelerometer. Furthermore, since the panel is driven from only one point, the vibration response at any one point on the panel is representative of the vibration at all points.

Identification of Propagation Paths

Another analysis of great importance in acoustical noise and vibration control problems is the identification of the physical path or paths by which energy from a source of excitation travels to a receiver location. For those cases involving broadband random energy that propagates in a nondispersive manner (with a frequency-independent propagation speed), such as airborne noise, the identification of propagation paths can often be accomplished by a cross-correlation analysis. Specifically, assume a source signal $x(t)$ propagates in a nondispersive manner through r paths to produce a receiver signal $y(t)$. For simplicity, further

assume the propagation paths have uniform (frequency-independent) gain factors denoted by H_i, $i = 1, 2, \ldots, r$. It follows that

$$y(t) = H_1 x(t - \tau_1) + H_2 x(t - \tau_2) + \cdots + H_r x(t - \tau_r) \tag{3.30}$$

where τ_i, $i = 1, 2, \ldots, r$, are the propagation times through each of the paths. Then, from Eqs. (3.18) and (3.19),

$$R_{xy}(\tau) = H_1 R_{xx}(\tau - \tau_1) + H_2 R_{xx}(\tau - \tau_2) + \cdots + H_r R_{xx}(\tau - \tau_r) \tag{3.31}$$

In words, the cross-correlation function between the source and receiver signals will be a series of superimposed autocorrelation functions, each associated with a nondispersive propagation path and centered on a time delay equal to the propagation time along that path. Referring to Eq. (3.20), if the source signal has a wide bandwidth, these autocorrelation peaks will decay rapidly when τ deviates from τ_i and will be sharply defined in the cross-correlation estimate, as illustrated in Fig. 3.14. Noting that the propagation time for each path is the ratio of distance to propagation speed, the physical path associated with each correlation peak can usually be identified from a knowledge of the length of the path and the propagation speed of the nondispersive waves in the medium forming the path. Finally, the portion of the receiver signal ms value that propagated through a specific path is proportional to the square of the magnitude of the correlation peak associated with that path. The normalized random error associated with the estimate of $R_{xy}(\tau)$ in Eq. (3.31) is given by Eq. (3.24).

For a cross-correlation analysis to be effective in identifying different nondispersive propagation paths, several requirements must be met, as follows.

1. The source $x(t)$ must be a broadband random signal.
2. The propagation paths must have reasonably uniform gain factors.
3. The propagation time through each path must be different from all other paths.

As a rule of thumb,[9] the difference in the propagation times through any pair of paths must be $\Delta t > 1/B_s$, where B_s is the spectral bandwidth of the receiver

FIGURE 3.14 Cross-correlation function between source and receiver signals with two nondispersive propagation paths.

signal, as defined in Eq. (3.7). As the spectral bandwidth becomes small, the peaks in the cross-correlation function spread, and the ability to identify peaks representing individual propagation paths diminishes. There are a number of other signal-processing operations that will enhance the ability to detect individual propagation paths between two signals when the bandwidth is not wide.[9] Also, the use of envelope functions generated by Hilbert transforms can further enhance such detections.[1] Nevertheless, in the limiting narrow-band case where the source signal is a sine wave (or any periodic function), the identification of individual propagation paths cannot be achieved by any signal-processing procedure no matter how large a difference there is between the propagation times through the various paths.

To illustrate this application of cross-correlation analysis to a propagation path identification problem, consider the experiment shown in Fig. 3.15, which involves a speaker that produces acoustical noise with a bandwidth of approximately 8 kHz. Two microphones are used to measure the noise, one located in front of the speaker and another located 0.68 m from the speaker. There is a wall behind the receiver microphone that causes a back reflection producing a second path between the source and receiver microphones with a length of 1.7 m. The computed cross-correlation function between the source and receiver signals is shown in Fig. 3.16. It is seen that two maxima appear in the cross-correlation estimate at 2 and 5 ms. Noting that the speed of sound in air at room

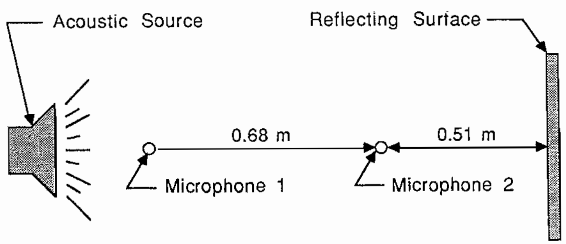

FIGURE 3.15 Acoustical propagation path experiment with back reflection.

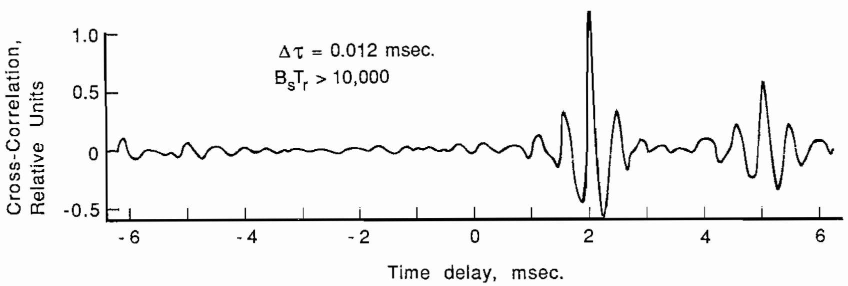

FIGURE 3.16 Cross-correlation function between two microphone signals with back reflection. (From Ref. 9 with the permission of the authors.)

temperature is about 340 m/s, these two peaks clearly identify the direct path and the back reflection. The magnitude of the correlation peak corresponding to the back reflection is only about 40% of the magnitude of peak corresponding to the direct path, as would be expected due to spherical spreading loss; that is, the reflected path is 2.5 times longer than the direct path and, hence, should be about 8 dB lower in level.

The cross-correlation analysis procedure often works well in multipath acoustical problems where the propagation is in the form of longitudinal waves that are nondispersive. In structural vibration problems, there may also be some nondispersive longitudinal wave propagation, but most vibratory energy in structures propagates in the form of flexural waves, which are dispersive,[15] that is, the propagation velocity is a function of frequency. Also, flexural waves strongly reflect and/or scatter at locations where there are changes in either the material properties or the geometry of the structural path. These facts greatly complicate the detection of individual propagation paths in multipath structural vibration problems. Nevertheless, meaningful results can sometimes be obtained through the judicious use of bandwidth-limited cross-correlation analyses[1,9] if the structural paths are reasonably homogeneous.

REFERENCES

1. J. S. Bendat and A. G. Piersol, *RANDOM DATA: Analysis and Measurement Procedures*, 3rd ed., Wiley, New York, 2000.
2. L. L. Beranek, *Acoustical Measurements*, rev. ed., Acoustical Society of America, Woodbury, NY, 1988.
3. H. Himelblau et al., *Handbook for Dynamic Data Acquisition and Analysis*, IEST-RP-DTE012.1, Institute of Environmental Sciences and Technology, Rolling Meadows, IL, 1994.
4. J. W. Cooley and J. W. Tukey, "An Algorithm for the Machine Calculation of Complex Fourier Series," *Math. Computat.*, **19**, 297–301 (1965).
5. F. J. Harris, "On the Use of Windows for Harmonic Analysis with the Discrete Fourier Transform," *Proc. IEEE*, **66**(1), 51–83, (1978).
6. S. Rubin, "Concepts in Shock Data Analysis," in C. M. Harris and A. G. Piersol (Eds.), *Harris' Shock and Vibration Handbook*, 5th ed., McGraw-Hill, New York, 2002.
7. P. D. Welch, "The Use of Fast Fourier Transforms for the Estimation of Power Spectra: A Method Based on Time Averaging Over Short, Modified Periodograms," *IEEE Trans. Audio Electroacoust.*, **AU-15**(2), 70–73 (1967).
8. A. H. Nuttall, "Spectral Estimates by Means of Overlapped Fast Fourier Transformed Processing of Windowed Data," NUSC TR-4169, Naval Underwater Systems Center, New London, CT, October 1971.
9. J. S. Bendat and A. G. Piersol, *Engineering Applications of Correlation and Spectral Analysis*, 2nd ed. Wiley, New York, 1993.
10. H. Schmidt, "Resolution Bias Errors in Spectral Density, Frequency Response and Coherence Function Estimates," *J. Sound Vib.*, **101**(3), 347–427 (1985).

11. A. G. Piersol, "Time Delay Estimation Using Phase Data," *IEEE Trans. Acoust. Speech Signal Proc.*, **ASSP-29**(3), 471–477 (1981).
12. R. J. Allemang and D. L. Brown, "Experimental Modal Analysis," in C. M. Harris and A. G. Piersol (Eds.), *Harris' Shock and Vibration Handbook*, 5th ed., McGraw-Hill, New York, 2002.
13. M. W. Trethewey and H. A. Evensen, "Time-Delay Bias Errors in Estimating Frequency Response and Coherence Functions from Windowed Samples of Continuous and Transient Signals," *J. Sound Vib.*, **97**(4), 531–540 (1984).
14. K. Verhulst and J. W. Verheij, "Coherence Measurements in Multi-Delay Systems," *J. Sound Vib.*, **62**(3), 460–463 (1979).
15. L. Cremer, M. Heckl, and E. E. Ungar, *Structure-Borne Sound*, 2nd ed., Springer-Verlag, New York, 1988.

BIBLIOGRAPHY

Brigham, E. O., *The Fast Fourier Transform and Its Applications*, Prentice-Hall, Englewood Cliffs, NJ, 1988.

Crocker, M. J., *Handbook of Acoustics*, Wiley, New York, 1998.

Doebelin, E. O., *Measurement Systems: Application and Design*, 5th ed., McGraw-Hill, New York, 2004.

Harris, C. M., *Handbook for Acoustic Measurements and Noise Control*, 3rd ed., McGraw-Hill, New York, 1991.

Harris, C. M., and A. G. Piersol, *Harris' Shock and Vibration Handbook*, 5th ed., McGraw-Hill, New York, 2002.

Hassall, E. R., and K. Zaven, *Acoustic Noise Measurements*, 5th ed., Bruel & Kjaer, Naerum, Denmark, 1989.

Mitra, S. K., and J. F. Kaiser, *Handbook for Digital Signal Processing*, Wiley, New York, 1993.

Newland, D. E., *Random Vibrations, Spectral and Wavelet Analysis*, 3rd ed., Wiley, New York, 1993.

Oppenheim, A. V., and R. W. Schafer, *Discrete-Time Signal Processing*, 2nd ed., Prentice-Hall, Englewood Cliffs, NJ, 1999.

Smith, S. W., *The Scientist and Engineer's Guide to Digital Signal Processing*, 2nd ed., California Technical Publishing, San Diego, CA, 2002. (Online: http://www.dspguide.com/pdfbook.htm)

Wirsching, P. H., T. L. Paez, and H. Ortiz, *Random Vibrations, Theory and Practice*, Wiley, New York, 1995.

Wright, C. P., *Applied Measurement Engineering*, Prentice-Hall, Englewood Cliffs, NJ, 1995.

CHAPTER 4

Determination of Sound Power Levels and Directivity of Noise Sources

WILLIAM W. LANG
Noise Control Foundation
Poughkeepsie, New York

GEORGE C. MALING, JR
Harpswell, Maine

MATTHEW A. NOBILE
IBM Hudson Valley Acoustics Laboratory
Poughkeepsie, New York

JIRI TICHY
The Pennsylvania State University
University Park, Pennsylvania

4.1 INTRODUCTION

Noise control can be considered as a system problem, the system containing three major parts: the source, the path, and the receiver.[1]

In any noise control problem, sound energy from the source or sources travels over a multiplicity of paths, both in solid structures and in air, to reach the receiver—an individual, a group of people, a microphone or other instrument, or a structure that is affected by the noise. Three action words are associated with the source–path–receiver model: *emission, transmission*, and *immission*. Sound energy that is emitted by a noise source is transmitted to a receiver where it is immitted. Transmission is treated in Chapters 5–7, 10, and 11. Immission is treated in Chapter 19.

Sound pressure level is the physical quantity usually used to describe a sound field quantitatively because the ear responds to sound pressure. A sound-level meter may be used to readily measure the sound pressure level at the location in the sound field occupied by the receiver. Therefore, the preferred descriptor of immission is the sound pressure level in decibels. However, the sound pressure

11. A. G. Piersol, "Time Delay Estimation Using Phase Data," *IEEE Trans. Acoust. Speech Signal Proc.*, **ASSP-29**(3), 471–477 (1981).
12. R. J. Allemang and D. L. Brown, "Experimental Modal Analysis," in C. M. Harris and A. G. Piersol (Eds.), *Harris' Shock and Vibration Handbook*, 5th ed., McGraw-Hill, New York, 2002.
13. M. W. Trethewey and H. A. Evensen, "Time-Delay Bias Errors in Estimating Frequency Response and Coherence Functions from Windowed Samples of Continuous and Transient Signals," *J. Sound Vib.*, **97**(4), 531–540 (1984).
14. K. Verhulst and J. W. Verheij, "Coherence Measurements in Multi-Delay Systems," *J. Sound Vib.*, **62**(3), 460–463 (1979).
15. L. Cremer, M. Heckl, and E. E. Ungar, *Structure-Borne Sound*, 2nd ed., Springer-Verlag, New York, 1988.

BIBLIOGRAPHY

Brigham, E. O., *The Fast Fourier Transform and Its Applications*, Prentice-Hall, Englewood Cliffs, NJ, 1988.

Crocker, M. J., *Handbook of Acoustics*, Wiley, New York, 1998.

Doebelin, E. O., *Measurement Systems: Application and Design*, 5th ed., McGraw-Hill, New York, 2004.

Harris, C. M., *Handbook for Acoustic Measurements and Noise Control*, 3rd ed., McGraw-Hill, New York, 1991.

Harris, C. M., and A. G. Piersol, *Harris' Shock and Vibration Handbook*, 5th ed., McGraw-Hill, New York, 2002.

Hassall, E. R., and K. Zaven, *Acoustic Noise Measurements*, 5th ed., Bruel & Kjaer, Naerum, Denmark, 1989.

Mitra, S. K., and J. F. Kaiser, *Handbook for Digital Signal Processing*, Wiley, New York, 1993.

Newland, D. E., *Random Vibrations, Spectral and Wavelet Analysis*, 3rd ed., Wiley, New York, 1993.

Oppenheim, A. V., and R. W. Schafer, *Discrete-Time Signal Processing*, 2nd ed., Prentice-Hall, Englewood Cliffs, NJ, 1999.

Smith, S. W., *The Scientist and Engineer's Guide to Digital Signal Processing*, 2nd ed., California Technical Publishing, San Diego, CA, 2002. (Online: http://www.dspguide.com/pdfbook.htm)

Wirsching, P. H., T. L. Paez, and H. Ortiz, *Random Vibrations, Theory and Practice*, Wiley, New York, 1995.

Wright, C. P., *Applied Measurement Engineering*, Prentice-Hall, Englewood Cliffs, NJ, 1995.

CHAPTER 4

Determination of Sound Power Levels and Directivity of Noise Sources

WILLIAM W. LANG
Noise Control Foundation
Poughkeepsie, New York

GEORGE C. MALING, JR
Harpswell, Maine

MATTHEW A. NOBILE
IBM Hudson Valley Acoustics Laboratory
Poughkeepsie, New York

JIRI TICHY
The Pennsylvania State University
University Park, Pennsylvania

4.1 INTRODUCTION

Noise control can be considered as a system problem, the system containing three major parts: the source, the path, and the receiver.[1]

In any noise control problem, sound energy from the source or sources travels over a multiplicity of paths, both in solid structures and in air, to reach the receiver—an individual, a group of people, a microphone or other instrument, or a structure that is affected by the noise. Three action words are associated with the source–path–receiver model: *emission, transmission*, and *immission*. Sound energy that is emitted by a noise source is transmitted to a receiver where it is immitted. Transmission is treated in Chapters 5–7, 10, and 11. Immission is treated in Chapter 19.

Sound pressure level is the physical quantity usually used to describe a sound field quantitatively because the ear responds to sound pressure. A sound-level meter may be used to readily measure the sound pressure level at the location in the sound field occupied by the receiver. Therefore, the preferred descriptor of immission is the sound pressure level in decibels. However, the sound pressure level by itself is not a satisfactory quantity to describe the strength of a noise source (emission) because the sound pressure level varies with distance from the source and with the acoustical environment in which the source operates.

Two quantities are needed to describe the strength of a noise source, its *sound power level* and its *directivity*. The sound power level is a measure of the total sound power radiated by the source in all directions and is usually stated as a function of frequency, for example, in one-third-octave bands. The sound power level is then the preferred descriptor for the emission of sound energy by noise sources. The sound power level is usually expressed in decibels.*

The directivity of a source is a measure of the variation in its sound radiation with direction. Directivity is usually stated as a function of angular position around the acoustical center of the source and also as a function of frequency. Some sources radiate sound energy nearly uniformly in all directions. These are called nondirectional sources (see Fig. 4.1). Generally, such sources are small in size compared to the wavelength of the sound radiated. Most practical sources are somewhat directional (see Fig. 4.2); that is, they radiate more sound in some directions than in others. Measures of source directivity are presented in Section 4.12.

From the sound power level and directivity, it is possible to calculate the sound pressure levels produced by the source in the acoustical environment in which it operates. This is not an easy task, however, because the resulting sound

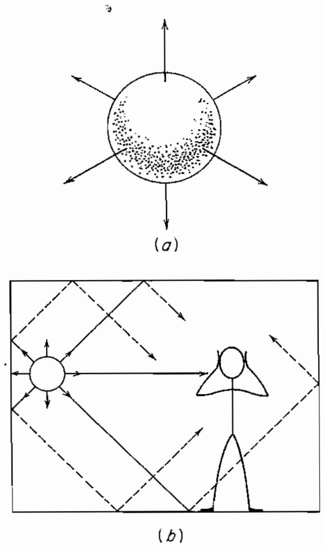

FIGURE 4.1 Sound source that radiates uniformly in all directions: *(a)* sound source in free space; *(b)* same source in enclosure showing reflections from interior surfaces. Solid lines show the direct sound; dashed lines show the reflected (reverberant) sound.

*Some industries have adopted the use of the bel, where 1 bel = 10 dB, as the unit of sound power level to distinguish clearly between sound pressure level in decibels and sound power level in bels.

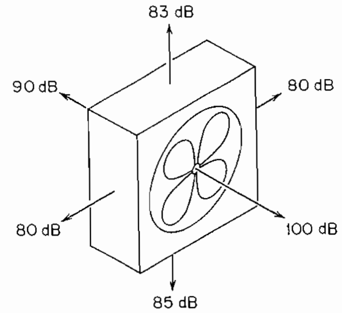

FIGURE 4.2 Sound source with directive radiation into free space. This behavior is typical of equipment noise.

pressure levels at points in the room depend not only on the characteristics of the source but also on the characteristics of the room itself. The sound energy from the source is reflected, absorbed, and scattered by the room boundaries, and some energy is transmitted through these boundaries to adjacent spaces. Thus, the same source could produce quite different sound pressure levels in different rooms or environments. This underscores the difference between *emission* and *immission* and illustrates why sound pressure level is not a good descriptor for noise emission from a source. Sound fields outdoors and in rooms are discussed in detail in Chapters 5–7.

A source may set a nearby surface into vibration if it is rigidly attached to that surface, causing more sound power to be radiated than if the source were vibration isolated. Both the operating and mounting conditions of the source therefore influence the amount of sound power radiated as well as the directivity of the source. Nonetheless, the sound power level alone is useful for comparing the noise radiated by machines of the same type and size as well as by machines of different types and sizes; determining whether a machine complies with a specified upper limit of noise emission; planning in order to determine the amount of transmission loss or noise control required; and engineering work to assist in developing quiet machinery and equipment.

4.2 SOUND POWER LEVELS OF SOURCES

Even though the sound power produced by a noisy machine is only a very small fraction of the total mechanical power that the machine produces, the range of sound powers produced by sources of practical interest is enormous—from less than a microwatt to megawatts. Shaw[2] has estimated the radiation ratio of a wide variety of noise sources.

A single-number descriptor for noise source emission is obtained when the sound power as a function of frequency is weighted using the A-frequency weighting curve. The result is the A-weighted sound power (Table 1.4). The

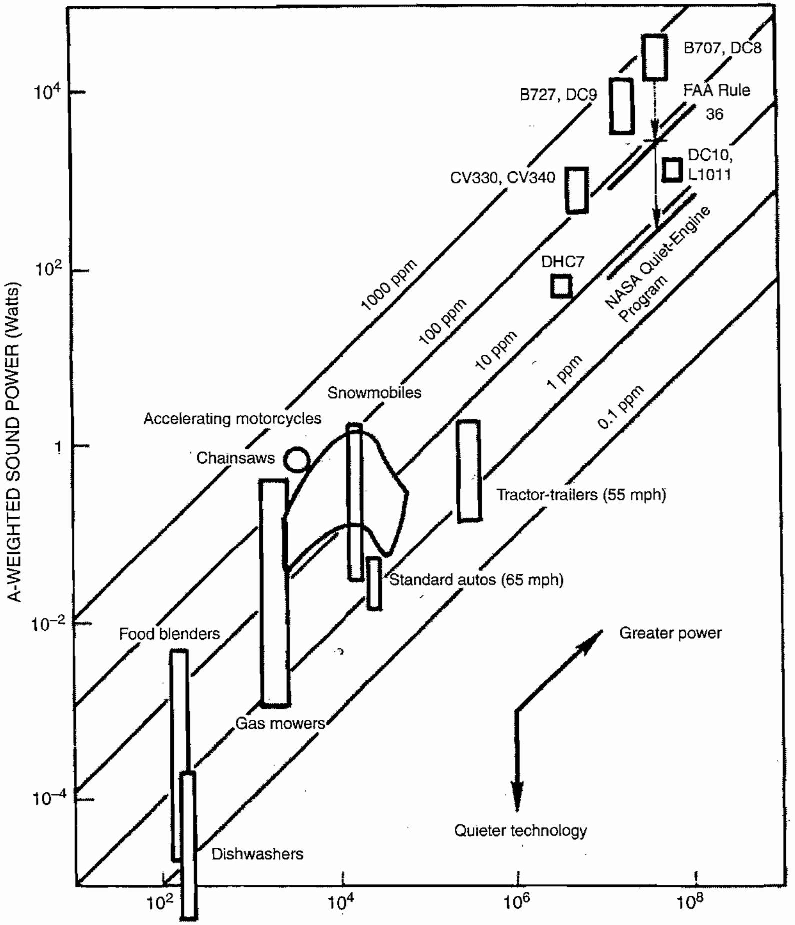

FIGURE 4.3 Estimated values of A-weighted sound power versus mechanical power for various machines. The diagonal lines are lines of constant mechanoacoustical efficiency (sound power per mechanical power) in parts per million. The line labeled FAA Rule 36 approximates 1975 noise levels for new aircraft designs, while the goal of a research program in progress at the time the figure was published is labeled NASA Quiet-Engine Program.

radiation ratio is the ratio of the A-weighted sound power level of the source and the mechanical power.

Estimates of the conversion ratio are shown in Fig. 4.3. The diagonal lines in the figure give conversion ratios ranging from 10^{-3} to 10^{-7}.

The sound powers of sources of practical interest cover a range of more than 12 orders of magnitude. Hence, it is convenient to express a sound power on a

logarithmic scale using an internationally agreed-upon sound power, 10^{-12} W (watts), as the reference for the logarithm (see Chapter 1). The A-weighted sound power level* in decibels is defined as

$$L_{WA} = 10 \log \left(\frac{W_A}{W_0} \right) \tag{4.1}$$

where W_A = A-weighted sound power
L_{WA} = A-weighted sound power level, dB
W_0 = reference sound power, internationally agreed upon as 10^{-12} W

Consequently

$$L_{WA} = 10 \log W_A + 120 \quad \text{dB re } 10^{-12} \text{ W} \tag{4.2}$$

The A-weighted sound power level (L_{WA}) is usually expressed in decibels but may be expressed in bels. Since there is an order-of-magnitude difference between sound power levels in bels (emission) and sound pressure levels in decibels (immission), the ambiguity of expressing both emission and immission values in decibels is avoided. Use of this convention is particularly important in dealing with the public. In many countries, people who are unfamiliar with the technical details of acoustics are unable to distinguish between different quantities that are expressed in decibels. Nonetheless, noise control engineers and other practitioners in the field usually find it convenient to express sound power levels in decibels.

Example 4.1. A sound source radiates an A-weighted sound power of 3 W. Find the A-weighted sound power level in decibels.

Solution

$$L_{WA} = 10 \log 3 + 120$$
$$= 4.8 + 120 = 124.8 \text{ dB re } 10^{-12} \text{ W}$$

A level is a dimensionless quantity, and it is imperative that the reference be stated to avoid confusion.

4.3 RADIATION FIELD OF A SOUND SOURCE

Near Field, Far Field, and Reverberant Field

Since the sound power emitted by a source must be determined by measurement of a field quantity such as sound pressure or sound intensity (the sound energy

*In the past, the A-weighted sound power level was sometimes designated by the term *noise power emission level*, abbreviated NPEL. This usage is no longer common.

flowing through a unit area in a unit time), it is important to understand the radiation field of a sound source when it is placed in various acoustical environments. The character of the radiation field of a typical noise source usually varies with distance from the source. In the vicinity of the source, the particle velocity is not necessarily in the direction of propagation of the sound wave, and an appreciable tangential velocity component may exist at any point. This is the near field. It is characterized by appreciable variations of the sound pressure with distance from the source along a given radius, even when the source is in a free unbounded space commonly referred to as a free field. Moreover, in the near field, the sound intensity is not simply related to the mean-square value of the sound pressure.

The distance from the source to which the near field extends is dependent on the frequency, on a characteristic source dimension, and on the phases of the radiating parts of the surface of the source. The characteristic dimension may vary with frequency and angular orientation. It is difficult, therefore, to establish limits for the near field of an arbitrary source with any degree of accuracy. It is often necessary to explore the sound field experimentally.

In the far field, the sound pressure level decreases by 6 dB for each doubling of the distance from the source, provided that either the source is in free space (no boundaries to reflect the sound) or the reverberant field has not yet been reached (see Fig. 4.4). In this free-field part of the far field, the particle velocity is primarily in the direction of propagation of the sound wave.

If the source is radiating inside an enclosure, fluctuations of sound pressure with position are observed in the reverberant part of the far field, that is, in the region

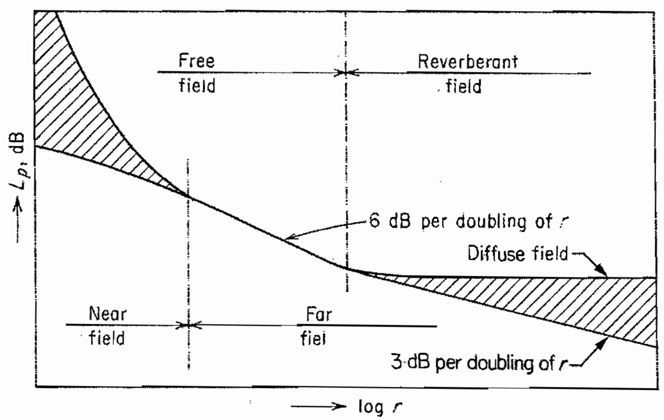

FIGURE 4.4 Variation of sound pressure level in an enclosure along a radius r from a typical noise source. The free field, reverberant field, near field, and far field are shown. The free far field indicates the region where the sound pressure level L_p decreases at the rate of 6 dB for each doubling of distance from the acoustical center of the source, although this region is often very short. In the reverberant far field, the sound pressure level in a highly reverberant room is constant. The lower edge of the shaded region is typical of sound fields in furnished rooms of dwellings and offices.

where the waves reflected from the boundaries of the enclosure are superimposed upon the direct field from the source (see Fig. 4.4). In a highly reverberant room in the region where the direct sound pressure from the source is considerably smaller than the contribution from the reflected sound, the sound pressure level reaches a value essentially independent of the distance from the source. This region may approximate an ideal *diffuse field* in which reflected energy propagates equally in all directions and the sound energy density is uniform.

As discussed in more detail in Chapter 7, in furnished rooms in dwellings and offices where the sound field is neither a free field nor a diffuse field, the sound pressure level decreases by about 3 dB for each doubling of distance from the source.

4.4 SOUND INTENSITY, SOUND POWER, AND SOUND PRESSURE

Sound Intensity and Sound Power

The sound energy (in joules, 1 J = 1 N · m) or the sound power (in joules per second or watts) radiated into free space by a source spreads out over a larger and larger area as the sound wave travels outward from the source. As a result, the sound intensity (in watts per square meter) and the sound pressure (in pascals) at a point in the sound field decreases as the distance from the source increases. Sound intensity, defined in Section 2.2 as the amount of sound energy flowing through a unit area per unit time, is a vector quantity $\mathbf{I}$ having magnitude $I = |\mathbf{I}|$ and direction $\hat{\mathbf{r}}$ pointing in the direction of sound energy propagation. If a closed surface that surrounds the source is selected, the sound power radiated by the source can be calculated from the following integral:

$$W = \int_S \mathbf{I} \cdot d\mathbf{S} \tag{4.3}$$

where W = sound power, W
$\mathbf{I}$ = time-average sound intensity vector, W/m^2
$d\mathbf{S}$ = infinitesimal element of surface area (a vector oriented normal to surface)
S = area of closed surface that surrounds source

Expanding the dot product in Eq. (4.3) allows the surface integral to be written in terms of scalar quantities as follows:

$$\begin{aligned} W &= \int_S \mathbf{I} \cdot d\mathbf{S} = \int_S (|\mathbf{I}|\hat{\mathbf{r}}) \cdot (|d\mathbf{S}|\hat{\mathbf{n}}) \\ &= \int_S (I\, dS) \times (\hat{\mathbf{r}} \cdot \hat{\mathbf{n}}) = \int_S I\, dS \cos\theta = \int_S I_n\, dS \end{aligned} \tag{4.4}$$

where $I_n = I\cos\theta$ is the component of sound intensity *normal* to the surface at the location of $d\mathbf{S}$; dS is the magnitude of the elemental surface area vector;

$\hat{\mathbf{r}}$ is the unit vector in the direction of sound propagation; $\hat{\mathbf{n}}$ is the unit vector normal to the surface; and θ is the angle between $\hat{\mathbf{r}}$ and $\hat{\mathbf{n}}$. It should be noted that the maximum value of the intensity is equal to its magnitude, $I_{\max} = I$, and is attained in the direction $\hat{\mathbf{r}}$; in general, components of the intensity vector, such as I_n (or components in the Cartesian directions $\hat{\mathbf{x}}$, $\hat{\mathbf{y}}$, or $\hat{\mathbf{z}}$) are less than $I_{\max}$.

The integral may be carried out over a spherical or hemispherical surface that surrounds the source. Other regular surfaces, such as a parallelepiped or a cylinder, are also used in practice, and, in principle, any closed surface can be used. If the source is nondirectional and the integration is carried out over a spherical surface having a radius r and centered on the source, sound intensity and sound power are related by

$$I\,(\text{at } r) = I_n\ (\text{at } r) = \frac{W}{S} = \frac{W}{4\pi r^2} \quad \text{W/m}^2 \tag{4.5}$$

where I = magnitude of intensity on the surface (at radius r)
I_n = normal component of intensity on the surface (at radius r)
W = sound power, W
S = area of spherical surface, $= 4\pi r^2$, m^2
r = radius of sphere, m

In general, a source is directional, and the sound intensity is not the same at all points on the surface. Consequently, an approximation must be made to evaluate the integral of Eq. (4.4). It is customary to divide the measurement surface into a number of subsegments each having an area S_i and to approximate the normal component of the sound intensity on each surface subsegment. The sound power of the source may then be calculated by a summation over all of the surface subsegments:

$$W = \sum_i I_{n_i} S_i \quad \text{W} \tag{4.6}$$

where I_{n_i} = normal component of sound intensity averaged over ith segment of area, W/m ^{2}
S_i = ith segment of area, m^2
i = number of segments

Equation (4.6) may be expressed logarithmically as

$$L_W = 10 \log \sum_i S_i \times 10^{L_{I_i}/10} \tag{4.7}$$

where L_W = sound power level, dB re 10^{-12} W
S_i = area of the ith segment, m^2
L_{I_i} = normal sound intensity level averaged over the ith area segment, dB re 10^{-12} W/m^2 (where the subscript n has been omitted for simplicity)

When each of the subareas S_i on the measurement surface has the same area, S_ε, Eq. (4.7) reduces to

$$W = \sum_{i=1}^{N} I_{n_i} S_i = S_\varepsilon \sum_{i=1}^{N} I_{n_i} = \left(\frac{1}{N}\sum_{i=1}^{N} I_{n_i}\right) \times (N \times S_\varepsilon) = \overline{I}_n \times S \quad \text{W} \tag{4.8}$$

where $\overline{I}_n = (1/N)\sum_{i=1}^{N} I_{n_i}$, average normal sound intensity over the measurement surface, W/m^2
S = total area of the measurement surface, m^2

Equation (4.8) may be expressed logarithmically as

$$L_W = 10 \log \frac{\overline{I}_n}{I_0} + 10 \log \frac{S}{S_0} \tag{4.9}$$

$$L_W = L_I + 10 \log \frac{S}{S_0} \tag{4.10}$$

where L_W = sound power level, dB re 10^{-12} W
L_I = normal sound intensity level, dB re 10^{-12} W/m^2
S = area of measurement surface, m^2
S_0 = 1 m^2
I_0 = reference sound intensity, internationally agreed upon as 10^{-12} W/m^2

Equation (4.10) is usually used to determine the sound power level of a source from the sound intensity level except when the source is highly directional. For directional sources, the subareas of the measurement surface may be selected to be unequal and Eq. (4.7) should be used.

Free-Field Approximation for Sound Intensity

From Eq. (2.24) or (2.30), for the far field of a source radiating into free space, the magnitude of the intensity at a point a distance r from the source is

$$I\,(\text{at } r) = \frac{p_{\text{rms}}^2(\text{at } r)}{\rho c} \quad \text{W/m}^2 \tag{4.11}$$

where ρc = characteristic resistance of air (see Section 2.5), N · s/m^3, equal to about 406 mks rayls at normal room conditions
p_{rms} = rms sound pressure at r, N/m^2

Strictly speaking, this relationship is only correct in the far field of a source radiating into free space. Good approximations to free-space, or "free-field," conditions can be achieved in properly designed anechoic or hemi-anechoic rooms, or outdoors. Hence, Eq. (4.11) is approximately correct in the far field of a source over a reflecting plane provided that the space above the reflecting plane remains essentially a free field at distance r (see Section 4.3). Even if the free field is not perfect and a small fraction of the sound is reflected from the walls and ceiling of the room, an "environmental correction" may be introduced to allow valid measurements to be taken in the room. Environmental corrections are introduced in Section 4.9. The relations below are widely used in standards that determine the sound power of a source from a measurement of sound pressure level.

If a closed measurement surface is placed around a source so that all points on the surface are in the far field and the intensity vector is assumed to be essentially normal to the surface so that $I = I_n$ at all points on the surface, then Eqs. (4.7) and (4.11) can be combined to yield

$$W = \frac{1}{\rho c}\sum_i p_i^2 S_i \tag{4.12}$$

where p_i = average rms sound pressure over area segment S_i, N/m^2

We may express Eq. (4.12) logarithmically as

$$L_W = 10 \log \sum_i S_i \times 10^{L_{pi}/10} - 10 \log D \tag{4.13}$$

where
L_W = sound power level, dB re 10^{-12} W
L_{pi} = sound pressure level over the ith area segment, dB re 2×10^{-5} N/m²
S_i = area of ith segment, m²
$10^{L_{pi}/10} = p_i^2/p_{\text{ref}}^2$
$p_{\text{ref}} = 2 \times 10^{-5}$ N/m²
$D = \rho c W_0/p_{\text{ref}}^2 = \rho c/400$

and values for 10 log D may be found from Fig. 1.7; at normal temperatures and pressures, the 10 log D term is negligible.

Note that in Eq. (4.13), if the A-weighted sound power level in bels were being computed, the constant 10 in front of the logarithm would disappear, and the result (with $D = 1$) would be

$$L_{WA} = \log \sum_i S_i \times 10^{L_{pAi}/10} \tag{4.14}$$

When each subsegment S_i has an equal area and 10 log $D = 0$, in analogy with Eqs. (4.8)–(4.10), Eq. (4.13) can be expressed as

$$L_W = \langle L_p \rangle_S + 10 \log \left(\frac{S}{S_0}\right) \tag{4.15}$$

where
L_W = sound power level, dB re 10^{-12} W
$\langle L_p \rangle_S$ = sound pressure level averaged on a mean-square basis over the measurement surface (surface sound pressure level, dB re 2×10^{-5} N/m²)
S = area of the measurement surface, m²
S_0 = 1 m²

Equation (4.15) is usually used to determine the sound power level of a source from the sound pressure level except when the source is highly directional. For directional sources, the subareas of the measurement surface may be selected to be unequal; Eq. (4.13) should be used (usually with 10 log $D = 0$).

Hence, the sound power level of a source can be computed from sound pressure level measurements made in a free field. Equations (4.13) and (4.15) are widely used in standardized methods for determination of sound power levels in a free field or in a free field over a reflecting plane.

Sound Power Determination in a Diffuse Field

The sound power level of a source can also be computed from sound-pressure-level measurements made in an enclosure with a diffuse sound field because in such a field the sound energy density is constant; it is directly related to the mean-square sound pressure and, therefore, to the sound power radiated by the source. The sound pressure level in the reverberant room builds up until the total sound power absorbed by the walls of the room is equal to the sound power generated by the source. The sound power is determined by measuring the mean-square sound pressure in the reverberant field. This value is either compared with the mean-square pressure of a source of known sound power output *(comparison method)* or calculated directly from the mean-square pressure produced by the source and a knowledge of the sound-absorptive properties of the reverberant room *(direct method)*. Depending on the method used, either Eq. (4.16) or Eq. (4.18) is used to determine the sound power level of the source in a diffuse field.

Diffuse sound fields can be obtained in laboratory reverberation rooms. Sufficiently close engineering approximations to diffuse-field conditions can be obtained in rooms that are fairly reverberant and irregularly shaped. When these environments are not available or when it is not possible to move the noise source under test, other techniques valid for in situ determination of sound power level may be used and are described later in this chapter.

All procedures described in this chapter apply to the determination of sound power levels in octave or one-third-octave bands. The techniques are independent of bandwidth. The A-weighted sound power level is obtained by summing (on a mean-square basis) the octave-band or one-third-octave-band data after applying the appropriate A-weighting corrections. A-weighting values are listed in Table 1.4.

Nonsteady and impulsive noises are difficult to measure under reverberant-field conditions. Measurements on such noise sources should be made either under free-field conditions or using one of the techniques described in Chapter 18.

4.5 MEASUREMENT ENVIRONMENTS

Three different types of laboratory environments in which noise sources are measured are found in modern laboratories: anechoic rooms (free field), hemi-anechoic rooms (free field over a reflecting plane), and reverberation rooms (diffuse field). In an anechoic room, all of the boundaries are highly absorbent, and the free-field region extends very nearly to the boundaries of the room. Because the "floor" itself is absorptive, anechoic rooms usually require a suspended wire grid or other mechanism to support the sound source, test personnel, and measurement instruments. A hemi-anechoic room has a hard, reflective floor, but all other boundaries are highly absorbent. Both anechoic and hemi-anechoic environments are used to determine the sound power level of a source, but the hemi-anechoic room is clearly more practical for testing large, heavy sources. The sound power level is derived from Eq. (4.7) if the sound intensity on a surface surrounding the source is measured directly or from Eq. (4.13) if the sound pressure level is measured on a surface surrounding the source and located in the far field.

In a reverberation room, where all boundaries are acoustically hard and reflective, the reverberant field extends throughout the volume of the room except for a small region in the vicinity of the source. The sound power level of a source may be determined from an estimate of the average sound pressure level in the diffuse-field region of the room coupled with a knowledge of the absorptive properties of the boundaries.

The sound pressure field in an ordinary room such as an office or laboratory space that has not been designed for acoustical measurements is neither a free field nor a diffuse field. Here the relationship between the sound intensity and the mean-square pressure is more complicated. Instead of measuring the mean-square pressure, it is usually more advantageous to use a sound intensity analyzer that measures the sound intensity directly (see Section 4.10). By sampling the sound intensity at defined locations in the vicinity of the source, the sound power level of the source can be determined. Equation (4.10) is used to determine the sound power levels from the sound intensity levels. If the subareas of the measurement surface are unequal, Eq. (4.7) may be used.

4.6 INTERNATIONAL STANDARDS FOR DETERMINATION OF SOUND POWER USING SOUND PRESSURE

ISO Standards

The International Organization for Standardization (ISO) has published a series of international standards, the ISO 3740 series,[3–13] which describes several methods for determining the sound power levels of noise sources. Table 4.1 summarizes the applicability of each of the basic standards of the ISO 3740 series. The most important factor in selecting an appropriate noise measurement method is the ultimate use of the sound-power-level data that are to be obtained.

TABLE 4.1 Description of the ISO 3740 Series of Standards for Determination of Sound Power

ISO Standard	Test Environment	Criteria for Suitability of Test Environment	Volume of Source	Character of Noise	Limitation on Background Noise	Sound Power Levels Obtainable	Optional Information Available
ISO 3741 Precision (Grade 1)	Reverberation room meeting specified requirements	Room volume and reverberation time to be qualified	Preferably less than 2% of room volume	Steady, broadband, narrow-band, or discrete frequency	$\Delta L \geq 10$ dB, $K_1 \leq 0.5$ dB	A weighted and in one-third-octave or octave bands	Other frequency-weighted sound power levels
ISO 3743-1 Engineering (Grade 2)	Hard-walled room	Volume ≥ 40 m^3, $\alpha \leq 0.20$	Preferably less than 1% of room volume	Any, but no isolated bursts	$\Delta L \geq 6$ dB, $K_1 \leq 1.3$ dB	A weighted and in octave bands	Other frequency-weighted sound power levels
ISO 3743-2 Engineering (Grade 2)	Special reverberation room	70 m$^3 \leq V \leq$ 300 m^3, 0.5 s $\leq T_{nom} \leq$ 1.0 s	Preferably less than 1% of room volume	Any, but no isolated bursts	$\Delta L \geq 4$ dB, $K_1 \leq 2.0$ dB	A weighted and in octave bands	Other frequency-weighted sound power levels
ISO 3744 Engineering (Grade 2)	Essentially free field over a reflecting plane	$K_2 \leq 2$ dB	No restrictions; limited only by available test environment	Any	$\Delta L \geq 6$ dB, $K_1 \leq 1.3$ dB	A weighted and in one-third-octave or octave bands	Source directivity; SPL as a function of time; single-event SPL; other frequency-weighted sound power levels

(continued overleaf)

TABLE 4.1 (*continued*)

ISO Standard	Test Environment	Criteria for Suitability of Test Environment	Volume of Source	Character of Noise	Limitation on Background Noise	Sound Power Levels Obtainable	Optional Information Available
ISO 3745 Precision (Grade 1)	Anechoic or hemi-anechoic room	Specified requirements; measurement surface must lie wholly inside qualified region	Characteristic dimension not greater than 1/2 measurement surface radius	Any	$\Delta L \geq 10$ dB, $K_1 \leq 0.5$ dB	A weighted and in one-third-octave or octave bands	Same as above plus sound energy level
ISO 3746 Survey (Grade 3)	No special test environment	$K_2 \leq 7$ dB	No restrictions; limited only by available test environment	Any	$\Delta L \geq 3$ dB, $K_1 \leq 3$ dB	A weighted	Sound pressure levels as a function of time
ISO 3747 Engineering or Survey (Grade 2 or 3)	Essentially reverberant field in situ, subject to stated qualification requirements	Specified requirements	No restrictions; limited only by available test environment	Steady, broadband, narrow-band, or discrete frequency	$\Delta L \geq 6$ dB, $K_1 \leq 1.3$ dB	A weighted from octave bands	Sound pressure levels as a function of time

Notes: ΔL is the difference between the sound pressure levels of the source-plus-background noise and the background noise alone; K_1 is the correction for background noise, defined in the associated standard; V is the test room volume; α is the sound absorption coefficient; T_{nom} is the nominal reverberation time for the test room, defined in the associated standard; K_2 is the environmental correction, defined in the associated standard; SPL is an abbreviation for "sound pressure level."

The principal uses of sound-power-level data include the development of quieter machines and equipment, compliance testing of products in production, acoustical comparisons of several products that may be of the same or different type and size, and preparing acoustical noise declarations for the general public.

In making a decision on the appropriate measurement method to be used, several factors should be considered: (a) the size of the noise source, (b) the movability of the noise source, (c) the test environments available for the measurements, (d) the character of the noise emitted by the noise source, and (e) the grade (classification) of accuracy required for the measurements. The methods described in this chapter are consistent with those of the ISO 3740 series. A set of standards with the same objectives is available from the ANSI or the Acoustical Society of America (ASA).

4.7 DETERMINATION OF SOUND POWER IN A DIFFUSE FIELD

Characteristics of Reverberation Rooms

Measurements of the sound power level of a device or machine may be performed in a laboratory reverberation room (see Section 7.8). The determination of the sound power level of a noise source in such a room is based on the premise that the measurements are performed entirely in the diffuse (reverberant) sound field (see Fig. 4.4). In the reverberant field, the average sound pressure level is essentially uniform, although there are fluctuations from point to point, and it is related to the sound power radiated by the source [see (Eq. 4.18)]. Information in regard to the directivity of the source cannot be obtained in a diffuse sound field.

The minimum volume of the room depends on how low in frequency valid measurements are to be taken. For example, if measurements in the 100-Hz one-third-octave band are desired, the minimum volume is recommended to be 200 m^3 in ISO 3741. On the other hand, if measurements are only needed down to the 200-Hz band, 70 m^3 will be adequate. Maximum room volume is constrained by the adverse effects of air absorption and the ability to make valid high-frequency measurements; a volume less than 300 m^3 is generally recommended. The equipment being tested should have a volume no greater than 2% of the room volume. The absorption coefficient of the surface that is closest to the equipment being evaluated (usually the floor) should not exceed 0.06, and the remaining surfaces of the room should be highly reflective, such that the reverberation time (in seconds) is greater than the ratio of volume V (m^3) to surface area S (m^2): $T_{60} > V/S$. In addition to these requirements on room volume and absorption, ISO 3741 includes requirements for background noise levels; temperature, humidity, and atmospheric pressure; instrumentation and calibration; installation and operation of the source under test; minimum distance between microphone and source; and performance requirements for the reference sound source, if used.

If the room is to be used to measure equipment that has discrete-frequency components in its noise emissions, it is often necessary to use additional microphone positions and additional source positions, and ISO 3741 includes detailed procedures to determine whether or not such positions are required. These procedures must be followed for each source tested, or, alternatively, the reverberation room itself can be "qualified" for the measurement of discrete-frequency components (see below). The need for additional source positions may be reduced by adding low-frequency sound absorption to the room or through the use of rotating diffusers.

Room Qualification

The ISO 3741 standard contains two detailed procedures for the qualification of reverberation rooms for the determination of sound power levels, one for qualifying the room for the measurement of broadband sound (Annex E) and one for qualifying the room for the measurement of discrete-frequency components (Annex A). For sources of broadband sound, the room is qualified by using a reference sound source placed at different positions in the room and determining the standard deviation of the measured space-averaged sound pressure levels in the room for each position. A minimum of six positions of the source are required, each with specified constraints on the distance between them, the distance from walls, and the distance from the microphone. The room is qualified according to ISO 3741 for the measurement of broadband sound if the standard deviation does not exceed the values given in Table 4.2.

The qualification of reverberation rooms for the measurement of noise that contains discrete-frequency components in the spectrum is complicated and time consuming. However, this only has to be performed once, and the benefit can be great. If the chamber is qualified for the measurement of discrete tones, there is no longer a need to perform initial tests to determine the number of microphone and source positions for each source under investigation.

Essentially, a "calibrated" loudspeaker is placed in the reverberation room and is driven by a series of discrete-frequency tones in each one-third-octave band. For example, there are 22 frequencies spaced 1 H apart in the 100-Hz one-third-octave band and 23 frequencies spaced 5 H apart in the 500-Hz octave band. The average sound pressure level in the room is determined at each frequency and corrected for the loudspeaker response (previously determined in a hemi-anechoic room). The room is qualified according to ISO 3741 if the standard deviation of the level in each one-third-octave band does not exceed the values given in Table 4.3.

TABLE 4.2 Qualification Requirements for Reverberation Room Used for Measurement of Broadband Noise Sources

Octave-Band Center Frequencies, Hz	One-Third-Octave-Band Center Frequencies, Hz	Maximum Allowable Standard Deviation, dB
125	100–160	1.5
250, 500	200–630	1.0
1000, 2000	800–2500	0.5
4000, 8000	3150–10,000	1.0

Source: ISO 3741: 1999.
Note: Annex A of ISO 3741 contains detailed procedures for the discrete-frequency qualification.

TABLE 4.3 Qualification Requirements for Reverberation Room Used for Measurement of Narrowband Noise Sources

Octave Band Center Frequency, Hz	One-Third-Octave-Band Center Frequency, Hz	Maximum Allowable Standard Deviation, dB
125	100–160	3.0
250	200–315	2.0
500	400–630	1.5
1000, 2000	800–2500	1.0

Experimental Setup

An array of fixed microphone positions or a single microphone that traverses a path (often circular) in the reverberant room may be used to determine the average sound pressure level in the reverberant field. The number of fixed microphone positions, N_M, required depends on the results of an initial series of sound-pressure-level measurements using six positions. If the standard deviation of these initial measurements, s_M, is less than or equal to 1.5, then the original six microphone positions will suffice (i.e., the noise is essentially broadband). If $s_M > 1.5$, it is assumed that the source emits discrete tones and a larger number of microphone positions is usually required to obtain an adequate sampling of the sound field. In this case, N_M could range anywhere from 6 to 30 depending on the frequency and the magnitude of s_M. When a traversing microphone is used, the path length l must be at least $(\lambda/2)N_M$, where λ is the wavelength of sound at the lowest midband frequency of interest. The microphone path or array should be positioned in the room so that no microphone position is within a minimum distance $d_{\min}$ of the equipment being evaluated. The distance $d_{\min}$ is determined differently in the comparison method and the direct method for determination of sound power. These requirements are discussed below.

If the noise source under test is typically associated with a hard floor, wall, edge, or corner, it should be placed in a corresponding position in the reverberation room. Otherwise, it should be placed no closer than 1.5 m from any wall of the room. The source should not be placed near the geometric center of the room since in that location many of the resonant modes of the room would not be excited. For rectangular reverberation rooms, the source should be placed asymmetrically relative to the boundaries. ISO 3741 gives further information for special source locations and installation conditions.

Near the boundaries of the room and close to other reflecting surfaces such as stationary or rotating diffusers, the sound field will depart from the ideal state of diffusion. ISO 3741 prescribes the following conditions on the microphone positions used during the measurements:

When using fixed microphone positions:

1. No position shall be closer than 1.0 m from any surface of or within the room.
2. No position shall be closer than d_{min} from the source (defined below).
3. The distance between microphone positions shall be at least $\lambda/2$, where λ is the wavelength of sound at the lowest midband frequency of interest.

When using one or more continuous microphone traverses:

1. No point on the traverse shall be closer than 1.0 m from any surface of the room.
2. No point on the traverse shall be closer than 0.5 m from any surface of a rotating diffuser.
3. No position shall be closer than d_{min} from the source (defined below).
4. The microphone traverse should not lie in any plane within 10° of a room surface.
5. The length of the traverse shall be at least $l \geq 3\lambda$, where λ is the wavelength of sound at the lowest midband frequency of interest.
6. If multiple traverses are used, the minimum distance between their paths shall be at least $\lambda/2$.

Comparison Method

The procedure for determining the sound power level of a noise source by the comparison method[6] requires the use of a reference sound source (see Fig. 4.5 and ref. 13) of known sound power output. Using microphone positions that meet the above requirements, the procedure is essentially as follows:

1. With the equipment being evaluated at a suitable location in the room, determine, in each frequency band, the average sound pressure level (on a mean-square basis) in the reverberant field using the microphone array or traverse described above.
2. Replace the source under test with the reference sound source and repeat the measurement to obtain the average level for the reference sound source.

The sound power level of the source under test, L_W, for a given frequency band is calculated as

$$L_W = L_{Wr} + (\langle L_p \rangle - \langle L_p \rangle_r) \tag{4.16}$$

where L_W = one-third-octave-band sound power level for source being evaluated, dB re 10^{-12} W

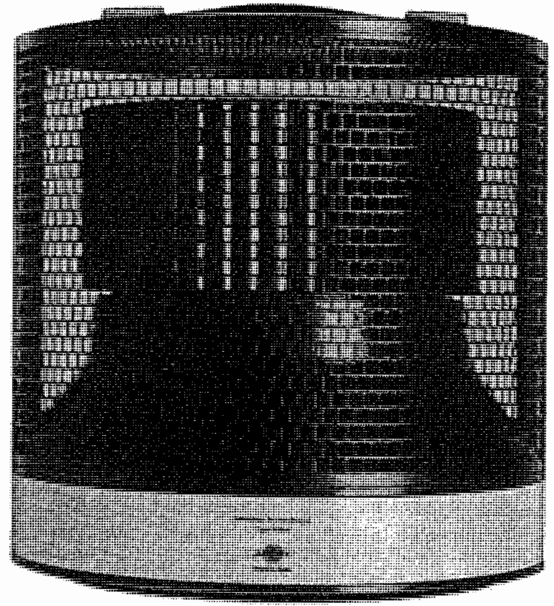

FIGURE 4.5 Reference sound source, Brüel and Kjær Type 4204. (Courtesy of Brüel and Kjær, Inc.)

$\langle L_p \rangle$ = space-averaged one-third-octave-band sound pressure level of source being evaluated, dB re 2×10^{-5} N/m^2

L_{Wr} = calibrated one-third-octave-band sound power level of reference source, dB re 10^{-12} W

$\langle L_p \rangle_r$ = space-averaged one-third-octave-band sound pressure level of reference sound source, dB re 2×10^{-5} N/m^2

To make certain that the reverberant sound field predominates in the determination of the average sound pressure level, the minimum distance d_{min} between the microphone(s) and the equipment being evaluated should be at least

$$d_{min} = 0.4 \times 10^{(L_{Wr} - L_{pr})/20} \tag{4.17}$$

where L_{Wr} and L_{pr} are as defined for Eq. (4.16). [Note that although Eq. (4.17) states the actual requirement, ISO 3741 also recommends that the constant be 0.8 instead of 0.4 to ensure that the microphone is in the reverberant field.]

Direct Method

The direct method does not use a reference sound source. Instead, this method requires that the sound-absorptive properties of the room be determined by measuring the reverberation time in the room for each frequency band. Measurement of T_{60} is described in ISO 3741.

With this method, the space-averaged sound pressure level for each frequency band of the source being evaluated is determined as described above for the comparison method. The sound power level of the source is found from[4]

$$L_W = \overline{L_p} + \left\{10\log\frac{A}{A_0} + 4.34\frac{A}{S} + 10\log\left(1 + \frac{S\times c}{8\times V\times f}\right)\right.$$
$$\left. -25\log\left[\frac{427}{400}\sqrt{\frac{273}{273+\theta}}\times\frac{B}{B_0}\right] - 6\right\} \quad \text{dB re } 10^{-12}\text{ W} \qquad (4.18)$$

where L_W = band sound power level of sound source under test
$\overline{L_p}$ = band space-averaged sound pressure level of sound source under test, dB re 2×10^{-5} N/m^2
A = equivalent absorption area of the room, $= (55.26/c)(V/T_{\text{rev}}), m^2$
V = room volume, m^3
T_{rev} = reverberation time for particular band
A_0 = reference absorption area, 1 m^2
S = total surface area of room, m^2
V = room volume, m^3
f = midband frequency of measurement, Hz
c = speed of sound at temperature θ, $= 20.05\sqrt{273+\theta}$, m/s
θ = temperature, °C
B = atmospheric pressure, Pa
$B_0 = 1.013\times 10^5$ Pa
$V_0 = 1$ m^3
$T_0 = 1$ s

To make certain that the reverberant sound field predominates in the determination of the average sound pressure level, the minimum distance $d_{\min}$ between the microphone(s) and the equipment being evaluated should be at least[4]

$$d_{\min} = 0.08\sqrt{\frac{V/V_0}{T/T_0}} \quad \text{m} \qquad (4.19)$$

where V and T_{rev} are as defined above. [Note that although Eq. (4.19) states the actual requirement, ISO 3741 also recommends that the constant be 0.16 instead of 0.08 to ensure that the microphone is in the reverberant field.]

Example 4.2. Assume a room at temperature 21.4°C with a volume of 200 m^3, a surface area $S = 210$ m^2, and a reverberation time at 100 Hz of 3 s. The space-averaged sound pressure level $\langle L_p\rangle$ in the diffuse field with a given machine operating is 100 dB. Find the sound power level for this machine. Assume a discrete-frequency spectrum and an atmospheric pressure of 1000 mbars.

Solution Use Eq. (4.18) to determine the sound power. The wavelength corresponding to 100 Hz is 3.44 m:

$$c = 20.05\sqrt{273+21.4} = 344 \text{ m/s}$$
$$A = \frac{55.26}{344}\left(\frac{200}{3}\right) = 10.7 \text{ m}^2$$

The sound power level is

$$L_W = 100 + \left\{10\log\frac{10.7}{1} + 4.34\frac{10.7}{210} + 10\log\left(1 + \frac{210\times 344}{8\times 200\times 100}\right)\right.$$
$$\left. -25\log\left[\frac{427}{400}\sqrt{\frac{273}{273+21.4}}\right] - 6\right\}$$
$$= 100 + (10.3 + 0.22 + 1.62 - 0.3 - 6)$$
$$= 106.4 \text{ dB re } 10^{-12}\text{ W(100 Hz mean frequency)}$$

4.8 DETERMINATION OF SOUND POWER IN A FREE FIELD USING SOUND PRESSURE MEASUREMENTS

Determination of the sound power level produced by a device or a machine may be performed in a laboratory anechoic or hemi-anechoic room. Alternatively, a hemi-anechoic environment may be provided at an open-air site above a paved area, distant from reflecting surfaces such as buildings, and with a low background noise level. This environment approximates a large room with sound-absorptive treatment on ceilings and walls with the equipment under test mounted on the hard, reflecting floor. Detailed information on anechoic and hemi-anechoic rooms is presented in Section 7.9.

The determination of the sound power level radiated in an anechoic or hemi-anechoic environment is based on the premise that the reverberant field is negligible at the positions of measurement for the frequency range of interest. Thus, the total radiated sound power may be obtained by a spatial integration, over a hypothetical surface that surrounds the source, of the component of sound intensity normal to the surface of the source [see Eq. (4.3)]. When all points of the measurement surface are in the far field of the source, the magnitude of the intensity can be assumed to be equal to $p^2/\rho c$ [see Eq. (4.11)]. With the additional assumption that the magnitude of the intensity is equal to the normal component of sound intensity (i.e., the direction of sound propagation is essentially normal to the surface at the measurement points), the relationships given in Eqs. (4.12) and

(4.13) can be used to determine the sound power level of a source from simple measurements of sound pressure level. This is the basis for two key international standards for the determination of sound power levels of noise sources, ISO 3744[8] and ISO 3745,[9] discussed below. Essentially, a measurement surface is chosen and microphone positions are defined over this surface. Sound-pressure-level measurements are taken at each microphone position for each frequency band, and from these, the sound power levels are computed.

Selection of a Measurement Surface

The international standards discussed below allow a variety of measurement surfaces to be used; some are discussed here. In selecting the shape of the measurement surface to be used for a particular source, an attempt should be made to choose one where the direction of sound propagation is approximately normal to the surface at the various measurement points. For example, for small sources that approximate a point source, the selection of a spherical or hemispherical surface may be the most appropriate—the direction of sound propagation will be essentially normal to this surface. For machines in a hemi-anechoic environment that are large and in the shape of a box, the parallelepiped measurement surface may be preferable. For "tall" machines in a hemi-anechoic environment having a height much greater than the length and depth, a cylindrical measurement surface[14,15] may be the most appropriate.

Measurement in Hemi-Anechoic Space

The sound power determination in a hemi-anechoic space may be performed according to ISO 3744[8] for engineering-grade accuracy or according to ISO 3745[9] for precision-grade accuracy. ISO 3744 is strictly for hemi-anechoic environments, while ISO 3745 includes requirements for both hemi-anechoic and fully anechoic environments. These standards specify requirements for the measurement surfaces and locations of microphones, procedures for measuring the sound pressure levels and applying certain corrections, and the method for computing the sound power levels from the surface-average sound pressure levels. In addition, they provide detailed information and requirements on criteria for the adequacy of the test environment and background noise, calibration of instrumentation, installation and operation of the source, and information to be reported. Several annexes in each standard include information on measurement uncertainty and the qualification of the test rooms.

In terms of allowable measurement surfaces, ISO 3744 currently specifies the hemisphere and the parallelepiped,* while ISO 3745 explicitly defines only the hemisphere and the sphere. However, ISO 3745 includes a clause for "other microphone arrangements" and cites as an example papers describing the cylindrical measurement surface.[14,15] If a hemisphere is used to determine the location

*At the time of this writing, a revision to ISO 3744 was under consideration, which included the cylindrical measurement surface as well.

of the microphone positions, it has its center on the reflecting plane beneath the acoustical center of the sound source. To ensure that the measurements are carried out in the far field, the radius of the hemisphere for ISO 3744 measurements should be equal to at least two "characteristic" source dimensions and generally not less than 1.0 m. For ISO 3745, the requirements are slightly more stringent with the radius being at least twice the *largest* source dimension or three times the distance of the acoustical center of the source from the reflecting plane (whichever is larger) and at least $\lambda/4$ of the lowest frequency of interest. No microphone position can lie outside of the region qualified for measurements (the free-field region), and this requirement generally prevents microphones from being located too close to the walls. Outdoors, atmospheric effects are likely to influence the measurements if the radius of the test hemisphere is much greater than about 15 m, even in favorable weather.

Figure 4.6 gives an array of 20 microphone positions that may be used for measurements according to ISO 3744[8] for sources that emit predominantly broadband sound. The concern when measuring in a hemi-anechoic room is that reflections of sound from the hard floor may cause far-field interference at the microphone positions. This becomes more problematic when the noise emissions contain discrete tones; a small change in the position of the microphone may result in large variations in measured sound pressure level in those bands containing the tones. Therefore, for sources that emit discrete tones, ISO 3744 specifies a different microphone array, one having a greater distribution in the vertical direction. For precision measurements made in a hemi-anechoic environment according to ISO 3745,[9] a microphone array of at least 20 positions, each with a different vertical height, is required. The coordinates of this array are given in Table 4.4. Procedures are specified in both standards for determining whether or not the number of microphones is sufficient and for defining additional positions, if required. Note that the simultaneous deployment of a very large number of microphones may result in a situation where the support structures of these microphones become effective scatterers of the direct sound at high frequencies and can introduce substantial errors. Scanning the sound field with a single microphone can eliminate this error.

A parallelepiped array of microphone positions is frequently used for the determination of sound power levels for box-shaped machines and equipment. Detailed requirements for the selection of microphone positions and the criteria for the sufficiency of the number of microphones are given in ISO 3744.[8] A minimum of nine positions is required, but this number rapidly increases as the size of the source under test increases. The basic nine-position parallelepiped arrangement is illustrated in Fig. 4.7. As can be seen, this array is limited in its sampling in the vertical direction and so should be used with caution if the source is directional or emits discrete tones.

Another convenient measurement surface standardized in at least one industry test code[16] is the cylindrical microphone array illustrated in Fig. 4.8. The use of this array facilitates the measurement of tall-aspect-ratio sound sources such as data-processing equipment installed in racks. Since the array is usually

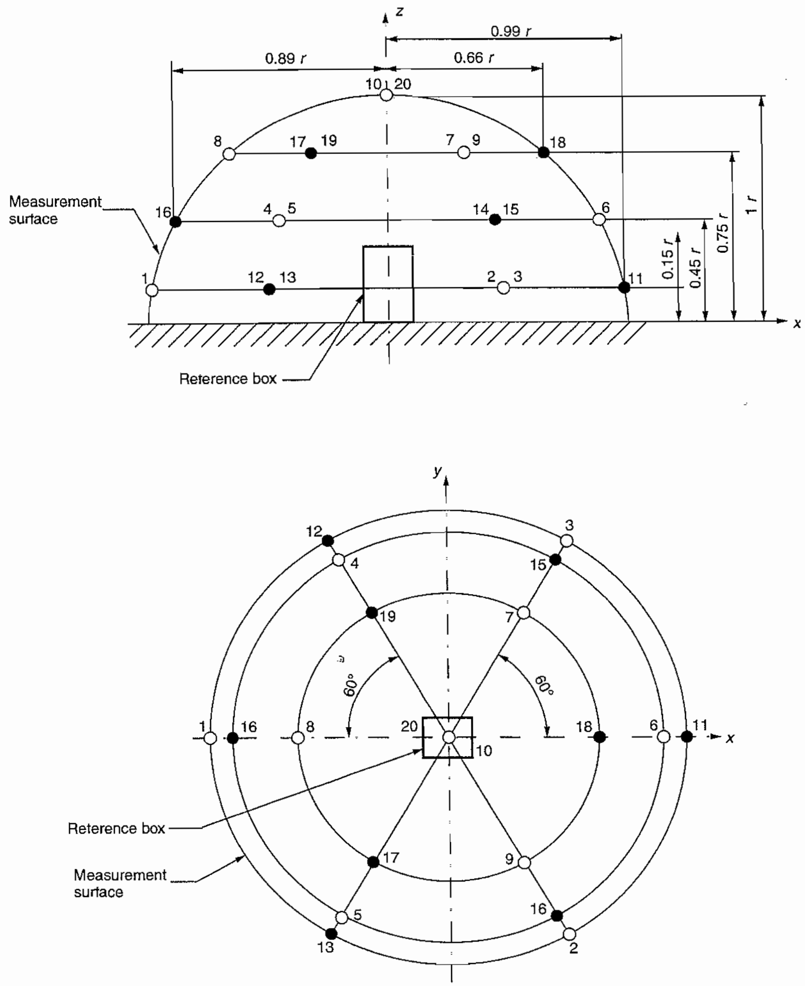

FIGURE 4.6 Microphone positions for a hemispherical measurement surface according to ISO CD 3744 (N1497). (Courtesy of the International Organization for Standardization, Geneva, Switzerland.)

implemented using continuously traversing microphones and a sufficient number of vertical heights, the accuracy is generally improved over that of the parallelepiped.[14,15]

The general procedure for determining the sound power level of the source according to either ISO 3744 or ISO 3745 can be summarized as follows:

1. The test room is set up and checked out and all environmental conditions are recorded.

TABLE 4.4 Twenty Microphone Positions on Surface of Hemisphere As Defined in ISO 3745

Position Number	x/r	y/r	z/r
1	−1.00	0	0.025
2	0.50	−0.86	0.075
3	0.50	0.86	0.125
4	−0.49	0.85	0.175
5	−0.49	−0.84	0.225
6	0.96	0	0.275
7	0.47	0.82	0.325
8	−0.93	0	0.375
9	0.45	−0.78	0.425
10	0.88	0	0.475
11	−0.43	0.74	0.525
12	−0.41	−0.71	0.575
13	0.39	−0.68	0.625
14	0.37	0.64	0.675
15	−0.69	0	0.725
16	−0.32	−0.55	0.775
17	0.57	0	0.825
18	−0.24	0.42	0.875
19	−0.38	0	0.925
20	0.11	−0.19	0.975

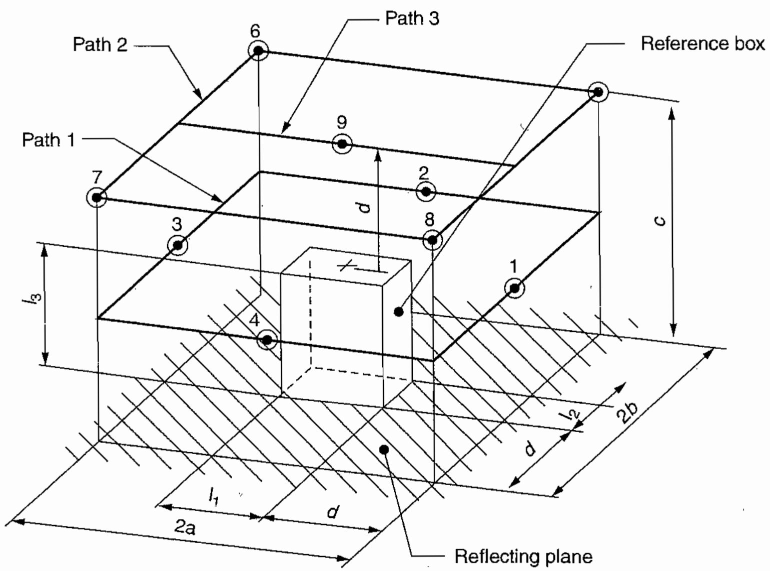

FIGURE 4.7 Microphone positions for a rectangular measurement surface according to ISO CD 3744 (N1497). (Courtesy of the International Organization for Standardization, Geneva, Switzerland.)

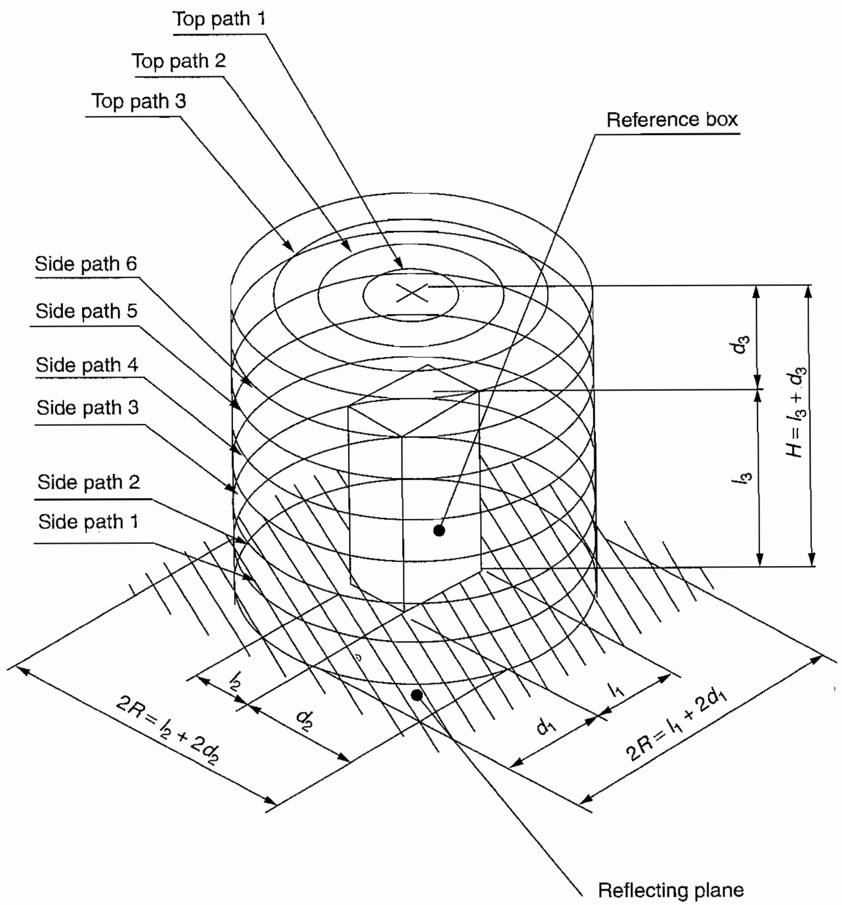

FIGURE 4.8 Microphone positions for a cylindrical measurement surface according to ISO CD 3744 (N1497). (From ISO CD 9997: 1999 Amended, Revision of Annex B (N1479). Courtesy of the International Organization for Standardization, Geneva, Switzerland.)

2. The microphones and instrumentation are calibrated.
3. The sound source is installed.
4. The measurement surface is selected and the microphones are set up in their proper positions.
5. The sound source under test is operated under specified conditions and sound pressure levels are measured at each microphone position for each frequency band of interest.
6. The sound source is turned off and the background noise levels are measured.

7. The sound pressure data are corrected for background noise and for environmental conditions (see below), if necessary.
8. The surface average band sound pressure levels are calculated.
9. The band sound power levels are calculated from the latter, taking into account corrections for meteorological conditions.

Equation (4.15) is used to determine the sound power level of the source when the subareas of the measurement surface associated with each microphone position are all equal. For highly directional sources, the standards require to increase the number of subareas of the measurement surface in the region of high directivity and to measure the sound pressure levels associated with each subarea. The sound power level can then be determined by using Eq. (4.13) for unequal subareas. The correction for background noise, denoted K_1, is specified in terms of the difference between the sound pressure levels measured with and without the source running, ΔL_i, as

$$K_1 = -10 \log(1 - 10^{-0.1\Delta L_i}) \quad \text{dB} \tag{4.20}$$

Measurement in Anechoic Space

In certain instances, the sound power level of a noise source must be determined in a totally free field, without the influence of a reflecting plane beneath the source. The reflecting plane not only causes constructive and destructive interference patterns in the far field—especially pronounced when the noise emissions contain discrete frequency components—but also may affect the radiated sound power of the source itself, especially at low frequencies.[17] Thus for critical measurements of tonal sources, measurements of noise sources that in normal use are not mounted over a hard surface, measurements of directivity, and other specialized measurements, a fully anechoic test environment may be desirable. In this case, the space-averaged mean-square sound pressure level is generally determined over a spherical measurement surface, and measurements are made according to ISO 3745.[9] Most of the procedures and requirements discussed above for hemi-anechoic measurements apply here also, with the exception of the measurement surfaces.

An array of at least 20 microphone positions is specified in ISO 3745, defined over the spherical surface by the Cartesian coordinates given in Table 4.5. If requirements on the sufficiency of the number of microphones given in ISO 3745 are not met, then the number of positions must be doubled, to 40. If the sound source is highly directional, the number of subareas in the regions of high directivity should be increased, as mentioned above. When measurements are made in an anechoic space according to ISO 3745, the sound power level of each frequency band is computed according to either Eq. (4.15) for equal subareas or Eq. (4.13) for unequal subareas. For the precision measurements of ISO 3745, however, two constants are included (instead of the single constant D), one to correct for meteorological conditions and one to "normalize" the measurements to specified "reference" meteorological conditions.

4.9 ENVIRONMENTAL CORRECTIONS AND DETERMINATION OF SOUND POWER LEVEL

In the previous sections, the only corrections applied for the determination of the average sound pressure level on the measurement surface were for the presence of background noise. However, if reflections from the room surfaces affect the measured surface sound pressure levels in any of the frequency bands of interest, a second correction may be required to account for these reflections. This so-called environmental correction, denoted K_2, is computed for both A-weighted values and individual frequency bands and is subtracted directly from the measured sound pressure level (after corrections for background noise are applied). The ISO 3744 standard[8] generally limits the environmental correction to a maximum of 2 dB. The correction may be determined in several ways:

1. By comparing the calibrated sound power level of a reference source, L_{Wr}, with the measured sound power level of the same source in the room, L_W. The environmental correction is then computed as $K_2 = L_W - L_{Wr}$.

TABLE 4.5 Twenty Microphone Positions on Sphere As Defined in ISO 3745

Position Number	x/r	y/r	z/r
1	−1.00	0	0.05
2	0.49	−0.86	0.15
3	0.48	0.84	0.25
4	−0.47	0.81	0.35
5	−0.45	−0.77	0.45
6	0.84	0	0.55
7	0.38	0.66	0.65
8	−0.66	0	0.75
9	0.26	−0.46	0.85
10	0.31	0	0.95
11	1.00	0	−0.05
12	−0.49	0.86	−0.15
13	−0.48	−0.84	−0.25
14	0.47	−0.81	−0.35
15	0.45	0.77	−0.45
16	−0.84	0	−0.55
17	−0.38	−0.66	−0.65
18	0.66	0	−0.75
19	−0.26	0.46	−0.85
20	−0.31	0	−0.95

2. By first determining the "equivalent sound absorption area" of the room, A, and computing the environmental correction as $K_2 = 10\ \log[1 + 4(S/A)]$ decibels, where S is the area of the measurement surface. There are two methods currently specified in ISO 3744 for determining the value of A: a method using the measured reverberation time in the room and the so-called two-surface method. There is also a third method under consideration for standardization, a direct method using a calibrated reference sound source. The latest version of ISO 3744 should be consulted for details of using these methods.
3. By using the "approximate" method for determining A, which is then used only for determining an A-weighted value of the environmental correction, $K_{2A} = 10\ \log[1 + 4(S/A)]$. Here the mean sound absorption coefficient α is estimated from Table 4.6.[10] The equivalent sound absorption area A is then calculated from $A = \alpha S_V$, where S_V is the total area of the boundary surfaces of the test room (walls, floor, ceiling) in square meters.

Reference should also be made to ISO 3746[10], a survey-grade standard for the determination of A-weighted sound power in rooms where the environmental correction may range up to 7 dB. This standard may be useful for taking measurements in situ, that is, when the source cannot be moved into a laboratory environment. The uncertainty of the A-weighted sound power level determined according to ISO 3746 is greater than that obtained when ISO 3744 or ISO 3745 is used. The average A-weighted sound pressure level is determined either on the parallelepiped measurement surface of Fig. 4.9 or the hemispherical measurement surface of Fig. 4.10, each shown with the minimum number of microphones required. Table 4.7 gives the coordinates for the four key microphone positions

TABLE 4.6 Approximate Values of Mean Sound Absorption Coefficient α

Mean Sound Absorption Coefficient α	Description of Room
0.05	Nearly empty room with smooth hard walls made of concrete, brick, plaster, or tile
0.1	Partly empty room; room with smooth walls
0.15	Room with furniture; rectangular machinery room; rectangular industrial room
0.2	Irregularly shaped room with furniture; irregularly shaped machinery room or industrial room
0.25	Room with upholstered furniture; machinery or industrial room with a small amount of sound-absorbing material on ceiling or walls (e.g., partially absorptive ceiling)
0.35	Room with sound-absorbing materials on both ceiling and walls
0.5	Room with large amounts of sound-absorbing materials on ceiling and walls

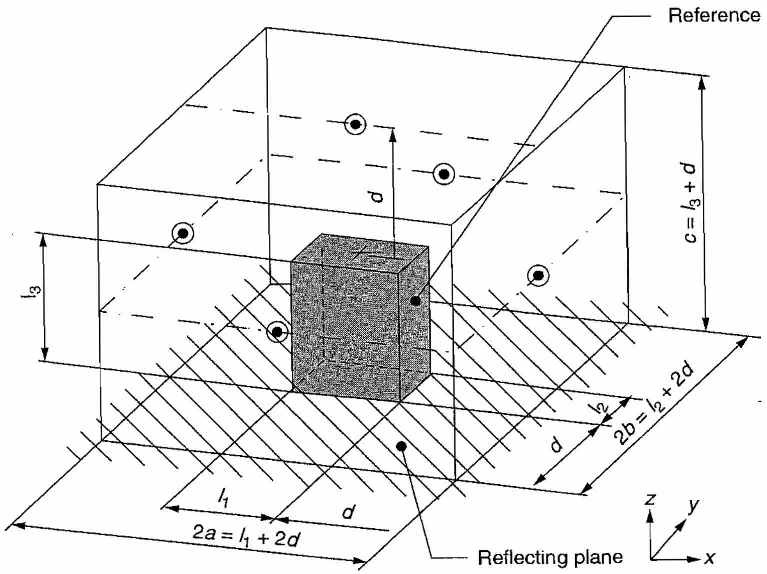

FIGURE 4.9 Microphone positions for a rectangular measurement surface according to ISO 3746. (Courtesy of the International Organization for Standardization, Geneva, Switzerland.)

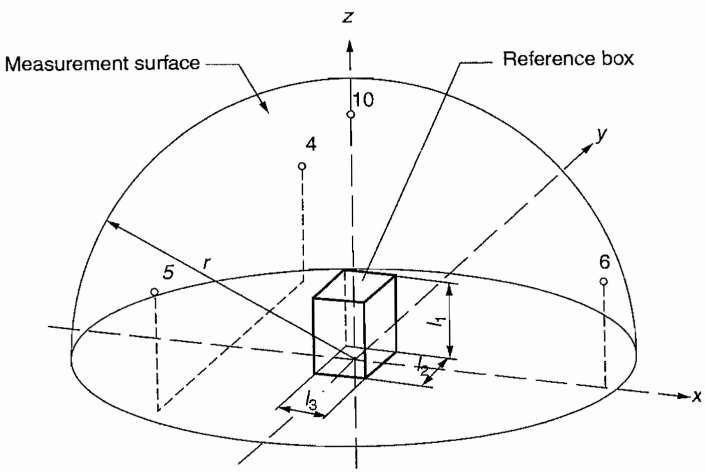

FIGURE 4.10 Microphone positions for a hemispherical measurement surface according to ISO 3746. (Courtesy of the International Organization for Standardization, Geneva, Switzerland.)

TABLE 4.7 Microphone Positions on Hemisphere for Survey Measurements According to ISO 3746

Microphone Position	Microphone Positions (All Heights, $z = 0.6R$)		
	x/r	y/r	z/r
4	−0.45	0.77	0.45
5	−0.45	−0.77	0.45
6	0.89	0	0.45
10	0	0	1.0
14	0.45	−0.77	0.45
15	0.45	0.77	0.45
16	−0.89	0	0.45
20	0	0	1.0

Note: The key microphone positions are 4, 5, 6, and 10. Additional microphone positions are 14, 15, 16, and 20.

shown in Fig. 4.10 for the hemisphere, along with the four additional positions that might be required under certain circumstances.

The measured sound pressure levels are first corrected for background noise according to Eq. (4.20), but for ISO 3746 only the A-weighted value, K_{1A}, is needed. The environmental correction, K_{2A}, is determined using methods similar to those mentioned above for ISO 3744, including the approximate method. The value of K_{2A} should not exceed 7 dB (or, the ratio *S/A* should be less than or equal to 1). The A-weighted sound power level is finally calculated according to Eq. (4.15).

4.10 DETERMINATION OF SOUND POWER USING SOUND INTENSITY

The fundamental procedures for the determination of sound power from sound intensity are formulated in Section 4.4. The sound intensity is measured over a selected surface enclosing the source. In principle, the integral over any surface totally enclosing the source of the scalar product (dot product) of the sound intensity vector and the associated elemental area vector provides a measure of the sound power radiated directly into the air by all sources located within the enclosing surface.

The precision of sound power determination based on sound intensity when the value of the intensity is calculated from measurements of sound pressure in a free field strongly depends on a number of factors. These include source type, measurement area related to source size, and presence of standing waves. The relationship between sound intensity and sound pressure in Eq. (4.11) is valid only in the far field of the free waves radiated by a source. Experience with the measurements on real sources has revealed that errors as large as 10 dB can occur if the selection of the measurement surface is unsuitable or if standing waves affect the measured sound pressure.

In recent years, methods and techniques for direct measurement of sound intensity have been developed. This direct measurement has made it possible to determine the sound power of a variety of source configurations and to make measurements in environments which are not suitable for use in sound power determinations based on measurement of sound pressure. These include sound power determination from measurements in the near field of large sources on test stands, elimination of the adverse effects of standing waves when measuring in enclosures, partial sound power determination of parts of the source with the entire source operating, and the analysis of the source behavior by finding the areas of sound radiation and absorption.

Other acoustical quantities are, by definition, based on sound power. These quantities include sound transmission coefficient, sound absorption coefficient, and radiation efficiency. Either the direct or indirect method described here can be used to determine the sound power for these purposes.

Sound intensity is defined as the sound power that propagates perpendicularly through a unit area. The sound power radiated by a source can be calculated using Eq. (4.5). Sound intensity can be calculated from the product of the sound pressure and particle velocity at a given field point. Because both of these quantities are functions of time, the sound intensity calculated from this time-dependent product is called instantaneous intensity. However, in noise control, it is more practical to work with time-averaged quantities so that acoustic intensity for periodic sound of frequency f and period $T = 1/f$ is defined at point r by

$$\mathbf{I}(r) = \frac{1}{T}\int_0^T p(r,t)\,\mathbf{u}(r,t)\,dt \qquad (4.21)$$

where $\mathbf{u}$ is the particle velocity and p is the sound pressure. The sound intensity $\mathbf{I}$ is a vector describing the time-averaged flow of power per unit area in watts per square meter normal to the intensity direction. This is typically applicable to the tonal components of the noise spectrum. The random components of the noise spectra usually consist of stationary noise and the length of the averaging time T is, in principle, related to the required measurement precision. In most situations, the sound power is determined in octave bands or one-third-octave bands, and the averaging time depends on the filter response—as specified in the instrumentation standards.

To determine the sound intensity, both the pressure and the particle velocity have to be measured. While good pressure microphones are available, precision measurement microphones for the particle velocity are not available. Recently, prototypes of velocity microphones that can measure all three components of the velocity vector by means of a hot-wire technique have been developed.[18] However, the standards for sound power measurements are based on a two-microphone (pressure microphones) technique for the velocity determination. This is based on Euler's equation, which links the particle velocity with the sound pressure

gradient. This equation has the form

$$\mathbf{u} = -\int_0^t \frac{1}{\rho}\nabla p\,dt \qquad (4.22)$$

where ρ is the density of the medium, ∇p is the pressure gradient, and t is the integration time, which, as before, depends on the time function defining the noise. When measuring sound power, we are usually interested in the intensity vector component that is normal to the measurement surface. In this case, the gradient of p is replaced by $\partial p/\partial x$, where x is the direction of the normal to the measurement surface. The measurement of this gradient is approximated by $\partial p/\partial x \cong \Delta p/\Delta x \cong (p_1 - p_2)/\Delta x$. The pressure difference $p_1 - p_2$ is measured using two microphones spaced a distance Δx apart, which must be much smaller than the wavelength of sound. Figure 4.11 shows a two-microphone probe used to measure the pressure gradient. The magnitude of the measured sound intensity vector component $\hat{I}_x$ in the direction x is determined from

$$\hat{I}_x = -\frac{1}{2\rho\,\Delta x}E\left\{[p_2(t) + p_1(t)]\int_0^t [p_2(t) - p_1(t)]\,dt\right\} \qquad (4.23)$$

where E is the expected value representing the time averaging and the pressures are on the two microphone diaphragms spaced a distance Δx apart. Figure 4.12 shows a block diagram of an intensity measurement instrument which calculates the intensity component $\hat{I}_x$ using Eq. (4.23).

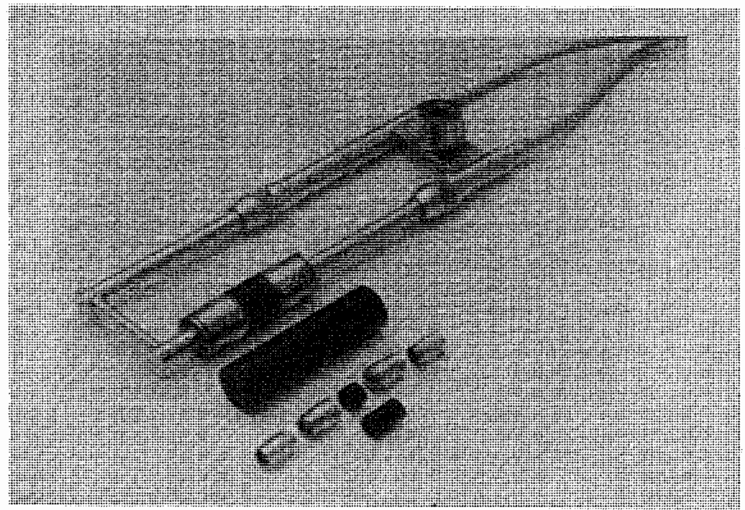

FIGURE 4.11 Sound intensity probe showing two $\frac{1}{2}$-in.-diameter microphones separated precisely by a 1.2-cm spacer. Just beneath is a 5-cm spacer. Below are two $\frac{1}{4}$-in. microphones separated by a 0.6-cm spacer. (Courtesy of Brüel and Kjær, Inc.)

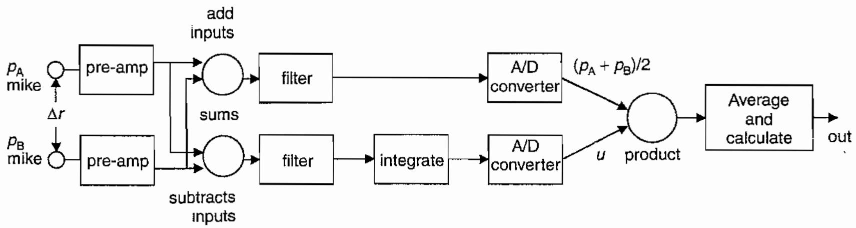

FIGURE 4.12 Block diagram of an analog/digital sound intensity analyzer using octave-band filters. Alternatively, the preamplifier outputs could be suitably amplified and converted to digital format. Then all further processing would be done digitally.

The instrument is also provided with filters with selectable bandwidths to be able to measure the sound power in frequency bands and also to calculate the total power with A-frequency weighting, as required by some standards. Because sound intensity is often used to locate the areas of sound energy radiation or absorption from the surface of a noise source, it is also very practical to measure the sound intensity in very narrow bands. This is conveniently accomplished by using a dual-channel FFT analyzer. The sound intensity measurement is based on a Fourier transform of Eq. (4.23):

$$\hat{I}_x(\omega) = \frac{1}{\omega\rho\ \Delta x}\mathrm{Im}[S_{p_1p_2}(\omega)] \tag{4.24}$$

where $\mathrm{Im}[S_{p_1p_2}(\omega)]$ is the imaginary part of the cross-spectra of the output from the two microphones as measured by the FFT analyzer. This measurement is particularly suitable to analyze the sound power radiation from sources with pronounced line spectra. All sound sources which operate with mechanical periodicity such as rotating engines, fans, vehicles, and similar equipment usually have strong line spectra. The output of the FFT analyzer is usually connected to a computer, which executes the desired postprocessing. The most common calculations are the energy in the lines, in octave or one-third-octave bands, and the total energy, either linear or with A-frequency weighting, as required by some standards. To determine the energy in a band, at least 10 lines of the FFT analysis are generally needed.

The precision of intensity measurements depends on many factors, which can be summarized into two groups: the precision of the instrumentation and the precision of the sampling of the radiated intensity and subsequent calculation of the total radiated power.

There are two standards that define instrumentation requirements for intensity measurements: International Electrotechnical Commission (IEC) 1043[19] and ANSI 1.9–1996.[20] In principle, the intensity measured by an intensity meter should be the same as the intensity in a plane wave measured by a pressure microphone and calculated from the equation $I = p^2/\rho c$. An intensity meter consists

of an intensity probe and a processor. The standards define allowable tolerances for both the probe and the processor for class 1 and 2 intensity instruments.

The probe shown in Fig. 4.11 consists of two pressure microphones separated by a spacer of a length selected by the user. The sound pressure is calculated from the arithmetic average of the microphone pressures. As shown in Eq. (4.23), the particle velocity is approximated by the pressure gradient, which depends on the difference of the microphone pressures. The selected microphone distance must be small enough to avoid a bias error at high frequencies. Figure 4.13 shows the bias error as a function of frequency and microphone distance. This type of bias error cannot be corrected.

Another bias error can occur at low frequencies if the microphones are too close together and not sufficiently phase matched. Figure 4.14 shows the bias error for a 0.3° microphone phase mismatch. The lower the frequency, the greater is the error. Increasing the microphone distance will decrease this error, but a large distance will cause, as mentioned above, a finite distance bias error. Fortunately, modern processors and signal processing can compensate for the phase mismatch error. Essential details are provided in the standards. Due to the existence of these two different bias errors, when the frequency range of the measured noise is large, the measurement usually needs to be repeated using two different microphone separations.

Another important quantity defining the useful frequency range of the instrument is the dynamic capability L_d, defined as

$$L_d = \theta_{pIR} - K \tag{4.25}$$

where θ_{pIR} is the pressure minus residual intensity index and $K = 7$ for a 1-dB allowable measurement error. The importance and usefulness of L_d are shown and

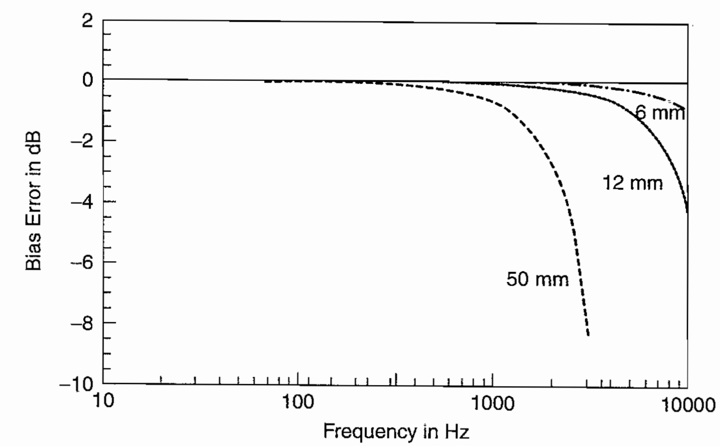

FIGURE 4.13 Intensity probe bias error as a function of frequency with different microphone distances as a parameter.

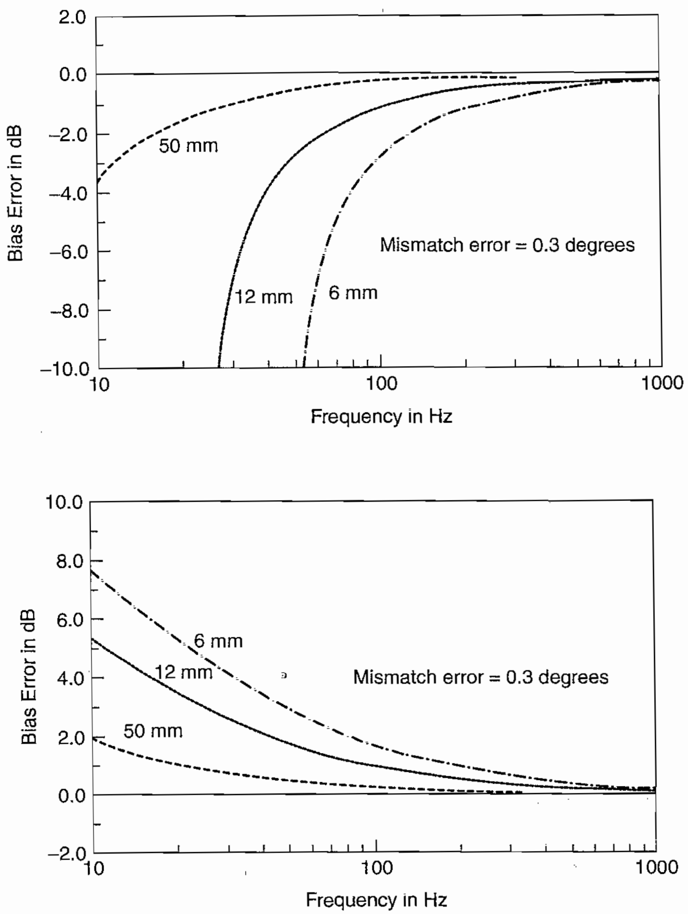

FIGURE 4.14 Intensity probe relative bias error as a function of frequency for different microphone distances as a parameter and mismatch error of 0.3° (plus and minus).

explained in Fig. 4.15. The pressure–residual intensity index θ_{pIR} can be obtained by placing both microphones in a small cavity in which the sound field is excited by an external source. In this way, both microphones are exposed to an identical sound pressure level L_p and the residual intensity level L_{IR} is measured using the intensity meter (usually a FFT analyzer). Ideally, the measured residual intensity should be zero, but due to the microphone mismatch, noise, and measurement instrumentation channel mismatch and other factors, L_{IR} is finite (see Fig. 4.15).

Both L_p and L_I are measured for an actual noise source and the pressure minus intensity index $L_{pI} = L_p - L_I$ is calculated. The intersection of the dynamic capability curve with L_I determines the lowest usable frequency. A phase mismatch will increase L_{IR} and shift the lowest usable frequency higher.

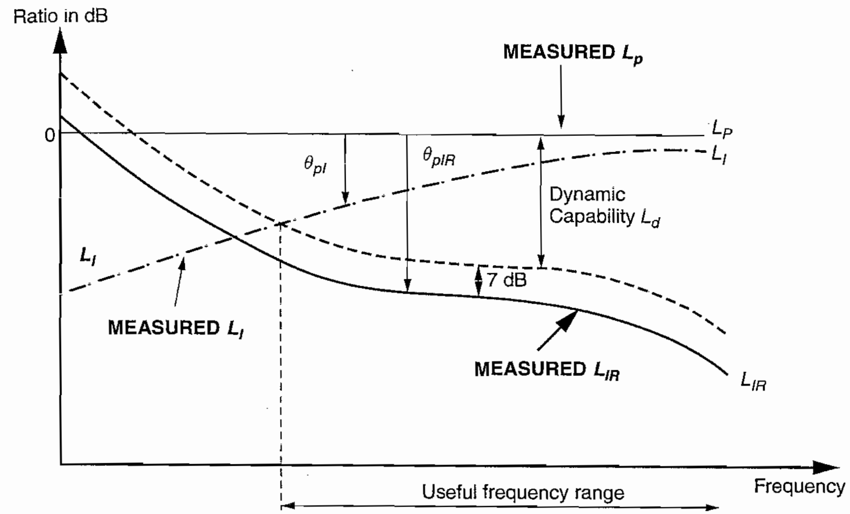

FIGURE 4.15 Dynamic capability of a sound intensity measurement system for 1-dB error as obtained from the pressure–intensity index. The values of L_p and L_I measured with the microphone in a small cavity are used to determine the residual pressure minus intensity index $\theta_{pIR} = L_p - L_{IR}$. The values of L_p and L_I on an actual noise source are used to determine the pressure minus intensity index, $\theta_{pI} = L_p - L_I$.

The pressure minus intensity index $L_{pI} = L_p - L_I$ obtained from the measurement of the actual noise source is an important quantity that characterizes at the measurement point the combination of the source properties and the sound field properties, particularly the effects of the wall reflections. The standards for the sound power measurements and other literature[21] provide essential details.

A typical machine (e.g., an engine) usually operates under conditions different from those under which it would be tested in a reverberant or anechoic room. Moreover, the radiation impedance "seen" by the source may be different from that in a controlled acoustical environment. Hence, its radiated power may be somewhat dependent on how it is mounted and on the proximity of surrounding surfaces.

The intensity technique permits, in most situations, measurement of the sound power of a source of any size operating in its natural environment or on a test stand. In many situations, the sound power radiated from parts of a source can be measured while the whole source is operating. In addition, the intensity technique has become an analytical tool to determine the sound power radiation from different regions of the surface of the source so that the areas of major power radiation can be found. These tasks require an extensive general knowledge of the characteristics of the sound fields, near and far, from the source, wave interference, reflected wave fields, and diffuse sound fields. The details of these important subjects can be found in the literature.[21,22]

Standards which use the direct measurement of sound intensity have been prepared by the ISO and are based on extensive research as well as practical experience gained from measurements. Part 1 of ISO 9614[23] is based on the sampling of sound intensity at discrete points. The intensity probe is moved from point to point and held at each point for a time sufficiently long to make the temporal averaging error small. Part 2 of the same standard uses a scanning technique. The intensity probe is moved over a prescribed path with a sufficiently low speed to satisfy the temporal averaging criterion. The measurement surface is subdivided into smaller sampling areas to secure the required uniformity in the motion of the hand-held probe. Part 3 of the same standard defines the conditions for using the scanning technique for more exact measurements than in Part 2. In practice, the intensity probe is held perpendicular to the measurement surface so that the scalar product converts into an algebraic product.

One of the principal advantages of using the intensity method in field situations is that the results are, in principle, independent of sources outside the measurement surface. The sound energy of external sources propagates through the measurement surface without contributing to the measured power of the sources within the surface—provided that no sound energy due to external sources is absorbed within the surface. Similarly, sound waves reflected from room boundaries or standing waves, unless they are too strong, do not affect the results of a sound power measurement. The standards are applicable to stationary sources located in a nonmoving medium. Because of instrumentation limitations, the frequency range is generally limited to the one-third-octave bands from 50 Hz to 6.3 kHz. A-frequency weighted data are calculated from one-third-octave-band data in this frequency range or from octave-band levels in the frequency range 63 Hz–4 kHz. The correction factors are given in Table 1.4.

Determination of the measurement uncertainty is an important component of the measurements. All standards define the methods and procedures for its determination. Before starting the measurement, the acoustical environment has to be examined for extraneous intensity, wind, gas flow, vibrations, and temperature. The next step consists of the calibration and field check of the instrumentation as specified in IEC 1043[19] or ANSI 1.9–1996.[20] The selection of the measurement surface is important. This is usually performed in two steps. First, an initial surface is selected and an initial measurement performed. The results are tested using a set of indicators that define the characteristics of both the pressure and intensity fields on the measurement surface.[23,24] If the values of these "field indicators" as specified in the standard are not satisfactory, the steps above have to be modified and the measurement repeated. Important field indicators are defined below.

The initial measurement surface is usually selected following the shape of the source at a distance greater than 0.5 m, unless that position is over an area that radiates an insignificant proportion of the sound power of the source under test. The selection of the number of measurement points depends on the shape, segments, and size of the measurement surface. A minimum of 10 points must be selected (greater number obviously leads to better precision, particularly at higher frequencies). If the source is large, one point per square meter of the measurement surface is usually selected, provided that the total number is not less than 50. If extraneous sound penetrates into the measurement area, the number of measurement points must be increased.

After both the sound pressure and the sound intensity are measured at all points, the results are tested by the field indicators in all frequency bands. Depending on the outcome from these indicators, the number and distribution of the measurement points and the distance of the measurement surface from the source may have to be changed. The standards provide tables and flow charts that define the actions to be taken.

The purpose of the indicators is to ensure a sufficient precision of the measurement. The statistical distributions of both the sound pressure and the sound intensity over the measurement surface depend on the source shape and its environment, primarily standing waves caused by sound reflections. Therefore, a general formula for the measurement error does not exist and the error must be determined experimentally. Figure 4.16 shows the flow diagram for the implementation of ISO 9614-1.

The field indicators as defined in ISO 9614 are as follows: F_1, temporal variability of the sound field; F_2, surface pressure–intensity; F_3, negative partial power; and F_4, field nonuniformity. The field indicators require measuring both the sound pressure and intensity. If the criteria for the indicators are not satisfied, the measurement arrangements must be modified. This concerns mainly the change of distance from the measurement surface and increase of the number of measurement points. The flow diagram indicates the actions to be taken. Table 4.8 provides detailed information on these actions.

Indicator F_1 checks the stationarity of the intensity field from several short time-average estimates of the sound intensity at one point of the measurement surface. Its value should be less than 0.6. This should assure that the source operation is steady and the environmental effects are not time variable.

Indicator F_2 is calculated from pressure square averages over the measurement area, converted into a pressure level L_p. Similarly, the intensity level L_I is determined from the arithmetic average of the sound intensities in individual points, all taken with positive sign, irrespective of the power flow out or the measurement surface at a particular point. Indicator F_2 must be smaller than the dynamic capability indicator L_d as defined by Eq. (4.25) and shown in Fig. 4.15 in order to keep the error caused by the instrumentation less than 1 dB for $K = 7$. This indicator is particularly important at low frequencies, as it is apparent in Fig. 4.15.

Indicator F_3 is similar to indicator F_2 except that the intensity level L_I is determined from intensity values with respect to its sign, which means that I is negative at the points where the sound power flows into the measurement surface. This can be caused by extraneous sources or strong reflections due to source environment. Thus $F_3 - F_2$, which is supposed to be less than 3 dB, is linked to the ratio of the sound power radiated out of the measurement surface to the sound power entering the measurement surface. Because both bias and

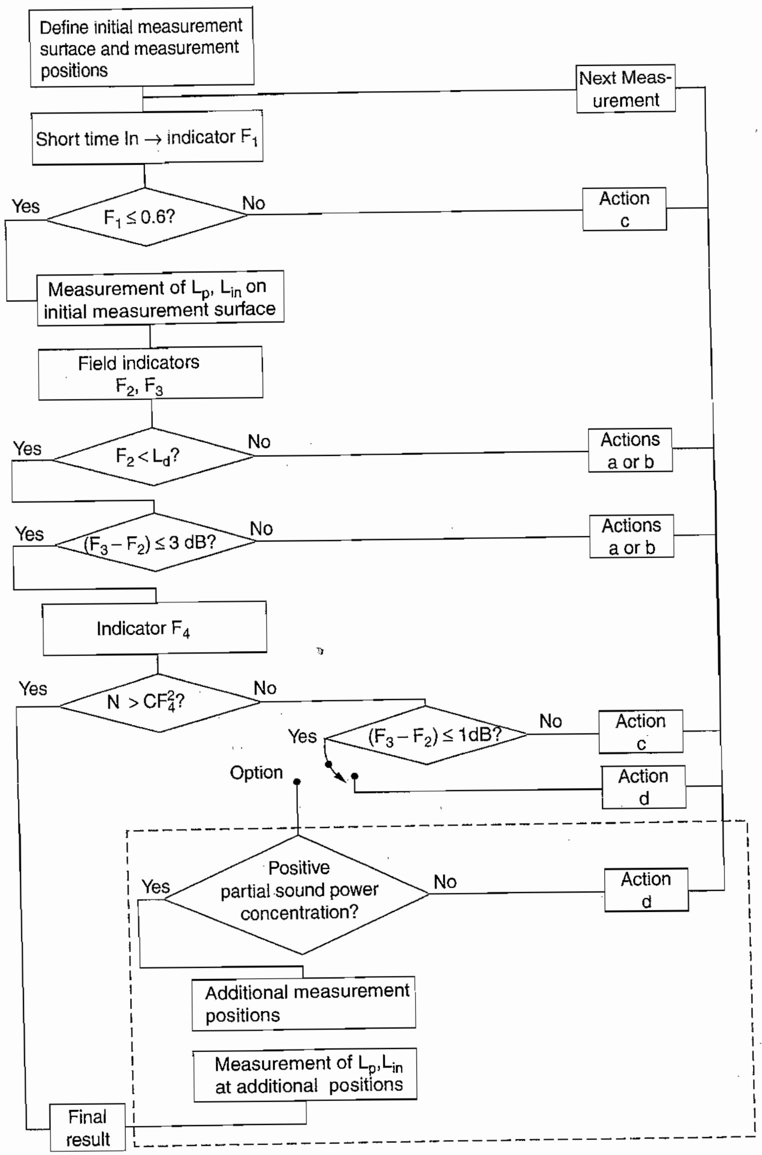

FIGURE 4.16 Flow diagram for the implementation of ISO 9614. The action codes defined in the center column of this figure are defined in Table 4.8. Calculation of the required number of measurement points requires a factor, C, which is defined in Table 4.9. The path enclosed in dashed lines represents an optimal procedure designed to minimize the number of additional measurement positions required on the initial measurement surface. (Courtesy of the International Organization for Standardization, Geneva, Switzerland.)

TABLE 4.8 Actions to Be Taken to Increase Grade of Accuracy of Determination

Criterion	Action Code[a]	Action
$F_1 > 0.6$	e	Take action to reduce the temporal variability of extraneous intensity, or measure during periods of less variability, or increase the measurement period at each position (if appropriate)
$F_2 > L_d$ or $(F_3 - F_2) > 3$ dB	a	In the presence of significant extraneous noise and/or strong reverberation, reduce the average distance of the measurement surface from the source to a minimum average value of 0.25 m; in the absence of significant extraneous noise and/or strong reverberation, increase the average measured distance to 1 m
	or b	Shield measurement surface from extraneous noise sources or take action to reduce sound reflections toward the source
Criterion 2 not satisfied and 1 dB $\leq (F_3 - F_2) \leq 3$ dB	c	Increase the density of measurement positions uniformly to satisfy criterion 2
Criterion 2 not satisfied and $(F_3 - F_2) \leq 1$ dB, and the procedure of ISO 9614 Section 8.3.2 either fails or is not selected	d	Increase average distance of measurement surface from source using the same number of measurement positions or increase the number of measurement positions on the same surface

[a]See Fig. 4.16.

random errors depend on $F_3 - F_2$, the 3-dB criterion satisfies the requirement to keep the bias errors low.

Indicator F_4 is the spatial variance of sound intensity measured at discrete points normalized to the average. The signs of intensity values are considered. This indicator reflects the variability of the power flow over the measurement surface. The higher is F_4, the more measurement points are needed. The number of the measurement points N is given by $N > C \times F_4^2$, where C is a factor which depends on frequency and required precision grade, as shown in Table 4.9.

Part 2 of ISO 9614 defines the measurement of both the sound pressure and intensity by scanning. The measurement area is subdivided into usually plane segments over which the probe is moved ("scanned") perpendicularly to the surface so that spatial averages of the measured quantities are obtained. The recommended moving pattern and speed are specified in the standard. Experimental evidence indicates that the results using the scanning technique are generally more precise than using point measurements.

TABLE 4.9 Values for Factor C

Octave Band Center Frequencies, Hz	One-Third-Octave-Band Center Frequencies, Hz	C: Precision (Grade 1)	C: Engineering (Grade 2)	C: Survey (Grade 3)
63–125	50–160	19	11	
250–500	200–630	29	19	
1000–4000	800–5000	57	29	
	6300	19	14	
A weighted[a]				8

[a] 63 Hz–4 kHz or 50 Hz–6.3 kHz.

Part 3 of ISO 9614 is also based on the scanning technique. The requirements for the measurements and the tolerances to be satisfied are more strict than in Part 2.

In addition to the cited international standards, the ANSI has developed a standard, ANSI S12.12-1992,[25] which mirrors, in its fundamental concept and measurement procedures, the ISO standards. This standard contains a greater number of field indicators and provides more details on the measurement procedures. The selection of any of these standards depends on the product to be measured, the purpose of the sound power determination, and commercial criteria.

ECMA International has also issued a standard for determining sound power from sound intensity using a scanning technique.[26] The standard is intended for use with computer and business equipment.

After substantial experience with the determination of sound power via sound intensity has been achieved, it is expected that these standards will be revised.

4.11 SOUND POWER DETERMINATION IN A DUCT

The most common application of in-duct measurements is to determine the sound power radiated by air-moving devices. The sound power level of a source in a duct can be determined according to ISO 5136[27] from sound-pressure-level measurements, provided that the sound field in the duct is essentially a plane progressive wave, using the equation

$$L_W = L_p + 10 \log \frac{S}{S_0} \tag{4.26}$$

where L_W = level of total sound power traveling down duct, dB re 10^{-12} W
L_p = sound pressure level measured just off centerline of duct, dB re 2×10^{-5} N/m^2
S = cross-sectional area of duct, m^2
S_0 = 1 m^2

The above relation assumes not only a nonreflecting termination for the end of the duct opposite the source but also a uniform sound intensity across the duct. At frequencies near and above the first cross resonance of the duct, the latter assumption is no longer satisfied. Also, when following the measurement procedures of ISO 5136, several correction factors are incorporated into Eq. (4.26) to account for microphone response and atmospheric conditions.

Equation (4.26) can still be used provided L_p is replaced by a suitable space average $\langle L_p \rangle$ obtained by averaging the mean-square sound pressures obtained at selected radial and circumferential positions in the duct or by using a traversing circumferential microphone. The number of measurement positions across the cross section used to determine $\langle L_p \rangle$ will depend on the accuracy desired and the frequency. (See ref. 27, Section 6.2.)

In practical situations, reflections occur at the open end of the duct, especially at low frequencies. The effect of branches and bends must be considered.[28] When there is flow in the duct, it is also necessary to surround the microphone by a suitable windscreen (see Chapter 14). This is necessary to reduce turbulent pressure fluctuations at the microphone, which can cause an error in the measured sound pressure level.

4.12 DETERMINATION OF SOURCE DIRECTIVITY[29,30]

Most sources of sound of practical interest are directional to some degree. If one measures the sound pressure level in a given frequency band a fixed distance away from the source, different levels will generally be found for different directions. A plot of these levels in polar fashion at the angles for which they were obtained is called the *directivity pattern* of the source. A directivity pattern forms a three-dimensional surface, a hypothetical example of which is sketched in Fig. 4.17. The particular pattern shown exhibits rotational symmetry about the direction of maximum radiation, which is typical of many noise sources. At low frequencies, many sources of noise are nondirectional—or nearly so. As the frequency increases, directivity also increases. The directivity pattern is usually determined in the far (free) field (see Fig. 4.4). In the absence of obstacles and reflecting surfaces other than those associated with the source itself, L_p decreases at the rate of 6 dB per doubling of distance.

Directivity Factor

A numerical measurement of the directivity of a sound source is the directivity factor Q, a dimensionless quantity. To understand the meaning of the directivity factor, we must first compare Figs. 4.17 and 4.18. We see in Fig. 4.18 the directivity pattern of a nondirectional source. It is a sphere with a radius equal in length to L_{pS}, the sound pressure level in decibels measured at distance r from a source radiating a total sound power W. The sources of Figs. 4.17 and 4.18 both radiate the same total sound power W, but because the source of Fig. 4.17

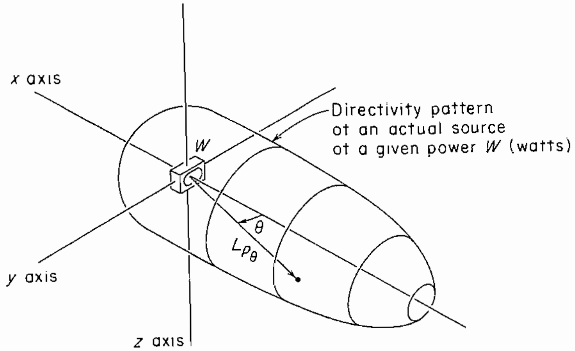

FIGURE 4.17 Directivity pattern of a noise source radiating sound power W into free space. A particular sound pressure level L_p is shown as the length of a vector terminating on the surface of the directivity pattern at angle θ. Sound pressure levels were measured at various angles θ and at a fixed distance r from the actual source in free space.

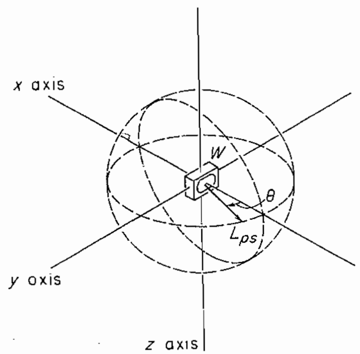

FIGURE 4.18 Spherical directivity pattern of a nondirectional source radiating acoustic power W into free space. At all angles θ and distance r, the sound pressure level equals L_{pS}, where $L_{pS} = 10\log(10^{12} \times W/4\pi r^2)$.

is directional, it radiates more sound than that of Fig. 4.18 in some directions and less in others.

To derive a directivity factor Q, we must assume that the directivity pattern does not change shape regardless of the radius r at which it is measured. For example, if L_p at a particular angle is 3 dB greater than at a second angle, the 3-dB difference should be the same whether r is 1, 2, 10, or 100 m. This can only be determined in the far field of a source located in anechoic space.

The directivity factor Q_θ is defined as the ratio of (1) the mean-square sound pressure p_θ^2 [(N/m^2)^2] at angle θ and distance r from an actual source radiating W watts to (2) the mean-square sound pressure p_s^2 at the same distance from a nondirectional source radiating the same acoustic power W. Alternatively, Q_θ

is defined as the ratio of the intensity in the direction of propagation (W/m^2) at angle θ and distance r from an actual source to the intensity at the same distance from a nondirectional source, both sources radiating the same sound power W. Thus

$$Q_\theta = \frac{p_\theta^2}{p_s^2} = \frac{I_\theta}{I_s} = \frac{10^{L_{p\theta}/10}}{10^{L_{pS}/10}} \quad \text{(dimensionless)} \tag{4.27}$$

or

$$Q_\theta = 10^{(L_{p\theta} - L_{pS})/10} \tag{4.28}$$

where $L_{p\theta}$ = sound pressure level measured a distance r and an angle θ from a source radiating power W into an anechoic space (see Fig. 4.17)
L_{pS} = sound pressure level measured at a distance r from a nondirectional source of power W radiating into anechoic space (see Fig. 4.18)

Note that Q_θ is for the angle θ at which $L_{p\theta}$ was measured and that L_{pS} and $L_{p\theta}$ are for the same distance r.

Directivity Index

The directivity index (DI) is simply defined as

$$\mathrm{DI}_\theta = 10\log Q_\theta \quad \mathrm{dB} \tag{4.29}$$

or

$$\mathrm{DI}_\theta = L_{p\theta} - L_{pS} \tag{4.30}$$

Obviously, a nondirectional source radiating into spherical space has $Q_\theta = 1$ and $\mathrm{DI} = 0$ at all angles θ.

Relations between $L_{p\theta}$, Directivity Factor, and Directivity Index

The sound pressure level for the nondirectional source of Fig. 4.18 is

$$L_{pS} = 10\log\frac{p^2 \text{ at distance } r}{4 \times 10^{-10}} \quad \mathrm{dB} \tag{4.31}$$

From Eqs. (4.5) and (4.11) and taking the quantity $D = \rho c W_0/p_{\text{ref}}^2$ to be small, L_{pS} is given by (see Fig. 4.18)

$$L_{pS} = 10\log\frac{W \times 10^{12}}{4\pi r^2} \quad \mathrm{dB} \tag{4.32}$$

From Eqs. (4.28) and (4.32), we find that

$$L_{p\theta} = 10 \log \frac{WQ_\theta \times 10^{12}}{4\pi r^2} \tag{4.33}$$

where W is in watts and r is in meters. In logarithmic form

$$L_{p\theta} = L_W + \mathrm{DI}_\theta - 20 \log r - 11 \text{ dB} \tag{4.34}$$

where r is the distance from the acoustical center of the source in meters.

Determination of Directivity Index in Spherical Space

The directivity index DI_θ of a sound source in free space at angle θ and for a given frequency band is computed from

$$\mathrm{DI}_\theta = L_{p\theta} - \langle L_p \rangle_S \tag{4.35}$$

where $L_{p\theta}$ = sound pressure level measured at distance r and angle θ from source, dB

$\langle L_p \rangle_S$ = sound pressure level averaged over test sphere of radius r (and area $4\pi r^2$) centered on and surrounding source

Determination of Directivity Index in Hemispherical Space

The directivity index DI_θ of a sound source on a rigid plane at angle θ and for a given frequency band is computed from

$$\mathrm{DI}_\theta = L_{p\theta} - \langle L_p \rangle_H + 3 \text{ dB} \tag{4.36}$$

where $L_{p\theta}$ = sound pressure level measured distance r and angle θ from source, dB

$\langle L_p \rangle_H$ = sound pressure level of space-averaged mean-square pressure averaged over a test hemisphere of radius r (and area $2\pi r^2$) centered on and surrounding source

The 3 dB in this equation is added to $\langle L_p \rangle_H$ because the measurement was made over a hemisphere instead of a full sphere, as defined in Eq. (4.37). The reason for this is that the intensity at radius r is twice as large if a source radiates into a hemisphere as compared to a sphere. That is, if a nondirectional source were to radiate uniformly into hemispherical space, $\mathrm{DI}_\theta = \mathrm{DI} = 3$ dB.

Determination of Directivity Index in Quarter-Spherical Space

Some pieces of equipment are normally associated with more than one reflecting surface, for example, an air conditioner standing on the floor against a wall. The power level of noise sources of this type may be measured with those surfaces in place. This is done best in a test room with anechoic walls but with one hard wall forming an "edge" with the hard floor. The general considerations of the

preceding paragraphs apply here as well. One determines the sound pressure level averaged over the quarter-sphere, $\langle L_p \rangle_H$, and also determines $L_{p\theta}$ as before. The directivity index is given by

$$\mathrm{DI}_\theta = Lp_\theta - \langle L_p \rangle_Q + 6 \text{ dB} \tag{4.37}$$

REFERENCES

1. R. H. Bolt and K. U. Ingard, "System Considerations in Noise-Control Problems," in C. M. Harris (Ed.), *Handbook of Noise Control*, 1st ed., McGraw-Hill, New York, 1957, Chapter 22.
2. E. A. G. Shaw, "Noise Pollution—What Can Be Done?" *Phys. Today*, **28**(1), 46 (1975).
3. ISO 3740, *"Acoustics—Determination of Sound Power Levels of Noise Sources—Guidelines for the Use of Basic Standards,"* International Organization for Standardization, Geneva, Switzerland, 2000.
4. ISO 3741, *"Acoustics—Determination of Sound Power Levels of Noise Sources Using Sound Pressure—Precision Methods for Reverberation Rooms,"* International Organization for Standardization, Geneva, Switzerland, 1999.
5. ISO 3741, *"Acoustics—Determination of Sound Power Levels of Noise Sources Using Sound Pressure—Precision Methods for Reverberation Rooms,"* International Organization for Standardization, Geneva, Switzerland, 1999. Correction 1:2001.
6. ISO 3743-1, *"Acoustics—Determination of Sound Power Levels of Noise Sources—Engineering Methods for Small, Movable Sources in Reverberant Fields—Part 1: Comparison Method for Hard-Walled Test Rooms,"* International Organization for Standardization, Geneva, Switzerland, 1994.
7. ISO 3743-2, *"Acoustics—Determination of Sound Power Levels of Noise Sources Using Sound Pressure—Engineering Methods for Small, Movable Sources in Reverberant Fields—Part 2: Methods for Special Reverberation Test Rooms,"* International Organization for Standardization, Geneva, Switzerland, 1994.
8. ISO 3744, *"Acoustics—Determination of Sound Power Levels of Noise Sources Using Sound Pressure—Engineering Method in an Essentially Free Field over a Reflecting Plane,"* International Organization for Standardization, Geneva, Switzerland, 1994.
9. ISO 3745, *"Acoustics—Determination of Sound Power Levels of Noise Sources Using Sound Pressure—Precision Methods for Anechoic and Hemi-Anechoic Rooms,"* International Organization for Standardization, Geneva, Switzerland, 2003.
10. ISO 3746, *"Acoustics—Determination of Sound Power Levels of Noise Sources Using Sound Pressure—Survey Method Using an Enveloping Measurement Surface over a Reflecting Plane,"* International Organization for Standardization, Geneva, Switzerland, 1995.
11. ISO 3746, *"Acoustics—Determination of Sound Power Levels of Noise Sources Using Sound Pressure—Survey Method Using an Enveloping Measurement Surface over a Reflecting Plane,"* International Organization for Standardization, Geneva, Switzerland, 1995. Correction 1:1995.
12. ISO 3747, *"Acoustics—Determination of Sound Power Levels of Noise Sources Using Sound Pressure—Comparison Method in Situ,"* International Organization for Standardization, Geneva, Switzerland, 2000.

13. ISO 6926, *"Acoustics—Requirements for the Performance and Calibration of Reference Sound Sources Used for the Determination of Sound Power Levels,"* International Organization for Standardization, Geneva, Switzerland, 1999.
14. M. A. Nobile, B. Donald, and J. A. Shaw, "The Cylindrical Microphone Array: A Proposal for Use in International Standards for Sound Power Measurements," Proc. NOISE-CON 2000 (CD-ROM), paper 1pNSc2, 2000.
15. M. A. Nobile, J. A. Shaw, and R. A. Boyes, "The Cylindrical Microphone Array for the Measurement of Sound Power Level: Number and Arrangement of Microphones," Proc. INTER-NOISE 2002 (CD-ROM), paper N318, 2002.
16. ISO 7779, *"Acoustics—Measurement of Airborne Noise Emitted by Information Technology and Telecommunications Equipment (Second Edition),"* International Organization for Standardization, Geneva, Switzerland, 1999.
17. R. V. Waterhouse, "Output of a Sound Source in a Reverberation Chamber and Other Reflecting Environments," *J. Acoust. Soc. Am.*, **30**, 4–13 (1958).
18. Hans-Elias de Bree, *"The Microflown Report,"* Amsterdam, The Netherlands, www.Microflown.com, April 2001.
19. IEC 1043, *"Instruments for the Measurement of Sound Intensity—Measurement with Pairs of Pressure Sensing Microphones,"* International Electrotechnical Commission, Geneva, Switzerland, 1993.
20. ANSI S1.9, *"Instruments for the Measurement of Sound Intensity,"* Acoustical Society of America, Melville, NY, 1996.
21. F. J. Fahy, *Sound Intensity*, 2nd ed., E&FN SPON, Chapman & Hall, London, 1995.
22. J. Adin Man III and J. Tichy, "Near Field Identification of Vibration Sources, Resonant Cavities, and Diffraction Using Acoustic Intensity Measurements," *J. Acoust. Soc. Am.*, **90**, 720–729 (1991).
23. ISO 9614, *"Determination of Sound Power Levels of Noise Sources Using Sound Intensity Part 1: Measurement at Discrete Points"—1993; "Part 2: Measurement by Scanning"—1994; "Part 3: Precision Method for Measurement by Scanning"—2000,* International Organization for Standardization, Geneva, Switzerland.
24. F. Jacobsen, "Sound Field Indicators: Useful Tools." *Noise Control Eng. J.*, **35**, 37–46 (1990).
25. ANSI S12.12, *"Engineering Method for the Determination of Sound Power Levels of Noise Sources Using Sound Intensity,"* Acoustical Society of America, Melville, NY, 1992.
26. ECMA-160: *"Determination of Sound Power Levels of Computer and Business Equipment using Sound Intensity Measurements; Scanning Method in Controlled Rooms,"* 2nd edition, ECMA International, Geneva, Switzerland, December 1992. A free download is available from www.ecma-international.org.
27. ISO 5136, *"Acoustics—Determination of Sound Power Radiated into a Duct by Fans and Other Air Moving Devices—In-Duct Method,"* International Organization for Standardization, Geneva, Switzerland, 2003.
28. P. K. Baade, "Effects of Acoustic Loading on Axial Flow Fan Noise Generation," *Noise Control Eng. J.*, **8**(1), 5–15 (1977).
29. L. L. Beranek, *Acoustical Measurements*, Acoustical Society of America, Woodbury, NY, 1988.
30. L. L. Beranek, *Acoustics*, Acoustical Society of America, Woodbury, NY, 1986.

CHAPTER 5

Outdoor Sound Propagation

ULRICH J. KURZE
Mueller-BBM GmbH
Planegg near Munich, Germany

GRANT S. ANDERSON
Harris Miller Miller, & Hanson Inc.
Burlington, Massachusetts

5.1 INTRODUCTION

This chapter deals with the description and prediction of sound due to sources in an outdoor environment. Specifically, it deals with the propagation path from source to receiver. Propagation is affected by geometrical spreading, ground effects including reflection and refraction due to temperature and wind speed vertical gradients, attenuation from intervening barriers, general reflections and reverberation, atmospheric absorption, and attenuation from intervening vegetation.

5.2 GENERAL DISCUSSION

The atmosphere is in constant motion due to wind and sun at amplitudes that are large compared to the amplitudes of sound–particle velocity. This constant motion results in considerable distortion of sound waves and considerable variability of propagation conditions. Ever since the careful observations and first scientific modeling of outdoor sound propagation by O. Reynolds, Lord Rayleigh, and Lord Kelvin in the nineteenth century,[1] numerous experimental and mathematical studies have provided detailed understanding of the effects of mechanical and thermal turbulence, humidity (including fog), boundary conditions at the ground surface, and obstacles such as trees, walls, and buildings in the propagation path.

Unfortunately, much of the vast amount of information published on outdoor sound propagation in scientific papers is not relevant to the practical control of noise from recreational and industrial facilities or from road, rail, and air

13. ISO 6926, *"Acoustics—Requirements for the Performance and Calibration of Reference Sound Sources Used for the Determination of Sound Power Levels,"* International Organization for Standardization, Geneva, Switzerland, 1999.
14. M. A. Nobile, B. Donald, and J. A. Shaw, "The Cylindrical Microphone Array: A Proposal for Use in International Standards for Sound Power Measurements," Proc. NOISE-CON 2000 (CD-ROM), paper 1pNSc2, 2000.
15. M. A. Nobile, J. A. Shaw, and R. A. Boyes, "The Cylindrical Microphone Array for the Measurement of Sound Power Level: Number and Arrangement of Microphones," Proc. INTER-NOISE 2002 (CD-ROM), paper N318, 2002.
16. ISO 7779, *"Acoustics—Measurement of Airborne Noise Emitted by Information Technology and Telecommunications Equipment (Second Edition),"* International Organization for Standardization, Geneva, Switzerland, 1999.
17. R. V. Waterhouse, "Output of a Sound Source in a Reverberation Chamber and Other Reflecting Environments," *J. Acoust. Soc. Am.*, **30**, 4–13 (1958).
18. Hans-Elias de Bree, *"The Microflown Report,"* Amsterdam, The Netherlands, www.Microflown.com, April 2001.
19. IEC 1043, *"Instruments for the Measurement of Sound Intensity—Measurement with Pairs of Pressure Sensing Microphones,"* International Electrotechnical Commission, Geneva, Switzerland, 1993.
20. ANSI S1.9, *"Instruments for the Measurement of Sound Intensity,"* Acoustical Society of America, Melville, NY, 1996.
21. F. J. Fahy, *Sound Intensity*, 2nd ed., E&FN SPON, Chapman & Hall, London, 1995.
22. J. Adin Man III and J. Tichy, "Near Field Identification of Vibration Sources, Resonant Cavities, and Diffraction Using Acoustic Intensity Measurements," *J. Acoust. Soc. Am.*, **90**, 720–729 (1991).
23. ISO 9614, *"Determination of Sound Power Levels of Noise Sources Using Sound Intensity Part 1: Measurement at Discrete Points"—1993; "Part 2: Measurement by Scanning"—1994; "Part 3: Precision Method for Measurement by Scanning"—2000,* International Organization for Standardization, Geneva, Switzerland.
24. F. Jacobsen, "Sound Field Indicators: Useful Tools." *Noise Control Eng. J.*, **35**, 37–46 (1990).
25. ANSI S12.12, *"Engineering Method for the Determination of Sound Power Levels of Noise Sources Using Sound Intensity,"* Acoustical Society of America, Melville, NY, 1992.
26. ECMA-160: *"Determination of Sound Power Levels of Computer and Business Equipment using Sound Intensity Measurements; Scanning Method in Controlled Rooms,"* 2nd edition, ECMA International, Geneva, Switzerland, December 1992. A free download is available from www.ecma-international.org.
27. ISO 5136, *"Acoustics—Determination of Sound Power Radiated into a Duct by Fans and Other Air Moving Devices—In-Duct Method,"* International Organization for Standardization, Geneva, Switzerland, 2003.
28. P. K. Baade, "Effects of Acoustic Loading on Axial Flow Fan Noise Generation," *Noise Control Eng. J.*, **8**(1), 5–15 (1977).
29. L. L. Beranek, *Acoustical Measurements*, Acoustical Society of America, Woodbury, NY, 1988.
30. L. L. Beranek, *Acoustics*, Acoustical Society of America, Woodbury, NY, 1986.

CHAPTER 5

Outdoor Sound Propagation

ULRICH J. KURZE
Mueller-BBM GmbH
Planegg near Munich, Germany

GRANT S. ANDERSON
Harris Miller Miller, & Hanson Inc.
Burlington, Massachusetts

5.1 INTRODUCTION

This chapter deals with the description and prediction of sound due to sources in an outdoor environment. Specifically, it deals with the propagation path from source to receiver. Propagation is affected by geometrical spreading, ground effects including reflection and refraction due to temperature and wind speed vertical gradients, attenuation from intervening barriers, general reflections and reverberation, atmospheric absorption, and attenuation from intervening vegetation.

5.2 GENERAL DISCUSSION

The atmosphere is in constant motion due to wind and sun at amplitudes that are large compared to the amplitudes of sound–particle velocity. This constant motion results in considerable distortion of sound waves and considerable variability of propagation conditions. Ever since the careful observations and first scientific modeling of outdoor sound propagation by O. Reynolds, Lord Rayleigh, and Lord Kelvin in the nineteenth century,[1] numerous experimental and mathematical studies have provided detailed understanding of the effects of mechanical and thermal turbulence, humidity (including fog), boundary conditions at the ground surface, and obstacles such as trees, walls, and buildings in the propagation path.

Unfortunately, much of the vast amount of information published on outdoor sound propagation in scientific papers is not relevant to the practical control of noise from recreational and industrial facilities or from road, rail, and air traffic. Relevance is determined by the rating criteria required by governmental agencies for assessment of community environments, such as described in the ISO 1996 series and various governmental regulations. Relevant criteria most often are given in the form of two acoustical descriptors: the equivalent continuous and the average maximum A-weighted sound pressure level, L_{eq} (as defined in Chapter 2) and $L_{A,max}$ (e.g., during a single-vehicle pass-by).

For that purpose, mainly average favorable conditions for sound propagation (plus the frequency of such conditions) need to be considered. Unfavorable conditions, which result in a large and uncertain range of low sound pressure levels, play a minor role in Europe.

For example, when favorable conditions occur during 50% of the time and unfavorable conditions result in at least 5-dB lower levels, then the equivalent continuous level

$$\begin{aligned} L_{eq} &= 10 \lg \left(\frac{50}{100} 10^{L_{fav}/10} + \frac{50}{100} 10^{L_{unfav}/10} \right) \text{ dB} \\ &< L_{fav} - 3 \text{ dB} + 10 \lg(1 + 10^{-5/10}) \text{ dB} = L_{fav} - 1.8 \text{ dB} \qquad (5.1) \\ &> L_{fav} - 3 \text{ dB} \end{aligned}$$

lies some 2–3 dB below the average maximum level L_{fav} that occurs under favorable propagation conditions. It never lies outside that range, independent of the actual distribution of levels L_{unfav} for unfavorable propagation conditions.

The techniques in this chapter concentrate on such average favorable conditions for sound propagation to receiver positions about 4 m above the ground (first story above the ground story or higher). Additional techniques will be needed in governmental jurisdictions that require assessment of somewhat lower levels received 1.5 m above the ground—as is common within the United States and Canada.

In general, the level of outdoor sound decays with increasing distance between source and receiver. This geometrical divergence is most important for attenuation near the source, while meteorological conditions dominate attenuation further away.

Barriers, buildings, and hills that interrupt direct propagation from source to receiver are most important for excess attenuation. Of less importance are the effects of atmospheric absorption, porous ground (with receivers above 3–5 m), trees, single reflections from buildings, and reverberation in forests, valleys, and street canyons. Even though such effects are well understood, their computation requires input that is often not available in engineering practice—such as the spatial distribution of relative humidity or the effective flow resistivity of the ground between source and receiver. For planning purposes, engineering estimates or conventions have to be employed, rather than detailed models, to account for such effects.

In a homogeneous atmosphere at rest, geometrical divergence of sound from point sources is described by rigorous solutions of the wave equation in spherical

coordinates. In these solutions, sound travels on a straight course in all directions at the same speed.

In reality, however, sound paths are not straight, because sound speed varies with temperature and wind velocity, mainly as a function of height above the ground. Underwater sound propagation is similarly dependent on height, due to the variation of salt content with height. To account for refraction of sound under water, various specialized mathematical models have been developed: ray theory, the spectral method or fast-field program (FFP), the normal mode, and the parabolic equation (PE).[2] Except for the normal-mode model, which is based on essentially two-dimensional fields between the bottom and the surface of an ocean, all these models have been proposed for airborne sound as well.

In addition, for airborne sound propagation the particular effects of ground impedance can be computed with a boundary element model (BEM)—although that model is limited to a nonrefracting (homogeneous) atmosphere. Also in the acoustical literature is a Meteo-BEM (presently limited to linear sound speed profiles) and a generalized-terrain PE. The latter is limited to axis-symmetric cases, just like the PE, but is also applicable to terrain profiles with moderate slope.[3]

In spite of these advanced models, the much-simpler ray theory has now gained engineering importance, exclusively. In the past, ray theory was dominant because of excessive computation-time requirements for FFP- and PE-like models. At present, the comparison of results obtained with FFP (within the limits of reliable atmospheric input data involving the Monin-Obukhov boundary layer theory) has shown no particular advantage to FFP over ray theory. Instead, the two models show surprising consistency for downwind conditions up to a distance of 2000 m.[4,5]

At a reception point outdoors, only the A-weighted overall sound pressure level is considered in most practical cases. Further calculation of sound transmission into buildings, which requires information about the spectral distribution, is limited to special problems of building acoustics. Consequently, older engineering estimates neglect the frequency dependence of propagation losses. Instead, they assume a single frequency band that represents the attenuation of A-weighted overall sound pressure from sources with typical spectra. Due to increased computer capabilities, advanced engineering models now include calculations in frequency bands. Except for distant propagation to receiver heights of 1.5 m, full-octave bands are sufficient—both for the precision obtainable and the requirement for traceable details. One-third-octave bands are needed for special cases only.

Regulations that allow various calculation procedures with frequency bands of different widths have a great disadvantage. The simpler procedure is not always on the safe side, and so users quickly learn to choose the procedure that yields "better" results, from their point of view. To avoid ambiguous results of this type, one should follow well-established governmental regulations and conventions—such as ISO 9613-2[6] in Europe and the regulations of funding authorities in the United States and Canada.

5.3 SOURCES

Point Sources at Rest

Historically, acousticians distinguished between point, line, and area sources. Modern computer capabilities allow for the exclusive use of large numbers of point sources to approximate lines and areas. Such approximation is officially considered satisfactory in Europe, but not in the United States, where federal regulations generally require use of line source algorithms and computer programs. Such line source programs eliminate the possibility that gaps in noise barriers, for example, will be ignored by computations when the approximating point sources are not sufficiently dense along the roadway.

European computer programs automatically break up extended sources into sufficiently small elements, which can be described as point sources. For this purpose, it is generally sufficient that

- the largest dimension of a source element be less than half the distance between source and receiver,
- the sound power be about equally distributed over the source element, and
- about the same propagation conditions exist from all points on the source element to the receiver.

The last requirement pertains to effects of the ground and obstacles in the propagation path. If they are relevant, the permissible difference in height above the ground between two source elements is typically less than 0.3 m. Whether a particular computer program follows these rules needs to be carefully determined by test cases.

Point sources are described by

- the location (x,y,z) of the center,
- the sound power level L_W in frequency bands (relative to 1 pW), and
- the directivity index D_I in frequency bands (in one or two dimensions).

Preferred frequency bands are octave bands with center frequencies from 63 to 8000 Hz. Lower frequencies may be important—for example, in the vicinity of jet engine test cells. They need special consideration. Higher frequencies are subject to strong and variable atmospheric attenuation. They can be neglected outdoors.

When available, one should use measured sound spectra and directivity of specific noise sources. If these are not available but the A-weighted overall sound power level is known, Table 5.1 contains an estimate of the octave-band spectra applicable to a surprising number of sound sources—such as roadway, railway and aircraft traffic, rifle fire, muffled diesel engines, and many industrial noise sources. For comparatively large and slow sources or for substantial vibration damping, the spectrum may be shifted to lower frequencies by one octave. On the other hand, comparatively small and fast-moving sources with little vibration

TABLE 5.1 Typical Unweighted and A-Weighted Octave-Band Source Spectra Relative to A-Weighted Overall Sound Power

Octave-Band Center frequency, Hz	63	125	250	500	1000	2000	4000	8000
Unweighted: $L_{W,\text{oct}} - L_{WA}$, dB	−2	1	−1	−3	−5	−8	−12	−23
A weighted: $L_{WA,\text{oct}} - L_{WA}$, dB	−28	−15	−10	−6	−5	−7	−11	−24

damping may have a spectrum that is shifted to higher frequencies by one octave. When the frequency band around 500 Hz is taken as an equivalent for the attenuation of A-weighted overall sound, this simplifying assumption is relative to one octave band below the average maximum of A-weighted octave-band noise.

The directivity index is normalized so that the average value of $10^{D_I/10}$ in all directions is unity. In many cases of rotational symmetry, the directivity index is sufficiently described in one dimension. Examples are smoke stacks and gunfire. For receivers on level ground, the directivity index is often described in the horizontal plane only. A practical example is the directivity of sound from aircraft engines during ground run-up tests. For turbo-jet aircraft on the ground, a typical dependence of directivity on angle and frequency is plotted in Fig. 5.1. Highest values occur in the direction $\phi = 120°$ from the forward direction and in the 1000-Hz frequency band.

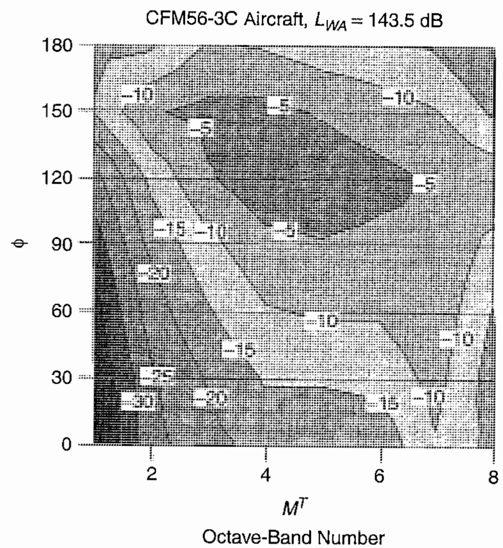

FIGURE 5.1 Combination of directivity and octave-band weighting for a turbojet engine with high bypass ratio at takeoff power setting. Octave-band number 2 is centered at 125 Hz and number 8 at 8000 Hz. Data are for a CFM-56-3C aircraft engine with $L_{WA} = 143.5$ dB.

The basic relation between the sound pressure level L_p at a distance d from a source and the sound power level L_W of the source is given by

$$L_p(d, \phi) = L_W + D_I(\phi) + D_\Omega - A(d, \phi) \tag{5.2}$$

where $A(d, \phi)$ = transfer function due to effect of all elements in propagation path; attenuating or enhancing effects are discussed in Section 5.4

$D_I(\phi)$ = directivity index

D_Ω = index that accounts for sound propagation into solid angles less than 4π steradians

When the sound power output of a source is determined from outdoor measurements of the sound pressure level $L_p(d, \phi)$ in various directions ϕ at a certain distance d from the source, it is important to apply the same transfer function $A(d, \phi)$ from the sound power level to the sound pressure level as is applied in the opposite direction.

The description of sound emission in terms of the sound power level generally includes the assumption that the source radiates into free space (solid angle $\Omega = 4\pi$). Instead, when the source is located on the ground, and therefore the solid angle of radiation is 2π, two equivalent assumptions can account for the ground: (1) an additional incoherent image source beneath the ground, with the same sound power, or (2) a correction of the sound power level L_W by D_Ω = 3 dB in Eq. (5.2). In general, when the source is located at a height h_S and the receiver at a height h_R above reflecting ground, the correcting index is

$$D_\Omega = 10 \lg \left[1 + \frac{d^2 + (h_S - h_R)^2}{d^2 + (h_S + h_R)^2}\right] \quad \text{dB} \tag{5.3}$$

from geometrical consideration of incoherent image sources.[6] Furthermore, in some cases the ground effect A_{gr} from source to receiver, which is part of $A(d)$ in Eq. (5.2), must be taken into account.

When the source is located close to a wall or in a corner formed by two walls, sound pressure at some distance would include reflections from these walls as well. Similar to Eq. (5.3), the effect of these reflections is a level difference of about D_Ω = 6 dB for a wall and about 9 dB for a corner. Alternatively—and necessarily for sound-absorbing walls—image sources may be considered separately.

Moving Sources

For traffic noise, it is common practice to consider the motion of sources along straight lines. Compared to continuous sources at rest, moving sources yield

- variable sound pressure levels at a stationary receiver,
- variable pitch of tonal components at a stationary receiver (Doppler effect), and
- different radiation due to different acoustical loading of the surrounding air.

The last of these effects is well described by theory, but in practice either included in the overall description of sound emission or neglected at low velocities.

The variation in pitch, from a higher pitch during vehicle approach to a lower pitch after passage, is determined by the factor $(1 + M)/(1 - M)$, in which $M = V/c$ is the Mach number resulting from the vehicle velocity V and the sound velocity c. For road traffic, this multiplicative factor roughly corresponds to one-third of an octave, but for high-speed maglev trains, it may reach a full octave. In addition, for maglev trains, the sinusoidal excitation of the track, which is due to the groove-passage frequency of magnets over the long-stator, results in a broadband maximum noise at receivers close to the track—when radiated frequencies shift upward from some parts of the track and downward from other parts (see Fig. 5.2). Pure tones from the vibration signal of the magnets are not audible during train passage.

For moving vehicles of any type, the variation in sound pressure level during approach and pass-by is generally not taken into account, except for its energy mean and, in some cases, its maximum value. An integrating sound-level meter is used to determine the total sound energy and then to report the pass-by's sound exposure level (SEL), which is the level of the integrated sound energy referred to a time interval of 1 s and is also called the single-event level. Since the direction of sound approach to a receiver from a long, straight track is equally distributed horizontally over 180°, Eq. (5.2) can be used without its directivity index to convert the SEL into a sound power level. Spreading this sound power over the distance the source travels in 1 h results in a sound power per unit length of track—the strength of a line source for one vehicle per hour. For further calculations, the line source is broken up into straight-line segments in the United States and Canada or into point sources in Europe.

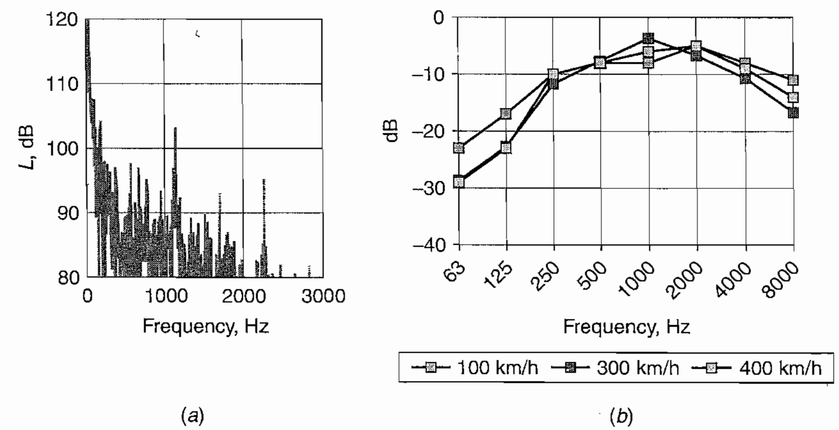

FIGURE 5.2 (*a*) Narrow-band spectrum of sound pressure level measured close to the magnets of a maglev train at 355 km/h. (*b*) A-weighted octave-band spectrum relative to A-weighted overall sound pressure level at some distance from a maglev train.

Although this procedure is normally applied to individual road and rail vehicles, the emission from the homogeneous section of a long train is usually evaluated differently. In such cases, the time integral of the squared sound pressure may be limited, without significant energy loss, to just when the center part of the homogeneous section passes by. This integral describes the sound emission from the homogeneous section in the same way as the SEL describes it for the entire train. Consequently, the same procedure can be used here (distribute the sound power over the distance the source travels in one hour) to determine the sound power per unit length of track for the train section selected. Sound power contributions from rolling noise of different vehicles are then added together. Contributions from sources at different heights need to be considered as separate line sources.

5.4 ELEMENTS IN PROPAGATION PATH

Overview

The transfer function of sound from a source to a receiver is determined by the sum of all attenuations along a particular ray path and by the contribution from all paths of direct and reflected sound. Attenuations account for spherical spreading A_{div}, ground effect A_{gr}, diffraction by barriers A_{bar}, partial reflections A_{refl}, atmospheric absorption A_{atm}, and miscellaneous others A_{misc}. They are described in the following.

Sound Propagation in Homogeneous Free Space over Ground

In the geometrical, high-frequency approximate solution of the Helmholtz equation for sound pressure p,

$$\Delta p + \left(\frac{2\pi f}{c}\right)^2 p = -\delta^2(\mathbf{r} - \mathbf{r}_S) \tag{5.4}$$

propagation of sound with frequency f from a point source at $\mathbf{r} = \mathbf{r}_S$ is described by ray theory. Rapid variations in phase are distinguished from slow variations in amplitude due to geometrical spreading and energy loss mechanisms. The ray trajectories are perpendicular to the surface of constant phase, which forms the wave front. The direction of average energy flux follows that of the trajectories. The amplitude of the field at any point can be obtained from the density of rays.

At short ranges, it is reasonable to assume straight rays. In free space, spherical spreading over a distance d results in an attenuation of

$$A_{\text{div}} = 10 \text{ lg } \frac{4\pi d^2}{d_0^2} \text{ dB} \tag{5.5}$$

where $d_0 = 1$ m. An observer above partially reflecting ground receives not only the direct ray but also a ground reflection, as sketched in Fig. 5.3. For simplicity,

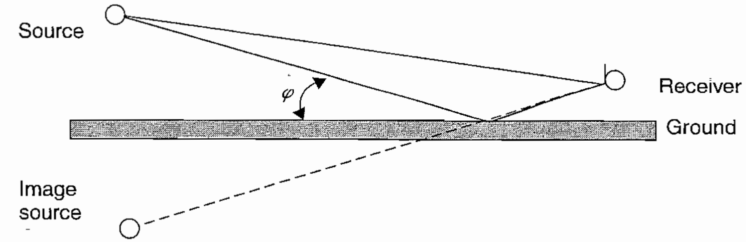

FIGURE 5.3 Ground reflection of a straight ray.

the plane-wave reflection coefficient

$$R_p = \frac{Z_s \sin\varphi - Z_0}{Z_s \sin\varphi + Z_0} \tag{5.6}$$

of a locally reacting surface of the ground, with impedance Z_s, may be used to determine the magnitude/phase effect of the reflection. The characteristic wave impedance of air, $Z_0 = \rho_0 c_0$, is generally very small compared to the magnitude of the ground impedance Z_s. Therefore, the reflection coefficient is usually about 1, except for very small angles φ—that is, when $|Z_s| \sin\varphi \ll Z_0$ and the reflection coefficient is about -1. Under the latter condition, the direct ray destructively interferes with the ground reflection and causes relatively low sound pressure close to the ground. In essence, the source and image source form a dipole, causing little radiation parallel to the ground. When the source is much closer to the ground than the receiver—e.g., for road traffic noise—the ground effect near the source can be attributed to a vertical radiation characteristic of the source. According to measurements over grassland near the shoulder of highways, the directivity index $D_I(\phi)$ of A-weighted road traffic noise drops from 0 dB at an elevation angle of 15° to about -5 dB at 0°. Generalized per reciprocity for arbitrary source and receiver heights, this relation converts to a reduction in overall A-weighted sound level[6]:

$$A_{\text{gr},D} = \left[4.8 - \frac{h_{\text{av}}}{d}\left(34 + \frac{600 \text{ m}}{d}\right)\right] \text{ dB} > 0, \tag{5.7}$$

where d is the source–receiver distance and

$$h_{\text{av}} = \tfrac{1}{2}(h_S + h_R) \tag{5.8}$$

is the average height of the sound ray from a source at height h_S to a receiver at height h_R.

Within a receiver distance of less than 200 m, this description is quite consistent with calculations of the Ontario noise regulation[7] from the equation

$$A_{\text{gr},O} = 10G \text{ lg}\frac{r}{15 \text{ m}} \text{ dB} > 0 \tag{5.9}$$

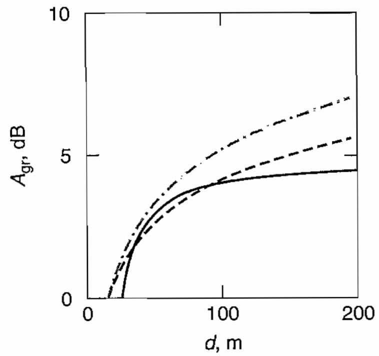

FIGURE 5.4 Excess attenuation A_{gr} over grassland as a function of distance d for an average height of 2 m: (—) according to Eq. (5.7); (- - -) according to Eq. (5.9) with $G = 0.5$; (-·-) according to Eqs. (5.9) and (5.10).

with

$$0 \leq G \equiv 0.75 \left(1 - \frac{h_{av}}{12.5 \text{ m}}\right) \leq 0.66 \tag{5.10}$$

for an average height of 2 m (or a receiver height of 4 m for a source close to the ground), as shown in Fig. 5.4.

More precise models have been developed to account for the curvature of wave fronts using a spherical reflection factor and possibly for an extended reaction of soft ground (e.g., fresh-fallen snow).[8] Such models explain a pronounced interference dip of sound pressure for sources and receivers within 2 m above the ground. This dip typically occurs in octave bands centered at 250 and 500 Hz. A dominant parameter of these more precise models is the effective flow resistivity of the ground. United States and Canadian agencies generally require the application of such models to properly account for this dip to receivers 1.5 m above the ground (the required receiver height). Note that this dip is caused by interference, not energy absorption at the ground.

However, near-complete destructive interference of two rays requires about equal amplitude and opposite phases. Diffuse rather than specular ground reflection, plus phase distortion due to thermal and wind turbulence in the propagation path, reduces or inhibits such near-complete interference, especially at large distances. Predicted ground attenuation A_{gr} of more than 20 dB for average lawn surface is unrealistic.

From an engineering point of view (especially in Europe), this interference effect is of little use. Some sound-level reduction may be experienced on a terrace surrounded by a lawn. But neighbors to industrial plants cannot be protected from sound impinging on their bedroom windows (4 m or more above the ground) by interfering reflections from a substantially lower ground. In Europe, planning of new roadways or commercial activities does not depend on the ground conditions of adjacent property, as it does in the United States and Canada.

Refraction of Sound in Inhomogeneous Atmosphere

Very important for outdoor sound propagation is the inhomogeneity of the atmosphere. The normal state of air is one of "convective equilibrium," in which the sound velocity c varies with temperature and wind velocity as a function of height above the ground. Higher temperature close to the ground results in higher sound velocity there and therefore in curvature of sound rays toward the sky. A component of wind in the direction of sound propagation causes refraction of sound rays toward the ground, because wind speed always increases with height. Linear wind and temperature profiles result in rays following a catenary curve that can be approximated by a circular arc with radius

$$R = \frac{1}{a \cos\phi} \tag{5.11}$$

as already described by Lord Rayleigh,[1] where a denotes the sound speed gradient due to vertical temperature and wind gradients. In the Nordic countries of Europe, measurements of wind and temperature are specified at heights of 0.5 and 10 m above level ground, expressly to determine a from the relation[9]

$$a = \frac{10^{-3}}{3.2 \text{ m}} \left(\frac{0.6\ \Delta T}{1°\text{C}} + \frac{\Delta u}{1 \text{ m/s}}\right) \tag{5.12}$$

where $\Delta T = T(10 \text{ m}) - T(0.5 \text{ m})$ is the difference in temperature and $\Delta u = u(10 \text{ m}) - u(0.5 \text{ m})$ is the difference in wind speed component at those two heights.

For negative values of a, causing upward refraction, there is a limiting arc between source and receiver at a distance

$$D = \sqrt{\frac{2}{|a|}} \left(\sqrt{h_S} + \sqrt{h_R}\right) \tag{5.13}$$

that just grazes the ground (see Fig. 5.5). Beyond this distance, sound can reach the receiver not along a ray but only by diffraction. The limiting arc determines the boundary of an acoustical shadow zone. For source and receiver height $h_S = 0$ m and $h_R = 4$ m, respectively, and a moderate gradient $a = -10^{-4}$ m^{-1}, this distance $D = 282$ m. Stronger gradients reduce the distance, but typically not below 100 m. Consequently, meteorological conditions are often neglected for sound propagation over less than 100 m. To ensure reliable measurements of industrial noise at a minimum height of 4 m, the Nordic countries specify a minimum value $a = -10^{-4}$ m^{-1} at distances from 50 to 200 m and $a > -10^{-4}$ m^{-1} at larger distances.

Most noticeable is the case of temperature inversion ($a > 0$), which happens on calm days during dawn and dusk when dampness covers the ground and sunshine is restricted to the upper layers of the atmosphere. With temperature inversion, traffic noise is trapped in the lowest layer by downward refraction

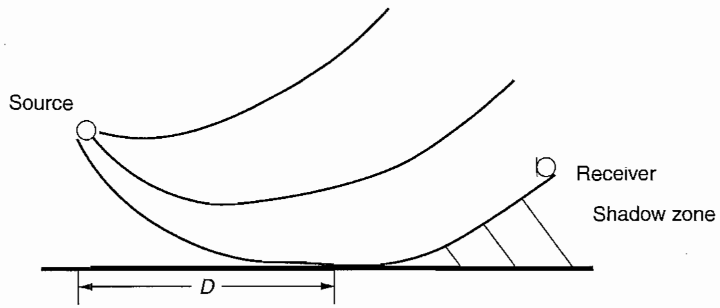

FIGURE 5.5 Sound rays and shadow formation for negative values of a.

and repeated reflections from the ground. As a result, sound can be heard over very large distances, due to divergence in only two (rather than three) dimensions—that is, no divergence upward. Even stronger effects can be observed for sound propagation over lakes and wide rivers.

Opposite effects occur from sound propagation over hot spots, as is well known from the poor quality of communication over an open fire. Ground surfaces warmed up by the sun or by industrial facilities may cause upward refraction and scattering of sound out of straight rays, both effects resulting in excess attenuation.

The combined effects of ground and micrometeorology have been studied in detail for the development of a heuristic model for outdoor sound propagation.[10] This model accounts for

- ray theory for the fastest path in air from source to receiver;
- one or more ground reflections during sound propagation downwind or for temperature inversion conditions, the number depending on the magnitude of the positive sound speed gradient;
- diffraction of sound into the shadow zone for a negative sound speed gradient;
- spherical reflection coefficient for refracted sound rays incident on the ground, depending on the effective flow resistivity of the ground; and
- reduced coherence of the various contributions to the sound pressure at the receiver, due to different travel times of these components and turbulence of the atmosphere.

Data calculated from this model have been compared to data measured over grassland at relatively low receiver positions with the following results:

- High excess attenuations calculated for negative gradients a at distances of more than 400 m have not been observed. Up to 1600 m, the average attenuation values were limited to approximately 20 dB in the frequency band centered at 630 Hz.

- For positive gradients a, average measured excess attenuations were limited to a few decibels and did not increase significantly with distance from 400 to 1600 m in the frequency bands below 200 Hz and above 630 Hz. Calculated values of excess attenuation came out higher.
- A pronounced excess attenuation in the frequency bands from 200 to 1000 Hz was both calculated and measured for low wind and a small positive gradient a.

A much simpler model for the ground effect on sound propagation outdoors has been adopted in ISO 9613-2[6]:

- Downwind (or a positive gradient a) is considered exclusively.
- The ground is either hard ($G = 0$) or porous ($G = 1$). If only a fraction of the ground is porous, G takes on a value between 0 and 1, the value being the fraction of the region that is porous.
- Three regions for ground reflection are distinguished: (1) the source region stretching $30h_S$ (maximum) toward the receiver, (2) the receiver region stretching $30h_R$ (maximum) toward the source, and (3) if the source and receiver regions do not overlap, a middle region in between.
- Similar to the angular parameter involved in Eq. (5.7), a parameter

$$q = \left(1 - 60\frac{h_{\text{eff}}}{d}\right) \text{dB} > 0 \tag{5.14}$$

is introduced to account for reflections in the middle region by a ground attenuation equal to $-3q$ in the octave band centered at 63 Hz and equal to $-3q(1 - G_m)$ in all the higher octave bands up to 8 kHz center frequency, where G_m is the value of G in the middle region. Together with the assumption that sound is radiated into a half-space with solid angle 2π, there is a 6-dB increase in sound pressure level due to correlated ground reflection at 63 Hz, independent of ground porosity, and at higher frequencies for hard ground. Over porous ground, a 3-dB increase at higher frequencies is due to uncorrelated reflections.
- For the source and the receiver region, $q = 0.5$ accounts for the splitting of regions and G_m is replaced by G_S or G_R, where the indices S and R refer to the source and receiver regions, respectively. In addition, the following attenuations are taken into account for both regions in four octave bands:

Midband Frequency, Hz	Attenuation Contribution, dB	
125	$3Ge^{-[(h-5\text{m})/2.9\text{m}]^2}\left(1 - e^{-d/50\text{m}}\right)$	
	$+5.7Ge^{-(h/3.3\text{m})^2}\left(1 - e^{-(d/600\text{m})^2}\right)$	(5.15)
250	$8.6Ge^{-(h/3.3\text{m})^2}\left(1 - e^{-d/50\text{m}}\right)$	
500	$14Ge^{-(h/1.5\text{m})^2}\left(1 - e^{-d/50\text{m}}\right)$	
1000	$5Ge^{-(h/1.05\text{m})^2}\left(1 - e^{-d/50\text{m}}\right)$	

Largest attenuation occurs over porous ground in the octave band with center frequency 500 Hz. Consequently, the simplifying assumption that this frequency band is representative for the attenuation of A-weighted overall sound may not be conservative. Instead, it could actually underestimate the sound pressure level at the receiver.

The attenuation linearly increases with distance d up to about $d = 50$ m and then approaches a limit, except for the low-frequency band around 125 Hz, where a further extending ground wave is assumed.

Equations (5.15) show an exponential decay of attenuation with the square of receiver height. For the octave band at 500 Hz, the normalizing height in that band's equation is 1.5 m, roughly two wavelengths of sound. At 1000 Hz, this normalizing height is 1.05 m. The ratio of height to wavelength is similar in the relevant octave bands around 250 and 1000 Hz, indicating that the model is based on physical considerations together with experimental findings.

Despite essential simplifications compared to the heuristic model, the procedure described in ISO 9613-2 for octave-band calculations of ground attenuation is often replaced in practice by the procedure of Eq. (5.7) for A-weighted overall sound, mainly because ground factors G are often ambiguous.

The application of Eq. (5.15) to road and rail traffic noise with low source height is questionable. Ground effects near the source are already included in measured data. Uneven surfaces due to ditches for drainage are not covered by the model. Ground effects near the receiver can be excluded by an appropriate minimum height. Consequently, it has been decided that German guidelines for prediction of rail traffic noise, presently under revision, shall not account for frequency-dependent ground effects.

In contrast, U.S. requirements for road traffic computations consist of a more detailed computer model based on acoustical theory—the U.S. Federal Highway Administration (FHWA) Traffic Noise Model (TNM).[11] Version 2.5 of this model has been compared with more than 100 h of measured sound levels (L_{eq}) at 17 highway sites, most with flat terrain, with and without noise barriers. Measurements ranged to 400 m from the roadway during daytime hours under varying wind conditions. Under these conditions, the average difference between results of computations and measurements was within approximately 1 dB.[12]

Barriers

Any large and dense object that causes an acoustical shadow zone in the path of a sound ray is considered as a sound barrier. Such objects include walls, roofs, buildings, or the ground itself if it forms an edge or a hill. Sound penetrates into such shadow zones by diffraction and thereby suffers barrier attenuation D_z. The amount of attenuation is primarily determined by the Fresnel number

$$N = \frac{2z}{\lambda} \tag{5.16}$$

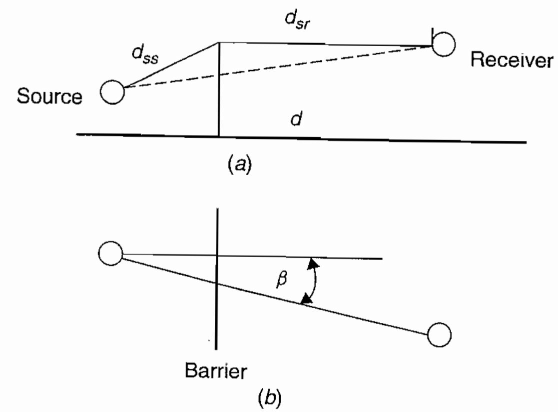

FIGURE 5.6 Barrier between source and receiver: (*a*) cross sectional view; (*b*) plan view.

where z is the increase in path length (the extension of a hypothetical rubber band between source and receiver) caused by one or more of the barrier edges and $\lambda = c/f$ is the wavelength of sound at frequency f. Note that z decreases with increasing angle of sound incidence β (see Fig. 5.6).

For $z = 0$ there is already a small barrier attenuation of about 5 dB plus an interference pattern at the edge of the shadow zone. Details of this interference pattern require a substantial computational effort that is not needed for engineering purposes. Therefore, preferred are simple approximations that are derived from extrapolations of the diffraction model and the ray-tracing model. When both models provide the same result for the line of sight over a hill or over undulating ground, the calculation of barrier insertion loss should be based on a limiting ($z = 0$) ground attenuation of about 5 dB independent of frequency, as described by Eq. (5.7). This consideration leads to the barrier insertion loss:

$$A_{\text{bar}} = \begin{cases} D_z - A_{\text{gr}} > 0 & \text{for diffraction over top edge of barrier} \\ D_z > 0 & \text{for diffraction around vertical edge of barrier} \end{cases} \tag{5.17}$$

where D_z is defined in Eq. (5.18).

Inclined barrier edges are considered to be top edges whenever the angle of inclination against the ground is less than 45°. Otherwise they are considered to be vertical edges.

Note in Eq. (5.17) that an intervening barrier causes the loss of all ground effects. At a height of 4 m or more over porous ground, this approximation is relatively accurate. Close to hard ground, however, it is not correct. Pressure doubling due to hard ground, which results in negative values of A_{gr}, persists even with intervening noise barriers and cannot result in larger values of A_{bar} than for porous ground.

The calculation of barrier attenuation is based on Huygens' model for wave fields, which takes all insonified points in a plane perpendicular to the ray from source to receiver as new sound sources. Points on a radius around the ray radiate with the same phase, varying between positive and negative values with increasing radius. Intervals between "phase zeros" in the hypothetical plane are called Fresnel zones. In free space, the contributions from neighboring Fresnel zones cancel each other, except for the center zone with the Fresnel radius $\sqrt{\lambda d_{so}}$, where d_{so} is the distance from the source to the plane. This center zone is the only uncanceled portion of the secondary wave front of Huygens' model and therefore is responsible for the entire sound field at the receiver. When this center zone is blocked by a barrier, the direct ray disappears.

In addition, a barrier partially blocks outer Fresnel zones and thereby inhibits the complete cancellation of their contributions. In the limit of many blocked Fresnel zones both above and on either side of the direct ray from the source to the receiver by a sufficiently high and long barrier, the intensity of the uncanceled portion decays with $1/N$; that is, the barrier attenuation increases with increasing path length difference over the top edge and with frequency.

Refined calculations of barrier attenuation include sound reflection at the barrier surface. When either the source or the receiver is close to a reflecting barrier surface, then the image source behind the barrier contributes almost as much to the sound field as does the actual source. This effect reduces the barrier attenuation but is often negligibly small.

Ground reflections can be important. When either the source or the receiver is high above the ground, ground-reflected contributions are relatively small due to relatively large path length differences z. But such high sources and receivers are generally not the case. Consequently, barrier attenuation over ground is computed 3 dB lower than the attenuation by a diffracting half-plane.

For outdoor sound propagation, the coherence of sound at different points in the sound field is reduced by wind and temperature fluctuations. This sets a limit for interference, depending upon the Fresnel radius and Fresnel number. Furthermore, one has to account for the curvature of rays due to gradients of wind and temperature. In the downwind direction, this curvature reduces the effective barrier height and the diffraction angle and, consequently, reduces the barrier attenuation—depending on the distance between the source, barrier, and receiver.

Theoretical and heuristic models have been developed to account for many or all of the effects just described. For prediction purposes, they suffer from the need for extremely detailed or unavailable input. In contrast, ISO 9613-2 requires less input—perhaps the upper limit of detail that can typically be obtained. In that standard, barrier attenuation is approximated by

$$D_z = 10 \lg (3 + 2NC_2C_3K_{\text{met}})\,\text{dB} < 20 \text{ dB for } C_3 = 1 (<25 \text{ dB for } C_3 > 1) \tag{5.18}$$

where $C_2 = 20$ and includes the effects of (1) sound rays from the source via the barrier edge to the receiver, (2) sound rays from the image source in the ground, and (3) sound rays to the image receiver in the ground (if ground reflections are taken into account separately in special cases, then $C_2 = 40$); $C_3 = 1$ for diffraction at a single edge but can increase to 3 for diffraction at two or more edges in series, according to

$$C_3 = \frac{1 + (5\,\lambda/e)^2}{1/3 + (5\,\lambda/e)^2} \tag{5.19}$$

with e as the path length from the first to the last diffracting edge; and K_{met} is a meteorological correction factor which accounts for down-wind ray curvature and is calculated from

$$K_{\text{met}} = \exp\left(-\frac{1}{2000\text{m}}\sqrt{\frac{d_{ss}d_{sr}d}{2z}}\right) \tag{5.20}$$

where d_{ss} is the path length from the source to the first diffracting edge, d_{sr} is the path length from the last diffracting edge to the receiver, and d is the path length without the barrier.

All of Eqs. (5.17)–(5.20) are conventions that are based on first-order approximations of theoretical relations, plus field experience, for sound propagation in a refracting atmosphere with curvature parameter $a > 0$. They can be applied for barriers of infinite or finite length on the ground, with one to three perpendicular diffracting edges. The barrier length must be large enough to meet the requirements for reflectors (see below). For example, this is true for typical railway barriers of 2 m height above the railhead. At a distance of 25 m and a height of 3.5 m above the railhead, the A-weighted sound pressure level of freight cars is reduced by about 11 dB.

Calculations of ISO 9613-2 do not include the case of barriers aloft, like shelter roofs at gas stations. If diffraction at a single edge is dominant for the received sound, the calculation should still be applicable, however. Contributions from more than one edge may be assumed as incoherent for sufficiently large barriers. Minimum dimensions must meet the requirements for reflectors.

Reflectors and Reverberation

Any large object—a wall, roof, building, or road sign, for example—that has plane surfaces in the path of a sound ray and that blocks an area with Fresnel radius at least $\sqrt{\lambda d_{so}}$ is considered to be a reflector. More specifically according to ISO 9613-2, the projection of the minimum dimension of the object in the direction of sound incidence shall meet the requirement

$$l_{\min} \cos\beta > \sqrt{\frac{2\lambda}{1/d_{so} + 1/d_{or}}} \tag{5.21}$$

where β is the angle of sound incidence on the reflecting plane and d_{so} and d_{or} are the path lengths from the reflection point to the source and to the receiver, respectively. Planes approximate nonplanar surfaces. Specular reflections are considered exclusively in terms of an image source (see Fig. 5.7).

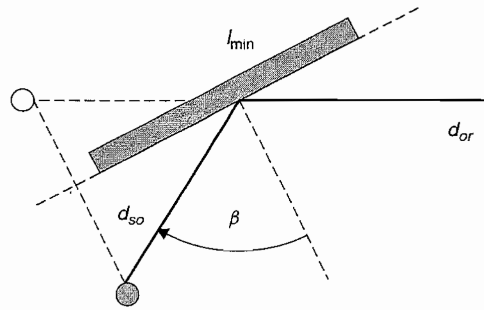

FIGURE 5.7 Specular reflection from a plane with minimum dimension l_{min}.

A reflection coefficient* $R < 1$ of the reflector reduces the sound power level of the image source by $-10\ \lg(R)$ dB. Diffuse reflections from rough building facades, which result in scattering of sound toward the sky, are generally taken into account with a reflection loss of 1 or 2 dB. The directivity of a source needs to be considered in the direction of a receiver image.

Atmospheric Absorption

The attenuation due to atmospheric absorption

$$A_{atm} = \alpha d \tag{5.22}$$

is theoretically well understood and fully described in ISO 9613-1.[13] For prediction purposes, one has to select the appropriate conditions of relative humidity, temperature, and ambient pressure. When low temperature and high humidity are assumed, the attenuation is relatively low around 500 Hz. In contrast, in the frequency bands at and above 4000 Hz, attenuation is high enough to reduce contributions to the A-weighted overall level to negligible values at distances of a few hundred meters. On the other hand, A_{atm} itself is mostly negligible in the frequency bands at and below 125 Hz. Table 5.2 contains selected values.

TABLE 5.2 Atmospheric Attenuation Coefficient α for Octave Bands of Noise at Selected Nominal Midband Frequencies[6]

		Atmospheric Attenuation Coefficient α, dB/km							
Temperature, °C	Relative Humidity, %	63 Hz	125 Hz	250 Hz	500 Hz	1000 Hz	2000 Hz	4000 Hz	8000 Hz
10	70	0.1	0.4	1.0	1.9	3.7	9.7	33	117
20	70	0.1	0.3	1.1	2.8	5.0	9.0	23	77
15	50	0.1	0.5	1.2	2.2	4.2	10.8	36	129
15	80	0.1	0.3	1.1	2.4	4.1	8.3	24	83

*ISO 9613-2 uses ρ instead of R.

Effects of Ground Cover and Trees

The consideration of ground cover and trees is often excluded from engineering prediction of excess attenuation in the propagation path of sound. The reason is twofold. The effect is small and unreliable. The situation is not only subject to seasonal variations but may change with different land use.

However, much money can be wasted building roadway noise barriers longer than truly needed if tree attenuation is ignored. This happens when barrier lengths are needlessly extended to reduce sound coming from far up and down the roadway—needlessly because trees adequately reduce that flanking sound by themselves. Note that sound arriving perpendicularly from the roadway might typically pass through only 50 m of trees, whereas sound arriving from far up and down the roadway passes through 500–1000 m of trees—for significant attenuation.

5.5 INTERACTION OF ELEMENTS AND CONTRIBUTIONS FROM VARIOUS PATHS

Standard Regulations for Consideration of Interactions

The attenuations discussed for individual elements in the propagation path of a sound ray are added to yield the total attenuation:

$$A = A_{div} + A_{gr} + A_{bar} + A_{atm} \tag{5.23}$$

where A_{div} = attenuation due to spherical spreading, predicted according to Eq. (5.5)
A_{gr} = attenuation due to ground effects, predicted according to Eqs. (5.7)–(5.10) and (5.14)–(5.15)
A_{bar} = attenuation due to diffraction at barrier edge, predicted according to Eqs. (5.16)–(5.20)
A_{atm} = attenuation due to atmospheric absorption, predicted according to Eq. (5.22)

The only interaction taken into account is that of barriers and ground, as described by Eq. (5.17). Reflections are assumed to result in incoherent contributions at the receiver.

Interaction of Barriers and Ground at Various Distances

Barriers on both sides of a roadway or railway provide at least two contributions to the total sound field at a receiver outside of the barriers—one by diffraction over the barrier at the receiver side and the second by reflection from the barrier on the other side—which may also suffer diffraction over the barrier on the receiver side (see Fig. 5.8). The second contribution is lower due to higher geometrical attenuation A_{div} but possibly higher due to lower barrier attenuation

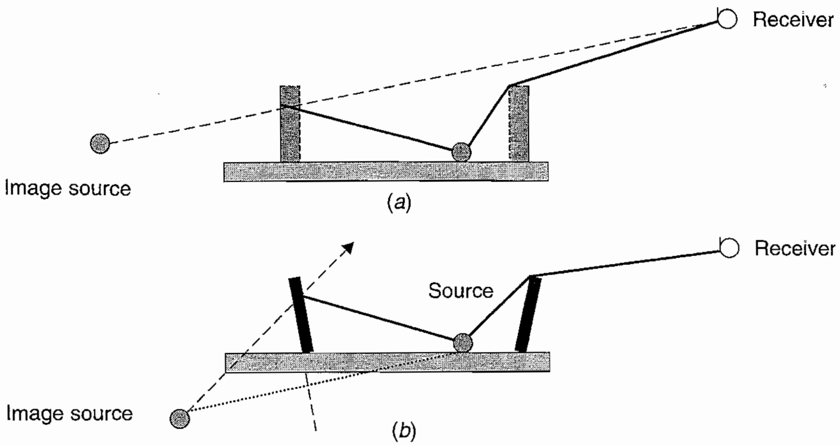

FIGURE 5.8 Sound rays from traffic lane shielded on both sides by (*a*) absorptive barriers and (*b*) inclined barriers.

A_{bar}. It generally needs to be reduced by absorptive or inclined barrier surfaces, which reduce the reflection toward the receiver.

Frequently discussed is the question of whether ground attenuation should be completely neglected for sound diffracted over the top of a barrier, as in Eq. (5.17). The reasoning to account for some ground attenuation in the barrier shadow zone is based on the assumption of an equivalent source at the diffracting edge. However, this assumption is not consistent with diffraction theory. There is no ray going out from the edge suffering attenuation just from divergence, but the diffracted field penetrates deeper and deeper into the shadow zone until it reaches the receiver. Since the ground effect on the receiver side is mostly determined by interference with a ground reflection close to the receiver, one has to consider two differently diffracted contributions, which are differently attenuated. Thus, the chance for considerable interference is reduced, particularly at high receiver positions. Of course, such an argument is valid only for meteorological conditions that provide no shadow formation. For greater accuracy at receiver positions near the ground, this interference is not neglected in the United States and Canada.

Barriers Close to Trees, with Gaps and Slots

The attenuation performance of barriers can be reduced by various influences. Past concern centered on trees or bushes that exceed the height of a nearby barrier. Experiments have shown that high-frequency components of noise are scattered by leaves into the barrier shadow zone.[14] However, this effect seems to be small compared to the better acceptability of "green" barriers.

Calculations with Eq. (5.18) assume that diffracted sound dominates in the barrier shadow zone. For this to be true, sound passing through the barrier must be negligible (down 5 dB or more) compared to the diffracted sound, which holds for a barrier relatively free of holes in its face and also free of a continuous gap between it and the ground. More sound energy gets through such holes/gaps than geometrically incident on the openings. Also required is a sufficiently large transmission loss through the surface material of the barrier. A mass per unit surface area (excluding framing) of 20 kg/m^2 is usually sufficient to provide a transmission loss of 25 dB or more at 500 Hz. Such weight is easily achievable with thickness and materials needed for mechanical stability of the barrier.

Procedures Applied by Computer Software

Engineering computer software for noise mapping is based on geometrical data provided by geographical information systems. The ground is often described by plane triangles; roads, railways, and barriers by sections of straight lines; and individual sources by points. Houses are modeled by rectangles. The handling of numerous data for larger areas requires a high degree of sophistication.

A sound ray may experience several reflections and may be diffracted on the path from source to receiver. Because of computer speed, current computer software can deal with many reflections with reasonable computation times. However, current software is not necessarily precise, due to approximate modeling of reflectors and reflection losses. Normally only three reflections are taken into account. Former consideration of reverberation in street canyons is excluded from current computations.

An essential part of the software is its validation by test cases[15]. This task does not aim for physical correctness but for consistency with the referenced calculation schemes. For this purpose, the program must be run in the same mode for test cases as for real applications—for example, the setting of software switches for accelerated computation.

5.6 ENGINEERING APPROACHES TO ACCOUNT FOR METEOROLOGY

Correction Terms C_{met} and C_0

The transfer function of Eq. (5.2), as specified by the attenuation in Eq. (5.23), leads from source properties to the equivalent continuous A-weighted sound pressure level L_{AT}(DW) for meteorological conditions that are favorable to sound propagation. This may be appropriate to meet specific restrictive requirements. A slightly better balance between interests of industry and neighborhood is the long-term A-weighted sound pressure level L_{AT}(LT), where the time interval T is several months or a year. Such a period will normally include a variety of sound propagation conditions, both favorable and unfavorable.

According to ISO 9613-2, a value L_{AT}(LT) may be obtained from the value of L_{AT}(DW) by subtraction of a meteorological correction term,

$$C_{\mathrm{met}} = \begin{cases} 0 & \text{if } d \leq 10(h_S + h_R) \\ C_0\left(1 - 10\dfrac{h_S + h_R}{d}\right) & \text{if } d > 10(h_S + h_R) \end{cases} \tag{5.24}$$

where C_0 (in decibels) depends on local meteorological statistics for wind speed and directions plus temperature gradients. Similar to Eq. (5.7), this subtracted term depends on the ratio of the effective height of the sound ray and distance, so that Fig. 5.4 gives a qualitative impression, except for distance. The correction term C_{met} is applied at somewhat larger distances. Experience indicates that values of C_0 are limited in practice between 0 and approximately 5 dB, with values in excess of 2 dB being exceptional.

Local Weather Statistics

Among the various procedures proposed for the calculation of C_0 from weather statistics is the following:

$$C_0(\alpha, g) = -10 \lg\left(\sum_{i=0}^{I-1} Q\frac{W_i(\theta_i)}{2}[1 + g - (1 - g)\cos(\theta_{\mathrm{rec}} - \theta_i)] + 1 - Q\right) \text{ dB} \tag{5.25}$$

where θ_{rec} = angle between North and the source-receiver line
g = parameter between 0.01 and 0.1 that accounts for attenuation in upwind direction
θ_i = angle between North and ith wind direction
W_i = probability for ith direction of wind
I = number of wind directions
$1 - Q$ = probability for no wind (calm)

Values of $g = 0.1$ and $g = 0.01$ correspond to a maximum upwind attenuation of 10 and 20 dB, respectively. Crosswind attenuation is less than 3 dB. Such values are effective for single point sources and wind always from the same direction. For extended sources (e.g., traffic lines or larger industrial areas), the appropriate averaging procedure typically results in values slightly smaller than 2 dB.

5.7 UNCERTAINTIES

General

The uncertainty of sound pressure levels calculated for a receiver position results from the uncertainty ΔL_W of the source level, determined, among other matters, by uncertain assumptions about the operating conditions of a sound source, the number of vehicles on a road, the roughness of rail heads, and the uncertainty

ΔA of the propagation losses. In the following, the uncertainty ΔA is discussed exclusively. However, note that uncertainties about source levels cannot always be neglected.

Elements

Uncertainty about spreading losses is generally small. Except for air traffic, distances between source and receiver can be determined very precisely. Effects of road traffic distribution on several parallel lanes are generally small if the most inner and outer lanes are modeled separately.

Uncertainty is significantly affected by effects of ground and meteorology. Very pronounced uncertainty has been obtained by Schomer[16] from long-term measurements with a loudspeaker centered at a height of 0.6 m above grassland and receivers at 1.2 m at distances up to 800 m. The standard deviation describing high portions of received octave-band levels is shown in Fig. 5.9.

At low frequencies up to 125 Hz and also at high frequencies above 2000 Hz, the standard deviation increases approximately continuously with distance and frequency, as one would expect. Anomalies can be seen in the intervening frequency bands. These anomalies can be attributed to variable ground interference. The low measurement height of 1.2 m may exaggerate the effect, though this receiver height is important to computations in the United States and Canada.

For special barrier-top design, a considerable uncertainty about barrier attenuation is found in the comparison of standard calculations with results calculated or measured in laboratories. However, in field tests such designs have hardly ever shown level differences of more than 1 dB at a distance of more than 25 m from a roadside or railway barrier. Source or receiver positions close to a barrier,

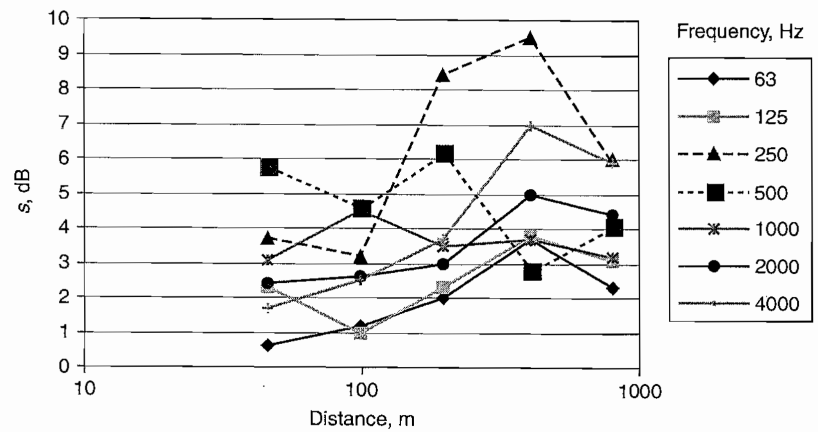

FIGURE 5.9 Standard deviation s of octave-band sound pressure levels for downwind condition at various distances from a loudspeaker centered at a height of 0.6 m and receiver height 1.2 m above grassland.

where reflections from the barrier surface or deep shadow zones play a role, are rarely met in practice, and therefore the laboratory effects are not observed in the field.

There is substantial uncertainty about the validity of the factor C_3 in Eq. (5.19). In many laboratory cases, multiple diffraction has shown an increase in barrier attenuation by more than 5 dB. But these cases are often related to barrier attenuations in excess of 20 dB. In practice, they depend significantly upon specific propagation paths from source to receiver.

Significant uncertainty exists for the meteorological correction factor of Eq. (5.20). It is matched to numerous data obtained for downwind situations at distances up to 1000 m over porous ground. Estimates for this uncertainty are about 2 dB, independent of distance, since the magnitude of barrier attenuation decreases with distance.

Uncertainty due to the roughness and absorption of reflecting surfaces is approximately 1 dB. In addition, limiting the number of reflections to three is sometimes not sufficient to let even a single computed sound ray enter through a passageway into a courtyard. It is obvious from such considerations that ray theory and specular reflections are limited to relatively open areas. Otherwise, standard deviations of more than 5 dB may occur. It is this consideration that partially argues for the U.S. and Canadian retention of line segment sources instead of point source approximations.

Uncertainty about atmospheric absorption may be calculated from the uncertainties of relative humidity, temperature, and ambient pressure. At low frequencies, that uncertainty is very small. At high frequencies, it is of little concern for engineering purposes. At frequencies around 500 Hz, the standard deviation is usually small compared to that of ground effects.

Overall A-Weighted Sound Pressure Level

The uncertainty for sound attenuation along the path of a ray in any frequency band increases with the square root of the sum of variances due to geometry, ground effects, barriers, reflectors, and atmospheric absorption. When several rays contribute to the sound pressure level at the receiver, the variances must be weighted according to their energy and the sum is divided by the total energy. This summation of uncorrelated partial uncertainties results in a reduction of the total uncertainty.

The uncertainty for the A-weighted overall sound pressure level may be calculated from the variances in octave bands, weighted according to their energy. When a number of n frequency bands equally contribute to the overall level, the uncertainty is reduced by a factor $1/\sqrt{n}$.

Approximately consistent with estimated accuracies in ISO 9613-2 is the standard deviation reported by Schomer[16] for the A-weighted overall sound pressure level received from a source of pink noise.[14] At distances from 100 to 800 m and an average height above grassland of 0.9 m, that standard deviation was about 3 dB. At an average height above 5 m, ISO 9613-2 estimates an accuracy of 1 dB. Advanced procedures for calculation of outdoor noise levels aim for an accuracy with a standard deviation of 1 dB up to a distance of 1000 m over flat terrain and of 2.5 dB over hilly terrain.[3]

REFERENCES

1. Lord Rayleigh, *Theory of Sound*, 2nd ed., Dover, New York, 1877, reissued 1945, Vol. 2, p. 128 ff.
2. W. A. Kuperman, "Propagation of Sound in the Ocean," in M. J. Crocker (Ed.), *Encyclopedia of Acoustics*, Wiley, New York, 1997, Chapter 36.
3. F. de Roo and I. M. Noordhoek,"Harmonoise WP2—Reference Sound Propagation Model," Proc. DAGA 03, Aachen, Germany, pp. 354–355
4. K. Attenborough et al., "Benchmark Cases for Outdoor Sound Propagation," *J. Acoust. Soc. Am.*, **97**(1), 173–191 (1995).
5. R. Matuschek and V. Mellert, "Vergleich von technischen Prognoseprogrammen für die Schallimmission mit physikalischen Berechnungen der Schallausbreitung im Freien" ("Comparison of Technical Prediction Programs for Sound Immission with Physical Calculations of Sound Propagation Outdoors"), Proc. DAGA 03, Aachen, Germany, pp. 428–429.
6. ISO 9613-2, *"Acoustics—Attenuation of Sound During Propagation Outdoors—Part 2: General Method of Calculation,"* International Organization for Standardization, Geneva, Switzerland, 1996.
7. H. Gidamy, C. T. Blaney, C. Chiu, J. E. Coulter, M. Delint, L. G. Kende, A. D. Lightstone, J. D. Quirt, and V. Schroter, "ORNAMENT: Ontario Road Noise Analysis Method for Environment and Transportation," Environment Ontario, Noise Assessment and Systems Support Unit, Advisory Committee on Road Traffic Noise, 1988.
8. L. C. Sutherland and G. A. Daigle, "Atmospheric Sound Propagation," in M. J. Crocker (Ed.), *Encyclopedia of Acoustics*, Wiley, New York, 1997, Chapter 32.
9. J. Kragh, "A New Meteo-Window for Measuring Environmental Noise from Industry," Technical Report LI 359/93, Danish Acoustical Institute, Lyngby, Denmark, 1993.
10. A. L'Espérance, P. Herzog, G. A. Daigle, and J. R. Nicolas, "Heuristic Model for Outdoor Sound Propagation Based on an Extension of the Geometrical Ray Theory in the Case of a Linear Sound Speed Profile," *Appl. Acoust.* **37**, 111–139, (1992).
11. G. S. Anderson, C. S. Y. Lee, G. G. Fleming, and C. W. Menge, *FHWA Traffic Noise Model, Version 1.0: User's Guide*, Report FHWA-PD-96-009 and DOT-VNTSC-FHWA-98-1, U.S. Department of Transportation, Federal Highway Administration, Washington, DC, January 1998.
12. J. L. Rochat and G. G. Fleming, *Validation of FHWA's Traffic Noise Model (TNM): Phase 1, Addendum*, Addendum to Report No. FHWA-EP-02-031 and DOT-VNTSC-FHWA-02-01 U.S. Department of Transportation, Federal Highway Administration, Washington, DC (in publication).
13. ISO 9613-1, *"Acoustics—Attenuation of Sound During Propagation Outdoors—Part 1: Calculation of the Absorption of Sound by the Atmosphere*, International Organization for Standardization, Geneva, Switzerland, 1993.
14. T. van Renterghem and D. Botteldooren, "Effect of a Row of Trees Behind Noise Barriers in Wind," *Acta Acustica* united with *Acustica*, **88**, 869–878 (2002).

15. DIN 45687, *"Acoustics—Software Products for the Calculation of the Sound Propagation Outdoors—Quality Requirements and Test Conditions" (draft)*, Deutsches Institut für Normung, Berlin, Germany, 2004.
16. P. D. Schomer, "A Statistical Description of Ground-to-Ground Sound Propagation," *Noise Control Eng. J.*, **51**(2), 69–89 (2003).

CHAPTER 6

Sound in Small Enclosures

DONALD J. NEFSKE AND SHUNG H. SUNG

Vehicle Development Research Laboratory
General Motors Research & Development Center
Warren, Michigan

6.1 INTRODUCTION

Only in an anechoic room may sound waves travel outwardly in any direction without encountering reflecting surfaces. In practice, one must deal with every shape and size of enclosure containing an infinite variety of sound-diffusing, sound-reflecting, and sound-absorbing objects and surfaces. However, in small rooms of fairly regular shape, with smooth walls, the sound is not statistically diffuse and will depend on the acoustical modal response in the room. Typical examples where this is the case are the passenger compartments of transportation vehicles, ductwork and small rooms in buildings, enclosures used to enhance the response of audio equipment, and enclosures designed for sound isolation. Because of the need to understand the modal nature of sound in such enclosures, this chapter will describe the governing equations, the modal theory, and its application for determining and controlling the interior acoustical response. While the modal theory for rectangular enclosures is described in most standard textbooks on acoustics,[1–5] the extended approach for irregular geometries and the use of advanced numerical techniques are more amenable to practical application and are also described here.

6.2 SOUND IN A VERY SMALL ENCLOSURE

Before considering the more general case, it will be instructive to consider the sound pressure response in a very small enclosure. Frequently, in noise control problems, a noise source is enclosed in a very small box to prevent it from radiating noise to the exterior, as conceptually represented in Fig. 6.1*a*. When the noise source has a frequency low enough so that the wavelength of the

15. DIN 45687, *"Acoustics—Software Products for the Calculation of the Sound Propagation Outdoors—Quality Requirements and Test Conditions" (draft)*, Deutsches Institut für Normung, Berlin, Germany, 2004.
16. P. D. Schomer, "A Statistical Description of Ground-to-Ground Sound Propagation," *Noise Control Eng. J.*, **51**(2), 69–89 (2003).

CHAPTER 6

Sound in Small Enclosures

DONALD J. NEFSKE AND SHUNG H. SUNG

Vehicle Development Research Laboratory
General Motors Research & Development Center
Warren, Michigan

6.1 INTRODUCTION

Only in an anechoic room may sound waves travel outwardly in any direction without encountering reflecting surfaces. In practice, one must deal with every shape and size of enclosure containing an infinite variety of sound-diffusing, sound-reflecting, and sound-absorbing objects and surfaces. However, in small rooms of fairly regular shape, with smooth walls, the sound is not statistically diffuse and will depend on the acoustical modal response in the room. Typical examples where this is the case are the passenger compartments of transportation vehicles, ductwork and small rooms in buildings, enclosures used to enhance the response of audio equipment, and enclosures designed for sound isolation. Because of the need to understand the modal nature of sound in such enclosures, this chapter will describe the governing equations, the modal theory, and its application for determining and controlling the interior acoustical response. While the modal theory for rectangular enclosures is described in most standard textbooks on acoustics,[1–5] the extended approach for irregular geometries and the use of advanced numerical techniques are more amenable to practical application and are also described here.

6.2 SOUND IN A VERY SMALL ENCLOSURE

Before considering the more general case, it will be instructive to consider the sound pressure response in a very small enclosure. Frequently, in noise control problems, a noise source is enclosed in a very small box to prevent it from radiating noise to the exterior, as conceptually represented in Fig. 6.1*a*. When the noise source has a frequency low enough so that the wavelength of the

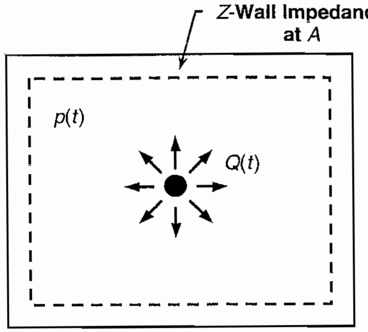

(*a*) Interior Noise Source

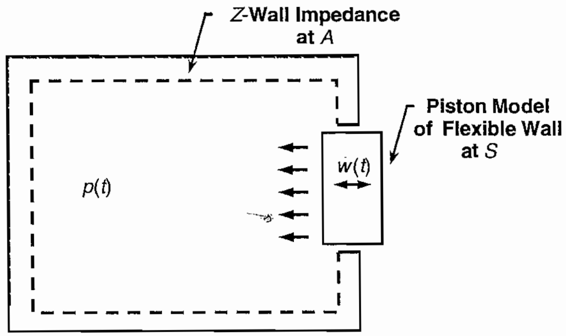

(*b*) Vibrating Flexible Wall

FIGURE 6.1 Sound in small enclosure with impedance boundaries generated by (*a*) interior noise source and (*b*) piston model of flexible-wall vibration. Symbols: $p(t)$, sound pressure; $Q(t)$, volume velocity; Z, wall impedance; A, impedance wall area; $\dot{w}(t)$, piston velocity; S, piston area.

sound is long compared to the largest distance of the box, the sound pressure produced by the source will be uniform throughout the entire cavity. A uniform sound pressure field will also be created in an enclosure when the walls of the enclosure are forced to vibrate at low frequency by the pressures of an external sound source, as conceptually represented by the vibrating piston in Fig. 6.1*b*. Frequently, the walls of the enclosure will be damped by applying panel-damping treatment or absorption material over the walls.

The uniform sound pressure $p(t)$ in such an enclosure will satisfy an extended form of Eq. (2.9) as $(1/P)dp/dt + (\gamma/V)d\tau/dt = (\gamma/V)Q(t)$, where $Q(t)$ is the *volume velocity* of the sound source (m^3/s), V is the enclosure volume, P is the ambient air pressure, and $\tau(t)$ is the volume variation. At the wall area A (m^2)

in Fig. 6.1*a* or *b*, the specific acoustical impedance is $Z = p/u$ and the particle velocity is $u(t)$, so $d\tau/dt = Au = Ap/Z$. Since $c^2 = \gamma P/\rho$ by Eq. (2.12), the uniform sound pressure in the enclosure satisfies

$$\frac{dp}{dt} + 2\delta p = \left(\frac{\rho c^2}{V}\right) Q(t) \qquad (6.1)$$

where $\delta = \rho c^2 A/(2VZ)$. For steady-state excitation, $Q(t) = \hat{Q}\cos(\omega t + \phi)$, which is the volume velocity of the source operating at the forcing frequency $f = \omega/2\pi$ (hertz) with the volume velocity amplitude $\hat{Q}$ and phase ϕ. The steady-state sound pressure in the enclosure is then $p(t) = p_0 \cos(\omega t + \theta_0)$, with the sound pressure amplitude and phase given by

$$p_0 = \frac{\rho c^2 \hat{Q}}{V[(\omega + 2\delta_i)^2 + (2\delta_r)^2]^{1/2}} \quad \text{N/m}^2$$
$$\theta_0 = \phi - \tan^{-1}\frac{\omega + 2\delta_i}{2\delta_r} \quad \text{rad} \qquad (6.2)$$

Here $\delta = \delta_r + i\delta_i$ is a complex damping factor ($i = \sqrt{-1}$) that accounts for the acoustical impedance $Z = R + iX$ of the wall area A, where

$$\delta_r = \frac{cA}{2V}\mathrm{Re}\frac{\rho c}{Z} \qquad \delta_i = \frac{cA}{2V}\mathrm{Im}\frac{\rho c}{Z} \quad \text{s}^{-1} \qquad (6.3)$$

For the interior noise source in Fig 6.1*a*, $Q(t)$ is taken as positive for outward volume flow, while for the flexible-wall vibration in Fig. 6.1*b*, $Q(t) = -S\dot{w}(t)$ is an *equivalent* volume velocity with outward piston velocity $\dot{w}(t)$ taken as positive.

From Eq. (6.2), we see that the amplitude p_0 of the sound pressure in the enclosure depends, not only on the noise source amplitude $\hat{Q}$ and forcing frequency $f = \omega/2\pi$, but also on the enclosure volume V and total wall impedance in δ. For a rigid-wall enclosure, $|Z| \to \infty$, so that $\delta_r, \delta_i = 0$, and

$$p_0 = \frac{\rho c^2 \hat{Q}}{\omega V} \quad \text{N/m}^2$$
$$\theta_0 = \phi - \tfrac{1}{2}\pi \quad \text{rad} \qquad (6.4)$$

In this case, the sound pressure depends only on the amplitude and frequency of the volume velocity of the source and on the enclosure volume. The sound pressure lags the volume velocity by exactly 90°, indicating that the source does not radiate any acoustical power.

Example 6.1. The piston of Fig. 6.1*b* has an area of 1 cm^2 and is driven harmonically with a peak-to-peak displacement of 4 mm at a frequency of 100 Hz.

The volume of the cavity is 0.0125 m^3 and it has rigid walls. What is the sound pressure level in the cavity?

Solution For harmonic displacement excitation $w = \hat{w} \sin \omega t$, and we obtain $\dot{w} = (\omega\hat{w}) \cos \omega t = \hat{\dot{w}} \cos \omega t$, so that $\hat{\dot{w}} = \omega\hat{w}$. Therefore, $\hat{Q} = S\hat{\dot{w}} = S\omega\hat{w}$ and from Eq. (6.4),

$$p_0 = \frac{\rho c^2 S\hat{w}}{V} = \rho c^2 \frac{\Delta\hat{V}}{V} \quad \text{N/m}^2 \tag{6.5}$$

where $\Delta\hat{V} = S\hat{w}$ is the volume change of the enclosure due to the piston displacement. Inserting the appropriate numerical values, we have $\Delta\hat{V} = 10^{-4} \times 2 \times 10^{-3} = 2 \times 10^{-7}$ m^3, so that

$$p_0 = 1.21 \times 343^2 \times \frac{2 \times 10^{-7}}{1.25 \times 10^{-2}} = 2.28 \text{ N/m}^2$$

The sound pressure level is then

$$L_p = 20 \log_{10} \frac{p_{\text{rms}}}{p_{\text{ref}}} = 20 \log_{10} \frac{0.707 \times 2.28}{2 \times 10^{-5}} = 98 \text{ dB}$$

Example 6.2. A noise source is enclosed in a very small box, as in Fig. 6.1*a*, that has flexible but very stiff walls. Determine the formula for the interior sound pressure.

Solution For a mass–spring–dashpot model of the box walls, the acoustical impedance is $Z = A^{-1}[C + i\omega(M - K/\omega^2)]$, where A is the wall surface area and C, M, K are overall values of wall damping, mass, and stiffness. For very stiff walls, $Z \approx -iK/A\omega$ so that, from Eq. (6.3),

$$\delta_r = 0 \qquad \delta_i = \frac{\omega}{2}\frac{\rho c^2 A^2/V}{K} = \frac{\omega}{2}\frac{K_{\text{air}}}{K} \quad \text{s}^{-1}$$

where $K_{\text{air}} = \rho c^2 A^2/V$ (N/m) is the *stiffness* of the air and K (N/m) is the wall stiffness. Substituting δ_r and δ_i into Eq. (6.2) then gives

$$p_0 = \frac{1}{1 + K_{\text{air}}/K}\frac{\rho c^2 \hat{Q}}{\omega V} \quad \text{N/m}^2 \tag{6.6}$$
$$\theta_0 = \phi - \tfrac{1}{2}\pi \quad \text{rad}$$

Note that the sound pressure in an enclosure with compliant walls is lower than the sound pressure in an equivalent rigid-wall enclosure given by Eq. (6.4), and the addition of damping to the walls can be shown to produce a similar effect.

Example 6.3. A *Helmholtz resonator* is a rigid-wall enclosure with a small aperture of cross-sectional area S that connects the enclosure to a column of air of length L that oscillates as the piston in Fig. 6.1*b*. Determine the natural frequency.

Solution The mass of the column of air is $M = \rho SL$ and the force on it is pS. Hence we must have $M\ddot{w} = pS$, where $\dot{w}$ is the velocity of the air column. Since $\hat{\dot{w}} = \omega\hat{w}$, we obtain $\hat{Q} = S\hat{\dot{w}} = S^2 p_0/\omega M$. Substituting this for $\hat{Q}$ in Eq. (6.4) gives $(1 - \rho c^2 S^2/\omega^2 MV)p_0 = 0$ or $(1 - K_{\text{air}}/\omega^2 M)p_0 = 0$, where $K_{\text{air}} = \rho c^2 S^2/V$ is the air stiffness. The natural frequency is then $\omega_0 = \sqrt{K_{\text{air}}/M} = c\sqrt{S/LV}$.

6.3 GOVERNING EQUATIONS FOR ACOUSTICAL MODAL RESPONSE

For larger enclosures or for higher frequencies, the sound pressure field in the enclosure is no longer uniform but depends on the acoustical modal response in the enclosure. More importantly, the sound pressure can be amplified considerably near discrete frequencies corresponding to the acoustical cavity resonances. This modal nature of sound in an enclosure results from the superposition of sound waves that propagate according to the well-known *acoustical wave equation* [Eq. (2.13)],

$$\nabla^2 p - \frac{\ddot{p}}{c^2} = 0 \quad \text{N/m}^4 \tag{6.7}$$

where $\ddot{p}$ denotes the second partial derivative with respect to time t.

Noise sources interior to an enclosed cavity can be included as forcing terms in the wave equation. For the example of a monopole source (e.g., a loudspeaker in a cabinet) as in Fig. 6.1*a*, the time-varying mass flow rate is $\dot{m}(x, y, z, t) = \rho Q(x, y, z, t)$ (kg/s), so that

$$\nabla^2 p - \frac{\ddot{p}}{c^2} = -\frac{\rho\dot{Q}}{V} \quad \text{N/m}^4 \tag{6.8}$$

where $\dot{Q} = \partial Q/\partial t$. Other interior sources can be represented as combinations of monopole sources or else can be included directly in the wave equation in a similar manner. For simple harmonic motion, $p(x, y, z, t) = \text{Re}[\hat{p}(x, y, z)\exp(i\omega t)]$ and $Q(x, y, z, t) = \text{Re}[\hat{Q}(x, y, z)\exp(i\omega t)]$, and we obtain the inhomogeneous *Helmholtz equation* for the steady-state sound pressure response,

$$\nabla^2\hat{p} + \left(\frac{\omega}{c}\right)^2 \hat{p} = -\frac{i\omega\rho\hat{Q}}{V} \quad \text{N/m}^4 \tag{6.9}$$

where $f = \omega/2\pi$ (Hz) is the forcing frequency of the vibration and $\lambda = c/f$ (m) is the wavelength of the sound produced by the source.

The boundary conditions for p determine the reflection, absorption, and transmission of the sound waves at the enclosure's surfaces and are derived from fluid mechanical considerations.[6] For small-amplitude motions, a momentum balance at the boundary requires that the air particle velocity u normal to the boundary surface be related to p through

$$\frac{1}{\rho}\frac{\partial p}{\partial n} = -\dot{u} \quad \text{m/s}^2 \tag{6.10}$$

where $\partial/\partial n$ is the outward surface-normal derivative. For an impervious wall surface, u is the normal-velocity component of the air into the pores of the surface. Table 6.1 lists the boundary conditions for different wall surfaces and air interfaces that are characterized by their acoustical impedance Z and surface-normal vibration velocity $\dot{w}$. In what follows, we will investigate the steady-state, random, and transient sound pressure response in enclosures with flexible, absorbent boundaries where Z and $\dot{w}$ are defined as in Table 6.1.

6.4 NATURAL FREQUENCIES AND MODE SHAPES

Acoustical resonances that result in high sound pressure occur at discrete natural frequencies in an enclosed cavity. The acoustical resonances are found from the free-vibration solution of the wave equation by substituting $p_n = p_{n0}\Psi_n(x, y, z)\exp(i\omega_n t)$, which gives

$$\nabla^2\Psi_n + \left(\frac{\omega_n}{c}\right)^2\Psi_n = 0 \quad \text{m}^{-2} \tag{6.11}$$

with free-vibration boundary conditions for the walls. The nondimensional pressure distributions $\Psi_n(x, y, z)$ for $n = 0, 1, 2, \ldots$ are the *mode shapes*, with $f_n = \omega_n/2\pi$ (Hz) being the corresponding *natural frequencies*. For absorbent boundaries, the mode shapes and natural frequencies are complex, and the acoustical modes are damped. However, for rigid boundaries ($|Z| \to \infty$) or for fully reflective open boundaries ($|Z| = 0$), one obtains real, undamped modes, or *standing waves*, that depend only on the geometrical shape of the cavity.

Table 6.2 gives formulas for the natural frequencies and mode shapes of the undamped acoustical modes of a few regular-shape enclosures with rigid walls as well as those of a tube with fully reflective and open boundaries. (A more complete list can be found in ref. 7.) One can show that the acoustical modes are orthogonal over the cavity volume such that

$$\int_V \Psi_m\Psi_n\,dV = \begin{cases} 0 & m \neq 0 \\ V_n & m = n \end{cases} \quad \text{m}^3 \tag{6.12}$$

and constitute *normal modes* of the enclosure. In Table 6.2, the number of indices used to identify each mode is based on the dimensionality of the enclosure, whereas we have used a single index to identify a mode, so the equivalence for a three-dimensional enclosure would be $f_n \equiv f_{ijk}$ and $\Psi_n \equiv \Psi_{ijk}$.

TABLE 6.1 Acoustical Boundary Conditions

Type	Boundary Condition	Air Particle Velocity
1. Rigid wall 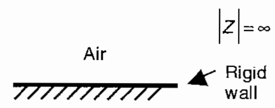	$\frac{\partial p}{\partial n} = 0$	$u = 0$
2. Flexible wall 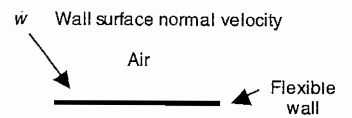	$\frac{1}{\rho}\frac{\partial p}{\partial n} = -\ddot{w}$	$u = \dot{w}$
3. Absorber on rigid wall 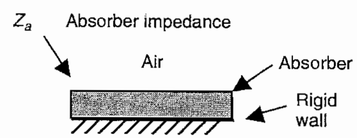	$\frac{1}{\rho}\frac{\partial p}{\partial n} = -\frac{1}{Z_a}\frac{\partial p}{\partial t}$	$u = \frac{p}{Z_a}$
4. Absorber on flexible wall 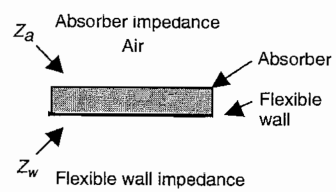	$\frac{1}{\rho}\frac{\partial p}{\partial n} = -\frac{1}{Z_a}\frac{\partial p}{\partial t} - \ddot{w}$ $= -\left(\frac{1}{Z_a} + \frac{1}{Z_w}\right)\frac{\partial p}{\partial t}$	$u = \frac{p}{Z_a} + \dot{w}$ $= \frac{p}{Z_a} + \frac{p}{Z_w}$
5. Open pressure release 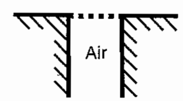	$p = 0$	Determine from analysis
6. Open plane wave 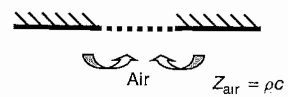	$\frac{1}{\rho}\frac{\partial p}{\partial n} = -\frac{1}{Z_{\text{air}}}\frac{\partial p}{\partial t}$	$u = \frac{p}{Z_{\text{air}}}$

TABLE 6.2 Acoustical Modes and Natural Frequencies[a]

Description	Figure	Natural Frequency, f_{ijk} (Hz)	Mode Shape, Ψ_{ijk}
1. Slender tube both ends closed	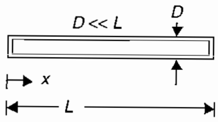	$\frac{ic}{2L}$ $D \ll \lambda$ where $\lambda = c/f$	$\cos \frac{i\pi x}{L}$ $\quad i = 0, 1, 2, \ldots$
2. Slender tube one end closed one end open	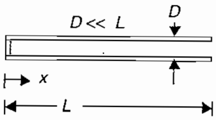	$\frac{ic}{4L}$ $D \ll \lambda$ where $\lambda = c/f$	$\cos \frac{i\pi x}{L}$ $\quad i = 1, 3, 5, \ldots$
3. Slender tube both ends open	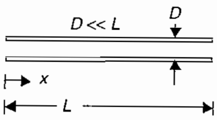	$\frac{ic}{2L}$ $D \ll \lambda$ where $\lambda = c/f$	$\sin \frac{i\pi x}{L}$ $\quad i = 1, 2, 3, \ldots$
4. Closed rectangular volume	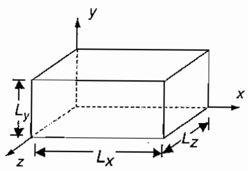	$\frac{c}{2}\left(\frac{i^2}{L_x^2} + \frac{j^2}{L_y^2} + \frac{k^2}{L_z^2}\right)^{1/2}$	$\cos \frac{i\pi x}{L_x} \cos \frac{j\pi y}{L_y} \cos \frac{k\pi z}{L_z}$ $i, j, k = 0, 1, 2, \ldots$
5. Closed cylindrical volume	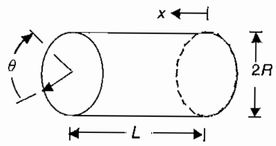	$\frac{c}{2\pi}\left(\frac{\lambda_{jk}^2}{R^2} + \frac{i^2\pi^2}{L^2}\right)^{1/2}$ λ_{jk} from Table 6.2a below	$J_j\left(\lambda_{jk}\frac{r}{R}\right) \cos \frac{i\pi x}{L} \begin{cases} \sin j\theta \\ \text{or} \\ \cos j\theta \end{cases}$ $i, j, k = 0, 1, 2, \ldots$
		Modes Symmetric about Center	
6. Closed spherical volume	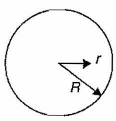	$\frac{\lambda_i c}{2\pi R}$ λ_i from Table 6.2b below	$\frac{R}{\lambda_i r} \sin \frac{\lambda_i r}{R}$ $i = 0, 1, 2, \ldots$
7. Arbitrary closed volume	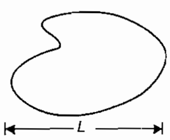	L—Maximum linear dimension fundamental natural frequency (approximate): $\frac{c}{2L}$	Finite-element analysis Boundary element analysis

Table 6.2a

λ_{jk}	j						
k	0	1	2	3	4	5	6
0	0	1.8412	3.0542	4.2012	5.3176	6.4156	7.5013
1	3.8317	5.3314	6.7061	8.0152	9.2824	10.5199	11.7349
2	7.0156	8.5363	9.9695	11.3459	12.6819	13.9872	15.2682
3	10.1730	11.7060	13.1704	14.5859	15.9641	17.3128	18.6374

$\lambda_{j=0,k} = \pi(k + 1/4)$ for $k \geq 3$ $(J_j'(\lambda_{jk}) = 0)$

Table 6.2b

i	0	1	2	3	4
λ_i	0	4.4934	7.7253	10.9041	14.0662

$\lambda_i = \pi(i + 1/2)$ for $i \geq 4$ $(\tan \lambda_i = \lambda_i)$

[a]From Ref. 6.

It is noteworthy that the first natural frequency of a cavity that is completely enclosed by rigid walls is zero, $f_0 = 0$, and is a *uniform pressure mode* (sometimes called a *Helmholtz mode*) with $\Psi_0 = 1$ and

$$V_0 = \int_V \Psi_0^2 \, dV = V \quad \text{m}^3 \tag{6.13}$$

where V is the volume of the enclosure. Also, the fundamental frequency of the first spatially varying mode in an enclosed cavity is approximately $f_1 = c/2L$ (Hz), where L is the maximum linear dimension of the cavity.

For a cavity with an open boundary, the $n = 0$ mode is absent because a (nonzero) uniform pressure cannot be sustained. Also, the natural frequencies and mode shapes in Table 6.2 for a tube with an open boundary are approximate because the boundary condition ($p \approx 0$) does not fully model the exact physics of the acoustical behavior at an open boundary. The accuracy of the formulas in Table 6.2 for an open tube increases with increasing slenderness of the tube. In general, the dimension of the open boundary must be small compared with the acoustical wavelength so that the sound is fully reflected from the open boundary.

Example 6.4. A closed rectangular cavity has dimensions $0.41 \times 0.51 \times 0.61$ m. From Table 6.2, frame 4, the formulas for the normal-mode frequencies and mode shapes are

$$\begin{aligned} f_{ijk} &= \frac{c}{2}\sqrt{\left(\frac{i}{L_x}\right)^2 + \left(\frac{j}{L_y}\right)^2 + \left(\frac{k}{L_z}\right)^2} \quad \text{Hz} \\ \Psi_{ijk} &= \cos\frac{i\pi x}{L_x}\cos\frac{i\pi y}{L_y}\cos\frac{i\pi z}{L_z} \end{aligned} \tag{6.14}$$

Let $L_x = 0.61$ m, $L_y = 0.51$ m, and $L_z = 0.41$m. (a) Find the natural frequencies of the $i = 2$, $j = 0$, $k = 0$; the $i = 1$, $j = 1$, $k = 0$; and the $i = 2$, $j = 1$, $k = 0$ normal modes of vibration. (b) Plot the sound pressure distribution for these three normal modes of vibration. The speed of sound, adjusted for temperature, is 347.3 m/s.

Solution

(a) From Eq. (6.13) we have

$$f_{2,0,0} = \frac{347.3}{2}\sqrt{\left(\frac{2}{0.61}\right)^2} = 569.3 \text{ Hz}$$

$$f_{1,1,0} = \frac{347.3}{2}\sqrt{\left(\frac{1}{0.61}\right)^2 + \left(\frac{1}{0.51}\right)^2} = 443.8 \text{ Hz}$$

$$f_{2,1,0} = \frac{347.3}{2}\sqrt{\left(\frac{2}{0.61}\right)^2 + \left(\frac{1}{0.51}\right)^2} = 663.4 \text{ Hz}$$

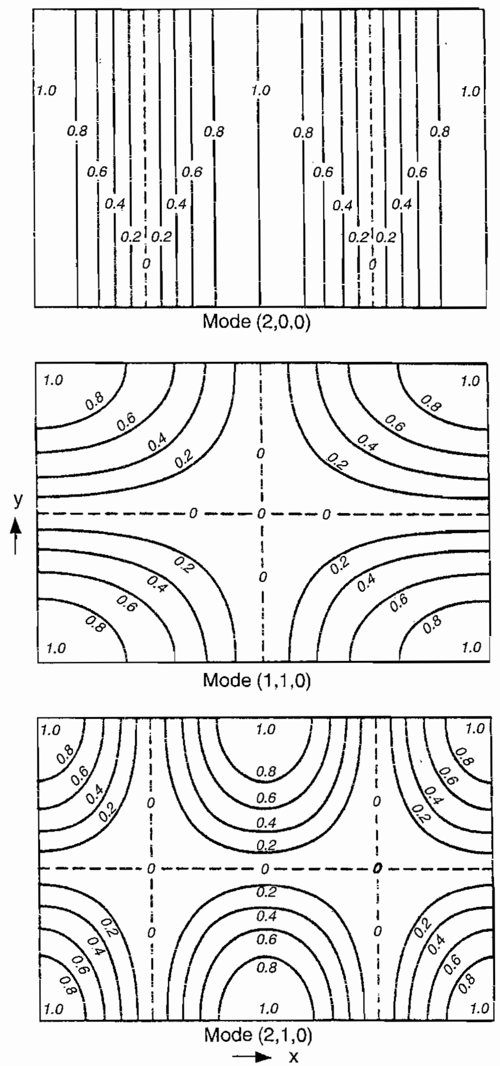

FIGURE 6.2 Sound pressure contour plots of a section through a rectangular enclosure for three different modes of vibration. The numbers on the plots indicate the relative sound pressure amplitude.

(b) The pressure distributions $|\Psi_{ijk}|$ of the modes are shown in Fig. 6.2, where the normalization is such that the maximum pressure at the corners is $|\Psi_{ijk}| = 1$. The minimum sound pressure occurs at the nodal surfaces for which $|\Psi_{ijk}| = 0$. Since $k = 0$ for all three modes, the pressure distributions are uniform in the z direction.

6.5 NUMERICAL METHODS FOR ACOUSTICAL ANALYSIS

For simple geometries and boundary conditions, the acoustical modes can be expressed analytically as in Table 6.2, but for more complicated geometries and boundary conditions numerical approaches such as the finite-element method or the boundary-element method are required.[8] The finite-element method is based upon the representation of the interior of the enclosure by a finite number of interconnected *volume* elements. The boundary-element method is based upon the representation of only the boundary surface of the enclosure by a finite number of interconnected *planar* elements. While both the finite-element method and the boundary-element method were originally developed for structural analysis, they are applicable to numerous nonstructural problems, and the acoustical cavity problem falls into this category. The major advantage of the boundary-element method is the reduction in modeling effort that is required because only the surface of the enclosure needs to be meshed. On the other hand, the finite-element method generally results in banded, frequency-independent, real matrices that require significantly less computational time when solving for the acoustical response.

To illustrate a numerical acoustical modal analysis of a complex-shaped enclosure, Fig. 6.3 shows the application of the acoustical finite-element method to an automobile passenger compartment. The acoustical finite-element model in Fig. 6.3*a* was developed from linear hexahedral and pentahedral elements, where only a half-model is required because of symmetry.[9] The model can be solved to obtain the acoustical modes by implementing a structural finite-element code and using the *structural–acoustical analogy*[10] outlined in Table 6.3. By specifying the structural material properties in terms of the acoustical material properties as shown in Table 6.3, the structural equations of motion reduce to the acoustical wave equation and the structural boundary conditions reduce to the required acoustical boundary conditions. The accuracy of the modal solution will be proportional to $(n/N)^2$ when using linear elements, where n is the mode number and N is the number of elements in a particular direction. Generally, accuracy to within 10% in frequency can be expected for the first four modes in a particular direction when there are about 10 linear elements in that direction.

The first acoustical mode predicted by the passenger compartment finite-element model in Fig. 6.3*a* is shown in Fig. 6.3*b*. It is a longitudinal mode with the nodal surface passing vertically through the passenger compartment. The nodal surface on which $|\Psi_n| = 0$ and the antinodal surfaces on which $|\Psi_n|$ is a local maximum are of practical importance because they indicate low- and high-noise regions, respectively, which result from excitation of the mode. For the example in Fig. 6.3*b*, excitation of the mode may go unnoticed by a front-seat occupant because of the proximity of the nodal surface, but it may be heard by a rear-seat occupant. The situation is just the opposite for the second mode illustrated in Fig. 6.3*c*. Because of the irregular geometrical shape of the compartment, these modes could not be predicted by simple formulas like those presented in Table 6.2. However, the numerical approach provides a method to predict the

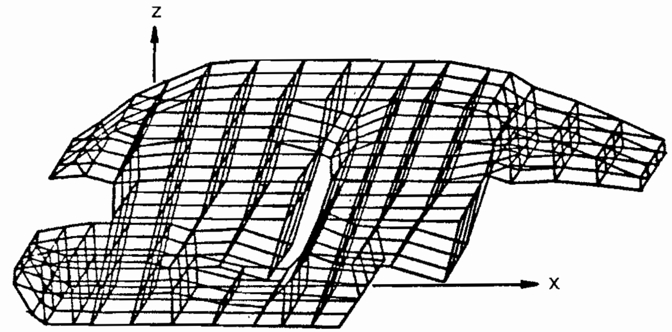

(a) Acoustic Finite Element Model

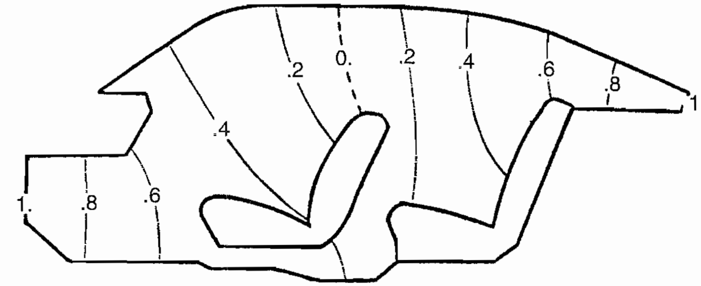

(b) First Resonant Mode at 73 Hz

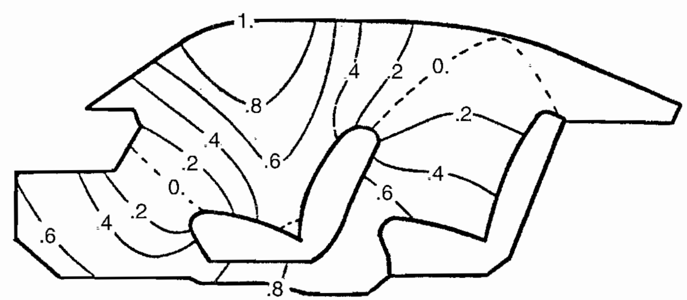

(c) Second Resonant Mode at 130 Hz

FIGURE 6.3 Acoustical finite-element analysis of automobile passenger compartment to determine the acoustical mode shapes and natural frequencies. The mode shapes become increasingly more complex as the natural frequency increases and as the complexity of the enclosure geometry increases.

TABLE 6.3 Structural–Acoustical Analogy

Description	Structure	Analogy	Acoustical Cavity
Finite element	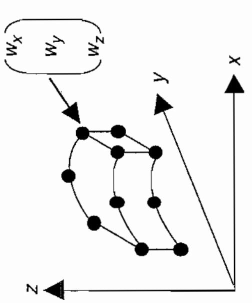 $w_k = \sum_{I=1}^{N} (W_k)_I N_I^k \quad k = x, y, z$	$w_x = p$ $N_I^z = N_I$	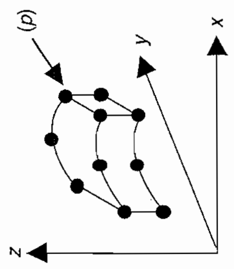 $p = \sum_{l=1}^{N} p_l N_l$
Constitutive equations	$\begin{pmatrix} \sigma_{xx} \\ \tau_{xy} \\ \tau_{xz} \end{pmatrix} = \begin{pmatrix} G_{11} & G_{14} & G_{16} \\ G_{14} & G_{44} & G_{46} \\ G_{16} & G_{46} & G_{66} \end{pmatrix} \begin{pmatrix} \varepsilon_{xx} \\ \gamma_{xy} \\ \gamma_{xz} \end{pmatrix}$	$\sigma_{xx} = u_x \quad \dfrac{\partial w_x}{\partial x} = \dfrac{\partial p}{\partial x}$ $\tau_{xy} = u_y \quad \dfrac{\partial w_x}{\partial y} = \dfrac{\partial p}{\partial y}$ $\tau_{xz} a = u_z \quad \dfrac{\partial w_x}{\partial z} = \dfrac{\partial p}{\partial z}$	$\begin{pmatrix} u_x \\ u_y \\ u_z \end{pmatrix} = \begin{pmatrix} -1/\rho & 0 & 0 \\ 0 & -1/\rho & 0 \\ 0 & 0 & -1/\rho \end{pmatrix} \begin{pmatrix} \partial p/\partial x \\ \partial p/\partial y \\ \partial p/\partial z \end{pmatrix}$
Equilibrium equations	$\dfrac{\partial \sigma_{xx}}{\partial x} + \dfrac{\partial \tau_{xy}}{\partial y} + \dfrac{\partial \tau_{xz}}{\partial z} = -\rho_s \ddot{w}_x$	Material properties $G_{11} = 1/\rho$ $G_{44} = 1/\rho$ $G_{66} = 1/\rho$ $G_{14} = 0$ $G_{16} = 0$ $G_{46} = 0$ $\rho_s = 1/\rho c^2$	$\dfrac{\partial u_x}{\partial x} + \dfrac{\partial u_y}{\partial y} + \dfrac{\partial u_z}{\partial z} = -\dfrac{1}{\rho c^2} \ddot{p}$
Finite-element equations	$([K] - \omega^2[M])\{w\} = \{0\}$ $K_{ij} = \int_V \{\nabla N_i^x\}^{\mathrm{T}} [G] \{\nabla N_i^x\}\, dV$ $M_{ij} = \int_V \rho_s N_i N_j \, dV$		$([K] - \omega^2[M])\{p\} = \{0\}$ $K_{ij} = \int_V \dfrac{1}{\rho} \{\nabla N_i\}^{\mathrm{T}} \{\nabla N_j\}\, dV$ $M_{ij} = \int_V \dfrac{1}{\rho c^2} N_i N_j \, dV$

acoustical modes, which can then be used to predict the forced sound pressure response by the methods of the following sections.

6.6 FORCED SOUND PRESSURE RESPONSE IN ENCLOSURE

Often the sound pressure response in an enclosure for known sound sources is of interest. The enclosure may be complicated in shape, and it may have walls that are both flexible and absorbent as well as multiple interior surfaces. If the undamped modes $\Psi_n(x, y, z)$ and natural frequencies $f_n = \omega_n / 2\pi$ for $n = 0, 1, 2, \ldots$ are known, the forced acoustical response in such an enclosure can be directly expressed using the *modal analysis* technique as the *normal-mode expansion*,[11,12]

$$p(x, y, z, t) = \sum_n P_n(t) \Psi_n(x, y, z) \quad \mathrm{N/m^2} \tag{6.15}$$

where the P_n are time-varying coefficients that must be determined to satisfy the acoustical wave equation, the boundary conditions, and the initial conditions.

For flexible and absorbent boundaries described by the boundary conditions in Table 6.1, the modal coefficients $P_n(t)$ are determined from

$$\ddot{P}_n + 2\delta_n \dot{P}_n + \omega_n^2 P_n = \frac{\rho c^2}{V_n} F_n(t) \quad \mathrm{N/m^2 \cdot s^{-2}} \tag{6.16}$$

where V_n is given by Eq. (6.12) and $F_n(t)$ is the *modal force*,

$$F_n(t) = \int_V \frac{\dot{Q}}{V} \Psi_n \, dV - \int_S \ddot{w} \Psi_n \, dS \quad \mathrm{m^3/s^2} \tag{6.17}$$

Q is the volume velocity of interior noise sources, and $\dot{w}$ is the vibration velocity of the wall panels at the boundary surface S. The integrations are carried out over the enclosure volume V and the wall panel surface S, respectively. In Eq. (6.16), δ_n is the *modal damping constant* or *modal damping decrement*, which as defined here is complex and given by

$$\delta_n = \delta_n^r + i\delta_n^i = \frac{\rho c^2}{2V_n} \int_A \frac{\Psi_n^2}{Z} \, dA \quad \mathrm{s^{-1}} \tag{6.18}$$

where $Z = R + iX$ is the complex wall impedance and the integration is carried out over the impedance wall area A. Table 6.1 determines the particular interpretation of $\dot{w}$ and Z in Eqs. (6.17) and (6.18) for different boundaries. The undamped modes Ψ_n are assumed to satisfy the rigid-wall boundary condition $(\partial \Psi_n / \partial n = 0)$ on both the wall panel surface S and the impedance boundary A.

From Eq. (6.18), the real and imaginary parts of δ_n can be expressed as [cf. Eq. (6.3)]

$$\delta_n^r = \frac{cA_n}{2V_n} \mathrm{Re} \frac{\rho c}{Z_n} \qquad \delta_n^i = \frac{cA_n}{2V_n} \mathrm{Im} \frac{\rho c}{Z_n} \quad \mathrm{s^{-1}} \tag{6.19}$$

where Z_n is an average impedance for the nth mode and

$$\frac{\rho c}{Z_n} = \frac{1}{A_n}\int_A \frac{\rho c}{Z}\Psi_n^2\, dA \qquad \text{where} \qquad A_n = \int_A \Psi_n^2 dA \tag{6.20}$$

When the wall impedance Z does not vary over the wall surface area A, Eq. (6.20) results in $\rho c/Z_n \equiv \rho c/Z$, as expected. Recalling the real and imaginary interpretation of the acoustical impedance in Eq. (6.19), we observe that δ_n^r relates to the wall resistivity ($\sim$ damping) and δ_n^i relates to the wall reactance ($\sim$ flexibility). In the above formulation, we have assumed that "light damping" exists such that $|\delta_n^r| \ll \omega_n$ and $|\delta_n^i| \ll \omega_n$. For more "heavily damped" enclosures that often occur in practice, the modal equations (6.16) are coupled through the boundary impedance and the wall flexibility, and they must be solved simultaneously. A complete discussion of the procedure is given in references 12 and 13.

Example 6.5. The acoustical modes Ψ_n and natural frequencies ω_n are given by the finite-element analysis in Table 6.3. Determine the normal-mode expansion for the forced sound pressure response.

Solution From the finite-element analysis, the acoustical modes are given as the $M \times N$ matrix

$$\{\Psi_1\Psi_2\cdots\Psi_n\cdots\Psi_N\} = \begin{bmatrix} \psi_{11} & \psi_{12} & \cdots & \psi_{1n} & \cdots & \psi_{1N} \\ \psi_{21} & \psi_{22} & \cdots & \psi_{2n} & \cdots & \psi_{2N} \\ \vdots & \vdots & \ddots & \vdots & \ddots & \vdots \\ \psi_{m1} & \psi_{m2} & \cdots & \psi_{mn} & \cdots & \psi_{mN} \\ \vdots & \vdots & \ddots & \vdots & \ddots & \vdots \\ \psi_{M1} & \psi_{M2} & \cdots & \psi_{Mn} & \cdots & \psi_{MN} \end{bmatrix} \tag{6.21}$$

where each row m corresponds to the response at a particular grid point of the finite-element model and each column n corresponds to the response of a particular mode. In matrix form, the normal-mode expansion in Eq. (6.15) for the forced sound pressure response then becomes

$$\begin{bmatrix} p_1(t) \\ p_2(t) \\ \vdots \\ p_m(t) \\ \vdots \\ p_M(t) \end{bmatrix} = \begin{bmatrix} \psi_{11} & \psi_{12} & \cdots & \psi_{1n} & \cdots & \psi_{1N} \\ \psi_{21} & \psi_{22} & \cdots & \psi_{2n} & \cdots & \psi_{2N} \\ \vdots & \vdots & \ddots & \vdots & \ddots & \vdots \\ \psi_{m1} & \psi_{m2} & \cdots & \psi_{mn} & \cdots & \psi_{mN} \\ \vdots & \vdots & \ddots & \vdots & \ddots & \vdots \\ \psi_{M1} & \psi_{M2} & \cdots & \psi_{Mn} & \cdots & \psi_{MN} \end{bmatrix} \begin{bmatrix} P_1(t) \\ P_2(t) \\ \vdots \\ P_n(t) \\ \vdots \\ P_N(t) \end{bmatrix} \tag{6.22}$$

Each modal coefficient $P_n(t)$ is determined from Eq. (6.16) with ω_n known and $V_n = \{\Psi_n\}^{\mathrm{T}}[M]\{\Psi_n\}$, where superscript T indicates the transpose and $[M]$ is developed in the finite-element analysis as in Table 6.3. The modal forcing in Eq. (6.16) is

$$\{F_n(t)\} = [\Psi]^{\mathrm{T}}(\{\dot{Q}\} - [S]\{\ddot{w}\}) \tag{6.23}$$

where $\{\dot{Q}\}$ and $\{\ddot{w}\}$ are vectors of the grid point volume acceleration and wall panel acceleration and $[S]$ is a matrix of surface areas associated with each wall panel grid. Similarly, the damping constant in Eq. (6.16) is

$$\{\delta_n\} = \frac{\rho c^2}{2V_n}[\Psi]^{\mathrm{T}}\left[\frac{A}{Z}\right][\Psi] \tag{6.24}$$

where $[A/Z]$ is a matrix of grid point impedance values weighted by the surface area A_m associated with each grid point m. Most structural finite-element computer codes, when adapted for acoustical normal-mode analysis according to Table 6.3, also have capabilities for modal frequency response and modal transient response to give the forced sound pressure response in the form of Eq. (6.22).

6.7 STEADY-STATE SOUND PRESSURE RESPONSE

The steady-state sound pressure in an enclosure is often of interest where the noise emanates from a point source, as in Fig. 6.1*a*. For a point source located at (x_0, y_0, z_0) and having a steady-state volume velocity $\hat{Q}\cos(\omega t + \phi)$, the mass flow rate from the source can be mathematically represented using the Dirac delta function as $\dot{m}(x, y, z, t) = \rho\hat{Q}\delta(x - x_0)\delta(y - y_0)\delta(z - z_0)\cos(\omega t + \phi)$. At a particular forcing frequency $f = \omega/2\pi$, the sound pressure response in the enclosure can then be obtained from Eqs. (6.15)–(6.17) by using the *frequency response function* technique,

$$p(x, y, z, t) = \sum_n p_n(x, y, z, \omega)\cos(\omega t + \theta_n) \qquad \mathrm{N/m^2} \tag{6.25}$$

where

$$p_n(x, y, z, \omega) = \frac{\rho c^2\omega\hat{Q}\Psi_n(x, y, z)\Psi_n(x_0, y_0, z_0)}{V_n[(\omega^2 - \omega_n^2 + 2\delta_n^i\omega)^2 + (2\delta_n^r\omega)^2]^{1/2}} \qquad \mathrm{N/m^2} \tag{6.26}$$

and

$$\theta_n(\omega) = \phi - \tan^{-1}\frac{\omega^2 - \omega_n^2 + 2\delta_n^i\omega}{2\delta_n^r\omega} \qquad \mathrm{rad} \tag{6.27}$$

The amplitude of the modal sound pressure is $|p_n|$. When $\hat{Q} = 1$, $|p_n|$ is the amplitude of the modal frequency response function.

Equation (6.25) shows that the steady-state sound pressure at one point in the enclosure can be considered as the superposition of numerous components of the same frequency ω but with different amplitudes $|p_n|$ and phase angles θ_n. If the source location (x_0, y_0, z_0) or the observer location (x, y, z) in Eq. (6.26) is on the nodal surface of a particular mode n, then the minimum participation of that mode will be observed in the response. It is also noteworthy that the solution is symmetric in the coordinates (x_0, y_0, z_0) of the sound source and the point of observation (x, y, z). If we put the sound source at (x, y, z), we observe at point (x_0, y_0, z_0) the same sound pressure as we did at (x, y, z) when the source was at (x_0, y_0, z_0). This is the famous reciprocity theorem (see Chapter 10) that can sometimes be applied with advantage to measurements in room acoustics.

When only the uniform-pressure mode $(\omega_0 = 0)$ is excited, Eqs. (6.25)–(6.27) reduce to $p = p_0 \cos(\omega t + \theta_0)$, where

$$p_0(\omega) = \frac{\rho c^2 \hat{Q}}{V[(\omega + 2\delta_0^i)^2 + (2\delta_0^r)^2]^{1/2}} \quad \text{N/m}^2$$
$$\theta_0(\omega) = \phi - \tan^{-1}\frac{\omega + 2\delta_0^i}{2\delta_0^r} \quad \text{rad} \tag{6.28}$$

which are equivalent to Eqs. (6.2). The uniform-pressure mode applies to the case of sound sources operating at very low frequencies, well below the first $(n = 1)$ resonance of the enclosure. This requirement is generally met if $L < \lambda/10$, where L is the maximum linear dimension of the cavity and $\lambda = c/f$ is the wavelength of sound generated by the source operating at the forcing frequency $f = \omega/2\pi$.

Example 6.6. For the rectangular cavity of Example 6.4, determine the steady-state sound pressure response in the cavity for loudspeaker excitation when (a) the enclosure walls are rigid and there is no damping, (b) one wall is covered uniformly with absorption material of known impedance Z, and (c) the damping is expressed in terms of the *critical damping ratio* ζ_n. Assume the loudspeaker acts as a simple monopole source.

Solution

(a) For an undamped $(\delta_n^r = 0)$ and rigid-wall $(\delta_n^i = 0)$ enclosure, we obtain, from Eqs. (6.25)–(6.27),

$$p(x, y, z, t) = \rho c^2 \hat{Q} \sum_{i=0}^{I}\sum_{j=0}^{J}\sum_{k=0}^{K} \frac{\omega \Psi_{ijk}(x, y, z)\Psi_{ijk}(x_0, y_0, z_0)}{V_{ijk}|\omega^2 - \omega_{ijk}^2|}$$
$$\times \cos\left(\omega t + \phi - \frac{\pi}{2}\right) \quad \text{N/m}^2 \tag{6.29}$$

where Ψ_{ijk} and $f_{ijk} = \omega_{ijk}/2\pi$ are given in Eq. (6.14), V_{ijk} is determined from Eq. (6.12), and I, J, K are the number of modes we include to obtain a converged solution. For a closed rectangular enclosure,

$$\frac{V_{ijk}}{V} = \varepsilon_i \varepsilon_j \varepsilon_k \qquad \text{where} \qquad \varepsilon_n = \begin{cases} 1 & \text{for } n = 0 \\ \frac{1}{2} & \text{for } n \geq 1 \end{cases} \tag{6.30}$$

with $V = L_x L_y L_z$. Note from Eq. (6.14) that for every mode of vibration the sound pressure is a maximum at the corners of the rectangular enclosure. Also, for every mode of vibration for which one of the indexes i, j, or k is *odd*, the sound pressure is zero at the *center* of the enclosure; hence at the geometrical center of the enclosure only one-eighth of the modes of vibration produce a finite sound pressure. Extending this further, at the center of any one wall, the modes for which two of the indexes (i, j, k) are odd will have zero pressure, so that only one-fourth of them will participate. Finally, at the center of one edge of the enclosure, the modes for which one index is odd will have zero pressure, so that only one-half of them participate there.

(b) Assume the uniform absorption material is on the $z = 0$ wall. Then, from Eqs. (6.19) and (6.20),

$$\delta_{ijk}^r = \frac{cA_{ijk}}{2V_{ijk}} \operatorname{Re}\frac{\rho c}{Z_{ijk}} = \frac{c}{2L_z\varepsilon_k} \operatorname{Re}\frac{\rho c}{Z} \quad \text{s}^{-1}$$
$$\delta_{ijk}^i = \frac{cA_{ijk}}{2V_{ijk}} \operatorname{Im}\frac{\rho c}{Z_{ijk}} = \frac{c}{2L_z\varepsilon_k} \operatorname{Im}\frac{\rho c}{Z} \quad \text{s}^{-1} \tag{6.31}$$

where $\rho c/Z_{ijk} = \rho c/Z$ and $A_{ijk} = \varepsilon_i \varepsilon_j A_z$ with $A_z = L_x L_y$. Substituting Eq. (6.31) into Eqs. (6.25)–(6.27), one can evaluate the series solution for the sound pressure when Z is known.

(c) From the theory of vibration (Chapter 13), the critical damping ratio ζ_n is related to the damping constant through $\delta_n = \zeta_n \omega_n$. In complex form, $\zeta_n = \zeta_n^r + i\zeta_n^i$, so that $\delta_n^r = \zeta_n^r \omega_n$ and $\delta_n^i = \zeta_n^i \omega_n$, which can be substituted into Eqs. (6.25)–(6.27) to evaluate the sound pressure for given ζ_n.

Figure 6.4 shows the predicted versus measured sound pressure level in a rectangular enclosure for volume–velocity (loudspeaker) excitation. The response was predicted by using Eqs. (6.25)–(6.27) as developed in Example 6.6. Figure 6.4*a* is the response in the undamped, rigid-wall enclosure, where the resonance peaks resulting from the excitation of the rigid-wall cavity modes are identified. Theoretically, the response at these resonances in an undamped enclosure should be infinite. In practice, however, damping is present even in an enclosure with very rigid walls since viscous and thermal losses occur in the air and at the boundaries. Modal damping provides a convenient method of accounting for these losses, and it is easily included in the solution as described in Example 6.6(c). Since the losses are primarily resistive, a real value of modal damping is used. Figure 6.4*b* shows the sound pressure response when sound-absorptive material of known impedance covers the bottom wall of the enclosure. The predicted response is obtained using the complex "damping" formulas given

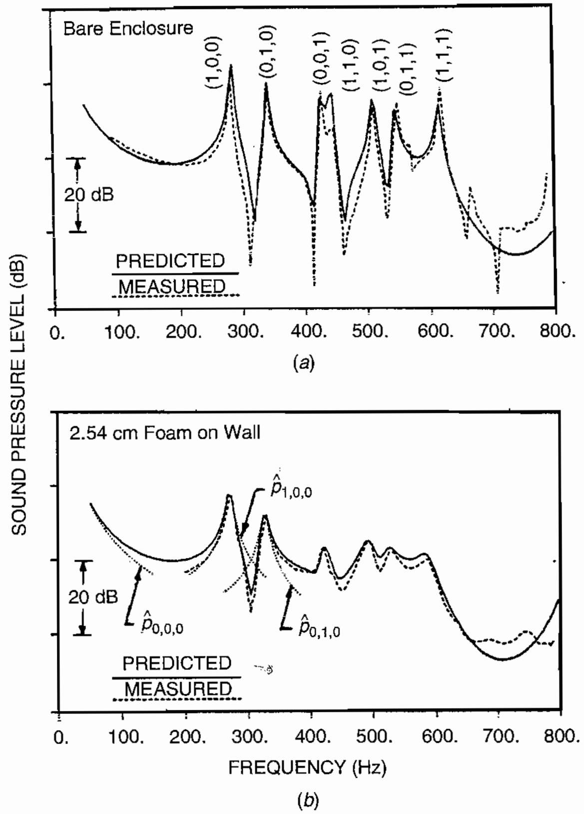

FIGURE 6.4 Comparisons of predicted versus measured of sound-pressure-level curves for a constant volume–velocity source in a rectangular enclosure of dimensions 0.61 × 0.51 × 0.41 m. The microphone was at (0.51 m, 0.10 m, 0.30 m) and the source was at (0.0 m, 0.10 m, 0.10 m). (*a*) Bare enclosure with 0.5% modal damping. (*b*) Acoustical foam 2.54 cm thick with measured impedance $\rho c/Z = (0.12 + 0.47i)(f/800)$ for $0 \le f < 800$ Hz covering the 0.61 × 0.51-m wall.

in Eq. (6.31) and by using the modes based on the reduced height of the enclosure due to the absorption material thickness. The resonant responses of the $|p_{0,0,0}|$, $|p_{1,0,0}|$, and $|p_{0,1,0}|$ terms in the series in Eq. (6.25) are also shown. The attenuation and frequency shift of the resonant peaks are evident by comparing Figs. 6.4*a* and 6.4*b*, and these are due to the resistive and reactive nature of the absorption material.

6.8 ENCLOSURE DRIVEN AT RESONANCE

If a point source of volume velocity Q is driven by a steady-state generator of frequency ω and if that frequency equals a normal-mode frequency ω_n, then the

modal sound pressure from Eq. (6.26) is

$$p_n(x, y, z, \omega_n) = \frac{\rho c^2 \hat{Q} \Psi_n(x, y, z) \Psi_n(x_0, y_0, z_0)}{V_n[(2\delta_n^i)^2 + (2\delta_n^r)^2]^{1/2}} \quad \text{N/m}^2 \tag{6.32}$$

From this we conclude that $|p_n| \to \infty$ when both $\delta_n^r = 0$ and $\delta_n^i = 0$, so that ω_n is the *resonance frequency* when we have an enclosure with undamped and rigid walls.

For an enclosure with reactive walls ($\delta_n^i \neq 0$, $\delta_n^r \equiv 0$), the frequency dependence in the denominator of Eq. (6.26) can be approximated by

$$\omega^2 - \omega_n^2 + 2\delta_n^i \omega \approx \omega^2 - \omega_n^2 \left(1 - \frac{2\delta_n^i}{\omega_n}\right) = \omega^2 - \omega_{n0}^2 \tag{6.33}$$

where

$$\omega_{n0} = \omega_n \sqrt{1 - \frac{2\delta_n^i}{\omega_n}} \quad \text{rad/s} \tag{6.34}$$

Since now $|p_n| \to \infty$ when $\omega \to \omega_{n0}$, we see that the new resonance frequency of an enclosure with undamped, reactive walls is ω_{n0}. The resonance frequency *shifts* from the rigid-wall resonance value ω_n due to the reactance δ_n^i of the walls, and ω_{n0} can be either higher or lower than the rigid-wall frequency ω_n, depending on whether $\delta_n^i < 0$ or $\delta_n^i > 0$, respectively. From Eq. (6.27), the phase angle between the modal pressure and the volume velocity source at resonance (i.e., when $\omega = \omega_{n0}$) is either 0° or 180°, and this provides a means of experimentally identifying the resonance frequency ω_{n0} and the enclosure reactance δ_n^i.

The enclosure dissipation δ_n^r controls the amplitude of the resonant peak when $\omega = \omega_{n0}$ since

$$p_n(x, y, z, \omega_{n0}) = \frac{\rho c^2 \, \hat{Q} \Psi_n(x, y, z) \Psi_n(x_0, y_0, z_0)}{2\delta_n^r V_n} \quad \text{N/m}^2 \tag{6.35}$$

The dissipation also shifts the resonance frequency an additional amount. The actual resonance frequency ω_{res} at which $|p_n|$ becomes a maximum can be shown to be

$$\omega_{\text{res}} = \sqrt{\omega_{n0}^2 - 2(\delta_n^r)^2} = \sqrt{\omega_n^2 - 2\delta_n^i \omega_n - 2(\delta_n^r)^2} \quad \text{rad/s} \tag{6.36}$$

The dissipative effect (δ_n^r) is always to reduce the resonance frequency, but this effect is of second order and generally less important than the reactive effect (δ_n^i), which is of first order, unless δ_n^r is large. In general, therefore, to first order, the resonance frequency of an enclosure is $\omega_{\text{res}} = \omega_{n0}$ with ω_{n0} given by Eq. (6.34). The *half-power bandwidth* of the resonant peak is the width of the resonance curve at 3 dB below the peak power (6 dB below the peak pressure) and is

$$\Delta\omega_{\text{res}} = 2\delta_n^r \quad \text{rad/s} \tag{6.37}$$

This provides a means of experimentally determining the enclosure dissipation δ_n^r.

Example 6.7. Determine the resonance frequency of the first mode in Fig. 6.4*b*. The measured wall impedance is $\rho c/Z = (0.12 + 0.47i)(f/800)$.

Solution For the (1, 0, 0) mode, we have $f_{1,0,0} = 284.8$ Hz from Eq. (6.14). For this frequency, $\rho c/Z = (0.12 + 0.47i)(284.8/800) = 0.043 + 0.167i$. Noting that the thickness of the absorption material is 2.54 cm, we have $L_z = 0.41 - 0.0254 = 0.3846$ m, and from Eq. (6.31),

$$\delta_{1,0,0}^r = \frac{347.3}{2 \times 0.3846 \times 1} \times 0.043 = 19.6$$

$$\delta_{1,0,0}^i = \frac{347.3}{2 \times 0.3846 \times 1} \times 0.167 = 76.2$$

Substituting these into Eq. (6.36) gives the resonance frequency

$$f_{\text{res}} = \frac{\omega_{\text{res}}}{2\pi} = f_n\sqrt{1 - \frac{2\delta_n^i}{\omega_n} - 2\left(\frac{\delta_n^r}{\omega_n}\right)^2}$$

$$= 284.8(1 - 0.085 - 0.00024)^{1/2} = 272.4 \text{ Hz}$$

Actually, the calculated frequency should be slightly greater than this because the impedance is frequency dependent and should be evaluated at f_{res}. An iterative calculation gives $f_{\text{res}} = 273$ Hz, while the measured resonance frequency in Fig. 6.4*b* is 274 Hz.

6.9 FLEXIBLE-WALL EFFECT ON SOUND PRESSURE

A flexible wall may exhibit structural resonances and affect the sound pressure in two ways: (a) by acting as a noise source when exterior structural or pressure loads excite vibrations of the wall and (b) by acting as a boundary impedance that can alter the cavity sound pressure. Both of these effects may occur simultaneously in a room with flexible walls, in which case a coupled *structural–acoustical analysis* is required to predict the sound pressure response. We shall first consider each of the two effects of a flexible wall separately and then consider the coupled structural–acoustical response.

Flexible Wall as Noise Source

When the vibration velocity $\dot{w}(x, y, z, t)$ of a flexible wall is known, the boundary condition in Table 6.1, frame 2 or 4, can be applied to Eqs. (6.16) and (6.17). The forcing is through the equivalent modal volume–velocity of the wall vibration,

$$Q_n = \hat{Q}_n \cos(\omega t + \phi_n) = -\int_S \dot{w}\Psi_n \, dS \quad \text{m}^3/\text{s} \qquad (6.38)$$

where the vibration velocity of the wall $\dot{w} = \hat{\dot{w}} \cos(\omega t + \phi_w)$ is assumed to have a known amplitude $\hat{\dot{w}}(x, y, z)$ and phase $\phi_w(x, y, z)$. The steady-state sound pressure response is then obtained as in Eqs. (6.26) and (6.27),

$$p_n(x, y, z, \omega) = \frac{\rho c^2 \omega \hat{Q}_n \Psi_n(x, y, z)}{V_n[(\omega^2 - \omega_n^2 + 2\delta_n^i\omega)^2 + (2\delta_n^r\omega)^2]^{1/2}} \quad \text{N/m}^2 \qquad (6.39)$$

$$\theta_n(\omega) = \phi - \tan^{-1}\frac{\omega^2 - \omega_n^2 + 2\delta_n^i\omega}{2\delta_n^r\omega} \quad \text{rad} \qquad (6.40)$$

where δ_n^r, δ_n^i relate to the layer of absorption material of acoustical impedance Z_a covering the flexible wall.

Figure 6.5*a* shows the calculation of the forced acoustical response in the automobile passenger compartment using the above method with measured panel acceleration amplitude and phase data to represent the wall vibration and with measured wall impedance data to represent the absorption materials. The solution is expressed in matrix form as in Eq. (6.22) with the acoustical modes obtained from a finite-element analysis (Fig. 6.3). Figure 6.5*a* shows that a large spatial variation in sound pressure level occurs in the passenger compartment because of the modal nature of the acoustical response. Figure 6.5*b* shows the sound pressure computed separately for the vibration of each individual wall panel. The individual sound pressures can be combined, by considering their magnitude and phase, to obtain the resultant sound pressure, which is shown in Fig. 6.5*b*. This provides a method to identify the major noise sources and the extent to which they must be controlled to yield a specified noise reduction. For example, Fig. 6.5*b* illustrates the large amplitude of the sound pressure due to the back-window vibration. Also note that the elimination of the roof vibration would increase the noise at the driver's ear.

Flexible Wall as Reactive Impedance

Wall panel vibration can generally be expressed in the normal-mode expansion form

$$w = \sum_m W_m(t)\Phi_m(x, y, z) \quad \text{m} \qquad (6.41)$$

where Φ_m are the structural vibration mode shapes and W_m are the modal amplitudes. If we consider the coupling between the wall panel and the cavity, for the mth structural mode and the nth acoustical mode, the modal acoustical impedance of the wall can be expressed as

$$Z_{mn} = (S_{mn})^{-1}\left[C_m + i\omega\left(M_m - \frac{K_m}{\omega^2}\right)\right] \quad \text{N/m}^3 \cdot \text{s}^{-1} \qquad (6.42)$$

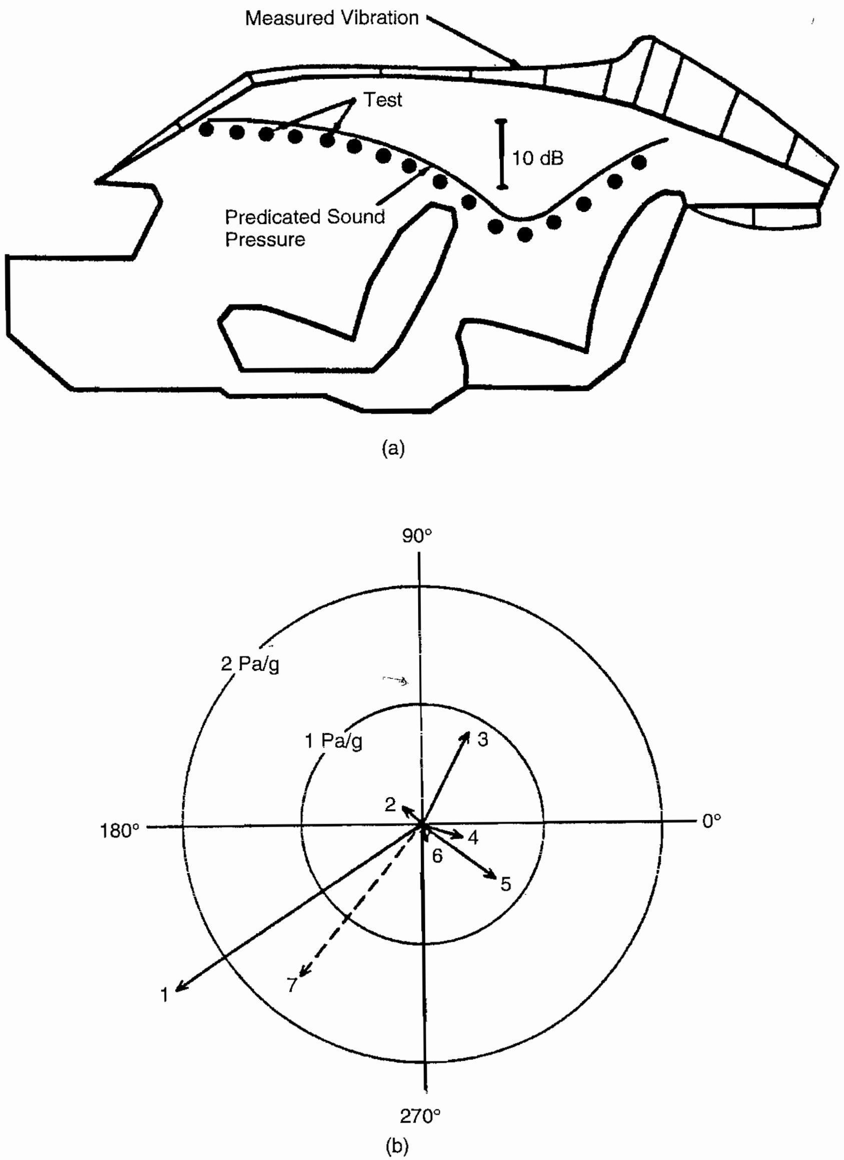

FIGURE 6.5 (*a*) Comparison of measured versus predicted sound-pressure-level spatial variation in automobile passenger compartment for 40-Hz structural excitation. (*b*) Polar amplitude–phase diagram indicating panel contributions to resultant sound pressure at driver's ear (1, back window; 2, rear floor; 3, roof; 4, windshield; 5, rear shelf; 6, front floor; 7, resultant).

where M_m, C_m, and K_m are the modal mass, damping, and stiffness of the mth wall mode, and

$$S_{mn} = \int_S \Phi_m \Psi_n \, dS \quad \text{m}^2 \tag{6.43}$$

where S_{mn} is the *structural–acoustical coupling*. [Note that when $S_{mn} = 0$, there is no coupling between the structural mode m and the acoustical mode n, and Eq. (6.42) does not apply. In practice, when S_{mn} is sufficiently small, the coupling can be neglected to simplify the solution.]

For an undamped enclosure, the structural–acoustical coupling modifies Eq. (6.26) to

$$p_n(x, y, z, \omega) = \frac{\rho c^2 \omega \hat{Q} \Psi_n(x, y, z) \Psi_n(x_0, y_0, z_0)}{V_n |\omega^2 - \omega_{n0}^2|} \left| \frac{\omega^2 - \Omega_m^2}{\omega^2 - \Omega_{m0}^2} \right| \quad \text{N/m}^2 \tag{6.44}$$

where $\Omega_m = \sqrt{K_m/M_m}$ (rad/s) is the natural frequency of the mth wall mode and ω_{n0}^2 and Ω_{n0}^2 are solutions of

$$(\omega^2 - \omega_n^2)(\omega^2 - \Omega_m^2) - D^2\omega^2 = 0 \tag{6.45}$$

where $D = \sqrt{K_{\text{air}}/M_m}$ with $K_{\text{air}} = \rho c^2 S_{mn}^2 / V_n$ (N/m) being the *stiffness* of the nth acoustical mode relative to the mth structural mode.

Equation (6.44) shows that the flexible wall introduces an additional resonance at $\omega = \Omega_{m0}$, which will appear as a resonance peak in the sound pressure response and corresponds to the wall resonance. It can be shown from Eq. (6.45) that, with wall modes at frequencies below the rigid-wall cavity resonance ($\Omega_m < \omega_n$, the case of *mass-controlled* boundaries), the cavity resonance is raised ($\omega_{n0} > \omega_n$) and the wall resonance is lowered ($\Omega_{m0} < \Omega_m$). With wall modes at frequencies above the rigid-wall cavity resonance ($\Omega_m > \omega_n$, the case of *stiffness-controlled* boundaries), the cavity resonance is lowered ($\omega_{n0} < \omega_n$) and the wall resonance is raised ($\Omega_{m0} > \Omega_m$). In addition, the wall acts as a vibration absorber when $\omega = \Omega_m$, so that the modal sound pressure $p_n = 0$. However, the total sound pressure p may not be zero because of the participation of other acoustical modes. A Helmholtz resonator used as a vibration absorber as described in Chapter 8 has impedance Z_R and performs in a similar manner.

Coupled Structural–Acoustical Response

Above we have considered the coupling of one acoustical mode n with one structural mode m, which is the case when a single coupling coefficient S_{mn} dominates for the mode pair (m, n). In practice, however, each acoustical mode n may couple with several structural modes, and the general case can be treated by substituting Eq. (6.41) into the second integral of Eq. (6.17) to obtain, from Eq. (6.16),

$$\ddot{P}_n + 2\delta_n \dot{P}_n + \omega_n^2 P_n + \frac{\rho c^2}{V_n} \sum_m S_{mn} \ddot{W}_m = \frac{\rho c^2}{V_n} F_n(t) \quad \text{N/m}^2 \cdot \text{s}^2 \tag{6.46}$$

where the summation is carried out over all coupled structural modes m. Similarly, each structural mode m may in general couple with several acoustical modes, and the corresponding equation for the structural modal amplitude $W_m(t)$ in Eq. (6.41) is

$$\ddot{W}_m + 2\Delta_m \dot{W}_m + \Omega_m^2 W_m - \frac{1}{M_m} \sum_n S_{mn} P_n = \frac{R_m(t)}{M_m} \quad \text{m/s}^2 \tag{6.47}$$

where the summation is carried out over all coupled acoustical modes n. In this latter equation for the structure, Δ_m is the modal damping constant, Ω_m is the natural frequency, M_m is the modal mass, and $R_m(t)$ is the modal force. The coupling between the acoustical and structural systems makes it necessary to solve Eqs. (6.46) and (6.47) simultaneously for all coupled P_n and W_m. A complete derivation of the equations and discussion of the procedure can be found in reference 12, and its finite-element implementation is described in references 14 and 15.

To illustrate a typical coupled structural–acoustical response, Fig. 6.6 shows an application to a small metallic box used to isolate instruments from an external noise field (cf. Fig. 6.1*b*). The analysis of such enclosures to predict their noise attenuation is discussed in detail in Chapter 11. The finite-element method can be used to model the box wall panels and the acoustical cavity (Figs. 6.6*b, c*) in order to compute the uncoupled structural and acoustical modes. Equations (6.46) and (6.47) are then solved for the coupled frequency response, where the exterior noise field in Fig. 6.6*a* is specified as an oscillating external pressure $\hat{p}_E \cos \omega t$ applied uniformly to the wall panels. The noise attenuation inside the enclosure is characterized by its *insertion loss*, defined in Chapter 11 as 20 $\log_{10}(\hat{p}_I/\hat{p}_E)$, where $\hat{p}_I$ is the interior sound pressure. The predicted versus measured insertion loss is shown in Fig. 6.6*d*. The structural–acoustical coupling effect is particularly evident in the rms panel vibration shown in Fig. 6.6*e*, which compares the coupled versus the uncoupled (i.e., in vacuo) panel response and illustrates the significant effect that the acoustical cavity modes have on the structural vibration response.

6.10 RANDOM SOUND PRESSURE RESPONSE

For steady-state, deterministic sound source excitation, the sound pressure response can be obtained by the frequency response function technique of Eqs. (6.25)–(6.27). However, for sound source excitation that is nondeterministic, it is generally necessary to utilize a random-analysis technique

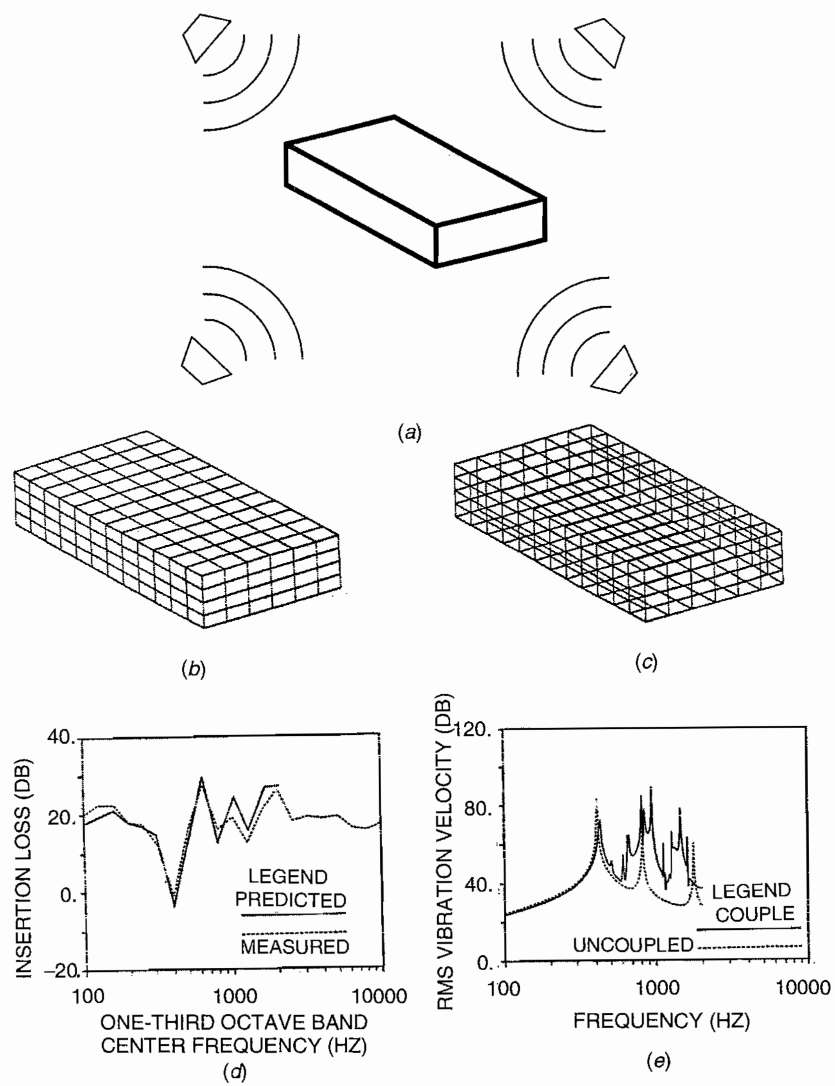

FIGURE 6.6 Structural–acoustical analysis to predict insertion loss of a 30 × 15 × 5-cm unlined aluminum box with 0.16-cm-thick walls: (*a*) box in uniform noise environment; (*b*) structural finite-element model of box wall panels; (*c*) acoustical finite-element model of box cavity; (*d*) predicted versus measured insertion loss at box center; (*e*) coupled versus uncoupled surface-averaged vibration of 30 × 15-cm wall panel. [Measured data in (*d*) from Chapter 11].

to obtain the sound pressure response. For example, irregular pressure fluctuations generated by turbulence can result in complicated sound sources that are more readily measured or defined as random excitations than as deterministic excitations. Also, interactions with irregular surfaces such as roads, runways, and pathways are more readily represented as random loads than as deterministic loads. Under certain conditions (stationarity) the average frequency content of these excitations may be represented by a spectral density function (Chapter 3). Then by using the spectral density representation of the input and the frequency response function technique to determine the sound pressure output, conventional random-analysis theory may be utilized to obtain the sound pressure spectral density response.

From random-analysis theory, nondeterministic stationary processes can be characterized by their auto- (power) spectral density function and their cross-spectral density function.[16] The power spectral density (PSD) function of a physical variable such as sound pressure $p(t)$ is defined as a real-magnitude function $S_p(\omega)$, where

$$S_p(\omega) = \lim_{T\to\infty} \frac{2}{T} \left| \int_0^T e^{-\iota\omega t} p(t)\, dt \right|^2 \quad (\text{N/m}^2)^2/\text{Hz} \tag{6.48}$$

Similarly, the PSD function $S_Q(\omega)$ for a volume–velocity point source $Q(t)$ is

$$S_Q(\omega) = \lim_{T\to\infty} \frac{2}{T} \left| \int_0^T e^{-\iota\omega t} Q(t)\, dt \right|^2 \quad (\text{m}^3/\text{s})^2/\text{Hz} \tag{6.49}$$

The PSD functions of the sound pressure response and sound source excitation are related via the frequency response function as

$$S_p(x,y,z,\omega) = \sum_n p_n^2(x,y,z,\omega) S_Q(\omega) \quad (\text{N/m}^2)^2/\text{Hz} \tag{6.50}$$

where $S_p(x,y,z,\omega)$ is the sound pressure PSD response and $p_n(x,y,z,\omega)$ is the modal frequency response function in Eq. (6.26) for unit sound source excitation $\hat{Q} = 1$. Equation (6.50) is the random-response equivalent of Eq. (6.25) for the steady-state response. However, for random response, only the amplitude of the modal frequency response function is required and not the phase information in $\theta_n(\omega)$ in Eq. (6.27).

Another useful result from random-analysis theory is that, if several sound sources $Q_1(t), Q_2(t), \ldots, Q_a(t), \ldots$ are statistically independent, then the cross-correlation between any pair of sources is zero, and the total sound pressure PSD response is equal to the sum of the PSD responses due to the individual sources. That is,

$$\begin{aligned} S_p(x,y,z,\omega) &= \sum_a S_{p_a}(x,y,z,\omega) \\ &= \sum_a \sum_n p_{an}^2(x,y,z,\omega) S_{Q_a}(\omega) \quad (\text{N/m}^2)^2/\text{Hz} \end{aligned} \tag{6.51}$$

Finally, when two sound sources $Q_a(t), Q_b(t)$ are statistically correlated, the degree of correlation is related by a cross-spectral density function $S_{Q_aQ_b}(\omega)$ given by

$$S_{Q_aQ_b}(\omega) = \lim_{T\to\infty} \frac{2}{T} \left[\left(\int_0^T e^{-\iota\omega t} Q_a(t)\, dt \right)^* \left(\int_0^T e^{-\iota\omega t} Q_b(t)\, dt \right) \right] \quad (\text{m}^3/\text{s})^2/\text{Hz} \tag{6.52}$$

where the asterisk denotes complex conjugate. Unlike the PSD function, the cross-spectral density function is generally a complex number that includes both amplitude and phase information. For correlated sound sources, the spectral density of the sound pressure response is then a complex number given by

$$S_p(x,y,z,\omega) = \sum_a \sum_b \sum_m \sum_n (p_{am}(x,y,z,\omega) e^{i\theta_m(\omega)})(p_{bn}(x,y,z,\omega) e^{i\theta_n(\omega)})^* \times S_{Q_aQ_b}(\omega) \quad (\text{N/m}^2)^2/\text{Hz} \tag{6.53}$$

where the phase relationships $\theta_m(\omega), \theta_n(\omega)$ are from Eq. (6.27) with $\phi = 0$. In the case where the sound sources are uncorrelated, Eq. (6.53) reduces to the previous real-magnitude sound pressure PSD functions in Eqs. (6.50) and (6.51).

Example 6.8. Determine the sound pressure PSD response in the very small enclosure in Fig. 6.1*a* with rigid walls when (a) there is a single sound source Q_a in the enclosure with PSD amplitude $S_{Q_a} = S(\omega)$; (b) there are two uncorrelated interior sound sources Q_a, Q_b in the enclosure with PSD amplitudes $S_{Q_a} = S(\omega)$, $S_{Q_b} = S(\omega)$; and (c) there are two interior sound sources with $S_{Q_a} = S(\omega)$, $S_{Q_b} = S(\omega)$ but perfectly correlated so that $S_{Q_aQ_b} = S(\omega)$.

Solution

(a) For a rigid-wall enclosure with a single sound source, substituting Eq. (6.4) into Eq. (6.50) gives

$$S_p(x,y,z,\omega) = p_0^2(x,y,z,\omega) S_{Q_a} = \left(\frac{\rho c^2}{\omega V}\right)^2 S_{Q_a} = \left(\frac{\rho c^2}{\omega V}\right)^2 S(\omega)$$

(b) For two uncorrelated sound sources in the enclosure, Eq. (6.51) gives

$$S_p(x,y,z,\omega) = \left(\frac{\rho c^2}{\omega V}\right)^2 (S_{Q_a} + S_{Q_b}) = 2\left(\frac{\rho c^2}{\omega V}\right)^2 S(\omega)$$

(c) For two correlated sound sources in the enclosure, Eq. (6.54) gives

$$S_p(x,y,z,\omega) = \left(\frac{\rho c^2}{\omega V}\right)^2 (S_{Q_a} + S_{Q_b} + 2S_{Q_aQ_b}) = 4\left(\frac{\rho c^2}{\omega V}\right)^2 S(\omega)$$

Thus, for uncorrelated sound sources, doubling the number of the sound sources in the enclosure *doubles* the sound pressure PSD response (3 dB increase), as in (b). On the other hand, for perfectly correlated sound sources, doubling the number of the sound sources *quadruples* the sound pressure PSD response (6 dB increase), as in (c).

The random-analysis formulas in Eqs. (6.50)–(6.53) are also applicable to structural analysis, by replacing the acoustical frequency response functions and sound source excitations with the corresponding structural frequency response functions and structural excitations.[16] Also, the coupled structural–acoustical analysis provided by Eqs. (6.46) and (6.47) can be applied to predict the sound pressure PSD response for random excitations.[17] As an example, Fig. 6.7 illustrates the predicted interior sound pressure PSD response in an automobile passenger compartment for the vehicle traveling at constant speed V over a randomly rough road. In this example, random road excitation occurs at the tire patch (Fig. 6.7*a*) and the sound pressure response in the passenger compartment results from the transmitted vibration to the vehicle body panels. Equations (6.46) and (6.47) can be used to obtain the sound pressure frequency response functions by employing the vehicle finite-element models in Figs. 6.7*b,c*. Equation (6.51) is then used to predict the sound pressure PSD response by applying the road profile PSD function in Fig. 6.7*d* as excitation at each tire patch at the vehicle speed V. Figure 6.7*e* shows the predicted sound pressure PSD response in the passenger compartment versus the 95% confidence band based on the measured responses in nominally identical vehicles. The relative participation of the sound sources and body panels to the sound pressure PSD response can also be identified by the methods in Chapter 3 and reference 17.

6.11 TRANSIENT SOUND PRESSURE RESPONSE

When the source of sound in a room is turned off, the sound dies out, or decays, at a rate that depends on the dissipation, or damping, in the room. The acoustical response that exists in the room can be found from the transient solution of Eq. (6.16), which is

$$P_n(t) = \frac{\rho c^2}{V\omega_{nD}} \int_0^t F_n(\tau) e^{-\delta_n^r(t-\tau)} \sin[\omega_{nD}(t-\tau)]\, d\tau \quad \text{N/m}^2 \qquad (6.54)$$

where $\omega_{nD} = \sqrt{\omega_n^2 - (\delta_n^r)^2 + (\delta_n^i)^2}$ is the "damped" modal frequency of the acoustical response in the enclosure. Equation (6.54) is the particular solution that satisfies zero initial conditions. For general initial conditions, the following free-vibration response must be added to the above equation:

$$P_n(t) = e^{-\delta_n^r t}\left[\frac{\dot{P}_n(0) + P_n(0)\delta_n^r}{\omega_{nD}} \sin \omega_{nD} t + P_n(0) \cos \omega_{nD} t\right] \quad \text{N/m}^2 \quad (6.55)$$

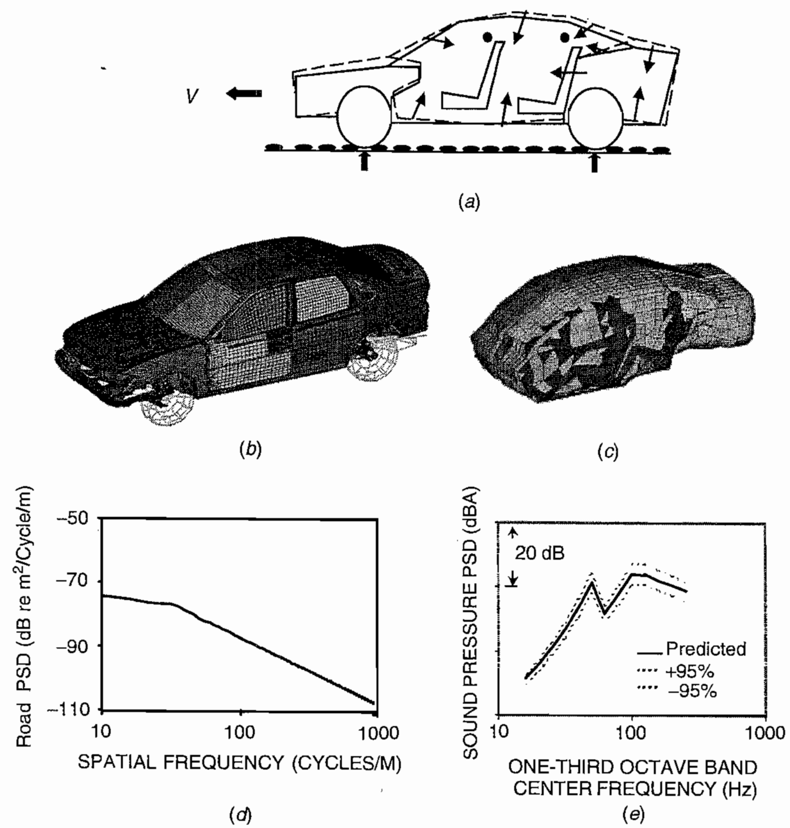

FIGURE 6.7 Structural–acoustical analysis to predict sound pressure PSD response in vehicle traveling at constant speed V on randomly rough road: (*a*) interior road noise generation; (*b*) structural finite-element model of vehicle; (*c*) acoustical finite-element model of passenger-trunk compartment; (*d*) road profile power spectral density; (*e*) predicted A-weighted sound pressure PSD response at front seat occupant ear location versus 95% confidence interval.

Equation (6.55) can be used to determine the decay of the modes after the sound source is turned off at $t = 0$, when the initial conditions $P_n(0)$ and $\dot{P}_n(0)$ are known. For light damping, each mode of vibration behaves independently of the others, and the total process of sound decay is the summation in Eq. (6.15) of the sound pressures associated with all of the individual modes of vibration that fall within the frequency band of interest. The long-time sound decay may be different than the short-time sound decay because of the different damping factors and initial conditions for the modes.

The *reverberation time* T is defined as the time in seconds required for the level of sound to drop by 60 dB or for the pressure to drop to $\frac{1}{1000}$ of its initial value (see Chapter 7). One can similarly define a *modal* reverberation time T_n as that for which the sound pressure decays in that mode by 60 dB or $\frac{1}{1000}$ of its initial value. Since the reverberation time is that associated with the decaying part $(-\delta_n^r t)$ of the solution in Eq. (6.55),

$$T_n = \frac{6.91}{\delta_n^r} = \frac{13.82 V_n}{cA_n \operatorname{Re}(\rho c/Z_n)} \quad \text{s} \tag{6.56}$$

where we have substituted for δ_n^r from Eq. (6.19). With $c = 343$ m/s (20°C) and expressed in terms of the random-incidence absorption coefficient, $\alpha_n = 8\operatorname{Re}(\rho c/Z_n)$, with V in cubic meters and A in square meters, one obtains the modal reverberation time $(n > 0)$

$$T_n = 0.322 \frac{V_n}{\alpha_n A_n} \quad \text{s} \tag{6.57}$$

which can be evaluated for a given Z by using the formulas in Eqs. (6.20) and (6.12). The uniform-pressure mode $(n = 0)$ must be treated separately. The general transient solution of Eq. (6.16) when $n = 0$ reduces to

$$P_0(t) = P_0(0)e^{-2\delta_0^r t} + \frac{\rho c^2}{V} \int_0^t \int_0^\tau F_0(\sigma)\, d\sigma \; e^{-2\delta_0^r (t-\tau)}\, d\tau \quad \text{N/m}^2 \tag{6.58}$$

and the reverberation time for the decay of a uniform sound pressure is $T_0 = 6.91/2\delta_0^r = 6.91V/cA\operatorname{Re}(\rho c/Z)$ so that, for V in cubic meters and A in square meters,

$$T_0 = 0.161 \frac{V}{\alpha A} \quad \text{s} \tag{6.59}$$

In this case, the formula for the reverberation time of a uniform sound pressure is identical to the formula of Sabine for the reverberation time of a diffuse sound field.

If the pressure–time history is dominated by a single mode, then the reverberation time is equal to the appropriate modal reverberation time. If the sound source is turned off at $t = 0$, the magnitude of the sound pressure associated with a particular mode at a response location (x, y, z) is given by Eq. (6.55). The decay of the response from its maximum amplitude $[\dot{P}_n(0) = 0]$ can then be written as

$$p_n(x, y, z, t) = P_n(0)\Psi_n(x, y, z)e^{-\delta_n^r t} \cos(\omega_n t + \theta_n) \quad \text{N/m}^2 \tag{6.60}$$

where $\theta_n = \tan^{-1}(\delta_n^r/\omega_{nD})$ is the modal phase. If we take the rms time average of $\cos(\omega_n t + \theta_n)$ and the rms spatial average of $\Psi_n\,(x, y, z)$ and we designate the resultant as $\overline{p}_n(t)$, then Eq. (6.60) indicates that on a plot of $\log \overline{p}_n$ versus

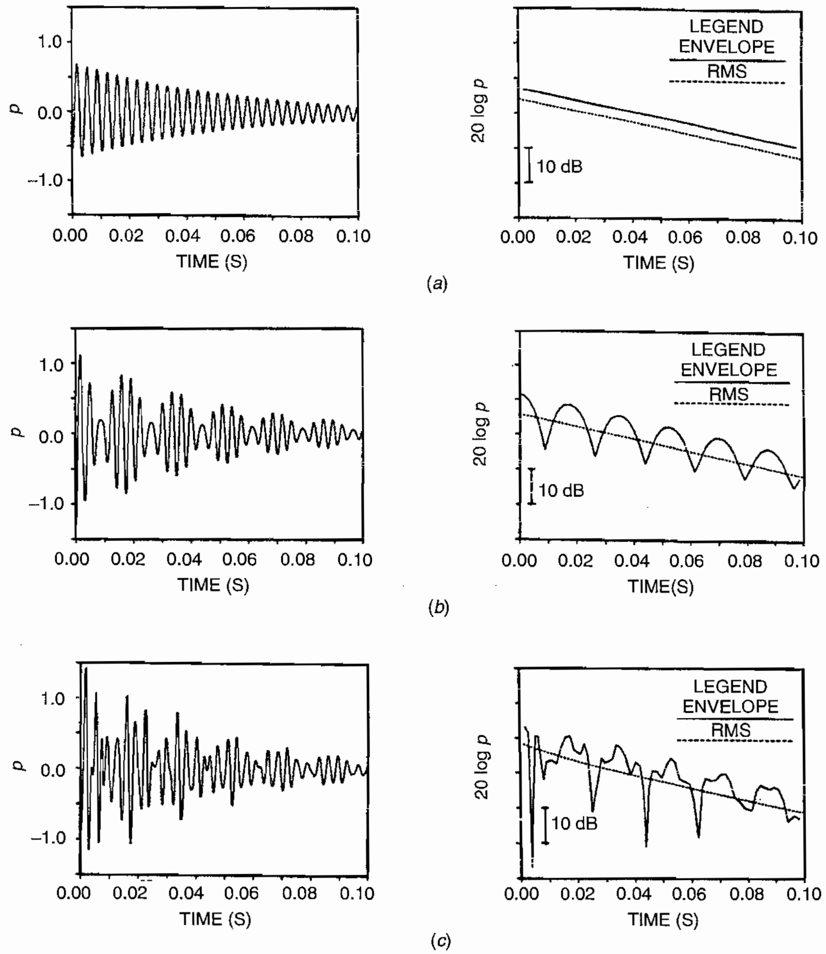

FIGURE 6.8 Sound pressure decay curves for rectangular enclosure of Fig. 6.6: (*a*) for the (1, 0, 0) mode of vibration; (*b*) for the (1, 0, 0) and (0, 1, 0) modes together; (*c*) for all modes up to 800 Hz. The graphs on the left show the course of the instantaneous sound pressure at the microphone location, and those on the right show the curve of the envelope of the left graphs and the rms pressure of Eq. (6.61) plotted on a log p-versus-t coordinate system.

time, as in Fig. 6.8*a*, both the envelope of the sound pressure and the rms sound pressure decay linearly with time and have the constant reverberation time T_n.

When many normal modes of vibration (each with its own amplitude, phase, resonance frequency, and damping constant) decay simultaneously, the total rms (spatial and temporal) sound pressure is obtained from Eq. (6.15) as

$$\overline{p}(t) = \sqrt{\overline{p}_I^2 + \overline{p}_{I+1}^2 + \cdots + \overline{p}_{I+N}^2} \quad \text{N/m}^2 \tag{6.61}$$

where I is the first mode in the frequency band considered and $I + N$ is the last mode in the decay. In this case, the decay envelope is generally not linear as above, even when the modal reverberation times do not vary greatly from one mode to another so that all modes in the frequency band have a similar damping constant. The decay envelope is irregular, as in Figs. 6.8*b,c*, because the modes of vibration have different frequencies and beat with each other during the decay. However, the rms decay from Eq. (6.61) will be nearly linear if the modal reverberation times are similar (Fig. 6.8*b*) or if the long-time decay is governed by a least-damped mode, which may occur when the modal reverberation times or initial conditions differ (Fig. 6.8*c*).

This brief description of sound decay in small rooms is applicable to rooms of any size and shape, and it can be extended to include the effects of structural–acoustical coupling. The fact that sound fields in large enclosures involve too many modes for the calculations to be practical does not mean that there are not distinct normal modes of vibration, each with its own natural frequency and damping constant. Alternate and more practical methods for handling large enclosures involving large numbers of modes are discussed in the next chapter.

REFERENCES

1. P. M. Morse and K. U. Ingard, *Theoretical Acoustics*, Princeton University Press, Princeton, NJ, 1986.
2. L. L. Beranek (Ed.), *Noise and Vibration Control*, rev. ed., Institute of Noise Control Engineers, Poughkeepsie, NY, 1988.
3. H. Kutruff, *Room Acoustics*, Applied Science, London, 1979.
4. L. E. Kinsler, A. R. Frey, A. B. Coppins, and J. V. Saunders, *Fundamentals of Acoustics*, 4th ed., Wiley, New York, 1999.
5. L. L. Beranek and I. L. Ver, *Noise and Vibration Control Engineering*, Wiley, New York, 1992.
6. E. H. Dowell, C. F. Chao, and D. A. Bliss, "Absorption Material Mounted on a Moving Wall-Fluid/Wall Boundary Condition," *J. Acoust. Soc. Am.*, **70**(1), 244–245 (1981).
7. R. D. Blevins, *Formulas for Natural Frequency and Mode Shape*, Krieger, Malabar, FL, 1995.
8. M. J. Crocker (Ed.), *Handbook of Noise and Vibration Control*, Chapter 6: "Numerical Acoustical Modeling (Finite Element Modeling)" and Chapter 7: "Numerical Acoustical Modeling (Boundary Element Modeling)," Wiley, New York, 2006.
9. M. M. Kamal and J. A. Wolf, Jr. (Eds.), *Modern Automotive Structural Analysis*, Van Nostrand Reinhold, New York, 1982.
10. G. C. Everstine, "Structural Analogies for Scalar Field Problems," *Int. J. Numer. Methods Eng.*, **17**, 471–476 (1981).

11. P. M. Morse and R. H. Bolt, "Sound Waves in Rooms," *Rev. Modern Phys.*, **16**(2), 69–150 (1944).
12. E. H. Dowell, G. F. Gorman III, and D. A. Smith, "Acoustoelasticity: General Theory, Acoustic Natural Modes and Forced Response to Sinusoidal Excitation, Including Comparisons with Experiment," *J. Sound Vib.*, **52**(4), 519–542 (1977).
13. E. H. Dowell, "Reverberation Time, Absorption, and Impedance," *J. Acoust. Soc. Am.*, **64**(1), 181–191 (1978).
14. D. J. Nefske, J. A. Wolf, Jr., and L. J. Howell, "Structural-Acoustic Finite Element Analysis of the Automobile Passenger Compartment: A Review of Current Practice," *J. Sound Vib.*, **80**(2), 247–266 (1982).
15. S. H. Sung and D. J. Nefske, "A Coupled Structural-Acoustic Finite Element Model for Vehicle Interior Noise Analysis," *ASME J. Vib. Acoust. Stress Reliabil. Design*, **106**, 314–318 (1984).
16. D. E. Newland, *An Introduction to Random Vibration, Spectral and Wavelet Analysis*, Wiley, New York, 1994.
17. S. H. Sung and D. J. Nefske, "Component Mode Synthesis of a Vehicle Structural-Acoustic System Model," *Am. Inst. Aero. Astro. J.*, **24**(6), 1021–1026 (1986).

CHAPTER 7

Sound in Rooms

MURRAY HODGSON

University of British Columbia
Vancouver, Canada

JOHN BRADLEY

National Research Council of Canada
Ottawa, Canada

Acoustical problems experienced by room users include difficult verbal communication in classrooms and conference rooms, impaired student learning and teacher voice problems in classrooms, hearing loss in industrial workshops, and inadequate speech privacy in open-plan offices. Room sound fields comprise both "signals" (useful sounds, such as speech) and detrimental "noise". To modify room sound fields and improve acoustical conditions, the acoustician must understand the relationship between the room user and activity, the sound sources, the room and its contents, and the characteristics of room sound fields. Models for predicting room sound fields are of primary importance. They allow the acoustical conditions to be optimized during design and permit sound control measures to be evaluated for cost effectiveness in new or existing rooms. In this chapter, we take an energy-based approach, ignoring phase, interference, and modal effects discussed in Chapter 6. This is justified, except perhaps at low frequencies, since we are interested in rooms which are large compared with the sound wavelength, which are of complex shape and may not be empty. Further, we are interested in wide-band (total A-weighted, octave- or third-octave band) results. In this chapter, the sound field is quantified by the time-averaged, mean-square sound pressure p^2 in $(\mathrm{N/m^2})^2$ or the associated sound pressure level L_p in decibels ($L_p = 10\ \log_{10}[p^2/p_0^2]$, $p_0 = 2 \times 10^{-5}$ N/m^2). In the case of multiple sources or sound reflections, the total energy is the sum of the individual energy contributions: $p_{\text{tot}}^2 = \sum p_i^2$, $L_{p,\text{tot}} = 10\ \log_{10}\left(\sum 10^{L_{pi}/10}\right)$.

Sound sources radiate energy over some frequency range and, at each frequency, with a certain intensity. The rate of emission of energy is described by the sound power W in watts or the associated sound power level L_w in decibels ($L_w = 10\ \log_{10}(W/W_0)$, $W_0 = 10^{-12}$ W), usually measured in octave- or third-octave frequency bands. As discussed in Section 7.8, the presence of surfaces near a source effectively increases its sound power output. Depending on its physical characteristics and frequency, a source may radiate uniformly in all directions (omnidirectional source) or more or less in certain directions (directional source). Source directivity is quantified by the directivity factor Q, which is the ratio of the mean-square sound pressure radiated in the receiver direction to the average of that radiated in all directions (see also Chapter 4). Small sources with three similar major dimensions can often be modeled as compact sources. Most real sources (large machines, conveyors, building walls) are more complex than a compact source, being extended in space in one or more dimensions. Readers wishing to do further reading on more fundamental aspects of room acoustics should consult reference 1. Throughout this chapter, references are provided for the benefit of readers who wish to do more in-depth reading on the topic under discussion.

7.1 ROOM SOUND FIELDS AND CONTROLLING FACTORS

Propagation of Sound

Sound waves propagate away from a source, being reflected (or scattered) by room boundaries, barriers, and furnishings. The resulting sound field at the receiver is composed of two parts. Sound which propagates directly from the source to the receiver is the direct sound. Its amplitude decreases with increasing distance from the source, as in a free field (discussed in Chapters 1 and 2). Sound which reaches the receiver after reflection from room surfaces or furnishings is the reverberant sound. Its amplitude decreases with increasing source distance at a rate which depends on the source geometry and on the acoustical properties of the room and its contents, as will be discussed below. To examine sound propagation in rooms, independent of the source sound power, to which it is directly related, we define the sound propagation function $\mathrm{SPF}(r) = L_p(r) - L_w$ in decibels as the variable characterizing the effect of the room alone on the sound field. Sound pressure levels may then be obtained using $L_p(r) = \mathrm{SPF}(r) + L_w$. Thus, from Eqs. (1.27)–(1.31), for a compact source with $Q = 1$ in a free field, $\mathrm{SPF}(r) = -20 \log_{10} r - 11$ dB. In the case of multiple sources, the individual source contributions are obtained from the source sound power levels and the room sound propagation function values at the relevant source/receiver distances. The total sound pressure level at the receiver position is obtained by summing the individual levels on a power (p^2) basis.

Sound Decay

Shortly after a steady-state sound source begins to radiate, an equilibrium (or steady state) is established between the rate of energy absorption in the room and the rate of energy emission by the source. If the source then ceases to radiate, the energy in the room decreases with time at a rate determined by the rate of energy absorption. This is the room sound decay. It is usually characterized by

the reverberation time T_{60}, which is the time in seconds required for the sound pressure level to decrease by 60 dB. Calculations of T_{60} are based on the average rate of decay over some part of the decay curve—usually the −5- to −35-dB part. Also of interest, since it quantifies perceived reverberance, is the early-decay time (EDT), based on the average rate of decay over the first 10 dB.

Air Absorption

Energy is absorbed continuously as sound propagates in air. This process follows an exponential law, $E(r) = E_0 e^{-2mr}$, where the constant $2m$ in the exponent is called the energy air absorption exponent, expressed in nepers per meter (1 Np = 8.69 dB), with $e = 2.7173$. Air absorption depends on air temperature, relative humidity, ambient pressure, and sound frequency. Table 7.1 presents some typical values calculated using reference 2.

Surface Absorption and Reflection

The ability of a surface to absorb incident sound energy is characterized by the energy absorption coefficient α. This is the fraction of the energy striking the surface that is not reflected, as discussed in more detail in Chapters 8 and 11. It is usually measured in octave- or third-octave bands. If E_i is the energy incident on a surface with absorption coefficient α, the reflected energy is $E_r = E_i(1 - \alpha)$. Ignoring transmission, acoustical energy not absorbed by a surface that it strikes is reflected. If the surface is flat, hard, and homogeneous, reflection is specular; that is, the angle of reflection is equal to the incident angle. In practice, because of finite absorber size, surface roughness, as well as physical or impedance discontinuities, the energy is scattered or diffused (reflected into a range of angles). Such diffuse reflections usually result in a more rapid decay of sound and lower reverberation times in the room.

TABLE 7.1 Energy Air Absorption Exponents ($2m$ in Terms of 10^{-3} Np/m) Predicted Using Reference 2 Assuming Ambient Pressure of 101.3 kPa

Temperature, °C	Relative Humidity, %	Air Absorption Exponents at Selected Frequencies						
		125 Hz	250 Hz	500 Hz	1000 Hz	2000 Hz	4000 Hz	8000 Hz
10	25	0.1	0.2	0.6	1.7	5.8	18.7	43.0
	50	0.1	0.2	0.5	1.0	2.8	9.8	33.6
	75	0.1	0.2	0.5	0.9	2.0	6.5	23.6
20	25	0.1	0.3	0.6	1.2	3.5	12.4	41.6
	50	0.1	0.3	0.7	1.2	2.3	6.5	22.4
	75	0.1	0.2	0.6	1.3	2.2	5.0	15.8
30	25	0.1	0.4	0.9	1.5	3.0	8.3	28.8
	50	0.1	0.2	0.8	1.7	3.0	5.8	16.4
	75	0.0	0.2	0.6	1.7	3.3	5.8	13.4

Furnishings

Many rooms are not empty, containing furnishings (the various obstacles, such as desks in a classroom or machines in a workshop, also called fittings). Often furnishings occupy the lower region of a room and there are fewer objects at higher elevations. Of course, the density and horizontal distribution of room furnishings may vary considerably. Acoustical energy propagating in furnished regions is scattered as well as partially absorbed, significantly modifying the sound field. In particular, it increases the rate of sound decay, reducing reverberation times. It also causes a redistribution of steady-state sound energy toward sources, due to back scattering, resulting in higher sound pressure levels near sources and a higher rate of decrease of levels with distance from sources.

7.2 DIFFUSE-FIELD THEORY

By far the best known theoretical models for predicting room sound fields are based on diffuse-field theory. Diffuse-field theory is widely applied because of its simplicity. Often forgotten is the fact that it may be of limited applicability because of its restrictive assumption of a diffuse field. The sound field in a room is diffuse if it has the following attributes:

1. At any position in the room, energy is incident from all directions with equal intensities (and random phase, though we are ignoring phase in this chapter).
2. The reverberant sound does not vary with receiver position.

These conditions are approximated only in specially designed acoustical test rooms called reverberation chambers, discussed in Section 7.8.

Average Diffuse-Field Surface Absorption Coefficient

Diffuse-field theory uses the average rate of random-incidence surface sound absorption averaged over all of the room surfaces. Thus, we define the average diffuse-field surface absorption coefficient as

$$\overline{\alpha}_d = \frac{\sum S_i \overline{\alpha}_{di}}{\sum S_i} \qquad (7.1)$$

where S_i and α_d are the surface area and diffuse-field absorption coefficient of the ith surface. If α_d is to be useful, it is necessary that no part of the room be strongly absorbing, since in this case a diffuse sound field cannot exist. Absorbing objects such as seats, tables, and people must be included when calculating α_d, despite the fact that such objects have ill-defined surface areas. In such cases it is common practice to assign an absorption A_i in square meters to each object, where $A_i = \alpha_d S_i$, with S_i the surface area. The absorptions of all objects are

summed, and the total absorption is included in the calculation of α_d, with no modification made to the total area. In other words, the total area $\sum S_i$ in Eq. (7.1) is taken to be that of the room boundaries, excluding objects and people. In the case of closely spaced absorbers, such as auditorium seats or suspended ceiling baffles, caution is necessary, since the total absorption may depend on the total area covered and may not be the sum of the absorptions of the individual objects. Also, the absorption coefficients of small patches of absorbing material (e.g., as measured in a reverberation room) are higher than those of a large area of the material (e.g., covering all of a room surface), due to the effects of diffraction at the material's edges. In the former case, the absorption coefficients of highly absorptive materials can exceed 1.0 (see also Section 7.7).

Sabine and Eyring Approaches

Several diffuse-field approaches exist; two are considered here. Both are expressed by the following equations, where Eq. (7.3) is applicable only for a compact source:

$$T_{60} = \frac{55.3V}{cA} \quad \text{(sound decay)} \qquad (7.2)$$

$$L_p(r) = L_w + 10\log_{10}\left(\frac{Q}{4\pi r^2} + \frac{4}{R}\right) \quad \text{(steady-state conditions)} \qquad (7.3)$$

where T_{60} = reverberation time, s
L_w = source sound power level, dB re 10^{-12} W
L_p = sound pressure level, dB re 2×10^{-5} N/m^2
c = speed of sound in air, $\approx$344 m/s at standard temperature and pressure (STP), m/s
R = room constant, $= A/(1-\alpha_d)$, m^2
A = total room absorption, $= -S\ln(1-\alpha_d) + 4mV$ (Eyring) $\approx \alpha_d S + 4mV$ (Sabine), m^2
r = source/receiver distance, m
Q = directivity factor
$2m$ = energy air absorption coefficient, Np/m
V = room volume, m^3
α_d = average diffuse-field surface absorption coefficient
S = total room (surface and barrier) surface area, m^2

The Eyring approach is applicable to rooms with arbitrary average surface sound absorption coefficient. It should be used, for example, to determine absorption coefficients of room surfaces from measured reverberation times. If, however, the average surface absorption coefficient is sufficiently low (say, $\alpha_d < 0.30$), it is accurate to use the Sabine approach; that is, Eqs. (7.2) and (7.3) with $-\ln(1-\alpha_d)$ replaced by α_d. Thus, the Sabine approach can be used when determining the sound absorption coefficients of materials in reverberation rooms. Of course, the approach applied in a particular sound field prediction must be consistent with that used to obtain the sound absorption coefficient data used in the prediction. Refer to reference 1 for further discussion of the relative merits of the Sabine, Eyring, and other diffuse-field theories.

Diffuse-field theory predicts the following characteristics of the sound field:

1. *Sound Decay/Reverberation Time.* After a sound source ceases to radiate, the mean-square pressure at the receiver decays exponentially with time. The corresponding sound pressure level decreases linearly with time. To a first approximation, the reverberation time is directly proportional to V/S and inversely proportional to α_d.
2. *Steady State.* The total field is the sum of direct and reverberant components described, respectively, by the first and second terms in parentheses of Eq. (7.3). The direct field, which dominates near the source, is independent of the room's properties. Its sound pressure level decreases at 6 dB/dd (dd = distance doubling). The reverberant field, which dominates far from the source, does not vary with source/receiver distance. Its sound pressure level is, to a first approximation (when both α_d and m are small), inversely proportional to α_d and S. The sound propagation function is as shown in Fig. 7.1.

Note that diffuse-field theory accounts for only some of the relevant room acoustical parameters and for some of these in an approximate manner. In particular, room geometry and source directivity are modeled only approximately. Neither the distribution of the surface absorption nor the presence of barriers or furnishings is modeled. This and the related fact that the theory is based on restrictive hypotheses seriously limit its applicability. To give one concrete example, the constant

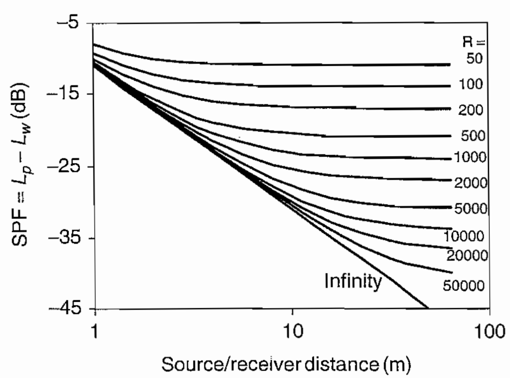

FIGURE 7.1 Sound propagation function curves predicted by diffuse-field theory for various values of the room constant R in m^2.

sound pressure level at sufficiently large distances from sources that is predicted by diffuse-field theory is only (approximately) found in practice in small rooms with low surface absorption (e.g., reverberation rooms, discussed in Section 7.8). Noise levels due to a single source in most rooms—especially large or absorptive ones—decrease monotonically with distance from the source (see, e.g., Fig. 7.4*b* below). Reference 3 discusses the applicability of diffuse-field theory more fully.

Diffuse-field theory, when applicable, can be used to estimate the reductions of reverberation time and noise level that occur when absorptive material is added to a room. Let A_b and A_a be the total room absorptions before and after treatment; $A_a = A_b + \Delta A$, where ΔA is the increase in room absorption. If A_b and ΔA are known, values of A_b and A_a can be used directly in Eqs. (7.2) and (7.3). Alternatively, if $T_{60,b}$ before treatment is known, $T_{60,a}$ after treatment can be determined from Eq. (7.2) as follows: since $T_{60,b} = 55.3V/(cA_b)$, then $A_b = 55.3V/(cT_{60,b})$. Now, $T_{60,a} = 55.3V/(cA_a) = 55.3V/[c(A_b + \Delta A)]$, and thus

$$T_{60,a} = \frac{55.3V}{c\left\{[55.3V/(cT_{60,b})] + \Delta A\right\}} \tag{7.4}$$

The steady-state sound pressure level $L_{p,a}$ after treatment can be calculated from that before treatment, $L_{p,b}$, as follows:

$$L_{p,a}(r) = L_{p,b}(r) + 10 \log_{10}\left[\frac{Q/(4\pi r^2) + 4/R_a}{Q/(4\pi r^2) + 4/R_b}\right] \tag{7.5}$$

At positions near sources, where the direct field dominates, the reduction in sound pressure level is small. At large distances from all sources, where the reverberant field dominates, the reduction approaches that of the reverberant sound pressure level alone. This, to a first approximation (when both α_d and m are small), is given by $10 \log_{10}(A_a/A_b)$. Doubling the room absorption reduces the sound pressure level of the reverberant field by 3 dB. Similarly, using Eq. (7.2), the reverberation time after treatment is $T_{60,a} = T_{60,b}(A_b/A_a)$. Doubling the sound absorption halves the reverberation time.

As an example, consider a room with dimensions 10 m × 5 m × 2.4 m (volume $V = 120$ m^3, surface area $S = 172$ m^2) and all concrete surfaces with $\alpha_b = 0.05$. Thus, ignoring air absorption and using the Sabine approach, we have $A_b = \alpha_b S = 0.05 \times 172 = 8.6$ m^2 and $T_{60,b} = 55.3V/(cA_b) = 55.3 \times 120/(344 \times 8.6) = 2.2$ s. A suspended acoustical ceiling with $\alpha_c = 0.9$ and surface area of 50 m^2 is installed to improve the acoustical environment. After treatment, $A_a = 8.6 + (0.9 - 0.05) \times 50 = 51.1$ m^2, so $T_{60,a} = 2.2 \times 8.6/51.1 = 0.4$ s.

7.3 OTHER PREDICTION APPROACHES

When diffuse-field theory cannot be applied, alternative approaches can be used to predict the steady-state sound pressure level, sound decay, and reverberation times in a room. These models apply only to compact sources. Extended sources must be approximated by an array of compact sources and the prediction model applied to each source. Two main approaches are available to accomplish this objective: computer algorithms (the method of image sources, ray or beam tracing, radiosity, hybrid models, etc.) and empirical models. The different approaches make assumptions which define and limit their applicabilities and accuracies. Furthermore, they take the various room acoustical parameters into account to a greater or lesser extent. To take advantage of the strengths of the different approaches and avoid their weaknesses, hybrid models combining several approaches into one model have been developed. Empirical prediction models are usually limited in application to specific building types.

Method of Image Sources

The method of image sources is based on the assumption that reflections from surfaces, assumed specular, can be replaced by the direct sound contributions of image sources. Figure 7.2 shows the simple example of a partial two-dimensional array of image rooms and sources. The simplest implementation of the method of image sources applies to empty, rectangular–parallelepiped rooms with no barriers.[4] In this case, the image sources corresponding to the infinite number of reflections are located on a three-dimensional grid. The total mean-square pressure is the sum of the contributions of all of the image sources, allowing for spherical divergence and energy losses due to absorption by the air and at each surface encountered by the ray from the image source. For decaying sound, the sound pressure at time t after the cessation of sound generation is calculated by summing over all image sources located at distances greater than ct from the receiver, where c is the speed of sound. The method of image sources can be extended to empty rooms of arbitrary shape bounded by planes; however, calculation times are greatly increased and become impracticable. The method of image sources can also account for the presence of furnishings, under the assumption that they are isotropically distributed in random fashion throughout

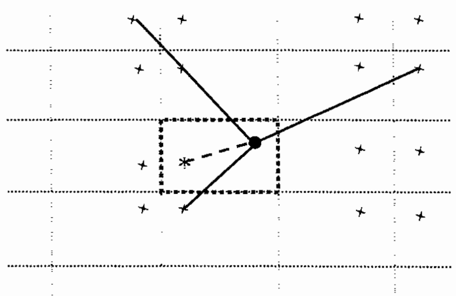

FIGURE 7.2 Image space of an empty two-dimensional room, showing the source (✱) and receiver (●), the image sources (⋆), the image surface planes (·········), the direct sound (- - - -), and the propagation paths of sound from three of the image sources (——).

the room.[5] In this case, the furnishings, as well as the sources, are mirrored in the room surfaces. The steady-state and decaying sound fields are formed as before. However, the contribution of each image source is modified due to scattering and absorption by the furnishings; absorption at surfaces is also increased due to scattering.

Ray and Beam Tracing

Ray-tracing techniques[6] can be used to predict sound fields in rooms of arbitrary shape with arbitrary surface absorption distributions, different surface reflection properties, and variable furnishing density. Source directivity can also be modeled. A computer program simulates the emission of a large number of rays (or beams) from each source in either random or deterministic fashion. Each ray is followed as it propagates in the room, being reflected and scattered by surfaces, barriers, and furnishings until it reaches a receiver position. The energy of a ray is attenuated according to spherical divergence as well as surface, furnishing, and air absorption. In principle, any surface reflection law (specular, diffuse, etc.) can be modeled. Ondet and Barbry[7] proposed an algorithm for accounting for quasi-arbitrary furnishing distributions in a ray-tracing model. Figure 7.3, taken from reference 8, illustrates the potential of ray-tracing techniques. It shows the contour map of the predicted reductions of total A-weighted noise levels over the floor of a furnished workshop containing eight machinery sources, which result from the introduction of an acoustical barrier around a noise-sensitive assembly bench and a partial ceiling absorption treatment suspended over the region of the sources. Of course, the program must be run for each frequency band (i.e.,

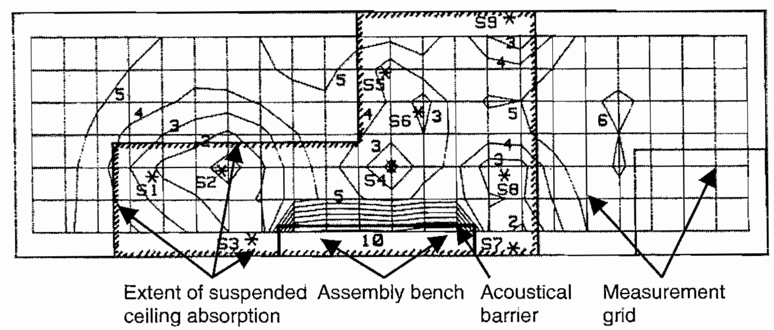

FIGURE 7.3 Floor layout of a furnished workshop (dimensions 46.0 × 15.0 × 7.2 m) showing a contour map of the predicted reductions of total A-weighted noise levels which result from the introduction of an acoustical barrier around a noise-sensitive assembly bench and of an absorptive treatment suspended below the ceiling over the region of the eight machinery sources (the shaded, L-shaped, enclosed area). The map was produced from noise levels predicted before and after treatment at positions on an imaginary 2 × 2-m grid, 1.5 m above the floor, as shown. Also shown are the noise sources (e.g., S4*) and the contour lines and their values (e.g., 5).

octave- or third-octave bands) to account for the frequency-dependent nature of the sound absorption coefficient of the room surfaces and that of the barrier insertion loss. This kind of detailed analysis is not possible using diffuse-field theory. It would only be possible to estimate noise reductions from the increase in absorption. These reductions could then be corrected as a function of the proximity of the receiver to the acoustical treatment and of the estimated insertion loss of the barrier.

Empirical Models

Empirical models are developed from experimental data. They usually focus on a particular category of room—models for offices, classrooms, and industrial workshops are discussed below. Measurements are made, in a number of rooms of some category, of the acoustical quantities to be predicted. Empirical algorithms or equations which predict the experimental results from appropriate predictor parameters describing the rooms are developed. This can, for example, involve multivariable regression modeling, whereby statistical modeling software is used to find the minimum set of mutually statistically independent predictors, each of which is highly correlated with the data to be predicted, that most accurately predicts the measured data. For further information on multivariable regression modeling, consult reference 9.

Auralization

Auralization is the process of rendering audible sounds "played" in a virtual room for which the acoustical response has been predicted. It allows subjective evaluation of the room. If done accurately, auralization allows full three-dimensional sound perception, with source externalization (i.e., the sound is perceived to be outside the head), spatial localization, and spatiousness. Auralization involves predicting the combined response of a virtual room and a virtual listener in it. The listener response is quantified by head-related transfer functions (HRTFs) quantifying how the acoustical response of the human external auditory system varies with frequency and angle. The room response is predicted using models, such as ray tracing, which predict the individual sound path contributions arriving at the receiver; since impulse responses involving phase effects are required, the room's phase response must also be considered. The result is the binaural impulse response (comprising the impulse responses at the left and right eardrums) of the room–listener combination. This is convolved with a sound signal for replay to a real listener. Readers interested in further details of this technique should consult reference 10.

7.4 DOMESTIC ROOMS AND CLOSED OFFICES

Schultz[11] investigated the prediction of sound pressure levels in domestic rooms and closed offices. He measured the variation of sound pressure level with distance from a source in a variety of small rooms, observing that levels never

become constant at larger distances as predicted by diffuse-field theory. In fact, he found that the curves always had a slope of about −3 dB/dd, though the absolute levels of the curves varied considerably. He further found that existing models developed for predicting sound propagation in, for example, workshops and corridors could not predict his experimental results. Schultz therefore proposed the following empirical formula:

$$L_p(r) = L_w - 10\log_{10} r - 5\log_{10} V - 3\log_{10} f + 12 \text{ dB} \qquad (7.6)$$

where r is the source–receiver distance in meters, V is the room volume in cubic meters, and f is the frequency in hertz. Note that this formula does not explicitly contain a room absorption term. Such behavior contrasts markedly with that predicted by diffuse-field theories and is an excellent example of their limitations.

7.5 CLASSROOMS

Relevance and Characteristics

Classrooms are acoustically critical spaces in which verbal communication is crucial for teaching and learning. Acoustically, conference rooms, gymnasiums, and other rooms for speech have much in common with classrooms. Many classrooms are built with little or no attention paid to the acoustical design. Studies have shown that nonoptimal acoustical conditions in classrooms result in impaired verbal communication between teachers and students, impaired student language development and learning, and teacher voice and other problems.[12,13] The problems are particularly acute for "acoustically challenged" listeners, including young and hearing-impaired people and those using a second language.

Classrooms vary from small seminar rooms for a few occupants to school classrooms for several tens of children to larger university lecture rooms and auditoria accommodating hundreds of listeners. Smaller classrooms are usually of rectangular shape. Larger lecture rooms can have, for example, fan plan shape, inclined seating, and nonflat ceiling profiles. In smaller classrooms, talkers and listeners can be anywhere in the classroom, and source–receiver distances can vary from less than a meter to several meters. In lecture rooms, the talker is usually at one end of the room, with the listeners spread out in front; source–receiver distances can vary from several meters to several tens of meters. For hygiene reasons, classrooms may have hard, nonabsorptive surfaces, though carpets and wall and ceiling absorption are not uncommon. Lecture and conference rooms can have nonabsorptive or padded, sound-absorptive seating. Of course, the occupants themselves contribute significant absorption to the classroom. This and the fact that classroom occupancy can vary considerably must be considered in the acoustical design. A detailed discussion of the physical and acoustical characteristics of (university) classrooms is found in reference 14. Of particular interest is the rate at which speech and noise levels decrease with distance from their sources, which is small in small, nonabsorptive classrooms. It increases with classroom size and absorption and can be large in large, absorptive (e.g., occupied) classrooms. One consequence of this is that speech levels in large classrooms may decrease by 10 or more decibels from the front to the back of the seating area.

Speech Intelligibility

In classrooms, as in other rooms for speech, quality and ease of verbal communication are prime concerns (see also Section 7.7). The quality can be quantified in human terms by speech intelligibility, the percentage of words correctly identified by the listener. Here, in general, we consider the effect of the room on the accurate transmission of speech signals from a talker to a listener and not, for example, the effects of individual talker and listener characteristics. Verbal communication is considered to be affected by two main factors—the classroom reverberation and the speech-signal-to-background-noise-level difference (often called the signal-to-noise ratio). The effect of reverberation can be quantified by the early-to-late energy ratio C_{50} (which is highly correlated with early decay time and reverberation time in many cases). This frequency-dependent ratio is usually measured in octave bands. The signal-to-noise level difference depends on the levels of speech and the levels of noise at the listener position. Total A-weighted or octave- or third-octave-band equivalent continuous levels are often considered. If the voice levels remain constant, the speech intelligibility decreases with increased reverberation and increases with increased signal-to-noise level difference. A number of physical metrics exist which combine these two quantities into a single speech intelligibility measure; these include the useful-to-detrimental energy ratio U_{50}, articulation index AI (discussed in Section 7.7), speech transmission index STI, and speech intelligibility index SII.

Numerous studies have found that many classrooms have nonoptimal acoustical conditions, with excessive noise levels and reverberation. A review of published data and of the many complex issues associated with speech intelligibility in classrooms is contained in reference 15. The classroom speech sources are the teachers' and the students' voices. Classroom noise sources include mechanical services (e.g., ventilation outlets), classroom equipment (projectors, computers), and the teachers' or students' voices when another person is generating the signal to be heard. Noise breaking into the classroom from outside can be significant when the classroom is located near transportation (such as highways and airports) or in cases when children are active in nearby corridors or play areas. Finally, classroom activity itself generates significant noise, including impact noise from furniture, toys, and so on. Data on the typical sound pressure levels generated by human talkers and classroom noise sources are available.[16] It is likely that a number of complex factors, including room acoustics, affect what these levels are at listener positions in a given classroom at a given time.

It is generally considered that, for excellent speech intelligibility, background noise levels should not exceed about 40 dBA for acoustically unchallenged listeners and 30 dBA for acoustically challenged listeners. The question of what is the optimal reverberation for speech intelligibility is a complex one. One body of opinion considers that reverberation should always be minimized. However, this is based on the results of speech intelligibility tests that were done under conditions that did not account for the acoustical behavior of classrooms. Investigations involving the useful-to-detrimental energy ratio speech intelligibility metric and realistic room acoustical modeling show that some reverberation can be beneficial (since it increases reverberant speech levels). The results indicate that the reverberation should be optimized as a function of the classroom volume and background noise. Optimal reverberation times vary from low values in small, quiet classrooms to over 1 s in large, noisy ones. For a full discussion of this issue, refer to reference 17. In any case, reverberation should be minimized in classrooms with high signal-to-noise level differences (e.g., resulting from voice amplification). Moreover, it is likely that less reverberation can be tolerated by acoustically challenged listeners. It has been shown that speech intelligibility is not very sensitive to variations in reverberation, and it has been suggested that a classroom reverberation time of about 0.5 s is usually appropriate.[18]

Standards and guidelines exist to help design professionals achieve high acoustical quality in classrooms and other educational spaces. They specify the acoustical conditions to be achieved in new and renovated rooms. They discuss reverberation times and background noise levels to be achieved in the unoccupied room. They also provide advice on how to achieve the design targets. Two recent examples of such standards are ANSI S12.60—2002 in the United States[19] and Building Bulletin 93 in the United Kingdom.[20]

Predicting Classroom Acoustics

Predicting acoustical quality in a classroom involves predicting room reverberation and steady-state sound pressure levels generated by the speech and noise sources, including student activity. Prediction should take into account the absorption contributed by the room occupants and furnishings (e.g., absorptive seating). This involves an appropriate prediction model and accurate input data. In the case of small, untreated classrooms, it is likely that diffuse-field theory is reasonably accurate. For treated and larger classrooms, comprehensive techniques such as ray tracing can be used. Empirical models are also available and inherently incorporate realistic data. Based on measurements of reverberation times and steady-state levels generated by a speech source in a wide variety of typical university classrooms and on published information, empirical models for predicting octave-band reverberation times and total A-weighted speech levels have been developed.[21] Approximate values of $T_{60,u}$ in the unoccupied classroom can be determined using Eq. (7.2), with the average surface absorption coefficient calculated as the sum of contributions (presented in Table 7.2) to the room average value, which are associated with the sound-absorbing features present in the classroom. An alternative empirical formula for predicting the 1-kHz octave-band $T_{60,u}$ is

$$T_{60,u} = 0.874 + 0.0021(LW) + 0.303\text{refl} + 0.412\text{basic} - 0.384\text{absorb} - 0.804\text{upseat} \qquad (7.7)$$

TABLE 7.2 Typical Octave-Band Contributions of Classroom Sound-Absorptive Features to Room-Average Surface Absorption Coefficient

Surface Feature	125 Hz	250 Hz	500 Hz	1000 Hz	2000 Hz	4000 Hz	8000 Hz
Basic	0.12	0.10	0.10	0.09	0.10	0.09	0.10
Carpeted floor	0.00	0.00	0.02	0.04	0.07	0.09	0.17
Wall/ceiling absorption	0.01	0.04	0.08	0.10	0.10	0.10	0.10
Upholstered seats	0.20	0.20	0.16	0.12	0.09	0.07	0.05

TABLE 7.3 Octave-Band Values of Average Absorption per Person

Band, Hz	125	250	500	1000	2000	4000	8000
A_p, m^2	0.25	0.45	0.67	0.81	0.82	0.83	1.14

where the parameters are defined following Eq. (7.10). The absorption of the classroom occupants can be included using the data in Table 7.3, and the number of occupants can be used to estimate the associated increase in classroom absorption. For an average talker speaking between a normal and a raised voice (total A-weighted sound power level $\approx$74 dBA), total A-weighted speech levels in the unoccupied classroom can be predicted from

$$\mathrm{SLA}_u(r) = I_u + s_u \frac{\log_{10}(r)}{\log_{10}(2)} \tag{7.8}$$

with

$$I_u = 65.8 - 0.0105(LW) + 1.52\mathrm{fwdist} - 1.41\mathrm{absorb} - 4.32\mathrm{upseat} \tag{7.9}$$

and

$$s_u = -1.21 - 0.088\ L + 1.14\mathrm{basic} \tag{7.10}$$

where $T_{60,u}$ = 1-kHz octave-band reverberation time, s
SLA_u = total A-weighted speech level, dBA
I_u = intercept of total A-weighted sound propagation curve, dBA
s_u = slope of total A-weighted sound propagation curve, dBA/dd
r = source–receiver distance, m
L = average classroom length, m
W = average classroom width, m
fwdist = distance from source to nearest wall, m
refl = 1 if classroom contains beneficial reflectors, = 0 if not

absorb = factor quantifying extent of sound-absorptive wall or ceiling treatment
absorb = 1 corresponds to full-coverage wall or ceiling treatment; in other cases, values should be scaled proportionately
upseat = 0 for nonabsorptive seating; = 1 for padded, sound-absorptive seating
basic = 1 if all classroom surfaces and seats are not sound absorptive; = 0 otherwise

As an example, consider a large classroom with average dimensions of $L = 20$ m long, $W = 10$ m wide, and 6 m high (volume $V = 1200$ m^3, surface area $S = 760$ m^2). The distance from the typical lecturing position to the nearest (front) wall is fwdist = 2.5 m. The classroom has a profiled ceiling directing sound to the back (i.e., beneficial reflectors, refl = 1). Consider the cases where N_p is 50 or 200 occupants. Before treatment, the classroom has no sound-absorptive surfaces (absorb = 0, basic = 1) and nonabsorptive seating (upseat = 0). Thus, the average surface absorption coefficient is that corresponding to the "basic" configuration in Table 7.2 ($\alpha = 0.09$). Equation (7.2) gives the corresponding $T_{60,u}$'s. Assuming air absorption exponents for a temperature of 20°C and a relative humidity of 50% ($m = 0.0012$ Np/m; see Table 7.1) and using the Eyring approach, the total absorption in the unoccupied room at 1 kHz is $A_u = -S\ \ln(1-\alpha) + 4mV = -760\ \ln(1 - 0.09) + 4 \times 0.0012 \times 1200 = 77.4$ m^2. From Eq. (7.2) the 1-kHz $T_{60,u} = 55.3V/(cA_u) = 55.3 \times 1200/(344 \times 77.4) = 2.49$ s. With 50 occupants, the total room absorption $A_o = A_u + N_pA_p = 77.4 + 50 \times 0.81 = 117.9$ m^2, and $T_{60,o} = 55.3V/(cA_o) = 55.3 \times 1200/(344 \times 117.9) = 1.64$ s. Similarly, with 200 occupants $T_{60,o} = 0.81$ s. Here, T_{60} is excessive with low occupancy and decreases sharply with the number of occupants. To control the reverberation, the classroom is treated with full-coverage wall absorption (absorb = 1) and padded, sound-absorptive seating (upseat = 1); thus, basic = 0. The average surface absorption coefficients are now the sum of the values for basic, wall/ceiling absorption, and upholstered seats given in Table 7.2 (e.g., $0.09 + 0.10 + 0.12 = 0.31$ at 1 kHz). The 1-kHz T_{60}'s in the classroom when unoccupied and with 50 or 200 occupants are 0.67, 0.63, and 0.52 s. The treatment significantly reduces T_{60}—in the unoccupied classroom by as much as 200 occupants do—and decreases the variation of T_{60} with the number of occupants.

As for speech levels, consider listeners seated at the front and back of the classroom at distances of 3 and 12 m from the talker. Before treatment, from Eq. (7.9), $I_{u,b} = 65.8 - 0.0105LW + 1.52\mathrm{fwdist} - 1.41\mathrm{absorb} - 4.32\mathrm{upseat} = 65.8 - 0.0105 \times 20 \times 10 + 1.52 \times 2.5 - 1.41 \times 0 - 4.32 \times 0 = 67.5$ dBA and, from Eq. (7.10), $s_{u,b} = -1.21 - 0.088L + 1.14\mathrm{basic} = -1.21 - 0.088 \times 20 + 1.14 \times 1 = -1.83$ dBA/dd. Using Eq. (7.8), the speech level at any position is $\mathrm{SLA}_{u,b}(r) = 67.5 - 1.83\ \log_{10}(r)/\log_{10}(2)$; thus, at 3 and 12 m speech levels are 64.6 and 61.0 dBA. Levels in the occupied classroom can be calculated using Eq. (7.5). Assuming $Q = 2$ to the front of a talker, at the front and back of the classroom speech levels are 63.1 and 59.2 dB with 50 occupants and 60.9 and 56.2 dBA with 200 occupants. After treatment, $I_{u,a} = 65.8 - 0.0105 \times 20 \times 10 + 1.52 \times 2.5 - 1.41 \times 0 - 4.32 \times 1 = 63.2$ dBA and $s_{u,a} = -1.21 - 0.088 \times 20 + 1.14 \times 0 = -3.0$ dBA/dd, giving speech levels of 57.1 and 51.1 dBA unoccupied at the front and back seats; occupants decrease levels by no more than 1 dB. Acoustical treatment causes speech levels at the front and back of the unoccupied classroom to decrease by 7.5 and 9.9 dBA for 50 occupants and with 200 occupants by 4.5 and 6.1 dB. These results must be interpreted with care, as they do not account for certain relevant nonacoustical factors. For example, they assume that the talker's vocal output is invariant, as would be the case for a loudspeaker. In fact, research suggests that a talker's vocal output varies with the prevailing classroom acoustical conditions; a preliminary empirical model for predicting this phenomenon is presented in reference 16.

Noise levels generated by classroom noise sources (e.g., projectors or ventilation outlets) can be estimated from their output power levels and receiver distances using the above empirical model after adjusting for the difference between the actual and the assumed output power levels. Student activity noise should also be considered; a preliminary empirical model for predicting this is presented in reference 16. Then signal-to-noise level differences can be determined. Classroom early-decay times and signal-to-noise level differences can then be used to determine values of speech intelligibility metrics.

Controlling Classroom Sound

Controlling and optimizing the acoustical conditions in a classroom or other rooms for speech involve three fundamental considerations:

1. *Promoting High Speech Levels.* Avoid excessive classroom cubic volume due, for example, to high and vaulted ceilings. Use room geometries which direct sound to the back of the room. In large lecture rooms, this can include angled reflectors around teaching areas and profiled ceilings. Keep at least the central part of the ceiling sound reflective to promote the reflection of speech sounds to the back of the classroom. Use approximately square floor plans to avoid long and wide rooms. Amplification by a speech reinforcement system or a sound field enhancement system may be an option; their design is beyond the scope of this chapter; see reference 22. One important issue to consider at the classroom design stage is that the optimal acoustical conditions for unaided speech may not be the same as with a speech reinforcement system.

2. *Controlling Background Noise.* Avoid open-plan design. Control the noise and vibration of mechanical services (see Chapter 16). Locating ventilation outlets toward the front of lecture rooms where speech levels are highest helps optimize signal-to-noise level differences throughout the room. Avoid high terminal velocities of supply air terminal devices and place air-volume control devices at distances of 0.5 m or more upstream to minimize noise generated by turbulent flow. Choose quiet equipment for use in the classroom. Impact noise due to student activity can be reduced by the use of carpets and cushioning materials (split tennis balls on desk, table, and chair legs are widely used). The partitions bounding the classroom must provide adequate sound isolation (see Chapter 10); in critical cases, this might require the use of nonopenable windows.

3. *Optimizing Reverberation.* Apply appropriate sound-absorptive materials to the room surfaces. Avoid applying sound absorption to the central part of the ceiling, which provides useful reflections between talkers and listeners. Using sound-absorptive seating allows the ceiling to be left reflective and reduces the sensitivity of the classroom's acoustical conditions to the number of occupants.

7.6 INDUSTRIAL WORKSHOPS

Relevance and Characteristics

Industrial workshops often have serious acoustical problems due to excessive noise and reverberation. Most jurisdictions have regulations aimed at limiting the risk of hearing damage by limiting the noise exposure of industrial workers. Excessive reverberation can also lead to poor verbal communication and a reduced ability to identify warning signals, and thus danger, as well as to stress and fatigue.

Industrial buildings come in every shape and size. However, many are rectangular in floorplan (with widely varying dimension ratios and floorplan sizes), with flat or nonflat (e.g., pitched or sawtooth) roofs. The floors of most workshops are made of concrete. The walls are often of brick or blockwork, sometimes of metal cladding. Workshop roofs are usually of suspended-panel construction, consisting of metal or other panels supported by metal trusswork or portal frames. A common modern construction is the steel deck, consisting of, for example, profiled metal as the internal surface, a vapor barrier, several centimeters of thermal insulation, tar paper, and gravel ballast as the external surface, again supported by metal trusswork. Acoustical steel decks exist; the inner metal layer is perforated, and its profiles are filled with sound-absorptive material, providing high sound absorption over a broad range of frequencies. Acoustical decks can support loads almost as great as normal decks, cost only about 10% more, and should always be considered at the design stage. The average surface absorption coefficients of untreated industrial buildings are 0.08–0.16 in the 125- and 250-Hz octave bands, varying with construction, and 0.06–0.08 in the 500–4000-Hz octave bands.

Figures 7.4*a* and *b* show the reverberation times and 1-kHz sound propagation function curves measured in an empty, untreated workshop with average dimensions of 45 m × 42.5 m and height of 4 m and a double-panel roof.[23] It is often the case that the sound propagation function—$L_p(r) - L_w$ as defined in Eq. (7.3)—at most source–receiver distances and the reverberation time are found to be highest at midfrequencies. The values of both quantities decrease at low and high frequencies due to increased panel and air absorption.

The effects of workshop furnishings are also illustrated in Figs. 7.4*a* and *b*, showing the reverberation times and sound propagation function curves after first 25 and then an additional 25 printing machines were introduced. These

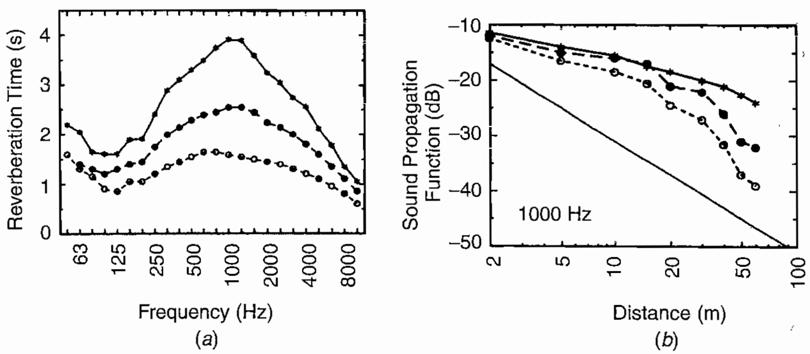

FIGURE 7.4 Measured (*a*) third-octave-band reverberation times and (*b*) 1-kHz sound propagation curves in an industrial workshop when empty (×——×) and containing 25 (•- - -•) and 50 (⊙····⊙) metal machines; (——) free-field sound.

metal machines had average dimensions of 3 m × 3 m and height of 2 m. Introduction of the furnishings significantly decreased reverberation times and sound propagation function values. According to diffuse-field theory, the decreases of reverberation time for this particular workshop correspond to the introduction of as much as 900 m^2 of acoustical absorption.[23] In fact, they are related to increased diffusion, not increased absorption. The percentage changes of reverberation time and the magnitudes of the changes of the sound propagation function with increasing furnishing density vary little with frequency. These results are supported by similar measurements in other workshops. They again illustrate the limitations of diffuse-field theory, which cannot accurately predict the effects of complex room geometry or furnishings.

Workshop Noise Prediction

Models developed for predicting noise levels and reverberation times in industrial workshops fall into two categories—*comprehensive* models, based on approaches such as ray tracing and the method of image sources, and *simplified*, based on simple theoretical or empirical approaches. Comprehensive models have been evaluated experimentally, concluding that the ray-tracing model of Ondet and Barbry[7] was most inherently accurate.[24] Ray tracing can account for complex room shape, barriers, and nonisotropic absorption and furnishing distributions. Simplified models have also been evaluated experimentally, concluding that a model developed by Kuttruff was inherently accurate in furnished workshops.[26]

Kuttruff[26] developed a simplified model for long and wide furnished workshops based on radiosity theory; the numerous furnishings on the floor and the ceiling were modeled as diffusely reflecting surfaces. According to this model, in a workshop of height h and with average absorption coefficient α, the sound pressure level $L_p(r)$ generated by an omnidirectional compact source of sound power level L_w at a distance r is given by

$$L_p(r) = L_w + 10\log_{10}\left\{\frac{1}{4\pi r^2} + \frac{1-\alpha}{\pi h^2}\left[\left(1+\frac{r^2}{h^2}\right)^{-1.5} + \frac{\beta(1-\alpha)}{\alpha}\left(\beta^2+\frac{r^2}{h^2}\right)^{-1.5}\right]\right\} \quad (7.11)$$

where $\beta \approx 1.5\alpha^{-0.306}$. Despite the assumption of infinite length and width, the model performed well in comparison with measurements made in workshops of a wide range of lengths and widths.[25] One disadvantage of the model is that it does not include a parameter that can be varied to account for variations in the number of furnishings. However, as can be seen from Fig. 7.4*b*, the variations are small at the smaller source–receiver distances that dominate noise levels in many practical cases. An alternative is empirical models for predicting workshop noise levels and reverberation times.[27]

When dealing with multiple sources in workshops, the effect of noise control measures may be determined to a first approximation by considering what happens at a distance corresponding to the average source–receiver distance. Changes in total noise levels due to noise control measures are approximated by changes in the sound propagation function at this distance. For machine operator positions, the average source–receiver distance is small—typically 1–2 m. For a room with a more or less square floorplan and with sound sources uniformly distributed over the floor, the average source–receiver distance is about one-half the average horizontal dimension.

As an example, let us use the Kuttruff model to calculate the 1-kHz noise level in the workshop illustrated in Fig. 7.3 (but without the acoustical screen and partial suspended ceiling shown) before and after introduction of full-coverage suspended ceiling absorption. Consider a position midway along the assembly bench and 1.5 m above the floor. The workshop dimensions are length 48.0 m, width 16.0 m, and height 7.2 m. Assume that the average midfrequency absorption coefficients of the workshop surfaces are 0.07 (untreated) and 0.4 (treated). The workshop contains nine noise sources located as shown in Fig. 7.3, with 1-kHz sound power levels and source–receiver distances as shown in Table 7.4. Table 7.4 shows the individual noise-level contributions of the sources before and after treatment. Total levels are determined by energy-based addition of the individual source contributions. The result is 82.4 dB before treatment and 78.7 dB after treatment. Introduction of the ceiling treatment is predicted to reduce the 1-kHz noise level at the assembly bench by 3.7 dB (confirming that the treatment illustrated in Fig. 7.3 is highly cost-effective).

Accurate prediction relies on an inherently accurate model and accurate input data. Workshop surface absorption coefficients were discussed above. Many workshop prediction models also include a parameter describing the workshop furnishing density. It is not known how to determine this quantity accurately. In theory, it can be estimated as the total surface area of the furnishings (or, more practically, of imaginary boxes that would fit around the individual objects)

TABLE 7.4 Details of Calculation of 1-kHz Noise Levels in Workshop before and after Acoustical Treatment Using Kuttruff Simplified Prediction Model[a]

Source Number	L_w, dB	Distance, r (m)	Before $L_{p,a}(r)$, dB	After $L_{p,b}(r)$, dB
1	94	13.5	70.7	65.3
2	101	9.8	79.1	74.8
3	92	7.6	71.1	67.5
4	94	3.9	75.6	73.5
5	86	9.5	64.2	60.0
6	90	7.6	69.1	65.5
7	91	8.7	69.6	65.6
8	89	8.5	67.6	63.8
9	93	15.5	69.0	63.2
Total noise level			82.4	78.7

[a] Reference 26.

divided by 4 times the volume of the furnished region.[24] However, there is some evidence that this procedure underestimates the correct value.[8] Research has shown that average workshop furnishing densities may attain 0.2 m^{-1} or higher, those of a workshop's furnished regions 0.5 m^{-1} or higher.[28] In any case, no simplified model will ever predict noise levels in workshops of complex shape or furnishing distributions or that contain, for example, barriers with high accuracy. In such cases, ray tracing may be the only viable option. Finally, a problem shared by all prediction models is the accurate estimation of the sound power levels of the noise sources. This problem is discussed in Chapter 4.

Workshop Noise Control

To achieve the reduction of workshop noise levels (as required by modern occupational noise regulations) in a cost-effective manner, the application of noise control principles should be incorporated into new designs and renovation in the following order of priority:

1. *Control at Source.* Reduce the sound power outputs of the equipment by design or by retrofit acoustical treatment.
2. *Control of Direct Field.* Isolate receiver positions from noisy sources by increasing the distance between them, by the use of source enclosures (see Chapter 12), and by surrounding the receiver by a cabin or screen. Barriers and screens are often not practical or cost-effective alternatives in workshops. Often separation can be achieved by appropriate planning of the workshop layout, taking full advantage of the building geometry, natural barriers such as stockpiles, and furnishings at the design stage.
3. *Control of Reverberant Field.* Apply sound-absorptive materials to the room surfaces. Such treatments should be accorded lower priority since they tend to be expensive and not very effective near noise sources, such as at operator positions. In practice, reductions of 0–6 dBA are possible. The best surfaces to treat are those closest to noise sources and/or receiver positions. In low-height industrial workshops, this usually implies the ceiling. Consider an acoustical steel deck at the design stage or acoustical treatments consisting of sound-absorptive materials applied to or suspended from the ceiling—for example, acoustical baffles (rectangular pieces of absorptive material) hung in appropriate patterns at appropriate densities. A particularly cost-effective treatment consists of suspending sound absorbers directly above noise sources. Difficulties may arise due to interference with overhead cranes and lighting and sprinkler systems and with respect to fire regulations and hygiene requirements. The treatment of walls may be warranted in more regularly shaped enclosures and where noise sources are located close to walls when it is important to absorb the strong wall reflections. Note that in workshops of any shape surface absorption, even when it has little effect on the total noise levels, may significantly reduce reverberation, reducing the perceived "noisiness" of the work environment and improving verbal communication.

Readers interested in the low-noise design of industrial workshops should be aware of relevant ISO standards available to help in the task. ISO 11688[29,30] provides advice on the design of low-noise machinery and equipment. Part 1 discusses planning, and Part 2 discusses the principles of low-noise design. ISO 14257[31] defines criteria for evaluating the acoustical quality of workshops with respect to noise control and describes how to perform the measurements to evaluate an existing workshop.

7.7 OPEN-PLAN OFFICES

Open-plan offices are one of the most common modern work environments. In these large spaces, many seated workers are separated by low barriers that provide partial visual and acoustical separation between workstations. The barriers may be free-standing but today are usually in the form of integrated furniture or cubicles. The ceiling and the carpeted floor form two large, extended sound-absorbing planes; their horizontal dimensions are much greater than the height of the ceiling. The space between these surfaces is filled with office furniture and barriers that are usually sound absorbing. Diffuse-field theory certainly does not apply in such a space; the sound pressure level decreases continuously with distance from sources (an example is shown in reference 3). The principal problem in an open-plan office is not propagation to large distances but the provision of privacy between neighboring workstations. The important sound paths are, therefore, the short-range ones. Sound from one work position reflects from extended surfaces (ceiling, walls, and windows) and diffracts over or around the edges of barriers, as illustrated in Fig. 7.5. These sound paths must be controlled to provide acoustical privacy for workers.

Open-plan offices can provide a reasonable degree of acoustical privacy if they are carefully designed as a complete system and if adjacent work functions are

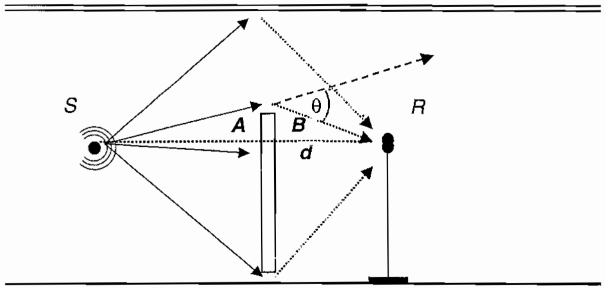

FIGURE 7.5 Possible sound paths between workstations in an open-plan office cross section. Reflection from the ceiling is reduced by using highly absorptive ceiling materials, transmission through the barrier by selecting a sufficiently heavy panel with adequate sound transmission loss, and diffraction over the barrier by increasing the barrier height.

compatible and not too close together. If any aspect of the system is neglected, then adequate acoustical privacy will not be achieved. Obtaining adequate acoustical privacy is first a question of attenuating unwanted speech sounds from adjacent work spaces, because speech sounds are much more distracting than most other types of noises. It is usually also necessary to include masking sound to render intruding speech sounds less intelligible while not being a source of annoyance. Special protection should be provided against noisy devices such as printers and copiers—for example, by locating them in a shielded area. Conference rooms with full-height partitions, providing good sound insulation, should be available for activities which require low background noise levels and particularly high privacy.

Open-Plan Office Barriers

Barriers (also called screens, partial-height partitions, workstation panels, or office dividers) provide sound attenuation and visual privacy between workstations for seated persons. They are the basic component of systems furniture (usually forming cubicles) that combines the functions of a barrier and supporting amenities such as storage compartments, lighting, power, communications, and work surfaces into a single unit. A barrier should attenuate sound that passes through it so that the transmitted sound is negligible.

Sound diffracts over the top of the barrier to reach the next workstation. For an infinitely wide barrier between a source and a receiver position, the insertion loss IL relative to the level at the receiver in the absence of the barrier can be approximated by[32]

$$\mathrm{IL} = 13.9 + 7\log_{10} N + 1.4(\log_{10} N)^2 \quad \mathrm{dB} \qquad \text{for } N \geq 0.001 \tag{7.12}$$

where the Fresnel number $N = 2f(A + B - d)/c$, d is the straight-line distance from the source to the receiver in meters, A is the distance from the source to the top of barrier in meters, B is the distance from the top of the barrier to the receiver in meters, and c is the sound speed (Fig. 7.5 shows A, B, and d). The greater the angle that sound has to bend to reach the receiver position on the other side of the barrier (θ in Fig. 7.5), the greater is the insertion loss of the barrier. Thus, higher barriers are more effective than lower ones, and barriers placed close to the talker or listener are more effective than those equidistant from both.

The effects of diffraction around and transmission through a barrier can be combined to determine the total insertion loss of a barrier. Sound transmitted through the screen should be negligible relative to the sound diffracted around it, especially at those frequencies important for speech intelligibility. Specifying that, at 1000 Hz, the normal-incidence sound transmission loss should be 6 dB greater than the theoretical insertion loss due to diffraction is a satisfactory criterion. This criterion leads to the requirement that the minimum mass per unit area of the barrier, ρ_s in kilograms per square meter, should be $\rho_s \geq 2.7(A + B - d)$. For an isolated screen, the total effect of the barrier can be calculated by applying Eq. (7.12) to each edge in turn and then summing the acoustical energies.

Maximum barrier dimensions are usually limited by physical convenience, possible interference with airflow, and preservation of the open look. Recommended minimum dimensions are height 1.7 m and width 1.8 m. Of course, a complete cubicle is equivalent to a long barrier, for which there is negligible propagation around the ends. If the attenuation of a high barrier is desired but visual openness must be maintained, a plate of glass or transparent plastic panel can be fitted to the top of a low barrier to increase its "acoustical height." The gap between the bottom edge of the barrier and the floor should be small; otherwise sound can reflect under the barrier to the opposite side. This is not critical, because sound following this path tends to be diffused or absorbed by furniture and carpets; a gap of up to 100 mm can be left when the floor is carpeted.

Measures for Rating Acoustical Privacy

Acoustical privacy is usually referred to as speech privacy because it is speech sounds that are usually the most disturbing (see also Section 7.5). Speech privacy is essentially the opposite of speech intelligibility. That is, the lower the intelligibility of the speech, the greater the speech privacy. Speech privacy (and speech intelligibility) is related to the level of the intruding speech sounds relative to the less meaningful ambient noise. Hence, speech privacy is related to measures involving the signal-to-noise level difference, where speech is the signal and the general ambient noise is the noise component.

Articulation index (AI) is a frequency-weighted signal-to-noise level difference measure which indicates the expected speech intelligibility in particular conditions. The signal-to-noise level differences in each frequency band are weighted according to their relative importance to the intelligibility of speech. These weighted signal-to-noise level differences are summed to obtain the AI value, between 0 and 1. An AI of 1 is intended to indicate conditions in which near-perfect intelligibility is expected. An AI close to 0 is expected to indicate conditions of near-perfect speech privacy. The AI has been widely used as a measure of speech privacy; AI $\leq$ 0.15 is considered to provide *normal* or *acceptable* speech privacy in open-plan office situations. The AI has now been replaced by the SII. It is similar to the AI but has slightly larger values, so the criterion for acceptable speech privacy becomes SII $\leq$ 0.20. Both have been described in ANSI standards.[33,34]

Figure 7.6 illustrates the suitability of this criterion. In this figure, median speech intelligibility scores are plotted versus SII for situations simulating conditions in open-plan offices. It is seen that SII = 0.2 represents the point below which privacy increases rapidly with decreasing SII. One can think of it as the point at which improvements to the acoustical design start to improve speech privacy. In practice, it is also a practically achievable goal if all aspects of the acoustical design are carefully considered.

Acoustical Design of Complete Workstations

Sound propagation between workstations in an open-plan office with modular workstations (cubicles) involves many different sound paths, not just propagation over a simple screen as described above. There are reflections from the ceiling and the other panels of the workstation as well as from nearby walls. These consist of not only simple first-order reflections but also paths with multiple reflections, such as those involving the floor and the ceiling or the vertical surfaces of the workstation. The problem of sound propagation between workstations has been addressed using the method of image sources (see Section 7.3) and implemented as a computer algorithm. Diffraction over the screen was modeled using Maekawa's results described in Eq. (7.12). The method of image sources assumes that all reflections are specular, so the angle of incidence equals the angle of reflection. However, the model includes an empirical correction to the

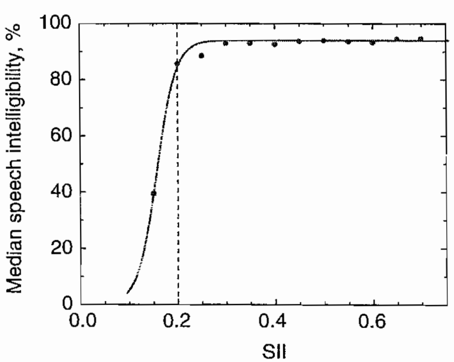

FIGURE 7.6 Variation of median speech intelligibility score with SII for situations simulating a range of conditions in open-plan offices.[35]

absorption coefficients of ceiling materials (obtained from standard reverberation room tests) to account for the limited range of angles of incidence for sound propagation between workstations, compared to that in a diffuse reverberant test room. The model has been validated with respect to a wide range of measurement conditions and is used here to illustrate the effects of various design parameters. See references 36–39 for details of the model.

Speech and Noise Levels

Two factors that have very large effects on speech privacy are the speech levels of the talkers in the open offices and the general ambient noise levels. These cannot be ignored when striving for acceptable speech privacy. Fortunately, people do not usually talk with *normal* vocal effort in open-plan offices. Measurements of talkers in open-plan offices have found mean voice levels close to those described as *casual* vocal effort. Using normal voice levels to calculate expected speech privacy greatly exaggerates the lack of speech privacy. The intermediate office speech level (IOSL) shown in Fig. 7.7 is recommended as the speech source level for calculating speech privacy in open-plan offices. It was obtained by averaging the mean speech levels measured in open-plan offices and the casual voice data and then adding 3 dB, corresponding to one standard deviation above the average talker level. The IOSL spectrum is therefore representative of louder talkers in open-office situations and corresponds to a speech source level at a distance of 1 m in a free field of 53.1 dBA. References 40–42 provide more details of speech levels.

One important aspect of achieving speech privacy is to encourage the use of lower voice levels as a form of open-plan office etiquette. Extended discussions should not be held in open-office areas but should be moved to closed meeting rooms.

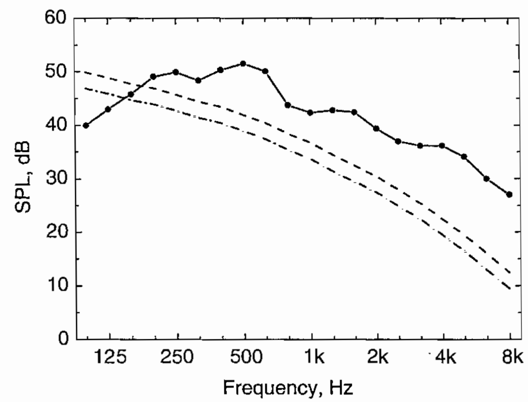

FIGURE 7.7 The IOSL spectrum and noise-masking spectra for open-office design calculations: (—●—) IOSL; (-·-·-·-) optimum masking; (- - - - -) maximum masking.

It is difficult to obtain acceptable speech privacy if the general ambient noise level is low. On the other hand, if ambient noise levels are high, they can become annoying and cause people to talk louder. There is a narrow range of ambient noise levels that are expected to be acceptable and that can also partially mask intruding speech sounds from adjacent workstations. (The masking of speech by noise is a well-researched field, and ANSI S3.5[34] includes many references on this topic.) For this reason, electronic sound-masking systems are often included in successful open-office designs. They can be designed to provide nearly ideal noise levels to mask speech sounds and enhance privacy without being unduly disturbing. The masking noise should be adjusted to sound like natural ventilation system noise and to be evenly distributed throughout the office. Figure 7.7 includes an example of a noise-masking spectrum that was judged to be at an optimal level, corresponding to 45 dBA. It has been found that the maximum acceptable level for masking sound is approximately 48 dBA. Hence, the maximum masking spectrum in Fig. 7.7 represents an example of such a maximum noise-masking spectrum. These two noise spectra are indicative of the narrow range of masking noises that provides *acceptable* speech privacy. Spatial variations of masking noise should be less than 3 dBA.

Conventional sound-masking systems have included those with centrally located electronics and others with distributed units. Distributed systems, with many small independent units, have the advantage of avoiding correlated sources, which can lead to annoying spatial variations in the masking sound. Manufacturers of both types claim various practical advantages. Although propagation into the ceiling void may aid the homogeneity of the masking sound in the office below, the masking sound will be modified by propagation through the ceiling tiles, and transmission through lighting fixtures can lead to localized areas of higher sound levels below. More recently, sound-masking systems with loudspeakers mounted in the ceiling tiles and on the panels of workstations have been introduced to provide better control over the resulting masking sound. The installation of noise-masking systems is best left to experienced professionals.

Important Design Parameters

In the design of an open-plan office, it is first assumed that the transmission loss of the workstation panels is sufficient to attenuate, to an insignificant level, the sound propagating directly through the panels. The requirement for surface density given by Eq. (7.12) usually leads to a minimum value corresponding to STC $\geq$ 20 (STC is the sound transmission class, obtained from a standard sound transmission loss test[43]; see also Chapter 10). After this, the two most important parameters are the sound absorption of the ceiling and the height of the separating barriers or panels. If these are not adequate, it will not be possible to achieve acceptable speech privacy.

The shaded area of Fig. 7.8 indicates combinations of ceiling absorption and panel height that can provide SII $\leq$ 0.20 if the other details considered below are also acceptable. Ceiling absorption is described in terms of the sound absorption

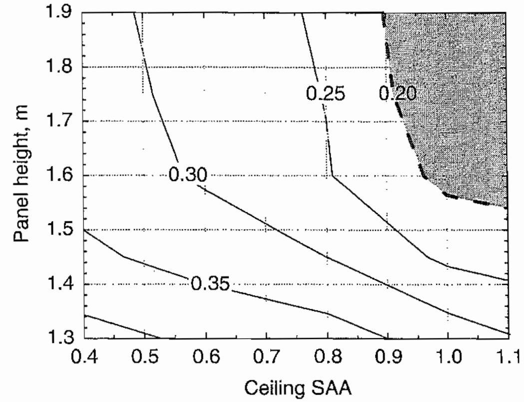

FIGURE 7.8 Shaded area shows combinations of workstation panel height and ceiling absorption that lead to *acceptable* speech privacy corresponding to SII $\leq$ 0.20.[44] Contours in unshaded part indicate degrees of unacceptable speech privacy. SAA is the average of the absorption coefficients in the third-octave bands from 250 Hz to 2.5 Hz.

average (SAA), which is the average of the absorption coefficients in the third-octave frequency bands from 250 Hz to 2.5 kHz. It replaces the older noise reduction coefficient (NRC) and has very similar values. Values of SAA greater than 1.0 are included in Fig. 7.8 because such values can result from the standard test procedure, due to the effects of edge diffraction (as mentioned in Section 7.2). It is seen that the sound absorption of the ceiling should correspond to SAA $\geq$ 0.90 and the separating panels should be $\geq$1.7 m high. Since the results in Fig. 7.8 were calculated with other details set to nearly ideal values, combinations of ceiling absorption and screen height outside of the shaded area make it impossible to achieve acceptable speech privacy.

A third key design parameter is the size of the workstation plan. The results in Fig. 7.8 are for a workstation with dimensions of 3 m $\times$ 3 m. If the workstation length and width each decrease by 1 m, then the resulting SII increases by 0.05. That is, for a 2 m $\times$ 2 m workstation plan, meeting the SII $\leq$ 0.20 criterion would require very high screens and the most absorptive ceiling materials.

Other Design Parameters

The sound-absorptive properties of the workstation panels and the floor have smaller effects on speech privacy. The height of the ceiling and the presence of lighting fixtures in the ceiling can also influence speech privacy.

The results shown in Fig. 7.8 were calculated for workstation panels with SAA = 0.9. If this were reduced to 0.75, the corresponding SII values would decrease by 0.01. If the panel absorption were decreased to 0.6, SII values would decrease by 0.02. These seem to be small degradations in the overall performance, but one must always remember that most designs will at best be on the edge of just providing acceptable speech privacy; even these small improvements may help to meet the SII ≤ 0.20 criterion. Of course, if the panels were not highly absorptive (i.e., SAA < 0.60), there would be a more significant increase in the resulting SII values. For example, if the workstation panels were nonabsorptive in an otherwise ideal workstation design, SII would increase from 0.2 to 0.3.

Varying floor absorption and varying ceiling height generally have very small effects on the resulting SII values. In most cases, varying these parameters changes SII by no more than about 0.01. On the other hand, lighting fixtures in the ceiling can degrade the speech privacy of the open-office design. The effect of a lighting fixture depends on the type of lighting unit and its location. Lights with a flat plastic or glass surface produce the strongest unwanted reflections and are most troublesome when located over the separating panel between two workstations. They will change SII values most when installed in a highly absorptive ceiling. Evaluation of the effects of several types and locations of lighting fixtures has shown that, for a ceiling with SAA $= 0.90$, SII values could increase by up to 0.08. Open-grill lighting fixtures have smaller effects but still reduce the effectiveness of a highly absorptive ceiling.

Practical Issues and Other Problems

Sound propagating in the horizontal plane can bypass barriers by reflection from vertical surfaces and hence reduce the sound attenuation between work positions. To minimize these effects, surfaces such as walls, office barriers, square columns, backs of cabinets, and systems furniture, as well as bookcases, should be covered with sound-absorptive material having SAA values of 0.7 or higher. A thickness of 2.5 cm or more of glass fiber with a porous fabric cover will satisfy this requirement. The application of carpets directly to hard surfaces is not an effective solution, since typical carpets have low sound absorption coefficients. Round columns with diameters of 0.5 m or less may be left uncovered. A simple way to avoid wall reflections is to avoid gaps between the wall and barriers. To prevent reflections from their surfaces, office barriers should be covered with sound-absorptive material on both faces.

Where workstations are adjacent to windows, there are often large gaps between the workstation panels and the window. To provide adequate acoustical privacy between these workstations, this gap must be filled with additions to the workstation panels. This problem cannot easily be solved using drapes, which would need to be heavy and closed; furthermore, most slatted blinds do not reduce reflections. Using the area next to the windows as a corridor is another solution to this problem.

Standard procedures exist for the evaluation of the degree of speech privacy in an existing office, in a mock-up of a proposed office,[45] or for the evaluation of open-plan noise-masking systems.[46] It is very important to evaluate the speech and noise in the office to completely determine the existing degree of speech privacy.

7.8 REVERBERATION ROOMS

Reverberation rooms are designed and equipped to give a close approximation to a diffuse sound field. Measurements in these rooms are used to characterize the sound-absorptive properties of materials, the sound power of sources, and the sound transmission through building elements, among other things, under standard diffuse-field conditions according to various standards.[43,47–52] A typical reverberation room has a volume of about 200 m^3; some are constructed with nonparallel walls. The walls and surfaces of the room are made highly reflective so that reverberation times are high and the region dominated by the direct field of a source is as small as possible.

At low frequencies, the frequency response to wide-band noise shows peaks corresponding to individual room modes. As frequency increases, the spacing between modes becomes less, the modes begin to overlap, and the individual modes are less obvious. At some transition frequency the room response for bands of noise becomes approximately constant, the properties of the sound field become more uniform, and the room response may be described in statistical terms. This transition point is usually defined by the Schroeder frequency[53] $f_S = 2000(T_{60}/V)^{1/2}$ hertz. For a $V = 250$ m^3 room with $T_{60} = 5$ s, $f_S =$ 282 Hz.

To make the response of the room more uniform at low frequencies, it is usually advisable to add low-frequency sound-absorbing elements. Even in rooms of approximately 200 m^3 volume, correctly chosen dimensions, and the recommended amount of sound absorption, the spatial variations of pressure and the sound decay rate are often too large to satisfy the precision requirements of standards. It is therefore common to add fixed panels suspended at random positions and orientations throughout the room to perturb the room modes and to create more diffuse conditions. In many cases rotating diffusers are also used for this purpose.

Fixed diffusers are most important in rectangularly shaped rooms used for sound absorption measurements. They may not be necessary in rooms that are sufficiently nonrectangular in shape. They help to create a more diffuse sound field during the measurement of sound decays by ensuring that, throughout the sound decay, a portion of the decaying sound energy is redirected toward the sound-absorbing sample. When commissioning a new reverberation room for sound absorption measurements, it is necessary to systematically increase the number of diffusers until measured absorption coefficients just reach maximum values due to the increasingly diffuse conditions in the chamber. Of course, adding too many diffusers can limit the number of valid positions for microphones, which must always be located more than a half wavelength (at the lowest frequency of interest) from reflecting surfaces such as walls and diffusing panels.

Rotating diffusers are particularly useful in reverberation rooms used for measuring the sound power levels of devices with strong tonal components. These types of sound sources lead to large spatial variations in sound levels that can be effectively reduced using a rotating diffuser. By continuously changing the geometry of the room, they shift the modal patterns and hence average out some of the spatial variations of the sound levels. Making the rotating diffuser in the form of panels of revolution can reduce the required drive power and aerodynamic noise.

In addition to such measures, it is still necessary to sample the room volume in order to measure mean-squared sound pressures and decay rates accurately. To provide statistically independent samples of the sound field, microphone positions must be more than one-half wavelength apart (at the lowest frequency of interest) as well as be located more than one-half wavelength away from reflecting objects to avoid nonrepresentative measures of the room average sound level.

It has been shown that close to one, two, or three infinite reflecting planes the sound pressure and energy increase. The mean-squared pressure p^2 can be expressed as

$$p^2 = 1 + \sum_{n=1}^{N_{\text{im}}} \frac{\sin(kr_n)}{kr_n} \quad (\text{N/m}^2)^2 \tag{7.13}$$

where $k = 2\pi/\lambda (\lambda = \text{wavelength})$
p^2 = mean-square pressure normalized to unity in absence of images or far from reflecting surfaces
r_n = distances from images of measurement point to measurement point
N_{im} = number of images: 1 for measurement near a plane surface, 3 near an edge, and 7 near a corner

Closer than $\lambda/2$ to highly reflecting surfaces, sound pressure increases significantly because of these positive interference effects. To account for the increase in sound energy close to surfaces, an adjustment term $(1 + S\lambda/8V)$ is included in the calculation of the sound power W from the space-averaged mean-square sound pressure. Thus, the relationship used to determine the sound power W of a source from the space-averaged mean-square sound pressure p^2 that it creates in the room is[54]

$$W = \frac{55.3 p^2 V}{4\rho c^2 T_{60}} (1 + S\lambda/8V) \qquad \text{N}\cdot\text{m/s} \tag{7.14}$$

where ρ = density of air, kg/m^2
c = speed of sound in air, m/s
V = room volume, m^3
T_{60} = reverberation time, s

It is assumed that sampling of the sound field in the room is confined to the central regions away from room surfaces. The Sabine formula, Eq. (7.2), relating reverberation time to room absorption is assumed to hold and is the basis for determinations of sound absorption in reverberation rooms.[47,48]

The planning and qualification of reverberation rooms are complex and best done by experienced professional acousticians.

7.9 ANECHOIC AND HEMI-ANECHOIC CHAMBERS

An anechoic chamber is a room with all of its interior surfaces highly absorptive such that a source in the room radiates in essentially free-field conditions. The resulting sound field has only a direct component. Hemi-anechoic chambers have a hard floor with all other interior surfaces highly sound absorptive. They are used for measuring the sound power level and radiation pattern of equipment (such as road vehicles, appliances, etc.) that are operated over a hard surface. The acoustical performance of an anechoic or hemi-anechoic room can be evaluated by determining how closely conditions in the room approximate those in a free field. This is usually done by measuring the variation of sound levels with distance from an approximately omnidirectional source; it should ideally be −6 dB per doubling of distance; see Eq. (7.3) and Fig. 7.1.

Tests are made in an anechoic room when it is necessary to accurately measure the unperturbed sound radiated by a source—for example, when measuring its radiation pattern (directivity) or sound power. The surfaces of anechoic chambers are made highly absorptive by lining them with deep, sound-absorptive materials. The lining typically consists of wedges of mineral wool or glass fiber.[55] All anechoic chambers are more anechoic at high than at low frequencies. The lowest frequency at which an anechoic chamber can be used depends primarily on the chamber volume and the depth of the wedges. This cutoff frequency, at which the wedges absorb 99% of the incident sound energy, is usually achievable with a wedge depth (including any air space between the base of the wedge and the hard wall) of approximately one-quarter wavelength. A large chamber with 1-m-deep wedges may be effective down to 80–100 Hz. To provide a walking surface to facilitate setting up experiments in an anechoic chamber, an open-metal-floor grid that is removed after the setup or a permanent wire-mesh floor can be provided. The perimeter frame of such a wire-mesh floor and to a lesser extent the wire mesh itself may degrade the high-frequency performance of the chamber.

REFERENCES

1. L. Cremer, H. A. Müller, and T. J. Schultz, *Principles and Applications of Room Acoustics*, Applied Science, New York, 1982; H. Kuttruff, *Room Acoustics*, 4th ed., Spon, London, 2000.
2. ANSI S1.26, "Method for the Calculation of the Absorption of Sound by the Atmosphere," Acoustical Society of America, Melville, New York.
3. M. R. Hodgson, "When Is Diffuse-Field Theory Applicable," *Appl. Acoust*, **49**(3), 197–207 (1996).
4. J. B. Allen and D. A. Berkeley, "Image Method for Efficiently Simulating Small-Room Acoustics," *J. Acoust. Soc. Am.*, **65**(4), 943–950 (1979).
5. E. A. Lindqvist, "Noise Attenuation in Factories," *Appl. Acoust.*, **16**, 183–214 (1983).
6. A. Krokstad, S. Strom, and S. Sorsdal, "Calculating the Acoustical Room Response by the Use of a Ray-Tracing Technique," *J. Sound Vib.*, **8**(1), 118–125 (1968).

7. A. M. Ondet and J. L. Barbry, "Modeling of Sound Propagation in Fitted Workshops Using Ray Tracing," *J. Acoust. Soc. Am.*, **85**(2), 787–796 (1989).
8. M. R. Hodgson, "Case History: Factory Noise Prediction Using Ray Tracing—Experimental Validation and the Effectiveness of Noise Control Measures," *Noise Control Eng. J.*, **33**(3), 97–104 (1989).
9. J. Neter, W. Wasserman, and G. A. Whitmore, *Applied Statistics*, 4th ed., Allyn and Bacon, Boston, 1993.
10. M. Kleiner, B.-I. Dalenbäck, and P. Svensson, "Auralization—An Overview," *J. Audio Eng. Soc.*, **41**(11), 861–875 (1993).
11. T. J. Schultz, "Improved Relationship between Sound-Power Level and Sound-Pressure Level in Domestic and Office Spaces," Report No. 5290, Bolt Beranek and Newman, Cambridge, MA, 1983.
12. B. M. Shield and J. E. Dockrell, "The Effects of Noise on Children at School: A Review," *J. Building Acoust.*, **10**(2), 97–116 (2003).
13. P. B. Nelson, S. D. Soli, and A. Seltz, *Acoustical Barriers to Learning*, Acoustical Society of America, Melville, NY, 2002.
14. M. R. Hodgson, "Experimental Investigation of the Acoustical Characteristics of University Classrooms," *J. Acoust. Soc. Am.*, **106**(4), 1810–1819 (1999).
15. M. Picard and J. S. Bradley, "Revisiting Speech Interference in Classrooms," *Audiology*, **40**(5), 221–244 (2001).
16. M. R. Hodgson, R. Rempel, and S. Kennedy, "Measurement and Prediction of Typical Speech and Background-Noise Levels in University Classrooms during Lectures," *J. Acoust. Soc. Am.*, **105**(1), 226–233 (1999).
17. M. R. Hodgson and E.-M. Nosal, "Effect of Noise and Occupancy on Optimum Reverberation Times for Speech Intelligibility in Classrooms," *J. Acoust. Soc. Am.*, **111**(2), 931–939 (2002).
18. S. R. Bistafa and J. S. Bradley, "Reverberation Time and Maximum Background-Noise Level for Classrooms from a Comparative Study of Speech Intelligibility Metrics," *J. Acoust. Soc. Am.*, **107**(2), 861–875 (2000).
19. ANSI S12.60, "Acoustical Performance Criteria, Design Requirements and Guidelines for Schools," Acoustical Society of America, Melville, New York.
20. Building Bulletin 93, *Acoustic Design of Schools*, Department of Education and Skills, UK, 2004.
21. M. R. Hodgson, "Empirical Prediction of Speech Levels and Reverberation in Classrooms," *J. Building Acoust.*, **8**(1), 1–14 (2001).
22. D. Davis and C. Davis, *Sound System Engineering*, 2nd ed., Focal Press, Burlington, MA, 1997.
23. M. R. Hodgson, "Measurement of the Influence of Fittings and Roof Pitch on the Sound Field in Panel-Roof Factories," *Appl. Acoust.*, **16**, 369–391 (1983).
24. M. R. Hodgson, "On the Accuracy of Models for Predicting Sound Propagation in Fitted Rooms," *J. Acoust. Soc. Am.*, **88**(2), 871–878 (1989).
25. M. R. Hodgson, "Experimental Evaluation of Simplified Methods for Predicting Sound Propagation in Industrial Workrooms," *J. Acoust. Soc. Am.*, **103**(4), 1933–1939 (1998).
26. H. Kuttruff, "Sound Propagation in Working Environments," *Proc. 5th FASE Symp.*, 17–32 (1985).

27. N. Heerema and M. R. Hodgson, "Empirical Models for Predicting Noise Levels, Reverberation Times and Fitting Densities in Industrial Workrooms," *Appl. Acoust.*, **57**(1), 51–60 (1999).
28. M. R. Hodgson, "Effective Fitting Densities and Absorption Coefficients of Industrial Workrooms," *Acustica*, **85**, 108–112 (1999).
29. ISO/TR 11688-1, "Recommended Practice for the Design of Low-Noise Machinery and Equipment—Part 1: Planning," International Organization for Standardization, Geneva, Switzerland, 1995.
30. ISO/TR 11688-2, "Recommended Practice for the Design of Low-Noise Machinery and Equipment—Part 2: Introduction to the Physics of Low-Noise Design," International Organization for Standardization, Geneva, Switzerland, 1998.
31. ISO 14257, "Measurement and Parametric Description of Spatial Sound Distribution Curves in Workrooms for Evaluation of Their Acoustical Performance," International Organization for Standardization, Geneva, Switzerland, 2001.
32. Z. Maekawa, "Noise Reduction by Screens," *Appl. Acoust.*, **1**(3), 157–173 (1968).
33. ANSI S3.5, "American National Standard Methods for the Calculation of the Articulation Index," Acoustical Society of America, Melville, New York, 1969.
34. ANSI S3.5, "Methods for Calculation of the Speech Intelligibility Index," Acoustical Society of America, Melville, New York, 1997.
35. J. S. Bradley and B. N Gover, "Describing Levels of Speech Privacy in Open-Plan Offices," Report IRC-RR-138, Institute for Research in Construction, National Research Council, Ottawa, 2003.
36. C. Wang and J. S. Bradley, "Sound Propagation between Two Adjacent Rectangular Workstations in an Open-Plan Office, I: Mathematical Modeling," *Appl. Acoust.*, **63**(12), 1335–1352 (2002).
37. C. Wang and J. S. Bradley, "Sound Propagation between Two Adjacent Rectangular Workstations in an Open-Plan Office, II: Effects of Office Variables," *Appl. Acoust.*, **63**(12), 1353–1374 (2002).
38. C. Wang and J. S. Bradley, "Prediction of the Speech Intelligibility Index behind a Single Screen in an Open-Plan Office," *Appl. Acoust.*, **63**(8), 867–883 (2002).
39. J. S. Bradley and C. Wang, "Measurements of Sound Propagation between Mock-Up Workstations," Report IRC-RR 145, Institute for Research in Construction, National Research Council, Ottawa, 2001.
40. A. C. C. Warnock and W. Chu, "Voice and Background Noise Levels Measured in Open Offices," Report IR-837, Institute for Research in Construction, National Research Council, Ottawa, 2002.
41. W. O. Olsen, "Average Speech Levels and Spectra in Various Speaking/Listening Conditions: A Summary of the Pearson, Bennett, and Fidell (1977) Report," *J. Audiol.*, **7**, 1–5 (October 1998).
42. J. S. Bradley, "The Acoustical Design of Conventional Open-Plan Offices," *Can. Acoust.*, **27**(3), 23–30 (2003).
43. ASTM E90, "Standard Test Method for Laboratory Measurement of Airborne Sound Transmission Loss of Building Partitions," American Society for Testing and Materials, Conshohocken, PA, 2004.
44. J. S. Bradley, "A Renewed Look at Open Office Acoustical Design," Paper N1034, Proceedings Inter Noise 2003, Seogwipo, Korea, August 25–28, 2003.

45. ASTM E1130, "Standard Test Method for Objective Measurement of Speech Privacy in Open Offices Using the Articulation Index," American Society for Testing and Materials, Conshohocken, PA, 2002.
46. ASTM E1041, "Standard Guide for Measurement of Masking Sound in Open Offices," American Society for Testing and Materials, Conshohocken, PA, 1985.
47. ASTM C423, "Standard Test Method for Sound Absorption and Sound Absorption Coefficients by the Reverberation Room Method," American Society for Testing and Materials, Conshohocken, PA, 2002.
48. ISO 354, "Measurement of Sound Absorption in a Reverberation Room," International Organization for Standardization, Geneva, Switzerland, 2003.
49. ANSI S1.31, "Precision Methods for the Determination of Sound-Power Levels of Broad-Band Noise Sources in Reverberation Rooms," and ANSI S1.32, "Precision Methods for the Determination of Sound-Power Levels of Discrete-Frequency and Narrow-Band Noise Sources in Reverberation Rooms," Acoustical Society of America, Melville, New York.
50. ISO 3740, 3741, 3742, "Determination of Sound-Power Levels of Noise Sources," International Organization for Standardization, Geneva, Switzerland, 2000.
51. ISO 140/III, "Laboratory Measurements of Airborne Sound Insulation of Building Elements," International Organization for Standardization, Geneva, Switzerland, 1995.
52. ASTM E492, "Standard Method of Laboratory Measurement of Impact Sound Transmission Through Floor-Ceiling Assemblies Using the Tapping Machine," American Society for Testing and Materials, Conshohocken, PA, 1992.
53. M. R. Schroeder, "Frequency-Correlation Functions of Frequency Responses in Rooms," *J. Acoust. Soc. Am.*, **34**(12), 1819–1823 (1962).
54. R. V. Waterhouse, "Output of a Sound Source in a Reverberation Chamber and in Other Reflecting Environments," *J. Acoust. Soc. Am.*, **30**(1), 4–13 (1958).
55. L. L. Beranek and H. P. Sleeper, Jr., "Design and Construction of Anechoic Sound Chambers," *J. Acoust. Soc. Am.*, **18**, 140–150 (1947).

CHAPTER 8

Sound-Absorbing Materials and Sound Absorbers*

KEITH ATTENBOROUGH
University of Hull
United Kingdom

ISTVÁN L. VÉR
Consultant in Acoustics, Noise, and Vibration Control
Stow, Massachusetts

8.1 INTRODUCTION

One of the most frequent problems faced by noise control engineers is how to design sound absorbers that provide the desirable sound absorption coefficient as a function of frequency in a manner that minimizes the size and cost, does not introduce any environmental hazards, and stands up to hostile environments such as high temperatures, high-speed turbulent flow, or contamination. The designer of sound absorbers must know how to choose the proper sound-absorbing material, the geometry of the absorber, and the protective facing. The theory of sound-absorbing materials and sound absorbers has progressed considerably during the last 10 years. Much of this progress is documented in K. U. Ingard's *Notes on Sound Absorption Technology*[1] and in F. P. Mechel's *Schall Absorber* (*Sound Absorbers*)[2] and the separately sold computer program on CD-ROM.[3] Ingard's book is a paperback edition of modest length and price and comes with a CD-ROM that allows the reader to make easy numerical predictions from almost all of the equations used in the book. The underlying physical processes are explained with great clarity and the mathematical treatment is kept simple. Derivations and difficult explanation are presented in appendices. The books cover all aspects of sound absorption in great detail. To derive full benefit, it helps if the reader has a reasonably strong mathematical background. However, even those with no such background will find the figures, which give the

*The authors acknowledge the contributions of Dr. Fridolin P. Mechel to the several parts of this chapter retained from the 1992 edition.

45. ASTM E1130, "Standard Test Method for Objective Measurement of Speech Privacy in Open Offices Using the Articulation Index," American Society for Testing and Materials, Conshohocken, PA, 2002.
46. ASTM E1041, "Standard Guide for Measurement of Masking Sound in Open Offices," American Society for Testing and Materials, Conshohocken, PA, 1985.
47. ASTM C423, "Standard Test Method for Sound Absorption and Sound Absorption Coefficients by the Reverberation Room Method," American Society for Testing and Materials, Conshohocken, PA, 2002.
48. ISO 354, "Measurement of Sound Absorption in a Reverberation Room," International Organization for Standardization, Geneva, Switzerland, 2003.
49. ANSI S1.31, "Precision Methods for the Determination of Sound-Power Levels of Broad-Band Noise Sources in Reverberation Rooms," and ANSI S1.32, "Precision Methods for the Determination of Sound-Power Levels of Discrete-Frequency and Narrow-Band Noise Sources in Reverberation Rooms," Acoustical Society of America, Melville, New York.
50. ISO 3740, 3741, 3742, "Determination of Sound-Power Levels of Noise Sources," International Organization for Standardization, Geneva, Switzerland, 2000.
51. ISO 140/III, "Laboratory Measurements of Airborne Sound Insulation of Building Elements," International Organization for Standardization, Geneva, Switzerland, 1995.
52. ASTM E492, "Standard Method of Laboratory Measurement of Impact Sound Transmission Through Floor-Ceiling Assemblies Using the Tapping Machine," American Society for Testing and Materials, Conshohocken, PA, 1992.
53. M. R. Schroeder, "Frequency-Correlation Functions of Frequency Responses in Rooms," *J. Acoust. Soc. Am.*, **34**(12), 1819–1823 (1962).
54. R. V. Waterhouse, "Output of a Sound Source in a Reverberation Chamber and in Other Reflecting Environments," *J. Acoust. Soc. Am.*, **30**(1), 4–13 (1958).
55. L. L. Beranek and H. P. Sleeper, Jr., "Design and Construction of Anechoic Sound Chambers," *J. Acoust. Soc. Am.*, **18**, 140–150 (1947).

CHAPTER 8

Sound-Absorbing Materials and Sound Absorbers*

KEITH ATTENBOROUGH
University of Hull
United Kingdom

ISTVÁN L. VÉR
Consultant in Acoustics, Noise, and Vibration Control
Stow, Massachusetts

8.1 INTRODUCTION

One of the most frequent problems faced by noise control engineers is how to design sound absorbers that provide the desirable sound absorption coefficient as a function of frequency in a manner that minimizes the size and cost, does not introduce any environmental hazards, and stands up to hostile environments such as high temperatures, high-speed turbulent flow, or contamination. The designer of sound absorbers must know how to choose the proper sound-absorbing material, the geometry of the absorber, and the protective facing. The theory of sound-absorbing materials and sound absorbers has progressed considerably during the last 10 years. Much of this progress is documented in K. U. Ingard's *Notes on Sound Absorption Technology*[1] and in F. P. Mechel's *Schall Absorber* (*Sound Absorbers*)[2] and the separately sold computer program on CD-ROM.[3] Ingard's book is a paperback edition of modest length and price and comes with a CD-ROM that allows the reader to make easy numerical predictions from almost all of the equations used in the book. The underlying physical processes are explained with great clarity and the mathematical treatment is kept simple. Derivations and difficult explanation are presented in appendices. The books cover all aspects of sound absorption in great detail. To derive full benefit, it helps if the reader has a reasonably strong mathematical background. However, even those with no such background will find the figures, which give the

*The authors acknowledge the contributions of Dr. Fridolin P. Mechel to the several parts of this chapter retained from the 1992 edition.

difficult mathematical results in graphical form, useful and practical. Mechel's book consists of three hard-covered volumes totaling 2866 pages. The associated computer program is available in MAC and Window versions but is expensive. The classical book of H. Kutruff, *Room Acoustics*,[4] deals predominantly with the room acoustics aspects of sound absorption and should be studied by acousticians designing buildings for the performing arts. Beranek's recently updated classic book *Acoustic Measurements*[5] describes the methods and experimental hardware for measuring all acoustical descriptors of sound-absorbing materials and sound absorbers. The reader with serious interest in sound absorption technology is advised to study all of these texts.

How Sound Is Absorbed

Sound is the organized superposition of particle motion on the random thermal motion of the molecules. The speed of the organized particle motion in air is typically six orders of magnitude smaller than that of the thermal motion. All sound absorbers facilitate the conversion of the energy carried by the organized particle motion into random motion. All forces, other than those that compress and accelerate the fluid, caused by the oscillatory particle flow in the presence of solid material result in loss of acoustical energy. The most important contribution to the conversion is associated with the drag forces caused by friction between the interface of a rigid or flexible wall or the skeleton of the porous or fibrous sound absorber material and the fluid in the thin acoustical boundary layer. For porous and fibrous sound-absorbing materials the acoustical flow speed is low and the flow remains laminar, and the drag force is proportional to the acoustical particle velocity. At high velocities, which occur at the mouth of resonators, the flow separates, turbulence is created, and the friction force becomes proportional to the square of the velocity. Other loss mechanisms, discussed in more detail elsewhere,[1,2] include the isothermal compression of air at low frequencies, direct conversion of acoustical energy into heat owing to a time lag between compression, and heat flow that takes place in closed cell foams. In the case of plate and foil (very thin plate) absorbers the acoustical energy is converted into heat in the vibrating flexible plate and radiated as sound from the rear of the plate or is transmitted in the form of vibration energy into connected structures.

A sound absorber can absorb only that part of the incident sound energy not reflected at its surface. Consequently, it is important to keep the reflection at the surface as low as possible. Essentially, the part of the incident acoustical energy that enters the absorber should be dissipated before it returns to the surface after traversing the absorber and reflecting from a rigid backing. Otherwise, the absorber gives back acoustical energy to the fluid on the receiver side that is in addition to the initial reflection. This requires a sufficient thickness. The challenge in sound absorber design is to keep the absorber thickness to a minimum.

Sound Absorption Coefficients

The acoustical performance of flat sound absorbers is characterized by their sound absorption coefficient α, defined as the ratio of the sound power, W_{nr}, that is not

reflected (i.e., dissipated in the absorber, transmitted through the absorber into a room to its rear, or conducted, in the form of vibration energy, to a connected structure) and the sound power incident on the face of the absorber, W_{inc}:

$$\alpha \equiv \frac{W_{nr}}{W_{inc}} \tag{8.1}$$

For convenience in analyses, the absorption coefficient is defined in terms of sound pressure reflection factor R of the absorber interface, namely

$$\alpha = 1 - |R|^2 \tag{8.2}$$

The vertical lines bracketing R indicate the absolute value. The reflection factor R is usually a function of the angle of sound incidence, the frequency, the material, and the geometry of the absorber. The absorber is characterized by its wall impedance (otherwise known as surface impedance) Z_w, defined as

$$Z_w = \frac{p}{v_n} \quad \text{N} \cdot \text{s/m}^3 \tag{8.3}$$

where p is the sound pressure and v_n is the normal component of the particle velocity, both evaluated at the interface. A substantial part of this chapter concerns the prediction of the wall impedance offered by a large variety of sound absorbers. The sound absorption coefficient as defined in Eqs. (8.1) and (8.2) is further differentiated according to the angular composition of the incident sound field, such as *normal incidence, oblique incidence, and random incidence*, and whether the absorber is *locally reacting* (sound cannot propagate in it parallel to the interface) or *non–locally reacting* (where sound can propagate in it parallel to the interface). At normal incidence there is no difference between locally and non–locally reacting materials.

Measurement of Normal-Incidence Sound Absorption Coefficient α_0. The normal incidence sound absorption coefficient α_0 can be measured in an impedance tube according to the American Society for Testing and Materials (ASTM) standard C384-98 as $\alpha_0 = 4\zeta/(\zeta+1)^2$, where $\zeta = p_{max}/p_{min}$ is the ratio of the maximum and minimum standing-wave sound pressure pattern in the tube upstream of the sample. Normal-incidence sound absorption coefficients, measured in an impedance tube, never exceed unity.

Measurement of Random-Incidence Sound Absorption Coefficient α_R(rev) in Reverberation Room. The random-incidence sound absorption coefficient α_R(rev), which is also referred to as the *Sabine absorption coefficient*, can be measured directly in a reverberation room according to ASTM C423-02. It is defined as $\alpha_R(\text{rev}) \equiv (55.3V/S)[(1/T_S) - (1/T_0)]$, where V is the volume of the reverberation chamber in m^3, $S = 6.7$ m^2 is the standardized surface area of the test sample, and T_S and T_0 are the reverberation times in seconds (see

Chapter 7) measured with and without the sample, respectively. It is important to distinguish between the two random-incidence sound absorption coefficients α_R(rev) and α_R. The coefficient α_R(rev), measured in the reverberation room, can yield values which exceed unity (measured values up to 1.2, as can be seen in Fig. 8.10). Such values obviously violate the theoretical definition of α given in Eq. (8.36) implying that the panel absorbs more energy than is incident on it. This fact that measured values of $\alpha_R(\text{rev}) > 1$ results from the finite size of the test sample, which means that there is diffraction at the edges of the sample. In design calculations, it is customary to replace all values of $\alpha_R(\text{rev}) > 1$ with unity. The random-incidence sound absorption coefficient α_R is computed from the wall impedance and never yields absorption coefficients that exceed unity. Based on the analyses of α_R(rev) measured according ASTM C423-02 for a large variety of thicknesses and flow resistivity of Owens Corning series 700 fiberglass boards, Godfrey[6] has proposed an empirical prediction scheme to relate α_R(rev) of a standard size (6.7 m^2) sample to α_R predicted theoretically from the computed wall impedance of the samples as

$$\alpha'_R(\text{rev}) = \left(\frac{21.3}{f^{0.5}} + 0.73\right)\alpha_R$$

where α'_R(rev) is the empirically predicted Sabine absorption coefficient of a standard size sample and f is the frequency in hertz. This formula provides reasonably accurate predictions for low-flow resistivities (in the range of 9000 N · m/s^4 = 0.56 $\rho_0 c_0$/in. to 17,000 N · m/s^4 = 1.1 $\rho_0 c_0$/in.) and small layer thicknesses from 1 to 3 in. (2.5–7.5 cm). For flow resistivities greater than 32,000 N · m/s^4 = 2 $\rho_0 c_0$/in. and layer thicknesses ≥76 mm = 3 in., the analytical method[7] yields the best prediction.

8.2 SOUND ABSORPTION BY NON–SOUND ABSORBERS

Although inefficiently, all rigid and flexible structures absorb sound. If efficient sound absorbers are present in the room, the contribution of these marginal sound absorbers may be neglected. However, if they represent the only sound-absorbing mechanism (such as is in the case of reverberation rooms without low-frequency absorbers), they, and at high frequencies the air absorption, account for the total sound absorption and set an upper limit for the maximum achievable reverberation time and for the buildup of reverberant sound pressure in these special rooms.

Sound Absorption of Rigid Nonporous Wall

The general assumption that a rigid, nonporous wall, however massive, gives rise to total reflection of the incident sound is not valid. In the immediate vicinity of the interface there are two phenomena that cause small but finite dissipation of sound energy. The first is that the wall-parallel component of the particle velocity of the incident sound results in shear forces in the acoustical boundary

layer. The acoustical boundary layer is identical to that which would develop at the interface between a stationary fluid and a plane, rigid wall oscillating with the frequency and velocity amplitude of the wall-parallel component of the sound-induced particle motion. The second component of the unavoidable dissipation results from the large thermal capacity of the wall, which makes it impossible to fully recover the heat energy in the rarefaction phase that was built up in the compression phase. According to reference 4, for randomly incident sound, the combined effect of these two dissipation processes results in a lower limit of the sound absorption coefficient of

$$\alpha_{\min} = 1.8 \times 10^{-4}(f)^{1/2} \tag{8.4}$$

where f is the frequency in hertz. For frequencies of 1 and 10 kHz, Eq. (8.4) yields values of $\alpha_{\min}$ of 0.006 and 0.018, respectively.

Sound Absorption of Flexible Nonporous Wall

Building partitions such as walls, windows, and doors absorb low-frequency sound. The sound power lost, W^{Loss}, when the incident sound interacts with a nonporous, flexible, homogeneous, and isotropic single partition that has another room or the outdoors on the receiver side is made up of three components:

$$W^{\text{Loss}} = W^{\text{ForcedTrans}} + W^{\text{ResTrans}} + W^{\text{ResDiss}} \quad \text{N} \cdot \text{m/s} \tag{8.5}$$

where $W^{\text{ForcedTrans}}$ is the sound power transmitted by the forced bending waves (i.e., mass law portion radiated from the receiver side by the forced bending waves), W^{ResTrans} is the sound power transmitted by the free resonant bending waves, and W^{ResDiss} is the sound power dissipated in the partition by the free resonant bending waves. The first two terms in Eq. (8.5) can be expressed in the form of sound transmission loss, TL, of the partition and the third term as a function of the space–time mean-square value of the sound-induced resonant vibration velocity $\langle v^2 \rangle$ of the plate, yielding

$$W^{\text{Loss}} = W^{\text{inc}}\, 10^{-\text{TL}/10} + \langle v^2 \rangle \rho_S \omega \eta S \quad \text{N} \cdot \text{m/s} \tag{8.6}$$

where η is the composite loss factor of the plate accounting for energy loss through dissipation in the plate as well as for that lost through structural coupling to neighboring structures at the plate boundaries and S is the surface area of the plate in square meters. The sound absorption coefficient is defined as

$$\alpha = \frac{W^{\text{Loss}}}{W^{\text{inc}}} \tag{8.7}$$

where W^{inc} is the sound power incident on the source side of the partition. As shown in Chapter 10, for random incidence, where the sound energy has equal probability of angle of incidence, the incident sound power is

$$W^{\text{inc}} = S\left(\frac{\langle p^2 \rangle}{4\rho_0 c_0}\right) \quad \text{N} \cdot \text{m/s} \tag{8.8}$$

where S is the surface area of the partition (one side) in square meters, $\langle p^2 \rangle$ (N^2/m^4) is the mean-square space–time average sound pressure in the source room, ρ_0 is the density of air in kilograms per cubic meter, and c_0 is the speed of sound of the gas at design temperature in meters per second. Using the results of the analyses in Chapter 10, for the power dissipated in the partition by the free bending waves, one obtains the following approximate formula for the random-incidence sound absorption coefficient α^{rand} of a single, flexible, homogeneous, isotropic, nonporous partition:

$$\alpha^{\text{rand}} \approx 10^{(-\text{TL}_{\text{rand}}/10)} + \frac{2\pi\sqrt{12}\rho_0 c_0^3 \sigma_{\text{rad}}}{\rho_M h^2 c_L \omega^2} \tag{8.9}$$

where TL_{rand} = random-incidence sound transmission loss of panel (measured or predicted according to Chapter 10)
ω = angular frequency, $= 2\pi f$
f = frequency, Hz
σ_{rad} = radiation efficiency of free bending waves (see Chapter 10)
ρ_M = density of plate material, kg/m^3
h = plate thickness, m
c_L = speed sound in plate material, in m/s

The second term on the right side of Eq. (8.9) is strictly valid only if the ratio of the power loss through dissipation and sound radiation by the free bending waves exceeds unity, $(h\rho_M\omega\eta_C/\rho_0 c_0 \sigma_{\text{rad}}) > 1$, which is almost always the case because σ_{rad} strongly decreases with decreasing frequency below the coincidence frequency of the plate. In Eq. (8.9) the first term represents the loss of energy by the transmission of sound into the receiver space as defined in Chapter 10. The second term represents the combined contribution of the dissipation of the free resonant bending waves in the plate and energy loss in the form of vibration energy transmission to neighboring structures at the boundaries. It is interesting to note that this second term does not depend of the composite loss factor η_C of the plate (the TL of the plate of course depends on η_C in the frequency range at and above the critical frequency where the free bending waves control the sound radiation). The physical reason for this is that in the case of a small loss factor the plate vibrates more vigorously and the combination of the increased vibration and decreased loss factor results in the same dissipation as happens in the case of a larger loss factor and less vigorous vibration response.

While the first term in Eq. (8.9) is valid for any type of partition (including, e.g., double walls and inhomogeneous and non isotropic plates), the second term is valid only for single, homogeneous, isotropic, platelike partitions. In case of

double walls or double windows the first term will exhibit a peak at the double-wall resonance frequency where the TL has a sharp minimum. In the case of double partitions made of two isotropic, homogeneous plates with air space in between, the second term in Eq. (8.9) can be crudely approximated by entering the parameters of the source-side plate into the second term.

8.3 SOUND ABSORBERS USING THIN LAYERS

For the purposes of this chapter, we call those constructions "sound absorbers" which have been designed on purpose to yield high sound absorption in a narrow or wide frequency band. The rest of this chapter deals with the design of such absorbers. We start with those absorber configurations which can be described by a few directly measurable parameters, such as a thin, flow-resistive layer in front of an air space backed by a rigid wall that can be fully characterized by its flow resistance and mass per unit surface area, and will proceed to configurations utilizing thick porous layers and to tuned absorbers.

Thin, Flow-Resistive Layer in Front of Rigid Wall

A sound absorber that consists of a thin, flow-resistive material in front of a rigid wall with an air space in between, such as shown in Fig. 8.1, is the configuration for which it is the easiest to predict acoustical performance. Accordingly, it is logical to treat it first. The flow-resistive layer might be rigid or flexible.

The sketch on the left in Fig. 8.1 depicts a configuration where the air space between the rigid porous layer and the rigid wall is partitioned in a honeycomb pattern to prohibit propagation of sound parallel to the plane of the porous layer. This absorber configuration is called *locally reacting* because the sound field in the absorber depends only on the sound pressure on the interface at the location of the particular honeycomb cell. The sound in the absorber can propagate only perpendicular to the plane of the interface. The sketch on the right in Fig. 8.1 has no partitioning of the air space and the sound can propagate within the absorber parallel to the plane of the interface. The sound pressure at any particular location in the air space depends on the sound pressure on all the locations on the sound-exposed face of the absorber. This configuration is called a *non–locally reacting* sound absorber.

Rigid Porous Layer

A thin, rigid, flow-resistive layer can be fully characterized by a single parameter, namely its flow resistance R_f or its normalized impedance $z' = R_f/(\rho_0 c_0)$, where ρ_0 is the density and c_0 is the speed of sound of the fluid. The normalized impedance of the partitioned air space is $z'' = j\cot(kt)$, where $k = 2\pi/\lambda$ is the wavenumber, λ is the wavelength of the sound, and t is the depth of the air space.

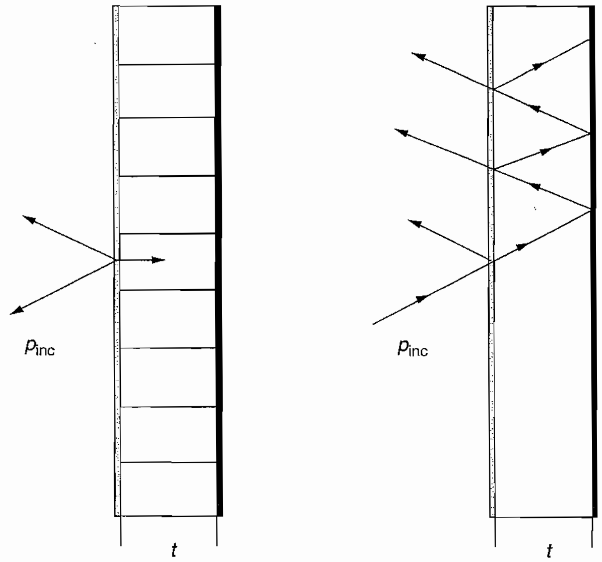

FIGURE 8.1 Thin porous sound-absorbing layer in front of an air space backed by a rigid wall. Left: Partitioned, locally reacting air space. Right: Not partitioned, non–locally reacting air space.

The normalized wall impedance for normal incidence, $\theta = 0$, is then given by

$$z_{w0} = z' + jz'' = \frac{R_f}{\rho c} + j\ \cot(kt) \tag{8.10}$$

The impedance of the air space is zero when $\cot(kt) = 0$, which is the case at those frequencies where the depth of the air space is an odd number of quarter wavelengths. The maximum value of the normal-incidence sound absorption coefficient is

$$\alpha_{0,\max} = \frac{4z'}{(1+z')^2} \tag{8.11}$$

indicating that total absorption occurs for $z' = 1$. According to reference 4, the normal-incidence sound absorption coefficient is given by

$$\alpha_0(f) = \left\{\left[\left(\frac{R_f}{\rho_0 c_0}\right)^{0.5} + \left(\frac{\rho_0 c_0}{R_f}\right)^{0.5}\right]^2 + \frac{\rho_0 c_0}{R_f}\cot^2\left(\frac{2\pi f t}{c_0}\right)\right\}^{-1} \tag{8.12}$$

Ingard[1] has computed the sound absorption coefficient of a rigid, flow-resistive layer in front of a locally reacting (partitioned) and non–locally reacting (unpartitioned) air space backed by a rigid wall for both normal and random incidence, as shown in Fig. 8.2.

Figure 8.2 shows that for a locally reacting air space the maximum normal-incidence sound absorption coefficient occurs at those frequencies where the depth of the air space corresponds to an odd multiple of quarter wavelengths [$t = (n+1)\lambda/4$, where $n = 0, 1, 2, \ldots$]. The physical reason for this is that the sound pressure in the partitioned air space just behind the porous layer is zero at these frequencies (the sound that is fully reflected from the hard wall is 180° out of phase with the incident sound). Consequently, the sound pressure gradient across the porous layer, Δp, reaches its maximum value that is numerically equal to the sound pressure on the incident side of the layer, namely $\Delta p = p_{\text{inc}}(1+R)$, where p_{inc} is the amplitude of the incident sound and R is the reflection factor:

$$R = \frac{R_f - \rho_0 c_0}{R_f + \rho_0 c_0}$$

This pressure gradient produces a particle velocity $v = \Delta p / R_f$ through the porous layer and the sound power dissipated per unit surface area of the absorber,

$$W^{\text{diss}} = v\,\Delta p = \frac{(p_{\text{inc}})^2(1+R)^2}{R_f}$$

In the case of $R_f = \rho_0 c_0$, $R = 0$ and $W^{\text{diss}} = (p_{\text{inc}})^2/(\rho_0 c_0) = W^{\text{inc}}$, indicating that all of the incident sound energy is dissipated in the porous layer. For values of $R_f \neq \rho_0 c_0$, the sound absorption coefficient still is a maximum but less than unity. The more R_f differs from $\rho_0 c_0$, the smaller is the sound absorption coefficient.

The maxima of the random-incidence sound absorption coefficient for a partitioned air space occur at the same frequencies as those at normal incidence. However, there is no value of R_f that would yield total absorption.

Another significant feature to be noted from Fig. 8.2 is that for a partitioned, locally reacting air space curves for both the normal and random-incidence sound absorption coefficients versus frequency have notches (zero absorption) at frequencies that correspond to an even multiple of half wavelengths. This occurs because at the corresponding frequencies the sound reflected from the hard wall combines at the rear of the porous layer with the incident sound in such a manner that there is no sound pressure gradient across the porous layer and consequently no sound is absorbed at these frequencies. This does not affect the random-incidence sound absorption coefficient obtained for the not partitioned (non–locally reacting) air space, as shown in the curves marked c. The advantage of not having notches in curves of the random-incidence sound absorption coefficient versus frequency must be "paid for" by having substantially lower sound absorption at low frequencies. The most important observation from Fig. 8.2 is that it is not possible to achieve a high sound absorption coefficient with a rigid porous layer in front of an air space backed by a rigid wall unless the thickness

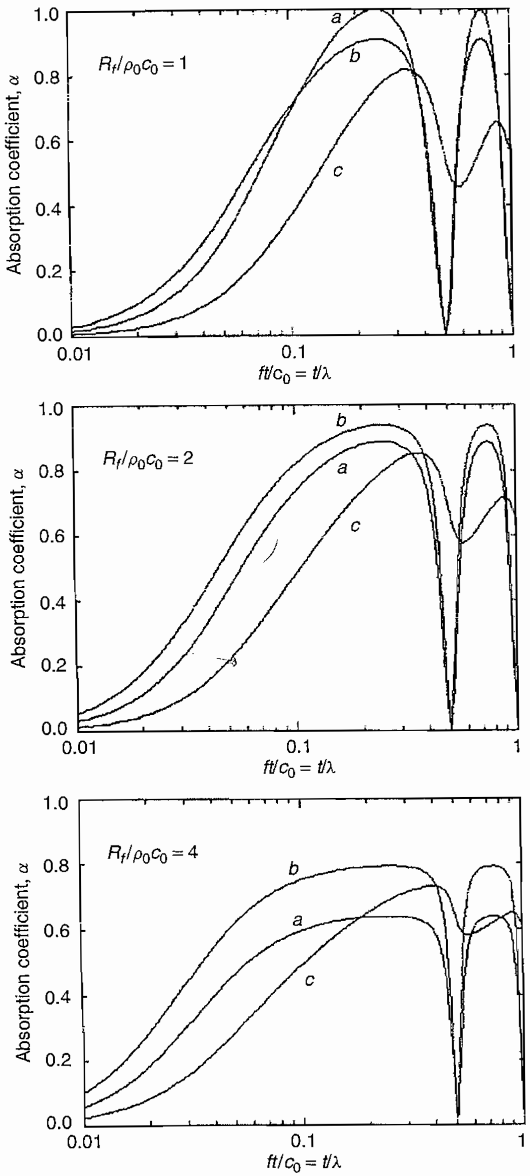

FIGURE 8.2 Sound absorption coefficient of a single, rigid, flow-resistive layer in front of an air space of thickness t backed by a hard wall as a function of the normalized frequency in the form of air space thickness–wavelength ratio $t/\lambda = tf/c_0$ with the normalized flow resistance of the layer, $R_f/\rho_0 c_0$, as the parameter: a, normal incidence; b, random-incidence, locally reacting air space; c, random-incidence, non–locally reacting air space. (After Ref. 1.)

of the air space exceeds one-eighth of the wavelength. For example, an air space thickness of 0.4 m (17 in.) or more is necessary to achieve a high degree of sound absorption at 100 Hz.

As we will discuss below, substantial low-frequency sound absorption can be achieved with an air space thickness of less than one-eighth of the wavelength if the porous layer is not rigid.

Limp Porous Layer

It is little known that sound absorbers using a limp, flow-resistive layer can provide high sound absorption at much lower frequencies than those with a rigid layer. However, caution should be exercised in designing such absorbers for applications where the sound pressure is very high. The limp, flow-resistive layer (e.g., heavy glass fiber cloth or stainless steel wire mesh) should be able to withstand the stresses owing to the high-amplitude sound-induced motion without fatigue. If the porous sound-absorbing layer is limp instead of being rigid, the mass per unit area of the layer and the stiffness per unit area of the air space between the layer and the hard wall result in a resonant system. Near the resonance frequency the limp porous layer will exhibit large-amplitude motion. Approximately, the resonance frequency f_{res} is given by[1]

$$f_{\text{res}} \approx \frac{1}{2\pi}\left(\frac{\kappa\rho_0(c_0)^2}{tm''}\right)^{1/2} \quad \text{Hz} \tag{8.13}$$

where $\kappa = 1.4$ is the adiabatic compression coefficient, t is the thickness of the air space in meters, and m'' is the mass per unit area of the limp porous layer in kilograms per square meter. The analytical model to predict the sound absorption coefficient of sound absorbers utilizing a limp porous screen is documented in reference 1. The computer program on the CD included in reference 1 allows prediction of the normal- and random-incidence sound absorption coefficient of such absorbers with locally reacting and non–locally reacting air space. The data in Figs. 8.3–8.5 were computed this way and show the sound absorption coefficient as a function of the normalized frequency, $f_n = t/\lambda = tf/c_0$, with the normalized flow resistance of the limp porous layer ($R_f/\rho_0 c_0$) as a parameter for various ratios of the mass of the limp layer and the mass of air in the air space behind, $\text{MR} = m''/t\rho_0$.

Figure 8.3 shows that the first maximum of the normal-incidence sound absorption coefficient occurs close to the mass–spring resonance frequency given by Eq. (8.13). The higher is the mass ratio $\text{MR} = m''/\rho_0 t$, the lower is the frequency of the peak sound absorption. For $\text{MR} = 16$ the frequency of the peak occurs at a frequency that corresponds to a normalized frequency $f_n = 0.03$. This is more than a factor of 8 lower than the peak at $f_n = 0.25$ one would obtain with a rigid porous layer. Also note that the first peak of the normal-incidence sound absorption coefficient is unity (100% absorption) if the mass ratio equals the normalized flow resistance (i.e., when $\text{MR} = R_f/\rho_0 c_0$). To achieve a relatively high

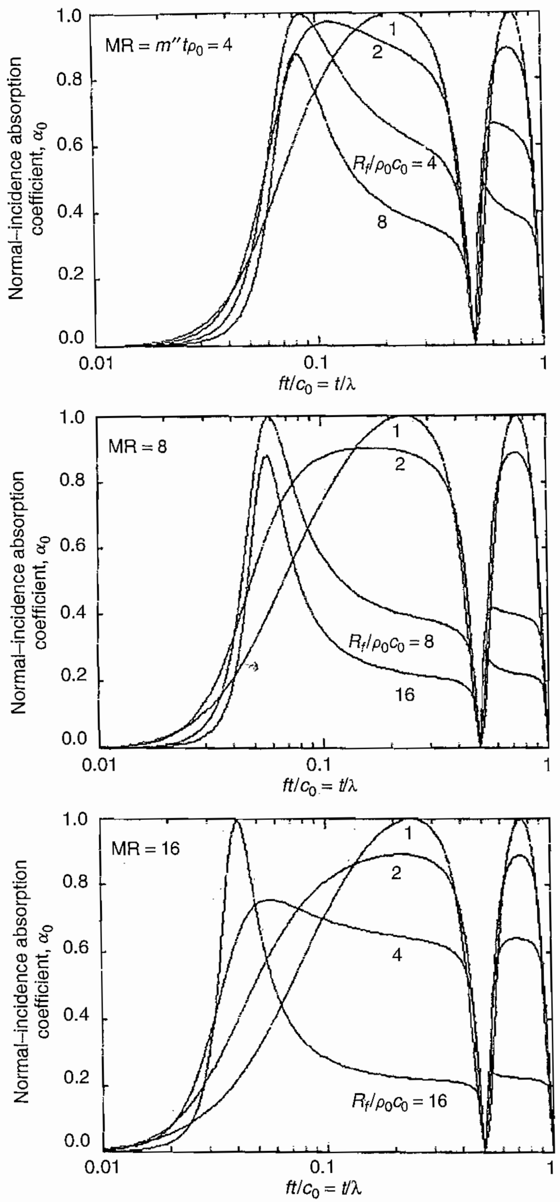

FIGURE 8.3 Normal-incidence absorption coefficient of a single, limp, flow-resistive layer in front of an air space of thickness t backed by a rigid wall as a function of the normalized frequency in the form of the thickness–wavelength ratio $t/\lambda = tf/c_0$ with the normalized flow resistance of the layer, $R_f/\rho_0 c_0$, as the parameter for mass ratios MR. (After Ref. 1.)

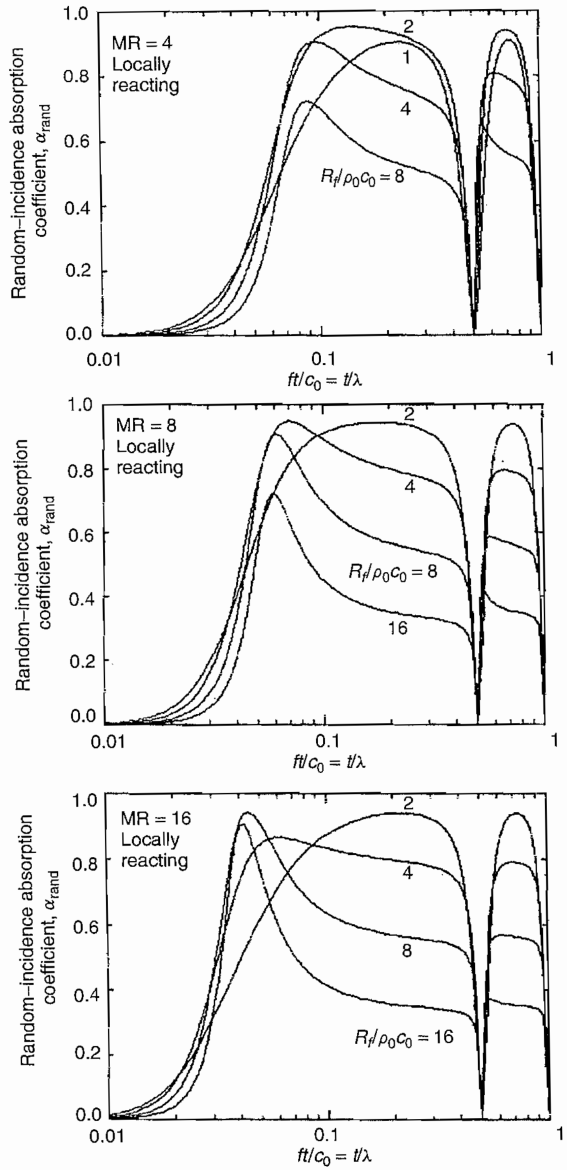

FIGURE 8.4 Random-incidence absorption coefficient of a single, limp, flow-resistive layer in front of a partitioned (locally reacting) air space of thickness t backed by a rigid wall as a function of the normalized frequency in the form of the thickness–wavelength ratio $t/\lambda = tf/c_0$ with the normalized flow resistance of the layer, $R_f/\rho_0 c_0$, as the parameter for mass ratios MR. (After Ref. 1.)

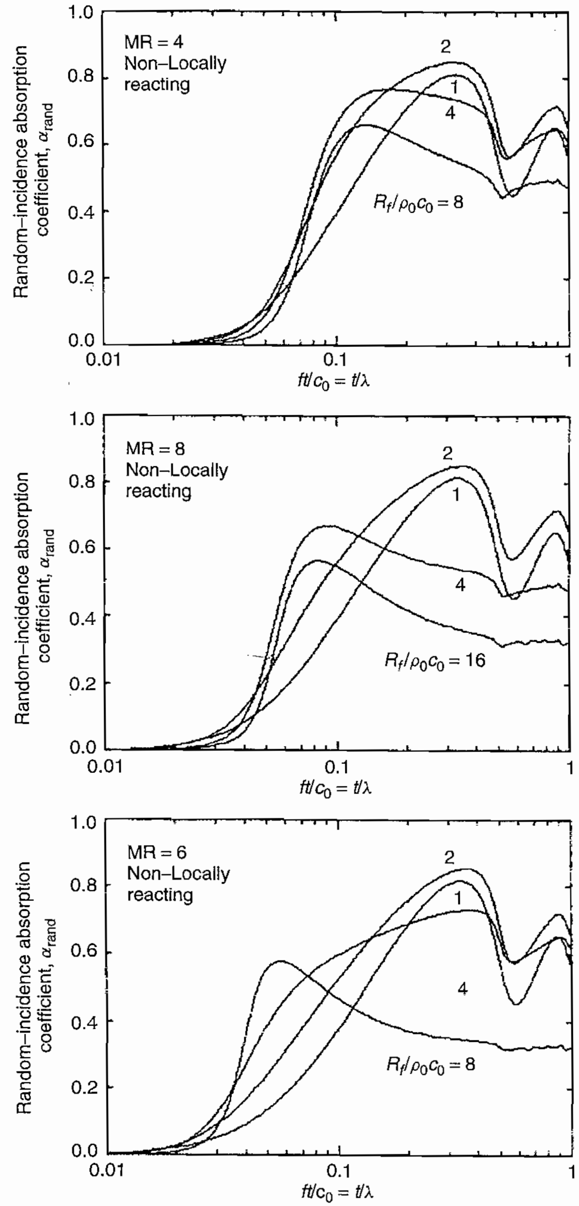

FIGURE 8.5 Random-incidence absorption coefficient of a single, limp, flow-resistive layer in front of a not-partitioned (non–locally reacting) air space of thickness t backed by a rigid wall as a function of the normalized frequency in the form of the thickness–wavelength ratio $t/\lambda = tf/c_0$ with the normalized flow resistance of the layer, $R_f/\rho_0 c_0$, as the parameter for mass ratios MR. (After Ref. 1.)

low-frequency absorption in a wide frequency band, a normalized flow resistance $R_f/\rho_0 c_0$ of between 2 and 3 seems to be a good choice.

Figure 8.4 shows the random-incidence sound absorption coefficient as a function of the normalized frequency computed for a locally reacting (partitioned) air space. Sufficient distance must be provided between the limp porous layer and the honeycomb configuration used to partition the air space to prevent the limp layer from hitting the honeycomb layer at the largest expected displacement amplitude. Curves of the absorption coefficient versus the normalized frequency have similar shape as those in Fig. 8.3 for normal incidence, except that no combination of the design parameters results in total absorption. To obtain substantial low-frequency sound absorption, the mass ratio MR ≈ 2 seems to be a good choice.

Figure 8.5 shows the random-incidence sound absorption coefficients for a non–locally reacting (unpartitioned) air space. Note the very different behavior from that observed for the partitioned air space in Figs. 8.2 an 8.3. The first, and undesirable, difference is that no combinations of parameters yield random-incidence sound absorption coefficients much above $\alpha_{rand} = 0.8$. The second, and desirable, attribute of the nonpartitioned air space is that there are no notches in the frequency response where the absorption coefficient would go to zero, as was the case for the partitioned air space.

Multiple Limp Porous Layers

As documented in reference 1, very high sound absorption at low frequencies can be achieved over nearly four octaves by placing a large number (up to 16) of limp, porous layers of low-flow resistance in front of a rigid wall. The computer program supplied with reference 1 allows the prediction of the normal- and random-incidence sound absorption coefficients of such absorbers and the optimization of performance by trial and error varying the flow resistance, mass per unit area, and number and position of the layers.

8.4 POROUS BULK SOUND-ABSORBING MATERIALS AND ABSORBERS

Porous bulk sound-absorbing materials are utilized in almost all areas of noise control engineering. This section deals with the following aspects:

1. description of the key physical attributes and parameters that cause a porous material to absorb sound,
2. description of the acoustical performance of porous sound absorbers used to perform specific noise control functions,
3. compilation of acoustical parameters that allow the quantitative design of sound-absorbing configurations on the bases of material and geometric parameters, and

4. experimental methods for measuring the acoustical parameters of porous sound-absorbing materials and the acoustical performance of porous sound absorbers.

Porous materials used for sound absorption may be fibrous, cellular, or granular. Fibrous materials may be in the form of mats, boards, or preformed elements manufactured of glass, mineral, or organic fibers (natural or man made) and include felts and felted textiles. Applications of fibrous materials in silencers require some form of protective covering. The most common covering consists of perforated metal with a fiberglass cloth behind. Sometimes metal screens are inserted between the perforated metal and fiberglass cloth. Cellular materials include polymer foams of varying degrees of rigidity and porous metals. For special applications increasing use is being made of porous metals (e.g., aluminum foams) as sound absorbers. During manufacture, before solidification, metal foams have closed cells, that is, without interconnections. At this stage such materials are poor sound absorbers. However, as liquid-metal foams solidify, thermal stresses occur. The solidified foams usually have cracked cell walls, which significantly increases sound absorption. In addition, by slightly rolling thin sheets of foam from, say, a thickness of 10 to 9 mm, further mechanical cracking occurs, and the interconnections between adjacent cells widen. This increases sound absorption even more. The result is an absorption coefficient versus frequency that has a maximum between 1 and 5 kHz and a peak value of up to 95%. By placing an air gap between metal foam and a rigid wall, one can shift the frequency curve to lower frequencies. In comparison with other materials, glass wool, for example, which gives high absorption over a wide frequency range, metal foams are not very good sound absorbers. However, the high weight-specific stiffness, good crash-energy absorption ability, and fire resistance of porous metals make them suitable for sound absorption panels in the aircraft and automotive industries.

Granular materials can be regarded as an alternative to fibrous and foam absorbers in many indoor and outdoor applications.[8] Sound-absorbing granular materials combine good mechanical strength and very low manufacturing costs. Granular materials may be unconsolidated (loose) or consolidated through use of some form of binder on the particles as in wood-chip panels, porous concrete, and pervious road surfaces. As well as man-made granular materials, there are many naturally occurring granular materials, including sands, gravel, soils, and snow. The acoustical properties of such materials are important for outdoor sound propagation.

A common feature of porous sound-absorbing materials is that the pores are interconnected and have typical dimensions below 1 mm, that is, much less than the wavelengths of the sounds of interest in noise control.

Porous materials must be considered to be elastic if they are in the form of flexible sheets. However, in many cases, the stiffness of the solid frame of the material is much greater than that of air so that the material may be treated as if it were rigid over a wide range of frequencies. This means that such materials can be treated as lossy, homogeneous media. This chapter will be confined to porous materials that may be treated as rigid framed.

How Rigid Porous Materials Absorb Sound

When excited by an incident sound wave, the air molecules in the pores of a porous material are made to oscillate. The proximity of the surrounding solid means that the oscillations result in frictional losses. An important factor that determines the relative contribution of frictional losses is the size (width) of the pores relative to the thickness of the viscous boundary layer. At low frequencies the viscous boundary layer thickness might be comparable with the pore width and the viscous loss is high. At high frequencies the viscous boundary layer thickness may be significantly less than the pore size and the viscous loss is small. At such high frequencies the oscillating flow is "pluglike." However, the presence of the solid causes changes in the flow direction and expansions and contractions of the flow through irregular pores, resulting in loss of momentum in the direction of wave propagation. This mechanism is relatively important at higher frequencies. In the larger pores and at lower frequencies heat conduction also plays a part in energy loss. During the passage of a sound wave, the air in the pores undergoes periodic compression and decompression and an accompanying change of temperature. If the solid part of the material is relatively heat conducting, then the large surface-to-volume ratio means that during each half-period of oscillation there is heat exchange and the compressions are essentially isothermal. At high frequencies the compression process is adiabatic. In the frequency range between isothermal and adiabatic compression the heat exchange process results in further loss of sound energy. In a fibrous material this loss is especially high if the sound propagates parallel to the plane of the fibers and may account for up to 40% of sound attenuation (energy lost per meter of propagation). The losses from forced mechanical oscillations of the skeleton of a porous material are generally so low that it is reasonable to neglect them.

Physical Characteristics of Porous Materials and Their Measurement

Porosity. The gravimetric measurement of porosity requires the weighing of a known volume of dry material. Since in inexpensive fibrous materials, such as mineral wool, the large droplets (or shot with diameter over 100 μm) may constitute up to 30% of the weight, their contribution to the acoustical porosity should be disregarded. Shot can be separated from fiber by a centrifuge process. The dry weight can be used together with the sample volume to calculate the bulk density ρ_B. Subsequently an assumed solid density is used to calculate the porosity h from

$$h = 1 - \frac{\rho_A}{\rho_B} \tag{8.14}$$

For glass fiber and mineral wool products the density of the fiber material is $\rho_B =$ 2450 kg/m^3. For silica sand, the density of the mineral grains is 2650 kg/m^3. A gravimetric method which may be used with some consolidated granular materials is to saturate the sample with water and deduce the porosity from the relative weights of the saturated and unsaturated samples. Mercury has been used as the pore-filling fluid in some applications (e.g., soils), but for many materials the introduction of liquids affects the pores. Following a proposal of Cremer and Hubert,[9] Champoux et al.[10] have developed a *dry* method of porosity determination which is based on the measurements of the change in pressure within a sample container subject to a small known change in volume. The lid of the container is a plunger, which is driven by a precise micrometer. The pressure inside the chamber is monitored by a sensitive pressure transducer and an air reservoir connected to the container through a valve serves to isolate the system from fluctuations in atmospheric pressure. The system has been estimated to deliver values of porosity accurate to within 2%. An important feature of the method from the point of view of acoustical properties is that it measures the porosity of connected air-filled pores. However, the gravimetric methods do not differentiate between sealed pores and connected pores. Recently a new method for determining porosity based on a simple measurement of displaced air volume has been proposed.[11] This has the advantage that it does not require compensation for temperature, as does the method of Champoux et al.[10]

An alternative method which may be used with some consolidated materials is to saturate the sample with water and deduce the porosity from the relative weights of the saturated and unsaturated samples.

An acoustical (ultrasonic) impulse method for measuring porosity using the impulse reflected at the first interface of a slab of air-saturated porous material has been proposed and has been shown to give good results for plastic foams[12–14] and random bead packing.[15]

The porosity of a stack of spherical particles depends on the form of the packing, ranging from 0.26 for the densest packing (face-centered-cubic) to 0.426 for simple-cubic packing.[16] A random packing of spheres has a porosity of 0.356.[17] An approximate value that may be assumed for the porosity of a granular material is 0.4.

Typical ranges of values of porosity are listed in Table 8.1.

Tortuosity. The tortuosity of a porous solid is a measure of the irregularity of the fluid-filled paths through the solid matrix. At very high frequencies, it is responsible for the difference between the speed of sound in air and the speed of sound through a rigid porous material. Tortuosity is related to the formation factor used to describe the electrical conductivity of a porous solid saturated with a conducting fluid. Indeed, tortuosity can be measured using an electrical conduction technique in which the electrical resistivity of such a saturated porous sample is compared to the resistivity of the saturating fluid alone. Thus

$$T = \frac{F}{h} \tag{8.15}$$

TABLE 8.1 Measured and Calculated Values of Porosity and Tortuosity

Material	Porosity, h	Method of Determination	Tortuosity, T	Method of Determination
Lead shot, 3.8 mm particle size	0.385	Measured by weighing	1.6	Estimated as $\alpha = 1/\phi^{0.5}$ (fits acoustic data)
			1.799	Cell model predictions[a]
Gravel, 10.5 mm grain size	0.45	Measured by weighing	1.55	Deduced by fitting surface admittance data
Gravel, 5–10 mm grain size	0.4	Measured by weighing	1.46	Deduced by fitting surface admittance data
Glass beads, 0.68 mm[b]	0.375	Unspecified	1.742	Measured[c]
			1.833	Cell model predictions[a]
Coustone[b]	0.4	Unspecified	1.664	Measured[c]
Foam YB10[b]	0.61	Unspecified	1.918	Measured[c]
Porous concrete	0.312	Measured	1.8	Deduced by fitting surface admittance data
Clay granulate, Laterlite, 1–3 mm grain size	0.52		1.25	Deduced by fitting surface admittance data (assuming porosity of 0.52)
Olivine sand	0.444	Measured	1.626	Cell model predictions[a]
Aluminum foam	0.93	Measured by weighing	1.1	Ultrasonic measurements (laser-generated pulses)
			1.07	Deduced by fitting surface admittance data
Polyurethane foam (Recticel Wetter, Belgium)				
Sample w1[d]	0.98	Measured	1.06	Measured
Sample w2[d]	0.97	Measured	1.12	Measured

[a]From Ref. 20.
[b]From Ref. 26.
[c]From Ref. 11.
[d]From Ref. 27.

where F is the formation factor defined by

$$F = \frac{\sigma_S}{\sigma_f} \tag{8.16}$$

where σ_f and σ_S are the electrical conductivities of the fluid and the fluid-saturated sample, respectively. These in turn are defined by

$$\sigma = \frac{GL}{A} \tag{8.17}$$

where L is the length of the sample, A is the area of the end of the sample, and G is the ratio of the resulting current to the voltage applied across the sample.

To measure the formation factor, first a cylindrical sample of the material is saturated with a conducting fluid (brine solution is convenient). Saturation is achieved by drawing the fluid through the sample after forming a vacuum above it. Agitation of the sample is also required if the pore sizes are small. A voltage is applied across the saturated sample placed between two similarly shaped electrodes at a known separation. The conductivity of the fluid is measured at similar voltages within a separate fluid-tight unit. The use of separate current and voltage probes assures a good contact between the end of the sample and the electrodes, eliminates problems associated with voltage drop at the current electrodes, and allows the simultaneous measurement of the electrical resistivities of the fluid and the saturated porous material.

The tortuosity of a random stacking of glass spheres is given by $1/\sqrt{h}$.[18] This has been verified for a range of porosities from 0.33 to 0.38 and is a special case of the relationship

$$T = h^{-n'} \tag{8.18}$$

where n' depends on grain shape and has the value 0.5 for spheres.[19]

An alternative derivation for stacked identical spheres[20] gives

$$T = 1 + \frac{1-h}{2h} \tag{8.19}$$

The equivalent formula for the tortuosity of a system of identical parallel fibers is

$$T = \frac{1}{h} \tag{8.20}$$

This means that the tortuosity of a typical fibrous material used in noise control is a little larger than 1 since the porosity is close to (but never greater than) 1. In a rigid porous material, tortuosity is one of the properties that contribute to the "structure factor" used in classical descriptions and is related to the "added mass" that is used in the theory of propagation of sound in porous and elastic materials.[21] The structure factor, introduced in classical texts, is intended to include frequency-dependent thermal effects (complex bulk modulus) and frequency-dependent effects due to fiber motion. This means it can *only* be determined by acoustical means. For characterizing the acoustical properties of a bulk porous material, tortuosity is preferred over the structure factor since it has clear physical meaning and can be deduced by nonacoustical means in many cases.

At the highest frequencies, the speed of sound inside the rigid porous material is equal to the speed of sound in air divided by the square root of tortuosity. Since it is primarily responsible for the acoustical properties of porous materials at high audible or ultrasonic frequencies, tortuosity can be deduced from ultrasonic measurements.[22]

Some representative values of tortuosity are listed in Table 8.1.

Flow Resistance and Flow Resistivity. The most important parameter in determining the acoustical behavior of thin porous materials is the airflow resistance R_f. For bulk-, blanket-, or board-type porous materials the flow resistivity (specific flow resistance per unit thickness) $R_1 = R_f/\Delta x$, where Δx is the thickness of the layer, is the key acoustical parameter. The flow resistivity is a measure of the resistance per unit thickness inside the material experienced when a steady flow of air moves through the test sample. Flow resistance R_f represents the ratio of the applied pressure gradient to the induced volume flow rate and has units of pressure divided by velocity. If a material has a high flow resistivity (high flow resistance per unit thickness), it means that it is difficult for air to flow through the surface. In disciplines other than noise control engineering (e.g., geophysics), it is more common to refer to air permeability (k), which is related to the inverse of flow resistivity ($k = \eta/R_1$, where η is the dynamic coefficient of air viscosity). Since flow resistivity is related to the inverse of permeability, high flow resistivity implies low permeability. Typically, low permeability results from very low surface porosity.

Flow resistance is measured as

$$R_f = \frac{\Delta p}{v} = \frac{TS\,\Delta p}{V} \quad \mathrm{N \cdot s \cdot m^{-3}} \text{ or } \mathrm{Pa \cdot s \cdot m^{-1}} \text{ (mks rayls)} \tag{8.21}$$

From this the flow resistivity is obtained as

$$R_1 = \frac{R_f}{\Delta x} \quad \mathrm{N \cdot s \cdot m^{-4}} \text{ or } \mathrm{Pa \cdot s \cdot m^{-2}} \text{ (mks rayls/m)} \tag{8.22}$$

where Δp is the static pressure differential across a homogeneous layer of thickness Δx, v is the velocity of the steady flow through the material, V *is* the volume of air passing through the test sample during the time period T, and S is face area (one side) of the sample.

Since R_f generally depends on the velocity v, it is customary to measure it at a number of different flow rates and extrapolate measured R_f versus v to R_f ($v = 0.05$ cm/s) because below this particle velocity the flow resistance of most fibrous materials does not depend any more on the velocity. The fact that, in general, flow resistivity depends on particle velocity becomes important when considering the behavior of porous absorbers at high sound levels.

The measurement of the flow resistance and flow resistivity of porous building materials has been standardized on a compressed-air apparatus.[23] A similar apparatus may be used to determine the flow resistivity of soils or granular materials (Fig. 8.6). In this measurement the pressure gradient across the sample in a fixed sample holder is monitored together with various (low) flow rates. Compressed air is passed through a series of regulating valves and a very narrow opening into chamber E. This creates an area of low pressure immediately in front of the three tubes connected to the rest of the system. Air is drawn from the environment through the sample as a result of the pressure differential. The rate of airflow through the system is controlled by three flowmeters, giving a total measurement

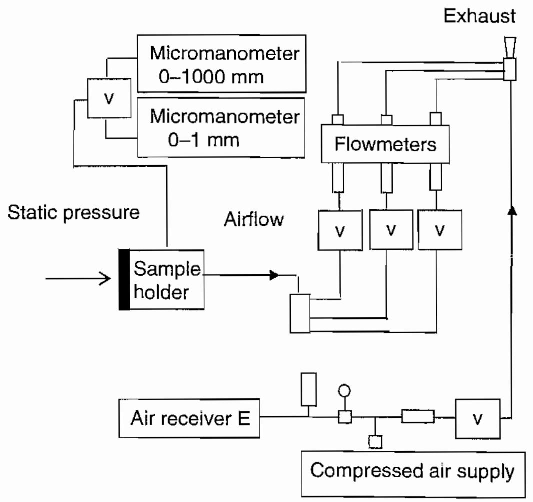

FIGURE 8.6 Concept sketch of a compressed-air apparatus for laboratory measurement of flow resistance.

range between 8.7 and 0.1 L/min. Typically the flow rate must be kept below 3 L/min to avoid structural damage to the sample.

A comparative method[24] makes use of a calibrated known resistance (a laminar-flow element) placed in series with the test sample. Variable-capacitance pressure transducers are used to measure pressure differences across both the test sample and the calibrated resistance. For steady, nonpulsating flow, the ratio of flow resistances equals the ratio of measured pressure differences. The airflow may also be controlled electronically. A unique method of measuring flow resistance by Ingard[1] does not require any flow-moving device, flow-rate meter, or static pressure differential sensor, just a stop watch. In this test setup the airflow (after the piston reaches its terminal velocity) is forced trough the sample, located at the open bottom end of the tube, at a constant rate driven by the static pressure differential $\Delta p = Mg/S$, determined by the weight, Mg, of a tightly sliding piston in the sample holder tube and by the cross-sectional area S of the piston. The factor $g = 9.81$ m/s^2 is the acceleration due to gravity. The flow resistance of the sample is then inversely proportional to the time T_L required for the piston to travel a specific distance L. The flow resistance of the sample is determined as $R_f = C[Mg\cos(\Phi)/LA^2]\,ST_L$, where A is the free surface area of the sample and Φ is the angle of tube axis with the vertical. For vertical tube orientation $\Phi = 0$. The small leakage flow between the piston and the tube wall, which is of consequence only if the sample has a very high flow resistance, is accounted for by the correction factor

$$C = \frac{1 + T_{L0}/T_L}{1 - T_L/T_{\text{Closed}}}$$

where T_{L0} and T_{Closed} are respectively the piston travel times with the sample removed and when the end of the tube is air tightly closed. The variation of the flow rate through the sample (needed to extrapolate the flow resistance to 5×10^{-4} m/s) can be accomplished by either changing the tube axis angle Φ or increasing the mass of the piston.

Empirical Prediction of Flow Resistivity. According to private communications with Richard Godfrey[6] of Owens Corning Corporation, the flow resistivity of fibrous sound-absorbing materials can be approximately predicted by a slightly modified version of Eq. 10.4 of the 1971 edition of this book. The modified equation is

$$R_1 \approx \frac{3450}{d^2}\left[\left(\frac{\text{SpGrGlass}}{\text{SpGrFiber}}\right)\rho_{\text{bulk}}\right]^{1.53} \quad \text{N} \cdot \text{m/s}^4 \qquad (8.23)$$

where d is the average fiber diameter in micrometers (10^{-6} m), SpGrGlass and SpGrFiber are the specific gravities of glass and that of the actual fiber material, and ρ_{bulk} is the bulk density (with shot contribution deducted) of the fibrous material in kilograms per cubic meter. Note that 1 μm $= 4 \times 10^{-5}$ in. and that $\rho_{\text{bulk}} \approx \rho_M h$, where ρ_M is the density of the fiber material and h is the porosity. It has been found that flow resistivity values measured according to the American Society of Mechanical Engineers (ASME) Standard E 522 for the entire glass fiber-based product line of different bulk densities and fiber diameters are successfully predictable by Eq. (8.23) with a correlation coefficient of 0.93. Equation (8.23) also can be used for predicting the flow resistivity of polymer-based fibrous sound-absorbing materials. For the same bulk density, the polymer fibers have approximately 2.5 times as much surface area and flow resistivity as glass fibers.

Theoretical Prediction of Flow Resistivity. For almost all granular or fibrous sound-absorbing materials, the flow resistivity cannot be predicted analytically on the basis of the geometry of the skeleton. It must be measured. For a few idealized absorber materials, such as materials made of identical spheres or parallel identical fibers, it is possible to make such a prediction. Since the prediction formulas identify important parameters that might be used to scale flow resistivity data measured for a specific material composition to other compositions in cases where direct measurement of the flow resistivity is not feasible, it is instructive to consider at least one idealized case where theoretical prediction is possible.

For stacked identical spheres with radius r it can be shown that[20]

$$R_1 = \frac{\eta}{k} = \frac{9\eta(1-h)}{2r^2h^2}\,\frac{5(1-\Theta)}{5 - 9\Theta^{1/3} + 5\Theta - \Theta^2} \qquad (8.24)$$

where h is the porosity and

$$\Theta = \frac{3}{\sqrt{2\pi}}(1-h) \cong 0.675(1-h) \qquad (8.25)$$

The equivalent formula for the flow resistivity of a system of identical parallel fibers of radius r is[25]

$$R_1 = \frac{16\eta h(1-h)}{r^2h^2\left[(1-8\Gamma)+8\Gamma(1-h)-(1-h)^2-2\,\ln(1-h)\right]} \tag{8.26}$$

where $\Gamma \approx 0.577$. This formula overestimates the flow resistivity of fibrous materials as a consequence of shot content, random fiber orientation, and distribution of fiber diameters in a real material.

Analytical Characterization of Porous Granular or Fibrous Sound-Absorbing Materials. For certain idealized microstructures such as parallel, identical cylindrical or slitlike pores, it is possible to make straightforward analytical predictions of the acoustical properties.[1,19,21] Although analytical characterization of porous granular or fibrous sound-absorbing materials with arbitrary microstructures is possible, it is a relatively complex procedure.[27–31] Moreover, at present, many of the required parameters are not routinely available to practicing noise control engineers. Consequently, the analysis is not reviewed in this chapter. For a comprehensive introduction to recent analytical treatments, the reader should consult reference 21. Semiempirical formulas for the acoustical properties of fibrous materials have been derived based on such a sophisticated analytical treatment.[32] It should be noted, also, that empirical formulas have been derived that predict the acoustical properties of granular media from knowledge only of porosity, grain density, and mean grain size.[33]

Acoustical Properties of Porous Materials. The acoustical properties of porous sound-absorbing materials are characterized by their complex propagation constant k_a and complex characteristic impedance Z_{Ca}, which are defined by

$$p(x,t) = \hat{p}e^{-jk_ax}e^{j\omega t} \quad \text{N/m}^2 \tag{8.27}$$

$$\langle p(x,t)\rangle_y = Z_{Ca}\langle v_x(x,t)\rangle_y \quad \text{N/m}^2 \tag{8.28}$$

where $\hat{p}$ represents the amplitude at $x = 0$ and $\langle\cdots\rangle$ represents an average perpendicular to the propagation direction (x) over an area that is small compared with the wavelength but large compared with the size of pores. The propagation constant

$$k_a = \beta - j\alpha$$

includes the attenuation constant α, which may be obtained by using a probe tube microphone to measure the decrease of the sound pressure level (in nepers per meter) of a plane sound wave propagating in a very thick layer of material. The phase constant β is obtained by measuring the change of phase with distance. It is equal to the angular frequency divided by the frequency-dependent sound speed within the material. The complex characteristic impedance $Z_{Ca} = R_{Ca} - jX_{Ca}$ is obtained by measuring the surface impedance of a thick layer (sufficiently thick

that reflection from the end is not detectable) of the absorber material placed in an impedance tube.

An alternative to use of a thick sample with a practically "infinite length" is to use a sample of known finite length and to measure the transfer function between two microphones located in an impedance tube with the loudspeaker source at one end and the sample at the other (closed) end.[34] A broadband input signal such as white noise or a sine sweep can be used. By means of a frequency analysis, output signals from the microphones are used to calculate the transfer function, which is converted to the surface impedance of a sample. The characteristic impedance and propagation constant of a sample can be obtained as long as two distinct sets of surface impedance are measured. This can be realized by using either two samples of different thicknesses[35] or a single sample backed with two different lengths of air cavities.[36] For the former, the two-thickness method, it is convenient if the length of the second sample is double that of the first. In the two-cavity method, the difference in the lengths of the air cavities needs to be tuned to fit the frequency range of interest together with the tube diameter and the microphone spacing.

Empirical Predictions from Regression Analyses of Measured Data

There are two families of parameters that determine the sound absorption coefficient. The characterization would be simplest if both k and Z_C could be expressed in terms of a single parameter. Figure 8.7a shows the measured[37] normal-incidence sound absorption coefficient α_0 of different Rockwool materials of practically infinite thickness (between 0.5 and 1 m, depending on the bulk density of the absorber material) as a function of frequency with bulk density of the material as parameter. Figure 8.7a clearly indicates that the bulk density is not the parameter that would collapse the measured data points into a single curve.

In 1970, Delany and Bazley[38] used many measurements on fibrous materials to deduce semiempirical formulas based on the dimensioned parameter (f/R_1). Equations (8.29a) and (8.29b) are valid only if the frequency f is entered in hertz (s^{-1}) and the flow resistivity R_1 in mks rayls per meter ($\text{N}\cdot\text{s}\cdot\text{m}^{-4}$). Although they have been used widely and successfully, Delany and Bazley's formulas give rise to unphysical results at low frequencies. In particular, the real part of the surface impedance of a rigid-backed layer goes negative. Miki's model[39] represents a modification of these formulas based on Delany–Bazley's data and an electrical analogy for the acoustical properties of porous materials. Miki's formulas are as follows:

$$k_{an} = \frac{k}{k_0} = 1 + 0.109\left(\frac{\rho_0 f}{R_1}\right)^{-0.618} - j0.160\left(\frac{\rho_0 f}{R_1}\right)^{-0.618} \tag{8.29a}$$

$$Z_{Cn} = \frac{Z_C}{Z_0} = 1 + 0.070\left(\frac{\rho_0 f}{R_1}\right)^{-0.632} - j0.107\left(\frac{\rho_0 f}{R_1}\right)^{-0.632} \tag{8.29b}$$

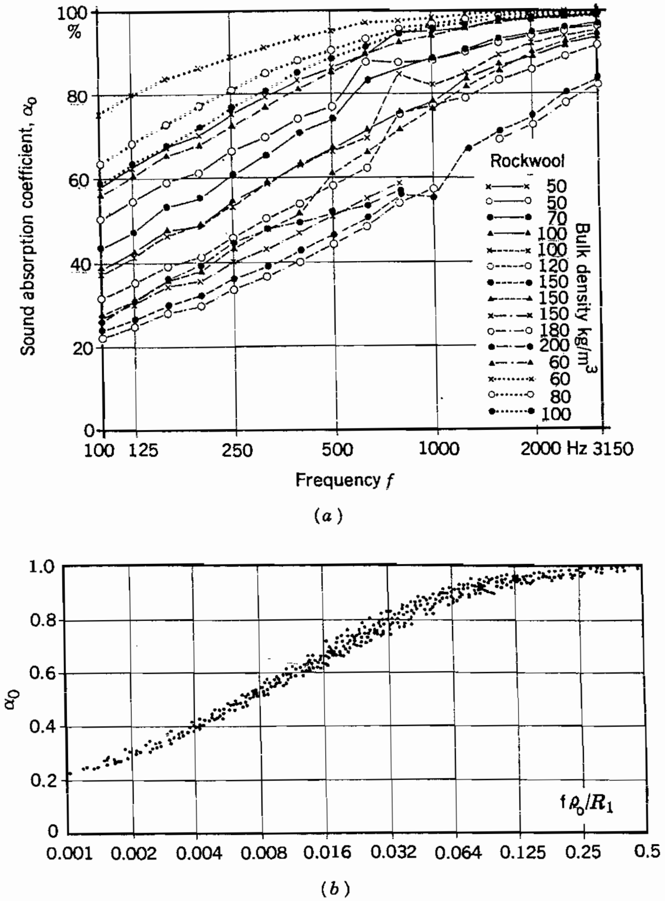

FIGURE 8.7 Normal-incidence sound absorption coefficients of different rock wool materials of practically infinite thickness (0.5–1 m) measured in an impedance tube plotted as a function of (*a*) frequency with bulk density ρ_A as parameter and (*b*) nondimensional frequency parameter $\rho_0 f/R_1 = \rho_0 c_0/(R_1\lambda)$.

Figure 8.7*b* shows the same data points as Fig. 8.7*a* but now as a function of the *dimensionless* variable $E = \rho_0 f/R_1$ on the horizontal scale, where ρ_0 is the density of air, f is the frequency, and R_1 is the flow resistivity of the bulk material at the density at which α_0 was measured. Clearly $E = \rho_0 f/R_1 = \rho_0 c_0/\lambda R_1$ is the single parameter that collapses all measured data. According to Fig. 8.7*b*, even for a layer of practically infinite thickness, very high sound absorption is obtainable only in the frequency range where $(\lambda/4)R_1 < \rho_0 c_0$. To fulfill this requirement at low frequencies, where λ is large, requires the use of a sound-absorbing material of low flow resistivity. The normalized, dimensionless frequency variable

$E = \rho_0 f/R_1$ is useful in describing not only the sound-absorbing capability of the semi-infinite layer of fibrous material but also the propagation constant and characteristic impedance of the bulk material.

It is useful to present the propagation constant and characteristic impedance in a dimensionless manner as

$$k_{an} = \frac{k}{k_0} = \frac{a - jb}{k_0} = a_n - jb_n \tag{8.30a}$$

$$Z_{Cn} = \frac{Z_C}{Z_0} = R - jX \tag{8.30b}$$

where $k_0 = \omega/c_0$ is the wavenumber in air and $Z_0 = \rho_0 c_0$ is the characteristic impedance of the gas filling the voids between the fibers for plane waves.

Figures 8.8 and 8.9 show plots of the real and imaginary parts of the normalized propagation constant k_{an} and that of the normalized characteristic impedance Z_{Cn} for a large variety of mineral wool sound-absorbing materials plotted as a function of the normalized frequency parameter, indicating that indeed the normalized frequency parameter $E = \rho_0 f/R_1$ is a universal descriptor of fibrous porous sound-absorbing materials. The data presented in Figs. 8.8 and 8.9 and similar curves for glass fiber materials were obtained by careful measurements of the acoustical and material characteristics (*a, b, R, X*, and R_1) of over 70 different types of materials.[38]

The solid lines in Figs. 8.8 and 8.9 result from the regression analyses of the data and have the form

$$k_{an} = \frac{k}{k_0} = (1 + a''E^{-\alpha''}) - ja'E^{-\alpha'} \tag{8.31a}$$

$$Z_{Cn} = \frac{Z_C}{Z_0} = (1 + b'E^{-\beta'}) - jb''E^{-\beta''} \tag{8.31b}$$

The regression parameters a', a'', b', b'', α', α'', β', and β'' in Eqs. (8.31) are compiled in Table 8.2 There are different regression parameters for the normalized frequency regions below and above $E = 0.025$. It was found that measured fibrous materials could be divided into two categories: (1) mineral wool and basalt wool and (2) glass fiber.

Polyester Fiber Materials

Polyester fiber materials are used increasingly to replace glass and mineral fiber materials in situations where there is concern to keep the air completely free of fibers suspected to have an adverse influence on health. An example material consists of a mix of two kinds of fibers: (1) polyethylenterephtalate and (2) a core of polyethylenterephtalate and a lining of copolyester. The raw mix is treated at 150°C to melt the external lining of the "bicomponent" fibers and hence form a skeleton of thermally bound fibers. The fiber diameters are between

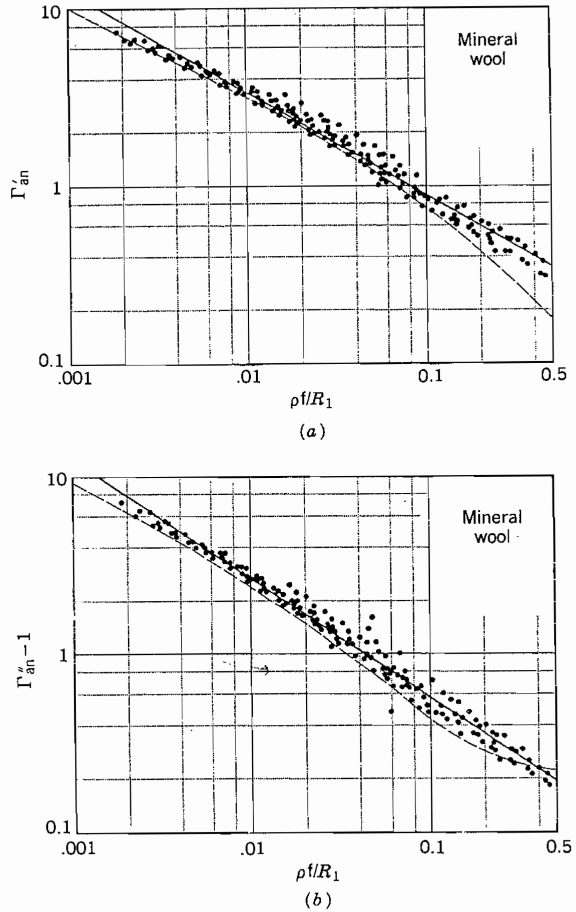

FIGURE 8.8 Measured normalized propagation constant $k_{an} = k/k_0 = a_n + ib_n$ for mineral wool as a function of normalized frequency parameter $E = \rho_0 f/R_1$: (——) regression line: Eq. (8.31a) and Table 8.2; (- - - -) prediction for cylindrical pores.[19,21,27]

TABLE 8.2 Regression Coefficients for Predicting Propagation Constant and Characteristic Impedance of Fibrous Sound-Absorbing Materials

Material	E Region	b'	β'	b''	β''	a''	α''	a'	α'
Mineral and basalt wool	$E \leq 0.025$	0.081	0.699	0.191	0.556	0.136	0.641	0.322	0.502
	$E > 0.025$	0.0563	0.725	0.127	0.655	0.103	0.716	0.179	0.663
Glass fiber	$E \leq 0.025$	0.0668	0.707	0.196	0.549	0.135	0.646	0.396	0.458
	$E > 0.025$	0.0235	0.887	0.0875	0.770	0.102	0.705	0.179	0.674

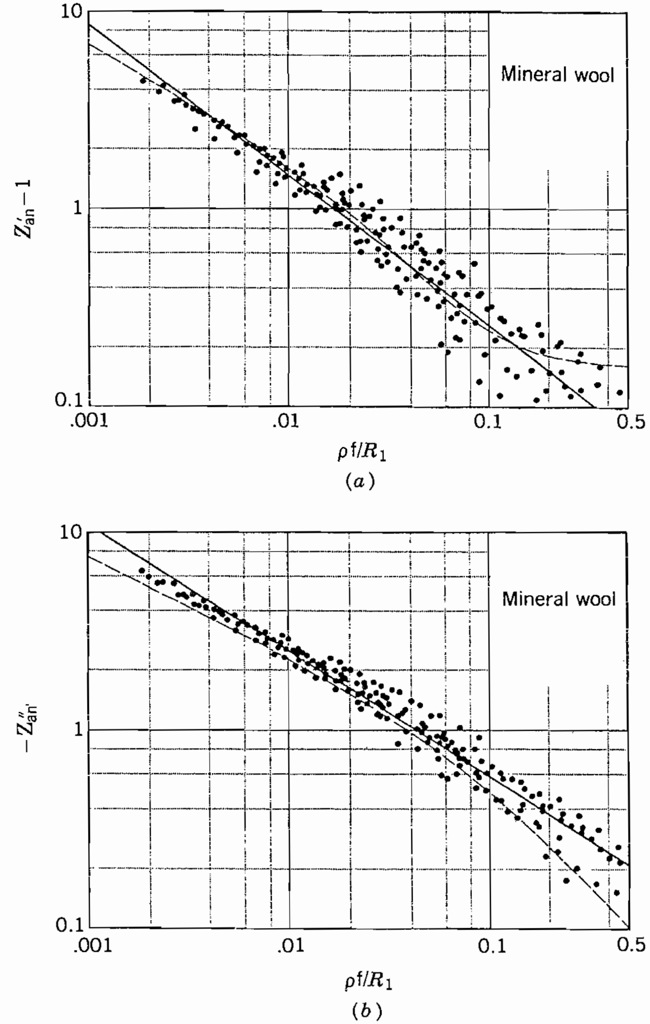

FIGURE 8.9 Measured normalized characteristic impedance $Z_{Cn} = Z_C/Z_0 = R + iX$ for mineral wool as a function of normalized frequency parameter $E = \rho_0 f/R_1$: (——) regression line: Eq. (8.29b); (- - - -) prediction for cylindrical pores.

17.9 and 47.8 μm (mean 33 μm) and have a mean length of 55 mm. Based on measurements of 38 samples, the flow resistivity has been found to obey the relationship[40]

$$R_1 D^2 = 26\rho_A^{1.404} \tag{8.32}$$

where D is the mean diameter in micrometers and ρ_A the bulk density in kg/m^3.

TABLE 8.3 Regression Coefficients for Predicting Propagation Constant and Characteristic Impedance of Polyester Fiber Materials

Material	b'	β'	b''	β''	a'	α'	a''	α''
Polyester fiber	0.159	0.571	0.121	0.530	0.078	0.623	0.074	0.660

Regression coefficients for predicting acoustical properties of polyester fiber materials are given in Table 8.3.[38]

Plastic Foams

Since concerns about fire hazard and release of toxic combustion products can be overcome largely by suitable treatments, plastic foams are used increasingly for noise control applications. A large variety of plastic foams are available with several different types of physical structure. Polyurethane foams, based on polyester or polyether polyols, are used most commonly. These foams can be fully or partially reticulated, that is, with all membranes or with varying proportions of membranes between cells removed. Formulas (8.31) with similar regression coefficients to those for fibrous materials are applicable to plastic foams.[41,42] However, unlike with fibrous materials, it has not been found necessary to distinguish between E-regions. The relevant regression coefficients are listed in Table 8.4.

The first row of Table 8.4 also shows the comparable values obtained from the empirical formulas of Delany and Bazley (ref. 38). Although these formulas have been superseded by those due to Mechel (ref. 37) and Miki (ref. 39), they serve to indicate that the coefficient values for plastic foams are significantly different and that the Delany and Bazley relationships would not generally give satisfactory predictions for the bulk properties of plastic foams.

TABLE 8.4 Regression Coefficients for Predicting Propagation Constant and Characteristic Impedance of Plastic Foams

Material	b'	β'	b''	β''	a'	α'	a''	α''
Mineral and glass fiber	0.0571	0.754	0.087	0.732	0.0978	0.700	0.189	0.595
Fully reticulated polyurethane foam, $60 \le R_1 \le 6229$ (Cummings/Beadle)	0.0953	0.491	0.0986	0.665	0.174	0.372	0.167	0.636
Mixed plastic foams,[42] $2900 \le R_1 \le 24300$	0.209	0.548	0.105	0.607	0.188	0.554	0.163	0.592
Fully reticulated polyurethane foam, $380 \le R_1 \le 3200^a$	0.114	0.369	0.0985	0.758	0.136	0.491	0.168	0.795
Partly reticulated polyurethane foam, $R_1 = 10{,}100^b$	0.279	0.385	0.0881	0.799	0.267	0.461	0.158	0.700

[a] From ref. 43.
[b] From ref. 44.

Effects of Temperature

In sound absorbers or silencers designed to operate at high temperatures, it is important to know the acoustical characteristics of the fibrous porous sound-absorbing materials at design temperature. Fortunately, it is not necessary to measure the propagation constant k and characteristic impedance Z_C at design temperature T because the values of these acoustical characteristics measured at room temperature, T_0, can be scaled. The dimensionless frequency variable $E = \rho_0 f/R_1$ must be evaluated at design temperature. Consider that the influence of temperature on ρ and η is

$$\rho(T) = \rho(T_0)\frac{T_0}{T} \tag{8.33}$$

$$\eta(T) = \eta(T_0)\left(\frac{T}{T_0}\right)^{0.5} \tag{8.34}$$

where T and T_0 are the design temperature and room temperature, respectively, measured on an absolute scale (i.e., Kelvin and Rankine; $\mathrm{K} = {}^\circ\mathrm{C} + 273$). Considering that $\rho = \rho_0(T/T_0)^{-1}$ and $c = c_0(T/T_0)^{1/2}$, the acoustical characteristics at design temperature T (in Kelvin) are determined as follows:

$$b(T) = b[E(T)]\frac{\omega}{c_0}\left(\frac{T}{T_0}\right)^{-1/2} \tag{8.35a}$$

$$Z_C(T) = Z_{Cn}[E(T)](\rho c_0)\left(\frac{T}{T_0}\right)^{-1/2} \tag{8.35b}$$

where $b[E(T)]$ and $Z_{Cn}[E(T)]$ are the normalized attenuation constant and normalized characteristic impedance according to Eqs. (8.30) computed for $E = E(T)$ determined from Eqs. (8.34) and (8.35). When fibrous sound-absorbing materials are first used in high-temperature applications, the material undergoes changes. For mats and boards the binder burns off. This decreases the bulk density to a negligible amount. The burning off of the binder does not appreciably change the flow resistivity. After the first high-temperature exposure the glass or mineral fibers thicken. Their virgin diameter d_V increases to the burned-off diameter $d_{BOF} = d_V + 0.5$. This increase is approximately 0.5 μm. This increase in fiber diameter and corresponding decrease in flow resistivity can be accounted for by correcting flow resistivity measured at room temperature by multiplying it by the factor $(1 + 0.5/d_V)^{-2}$ when calculating $E_{BOF}(T_0) = f\rho_0/R_1(1 + 0.5/d_V)^{-2}$.

Example 8.1. Compute the real and imaginary parts of the normalized propagation constant and characteristic impedance of a very (practically infinite) thick layer of glass fiber at a frequency of 100 Hz at 20°C and for 500°C and determine α_N using the regression parameter values in Table 8.2. The flow resistivity of the fibrous material at 20°C is $R_1(T_0) = 16{,}000\ \mathrm{N \cdot s/m^4}$ and $\rho_0 = 1.2\ \mathrm{kg/m^3}$.

Solution

$$T_0 = 273 + 20 = 293\ \mathrm{K} \qquad T = 273 + 500 = 773\ \mathrm{K}$$

$$E(T_0) = \frac{\rho_0 f}{R_1} = 1.2 \times \frac{100}{16{,}000} = 0.0075, \quad \text{which is} < 0.025$$

$$E(T) = E(T_0)\left(\frac{T}{T_0}\right)^{-1.65} = 0.0075\left(\frac{773}{293}\right)^{-1.65} = 1.5 \times 10^{-3},$$

which is <0.025

The regression parameters from Table 8.2 are

$$a' = 0.396 \qquad a'' = 0.135 \qquad \alpha' = 0.458 \qquad \alpha'' = 0.646$$
$$b' = 0.0668 \qquad b'' = 0.196 \qquad \beta' = 0.707 \qquad \beta'' = 0.549$$

According to Eqs. (8.35), we obtain the following:

Parameter	At 20°C	At 500°C
$b = a'E^{-\alpha'}$	3.72	7.78
$a = 1 + a''E^{-\alpha''}$ a	4.18	10.0
$R = 1 + b'E^{-\beta'}$ R	3.12	7.62
$X = b''E^{-\beta''}$	2.88	6.9

The normal-incidence sound absorption coefficient according to Eq. (8.36) is

$$\alpha_N = 4\frac{Z'_{an}}{Z'^2_{an} + 2Z'_{an} + 1 + Z''^2_{an}}$$

yielding

$$\alpha_N = \begin{cases} 0.49 & \text{for } 20^\circ\mathrm{C} \\ 0.25 & \text{for } 500^\circ\mathrm{C} \end{cases}$$

8.5 SOUND ABSORPTION BY LARGE FLAT ABSORBERS

When considering sound absorption, the portion of a sound wave incident on the absorber that is absorbed is a quantity of interest. This is easiest to define when

the surface of the absorber is flat and sufficiently large that sound waves scattered at the edges of the absorber can be neglected. For a plane incident sound wave, it is possible to assign a sound energy absorption coefficient α for each point on the absorber surface given by

$$\alpha = \frac{\text{absorbed energy}}{\text{incident energy}} = 1 - |R^2| \tag{8.36}$$

where R is the reflection factor, which is defined as the ratio of the reflected and incident sound pressures at the interface. A high sound absorption coefficient ($\alpha \to 1$) requires that $|R| \to 0$. Note that $|R| = 0.1$ corresponds to $\alpha = 0.99$. In this chapter we shall deal only with infinitely large, flat, homogeneous absorbers. Edge effects manifest themselves in increased sound absorption with increasing perimeter–surface area ratio of the absorber.[45] Edge effects are involved also when numerical values greater than 1 are obtained for random-incidence absorption coefficients measured in reverberation rooms.

Plane Sound Waves at Normal Incidence

For plane waves of sound incident perpendicularly to an absorber it is sufficient to know the complex normal specific *surface impedance* $Z_1 = Z_1' - jZ_1''$ of the absorber, which is the ratio of sound pressure to the *normal* component of the particle velocity at the interface (see Chapter 1). The reflection factor and absorption coefficient are related by

$$R = \frac{Z_1 - Z_0}{Z_1 + Z_0} \qquad \alpha = \frac{4Z_1'Z_0}{(Z' + Z_0)^2 + Z_1''^2} \tag{8.37}$$

where $Z_0 = \rho_0 c_0$ is the characteristic impedance of air for plane waves and ρ_0 is the density and c_0 the speed of sound in air.

For sound absorbers consisting of highly porous layers with perforated or cloth facings of smaller porosity, a modified air-side surface impedance must be used in Eq. (8.37). This is obtained by taking the air-side volume velocity averaged over the face area of the absorber. If an absorber with surface impedance Z_i is covered by a perforated facing with porosity h, then $Z_1 = Z_i/h$.

If $|R| \to 0$, Eq. (8.37) indicates that $Z_1 \to Z_0$. This means that the ideal absorber should have a surface impedance similar to that of unbounded air. For a thick (effectively semi-infinite) layer, this requires that the characteristic impedance of porous sound-absorbing materials, Z_C, should be only slightly above that for air, Z_0, and so it is imperative to keep the porosity high. For fibrous sound-absorbing materials, the porosity should be in the range of 0.95–0.99 and for perforated facings the porosity should be above 0.25.

This is illustrated in Fig. 8.10, which shows random-incidence absorption coefficients σ_R(rev) for various configurations with a glass fiber fabric or perforated plate covering measured in a reverberation room. Note the relatively

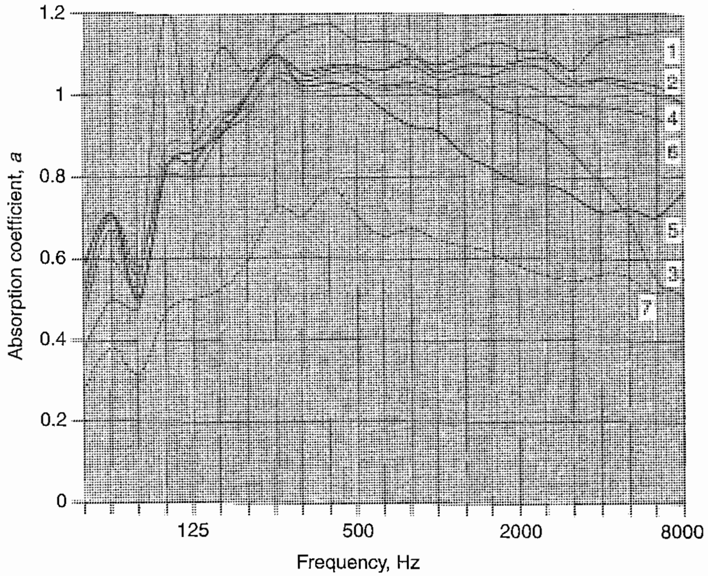

FIGURE 8.10 Random-incidence sound absorption coefficients of 200-mm-thick exhaust silencer pillows (basalt fiber core, density 125 kg/m^3) as a function of frequency measured in a reverberation room: (1) high-porosity fabric covering, equivalent flow resistivity 12 kPa · s · m^{-2}; (2) perforated sheet (32% open area) over high-porosity fabric covering; (3) perforated sheet (17% open area) over high-porosity covering; (4) high-porosity fabric covering and fiberglass facing over basalt fiber core; (5) low-porosity fabric covering, equivalent flow resistivity 43 kN · m · s^{-4}; (6) perforated sheet (32% open area) and fiberglass facing over basalt fiber core; (7) perforated sheet (17% open area), low-porosity fabric covering and fiberglass facing. (Courtesy of John Bowman, Lancaster Glass Fiber, Ltd.)

poor results for the configurations of low-percentage open-area perforated-plate (17%), low-porosity, high-flow-resistivity fabric covering (43,000 mks rayls/m = 100 $\rho_0 c_0$ per meter = 2.4 $\rho_0 c_0$ per inch). Further note that the measured values of α_R(rev) exceed unity. The reasons for this behavior have been discussed in the introductory part of this chapter.

Normal Incidence on a Porous Layer in Front of a Rigid Wall

A rigid wall represents a nearly [see Eq. (8.4)] perfect acoustical reflector. It is an acoustically hard surface. When a porous layer is placed on such an acoustically hard backing, the surface impedance is controlled by the combination of the incident and (multiple) reflected sound waves in the layer, yielding

$$Z_1 = Z_{Ca} \coth(jk_a d) = -jZ_{Ca} \cot(k_a d) \quad \text{N} \cdot \text{s/m}^3 \tag{8.38a}$$

where d is the layer thickness and Z_{Ca} is the characteristic impedance.

Equation (8.38a) may be expressed as

$$Z_1 = Z_{Ca} \frac{\sinh(bd)\cosh(bd) - j\,\sin(ad)\cos(ad)}{\cosh^2(bd) - \cos^2(ad)} \quad \text{N} \cdot \text{s/m}^3 \tag{8.38b}$$

The impedance given by Eqs. (8.38) exhibits the following behavior:

(a) When $d \ll \frac{1}{4}\lambda_a$ [$\lambda_a = 2\pi/a$ is the wavelength in the absorbing material, and a is defined in Eq. (8.30a)], which is the case when the layer is thin or the frequency is low, the magnitude of $\coth(jk_{an}d)$ is always large and the lack of impedance matching between Z_1 and Z_0 leads to a small sound absorption coefficient. This is the reason there is no "sound-absorbing paint" and that rugs absorb sound only modestly.

(b) When d is sufficiently large compared with the wavelength inside the material and the attenuation constant is not too small, the acoustical behavior of the layer approximates that of an "infinitely thick" layer. In this case $\coth(jk_{an}d) \to 1$ and the surface impedance is the same as the characteristic impedance.

(c) When $\coth(jk_{an}d)$ is minimum, the surface impedance of the hard-backed layer is minimum and the absorption coefficient takes its maximum value. Consideration of the expanded form in Eq. (8.38b) indicates that, for $bd > 0$, which is the only situation of interest, the real part is never zero. So the normalized surface impedance is minimum approximately when the imaginary part is zero. In fact, this condition gives a slight underestimate of the frequency of maximum absorption, whereas $\cos(ad) = 0$, corresponding to $d = \frac{1}{4}\lambda_a$, gives an overestimate.

In general the absorption coefficient is maximum at a frequency that is somewhat less than the frequency at which the layer is a quarter-wavelength thick. Doubling the layer thickness halves the frequency of maximum absorption.

For practical purposes a layer of thickness d can be considered "infinitely thick" if $bd > 2$. For such conditions $Z_1 = Z_{Ca}$. The higher the flow resistivity of the porous material, the more Z_1 exceeds Z_0. Even in the extreme case of practically infinite layer thickness (which at low frequencies and low flow resistivity becomes very large), the sound absorption coefficient will be small. As frequency increases, the general tendency is $Z_{Ca} \to Z_0/h$, and for highly porous absorbers where $h \approx 1$, the good impedance matching results in a high absorption coefficient.

Sound-Absorbing Layer Separated from a Rigid Wall by an Air Space. The sound-absorbing configuration depicted in Fig. 8.11 is frequently used in practical applications (e.g., hung acoustical ceilings). The impedance of a layer of air of thickness t in front of a rigid wall is

$$Z_2 = -jZ_0 \cot(k_0 t) \quad \text{N} \cdot \text{s/m}^3 \tag{8.39}$$

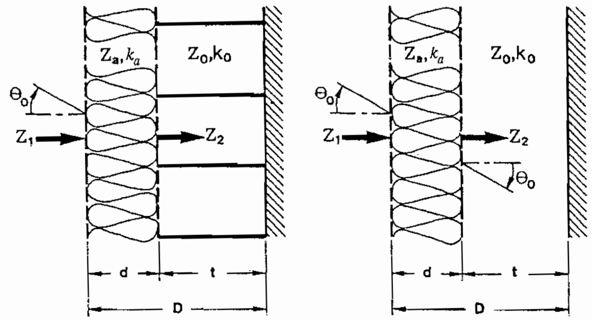

(a) (b)

FIGURE 8.11 Combination of a bulk-reacting absorber layer with (*a*) an air gap such that sound can only travel perpendicular to the hard wall and (*b*) an air gap such that sound can travel parallel to the hard wall.

where $k_0 = \omega/c_0 = 2\pi\lambda_0/c_0$ is the acoustical wavenumber for air. The internal reflection coefficient at the back of the layer is $R_B = (Z_2 - Z_{Ca})/(Z_2 + Z_{Ca})$ and the surface impedance at the front of the layer is

$$Z_1 = Z_C\left(\frac{Z_2 + jZ_{Ca}\tan(k_a d)}{Z_{Ca} + jZ_2\tan(k_a d)}\right) \quad \text{N}\cdot\text{s/m}^3 \tag{8.40a}$$

where Z_C is the normalized characteristic impedance of the porous layer, k_a is the (not-normalized) propagation constant in the porous layer, and d is the layer thickness. Note that Z_2 is zero when $t = \frac{1}{4}\lambda_0$; that is, the impedance Z_s of the absorbing layer backed by zero impedance is given by $Z_s = jZ_C\tan(k_a d) = Z_C\tanh(jk_a d)$. If the impedance of the absorbing layer backed by a hard wall [i.e., with $Z_2 \to \infty$ in Eq. (8.40a) or from Eq. (8.38a)] is denoted by Z_h, then $Z_{Ca} = \sqrt{Z_h Z_s}$. So Eq. (8.40a) can be written in the form

$$Z_1 = \frac{Z_h(Z_2 + Z_s)}{Z_2 + Z_s} = Z_h\frac{1 + Z_s/Z_2}{1 + Z_s/Z_2} \quad \text{N}\cdot\text{s/m}^3 \tag{8.40b}$$

The reflection factor and absorption coefficient a are computed by using Z_1 in Eq. (8.37). For small air space thickness such that $t/\lambda_0 < \frac{1}{8}$, $|Z_h| \gg |Z_w|$ and the following approximation is valid:

$$Z_1 \approx \frac{Z_h}{1 + Z_h/Z_2} \quad \text{N}\cdot\text{s/m}^3 \tag{8.41}$$

When the thickness of the absorbing layer is not too small, that is, $|Z_h| \ll |Z_2|$, Eq. (8.41) results in $Z_1 \approx Z_h$. Consequently at low frequencies a very thin air space between the absorbing layer and the rigid wall is ineffective.

As long as the layer thickness is small compared with the wavelength ($d < \frac{1}{8}\lambda_a$), the air space behind the absorbing layer results in a reduction of the surface impedance and at low frequencies the magnitude of the surface impedance shifts toward the characteristic impedance of air Z_0. This results in a decrease of the reflection factor R and a corresponding increase of the normal-incidence sound absorption coefficient. The largest improvement is observed when the thickness of the air space is a quarter of a wavelength, $t = \frac{1}{4}\lambda_0$.

When the air space thickness corresponds to a multiple of $\frac{1}{2}\lambda_0$, $\sin(k_0 t) \to 0$ and Z_2 is very large [see Eq. (8.39)]. At such frequencies, the air space becomes totally ineffective.

Oblique Sound Incidence

For oblique sound incidence one must distinguish between locally reacting and bulk-reacting absorbers. Locally reacting absorbers are those where sound propagation parallel to the absorber surface is prohibited, as, for example, in partitioned porous layers, porous layers backed by a partitioned air space as depicted on the left in Fig. 8.1, in Helmholtz resonators with partitioned volumes, and in small plate absorbers. Local reaction is a good approximation to absorber behavior also when the flow resistivity is relatively high, causing the transmitted wave to bend toward the normal to the surface. This is true, for example, at high densities or in granular media consisting of small particles. In bulk-reacting absorbers, such as a low-flow-resistivity porous layer, possibly with an unpartitioned air space behind it (Fig. 8.11*b*), sound propagation in the direction parallel to the absorber surface is possible in the sound-absorbing layer or in the air space behind it. The term "locally reacting" results from the fact that the particle velocity at the interface depends only on the *local* sound pressure. For bulk-reacting absorbers, the particle velocity at the interface depends not only on the local sound pressure but also on the particular distribution of the sound pressure in the entire absorber volume. Certain materials are inherently anisotropic; that is, the properties vary with direction through the material. This is true, for example, of fibrous materials where the fibers lie in planes parallel to the surface. Strictly, in such materials the propagation constant and characteristic impedance are a function of angle. However, this complication will not be considered further here.

Oblique-Incidence Sound on Locally Reacting Absorber. Locally reacting absorbers are characterized by a surface impedance Z_1 that is independent of the angle of incidence θ_0. The reflection factor $R(\theta_0)$ for locally reacting absorbers is determined by how well the surface impedance Z_1 matches the field impedance of $Z_0/\cos\theta_0$ and is given by

$$R(\theta_0) = \frac{Z_1\cos\theta_0 - Z_0}{Z_1\cos\theta_0 + Z_0} \tag{8.42}$$

Equation (8.42) indicates that best impedance match, and correspondingly the lowest reflection factor for a given incidence angle θ_0, is achieved by $|Z_1| > Z_0$

and that such "overmatched" surface impedances will yield absorption maxima at a specific angle of incidence.

Oblique-Incidence Sound on Bulk-Reacting Absorber. Mineral-fiber and open-pore foams are the most frequently used bulk-reacting sound-absorbing materials. As long as the materials may be treated as isotropic, the acoustical behavior of these materials can be fully characterized by their propagation constant k_a and characteristic acoustical impedance Z_a. Methods for measuring and predicting these key acoustical parameters are given in Section 8.4 under Physical Characteristics of Porous Materials and their Measurement.

Semi-Infinite Layer. Figure 8.12 shows the incident, reflected, and transmitted waves at the interface. The combination of these waves must satisfy the following boundary conditions: (1) equal normal components of the impedances and (2) equality of the wavenumber components parallel to the interface. The second of these requirements yields the refraction law

$$\frac{\sin\theta_1}{\sin\theta_0} = \frac{k_0}{k_a} \tag{8.43}$$

where θ_1 is the complex propagation angle of the sound inside the absorber. The complex reflection factor is given by

$$R(\theta_0) = \frac{1 - (Z_0/Z_1)\cos\theta_0}{1 + (Z_0/Z_1)\cos\theta_0} \tag{8.44a}$$

and

$$Z_1 = \frac{Z_{Ca}}{[1 - (k_0/k_a)^2 \sin\theta_0^2]^{1/2}} \quad \mathrm{N\cdot s/m^3} \tag{8.44b}$$

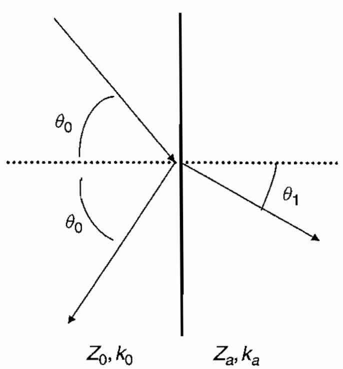

FIGURE 8.12 Reflection and transmission of an oblique-incidence sound wave by a semi-infinite, bulk-reacting absorber.

Finite-Layer Thickness. For a finite layer of bulk-absorbing material of thickness d in front of a hard wall, the reflection factor is

$$R(\theta_0) = \frac{1 - (Z_0/Z_{1d})/\cos\theta_0}{1 + (Z_0/Z_{1d})\cos\theta_0} \tag{8.45}$$

where $Z_{1d} = (Z_{Ca}/\cos\theta_1)\coth(jk_a d\cos\theta_1)$ and θ_1 is defined in Eq. (8.43),

Multiple Layers. Absorbers may consist of a porous sound-absorbing layer with an air space behind, as illustrated in Fig. 8.11, or a number of porous layers of different thicknesses and different acoustical characteristics (Fig. 8.13). Analytical expressions describing the absorber functions and design charts to predict the sound absorption coefficients for those multiple-layer absorbers are provided in reference 46.

Random Incidence. In a diffuse sound field where the intensity $I(\theta) = I$ is independent of the incident angle θ, the sound power incident on a small surface area dS of an absorber is given as

$$dW_{\mathrm{inc}} = I\,dS \int_0^{2\pi} d\phi \int_0^{\pi/2} \cos\theta\,\sin\theta\,d\theta = \pi I\,dS \tag{8.46}$$

and the absorbed portion as

$$\begin{aligned} dW_a &= I\,ds \int_0^{2\pi} d\phi \int_0^{\pi/2} \alpha(\theta)\cos\theta\,\sin\theta\,d\theta \\ &= 2\pi I\,dS \int_0^{\pi/2} \alpha(\theta)\cos\theta\,\sin\theta\,d\theta \end{aligned} \tag{8.47}$$

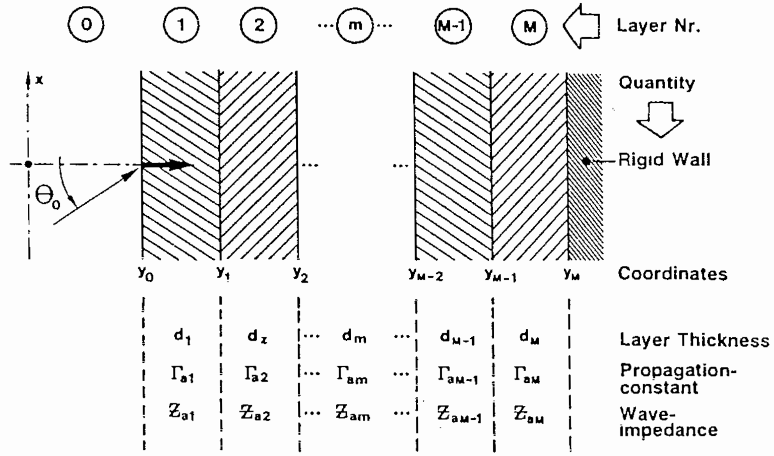

FIGURE 8.13 Multiple-layer absorber.

So the random-incidence sound absorption coefficient is given by

$$\alpha_R = \frac{dW_a}{dW_{\mathrm{inc}}} = 2\int_0^{\pi/2} \alpha(\theta)\cos\theta\,\sin\theta\,d\theta \qquad (8.48)$$

Random-Incidence Sound Absorption Coefficient of Locally Reacting Absorbers. When the constituent materials of a multiple-layer absorber are locally reacting, the combination of Eqs. (8.2), (8.42), and (8.48) will yield the random-incidence sound absorption coefficient. The surface impedance Z_1 that is required for the computation of the random-incidence absorption coefficient can be measured in an impedance tube or computed, and the true random-incidence sound absorption coefficient α_R can be determined as[4]

$$\alpha_R = \frac{8}{|z|}\cos(\beta)\left\{1 + \frac{\cos 2\beta}{\sin\beta}\arctan\left(\frac{|z|\sin\beta}{1+|z|\cos\beta}\right) - \frac{\cos\beta}{|z|}\ln(1+2|z|\cos\beta+|z|^2)\right\} \qquad (8.49)$$

where $z = Z/\rho_0 c_0$ is the normalized wall impedance and
$\beta = \arctan[\mathrm{Im}(z)/\mathrm{Re}(z)]$.

The maximum value of the true $\alpha_R(\max) = 0.955$ that occurs at a normalized wall impedance of $|z| = 1.6$ and $\beta \approx \pm 30°$ indicates that no locally reacting sound absorber can achieve total absorption or even the 99% absorption that is required as a minimum for the walls of anechoic chambers. The random-incidence sound absorption coefficient measured in a reverberation room, $\alpha_R(\mathrm{rev})$, as described in Chapter 7, can yield physically impossible values above unity (sometimes in excess of 1.2). To avoid confusion, the computed physically correct random-incidence coefficient represented by α_R and that measured with the reverberation room method should have a different symbol, namely $\alpha_R(\mathrm{rev})$.

Random-Incidence Sound Absorption Coefficient of Bulk-Reacting Absorbers. For bulk-reacting absorbers the integration in Eq. (8.48) can only be evaluated numerically. It is more appropriate to use the geometric and acoustical characteristics of the porous liner than its impedance to generate design charts for general use.

8.6 DESIGN CHARTS FOR FIBROUS SOUND-ABSORBING LAYERS

For design use it is useful to have charts where the sound absorption coefficient is plotted as a function of the first-order parameters of the absorber, such as thickness *d*, flow resistivity R_1, and frequency *f*. This section contains such design charts. Design charts for a multiple-layered absorber, such as shown in Fig. 8.13, are given in reference 46.

Monolayer Absorbers

As shown in Fig. 8.7*b*, the key acoustical parameters k_a and Z_{Ca} of fibrous sound-absorbing materials depend only on a single material parameter, namely the flow resistivity R_1 (specific flow resistance per unit thickness). Consequently, the absorption coefficient can be computed and plotted as a function of two dimensionless variables:

$$F = \frac{d}{\lambda} = \frac{fd}{c_0} \quad \text{and} \quad R = \frac{R_1 d}{Z_0} \qquad (8.50)$$

Then $k_0 d = 2\pi F$ and $E = \rho_0 f/R_1 = F/R$. At oblique incidence, the angle θ is the third input variable. In the design charts contour lines of constant values of α are plotted on a log-log chart of R versus F. A variation of frequency f produces a horizontal path, an increase of the flow resistivity R_1 causes an upward move, and an increase in layer thickness d leads to a diagonally upward shift to the right. Frequency curves for an absorber layer may be derived by a horizontal intersection, with a starting point determined by the individual parameter values.

Figure 8.14 shows lines of constant absorption of a monolayer absorber for *normal incidence* (the absorber may be bulk or locally reacting). The maximum absorption is reached at about $R = 1.2$ for $F = 0.25$, that is, at a thickness d equal to a quarter of a free-field wavelength and at the flow resistance of the layer of $1.2Z_0$. Higher resonances at odd multiples of a quarter wavelength are visible for a small flow resistance. The "summit line" of the first maximum, which goes through the points of relative maxima of a at the first resonance, is inclined so

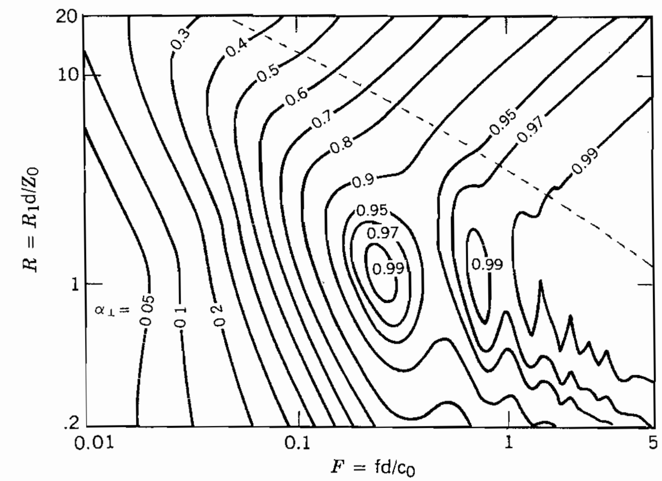

FIGURE 8.14 Lines of constant absorption at normal-incidence sound; absorption coefficient for fibrous absorbers of thickness d and flow resistivity R_1; no air space.

that the first relative maximum will occur below $F = 0.25$ for flow resistances such that $R > 1$, and the first relative maximum of the frequency curve will occur at somewhat higher frequencies than $F = 0.25$ for flow resistances such that $R < 1$. The higher orders of resonances are relatively stationary in frequency as R varies.

At *oblique incidence* the sound absorption for small angles, below about $\theta = 30°$, is only modified slightly. The modifications in $\alpha(\theta)$ are pronounced for larger angles with locally reacting absorbers. The curves on the left in Figs. 8.15 *a–c* were computed for a locally reacting absorber for θ values of 30°, 45°, and 60°. The resonance structure of the contour plots becomes very distinct at low flow resistances and high frequencies.

Curves on the right in Figs. 8.15*a–c* show the analogous contour plots of $\alpha(\theta)$ for the same values of θ but now for bulk-reacting (isotropic) absorber layers. Compared to those for a local-reacting absorber, the contours are relatively continuous. The maxima of absorption are shifted downward toward smaller R values for larger angles.

The *random-incidence* absorption coefficients α_R for locally reacting and bulk-reacting absorbers are plotted on the left and right, respectively, in Fig. 8.16. For locally reacting absorbers the absolute maximum of $\alpha_R = 0.95$ is attained for a matched flow resistance $R = 1$ at $F = 0.367$, that is, at a thickness $d = 0.367\lambda_0$, which is larger than a free-field quarter wavelength $\frac{1}{4}\lambda_0$. With homogeneous isotropic absorbers, the absorption coefficient α_R becomes larger than with locally reacting absorbers. Only a weak resonance maximum (belonging to the second resonance) is observed with homogeneous absorbers. The contour lines of absorption are smooth and steady.

Key Information Contained in Design Charts. Many of the general conclusions that were known qualitatively can be answered now in a quantitative manner by studying Figs. 8.14–8.16.

Determining Thickness of Absorber. What is the thickness d_∞ from which an absorber layer starts to behave acoustically as infinitely thick and yields no further increase in absorption? This thickness starts where the contour lines become 45° diagonally straight lines. The exact position of the curve for thickness d_∞ will depend on the criterion chosen and on the tolerance allowed. If, at this limit, the final value of α is supposed to be reached with a deviation between 1 and 3%, then the limit curve for normal incidence (in Fig. 8.14) is defined by

$$F = 7.45R^{-1.67} \tag{8.51}$$

The layer becomes practically infinite when the sound attenuation during propagation of the sound wave through the layer from the surface to the rigid rear wall is $8.68\Gamma_a' d_\infty = 24$ dB, as first derived in reference 2. This is a much higher attenuation than usually assumed as sufficient (about 6–10 dB) for neglecting the influence of the reflection from the rigid wall on the sound absorption at the front side of the absorber layer.

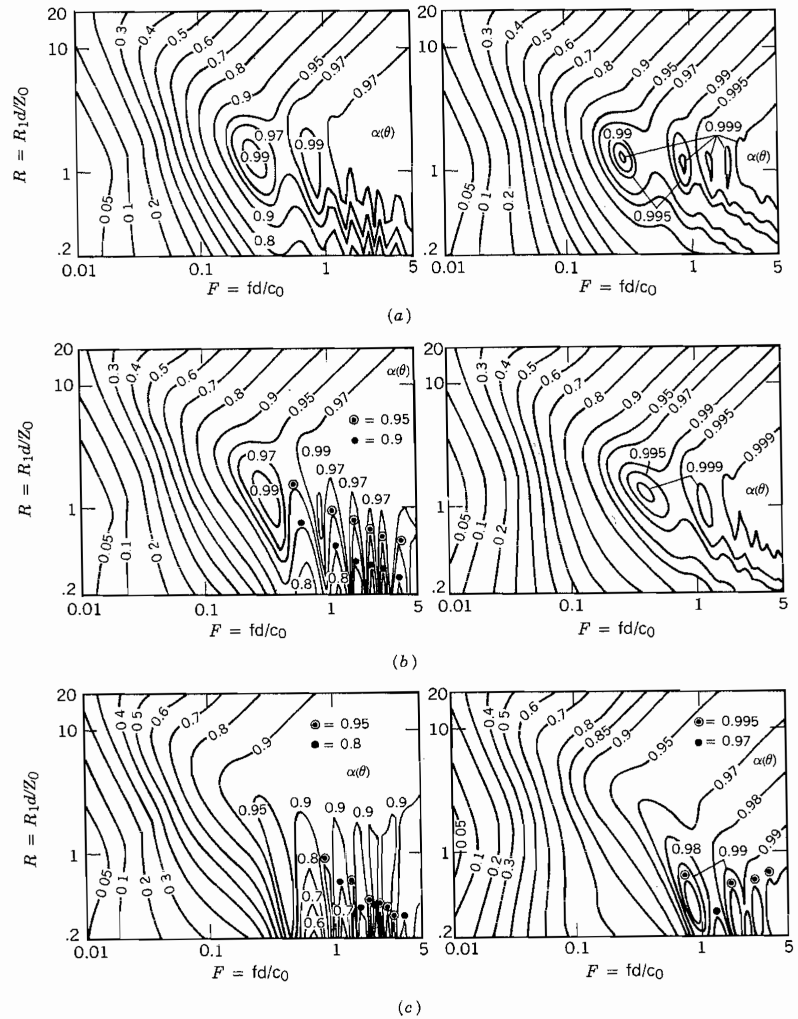

FIGURE 8.15 Lines of constant absorption $\alpha(\theta)$ for fibrous absorbers of thickness d and flow resistivity R_1 for discrete angles of incidences θ; no air space. Left: locally reacting. Right: bulk reacting. *(a)* $\theta = 30°$; *(b)* $\theta = 45°$; *(c)* $\theta = 60°$.

The relationships for "practically infinite" layer thickness d_∞ for which $\Delta L(d_\infty) = 24$ dB can be formulated as

$$f d_\infty^{2.67} R_1^{1.67} = 59 \times 10^6 \quad \text{for } \theta = 0° \tag{8.52a}$$

$$f d_\infty^{2.56} R_1^{1.56} = 34.3 \times 10^6 \quad \text{for } \theta = 45°, \quad \text{locally reacting and random incidence} \tag{8.52b}$$

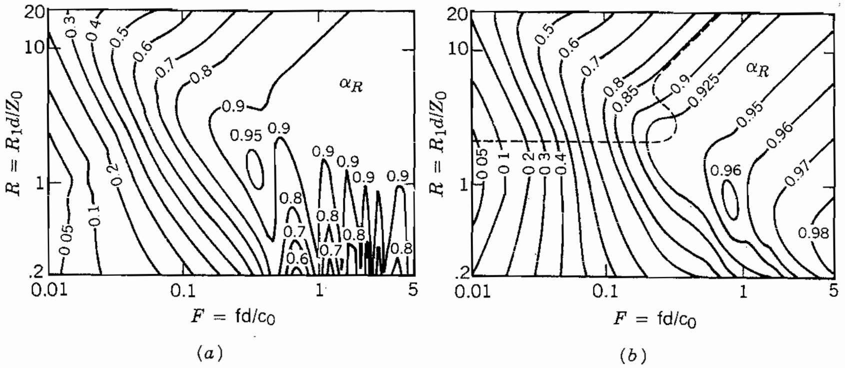

FIGURE 8.16 Lines of constant random-incidence absorption coefficient α_R for fibrous absorbers of thickness d; no air space: (*a*) locally reacting liner; (*b*) bulk-reacting liner.

$$f d_\infty^{2.4} R_1^{1.4} = 7.7 \times 10^6 \quad \text{for } \theta = 45°\text{, bulk reacting} \tag{8.52c}$$

$$f d_\infty^{2.2} R_1^{1.2} = 1.1 \times 10^6 \quad \text{for random-incidence bulk reacting} \tag{8.52d}$$

where f = frequency, Hz
d_∞ = layer thickness, m
R_1 = flow resistivity, N · s/m^4

Optimal Choice of Flow Resistance. Optimal values for the normalized specific flow resistance of the layer, $R = R_1 d/Z_0$, plotted on the vertical scale of Figs. 8.14–8.16, depend on what the designer wants to accomplish.

If the aim is to maximize the sound absorption coefficient, then the optimal choice of normalized specific flow resistance R is in the range of 1–2 for both locally reacting and bulk-reacting absorbers and for normal, oblique, or random angles of sound incidence with the exception of bulk-reacting absorbers for $\theta > 45°$ incidence where $R = 0.7$ yields the best results.

The absorption coefficient depends strongly on flow resistivity R_1, where the curves in Figs. 8.14–8.16 have nearly horizontal contours. The design charts reveal that the typical orientation of the curves of constant α is nearly vertical, indicating only a slight dependence on R_1. This is fortunate because our ability to determine R_1 and our accurate control over its value in the manufacturing process are limited.

Bulk-Reacting versus Locally Reacting Absorbers. A comparison of two graphs in Fig. 8.16 indicates that the random-incidence sound absorption coefficient of locally reacting and bulk-reacting absorbers of the same thickness is practically identical (within 10%) in the left upper quadrant, where $R > 2$ and $F = fd/c_0 < 0.25$, above the dotted line in the graph on the right in Fig. 8.16.

A comparison of $\theta = 45°$ curves in Fig. 8.15*b* with the random-incidence curves presented in Fig. 8.16 indicates that the $\theta = 45°$ curves for both locally reacting and bulk-reacting absorbers agree with the random-incidence curves within an error of 5%, except in the range where $\alpha > 0.9$, which is of little practical interest. This close agreement between $\alpha(45°)$ and α_R indicates that it is permissible to compute $\alpha(45°)$ instead of the much more difficult α_R.

Two-Layer Absorbers

The two-layer absorbers shown in Fig. 8.11 have a layer of fibrous sound-absorbing material of thickness d backed by an air space of thickness t, with total thickness $D = d + t$. Figure 8.11*a* shows a partitioned (e.g., in a honeycomb pattern) air space resulting in a locally reacting absorber, and Fig. 8.11*b* shows an unpartitioned air space resulting in a bulk-reacting absorber. The sound absorber types shown in Fig. 8.11 are usually employed when it is impractical to fill the entire absorber thickness with porous material because no fibrous material of sufficiently low flow resistivity is available to keep the normalized flow resistance $R = R_1 d/Z_0 < 2$. Based on the analyses described in reference 5, design charts similar to those presented in a preceding section for monolayer absorbers were computed.

Figure 8.17 shows contour maps of the random-incidence sound absorption coefficient α_R in a diffuse sound field for a bulk absorber layer of thickness d in front of a locally reacting air gap of thickness t (see Fig. 8.11*a*) for three fractions, $d/D = 0.25, 0.5, 0.75$, absorber thickness d, and total thickness $D = d + t$. Because the two-layer design curves in Fig. 8.17 are not plotted as functions of the total layer thickness D, they are not directly comparable with the monolayer design curves presented in Fig. 8.16. Some differences may be noticed by comparing these figures with Fig. 8.16, which applies to the bulk monolayer absorber.

First, the variable $F = fd/c_0$ for maximum absorption in the first resonance maximum is shifted toward smaller values with decreasing d/D, which results in higher absorption at low frequencies for less absorber material thickness. Generally, however, the reduction in weight of the material is not as large. The horizontal shift of the absorption maximum toward lower F values, when realized by a reduction in d, makes a larger flow resistivity necessary on the ordinate in order to hold R on a constant value. The increase in R_1 is achieved mostly by an increase of the material bulk density ρ_A. For most fibrous absorber materials R_1 is proportional to about $\rho_A^{1.5}$. Hence, only a small net reduction in absorber material is possible by the addition of an air gap.

For thick absorber layers, that is, for large d, the air gap has no effect, as expected. The limit for the onset of an "infinite" thickness is the same as with the monolayer absorber.

The resonance structure of the layered absorber with small d/D resembles more that of the locally reacting monolayer absorber (see Fig. 8.16*a*). The character of the bulk-reacting monolayer absorber plot (see Fig. 8.16*b*), which must be the asymptotic limit for increasing d/D, becomes dominant for $d/D \geq 0.5$.

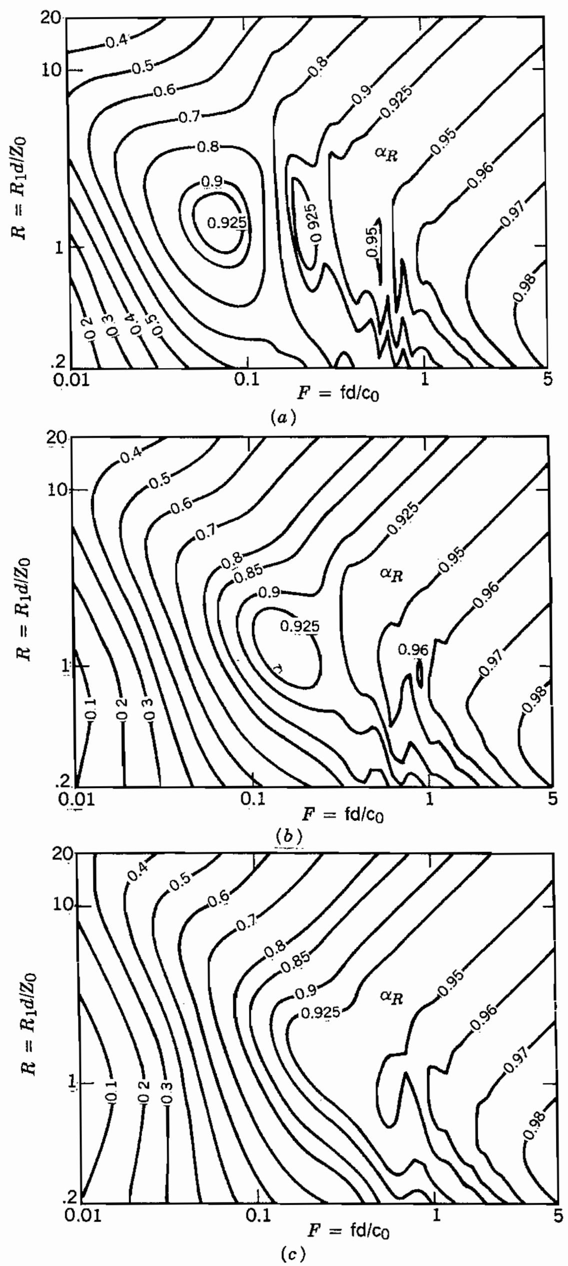

FIGURE 8.17 Lines of constant random-incidence absorption coefficient α_R for a bulk-reacting absorber layer of thickness d in front of a locally reacting air gap of thickness t for thickness ratios $d/D = d/(d+t)$ of (*a*) 0.25, (*b*) 0.5, and (*c*) 0.75.

The sound absorption coefficient of a porous layer of thickness d with an air gap behind it is generally higher than that of a monolayer with equal d. However, the absorption of the layered absorber is smaller than that of a monolayer absorber with equal total thickness $d' = D$. In the range $R > 1$, the absorption of a layered absorber with $d/D = 0.75$ corresponds to that of a monolayer absorber with thickness $d' = 1.25d$ and the absorption of a layered absorber with $d/D = 0.5$ corresponds to that of a monolayer having a thickness $d' = 1.67d$. The quite different character of the plot for $d/D = 0.25$ excludes a similar equivalence.

Finally, the lines of constant α_R of the layered absorber have strong deflections toward the left for values of α_R between about 0.7 and 0.9. As a consequence, the optimum flow resistance $R_1 d$ (which is defined by the leftmost point of a curve) has a more distinct meaning than with monolayer absorbers.

Design graphs for layered absorbers with bulk-reacting absorber layers in front of a bulk-reacting air gap (see Fig. 8.7*b*) are given in reference 45.

Multilayer Absorbers

Multilayer absorbers, such as shown in Fig. 8.13, have been treated in reference 4. Best results are obtained if the flow resistivity of the layers, R_1, increases from the interface toward the rigid wall. These results obtained with such multilayer absorbers are somewhat better than those obtained with a monolayer absorber of equal thickness. However, the improvements seldom justify the added cost and complexity. Of course, Fig. 8.13 represents an idealization of practical constructions (see Fig. 8.18) which combine multiple porous layers with perforations and slots.

It should be noted, however, that even the most elaborate multiple-layer absorber cannot match the random-incidence sound absorption performance of anechoic wedges.

Thin Porous Surface Layers

Thin porous surface layers such as mineral wool felt sprayed on plastic, steel wool, mineral wool, or glass fiber cloth; wire mesh cloth; and thin perforated metal are frequently used to provide mechanical protection. They also reduce the

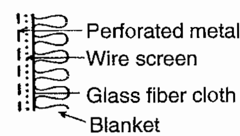

FIGURE 8.18 Multilayered absorber with perforated porous layer structure.

loss of fibers. The acoustical properties of such thin layers are characterized by their flow resistance $R_s = \Delta p/v$ and their mass per unit area ρ_s. The surface impedance is

$$Z_s = \begin{cases} R_s & \text{(fixed)} \quad (8.53a) \\ \dfrac{(j\omega\rho_s)R_s}{j\omega\rho_s + R_s} & \text{(free)} \quad (8.53b) \end{cases}$$

which must be added to the wall impedance of the absorber. If the porous surface layer is not free to move, Eq. (8.53a) is used. For surface layers that are free to move due to the pressure differential produced by their flow resistance, Eq. (8.53b) is used.

Tables 8.5 and 8.6 provide design information on wire mesh cloth and glass fiber cloth, respectively. The flow resistance values listed in these tables represent the linear part of the flow resistance, which is appropriate for design use only if the particle velocity is low. At high sound pressure levels (above 140 dB), the nonlinear behavior of the flow resistance must be determined by measuring the flow resistance as a function of the face velocity.

Sintered porous metals have been developed for silencers in jet engine inlets. If backed by a honeycomb-partitioned air space, they provide good sound absorption and remain linear up to high sound pressure levels and for high-Mach-number grazing flow. Their additional advantage is that they do not require any surface protection. Table 8.7 gives the flow resistance R_s and mass per unit area ρ_s for some commercially available porous metal sheets.

Steel wool mats typically have a thickness from 10 to 45 mm, mass per unit area ρ_s from 1 to 3.8 kg/m^2, and a specific flow resistance R_s from 100 to 500 N · s/m^3. Recently, such steel wool mats needled on mineral wool of specified thickness and density have become available on special order.

Perforated metal facings, when they rest directly on a porous sound-absorbing layer, can be accounted for by a series impedance Z_s given by

$$Z_s = \frac{j\omega\rho_0}{\varepsilon}\left\{l + \Delta l\left[H(1 - |v_h|) - j\frac{\Gamma_a}{k_0}\frac{Z_a}{Z_0}\right]\right\} \quad (8.54)$$

TABLE 8.5 Mechanical Characteristics and Flow Resistance R_s of Wire Mesh Cloths

		Wire Diameter		Mass per Unit Area		Flow Resistance R_s	
Wires/cm	Wires/in.	μm (10^{-6} m)	mils (10^{-3} in.)	kg/m^2	lb/ft^2	N · s/m^3	$\rho_0 c_0$
12	30	330	13.0	1.6	0.32	5.7	0.014
20	50	220	8.7	1.2	0.25	5.9	0.014
40	100	115	4.5	0.63	0.13	9.0	0.022
47	120	90	3.6	0.48	0.1	13.5	0.033
80	200	57	2.25	0.31	0.63	24.6	0.06

TABLE 8.6 Mechanical Characteristics and Flow Resistance R_s of Glass Fiber Cloth

		Surface Density[a]			
Manufacturer[b]	Cloth Number	oz/yd^2	g/m^2	Construction, Ends × Picks	Flow Resistance, mks rayls (N · s/m^3)
1, 2, 3	120	3.16	96	60 × 58	300
1, 2, 3	126	5.37	164	34 × 32	45
1, 2, 3	138	6.70	204	64 × 60	2200
1, 2, 3	181	8.90	272	57 × 54	380
3	1044	19.2	585	14 × 14	36
2	1544	17.7	535	14 × 14	19
3	3862	12.3	375	20 × 38	350
1	1658	1.87	57	24 × 24	10
1	1562	1.94	59	30 × 16	<5
1	1500	9.60	293	16 × 14	13
1	1582	14.5	442	60 × 56	400
1	1584	24.6	750	42 × 36	200
1	1589	12.0	366	13 × 12	11

[a] Averaged over a large sample.
[b] Code numbers for manufacturers are as follows: (1) Burlington Glass Fabrics Company; (2) J. P. Schwebel and Company; (3) United Merchants Industrial Fabrics.

TABLE 8.7 Specific (Unit-Area) Flow Resistance R_s, Thickness, and Mass per Unit Area of Sintered Porous Metals Manufactured by the Brunswick Corporation[a]

Specific Flow Resistance Air, 70°F		NLF[b]		Thickness		Mass per Unit Area	
$\rho_0 c_0$	N · s/m^3	500/20	Designation	mm	in.	kg/m^2	lb/ft^2
0.25	100	3.6	FM 125	1.0	0.04	3.9	0.79
		5.0	FM 127	0.76	0.03	3.3	0.67
		2.6	FM 185	0.5	0.02	2.0	0.4
		2.0	347-10-20-AC3A-A	0.5	0.02	1.32	0.27
		2.0	347-10-30-AC3A-A	0.76	0.03	1.1	0.23
		2.0	FM 802	0.5	0.02	1.3	0.27
0.88	350	4.7	FM 134	0.89	0.035	3.8	0.77
1.25	500	1.8	FM 122	0.76	0.03	1.4	0.28
		3.6	FM 126	0.66	0.026	3.7	0.76
		3.3	FM 190	0.41	0.016	2.0	0.4
		2.0	347-50-30-AC3A-A	0.76	0.03	1.4	0.29

[a] Except FM 802, which is made of Hastelloy X, all materials are type 347 stainless steel. (Courtesy of Brunswick Corporation.)
[b] Nonlinearity factor, calculated as the ratio of flow resistances obtained at flow velocities of 500 and 20 cm/s, respectively.

where ε is the fractional open area of the perforated facing, l is the plate thickness, Δl is the end correction length of the perforations given in Section 8.5, H is a step function that is unity for $|v_h| \leq 1$ m/s and zero for $|v_h| > 1$ m/s, and v_h is the particle velocity in the holes of the perforations. For thin, unrestrained perforated surface protection plates, it is necessary to take the parallel combination of Z_s and $j\omega\rho_s$ according to Eq. (8.53b).

8.7 RESONANCE ABSORBERS

In building acoustics the most frequently used type of resonant absorber is the Helmholtz resonator, consisting of the mass of an air volume in a cross-sectional area restriction (such as holes or slits in a covering plate) and the compliance of the air volume behind the covering plate. In the narrow frequency range, centered at their resonance frequency, the resonators "soak in" the acoustical energy from a large room volume in the vicinity of the neck. This high energy concentration results in high local sound pressures at the neck (and in the internal volume) which are much higher than that one would register with the resonator opening closed. On the room side, this near-field sound pressure decays exponentially with increasing distance. In architectural application of resonance absorbers care should be exercised not to locate them too near to any member of the audience to avoid distortion of the auditory experience. The open bottles embedded in the vertical portion of the seats in ancient Greek amphitheaters indicate that this local amplification of the sound field in the vicinity of acoustical resonators was known more than 2000 years ago. What was not known, which misguided their application, was that the amplification occurs only in a narrow frequency band and cannot locally amplify such broadband signals as speech. Such a Helmholtz resonator (named after the nineteenth-century German physicist Ludwig Helmholtz, who was first to utilize its narrow-band tuning to analyze the spectral composition of complex sounds) is shown in Fig. 8.19. In the following treatment it is assumed that all dimensions of a single resonator are small compared with the acoustical wavelength (except in the case of two-dimensional resonators with slits) and that the skeleton of the resonator is rigid.

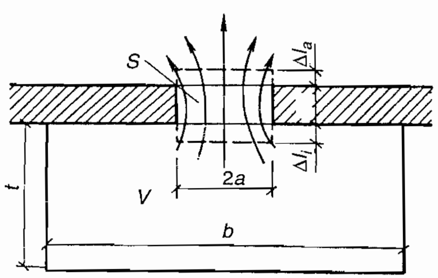

FIGURE 8.19 Key geometric parameters of a Helmholtz resonator.

Acoustical Impedance of Resonators

The specific acoustical impedance of the resonator opening Z_R is the sum of the impedance of the enclosed air volume Z_v and that of the air volume that oscillates in and around the resonator mouth Z_m, namely,

$$Z_R = Z_v + Z_m = (Z'_v + jZ''_v) + (Z'_m + jZ''_m) \quad \text{N} \cdot \text{s/m}^3 \tag{8.55}$$

The volume impedance $Z_v = jZ''_v$ is purely imaginary and predominantly of spring character while the mouth impedance has a real part Z'_m and an imaginary part Z''_m and is predominantly of mass character.

The impedance of a rectangular resonator volume is

$$Z_v = jZ''_v = -j\rho_0 c_0 \cot(k_0 t)\frac{S_a}{S_b} \quad \text{N} \cdot \text{s/m}^3 \tag{8.56a}$$

where S_b is the surface area of the resonator cover plate, $S_a = \pi a^2$ is the area of the resonator mouth, t is the depth of the resonator cavity, and $V = S_b t$ is the resonator volume. If the resonator dimensions are small compared with the wavelength ($k_0 t \ll 1$), Eq. (8.56a) yields

$$Z_v = jZ''_v = -j\frac{\rho_0 c_0^2}{\omega}\frac{S_a}{V} \quad \text{N} \cdot \text{s/m}^3 \tag{8.56b}$$

Thus, when all the dimensions are smaller than the wavelength of interest, the shape of the air cavity does not matter.

The impedance of the resonator mouth Z_m consists of components related to the oscillations of air internal to the mouth, within the mouth, and external to the mouth of the resonator plus the impedance of the screen (Z_s) that may be placed across the resonator mouth to provide resistance. For circular resonator openings of radius a and orifice plate thickness l, the resulting total impedance is given by

$$Z'_m = \rho_0\left[\sqrt{8\nu\omega}\left(1 + \frac{l}{2a}\right) + \frac{(2\omega a)^2}{16c_0}\right] + Z_s \quad \text{N} \cdot \text{s/m}^3 \tag{8.57a}$$

$$Z''_m = \omega\rho_0\left[l + \left(\frac{8}{3\pi}\right)2a\right] + \left(l + \frac{1}{2a}\right)\sqrt{8\nu\omega} \quad \text{N} \cdot \text{s/m}^3 \tag{8.57b}$$

where ν is the kinematic viscosity ($\nu = 1.5 \times 10^{-6}$ m^2/s for air at room temperature). The quantity $0.5(8\nu/\omega)^{1/2}$ is the viscous boundary layer thickness.[1]

In general, the first term in Eq. (8.57a) applies only for smooth orifice edges. For sharp orifice edges it can be many times higher. Also note that the second term in Eq. (8.57b) is usually small compared with the first term and can be neglected.

The results of Eqs. (8.57) for circular orifices and for a single resonator can be generalized for other orifice shapes and for situations where the orifice is located on a large wall or at a two- or three-dimensional corner. This generalized form is

$$Z'_m = \frac{P(l + P/2\pi)}{4S_a}\rho_0\sqrt{8\nu\omega} + \rho_0 c_0 \frac{k_0^2 S_a/\Omega}{1 + k_0^2 S_a/\Omega} + Z_s \quad \text{N s/m}^3 \tag{8.58a}$$

$$Z''_m = j\omega\rho_0\left[l + 2\,\Delta l + \frac{P(l + P/2\pi)}{4S_a}\sqrt{8\nu/\omega}\right] \quad \text{N}\cdot\text{s/m}^3 \tag{8.58b}$$

where P is the perimeter of the orifice, S_a is its surface area, and Ω is the spatial angle the resonator "looks into":

$$\Omega = \begin{cases} 4\pi & \text{for resonator away from all walls} \\ 2\pi & \text{flush mounted on wall far from corners} \\ \pi & \text{flush mounted on wall at two-dimensional corners} \\ \frac{1}{2}\pi & \text{flush mounted on wall at three-dimensional corners} \end{cases}$$

The quantity $\Delta l = 16a/3\pi$ represents the combined internal and external end corrections.

Resonance Frequency

The resonance frequency f_0 of the Helmholtz resonator occurs where Z''_m and Z''_v are equal in magnitude. Combination of Eqs. (8.56b) and (8.57b) yields

$$f_0 = \frac{c_0}{2\pi}\sqrt{\frac{S_a}{V\langle\cdots\rangle}} \cong \frac{c_0}{2\pi}\sqrt{\frac{S_a}{V(l + 16a/3\pi)}} \tag{8.59}$$

where $\langle\cdots\rangle = l + \Delta l$ represents the quantity in square brackets in Eq. (8.58b).

The viscous terms in (8.57b) are ignored in (8.59). However, this is usual when calculating a resonance frequency because the viscous contribution is small. For resonators where the area of the mouth, S_a, is not much smaller than the area of the top plate of the resonator, the proximity of the side walls of the cavity influences the flow in the resonator mouth. In this case it is necessary to determine the combined end correction from $\Delta l = 8a/3\pi + \Delta l_{\text{int}}$.[47]

Absorption Cross Section of Individual Resonators

For individual resonators (or groups of resonators where the distance between the individual resonators is large enough that interaction is negligible), the absorption coefficient α is meaningless. In this case, the sound-absorbing performance must be characterized by the absorption cross section A of the individual resonator. The absorption cross section is defined as that surface area (perpendicular to the direction of sound incidence) through which, in the undisturbed sound wave (resonator not present), the same sound power would flow through as the sound power absorbed by the resonator.

The power dissipated in the mouth of a resonator is

$$W_m = 0.5|v_a|^2 S_a R_T = \frac{0.5 \times 2^n |p_{\text{inc}}|^2 S_a R_T}{|Z_R|^2} \quad \text{W} \tag{8.60}$$

Accordingly, the absorption cross section is

$$A = \frac{2^n \rho_0 c_0 S_a R_T}{|Z_R|^2} \quad \text{m}^2 \tag{8.61}$$

where $n = 0$ for resonators placed in free space, $n = 1$ if the resonators are flush mounted in a wall, $n = 2$ if the resonators are at the junction of two planes, and $n = 3$ if the resonators are in a corner; $R_T = Z'_m + Z_{\text{rad}}$ is the total resistance.

At the resonance frequency f_0, where $Z''_v + Z''_m = 0$, the absorption cross section reaches its maximum value A_0:

$$A = 2^n \frac{S_a \rho_0 c_0}{R_{\text{rad}}}\left[\frac{R_T/R_{\text{rad}}}{|1 + R_T/R_{\text{rad}}|^2}\right] \quad \text{m}^2 \tag{8.62a}$$

For a flush-mounted ($n = 1$) circular resonator area $S_a = \pi a^2$, the radiation resistance is $R_{\text{rad}} = 2(\pi a)^2 \rho_0 c_0/\lambda_0^2$, and Eq. (8.62a) yields

$$A = \frac{1}{\pi}\lambda_0^2\left[\frac{R_T/R_{\text{rad}}}{|1 + R_T/R_{\text{rad}}|^2}\right] \quad \text{m}^2 \tag{8.62b}$$

where λ_0 is the wavelength at the resonance frequency of the resonator. The maximum value of the absorption cross section is obtained by matching the *internal* resistance to the radiation resistance at the resonance frequency, yielding ($R_T = R_{\text{rad}}$)

$$A_0^{\max} = \frac{\lambda_0^2}{4\pi} \quad \text{m}^2 \tag{8.63}$$

According to Eq. (8.63), a matched resonator tuned to 100 Hz can achieve absorption cross section $A_0^{\max} = 0.92\ \text{m}^2$.

According to Eq. (8.61), the frequency dependence of A can be presented in generalized form as

$$\frac{A(f)}{A_0} = \frac{1}{1 + Q^2\phi^2} \tag{8.64}$$

where the Q of the resonator and the normalized frequency parameter ϕ are given as

$$Q = \frac{Z''_m(\omega_0)}{Z'_m(\omega_0)} \qquad \phi = \frac{f}{f_0} - \frac{f_0}{f}$$

Figure 8.20 shows the normalized absorption cross section A/A_0 as a function of the normalized frequency ϕ with Q as the parameter, indicating that the

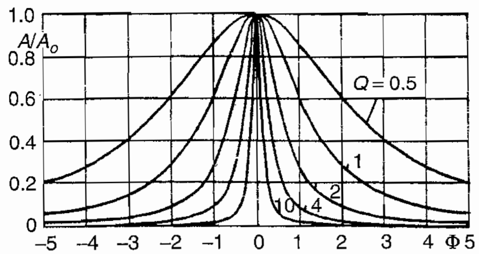

FIGURE 8.20 Normalized absorption cross section A/A_0 as function of normalized frequency ϕ with Q as parameter.

normalized bandwidth of the absorption cross section f_0/Q corresponds to the relative bandwidth $\Delta f/f_0 = 1/Q$.

Consequently, the choice of Q determines the relative shape of the absorption curve and the factor in the square brackets in Eq. (8.62b) determines the height of the curve at resonance. To obtain optimal absorption characterized by high absorption at resonance A_0 and wide bandwidth requires resistance matching $R_T = R_{\text{rad}}$ and a relatively low value of Q.

Nonlinearity and Grazing Flow

The oscillating air mass (that includes the end-correction term) is a measure for the reversible kinetic energy of the acoustical resonator. Reversibility and spatial coherence diminish with increasing turbulence due to jet flow through the orifice caused by high-amplitude sound and by the grazing flow of velocity U_∞. Both reduce the air mass that participates in the oscillating motion and consequently increase resonance frequency and increase the losses of the resonator.

Nonlinearity and grazing flow affect only the mouth impedance Z_m of the resonator orifice. Table 8.8 is a compilation of the nonlinear effects owing to high sound pressure level and grazing flow for a perforated plate. The round holes are regularly distributed. The porosity of the perforated plate is $\varepsilon = \pi a^2/b^2$, where a is the hole radius and b the hole spacing. The amplitude nonlinearity is characterized by the particle-velocity-based Mach number $M_0 = v/c_0$, which is the ratio of the particle velocity in the resonator orifice and the speed of sound in air. The grazing flow nonlinearity is characterized by the flow-velocity-based Mach number $M_\infty = U_\infty/c_0$, where U_∞ is the velocity of the grazing flow far from the wall. The formulas presented in Table 8.8 are analytical results adjusted to yield agreement with measured data.[48] The impedances in Table 8.8 are values averaged over the plate surface.

Internal Resistance of Resonators

The most difficult part of resonator design is the prediction of the internal resistance. In the earlier section Acoustical Impedance of Resonators (page 265) formulas were given to predict the friction loss resistance [first term in Eq. (8.57a)], which is valid only for rounded orifice perimeter. Additional resistance due to sharp edges cannot be predicted analytically. Table 8.8 contains formulas to predict resonator resistance due to nonlinear effects owing to high sound pressure level and grazing flow.

Should it be desirable to obtain higher loss resistance than provided by friction and nonlinear effects (e.g., obtaining larger absorption bandwidth), porous materials such as a screen, felt, or layer of fibrous sound-absorbing material must be placed in (or behind) the resonator orifice. Figure 8.21 shows some of the more frequently used ways to increase resonator resistance. In Fig. 8.21, R_1 is the flow resistivity of the porous material, d is its thickness, t_1 is its distance from the back side of the cover plate, t is the depth of the resonator cavity, $2a$ is the diameter of the holes, Δl is the end correction, and ε is the porosity of the cover plate.

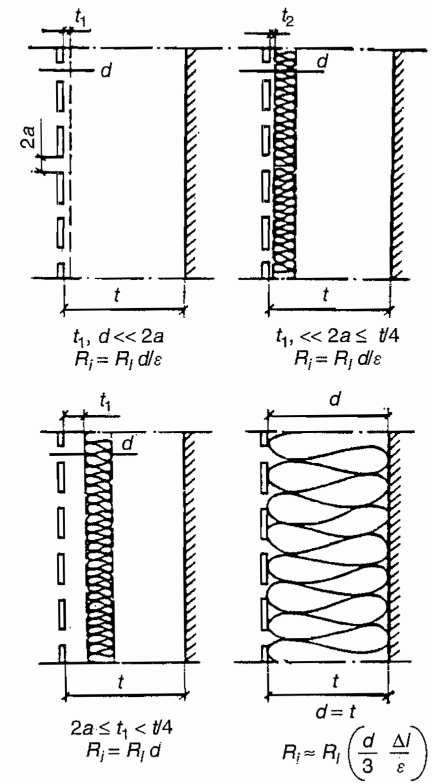

FIGURE 8.21 Methods to increase resonator resistance and the achieved specific acoustical resistance R_i (R_1 = flow resistivity of porous material, d is its thickness, and $\Delta l = 16a/3\pi$).

TABLE 8.8 Nonlinearity of Orifice Impedance $Z_m = Z'_m + jZ''_m$ of Perforated-Plate Resonator Covers Caused by High Sound Pressure Level L_p and Grazing Flow U_∞[a]

Grazing Flow	Low SPL, $L_p < L_{0l}$	Medium SPL, $L_{0l} \le L_p \le L_{0h}$	High SPL, $L_p > L_{0h}$
No flow or very low flow, $M_\infty \le 0.025$, $U_\infty \le 8$ m/s	$L_{0l} = 107 + 27\log[4(1-\epsilon^2)\omega\rho_0 v(1 + l/2a)^2]$ dB		$L_{0h} = L_{0l} + 30$ dB
	$Z'_m = R_0 \quad Z''_m = X_0(\delta)$ $R_0 = \frac{\rho_0}{\epsilon}\sqrt{8v\omega}\left(1 + \frac{l}{2a}\right) + (\rho_0/8\epsilon c_0)(2a\omega)^2$ $X_0 = \frac{\omega\rho_0}{\epsilon}\left[\sqrt{\frac{8v}{\omega}}\left(1+\frac{l}{2a}\right) + l + \delta\right]$ $\delta = \delta_0 = 0.85(2a)\phi_0(\epsilon)$ $\phi_0(\epsilon) = 1 - 1.47\sqrt{\epsilon} + 0.47\sqrt{\epsilon^3}$	$Z'_m = \sqrt{R_h^2 - R_0^2} \quad Z''_m = X_0(\delta)$ $\delta = \delta_0\phi_1(M_0)$ $M_0 = \frac{10^{(-2.25+0.025L_p)}}{\sqrt{0.5\,\rho_0 c_0^2(1+\epsilon^2)}}$	$Z'_m = R_h \quad Z''_m = X_0(\delta)$ $R_h = \frac{1}{\epsilon}\sqrt{2\rho_0(1-\epsilon^2)} \times 10^{(-2.25+0.018L_p)}$ $\delta = \delta_0\phi_1(M_0)$ $\phi_1(M_0) = \frac{1 + 5\times 10^3 M_0^2}{1 + 10^4 M_0^2}$
With flow, $M_\infty \ge 0.025$, $U_\infty \ge 10$ m/s	$L_p \le L_{ml} \quad L_{ml} = 175 + 40\log M_\infty$ dB $Z'_m = R_m \quad Z''_m = X_0(\delta)$ $R_m = 0.6\,\rho_0 c_0 \frac{1-\epsilon^2}{\epsilon}(M_\infty - 0.025) - 40R_0(M_\infty - 0.05)$; $M_\infty \le 0.05$ $R_m = 0.3\,\rho_0 c_0 \frac{1-\epsilon^2}{\epsilon} M_\infty$ $\delta = \delta_0\phi_2(M_\infty)$ $\phi_2(M_\infty) = 1/(1 + 305M_\infty^3)$	$L_{ml} \le L_p \le L_{mh}$ $Z'_m = \sqrt{R_m^2 + R_h^2} \quad Z''_m = X_0(\delta)$ $M_\infty > 0.05$ $\delta = \delta_0\phi_2(M_\infty)$	$L_p > L_{mh} \quad L_{mh} = L_{ml} + 18$ dB $Z'_m = R_h \quad Z''_m = X_0(\delta)$ $\delta = \delta_0\phi_1(M_\infty)$

[a] L_p is octave-band SPL in dB re 20 μPa at the peak of the spectrum.

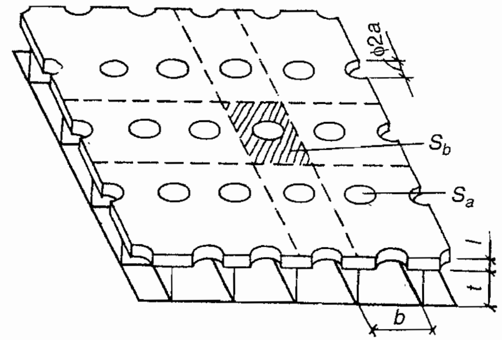

FIGURE 8.22 Resonators arranged on a raster to form a surface array.

Placing of flow-resistive materials in or behind the resonator opening reduces nonlinearity and sensitivity to grazing flow.

Spatial Average Impedance of Resonator Arrays

Locally reacting absorbers such as resonators are frequently used in the form of a surface array, shown in Fig. 8.22, where the individual resonators are arranged periodically. If the dimension b or $\sqrt{S_b}$ in Fig. 8.22 is much smaller than the acoustical wavelength, it is not necessary to take into account the interaction of the individual elements (resonators) with the sound field. To characterize the absorber, it is sufficient in this case to compute the spatial average wall impedance Z_1:

$$Z_1 = \frac{\langle p \rangle}{\langle v \rangle} = \frac{S_b}{S_a}\frac{p_a}{v_a} = \frac{S_b}{S_a} Z_R = \frac{Z_R}{\varepsilon} \quad \mathrm{N \cdot s/m^3} \tag{8.65}$$

where Z_R is the impedance of the resonator as given in Eqs. (8.55) "measured" in the orifice of the resonator and $\varepsilon = S_a/S_b$ is the surface porosity. The effective wall impedance Z_1 is then used in Eq. (8.37) to determine the absorption coefficient. The impedances Z_m in Table 8.8 are effective impedances averaged over the plate surface (resonator mass impedance divided by porosity).

8.8 PLATE AND FOIL ABSORBERS

Plate absorbers are used in absorbing low-frequency tonal noise in situations where Helmholtz resonators are not feasible. The resonator consists of the mass of a thin plate and usually the stiffness of the air space between the plate and the elastic mounting at the perimeter of the plate. Foils are a special case of a thin limp plate.

Limp Thin Plate or Foil Absorber

The resonance frequency of a foil absorber is

$$f_0 = \frac{\sqrt{\rho_0 c_0^2 / m'' t}}{2\pi} \tag{8.66}$$

where t is the depth of the partitioned air space in meters and m'' is the mass per unit area of the limp foil in kilograms per square meter. If the air space depth is not small ($t > \frac{1}{8}\lambda$), there will be many resonance frequencies ω_n ($n = 0, 1, 2, \ldots$) given by

$$\frac{\omega_n t}{c_0} \tan \frac{\omega_n t}{c_0} = \frac{\rho_0 t}{m''} \tag{8.67}$$

For an unpartitioned air space behind the foil the resonance frequency depends on the angle of sound incidence θ_0. In this case t must be replaced in Eqs. (8.66) and (8.67) by $t \cos \theta_0$. If the air space is filled (without obstructing the movement of the foil) with a porous sound-absorbing material, then $(t/c_0)\Gamma_a''$ is used instead of t/c_0 in Eq. (8.67).

Foil-Wrapped Porous Absorber

Sound absorbers consisting of a protective layer of thin foil, a porous layer, and an air space behind are frequently used where the porous material must be protected from dust, dirt, and water. The effect of the thin foil can be taken into account by a series impedance $Z_s = j\omega m''$ that is added to the surface impedance Z_1 [see Eq. (8.37)]. It is essential that the foil is not stretched so that its inertia and not its membrane stress controls its response. Inserting a large-mesh (≥ 1 cm) wire cloth between the porous sound-absorbing material and the protective foil is a practical way to assure this.

Elastically Supported Stiff Plate

A form of resonant plate absorber that can be easily treated analytically is the elastically supported stiff plate. The elastic support may be localized by discrete points to occur along the perimeter in the form of a resilient gasket strip. The effective stiffness of such a resonator is

$$s'' = \frac{s_e}{S_p} + \frac{\rho_0 c_0^2}{t} \quad \text{N/m}^3$$

and the resonance frequency is

$$f_0 = \frac{1}{2\pi}\sqrt{\frac{s''}{m''}} = \frac{1}{2\pi}\sqrt{\frac{s_e/S_p + \rho_0 c_0^2/t}{m''}} \quad \text{Hz} \tag{8.68}$$

where $s_e = S_p \, \Delta p / \Delta x$ is the dynamic stiffness of resilient plate mounting and S_p is the surface area of the plate. Note that the elastic mounting increases the

resonance frequency (compared with that obtainable with a limp foil of the same m''). This can be compensated for by an appropriate increase of m''. However, an increase of m'' increases the Q of the resonator ($Q = \sqrt{s''/m''}/R$) resulting in a narrower bandwidth.

Elastic Foil Absorber

Elastic foil absorbers consist of small air volumes enclosed in thin (200–400-μm) foil coffers. The coffers have typical dimensions of a few centimeters. A typical

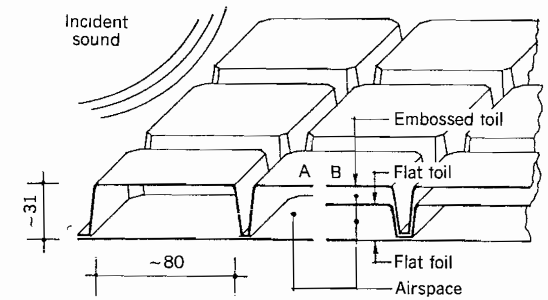

FIGURE 8.23 Construction of a foil absorber made of cold-drawn PVC foil.

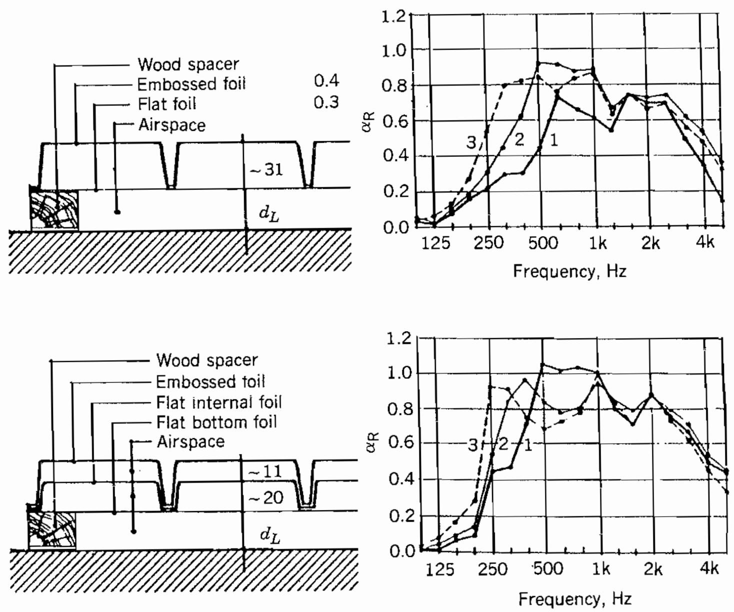

FIGURE 8.24 Random-incidence sound absorption coefficient α_R of absorbers made of cold-drawn PVC foil: (1) $d_L = 0$; (2) $d_L = 25$ mm; (3) $d_L = 50$ mm.

foil absorber is shown in Fig. 8.23. The wavelength of the incident sound is large compared with the typical dimensions of the coffers. Consequently, the incident sound periodically compresses the air in the individual coffers by exiting all of the volume-displacing modes of vibration of the various coffer walls. Because of the small thickness of the coffer walls, these resonances fall into the frequency range of 200–3150 Hz, which is of primary interest in building applications.[49] The foil material can be plastic (PVC) or metal. It is beneficial to emboss the foil because this leads to a more even distribution of the resonance frequencies. Figure 8.24 shows the measured random-incidence sound absorption coefficient obtained with two different foil absorber configurations, indicating that significant broadband sound absorption is achievable.

The key advantage of these foil absorbers is that they are nonporous, do not support bacterial growth, are lightweight, and can be made light transparent. Their main application is in breweries, packaging plants, hospitals, and computer chip manufacturing areas, where high emphasis is placed on hygiene and dust cannot be tolerated. They also lend themselves as sound absorbers in high-moisture environments such as swimming pools and as muffler baffles in cooling towers. Their light transparency is a distinct advantage in industrial halls. Considerable experience has been gained in such applications in Europe.[49]

REFERENCES

1. K. U. Ingard, *Notes on Sound Absorption Technology*, Version 94-02, Noise Control Foundation, Poughkeepsie, NY, October 1994.
2. F. P. Mechel, *Schall Absorber [Sound Absorbers]*, Vol. 1: *Aeussere Schallfelder, Wechselwirkungen [Outer Sound Fields, Interactions]*; Vol. 2: *Innere Schallfelder, Structuren [Internal Sound Fields, Structures]*; Vol. 3: *Anwendungen [Application]*, S. Hirzel Verlag, Stuttgart, 1989.
3. F. P. Mechel, *MAPS-Mechels Acoustic Program System*, CD-ROM for Windows, S. Hirzel, Stuttgart, Germany, 2001.
4. H. Kutruff, *Room Acoustics*, Applied Science, London, 1973.
5. L. L. Beranek, *Acoustic Measurements*, Acoustical Society of America, Melville, New York, 1988.
6. R. D. Godfrey, Owens Corning Fiberglass Company, private communication, June 2004.
7. T. Northwood, *J. Acoust. Soc. Am.*, **31**, 596 (1959); **35**, 1173 (1963).
8. M. J. Swift, "The Physical Properties of Porous Recycled Materials," Ph. D. Thesis, University of Bradford, United Kingdom, 2000.
9. L. Cremer and M. Hubert, *Vorlesungen Ueber Technische Akustik [Lectures on Technical Acoustics]*, 3rd ed., Springer, Berlin, 1985.
10. Y. Champoux, M. R. Stinson, and G. A. Daigle, "Air-Based System for the Measurement of Porosity," *J. Acoust. Soc. Am.*, **89**, 910–916 (1991).

11. P. Leclaire, O. Umnova, K. V. Horoshenkov, and L. Maillet, "Porosity Measurement by Comparison of Air Volumes," *Rev. Sci. Instrum.*, **74**, 1366–1370 (2003).
12. Z. E. A. Fellah, S. Berger, W. Lauriks, C. Depollier, C. AristBgui, and J.-Y. Chapelon, "Measuring the Porosity and the Tortuosity of Porous Materials via Reflected Waves at Oblique Incidence," *J. Acoust. Soc. Am.*, **113**, 2424–2433 (2003).
13. Z. E. A. Fellah, S. Berger, W. Lauriks, C. Depollier, and M. Fellah, "Measuring the Porosity of Porous Materials Having a Rigid Frame via Reflected Waves: A Time Domain Analysis with Fractional Derivatives," *J. Appl. Phys.*, **93**, 296–303 (2003).
14. Z. E. A. Fellah, S. Berger, W. Lauriks, C. Depollier, and J. Y. Chapelon, "Inverse Problem in Air-Saturated Porous Media via Reflected Waves," *Rev. Sci. Int.*, **74**, 2871–2879 (2003).
15. Z. E. A. Fellah, S. Berger, W. Lauriks, C. Depollier, W. Lauriks, P. Trompette, and J. Y. Chapelon, "Ultrasonic Measurement of the Porosity and Tortuosity of Air-Saturated Random Packings of Beads," *J. Appl. Phys.* to appear.
16. A. S. Sangani and A. Acrivos, "Slow Flow through Periodic Array of Spheres," *Int. J. Multiphase Flow*, **8**, 343–360 (1982).
17. W. S. Jodrey and E. M. Tory, "Computer-Simulation of Close Random Packing of Equal Spheres," *Phys. Rev. A*, **32**, 2347–2351 (1985).
18. N. Sen, C. Scala, and M. H. Cohen, "A Self-Similar Model for Sedimentary Rocks with Application to the Dielectric Constant of Fused Glass Beads," *Geophysics*, **46**, 781–795 (1981).
19. K. Attenborough, "Acoustical Characteristics of Rigid Absorbents and Granular Media," *J. Acoust. Soc. Am.*, **83**(3), 785–799 (March 1983).
20. O. Umnova, K. Attenborough, and K. M. Li, "Cell Model Calculations of Dynamic Drag Parameters in Packings of Spheres," *J. Acoust. Soc. Am.*, **107**(3), 3113–3119 (2000).
21. J. F. Allard, *Propagation of Sound in Porous Media*, Elsevier Applied Science, London, 1993.
22. J. F. Allard, B. Castagnede, M. Henry, and W. Lauriks, "Evaluation of Tortuosity in Acoustic Porous Materials Saturated by Air," *Rev. Sci. Instrum.*, **65**, 754–755 (1994).
23. ASTM C 522-87, *"Standard Test Method for Airflow Resistance of Acoustical Materials,"* American Society for Testing and Materials, West Conshohocken, PA, pp. 169–173.
24. M. R. Stinson and G. A. Daigle, "Electronic System for the Measurement of Flow Resistance," *J. Acoust. Soc. Am.*, **83**, 2422–2428 (1988).
25. O. Umnova, University of Salford, United Kingdom, September, 2004. private communication.
26. P. Leclaire, M. J. Swift, and K. V. Horoshenkov. "Determining the Specific Area of Porous Acoustic Materials from Water Extraction Data," *J. Appl. Phys.*, **84**, 6886–6890 (1998).
27. K. Attenborough, "Models for the Acoustical Properties of Air-Saturated Granular Media," *Acta Acustica*, **1**, 213–226 (1993).
28. K. V. Horoshenkov, K. Attenborough, and S. N. Chandler-Wilde, "Pade Approximants for the Acoustical Properties of Rigid Frame Porous Media with Pore Size Distribution," *J. Acoust. Soc. Am.*, **104**, 1198–1209 (1998).

29. K. V. Horoshenkov and M. J. Swift, "The Acoustic Properties of Granular Materials with Pore Size Distribution Close to Log-normal," *J. Acoust. Soc. Am.*, **110**, 2371–2378 (2001).
30. D. L. Johnson, J. Koplik, and R. Dashen, "Theory of Dynamic Permeability and Tortuosity in Fluid-Saturated Porous Media," *J. Fluid Mech.*, **176**, 379–402 (1987).
31. O. Umnova, K. Attenborough, and K. M. Li, "A Cell Model for the Acoustical Properties of Packings of Spheres," *Acustica* combined *with Acta Acustica*, **87**, 26–235 (2001).
32. J. F. Allard and Y. Champoux, "New Empirical Relations for Sound Propagation in Rigid Frame Fibrous Materials," *J. Acoust. Soc. Am.*, **91**, 3346–3353 (1992).
33. N. N. Voronina and K. V. Horoshenkov, "A New Empirical Model for the Acoustic Properties of Loose Granular Media," *Appl. Acoust.*, **64**(4), 415–432 (2003).
34. J. Y. Chung and D. A. Blaser, "Transfer Function Method of Measuring In-Duct Acoustic Properties. I. Theory, II Experiment," *J. Acoust. Soc. Am.*, **68**(3), 907–921 (1980).
35. C. D. Smith, and T. L. Parrott, "Comparison of Three Methods for Measuring Acoustic Properties of Bulk Materials," *J. Acoust. Soc. Am.*, **74**(5), 1577–1582 (1983).
36. H. Utsuno et al., "Transfer Function Method for Measuring Characteristic Impedance and Propagation Constant of Porous Materials," *J. Acoust. Soc. Am.*, **86**(2), 637–643 (1989).
37. P. Mechel, *Akustische Kennwerte von Faserabsorbem [Acoustic Parameters of Fibrous Sound Absorbing Materials]*, Vol. I, *Bericht* BS 85/83; Vol. II, *Bericht* BS 75/82, Fraunhofer Inst. Bauphysik, Stuttgart, Germany.
38. M. E. Delany and E. N. Bazley, "Acoustical Properties of Fibrous Absorbent Materials," *Appl. Acoust.*, **3**, 105–116 (1970).
39. Y. Miki, "Acoustical Properties of Porous Materials—Modifications of Delany-Bazley Models," *J. Acoust. Soc. Jpn. (E)*, **11**, 19–24 (1990).
40. M. Garai and F. Pompoli, "A Simple Empirical Model of Polyester Fibre Materials for Acoustical Applications," *Appl. Acoust.* (in press).
41. A. Cummings and S. P. Beadle, "Acoustic Properties of Reticulated Plastic Foams," *J. Sound Vib.*, **175**(1), 115–133 (1993).
42. Q. Wu, "Empirical Relations between Acoustical Properties and Flow Resistivity of Porous Plastic Open-Cell Elastic Foams," *Appl. Acoust.*, **25**, 141–148 (1988).
43. L. P. Dunn and W. A. Davern "Calculation of Acoustic Impedance of Multilayer Absorbers," *Appl. Acoust.*, **19**, 321–334 (1986).
44. R. J. Astley and A. Cummings, "A Finite Element Scheme for Attenuation in Ducts Lined with Porous Material: Comparison with Experiment," *J. Sound Vib.*, **116**, 239–263 (1987).
45. J. Royar, "Untersuchungen zum Akustishen Absorber-Kanten-Etfekt an einem zweidimensionalen Modell" ["Investigation of the Acoustic Edge-Effect Utilizing a Two-Dimensional Model"], Ph.D. Thesis, Faculty of Mathematics and Nature Sciences, University of Saarbrueken, Germany, 1974.
46. F. P. Mechel, "Design Charts for Sound Absorber Layers," *J. Acoust. Soc. Am.*, **83**(3), 1002–1013 (1988).

47. F. Mechel, "Sound Absorbers and Absorber Functions," in G. L. Osipova and E. J. Judina, (Eds.), *Reduction of Noise in Buildings and Inhabited Regions* (in Russian), Strojnizdat, Moscow, 1987.
48. J. L. B. Coelho, "Acoustic Characteristics of Perforate Liners in Expansion Chambers," Ph.D. Thesis, Institute of Sound Vibration, Southampton, 1983.
49. F. Mechel and N. Kiesewetter, "Schallabsorberaus Kunstotf-Folie" ["Plastic-Foil Sound Absorber"], *Acustica*, **47**, 83–88 (1981).

CHAPTER 9

Passive Silencers

M. L. MUNJAL

Indian Institute of Science
Bangalore, India

ANTHONY G. GALAITSIS

BBN Systems and Technologies Corporation
Cambridge, Massachusetts

ISTVÁN L. VÉR

Consultant in Acoustics, Noise, and Vibration Control
Stow, Massachusetts

9.1 INTRODUCTION

Chapter Organization

This chapter is organized in seven sections. The present section reviews some of the significant milestones in silencer design, citing relevant references. Section 9.2 reviews the acoustical criteria commonly used to determine silencer performance. Section 9.3 discusses the decomposition of a silencer into basic acoustical transmission elements, presents transmission matrix expressions for some elements used in the Section 9.4 examples, and provides references for additional elements not explicitly covered in this chapter. Section 9.4 discusses the predicted performance of several silencer designs and provides selected examples of designs aimed at achieving specific acoustical goals. Section 9.5 provides a more qualitative discussion of perforated-element mufflers along with a few muffler design examples. Section 9.6 considers dissipative silencers most widely used to attenuate broadband noise in ducts with gas flow with a minimum of pressure drop across the silencer. Section 9.7 discusses designs that combine reactive silencer low-frequency tonal performance with passive silencer high-frequency broadband performance. A reader solely interested in designing a silencer for a specific application may proceed directly to Sections 9.3–9.7.

Background Information

The noise generated by air/gas handling/consuming equipment, such as fans, blowers, and internal combustion engines, is controlled through the use of two types of devices: (1) passive silencers and lined ducts whose performance is a function of the geometric and sound-absorbing properties of their components and (2) active noise control silencers whose noise cancellation features are controlled by various electromechanical feed-forward and feedback techniques. This chapter focuses on passive silencers while active noise control is discussed in Chapter 17 and lined ducts are covered in Chapter 16.

In the remainder of this chapter, the term *silencer* is often used generically to refer to any type of passive noise control device. Specific names are introduced primarily in cases where the use of "silencer" may lead to ambiguities.

Over the last four decades silencers have been the focus of many research programs that improved the understanding of the basic phenomena and resulted in more accurate design methods. The groundwork for the behavior of lined ducts with no flow was laid even earlier by Morse[1] and Cremer,[2] and the first systematic evaluation of mufflers with no flow was conducted by Davis et al.[3] Those works were followed by numerous theoretical and experimental investigations which addressed additional important issues such as uniform flow, temperature gradient, and the behavior of new silencer components that are common in modern applications. Reviews of the major accomplishments in this area have been presented periodically in the form of individual articles in professional journals, chapters in engineering handbooks,[4–7] and, more recently, books by Munjal[8,9] solely devoted to mufflers.

The analytical work on this subject benefited substantially from the early adaptation of the transfer matrix approach to silencer modeling. This method, which was promoted for the description of mechanical systems early on,[10] was used along with electrical analogs to describe the behavior of basic silencer components[11] for plane-wave sound propagation in the absence of flow. Subsequent investigations began addressing the effects of flow on the response of elements consisting of area discontinuities[12,13] and generating transfer matrix models for silencer elements. The predicted performance of various reactive silencers using transfer matrices with convective and dissipative effects in the presence of flow agreed well with measured data.[14]

Concurrently, systematic studies were initiated on the behavior of perforated plates (perforates) to take advantage of their dissipative properties[15–17] for general applications in the transportation industry. Such perforates are used in automotive applications as part of the two- and three-pipe elements featuring one and two perforated pipes, respectively, contained within a larger diameter rigid-wall cylindrical cavity. Such configurations were investigated[18–23] by combining an orifice model with the transfer matrices of the axially segmented perforated tube or tubes and the unpartitioned cavity.

At higher frequencies or for large mufflers, three-dimensional effects become significant. The approaches used in three-dimensional silencer analysis include the finite-element, boundary-element, and acoustical-wave finite-element methods. Each has some inherent advantages at higher frequencies where higher order modes will start propagating, but on the average they are much more complex and time consuming to implement. Therefore, the plane-wave transfer matrix

method is presently the most widely used approach, particularly for synthesis of an initial configuration of a passive silencer.[24–26]

Experimental work conducted in parallel with the analysis validated the developed models and pointed out areas requiring further investigation. Methods for the direct measurement of transfer matrices were developed[27–31] to validate/modify the models of existing silencer elements. Substantial attention was also paid to the source impedance, which was expected to influence the insertion loss of a silencer and the net radiated acoustical power of the system. The source impedance of a six-cylinder engine was measured with an impedance tube using pure tones,[32,33] and the impedance of electroacoustical drivers and multicylinder engines was subsequently measured[34–37] using the much quicker two-microphone methods.[38–40] More recent indirect methods characterized the source impedance through measurements using two, three, or four different acoustical loads.[41–46]

The research performed and the knowledge developed in the field of passive silencers are very extensive and cannot be adequately covered in a single chapter. Accordingly, this chapter reviews the basic background information, summarizes the methodologies for silencer design, demonstrates these approaches through selected examples, and discusses additional topics and references useful to general applications. A reader wishing to acquire more information on internal combustion engine silencers is urged to review references 47–50 for a summary of a general automotive silencer development approach and of typical predicted and measured results, references 51 and 52 for condensed qualitative reviews of the accomplishments in this field, and references 8 and 9 for an extensive bibliography on and a detailed discussion of most silencer-related topics.

9.2 SILENCER PERFORMANCE METRICS

The majority of noise sources have an intake and an exhaust and, generally, they require both intake and exhaust silencers. The two cases are characterized by different flow direction, back pressure, average gas temperature, and average sound pressure levels, but the corresponding hardware is developed using the same principles and design methods. The following discussion is tailored to exhaust silencers but it is equally applicable to intake silencers.

Silencer Selection Factors

The use of a silencer is prompted by the need to reduce the radiated noise of a source but, in most applications, the final selection is based on trade-offs between the predicted acoustical performance, mechanical performance, volume/weight, and cost of the resulting system.

During development, the acoustical performance (insertion loss) of a candidate silencer is determined from the free-field sound pressure levels measured at the same relative locations with respect to the noise outlet of the unsilenced and silenced sources. If the noise outlet is inserted into a reverberant space, then the difference can be measured anywhere within the reverberant field, and the difference sound pressure level represents the power-based insertion loss.

The impact of the silencer on the mechanical performance of the source is determined from the change in the silencer back pressure. For a continuous-flow source, such as a fan or a gas turbine, the impact is determined from the increase in the average back pressure; by contrast, for an intermittent-flow source, such as a reciprocating engine, the impact is a function of the increase in the exhaust manifold pressure when an exhaust valve is open.

Most silencers are subject to volume/weight constraints, which also influence the silencer design process. In addition, the initial purchase/installation cost and the periodic maintenance cost are other important factors that influence the silencer selection process.

Since noise is the root cause of silencer design, the remainder of this chapter focuses on the prediction of a silencer's acoustical performance and also on the estimation of back pressure. The additional performance criteria associated with hardware volume, weight, and cost are trade-off parameters to be determined separately for each application.

Factors Influencing Acoustical Performance

Reactive and Dissipative Silencers. The net change ΔW in the acoustical power radiated from a source can be expressed as

$$\Delta W = W_1 - W_2 = W_1 - (W_1' - W_d) = (W_1 - W_1') + W_d \quad \text{N} \cdot \text{m/s} \qquad (9.1)$$

where W_1 and W_2 correspond to the unsilenced and silenced sources (Fig. 9.1), $W_1 - W_1'$ is the net change in the acoustical power output of the source resulting from changes in the silencer's reflection coefficient, and W_d is attributable to the dissipative properties of the silencer.

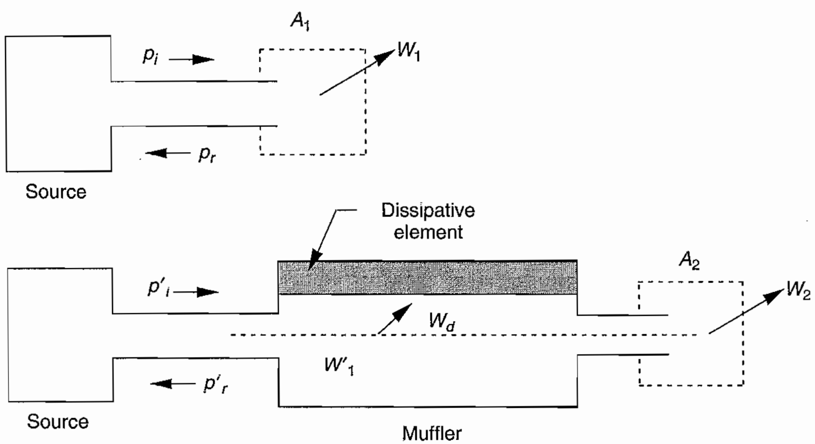

FIGURE 9.1 Radiated noise reduction mechanisms of a silencer.

The reflection coefficient is manipulated primarily by introducing cross-sectional discontinuities in the piping system, and the dissipated part W_d depends largely on the dissipative properties of the silencer elements. In practice, all silencer elements reflect and dissipate acoustical energy to some extent. However, traditionally, they have been categorized into reactive and dissipative silencers when their insertion loss is dominated by reflective and dissipative mechanisms, respectively. This convention has also been adopted in this chapter, but the reader should be aware that most common applications involve various degrees of overlap between the two extremes.

Flanking Paths and Secondary Source Mechanisms. The acoustical power radiated from a silenced source, such as an engine, includes airborne noise (W_{EX}) from the exhaust pipe outlet, silencer shell noise (W_{SH}) radiated from the vibrating walls of the silencer and exhaust line pipes, and a contribution (W_{AD}) from additional sources, such as source shell and source intake, located upstream of the silencer.

The shell noise results from the excitation of silencer components by the vibrating engine, by the intense internal acoustical pressure fields, and by aerodynamic forces. These contributions can be reduced substantially through various methods, but they cannot be totally eliminated and, eventually, they set the limit for the achievable insertion loss for high-performance silencers.

The acoustical power contributions W_{SH} and W_{AD} are excluded from further consideration in the remainder of the chapter; that is, the discussion is focused on the impact of silencers on the airborne noise contributions W_{EX}. However, one should be aware of their existence and significance, particularly in experimental applications where limited resources may lead to the measurement of W_{EX} in the presence of W_{SH} and W_{AD}.

Silencer System Modeling

Silencer Component Representation. The basic components of a typical silencer system comprise the noise source, silencer, connecting pipes, and surrounding medium (Fig. 9.2*a*). The pipe connecting the source to the silencer is treated as part of the source. Figure 9.2*b* shows the corresponding electrical analog of the acoustical system, which is widely used to facilitate the representation and handling of acoustical transmission lines. This analog model, which uses acoustical pressure p and mass velocity $\rho_0 S u$ in kg/s, instead of voltage and current, represents the noise source with a source pressure p_s and an internal impedance Z_s, the silencer and pipe segment with four-pole elements (T_{ij} and D_{ij}), and the surrounding medium with a termination (or radiation load) impedance Z_T. Analytical expressions for the transfer matrices of pipes and selected silencer elements are presented in references 8 and 9. Some of them are given later in Section 9.3.

Let p_i, u_i, $i = 1, 2, 3$, designate the acoustical pressure and particle velocity at the interfaces of acoustical components of the source–silencer–load system illustrated in Fig. 9.2*b*. These quantities may be obtained by solving the system

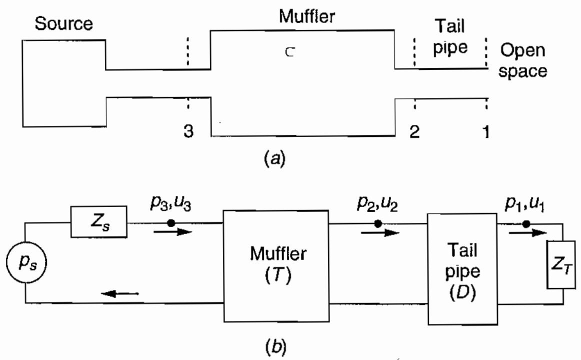

FIGURE 9.2 (*a*) Acoustical and (*b*) electrical analog components of a silencer.

of equations describing the response of the components depicted in Fig. 9.2*b*, namely,

$$p_s = p_3 + \rho_0 Z_s S_3 u_3 \tag{9.2}$$

$$\begin{bmatrix} p_3 \\ \rho_0 S_3 u_3 \end{bmatrix} = \begin{bmatrix} T_{11} & T_{12} \\ T_{21} & T_{22} \end{bmatrix} \begin{bmatrix} p_2 \\ \rho_0 S_2 u_2 \end{bmatrix} \tag{9.3}$$

$$\begin{bmatrix} p_2 \\ \rho_0 S_2 u_2 \end{bmatrix} = \begin{bmatrix} D_{11} & D_{12} \\ D_{21} & D_{22} \end{bmatrix} \begin{bmatrix} p_1 \\ \rho_0 S_1 u_1 \end{bmatrix} \tag{9.4}$$

$$p_1 = Z_T \rho_0 S_1 u_1 \tag{9.5}$$

where ρ_0 is the mean gas density and S_i is the duct cross-sectional area at the ith location. The calculated quantities p_i, $\rho_0 S_i u_i$, $i = 1, 2, \ldots$, can then be combined with the selected performance criterion to determine the effectiveness of the silencer.

Acoustical Performance Criteria. The most frequently used performance criteria are the insertion loss (IL), noise reduction (NR), and transmission loss (TL). All three use a sound-pressure-level difference as a performance indicator; therefore, they require no explicit knowledge of the source strength p_s, of Eq. (9.2). The number of required system parameters (source impedance Z_s, transfer matrix elements D_{ij}, and termination impedance Z_T*) other than the silencer matrix T_{ij} can be further reduced by the specific choice of the performance criterion.

The IL is defined as the change in the radiated sound pressure level resulting from the insertion of the muffler, that is, the replacement of a pipe segment of length l_1 (Fig. 9.3*a*) located downstream from the source by the silencer and a new tail-pipe segment of length l_2 (Fig. 9.3*b*). Insertion loss is expressed as

$$\mathrm{IL} = L_b - L_a = 20 \log \left| \frac{p_b}{p_a} \right| \tag{9.6}$$

*The impedance Z in this chapter is defined as $p_i/(\rho_0 S_i u_i)$.

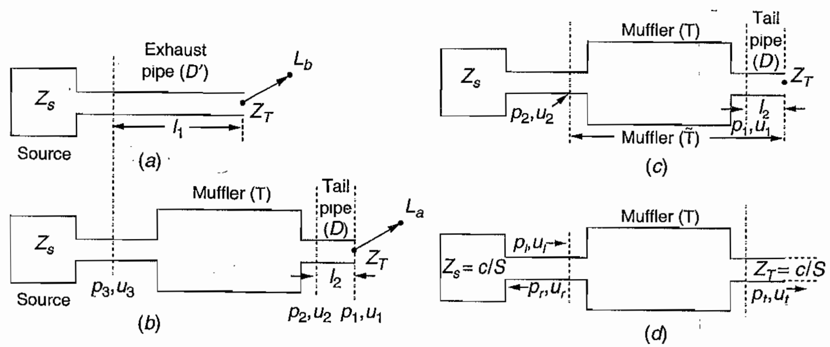

FIGURE 9.3 Quantities use for the determination of (*a,b*) insertion loss, (*c*) noise reduction, and (*d*) transmission loss.

where p_b, p_a and L_b, L_a are the measured sound pressures and sound pressure levels at the same relative location (distance and orientation) with respect to the exhaust outlet (Fig. 9.3*a*) before and after the installation of the muffler and "log" refers to a logarithm with respect to the base 10. Mathematically,

$$\mathrm{IL} = 20 \log \left| \frac{\tilde{T}_{11} Z_T + \tilde{T}_{12} + \tilde{T}_{21} Z_s Z_T + \tilde{T}_{22} Z_s}{D_{11} Z_T + D_{12} + D_{21} Z_s Z_T + D_{22} Z_s} \right| \tag{9.7}$$

where $\tilde{T}_{ij}$ is the combined transfer matrix element of the silencer and its tail pipe ($\tilde{T} = TD$), and D'_{ij} is the transfer matrix element of the replaced exhaust pipe segment. If the silencer is simply added to the end of the source ($l_1 = l_2 = 0$ in Figs. 9.3*a* and *b*), then both D' and D are identity matrices (see Transfer Matrices for Reactive Elements in Section 9.3) and Eq. (9.7) is reduced to

$$\mathrm{IL}(l_1 = l_2 = 0) = 20 \log \left| \frac{T_{11} Z_r + T_{12} + T_{21} Z_r Z_s + T_{22} Z_s}{Z_T + Z_s} \right| \tag{9.8}$$

The noise reduction is given by

$$\mathrm{NR} = L_2 - L_1 = 20 \log \left| \frac{p_2}{p_1} \right| \tag{9.9}$$

that is, it is the difference between the sound pressure levels measured at two points 1 and 2 (Fig. 9.3*c*) of the silenced system located upstream and downstream of the silencer, respectively. If D_{ij} and $\tilde{T}_{ij}$ represent the transfer matrix elements for the silencer portions downstream of points 1 and 2, respectively, the noise reduction is given by

$$\mathrm{NR} = 20 \log \left| \frac{\tilde{T}_{11} Z_T + \tilde{T}_{12}}{D_{11} Z_T + D_{12}} \right| \tag{9.10}$$

The TL is the acoustical power-level difference between the incident and transmitted waves of an anechoically terminated silencer (see Fig. 9.3d). In terms of the corresponding transfer matrix, the transmission loss is given by

$$\mathrm{TL} = 20\ \log\left|\frac{T_{11} + (S/c)T_{12} + (c/S)T_{21} + T_{22}}{2}\right| \tag{9.11}$$

where c is the speed of sound at design temperature and S is the cross-sectional area of the reference pipe.

This expression assumes that (a) the area of cross section of the exhaust pipe upstream of the silencer is the same as that of the tailpipe, that is, S; (b) the silencer is simply added at the end of the source ($l_1 = l_2 = 0$); and (c) the tail pipe end (or radiation end) is anechoic ($Z_T = c/S$).

The IL is the most appropriate indicator of a silencer's performance because it is the level difference of the acoustical power radiated from the unsilenced and silenced systems. It is easy to quantify from pre- and postsilencing data, but it is hard to predict because it depends on Z_s and Z_T, which vary from one application to another. By contrast, the TL is easy to predict but is only an approximation of the silencer's actual performance because it does not account for the source impedance and it models all silencer outlets with anechoic terminations. Equations (9.7) and (9.11) show that the TL and IL of a silencer become identical when the noise source and silencer termination are anechoic, that is, $Z_s = Z_T = c/S$. Similarly, it can readily be shown[8] that for a constant-pressure source ($Z_s = 0$), the NR and IL become identical, provided the cross-sectional area of the exhaust pipe upstream of the silencer is the same as that of the tailpipe.

The ultimate selection of an evaluation criterion is based on trade-offs between the desired accuracy in the predictions and the amount of available resources. For example, Z_s, required for IL predictions, can be determined experimentally through various methods,[32–46] but the procedure is too costly for the majority of applications. As a result, the silencer design is, generally, based on predicted TL, with a clear understanding of the associated approximations, while the final evaluation of the hardware during field tests is based on the measured IL.

9.3 REACTIVE SILENCER COMPONENTS AND MODELS

Reactive silencers consist typically of several pipe segments that interconnect a number of larger diameter chambers. These silencers reduce the radiated acoustical power primarily through impedance mismatch, that is, through the use of acoustical impedance discontinuities to reflect sound back toward the source. In essence, the more pronounced the discontinuities, the higher the amount of reflected power. Acoustical impedance discontinuities are commonly achieved through (a) sudden cross-sectional changes (i.e., expansions or contractions), (b) wall property changes (i.e., transition from a rigid-wall pipe to an equal-diameter absorbing wall pipe), or (c) any combination thereof.

Silencer Representation by Basic Silencer Elements

Every silencer can be divided into a number of segments or elements each represented by a transfer matrix. The transfer matrices can then be combined to obtain the system matrix, which may then be substituted into Eqs. (9.7), (9.10), or (9.11) to predict the corresponding acoustical performance for the silencer system.

The procedure is illustrated by considering the silencer of Fig. 9.4, which is divided into the basic elements, labeled 1–9, indicated by the dashed lines. Elements 1, 3, 5, 7, and 9 are simple pipes of constant cross section. Element 2 is a simple area expansion, element 4 is an area contraction with an extended outlet pipe, element 6 is an area expansion with an extended inlet pipe, and element 8 is a simple area contraction. The nine elements are characterized by the transfer matrices $T^{(1)}$ through $T^{(9)}$; therefore, the system matrix $T^{(S)}$ for the entire silencer is obtained from

$$T^{(S)} = T^{(1)} \cdot T^{(2)} \cdot \cdots \cdot T^{(9)} \tag{9.12}$$

through matrix multiplication. The matrices for each of the above elements may be derived from the formulas presented later in this section.

A few of the most common reactive muffler elements are discussed in this section and some are used in illustrative design examples. Additional elements that were the subject of previous investigations include gradually varying area ducts (such as horns), uniform-area compliant-wall ducts (such as hoses), Quincke tubes, inline cavities, inline bellows, catalytic converter elements, branch sub systems, side inlets/outlets, cavity-backed resistive-wall elements, and perforated-duct elements with and without mean flow through the perforations. Transfer matrices for each of these elements have been derived over the last three decades by different researchers,[53–70] and explicit expressions for their four-pole parameters are given in detail in references 8 and 9.

The variety of silencer elements and the multitude of elements per silencer result in numerous silencer configurations; therefore, a comprehensive study of all possible silencer applications is beyond the scope of this work. For this

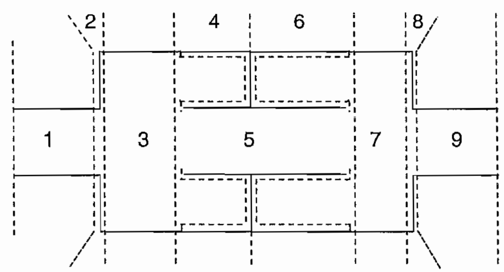

FIGURE 9.4 Decomposition of a silencer into basic elements.

reason, the remainder of this chapter uses selected silencer configurations to demonstrate

(a) the typical process for modeling a basic silencer element with a (four-pole parameter) transmission matrix,
(b) the process for predicting the acoustical performance of a given silencer configuration from the properties (transmission matrices) of its constituent elements, and
(c) the process for selecting a silencer design to achieve approximately a specified acoustical performance.

Furthermore, Section 9.5 provides additional information and sketches for perforated-tube elements and analyzes the performance of selected perforated-tube muffler configurations. The reader could also apply the demonstrated design process to any other silencer configurations by obtaining and utilizing the relevant transmission matrix information from the corresponding references 8, 9, 53–69.

Transfer Matrices for Reactive Elements

The transfer matrix of a silencer element is a function of the element geometry, state variables of the medium, mean flow velocity, and properties of duct liners, if any. The results presented below correspond to the linear sound propagation of a plane wave in the presence of superimposed flow. In certain cases, the matrix may also be influenced by nonlinear effects, higher order modes, and temperature gradients; these latter effects, which can be included in special cases, are discussed qualitatively later in this section, but they are excluded from the analytical procedure described below. The following is a list of variables and parameters that appear in most transfer matrix relations of reactive elements:

p_i = acoustical pressure at ith location of element
u_i = particle velocity at ith location of element
ρ_0 = mean density of gas, kg/m^3
c = sound speed m/s, $= 331\sqrt{\theta/273}$
θ = absolute temperature, K = °C + 273
S_i = cross section of element at ith location, m^2
$Y_i = c/S_i$
A, B = amplitudes of right- and left-bound fields
$k_c = k_0/(1 - M^2)$ assuming negligible frictional energy loss along straight pipe segments
$k_0 = \omega/c = 2\pi f/c$
$\omega = 2\pi f$
f = frequency, Hz
$M = V/c$
V = mean flow velocity through S
T_{ij} = (ij)th element of transmission matrix or transfer matrix

Symbols without subscripts, such as V, c, and M, describe quantities associated with the reference duct.

Pipe with Uniform Cross Section. The acoustical pressure and mass velocity fields p, $\rho_0 Su$ in a pipe with uniform cross section S and a mean flow V_0 are given by

$$p(x) = (Ae^{-jk_c x} + Be^{jk_c x})e^{j(Mk_c x+\omega t)} \tag{9.13a}$$

$$\rho_0 Su(x) = (Ae^{-jk_c x} - Be^{jk_c x})\frac{e^{j(Mk_c x+\omega t)}}{Y} \tag{9.13b}$$

where S is the cross section of the pipe. Equations (9.13a) and (9.13b) can be evaluated at $x = 0$ and $x = l$ to obtain the corresponding fields p_2, $\rho_0 Su_2$ and p_1, $\rho_0 Su_1$, respectively. Upon elimination of the constants A and B, one obtains[8,13]

$$\begin{bmatrix} p_2 \\ \rho_0 Su_2 \end{bmatrix} = \begin{bmatrix} T_{11} & T_{12} \\ T_{21} & T_{22} \end{bmatrix} \begin{bmatrix} p_1 \\ \rho_0 Su_1 \end{bmatrix} \tag{9.14}$$

where the transmission matrix T_{pipe} is given by

$$T_{\text{pipe}} = \begin{bmatrix} T_{11} & T_{12} \\ T_{21} & T_{22} \end{bmatrix}_{\text{pipe}} = e^{-jMk_c l} \begin{bmatrix} \cos k_c l & jY_0 \sin k_c l \\ \frac{j}{Y} \sin k_c l & \cos k_c l \end{bmatrix} \tag{9.15}$$

In the transfer matrix of Eq. (9.15) the acoustical energy dissipation that may result from friction between the gas and the rigid wall as well as from turbulence is neglected. These effects, which would result in a slightly different matrix,[8] may be noticeable in very long exhaust systems but they are negligible for most silencer applications.

Cross-Sectional Discontinuities. The transition elements used to model most cross-sectional discontinuities are shown in Figs. 9.5*b,c,e,f* and in the first column of Table 9.1. Using decreasing element-subscript values with distance from the noise source, the cross-sectional areas upstream, at, and downstream of the transition (S_3, S_2, and S_1) are related through[8]

$$C_1 S_1 + C_2 S_2 + S_3 = 0 \tag{9.16}$$

where the constants C_1 and C_2 (Table 9.1) are selected so as to satisfy the compatibility of the cross-sectional areas across the transition.

For each configuration, Table 9.1 also shows the pressure loss coefficient K, which accounts for the conversion of some mean-flow energy and acoustical field energy into heat at the discontinuities. As indicated, $K \le 0.5$ for area contractions, while $K \to (S_1/S_3)^2$ for area expansions at large values of S_1/S_3.

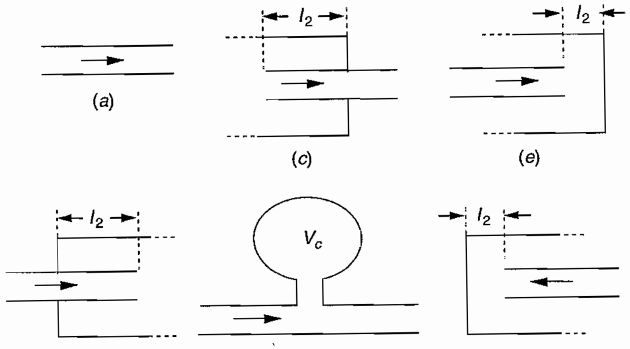

FIGURE 9.5 Basic silencer element: (*a*) plain pipe; (*b,c*) extended tube inlet/outlet; (*d*) resonator; (*e,f*) reversal expansion/contraction.

TABLE 9.1 Parameter Values of Transition Elements

Element Type	C_1	C_2	K
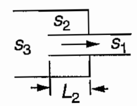	-1	-1	$\dfrac{1-S_1/S_3}{2}$
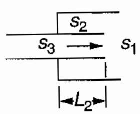	-1	1	$\left(\dfrac{S_1}{S_3}-1\right)^2$
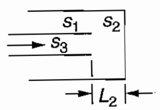	1	-1	$\left(\dfrac{S_1}{S_3}\right)^2$
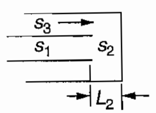	1	-1	0.5

Transfer matrices for cross-sectional discontinuities (csd) in the presence of mean flow that include terms proportional up to the fourth power (M^4) of the Mach number are presented in reference 8. However, in most silencer design applications, $M \ll 1$; therefore, terms of the form $1+M^n, n \geq 2$, are set to unity. This simplification reduces the matrix T_{csd}, which relates the upstream and

downstream acoustical fields p_3, $\rho S u_3$ and p_1, $\rho S u_1$ through

$$\begin{bmatrix} p_3 \\ \rho_0 S_3 u_3 \end{bmatrix}_{\text{upstream}} = T_{\text{csd}} \begin{bmatrix} p_1 \\ \rho_0 S_1 u_1 \end{bmatrix}_{\text{downstream}} \tag{9.17}$$

to

$$[T_{\text{csd}}] = \begin{bmatrix} 1 & \dfrac{kM_1Y_1}{C_2S_2Z_2 - M_1Y_1(C_1S_1+S_3K)} \\ \dfrac{C_2S_2}{C_1S_2Z_2+S_2M_3Y_3} & \dfrac{C_2S_2Z_2+S_3M_3Y_3}{} \end{bmatrix} \tag{9.18}$$

where $Z_2 = -j(c/S_2)\cot k_0 l_2$

l_2 = length of extended inlet/outlet pipe, m (9.19)

Letting length l_2 tend to zero (as in the case of sudden expansion and contraction shown in Fig. 9.5) yields the transfer matrix

$$\begin{bmatrix} 1 & KM_1Y_1 \\ 0 & 1 \end{bmatrix} \tag{9.20}$$

Resonators. A resonator is a cavity-backed opening in the sidewall of a pipe Fig. (9.5*d*). The opening may consist of a single hole on the pipe wall (Fig. 9.6*a*) or a closely distributed group of holes (Fig. 9.6*b*). The volume behind this opening can comprise a throat of length l_t and cross section S_n terminated by a straight pipe of cross-sectional area S_c and depth l_c (Fig. 9.6*c*), a concentric cylinder extending a length l_u and l_d upstream and downstream of the opening (Fig. 9.6*d*), an odd-shaped chamber of total volume V_c (Fig. 9.6*e*), or an extended-tube (quarter-wave) resonator of length l_2 (Figs. 9.5*b,c,e,f*).

The resonator opening in the wall of the main duct is assumed to be well localized; that is, the axial dimension of the perforated section is much smaller than the wavelength and typically smaller than a duct diameter. This requirement ensures that the duct–cavity interaction is in phase over the entire surface of the connecting opening. Transmission matrices for multihole openings with substantial axial dimensions requiring modeling by perforated-tube elements may be found in references 8 and 9.

The transfer matrix for a resonator for a stationary medium is given by[9]

$$T_r = \begin{bmatrix} 1 & 0 \\ \dfrac{1}{Z_r} & 1 \end{bmatrix} \tag{9.21}$$

where $Z_r = Z_t + Z_c$, Z_t is the impedance of the throat connecting the pipe to the cavity, and Z_c is the impedance of the cavity. Here, Z_c is independent of the flow in the main duct and is given by one of the following expressions:

$$Z_c = \begin{cases} Z_{tt} = -j\dfrac{c}{S_c}\cot k_0 l_c \\ Z_{cc} = -j\dfrac{c}{S_c}\dfrac{1}{\tan k_0 l_u + \tan k_0 l_d} & (\text{m} \cdot \text{s})^{-1} \\ z_{gv} = -j\dfrac{c}{k_0 V_c} \end{cases} \tag{9.22}$$

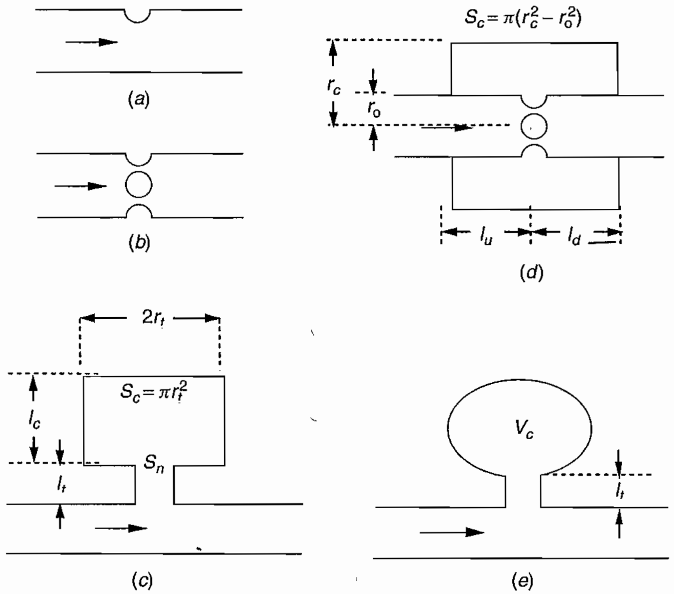

FIGURE 9.6 Resonator components and configurations.

where the subscripts tt, cc, and gv refer to the transverse-tube (quarter-wave resonator), concentric-cylinder, and general-volume cavities. These quantities and the lengths l_u, l_d, and l_c, the cross section S_c, and the volume V_c are illustrated in Fig. 9.6. It should be noted that at low frequencies ($k_0 l_c \ll 1$ and $k_0 l_u$, $k_0 l_d \ll 1$) both Z_{tt} and Z_{cc} are reduced to the expression of Z_{gv}.

The impedance Z_t of the throat connecting the duct to the cavity changes dramatically with grazing flow; therefore, it is characterized by two sets of values. For $M = 0$, this quantity is given by

$$Z_t^{[M=0]} = \frac{1}{n_h}\left(\frac{ck_0^2}{\pi} + j\frac{ck_0(l_t + 1.7r_0)}{S_0}\right) \quad (\mathrm{m \cdot s})^{-1}, \qquad (9.23)$$

where l_t is the length of the connecting throat, r_o the orifice radius, S_o the area of a single orifice, and n_h the total number of perforated holes. In the absence of mean flow, this expression has yielded good agreement between predicted and measured results for single-hole and well-localized multihole resonators.

The presence of grazing flow ($M \neq 0$ in the duct) has a strong effect on the impedance Z_t of the resonator throat. Measurements conducted using single- and multihole throats[15,57] have led to the empirical expression

$$Z_t^{[M\neq 0]} = \frac{c}{\sigma S_0}[7.3 \times 10^{-3}(1 + 72M) + j2.2$$
$$\times 10^{-5}(1 + 51l_t)(1 + 408r_0)f] \quad (\mathrm{m \cdot s})^{-1} \qquad (9.24)$$

where the parameters l_t and r_o in Eq. (9.23) are in meters and σ is the porosity. The expression of Eq. (9.24) is more appropriate for predictions in the presence of grazing flow.

Transmission Matrices for Other Elements. The mass and momentum conservation laws used to derive the transmission matrices for a pipe segment, area discontinuities, and resonators can be similarly deployed to obtain similar expressions for other elements. The reader may find additional information on transmission matrices in references 8, 9, and 53–69.

9.4 PERFORMANCE PREDICTION AND DESIGN EXAMPLES FOR EXPANSION CHAMBER MUFFLERS

Simple Expansion Chamber Muffler (SECM)

This silencer consists of an exhaust pipe, an expansion chamber, and a tail pipe of different transverse dimensions as shown in Fig. 9.7. The TL for this simple configuration may be obtained by substituting into Eq. (9.11) the transmission matrices for these elements obtained from Eqs. (9.15) and (9.18).

In a simplified case, where the flow is or is assumed to be insignificant, the product of the three matrices is reduced to the expression

$$\mathrm{TL} = 10 \log \left[1 + 0.25\left(N - \frac{1}{N}\right)^2 \sin^2 kL\right] \quad \mathrm{dB} \qquad (9.25)$$

where k is the wavenumber, L is the chamber length, and N is the area ratio given by $N = S_2/S_1$, where S_2 is the area of cross section of the chamber and S_1 that of the tail pipe or exhaust pipe (assumed to be equal).

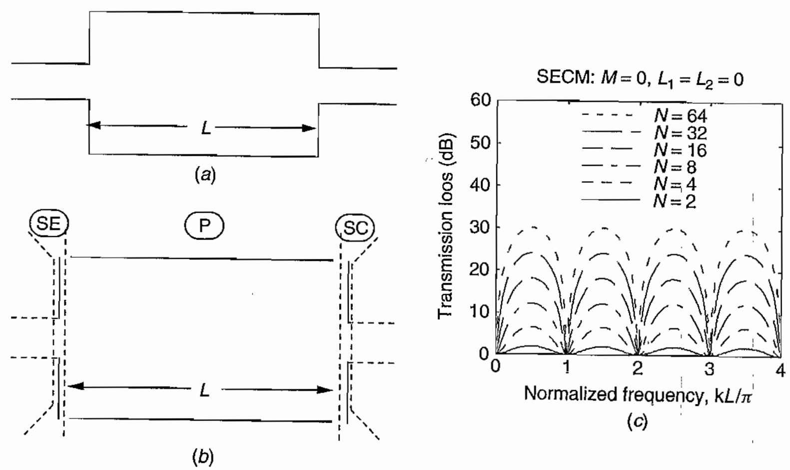

FIGURE 9.7 Simple expansion chamber muffler: (*a*) typical cross section; (*b*) muffler elements; (*c*) predicted transmission loss for different area ratios.

The predicted TL is presented in Fig. 9.7*c* for a few values of the area ratio N and displayed versus the dimensionless quantity $q = kL/\pi$. The troughs of the TL curve occur at $kL/\pi = n$, while the peaks occur at $kL/\pi = (2n-1)/2$, where $k = \omega/c$ is the wave number and n is an integer.

Example 9.1. The predicted curves of Fig. 9.7*c* can be used to develop a starting design of a SECM with a given performance goal. For example, assume that we need a 10-dB reduction for a 180-Hz tone generated by the exhaust of a small engine venting through a pipe with a diameter $d = 2$ in. (5.1 cm) at a temperature of 50°C and at a negligible flow speed.

The typical design process aligns the 180-Hz tone with one of the predicted acoustical performance peaks. Generally, alignment with a peak on a low-area-ratio (S_2/S_1) curve will minimize the muffler diameter and alignment with a peak at a low value of kL/π will minimize the length of the resulting muffler. In the present example, the design may proceed along the following steps:

- Step 1: The 180-Hz tone is aligned with the predicted 12-dB peak of the $S_2/S_1 = 8$ curve at $kL/\pi = 0.5$ (Fig. 9.7*c*).
- Step 2: At 50°C (323 K), the sound speed $c = 331$ radical $\sqrt{323/273} =$ 360 m/s.
- Step 3: The corresponding wavenumber $k = 2\pi f/c = 2\pi \times 180/360 =$ 3.14 rad/m.
- Step 4: The required muffler length L (given by $kL/\pi = 0.5) = 0.5\pi/k =$ $0.5\pi/3.14 = 0.5$.
- Step 5: The required muffler diameter $D = d\sqrt{S_2/S_1} = 5.1\sqrt{8} = 14.4$ cm.

One important implication of antilog addition and subtraction is that raising the trough levels of the IL (or, for that matter, the TL) by an amount DL has a more favorable impact than raising the peaks by the same amount DL. Therefore, it is desirable to try to raise the troughs (particularly, the first few at the lower end frequency range) through design adjustments, even at the expense of some reduction in the peaks of the revised muffler configuration.

A major disadvantage of the simple expansion chamber silencer is that in certain applications time-varying tones and their harmonics may align simultaneously with the periodic troughs and cause a severe deterioration in acoustical performance. This problem may be resolved to varying degrees by using extended-tube (inlet and/or outlet) elements.

Extended-Outlet Mufflers

An extended-outlet muffler (Fig. 9.8*a*) represents the first incremental step toward improving the performance of a single-chamber muffler. This configuration is decomposed into the three basic elements illustrated in Fig. 9.8*b*:

- a sudden expansion element (SE) at the inlet, flush with the left wall of the chamber;

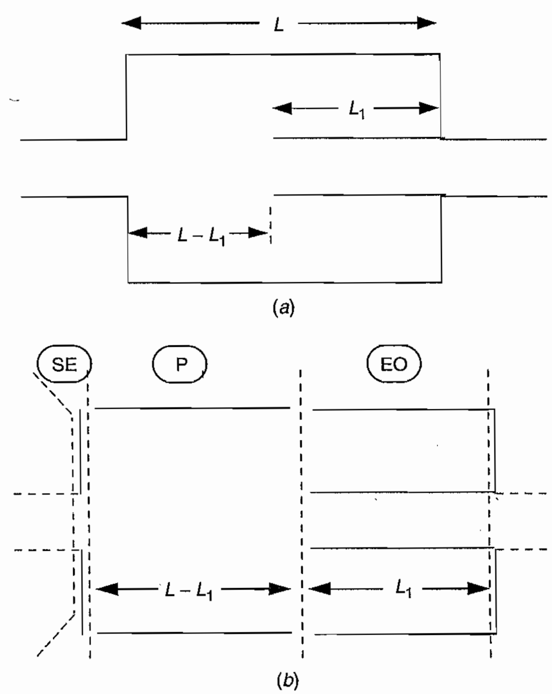

FIGURE 9.8 Extended-outlet expansion chamber: (*a*) typical configuration; (*b*) constituent muffler elements.

- a pipe element (P); and
- an extended-outlet element (EO) at the right end of the chamber.

The extended-outlet muffler design introduces a new length, L_1, which increases by 1 the number of dimensionless parameters (L/d, S_2/S_1, and L_1/L) that can be used to optimize the muffler's TL.

Transmission matrices for the silencer elements shown in Fig. 9.8*b* are obtained from Eq. (9.15) (for the pipe element P), Eq. (9.18) (extended-outlet element EO), and Eq. (9.20) (sudden expansion element SE).

It should be noted that at certain frequencies the impedance Z_2, introduced by the transmission matrix of Eq. (9.19) for the extended-outlet element, would approach zero, and the branch element would generate a pressure release condition. Under these conditions, the incident wave would appear to interact with a closed-end cavity, and no acoustical power would be transmitted downstream. For rigid end plates, this condition would occur when $\cot(kL_1) = 0$, corresponding to $kL_1/\pi = (2n-1)/2$. Accordingly, a dominant peak in the source spectrum can be reduced significantly by proper selection of the tube length extended into the chamber.

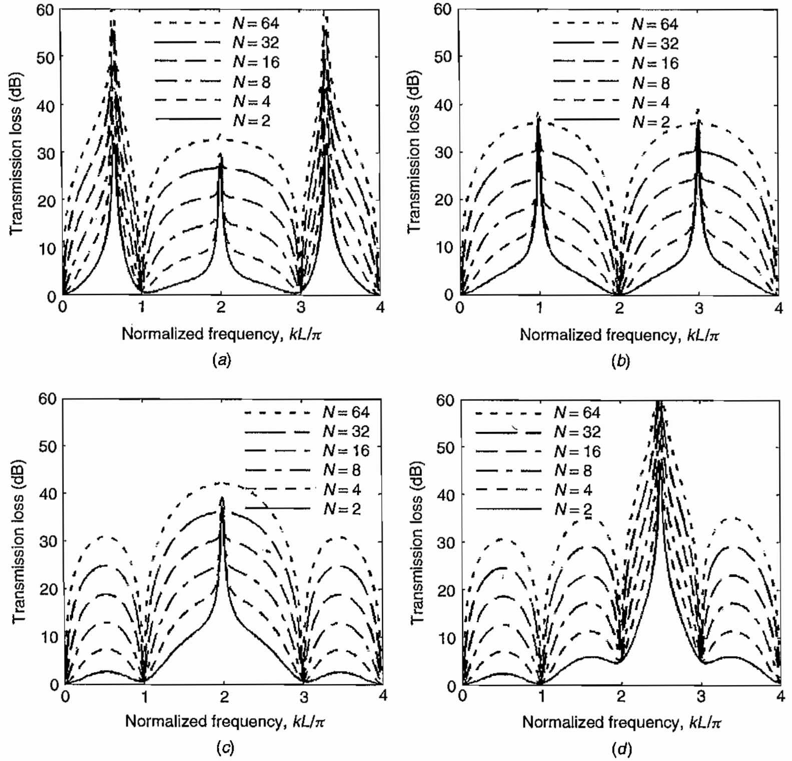

FIGURE 9.9 Transmission loss of extended-outlet muffler for different outlet pipe lengths: $M = 0$; L_1/L equals (*a*) 0.75, (*b*) 0.5, (*c*) 0.25, and (*d*) 0.2.

Figures 9.9*a*–9.9*d* illustrate the variation of the TL for an extended-outlet expansion chamber for four values of the dimensionless parameter L_1/L. As expected, the maximum peak of TL shifts toward higher frequencies as L_1/L decreases. Furthermore, a suitable choice of L_1/L, resulting in $kL_1/\pi = (2n-1)/2$, n being an integer, relocates some performance peaks so as to eliminate some of the troughs that would otherwise occur at $kL = n\pi$ (Fig. 9.7*c*) for the simple expansion chamber muffler. This behavior is exploited in the following two design examples.

Example 9.2. Consider the application requiring a 15-dB reduction of a steady 120-Hz tone generated by the exhaust of a small engine venting through a pipe with a diameter $d = 1.5$ in. (3.8 cm) at a temperature of 100°C and at a negligible flow speed.

Since the tone is steady, that is, its does not vary appreciably versus time, we can consider aligning it with one of the sharp peaks in the predicted TL. This

suggests selection of the Fig. 9.9*a* configuration, characterized by $L_1/L = 0.75$, which has a family of relatively sharp peaks at $kL/\pi = 0.75$.

In the present example, the design may proceed along the following steps:

- Step 1: The 120-Hz tone is aligned with the predicted >12-dB peak of the $S_2/S_1 = 8$ curve at $kL/\pi = 0.75$ (Fig. 9.9*a*).
- Step 2: At 100°C (373 K), the sound speed $c = 331\sqrt{373/273} = 387$ m/s.
- Step 3: The corresponding wavenumber $k = 2\pi f/c = 2\pi \times 120/387 = 1.95$ rad/m.
- Step 4: The required muffler length (given by $kL/\pi = 0.75$) $L = 0.75\pi/1.95 = 1.2$ m.
- Step 5: The required muffler diameter $D = d\sqrt{S_2/S_1} = 3.8\sqrt{8} = 10.8$ cm.

Example 9.3. Consider the application requiring a 10-dB reduction of a time-varying 150-Hz tone generated by the exhaust of a small engine venting through a pipe with diameter $d = 2.5$ in. (6.3 cm) at a temperature of 80°C and at a negligible flow speed. Furthermore, assume that the a variable load in the engine causes its frequency to vary ±15%, that is, operating anywhere in the $127 < f < 172$-Hz range.

Since the frequency of the tone is unsteady, we can consider aligning it with one of the "broad" peaks in the predicted TL. This suggests selection of the Fig. 9.9*b* configuration, characterized by $L_1/L = 0.5$, which has a family of relatively "broad hill peaks" around the spikes occurring at $kL/\pi = 1$.

All curves with $S_2/S_1 \geq 4$ appear to have TL > 10 dB within 15% of $kL/\pi = 1$. For a conservative result, we select the curve with $S_2/S_1 = 8$ and complete the muffler design using the following steps:

- Step 1: The 150-Hz tone is aligned with the predicted >10-dB peak of the $S_2/S_1 = 8$ curve at $kL/\pi = 1$ (Fig. 9.9b).
- Step 2: At 80°C (353 K), the sound speed $c = 331\sqrt{353/273} = 376$ m/s.
- Step 3: The corresponding wavenumber $k = 2\pi f/c = 2\pi \times 150/376 = 2.5$ rad/m.
- Step 4: The required muffler length (given by $kL/\pi = 1$) $L = 1.0\pi/2.5 = 1.25$ m.
- Step 5: The required muffler diameter $D = d\sqrt{S_2/S_1} = 6.3\sqrt{8} = 18$ cm.

The TL for extended-inlet silencers can be derived in a similar manner. For negligible values of flow, their acoustical performance is similar to that of the extended-outlet silencers; in other words, for negligible inflow, either side of the muffler can be used as the inlet with no appreciable change in the TL.

Double-Tuned Expansion Chamber (DTEC)

The "filling up" of the troughs achieved through the extended-outlet muffler can be further enhanced through the simultaneous deployment of an extended-inlet pipe of length L_2 (double tuning). An extended inlet introduces an additional parameter, L_2/L, which used in conjunction with the extended-outlet parameter L_1/L can fill up additional troughs and further improve the achievable TL over a broader frequency range. For optimum results, L_1 and L_2 are selected so as to neutralize different sets of troughs to the extent possible.

The new double-tuned expansion chamber (DTEC) silencer design (Fig. 9.10*a*) is decomposed into three basic elements (Fig. 9.10*b*):

- an extended-inlet element (EI) at the left end of the chamber,
- a pipe element (P), and
- an extended-outlet element (EO) at the right end of the chamber

Thus, the introduction of the new length, L_2, for the extended inlet enhances the optimization of the DTEC's transmission loss through an increased number of dimensionless parameters, which now include d/L, S_2/S_1, L_1/L, and L_2/L.

Transmission matrices for the Fig. 9.10*b* silencer elements are obtained from Eq. (9.15) (for the pipe element P) and from Eq. (9.18) (extended-inlet and extended-outlet elements EI and EO).

Of the infinite number of $(L_2/L,\ L_1/L)$ combinations, a selection of $L_1 = L/2$ and $L_2 = L/4$ leads to a particularly favorable TL. Specifically, since the extended-inlet element includes a term proportional to $\cot(kL_2)$ [see Eqs. 9.18 and 9.19], it produces stop bands at $kL_2 = (2n-1)\pi/2$ or, equivalently, at $kL = 2(2n-1)\pi$, filling up the troughs at $kL/\pi = 2, 6, 10, \ldots$. Similarly, since the EO element includes a term proportional to $\cot(kL_1)$, it produces stop bands at

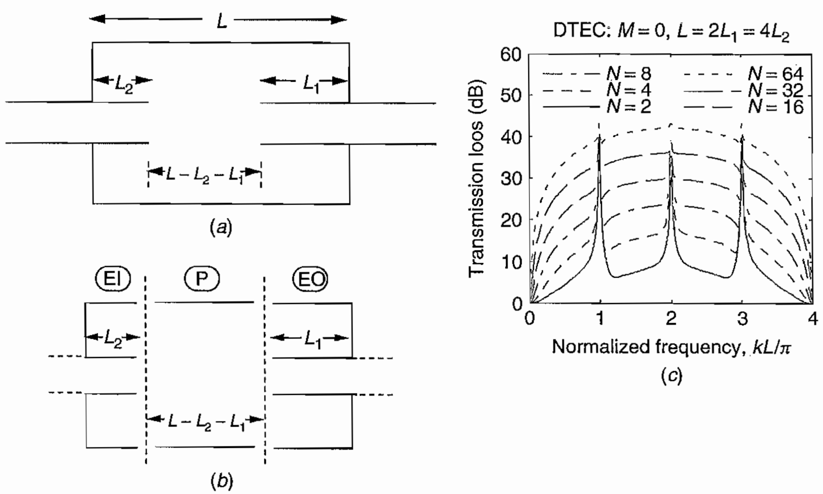

FIGURE 9.10 Double-tuned expansion chamber: (*a*) typical configuration; (*b*) constituent elements; (*c*) predicted TL for $L_2 = L/4$, $L_1 = L/2$.

$kL_1 = (2n-1)\pi/2$ or, equivalently, at $kL = (2n-1)\pi$, filling up the troughs at $kL/\pi = 1, 3, 5, \ldots$. In other words, this design features troughs only at $kL/\pi = 0, 4, 8, 12, \ldots$.

The corresponding predicted TL for a few area ratio values is shown in Fig. 9.10*c*. Its most prominent feature is the lack of troughs at locations other than at $kL/\pi = 4n$, n being an integer. Accordingly, this design offers a better solution for broadband performance than any of the previous configurations. High reduction limited to a narrow band (like Fig. 9.9*a*) can be achieved by adjusting the inlet/outlet lengths away from their $(L_1/L, L_2/L) = (\frac{1}{2}, \frac{1}{4})$ values.

Example 9.4. Consider the application requiring a 10-dB reduction of 200–600-Hz broadband noise generated by a noise source venting through a pipe with diameter $d = 2$ in. (5.1 cm) at a temperature of 120°C and at a negligible flow speed. Because of the broadband requirements, a DTEC muffler design is selected through the following steps:

- Step 1: The 400-Hz center of the subject frequency band is aligned with the center, $kL/\pi = 2$ of the broad TL peaks of Fig. 9.10*c*; this places the upper and lower frequency bounds (200 and 600 Hz) at kL/π values of 1 and 3, respectively.
- Step 2: The $S_2/S_1 = 4$ curve (Fig. 9.10*c*) is selected because it provides > 10 dB TL in the $1 < kL/\pi < 3$ range.
- Step 3: The required muffler diameter $D = d\sqrt{S_2/S_1} = 5.1\sqrt{4} = 10.1$ cm.
- Step 4: At 120°C (393 K), the sound speed $c = 331\sqrt{393/273} = 397$ m/s.
- Step 5: Given that $kL/\pi = 1$ corresponds to 200 Hz, the required muffler length $L = k = \pi c/(2\pi f) = 397/(2 \times 200) = 0.99$ m, $L_1 = L/2 = 0.495$ m and $L_2 = L/4 = 0.247$ m.

General Design Guidelines for Expansion Chamber Mufflers

Transmission loss curves with higher levels and fewer or less pronounced troughs can be obtained with more complex muffler configurations. Specifically, one can cascade two or more DTECs to further optimize performance through an increased number of system parameters. However, an increasing system complexity is not without limits, since muffler size and weight are important design parameters in practical applications. For example, increasing the number of elements reduces the average length/diameter of individual elements, which reduces low-frequency performance, and increases the number of partitions, which increases weight. These competing factors improve certain features while degrading others and lead to design trade-offs that are specific to each application.

A close examination of a number of designs (not detailed here) featuring one to three DTECs leads to the following observations or design considerations:

- The TL of a SECM features nulls (troughs) at $kL/\pi = 1, 2, 3, 4, 5$.

- If an SECM is augmented with an extended-inlet (or outlet, for that matter) pipe equal in length to half the chamber length, then the troughs corresponding to $kL/\pi = 1, 3, 5, 7, 9, \ldots$ are eliminated.
- If an SECM is augmented with an extended-inlet (or outlet, for that matter) pipe equal in length to quarter the chamber length, then the troughs corresponding to $kL/\pi = 2, 6, 10, 14, \ldots$ are eliminated.
- If an SECM is augmented with extended-inlet and extended-outlet pipes equal in length to half and quarter the chamber length, respectively (DTEC), then the TL retains troughs only at $kL/\pi = 4, 8, 12, 16, \ldots$.
- The TL of two identical cascaded DTECs occupying the same envelope as a single DTEC features less pronounced troughs and generally higher levels, except at low frequencies ($kL/\pi < 0.5$), where some degradation is observed.
- The TL of two unequal cascaded DTECs can be further improved over the TL of two identical cascaded DTECs occupying the same envelope.

Additional TL improvements can be achieved through the use of three or more cascaded DTECs occupying the same total envelope as one DTEC. However, such improvements lead to further degradation of low-frequency performance; therefore, commercial application mufflers generally include no more than two or three cascaded DTEC chambers. Nevertheless, a designer who is forced to use a larger number of chambers by the needs of a specific application may recover low-frequency performance through the use of other types of elements, as discussed in the next section.

9.5 REVIEW OF PERFORATED-ELEMENT MUFFLERS

Perforated-element silencers have long been known to be acoustically more efficient than the corresponding simple tubular-element silencers. However, a systematic aeroacoustical analysis of perforated elements began only in late 1970s, when Sullivan introduced his segmentation model.[18–20] This was followed by the distributed-parameter model of Munjal et al., which produced experimentally verified four-pole parameters for perforated elements, namely, concentric-tube resonators (Fig. 9.11*a*), plug chambers (Fig. 9.11*b*), and three-duct cross-flow (Fig. 9.11*c*) and reverse-flow chambers.[8,9,21–23].

This section conducts a parametric study on some perforated-element mufflers to identify representative trends and to develop basic design guidelines.[25] Again, TL has been selected as an appropriate performance index. Explicit expressions for the impedance and the transfer matrix parameters of perforated muffler elements in terms of the geometric and operating variables and formulas for TL and IL are given in Chapter 3 of reference 8.

Range of Variables

Perforated-tube mufflers share several parameters with the expansion chamber mufflers discussed earlier, but they also include additional parameters accounting

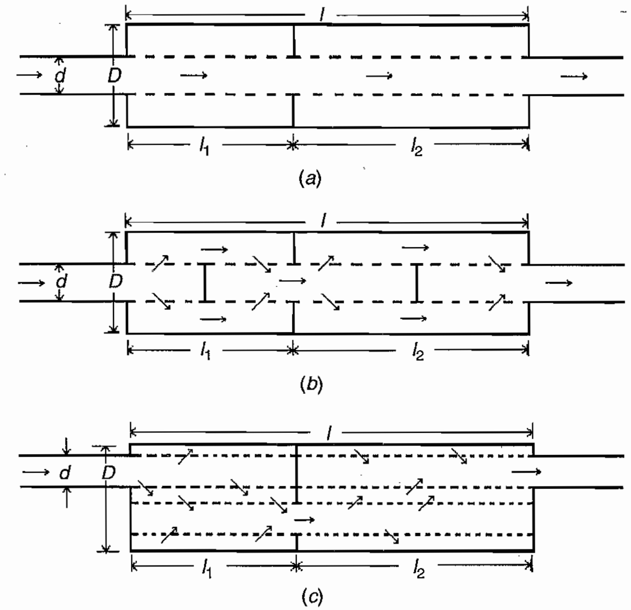

FIGURE 9.11 Schematic of the two-chamber configurations of three types of perforated-tube mufflers: (*a*) Concentric-tube resonator; (*b*) plug muffler; (*c*) three-duct cross-flow muffler.

for the additional features of the perforated tubes. Thus, the physical parameters influencing the performance of the Fig. 9.11 perforated mufflers include the following:

M = mean-flow Mach number in exhaust pipe
l = total length of muffler shell
D = internal diameter of muffler shell
d = internal diameter of exhaust pipe and tail pipe
d_h = diameter of perforated holes (Fig. 9.12)
C = center-to-center distance between consecutive holes (Fig. 9.12)
N_c = number of chambers within fixed-length muffler shell
t_w = wall thickness of perforated tube

Another parameter, often used instead of explicit values of d_h or C, is the porosity (or open-area ratio) of the perforated-tube wall, which is defined by

$$\sigma = \frac{\pi d_h^2}{4C^2} \tag{9.26}$$

Extensive simulations conducted for representative configurations encountered in most practical applications showed that the performance of perforated-tube

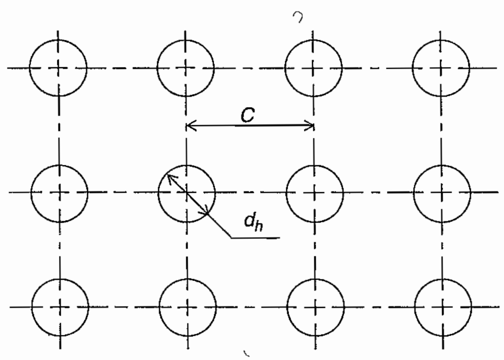

FIGURE 9.12 Parameters d_h and C of perforated-tube walls.

mufflers is relatively insensitive (within ±1 dB) to the hole diameter d_h and wall thickness t_w. For this reason, all of the following predictions have been conducted at the typically encountered values of $d_h = 4$ mm and $t_w = 1$ mm.

Furthermore, to reduce the simulations to a manageable number, the pipe diameter was fixed to a commonly encountered value of $d = 30$ mm for all cases considered in this section. This constraint does not influence the corresponding predicted TL curves, because they are invariant with respect to the specific value of d when plotted against the nondimensional frequency parameter kR ($R = D/2$ is the shell radius and $k = \omega/c$).

Despite the simplification resulting from the fixed values of d, d_h, and t_w, the number of perforated-tube muffler configurations is still too large for a comprehensive study. Under the circumstances, the influence of each parameter on muffler performance is demonstrated by selecting a reference (default) configuration and then by changing individual parameters (one at a time) about the default values. Table 9.2 shows the range of parameter values investigated including the default values (last column).

The TL was calculated as a function of the dimensionless frequency kR to extend the validity of the predictions over all geometrically similar hardware, that is, mufflers differing only by a length scale. The nondimensional frequency parameter kR was varied in steps of 0.025 from 0.025 to 3, which is well

TABLE 9.2 Parameter Values Used in Perforated Tube Muffler Performance Predictions

Parameter Name	Description	Range	Default
M	Mach number	0.05, 0.1, 0.15, 0.2	0.15
D/d	Expansion ratio	2, 3, 4	3
C/d_h	Center-to-center distance	3, 4, 5, 6	4
N_c	Number of chambers	1, 2, 3	2
L_2/L	Chamber size	$1, \frac{1}{2}, \frac{1}{3}$	$\frac{1}{2}$
L/d	Muffler length–pipe diameter	15, 20, 25	20

within the plane-wave cutoff limit of 3.83 for the axisymmetric mufflers of Figs. 9.11*a*,*b*. By comparison, the cutoff limit of kR for the asymmetric configuration of Fig. 9.11*c* is 1.84.

Acoustical Performance

Figures 9.13–9.17 show the computed TL for the Fig. 9.11 mufflers as a function of the normalized frequency kR. The three plots (a, b, and c) in each figure display the TL of a concentric-tube resonator muffler, plug muffler, and three-duct cross-flow muffler, respectively, and the different traces within each plot correspond to different combinations of muffler parameter values listed in Table 9.2.

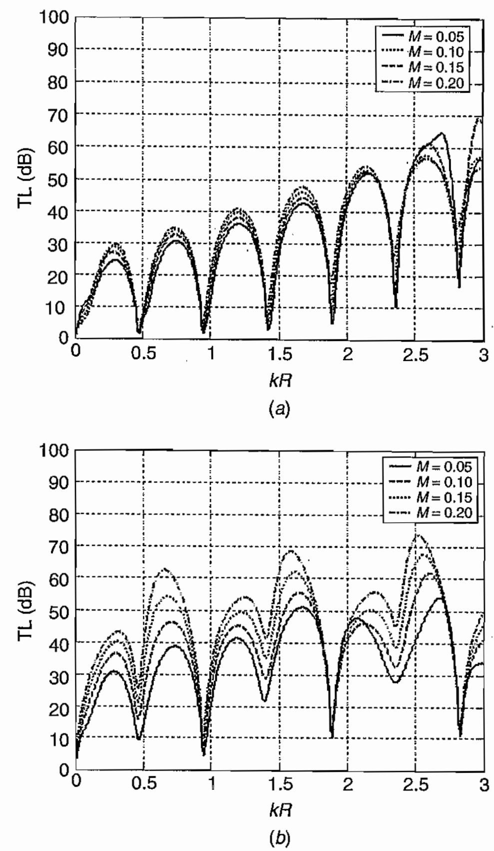

FIGURE 9.13 Effect three of mean flow Mach number on TL of (a) CTR, (b) plug muffler, and (c) duct muffler: (—) $M = 0.05$; (- - -) $M = 0.1$; (. . .) $M = 0.15$; (-·-·-) $M = 0.2$.

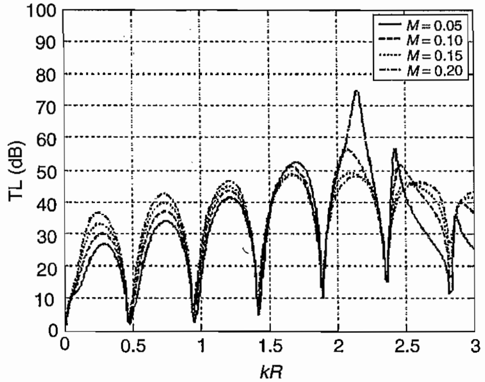

(c)

FIGURE 9.13 *(continued)*

Figure 9.13 shows the effect of the mean-flow Mach number on the acoustical performance of three perforated-element muffler designs. These predictions show a general increase in TL when the mean-flow Mach number increases. The effect is minimum for the concentric-tube resonator (CTR) and maximum for the plug muffler; this is not surprising given that (because of their intrinsic geometric features) the former and latter configurations present the minimum and maximum "blockages," respectively, to the mean flow through the muffler.

Clearly, the choice of the Mach number is not in the designer's control, as it is determined by the engine displacement, speed, and exhaust pipe diameter. Nevertheless, the designer may combine the information in Fig. 9.13 with back-pressure information (discussed in the next section) in the selection of a muffler design appropriate for the specific application.

The effect of the expansion ratio, or the diameter ratio D/d, is illustrated in Fig. 9.14. The TL of all three perforated-element mufflers improves considerably with higher diameter ratio.

In most practical applications, the shell diameter D is directly related to muffler volume, weight, and cost and influences the choice of the expansion ratio D/d and the type of muffler. The alternate troughs in the TL curves are higher for a plug muffler (Fig. 9.14*b*) than for the other two designs; therefore, when space is constrained, the plug muffler typically offers a higher acoustical performance. Unfortunately, it also leads to a typically higher back pressure, as discussed later. As a result, the final choice is usually based on a trade-off between acoustical and mechanical performance.

The effect of the center-to-center spacing between consecutive holes (which determines the porosity) on the TL of the mufflers is illustrated in Fig. 9.15. As can be seen, the performance of all perforated mufflers tends to that of the simple expansion chamber muffler for sufficiently high values of porosity ($\sigma > 0.1$) but is considerably better for lower values of porosity, particularly for the plug

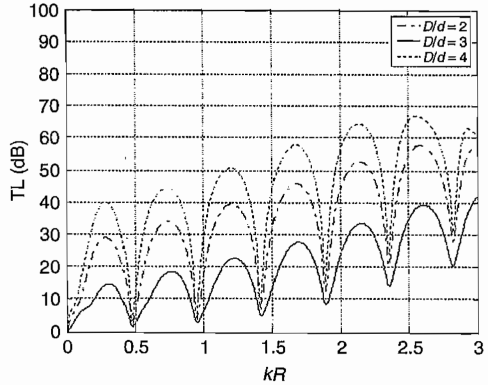

(a)

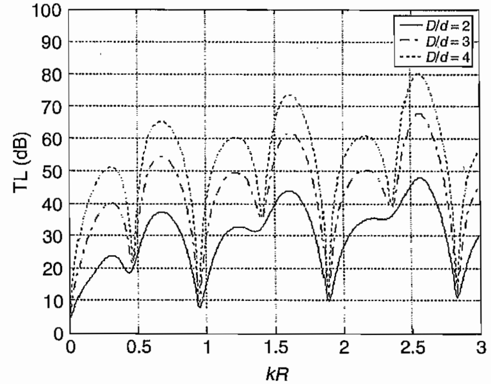

(b)

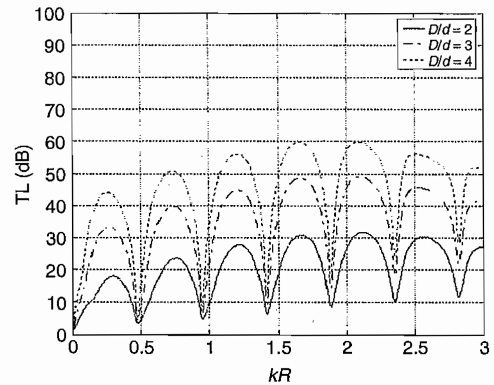

(c)

FIGURE 9.14 Effect of expansion ratio on TL of (*a*) CTR, (*b*) plug muffler, and (*c*) three-duct muffler: (—) $D/d = 2$; (- - -) $D/d = 3$; (. . .) $D/d = 4$.

muffler and the three duct muffler configurations. On the other hand, a reduced porosity raises back pressure, except for the CTR, where the back pressure is nearly independent of porosity, as demonstrated later in this section. Consequently, the porosity provides another parameter that can be used to trade off between acoustical and mechanical performance.

Another, and perhaps more meaningful, parameter often used instead of the porosity is the open area ratio x, defined as

$$x = \frac{\text{total area of perforations}}{\text{cross-sectional area of pipe}} \tag{9.27}$$

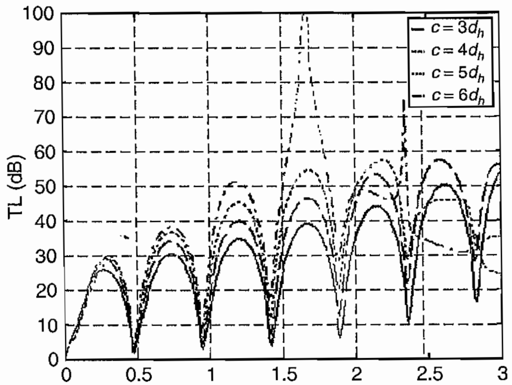

(a)

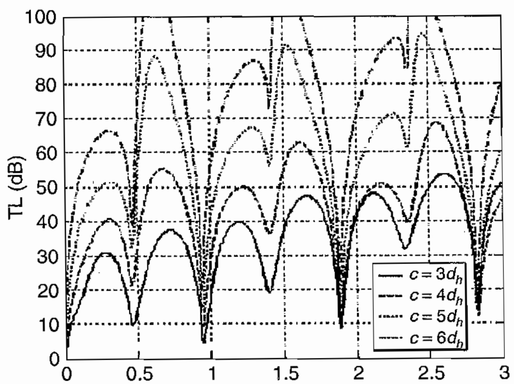

(b)

FIGURE 9.15 Effect of center-to-center distance between consecutive holes on TL of (*a*) CTR, (*b*) plug muffler, and (*c*) three-duct muffler: (—) $C = 3d_h$; (- - -) $C = 4d_h$; (. . .) $C = 5d_h$; (-·-·-) $C = 6d_h$.

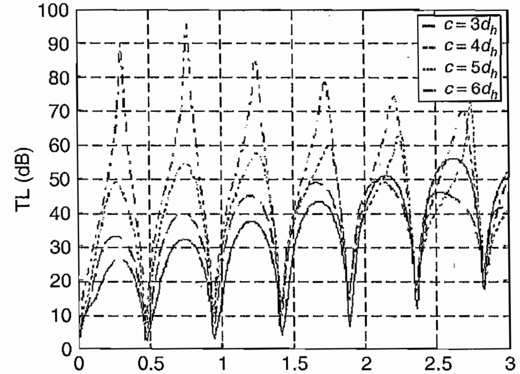

(c)

FIGURE 9.15 (*continued*)

The denominator refers to the inlet/outlet pipe cross section that accommodates the entire mean flow. For example, the CTR (Fig. 9.15*a*) and three-duct muffler (Fig. 9.15*c*), may be described in terms of either the porosity associated with the indicated $C = 3d_h, 4d_h, 5d_h, 6d_h$ or in terms of the corresponding open-area ratio values of 3.49, 1.78, 1.25, and 0.87, respectively. The corresponding values of x for the plug muffler (Fig 9.15*b*) are half as much.

The plot in Fig. 9.16 shows the effect of multiple equal partitioning of a muffler of overall length l on the TL. The normalized frequency spacing between the consecutive troughs is proportional to the number of partitions and, as in the case of the simple expansion chamber mufflers, the troughs occur at frequencies given by

$$\sin kl_{1,2} = 0 \qquad kl_{1,2} = n\pi \qquad n = 1, 2, 3 \ldots \tag{9.28}$$

In general, the partitioning improves the TL of all three mufflers, except at the low-frequency end of the CTR curves, where the TL decreases. An increased number of partitions N_c would be particularly desirable for a CTR, where an increase in partitions would not increase the back pressure. However, the back pressure will be proportional to the cube of the number of chambers for the other two types of mufflers. Therefore, increased partitioning must be closely considered with an increased porosity to optimize acoustical performance while maintaining the back pressure within acceptable levels.

Figure 9.17 illustrates the effect of unequal partitioning of a muffler of overall length l on the TL by comparing the results of an equally and an unequally partitioned muffler for each of the three designs. One can observe that unequal partitioning (a) has no significant impact on the envelope of the TL peaks, (b) influences significantly the location of individual peaks and troughs, and (c) raises noticeably the level of each alternate trough. On average, the additional

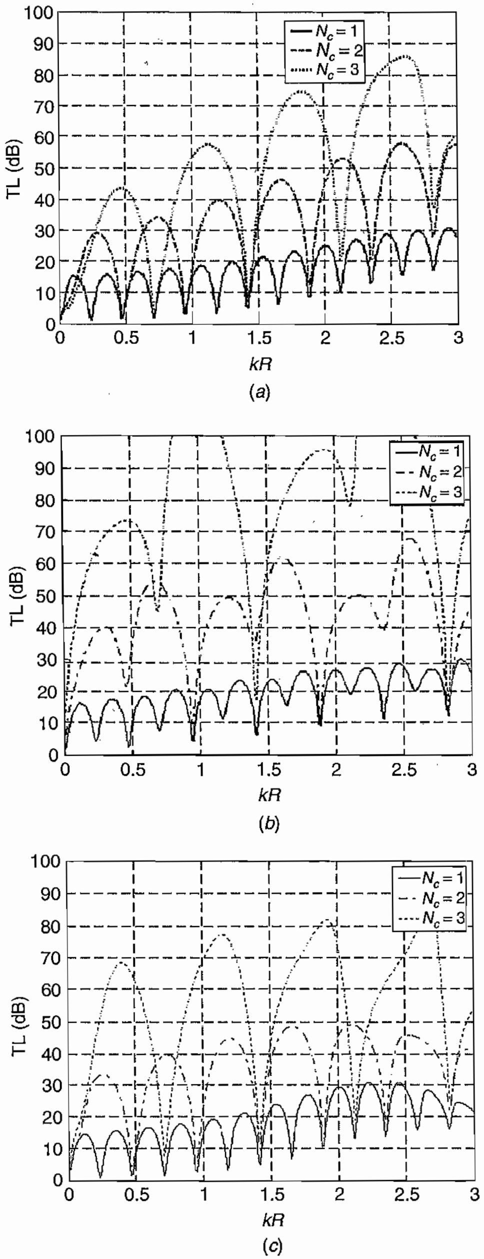

FIGURE 9.16 Effect of number of chambers within the same overall length on TL of (*a*) CTR, (*b*) plug muffler, and (*c*) three-duct muffler: (—) $N_c = 1$; (- - -) $N_c = 2$; (. . .) $N_c = 3$.

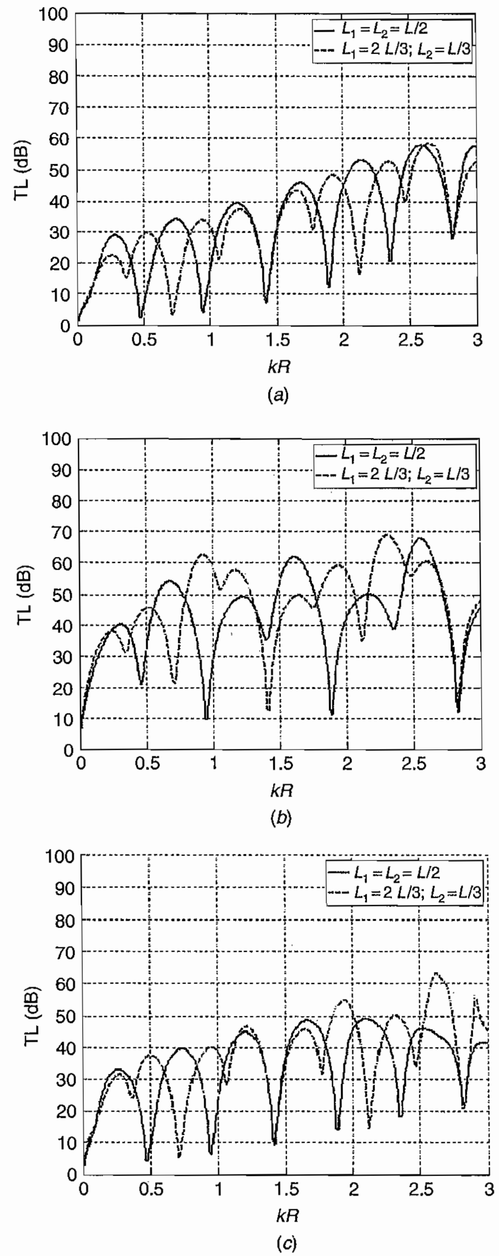

FIGURE 9.17 Effect of unequal partitioning of (*a*) CTR, (*b*) plug muffler, and (*c*) three-duct muffler: (—) $l_1 = l_2 = \frac{1}{2}$; (- - -) $l_1 = 2l/3$; $l_2 = l_3$.

tuning enabled by the unequal partitioning will enhance the overall acoustical performance of mufflers.

Back Pressure

The static pressure drop resulting from energy dissipation in sheared flow regions of the muffler elements results in a substantial back pressure on the piston of a reciprocating engine. This generally has an adverse effect on the volumetric efficiency, power, and specific fuel consumption of a multicylinder engine.

A systematic experimental study was undertaken[25] to derive empirical expressions for pressure drop or head loss across all the three types of perforated-element chambers of Fig. 9.11. The results were expressed as a coefficient that normalized the pressure drop with respect to the incoming dynamic head in the pipe, namely,

$$y \equiv \frac{\Delta p}{H} \qquad H = \tfrac{1}{2}\rho U^2 \tag{9.29}$$

The parameter y was dependent on the open-area ratio x of the perforate defined by Eq. (9.27), and its value was determined to vary as follows:

Concentric-tube resonator:

$$y_{\text{ctr}} = 0.06x \qquad 0.6 < x \tag{9.30}$$

Plug muffler:

$$y_{\text{pm}} = 5.6e^{-0.23x} + 67.3e^{-3.05x} \qquad 0.25 < x < 1.4 \tag{9.31}$$

Three-duct cross-flow chamber:

$$y_{\text{cfc}} = 4.2e^{-0.06x} + 16.7e^{-2.03x} \qquad 0.4 < x < 5.8 \tag{9.32}$$

During the measurements of the parameter y,[25] the desired variation in the open-area ratio x was achieved by varying the length l_2 (see Fig. 9.11). The measured y [Eqs. (9.30)–(9.32)] was found to be independent of the mean-flow velocity U (for Mach number $M \leq 0.2$) and very weakly dependent on the expansion ratio D/d and lengths l_1 and l_3 for values of x in the range indicated by Eqs. (9.30)–(9.32). However, the expressions for y in these equations are least-squares fits and therefore are not limited to the indicated range; they cover the entire practical range ($0.2 < x < 6.0$).

The back-pressure coefficient y_{ec} for the expansion chamber mufflers of Section 9.3 is analogously given by[8]

$$y_{\text{ec}} = (1-n)^2 + \tfrac{1}{2}(1-n) \qquad n = \left(\frac{d}{D}\right)^2 \tag{9.33}$$

Equations (9.30)–(9.32) show that the static pressure drop across a CTR, which involves no net flow through the perforated-tube walls, is much smaller than that across the corresponding plug muffler and the three-duct cross-flow chamber. Similarly, Equations (9.30) and (9.33) indicate that the pressure drop across a CTR is less than that across a simple expansion chamber of identical shell size and pipe diameter.

9.6 DISSIPATIVE SILENCERS

Dissipative silencers are the most widely used devices to attenuate the noise in ducts through which gas flows and in which the broadband sound attenuation must be achieved with a minimum of pressure drop across the silencer. They are frequently used in the intake and exhaust ducts of gas turbines, air conditioning and ventilation ducts connected to small and large industrial fans, cooling-tower installations, and the ventilation and access openings of acoustical enclosures, and they have an allowed pressure drop that typically ranges from 125 to 1500 Pa (0.5–6 in. H_2O). Unlike reactive silencers, which mostly reflect the incident sound wave toward the source, dissipative silencers attenuate sound by converting the acoustical energy propagating in the passages into heat caused by friction in the voids between the oscillating gas particles and the fibrous or porous sound-absorbing materials, as described in detail in Chapter 8.

The theories of dissipative silencers were developed long ago,[1,2,71–74] and they are highly complex. This chapter provides design information in a form that can be readily used by engineers not thoroughly trained in acoustics. Though there are a large variety of geometries used, the most common configurations include parallel-baffle silencers, round silencers, and lined ducts.

Lined Ducts

The sound attenuation of lined and unlined ducts and lined and unlined bends are treated in Chapter 16. The geometry of frequently used dissipative silencers is shown schematically in Fig. 9.18.

Figure 9.19 shows some of the baffle constructions that have been used in typical applications. Only the acoustically significant features are shown. Protective treatments such as perforated facing, fiberglass cloth, and porous screens are omitted. If the same concepts depicted in Figs. 9.19*a*–*i* are applied as a duct lining, one-half of the baffles depicted in Fig. 9.19 constitutes the lining.

Figure 9.19 illustrates the cross sections of frequently used silencer baffle configurations.

The full-depth porous baffle depicted in Fig. 9.19*a* is the most frequently used in parallel-baffle silencers. The other baffle configurations are used in special-purpose silencers custom deigned to yield high attenuation in specific

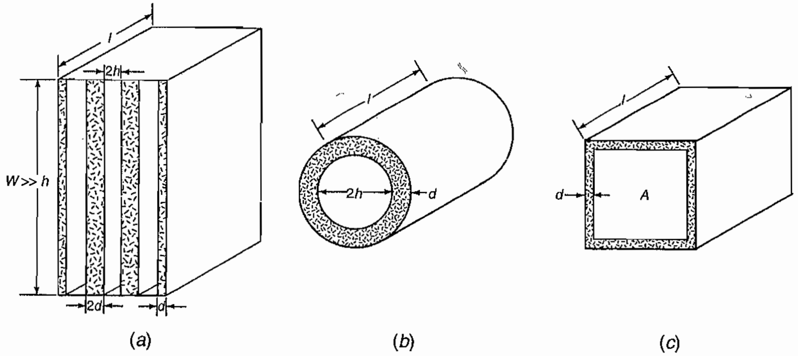

FIGURE 9.18 Geometry of frequently used silencer types: (*a*) parallel baffle; (*b*) round; (*c*) lined ducts.

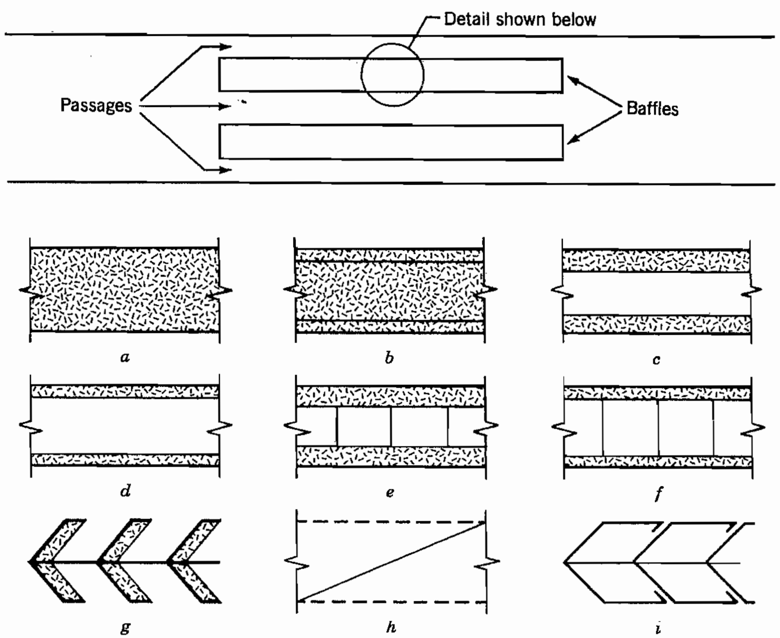

FIGURE 9.19 Cross section of frequently used silencer baffle configurations: (*a*) full-depth porous; (*b*) porous center layer with thin resistive facing on both sides; (*c*) thick porous surface layer with unpartitioned center air space; (*d*) thin porous surface layers with unpartitioned air space; (*e*) thick porous layer with partitioned center air space; (*f*) thin porous surface layers with partitioned center air space; (*g*) tuned cavity (Christmas tree), porous material in cavities protected from flow; (*h*) small percentage open-area perforated surface plates exposed to grazing flow, partitioned center air space; (*i*) Helmholtz resonators.

frequency ranges or to work in hostile environments of contaminated flow or high temperatures.

Key Performance Parameters

The key design parameters of silencers are acoustical insertion loss (IL), pressure drop (Δp), flow-generated noise, size cost, and life expectancy. The challenge of silencer design is to obtain the needed IL without exceeding the allowable pressure drop and size for a minimum of cost. These are frequently opposing requirements, and the optimal design represents a balance compromise between them.

Insertion Loss. The IL of a silencer is defined as

$$\mathrm{IL} = 10 \log \frac{W_0}{W_M} \tag{9.34}$$

where W_0 and W_M represent the sound power in the duct without and with the silencer, respectively. Provided that structure-borne flanking along the muffler casing and sound radiation from the casing is kept low, the sound power in the duct with the silencer in place is given by

$$W_M = W_0 \times 10^{-(\Delta L_l + \Delta L_{\mathrm{ENT}} + \Delta L_{\mathrm{EX}})/10} + W_{\mathrm{SG}} \tag{9.35}$$

where W is in watts (N·m/s); ΔL_l represents the attenuation of the silencer of length l; ΔL_{ENT} and ΔL_{EX} are the entrance and exit losses, respectively; and W_{SG} is the sound power generated by the flow exiting the silencer.

Combining Eqs. (9.34) and (9.35) yields

$$\mathrm{IL} = -10 \log \left(\frac{W_{\mathrm{SG}}}{W_0} + 10^{-(\Delta L_l + \Delta L_{\mathrm{ENT}} + \Delta L_{\mathrm{EX}})/10} \right) \tag{9.36}$$

In the extreme case of very high silencer attenuation, the second term on the right-hand side of Eq. (9.36) becomes comparable to the first, and the achievable IL is affected by the self-generated noise of the silencer, and in this case Eq. (9.36) is nonlinear. When the flow velocity in the silencer passages is sufficiently low, flow noise is negligible. In this case, Eq. (9.36) is linear and simplifies to

$$\mathrm{IL} \cong \Delta L_l + \Delta L_{\mathrm{ENT}} + \Delta L_{\mathrm{EX}} \quad \mathrm{dB} \tag{9.37}$$

Entrance Loss ΔL_{ENT}. In most dissipative silencers, the entrance losses ΔL_{ENT} are small if the incident sound energy is in the form of a plane wave normally incident on the silencer entrance. This is always the case for straight ducts at low frequencies. The small entrance loss should be considered as a safety factor.

However, if the cross dimensions of the duct are much larger than the wavelength, the incident sound field usually contains a very large number of higher order modes. The conversion of the semidiffuse sound field in the entrance duct into a plane-wave field in the narrow silencer passages typically results in an entrance loss of 3–6 dB. The engineer can also assign any entrance loss between 0 dB at low frequencies and up to 8 dB at high frequencies on the basis of prior experience with similar situations or on the basis of scale model measurements. If no such information is available, Fig. 9.20 can be used to estimate the entrance loss.

***Exit Loss* ΔL_{EX}.** Most exit losses ΔL_{EX} are generated when the silencer is located at the open end of a duct and the typical cross dimensions of the opening are small compared with the wavelength. In this case, the exit loss is predominantly determined by the end reflection. Exit losses for silencers inserted in ducts are usually small and can either be neglected or considered as part of the safety margin.

It should be noted that the relative importance of the entrance and exit losses diminishes as the silencer length increases because both quantities are independent of this length. Figure 9.21 shows qualitatively a typical sound pressure level versus distance recorded by a microphone traveling through the silencer and indicates the three components of IL.

***Silencer Attenuation* ΔL_l.** The silencer attenuation ΔL_l is proportional to its length (tail and nose of baffle not included) and to the lined perimeter of the passage, P, and inversely proportional to the cross-sectional area of the passage,

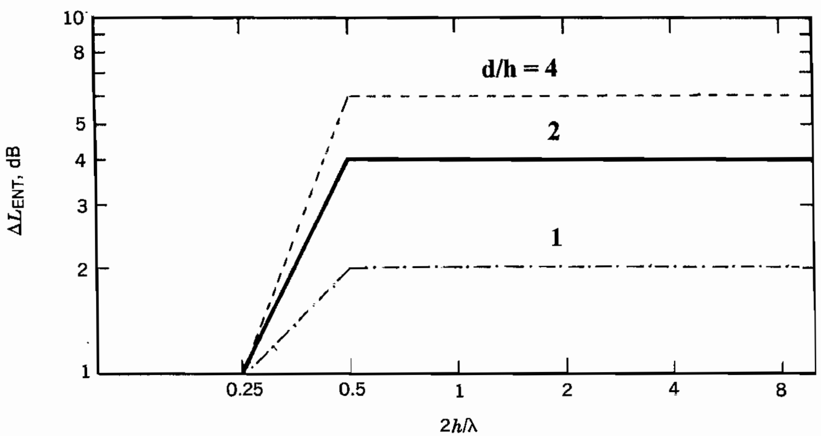

FIGURE 9.20 Acoustical entrance loss coefficient, ΔL_{ENT}, of silencers in a large duct with a semireverberant sound field in the entrance duct: $2h$ = silencer passage cross dimension.

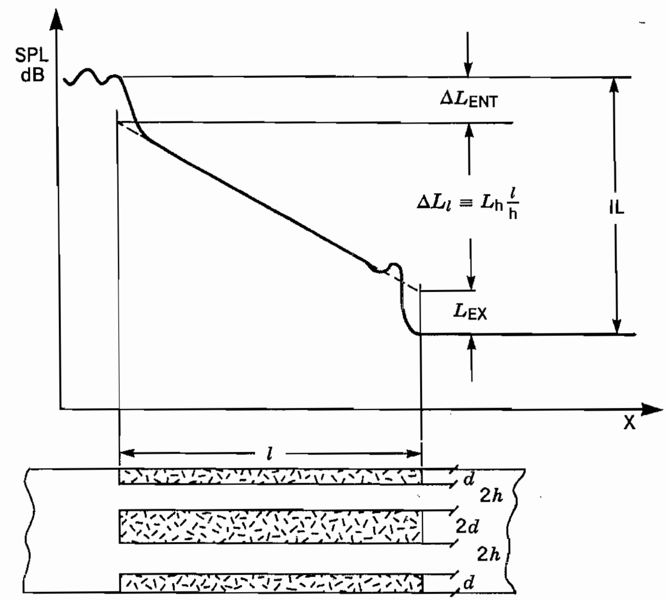

FIGURE 9.21 Typical SPL-versus-distance curve obtained when microphone traverses through a silencer.

A. It can be expressed as

$$\Delta L_l = \left(\frac{P}{A}\right) l L_h \tag{9.38}$$

where L_h is the parameter that depends in a complex manner on the geometry of the passage and the baffle, acoustical characteristics of the porous sound-absorbing material filling the baffles, frequency, and temperature. The quantity L_h, which also depends on the velocity of the flow in the passage, is usually referred to as the attenuation per channel height. The major part of this section is devoted to the determination of this important normalized sound attenuation parameter.

***Pressure Drop* Δp.** The total pressure drop Δp_T across a muffler is made up of entrance, exit, and friction losses:

$$\Delta p_T = 1/2\rho v_P^2 \left[K_{ENT} + K_{EX} + \left(\frac{P}{A}\right) l K_F\right] = \Delta p_{ENT} + \Delta p_{EX} + \Delta p_F \quad \text{N/m}^2 \tag{9.39}$$

where ρ is the density of the gas and v_P its face velocity in the passage of the silencer. The constants K_{ENT} and K_{EX} are the entrance and exit head loss coefficients, which depend only on the geometry of the baffle/passage configuration.

The third term on the right-hand side of Eq. (9.39) represents the friction losses, given by

$$\Delta p_F = \frac{P}{A} l (K_F \tfrac{1}{2} \rho v_P^2) \quad \mathrm{N/m^2} \tag{9.40}$$

Comparing Eq. (9.38) with Eq. (9.40), one notes that baffle configurations that tend to yield high acoustical attenuation ΔL_l also tend to yield high frictional pressure losses Δp_F. Both ΔL_l and Δp_F are proportional to $(P/A)l$, indicating that high silencer attenuation and low frictional pressure drop are contradictory requirements. This finding emphasizes the need to optimize L_h by beneficial choice of the acoustical parameters of the baffles before one resorts to obtaining increased sound attenuation by increasing the factor $(P/A)l$.

Parallel-Baffle Silencers

The parallel-baffle-type silencer shown in Fig. 9.18*a* is the most frequently used because of its good acoustical performance and low cost. The attenuation of such a silencer is proportional to the perimeter–area ratio P/A, the length l, and L_h. Therefore, it is maximized by maximizing $(P/A)L_h$. The largest perimeter–area ratio obtained for narrow passages is $1/h$. Allowing for entrance losses, Eq. (9.38) yields the following simple formula for silencer attenuation:

$$\Delta L_l = L_h \frac{l}{h} + \Delta L_{\mathrm{ENT}} \quad \mathrm{dB} \tag{9.41}$$

where ΔL_{ENT} can be approximated from Fig. 9.20. The following discussion shows how to obtain L_h from the geometric and acoustical parameters of the silencer.

Prediction of Attenuation. The sound energy traveling in the passages of a parallel-baffle silencer, depicted in Fig. 9.19, is attenuated effectively in a wide bandwidth if (1) the sound enters the porous sound-absorbing material in the baffles and (2) a substantial part of the energy of the sound wave entering the baffle is dissipated before it can reenter the passage. Formulas for wall impedance that yield maximum attenuation in a narrow-frequency band are given in reference 2.

Requirement 1 is fulfilled if the passage height is small compared with wavelength (i.e., $2h < \lambda$) and the porous sound-absorbing material is open enough and has sufficiently low flow resistivity so that the sound wave enters the baffle rather than being reflected at the interface. This requires a "fluffy" material of low flow resistivity. Requirement 2 is fulfilled by a porous material of moderate flow resistivity. The requirements of easy sound penetration and high dissipation are contradictory unless the baffle is very thick and is packed with porous sound-absorbing material of low flow resistivity. Consequently, the choice of baffle thickness and flow resistivity of the porous sound-absorbing material is always a compromise.

Generally, the silencer geometry is controlled by the shape of the attenuation-versus-frequency curve we aim to achieve. To provide reasonable attenuation at the low end of the frequency spectrum, the baffle thickness $2d$ must be on the order of one-eighth of the wavelength. To provide reasonable attenuation at the high end of the frequency spectrum, the passage height $2h$ must be not much larger than the wavelength. To allow reasonable penetration of the sound and yield the needed dissipation, the total flow resistance $R_1 d$ of a baffle of thickness $2d$ must be 2–6 times the characteristic impedance of the gas in the silencer passages at design temperature.

Quantitative Considerations. The normalized attenuation constant L_h is obtained by solving the coupled wave equation in the passage and in the porous material of the baffle and requiring that (1) the coupled wave, which propagates axially in both the passage and baffle, has a common propagation constant Γ_c and (2) both particle velocity and the sound pressure are continuous at the passage baffle interface.

The coupled wave equation[1,71–74] can be solved by numerical iteration methods to yield the common propagation constant Γ_c. The normalized attenuation L_h is then obtained from

$$L_h = 8.68h \; \mathrm{Re}\{\Gamma_c\} \quad \mathrm{dB/m} \tag{9.42}$$

where Γ_c depends on the characteristic impedance ρc of the gas in the passage, the characteristic impedance Z_a and the propagation constant Γ_c of the porous material in the baffle, and the geometry.

The characteristic impedance Z_a and the propagation constant Γ_c of the porous sound-absorbing materials (which are complex quantities and vary with frequency) are generally not available. As discussed in Chapter 8, one can approximate these important parameters with reasonable accuracy if the flow resistivity of the porous sound-absorbing material R_1 is known. For fibrous sound-absorbing materials the characteristic impedance Z_a and propagation constant Γ_a in the bulk porous material can be estimated using the empirical formulas presented in Chapter 8.

The most accurate characterization of the porous materials is achieved by measuring the characteristic impedance and propagation constant on a sufficiently large number of samples as a function of frequency at room temperature and by scaling these data to design temperature. Note that this attenuation, which is computed on the basis of the acoustical parameters of the porous material predicted from flow resistivity by employing the formulas given in Chapter 8, compares very well with experimental data if the porous sound-absorbing material is homogeneous.

Normalized Graphs to Predict Acoustical Performance of Parallel-Baffle Silencers. The normalized attenuation L_h has been computed for various percentages of open area of the silencer cross section (i.e., for various h/d) and for various values of the normalized flow resistance $R = R_1 d/\rho c$ of isotropic porous sound-absorbing material in the baffles. It is presented in Figs. 9.22*a–c* for open-area ratios of 66, 50, and 33%, respectively. The effect of nonisotropic material is covered in reference 72. The vertical axis in Fig 9.22 represents the normalized attenuation L_h in decibels on a logarithmic scale. The lower horizontal scale represents the normalized frequency parameter $\eta = 2h/c$. It is valid for all temperatures and gases provided that the speed of sound c is taken at the actual temperature. *The upper horizontal scale, which is valid only for air at room* temperature, represents the product of the half-passage height h in centimeters and the frequency f in kilohertz.

Figures 9.22*a*–*c* show that the attenuation starts to decrease rapidly above the frequency where the passage height $2h$ becomes large compared to the wavelength (i.e., $\eta > 1$). The attenuation in this frequency region can be increased by up to 10 dB by utilizing a two-stage silencer with staggered-baffle arrangement. Note that the bandwidth of appreciable attenuation increases with decreasing percentage of open area of the silencer cross section.

Figure 9.22 shows that in the range of $R = R_1 d/\rho c$ from 1 to 5, the attenuation does not depend strongly on the specific choice of the flow resistance; this coincidence is welcome because the present lack of adequate knowledge of and control over the material characteristics represents the weakest link in the prediction process. Note that if the normalized flow resistance becomes too large

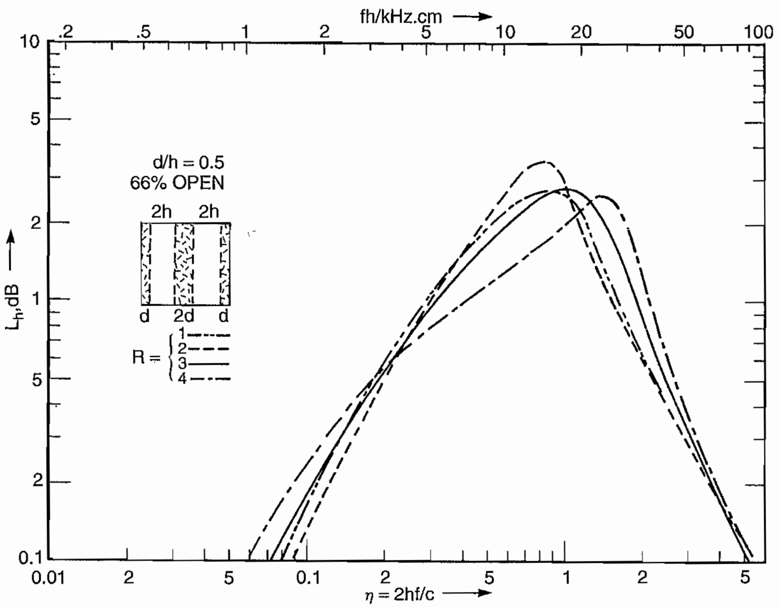

(*a*)

FIGURE 9.22 Normalized attenuation-versus-frequency curves for parallel-baffle silencers with normalized baffle flow resistance $R = R_1 d/\rho c$ as parameter: (*a*) 66% open; (*b*) 50% open; (*c*) 33% open.

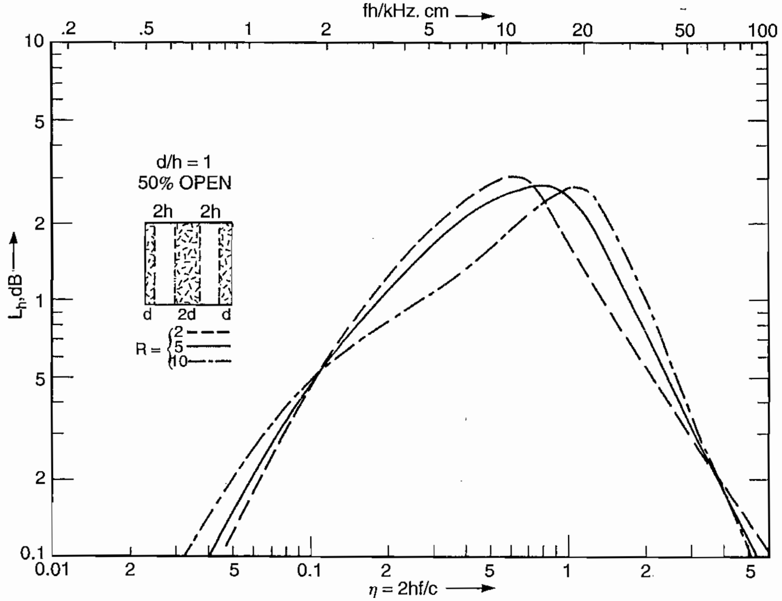

(*b*)

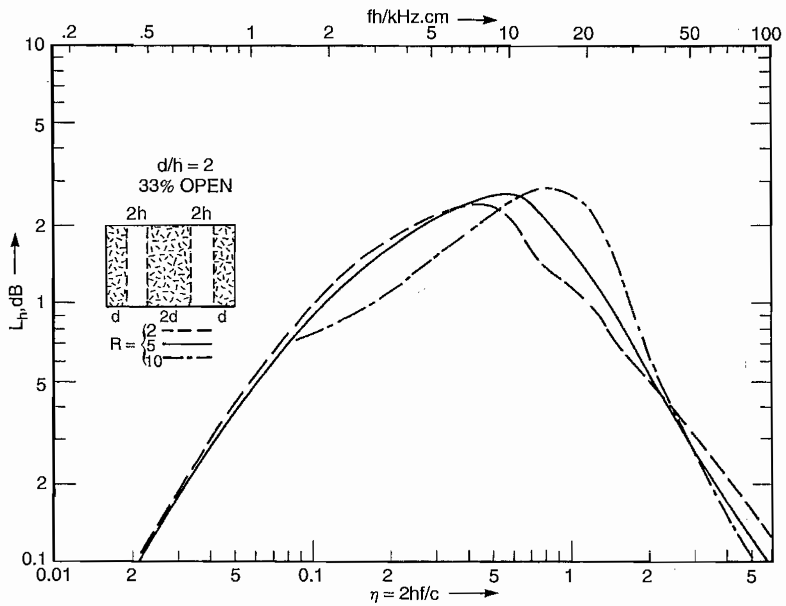

(*c*)

FIGURE 9.22 (*continued*)

($R \geq 10$), a substantial decrease of attenuation occurs in the frequency region from $\eta = 0.2$ to $\eta = 1$ accompanied by a modest increase of attenuation at very low and at high frequencies.

The normalized attenuation-versus-frequency curves presented in Figs. 9.22*a*–*c* correspond to zero flow; corrections to account for flow are presented in a later section.

The use of the design information presented in Figs. 9.22*a*–*c* is illustrated by a few examples.

Example 9.5. Predict the attenuation-versus-frequency curve of a parallel-baffle silencer consisting of 200-mm- (8-in.-) thick parallel baffles 1 m (40 in.) long spaced 400 mm (16 in.) off center when the flow resistance of the baffle $R_1 d = 5\rho c$ and the duct carries a very low velocity air at 20°C; $h = 0.1$ m; $d = 0.1$ m; $L = 1$ m; $c = 340$ m/s; $\rho = 1.2$ kg/m^3; $R = R_1 d/\rho c = 5$.

Solution

1. Determine frequency f^*, which corresponds to $\eta = 1$:

$$f^* = \frac{c}{2h} = \frac{340 \text{ m/s}}{0.2 \text{ m}} = 1700 \text{ Hz}$$

2. Determine $1/h = 1$ m/0.1 m $= 10$.
3. Determine the applicable normalized attenuation-versus-frequency curve for $d/h = 1$ and $R = 5$; the solid curve in Fig. 9.22*b* is applicable.
4. Mark the frequency $f^* = 1700$ Hz on the horizontal scale of a sheet of transparent graph paper that has the same horizontal and vertical scales as Fig. 9.22*b* and align it with $\eta = 1$ in Fig 9.22*b*.
5. Shift the transparent graph paper vertically until the mark $L_h = 1$ in Fig. 9.22*b* corresponds to 10 ($1/h = 10$) on the transparent overlay.
6. Copy the solid curve in Fig. 9.22*b* that corresponds to $R = 5$ on the overlay.
7. The copied curve then corresponds to the attenuation-versus-frequency curve of the silencer according to $\Delta L_l = L_h(1/h)$; the above procedure is sketched in Fig. 9.23.

Example 9.6. Design a parallel-baffle silencer that yields the attenuation listed below:

f, Hz	100	200	500	1000	2000	4000
ΔL, dB	4	9	19	26	10	5

Design Steps

1. Find the graph in Figs. 9.22*a*–*c* that best matches the shape of the desired attenuation-versus-frequency curve plotted in Fig. 9.23. Overlay the transparent paper of Fig. 9.23 on the curve that yields the best match and shift the transparent overlay horizontally and vertically until all of the desired attenuation-versus-frequency points fall below the chosen normalized attenuation-versus-frequency curve. In this case, the solid curve in Fig. 9.22*c* gives the best match.

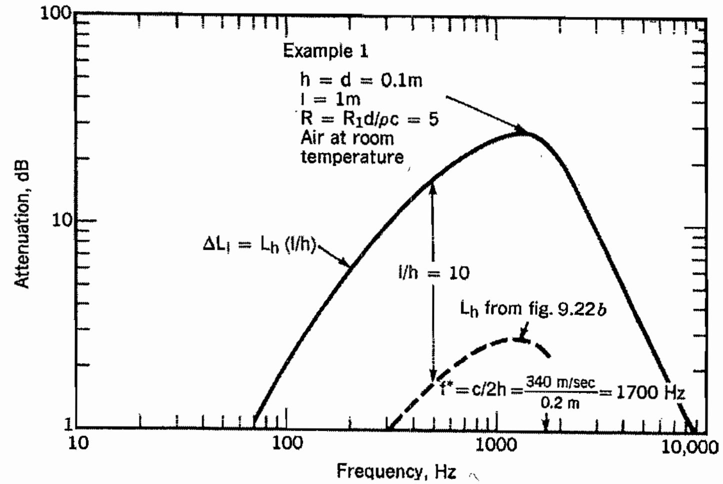

FIGURE 9.23 Attenuation prediction for parallel-baffle silencer, Example 9.5.

2. On the overlay, mark the frequency f^* that corresponds to $\eta = 1$ on the horizontal scale of the appropriate design curve under the overlay, and on the vertical scale, mark the attenuation ΔL^*, which corresponds to $L_h = 1$ on the design curve below the overlay, as shown in Fig. 9.24. In this case, these will be $f^* = 2000$ Hz and $\Delta L^* = 10$ dB.
3. From the design curve below the overlay, note the values of the parameters d/h and R that correspond to the curve that provides the best match. In this case, these are $d/h = 2$ and $R = R_1 d/\rho c = 5$.
4. On the basis of the information obtained in steps 3 and 4, one obtains the geometric and acoustical parameters of the silencer that will yield the specified attenuation as follows:
   - Passage height $2h$:

$$\eta = 1 = \frac{2hf^*}{c} \quad \text{yields} \quad 2h = \frac{340 \text{ m/s}}{2000 \text{ s}^{-1}} = 0.17 \text{ m}$$

   - Baffle thickness $2d$:

$$2d = 2(2h) = 2 \times 0.17 \text{ m} = 0.34 \text{ m}$$

   - Silencer length:

$$\Delta L^* = 10 = \frac{l}{h} \quad \text{yields} \quad l = \Delta L^* h = 10 \times \frac{0.17}{2} \text{ m} = 0.85 \text{ m}$$

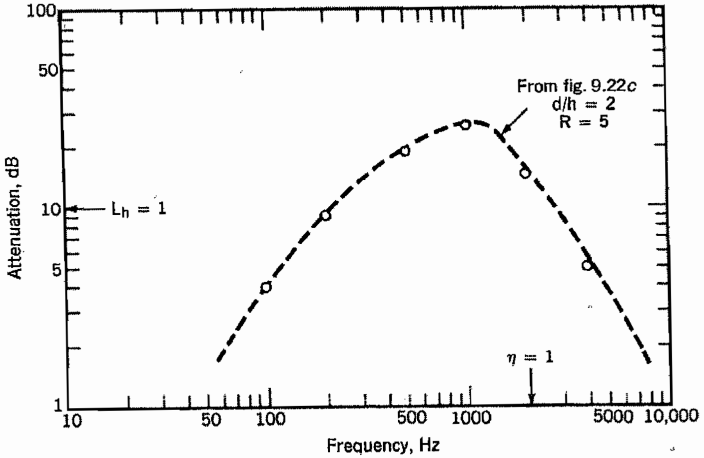

FIGURE 9.24 Acoustical design of a parallel-baffle silencer, Example 9.6: (o) design requirements; (- - - - - -) curve of matching attenuation versus frequency from Fig. 9.22*c*.

- Flow resistance per unit thickness of porous material:

$$\frac{R_1 d}{\rho c} = 5 \quad \text{yields} \quad R_1 = \frac{5\rho c}{d} = \frac{5}{0.17\ \text{m}}\rho c = 29.4\rho c/\text{m}$$

or

$$R_1 = 0.7\rho c/\text{in.} \quad \text{or} \quad R_1 = 1.2 \times 10^4\ \text{N} \cdot \text{s/m}^4$$

Cross-Sectional Area. The cross-sectional area of the muffler is determined by the maximum allowable pressure drop and self-generated noise as discussed later.

Effect of Temperature. The design temperature affects the acoustical and aerodynamic performance of the silencers because the following key parameters depend on the temperature: (1) speed of sound, (2) density of the gas, and (3) viscosity. The effects of temperature are taken into account as follows:

$$c(T) = c_0\sqrt{\frac{273+T}{293}} \quad \text{m/s} \tag{9.43}$$

$$\rho(T) = \rho_0 \frac{293}{273+T} \quad \text{kg/m}^3 \tag{9.44}$$

$$R(T) = R_0\left(\frac{273+T}{293}\right)^{1/2} \tag{9.45}$$

where T is the design temperature in degrees Celsius, c_0 is the speed of sound, ρ_0 is the density of the gas (usually air) at 20°C, and

$$R_0 = \frac{R_1(20^\circ\text{C})d}{\rho_0 c_0} \tag{9.46}$$

where $R_1(20^\circ\text{C})$ is the flow resistivity of the porous bulk material at 20°C. This material parameter is usually provided by the manufacturer or is measured.

Example 9.7. To illustrate how to account for the effect of temperature, let us predict the attenuation provided by the silencer of Example 9.5 at $T = 260^\circ\text{C}$ (500°F).

Solution The effect of temperature must be accounted for in the flow resistivity and in the speed of sound according to Eqs. (9.45) and (9.43), yielding $c(T) =$ 457 m/s and $R(T) = 10$. From now on, the solution proceeds according to the same steps followed in Example 9.5.

1. $f^* = c(T)/2h = (457\ \text{m/s})/0.2\ \text{m} = 2285\ \text{Hz}; l/h = (1\ \text{m}/0.1\ \text{m}) = 10.$
2. The applicable normalized attenuation curve that corresponds to $d/h = 1$ and $R = 10$ is the short/long-dashed curve in Fig. 9.22*b*.

This results in the attenuation-versus-frequency curve shown as the solid line in Fig. 9.25. The dashed curve in Fig. 9.25 is the attenuation of the same silencer at room temperature (20°C), as determined in Example 9.5.

Comparing the solid curve obtained for 260°C with the dashed curve obtained for 20°C, one notes a shift in the attenuation-versus-frequency curve toward higher frequencies with increasing temperature. This shift is mainly due to the increase of propagation speed of sound with increasing temperature. In addition, one also observes distortion in the shape of the attenuation-versus-frequency curve. This is caused by the increase in the flow resistivity of the porous material,

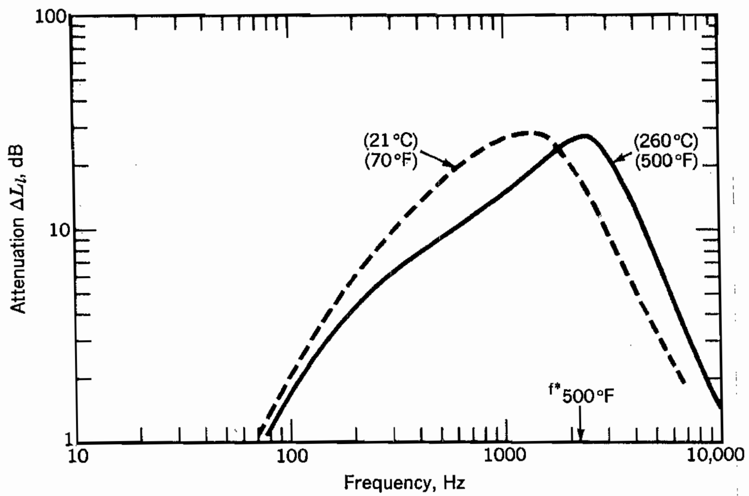

FIGURE 9.25 Attenuation of silencer of Example 9.5 at 260°C (500°F), Example 9.7.

which in turn is due to the increasing viscosity with increasing temperature. This effect has also been predicted by Mechel.[75]

Baffle Thickness Considerations. A particular percentage of open area of a silencer can be accomplished either by a small number of thick baffles or by a large number of thin baffles. Figure 9.26 shows the attenuation-versus-frequency curves computed for a 2-m- (6.5-ft-) long silencer of 50% open area with baffle thickness $2d = 2h$ of 152 mm (5 in.), 203 mm (8 in.), 254 mm (10 in.), and 305 mm (12 in.). The baffles are filled with a fibrous sound-absorbing material that has a flow resistivity $R_1 = 51,500$ N · s/m^4 at 500°C ($1\rho c$/in. at 20°C). The outstanding feature of the data presented in Fig. 9.26 is that in the midfrequency region, the sound attenuation decreases with increasing baffle thickness. At 500 Hz, the 152-mm- (6-in.-) thick baffles yield 25 dB attenuation while the 305-mm- (12-in.) thick baffles yield only 11 dB. This is because the sound does not fully penetrate into the fibrous sound-absorbing material in the thick baffles. Consequently, the material and the space in the center of the thick baffles are wasted.

Figure 9.27 shows the predicted sound attenuation of a silencer of the same geometry as that in Fig. 9.26, but the baffles in this case are filled with fibrous sound-absorbing material of low flow resistivity such that the total normalized flow resistance of each baffle was $R = R_1 d/\rho c = 2$, which allows full penetration of the sound into even the thickest baffle. Consequently, the sound attenuation at

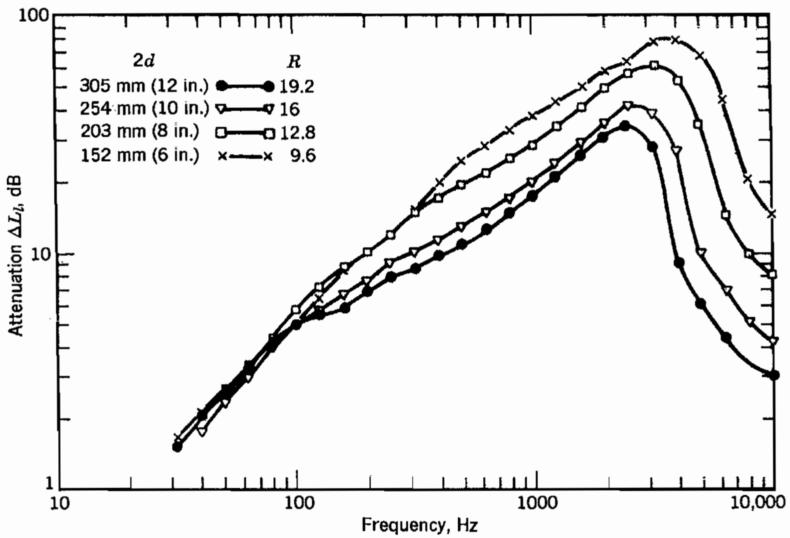

FIGURE 9.26 Computed attenuation-versus-frequency curves for a 2-m- (6.6-ft-) long parallel-baffle silencer of 50% open area with baffle thickness $2d$ as parameter.

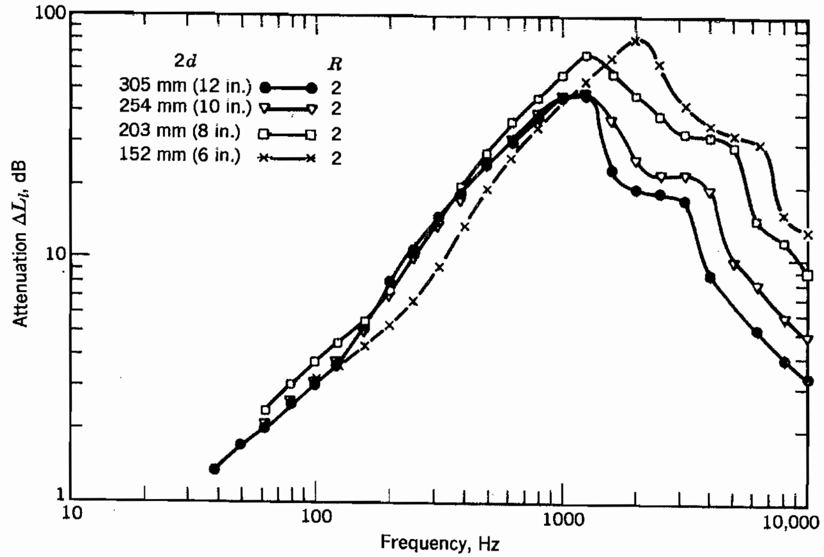

FIGURE 9.27 Computed attenuation-versus-frequency curves of the same silencer as Fig. 9.26 but fibrous fill is chosen to yield $R = R_1 d/\rho c = 2$ for all baffle thicknesses.

low and midfrequencies depends only slightly on the baffle thickness. Comparing Figs. 9.26 and 9.27 reveals that using a few thick baffles (which is more economical than using many thinner baffles) results in decreased sound attenuation at midfrequencies unless the baffles are filled with a sound-absorbing material of low enough resistivity so that the normalized baffle flow resistance at design temperature, $R = R_1 d/\rho c$, is much less than 10. Fibrous sound-absorbing materials that fulfill this requirement for thick baffles used in elevated temperatures may not be readily available. Consequently, silencer baffles of traditional design in high-temperature applications should be kept at a thickness that seldom exceeds $2d = 200$ mm (8 in.).

Note that the attenuation-versus-frequency curve of parallel-baffle silencers increases monotonically up to a frequency $f = c/2d$, where the passage width corresponds to a wavelength, and decreases sharply above it.

Round Silencers

Round silencers, as depicted in Fig. 9.18b, are used in connection with round ducts. The curvature of the duct casing results in a high form stiffness that yields high sound transmission loss of the silencer wall at low frequencies. The acoustical performance of round silencers with respect to normalized attenuation L_h is very similar to that of parallel-baffle silencers. The diameter of the round passage, $2h$, and the thickness of the homogeneous isotropic lining, d, resemble the passage width $2h$ and the half-baffle thickness d of a parallel-baffle silencer. The silencer attenuation $\Delta L^r(l)$ of a round muffler of length l is obtained from

$$\Delta L^r(l) = L_h^r \frac{l}{h} \tag{9.47}$$

The sound attenuation in round ducts has been studied by Scott[71] and Mechel.[74] Their work forms the theoretical foundations for computing their performance.

Figure 9.28 shows curves of normalized attenuation L_h^r versus normalized frequency $\eta = 2hf/c$ for round silencers with homogeneous isotropic lining for thickness–passage radius ratios d/h of 0.5, 1, and 2, respectively, with the normalized lining flow resistance $R = R_1 d/\rho c$ as parameter. The lower horizontal scale is valid for all temperatures, while the upper scale is valid only for air at room temperature. Figure 9.28 shows that the normalized attenuation increases monotonically with frequency until the wavelength corresponds to the diameter of the passage ($\eta = 2hf/c = 2h/\lambda = 1$). Above this frequency the attenuation decreases rapidly with increasing frequency, as was the case for parallel-baffle silencers. Note that the maximum normalized attenuation is about $L_{h,\max}^r \approx 6$ dB

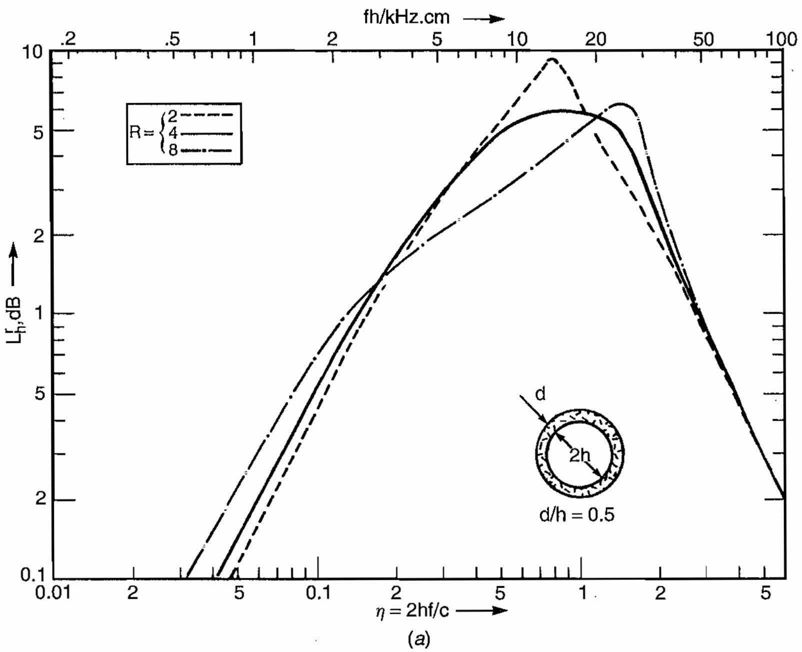

(a)

FIGURE 9.28 Curves of normalized attenuation L_h^r versus frequency for round silencers with normalized lining flow resistance $R = R_1 d/\rho c$ as parameter: (a) $d/h = 0.5$; (b) $d/h = 1$; (c) $d/h = 2$.

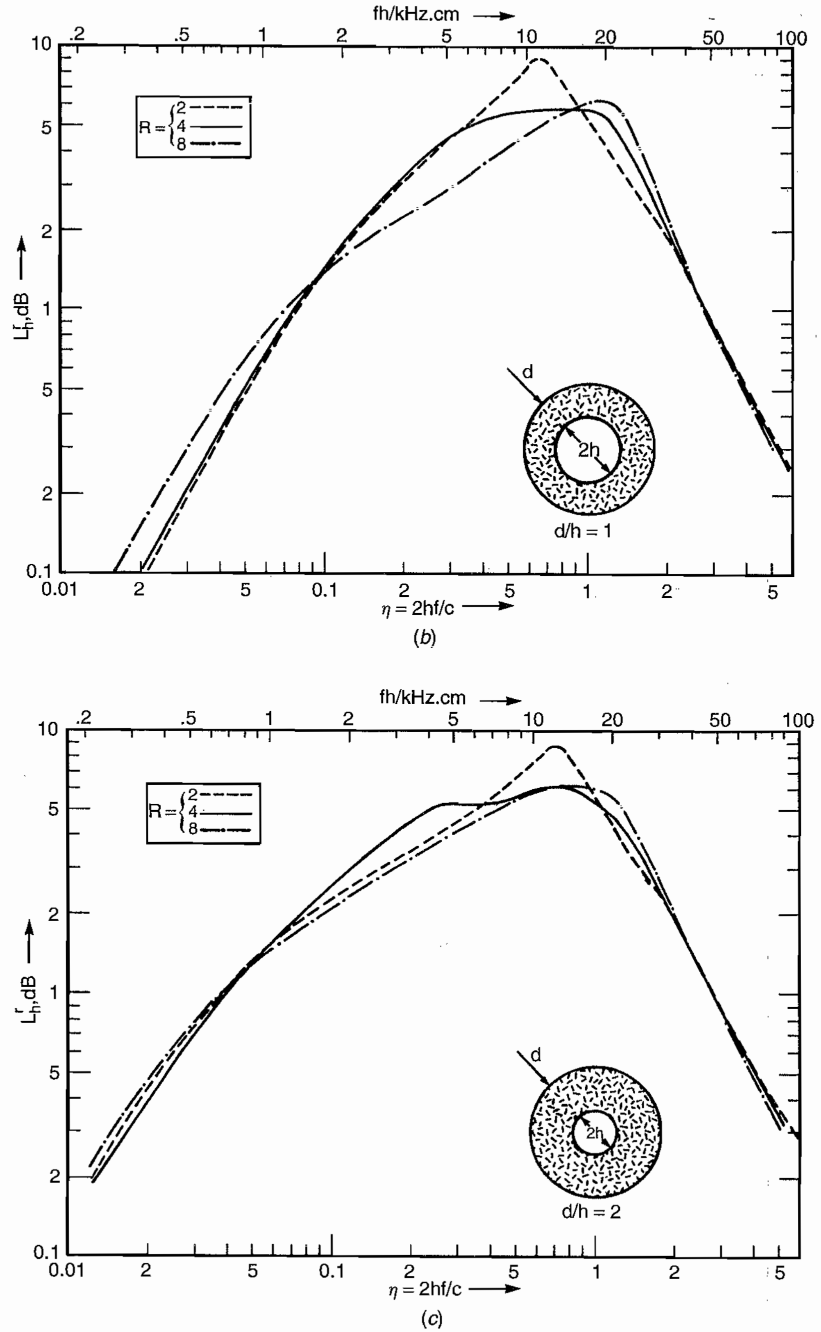

FIGURE 9.28 *(continued)*

for round silencers compared to $L^r_{h,\max} \approx 3$ dB for parallel-baffle silencers. This is because a round passage has twice as high perimeter–area ratio $(2/h)$ than a narrow passage of a parallel-baffle silencer $(1/h)$. As expected, the attenuation bandwidth increases toward low frequencies with increasing lining thickness d. The curves presented in Fig. 9.28 are used in the same way as the corresponding curves for parallel-baffle silencers by applying the design steps listed earlier in the Examples 9.5 and 9.7. Incidentally, similar curves and trends have been predicted by Mechel.[75]

Pod Silencers

Round silencers have a generic disadvantage of providing poor high-frequency performance when the passage diameter is large compared with the wavelength. This disadvantage can be overcome by inserting a center body or pod into the passage[76]. With the center body in place, the round silencer has a narrow annular passage, just like a parallel-baffle silencer, and the attenuation will continue to increase monotonically until the wavelength of the sound becomes equal to the width of the narrow annular passage, as illustrated in the example of Fig. 9.29. Both the rigid and absorbing center bodies result in a modest increase in attenuation at low and midfrequencies, which is mostly due to reduction of the passage cross-sectional area. The attenuation of this silencer without center body

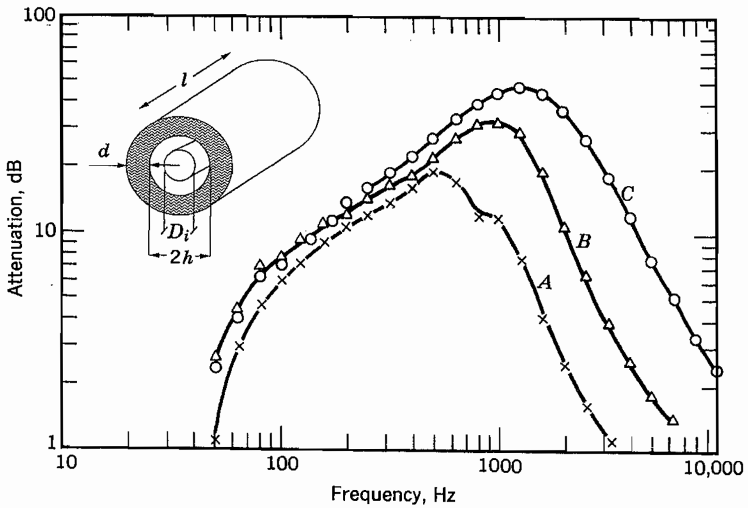

FIGURE 9.29 Effect of center body on the attenuation-versus-frequency curve of a round silencer, passage diameter $2h = 0.6$ m (24 in.), center body diameter $D_i = 0.3$ m (12 in.), lining thickness $d = 0.2$ m (8 in.), length $l = 1.2$ m (48 in.), $T = 20°$C (68°F), $R_1 = 16{,}000$ N · s/m^4 (1ρc/in.): A, no center body; B, rigid center body; C, absorbing center body.

decreases sharply above 560 Hz, the frequency where the wavelength equals the diameter of the passage. With the rigid center body the attenuation continues to increase up to 1130 Hz and with the porous center body up to 2260 Hz.

If center bodies are impractical, the high-frequency attenuation of round silencers can also be increased by inserting parallel baffles into the round passage. Similarly, the high-frequency attenuation of silencers with rectangular cross section can be increased by inserting parallel baffles (oriented perpendicular to the plane of the thick, low-frequency liner, or side branches on the sidewalls) into the rectangular passage. As described in detail by Kurze and Ver[77], the inserted parallel baffles also increase the low-frequency attenuation by a beneficial interaction with the low-frequency part of the silencer located at the walls. The mechanism of this interaction is that the reduction of the wave speed owing to the structure factor of the parallel baffles increases the attenuation performance of the low-frequency liner on the sidewalls. Similarly, the structure factor of the low-frequency liner on the sidewalls increases the attenuation of the parallel baffles. Consequently, the beneficial interaction results in increased sound attenuation at both low and high frequencies. This type of insert silencer also has the benefit of requiring substantially less total silencer length than the traditional series combination of a low- and high-frequency silencer section.

Effect of Flow on Silencer Attenuation

The flow affects the attenuation of sound in silencers in three ways:

1. It changes slightly the effective propagation speed of the sound.
2. By creating a velocity gradient near the passage boundaries, it refracts the sound propagating in the passage toward the lining if the propagation is in the flow direction (exhaust silencers) and "focuses" the sound toward the middle of the passage if the propagation is opposite to the flow direction (intake silencers).
3. It increases the effective flow resistance of the baffle.

Figure 9.30*a* shows the effect of flow on the attenuation performance of an exhaust silencer when the flow direction coincides with the direction of sound propagation. Note that the attenuation is decreased at low frequencies and is increased slightly at high frequencies. In most cases, a Mach number $M > 0.1$ is not permissible because of material deterioration or self-noise.

Figure 9.30*b* shows what happens when the sound propagates against the flow. In this case the attenuation at low frequencies increases because it takes the sound a longer time to traverse through the *muffler* passage. The high-frequency attenuation decreases because the velocity gradients in the passage "channel" the sound toward the center of the passage. The effect of flow on attenuation can be approximated by appropriate shift of the attenuation-versus-frequency curve obtained without flow $(M = 0)$.

The attenuation in the presence of flow is obtained by shifting the no-flow $(M = 0)$ attenuation curve as illustrated in Fig. 9.31*a* when the direction of sound

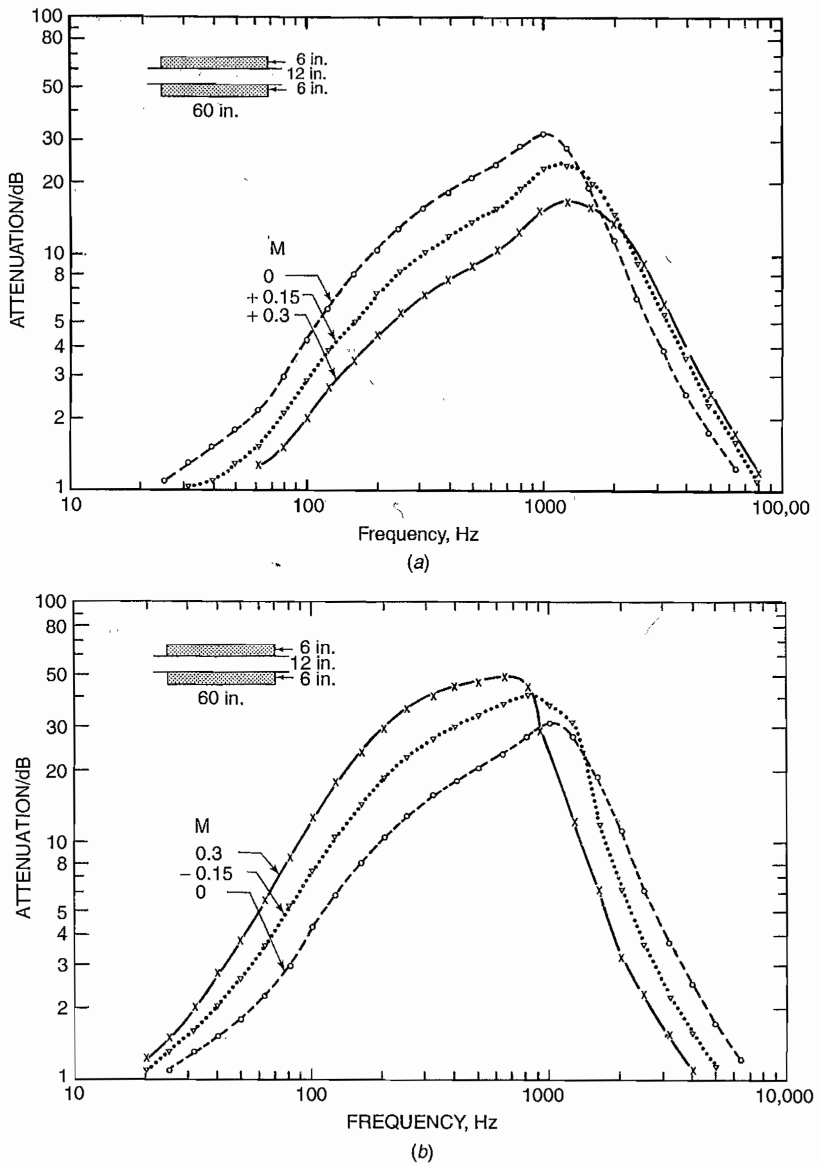

FIGURE 9.30 Effect of flow on sound attenuation for Mach numbers $M = 0$, 0.15, 0.3: sound propagation (*a*) in flow direction and (*b*) against flow direction.

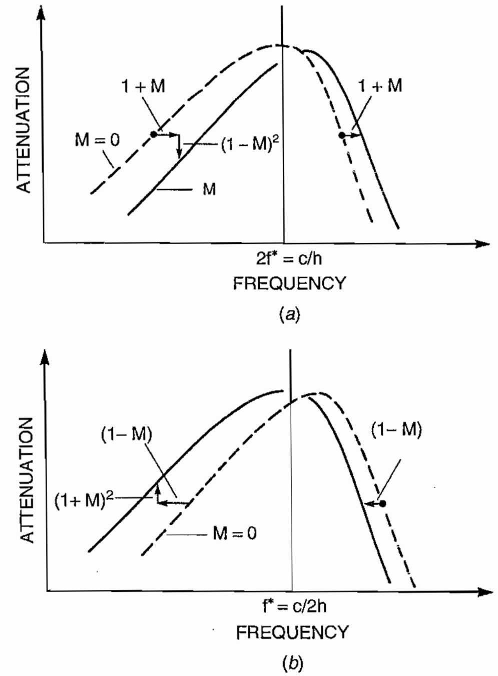

FIGURE 9.31 Rules for shifting the no-flow ($M = 0$) attenuation-versus-frequency curve to account for flow effects: sound propagation (*a*) in flow direction and (*b*) against flow direction.

propagation and the gas flow are the same and in Fig. 9.31*b* when they are opposite.

Figure 9.32 shows the attenuation-versus-frequency curve of a silencer with $M = 0.15$ flow in the direction of sound propagation. The values represented by the crosses are those directly computed for $M = +0.15$ (dotted line in Fig. 9.30*a*) and those represented by the open circles were obtained by shifting the $M = 0$ curve in Fig. 9.30*a* according to the guidelines discussed in conjunction with Fig. 9.31 The agreement between the curve obtained by shifting and by computations (which takes into account flow effects in the wave equation) is good.

The empirical flow correction procedure illustrated in Fig. 9.31 is based on experience with parallel-baffle silencers. We have no experience at present to gauge its applicability and accuracy for other silencer geometries.

Flow-Generated Noise

At present there is no universally accepted method for predicting the flow-generated noise of silencers. Information provided by silencer manufacturers shall be used wherever available. The empirical predictive scheme presented here

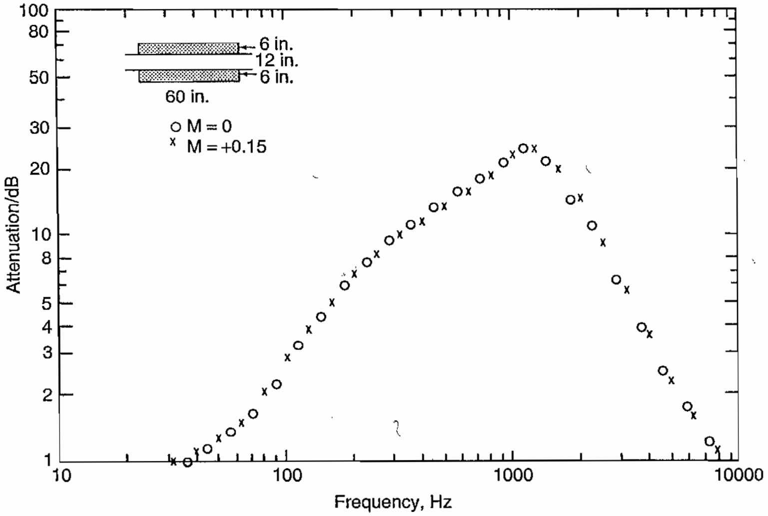

FIGURE 9.32 Attenuation-versus-frequency curve of a silencer for sound propagation in flow direction, $M = +0.15$: (×) computed; (○) obtained by shifting the $M = 0$ curve according to Fig. 9.31*a*.

is based on a broad range of experimental data on flow-generated noise of duct silencers and is reproduced from ISO 14163:1998(E).[78]

An estimate for the octave-band sound power level of regenerated sound can be obtained from Eq. (9.48):

$$L_{W,\text{oct}} = B + \left\{ 10 \lg \frac{PcSn}{W_0} + 60 \lg \text{Ma} + 10 \lg \left[1 + \left(\frac{c}{2fH} \right)^2 \right] - 10 \lg \left[1 + \left(\frac{f\delta}{v} \right)^2 \right] \right\} \quad (9.48)$$

where B = a value depending on type of silencer and frequency, dB
v = flow velocity in narrowest cross section of silencer, m/s
c = speed of sound in medium, m/s
Ma = Mach number (Ma = v/c)
P = static pressure in duct, Pa
S = area of narrowest cross section of passage, m^2
n = number of passages
f = octave-band center frequency, Hz
H = maximum dimension of duct perpendicular to baffles, m
δ = length scale characterizing high-frequency spectral content of regenerated noise, m
$W_0 = 1$ W $= 1$ N · m/s

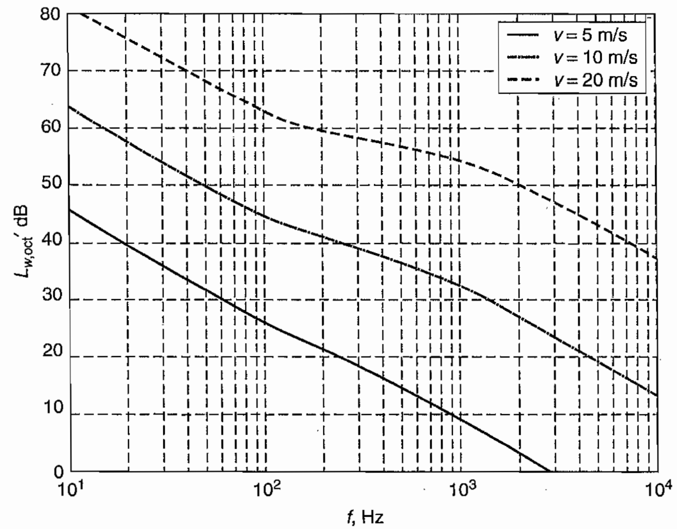

FIGURE 9.33 Octave-band sound power level $L_{W,\text{oct}}$ of regenerated sound versus frequency f for air under ambient conditions in a ducted silencer with narrowest cross section $S = 0.5\ \text{m}^2$, maximum transverse dimension $H = 1$ m, and different flow velocities v.

The sound power level of regenerated sound will vary with the temperature T approximately with $-25 \lg(T/T_0)$ decibels. For smooth-walled dissipative splitter silencers used in heating, ventilation, and air-conditioning equipment, an approximation is given by $B = 58$ and $\delta = 0.02$ m. For this case, a graph of Eq. (9.48) is shown in Fig. 9.33, and the A-weighted sound power level of a duct cross section of 1 m^2 is then calculated from

$$L_{WA} = \left(-23 + 67 \lg \left[\frac{v}{v_0} \right] \right) \quad \text{dB} \quad (9.49)$$

where $v_0 = 1$ m/s. For other types of silencers, particularly for resonator silencers, B may be larger in certain frequency bands. However, no general information can be given on the values of B and δ.

Prediction of Silencer Pressure Drop

The maximum permissible pressure drop at design flow rates and at design temperatures, together with the flow-generated noise, determines the cross-sectional dimensions of a silencer. It is important that the silencer designer makes good use of all the available pressure drop, though with an adequate factor of safety. The maximum permissible pressure drop $\Delta p_{\max}$ must be carefully allocated among the pressure drop of transition ducts (Δp_{trans}) and the total pressure drop of the silencer, Δp_{tot}:

$$\Delta p_{\max} \geq F_s(\Delta p_{\text{trans}} + \Delta p_{\text{tot}}) \quad \text{N/m}^2 \quad (9.50)$$

The specific choice of the safety factor ($F_s > 1$) is influenced by the degree of inhomogeneity of the inflow and by guaranty obligations regarding pressure drop performance of the silencer system. The silencer system usually includes the transition ducts both upstream and downstream of the silencer.

Detailed information on how to predict the pressure drop of inlet and exit transitions has been compiled by Idel'chik.[79] The silencer pressure losses are expressed as a product of the dynamic head in the muffler passage, $0.5\rho v_p^2$, and a loss coefficient. The terms K_{ENT}, K_F, and K_{EX} represent the entrance, friction, and exit loss coefficients. They are predicted according to the formulas given in Table 9.3

The required silencer face area is determined by an iteration process. First, Eq. (9.39) is solved for the passage velocity v_p. The initial face area A'_F is obtained as

$$A'_F = \frac{Q}{v_p}\left(\frac{100}{\mathrm{POA}}\right) \quad \mathrm{m}^2 \tag{9.51}$$

TABLE 9.3 Pressure Loss Coefficient for Parallel Baffle Silencers

Geometry	Loss Coefficient
Square-edge nose 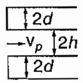	$K_{\mathrm{ENT}} = \dfrac{0.5}{1 + h/d}$
Rounded nose 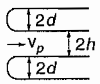	$K_{\mathrm{ENT}} \simeq \dfrac{0.05}{1 + h/d}$
Typical perforated metal facing 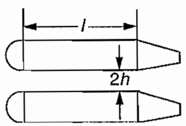	$K_F \simeq 0.0125$ ℓ = baffle length, tail and nose not included
Square tail 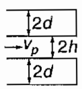	$K_{\mathrm{EX}} = \left(\dfrac{1}{1 + h/d}\right)^2$
Rounded tail 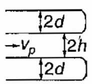	$K_{\mathrm{EX}} = 0.7\left(\dfrac{1}{1 + h/d}\right)^2$
Faired tail, 7.5° 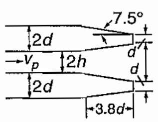	$K_{\mathrm{EX}} = 0.6\left(\dfrac{1}{1 + h/d}\right)^2$

where Q is the volume flow rate through the silencer (in cubic meters per second) v_p is the passage velocity (in meters per second), and POA is the percentage of open area of the silencer cross section (e.g., for parallel-baffle muflers POA = 50 means that $h/d = 1$; the passage height is the same as the baffle thickness). Based on this initial value of $A_F = A'_F$, the pressure loss of the inlet and exit transitions is calculated and added to the muffler pressure drop. The total $F_s(\Delta p_{\mathrm{trans}} + \Delta p_T)$ is compared with maximum permissible pressure drop $\Delta p_{\max}$ according to Eq. (9.50). If $F_s(\Delta p_{\mathrm{trans}} + \Delta p_T) > \Delta p_{\max}$, the face area of the silencer must be increased. This results in a decrease of Δp_T and a relatively smaller increase in $\Delta p_{\mathrm{trans}}$, and the iteration is continued until the inequality, expressed in Eq. (9.50), is satisfied.

Economic Considerations

For large silencers such as used in electric power plants, the product of the pressure drop and volume flow rate, $Q\Delta p$, represents a substantial power that is lost (converted to heat). The cost to produce this power during the entire design life of the installation usually far exceeds the purchase cost of the silencer. Therefore, it is important to specify a silencer pressure drop that yields the lowest total cost. The total cost includes the present worth of revenue requirements to purchase and install the silencer (which decreases with increasing pressure drop allowance) and the present worth of revenue requirements of the energy cost caused by operating the silencer (which increases with increasing pressure drop allowance). The optimal pressure drop is that which yields the lowest total cost. Information on how to predict the optimal silencer pressure drop is given in reference 80.

9.7 COMBINATION MUFFLERS

It is clear from Sections 9.1–9.3 that the TL of reactive mufflers is generally characterized by several troughs that limit the overall value of TL notwithstanding the peaks, owing to the arithmetic of antilog summation. The acoustically lined ducts and parallel-baffle mufflers (or splitter silencers) do not suffer from this characteristic; they are characterized by a wide-band TL curve. However, they have rather poor performance (attenuation) at low frequencies where the reactive mufflers have a relative edge. One way out of these limitations is to combine reflective or reactive elements and dissipative elements into a combination muffler (or hybrid muffler). An acoustically lined plenum chamber is one obvious example of a combination muffler. Figures 9.34–9.37 illustrate the concept and present some design guidelines in the process.[81]

Figure 9.34a is an unlined simple axisymmetric expansion chamber. Figures 9.34b,c show the chamber with lining (with resistivity of 5000 Pa · s/m^2) of 18.2 and 36.4 mm thickness, respectively. The plots in Fig. 9.34 compare the computed values of their axial transmission loss TL$_a$ (assuming rigid shell). Clearly, the role of lining is to raise and even out the troughs, particularly at the medium and high frequencies.

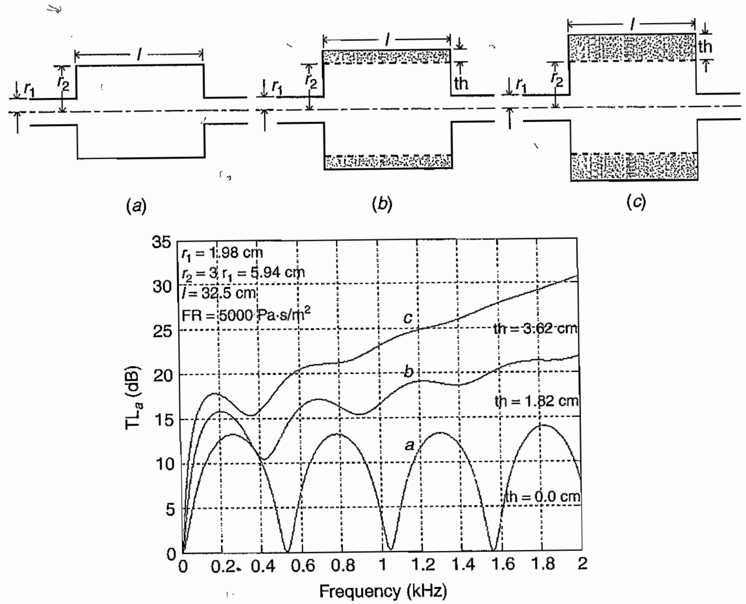

FIGURE 9.34 Use of acoustical lining in combination with a simple expansion chamber or plenum; th = lining thickness in centimeters.

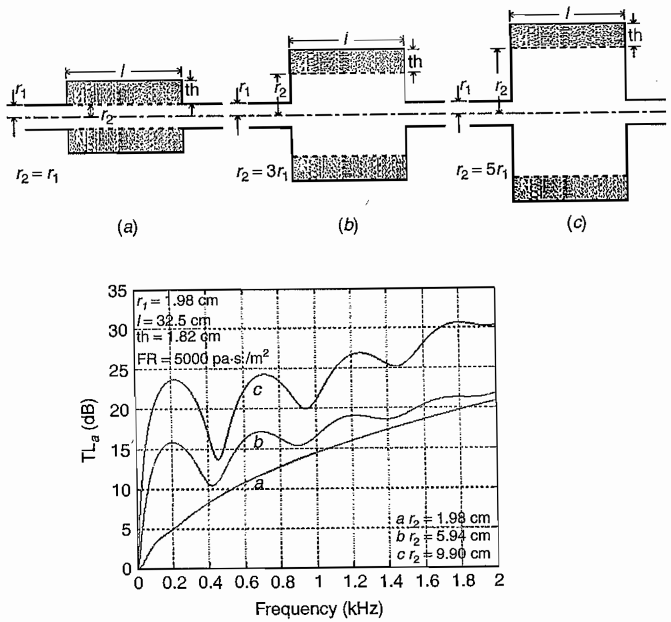

FIGURE 9.35 Use of sudden area discontinuities in combination with lined duct.

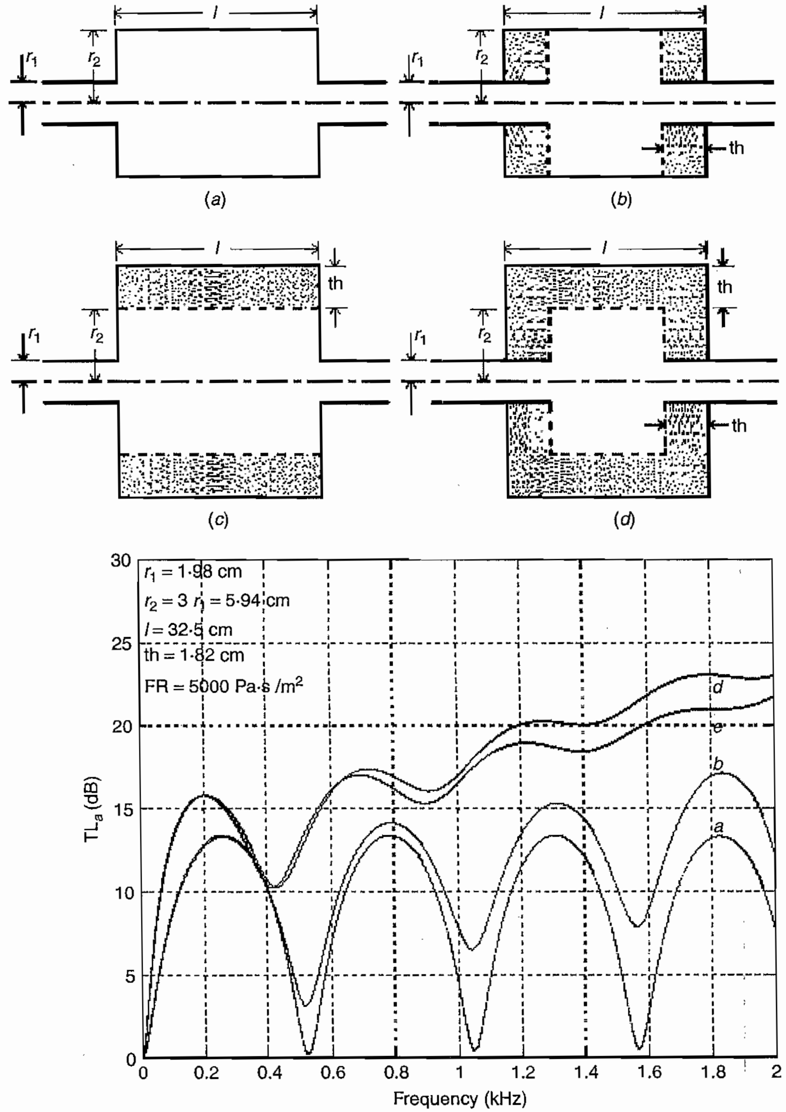

FIGURE 9.36 Effect of lined walls and lined shell.

Figure 9.35 shows the effect of building a sudden expansion and contraction into an acoustically lined circular duct, keeping the radial thickness of the lining constant. As can be noticed, the area discontinuities (sudden impedance mismatch) increase TL, particularly at the low frequencies ($\leq$ 400 Hz).

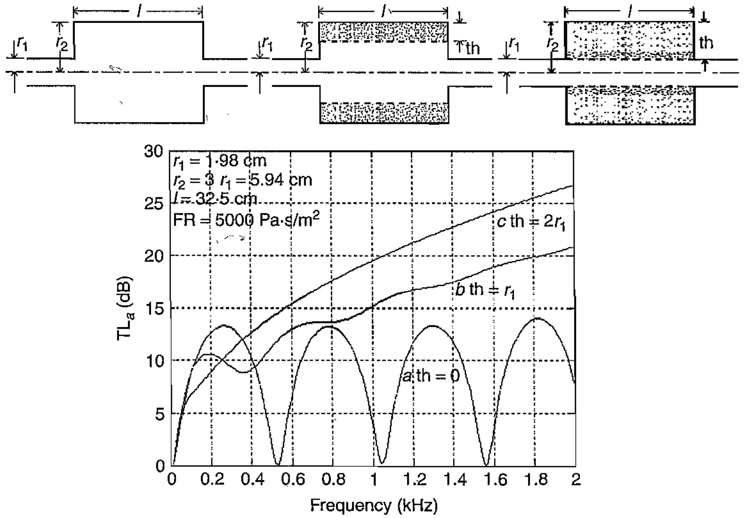

FIGURE 9.37 Reactive elements versus dissipative elements within the same overall shell radius.

A plenum chamber has lining not only on the shell but also on the sidewalls/plates. Figure 9.36 shows (a) a simple expansion chamber (plenum), (b) one with lined sidewalls, (c) one with lined shell only, and (d) one with lined shell as well as lined sidewalls (or end plates). It may be noticed that while the sidewall lining has considerable effect (in raising the troughs), the effect of shell lining is much more pronounced. In fact, a comparison of curves *b* and *c* of Fig. 9.36 shows that the relative effect of sidewall lining is only marginal.

In all the three foregoing figures, provision of lining has increased the overall radius of the muffler shell. Sometimes, it may not be feasible or advisable to increase the shell radius. Then, the internal lining of the shell would decrease the ratio of sudden expansion and sudden contraction. Figure 9.37 shows the effect of this compromise (between reaction and dissipation), keeping the overall shell radius constant. It may be observed that the performance of lined ducts is relatively poor at very low frequencies, when a simple unlined chamber has an edge. The two can supplement each other in a combination muffler (configuration *b* in Fig. 9.37).

REFERENCES

1. P. M. Morse, "Transmission of Sound in Pipes," *J. Acoust. Soc. Am.*, **11**, 205–210 (1999).
2. L. Cremer, "Theory of Attenuation of Airborne Sound in a Rectangular Duct with Sound-Absorbing Walls and the Maximum Achievable Attenuation" (in German), *Acustica*, **3**, 249–263 (1953).

3. D. D. Davis, Jr., M. Stokes, D. Moore, and L. Stevens, "Theoretical and-Experimental Investigation of Mufflers with Comments on Engine Exhaust Design," NACA Report 1192, 1954.
4. D. Davis, "Acoustical Filters and Mufflers," in C. Harris (Ed.), *Handbook of Noise Control*, McGraw-Hill, New York, 1957, Chapter 21.
5. N. Doelling, "Dissipative Mufflers," in L. Beranek (Ed.), *Noise Reduction*, McGraw-Hill, New York, 1960, Chapter 17.
6. T. Embleton, "Mufflers," in L. Beranek (Ed.), *Noise and Vibration Control*, McGraw-Hill, New York, 1971, Chapter 12.
7. L. Ericsson, "Silencers," in D. Baxa (Ed.), *Noise Control in Internal Combustion Engines*, Wiley, New York, 1982, Chapter 5.
8. M. L. Munjal, *Acoustics of Ducts and Mufflers*, Wiley, New York, 1987.
9. M. L. Munjal, "Muffler Acoustics," in F. P. Mechel (ed.), *Formulas of Acoustics*, Springer-Verlag, Berlin, 2002, Chapter K.
10. C. L. Molloy, "Use of Four Pole Parameters in Vibration Calculations," *J. Acoust. Soc. Am.*, **29**, 842–853 (1957).
11. M. Fukuda and J. Okuda, "A Study on Characteristics of Cavity-Type Mufflers," *Bull. Jpn. Soc. Mechan. Eng.*, **13**(55), 96–104 (1970).
12. R. J. Alfredson and P. O. A. L. Davies, "Performance of Exhaust Silencer Components," *J. Sound Vib.*, **15**(2), 175–196 (1971).
13. M. L. Munjal, "Velocity Ratio Sum Transfer Matrix Method for the Evaluation of a Muffler with Mean Flow," *J. Sound Vib.*, **39**(1), 105–119 (1975).
14. P. T. Thawani and A. G. Doige, "Effect of Mean Flow and Damping on the Performance of Reactive Mufflers," *Can. Acoust.*, **11**(1), 29–47 (1983).
15. D. Ronneberger, "The Acoustical Impedance of Holes in the Wall of Flow Ducts," *J. Sound Vib.*, **24**, 133–150 (1972).
16. T. Melling, "The Acoustic Impedance of Perforates at Medium and High Sound Pressure Levels," *J. Sound Vib.*, **29**(1), 1–65 (1973).
17. P. D. Dean, "An In Situ Method of Wall Acoustic Impedance Measurement in Flow Ducts," *J. Sound Vib.*, **34**(1), 97–130 (1974).
18. J. W. Sullivan and M. Crocker, "Analysis of Concentric-Tube Resonators Having Unpartitioned Cavities," *J. Acoust. Soc. Am.*, **64**(1), 207–215 (1978).
19. J. W. Sullivan, "A Method for Modeling Perforated Tube Mufflers Components. I. Theory." *J. Acoust. Soc. Am.*, **66**(3), 772–778 (1979).
20. J. W. Sullivan, "A Method for Modeling Perforated Tube Mufflers Components. II. Applications." *J. Acoust. Soc. Am.*, **66**(3), 779–788 (1979).
21. K. Jayaraman and K. Yam, "Decoupling Approach to Modeling Perforated Tube Muffler Components," *J. Acoust. Soc. Am.*, **69**(2), 390–396 (1981).
22. P. T. Thawani and K. Jayaraman, "Modeling and Applications of Straight-Through Resonators," *J. Acoust. Soc. Am.*, **73**(4), 1387–1389 (1983).
23. M. L. Munjal, K. N. Rao, and A. D. Sahasrabudhe, "Aeroacoustic Analysis of Perforated Muffler Components," *J. Sound Vib.*, **114**(2), 173–188 (1987).
24. M. L. Munjal, M. V. Narasimhan, and A. V. Sreenath, "A Rational Approach to the Synthesis of One-Dimensional Acoustic Filters," *J. Sound Vib.*, **29**(3), 148–151 (1973).

25. M. L. Munjal, S. Krishnan, and M. M. Reddy, "Flow-Acoustic Performance of the Perforated Elements with Application to Design," *Noise Control Eng. J.*, **40**(1), 159–167 (1993).
26. M. L. Munjal, "Analysis and Design of Pod Silencers," *J. Sound Vib.*, **262**(3), 497–507 (2003).
27. C. W. S. To and A. G. Doige, "A Transient Testing Technique for the Determination of Matrix Parameters of Acoustic Systems, I: Theory and Principles," *J. Sound Vib.*, **62**(2), 207–222 (1979).
28. C. W. S. To and A. G. Doige, "A Transient Testing Technique for the Determination of Matrix Parameters of Acoustic Systems, II: Experimental Procedures and Results," *J. Sound Vib.*, **62**(2), 223–233 (1979).
29. C. W. S. To and A. G. Dogie, "The Application of a Transient Testing Method to the Determination of Acoustic Properties of Unknown Systems," *J. Sound Vib.*, **71**(4), 545–554 (1980).
30. T. Y. Lung and A. G. Doige, "A Time-Averaging Transient Testing Method for Acoustic Properties of Piping Systems and Mufflers with Flow," *J. Acoust. Soc. Am.*, **73**(3), 867–876 (1983).
31. M. L. Munjal and A. G. Doige, "Theory of a Two Source Location Method for Direct Experimental Evaluation of the Four-Pole Parameters of an Aeroacoustic Element," *J. Sound Vib.*, **141**(2), 323–334 (1990).
32. A. Galaitsis and E. K. Bender, "Measurement of Acoustic Impedance of an Internal Combustion Engine," *J. Acoust. Soc. Am.*, **58**(Suppl. 1) (1975).
33. M. L. Kathuriya and M. L. Munjal, "Experimental Evaluation of the Aeroacoustic Characteristics of a Source of Pulsating Gas Flow," *J. Acoust. Soc. Am.*, **65**(1), 240–248 (1979).
34. M. G. Prasad and M. J. Crocker, "Insertion Loss Studies on Models of Automotive Exhaust Systems," *J. Acoust. Soc. Am.*, **70**(5), 1339–1344 (1981).
35. M. G. Prasad and M. J. Crocker, "Studies of Acoustical Performance of a Multi-Cylinder Engine Exhaust Muffler System," *J. Sound Vib.*, **90**(4), 491–508 (1983).
36. M. G. Prasad and M. J. Crocker, "Acoustical Source Characterization Studies on a Multicylinder Engine Exhaust System," *J. Sound Vib.*, **90**(4), 479–490 (1983).
37. D. F. Ross and M. J. Crocker, "Measurement of the Acoustic Source Impedance of an Internal Combustion Engine," *J. Acoust. Soc. Am.*, **74**(1), 18–27 (1983).
38. A. F. Seybert and D. F. Ross, "Experimental Determination of Acoustic Properties Using a Two-Microphone Random Excitation Technique," *J. Acoust. Soc. Am.*, **61**, 1362–1370 (1977).
39. J. Y. Chung and D. A. Blaser, "Transfer Function Method of Measuring In-Duct Acoustic Properties II. Experiment," *J. Acoust. Soc. Am.*, **68**, 914–921 (1980).
40. M. L. Munjal and A. G. Doige, "The Two-microphone Method Incorporating the Effects of Mean Flow and Acoustic Damping," *J. Sound Vib.*, **137**(1), 135–138 (1990).
41. H. S. Alves and A. G. Doige, "A Three-Load Method for Noise Source Characterization in Ducts," in J. Jichy and S. Hay, (Eds.), *Proceedings of NOISE-CON*, National Conference on Noise Control Engineering, State College, PA, Noise Control Engineering, New York, 1987, pp. 329–339.
42. M. G. Prasad, "A Four Load Method for Evaluation of Acoustical Source Impedance in a Duct," *J. Sound Vib.*, **114**(2), 347–356 (1987).

43. H. Boden, "Measurement of the Source Impedance of Time Invariant Sources by the Two-Microphone Method and the Two-Load Method," Department of Technical Acoustics Report TRITA-TAK-8501, Royal Institute of Technology, Stockholm, 1985.
44. H. Boden, "Error Analysis for the Two-Load Method Used to Measure the Source Characteristics of Fluid Machines," *J. Sound Vib.*, **126**(1), 173–177 (1988).
45. V. H. Gupta and M. L. Munjal, "On Numerical Prediction of the Acoustic Source Characteristics of an Engine Exhaust System," *J. Acoust. Soc. Am.*, **92**(5), 2716–2725 (1992).
46. L. Desmonds, J. Hardy, and Y. Auregan, "Determination of the Acoustical Source Characteristics of an Internal Combustion Engine by Using Several Calibrated Loads," *J. Sound Vib.*, **179**(5), 869–878 (1995).
47. P. T. Thawani and R. A. Noreen, "Computer-Aided Analysis of Exhaust Mufflers," ASME paper 82-WA/NCA-10, American Society of Mechanical Engineers, New York, 1982.
48. L. J. Eriksson, P. T. Thawani, and R. H. Hoops, "Acoustical Design and Evaluation of Silencers," *J. Sound Vib.*, **17**(7), 20–27 (1983).
49. L. J. Eriksson and P. T. Thawani, "Theory and Practice in Exhaust System Design," SAE Technical paper 850989, Society of Automotive Engineers, Warrendale, PA, 1985.
50. M. L. Munjal, "Analysis and Design of Mufflers—An Overview of Research at the Indian Institute of Science," *J. Sound Vib.*, **211**(3), 245–433 (1998).
51. A. Jones, "Modeling the Exhaust Noise Radiated from Reciprocating Internal Combustion Engines—A Literature Review," *Noise Control Eng. J.*, **23**(1), 12–31 (1984).
52. M. L. Munjal, "State of the Art of the Acoustics of Active and Passive Mufflers," *Shock Vib. Dig.*, **22**(2), 3–12 (1990).
53. V. Easwaran and M. L. Munjal, "Plane Wave Analysis of Conical and Experimental Pipes with Incompressible flow," *J. Sound Vib.*, **152**, 73–93 (1992).
54. E. Dokumaci, "On Transmission of Sound in a Non-uniform Duct Carrying a Subsonic Compressible Flow," *J. Sound Vib.*, **210**, 391–401 (1998).
55. M. L. Munjal and P. T. Thawani, "Acoustic Performance of Hoses—A Parametric Study," *Noise Control Eng. J.*, **44**(6), 274–280 (1996).
56. K. S. Peat, "A Numerical Decoupling Analysis of Perforated Pipe Silencer Element," *J. Sound Vib.*, **123**, 199–212 (1988).
57. K. N. Rao and M. L. Munjal, "Experimental Evaluation of Impedance of Perforates with Grazing Flow," *J. Sound Vib.*, **108**, 283–295 (1986).
58. M. L. Munjal, B. K. Behera, and P. T. Thawani, "Transfer Matrix Model for the Reverse-Flow, Three-Duct, Open End Perforated Element Muffler," *Appl. Acoust.*, **54**, 229–238 (1998).
59. M. L. Munjal, B. K. Behera, and P. T. Thawani, "An Analytical Model of the Reverse Flow, Open End, Extended Perforated Element Muffler," *Int. J. Acoust. Vib.*, **2**, 59–62 (1997).
60. M. L. Munjal, "Analysis of a Flush-Tube Three-Pass Perforated Element Muffler by Means of Transfer Matrices," *Int. J. Acoust. Vib.*, **2**, 63–68 (1997).
61. M. L. Munjal, "Analysis of Extended-Tube Three-Pass Perforated Element Muffler by Means of Transfer Matrices," in C. H. Hansen (Ed.), *Proceedings of ICSV-5*,

International Conference on Sound and Vibration, Adelaide, Australia, International Institute of Acoustics and Vibration, Auburn, AL, 1997.

62. A. Selamet, V. Easwaran, J. M. Novak, and R. A. Kach, "Wave Attenuation in Catalytical Converters: Reactive versus Dissipative Effects," *J. Acoust. Soc. Am.*, **103**, 935–943 (1998).
63. M. L. Munjal and P. T. Thawani, "Effect of Protective Layer on the Performance of Absorptive Ducts," *Noise Control Eng. J.*, **45**, 14–18 (1997).
64. M. E. Delany and B. N. Bazley, "Acoustical Characteristics of Fibrous Absorbent Materials," *Appl. Acoust.*, **3**, 106–116 (1970).
65. F. P. Mechel, "Extension to Low Frequencies of the Formulae of Delany and Bazley for Absorbing Materials" (in German), *Acustica*, **35**, 210–213 (1976).
66. V. Singhal and M. L. Munjal, "Prediction of the Acoustic Performance of Flexible Bellows Incorporating the Convective Effect of Incompressible Mean Flow," *Int. J. Acoust. Vib.*, **4**, 181–188 (1999).
67. A Selamet, N. S. Dickey, and J. M. Novak, "The Herchel–Quincke Tube: A Theoretical, Computational, and Experimental Investigation," *J. Acoust Soc. Am.*, **96**, 3177–3199 (1994).
68. M. L. Munjal and B. Venkatesham, "Analysis and Design of an Annular Airgap Lined Duct for Hot Exhaust Systems," in M. L. Munjal (Ed.), *IUTAM Symposium on Designing for Quietness*, Kluwer, Dordrecht, 2002.
69. M. O. Wu, "Micro-Perforated Panels for Duct Silencing," *Noise Control Eng. J.*, **45**, 69–77 (1997).
70. P. O. A. L. Davies, "Plane Acoustic Wave Propagation in Hot Gas Flows," *J. Sound Vib.*, **122**(2), 389–392 (1998).
71. R. A. Scott, "The Propagation of Sound between Walls of Porous Material," *Proc. Phys. Soc. Lond.*, **58**, 338–368 (1946).
72. U. J. Kurze and I. L. Ver, "Sound Attenuation in Ducts Lined with Non-Isotropic Material," *J. Sound Vib.*, **24**, 177–187 (1972).
73. F. P. Mechel, "Explicit Formulas of Sound Attenuation in Lined Rectangular Ducts" (in German), *Acustica*, **34**, 289–305 (1976).
74. F. P. Mechel, "Evaluation of Circular Silencers" (in German), *Acustica*, **35**, 179–189 (1996).
75. F. P. Mechel, *Schallabsorber* (Sound Absorbers), Vol. III, *Anwendungen* (Applications), S. Hirzel, Stuttgart 1998.
76. M. L. Munjal, "Analysis and Design of Pod Silencers," *J. Sound Vib.*, **262**(3), 497–507 (2003).
77. U. J. Kurze and I. L. Ver, "Sound Silencing Method and Apparatus," U.S. Patent No. 3,738,448, June 12, 1973.
78. ISO 14163-1998(E), "Acoustics—Guidelines for Noise Control by Silencers," International Organization for Standardization, Geneva, Switzerland, 1998.
79. I. D. Idel'chik, *Handbook of Hydrodynamic Resistance, Coefficients of Local Resistance and of Friction*, translation from Russian by the Israel Program for Scientific Translations, Jerusalem, 1966 (U. S. Development of Commerce, Nat. Tech. Inf. Service AECTR-6630).

80. I. L. Ver and E. J. Wood, *Induced Draft Fan Noise Control*, Vol. 1: *Design Guide*, Vol. 2: *Technical Report*, Research Report EP 82-15, Empire State Electric Energy Research Corporation, New York January 1984.
81. S. N. Panigrahi and M. L. Munjal, "Combination Mufflers—A Parametric Study," *Noise Control Eng. J.*, Submitted for publication.

CHAPTER 10

Sound Generation

ISTVÁN L. VÉR

Consultant in Acoustics, Noise, and Vibration Control
Stow, Massachusetts

Acoustical engineers can be grouped into two categories: those who try to *minimize* the efficiency of sound radiation and are called *noise control engineers* and those who try to *maximize* it and are called *audio engineers*. This book addresses the first group exclusively.

The main duty of noise control engineers is to know how to reduce, in a cost-effective manner, the noise produced by equipment at the location of an observer. The noise reduction can be achieved (1) *at the source*; (2) *along the propagation path* by building extensive barriers between the source and receiver, installing silencers, and so on, as discussed in Chapters 5 and 9; and (3) *at the receiver* by enclosing it, as discussed in Chapter 12, or by creating a limited "zone of silence" around it by active noise control, as described in Chapter 18.

The most effective, and by far the least expensive, noise control can be achieved at the source by reducing its sound radiation efficiency. A reduction of the efficiency of noise generation of the source results in a commensurate *reduction of the noise at all observer locations*. In comparison, the erection of barriers, enclosing the receiver, and creating a localized "zone of silence" at the receiver are *effective only in limited spatial regions*. Putting silencers on the noisy equipment is cumbersome and usually increases the size and weight and reduces the mechanical efficiency of the equipment. The last two measures are often referred to as the *brute-force* methods.

The reduction of the efficiency of noise radiation at the source can be achieved passively by changing the shape of the body if its vibration velocity is given and by changing both the shape and mass of the body if the vibratory force acting on it is given. Reducing the efficiency of sound radiation by active means is generally accomplished by placing a secondary sound source of the same volume displacement magnitude but opposite phase in the immediate vicinity of the body, as discussed in detail in Chapter 18, or by a combination of these passive and active measures.

If constructional changes are possible, always the passive measures should be implemented first, even if the needed additional reduction will be achieved by active means. Even if they do not achieve all the needed noise reduction, passive noise control measures reduce the demand on the power-handling capability of the noise-canceling loudspeakers. In addition, passive noise control measures remain effective in case the active control fails. The most desirable, but also the most difficult to achieve, passive noise control measures are those which require constructional changes of the equipment. Not infrequently, the same constructional changes that reduce the efficiency of sound radiation also may improve the mechanical efficiency of the equipment. The primary purpose of every machine is to perform a specific, usually mechanical, function. The noise is an unwanted by-product. The reduction of the efficiency of sound radiation at the source must always be accomplished without interfering with the primary function of the equipment. As we will show later, the reduction in the efficiency of sound radiation of any noise source is always achieved by reducing the force or forces that act on the surrounding fluid.

10.1 BASICS OF SOUND RADIATION

This chapter deals with the sound radiation of small pulsating and oscillating rigid bodies. Throughout this chapter the adjective *small* means that the dimensions of the body are small *compared with the acoustical wavelength*. Sound radiation of large bodies is treated in Chapter 11. An exhaustive treatment of the sound radiation of all types of bodies is given in reference 1.

Historical Overview

Technical acoustics is a branch of applied physics. All acoustical phenomena can be derived from Newton's basic laws. During the early part of the last century the science of technical acoustics has been developed mainly by physicists with a strong background in electromagnetism or by electronics engineers. The reason for this is that only they had the mathematical background to deal with dynamic phenomena in general and, most importantly, with the wave equation. In those days, the education of mechanical engineers was almost exclusively in static deformation of structures and *slow* phenomena in hydrodynamics. Physicists often describe the acoustical phenomena by mathematical formalisms that facilitate the mathematical analyses. Unfortunately, these formalisms, such as *monopoles, dipoles, quadrupoles, "equivalent electric circuits," and "short circuiting,"* were often not familiar to mechanical engineers. This built artificial barriers for the mechanical engineers which have been overcome only in the last few decades due to the dramatic increase in the education of mechanical engineers in dynamic phenomena.

This chapter attempts to explain the important phenomena of sound generation in a form, the author believes, that might have been done if the theory of sound generation had been developed by mechanical engineers. As we will show in the remainder of the chapter, the sound radiation phenomena can be fully described without knowing anything about monopoles, dipoles, quadrupoles, and equivalent electric circuits.

The added advantage of characterizing the sound sources by the force and the moment they exert on the fluid rather than assigning abstract descriptors such as *equivalent point sound source, dipole strength,* and *quadrupole strength* means that such characterization gives a better understanding of the physical phenomena involved and identifies the actual physical parameters that control all types of sound generation processes.

Qualitative Description of Sound Radiation of Small Rigid Bodies

Small rigid bodies oscillating in an unbounded fluid experience three types of reaction forces; (1) inertia force needed to accelerate the fluid to move out of the way of the body, (2) force to compress the fluid, (3) friction forces owing to the viscosity of the fluid.

The inertia force, which is by far the largest of them, is 90° out of phase with the velocity of the body. The compressive force is in phase with the velocity and is much smaller than the inertia force. However, it has to be considered because it determines the sound radiation. The friction force is usually small enough compared with the two other components that it can be neglected by assuming that the fluid has no viscosity.

Sound is generated by phenomena that cause a localized compression of the fluid (gases or liquids). This chapter deals with the most common sources of sound generated by pulsation and oscillatory motion of small rigid bodies and by pointlike forces and moments acting on the fluid.

Anyone who has operated a bicycle pump can attest to it that it takes considerable force to maintain a repetitive pumping motion of the piston when the valve is closed. The compression of the air in the closed cavity generates a large reaction force that opposes the motion of the piston. The opposing force depends only on the magnitude of the stroke and does not depend on the rapidity of the pumping.

It takes considerably less force to perform the same repetitive pumping motion when the valve is open and the hose is not connected to the tire. The force that resists the stroke in this case is the inertia force needed to push the air mass (stroke times surface area of the piston times the density of the air) through the open valve. The inertia force is proportional to the acceleration (i.e., the rapidity of the pumping motion) of this mass. The reaction force is very small if the rate of repetition is low and increases with increasing repetition rate. At sufficiently high repetition rate it becomes harder to accelerate the air mass that must be pushed through the open valve during increasingly shorter time periods than to compress the air in the pump's cavity. In this case the force needed to operate the leaky pump approaches that needed to operate the pump with the valve closed.

As we will see, similar behavior is observed in the sound radiation of small rigid bodies where the surrounding fluid is compressed in earnest only when the force needed to move the fluid in the vicinity of the pulsating or oscillating body out of the way becomes the same order of magnitude as that required to compress it.

Pulsating Small Rigid Bodies. If a small body, exemplified by a pulsating sphere, operates at low frequencies where the wavelength of the sound is large compared with the acoustical wavelength, the pressure has two components. One is 90° out of phase with the velocity of the pulsating surface and a much smaller component is in phase with it. The former component is owing to the inertia of the surrounding fluid that is pushed into a larger spherical area during the outward motion of the pulsating surface and pulled back during the inward movement without much compression. The latter component of the pressure, which is in phase with the surface velocity, is owing to the compression of the surrounding fluid.

The force needed to overcome the inertia of this back-and-forth sloshing fluid volume increases with increasing frequency and so does the in-phase component of the surface pressure. Above a frequency where the wavelength becomes smaller than six times the radius of the sphere, it becomes easier to compress the fluid than to accelerate the fluid volume and the pulsating sphere becomes an efficient radiator of sound. Both the in-phase and 90° out-of-phase components of the pressure are evenly distributed over the surface of the sphere and the pulsating sphere radiates sound omnidirectionally.

At low frequencies not only the pulsating sphere but also all pulsating small bodies have an omnidirectional sound-radiating pattern and both the far-field sound pressure and radiated sound power depend only on the net volume flux and the frequency irrespective of how the vibration pattern is distributed over their surface. Because of these unique properties, pulsating small bodies are referred to as monopoles.

Oscillating Small Rigid Bodies. In the case of an oscillating rigid body, exemplified by an oscillating sphere, the fluid pushed aside by the forward-moving half of the sphere is "sucked in" by the void created by the receding half of the sphere. The fluid moves back and forth around the sphere between the two poles. The velocity of the fluid is highest near the surface of the sphere and decreases exponentially with increasing radial distance. This exponentially decreasing velocity field is referred to as the near field. The kinetic energy flux of the near field depends on the geometry of the body, the direction of the oscillatory motion, and the density of the fluid surrounding the body. The quantity *added mass/fluid density* is a property of the body and its motion. It is referred to in the acoustical literature as the *added volume*. In the hydrodynamic literature the *added mass coefficient* is defined as the ratio of the added volume, V_{ad}, and volume of the body, V_b.

Push–pull action between the poles (located in the direction of the oscillatory motion) makes it easy to move the fluid back and forth and the surface of the oscillating small rigid sphere, for the same surface velocity, experiences much smaller reaction pressure than the pulsating sphere and radiates substantially less sound. The magnitude of the reaction pressure on the surface of the oscillating sphere has its maxima at the poles where the radial velocity has its maxima and zero at the equator where the radial velocity is zero. Consequently, the sound radiation pattern is maximum in the direction of the oscillatory motion and zero in the direction perpendicular to it. This behavior is not restricted to the oscillating sphere but holds for small oscillating rigid bodies of any shape. In analogy to the similar radiation patter of the magnetic field caused by an oscillating charge, oscillating small rigid bodies are referred to as dipole sound sources.

The net oscillatory force exerted on the fluid is obtained by integrating the pressure distribution over the surface of the sphere. The force points in the direction of the oscillatory motion. As we will show later, with respect to sound radiation, a small, oscillating rigid body is equivalent to a pointlike force (i.e., pressure exerted by a small surface) acting on the fluid. The radiated sound power is obtained as the product of the body's velocity and the component of the net reaction force that is in phase with the velocity.

The distribution of the reaction pressure on the surface is known only for a few bodies. Consequently, the net oscillatory force they exert on the fluid (and consequently the radiated sound field) cannot be obtained directly. As we will show later, the force exerted on the fluid by such bodies—and consequently also their sound radiation pattern—can be predicted on the bases of the oscillatory velocity and geometry of the body and its added mass in the direction of the oscillatory motion. The latter can be found frequently in the hydrodynamic literature or can be determined experimentally by measuring the resonance frequency of the body supported on a spring; first in a vacuum then immersed in a fluid (preferably a liquid).

Moment Excitation: Lateral Quadrupole. Two closely spaced identical small rigid bodies oscillating in the same direction but 180° out of phase, or the equivalent two closely spaced parallel pointlike forces acting on the fluid 180° out of phase, are referred to as a *lateral quadrupole*. The forces constituting the moment are frequently due to shear strain. Both of these descriptions are helpful in understanding the sound radiation properties.

If we consider the representation of the two closely spaced small rigid bodies oscillating in opposite directions, it becomes apparent that the fluid pushed aside by the pole of one of the bodies does not need to be moved around to the opposite pole but is easily moved into the void created by the receding pole of the second body. The reaction pressure on the surface of each of the bodies, and consequently the sound field they produce, is substantially smaller than would result when only one of the bodies would oscillate.

If we consider the model of two parallel closely spaced pointlike forces, we realize that the lateral quadrupole represents excitation of the fluid by a moment.

The source strength is characterized by the moment, regardless of whether the moment is constituted by large forces spaced very close to each other or by smaller forces spaced at a larger distance apart, provided that the distance is still much smaller than the wavelength.

The sound radiation pattern of a lateral quadrupole is zero in two planes. The first of this is perpendicular to the plane defined by the two parallel forces and cuts the plane of the forces halfway between them. All points located in this plane have an equal distance from the two bodies moving in opposite directions and their contribution to the sound field cancels each other.[2] The second plane of zero sound pressure is perpendicular to the direction of the motion of the oscillating bodies and cuts through their center. The sound pressure is zero at all points on this plane because the two oscillating bodies constituting the lateral dipole have zero radial velocity in these directions.

The sound radiation pattern has maxima in two planes. Both of these planes cut the zero planes at 45° angles. In two dimensions the radiation pattern resembles an old-fashioned, four-bladed propeller where the four maxima are represented by the four blades and the minima by the void between the blades.

If the two opposing forces are of different magnitude, the sound radiation pattern is the superposition of the quadrupole radiation pattern associated with a moment constituted by two opposing forces having the same magnitude as the smaller force and a dipole pattern associated with a single pointlike force that equals the difference between the two forces.

Because the maxima of the dipole pattern "fill" the zero planes of the quadrupole pattern, the resulting radiation pattern has no zero value in any direction.

Sound Excitation by Two Opposing Forces Aligned Along a Line: Longitudinal Quadrupole. If two equal-magnitude but opposing dynamic forces are placed on a line a small distance apart (or the equivalent of two identical small rigid bodies are oscillating 180° out of phase), the sound radiation pattern resembles that of a single pointlike force. However, the two maximum lobes, pointing in the direction of the forces, are much narrower and the radiated sound power is much smaller than if only one of the forces acted on the fluid. In analogy to the directivity pattern of the magnetic field generated by two closely spaced charges oscillating in the opposite direction, this type of sound source is referred to as a longitudinal quadrupole. This type of radiation pattern occurs when a small rigid body oscillates in water near to and perpendicular to the water–air interface. In this case the mirror image represents the identical second body that oscillates 180° out of phase.

If the two opposing forces are not equal, then the resulting radiation pattern is the superposition of the pattern of a longitudinal quadrupole and a dipole. Because both radiation patterns have zero value in a plane that is perpendicular to the forces and cuts through the center of the force pair, the resulting radiation pattern has zero value in this plane. The contribution of the dipole component widens the two maximum lobes.

Radiated Sound Power. The sound power radiated by all of the above-discussed sound sources can also be determined by integrating the intensity $p^2_{\text{rms}}(r, \vartheta, \theta)/\rho_0 c_0$ over a large radius ($kr \gg 1$) sphere centered at the acoustical center of the source, where $p^2_{\text{rms}}(r)$ is the mean-square value of the sound pressure at distance r in the direction designated by the angles ϑ and θ.

Acoustical Parameters of Sound Radiation

This section contains a brief introductory discussion of the acoustical parameters of fluids, including the speed of sound, density, and plane-wave acoustical impedance.

Propagation Speed of Sound in Fluids. The molecules of fluids and gases in equilibrium undertake a random motion with equal probability of direction, c_t, and the propagating speed in a stationary fluid, c_0, given by[2]

$$c_0 = c_t\sqrt{\gamma} = \sqrt{\frac{\gamma RT}{M}} \quad \text{m/s} \tag{10.1}$$

where $\gamma = c_p/c_v$ is the specific heat ratio with $\gamma \approx 1.4$ for air and $\gamma \approx 1.3$ for steam, R is the universal gas constant ($R = 8.9$ J/K), T is the absolute temperature in degrees Kelvin (K), (0 K = −273°C), and M is the molar mass equal to 0.029 kg/mole for air and 0.018 kg/mole for steam. For air Eq. (10.1) yields

$$c_0 = 20.02\sqrt{T\,(\text{K})} = 342.6\sqrt{\frac{T\,(\text{K})}{293}} = 342.6\sqrt{\frac{T\,(^\circ\text{C}) + 273}{293}} \quad \text{m/s} \tag{10.2}$$

For air at 20°C = 68°F = 293 K the propagating speed is $c_0 = 342.6$ m/s, at which a sound wave travels in air. The individual molecules collide with each other in a random fashion exchanging momentum with each other. If they impinge on a solid impervious wall, they rebound back from it. Sound is generated when dynamic forces acting on the fluid superimpose a very small but organized dynamic velocity on the very large random velocity of the molecules. The word "organized" means that in the case of periodic motion the superimposed velocity has a specific direction and a specific frequency and in the case of random motion it has a direction and its frequency composition can be described either by its power spectrum or autocorrelation function, as described in Chapter 3. In a stationary fluid the kinetic energy of the molecules acquired through the excitation causes compression and the compression then accelerates the molecules. In a stationary fluid the kinetic energy and potential energy are in balance in any small volume of the fluid. If the sound source acts on a moving media, the kinetic energy depends on the velocity and the direction of the fluid movement. In this chapter we will deal with stationary media only. Sound radiation in moving media is covered in Chapter 15.

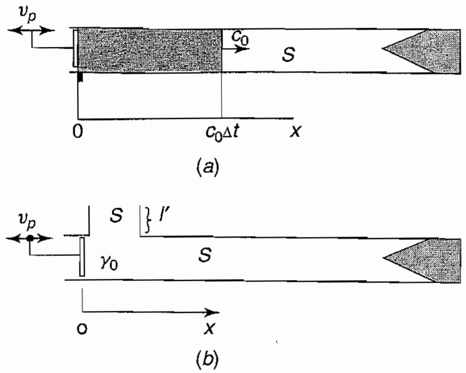

FIGURE 10.1 Oscillating plane rigid piston radiating sound into a small-diameter rigid pipe that is either infinitely long or anechoically terminated: (*a*) Hypothetical experiment to determine the plane wave impedance of fluids, No side branch; (*b*) open side branch of the same cross section area S as the face area of the piston and effective length l'.

The superimposed organized particle velocity of sound we experience is usually in the range 10^{-8} m/s (corresponding to a sound pressure level of 14 dB re 20 μPa) to 10^{-4} m/s (corresponding to 94 dB re 20 μPa).

Plane-Wave Impedance. The plane-wave impedance can be obtained by performing a hypothetical experiment similar to that suggested by Ingard,[2] as shown in Fig. 10.1*a*.

Hypothetical Experiment 1. Assume, as sketched in Fig. 10.1*a*, that a plane, rigid piston of surface area S is located on the left end of a small-diameter (much smaller than the wavelength), infinitely long or anechoically terminated tube with rigid walls filled with a fluid of density ρ_0 and speed of sound c_0. If the piston moves to the right with a constant speed of v_p, the face of the piston experiences a reaction pressure. To determine the plane-wave impedance defined as $Z_0 = p(x = 0)/v_p$, we need to find that particular pressure $p(x = 0)$ at the piston–fluid interface (at position $x = 0$) that results from the piston velocity v_p. At the time Δt, the shaded volume of the fluid on the left, $S_0 c_0 \,\Delta t$, has acquired the particle velocity v_0 and the rest of the fluid on the right is motionless. The momentum M acquired by the fluid during the time Δt is then $M = v_0 \rho S_0 c_0 \,\Delta t$. According to Newton's law the force on the interface is

$$F(x = 0) = Sp(x = 0) = \frac{d}{dt} M \,\Delta t = v_p \rho_0 S c_0 \quad \text{N} \qquad (10.3)$$

yielding the plane wave impedance Z_0,

$$Z_0 \equiv \frac{p(x = 0)}{v_p} = \rho_0 c_0 \quad \text{N} \cdot \text{s/m}^3 \qquad (10.4)$$

Performing the same thought experiment on a solid bar yields the plane-wave impedance of a solid as

$$Z_0 \approx \rho_M c_L \quad \text{N} \cdot \text{s/m}^3 \qquad (10.5)$$

where c_L = propagation speed of longitudinal waves in bar, $(E/\rho)^{1/2}$ m/s
ρ_M = density of solid material, kg/m^3
E = Young's modulus, N/m^2

If the piston oscillates with a velocity of the form $v_p\, e^{j\omega t}$, starting at $t = 0$, the sound pressure in the tube filled with a fluid (air) is

$$p(x, t) = v_p \rho_0 c_0 \, e^{-jkx} \, e^{j\omega t} \quad \text{N/m}^2 \qquad (10.6)$$

and the sound power radiated by the piston, W_{rad}, is

$$W_{\text{rad}} = \tfrac{1}{2} \hat{v}_p \,\text{Re}[\hat{p}_p(x = 0)]\, S \rho_0 c_0 \quad \text{N} \cdot \text{m/s} \qquad (10.7)$$

where in Eqs. (10.6) and (10.7) $\omega = 2\pi f$, f is the frequency in hertz, $k = \omega/c_0$ is the wavenumber, and the hat above the symbol signifies the peak value. Observing Eqs. (10.6) and (10.7), note that the higher is the product of density and speed of sound, the larger are the sound pressure and the radiated power that a given excitation velocity v will generate.

For example, when plane waves are generated in a column of air, water, and steel, an enforced velocity v = 1 mm/s = 10^{-3} m/s will produce the sound pressure p, sound pressure level SPL (in dB re 2×10^{-5} N/m^2) listed below. Assuming that the cross-sectional area is 10^{-4} m^2, we also can predict the radiated sound power W_{rad} in watts:

Material	ρ (kg/m^3)	c (m/s)	p (N/m^2)	SPL (dB)	W_{rad} (W)
Air inside rigid tube	1.21	344	0.42	86	4.2×10^{-8}
Water inside rigid tube	998	1481	1478	157	1.5×10^{-4}
Steel bar in air	7700	5050	3.9×10^4	186	3.9×10^{-3}

In plane waves all of the volume displacement produced by the vibratory excitation at the interface is converted into compression and the resulting sound pressure at the interface is in phase with the excitation velocity. In this case, the sound radiation is that which is the maximum achievable. In other situations, where the volume displaced by the vibratory excitation is mainly used for "pushing aside" rather compressing the fluid, the resulting sound pressure at the interface is much smaller. That is, the pressure has only a small component that is in phase with the vibration velocity of the excitation, which is the reason for the inefficient low-frequency sound radiation of small bodies. For such small sound sources, maintaining the same velocity with increasing frequency means that it is increasingly more difficult to push aside the fluid. When it becomes much easier to compress the fluid than to push it aside, the pressure produced at the interface reaches its maximum and is nearly in phase with the excitation velocity and the efficiency of sound radiation approaches that of a plane wave. The remaining very small but finite phase difference is essential because it determines the radius of curvature of the wave front.

Piston Generating Sound in Rigid Tube with Open Side Branch. To illustrate the effect in a quantitative manner that the efficiency of sound generation is decreased if it is easier to push the fluid aside than to compress it, consider the situation shown in Fig. 10.1*b*. It differs from the situation depicted in Fig. 10.1*a* by the addition of an open side branch to the pipe in the immediate vicinity of the piston. Let assume that the piston, the main pipe, and the side-branch pipe all have the same cross-sectional area S and that the effective length of the open-ended side branch is l'. The mass of the air in the side branch is $\rho_0 S l'$. The force needed to push this mass aside, $j\omega v_p \rho_0 S l'$, is smaller than the force $v_p \rho_0 c_0 S$ needed to compress the fluid, and the presence of the open side branch will reduce the ability of the piston to exert force on the fluid.

The sound pressure that the oscillating piston with peak velocity amplitude $\hat{v}_p$ produces is given by

$$\hat{p}(x=0) = \hat{v}_p \frac{1}{1/(j\omega\rho_0 l') + 1/(\rho_0 c_0)} \quad \text{N/m}^2 \tag{10.8}$$

Separating the real and imaginary parts in Eq. (10.7) yields

$$\hat{p}(x=0) = \hat{v}_p \frac{(\omega\rho_0 l')^2 \rho_0 c_0 + (j\omega\rho_0 l')(\rho_0 c_0)^2}{(\rho_0 c_0)^2 + (\omega\rho_0 l')^2} \quad \text{N/m}^2 \tag{10.9}$$

At low frequencies where $\omega\rho_0 l' \ll \rho_0 c_0$, Eq. (10.8) yields

$$\hat{p}(x=0) \approx \hat{v}_p(j\omega\rho_0 l') \quad \text{N/m}^2 \tag{10.10}$$

At high frequencies where $\omega\rho_0 l' \gg \rho_0 c_0$, Eq. (10.8) yields

$$\hat{p} \approx \hat{v}_p \rho_0 c_0 \quad \text{N/m}^2 \tag{10.11}$$

Inspecting Eqs. (10.9) and (10.10), note that the sound pressure produced by the piston is small, is nearly 90° out of phase of the velocity of the piston, and increases linearly the frequency ω. Using the vocabulary of electric engineers, the low impedance of the mass in the open side branch, $j\omega\rho_0 l'$, "shunts" $\rho_0 c_0$, the plane-wave impedance of the fluid in the tube.

More specifically at low frequencies most of the volume displaced by the oscillating piston flows into the open side branch, where it encounters little "resistance," and only a very small portion flows into the main tube. Consequently,

the magnitude of the reaction force exerted on the piston owing to the presence of both the side branch and the main pipe is only a minute amount larger than the small force needed to keep the fluid mass in the side branch oscillating. The same small force is exerted on the fluid in the main pipe. This force is substantially smaller than it would be if the entrance of the side branch were closed. Accordingly, the sound pressure in the main tube is also substantially smaller.

The sound power that the piston is radiating into the main tube is the product of the velocity of the piston and the small component of the reaction force that is in phase with the velocity and is given by

$$W_{\text{rad}} = \tfrac{1}{2}\hat{v}_p \operatorname{Re}[\hat{p}(x=0)]\, S = \tfrac{1}{2}\hat{v}_p^2 S \frac{\rho_0 c_0 (\omega\rho_0 l')^2}{(\rho_0 c_0)^2 + (\omega\rho_0 l')^2} \quad \text{N}\cdot\text{m/s} \tag{10.12}$$

The hat above the variables indicates peak amplitude. If the rms value of the piston' velocity were used, the factor $\frac{1}{2}$ would be omitted in Eq. (10.12).

Inspecting Eq. (10.12), note that at low frequencies where $\omega\rho_0 l' \ll \rho_0 c_0$, the radiated sound power approaches zero with decreasing frequency. At high frequencies where $\omega\rho_0 l' \gg \rho_0 c_0$, the radiated sounds power becomes independent of frequency and approaches that obtained in Eq. (10.7) for the pipe without an open side branch.

Pipe with Open Side Branch Representing Sound Radiation of Pulsating Sphere. Following the qualitative suggestion by Cremer and Hubert,[3] we are assigning the specific values for S and l' in Eqs. (10.9) and (10.12), namely, $S = 4\pi a^2$, $\hat{v}_p = \hat{v}_s$, and $l' = a$, and considering that the wavenumber $k = \omega/c_0$ and $\hat{v}_p S = \hat{v}_s 4\pi a^2 = \hat{q}$ is the peak volume velocity of our sound source, Eq. (10.9) yields the well-known[3] formula for the peak value of the sound pressure on the surface of the sphere:

$$\hat{p}(a) = \hat{v}_s \frac{j\omega\rho_0 a}{1 + jka} \quad \text{N/m}^2 \tag{10.13}$$

Also note that the volume of fluid in the side branch is $V_{\text{ad}} = 4\pi a^3$ and the added mass of the fluid is $M_{\text{ad}} = 4\pi a^3 \rho_0$. For a pulsating sphere the volume V_{ad} is three times the volume of the sphere and is called the *added volume* in the acoustical literature and in M_{ad} is called the *added mass*. The added mass plays a central role in the sound radiation of small pulsating and oscillating rigid bodies. The added mass is a measure of the ability of these bodies to exert a dynamic force on the surrounding fluid.

Substituting the same values into Eq. (10.12) yields the well-known formula[4] for the sound power radiated by the a pulsating sphere of radius a and peak surface velocity $\hat{v}_s$:

$$W_{\text{rad}} = \hat{v}_s^2 4\pi a^2 \left(\frac{\rho_0 c_0}{2}\right) \frac{(ka)^2}{1 + (ka)^2} = \hat{q}^2 \left(\frac{\rho_0 c_0}{2}\right) \frac{(ka)^2}{1 + (ka)^2} \quad \text{N/m}^2 \tag{10.14}$$

Sound Radiation by Volume-Displacing Sound Sources

To describe the sound radiation of small volume-displacing sound sources, we take the unusual approach of starting with the case where the source operates in the most restrained environment and then gradually weakening the restraints to arrive at the unrestrained case where the sound source operates in an undisturbed infinite fluid.

On the top of Figure 10.2 is shown the starting point where the volume-displacing sound source is represented by a piston that vibrates with an axial velocity v_p in the mouth of a rigid linear horn. The horn represents the restraint. The linear horn is a rigid hollow cone with the tip cut off. The cutoff end becomes the mouthpiece of the horn. The diameter of the cross-sectional area of the linear horn increases linearly with increasing distance r from the tip and its cross-sectional area increases with r^2. The cross-sectional area of the horn at its mouth, $l\theta$, is chosen to fit the mouth of a human speaker. The symbol θ is the solid angle (θ equals π for a quarter space, 2π for a half space, and 4π for a full space, as illustrated in Fig. 10.3).

The cross-sectional area at the large end of the horn is chosen to be $S_{\text{End}} \geq \lambda^2 \geq c_0^2/f_{\text{int}}^2$, where f_{int} is the lowest frequency of interest (usually 500 Hz for voice communication) so that practically no sound is reflected from the far end of the horn. If this condition is fulfilled, the use of the linear horn is equivalent to increasing the size of the mouth of the human speaker by the ratio of the end and mouthpiece cross-sectional areas of the horn, as illustrated by the lower sketch in Fig. 10.11.

The cross-sectional area of the horn can be expressed as

$$S(r) = \theta r^2 \quad \text{m}^2 \qquad (10.15)$$

According to Cremer and Hubert,[3] the sound pressure inside the horn as a function of distance from the tip can be expressed as

$$\tilde{p}(r) = \frac{\tilde{v}_p\,(l/r)}{1/(\rho_0 c_0) + 1/(j\omega\rho_0 l)} \quad \text{N/m}^2 \qquad (10.16)$$

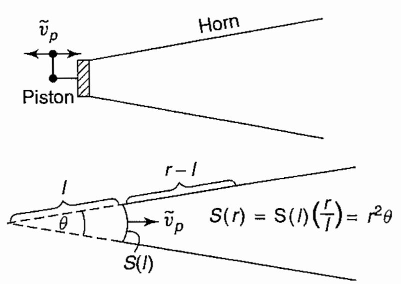

FIGURE 10.2 Vibrating piston sound source driving a linear acoustical horn (see text for explanation of symbols).

where v_p is the vibration velocity of the piston at the mouth of the horn and l is the radial length from the cutoff tip of the cone to the mouthpiece end, as illustrated in Fig. 10.2. Observing Eq. (10.16), note the following:

1. The term $j\omega\rho_0 l$ represents the added mass that is the consequence of the expansion of the cross section, which makes it possible to push the fluid off axis. In the extreme case when $\theta \to 0$ the horn turns into a rigid pipe and the added mass becomes infinite. This means that the near field in the pipe extends to infinity.
2. The sound propagates in the linear horn at all frequencies (which is not the case in an exponential horn, where no sound propagates below its cutoff frequency).
3. At low frequencies when $kl = (\omega/c_0)l \ll 1$ the sound pressure increases linearly with frequency as $p(r) \cong j\omega\rho_0(l^2/r)\tilde{v}_p$.
4. Above the frequency $\omega \geq c_0/l$ the linear horn works at full efficiency and the sound pressure as a function of distance becomes $p(r) \cong v_p(l/r)\rho_0 c_0$.

Considering that the volume velocity at the mouth of the horn is $q = v_p\theta l^2$, the radiated sound power takes the form

$$W_{\text{rad}} = q^2\rho_0 c_0\left(\frac{k^2}{\theta}\right)\frac{1}{1+(kl)^2} = q^2\frac{\rho_0\omega^2}{c_0\theta}\left[\frac{1}{1+\pi(S/\lambda^2)(4\pi/\theta)}\right] \quad \text{N}\cdot\text{m/s} \qquad (10.17)$$

Figure 10.3 shows what happens if we gradually weaken the restraint by increasing the solid angle θ from zero to 4π. In the extreme case, when the solid angle

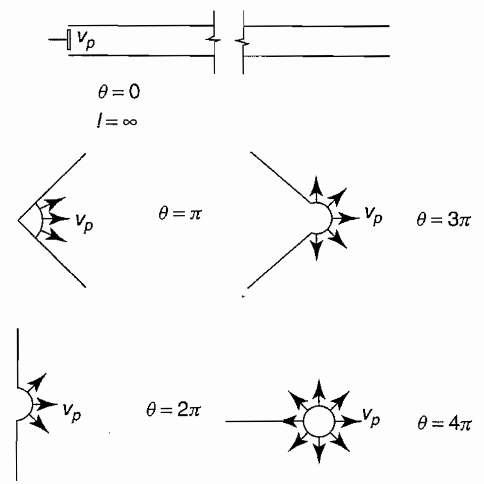

FIGURE 10.3 Increasing the solid angle θ of the horn; Top left: $\theta = 0$, pipe. Middle left: $\theta = \pi$, quarter space. Bottom left: $\theta = 2\pi$, half space. Middle right: $\theta = 3\pi$, three-quarter space. Bottom right: pulsating sphere in unbounded space.

of the horn θ is zero and tip length l approaches infinity, the horn becomes a cylindrical pipe, as shown in the top sketch. In this extreme case the sound pressure in the pipe is

$$p(r,t) = (q/S)\, e^{-jkr}\, e^{j\omega t} \quad \text{N/m}^2 \tag{10.18}$$

indicating that theoretically the amplitude of the sound pressure would not decrease with distance. A practical use of this attribute is shown on the left in Fig. 10.11.

Consider now the effect of increasing the solid angle of the horn from $\theta = 0$ by an infinitesimally small $\Delta\theta$. Consequence of this is a phenomenological change in the behavior of the sound field, namely the sound pressure approaches zero at an infinitely large axial distance while for the pipe it would remain just as high as on the surface of the piston. Such quantum jumps are not allowed in Newtonian physics. The change in the behavior of the sound field is rapid but continuous. In the constant cross-sectional area of the pipe the near field extends infinitely. In the linear horn with infinitesimally small solid angle the near field extends nearly infinitely. Since in practice there are only finite-length pipes and horns, a microphone near the end of the anechoically terminated finite-length horn with an infinitesimally small solid angle would practically sense the same sound pressure as it would in a pipe.

Let us now explore the behavior of our linear horn given in Eq. (10.17) at solid angles of practical interest. Equation (10.17) yields

$$W_{\text{rad}} = q^2(\rho_0 c_0)\left(\frac{k^2}{4\pi}\right) n \quad \text{N}\cdot\text{m/sec} \tag{10.19}$$

where $n = 1$ when the volume source is located in an infinite, undisturbed fluid;
$n = 2$ when the volume source is flash mounted in an infinite, hard, flat baffle and radiates into a half space;
$n = 4$ when the sound source is located in a two-dimensional corner and radiates into a quarter space; and
$n = 8$ when located in a three-dimensional corner and radiating into an eighth space.

If there is a net volume displacement (as far as the far-field sound pressure and the radiated sound power are concerned), the specific distribution of the velocity over the vibrating surface is unimportant. This is because the non–volume-displacing vibration patterns (dipole, quadrupole, etc.) radiate low-frequency sound much less efficiently than volume-displacing patterns.

Figure 10.4 shows volume sources with different distributions of the vibration velocity but having the same net volume velocity. The solid and dashed lines represent the location of the vibrating surface at two time instances. The solid line shows the maximum and the dashed line the minimum volume displacement positions, respectively.

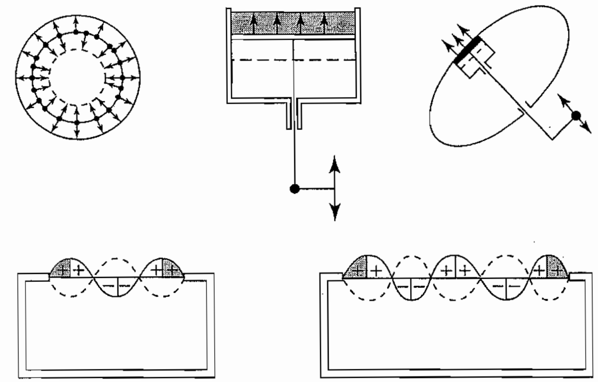

FIGURE 10.4 Small volume sources with different distributions of the vibration velocity but the same net volume velocity.

Limits of Maximum Achievable Volume Velocity of Pulsating Sphere. The maximum peak volume velocity $\hat{q}_{\max}$ achievable with a small pulsating sphere of volume $V_{\text{sphere}} = 4\pi a^3/3$ is limited by (1) the impossibility of having a larger volume displacement than the volume of the sphere, (2) the desire of not having supersonic surface velocity, and (3) the desire of keeping nonlinear distortion within acceptable limits. These requirements are accounted for in Eq. (10.20) below.

$$\frac{\hat{q}_{\max}}{V_{\text{sphere}}} \le \frac{n}{a/(3c_0) + 1/(12\pi\omega)} \quad \text{s}^{-1} \tag{10.20}$$

where the first summand in the denominator accounts for the first limit, the second for the second limit, and the factor $n \ll 1$ in the numerator for the third limit.

Combining Eqs. (10.19 and (10.20) and solving for $\hat{W}_{\text{rad}}$ yield the maximum peak acoustical power a pulsating sphere of radius a can produce:

$$\begin{aligned} \hat{W}_{\text{rad}}(\max) &\le 2\pi\left(\frac{\rho_0 c_0^3 a^4 k^2 n^2}{\{1 + [3/(12\pi)][1/(ka)]\}^2}\right) \\ &= 2\pi\left(\frac{\rho_0 \omega^2 c_0 a^4 n^2}{1 + [3/(12\pi)][c_0/(\omega a)]}\right) \quad \text{N}\cdot\text{m/s} \end{aligned} \tag{10.21}$$

If we use the pulsating sphere as a loudspeaker to reproduce voice and music, it would be appropriate to choose n in the range of 0.001–0.01 to keep distortion at peak events within tolerable limits.

A dodecahedron-shaped enclosure with a loudspeaker flash mounted on each of the 12 faces of the enclosure is often used to simulate an omnidirectional volume sound source. The top photograph in Fig. 10.5 shows such a special reciprocity transducer[5–7] (loudspeaker) that the author has developed for the NASA

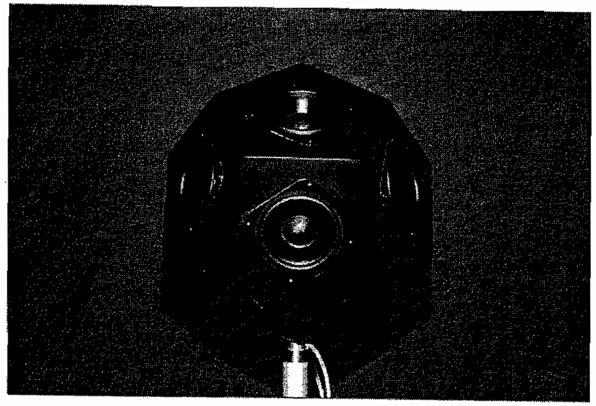

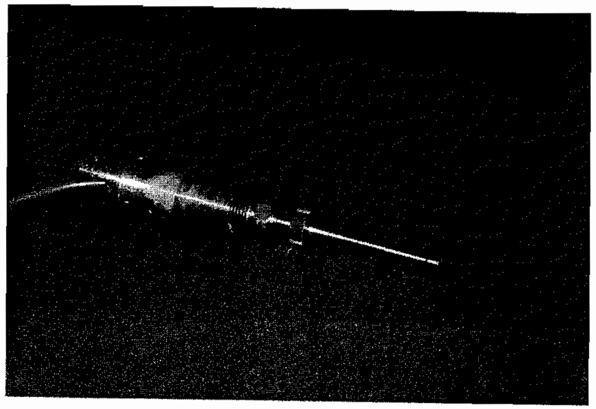

FIGURE 10.5 Photographs of a 4-in. edge-length dodecahedron loudspeaker to simulate a pulsating sphere as an omnidirectional sound source with volume velocity calibration and compensation for acoustical loading. Top: View of the loudspeaker. Bottom: Removed internal $\frac{1}{4}$-in. microphone used for volume velocity calibration and for correcting the acoustical loading when the source is placed in a confined environment.

Langley Research Center. The lower photograph in Fig. 10.5 shows the internal microphone removed from the center of the speaker. The internal microphone is used for volume velocity calibration at low frequencies, for measuring and compensating for the effect of acoustical loading (when the loudspeaker is placed in a small, confined environment such as inside an automobile or in the cockpit of an airplane or placed near a boundary) on the volume velocity, and for measuring nonlinear distortion at low frequencies. The volume velocity calibration of the transducer at mid- and high frequencies was accomplished experimentally by calibrating the transducer as a microphone and utilizing the principle of

reciprocity to obtain the volume velocity as a function of the applied voltage to the loudspeakers.

Example 10.1. determine the minimum radius $a_{\min}$ of a pulsating sphere that should radiate 1 W peak acoustical power at 100 Hz for a distortion parameter $n = 0.005$ and $n = 0.01$.

Solution solving Eq. (10.21) for the radius a yields

$$a_{\min} = \begin{cases} 0.088 \text{ m} \cong 3.5 \text{ in.} & \text{for } n = 0.005 \\ 0.075 \text{ m} \cong 3 \text{ in.} & \text{for } n = 0.01 \end{cases}$$

The investigations above indicates that to radiate a practically meaningful amount of sound power at low frequencies requires a sizable sound source. Consequently, a *point sound source* is a practical impossibility. Furthermore, if the point sound source does not exist, then there are no physically meaningful acoustic dipoles and quadrupoles.

Consequently, it wound be physically more meaningful to substitute the following in the engineering acoustical vocabulary:

small-volume sound source instead of *monopole* or *point source*,
force (acting on the fluid) instead of *dipole*, and
moment (acting on the fluid) instead of *quadrupole*.

Sound Radiation by Non-Volume-Displacing Sound Sources

Parts (a) and (b) in Figure 10.6 show the response of an unbounded fluid to rigid, non-volume-displacing sound sources and parts (c) and (d) that of volume-displacing sound sources. All of the sources are small compared with the acoustical wavelength. The upper row depicts the body and shows the variables that are responsible for the sound generation. The lower row shows, in a schematic manner, how the fluid particles are pushed aside, creating a near field. The symbol $\tilde{v}_b$ represents the dynamic velocity of the body and $\tilde{v}_n$ the particle velocity in the near field. As we will show latter, the kinetic energy flux of this near field, $\omega(0.5\rho_0\tilde{v}_n)$, integrated over the entire fluid volume outside the body represents the added mass, which is a measure for the vibrating body's ability to exert a dynamic force on the fluid ("grab onto it").

In Fig. 10.6 (a) and (b) are examples of non-volume-displacing sound sources and (c) and (d) of volume-displacing sound sources.

In Fig. 10.6a the upper sketch depicts a small rigid body that exhibits random motion in one dimension with a velocity $\tilde{v}_b$ and the lower sketch depicts the direction and path of the particle velocity in the near field at a given moment in time. Note that the fluid "pushed aside" by the forward face of the body is

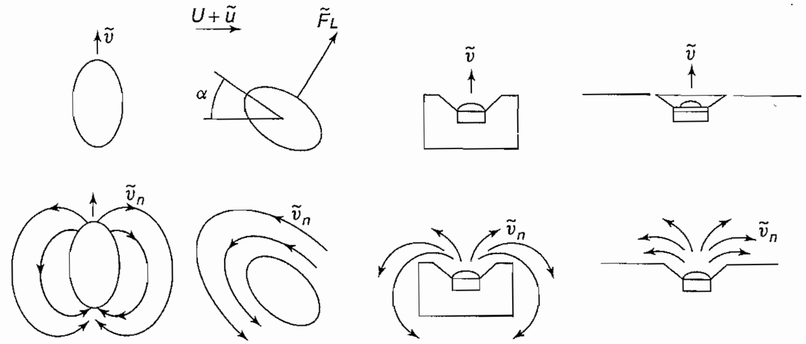

(a) (b) (c) (d)

FIGURE 10.6 Schematic representation of various non-volume-displacing and volume-displacing sound sources and the associated particle velocity in the near field. The symbol $\tilde{v}$ is the vibration velocity of the body and $\tilde{v}_n$ is the particle velocity in the near field. (*a*) Non-volume-displacing sound source; small, rigid body of arbitrary shape moving with a velocity $\tilde{v}$ in an unbounded fluid. (*b*) Stationary, small, rigid body exposed to a flow field of stationary velocity U with a fluctuating component $\tilde{u}$. The angle of attack is α and the resulting dynamic force is $\tilde{F}_L = C_L\left(\frac{1}{2}\rho_0\tilde{u}^2\right)$ and C_L is the lift coefficient of the body. (*c*) Volume-displacing small sound source typified by a loudspeaker mounted on the face of an airtight, rigid enclosure. (*d*) Volume-displacing small sound source flash mounted in an infinitely large, plane, rigid baffle.

"sucked in" by the void created by the receding backward face of the body. This "push–pull" situation results in a very small force. Borrowing from the vocabulary of electronic engineers, this situation is referred to as an "acoustical short circuit."

In Fig. 10.6*b* the upper sketch depicts a small stationary body exposed to a flow field of average velocity U and a fluctuating component $\tilde{u}$. The fluctuating component of the flow produces a fluctuating lift force $\tilde{F}_L$ and a fluctuating drag force $\tilde{F}_D$ (the drag force is not shown to preserve clarity).

In Fig. 10.6*c* the upper sketch shows a loudspeaker mounted on a face of a rigid-walled enclosure. In this case the rigid enclosure prevents the "pulling" by the receding back face of the speaker. Moving aside the fluid by "push" alone, without the help of the "pull," requires more force. More force acting on the fluid translates into higher sound radiation. This is the reason that a small oscillating surface radiates sound more efficiently if its back side is enclosed than the same surface would radiate if the back side is not enclosed.

Sound sources with an enclosed back side displace the same volume in the back side as on the front side. However, the volume displaced by the back side is prevented from "communicating" with the surrounding fluid by the rigid enclosure. If a dynamic force of constant amplitude drives the vibration velocity (which is the case for our loudspeaker shown in the upper sketch in Fig. 10.6*c*),

the obtainable vibration velocity is limited either by the volume stiffness of the air in the enclosure volume or by the mass of the moving part of loudspeaker.

If the enclosure is small compared with the acoustical wavelength, the sound pressure that is produced at the surface of the active part has time to spread around the outside wall of the enclosure during each vibration cycle. As a direct consequence of this, all small volume-displacing sound sources, independent of their geometry, have an omnidirectional sound radiation pattern in the far field.

In Fig. 10.6*d* the upper sketch shows a vibrating surface (in the form of a loudspeaker membrane) flush mounted in a flat infinite rigid baffle. This is a situation that basically resembles the configuration in Fig. 10.6*c*, except that the sound radiation must take place in a hemisphere (half space). Consequently, for the same volume displacement the mean-square sound pressure p^2_{rms} at a given radial distance r will be twice as large as an omnidirectionally radiating source would produce.

Response of Unbounded Fluid to Excitation by Oscillating Small Rigid Body. The dynamic "near-point" force acting on the fluid is always in the form of a dynamic pressure over a small area. By *small*, we mean here and in the rest of this chapter that the body is small compared with the acoustic wavelength ($\lambda = c_0/f$).

The quintessential question is, "How does the organized motion that a small rigid body imparts on the fluid spread out, that is, diffuse in various directions with increasing distance through the molecular collision process.

Diffusion of Sound Energy in Response to Excitation of Fluid by Oscillating Small Rigid Sphere. This section deals with the prediction of the sound radiation pattern and the radiated sound power of small, rigid, oscillating bodies for one-dimensional, harmonic, and random motion.

Harmonic Excitation. The sound field that the harmonic, one-dimensional, oscillatory velocity $v(\omega) = \hat{v}_b\, e^{j\omega t}$ of a small rigid sphere generates is well known and for $r \geq a$ is given by[4]

$$\hat{p}(r,\varphi,\omega) = \hat{v}_b(\omega)\cos(\varphi)\left(\frac{j\omega\rho_0 a^3}{2 - k^2a^2 + j2ka}\right)\left(\frac{1+jkr}{r^2}\right)e^{-jk(r-a)}\,e^{j\omega t}\ \text{N/m}^2 \tag{10.22}$$

where
$\hat{p}(r,\varphi,\omega)$ = peak sound pressure (N/m^2) at distance r (m) in direction ϕ
$\hat{v}_b$ = peak velocity of body in $\phi = 0$ direction, m/s
ω = radian frequency, $2\pi f$ Hz
f = frequency of oscillation, Hz
ρ_0 = density fluid, kg/m^3
a = radius of sphere, m
k = wavenumber, ω/c_0, m^{-1}
c_0 = propagation speed of sound, m/s

It is instructive to evaluate Eq. (10.22) at the two extreme cases, namely on the surface of the sphere ($r = a$) and in the geometric far field where $kr \gg 1$.

On the surface of the oscillating sphere Eq. (10.22) yields the reaction pressure of the fluid

$$\hat{p}(a, \varphi, \omega) = \hat{v}_b(\omega)\cos(\varphi)\, e^{j\omega t}\frac{k^4a^4 + jka(2 + k^2a^2)}{4 + k^4a^4} \quad \text{N/m}^2 \tag{10.23}$$

The radiation impedance of the sphere, defined as the ratio of the surface pressure and the radial velocity $\hat{v}_b\cos(\varphi)$, is

$$Z_{\text{rad}} = \begin{cases} \rho_0 c_0 \left\{\dfrac{k^4a^4 + jka(2 + k^2a^2)}{4 + k^4a^4}\right\} \quad \text{Ns/m}^3 & (10.24\text{a}) \\[2ex] \rho_0 c_0 \left(\dfrac{k^4a^4}{4} + \dfrac{jka}{2}\right) \quad \text{for } ka \ll 1 & (10.24\text{b}) \\[2ex] \rho_0 c_0 \quad \text{for } ka \gg 1 & (10.24\text{c}) \end{cases}$$

The dynamic force exerted on the fluid in the direction of the oscillation, F_{ax}, is obtained by integrating the axial component of the elementary radial force, $dF_x = \cos(\varphi)\, dF_{\text{rad}} = p(a, \varphi)\cos(\varphi)\, dS$ over the surface of the sphere, yielding

$$\hat{F}_{\text{ax}} = \begin{cases} \dfrac{2}{3}\hat{v}_0\rho_0 c_0(2\pi a^2)\dfrac{k^4a^4 + jka(2 + k^2a^2)}{4 + k^4a^4} \quad N & (10.25\text{a}) \\[2ex] j\omega\rho_0\hat{v}_0\dfrac{2\pi a^2}{3} = j\omega\hat{v}_0\rho_0 V_{\text{ad}} \quad \text{for } ka \ll 1 & (10.25\text{b}) \\[2ex] \dfrac{4\pi a^2}{3}\rho_0 c_0\hat{v}_0 \quad \text{for } ka \gg 1 & (10.25\text{c}) \end{cases}$$

where V_{ad} is the added volume and $\rho_0 V_{\text{ad}}$ is the added mass (as we will define latter on). Observing Eq. (10.24b) note that at low frequencies $\hat{F}_{\text{ax}}$ is the force needed to produce the same acceleration as that of the sphere ($j\omega\hat{v}_0$) on a concentrated mass that is equal the added mass.

The radiated sound power, W_{rad}, is obtained as a product of the oscillatory velocity and the component of the axial force that is in-phase with it, yielding

$$W_{\text{rad}} = \begin{cases} \dfrac{1}{2}|\hat{v}_0|\text{Re}\{F_{\text{ax}}\} = \dfrac{1}{2}|\hat{v}_0|^2\rho_0 c_0(4\pi a^2)\dfrac{k^4a^4}{4 + k^4a^4} \quad \text{Nm/s} & (10.26\text{a}) \\[2ex] \dfrac{1}{2}|\hat{v}_0|^2\rho_0 c_0(\pi a^2/3)k^4a^4 \quad \text{for } ka \ll 1 & (10.26\text{b}) \\[2ex] \dfrac{1}{2}|\hat{v}_0|^2\rho_0 c_0(4\pi a^2/3) \quad \text{for } ka \gg 1 & (10.26\text{c}) \end{cases}$$

Equation (10.25) indicates that at low frequencies ($ka \ll 1$) the radiated sound power is small and increases with the fourth power of the frequency and at high frequencies ($ka \gg 1$) reaches a frequency-independent value.

In the far field ($kr \gg 1$) Eq. (10.22) takes the form

$$\hat{p}(r, \varphi, \omega) = \begin{cases} -\dfrac{\hat{v}_0}{r}\cos(\varphi)\rho_0 c_0 k^3 a^3\dfrac{(2 - k^2a^2) + j2ka}{4 + k^4a^4} \quad \text{N/m}^2 & (10.27\text{a}) \\[2ex] -\dfrac{\hat{v}_0(\omega)\cos(\varphi)}{4\pi c_0 r}\omega^2\rho_0 2\pi a^3 \quad \text{for } ka \ll 1 & (10.27\text{b}) \\[2ex] -\hat{v}_b\rho_0 c_0\left(\dfrac{a}{r}\right)\cos(\varphi) \quad \text{for } ka \gg 1 & (10.27\text{c}) \end{cases}$$

Sound Radiation of Oscillating Small Rigid Nonspherical Bodies. Realizing that $2\pi a^3/2 = 4\pi a^3/3 + 2\pi a^3/3$ and that $V_b = 4\pi a^3/3$ is the volume of the sphere and $V_{\text{ad}} = 2\pi a^3/3$ is the added mass of an oscillating rigid sphere, we can write Eq. (10.24) in the form

$$\hat{p}(r, \varphi, \omega) \approx -\frac{\omega^2\rho_0}{4\pi rc}\hat{v}_b(\omega)\cos(\varphi)[V_b + V_{\text{ad}}(\square, \Psi)]\, e^{j(\omega t - kr)} \quad \text{N/m}^2 \tag{10.28}$$

where the symbols $\square$ and Ψ in the argument of V_{ad} signify that the added mass depends on the geometry of the body and the specific direction of its oscillatory motion.

While Eq. (10.27b) is valid only for a small oscillating rigid sphere, Eq. (10.28) is exact for an oscillating sphere and is a good engineering approximation for small rigid bodies of any shape. It is instructive to rewrite Eq. (10.28) in the form

$$\hat{p}(r, \varphi, \omega) \simeq -\frac{\omega^2\rho_0}{4\pi rc_0}\hat{v}_b(\omega)\cos(\varphi)(S_p l_v)\, e^{j(\omega t - kr)} \quad \text{N/m}^2 \tag{10.29}$$

where S_p is the projected area of the body on a plane perpendicular to the oscillatory motion and

$$l_v \equiv \frac{V_b + V_{\text{ad}}(\square, \Psi)}{S_p} \quad \text{m} \tag{10.30}$$

is a length defined by the author in Eq. (10.30), where the angle Ψ corresponds to the direction of the oscillation of the body. The importance of the length l_v is that it defines the frequency range to $ka \ll 1$, where the body can be considered small and where Eq. (10.29) is valid.

The $\cos(\varphi)$ dependence of the directivity pattern in the vicinity of the oscillating body is strictly valid only for spheres. However, in the far field of any oscillating small rigid body (i.e., $kr \gg 1$ and $kl_v \ll 1$) the same $\cos(\varphi)$ dependence applies provided that the fluid displaced by the forward-moving face of the body is free to move to the void left by the opposite face. A detailed mathematical proof of this is given by Koopmann and Fahnline.[8]

Prediction of l_v. The length l_v of various three-dimensional and two-dimensional bodies are listed in Table 10.1. The l_v values in Table 10.1 where computed utilizing the formulas for V_{ad} given by Newman[9]

For the spheroid with major axis $2a$ and minor axes $2b$ and aspect ratio b/a, the *Ver-lengths* l_{vx}, l_{vy}, and l_{vz} are obtained by finding $m''_{11} = V_{ad}(x)/V_b$ and $m''_{22} = V_{ad}(y)/V_b = V_{ad}(z)/V_b$ in Fig. 10.7 at the desired b/a ratio and performing the operation indicated in Table 10.1. The increase in moment of inertia (in addition to that measured in a vacuum) when the ellipsoid body rotates around any of the minor axes is obtained by finding the numerical value of m'_{55} that belongs to the appropriate b/a ratio and performing the operation indicated in Table 10.1.

Predicting Radiated Sound Power. The sound power radiated by small oscillating rigid bodies is obtained by integrating the far-field intensity $I = p^2(r, \varphi, \omega)/\rho_0 c_0$ over the surface of a large sphere of radius r centered at the oscillating small rigid body, namely

$$W_{rad} \simeq \int_0^{\pi} \frac{|\hat{p}|^2(r, \varphi, \omega)}{\rho_0 c_0} 2\pi r^2 \sin(\varphi)\, d\varphi \quad \text{N} \cdot \text{m/s} \tag{10.31}$$

Combining Eqs. (10.29) and (10.31) yields

$$W_{rad} \simeq \frac{k^4 \rho_0 c_0 S_p^2 (l_v)^2}{12\pi} v_{b,\text{rms}}^2 \quad \text{N} \cdot \text{m/s} \tag{10.32}$$

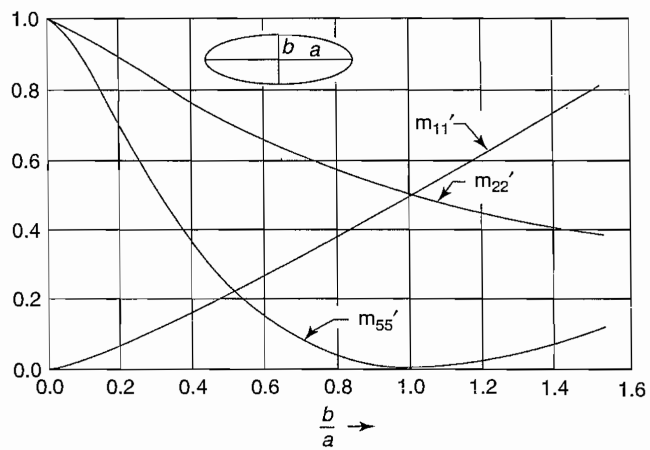

FIGURE 10.7 Added-mass coefficient V_{ad}/V_b for a spheroid, of length $2a$ and maximum diameter $2b$. The added-mass coefficient m'_{11} corresponds to longitudinal acceleration, m'_{22} corresponds to lateral acceleration in the equatorial plane, and m'_{55} denotes the added moment of inertia coefficient for rotation about an axes in the equatorial plane representing the ratio of the added moment of inertia and the moment of inertia of the displaced volume of the fluid. After Ref. 9. Reproduced by permission of the MIT Press.

TABLE 10.1 Added Volume, V_{ad}, Ver-length, l_v, and Added Moment of Inertia M of Oscillating and Rotating Rigid Bodies

Name and Sketch	V_{ad} and l_v	M
Sphere of Radius a 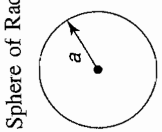	$V_{ad}(x) = V_{ad}(y) = V_{ad}(z) = 2\pi a^3/3$ $l_{vx} = l_{vy} = l_{vz} = 2a$	$M_x = M_y = M_z = 0$
Spheroid of aspect ratio a/b 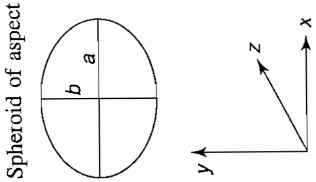	$V_{ad}(x) = (\frac{4}{3})\pi ab^2 m'_{11}$ $V_{ad}(y) = V_{ad}(z) = (\frac{4}{3})\pi ab^2 m'_{22}$ $l_{vx} = (\frac{4}{3})a(1 + m'_{11})$ $l_{vy} = l_{vz} = (\frac{4}{3})\left(\frac{b^2}{a}\right)(1 + m'_{22})$	$M_x = 0$ $M_y = M_z = (\frac{4}{15})\pi\rho_0 ab^2(a^2 + b^2)$

(*continued overleaf*)

TABLE 10.1 (*continued*)

Name and Sketch	V_{ad} and I_v	M
Long thin plate strip $L \gg 2a; kL \ll 1$ 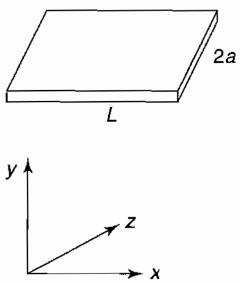	$V_{ad}(x) = V_{ad}(z) = 0$ $V_{ad}(y) = \pi a^2 L$ $I_{vx} = I_{vz} = 0$ $I_{vy} = (\pi/2)a$	$M_x = (\frac{1}{8})\pi\rho_0 a^4 L$
Long round finned rod $L \gg 2a; kL \ll 1$ 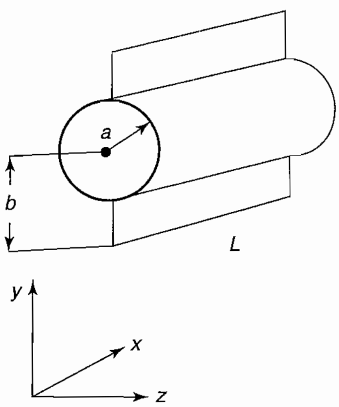	$V_{ad}(x) =$ NPI[a] $V_{ad}(y) = \pi a^2 L$ $V_{ad}(z) = \pi[a^2 + (b^2 - a^2)^2/b^2]L$ $I_{vx} =$ NPI[a] $I_{vy} = \pi a$ $I_{vz} = \pi[a^2/b + (b^2 - a^2)^2/2b^3]$	$M_x =$ see footnote *b*
Long rectangular plates crossing perpendicularly $L \gg 2a; kL \ll 1$ 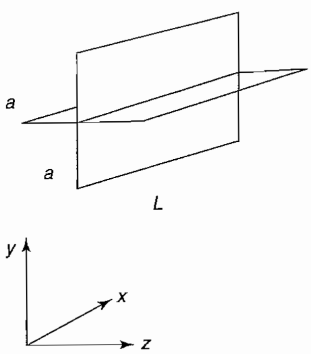	$V_{ad}(x) =$ NPI[a] $V_{ad}(y) = V_{ad}(z) = \pi a^2 L$ $I_{vx} =$ NPI[a] $I_{vy} = I_{vz} = (\pi/2)a$	$M_x = (2/\pi)a^4 L$
Long cylindrical rod of radius a $L \gg 2a; kL \ll 1$ 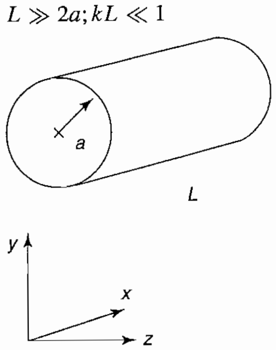	$V_{ad}(x) =$ NPI[a] $V_{ad}(y) = V_{ad}(z) = \pi a^2 L$ $I_{vx} =$ NPI[a] $I_{vy} = I_{vz} = \pi a$	$M_x = 0$

(*continued overleaf*)

TABLE 10.1 (continued)

Name and Sketch	V_{ad} and I_v	M
Long rod with elliptical cross section $L \gg 2a; kL \ll 1$ 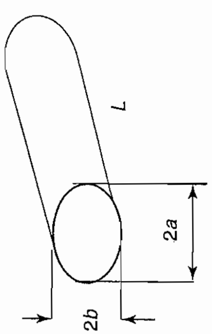 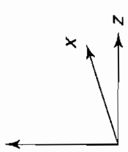	$V_{ad}(x) = \text{NPI}^a$ $V_{ad}(y) = \pi a^2 L$ $V_{ad}(z) = \pi b^2 L$ $I_{vx} = \text{NPI}^a$ $I_{vy} = I_{vz} = (\pi/2)(a+b)$	$M_x = (\frac{1}{8})\pi \rho_0 a^4 L$
Long rod of square cross section $L \gg 2a; kL \ll 1$ 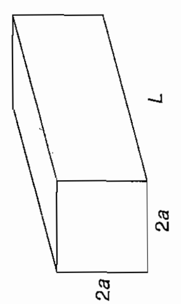	$V_{ad}(x) = \text{NPI}^a$ $V_{ad}(y) = V_{ad}(z) = 4.754a^2 L$ $I_{vx} = \text{NPI}^a$ $I_{vy} = I_{vz} = 2.38a$	$M_x = 0.725a^4 L$

[a] NPI = not of practical interest

[b] $M_x = [\pi^{-1}\csc^4(\alpha)][2\alpha^2 - \alpha \sin(4\alpha) + (1/2)\sin^2(2\alpha)] - \pi/2]$, $\sin(\alpha) = 2ab/(a^2+b^2)$, and $\pi/2 < \alpha < \pi$

For a oscillating, small, rigid spherical body of radius a the area projected on the plane perpendicular to the direction of the oscillatory motion $S_p = \pi a^2$ and $l_v = 2a$ and Eq. (10.32) yield

$$W_{\text{rad}}(\text{Sphere}) = \frac{\rho_0 c_0 (4\pi a^2)(ka)^4}{24} |v_b|^2 \quad \text{N} \cdot \text{m/s} \tag{10.33}$$

This is the well-known[3,4] formula for the sound power radiated by a small ($ka \ll 1$) sphere of radius a oscillating with an rms velocity amplitude of $v_{b,\text{rms}}$.

Random Excitation. Let us investigate the case where a small rigid sphere exhibits random motion in one dimension (e.g., in the x direction). As described in Chapter 3, the random motion is characterized by the power spectrum of its velocity in the x direction, $S_{vv}(x)$.

The *power spectrum*, as defined in Chapter 3, represents the quantity obtained by filtering the random time signal in a 1-Hz bandwidth multiplying by itself and time averaging the product. In this chapter we use the symbol S with a double subscript to represent a power spectrum or cross spectrum. The double-letter subscript of S identifies which of the two filtered signal are multiplied with the other before time averaging. For example the symbol $S_{vv}(\omega)$ represents the autospectrum of the random velocity signal filtered in a 1-Hz bandwidth centered at the angular frequency $\omega = 2\pi f$, where f is the frequency in hertz. The symbol $S_{xy}(\omega)$ represents a cross spectrum of two random signals $x(t)$ and $y(t)$ obtained by filtering both signals in a 1-Hz bandwidth, multiplying them, and time averaging the product. The power spectrum of a signal resulting from the superposition of two signals $z(t) = x(t) + y(t)$ is computed as $S_{zz}(\omega) = S_{xx}(\omega) + S_{yy}(\omega) + 2S_{xy}(\omega)$. If the two random processes $x(t)$ and $y(t)$ are not correlated, $S_{xy}(\omega) = 0$. If the two random processes of the same power spectral density are fully correlated (i.e., they have the same cause), the cross spectrum is identical to the autospectrum, $S_{xy}(\omega) = S_{xx}(\omega) = S_{yy}(\omega)$ and $S_{zz}(\omega) = 4S_{xx}(\omega) = 4S_{yy}(\omega)$.

If the velocity of the vibrating body is exclusively in the x direction and is a random function of time, with a power spectrum of $S_{v_x v_x}(\omega)$ the power spectrum of the sound at distance r in the direction ϕ from the positive x axis, $S_{pp}(r, \varphi, \omega)$, is

$$S_{pp}(\omega, r, \varphi) = S_{v_x v_x}(\omega) |h_1(\omega, \rho_0, k, a, r, \varphi)|^2 \quad \text{N}^2/\text{m}^4 \tag{10.34}$$

where

$$h_1(\omega, \rho_0, k, l_v, r, \varphi) = \frac{\omega^2 \rho_0}{4\pi r c_0} \cos(\varphi)(S_p l_v) e^{jkr} \tag{10.35}$$

Hypothetical Experiment 2: Force Acting on Fluid. To find the dynamic force acting on the fluid F_f, let us perform the thought experiment shown in Fig. 10.8. Let a dynamic force $\mathbf{F}_b$ act on a small, rigid, hollow body of arbitrary shape at its center of gravity and determine the oscillatory velocity $\mathbf{v}_b$ of the

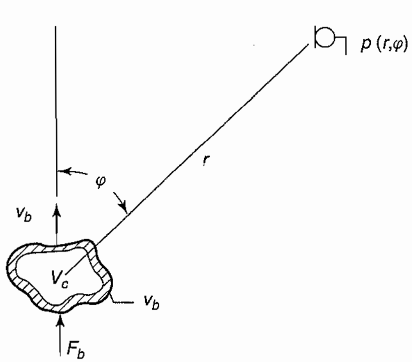

FIGURE 10.8 Hypothetical experiment to determining the force F_f that acts on the fluid and the sound field it produces by letting the wall thickness of an oscillating, hollow rigid body approach zero.

body responding to the force as

$$\mathbf{F}_b = \mathbf{v}_b(j\omega m_b + Z_{\text{rad}}) \quad \text{N} \tag{10.36}$$

where m_b is the mass of the body and $Z_{\text{rad}} = F_f/v_b$ is the radiation impedance:

$$\mathbf{F}_b = j\omega \mathbf{v}_b[\rho_M(V_b - V_c) + \rho_0 V_c + \rho_0 V_{\text{ad}}(\square, \Psi)] \quad \text{N} \tag{10.37}$$

where V_b is the volume of the oscillating, hollow, rigid body and V_c is the volume of the inside cavity, filled with the same fluid that surrounds the body. Both volumes are in cubic meters. The symbol ρ_M represents the density of the solid part of the body in kilograms per cubic meter. The symbol V_{ad}, in cubic meters, is the added volume, or in the hydrodynamic vocabulary the added mass coefficient. The symbols $\square$ and Ψ in the argument of V_{ad} is to remind us that it is a function of the body's geometry and the particular angle of its oscillatory motion to one of the designated axes of the body.

Let us now investigate the very important extreme case of Eq. (10.37) where the wall thickness of the hollow body approaches zero (and still remains rigid) by setting $V_c \to V_b$. In this case the entire applied dynamic excitation force $F_b = F_f$ is acting directly on the fluid, yielding

$$\mathbf{F}_f = v_b j\omega\rho_0 V_b + \mathbf{v}_b j\omega\rho_0 V_{\text{ad}}(\square, \Psi) \quad \text{N} \tag{10.38}$$

The first term in Eq. (10.38) represents the flux of the momentum of the fluid volume displaced by the body, $\rho_0 V_b[\partial(v_b)/dt]$, and the second term, $\rho_0 V_{\text{ad}}\,(\square, \Psi)[\partial(v_b)/dt]$, the flux of the momentum of the near field obtained by integrating the component of the particle velocity that is out phase with the velocity of the body over the entire volume outside of the body. Fortunately, we do not need to perform this integration to obtain $V_{\text{ad}}(\square, \Psi)$ because

(a) hydrodynamists have computed it for many body geometries of interest (see Table 10.1 and Fig. 10.7),
(b) for most bodies of practical interest it can be well approximated by spheroids of the appropriate aspect ratio (see Fig.10.7), and
(c) it can be determined experimentally.

Equation (10.38) is of fundamental importance. It signifies the following:

1. The force acting on the fluid acts in the direction of the oscillatory motion.
2. Two-dimensional bodies, which have no volume ($V_b = 0$) can exert force on the fluid provided their velocity has a component perpendicular to their plane and, consequently, $V_{\text{ad}} \neq 0$.
3. No force can be exerted on the fluid without a finite added mass (i.e., $V_{\text{ad}} \neq 0$).

The far-field sound pressure as a function of distance r, direction φ, and frequency ω produced by a pointlike force F_f is obtained by solving Eq. (10.38) for v_b and inserting this value into Eq. (10.25), yielding

$$p(r, \varphi, \omega) = -j\frac{kF_f\cos(\varphi)}{4\pi r}e^{j(\omega t - kr)} = -j\frac{F_f\cos(\varphi)}{2r\lambda}e^{j(\omega t - kr)} \quad \text{N/m}^2 \tag{10.39}$$

The radiated sound power W_{rad} is obtained by integrating the intensity $I = p^2(r, \vartheta, \omega)/\rho_0 c_0$ over the surface of a sphere of radius $r \gg (1/k)$ centered on the excitation point. Carrying out the integration yields

$$W_{\text{rad}} = \frac{k^2 F_{f,\text{rms}}^2}{12\pi\rho_0 c_0} = \frac{\omega^2 F_{f,\text{rms}}^2}{12\pi\rho_0 c_0^3} \quad \text{N}\cdot\text{m/s} \tag{10.40}$$

If the excitation is random, the excitation and response parameters have to be replaced by their respective power spectra.

Equation (10.39) describes the diffusion law of acoustics. It gives the full answer to the question "How does this organized motion—that is, in the direction of the force at the application point—diffuse with increasing distance in other directions through the molecular collision process?"

Equation (10.39)signifies that:

1. The sound pressure in any particular direction is proportional the projection of the force vector in that direction, $F_f\cos(\phi)$, indicating that the strength of the diffusion varies as $\cos(\phi)$. The radiated sound pressure has its maximum in the direction of the force and it is zero perpendicular to it. This is consistent with the fact that the oscillatory motion of the body exerts on the fluid the maximum force in the motion direction and no force at all in the direction perpendicular to it. The directivity pattern $\cos(\phi)$ in three dimensions is represented by two spheres of unit diameter aligned in the

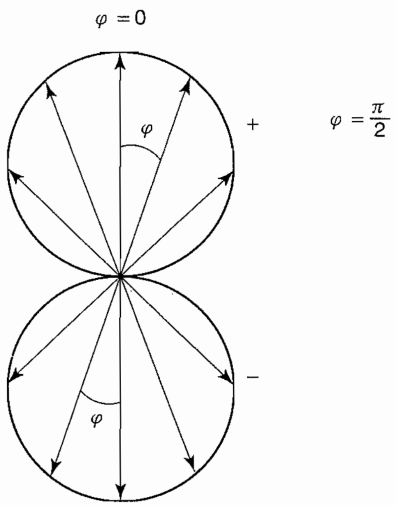

FIGURE 10.9 Far-field sound radiation pattern of a small rigid body oscillating in the $\phi = 0$ direction or an oscillatory force acting on the fluid in the $\phi = 0$ direction.

direction of the oscillatory motion or the direction of the force and centered on the line of the oscillating body or on the point where the force acts on the fluid, as shown (in two dimensions) in Fig. 10.9.

2. The sound pressure in any direction is inversely proportional to the source–receiver distance r.
3. Independent of what causes the dynamic force F_f which acts on the fluid, the sound pressure fully determines the sound radiation pattern and sound power output of small rigid bodies. The force can be, for example, the reaction force to the oscillatory movement of the body or that caused by fluctuating lift or drag forces generated on small stationary bodies by the fluctuation of the inflow velocity or by vortex shedding at the trailing edge of airfoils. Fluctuating inflow is caused by incoming turbulence of a scale that is large compared with the size of the body. If the scale of the convected pressure fluctuations (turbulence) is large compared with the size of the rigid body, the force would be identical to that obtained by moving the body in a stationary fluid in the direction and with the velocity of the fluctuating component of the unsteady inflow and predicting lift and drag forces.
However, a rigid stationary body exposed to fluctuating aerodynamic forces radiates sound into a moving media. Consequently, the radiated sound pressure and sound power is different from that an oscillating rigid body, that exerts the same dynamic force on the fluid, would produce in a stationary media. The effect of moving media on sound radiation is treated in Chapter 15.

4. The sound pressure is independent of the density of the surrounding fluid. This is because the acceleration of the fluid caused by the force is inversely proportional to the density and the sound pressure is proportional to the product of the density and acceleration.

If the force applied to the F_f is of random nature, it is characterized by its power spectral density $S_{FF}(\omega)$ and the sound pressure it produces by its power spectral density $S_{pp}(r, \varphi, \omega)$, as defined in Chapter 3. In this case Eq. (10.39) takes the form

$$S_{pp}(\omega, r, \varphi) = S_{FF}(\omega,) \left| \frac{\omega \cos(\varphi)}{4\pi r c_0} \right|^2 \quad (\text{N/m}^2)^2 \qquad (10.41)$$

and the power spectrum of the radiated sound power takes the form

$$S_w(\omega) = S_{FF}^2(\omega) \left| \frac{\omega^2}{12\pi \rho_0^2 c_0^3} \right|^2 \quad (\text{N} \cdot \text{m/s})^2 \qquad (10.42)$$

Response of Bounded Fluid to Point Force Excitation. It is instructive to investigate briefly what effects nearby boundaries have on the sound radiation pattern and on the sound power radiated by a point force. We will consider

1. the most severe restricting boundaries, surrounding the oscillating rigid body by an infinitely long (or finite-length but at both ends anechoically terminated) small-diameter rigid pipe;
2. rigid plane boundaries; and
3. yielding plane boundaries.

Rigid Pipe Surrounding Point Force. Figure 10.10 shows the situation where a point force of arbitrary orientation is acting in a fluid inside of a pipe of diameter d and cross-sectional area $S = d^2\pi/4 = r^2\pi$ that is anechoically terminated at both ends. Let the axis of the pipe coincide with the x axis of the Cartesian coordinate system and let the point force, which acts at $x = 0$, have components F_x, F_y, and F_z. [If we place a small rigid oscillating body with known velocity v_b into the tube, we must first determine the oscillatory force F_f according to Eq. (10.38).] Let restrict our analysis to the frequency range where the acoustical wavelength is large compared with the internal diameter of the pipe (i.e., $\lambda \gg d$) when only plain sound waves can propagate in the pipe and assume that

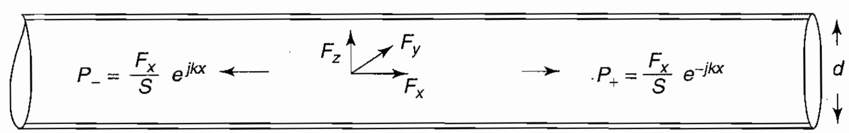

FIGURE 10.10 Force exerted on the fluid inside of a small-diameter, infinitely long, or on both ends anechoically terminated rigid pipe.

the near field of the body giving rise to the force is not influenced by the presence of the pipe (i.e., $kl_v \ll d$). This is not an unreasonable assumption because we can always choose a reasonably small size body and compensate for it by appropriately increasing its oscillatory velocity (as long as $v_b \ll c_0$) to produce the same force on the fluid. With these minor restrictions, the sound pressure at a distance $x \gg d$ the sound pressure $p(x)$ and the power spectrum S_{pp} for any $x \gg d$ will be

$$p(x) = -p(-x) = \left(\frac{F_x}{S}\right) e^{-kx} e^{j\omega t} \quad \text{N/m}^2 \tag{10.43}$$

$$S_{pp}(f) = \left(\frac{S_{FF}(f)}{S}\right) \quad \text{N/m}^2 \tag{10.44}$$

Note that Eq. (10.40) signifies that the amplitude of the sound propagating inside the rigid pipe does not diminish with increasing distance, as was the case when the point force was acting on an unbounded fluid [see Eq. (10.39)]. Before electroacoustical communication was invented, sea captains communicated with distant crew in the belly of a ship through pipes, as shown in Fig. 10.11a, and on the deck by using an acoustical horn, as depicted in Fig. 10.11b.

Equal sound power is radiated toward the right and left and the total sound power is

$$W'_{\text{rad}} = \frac{2[(F_x)^2/S]}{\rho_0 c_0} \quad \text{N/m}^2 \tag{10.45}$$

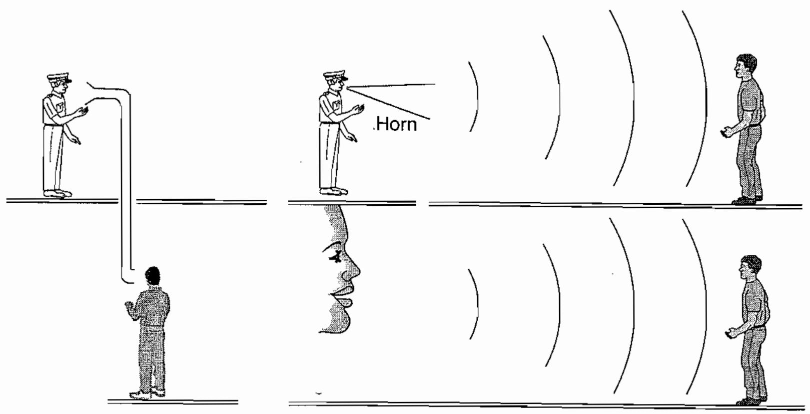

(a) (b)

FIGURE 10.11 Passive devices used for voice communication to large distances before the invention of electroacoustical devices. (a) Captain gives orders to crew member located in a lower deck. (b) Top: Captain gives orders to distant crew member on deck using an acoustical horn. Bottom: Using a horn is equivalent to enlarging the mouth of the speaker to the size of the downstream cross-sectional area of the horn.

$$S'_{ww}(f) = \frac{S^2_{F_x F_x}(f)}{|S(\rho_0 c_0)|^2} \quad \text{N/m}^2 \tag{10.46}$$

where $S'_{ww}(f)$ is the power spectrum density of the radiated sound power. The prime notation signifies that the parameter is obtained when the point force is acting inside a small-diameter ($kr \ll 1$) rigid pipe.

The ratio $W'_{\text{rad}}/W_{\text{rad}}$ is a measure of the effect that enclosing the force with a rigid pipe has on the radiated sound power. It is obtained by dividing Eq. (10.45) by Eq. (10.39), yielding

$$\frac{W'_{\text{rad}}}{W_{\text{rad}}} = \left(\frac{6\pi}{S}\right)\left(\frac{1}{k^2}\right)\left\{\frac{1}{1 + (F_y/F_x)^2 + (F_z/F_x)^2}\right\} \tag{10.47}$$

Equation (10.47) indicates that no sound power is radiated if $F_x = 0$, independent of how large F_y and F_z might be. The effect of placing the force inside the pipe reaches its maximum if the force is aligned with the axis of the tube (i.e., $F_y = F_z = 0$) and the value inside the curly brackets is unity. In this case Eq. (10.47) simplifies to

$$\frac{W'_{\text{rad}}}{W_{\text{rad}}} = \left(\frac{3}{2\pi}\right)\frac{c_0^2}{sf^2} \tag{10.48}$$

Example 10.2. Calculate the increase in radiated sound power and the sound power level when an axially oriented force located in a rigid pipe of $a = 2.5$ cm $= 0.025$ m internal radius at a frequency $f = 100$ Hz at a temperature of 20°C = 68°F.

Solution Utilizing Eq. (10.2), we find $c_0 = 342.6$ m/s and with the above values Eq. (10.48) yields

$$\frac{W'_{\text{rad}}}{W_{\text{rad}}} = \frac{(3/2\pi)(342.6)^2}{\pi(0.025)^2(100)^2} = 2854$$

indicating that the same point force oriented axially in this rigid tube radiates 2854 times as much sound power than it does in a unbounded fluid. This corresponds to a $10\log_{10}(2854) = 34.6$ dB increase of the sound power level.

10.2 EFFECT OF NEARBY PLANE BOUNDARIES ON SOUND RADIATION

In this section we only consider entirely rigid and fully yielding plane boundaries. Other boundaries of practical interest, such as lining the rigid boundary with a porous sound-absorbing material of finite thickness, is beyond the scope of this chapter. For guidance in this situation see Chapter 6. The infinitely rigid plane boundary is approached by an infinitely large, nonporous wall and the fully yielding plane boundary by the undisturbed horizontal air–water interface. With regard to their effect on the sound power radiated by a point force (or by an oscillating small rigid body), the plane boundaries do not need to be infinitely large. For practical purposes it is sufficient that they extend, in each direction from the position of the force, many acoustical wavelengths.

A water tank with practically all boundaries pressure releasing (pressure reflection coefficient $R \simeq -1$) is realized by lining the retaining sidewalls and the bottom of the pool with a thin impervious foil with an elastic layer behind. These pools are the equivalent of reverberation chambers with the important exception that in this case the sound pressure reflection coefficient $R \approx -1$ instead of $R \approx +1$ in the case of the (air-filled) reverberation chamber. In both cases the walls have theoretically zero sound absorption coefficient, $\alpha \cong [1 - |R^2|]$ (see Chapter 8). As we will show latter, the vicinity of a rigid boundary increases the sound power output and that of a yielding boundary decreases the sound power output provided that the sound source is less than a half wavelength from the plain boundary.

Effect of Nearby Plane Rigid Boundaries. Rigid plane boundaries are places where the particle velocity is zero and the sound pressure doubles. If the sound source is a small, oscillating, rigid body or a dynamic force acting on the fluid, the directivity pattern of the image source must have the same strength but a mirrored directivity pattern of the actual sound source to produce zero particle velocity in the direction perpendicular to the plane of the boundary and, at the same time, double the sound pressure at all locations in the plane of the rigid boundary, as illustrated in Fig. 10.12.

The sound field in the receiver side of the rigid plane boundary can be constructed as the superposition of the sound fields that would result from the real sound source and its mirror image if both were placed in an infinite fluid. Then, as the sound source approaches the plane rigid interface, the sound field on the source side approaches that of a single source with doubled sources strength.

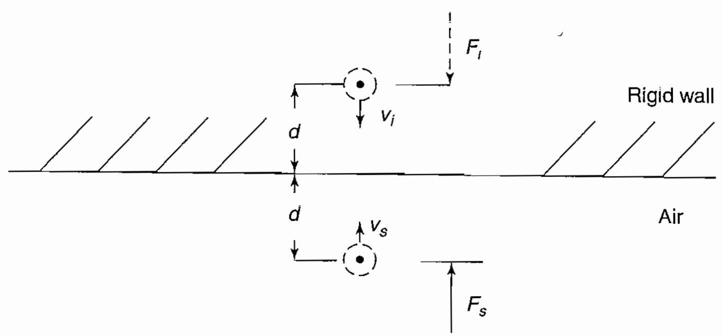

FIGURE 10.12 Representation of a plane rigid boundary, such as at air–hard wall interface, by mirroring the original sound source and superimposing the sound field of the real and in–phase image source in the source-side half space.

If it approaches a rigid two-dimensional corner (i.e., the intersection of two perpendicular plane rigid surfaces), there will be three collapsing mirror images and the sound field in the source-side quarter space approaches that of a single source with 4 times larger source strength. Finally, if the sound source approaches a three-dimensional corner (the intersection of three perpendicular rigid plane surfaces), there will be seven collapsing mirror images and the sound field in the source-side one-eighth space approaches that of a single source with 8 times the source strength.

Effect of Nearby Plane Pressure-Release Boundaries. The pressure-release boundary is well approximated by the plane water–air interface shown schematically in Fig. 10.13 for the force acting perpendicular to the interface and Fig. 10.14 when it acts parallel to the interface. For an oblique-incidence force, the force vector can be decomposed into a component that is perpendicular to the interface and into components that are parallel to the interface. Consequently, we will investigate the perpendicular and parallel cases only. If the sound source is a small, oscillating, rigid body or a dynamic force acting on the fluid, the directivity pattern of the image source must have the same strength but opposite phase and a mirrored directivity pattern of the actual sound source to produce zero sound pressure on the entire interface and, at the same time, double the sound particle velocity at all locations in the plane of the pressure release boundary.

Excitation Is Perpendicular to Pressure-Release Boundary. For the case shown in Fig. 10.13, where the distance to the interface is small compared to the wavelength ($kd \ll 1$) and the body exerting the force is small ($kl_v \ll 1$) and the direction of motion and the force exerted on the fluid are perpendicular to the plane pressure-release interface, the superposition of the sound pressures produced by the real source and that produced by its negative mirror image yields

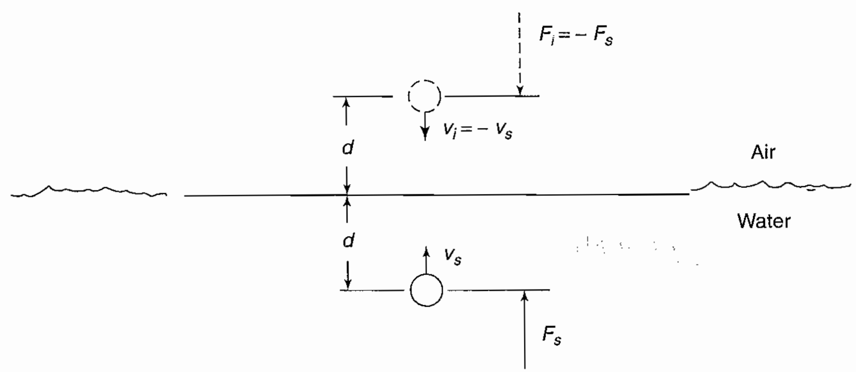

FIGURE 10.13 Representation of a plane pressure-release boundary, such as the water–air interface, by mirroring the original sound source and the 180° out-of-phase mirror image superimposing the sound field of the real and image sources in the source-side half space. Motion is perpendicular to the interface.

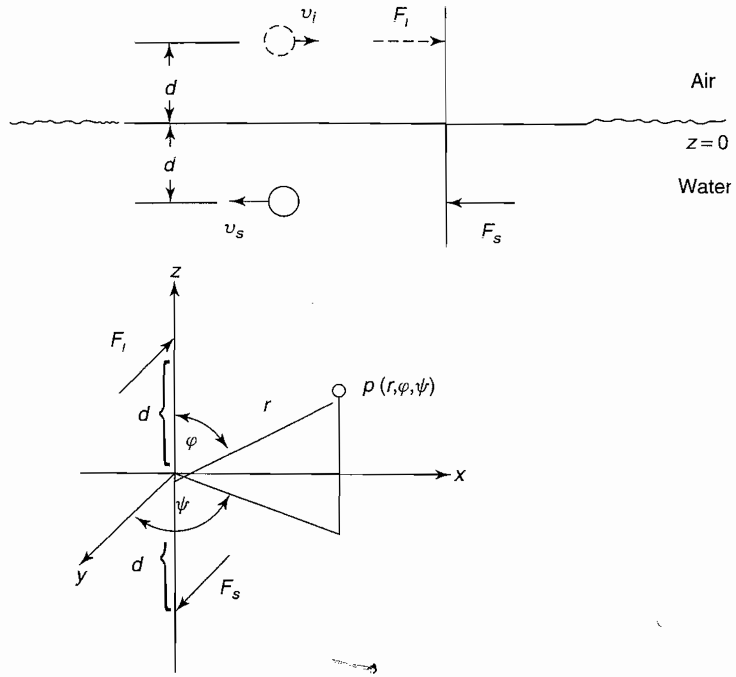

FIGURE 10.14 Representation of a plane pressure-release boundary, such as the water–air interface, by mirroring the original sound source 180° out of phase and superimposing the sound field of the original sound source and the image in the source-side half space. Motion is parallel to the interface.

the sound pressure, intensity, and radiated sound power in the liquid obtained by substituting $F = \rho_0 \omega Q h$ in the respective formulas given by Bies and Hansen[10] for the sound radiation of longitudinal quadrupoles constituted from two dipoles of strength Qh, where Q is the volume velocity of the monopoles that make up the dipole and 2 h is the distance between them:

$$p(r,\varphi,\omega) = \left(\frac{1}{\pi r}\right)\left(\frac{\omega^2}{c_0^2}\right) Fd\cos^2(\varphi) = \left(\frac{1}{\pi r}\right) k^2 Fd\cos^2(\varphi) \quad \mathrm{N/m^2} \qquad (10.49)$$

$$I(r,\varphi,\omega) = \left(\frac{F^2 d^2 k^4 \cos^4(\varphi)}{(\pi r)^2 \rho_0 c_0}\right) = \frac{F^2 d^2 \omega^4 \cos^4(\varphi)}{(\pi r)^2 \rho_0 c_0^5} \quad \mathrm{N/m\cdot s} \qquad (10.50)$$

$$W_{\mathrm{rad}} = \left(\frac{4}{5\pi}\right)\frac{F^2 d^2 k^4}{\rho_0 c_0} = \left(\frac{4}{5\pi}\right) F^2 d^2 \omega^4 \cos^4(\varphi) \quad \mathrm{N\cdot m/s} \qquad (10.51)$$

where $p(r,\varphi,\omega)$ is the sound pressure at distance r at an angle φ from the direction of the motion or from the force at the angular frequency $\omega = 2\pi f$, $I(r,\varphi,\omega)$ is the sound intensity in the radial direction from the excitation point,

W_{rad} is the radiated sound power, F is the rms value of the force, and d is the distance between the excitation point and the plain pressure-release boundary (i.e., the depth of the excitation point in the water.

Note that Eqs. (10.49)–(10.51) are valid for both cases:

(a) A single excitation source is at a distance d from the plane pressure-release boundary.
(b) Two identical small bodies at a distance $2d$ oscillate with the same amplitude but opposite phase in an infinite fluid (for practical purposes far enough from the interface).

Observing Eq. (10.49), note that (1) the radiation pattern is much more directional than that obtained when the body radiates into an infinite fluid [$\cos^2(\varphi)$ vs. $\cos(\varphi)$]; (2) here again the sound pressure is independent of the density of the fluid; and (3) comparing Eq. (10.49) to Eq. (10.39) reveals that the vicinity of the pressure-release boundary substantially reduces the efficiency of the sound radiation at low frequencies. Those familiar with quadrupoles will realize that Eqs. (10.49)–(10.51) describe a longitudinal quadrupole constituted either by two opposing forces of equal magnitude acting on the fluid a short distance $2d$ apart or by two equal-size small rigid bodies oscillating in opposite directions in a small distance $2d$ apart.

Excitation Is Parallel to Pressure-Release Boundary. Figure 10.14 shows the situation where the excitation is parallel to the plane pressure-release boundary. For this case the sound field descriptors, obtained in a similar manner as for the longitudinal quadrupole above, are

$$p(r,\varphi,\omega) = \left(\frac{1}{\pi c_0^2 r}\right)\omega^2 Fd\cos(\varphi)\sin^2(\psi) \quad \mathrm{N/m^2} \qquad (10.52)$$

$$I(r,\varphi,\psi,\omega) = \left(\frac{1}{\rho_0 c_0^5}\right)\left(\frac{1}{\pi r}\right)^2 \omega^4 (Fd)^2 \cos^2(\varphi)\sin^4(\psi) \quad \mathrm{N/m\cdot s} \qquad (10.53)$$

$$W_{\mathrm{rad}} = \left(\frac{4}{15\pi}\right)\left[\frac{(Fd)^2 k^4}{\rho_0 c_0}\right] = \left(\frac{4}{15\pi}\right)\left[\frac{(Fd)^2 \omega^4}{\rho_0 c_0^5}\right] \quad \mathrm{N\cdot m/s} \qquad (10.54)$$

Those familiar with quadrupoles will realize that Eqs. (10.52)–(10.54) describe a lateral quadrupole.

Sound Radiation of Oscillating Moment in Infinite Liquid. An oscillating moment consists of a pair of oscillating forces which (a) act in the same plane, (b) have the same magnitude but opposite direction and phase, and (c) are at a short distance apart.

Observing Fig. 10.14, we realize that the force pair has all the above attributes. Consequently, if we substitute M in place of Fd in Eqs. (10.52)–(10.54), the

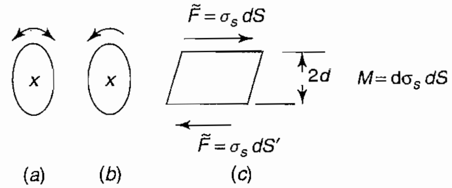

FIGURE 10.15 Different ways of exerting a moment on a fluid: (*a*) rotary oscillation around axes of nonrevolution; (*b*) rotation around axes of nonrevolution; (*c*) by shear stresses.

equations describe the sound radiation of an oscillating moment, yielding

$$p(r,\varphi,\omega) = \left(\frac{1}{\pi c_0^2 r}\right)\omega^2 M\cos(\varphi)\sin^2(\psi)\quad \text{N/m}^2 \tag{10.55}$$

$$I(r,\varphi,\psi,\omega) = \left(\frac{1}{\rho_0 c_0^5}\right)\left(\frac{1}{\pi r}\right)^2 \omega^4 M^2\cos^2(\varphi)\sin^4(\psi)\quad \text{N/m}\cdot\text{s} \tag{10.56}$$

$$W_{\text{rad}} = \left(\frac{4}{15\pi}\right)\left[\frac{M^2 k^4}{\rho_0 c_0}\right] = \left(\frac{4}{15\pi}\right)\left[\frac{M^2\omega^4}{\rho_0 c_0^5}\right]\quad \text{N}\cdot\text{m/s} \tag{10.57}$$

The moment can be any combination of F and d provided that $kd \ll 1$.

As shown in Fig. 10.15, the moment M can be the result of the oscillatory rotation of solid bodies around axes of nonrotational symmetry, shear stresses acting on the fluid (as it is the main source of noise of high-speed jets), or any other acceleration motion that results in a increase of the rotary inertia of the body above that which would exist if the oscillatory rotation would be taking place in a vacuum. For a large number of body shapes this additional moment of rotary inertia M that acts on the fluid is given in Table 10.1 under heading M_x and for ellipsoids of different aspect ratios in Fig. 10.7.

Figure 10.15 shows various ways for the moment excitation of a fluid. Figure 10.15*a* depicts moment excitation by an oscillatory rotation of a body around a nonsymmetric axis, and Fig. 10.15*b* shows excitation by steady rotation along the same axes. Figure 10.15*c* shows moment excitation by shear forces, where $\tilde{F} = \tilde{\sigma}\, dS$ acts on a small fluid volume $dV = 2(dS)d$. The symbol $\tilde{\sigma}$ is the fluctuating shear stress in newtons per square meter. This is the type of moment excitation found in the shear layer of high-speed jets and is treated in Chapter 15.

10.3 MEASURES TO REDUCE SOUND RADIATION

In this section we will discuss some of the measures noise control engineers and machine designers might employ to minimize the sound radiation of vibrating bodies. Most of these measures have been already discussed in a qualitative manner in Section 10.1. In this section we will show certain specific measures in

the form of conceptual sketches and give references where the reader can find more detailed design information.

Fish as Example for Minimized Added Mass. Through evolutionary development, fish have developed body shapes that minimize the reaction force on them when they accelerate their motion in the forward direction. If not in motion, most fish have their pectoral fins deployed perpendicular to their body. If they sense danger and want to dart away as fast as possible, the pectoral fins move rapidly backward (just like the oars of a paddleboat). For moving their pectoral fin in this direction they have a large added mass and can produce a large impulsive force on the water, which propels them forward. As the pectoral fins come near their body, the fins rotate 90° to align their body so that they contribute only a negligible amount to the friction coefficient. After this first impulsive burst, the pectoral fins are not deployed again until the fish want to use them to rapidly stop forward motion. With pectoral fins aligned the forward motion is propelled by the movement of the tail. At rest they deploy the pectoral fins again to be ready for the next dart.

To survive, predator fish must develop a body that minimizes the added mass for swimming in the forward direction so that they can generate a minimum of waterborne sound when they increase their speed (accelerate) when closing in on their prey. Otherwise the prey would sense the sound generated by their acceleration early enough to dart into a safe hiding space. In choosing body shapes that, for a given oscillatory velocity, radiate the least amount of sound in the direction of the body's motion, noise control engineers are well advised to choose the shape of the vibrating body to resemble the body of a fish.

As shown in Fig. 10.16, the most promising body shape would resemble that obtained by cutting two identical-size fish perpendicularly at the location of their largest cross-sectional area and fitting the two head-parts together so that the two mouths point in the opposite direction. For motion in a direction different

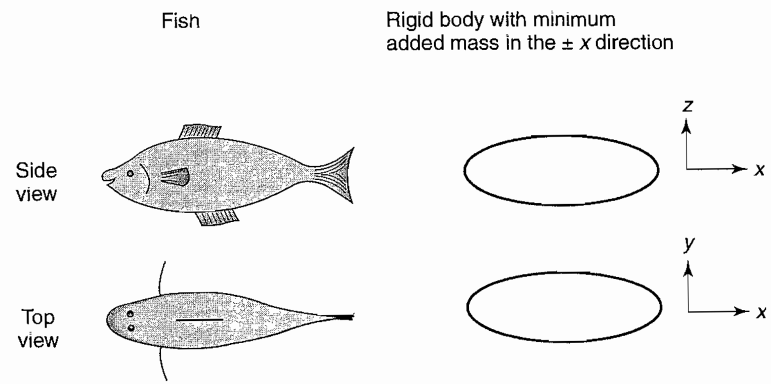

FIGURE 10.16 Learning from fish how to design bodies of minimum sound radiation owing to minimum added mass when oscillating in a specific direction.

from forward, especially in the direction perpendicular to it, the added mass of the fish is much larger, indicating the importance of the directional and shape dependence of the added mass of vibrating bodies of a geometry that is different from a sphere. The sphere has the distinction of having the same, large added mass for accelerating in any direction of motion. This large added mass is the reason that fish do no have a spherelike body (except some slow- swimming variety that inflate themselves to deceive their would-be predator). If fish would rotate instead of swim (mostly along straight paths), all of them would have a near-sphere-like body. On the other hand, if we wish to reduce the noise generated by the spinning of a rigid body, the sphere is the best choice. Surrounding a rotating nonspherical body with a spherical shell that rotates with the body will substantially reduce the noise radiation.

Reduction of Sound Radiation at Specific Frequencies. There is a class of noise sources, such as power transformers and turbine-generators, that radiate exclusively or predominantly tonal noise. Figures 10.17 and 10.18 show how the tonal noise produced by such equipment can be controlled by lining their radiating surface with Helmholtz resonator arrays tuned to the frequency (or frequencies) of their tonal noise output.

As shown in the lower sketch in Fig. 10.18, the noise radiation at the tuning frequency of the resonators is achieved by the low impedance of the resonator mouth in the vicinity of its resonance frequency. The fluid displaced by the solid part of the face of the resonator finds it easier to enter the resonator volume than to undergo compression. The smaller the compression, the lower is the radiated sound. Information on how to design Helmholtz resonators can be found in Chapter 8.

In the case of power transformers these tonal frequencies are 120, 240, 360, and 480 Hz in the United States and 100, 200, 300, and 400 Hz in Europe. Noise

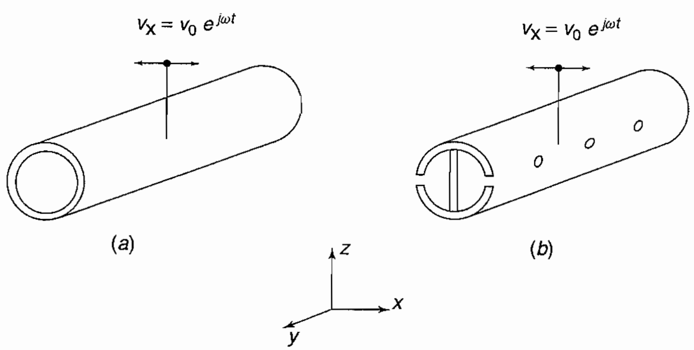

FIGURE 10.17 Frequency-selective reduction of sound generation owing to incorporation of Helmholtz resonators into the body: stiffened structural pipe beam vibrating perpendicular to its axes or rotating at constant rate as a spoke of a wheel.

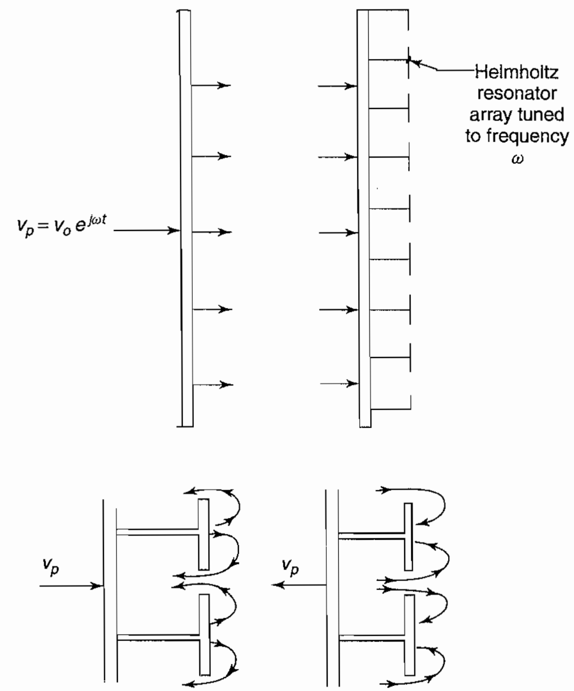

FIGURE 10.18 Frequency-selective reduction of sound radiation of a large flat surface, such as the outside wall of transformer tank, by lining it with a Helmholtz resonator array.

control measures for such noise sources and their advantages, disadvantages, and cost are compiled in reference 11.

Vacuum Bubbles. Figure 10.19 shows the concept of reducing the sound radiation of a transformer tank by lining the oil-side surface of the transformer tank with vacuum bubbles and how the presence of the vacuum bubbles, owing to their very large compliance, relieves the dynamic pressure on the tank wall and, consequently, reduces the sound radiation. As shown schematically in Fig. 10.20*a*, vacuum bubbles are twin curved thin shells with a small volume in between. When the cavity is evacuated, the shell nearly flattens out. In this evacuated final state they yield a compliance (inverse of the dynamic volume stiffness) that can be up to 50 times larger than the compliance of the air volume they replace and up to 1000 times that of the compliance of oil volume they replace. A unique feature of the vacuum bubbles is that there is vacuum in the cavity and there is no limit for the dynamic compliance, as there would be if the cavity were filled with a fluid. Below their resonance frequency, which is determined by the surface mass of the shell and its dynamic volume compliance, their volume compliance is independent of frequency. They work well even if the frequency approaches

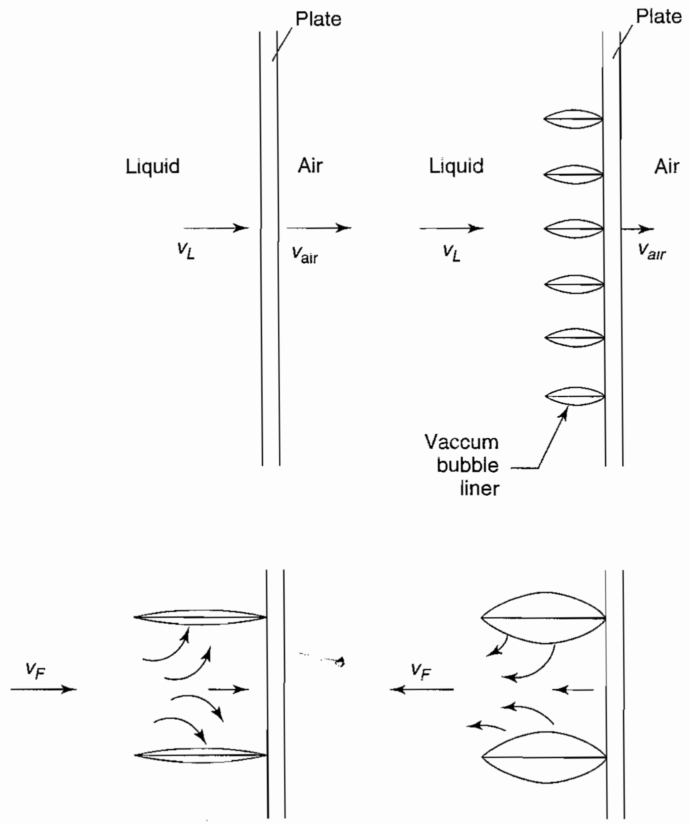

FIGURE 10.19 Reduction of the sound radiation from a transformer tank by lining the oil-side face of the tank wall with an array of vacuum bubbles of extremely high volume compliance. The vacuum bubbles can be oriented either perpendicular to the wall (as shown here) or parallel to it. Lower sketches indicate how the vacuum bubbles, which are much more compliant than either the oil or the tank wall, "soaks up" the momentum of the periodically approaching and receding oil. The velocity of the oil is due to the vibration of the transformer core driven by magnetostrictive forces.

zero. Information on how to design a vacuum bubbles for specific applications is given in references 12–14.

Figure 10.20 shows the geometry of a vacuum bubble (also called Scillator by its inventor Dr. Bschorr[12]) before and after evacuation of the cavity. As the name vacuum bubble implies, it is useful only in the evacuated state.

Vacuum bubbles are very sensitive to changes in static pressure (barometric pressure in air and depth-dependent pressure in liquids). Consequently, their most promising application would be in space stations, where the static air pressure can be controlled accurately.

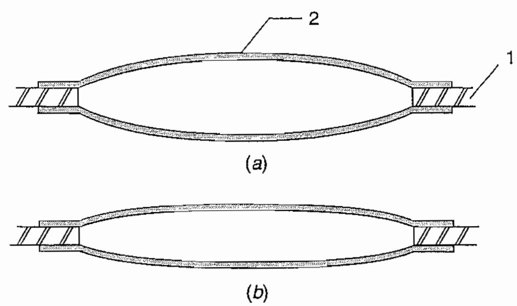

FIGURE 10.20 Conceptual sketch of a vacuum bubble. (*a*) Cross-sectional shape before evacuation of the cavity: 1, double-curved thin shell in the form of a top segment of a large-radius hollow sphere; 2, flat-plate strip base with punched holes. (*b*) Shape after evacuation of the cavity.

REFERENCES

1. M. C. Junger and D. Feit, *Sound Structures and Their Interaction*, 2nd ed., MIT Press, Cambridge, MA, 1986.
2. U. K. Ingard, *Notes on Sound Absorption Technology*, Version 94-02, Noise Control Foundation, Arlington Branch, Poughkeepsie, NY, pp B-5 (out of print). A CD version can be purchased from the author at www.ingard.com.
3. L. Cremer and M. Hubert, *Vorlesungen ueber Technische Akustik*, [Lectures about Technical Acoustics], 3rd ed., Springer, Berlin, 1985.
4. M. Heckel and H. A Mueller, *Taschenbuch der Technischen Akustik*, 2nd ed., Springer, Berlin, 1994.
5. I. L. Ver, "Reciprocity as a Prediction and Diagnostic Tool in Reducing the Transmission of Structureborne and Airborne Noise into an Aircraft Fuselage," BBN Report No. 4985, NASA Contract No. NASI-16521, January 3, 1982, Bolt Beranek and Newman Inc., Cambridge MA.
6. I. L. Ver "Using Reciprocity and Superposition as a Diagnostic and DesignTool in Noise Control," *Acustica, Acta Acoustica*, **82**, 62–69 (1996).
7. I. L. Ver and R. W. Oliphant, "Acoustic Reciprocity for Source-Path-Receiver Analyses," *Noise Vibration*, March 1996, pp. 14–17.
8. G. H. Koopmann and J. B. Fahnline, *Designing Quiet Structures; A Sound Power Minimization Approach*, Academic, New York, 1997.
9. J. N. Newman, *Marine Hydrodynamics*, MIT Press, Cambridge, MA, 1980, p. 144.
10. D. A. Bies and C. H. Hansen, *Engineering Noise Control Theory and Practice*, Unwin Hyman, Boston, 1988.
11. I. L. Ver, C. L. Moore, et al., "Power Transformer Noise Abatement," BBN Report No. 4863, October 1981. Submitted to the Empire State Electric Energy Research Corporation (ESEERCO).
12. O. Bschorr and E. Laudien, "Silatoren zur Daempfung und Daemmung von Schall" [Vacuum Bubbles for Absorption and Reduction of Sound], *Automobil-Industrie*, **2**, 159–166 (1988).

13. I. L. Ver, "Potential Use of Vacuum Bubbles in Noise Control," BBN Report No. 6938, NASA CR-181829, December 1988, Bolt Beranek and Newman, Inc., Cambridge MA.
14. I. L. Ver, "Noise Reduction from a Flexible Transformer Tank Liner," Phase I, Feasibility Study, BBN Report No. 6240, February 1987, Bolt Beranek and Newman, Inc., Cambridge MA.

CHAPTER 11

Interaction of Sound Waves with Solid Structures

ISTVÁN L. VÉR

Consultant in Acoustics, Noise, and Vibration Control
Stow, Massachusetts

The response of structures to dynamic forces or dynamic pressures is the subject of structural dynamics and acoustics. Structural dynamics is concerned predominantly with dynamic stresses severe enough to endanger structural integrity. Structural acoustics deals with low-level dynamic processes in structures resulting from excitation by forces, moments, and pressure fields. The primary interest in airborne and structure-borne noise problems is the prediction of

1. power input into the structure,
2. the response of the excited structure,
3. propagation of structure-borne sound to connecting structures, and
4. sound radiated by the vibrating structure.

The subject matter of this chapter is specific to noise control problems and thus is restricted to the audible frequency range and to air as the surrounding medium, though many of the concepts are directly applicable to liquid media or to higher or lower frequencies.

A typical noise control problem is illustrated in Fig. 11.1. A resiliently supported floor slab in the room to the left (source room) is excited by the periodic impacts of a tapping machine, while the microphone in the receiving room to the right registers the resulting noise. A part of the vibrational energy is dissipated in the floating slab, a part is radiated directly as sound into the source room, and the remainder is transmitted through the resilient layer into the building structure.

The radiated sound energy builds up a reverberant sound field in the source room that in turn excites the walls. The vibrations in the wall separating the two rooms, identified as path 1 in Fig. 11.1, radiate sound directly into the receiver room. The vibrations in the other partitions of the source room travel in the form of structure-borne sound to the six partitions of the receiving room and radiate

13. I. L. Ver, "Potential Use of Vacuum Bubbles in Noise Control," BBN Report No. 6938, NASA CR-181829, December 1988, Bolt Beranek and Newman, Inc., Cambridge MA.
14. I. L. Ver, "Noise Reduction from a Flexible Transformer Tank Liner," Phase I, Feasibility Study, BBN Report No. 6240, February 1987, Bolt Beranek and Newman, Inc., Cambridge MA.

CHAPTER 11

Interaction of Sound Waves with Solid Structures

ISTVÁN L. VÉR
Consultant in Acoustics, Noise, and Vibration Control
Stow, Massachusetts

The response of structures to dynamic forces or dynamic pressures is the subject of structural dynamics and acoustics. Structural dynamics is concerned predominantly with dynamic stresses severe enough to endanger structural integrity. Structural acoustics deals with low-level dynamic processes in structures resulting from excitation by forces, moments, and pressure fields. The primary interest in airborne and structure-borne noise problems is the prediction of

1. power input into the structure,
2. the response of the excited structure,
3. propagation of structure-borne sound to connecting structures, and
4. sound radiated by the vibrating structure.

The subject matter of this chapter is specific to noise control problems and thus is restricted to the audible frequency range and to air as the surrounding medium, though many of the concepts are directly applicable to liquid media or to higher or lower frequencies.

A typical noise control problem is illustrated in Fig. 11.1. A resiliently supported floor slab in the room to the left (source room) is excited by the periodic impacts of a tapping machine, while the microphone in the receiving room to the right registers the resulting noise. A part of the vibrational energy is dissipated in the floating slab, a part is radiated directly as sound into the source room, and the remainder is transmitted through the resilient layer into the building structure.

The radiated sound energy builds up a reverberant sound field in the source room that in turn excites the walls. The vibrations in the wall separating the two rooms, identified as path 1 in Fig. 11.1, radiate sound directly into the receiver room. The vibrations in the other partitions of the source room travel in the form of structure-borne sound to the six partitions of the receiving room and radiate

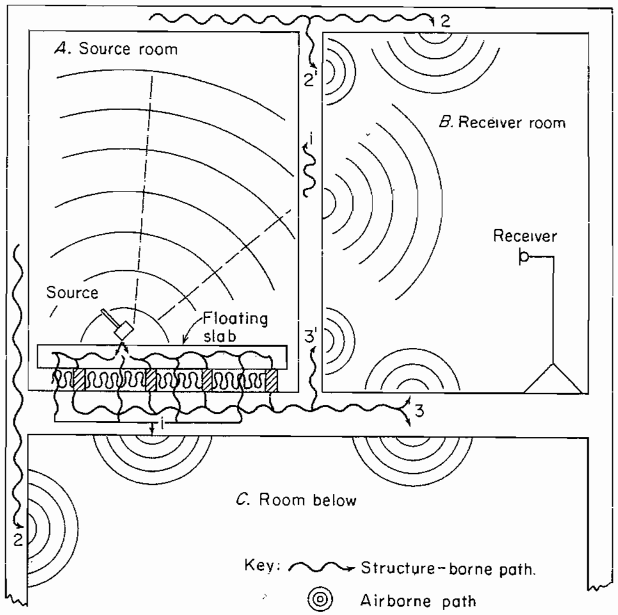

FIGURE 11.1 Sound transmission paths between an impact source in room A and a receiver in room B. Also shown are the paths to room C below.

sound into the receiver room. The structure-borne paths are identified by waves, 2, 2′ and 3, 3′.

To reduce the noise level in the receiving room by a desired amount, the acoustical engineer must estimate the sound power transmitted from the source room to the receiver room through each path and then design appropriate measures to (1) reduce power input to the floating slab, (2) increase power dissipation in the slab, (3) increase vibration isolation, (4) reduce the structure-borne noise along its propagation path between source and receiver room, (5) reduce the sound radiated by the partitions of the source room, and (6) reduce the reverberation buildup of the sound in the receiver room by increasing sound absorption.

The aim of this chapter is to provide the information needed to solve such typical noise control engineering problems.

11.1 TYPES OF WAVE MOTION IN SOLIDS

Wave motion in solids can store energy in shear as well as in compression. The types of waves possible in solids include compressional waves, flexural waves, shear waves, torsional waves, and Rayleigh waves. Compressional waves are of practical importance in gases and liquids, which can store energy only in

compression. The different types of waves in solids result from different ways of stressing. For a wave to propagate in solids, liquids, and gases, the medium must be capable of storing energy alternatively in kinetic and potential form. Kinetic energy is stored in any part of a medium that has mass and is in motion, while potential energy is stored in parts that have undergone elastic deformation.

Solid materials are characterized by the following parameters:

Density	ρ_M	kg/m^3
Young's modulus	E	N/m^2
Poisson's ratio	ν	
Loss factor	η	

The shear modulus G is related to Young's modulus as

$$G = \frac{E}{2(1+\nu)} \quad \text{N/m}^2 \tag{11.1}$$

The sketches on the left of Table 11.1 illustrate the deformation pattern typical for compressional, shear, torsional, and bending waves in bars and plates. Acoustically important parameters of solid materials are compiled in Table 11.2. Note that all tables in this chapter are placed at the end of the text. Thickness and weight per unit surface area of steel plates are listed in Table 11.10. Percentage open area of perforated metal is given in Table 11.11.

In dealing with structure-borne sound, we must distinguish between velocity and propagation speed. The term *velocity* refers to vibration velocity of the structure (i.e., the time derivative of the local displacement), which is linearly proportional to the excitation and will be designated by the letter v. As illustrated on the left of Table 11.1, the displacement and velocity are in the direction of wave propagation for longitudinal waves and perpendicular to it for shear and bending waves.

The term *speed* refers to the propagation speed of structure-borne sound, which is a characteristic property of the structure for each type of wave motion and is independent of the strength of excitation provided that the deformations are small enough to avoid nonlinearities. Propagation speeds will be designated by the letter c. We must distinguish between *phase speed* and *group speed* (or energy speed).

The phase speed c is defined in terms of (1) the wavelength λ, which is the distance in the propagation direction for which the phase of a sinusoidal wave changes 360°, and (2) the frequency f of the sinusoid. Consequently, $c = \lambda f$. Formulas to calculate phase speed of the various wave types are given on the right side of Table 11.1. Note that the phase speed for longitudinal, shear, and torsional waves is independent of frequency. Consequently, they are referred to as nondispersive waves. This means that the time history of an impulse, such as caused by a hammer blow striking axially on one end of a semi-infinite bar, as illustrated in Fig. 11.2a, will have the same shape regardless of where the

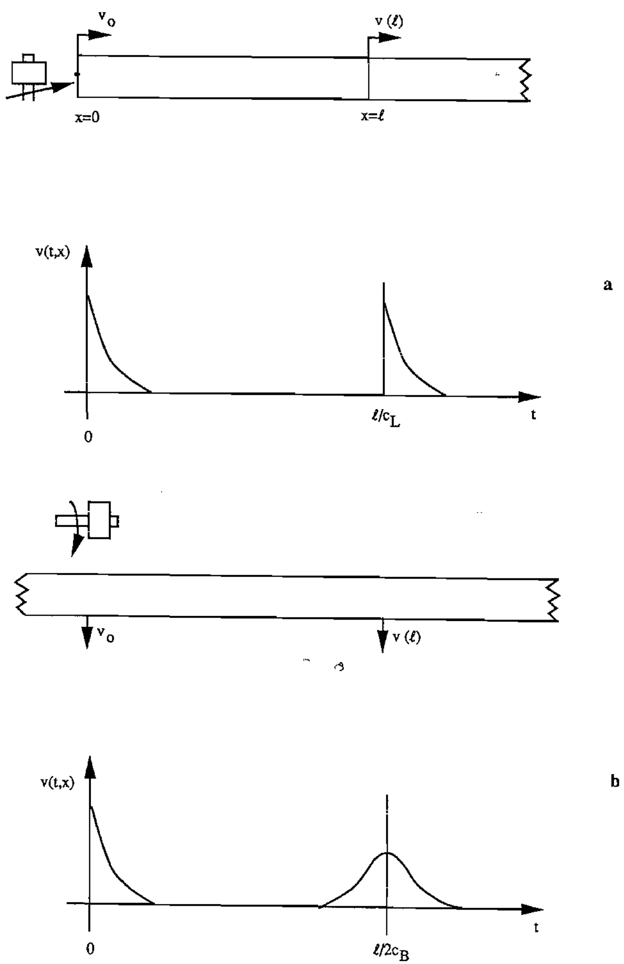

FIGURE 11.2 Time history of beam motion for impulsive excitation: (*a*) axial impact-generating nondispersive compressional waves; (*b*) normal impact-generating dispersive bending waves.

axial motion is sensed. Because the pulses sensed at different locations are time-delayed versions of each other, the propagation speed of the longitudinal wave can be determined experimentally as the ratio of the axial distance and the difference of arrival time. Since all frequency components travel at the same speed, the phase speed (which is defined only for a steady-state sinusoidal excitation) is identical with the speed of energy transport.

The phase speed of the bending wave can be easily measured by exciting the infinite beam with a steady-state sinusoidal force acting normal to the beam

axis and measuring the gradient of the phase $d\phi/dx$ along the beam. The phase velocity c_B is defined as

$$c_B = \frac{2\pi f}{|d\phi/dx|} \quad \text{m/s} \tag{11.2}$$

However, the situation is much more complicated in the case of a complex waveform such as illustrated in Fig. 11.2*b*, where an infinite beam is impacted normally and a bending-wave pulse that contains a wide band of frequencies is created. Because of their higher phase speed, high-frequency components speed ahead of the low-frequency component. Consequently, the width of the pulse increases as it travels along the beam. The speed of energy transport for the bending-wave pulse is not obvious. In case of light fluid loading (when the energy carried in the surrounding fluid is negligible), it is meaningful to define the energy transport speed as the ratio of transmitted power W and the energy density E'' (per unit length of beam). For a pulse whose spectrum peaks at frequency f the energy speed c_{BG} is twice the phase speed[1]:

$$c_{BG}(f) = 2c_B(f) \quad \text{m/s} \tag{11.3}$$

Accordingly, the power transmitted by a plane bending wave in the direction of propagation per unit area of a structure normal to that direction is

$$W_S = c_{BG}E'' = 2c_B\rho_M v^2 \quad \text{W/m}^2 \tag{11.4}$$

where v is the rms value of the bending-wave velocity and ρ_M is the density of the material. According to Eq. (11.4), the bending-wave power in an infinite beam of cross section S is given by

$$W = 2c_B S\rho_M v^2 \quad \text{W} \tag{11.5}$$

and power transmitted by a plate of thickness h across a line length l aligned parallel to the wave front is

$$W = 2c_B hl\rho_M v^2 \quad \text{W} \tag{11.6}$$

11.2 MECHANICAL IMPEDANCE AND POWER INPUT

Except for the initial transient, the velocity at the excitation point is zero if a structure is subjected to a static force. Accordingly, a static force does not transmit power into a fixed structure. For dynamic excitation by a point force or moment [the moment $M = Fl_m$ is defined as a pair of forces (F) of equal magnitude but opposite direction acting simultaneously at a short distance ($\frac{1}{2}l_M$) on both sides of the excitation point], there is always a finite dynamic velocity or dynamic rotation at the excitation point. If the velocity at the excitation point has a component that is in phase with the force, or the angular velocity has a component that is in phase with the moment, then power is fed continuously into the structure.

Mechanical Impedance

The mechanical impedance is a measure of how a structure "resists" outside forces or moments. A thorough understanding of mechanical impedances is a necessary requirement for understanding and for solving most noise control problems. The concept of mechanical impedance is best introduced by considering a harmonic force $F = \hat{F}e^{j\omega t}$ acting on an ideal lumped-parameter system such as a rigid unrestrained mass, a massless spring, or a dashpot. The velocity response is also a harmonic function of the form $v = \hat{v}e^{j\omega t}$. The force impedance Z_F is defined as

$$Z_F = \frac{\hat{F}}{\hat{v}} \quad \text{N} \cdot \text{s/m} \tag{11.7}$$

and the moment impedance Z_M as

$$Z_M = \frac{\hat{M}}{\hat{\dot{\theta}}} \quad \text{N} \cdot \text{s/m} \tag{11.8}$$

where M is the exciting moment (torque) and $\dot{\theta}$ is the angular velocity at the excitation point.

The point force impedance for these basic lumped elements are listed below:

Element	Z_F	
Mass	$j\omega m$	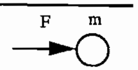
Spring	$-js/\omega$	
Dashpot	r	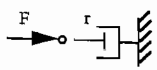

where m is the mass of a rigid body, s is the stiffness of the spring, and r is the resistance of the dashpot. Note that the direction of the force must go through the center of gravity of the mass so that the velocity response is free of rotation and is in the direction of the force. For the rigid mass and the massless spring the force impedance is imaginary, indicating that the force and velocity are in quadrature and the power input is zero.

Formulas for computing the point force and moment impedances of infinite structures are given in references 2–12 and in Tables 11.3 and 11.4, respectively. Both force and moment impedances are idealized concepts, defined for point

forces and point moments. Forces or moments can be considered applied at a point, provided that the surfaces over which they act are smaller than one-sixth of the structural wavelength. Naturally, the excited surface area must be large enough so that the force does not cause plastic deformation of the structure. There is proportionality between force and moment impedances in the form of

$$Z_M = l_M^2 Z_F \quad \text{N} \cdot \text{m/s} \tag{11.9}$$

where l_M is the effective length given in Table 11.5.

Power Input

For the dashpot the force impedance is real. The velocity is in phase with the force and the power that is fed continuously into the dashpot and dissipated in it is given by $\frac{1}{2}|\hat{F}|^2/r$. More generally, for a system with a complex force impedance Z_F, the input power is

$$W_{\text{in}} = \frac{\omega}{2\pi}\int_0^{2\pi/\omega} F(t)v(t)\, dt = \tfrac{1}{2}|\hat{F}|\ |\hat{v}|\cos\phi = \tfrac{1}{2}|\hat{F}|^2\, \text{Re}\left\{\frac{1}{Z_F}\right\} \quad \text{W} \tag{11.10}$$

where $\hat{F}$ and $\hat{v}$ are the peak amplitude of the exciting force and the velocity, ϕ is the relative phase between $F(t)$ and $v(t)$, and Re{} refers to the real part of the bracketed quantity. Equation (11.10) is valid for any situation, not only for the dashpot.

Rigid masses, massless springs, and dashpots are useful abstractions that represent the dynamic properties of structural elements. At sufficiently low frequencies, the housing of a resiliently mounted pump behaves like a rigid mass, while the resilient rubber mount that supports it behaves like a spring. This lumped-parameter characterization of mechanical elements becomes invalid when, with increasing frequency, the structural wavelength becomes smaller than the largest dimensions of the structural element.

To deal with finite structures that are large compared with the structural wavelength, we need another useful abstraction. Regarding their input impedance—which governs power input—it is useful to consider such structures as infinite. The strategy for predicting the vibration response and sound radiation for these structures is to estimate the power input as if they were infinite and then predict the average vibration that such input power will cause in the actual finite structure. Because most structures are made of plates and beams, our strategy requires us to characterize the impedance of infinite plates and beams. The abstraction of infinite size is invoked so that no structural waves reflected from the boundaries come back to the excitation point. In this respect, structures can be considered infinite if no reflected waves that are coherent with the input come back to the excitation point because the boundaries are completely absorbing or because there is sufficient damping so that the response attributable to the reflected waves is small compared to that attributable to the local excitation.

In respect to point force excitation, infinite structures are characterized by their point force impedance $\tilde{Z}_{F\infty}$ or point input admittance (also called mobility) $\tilde{Y}_{F\infty}$, defined as

$$\tilde{Z}_{F\infty} = \frac{\tilde{F}_0}{\tilde{v}_0} \quad \mathrm{N \cdot s/m} \tag{11.11}$$

$$\tilde{Y}_{F\infty} = \frac{1}{\tilde{Z}_{F\infty}} = \frac{\tilde{v}_0}{\tilde{F}_0} \quad \mathrm{m/N \cdot s} \tag{11.12}$$

where $\tilde{F}_0$ is the applied point force and $\tilde{v}_0$ is the velocity response at the excitation point. The tilde above the symbols (which we will drop in further considerations) signifies that F_0 and v_0 are complex scalar quantities characterized by a magnitude and phase. Since $\tilde{v}_0$ usually has a component that is in phase with $\tilde{F}_0$ and one that is out of phase with $\tilde{F}_0$, the parameters $\tilde{Z}_F$ and $\tilde{Y}_F$ usually have both real and imaginary parts.

The power inputs to infinite structures excited by a point force or by a point velocity source (i.e., a vibration source of high internal impedance) are, respectively,

$$W_{\text{in}} = |\tfrac{1}{2}\hat{F}_0^2| \,\mathrm{Re}\left\{\frac{1}{Z_{F\infty}}\right\} \quad \mathrm{W} \tag{11.13a}$$

$$W'_{\text{in}} = G_{FF} \,\mathrm{Re}\left\{\frac{1}{Z_{F\infty}}\right\} \quad \mathrm{W/Hz} \tag{11.13b}$$

$$W_{\text{in}} = (\tfrac{1}{2}\hat{v}_0^2) \,\mathrm{Re}\{Z_{F\infty}\} \quad \mathrm{W} \tag{11.14a}$$

$$W'_{\text{in}} = G_{VV} \,\mathrm{Re}\{Z_{F\infty}\} \quad \mathrm{W/Hz} \tag{11.14b}$$

where $\hat{F}_0$ and $\hat{v}_0$ are peak amplitudes of the exciting sinusoidal force and velocity and G_{FF} and G_{VV} are the force and velocity spectral densities when the excitation is of broadband random nature. For excitation by a moment of peak amplitude $\hat{M}$ or by an enforced angular velocity of peak amplitude $\hat{\theta}$, the corresponding expressions are

$$W_{\text{in}} = |\tfrac{1}{2}\hat{M}_0^2| \,\mathrm{Re}\left\{\frac{1}{Z_M}\right\} \quad \mathrm{W} \tag{11.15a}$$

$$\frac{W'_{\text{in}}}{\mathrm{Hz}} = G_{MM} \,\mathrm{Re}\left\{\frac{1}{Z_M}\right\} \quad \mathrm{W/Hz} \tag{11.15b}$$

$$W_{\text{in}} = |\tfrac{1}{2}\hat{\theta}| \,\mathrm{Re}\{Z_M\} \quad \mathrm{W} \tag{11.16a}$$

$$W'_{\text{in}} = G_{\theta\theta} \,\mathrm{Re}\{Z_M\} \quad \mathrm{W/Hz} \tag{11.16b}$$

Table 11.3 lists the point force impedance $Z_{F\infty}$ and Table 11.4 the moment impedance $Z_{M\infty}$ for semi-infinite and infinite structures. Table 11.5 lists the effective length l_M that connects the point force and moment impedances according

to Eq. (11.9). Information regarding power input to infinite structures for force, velocity, moment, and angular velocity excitation is compiled in Table 11.6. The most complete collection of impedance formulas, which includes beams, box beams, orthotropic and sandwich plates with elastic or honeycomb core, grills, homogeneous and rib-stiffened cylinders, spherical shells, plate edges, and plate intersections and transfer impedances of various kinds of vibration isolators, is presented in reference 12.

For approximate calculations or for cases where no formulas are given in Tables 11.3–11.6, the power input to infinite structures can be estimated according to Heckl[10,11] as

$$W_{\text{in}} = \frac{\tfrac{1}{2}\hat{F}_0^2}{Z_{\text{eq}}} \quad \mathrm{W} \tag{11.17}$$

$$W_{\text{in}} = (\tfrac{1}{2}\hat{v}_0^2) Z_{\text{eq}} \quad \mathrm{W} \tag{11.18}$$

where Eq. (11.17) is used for localized force excitation (i.e., low-impedance vibration source) and Eq. (11.18) for localized velocity excitation (i.e., high-impedance vibration source) and Z_{eq} is estimated as

$$Z_{\text{eq}} = \omega\rho_M S\epsilon[\alpha\lambda] \quad \mathrm{N \cdot s/m} \quad \text{(beam)} \tag{11.19a}$$

$$Z_{\text{eq}} = \omega\rho_M h\epsilon[\pi(\alpha\lambda)^2] \quad \mathrm{N \cdot s/m} \quad \text{(plate)} \tag{11.19b}$$

$$Z_{\text{eq}} = \omega\rho_M \epsilon[\tfrac{4}{3}\pi(\alpha\lambda)^3] \quad \mathrm{N \cdot s/m} \quad \text{(half space)} \tag{11.19c}$$

where ρ_M is the density of the material, S is the cross-sectional area of the beam, h is the plate thickness, λ is the wavelength of the motion excited most strongly (bending, shear, torsion, or compression), and ϵ is 1 when the structure is excited in the "middle" and 0.5 when it is excited at the end or at the edge (semi-infinite structure) and α is a number in the range of 0.16–0.6. If not known, it is customary to use $\alpha = 0.3$.

The equivalent impedance Z_{eq} in Eq. (11.19) has an instructive and easy-to-remember interpretation, namely that the magnitude of the point input impedance is roughly equal to the impedance of a lumped mass that lies within a sphere of radius $r \simeq \frac{1}{3}\lambda$ centered at the excitation point. This portion of the structure is shown in the third column of Table 11.3. This principle can be extended to composite structures[10] such as beam-stiffened plates where the combination of Eqs. (11.19a) and (11.19b) yields

$$Z_{\text{eq}} \cong \omega\rho_B S_B(\tfrac{1}{3}\lambda_{BB}) + \omega\rho_p h(\tfrac{1}{3}\lambda_{BP}) \quad \mathrm{N \cdot s/m} \tag{11.20}$$

Another useful rule of thumb is that, regarding power input, excitation by a moment $\hat{M}$ and by an enforced angular velocity $\hat{\theta}$ can be represented by an equivalent point force $\hat{F}_{\text{eq}}$ or equivalent velocity $\hat{v}_{\text{eq}}$,[11]

$$\hat{F}_{\text{eq}} \cong \frac{\hat{M}}{0.2\lambda_B} \quad \text{N} \tag{11.21}$$

$$\hat{v}_{\text{eq}} \cong \hat{\dot{\theta}}(0.2\lambda_B) \quad \text{m/s} \tag{11.22}$$

If the excitation force extends over an area that is large compared with the bending wavelength, the power transmitted into the structure becomes substantially less than it would be for a concentrated force. For extended velocity source the power transmitted becomes significantly larger than it would be for a concentrated velocity excitation.

According to reference 5, the real part of the point force impedance, Re $\{Z_{F\infty}\}$, can be predicted according to Bode's theorem as

$$\text{Re}\{Z_{F\infty}\} \cong |Z_{\text{eq}}| \cos(\tfrac{1}{2}\epsilon\pi) \quad \text{N}\cdot\text{s/m} \tag{11.23}$$

where ϵ is defined here as an exponent of the Z_{eq}-versus-frequency curve (i.e., $Z_{\text{eq}} \sim \omega^{\epsilon}$), where $\epsilon = 0$ for homogeneous isotropic thick plates, $\epsilon = 0.5$ for beams in bending, and $\epsilon = \frac{2}{3}$ for cylinders below the ring frequency.

Parameters Influencing Power Input. When the excitation point is near a structural junction, part of the incident vibration wave is reflected. This reflected wave influences the velocity at the excitation point and thereby also the driving point impedance and consequently the power input. Fig. 11.3*a* shows the effect of the vicinity of a T-junction comprised of identical, anechoically terminated beams on the point force impedance $Z_2(x_0)$ as a function of the distance x_0 between the junction and the excitation point.[13] As expected, the impedance increases rapidly with decreasing distance when $x_0 < \frac{1}{3}\lambda_B$. The junction has a considerable effect even for large x_0, causing approximately a 2 : 1 fluctuation in the magnitude of the impedance. Figure 11.3*b* shows the measured distribution of the beam vibration velocity $|v(x)|$ along each of the three beam branches, indicating that the observed strong standing-wave pattern is limited to that part of beam 2 that lies between the junction and the excitation point.

The impedance formulas presented in Tables 11.3–11.6 are strictly valid only when the surrounding fluid medium has no appreciable effect on the response of the structure. This is generally true for air as the surrounding medium but not for water, which is 800 times more dense than air. The effect of fluid loading at low frequencies is equivalent[14] to adding a virtual mass per unit area ρ_s',

$$\rho_s' = \frac{\rho_0 c_B(f)}{\omega} \cong \rho_0[\tfrac{1}{6}\lambda_B(f)] \quad \text{kg/m}^2 \tag{11.24}$$

to the mass per unit area of the plate. In Eq. (11.24), ρ_0 is the density of the fluid and $c_B(f)$ and $\lambda_B(f)$ are the bending-wave speed and the wavelength of the free bending waves in the unloaded plate (see Table 11.1). Because ρ_s' is inversely proportional to $\omega^{1/2}$, fluid loading results in greater reduction of the response

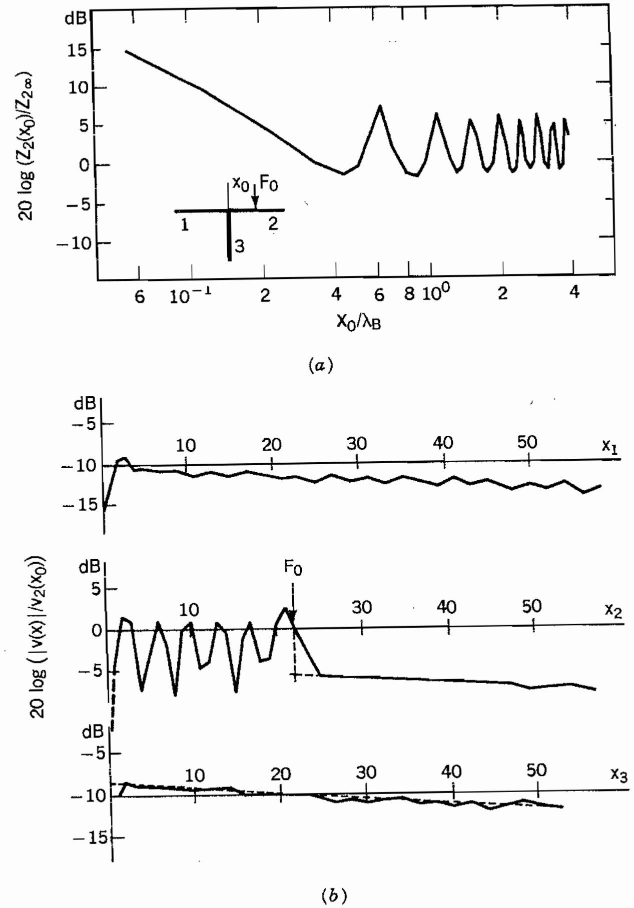

FIGURE 11.3 Effect of the vicinity of T-junction on the measured point force impedance and velocity response[13]: (*a*) normalized force impedance $Z_1(x_0)/Z_{1\infty}$ as a function of the normalized distance x_0/λ_B and x_i is the distance from the junction along beam i; (*b*) distribution of normalized velocity, $v(x)/v_0$, along the three beam branches as numbered in (*b*).

at the excitation point at low than at high frequencies. Fluid-loading effects are treated in references 14–17.

11.3 POWER BALANCE AND RESPONSE OF FINITE STRUCTURES

For finite structures, the response at the excitation point, and accordingly also the input admittance, $Y = 1/Z$, depends on the contribution of the waves reflected from the boundaries or discontinuities. Consequently, Y varies with the location of the excitation point and with frequency. However, both the space-averaged and frequency-averaged input admittances of the finite structure $\langle Y(x, f)\rangle_x$ and $\langle Y(x, f)\rangle_f$ equal the point input admittance of the equivalent infinite structure,[18] namely,

$$\langle Y(x, f)\rangle_x = \langle Y(x, f)\rangle_f = Y_\infty \quad \text{m/N} \cdot \text{s} \tag{11.25}$$

Figures 11.4*a* and 11.4*b* show the typical variation of the real and imaginary parts of the point input admittance of a finite plate with location x and frequency f, respectively. This particular behavior has considerable practical importance:

1. The power introduced into a finite structure by a point force of random-noise character can be well approximated by the power that the same force would introduce into an equivalent infinite structure.
2. The power introduced into a finite structure by a large number of randomly spaced point forces can be approximated by the power the same forces would introduce into an equivalent infinite structure.

Resonant Modes and Modal Density

The peaks in Fig. 11.4*a* correspond to resonance frequencies of the finite structure, where waves reflected from the boundaries travel in closed paths such that they arrive at their starting point in phase. The spatial deformation pattern that corresponds to such a particular closed path is referred to as the *mode shape* and the frequency where it occurs as the *eigenfrequency* or *natural frequency* of the finite structure. The importance of such resonances lies in the high transverse velocity caused by the in-phase superposition of the multiple reflections that may result in increased sound radiation or fatigue.

Exact calculation of the natural frequencies is possible only for a few highly idealized structures. Fortunately, the modal density $n(f)$, which is defined as the average number of natural frequencies in a 1-Hz bandwidth, depends not too strongly on the boundary conditions. Accordingly, one can make a reliable statistical prediction of the modal density using the formulas obtained for the equivalent idealized system.

For example, the modal density of a thin, flat, homogeneous, isotropic plate of not too high aspect ratio two octaves above the first plate resonance is already well approximated by the modal density of a rectangular plate of equal surface area, which is given by[1]

$$n(f) \approx \frac{\sqrt{12}S}{2c_L h} \quad \text{s} \tag{11.26}$$

where S is the area (one side) and h is the thickness. Note that $n(f)$ is independent of frequency and that it is large for large and thin plates.

The modal density of rooms of volume V one octave above the first room resonance is usually well approximated by the first term of the modal density of

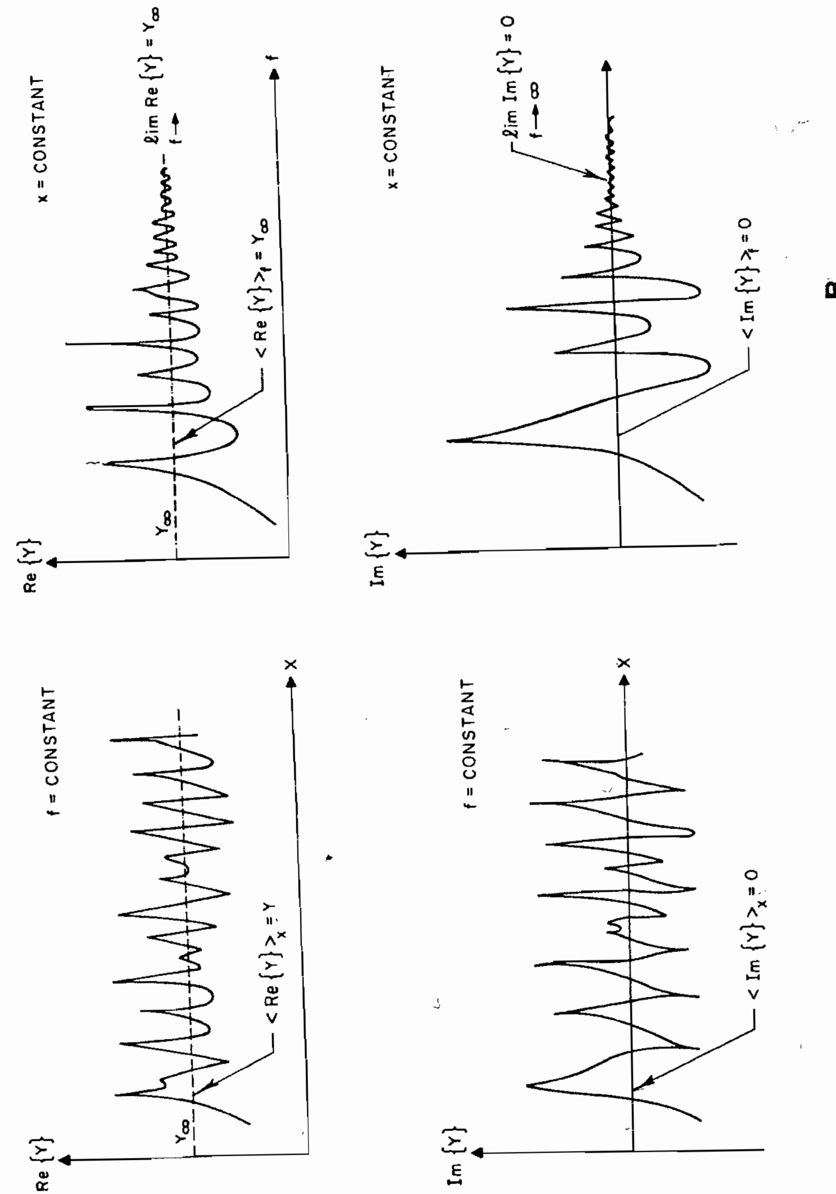

FIGURE 11.4 Typical fluctuations of the real part, Re{Y}, and imaginary part, Im{Y}, of the point input admittance of a finite plate as a function of (*a*) location x, $\langle \cdots \rangle_x$ is spatial average at a fixed frequency; (*b*) frequency f, $\langle \cdots \rangle_f$ is frequency average at a fixed location

a rectangular room with hard walls,

$$n(f) = \frac{4\pi V}{c_0^3} f^2 + \frac{\pi S}{c_0^2} + \frac{L}{8c_0} \quad \text{s} \tag{11.27}$$

where S is the total wall surface area and L is the longest dimension of the rectangular room. The first resonance frequency, modal densities, and mode shapes of a number of finite structures and the point input impedance (the inverse of the admittance) of the equivalent infinite structure are compiled in Table 11.7. More detailed information on mode shapes, natural frequencies, and modal densities are given in reference 19. The following important relationship exists between the modal density and the real part of the point force admittance of the equivalent infinite system[1]:

$$\operatorname{Re}\{Y_\infty\} = \frac{n(f)}{iM} \quad \text{m/N} \cdot \text{s} \qquad i = \begin{cases} 4 \text{ for thin plate} \\ 2 \text{ for thin cylinder} \\ 1 \text{ for thin sphere} \end{cases} \tag{11.28}$$

where M is the total mass of the finite system.

Power Balance

The power balance given in Eq. (11.29),

$$W_{\text{in}} = W_d + W_{\text{tr}} + W_{\text{rad}} \quad \text{W} \tag{11.29}$$

states that, in steady state, the power introduced, W_{in}, equals the power dissipated in the structure, W_d, the power transmitted to connected structures, W_{tr}, and the power radiated as sound into the surrounding fluid, W_{rad}. If the excitation is by a point force of peak amplitude $\hat{F}_0$ and the structure is a homogeneous isotropic thin plate of thickness h, area S (one side), density ρ_M, with longitudinal wave speed c_L, immersed in a fluid of density ρ_0, and speed of sound c_0, Eq. (11.29) takes the form

$$\tfrac{1}{2}\hat{F}^2 \operatorname{Re}\{Y_F\} = \langle v^2 \rangle S[\rho_s \omega \eta_d + \rho_s \omega \eta_{\text{tr}} + 2\rho_0 c_0 \sigma] \quad \text{W} \tag{11.30}$$

where $\rho_s = \rho_M h$ is the mass per unit area of the plate, $\omega = 2\pi f$ is the radian frequency, η_d and η_{tr} are the dissipative and transmissive loss factors, and σ is the sound radiation efficiency of the plate (see Section 11.6). Combining dissipative and transmissive losses into a single composite loss factor $\eta_c = \eta_d + \eta_{\text{tr}}$ and assuming $\operatorname{Re}\{Y_F\} = Y_{F\infty} = 1/Z_{F\infty} = 1/(2.3\rho_s C_L t)$, as given in Table 11.3, and solving for the space–time averaged mean-square plate velocity $\langle v^2 \rangle$ yield

$$\langle v^2 \rangle = \frac{\hat{F}_0^2}{4.6\rho_s^2 c_L t \omega \eta_c S(1 + 2\rho_0 c_0 \sigma/\rho_s \omega \eta_c)} \quad \text{m}^2/\text{s}^2 \tag{11.31}$$

Example 11.1. Predict the space–time averaged velocity response $(\langle v^2 \rangle)^{1/2}$ of a 2-mm-thick, 1×2-m steel plate to a point force $\hat{F}_0 = 10$ N peak amplitude at a frequency of 10 kHz when $\sigma = 1$ and $\eta_c = 0.01$. Compare $\langle v^2 \rangle$ with the mean-square velocity at the excitation point v_0^2. The input parameters to be used in connection with Eq. (11.31) and Table 11.2 are

$$\begin{aligned} &\hat{F}_0 = 10 \text{ N} \qquad \rho_s = \rho_M t = 7700 \text{ kg/m}^3 \times 2 \times 10^{-3} \text{ m} = 15.4 \text{ kg/m}^2 \\ &c_L = 5050 \text{ m/s} \qquad \omega = 2\pi f = 2\pi \times 10^4 \text{ rad/s} \qquad \eta_c = 0.01 \\ &S = 2 \text{ m}^2 \qquad \rho_0 = 1.2 \text{ kg/m}^3 \qquad c_0 = 340 \text{ m/s} \qquad \sigma = 1 \end{aligned}$$

yielding

$$\begin{aligned} \langle v^2 \rangle &= \frac{10^2}{4.6 \times (15.4)^2 \times 5.05 \times 10^3 \times 2 \times 10^{-3} \times 2\pi \times 10^4 \times 10^{-2}} \\ &\quad \times \frac{1}{2(1 + 2 \times 1.2 \times 340/15.4 \times 2\pi \times 10^4 \times 2 \times 10^{-2})} \\ &= 6.7 \times 10^{-6} \text{ m/s}^2 \\ \sqrt{\langle v^2 \rangle} &= 2.6 \times 10^{-3} \text{ m/s} \\ v_0^2 &= \frac{1}{2}\hat{F}_0^2 Y_\infty = \frac{\hat{F}^2}{4.6\rho_s c_L t} = \frac{10^2}{4.6 \times 15.4 \times 5.03 \times 10^3 \times 2 \times 10^{-3}} \\ &= 0.14 \text{ m/s} \\ \frac{v_0^2}{\langle v^2 \rangle} &= \frac{(0.14)^2}{6.7} \times 10^6 = 2925 \qquad \sqrt{\frac{\langle v^2 \rangle}{v_0^2}} = 54 \end{aligned}$$

11.4 REFLECTION AND TRANSMISSION OF SOUND AT PLANE INTERFACES

When a plane sound wave traveling in a homogeneous medium encounters a plane interface with another medium, it may be (1) totally reflected, (2) partially reflected, or (3) totally transmitted depending upon the angle of incidence, the propagation speed of sound, and the density of the materials on both sides of the interface. Interfaces of practical importance are between air and water, between air and solid materials, between air and porous materials (such as ground or sound-absorbing materials), and between layers of fibrous sound-absorbing material such as treated in Chapter 8.

The simplest case is when the wave front of the incident plane wave is parallel to the plane of the interface (i.e., the wave propagates normal to the interface), as shown schematically in Fig. 11.5. In this simple case the transmitted wave p_{tran} retains the propagation direction of the incident wave p_{inc} and the following

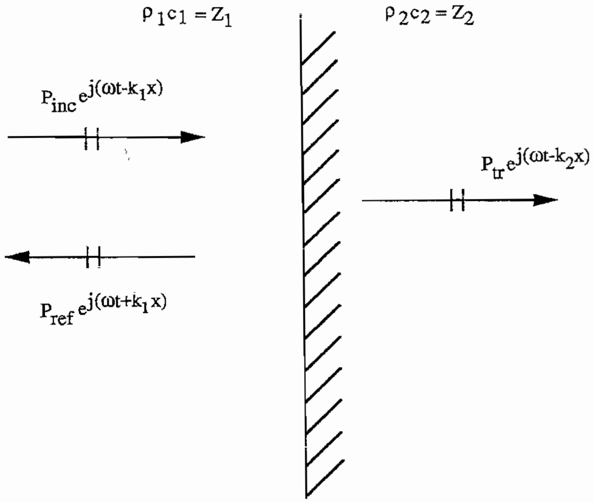

FIGURE 11.5 Reflection and transmission of a plane sound wave normally incident on the plane interface of an infinitely thick medium: p_{inc}, p_{ref}, p_{tr}, peak amplitudes of incident, reflected, and transmitted pressure; ρ, c, density and speed of sound of respective media.

relationships apply:

$$\frac{p_{tran}}{p_{inc}} = \frac{4R_e\{Z_2\}/R_e\{Z_1\}}{|Z_2/Z_1 + 1|^2} = \frac{2Z_2}{Z_2 + Z_1} \tag{11.32}$$

$$\frac{p_{ref}}{p_{inc}} = 1 - \frac{W_{tran}}{W_{ref}} = \frac{Z_2 - Z_1}{Z_2 + Z_1} \tag{11.33}$$

and for the power transmission and reflections

$$\frac{W_{tran}}{W_{inc}} = 1 - \left|\frac{Z_2 - Z_1}{Z_2 + Z_1}\right|^2 \tag{11.34}$$

$$\frac{W_{ref}}{W_{inc}} = \left|\frac{Z_2 - Z_1}{Z_2 + Z_1}\right|^2 \tag{11.35}$$

where $Z_i = \rho_i c_i$ is the characteristic impedance of media i for plane waves and ρ_i and c_i are the density and sound speed of the medium. For an air–steel interface and for a water–steel interface where $Z_2/Z_1 = 3.9 \times 10^7/4.1 \times 10^2$ and $Z_2/Z_1 = 3.9 \times 10^7/1.5 \times 10^6$, respectively, Eqs. (11.32)–(11.35) yield

Interface	p_{tran}/p_{inc}	p_{ref}/p_{inc}	W_{tran}/W_{inc}	W_{ref}/W_{inc}
Air–steel	1.99998	0.99998	0.00004	0.99996
Water–steel	1.927	0.927	0.141	0.859

indicating that plane waves normally incident from air onto bulk solid materials transmit only an extremely small portion of the incident energy while those incident from liquids are able to transmit an important fraction of the incident sound energy.

If the plane wave arrives at the plane interface at an oblique angle ϕ_1 ($\phi_1 = 0$ is normal incidence), the angle of the reflected wave $\phi_r = \phi_i$ but the angle of the transmitted wave ϕ_2 depends on the ratio of the propagation speeds in the two materials according to Snell's law:

$$\frac{c_1}{c_2} = \frac{\sin\phi_1}{\sin\phi_2} \tag{11.36}$$

If the plane interface is between two semi-infinite fluids or between a fluid and a porous sound-absorbing material, only compressional waves are generated. However, at interfaces between a fluid and a solid the energy transmitted into the semi-infinite solid contains both compressional and shear waves. As illustrated in Fig. 11.6, the transmitted wave breaks toward the normal of the interface if $c_2 < c_1$ and away from the normal if $c_2 > c_1$.

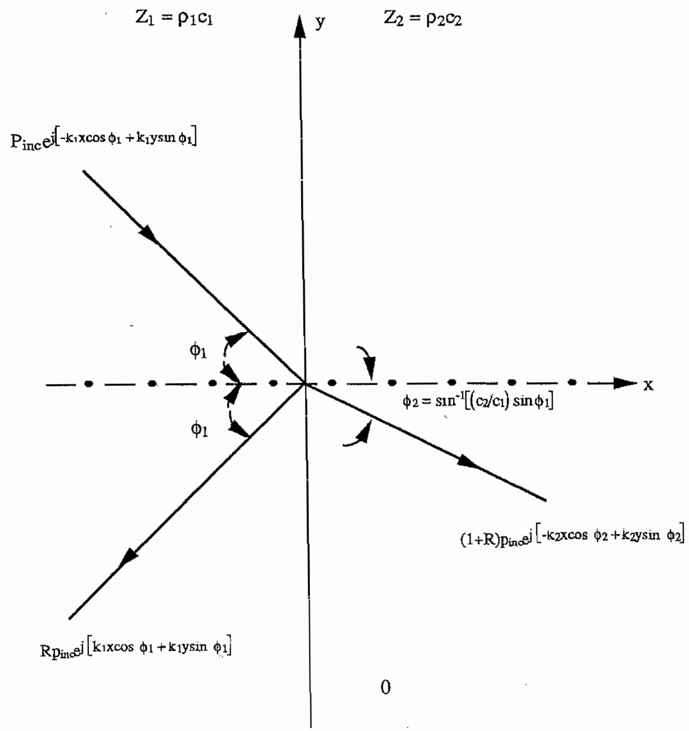

FIGURE 11.6 Reflection and transmission of an oblique-incidence plane sound wave at the plane interface of two semi-infinitely thick medium, $k_1 = \omega/c_1$, $k_2 = \omega/c_2$.

If $c_2 < c_1$, there is always a transmitted wave even for grazing incidence ($\phi_1 = 90°$), and for lossless media the power transmission reaches 100% at an oblique-incidence angle ϕ_1 when

$$\left(\frac{Z_1}{Z_2}\right)^2 = \frac{1 - (c_2/c_1)^2 \sin^2 \phi_1}{\cos^2 \phi_1} \tag{11.37}$$

If $c_2 > c_1$ sound transmission occurs only in a limited incidence angle range $0 < \phi_1 < \phi_{1L} = \sin^{-1}(c_1/c_2)$. For angles $\phi_1 > \phi_{1L}$ there is a total reflection and the sound wave penetrates into the second medium only in the form of a near field that exponentially decays with distance from the interface. The pressure reflection coefficient for oblique-incidence sound is given by

$$R(\phi_1) = \frac{p_{\text{ref}}(\phi_1)}{p_{\text{inc}}(\phi_1)} = \begin{cases} \dfrac{Z_2/\sqrt{1 - [(c_2/c_1)\sin\phi_1]^2} - Z_1/\cos\phi_1}{Z_2/\sqrt{1 - [(c_2/c_1)\sin\phi_1]^2} + Z_1/\cos\phi_1} \\ \quad \text{for } c_2 < c_1 \text{ or } c_2 > c_1 \text{ and } \phi_1 < \phi_{1L} \\ 1 \text{ for } c_2 > c_1 \text{ and } \phi_1 > \phi_{1L} \end{cases} \tag{11.38}$$

The limiting angle for plane-wave sound transmission from air to steel is $\phi_{LC} = \sin^{-1}(c_0/c_s) = 3.8°$ for compressional waves and $\phi_{LS} = \sin^{-1}(c_0/c_s) = 4.5°$ for shear waves. For sound transmission from water to steel, the corresponding limiting angles are $\phi_{LC} = 13°$ and $\phi_{LS} = 15°$, respectively. For angles larger than these, there is total reflection and only exponentially decaying near fields exist in the solid.

11.5 POWER TRANSMISSION BETWEEN STRUCTURAL ELEMENTS

In the preceding sections, the power lost to a connected structure was considered only as an additional mechanism that increases the loss factor of the excited structure. In many practical problems, however, the power transmitted to a neighboring structure is the prime reason for a noise reduction program.

The power balance equation states that the power introduced into the directly excited structure is either dissipated in it or is transmitted to neighboring structures. Accordingly, if in a noise reduction problem the power is to be *confined* to the excited structure, the power *dissipated* in the structure must greatly exceed the power *transmitted* to the neighboring structures. This requires a *high loss factor* for the excited structure and a construction that *minimizes the power transmission* to neighboring structures. Methods to achieve high damping are the subject of Chapter 14.

Reduction of Power Transmission through a Change in Cross-Sectional Area

The simplest construction that causes a partial reflection of an incident compression or bending wave is a sudden change in cross-sectional area, as shown schematically in Fig. 11.7.

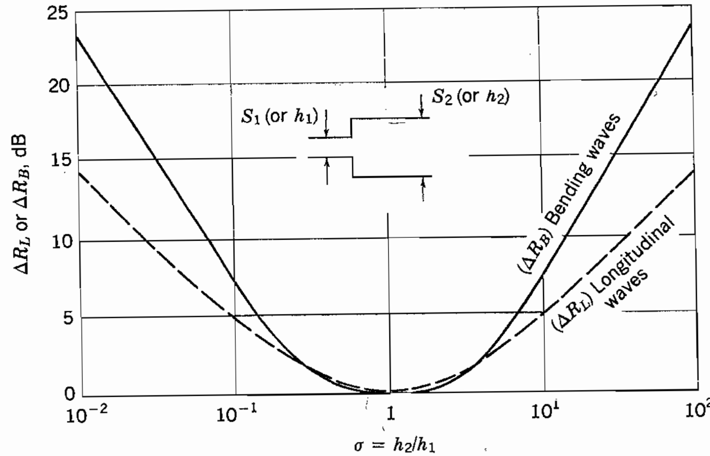

FIGURE 11.7 Attenuation at discontinuity in cross section as a function of thickness ratio. (After reference 1.)

Reflection Loss of Compression Waves. The *reflection loss* ΔR_L, defined as the logarithmic ratio of the incident to the transmitted power (for both sections of the same material), is calculated as[1]

$$\Delta R_L = 20 \log[\tfrac{1}{2}(\sigma^{1/2} + \sigma^{-1/2})] \quad \text{dB} \tag{11.39}$$

where $\sigma = S_2/S_1$ is ratio of the cross-sectional areas (see Fig. 11.7).

The reflection loss as a function of cross-sectional area ratio is plotted as the dashed line in Fig. 11.7. Since Eq. (11.39) is symmetrical for S_1 and S_2, the reflection loss is independent of the direction of the incident wave. This equation is also valid for plates where $\sigma = h_2/h_1$ is the ratio of the thicknesses. Note that a 1 : 10 change in cross-sectional area yields only 4.8 dB reflection loss. To achieve 10 dB reflection loss, a 1 : 40 change in cross-sectional area would be necessary!

Reflection Loss of Bending Waves. The reflection loss for bending waves of perpendicular incidence at low frequencies is independent of frequency and is given by[1]

$$\Delta R_B = 20 \log \frac{\frac{1}{2}(\sigma^2 + \sigma^{-2}) + (\sigma^{1/2} + \sigma^{-1/2}) + 1}{(\sigma^{5/4} + \sigma^{-5/4}) + (\sigma^{3/4} + \sigma^{-3/4})} \quad \text{dB} \tag{11.40}$$

The equation is also plotted in Fig. 11.7 (solid line).

We conclude from Fig. 11.7 that a change in cross-sectional area is not a practical way to achieve high reflection loss in load-bearing structures.

Reflection Loss of Free Bending Waves at an *L*-Junction

Structural elements that necessitate a change in the direction of a bending wave play an important role in structures. We consider here normally incident bending waves at a junction between two plates (or beams) at right angles: For low frequencies both the transmitted and reflected energy is predominantly in the form of bending waves. In this frequency range the reflection loss (logarithmic ratio of incident to transmitted power) for plates and beams of the same materials is given by[1]

$$\Delta R_{BB} = 20 \log \left[\frac{\sigma^{5/4} + \sigma^{-5/4}}{\sqrt{2}} \right] \quad \text{dB} \tag{11.41}$$

This equation is plotted in Fig. 11.8. Because ΔR_{BB} is symmetric in σ, the reflection factor does not depend upon whether the original bending wave is incident from the thicker or from the thinner beam or plate. Note that the lowest reflection loss of 3 dB occurs for equal thicknesses ($\sigma = 1$). If the two plates or beams constituting the junction are of different material, replace the ratio $\sigma = h_2/h_1$ by

$$\sigma = \left(\frac{B_2 c_{B1}}{B_1 c_{B2}} \right)^{2/5} \tag{11.42}$$

where B and c_B are the bending stiffness and propagation speed of free bending waves, respectively (see Table 11.1). At higher frequencies the incident bending wave also excites longitudinal waves in the second structure.[1]

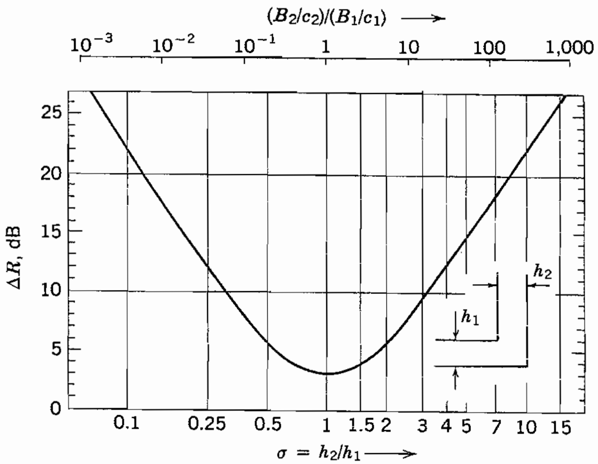

FIGURE 11.8 Attenuation of bending waves at corners (in absence of longitudinal wave interactions) as a function of thickness ratio. (After reference 1.)

Reflection Loss of Bending Waves through Cross Junctions and T-Junctions

Other structures that may provide a substantial reflection of an incident bending wave are the *cross junction* of walls shown schematically in Fig. 11.9 and the *T-junction* in Fig. 11.10. If a bending wave of perpendicular incidence reaches

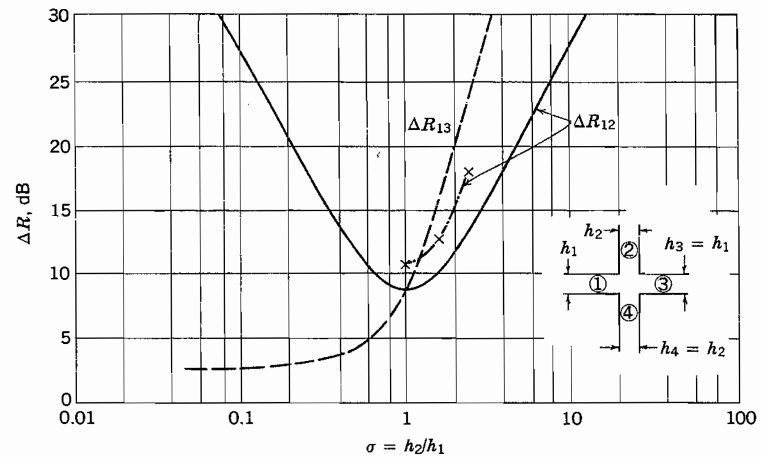

FIGURE 11.9 Attenuation of bending waves at plate intersections (in absence of longitudinal wave interactions) as a function of thickness ratio. (After reference 1.) (—·—) ΔR_{12} for random incidence computed by Kihlman.[20]

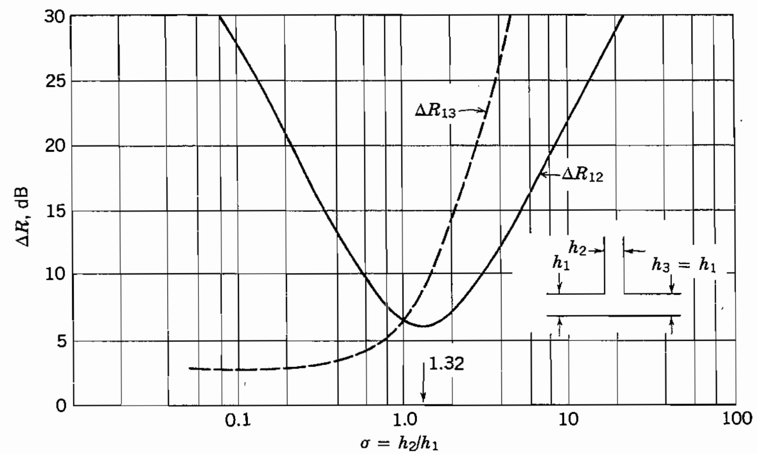

FIGURE 11.10 Attenuation of bending waves at plate intersections (in absence of longitudinal wave interactions) as a function of thickness ratio. (After reference 1.)

the cross junction from plate 1, it is partially reflected and partially transmitted to the other plates. The transmitted power splits into a number of different wave types, namely, bending waves in plate 3 and longitudinal and bending waves in plates 2 and 4. Because of the symmetry in the geometry, plates 2 and 4 will have the same excitation.[1]

The reflection loss (defined as the logarithmic ratio of the power in the incident to that in the transmitted bending wave) is given as a function of the ratio of the plate thickness for plates or beams of the same material and is shown in Figs. 11.9 and 11.10. When the plates are made of different material, the ratio $\sigma = h_2/h_1$ is given by Eq. (11.42). The amplitudes of the bending waves transmitted without a change in direction are restrained by the perpendicular plate, and the reflection loss in this direction, ΔR_{13}, increases monotonically with increasing thickness of the restraining plate, h_2. Since this plate effectively stops the vertical motion of the horizontal plate at the junction, even for very thin vertical walls, ΔR_{13} remains level at 3 dB, indicating that only the power carried by the bending moment can pass the junction. For those bending waves that change direction at the junction, the reflection loss becomes a minimum ($\Delta R_{12} =$ 9 dB) at a thickness ratio $\sigma = h_2/h_1 = 1$ for the cross junction; corresponding numbers for the T-junction are 6.5 dB at a thickness ratio $\sigma = h_2/h_1 = 1.32$. The reflection loss then increases symmetrically for increasing or decreasing thickness ratio (h_2/h_1).

The transmission of free bending waves at cross junctions for random incidence has been computed and the reflection loss for a number of combinations of dense and lightweight concrete plates determined.[20] The results for ΔR_{12} are plotted in Fig. 11.9 (as x's), which indicate that ΔR_{12} for random incidence is somewhat higher than that for normal incidence. It was also found that for random incidence ΔR_{12} is independent of frequency but ΔR_{13} decreases with increasing frequency.

Power Transmission from a Beam to a Plate

The structural parts of a modern building frequently include columns and structural floor slabs. Consequently, the power transmission from a beam to a plate, which models this situation, is of practical interest. Let us first consider the reflection loss for longitudinal and bending waves incident *from* the beam onto an infinite homogeneous plate.

Reflection Loss for Longitudinal Waves. When a longitudinal wave in the beam reaches the plate, its energy is partly reflected back up the beam and is partly transmitted to the plate in the form of a bending wave. The reflection loss (equal to the logarithmic ratio of the incident to the transmitted power) is given by[21]

$$\Delta R_L = -10 \log \left(1 - \left| \frac{Y_b - Y_p}{Y_b + Y_p} \right|^2 \right) \quad \text{dB} \tag{11.43}$$

where $Y_b = 1/Z_b$ = admittance of semi-infinite beam for longitudinal waves, m/N · s

Y_p = point admittance of infinite plate, $1/Z_p$, m/N · s

Both Y_p and Y_b are real and frequency independent and can be found for infinite beams and plates from Table 11.3 by taking the reciprocal of the impedances, that is, $Y_b = 1/\rho_b c_{Lb} S_b$ and $Y_p = 1/2.3\rho_p c_{Lp} h^2$.

Complete Power Transmission between Beam and Plate for Longitudinal Waves. Inspecting Eq. (11.43), we note that the reflection factor is zero (all the incident energy is transmitted to the plate) when $Y_b = Y_p$. Equating the values for Y_p and Y_p given above yields the requirements for complete power transmission from the beam to the plate:

$$S_b = 2.3 \frac{\rho_p c_{Lp} h^2}{\rho_b c_{Lb}} \quad \text{m}^2 \tag{11.44}$$

If the column and the slab are of the same material so that $\rho_p c_{Lp} = \rho_b c_{Lb}$, Eq. (11.44) simplifies to

$$S_b = 2.3 h^2 \quad \text{m}^2 \tag{11.45}$$

This equation says that for perfect power transfer from a beam of square cross section to a large plate, the cross dimension of the beam must be 1.52 times the thickness of the plate and for a beam of circular cross section the radius must be 0.86 times the plate thickness. Actually, this is well within the range of slab thicknesses–column cross section ratios commonly found in architectural structures. The reflection factor for different geometries of steel beam and plate connections has been measured.[21] The results for a substantial mismatch (a) and for a near matching (b) are plotted in Fig. 11.11.

Reflection Loss for Bending Waves. When a beam carries a free bending wave, a part of the energy carried by the wave is transmitted to the plate by the effective bending moment and excites a radially spreading free bending wave in the plate. A part of the incident energy is reflected from the junction. Here the reflection loss is determined by the respective moment impedances[1,21] of the plate and the beam:

$$\Delta R_b = -10 \log \frac{Y_b^M - Y^M}{Y_b^M + Y_p^M} \quad \text{dB} \tag{11.46}$$

where the moment admittances Y_b^M and Y_p^M are given by[1,20]

$$Y_b^M = \frac{2}{1+j} \frac{k_b^2}{\rho_b S_b c_{B_b}} \quad \text{m/N} \cdot \text{s} \tag{11.47}$$

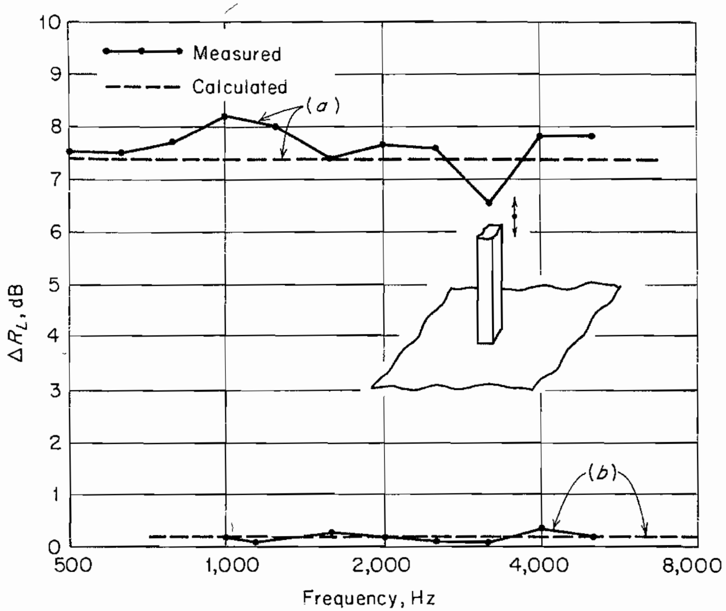

FIGURE 11.11 Reflection loss for longitudinal waves, ΔR_L, for a steel beam plate system: (*a*) plate thickness 2 mm, beam cross section 10 × 20 mm; (*b*) plate thickness 4 mm, beam cross section 5 × 10 mm. (After reference 21.)

and

$$Y_b^M = \frac{\omega}{16B_p}\left(1 + j\frac{4}{\pi}\ln\frac{1.1}{k_p a}\right) \quad \text{m/N} \cdot \text{s} \tag{11.48}$$

where k = wavenumber, m^{-1}
B_p = bending stiffness per unit width of plate, N · m
a = effective distance of pair of point forces making up moment on plate, m; for rectangular and circular beam cross section $a_r = \frac{1}{3}d$ and $a_c = 0.59r$
d = side dimension of rectangular beam cross section (in direction of bending), m
r = radius of circular beam cross section, m

The reflection loss obtained[21] for the bending-wave excitation of a steel rod of 1 × 2 cm cross-sectional area attached to a 0.2-cm-thick semi-infinite steel plate for two perpendicular directions of bending of the rod is plotted in Fig. 11.12.

Complete Power Transmission for Bending Waves. Since the moment impedances of the plate and beam are both frequency dependent, complete power transmission ($\Delta R_B = 0$) can occur only at a single frequency. The criteria for

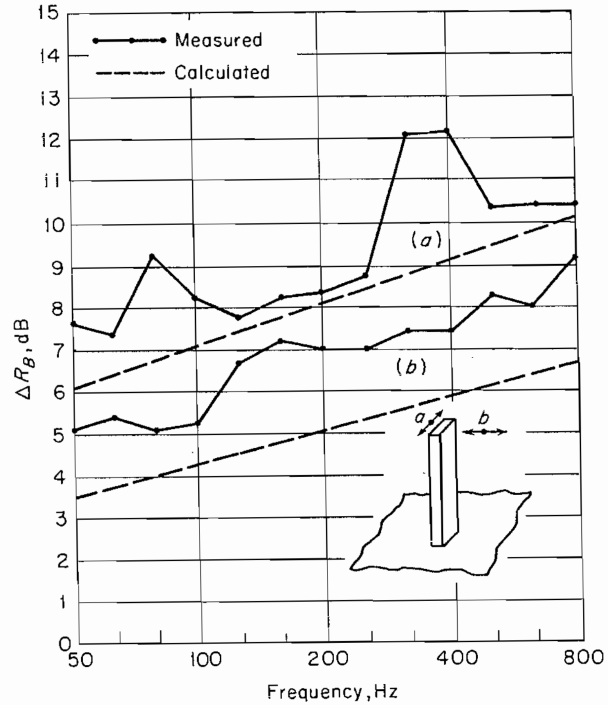

FIGURE 11.12 Reflection loss for bending waves, ΔR_B, for a steel beam plate system for two different directions of bending of the beam (*a* and *b*). Plate thickness 2 mm, beam cross section 10 × 20 mm. (After reference 21.)

perfect power transmission is achieved when both the real and imaginary parts of the moment impedances of the beam and plate are equal, which requires that

$$\lambda_b = 0.39\frac{B_b}{B_p} \quad \text{m} \tag{11.49}$$

$$\lambda_p = 2.6a \quad \text{m} \tag{11.50}$$

where B_p = bending stiffness of beam, N · m^2
λ_b = bending wavelength in beam, m
λ_p = bending wavelength in plate, m

Reduction of Power Transmission between Plates Separated by Thin Resilient Layer

In architectural structures it is customary to provide a so-called vibration break by inserting a thin layer of resilient material between structural elements. The

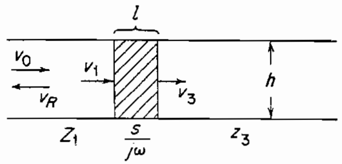

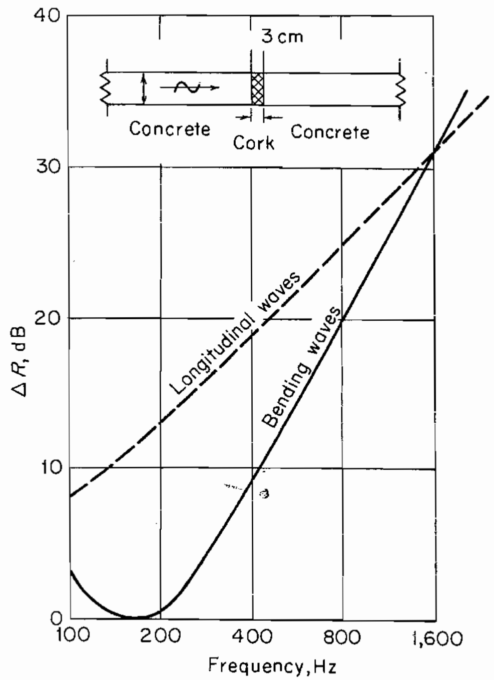

FIGURE 11.13 Attenuation due to an elastic interlayer of 3-cm-thick cork between 10-cm-thick slabs of concrete as a function of frequency. (After reference 1.)

geometry of such a vibration break is shown in Fig. 11.13. Often this construction serves also as an expansion joint.

Reflection Loss for Compression Waves. The reflection loss is given by[1]

$$\Delta R_L = 10 \log \left[1 + \left(\frac{\omega Z_1}{2 s_i} \right) \right] \quad \text{dB} \qquad (11.51)$$

where Z_1 = impedance of solid structure for compressional waves, N · s/m
s_i = stiffness of resilient layer in compression, N/m

Above a certain frequency ($\omega = 2s_i/Z_1$) the ΔR_L-versus-frequency curve increases with a 20-dB/decade slope with increasing frequency. Below this frequency the resilient layer transmits the incident wave almost entirely. As an example,[1] the ΔR_L-versus-frequency curve for a 3-cm-thick layer of cork inserted between two 10-cm-thick concrete slabs (or columns) is shown in Fig. 11.13.

To achieve a high reflection loss, the resilient layer must be as soft as is permitted by the load-bearing requirements ($s_i/\omega \ll Z_1$). However, the stiffness of the layer cannot be reduced indefinitely by increasing the thickness. For frequencies where the thickness of the layer is comparable with the wavelength of compressional waves in the resilient material, the layer can no longer be considered as a simple spring characterized by its stiffness alone. The reflection loss in this frequency region is given by[1]

$$\Delta R_L = 10 \log \left[\cos^2 k_i l + \frac{1}{4} \left(\frac{Z}{Z_i} + \frac{Z_i}{Z} \right)^2 \sin^2 k_i l \right] \quad \text{dB} \qquad (11.52)$$

where k_i = wavenumber for compressional waves in resilient material, m^{-1}
Z = impedance of equivalent infinite structure for compression waves, $= Z_1 = Z_3$, N · s/m
Z_i = impedance of equivalent infinite (length) resilient material for compression waves, N · s/m
l = length of resilient layer, m

The impedances Z, Z_i and the wavenumber k_i are assumed real; thus Eq. (11.52) does not account for wave damping in the resilient material. As expected, $\Delta R_L = 0$ for $Z_i = Z$. The maximum of ΔR_L is reached when $k_i l = (2n + 1)(\frac{1}{2}\pi)$; here the reflection loss becomes

$$\Delta R_{L,\max} = 20 \log \frac{Z_i^2 + Z^2}{2 Z Z_i} \quad \text{for } l = \tfrac{1}{2}(2n+1)\lambda_i \qquad (11.53)$$

For $k_i l = n\pi (l = \frac{1}{2} n \lambda_i)$, the denominator of Eq. (11.51) becomes unity independent of the magnitude Z, yielding

$$\Delta R_{L,\min} = 0 \quad \text{for } l = \tfrac{1}{2} n \lambda_i$$

Finally for $k_i l \ll 1$ and $Z_i \ll Z$, Eq. (11.52) simplifies to Eq. (11.51).

Reflection Loss for Bending Waves. The geometry in Fig. 11.13 suggests that for bending waves of perpendicular incidence the moments and forces acting on both sides of the junction must be equal. However, the transverse velocity and angular velocity on both sides of the junction are different because of shear and compressional deformation of the resilient layer. The elastic layer behaves quite differently for bending waves than it does for compressional waves.[1] The most striking difference is the *complete transmission* of the incident bending wave at a certain frequency and a *complete reflection* of it at another, higher frequency. Unfortunately, it turns out that the frequency of complete transmission for architectural structures of interest usually occurs in the audio frequency range. As an example, Fig. 11.13 shows the reflection factor for bending waves as a function of frequency for a layer of 3-cm-thick cork between 10-cm-thick concrete slabs. The transmission is complete at a frequency of 170 Hz and then decreases with increasing frequency. The reflection loss for bending waves can be approximated by[1]

$$\Delta R_B \cong 10 \log \left[1 + \frac{1}{4} \left(1 - \frac{E}{E_i} \frac{2\pi^3 l h^2}{\lambda_B^3} \right)^2 \right] \quad \text{dB} \tag{11.54}$$

where E = Young's modulus of structural material
E_i = Young's modulus of elastic material
l = length of elastic layer, m
h = thickness of structure, m
λ_B = wavelength of bending waves in structure, m

The bending wavelength in the structure for which the elastic layer provides a complete transmission of bending waves is given by

$$\lambda_{B,\text{trans}} = \pi \left(\frac{E}{E_i} h^2 l \right)^{1/3} \quad \text{m} \tag{11.55}$$

If one wishes to reduce the frequency of complete transmission, the ratio E/E_i and the length of the resilient layer must be large. However, the length of the resilient material should always be small compared with the wavelength of bending waves in the elastic layer to avoid resonances.

A complete reflection of the incident bending wave occurs when the bending wavelength in the plate equals π times the plate thickness, $\lambda_{Bs} = c_b/f_s = \pi h$. Consequently, the frequency where *complete reflection* occurs is *independent* of the dynamic properties and the length of the elastic layer and is given by the thickness and the dynamic properties of the plate or beam.

11.6 SOUND RADIATION

The sound radiation of small rigid bodies is treated in Chapter 10. This section deals exclusively with the sound radiation of thin flexible plates excited to vibration by point forces or by sound fields. Sound radiation of small rigid bodies is treated in Chapter 10.

Vibration of rigid and elastic structures forces the surrounding fluid or gas particles at the interface to oscillate with the same velocity as the vibrating structure and thus causes sound. The sound waves propagate in the form of compressional waves that travel with the speed of sound in the surrounding medium.

Infinite Rigid Piston

Conceptually the simplest sound-radiating structure is an infinite plane rigid piston. The motion of the piston forces the fluid particles to move along parallel lines that are perpendicular to the plane of the piston. There is no divergence that could lead to inertial reaction forces, such as those that can occur along the edges of a finite piston where the fluid can move to the side. Consequently, the reaction force per unit area (i.e., the sound pressure) is fully attributable to compression effects. This is the same situation as if the piston would be placed in a tube of rigid walls, as discussed already in Chapter 10. If the piston vibrates with velocity $\hat{v} \cos \omega t$, it generates a plane sound wave traveling perpendicular to the plane of the piston. The sound pressure as a function of distance is

$$p(x, t) = \hat{v} \rho_0 c_0 \cos(\omega t - k_0 x) \quad \text{N/m}^2 \tag{11.56}$$

and the radiated sound power per unit area is

$$W'_{\text{rad}} = 0.5 \hat{v}^2 \rho_0 c_0 = \langle v^2 \rangle_t \rho_0 c_0 \quad \text{W/m}^2 \tag{11.57}$$

where ρ_0 and c_0 are the density and speed of sound of the medium, $\omega = 2\pi f$ is the radian frequency, $k_0 = \omega/c_0 = 2\pi/\lambda_0$ is the wavenumber, $\lambda_0 = c_0/f$ is the wavelength of the radiated sound, and $\langle v^2 \rangle_t$ is the time-averaged mean-square velocity (i.e., $v = v_{\text{rms}}$).

Infinite Thin Plate in Bending

If a plane bending wave of velocity amplitude $\hat{v} = \sqrt{2} v$ and bending wave speed c_B travels on a thin plate in the positive x direction, the sound pressure as a function of x and perpendicular distance z is given by[1]

$$\hat{p}(x, y) = \frac{j \hat{v} \rho_0 c_0 e^{j\omega t}}{\sqrt{(k_B/k_0)^2 - 1}} e^{-jk_B z} \exp(-z \sqrt{k_B^2 - k_0^2}) \quad \text{N/m}^2 \tag{11.58}$$

where $k_B = 2\pi f/c_B = 2\pi/\lambda_B$ and $k_0 = 2\pi f/c_0 = 2\pi/\lambda_0$ are the bending wavenumber in the plate and the wavenumber in the air, respectively. Inspecting Eq. (11.58), one finds that for $c_B \langle c_0$ $(k_B/k_0 \rangle 1)$ the sound pressure is 90° out of phase with the velocity at the interface so that no sound power is radiated by the plate. The sound pressure constitutes a near field that decays exponentially with increasing z. For $c_B > c_0$; $k_B/k_0 < 1$, Eq. (11.58) has the form

$$\hat{p}(x, y) = \frac{\hat{v} \rho_0 c_0 e^{-j\omega t}}{\sqrt{1 - (k_B/k_0)^2}} e^{-jk_B x} \exp\left(-jk_0 z \sqrt{1 - \left(\frac{k_B}{k_0}\right)^2} \right) \quad \text{N/m}^2 \tag{11.59}$$

where the pressure and velocity are in phase at the interface ($z = 0$) and the sound power radiated by a unit area of the plate is

$$W'_{\text{rad}} = \begin{cases} \dfrac{0.5\hat{v}^2 \rho_0 c_0}{\sqrt{1-(\lambda_0/\lambda_B)^2}} \quad \text{W/m}^2 & \text{for } \lambda_B > \lambda_0 \\ 0 & \text{for } \lambda_B < \lambda_0 \end{cases} \tag{11.60}$$

which, with increasing frequency ($\lambda_0/\lambda_B \ll 1$), approaches that of an infinite rigid piston as given in Eq. (11.57).

Radiation Efficiency

It is customary to define the radiation efficiency of a vibrating body as

$$\sigma_{\text{rad}} = \frac{W_{\text{rad}}}{\langle v_n^2 \rangle \rho_0 c_0 S} \tag{11.61}$$

where $\langle v_n^2 \rangle$ is the normal component of the space–time average mean-square vibration velocity of the radiating surface of area S and W_{rad} is the radiated sound power. With this definition, Eqs. (11.57) and (11.60) yield for the piston

$$\sigma_{\text{rad}} = \begin{cases} 1 & \text{for infinite rigid piston} \\ 0 & \text{for } \lambda_B < \lambda_0 \text{ for infinite plate in bending} \\ [1-(\lambda_0/\lambda_B)]^{-1/2} & \text{for } \lambda_B > \lambda_0 \text{ for infinite plate in bending} \\ (k_0 a)^2/[1+(k_0 a)^2] & \text{for pulsating sphere} \end{cases} \tag{11.62}$$

It is important to know that the radiation efficiency depends not only on the size and shape of the radiating body as compared with the wavelength but also on the manner the body is vibrating. If a sphere vibrates back and forth instead of pulsating, then the net volume displacement is zero and the radiation efficiency is[22]

$$\sigma_{\text{rad}} = \frac{(k_0 a)^4}{4 + (k_0 a)^4} \tag{11.63}$$

Comparing Eqs. (11.62) and (11.63) reveals that at low frequencies a rigid body vibrating in translation radiates much less (approximately $\frac{1}{4}(k_0 a)^2$ times) sound power than a pulsating body of the same surface area. Radiation efficiencies of some typical structural elements are given in Table 11.8 (see references 22 and 23 for a more extensive collection). Radiation efficiencies for oscillating three-dimensional bodies of near-unity aspect ratio (such as a sphere or cube) are plotted in Fig. 11.14 and those of pipes of circular rods oscillating as rigid bodies in Fig. 11.15. Note that with increasing frequency, when the distance between the neighboring, out-of-phase moving parts of the vibrating body becomes larger than the wavelength of the radiated sound (i.e., $2\pi a > \lambda_0$ for oscillating bodies and $\lambda_B > \lambda_0$ for plates in bending), it becomes more difficult to push the air

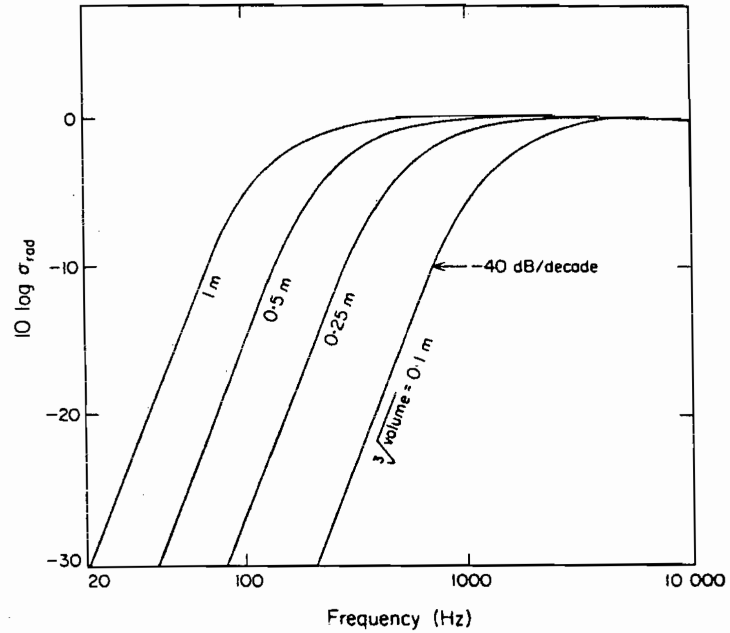

FIGURE 11.14 Radiation efficiency of oscillating three-dimensional bodies. (After reference 22.)

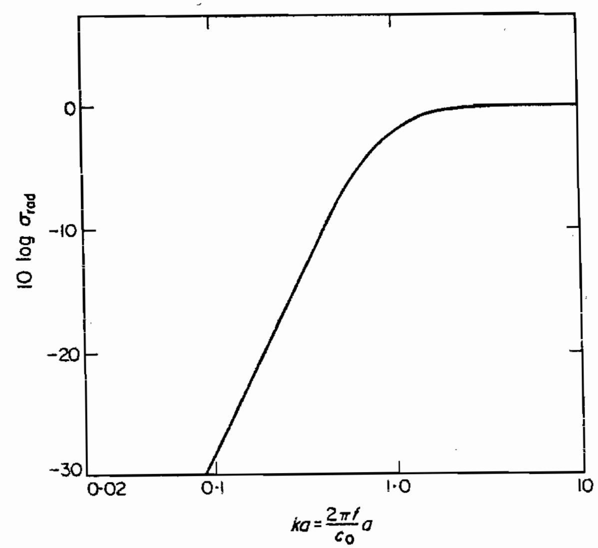

FIGURE 11.15 Radiation efficiency of oscillating rigid pipes and rods of radius a. (After reference 22.)

rapidly enough aside then to compress it, and the radiation efficiency approaches unity.

Point-Excited Infinite Thin Plate

When a very large homogeneous isotropic thin plate is excited by a point force of amplitude $\hat{F}_0$ or by an enforced local velocity of amplitude $\hat{v}_0$, free bending waves with a propagation speed of $c_B(f) \sim \sqrt{f}$ propagate radially from the excitation point. At low frequencies, where $c_B < c_0$, the free bending waves radiate no sound. Far from the excitation point, where the wave front approaches a straight line, the sound radiation that does occur is due to the in-phase vibration of the plate in the vicinity of the excitation point. The sound intensity radiation pattern has a $\cos^2\phi$ dependence, where ϕ is the angle to the normal of the plate. The mechanical power input W_{in}, the radiated sound power W_{rad}, and the acoustical–mechanical conversion efficiency $\eta_{\text{am}} = W_{\text{rad}}/W_{\text{in}}$ are listed below:

	Point Force Excitation	Point Velocity Excitation	
$W_{\text{in}} =$	$\frac{1}{2}\hat{F}_0^2 \dfrac{1}{2.3\rho_s c_L h}$	$(\frac{1}{2}\hat{v}_0^2)2.3\rho_s c_L h$	(11.64)
$W_{\text{rad}}(f < f_c) =$	$\hat{F}^2 \dfrac{\rho_0}{4\pi\rho_s^2 c_0}$	$\hat{v}^2 \dfrac{c_L^2 h^2 \rho_0}{2.38 c_0}$	(11.65)
$\eta_{\text{am}}(f < f_c) =$	$0.37\dfrac{\rho_0}{\rho_M}\dfrac{c_L}{c_0}$	$0.37\dfrac{\rho_0}{\rho_M}\dfrac{c_L}{c_0}$	(11.66)

where $\rho_s = \rho_M h$ is the mass per unit of the plate, ρ_M is the density and c_L the speed of longitudinal waves in the plate material, h is the plate thickness, and ρ_0 and c_0 are the density and speed of sound in the surrounding fluid.

Equations (11.64)–(11.66) contain the following, quite surprising, information:

1. W_{in}, W_{rad}, and η_{am} are independent of frequency and plate loss factor.
2. For point force excitation, the radiated sound power depends only on the mass per unit area of the plate ($W_{\text{rad}} \sim 1/\rho_s^2$) and not on stiffness.
3. For point velocity excitation, the radiated sound power depends only on stiffness ($W_{\text{rad}} \sim c_L^2 h^2$) and not on the plate material density.
4. The acoustical–mechanical conversion efficiency is the same for point force or point velocity excitation, and it is independent of plate thickness h and is a material constant [$\eta_{\text{am}} \sim (c_L/\rho_M)(\rho_0/c_0)$].

For noise control engineers, observations 2 and 3, embodied in Eq. (11.65), are very important. To minimize sound radiation from highly damped, point-excited, thin, platelike structures, the plate should have large mass per unit area for force excitation (e.g., by a low-impedance vibration source) and low stiffness (low E/ρ_M) for velocity excitation (by a high-impedance vibration source).

Equation (11.66) supplies the rationale for violin makers, who want to convert as large a portion of the mechanical power of the vibrating string as possible into radiated sound, to use wood ($\eta_{\text{am}} = 0.024$) and not steel ($\eta_{\text{am}} = 0.0023$) or lead ($\eta_{\text{am}} = 0.0004$) for the body of the violin.

Note also that the radiated sound power given in Eq. (11.65) usually represents the minimum achievable for a finite-size plate since it accounts only for the sound radiated from the vicinity of the excitation point.

Point-Excited Finite Plates

For finite-size plates, the sound power radiated has two components. The first component is radiated from the vicinity of the excitation point given in Eq. (11.65). The second component is radiated by the free bending waves as they interact with plate edges and discontinuities. The contribution of these two components to total radiated noise is represented by the first and second terms in Eqs. (11.67a) and (11.67b), where the first equation is valid for point force and the second for point velocity excitation:

$$W_{\text{rad}}^F \cong \hat{F}^2\left[\frac{\rho_0}{4\pi\rho_s^2 c_0} + \frac{\rho_0 c_0 \sigma_{\text{rad}}}{4.6\rho_s^2 c_L h\omega\eta_c}\right] \quad \text{W} \tag{11.67a}$$

$$W_{\text{rad}}^v \cong \hat{v}^2\left[\frac{\rho_0 c_L^2 h^2}{2.38 c_0} + 1.15\left(\frac{c_L h}{\omega\eta_c}\right)\rho_0 c_0 \sigma_{\text{rad}}\right] \quad \text{W} \tag{11.67b}$$

where η_c is the composite loss factor and σ_{rad} is the radiation efficiency of the plate for free bending waves. The second term in Eqs. (11.67) has been derived by the power balance (see Section 11.3) of the finite plate, assuming that the mechanical power input to the finite plate can be well approximated by the power input to the equivalent infinite plate.

Equations (11.67a) and (11.67b) can be used to assess the useful upper limit of the composite loss factor ($\eta_c^{\max}$) which, if exceeded, results only in added expense but no meaningful reduction of the radiated noise. This is done by equating the first and second terms in the square brackets and solving for η_c.

11.7 SOUND EXCITATION AND SOUND TRANSMISSION

The sound transmission process has the following three components: (1) description of the sound field at the source side, (2) prediction of the vibration response, and (3) sound radiation from the receiver side of the partition into the receiver room. Item 1 is treated in Chapter 7. Items 2 and 3 will be treated in this section. Regarding the appropriate way of analysis, partitions can be classified as either small or large compared with the acoustical wavelength.

Sound Transmission of Small Partitions

In the following analyses we define a partition small if its dimensions are small compared with the acoustical wavelength. Consequently, if the frequency is sufficiently low, even partitions of large size are considered "acoustically small."

The subject of sound transmission of acoustically small plates has been mostly ignored or treated only qualitatively in books on noise control engineering. The reason for this is that the traditional definition of sound transmission loss, which is based on the ratio of the incident and transmitted sound power, does not make sense in this low-frequency region where the sound power radiated into the receiver room is independent of the angle of incidence of the sound striking the source side of the partition. In this low-frequency region the partition will radiate the same sound power for grazing incidence (sound wave on the source side propagates parallel to the partition) than it does at normal incidence (where it propagates perpendicular to the plane of the partition).

It is instructive to start the investigation of sound transmission with a small, single, homogeneous, isotropic plate that is flash mounted in the test section between two reverberation rooms, as shown schematically in Fig. 11.16.

Let our investigation start at very low frequencies and proceed by gradually increasing the frequency of the incident sound. We will investigate the following cases:

1. The size of the panel, L, is small compared with the acoustical wavelength λ and the frequency of the incident sound wave, f, is small compared with the frequency of the first mechanical resonance of the plate, f_{M1}:

$$L \ll \lambda \qquad \text{and} \qquad f \ll f_{M1}$$

2. The size of the panel, L, is small compared with the acoustical wavelength λ and the frequency of the incident sound wave, f, matches the frequency of the first mechanical resonance of the plate, f_{M1}.

$$L \ll \lambda \qquad \text{and} \qquad f = f_{M1}$$

3. The size of the panel, L, is small compared with the acoustical wavelength λ and the frequency of the incident sound wave, f, is much larger than the frequency of the first mechanical resonance of the plate, f_{M1}.

$$L \ll \lambda \qquad \text{and} \qquad f \gg f_{M1}$$

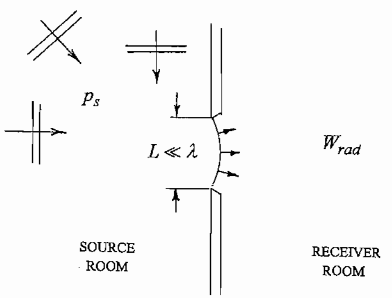

FIGURE 11.16 Sound Transmission of a small homogeneous isotropic partition.

Case 1 ($L \ll \lambda$ *and* $f \ll f_{M1}$). If the size of the partition is much smaller than the acoustical wavelength, the sound pressure, even at grazing incidence (i.e. the sound wave propagates parallel to the plate), is nearly constant across the source side of the plate. At any other angle of incidence, the sound pressure is even more evenly distributed across the plate than at grazing. At normal incidence, where the sound wave propagates perpendicular to the plane of the plate, the sound pressure is absolutely evenly distributed over the surface of the plate independent of the wavelength (for normal incidence the trace wavelength is infinitely large at all frequencies). In the case 1 frequency range the sound transmission of the plate is controlled by its volume compliance C_v defined as

$$C_v \equiv \frac{\Delta V}{p} \quad \text{m}^5/\text{N} \tag{11.68}$$

where C_v = volume compliance of plate, m^5/N
$p \approx$ sound pressure on source side of plate, N/m^2

As long as the dimensions of the plate are small compared with the acoustical wavelength, $p_s = 2p_{\text{inc}}$, where p_{inc} is the amplitude of the incident sound wave.

Considering now that the volume velocity $q = d\,\Delta V/dt = j\omega C_v p_s$ and using Eq. (10.49) from Chapter 10 the formula for the radiated sound power yields

$$W_{\text{rad}} = q^2(\rho_0 c_0)\left(\frac{k^2}{2\pi}\right) = \frac{\omega^4 C_v^2(\rho_0/c_0)}{2\pi} p_s^2 \quad \text{N} \cdot \text{m/s} \tag{11.69}$$

where ρ_0 = density of gas, kg/m^3
c_0 = speed of sound in gas, m/s.

Considering that our small plate radiates omnidirectionally into a half space, the sound pressure as a function of distance is

$$p(r) = \frac{p_s}{2\pi r}(\omega^2 C_v \rho_0) \quad \text{N/m}^2 \tag{11.70}$$

where r is the radial distance in meters from the center of the panel.

Formulas to predict the volume compliance C_v and resonance frequency f_{M1} for rectangular plates with simply supported and clamped edges are given in Chapter 12. Panels found in practical applications have a C_v that is larger than predicted for clamped edges and smaller than that predicted for simply supported edges. Also the resonance frequency of practical panels falls between those resonance frequencies predicted for clamped and simply supported edges.

Case 2 ($L \ll \lambda$ *and* $f \approx f_{M1}$). At the first resonance frequency of the panel, f_{M1}, the mass part of the panel impedance (which increases with increasing frequency) becomes equal in magnitude but opposite in phase to the stiffness part of the panel impedance, which is decreasing with increasing frequency. At and in the vicinity of the resonance frequency even a small sound pressure on the source side can cause a large volume velocity and the panel motion is limited only by energy dissipation in the panel and by its radiation resistance. In the vicinity of f_{M1} the sound power radiated by the receiver side of the panel reaches a maximum. The dissipative losses in the panel cannot be predicted analytically. Consequently, the sound transmission cannot be predicted with satisfactory accuracy. In designing enclosures for equipment with a high-intensity tonal component at low frequencies the panels or subpanels should be chosen that their first resonance frequency should be substantially higher than the frequency of the low-frequency tonal component of the enclosed equipment. The first resonance frequency of platelike elements can be increased by curving them in two perpendicular directions to gain form stiffness.

Case 3 ($L \ll \lambda$ *and* $f \gg f_{M1}$). Above the first mechanical resonance frequency the velocity of the plate is controlled by the mass per unit area $\rho_s = \rho_M h$
ρ_M = density of plate material, kg/m^3
h = plate thickness, m

The volume velocity of the plate in this frequency region can be approximated by

$$q \approx p_s \frac{S}{j\omega\rho_s} \quad \text{m}^3/\text{s} \tag{11.71}$$

the radiated sound power by

$$W_{\text{rad}} \approx p_s^2 \frac{\omega^2 S^2(\rho_0 c_0)}{2\pi} \quad \text{N} \cdot \text{m/s} \tag{11.72}$$

and the sound pressure at a distance r by

$$p(r) \approx p_s \frac{\omega^2 \rho_0^2 S}{2\pi r} \quad \text{N/m}^2 \tag{11.73}$$

where S is surface area (one side) of the plate in square meters.

More accurate prediction of the transmitted sound power can be obtained by determining the response of each of the volume-displacing modes of the plate responding to the spatially uniform sound pressure on the source side of the plate and determining the net volume velocity as the sum total of the volume velocities of all modes, as done in Chapter 6.

If the spatial distribution of the plate vibration $v(x, y)$ is known, the sound pressure in the receiver-side half space $p(x, y, z, \omega)$ can be computed as[1]

$$p(x, y, z, \omega) = \frac{j\omega\rho_0}{2\pi} \int v(x, y, \omega) \frac{e^{-jkr}}{r} \, dS \quad \text{N/m}^2 \tag{11.74}$$

where r is the distance between the small surface element of the plate and the observation point. Equation (11.74) is valid only for a flat plate flash mounted in an infinite, flat, hard wall.

In the low-frequency region, where the plate dimensions are small compared with the acoustical wavelength ($\sqrt{S} \ll \lambda$), the transmitted sound power depends only on the sound pressure on the source side of the plate p_s and does not depend on the angle of incidence or the sound power incident on the source side of the plate, W_{inc}. Consequently, the traditional definition of the sound transmission loss given in Eqs. (11.79) and (11.80) makes no sense in this frequency region.

Sound Transmission of Large Partitions

This section deals with the sound transmission loss of acoustically large partitions, where it is meaningful to characterize the excitation by the sound power incident on the source side of the partition and define the transmission coefficient τ and the sound transmission loss R as given in Eqs. (11.75) and (11.76), respectively.

The most common problem that noise control engineers have to deal with is the transmission of sound through solid partitions such as windows, walls, and floor slabs. The problem may be either prediction or design. The prediction problem is typically this: Given a noise source, a propagation path up to the partition, and the size and construction of the partition and the room acoustics parameters of the receiver room, predict the noise level in the receiver room. The design problem is typically stated as: Given a source, a propagation path, the room acoustics parameters of the receiver room, and a noise criterion (in the form of octave-band sound pressure levels), determine the construction of those partitions that would assure that the noise criteria are met with a sufficient margin of safety.

The transmission coefficient τ and sound transmission loss R, which characterize sound transmission through partitions, are defined as

$$\tau(\phi, \omega) = \frac{W_{\text{trans}}(\phi, \omega)}{W_{\text{inc}}(\phi, \omega)} \tag{11.75}$$

$$R(\phi, \omega) = 10 \log \frac{1}{\tau(\phi, \omega)} = 10 \log \frac{W_{\text{inc}}(\phi, \omega)}{W_{\text{trans}}(\phi, \omega)} \quad \text{dB} \tag{11.76}$$

where $W_{\text{inc}}(\phi, \omega)$ is the sound power incident at angle ϕ at frequency $\omega = 2\pi f$ on the source side and $W_{\text{trans}}(\phi, \omega)$ is the power transmitted (radiated by the receiver side).

Though knowledge of the sound transmission loss of a window or curtain wall for a particular angle of incidence may be desirable sometimes, it is a more common problem to characterize the transmission of sound between two adjacent rooms where the sound is incident on the separating partition from all angles with approximately equal probability. In such "random incident" sound fields, the sound intensity (energy incident on a unit area) I_{random} is related to the space-averaged mean-square sound pressure in the source room $\langle p^2 \rangle$ as

$$I_{\text{random}} = \frac{\langle p^2 \rangle}{4\rho_0 c_0} \quad \text{W/m}^2 \tag{11.77}$$

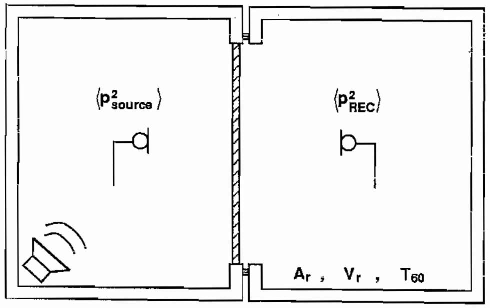

FIGURE 11.17 Experimental setup for laboratory measurements of the sound transmission loss of partitions (see text for definition of symbols).

Laboratory procedures ASTM E90-02[24] and ISO 140-1 : 1997,[25] adopted for measuring the sound transmission loss of partitions, are based on such a diffuse sound field obtained by utilizing large reverberation rooms (see Chapter 7) as source and receiver rooms. The measurement procedure depicted in Fig. 11.17 has three steps. The first step is to measure the sound power incident on the source-side face of the test partition of area S_w:

$$W_{\text{inc}} = I_{\text{inc}} S_w = \frac{\langle p^2_{\text{source}} \rangle S_w}{4\rho_0 c_0} \quad \text{W} \tag{11.78}$$

by measuring the space–time average mean-square sound pressure level $\langle p^2_{\text{source}} \rangle$ in the source room by spatially sampling the sound field. The second step is to measure the transmitted sound power W_{trans} from the power balance of the receiver room,

$$W_{\text{trans}} = \frac{\langle p^2_{\text{rec}} \rangle A_r}{4\rho_0 c_0} \quad \text{W} \tag{11.79}$$

yielding the laboratory sound transmission loss

$$R_{\text{lab}} = 10 \log \frac{W_{\text{inc}}}{W_{\text{trans}}} = \langle L_p \rangle_s - \langle L_p \rangle_R + 10 \log \frac{S_w}{A_r} \quad \text{dB} \tag{11.80}$$

where A_r is the total absorption in the receiving room. The third step is to determine A_r from the known volume and the measured reverberation time T_{60} of the receiver room, as described in Chapter 7.

Once R_{lab} has been measured, it can be used for predicting the mean-square sound pressure in a particular receiver room acoustically characterized by its total absorption A_r through a partition of surface area S_w for an incident sound field of intensity I_{inc} as

$$\langle p_r^2 \rangle = \frac{\overline{\tau} I_{\text{inc}} S_w (4\rho_0 c_0)}{A_r} = \frac{\overline{\tau} S_w < p^2_{\text{source}}}{A_r} \quad \text{N}^2/\text{m}^4 \tag{11.81a}$$

$$\langle \text{SPL}_R \rangle = \langle \text{SPL}_s \rangle - R_{\text{lab}} + 10 \log \frac{S_w}{A_r} \quad \text{dB} \tag{11.81b}$$

provided that the partition is not much smaller than tested and that edge conditions are not much different. Curves of measured random-incidence sound transmission loss versus frequency for standard windows, doors, and walls are available from manufacturers and should be used in design and prediction work. Measured sound transmission losses of some selected partitions are given by Bies and Hansen in their Table 8.1 (see the Bibliography).

The purpose of the discussion that follows is to identify the physical processes and the key parameters that control sound transmission through partitions and to provide analytical methods that further the development of an informed judgment needed for working with data obtained in laboratory measurements. Most importantly, however, this will focus on predicting sound transmission loss for situations that are different from those employed in the standardized laboratory measurements (i.e., for near-grazing incidence) and for the task of designing nonstandard partitions for unique applications.

Excitation of structures by an incident sound wave is significantly different from excitation by localized forces, moments, enforced velocities, or angular velocities. As discussed in the previous sections, the response of thin, platelike structures to localized excitation results in radially spreading free bending waves. The propagation speed of these waves, $c_B(f)$, is as unique a characteristic of the plate as is the period of a pendulum. The thinner the plate and the lower the frequency, the lower is the propagation speed.

If the structure is excited by an incident sound wave, forcing occurs simultaneously over the entire exposed surface of the plate. The incident sound enforces its spatial pattern on the plate, causing it to instantaneously conform to its trace. The trace "runs" along the plate with a speed that approaches the speed of sound in the source-side media when the sound runs nearly parallel to the plate (grazing incidence) and approaches infinity as the sound incidence approaches normal. This "sound-forced" response of the thin plate to sound excitation is referred to as the "forced wave." In contrast to the free bending waves, the speed of the forced bending wave is independent of frequency, plate thickness, and mass per unit area (though the amplitude of the response depends on them). Because of their supersonic speed, forced waves radiate sound very efficiently at all frequencies (e.g., their radiation efficiency $\sigma_F \geq 1$), except for panels that are small compared with the acoustical wavelength.

Transmission of Normal-Incidence Plane Sound Waves through an Infinite Plate

It is advisable to introduce the complex process of sound transmission by considering first the least complicated case when a plane sound wave is normally incident on a uniform homogeneous, isotropic, flat plate of thickness h, as shown in Fig. 11.18. Because the pressure exerted on the plate is in phase over the

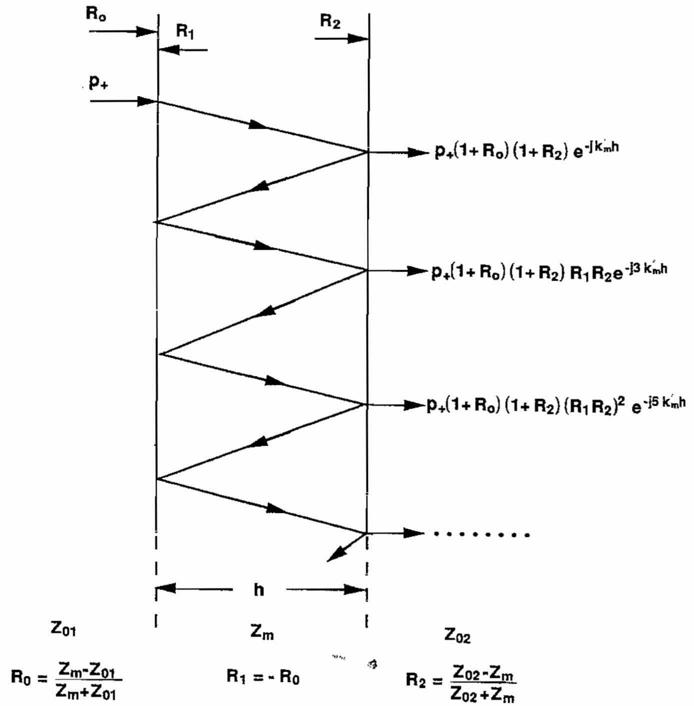

FIGURE 11.18 Transmission of a normally incident sound wave through a flat, homogeneous, isotropic plate. The transmitted pressure p_T is the sum of all the infinite components on the right. (See text for definition of symbols.)

entire surface of the plate, only compressional waves are excited. The sound wave of pressure amplitude p_+ propagates in a gas of characteristic plane-wave impedance $Z_{01} = \rho_{01}c_{01}$. It encounters the solid plate of characteristic impedance $Z_M = \rho c_L$ and on the transmitting side (right) will radiate sound into another gas of characteristic impedance $Z_{02} = \rho_{02}c_{02}$. The multiple reflection and transmission phenomena at the interfaces are governed by Eqs. (11.32) and (11.33). The amplitude of the transmitted sound pressure p_T in the receiver-side media is obtained by the summation of the transmitted components, as illustrated in Fig. 11.18, yielding[26]

$$p_T = p_+ \frac{(1 + R_0)(1 + R_2)e^{-jk_m h}}{1 - R_1 R_2 e^{-j2k_m h}} \quad \text{N/m}^2 \qquad (11.82)$$

where R_0, R_1, and R_2 are the reflection factors at the interfaces and directions indicated in Fig. 11.18 and h is the plate thickness. Propagation losses can be taken into account by a complex wavenumber $k'_m = k_m(1 + \frac{1}{2}j\eta)$, where $k_m = \omega/c_L$ is the wavenumber of compressional waves in the plate and η is the loss

factor. The normal-incidence sound transmission loss is defined as

$$R_N = 10 \log \frac{W_{\text{inc}}}{W_{\text{rad}}} = 10 \log \frac{p_+^2}{p_T^2} \quad \text{dB} \qquad (11.83a)$$

Assuming that the same gas is on both sides of the plate, Eq. (11.82) yields

$$R_N = 10 \log \left[\cos^2 k'_m h + 0.25 \left(\frac{Z_0}{Z_m} + \frac{Z_m}{Z_0} \right)^2 \sin^2 k'_m h \right] \quad \text{dB} \qquad (11.83b)$$

which for $|k'_m h| \ll 1$ yields the simple expression

$$R_N \cong 10 \log \left[1 + \left(\frac{\rho_s \omega}{2\rho_0 c_0} \right)^2 \right] \quad \text{dB} \qquad (11.83c)$$

known as the normal-incidence mass law. In Eq. (11.83c), $\rho_s = \rho h$ is the mass per unit area of the plate and $\rho_0 c_0 = Z_0$ is the characteristic impedance of the gas, assumed the same on both sides.

Figure 11.19 shows the computed normal-incidence sound transmission loss of a 0.6-m- (2-ft-) thick dense concrete wall. At low frequencies where the plate thickness is less than one-sixth of the compressional wavelength ($f < c_L/6h$) the sound transmission loss follows the normal-incidence mass law of Eq. (11.83c), increasing by approximately 6 dB for each doubling of the frequency or the mass per unit area. At high frequencies compressional wave resonances in the plate

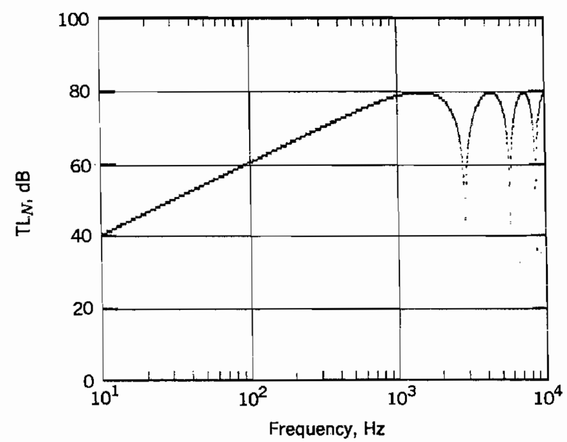

FIGURE 11.19 Normal-incidence sound transmission loss R_0 of a 0.6-m-thick dense concrete wall computed according to Eq. (11.83b) assuming $\eta = 0$.

occur and the R_N-versus-frequency curve exhibit strong minima at $f_n = nc_L/2h$, yielding

$$R_N^{\min} = 20 \log \left(1 + \frac{\pi}{4} \frac{Z_m}{Z_0} \eta n\right) \quad \text{dB} \tag{11.84a}$$

and the maximal achievable sound transmission loss can be approximated as

$$R_N^{\max} \cong 20 \log \frac{Z_m}{2Z_0} \quad \text{dB} \tag{11.84b}$$

Equation (11.84a) indicates complete transmission of the incident sound ($R_N^{\min} = 0$ dB) at compressional wave resonances if $\eta = 0$. However, Eq. (11.84a) indicates that even a small loss factor of $\eta = 0.001$ ensures that the normal-incidence transmission loss of a concrete partition does not dip below 24 dB at compressional wave resonances. Note, however, that no such dips are observed for random incidence because different incident angles correspond to different frequencies where such dips occur. As indicated in Eq. (11.84b), the maximum achievable normal-incidence sound transmission loss of homogeneous, isotropic single plates of any thickness is limited by the ratio of the characteristic impedances and is 80 dB for dense concrete, 94 dB for steel, and 68 dB for wood.

Transmission of Oblique-Incidence Plane Sound Waves through an Infinite Plate

The transmission of oblique-incidence sound through infinite plane plates can be formulated either in terms of shear and compressional waves, where the bending of the plate is considered as a superposition of these two wave types, or by utilizing the bending-wave equation of the plate. Both formulations are discussed below.

Combined Compressional and Shear Wave Formulation. The combined shear and compression wave formulation, which is valid also for thick plates, has been treated in Chapter 9 of the 1992 edition. It is too involved to present it here. The interested reader is referred to references 27 and 28 or to pages 248–288 of the 1992 edition of this book.

Separation Impedance Formulation. Sound transmission through plates can be conveniently characterized by the separation impedance Z_s defined as[1,26]

$$Z_s = \frac{p_s - p_{\text{rec}}}{v_n} \quad \text{N} \cdot \text{s/m}^3 \tag{11.85}$$

where p_s is the complex amplitude of the sound pressure at the source-side face of the plate representing the sum of the incident and reflected pressures ($p_s = p_{\text{inc}} + p_{\text{refl}}$), p_{rec} is the complex amplitude of sound pressure on the receiver-side face, and v_n is the complex amplitude of normal velocity of the receiver-side face of the plate. In the case of single panels, it is generally assumed that both faces of the panel vibrate in phase with the same velocity. The sound transmission coefficient of the plate τ and its sound transmission loss R are given by[1,26]

$$\tau(\phi) = \frac{I_{\text{trans}}}{I_{\text{inc}}} = \left|1 + \frac{Z_s \cos\phi}{2\rho_0 c_0}\right|^2 \tag{11.86}$$

$$R(\phi) = 10 \log \frac{1}{\tau(\phi)} = 10 \log \left(\left|1 + \frac{Z_s}{2\rho_0 c_0/\cos\phi}\right|^2\right) \quad \text{dB} \tag{11.87}$$

where ϕ is the angle of sound incidence ($\phi = 0$ for normal incidence).

The formulation of the sound transmission in terms of the separation impedance of Eq. (11.87) lends itself exceptionally well to predicting the sound transmission loss of multilayer partitions where the constituent layers may be thin plates separated by air spaces with and without porous sound-absorbing material (such as double and triple walls), windows, and so on. The reason for this is that the separation impedance of such multilayer partitions can be expeditiously obtained by appropriately combining the separation impedances of the constituent layers.

The separation impedance for a thick isotropic plate is obtained by solving the bending-wave equation of the plate as formulated by Mindlin[29]:

$$\left(\nabla^2 - \frac{\rho_M}{G}\frac{\partial^2}{\partial t^2}\right)\left(B\,\nabla^2 - \frac{\rho_M h}{12}\frac{\partial^2}{\partial t^2}\right)\xi(x,y) + \rho_M h \frac{\partial^2}{\partial t^2}\xi(x,y)$$
$$= \left(1 - \frac{B}{Gh}\nabla^2 + \frac{\rho_M h^2}{12G}\frac{\partial^2}{\partial t^2}\right)\Delta p\ (x,y,0) \tag{11.88}$$

where $\Delta p(x, y, 0)$ is the pressure differential across the plate, $\zeta(x, y)$ is the plate displacement in the z direction normal to the plate surface, $\nabla^2 = \partial^2/\partial x^2 + \partial^2/\partial y^2$ is the Laplacian operator, ρ_M is the density, G is the shear modulus, B is the bending stiffness, and h is the thickness of the panel. The solution of Eq. (11.88) for a plane sound wave of incidence angle ϕ yields[30]

$$Z_s = \frac{j\left\{[\rho_M h + (\rho_M h^3/12 + \rho_M B/G)(\omega^2/c_0^2)\sin^2\phi]\omega - [(B/c_0^4)\sin^4\phi + \rho_M^2 h^3/(12G)]\omega^3\right\}}{1 + B\omega^2\sin^2\phi/(Gc_0^2 h) - \rho_M h^2\,\omega^2/(12G)} \quad \text{N} \cdot \text{s/m}^3 \tag{11.89}$$

Equation (11.89) can be approximated by

$$Z_s \cong Z_m + \left(\frac{1}{Z_B} + \frac{1}{Z_{\text{sh}}}\right)^{-1} \quad \text{N} \cdot \text{s/m}^3 \tag{11.90}$$

where $Z_m = j\omega\rho_M h$ is the mass impedance of the plate per unit area and $Z_B = -jB\omega^3\sin^4\phi/c_0^4$ and $Z_{\text{sh}} = -jGh\omega\sin^2\phi/c_0^2$ are the bending-wave and shear wave impedances of the plate per unit area.

If $|Z_{sh}| \ll |Z_B|$, the plate responds predominantly in shear and $Z_s \cong Z_m + Z_{sh}$. In this case, Eq. (11.89) yields

$$R_{sh}(\phi) = 20\log\left|1 + \frac{j\omega\rho_M h[1-(c_s/c_0)^2\sin^2\phi}{2\rho_0 c_0/\cos\phi}\right| \quad \text{dB} \tag{11.91}$$

Equation (11.91) indicates that trace coincidence between the incident sound wave and the free shear waves in the plate (which would lead to complete transmission) can be avoided at all incident angles provided that the panel is specifically designed to yield a low shear wave speed such that $c_s^2 = G/\rho < c_0^2 = P_0\kappa/\rho_0$. Unfortunately, this desirable condition cannot be met with homogeneous plates made of any construction-grade material. As we will discuss later, however, it is possible to satisfy the $c_s < c_0$ criterion with specially designed[31] inhomogeneous sandwich panels without compromising the static strength of the panel and thereby preserving the mass law behavior described by

$$R_{sh}(\phi) \cong R_{mass}(\phi) = 20\log\left(1 + \frac{\rho_2\ \omega\cos\phi}{2\rho_0 c_0}\right) \quad \text{dB} \tag{11.92}$$

which is representative of a limp panel of the same mass per unit area $\rho_s = \rho_M h$ as the shear panel.

Thin homogeneous panels are easier to bend than to shear so that $Z_B \ll Z_{sh}$. It follows that $Z_s \cong Z_m + Z_B$ and Eqs. (11.87) and (11.89) yield

$$R(\phi) = 10\log\frac{1}{\tau(\phi)} = 10\log\left|1 + \frac{j\rho_s\omega[1-(f/f_c)^2\sin^4\phi]}{2\rho_0 c_0/\cos\phi}\right|^2 \quad \text{dB} \tag{11.93}$$

where f_c is the critical frequency where the speed of the free bending waves in the plate, $c_B(f_c)$, equals the speed of sound in the media. It is given by

$$f_c = \left(\frac{\omega_c}{2\pi}\right) = \left(\frac{c_0^2}{2\pi}\right)\left(\frac{\rho_s}{B}\right)^{1/2} \quad \text{Hz(s)}^{-1} \tag{11.94}$$

where ρ_s = mass per unit are, $\rho_M h$ kg/m^2
h = plate thickness, m
B = bending stiffness of plate, $Eh^3/[12(1-\nu^2)]$ N · m

Consequently, the product $f_c\rho_s$ is a constant for a specific plate material and liquid (usually air). It is given by

$$f_c\rho_s = \left(\frac{c_0^2}{2\pi}\right)\sqrt{12(1-\nu^2)}\sqrt{\frac{\rho_M}{E}} \quad \text{Hz(s)}^{-1} \tag{11.95}$$

This product is listed in Table 11.2 for air as a surrounding medium. It is used to determine f_c as $f_c = \rho_s f_c/f_c$.

The coincidence frequency in air of homogeneous isotropic plates can be easily determined by cutting a narrow strip of length l in meters, supporting the two ends of the strip on a knife edge (to simulate simple supported edge conditions), and measuring the sag d in millimeters at the midpoint of the strip. The coincidence frequency is computed as

$$f_c = 1.65(10^2)\sqrt{\frac{d/\text{mm}}{l/\text{m}}} \quad \text{Hz(s)}^{-1} \tag{11.96}$$

Equation (11.93) indicates that above the critical frequency f_c given in Eq. (11.94), trace coincidence between the incident sound wave and the free bending waves in the plate occurs when $f = f_c/\sin^2\phi$ (which is called the coincidence frequency) and would result in complete transmission if the plate had no internal damping.

It is customary to account for internal damping in Eq. (11.88) by introducing a complex Young's modulus $E' = E(1 + j\eta)$ that results in complex wavenumbers $k_c' = k_c(1 + \frac{1}{2}j\eta)$ and $k_s' = k_s(1 + \frac{1}{2}j\eta)$ and yields the following modified form of the sound transmission loss:

$$\begin{aligned} R(\phi) &= 10\log\frac{1}{\tau(\phi)} \\ &= 10\log\left\{\left|1 + \frac{\rho_s\omega}{2\rho_0 c_0/\cos\phi}\right.\right. \\ &\qquad \left.\left.\left\{\eta\left(\frac{f}{f_c}\right)^2\sin^4\phi + j\left[1-\left(\frac{f}{f_c}\right)^2\sin^4\phi\right]\right\}\right|^2\right\} \quad \text{dB} \end{aligned} \tag{11.97}$$

Equation (11.97) indicates that in the vicinity of $f = f_c/\sin^2\phi$ the curves of sound transmission loss versus frequency exhibit a minimum that is controlled by the damping.

Figure 11.20 shows the curve of sound transmission loss versus frequency for a 4.7-mm-($\frac{3}{16}$-in.-) thick glass plate for normal ($\phi = 0°$), $\phi = 45°$, and near-grazing ($\phi = 85°$) angles of incidence computed according to Eq. (11.97). Figure 11.20 illustrates the decrease in sound transmission loss that occurs with increasing angle of incidence (owing to the $\cos\phi$ term) and the trace-matching dip that occurs at $f = f_c/\sin^2\phi$.

Transmission of Random-Incidence (Diffuse) Sound through an Infinite Plate

A plane wave impinging on the plate at one particular angle is not a typical problem. The sound field in a room is better modeled as a diffuse sound field, which is an ensemble of plane sound waves of the same average intensity traveling with equal probability in all directions. A region of unit area on the plate will be exposed, at any instant, to plane sound waves incident from all areas on

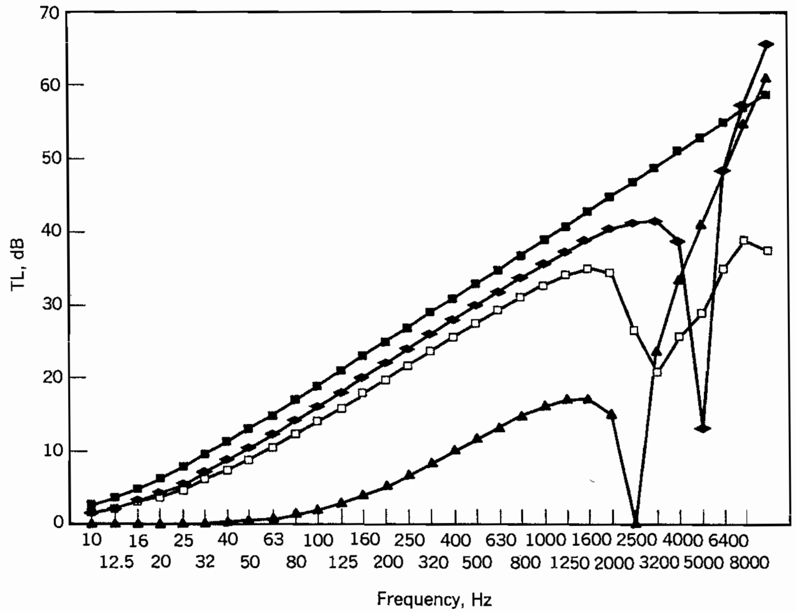

FIGURE 11.20 Computed TL-versus-frequency curve of a 3.7-mm-($\frac{3}{16}$-in.-) thick infinite glass plate for various angles of incidence: (■) normal ($\phi = 0°$); (♦) $\phi = 45°$; (►) $\phi = 85°$; (□) random.

a hemisphere whose center is the area on the plate. These waves are uncorrelated and have equal intensity. The sound intensity incident on the unit area of the plate from any particular angle will be the intensity of the plane wave at angle I_{inc} multiplied by the cosine of the angle of incidence. The total transmitted intensity is then

$$I_{\text{trans}} = \int_{\Omega} \tau(\phi) I_{\text{inc}} \cos\theta \, d\Omega \quad \text{W/m}^2 \tag{11.98}$$

The integration is over a hemisphere of solid angle Ω, where $d\Omega = \sin\phi \, d\phi \, d\theta$. Because I_{inc} is the same for all plane waves and τ is independent of the polar angle θ, an average transmission coefficient may be defined by

$$\overline{\tau} = \frac{\int_0^{\phi\,\text{lim}} \tau(\phi) \cos\phi \sin\phi \, d\phi}{\int_0^{\phi\,\text{lim}} \cos\phi \sin\phi \, d\phi} \tag{11.99}$$

where ϕ_{lim} is the limiting angle of incidence of the sound field. For random incidence, ϕ_{lim} is taken as $\frac{1}{2}\pi$, or 90°. The sound transmission coefficient $\tau(\phi)$ is that given in Eq. (11.97), and the random-incidence sound transmission loss is given by

$$R_{\text{random}} = 10 \log \frac{1}{\overline{\tau}} \quad \text{dB} \tag{11.100a}$$

At low frequencies ($f \ll f_c$) the random-incidence sound transmission loss (for $\text{TL}_N > 15$ dB) is found by averaging the argument of Eq. (11.97) over a range of ϕ from 0° to 90° to yield[32,33]

$$R_{\text{random}} \cong R_0 - 10 \log(0.23 R_0) \quad \text{dB} \tag{11.100b}$$

which is commonly referred to as the random-incidence mass law.

It has become common practice to use the *field-incidence mass law*, which is defined (for $R_0 \geq 15$ dB) as[34]

$$R_{\text{field}} \cong R_0 - 5 \quad \text{dB} \tag{11.101}$$

This result, which yields better agreement with measured data than Eq. (11.100b), approximates a diffuse incident sound field with a limiting angle ϕ_{lim} of about 78° in Eq. (11.99).[34]

The mass law transmission losses R_0, R_{field}, and R_{random}, valid for frequencies well below coincidence, are plotted versus $f\rho_s$ in Fig. 11.21.

Field-Incidence Sound Transmission for Thin Isotropic Plates, R_{field}. Equations (11.98) and (11.99) must be solved by numerical integration.

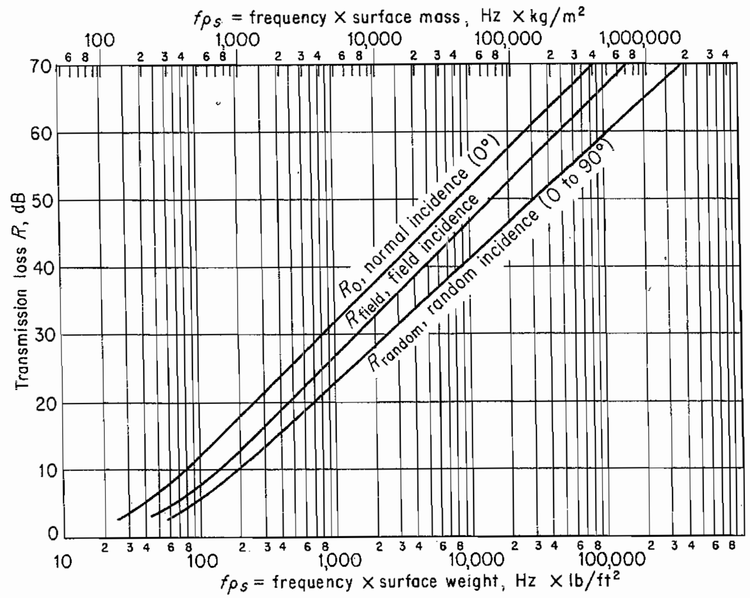

FIGURE 11.21 Theoretical sound transmission loss of large panels for frequencies well below coincidence ($f \leq 0.5 f_c$). Field incidence assumes a sound field that allows all angles of incidences up to 78° from normal.

The results of such an integration of the transmission coefficient between the angles 0° and 78° and application of Eq. (11.100a) to give the *field-incidence transmission loss* are presented in Fig. 11.22 for all values of f/f_c. The ordinate is the difference between the field-incidence transmission loss R_{field} and the normal-incidence mass law transmission loss at the critical frequency $R_0(f_c)$. The latter is easily determined from Eq. (11.83c) or from Fig. 11.21 when the mass per unit area and the critical frequency of the panel are known. Note that predicted transmission losses of less than about 15 dB for $f \ll f_c$ or less than 25 dB for $f \simeq f_c$ from Fig. 11.22 are not accurate.

Example 11.2. Calculate the normal-incidence mass law for an aluminum panel weighing 10 lb/ft^2 at a frequency of 500 Hz. Also determine the random-incidence and field-incidence mass laws. What is R_{field} at 2800 Hz when $\eta = 10^{-2}$?

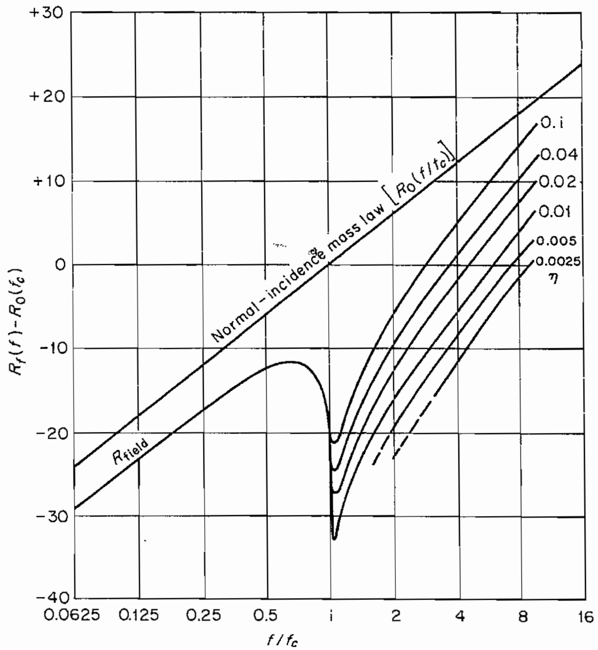

FIGURE 11.22 Field-incidence forced-wave transmission loss. The ordinate is the difference between the field-incidence transmission loss at the frequency f and the normal-incidence transmission loss at the *critical frequency* ($f/f_c = 1$). Note that for a predicted transmission loss of less than 15 dB or for the dashed areas on the figure, the transmission loss depends on both the surface weight and the loss factor, and the curves provide only a lower bound estimate to the actual transmission loss. Use of curve: (1) determine $\rho_s f_c$ from Table 11.2, (2) determined f_c, (3) determine $R_0(f_c)$ from Fig. 11.21 or Table 11.2, (4) read $R_f(f) - R_0(f_c)$ from Fig. 9.21 at the required η, and (5) $R_f(f) = [R_f(f) - R_0(f_c)] + R_0(f_c)$. Top curve is the normal-incidence mass law defined in Eq. (11.83c).

Solution The normal-incidence mass law is given by Eq. (11.83c) and the upper curve of Fig. 11.21. We have $f\rho_s = 500 \times 10 = 5000$ Hz · lb/ft^2. From Fig. 11.21, $R_0 = 45.5$ dB. The random-incidence mass law is given by Eq. (11.100b) and the lower curve of Fig. 11.21; that is, $R_{\text{random}} = 35$ dB. The field-incidence mass law is given by Eq. (11.101) and the middle curve of Fig. 11.21, that is, $R_{\text{field}} = 45.5 - 5 = 40.5$ dB.

From Table 11.2, $\rho_s f_c = 7000$ Hz · lb/ft^2; $f_c = 7000/10 = 700$ Hz and $R_0(f_c) = 48$ dB from Fig. 11.21. Evaluating Fig. 11.22 at $f/f_c = 2800/700 = 4$ and $\eta = 0.01$, we get $R_f(f) - R_0(f_c) = -6$ dB, yielding $R_r(f) = [R_r(f) - R_0(f_c)] + R_0(f) = -6 + 48 = 42$ dB.

Sound Transmission for Orthotropic Plates. Sound transmission for orthotropic plates differs from that of isotropic plates because orthotropic plates have markedly different bending stiffnesses in the different principal directions. The difference in bending stiffness for plane plates may result from the anisotropy of the plate material (such as for wood caused by grain orientation) or from the construction of the plate such as corrugations, ribs, cuts, and so on. Consequently, the speed of free bending waves is different for these two directions and the orthotropic panel has two coincidence frequencies given by[35]

$$f_{c1} = \frac{c_o^2}{2\pi}\sqrt{\frac{\rho_s}{B_x}} \quad \text{Hz} \tag{11.102a}$$

$$f_{c2} = \frac{c_o^2}{2\pi}\sqrt{\frac{\rho_s}{B_y}} \quad \text{Hz} \tag{11.102b}$$

where B_x is the bending stiffness for the stiffest direction and B_y the direction perpendicular to this. The random-incidence sound transmission loss of an orthotropic plate is predicted by[35]

$$R_{\text{random}} \cong \begin{cases} 10\log\left[\left(\dfrac{\rho_s\omega}{2\rho_0 c_0}\right)^2\right] - 5 & \text{for } f \ll f_{c1} \\ 10\log\left[\left(\dfrac{\rho_s\omega}{2\rho_0 c_0}\right)^2\right] - 10\log\left[\dfrac{1}{2\pi^3\eta}\dfrac{f_{c1}}{f}\sqrt{\dfrac{f_{c1}}{f_{c2}}}\left(\ln\dfrac{4f}{f_{c1}}\right)^4\right] & \text{for } f_{c1} < f < f_{c2} \\ 10\log\left[\left(\dfrac{\rho_s\omega}{2\rho_0 c_0}\right)^2\right] - 10\log\dfrac{\pi f_{c2}}{2\eta f} & \text{for } f > f_{c2} \end{cases} \tag{11.103}$$

where η is the loss factor. For corrugated plates, as shown in Fig. 11.23, the bending stiffnesses can be approximated by

$$B_y = \frac{Eh^3}{12(1 - \nu^2)} \quad \text{N} \cdot \text{m} \tag{11.104a}$$

$$B_x = B_y \left(\frac{s}{s'}\right) \quad \mathrm{N \cdot m} \tag{11.104b}$$

where s and s' are defined in Fig. 11.23. Note that the increase in bending stiffness caused by corrugations, ribs, and stiffeners always results in a reduction of the sound transmission loss, while measures such as partial-depth saw cuts, which decrease bending stiffness, result in an increase of the sound transmission loss of plates.

Sound Transmission Loss for Inhomogeneous Plates. Sound transmission loss for inhomogeneous plates, such as appropriately designed sandwich panels, can be substantially higher than for homogeneous panels of the same mass per unit area, provided that such plates favor the propagation of the free shear waves (with frequency-independent propagation speed) rather than free bending waves for which the propagation speed increases with increasing frequency. However, they must be designed such that the shear wave speed remains below the speed of sound in air so that no trace coincidence occurs. Consequently, the sound transmission loss of such so-called shear wall panels closely approximates the field-incidence mass law. Information for designing such panels is given in reference 31. However, ordinary sandwich panels are very poor sound barriers because

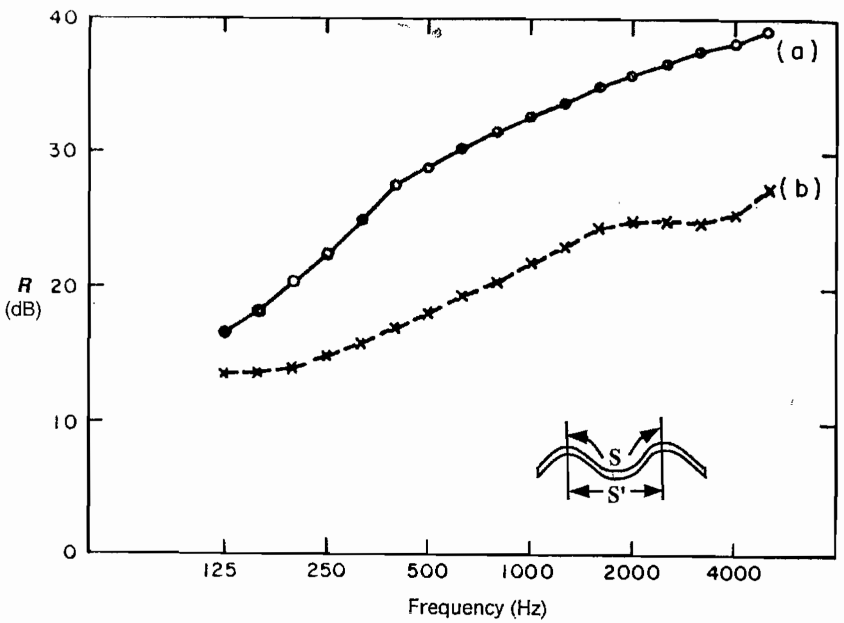

FIGURE 11.23 Measured sound transmission loss of steel plates (after Ref. 28): (*a*) plane plate, $\rho_s = 8$ kg/m^2; (*b*) corrugated plate, $\rho_s = 11$ kg/m^2; s, distance between corrugations along surface; s', distance along straight line.

of their low mass and high bending stiffness that result in a coincidence frequency that usually falls in the middle of the audio frequency range. Dilation resonance, which occurs at the frequency where the combined stiffness impedance of the face plate and that of the enclosed air equals the mass impedance of the plate, also leads to further deterioration of the sound transmission loss of sandwich panels.

Sound Transmission through a Finite-Size Panel

For most architectural applications, where the first resonance frequency of typical platelike partitions is well below the frequency range of interest and the plate size is much larger than the acoustical wavelength, Eq. (11.97) or Fig. 11.22 (which are strictly valid only for infinitely large panels) can be used to predict the sound transmission loss of finite panels. In many industrial applications, the finite size of the panel must be taken into account.[36]

In finite panels the sound-forced bending waves encounter the edges of the plate and generate free bending waves, such that the sum of the incident forced bending wave and the generated free bending wave satisfies the particular plate edge condition (e.g., zero displacement and angular displacement at a clamped edge). Consequently, the sound-forced bending waves continuously feed free bending wave energy into the finite panel and build up a reverberant, free bending wave field. The mean-square vibration velocity of this free bending wave field, $\langle v_{\mathrm{FR}}^2 \rangle$ can be obtained using a power balance for the finite plate. The power introduced into the finite plate at the edges equals the power lost by the plate owing to viscous losses in the plate material, energy flow into connected structures, and sound radiation. The transmitted sound radiated by the finite panel is given by

$$W_{\mathrm{rad}} = \langle v_{\mathrm{FO}}^2 \rangle\, \rho_0 c_0 S \sigma_{\mathrm{FO}} + \langle v_{\mathrm{FR}}^2 \rangle\, \rho_0 c_0 S \sigma_{\mathrm{FR}} \quad \mathrm{W} \tag{11.105}$$

where $\langle v_{\mathrm{FO}}^2 \rangle$ is the mean-square velocity of the sound-forced supersonic bending waves, $\sigma_{\mathrm{FO}} \geq 1$ is the radiation efficiency of the forced waves, S is the surface area of the panel, and σ_{FR} is the radiation efficiency of the free bending waves. Since $\sigma_{\mathrm{FR}} \ll 1$ below the critical frequency of the panel ($f \ll f_c$), it is frequently the case that the vibration response of the panel is controlled by the free bending waves (i.e., $\langle v_{\mathrm{FR}}^2 \rangle \gg \langle v_{\mathrm{FO}}^2 \rangle$) but the sound radiation is controlled by the less intense but more efficiently radiating forced waves.

The classical definition of sound transmission loss is $R = 10 \log(W_{\mathrm{inc}}/W_{\mathrm{trans}})$, where W_{inc} is the sound power incident at the source side and W_{trans} is that radiated from the receiver side of the panel. If the incident sound is a plane wave arriving at an incident angle ϕ ($\phi = 90°$ for grazing incidence), then it is assumed that

$$W_{\mathrm{inc}} = \frac{0.5 |\hat{p}_{\mathrm{in}}|^2 S \cos\phi}{\rho_0 c_0} \quad \mathrm{W} \tag{11.106}$$

This assumption leads to the dilemma that at grazing incidence ($\phi = 90°$) no power is incident on the panel. It is common knowledge that grazing incidence sound excites the panel to forced vibrations, and the panel radiates sound into the receiver room when the forced bending waves in the panel and the sound wave at the receiver side, which run parallel to the panel, encounter the edges of the finite panel. This unresolved conceptual problem has been avoided[34] by limiting the incident angle range to 78°, in computing the field incidence sound transmission loss for the infinite panel according to Eq. (11.101), so as to yield reasonable agreement with laboratory measurements for panel sizes typically employed in such tests.

Obviously, it is not the incident sound power but the mean-square sound pressure on the source side that is forcing the panel. Since this quantity is proportional to the sound energy density in the source room $E_s = \langle p_s^2 \rangle / \rho_0 c_0^2$, it has been suggested[37,38] that the sound transmission loss of a finite partition be defined as

$$R_E \equiv 10 \log \left(\frac{E_s}{E_R} \frac{S}{A} \right) \quad \text{dB} \qquad (11.107)$$

where $E_R = 4\ W_{\text{trans}}/c_0 A$ is the energy density in the receiver room, S is the surface area of the panel (one side), and A is the total absorption in the receiver room. The transmitted sound power $W_{\text{trans}} = \frac{1}{4} c_0 A E_R$ is owing to the velocity of the plate. The forced response is dominated by the mass-controlled separation impedance $Z_s \simeq j\omega\rho_s$. The sound radiation of the sound-forced finite plate is controlled by its radiation impedance $Z_{\text{rad}} \cong \text{Re}\{Z_{\text{rad}}\} = \rho_0 c_0 \sigma_F$. Consequently, the low-frequency sound transmission loss of the finite partition is predicted is predicted as[38]

$$R_E \cong R_0 - 3 - 10 \log \sigma_F \quad \text{dB} \qquad (11.108)$$

where R_0 is the normal-incidence mass law sound transmission loss given in Eq. (11.83c) and σ_F is the forced-wave radiation efficiency of the finite panel given in Table 11.8. Note that σ_F depends on panel size as well as on incidence angle and can be smaller or larger than unity. This implies that the sound transmission loss of finite panels can be larger than the normal-incidence mass law even for grazing incidence if the size of the panel is small compared with the wavelength. When the panel size is much larger than the acoustical wavelength, σ_F approaches $1/\cos\phi$. For predicting the sound transmission loss of finite partitions over the entire low-frequency range ($f \ll f_c$), Eq. (11.108) should be used.

According to reference 38, the classical sound transmission formulas for infinite panels can be used to approximate the sound transmission loss of finite partitions by substituting $1/\sigma_F$ instead of $\cos\phi$ and $\sqrt{1 - 1/\sigma_F^2}$ instead of $\sin\phi$ in Eq. (11.97) and carrying out the integration in Eq. (11.99) from $\phi = 0$ to $\phi = 90°$ to obtain an estimate of the random-incidence sound transmission loss that agrees well with laboratory measurements. There is no need to resort to limiting the incident angle range to 78°. The radiation efficiency for random-incidence (diffuse-field) sound-forced excitation is given in Table 11.8, and this expression

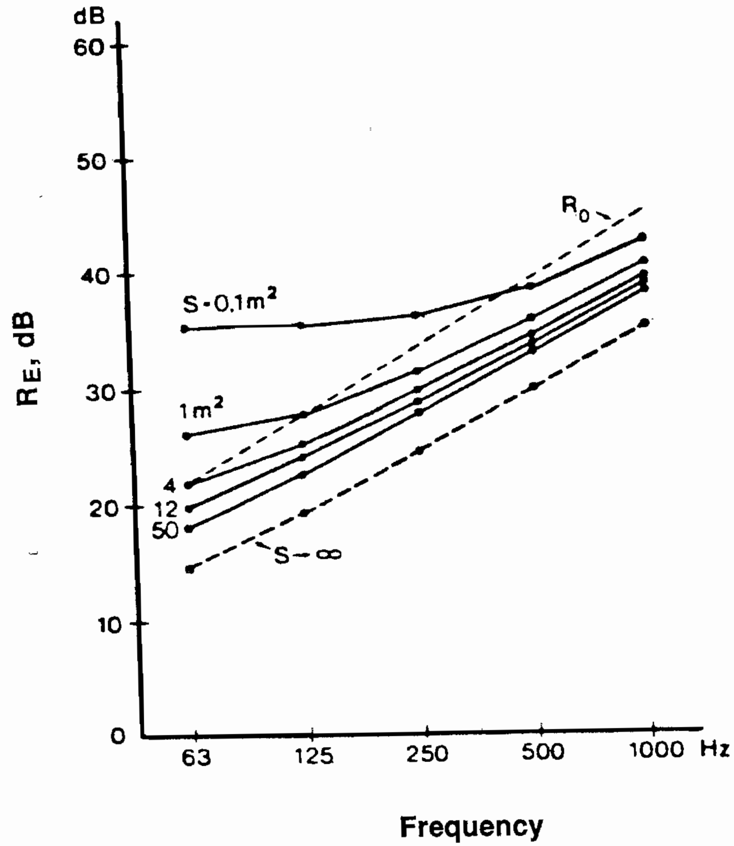

FIGURE 11.24 Random-incidence sound transmission loss of 25-kg/m² panels as a function of frequency with panel surface area S as a parameter, mass-controlled low-frequency region; computed according to Eq. (11.110). (After References 37 and 38.)

should be used in Eq. (11.108). As shown in Fig. 11.24, the random-incidence sound transmission loss of partitions of approximately 4 m² surface area, which are typically used in laboratory measurements, yield predicted values that are 5 dB below the normal-incidence mass law, giving theoretical justification for using the field-incidence mass law defined in Eq. (11.101) for partitions of this size. Note, however, that for small partitions Eq. (11.108) is more accurate. It should be pointed out that all of the sound transmission loss prediction formulas are valid only in the frequency region well above the first bending wave resonance of the panel where the forced response is mass controlled. For small, very stiff partitions the frequency range of interest may extend into the stiffness-controlled region below the frequency of the first bending wave resonance.* In this case,

*For prediction in this frequency region use Eqs. (11.70)–(11.73).

the volume compliance of the panel, as described in the beginning of this section in Chapter 12, should be used to predict sound transmission.

Empirical Method for Predicting Sound Transmission Loss of Single Partitions. An alternate technique useful in preliminary design is illustrated in Fig. 11.25. In essence, it considers the loss factor of the material to be determined completely by the material selection and substitutes a "plateau" or horizontal line for the peak and valley of the forced-wave analysis in the region of the critical frequency.[34,39] Its use will be demonstrated in Example 11.3.

Example 11.3. Calculate the transmission loss of a $\frac{1}{8}$-in.- (3-mm-) thick, 5×6.5-ft (1.52×2-m) aluminum panel by the alternate (plateau) method.

Solution From Table 11.2, the product of surface mass and critical frequency is $\rho_s f_c = 34,700$ Hz $\cdot$ kg/m^2. The $\frac{1}{8}$-in.-thick aluminum plate has a surface density

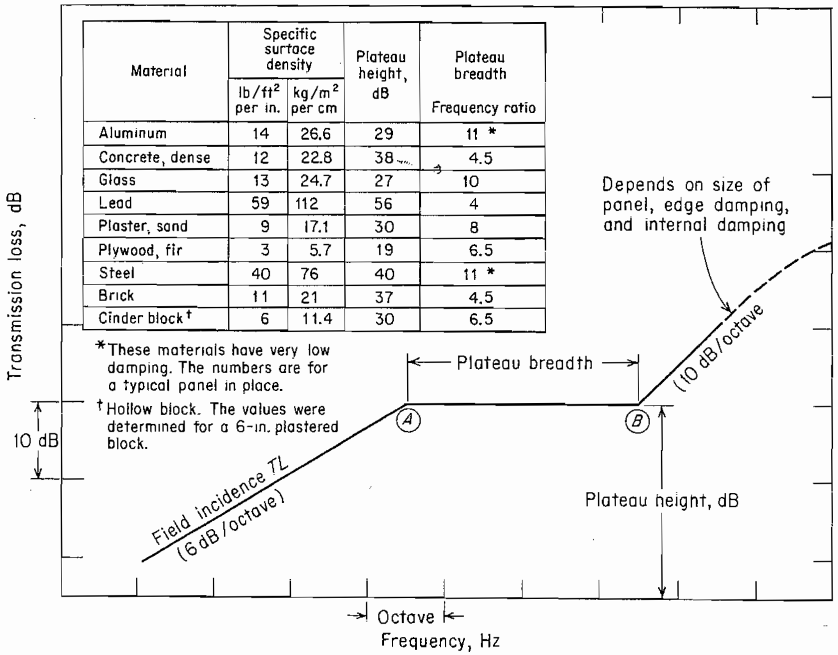

Material	Specific surface density lb/ft^2 per in.	Specific surface density kg/m^2 per cm	Plateau height, dB	Plateau breadth Frequency ratio
Aluminum	14	26.6	29	11 *
Concrete, dense	12	22.8	38	4.5
Glass	13	24.7	27	10
Lead	59	112	56	4
Plaster, sand	9	17.1	30	8
Plywood, fir	3	5.7	19	6.5
Steel	40	76	40	11 *
Brick	11	21	37	4.5
Cinder block†	6	11.4	30	6.5

*These materials have very low damping. The numbers are for a typical panel in place.

†Hollow block. The values were determined for a 6-in. plastered block.

FIGURE 11.25 Approximate design chart for estimating the sound transmission loss of single panels. The chart assumes a reverberant sound field on the source side and approximates the behavior around the critical frequency with a horizontal line or plateau. The part of the curve to the left of A is determined from the field-incidence mass law curve (Fig. 11.21). The plateau height and length of the line from A to B are determined from the table. The part above B is an extrapolation. This chart is fairly accurate for large panels. Length and width of the panel should be at least 20 times the panel thickness.[34]

of 8.5 kg/m^2. From Fig. 11.21 we find that the normal-incidence transmission loss at the critical frequency is $R_0(f_c) = 48.5$ dB and that the field-incidence transmission loss at 1000 Hz is R_{field} (8500 Hz $\cdot$ kg/m^2) = 31.5 dB.

The procedure by the plateau method is as follows[34,39]:

1. Using semilog paper (with coordinates decibels versus log frequency), plot the field-incidence mass law transmission loss as a line with a 6-dB/octave slope through the point 31.5 dB at 1000 Hz.
2. From Fig. 11.25, the plateau height for aluminum is 29 dB. Plotting the plateau gives the intercept of the plateau with the field-incidence mass law curve at approximately 750 Hz.
3. From Fig. 11.25, the plateau width is a frequency ratio of 11. The upper frequency limit for the plateau is therefore 11×750 Hz = 8250 Hz.
4. From the point 29 dB, 8250 Hz, draw a line sloping upward at 10 dB/octave. This completes the plateau method estimate (see curve b in Fig. 11.34).

Sound Transmission through Double- and Multilayer Partitions

The highest sound transmission loss obtainable by a single partition is limited by the mass law. The way to "break this mass law barrier" is to use multilayer partitions such as double walls, where two solid panels are separated by an air space that usually contains fibrous sound-absorbing material and double windows where light transparency requirements do not allow the use of sound-absorbing materials.

The transmission of sound through a multilayer partition can be computed in a similar manner as the sound absorption coefficient of multilayer sound absorbers treated in Chapter 8. Figure 11.26 shows the situation where a plane sound wave of frequency $f = \omega/2\pi$ is incident at an angle ϕ on a panel that has N layers and $N+1$ interfaces. The important boundary conditions are that the wavenumber component parallel to the panel surface $k_x = k \sin\phi$ must be the same in all of the layers and that the acoustical pressure and particle velocity at the interfaces of the layers must be continuous.[40–42]

The layers are characterized by their wave impedance formula, which relates the complex wave impedance at the input-side interface Z_I with that at the termination-side interface Z_T and by their pressure formula that relates the complex sound pressure at the input-side interface p_I to that at the terminal-side interface p_T.

The impedance and pressure formulas for an impervious orthotropic thin plate are given by[42]

$$Z_I = Z_T + Z_S$$

$$= Z_T + j\left[\omega\rho_s - \frac{1}{\omega}(B_x k_x^4 + 2B_{xy}k_x^2k_y^2 + B_y k_y^4)\right] \quad \text{N} \cdot \text{s/m}^3 \qquad (11.109)$$

$$p_I = p_T \frac{Z_I}{Z_T} \quad \text{N/m}^2 \qquad (11.110)$$

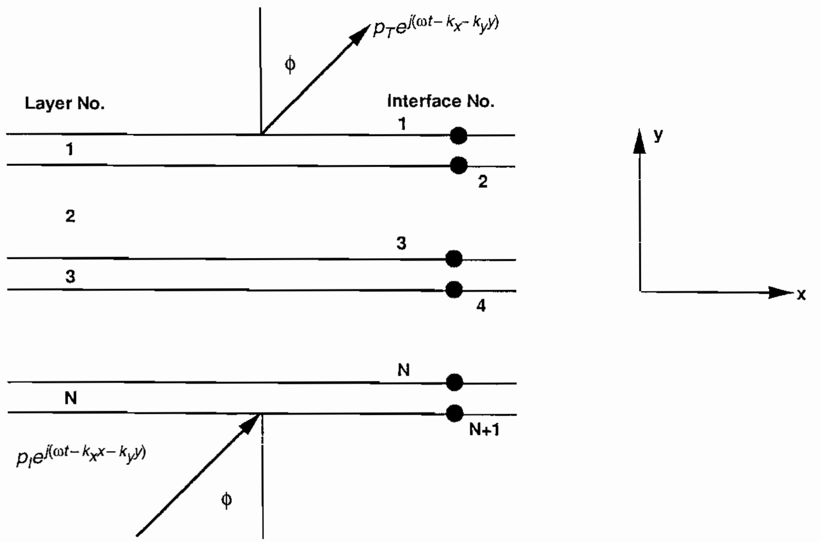

FIGURE 11.26 Transmission of a plane oblique incident sound wave through an infinite lateral dimension multilayer panel.

where ρ_s is the mass per unit area and B is the bending stiffness of the orthotropic plate.

For isotropic plates the second term in Eq. (11.109) reduces to $Z_s = Z_m + Z_B = j(\omega\rho_s - Bk_x^4/\omega)$. If the impervious layer is a composite of an isotropic homogeneous plate with a bonded damping material of thickness h_D, Young's modulus E_D, Poisson ratio ν_D, and damping loss factor η_D and the plate characteristics are thickness h_p, Young's modulus E_p, Poisson ratio ν_p, and loss factor η_p, then the complex bending stiffness $B = B_{\text{comp}}(1 + j\eta_{\text{comp}})$ is obtained[1,42] from

$$B_{\text{comp}} = \frac{E_p h_p^3}{12(1-\nu_p^2)} + \frac{E_D h_D (h_p + h_D)^2}{4(1-\nu_D^2)} \quad \text{Nm} \tag{11.111}$$

$$\eta_{\text{comp}} = \tfrac{1}{4} B_{\text{comp}} (\eta_p E_p h_p + \eta_D E_D h_D)(h_p + h_D)^2 \tag{11.112}$$

For a porous sound-absorbing layer of thickness h the impedance and pressure formulas are given by[42]

$$Z_I = Z_a \frac{k_a}{k_{ay}} \frac{(1 + Z_a\Gamma_a/Z_T\Gamma_{ay})e^{j\Gamma_{ay}h} + (1 - Z_a\Gamma_a/Z_T\Gamma_{ay})e^{-j\Gamma_{ay}h}}{(1 + Z_a\Gamma_a/Z_T\Gamma_{ay})e^{j\Gamma_{ay}h} - (1 - Z_a\Gamma_a/Z_T\Gamma_{ay})e^{-j\Gamma_{ay}h}} \quad \text{N} \cdot \text{s/m} \tag{11.113}$$

$$p_T = \frac{p_I}{2}\left[\left(1 + \frac{Z_a\Gamma_a}{Z_I\Gamma_{ay}}\right)e^{-j\Gamma_{ay}h} + \left(1 - \frac{Z_a\Gamma_a}{Z_I\Gamma_{ay}}\right)e^{j\Gamma_{ay}h}\right] \quad \text{N/m}^2 \tag{11.114}$$

where $Z_a = \rho_0 c_0 Z_{an}$ is the complex characteristic acoustical impedance of the porous bulk material for plane waves and Z_{an} is its normalized value while $\Gamma_a = \Gamma_{an} k_0$ is the complex wavenumber of plane sound waves in the bulk porous material; $\Gamma_{ay}^2 = \Gamma_a^2 - k_x^2$. Formulas for computing Γ_{an} and Z_{an} on the basis of the flow resistivity of the porous material R_1 are given in Chapter 8 [see Eqs. (8.22) and (8.19)]. The simpler approximate formulas for Γ_a and Z_a given in reference 42 are less accurate and their use is not recommended.

In the special case of an air layer without porous sound-absorbing material, substitute $Z_a = \rho_0 c_0$ and $k_a = k_0$ into Eqs. (11.113) and (11.114).

The computation of the sound transmission loss of a layered partition proceeds as follows:

1. Set the termination impedance at the receiver-side interface (interface 1 in Fig. 11.26) to $Z_T = \rho_0 c_0 / \cos\phi$.
2. Apply the appropriate impedance formula for layer 1 and compute the input impedance at interface 2.
3. Using the impedance computed in step 2 as the termination impedance for layer 2, compute the input impedance at interface 3 and proceed down the chain of impedance calculations until the input impedance at the source-side interface (interface $N+1$ in Fig. 11.26), Z_{N+1}, is obtained.
4. Compute the sound pressure at the source-side interface as the sum of the incident and reflected pressures $p_{N+1} = p_I[2\alpha/(\alpha+1)]e^{j(\omega t - k_x x - k_y y)}$, where $\alpha = Z_{N+1}/(\rho_0 c_0/\cos\phi)$.
5. Apply the appropriate pressure formulas in succession until the sound pressure at the receiver-side interface, p, is obtained.
6. Determine the transmission coefficient $\tau(\omega, \phi) = p_1^2/p_I^2$ for all frequencies of interest.
7. Perform computational steps 1–6 for the incident angle range from $\phi = 0°$ to $\phi = 90°$ in one-third-degree increments.
8. Compute the random-incidence sound transmission coefficient for isotropic layers (see ref. 42 for orthotropic impervious layers) as

$$\tau_R(\omega) = \int_0^{\pi/2} \tau(\omega, \phi) \sin 2\phi \, d\phi$$

9. Compute the random-incidence sound transmission loss of the infinite layered partition as

$$R_{\text{random}}(\omega) = 10 \log \frac{1}{\tau_R(\omega)}$$

Figure 11.27 shows the random-incidence sound transmission loss of an infinite three-layer partition as well as that of its constituent layers, computed according to Eqs. (11.109)–(11.114). The partition consists of two 1-mm-thick steel plates and a 100-mm-thick air space that may or may not contain a fibrous sound-absorbing material. Figure 11.27 illustrates the benefit of using sound-absorbing

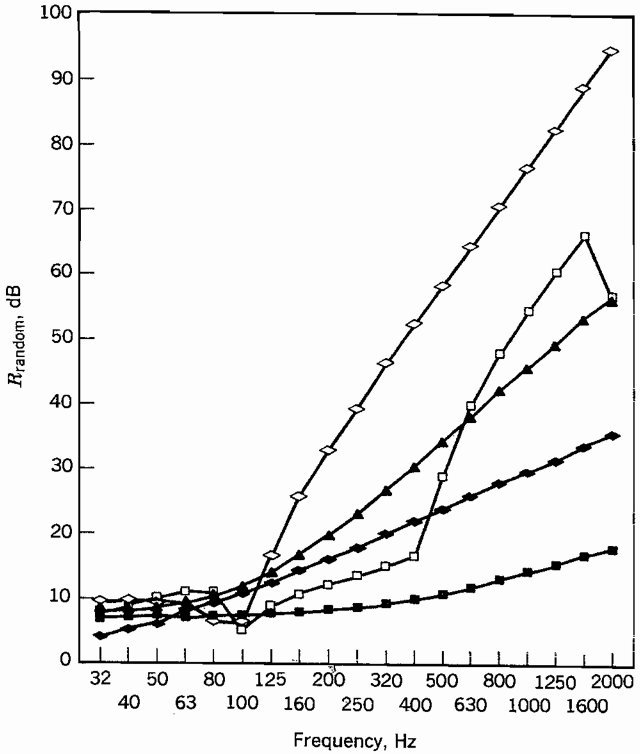

FIGURE 11.27 Computed random-incidence sound transmission loss of a double wall and its constituent layers: (■) 100-mm-thick fibrous absorber, flow resistivity $R_1 = 16{,}700$ N/s · m^4; (◆) 1-mm steel plate; (▲) 1-mm steel plate and 100-mm fibrous absorber. Double wall consisting of two 1-mm-thick steel plates: (□) 100-mm air space, no fibrous absorber; (◇) 100-mm air space with fibrous absorber.

layers. Note that below 500 Hz the double wall without sound-absorbing material in the air space provides substantially lower random-incidence sound transmission loss than a single 1-mm steel plate or the single plate combined with the sound-absorbing layer. The highest sound transmission loss is obtained when the air space is filled with the porous sound-absorbing material. In practical situations, leaks and structure-borne connections between the face plates at edges of the partition usually limit the maximally achievable sound transmission loss at high frequencies to a range of 40–70 dB. At low frequencies the finite size of the partition results in higher values than predicted for infinite partitions. The effect of the sound-absorbing material in the air space results in refraction of the oblique-incidence sound toward the normal, thereby reducing the dynamic stiffness of the air between the plates. The sound-absorbing material also prevents high sound energy buildup in the cavity. These result in a substantial

increase in sound transmission loss. The flow resistivity of the sound-absorbing material should be about $R_1 = 5000$ N · s/m^4.[43] Higher values of R_1 yield only diminishing returns.

The filling of the air space with a gas of 50% lower speed of sound than air (such as SF_6 or CO_2) has the same effect as the sound-absorbing material,[44,45] as illustrated in Fig. 11.28. Using a light gas such as helium, which has three times higher speed of sound than air, also improves sound transmission loss to the same extent as a heavy-gas fill. In this case, the improvement is due to the higher speed of sound in the gas fill, which makes it easier to push the gas tangentially than to compress it. Double windows, which can be hermetically sealed and must be light transparent, are partitions where this beneficial effect can be exploited.

Empirical Method for Predicting Sound Transmission Loss of Double Partitions. Goesele[46] has proposed a simplified method to predict the sound transmission loss R of a double partition when the measured sound transmission losses of the two constituent single partitions R_{I} and R_{II} are available, there are no structure-borne connections, and the gap is filled with porous sound-absorbing material. The prediction is given as

$$R \cong R_{\mathrm{I}} + R_{\mathrm{II}} + 20\log\left(\frac{4\pi f \rho_0 c_0}{s'}\right) \quad \text{dB} \tag{11.115}$$

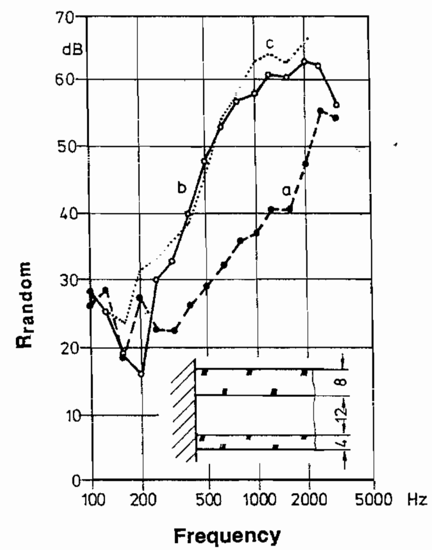

FIGURE 11.28 Improvement of the sound transmission loss of a double glass partition (no contact at the edges) owing to heavy gas (SF_6) fill of the gap: a, measured with air-filled gap; b, measured with SF_6-filled gap; c, computed for mineral wool fill. (After Ref. 44.)

where

$$s' = \begin{cases} \dfrac{\rho_0 c_0^2}{d} & \text{for } f < f_d = \dfrac{c_0}{2\pi\, d} \quad \text{N/m}^3 \quad (11.116\text{a}) \\ 2\pi f \rho_0 c_0 & \text{for } f > f_d \quad \text{N/m}^3 \quad (11.116\text{b}) \end{cases}$$

is the dynamic stiffness per unit area of the gap and d is the gap thickness.

If no measured sound transmission loss data for the constituent single partitions are available, the sound transmission loss of the double wall made of two identical panels can be predicted on the basis of material properties as

$$R(f_R < f < f_c) \cong 20 \log \frac{\pi f \rho_{s1}}{\sqrt{2}\rho_0 c_0} + 40 \log \left(\frac{\sqrt{2} f}{f_R} \right) \quad \text{dB} \qquad (11.117\text{a})$$

$$R(f > f_R, f > f_c) \cong 40 \log \left[\frac{\pi f \rho_{s1}}{\rho_0 c_0} \sqrt{2\eta} \left(\frac{f}{f_c} \right)^{1/4} \right] + 20 \log \frac{4\pi f \rho_0 c_0}{s'} \quad \text{dB} \qquad (11.117\text{b})$$

where f_c is the critical frequency of the panels and f_R is the double-wall resonance frequency

$$f_R = \frac{1}{2\pi} \sqrt{\frac{2\sqrt{2} s'}{\rho_{s1}}} \quad \text{Hz} \qquad (11.118)$$

Figure 11.29 shows that Eq. (11.115) yields good agreement with measured data in the entire frequency region, while Eqs. (11.117a) and (11.117b) give good agreement only well below and well above the critical frequency but fail in the frequency region near the critical frequency. Prediction methods for the sound transmission loss of double walls with point and line bridges are given by reference 30 and by Bies and Hansen (see Bibliography).

Sound Transmission Loss of Ducts and Pipes

Pipes and ducts that carry high-intensity internal sound are excited into vibration and radiate sound to the outside. This sound transmission in the breakout direction (i.e., from inside to outside) is characterized by breakout sound transmission loss R_{io}, which is a measure of the rate at which sound energy from the interior of the duct radiated to the outside. When pipes and ducts traverse areas of high-intensity sound such as found in mechanical equipment rooms, the exterior sound field excites ductwall vibrations and the vibrating walls generate an internal sound field that can travel to distant quiet areas. This sound transmission from the outside to the inside direction is characterized by the breakin sound transmission loss R_{oi}, which is a measure of the rate at which sound energy from the exterior sound field enters the duct.

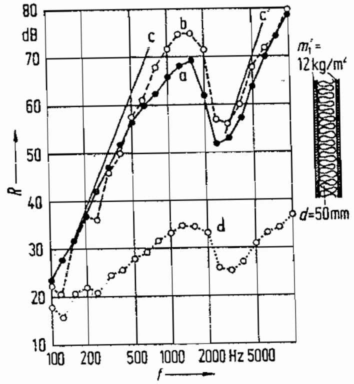

FIGURE 11.29 Sound transmission loss of a double partition consisting of two identical, 12.5-mm-thick gypsum boards separated by a 50-mm-thick gap filled with fibrous sound-absorbing material: *a*, measured values; *b*, predicted by Eq. (11.117); *c*, predicted by Eqs. (11.116a) and (11.116b); *d*, measured sound transmission loss of a single gypsum board wall. (After reference 46.)

The sound power level radiated by a duct or pipe of length l, L_w^{io}, is predicted as[47]

$$L_w^{io}(l) = L_w^i(0) - R_{io} + 10 \log \left(\frac{Pl}{S} \right) + 10 \log(C) \quad \text{dB re} 10^{-12} \text{ W} \qquad (11.119\text{a})$$

where

$$C = \frac{1 - e^{-(\tau + \beta)l}}{(\tau + \beta)l} \qquad (11.119\text{b})$$

$$\tau = \frac{P}{S} \times 10^{-R_{io}/10} \qquad (11.119\text{c})$$

$$\beta = \frac{\Delta L_1}{4.34} \qquad (11.119\text{d})$$

where $L_w^i(0)$ is the sound power level in the duct at the source side, S is the cross-sectional area in square meters, P is the perimeter of the duct cross section in meters, and ΔL_1 is the sound attenuation in decibels per unit length inside the duct due to porous lining. Equation (11.119a) contains only measurable quantities and is used as a basis for the experimental evaluation of the breakout sound transmission loss R_{io}, by measuring the sound power $W_{io}(l)$ radiated by a test duct of length l into a reverberation room, the sound power in the duct at the source side, $W_i(0)$, and the sound attenuation inside the duct, ΔL_1, and solving Eq. (11.119a) for R_{io} by iteration.

The sound power level of the sound propagating in one direction, $L_w^{io}(l)$ when a duct of length l traverses through a noisy area (and sound breaks into the duct is predicted by[47]

$$L_w^{io}(l) = L_w^{\text{inc}} - R_{io} - 3 + C \quad \text{dB re}10^{-12}\ \text{W} \tag{11.120}$$

where L_w^{inc} is the sound power level of the sound incident on the duct of length l, R_{io} is the breakin sound transmission loss, and C is as defined in Eq. (11.119b). On the basis of reciprocity,[48] the following relationship exists between breakout and breakin sound transmission loss:

$$R_{oi} \cong R_{io} - 10\log\left\{4\gamma\left[1 + 0.64\frac{a}{b}\left(\frac{f_{\text{cut}}}{f}\right)^2\right]\right\} \quad \text{dB} \tag{11.121}$$

where a and b are the larger and smaller sides of a rectangular duct cross section, f is the frequency, f_{cut} is the cutoff frequency of the duct, and γ is 1 below cutoff and 0.5 above cutoff. Empirical methods for predicting the breakout sound transmission loss of unlined, unlagged rectangular sheet metal ducts are given in references 48–50. Chapter 17 contains predicted values of octave-band breakout sound transmission loss versus frequency for rectangular sheet metal ducts of sizes most frequently used in low-velocity HVAC systems. Sound transmission loss predictions for round and flat-oval ducts are given elsewhere.[49,50] Figure 11.30 shows the breakin sound transmission loss of an unlined, unlagged

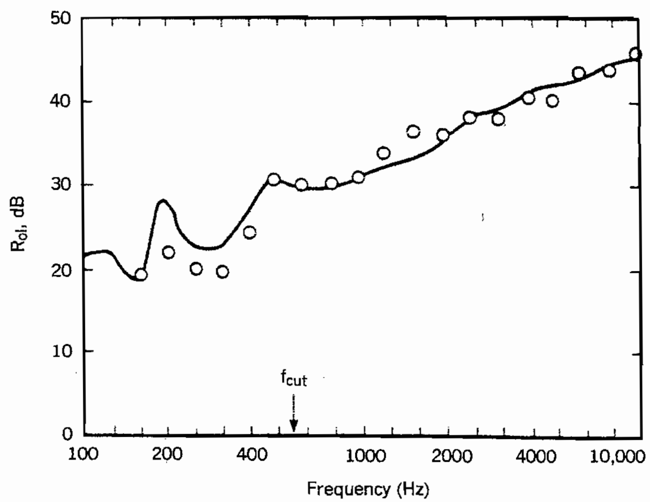

FIGURE 11.30 Breakin sound transmission loss R_{io} of a 0.3 m × 0.91 mm thick sheet metal duct (after Ref. 48): (——) measured: (○ ○ ○) predicted from measured R_{io} using Eq. (11.121).

sheet metal duct. The solid curve was obtained by directly measuring the breakin sound transmission loss while the open circles represent data points obtained by applying the reciprocity relationship embodied in Eq. (11.121) for the measured breakout sound transmission loss. The importance of Eq. (11.121) is that it makes it unnecessary to measure both R_{oi} and R_{io} separately because if one has been measured, the other can be predicted.

Sound Transmission through a Composite Partition

Partitions that separate adjacent rooms frequently consist of areas that have different sound transmission losses, such as a wall that contains a door with an uncovered key hole. If all parts of the composite partition are exposed to the same average sound intensity, I_{inc}, on the source side, then the sound power transmitted is

$$W_{\text{trans}} = I_{\text{inc}} \sum_{i=1}^{n} S_i \times 10^{-R_i/10} = I_{\text{inc}} \sum_{i=1}^{n} S_i \tau_i \quad \text{W} \tag{11.122a}$$

and the transmission loss of the composite partition is

$$R_{\text{comp}} = 10\log\frac{W_{\text{inc}}}{W_{\text{trans}}} = -10\log\sum_{i=1}^{n}\frac{S_i}{S_{\text{tot}}} \times 10^{-R_i/10} \quad \text{dB} \tag{11.122b}$$

where S_i is the surface area of each component, S_{tot} is the total area of all components, and R_i is the sound transmission loss of the ith component. The sound transmission loss of a small hole radius $a \ll \lambda_0$ in a thin plate of thickness h is well approximated by[26]

$$R_{\text{hole}} \cong 20\log\frac{h + 1.6a}{\sqrt{2}a} \quad \text{dB} \tag{11.123}$$

indicating that small holes in thin partitions ($h < a$) yield a frequency-independent sound transmission loss of $R_{\text{hole}} \simeq 0$ dB. Note, however, that Eq. (11.123) is valid only for small round holes. Long narrow slits can have a "negative sound transmission loss."[51] The sound transmission loss of holes and slits can be increased substantially by sealing them with either porous sound-absorbing material or an elastomeric material or designing them as silencer joints. Prediction of the sound transmission loss of such acoustically sealed openings are given in references 52 and 53.

Flanking Sound Transmission

The sound transmission loss of partitions is measured in acoustical laboratories where sound transmission from the source room to the receiver room occurs only through the partition under test. However, if the same partition constitutes a part of a building, then sound can be transmitted through many paths, as shown schematically in Fig. 11.31. Path 1 represents the primary path, which is

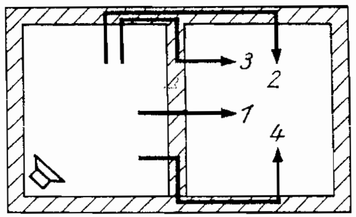

FIGURE 11.31 Sound transmission paths between two adjacent rooms in a typical building (after Reference 54): 1, primary path; 2–4, flanking paths.

characterized by sound transmission loss of the separating partition R_1, usually available from laboratory measurements. The sound transmission loss for each of the $n = 4$ paths (1 the direct and 2, 3, and 4 the flanking paths) is defined as[54]

$$R_n \equiv 10 \log \frac{W_1^{\text{inc}}}{W_{\text{trans}}^n} \quad \text{dB} \tag{11.124}$$

and the composite sound transmission loss, which combines sound transmission along each of the four paths, as

$$R_{\text{comp}} \equiv -10 \log \left(10^{-R_1/10} + \sum_{n=2}^{4} \sum_{m=1}^{4} 10^{-R_{mn}/10} \right) \quad \text{dB} \tag{11.125}$$

where $m = 4$ represents the four sound-excited flanking partitions (i.e., the two sidewalls, floor, and ceiling of the receiver room) each of which transmit sound along each of the three flanking paths $n = 2$, 3, 4. Usually flanking path $n = 2$ contributes as much to the receiver room sound power as do the two other flanking paths $n = 3$ and $n = 4$ together. The contribution of the back wall of the source and receiver room is usually negligible. The process of flanking transmission along flanking paths $n = 2$, 3, 4 is as follows: (1) the sound field in the source room excites the flanking walls to vibration, (2) the vibration is transmitted through the wall junctions to the receiver room walls, and (3) the receiver room walls radiate sound power into the receiver room that adds to that transmitted by the separating partition through the direct path. If the source and receiver rooms have no common wall, the entire sound transmission takes place through flanking paths. For adjacent rooms with a common wall, the composite sound transmission loss given in Eq. (11.125) should be used to predict the sound pressure level in the receiver room. The component flanking transmission losses R_{mn} for homogeneous isotropic single-wall construction can be approximated by[54]

$$R_{mn} = 10 \log \left[\frac{1}{4\pi\sqrt{12}} \left(\frac{\rho_M}{\rho_0} \right)^2 \frac{c_L h^3}{c_0^4} \frac{\omega^2}{} \eta_m \right] + \Delta L_{\text{junct}}$$

$$+ 10 \log \frac{S_1}{S_{\text{rad}}} - 10 \log(\sigma_m \sigma_{\text{rad}}) \quad \text{dB} \tag{11.126}$$

where ρ_M is density and c_L the longitudinal wave speed of the wall material, h is the thickness, η_m is the composite loss factor of the mth partition in the source room, and ΔL_{junct} is the attenuation of the structure-borne sound amplitude at the wall junction along the transmission path n. The symbol S_1 is the surface area of the separating partition and S_{rad} is the surface area of the partition in the receiver room involved in the transmission along path n. The symbols σ_m and σ_{rad} are the radiation efficiencies of the mth partition in the source room and the radiation efficiency of the partition in the receiver room that radiates sound owing to the sound-induced vibration of the mth partition in the source room transmitted through the nth path. A more accurate prediction of the effect of flanking paths on sound transmission loss can be made utilizing the statistical energy analysis method discussed in the next section.

11.8 STATISTICAL ENERGY ANALYSES

Statistical energy analysis (SEA) is a point of view in dealing with the vibration of complex resonant systems. It permits calculation of the energy flow between connected resonant systems, such as plates, beams, and so on, and between plates and the reverberant sound field in an enclosure.[55–59]

System of Modal Groups

In respect to the energy E stored in a structure or in an acoustical volume, may be thought of as a *system of* resonant modes or resonators. First, let us consider the power flow between two groups of resonant modes of two coupled structures having their modal resonance frequencies within the same narrow frequency band $\Delta\omega$ (see Fig. 11.32).

We assume that each resonant mode of the first system (box 1 in Fig. 11.32) has the same energy. Also, assume that the coupling of the individual resonant modes of the first system with each resonance mode of the second system is approximately the same.

If we further assume that the waves carrying the energy in one system are uncorrelated with the waves carrying the energy gained through coupling to the

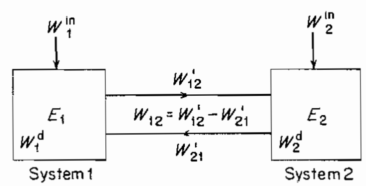

FIGURE 11.32 Block diagram illustrating power flow between two nondissipatively coupled systems.

other system, we can separate the power flow (each equation is written for a narrow frequency band $\Delta\omega$) as

$$W'_{12} = E_1\omega\eta_{12} \quad \text{W} \tag{11.127}$$

$$W'_{21} = E_2\omega\eta_{21} \quad \text{W} \tag{11.128}$$

where W'_{12} = power system 1 transmits to system 2, W
W'_{21} = power system 2 transmits to system 1, W
E_1 = total energy in system 1, m · kg/s
E_2 = total energy in system 2, m · kg/s
ω = center frequency of band, rad/s
η_{12} = coupling loss factor from system 1 to system 2, as defined in Eq. (11.127)
η_{21} = coupling loss factor from system 2 to system 1, as defined in Eq. (11.128)

The net power flow between the two systems is, accordingly,

$$W_{12} = W'_{12} - W'_{21} = E_1\omega\eta_{12} - E_2\omega\eta_{21} \quad \text{W} \tag{11.129}$$

Modal Energy E_m

Let us define modal energy as

$$E_m = \frac{E(\Delta\omega)}{n(\omega)\ \Delta\omega} \quad \text{W} \cdot \text{s/Hz} \tag{11.130}$$

where $E(\Delta\omega)$ = total energy in system in angular frequency band $\Delta\omega$
$n(\omega)$ = modal density, = number of modes in unit bandwidth ($\Delta\omega = 1$) centered on ω, the angular frequency
$\Delta\omega$ = bandwidth, rad/s

If the previously made assumptions about the equal distribution of energy in the modes and the same coupling loss factor are valid, then it may be shown that

$$\frac{\eta_{21}}{\eta_{12}} = \frac{n_1(\omega)}{n_2(\omega)} \tag{11.131}$$

where $n_1(\omega)$ = modal density of system 1 at frequency ω, s
$n_2(\omega)$ = modal density of system 2 at frequency ω, s

Equation (11.131) implies that for equal total energies in the two systems, $E_1 = E_2$, the system that has the *lower* modal density [lower $n(\omega)$] transfers more energy to the second system than is transferred from the second to the first system.

Combining Eqs. (11.129) and (11.131) yields*

$$W_{12} = \omega\eta_{12}n_1(\omega)[E_{m1} - E_{m2}]\ \Delta\omega \quad \text{W} \tag{11.132}$$

where W_{12} = net power flow between systems 1 and 2 in band $\Delta\omega$, centered at ω, W
E_{m1}, E_{m2} = modal energies for systems 1 and 2, respectively [see Eq. (11.130)], W · s/Hz

This equation is positive if the first term in the brackets is greater than the second.

The principle of the SEA method is given by Eq. (11.132), which is a simple algebraic equation with energy as the independent dynamic variable. It states that *the net power flow between two coupled systems in a narrow frequency band, centered at frequency ω, is proportional to the difference in the modal energies of the two systems at the same frequency. The flow is from the system with the higher modal energy to that with the lower modal energy.*

It may help to understand Eq. (11.132) if we use the thermodynamical analogy of heat transfer between two connected bodies of different temperature, where the heat flow is from the body of higher temperature to that of lower temperature and the net heat flow is proportional to the difference in temperature of the two bodies. Consequently, the modal energy E_m is analogous to temperature, and the net power flow W_{12} is analogous to heat flow. The case of equal modal energies of the two systems where the net power flow is zero is analogous to the equal temperature of the two bodies.

Equal Energy of Modes of Vibration

Equal energy of the modes within a group will usually exist if the wave field of the structure is diffuse. Also, since the frequency-adjacent resonance modes of a structure are coupled to each other by scattering and damping, there is always a tendency for the modal energy of resonant modes to equalize within a narrow frequency band even if the wave field is not diffuse.

Noncorrelation between Waves in the Two Systems

In sound transmission problems usually only one system is excited. The power W'_{12} transmitted to the nonexcited system builds up a semidiffuse vibration field in that system. Accordingly, the waves that carry the transmitted power W'_{21} back to the excited system are almost always sufficiently delayed and randomized in phase with respect to the waves carrying the incident power W'_{12} that there is little correlation between the two wave fields.

*Note that Eq. (11.131) is a necessary requirement if Eq. (11.132) is to obey the consistency relationship $W_{12} = -W_{21}$.

Realization of Equal Coupling Loss Factor

Equality of the coupling loss factors between individual modes within a group is a matter of grouping modes of similar nature. If the coupled system is a plate in a reverberant sound field, the *acoustically slow edge and corner modes* and *acoustically fast surface modes* are grouped separately.

Composite Structures

Composite structures generally consist of a number of elements such as plates, beams, stiffeners, and so on. We may divide a complex structure into its simpler member provided the wavelength of the structure-borne vibration is small compared with the characteristic dimensions of the elements. Where this is true, the modal density of a complex structure is approximately that of the sum of the modal densities of its elements. If the power input, the various coupling loss factors, and the power dissipated in each element are known, the power balance equations will yield the vibrational energy in the respective elements of the structure.

The dissipative loss factor for an element of a structure is obtained by separating that element from the rest of the structure and measuring its decay rate, as discussed in Chapter 14. The coupling loss factor can be determined experimentally from Eq. (11.132); however, the procedure is difficult. Theoretical solutions are available for the coupling loss factors of a few simple structural connections.[59] When the coupling loss factor between a sound field and a simple structure is desired, such a loss factor can be calculated from Eq. (11.131) if the radiation ratio of the structure is known, as shown in the next section.

Power Balance in a Two-Structure System

The power balance of the simple two-element system of Fig. 11.32 is given by the following two algebraic equations:

$$W_1^{\text{in}} = W_1^d + W_{12} \quad \text{W} \tag{11.133}$$

$$W_2^{\text{in}} = W_{12} + W_2^d \quad \text{W} \tag{11.134}$$

where W_1^{in} = input power to system 1, W
W_1^d = power dissipated in system 1, W
W_{12} = net power lost by system 1 through coupling* to system 2, = W'_{12} - W'_{21}, W
W_2^{in} = input power to system 2, W
W_2^d = power dissipated in system 2, W

*As in our previous analysis, we assume that the coupling is nondissipative.

The power dissipated in a system is related to the energy stored by that system, E_i, through the dissipative loss factor η_i, namely,

$$W_i^d = E_i \omega \eta_i \quad \text{W} \tag{11.135}$$

where E_i is energy stored in system i in newton-meters.

Assuming that the second system does not have direct power input ($W_2^{\text{in}} = 0$), the combination of Eqs. (11.130)–(11.132), (11.134), and (11.135) (with $i = 2$) yields the ratio of the energies stored in the two respective systems:

$$\frac{E_2}{E_1} = \frac{n_2}{n_1} \frac{\eta_{21}}{\eta_{21} + \eta_2} \tag{11.136}$$

If the coupling loss factor is very large compared to the loss factor in system 2, that is, if $\eta_{21} \gg \eta_2$, Eq. (11.136) yields the equality of the modal energies ($E_1/n_1\ \Delta\omega = E_2/n_2\ \Delta\omega$).

Diffuse Sound Field Driving a Freely Hung Panel

Let us now examine the special case of the excitation of a homogeneous panel (system 2) that hangs freely, exposed to the diffuse sound field of a reverberant room (system 1).

For this case, the total energies for each system are given by

$$E_1 = DV = \frac{\langle p^2 \rangle}{\rho_0 c_0^2} V \quad \text{N} \cdot \text{m} \tag{11.137}$$

$$E_2 = \langle v^2 \rangle \rho_s S \quad \text{N} \cdot \text{m} \tag{11.138}$$

where D = average energy density in reverberant room, N/m^2
$\langle p^2 \rangle$ = mean-square sound pressure (space–time average), N^2/m^4
V = room volume, m^3
$\langle v^2 \rangle$ = mean-square plate vibration velocity (space–time average), m^2/s^2
S = plate surface area (one side), m^2
ρ_s = mass per unit area of panel, kg/m^2

To find the coupling loss factor η_{21}, we must first recognize that W'_{21} equals the power that the plate, having been excited into vibration, radiates back into the room. Thus

$$W_{\text{rad}} = W'_{21} = 2\langle v^2 \rangle \rho c \sigma_{\text{rad}} S \equiv E_2\ \omega\eta_{21} = \langle v^2 \rangle \rho_s S \omega \eta_{21} \quad \text{W} \tag{11.139}$$

where σ_{rad} = radiation ratio for plate, dimensionless
W_{rad} = acoustical power radiated by both sides of plate, which accounts for factor 2, W

Solving for η_{21} yields

$$\eta_{21} = \frac{2\rho_0 c_0 \sigma_{\text{rad}}}{\rho_s \omega} \tag{11.140}$$

The modal density of the reverberant sound field in the room $n_1(\omega)$ and that of the thin homogeneous plate $n_2(\omega)$ are given in Table 11.7, namely,

$$n_1(\omega) \simeq \frac{\omega^2 V}{2\pi^2 c_0^3} \quad \text{s} \tag{11.141}$$

$$n_2(\omega) = \frac{\sqrt{12}\, S}{4\pi c_L h} \quad \text{s} \tag{11.142}$$

where c_L = propagation speed of longitudinal waves in plate material, m/s
h = plate thickness, m

Inserting Eqs. (11.137)–(11.142) into Eq. (11.135) yields the desired relation between the sound pressure and plate velocity:

$$\langle v^2 \rangle = \langle p^2 \rangle \frac{\sqrt{12}\pi c_0^2}{2\rho_0 c_0 h c_L \rho_s \omega^2} \frac{1}{1 + \rho_s \omega \eta_2 / 2\rho c \sigma_{\text{rad}}} \quad \text{m}^2/\text{s}^2 \tag{11.143}$$

The mean-square (space–time average) acceleration of the panel is simply

$$\langle a^2 \rangle = \omega^2 \langle v^2 \rangle = \langle p^2 \rangle \frac{\sqrt{12}\pi c_0^2}{2\rho_0 c_0 h c_L \rho_s} \frac{1}{1 + \rho_s \omega \eta_2 / 2\rho_0 c_0 \sigma_{\text{rad}}} \quad \text{m}^2/\text{s}^4 \tag{11.144}$$

It can be shown that as long as the power dissipated in the plate is small compared with the sound power radiated by that plate ($\rho_s \omega \eta_2 \ll 2\rho_0 c_0 \sigma_{\text{rad}}$), the equality of the modal energies of the sound field and the plate yields the proper plate velocity and acceleration. Also, under this condition, the ratio of the mean-square plate acceleration to the mean-square sound pressure is independent of frequency.

In general, *the plate response is always smaller than that calculated by the equality of the modal energies by the last factor on the right of Eq. (11.143) or (11.144), which equals the ratio of the power loss by acoustical radiation to the total power loss.* In dealing with the excitation of structures by a sound field, the concept of equal modal energy often enables one to give a simple estimate for the upper bound of the structure's response.

Example 11.4. Calculate the rms velocity and acceleration of a 0.005-m- ($\frac{1}{10}$-in.-) thick homogeneous aluminum panel resiliently suspended in a reverberant room. The space-averaged sound pressure level $\overline{L}_p = 100$ dB ($\sqrt{\langle p^2 \rangle} = 2$ N/m^2) as measured in a one-third-octave band centered at a frequency $f = \omega/2\pi = 1000$ Hz. The appropriate constants of the panel and surrounding media are $\rho_s = 13.5$ kg/m^2; $c_L = 5.2 \times 10^3$ m/s; $h = 5 \times 10^{-3}$ m; $\rho_0 = 1.2$ kg/m^3; $c_0 = 344$ m/s; and $\eta_2 = 10^{-4}$.

Solution First, calculate the factor

$$\frac{\rho_s \omega \eta_2}{2\rho_0 c_0 \sigma_{\text{rad}}} = \frac{13.5 \times 2\pi \times 10^3 \times 10^{-4}}{2 \times 1.2 \times 344 \times \sigma_{\text{rad}}} = \frac{8.5}{820\sigma_{\text{rad}}} \ll 1$$

According to the above inequality the mean-square acceleration of the panel given by Eq. (11.144) simplifies to

$$\langle a^2 \rangle \approx \langle p^2 \rangle \frac{\sqrt{12}\pi c_0^2}{2\rho_0 c_0 h c_L \rho_s} = 19 \quad \text{m}^2/\text{s}^4$$

or $a_{\text{rms}} = \sqrt{\langle a^2 \rangle} = 4.34$ m/s^2, an acceleration level of 113 dB re 10^{-5} m/s^2.

The mean-square velocity is

$$\langle v^2 \rangle = \frac{\langle a^2 \rangle}{\omega^2} = \frac{19}{4\pi^2 \times 10^6} = 4.76 \times 10^{-7} \ \text{m}^2/\text{s}^2$$

or $v_{\text{rms}} = \sqrt{\langle v^2 \rangle} = 6.9 \times 10^{-4}$ m/s, a velocity level of 97 dB re 10^{-8} m/s.

Sound Transmission Loss of a Simple Homogeneous Structure by the SEA Method

The SEA method may be used to analyze the transmission of sound between two rooms coupled to each other by a single common, thin homogeneous wall.[58] (i.e., there are no flanking paths). System 1 is the ensemble of modes of the diffuse, reverberant sound field in the source room, resonant within the frequency band $\Delta\omega$. System 2 is an appropriately chosen group of vibration modes of the wall. System 3 is the ensemble of modes of the diffuse reverberant sound field in the receiving room, resonant within the frequency band $\Delta\omega$. A loudspeaker in the source room is the only source of power, and the power dissipated in each system is assumed to be large compared with the power lost to the other two systems through the coupling (see Fig. 11.33).

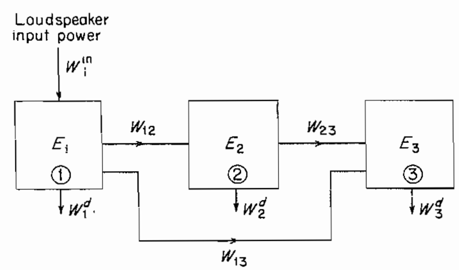

FIGURE 11.33 Block diagram illustrating the power flow in three-way coupled systems: W_{13}, transmission of sound by those modes whose resonance frequency lies outside the source band. The "nonresonant" modes are important below the critical frequency.

The procedure is as follows:

1. Relate W_1^{in} to the power lost by sound absorption in the room. This yields $\langle p_1^2 \rangle$, the space-averaged mean-square sound pressure in the source room.
2. Calculate $E_1 = \langle p_1^2 \rangle V_1/\rho c^2$, where V_1 is the volume of the source room.
3. The reverberant sound power incident on the dividing wall of area S_2 is $W_{\text{inc}} = E_1 c S_2/4V_1 = p_1^2/4\rho c$.
4. From the power balance of the wall for resonant modes within the bandwidth, $\Delta\omega$ is next determined, that is, $W_{12} = W_2^d + W_{23}$, so that

$$W_{12} = \text{Eq.}(11.135) + 0.5\ [\text{Eq.}(11.139)]$$

This sum equals Eq. (11.132). Because η_{12} of Eq. (11.32) is not well known, it is replaced by using Eq. (11.131) and the definition of loss factor η_{21}, which yields $\eta_{21} = \rho_0 c_0 \sigma_{\text{rad}}/\rho_s \omega$.

5. The vibrational energy of the wall is $E_2 = \langle v^2 \rangle \rho_s S_2$.
6. Combining steps 3, 4, and 5 yields the mean-square wall velocity $\langle v^2 \rangle$ as a function of mean-square source room pressure $\langle p_1^2 \rangle$.
7. The power radiated into the receiving room is

$$W_{23} = \rho_0 c_0 S_2 \sigma_{\text{rad}} \langle v^2 \rangle$$

8. Finally, the resonance transmission coefficient τ_r is found by dividing step 7 by step 3.
9. The *resonance transmission loss*, defined as $R_r = 10\log(1/\tau_r)$, is computed from step 8 using Eq. (11.97) and assuming that $\rho_s \omega \eta_2 \gg 2\rho_0 c_0 \sigma_{\text{rad}}$ to yield

$$R_r = 20\log\left(\frac{\rho_s \omega}{2\rho_0 c_0}\right) + 10\log\left(\frac{f}{f_c}\frac{2}{\pi}\frac{\eta_2}{\sigma_{\text{rad}}^2}\right) \quad \text{dB} \tag{11.145}$$

The first term in Eq. (11.145) is approximately the normal-incidence mass law transmission loss R_0, so that Eq. (11.145) becomes

$$R_r = R_0 + 10\log\left(\frac{f}{f_c}\frac{2}{\pi}\frac{\eta_2}{\sigma_{\text{rad}}^2}\right) \quad \text{dB} \tag{11.146}$$

where f_c = critical frequency [see Eq. (11.94)], Hz
η_2 = total loss factor of wall, dimensionless
σ_{rad} = radiation efficiency for wall, dimensionless

Thus we have obtained the transmission loss between two rooms separated by a common wall using the SEA method.

Below the critical frequency and when the dimensions of the wall are large compared with the acoustical wavelength, the radiation factor σ_{rad} can be taken from Table 11.8.

It is important to note that if the sound transmission loss of an equivalent *infinite* wall is compared with the data measured and predicted by the SEA method, it is found that *above the critical frequency*, the transmission loss R for the infinite wall yields the same results as Eq. (11.146), which takes into account only the resonance transmission of a finite wall.

Below the critical frequency the sound transmission loss of a finite panel is more controlled by the contribution of those modes that have their resonance frequencies outside of the frequency band of the excitation signal than by those with resonance frequencies within that band. Since only the contributions of the latter are included in the previous SEA calculation, Eq. (11.146) usually overestimates the sound transmission loss of a finite panel below the critical frequency. Figure 11.34 shows that below the critical frequency for a $\frac{1}{8}$-in.-thick aluminum panel the sound transmission loss of the resonant modes alone (curve a) is approximately 10 dB higher than that measured on the actual panel (curve d).

A *composite transmission factor* that approximately takes into account both the forced and resonance waves is closely approximated by

$$\begin{aligned}\frac{1}{\tau} &= \frac{W_{\text{inc}}}{W_{\text{forced}} + W_{\text{res}}} \\ &= \frac{(\langle p^2 \rangle/4\rho c)S_2}{\langle p^2 \rangle(\pi\rho c S_2/\rho_s^2\,\omega^2) + \langle p^2 \rangle(\sqrt{12}\pi c^3 \rho \sigma_{\text{rad}}^2 S_2/2\,\omega^3 \rho_s^2 c_L h \eta_2)}\end{aligned} \tag{11.147}$$

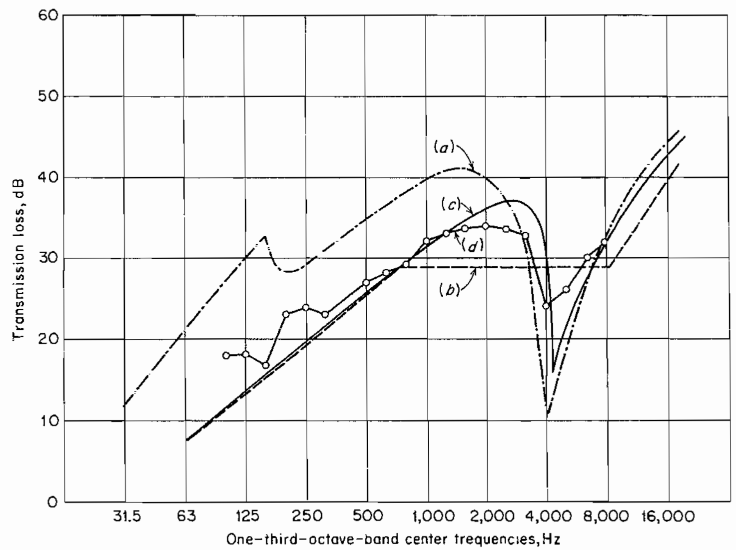

FIGURE 11.34 Comparison of experimental and theoretical transmission loss of a 5 ft × 6.5 ft × $\frac{1}{8}$ in. aluminum panel. The theoretical calculations are based on (a) resonance mode calculation, (b) plateau calculation, and (c) forced-wave calculation. Curve d shows the experimental results. (After Reference 58.)

At low frequencies where the first term in the denominator dominates, the transmission factor becomes

$$\frac{1}{\tau} \approx \frac{1}{\pi}\left(\frac{\rho_s \omega}{2\rho c}\right)^2 \qquad (11.148)$$

and the sound transmission loss is [see Eq. (11.101)]

$$R = 10 \log \frac{1}{\tau} \approx R_0 - 5 = R_{\text{field}} \quad \text{dB} \qquad (11.149)$$

At high frequencies where the second term in the denominator becomes dominant, the sound transmission loss is given by Eq. (11.146).

11.9 EQUIVALENCY BETWEEN THE EXCITATION OF A STRUCTURE SOUND FIELD AND POINT FORCE

In the mechanical equipment room of buildings, ships, and engine compartment of vehicles the boundaries (such as the walls, floor, and ceiling) are excited simultaneously by airborne noise and by dynamic forces. The airborne noise might emanate from the casing of machines and the dynamic forces might be those acting at the rigid or resilient attachment points of the machine to the floor or at the attachment points of pipes, conduits, or ducts (which are rigidly connected to the vibrating machine) to the wall or to the ceiling.

The noise control engineer is faced with the dilemma of predicting whether the airborne noise or the dynamic forces at the attachment points control the vibration response of the structure. The type of excitation that controls the vibration response of the structure will also control the airborne noise and vibration at distant noise- and vibration-sensitive receiver locations.

In his noise control engineering practice the author has been called upon to predict whether the ramble (low-frequency random noise) generated by the passage of subway trains in a nearby tunnel will be above or below the threshold of human hearing in a planned concert hall. In another project, he had to predict whether eye surgeons would be able to perform retina operations in a hospital located near another subway tunnel.

The dynamic forces acting in the tunnel floor owing to the wheel–rail interaction can be reduced substantially by mounting the track on a "floating slab" consisting of a thick concrete slab that is supported by resilient rubber mounts laid on the tunnel floor. However, the floating slab has no beneficial effect on reducing the airborne noise exposure of the walls and the roof of the tunnel. Actually, the floating slab results in an increase of the airborne noise, especially in the frequency range near its coincidence frequency where the propagation speed of bending waves in the floating slab coincides with the propagation speed of sound in air and the slab becomes a very efficient sound radiator. Consequently, the airborne sound excitation of the tunnel structure might be controlling the low-frequency vibration response of the tunnel walls and the noise and vibration at a distant observer location.

To enable him to make a quantitative judgment on the relative importance of the airborne noise versus the force excitation of a platelike structure, the author has derived the relationship[60]

$$F_{\text{eq}} = p\left(\frac{c_0}{f}\right)\sqrt{\frac{\sigma_{\text{rad}} S_f}{\pi}} = p\lambda\sqrt{\frac{\sigma_{\text{rad}} S_f}{\pi}}[2(10^{-5})]10^{L_p/20} \quad \text{N} \qquad (11.150)$$

where F_{eq} is the point force in newtons that generates the same free bending wave response on a partition of surface area S_f as a random-incidence sound field with a space–time average sound pressure p. The symbol σ_{rad} is the radiation efficiency of the partition. It is unity at frequencies above the coincidence frequency. The principle of reciprocity requires that σ_{rad} is also a measure of the degree of coupling of the sound waves to the vibration response of the structure. The symbol $\lambda = c_0/f$ is the acoustical wavelength in meters, c_0 is the speed of sound in air in meters per second, and f is the frequency in hertz (reciprocal seconds). The symbol L_p is the sound pressure level in decidels re 2×10^{-5} N/m^2.

Equation (11.150) can be written in a form that is easy to remember:

$$F_{\text{eq}}^2 = \left(\frac{4}{\pi}\right)\left(\frac{(pS)^2}{S/(\lambda/2)^2}\right) \simeq \left(\frac{(pS)^2}{S/(\lambda/2)^2}\right) \quad \text{N}^2 \qquad (11.151)$$

The numerator of Eq. (11.151) is a force squared (the product sound pressure and the area) and the denominator is the number of areas, each a half wavelength squared, that would fill the entire surface area S. The area $(\lambda/2)^2$ is where the sound pressure on the surface of the partition is in phase.

Equations (11.150) and (11.151) are extremely simple and universally useful because:

1. The force/sound pressure equivalency does not implicitly depend on the material properties of the partition such as the density, Young's modulus, loss factor, and geometry.
2. They do not depend on the density of the fluid:
3. They are also valid for partitions with fluid loading such as concrete slabs embedded in soil or steel plates with a liquid on the other side.

The reason for these unique properties of Eqs. (11.150) and (11.151) is that the vibration response to both sound and point force depends the same way on these properties. For example, a lightly damped structure will respond equally vigorously to sound and point force excitation, a plate made out of a material with high density will respond equally less vigorously to both sound and force excitation than one that is made of a less dense material, and so on. Equations (11.150) and (11.151) have been derived by assuming that the partition is large compared with the bending wavelength and the room where the sound field is generated is large compared with the acoustical wavelength. Both the structure and the sound field respond in a multimodal fashion and their response is dominated by the resonant modes.

In noise control design the airborne noise strength of machines and equipment is given in the form of their sound power $W(f)$ or sound power level spectrum $L_w(f)$. The diffuse-field sound pressure in a room, resulting from the injected sound power, is given by

$$\frac{p^2}{4\rho_0 c_0} S_{\text{tot}}\overline{\alpha} = W_f \quad \text{N/m}^2 \tag{11.152}$$

Combining Eqs. (11.150) and (11.152) yields

$$F_{\text{eq}}(f) = W(f)\frac{\rho_0 c_0^3 \sigma_{\text{rad}}(f)}{f^2}\left(\frac{1}{\alpha}\right)\left(\frac{S_i}{S_{\text{tot}}}\right)\left(\frac{4}{\pi}\right) \quad \text{N}^2 \tag{11.153}$$

where $W(f)$ = sound power of machine, W

$F_{eq}(f)$ = equivalent point force acting on solid boundary that produces same resonant (i.e., free bending wave) vibration response of boundary as the sound field produced in room owing to sound power output of the machine, N/m^2,

S_i = surface area (one side) of boundary directly excited by force, m^2,

S_{tot} = total surface area of all boundaries of room, m^2,

α = sound absorption coefficient of internal boundary surfaces

The validity of Eqs. (11.150), (11.151), and (11.153) have been briefly checked[61] experimentally by exciting the boundaries of an underground fan room. First one wall was excited with a shaker and the point force $F(f)$ was measured with a force gauge built into the impedance head that connected the shaker to the fan room wall. Then, a sound field was generated in the fan room by a loudspeaker and the sound pressure level SPL(f) was measured with a calibrated microphone. For both types of excitation the force and the sound pressure level was generated at an identical series of pure-tone frequencies to maximize the signal–noise ratio. The response was measured by a geophone in the form of the ground vibration at a distant location.

Example 11.5. Predict whether a planned concert hall can be located on a site near an existing subway line without imposing speed limits on the subway train and without supporting the entire concert hall on resilient vibration isolation pads. The design goal is to keep the ramble noise in the concert hall below the threshold of human hearing, which is 35 dB in the 63-Hz center-frequency octave band.

The subway tunnel has a 10 ft × 10 ft cross section and the subway train is 100 ft long. The tunnel walls, roof, and floor are poured concrete of 0.4 m thickness. Analytical predictions carried out have indicated that mounting the

rails on a floating slab would reduce the total force acting on the tunnel floor to 200 N in the 63-Hz center-frequency octave band and that this dynamic force was expected to produce a sound pressure level of 30 dB in the concert hall. This is 5 dB lower than the human threshold of hearing. Sound-level measurements carried out in the tunnel during the passage of a subway train yielded a sound pressure level of 110 dB in the 63-Hz center-frequency octave band. Predict whether this airborne excitation will produce noise levels in the concert hall above the 35-dB threshold of hearing.

Solution The critical frequency f_c is predicted from Table 11.2. The density of concrete $\rho = 2300$ kg/m^3, the mass per unit area $\rho_s = \rho h = 2300 \times 0.4 = 920$ kg/m^2, $f_c\rho_s = 43,000$, and $f_c = 43,000/920 = 47$ Hz; consequently, $\sigma_{\text{rad}(f=63\text{ Hz})} \simeq 1$. The surface area ot the tunnel exposed to the high-level airborne noise excitation $S_{\text{tot}} = 10 \times 10 \times 100 = 10,000\ \text{ft}^2 = 929\ \text{m}^2$. With these values Eq. (11.150) yields

$$F_{\text{eq}} = \left(\frac{c_0}{f}\right)\sqrt{\frac{S_{\text{tot}}}{\pi}}2(10^{-5})10^{\text{SPL}/20} = \left(\frac{340}{63}\right)\sqrt{\frac{929}{\pi}}2(10^{-5})10^{110/20} = 586\ \text{N}$$

Consequently, the noise level in the concert hall that is attributable to the airborne sound excitation of the tunnel walls is predicted to be

$$\text{SPL}_{\text{Hall}}(f = 63\ \text{Hz}) = 30 + 20\log\left(\frac{586}{200}\right) \simeq 39\ \text{dB}$$

This is 4 dB above the design goal, indicating that the design goal cannot be achieved without restricting the train speed or putting the concert hall on vibration isolators that would need to provide a high degree of isolation at 63 Hz.

11.10 RECIPROCITY AND SUPERPOSITION

The principles of reciprocity and superposition apply to linear systems with time-invariant parameters. Not only solid structures but fluid volumes at rest fall into this category. Consequently, reciprocity and superposition apply to systems that consist of solid structures surrounded by acoustical spaces and can be used to great advantage not only in structure-borne noise and airborne noise but also in structural acoustics, which deals with the interaction of sound waves with solid structures.

The principle of superposition, illustrated in Fig. 11.35, allows the use of the simplest excitation sources such as a point force source or a point-monopole sound source to explore the response to more complex excitation sources such as a moment acting on a structural element or an acoustical dipole radiating into an acoustical volume. The principle of reciprocity, which can be traced back to Lord Rayleigh,[62] is illustrated in the upper three sketches in Fig. 11.36. It states that

$$F_2 v_2 = F_1 v_1 \quad \text{W} \tag{11.154a}$$

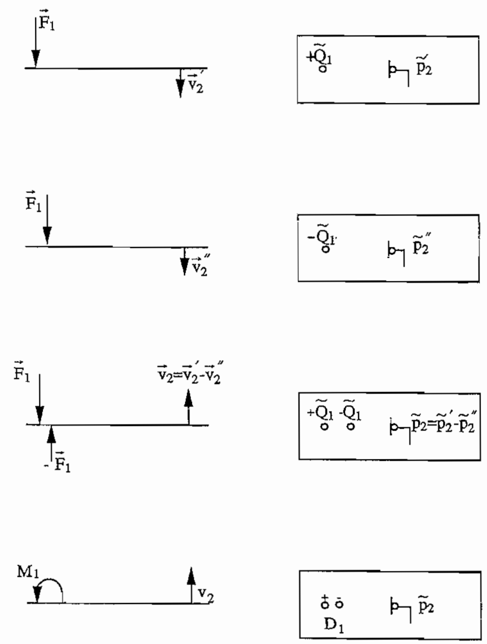

FIGURE 11.35 Use of superposition to predict the response of structures and acoustical spaces (v_2 and p_2) to complex excitation sources such as moments (M_1) and dipoles (D_1) on the basis of point force (F_1) and acoustical monopole (Q_1). Note that the structure and the acoustical space may be of arbitrary shape and the acoustical space may be unbound or bound by elastic or sound-absorbing boundaries and may contain an arbitrary number and size of rigid or elastic scatterers.

The symbol F_1 is (generalized) force when point 1 is source and point 2 is receiver and v_1 is (generalized) velocity when point 1 is receiver and point 2 is source. The vector product $F_1 v_1$ must yield the instantaneous power, or in complex notation $\text{Re}\{\frac{1}{2}F_1 v_1^*\} = \text{Re}\{\frac{1}{2}F_2 v_2^*\}$ must yield the time-averaged power. Note that F and v are vector quantities as signified in the figure by the arrow above the symbols. If v_1 and F_1 and v_2 and F_2 are measured or applied in the same direction, as illustrated by the sketch in the lower left side of Fig. 11.36, the vector notation can be exchanged for the less complicated scalar notation, where force and velocity are characterized by a magnitude and phase (i.e., $\tilde{F} = Fe^{j\phi f}$, $\tilde{v} = ve^{j\phi r}$). In this case, the reciprocity takes the form of the equality of transfer functions

$$\frac{\tilde{v}_2}{\tilde{F}_1} = \frac{\tilde{v}_1}{\tilde{F}_2} \quad \text{m/N} \cdot \text{s} \tag{11.154b}$$

This should be kept in mind in our latter deliberations, where the special vector notation is not carried through. Since monopole strength $\tilde{Q}$ and sound pressure

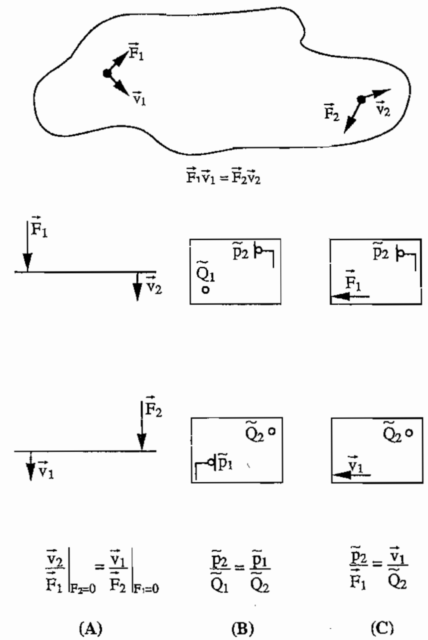

FIGURE 11.36 Principle of reciprocity as applied to a complex structure. Top sketch illustrates general principle. Lower sketches apply in special situations: (a) structure; (b) an acoustical space; (c) a structure coupled to an acoustical space. Symbols: F, point force vector; v, velocity response vector (measured by the same direction as F); $\tilde{Q}$, volume velocity of acoustical point source; $\tilde{p}$, sound pressure.

$\tilde{p}$ are scalar quantities (defined by their magnitude and phase), no directional restraints exist in the acoustical case illustrated in Fig. 11.36b.[63,64] However, dipole and quadrupole sound sources (constructed from adjacent out-of-phase monopoles) have highly directional radiation characteristics and must be connected to directional quantities of the sound field such as pressure gradients dp/dx and d^2p/d^2x measured in the same direction relative to the orientation of the dipole or quadrupole sound source for the reciprocity to apply.

Table 11.9 contains useful reciprocity relationships applicable to higher order excitation sources and responses. These relationships automatically follow from the joint application of superposition and reciprocity to the appropriate combination of simple sources such as point forces and acoustical monopoles.

The principle of reciprocity can be used to considerable advantage in both experimental and analytical work. In experimental work it is difficult and cumber some to excite complex structures by point forces and moments and to measure the sound pressure such excitation causes in the interior of a vehicle. It is almost always easier to obtain the sought transfer function between the acoustical pressure and the exciting force or moment by placing a small acoustical source of known volume velocity at the microphone location and measuring the vibration response at the position and in the direction of the applied force and applying the reciprocity relationship illustrated in Fig. 11.36*c*.

The form of reciprocity illustrated in Fig. 11.36*c* is the most useful in structural acoustics. Its practical application is described in reference 64. In the direct experiment the force $\tilde{F}_1$ is applied to the structure by a shaker (and its magnitude and phase are measured by a force gauge inserted between the shaker and the structure), and the magnitude and phase of the sound pressure p_2 are measured by a microphone. The phase of F_1 and p_2 are referenced to the voltage U applied to the shaker. In the reciprocal experiment—which is much easier to perform than the direct experiment—a small omnidirectional sound source (an enclosed loudspeaker whose diameter is smaller than one-quarter acoustical wavelength) with calibrated volume velocity response Q is placed at the former microphone location and the velocity response of the structure at the former excitation point v_2 is measured (in the same direction as the force was applied) by a small accelerometer. The phases of Q and v_2 are referenced to the voltage U applied to the loudspeaker sound source. The volume velocity calibration of the sound source (Q/U) is obtained by placing it in an anechoically terminated rigid tube, baffling it so it radiates only toward the anechoic termination, sweeping the loudspeaker voltage through the frequency range of interest, and measuring the transfer function (p/U), where U is the voltage applied to the loudspeaker and p is the sound pressure measured by a microphone located two tube diameters or further away from the source. The sought volume velocity calibration of the source is then computed as[65] $|Q/U| = |P/U|(S/\rho_0 c_0)$, where S is the cross-sectional area of the tube, ρ_0 is the density of air, and c_0 is the speed of sound in air. When phase information is important, the sound source can be calibrated in an anechoic chamber by measuring the sound pressure $p(r)$ at a large distance $r \gg \lambda_0$ away from the source and computing the volume velocity calibration $Q/U = [p(r)/U](4\pi r^2/\rho_0 c_0)e^{-j2\pi f r/c_0}$.

Figure 11.37 illustrates the application of reciprocity on a complex structural acoustical problem, namely, the prediction of the interior noise of an automobile to point force excitation of the shock tower. First, the shock tower was excited by a point force, and sound pressure generated at the driver's head position was measured to obtain the direct transfer function $\tilde{p}/F$ identified by the solid line. Next, the reciprocal experiment was carried out by placing a point sound source of known volume velocity $\tilde{Q}$ at the former location of the microphone and measuring the vibration velocity response of the shock tower. The transfer function $v/\tilde{Q}$ obtained this way is shown as the dotted curve in Fig. 11.37*a*. Referencing the phases of $\tilde{p}$ and F to the voltage applied to the shaker and that of v and $\tilde{Q}$ to the voltage applied to the loudspeaker source, not only the magnitude but also the phase of the reciprocal transfer functions $\tilde{p}/F$ and $v/\tilde{Q}$ can be retained so that the interior noise caused by many simultaneously acting forces and moments can be predicted. Figure 11.37*b* shows the unrolled phase of the transfer function pair.

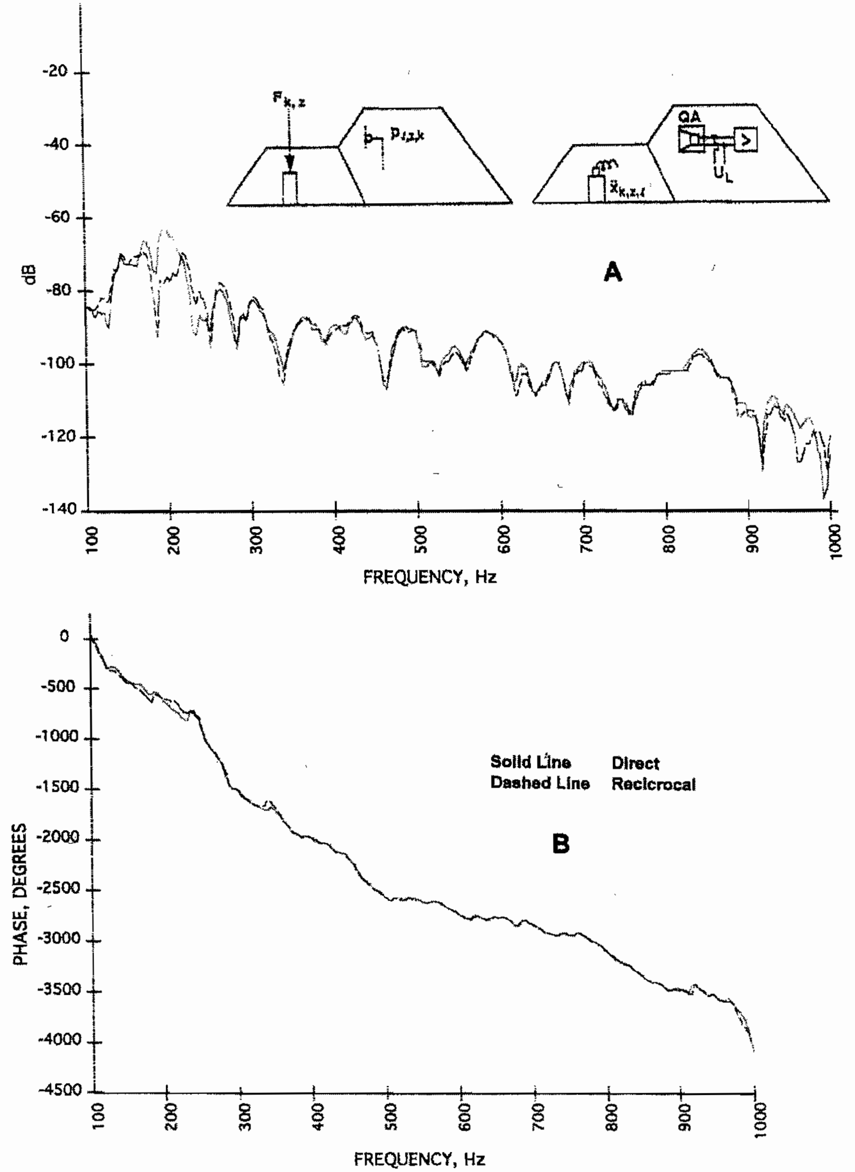

FIGURE 11.37 Pair of reciprocal transfer functions measured in a passenger vehicle: (*a*) direct, $\tilde{p}/\tilde{F}$; (*b*) reciprocal, $\tilde{v}/\tilde{Q}$.

Prediction of Noise Caused by Multiple Correlated Forces

The use of reciprocity and superposition in the case of multiple correlated force input is illustrated in Fig. 11.38. The problem is to predict the sound pressure p_R in the receiver room below after installation of a vibrating machine in the source room above. The building is constructed, and the machine manufacturer provides the magnitude, the direction, and the mutual phase ϕ_{12} of forces F_1 and F_2 the machine—when installed on soft springs—will impart to the floor. The prediction of p_R proceeds as illustrated in the lower part of Fig. 11.38 by measuring the reciprocal transfer functions $-v_1/\tilde{Q}_R = \tilde{p}_R/F_1$ and $-v_2/\tilde{Q}_R = \tilde{p}_{R2}/F_2$ and utilizing the principle of superposition. The forces and velocities must be measured in the same direction. Performing the reciprocity prediction for a number of different loudspeaker positions in the receiver room, the spatial

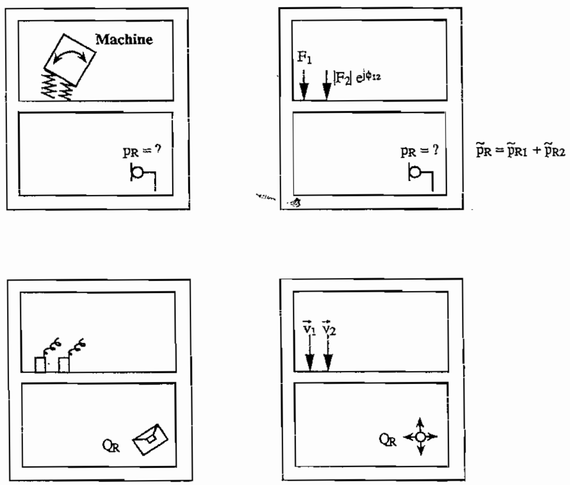

$$-\frac{p_{R1}}{\vec{F}_1} = \frac{\vec{v}_1}{Q_R}, \quad -\frac{p_{R2}}{\vec{F}_2} = \frac{\vec{v}_2}{Q_R}$$

$$-p_R = \left\{ |F_1| \frac{|v_1|}{|Q_R|} e^{j\phi_{1Q}} + |F_2| e^{j\phi_{12}} \frac{|v_2|}{|Q_R|} e^{j\phi_{2Q}} \right\}$$

FIGURE 11.38 Use of reciprocity and superposition to predict the sound pressure in a room caused by two correlated forces $\tilde{F}_1$ and $\tilde{F}_2$ acting on the building structure. Top sketch represents actual situation and lower sketch the reciprocity prediction: ϕ_{1Q} and ϕ_{2Q} represent the phases of the transfer functions $\tilde{v}_1/\tilde{Q}_R$ and $\tilde{v}_2/\tilde{Q}_R$, respectively; each is conveniently referenced to the excitation voltage of the loudspeaker sound source.

variation of p_R can also be predicted. The methodology can be easily extended to more than two simultaneously acting, correlated forces.[66]

The reciprocity is most useful in the early stages of design of aircraft and ground vehicles, well before a flightworthy version of the aircraft or a roadworthy version of the ground vehicle is available. Reciprocity helps the noise control engineer to find answers to some difficult questions:

1. What will be the contribution of the structure-borne noise at the engine firing rate to the noise in the passenger compartment?
2. Which engine mount transmits most of the structure-borne noise?
3. Which direction of vibration force is most critical?
4. Which mutual phasing of forces acting on the individual engine-mounting points is most critical?
5. Most importantly, what is the effect of changing the design of engine-mounting brackets on cabin noise?

All these questions can be answered without applying known forces in three orthogonal directions to each of the engine-mounting brackets.

Source Strength Identification by Reciprocity

When it is not feasible to measure directly the strength of noise and vibration sources during the operation of vehicles, equipment, and machinery, reciprocity can be used to obtain them indirectly. This is accomplished by measuring the noise or vibration during the operation of the equipment at a distant, accessible receiver location and—when the equipment is not operating—exciting it at these distant receiver locations and measuring the acoustical or structural response at the source location, which is now accessible. The principle is illustrated in Fig. 11.39. Common in the three problems shown in Fig. 11.39 is the knowledge of the location and nature of the excitation sources. Unknown are their magnitude and mutual phase, which must be determined by observation of response to these sources at distant locations and by reciprocity experiments as described below.

The upper left-hand side of Fig. 11.39 represents the case where the sound field in an enclosure is excited by two monopole sound sources of unknown strength and mutual phase $\tilde{Q}_1(?)$ and $\tilde{Q}_2(?)$ (e.g., the openings of the inlet pipe leading to two cylinders of a reciprocating compressor). The first experiment, illustrated in the upper sketch, is the measurement of the magnitude and mutual phase of the sound pressure $\tilde{p}_3$ and $\tilde{p}_4$ at accessible distant locations 3 and 4 obtained when both sources were operating simultaneously. The reciprocal experiments, illustrated in the two lower sketches, are performed when the sources are not operational by placing a monopole sound source of known volume velocity Q at the former microphone locations 3 and 4 and measuring the magnitude and phase of the sound pressure produced at the two former source locations $\tilde{p}_{13}$, $\tilde{p}_{23}$,

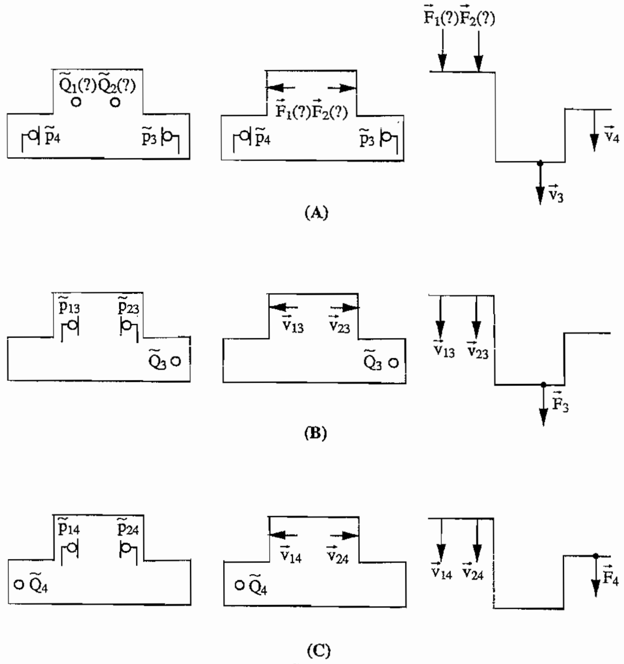

FIGURE 11.39 Source strength identification utilizing reciprocity and superposition: (*a*) response measurements at distant locations with sources active and (*b, c*) reciprocity measurements, sources inactive. (See text for explanation of symbols.)

$\tilde{p}_{14}$, and $\tilde{p}_{24}$. The phase of the sound pressure is referenced to the loudspeaker voltage.

The sketches in the middle column in Fig. 11.39 illustrate a case where the sound field in an enclosure is produced by two forces $\tilde{F}_1$ and $\tilde{F}_2$ of known location and direction but unknown magnitude and mutual phase, both acting simultaneously at the enclosure wall (e.g., forces caused by a vibration isolation-mounted reciprocating or rotating machine). In this case, the reciprocal experiment yields the vibration velocity responses at the former force application points $\tilde{v}_{13}$, $\tilde{v}_{23}$, $\tilde{v}_{14}$, and $\tilde{v}_{24}$, measured in the same direction as the force.

The situation shown in the sketch on the upper right-hand side in Fig. 11.39 illustrates the situation when the determination of the unknown magnitude and mutual phase of the two forces $\tilde{F}_1(?)$ and $\tilde{F}_2(?)$ must be diagnosed (e.g., forces transmitted to a structural floor by a vibration-isolated machine). In this case, the reciprocal experiment is carried out by exciting the building structure at the two distant observation points 3 and 4 by known forces $\tilde{F}_3$ and $\tilde{F}_4$ and measuring the velocity responses $\tilde{v}_{13}$, $\tilde{v}_{23}$, $\tilde{v}_{14}$, and $\tilde{v}_{24}$ at the former force excitation points 1 and 2. Utilizing the principle of reciprocity and superposition yields the following pairs of linear equations:

$$\tilde{p}_3 = \tilde{Q}_1(?)\left[\frac{\tilde{p}_{13}}{\tilde{Q}_3}\right] + \tilde{Q}_2(?)\left[\frac{\tilde{p}_{23}}{\tilde{Q}_3}\right] \quad \text{N/m}^2 \tag{11.155a}$$

$$\tilde{p}_4 = \tilde{Q}_1(?)\left[\frac{\tilde{p}_{14}}{\tilde{Q}_4}\right] + \tilde{Q}_2(?)\left[\frac{\tilde{p}_{24}}{\tilde{Q}_4}\right] \quad \text{N/m}^2 \tag{11.155b}$$

which can be solved for the two unknowns $\tilde{Q}_1(?)$ and $\tilde{Q}_2(?)$. Similarly, the set of equations for obtaining $\tilde{F}_1(?)$ and $\tilde{F}_2(?)$ in the situation illustrated in the center sketches in Fig. 11.39 are

$$\tilde{p}_3 = \tilde{F}_1(?)\left[\frac{\tilde{v}_{13}}{\tilde{Q}_3}\right] + \tilde{F}_2(?)\left[\frac{\tilde{v}_{23}}{\tilde{Q}_3}\right] \quad \text{N/m}^2 \tag{11.155c}$$

$$\tilde{p}_4 = \tilde{F}_1(?)\left[\frac{\tilde{v}_{14}}{\tilde{Q}_4}\right] + \tilde{F}_2(?)\left[\frac{\tilde{v}_{24}}{\tilde{Q}_4}\right] \quad \text{N/m}^2 \tag{11.155d}$$

and for that illustrated in the sketches on the right

$$\tilde{p}_3 = \tilde{F}_1(?)\left[\frac{\tilde{v}_{13}}{\tilde{F}_3}\right] + \tilde{F}_2(?)\left[\frac{\tilde{v}_{23}}{\tilde{F}_3}\right] \quad \text{N/m}^2 \tag{11.155e}$$

$$\tilde{p}_4 = \tilde{F}_1(?)\left[\frac{\tilde{v}_{14}}{\tilde{F}_4}\right] + \tilde{F}_2(?)\left[\frac{\tilde{v}_{24}}{\tilde{F}_4}\right] \quad \text{N/m}^2 \tag{11.155f}$$

In the case of n unknown excitation sources, the prediction equations represent an $n \times n$ matrix.

Extension of Reciprocity to Sound Excitation of Structures

As illustrated in Fig. 11.40, the reciprocity relationship can be extended for surface excitation of structures (e.g., by an incident sound wave). Consider first a small part of the surface of a cylindrical body (such as an aircraft fuselage) with surface area dA exposed to a local sound pressure of $\tilde{p}_1$ as illustrated in the upper left sketch in Fig. 11.40 resulting in a local force of $\tilde{F}_1 = \tilde{p}_1\, dA$. For this force the reciprocity relationship shown in Fig. 11.36*c* yields $\Delta\tilde{p}_{R1}/\tilde{F}_1 = \Delta\tilde{v}_{1R}/Q_R$, which for $\tilde{F}_1 = \tilde{p}_1\, dA$ and $\Delta\tilde{Q}_{1R} = \Delta\tilde{v}_{1R}\, dA$ becomes

$$\frac{\Delta\tilde{p}_R}{\tilde{p}_1} = \frac{\Delta\tilde{Q}_{1R}}{\tilde{Q}_R} \tag{11.156a}$$

When the structure is exposed to a complex sound field distribution $\tilde{p}_1, \tilde{p}_2, \ldots, \tilde{p}_n$, as illustrated in the lower sketch, the resulting interior sound pressure at the receiver location, $\tilde{p}_R$, is given by

$$\tilde{p}_R = \sum_{i=1}^{n} \tilde{p}_i \left(\frac{\Delta\tilde{Q}_{iR}}{\tilde{Q}_R}\right) \quad \text{N/m}^2 \tag{11.156b}$$

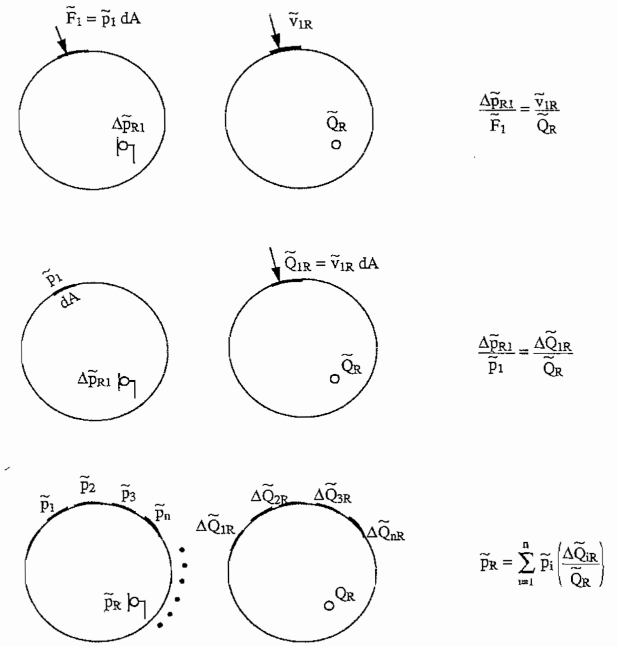

FIGURE 11.40 Extension of reciprocity to sound excitation of structures. Top: Reciprocity relationship for external pressure, $\tilde{p}_1$, acting on a small area (dA) of the structure and the resulting internal sound pressure, $\Delta\tilde{p}_{R1}$, and structural response v_{1R} produced by an internal point sound source of volume velocity Q_R located at the former receiver position. Middle: Substitution of volume velocity response $\Delta\tilde{Q}_{1R} = d\tilde{v}_{1R}\,dA$ into the reciprocity relationship. Bottom: Reciprocity relationship for external incident sound excitation p_i and internal sound pressure $\tilde{p}_R$ and volume velocity responses of the structure $\Delta\tilde{Q}_{1R}$ produced by an internal point sound source of volume velocity $\tilde{Q}_R$.

where the transfer functions $\Delta\tilde{Q}_{1R}/\tilde{Q}_R$ represent the reciprocity calibration of the structure as a transducer. This extension of reciprocity by Fahy[67] has the advantage that the reciprocity calibration of the structure (in the form of discretized transfer functions $\Delta\tilde{Q}_{iR}/\tilde{Q}_R$) can be carried out with a capacitive transducer that directly measures the structure's local volume displacement $\Delta\tilde{Q}_{iR}/j\omega$. To obtain sufficient resolution, the side length of the square-shaped capacitive transducer used in measuring the volume displacement must not exceed one-eighth of the acoustical wavelength. Note that the bending wavelength in thin, plate-like structures is usually much smaller than the transducer size so that the capacitive transducer acts as a wavenumber filter, accounting only for those components of the vibration field that results in a net volume displacement. The high-wavenumber components, which result only in local near fields, are "averaged out." The additional advantage of the capacitive transducer is that it does not influence the vibration response of the structure.

Reciprocity can also be used in predicting the sound pressure attributable to the complex vibration pattern of a vibrating body in case where the radiated sound cannot be measured directly (e.g., other correlated vibration sources dominate the sound field). The reciprocity prediction proceeds in two steps. First the vibration pattern of the body is mapped during the operation of the equipment by measuring the vibration velocity $\tilde{v}_i$ at a large number of locations. The phase of the velocity responses is referenced to the velocity measured at a designated reference location. Next the machine is shut off and a point sound source of known volume velocity Q is placed at the receiver location where the sound pressure should be predicted and the sound pressure $\tilde{p}_i$ produced by the point sound source at the various locations along the stationary surface of the body is measured. The phase of the pressure responses is conveniently referenced to the voltage applied to the loudspeaker sound source. The sound pressure at the receiver location, $\tilde{p}_R$, attributable to the periodic vibration of body is predicted as

$$\tilde{p}_R = \sum_{i=1}^{n} \tilde{v}_i\, dA_i \frac{\tilde{p}_i}{Q} \cong \sum_{i=1}^{n} \Delta\tilde{Q}_i \frac{\tilde{p}_i}{Q} \quad \text{N/m}^2 \tag{11.156c}$$

where dA_i is the area and $\Delta\tilde{Q}_i = \tilde{v}_i dA_i$ is the volume velocity of the ith sample of the vibrating surface.

The solid line in Fig. 11.41 represents the directly measured sound pressure $\tilde{p}_R$ at a specific location in a room when a thin plate was excited by a shaker to a

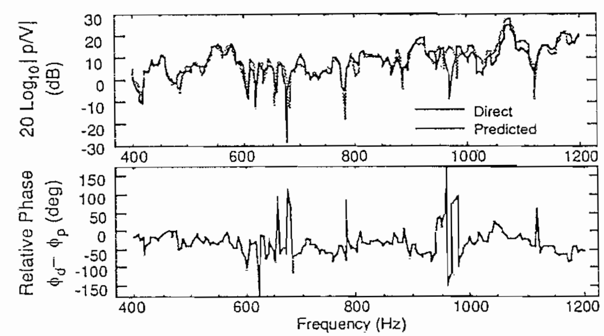

FIGURE 11.41 Sound pressure response at a specific location in a room produced by a thin plate excited by a shaker to complex vibration pattern. Solid line: Directly measured transfer function between sound pressure $\tilde{p}_R$ and excitation force F, phase is referenced to shaker voltage $\tilde{U}$ Dotted line: Transfer function predicted by measuring the magnitude and relative phase of the plate response, $\Delta\tilde{Q}_i = \tilde{v}_i\, dA$ at $i = 81$ position during shaker excitation and the magnitude and phase of the sound pressure $\tilde{p}_i$ at the surface of the stationary plate when a point sound source of volume velocity $\tilde{Q}_R$ is placed at the former receiver position and applying the reciprocity relationship $\tilde{p}_R = \Sigma_{i=1}^{81}\Delta\tilde{Q}_i(\tilde{p}_i/\tilde{Q}_R)$ (after Reference[67]). Top curve, magnitude of pressure; lower curve, phase spectrum of directly measured minus phase spectrum of predicted pressure.

complex vibration pattern. The dotted curve represents the reciprocity prediction according to Eq. (11.156a) utilizing $n = 81$ sampling points on the plate.[67] The experimental results indicate the feasibility of using reciprocity predictions in engineering applications.

Reciprocity in Moving Media

Reciprocity requires that exchanging the function of the source and receiver should not result in any change in the sound propagation path. This is true only if the acoustical medium is at rest. As illustrated in Fig. 11.42, the propagation path between source and receiver remains the same if the exchange of source and receiver positions is accompanied by a reversal of the direction of the uniform mean flow. In this case, or in the case of low-Mach-number potential flow where the shear layer is small compared with the acoustical wavelength, the reciprocity also applies in moving media.[68] Reversal of potential flow is usually easy to accomplish in analytical calculations. However, in many experimental situations where the shear layer is not small compared with the acoustical wavelength, reciprocity does not apply.

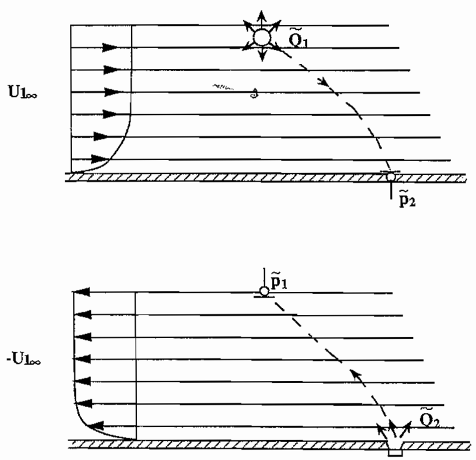

$$\left(\frac{\tilde{p}_2}{\tilde{Q}_1}\right)_{U_{1\infty}} = \left(\frac{\tilde{p}_1}{\tilde{Q}_2}\right)_{-U_{1\infty}}$$

FIGURE 11.42 Reciprocity in moving media. Reversal of the function of source and receiver must be accompanied by reversing the flow direction. Streamlines must remain unchanged to assure that the propagation path between source and receiver remains the same.

Fundamental questions regarding reciprocity are dealt with in references 69–71. Analytical applications of reciprocity and superposition for predicting power input structures excited by complex airborne or structure-borne sources is presented in references 66, 72, and 73. Ship acoustics application of reciprocity are treated in references 74 and 75.

11.11 IMPACT NOISE

There are many practical cases where the excitation of a structure can be represented reasonably well by the periodic impact of a mass on its surface. Footfall in dwellings, punch presses, and forge hammers fall into this category. This section deals only with footfall noise in buildings. For the prediction and control of impact noise of machines and equipment, the reader is referred to a series of 10 papers[76–85] that covers all aspects of impact noise of machinery.

Standard Tapping Machine

A standard tapping machine[86] is used to rate the impact noise isolation of floors in dwellings. This machine consists of five hammers equally spaced along a line, the distance between the two end hammers being about 40 cm. The hammers successively impact on the surface of the floor to be tested at a rate of 10 times per second. Each hammer has a mass of 0.5 kg and falls with a velocity equivalent to a free-drop height of 4 cm. The area of the striking surface of the hammer is approximately 7 cm^2; the striking surface is rounded as though it were part of a spherical surface of 50 cm radius. The impact noise isolation capability of a floor is rated by placing the standard tapping machine on the floor to be tested and measuring the one-third-octave-band sound pressure level L'_p averaged in space in the room below.

$$L_n \equiv L_p - 10\log\frac{A_0}{S\overline{\alpha}_{S,\mathrm{ab}}} \quad \text{dB re} 2\times10^{-5}\ \text{N/m}^2 \tag{11.157a}$$

where L_p = one-third-octave-band sound pressure level as measured, dB
$S\overline{\alpha}_{S,\mathrm{ab}}$ = total absorption in receiving room (see Chapter 7), m^2
A_0 = reference value of absorption, =10 m^2

The physical formulation of the problem of impact noise is that of the excitation of a plate by periodic force impulses. Such periodic forces can be presented by a Fourier series consisting of an infinite number of discrete-frequency components, each with amplitude F_n, given by

$$F_n = \frac{2}{T_r}\int_0^{T_r} F(t)\cos\frac{2\pi n}{T_r}t\,dt \quad \text{N} \tag{11.157b}$$

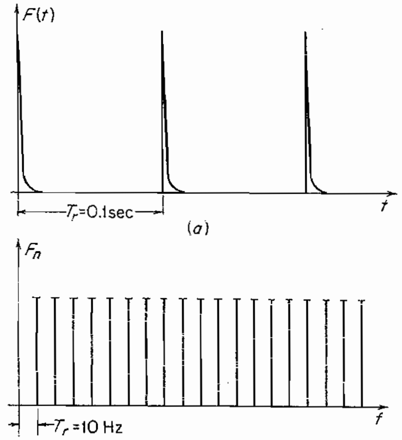

FIGURE 11.43 (*a*) Time function and (*b*) Fourier components of the force that a standard tapping machine exerts on a massive rigid floor.

where $T_r = 1/f_r = 0.1$ is the time interval between hammer strikes and $n = 1, 2, 3, \ldots$. The curve in Fig. 11.43*a* shows the time function of the force $F(t)$, and that in Fig. 11.43*b* shows the amplitude of its Fourier components.

It is an experimental fact that when the hammer strikes a hard concrete slab, the duration of the force impulse is small compared even with the period of the highest frequency of interest in impact testing. For less stiff structures, like wooden floors, this assumption is not valid and the exact shape of $F(t)$ has to be determined and used in Eq. (11.157b). For a thick concrete slab the effective length of the force impulse is short enough so that $\cos[(2\pi n/T_r)t] \approx 1$, and all components have the same amplitude. Because the integral in Eq. (11.157b) is the momentum of a single hammer blow (assuming no rebound) equal to mv_0 (in kg · m/s), the amplitudes of the Fourier components of the force for a repetition frequency f_r are

$$F_n = 2 f_r m v_0 \quad \text{N} \tag{11.158}$$

The velocity of the hammer at the instant of impact is

$$v_0 = \sqrt{2gh} \quad \text{m/s} \tag{11.159}$$

where h = falling height of hammer, m
g = acceleration of gravity (9.8 m/s²)

Let us define a mean-square-force spectrum density S_{f0} that when multiplied by the bandwidth will yield the value of the mean-square force in the same bandwidth,

$$S_{f0} = \tfrac{1}{2} T_r F_n^2 = 4 f_r m^2 g h \quad \text{N}^2/\text{Hz} \tag{11.160}$$

For the standard tapping machine the numerical value of S_{f0} is 4 N²/Hz. Accordingly, the mean-square force in an octave band $\Delta f_{\text{oct}} = f/\sqrt{2}$ is

$$F_{\text{rms}}^2(\text{oct}) = \frac{4}{\sqrt{2}} f \quad \text{N}^2 \tag{11.161}$$

The octave-band sound power level radiated by the impacted slab (which is assumed to be isotropic and homogeneous) into the room below is calculated by inserting Eq. (11.161) into Eq. (11.67a), which yields

$$L_w(\text{oct}) \approx 10 \log_{10} \left(\frac{\rho c \sigma_{\text{rad}}}{5.1 \rho_p^2 c_L \eta_p t^3} \right) + 120 \quad \text{dB re} 10^{-12} \text{ W} \tag{11.162}$$

where ρ = density of air, kg/m³
c = speed of sound in air, m/s
σ_{rad} = radiation factor of slab
ρ_p = density of slab material, kg/m³
c_L = propagation speed of longitudinal waves in slab material, m/s
η_p = composite loss factor of slab
t = thickness of slab, m

Note that the *sound power level is independent of the center frequency of the octave*, that *doubling the slab thickness decreases the level of the noise radiated into the room below by 9 dB*, and that the *sound power level decreases with increasing loss factor*.

Improvement of Impact Noise Isolation by an Elastic Surface Layer

Experience has shown that the impact noise level of even an 8–10-in.-thick dense concrete slab is too high to be acceptable. A further increase of thickness to reduce impact noise is not economical.

Impact noise may be reduced effectively by an elastic surface layer, much softer than the surface of the slab, applied to the structural slab. The resilient layer changes the shape of the force pulse and the amount of mechanical power introduced into the slab by the impacting hammer, as shown in Fig. 11.44.

We would expect, if the elastic layer is linear and nondissipative, that the velocity will be at its maximum v_0 at the instant of impact $t = 0$. It will then decrease to zero and the mass will rebound to nearly the same velocity (it is assumed the hammer is not permitted to bounce a second time) according to the function shown by curve *a* of Fig. 11.44. The force function is shown by curve *b*.

The improvement in impact noise isolation achieved by the addition of the soft surface layer is defined in terms of the logarithmic ratio[87]

$$\Delta L_n = 20 \log \frac{F}{F'} = 20 \log \left(\left| \frac{1 - n f_r / f_0}{\cos[(\pi/2) n (f_r/f_0)]} \right| \right) \quad \text{dB} \tag{11.163}$$

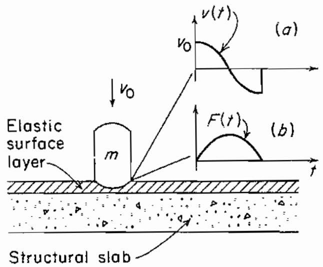

FIGURE 11.44 Velocity and force pulse of a single hammer blow on an elastic surface layer over a rigid slab: (*a*) velocity pulse; (*b*) force pulse.

where

$$n = 1, 2, 3, \ldots \tag{11.164}$$

$$f_0 = \frac{1}{2\pi}\sqrt{\frac{A_h}{m}}\sqrt{\frac{E}{h}} \quad \text{Hz} \tag{11.165}$$

F', F = forces acting on slab with and without resilient surface layer, respectively, N
A_h = striking area of hammer, m^2
m = mass of hammer, kg
E = dynamic Young's modulus of elastic material, N/m
h = thickness of layer, m

The characteristic frequency f_0 of an elastic surface layer for the standard tapping machine is plotted in Fig. 11.45 as a function of E/h.

Equation (11.163), which assumes no damping, is plotted in Fig. 11.46 as a function of the normalized frequency f/f_0. Below $f/f_0 = 1$, the improvement is zero. Above $f/f_0 = 1$ the improvement increases with an asymptotic slope of 40 dB/decade.

Figures 11.45 and 11.46 (use the 40-dB/decade asymptote) permit one to select an elastic surface layer to achieve a specified ΔL_n.

Example 11.6. The required improvement in impact noise isolation should be 20 dB at 300 Hz. Design a resilient covering for the concrete slab.

Solution From Fig. 11.46 we obtain $f/f_0 \approx 3$, which gives $f_0 = 100$ Hz. Entering Fig. 11.45 with this value of f_0 yields $E/h = 2.8 \times 10^8$ N/m^3 (or $E/h \approx$ 1000 psi/in.). Any material having this ratio of Young's modulus to thickness will provide the required improvement. If we wish to select a 0.31-cm- ($\frac{1}{8}$-in.-) thick layer, the dynamic modulus of the material should be 8.7×10^5 N/m^2 (8000 psi). Since the dynamic modulus of most elastic materials is about twice the statically

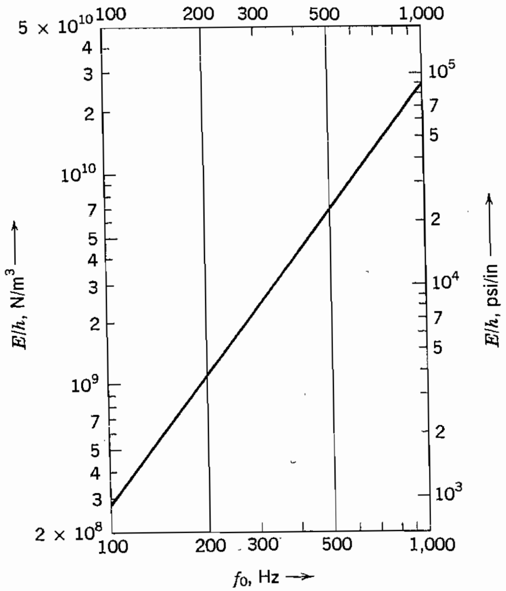

FIGURE 11.45 Chart for the selection of an elastic surface layer, where f_0 = characteristic frequency, E = Young's modulus, and h = thickness of layer.

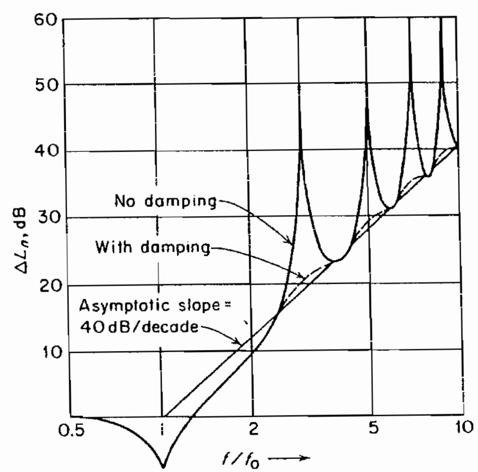

FIGURE 11.46 Improvement in impact noise isolation ΔL_n versus normalized frequency for a resilient surface layer (select f_0 to yield desired improvement).

measured Young's modulus,[88] a material with $E \leq 4.35 \times 10^5$ N/m^2 (4000 psi) should be selected.

Frequently used materials for the elastic surface layer are rubberlike materials, vinyl-cork tile, or carpet. The impact isolation improvement curve (ΔL_n vs. frequency) has been measured and reported[89] for a large variety of elastic surface layer configurations.

The expected normalized impact sound level in the room below (see Fig. 11.1) for a composite floor (with a heavy structural slab) is that of the bare concrete structural floor minus the improvement caused by the elastic surface layer, that is,

$$L_{n,\text{comp}} = L_{n,\text{bare}} - \Delta L_n \tag{11.166}$$

where

$$L_{n,\text{bare}}(\text{oct}) = 116 + 10 \log \left(\frac{\rho c \sigma_{\text{rad}}}{5.1 \rho_p^2 c_L \eta_p t^3} \right) \quad \text{dB re} 2 \times 10^{-5}\ \text{N/m}^2 \tag{11.167}$$

for homogeneous isotropic slabs.

Measured values of impact noise isolation of a large number of floor constructions and improvement of impact noise isolation by various surface layers are presented in reference 89.

Improvement through Floating Floors. It is often more practical to use a floating floor above a structural slab than a soft resilient surface layer. The advantages are that (1) both the impact noise isolation and the airborne sound transmission loss of the composite floor are improved and (2) the walking surface is hard. For analysis, floating floors can be categorized as either (1) locally reacting or (2) resonantly reacting, as defined below.

Locally Reacting Floating Floors. A locally reacting floor is one where the impact force of the hammer on the upper slab (slab 1) is transmitted to the structural slab (slab 2), primarily in the immediate vicinity of the excitation point, and where there is no spatially homogeneous reverberant vibration field on slab 1. In this case the bending waves in the floating slab are highly damped. If the Fourier amplitude of the force acting on plate 1 is given by Eq. (11.158), the reduction in transmitted sound level is[87]

$$\Delta L_n = 20 \log \left[1 + \left(\frac{f}{f_0} \right)^2 \right] \approx 40 \log \frac{f}{f_0} \tag{11.168}$$

where

$$f_0 = \frac{1}{2\pi} \sqrt{\frac{s'}{\rho_{s_1}}} \tag{11.169}$$

and ρ_{s_1} = mass per unit area of floating slab, kg/m^2
s' = dynamic stiffness per unit area of resilient layer between slab 1 and slab 2 including trapped air, N/m^3

Resonantly Reacting Floating Floors. If the floating slab is thick, rigid, and lightly damped, the impact force of the hammers excites a more-or-less spatially homogeneous reverberant bending wave field.

The improvement in impact noise isolation at higher frequencies, where the power dissipated in slab 1 exceeds the power transmitted to slab 2, can be approximated by[87,90]

$$\Delta L_n \approx 10 \log \frac{2.3 \rho_{s_1}^2 \omega^3 \eta_1 c_{L_1} h_1}{n' s^2} \tag{11.170}$$

where h_1 = thickness of floating slab, m
c_{L_1} = propagation speed of longitudinal waves in floating slab, m/s
ρ_{s_1} = mass per unit area of floating slab, kg/m^2
η_1 = loss factor of floating slab
n' = number of resilient mounts per unit area of slab, m^2
s = stiffness of mount, N/m

Equation (11.170) indicates that, in contrast to the locally reacting case where ΔL_n increases at a rate of 40 dB for each decade increase in frequency, the increase is only 30 dB/decade if the loss factor of the floating slab η_1 is frequency independent. Another difference is the marked dependence of ΔL_n on this loss factor. The loss factor is determined both by the energy dissipated in the slab material itself and by the energy dissipated in the resilient mounts.

Figure 11.47 shows the improvement of a floating-floor system under impacting by a standard tapping machine and high-heel shoes, respectively.[91] The negative improvement in the vicinity of the resonance frequency f_0 can be observed.

Impact Noise Isolation versus Sound Transmission Loss

Whether a floor is excited by the hammers of a tapping machine or by an airborne sound field in the source room, it will in both cases radiate sound into the receiving room. There is a close relation between the airborne sound transmission loss R and the normalized impact noise level L_n for a given floor.

In the case of acoustical excitation, the sound power transmitted to the receiver room comprises the contribution of forced waves and of resonance waves. The forced waves usually dominate below the critical frequency of the slab and the resonance waves above. The sound power transmitted by exciting the slab by a standard tapping machine is made up of the contributions of the near-field component and of the reverberant component.

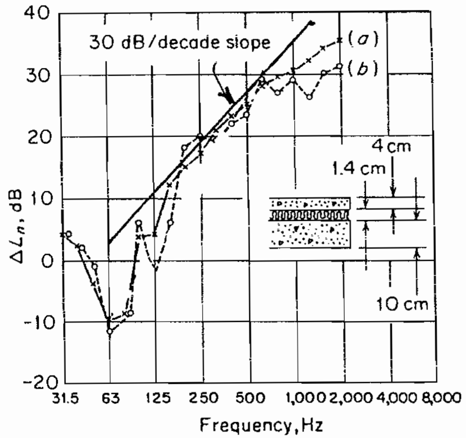

FIGURE 11.47 Improvement in impact noise isolation ΔL_n for a resonantly reacting floating floor for excitation by (*a*) a standard tapping machine and (*b*) high-heeled shoes. Note the negative ΔL_n in the vicinity of the resonance frequency. (After Ref. 91.)

The relation between sound transmission loss R and normalized impact noise level, assuming measurement in octave bands, is[92]

$$L_n + R$$
$$= 84 + 10 \log \left[\frac{S_{f0} f}{\sqrt{2}} \left(\frac{\rho/(2\pi\rho_s^2 c) + \rho c \sigma_{\text{rad}}/(2.3\rho_s^2 c_L \omega \eta_p h)}{\pi \rho c/(\omega^2 \rho_s^2) + \pi\sqrt{12} c^3 \rho \sigma_{\text{rad}}^2/(2\rho_s^2 c_L \omega^3 \eta_p h)} \right) \right] \text{dB} \tag{11.171}$$

where ρ_s = mass per unit area of slab, kg/m^2
c_L = propagation speed of longitudinal waves in slab, m/s
σ_{rad} = radiation factor of slab
h = thickness of slab, m
η_p = composite loss factor of slab
S_{f0} = mean-square force spectrum density as given in Eq. (11.160), N^2/Hz

In the special case of a thick, lightly damped slab,

$$L_n + R = 43 + 30 \log f - 10 \log \sigma_{\text{rad}} - \Delta L_n \tag{11.172}$$

where ΔL_n represents the effect of the surface layer only. For a bare structural slab, by definition, $\Delta L_n = 0$.

Equation (11.172) states that the *sum of the airborne sound transmission loss and the normalized impact noise level is independent of the physical characteristics of the structural slab above the critical frequency of the slab where* $\sigma_{\text{rad}} \approx 1$.

Below the coincidence frequency where the forced waves control the airborne sound transmission loss but the impact noise isolation is still controlled by the resonant vibration of the impacted slab, Eq. (11.171) yields[92]

$$R + L_n = 39.5 + 20 \log f - \Delta L_n - 10 \log \frac{\eta_p}{f_c \sigma_{\text{rad}}} \quad \text{dB} \tag{11.173}$$

where ΔL_n = effect of surface layer only (zero for structural slab), dB
f_c = critical frequency of structural slab, Hz

In this case, the sum $R + L_n$ decibels depends on the physical characteristics of the slab and frequency. Figure 11.48 shows the measured sound transmission loss R and normalized impact sound level L_n as well as their sum for a typical floating floor. The measured and predicted values for the sum are in good agreement,

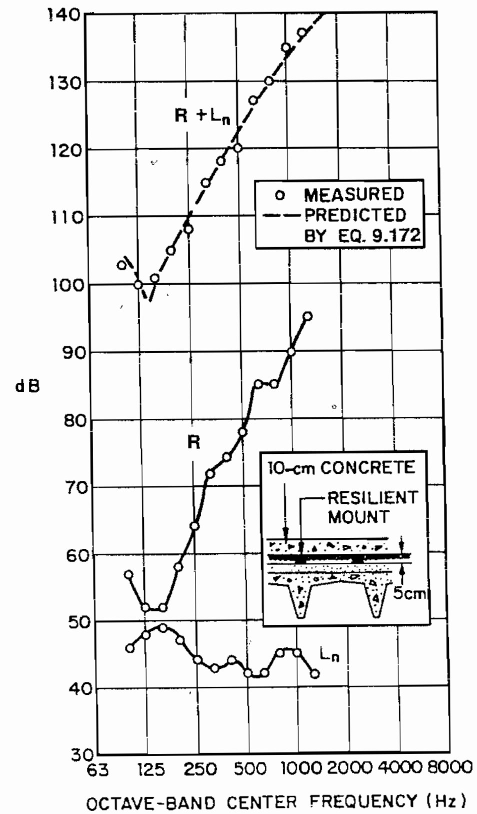

FIGURE 11.48 Measured sound transmission loss R and normalized impact sound level L_n and their sum ($R + L_n$) of a resonantly reacting floating floor assembly. Dotted curve: $R + L_n$ predicted by Eq. (11.172). (After reference 92.)

indicating that the precautionary measures taken to eliminate flanking have been successful.

In checking out the performance of floating floors in the field, it is advisable to measure both R and L_n. The discrepancy between the measured R and that calculated from Eq. (11.173) is a direct indication of flanking. By measuring the acceleration level on the wall surfaces in the source and receiving rooms during acoustical and impact excitation, the flanking paths can be immediately identified.

The measurement and rating of the impact noise isolation of floor assemblies is prescribed in ASTM E492–90 (1996), ASTM E989–89 (1999), and ASTM E1007–97.

REFERENCES

1. L. Cremer, M. Heckl, and E. E. Ungar, *Structureborne Sound*, 2nd ed., Springer Verlag, Berlin 1988.
2. M. Heckl, "Compendium of Impedance Formulas," Report No. 774, Bolt Beranek and Newman, Cambridge, MA, May 26, 1961.
3. I. Dyer, "Moment Impedance of Plate," *J. Acoust. Soc. Am.*, **32**, 247–248 (1960).
4. E. Eichler, "Plate Edge Admittances," *J. Acoust. Soc. Am.*, **36**(2), 344–348 (1964).
5. H. G. D. Goyder and R. G. White, "Vibrational Power Flow from Machines into Builtup Structures, Part I: Introduction and Approximate Analyses of Beam and Plate-Like Foundations," *J. Sound Vib.*, **68**(1), 59–75 (1980); "Part II: Wave Propagation and Power Flow in Beam-stiffened Plates," *J. Sound Vib.*, **68**(1), 77–96 (1980); "Part III: Power Flow through Isolation Systems," *J. Sound Vib.*, **68**(1), 97–117 (1980).
6. U. J. Kurze, *Laermarm Konstruieren XII; Mechanische Impedance [Low Noise Design XII; Mechanical Impedance], Bundesanstalt fuer Arbeitschutz*, FB Nr. 398, Wirtschaftverlag NW, Bremerhaven, 1985.
7. K. -P. Schmidt *Laermarm Konstruieren (III); Aenderung der Eingangsimpedanz als Massnahme zur Laermminderung [Low Noise Design (III); Reducing Noise by Changing the Input Impedance] Bundesanstalt fuer Arbeitschutz*, FB Nr. 169, Wirtschaftsverlag NW, Bremerhaven, 1979.
8. VDI 3720, Blatt 6 (Preliminary, July 1984), *Noise Abatement by Design; Mechanical Input Impedance of Structural Elements, Especially Standard-Section Steel*, VDI-Verlag, Dusseldorf, 1984 (in German).
9. M. Heckl, "Bending Wave Input Impedance of Beams and Plates," in *Proceedings 5th ICA*, Liége, Paper L67, 1965 (in German).
10. M. Heckl, "A Simple Method for Estimating the Mechanical Impedance," in *Proceedings DAGA*, VDI Verlag, 1980, pp. 828–830 (in German).
11. M. Heckl, "Excitation of Sound in Structures," *Proc. INTER-NOISE*, 1988, pp. 497–502.
12. R. J. Pinnington, "Approximate Mobilities of Builtup Structures," Report No. 162, Institute of Sound and Vibration Research, Southampton, England, 1988.
13. H. Ertel and I. L. Vér, "On the Effect of the Vicinity of Junctions on the Power Input into Beam and Plate Structures," *Proc. INTER-NOISE*, 1985, pp. 684–692.

14. P. W. Smith Jr., "The Imaginary Part of Input Admittance: A Physical Explanation of Fluid-Loading Effects on Plates," *J. Sound Vib.*, **60**(2), 213–216 (1978).
15. M. Heckl, "Input Impedance of Plates with Radiation Loading," *Acustica*, **19**, 214–221 (1967/68) (in German).
16. D. G. Crighton, "Force and Moment Admittance of Plates under Arbitrary Fluid Loading," *J. Sound Vib.*, **20**(2), 209–218 (1972).
17. D. G. Crighton, "Point Admittance of an Infinite Thin Elastic Plate under Fluid Loading," *J. Sound Vib.*, **54**(3), 389–391 (1977).
18. R. H. Lyon, "Statistical Analysis of Power Injection and Response in Structures and Rooms," *J. Acoust. Soc. Am.*, **45**(3), 545–565, (1969).
19. R. D. Blevins, *Formulas for Natural Frequency and Mode Shape*, Van Nostrand Reinhold, New York, 1979.
20. T. Kihlman, "Transmission of Structureborne Sound in Buildings," Report No. 9. National Swedish Institute of Building Research, Stockholm, 1967.
21. M. Paul, "The Measurement of Sound Transmission from Bars to Plates," *Acustica*, **20**, 36–40 (1968) (in German).
22. E. J. Richards et al. "On the Prediction of Impact Noise, II: Ringing Noise," *J. Sound Vib.*, **65**(3), 419–451 (1979).
23. R. Timmel, "Investigation on the Effect of Edge Conditions on Flexurally Vibrating Rectangular Panels on Radiation Efficiency as Exemplified by Clamped and Simply Supported Panels," *Acustica*, **73**, 12–20 (1991) (in German).
24. ASTM E90-02 1990, "Laboratory Measurement of Airborne-Sound Transmission Loss of Building Partitions," American Society for Testing and Materials, Philadelphia, PA.
25. ISO 140-1 : 1997 "Laboratory Measurement of Airborne Sound Insulation of Building Elements," American National Standards Institute, New York.
26. L. Cremer, *Vorlesungen ueber techische Akustik*, *[Lectures on Technical Acoustics]*, Springer-Verlag, Berlin, 1971.
27. H. Reissner, "Der senkrechte und schräge Durchtritt einer in einem fluessigen Medium erzeugten ebenen Dilations(Longitudinal)–Welle durch eine in diesem Medium befindliche planparallele feste Platte" ["Transmission of a Normal and Oblique-Incidence Plane Compressional Wave Incident from a Fluid on a Solid, Plane, Parallel Plate"] *Helv. Phys. Acta*, **11**, 140–145 (1938).
28. M. Heckl, "The Tenth Sir Richard Fairey Memorial Lecture: Sound Transmission in Buildings," *J. Sound Vib.*, **77**(2), 165–189 (1981).
29. R. D. Mindlin, "Influence of Rotary Inertia and Shear on Flexural Motion of Elastic Plates," *J. Appl. Mech.*, **18**, 31–38 (1951).
30. B. H. Sharp, "A Study of Techniques to Increase the Sound Insulation of Building Elements," Report WR-73-5, HUD Contract No. H-1095, Wyle Laboratories, Arlington, VA June 1973.
31. G. Kurtze and B. G. Watters, "New Wall Design for High Transmission Loss or High Damping," *J. Acoust. Soc. Am.*, **31**(6), 739–748 (1959).
32. H. Feshbach, "Transmission Loss of Infinite Single Plates for Random Incidence," Report No. TIR 1, Bolt Beranek and Newman, Cambridge Mass. October 1954.

Idaho Power/1206
Ellenbogen/257

33. L. L. Beranek, "The Transmission and Radiation of Acoustic Waves by Structures" (the 45th Thomas Hacksley Lecture of the British Institution of Mechanical Engineers), *J. Inst. Mech. Eng.*, **6**, 162–169 (1959).
34. L. L. Beranek, *Noise Reduction*, McGraw-Hill, New York, 1960.
35. M. Heckl, "Untersuchungen an Orthotropen Platten" ["Investigations of Orthotropic Plates"] *Acustica*, **10**, 109–115 (1960).
36. M. Heckl, "Die Schalldaemmung von homogene Einfachwaenden endlicher Flaeche" ["Sound Transmission Loss of the Homogeneous Finite Size Single Wall"], *Acustica*, **10**, 98–108 (1960).
37. H. Sato, "On the Mechanism of Outdoor Noise Transmission through Walls and Windows; A Modification of Infinite Wall Theory with Respect to Radiation of Transmitted Wave," *J. Acoust. Soc. Jpn.*, **29**, 509–516 (1973) (in Japanese).
38. J. H. Rindel, "Transmission of Traffic Noise through Windows; Influence of Incident Angle on Sound Insulation in Theory and Experiment," Ph.D. Thesis, Technical University of Denmark, Report No. 9, 1975 (also see *Proc. DAGA*, pp. 509–512), 1975; also private communications.
39. B. G. Watters, "Transmission Loss of Some Masonry Walls," *J. Acoust. Soc. Am.*, **31**(7), 898–911 (1959).
40. Y. Hamada and H. Tachibana, "Analysis of Sound Transmission Loss of Multiple Structures by Four-Terminal Network Theory," *Proc. INTER-NOISE*, 1985, pp. 693–696.
41. A. C. K. Au and K. P. Byrne "On the Insertion Loss Produced by Plane Acoustic Lagging Structures," *J. Acoust. Soc. Am.*, **82**(4), 1325–1333 (1987).
42. A. C. K. Au and K. P. Byrne, "On the Insertion Loss Produced by Acoustic Lagging Structures which Incorporate Flexurally Orthotropic Impervious Barriers," *Acustica*, **70**, 284–291 (1990).
43. K. Goesele and U. Goesele, "Influence of Cavity-Volume Damping on the Stiffness of Air Layer in Double Walls," *Acustica*, **38**(3), 159–166 (1977) (in German).
44. K. W. Goesele, W. Schuele, and B. Lakatos. *(Glasfuellung bei Isolierglasscheiben) Forschunggemeinschaft Bauen und Wohen* [*Gas Filling of Isolated Glass Windows*], FBW Blaetter, Vol. 4, 1982 Stuttgart.
45. H. Ertel and M. Moeser, *Effects of Gas Filling on the Sound Transmission Loss of Isolated Glass Windows in the Double Wall Resonance Frequency Range*, FBW Blaetter, Stuttgart, Vol. 5, 1984 (in German).
46. K. Goesele, "Prediction of the Sound Transmission Loss of Double Partitions (without Structureborne Connections)," *Acustica*, **45**, 218–227 (1980) (in German).
47. I. L. Vér, "Definition of and Relationship between Breakin and Breakin Sound Transmission Loss of Pipes and Ducts," *Proc. INTER-NOISE*, 1983, pp. 583–586.
48. L. L. Vér, "Prediction of Sound Transmission through Duct Walls: Breakout and Pickup," ASHRAE Paper 2851 (RP-319), *ASHRAE Trans.*, **90**(Pt. 2), 391–413 (1984).
49. Anonymous, "Sound and Vibration Control," in *ASHRAE Handbook, Heating, Ventilating, and Air-Conditioning Systems and Applications*, American Society of Heating, Refrigerating and Air Conditioning Engineers, Atlanta, GA, 1987, Chapter 52.
50. A. Cummings, "Acoustic Noise Transmission through Duct Walls," *ASHRAE Trans.*, **91**(Pt. 2A), 48–61 (1985).

51. M. C. Gomperts and T. Kihlman, "Transmission Loss of Apertures in Walls," *Acustica*, **18**, 140 (1967).
52. F. P. Mechel, "The Acoustic Sealing of Holes and Slits in Walls," *J. Sound Vib.*, **111**(2), 297–336 (1986).
53. F. P. Mechel, "Die Schalldaemmung von Schalldaempfer-Fugen" ["Acoustical Insulation of Silencer Joints"], *Acustica*, **62**, 177–193 (1987).
54. W. Fasold, W. Kraak, and W. Schirmer, *Pocketbook Acoustic*, Part 2, Section 6.2, VEB Verlag Technik, Berlin, 1984 (in German).
55. R. H. Lyon and G. Maidanik, "Power Flow between Linearly Coupled Oscillators," *J. Acoust. Soc. Am.*, **34**(5), 623–639 (1962).
56. E. Skudrzyk, "Vibrations of a System with a Finite or Infinite Number of Resonances," *J. Acoust. Soc. Am.*, **30**(12), 1114–1152 (1958).
57. E. E. Ungar, "Statistical Energy Analysis of Vibrating Systems," *J. Eng. Ind. Trans. ASME Ser. B*, **87**, 629–632 (1967).
58. M. J. Crocker and A. J. Price, "Sound Transmission Using Statistical Energy Analysis," *J. Sound Vib.*, **9**(3), 469–486 (1969).
59. R. H. Lyon, *Statistical Energy Analysis of Dynamical Systems; Theory and Application*, MIT Press, Cambridge, MA, 1975.
60. I. L. Ver, Equivalent Dynamic Force that Generates the same Vibration Response as a Sound Field, Proceedings of Symposium on International Automotive Technology, SIAT 2005-SAE Conference, Pune, India, 19–22 January 2005, pp 81–86.
61. Private communications. J. Barger of BBN LLC.
62. Lord Rayleigh, *Theory of Sound*, Vol. I, Dover, New York, 1945, pp. 104–110.
63. M. Heckl, "Some Applications of Reciprocity Principle in Acoustics," *Frequenz*, **18**, 299–304 (1964) (in German).
64. I. L. Vér, "Uses of Reciprocity in Acoustic Measurements and Diagnosis," *Proc. INTER-NOISE*, 1985, pp. 1311–1314.
65. I. L. Vér, *Reciprocity as a Prediction and Diagnostic Tool in Reducing Transmission of Structureborne and Airborne Noise into an Aircraft Fuselage*, Vol. 1: *Proof of Feasibility*, BBN Report No. 4985 (April 1982); Vol. 2: *Feasibility of Predicting Interior Noise Due to Multiple, Correlated Force Input*, BBN Report No. 6259 (May 1986), NASA Contract No. NAS1-16521, Bolt Beranek and Newman.
66. I. L. Vér, "Use of Reciprocity and Superposition in Predicting Power Input to Structures Excited by Complex Sources," *Proc. INTER-NOISE*, 1989, pp. 543–546.
67. F. J. Fahy, "The Reciprocity Principle and Its Applications in Vibro-Acoustics," *Proc. Inst. Acoust. (UK)*, **12**(1), 1–20 (1990).
68. L. M. Lyamshev, "On Certain Integral Relations in Acoustics of a Moving Medium," *Dokl. Akad. Nauk SSSR*, **138**, 575–578 (1961); *Sov. Phys. Dokl.*, **6**, 410 (1961).
69. Yu I. Belousov and A. V. Rimskii-Korsakov, "The Reciprocity Principle in Acoustics and Its Application to the Calculation of Sound Fields of Bodies," *Sov. Phys. Acoust.*, **21**(2), 103–109 (1975).
70. L. Cremer, "The Law of Mutual Energies and Its Application to Wave-Theory of Room Acoustics," *Acoustica*, **52**(2), 51–67 (1982/83) (in German).
71. M. Heckl, "Application of the Theory of Mutual Energies," *Acustica*, **58**, 111–117 (1985) (in German).

72. J. M. Mason and F. J. Fahy, "Development of a Reciprocity Technique for the Prediction of Propeller Noise Transmission through Aircraft Fuselages," *Noise Control Eng. J.*, **34**, 43–52 (1990).
73. P. W. Smith, "Response and Radiation of Structures Excited by Sound," *J. Acoust. Soc. Am.*, **34**, 640–647 (1962).
74. H. F. Steenhock and T. TenWolde, "The Reciprocal Measurement of Mechanical-Acoustical Transfer Functions," *Acustica*, **23**, 301–305 (1970).
75. T. TenWolde, "On the Validity and Application of Reciprocity in Acoustical, Mechano-Acoustical and other Dynamical Systems," *Acustica*, **28**, 23–32 (1973).
76. E. J. Richards, M. E. Westcott, and R. K. Jeyapalan, "On the Prediction of Impact Noise, I: Acceleration Noise," *J. Sound Vib.*, **62**, 547–575 (1979).
77. E. J. Richards, M. E. Westcott, and R. K. Jeyapalan, "On the Prediction of Impact Noise, II: Ringing Noise," *J. Sound Vib.*, **65**, 419–451 (1979).
78. E. J. Richards, "On the Prediction of Impact Noise, III: Energy Accountancy in Industrial Machines," *J. Sound Vib.*, **76**, 187–232 (1981).
79. J. Cuschieri and E. J. Richards, "On the Prediction of Impact Noise, IV: Estimation of Noise Energy Radiated by Impact Excitation of a Structure," *J. Sound Vib.*, **86**, 319–342 (1982).
80. E. J. Richards, I. Carr, and M. E. Westcott, "On the Prediction of Impact Noise, Part V: The Noise from Drop Hammers," *J. Sound Vib.*, **88**, 333–367 (1983).
81. E. J. Richards, A. Lenzi, and J. Cuschieri, "On the Prediction of Impact Noise, VI: Distribution of Acceleration Noise with Frequency with Applications to Bottle Impacts," *J. Sound Vib.*, **90**, 59–80 (1983).
82. E. J. Richards and A. Lenzi, "On the Prediction of Impact Noise, VII: Structural Damping of Machinery," *J. Sound Vib.*, **97**, 549–586 (1984).
83. J. M. Cuschieri and E. J. Richards, "On the Prediction of Impact Noise, VIII: Diesel Engine Noise," *J. Sound Vib.*, **102**, 21–56 (1985).
84. E. J. Richards and G. J. Stimpson, "On the Prediction of Impact Noise, IX: The Noise from Punch Presses," *J. Sound Vib.*, **103**, 43–81 (1985).
85. E. J. Richards and I. Carr, "On the Prediction of Impact Noise, X: The Design and Testing of a Quietened Drop Hammer," *J. Sound Vib.*, **104**(1), 137–164 (1986).
86. ASTM E492-90, "Standard Test Method for Laboratory Measurement of Impact Sound Transmission through Floor-Ceiling Assemblies Using the Tapping Machine," American Society for Testing and Materials, Philadelphia, PA, 1996.
87. I. L. Vér, "Impact Noise Isolation of Composite Floors," *J. Acoust. Soc. Am.*, **50**(4, Pt. 1), 1043–1050 (1971).
88. K. Gösele, "Die Bestimmung der Dynamischen Steifigkeit von Trittschall-Dämmstoffen," Boden, Wand und Decke, Heft 4 and 5, Willy Schleunung, Markt Heidenfeld, 1960.
89. I. L. Vér and D. H. Sturz "Structureborne Sound Isolation," in C. M. Harris (ed.), *Handbook of Acoustical Measurements and Noise Control*, 3rd ed., McGraw-Hill, New York, 1991, Chapter 32.
90. I. L. Vér, "Acoustical and Vibrational Performance of Floating Floors," Report No. 72, Bolt Beranek and Newman, Cambridge, MA, October 1969.

91. R. Josse and C. Drouin, "Étude des impacts lourds a l'interieur des bâtiments d'habitation," Rapport de fin d'étude, Centre Scientifique et Technique du Bâtiment, Paris, February 1, 1969, DS No. 1, 1.24.69.
92. I. L. Vér, "Relationship between Normalized Impact Sound Level and Sound Transmission Loss," *J. Acoust. Soc. Am.*, **50**(6, Pt. 1), 1414–1417 (1971).
93. L. Cremer, "Theorie des Kolpfschalles bei Decken mit Schwimmenden Estrich," *Acustica*, **2**(4), 167–178 (1952).

BIBLIOGRAPHY

Beranek, L. L., *Acoustical Measurements*, rev. ed., Acoustical Society of America, Woodbury, NY, 1988.

Bies, D. A., and C. H. Hansen, *Engineering Noise Control*, Unwin Hyman, London/Boston/Sydney, 1988.

Cremer, L., M. Heckl, and E. E. Ungar, *Structureborne Sound*, 2nd ed., Springer-Verlag, Berlin, Heidelberg, New York, London, Paris, Tokyo, 1988.

Fahy, F., *Sound and Structural Vibration*, Academic, London, 1989, revised, corrected paperback edition.

Fasold, W., W. Kraak, and W. Shirmer, *Taschenbuch Akustik* [*Pocket Book Acoustics*] Vols. 1 and 2, VEB Verlag Technik, Berlin, 1984.

Harris, C. M. (Ed.), *Handbook of Acoustical Measurements Noise and Control*, 3rd ed., McGraw-Hill, New York, 1991.

Junger, M. C., and D. Feit, *Sound Structures and Their Interaction*, 2nd ed., MIT Press, Cambridge, MA, 1986.

Reichardt, W., *Technik-Woerterbuch, Technische Akustik* [*Dictionary of Technical Acoustics*; English, German, French, Russian, Spanish, Polish, Hungarian, and Slowakian], VEB Verlag, Technik, Berlin, 1978.

Mechel, F. P. (Ed.), *Formulas of Acoustics*, Springer, Berlin, 2002.

Heckl, M., and H. A. Mueller, *Taschenbuch der Technischen Akustik* [*Pocketbook of Technical Acoustics*], 2nd ed., Springer, Berlin, 1997.

TABLE 11.1 Speeds of Sound in Solids, Deformation of Solids for Different Wave Types, and Formulas for Propagation Speed

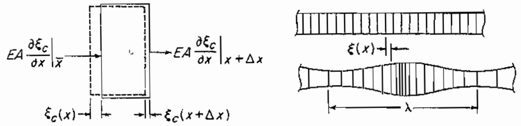

Longitudinal Waves Bar

$c_L = \sqrt{E/\rho_M}$

Infinite plate

$c'_L = \sqrt{E/[\rho_M(1-\nu^2)]}$

Infinite solid

$$c''_L = \sqrt{\frac{(E/\rho_M)(1-\nu)}{(1+\nu)(1-2\nu)}}$$

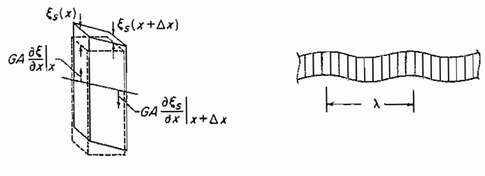

Shear Wave

$c_s = \sqrt{G/\rho_M} \quad G = E/(2+2\nu)$

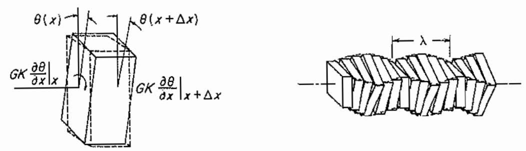

Torsional Wave Bar

$c_T = \sqrt{GK/\rho_M I}$
$= c_s$ for rods of circular cross section

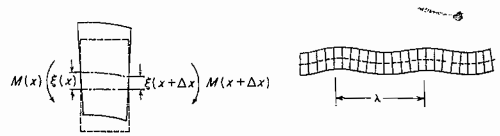

Bending Wave Plate

$c_B = \sqrt[4]{\omega^2 B/\rho_s}$

Young's modulus E, N/m^2, relates the stress S (force per unit area) to the strain (change in length per unit length). *Poisson's ratio* ν is the ratio of the transverse expansion per unit length of a circular bar to its shortening per unit length, under a compressive stress, dimensionless. It equals about 0.3 for structural materials and nearly 0.5 for rubberlike materials. The *density* of the material is ρ_M, kg/m^3. ρ_s is mass per unit area (kg/m^2) for plates and mass per unit length (kg/m) for bars, rods, or beams. The *shear modulus G* is the ratio of shearing stress to shearing strain, N/m^2. I is the *polar moment* of inertia, m^4. The *torsional stiffness factor K* relates a twist to the shearing strain produced, m^4. The *bending stiffness* per unit width B equals $Eh^3/[12(1-\nu^2)]$ for a homogeneous plate, N·m, where h is the thickness of the bar (or plate) in the direction of bending, m. For rectangular rods $B = Eh^3w/12$, where h is the cross-sectional dimension in the plane of bending and w that perpendicular to it (and width), m.

TABLE 11.2 Key Acoustical Parameters of Solid Materials

Material	Density ρ_M, kg/m^3	Young's Modulus E, N/m^2	Poisson Ratio ν	Speed of Sound c_L, m/s	Product of Surface Density and Critical Frequency $\rho_s f_c$: Hz·kg/m^2	Hz·lb/ft^2	TL at Critical Frequency $R(f_c)$, dB	Internal Damping Factor for Bending at 1000 Hz, η[a]	Acoustical–Mechanical Conversion Efficiency η_{am}, Eq. (11.66)
Aluminum	2,700	7.16×10^{10}	0.34	5,150	34,700	7,000	48.5	10^{-4}–10^{-2}[b]	2.5×10^{-3}
Copper	8,900	1.3×10^{11}	0.35	3,800					3.3×10^{-4}
Glass	2,500	6.76×10^{10}		5,200	38,000	7,800	49.5	0.001–0.01[b]	2.7×10^{-3}
Lead (chemical or tellurium)	11,000	1.58×10^{10}	0.43	1,200	605,000	124,000	73.5	0.015	1.4×10^{-4}
Plexiglas or Lucite	1,150	3.73×10^{9}	—[c]	1,800	35,400	7,250	49.0	0.002[b]	2×10^{-3}
Steel	7,700	1.96×10^{11}	0.31	5,050	97,500	20,000	57.5	10^{-4}–10^{-2}[b]	8.5×10^{-4}
Brick	1,900–2,300	—[c]	—[c]	—[c]	34,700–58,600	7,000–12,000	48.5 to 53	0.01	—[c]
Concrete, dense poured	2,300	2.61×10^{10}	—[c]	3,400	43,000	9,000	50.5	0.005–0.02	1.9×10^{-3}
Concrete (Clinker) slab, plastered on both sides 5 cm thick	1,500	—	—	—	48,800	10,000	51.5	0.005–0.02	—[c]
Masonry block	750	—	—	—	23,200	4,750	45.0	0.005–0.02	

(continued overleaf)

TABLE 11.2 (*continued*)

Material	Density ρ_M, kg/m^3	Young's Modulus E, N/m^2	Poisson Ratio ν	Speed of Sound c_L, m/s	Product of Surface Density and Critical Frequency $\rho_s f_c$: Hz kg/m^2	Product of Surface Density and Critical Frequency $\rho_s f_c$: Hz lb/ft^2	TL at Critical Frequency $R(f_c)$, dB	Internal Damping Factor for Bending at 1000 Hz, η[a]	Acoustical–Mechanical Conversion Efficiency η_{am}, Eq. (11.66)
Hollow cinder with 1.6 cm sand plaster, nominal thickness 15 cm (6 in.)	900	—	—	—	25,500	5,220	46.0	0.005–0.02	—[c]
Hollow dense concrete, nominal 15 cm (6 in.) thick	1100	—	—	—	23,000	4,720	45.0	0.007–0.02	—[c]
Hollow dense concrete, sand-filled voids, nominal 15 cm (6 in.) thick	1,700	—[c]	—[c]	—[c]	42,200	8,650	50.0	Varies with frequency	—[c]
Solid dense concrete, nominal 10 cm (4 in.) thick	1,700	—[c]	—[c]	—[c]	54,100	11,100	52.5	0.012	—[c]
Gypsum board 1.25–5 cm ($\frac{1}{2}$–2 in.) thick	650	—[c]	—[c]	6,800	20,000	4,500	45.0	0.01–0.03	—[c]
Plaster, solid, on metal or gypsum lathe	1,700	—[c]	—[c]	—[c]	24,500	5,000	45.5	0.005–0.01	—[c]
Fir timber	550	—[c]	—[c]	3,800	4,880	1,000	31.5	0.04	9×10^{-3}
Plywood 0.6–3.12 cm ($\frac{1}{2}$–2 in.) thick	600	—[c]	—[c]	—[c]	12,700	2,600	40	0.01–0.04	—[c]
Wood waste material bonded with plastic 23 kg/m^2 (5 lb/ft^2)	750	—[c]	—[c]	—[c]	73,200	15,000	55.0	0.005–0.01	—[c]

[a]The range in values of η are based on limited data. The lower values are typical for material alone while the higher values are the maximum observed on panels in place.
[b]The loss factors for structures of these materials are sensitive to construction techniques and edge conditions.
[c]The parameter either is not meaningful or is not available.

TABLE 11.3 Driving Force Point Impedance of Infinite Structures

Element	Picture	Equivalent Mass [see Eq. (11.19)]	Driving Point Force Impedance	Range of Validity	Auxiliary Expressions and Notes
Beam, in compression Semi-infinite Infinite	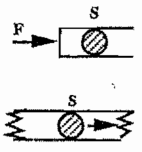	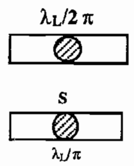	$Z_F = \rho_M c_L S$ $Z_F = 2\rho_M c_L S$	$S < (\lambda_s/4)^2$	$c_L = \sqrt{\dfrac{E}{\rho_M}}$ $S =$ cross-sectional area $\lambda_s = \dfrac{1}{f}\sqrt{\dfrac{E}{2(1+\nu)\rho_M}}$
Beam in bending Semi-infinite Infinite	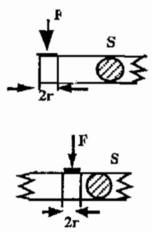	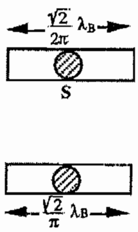	$Z_F = \frac{1}{2}(1+j)\rho_M S c_B$ $Z_F = 2(1+j)\rho_M S c_B$	$S < (\lambda_B/6)^2$ $2r > 9S/\lambda_S$	$r =$ radius of contact area $c_B = \left(\dfrac{EI\omega^2}{\rho_M S}\right)^{1/4}$ $\nu =$ Poisson Ratio $\lambda_B = c_B/f$ $I =$ polar moment of inertia
Thin infinite plate Vertical force Horizontal force (in plane)	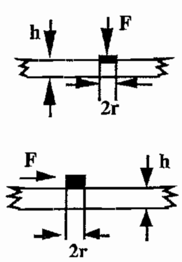	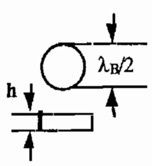	$Z_F = 8\sqrt{B'\rho_M c_L h}$ $= 2.3\rho_M c_L h^2$ $\dfrac{1}{Z_F} = \dfrac{\pi f}{4Gh} \times \left(\dfrac{3-\mu}{2} + jH\right)$ $\mathrm{Re}\{1/Z_F\} = [n_L(f) + n_s(f)]/8M$	$h < \lambda_B/6$ $2r > 3h$ $\lambda_s \gg 2\pi r > 10h$	$B' = \left(\dfrac{Eh^3}{12(1-\nu^2)}\right)$ $\lambda_s = \dfrac{1}{f}\sqrt{\dfrac{E}{2(1+\nu)\rho_M}}$ $H = K + L$ $K = (1-\mu)\ln\left(\dfrac{\lambda_l}{\pi r}\right)$ $L = 2\ln\left(\dfrac{\lambda_s}{\pi r}\right)$
Thin semi-infinite plate	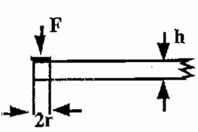	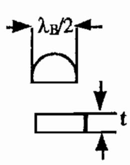	$Z_F = 3.5\sqrt{B'\rho_M h}$ $\approx \rho_M c_L h^2$	$h < \lambda_B/6$ $2r > 3h$	$n_L(f) =$ longitudinal modal density $n_L(f) =$ shear modal density $M =$ total mass $\lambda_l = c_L/f$ $\lambda_s = c_s/f$ $\lambda_B = c_B/f$

(continued overleaf)

TABLE 11.3 (*continued*)

Element	Picture	Equivalent Mass [see Eq. (11.19)]	Driving Point Force Impedance	Range of Validity	Auxiliary Expressions and Notes
Beam-stiffened infinite thin plate	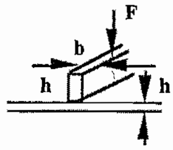	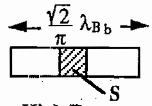 **High Frequency Approximation**	$Z_F = \frac{(1-j)k'}{4\rho_s'\omega}$ $Z_F \cong Z_{FB}$ $= 2(1+j)\rho_M S_b c_B$	$S_b < (\lambda_B/6)^2$ $2r > 9S_b/\lambda_B$	$\rho_s' = \rho_M S_B + 2\rho_M h/k_p$ $k' = \left(\frac{\rho_s'}{B}\right)^{1/4} \omega^{1/2} A$ $A = 1 - j\frac{\rho_M h}{2\rho_s' k_p}$ k_p = plate-bending wavenumber $B = Eh^3b/3$ $s = k_b/k_p$
Infinite string	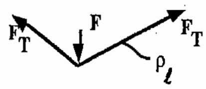	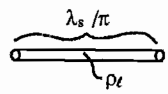	$Z_F = 2\sqrt{\rho_l F_T}$		$c_s = \sqrt{F_T/\rho_l}$ ρ_l = mass per unit length F_T = tension force
Semi-infinite plate, in-plane edge force	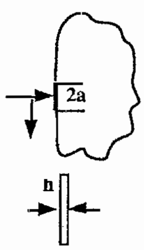	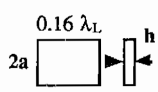	$\frac{1}{Z_F} = -\frac{j\omega^2}{\pi E h}\log a$ $+\frac{\omega}{4}\left(\frac{1}{D}+\frac{1}{S}\right)$		$D = \frac{Eh(1-\nu)}{(1-\nu)(1-2\nu)}$ $S = Gh$ G = shear modulus
Infinite corrugated plate	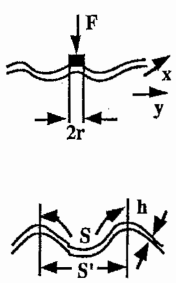	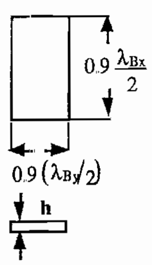	$Z_F = 8[(\rho_M h)^2$ $\times B_x B_y]^{1/4}$	$S \ll \lambda_B$	$B_y = \frac{Eh^3}{12(1-\nu^2)}$ $B_x \cong \left(\frac{1-\nu}{1+\nu}\right)^2 \frac{S}{S'} B_y$ $f_{c1} = \frac{c_0^2}{2\pi}\sqrt{\frac{\rho_M h}{B_x}}$ $f_{c2} = f_{c1}\sqrt{\frac{B_x}{B_y}}$

(*continued overleaf*)

TABLE 11.3 (continued)

Element	Picture	Equivalent Mass [see Eq. (11.19)]	Driving Point Force Impedance	Range of Validity	Auxiliary Expressions and Notes
Elastic half space			$Z = \dfrac{-j0.64Gr}{f(1-\nu/2)} + 1.79r^2\sqrt{\dfrac{4G\rho_M}{1-\nu}}$	$2r < \lambda_s/6$	ρ_M = density; G = shear modulus; ν = Poisson's ratio
Infinite cylindrical shell	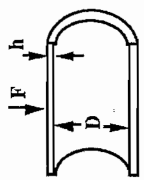	—	$Z_\infty \cong 2.3\rho_M c_L h$; $\mathrm{Re}\left(\dfrac{1}{Z_\infty}\right) = \dfrac{\sqrt{12}}{8\rho_M c_L h^2} \times \left(\dfrac{f}{f_R}\right)^{2/3}$	$f > 1.5 f_R$; $f < 0.7 f_R$	$f_R = c_L/\pi D$ ring frequency

TABLE 11.4 Moment Impedance Z_M of Infinite and Semi-Infinite Structures

Element	Picture	Driving Point Moment Impedance
Semi-infinite beam		
Free end	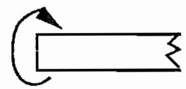	$\dfrac{(1-j)\rho_l c_B^3(f)}{8\pi^2 f^2}$
Pinned end	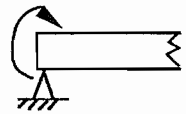	$\dfrac{(1-j)\rho_l c_B^3(f)}{4\pi^2 f^2}$
Infinite beam		$\dfrac{(1-j)\rho_l c_B^3(f)}{2\pi^2 f^2}$
Infinite homogeneous isotropic plate	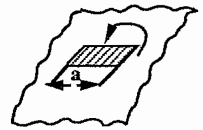	$\dfrac{16\rho_M h c_L^2 k_B^{-2}(f)}{2\pi f[(1-j)1.27\ \ln(k_B a/2.2)]}$
Semi-infinite homogeneous isotropic plate	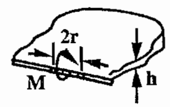	$\dfrac{12\rho_M h c_L^2 k_B^{-2}(f)}{2\pi f[(1-j)3.35\ln(kr/3.5)]}$
At joint of homogeneous, isotropic plates	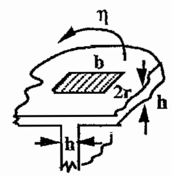	$\dfrac{\rho_M c_L^2 h^3}{75.4 f}\left\{16\left[\dfrac{(1+j)1.27\ln(kb/2.2)}{1+(1.27\ln kb/2.2)^2}\right] + 12\left[\dfrac{(1+j)3.35\ln(kr/3.5)}{1+(3.35\ln kr/3.5)^2}\right]\right\}$

Auxiliary expressions and notes:

ρ_l = mass per unit length (kg/m)
$c_B(f)$ = bending wave speed (m/s) in bending, $= \sqrt{2\pi f}(EI/\rho_l)^{1/4}$
E = Young's modulus(N/m^2)
I = area moment of inertia in bending(m^4)
f = frequency
ρ_M = material density(kg/m^3)
$k_B(f) = 2\pi f/c_B(f)$ bending wavenumber
h = plate thickness

TABLE 11.5 Effective Length l_M Connecting Force and Moment Impedance, $Z_M = l_M^2 Z_f$ for Infinite Beams and Plates

Element	Picture	Equivalent Force Pair	Effective Length l_M	Auxiliary Expressions
Beam in bending		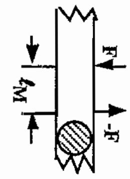	$\frac{\lambda_B}{2\pi}/\sqrt{j}$	$j = \sqrt{-1}$
Beam in torsion	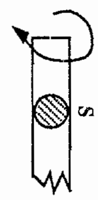	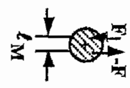	$0.79i$	For hollow beams: $i = \sqrt{\frac{d_o^2 - d_i^2}{2}}$ d_o = outside diameter d_i = inside diameter
Plate, vertical moment	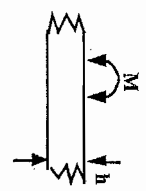	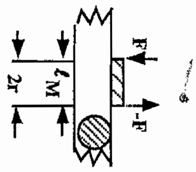	$\frac{\lambda_B/\sqrt{8\pi j}}{\sqrt{\ln(\lambda_B/\pi r)}}$	Bending waves: $3h < 2r \ll \lambda_B/\pi$
Plate, in-plane torsional moment	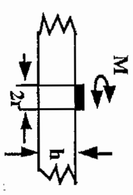	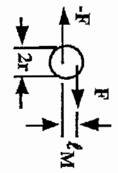	$\frac{r}{\sqrt{\ln(\lambda_s/\pi r)}}$	Shear waves: $3h < 2r \ll \lambda_s/\pi$ λ_s = shear wavelength

Source: After reference 6.

TABLE 11.6 Power Input to Structures

Element	Picture	Power Input to Infinite Element: Force or Moment Excitation	Power Input to Infinite Element: Velocity or Angular Velocity Excitation	Finite Elements: Onset of Infinite Behavior	Finite Elements: $W_{\text{fin}}/W_{\text{inf}}$	Auxiliary Expressions
Beam in longitudinal wave motion; force or velocity excitation	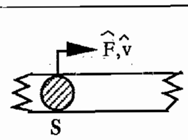	$\frac{\lvert\hat F\rvert^2}{4\rho_M S c_L}$	$4\lvert\hat v\rvert^2 S\rho_M c_L$	$\omega > \frac{\pi c_L}{\eta l}$	$\frac{4}{\pi\eta}$	$c_L = \sqrt{E/\rho_M}$ l = length η = loss factor Q = torsion constant G = shear modulus J = mass moment of inertia per unit length $c_T = \sqrt{\frac{E/\rho_M}{GQ/J}}$ = torsional wave speed ρ_M = density E = Young's modulus I = second moment of inertia $\dot\theta$ = angular velocity $c_B = \sqrt{\omega}\sqrt{\frac{E/I}{\rho_M S}}$ = bending wave speed $B_p = \frac{h^3 E}{12(1-\upsilon^2)}$ S = area
Beam in torsion moment or angular velocity excitation	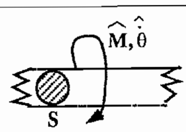	$\frac{\lvert\hat M\rvert^2}{4GQJ}$	$4\lvert\hat{\dot\theta}\rvert^2\sqrt{GQJ}$	$\omega > \frac{\pi c_T}{\eta l}$	$\frac{4}{\pi\eta}$	
Beam in bending; force or velocity excitation	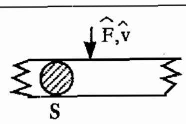	$\frac{\lvert\hat F\rvert^2}{8\rho_M S c_B(f)}$	$\lvert\hat v\rvert^2 S\rho_M c_B(f)$	$\omega > \frac{4\pi c_B(f)}{\eta l}$	$\frac{4\sqrt{2}}{\pi\eta}$	
Beam in bending; moment or angular velocity excitation	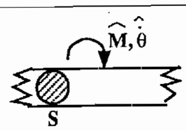	$\frac{\lvert\hat M\rvert^2 c_B(f)}{8EI}$	$\frac{\lvert\hat{\dot\theta}\rvert^2 EI}{c_B(f)}$	$\omega > \frac{4\pi c_B(f)}{\eta l}$	$\frac{2\sqrt{2}}{\pi\eta}$	
Plate in bending; force or velocity excitation	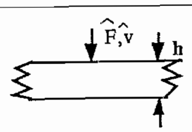	$\frac{\lvert\hat F^2\rvert}{16\sqrt{B_p\rho_M h}} = \frac{\lvert\hat F^2\rvert}{4.6\rho h^2 c_L}$	$4\hat v^2\sqrt{B_p\rho_M h} = 1.15\hat v^2\rho_M h^2 c_L$	$\omega > \frac{8}{\eta l_1 l_2}\sqrt{\frac{B_p}{\rho_M h}}$	$\frac{32 l_1 l_2}{\pi^2\eta(l_1^2 + l_2^2)}\frac{\omega}{c_B}$	

(continued overleaf)

TABLE 11.6 (*continued*)

Element	Picture	Power Input to Infinite Element: Force or Moment Excitation	Power Input to Infinite Element: Velocity or Angular Velocity Excitation	Finite Elements: Onset of Infinite Behavior	Finite Elements: W_{fin}/W_{inf}	Auxiliary Expressions
Plate in bending; moment or angular velocity excitation	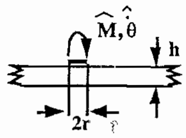	$\sim \dfrac{\omega\lvert\hat{M}\rvert^2}{16B_p}$ for $r > h$	$\dfrac{4\lvert\hat{\dot{\theta}}\rvert^2 B_p}{\omega\left\{1+\left[\dfrac{4}{\pi}\ln\left(\dfrac{\omega r}{c_B}\right)-\dfrac{8}{\pi(1-v)}\left(\dfrac{h}{\pi r}\right)^2\right]^2\right\}}$	$\omega > \dfrac{8}{\eta l_1 l_2}\sqrt{\dfrac{B_p}{\rho_M h}}$		
Thin-walled pipe in bending; force excitation	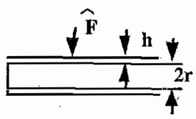	$\hat{F}^2/(16\pi\rho_M r h\sqrt{c_L r\omega})$ for $f < 0.123c_L h/r$ $\hat{F}^2\sqrt{V/(2+V)}/(\omega\rho_s 2\lambda^2/\pi^2)$ for $f > 0.123c_L h/r$				$V = \omega r/c_L$ λ_p = bending wavelength in equivalent thickness plate $\rho_s = \rho_M h$
Plate in bending; multiple force excitation, equally spaced	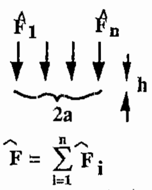	$\hat{F}^2[2J_1(z)/z]^2/(16\sqrt{B_p\rho_M h})$				$Z = 2\pi a/\lambda_B$ J_1 = Bessel function of order 1

TABLE 11.6 (*continued*)

Element	Picture	Power Input to Infinite Element: Force or Moment Excitation	Power Input to Infinite Element: Velocity or Angular Velocity Excitation	Finite Elements: Onset of Infinite Behavior	Finite Elements: W_{finite}/W_{inf}	Auxiliary Expressions
Plate in bending; large area velocity excitation	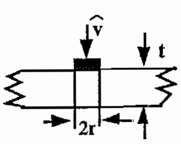	$\hat{v}^2\dfrac{\pi}{2}\rho_M c_B(r+0.8\lambda_B)h$				
Elastic half space; single force	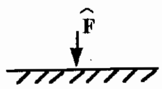	$\dfrac{48\hat{F}^2}{\omega\rho_M\pi\lambda_s^3}$				$\lambda_s = \sqrt{G/\rho_M}/f$ shear wavelength
Elastic half space equal multiple forces along a line, equally spaced	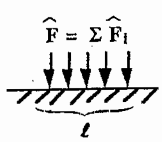	$\dfrac{16\hat{F}^2}{\omega\rho_M l\lambda_s^2}, l > \lambda_s/2$				

(*continued overleaf*)

TABLE 11.6 (*continued*)

Element	Picture	Power Input to Infinite Element Nearby Monopole and Dipole Excitation	Auxiliary Expressions
Infinite plate excited by nearby: Monopole	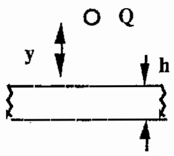	$W_{\text{mon}} \cong \dfrac{Q^2(\rho_o c_0)^2\ \text{Re}\{Y_\infty\}}{(f_c/f)-1} \times \exp\left(\dfrac{4\pi f}{c_0} y\sqrt{f_c/f - 1}\right),\ f < f_c$ $y \ll \lambda_0/4$ light fluid loading	Q = rms volume velocity Y_∞ = point force admittance k_B = free plate bending wavenumber f_c = critical coincidence frequency
Lateral dipole	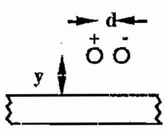	$W_{\text{LD}} \cong 0.5(k_B d)^2\ W_{\text{mon}},\ f < f_c$	
Perpendicular dipole	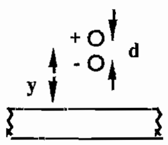	$W_{\text{PD}} \cong W_{\text{mon}}(k_B d)^2[1-(f/f_c)]^2$ (for $f < f_c$ and light fluid loading)	

TABLE 11.7 **First Resonance Frequency, Mode Shape and Modal Density of Finite Structures**

Element	Picture	Boundary Conditions[a]	First Resonance Frequency	Mode Shape $\phi(x, y, z)$	Modal Density[b] $n(\omega)$	Auxiliary Formulas
Beam in compression	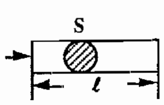	f–f c–c	$c_L/2l$	$\cos(n\pi x/l)$ $\sin(n\pi x/l)$	$l/\pi c_L$	$\kappa = \sqrt{I/S}$ radius of gyration
Beam in bending	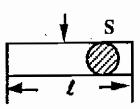	p–p f–f c–c c–f	$(\pi/2)(\kappa c_L/l^2)$ $(1/2\pi)(4.73/l)^2\kappa c_L$ $(1/2\pi)(4.73/l)^2\kappa c_L$ $(1/2\pi)(1.875/l)^2\kappa c_L$	$\sqrt{2}\ \sin(k_n X)$ See ref 19	$\dfrac{l}{2\pi}\dfrac{1}{\sqrt{\omega\kappa c_L}}$	$k_n = \sqrt{2\pi f_n/c_L\kappa}$ a/b = aspect ratio h = plate thickness, m
Rectangular plate in bending	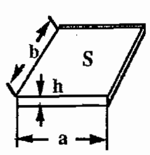	ffff ssss cccc	a/b: 1, 1.5, 2.5 3.33, 3.31, 2.13 C_1: 4.88, 5.28, 7.1 8.89, 10.0, 14.6 $f_1 = 10^3 C_1(h/S)(c_L/c_{L_{st}})$	See ref. 19	$\dfrac{\sqrt{12}S}{4\pi c_L h}$	S = area, m^2 $c_{L_{st}}$ = 5050 m/s c_L = longitudinal wave speed

(continued overleaf)

TABLE 11.7 (*continued*)

Element	Picture	Boundary Conditions[a]	First Resonance Frequency	Mode Shape $\phi(x, y, z)$	Modal Density[b] $n(\omega)$	Auxiliary Formulas
Membrane	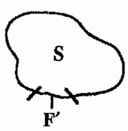		See ref. 18	See ref. 19	$\frac{S}{2\pi c_m}$	F' = tension per unit length; ρ_s = mass per unit area; $c_m = \sqrt{F'/\rho_s}$
String	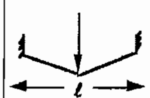	c–c	$\pi c_s/l$	$\sin(n\pi x/l)$	$l/\pi c_s$	$c_s = \sqrt{F'/\rho_l}$; F = tension force; ρ_l = mass per unit length
Rectangular air volume	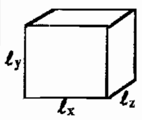	Hard walls	$c_0/2l_{max}$	$\cos\left(\frac{n_x\pi x}{l_x}\right)\cos\left(\frac{n_y\pi y}{l_y}\right)\cos\left(\frac{n_z\pi z}{l_z}\right)$ $n(\omega) = \frac{\omega^2 V}{2\pi^2 c_0^3} + \frac{S\omega}{4\pi c_0} + \frac{L}{16\pi c_0}$		$V = l_x l_y l_z$; c_0 = speed of sound; $n = 1, 2, 3, \ldots$

[a] f = free; s = simply supported; c = clamped; p = pinned

[b] $n(\omega) = n(f)/2\pi$, $S = 2(l_x ly + l_x l_z + l_y l_z)$, $L = 4(l_x + l_y + l_z)$.

Source: After reference 19.

TABLE 11.8 Radiation Efficiency of Vibrating Bodies

Body	Picture	σ_{rad}	Auxiliary Expressions
Small pulsating body	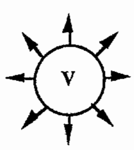	$\frac{(ka)^2}{1+(ka)^2}$	c_0 = speed of sound; $k_0 = 2\pi f/c_0$; a = source radius
Small oscillating rigid body	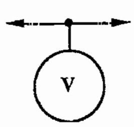	$\frac{(ka)^4}{4+(ka)^4}$, see Fig. 11.14	
Pulsating pipe	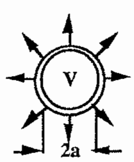	$2/\pi k_0 a \lvert H_1(k_0 a)\rvert^2$ for $(\pi/2)k_0 a \le 2/\pi$	H_1 = Hankel function, second kind, order 1; $k_0 = 2\pi f/c_0$
Oscillating pipe or rod	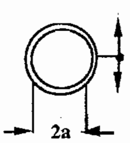	$2/\pi k_0 a \lvert H_1(k_0 a)\rvert^2$, see Fig. 11.15	H_1' = first derivative of H_1 in respect of its argument

(*continued overleaf*)

TABLE 11.8 (*continued*)

Body	Picture	σ_{rad}	Auxiliary Expressions
Circular pipes in bending	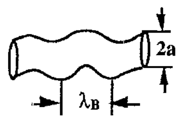	zero; $f < f_c$ $(k_0a)^3[1-(f_c/f)]$; $f > f_c; k_d a \ll 1$ 1; $f > f_c; k_0 a \gg 1.5$	$k_d^2 = k_0^2 - k_B^2$ $k_B = 2\pi/\lambda_B$ f_c = critical frequency where $k_B = k_0$
Rectangular and elliptic beams in bending	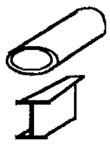	See ref. 22	
Infinite thin plate supporting free bending waves		0 for $f < f_c$ $1/[1-(f_c/f)]^{1/2}$ for $f > f_c$	
Finite thin plate supporting free bending waves; plate surrounded by rigid baffle	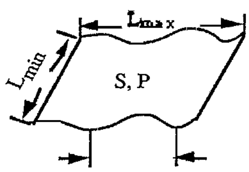	$\frac{Pc_0}{\pi S f_c}\sqrt{f/f_c}\,c_1$; $f < f_c$ $0.45(P/\lambda_c)^{1/2}(L_{min}/L_{max})^{1/4}$; $f = f_c$ $(1 - f_c/f)^{-1/2}$; $f > 1.3 f_c$ 1; $f \geq 1.3 f_c$	f_c = critical frequency. See Eq. 11.94 $\lambda_c = c_0/f_c$ $S = L_{max}L_{min}$ = area (one side) $P = 2(L_{max} + L_{min})$ = perimeter $\beta = (f/f_c)^{1/2}$

TABLE 11.8 (*continued*)

Body	Picture	σ_{rad}	Auxiliary Expressions
		$g_1(\beta) = \begin{cases} ((4/\pi^4)[(1-2\beta^2)/\beta(1-\beta^2)^{1/2}]) & ; f < 0.5 f_c \\ 0 & ; f > 0.5 f_c \end{cases}$ $g_2(\beta) = \left(\frac{1}{4\pi^2}\right)\frac{(1-\beta^2)\ln[(1+\beta)/(1-\beta)] + 2\beta}{(1-\beta^2)^{3/2}}$; $C_1 = \begin{cases} \text{1 for simple supported edges} \\ \beta^2 \exp(10\lambda_c/P) \text{ for clamped edges} \end{cases}$ $\sigma_{rad} = \frac{P}{S}\frac{c_0}{\pi^2}\sqrt{\frac{f}{f_c^3}}$	
Thick finite plate supporting free bending waves		$0.45\sqrt{P/\lambda_0}$ for $f \leq f_b$ 1 for $f \gg f_b$	$f_b = f_c + \frac{5c_0}{P}$ P = perimeter
Infinite plate sound-forced waves		$\sigma_F = 1/\cos\phi$	ϕ = incidence angle, degrees
Finite square-plate oblique-incidence plane sound wave excitation		$\sigma_F = \min\begin{cases} A[(k_o/2)\sqrt{S}] \\ 1/\cos\phi \end{cases}$ for $0.1\lambda_0^2 < S < 0.4\lambda_0^2$ $\sigma_F = \min\begin{cases} [(0.5)^{(\phi/90)}\sqrt{k_0/2\sqrt{S}}] \\ 1/\cos\phi \end{cases}$ for $S > 0.4\lambda_0^2$	$A = (0.5)(0.8)^{(\phi/90)}$ $\alpha = 1 - 0.34\phi/90$ $k_o = 2\pi/\lambda_0 = 2\pi f/c_0$
Finite square-plate diffuse-sound-field excitation		$\sigma_F = 0.5[0.2 + \ln(k_0\sqrt{S})]$ for $k_0\sqrt{S} > 1$	

Source: After references 1, 23, and 28.

Idaho Power/1206
Ellenbogen/268

TABLE 11.9 Reciprocity Relationships for Higher Order Excitation Sources and Responses

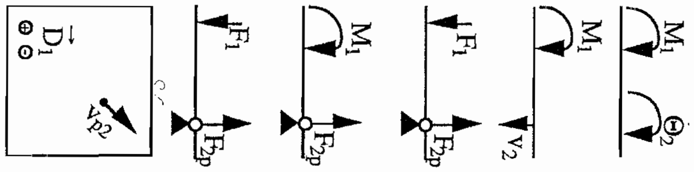

$$\frac{\dot{\Theta}_2}{M_1} = \frac{\dot{\Theta}_1}{M_2}$$

$$\frac{v_2}{M_1} = \frac{\dot{\Theta}_2}{F_2}$$

$$\frac{F_{2p}}{F_1} = \frac{F_{1p}}{F_2}$$

$$\frac{F_{2p}}{M_1} = \frac{\dot{\Theta}_1}{v_2}$$

$$\frac{F_{2p}}{F_1} = \frac{v_1}{v_2}$$

$$\frac{\vec{v}_{p2}}{D_1} = \frac{\vec{v}_{p1}}{D_2}$$

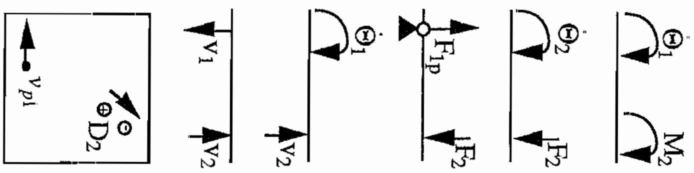

Note: M = moment, v = velocity, v_p = particle velocity, $\dot{\Theta}$ = angular velocity, F = force, F_p = force acting at pinned restraints, D = dipole sound source.
Source: After reference 63.

TABLE 11.10 USS Gauges and Weigthts of Steel Plates

	Steel USS Gauge Rev.				Galvanized Steel USS Gauge				Stainless Chrome Alloy USS Gauge				Stainless Chrome Nickel USS Gauge		Monel USS Gauge			
	Thickness		Surface Weight		Thickness		Surface Weight		Thickness		Surface Weight		Surface Weight		Thickness		Surface Weight	
Gauge	in.	mm	lb/ft^2	kg/m^2	in.	mm	lb/ft^2	kg/m^2	in.	mm	lb/ft^2	kg/m^2	lb/ft^2	kg/m^2	in.	mm	lb/ft^2	kg/m^2
32	0 01	0 254			0 013	0 330	0 563	2 75	0.01	0 254	0 418	2.04	0.427	2 08				
31	0.011	0.279			0.014	0 356	0 594	2.90	0.0109	0 277	0.45	2.20	0.459	2 24				
30	0.012	0.305	0.5	2.44	0.0157	0.399	0.656	3.20	0 0125	0.318	0.515	2.51	0.525	2.56				
29	0.0135	0.343	0 563	2.75	0.0172	0.437	0.719	3.51	0 014	0.356	0.579	2 83	0.591	2.89				
28	0 0149	0 378	0.625	3.05	0.187	4 750	0.781	3 81	0.0156	0 396	0.643	3.14	0.656	3 20				
27	0.0164	0 417	0.688	3.36	0 0202	0 513	0 844	4 12	0.0171	0.434	0.708	3.46	0 721	3.52				
26	0 0179	0 455	0.75	3.66	0.0217	0.551	0.906	4.42	0.0187	0.475	0.772	3 77	0.787	3.84	0 0187	0.475	0.827	4.04
25	0 0209	0.531	0.875	4 27	0.0247	0.627	1.031	5.03	0 0218	0.554	0.901	4 40	0.918	4.48	0.0218	0.554	0.965	4 71
24	0.0239	0.607	1	4.88	0.0276	0.701	1.156	5 64	0.025	0 635	1.03	5.03	1.05	5.13	0.025	0 635	1.148	5.60
23	0.0269	0.683	1.125	5.49	0.0306	0.777	1.281	6 25	0.0281	0.714	1 158	5.65	1 181	5.77	0.0281	0.714	1.1286	5 51
22	0.0299	0.759	1.25	6 10	0.0336	0 853	1.406	6.86	0 0312	0.792	1.287	6.28	1.312	6 41	0.0312	0.792	1 424	6 95
21	0 0329	0 836	1.375	6 71	0.0366	0 930	1.531	7.47	0.0343	0.871	1.416	6.91	1.443	7.04	0.0343	0.871	1.562	7.63
20	0.0359	0.912	1.5	7.32	0.0396	1.006	1.656	8.08	0.0375	0.953	1 545	7 54	1.575	7.69	0.0375	0.953	1.7	8 30
19	0.0418	1.062	1 75	8.54	0.0456	1 158	1.906	9.31	0.0437	1.110	1.802	8.80	1.837	8 97	0.0437	1.110	1 975	9.64
18	0.0478	1.214	2	9.76	0.0516	1.311	2.156	10.53	0 05	1.270	2.06	10.06	2.1	10.25	0.05	1 270	2.297	11.21
17	0 0538	1.367	2.25	10.98	0.0575	1.461	2.406	11.75	0 0562	1.427	2 317	11.31	2.362	11.53	0.0562	1.427	2.572	12.56

(*continued overleaf*)

TABLE 11.10 (*continued*)

	Steel USS Gauge Rev.				Galvanized Steel USS Gauge				Stainless Chrome Alloy USS Gauge				Stainless Chrome Nickel USS Gauge		Monel USS Gauge			
	Thickness		Surface Weight		Thickness		Surface Weight		Thickness		Surface Weight		Surface Weight		Thickness		Surface Weight	
Gauge	in.	mm	lb/ft^2	kg/m^2	in.	mm	lb/ft^2	kg/m^2	in.	mm	lb/ft^2	kg/m^2	lb/ft^2	kg/m^2	in.	mm	lb/ft^2	kg/m^2
16	0 0598	1 519	2.5	12 21	0.0635	1.613	2.656	12.97	0.0625	1.588	2 575	12.57	2.625	12.82	0 0625	1.588	2.848	13.90
15	0 0673	1 709	2.812	13.73	0.071	1.803	2.969	14.49	0.0703	1.786	2 896	14 14	2.953	14.42	0 0703	1 786	3 216	15.70
14	0.0747	1.897	3.125	15.26	0 0785	1.994	3 281	16.02	0 0781	1.984	3.218	15.71	3 281	16.02	0.0781	1.984	3.583	17 49
13	0.0897	2.278	3.75	18.31	0 0934	2.372	3.906	19.07	0.0937	2.380	3.862	18.85	3.937	19.22	0.0937	2 380	4.272	20.86
12	0.1046	2.657	4.375	21 36	0.1084	2 753	4.531	22 12	0.1093	2.776	4.506	22 00	4.593	22.42	0.1093	2 776	5.007	24.44
11	0 1196	3.038	5	24.41	0.1233	3.132	5.156	25 17	0.125	3.175	5 15	25 14	5.25	25.63	0.125	3.175	5.742	28.03
10	0.1345	3.416	5.625	27.46	0.1382	3.510	5 781	28.22	0 1406	3.571	5.793	28.28	5.906	28 83	0.1406	3.571	6 431	31.40
9	0.1497	3.802	6.25	30.51	0.1532	3.891	6.406	31.27	0.1562	3.967	6.437	31.43	6.562	32.04	0 1562	3.967	7 166	34.98
8	0 1644	4.176	6.875	33.56	0.1681	4.270	7.031	34 33	0 1718	4 364	7 081	34 57	7 218	35 24	0 1718	4 364	7 855	38.35
7	0.1793	4.554	7.5	36.62					0 1875	4.763	7.59	37.05	7.752	37.85	0.1875	4.763	8 59	41.94

TABLE 11.11 Percentage Open Area of Perforated Plates

Diameter Divided by Centers or side of square divided by centers D/C or S/C	Round Holes, Standard Staggered	Round Holes, Standard Staggered	Square Holes, Straight Or
.200	3.6	3.1	4.0
.225	4.6	4.0	5.1
.250	5.7	4.9	6.3
.275	6.9	5.9	7.6
.300	8.1	7.1	9.0
.325	9.6	8.3	10.6
.350	11.1	9.6	12.3
.375	12.8	11.0	14.1
.400	14.5	12.6	16.0
.425	16.4	14.2	18.1
.450	18.4	15.9	20.3
.475	20.5	17.7	22.6
.500	22.7	19.6	25.0
.525	25.0	21.6	27.6
.550	27.4	23.8	30.3
.575	30.0	26.0	33.1
.600	32.7	28.3	36.0
.625	35.4	30.7	39.1
.650	38.3	33.2	42.3
.675	41.3	35.8	45.6
.700	44.4	38.5	49.0
.725	47.7	41.3	52.6
.750	51.0	44.2	56.3
.775	54.4	47.2	60.0
.800	58.0	50.3	64.0
.825	61.7	53.5	68.0
.850	65.5	56.7	72.3
.875	69.5	60.1	76.6
.900	73.5	63.6	81.0
.925	77.6	67.2	85.6
.950	81.9	70.9	90.3

CHAPTER 12

Enclosures, Cabins, and Wrappings

ISTVÁN L. VÉR

Consultant in Acoustics, Noise, and Vibration Control
Stow, Massachusetts

This chapter deals with the acoustical design of enclosures, cabins, and wrappings. Acoustical enclosures are structures that house a noise source (usually a machine) for protection of the environment from the noise emitted by the source. Cabins are fully enveloping structures specifically designed for protecting a human being from environmental noise. The human being protected by the cabin may be the operator of a noisy machine, supervisor of a manufacturing operation, or attendant of a road toll booth. Wrappings are acoustical structures which closely envelop the casing of machines, valves, and connected piping to provide a high degree of noise reduction at high frequencies, practically no reduction at low frequencies, and modest reduction in the frequency range in-between.

The recently issued international standard ISO 15667:2000E,[1] entitled "Guidelines for Noise Control by Enclosures and Cabins," defines a large number of acoustical performance ratings and specifies the measurement procedure of how to obtain them in the laboratory or in situ. These performance measures, which include single-number and spectral and directivity information, are listed in Table 12.1 for enclosures and in Table 12.2 for cabins. For purposes of easy comparison, these tables retain the somewhat cumbersome nomenclature used in the standard.

The technical content of ISO 15667:2000E is based, to a large extent, on the content of Chapter 13 of the 1992 edition of this book[2] and, consequently, the reader will find much of the information in this chapter. The standard contains excellent suggestions about the collection of input information, planning, and performance verification of acoustical enclosures and cabins.

Annex A provides a large number of sketches depicting (1) details for joining wall panels, (2) mounting the enclosure airtight to the floor, (3) seals around doors and observation windows, (4) vibration isolation of the enclosed machines, (5) pipe and shaft penetrations, (6) ventilation possibilities, and so on. Though the information contained in these sketches is useful, the author cautions the purchaser of acoustical enclosures to contract with an experienced provider of noise control hardware who has similar proven details and the necessary experience to

TABLE 12.1 Acoustical Performance Measures of Enclosures

Sound Power Insulation[a] D_W	Weighted Sound Power Insulation[b] D_{WW}	Sound Pressure Insulation[c] D_P	A-Weighted Sound Pressure Insulation[d] D_{PA}
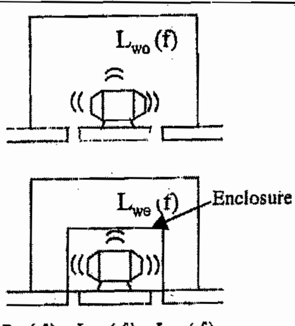 $D_w(f) \equiv L_{wo}(f) - L_{we}(f)$	$D_{WW}(f)$ is obtained from $D_W(f)$ according to ISO 717-1, resulting in a single-number value	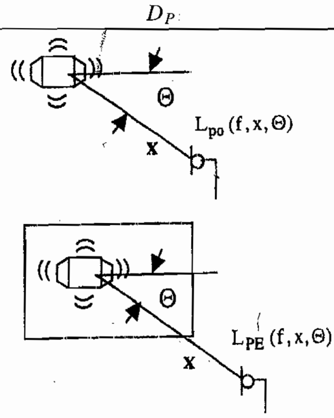	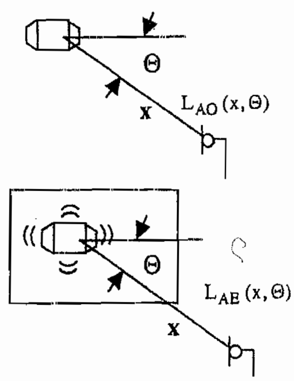
L_{w0} = Sound power level of unenclosed source L_{we} = Sound power level of enclosed source according to ISO 11546-1 or ISO 110546-2 $D_w(f) = R(f) + 10 \log[\alpha(f)]$ $R(f)$ = sound transmission loss of enclosure wall according to ISO 140-3 $\alpha(f)$ = average absorption coefficient of internal side of enclosure panels		$D_p(f, x, \theta) = L_{\text{po}}(f, x, \theta) - L_{\text{pe}}(f, x, \theta)$ $L_{po}(f, x, \theta)$ = sound-pressure-level spectrum of unenclosed source at distance x, direction θ $L_{pe}(f, x, \theta)$ = sound-pressure-level spectrum of enclosed source at distance x, direction θ	$D_{PA}(X, \theta) = L_{\text{AO}}(X, \theta) - L_{\text{AE}}(X, \theta)$ L_{AO} = dBA for unenclosed source L_{AE} = dBA for enclosed source

[a]Contains no information about directivity. Limited usefulness if (1) source is highly directional and (2) source is much nearer to one wall than to others.
[b]Used for rough comparison of different enclosures in cases where source spectrum is not known
[c]Best suited for detailed analyses of enclosure performance for different directions.
[d]Single-number rating for particular machine of known sound power spectrum.
Note: According ISO 15667:2000.

Idaho Power/1206
Ellenbogen/273

TABLE 12.2 Acoustical Performance Measures of Cabins

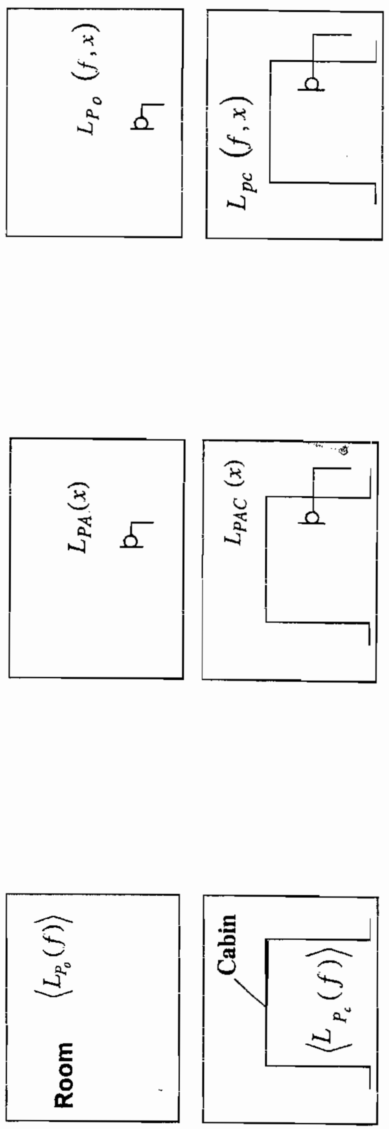

Sound Pressure Insulation[a] D_P	A-Weighted Sound Pressure Insulation[b] D_{PA}	Apparent Sound Pressure Insulation[c] D'_P
$D_P \equiv \langle L_{p_o}(f)\rangle - \langle L_{p_c}(f)\rangle$	$D_{PA} \equiv L_{PA}(x) - L_{PAC}(x)$	$D'_P \equiv L_{p_o}(f,x) - L_{pc}(f,x)$
$\langle L_{p_o}(f)\rangle$ = space-average sound pressure level in a room with semi diffuse sound field	$L_{PA}(x)$ = A-weighted sound pressure level in room at position x, without cabin	$L_{p_o}(f,x)$ = sound pressure level at frequency f in position x, arbitrary sound field distribution
$\langle L_{p_c}(f)\rangle$ = space-average sound pressure level inside the cabin	$L_{PAC}(x)$ = A-weighted sound pressure level in cabin at the same position x	$L_{pc}(f,x)$ = Sound pressure level at frequency f in position x inside cabin

[a] $\langle L_{p_o}(f)\rangle$ assumed to be semidiffuse field
[b] $L_{PA}(x)$ is the actual A-weighted level in the Room.
[c] L_{po} is produced by an arbitrary sound pressure distribution
Note: According ISO 15667:2000

integrate them into the total design and successfully install them onsite. Giving the construction details included in Annex A to a local sheet metal shop without prior experience in producing noise control hardware may result in a low bid but it is very likely that the end result will be disappointing.

In Annex B the standard provides informative case studies where the non-expert reader can find typical ranges of acoustical performance of functional enclosures and cabins which have operable doors, inlet and discharge openings for ventilation, and so on.

The key difference between enclosures and wrapping is that in the case of enclosures, the sound-absorbing layer is not in contact with the surface of the vibrating equipment, while in the case of wrappings, the porous sound-absorbing layer is in full surface contact with the vibrating body it surrounds. Because the porous sound-absorbing material of wrappings provides a full-surface, structure-borne connection between the vibrating equipment and the exterior layer, it must not only be a good sound absorber but also be highly resilient so as to prevent the transmission of vibration to the outer impervious layer where it can be radiated as sound. Sound-absorbing materials used in enclosures, where there is no contact between the porous material and the vibrating equipment, can have a fairly rigid skeleton. Wrappings are most frequently used to decrease the sound radiation of vibrating surfaces such as ducts and pipes and sometimes also to gain extra sound attenuation of acoustical enclosures. Since fibrous sound-absorbing materials, such as glass fiber and mineral wool, are good heat insulators, properly designed wrappings can provide both substantial acoustical and heat insulation. On the other hand, the heat-insulating properties of the enclosure may be detrimental and require that provision be made for auxiliary cooling of the interior of the enclosure to prevent the buildup of excessively high temperatures. Only the acoustical design aspects of enclosures and wrappings are treated in this chapter.

12.1 ACOUSTICAL ENCLOSURES

Depending on their size (compared with the acoustical and bending wavelength) acoustical enclosures can be termed either small or large. The enclosure is considered small* if both the bending wavelength is large compared with the largest wall panel dimensions and the acoustical wavelength is large compared with the largest interior dimension of the enclosure volume. In small acoustical enclosures, the interior volume has no acoustical resonances. If the largest dimension of the acoustical volume is $L_{\max} \leq \frac{1}{10}\lambda$, the sound pressure is evenly distributed within the volume. The enclosure is considered large if all of its interior dimensions are large compared with the acoustical wavelength and there are a large number of acoustical resonances in the interior volume in the frequency range of interest. Accordingly, even enclosures with large physical dimensions are acoustically small at very low frequencies while enclosures of small physical size are acoustically large at very high frequencies. In almost all acoustical enclosures the

*Small enclosures are also treated in Chapter 6.

enclosure walls already exhibit numerous structural resonances in the frequency range where the first acoustical resonance occurs.

If the enclosure has no mechanical connections to the enclosed equipment, it is termed *free standing*. If there are mechanical connections, then the enclosure is *equipment mounted*. Enclosures that very closely surround the enclosed equipment and the volume of the machine is comparable to the volume of the enclosure are called *close fitting*. Enclosures without acoustically significant openings are referred to as *sealed enclosures*, and those with significant acoustical leaks (intentional or unintentional) as *leaky* acoustical enclosures. Figure 12.1 shows various configurations of sealed acoustical enclosures. This chapter deals with the acoustical design of enclosures. Nonacoustical aspects—such as ventilation, safety, and economy—are treated in a handbook by Miller and Montone (see Bibliography). Construction details and advice for writing purchase specifications are given in a VDI guideline (also see Bibliography).

Insertion Loss as Acoustical Performance Measure

The insertion loss is the most appropriate descriptor for the acoustical performance of enclosures of all types. The operational definition of the insertion loss (IL) of an acoustical enclosure is illustrated in Fig. 12.2. For noise sources that will be positioned indoors, such as machinery in factory spaces, the sound-power-based insertion loss of the enclosure as indicated in Fig. 12.2*a* is the most meaningful. It is defined as

$$\mathrm{IL}_w = 10 \log \left(\frac{W_0}{W_E} \right) = L_{w0} - L_{WE} \quad \mathrm{dB} \tag{12.1}$$

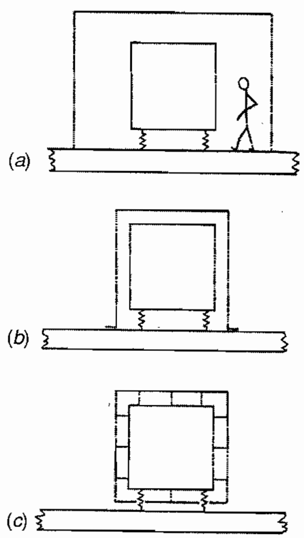

FIGURE 12.1 Enclosure types: (*a*) free standing, large; (*b*) free standing, close fitting; (*c*) equipment mounted, close fitting.

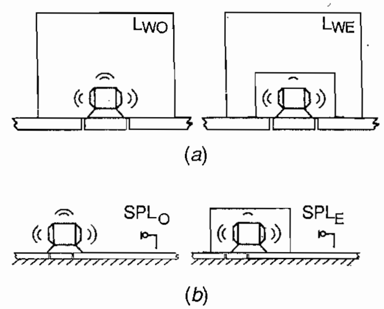

FIGURE 12.2 Operational definition of enclosure insertion loss IL: (*a*) power based; $\mathrm{IL}_w \equiv L_{w0} - L_{WE}$, (*b*) sound pressure based; $\mathrm{IL}_P \equiv \mathrm{SPL}_O - \mathrm{SPL}_E$.

where W_0 is the sound power radiated by the unenclosed source and L_{W0} the corresponding sound power level and W_E is the sound power radiated by the enclosed source and L_{WE} the corresponding sound power level. Both W_0 and W_E are measured in a reverberation room (see Chapter 4) or with the aid of a sound intensity meter.

For enclosures used with equipment deployed outdoors, a less precise but more easily implemented definition of insertion loss, the so-called pressure-based insertion loss, or IL_p, illustrated in Fig. 12.2*b* is most appropriate. It is defined as

$$\mathrm{IL}_p = \mathrm{SPL}_O - \mathrm{SPL}_E \quad \mathrm{dB} \tag{12.2}$$

where SPL_O is the average sound pressure level measured at a number of locations around the source without the enclosure and SPL_E is that measured with the source surrounded by the enclosure. The measurement positions may be chosen on a circle that is centered at the source location. The measurement distance should be at least three times the longest dimension of the enclosure. Equations (12.1) and (12.2) represent definitions readily implemented in the field or laboratory. Using these definitions one can readily determine whether a specific enclosure will or will not meet specific performance requirements stated in the form of a sound-power-level reduction, a sound-pressure-level reduction for a specified distance, or a sound-pressure-level reduction at a specified distance and direction. If the laboratory facilities are available, the sound-pressure-based insertion loss may also be measured in a large hemianechoic chamber.

Note that if the radiation patterns of both the unenclosed and enclosed source is omnidirectional, the two measures yield the same result ($\mathrm{IL}_w = \mathrm{IL}_p$).

Qualitative Description of Acoustical Performance

Figure 12.3 shows the typical shape of a curve of the acoustical insertion loss versus frequency of a free-standing, sealed acoustical enclosure. Region I is the small-enclosure region where neither the interior air volume nor the enclosure

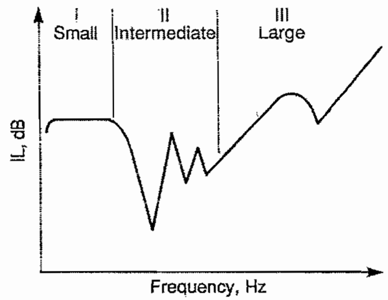

FIGURE 12.3 Typical curve of insertion loss versus frequency of a sealed, free-standing acoustical enclosure. Region I: panel stiffness controlled; damping and interior absorption are ineffective. Region II: resonance controlled; damping and interior absorption are effective. Region III: controlled by sound transmission loss; sound transmission loss and interior absorption are effective; usually limited by leaks.

wall panels exhibit any resonances. In this frequency region the insertion loss is frequency independent and is controlled by the ratio of the volume compliance (inverse of volume stiffness) of the enclosure walls and that of the enclosed air volume.

Region II in Fig. 12.3 is the intermediate region where the insertion loss is controlled by the resonant interaction of the enclosure structure with the enclosed acoustical volume. The region is characterized by a number of alternating maxima and minima in the insertion loss. Typically, the first and most important minima in the insertion loss occurs when the combined volume compliance of the interior air volume and the volume compliance of the wall panels matches the mass compliance of the wall panels. The insertion loss at this resonance frequency usually controls the low-frequency insertion loss of the enclosure and in some instances can become negative, signifying that the equipment with the enclosure may radiate more noise than without the enclosure. Additional minima of the insertion loss occur at acoustical resonances of the enclosure volume. Further minima in insertion loss occur when the frequencies of structural resonances of a wall panel and the frequencies of acoustical resonances of the enclosure volume coincide. It is imperative that enclosures designed for sound sources that radiate noise of predominantly tonal character (such as transformers, gears, reciprocating compressors and engines, etc.) should have no structural or acoustical resonances that correspond to the frequencies of the predominant components of the source noise.

Region III in Fig. 12.3 is the large-enclosure region where both the enclosure wall panels and the interior air volume exhibit a very large number of acoustical resonances. Here, statistical methods of room acoustics can be used to predict the sound field inside the enclosure (see Chapter 7) and the sound transmission through the enclosure walls (see Chapter 11). In this frequency region, the insertion loss is controlled by the interior sound absorption and by the sound

transmission loss (R) of the enclosure wall panels. The dip in the curve of insertion loss versus frequency in region III corresponds to the coincidence frequency of the wall panel (see Chapter 11), which for the most frequently used wall panels (1–2 mm steel or aluminum) falls above the frequency region of interest. The coincidence frequency may fall into the region of interest if the ratio of stiffness of the panel to its mass per unit area is high (e.g., a honeycomb panel).

The prediction of the insertion loss of small and large acoustical enclosures is treated in the following sections. Performance prediction in the intermediate frequency region requires a detailed finite-element analysis of the coupled mechanical acoustical system such as outlined in Chapter 6.

Small Sealed Acoustical Enclosures

For a small, sealed acoustical enclosure, where the sound pressure inside the cavity is evenly distributed, the insertion loss is given by[4–5]

$$\mathrm{IL_{SM}} = 20 \log \left(1 + \frac{C_v}{\sum_{i=1}^{n} C_{wi}}\right) \quad \text{dB} \tag{12.3}$$

where

$$C_v = \frac{V_0}{\rho c^2} \quad \mathrm{m^5/N} \tag{12.4}$$

is the compliance of the gas volume inside the enclosure, V_0 is the volume of the gas in the enclosure volume, ρ is the density of the gas, c is the speed of sound of the gas, and C_{wi} is the *volume compliance* of the ith enclosure wall plate defined as

$$C_{wi} = \frac{\Delta V_{pi}}{p} \quad \mathrm{m^5/N} \tag{12.5}$$

where ΔV_{pi} is the volume displacement of the ith enclosure wall plate in response to the uniform pressure p. It is assumed here that the enclosure is rectangular and is made of n separate, homogeneous, isotropic plates, each with its own volume compliance.

At frequencies below the first mechanical resonance of the isotropic enclosure wall panel, the volume compliance of a homogeneous, isotropic panel C_{pi} is given by[3]

$$C_{wi} = \frac{10^{-3} A_{wi}^3 F(\alpha)}{B_i} \quad \mathrm{m^5/N} \tag{12.6}$$

where A_{wi} is the surface area of the ith wall panel and $F(\alpha)$ is given in Fig. 12.4 as a function of the aspect ratio $\alpha = a/b$ of the panel, where a is the longest and b is the smallest edge dimension of the wall panel. For homogeneous, isotropic wall panels, the bending stiffness per unit length of the panel is

$$B = \frac{Eh^3}{12(1-\nu^2)} \quad \mathrm{N \cdot m} \tag{12.7}$$

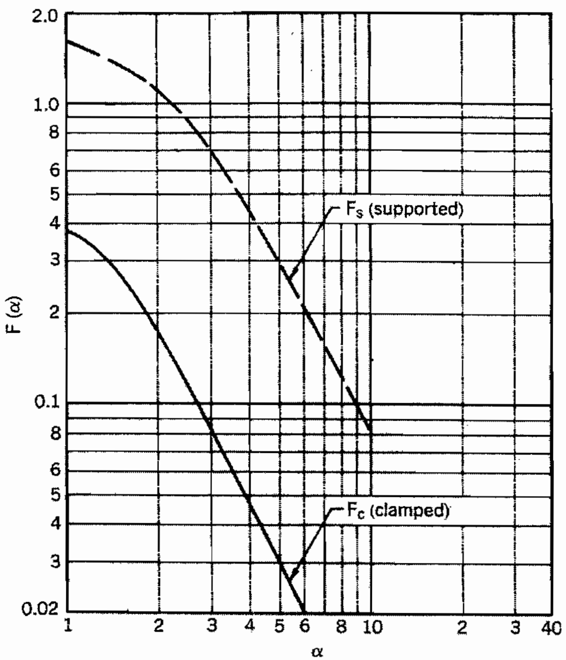

FIGURE 12.4 Plate volume compliance function $F(\alpha)$ plotted versus the aspect ratio $\alpha = a/b$ for homogeneous isotropic panels either with clamped or simply supported edges. (After Ref. 3).

where E is Young's modulus and h is the thickness and ν the Poisson ratio of the wall panel. For a rectangular enclosure combining Eqs. (12.3)–(12.7) yields

$$\mathrm{IL_{SM}} = 20\log\left[1 + \frac{V_0 E h^3}{12\times 10^{-3}(1-\nu^2)\rho c^2}\sum_{i=1}^{6}\frac{1}{A_{wi}^3 F(\alpha_i)}\right]\ \mathrm{dB} \qquad (12.8)$$

For the special case of a cubical enclosure with clamped walls of edge length a Eq. (12.8) yields

$$\mathrm{IL}_s = 20\log\left[1 + 41\left(\frac{h}{a}\right)^3\frac{E}{\rho c^2}\right]\ \mathrm{dB} \qquad (12.9)$$

Equation (12.8) indicates that high insertion loss is achieved if the enclosure has small edge length, high aspect ratio, and large wall thickness, edge conditions are clamped, and the panels are made of a material of high Young's modulus. In short, for an enclosure with high insertion loss at low frequencies, the wall must be made as stiff as possible. According to Eq. (12.9), the low-frequency insertion

loss of a cubical steel enclosure of edge length $a = 300$ mm, $E = 2\times10^{11}$ N/m^2, $\rho = 1.2$ kg/m^3, and $c = 340$ m/s is for two different wall thicknesses h:

	Clamped		Simply Supported	
Wall Thickness h	IL_s	f_0	IL_s	f_0
3 mm	35.5 dB	296 Hz	24 dB	162 Hz
1.5 mm	18.5 dB	148 Hz	9 dB	81 Hz

Here f_0 is the resonance frequency of each of the identical homogeneous isotropic clamped panels. The insertion loss values listed in the table above are valid only at frequencies well below f_0. Note in the table that much higher insertion loss is achieved with a clamped-edge condition than with simply supported edge conditions. In practice, clamped edges are almost impossible to achieve. Consequently, one should use the simply supported edge condition in the initial design to ensure that the designed performance will be achieved.

It is of considerable practical interest to know which material should be used for a small sealed cubical enclosure to yield the highest insertion loss at low frequencies for the same enclosure volume and same total weight. Considering that the total mass M of a cubical enclosure of edge length a is $M = 6\rho_M a^2 h$, Eq. (12.9) can be expressed as

$$\mathrm{IL}_s = 20\log\left[1 + 0.19\frac{M^3}{a^9\rho c^2}\left(\frac{c_L}{\rho_M}\right)^2\right]\ \mathrm{dB} \qquad (12.10)$$

where $c_L = \sqrt{(E/\rho_M)}$ is the speed of longitudinal waves in the bulk enclosure material and ρ_M is the density of the enclosure material. Equation (12.10) indicates that for all materials giving the same enclosure mass M, the material with the highest c_L/ρ_M ratio yields the highest insertion loss. Table 12.3 lists the c_L/ρ_M ratio and the normalized low-frequency insertion loss $\Delta\mathrm{IL}$ for frequently used materials, where $\Delta\mathrm{IL}$ is defined as the low-frequency insertion loss of an enclosure made out of a specific material minus the insertion loss of an enclosure of the same volume and weight built of steel. Table 12.3 indicates that, in regard to low-frequency insertion loss, aluminum and glass are superior to steel and lead is the worst possible choice! Note, however, that this conclusion can be exactly opposite for a large enclosure if the coincidence frequency falls within the frequency range of interest.

Formstiff Small Enclosures. Because the insertion loss of small, sealed enclosures at very low frequencies ($L_{\max} < \frac{1}{10}\lambda$) is controlled by the volume compliance of the enclosure walls, it is desirable to select constructions that provide the highest wall stiffness for the allowable enclosure weight. An enclosure consisting of a round, cylindrical body and two half-spherical end caps yields a very

TABLE 12.3 Difference in Low-Frequency Insertion Loss ΔIL and c_L/ρ_M Ratio for Different Construction Materials[a]

	Lead	Steel	Concrete	Plexiglass	Aluminum	Glass
c_L/ρ_M, m^4/kg·s	0.11	0.65	1.5	1.6	1.9	2.1
ΔIL, dB	−31	0	+14	+15	+19	+20

[a] ΔIL is for a cubical enclosure with identical sides.

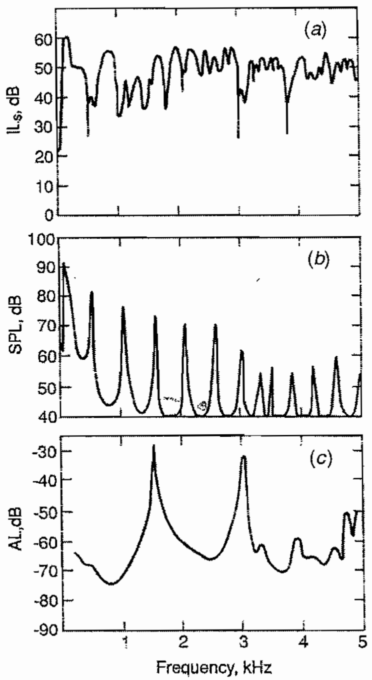

FIGURE 12.5 Acoustical characteristics of a small, sealed, round cylindrical enclosure without interior absorption: (*a*) insertion loss IL; (*b*) resonant acoustical response of interior volume, SPL; (*c*) sound-induced vibration acceleration response of enclosure wall, AL.

stiff construction and much higher insertion loss than a rectangular enclosure of the same volume and weight. Figure 12.5 shows the acoustical characteristics of such a particular small, cylindrical enclosure with no internal sound-absorbing treatment. Curve *A* represents insertion loss versus frequency measured with an external source, indicating that insertion loss at most frequencies exceeds 55 dB. Curve *B* represents the sound pressure levels in the enclosed air volume when excited with an external source, indicating the presence of strong acoustical resonances at 550 Hz and above. Curve *C* represents the sound-induced vibration

acceleration of the cylindrical shell caused by an external sound source. Strong structural resonances are seen at 1.5, 3, and 3.75 kHz. Observing the three curves in Fig. 12.5, it is noted that the frequencies where the insertion loss is minimum coincide either with acoustical resonances of the interior volume or with structural resonances of the enclosure shell. The strong minima of the curve of insertion loss versus frequency in the vicinity of 1.5, 3, and 3.75 kHz are caused by coincidence of the structural resonance of the shell with acoustical resonances of the interior air volume.

Another way to achieve a low wall compliance for a given total weight is to make the enclosure walls out of a composite material consisting of a honeycomb core sandwiched between two lightweight plates. A special form of such high-stiffness, low-weight panel, described by Fuchs, Ackermann, and Frommhold,[6] also provides high sound absorption at low frequencies in addition to the low volume compliance. In this case, the panel on its interior side has two double membranes. The first, thicker membrane, which is rigidly bonded to the honeycomb core, has round openings to make an inward-facing Helmholtz resonator out of each honeycomb cavity. A second, thin, membrane that is covering the first one is free to move over the resonator openings. The presence of this second, thin membrane lowers the resonance frequency of the Helmholtz resonators owing to the mass of the membrane covering the opening and increases the dissipation owing to air pumping. Such Helmholtz plates can be constructed from stainless steel, aluminum, or light-transparent plastic. They are fully sealed and can be hosed down for cleaning. Figure 12.6 shows the curve of insertion loss versus frequency of a cubical enclosure of 1 m edge length. The solid curve was obtained with enclosure walls made of the above-described Helmholtz plates of

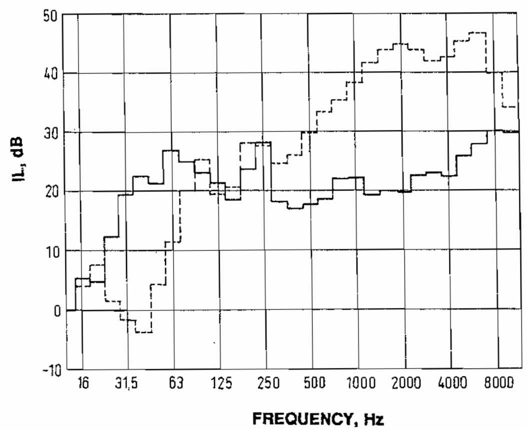

FIGURE 12.6 Measured insertion loss of two 1 × 1 × 1-m enclosures. (After Ref. 6.) Solid curve: Helmholtz plate walls, 10 cm thick, 8.5 kg/m^2, no sound-absorbing treatment. Dashed curve: Woodchip board walls, 1.3 cm thick, 5-cm-thick sounding-absorbing layer, 10 kg/m^2.

10 cm thickness with a mass per unit area of 8.5 kg/m^2 without any additional sound-absorbing lining. The dotted curve was obtained with an enclosure of the same size, made of 1.3-cm-thick wood chip board with 5-cm sound-absorbing lining, yielding a mass per unit area of 10 kg/m^2. The Helmholtz plate enclosure yields superior low-frequency performance and does not require extra sound-absorbing lining. However, the insertion loss of this enclosure at midfrequencies (above 250 Hz) is low because of the low coincidence frequency of the light and stiff panels.

Small Leaky Enclosures. Except for special constructions, such as hermetically sealed compressors, all enclosures are likely to be leaky and provide zero insertion loss as the frequency approaches zero. If an enclosure has a leak in the form of a round opening of radius a_L in a wall of thickness h, the leak represents a compliance $C_L = 1/j\omega Z_L$, where Z_L is the acoustical impedance of the leak given as

$$C_L = \frac{(\pi a_L^2)^2}{-\omega^2 \rho (h + \Delta h)\pi a_L^2 + j\omega R} \quad \text{m}^5/\text{N} \qquad (12.11)$$

where h is the plate thickness, $\Delta h \simeq 1.2 a_L$ represents the end correction, and R is the real part of the impedance of the leak. The sound pressure inside the small, leaky enclosure owing to the operation of a source of volume velocity q_0 is

$$p_{\text{ins}}^{\text{leaky}} = \frac{q_0}{j\omega} \frac{1}{C_L + C_v + \sum_i C_{wi}} \quad \text{N/m}^2 \qquad (12.12)$$

and the insertion loss of the small leaky enclosure is

$$\text{IL}_{\text{leaky}} = \text{IL}_L = 20 \log \frac{C_L + C_v + \sum_i C_{wi}}{C_L + \sum_i C_{wi}} \quad \text{dB} \qquad (12.13)$$

where C_v and C_{wi} are given in Eqs. (12.4) and (12.5), respectively. Since C_L approaches infinity as the frequency approaches zero, the insertion loss of leaky enclosures approaches zero for any form of leak. The insertion loss becomes negative in the vicinity of the Helmholtz resonance frequency of the compliant leaky enclosure given by

$$f_{0L} = \frac{a_L c}{2} \sqrt{\frac{1}{\pi (h + \Delta h)\left(V_0 + \rho c \sum_i C_{wi}\right)}} \quad \text{Hz} \qquad (12.14)$$

As $C_L/\Sigma C_{wi}$ becomes small with increasing frequency, the insertion loss of the small, leaky enclosure, IL_L, approaches that of the sealed enclosure, IL_s. This behavior is illustrated in Fig. 12.7.

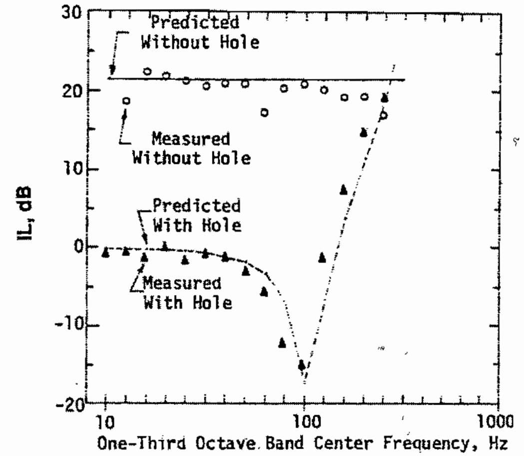

FIGURE 12.7 Measured and predicted sound-pressure-based insertion loss (outside–inside direction) of a 50 × 150 × 300-mm aluminum enclosure of 1.5-mm-thick wall with a single 9.4-mm-diameter hole (after Ref. 5): (——) predicted, sealed; (- - - -) predicted, leaky; (○) measured, sealed; (▲) measured, leaky.

Close-Fitting, Sealed Acoustical Enclosures

A close-fitting acoustical enclosure is one in which a considerable portion of the enclosed volume is occupied by the equipment being quieted. Such enclosures are used in cases where the radiated noise must be reduced using a minimum of added volume. Vehicle engine enclosures, portable compressors, and transportable transformers fall into this category.

Free-standing, close-fitting enclosures, such as shown in Fig. 12.1*b*, have no mechanical connections to the vibrating source and the enclosure walls are excited to vibration only by the airborne path. Conversely, the walls of machine-mounted, close-fitting enclosures, such as depicted in Fig. 12.1*c*, are excited by both airborne and structure-borne paths.

The characteristic property of a close-fitting enclosure is that the air gap (the perpendicular distance between the vibrating surface of the machine and the enclosure wall) is small compared with the acoustical wavelength in most of the frequency range. The walls of the close-fitting enclosures are usually made of thin, flat sheet metal with a layer of sound-absorbing material such as glass fiber or acoustical foam on the interior face. The purpose of the sound-absorbing lining is to damp out the acoustical resonances in the air space.

Free-Standing, Close-Fitting Acoustical Enclosures. Free-standing, close-fitting enclosures, which have no structure-borne connection to the vibrating equipment, always achieve higher insertion loss than a similar machine-mounted enclosure can provide. If the enclosure is perfectly sealed, then its insertion loss depends on (1) thickness, size, and material of the enclosure wall; (2) edge-joining conditions of the wall plates and their loss factors; (3) vibration pattern of the machine surface; (4) average thickness of the air gap between the wall and the machine; and (5) type of sound-absorbing material in the air gap.

Figure 12.8 shows the measured dependence of the power-based insertion loss of a model close-fitting enclosure consisting of 0.6×0.4-m enclosure walls of thickness h and a variable spacing gap of thickness T. To obtain these data, an array of loudspeakers, which represented the vibrating surface of the enclosed machine, was phased to simulate various vibration patterns.[8] Figure 12.8a shows

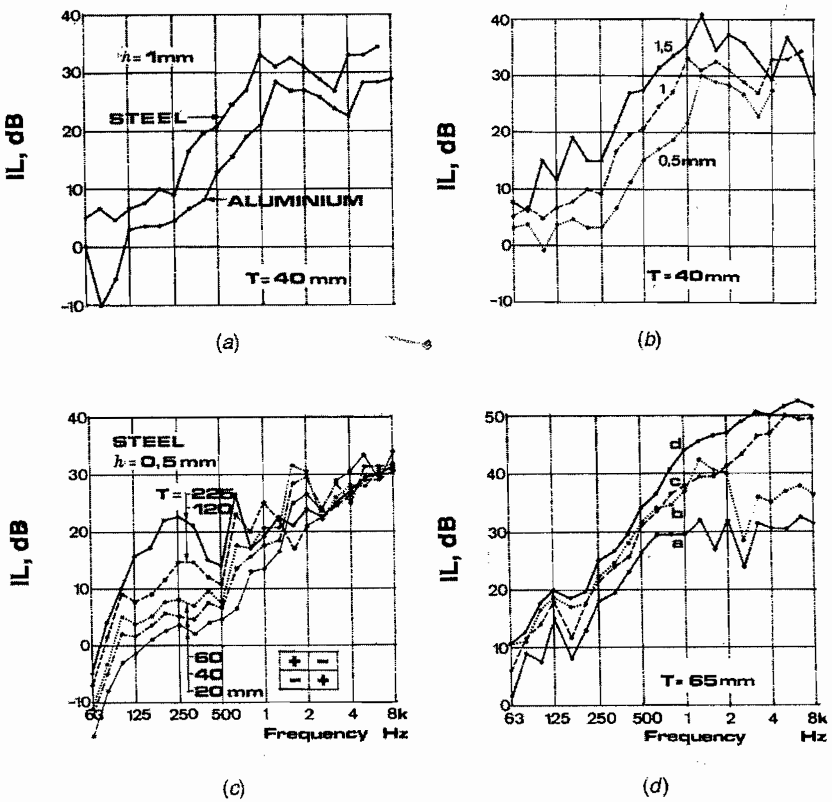

FIGURE 12.8 Effect of key parameters on the power-based insertion loss of a model close-fitting enclosure. Wall panel 0.6×0.4. (After Ref. 8.) (a) Effect of the wall material; 4-cm air gap, in-phase excitation. (b) Effect of wall panel thickness, 4-cm air gap, in-phase excitation. (c) Effect of average air gap thickness; 0.5-mm steel plate, quadrupole excitation. (d) Effect of sound-absorbing material and structural damping; 1-mm steel plate, 6.5-cm air gap, in-phase excitation; a, no damping, no absorption in air space; b, with damping treatment; c, no damping, but absorption in air space; d, with damping and absorption.

the dependence of the measured insertion loss on frequency obtained for 1-mm-thick aluminum and steel wall plates, respectively. Because the steel and aluminum plates have practically the same dynamic behavior, the higher insertion loss of the steel wall panel is attributable to its higher mass. In the frequency range between 300 Hz and 1 kHz, the 9-dB average difference corresponds to the difference in density of the two materials. Figure 12.8b shows the effect of wall thickness. Here again the insertion loss increases with increasing wall thickness. Below 250 Hz, where the insertion loss is controlled by the stiffness of the air and the stiffness and damping of the wall panels, the IL_w changes little with increasing frequency. In the frequency range between 200 Hz and 1 kHz, where the IL_w is controlled by the volume stiffness of the air and by the mass per unit area of the wall, the IL_w increases with a slope of 40 dB/decade. Above 1 kHz, the insertion loss is limited by the acoustical resonances in the air space. Figure 12.8c shows that the insertion loss increases with increasing air gap thickness. Figure 12.8d shows the effect of sound-absorbing material in the air space and damping treatment of the enclosure wall on the achieved insertion loss. The sound-absorbing treatment in the air space prevents the acoustical resonances in the air space and results in a substantial increase of the insertion loss above 1 kHz. Structural damping helps to reduce the deleterious effect of the efficiently radiating plate resonance at 160 Hz. A combination of sound-absorbing treatment and structural damping results in a smooth, steeply increasing insertion loss with increasing frequency and provides a very high degree of acoustical performance.

One-Dimensional Model. According to Bryne, Fischer, and Fuchs,[9] the insertion loss of free-standing, sealed, close-fitting acoustical enclosures can be predicted with reasonable accuracy with the simple one-dimensional model shown in Fig. 12.9. It is assumed that the machine wall (A) vibrates in phase (like a rigid piston) with velocity v_M and that the motion of the machine is not affected by the presence of the enclosure. The vibrating machine is surrounded by a

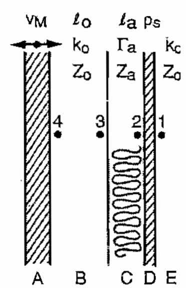

FIGURE 12.9 One-dimensional model for predicting the power-based insertion loss IL of free-standing, sealed close-fitting acoustical enclosures; A machine wall vibrating with velocity v_M; B, air gap thickness l_0; C, sound-absorbing layer thickness l_a; D, impervious enclosure wall of mass per unit area ρ_s; E, free space into which sound is radiated. (After Ref. 9).

flat, limp, impervious enclosure wall (D) which has an internal sound-absorbing lining (C) of thickness l_a and there is an air gap (B) of thickness l_0 between the machine and the sound-absorbing layer. The sound pressure on the outside surface of the enclosure (point 1 in Fig. 12.9) is given by

$$p_1 = p_2\left(1 - \frac{j\omega\rho_s}{Z_0}\right) \quad \text{N/m}^2 \tag{12.15}$$

where $Z_0 = \rho c$ is the characteristic impedance of air. The following equations are used to obtain p_1 as a function of the machine wall vibration velocity v_M:

$$p_3 = 0.5p_2\left[\left(1+\frac{Z_a}{Z_3}\right)e^{-j\Gamma_a l_a} + \left(1-\frac{Z_a}{Z_3}\right)e^{j\Gamma_a l_a}\right] \quad \text{N/m}^2 \tag{12.16}$$

$$p_4 = v_M Z_4 = 0.5p_3\left[\left(1+\frac{Z_0}{Z_4}\right)e^{-jk_0 l_0} + \left(1-\frac{Z_0}{Z_4}\right)e^{jk_0 l_0}\right] \quad \text{N/m}^2 \tag{12.17}$$

$$Z_2 = Z_0 + j\omega\rho_s \quad \text{N}\cdot\text{s/m}^3 \tag{12.18}$$

$$Z_3 = Z_a\frac{(1+Z_a/Z_2)e^{j\Gamma_a l_a} + (1-Z_a/Z_2)e^{-j\Gamma_a l_a}}{(1+Z_a/Z_2)e^{j\Gamma_a l_a} - (1-Z_a/Z_2)e^{-j\Gamma_a l_a}} \quad \text{N}\cdot\text{s/m}^3 \tag{12.19}$$

$$Z_4 = Z_0\frac{(1+Z_0/Z_3)e^{jk_0 l_0} + (1-Z_0/Z_3)e^{-jk_0 l_0}}{(1+Z_0/Z_3)e^{jk_0 l_0} - (1-Z_0/Z_3)e^{-jk_0 l_0}} \quad \text{N}\cdot\text{s/m}^3 \tag{12.20}$$

where $k_0 = 2\pi f/c$ is the wavenumber, ρ the density, and c the speed of sound in air; Z_a is the complex characteristic impedance and Γ_a the complex propagation constant of the porous sound-absorbing material as given in Chapter 8.

The sound power radiated by the unenclosed machine wall is given by

$$W_0 = v_M^2\rho c A \quad \text{W} \tag{12.21a}$$

and when it is enclosed with a free-standing, close-fitting enclosure

$$W_A = \frac{p_1^2}{\rho c}A \quad \text{W} \tag{12.21b}$$

yielding for the insertion loss

$$\text{IL}_F = 10\log\frac{W_0}{W_A} = 20\log\frac{v_M\rho c}{p_1^2} \quad \text{dB} \tag{12.22}$$

In deriving this equation, no account is taken of possible change in surface area or radiation efficiency between the enclosure surface and machine surface.

If the angle of sound incidence on the enclosure wall is known (i.e., a specific oblique angle or random), the power-based insertion loss of free-standing, close-fitting enclosures can be predicted on the basis of the two-dimensional model of sound transmission through layered media presented in Chapter 11.

Machine-Mounted, Close-Fitting Acoustical Enclosure. If the close-fitting enclosure is machine mounted, the rigid or resilient connections between the machine and the enclosure wall give rise to additional sound radiation of the enclosure wall. Assuming that the vibration velocity of the machine v_M is not affected by the connected enclosure, the additional sound power W_M radiated owing to the structural connections is

$$W_M = \sum_{i=1}^{n} F_i^2\left(\frac{\rho}{\rho_s^2 c} + \frac{\rho c\sigma}{2.3\rho_s^2 c_L h\omega\eta}\right) \quad \text{W} \tag{12.23}$$

where

$$F_i^2 = \frac{v_{mi}^2}{|1/2.3\rho_s^2 c_L h + j\omega/s|^2} \quad \text{N}^2 \tag{12.24}$$

In Eq. (12.24), F_i is the force transmitted by the ith attachment point, v_{Mi} is the vibration velocity of the machine at the ith attachment point, n is the number of point attachments between the machine and the homogeneous, isotropic enclosure wall, ρ_s is the mass per unit area of the enclosure wall, h is the wall thickness, c_L is the speed of longitudinal waves in the wall material, η is the loss factor, σ is the radiation efficiency, and s is the dynamic stiffness of the resilient mount connecting the enclosure wall to the machine ($s = \infty$ for rigid point connections). To minimize structure-borne transmission, it is advantageous to select attachment points at those locations on the machine that exhibit the lowest vibration. The insertion loss of the machine-mounted, close-fitting enclosure is

$$\text{IL}_{\text{MM}} = 10\log_{10}\frac{W_0}{W_A + W_M} \quad \text{dB} \tag{12.25}$$

where W_0 and W_A are given in Eqs. (12.21a) and (12.21b).

Figure 12.10 shows a close-fitting enclosure investigated experimentally and analytically by Byrne, Fischer, and Fuchs[9] in three configurations: (1) free standing, (2) rigidly machine mounted, and (3) resiliently machine mounted. Figure 12.11 shows the measured insertion loss obtained for each of the three configurations. The machine-mounted enclosure, which was supported from the machine at four points at each side, yield substantially lower insertion loss at high frequencies than the free-standing enclosure. Elastic mounting yields higher insertion loss than rigid mounting.

As shown by reference 9, the simple one-dimensional analytical model based on Eqs. (12.15)–(12.25) yields predictions that are in good agreement with measured data. The reason for this surprisingly good agreement is that the sound-absorbing treatment effectively prevents sound propagation (and the occurrence of acoustical resonances) in the plane parallel to the enclosure wall and also provides structural damping to the thin enclosure wall. Replacing the effective glass fiber sound-absorbing treatment with a thinner, less effective acoustical foam has resulted in substantial decrease in the insertion loss, indicating the crucial importance of an effective sound-absorbing treatment. Figure 12.12 shows

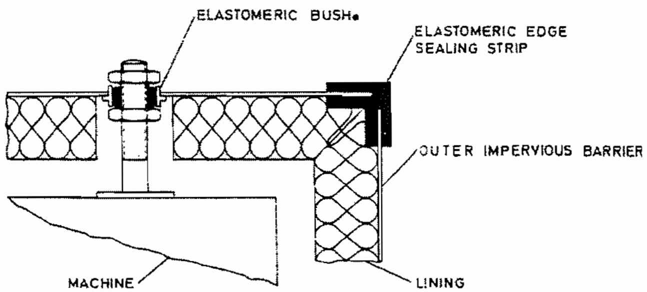

FIGURE 12.10 Machine-mounted, close-fitting enclosure; resilient mounting, resilient panel edge connections. (After Ref. 9).

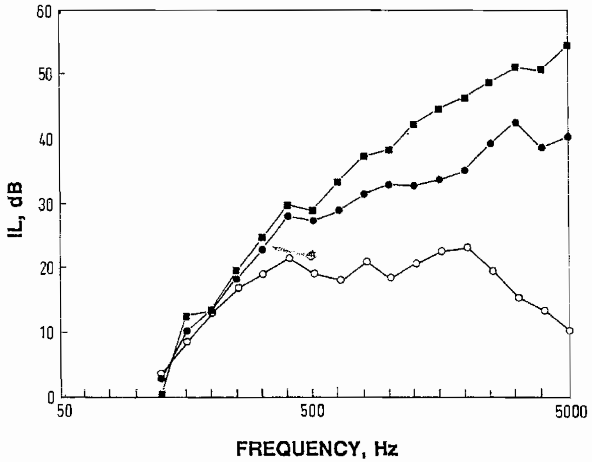

FIGURE 12.11 Insertion loss (IL_s) of a sealed, close-fitting enclosure made of 1-mm steel plates. (After Refs. 7 and 10.) Dimensions: $1 \times 0.6 \times 0.8$ m; machine, enclosure wall distance 50 mm; interior lining 50 mm thick; flow resistivity $R_1 = 2 \times 10^4 \mathrm{N \cdot s/m^4}$. (■) Free standing; (•) machine mounted, resilient mounting (see Fig. 12.10); (O) machine mounted, rigid mounting.

how the specific choice of edge connections of the enclosure plates affected the insertion loss of the machine-mounted, close-fitting enclosure. Elastically sealed edges, such as shown in Fig. 12.10, yield higher insertion loss than rigidly connected (welded) edges. The better performance obtained with elastically sealed edges is due to the reduced coupling between the in-plane motion of one plate (which radiates no sound) with the normal motion of the connected plate (that radiates sound efficiently). The elastic edge seal also increases the loss factor of the enclosure plates, thereby reducing their resonant vibration response.

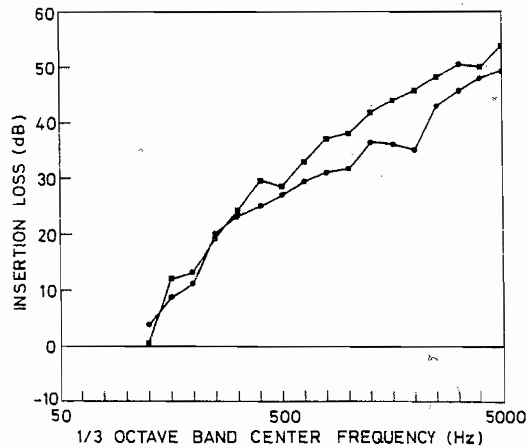

FIGURE 12.12 Effect of plate edge connection on the insertion loss of sealed, resiliently machine-mounted, close-fitting enclosure: (■) elastically sealed edge; (●) welded edge.

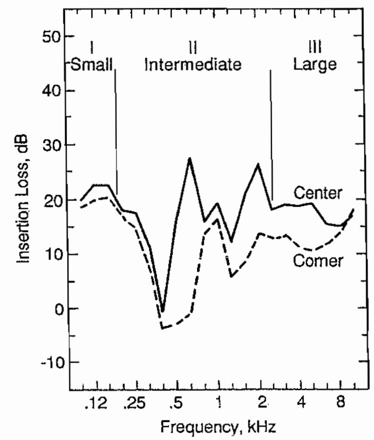

FIGURE 12.13 Effect of microphone position on the sound-pressure-based insertion loss measured in the outside–inside direction of a $50 \times 150 \times 300$-mm (1.6-mm-thick) empty, plane, sealed, unlined aluminum acoustical enclosure. (After Ref. 11.) Solid line: center microphone location. Dashedline: corner microphone location.

Intermediate-Size Enclosures

The intermediate frequency region, designated as region II in Figs. 12.3 and 12.13, is defined as the frequency region where the enclosure walls, the enclosure air volume, or both exhibit resonances; but the resonances do not overlap so that statistical methods are not yet applicable.

Comparison of the solid and dashed curves in Fig. 12.13 show how the insertion loss, measured in the outside–inside direction (such as in a quiet control room in a noisy test facility), depends on the location of the microphone. Below 400 Hz, the sound pressure is uniformly distributed in the enclosure and the microphone in the corner measures the same sound pressure as that placed at the center. The first acoustical resonance occurs at 565 Hz, which results in a very low insertion loss at the enclosure corner in the 500- and 800-Hz center-frequency one-third-octave bands, as illustrated by the dashed curve, but in a high insertion loss in the same bands for the enclosure center location, as depicted by the solid curve. Fluctuations owing to structural resonances can be reduced by application of damping treatment to the panels (see Chapter 14) and those owing to acoustical resonances by internal sound-absorbing lining (see Chapter 8).

Because the insertion loss in this intermediate frequency range fluctuates widely with frequency and position, it is very difficult to make accurate analytical predictions of the insertion loss. Frequently, involved finite-element analysis (see Chapter 6), model-scale or full-scale experiments, or crude approximations must be employed. For crude approximations one connects the low- and high-frequency predictions to cover the intermediate range.

Enclosures without Internal Sound-Absorbing Treatment

There are cases where the danger of bacterial growth or the accumulation of combustible particles precludes the use of porous or fibrous sound-absorbing materials inside of acoustical enclosures. In such cases bare enclosures must be used. Simple analytical models yield zero insertion loss for such enclosures. Consequently, it is also of theoretical interest to treat this extreme case.

Acoustical Performance Prediction of Large, Bare Enclosures. Even if the enclosure is built from homogeneous, isotropic panels without any interior sound-absorbing treatment, the interior sound pressure will not be infinitely high and the insertion loss of the enclosure will not be zero.

The interior sound pressure does not go to infinity because the interior sound field loses power through (1) sound radiation of the walls by the forced bending waves, (2) sound radiation of the walls by the free bending waves, (3) energy dissipation in the panel by the free bending waves, and (4) the inevitable acoustical energy dissipation at the interior surfaces of the impervious enclosure panels owing to the acoustical shear layer and heat conduction losses.

The insertion loss of the enclosure will be finite because of the energy dissipation by processes 3 and 4 above.

The power balance of the interior sound field is given as

$$W_{\text{source}} = W_{\text{rad}}^{\text{forced}} + W_{\text{rad}}^{\text{free}} + W_{d}^{\text{free}} + W_{d}^{\text{shear}} \quad \text{W} \tag{12.26}$$

where W_{source} = sound power of enclosed source
$W_{\text{rad}}^{\text{force}}$ = sound power radiated by forced bending waves

$W_{\text{rad}}^{\text{free}}$ = sound power radiated by free bending waves
W_{d}^{free} = sound power dissipated in plate by free bending waves
W_{d}^{shear} = sound power lost through shear and heat conduction at interior surface of impervious, solid walls

Unless the panel is very heavily damped, the power dissipated by the forced bending waves is small compared with that dissipated by the free bending waves and can neglected.

Inserting into Eq. (12.26) the appropriate relationships from Section 11.8 and for α_{min} from reference 12 yields for the random-incidence sound absorption coefficient of the bare enclosure walls,

$$\overline{\alpha}_{\text{rand}} = \frac{W_{\text{loss}}^{\text{tot}}}{W_{\text{inc}}} = A + B + C + D \tag{12.27}$$

for the space-average mean-square sound pressure in the enclosure,

$$\overline{p}^2 = \frac{4\rho_0 c_0 \, W_{\text{source}}}{S_{\text{tot}}(A + B + C + D)} \quad \text{N}^2/\text{m}^4 \tag{12.28}$$

and for the insertion loss of the bare enclosure,

$$\text{IL}_{\text{bare}} = 10 \log \left(\frac{A + B + D}{A + BC} \right) \quad \text{dB} \tag{12.29}$$

where

$$A = \frac{1}{1 + (1/52)[\omega\rho_s/(\rho_0 c_0)]^2} \qquad B = \frac{2\pi\sqrt{12} c_0^2 \rho_0 c_0 \sigma_{\text{rad}}}{c_L \rho_M h^2 \, \omega^2}$$

$$C = \frac{\rho_0 c_0 \sigma_{\text{rad}}}{\rho_0 c_0 \sigma_{\text{rad}} + \rho_s \omega \eta} \qquad D = \alpha_{\text{min}} = 0.72(10^{-4})\sqrt{\omega}$$

where S_{tot} = total interior surface area of enclosure, m^2 (assuming that all six partitions are made from the same panels)
ρ_s = mass per unit area of plate, $h\rho_M$, kg/m^2
ρ_M = density of plate material, kg/m^3
h = plate thickness, m
ω = radian frequency, $2\pi f$, Hz
ρ_0 = density of air, kg/m^3
c_0 = speed of sound, m/s
σ_{rad} = radiation efficiency of free bending waves on plate (see Chapter 11)
η_c = loss factor of plate (see Chapter 14)

Inspecting Eq. (12.29), note that for $\eta = 0, C = 1$, and $D \approx 0$, Eq. (12.29) yields IL = 0, as it should be. In the vicinity of the coincidence frequency (i.e., in the plateau region of the transmission loss), where $B \gg A$, the insertion loss of the bare enclosure approaches

$$\mathrm{IL} \approx 10 \log\left(\frac{1}{C}\right) = 10 \log\left(\frac{\rho_0 c_0 \sigma_{\mathrm{rad}} + \rho_s \omega \eta}{\rho_0 c_0 \sigma_{\mathrm{rad}}}\right) \simeq 10 \log\left(\frac{\rho_s \omega \eta}{\rho_0 c_0 \sigma_{\mathrm{rad}}}\right) \quad (12.30)$$

Figure 12.14 compares the insertion loss predicted for an unlined, sealed enclosure [using Eq. (12.8) at low frequencies and Eq. (12.27) at high frequencies] with experimental data obtained by reference 11. There is a reasonably good agreement between the predicted and measured values at both low and high frequencies not only for this specific enclosure but also for a large variety of unlined sealed enclosures of different size and wall panel thickness, indicating that the prediction formulas embodied in Eqs. (12.8) and (12.27) yield reasonable estimates for engineering design. Figure 12.14 also indicates that without internal sound-absorbing treatment the insertion loss remains very modest even at high frequencies, highlighting the importance of sound absorption in enclosure design.

Large Acoustical Enclosures with Interior Sound-Absorbing Treatment

Acoustical enclosures are termed large at frequencies where both the enclosure wall panels and the enclosure volume exhibit a large number of resonant modes in a given frequency band and statistical methods for predicting the level of the interior sound field and the vibration response and sound radiation of the enclosure wall panels can be applied. Large acoustical enclosures used in industrial noise control have many paths for transmitting acoustical energy, as illustrated schematically in Fig. 12.15. These paths can be grouped into three basic categories: (1) through the enclosure walls, (2) through openings, and (3) through structure-borne paths. The first group is characterized by the sound excitation of the enclosure wall by the interior sound field, resulting in sound radiation from the exterior wall surfaces. Sound transmission by this path is relatively well understood, and in most cases the sound power transmitted can be predicted with good engineering accuracy (see Chapter 11). The second group is characterized by sound energy escaping through openings in the enclosure wall such as air intake and exhaust ducts, gaps between panels, and gaps around the gasketing at the floor and doors. These are also fairly well understood[13–15] but not so easily controlled. The third group is characterized by radiation of solid surfaces excited to vibration by dynamic forces, such as the enclosure walls when rigidly connected to the enclosed vibrating equipment, shafts and pipes that penetrate the enclosure wall, and the vibration of the uncovered portion of the floor. This path is difficult to predict without detailed information about the motion of the enclosed machine and its dynamic characteristics. Consequently, all possible efforts should be made to prevent any solid connections to the source. To obtain a balanced design, one must control each of these transmission paths and avoid overdesigning any one of them.

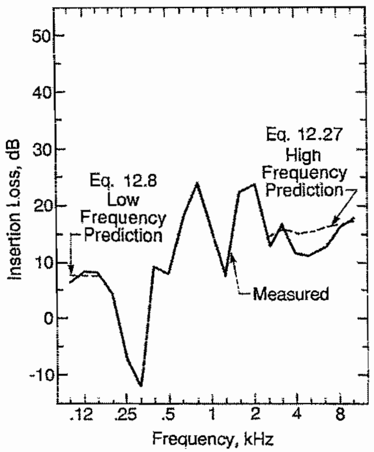

FIGURE 12.14 Comparison of measured and predicted pressure-based IL of a 50 × 150 × 300-mm (0.8-mm-thick) sealed, unlined aluminum enclosure, with source outside. (After Ref. 11).

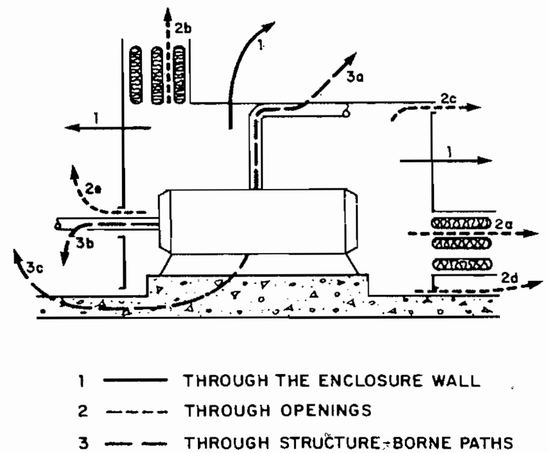

FIGURE 12.15 Paths of noise transmission from a typical acoustical enclosure.

Analytical Model for Predicting Insertion Loss at High Frequencies. A sound source enclosed in a large, acoustically lined enclosure will radiate approximately the same sound power as it would in the absence of the enclosure. To achieve a high power-based insertion loss, a high percentage of this radiated sound power must be dissipated (i.e., converted into heat) within the enclosure proper. This is accomplished by providing walls of high sound transmission loss to contain the sound waves and by covering the interior with sound-absorbing treatment to convert the trapped acoustical energy into heat.

In analyzing the acoustical behavior of an enclosure at high frequencies, the first step is to predict the space–time average mean-square pressure of the diffuse sound field, $\langle p^2 \rangle$, within the enclosure proper. Once the interior sound field is predicted, one can determine the sound power escaping from the enclosure through the various paths. The mean-square value of the diffuse sound pressure in the interior of the enclosure is obtained by balancing (a) the sound power injected into the enclosure from all the noise sources with (b) the power loss through dissipation (in the sound-absorbing lining, in the air, and in the wall structure) and the sound transmission through the walls of the enclosure and through diverse openings. According to reference 4, a sound source of power output W_0 generates in the enclosure a reverberant field with a space–time average mean-square sound pressure $\langle p^2 \rangle$ given by

$$\langle p^2 \rangle = W_0 \frac{4\rho c}{\left\{ \begin{array}{c} S_w \left[\alpha_w + \sum_i (S_{wi}/S_w) 10^{-R_{wi}/10} + D \right] \\ + S_i\alpha_i + \sum_k S_{sk} + mV + \sum_j S_{Gj} 10^{-R_{Gj}/10} \end{array} \right\}} \quad \mathrm{N^2/m^4} \tag{12.31}$$

where

$$D = \left(\frac{4\pi \sqrt{12} \rho c^3 \sigma}{c_L h \rho_s \omega^2} \right) \left(\frac{\rho_s \omega \eta}{\rho_s \omega \eta + 2\rho c \sigma} \right) \tag{12.32}$$

and S_w is the total interior wall surface, S_{wi} is the surface area of the ith wall, α_w is the average energy absorption coefficient of the walls, R_{wi} is the sound transmission loss of the ith wall, ρ_s is the mass per unit area of a typical wall panel, η is the loss factor of a typical wall panel in place, σ is the radiation efficiency of a typical panel, c_L is the propagation speed of longitudinal waves in the plate material, h is the wall panel thickness, $S_i\alpha_i$ is the total absorption in the interior in excess of the wall absorption (i.e., the machine body itself), S_{Gj} is the area of the jth leak or opening, R_{Gj} is the sound transmission loss of the jth leak or opening, S_{sk} is the face area of the kth silencer opening (assumed completely absorbing), m is the attenuation constant for air absorption, and V is the volume of the free interior space. The sound power incident on the unit surface area is given by

$$W_{\text{inc}} = \frac{\langle p^2 \rangle}{4\rho c} = \frac{W_0}{\{\cdots\}} \quad \mathrm{W} \tag{12.33}$$

where $\{\cdots\}$ represents the expression in the denominator in Eq. (12.31) and W_0 is the sound power output of the enclosed machine.

The terms in the denominator of Eq. (12.31) from left to right stand for (1) power dissipation by the wall absorption ($S_w\alpha_w$), (2) power loss through sound radiation of the enclosure walls ($\sum_i S_{wi} \times 10^{-R_{wi}/10}$), (3) power dissipation in the walls through viscous damping effects ($S_w D$), (4) power dissipation by sound-absorbing surfaces in addition to the walls ($S_i\alpha_i$), (5) sound power loss to silencer terminals ($\sum_k S_{sk}$), (6) sound absorption in air (mV), and (7) sound transmission to the exterior through openings and gaps ($\sum_j S_{Gj} \times 10^{-R_{Gj}/10}$).

The relative importance of the various terms may differ widely for different enclosures and even for the same enclosure in the different frequency ranges. For example, for a small airtight enclosure without any sound-absorbing treatment, the power dissipation in the wall panels may be of primary importance, while it is usually negligible for enclosures with proper interior sound-absorbing treatment. Air absorption is important in large enclosures at frequencies above 1000 Hz. The sound power transmitted through the enclosure walls, W_{TW}, that through gaps and openings, W_{TG}, and that through silencers, W_{TS}, are given in Eqs. (12.34)–(12.36), respectively:

$$W_{\text{TW}} = \frac{W_0(\sum_i S_{wi} \times 10^{R_{wi}/10})}{\{\cdots\}} \quad \mathrm{W} \tag{12.34}$$

$$W_{\text{TG}} = \frac{W_0(\sum_j S_{Gj} \times 10^{-R_{Gj}/10})}{\{\cdots\}} \quad \mathrm{W} \tag{12.35}$$

$$W_{\text{TS}} = \frac{W_0(\sum_k S_{sk} \times 10^{-\Delta L_k/10})}{\{\cdots\}} \quad \mathrm{W} \tag{12.36}$$

where ΔL_k is the sound attenuation through the silencer over opening k. The power-based insertion loss of the enclosure in the inside–outside direction is defined as

$$\mathrm{IL} \equiv 10 \log_{10} \frac{W_0}{W_{\text{TW}} + W_{\text{TG}} + W_{\text{TS}} + W_{\text{SB}}} \quad \mathrm{dB} \tag{12.37}$$

which takes the form

$$\mathrm{IL} = 10 \log_{10} \frac{\{\cdots\}}{\sum_i S_{wi} \times 10^{-R_{wi}/10} + \sum_k S_{sk} \times 10^{-\Delta L_k/10}} \times \frac{1}{\sum_j S_{Gj} \times 10^{-R_{Gj}/10} + W_{\text{SB}}(\{\cdots\}/W_0)} \quad \mathrm{dB} \tag{12.38}$$

where W_{SB} is the sound power transmitted through structure-borne paths considered separately according to Eqs. (12.23) and (12.24).

The denominator of Eq. (12.38) reveals that if full advantage is to be taken of the high transmission loss of the enclosure walls, the air paths through gaps, openings, and air intake and exhaust silencers and structure-borne paths must be controlled to a degree that their contribution to the sound radiation is small compared with the sound radiation of the walls. If these paths are well controlled and the dissipation is achieved by the sound-absorbing treatment of the interior wall surfaces and by the absorption in the interior, then for $R_{wi} = R_w$ the insertion loss of the enclosure is well approximated by

$$\mathrm{IL} \cong 10 \log \left(1 + \frac{S_w\alpha_w + S_i\alpha_i}{S_w} \times 10^{R_w/10} \right) \quad \mathrm{dB} \tag{12.39}$$

If we further assume that the second term in Eq. (12.39) is much larger than unity and call the total absorption in the interior of the enclosure $S_w\alpha_w + S_i\alpha_i = A$, Eq. (12.39) simplifies to

$$\mathrm{IL} \cong R_w + 10 \log \frac{A}{S_w} \quad \mathrm{dB} \qquad (12.40)$$

This approximate formula would yield negative insertion loss for very small values of interior absorption. It has been widely promulgated in the acoustical literature without mention of its limited validity. Note that the insertion loss of a large enclosure can approach the sound transmission loss of the enclosure wall panels only if there are no leaks and α_w approaches unity.

Key Parameters Influencing the Insertion Loss of Acoustical Enclosures. The primary paths for the transmission and dissipation of sound in large acoustical enclosures are shown in the block diagram in Fig. 12.16. The key parameter affecting enclosure insertion loss are summarized in Table 12.4. Fisher and Veres[10] and Kurtze and Mueller[16] have carried out systematic experimental investigations on how (1) choice of wall panel parameters, (2) internal sound-absorbing lining, (3) leaks, and (4) vicinity of the enclosed machine to the enclosure walls and its vibration pattern influence the acoustical performance of enclosures. The model–machine sound source employed in reference 10 consisted of 1 × 1.5 × 2-m steel boxes of 1 mm wall thickness and were combined to yield a small (3 × 2 × 1.5-m) and a large (4 × 2 × 1.5-m) model machine. The

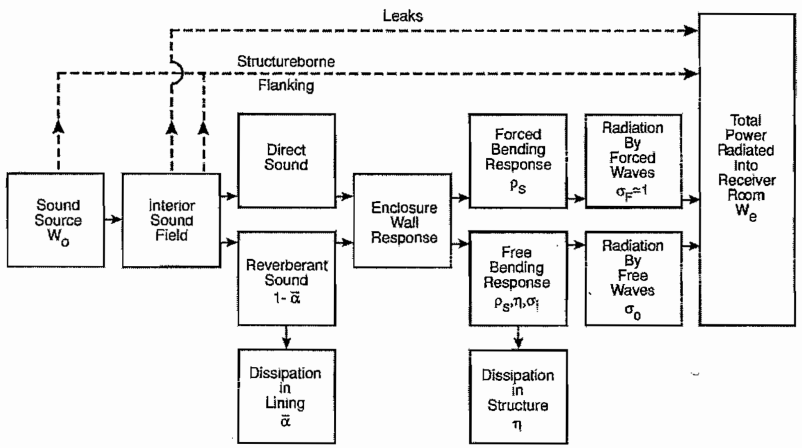

FIGURE 12.16 Block diagram of key components controlling the sound attenuation process in acoustical enclosures: W_0, source sound power output; $\bar{\alpha}$, average sound absorption coefficient; ρ_s, mass per unit area; η, loss factor; σ_i, radiation efficiency of wall panels for radiation for inside direction; σ_0, radiation efficiency of wall panels for radiation for outside direction; σ_F, 1 radiation efficiency of forced waves; W_e, total sound power radiated by the enclosure.

TABLE 12.4 Effect of Key Parameters on Sound Insertion Loss of Large Enclosures

Parameter	Symbol	Effect on Insertion Loss
Absorption coefficient of lining	$\bar{\alpha}$	Increases IL by reducing reverberant buildup
Distance between machine and enclosure wall	d	If d decreases beyond a certain limit, IL decreases at low frequencies (close-fitting enclosure behavior)
Thickness of wall panel	h	Increases IL
Density of wall panel material	ρ_M	Increases IL
Speed of longitudinal waves in panel material	$c_L = \sqrt{E/\rho_M}$	Decreases IL below critical frequency
Loss factor of wall panel	η	Increases IL, especially near and above critical frequency and at first panel resonance
Critical frequency of wall panel	$f_c = c^2/1.8c_L h$	The higher is f_c for a given mass per unit area, the higher is IL
Radiation efficiencies of wall panels	σ_i, σ_0	The higher is the radiation efficiency for inside direction, σ_i, and for outside direction, σ_0, the smaller is IL
Stiffeners	—	Decrease IL by increasing σ
Leaks	—	Limit achievable IL, watch out for door gaskets and penetrations
Structure-borne flanking	—	Limit achievable IL, watch out for solid connections between vibrating machine and enclosure and for floor vibration

walls of the model machines could be excited by either an internal loudspeaker or an internal tapping machine to simulate both sound and structure-borne excitation. The investigated rectangular walk-in enclosure had 4.5 × 2.5 × 2 m inside dimensions and was equipped with an operational personal-access door. The thickness and material of the wall panels as well as the thickness of the interior lining could be varied.

Wall Panel Parameters. Figure 12.17 shows the measured insertion loss versus frequency for three different values of the wall thickness h, indicating that above 1.5 mm, a further increase of the wall thickness brings only slight improvement at low frequencies and a slight deterioration at high frequencies near coincidence. Figure 12.17 also includes, as the dashed line, the field-incidence

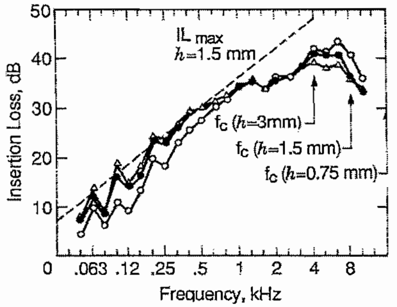

FIGURE 12.17 Curves of power-based insertion loss versus frequency measured (inside–outside direction) for a large walk-in enclosure for various thicknesses of steel plate, h. (After Ref. 10.) Sound-absorbing treatment, 70 mm thick, door sealed; f_c, coincidence frequency; $\mathrm{IL}_{\max} = R_f$ represents the maximum achievable insertion loss. (Δ) $h = 3$ mm; ($\bullet$) $h = 1.5$ mm; ($\circ$) $h = 0.75$ mm.

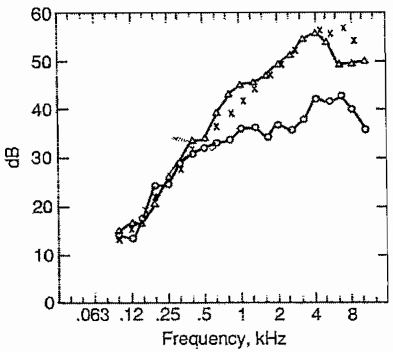

FIGURE 12.18 Comparison of measured enclosure insertion loss IL and panel sound transmission loss R (after Ref. 10): 1.5-mm-thick steel plate, 70-mm-thick sound-absorbing treatment; (Δ) R, measured; ($\times$) R, predicted according to Chapter 11; ($\circ$) IL measured.

sound transmission loss for a 1.5-mm-thick steel plate for comparison, indicating that up to 500 Hz, the insertion loss matches well the field-incidence sound transmission loss of the panel.

Figure 12.18 compares the measured sound transmission loss of a typical 2.1 × 1.2-m wall panel and predicted sound transmission loss of an identical infinite-enclosure panel with the measured insertion loss obtained with an enclosure built with the same panels. The data indicate that the prediction formulas presented in Chapter 11 for infinite panels can be used to predict accurately the sound transmission loss of the finite panels of this specific size and that above 500 Hz the insertion loss is dominated by unintentional small leaks. According to reference 10, the sound-absorbing interior liner provides sufficient structural

damping of the wall panels so that additional damping treatment did not result in improved performance.

Stiffening the wall panels with exterior L-channels, which increase the radiation efficiency, resulted in slight deterioration of the acoustical performance. Using steel and wood chipboard of equal mass per unit area yielded different transmission loss but resulted in practically the same insertion loss because in the frequency range where the chipboard had its coincidence frequency the insertion loss was already controlled by leaks.

As a general rule, wall panels should be selected to have *high enough coincidence frequency* to be above the frequency region of interest and be *large enough that their first structural resonance occurs below the frequency region of interest* but heavy enough to yield a field-incidence mass law sound transmission loss that matches the insertion loss requirements. Steel plates 1.5 mm thick usually fulfill most of these requirements.

Stiff, lightweight panels (such as honeycombs) usually yield a critical frequency as low as 500 Hz and provide a very low sound transmission loss in this frequency region. Consequently, such panels should not be used in enclosure design unless the enclosure is required to provide high insertion loss at only very low frequencies and mid- and high-frequency performance is not required.

Effect of Sound-Absorbing Treatment. The proper choice of sound-absorbing treatment plays a more crucial role than the specific choice of wall material or wall thickness, as shown in Fig. 12.19. The sound-absorbing treatment helps to increase insertion loss by (1) reducing reverberant buildup in the enclosure at mid- and high frequencies, (2) increasing the transmission loss of the enclosure walls at high frequencies, and (3) covering up some of the unintentional leaks between adjacent panels and between panels and frames. Whenever feasible, the thickness of the interior sound-absorbing treatment should be chosen to yield a normal-incidence absorption coefficient $\alpha \geq 0.8$ in the frequency region of interest. As shown in Chapter 8, this can be achieved by a layer thickness $d \geq \frac{1}{10}\lambda$, where λ_L is the acoustical wavelength at the lower end of the frequency region, and by choosing a porous material of normalized flow resistance of $1.5 \leq R_1 d/\rho c < 3$.

Leaks. Leaks reduce the insertion loss of large enclosures just as they reduce it for small enclosures [see Eq. (12.13)]. The reduction in insertion loss due to leaks, $\Delta\mathrm{IL}_L$, is defined as

$$\Delta\mathrm{IL}_L \equiv \mathrm{IL}_s - \mathrm{IL}_L \cong 10\log(1 + \beta \times 10^{R_w/10}) \quad \mathrm{dB} \qquad (12.41)$$

where IL_s and IL_L are the insertion losses of the sealed and leaky enclosures, respectively, R_w is the sound transmission loss of the enclosure wall, and $\beta = (1/S_w)\Sigma_j S_{Gj} \times 10^{-R_{Gj}/10}$ is the leak ratio factor, S_{Gj} is the face area, and R_{Gj} is the sound transmission loss of the jth leak. The sound transmission loss of leaks can be positive or, in the case of longitudinal resonances in wide, rigid-walled gaps, also negative. For preliminary calculations it is customary to assume

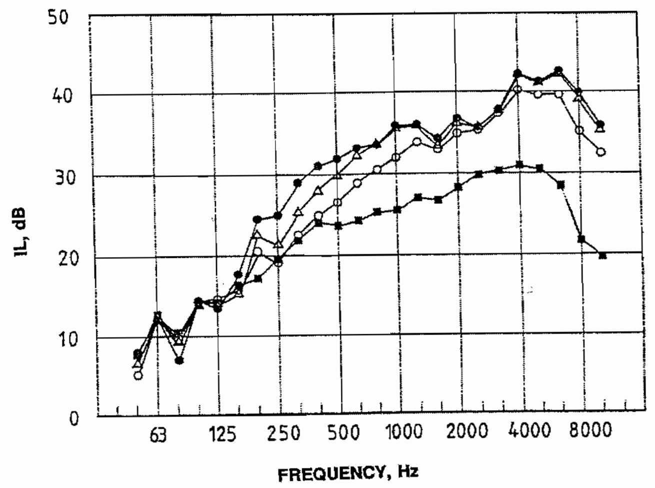

FIGURE 12.19 Measured insertion loss of the enclosure with 1.5-mm-thick steel plates for various thicknesses of the sound-absorbing material (after Ref. 10): (■) 0 mm (no absorption); (○) 20 mm; (△) 40 mm; (•) 70 mm.

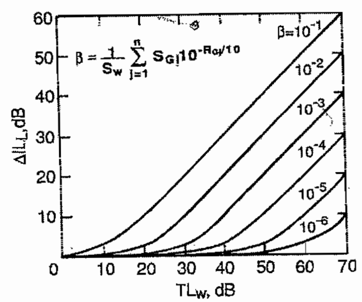

FIGURE 12.20 Decrease of enclosure insertion loss, ΔIL, as a function of the wall sound transmission loss R_w with the leak ratio factor β as parameter; S_w is the wall surface area and R_{Gj} and S_{Gj} are the sound transmission loss and face area of the jth leak, respectively.

$R_{Gj} = 0$. In this case, $\beta = \sum_j S_{Gj}/S_w$ is the ratio of the total face area of the leaks and gaps and the surface area (one side) of the enclosure walls.

Figure 12.20 is a graphical representation of Eq. (12.41) indicating that the higher is the sound transmission loss of the enclosure walls, the higher is the reduction in insertion loss caused by leaks. For example, for an enclosure assembled from wall panels that provide a R_w of 50 dB, the total area of all leaks must be less than 1/1000 percent ($\beta = 10^{-5}$) of the total enclosure surface area if the insertion loss is not to be decreased by more than 3 dB!

Machine Position. Experimental investigations by Fischer and Veres[10] have shown that the insertion loss of an enclosure at low frequencies also depends on the specific position of the enclosed machine within the enclosure. At low frequencies, where the distance between the flat machine wall and the flat enclosure wall panel, d, becomes smaller than one-eighth of the acoustical wavelength ($d < \frac{1}{8}\lambda$), the observed decrease of the insertion loss (from its value obtained when the machine was positioned centrally so that all wall distances were large compared with $\frac{1}{8}\lambda$) was as high as 5 dB. Note that the machine–wall distance d includes the thickness of the internal lining. As a general rule, machines with omnidirectional sound radiation should be positioned centrally. It is especially important to avoid positioning the noisy side of machines very close to enclosure walls, doors, windows, and ventilation openings.

Machine Vibration Pattern. The insertion loss of an enclosure also depends on the specific vibration pattern of the machine, although that dependence appears to not be very strong. Experimental investigations[10] have shown that variation of the insertion loss was about ± 2.5 dB when measured with a loudspeaker inside the model machine and with excitation of the model machine by an ISO tapping machine.

Flanking Transmission through the Floor. The potential insertion loss of an enclosure can be limited severely by flanking if the floor is directly exposed to vibration forces, the internal sound field of the enclosure, or both. Figure 12.21 shows typical enclosure installations ranging from the best to the worst with regard to flanking transmission via the floor. For most equipment it is imperative to provide vibration isolation, a structural break in the floor, or both to reduce the transmission of structure-borne excitation of the floor. Applicable prediction tools and isolation methods are described in Chapters 11 and 13. For the cases depicted in Figs. 12.21*c,d*, where the interior sound field directly impinges on the floor, the sound-induced vibration of the floor sets a limit to the achievable insertion loss of the enclosure. This limit can be estimated roughly from

$$\mathrm{IL}_L \cong R_F + 10 \log \sigma_F \quad \mathrm{dB} \qquad (12.42)$$

where R_F is the sound transmission loss and σ_F is the radiation efficiency of the floor slab.

Relationship between Inside–Outside and Outside–Inside Transmission. Acoustical enclosures are most frequently used to surround a noisy equipment for reducing the noise exposure of a receiver located outside of the enclosure. Less frequently, the enclosure surrounds the receiver (i.e. it is a cabin) to reduce its noise exposure to a sound source located outside of the enclosure. The acoustical performance of the enclosure in the former case is given by its insertion loss in the inside–outside direction, IL_{io}, while the latter is given by its insertion loss in the outside–inside direction, IL_{oi}. All of

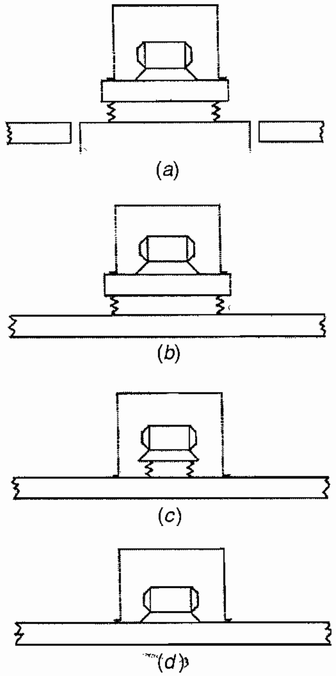

FIGURE 12.21 Rating of enclosure installations with regard to flanking transmission of the floor: (*a*) best; (*b*) good; (*c*) bad; (*d*) worst.

our considerations in this chapter have dealt with sound transmission from the inside to the outside. According to the principle of reciprocity (see Chapter 11), exchanging the position of the source and receiver does not affect the transfer function. Though it is strictly true only for point sound sources and receivers, it also can be applied to extended sound sources and averaged observer positions in an enclosure, yielding $\mathrm{IL}_{io} = \mathrm{IL}_{oi}$.

Example. To demonstrate the use of the previously provided design information, predict the insertion loss of the large, acoustically lined, walk-in enclosure investigated experimentally in reference 10. The enclosure is 4.5 × 2.5 × 2.0 m high and is constructed of 1.5-mm-thick steel plates and has a 70-mm-thick interior sound-absorbing lining. The sound transmission loss of the wall panels, R_w, given in Fig. 12.18 by the triangular data points, and the sound absorption coefficient of the interior panel surfaces, $\overline{\alpha}$, taken from reference 10, as a curve that monotonically increases from 0.16 at 100 Hz and reaches a plateau of 0.9 at 600 Hz. The insertion loss is predicted by Eq. (12.38) using the following values: $S_{wi} = S_w = 39\ \mathrm{m}^2$, $\sum_j S_{Gj} \times 10^{-R_{Gj}/10} = 10^4$, $S_{Gj} = 3.9 \times 10^{-3}$, assuming that leaks account for 1/100 percent of the wall surface area, that there are no silencer openings ($S_s = 0$) and no structure-borne connections ($W_{\mathrm{SB}} = 0$), and

that air absorption (mV), the sound absorbed by the machine ($S_i\alpha_i$), and power lost due to dissipation in the panels ($S_w D$) and due to sound radiation ($10^{-R_w/10}$) are small compared with the power dissipated in the sound-absorbing treatment on the interior wall surfaces.

Then Eq. (12.38) simplifies to

$$\mathrm{IL}_L \cong 10 \log \frac{S_w\overline{\alpha}}{\sum_i S_{wi} \times 10^{-R_{wi}/10} + \sum_j S_{Gj} \times 10^{-R_{Gj}/10}} \quad \mathrm{dB} \qquad (12.43)$$

The curve of insertion loss versus frequency predicted by Eq. (12.43) is represented by the open circles in Fig. 12.22, while the solid curve represents the measured data. The measured sound transmission loss of the wall panels, R_w, is the dashed line and represents the limiting insertion loss that could be achieved only if there would be no leaks and the random-incidence sound absorption coefficient $\overline{\alpha}_w$ would approach unity. Observing Fig. 12.22, note that the assumption of 1/100 percent leaks ($\beta = 10^{-4}$) yielded a prediction that matches reasonably well the measured data, which indicates that even such a very small percentage of leaks, which can be realized only if extreme care is exercised during erecting the enclosure and careful caulking of all leaks detected during the initial performance checkout and careful adjustment of door gaskets, can substantially decrease the potential insertion loss of an enclosure.

Partial Enclosures

When the work process of the machine or safety and maintenance requirements do not allow a full enclosure, a partial enclosure (defined as those with more than 10% open area) is used to reduce radiated noise. When a partial enclosure is far enough from the sound source not to cause an increase in source sound

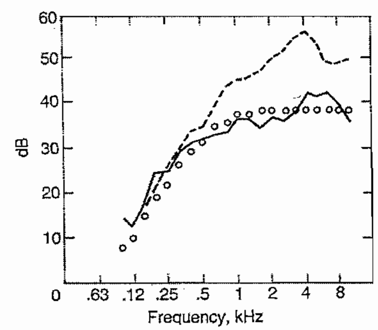

FIGURE 12.22 Typical acoustical performance of a leaky enclosure: (——) IL, measured by Ref. 10; (- - - -) R_w, measured by Ref. 10; (O) IL, predicted by Eq. (12.43) for

$$\beta = \left(\sum_j \left(\frac{S_{Gj}}{S_w} \right) \times 10^{-R_{Gj}/10} \right) = 10^{-4}$$

power by hydrodynamic interactions of the near field of the source with edges of the opening and the walls of the partial enclosure are not rigidly connected to the vibrating machine to serve as a sounding board, a partial enclosure can provide a modest insertion loss of 5 dB or less. According to reference 17, the power-based insertion loss of partial enclosure can be estimated by

$$\mathrm{IL} = 10 \log \left[1 + \alpha \left(\frac{\Omega_{\text{tot}}}{\Omega_{\text{open}}} - 1 \right) \right] \quad \text{dB} \tag{12.44}$$

where Ω_{tot} is the solid angle of sound radiation of the unenclosed source and $\Omega_{\text{open}} = S_{\text{open}}/r$ is the solid angle at which the enclosed source (located at a distance r) "sees" the opening of area S_{open}. Reference 17 contains construction details, curves of measured insertion loss versus frequency, and cost information of 54 different partial enclosures.

12.2 WRAPPINGS

Many machines and pipes need thermal insulation to provide protection of operating personnel or to prevent excessive heat loss. Typically, they need a minimum of 25-mm- (1-in.-) thick glass or ceramic fiber blanket to achieve proper protection. Since many hot equipment, such as turbines, boiler feed pumps, compressor valves, and pipelines, are also sources of intense noise, it is frequently feasible to achieve both heat and acoustical insulation by providing a (preferably) limp, impervious surface layer on top of the porous blanket. The impervious surface layer also provides protection for the porous blanket. Acoustically, the combination of the resilient blanket and the heavy, limp, impervious surface layer provide a spring–mass isolation system. At frequencies where the mass impedance of the surface layer exceeds the combined stiffness impedance of the skeleton of these flexible blankets and the entrapped air, the vibration amplitude of the surface layer becomes smaller than that of the machine surface and wrapping results in an insertion loss that monotonically increases with increasing frequency. The insertion loss of the wrapping is defined the same way as the insertion loss of a close-fitting enclosure and for flat wrappings can be predicted in a manner similar to that of the close-fitting enclosure.

The major difference between wrappings and close-fitting enclosures is that for wrappings the skeleton of the porous layer is in full surface contact with the vibrating surface of the machine, but for the close-fitting enclosures there is no such contact. Consequently, for wrappings the vibrating machine surface transmits a pressure to the impervious surface layer not only through sound propagation in the voids between the fibers but also through the skeleton of the porous material. At low frequencies where the thickness of the porous layer, L, is much smaller than the acoustical wavelength, the porous layer can be represented by a stiffness per unit area, S_{tot}, that according to Mechel[18] can be estimated as

$$S_{\text{tot}} = S_M + S_L \left(1 - \frac{P}{A} \sqrt{\frac{\rho c^2}{L \pi f \gamma R_1 h'}} \right) \quad \text{N/m}^3 \tag{12.45}$$

where S_L is the stiffness of the trapped air,

$$S_L \cong \frac{\rho c^2}{\gamma L h'} \quad \text{N/m}^3 \tag{12.46}$$

γ the adiabatic exponent, h' the porosity, f the frequency, and R_1 the flow resistivity of the material, and S_M is given by

$$S_M = (2\pi f_0)^2 \rho_s \quad \text{N/m}^3 \tag{12.47}$$

In Eq. (12.47) the symbol f_0 represents the measured resonance frequency of a mass–spring system consisting of a small rectangular or square-shaped sample of the porous material covered with a metal plate of mass per unit area ρ_s. The resonance frequency is measured by putting the mass–spring system on top of a shaker table and performing a frequency sweep. The second term in Eq. (12.45) accounts for the air that escapes along the perimeter P of a test sample of surface area A, used in the experiment to determine the resonance frequency f_0 according to Eq. (12.47). Young's modulus of the porous material is then determined as $E = S_{\text{tot}}/L$, the speed of longitudinal waves in the porous layer as $c_L = \sqrt{E/\rho_M}$, where ρ_M is the density of the porous material, and the wavenumber as $k = 2\pi f/c_L$. Characteristics of some frequently used thermal insulation materials reported by Wood and Ungar[19] are given below:

Material	Dynamic Stiffness per Unit Area, S_M (N/m^3)	Density, ρ_M (kg/m^3)
Erco-Mat[a]	1.3×10^7	138
Erco-Mat F[a]	2×10^6	104
Glass fiber[b]	4×10^4	12

[a] Nedled glass fiber insulation.
[b] Low-density Owens Corning Fiberglas blanket.

Considering the porous heat insulating layer as a wave-bearing medium of density ρ and a complex Young's modulus $E' = E(1 + j\eta)$ and characterizing the impervious, limp surface layer by its mass per unit area ρ_s, Wood and Ungar[19] derived the analytical formula

$$\mathrm{IL} = 20 \log \left| \cos(kL) - \frac{\rho_s}{\rho_M L}(kL)\sin(kL) \right| \quad \text{dB} \tag{12.48}$$

where $k = \omega/\sqrt{E(1 + j\eta)/\rho_M}$ is the complex propagation constant of the porous layer, $\eta = 1/Q$ the loss factor, and $\rho_s \omega$ the mass impedance per unit area of the covering layer.

At very low frequencies, where $kL \ll 1$, Eq. (12.48) can be approximated by

$$\mathrm{IL}_L = 20 \log \left[1 - \left(\frac{\omega}{\omega_n} \right)^2 \right] \quad \text{dB} \tag{12.49}$$

where $\omega_n = E/\rho_s L$ is the resonance frequency of a system consisting of a massless spring of stiffness E/L and a mass ρ_s (per unit area). According to Eq. (12.49), the cladding provides no insertion loss for $\omega \ll \omega_n$ and yields a negative insertion loss (amplifies the radiated sound) if $\omega \cong \omega_n$.

For frequencies above the resonance frequency ($\omega \gg \omega_n$) the blanket provides an attenuation that increases monotonically with increasing frequency. Noting that in Eq. (12.48) neither the cosine nor the sine term can exceed unity, an upper bound for the curve of insertion loss versus frequency at high frequencies is obtained by[19]

$$\mathrm{IL}_L \le 20 \log \left[1 + \frac{\rho_s}{\rho_L} (kL)^2 \right] \quad \mathrm{dB} \tag{12.50}$$

Pipe Wrappings

Pipe wrappings consist of a resilient porous layer and an impervious jacket. The impervious jacket is usually sheet metal or loaded plastic. They achieve their acoustical performance in a similar manner as flat wrappings. However, there is an important difference. While flat wrappings do not increase the sound-radiating surface, when a wrapping is applied to a small-diameter pipe, the diameter of the impervious jacket can be substantially larger than that of the bare pipe. This increases both the radiating surface and the radiation efficiency. Accordingly, at low frequencies, below or slightly above the resonance frequency of the pipe wrapping, the insertion loss is negative. Positive insertion loss is usually achieved only above 200 Hz.

According to Michelsen, Fritz, and Sazenhofen,[20] the maximal achievable insertion loss of wrappings can be estimated by the empirical formula

$$\mathrm{IL}_{\max} = \frac{40}{1 + 0.12/D} \log \frac{f}{2.2 f_0} \quad \mathrm{dB} \tag{12.51}$$

where

$$f_0 = 60/\sqrt{\rho_s L} \quad \mathrm{Hz} \tag{12.52}$$

where L is the thickness of the porous resilient layer and D is the pipe diameter, both in meters, and ρ_s is the mass per unit area of the impervious jacket in kilograms per square meter.

Equation (12.51) is valid only if there are no structure-borne connections between the pipe and jacket and for frequencies $f \ge 2 f_0$. Figure 12.23 shows curves of measured insertion loss versus frequency obtained in reference 20 for typical pipe wrapping consisting of a galvanized steel jacket, thickness 0.75–1 mm, and a porous resilient layer with the following parameters:

Thickness L	30, 60, 80, and 100 mm
Density	85–120 kg/m^3
Flow resistivity	3×10^4 N · s/m^4
Dynamic Young's modulus	2×10^5 N/m^2

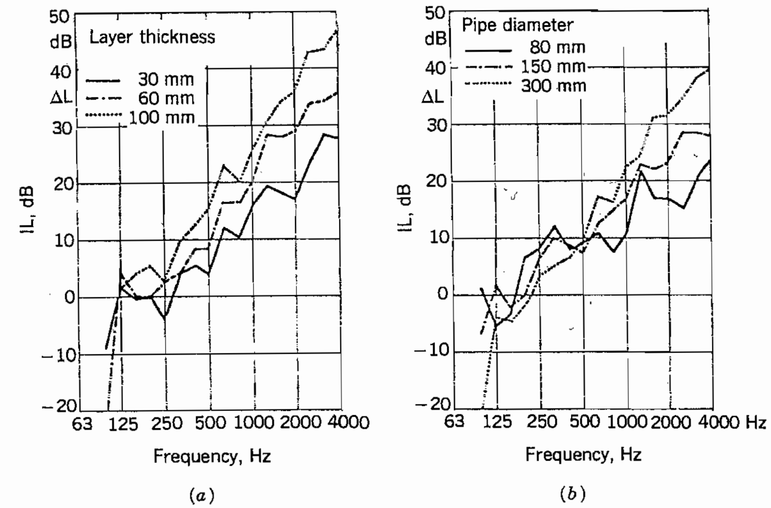

FIGURE 12.23 Curves of measured insertion loss versus frequency of pipe wrappings. (After Ref. 20.) (*a*) Effect of layer thickness. (*b*) Effect of pipe diameter.

Figure 12.23*a* shows the effect of layer thickness L on the insertion loss for a pipe of diameter $D = 300$ mm while Fig. 12.23*b* illustrates the effect of pipe diameter D for a constant layer thickness $L = 60$ mm. The insertion loss above 250 Hz increases with increasing thickness of the porous layer and with increasing diameter of the bare pipe. The standard deviation of the measured insertion loss around that predicted by Eq. (12.52) was 4 dB.

Note that spacers between the pipe and jacket result in insertion loss values that may be substantially lower than those predicted by Eq. (12.50) unless the spacers are less stiff dynamically than the porous layer.

REFERENCES

1. ISO 15667: 2000E, "Guidelines for Noise Control by Enclosures and Cabins," International Organization for Standardization, Geneva, Switzerland, 2000.
2. I. L. Ver, "Enclosures and Wrappings," in L. L. Beranek and I. L. Ver (Eds.), *Noise and Vibration Control Engineering*, J. Wiley, New York, 1992.
3. R. H. Lyon, "Noise Reduction of Rectangular Enclosures with One Flexible Wall," *J. Acoust. Soc. Am.*, **35**(11), 1791–1797 (1963).
4. I. L. Vér, "Reduction of Noise by Acoustic Enclosures," in *Isolation of Mechanical Vibration, Impact and Noise*, Vol. 1, American Society of Mechanical Engineers, New York, 1973, pp. 192–220.
5. J. B. Moore, "Low Frequency Noise Reduction of Acoustic Enclosures," *Proc. NOISE-CON*, (1981) pp. 59–64.

6. H. M. Fuches, U. Ackermann, and W. Frommhold, "Development of Membrane Absorbers for Industrial Noise Abatement," *Bauphysik*, **11**(H.1), 28–36 (1989) (in German).
7. M. H. Fischer, H. V. Fuchs, and U. Ackermann, "Light Enclosures for Low Frequencies," *Bauphysik*, **11**(H.1), 50–60 (1989) (in German).
8. I. L. Vér and E. Veres, "An Apparatus to Study the Sound Excitation and Sound Radiation of Platelike Structures," *Proc. INTER-NOISE*, (1980) pp. 535–540.
9. K. P. Byrne, H. M. Fischer, and H. V. Fuchs "Sealed, Close-Fitting, Machine-Mounted Acoustic Enclosures with Predictable Performance," *Noise Control Eng. J.*, **31**, 7–15 (1988).
10. M. H. Fischer and E. Veres, "Noise Control by Enclosures" Research Report 508, Bundesanstalt fuer Arbeitschutz, Dortmund, 1987 (in German); also Fraunhofer Institute of Building Physics Report, IBP B5 141/86, 1986.
11. J. B. Moreland, Westinghouse Electric Corporation, private communication.
12. L. Cremer, M. Heckl, and E. E. Ungar, *Structureborne Sound*, Berlin, Springer, 1988.
13. K. Goesele, *Berichte aus der Bauforschung* [*Sound Transmission of Doors*], H. 63 Wilhelm Ernst & Sohn Publishers, Berlin, 1969, pp. 3–21.
14. F. P. Mechel, "Transmission of Sound through Holes and Slits Filled with Absorber and Sealed," *Acustica*, **61**(2), 87–103 (1986).
15. F. P. Mechel, "The Acoustic Sealing of Holes and Slits in Walls," *J. Sound Vib.*, **III**(2), 297–336 (1986).
16. G. Kurtze and K. Mueller "Noise Reducing Enclosures," Research Report BMFT-FB-HA 85-005, Bundesministerium fuer Forschung und Technologie, Berlin, 1985 (in German).
17. U. J. Kurze et al., "Noise Control by Partial Enclosures; Shielding in the Nearfield," Research Report No. 212, Bundesanstalt fuer Arbeitschutz und Unfallforshung, 1979 (in German).
18. F. P. Mechel, "Sound Absorbers and Absorber Functions" in *Reduction of Noise in Buildings and Inhabited Regions*, Strojnizdat, Moscow, 1987 (in Russian).
19. E. W. Wood and E. E. Ungar, BBN Systems and Technologies Corporation, private communications.
20. R. Michelsen, K. R. Fritz, and C. V. Sazenhofen, "Effectiveness of Acoustic Pipe Wrappings" in *Proc. DAGA '80*, VDE-Verlag, Berlin, 1980, pp. 301–304 (in German).

BIBLIOGRAPHY

Miller, R. K., and W. V. Montone, *Handbook of Acoustical Enclosures and Barriers*, Fairmont, Atlanta, GA, 1978.

"Noise Reduction by Enclosures," VDI Guideline 2711, VDI-Verlag GmbH, Dusseldorf, Germany (in German).

CHAPTER 13

Vibration Isolation

ERIC E. UNGAR AND JEFFREY A. ZAPFE

Acentech, Inc.
Cambridge, Massachusetts

13.1 USES OF ISOLATION

Vibration isolation refers to the use of comparatively resilient elements for the purpose of reducing the vibratory forces or motions that are transmitted from one structure or mechanical component to another. The resilient elements, which may be visualized as springs, are called vibration isolators. Vibration isolation is generally employed (1) to protect a sensitive item of equipment from vibrations of the structure on which it is supported or (2) to reduce the vibrations that are induced in a structure by a machine it supports. Vibration isolation may also be used to reduce the transmission of vibrations to structural components whose attendant sound radiation one wishes to control.

13.2 CLASSICAL MODEL

Mass–Spring–Dashpot System

Many aspects of vibration isolation can be understood from analysis of an ideal, linear, one-dimensional, purely translational mass–spring–dashpot system like that sketched in Fig. 13.1. The isolator is represented by the parallel combination of a massless spring of stiffness k (which produces a restoring force proportional to the displacement) and a massless damper with viscous damping coefficient c (which produces a force proportional to the velocity and opposing it). The rigid mass m, which here is taken to move only vertically and without rotation, corresponds either to an item to be protected (Fig. 13.1a) or to a machine frame on which a vibratory force acts (Fig. 13.1b).

Transmissibility

Although the mass–spring–dashpot diagrams of Figs. 13.1a and b are similar, they describe physically different situations. In Fig. 13.1a, the support S is

6. H. M. Fuches, U. Ackermann, and W. Frommhold, "Development of Membrane Absorbers for Industrial Noise Abatement," *Bauphysik*, **11**(H.1), 28–36 (1989) (in German).
7. M. H. Fischer, H. V. Fuchs, and U. Ackermann, "Light Enclosures for Low Frequencies," *Bauphysik*, **11**(H.1), 50–60 (1989) (in German).
8. I. L. Vér and E. Veres, "An Apparatus to Study the Sound Excitation and Sound Radiation of Platelike Structures," *Proc. INTER-NOISE*, (1980) pp. 535–540.
9. K. P. Byrne, H. M. Fischer, and H. V. Fuchs "Sealed, Close-Fitting, Machine-Mounted Acoustic Enclosures with Predictable Performance," *Noise Control Eng. J.*, **31**, 7–15 (1988).
10. M. H. Fischer and E. Veres, "Noise Control by Enclosures" Research Report 508, Bundesanstalt fuer Arbeitschutz, Dortmund, 1987 (in German); also Fraunhofer Institute of Building Physics Report, IBP B5 141/86, 1986.
11. J. B. Moreland, Westinghouse Electric Corporation, private communication.
12. L. Cremer, M. Heckl, and E. E. Ungar, *Structureborne Sound*, Berlin, Springer, 1988.
13. K. Goesele, *Berichte aus der Bauforschung* [*Sound Transmission of Doors*], H. 63 Wilhelm Ernst & Sohn Publishers, Berlin, 1969, pp. 3–21.
14. F. P. Mechel, "Transmission of Sound through Holes and Slits Filled with Absorber and Sealed," *Acustica*, **61**(2), 87–103 (1986).
15. F. P. Mechel, "The Acoustic Sealing of Holes and Slits in Walls," *J. Sound Vib.*, **III**(2), 297–336 (1986).
16. G. Kurtze and K. Mueller "Noise Reducing Enclosures," Research Report BMFT-FB-HA 85-005, Bundesministerium füer Forschung und Technologie, Berlin, 1985 (in German).
17. U. J. Kurze et al., "Noise Control by Partial Enclosures; Shielding in the Nearfield," Research Report No. 212, Bundesanstalt fuer Arbeitschutz und Unfallforshung, 1979 (in German).
18. F. P. Mechel, "Sound Absorbers and Absorber Functions" in *Reduction of Noise in Buildings and Inhabited Regions*, Strojnizdat, Moscow, 1987 (in Russian).
19. E. W. Wood and E. E. Ungar, BBN Systems and Technologies Corporation, private communications.
20. R. Michelsen, K. R. Fritz, and C. V. Sazenhofen, "Effectiveness of Acoustic Pipe Wrappings" in *Proc. DAGA '80*, VDE-Verlag, Berlin, 1980, pp. 301–304 (in German).

BIBLIOGRAPHY

Miller, R. K., and W. V. Montone, *Handbook of Acoustical Enclosures and Barriers*, Fairmont, Atlanta, GA, 1978.
"Noise Reduction by Enclosures," VDI Guideline 2711, VDI-Verlag GmbH, Dusseldorf, Germany (in German).

CHAPTER 13

Vibration Isolation

ERIC E. UNGAR AND JEFFREY A. ZAPFE

Acentech, Inc.
Cambridge, Massachusetts

13.1 USES OF ISOLATION

Vibration isolation refers to the use of comparatively resilient elements for the purpose of reducing the vibratory forces or motions that are transmitted from one structure or mechanical component to another. The resilient elements, which may be visualized as springs, are called vibration isolators. Vibration isolation is generally employed (1) to protect a sensitive item of equipment from vibrations of the structure on which it is supported or (2) to reduce the vibrations that are induced in a structure by a machine it supports. Vibration isolation may also be used to reduce the transmission of vibrations to structural components whose attendant sound radiation one wishes to control.

13.2 CLASSICAL MODEL

Mass–Spring–Dashpot System

Many aspects of vibration isolation can be understood from analysis of an ideal, linear, one-dimensional, purely translational mass–spring–dashpot system like that sketched in Fig. 13.1. The isolator is represented by the parallel combination of a massless spring of stiffness k (which produces a restoring force proportional to the displacement) and a massless damper with viscous damping coefficient c (which produces a force proportional to the velocity and opposing it). The rigid mass m, which here is taken to move only vertically and without rotation, corresponds either to an item to be protected (Fig. 13.1a) or to a machine frame on which a vibratory force acts (Fig. 13.1b).

Transmissibility

Although the mass–spring–dashpot diagrams of Figs. 13.1a and b are similar, they describe physically different situations. In Fig. 13.1a, the support S is

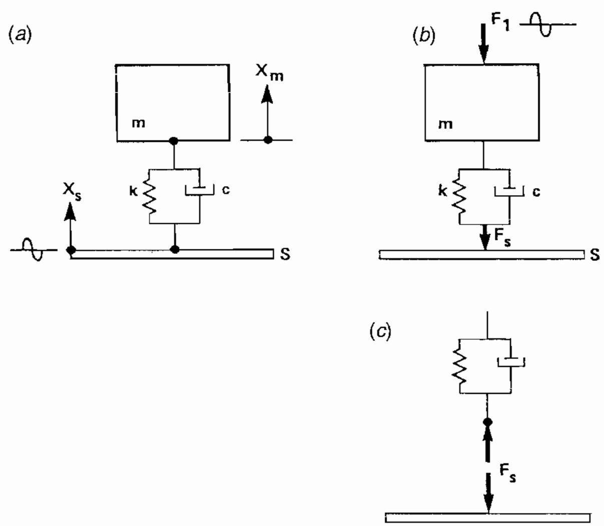

FIGURE 13.1 One-dimensional translational mass–spring–dashpot system: (*a*) excited by support motion; (*b*) excited by force acting on mass; (*c*) force F_s between isolator and support.

assumed to vibrate vertically with a prescribed amplitude X_s at a given frequency; the purpose of the isolator is to keep the displacement amplitude X_m of mass m acceptably small. In Fig. 13.1*b*, a force of a prescribed amplitude F_1 at a given frequency is assumed to act on mass m; the purpose of the isolator is to keep the amplitude F_s of the force that acts on the support within acceptable limits, thereby also keeping the support's resulting motion adequately small.

For the situation represented by Fig. 13.1*a*, the ratio $T = X_m/X_s$ of the amplitude of the mass' displacement to that of the disturbing displacement of the support S is called the (motion) transmissibility. For the situation represented by Fig. 13.1*b*, the ratio $T_F = F_s/F_1$ of the amplitude of the force transmitted to the support S to that of the disturbing force is called the force transmissibility. In many practical instances corresponding to force excitation as represented by Fig. 13.1*b*, the support is so stiff or massive that its displacement may be taken to be zero. It turns out that the force transmissibility T_{F0} obtained with an immobile support (for the case of Fig. 13.1*b*) is given by the same expression as the motion transmissibility (for the case of Fig. 13.1*a*),* namely,[1,2]

$$T = T_{F0} = \sqrt{\frac{1 + (2\zeta r)^2}{(1 - r^2)^2 + (2\zeta r)^2}} \tag{13.1}$$

*This equality holds not only for the simple system of Fig. 13.1, but also for any mathematically linear system.[3] Because of this equality, the literature generally does not differentiate between the two types of transmissibility.

where $r = f/f_n$ is the ratio of the excitation frequency to the natural frequency of the mass–spring system and $\zeta = c/c_c$, which is called the *damping ratio*, is the ratio of the system's viscous damping coefficient c to its critical damping coefficient c_c.

The critical damping coefficient is given by $c_c = 2\sqrt{km} = 4\pi f_n m$. The natural frequency f_n of a spring–mass system obeys[1,2]

$$2\pi f_n = \sqrt{\frac{k}{m}} = \sqrt{\frac{kg}{W}} = \sqrt{\frac{g}{X_{st}}} \tag{13.2}$$

where g denotes the acceleration of gravity, W the weight associated with the mass m, and X_{st} the static deflection of the spring due to this weight. In customary units,

$$f_n(\text{Hz}) \approx \frac{15.76}{\sqrt{X_{st}(\text{mm})}} \approx \frac{3.13}{\sqrt{X_{st}(\text{in.})}} \tag{13.3}$$

The relation $X_{st} = k/W$ and Eq. (13.3) hold only if the spring is mathematically linear—that is, if the slope of the spring's force–deflection curve (which slope corresponds to the stiffness k) is constant. For small-amplitude vibrations about an equilibrium deflection one may take k in the first form of Eq. (13.2) as the slope dF/dx of the spring's force–deflection curve* at the spring's static deflection under an applied load W. However, for some practical isolators, notably those incorporating elastomeric materials, the effective dynamic stiffness may be considerably greater than that obtained from a quasi-static force–deflection curve.[4]

Figure 13.2 shows curves based on Eq. (13.1) for several values of the damping ratio. For small frequency ratios, $r \ll 1$, the transmissibility T is approximately equal to unity; the motion or force is transmitted essentially without attenuation or amplification. For values of r near 1.0, T becomes large (at $r = 1$ or $f = f_n$, $T = 1/2\zeta$); the system responds at resonance, resulting in amplification of the motion or force. All curves pass through unity at $r = \sqrt{2}$.

For $r > \sqrt{2}$, T is less than unity and decreases continually with increasing r. In this high-frequency range, which may be called the *isolation range*, the inertia of the mass plays the dominant role in limiting the mass excursion and thus in limiting the mass' response to support displacement or to forces acting on the mass. Thus, if one desires to achieve good isolation, which corresponds to small transmissibility, one needs to choose an isolator with the smallest possible k (i.e., with the largest practical static deflection X_{st}) in order to obtain the smallest f_n and the greatest value of $r = f/f_n$ for a given excitation frequency.

*Nonlinear spring elements for which $k = dF/dx$ is proportional to the applied load W in a given range are the basis for isolators which have the practical advantage of providing the same natural frequency for all loads in the given range.[4]

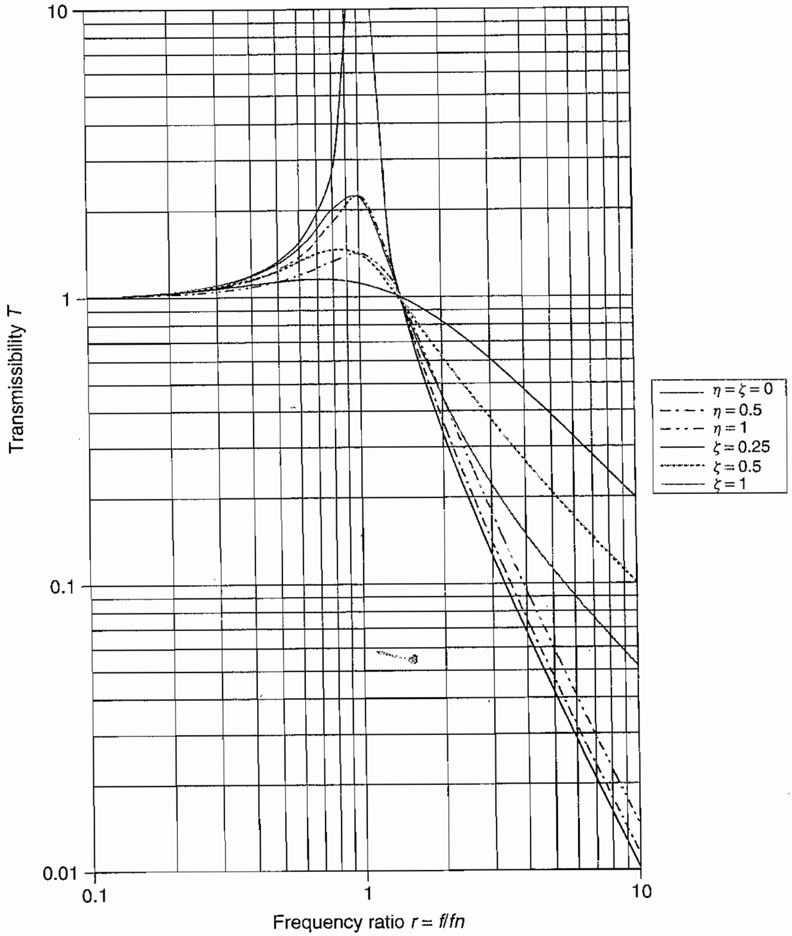

FIGURE 13.2 Transmissibility of mass–spring–damper system of Fig. 13.1 from Eqs. (13.1) and (13.4).

Isolation Efficiency

The performance of an isolation system is sometimes characterized by the isolation efficiency I, which is given by $I = 1 - T$. Whereas the transmissibility indicates the fraction of the disturbing motion or force that is transmitted, the isolation efficiency indicates the fraction by which the transmitted disturbance is less than the excitation. Isolation efficiency is often expressed in percent. For example, if the transmissibility is 0.0085, the isolation efficiency is 0.9915, or 99.15%, indicating that 99.15% of the disturbance does not "get through" the isolator.

Effect of Damping

In the isolation range, that is, for frequency ratios $r > \sqrt{2}$, increased viscous damping results in increased transmissibility, as evident from Fig. 13.2 or Eq. (13.1). Although this fact is mentioned in many texts, it is of little practical consequence for two reasons. First, in practice one rarely encounters systems with damping ratios that are greater than 0.1 unless high damping is designed into a system on purpose—and small values of the damping ratio, and certainly small changes in that damping ratio, have little effect on transmissibility. Second, Eq. (13.1) and Fig. 13.2 pertain only to viscously damped systems, in which a damper produces a retarding force that is proportional to the velocity. Although such systems have been studied most extensively (largely because they are relatively easy to analyze mathematically), the retarding forces in practical systems generally have other parameter dependences.

The effect of damping in practical isolators is generally better represented by *structural damping* than by viscous damping. In structural damping, the retarding force acts to oppose the motion, as in viscous damping, but is proportional to the displacement. For structurally damped systems,[2]

$$T = F_{F0} = \sqrt{\frac{1+\eta^2}{(1-r^2)^2+\eta^2}} \tag{13.4}$$

where η denotes the *loss factor* of the system.*

If a structurally damped system has the same amplification at the natural frequency as a similar viscously damped system, then $\eta = 2\zeta$. The transmissibility of a structurally damped system in the isolation range increases much less rapidly with increasing damping than does that of a system with viscous damping, as evident from Fig. 13.2.

In practical isolation arrangements the damping typically is very small, that is, $\zeta < 0.1$. For such small amounts of damping, the transmissibility in the isolation range differs little from that for zero damping, so that one may approximate the transmissibility in that range by

$$T = T_{F0} = \frac{1}{|r^2-1|} \approx \left(\frac{f_n}{f}\right)^2 \tag{13.5}$$

where the rightmost expression applies for $r^2 = (f/f_n)^2 \gg 1$.

Effects of Inertia Bases

An isolated machine is often mounted on a massive support, generally called an *inertia base*, to increase the isolated mass. If the isolators are not changed as

*The loss factor η in Eq. (13.4) may be taken to vary with frequency as determined from experimental data. See Chapter 14.

the mass is increased, then the natural frequency of the system is reduced, the frequency ratio r corresponding to a given excitation frequency is increased, and the transmissibility is reduced; that is, isolation is improved.

However, practical considerations, such as the load-carrying capacities of isolators, usually dictate that the total isolator stiffness be increased* as the mass is increased, with the static deflection changing little. (In fact, conventional commercial isolators typically are specified in terms of the loads they can carry and the corresponding static deflection.) As evident from Eq. (13.3), the natural frequency remains unchanged if the static deflection remains unchanged, and addition of an inertia base then does not change the transmissibility.

Thus, inertia bases in practice typically do not improve isolation significantly. They are of some benefit, however: With a greater mass supported on stiffer springs, forces that act directly on the isolated mass produce smaller static and vibratory displacements of that mass.

Effect of Machine Speed

In a rotating or reciprocating machine, the dominant excitation forces generally are due to dynamic unbalance and occur at frequencies that correspond to the machine's rotational speed and/or multiples of that speed. Greater speed thus corresponds to increased excitation frequencies and larger values of r—and therefore to reduced transmissibility (or improved isolation). As evident from Eq. (13.1) or (13.5), the transmissibility[3]—the ratio of the transmitted to the excitation force—becomes smaller as the speed (and the excitation frequency) is increased; in the isolation range, the transmissibility is very nearly inversely proportional to the square of the excitation frequency. However, the excitation forces associated with unbalance vary as the square of speed (and frequency) and thus increase with speed about as much as the transmissibility decreases. The net result is that the magnitudes of the forces that are transmitted to the supporting structure are virtually unaffected by speed changes, although speed changes do affect the frequencies at which these forces occur.

Limitations of Classical Model

Although the linear single-degree-of-freedom model provides some useful insights into the behavior of isolation systems, it obviously does not account for many aspects of realistic installations. Clearly, real springs are not massless and may be nonlinear, and real machine frames and supporting structures are not rigid. Resiliently supported masses generally move not only vertically but also horizontally—and they also tend to rock.

In simple classical analyses, furthermore, the magnitude of the exciting force or motion is taken as constant and independent of the resulting response, whereas

*Note that the single spring and dashpot in the schematic diagrams of Fig. 13.1 represent the entire isolation system, which in reality may consist of many isolators. Addition of isolators amounts to an increase in the stiffness of the isolation system.

in actual situations the excitation often depends significantly on the response, as discussed in Section 13.4 under Loading of Sources.

13.3 ISOLATION OF THREE-DIMENSIONAL MASSES

General

Unlike the simple model shown in Fig. 13.1, where the mass can only move vertically without rotation and the system has only one natural frequency, an actual rigid three-dimensional mass has six degrees of freedom; it can translate in three coordinate directions and rotate about three axes. An elastically supported rigid mass thus has six natural frequencies. A nonrigid mass has many additional ones associated with its deformations. Obtaining effective isolation here requires that all of the natural frequencies fall considerably below the excitation frequencies of concern. Descriptions of the natural frequencies and responses of general isolated rigid masses are available[3,5] but are so complex that they provide little practical insight and tend to be used only rarely for design purposes.

Coupling of Vertical Motion and Rocking

Figure 13.3 is a schematic diagram of a mass m supported on two isolators in a plane through its center of gravity, parallel to the plane of the paper (or on two rows of isolators extending in the direction perpendicular to the plane of the paper) with stiffnesses k_1 and k_2 located at distances a_1 and a_2 from the mass' center of gravity. One may visualize easily that a downward force applied at the center of gravity of the mass in general would produce not only a downward displacement of the center of gravity but also a rotation of the mass, the latter due to the moment resulting from the isolator forces. Similarly, purely vertical up-and-down motion of the support S would in general result in rocking of the mass, in addition to its vertical translation. Vertical and rocking motions here are said to be "coupled."

The natural frequency f_v at which pure vertical vibration would occur if the mass would not rock (i.e., the "uncoupled" vertical natural frequency) is given by

$$2\pi f_v = \sqrt{\frac{k_1 + k_2}{m}} \tag{13.6}$$

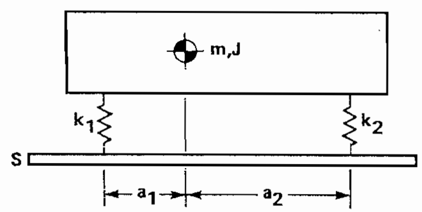

FIGURE 13.3 Mass m with moment of inertia J supported on two isolators.

The natural frequency f_r at which the mass would rock if its center of gravity would not move vertically (i.e., the uncoupled rocking frequency) is given by

$$2\pi f_r = \sqrt{\frac{k_1 a_1^2 + K_2 a_2^2}{J}} \tag{13.7}$$

where J denotes the mass polar moment of inertia about an axis through the mass' center of the gravity and perpendicular to the plane of the paper.

The rocking frequency f_r may be either smaller or larger than f_v. In the general case, the two natural frequencies of the system differ from both of these frequencies and correspond to motions that combine rotation and vertical translation (but without rotation out of the plane of the paper). These "coupled" motion frequencies always lie above and below the foregoing uncoupled motion frequencies; that is, one of the coupled motion frequencies lies below both f_v and f_r and the other lies above both f_v and f_r; coupling in effect increases the spread between the natural frequencies.[6,7]

The presence of coupled motions complicates the isolation problem because one needs to ensure that both of the coupled natural frequencies fall considerably below the excitation frequencies of concern. To eliminate this complication, one may select the locations and stiffnesses of the isolators so that the forces produced by them when the mass moves downward without rotation result in zero net moment about the center of gravity. This situation occurs if the isolators are linear and designed so that they have the same static deflection under the static loads to which they are subject. (Selection of isolators that have the same unloaded height as well as the same static deflection results also in keeping the isolated equipment level.) Then f_v and f_r of Eqs. (13.6) and (13.7) are the system's actual natural frequencies, and vertical forces at the center of gravity or vertical support motions produce no rocking.

Effect of Horizontal Stiffness of Isolators

In the foregoing discussion, horizontal translational motions and the effects of horizontal stiffnesses of the isolators were neglected. However, any real isolator that supports a vertical load also has a finite horizontal stiffness, and in some systems separate horizontally acting isolators may be present. Figure 13.4 is a schematic diagram of a mass on two vertical isolators (or on two rows of such isolators extending perpendicular to the plane of the paper) with stiffnesses k_1 and k_2. The effects of the horizontal stiffnesses of these isolators or of separate horizontally acting isolators are represented by the horizontally acting spring elements with stiffnesses h_1 and h_2, here assumed to act in the same plane at a distance b below the center of gravity of the mass.

The system of Fig. 13.4 has three degrees of freedom and therefore three natural frequencies. If the vertically acting isolators are selected and positioned so that they have the same static deflection, then (as discussed in the foregoing section) there is very little coupling between the vertical translational and the

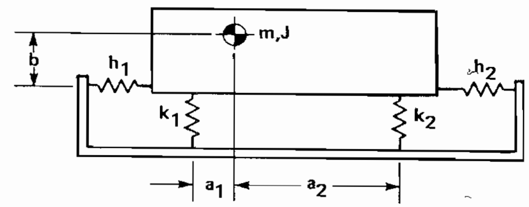

FIGURE 13.4 Mass m with moment of inertia J supported by two vertically and two collinear horizontally acting isolators.

rocking motions, and the natural frequency corresponding to vertical translation is given by Eq. (13.6). The other two natural frequencies, which are associated with combined rotation and horizontal translation, are given by the two values of f_H one may obtain from[6,7]

$$\frac{f_H}{f_v} = (N \pm \sqrt{N^2 - SB})^{1/2} \tag{13.8}$$

where

$$N = \frac{1}{2}\left[S\left(1 + \frac{b^2}{r^2}\right) + B\right] \qquad B = \frac{a_1^2 k_1 + a_2^2 k_2}{r^2(k_1 + k_2)} \qquad S = \frac{h_1 + h_2}{k_1 + k_2} \tag{13.8a}$$

Here, $r^2 = J/m$ represents the square of the radius of gyration of the mass about an axis through its center of gravity.

For a rectangular mass of uniform density, the center of gravity is in the geometric center and the radius of gyration r obeys $r^2 = \frac{1}{12}(H^2 + L^2)$, where H and L represent the lengths of the vertical and horizontal edges of the mass (in the plane of Fig. 13.4).

Nonrigidity of Mass or Support

If the mass of Fig. 13.1a is flexible instead of rigid and has a resonance at a certain frequency, then it will deflect (by deforming) considerably in response to excitation at that frequency, resulting in large transmissibility and thus in poor isolation. An analogous situation occurs if the system of Fig. 13.1b is excited at a resonance frequency of the support.

Figure 13.5 is a schematic diagram representing the vertical translational motion of a machine isolated from a nonrigid support, where the support is represented by a spring–mass system, corresponding, for example, to the static stiffness of a building's floor and to the effective mass that participates in the floor's vibration at its fundamental resonance. Isolator and floor damping have little effect on the off-resonance vibrations and may be neglected for the sake of simplicity. If f_M denotes the natural frequency of the isolated machine on a

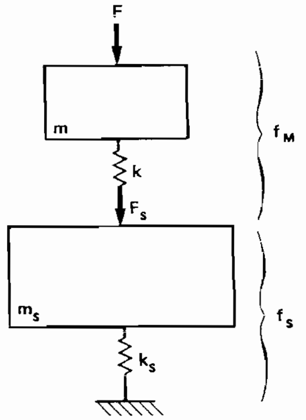

FIGURE 13.5 Schematic representation of isolated machine on nonrigid support structure. Machine is represented by mass m subject to oscillatory force F; isolator is represented by spring k. Support structure is represented by effective mass m_s on spring k_s.

rigid support and f_S represents the natural frequency of the support without the machine in place, so that

$$2\pi f_M = \sqrt{\frac{k}{m}} \qquad 2\pi f_S = \sqrt{\frac{k_s}{m_s}} \tag{13.9}$$

then the force transmissibility, that is, the ratio of the magnitude of the force F_S transmitted to the support to that of the excitation force F, may be written as

$$T_F = \frac{F_S}{F} = \left| \frac{1 - R^2}{(1 - R^2)(1 - R^2G^2) - R^2/M} \right| \tag{13.10}$$

where $R = f/f_S$, $G = f_S/f_M$, and $M = m/m_s$ with f representing the excitation frequency.

Figure 13.6 shows a plot of the transmissibility calculated from Eq. (13.10) for the illustrative case where $M = \frac{1}{2}$, $G = 2$, together with a corresponding plot of the transmissibility that would be obtained with an immobile (infinitely rigid) support. For excitation frequencies that fall between the two resonance frequencies of the system with the nonrigid support, the transmissibility obtained with the nonrigid support is less than that with the rigid support; the reverse is true for excitation frequencies above the upper of the two resonance frequencies. For sufficiently high excitation frequencies, the difference between the two transmissibilities becomes negligible.

The two resonance frequencies f_c of the system with the nonrigid support may be found from

$$\left(\frac{f_c}{f_M}\right)^2 = P \pm \sqrt{P^2 - G^2} \qquad P = \tfrac{1}{2}(1 + G^2 + M) \tag{13.11}$$

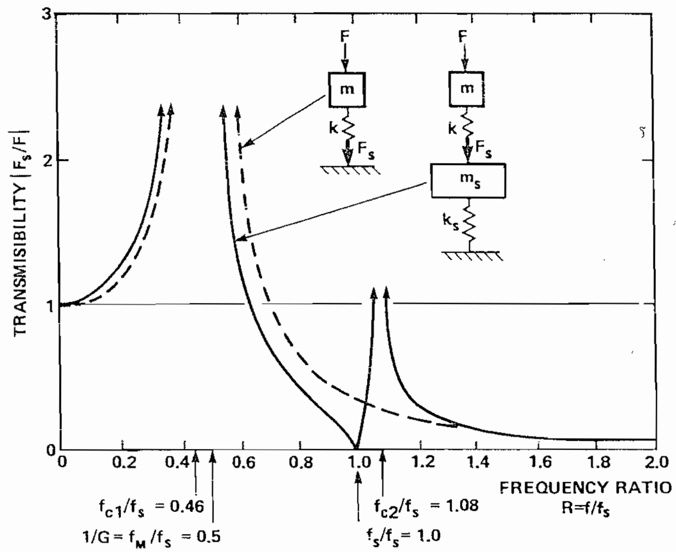

FIGURE 13.6 Comparison of transmissibilities obtained with rigid and nonrigid supports. Curves were obtained from Eqs. (13.1) and (13.10) for zero damping and for mass ratio $M = m/m_s = \frac{1}{2}$ and system frequency ratio $G = f_S/f_M = 2$. Resonance frequencies f_{c1} and f_{c2} of coupled system and f_M and f_S of uncoupled machine and support are indicated on the frequency scale.

with G and M defined as indicated after Eq. (13.10). The higher resonance frequency, obtained with the plus sign in Eq. (13.11), always lies above both f_M and f_S; the lower resonance frequency, obtained with the minus sign, always lies below both f_M and f_S.

13.4 HIGH-FREQUENCY CONSIDERATIONS

Although the relations discussed in the foregoing sections usually suffice for analysis and design in cases where only relatively low frequencies are of concern (i.e., for frequencies that are generally below the resonance frequencies of the machine and support structures themselves), at higher frequencies there occur complications that may need to be taken into account. At high frequencies, the isolated item and the support structure cease to behave as rigid masses, isolators may exhibit internal resonances, and vibration sources tend to be affected by "loading."

Loading of Sources

Loading of a source refers to the reduction of the source's vibratory motion that results from a force that opposes this motion. For example, the vibrations of a sheet metal enclosure tend to be reduced by the opposing forces produced when a hand is placed against it. Similarly, a factory floor that vibrates with a certain amplitude tends to vibrate less when a (nonvibrating) machine is bolted to it as the result of reaction forces produced by the machine.

In the latter example, if the machine is isolated from the floor, it is likely to produce smaller reaction forces on the floor than it would produce if it is bolted rigidly to the floor, and the floor may be expected to vibrate more if the machine is isolated than if it is rigidly fastened to the floor. Since greater floor vibrations then are transmitted to the machine, use of isolation will protect the machine less than anticipated from transmissibility considerations.

To be able to evaluate how much protection of the machine the isolator provides in this case, one needs a quantitative description of the source's response to loading. One may obtain such a description by measuring the motion produced by the source as it acts on several different masses or structures with different dynamic characteristics (impedances), which produce different (known or measurable) reaction forces. For prediction purposes, it often suffices to assume that the source's response to loading at any given frequency is "linear"; that is, the motion amplitude produced by the source decreases in proportion to the amplitude F_0 of the reaction force (which is equal to the amplitude of the force that the source generates). One may describe source motions at a given frequency equally well in terms of acceleration, displacement, or velocity, but use of velocity has become customary. For a linear source one may express the dependence of the source's velocity amplitude V_0 on the force as[8]

$$V_0 = V_{\text{free}} - M_s F_0 \tag{13.12}$$

Here V_{free} represents the velocity amplitude that the source generates if it is free of reaction forces, that is, if it produces zero force. (In general, the parameters V_{free} and M_s for a given source may be different for different frequencies.) The quantity M_s, which indicates how rapidly V_0 decreases with increasing F_0, is known as the *source mobility* and may be found from $M_s = V_{\text{free}}/F_{\text{blocked}}$, where F_{blocked} denotes the force amplitude obtained if the source is "blocked" so that it has zero velocity V_0.

One may readily verify that $M_s = 0$ corresponds to a *velocity source*, that is, to a source whose output velocity amplitude is constant, regardless of the magnitude of its output force F_0. Similarly, infinite M_s corresponds to a *force source*, whose output force F_0 is constant and independent of its output velocity.[8] (For example, a rotating unbalanced mass generates forces that are virtually independent of its support motions and thus acts essentially like a force source. On the other hand, a piston driven by a shaft with a large flywheel moves at essentially the same amplitude regardless of the force acting on it and thus behaves like a velocity source.)

Isolation Effectiveness[3,8]

In the presence of significant source loading, one cannot evaluate the performance of an isolation system on the basis of transmissibility because in the definition

of transmissibility the magnitudes of the disturbances are prescribed and thus, in effect, are taken as constant. A measure of isolation performance that is useful in the presence of loading is the so-called *isolation effectiveness E*. Isolation effectiveness is defined as the ratio of the magnitude of the vibrational velocity of the item to be protected (called the "receiver") that results if the item is rigidly connected to the source to the magnitude of the receiver's velocity that is obtained if the isolator is inserted between the source and the receiver in place of the rigid connection. The definition of isolation effectiveness is analogous to that of insertion loss in airborne acoustics.

If the receiver velocity V_R is proportional to the force F_R that acts on the receiver, so that $V_R = M_R F_R$, where M_R is called receiver mobility,* then the isolation effectiveness may be expressed in terms of a ratio of forces acting on the receiver as well as of a ratio of receiver velocities, namely,

$$E = \frac{V_{Rr}}{V_{Ri}} = \frac{F_{Rr}}{F_{Ri}} \tag{13.13}$$

where the added subscript r refers to the case in which a rigid connection replaces the isolator and the subscript i refers to the situation where the isolator is present.

Whereas small transmissibility T corresponds to good isolation, it is large values of E that imply effective isolation. For this reason, the reciprocal of the effectiveness is sometimes used to characterize the performance of an isolation system. Although this reciprocal differs from the transmissibility T in the general situation where the source is affected by loading, in the special case of sources that are unaffected by loading (i.e., for sources that generate load-independent velocity or force amplitudes), $E = 1/T$.

Effectiveness of Massless Linear Isolator

An isolator may be considered as "massless" if it transmits whatever force is applied to it. (Equal and opposite forces must act on the two sides of a massless isolator if it is not to accelerate infinitely.) A "linear" isolator is one whose deflection is proportional to the applied force. The velocity difference across such an isolator at any frequency then is also proportional to the applied force, and the ratio of the magnitude of this velocity difference to that of the applied force is called the isolator's mobility M_I. Like the reciprocal of isolator stiffness, M_I is large for a soft isolator and zero for a rigid isolator.

For a massless linear isolator, the effectiveness obeys[8,11]

$$E = \left|1 + \frac{M_I}{M_S + M_R}\right| \tag{13.14}$$

*Mobilities of receivers at their attachment points may be estimated analytically for simple configurations (e.g., refs. 9 and 10) or may be measured (as functions of frequency). The velocities and forces usually are expressed in terms of complex numbers, or *phasors*, which indicate both the magnitudes and the relative phases of sinusoidally varying quantities. Mobilities then also are complex quantities in general.

At a resonance of the receiver, the receiver's vibratory velocity V_R resulting from a given force F_R is large, so that the receiver's mobility is large. In view of Eq. (13.14), the effectiveness of an isolator is small in the presence of such a resonance.

Equation (13.14) also indicates that the effectiveness is small if the source mobility M_S is large. For a force source, for which M_S is infinite, the effectiveness is equal to unity, implying that the receiver vibrates just as much with the isolator in place as it does if the isolator is replaced by a rigid connection. This initially somewhat surprising result is correct: After all, the force source generates the same force, regardless of the velocity or displacement it produces, and the isolator transmits all of this force, with a softer isolator merely leading to greater displacement of the source at its output point.

Consequences of Isolator Mass Effects

Isolator mass effects may be neglected—that is, an isolator may be considered as massless—as long as the frequencies under consideration are appreciably lower than the first internal or *standing-wave* resonance frequency of the isolator.* Such standing-wave resonances tend to reduce the isolator's effectiveness severely, as illustrated by Fig. 13.7. This figure shows the calculated transmissibility of a leaf spring modeled as a uniform cantilever beam. The upper left-hand corner of the plot may be recognized as the usual transmissibility curve (similar to Fig. 13.2) in the vicinity of the resonance frequency $f_n = (1/2\pi)\sqrt{k/m}$ obtained for a massless isolator. With increasing excitation frequency the transmissibility does not decrease monotonically, as it would for a massless spring (see curve for $m_{sp} = 0$); instead, there occur secondary peaks associated with standing-wave resonances of the beam. The frequency at which these peaks begin to occur increases as the ratio of the isolated mass m to the mass m_{sp} of the spring increases. Although in the figure only two peaks are shown for each mass ratio, there actually occurs a succession of peaks that become more closely spaced with increasing frequency. The magnitude of these peaks decreases with increasing damping.

To reduce the effects of standing-wave resonances, one thus needs to select an isolator with relatively high damping and a configuration for which the onset of standing-wave resonances occurs at comparatively high frequencies. This implies use of a material with high stiffness-to-weight ratio or, equivalently, with a high longitudinal wave velocity $\sqrt{E/\rho}$ (where E denotes the material's modulus of elasticity and ρ its density), and also use of a configuration with small overall dimensions.

*At lower frequencies, the only effect of the mass of the isolator is to reduce slightly the fundamental resonance frequency of the system. The modified resonance frequency may be calculated from the isolator stiffness and a mass consisting of the isolated mass plus a fraction of the mass of the isolator. If the isolator consists of a uniform spring or pad in compression or shear, the fraction is $\frac{1}{3}$; if the isolator consists of a uniform cantilever beam, the fraction is approximately 0.24.

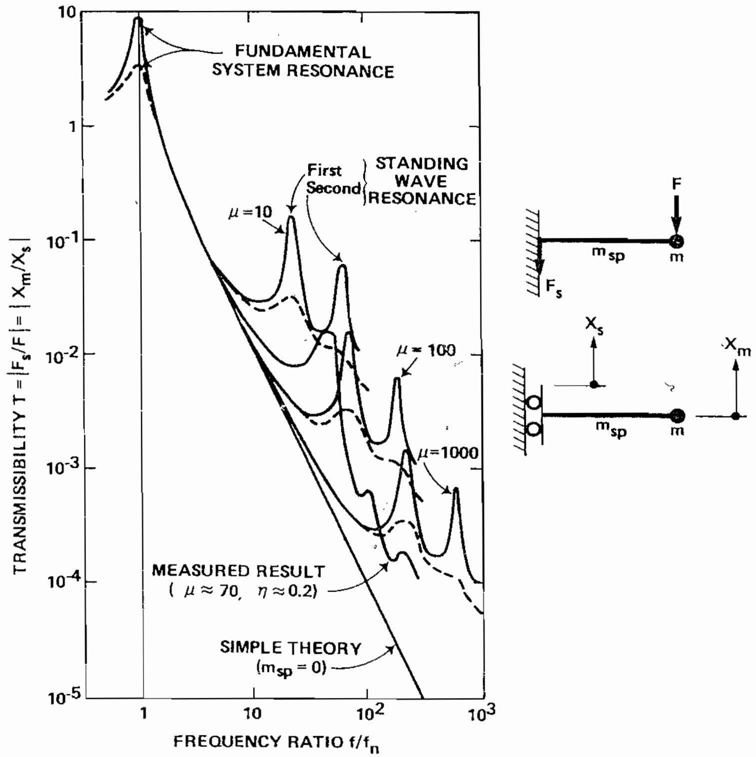

FIGURE 13.7 Effect of isolator mass and damping on transmissibility of uniform cantilever for three values of ratio $\mu = m/m_{sp}$ of isolated mass to mass of cantilever spring. (After Refs. 11 and 12.) Solid calculated lines are for loss factor $\eta = 0.1$; dashed lines for $\eta = 0.6$. (Measured result shown is from Ref. 13.) Frequency is normalized to f_n, the fundamental resonance frequency obtained with a massless spring.

The isolation effectiveness at any specified frequency of a system in which isolator mass effects are not negligible is given by[8]

$$E = \left|\frac{\alpha}{M_S + M_R}\right| \left|1 + \frac{M_S}{M_{Isb}} + \frac{M_R}{M_{Irb}}\left(1 + \frac{M_S}{M_{Isf}}\right)\right| \qquad (13.15)$$
$$\frac{1}{\alpha^2} = \frac{1}{M_{Irb}}\left(\frac{1}{M_{Isb}} - \frac{1}{M_{Isf}}\right)$$

where M_{Isb} denotes the isolator mobility (i.e., the velocity-to-force ratio) measured on the source side of the isolator if the receiver side of the isolator is "blocked" (i.e., prevented from moving), M_{Irb} denotes the mobility measured on the receiver side of the isolator if the source side is blocked, and M_{Isf} denotes the mobility measured on the source side if the receiver side is "free" or unconstrained. One may readily verify that Eq. (13.15) reduces to Eq. (13.14) for massless isolators, for which $M_{Isb} = M_{Irb} = M_I$ and M_{Isf} is infinite.

13.5 TWO-STAGE ISOLATION

A force applied to one side of a massless isolator, as has been mentioned, must be balanced by an equal and opposite force at the other side of the isolator. This is not the case for an isolator that incorporates some mass, because the force applied to one side then is balanced by the sum of the inertia force and the force acting on the other side of the isolator. Thus, unlike for a massless isolator, the force transmitted by an isolator with mass can be less than the applied force.

One may realize such a force reduction benefit, even at low frequencies at which mass effects in isolators themselves are negligible, by adding a lumped mass "inside" an isolator. One may visualize this concept by considering a spring that is cut into two lengths with a rigid block of mass welded in place between the two parts, resulting in an isolator consisting of two lengths of spring with a mass between them. If a mass m is mounted atop this isolator, one obtains a system that may be represented by a diagram like that of Fig. 13.8a. Because this system consists of a cascade of two spring–mass systems, it is said to have two stages of isolation.

Transmissibility

The system of Fig. 13.8a has two natural frequencies f_b that may be found from

$$\left(\frac{f_b}{f_0}\right)^2 = Q \pm \sqrt{Q^2 - B^2} \qquad Q = \frac{1}{2}\left(B^2 + 1 + \frac{k_2}{k_1}\right) \tag{13.16}$$

where

$$B = \frac{f_I}{f_0} \qquad 2\pi f_I = \sqrt{\frac{k_1 + k_2}{m_I}} \qquad 2\pi f_0 = \frac{1}{\sqrt{m(1/k_1 + 1/k_2)}} \tag{13.16a}$$

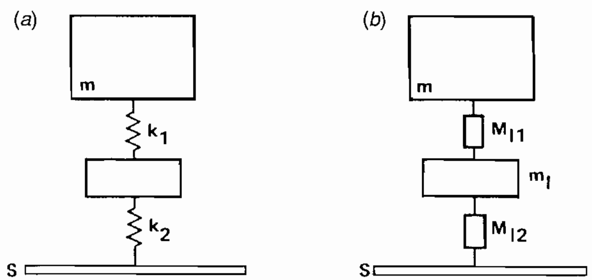

FIGURE 13.8 Two-stage isolation with intermediate mass m_I: (a) springs; (b) general isolation elements.

The frequency f_0 is the natural frequency of the system in the absence of any included mass m_I; that is, it is the natural frequency of a conventional simple single-stage system. The frequency f_I is the natural frequency of mass m_I moving between the two springs, with mass m held completely immobile. The upper frequency f_b, which one obtains if one uses the plus sign before the square root, always is greater than both f_0 and f_I; the lower frequency f_b, corresponding to the minus sign, always falls below both f_0 and f_I.

The transmissibility of a two-stage system like that of Fig. 13.8a obeys

$$\frac{1}{T} = \frac{1}{T_{F0}} = \frac{1}{B^2}\left(\frac{f}{f_0}\right)^4 - \left[1 + \frac{1 + k_2/k_1}{B^2}\right]\left(\frac{f}{f_0}\right)^2 + 1 \approx \left(\frac{f^2}{f_0 f_I}\right)^2 \tag{13.17}$$

where the last approximate expression applies for high frequencies, namely, for excitation frequencies that are much greater than both f_0 and f_I.

Figure 13.9 shows an illustrative plot of the transmissibility of an undamped two-stage system with $B = f_I/f_0 = 5$ and $k_2/k_1 = 1$, together with a plot of the transmissibility of an (undamped) single-stage system. The second natural frequency of the two-stage system (at $f/f_0 \approx 5.1$) is clearly evident, as is the subsequent rapid decrease in that system's transmissibility with increasing frequency. At high frequencies, that is, a little above the aforementioned second natural frequency, the transmissibility of the two-stage system may be seen to be smaller than that of a single-stage system with the same fundamental natural frequency. As evident from Eq. (13.17), the high-frequency transmissibility of a two-stage system varies inversely as the fourth power of the excitation frequency, whereas Eq. (13.5) indicates that the transmissibility of a single-stage system varies inversely as only the second power of the excitation frequency.

The advantage of a two-stage system over a single-stage system is that it results in greatly reduced transmissibility at high frequencies (i.e., above the higher of its two natural frequencies). It has the disadvantage that it introduces an additional transmissibility peak at a low frequency (i.e., at its second natural frequency). Thus, two-stage isolation is beneficial in general only if the aforementioned second natural frequency is somewhat lower than the lowest excitation frequency of concern. Thus, to reap the benefit of a two-stage system, one typically needs a relatively large intermediate mass m_I. Where several items need to be isolated, it often is advantageous to support these on a common massive platform (often called a "subbase" or "raft"), to isolate each item from the platform, and to isolate the platform from the structure that supports it. In this arrangement the platform serves as a relatively large intermediate mass for each of the isolated items, resulting in efficient two-stage isolation performance with comparatively small weight penalty.

Isolation Effectiveness

Although the foregoing results apply strictly only to isolators without damping, they also provide a reasonable approximation to the behavior of lightly damped systems, except near the natural frequencies. To account for high damping or more

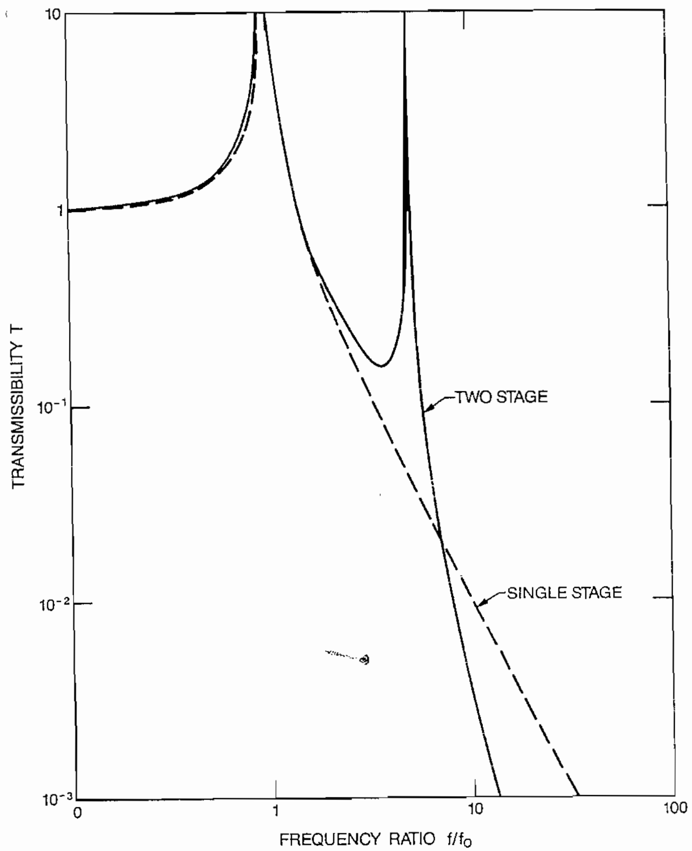

FIGURE 13.9 Transmissibility of two-stage system. Calculated from Eq. (13.17) for $k_2/k_1 = 1$ and $B = f_I/f_0 = 5$.

complicated linear isolator configurations (e.g., where each isolator is modeled by various series and parallel combinations of springs and dampers), it is convenient to represent each isolator by its mobility. A corresponding diagram appears in Fig. 13.8*b*. As has been discussed in Section 13.4, the source mobility M_S is a measure of a vibration source's susceptibility to loading effects, and the isolation effectiveness E is a measure of the isolation performance, which, unlike transmissibility, takes loading effects into account. If one takes S in Fig. 13.8*b* to represent a general linear source and replaces the mass m by a general linear receiver with mobility M_R, one obtains a general linear two-stage system whose effectiveness one may write as[8]

$$E = |E_1 + \Delta E| \qquad E_1 = 1 + \frac{M_I}{M_S + M_R} \tag{13.18}$$

where

$$M_I = M_{I1} + M_{I2} \qquad \Delta E = \frac{(M_{I1} + M_S)(M_{I2} + M_R)}{M_m(M_S + M_R)} \tag{13.18a}$$

One may recognize E_1 as corresponding to the effectiveness of a single-stage system [see Eq. (13.14)], that is, to a two-stage system with zero included mass, with M_I denoting the mobility of the two partial isolators in series. Thus, ΔE represents the effectiveness increase obtained by addition of the included mass m_I, whose mobility is M_m. Note that ΔE is inversely proportional to M_m, indicating that greater included masses generally result in greater effectiveness increases.

Optimization of Isolator Stiffness Distribution

Once one has selected the mobility M_I of the total isolator (or, equivalently, its compliance or stiffness), one needs to consider how to allocate this mobility among the components M_{I1} and M_{I2}. If one lets r_1 denote the fraction of the total mobility on the source side of the included mass, so that $M_{I1} = r_1 M_I$ and $M_{I2} = (1 - r_1)M_I$, it turns out that one may obtain the largest value of ΔE, namely,

$$\Delta E_{\max} = \frac{(M_I + M_s + M_R)^2}{4M_m(M_s + M_R)} \tag{13.19}$$

by making r_1 equal to its optimum value,*

$$r_{\text{opt}} = \frac{1}{2}\left(1 + \frac{M_R - M_S}{M_I}\right) \tag{13.20}$$

In view of Eq. (13.18a), in an efficient isolation system M_{I1} must be considerably greater than M_S, and also M_{I2} must be considerably greater than M_R. For such a system, one finds that $r_{\text{opt}} \approx \frac{1}{2}$ and that $\Delta E_{\max}$ may be approximated by replacing the expression in the parentheses of the numerator of Eq. (13.19) by M_I. Thus, if the total mobility of the isolator is sufficiently great, that is, if the total stiffness of the isolator is sufficiently small, one may generally obtain the greatest improvement $\Delta E_{\max}$ by allocating the same mobility or stiffness to the two isolator components.

It may be shown[8] that placing a given mass "within" the isolator as described above, so as to obtain a two-stage system with two like isolator mobility components, results in greater effectiveness than placement of the mass directly at the receiver as long as $M_I \gg M_R$. This inequality usually is likely to be satisfied in practice, except at resonances of the receiver at which M_R is very large. Similarly, as long as $M_I \gg M_S$, placing the mass within the isolator results in greater

*This result applies strictly only if the various mobilities or mobility ratios are real quantities. It suffices for development of an intuitive understanding, although more complicated expressions apply in the general case where the mobilities are represented by complex quantities.

effectiveness than placement of the mass directly at the source. The foregoing inequality generally is likely to be satisfied in practice, except for sources that behave essentially like force sources and thus have very high mobility.

13.6 PRACTICAL ISOLATORS

A great many different isolators are available commercially in numerous sizes and load capacities, with various attachment means, and with many types of specialized features.[4] Details concerning such isolators typically may be found in suppliers' catalogs.

Most commercial isolators incorporate metallic or elastomeric resilient elements. Metallic elements most often are in the form of coil springs but also occur in the form of flexural configurations such as leaf springs or conical Belleville washers. Coil springs are predominantly used in compression, usually because such tensile springs tend to involve configurations that give rise to stress concentrations and thus have lesser fatigue life. Coil spring isolator assemblies often involve parallel and/or series arrangements of springs in suitable housings, are designed to have the same stiffness in the lateral directions as in the axial direction, and may also incorporate friction devices (such as wire mesh inserts), snubbers to limit excursions due to large disturbances (such as earthquakes), and in-series elastomeric pads for enhanced damping and isolation at high frequencies. Spring systems in housings need to be installed with care to avoid binding between the housing elements and between these elements and the springs.

Some commercial metallic isolators employ pads or woven assemblies of wire mesh to provide both resilience and damping. Others use arrangements of coils or loops of wire rope not only to provide damping but also to serve as springs.

A great many commercially available isolators that employ elastomeric elements have these elements bonded or otherwise attached to support plates or sleeves that incorporate convenient means for fastening to other components. The isolators may be designed so that the elastomeric element is used in shear, torsion, compression, or a combination of these modes. There are also available a variety of elastomeric gaskets, grommets, sleeves, and washers, intended to be used with bolts or similar fasteners to provide both connection and isolation.

Elastomeric pads often are used as isolators by themselves, as are pads of other resilient materials, such as cork, felt, fiberglass, and metal mesh. Such pads often are convenient and relatively inexpensive; their areas can be selected to support the required loads, and their thicknesses can be chosen to provide the desired stiffness.

In the design and selection of pads of solid (in contrast to foamed) elastomeric materials, one needs to take into account that a pad's stiffness depends not only on its thickness and area but also on its shape and constraints. This behavior is due to the incompressibility of elastomeric materials, which essentially prevents a pad from changing its volume as it is compressed and thus in essence does not permit a pad to be compressed if it is confined so that its edges cannot bulge outward. A pad's freedom to compress may be characterized by its shape factor, defined as the ratio of its loaded area to the total area of the edges that are free to bulge; the greater the shape factor, the greater is the pad's effective stiffness. However, a pad's freedom to deform while maintaining constant volume also is affected by how easily the loaded surfaces can slip relative to the adjacent surfaces; the more restricted this slippage, the greater the pad's effective stiffness. Some commercial isolation pads are furnished with top and bottom load-carrying surfaces bonded to metal or other stiff plates to eliminate the stiffness uncertainties due to unpredictable slippage.

To avoid the need for considering the shape factor in pad selection, many commercial isolation pad configurations have a multitude of cutouts (e.g., closely spaced arrays of holes) or ribs, which provide roughly constant amounts of bulging area per unit surface area. If ribbed or corrugated pads or pads with cutouts are used in stacks, plates of a stiff material (e.g., metal sheets) generally are used between pads to distribute the load on the load-bearing surfaces and to avoid having protrusions on one pad extending into openings on the adjacent pad.

So-called pneumatic, or air spring, isolators, which have found considerable use, obtain their resilience primarily from the compressibility of confined volumes of air. They may take the form of air-filled pillows of rubber or plastic, often with cylindrical or annular shapes, or they may consist essentially of piston-in-cylinder arrangements. Air springs can be designed to have small effective stiffnesses while supporting large loads and to have smaller heights than metal springs of equal stiffness. Practical air springs typically can provide fundamental resonance frequencies that may be as low as about 1 Hz. Some air spring configurations are laterally unstable under some load conditions and require the use of lateral restraints; some are available with considerable lateral stability.

Air springs of the piston-and-cylinder type can be provided with leveling controls, which automatically keep the isolated item's static position at a predetermined distance from a reference surface and (by use of several air springs and a suitable control system) at a predetermined inclination. The stiffness of a piston-type air spring is proportional to PA^2/V, where P denotes the air pressure, A the piston face area, and V the cylinder volume. The product $(P - P_0)A$, where P_0 represents the ambient atmospheric pressure, is equal to the static load carried by the spring. Lower stiffnesses may be obtained with a given area at a given air pressure by use of larger effective volumes; for this reason, some commercial air spring isolators are available with auxiliary tanks that communicate with the cylinder volume via piping. In some instances, a flow constriction in this piping is used to provide low-frequency damping. If the pressure in a piston-and-cylinder-type air spring is considerably greater than the atmospheric pressure, the pressure in the spring is nearly proportional to the load it supports. Because the spring's stiffness is proportional to this pressure, the natural frequency one obtains with such an air spring isolation system is essentially independent of the load, making air springs (like other constant-natural-frequency systems[4]) particularly useful for applications in which the loads are variable or uncertain.

Pendulum arrangements often are convenient means for obtaining horizontally acting isolation systems with low natural frequencies. One may calculate the horizontal natural frequency of a pendulum system from Eq. (13.3) if one replaces X_{st} in that equation by the pendulum length. Some commercial isolation systems combine pendulum action for horizontal isolation with spring action for vertical isolation.

Various exotic isolation systems have also been investigated or employed for special applications. These include systems in which the spring action is provided by magnetic or electrostatic levitation or by streams or thin films of gases or liquids.

Active isolation systems (see Chapter 18) have recently received increased attention. Such systems essentially are dynamic control systems in which the vibration of the item to be protected is sensed by an appropriate transducer whose suitably processed output is used to drive an actuator that acts on the item so as to reduce its vibration. Active systems are relatively complex, but they can provide better isolation than passive systems under some conditions, notably, in the presence of low-frequency disturbances, attenuation of which by passive means generally tends to be most difficult.

REFERENCES

1. W. T. Thomson, *Theory of Vibration with Applications*, 2nd ed., Prentice-Hall, Englewood Cliffs, NJ, 1981.
2. J. C. Snowdon, *Vibration and Shock in Damped Mechanical Systems*, Wiley, New York, 1968.
3. D. J. Mead, *Passive Vibration Control*, Wiley, New York, 1998.
4. E. I. Rivin, *Passive Vibration Isolation*, American Society of Mechanical Engineers, New York, 2003.
5. H. Himelblau, Jr. and S. Rubin, "Vibration of a Resiliently Supported Rigid Body," in C. M. Harris and C. E. Crede (Eds.), *Shock and Vibration Handbook*, 2nd ed. McGraw-Hill, New York, 1976.
6. J. N. Macduff and J. R. Curreri, *Vibration Control*, McGraw-Hill, New York, 1958.
7. C. E. Crede and J. E. Ruzicka, "Theory of Vibration Isolation," in C. M. Harris and C. E. Crede (Eds.), *Shock and Vibration Handbook*, 2nd ed., McGraw-Hill, New York, 1976.
8. E. E. Ungar and C. W. Dietrich, "High-Frequency Vibration Isolation," *J. Sound Vib.*, **4**, 224–241 (1966).
9. L. Cremer, M. A. Heckl, and E. E. Ungar, *Structure-Borne Sound*, 2nd ed., Springer-Verlag, Berlin, 1988.
10. E. E. Ungar, "Mechanical Vibrations," in H. A. Rothbart (Ed.), *Mechanical Design and Systems Handbook*, 2nd ed., McGraw-Hill, New York, 1985, Chapter 5.
11. D. Muster and R. Plunkett, "Isolation of Vibrations," in L. L. Beranek (Ed.), *Noise and Vibration Control*, McGraw-Hill, New York, 1971, Chapter 13.
12. E. E. Ungar, "Wave Effects in Viscoelastic Leaf and Compression Spring Mounts," *Trans. ASME Ser. B*, **85**(3), 243–246 (1963).
13. D. Muster, "Resilient Mountings for Reciprocating and Rotating Machinery," Eng. Rept. No. 3, ONR Contract N70NR-32904, July 1951.

CHAPTER 14

Structural Damping

ERIC E. UNGAR AND JEFFREY A. ZAPFE

Acentech, Inc.
Cambridge, Massachusetts

14.1 THE EFFECTS OF DAMPING

The dynamic responses and sound transmission characteristics of structures are determined by essentially three parameters: mass, stiffness, and damping. Mass and stiffness are associated with storage of kinetic and strain energy, respectively, whereas damping relates to the dissipation of energy, or, more precisely, to the conversion of the mechanical energy associated with a vibration to a form (usually heat) that is unavailable to the mechanical vibration.

Damping in essence affects only those vibrational motions that are controlled by a balance of energy in a vibrating structure; vibrational motions that depend on a balance of forces are virtually unaffected by damping. For example, consider the response of a classical mass–spring–dashpot system to a steady sinusoidal force. If this force acts at a frequency that is considerably lower than the system's natural frequency, the response is controlled by a quasi-static balance between the applied force and the spring force. If the applied force acts at a frequency that is considerably above the system's natural frequency, the response is controlled by a balance between the applied force and the mass's inertia. In both of these cases, damping has practically no effect on the responses. However, at resonance, where the excitation frequency matches the natural frequency, the spring and inertia effects cancel each other and the applied force supplies some energy to the system during each cycle; as a result, the system's energy (and amplitude) increases until steady state is reached, at which time the energy input per cycle is equal to the energy lost per cycle *due to damping*.

In light of energy considerations like the foregoing, one finds that increased damping results in (1) more rapid decay of unforced vibrations, (2) faster decay of freely propagating structure-borne waves, (3) reduced amplitudes at resonances of structures subject to steady periodic or random excitation with attendant reductions in stresses and increases in fatigue life, (4) reduced response to sound and increased sound transmission loss (reduced sound transmission) above the coincidence frequency (at which the spatial distribution of the disturbing pressure the horizontal natural frequency of a pendulum system from Eq. (13.3) if one replaces X_{st} in that equation by the pendulum length. Some commercial isolation systems combine pendulum action for horizontal isolation with spring action for vertical isolation.

Various exotic isolation systems have also been investigated or employed for special applications. These include systems in which the spring action is provided by magnetic or electrostatic levitation or by streams or thin films of gases or liquids.

Active isolation systems (see Chapter 18) have recently received increased attention. Such systems essentially are dynamic control systems in which the vibration of the item to be protected is sensed by an appropriate transducer whose suitably processed output is used to drive an actuator that acts on the item so as to reduce its vibration. Active systems are relatively complex, but they can provide better isolation than passive systems under some conditions, notably, in the presence of low-frequency disturbances, attenuation of which by passive means generally tends to be most difficult.

REFERENCES

1. W. T. Thomson, *Theory of Vibration with Applications*, 2nd ed., Prentice-Hall, Englewood Cliffs, NJ, 1981.
2. J. C. Snowdon, *Vibration and Shock in Damped Mechanical Systems*, Wiley, New York, 1968.
3. D. J. Mead, *Passive Vibration Control*, Wiley, New York, 1998.
4. E. I. Rivin, *Passive Vibration Isolation*, American Society of Mechanical Engineers, New York, 2003.
5. H. Himelblau, Jr. and S. Rubin, "Vibration of a Resiliently Supported Rigid Body," in C. M. Harris and C. E. Crede (Eds.), *Shock and Vibration Handbook*, 2nd ed. McGraw-Hill, New York, 1976.
6. J. N. Macduff and J. R. Curreri, *Vibration Control*, McGraw-Hill, New York, 1958.
7. C. E. Crede and J. E. Ruzicka, "Theory of Vibration Isolation," in C. M. Harris and C. E. Crede (Eds.), *Shock and Vibration Handbook*, 2nd ed., McGraw-Hill, New York, 1976.
8. E. E. Ungar and C. W. Dietrich, "High-Frequency Vibration Isolation," *J. Sound Vib.*, **4**, 224–241 (1966).
9. L. Cremer, M. A. Heckl, and E. E. Ungar, *Structure-Borne Sound*, 2nd ed., Springer-Verlag, Berlin, 1988.
10. E. E. Ungar, "Mechanical Vibrations," in H. A. Rothbart (Ed.), *Mechanical Design and Systems Handbook*, 2nd ed., McGraw-Hill, New York, 1985, Chapter 5.
11. D. Muster and R. Plunkett, "Isolation of Vibrations," in L. L. Beranek (Ed.), *Noise and Vibration Control*, McGraw-Hill, New York, 1971, Chapter 13.
12. E. E. Ungar, "Wave Effects in Viscoelastic Leaf and Compression Spring Mounts," *Trans. ASME Ser. B*, **85**(3), 243–246 (1963).
13. D. Muster, "Resilient Mountings for Reciprocating and Rotating Machinery," Eng. Rept. No. 3, ONR Contract N70NR-32904, July 1951.

Idaho Power/1206
Ellenbogen/304

CHAPTER 14

Structural Damping

ERIC E. UNGAR AND JEFFREY A. ZAPFE

Acentech, Inc.
Cambridge, Massachusetts

14.1 THE EFFECTS OF DAMPING

The dynamic responses and sound transmission characteristics of structures are determined by essentially three parameters: mass, stiffness, and damping. Mass and stiffness are associated with storage of kinetic and strain energy, respectively, whereas damping relates to the dissipation of energy, or, more precisely, to the conversion of the mechanical energy associated with a vibration to a form (usually heat) that is unavailable to the mechanical vibration.

Damping in essence affects only those vibrational motions that are controlled by a balance of energy in a vibrating structure; vibrational motions that depend on a balance of forces are virtually unaffected by damping. For example, consider the response of a classical mass–spring–dashpot system to a steady sinusoidal force. If this force acts at a frequency that is considerably lower than the system's natural frequency, the response is controlled by a quasi-static balance between the applied force and the spring force. If the applied force acts at a frequency that is considerably above the system's natural frequency, the response is controlled by a balance between the applied force and the mass's inertia. In both of these cases, damping has practically no effect on the responses. However, at resonance, where the excitation frequency matches the natural frequency, the spring and inertia effects cancel each other and the applied force supplies some energy to the system during each cycle; as a result, the system's energy (and amplitude) increases until steady state is reached, at which time the energy input per cycle is equal to the energy lost per cycle *due to damping*.

In light of energy considerations like the foregoing, one finds that increased damping results in (1) more rapid decay of unforced vibrations, (2) faster decay of freely propagating structure-borne waves, (3) reduced amplitudes at resonances of structures subject to steady periodic or random excitation with attendant reductions in stresses and increases in fatigue life, (4) reduced response to sound and increased sound transmission loss (reduced sound transmission) above the coincidence frequency (at which the spatial distribution of the disturbing pressure matches that of the structural displacement), (5) reduced rate of buildup of vibrations at resonances, and (6) reduced amplitudes of "self-excited" vibrations, in which the vibrating structure accepts energy from an external source (e.g., wind) as the result of its vibratory motion.

14.2 MEASURES AND MEASUREMENT OF DAMPING

Most measures of damping are based on the dynamic responses of simple systems with idealized damping behaviors. Damping measurements typically involve observation of some characteristics of these responses.

Decay of Unforced Vibrations with Viscous Damping

Many aspects of the behaviors of vibrating systems can be understood in terms of the simple ideal linear mass–spring–dashpot system shown in Fig. 14.1. If this system is displaced by an amount x from its equilibrium position, the massless spring produces a force of magnitude kx tending to restore the mass m toward its equilibrium position, and the massless dashpot produces a retarding force of magnitude $c\dot{x}$. Here k and c are constants of proportionality; k is known as the spring constant and c as the *viscous damping coefficient.*

If this system is displaced from its equilibrium position by an amount X_0 and then released, the resulting displacement varies with time t as[1]

$$x = X_0 e^{-\zeta\omega_n t} \cos(\omega_d t + \phi) \tag{14.1}$$

provided that $\zeta < 1$. Here ϕ represents a phase angle, which depends on the velocity with which the mass is released, and ω_n and ω_d represent the undamped and damped radian natural frequencies of the system. These obey

$$\omega_n = \sqrt{\frac{k}{m}} = 2\pi f_n \qquad \omega_d = \omega_n\sqrt{1-\zeta^2} \tag{14.2}$$

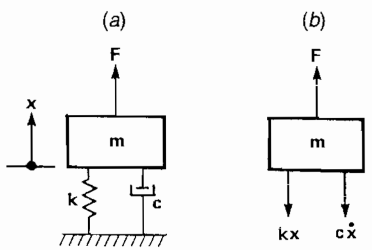

FIGURE 14.1 System with single degree of freedom: (*a*) schematic representation of mass–spring–dashpot system or of a vibrational mode of a structure; (*b*) free-body diagram of mass. Spring produces restoring force kx; dashpot produces retarding force $c\dot{x}$.

with f_n representing the cyclic (undamped) natural frequency. The constant ζ is called the *damping ratio* or *fraction of critical damping*; it is defined as

$$\zeta = \frac{c}{c_c} \qquad c_c = 2\sqrt{km} = 2m\omega_n \tag{14.3}$$

where c_c is known as the *critical damping coefficient*. For the small values of ζ one usually encounters in practice, ω_d is sufficiently close to ω_n so that one rarely needs to distinguish between the damped and the undamped natural frequencies. Furthermore, the foregoing expression for ω_d applies only for viscous damping; other relations hold for other damping models.

The right-hand side of Eq. (14.1) represents a cosine function with an amplitude $X_0 e^{-\zeta\omega_n t}$ that decreases as time t increases (see Fig. 14.2); its rate of decrease is $\zeta\omega_n$ and thus is proportional to ζ. However, Eq. (14.1) does not apply for values of ζ that equal or exceed unity (or for values of c that equal or exceed c_c). For such large values of ζ or c one obtains a nonoscillatory decay represented by pure exponential expressions instead of the decaying oscillation represented by Eq. (14.1). The critical damping coefficient c_c constitutes the boundary between oscillatory and nonoscillatory decays.

The *logarithmic decrement* δ is a convenient, time-honored representation of how rapidly a free oscillation decays. It is defined by[1]

$$\delta = \frac{1}{N}\ln\frac{X_i}{X_{i+N}} \tag{14.4}$$

where X_i represents the value of x at any selected peak and X_{i+N} represents the value at the peak at N cycles from the aforementioned one. It follows from Eq. (14.1) that $\delta = 2\pi\zeta$.

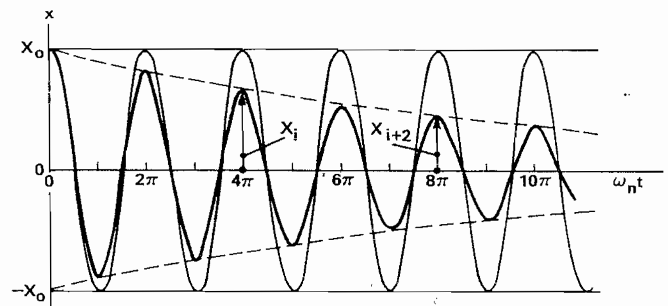

FIGURE 14.2 Time variation of displacement of mass–spring–dashpot system released with zero velocity from initial displacement X_0. *Light curve*: Undamped system ($c = \zeta = 0$); amplitude remains constant at X_0. *Heavy curve*: Damped system ($0 < c < c_c$; $0 < \zeta < 1$); amplitude decreases according to $x = X_0 e^{-\zeta\omega_n t}$, which is represented by upper dashed curve. Lower dashed curve corresponds to $x = -X_0 e^{-\zeta\omega_n t}$. Amplitudes X_i and X_{i+2} illustrate values that may be used to calculate logarithmic decrement from Eq. (14.4) for $N = 2$.

The utility of logarithmic measures of oscillatory quantities has long been recognized in acoustics, and definitions analogous to acoustical levels have come into use in the field of vibrations, particularly in regard to measurement. For example, one may define the displacement level L_x, in decibels, corresponding to an oscillatory displacement $x(t)$ in analogy to sound pressure level, as

$$L_x = 10 \log_{10} \frac{x^2(t)}{x_{\text{ref}}^2} \tag{14.5}$$

where x_{ref} denotes a (constant) reference value of displacement. One may then define a decay rate Δ, in decibels per second, and find that for a viscously damped system[2]

$$\Delta = -\frac{dL_x}{dt} = 8.69\zeta\omega_n = 54.6\zeta f_n \tag{14.6}$$

Also in analogy to acoustics, one may define the reverberation time T_{60} as the time it takes for the displacement level to decrease by 60 dB; thus,

$$T_{60} = \frac{60}{\Delta} = \frac{1.10}{\zeta f_n} \tag{14.7}$$

Because velocity and acceleration levels may be defined in full analogy to the definition of displacement level in Eq. (14.5), the decay rate and reverberation time expressions of Eqs. (14.6) and (14.7) also apply to these other vibration levels.

If any extended structure that is not too highly damped vibrates in the absence of external forces at one of its natural frequencies, all points on that structure move either in phase or in opposite phase with each other, and the structure is said to vibrate in one of its modes. In addition to the modal natural frequency, there corresponds to each mode a modal mass, a modal stiffness, and a modal damping value. With the aid of these parameters the behavior of a modal vibration may be described in terms of that of an equivalent simple mass–spring–dashpot system.[1,3,4] Thus, all of the foregoing discussion concerning this simple system also applies to structural modes.

Of course, extended structures also can exhibit wave motions at a given frequency in which all points are not in or out of phase with each other. Such motions, which can be described in terms of freely propagating waves, also decrease due to damping. For flexural waves on a beam or for nonspreading (straight-crested) flexural waves on a plate, the *spatial decay rate* Δ_λ, defined as the reduction in vibration level per wavelength, obeys[2] $\Delta_\lambda = 27.2\zeta$ in decibels per wavelength.

Steady Forced Vibrations

If the system of Fig. 14.1 is subject to a sinusoidal force $F(t) = F \cos \omega t$, then its equation of motion may be written as

$$m\ddot{x} + c\dot{x} + kx = F(t) = F \cos \omega t \tag{14.8}$$

One may find its steady-state solution by substituting $x(t) = X\cos(\omega t - \phi)$ and solving for X and ϕ. Alternatively, one may obtain this solution by taking $x(t) = \text{Re}\lfloor \overline{X} e^{j\omega t} \rfloor$, where $j = \sqrt{-1}$ and the complex amplitude or *phasor* $\overline{X} = Xe^{-j\phi}$ indicates both the amplitude and the phase of the vibration.* In terms of phasors (and omitting the writing of "Re"), the equation of motion may be written as

$$(-m\omega^2 + j\omega c + k)\overline{X} = (\overline{k} - m\omega^2)\overline{X} = F \tag{14.9}$$

In the foregoing there has been introduced the complex stiffness

$$\overline{k} = k + j\omega c = k + k_i = k\left(1 + \frac{jk_i}{k}\right) \tag{14.10}$$

which includes information about the system's damping as well as about it stiffness. By means of either solution approach one may determine that

$$\frac{X}{F/k} = \frac{X}{X_{\text{st}}} = \frac{1}{\sqrt{(1-r^2)^2 + (2r\zeta)^2}} \qquad \tan\phi = \frac{2r\zeta}{1-r^2} \tag{14.11}$$

where $r \equiv \omega/\omega_n$.

The deflection $X_{\text{st}} = F/k$, which was introduced in order to obtain a nondimensional expression, is the quasi-static or zero-frequency deflection that the system would experience due to a statically applied force of magnitude F. The ratio X/X_{st}, which indicates by what factor the amplitude under dynamic excitation exceeds the quasi-static deflection, is called the *amplification*.

The foregoing response expressions (and related ones that involve velocity V or acceleration A instead of displacement) depend on damping; thus, damping data may be extracted from corresponding measurements. Two widely used measures of damping may be derived readily from the amplification expressions of Eq. (14.11), a plot of which is shown in Fig. 14.3. One is the *amplification at resonance*, conventionally represented by the letter Q and often simply called "the Q" of the system.[2] This corresponds to the value of X/X_{st} that results if the excitation frequency ω is equal to the natural frequency ω_n and is related to the viscous damping ratio by $Q = 1/2\zeta$. The second commonly used measure is the *relative bandwidth* $b = \Delta\omega/\omega_n \approx 1/Q$, where $\Delta\omega$ represents the difference between the two frequencies† (one below and one above ω_n; see Fig. 14.3) at which the amplification is equal to $Q/\sqrt{2}$.

In view of Eq. (14.11), the phase lag ϕ also provides a measure of damping. It is particularly convenient to use phase information in "Nyquist plots," that is, in plots of the real and imaginary parts of responses at a number of frequencies, as illustrated in Fig. 14.4. These plots are circles or nearly circles, with a diameter that is equal to Q if the plots are appropriately nondimensionalized.[5,6]

*Note that $e^{jz} = \cos z + j \sin z$ for any real number z. The amplitude X is equal to the absolute value of the phasor; that is, $X = |\overline{X}|$.

†These frequencies often are called the *half-power points* because at these the energy stored in the system (and that dissipated by it), which is proportional to the square of the amplitude [see Eq. (14.6)], is half of the maximum value.

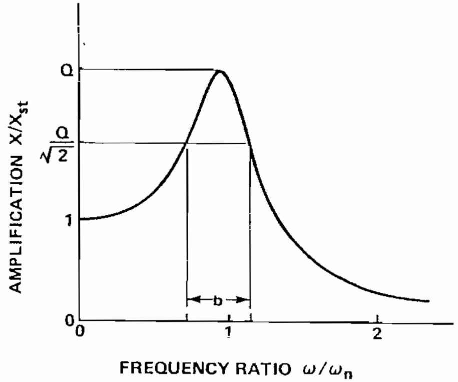

FIGURE 14.3 Steady-state response of mass–spring–dashpot system to sinusoidal force. See Eq. (14.11): Q = value of amplification X/X_{st} at resonance. Relative bandwidth $b = \Delta\omega/\omega_n$ is determined from "half-power points," that is from frequencies at which response amplitude is $1/\sqrt{2}$ times the maximum.

If the system of Fig. 14.1 (or a structural mode modeled by it) is subject to a broadband force (or broadband modal force) rather than a single-frequency sinusoidal force, then the mean-square displacement $\overline{x}^2$ of the mass is given by[7]

$$\frac{\overline{x}^2}{\pi S_F(\omega)\omega_n/k^2} = \frac{1}{2\zeta} \tag{14.12}$$

where $S_F(\omega)$ denotes the spectral density of the force in terms of radian frequency (i.e., the value of excitation force squared per unit radian frequency interval). Note that the spectral density in cyclic frequency obeys $S_F(f) = 2\pi S_F(\omega)$. The foregoing equation is exact for excitations with spectral densities that are constant for all frequencies. It is a good approximation for excitations with spectral densities that vary only slowly in the vicinity of the system's natural frequency ω_n; the spectral density value to be used in the equation then is that corresponding to ω_n.

Energy; Complex Stiffness

All of the measures of damping discussed so far are based on the motions of simple systems. However, since damping pertains to the dissipation of energy, damping measures that relate to energy are more basic and more general.

The *damping capacity* ψ is defined as the ratio of the energy that is dissipated per cycle to the total energy present in the vibrating system. The *loss factor* η is defined similarly as the ratio of the energy that is dissipated per radian to the total energy. If D denotes the energy dissipated per cycle and W the total energy in the system, then

$$\eta = \frac{\psi}{2\pi} = \frac{D}{2\pi W} \tag{14.13}$$

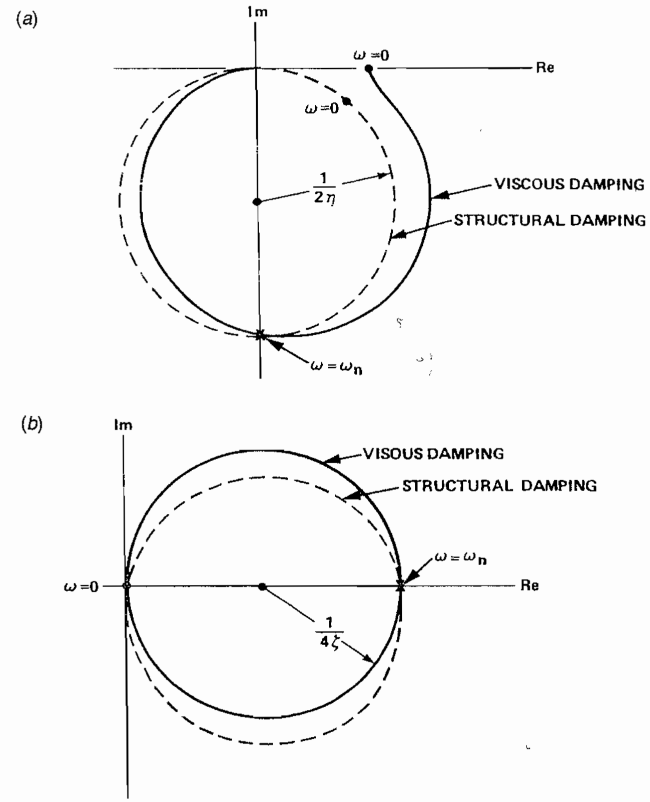

FIGURE 14.4 Nyquist plots of nondimensional responses of viscously and structurally damped mass–spring–damper systems. (*a*) Real and imaginary parts of amplification X/X_{st}. (*b*) Real and imaginary parts of mobility $Vk/F\omega_n = Vc_c/2F$. Amplification plot for structural damping and mobility plot for viscous damping are exact circles; others are approximate circles that become more nearly circular with decreased damping. Diameter is exactly or approximately equal to Q. Figure plots correspond to $\zeta = 0.2$, $\eta = 0.4$.

These expressions apply for any damping mechanism. However, it is interesting to relate them to the special case of a viscously damped mass–spring–dashpot system like that of Fig. 14.1. In this system the energy dissipated corresponds to the work that is done on the dashpot, and one may readily determine that the energy dissipated per cycle in a steady vibration at radian frequency ω and displacement amplitude X obeys $D = \pi\omega c X^2$. The total energy W stored by the system consists of the kinetic energy W_{kin} of the mass and the potential (or strain) energy W_{pot} in the spring. If the energy dissipated is small compared to the total energy stored, then W is approximately equal to the energy stored in the spring when the kinetic energy is zero—that is, when the spring is displaced to the full extent of its amplitude—and $W = W_{kin} + W_{pot} \approx kX^2/2$.

Thus, one finds by use of Eqs. (14.3) and (14.13) that for a viscously damped system

$$\eta \approx \frac{\omega c}{k} = \frac{2\zeta\omega}{\omega_n} = 2r\zeta \tag{14.14}$$

From Eq. (14.10) one finds that

$$\overline{k} = k(1 + j\eta) \qquad k_i/k = \eta \tag{14.15}$$

Equation (14.14) indicates that for the particular case of a viscously damped system the loss factor is proportional to the frequency. In cases where the loss factor exhibits some other frequency dependence, Eqs. (14.13) and (14.15) still apply—and Eq. (14.11) holds if $2r\zeta$ is replaced by η. These equations then permit one not only to consider the case of *structural damping*, which is characterized by a constant loss factor, but also to take into account experimentally determined frequency variations of the loss factor.

Interrelation of Measures of Damping

The following relations apply at all frequencies:

$$\eta = \frac{\psi}{2\pi} = \frac{k}{k_i} = |\tan\phi|_{r=0} \tag{14.16a}$$

but the relations of Eq. (14.16b) are exact only at resonance:

$$\eta = \frac{1}{Q} = 2\zeta \qquad \text{and} \qquad \eta \approx b \text{ for small damping} \tag{14.16b}$$

For systems with viscous damping,

$$2\zeta = \frac{\delta}{\pi} = \frac{2.20}{f_n T_{60}} = \frac{\Delta}{27.3 f_n} = \frac{\Delta_\lambda}{13.6} \tag{14.16c}$$

For systems with small damping, one may take $\eta \approx 2\zeta$, consider that the system behaves approximately like a viscously damped one, and use the relations of Eq. (14.16c).

Measurement of Damping

Most approaches to measurement of the damping of structures are based on the previously discussed responses of simple systems, which, as has been mentioned, also correspond to those of structural modes. However, unlike mass–spring–dashpot systems, structures have a multiplicity of modes and corresponding natural frequencies. Therefore, many of the approaches applicable to simple systems can be applied only to structural modes whose responses can be separated adequately from those of all others because of differences in their natural frequencies or mode shapes.

Measurement of logarithmic decrement δ typically is applicable only to the fundamental modes of structures for which a clear record of the amplitude-versus-time trace can be obtained. If more than one mode is present, their decaying responses are superposed and the record becomes difficult to interpret.

The counting of peaks that is required for determination of the logarithmic decrement from Eq. (14.4) is not needed if one focuses on the decaying signal's envelope. For purposes of evaluating this envelope it is particularly convenient to use a display of the logarithm of the rectified amplitude versus time. Rectification is needed because the logarithm of negative numbers is undefined. In such a logarithmic display the envelope becomes a straight line whose slope is proportional to $\zeta\omega_n$ and thus to the decay rate. Not only does measurement of the slope enable one to evaluate the damping, but also observation of deviations of the envelope from a straight line permit one to judge whether the structure's damping is indeed viscous and amplitude-independent and whether a superposition of responses with different decay rates is present.

Determination of decay rates is useful also in frequency bands in which a multitude of modes are excited. A typical measurement here involves excitation of a structure by a broadband force in a given frequency band, cutting off the excitation, then observing the envelope of the logarithm of the rectified signal obtained by passing the output of a transducer (usually an accelerometer) through a bandpass filter* tuned to the excitation band. The center frequency of this passband may be taken to represent ω_n for all modes in the band. Some judgment in interpreting the resulting envelopes and averaging of results from repeated measurements is generally required because different modes in the band may exhibit somewhat different decays.

A conceptually straightforward approach to measuring the damping of a structure involves the application of Eq. (14.13) to observed values of the energy dissipation and total vibrational energy W present in a structure in the steady state.[8] The structure is excited via an impedance head or a similar transducer arrangement that measures the force and motion at the excitation point. The instantaneous force and velocity values are multiplied and the product is time averaged to yield the average energy input per unit time, which is equal to the energy dissipated per unit time under steady-state conditions. For a given excitation frequency f, the energy D dissipated per cycle is equal to $1/f$ times the energy dissipated per unit time.

The energy W stored in the structure may be determined from its kinetic energy, which may be calculated from information on its mass distribution and from velocity values measured by a suitable array of accelerometers or other motion transducers. This measurement approach requires particular care in instrumentation selection and calibration, but it has a significant advantage: Because it involves direct measurement of the dissipated energy, it does not rely on any

*The filter's response must be fast enough so that it can follow the decaying signal; otherwise one observes the decay of the filter response instead of that of the structural vibration. Filters with wider passbands need to be used to observe the more rapid decays associated with greater damping.

particular model of dissipation. It also permits one, for example, to investigate how the loss factor varies with amplitude.

Force-and-motion transducer combinations may also be employed for the direct measurement of complex impedance or mobility (or of other force–motion ratios), from which damping information may be extracted, typically on the basis of Nyquist plots. Much corresponding specialized *modal testing* or *modal parameter extraction* instrumentation and software has recently become available.

Simple steady sinusoidal response measurements may also be made to measure Q and the half-power point bandwidth b directly on the basis of their definitions. These measurements require particular care to ensure that the near-resonance response of the mode of interest is not affected significantly by the responses of other modes with resonance frequencies near that of the mode of interest.

14.3 DAMPING MODELS

Analytical Models

Most of the foregoing discussion has dealt with "viscous" damping, where energy dissipation results from a force that is proportional to the velocity of a vibrating system and that acts opposite to the velocity. This viscous model of damping action has been used most widely because it results in relatively simple linear differential equations of system motion and because it yields a reasonable approximation to the action of some real systems, particularly at small amplitudes.

Among the many other models that have received considerable attention, most also involve a motion-opposing force that is a function of velocity. In *dry friction* or *Coulomb* damping, the force is constant in magnitude (but changes its algebraic sign when the velocity does). In *square law* and *power law* damping the force magnitude is proportional to the square or to some other power of velocity. Of course, modern numerical methods also permit one readily to analyze models involving other velocity dependences, such as one might obtain from corresponding experiments.

Whereas in viscous damping the retarding force is proportional to the velocity, in *structural damping* the retarding force is proportional to the displacement. As has been mentioned, structural damping is characterized by a constant loss factor η and the dimensionless response relation for a system with structural damping is given by Eq. (14.11) with $2r\zeta$ replaced by η. Because of the difference in the retarding forces, a structurally damped system behaves differently from a viscously damped one, except near the natural frequency. The structural damping model is often extended to loss factors that vary with frequency as determined from experimental data. With the appropriate frequency dependence of the loss factors, the structural damping model can be made to represent the sinusoidal response of viscously damped systems—and, indeed, of any system whose loss factor is independent of amplitude.*

*Caution is required if one wants to undertake transformations from the frequency to the time domain. Not all conceivable frequency variations of the loss factor lead to physically realizable results; e.g., some imply system motions that begin before application of a force.[9]

Applicability of Models

If one desires to determine the precise response of a system to a prescribed excitation, one generally needs to have a complete description of all forces, including the damping forces; that is, one needs a damping model that corresponds to the actual system. This is true, for example, if one wants to study the "wave shape" of the motion of a screeching brake or a chattering tool or if one needs to determine the response of a system to a transient, such as a shock.

In many practical instances, however, the details of the system's motion are of no interest and only the amplitudes are of concern. As has been mentioned, under steady resonant or free decay conditions (and in a few other situations), the amplitudes are established essentially by the energy in the system. For such conditions, the details of the damping model are unimportant as long as the model gives the correct energy dissipation per cycle. It is for this reason that measures of damping that involve only energy considerations have found wide acceptance.*

14.4 DAMPING MECHANISMS AND MAGNITUDES

Since damping involves the conversion of energy associated with a vibration to other forms that are unavailable to the vibration, there are as many damping mechanisms as there are ways to remove energy from a vibrating system. These include mechanisms that convert mechanical energy into heat, as well as others that transport energy away from the vibrating system of concern.

Energy Dissipation and Conversion

Material damping, mechanical hysteresis, and internal friction refer to the conversion of mechanical energy into heat that occurs within materials due to deformations that are imposed on them. This conversion may result from a variety of effects on the molecular, crystal lattice, or metal grain level, including magnetic, thermal, metallurgical, and atomic phenomena.[10] Figure 14.5 indicates the ranges of the loss factors reported for some common materials.

Damping of a vibrating structure may also result from friction associated with relative motion between the structure and solids or fluids that are in contact with it. Also, an electrically conductive structure moving in a magnetic field is subject to damping due to eddy currents that result from the motion and that are converted into heat.

A granular material, such as sand, placed in contact with a vibrating structure tends to produce damping by two different mechanisms. At small amplitudes, damping results predominantly from interaction of asperities on adjacent grains and the attendant energy loss due to mechanical hysteresis. At large amplitudes,

*Equivalent viscous damping, defined as viscous damping that results in the same energy dissipation as the damping actually present in the system, is often used in analyses. This damping model obviously should not be used where details of the system motion are of concern.

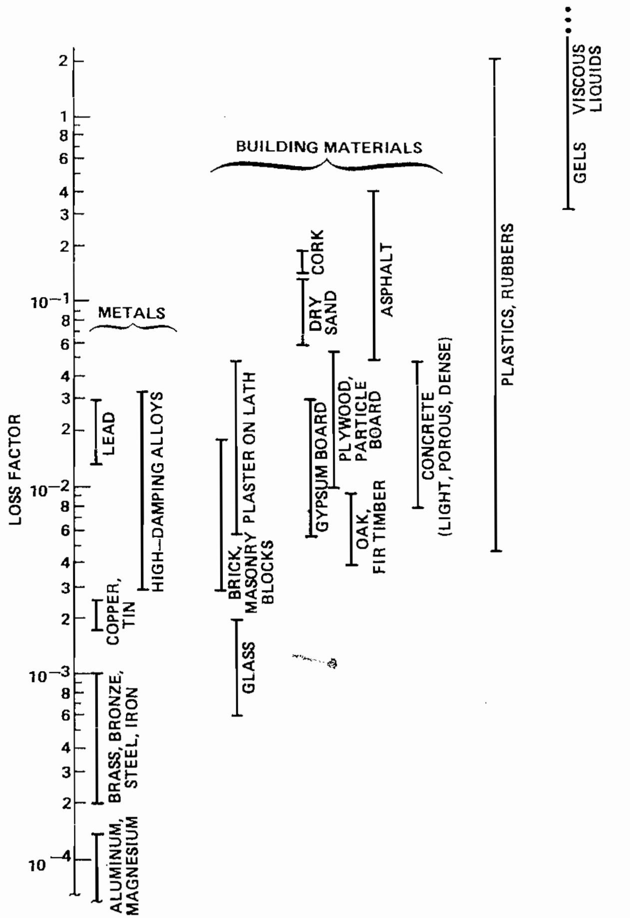

FIGURE 14.5 Typical ranges of material loss factors at small strains, near room temperature, at audio frequencies. The loss factors of metals tend to increase with strain amplitude, particularly near the yield point, but the loss factors of plastics and rubbers tend to be relatively independent of strain amplitude up to strains of the order of unity. The loss factors of some materials, particularly those that can flow or creep, tend to vary markedly with temperature and frequency.

damping results predominantly from impacts between the structure and the grains or between grains; these impacts produce high-frequency vibrations of the structure and of the granular material, and the energy that goes into these vibrations (which eventually is converted to heat) is no longer available to the structural vibrations of concern.[11] Impact dampers, in which a small element is made to rattle against a vibrating structure, similarly rely on conversion of the energy of the vibrating structure to higher frequency vibrations.

Damping due to Boundaries and Reinforcements

For panels or other structural components that may be considered as uniform plates, one may estimate the loss factor η_b associated with energy loss at the panel boundaries, due to both energy transport to adjacent panels and dissipation at its boundaries, from information on the boundary absorption coefficients.[12] For a panel of area A vibrating at a frequency at which the flexural wavelength λ on the panel is considerably shorter than a panel edge, this loss factor is given by

$$\eta_b = \frac{\lambda}{\pi^2 A} \sum \gamma_i L_i \tag{14.17}$$

where γ_i denotes the absorption coefficient of the ith boundary increment whose length is L_i and where the summation extends over all boundary increments.

At frequency f the flexural wavelength on a homogeneous plate of thickness h of a material with longitudinal wave speed c_L and Poisson's ratio ν is given by $\lambda = \sqrt{(\pi/\sqrt{3})hc_L/f(1-\nu^2)}$.

The absorption coefficient γ of a boundary element is defined as the fraction of the panel bending-wave energy impinging on the boundary element that is not returned to the panel. Although the absorption coefficient values associated with a given boundary element rarely can be predicted well analytically, they can often be determined experimentally. For example, one might add a boundary element of length L_0 to a panel, measure the resulting loss factor increase $\Delta\eta$ at various frequencies, and calculate the absorption coefficient values γ_0 of this boundary element from $\gamma_0 = (\Delta\eta)\pi^2 A/\lambda L_0$, which follows from Eq. (14.17). Both Eq. (14.17) and the expression for γ_0 are based on the assumption that the absorption coefficient of a boundary element is independent of its length, an assumption that generally holds true if the wavelength λ is considerably smaller than the element length.

Equation (14.17) also permits one to account for the damping effects of linear discontinuities, such as seams or attached reinforcing beams, on panels, provided one knows the corresponding absorption coefficients. Since plate waves can impinge on both sides of a discontinuity located within the panel area, for such a discontinuity location one needs to use in Eq. (14.17) twice the actual discontinuity length.

The energy that beams or reinforcements attached to a panel can dissipate, and thus the damping they can produce, depends markedly on the fastening method used. Metal beams attached to metal panels or seams in such panels generally produce little damping if they are continuously welded or joined by means of a rigid adhesive. However, they can contribute significant damping if they are fastened by a flexible, dissipative adhesive or if they are fastened at only a number of points, for example, by rivets, bolts, or spot welds. At high frequencies, at which the flexural wavelength on the panel is smaller than the distance between fastening points, damping results predominantly not from interface friction but from an "air-pumping" effect produced as adjacent surfaces (at locations between the connection points) move away from and toward each other. Energy loss here is due to the viscosity of the air or other fluid present between the surfaces.[13–15]

The high-frequency absorption coefficient corresponding to a beam that is fastened to a panel at a multitude of points may be estimated from the experimental results summarized in Fig. 14.6, which shows how the beam's reduced absorption coefficient γ_r varies with reduced frequency f_r or with the ratio d/λ of fastener spacing to plate flexural wavelength. These reduced quantities, definitions of which are given in the figure, account for the absorption coefficients' dependence on beam width w, plate thickness h, fastener spacing d, and longitudinal wave speed c_L in the plate material by relating these to reference values of these parameters (indicated by the subscript 0). It should be noted that Fig. 14.6 pertains to panels immersed in air at atmospheric pressure; lesser absorption coefficient values apply for panels at reduced pressure and higher values for panels at greater pressures. A theory is available[13] to account for the effects of atmospheric pressure changes and for other gases or liquids present between the contacting surfaces.

Damping due to Energy Transport

Structural Transmission. Energy that is transported away from a vibrating structure constitutes energy lost from that structure and thus contributes damping. Energy transport may occur to neighboring structural elements or to fluids in contact with the vibrating structure.

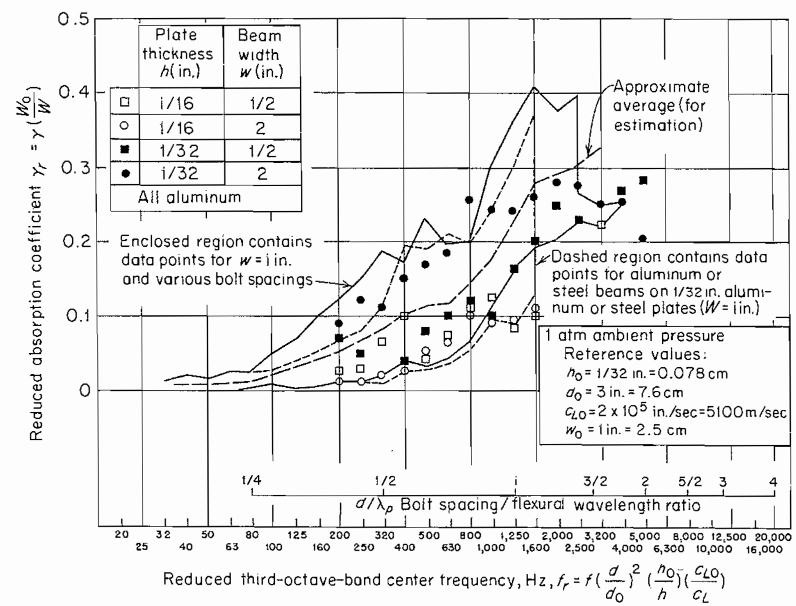

FIGURE 14.6 Summary of reduced absorption coefficient data for beams fastened to plates by rows of rivets, bolts, or spot welds.[15]

For example, a panel that is part of a multipanel array (such as an aircraft fuselage) is damped not only due to energy dissipation within the panel but also due to energy transport to adjacent panels. Energy transport makes it very difficult in practice to measure the dissipative damping of a structural component that is connected to others. Energy transported via the supports of test samples also tends to contaminate laboratory measurements of dissipative damping, potentially introducing large errors in measurements on samples with small inherent damping.

If a structural element is attached to a vibrating structure at a given point, then the energy D that is transported to the attached structure per cycle at frequency f is given by

$$D = \frac{V_S^2 \operatorname{Re}[Z_A]}{2f}\left|1 + \frac{Z_A}{Z_S}\right|^{-2} \tag{14.18}$$

Here V_S denotes the amplitude of the velocity of the vibrating structure at the attachment point before the added structure is attached; Z_A denotes the driving-point impedance of the attached structure, and Z_S denotes the impedance of the vibrating structure at the attachment point (with both impedances measured in the direction of V_S). The loss factor contribution due to an attached structure then may be found by use of Eq. (14.13).

A *waveguide absorber* is a damping device that is intended to conduct energy away from its attachment point and to dissipate that energy. Such an absorber consists essentially of a structural element along which waves can travel and which includes means for dissipating the energy transported by these waves. For example, a long slender beam (which may be straight or coiled in some fashion) that is made of a highly damped plastic or coated with a high-damping material may serve as a waveguide absorber at frequencies considerably above its fundamental resonance. To be effective, a waveguide absorber must support waves in the frequency range of interest, it must be attached at a point where the vibrating structure moves with considerable amplitude, and its impedance must be such that it does not excessively reduce the vibrating structure's motion at the attachment point.[16]

A *tuned damper*, often also called a *dynamic absorber* or *neutralizer*, may be visualized as a mass–spring–damper system whose spring base is attached to a point on a vibrating structure. In the region near its natural frequency a tuned damper tends to impede the motion of the attachment point and to dissipate considerable energy; outside this frequency region, the damping effect of such a damper typically is small. Any system, such as a beam or plate, which exhibits a resonance at the frequency of concern, can act as a tuned damper at that frequency. Considerable damping of a plate over a relatively wide frequency range can be obtained by distributing a number of small tuned dampers with slightly different natural frequencies over the plate surface.[17]

Sound Radiation. Sound radiated by a vibrating structure transports energy from the structure and thus contributes damping. For a homogeneous panel of thickness h and material density ρ_p, one may calculate the panel's loss factor η_R at frequency f due to sound radiation from one side of the panel from its radiation efficiency σ by use of the relation[14]

$$\eta_R = \frac{\rho}{\rho_p}\frac{c}{2\pi f h}\sigma \tag{14.19}$$

where ρ and c denote the density of the ambient medium and the speed of sound in it, respectively. If the panel can radiate from both of its sides, η_R is twice as great as indicated by Eq. (14.19). The magnitude of the radiation efficiency σ depends on the vibratory velocity distribution on the panel, as well as on frequency, and thus generally is different for different excitation distributions.

For a plate that has little inherent damping and that is excited at a single point, the radiation efficiency σ obeys[18]

$$\sigma = \begin{cases} (Uc/\pi^2 A f_c)\sqrt{f/f_c} & \text{for } f \ll f_c \\ 0.45\sqrt{U f_c/c} & \text{for } f = f_c \\ 1.0 & \text{for } f \gg f_c \end{cases} \tag{14.20}$$

where A denotes the panel's surface area (one side), U its circumference, and f_c the coincidence frequency. This frequency, which is defined as that at which the plate flexural wavelength is equal to the acoustical wavelength in the ambient medium, is given by $f_c \approx c^2/1.8hc_L$, where c_L represents the longitudinal wave speed in the plate material. More detailed information on radiation efficiency is provided in Chapter 11. Equation (14.20) may be used for the general estimation of radiation efficiency values for plates that are not too highly damped. This equation also provides a reasonable estimate of the radiation efficiency of rib-stiffened plates if twice the total rib length is included in the circumference U.

14.5 VISCOELASTIC DAMPING TREATMENTS

Viscoelastic Materials and Material Combinations

Materials that have both damping (energy dissipation) and structural (strain energy storage) capability are called "viscoelastic." Although virtually all materials fall into this category, the term is generally applied only to materials, such as plastics and elastomers, that have relatively high ratios of energy dissipation to energy storage capability.

Structural materials with high strength-to-weight ratios typically have little inherent damping, as is evident from Fig. 14.5, whereas plastics and rubbers that are highly damped tend to have relatively low strength. This circumstance has led to the consideration of combinations of high-strength materials and high-damping viscoelastic materials for applications where both strength and damping are required. Additions of viscoelastic materials to structural elements have come to be known as viscoelastic damping treatments.

If a composite structure is deflected, it stores energy via a variety of deformations (such as shear, tension and compression, flexure) in each structural element. If η_i denotes the loss factor corresponding to the ith element deformation and W_i represents the energy stored in that deformation, then the loss factor η of the entire structure obeys[19]

$$\eta = \sum \eta_i \frac{W_i}{W_T} \tag{14.21}$$

where $W_T = \sum W_i$ denotes the total energy stored in the structure. The foregoing expression indicates that the loss factor η of the composite structure is equal to a weighted average of the loss factors corresponding to all of the element deformations, with the energy storages serving as the weighting factors. This expression also leads to an important conclusion: An element deformation can make a significant contribution to the total loss factor only if (1) the loss factor associated with it is significant *and* (2) the energy storage associated with it is a significant fraction of the total energy storage.*

Mechanical Properties of Viscoelastic Materials

Because viscoelastic materials have both energy storage and energy dissipation capability, it is convenient to describe their behavior in terms of elastic and shear moduli that are complex quantities, in analogy to the definition of the complex stiffness introduced in Eq. (14.10). The complex Young's modulus $\overline{E}$ of a material, defined as the ratio of the stress phasor to the strain phasor, may be written as[10] $\overline{E} = E_R + jE_I = E_R(1 + j\eta_E)$, where the real part E_R is called the storage modulus, the imaginary part E_I is called the loss modulus, and the loss factor η_E associated with Young's modulus is equal to E_I/E_R. A completely analogous definition applies to the complex shear modulus.†

For plastics and elastomers, the viscoelastic materials of greatest practical interest, the real and imaginary moduli as well as the loss factors vary considerably with frequency and temperature. However, these parameters usually vary relatively little with strain amplitude, preload, and aging.[10] The loss factor associated with the shear modulus typically is equal to that associated with the Young's modulus for all practical purposes, so that one generally need not distinguish between the two. Also, since most of the viscoelastic materials of practical interest are virtually incompressible, the shear modulus value is nearly equal to one-third of the corresponding Young's modulus value. One may also note that often $\eta_E^2 \ll 1$, so that $|\overline{E}| \approx E_R$.

*Equation (14.21) applies precisely only for cases where all energy storage elements are deflected in phase, so that they reach their maximum energy storages at the same instant.

†An advantage of the complex modulus representation is the ease with which it enables one to incorporate damping in an analysis. One merely needs to replace the real moduli in the undamped formulation of a problem by the corresponding complex moduli—or, equivalently, to replace the real stiffnesses by the corresponding complex stiffnesses—to obtain a formulation of the problem that includes damping. This approach applies for lumped-parameter dynamic systems as well as for continuous systems and can take account of different values of damping in different elements and materials.

Figure 14.7 shows how the (real) shear modulus and loss factor of a typical viscoelastic material vary with frequency and temperature. At low frequencies and/or high temperatures, the material is soft and mobile enough for the strain to follow an applied stress without appreciable phase shift so that the damping is small; the material is said to be in its "rubbery" state. At high frequencies and/or low temperatures, the material is stiff and immobile, may tend to be brittle, is relatively undamped, and behaves somewhat like glass; it is said to be in its "glassy" state. At intermediate frequencies and temperatures, the modulus takes on intermediate values and the loss factor is highest; the material is said to be in its "transition" state.

This material behavior may be explained on the basis of the interactions of the long-chain molecules that constitute polymeric materials. At low temperatures, the molecules are relatively inactive; they remain "locked together," resulting in high stiffness, and because they move little relative to each other, there is little intermolecular "friction" to produce damping. At high temperatures, the molecules become active; they move easily relative to each other, resulting in low stiffness, and because they interact little, there is again little energy dissipation due to intermolecular friction. At intermediate temperatures, where the molecules have intermediate relative motion and interaction, the stiffness also takes on an intermediate value and the loss factor is greatest. A similar discussion applies to the effect of frequency on the material properties, with the inertia of the molecules leading to their decreasing mobility and interaction with increasing frequency.

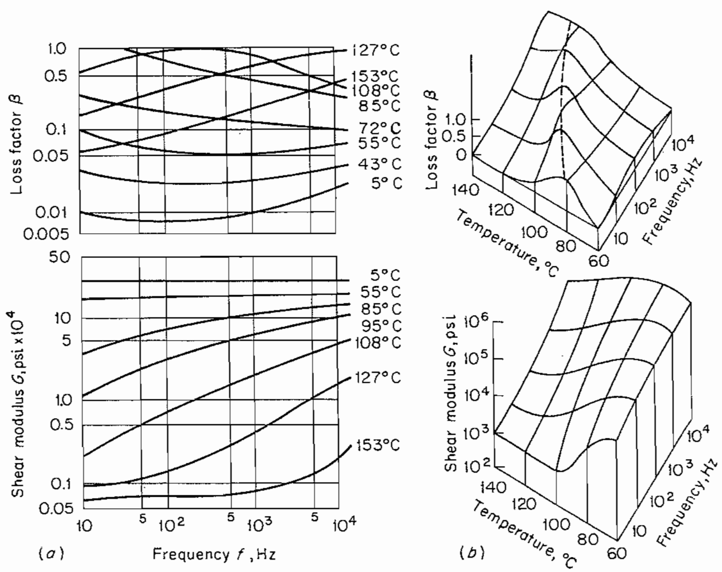

FIGURE 14.7 Dependence of shear modulus and loss factor of a polyester plastic on frequency and temperature[20]: (*a*) functions of frequency at constant temperature; (*b*) isometric plots on temperature–frequency plane. Note logarithmic frequency axes.

The observation that there exists a *temperature–frequency equivalence*, namely that an appropriate temperature decrease produces the same effect as a given frequency increase, has led to the development of convenient plots in which data for the frequency and temperature variations of each material modulus collapse onto single curves.[10,21] This collapse is achieved by plotting the data against a reduced frequency $f_R = f\alpha(T)$, where $\alpha(T)$ is an appropriately selected function of temperature T. In presentations of data in this form the function $\alpha(T)$ may be given analytically, in a separate plot or, as has recently been standardized[22,23], in the form of a nomogram that is superposed on the reduced data plot. Figure 14.8 is an illustration of such a plot and nomogram; its use is explained in the figure's legend.

Data on the properties of damping materials are available from knowledgeable suppliers of these materials. Compilations of data appear in references 10, 21, and 24. Key information on some of these materials appears in Table 14.1 in a form that is useful for preliminary material comparison and selection for specific applications in keeping with the concepts discussed in the later portions of this chapter. For each listed material the table shows the greatest loss factor value η_{max} exhibited by the material and the temperatures at which this value is obtained at three frequencies. The table also lists three values of the modulus of elasticity: E_{max}, the greatest value of Young's modulus, applies at low temperatures (i.e.,

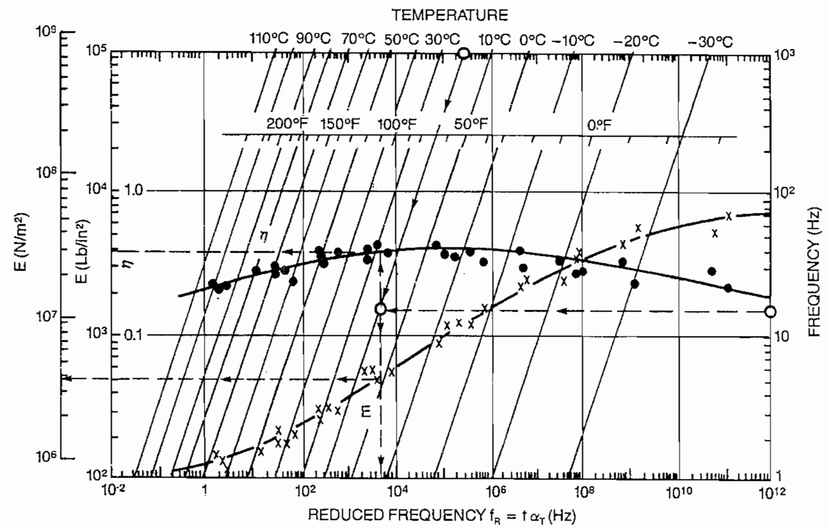

FIGURE 14.8 Reduced frequency plot of elastic modulus E and loss factor η of "Sylgard 188" silicone potting compound. (After Ref. 25) Points indicate measured data to which curves were fitted. Nomograph superposed on data plot facilitates determination of reduced frequency f_R corresponding to frequency f and temperature T. Use of nomogram is illustrated by dashed lines: For $f = 15$ Hz and $T = 20°C$, one finds $f_R = 5 \times 10^3$ Hz and $E = 3.8 \times 10^6$ N/m², $\eta = 0.36$.

TABLE 14.1 Properties of Some Commercial Damping Materials[a]

	Maximum Loss Factor	Temperature (°F)[b] for η_{max} at			Elastic Moduli (psi)[c]			
Material	η_{max}	10 Hz	100 Hz	1000 Hz	E_{max}	E_{min}	E_{trans}	$E_{I,max}$
Antiphon-13	1.8	25	75	120	3e5	1.2e3	1.9e4	3.e3e
blachford Aquaplas	0.5	50	80	125	1.6e6	3e4	2.2e5	1.1e5
Barry Controls H-326	0.8	−40	−25	−10	6e5	3e3	4.2e4	3.4e4
Dow Corning Sylgard 188	0.6	60	80	110	2.2e4	3e2	2.6e3	1.5e3
EAR C-1002	1.9	23	55	90	3e5	2e2	7.7e3	1.5e4
EAR C-2003	1.0	45	70	100	8e5	6e2	2.2e4	2.2e4
lord LD-400	0.7	50	80	125	3e6	3.3e3	1e5	7e4
Soundcoat DYAD 601	1.0	15	50	75	3e5	1.5e2	6.7e3	6.7e3
Soundcoat DYAD 606	1.0	70	100	130	3G5	1.2e2	6e3	6e3
Soundcoat DYAD 609	1.0	125	150	185	2e5	6e2	1.1e4	1.1e4
Soundcoat N	1.5	15	30	70	3e5	7e1	4.6e3	6.9e3
3M ISD-110	1.7	80	115	150	3e4	3e1	1e3	1.7e3
3M ISD-112	1.2	10	40	80	1.3e5	8e1	3.2e3	3.9e3
3M ISD-113	1.1	−45	−20	15	1.5e5	3e2	2.1e2	2.3e2
3m 468	0.8	15	50	85	1.4e5	3e1	2e3	1.6e3
3M ISD-830	1.0	−75	−50	−20	2e5	1.5e2	5.5e3	5.5e3
GE SMRD	0.9	50	80	125	e35	5e3	3.9e4	3.5e4

[a] Approximate values taken from curves in Ref. 11.

[b] To convert to °C, use the formula °C = $(\frac{5}{9})$(°F − 32) or the approximate table below:

°F	−80	−60	−40	−20	0	20	40	60	80	100	120	140	160	180	200
°C	−62	−51	−40	−29	−18	−7	4	16	27	38	49	60	71	82	93

[c] Numbers shown correspond to storage (real) values of Young's modulus, except that $E_{I,max}$ represents the maximum values of the loss (imaginary) modulus. E_{max} applies for low temperatures and/or high frequencies. E_{min} applies for high temperatures and/or low frequencies. E_{trans} and $E_{I,max}$ applies in the range of η_{max}. Divide by 3 to obtain the corresponding shear modulus values.
To convert to N/m², multiply tabulated values by 7×10^3. The number following e represents the power of 10 by which the number preceding e is to be multiplied; e.g., 1.2e3 represents 1.2×10^3

temperatures considerably below those corresponding to η_{max}); E_{min}, the smallest value of E, applies at high temperatures; the transition value E_{trans} applies in the η_{max} range; and $E_{I,max} \approx \eta_{max} E_{trans}$, the maximum value of the loss modulus, applies in the transition range.

It is important to keep in mind that the mechanical properties of polymeric materials, including plastics and elastomers, tend to be more variable than those of metals and other classical structural materials. Some of this variability results from a polymer's molecular structure and molecular weight distribution, which depend not only on the material's chemical composition but also on its processing. Additional variability results from the various types and amounts of plasticizers and fillers that are added to most commercial materials for a number of practical

purposes. Thus, it is quite common for nominally identical polymeric materials to exhibit considerably different mechanical behaviors. It may also occur that even material samples from the same production run have considerably different loss factors and moduli at frequencies and temperatures at which they are intended to be used, pointing toward the need for careful quality control and performance verification for critical applications.

Structures with Viscoelastic Layers

One may calculate the loss factor of a structure vibrating in a given mode by use of Eq. (14.21) if one knows the energies W_i stored in the various deformations of all of the component elements. Indeed, modern finite-element analysis methods[26–28] proceed by calculating the modal deflections, applying these to evaluate all the energy storage components, and then using Eq. (14.21) to find the loss factor.

Analytical results have been developed for flexure of uniform beam and plate structures under conditions that are often approximated in practice. These results, which are extremely useful for design guidance and for development of an understanding of the important parameters, apply to structures whose deflection distributions are sinusoidal.*

Two-Component Beams

In flexure of a uniform beam with an insert or added layer of viscoelastic material, as illustrated by Fig. 14.9, the energy storage (and dissipation) associated with shear and torsional deformations may generally be neglected. If contact between the components is maintained without slippage at all surfaces and if the loss factor of the basic structural (nonviscoelastic) component is negligible, then the

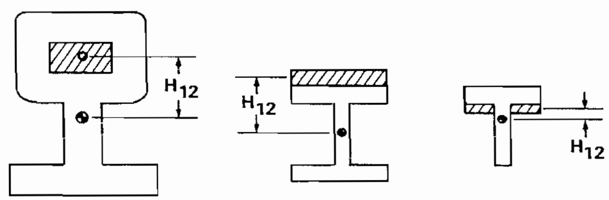

FIGURE 14.9 End views of beams with viscoelastic inserts or added layers. Structural material is unshaded, viscoelastic material is shown shaded; H_{12} represents distance between neutral axis of structural component and that of viscoelastic component. Beam deflection is vertical, with wave propagation along the beam length, perpendicular to the plane of the paper.

*The deflection distribution of any beam (or plate) vibrating in one of its natural modes is at least approximately sinusoidal (in one dimension for beams and in two dimensions for plates) at locations that are one wavelength or more from the boundaries, regardless of the boundary conditions. Therefore, the assumption of a sinusoidal deflection distribution is valid for a larger fraction of the structure as the frequency increases.

loss factor η of the composite beam is related to the loss factor β of the material of the viscoelastic component by[29,30]

$$\frac{\eta}{\beta} = \left[1 + \frac{k^2(1+\beta^2) + (r_1/H_{12})^2\alpha}{k[1 + (r_2/H_{12})^2\alpha]}\right]^{-1} \tag{14.22}$$

where $\alpha = (1+k)^2 + (\beta k)^2$ and H_{12} denotes the distance between the neutral axes of the two components. With subscript 1 referring to the structural (undamped) component and subscript 2 referring to the viscoelastic component, $k = K_2/K_1$, where $K_i = E_i A_i$ denotes the extensional stiffness of component i, expressed in terms of its Young's modulus (real part) E_i and cross-sectional area A_i. Furthermore, $r_i = \sqrt{I_i/A_i}$ represents the radius of gyration of A_i, where I_i denotes the centroidal moment of inertia of A_i.

For the often-encountered case where the structural component's extensional stiffness is much greater than that of the viscoelastic component, $k \ll 1$ and Eq. (14.22) reduces to

$$\eta \approx \frac{\beta E_2 I_T}{E_1 I_1 + E_2 I_T} \approx \frac{\beta E_2}{E_1}\frac{I_T}{I_1} \tag{14.23a}$$

where $I_T = I_2 + H_{12}^2 A_2 = A_2(r_2^2 + H_{12}^2)$ denotes the moment of inertia of A_2 about the neutral axis of A_1.

The last expression in Eq. (14.23a) applies for $E_2 I_T \ll E_1 I_1$, which is generally true in practical structures where the area and elastic modulus of the viscoelastic component are small compared to those of the structural component. In this case the composite structure's neutral axis coincides very nearly with that of the structural component and the dominant energy storage is associated with flexure of the structural component (whose flexural stiffness is $E_1 I_1$). The dominant energy dissipation is associated with extension and compression of the viscoelastic component, with the average extension (equal to the extension at the viscoelastic component's neutral axis) resulting from the flexural curvature and the distance H_{12} between the neutral axes of the viscoelastic and the structural components.* The flexural curvature is greatest at the antinodes of the vibrating structure; most of the damping action thus occurs at these locations, with little damping resulting from the material near the nodes.

The second form of Eq. (14.23a) contains two ratios; the first involves only material properties and the second only geometric parameters. It indicates that the most important dynamic mechanical property of the viscoelastic material is its extensional loss modulus $E_I = \beta E_2$. In keeping with the conclusions based on the general energy expression [Eq. (14.21)], good damping of the composite structure can be obtained only from a viscoelastic material that has not only a high loss factor but also a considerable energy storage capability.

*A "spacer," a layer that is stiff in shear and soft in extension (e.g., like honeycomb), inserted between the structural and the viscoelastic component can increase H_{12} and thus the damping obtained with a given amount of viscoelastic material.[30]

Plates with Viscoelastic Coatings

A strip of a plate (see insert of Fig. 14.10) may be considered as a special case of a two-component beam, where the two components have rectangular cross sections. Thus Eqs. (14.22) and (14.23a) apply, with $r_i = H_i/\sqrt{12}$ and $H_{12} = \frac{1}{2}(H_1 + H_2)$, where H_i denotes the component thickness. The energy storage and dissipation considerations that were discussed in the foregoing section, as well as the foregoing remarks concerning the dominant damping material properties, apply here also.

Figure 14.10 is a plot based on Eq. (14.22) for $\beta^2 \ll 1$. It shows that for small relative thicknesses $h_2 = H_2/H_1$, the loss factor ratio η/β is proportional to the viscoelastic layer thickness, whereas for very large relative thicknesses the loss factor ratio approaches unity; that is, the loss factor of the coated plate approaches that of the viscoelastic coating, as one would expect.* As also is evident from

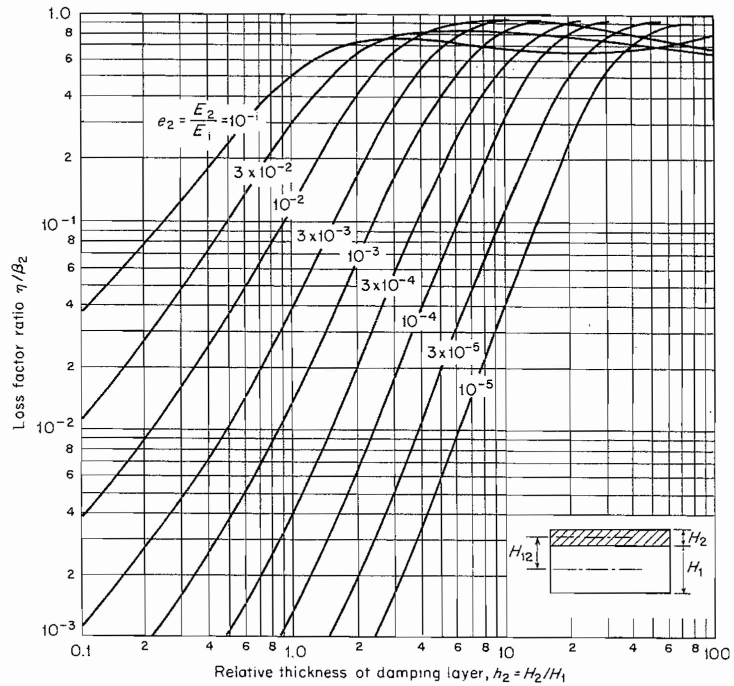

FIGURE 14.10 Dependence of loss factor η of plate strip with added viscoelastic layer on relative thickness and relative modulus of layer.[30] Curves apply for loss factors β of viscoelastic material that are small compared to unity.

*For very thick viscoelastic coatings, deformations in the thickness direction (which are not considered in this simplified analysis) also may play a significant role, particularly at frequencies at which standing-wave resonances may occur in the viscoelastic material.[31]

the figure, at small relative thicknesses the loss factor ratio is proportional to the modulus ratio $e_2 = E_2/E_1$. For small relative thicknesses, that is, in the regions where the curves of Fig. 14.10 are nearly straight, the loss factor of a coated plate may be estimated from[30]

$$\eta \approx \frac{\beta E_2}{E_1} h_2 \ (3 + 6h_2 + 4h_2^2) \tag{14.23b}$$

where $h_2 = H_2/H_1$.

If two viscoelastic layers are applied to a plate, one layer on each side, then the loss factor of the coated plate may be taken as the sum of the loss factors contributed by the individual layers, with each contribution calculated as if the other layer were absent, provided that each viscoelastic layer has low relative extensional rigidity, that is, that $E_2 H_2 \ll E_1 H_1$. If this inequality is not satisfied, a more complex analysis is required.

Three-Component Beams with Viscoelastic Interlayers

Figure 14.11 illustrates uniform beams consisting of two structural (nonviscoelastic) components interconnected via a relatively thin viscoelastic component. Such three-component beams may be preferable to two-component beams for practical reasons because the viscoelastic material is exposed only at its edges; however, such beams can also be designed to have higher damping than two-component beams of similar weight.*

In flexure of a three-component beam with a viscoelastic layer whose extensional and flexural stiffnesses are small compared to those of the structural components, the dominant energy dissipation is associated with shear in the viscoelastic component and the most significant energy storage occurs in connection with extension/compression and flexure of the two structural components. The shear in the viscoelastic component is greatest at the vibrating structure's nodes. Thus, most of the energy dissipation occurs in the viscoelastic material near

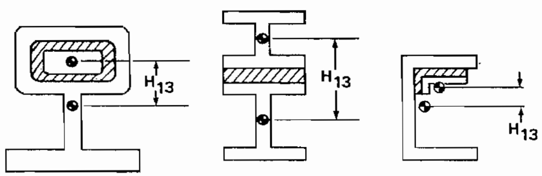

FIGURE 14.11 End views of composite beams made up of two structural components (unshaded) joined via a viscoelastic component (shaded); H_{13} is distance between neutral axes of structural components. Beam deflection is vertical, with wave propagation along the beam length, perpendicular to the plane of the paper.

*It should be noted that design changes to obtain increased damping generally also result in mass and stiffness changes, which tend to affect a structure's vibratory response and should be considered in the design process.[17,32,33]

the nodes, with relatively little resulting in that near the antinodes. For efficient damping, it is important that the shearing action in the viscoelastic material not be restrained (particularly at and near nodes) by structural interconnections, such as bolts.

The loss factor η corresponding to a spatially sinusoidal deflection shape of such a three-component beam is related to the loss factor β of the viscoelastic material by[29,30]

$$\eta = \frac{\beta Y X}{1 + (2 + Y)X + (1 + Y)(1 + \beta^2)X^2} \tag{14.24}$$

where

$$X = \frac{G_2 b}{p^2 H_2} S \qquad \frac{1}{Y} = \frac{E_1 I_1 + E_3 I_3}{H_{13}^2} S \qquad S = \frac{1}{E_1 A_1} + \frac{1}{E_3 A_3} \tag{14.25}$$

Here subscripts 1 and 3 refer to the structural components and 2 to the viscoelastic component; E_i, A_i, and I_i represent, respectively, the Young's modulus, cross-sectional area, and moment of inertia of component i; H_{13} denotes the distance between the neutral axes of the two structural components; and G_2 represents the shear modulus (real part) of the viscoelastic material, H_2 the average thickness of the viscoelastic layer, and b its length as measured on a cross section through the beam. The wavenumber p of the spatially sinusoidal beam deflection obeys

$$\frac{1}{p^2} = \left(\frac{\lambda}{2\pi}\right)^2 = \frac{1}{\omega}\sqrt{\frac{B}{\mu}} \tag{14.26}$$

where λ represents the bending wavelength and B denotes the flexural rigidity and μ the mass per unit length of the composite beam.

The *structural parameter* Y of three-component structures depends only on the geometry and Young's moduli of the two structural components, whereas the *shear parameter* X depends also on the properties of the viscoelastic layer and on the wavelength of the beam deflection. The shear parameter X is proportional to the square of the ratio of the beam flexural wavelength to the *decay distance*,[34] that is, the distance within which a local shear disturbance decays by a factor of e, where $e \approx 2.72$ denotes the base of natural logarithms; thus, X also is a measure of how well the viscoelastic layer couples the flexural motions of the two structural components.

The (complex) flexural rigidity of a three-component beam is given by

$$\overline{B} = (E_1 I_1 + E_3 I_3)\left(1 + \frac{X^* Y}{1 + X^*}\right) \qquad X^* = X(1 - j\beta) \tag{14.27}$$

Its magnitude is $B = |\overline{B}|$. Thus, for small X, the flexural rigidity B of the composite beam is equal to the sum of the flexural rigidities of the structural components, that is, to the total flexural rigidity that the two components exhibit if they are not interconnected. For $X \gg 1$, however B approaches $1 + Y$ times the foregoing value, which is equal to the flexural rigidity of a beam with rigidly interconnected structural components 1 and 3.

For a given value of β and Y, the loss factor η of the composite beam takes on its greatest value,

$$\eta_{\max} = \frac{\beta Y}{2 + Y + 2/X_{\text{opt}}} \tag{14.28}$$

at the optimum value of X, which is given by

$$X_{\text{opt}} = [(1 + Y)(1 + \beta^2)]^{-1/2} \tag{14.29}$$

With the aid of these definitions, one may rewrite Eq. (14.24) in terms of the ratio $R = X/X_{\text{opt}}$ in the following form, which provides a convenient view of the damping behavior of three-component beams:

$$\frac{\eta}{\eta_{\max}} = \frac{2(1 + N)R}{1 + 2NR + R^2} \qquad N = (1 + \tfrac{1}{2}Y)X_{\text{opt}} \tag{14.30}$$

Figure 14.12, which is based on Eqs. (14.28) and (14.29), shows how $\eta_{\max}/\beta$ increases monotonically with Y, indicating the importance of selecting a configuration with a large value of Y in the design of highly damped composite structures.* Figure 14.13 gives approximate values of Y for some often encountered

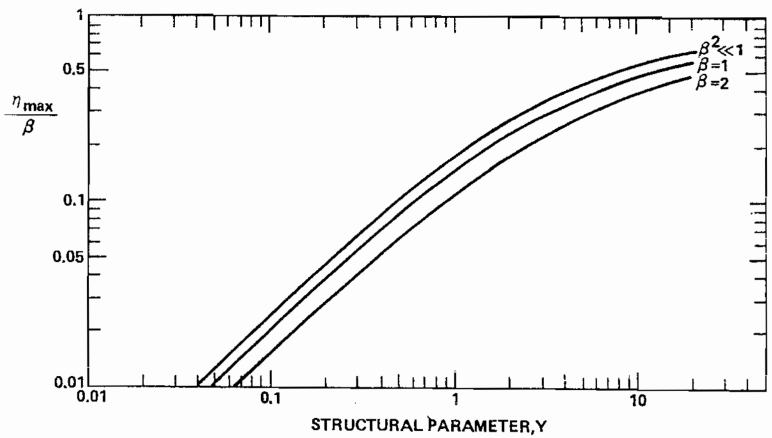

FIGURE 14.12 Dependence of maximum loss factor $\eta_{\max}$ of three-component beams or plates on structural parameter Y and loss factor β of viscoelastic material.

*A shear-stiff, extensionally soft "spacer" (e.g., honeycomb) inserted between the viscoelastic and one or both structural components can serve to increase H_{13} and, therefore, the value of Y. See Eq. (14.25). For a given deflection of the composite structure, a spacer increases the damping by increasing the shear strain—and thus the energy storage and dissipation—in the viscoelastic component.[30,34]

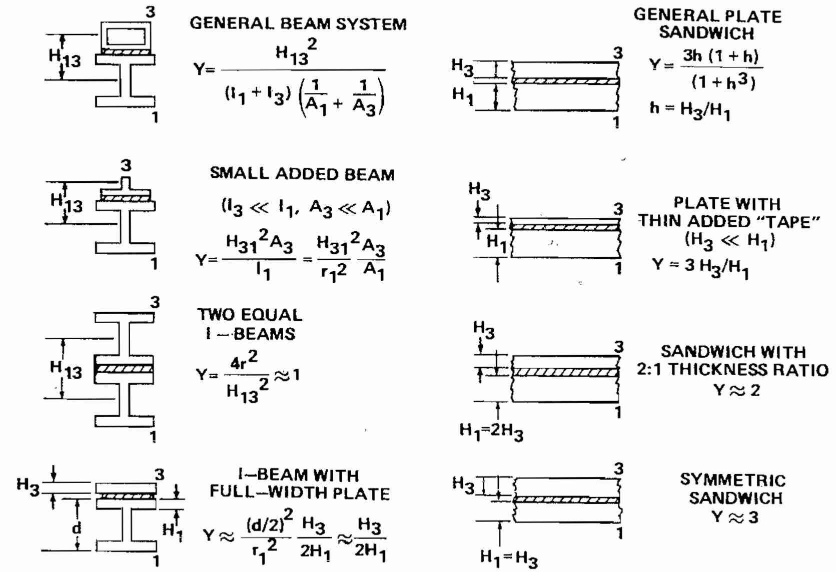

FIGURE 14.13 Values of structural parameter Y for three-component beam and plate configurations with thin viscoelastic components and with structural components of the same material; viscoelastic component is shown cross-hatched. I, moment of inertia; A, cross-sectional area; r, radius of gyration; H_{13}, distance between neutral axes.

configurations. Figure 14.14 shows how $\eta/\eta_{\max}$ varies with X/X_{opt}, indicating the importance of making the operating value of X of a given design match X_{opt} as closely as possible in order to obtain a loss factor that approaches $\eta_{\max}$.

If one knows the wavenumber $p = 2\pi/\lambda$ and the frequency associated with a given beam vibration, one may calculate the loss factor η of a composite beam simply by substituting the beam parameters and the material properties at any frequency (and temperature) of interest into Eqs. (14.24) and (14.25) or (14.28)–(14.30). The latter set of equations is particularly useful for judging how far from the optimum a given configuration may be operating.

If one knows only the frequency and not the wavenumber p corresponding to a beam vibration, one needs to use Eq. (14.26) to determine p. Substitution of B as calculated from Eq. (14.27) into Eq. (14.26), followed by substitution of the result into the first of Eqs. (14.25), leads to a cubic equation in X. Although one may solve this numerically, it is often more convenient to determine X by use of an iteration procedure like that indicated in Fig. 14.15.

In contrast to the previously discussed two-component beam, the loss factor η of a three-component beam does not depend primarily on the loss modulus (i.e., on the product of the loss factor β and storage modulus E_2 or G_2) of the viscoelastic material. The loss factor of a three-component beam depends on β and G_2 separately, and the separate dependences must be taken into account in

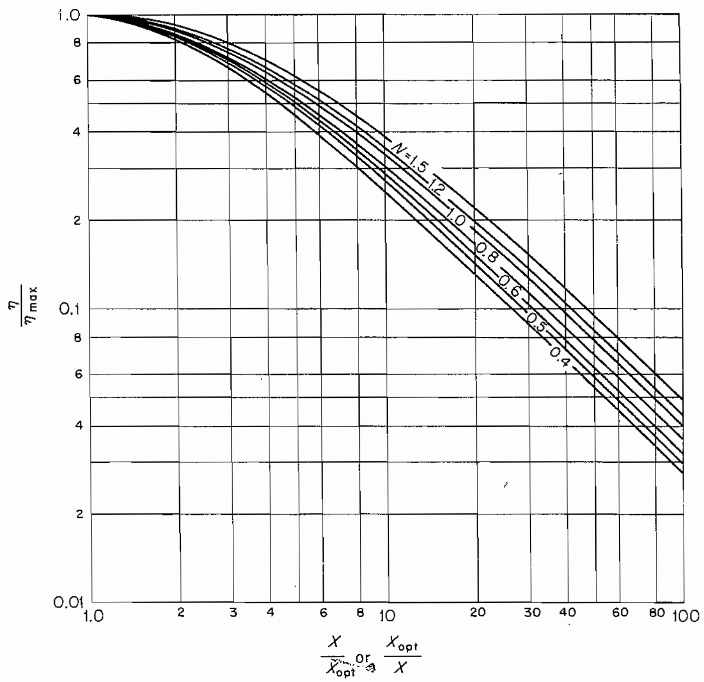

FIGURE 14.14 Dependence of loss factor η of three-component beam or plate on shear parameter X [from Eq. (14.30)].

the design of such a beam. Design of a highly damped three-component beam structure requires (1) choice of a configuration with a large structural parameter Y, (2) selection of a damping material with a large loss factor β in the frequency and temperature range of interest, and (3) adjustment of the damping material thickness H_2 and length b so as to make X [as calculated from Eq. (14.25) for the value of G_2 applicable to the frequency and temperature of concern] approximately equal to X_{opt} [given by Eq. (14.29)]. The resulting design then will have a loss factor approximately equal to η_{max} as given by Eq. (14.28).

The expected performance of any design should be checked for the frequency and temperature ranges of interest by means of the procedure described in the previous paragraph. Note that a given design may be expected to perform optimally—that is, to have X under operating conditions approximately equal to X_{opt}—only in a limited range of frequencies and temperatures, with reduced performance outside this range.

Plates with Viscoelastic Interlayers

A strip of a plate consisting of a viscoelastic layer between two structural layers may be considered as a special case of a three-component beam. In a plate strip,

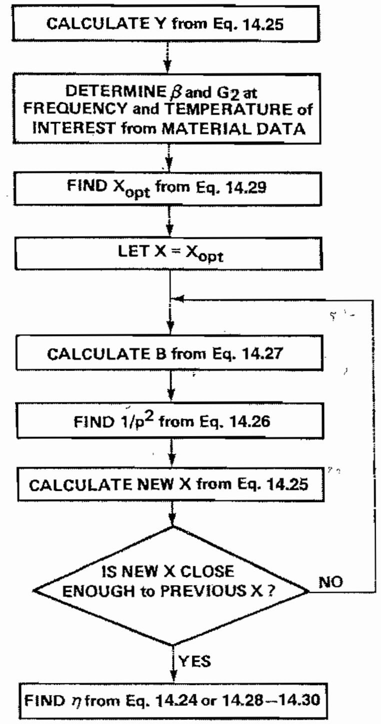

FIGURE 14.15 Iteration procedure for determination of loss factor of three-component beams or plates for which wavelength is not known initially.

all components have rectangular cross sections of the same width; Eqs. (14.25) accordingly become

$$X = \frac{G_2}{p^2 H_2} S \qquad \frac{1}{Y} = \frac{E_1 H_1^3 + E_3 H_3^3}{12 H_{31}^2} S \qquad S = \frac{1}{E_1 H_1} + \frac{1}{E_3 H_3} \tag{14.31}$$

If, furthermore, $E_1 I_1 + E_3 I_3$ in Eq. (14.27) is replaced by $\frac{1}{12}(E_1 H_1^3 + E_3 H_3^3)$ and if μ in Eq. (14.26) is interpreted as the mass per unit surface area of the plate, then all of the foregoing discussion pertaining to beams also applies to plates.

REFERENCES

1. W. T. Thomson, *Theory of Vibration with Applications*, 2nd ed., Prentice-Hall, Englewood Cliffs, NJ, 1981.
2. R. Plunkett, "Measurement of Damping," in J. F. Ruzicka (Ed.), *Structural Damping*, American Society of Mechanical Engineers, New York, 1959.

3. K. N. Tong, *Theory of Mechanical Vibration*, Wiley, New York, 1960.
4. E. E. Ungar, "Mechanical Vibrations," in H. A. Rothbart (Ed.), *Mechanical Design and Systems Handbook*, 2nd ed., McGraw-Hill, New York, 1985, Chapter 5.
5. D. J. Ewins, *Modal Testing: Theory and Practice*, Research Studies Press, Letchworth, Hertfordshire, England, 1986.
6. V. H. Neubert, *Mechanical Impedance: Modelling/Analysis of Structures*, Josens Printing and Publishing, State College, PA, distributed by Naval Sea Systems Command, Code NSEA-SSN, 1987.
7. B. L. Clarkson and J. K. Hammond, "Random Vibration," in R. G. White and J. G. Walker (Eds.), *Noise and Vibration*, Wiley, New York, 1982, Chapter 5.
8. B. L. Clarkson and R. J. Pope, "Experimental Determination of Modal Densities and Loss Factors of Flat Plates and Cylinders," *J. Sound Vib.*, **77**(4), 535–549 (1981).
9. S. H. Crandall, "The Role of Damping in Vibration Theory," *J. Sound Vib.*, **11**(1), 3–18 (1970).
10. A. D. Nashif, D. I. G. Jones, and J. P. Henderson, *Vibration Damping*, Wiley, New York, 1985.
11. G. Kurtze, "Körperschalldämpfung durch Körnige Medien" [Damping of Structure-Borne Sound by Granular Media], *Acustica*, **6**(Beiheft 1), 154–159 (1956).
12. M. A. Heckl, "Measurements of Absorption Coefficients on Plates," *J. Acoust. Soc. Am.*, **34**, 308–808 (1962).
13. G. Maidanik, "Energy Dissipation Associated with Gas-Pumping at Structural Joints," *J. Acoust. Soc. Am.*, **34**, 1064–1072 (1966).
14. E. E. Ungar, "Damping of Panels Due to Ambient Air," in P. J. Torvik (Ed.), *Damping Applications in Vibration Control*, AMD-Vol 38, American Society of Mechanical Engineers, New York, 1980, pp. 73–81.
15. E. E. Ungar and J. Carbonell, "On Panel Vibration Damping Due to Structural Joints," *AIAA J.*, **4**, 1385–1390 (1966).
16. E. E. Ungar and L. G. Kurzweil, "Structural Damping Potential of Waveguide Absorbers," *Trans. Internoise 84*, December 1985, pp. 571–574.
17. D. J. Mead, *Passive Vibration Control*, J Wiley, New York, 2002.
18. L. Cremer, M. Heckl, and E. E. Ungar, *Structureborne Sound*, 2nd ed., Springer-Verlag, New York, 1988.
19. E. E. Ungar and E. M. Kerwin, Jr., "Loss Factors of Viscoelastic Systems in Terms of Energy Concepts." *J. Acoust. Soc. Am.*, **34**(7), 954–957 (1962).
20. E. E. Ungar, "Damping of Panels," in L. L. Beranek (Ed.), *Noise and Vibration Control*, McGraw-Hill, New York, 1971, Chapter 14.
21. D. I. G. Jones, *Handbook of Viscoelastic Vibration Damping*, Wiley, New York, 2002.
22. ISO 10112, "Damping Materials—Graphic Presentation of the Complex Modulus," International Organization for Standardization, Geneva, Switzerland, 1991.
23. ANSI S2.24-2001, "Graphical Presentation of the Complex Modulus of Viscoelastic Materials," American National Standards Institute,Washington, DC, 2001.
24. J. Soovere and M. L. Drake, "Aerospace Structures Technology Damping Design Guide," AFWAL-TR-84-3089, Flight Dynamics Laboratory, Wright-Patterson Air Force Base, OH, December 1985.

25. D. I. G. Jones and J. P. Henderson, "Fundamentals of Damping Materials," Section 2 of Vibration Damping Short Course Notes, M. L. Drake (Ed.), University of Dayton, 1988.
26. M. L. Soni and F. K. Bogner, "Finite Element Vibration Analysis of Damped Structures." *AIAA J.*, **20**(5), 700–707 (1982).
27. C. D. Johnson, D. A. Kienholz, and L. C. Rogers, "Finite Element Prediction of Damping in Beams with Constrained Viscoelastic Layers," *Shock Vib. Bull.*, **51**(Pt. 1), 71–82 (1981).
28. M. F. Kluesner and M. L. Drake, "Damped Structure Design Using Finite Element Analysis," *Shock Vib. Bull.*, **52**(Pt. 5), 1–12 (1982).
29. E. E. Ungar, "Loss Factors of Viscoelastically Damped Beam Structures," *J. Acoust. Soc. Am.*, **34**(8), 1082–1089 (1962).
30. D. Ross, E. E. Ungar, and E. M. Kerwin, Jr., "Damping of Plate Flexural Vibrations by Means of Viscoelastic Laminae," in J. Ruzicka (Ed.), *Structural Damping*, American Society of Mechanical Engineers, New York, 1959, Section 3.
31. E. E. Ungar and E. M. Kerwin, Jr., "Plate Damping Due to Thickness Deformations in Attached Viscoelastic Layers," *J. Acoust. Soc. Am.*, **36**, 386–392 (1964).
32. D. J. Mead, "Criteria for Comparing the Effectiveness of Damping Materials," *Noise Control*, **1**, 27–38 (1961).
33. D. J. Mead, "Vibration Control (I)," in R. G. White and J. G. Walker (Eds.), *Noise and Vibration*, Ellis Horwood, Chichester, West Sussex, England, 1982.
34. E. M. Kerwin, Jr., "Damping of Flexural Waves in Plates by Spaced Damping Treatments Having Spacers of Finite Stiffness," in L. Cremer (Ed.), *Proc. 3rd Int. Congr. Acoust., 1959*, Elsevier, Amsterdam, Netherlands, 1961, pp. 412–415.

CHAPTER 15

Noise of Gas Flows

H. D. BAUMANN

Consultant
Rye, New Hampshire

W. B. CONEY

BBN Systems and Technologies Corporation
Cambridge, Massachusetts

15.1 INTRODUCTION

The sound produced by unsteady gas flows and by interactions of gas flows with solid objects is called *aerodynamic sound*. The same flows often excite structural modes of vibration in surfaces bounding the flow and are then said to generate *structure-borne sound*. Unwanted flow-generated sound, noise, is a common by-product of most industrial processes. It also accompanies the operation of ships, automobiles, aircraft, rockets, and so on, and can adversely affect structural stability and be an important source of fatigue.

A practical understanding of the sources of aerodynamic sound is necessary over the whole range of mean-flow Mach numbers, from the very lowest (0.01 or less) associated with flows in air conditioning systems and underwater applications to the high supersonic range occurring in jet engines and high-pressure valves. In subsonic flows, the sound may be attributed to three basic aerodynamic source types: monopole, dipole, and quadrupole.[1]

These fundamental source types are discussed in this chapter, together with a survey of noise mechanisms associated with turbulent jets, spoilers and airfoils, boundary layers and separated flow over wall cavities, combustion, and valves.

15.2 AEROACOUSTICAL SOURCE TYPES

Aerodynamic Monopole

Monopole radiation is produced by the unsteady introduction of mass or heat into a fluid. Typical examples are pulse jets (where high-speed air is periodically ejected through a nozzle), turbulent flow over a small aperture in a large wall (where the flow induces pulsating motion in the aperture), unsteady combustion processes, and heat release from boundaries or from a pulsed laser beam.

The radiation from a monopole source in an otherwise stationary fluid is equivalent to that produced by a pulsating sphere (Fig. 15.1*a*). Both the amplitude and phase of the acoustical pressure are spherically symmetric. When the monopole sound is generated by unsteady flow velocities, the dimensional relation between the radiated sound power and the flow parameters is

$$W_{\text{monopole}} \propto \frac{\rho L^2 U^4}{c} = \rho L^2 U^3 M \tag{15.1}$$

where W_{monopole} = radiated sound power, W
ρ = mean speed of gas, kg/m^3
c = speed of sound in gas, m/s
U = flow velocity in source region, m/s
L = length scale of flow in source region, m
M = Mach number, $= U/c$, dimensionless

Aerodynamic Dipole

Dipole sources arise when unsteady flow interacts with surfaces or bodies, when the dipole strength is equal to the force on the body, or when there are significant variations of mean fluid density in the flow. This source type is found in compressors where turbulence impinges on stators, rotor blades, and other control surfaces. Similarly, the unsteady shedding of vorticity from solid objects,

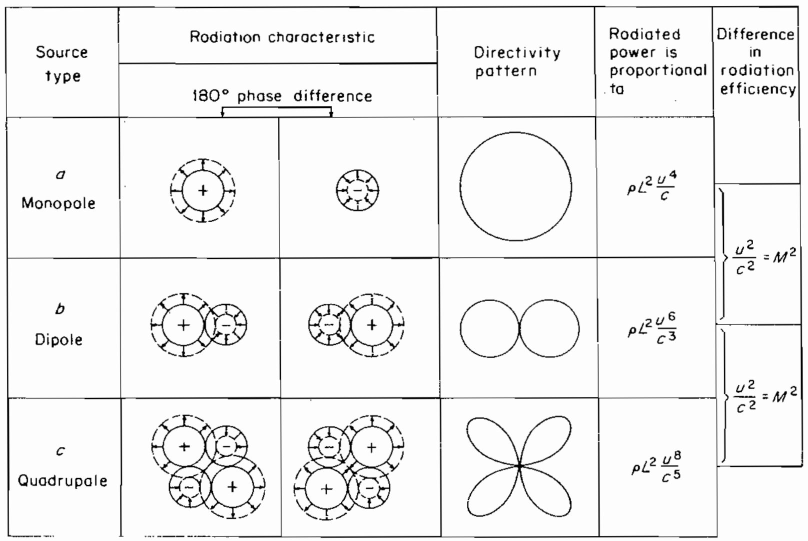

FIGURE 15.1 Aeroacoustical source types and their dimensional properties in fluid of uniform mean density. See also Fig. 1.2.

such as telegraph wires, struts, and airfoils, generates "singing" tones that are also attributable to dipole sources. Other examples include the noise generated by hot jets exhausting into a cooler ambient medium and by the acceleration of temperature (or "entropy") inhomogeneities in a mean pressure gradient, as in a duct contraction.

The dipole is equivalent to a pair of equal monopole sources of opposite phase separated by a distance that is much smaller than the wavelength of the sound. Destructive interference between the radiations from the monopoles reduces the efficiency with which sound is generated by the dipole relative to a monopole and produces a double-lobed, figure-eight radiation field shape proportional to the cosine of the angle measured from the dipole axis (Fig. 15.1*b*). In fluid of uniform mean density, the dimensional dependence of the aerodynamic dipole sound power is

$$W_{\text{dipole}} \propto \frac{\rho L^2 U^6}{c^3} = \rho L^2 U^3 M^3 \tag{15.2}$$

This differs by a factor M^2 from the power output of the monopole. In subsonic flow ($M < 1$) the dipole is a less efficient source of sound.

If the specific entropy or temperature of the flow in the source region is not uniform (e.g., in the shear layer of a hot jet exhausting into a cooler ambient atmosphere), the density must also be variable. The relatively strong pressure fluctuations in the turbulent flow are then scattered by the density variations and produce sound of the dipole type. The dipole strength is proportional to the difference between the actual acceleration of the density inhomogeneity in the turbulent pressure field and that which it would have experienced had the density been uniform.[2] The dimensional dependence of the corresponding sound power is

$$W_{\text{entropy}} \propto \frac{\rho L^2 (\delta T/T)^2 U^6}{c^3} = \rho L^2 \left(\frac{\delta T}{T}\right)^2 U^3 M^3 \tag{15.3}$$

where $(\delta T/T)^2$ is the mean-square fractional temperature fluctuation.

Aerodynamic Quadrupole

Quadrupole radiation is produced by the Reynolds stresses in a turbulent gas in the absence of obstacles. These arise from the convection of fluid momentum by the unsteady flow. The Reynolds stress forces must occur in opposing pairs, since the net momentum of the fluid is constant. Force pairs of this type are called quadrupoles and are equivalent to equal and opposite dipole sources (see Fig. 15.1*c*).

Aerodynamic quadrupoles and entropy dipoles are the dominant source types in high-speed, subsonic, turbulent air jets. The quadrupole strength is larger where both the turbulence and mean velocity gradients are high, for example, in the turbulent mixing layer of a jet.

The dimensional dependence of the radiated quadrupole sound power is

$$W_{\text{quadrupole}} \propto \frac{\rho L^2 U^8}{c^5} = \rho L^2 U^3 M^5 \tag{15.4}$$

This differs from the dipole power by a factor M^2. At subsonic speeds ($M < 1$), the quadrupole radiation efficiency is lower than that of the dipole because of the double cancellation illustrated in Fig. 15.1c.

The monopole, dipole, and quadrupole sources decrease in their respective radiation efficiencies for subsonic flows, but the dependencies of their radiated sound powers on flow velocity show the opposite trend, that is, the total radiated sound power varies as the fourth, sixth, and eighth powers of the flow speed U for monopole, dipole, and quadrupole sources, respectively. Thus, if the flow velocity is high enough, the radiation from the quadrupole sources may be the dominant source of sound even though the efficiency with which the sound is produced is small. This is usually the case for a jet engine at high subsonic exhaust velocities, although other internal sources caused by unsteady combustion or rough burning (predominantly monopole) or compressor noise (predominantly dipole) can also make a significant contribution to the total noise.

The value of the constant of proportionality for each type of source depends on both the sound-generating mechanism and the flow configuration. Thus, the constant for a singing wire differs from that of an edge tone, although both arise from unsteady surface forces (dipole sources). However, the proportionality relations (15.1)–(15.4) can be used to estimate the influence on radiated sound power of changes in one or more of the source parameters. A twofold increase in the exhaust velocity U of a jet (quadrupole-type source) causes the sound power level to increase by 24 dB (eighth power of flow velocity), whereas a doubling of the exhaust nozzle area A (proportional to L^2) increases the sound power level by only 3 dB. Because the thrust of a jet engine is proportional to AU^2, the increase in radiated sound will be smaller if a doubling of the thrust is achieved by increasing the nozzle area by a factor of 2 rather than the exhaust velocity by a factor of 1.4.

Aerodynamic Sources of Fractional Order

The efficiency with which sound is produced by aerodynamic dipole sources on surfaces whose dimensions greatly exceed the acoustical wavelength frequently differs from those implied by Eqs. (15.2) and (15.3). For example, the net dipole strength associated with turbulent flow over a smooth, plane wall is zero: The radiation is the same as that generated by the quadrupole sources in the flow when the wall is regarded as a plane reflector of sound. Similarly, the net strength of the dipoles induced by turbulence near the edge of a large wedge-shaped body varies with angle ν—being equivalent to that of a quadrupole when $\nu = 180°$ (i.e., for a plane wall) and to a *fractional* multipole order $\frac{3}{2}$ when $\nu = 0$ (knife edge). The latter case is important in estimating the leading and trailing edge noise of an airfoil, where at high enough frequency the sound power is proportional to $\rho L U^3 M^2$.

Influence of Source Motion

The directional characteristics of the radiation from acoustical sources are changed if the source moves relative to the fluid. Both the frequency and intensity of the sound are increased ahead of the source and decreased to its rear. It is usual to refer the observer to a coordinate system based on the source location at the time of emission of the received sound.

For a monopole source of strength $q(t)$ kilograms per second (equal to the product of the volume velocity and the fluid density) moving at constant speed U in the direction illustrated in Fig. 15.2, the acoustical pressure p in the far field is

$$p_{\text{monopole}} = \pm \left[\frac{dq/dt}{4\pi r(1 - M_{fr})^2}\right] \tag{15.5}$$

where the square brackets denote evaluation at the time of emission of the sound, (r, Φ) are coordinates defining the observer position relative to the source at the time of emission of the sound, and the plus and minus sign is taken according as $M_{fr} < 1$ or $M_{fr} > 1$, where

$$M_{fr} = \left(\frac{U}{c}\right) \cos \Phi \quad \text{(dimensionless)}$$

The frequency of the received sound is $f/(1 - M_{fr})$, where f, per second, is the frequency in a frame fixed relative to the source. The term $1/(1 - M_{fr})$ is called the *Doppler factor*. Its effect is to modify both the frequency and the amplitude of the acoustic field.

For a uniformly translating dipole of strength $f_i(t)$ (newtons), which is equivalent to an applied force in the i direction, and for a quadrupole $T_{ij}(t)$ (newtons-meters), specified by directions i, j (and equivalent to a force pair applied to the fluid), the respective acoustical pressure fields become

$$p_{\text{dipole}} = \pm \left[\frac{df_r/dt}{4\pi c r(1 - M_{fr})^2}\right] \qquad p_{\text{quadrupole}} = \left[\frac{d^2 T_{rr}/dt^2}{4\pi c^2 r|1 - M_{fr}|^3}\right] \tag{15.6}$$

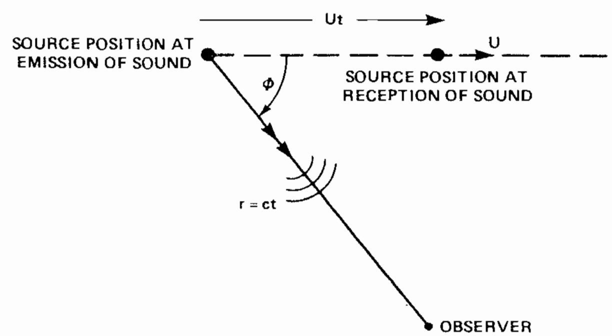

FIGURE 15.2 Coordinates defining the observer position at the time of emission of the received sound from a moving source.

where f_r, T_{rr} denote the components of the dipole and quadrupole source strengths in the observer direction at the time of emission of the sound and the plus and minus sign is taken according as $M_{fr} < 1$ or $M_{fr} > 1$.

These expressions are valid for ideal, point sources moving at constant velocity. The influence of source motion on real, aerodynamic sources is often much more complicated. For example, a pulsating sphere is a monopole source when at rest. In uniform translational motion, however, the radiation is amplified by a Doppler exponent of $\frac{7}{2}$ instead of the 2 of Eq. (15.5). This is because the monopole is augmented due to the motion by a dipole whose strength is proportional to the convection Mach number M_f. The interaction of the volume pulsations with the mean flow over the sphere produces a net fluctuating force on the fluid.

15.3 NOISE OF GAS JETS

The sound generated by high-speed jets is usually associated with several different sources acting simultaneously. *Jet mixing noise*, caused by the turbulent mixing of the jet with the ambient medium, and for imperfectly expanded supersonic jets *shock-associated noise*, produced by the convection of turbulence through shock cells in the jet, are the principal components of the radiation. The properties of sound sources in real jets differ considerably from those of the idealized models described in Section 15.2. Sources located within the "jet pipe" can also make a significant contribution to the noise. In the case of a gas turbine engine, the additional radiation includes combustion noise as well as tonal and broadband sound produced by interactions involving fans, compressors, and turbine systems. The following discussion is based on experimental data obtained and validated by several independent investigators and collated for prediction purposes by the Society of Automotive Engineers.[3] Formulas are given for predicting the *free-field* radiation from a jet in an ideal acoustical medium. In many applications it will be necessary to modify these predictions to account for atmospheric attenuation and interference caused by reflections from surfaces.

Jet Mixing Noise

Mixing noise is the most fundamental source of sound produced by a jet. The simplest free jet is an air stream issuing from a large reservoir through a circular convergent nozzle (Fig. 15.3). The gas accelerates from near-zero velocity in the reservoir to a peak velocity in the narrowest cross section of the nozzle. Sonic flow occurs at the nozzle exit when the pressure ratio p_0/p_s exceeds 1.89, where p_0 is the steady reservoir pressure and p_s is the ambient pressure downstream of the nozzle. An increase above this critical pressure ratio leads to the appearance of a shock cell structure downstream of the nozzle and "choking" of the flow unless the convergent part of the nozzle is followed by a divergent section in which the pressure decreases smoothly to p_s.

For the idealized, shock-free jet, no interaction is assumed between the gas flow and the solid boundaries. The noise is produced entirely by turbulent mixing

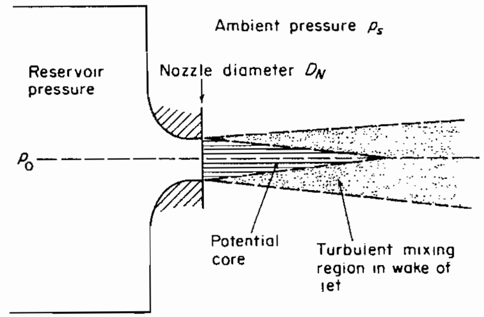

FIGURE 15.3 Subsonic turbulence-free jet.

in the shear layer. The sources extend over a considerable distance downstream of the nozzle. The high-frequency components of noise are generated predominantly close to the nozzle, where eddy sizes are small. Lower frequencies are radiated from sources further downstream where eddy sizes are much larger. The sources may be regarded as quadrupoles, whose strength and directivity are modified by the influences of nonuniform fluid density (temperature) and convection by the flow.

The total radiated sound power W in watts of the mixing noise may be expressed in terms of the mechanical stream power of the jet, equal to

$$W_{\text{mech stream}} = \tfrac{1}{2} m U^2 \qquad (15.7)$$

where m = mass flow of gas, kg/s
U = fully expanded mean jet velocity, m/s

The dependence of $W/\frac{1}{2}mU^2$ on jet Mach number $M = U/c$ and density ratio ρ_j/ρ_s, where c is the ambient sound speed and ρ_j, ρ_s are respectively the densities (in kilograms per cubic meter) of the fully expanded jet and the ambient atmosphere, is illustrated in Fig. 15.4. For $M < 1.05$ the sound power increases as ρ_j/ρ_s decreases (i.e., as the jet temperature increases) and decreases at higher Mach numbers. When $M < 1$, W may be estimated from

$$\frac{W}{W_{\text{mech stream}}} = \frac{4 \times 10^{-5} (\rho_j/\rho_s)^{(w-1)} M^{4.5}}{(1 - M_c^2)^2} \qquad M < 1 \qquad (15.8)$$

where $M_c = 0.62U/c$ and w is the jet density exponent given by[4]

$$w = \frac{3M^{3.5}}{0.6 + M^{3.5}} - 1 \qquad (15.9)$$

Equation (15.9) is applicable for M greater than about 0.35, including the supersonic region and is also used in the formulas given below.

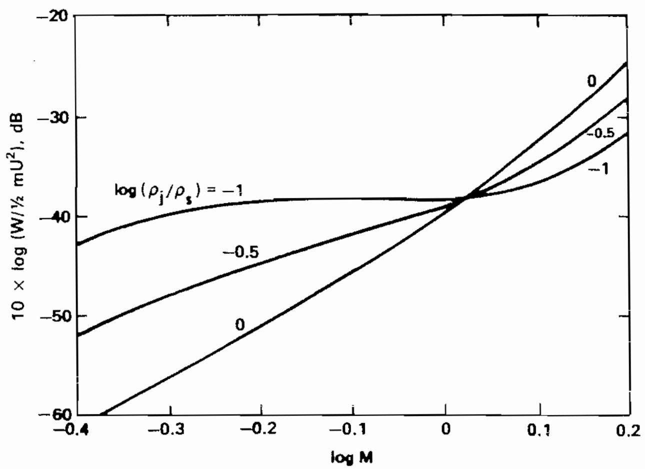

FIGURE 15.4 Ten times the logarithm of the ratio of acoustical power of jet mixing noise to mechanical stream power as a function of the fully expanded jet Mach number $M = U/c$ for different values of ρ_j/ρ_s.

The overall sound pressure level (OASPL) at any point in space is defined as

$$\text{OASPL} = 20 \times \log_{10} \frac{p_{\text{rms}}}{20\ \mu\text{Pa}} \qquad \text{dB} \tag{15.10}$$

where p_{rms} is the rms sound pressure in pascals (newtons per square meter) (see Chapter 2). Source convection and refraction in the shear layers causes the sound field to be directive, the maximum noise being radiated in directions inclined at angles θ to the jet axis between about 30° and 45°.

Typical field directivities at a fixed observer distance for an air jet at three different jet Mach numbers $M = U/c$ are shown in Fig. 15.5. The curves give the variation of OASPL(θ) − OASPL(90°), the sound pressure level relative to its value at $\theta = 90°$, and are approximated by the formula

$$\text{OASPL}(\theta) = \text{OASPL}(90°) - 30 \times \log\left[1 - \frac{M_c \cos\theta}{(1 + M_c^5)^{1/5}}\right]$$
$$- 1.67 \times \log\left[1 + \frac{1}{10^{(40.56-\theta')} + 4 \times 10^{-6}}\right] \tag{15.11}$$

where $M_c = 0.62U/c$
$\theta' = 0.26(180 - \theta)M^{0.1}$, degrees

The final term on the right of (15.11) is negligible unless $\theta < 180° - 150°/M^{0.1}$, that is, except in directions close to the jet axis.

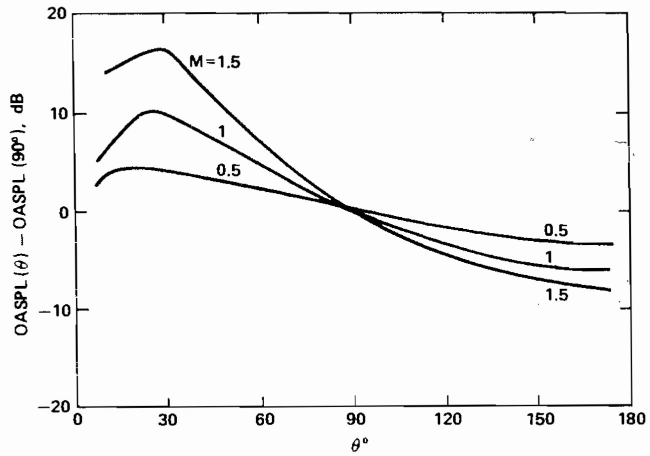

FIGURE 15.5 Directivity of jet mixing noise.

At $\theta = 90°$ the overall sound pressure level of jet mixing noise can be calculated from the formula

$$\text{OASPL} = 139.5 + 10 \times \log \frac{A}{R^2} + 10 \times \log\left[\left(\frac{p_s}{p_{\text{ISA}}}\right)^2 \left(\frac{\rho_j}{\rho_s}\right)^w\right]$$
$$+ 10 \times \log\left(\frac{M^{7.5}}{1 - 0.1M^{2.5} + 0.015M^{4.5}}\right) \tag{15.12}$$

where A = fully expanded jet area, $= \frac{1}{4}\pi D_N^2$ for a subsonic jet, m²
D_N = nozzle exit diameter, m
R = distance from center of nozzle exit, m
p_{ISA} = international standard atmospheric pressure at sea level, = 10.13 μPa

The dependence of OASPL(90°) − $10 \times \log(A/R^2)$ on jet Mach number M and density ratio ρ_j/ρ_s is illustrated in Fig. 15.6.

The sound-pressure-level (SPL) frequency spectrum of jet mixing noise is broadband and peaks at a frequency $f = f_p$ that is a function of the radiation direction θ, jet Mach number M, and temperature ratio T_j/T_s, where T_j (in kelvin) is the fully expanded jet temperature and T_s (kelvin) is the ambient gas temperature. The spectrum has a broad peak that occurs in the range $0.3 < S < 1$, where

$$S = \frac{f_p D_N}{U} \tag{15.13}$$

is the *Strouhal number* (dimensionless), tabulated in Table 15.1 for $\theta \geq 50°$ and for different values of T_j/T_s. For practical purposes the difference $\Delta =$

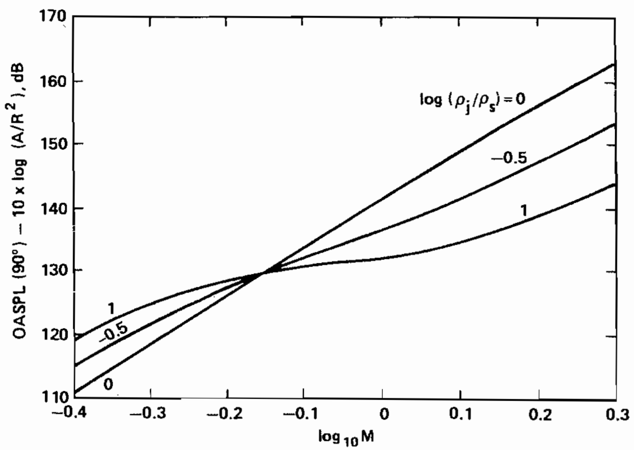

FIGURE 15.6 Overall sound pressure level at $\theta = 90°$.

TABLE 15.1 Values of Strouhal Number and $\Delta(\cdot)$ for Different Values of T_j/T_s[a]

T_j/T_s	$\theta = 50°$	$\theta = 60°$	$\theta = 70°$	$\theta = 80°$	$\theta \geq 90°$
1	0.7 (11 dB)	0.8 (11 dB)	0.8 (11 dB)	1.0	0.9
2	0.5 (10 dB)	0.4 (10 dB)	0.6 (11 dB)	0.5	0.6
3	0.3 (9 dB)	0.4 (10 dB)	0.4 (10 dB)	0.4	0.5

[a]Strouhal number $S = fD_N/U$ at the peak of the one-third-octave-band spectrum of jet mixing noise for $U/c \leq 2.5$ (left columns); Δ = OASPL − $\text{SPL}_{\text{peak}} \cong 11$ dB for all $\theta \geq 80°$ except as indicated in parentheses (right columns).

OASPL − SPL_{peak} between the peak of the one-third-octave-band spectrum and the overall SPL at the same value of θ may be taken to be 11 dB except as indicated in the table.

Figure 15.7 shows a typical relative one-third-octave-band SPL spectrum SPL(f) − OASPL for $\rho_j = \rho_s$ and angles $\theta \geq 90°$. The characteristic shape is the same for all temperatures and angles, although there is significant dependence on temperature and Mach number when θ is smaller than about 50° and $f > f_p$ when refraction of sound by the jet shear layer becomes important. For subsonic jets, the spectrum varies roughly as f^3 at low frequencies and decays like $1/f$ for $f > f_p$.

Figures 15.4–15.7 and Table 15.1, supplemented when necessary by Eqs. (15.8) and (15.9), comprise a general procedure for estimating the SPL, directivity, and spectrum of jet mixing noise.

Example 15.1. Find the total jet mixing noise sound-power- and sound-pressure-level spectrum at 60° from the jet axis and 3 m from the nozzle of a 0.03-m-diameter air jet. The jet exhausts into ambient air (15°C, $p_s = 10.13$ μPa, $\rho_s = 1.225$ kg/m³) at sonic ($U/c = 1$) exit velocity, that is, 340 m/s.

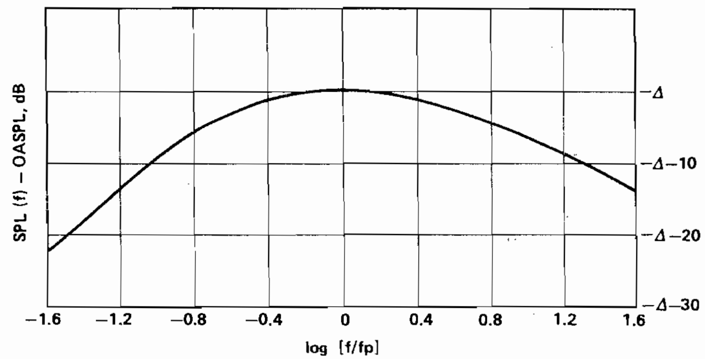

FIGURE 15.7 One-third-octave-band SPL − OASPL (dB) for radiation directions $\theta \geq 90°$ and $\rho_j = \rho_s$.

Solution The mechanical stream power $\frac{1}{2}mU^2$ is 1.70×10^4 W. The ratios ρ_j/ρ_s and U/c are unity. Therefore, from Fig. 15.3 [or Eqs. (15.8) and (15.9)] the ratio of sound power to mechanical stream power is 1.0×10^{-4}. The resulting overall sound power is 1.7 W. From Fig. 15.6 [or Eq. (15.12)] the OASPL at 90° to the jet axis and $R = 3$ m is 98.8 dB re 20 μPa. From Eq. (15.11) the OASPL at 60° to the jet axis and $R = 3$ m is 103.5 dB, and the peak Strouhal number is 0.8. The one-third-octave-band SPL spectrum is found from Fig. 15.6 by adding 103.5 dB to the ordinate with $\Delta = 11$ dB (from Table 15.1).

Realistic jets exhausting from pipes and engine nozzles do not provide smooth, low-turbulence entrainment of flow but rather flow that has been disturbed or spoiled before leaving the nozzle. In this case, the above procedure is not valid unless the jet velocity U exceeds about 100 m/s. Below this speed major portions of the aerodynamically generated noise emanate from internal sources.

Noise of Imperfectly Expanded Jets

Supersonic, underexpanded, or "choked" jets contain shock cells through which the flow repeatedly expands and contracts (see inset to Fig. 15.8). Seven or more distinct cells are often visible extending up to 10 jet diameters downstream of the nozzle. They are responsible for two additional components of jet noise: *screech tones* and broadband *shock-associated noise*. Screech is produced by a feedback mechanism in which a disturbance convected in the shear layer generates sound as it traverses the standing system of shock waves. The sound propagates upstream through the ambient atmosphere and causes the release of a new flow disturbance at the nozzle exit. This is amplified as it convects downstream, and the feedback loop is completed when it encounters the shocks. A notable feature of the screech tones is that the frequencies are independent of the radiation direction, the fundamental occurring at approximately $f = U_c/L(1 + M_c)$, where $M_c = U_c/c$, U_c is the convection velocity of the disturbance in the shear layer, L is the axial length

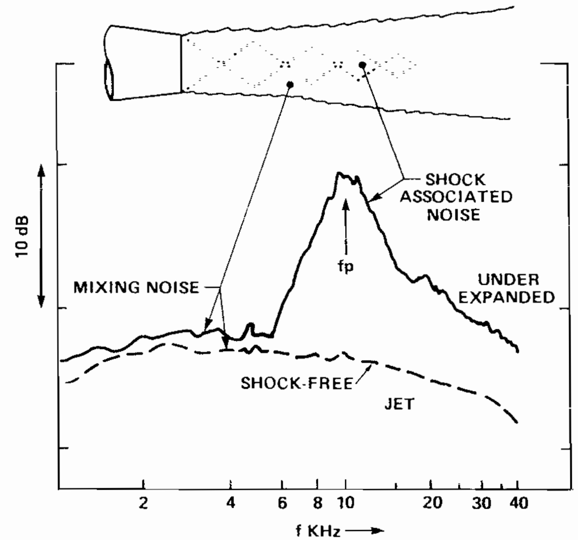

FIGURE 15.8 Jet noise spectra for shock-free and underexpanded jets at $\theta = 90°$, $\beta = 1$.

of the first shock cell, and c is the ambient speed of sound. Although screech is often present in model-scale experiments and can be important for choked jet engines, it is usually easy to eliminate by minor modifications to nozzle design, for example, by notching.

In practice, it is the broadband, shock-associated noise that is important for supersonic jet engines. It can be suppressed by proper nozzle design, but it is always present for a convergent nozzle. The dominant frequencies are usually higher than the screech tones and can range over several octave bands. For predictive purposes it is permissible to estimate separately the respective contributions of mixing noise and shock-associated noise to the overall sound power generated by the jet. The mixing noise predictions are the same as for a shock-free jet.

The overall SPL of shock-associated noise is approximately independent of the radiation direction and may be estimated from

$$\text{OASPL} = C_0 + 10 \times \log \frac{\beta^n A}{R^2}$$

$$C_0 = 156.5 \quad (\text{dB}) \quad n = \begin{cases} 4 & (\beta < 1) \\ 1 & (\beta > 1) \end{cases} \quad \frac{T_j}{T_s} < 1.1 \tag{15.14}$$

$$C_0 = 158.5 \quad (\text{dB}) \quad n = \begin{cases} 4 & (\beta < 1) \\ 2 & (\beta > 1) \end{cases} \quad \frac{T_j}{T_s} > 1.1$$

where T_j = total (reservoir) jet temperature, K
T_s = total ambient temperature, K
$\beta = \sqrt{M_j^2 - 1}$
M_j = fully (ideally) expanded jet Mach number, based on sound speed in jet

The shock-associated noise spectrum exhibits a well-defined peak in the vicinity of

$$f_p = \frac{0.9U_c}{D_N \beta (1 - M_c \cos \theta)} \tag{15.15}$$

where the convection velocity U_c meters per second is equal to $0.7U$ and θ is measured from the jet axis. When $T_j/T_s > 1.1$, the one-third-octave-band SPL (re 20 μPa) is given by

$$\begin{aligned} \text{SPL} = {} & 143.5 + 10 \times \log \frac{\beta^n A}{R^2} - 16.13 \times \log \left(\frac{5.163}{\sigma^{2.55}} + 0.096\sigma^{0.74} \right) \\ & + 10 \times \log \left\{ 1 + \frac{17.27}{N_s} \cdot \sum_{i=0}^{N_s - 1} \left[C(\sigma)^{(i^2)} \right. \right. \\ & \left. \left. \times \sum_{j=1}^{N_s - i - 1} \frac{\cos(\sigma q_{ij}) \sin(0.1158 \sigma q_{ij})}{\sigma q_{ij}} \right] \right\} \end{aligned} \tag{15.16}$$

where $C(\sigma) = 0.8 - 0.2 \times \log_{10}(2.239/\sigma^{0.2146} + 0.0987\sigma^{2.75})$
$\sigma = 6.91 \beta D_N f/c$, dimensionless
c = ambient speed of sound, m/s
N_s = 8 (number of shocks)
$q_{ij} = (1.7ic/U)\{1 + 0.06[j + \frac{1}{2}(i+1)]\}[1 - 0.7(U/c) \cos\theta]$

and n is defined as in (15.14). In the case of a "cold jet," for which $T_j/T_s < 1.1$, the prediction (15.16) should be reduced by 2 dB.

The prediction procedure for shock-associated noise is applicable over all angles θ where shock cell noise is important (say, $\theta > 50°$). When used in conjunction with the prediction procedure for jet mixing noise, the one-third-octave-band sound pressure spectrum for the overall jet noise may be estimated by adding the respective contributions to each frequency band of the mean-square acoustical pressures of the mixing noise and the shock-associated noise. The influence of shock-associated noise is illustrated in Fig. 15.8, which compares the spectrum of the jet mixing noise of a fully expanded, shock-free supersonic jet from a convergent–divergent nozzle at the same pressure ratio. In the latter case the spectral peak occurs at the frequency f_p given by Eq. (15.15).

Flight Effects

The noise generated by a jet engine in flight is modified because of the joint effects of Doppler amplifications (discussed in Section 15.2) and the reduction in mean shear between the jet flow and its environment. From an extensive series of experimental studies[3] empirical formulas have been developed to predict the SPL in flight in terms of the corresponding static levels.

In the Mach number range of $1.1 < M < 1.95$ jet mixing noise $\text{OASPL}(\theta)_{\text{flight}}$ is related to $\text{OASPL}(\theta)_{\text{static}}$ by

$$\text{OASPL}(\theta)_{\text{flight}} = \text{OASPL}(\theta)_{\text{static}} - 10 \times \log\left[\left(\frac{U}{U - V_f}\right)^{m(\theta)} (1 - M_f \cos \Phi)\right]$$

$$m(\theta) = \left[\left(\frac{6959}{|\theta - 125|^{2.5}}\right)^7 + \frac{1}{[31 + 18.5M - (0.41 - 0.37M)\theta]^7}\right]^{-1/7} \tag{15.17}$$

where θ = angle between jet axis and observer at retarded time of emission of sound, degrees
Φ = angle between flight direction and observer direction at retarded time of emission of sound, defined in Fig. 15.2
U = fully expanded jet velocity (relative to nozzle), m/s
V_f = aircraft flight speed, m/s
M_f = flight Mach number relative to sound speed in air, $= V_f/c$

The formula is applicable for $20° < \theta < 160°$. For $M < 1.1$ and $M > 1.95$, the relative velocity exponent $m(\theta)$ should be taken to be given by the above formula at $M = 1.1$, 1.95, respectively.

Estimates of the one-third-octave-band SPL spectrum in flight can be made by using Fig. 15.6 with the OASPL determined by (15.17) and the Strouhal number fD_N/U replaced by that based on the jet velocity: $fD_N/(U - V_f)$.

For shock-associated noise the influence of flight on both the spectrum and the OASPL is approximately given by

$$\text{SPL}_{\text{flight}} = \text{SPL}_{\text{static}} - 40 \log \times (1 - M_f \cos \Phi) \tag{15.18}$$

15.4 COMBUSTION NOISE OF GAS TURBINE ENGINES

Jet mixing noise and shock-associated noise of high-speed jet engines are the result of sources in the flow downstream of the nozzle. Their importance has progressively diminished in recent years with the introduction of large-diameter, high-bypass-ratio turbofan engines with much reduced mass efflux velocities. In consequence, greater attention has been given to noise generated within the engine (termed *core noise*), which tends to be predominant at frequencies less than 1 kHz. Combustion processes are a significant component of core noise, both directly in the form of thermal monopole sources and indirectly through the creation of temperature and density inhomogeneities ("entropy spots"), which behave as dipole sources when accelerated in nonuniform flow.

The noise prediction scheme outlined below is based on an analysis of combustion noise of turbojet, turboshaft, and turbofan engines as well as model-scale data[3]. Annular, can-type, and "hybrid" combusters were all included in the valuation studies.

The overall sound power level (OAPWL, in decibels) is a function of the operating conditions of the combuster and the turbine temperature extraction and may be estimated from the equation

$$\text{OAPWL} = -60.5 + 10 \times \log \frac{mc^2}{\Pi_{\text{ref}}} + 20 \times \log \frac{(\Delta T/T_I)(P_I/p_{\text{ISA}})}{[(\Delta T)_{\text{ref}}/T_s]^2} \tag{15.19}$$

where m = combuster mass flow rate, kg/s
P_I = combuster inlet total pressure, Pa
ΔT = combuster total temperature rise, K
$(\Delta T)_{\text{ref}}$ = reference total temperature extraction by engine turbines at maximum takeoff conditions, K
T_I = inlet total temperature, K
T_s = sea-level atmospheric temperature, 288.15 K
Π_{ref} = reference power, 10^{-12} W
p_{ISA} = sea-level atmospheric pressure, 10.13 kPa = 1.013×10^4 N/m^2
c = sea-level speed of sound, 340.3 m/s

This formula is expected to yield predictions that are accurate to within ±5 dB.

The one-third-octave-band power level spectrum PWL(f) is given in terms of the OAPWL by

$$\text{PWL}(f) = \text{OAPWL} - 16 \times \log[(0.003037f)^{1.8509} + (0.002051f)^{-1.8168}]\,\text{dB} \tag{15.20}$$

where f is frequency (in hertz) and the formula is applicable for 100 Hz $\le f \le$ 2000 Hz. The spectrum is essentially symmetric about a peak at $f = 400$ Hz (Fig. 15.9). In applications where the observed peak frequency f_p differs slightly from this value, the spectrum in the figure should be shifted, retaining its shape, so that the peak coincides with observation. In (15.20), f would be replaced by $400f/f_p$.

The one-third-octave-band sound power pressure spectrum may now be determined from the formula

$$\begin{aligned}\text{SPL} = {} & -10.8 + \text{PWL}(f) - 20 \times \log R \\ & - 2.5 \times \log\left[\frac{1}{(10^{(1.633-0.0567\theta)} + 10^{(19.43-0.233\theta)})^{0.4}} + 10^{(4.333-0.115\theta)}\right]\end{aligned} \tag{15.21}$$

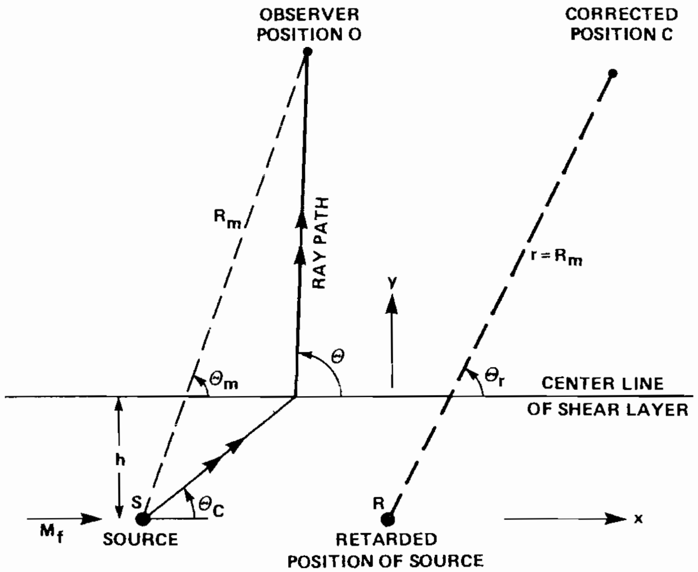

FIGURE 15.9 One-third-octave-band frequency power level spectrum of combuster noise.

where θ = angle from jet exhaust axis, degrees
R = observer distance, m

The peak radiation is predicted by (15.21) to occur at $\theta \approx 60°$, although at very low frequencies ($\leq$200 Hz) the peak may be shifted slightly toward the jet axis.

For an aircraft in flight at speed V_f, the modification of the predicted SPL may be estimated from Eq. (15.18).

15.5 TURBULENT BOUNDARY LAYER NOISE

The intense pressure fluctuations that can occur beneath a turbulent boundary layer are a source of sound and structural vibrations. The sound is produced directly by aerodynamic sources within the flow and indirectly by the *diffraction* at discontinuities in the wall (e.g., corners, ribs, support struts) of structural modes excited by the boundary layer pressures.

The pressure developed beneath a boundary layer on a *hard* wall is called the *blocked pressure* and is twice the pressure that a nominally identical flow would produce if the wall were absent. The rms wall pressure p_{rms} (in pascals) of the turbulent boundary layer can be estimated by[5]

$$\frac{p_{\text{rms}}}{q} \approx \sigma\varepsilon^* = \frac{\sigma}{\frac{1}{2}(1 + T_w/T) + 0.1(\gamma - 1)M^2} \tag{15.22}$$

where σ = 0.006, dimensionless
q = local dynamic pressure, $= \frac{1}{2}\rho U^2$, Pa
ρ = fluid density at outer edge of boundary layer, kg/m^3
U = free-stream velocity at outer edge of boundary layer, m/s
M = free-stream Mach number, $= U/c$, dimensionless
c = speed of sound at outer edge of boundary layer, m/s
T = temperature at outer edge of boundary layer, K
T_w = temperature of the wall, K
γ = ratio of specific heats of gas, dimensionless

The quantity $\sigma \equiv (p_{\text{rms}}/q)_{\text{incompressible}}$, and Eq. (15.22) represents a mapping from an incompressible flow to the compressible state by means of the compressibility factor, ε^*. Recent measurements[6] suggest that the currently accepted value $\sigma = 0.006$ may be too low and that a better approximation is $\sigma = 0.01$.

In many applications wall pressure fluctuations are substantially higher if the flow *separates*. For example, when separation occurs at the compression corner at a ramp or at an expansion corner, the rms wall pressure can typically exceed 2% of the local dynamic pressure q.

The structural response of a flexible wall to forcing by the boundary layer depends on both the temporal and spatial characteristics of the pressure fluctuations. When the wall is locally plane, these can be expressed in terms of the *wall pressure wavenumber–frequency spectrum* $P(\mathbf{k}, \omega)$. This is the two-sided Fourier transform $(1/2\pi)^3 \int_{-\infty}^{\infty} R_{pp}(x_1, x_3, t) \exp[-i(\mathbf{k} \cdot \mathbf{x} - \omega t)]\, dx_1\, dx_3\, dt$ of the space–time correlation function of the wall pressure R_{pp}. By convention, coordinate axes (x_1, x_2, x_3) are taken with x_1, x_3 parallel and transverse to the mean flow, respectively, x_2 measured outward of the wall, and the wavenumber $\mathbf{k} = (k_1, k_3)$ (in reciprocal meters) has components parallel to the x_1, x_3 axes only. The principal properties of the blocked-pressure spectrum $P_0(\mathbf{k}, \omega)$, say, are understood only for low-Mach-number flows ($M \ll 1$).

Wall Pressure Spectrum at Low Mach Number

Here, $P_0(\mathbf{k}, \omega)$ is an even function of ω, and its general features are shown in Fig. 15.10[7] for $\omega > 0$ The strongest pressure fluctuations are produced by eddies in the *convective ridge* of the wavenumber plane that convect along the wall at about 70% of the free-stream velocity. The region $k \equiv |\mathbf{k}| < \omega/c$ (c = speed of sound, in meters per second) is called the acoustical domain, and $k_0 = \omega/c$ is the acoustical wavenumber. The adjacent *subconvective* domain ($k_0 < k \ll \omega/U_c$) is important to determining the structural response of the wall to forcing by the turbulence pressures. In these regions $10 \times \log[P_0(\mathbf{k}, \omega)]$ is typically 30–60 dB below the levels in the convective domain.

Pressure fluctuations in the acoustical domain correspond to sound waves in the fluid. When the wall is smooth and flat, the generation of sound is dominated by quadrupole sources in the flow,[7] and the acoustical pressure frequency spectrum

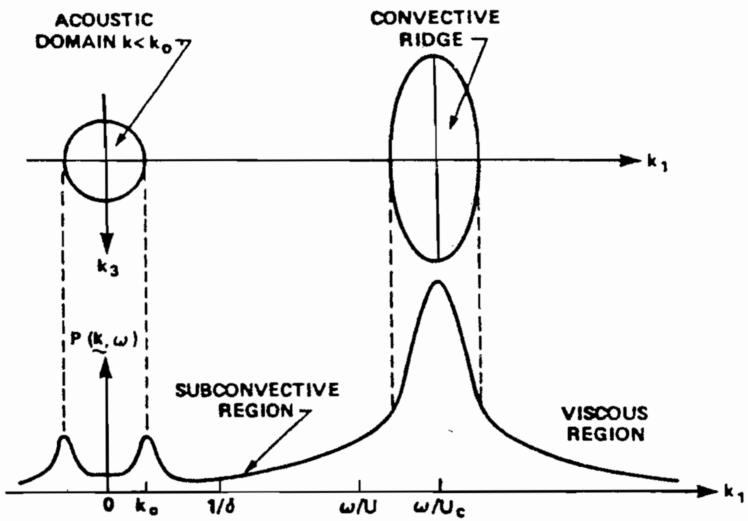

FIGURE 15.10 Turbulent boundary layer wall pressure spectrum at low Mach number for $\omega\delta/U \gg 1$, where δ is the boundary layer thickness (m).

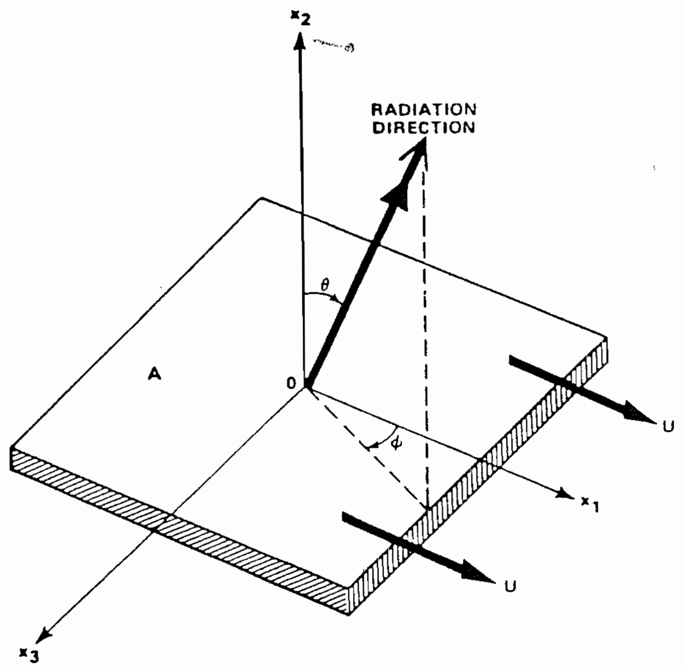

FIGURE 15.11 Coordinates defining the radiation of sound from a region of the wall of area A.

of sound produced by a fixed area of the wall (Fig. 15.11) is

$$\Phi(\omega) = 2\frac{A}{R^2}k_0^2 \cos^2\theta P_0(k_0 \sin\theta \cos\phi, k_0 \sin\theta \sin\phi, \omega) \qquad (15.23)$$

where OASPL $= 10 \times \log\left[\int_0^\infty \Phi(\omega)\, d\omega/(20\ \mu\text{Pa})^2\right]$, dB
A = area of wall region, m^2
R = observer distance from center of A, m
(θ, ϕ) = polar angles of observer defined in Fig. 15.11

Chase[8] has proposed the following representation of the blocked-pressure spectrum that is applicable over the whole range of wavenumbers and is based on an empirical fit to experimental data in the convective and subconvective domains:

$$\frac{P_0(\mathbf{k},\omega)}{\rho^2 v_*^2 \delta^3} = \frac{1}{[(k_+\delta)^2 + 1.78]^{5/2}} \left\{ \frac{0.1553(k_1\delta)^2 k^2}{|k_0^2 - k^2| + \beta^2 k_0^2} + 0.00078 \right.$$
$$\left. \times \frac{(k\delta)^2[(k_+\delta)^2 + 1.78]}{(k\delta)^2 + 1.78} \left(4 + \frac{|k_0^2 - k^2|}{k^2} + \frac{k^2}{|k_0^2 - k^2| + \beta^2 k_0^2} \right) \right\}$$
$$\frac{\omega\delta}{U} > 1 \qquad (15.24)$$

where δ = boundary layer thickness (distance from wall at which mean-flow velocity is equal to $0.99U$), m
ρ = mean fluid density, kg/m^3
v_* = friction velocity, $\approx 0.035U$, m/s
$U_c \approx 0.7U$, m/s
U = mainstream velocity at outer edge of boundary layer, m/s
ω = radian frequency, $= 2\pi f$, rad/s
$k_+ = \sqrt{(\omega - U_c k_1)^2/9v_*^2 + k^2}$, m^{-1}
$\beta \approx 0.1$, dimensionless

The first term in the curly brackets determines the behavior near the convective ridge and the second the low-wavenumber and acoustical domains. The numerical coefficient β controls the height of the spectral peak (Fig. 15.10) at the boundary $k = k_0$ of the acoustical domain and determines the intensity of the sound waves propagating parallel to the plane of the wall.

Example 15.2. Estimate the frequency spectrum $\Psi(\omega)$ of the power dissipated by flexural motion of a plane wall when the wall is excited by a low-Mach-number turbulent flow over a region of area A whose normal impedance $\mathbf{Z}(\mathbf{k}, \omega)$ (kg/m^2 · s) is independent of the orientation of $\mathbf{k}$.

Solution The impedance satisfies $Z(\mathbf{k},\omega) = -p(\mathbf{k},\omega)/v_2(\mathbf{k},\omega)$, where p and v_2, respectively, denote the Fourier components of the pressure and normal velocity on the wall. Let $Z = R - iX$, where R and X are the resistive and reactive components of the impedance, respectively. The total power delivered to the flexural motions is equal to $\int_0^\infty \Psi(\omega)\,d\omega$, where

$$\Psi(\omega) = 2A\int_{k>|k_0|}^{\infty} \frac{R(\mathbf{k},\omega)P_0(\mathbf{k},\omega)\,d^2\mathbf{k}}{R(\mathbf{k},\omega)^2 + [X(\mathbf{k},\omega) + \rho\omega/\sqrt{k^2-k_0^2}]^2}$$

The flexural-mode wavenumbers are the roots $\mathbf{k} = \mathbf{k}_n, n = 1, 2, 3, \ldots,$ of $X(\mathbf{k},\omega) + \rho\omega/\sqrt{k^2 - k_0^2} = 0$. In practice, these usually lie in the low-wavenumber region where $P_0(\mathbf{k},\omega) \equiv P_0(k,\omega)$, so that, when $R \ll X$ and Z is a function of $k \equiv \mathbf{k}$ and ω only,

$$\Psi(\omega) \approx \sum_n \frac{4\pi^2 A k_n P_0(k_n,\omega)}{\left|(\partial/\partial k)\left[X(k,\omega) + \rho\omega\Big/\sqrt{k^2-k_0^2}\right]\right|_{k_n}}$$

When the wall consists of a vacuum-backed, thin elastic plate of bending stiffness B (kg · m^2/s^2), mass density m (kg/m^2) per unit area, and negligible damping $R = 0$, we have $X = -(Bk^4 - m\omega^2)/\omega$, and there is only one flexural mode that occurs at $k = k_* > |k_0|$ such that

$$\Psi(\omega) = \frac{4\pi^2 A\omega(k_*^2 - k_0^2)P_0(k_*,\omega)}{5Bk_*^4 - 4B(k_0k_*)^2 - m\omega^2}$$

where k_* is the positive root of $Bk^4 - m\omega^2 - \rho\omega^2/\sqrt{k^2 - k_0^2} = 0$. Numerical estimates may be made by substituting for $P_0(k_*,\omega)$ from (15.24).

15.6 NOISE FROM FLUID FLOW IN PIPES

Piping system noise typically comes mainly from control valves (see Section 15.11) and high-speeds machines (see Chapter 18). However, under some circumstances the noise induced by flow through milder discontinuities (bends, tees, swags, and other components) may be significant. Here we describe an approximate approach for estimating this type of flow-induced noise.

Pressure fluctuations in the turbulent boundary layer drive the wall of the pipe, causing it to radiate sound. As described in Section 15.5, the structural response of a flexible wall to forcing by the boundary layer depends in a complex manner on both the temporal and spatial characteristics of the pressure fluctuations. Seebold[9] suggested the following approximate method for estimating the noise produced by fluid flow in piping systems. The method estimates the noise that results from boundary layer pressure fluctuations in fully developed turbulent flow in uninterrupted straight pipes[10] and then applies a loss factor correction for local discontinuities. This loss factor correction is based on the notion that the sound power radiated at a discontinuity is approximately proportional to the square of the pressure drop Δp there and can therefore be related to the pressure head loss factor K, where $\Delta p = K(\frac{1}{2}\rho U^2)$.

The sound pressure level at a distance of 1 m from the pipe in the octave band centered on frequency f_c is approximated by

$$\begin{aligned} \text{SPL} = &-3.5 + 40\log U + 20\log\rho + 20\log K \\ &- 10\log\left[\frac{t}{D}\left(1 + \frac{1.83}{D}\right)\right] - 5\log\left[\frac{f_c}{f_r}\left(1 - \frac{f_c}{f_r}\right)\right] + \Delta L(f_c) \end{aligned} \tag{15.25}$$

where U = gas flow velocity, m/s
ρ = fluid density, kg/m^3
t = pipe wall thickness, m
D = inside diameter of pipe, m
f_c = octave-band center frequency, Hz
f_r = ring frequency of pipe, Hz; = $1608/D$ for steel
K = total loss factor per 10-diameter pipe section, dimensionless

The spectral correction $\Delta L(f_c)$ depends on the ratio of the octave-band center frequency f_c to the Strouhal frequency of the pipe flow, $f_p = 0.2U/D$, as[11]

$$\Delta L = \begin{cases} 10.4 + 11.4\log\dfrac{f_c}{f_p} & \text{for } \dfrac{f_c}{f_p} < 0.5 \\ 7 & \text{for } 0.5 \le \dfrac{f_c}{f_p} < 5 \\ 14 - 10\log\dfrac{f_c}{f_p} & \text{for } 5 \le \dfrac{f_c}{f_p} < 12 \\ 41.9 - 36.1\log\dfrac{f_c}{f_p} & \text{for } \dfrac{f_c}{f_p} \ge 0.5 \end{cases} \tag{15.26}$$

When employing (15.25), the piping system should be thought of as being composed of segments 10 diameters in length. The total loss factor K is determined by adding the individual loss factors K_i for the flow fittings and elements present within each 10-diameter segment of pipe. This total loss factor is then entered in Eq. (15.25) to estimate the flow noise emanating from that segment (at a distance of 1 m from the pipe wall). Loss factors for various piping components are provided in Table 15.2. For example, the loss factor for a straight pipe is taken to be 0.12 velocity heads per 10-diameter segment. On the other hand, a 10-diameter-long segment of piping containing an expander (1.5 : 1), an elbow (90°, $R/D = 1.5$), and a tee (flow-through run) would have a total loss factor of approximately 1, $K \approx 0.1 + 0.33 + 0.5 \approx 1$.

15.7 SPOILER NOISE

The term *spoiler noise* is used to characterize the noise produced by an obstacle or other obstruction that spans a duct carrying a mean flow. We shall discuss the case of air flowing in a duct or pipe that may be regarded as "semi-infinite" when

TABLE 15.2 Pressure Head Loss Factors[a] K

Straight pipes (10-diameter-long segment)		0.12				
45° Elbow	Screwed	0.42	Welded, $R/D = 1$	0.29	Welded, $R/D = 1.5$	0.21
90° Elbow	Screwed	0.92	Welded, $R/D = 1$	0.45	Welded, $R/D = 1.5$	0.33
180° Elbow	Screwed	2.00	Welded, $R/D = 1$	0.60	Welded, $R/D = 1.5$	0.43
Tees (screwed)	Thru branch	1.80	Thru run	0.50		
Tees (welded)	Thru branch	1.40	Thru run	0.40		
Reducer	$D_2/D_1 = 0.3$	0.25	$D_2/D_1 = 0.5$	0.17	$D_2/D_1 = 0.7$	0.07
Expander	$D_2/D_1 = 3$	0.80	$D_2/D_1 = 2$	0.56	$D_2/D_1 = 1.25$	0.10
Sudden Contraction	$D_2/D_1 = 0.1$	0.48	$D_2/D_1 = 0.33$	0.41	$D_2/D_1 = 0.8$	0.12
Sudden Expansion	$D_2/D_1 = 10$	0.98	$D_2/D_1 = 3$	0.79	$D_2/D_1 = 1.25$	0.12

[a] After Ref. 9.

it is desired to estimate the acoustical radiation from the open end. A spoiler-noise-generating system is shown schematically in Fig. 15.12. In practice, the spoiler may be a strut, stringer, guide vane, or other flow control device. The nominally steady mean flow exerts unsteady lift and drag forces on the spoiler, which accordingly behaves as an acoustical source of *dipole* type.

The following idealizations will be made:

1. The spoiler can be of arbitrary shape, but its cross-flow dimensions are small relative to the pipe cross section. This ensures that the flow speeds near the spoiler are not significantly greater than the pipe mean flow speed and therefore that turbulence mixing noise (quadrupole) can be neglected. Thus, the case of a valve, which produces a severe throttling of the flow, is excluded (see Section 15.11).
2. The peak frequency of the noise spectrum is below the "cutoff" frequency f_{co} of the pipe, which is given by

$$f_{co} = \begin{Bmatrix} 0.293c/r & \text{Hz (circular pipe)} \\ 0.5c/w & \text{Hz (rectangular pipe)} \end{Bmatrix} \tag{15.27}$$

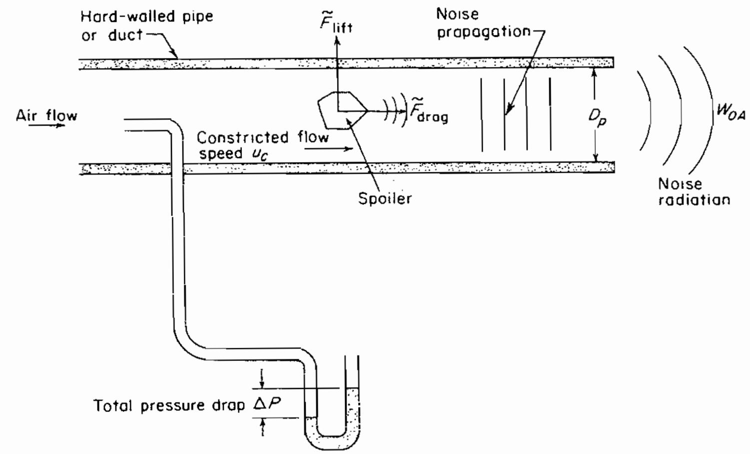

FIGURE 15.12 Flow spoiler system. The sound power is generated by the unsteady drag force on the spoiler and radiated from the open end of the pipe.

where c = sound speed, m/s
r = radius of circular pipe, m
w = largest transverse dimension of rectangular pipe, m

If this condition is not fulfilled, the propagated sound power near and above the peak frequency (which determines most of the overall sound power) will be influenced by transverse modes of the pipe.

3. The pipe wall is acoustically rigid. The fluctuating lift forces on the spoiler are then canceled by images in the wall, and sound is produced solely by the unsteady drag, which corresponds to an acoustical dipole whose axis is parallel to the mean flow. A low-noise spoiler system should therefore use bodies of low drag, such as airfoils, rather than grids or other oddly shaped bodies.

For several elementary flow spoiler configurations, such as the one shown in Fig. 15.12, the *fluctuating drag is directly proportional to the steady-state drag experienced by the body*. This depends on the pressure drop ΔP across the spoiler (as measured by an upstream and a downstream total-pressure probe), and the broadband noise radiated from the open end of the pipe is given by[12]

$$W_{OA} = \frac{k(\Delta P)^3 D_p^3}{\rho^2 c^3} \tag{15.28}$$

where W_{OA} = overall radiated sound power, W
k = constant of proportionality, dimensionless

ΔP = total pressure drop across spoiler, Pa
D_p = pipe diameter, m
ρ = atmospheric density, kg/m^3
c = atmospheric sound speed, m/s

Specific information about spoiler geometry is absent from Eq. (15.28) but is implicit in the pressure drop ΔP. From a variety of experimental spoiler configurations the constant k is found to be about 2.5×10^{-4} for air.

Equation (15.28) determines the broadband sound power. It should strictly be regarded as a lower bound that is applicable only if there are no *discrete-frequency* components of the noise. These are present in certain conditions (e.g., excitation of edge tones) and may well stand out against the broadband levels.[13] When such a mechanism has been identified, the discrete tones can usually be eliminated or controlled by detuning or rounding off sharp corners or edges or cutting feedback paths by treating reflecting surfaces with sound-absorbent materials.

The frequency spectrum measured outside the pipe for the noise generated by the spoiler exhibits a haystack structure (Fig. 15.13) with a peak frequency given by

$$f_p \approx \frac{u_c}{db} \quad \text{Hz} \tag{15.29}$$

where u_c = constricted flow speed, m/s
d = projected width of spoiler, m
b = constant that equals 0.2 for pressure differences ΔP of the order 4000 Pa and 0.5 for ΔP of the order of 40,000 Pa

The constricted flow speed u_c for cold air is given in Table 15.3 as a function of ΔP. Values in between those in the table can be interpolated.

Example 15.3. Find the sound-power-level spectrum of noise produced by a spoiler consisting of a flat plate of width 2 cm stretching across a circular pipe of internal diameter $D_p = 5$ cm. The pressure drop across the spoiler is $\Delta P = 10,000$ Pa.

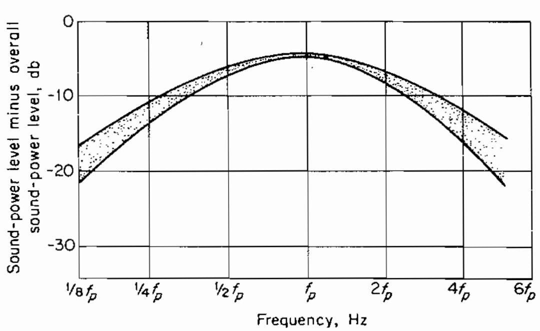

FIGURE 15.13 Generalized octave-band spectrum for in-pipe-generated spoiler noise referenced to the total power radiated from the open end and the peak frequency.

TABLE 15.3 Constricted Flow Speed u_c for Cold Air as Function of Pressure Drop

ΔP, Pa	2500	5000	10,000	20,000	30,000	40,000
u_c, m/s	63	90	124	173	209	238

Solution From Eq. (15.28) the total sound power $L_w \approx 101$ dB re 10^{-12} W. When $\Delta P = 10,000$ Pa, the peak frequency of the spectrum can be expected to be at $f_p \approx 0.35 u_c/d$.

From Table 15.3, we find $u_c = 124$ m/s; hence $f_p \approx 2170$ Hz. The sound power spectrum in octave bands is obtained form Fig. 15.13 with 101 dB added to the ordinate.

15.8 GRID OR GRILLE NOISE

The characteristics of noise produced by flow through grids, grilles, diffusers, guide vanes, or porous plates, which often terminate air conditioning ducts, are similar to those of spoiler-generated sound. The principal differences are that (1) the grid is located at the open end of the duct, (2) the duct cross-sectional area is typically quite large (say, 0.04–1 m^2), and (3) the velocity of the air in the duct is usually small, rarely exceeding 30 m/s. The speed of the "air jets" exhausting from the individual air passages (or orifices) in a diffuser is generally low enough (<100 m/s) that jet mixing noise can be neglected. The dominant sound source is of dipole type and is associated with the interaction of the flow with the diffuser elements (e.g., guide vanes).

When a duct is terminated by a grid of circular rods (Fig. 15.14*a*), periodic shedding of vortices can occur, producing a fluctuating lift force on each rod and an associated *tonal* component of the radiated sound. This source is a dipole (whose axis is parallel to the lift direction) and is in addition to the drag dipole. The frequency of the tone is given approximately by

$$f = \frac{0.2u}{D_R} \tag{15.30}$$

where u = mean flow speed, m/s
D_R = diameter of rods, m

Tonal oscillations produced by a feedback mechanism can also arise when the duct termination consists of a plate perforated with sharp-edged circular cylindrical apertures (Fig. 15.14b).

In general, however, the noise produced by typical air conditioner grids is almost always broadband and of conventional dipole character, with the sound power varying as the sixth power of the velocity. As in the case of spoiler noise, the overall sound power can be related to the pressure drop ΔP across the grid,

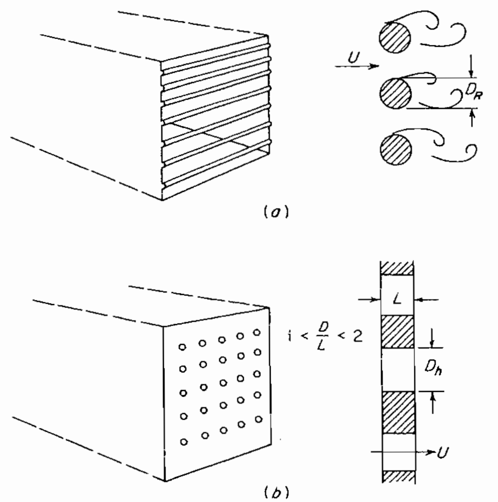

FIGURE 15.14 Special cases of duct terminations: (*a*) circular rods; (*b*) sharp-edge circular cylindrical holes.

independently of the specific grid geometry. To do this, we introduce the pressure drop coefficient

$$\xi = \frac{\Delta P}{\frac{1}{2}\rho u^2} \tag{15.31}$$

where ρ = density of air, kg/m^3
u = mean flow speed in duct prior to grid, m/s

Three typical diffuser configurations together with their pressure drop coefficients ξ are illustrated in Fig. 15.15.[14] The values of ξ for similar diffuser configurations are usually available from the manufacturer. If not, they may be estimated from this figure.

If not given by the manufacturer, the overall sound power level L_w from air conditioning diffusers can be estimated from the empirical formula[14]

$$L_w = 10 + 10 \times \log(S\xi^3 u^6) \quad \text{dB re } 10^{-12}\text{ W} \tag{15.32}$$

where S = area of duct cross section prior to diffuser, m^2
ΔP = pressure drop through diffuser, Pa

The noise spectra of different diffusers do not exhibit identical shapes even when normalized to similar flow speeds and exhaust areas. Construction differences tend to emphasize different frequency regimes, and poorly designed diffusers will radiate discrete-frequency sound. In practical noise control problems, however, a general spectrum shape $L_w - 10 \times \log_{10}(S\xi^3)$ (dB re 10^{-12} W) can be used for each duct velocity u (in meters per second) that fits most diffuser noise spectra to within about ±5 dB, as shown in Fig 15.16.

Configuration	Duct area, m^2	Comment	Pressure drop coefficient ξ
(a) 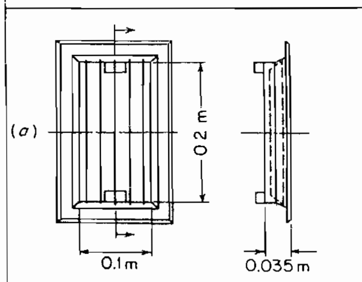 0.2 m; 0.1 m; 0.035 m	0.020	Parallel louvres	2.9
	0.020	Inclined louvres	2.7
(b) 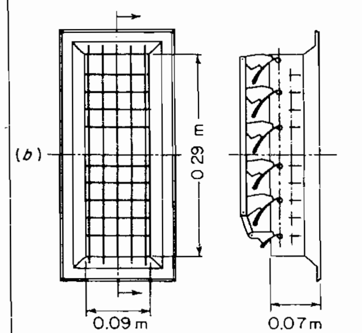 0.29 m; 0.09 m; 0.07 m	0.028	Parallel louvres Open damper	4.8
	0.028	Parallel louvres Partially closed damper	7.3
(c) 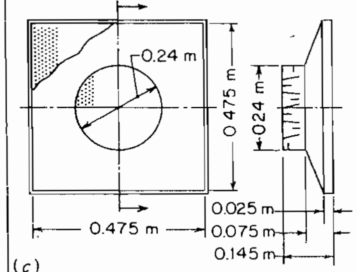 0.24 m; 0.475 m; 0.024 m; 0.475 m; 0.025 m; 0.075 m; 0.145 m	0.046	Open stagnation disk Parallel damper vanes	5.6
	0.046	Closed stagnation disk Parallel damper vanes	6.2
	0.046	Open stagnation disk Deflected damper vanes	19.8
	0.046	Closed stagnation disk Deflected damper vanes	19.9

FIGURE 15.15 Various duct terminations and their pressure drop coefficients $\xi = \Delta P / \frac{1}{2}\rho u^2$. The duct area S is in square meters. (After Ref. 14.)

To estimate the sound power spectrum of the radiation from a given diffuser, first determine the relevant curve from Fig. 15.16 for the particular flow speed. The ordinate in the figure is then increased by $10 \times \log_{10}(S\xi^3)$ decibels to yield the desired one-third-octave-band spectrum with a margin of error of about ±5 dB.

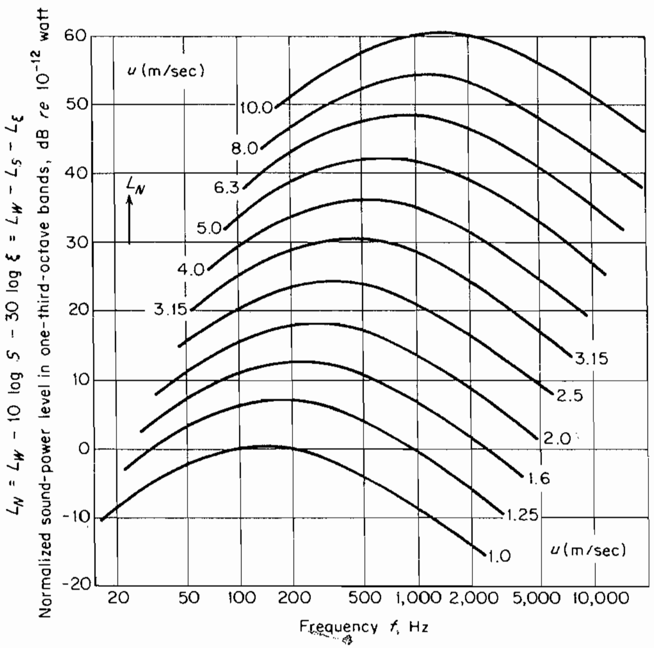

FIGURE 15.16 Normalized one-third-octave-band sound power level spectra for noise radiated from diffusers of various flow velocities. (After Ref. 14.)

15.9 SOUND GENERATION BY AIRFOILS AND STRUTS

Noise of a Strut in a Turbulent Stream

Long struts, airfoils, guide vanes, and so on, which offer negligible drag to a mean flow, frequently experience significant fluctuations in lift when exposed to a turbulent stream and behave as *dipole-type* sources of broadband sound. The strength of the radiation depends on the dimensions of the airfoil and on the turbulence intensity and correlation length of the velocity fluctuations.

A simple description of the radiation can be given when the mean flow is of low Mach number (say, <100 m/s in air) and when the distance to the nearest boundary (e.g., duct wall) is at least of the order of the acoustical wavelength. In these circumstances the *frequency spectral density* of the total radiated sound power $\Pi(\omega)$ is given approximately by

$$\Pi(\omega) = \frac{\pi l a^2 \rho u^2 M^3 (\omega\Lambda/U)^4}{4(1+\pi\omega a/U)[1+(\omega\Lambda/U)^2]^{5/2}[1+(\omega a/3c)^3]^{1/3}} \qquad (15.33)$$

where ω = radian frequency, $= 2\pi f$, f in Hz
a = chord of airfoil, m

l = span of airfoil, m
ρ = density of mean stream, kg/m^3
u = rms turbulence velocity in lift direction, m/s
U = velocity of mean stream, m/s
M = mean flow Mach number, $= U/c$, dimensionless
c = sound speed, m/s
Λ = integral scale of turbulence velocity, m

The total radiated sound power $W = \int_0^\infty \Pi(\omega)\, d\omega$, in watts, can be estimated from

$$W = \frac{1.78(la^2/\Lambda)\rho u^2 U M^3}{(1+10.71a/\Lambda)(1+1.79\, Ma/\Lambda)} \qquad 0 \le M \le 0.3 \qquad (15.34)$$

At low frequencies the acoustical intensity exhibits the characteristic dipole *field shape*, proportional to $\cos^2\theta$, where θ is measured from the direction of the mean lift. At higher frequencies (when the acoustical wavelength is much smaller than the chord of the airfoil but still exceeds the airfoil thickness), the field shape assumes a cardioid form, with a null in the forward direction and peaks close to the direction of the mean flow.

Airfoil Self-Noise

In addition to gust/inflow turbulence-induced noise, an airfoil can also generate *self-noise* when turbulence that arises from the natural instability of the boundary layers on the surface of the airfoil is swept past the trailing edge. This is usually important when the hydrodynamic wavelength of the turbulence eddies is larger than the airfoil thickness at the trailing edge. The mechanism of noise production tends to be weaker than at the leading edge, because the violence of the unsteady motion at the trailing edge is alleviated by vortex shedding into the wake, and to be more prominent at higher frequencies.[15]

The noise may be ascribed to a distribution of lift dipoles near the trailing edge. At low frequencies the acoustical intensity exhibits the characteristic dipole field shape, proportional to $\cos^2\theta$, with a null in the plane of mean motion of the airfoil. At higher frequencies (when the acoustical wavelength is smaller than the chord of the airfoil) the field shape assumes a cardioid form, with a null in the downstream direction and the peak in the forward direction. In either case, when the trailing edge is at right angles to the mean flow, the frequency spectral density of the overall sound power $\Pi(\omega)$ (in watt-seconds) is given approximately by

$$\Pi(\omega) = \frac{\pi l a \omega^2}{24\rho c^3[1+(\omega a/3c)^3]^{1/3}} \int_{-\infty}^{\infty} \frac{P_0(k_1, 0, \omega)}{|k_1|}\, dk_1 \qquad (15.35)$$

where $P_0(\mathbf{k}, \omega)$ = blocked-pressure wavenumber–frequency spectrum on airfoil just upstream of trailing edge (see Section 15.5)
k_1 = wavenumber component parallel to mean flow, m^{-1}

If the flow approaching the trailing edge is turbulent on both sides of the airfoil, $P_0(k_1, 0, \omega)$ in Eq. (15.35) should be replaced by the sum of the wall pressure spectra on the two sides.

When the Chase model [Eq. (15.24)] is used to estimate the integral in Eq. (15.35), the frequency spectral density of the sound power radiated by a section of the airfoil of spanwise length l (in meters) is

$$\Pi(\omega) = \frac{0.08 a l \delta \rho v_*^4 U_c (\omega\delta/U_c)^3}{c^3[1 + (\omega a/3c)^3]^{1/3}[(\omega\delta/U_c)^2 + 1.78]^2} \qquad (15.36)$$

where δ = boundary layer thickness, m
v_* = friction velocity, m/s
$U_c \approx 0.7 \times$ velocity of mean stream, m/s

and other quantities are defined after Eq. (15.35).[16] However, measured levels of $\Pi(\omega)$ frequently exceed predictions of this formula. More detailed empirical formulas are given in the references.[16,17]

When the frequency is high enough [beyond the range of applicability of Eq. (15.36)] that the *Strouhal number* $\omega h/U \approx 1$, where h is the thickness of the trailing edge of the airfoil, the shedding of discrete vortices from the trailing edge can occur, provided the Reynolds number Ua/ν based on the chord a of the airfoil (dimensionless; ν is kinematic viscosity in square meters per second) does not exceed 10^6–10^7. This produces a distinct contribution to trailing-edge noise, often called "airfoil singing," whose amplitude is not easily predicted.[16]

15.10 FLOWS PAST CAVITIES

Sheared flow passing over a hole or opening in a wall can be the source of intense acoustical tones. Instability of the mean flow over such a wall cavity not only can excite hydrodynamic self-sustained oscillations but also can couple with resonant acoustical modes of the cavity, as in the Helmholtz resonator. Cavity tones are a frequent source of unwanted noise and vibration in branched duct and piping systems, turbomachinery, and exposed openings on automobiles, aircraft, and other high-speed vehicles. In this section we provide relationships for determining when flow over an opening that can be approximated as either a rectangular cavity (Fig. 15.17*a*) or a Helmholtz resonator (Fig. 15.17*b*) might be expected to exhibit strongly resonant behavior.

Flow over Cavities of Uniform Cross Section

For cavities of the type shown in Fig. 15.17*a*, resonant cavity oscillation occurs when the frequency associated with the shedding of vorticity from the upstream edge of the cavity is sufficiently high and the acoustical wavelengths within the cavity are sufficiently short as to allow standing waves inside the cavity. Longitudinal wave resonance is possible when the acoustical wavelength is less

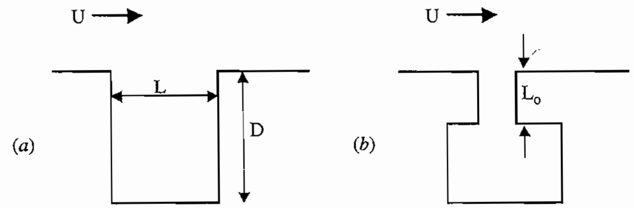

A_o = Orifice Cross-Sectional Area
V_c = Cavity Volume
A_c = Cavity Cross-Sectional Area

FIGURE 15.17 Examples of flows that sustain cavity resonances: (*a*) rectangular cavity of uniform cross section; (*b*) non-axisymmetric Helmholtz resonator.

than twice the cavity length, $c/f \leq 2L$, and depth resonance is observed when the acoustical wavelength is less than four times the cavity depth, $c/f \leq 4D$. For shallow cavities, where cavity length-to-depth ratio is large ($L/D > 1$), the longitudinal standing waves are dominant, while for deep cavities ($L/D < 1$) the depth resonance dominates.

Rossiter[18] derived the following equation for the Strouhal number associated with longitudinal cavity resonance modes:

$$\frac{fL}{U_\infty} = \frac{m - \xi}{M + 1/k_v} \qquad (15.37)$$

where k_v = ratio of shear layer velocity to free-stream velocity, $= U_c/U_\infty \cong 0.57$
m = mode number, $= 1, 2, 3, \ldots$, dimensionless
ξ = empirical constant, = 0.25, dimensionless
L = cavity length, m
M = free-stream Mach number, $= U_\infty/c$, dimensionless

Block[19] developed the following relation for the longitudinal cavity modes that accounts for the dependence of the Strouhal number on the cavity L/D ratio as observed in experimental data for shallow ($L/D > 1$) cavities:

$$\frac{fL}{U_\infty} = \frac{m}{1.75 + M\,(1 + 0.514/(L/D))} \qquad (15.38)$$

The following relation for depthwise modes of cavity oscillation was developed by East[20]:

$$\frac{fL}{U_\infty} = \left(\frac{1}{M}\right)\left(\frac{L}{D}\right)\left(\frac{0.25}{1 + 0.65(L/D)^{0.75}}\right) \qquad (15.39)$$

Lucas,[21] after comparing the ranges of validity of various cavity oscillation models, recommends, for low to moderate Mach number, the use of Block's formula (15.38) for shallow $(L/D > 1)$ cavities. For deep cavities he suggests use of East's formula (15.39) to determine the resonance of the depth mode and Rossiter's formula (15.37) for the longitudinal resonance mode. For such deep cavities the depth resonance will be the dominant mode.

Block[19] combined Eqs. (15.38) and (15.39) so that the frequency for the shallow acoustical waves coincides with the depthwise acoustical modes, providing the following formula for estimating the Mach number at which a cavity begins to oscillate in a given mode m:

$$M = \frac{1.75L/D}{4m[1 + 0.65(L/D)^{0.75}] - [(L/D) + 0.514]} \tag{15.40}$$

Equation (15.40) was shown by Block[19] to give adequate agreement with experimental data for Mach numbers in the range of 0.1–0.5 and for $L/D < 2$.

Flow over a Helmholtz Resonator

The natural frequency f_n of the Helmholtz resonator shown in Fig. 15.17b is given by

$$f_n = \frac{c}{2\pi}\sqrt{\frac{A_o}{V_c L_{\text{eff}}}} \tag{15.41}$$

where c = sound speed, m/s
A_o = orifice cross-sectional area, m^2
V_c = cavity volume, m^3
L_{eff} = effective neck length of orifice, m

The following approximate expression[22] for the effective neck length L_{eff} in the presence of a mean flow over the Helmholtz resonator accounts for an end correction due to the entrained mass of the virtual piston forming the interface between the neck and the exterior space (length ΔL_o):

$$\begin{aligned} L_{\text{eff}} &= L_o + \Delta L_o \\ &= L_o + 0.48\sqrt{A_0} \end{aligned} \tag{15.42}$$

where L_o is the length of the neck length of the orifice in meters.

An experimental study by Panton and Miller[23] indicates a strong response of the Helmholtz resonator excited by a turbulent boundary layer when

$$\frac{2d_o f_n}{U_c} \cong 1 \tag{15.43}$$

where d_o = Helmholtz resonator neck diameter, m
U_c = boundary layer convection velocity, $\approx 0.7U$, m/s
U = mainstream velocity at outer edge of boundary layer, m/s

In Eq. (15.43) f_n is either the Helmholtz resonance frequency in Eq. (15.41) or the fundamental standing-wave (organ pipe) resonance. For the latter, the natural frequency is approximately given by

$$f_n \cong \frac{c}{2L_{\text{eff}}} \tag{15.44}$$

Example 15.4. Many automobiles have a sunroof opening in their roof. Under some conditions the interior volume of the automobile cabin can act in combination with such an opening to create a Helmholtz resonator. If no measures are taken to prevent such an occurrence, at what speed might we expect the automobile's passengers to experience intense pressure fluctuations given a cabin interior volume of approximately 3 m^2, a square opening in the roof 0.4 m on a side, and a combined thickness of the roof and edging surrounding the opening of approximately 10 cm.

Solution Assuming an air temperature of 20°C, the speed of sound $c = 331.5 + 0.58T$ (in °C) = 343.1 m/s. The orifice cross sectional area $A_o = 0.4 \times 0.4 = 0.16$ m^2. The effective length of the opening is given by Eq. (15.42) as $L_{\text{eff}} = 0.1 + 0.48\sqrt{0.16} = 0.29$ m. Applying the above values and the cavity volume of $V_c = 3$ m^2, from Eq. (15.41) we expect the Helmholtz resonance to occur at $f_n = 23.4$ Hz. We take the neck diameter to be given by the length of the opening, $d_o = 0.4$ m. Substituting this value and that of the resonance frequency into Eq. (15.43), we can solve for the convection velocity, $U_c \approx 2 \times 0.4 \times 23.4 = 18.7$ m/s. The corresponding velocity of the mainstream, and thus our estimate of the vehicle speed at which we expect to strongly excite the Helmholtz resonance, is $U = U_c/0.7 = 26.7$ m/s, or 96 kph.

15.11 AERODYNAMIC NOISE OF THROTTLING VALVES

The noise of gas control or throttling valves may generally be associated with two sources: (1) mechanical vibration of the trim and (2) aerodynamic throttling. Noise generation by these mechanisms rarely occurs simultaneously, but when it does, the cure of one is usually the cure of the other.

Aerodynamic Noise

The prediction of the noise radiated from the body of a valve and from the downstream piping connected to it involves the following conceptual steps: (1) prediction of the magnitude and the spatial and spectral distribution of the noise inside the pipe based on the aerodynamic characteristics of the valve and the cross sectional area of the pipe, (2) prediction of the vibration response of the pipe to the internal sound field, (3) prediction of the sound radiation of the vibrating pipe.

In Step 1, the sound power generated by the valve has two components. The first is owing to the dynamic drag and lift forces (dipole) generated by the interaction of the turbulent flow with the valve, which are roughly proportional to the sixth power of the flow velocity. The second is sound power generated by the jet noise component (quadrupole), which is roughly proportional to the eighth power of the jet exit velocity. At very high pressure ratios, when the flow in the valve passage is supersonic, a shock pattern emerges downstream of the valve and generates intense screech noise. The dipole mechanism dominates the internal sound field at low Mach numbers and the quadrupole at high Mach numbers.

Based on the scaling of experimental data,[24] the lowest pipe wall attenuation occurs at $f_0 = (f_R/4)(c_{gas}(T)/c_0)$, where f_R is the ring frequency (Eq.15.58) and $c_{gas}(T)$ and $c_0 = 340$ m/s are the speed of sound of the gas in the pipe at local temperature and the that of air at room temperature respectively.

A fully analytical prediction procedure is too cumbersome. Consequently, the valve industry has adopted a prediction procedure based on both analytical and empirical methods that predicts the sound pressure level of the valve noise at 1 meter from the pipe wall directly from the aerodynamic properties of the valve and the geometric and material properties of the pipe. The rest of this chapter describes this semi-empirical prediction procedure.

Investigations of noise-induced pipe failures[25] have enabled maximum safe sound power levels to be established for given pipe sizes and wall thicknesses, as indicated in Fig. 15.18. The power levels shown in the figure correspond approximately to a sound level of 130 dBA at 1 m from the pipe wall downstream of the valve. Exceeding this level will most probably lead to piping failure, and a limit of 110 dBA at 1 m is recommended for safety and to maintain the structural integrity of valve-mounted accessories.

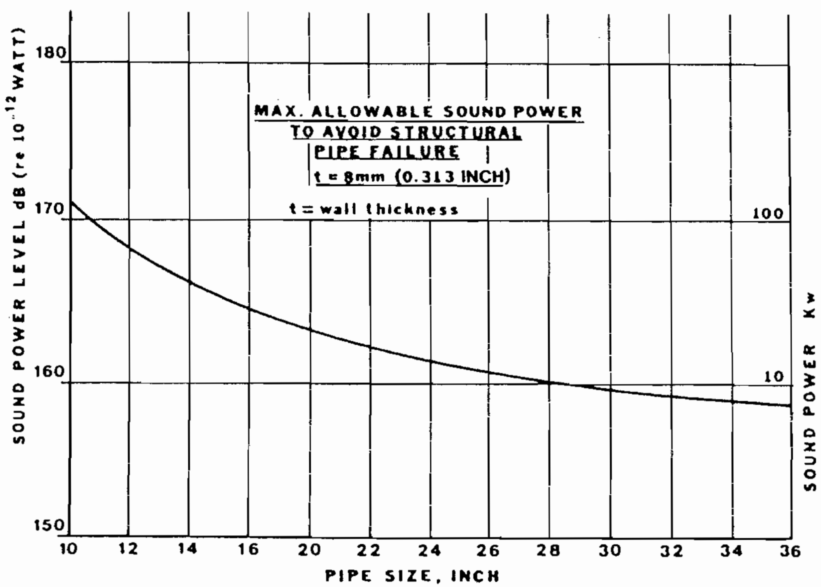

FIGURE 15.18 Suggested sound power level and sound power (Kw) limits inside pipe to avoid structural pipe failure based on actual occurrence.[24]

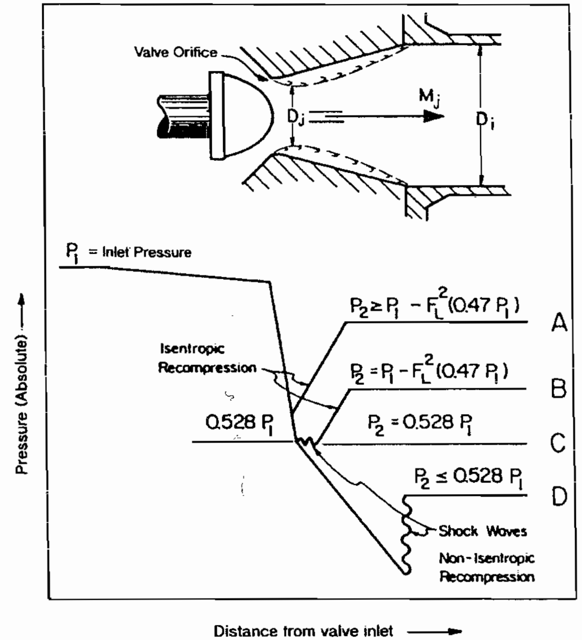

FIGURE 15.19 Schematic flow profile and static pressure diagram of throttling valve for various downstream pressures (P_2).

The aerodynamic noise is determined by the mechanical stream power $W_{\mathrm{mech\ strm}} = \frac{1}{2}mU^2$ (m being the mass flow and U the velocity; see Section 15.3) that is converted from potential energy (inlet pressure) to kinetic energy (velocity head) within the valve and subsequently to thermal energy (corresponding to reduced downstream pressure and an increase in entropy).[26] The pressure reduction (i.e., the conversion of kinetic into thermal energy) occurs via the generation of turbulence or, when the flow is supersonic, through shock waves. The sound power is equal to $\eta W_{\mathrm{mech\ strm}}$, where η is an acoustical efficiency factor. Unlike the case of a jet discharging into the atmosphere, the jet from a valve cannot expand freely, and only a fraction of the kinetic energy is converted by turbulence into thermal energy. This is illustrated in Fig. 15.19, which is a schematic view of a throttling valve and the associated pressure profile for various downstream pressures P_2.* On curve A the flow is subsonic, and turbulence-generated sound is predominantly of dipole type. At the critical pressure ratio ($P_1/P_2 = 1.89$ for air), curve B shows the presence of incipient shock waves followed by subsonic recompression, with both turbulence and shocks as noise sources. At higher pressure ratios recompression tends to be nonisentropic, and sound is produced predominantly by shock waves (curve D).

*In the rest of this chapter all pressures are absolute static pressures (in pascals).

Downstream of the vena contracta (D_j in Fig. 15.19) a portion of the velocity head is always recovered. The fraction lost is equal to F_L^2, where F_L is an experimentally determined pressure recovery coefficient that depends on valve type and size. The pressure drop $P_1 - P_2$ across the valve required to reach sonic velocity in the vena contracta is $F_L^2(P_1 - P_0)$, where P_0 is the static pressure in the vena contracta.[26] In subsonic flow the remaining portion of the jet power is recovered through isentropic recompression and is not converted to sound. If there were no pressure recovery at the valve orifice and assuming sonic flow at speed in c_0 meters per second (curve D in Fig. 15.19),

$$W_{\text{mech strm}} = \tfrac{1}{2} m c_0^2 \tag{15.45}$$

where m is the mass flow in kilograms per second, which also determines the valve flow coefficient C_v [see Eq. (15.50) or Table 15.4] together with the specific gravity G_f of the vapor or gas (relative to air = 1) and the valve inlet pressure P_1 (in pascals) such that

$$W_{\text{mech strm}} = 7.7 \times 10^{-11} C_v F_L c_0^3 P_1 G_f \quad \text{W} \tag{15.46}$$

The total sound power is then

$$W = \eta W_{\text{mech strm}} \quad \text{W} \tag{15.47}$$

$$L_W = 10 \times \log \frac{\eta W}{10^{-12}} \quad \text{dB} \tag{15.48}$$

When the pressure ratio is not sonic, η should be replaced by the acoustical power coefficient η_m determined below and (to simplify the calculations) should be used in conjunction with the sonic mechanical stream power given by Eq. (15.45). The acoustical power coefficient is further used in Eq. (15.53).

It may be remarked that the pressure recovery coefficient F_L can be used to predict the pressure P_0 in the vena contracta and also, to a satisfactory approximation, the area A_v of the vena contracta by

$$P_0 = P_1 - \frac{P_1 - P_2}{F_L^2} \tag{15.49a}$$

$$A_v = \frac{C_v F_L}{5.91 \times 10^4} \quad \text{m}^2 \tag{15.49b}$$

The valve's flow coefficient C_v can be calculated as follows:

$$C_v = \begin{Bmatrix} 2.14 \times 10^7 \dfrac{m}{\sqrt{\Delta P (P_1 + P_2) G_f}} & \Delta P \le \dfrac{1}{2} F_L^2 P_1 \\ 1.95 \times 10^7 \dfrac{m}{F_L P_1 \sqrt{G_f}} & \Delta P \ge \dfrac{1}{2} F_L^2 P_1 \end{Bmatrix} \tag{15.50}$$

TABLE 15.4 Factors for Valve Noise Prediction (Typical Values)

Valve Type	Flow To	Percentage of Capacity or Angle of Travel	$C_v/D^{2,a}$	F_L	F_d
Globe, single-port parabolic plug	Open	100%	0.020	0.90	0.46
Globe, single-port parabolic plug	Open	75%	0.015	0.90	0.36
Globe, single-port parabolic plug	Open	50%	0.010	0.90	0.28
Globe, single-port parabolic plug	Open	25%	0.005	0.90	0.16
Globe, single-port parabolic plug	Open	10%	0.002	0.90	0.10
Globe, single-port parabolic plug	Close	100%	0.025	0.80	1.00
Globe, V-port plug	Open	100%	0.016	0.92	0.50
Globe, V-port plug	Open	50%	0.008	0.95	0.42
Globe, V-port plug	Open	30%	0.005	0.95	0.41
Globe, four-port cage	Open	100%	0.025	0.90	0.43
Globe, four-port cage	Open	50%	0.013	0.90	0.36
Globe, six-port cage	Open	100%	0.025	0.90	0.32
Globe, six-port cage	Open	50%	0.013	0.90	0.25
Butterfly valve, swing-through vane	—	75° open	0.050	0.56	0.57
Butterfly valve, swing-through vane	—	60° open	0.030	0.67	0.50
Butterfly valve, swing-through vane	—	50° open	0.016	0.74	0.42
Butterfly valve, swing-through vane	—	40° open	0.010	0.78	0.34
Butterfly valve, swing-through vane	—	30° open	0.005	0.80	0.26
Butterfly valve, fluted vane	—	75° open	0.040	0.70	0.30
Butterfly valve, fluted vane	—	50° open	0.013	0.76	0.19
Butterfly valve, fluted vane	—	30° open	0.007	0.82	0.08
Eccentric rotary plug value	Open	50° open	0.020	0.85	0.42
Eccentric rotary plug value	Open	30° open	0.013	0.91	0.30
Eccentric rotary plug value	Close	50° open	0.021	0.68	0.45
Eccentric rotary plug value	Close	30° open	0.013	0.88	0.30
Ball valve, segmented	Open	60° open	0.018	0.66	0.75
Ball valve, segmented	Open	30° open	0.005	0.82	0.63

[a] D is the internal pipe diameter in mm.

Acoustical Efficiency

At Mach 1 a free jet has an acoustical efficiency $\eta \approx 10^{-4}$. If it is assumed that the sources of valve noise are dipoles and quadrupoles of equal magnitude (5×10^{-5}) at the Mach 1 reference point, then their respective efficiencies are represented by curves A and B in Fig. 15.20, and both curves can be combined to yield a subsonic slope C that originates at 1×10^{-4} and varies as $U^{3.6}$. This curve can be modified further to account for the decrease in $W_{\text{mech strm}}$ ($\propto U^3$) with subsonic velocities, leading to the final curve D for the effective efficiency (i.e., acoustical power coefficient) η_m that varies as $U^{6.6}$ or $(P_1/P_0 - 1)^{2.57}$ when $U \propto (P_1/P_0 - 1)^{0.39}$, P_0 being the static pressure in the vena contracta. This approximation gives satisfactory results for $0.38 \le M \le 1$ (i.e., down to $P_1/P_2 = 1.1$).

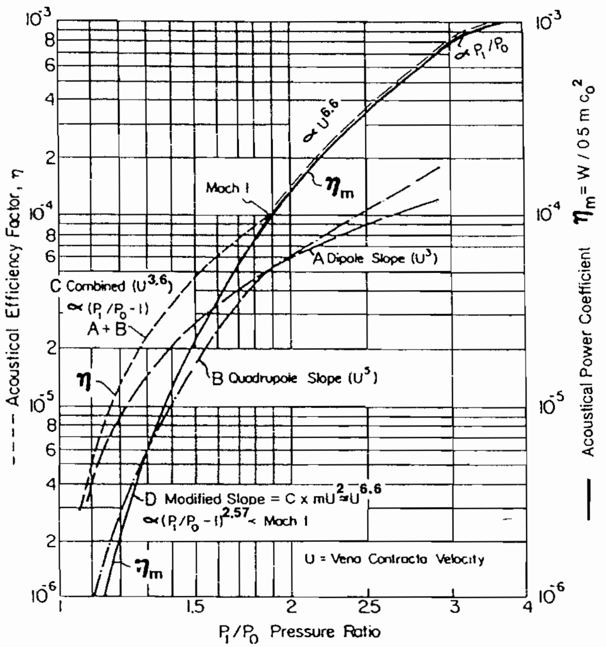

FIGURE 15.20 Slopes of dipole and quadrupole acoustical efficiency curves, assuming each has equal strength at Mach 1; their combined slope and the η_m curve after subtracting the effects of change in mass flow m and orificial velocity U for regions below Mach 1 from the combined curve.

For practical use it is convenient to express η_m in terms of P_1/P_2 = inlet pressure/outlet pressure. The following formulas[28,29] may be used for this purpose:

regime I: $P_1/P_2 < P_1/P_{2\text{critical}}$ (subsonic):

$$\eta_{mI} = 10^{-4} F_L^2 \left(\frac{P_1 - P_2}{P_1 F_L^2 - P_1 + P_2} \right)^{2.6} \tag{15.51a}$$

regimes II and III: $P_1/P_{2\text{critical}} < P_1/P_2 < 3.2\alpha$:

$$\eta_{mII} = 10^{-4} F_L^2 \left(\frac{P_1/P_2}{P_1/P_{2\text{critical}}} \right)^{3.7} \tag{15.51b}$$

regime IV: $3.2\alpha < P_1/P_2 < 22\alpha$ ($M_j > 1.4$):

$$\eta_{mIV} = 1.32 \times 10^{-3} F_L^2 \left(\frac{P_1/P_2}{P_1/P_{2\text{break}}} \right) \tag{15.51c}$$

regime V: $P_1/P_2 > 22\alpha$ (constant efficiency):

$$\eta_{mV} = \text{maximum value from regime IV} \tag{15.51d}$$

where
$\alpha = (P_1/P_{2\text{critical}})/1.89$
$P_1/P_{2\text{break}} = \alpha\gamma^{\gamma/(\gamma-1)}$ at $M = \sqrt{2}$
γ = ratio of specific heat of gas
$P_1/P_{2\text{critical}} = P_1/(P_1 - 0.5 P_1 F_L^2)$

The values of these parameters may be taken from Table 15.5.

When the downstream piping is straight and there are no sudden changes in cross-sectional area, the highest internal $\frac{1}{3}$-octave band sound pressure level L_{pi} (re 2×10^{-5} Pa) downstream of the valve is given by

$$L_{pi} = -61 + 10 \times \log \frac{\eta_m C_v F_L P_1 P_2 c_0^4 G_f^2}{D_i^2} \quad \text{dB} \tag{15.52}$$

where D_i = internal diameter of downstream pipe, m
G_f = specific gravity of gas relative to air at 20°C
$c_0 = \sqrt{\gamma P_0/\rho_0}$, m/s (speed of sound)
γ = ratio of specific heats
ρ_0 = gas density at vena contracta, kg/m³

Pipe Transmission Loss Coefficient

Knowledge of the peak internal sound frequency f_p is crucial for a proper prediction of the pipe transmission loss coefficient T_L. The coefficient T_L does not vary significantly between the first cutoff frequency f_0 [see Eq. (15.58)] and the ring frequency f_R of the pipe (see lower curve in Fig. 15.21), but variations can be large at other frequencies. The slope of T_L is about −6 dB per octave below f_0 and +6 dB per octave above f_r.[28]

For Mach numbers in the pipe less than about 0.3 and for relatively heavy pipes (as found in typical process plants) it may be assumed that the *minimum*

TABLE 15.5 Important Pressure Ratios for Air[a]

F_L	0.5	0.6	0.7	0.8	0.9	1.0
P_1/P_2 critical	1.13	1.20	1.30	1.43	1.61	1.89
P_1/P_2 break	1.95	2.07	2.24	2.40	2.76	3.25
α Ratio	0.60	0.64	0.68	0.76	0.85	1.0
22α	13	14	15	16	19	22

Note: P_1/P_0 critical = 1.89.
[a]May be used for other gases with reasonable accuracy.

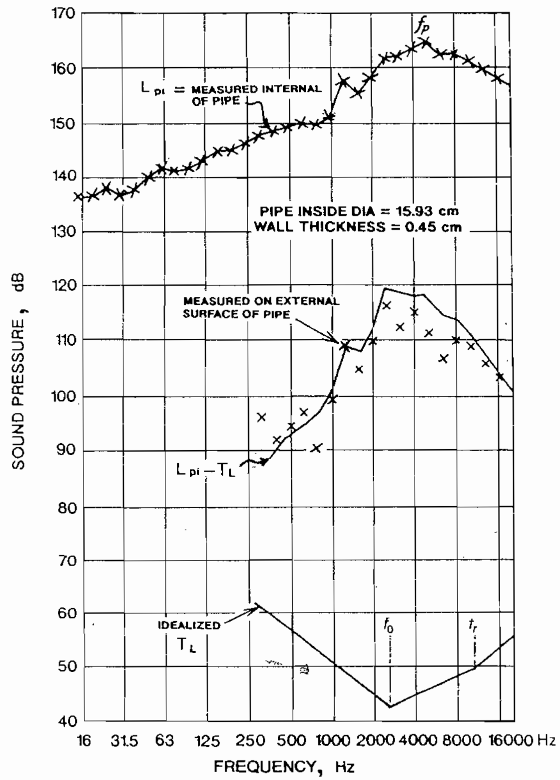

FIGURE 15.21 Test data taken on a 150-mm globe valve showing good agreement using the stated transmission loss equation. Notice the resultant shift in the peak sound frequency (f_p) from ~4.8 kHz inside the pipe to the first cutoff frequency of the pipe (f_0) at 2.5 kHz outside the pipe.

transmission loss occurs at f_0 and is given by[28]

$$T_{Lf_0} = 10 \times \log\left[9 \times 10^6 \frac{r t_p^2}{D_i^3}\left(\frac{P_2}{P_a} + 1\right)\right] \quad \text{dB} \tag{15.53}$$

where r = distance from pipe wall to observer, m
t_p = thickness of pipe wall, m
D_i = internal pipe diameter, m
P_2 = internal static pressure downstream of valve, Pa
P_a = external static pressure at same downstream distance, Pa

Typical values are given in Table 15.6. For fluids with higher sonic velocities and for thinner pipe walls, the minimum value of T_{Lf_0} shifts toward the ring frequency f_R [see Eq. (15.58)].

Idaho Power/1206
Ellenbogen/340

TABLE 15.6 Minimum Pipe Transmission Loss Coefficient T_{Lf_0}[a]

	Pipe Schedule	
Nominal Pipe Size, m	40	80
0.025	72	76
0.050	65	69
0.080	64	68
0.100	60	64
0.150	57	61
0.200	54	58
0.250	52	57
0.300	51	56
0.400	50	55
0.500	48	53

[a] At 1 m distance from steel pipe (dB) for 200 kPa internal and 100 kPa external air pressure. Pipe schedules per ANSI B36.10.

The total transmission loss coefficient for the valve is now expressed in the form

$$T_L = T_{Lf_0} + \Delta T_{Lf_p} \tag{15.54}$$

where the correction ΔT_{Lf_p} (in decibels) is determined by the peak noise frequency according to

$$\Delta T_{Lf_p} = \begin{cases} 20 \times \log \dfrac{f_0}{f_p} & f_p \le f_0 \\ 13 \times \log \dfrac{f_p}{f_0} & f_p \le 4 f_0 \\ 20 \times \log \dfrac{f_p}{4 f_0} + 7.8 & f_p > 4 f_0 \end{cases} \tag{15.55}$$

The peak frequency is estimated from[29]

$$f_p = \begin{cases} \dfrac{0.2 M_j c_0}{D_j} & M_j < 4 \\ \dfrac{0.28 c_0}{D_j \sqrt{M_j^2 - 1}} & M_j > 4 \end{cases} \tag{15.56}$$

where c_0 = speed of sound at vena contracta, m/s
D_j = jet diameter at valve orifice

and

$$M_j = \left\{\frac{2}{\gamma - 1}\left[\left(\frac{P_1}{\alpha P_2}\right)^{(\gamma-1)/\gamma} - 1\right]\right\}^{1/2} \tag{15.57}$$

$$f_R = \frac{c_L}{\pi D_i} = 4 f_0; \quad \text{for steel pipes and air} \quad f_R \approx \frac{5000}{\pi D_i} \tag{15.58}$$

For a gas other than air f_0 must be multiplied by $c_{0,\text{gas}}/c_{0,\text{air}}$.

The diameter D_j is difficult to determine because of the complex flow geometry in many valves. A reasonable approximation is to use the hydraulic diameter D_H as the jet diameter and make use of a valve-style modifier F_d (see Table 15.4) to obtain

$$D_j \approx 4.6 \times 10^{-3} F_d \sqrt{C_v F_L} \quad \text{m} \tag{15.59}$$

This formula is *not* applicable if jet portions combine downstream (usually at higher pressure ratios). This is common with multiple-hole valve cages,[30] short-stroke parabolic valve plugs in the "flow to close" direction, and butterfly valves at larger openings.

The external sound level (measured at 1 m from the wall) is now given by

$$L_a = 5 + L_{pi} - T_L - L_g \quad \text{dBA} \tag{15.60}$$

where L_g is a correction for fluid velocity in the pipe:

$$L_g = -16 \times \log\left(1 - \frac{1.3 \times 10^{-5} P_1 C_v F_L}{D_i^2 P_2}\right) \tag{15.61}$$

The laboratory test data shown in Fig. 15.21, taken with air on a DN150 globe valve, exhibits good agreement between predicted and measured external valve sound levels using T_L calculated from Eq. (15.54). In the absence of unusual phenomena such as jet "screech," Eq. (15.60) is found to be accurate to within ±3 dB assuming that all the valve coefficients are well established.

Accounting for Additional Noise due to High Velocities in Valve Outlet

Gas expanding in volume due to pressure reduction in a valve can cause high valve outlet velocities. These, in turn, can create secondary noise sources in the downstream pipe or pipe expander.[31,32]

The first step is to estimate the valve's outlet velocity (limited to sonic c_2):

$$U_R = 4 \frac{m}{\pi \rho_2 (d_i^2)} \tag{15.62}$$

where d_i is the valve diameter in meters.

The internal sound pressure level produced by this velocity is

$$L_{piR} = 65 + 10 \log\left(M_R^3 \frac{W_{mR}}{D_i^2}\right) \tag{15.63}$$

Here

$$W_{mR} = \frac{m}{2} U_R^2 \left[\left(1 - \frac{d_i^2}{D_i^2}\right) + 0.2\right] \tag{15.64}$$

and

$$M_R = \frac{U_R}{c_2} \tag{15.65}$$

Use Eq. (15.60) to calculate the external sound level L_R, substituting L_{piR} for L_{pi}, and using Eq. (15.54) to calculate TL, here substituting f_{pR} for f_p, where

$$f_{pR} = 0.2 \frac{U_R}{d_i} \tag{15.66}$$

The combined estimated external sound level at 1 m from the pipe from both the valve and the downstream piping now is

$$L_{ps} = 10 \log(10^{L_a/10} + 10^{L_R/10}) \tag{15.67}$$

The reader in encouraged to review reference 24, which illustrates the use of the prediction procedure in numerous examples.

Methods of Valve Noise Reduction

The two basic variables controlling the valve noise are the jet Mach number M_j and the internal peak frequency f_p. In subsonic flows lower jet velocities can be achieved by use of a valve trim that is less streamlined ($F_L \geq 0.9$, say).

At higher pressure ratios the only remedy is to use orifices or resistance paths in series, so that each operates subsonically. Such a "zig-zag" path valve is shown in Fig. 15.22. For example, for natural gas with an inlet pressure of 10,000 kPa that is to be throttled down to 5000 kPa and assuming a valve pressure recovery factor $F_L = 0.9$, the internal pressure ratio P_1/P_0 for a single-stage reduction would be $P_1/P_2\alpha = 2.35 : 1$. However, using the trim from Fig. 15.22 with 10 reduction steps, the orificial pressure ratio for each step is now only 1.603 : 1 with an acoustical power coefficient of only 1.1×10^{-7}. Ignoring the partial addition of 10 separate power sources, this represents a noise reduction of about 30 dB.

A less costly way to reduce "audible" valve noise is to increase the peak frequency by using multiorifice trim, as shown in Fig. 15.23. The throttling is still single stage, but the jets are divided into a number of parallel ports. This reduces the value of the valve style modifier $F_d \approx 1/\sqrt{n_o}$, where n_o is the number of equally sized parallel ports. Since F_d is proportional to jet diameter D_j, f_p can be shifted to higher levels. Thus if $n_o = 16$, as in Fig. 15.23, $F_d = 0.25$ and f_p is four times higher than for a single orifice ($F_d = 1$) with the same total flow area. If the peak frequency occurs in the mass-controlled region, an overall reduction in the external (audible) sound level of $\Delta T_{Lf_p} = 20 \times \log(f_{p1}/f_{p0}) = 20 \times \log(1/0.25) \approx 12$ dB is achieved.

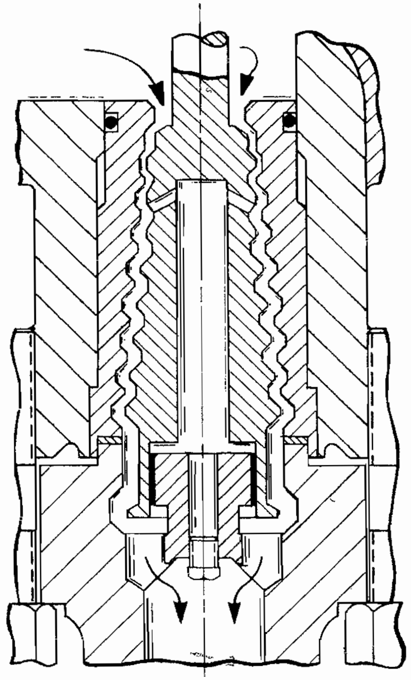

FIGURE 15.22 High-pressure reducing valve using multiple-step trim with a single flow path. Ideally each step will have subsonic orifice velocity.

The beneficial effects of a reduction in velocity combined with higher transmission loss caused by increased frequency are obtained with the elaborate arrangement shown in Fig. 15.24. This combines the multistep and multipath approach by use of a layer of disks having individually cast or etched channels.

A more economical solution is to couple a static downstream pressure-reducing device, such as a multihole restrictor, with a throttling valve with a fluted disk as indicated in Fig. 15.25. The fluted disk generates multiple jets with increased noise frequencies, although most of the energy is converted by the static pressure plate. At maximum design flow the valve is sized to have a low pressure ratio of 1.1 or 1.15 and the remainder of the pressure reduction occurs across the static plate having inherent low-noise throttling due to multistage, multihole design.

The most advanced and most compact form of a low noise valve trim is shown in Fig. 15.26. It consists of identical stamped or cut plates and constitutes a two-stage device, hence the narrow envelope. The device combines a supersonic first stage with a subsonic second stage for lowest overall acoustic efficiency, while retaining the final high frequency peak outlet sound level for high transmission losses.

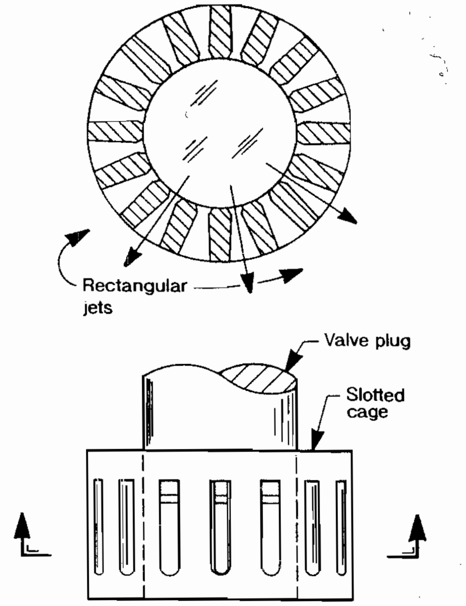

FIGURE 15.23 Slotted valve cage subdivides single-step flow path in 16 separate openings ($F_d = 0.25$) to increase peak frequency and thereby transmission loss.

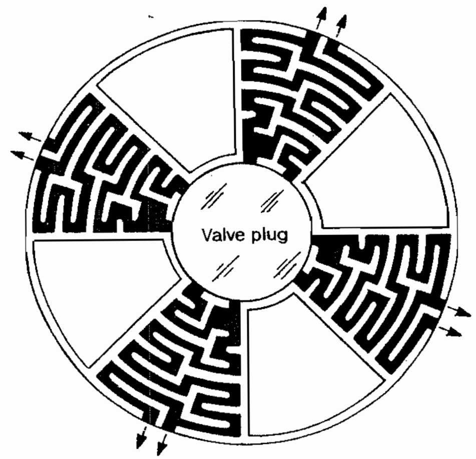

FIGURE 15.24 Labyrinth-type flow path cast or machined into each of a stack of metal plates surrounding a valve plug to provide a combination of multistep and multichannel flow paths in order to reduce throttling velocity and increase peak frequency.

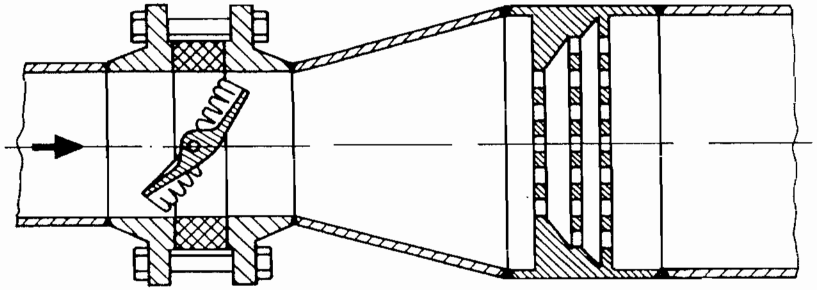

FIGURE 15.25 Modulating fluted butterfly valve cooperates with triple-stage static resistance plate for purposes of pressure reduction. Static plates see 90% of pressure drop at maximum design flow. Balance is handled by the valve.

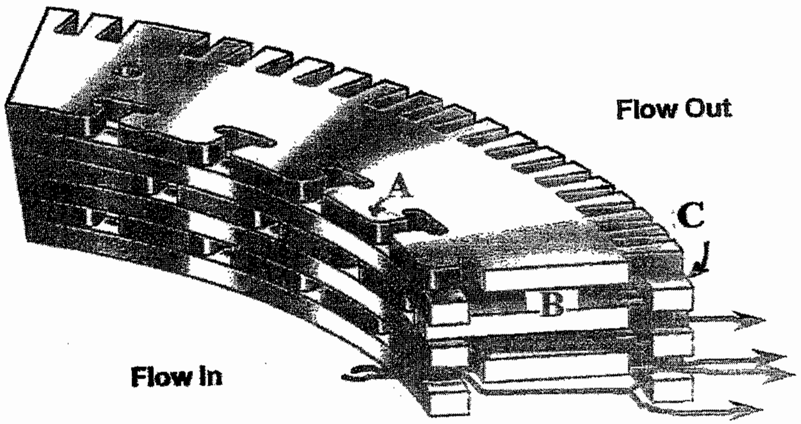

FIGURE 15.26 A stacked trim made from identical plates offers most advanced noise reduction. Here gas enters inlet orifices (A) configured as supersonic diffusers. These orifices convert about 95% of the stream power of the gas through a mechanism of shock waves; the gas then expands into sound-absorbing settling chambers (B) and finally exits the trim through a series of small subsonic passages (C).

Placing a silencer downstream of a valve is not cost effective because a good portion of the sound power travels upstream or radiates through the valve body and actuator, yielding noise reductions that typically do not exceed about 10 dB. Similar remarks apply to acoustical insulation of the pipe wall, where attenuations are limited to about 15 dB. The effectiveness of various abatement procedures is summarized below:

1. One-inch-thick pipe insulation: 5–10-dB reduction
2. Doubling thickness of pipe wall: 6-dB reduction

3. Silencer downstream: 10-dB reduction
4. Silencers upstream and downstream: 20-dB reduction
5. Multiport resistance plate downstream of valve: 15–20-dB reduction (use only 5–10% of valve inlet pressure as valve ΔP at maximum flow)
6. Special low-noise valve: 15–30-dB reduction

ACKNOWLEDGMENT

The authors wish to acknowledge the contribution of Dr. M. H. Howe for the portions of this chapter that have been retained from previous editions of this book.

REFERENCES

1. M. J. Lighthill, "On Sound Generated Aerodynamically. Part I: General Theory," *Proc. Roy. Soc. Lond.*, **A211**, 564–587 (1952).
2. M. S. Howe, "Contributions to the Theory of Aerodynamic Sound with Applications to Excess Jet Noise and the Theory of the Flute," *J. Fluid Mech.*, **71**, 625–673 (1975).
3. Society of Automotive Engineers, *"Gas Turbine Jet Exhaust Noise Prediction,"* Report No. SAE ARP 876C, Society of Automotive Engineers, Warrendale, PA, 1985.
4. J. R. Stone, "Prediction of In-Flight Exhaust Noise for Turbojet and Turbofan Engines," *Noise Control Eng.*, **10**, 40–46 (1977).
5. A. L. Laganelli and H. Wolfe, *"Prediction of Fluctuating Pressure in Attached and Separated Turbulent Boundary Layer Flow,"* Paper 89, American Institute of Aeronautics and Astronautics, Washington, DC, 1989, p. 1064.
6. M. S. Howe, "The Role of Surface Shear Stress Fluctuations in the Generation of Boundary Layer Noise," *J. Sound Vib.*, **65**, 159–164 (1979).
7. M. S. Howe, "Surface Pressures and Sound Produced by Low Mach Number Turbulent Flow over Smooth and Rough Walls," *J. Acoust. Soc. Am.*, **90**, 1041–1047 (1991).
8. D. M. Chase, "The Character of Turbulent Wall Pressure Spectrum at Subconvective Wavenumbers and a Suggested Comprehensive Model," *J. Sound Vib.*, **112**, 125–147 (1987).
9. J. G. Seebold, "Smooth Piping Reduces noise—Fact or Fiction?" *Hydrocarbon Process.*, September 1973, pp. 189–191.
10. D. A. Bies, *"A Review of Flight and Wind Tunnel Measurements of Boundary Layer Pressure Fluctuations and Induced Structural Response,"* NASA CR-626, NASA Langley Research Center, Hampton, VA, May 1966.
11. D. A. Nelson, *Reduced-Noise Gas Flow Design Guide*, NASA Glenn Research Center, Cleveland, OH, April 1999.
12. H. H. Heller and S. E. Widnall, "Sound Radiation from Rigid Flow Spoilers Correlated with Fluctuating Forces," *J. Acoust. Soc. Am.*, **47**, 924–936 (1970).
13. P. A. Nelson and C. L. Morfey, "Aerodynamic Sound Production in Low Speed Flow Ducts," *J. Sound Vib.*, **79**, 263–289 (1981).

14. M. Hubert, "Untersuchungen ueber Geraeusche durchstroemter Gitter," Ph.D. Thesis, Technical University of Berlin, 1970.
15. M. S. Howe, "The Influence of Vortex Shedding on the Generation of Sound by Convected Turbulence," *J. Fluid Mech.*, **76**, 711–740 (1976).
16. W. K. Blake, *Mechanics of Flow-Induced Sound and Vibration*, Vol. 2: *Complex Flow-Structure Interactions*, Academic, New York, 1986.
17. T. F. Brooks, D. S. Pope, and M. A. Marcolini, *"Airfoil Self-Noise and Prediction,"* NASA Reference Publication No. 1218, NASA Langley Research Center, Hampton, VA, 1989.
18. J. E. Rossiter, *"Wind Tunnel Experiments on the Flow over Rectangular Cavities at Subsonic and Transonic Speeds,"* RAE TR 64037, Royal Aircraft Establishment, Farnsborough, U.K., 1964.
19. P. J. W. Block, *"Noise Response of Cavities of Varying Dimensions at Subsonic Speeds,"* Technical Paper D-8351, NASA Langley Research Center, Hampton, VA, 1976.
20. L. F. East, "Aerodynamically Induced Resonance in Rectangular Cavities," *J. Sound Vib.*, **3**(3), 277–287 (1966).
21. M. J. Lucas, "Impinging Shear Layers," in M. J. Lucas et al., *Handbook of the Acoustic Characteristics of Turbomachinery Cavities*, American Society of Mechanical Engineers, New York, 1997, pp. 205–241.
22. M. C. Junger, "Cavity Resonators," in M. J. Lucas et al., *Handbook of the Acoustic Characteristics of Turbomachinery Cavities*, American Society of Mechanical Engineers, New York, 1997, pp. 13–38.
23. R. L. Panton and J. M. Miller, "Excitation of a Helmholtz Resonator by a Turbulent Boundary Layer," *J. Acoust. Soc. Am.*, **58**, 533–544 (1975).
24. IEC 60534-8-3, *"Control Valve Aerodynamic Noise Prediction Method,"* International Electrical Commission, Geneva, Switzerland, 2000.
25. V. A. Carucci and R. T. Mueller, *"Acoustically Induced Piping Vibration in High Capacity Pressure Reducing Systems,"* Paper No. 82-WA/PVP-8, American Society of Mechanical Engineers, New York, 1982.
26. H. D. Baumann, *"On the Prediction of Aerodynamically Created Sound Pressure Level of Control Valves,"* Paper No. WA/FE-28, American Society of Mechanical Engineers, New York, 1970.
27. ANSI/ISA S75.01-1985, *"Flow Equations for Sizing Control Valves,"* Instrument Society of America, Research Triangle Park, NC, 1985.
28. ANSI/ISA S75.17, *"Control Valve Aerodynamic Valve Noise Prediction,"* Instrument Society of America, Research Triangle Park, NC, 1989.
29. H. D. Baumann, *"A Method for Predicting Aerodynamic Valve Noise Based on Modified Free Jet Noise Theories,"* Paper No. 87-WA/NCA-7, American Society of Mechanical Engineers, New York, 1987.
30. C. Reed, "Optimizing Valve Jet Size and Spacing Reduces Valve Noise," *Control Eng.*, **9**, 63–64 (1976).
31. H. D. Baumann, "Predicting Control Valve Noise at High Exit Velocities," *INTECH*, February 1997, pp. 56–59.

CHAPTER 16

Prediction of Machinery Noise

ERIC W. WOOD AND JAMES D. BARNES

Acentech, Inc.
Cambridge, Massachusetts

Engineering information and prediction procedures are presented describing the sound power emission characteristics of various industrial machinery. The types of equipment addressed in this chapter include air compressors, boilers, coal-handling equipment, cooling towers, air-cooled condensers, diesel-engine-powered equipment, fans, feed pumps, gas turbines, steam turbines, steam vents, transformers, and wind turbines. The information has been extracted from consulting project files and the results of field measurement programs. The machinery noise prediction procedures are based on studies of empirical field data sponsored by numerous clients, including the Edison Electric Institute and the Empire State Electric Energy Research Corporation, for whom references 1–3 were prepared with the authors' colleagues: Robert M. Hoover, Laymon N. Miller, Susan L. Patterson, Anthony R. Thompson, and István L. Vér.

Characteristics identified and described for the noise produced by the machines discussed in this chapter include the estimated overall, A-weighted, and octave-band sound power levels (L_w) in dB re 1 pW, general directivity and tonal characteristics observed in the far field of the source, and temporal characteristics associated with the source operation. In addition, noise abatement concepts that have proven to be useful to the authors during previous consulting projects are described briefly. Successful noise control treatments often require a detailed understanding of site-specific operating and maintenance requirements as well as pertinent acoustical conditions at the site. We suggest that acoustical design handbooks or experienced acoustical engineering professionals be consulted when guidance is needed for specific design applications.

The information and procedures presented here can be used for numerous engineering applications requiring predictions of the approximate acoustical characteristics of new machinery installations and estimates of the noise attenuation that may be needed to meet local requirements. The prediction procedures are expected to provide A-weighted sound-power-level estimates that are generally accurate to within about ±3 dB. Individual octave-band sound-power-level estimates will necessarily be somewhat less accurate than A-weighted

14. M. Hubert, "Untersuchungen ueber Geraeusche durchstroemter Gitter," Ph.D. Thesis, Technical University of Berlin, 1970.
15. M. S. Howe, "The Influence of Vortex Shedding on the Generation of Sound by Convected Turbulence," *J. Fluid Mech.*, **76**, 711–740 (1976).
16. W. K. Blake, *Mechanics of Flow-Induced Sound and Vibration*, Vol. 2: *Complex Flow-Structure Interactions*, Academic, New York, 1986.
17. T. F. Brooks, D. S. Pope, and M. A. Marcolini, *"Airfoil Self-Noise and Prediction,"* NASA Reference Publication No. 1218, NASA Langley Research Center, Hampton, VA, 1989.
18. J. E. Rossiter, *"Wind Tunnel Experiments on the Flow over Rectangular Cavities at Subsonic and Transonic Speeds,"* RAE TR 64037, Royal Aircraft Establishment, Farnsborough, U.K., 1964.
19. P. J. W. Block, *"Noise Response of Cavities of Varying Dimensions at Subsonic Speeds,"* Technical Paper D-8351, NASA Langley Research Center, Hampton, VA, 1976.
20. L. F. East, "Aerodynamically Induced Resonance in Rectangular Cavities," *J. Sound Vib.*, **3**(3), 277–287 (1966).
21. M. J. Lucas, "Impinging Shear Layers," in M. J. Lucas et al., *Handbook of the Acoustic Characteristics of Turbomachinery Cavities*, American Society of Mechanical Engineers, New York, 1997, pp. 205–241.
22. M. C. Junger, "Cavity Resonators," in M. J. Lucas et al., *Handbook of the Acoustic Characteristics of Turbomachinery Cavities*, American Society of Mechanical Engineers, New York, 1997, pp. 13–38.
23. R. L. Panton and J. M. Miller, "Excitation of a Helmholtz Resonator by a Turbulent Boundary Layer," *J. Acoust. Soc. Am.*, **58**, 533–544 (1975).
24. IEC 60534-8-3, *"Control Valve Aerodynamic Noise Prediction Method,"* International Electrical Commission, Geneva, Switzerland, 2000.
25. V. A. Carucci and R. T. Mueller, *"Acoustically Induced Piping Vibration in High Capacity Pressure Reducing Systems,"* Paper No. 82-WA/PVP-8, American Society of Mechanical Engineers, New York, 1982.
26. H. D. Baumann, *"On the Prediction of Aerodynamically Created Sound Pressure Level of Control Valves,"* Paper No. WA/FE-28, American Society of Mechanical Engineers, New York, 1970.
27. ANSI/ISA S75.01-1985, *"Flow Equations for Sizing Control Valves,"* Instrument Society of America, Research Triangle Park, NC, 1985.
28. ANSI/ISA S75.17, *"Control Valve Aerodynamic Valve Noise Prediction,"* Instrument Society of America, Research Triangle Park, NC, 1989.
29. H. D. Baumann, *"A Method for Predicting Aerodynamic Valve Noise Based on Modified Free Jet Noise Theories,"* Paper No. 87-WA/NCA-7, American Society of Mechanical Engineers, New York, 1987.
30. C. Reed, "Optimizing Valve Jet Size and Spacing Reduces Valve Noise," *Control Eng.*, **9**, 63–64 (1976).
31. H. D. Baumann, "Predicting Control Valve Noise at High Exit Velocities," *INTECH*, February 1997, pp. 56–59.

CHAPTER 16

Prediction of Machinery Noise

ERIC W. WOOD AND JAMES D. BARNES

Acentech, Inc.
Cambridge, Massachusetts

Engineering information and prediction procedures are presented describing the sound power emission characteristics of various industrial machinery. The types of equipment addressed in this chapter include air compressors, boilers, coal-handling equipment, cooling towers, air-cooled condensers, diesel-engine-powered equipment, fans, feed pumps, gas turbines, steam turbines, steam vents, transformers, and wind turbines. The information has been extracted from consulting project files and the results of field measurement programs. The machinery noise prediction procedures are based on studies of empirical field data sponsored by numerous clients, including the Edison Electric Institute and the Empire State Electric Energy Research Corporation, for whom references 1–3 were prepared with the authors' colleagues: Robert M. Hoover, Laymon N. Miller, Susan L. Patterson, Anthony R. Thompson, and István L. Vér.

Characteristics identified and described for the noise produced by the machines discussed in this chapter include the estimated overall, A-weighted, and octave-band sound power levels (L_w) in dB re 1 pW, general directivity and tonal characteristics observed in the far field of the source, and temporal characteristics associated with the source operation. In addition, noise abatement concepts that have proven to be useful to the authors during previous consulting projects are described briefly. Successful noise control treatments often require a detailed understanding of site-specific operating and maintenance requirements as well as pertinent acoustical conditions at the site. We suggest that acoustical design handbooks or experienced acoustical engineering professionals be consulted when guidance is needed for specific design applications.

The information and procedures presented here can be used for numerous engineering applications requiring predictions of the approximate acoustical characteristics of new machinery installations and estimates of the noise attenuation that may be needed to meet local requirements. The prediction procedures are expected to provide A-weighted sound-power-level estimates that are generally accurate to within about ±3 dB. Individual octave-band sound-power-level estimates will necessarily be somewhat less accurate than A-weighted sound-power-level estimates. The prediction procedures estimate the equivalent (energy average) L_{eq} sound power level during operation of one machine. For equipment with intermittent operating cycles, the estimated sound power levels may be reduced by 10 log (operating cycle) if long-term equivalent values are required. When several identical machines are operating simultaneously, the sound power levels can be increased by 10 log (number of machines). When equipment is located within a large plant, other nearby large equipment may provide some shielding that will reduce the noise radiated to distant neighbors in shielded directions (see Chapter 7). When equipment is located within an enclosed plant, a portion of the acoustical energy will be dissipated inside the plant, leading to further reductions in the far-field noise. One should note that doors, windows, and ventilation openings can substantially diminish the acoustical performance (composite sound transmission loss) of building exterior walls (see Chapter 12).

The reader should try to obtain actual field data and/or manufacturers' information whenever possible for machines being studied. Information about the noise produced by gas flows and fans in buildings is presented in Chapters 15 and 17. Noise abatement information is provided in several other chapters. Indoor sound field characteristics are described in Chapters 6 and 7, and outdoor sound propagation is discussed in Chapter 5. The noise emission information provided in this chapter is representative of equipment presently available in the United States. Equipment in use in other countries may produce noise levels that are somewhat different than presented here. Prediction formulas for the overall sound power level are provided in the text of this chapter. Adjustments to predict the A-weighted and octave-band sound power levels are provided in Table 16.1.

16.1 AIR COMPRESSORS

The noise produced by air compressors is radiated from the filtered air inlet, the compressor casing, the interconnected piping and interstage cooler, as well as the motor or engine used to drive the compressor. The noise produced by air compressors can exhibit a distinctive duty cycle based on the demand for compressed air and is generally considered omnidirectional and broadband and absent prominent discrete tones. The air inlet noise of certain vacuum pumps sometimes includes high levels of low-frequency pulsating noise.

Noise-estimating procedures presented in this section are applicable to conventional industrial-, utility-, and construction-type air compressors without special noise abatement packages. Air compressors are often available from their manufacturer with special noise abatement packages that include various types of inlet mufflers, laggings, insulations, and enclosures that provide varying degrees of noise reduction. Acoustical data for these low-noise compressors should be obtained directly from the manufacturer's literature.

TABLE 16.1 Adjustments Used to Estimate A-Weighted and Octave-Band L_w[a]

Line	Equipment[b]	A-Weighted	31.5	63	125	250	500	1000	2000	4000	8000
1	RR compressor	2	11	15	10	11	13	10	5	8	15
2	C Compressor case	2	10	10	11	13	13	11	7	8	12
3	C Compressor inlet	0	18	16	14	10	8	6	5	10	16
4	S boilers	9	6	6	7	9	12	15	18	21	24
5	L boilers	12	4	5	10	16	17	19	21	21	21
6	CC shakers	9	5	6	7	9	12	15	18	21	24
7	R car open	12	4	5	10	13	17	19	21	21	21
8	R car enclosed	10	3	5	11	14	14	14	18	19	19
9	BL unloaders	9	8	5	8	10	12	13	18	23	27
10	CS unloaders	11	3	8	12	14	14	16	19	21	25
11	Coal crushers	9	6	6	6	10	12	15	17	21	30
12	T towers	7	7	7	7	9	11	12	14	20	27
13	C mill (13–36)	5			4	6	8	11	13	15	
14	C mill (37–55)	5			6	7	4	11	14	17	
15	ND C towers	0			12	13	11	9	7	5	7
16	MD C towers	10	9	6	6	9	12	16	19	22	30
17	MD C towers 1/2S	5	9	6	6	10	10	11	11	14	20
18	A-C condenser	12	5	6	6	10	14	17	24	29	34
19	D engine	5		11	6	3	8	10	13	19	25
20	C fan I + O	5	11	9	7	8	9	9	13	17	24
21	C fan case	13	3	6	7	11	16	18	22	26	33
22	R fan case	12	10	7	4	7	18	20	25	27	31
23	Axial fan	3	11	10	9	8	8	8	10	14	15
24	S Fd pumps	4	11	5	7	8	9	10	11	12	16
25	L Fd pumps	1	19	13	15	11	5	5	7	19	23
26	C-C plant	11	7	3	7	13	15	17	19	23	21
27	S St turbines	5	11	7	6	9	10	10	12	13	17
28	L St turbines	12	9	3	5	10	14	18	21	29	35
29	SL blow-out	11		2	6	14	17	17	21	18	18
30	Transformers	0		−3	−5	0	0	6	11	16	23

[a] Subtract values shown from estimated overall L_w; except for transformers, subtract values from A-weighted sound level.

[b] RR: rotary and reciprocating; C: casing; S: small, L: large, CC: coal car; R: rotary car dumpers; BL: bucket ladder; CS: clamshell; T: transfer; C. coal; ND C: natural-draft cooling; MD C: mechanical-draft cooling; A-C: air cooled; D: diesel; C-C plant: inside combined-cycle power plant main building; SL: steam line.

The overall sound power level radiated by the casing and air inlet of rotary and reciprocating air compressors can be estimated using Eq. (16.1) (see also line 1 of Table 16.1). These relations for rotary and reciprocating compressors assume that the air inlet is equipped with a filter and small muffler as normally provided by the manufacturer:

$$\text{Rotary and reciprocating compressor, overall } L_w = 90 + 10\log(\text{kW}) \quad \text{(dB)} \tag{16.1}$$

where kW is the shaft power in kilowatts. The casing and unmuffled air inlet overall sound power levels for centrifugal air compressors in the power range of 1100–3700 kW can be estimated using Eqs. (16.2) and (16.3) (see also lines 2 and 3 of Table 16.1). The insertion loss of any muffler installed at the air inlet should be deducted from the calculated inlet power levels:

$$\text{Centrifugal compressor casing, overall } L_w = 79 + 10 \log(\text{kW}) \quad (\text{dB}) \qquad (16.2)$$

$$\text{Centrifugal compressor inlet, overall } L_w = 80 + 10 \log(\text{kW}) \quad (\text{dB}) \qquad (16.3)$$

The term $\log(x)$ represents the common logarithm to base 10 of the value of x.

Equations (16.2) and (16.3) do not include the noise radiated by the motor or engine used to drive the compressor. Sound power levels calculated for the driving equipment should be added to the calculated sound power levels for the compressor.

Mufflers, laggings, barriers, and enclosures have all been used with varying degrees of success to control the noise radiated from compressors to nearby workspaces or neighborhoods. However, it is suggested that it is often most practical to specify and purchase a reduced-noise compressor from the manufacturer.

16.2 BOILERS

Two procedures are provided to predict the noise from boilers; one is for relatively small boilers in the range of about 50–2000 boiler horsepower (one boiler horsepower equals 15 kg of steam per hour). Another procedure is provided for large boilers of the type that serve electric-power-generating stations in the range of 100–1000 megawatts (MWe).

Small Boilers

The sound power output of small boilers is only weakly related to the thermal rating of the boiler. The combustion air fans and the burners probably radiate more noise than do the insulated sidewalls of small boilers. The overall sound power level of small boilers can be estimated using Eq. (16.4) (also see line 4 of Table 16.1):

$$\text{Small boiler, overall } L_w = 95 + 4 \log(\text{bhp}) \quad (\text{dB}) \qquad (16.4)$$

Large Boilers

Noise levels measured in work spaces adjacent to large central-station boilers that are not enclosed in a building (open boilers) are often in the range of 80–85 dBA at the lower half and 70–80 dBA at the upper half of the boiler. Noise levels measured in the vicinity of enclosed boilers (generally found in areas with cold climates) are often about 5 dBA higher. The overall sound power output of large central-station boilers can be estimated by the relation given in Eq. (16.5) (also see line 5 of Table 16.1):

$$\text{Large boiler, overall } L_w = 84 + 15 \log(\text{MWe}) \quad (\text{dB}) \qquad (16.5)$$

The noise from boilers is essentially omnidirectional and broadband in character. However, the combustion air or forced-draft fans, induced-draft fans, gas recirculation fans, overfire air fans, and drive motors sometimes produce tonal noise and may increase the noise levels on their side of the boiler. A small number of boilers have also been found to exhibit a strong discrete tone, usually at a frequency between about 20 and 100 Hz during operation at particular boiler loads. This can be caused by vortex shedding from heat exchanger tubes that excite an acoustical resonance within the boiler that in turn causes coherent (rather than random) vortex shedding to occur at a boiler resonance frequency. The low-frequency tonal noise that radiates from the boiler sidewalls has caused strong adverse reactions from residential neighbors. Boiler operators have also expressed concern about possible fatigue failure of vibrating tube sheets. Installation of one or more large metal plates to subdivide the interior of the boiler volume and thereby change its resonance frequency has successfully corrected this problem. Additional information about this resonant condition and its control is provided in references 4 and 5.

The typical broadband noise radiated by boiler sidewalls has been successfully reduced with the use of a well-insulated exterior enclosure, which also serves as weather protection for equipment and workers. The noise produced by fans serving the boiler can also be controlled as described in Section 16.6.

16.3 COAL-HANDLING EQUIPMENT

A wide variety of noise-producing equipment, such as railcar, ship and barge unloaders, transfer towers, conveyors, crushers, and mills, are used to unload, transport, and condition coal for use at large industrial and utility boilers. The results of numerous noise-level surveys have been studied and condensed to prepare the following general noise prediction procedures for this equipment.

Coal Car Shakers

Coal car shakers vibrate coal cars during bottom unloading. The unloading operation of each car often occurs for about 2–5 min when the coal is not frozen. When frozen coal is located in the car, the shake-out operation can last for up to 10 min or longer. Car shakers are often located inside a sheet metal or masonry building with little or no interior insulation for sound absorption. Shaker buildings include large openings at both ends and sometimes smaller openings and windows along the sidewalls. They also include dust collection and ventilation systems with fans that produce noise. The overall sound power produced during a coal car shake-out can be estimated using the following relation (also see line 6 of Table 16.1):

$$\text{Coal car shake-out, overall } L_w = 141 \text{ dB} \qquad (16.6)$$

Noise produced by the dust collection and ventilation fans can be estimated using the relations provided in Section 16.6 and in Chapter 17.

The far-field noise produced by car shake-outs can be reduced by enclosing the operation inside a metal or masonry building or by reducing the openings in any existing building. In addition, modern car-shaking equipment is sometimes available that produces measured A-weighted sound levels about 10 dB lower than are estimated with Eq. (16.6). Careful train movements can reduce the impact noise associated with indexing the train through the shaker operation. Limiting the shake-out operation to daytime hours also reduces the community noise impacts.

Rotary Car Dumpers

Rotary car dumpers are often used to unload long unit trains equipped with special rotary couplings. It typically takes 2–3 min to unload unfrozen coal from each car. A 100-car unit train can be unloaded in about 3–5 h unless delays are encountered. The overall sound power produced during rotary car unloading cycles can be estimated using Eqs. (16.7) and (16.8) for open and enclosed facilities (also see lines 7 and 8 of Table 16.1). However, short-duration impact sounds can be as much as 10–25 dB greater than the equivalent values given by these relations:

$$\text{Rotary car open unloading, overall } L_w = 131 \text{ dB} \tag{16.7}$$

$$\text{Rotary car enclosed unloading, overall } L_w = 121 \text{ dB} \tag{16.8}$$

Noise abatement methods for rotary car dumpers are similar to those discussed previously for car shakers.

Bucket Ladder and Clamshell Bucket Unloaders

Bucket ladder and clamshell bucket unloaders are often used to unload coal delivered by ship or barge. This equipment is located outdoors along the dock line with the electric motors and speed reduction gears often inside metal enclosures for weather protection. Acoustical data studied to prepare the prediction relations provided here were obtained at bucket ladder unloaders with free-digging rates in the range of 1800–4500 metric tons per hour and clamshell unloaders with free-digging rates in the range of 1600–1800 metric tons per hour. The energy-averaged overall sound power level produced during operation of bucket ladder and clamshell bucket unloaders can be estimated using Eqs. (16.9) and (16.10) (see also lines 9 and 10 of Table 16.1):

$$\text{Bucket ladder unloader, overall } L_w = 123 \text{ dB} \tag{16.9}$$

$$\text{Clamshell bucket unloader, overall } L_w = 131 \text{ dB} \tag{16.10}$$

Noise control treatments for bucket ladder and clamshell bucket unloaders generally employ insulated enclosures for the drive equipment and limiting unloading operations to daytime hours.

Coal Crushers

Coal is sometimes conveyed to a crusher building where the chunks are reduced in size in preparation for firing in a power plant boiler. Noise produced during crushing operations is a composite of the crusher, metal chutes, conveyors, drive motors, and speed reducers. Coal crushing is usually an intermittent operation and the noise is often omnidirectional without major tonal components. The overall sound power level produced during operation of the crusher can be estimated in accordance with the following relation (also see line 11 of Table 16.1):

$$\text{Coal crusher, overall } L_w = 127 \text{ dB} \tag{16.11}$$

The far-field noise associated with coal-crushing operations can be reduced by using a well-insulated and ventilated building to enclose the operation.

Coal Transfer Towers

Transfer towers reload coal from one conveyor to another as the coal is relocated within the coal yard on its way to the plant. Transfer tower noise is comprised of coal impacts, local conveyors, drive motors, and dust collection and ventilation system fans. Coal transfer is usually an intermittent operation, and the noise is often omnidirectional without major tonal components. The overall sound power level produced during coal transfer in open buildings can be estimated in accordance with the following relation (also see line 12 of Table 16.1):

$$\text{Transfer tower, overall } L_w = 123 \text{ dB} \tag{16.12}$$

Coal transfer operations can be enclosed in a well-ventilated building to reduce the far-field community noise. In this case, the estimated far-field noise can be mitigated by the composite sound transmission loss of the exterior building walls. Fan noise associated with the ventilation system should be estimated with the relations given in Section 16.6 or Chapter 17.

Coal Mills and Pulverizers

Coal mills and pulverizers crush and size coal in preparation for burning in a boiler. The resulting noise is associated with internal impacts, drive motors, speed reducers, and fans. The noise is essentially broadband, omnidirectional, reasonably steady, and continuous while the plant is operating. The overall sound power level produced by a coal mill in a building with large openings can be estimated in accordance with the following relations for mills in the size ranges of 13–36 and 37–55 metric tons per hour (also see lines 13 and 14 of Table 16.1). When coal mills are located in a closed building, the estimated far-field noise can be reduced by the composite sound transmission loss of the exterior building walls:

$$\text{Coal mill, overall } L_w = \begin{cases} 110 \text{ dB} & 13\text{–}36 \text{ metric tons per hour} \quad (16.13) \\ 112 \text{ dB} & 37\text{–}55 \text{ metric tons per hour} \quad (16.14) \end{cases}$$

16.4 COOLING TOWERS

The sound power output of wet cooling towers is caused primarily by the water splash in the fill and in the basin as well as by the fans, motors, and gears used to provide draft in mechanical towers. The noise is usually continuous and somewhat directive for rectangular towers. The noise produced by a specific pair of large natural-draft hyperbolic cooling towers has been observed to include a modest low-frequency discrete tone associated with aerodynamic vortex shedding at the base of each tower.

Methods that can be used to estimate the sound power output of natural-draft and mechanical induced-draft cooling towers are provided below. Major tower manufacturers can provide additional useful information regarding noise estimates and noise abatement.

Natural-Draft Cooling Towers

The overall sound power radiated from the rim of large hyperbolic natural-draft wet cooling towers can be estimated with Eq. (16.15) (see line 15 in Table 16.1). Noise radiated by the top of the tower is usually not significant at ground elevations compared to the rim-radiated noise:

$$\text{Natural-draft cooling tower rim, overall } L_w = 86 + 10 \log Q \quad \text{(dB)} \tag{16.15}$$

where Q is the water flow rate in gallons per minute (one cubic meter per minute is equal to 264 U.S. gallons per minute).

Inlet mufflers and fan assistance have been installed to control rim-radiated noise for hyperbolic cooling towers in Europe when located near residential neighbors. However, noise abatement is expensive and not common for large hyperbolic towers.

Mechanical Induced-Draft Cooling Towers

The sound power produced by mechanical induced-draft wet cooling towers operating at full fan speed and at half fan speed can be estimated using the following relations (also see lines 16 and 17 of Table 16.1):

Mechanical-draft tower full speed, overall

$$L_w = 96 + 10 \log(\text{fan kW}) \quad \text{(dB)} \tag{16.16}$$

Mechanical-draft tower half speed, overall

$$L_w = 88 + 10 \log(\text{fan kW}) \quad \text{(dB)} \tag{16.17}$$

where kW is the full-speed fan power rating in kilowatts for both relations.

The above relations apply in all horizontal directions from round towers and most directions away from the inlet face of rectangular towers. For directions away from the enclosed ends of rectangular towers, the far-field noise is several decibels less than estimated above due to the effects of shielding by the solid closed ends. For a line of as many as 6–10 rectangular towers, the far-field noise from the enclosed ends could be as much as 5–6 dB less than estimated, based on omnidirectional radiation using Eqs. (16.16) and (16.17).

Reduced fan speed is a common method used to mitigate the noise from mechanical-draft cooling towers during evening and nighttime hours when excess cooling capacity may be available due to reduced ambient air temperatures. In multiple-cell tower installations, it is preferable to reduce the fan speed for all cells rather than to shut down unneeded cells; the fans' speeds should be properly selected to avoid introducing a strong acoustical beat. Another common noise control method is to install wide-chord high-efficiency fan blades that can provide the necessary fan performance at reduced speeds. In addition, mechanical-draft towers with centrifugal fans may be selected because they can sometimes be designed to produce less noise than towers with propeller fans, although at some energy cost. Mufflers have also been installed at the air inlet and discharge to reduce both the fan and water noise. However, the mufflers must be protected from the wet environment, can become coated with ice during freezing weather, and introduce an additional aerodynamic restriction that must be overcome by the fan. Barrier walls and partial enclosures have successfully shielded neighbors from cooling-tower noise; however, barrier walls that avoid excessive restrictions to the airflow often limit their acoustical benefit for protecting far-field locations.

16.5 AIR-COOLED CONDENSERS

The sound power output of air-cooled condensers (dry cooling systems) is caused primarily by the fans used to move air across the condenser with some additional noise contribution from the motors and gears. The noise is usually continuous and somewhat directive for rectangular installations. The sound power output of dry air-cooled condensers does not, of course, include the water splash noise associated with wet cooling towers.

The need to reduce water consumption is causing the increasing trend to install air-cooled condensers even at large industrial facilities. When installed at a moderate to large new combined-cycle power plant, the fans for the forced-draft air-cooled condenser can contribute approximately the same sound power output as the balance of equipment at the plant. Fortunately, low-noise fans are now readily available for air-cooled condensers that produce comparable airflow rates and 3–6 dBA less noise than do conventional fans. These low-noise fans include high-efficiency wide-chord blades operating at reduced tip speeds. For some installations, noise reductions greater than 6 dBA can be available.

To avoid water consumption, power consumption, and fan noise generation, air-cooled systems are installed in hyperbolic natural-draft towers.

The sound power produced by air-cooled condensers with low-noise fans operating at full speed can be estimated using the following relation (also see line 18 of Table 16.1):

$$\text{Air-cooled condenser full speed, overall } L_w = 84 + 10\log(\text{fan kW}) \quad \text{(dB)} \tag{16.18}$$

where kW is the full-speed fan power rating in kilowatts.

The above relation applies in all horizontal directions from a low-noise unit; a standard unit will produce greater noise. It is suggested that fan- and air-cooled condenser manufacturers be contacted to obtain useful information regarding noise estimates and noise abatement for specific applications. See also references 6 and 7 for information about air-cooled condenser noise generation and propagation. Summary comparisons of the operating performance of wet, dry, and parallel condensing systems are provided in reference 8.

16.6 DIESEL-ENGINE-POWERED EQUIPMENT

When machinery such as compressors, generators, pumps, and construction equipment is powered by a diesel engine, it is usually the diesel engine that is the dominant noise source.

Mobile construction and coal yard equipment powered by diesel engines, such as dozers, loaders, and scrapers, often produces in-cab A-weighted noise levels as high as 95–105 dB. Methods to retrofit and reduce in-cab noise levels for several loaders and dozers have been developed, field tested, and documented in references 9 and 10. Well-designed cabs and noise control features are now often available from major manufacturers when purchasing new diesel-engine-powered mobile equipment.

A simple relation for estimating the maximum exterior overall sound power level for naturally aspirated and turbocharged diesel engines used to power equipment is provided in Eq. (16.19) (also see line 19 in Table 16.1):

$$\text{Diesel engine equipment, overall } L_w = 99 + 10\log(\text{kW}) \quad \text{(dB)} \tag{16.19}$$

The above relation assumes that the engine has a conventional exhaust muffler in good working condition as typically provided by the engine manufacturer and further assumes that the engine is operating at rated speed and power. Noise associated with material impacts during equipment operation is not included.

Equipment used on construction sites often operates at part power. Measurements obtained at the operating equipment indicate that work-shift-long equivalent L_{eq} sound levels are therefore typically about 2–15 dB less than the maximum values provided by Eq. (16.19). It is assumed that the following values could be subtracted from the Eq. (16.19) maximum levels to obtain work-shift-long equivalent L_{eq} levels. When project-long equivalent L_{eq} levels are required, the estimated values can be further reduced to account for the percentage of time that the equipment will actually operate on the construction site [10 log(operating time/project time)]:

3–4 dB	Backhoes, rollers
5–6 dB	Dozers, graders, haulers, loaders, scrapers
7–8 dB	Air compressors, concrete batch plants, mobile cranes, trucks
12–13 dB	Derrick cranes, paging systems

When stationary diesel-engine-driven equipment is located inside masonry or metal buildings, it is necessary to consider the sound power radiated by the engine inlet, the engine casing, the engine exhaust, and the engine cooling fan as well as the driven equipment. It is also necessary to account for the attenuation expected from the building walls and openings, the inlet filter/muffler, the exhaust muffler, and mufflers to be installed at building openings that serve ventilation and cooling systems. Additional information about the propagation of noise from equipment located inside buildings and about muffler systems is provided in Chapters 9 and 17.

16.7 INDUSTRIAL FANS

The noise produced by industrial fans is caused by the dynamic interaction of the gas flow with rotating and stationary surfaces of the fan. Noise produced by shear flow is usually not considered important. Broadband fan noise results from the random aerodynamic interactions between the fan and the gas flow. The prominent discrete tones produced by centrifugal fans result from the periodic interaction of the outlet flow and the cutoff located directly downstream of the blade trailing edges. Tonal noise produced by axial-flow fans results from periodic interactions between distorted inflow and the rotor blades as well as the rotor wakes and nearby downstream surfaces, including struts and guidevanes. This tonal noise is usually most prominent at the harmonics of the passing frequency of the fan blade (number of blades times the rotation rate in revolutions per second). Detailed information about the noise associated with gas flows and fans is provided in Chapters 15 and 17.

The noise produced by new forced-draft fans can be controlled most easily with the use of ducted and muffled inlets. Sometimes the ducted inlet is extended to a location in the plant where warm air is available and additional ventilation is needed. To provide further noise reduction, acoustical insulation lagging should be considered for the inlet and outlet ducts and the fan housing. Open-inlet forced-draft fans can be located within an acoustically treated fan room that contains the fan and its noise. However, workers inside the fan room during inspections and maintenance will be exposed to high levels of fan noise and should wear ear protection.

Discharge noise of large induced-draft fans radiated from the top of the stack to residential neighbors has caused serious community noise problems. The fan and duct system design should include provisions to control this noise if residential areas are located within $\frac{1}{2}$–1 mile of the plant. Mufflers used for induced-draft fan service at boilers and furnaces should be of the dissipative, parallel-baffle, open-cavity type tuned to the harmonics of fan blade passing frequency. These mufflers are built to avoid fly-ash clogging and include erosion protection to ensure adequate long-term performance. They can usually be designed to introduce a pressure loss in the range of about 10–40 mm water gauge. Consideration should also be given to the noise attenuation that will be provided by any flue gas scrubbers, filters, or precipitators that are to be located between the induced-draft fan and its stack. Alternatively, variable-speed fan drives can be installed to reduce nighttime noise at cycling plants that shed load during nighttime hours. This has the added benefit of also reducing the power consumed by the fans and reducing the erosion rates and stresses of rotating components. When multiple fans are installed, they should be operated at the same speed to avoid acoustical beats between the fan tones. (see references 3 and 11).

When an induced-draft centrifugal fan discharges directly to a stack, it is not uncommon for the tonal fan noise to radiate relatively long distances from the top of the stack. This tonal noise is generated by the fluid dynamic interaction of the gas flow leaving rotating fan blades and the stationary cutoff of the fan. This noise propagates with little attenuation up the stack and radiates from the stack top. Some success in reducing the magnitude of this tonal noise at large industrial centrifugal fan installations has been achieved by modifying the geometry of the cutoff. The fabrication and installation of "slanted" and rounded cutoffs, as described in reference 12, have been shown to reduce the tonal noise level by about 3–10 dB with no observed loss in fan performance.

Well-designed and sized inlet and outlet ducts that properly manage the flow are essential to avoid excessive fan noise. Inlet swirl, distorted inflow, and excessive turbulence can result in high noise levels and reduced system efficiency. Useful design guidelines have been established by the Air Movement and Control Association (AMCA) for large industrial fan installations.

Procedures are provided in this section to estimate the overall sound power output of large industrial fans operating at peak efficiency conditions with undistorted inflow. Experience indicates that fans operating with highly distorted inflow or at off-peak efficiency conditions often produce sound power levels that may be 5–10 dB higher than indicated below. Centrifugal- and axial-flow fans produce less sound power when operating at low speeds and reduced working points than during full-load, high-speed operation. For part-speed operation, the sound power levels estimated below can be reduced by about 55 log(speed ratio). Additional information about fan noise generation and attenuation is provided in reference 13.

Centrifugal-Type Forced-Draft and Induced-Draft Fans with Single-Thickness, Backward-Curved or Backward-Inclined Blades or Airfoil Blades

The overall sound power level radiated from the inlet of forced-draft centrifugal fans and the outlet of induced-draft centrifugal fans (with single-thickness, backward-curved or backward-inclined blades or airfoil blades) can be estimated with the relationship provided in Eq. (16.20) (also see line 20 of Table 16.1):

$$\text{Centrifugal fan, overall } L_w = 10 + 10\log Q + 20\log(\text{TP}) \quad \text{(dB)} \qquad (16.20)$$

where Q is fan flow rate in cubic meters of gas per minute and TP is fan total pressure rise in newtons per square meter at rated conditions.

To account for the tonal noise, 10 dB should be added to the octave bands containing the fan blade passing frequency and its second harmonic. For multiple-fan installations, the estimated sound power levels should be increased by 10 log N, where N is the number of identical fans.

The overall sound power level radiated from the uninsulated casing of centrifugal fans can be estimated with the relationship provided in Eq. (16.21) (also see line 21 of Table 16.1). To account for the tonal noise, 5 dB should be added to the octave band containing the fan blade passing frequency:

$$\text{Centrifugal fan casing, overall } L_w = 1 + 10\log Q + 20\log(\text{TP}) \quad \text{(dB)} \qquad (16.21)$$

where Q and TP are as defined for Eq. (16.20).

The sound power radiated by the uninsulated discharge breaching is about 5 dB less than the sound power estimated using Eq. (16.21) for the fan casing.

The overall sound power level radiated from the casings of radial-blade centrifugal fans with ducted inlets and outlets, such as are sometimes used for gas recirculation and dust collection service, can be estimated with the relationship provided in Eq. (16.22) (also see line 22 of Table 16.1):

$$\text{Radial fan casing, overall } L_w = 13 + 10\log Q + 20\log(\text{TP}) \quad \text{(dB)} \qquad (16.22)$$

where again Q and TP are as defined for Eq. (16.20).

To account for the tonal noise, 10 dB should be added to the octave bands containing the fan blade passing frequency and its second harmonic.

Axial-Flow Forced-Draft and Induced-Draft Fans

The overall sound power level radiated from the inlet of forced-draft axial-flow fans and the outlet of induced-draft axial-flow fans can be estimated with the following relation:

$$\text{Axial-flow fan, overall } L_w = 24 + 10\log Q + 20\log(\text{TP}) \quad \text{(dB)} \qquad (16.23)$$

where Q and TP have been defined in Eq. (16.20).

To account for the tonal noise, 6 dB should be added to the octave band containing the fan blade passing frequency and 3 dB should be added to the octave band containing its second harmonic. For multiple-fan installations, the above estimated values should be increased by 10 log N, where N is the number of identical fans.

Ventilation Fans

The sound power output of industrial ventilation fans can be estimated using Eq. (16.20) for centrifugal ventilation fans or Eq. (16.23) for axial-flow ventilation fans; also see Chapter 17.

16.8 FEED PUMPS

It is common for the noise radiated by a pump motor set to be dominated by the motor noise. One exception is the relatively high-flow, high-head pumps used for boiler and reactor feedwater service in large modern power-generating stations that operate in the United States. These feed pumps are usually driven by an electric motor, an auxiliary steam turbine, or the main turbine-generator shaft. Midsize pumps generally produce broadband noise without strong tonal components. The larger pumps, however, commonly produce both broadband noise and strong midfrequency tonal noise. Feed pump noise is omnidirectional and continuous during plant operation.

A high-performance thermal-acoustical blanket insulation, described in reference 14, has been developed and evaluated at field installations specifically for use with equipment such as noisy feedwater pumps, valves, and turbines. This thermal-acoustical insulation provides far better noise attenuation than conventional blanket insulations. It is also easier to remove and reinstall during maintenance and inspections than most rigid insulations. It has been successfully used as a retrofit insulation at installed pumps, turbines, valves, and lines and has been used by equipment manufacturers at new installations requiring reduced noise levels. The use of flexible thermal-acoustical insulation to control noise avoids the mechanical, structural, and safety problems associated with the large rigid enclosures that have sometimes been used at boiler feedwater pump installations. Note that experience in Germany indicates that it is possible to design and operate boiler feedwater pumps that produce relatively low noise levels without external means for controlling the noise.

The overall sound power level radiated by boiler and reactor feedwater pumps can be estimated using the information provided below for pumps in the power range of 1–18 MWe:

Rated Power (MWe)	Overall Sound Power (dB)
1	108
2	110
4	112
6	113
9	115
12	115
15	119
18	123

Octave-band and A-weighted sound power levels for boiler and reactor feedwater pumps can be estimated by subtracting the values provided in line numbers 24 and 25 of Table 16.1 from the overall power level estimated above.

16.9 INDUSTRIAL GAS TURBINES

Industrial gas turbines are often used to provide reliable, economic power to drive large electric generators, gas compressors, pumps, or ships. A prediction scheme for the combustion noise of flightworthy gas turbine engines used in aircraft operations (turbojet, turboshaft, and turbofan engines) is provided in Chapter 15. The noise produced by industrial gas turbine installations is radiated primarily from four general source areas: the inlet of the compressor; the outlet of the power turbine; the casing and/or enclosure of the rotating components; and various auxiliary equipment, including cooling and ventilating fans, the exhaust-heat recovery steam generator, poorly gasketed or worn access openings, generators, and electric transformers. Each of the above areas should receive considerable attention if an industrial gas turbine is to be located successfully near a quiet residential area.

Operation of unmuffled industrial gas turbines of moderate size would produce sound power levels of 150–160 dB or greater. Because the resulting noise levels would be unacceptable, essentially all industrial gas turbine installations include at least some noise abatement provided by the manufacturer. Noise abatement performance requirements may call for reducing the sound power output to levels as low as 100 dB for installations located near sensitive residential areas.

Noise radiated from the compressor inlet includes high levels of both broadband and tonal noise, primarily at frequencies above 250–500 Hz. This mid- and high-frequency noise is controlled with the use of (a) a conventional parallel-baffle or tubular muffler comprised of closely spaced thin baffles and (b) inlet ducting, plenum walls, expansion joints, and access hatches that are designed to contain the noise and avoid flanking radiation.

Noise radiated by the casings of rotating components is typically contained with the use of thermal insulation laggings and close-fitting steel enclosures that include interior sound absorption and well-gasketed access doors. It is not uncommon for the enclosure to be mounted directly on the structural steel base that supports the rotating components. This encourages the transmission of structure-borne noise to the enclosure and can limit its effective acoustical performance at installations requiring high degrees of noise reduction. Off-base mounting of the enclosure can be considered for installations where noise abatement performance must be improved. In addition, many large industrial gas turbines are being installed within a turbine-generator building that provides weather protection and additional reduction of noise radiated through the enclosure from the rotating components.

Noise radiated from the power turbine outlet includes high levels of both broadband and tonal noise at low, mid, and high frequencies, with the low-frequency noise being the most difficult and expensive to control at simple-cycle installations (without heat recovery boilers) located near residential areas. The wavelength of sound at about 30 Hz is on the order of 15–20 m in the gas stream at the back end of the power turbine, thereby increasing the required size of the discharge mufflers. Furthermore, low-frequency exhaust noise has caused significant community noise problems when the sound level in the 31-Hz octave band exceeded about 70 dB at sensitive residential areas. This low-frequency exhaust noise might be best controlled by the manufacturer with improved gas management designs behind the power turbine. The outlet noise is typically controlled with the use of (a) conventional parallel-baffle or tubular mufflers that include thick acoustical treatments; (b) additional dissipative or reactive muffler elements tuned to attenuate low-frequency noise; and (c) outlet ducts, plenum chamber, expansion joints, and access hatches that include adequate acoustical treatments to avoid flanking along these paths and their radiation of excessive noise.

At combined-cycle and cogeneration plants, heat recovery steam generators (HRSGs) are installed downstream of the power turbine to absorb waste heat from the exhaust stream. The HRSG also serves to attenuate the stack-radiated turbine exhaust noise, often by as much as 15–30 dBA, depending on the configurations and sizes of the gas turbine and HRSG. The HRSG can eliminate, or at least reduce, the performance requirements of the exhaust muffler. Also, the HRSG reduces the exhaust gas stream temperature, the wavelengths of the exhaust sounds, and the required size of an exhaust muffler. It is necessary to consider and account for the noise radiated from the surfaces and various steam vents of the HRSG. It is suggested that most HRSG manufacturers can provide technical information describing the noise radiated from their equipment. See also references 15–19 for additional information.

Noise produced by auxiliary cooling and ventilation fans can be controlled effectively with the use of high-performance low-speed fan blades, mufflers, or partial enclosures, depending on specific site and installation requirements. The control of transformer noise, if required for a specific installation, is discussed in Section 16.11. The control of noise radiated from the sidewalls of heat recovery steam generators can be accomplished with large barrier walls or an enclosing building.

Combined-cycle gas turbine power plants produce relatively steady noise as well as relatively brief intermittent loud noises often associated with steam venting and steam bypass operations. Noise levels of 75–80 dBA or greater at 300 m are not uncommon; however, these intermittent sources can usually be reduced 5–10 dBA or more. Further information about such intermittent loud noise from power plants is provided in reference 20.

Sound-power-level prediction procedures are not provided here specifically for industrial gas turbines because of the rather wide range of noise control treatments available within the industry. Many manufacturers offer their machines with a variety of optional noise abatement treatments, ranging from modest to highly effective. For example, 50–100-MWe installations, with or without heat recovery boilers, are readily available with noise abatement treatments resulting in A-weighted noise levels in the range of 50–60 dB at 120 m. Installations with lower noise levels are available from certain manufacturers and can be designed by several independent professionals who have specialized in the control of noise from industrial gas turbines. Combined-cycle plants in the range of 500–600 MWe have been designed and constructed to meet 43 dBA at 300 m.

The overall sound power level of the combined-cycle equipment located within the main power building, including the combustion turbine, HRSG, steam turbine, generators, and support equipment can be estimated with the following relation (also see line 26 of Table 16.1):

$$\text{Inside main power building, overall } L_w = 96 + 10\log(A) \qquad \text{(dB)} \qquad (16.24)$$

where A is the wall and roof area of the building in square meters.

This relationship is based on field measurements obtained near the outer wall and roof areas at numerous combined-cycle and cogeneration power plants. Equation (16.24) assumes that the interior surfaces of the building have sound absorption, with a resulting average sound level of 85 dBA at the outer wall and roof areas. For buildings without significant sound absorption treatment, the estimates should be increased by 5 dB. The interior sound level and the building shell transmission loss will determine the amount of noise that radiates to the outdoors from the main plant equipment. For additional discussion on these plants, see reference 21.

One early but important step in the design of a new gas turbine installation is the preparation of a reasonable and well-founded technical specification by the buyer or buyer's acoustical consultant that fully describes the site-specific noise requirements. Methods and procedures for preparing gas turbine procurement specifications that describe expected noise-level limits are included in ANSI/ASME B133.8-1977 (R1996). If residential neighbors are near the site, the reader is cautioned to consider fully the site-specific needs when planning control of the low-frequency exhaust noise. Several independent consultants with many years of gas turbine experience have suggested that the noise-level threshold of complaints resulting from low-frequency noise in the 31-Hz octave band is about 65–70 dB, measured at residential wood-frame homes. Higher levels of low-frequency noise can sometimes vibrate the walls and rattle the windows and doors of wood-frame homes and result in varying degrees of annoyance. Gas turbine manufacturers, however, correctly indicate that low-frequency noise control treatments are expensive and that many industrial gas turbines are operating that produce higher levels of low-frequency noise in residential areas without causing complaints.

16.10 STEAM TURBINES

Two procedures are provided to predict the sound power radiation from steam turbines; one is for the relatively small turbines in the power range of 400–8000 kW that operate at about 3600–6000 rpm and are often used to drive auxiliary equipment at a plant where steam is readily available. Another procedure is provided for large steam turbine generators in the range of about 200–1100 MWe used at central electricity-generating stations. Thermal-acoustical blanket insulation that has been developed to control noise radiated from equipment including steam turbines is discussed in Section 16.8 and reference 14.

Auxiliary Steam Turbines

The overall sound power output of auxiliary steam turbines, with common thermal insulation installed, can be estimated using Eq. (16.25) (see also line 27 of Table 16.1). This noise is considered to be omnidirectional, generally nontonal, and continuous when the driven equipment is operating:

$$\text{Auxiliary steam turbine, overall } L_w = 93 + 4 \log(\text{kW}) \qquad (\text{dB}) \qquad (16.25)$$

Large Steam Turbine-Generators

The overall sound power output of large steam turbine-generators can be estimated using Eq. (16.26). This includes the noise radiated by the low-pressure, intermediate-pressure, and high-pressure turbines as well as the generator and shaft-driven exciter. The turbine-generator produces both tonal and broadband noise. The tonal components produced by the generator are typically most noticeable at 60 and 120 Hz for 3600-rpm machines and 30, 60, 90, and 120 Hz for 1800-rpm machines:

$$\text{Large steam turbine-generator, overall } L_w = 113 + 4 \log(\text{MW}) \qquad (\text{dB}) \qquad (16.26)$$

Octave-band and A-weighted sound power levels for large steam turbine-generators can be calculated by subtracting the values provided in line 28 of Table 16.1 from the overall sound power level estimated using Eq. (16.26).

Most major manufacturers of large steam turbine-generators will provide their equipment with additional noise abatement features that reduce the noise by about 5–10 dBA, when required by a well-written purchase specification. The reverberant noise inside a turbine building can also be reduced through the proper selection of the building siding. The use of building siding with a fibrous insulation sandwiched between a perforated metal inner surface and a solid exterior surface will provide improved midfrequency sound absorption and thereby reduce the reverberant buildup of noise within the turbine building. It can also reduce the noise radiated to the outdoors.

16.11 STEAM VENTS

Atmospheric venting of large volumes of high-pressure steam is probably one of the loudest noise sources found at industrial sites. The overall sound power produced during steam line blow-outs at large central stations prior to starting a new boiler can be estimated using Eq. (16.27) (see also line 29 of Table 16.1).

This noise is broadband and only occurs for a few minutes during each blow-out for the first few weeks of boiler operation:

$$\text{Steam line blow-out, overall } L_w = 177 \text{ dB} \qquad (16.27)$$

The actual sound power level produced during the venting of high-pressure gas is, of course, related to various factors, including the conditions of the flowing gas and the geometry of the valve and pipe exit. However, the above relationship will provide a reasonable estimate of the noise associated with the blow-out of steam lines at large boilers used for utility service.

Large heavy-duty mufflers are sometimes purchased or rented that reduce the noise by about 15–30 dB during steam line blow-outs. The noise produced by the more common atmospheric vents and commonly encountered valves can be estimated using prediction procedures available from many valve manufacturers and their representatives. Many manufacturers offer valves with special low-noise trims, orifice plates, and inline mufflers that effectively reduce noise generation and radiation. The low-noise trim can also reduce the vibration and maintenance that are sometimes associated with valves used in high-pressure-drop service.

16.12 TRANSFORMERS

The noise radiated by electrical transformers is composed primarily of discrete tones at even harmonics of line frequency, that is, 120, 240, 360, ... Hz when the line frequency is 60 Hz and 100, 200, 300, ... Hz when the line frequency is 50 Hz. This tonal noise is produced by magnetostrictive forces that cause the core to vibrate at twice the electrical line frequency. The cooling fans and oil pumps at large transformers produce broadband noise when they operate; however, this noise is usually less noticeable and therefore less annoying to nearby neighbors. The tonal core noise should be considered omnidirectional and continuous while the transformer is operating. The broadband fan and pump noise occurs only during times when additional cooling is required.

The technical literature includes numerous relations and guidelines for the prediction of noise produced by transformers. Reference 22 reports the results of measurements obtained at 60 transformer banks and indicates that the space-averaged A-weighted sound level produced by the core of the average transformer (without built-in noise abatement) at an unobstructed distance of about 150 m is well represented by the relationship given in Eq. (16.28). Ninety-five percent of the A-weighted noise data reported in reference 22 lies within about ±7 dB of this relation for transformers with maximum ratings in the range of 6–1100 MVA:

Average A-weighted core sound level at 150 m,

$$L_p = 26 + 8.5 \log(\text{MVA}) \qquad (\text{dBA}) \quad (16.28)$$

where MVA is the maximum rating of the transformer in million volt-amperes.

The space-averaged sound pressure levels of the transformer core tones at 120, 240, 360, and 480 Hz at 150 m can be estimated by adding the following values to the A-weighted sound level of Eq. (16.28):

120	240	360	480
17	5	−4	−8

Another relation for transformer A-weighted sound levels versus distance, extracted from reference 23, is

$$\text{Space-averaged far-field sound level } L_p = L_n - 20(\log\ d/S^{1/2}) - 8 \qquad \text{(dBA)} \tag{16.29}$$

where L_n = circumferential average sound pressure levels measured at National Electrical Manufacturers Association (NEMA) close-in measurement positions (A-weighted or tonal)
S = total surface area of four sidewalls of transformer tank
d = distance from transformer tank (in units that are compatible with tank sidewall area), must be greater than $S^{1/2}$

Equation (16.29) can be used if L_p and L_n represent the A-weighted sound levels or the sound pressure levels of the discrete tones produced by the transformer tank. The octave-band sound pressure levels of the transformer core noise can be obtained directly from the sound pressure levels of the discrete tones estimated above. The octave-band sound pressure levels of the total transformer noise with the cooling fans operating can be estimated by subtracting the values provided in line 30 of Table 16.1 from the A-weighted sound level estimated with Eq. (16.29). This applies to conventional cooling-fan systems with motors in the power range of about 0.15–0.75 kW operating at about 1000–1700 rpm with two- or four-bladed propeller fans. Further information about special low-noise cooling systems should be obtained from the manufacturer. Excess attenuation should be considered (see Chapter 5) when estimating sound levels at distances beyond about 150 m.

NEMA has published standard tables of close-in noise levels for transformers; see reference 24. Experience indicates that the noise near most operating transformers is often equal to or somewhat less than the NEMA standard values, and the noise near new high-efficiency transformers can be significantly less than the NEMA values. However, the noise produced by converter transformers operating at AC-to-DC converter terminals can include discrete tones at frequencies up to about 2000 Hz and can be about 5–10 dB greater than the NEMA standard values. This additional high-frequency noise has been found to be unusually noticeable and disturbing to residential neighbors when the converter transformer is located in quiet rural-suburban areas.

Two basic methods are available for reducing the far-field noise produced by transformers. First, manufacturers are able to respond to custom noise requirements and produce transformers with reduced flux density that generate noise levels as much as 10–20 dB lower than the NEMA standard values. New high-efficiency transformers with low electrical losses usually produce core noise levels that are less than the NEMA standard values. For the quieted-design transformers, reductions of the higher frequency tones (e.g., 480 and 600 Hz) are typically 1–3 dB more than the reductions of the lower frequency tones (e.g., 120, 240, and 360 Hz). High-efficiency low-speed cooling fans and cooling-fan mufflers are also available from some manufacturers when needed for special siting applications. In some cases, the cooling fans are eliminated from the transformer tank and replaced with oil-to-water heat exchangers.

Second, barrier walls, partial enclosures, and full enclosures can be provided to shield or contain the transformer noise. They are usually fabricated with masonry blocks or metal panels. The interior surfaces of the barrier or enclosure walls should usually include sound absorption that is effective at the prominent transformer tones. Care must be used to ensure adequate strike distances and space for cooling-air flows. If the fin-fan oil coolers are to be located outside of the enclosure, some attention should be given to the structure-borne and oil-borne noise from the core that can be radiated by the coolers. Space and provisions must be provided for inspections, maintenance, and transformer removal. It is also important to ensure that the enclosure walls are structurally isolated from the transformer foundation to avoid radiation of structure-borne noise resulting transformer-induced vibration. Further information about the control of transformer noise is available from most major transformer manufacturers as well as from reference 25. And a promising passive means of canceling tonal noise radiated from transformer sidewalls by means of an attached mechanical oscillator is discussed in reference 26.

As energy efficiency becomes increasingly important, new transformers are being purchased with low electrical losses reducing operating costs. Experience at numerous large electrical facilities indicates that new high-efficiency low-loss transformers also often produce core noise levels 5–10 dB less than the NEMA standard values.

Instead of, or in addition to, reducing the noise radiated from a transformer substation, it is sometimes possible to site a transformer far from residential neighbors or within an existing noisy area, such as close to a well-traveled highway, where the ambient sounds partially mask the transformer noise.

16.13 WIND TURBINES

The installation of modern wind energy systems is growing rapidly throughout many areas of the world. Installed capacity by 2001 exceeded 30,000 MWe as the reliability and efficiency of modern wind turbines increased and the costs declined. It has been estimated that wind turbines will generate more than 10% of the world's energy, more than 1200 GW, by year 2020. Wind turbine capacity is generally rated based on rotor diameter, rotor swept area, or generator capacity in watts. Small-capacity wind turbines are generally rated at less than about 5 kW, medium turbines at about 5–300 kW, and large wind turbines at about 500 kW and above. Large turbines are now available rated at up to 1–5 MW, and with multiple turbines on a single tower, ratings can continue to increase. Wind turbine parks or farms are being developed onshore and offshore with rated capacities of 50–150 MWe and greater. The development of wind turbine rotors to operate with low wind speeds will increase the available resource area and will bring development closer to more people.

The main types of noise from wind turbines are aerodynamic, mechanical, and electrical. The principal sources of noise include the rotor blades, the gearbox, and the generator. Additional sources include the brakes, the electronics, and the tower. Earlier wind turbine installations produced both prominent tonal noise from the gear box and a strongly modulated "thumping" noise most often associated with the rotor blades passing through and interacting with the turbulent tower wake flow at downwind machines. Fortunately, the manufacturers of modern wind turbines have learned to avoid what were these most noticeable and annoying aspects of wind turbine noise.

Considerable progress in reducing noise generation and radiation continues to be made by the equipment manufacturers with ongoing technical support from research organizations (reference 27). Noise abatement for modern wind turbines includes increasingly efficient rotor blade profiles, variable-speed and variable-pitch rotors, advanced electronics, and low-noise gearboxes, as well as vibration isolation mounts and sound absorption within turbine nacelles. Noise from modern wind turbines is generally dominated by broadband rotor noise that is directly related to tip speed. Information about aeroacoustical noise generation is provided in Chapter 15.

Modern wind turbines are generally available that produce broadband noise without strong tonal components. The midfrequency aerodynamic rotor noise generally includes some noticeable time-varying amplitude modulation at the passing frequency of the rotor blade (number of blades times the rotation rate in revolutions per second). For a three-blade constant-speed turbine operating at 25 rpm, this is 1.25 Hz. For variable-rotor-speed turbines, the modulation frequency will often be in the range of 0.5–1 Hz.

The approximate A-weighted sound power level of modern medium to large wind turbines can be estimated with the relationships provided in Eq. (16.30) or (16.31), although the sound power level of some turbines will be as much as 10 dBA greater:

$$\text{Wind turbine, A-weighted sound power level} = \begin{cases} 86 + 10 \log D \quad (\text{dBA}) & (16.30) \\ 73 + 10 \log \text{kW} \quad (\text{dBA}) & (16.31) \end{cases}$$

where D is the rotor diameter in meters and kW is the rated turbine power.

Alternatively, the approximate footprint area surrounding a modern wind turbine within which the A-weighted sound level equals or exceeds 40 dBA can be estimated with the relationship provided in Eq. (16.32):

$$\text{Wind turbine 40 dBA footprint area in square meters} = 800 \times \text{kW} \quad (\text{m}^2) \qquad (16.32)$$

The operating characteristics, including noise generation under specific conditions, of most modern wind turbines have been certified in accordance with national and international standards. The special requirements associated with reliable measurements and specification of wind turbine noise are defined by International Standard IEC 61400-11, 1998, "Wind Turbine Generator Systems—Part 11: Acoustic Noise Measurement Techniques."

16.14 SUMMARY

The machinery noise prediction procedures and relations presented in this chapter are based primarily on extensive field measurement data collected by the authors and their colleagues during many years of consulting projects. The results obtained when using these relations should be useful for many engineering applications. The reader is cautioned, however, that site-specific installation conditions and individual equipment characteristics can cause noise levels to be somewhat higher or lower than predicted, and detailed knowledge of these exceptions can be important for critical applications. Also, many items of equipment can be purchased with reduced noise, can be installed so as to reduce noise, or can be fitted with effective noise control treatments.

The authors continue to add to and update their library of equipment noise emission data used in the preparation of this chapter. Readers with access to new or useful data or information on equipment noise characteristics or control and wanting to share their information are encouraged to send copies to the authors.

REFERENCES

1. L. N. Miller, E. W. Wood, R. M. Hoover, A. R. Thompson, and S. L. Patterson, *Electric Power Plant Environmental Noise Guide,* rev. ed., Edison Electric Institute, Washington, DC, 1984.
2. J. D. Barnes, L. N. Miller, and E. W. Wood, *Power Plant Construction Noise Guide*, BBN Report No. 3321, Empire State Electric Energy Research Corporation, New York, 1977.
3. I. L. Vér and E. W. Wood, *Induced Draft Fan Noise Control: Technical Report and Design Guide*, BBN Report Nos. 5291 and 5367, Empire State Electric Energy Research Corporation, New York, 1984.
4. I. L. Vér, "Perforated Baffles Prevent Flow-Induced Resonances in Heat Exchangers," in *Proceedings of DAGA*, Deutschen Arbeitsgemeinschaft fur Akustik, Göttingen, Germany, 1982, pp. 531–534.
5. R. D. Blevins, *Flow-Induced Vibrations*, Krieger Publishing Company, Melbourne, FL, 2001.
6. W. E. Bradley, "Sound Radiation from Large Air-Cooled Condensers," in *Proceedings of NoiseCon 2003*, June 2003, The Institute of Noise Control Engineering of the USA, Inc., Washington, DC, 2003.
7. J. Mann, A. Fagerlund, C. DePenning, F. Catron, R. Eberhart, and D. Karczub, "Predicting the External Noise from Multiple Spargers in an Air-Cooled Condenser Power

Idaho Power/1206
Ellenbogen/357

Plant," in *Proceedings of NoiseCon 2003*, June 2003, The Institute of Noise Control Engineering of the USA, Inc., Washington, DC, 2003.

8. L. De Backer and W. Wurtz, "Why Every Air-Cooled Steam Condenser Needs a Cooling Tower," *CTI J.*, **25** (1), 52–61 (Winter 2004).
9. *Bulldozer Noise Control*, manual prepared by Bolt Beranek and Newman for the U.S. Bureau of Mines Pittsburgh Research Center, Pittsburgh, PA, May 1980.
10. *Front-End Loader Noise Control*, manual prepared by Bolt Beranek and Newman for the U.S. Bureau of Mines Pittsburgh Research Center, Pittsburgh, PA, May 1980.
11. R. M. Hoover and E. W. Wood, "The Prediction, Measurement, and Control of Power Plant Draft Fan Noise," Electric Power Research Institute Symposium on Power Plant Fans—The State of the Art, Indianapolis, IN, October 1981.
12. J. D. Barnes, E. J. Brailey, Jr., M. Reddy, and E. W. Wood, "Induced Draft Fan Noise Evaluation and Control at the New England Power Company Salem Harbor Generating Station Unit No. 3," in *Proceedings of ASCE Environmental Engineering*, Orlando, FL, July 1987.
13. *Proceedings of Fan Noise Symposiums*, Senlis, France, 1992 and 2003.
14. C. C. Thornton, C. B. Lehman, and E. W. Wood, "Flexible-Blanket Noise Control Insulation-Field Test Results and Evaluation," in *Proc. INTER-NOISE* 84, June 1984, Noise Control Foundation, Poughkeepsie, NY, 1984, pp. 405–408.
15. G. F. Hessler, "Certifying Noise Emissions from Heat Recovery Steam Generators (HRSG) in Complex Power Plant Environments," in *Proceedings of NoiseCon 2000*, December 2000, The Institute of Noise Control Engineering of the USA, Inc., Washington, DC, 2000.
16. W. E. Bradley, "Integrating Noise Controls into the Power Plant Design," in *Proceedings of NoiseCon 2000*, December 2000, The Institute of Noise Control Engineering of the USA, Inc., Washington, DC, 2000.
17. J. R. Cummins and J. B. Causey, "Issues in Predicting Performance of Ducts and Silencers Used in Power Plants," in *Proceedings of NoiseCon 2003*, June 2003, The Institute of Noise Control Engineering of the USA, Inc., Washington, DC, 2003.
18. *Noise Prediction—Guidelines for Industrial Gas Turbines*, Solar Turbines, San Diego, CA, 2004.
19. R. S. Johnson, "Recommended Octave Band Insertion Losses of Heat Recovery Steam Generators Used on Gas Turbine Exhaust Systems," in *Proceedings of NoiseCon 1994*, May 1994, Noise Control Foundation, Poughkeepsie, NY, 1984, pp. 181–184.
20. D. Mahoney and E. W. Wood, "Intermittent Loud Sounds from Power Plants," in *Proceedings of NoiseCon 2003*, June 2003, The Institute of Noise Control Engineering of the USA, Inc., Washington, DC, 2003.
21. G. F. Hessler, "Issues In HRSG System Noise," in *Proceedings of NoiseCon 1997*, June 1997, The Institute of Noise Control Engineering of the USA, Inc., Washington, DC, 1997, pp. 297–304.
22. R. L. Sawley, C. G. Gordon, and M. A. Porter, "Bonneville Power Administration Substation Noise Study," BBN Report No. 3296, Bolt Beranek and Newman, Cambridge, MA, September 1976.
23. L. Vér, D. W. Anderson, and M. M. Miles, "Characterization of Transformer Noise Emissions," Vols. 1 and 2, BBN Report No. 3305, Empire State Electric Energy Research Corporation, New York, July 1977.

24. NEMA Standards Publication No. TR 1–1993 (R2000), "*Transformers, Regulators and Reactors*," National Electrical Manufacturers Association, Rosslyn, VA, 2000.
25. C. L. Moore, A. E. Hribar, T. R. Specht, D. W. Allen, I. L. Vér, and C. G. Gordon, "Power Transformer Noise Abatement," Report No. EP 9–14, Empire State Electric Energy Research Corporation, New York, October 1981.
26. J. A. Zapfe and E. E. Ungar, "A Passive Means for Cancellation of Structurally Radiated Tones," *J. Acoust. Soc. Am.*, **113** (1), 320–326 (January 2003).
27. P. Migliore, J. van Dam, and A. Huskey, "Acoustic Tests of Small Wind Turbines," AIAA-2004-1185, 23rd ASME Wind Energy Symposium, U.S. DOE National Renewable Energy Laboratory, Reno, NV, January 2004.

CHAPTER 17

Noise Control in Heating, Ventilating, and Air Conditioning Systems

ALAN T. FRY

Consultant
Colchester, Essex, United Kingdom

DOUGLAS H. STURZ

Acentech, Inc.
Cambridge, Massachusetts

This chapter provides guidelines, recommendations, and design tools useful in assessing and controlling noise and vibration stemming from mechanical systems serving buildings. Discussed are the transmission of noise along duct systems, airflow velocities at various points in duct systems that are consistent with particular noise goals, fan noise, terminal box noise, and special design features for especially quiet heating, ventilating, and air conditioning (HVAC) systems. Sound isolation for mechanical rooms and special consideration for the application of vibration isolation for mechanical equipment in buildings are also addressed. Further discussion and additional detailed design information can be found in references 1–5, and in Chapters 9–15 of this book.

17.1 DUCT-BORNE NOISE TRANSMISSION

It is of significant practical interest to predict the noise that transmits via a ducted system from a source to a receiver space to achieve a desired noise goal. This is typically done by starting with the noise of a known source (typically and primarily a fan) and subtracting from this the attenuation provided by each of the various duct elements that the noise encounters as it propagates along the duct path. Thus, from a known noise source level, one can predict the noise level that reaches the occupant of a space and can engineer any special attenuation treatments that may need to be incorporated in the duct system to help achieve a desired result. Alternatively, one can work backward from a desired noise goal in the receiving space to determine the permissible sound power level of a fan serving the system (or other source in the system). There are many acoustical complexities that are difficult to model precisely without exhaustive knowledge of the duct construction and the nature of the sound field entering a duct element, and such details are generally not well known. The prediction procedure is really a guide to make decisions in order to achieve designs that are in the correct neighborhood of the goal, and generally the procedure is a good guide in the moderately lower frequency range that is of greatest interest for ventilation systems. There are many aspects of ducted systems which are strongly frequency dependent in the higher frequency range, and the precision of the calculations may be questionable for extensive systems in this frequency range. Fortunately, in designing noise control for ducted systems, when the lower frequencies are suitably controlled, the predicted noise levels at higher frequencies are dramatically lower than the goal and there is no need to make precise predictions in this higher frequency range. The following presents some of the data necessary to assess attenuation in the path of sound propagation from source to receiver. Considerations for some relevant noise sources are presented later.

Sound Attenuation in Straight Ducts

Even the attenuation of sound propagating in simple, straight ducts is quite complex. The sound attenuation in straight ducts of uniform cross section and wall construction is usually given in attenuation per unit length, decibels per meter or decibels per feet, assuming that every unit of duct length provides the same amount of attenuation. This is a considerable simplification because the attenuation is a function of the character of the sound field entering the duct section and the character of the sound field is constantly changing along the length of even a straight-duct run. At frequencies high enough for the duct to support higher order modes, these higher order modes are much more rapidly attenuated by duct attenuation treatments than the plane-wave fundamental mode. Attenuation of sound along a duct is a function of the sound dissipation when the sound wave interacts with the walls of the duct and this is determined by the impedance of the duct wall. Sound attenuation in lined ducts and silencers is treated in detail in Chapter 9. At high frequencies, energy loss due to sound transmission through the bare sheet metal duct walls yields only very little sound attenuation for the duct path. However, with sound-absorptive lining of the walls, high-frequency sound attenuation along the ducts can be quite high. At low frequencies, a substantial portion of the sound attenuation along the duct path is provided by energy transmission through the sheet metal walls of the duct—breakout. Form, stiffness, and surface weight control the low-frequency sound attenuation. Consequently, unlined form-stiff round ducts yield much less sound attenuation (and also much higher breakout sound transmission loss) than do ducts with rectangular or oval cross section and with large aspect ratio. The sound attenuation values represented herein are for typical duct construction within the range of constructions typically allowed by the Sheet Metal and Air Conditioning National Association (SMACNA) for low-pressure ductwork.

Estimation of the attenuation provided by unlined and lined ducts of round and rectangular duct constructions typically found in the field is presented in Tables 17.1–17.6.

TABLE 17.1 Sound Attenuation in Unlined Rectangular Sheet Metal Ducts

Duct Size, in. × in.	P/A, ft^{-1}	Attenuation by Octave-Band Center Frequency, dB/ft			
		63 Hz	125 Hz	250 Hz	>250 Hz
6 × 6	8.0	0.30	0.20	0.10	0.10
12 × 12	4.0	0.35	0.20	0.10	0.06
12 × 24	3.0	0.40	0.20	0.10	0.05
24 × 24	2.0	0.25	0.20	0.10	0.03
48 × 48	1.0	0.15	0.10	0.07	0.02
72 × 72	0.7	0.10	0.10	0.05	0.02

Source: 1999 ASHRAE *Applications Handbook*, © American Society of Heating, Refrigerating and Air Conditioning Engineers, Inc., www.ashrae.org.

Sound Attenuation by Duct Divisions

When sound propagating along a duct encounters a duct branch, the acoustical energy divides into the two branches according to the fraction of the area that each represents to the total area leaving the division. This is probably a reasonable approximation of what happens at lower frequencies, but at higher frequencies there are likely to be directional effects for which this simple model does not account. Fortunately, for most practical HVAC noise control concerns, the low-frequency range is of the greatest interest. The attenuation in decibels that occurs at a duct division is given by

$$\text{Attenuation} = 10 \log \left(\frac{A_1}{A_T}\right) \quad \text{dB} \tag{17.1}$$

where A_1 is the area of the duct leaving the division on the path being studied and A_T is the total area of all branches leaving the division.

Sound Attenuation by Duct Cross-Sectional Area Changes

Sound propagating along a duct is reflected back if it encounters a sudden cross-sectional area change. The strength of reflection at low frequencies, where only the fundamental plane wave can propagate in the duct, depends only on the ratio of the cross-sectional areas. Whether the sound is coming from the duct of the larger or smaller cross-sectional area, the resulting sound attenuation is given by

$$\text{Attenuation} = 10 \log \left\{0.25\left[\left(\frac{A_1}{A_2}\right)^{0.5} + \left(\frac{A_2}{A_1}\right)^{0.5}\right]^2\right\} \quad \text{dB} \tag{17.2}$$

TABLE 17.2 Insertion loss for Rectangular Sheet Metal Ducts with 1-in. Fiberglass Lining[a]

	Insertion Loss by Octave Band Center Frequency, dB/ft					
Dimensions, in. × in.	125 Hz	250 Hz	500 Hz	1000 Hz	2000 Hz	4000 Hz
6 × 6	0.6	1.5	2.7	5.8	7.4	4.3
6 × 10	0.5	1.2	2.4	5.1	6.1	3.7
6 × 12	0.5	1.2	2.3	5.0	5.8	3.6
6 × 18	0.5	1.0	2.2	4.7	5.2	3.3
8 × 8	0.5	1.2	2.3	5.0	5.8	3.6
8 × 12	0.4	1.0	2.1	4.5	4.9	3.2
8 × 16	0.4	0.9	2.0	4.3	4.5	3.0
8 × 24	0.4	0.8	1.9	4.0	4.1	2.8
10 × 10	0.4	1.0	2.1	4.4	4.7	3.1
10 × 16	0.4	0.8	1.9	4.0	4.0	2.7
10 × 20	0.3	0.8	1.8	3.8	3.7	2.6
10 × 30	0.3	0.7	1.7	3.6	3.3	2.4
12 × 12	0.4	0.8	1.9	4.0	4.1	2.8
12 × 18	0.3	0.7	1.7	3.7	3.5	2.5
12 × 24	0.3	0.6	1.7	3.5	3.2	2.3
12 × 36	0.3	0.6	1.6	3.3	2.9	2.2
15 × 15	0.3	0.7	1.7	3.6	3.3	2.4
15 × 22	0.3	0.6	1.6	3.3	2.9	2.2
15 × 30	0.3	0.5	1.5	3.1	2.6	2.0
15 × 45	0.2	0.5	1.4	2.9	2.4	1.9
18 × 18	0.3	0.6	1.6	3.3	2.9	2.2
18 × 28	0.2	0.5	1.4	3.0	2.4	1.9
18 × 36	0.2	0.5	1.4	2.8	2.2	1.8
18 × 54	0.2	0.4	1.3	2.7	2.0	1.7
24 × 24	0.2	0.5	1.4	2.8	2.2	1.8
24 × 36	0.2	0.4	1.2	2.6	1.9	1.6
24 × 48	0.2	0.4	1.2	2.4	1.7	1.5
24 × 72	0.2	0.3	1.1	2.3	1.6	1.4
30 × 30	0.2	0.4	1.2	2.5	1.8	1.6
30 × 45	0.2	0.3	1.1	2.3	1.6	1.4
30 × 60	0.2	0.3	1.1	2.2	1.4	1.3
30 × 90	0.1	0.3	1.0	2.1	1.3	1.2
36 × 36	0.2	0.3	1.1	2.3	1.6	1.4
36 × 54	0.1	0.3	1.0	2.1	1.3	1.2
36 × 72	0.1	0.3	1.0	2.0	1.2	1.2
36 × 108	0.1	0.2	0.9	1.9	1.1	1.1
42 × 42	0.2	0.3	1.0	2.1	1.4	1.3
42 × 64	0.1	0.3	0.9	1.9	1.2	1.1
42 × 84	0.1	0.2	0.9	1.8	1.1	1.1
42 × 126	0.1	0.2	0.9	1.7	1.0	1.0
48 × 48	0.1	0.3	1.0	2.0	1.2	1.2
48 × 72	0.1	0.2	0.9	1.8	1.0	1.0
48 × 96	0.1	0.2	0.8	1.7	1.0	1.0
48 × 144	0.1	0.2	0.8	1.6	0.9	0.9

[a] Add to attenuation of bare sheet metal ducts.

Source: 1999 ASHRAE *Applications Handbook*, © American Society of Heating, Refrigerating and Air Conditioning Engineers, Inc., www.ashrae.org.

TABLE 17.3 Insertion loss for Rectangular Sheet Metal Ducts with 2-in. Fiberglass Lining[a]

	Insertion Loss by Octave-Band Center Frequency, dB/ft					
Dimensions, in. × in.	125 Hz	250 Hz	500 Hz	1000 Hz	2000 Hz	4000 Hz
6 × 6	0.8	2.9	4.9	7.2	7.4	4.3
6 × 10	0.7	2.4	4.4	6.4	6.1	3.7
6 × 12	0.6	2.3	4.2	6.2	5.8	3.6
6 × 18	0.6	2.1	4.0	5.8	5.2	3.3
8 × 8	0.6	2.3	4.2	6.2	5.8	3.6
8 × 12	0.6	1.9	3.9	5.6	4.9	3.2
8 × 16	0.5	1.8	3.7	5.4	4.5	3.0
8 × 24	0.5	1.6	3.5	5.0	4.1	2.8
10 × 10	0.6	1.9	3.8	5.5	4.7	3.1
10 × 16	0.5	1.6	3.4	5.0	4.0	2.7
10 × 20	0.4	1.5	3.3	4.8	3.7	2.6
10 × 30	0.4	1.3	3.1	4.5	3.3	2.4
12 × 12	0.5	1.6	3.5	5.0	4.1	2.8
12 × 18	0.4	1.4	3.2	4.6	3.5	2.5
12 × 24	0.4	1.3	3.0	4.3	3.2	2.3
12 × 36	0.4	1.2	2.9	4.1	2.9	2.2
15 × 15	0.4	1.3	3.1	4.5	3.3	2.4
15 × 22	0.4	1.2	2.9	4.1	2.9	2.2
15 × 30	0.3	1.1	2.7	3.9	2.6	2.0
15 × 45	0.3	1.0	2.6	3.6	2.4	1.9
18 × 18	0.4	1.2	2.9	4.1	2.9	2.2
18 × 28	0.3	1.0	2.6	3.7	2.4	1.9
18 × 36	0.3	0.9	2.5	3.5	2.2	1.8
18 × 54	0.3	0.8	2.3	3.3	2.0	1.7
24 × 24	0.3	0.9	2.5	3.5	2.2	1.8
24 × 36	0.3	0.8	2.3	3.2	1.9	1.6
24 × 48	0.2	0.7	2.2	3.0	1.7	1.5
24 × 72	0.2	0.7	2.0	2.9	1.6	1.4
30 × 30	0.2	0.8	2.2	3.1	1.8	1.6
30 × 45	0.2	0.7	2.0	2.9	1.6	1.4
30 × 60	0.2	0.6	1.9	2.7	1.4	1.3
30 × 90	0.2	0.5	1.8	2.6	1.3	1.2
36 × 36	0.2	0.7	2.0	2.9	1.6	1.4
36 × 54	0.2	0.6	1.9	2.6	1.3	1.2
36 × 72	0.2	0.5	1.8	2.5	1.2	1.2
36 × 108	0.2	0.5	1.7	2.3	1.1	1.1
42 × 42	0.2	0.6	1.9	2.6	1.4	1.3
42 × 64	0.2	0.5	1.7	2.4	1.2	1.1
42 × 84	0.2	0.5	1.6	2.3	1.1	1.1
42 × 126	0.1	0.4	1.6	2.2	1.0	1.0
48 × 48	0.2	0.5	1.8	2.5	1.2	1.2
48 × 72	0.2	0.4	1.6	2.3	1.0	1.0
48 × 96	0.1	0.4	1.5	2.1	1.0	1.0
48 × 144	0.1	0.4	1.5	2.0	0.9	0.9

[a] Add to attenuation of bare sheet metal ducts.

Source: 1999 ASHRAE *Applications Handbook*, © American Society of Heating, Refrigerating and Air Conditioning Engineers, Inc., www.ashrae.org.

TABLE 17.4 Sound Attenuation in Straight Unlined Round Ducts

	Attenuation by Octave-Band Center Frequency, dB/ft						
Diameter, in.	63 Hz	125 Hz	250 Hz	500 Hz	1000 Hz	2000 Hz	4000 Hz
$D \leq 7$	0.03	0.03	0.05	0.05	0.10	0.10	0.10
$7 < D \leq 15$	0.03	0.03	0.03	0.05	0.07	0.07	0.07
$15 < D \leq 30$	0.02	0.02	0.02	0.03	0.05	0.05	0.05
$30 < D \leq 60$	0.01	0.01	0.01	0.02	0.02	0.02	0.02

Source: 1999 ASHRAE *Applications Handbook*, © American Society of Heating, Refrigerating and Air Conditioning Engineers, Inc., www.ashrae.org.

TABLE 17.5 Insertion Loss for Acoustically Lined Round Ducts with 1-in. Lining[a]

	Insertion Loss by Octave-Band Center Frequency, dB/ft							
Diameter, in.	63 Hz	125 Hz	250 Hz	500 Hz	1000 Hz	2000 Hz	4000 Hz	8000 Hz
6	0.38	0.59	0.93	1.53	2.17	2.31	2.04	1.26
8	0.32	0.54	0.89	1.50	2.19	2.17	1.83	1.18
10	0.27	0.50	0.85	1.48	2.20	2.04	1.64	1.12
12	0.23	0.46	0.81	1.45	2.18	1.91	1.48	1.05
14	0.19	0.42	0.77	1.43	2.14	1.79	1.34	1.00
16	0.16	0.38	0.73	1.40	2.08	1.67	1.21	0.95
18	0.13	0.35	0.69	1.37	2.01	1.56	1.10	0.90
20	0.11	0.31	0.65	1.34	1.92	1.45	1.00	0.87
22	0.08	0.28	0.61	1.31	1.82	1.34	0.92	0.83
24	0.07	0.25	0.57	1.28	1.71	1.24	0.85	0.80
26	0.05	0.22	0.53	1.24	1.59	1.14	0.79	0.77
28	0.03	0.19	0.49	1.20	1.46	1.04	0.74	0.74
30	0.02	0.16	0.45	1.16	1.33	0.95	0.69	0.71
32	0.01	0.14	0.42	1.12	1.20	0.87	0.66	0.69
34	0	0.11	0.38	1.07	1.07	0.79	0.63	0.66
36	0	0.08	0.35	1.02	0.93	0.71	0.60	0.64
38	0	0.06	0.31	0.96	0.80	0.64	0.58	0.61
40	0	0.03	0.28	0.91	0.68	0.57	0.55	0.58
42	0	0.01	0.25	0.84	0.56	0.50	0.53	0.55
44	0	0	0.23	0.78	0.45	0.44	0.51	0.52
46	0	0	0.20	0.71	0.35	0.39	0.48	0.48
48	0	0	0.18	0.63	0.26	0.34	0.45	0.44
50	0	0	0.15	0.55	0.19	0.29	0.41	0.40
52	0	0	0.14	0.46	0.13	0.25	0.37	0.34
54	0	0	0.12	0.37	0.09	0.22	0.31	0.29
56	0	0	0.10	0.28	0.08	0.18	0.25	0.22
58	0	0	0.09	0.17	0.08	0.16	0.18	0.15
60	0	0	0.08	0.06	0.10	0.14	0.09	0.07

[a] Add to attenuation of bare sheet metal ducts.
Source: 1999 ASHRAE *Applications Handbook*, © American Society of Heating, Refrigerating and Air Conditioning Engineers, Inc., www.ashrae.org.

TABLE 17.6 Insertion Loss for Acoustically Lined Round Ducts with 2-in. Lining[a]

	Insertion Loss by Octave-Band Center Frequency, dB/ft							
Diameter, in.	63 Hz	125 Hz	250 Hz	500 Hz	1000 Hz	2000 Hz	4000 Hz	8000 Hz
6	0.56	0.80	1.37	2.25	2.17	2.31	2.04	1.26
8	0.51	0.75	1.33	2.23	2.19	2.17	1.83	1.18
10	0.46	0.71	1.29	2.20	2.20	2.04	1.64	1.12
12	0.42	0.67	1.25	2.18	2.18	1.91	1.48	1.05
14	0.38	0.63	1.21	2.15	2.14	1.79	1.34	1.00
16	0.35	0.59	1.17	2.12	2.08	1.67	1.21	0.95
18	0.32	0.56	1.13	2.10	2.01	1.56	1.10	0.90
20	0.29	0.52	1.09	2.07	1.92	1.45	1.00	0.87
22	0.27	0.49	1.05	2.03	1.82	1.34	0.92	0.83
24	0.25	0.46	1.01	2.00	1.71	1.24	0.85	0.80
26	0.24	0.43	0.97	1.96	1.59	1.14	0.79	0.77
28	0.22	0.40	0.93	1.93	1.46	1.04	0.74	0.74
30	0.21	0.37	0.90	1.88	1.33	0.95	0.69	0.71
32	0.20	0.34	0.86	1.84	1.20	0.87	0.66	0.69
34	0.19	0.32	0.82	1.79	1.07	0.79	0.63	0.66
36	0.18	0.29	0.79	1.74	0.93	0.71	0.60	0.64
38	0.17	0.27	0.76	1.69	0.80	0.64	0.58	0.61
40	0.16	0.24	0.73	1.63	0.68	0.57	0.55	0.58
42	0.15	0.22	0.70	1.57	0.56	0.50	0.53	0.55
44	0.13	0.20	0.67	1.50	0.45	0.44	0.51	0.52
46	0.12	0.17	0.64	1.43	0.35	0.39	0.48	0.48
48	0.11	0.15	0.62	1.36	0.26	0.34	0.45	0.44
50	0.09	0.12	0.60	1.28	0.19	0.29	0.41	0.40
52	0.07	0.10	0.58	1.19	0.13	0.25	0.37	0.34
54	0.05	0.08	0.56	1.10	0.09	0.22	0.31	0.29
56	0.02	0.05	0.55	1.00	0.08	0.18	0.25	0.22
58	0	0.03	0.53	0.90	0.08	0.16	0.18	0.15
60	0	0	0.53	0.79	0.10	0.14	0.09	0.07

[a] Add to attenuation of bare sheet metal ducts.
Source: 1999 ASHRAE *Applications Handbook*, © American Society of Heating, Refrigerating and Air Conditioning Engineers, Inc., www.ashrae.org.

Equation (17.2) yields an attenuation of only 0.5 dB for a cross-sectional area change of $A_1/A_2 = 2$ or $A_2/A_1 = 0.5$ and that of 2 dB for a 1 : 4 or 4 : 1 change. Since large abrupt changes in duct cross-sectional area do not occur very often for aerodynamic reasons, the attenuation attributable to duct cross-sectional area changes usually encountered in HVAC duct design is very small.

Sound Attenuation by Elbows

When sound propagating along a duct encounters an elbow, some of the sound is reflected back in the direction from which it was coming, some is dissipated, and some continues to propagate along the duct path. The fraction of sound energy that is reflected or dissipated determines the attenuation. The attenuation is a function of frequency and size of the elbow. The attenuation is also impacted by the type of elbow (mitered, mitered with vanes, and radiused) and the presence (or absence) of sound-absorbing lining in the duct (or on the turning vanes). Mitered elbows with vanes and radiused elbows tend to transmit more higher frequency energy around the bend than mitered elbows without vanes and so they provide less attenuation for the duct path. However, they yield lower pressure drop and therefore are commonly used. Tables 17.7–17.9 present the estimated sound attenuation for various elbow types.

TABLE 17.7 Insertion Loss of Unlined and Lined Rectangular Elbows without Turning Vanes

	Insertion Loss, dB	
	Unlined Elbows	Lined Elbows
$fw < 1.9$	0	0
$1.9 \le fw < 3.8$	1	1
$3.8 \le fw < 7.5$	5	6
$7.5 \le fw < 15$	8	11
$15 \le fw < 30$	4	10
$fw > 30$	3	10

Note: $fw = f \times w$, where f = center frequency, kHz, and w = width, in.
Source: 1999 ASHRAE *Applications Handbook*, © American Society of Heating, Refrigerating and Air Conditioning Engineers, Inc., www.ashrae.org.

TABLE 17.8 Insertion Loss of Unlined and Lined Rectangular Elbows with Turning Vanes

	Insertion Loss, dB	
	Unlined Elbows	Lined Elbows
$fw < 1.9$	0	0
$1.9 \le fw < 3.8$	1	1
$3.8 \le fw < 7.5$	4	4
$7.5 \le fw < 15$	6	7
$fw > 15$	4	7

Note: $fw = f \times w$, where f = center frequency, kHz, and w = width, in.
Source: 1999 ASHRAE *Applications Handbook*, © American Society of Heating, Refrigerating and Air Conditioning Engineers, Inc., www.ashrae.org.

TABLE 17.9 Insertion Loss of Unlined Round Elbows

	Insertion Loss, dB
$fw < 1.9$	0
$1.9 \le fw < 3.8$	1
$3.8 \le fw < 7.5$	2
$fw > 7.5$	3

Note: $fw = f \times w$, where f = center frequency, kHz, and w = width, in.
Source: 1999 ASHRAE *Applications Handbook*, © American Society of Heating, Refrigerating and Air Conditioning Engineers, Inc., www.ashrae.org.

Prefabricated Sound Attenuators

Prefabricated sound-attenuating devices (duct silencers) are available from a variety of manufacturers in a variety of styles, configurations, and constructions to fit virtually every HVAC system application and to meet every sound attenuation requirement. The sound-absorptive media may be conventional dissipative materials such as glass fiber, mineral wool, or nylon wool covered by a perforated metal facing sheet to provide physical protection for the fibrous sound-absorbing material from erosion by the turbulent flow. For low-velocity flows the sound-dissipating material may be protected only by a thin surface layer of flow-resistive facing such as applied on the surface of duct liners. For special applications, to prevent any fibrous material from getting into the air stream, the fill material can be sealed in thin plastic bagging. This typically will slightly increase the acoustical attenuation at specific low and midfrequencies and diminish it substantially at high frequencies compared to unfaced fill. Special construction details are typically required to prevent the film from sealing the holes in the perforated metal protective facing and to avoid chafing of the film on sharp edges formed on the back of the perforated metal in the punching process. Detailed information on the design and prediction of dissipative silencers is given in Chapter 9. There are also silencers without traditional dissipative fill but with special acoustically reactive surfaces lining the air channels which remove acoustical energy from the air stream.

Basic silencers have a straight-through air path with aerodynamic inlet and discharge geometry to help minimize pressure losses which are greatest at the flow transition points. Silencers are also available with special flow configurations for special applications. For HVAC system applications, elbow configuration silencers are particularly notable since these can help to avoid difficult flow conditions that could otherwise exist or even be caused by aerodynamically poor application of a straight silencer.

Manufacturers' information should be used for the prediction of the sound attenuation, pressure drop, and flow-generated noise. For a given application there are typically several silencers that might be able to provide the desired acoustical performance. The noise control and HVAC design engineers must select one that also yields a suitably low pressure drop and trade-offs will need to be considered between the length and the resistance class of the silencer. For most typical HVAC system applications the pressure drop across the silencer should be limited to about 0.30 in. water gauge (wg). The pressure loss can be higher, but the designer needs to be sure the extra pressure loss will not have undesirable impacts on the system. The energy consumed to overcome the pressure drop of the silencer should be considered in deciding what pressure loss is acceptable. Over the lifetime of the system, significant energy cost savings will result from having a silencer that has a particularly low pressure drop. The savings may be much more than the extra initial cost of the lower pressure drop model. Silencers should not be placed in the duct just upstream of a fan to avoid having the turbulent flow from the tail end of the baffles interact with the fan blade, which will increase the fan's broadband and blade passage tone noise.

Ideally, the airflow entering and leaving the silencer should be straight and smooth to approach the conditions under which the sound attenuation, pressure drop, and flow noise of the silencer are tested in accordance with ASTM E-477 or ISO 7235. In the field, such ideal conditions seldom occur, and there is some degree of excess pressure drop beyond the catalogued value for the application due to system effects. The system designer needs to consider these when making pressure drop predictions. To the extent that the silencers are placed in positions where the inflow is distorted and turbulent, there will be extra pressure drop. Figure 17.1 presents some common flow configurations and the associated extra pressure drop multiplier to be applied to the catalogued silencer pressure loss.

Because of the high velocity flows through the narrow silencer channels and the imperfect conversion of velocity pressure to static pressure at the discharge, turbulence is generated in the flow through silencers and this creates flow noise. The manufacturers typically tabulate the flow-generated noise of their silencers at various face velocities. The total flow-generated sound power is a function of the face velocity and the area of the silencers, and the noise generated by the silencer will typically be published for various face velocities and for a specific cross-sectional area. This data must be adjusted for the cross-sectional size of the silencer actually used when one predicts the flow-generated noise by adding $10 \log A_1/A_0$ to the published data (where A_1 is the actual silencer area and A_0 is the area that is the basis for the presented data, in consistent units). The noise generated by the silencer becomes another source of noise that propagates along the duct and needs to be addressed. The closer the silencer is placed to the receiving space and the quieter the receiving space, the more care needs to be taken in controlling flow-generated noise because there is less opportunity to attenuate it before it reaches the receiving space. For duct systems serving spaces where the noise goal is moderate (perhaps NC-35 to NC-40; NC = noise criterion) silencers located near the occupied space (such as on the room-side of a terminal box) typically need to be sized for less about 0.10 in. wg pressure drop. Where the noise goal is more stringent, the pressure loss through the silencer

DUCT ELEMENT	SILENCER SYSTEM EFFECT FACTOR DUCT ELEMENT ON... SILENCER INLET	SILENCER DISCHARGE
TRANSITIONS		
$7\frac{1}{2}$ degrees per side		
Distance of transition from silencer		
$D = i$	1.0	1.0
$D = 2$	1.1	1.1
$D = 3$	1.2	1.1
25 degrees per side		
Distance of transition from silencer		
$D = i$	1.3	1.1
$D = 2$	1.6	1.1
$D = 3$	1.8	1.1
45 degrees per side		
Distance of transition from silencer		
$D = i$	1.7	1.1
$D = 2$	1.9	1.1
$D = 3$	2.0	1.1
ELBOW-RADIUS TYPE		
Distance of radius elbow from silencer		
$D = 0$	1.2	1.4
$D = 1$	1.1	1.2
ELBOW-MITERED TYPE WITH SHORT TURNING VANES		
Distance of mitered elbow from silencer		
$D = 0$	1.2	1.1
$D = 1$	1.2	1.1
$D = 2$	1.2	1.2
ELBOW-MITERED TYPE WITH NO TURNING VANES		
Distance of mitered elbow from silencer		
$D = 0$	1.2	2.9
$D = i$	1.0	1.8
$D = 2$	1.1	1.4
ABRUPT ENTRY OR EXIT		
Smooth inlet or discharge		
Distance of entry or exit from silencer		
$D = 0$	1.1	1.8
$D = i$	1.0	1.4
$D = 2$	1.0	1.1
$D = 3$	1.0	1.0
ABRUPT ENTRY OR EXIT		
Sharp inlet or discharge		
Distance of entry or exit from silencer		
$D = 0$	1.2	2.0
$D = 1$	1.1	1.5
$D = 2$	1.0	1.2
$D = 3$	1.0	1.0
CENTRIFUGAL FAN		
Distance of centrifugal fan from silencer		
$D = 0$	1.5	2.0
$D = 1$	1.2	1.7
$D = 2$	1.1	1.5
$D = 3$	1.0	1.2
AXIAL FAN		
Distance of axial fan from silencer		
$D = 0$	1.5	2.0
$D = i$	1.2	1.7
$D = 2$	1.1	1.5
$D = 3$	1.0	1.2

D is the diameter of round duct or equivalent diameter of rectangular duct.

FIGURE 17.1 Factor by which catalogue silencer pressure loss is multiplied for various applications. (Reproduced with permission from Vibro-Acoustics.)

needs to be commensurately lower. When silencers are located near the fans, at the beginning of systems, the noise of the fan on the building side of the silencer will often still be substantially higher than the flow-generated noise of the silencer (if selected for reasonable pressure loss), so that flow noise is not of concern. The lower the noise goal, the more carefully this needs to be checked.

Poorly selected and positioned silencers, which produce excessive pressure drop, can cause more noise problems than they solve.

Sound Attenuation by Plenums

Plenums in duct systems can often provide significant sound attenuation for the ducted path. The extent of the attenuation depends upon the size of the plenum compared to the connecting ducts, the orientation of the inlets and outlets, and the absorptivity of the inner walls. Equations (17.3)–(17.5) as applied to Fig. 17.2 provide a method for estimating the attenuation provided by plenums:

$$\mathrm{TL} = -10\log_{10}\left[S_{\text{out}}\left(\frac{Q\cos\theta}{4\pi r^2} + \frac{1-\alpha_A}{S\alpha_A}\right)\right] \tag{17.3}$$

where (refer to Fig. 17.2)

where TL = transmission loss, dB

S_{out} = area of outlet section of plenum, ft^2

S = total inside surface area of plenum minus inlet and outlet area, ft^2

r = distance between centers of inlet and outlet sections of plenum, ft

Q = directivity factor, which may be taken as 4

α_A = average absorption coefficient of the plenum lining

θ = angle of vector representing r to long axis l of plenum

The average absorption coefficient α_A of the plenum lining is

$$\alpha_A = \frac{S_1\alpha_1 + S_2\alpha_2}{S} \tag{17.4}$$

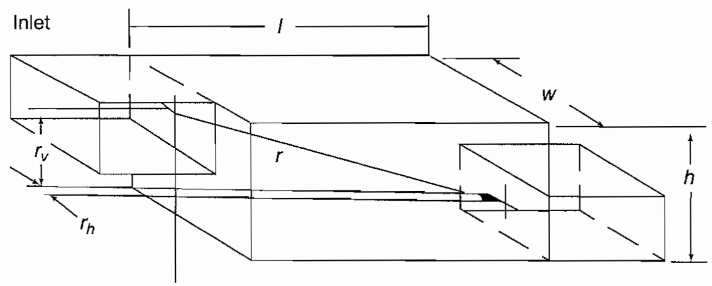

FIGURE 17.2 Schematic of plenum chamber. *Source*: 1999 ASHRAE *Applications Handbook*, © American Society of Heating, Refrigerating and Air Conditioning Engineers, Inc., www.ashrae.org.

where α_1 = sound absorption coefficient of any bare or unlined inside surfaces of plenum

S_1 = surface area of bare or unlined inside surface of plenum, ft^2

α_2 = sound absorption coefficient of any acoustically lined inside surfaces of plenum

S_2 = surface area of acoustically lined inside surface of plenum, ft^2

The value of cos θ is obtained from

$$\cos\theta = \frac{l}{r} = \frac{l}{(l^2 + r_v^2 + r_h^2)^{0.5}} \tag{17.5}$$

where l = length of plenum, ft

r_v = vertical offset between axes of plenum inlet and outlet, ft

r_h = horizontal offset between axes of plenum inlet and outlet, ft

The precision of plenum insertion loss predictions is generally not considered to be very good, and research is being conducted currently to improve the accuracy of the predicted attenuation of these duct elements. The results of the above equations are only valid where the wavelength of sound is small compared to the characteristic dimensions of the plenum. Equation (17.3) is not valid below the cutoff frequency of the entering and exiting ducts, given as

$$f_{\text{co}} = \frac{c_0}{2a} \quad \text{for rectangular ducts}$$

and

$$f_{\text{co}} = \frac{0.586c_0}{d} \quad \text{for circular ducts}$$

where f_{co} = cutoff frequency, Hz

c_0 = speed of sound in air, m/s

a = larger cross-sectional dimension of duct, m

d = diameter of duct, m

End-Reflection Loss

When sound propagating along ducts reaches an abrupt change in cross-sectional area (such as the termination of a duct system at a diffuser or grille) and there is no disturbance of the sound field as it makes the transition, some low-frequency sound reflects back from the point of the abrupt change and does not propagate on toward the receivers of concern. The end-reflection loss is a function of the size of the termination compared with the acoustical wavelength and the specific location of the duct termination within the room. Typical values of end reflections are given in Table 17.10. Note that these are for idealized conditions. If there is a grille or diffuser at the termination of the duct system or if the grille or diffuser is not in the middle of a large plane (like the ceiling) but is in a two- or three-dimensional corner of the room, the end reflection will be lower. For each factor that deviates

TABLE 17.10 Duct End-Reflection Loss

Duct Diameter, in.	End Reflection Loss by Octave-Band Center Frequency, dB 63 Hz	125 Hz	250 Hz	500 Hz	1000 Hz	2000 Hz
		Duct Terminated in Free Space				
6	20	14	9	5	2	1
8	18	12	7	3	1	0
10	16	11	6	2	1	0
12	14	9	5	2	1	0
16	12	7	3	1	0	0
20	10	6	2	1	0	0
24	9	5	2	1	0	0
28	8	4	1	0	0	0
32	7	3	1	0	0	0
36	6	3	1	0	0	0
48	5	2	1	0	0	0
72	3	1	0	0	0	0
		Duct Terminated Flush with Surface				
6	18	13	8	4	1	
8	16	11	6	2	1	
10	14	9	5	2	1	
12	13	8	4	1	0	
16	10	6	2	1	0	
20	9	5	2	1	0	
24	8	4	1	0	0	
28	7	3	1	0	0	
32	6	2	1	0	0	
36	5	2	1	0	0	
48	4	1	0	0	0	
72	2	1	0	0	0	

Source: 1999 ASHRAE *Applications Handbook*, © American Society of Heating, Refrigerating and Air Conditioning Engineers, Inc., www.ashrae.org.

from the ideal case, one might consider the effective duct emitting area to be 4 times the actual duct size when entering the chart.

Note that end-reflection losses are not limited to the duct terminations but can be a useful technique within a ducted system to get low-frequency attenuation, for instance where a duct abruptly enters a large highly sound absorptive plenum volume.

Room Effect

Room effect is the translation of the sound power emitted into the room from the duct system to the sound pressure level that results in the space at a given location. The process of predicting the sound pressure level from the sound power level is treated in detail in Chapter 7.

The classical method to relate the sound pressure that results in a room to the sound power emitted from a source is modeled by a point sound source for small-size sources, such as round or rectangular diffusers, and by a line sound source in the case of strip diffusers or duct breakout. Note that the amplitude of the reverberant sound field, which dominates at large distances from the source, is independent of the nature of the source. However, the amplitude of the direct sound, which dominates in the vicinity of the sound source, strongly depends on how the sound energy spreads from the source.

For a point sound source radiating into the room the sound pressure level at a distance r (resulting from the power-based addition of the direct and reverberant fields) is given in the equation

$$L_p(r) = L_w + 10 \log_{10}\left(\frac{Q}{4\pi r^2} + \frac{4}{R}\right) \tag{17.6}$$

where L_w = source sound power level, dB re 10^{-12}W
L_p = sound pressure level, dB re 2×10^{-5}N/m^2
R = room constant, = $S\alpha_A/(1-\alpha_A)$, m^2
S = total room absorption, m^2
α_A = average absorption coefficient of room surfaces
r = source–receiver distance, m
Q = inverse of fraction of sphere to which sound energy radiates

For a case where there is only one source of concern for design, using this equation is simple and sufficient. However, where there are multiple noise sources such as various diffusers or grills with close to the same noise emission level and producing close to the same noise level at the receiver position, some way to adjust the room effect for the multiple diffusers is needed. This might be done by adjusting the room effect by 10 log N decibels, where N is the effective number of outlets contributing to the sound at the critical receiver location. Other, more sophisticated, methods based of sound propagation modeling in rooms presented in Chapter 7 may be used when dealing with special situations.

17.2 FLOW NOISE IN DUCTED SYSTEMS

The noise generated by flow in duct systems is a concern for noise transmission inside the duct along the duct path and that radiated from the outside surface of the duct. Noise generated at particular fittings or duct elements can be estimated in accordance with the methods presented in Chapter 15. Flow-generated noise propagates down the ducts just like noise from any other sources in the duct system. It is typically in the mid- and higher frequency range and thus is relatively easily attenuated by dissipative treatments such as silencers or lining. When attenuating elements do not exist in the ductwork between the source and the occupied space, this noise can become a concern.

TABLE 17.11 Recommended Airflow Velocities in Lined Duct Systems[a,b]

	Airflow Velocities (fpm) Consistent with Indicated Noise Criterion (NC) through Net Free Area of Duct Section or Device							
	NC 15		NC 20		NC 25		NC 30	
Duct Element or Device	Supply	Return	Supply	Return	Supply	Return	Supply	Return
Terminal device[c] ($\frac{1}{2}$in. minimum slot width)	250	300	300	360	350	420	425	510
First 8–10 ft of duct	300	350	360	420	420	490	510	600
Next 15–20 ft of duct	400	450	480	540	560	630	680	765
Next 15–20 ft of duct	500	570	600	685	700	800	850	970
Next 15–20 ft of duct	640	700	765	840	900	980	1080	1180
Next 15–20 ft of duct	800	900	960	1080	1120	1260	1360	1540
Maximum within space[b]	1000	1100	1200	1320	1400	1540	1700	1870

Note: Fan noise must be considered separately. Reduce duct velocities (not diffuser/grille velocities) by 20% if ductwork is unlined.

[a] All ducts with 1-in.-thick internal sound absorptive lining.

[b] Above mineral fiber panel ceiling. Lower velocities 20% if open or acoustically transparent ceiling.

[c] No dampers, straighteners, deflectors, equalizing grids, etc. behind terminal devices.

The following guidelines are offered for duct sizing based on the location, type, and class of ductwork:

- <3000 feet per minute (fpm) velocity in round ducts in mechanical rooms and shafts,
- <2500 fpm velocity in rectangular ducts in mechanical rooms and shafts,
- <2000–2500 fpm velocity in the ceiling of occupied spaces with mineral fiber ceiling for NC-35 to NC-40 goal,
- <1500–2000 fpm velocity in the ceiling of occupied spaces with open or acoustically transparent ceiling for NC-35 to NC-40 goal,
- <1500 fpm velocity in larger final distribution ducts serving NC-35 to NC-40 spaces,
- <a friction rate (pressure loss rate) of 0.10 in. wg/100 ft of duct run in smaller final duct distribution for NC-40, and
- <a friction rate (pressure loss rate) of 0.08 in. wg/100 ft of duct run in smaller final duct distribution for NC-35.

Airflow velocity guidelines for the design of special low noise spaces (typically NC-30 and lower) are presented in Table 17.11 for lined duct systems.

17.3 SYSTEM DESIGN FOR ESPECIALLY QUIET SPACES

The lower the noise goal for a particular space, the more carefully the duct arrangement needs to be considered from the air balance and aerodynamic

standpoints. In particular, the duct system needs to be designed to be as naturally balanced as possible. That is, if the system is turned on, the airflow naturally delivered from each outlet would match the desired airflow with little or no damper throttling to control the flow. Creating systematically branching duct arrangements to an array of diffusers or grilles is typically a good approach. There should be suitably long straight ducts between the branches for the flow to straighten out and divide, as desired at the next branch. However, not all buildings and conditions can accommodate this design concept. Often there is a need to have a series of diffusers or branches to diffusers off the side of a large main duct. Having at least a modest length (a duct diameter) of straight duct run out to the diffuser is always preferred to improve the airflow presentation to the back of the diffuser and to create a more desirable position for a damper that can be used to control the flow at a point that is away from the diffuser. For these cases, it is often best to have the main duct that feeds the diffusers remain a constant size so that the pressure drop along the main "header" duct becomes small and the flow distribution is controlled by the pressure drop of the runouts. To achieve a naturally balanced design, it is generally best to have the diffusers and grilles be in a reasonably cohesive grouping rather than be widely spaced out.

It is recommended to avoid having a tight cluster of diffusers serving a critical space and then a long "tail" duct extending downstream, because to balance the system, it will be necessary to throttle dampers near the diffusers serving the critical space, and this will cause noise to be generated.

Dampers should be provided in duct systems as needed to control the flow, but they must be located sufficiently far from the terminal devices so that the turbulence and noise they generate can be sufficiently attenuated before it reaches the occupied space. For especially quiet systems, dampers should not be placed at or near the face of the diffusers and grilles. It is essential to use dampers well back in the duct system to adjust for major deviations from a natural air balance design.

The airflow velocity near diffusers and grilles needs to be appropriately slow to avoid excessive noise generation. As one moves back in the duct system away from the critical space, flow velocities can progressively increase. Ideally, the velocities would step down in moving toward the critical space in a manner that is consistent with the desired systematic branching pattern. The best correlation between airflow velocities and the noise resulting in the space of interest is for noise from grilles and diffusers in the room and for the ducts closest to the room. The correlation between noise reaching the space of interest and the flow velocity becomes less direct as one moves further into the duct system, away from the receiving space. Thus, there is not much room for compromise in velocities close to the occupied space, but there may be room for compromise from an ideal design at greater distances from the occupied space.

Table 17.11 presents suggested velocities in duct systems serving quiet spaces to help ensure achieving particular noise goals with acoustically lined ductwork. These suggested flow velocities generally assume that the duct configuration will be only average in terms of its aerodynamics. If very desirable airflow geometry is achieved, somewhat higher velocities can be allowed. The suggested velocities through the net free area of the diffusers and grilles, given in Table 17.11, assumes a nominal slot width of about 1/2 in. To the extent that wider slot widths are used, higher velocities can be allowed for a given noise goal. Typically, there might be an allowable increase in slot velocity of 15–20% for each doubling of the nominal slot width up to about 2-in.-wide slots. Special nozzle-type diffusers are available to operate more quietly so that they can throw the air further for a given noise level. The manufacturer's noise data should be reviewed for special diffuser applications, being sure that the noise generation is adjusted from the conditions under which the devices are tested to the actual conditions of use. Because, at the indicated velocities, it is difficult to blow the air very far, for quiet systems, supply air is often delivered using a distributed array of diffusers at the ceiling rather than from the sidewalls of a space. This is not to say that sidewall blow applications need to be avoided; they just need to be limited to covering a small zone at the sides of the space rather than trying to condition the entire space from this position. Using a combination of ceiling diffusers and sidewall blow diffusers can be a useful technique to divide the main ducts into smaller pieces that will fit through the building more easily than handling all the airflow in fewer large ducts. Note that to help fit ducts into buildings it is often better to avoid having diffusers or grilles directly off the sides of a main duct because the entire airflow in the main duct will have to run at a very low velocity and this duct will be very large. However, in applications where there is ample space for large ducts or where ducts are exposed, this may be a simple, neat, and clean approach to the design. Developing the duct distribution in a systematic branching pattern naturally allows the ducts that have the large airflow quantity to be sized at a higher velocity, which helps them fit in the building more easily. For quiet systems, the space required to handle the airflow at the desired velocities can be considerable and this can translate into requiring more building volume in which to maneuver the ducts. Considering the system design concept and velocities early in the design can allow the building to be more economical from the standpoint of the sheet metal that is used and the building volume that is constructed. Not considering the duct system requirements early in the design may result in an undesirable compromise in the design and/or the noise levels that can be achieved.

Note that about a 20% change in velocity is generally associated with a 5-NC point change in noise level in the occupied spaces. Thus, a compromise of increasing the airflow velocities in a project design by 20% will generally increase the noise by about 5 NC points. Also, lowering the noise level by about 5 NC points requires about 20% lower velocities; this translates into only about 10–15% increase in the dimensions and surface area of round and (reasonably square) rectangular ducts. Increasing the noise goal by 5 NC points will only save about 10–15% of the sheet metal cost.

The airflow velocity guidelines in Table 17.11 assume that there will be lining in the duct system, and this is generally recommended to control the noise generated by flow in the ducts at fittings and unexpected flow obstacles in systems that are to be especially quiet. For lower noise goals, more things need to be

done properly in the implementation of the design and there is less margin for error. If the ductwork does not have lining, it is suggested that the velocities in the ductwork (not at the diffusers and grilles) be about 20% lower than indicated to allow about a 5-dB margin for the lack of attenuation in the duct path.

17.4 DIFFUSER AND GRILLE SELECTION

The airflow velocities for low-noise spaces presented in Table 17.11 are only guidelines which include a number of assumptions, including that the nominal slot width is about 1/2 in. and the ductwork leading to the diffuser is only nominally configured. This also includes assumptions regarding the room effect and the number of diffusers that are contributing to the sound field at the receiving position. Note that the larger the room, the more likely it is that diffusers will be more numerous (and hence there will be more sources of noise), but in this case, it is also more likely that the diffusers will be further from the receiver and hence the room effect will be larger. These two factors tend to counter each other so that a single velocity guideline chart can cover a wide range of applications.

Manufacturers often provide data for the noise generated by their diffusers and typically these are boiled down to a single NC rating for the diffuser at a particular flow. Be careful in applying manufacturers' data because they are generated under ideal flow conditions and often include very favorable room effects so that the reported noise levels are as favorable as possible. Also, they typically are reported for one diffuser or for a short section of a linear diffuser where the application may have many more such elements contributing to the noise level at a receiver location. It is necessary to account for the sum of the noise that is generated by multiple diffusers/grilles which reach the receiver as well as to make other adjustments to correct the assumptions in the presented data to match the actual conditions of a project. It is also essential to make adjustments to the ideal flow condition used as the basis for the data to get to the actual applied flow condition. For especially quiet spaces, use of the velocity guidelines may be a preferable approach for establishing the selection parameters for the diffusers and grilles.

The noise produced by dampers needs to be assessed separately from diffuser and grille noise, but having two flow turbulence-producing devices closely spaced in series may add to the noise each device produces by itself.

Displacement ventilation systems which deliver air to the occupied zone through diffusers at the floor can often be very quiet. This is largely because air is introduced to the space in small quantities at any one location and the flow velocity at the diffuser needs to be particularly low for comfort reasons. The result can be a system with little diffuser-generated noise and this can be a favorable design approach for spaces that need to be very quiet.

17.5 NOISE BREAKOUT/BREAK-IN

When ducts containing high levels of noise pass though spaces with low or moderate noise goals, it is necessary to consider whether the noise that transmits out through the surface of the sheet metal duct (called the breakout noise) is suitably controlled. Similarly, when a duct in which the sound field inside has been quieted passes near a noisy piece of mechanical equipment prior to penetrating the mechanical room wall, noise may break into the duct and travel down the duct to a receiving space of concern. To minimize concern for noise breakout/break-in, it is usually best to position the high-insertion-loss elements in the duct system (the silencer) at or very near the penetration of the mechanical room boundary. However, it is not always possible to achieve this goal along with the goal of achieving good aerodynamics for the application of the silencer. Special elbow (or other configuration) silencers can help achieve the goal of the desired position of the silencer for breakout/break-in considerations while avoiding poor flow. This is a very good use of special silencers.

The noise that breaks out of and into ducts can be predicted using Eqs. (17.7) and (17.8), respectively:

$$L_{w(\text{out})} = L_{w(\text{in})} - \text{TL}_{\text{out}} + 10 \log \left(\frac{S}{A}\right) - C \tag{17.7}$$

$$L_{w(\text{in})} = L_{w(\text{out})} - \text{TL}_{\text{in}} - 3 \tag{17.8}$$

where $L_{w(\text{out})}$ = sound power level of sound radiated from outside surface of duct walls, dB
$L_{w(\text{in})}$ = sound power level of sound inside duct, dB
S = surface area of outside sound-radiating surface of duct, in.^{2}
A = cross-sectional area of inside of duct, in.^{2}
TL_{out} = duct breakout transmission loss, dB
C = correction factor as follows for values of $\Delta = \text{TL}_{\text{out}} - 10 \log(S/A)$

Δ	C
$> +10$	0
$+8$ to $+5$	1
$+4$ to $+2$	2
$+1$ to -1	3
-2 to -3	4
-4	5
-5	6
-6	7
-7	8
-8	9
<-9	$-\Delta$

Note: These breakout and break-in equations should not be used where $\Delta < -10$. Also, where Δ is a negative number, the precision of the result is questionable. The value of Δ tends to go negative with relatively long duct sections. This approach does not take into account any dissipative attenuation along the duct path, but at the low frequencies principally of concern for breakout and break-in issues, dissipative attenuation is usually small along the duct path in the length of duct sections for which the approach should be used.

The noise breakout formula can further lead to prediction of the sound pressure level in a receiving space by applying an appropriate room effect and including the sound isolation of any intervening construction. The noise break-in equation will determine the sound power that can then be used as a source level and the propagation of this noise can be traced along the duct system. Treatments for noise breakout/break-in typically include increasing the surface weight of the duct construction, stiffening the duct, applying a flexible mass barrier material on resilient backing (such as a glass fiber mat or foam), or enclosing the duct in gypsum board using a variety of possible details. Prediction of the insertion loss achieved by various types of wrappings is given in Chapter 13. The further the enclosing mass layer is from the duct surface and the heavier the enclosure material, the better this will control low-frequency sound, which is most typically the concern. Circular ducts are inherently stiffer than rectangular ducts made of flat metal sheets, and for this reason, distribution systems using circular ducts are often less prone to breakout/break-in noise problems. Note that there is a particular concern for breakout/break-in noise when glass fiber panel or other acoustically transparent ceilings are used in occupied spaces in buildings. Where there is a solid gypsum board ceiling, breakout noise is naturally less of a concern than where there is a conventional mineral fiber acoustical ceiling.

Ducts that drop out of the bottom of rooftop air-handling units into the ceiling plenums above occupied spaces are a classic case where duct breakout noise is a problem, and this typically is worst when the supply duct discharges directly down into the ducts rather than into a plenum within the unit. Elbow silencers with high-transmission-loss casings can be a convenient method of addressing this problem. If a straight silencer is used and is located well away from the elbow that turns in the ceiling space, there can be a significant amount of duct wall which can radiate noise to the occupied space and may need to be treated. This is discussed further under the rooftop unit section (Section 17.10). Most of the duct enclosure treatments to address this concern are very difficult to install, especially when there is limited space and the building is finished. Whenever possible, designs should be developed which avoid the need for this sort of treatment.

17.6 FANS

Fans are typically the major source of noise emission into duct systems. The various fan types have differing noise spectrum and magnitude characteristics and this is also a function of the duty. Certain fans are aerodynamically better suited for particular flow and pressure applications. This needs to be considered for the full operating range of the application. Many older references, such as older editions of the ASHRAE handbooks, include generic methods to predict the noise generated by fans, and such sources can provide useful guidance in the absence of more specific data from the manufacturer for the fans that are planned. If such data are used, remember that, due to changes in manufacturing methods, modern fans may not be made the same way as the fans used as the basis for the generic prediction methodology. Often new fans are made more economically and produce more noise that older fans. It is best to obtain the noise data for the fan from the prospective manufacturer, tested in accordance with the most current applicable standards. These data should be used as a guide in the selection of the fan and as a point of comparison between candidate fans for an application. In addition, the quietest of the reasonable fans should be selected for a given application. Such a process should help avoid selecting a particularly noisy fan, which could lead to unexpected noise problems or noise control treatment which could unduly burden the system.

The manufacturer's noise emission data for fans are based on a standard test which may or may not closely match the conditions of a particular field

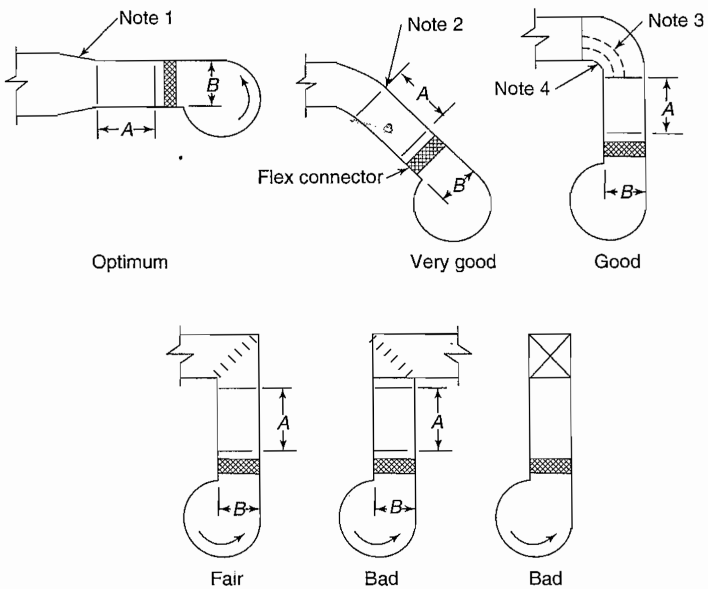

Notes:
1. Slopes of 1 in 7 preferred. Slopes of 1 in 4 permitted below 200 fpm.
2. Dimension *A* should be at least 1.5 times *B*, where *B* is the largest discharge duct dimension.
3. Rugged turning vanes should extend the full radius of the elbow.
4. Minimum 6-in, radius required.

FIGURE 17.3 Various outlet configurations for centrifugal fans and their possible rumble conditions. *Source*: 1999 ASHRAE *Applications Handbook*, © American Society of Heating, Refrigerating and Air Conditioning Engineers, Inc., www.ashrae.org.

application. The noise radiated by the fan into the duct will vary with the particular acoustical impedance of the connected ductwork. Consequently, the actual sound power of the fan that is emitted into a duct system may differ from the manufacturer's data.

Particular care should be given to the inlet and outlet flow conditions for fans. Poor inlet flow can unbalance the flow over a fan wheel, causing performance problems and excess noise generation at the anticipated speed for the application. The fan speed may need to be increased to compensate for unexpected pressure losses and thus generate more noise than expected. Inlet vanes or substantial flow distortion due to flexible connections protruding into the flow can easily cause an increase of noise on the order of 6 dB across the full frequency spectrum. The local airflow velocities on the discharge of fans can be quite high in some regions and probably will not be uniform over the outlet area. This needs to be taken into account in the system design and arrangement. It is often not possible to create ideal flow conditions, but it is important to create at least reasonable flow conditions and to avoid poor flow conditions which can create severe noise problems. Figure 17.3 illustrates some favorable fan discharge conditions as well as conditions that need to be avoided. It is always necessary to consider the flow arrangement on the discharge of a fan or air-handling unit to be sure that the duct and fan geometry work together as well as possible for the condition and, most essentially, to avoid poor conditions. Poor flow conditions at the fans can lead to low-frequency noise generation, either by the fan or due to large-scale turbulence in the ductwork which will drum the duct walls, causing a low-frequency noise problem that can be very difficult to solve.

17.7 TERMINAL BOXES/VALVES

Many HVAC systems serving buildings include a variety of terminal boxes or valves to control the amount of air delivered to the occupied zone. Some boxes are used to vary the airflow to the room in accordance with thermal load. Others provide a constant amount of flow to assure ventilation rates and control zone pressurization. Some boxes incorporate fans to mix plenum air with a variable amount of main system air to maintain a minimum amount of air movement while delivering variable heating/cooling. All of these boxes and valves have in common that they produce a pressure drop from the higher pressure in the main duct system to a low pressure in the final distribution ductwork on the room side of the box. In throttling the pressure from the main to the final distribution ductwork, noise is generated and this noise needs to be considered in the design to meet desirable noise levels in the occupied spaces. The greater the airflow quantity through the box, the greater the noise that is generated. However, the most significant factor is that the noise boxes generate is a strong function of the pressure drop across the valve. Boxes on a system that are near the fans naturally see a higher pressure in the main duct than boxes near the ends of the system, and boxes close to the beginning of the system will generate more noise than comparable boxes located toward the end of the system. Excess static pressure in the main ducts can be a significant factor in noisy systems as the terminal boxes in the system are throttling hard (have large pressure differential across them) to control the excess pressure.

The manufacturers of terminal boxes generally provide noise data for their boxes rated at various flow rates and pressure losses, and these data can be used for noise analysis of the ducted system just as fan noise propagation down the ducts is done. In such an analysis, the pressure loss that is of interest in determining the noise of the box is the actual pressure drop that the box is expected to produce in the field, not the minimum pressure at which the box will satisfactorily control flow or some arbitrary pressure loss that is assigned. Because of airflow control considerations, the boxes in many applications have inlet flow conditions that are reasonably close to the ideal flow condition under which the terminal box is tested for flow and noise. However, if there are adverse flow conditions, the noise generated by the boxes may be higher than the manufacturer's rating.

Noise radiation from the casings of the boxes can also impact the occupied spaces near them, and to enable assessment of this, manufacturers also publish casing radiated noise data. For fan-power boxes, these data include the noise that radiates from the fan out of the plenum air inlet and this can be a significant issue. In some cases it is necessary to provide attenuation for the plenum air inlet to the box. Most moderate-size terminal boxes operating at nominal pressures can be located in the ceilings of occupied spaces where the noise goal is NC-35 or higher when there is a conventional mineral fiber ceiling. Where boxes are in the ceilings of spaces with noise goals more stringent than NC-35, where system pressures are anticipated to be high, and/or where ceilings with lower transmission loss are used, special consideration should be given to the issue of casing radiated noise. In particular, be cautious of exposed box applications or where glass fiber, perforated, or open-slat ceilings are used.

The manufacturer's noise data should be reviewed for verification, but typically the frequency band of concern for flat-plate damper boxes is the 250-Hz octave band; for pneumatic-style boxes, the 500-Hz octave band; and for plunger-style valves, the 1000-Hz octave band. The type of noise control treatments that are applied in the duct systems should ideally be selected to treat the particular noise spectrum that is expected based on the box/valve type that is used.

For systems that utilize terminal boxes/valves it is usually a good idea to try to conceive the main duct system to be able to deliver the design airflow with the minimum overall pressure loss and the minimum differential in pressure arriving at the various boxes in the system. Consider gradually reducing the flow resistance in the main duct as the duct proceeds toward the end of the run and the magnitude of air being handled is reduced. The overall velocity in the duct system is often a significant factor determining the pressure drop from beginning to end, and the design velocities should be as low as reasonably possible. Use aerodynamically favorable fittings. Try to avoid particularly long duct runs by using more vertical shafts in the building to minimize the length of duct runs on the floors served. Where it is possible and acceptable to create ring ducts fed from both ends to serve the floor plate of a building, this can favorably reduce the pressure that is needed in the system. Consideration of these design features can help avoid noise problems and/or minimize the magnitude of attenuation treatments that are needed.

Always be sure that the final setup and balancing have the system operating at the lowest pressure that is consistent with delivering design airflow. This includes making sure that the system pressure cannot be further lowered without jeopardizing the required flow at the extremes of the duct system and making sure that the fan is operating at the lowest speed that will deliver design flow. If there are inlet vanes on the fan to control capacity, they should be nearly fully open when the system is demanding full design flow. The inlet vanes should not be constricting the airflow when the demand is full; if they are, the fan can probably be slowed, which should reduce noise emission.

17.8 MECHANICAL PLANT ROOM SOUND ISOLATION AND NOISE CONTROL

Good space planning is the best way to avoid sound isolation and noise problems at mechanical rooms. Avoid a common wall with a noise-sensitive space that would require a substantial and expensive wall construction. Very high sound isolation walls typically require discontinues in or special protection of the flanking structural paths; such treatments can be cumbersome and expensive. Having a common wall also invites penetration of that wall with ducts and pipes. Since creating a sufficiently tight seal around a single wall that is penetrated can often be difficult and risky, these should be avoided. Creating a buffer zone of less critical space between a mechanical room and noise-sensitive space allows simpler and less costly constructions to provide the desired isolation, and this minimizes the risk of noise leaks at penetrations. It is good practice to position particularly noisy equipment in mechanical rooms away from critical sound-isolating walls to avoid exposure of critical constructions to unnecessarily high levels of noise. Especially avoid locating equipment extremely close to walls where the sound has no opportunity to lose intensity owing to spreading losses.

Building constructions that provide a good deal of sound isolation can be constructed well, but there is always a door into the space, which is a weak sound isolation condition, and the location of doors needs special planning. Certainly it is necessary to avoid doors to mechanical rooms directly from noise-sensitive rooms. To the extent that it is possible to naturally create a double-door entrance vestibule ("noise-lock") to the mechanical room, such as by accessing the room off of a back-of-the-house corridor that is separated with another door from more public space, this is a good idea since good isolation can be reliably achieved with ordinary door construction.

Mechanical plant rooms often contain equipment which radiate relatively high levels of low-frequency noise, and it is necessary to have heavy constructions, such as masonry walls, surrounding the room. Lighter constructions such as gypsum board on stud can be used, but double-wall constructions with a substantial air space between the two sides of the wall will likely be required. Hence, light weight wall construction alternatives may take up more floor space. To the extent that there is auxiliary equipment associated with the main plant equipment that is wall mounted, it is often wise to have a double-wall construction so that minor vibration and structure-borne noise that might get coupled to the inner wall of the mechanical room will not get strongly transmitted to the side of the wall construction in the occupied space that is to be protected.

Creating an air-tight seal, as is always necessary for sound isolation, at the heads of walls can be particularly problematic. Necessary firestopping can be achieved for walls with fibrous packing and coating with intumescent material, but this is not a suitable seal for sound control purposes where the basic construction needs to close within a typical caulk joint of the abutting construction. Closing concrete block construction to the underside of fluted metal deck and beams can be very difficult. It is also difficult to create a seal when concrete block comes up under roof constructions that are sloped for drainage or need to accommodate structural deflection. The seals that are needed under these conditions need to be considered early in the design, and practical methods to accomplish the necessary seal in the field need to be detailed.

Floating concrete floors are sometimes required to separate mechanical spaces from noise-sensitive spaces that are above or below the mechanical room. Prediction of the insertion loss of floating floors is provided in Chapter 11. These constructions consist of a concrete slab (typically 4 in. thick) which is supported above the structural floor on resilient mounts. Systems to accomplish this are available from the various isolation product vendors. These constructions can and do provide effective control of sound transmission through floors, but they take up space that needs to be allocated from the start. They also require careful coordination and implementation in the field in order to function as planned. Floating floors are not generally designed as part of a vibration isolation scheme for plant equipment; their primary use is for airborne sound isolation. Concentrated loads such as from equipment can be accommodated on floated floors with appropriate planning and design of the floated floor, but it can also be acceptable to have such loads supported on small structural piers (housekeeping pedestals) that penetrate through the floated floor. To avoid a sound isolation concern at support points that penetrate the floors, these need to be kept as small as practical and typically complete housekeeping pads are not used. The sizes and positions of support piers need to be carefully coordinated in the field. Rather than use floating floors to provide high-level sound isolation to spaces above or below mechanical rooms, it is sometimes necessary to have special sound-isolating ceilings above or below the mechanical spaces. These can be complex to implement and require special coordination of the building services to avoid or minimize penetrations for supports through the ceiling. The timing of construction of the ceiling relative to installation of the building services needs forethought since it typically cannot follow the usual sequence.

17.9 VIBRATION ISOLATION CONSIDERATIONS FOR BUILDING MECHANICAL SYSTEMS

Technical aspects of isolation of vibration sources are treated in detail in Chapter 13. This section will provide some practical guidance regarding the application of vibration isolation systems and devices to building mechanical systems.

Numerous references, such as the sound and vibration control chapters of the ASHRAE *Applications Handbook*,[1] and vibration isolation equipment vendors provide guidance regarding the application of isolation devices for building equipment, and the reader is referred to such sources for specific isolation selections based on the type of equipment, the speed of the equipment, the location in the building, and the sensitivity of the application. For application to building equipment, the selection of vibration isolators is reduced to identifying the deflection of the isolation element under the static load. The deflection of the isolator under load is related to the natural frequency (the frequency at which resonance occurs) of the isolation system by the equation

$$f_n = 3.13 \left(\frac{1}{d}\right)^{0.5} \tag{17.9}$$

where f_n = isolator natural (resonance) frequency, Hz
d = isolator deflection, in.

Generally, to provide effective isolation, the natural frequency of the isolation system needs to be no more than 0.30–0.10 times the drive frequency (RPM/60) of the equipment. At ratios greater than 0.30 isolation efficiency will be minimal, and at a ratio of 0.70 there is theoretically no isolation at all. Clearly, it is necessary to avoid having the equipment operate at or near the natural frequency of the equipment. There is generally little point in an isolation system that has a ratio of isolation system natural frequency to equipment drive speed smaller than 0.10 since little additional effectiveness is gained for practical installations and the stability of the equipment on the isolation system can be marginal.

Many pieces or equipment are equipped with variable-speed drives and, in this case, it is generally appropriate to select the isolation system for the normal full speed of the equipment. As the equipment slows down and operates closer to the natural frequency of the isolation system, the isolation system will provide less isolation efficiency, but fortunately, the magnitude of the machine vibration force will be reduced at approximately the same rate. So, there are generally no problems with this. The natural frequency of the isolator should typically be no more than about half of the lowest operating frequency of the equipment to prevent operation too close to resonance, but for more difficult applications, this might be as high as 0.7. If it is not feasible to select large deflection springs, sometimes it is necessary to limit the operating range of the equipment to avoid operating too close to the isolation system natural frequency. This possibility should be considered early in the design. In some cases it might be worthwhile to judiciously increase the deflection of the springs to lower the natural frequency to avoid impacting equipment operation and efficiency. However, an isolation system should not be so flexible that it creates instability or operational problems such as with alignment or stress transfer.

Inertia bases are used with many pieces of equipment to lower the center of gravity and to reduce the vibratory movement of the equipment when it is resiliently supported. Movement due to starting torque, resistance to forces created by the static pressure a fan develops, and turbulent flow in large fan systems are also reasons such bases are recommended for equipment. The inertia bases only reduce the motion of the equipment on the isolation system. They do not change the inherent unbalanced forces of the equipment, even though the magnitude of vibratory movement of the equipment on the base will be lower. The vibratory displacement of the base and that of the equipment rigidly mounted on it will be lower because the mass that the forces are now acting on is the combined mass of the equipment and the inertia base compared with the mass of the equipment alone. Note that the inertia base does not change the vibration forces that are transmitted to the building assuming that the deflection of the isolation system remains the same. This is because, for the same static deflection, the springs need to be stiffer to support the additional weight of the equipment plus its inertia base.

In theory, the weight of the inertia base would be determined by the desired reduction of the magnitude of the vibratory movement, but the magnitude of the motion of the equipment is not well known, so it is difficult to tell what mass ratio to use. In practice, the weight of the inertia base for building mechanical equipment is often determined by the weight of concrete fill in a steel frame that approximates the rectangular outline of the equipment footprint (with allowance for fastening), and the depth is determined by the need to make the base suitably stiff. The depth of the base is often related to the length of the base and is typically about $\frac{1}{10}$ to $\frac{1}{12}$ the longest dimension. Experience indicates that for many pieces of mechanical equipment, the base weight that results from this methodology is sufficient to control excessive movement and prevent undue forces from being transmitted to connected pipes and appurtenances.

Spring isolators most typically are manufactured to achieve rated deflections of approximately 1, 2, 3, and 4 in. This means that when the full design load for the spring is applied, the spring will approximately deflect this rated distance, and at this condition, the spring will also achieve other desirable design features such as for lateral stability, horizontal stiffness, and deflection reserve to bottoming out. The rated deflection has nothing to do with the deflection actually achieved in the field under the actual equipment load applied. For example, a spring that has a rated deflection of 1 in. for a 1000-lb load will only deflect 0.10 in. if it is supporting 100 lb. The only thing that is important in terms of the isolation efficiency of the mounting is the actual static deflection that results under the applied load and, in the case of this example, the natural frequency would be determined by 0.1 in. deflection. Isolation devices need to be properly selected to achieve the desired minimum static deflection and hence the desired isolation

efficiency. Underloading an isolator can result in achieving less than the desired isolation efficiency and overloading can cause the spring to collapse (bottom out) so that it provides no isolation at all. If a spring is specified to achieve 1 in. minimum deflection under load, there is only one load that will exactly satisfy the requirement if a spring is selected from a 1-in. rated series of springs, and that is the maximum load that the mount can support; lower loads will achieve less than 1 in. deflection and will not meet the required minimum deflection, and greater loads will overload the spring. To achieve the required minimum deflection in this case, a 2-in. rated deflection spring would need to be used so that as long as it is loaded between half and full load, it will achieve the required minimum deflection. This can cause unnecessary expense for isolators that have substantially more capacity than needed. To clarify the performance desired and to avoid unnecessarily costly springs, it is often better to specify spring deflections of 0.75, 1.5, 2.5, and 3.5 in., as expected from 1,2, 3, and 4-in. rated static deflection springs, respectively, so that there is a reasonable selection range available.

For applications where the weight of the isolated equipment may vary substantially from time to time, such as for a cooling tower or chiller if the water is drained for maintenance, the isolation devices that are used need to incorporate some method to restrain the upward movement of the equipment as the weight is removed because this can put excessive stress on connecting pipes. Equipment that is located outdoors may be exposed to wind and exhibit lateral movement which needs to be restrained. Special travel-limited isolators have been developed for this application which will snub the movement of the equipment under such conditions, typically at about 1/4 in.

Many pieces of equipment need to be specially restrained to avoid damage to the equipment or the building if a seismic event occurs. This applies to many pieces of equipment, whether resiliently mounted or not, but clearly, equipment that is resiliently supported could easily fall off its mounts if there is a seismic event. Seismic restraint of equipment is an entirely separate issue from vibration isolation; it is essentially a structural issue. Isolation and seismic restraint become related because so many pieces of equipment that are resiliently supported need restraint. There are seismic restraints available from vendors which are completely separate devices from vibration isolators. In some cases it is convenient to incorporate seismic restraint into the isolators, and products that do this are available from vibration isolation vendors, but it may not be necessary to use combination devices. Where the equipment has no other point of attachment but the mounting points at which suitable support and restraint can be achieved, a combination device is necessary. It is essential that the seismic restraint not compromise the performance of the vibration isolation system, and this is not an easy task considering the relatively tight installation tolerances that are required for both seismic restraints and vibration isolators. Often isolators with combined seismic restraint can help achieve the desired level of installation more reliably, and this is another benefit that such devices provide.

Electrical connections to vibration isolated equipment need to be made flexible to avoid creating a problematic vibration transmission path to the building structure. These are typically made with either a section of flexible conduit or a special flexible electrical coupling. For small-size equipment and conduits, practical lengths of flexible conduit are effective and sufficient. As the size of the equipment and the connecting conduit increase, the flexibility of these systems may diminish and it may be necessary to use special flexible electrical couplings. The flexible connections should be installed in whatever manner creates a slack condition.

Piping that connects to isolated equipment also needs to avoid creating a vibration transmission path to the building. There are flexible pipe connections available for many applications, but because vibration can travel through the fluid in the pipes (which is often highly incompressible), vibratory energy is often not stopped sufficiently by them. Such connections are best used (or not) based on considerations other than vibration control (e.g., thermal expansion/contraction or alignment). To control vibration transmission to the building via pipes, it is usually necessary to resiliently support the pipes for some prescribed extent, but that extent is not easy to describe and could vary substantially from project to project. Many schemes have been devised to describe the scope of pipe isolation in buildings, such as a prescribed length of pipe or a certain multiple of the pipe diameter, and this is somewhat dependent on the designer's philosophical approach. The fixed length of pipe isolation from a vibration source approach does not account for variations of pipe stiffness based on size. Clearly, a 1-in. pipe for a particular duty is much more flexible over a given distance than a 12-in. pipe for a similar duty. Prescribing the length of isolation in pipe diameters partly addresses this issue, but this approach can be difficult to work with in the field. In practice, there needs to be some compromise between a practical scheme that can be implemented in the field, a system that makes sense economically, and a scheme which will provide the isolation that is needed for the size of pipes and the vibration sources involved. There are many possible approaches to this specification depending upon what is workable and cost effective. There may be a generic scheme that is appropriate for many applications, but this should be carefully considered for each project before finalizing the scheme. The designer should keep in mind that a resilient connection between a pipe and the building structure provides a reduction of the vibratory force only if the local impedance of the supporting structure is high compared to the impedance of the isolation device. Little isolation will be gained if a moderately stiff isolator like a neoprene pad is used to resiliently support a pipe from a lightweight and flexible gypsum board on stud wall.

Classic vibration isolation theory assumes that isolators sit on supports that are infinitely stiff and massive. This is reasonably the case for support conditions at slab-on-grade floors, but this may not be the case for support conditions at all structures above grade. Most isolation application guides take this into account and provide recommendations for a variety of less than perfect support conditions such as on above-grade structures. The implications of structural flexibility on vibration isolation for most above-grade support conditions are rather modest where the structure is reasonably massive (such as a concrete floor) and is suitably strong to support mechanical service equipment. This accommodation involves only slightly softer isolators than would be used on grade, but the isolators are still within the range of conventional products that are economically available. When the supporting structure is particularly lightweight, such as wood frame construction or a simple metal deck roof, special attention needs to be given to the support condition, and it may be necessary to create special load transfer schemes to transfer the load to more substantial points of structure such as columns.

17.10 ROOFTOP AIR CONDITIONING UNITS

Many HVAC systems employ a variety of types of packaged rooftop air conditioning units with circulating fan systems and sometimes with integral compressor/condenser sections. Because such equipment is often noisy and typically supported on a lightweight structure directly above occupied space, this equipment is one of the most common sources of noise problems in buildings. Because of space limitations and the magnitude and frequency of excess noise that results, problems with this equipment are often very difficult and expensive to address, especially once the equipment is installed. Sometimes it is not practical and economically feasible to fully resolve the problems presented by this equipment at the initially chosen location and major system changes are needed. The best way to address noise from this equipment is to have it installed at the outset according to a well-conceived noise and vibration control scheme. The necessary installation features to control noise and vibration may be new and unusual to some installers, and it is wise to take the extra steps to clearly document all the necessary details so they can be properly implemented.

The roof construction needs to extend fully under the equipment and needs to close tightly around any penetrating elements such as pipes and ducts. The roof construction needs to be appropriate to control airborne sound transmission to the occupied space, including sound that might transmit both through the roof deck directly under the unit and off to the side of the unit (for some distance from the unit). If concrete is used in the roof deck, this is very good and can help to address, in a simple manner, both airborne noise and vibration isolation issues. Concrete is not always necessary and lighter weight sound isolation alternatives can be conceived, but they may be unfamiliar to some installers.

Having the supply fan discharging directly down into the supply duct entering the ceiling of an occupied space is often a problem and does not allow easy opportunities to incorporate silencing devices. If possible, it is usually much better to have the fan discharge horizontally within the unit, into a discharge plenum (also in the unit), before the air is delivered to the duct system. The discharge plenum presents an opportunity to incorporate sound attenuation treatment before the air stream enters the duct in the ceiling of the occupied space. In some cases it is acceptable to run the ductwork across the roof before penetrating the roof, and this is always a favorable noise control approach since it allows space for turbulent airflow to smooth out, allows room for substantial silencing treatments before the ductwork gets into the ceiling of the occupied space, avoids what are often poor duct flow geometries at the fan discharge which occur when the duct drops directly out of the bottom of the unit, and allows low-frequency fan and duct rumble noise in the initial duct sections to dissipate outdoors rather than radiate in the ceiling of occupied space. However, such ducts may present practical and aesthetic design issues. The return/relief air path associated with rooftop units can present similar issues as discussed for the supply air path, but typically conditions at the return are not as severe because the flow conditions are not as bad and there is less fan noise. Similar noise control treatments might be considered for the return as for the supply.

Be sure that the duct geometry on the discharge of the supply fan is as reasonably advantageous as possible and avoid poor geometries as discussed above.

Silencers are often needed in the supply and return ducts and this attenuation should ideally happen before the ducts enter the occupied space, but if the ductwork from the unit drops directly into the ceiling and then has to turn into the horizontal ceiling plane, there is no aerodynamically appropriate location to put the silencer close to the unit discharge. Often, an elbow silencer can work well for these applications. When the silencer is moved away from the roof penetration, it is often necessary to encase the ductwork between the roof penetration and the silencer in a special noise barrier construction. The silencers for these applications also often need to have special high-transmission-loss casings or be encased along with the adjacent ductwork. All of these details are awkward, expensive, and difficult to construct within the limited ceiling space that typically exists. Sometimes, special curbs are created under the units to allow the return air to flow back to the units within the curb space, such as shown in Figure 17.4. With appropriate design and detailing, this can facilitate very good and practical ways to incorporate noise control treatments for both the supply and return paths.

Vibration isolation of packaged rooftop HVAC equipment can present problems, but this most often results when the units have integral compressor/condenser sections. When the unit just has basic supply and return/relief fans in the cabinet, vibration isolation can usually be satisfactorily accomplished with conventional, suitably soft, spring isolation for the fans within the unit. In this case, such units can externally be rigidly supported to the building in whatever manner is desired based on other considerations. When a unit has a compressor/condenser section, there is a concern for vibration isolation even though the compressor may be "internally" isolated. This is because the refrigerant piping within the unit is typically not adequately internally isolated, allowing vibration transmission to the equipment casing and hence to the building. In this case it is necessary to externally vibration isolate the entire unit with a spring isolation system. This is done in either of two ways, depending upon how the unit is intended to be supported and how the building designer plans to transfer the load to the building structure. There are special curb isolation devices available for equipment that requires curb support and closure of the space below the unit,

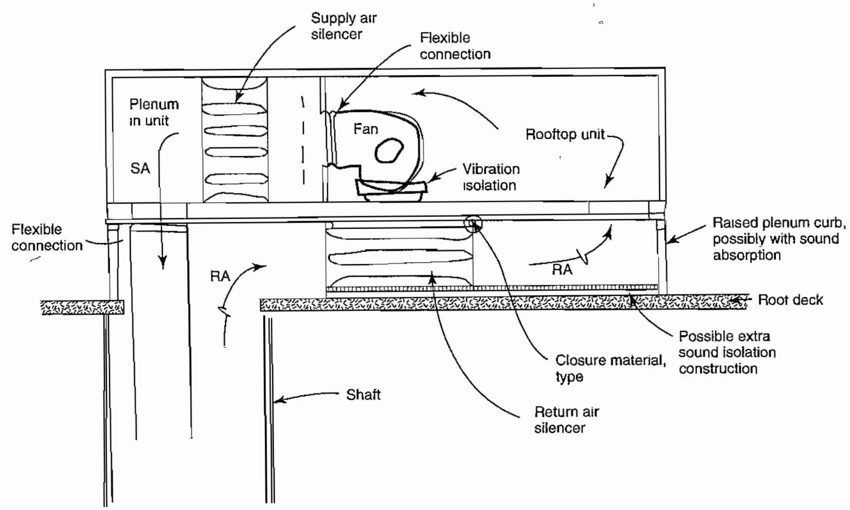

FIGURE 17.4 Rooftop unit with curb plenum return air. RA = return air, SA = supply air.

and some of these products can accommodate the aforementioned in-curb return airflow path scheme. If the load is to be transferred to the roof via a structural system raised above the roof, then point isolators are used. If the unit is intended for curb support but is raised above the roof in this manner, it may be necessary to mockup a structural curb for the unit to transfer its load to the point isolators.

17.11 OUTDOOR NOISE EMISSIONS

Many local authorities have noise regulations to control noise impact on neighboring properties and generally throughout the community. These need to be uncovered as part of the code searches at the outset of a building project so that they can be addressed in the mechanical system concept for the building. Typically, either fixed noise limits for specific receivers are established or the allowable noise level is based on the existing ambient noise level in the impacted area. If the noise requirement is based on the existing ambient noise condition, the existing noise has to be measured. Where neighbors are close by, requirements are stringent, and/or the receivers look down on the noise sources, meeting the noise requirements can be quite challenging.

Many pieces of equipment that are particularly economical (such as many air-cooled devices) are quite noisy and may not easily conform to noise regulations. Fortunately, equipment and mechanical schemes that produce less noise are often available, and, although they may be more expensive at the outset, they often provide some energy payback in the long run. Quieting the noise at the source is almost always the best approach to controlling outdoor noise emissions. Evaporative cooling equipment is usually quieter than air-cooled equipment. Equipment incorporating centrifugal fans is usually much quieter for a given duty than comparable equipment with propeller fans. Propeller fans can be quieted by using larger and/or slower moving fan blades, even if more fans are required for the duty. There are several degrees of propeller blade technology available (particularly for moderate to larger blade size applications) which can provide worthwhile noise reduction at an affordable cost. Typically, propeller blade noise reduction is achieved by having more aerodynamically efficient blades with wider chords so that they move more air with each rotation and can move a given quantity of air with lower fan speeds. Some equipment can be equipped with variable-speed drives so that when the demand on the equipment is low, the equipment (typically fans) can operate more slowly and therefore with lower noise emission levels. This is of course statistical noise reduction and will not produce noise reduction when full speed is required. However, this is particularly useful for equipment such as cooling towers where the heat rejection requirements at night are lower than the design condition and it is easier to reject heat to the cooler nighttime environment. The noise reduction that results with variable-speed drives often works naturally with the typical diurnal noise cycle which has lower noise conditions at night. It is best to avoid equipment which has a noise emission spectrum that is particularly tonal since many regulations prohibit or more strictly limit tonal sounds. Tonal sounds are typically judged to be more annoying than an equivalent level of broadband sound, so the likelihood of avoiding a noise complaint is better with broadband sources than with tonal sources. For a given level of satisfaction with the noise level achieved, a greater degree of noise control will need to be applied to tonal sources.

Sometimes equipment cannot be purchased suitably quiet within practical or economical limits, and it is necessary to apply noise control treatments. For many pieces of equipment and systems this can be reasonably and economically accomplished, such as with silencers or by building a noise barrier to block sound emissions in a particular direction. However, some pieces of equipment are not well suited to having noise control applied and treatments (such as barriers) can inhibit airflow. For instance, propeller fans produce dramatically lower airflow when working against even small degrees of extra pressure loss, and it is difficult to apply silencing devices to such equipment without degrading mechanical performance. Heat rejection equipment such as cooling towers and condensers need to avoid having the hot discharge air be recirculated back into the inlet because this can reduce efficiency and limit the mechanical capacity of the unit. Providing high levels of noise control to such equipment is often not possible and alternate equipment selection may become essential. The ability to adapt noise control treatments to equipment, if required, is a factor that should be considered in selecting the basic equipment and mechanical scheme. For small amounts of excess noise (typically less than about 10 dBA) it may be possible to create a noise barrier with sound-attenuating louvers which can allow some airflow to help mitigate the adverse airflow due to the barrier.

REFERENCES

1. *Applications Handbook*, American Society of Heating, Refrigerating and Air Conditioning Engineers, Inc., Atlanta, GA, 1999, Chapter 46.
2. C. Harris, *Handbook of Acoustical Measurements and Noise control*, 3rd ed., McGraw-Hill, New York, 1991.
3. A. T. Fry (Ed.), *Noise Control in Building Services*, Pergamon, Oxford, 1988.
4. M. E. Schaffer, *A Practical Guide to Noise and Vibration Control for HVAC Systems*, American Society of Heating, Refrigerating and Air Conditioning Engineers, Inc., Atlanta, GA, 1991.
5. R. S. Johnson, *Noise and Vibration Control in Buildings*, McGraw-Hill, New York, 1984.

CHAPTER 18

Active Control of Noise and Vibration

RONALD COLEMAN AND PAUL J. REMINGTON

BBN Technologies
Cambridge, Massachusetts

18.1 INTRODUCTION

The term active noise and vibration control (ANVC) refers to systems that use externally powered actuators to generate sound and/or vibration to reduce responses caused by unwanted disturbances. These systems consist of a set of reference sensors that monitor the source and a set of control, or residual, sensors that monitor system response. In some cases (e.g., feedback control) the reference and control sensors are the same. The signals from these sensors are inputs to an electronic controller, which filters the sensor signals to generate drive signals for the actuators. In a well-designed system the actuators excite a structure and/or sound field in such a way as to interfere with the disturbance and reduce the unwanted noise and/or vibration. The advent of modern digital signal processing hardware and software has allowed the controller in the system to be extremely flexible and even to adapt to changing conditions.

While ANVC has become a powerful tool for the noise control engineer, it is not a "silver bullet," and careful consideration must be given to passive mitigation approaches in any noise and vibration control problem. At low frequencies where the offending source consists of a small number of discrete frequencies and where the system to be controlled has only a small number of degrees of freedom, ANVC can be very cost effective. Passive treatments can also be utilized successfully on tonal sources at low frequency, but because the acoustic and structural wavelengths can be very long, the weight and size of the treatments must often be quite large to be effective.

Broadband sources of noise and vibration at high frequency, the other extreme, are often best controlled using passive techniques because many passive approaches are broadband in nature. In addition, because the acoustic and structural wavelengths in the system to be controlled are short, the treatments need not be large and heavy to be effective. On the other hand, active systems are usually less effective against broadband sources, and higher frequencies can place considerably higher demands on the controller hardware.

As the above discussion indicates, ANVC can be effectively employed against narrow-band disturbances at low frequencies where the system to be controlled has a small number of degrees of freedom. The term *degrees of freedom* refers to the number of ways that the system to be controlled can respond. The number of modes contributing significantly to the response of a system is an example of the number of degrees of freedom. It is important in ANVC because, as will be discussed later, the number of degrees of freedom corresponds to the number of actuators needed to provide effective control. As the number of input and output channels to the controller, the frequency range for control, and the performance goals increase, so do the risks associated with the stability, robustness, and costs of the resulting control system. In general, one wants to employ the system of minimum complexity to achieve the design goals. In many cases the use of a hybrid system employing both passive and active components is the best approach and the most likely to succeed.

This chapter is designed to provide the practicing noise control engineer with an overview of the technology currently employed in the application of ANVC. Enough detail is included in the hope of allowing readers to assess the applicability of the technology to their problem and to allow them to lay out an approach to the solution of that problem appropriate for ANVC. We begin with a brief discussion of some basic issues underlying ANVC technology, including conceptual overviews of several types of ANVC systems. Modern-day ANVC systems rely on digital signal processing technology, and the heart of digital signal processing technology is, of course, the digital filter. These are discussed in Section 18.3. The design of digital filters is a rich topic that has seen many years of development. Here we can only scratch the surface and hope to give the reader some appreciation of the power of the technology. Sections 18.4 and 18.5 deal with feedforward and feedback control architectures, respectively. The chapters compare the two architectures, provide guidelines for design of optimal controllers, including adaptation, and discuss system identification issues. For feedback a suboptimal heuristic design approach is also presented. The next section deals with practical design considerations. The topics include the determination of the number and location of actuators and sensors, selection of control architecture and hardware, performance simulations, and controller implementation and testing. The final section provides a detailed discussion of three ANVC systems that have been successfully implemented.

18.2 BASIC PRINCIPLES

Placement and Selection of Control Sources/Actuators

The basic concept behind active noise control is illustrated in Fig. 18.1. There a loudspeaker has been placed a distance L from an unwanted source of sound. The intent is to create sound from the *control* loudspeaker that will be out of phase with and will cancel the sound from the *disturbance* source. Ideally it would be desirable to control the sound radiation in all directions (global cancellation),

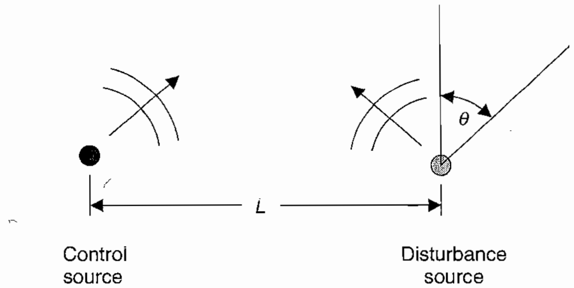

FIGURE 18.1 Disturbance source and control source.

and if the distance between the control source and disturbance source is small compared to a wavelength of sound, excellent global cancellation is possible. This comes about because the phases of the sound fields surrounding the two sources are very nearly the same at every location. Consequently, if one source is out of phase with the other two, the sound fields will cancel everywhere. On the other hand, if the separation distance is large compared to a wavelength, the two sound fields will have very different phases with the differences depending on location. As a result, the two sound fields will in some locations cancel and in others reinforce one another. This is illustrated in Fig. 18.2, where the change in the sound radiation from the disturbance source is shown as a function of angle θ. For $k_0L = 0.1$ in the figure, where k_0 is the acoustical wavenumber and L the distance between the disturbance source and the control source, the change is a reduction of 20 dB or more for all angles. However, as the frequency increases and k_0L increases, the global reductions decrease. For example, in the figure, for $k_0L = 1$ the reductions are limited to a small range of angles around $\pm 90°$ and for $k_0L = 10$ there is a 6-dB increase for most angles. The figure clearly shows that it is desirable to locate the control source as close as possible to the disturbance source. In some cases, however, when the physical dimensions of the source are comparable to or larger than a wavelength at the frequencies of interest, the control source cannot be located close enough to the disturbing source. Figure 18.3 shows the effect of source separation on the overall radiated acoustic power (the integral over all angles in Fig. 18.2). The figure shows that for separation distances greater than one-quarter of an acoustic wavelength the total radiated power will actually increase. This is a fundamental limitation on ANVC that can only be overcome through the use of additional control sources. The use of multiple sources in a prototype system for controlling locomotive exhaust noise is discussed in Section 18.7 under MIMO Feedforward Active Locomotive Exhaust Noise Control System with Passive Component.

One of the earliest demonstrations of active noise control was carried out by Conover[1] and Conover and Ringlee[2] of General Electric in the early 1950s to control the noise from a high-voltage transmission line transformer. Using a single loudspeaker, he utilized the electrical line signal to drive the speaker and

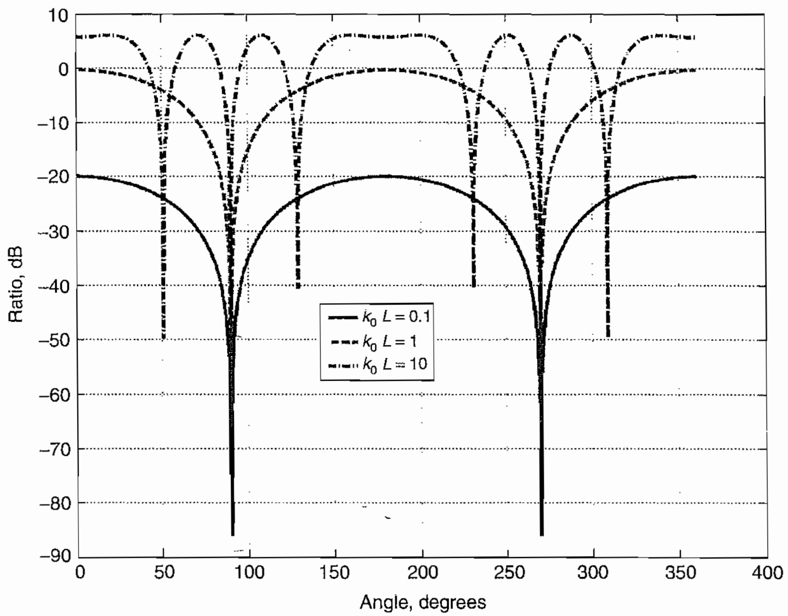

FIGURE 18.2 Change in the ratio of the controlled to the uncontrolled sound pressure level as a function of frequency and angle.

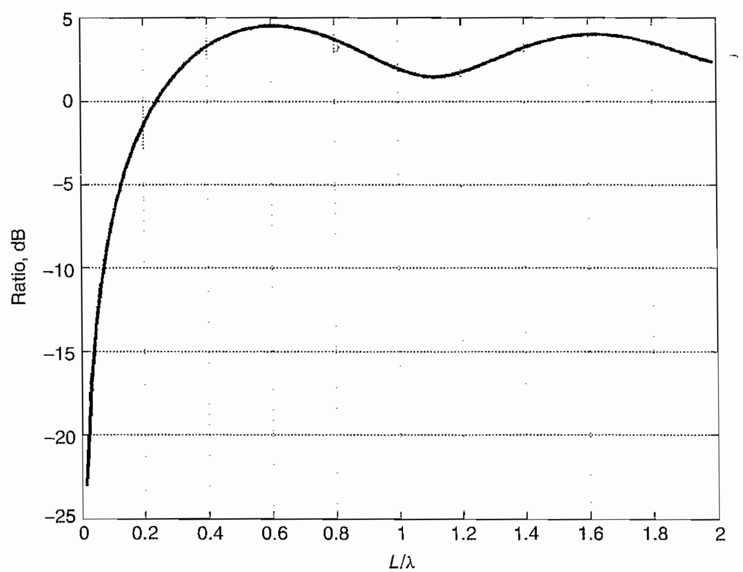

FIGURE 18.3 Change in the overall radiated output power as a function of the separation between sources.

appropriately amplified and phase shifted the harmonics of the line frequency to achieve the desired control. Because the system was not adaptive, occasional manual adjustment was required to correct for changes in sound propagation at the test site. In addition, because of the large size of the transformer, even at the low frequencies he was concerned with (120 Hz), he could not achieve global cancellation but had to be satisfied with ~10 dB of cancellation over a beam width of about 23°, corresponding to a point somewhere between the curves for $k_0L = 1$ and $k_0L = 10$ in Fig. 18.2. Remarkably, Conover was able to achieve this level of performance using purely analog hardware. Digital hardware did not come into use until the 1970s. Among the first to employ digital electronics were Kido[3] and Chaplin and Smith.[4] Kido used digital hardware to implement an active system to control transformer noise similar to Conover's and Chaplin and Smith developed a digital system for controlling tonal exhaust noise.

While the above discussion has focused on acoustical sources, similar principles apply to structural systems. Consider, for example, a plate with a point force disturbance applied as illustrated in Fig. 18.4 with a control actuator located as shown. In this example the plate is 10 × 5 ft and $\frac{1}{2}$-in-thick steel with a loss factor of 10% and the disturbance force and control actuator are about 1.4 ft apart. Because the plate in this example is finite in size, there will be resonant modes, which will add further complications to the selection of the number and location of the actuators. In this example, the control actuator is applying a force to the plate, the amplitude and phase of which is designed to control the first mode. Figure 18.5 shows the contribution of each mode to the plate response with and without activating the control actuator. Comparing the two plots in the figure, one can see that activating the control actuator has suppressed the first mode, and, in addition, the second and third modes have also been reduced. Higher

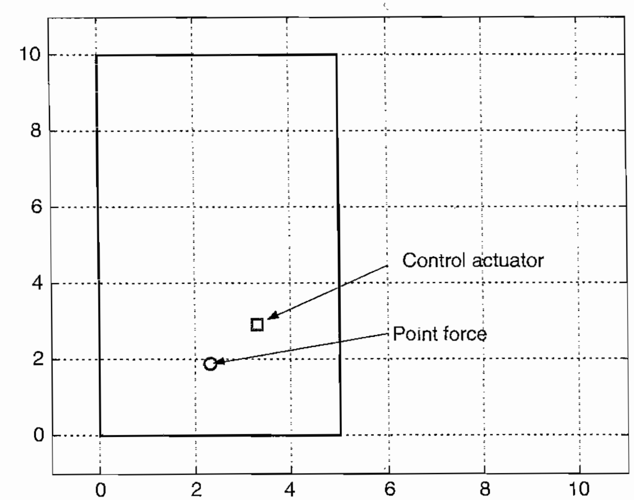

FIGURE 18.4 Plate with disturbance force and control actuator.

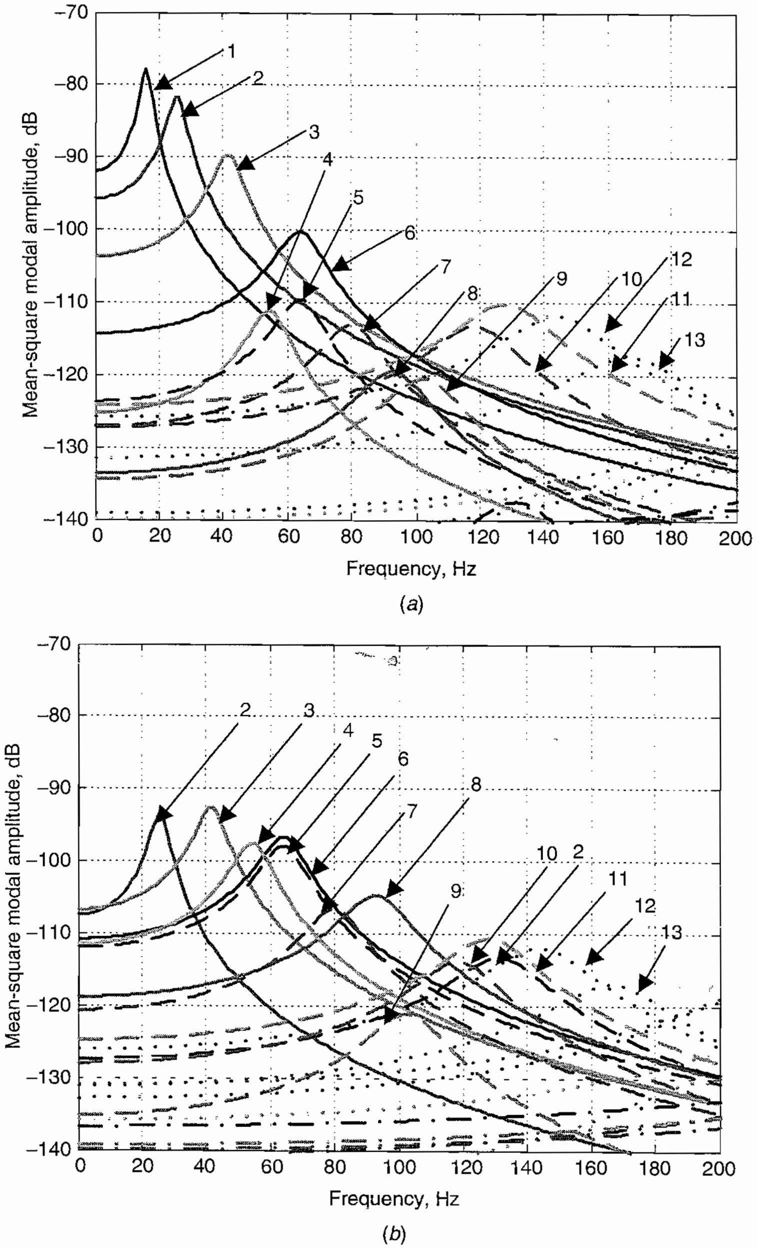

FIGURE 18.5 Modal amplitudes: (*a*) uncontrolled; (*b*) controlled.

order modes, however, have generally increased in amplitude. This increase in the amplitude of uncontrolled modes is referred to as *modal spillover*. Modes that are not targeted to be controlled can increase in amplitude. We can overcome this problem by moving the control actuator closer to the point of application of the disturbance force or we can add additional actuators, one for each mode that we wish to control. In general, placing the actuator as close as possible to the disturbance source will result in the best reduction in vibration. For example, in Fig. 18.6 the mean-square plate displacement averaged over the area of the plate is shown uncontrolled and controlled with a single actuator 1.4 ft away from the disturbance force and 0.28 ft away. When the actuator and disturbance are 1.4 ft apart, the vibration below 40 Hz is well controlled, but above about 50 Hz the control actuator increases the plate vibration due to modal spillover. When the control actuator is moved closer, spillover is virtually eliminated in the frequency range shown.

We can also increase the number of actuators, which will enable us to control additional modes and increase the frequency range over which the control will be effective. As an example consider the four control actuators located as shown in Fig. 18.7. These will be used to control the first four modes.* The result is shown in Fig. 18.8. While spillover has not been eliminated at all frequencies,

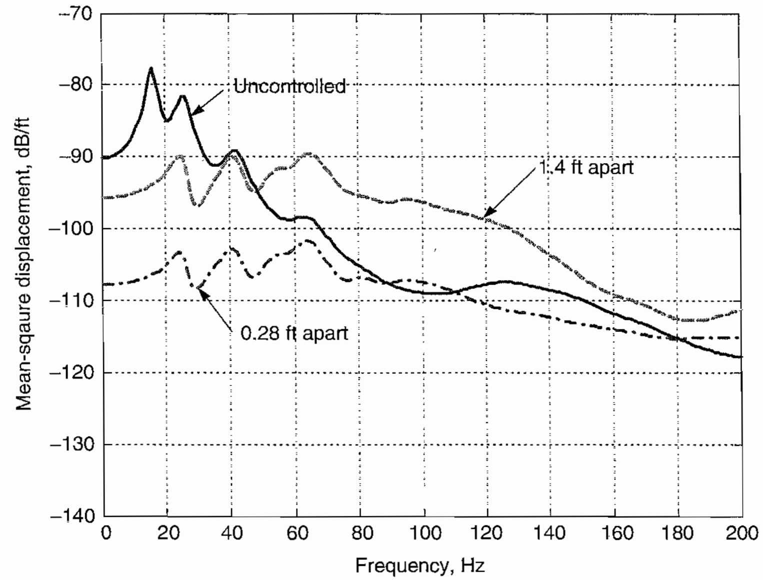

FIGURE 18.6 Controlled and uncontrolled plate response.

*Note that the actuator positions have been selected to ensure that at least one actuator is capable of exciting each of the four modes. If the actuators are placed near the node of a mode to be controlled, the actuator will be ineffective in controlling that mode.

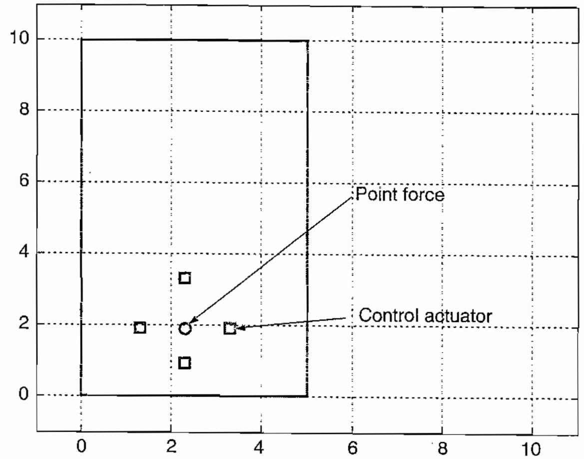

FIGURE 18.7 Location of four control actuators.

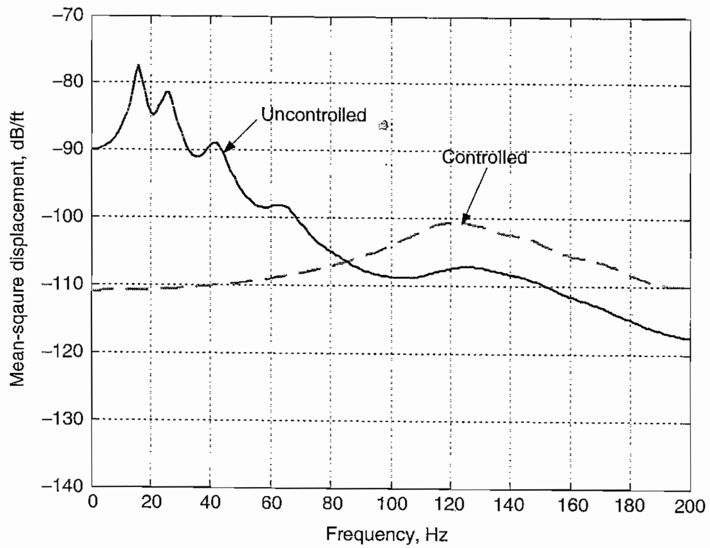

FIGURE 18.8 Change in mean-square plate vibration using four control actuators.

below 80 Hz the reduction in vibration is comparable to that achieved by bringing the control actuator very close to the disturbance point force. Good performance above 80 Hz can be achieved by continuing to increase the number of actuators and targeting more and more modes for control. Note that similar modal issues come into play in active noise control when the noise control is to be carried out in a confined space rather than in the free field in the first example.

The lesson to be learned from all of this is that, when possible, placing the control sources as close as feasible to the offending sources will provide the best noise and vibration reduction performance. When this is not possible due to the size of the source, lack of access, and so on, the loss in performance can be made up, in principle, by employing a larger number of control sources. However, increasing the number of control sources will increase the complexity of the controller needed to drive them and will certainly increase the cost of the entire system.

Control sources come in a wide variety of forms. For acoustic applications, loudspeakers are typically employed. The active elements in the speakers may be electrodynamic (voice coil), piezoelectric, or electromagnetic, to mention a few. The active element might be used to move a speaker cone, modulate airflow, or deform a structure. The most common configuration is a speaker cone driven by a voice coil. Whatever the configuration, the speaker usually needs to be enclosed for protection against physical damage, weather protection, and performance enhancement.[5] Figure 18.9 shows an enclosure arrangement developed for the active control system discussed in Section 18.7 under MIMO Feedforward Active Locomotive Exhaust Noise Control System with Passive Component. These enclosures are bandpass enclosures designed to enhance the speaker output between 40 and 250 Hz. Each contains 2–12-in. loudspeakers and 10 were employed to control the locomotive exhaust noise. Despite these efforts the

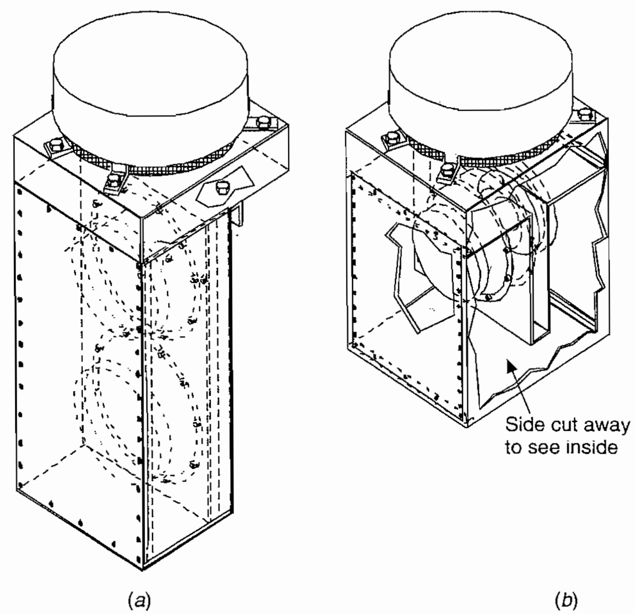

FIGURE 18.9 Typical loudspeaker enclosure arrangement.

performance of the active noise control system was limited by the output of these control sources. This is typically described as having insufficient *control authority*. Insufficient control authority is a problem often encountered in active noise control systems, and an assessment of the control source requirements is one of the first things that should be done before proceeding with any active noise and vibration control system design. If there is not sufficient space and power available to ensure adequate control authority, the active system is doomed to have inferior performance.

A wide variety of devices are available to be employed as structural control actuators. Typically these are devices that generate a force that is reacted against an inertial mass (inertial shaker) or against another part of the structure (interstructural shaker). The active element may be pneumatic,[6] hydraulic,[7] electrodynamic,[8] electromagnetic,[9] piezoelectric,[10] electrostatic,[11] or magnetostrictive,[12] to mention a few. A large-capacity electromagnetic inertially referenced shaker designed for use in an active control system is shown in Fig. 18.10.

In place of shakers piezoelectric[13] patches are sometimes applied directly to panels to control vibration or to radiate sound for noise control. Any of these devices can be very effective,* but the critical issue still remains. The device must provide sufficient control authority.

Control Sensors and Control Architectures

Sensors provide the input signals that the controller filters to drive the control sources and actuators. Sensors provide two functions, and to discuss those

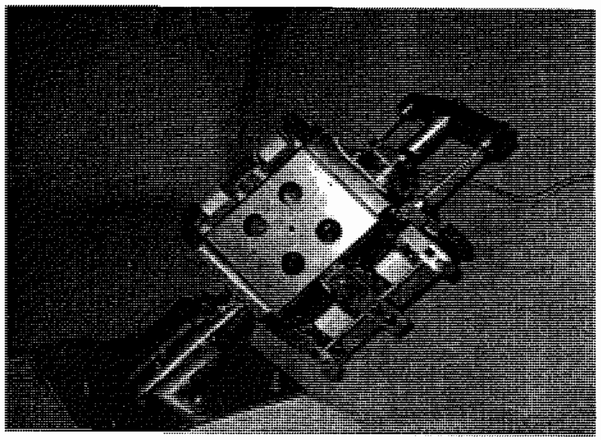

FIGURE 18.10 A 2000-lb-capacity electromagnetic inertial shaker.

*The inertial shaker usually provides better performance than the interstructural shaker, especially if the interstructural shaker creates a flanking path outside of the frequency range where the control system is functioning, but the interstructural device may be preferred when high control authority is needed with minimum weight.

functions, we need to describe the two commonly used control architectures: feedforward and feedback. The two architectures are illustrated in Fig. 18.11. In the feedforward system (Fig. 18.11*a*) one or more reference sensors measure a signal that is correlated with the disturbance to be controlled. The reference sensor output is sent to a control filter, which acts on the signal to generate an output signal that is used to drive the control actuators. The control actuators drive the system to be controlled (the plant function *P* in the figure) and the response of the plant is monitored by one or more residual sensors. The residual sensors are sometimes called the control sensors or error sensors. The purpose of the residual sensors is to monitor the performance of the control system. In later sections we will see how the reference and residual sensors are use to define and/or adapt the control filter.

In a feedback system (Fig. 18.11*b*) there are only residual sensors, or, to put it in other terms, the sensors in a feedback system provide both reference and residual functions. As in a feedforward system, the residual sensors monitor the performance of the control system. In addition, their signals are fed to the control filter, which acts on the signals to generate an output signal that is used to

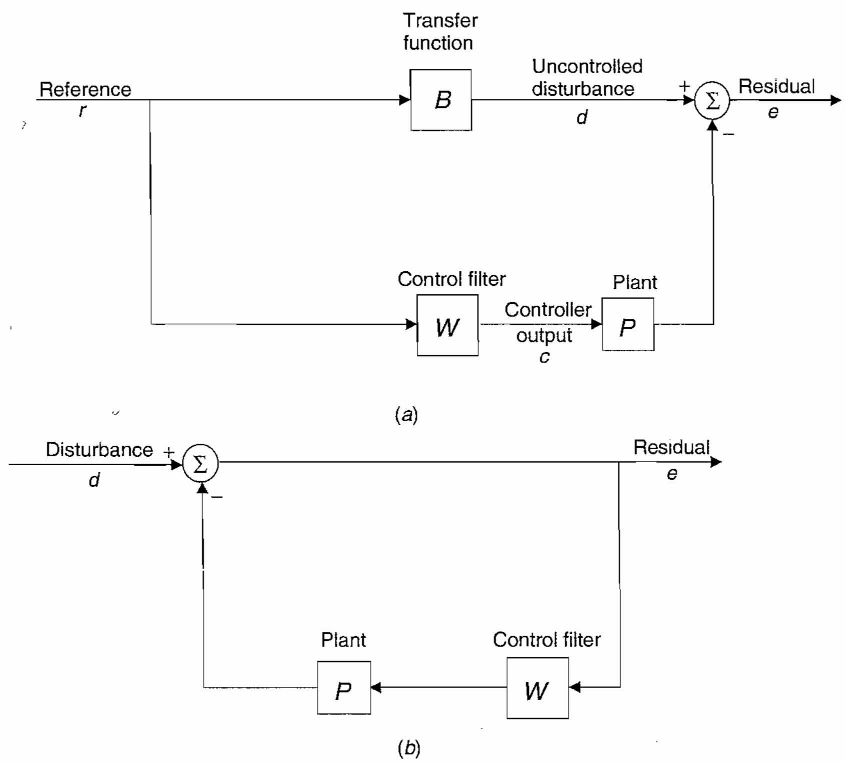

FIGURE 18.11 (*a*) Feedforward and (*b*) feedback architectures.

drive the control actuators. The control actuators drive the system and generate responses in the residual sensors through the plant transfer function, P.

The choice of whether to use feedback or feedforward architectures depends on a number of factors. In general, if reference sensors can be placed to measure a system response that is well correlated with the disturbance and residual sensors can be placed on the system such that there is sufficient delay between the reference and residual sensors (i.e., the reference sensors receive their signals before the residual sensors), then feedforward is the architecture of choice. This is especially true if the reference sensors are unaffected by the operation of the control actuators, such as would occur with a tachometer reference, for example. Feedforward is preferred (as we shall see in later sections of this chapter) because the algorithms are simple and easy to implement and the bandwidth requirements on a feedforward system are much less stringent than for feedback.

If a suitable set of reference and residual sensors satisfying the above requirements does not exist, then feedback must be used. As will be shown in later sections of this chapter, feedback control systems can present special problems. In particular, stability and out-of-band amplification requirements* can force the bandwidth of the system to be up to 100 times the control bandwidth.

As with actuators there is a wide variety of sensors used in active noise and vibration control systems. For systems designed to control only tones, a tachometer is often the reference sensor of choice, because in most cases the operation of the control system does not affect the tachometer, making the implementation of a feedforward system much easier. Other sensors that are commonly used include, accelerometers, force gauges, strain gauges and piezoelectric patches, proximity sensors, linear variable differential transformers (LVDTs), microphones, hydrophones, and pressure sensors. The requirements on the sensors are the same as for any high-quality instrumentation system: sufficient sensitivity to measure the phenomena of interest, low noise, stable operation, durability, and so on.

Performance Expectations

Active noise and vibration control systems can be powerful tools in the hands of a knowledgeable noise control engineer. In many cases, significant reductions in noise and vibration can be achieved with active systems that cannot be achieved using passive treatments with the same space and weight constraints. This is especially true at low frequencies. Despite the power of the technology, there are realistic limits on what reductions can be achieved. Figure 18.12 shows the performance achieved by the prototype active system described in Section 18.7 under Active Machinery Isolation. We present it here because it reflects the performance that is normally achievable in a properly designed active system. The figure shows the reduction in force transmitted by an active vibration isolation

*Outside of the frequency band where control is desired, the active system can amplify the disturbance unless great care is exercised in implementing the system filters to frequencies well beyond the frequency band for control.

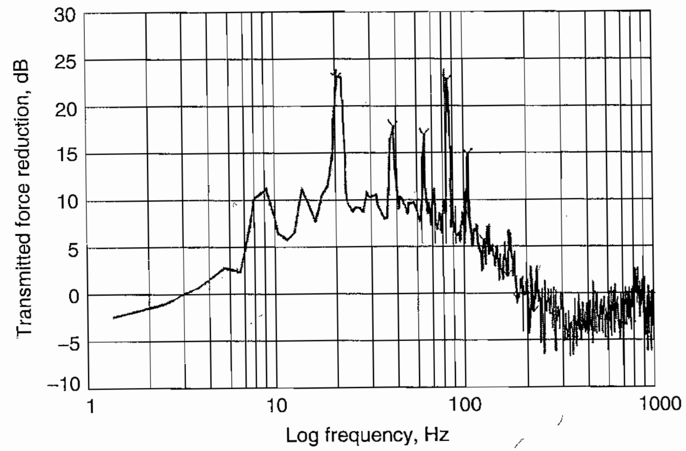

FIGURE 18.12 Typical performance of an active vibration control system.

mount. The system was a single-input, single-output (SISO) feedback control system designed for suppression of both broadband and narrow-band vibration. The narrow peaks in the figure with amplitudes of 15 to nearly 25 dB reflect the reduction in tonal components of the force transmitted by the mount. These values are what one would typically expect in tonal suppression from an active system. In addition to the peaks there is broad hill beneath them that in the frequency range of 10–100 Hz has an amplitude of from 6 to 10 dB. This too is typical of what one might expect from a system designed to provide control of broadband noise and vibration. Of course, there are many factors that go into determining the performance of an ANVC system, and there is no substitute for careful analytical/empirical modeling helping to direct the design process, but these values represent reasonable expectations for system performance when the technology is properly implemented.

Examples of Prototype ANVC Systems

There have been a vast number of ANVC prototype systems implemented over the past 50 years or so. Here we present a few examples of those systems to give the reader a sense of how the technology has been applied, where it has been most successful, and where additional technology and research is required. For a more detailed look at the early development of the technology the reader is referred to a number of review articles.[14–17]

The first patents proposing the use of a sound to cancel unwanted sound in the early 1930s proposed the type of system[18,19] illustrated in Fig. 18.13. These early proposals focused on the control of sound in a duct and involved the use of a reference microphone to sense the unwanted sound. In Fig. 18.13 the signal from that microphone was then acted on by appropriate electronics to synthesize

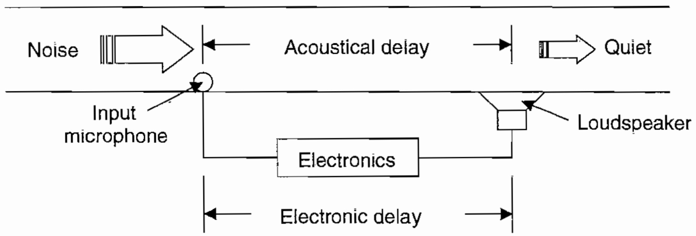

FIGURE 18.13 Schematic diagram of the active noise control concept for controlling sound in ducts.

a signal to drive a loudspeaker downstream from the microphone. The sound wave from the loudspeaker then cancels the unwanted sound. The use of active systems to control sound in ducts has received a great deal of attention over the years. Swinbanks[20] provided an extensive theoretical foundation in the early 1970s focusing on various arrangements of control sources at two different axial positions in a duct to minimize propagation of canceling sound back to the reference microphone. Other researchers[21,22] examined more complex control source configurations to deal with the control-source-to-reference coupling. Eventually laboratory experiments were carried out using analog electronics to confirm the predictions of the analysts[23] and to demonstrate both narrow-band and broadband control.[24] Eriksson's work in this area is particularly noteworthy.[25–28] His theoretical and experimental work eventually resulted in a commercially available active duct silencer utilizing digital electronics that was sold through Digisonix,* a subsidiary of Nelson Industries. The system configuration was very similar to that shown in Fig. 18.13.

Another early concept (1950s) for active noise control is illustrated in Fig. 18.14. This idea was developed by Olsen and May[29] while at the Radio

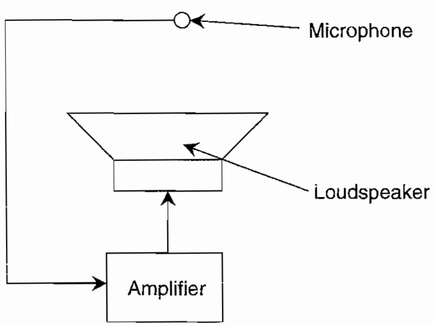

FIGURE 18.14 Olsen and May's "electronic sound absorber".

*Nelson Industries is currently owned by the Cummins Engine Company and Digisonix is no longer in business.

Corporation of America. The concept utilizes a microphone placed close to a loudspeaker in which the microphone detects the unwanted sound and the speaker generates a canceling signal that creates a zone of silence around the microphone. They assembled and successfully demonstrated their concept using only analog components. This basic concept has been extended and utilized in a number of applications, including control of automobile[30–34] and aircraft[35–38] interior noise and noise-reducing headsets.[39–41] The example in Section 18.7 under Active Control of Airborne Noise in a High-Speed Patrol Craft describes a system that uses this concept to reduce the noise in the berthing spaces of a high-speed patrol craft.

Figure 18.15 shows a schematic diagram of a notional active automotive interior noise control system. As shown, the system is designed to control noise generated by the propagation of vibration from the vehicle's suspension to the passenger compartment where it is radiated as sound to the vehicle interior (road noise) and engine noise. Feedforward active control architectures have usually been used to attack this problem. A number of reference accelerometers are placed on vehicle suspension components and in the engine compartment. Reference microphones might also be used. The reference signals are fed to a controller, which generates signals to drive the control loudspeakers in the passenger compartment. Residual microphones are located in the passenger compartment near the ears of the occupants so as to generate a zone of silence around the head of each occupant. Because of the nature of the interior noise, the control system must reduce both narrow-band and broadband noise. While the system concept is fairly simple, its successful implementation has proven difficult. First the number of residual sensors needed to sample all of the suspension sources can be quite large[42] (10–20). This can lead to significant costs due to the high channel count. In addition, the reductions achievable seem to be limited to about 6 dBA and the zone of silence around the control microphones is usefully large only at low

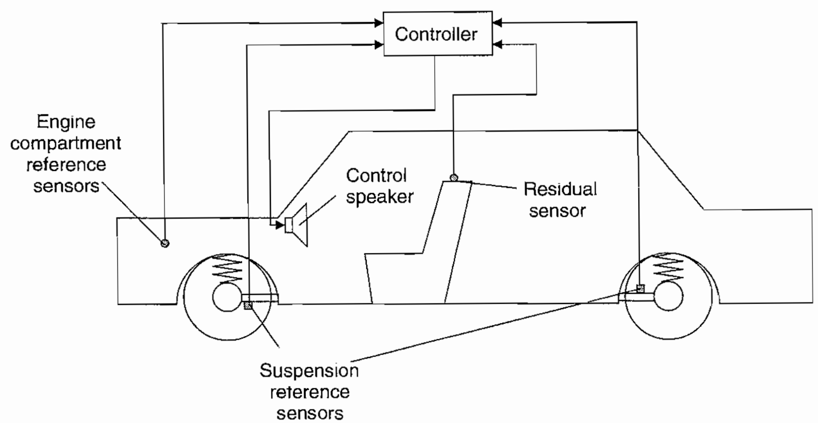

FIGURE 18.15 Schematic of an active automobile interior noise suppression system.

frequency (up to a few hundred hertz), limiting the useful frequency range of the system. Consequently, active systems providing broadband automobile interior noise control are not presently commercially available.

Systems for the control of aircraft interior noise have generally focused on tonal noise, that is, the propeller blade passage frequency and its harmonics. A schematic of a typical system is shown in Fig. 18.16. Experimental systems like that shown have generally provided about 10 dB of tonal interior noise control at the blade passage frequency and somewhat less at the higher harmonics. The system in the figure is similar to the automotive interior noise control system except that the reference is now a tachometer from the aircraft engine. The schematic shows control speakers as the actuators, but piezoelectric patches on the fuselage panels and inertial shakers on the ribs and stringers have also been tried, effectively turning the fuselage into a loudspeaker. Systems suitable for small propeller-driven business aircraft are presently commercially available from Ultra Electronics.

A number of manufacturers now provide reasonably priced active noise cancellation headsets. Figure 18.17 shows one arrangement. The figure shows the shell of one side of the headset in which there is a small speaker and colocated microphone. The signal that the wearer wishes to hear drives the speaker, the output of which is picked up by the microphone. The microphone also picks up any noise that passes through the shell. The microphone signal is then fed back, as shown in the block diagram in the figure. By increasing the gain of the filter,

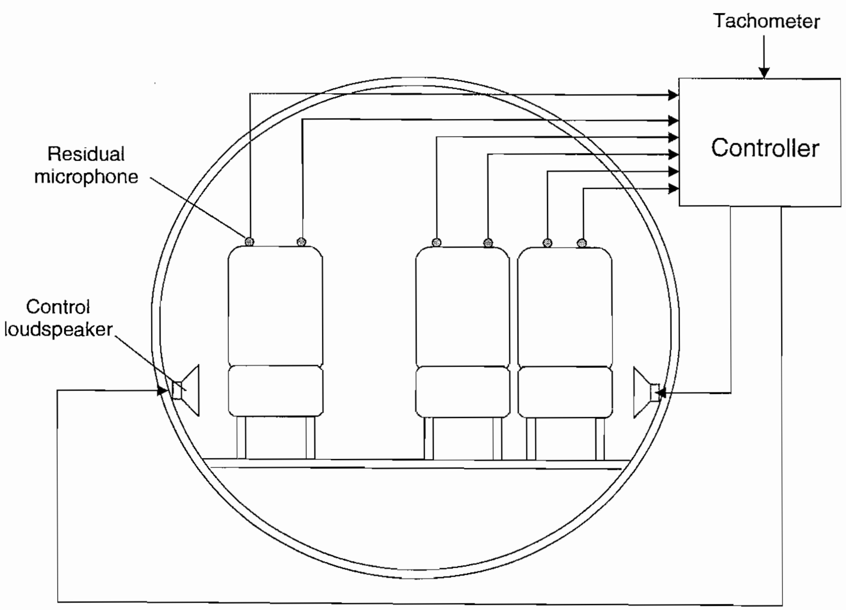

FIGURE 18.16 Schematic of an active aircraft interior noise control system.

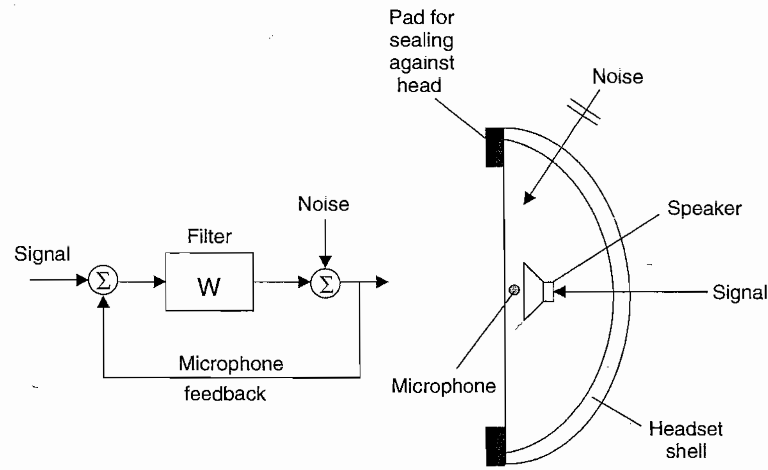

FIGURE 18.17 Typical noise cancellation headset.

W, in the block diagram* (typically an analog filter in commercial products rather than a digital one), the signal will pass through unchanged and the noise will be attenuated. Of course, this gain cannot be increased without limit, since too high a gain can result in instability and ringing. These devices produce noticeable improvement (10–15 dB) in the passive performance of hearing protection headsets above 100 Hz. The improvement gradually decreases with increasing frequency until at ~1 kHz most of the improvement has gone away. In very loud environments headsets can be limited in performance by the sound level the small speaker can generate within the shell.

Another area that has received considerable attention in recent years is the active control of tonal noise from turbofan engines.[43–50] Tonal noise from these engines is caused primarily by the interaction between the fan blade wakes and the stator vanes. The control systems for the most part have been feedforward systems utilizing a tachometer for a reference sensor. Since the fan and stator vanes are located in the bypass duct, the systems need to take into account the complex physics of the propagation of sound in ducts. The physics dictates that the fan–stator interaction noise will propagate down the duct as, so-called, spinning modes. These modes have a sinusoidal pressure variation in the circumferential directions that rotates as the mode propagates, hence the term *spinning mode*. Only a selected number of these modes are excited by the fan–stator interaction and a still smaller number propagate. Consequently, the control actuators must also generate spinning modes in order to cancel the fan–stator interaction noise without generating additional propagating modes in the duct. Figure 18.18 shows a schematic drawing of one such active noise control system. This particular

*In the block diagram *W* also contains the frequency response between the speaker input and the microphone output.

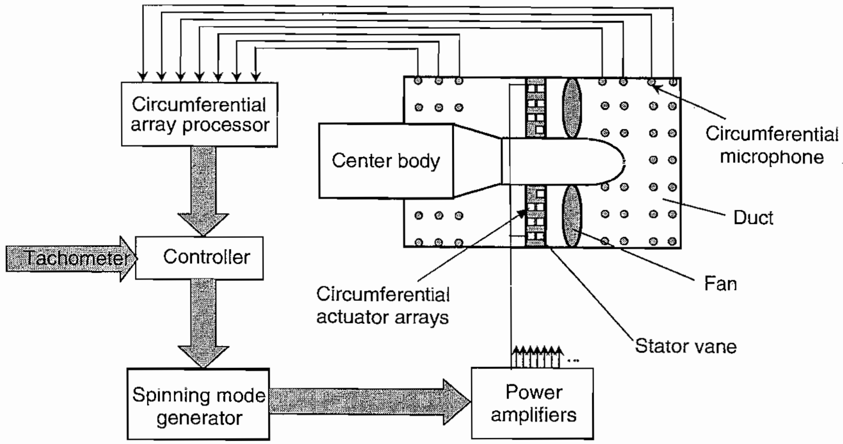

FIGURE 18.18 Schematic of the active noise control system for controlling fan-stator interaction noise.

system utilizes actuators in the stator vanes. Actuators have also been installed in the walls of the duct. The system must be designed with a sufficient number of actuators to ensure that the propagating modes to be controlled can be generated by the array without aliasing into other modes that will propagate.

Each array is driven by a single signal passed through analog or digital electronics (spinning-mode generator) that properly phase shifts the actuators in each array to produce a spinning mode of the desired circumferential order. Each actuator in the array must be the same. If there are large variations in amplitude and phase between actuators when driven by the same signal, then modes other than the desired mode will be generated, resulting in noise generation rather than suppression if the spurious modes propagate. The control sensors are typically wall-mounted microphones arranged in circumferential arrays and each array is steered (circumferential array processor) to accept a spinning mode of the circumferential mode order that is to be controlled. In a laboratory setting, systems of this type are capable of reducing the tonal noise from fan–stator interaction by 10–20 dB. In real high bypass turbofan engines, however, especially in modern-day large engines, none of the actuators tested to date have sufficient control authority to be able to overcome the disturbance. In addition, at the present time, while the controller channel count can be fairly low, typically equal to the number of modes to be controlled, the number of actuators and sensors needed to field a system can be quite large. It is very likely, however, that if active noise control is included early in the design process of an engine along with passive noise control treatments, the number of actuators and sensors needed could be substantially reduced. If more powerful actuation systems become available, commercially available active systems for the control of fan–stator interaction noise in turbofan engines may become a reality.

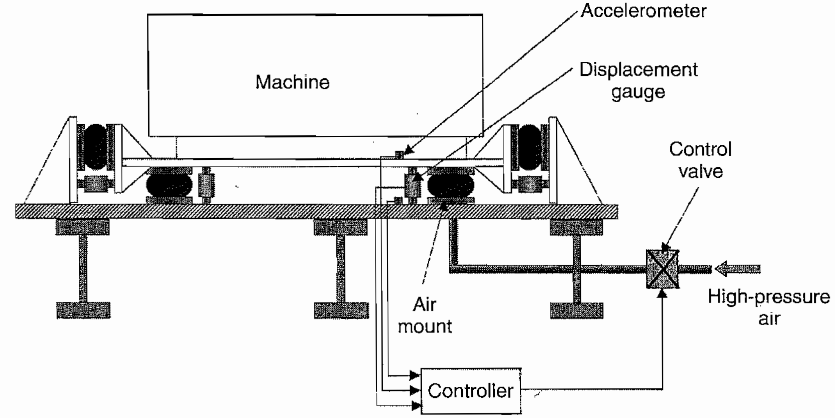

FIGURE 18.19 Notional activated vibration isolation mount.

In the 1950s Olsen[51] was the first to suggest extending active control to the control of machinery vibration. Since that time numerous studies have been carried out into the activation of vibration isolation mounts.[52–55] Figure 18.19 shows a schematic drawing of a notional active vibration isolation system. In this case, we envision a set of mounts supporting a vibrating machine on the deck of a ship. In the figure only one mount is shown activated. In actuality all (possibly 10 or 12 mounts) would be. It is desired to reduce the vibration excitation of the deck while maintaining the position of the machine, which is in a confined space, so that it does not strike any of the ship structure surrounding it during ship maneuvers. These two requirements are conflicting. Good vibration isolation performance requires a mount that is as compliant as possible while good position keeping requires a stiff mount. Two approaches can be taken to the activation of the mount. We can employ a mount that is stiff enough to ensure good position keeping and use an active system to increase the compliance of the mount at higher frequency where good vibration isolation performance is desired. We will refer to this type of system as the active isolation system. Another approach is to use a very compliant mount that provides the desired vibration isolation performance at high frequency and use the active system to provide position keeping at low frequency. We will refer to this system as the position-keeping system. For either concept to work the frequencies associated with ship maneuvers should be much lower than the frequencies where vibration isolation performance is desired. The notional system that we have shown in Fig. 18.19 incorporates air mounts. Since air mounts tend to be very compliant, they would be most appropriate for the position-keeping approach. The system would require 10–12 mounts to conveniently control all six rigid-body degrees of freedom. Each mount incorporates sensors for measuring relative displacement between the machine and the deck and for measuring the acceleration on the deck and the machine. These sensors would be used in the controller to generate a frequency-dependent linear combination of relative displacement, velocity, and acceleration at each mount. Those inputs would then be used by the controller in a feedback architecture to drive the control valves, which can inject high-pressure air into or vent it from the air mounts. Since the frequencies associated with ship maneuvers tend to be lie below 1 Hz, the machine would most likely act as a rigid body, significantly simplifying the system transfer functions and making the controller simpler as well. This approach does have some disadvantages. For example, it would require about 10–12 air mounts to conveniently implement it. In addition, all mounts must be coupled in the controller, making it a multiple-input, multiple-output (MIMO) system. On the other hand, there would only need to be six independent channels in the controller to control the six rigid-body degrees of freedom of the machine. Multi-degree-of-freedom systems of this type and of even greater complexity have been implemented in research programs, but none are commercially available. However, there remains considerable interest in active isolation systems and position-keeping systems for both military and civilian applications.

The above examples of types of ANVC systems represent only a taste of the many noise cancellation problems that have been addressed using the technology. In Section 18.7 we present three detailed examples of ANVC systems to provide the reader with a more in-depth look at the development, implementation, and performance of real prototype systems.

18.3 DIGITAL FILTERS

Advantages of Digital Filters

Active noise and vibration controllers are basically filters. The inputs are sensor signals and the outputs are the drive signals to the actuator electronics, which impart desired control forces to the physical system being controlled. For some ANVC applications, implementing these filters using analog electronics is an efficient and cost-effective approach. In particular, analog controllers should be considered for applications where the required magnitude and phase responses of the filters are a relatively simple function of frequency and when these filters are not required to change over time. An example of an application where analog controllers have been used effectively is active headsets. However, when the required magnitude and phase responses vary significantly as a function of frequency and the characteristics of these filters are required to change over time to maintain a desired level of performance, digital controllers are often the best choice. The filters implemented within these digital controllers are referred to as digital filters.

Digital controllers offer many advantages over analog controllers. As discussed by Nelson and Elliott,[56] these advantages include the following:

Flexibility. Digital controllers implement digital filters by running programs written to operate on digital signal processor (DSP) chips. The codes to implement these filters can be written to allow for these filters to change their characteristics over time (i.e., adapt). Further, these codes can be written to accommodate increases in the number of input and output channels. Additionally, the complexity of the digital filters can be increased or decreased by modifying the codes running on the DSPs.

Accuracy. Many DSPs support floating-point computations running in either single- or double-precision arithmetic. Although greater accuracy in the calculations can be achieved using double precision, this increased precision is seldom required and comes at the cost of increased memory requirements. The accuracy of single-precision controllers has been demonstrated for a wide variety of ANVC applications, including those with large numbers of input and output signals and digital filters requiring very complex magnitude and phase responses as a function of frequency.

Adaptability. Applications of ANVC often require the controller to alter filtering characteristics over time to maintain a desired level of performance. Controllers that satisfy this requirement are said to be "adaptive." An example of an adaptive controller is ANVC applied to systems whose dynamics (as a function of frequency) change over time. Digital controllers implemented using DSPs can be designed to adapt to these changes.

Cost. The cost of DSPs has continued to drop over the past 15 years. At the same time, the computational and memory capabilities of these chips have continued to increase. Currently available DSPs deliver up to 1×10^9 floating-point operations per second (1 gigaflop, abbreviated Gflop) and are equipped with up to 256 Mbytes of local, fast-access memory. In addition, the architecture of these chips has expanded to allow communications between DSPs to support efficient implementation of digital controllers employing multiple DSPs for large-scale applications. Both fixed- and floating-point DSPs are available. Fixed-point processors are cheaper than floating-point processors but are generally more difficult to program, resulting in increased software development costs.

In the following section the concepts of digital sampling and filtering are discussed. Subsequent sections use these concepts to summarize optimal digital and adaptive digital filter designs.

Description of Digital Filters

There are many good texts covering the concepts of digital sequences, sampling, and filtering.[56–59] For purposes here, we summarize these concepts following the developments of Nelson and Elliott[56] and Oppenheim and Schafer.[57] The interested reader should look to these references for more detailed discussions.

The input to a digital controller is typically an analog signal from a sensor that passes through an analog-to-digital (A/D) converter. The purpose of the A/D converter is to sample the input signal at regular time intervals (Δt) to produce a sequence of numbers corresponding to the amplitude of the input signal at each sample time. A schematic of the operation of an A/D converter is shown in

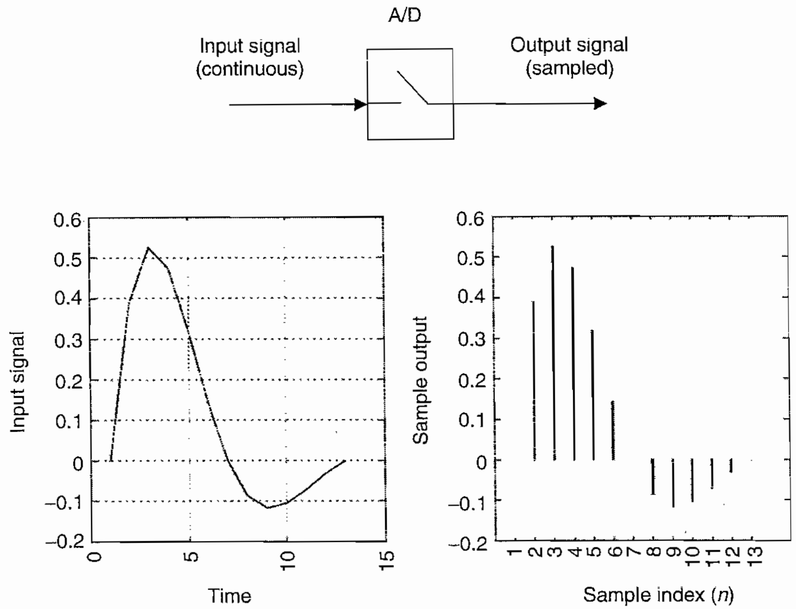

FIGURE 18.20 Digital sampling of an analog signal.

Fig. 18.20. The output of the A/D converter can be related to the continuous-time input signal through the following relationship:

$$f(n) = \sum_{i=-\infty}^{\infty} f(i)\delta(n-i) \tag{18.1}$$

where $\delta(n-i)$ is called the Kronecker delta function, or unit-sample sequence, and is defined as

$$\delta(n-i) = \begin{cases} 1 & n = i \\ 0 & n \neq i \end{cases} \tag{18.2}$$

The sampled signal in Eq. (18.1) is only defined for integer values of n. That is, $f(n)$ is only defined for $n = 0, \pm 1, \pm 2, \ldots$ An example of a continuous-time signal and the corresponding sampled signal $f(n)$ is shown in the lower portion of Fig. 18.20. The sample index n can be related to a discrete time by $t_n = n\ \Delta t$, where Δt is the fixed time interval between samples.

A digital system (e.g., digital filter) operates on a sequence of numbers to produce an output sequence. This is shown schematically in Fig. 18.21. The *impulse response* $w(n)$ of the digital system W is defined as the output corresponding to a unit-sample input [i.e., $\delta(n-i)$, $i = 0$]:

$$w(n) = W\{\delta(n)\} \tag{18.3}$$

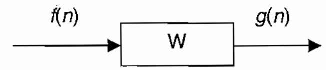

FIGURE 18.21 Digital filter operating on input $f(n)$ to produce an output $g(n)$.

where $w(i) = 0$ for $i < 0$ ensures that the output of the filter does not occur before the input sequence is applied. Filters that obey this constraint are referred to as *causal* filters.

The filter operation implied by the block diagram of Fig. 18.21 can be expressed mathematically as

$$g(n) = \sum_{i=0}^{I-1} w(i) f(n-i) \tag{18.4}$$

where the impulse response of the digital filter $w(i)$ in Eq. (18.4) is assumed to be a sequence of numbers of length I. It is common to refer to these numbers as the coefficients, taps, or weights of the digital filter. For example, $w(i)$ is called the ith coefficient of the digital filter w. Using this nomenclature, Eq. (18.4) states that the output of the digital filter w at time step n is equal to the summation over i of the ith coefficient of w times the input at time step $n - i$. In vector notation, this operation is equivalent to the inner product of a row vector and a column vector such that

$$g(n) = \mathbf{f}^{\mathrm{T}}(n)\mathbf{w} \tag{18.5}$$

where $(\cdot)^{\mathrm{T}}$ represents the vector transpose operator and $\mathbf{w}$ and $\mathbf{f}(n)$ are defined as

$$\begin{aligned} \mathbf{w}^{\mathrm{T}} &= [w(0), w(1), w(2), \ldots, w(I-1)] \\ \mathbf{f}^{\mathrm{T}}(n) &= [f(n), f(n-1), \ldots, f(n-I+1)] \end{aligned} \tag{18.6}$$

An example of this filtering process is shown schematically in Figs. 18.22 and 18.23. Figure 18.22 shows the input time sequence $f(n)$ and the impulse response of the digital filter $w(i)$. Figure 18.23 depicts the filtering of Eq. (18.4) at three increments in time during the filtering operation. The upper three charts plot the input sequence $f(n-i)$ for $n = 0, 4, 9$. The middle three charts plot the impulse response of the digital filter w. The lower three charts plot the output $g(n)$ at time step $n = 0, 4, 9$. As shown in these figures, the output of the filter is obtained by computing the summation of the time-reversed input signal as it slides past the impulse response of the filter.

The digital filter of Eq. (18.4) depends only on current and past values of the input sequence and is limited in length to I coefficients. These types of digital filters are referred to as finite impulse response (FIR) filters because their impulse response is zero after a finite number of taps or coefficients. These filters are also known as "tapped delay line," "moving-average" (MA), "nonrecursive," "all zero," or "transversal" filters.

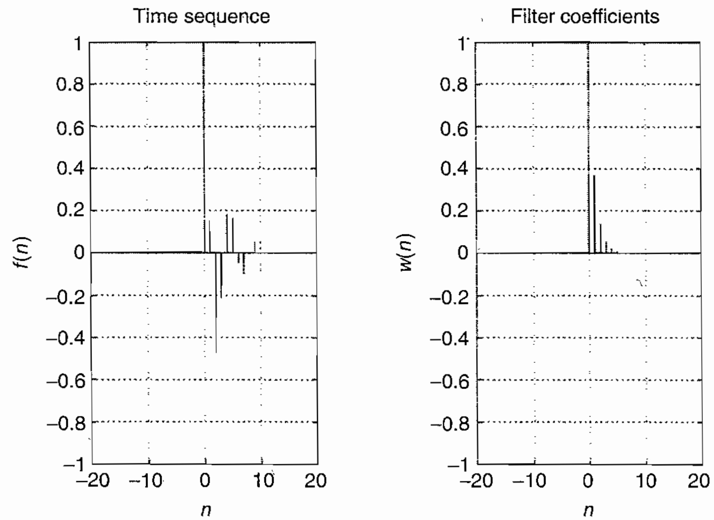

FIGURE 18.22 Example input sequence and impulse response.

A more general class of filters is defined as

$$g(n) = \sum_{i=0}^{I-1} a_i f(n-i) + \sum_{k=1}^{K} b_k g(n-k) \tag{18.7}$$

In addition to depending on current and past values of the inputs, the current output of the digital filter represented by Eq. (18.7) depends on past values of the output. Digital filters of this type are referred to as infinite impulse response (IIR) filters because, in general, the impulse response of these filters never decays to zero. These filters are also known as "recursive," "pole-zero," or "autoregressive moving average" (ARMA) filters. The general form of Eq. (18.7) reduces to a FIR filter when $b_k = 0$ for all k.

Implementations of FIR and IIR filters can be represented schematically if we define a delay operator z^{-k} such that

$$f(n-k) = z^{-k}\{f(n)\} \tag{18.8}$$

Using the property of the delay operator in Eq. (18.8) and the general filter representation in Eq. (18.7), a FIR filter can be implemented as shown in Fig. 18.24. A corresponding implementation for an IIR filter is shown in Fig. 18.25. A desired filter response can be approximated digitally using either the FIR or IIR filter structures discussed above. The choice between these two involves certain trade-offs, including the following:

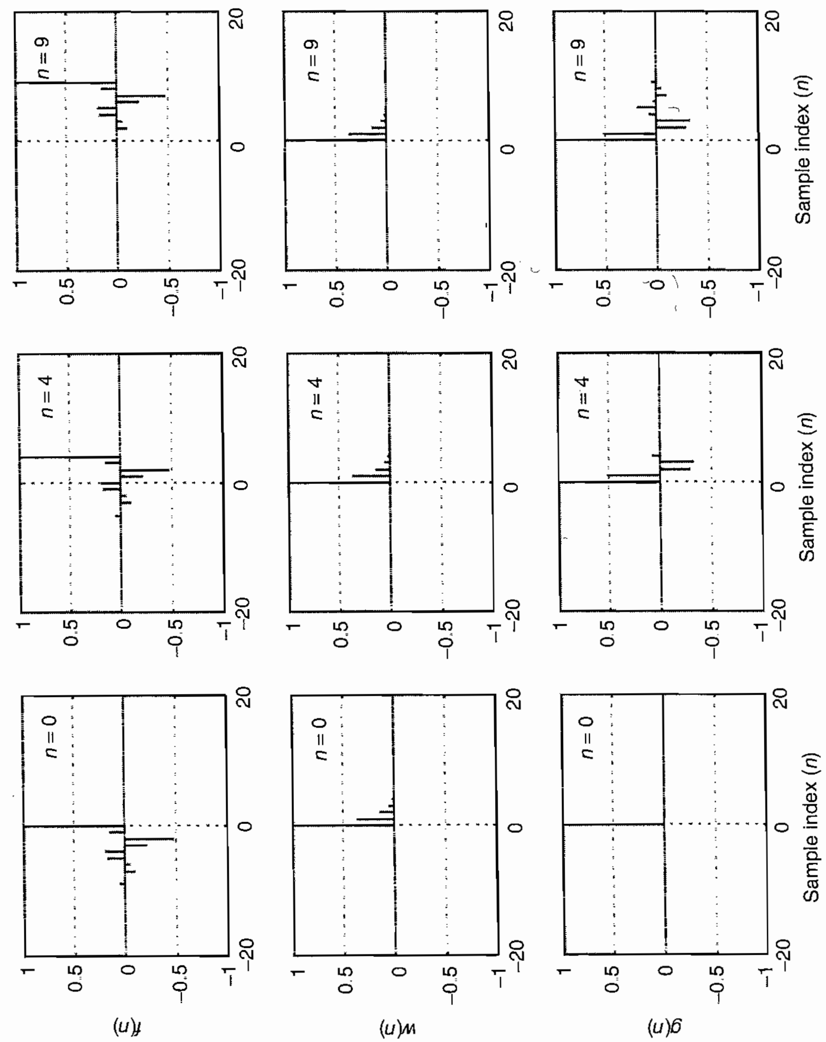

FIGURE 18.23 Representation of digital filtering as a discrete convolution.

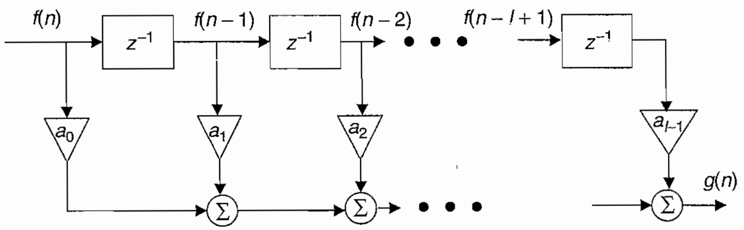

FIGURE 18.24 Implementation of a FIR filter using current and delayed values of the input.

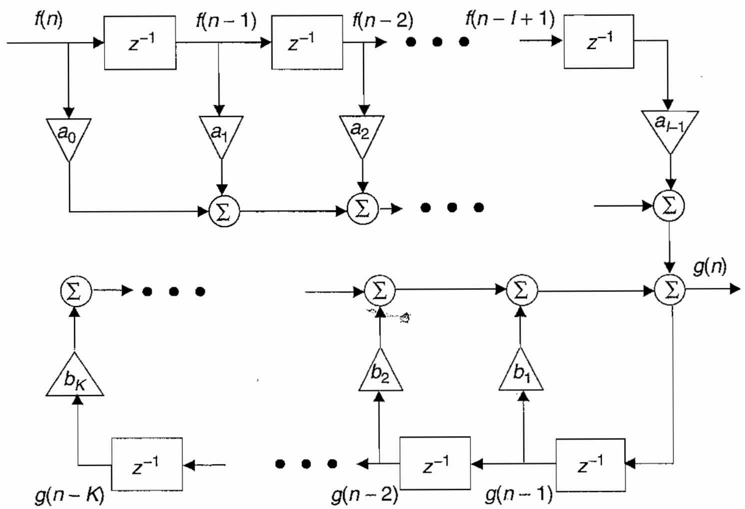

FIGURE 18.25 Implementation of an IIR filter using current input and delayed values of the inputs and outputs.

- FIR filters are guaranteed to be stable provided the coefficients are finite: Bounded inputs produce bounded outputs.
- IIR filters can be unstable even when all coefficients are finite: Bounded inputs can produce unbounded outputs.
- IIR filters may require fewer coefficients than FIR filters to approximate the frequency response necessary to provide active noise and vibration control: Typical transfer functions associated with structural acoustics include both poles and zeros, as do IIR filters, whereas FIR filters have only zeros.
- Design procedures to solve for FIR filter coefficients are generally numerically better behaved than those to solve for IIR filter coefficients.

Although there are advantages and disadvantages to both approaches, the vast majority of ANVC applications rely on the numerically stable design procedures and guaranteed stability associated with FIR filters and consequently implement the digital filters within ANVC controllers as FIR filters or composites of FIR filters.

Optimal Digital Filter Design

Having described the concept of digital filtering in the previous section, we focus in this section on design procedures to solve for the optimal coefficients of a digital filter for a particular class of problems. The class of problems considered is illustrated in Fig. 18.26. This problem is referred to as the electrical noise cancellation problem and is discussed in detail in references[56,58, and 59]. This is an important class of problems because it introduces the concept of minimizing a mean-square error metric and because it has strong parallels to problems encountered in ANVC applications; the main difference is that ANVC applications will have a nonunity transfer function relating the output of the control filter to the error signal response.

As shown in Fig. 18.26, the input signal $f(n)$, which is also referred to as the reference signal, is filtered by the FIR filter **w** to produce an output sequence $y(n)$. The desired signal, $\hat{d}(n)$, is contaminated by noise correlated with the input signal but presumably uncorrelated with the desired signal. The resulting signal plus noise is shown in the figure as $d(n)$. The correlation of the noise and the input signal is indicated by the unknown physical impulse response function h_i. The objective for this problem is to solve for the coefficients of the FIR filter that will take the input sequence $f(n)$ and generate the output sequence $y(n)$ that will remove the unwanted noise from the signal $d(n)$. In other words, we seek to design the optimal FIR filter to remove the part of $d(n)$ that is correlated with the input signal $f(n)$. If successful, the error signal $e(n)$ will be uncorrelated with the input signal when the filter is in place.

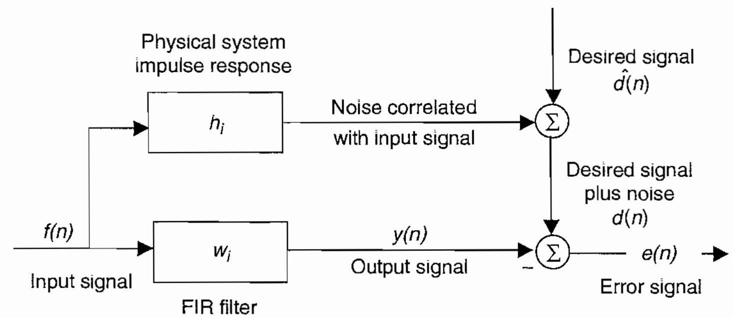

FIGURE 18.26 Electrical noise cancellation problem.

Following the developments in references 56 and 58 the error signal can be expressed in terms of the desired signal plus noise, the input signal, and the FIR filter coefficients:

$$\begin{aligned} e(n) &= d(n) - \sum_{i=0}^{I} w(i) f(n-i) \\ &= d(n) - \mathbf{w}^{\mathrm{T}}\mathbf{f}(n) = d(n) - \mathbf{f}^{\mathrm{T}}(n)\mathbf{w} \end{aligned} \tag{18.9}$$

where the lower equation has been used to express this relationship using vector inner products and $f(n)$ is defined in Eq. (18.6).

An expression for the mean-square error can be obtained by expanding terms in Eq. (18.9) and taking the expected value:

$$E\{e^2(n)\} = E\{d^2(n)\} - 2\mathbf{w}^{\mathrm{T}} E\{\mathbf{f}(n)d(n)\} + \mathbf{w}^{\mathrm{T}} E\{\mathbf{f}(n)\mathbf{f}^{\mathrm{T}}(n)\}\mathbf{w} \tag{18.10}$$

Equation (18.10) is a key result because it reveals that the mean-square error is a quadratic function of the weights of the FIR filter. The quadratic function will have a *global minimum* provided that the matrix $E\{\mathbf{f}(n)\mathbf{f}^{\mathrm{T}}(n)\}$ in the third term is *positive definite*,[56,58–60] which means that all of its eigenvalues are greater than zero. Assuming this requirement is met, if one were to plot the mean-square error as a function of any two of the coefficients of the FIR filters, the "error surface" would be a bowl, as shown in Fig. 18.27. As a consequence, the FIR filter coefficients that correspond to the minimum mean-square error can be determined by differentiating Eq. (18.10) with respect to each coefficient of the FIR filter and setting the resulting set of equations equal to zero.

This process of differentiating and equating the results to zero will produce a set of linear equations in terms of the unknown coefficients of the FIR filter. This matrix equation can be expressed as

$$[\mathbf{A}]\mathbf{w} = \mathbf{b} \tag{18.11}$$

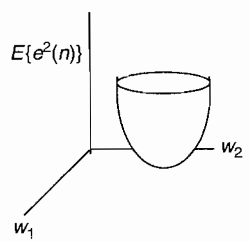

FIGURE 18.27 Error surface for a quadratic function in terms of coefficients w_1 and w_2.

where [**A**] is the *input correlation matrix* defined as

$$[\mathbf{A}] = \begin{bmatrix} R_{ff}(0) & R_{ff}(1) & \cdots & R_{ff}(I-1) \\ R_{ff}(1) & R_{ff}(0) & & \\ \vdots & & \ddots & \vdots \\ R_{ff}(I-1) & & & R_{ff}(0) \end{bmatrix} \tag{18.12}$$

where

$$R_{ff}(m) = E\{f(n)f(n-m)\} = E\{f(n)f(n+m)\} \tag{18.13}$$

The vector **b** in Eq. (18.11) corresponds to the lag values of the cross correlation between the reference sequence and the desired sequence given by

$$\mathbf{b} = [\, R_{fd}(0) \quad R_{fd}(1) \quad \cdots \quad R_{fd}(I-1)\,]^{\mathrm{T}} \tag{18.14}$$

where

$$R_{fd}(m) = E\{f(n)d(n+m)\} = E\{f(n-m)d(n)\} \tag{18.15}$$

With the above definitions for [**A**] and **b**, the coefficients of the optimal FIR filter can be expressed in terms of auto- and cross-correlation functions of the input and the desired signals. Provided that the input correlation matrix [**A**] is invertible, the optimal coefficients are given by

$$\mathbf{w}_{\mathrm{opt}} = [\mathbf{A}]^{-1}\mathbf{b} \tag{18.16}$$

where $[\mathbf{A}]^{-1}$ is the inverse of the matrix [**A**]. As discussed by Widrow and Stearns[59] and Elliott,[58] the solution of Eq. (18.16) is called the *Wiener filter*. It can be shown that using this filter will cause the cross correlation between the error signal and input signal to be zero over the length of the filter $(I-1)$. For the problem posed in Fig. 18.26, this implies that the Wiener filter will remove any portion of the signal, $d(n)$, that is correlated with the input signal $f(n)$.

The residual mean-square error can be determined by substituting Eq. (18.16) into Eq. (18.10):

$$E\{e^2(n)\}_{\min} = E\{d^2(n)\} - \mathbf{b}^{\mathrm{T}}[\mathbf{A}]^{-1}\mathbf{b} \tag{18.17}$$

Solving for $\mathbf{w}_{\mathrm{opt}}$ in Eq. (18.16), however, requires computing the inverse of the input correlation matrix [**A**], which can be computationally expensive and may be numerically ill-conditioned (i.e., singular). As a consequence, procedures have been developed to search for the minimum of Eq. (18.10) using iterative techniques. One of the most computationally efficient iterative techniques, the least mean-square (LMS) algorithm, is introduced in the next section.

Adaptive Digital Filter Design

Gradient Descent Algorithms. As discussed in the previous section, the mean-square error is a quadratic function in terms of the optimal weights of the FIR filter. As such, gradient descent algorithms are guaranteed to converge to the global minimum, provided [**A**] is positive definite and the algorithm is itself stable.

The basic concept of a gradient descent algorithm is to estimate the gradient (i.e., derivative) of the mean-square error with respect to the FIR filter coefficients and update the filter coefficients by moving in the direction of the negative of the local gradient. There are many different algorithms that can be used to adaptively determine the filter coefficients corresponding to the global minimum. These algorithms include Newton-based algorithms, steepest-descent algorithms, and the LMS algorithm, which was introduced by Widrow and Stearns.[59] These algorithms typically trade off convergence speed versus numerical stability (for IIR filters) and computational complexity. Details of these algorithms can be found in texts written by Widrow and Stearns[59] and Elliott.[58] While sometimes having performance advantages over FIR filters, IIR filters can encounter numerical stability problems during design and can converge to nonglobal minima, resulting in less than optimal performance. On the other hand, the LMS algorithm discussed in the next section (for FIR filter design) approximates the gradient term, thus significantly reducing the required number of computations while ensuring convergence to the optimal coefficient vector.

LMS Algorithm. Widrow and Stearns[59] developed an elegant algorithm that greatly simplifies the computational complexity yet still converges to the optimal coefficient vector (i.e., Wiener filter). This algorithm estimates the gradient term using the instantaneous value of the error, as opposed to performing a matrix inversion or estimating expected values as required by Newton's algorithm and steepest-descent algorithm, respectively. As a consequence, the gradient term is approximated as [see Eq. (18.10)]

$$\frac{\partial E\{e^2(n)\}}{\partial \mathbf{w}} \approx 2e(n)\frac{\partial e(n)}{\partial \mathbf{w}} \approx -2\mathbf{f}(n)e(n) \tag{18.18}$$

Using this expression for the gradient, the update equation of the filter coefficients using the LMS algorithm is given by

$$\mathbf{w}(n+1) = \mathbf{w}(n) + 2\mu\mathbf{f}(n)e(n) \tag{18.19}$$

where μ is a constant known as the adaptation coefficient, which characterizes the speed of convergence of the algorithm. This equation states that the vector of filter coefficients at time step $n+1$ can be determined from the vector of coefficients at time step n plus a correction term in the direction of the negative of the gradient of the error surface as estimated by Eq. (18.18).

Widrow and others have shown that this algorithm will converge to the optimal solution and is guaranteed to be stable provided that the value of the convergence parameter satisfies the relationship

$$0 < \mu < \frac{2}{m\overline{f^2}} \tag{18.20}$$

The denominator of the right-hand term is an approximation to the trace of the input correlation matrix, where m is the number of FIR filter coefficients and $\overline{f^2}$ is equal to the mean-square value of $f(n)$.

Another important parameter associated with the LMS algorithm is termed the *misadjustment*, which is the ratio of the excess mean-square error to the minimum mean-square error. Essentially, this is a measure of how close the algorithm will converge toward the bottom of the quadratic performance surface (see, e.g., Fig. 18.27) for a particular value of μ. It can be shown that the *misadjustment* is equal to the convergence parameter times the trace of the input correlation matrix for the LMS algorithm.[59] If we invoke the same approximation to this trace as in Eq. (18.20), we obtain an expression for the convergence parameter in terms of the misadjustment and mean-square value of the input sequence:

$$\mu_{\max} = \frac{\rho}{m\overline{f^2}} \tag{18.21}$$

where ρ is the misadjustment factor. This final expression provides a useful procedure for selecting the convergence parameter. In fact, it is often useful to specify the desired misadjustment (e.g., $\rho = 0.01$) and let the adaptation coefficient be calculated from Eq. (18.21). In this way, the resulting adaptation coefficient will be normalized by the power of the reference signal. When the adaptation coefficient is adjusted to be inversely proportional to the power of the input signal, the algorithm is referred to as the *normalized* LMS algorithm. In practice, the value of the convergence coefficient obtained in this way serves as a starting point and manual adjustment is often necessary to obtain the desired performance.

To preserve clarity, we have presented the LMS algorithm assuming a SISO error signal. However, the algorithm is easily extendable to the MIMO case. Details for the MIMO implementation can be found in Widrow and Stearns,[59] Nelson and Elliott,[16] and Elliott.[58]

Because of its computational simplicity and good convergence properties, the LMS algorithm has been used extensively in a variety of applications (e.g., in-wire cancellation, system identification) and is the basis for the filtered-x LMS algorithm that is most often used in ANVC applications. In fact, the LMS algorithm is typically used to estimate the impulse response between the filter output and the error signal (i.e., plant), which is needed for the implementation of the filtered-x LMS algorithm. Details and examples of the filtered-x LMS algorithm are covered in the next section.

18.4 FEEDFORWARD CONTROL SYSTEMS

Basic Architecture

The basic architecture of a feedforward active control system is shown in Fig. 18.28. The figure shows a disturbance d exciting a system which is to be controlled. A transfer function T relates the disturbance to the system output o.

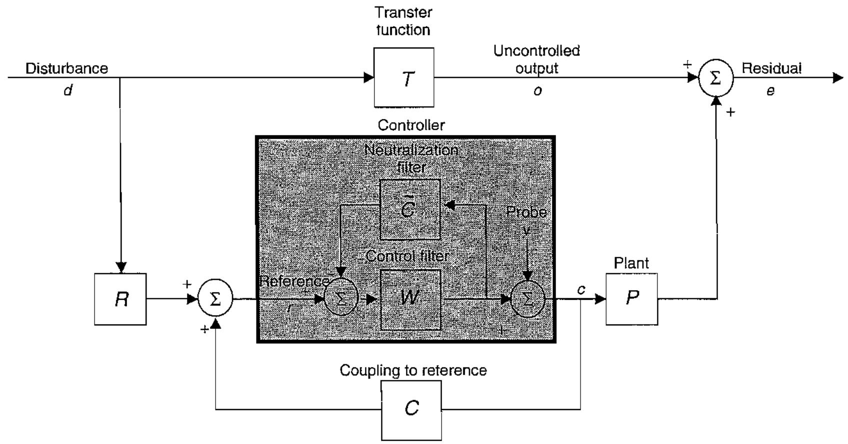

FIGURE 18.28 Basic feedforward architecture without adaptation.

A reference signal r correlated with the disturbance is used by the controller to generate a signal that drives a control actuator to excite the system and reduce the system response to the disturbance. The transfer function R is shown simply to indicate that the disturbance and the reference are correlated. The transfer function P, referred to as the plant, relates the controller output to the system output. The block diagram shows that the actuator, when driven by the controller output, is coupled not only to the system output but also to the reference through the transfer function C. The feedback to the reference signal is not desirable and the controller contains a filter $\tilde{C}$ the transfer function of which is a copy of the coupling transfer function between the control actuator and the reference sensor. The purpose of this neutralization filter is to cancel or neutralize the coupling between actuator and reference signal. In addition to $\tilde{C}$, the controller contains a second filter, W, the purpose of which is to take the reference signal and generate a signal to drive the actuator to reduce the system output o. If the neutralization filter performs properly, the coupling to the reference is removed and the block diagram simplifies to that shown in Fig. 18.29. Note that an alternate approach has been pioneered by Eriksson and his colleagues in which the designs of W and $\tilde{C}$ are combined in a slightly different architecture from that shown here. The interested reader is referred to references 25 and 61–63.

To see what the block diagram in Fig. 18.28 means physically, consider the duct problem described in Section 18.2. Figure 18.30 show a schematic of the duct with a reference microphone, controller, and control speaker. The disturbance, a sound wave of amplitude d, can be seen to the left propagating down the duct toward the control speaker. The transfer function T relates the disturbance pressure to the uncontrolled pressure, o, downstream of the speaker location in the duct. The reference microphone senses the disturbance pressure and sends a reference signal r to the controller. The control filter W operates

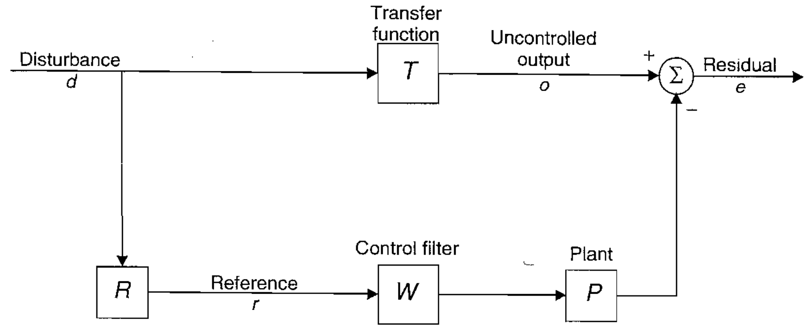

FIGURE 18.29 Simplified feedforward architecture with coupling to reference removed.

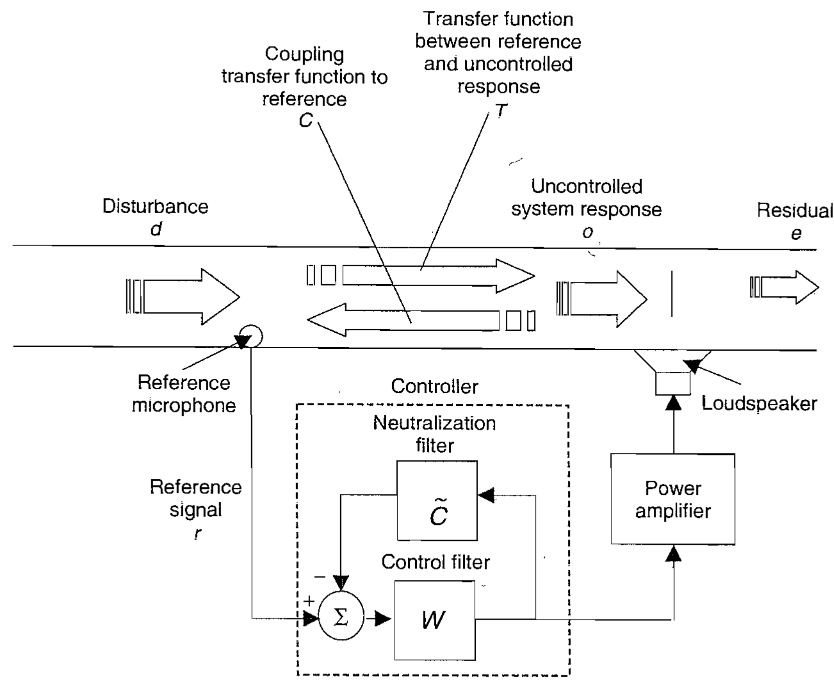

FIGURE 18.30 Feedforward architecture applied to the control of noise in a duct.

on the reference and sends the resulting signal to the power amplifier, which in turn drives the speaker. The transfer function relating the controller output signal to the pressure in the duct at the speaker is the plant transfer function P. The pressure generated by the speaker interacts with the disturbance propagating down the duct, reducing the amplitude and producing the residual sound wave of amplitude e. In an adaptive system there would be a microphone in the duct downstream of the control speaker to sense this residual. As we shall see later, this residual, or error, signal and the reference signal can then be used in the controller electronics to update, or adapt, the coefficients of the control filter. In addition to generating a sound wave that interferes with the sound propagating down the duct, the speaker also generates a sound wave which travels upstream to the reference microphone, contaminating the reference signal. The filter $\tilde{C}$ is a copy of the transfer function relating the controller output to the pressure at the reference microphone. It electronically removes the contamination from the control speaker in the reference microphone before it reaches the control filter W.

The architecture in Figs. 18.28 and 18.29 has been discussed as if there were only one reference signal and one residual. In fact, the controller need not be restricted to the SISO case. There commonly are cases with multiple references and multiple residuals. In fact, for feedforward systems the procedures for estimating the optimum control filter W for the MIMO case as well as the SISO case are well in hand. In addition the block diagrams in Figs. 18.28 and 18.29 are completely general and apply equally to SISO or MIMO systems. The only difference is that the blocks, which for SISO systems are transfer functions, for MIMO systems become transfer function matrices.

Optimal Control Filter Estimation

Tonal Disturbances. We will first consider the case of narrow-band, or tonal, disturbances. To do so, we will first modify the block diagram of Fig. 18.29 by showing a functional connection between the reference and the disturbance indicated by the transfer function B, as shown in Fig. 18.31. Mathematically this is equivalent to setting $T = 1$ and $B = R^{-1}$. A simple equation can be written for the residual e in terms of the controller transfer function in Fig. 18.31:

$$e(\omega) = d(\omega) - P(\omega)W(\omega)r(\omega) \tag{18.22}$$

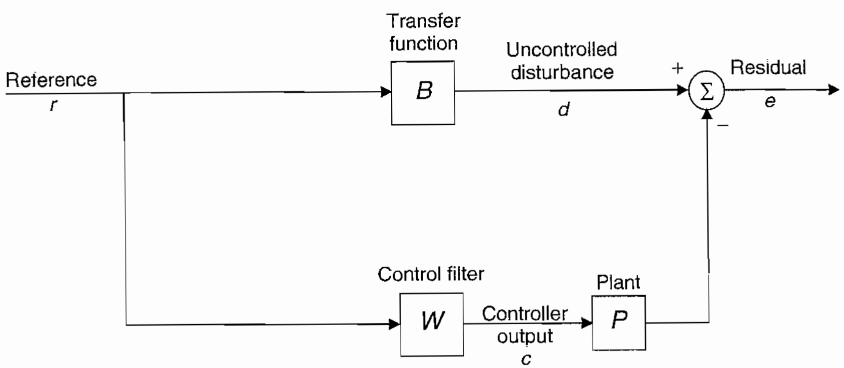

FIGURE 18.31 Simplified feedforward block diagram.

where ω is the frequency of the disturbance, the other variables are defined in Fig. 18.31, and all of the variables are scalars. We can use this equation to express the autospectrum of the residual as $S_{ee}(\omega) = E\{e(\omega)e^*(\omega)\}$, where $E\{\cdot\}$ means the expected value. Substituting Eq. (18.22) into this equation, we obtain

$$\begin{aligned} S_{ee}(\omega) &= S_{dd}(\omega) - P(\omega)W(\omega)S_{rd}(\omega) \\ &\quad - P^*(\omega)W(\omega)^*S_{dr}(\omega) + |P^2(\omega)|S_{rr}(\omega)|W(\omega)^2| \end{aligned} \tag{18.23}$$

where $(\cdot)^*$ means complex conjugate, S_{dd} is the autospectrum of the disturbance, S_{rr} is the autospectrum of the reference, $S_{dr} = E\{dr^*\}$ is the cross-spectra of the disturbance and the reference, and $S_{rd} = E\{rd^*\}$ is the complex conjugate of that cross-spectrum. If we take the derivative of Eq. (18.23) with respect to W and equate it to zero and solve for $W(\omega)$, we obtain

$$W(\omega) = \{|P^2(\omega)|S_{rr}(\omega)\}^{-1}P^*(\omega)S_{rd}(\omega) = P^{-1}(\omega)\left\{\frac{S_{rd}(\omega)}{S_{rr}(\omega)}\right\} = P^{-1}(\omega)B(\omega) \tag{18.24}$$

where we have taken advantage of the fact that $\{S_{rd}(\omega)/S_{rr}(\omega)\}$ is an estimate of the transfer function between the disturbance and the reference. In Eq. (18.24) W is the optimum control filter. It consists of the inverse of the plant times an estimate of the transfer function between the reference and the disturbance. Such a form for the control filter makes a lot of sense, because W is attempting to take the reference signal r and turn it into the disturbance d. To do so, the filter must first remove the influence of the plant transfer function, which is the purpose of the plant inverse. It then must include an estimate of the transfer function between the reference and the disturbance, which is the purpose of the term in brackets.

If we substitute Eq. (18.24) into Eq. (18.23), we can obtain an estimate of the spectrum of the residual when this control filter is used:

$$S_{ee}(\omega) = S_{dd}(\omega) - \frac{|S_{rd}(\omega)|^2}{S_{rr}(\omega)} \tag{18.25}$$

This equation shows that for perfect correlation between the reference and disturbance ($d = \gamma r$), where γ is constant, the spectrum of the residual goes to zero.

Note that this approach does not guarantee that the control filter will be causal. As discussed in Section 18.3, a causal filter is one whose impulse response is zero for $t < 0$. Causal filters can be formulated as FIR or stable IIR digital filters. Noncausal filters cannot. Consequently, a digital representation of a noncausal filter cannot be found for use in a control system. The filter is simply not realizable.

In some cases using the above control filter can result in excessive demands on the actuators, in which case it is useful to be able to limit the output of the control filter. Control effort weighting is one means of reducing the actuator effort. It can be included in the design equations for the filter by adding a term to Eq. (18.23), the equation for the residual. The term that is added is the weighted output of the controller given by

$$\alpha^2(\omega)|W(\omega)^2|S_{rr}(\omega) \tag{18.26}$$

where α^2 is a real positive scalar that might be a function of frequency. By selecting increasing values of α^2, the minimization of the residual can be adjusted. If α^2 is very small, the control filter will be designed as if there were no control effort weighting. If α^2 is large, the control effort will be reduced, and the performance of the control system will also be reduced. Including Eq. (18.26) in Eq. (18.23) results in a control filter given by

$$W(\omega) = \{[|P^2(\omega)| + \alpha^2(\omega)]S_{rr}(\omega)\}^{-1}P^*(\omega)S_{rd}(\omega) \tag{18.27}$$

and the residual is given by

$$S_{ee}(\omega) = S_{dd}(\omega) - \left\{\frac{|P^2(\omega)|}{|P^2(\omega)| + \alpha^2(\omega)}\right\}\left\{2 - \frac{|P^2(\omega)|}{|P^2(\omega)| + \alpha^2(\omega)}\right\}\frac{|S_{rd}(\omega)|^2}{S_{rr}(\omega)} \tag{18.28}$$

It is clear from this equation that as α^2 approaches zero the residual becomes the same as Eq. (18.25) with no control effort weighting. However, as α^2 becomes large, $S_{ee} \to S_{dd}$ and the control performance is reduced. Similarly the spectrum of the controller output c (see Fig. 18.31) is given by

$$S_{cc}(\omega) = |W^2(\omega)|S_{rr}(\omega) = \frac{|P^2(\omega)|}{\{|P^2(\omega)| + \alpha^2(\omega)\}^2}\frac{|S_{rd}(\omega)|^2}{S_{rr}(\omega)}$$

This equation shows that as α^2 increases the spectrum of the controller output will decrease, reducing the drive to the actuators. As a result increasing the control effort weighting will decrease the actuator drive at the cost of increasing the residual.

Broadband Disturbances. For a pure-tone disturbance, Eqs. (18.24) and (18.27) provide the proper control filter representation (amplitude and phase) at the frequency of the disturbance. For a broadband disturbance, if the broadband filter defined by these equations is noncausal, as it often is, then, a different approach that includes a constraint on causality needs to be employed to determine the optimum causal filter. We can ensure that the control filter is causal by inserting the form of a causal filter into Eq. (18.23) and carrying out the same optimization procedure. Because it results in a set of linear equations, we will use the form of an FIR digital filter given by

$$W(\omega) = \sum_{n=0}^{N-1} W_n e^{-j\omega n\Delta t} \tag{18.29}$$

where N is the number of taps in the filter, W_n is the real amplitude associated with each tap, and Δt is the sampling period (1/sampling rate). Before substituting Eq. (18.29) into (18.23) we need to modify Eq. (18.23) slightly. Since we are now concerned with a broadband disturbance, we need to integrate the residual spectrum over the frequency range where control is desired. Following the same procedure as for Eq. (18.23), we obtain for the optimum control filter the matrix equation

$$\begin{Bmatrix} W_0 \\ W_1 \\ \vdots \\ W_{N-1} \end{Bmatrix} = \begin{bmatrix} C_0 & C_{-1} & \cdots & C_{1-N} \\ C_1 & C_0 & \cdots & C_{2-N} \\ \vdots & & & \vdots \\ C_{N-1} & C_{N-2} & \cdots & C_0 \end{bmatrix}^{-1} \begin{Bmatrix} A_0 \\ A_1 \\ \vdots \\ A_{N-1} \end{Bmatrix} \tag{18.30}$$

where

$$A_p = \mathrm{Re}\left\{\sum_{k=0}^{K-1} P(k)S_{rd}(k)e^{-jpk(2\pi/K)}\right\}$$

$$C_{(p-m)} = \mathrm{Re}\left\{\sum_{k=0}^{K-1}\{|P^2(k)| + \alpha^2(k)\}\,S_{rr}(k)e^{-j(p-m)k(2\pi/K)}\right\} \tag{18.31}$$

and $p = 0, 1, \ldots, N-1$ and $m = 0, 1, \ldots, N-1$. In writing this equation, we have substituted a discrete sum for the integrals. The knowledgeable reader will recognize that Eq. (18.31) is in the form of the discrete Fourier transform (DFT), allowing for the efficient use of the fast Fourier transform algorithm in the evaluation of the vector and matrix elements in Eq. (18.30). In the equations K is the number of elements in the DFT.

Example. To illustrate these ideas, we will compute the noncausal and causal control filters for a simple example. We will use the following parameters:

$$S_{dd} = 1 \qquad S_{rr} = 1$$

$$S_{rd} = e^{-j\omega T}\left\{\frac{\omega_{\mathrm{BW}}^4}{\omega^4 + \omega_{\mathrm{BW}}^4}\right\} \tag{18.32}$$

$$P = \frac{\omega_0^2}{-\omega^2 + j\eta\omega_0\omega + \omega_0^2} \tag{18.33}$$

$$T = 0.02\ \mathrm{s} \qquad f_0 = \frac{\omega_0}{2\pi} = 25\ \mathrm{Hz}$$

$$\eta = 0.1 \qquad f_{\mathrm{BW}} = \frac{\omega_{\mathrm{BW}}}{2\pi} = 40\ \mathrm{Hz}$$

Sampling rate = 200 Hz Filter length = 100 taps

In this case the autocorrelations of the disturbance and reference are taken as unity. The cross-spectral density S_{rd} shows a delay of $T = 0.02$ s and includes a transfer function (in brackets) that decreases with increasing frequency. The plant P is a simple second-order system with a natural frequency of 25 Hz and a loss factor of 0.1. For the causal control filter estimation procedure we will use the indicated sampling rate and filter length.

Figure 18.32 compares the frequency responses of the control filters estimated using the noncausal and causal estimation procedures. The two estimation procedures give different filters but not markedly so. The difference is slightly more evident in Figs. 18.33a and 18.33b, where the impulse response of the control filter estimated using the noncausal approach and the filter tap coefficients of the filter from the causal procedure are compared. Bear in mind that if we plot the filter tap coefficients separated by the sampling period (0.005 s at 200 Hz sampling rate), we will obtain a graph corresponding to the impulse response of the filter. The two figures are similar except that in the noncausal impulse response there is a small increase near the end of the time interval. Because of the periodicity of the impulse response of the filter obtained using the DFT, the increase at the end of the time interval actually indicates that the filter is responding before $t = 0$ and consequently that the filter is noncausal. The effect in this

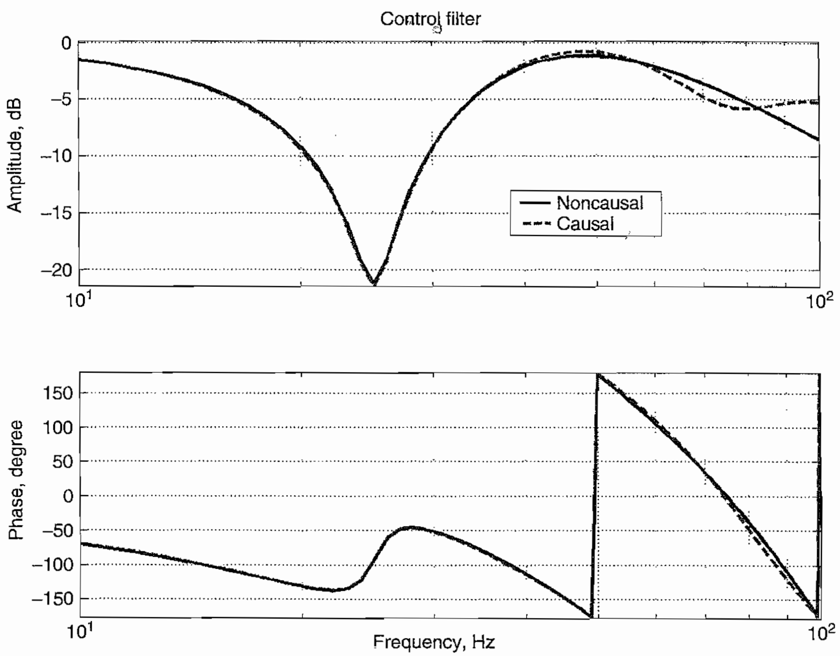

FIGURE 18.32 Control filter frequency response using the noncausal and causal estimation procedures.

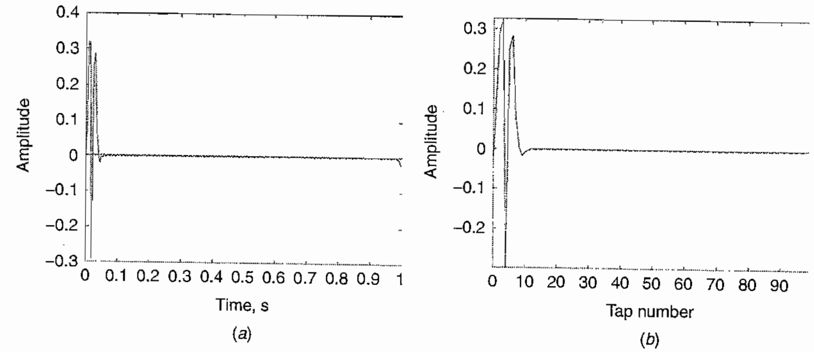

FIGURE 18.33 Comparison of the impulse response of (a) the noncausal control filter and (b) the tap coefficients of the causal filter.

instance is small; however, in later examples where we bring more realism into the calculation by including anti-aliasing filters and other practical considerations we will see much larger noncausal effects. Note that the tap coefficients of the filter estimated using the causal procedure show no such increase and the higher tap coefficients decrease to zero.

The performance of this system using the causal control filter is shown in Fig. 18.34. The figure shows the ratio of the spectrum of the controlled residual to the spectrum of the uncontrolled residual $\{S_{ee}(\omega)/S_{dd}(\omega)\}$ as a function of

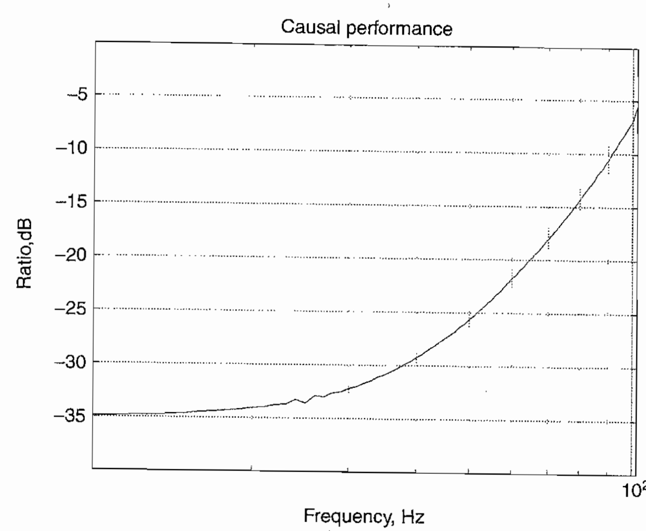

FIGURE 18.34 Ratio of the residual to the disturbance using the control filter in Fig. 18.32.

frequency out to the Nyquist frequency. Note that the performance of the non-causal filter (not shown in the graph) would be predicted to be perfect, that is, the residual would be zero for all frequencies.

The performance shown in the Fig. 18.34 is unrealistically large for a broadband active control system. This is a consequence of the fact that, at this stage, we have neglected to include other elements in the analysis that would add more realism to the estimate, such as system delays, anti-aliasing filters, sensor noise, and so on. In addition the figure only shows system performance up to the Nyquist frequency (one-half the sampling frequency). As we shall see in a later section, the digital control filter is periodic in frequency with a period equal to the sampling frequency. Consequently, the performance above the Nyquist frequency may also need to be controlled, especially if there is significant energy in the disturbance at those frequencies. We will see how this is done in a later section.

Adaptive Control

In the previous section we discussed the design of a control filter to reduce optimally a chosen residual in a least-squares sense. In that derivation the system to be controlled was assumed to be fixed. In reality the transfer functions defining dynamic systems often change with time. This means that those transfer functions must be measured periodically and the new results used to update the control filter coefficients. We will discuss this process of system identification in the next section. Here we examine an adaptive control algorithm based on the LMS algorithm that continuously updates the control filter coefficients in order to minimize the chosen residual sensor signals. The filtered-x algorithm, as it has come to be called, updates the control filter coefficients at each time step.

The filtered-x LMS algorithm, a modification of the LMS algorithm[59] commonly used for cancellation of electronic noise, was first proposed by Morgan.[64] If used unmodified in an active cancellation system, the LMS algorithm can lead to instabilities because the signal from the controller must pass through the plant dynamics where it will experience amplitude changes and phase shifts. The solution to this problem proposed by Morgan was also proposed independently by Widrow et al.[65] and Burgess.[66] Morgan's solution, which has come to be called the filtered-x LMS algorithm, is used extensively today and has been generalized to MIMO systems by Elliott and Nelson.[67]

Figure 18.35a shows a block diagram of a simplified feedforward control system. If we change the order of the plant and control filter in the block diagram, the response will be unchanged as long as the system is linear. The resulting block diagram is shown Fig. 18.35b. The result is a new reference signal u that is the original reference signal filtered by the plant transfer function P. The residual of this new system can be written as

$$e(n) = d(n) - \sum_{n=0}^{N_w-1} w(k)u(n-k) = d(n) - \mathbf{w}^{\mathrm{T}}\mathbf{u} \tag{18.34}$$

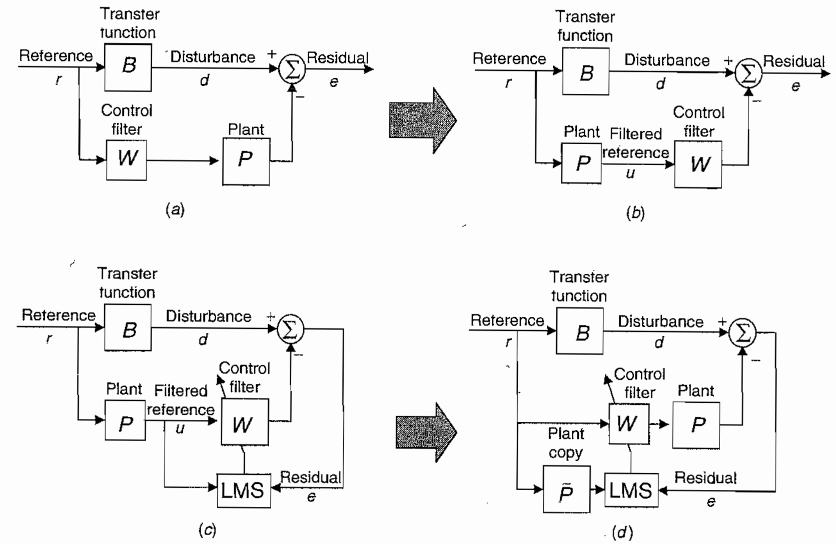

FIGURE 18.35 Feedforward block diagram with and without adaptation showing the progression to the LMS filtered-x algorithm: (a) original diagram; (b) changing the order of plant and control filter; (c) LMS algorithm; (d) filtered-x algorithm.

where $e(n)$ is the nth element of a time sequence $e, d(n)$ is similarly defined, $\mathbf{w}^{\mathrm{T}}$ is the transpose of a vector, the N_w elements of which are the control filter tap coefficients, and $\mathbf{u}$ is a column vector of the last N_w samples in the filtered reference, which is given by

$$u(n) = \sum_{m=0}^{N_w-1} p(m)r(n-m) \tag{18.35}$$

where p is the impulse response of the system estimate of the plant filter P and r is the reference signal time sequence. The block diagram showing the adaptation process is shown in Fig. 18.35c, and a slight rearrangement of the blocks in the block diagram in Fig. 18.35d results in the specialized LMS algorithm called the filtered-x LMS algorithm.

Unlike the direct-estimation approach in the previous section in which the filter coefficients are estimated in a single calculation, the filtered-x algorithm uses an iterative approach which updates the estimate at each time step. The update equation for the control filter is derived similarly to that for the LMS algorithm (see Adaptive Digital Filter Design in Section 18.3). The resulting equation to estimate the coefficients of w is typically written as

$$\mathbf{w}(n+1) = \mathbf{w}(n) + 2\mu e(n)\mathbf{u}(n) \tag{18.36}$$

where

$$\mathbf{w}(n) = \begin{Bmatrix} w(0) \\ w(1) \\ \vdots \\ w(N_w - 1) \end{Bmatrix}$$

is a column vector of the nth estimate of the N_w control filter coefficients, $w(0)$ is the first filter coefficient, $w(1)$ is the second, and so on,

$$\mathbf{u}(n) = \begin{Bmatrix} u(n) \\ u(n-1) \\ \vdots \\ u(n - N_w + 1) \end{Bmatrix}$$

is a column vector of the last N_w samples in the filtered reference, and μ is a scalar convergence coefficient set by the user to ensure stable convergence to the optimum filter coefficients. This equation is very similar to that derived for the LMS algorithm, the only difference being that the filtered reference $\mathbf{u}(n)$ is used in the update equation rather than the reference itself.

In Eq. (18.36) the larger is μ, the faster the algorithm will converge to the optimum filter coefficients. However, if μ is too large, the algorithm will go unstable and will not converge. The convergence coefficient can be selected using the following rule of thumb[58]:

$$0 < \mu \leq \frac{1}{N_w E\{u^2\}} \tag{18.37}$$

where N_w is the number of control filter coefficients and $E\{u^2\}$ is the mean-square value of the filtered reference. This is very similar to the rule of thumb for the LMS algorithm presented in Section 18.3 except that the mean-square value of the filtered reference, $E\{u^2\}$, is substituted for mean-square value of the reference itself, $E\{r^2\}$.

Equation (18.36) along with Eq. (18.35) states the SISO filtered-x algorithm. This algorithm has enjoyed a great deal of popularity because it is very easy to implement and functions well in the presence of errors in the plant estimate used to filter the reference. If the convergence rate is kept slow enough, the algorithm will still find the optimum filter coefficients even in the presence of plant phase errors of up to 90°.[64] In addition, the algorithm can be very effective in maintaining control even if the reference is nonstationary. Finally, it is possible to introduce something comparable to control effort weighting as discussed in the previous section. In the filtered-x algorithm this is referred to as *leakage*. By reducing the control filter coefficients by a small percentage at each time step,[59] the effect is similar to broadband control effort weighting.

Example. To illustrate the application of this algorithm, we will utilize it to design an optimum filter for the system of the previous section. To do so, we will require the impulse response function (IRF) associated with the cross-spectrum between disturbance and reference, S_{rd}, and the IRF of the plant, P. We obtain these by simply inverse Fourier transforming the FRF functions in Eqs. (18.32) and (18.33), respectively, and retaining a sufficient number of terms to ensure that we capture all of the impulse response. Figure 18.36 illustrates the two IRFs. The plant IRF is a decaying sinusoid with a frequency of 25 Hz, the natural frequency of the plant. The cross-spectrum IRF shows the delay of 0.02 s introduced into the model. We will retain the full 1 s duration (200 taps at a sampling rate of 200 Hz) of the IRFs in the figure, although it would probably be sufficient to retain substantially less. The filter coefficients obtained using the direct [Eq. (18.30)] and filtered-x [Eqs. (18.35) and (18.36)] estimation procedures are compared in Fig. 18.37, and the frequency response functions are compared in Fig. 18.38. There are clear differences between the two control filters that may be a consequence of the fact that the filtered-x procedure is still converging. That the procedure is still converging can be seen in Fig. 18.39, which shows a time history of the residual, or controlled disturbance. Even after over 80 s the residual still shows a tendency to decrease. Figure 18.40 shows the ratio of the spectrum of the controlled disturbance to the spectrum of the uncontrolled disturbance as a function of frequency at the end of the time interval in Fig. 18.39. Also shown in the figure is the same ratio for the direct-estimation procedure. In this case the two procedures give comparable results despite the differences in the control filters.

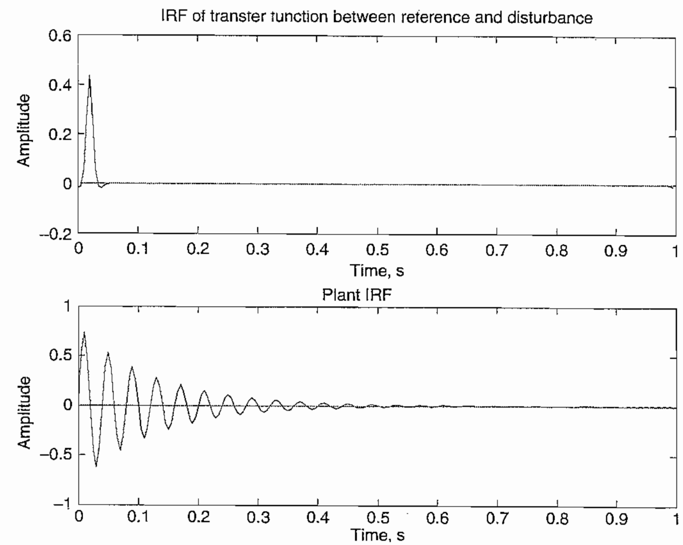

FIGURE 18.36 Impulse response functions for S_{rd} (top) and the plant, P (bottom).

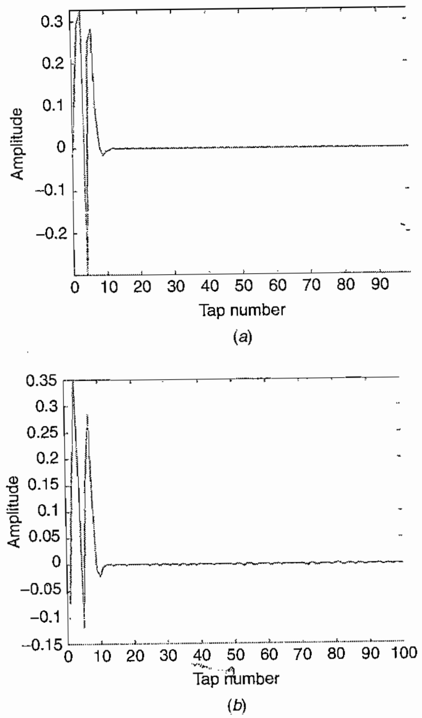

FIGURE 18.37 (*a*) Direct-estimation control filter coefficient compared to (*b*) filtered-x control filter coefficients.

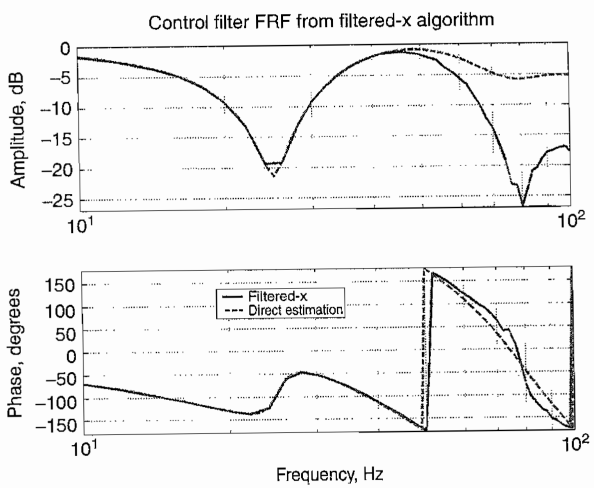

FIGURE 18.38 Filtered-x control filter frequency response compared to the direct estimation control filter frequency response.

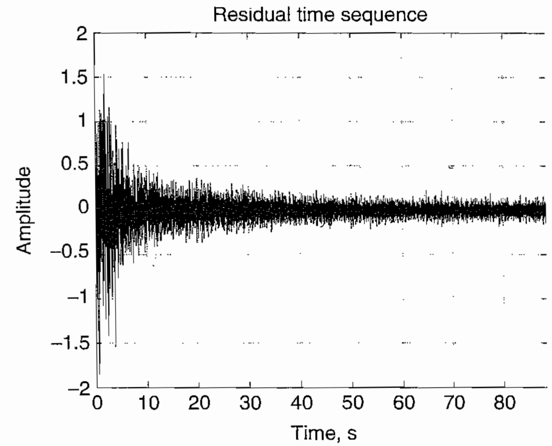

FIGURE 18.39 Time history of the residual.

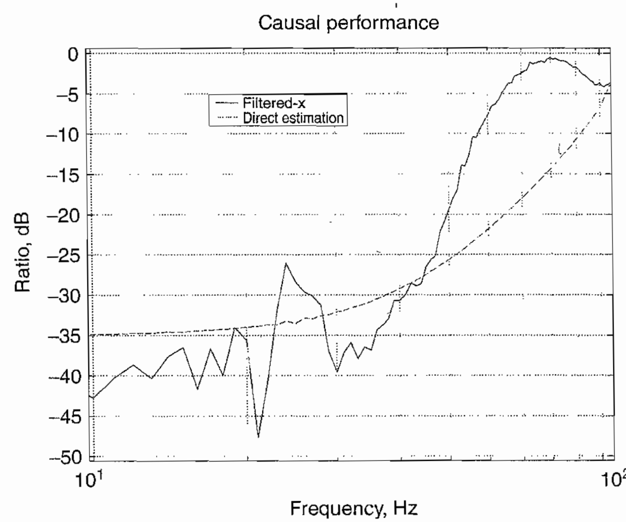

FIGURE 18.40 Ratio of controlled to uncontrolled disturbance.

Control of Aliasing Effects

In the previous sections we have focused on control of the disturbance below the Nyquist frequency. In fact, because digital filters are periodic in the frequency domain with a period equal to the sampling frequency, we must also concern ourselves with the performance above the Nyquist frequency, especially if the disturbance has significant amplitude there. Figure 18.41 shows the ratio

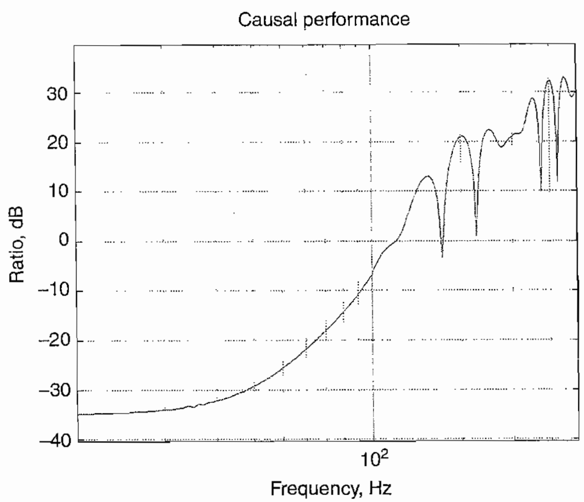

FIGURE 18.41 Change in the ratio of controlled to uncontrolled disturbance beyond the Nyquist frequency.

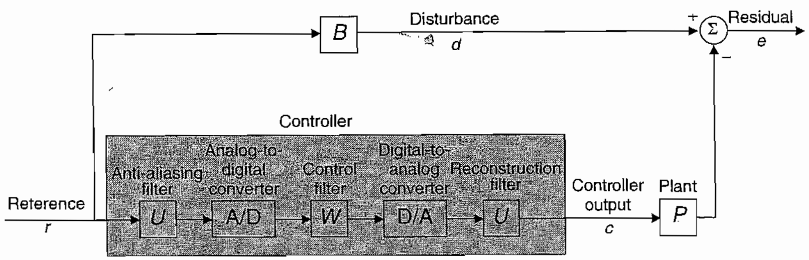

FIGURE 18.42 Feedforward block diagram further simplified (adaptation blocks not shown).

of the controlled-to-uncontrolled disturbance beyond the Nyquist frequency for the direct-estimation case in the previous section on optimal control filter estimation. Above ~125 Hz the figure shows that the control system will amplify the disturbance. To control this out-of-band amplification, one usually employs anti-aliasing filters, low-pass filters that minimize energy above the Nyquist frequency entering the controller. In addition, there are other low-pass filters and delays that should be included in a more realistic model of the active control system. To that end Fig. 18.42 shows the controller expanded into five blocks. First the analog reference signal needs to be digitized before the controller can utilize it. That is the function of the A/D converter shown as the second block in the controller. The first block is a low-pass filter called the anti-aliasing filter. Its cutoff frequency is usually set slightly below the Nyquist frequency in order

to reduce aliasing in the digital controller, as described above. The third block is the digital control filter, the output of which is fed to a D/A converter to convert the digital signals to analog signals. The D/A converter is usually a sample-and-hold device that produces a signal with discrete steps or jumps at the sampling rate. Consequently, there is usually a low-pass filter at the output of the D/A converter, typically called a reconstruction filter, to smooth or reconstruct the signal. This filter is typically the same as the anti-aliasing filter, although there is no requirement that the two filters be the same. The output of the reconstruction filter is an analog signal, c, that is applied to power electronics that will in turn drive a speaker or other actuator. The plant, P, accounts for all of the dynamics relating the controller output to the control signal, which cancels the disturbance d. In designing the control filter there may be significant delays associated with the anti-aliasing filter, the reconstruction filter, and the D/A converter, which need to be included in designing and evaluating the control filter. The delays associated with the A/D converter are usually small and can, in most cases, be neglected. The delays associated with the D/A converter, on the other hand, are on the order of half a sample period and usually need to be included in the design and evaluation process. To carry out the analysis, the anti-aliasing filter, reconstruction filter, and sample-and-hold delay (D/A converter) are usually lumped in with the plant transfer function. The D/A converter is typically modeled by a simple delay of one-half of the sample period. The total plant then becomes

$$U^2(\omega)P(\omega)e^{-j\omega\Delta T/2} \tag{18.38}$$

where ΔT is the sample period and $U^2(\omega)$ is the product of the frequency response functions of the anti-aliasing and reconstruction filters. To illustrate the impact on the design process and on the resulting performance, we will select an anti-aliasing filter and go through the design process once again using the same plant and disturbance-to-residual transfer function as used in Section 18.4 and given by Eqs. (18.32) and (18.33). As will be discussed in Section 18.6 under Hardware Selection, there is a wide variety of low-pass filter types that are commonly used for anti-aliasing and reconstruction, such as Butterworth, Bessel, and elliptical (Cauer), to name just a few. In this example we will use the third-order elliptical filter whose frequency response function is shown in Fig. 18.43. The filter has a cutoff frequency of 70 Hz, slightly below the Nyquist frequency, and the ratio of passband to stop-band amplitude is nominally 50 dB.

Using the direct-estimation procedure outlined in Section 18.4 under Optimal Control Filter Estimation, we obtain the causal control filter whose frequency response is shown in Fig. 18.44. Also shown in the figure is the noncausal control filter given by $B(\omega)\{U^2(\omega)P(\omega)\}^{-1}e^{j\omega\Delta T/2}$. The frequency response functions of the two filters are clearly quite different, but the difference is more clearly seen in Figs. 18.45a and b, where the impulse response function of the noncausal control filter and the filter coefficients of the causal control filter, respectively, are compared. The noncausal filter IRF shows a strong increase at the end of the time interval, which, as explained earlier, indicates that the filter responds before

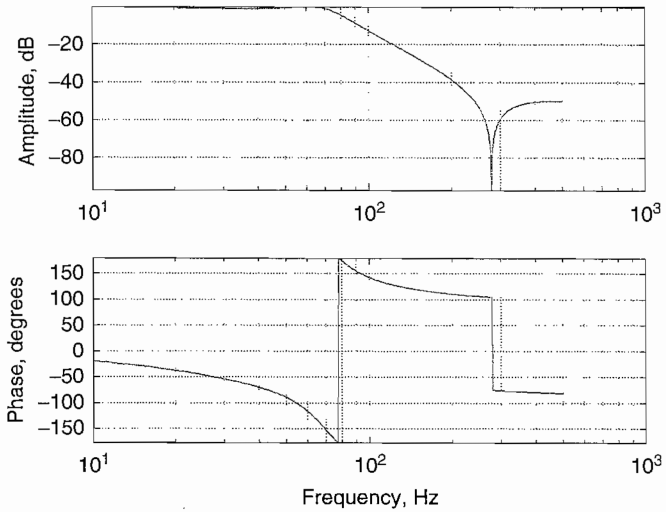

FIGURE 18.43 Frequency response function for a third-order elliptical filter with a cutoff frequency of 70 Hz and a passband–stop band ratio of 50 dB.

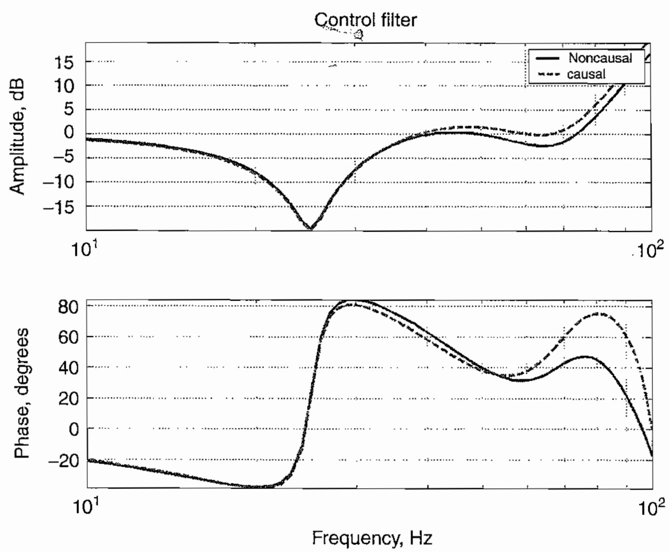

FIGURE 18.44 Comparison of the causal and noncausal control filter frequency response functions.

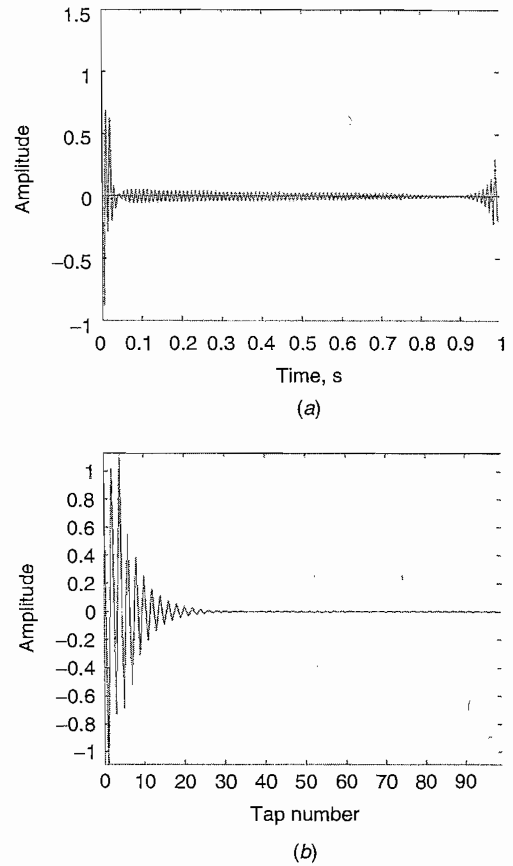

FIGURE 18.45 Comparison of (*a*) the noncausal control filter impulse response function and (*b*) the filter coefficients of the causal control filter.

it receives an input signal and is clearly noncausal. The filter coefficients of the causal filter, on the other hand, decay away to zero. The performance of the active control system is shown in Fig. 18.46. The figure shows the ratio of the controlled disturbance spectrum to the uncontrolled spectrum. The performance has clearly been degraded, especially in the vicinity of the Nyquist frequency. Nevertheless, the out-of-band amplification clearly visible in Fig. 18.41 has been completely removed through the use of the anti-aliasing and reconstruction filters.

System Identification

The control algorithms discussed in the previous sections require internal models of the transfer functions between the outputs of the controller (i.e., the signals sent

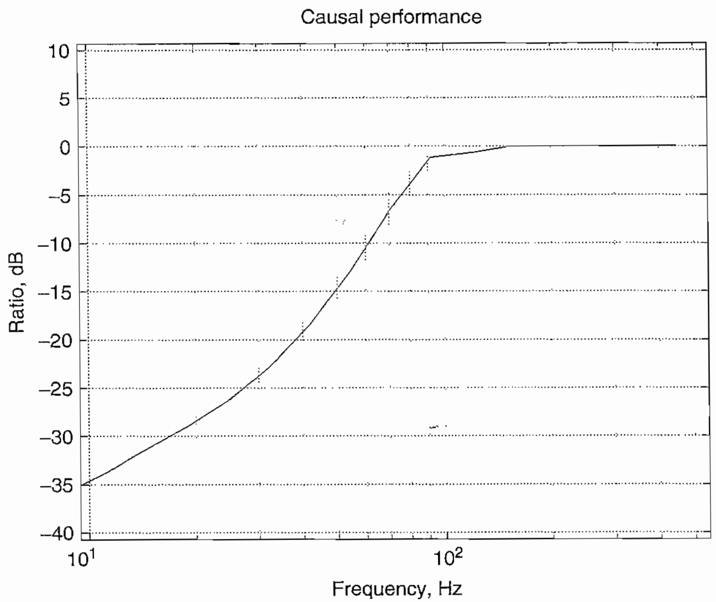

FIGURE 18.46 Ratio of controlled to uncontrolled disturbance with anti-aliasing filters, reconstruction filters, and D/A converter delays.

to the D/A converters) and the inputs to the controller from the residual sensors (i.e., outputs from the A/D converters). These transfer functions are commonly referred to as *plant* transfer functions. The procedure used to measure these transfer functions (or equivalently impulse response functions) is referred to as *system identification*. In this section, we discussed system identification approaches that apply to feedforward controllers.

Since most control algorithms require plant models for the control algorithms to converge to (or solve directly for) the optimal control filters,[58] system identification must be performed prior to any adjustments to the control filters. As such, when system identification is performed with control filters set to zero (i.e., all coefficients are equal to zero), it is referred to as "*open-loop*" system identification. It derives this name because the system identification algorithms are run when the control loop is open (i.e., no signals are allowed to pass through the control filters). The plant estimates obtained during open-loop system identification are used to initialize the plant models within the controller to support the control algorithms that subsequently adjust the control filter coefficients.

For systems where the plant transfer functions are expected to be time invariant (i.e., they do not change characteristics as a function of time), the plant estimates obtained during open-loop system identification can be held constant as the control filter coefficients are adjusted. It is more common, however, to expect that these transfer functions will change over time. These changes may

occur because of changes in environmental conditions (e.g., temperature, pressure), changes in the operating conditions of the system to be controlled (e.g., speed, load), or the presence of external factors (e.g., number and movement of passengers in an automobile).

There are two basic approaches to account for time-varying transfer functions that may be encountered in ANVC systems: the use of robust control algorithms and periodic system identification. Control algorithms are often formulated to allow for certain levels of uncertainty associated with the internal plant models. For example, the magnitude and phase response of the plant at a given frequency may only be known to within, say, ± 2 dB in magnitude and $\pm 10°$ in phase. In effect, these algorithms recognize that the internal plant model is "close" to the actual plant transfer function but not exact. Control algorithms that are stable and provide performance in the presence of this plant uncertainty are called "robust." For example, the filtered-x LMS algorithm is robust to errors in the plant model of up to 90°.[68] The second approach to account for time-varying transfer functions is to perform system identification at the same time that control filter coefficients are being adjusted. This approach provides *periodically updated* plant models to the control algorithms that track changes in the plant over time. System identification performed in this manner is referred to as *closed-loop* or *concurrent* since it occurs while the control loop is closed.

In practice, a combination of both approaches is often required to account for time-varying plants while at the same time maximizing achievable system performance. Control algorithms that rely on exact models of the plants to be controlled can offer maximum performance but are also very sensitive to slight changes in the plant transfer function. As such, small changes in the plant can lead to instability, and for this reason such systems are rarely used in practice. On the other hand, algorithms that make do with very inaccurate plant models will often provide very little performance. As such, there is a trade-off between control system robustness and performance. These trade-offs ultimately influence the approach chosen for system identification.

We now discuss procedures for open- and closed-loop system identification that are applicable to feedforward control systems. Consider first the feedforward system of Fig. 18.47. For this system, the plant, P, is the transfer function between the output of the control filter, y, and the response of the residual sensor, e. Though not shown explicitly, the plant transfer function P is assumed to include the following: D/A sample and hold, smoothing filters, transfer function through the structure to be controlled, anti-alias filters, and A/D converters. An open-loop estimate of P can be performed by setting the coefficients of the control filter, W, to zero and injecting a band-limited probe signal v into the output of the control filter. The probe signal is therefore a digital signal that adds to the output of the control filter y to produce a net signal c at the output of the controller.

The bandwidth of the probe signal is chosen to span the frequency range over which control performance is desired. For a tonal control problem, where the tone is nominally fixed in frequency, the probe signal may span only a few hertz.

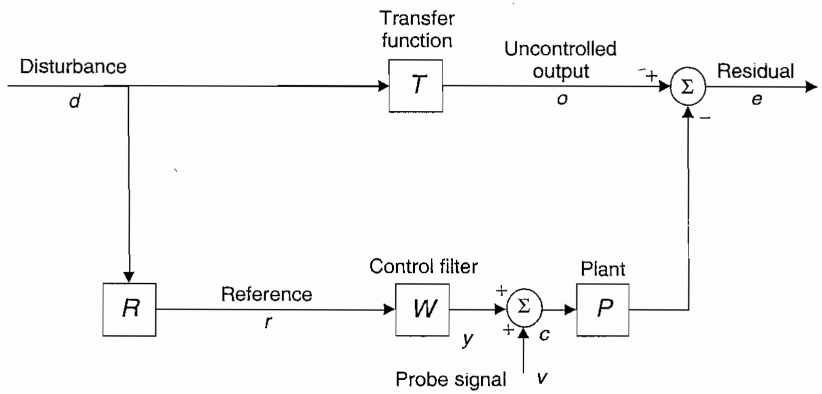

FIGURE 18.47 Probe signal injection for system identification in a feedforward system with no coupling between actuators and reference.

For broadband control, the probe signal bandwidth is often chosen to extend marginally beyond the control bandwidth to ensure an accurate plant estimate throughout the bandwidth for control.

The transfer function between the probe, v, and the residual, e, can be estimated in the frequency domain using the expression

$$\hat{P} = -S_{ve}S_{vv}^{-1} \tag{18.39}$$

where $\hat{P}$ = estimate of plant transfer function P
S_{ve} = cross-spectrum between probe and residual
S_{vv} = autospectrum of probe

This expression will provide an unbiased estimate of the plant transfer function for $W = 0$ (i.e., open-loop system identification) as well as for $W \neq 0$ (i.e., closed-loop system identification) provided the probe signal is uncorrelated with the disturbance and sufficient averaging time is allowed to obtain good estimates of S_{ve}.

An estimate of the plant transfer function in Fig. 18.47 can be made in the frequency domain using Fourier transforms of the probe and residual signals as outlined above. Alternatively, an estimate of the plant *impulse response* can be obtained using the optimal or adaptive FIR filter design procedures discussed in Section 18.3.

An example of system identification using the LMS algorithm integrated into a filtered-x control algorithm is depicted in Fig. 18.48. The filtered-x algorithm adapts the coefficients of the control filter W using the filtered reference signal and a modified residual signal (see later) as inputs. A separate LMS algorithm is used to identify the plant impulse response as shown in the lower portion of the figure. A probe signal v is injected into the control loop and sums with

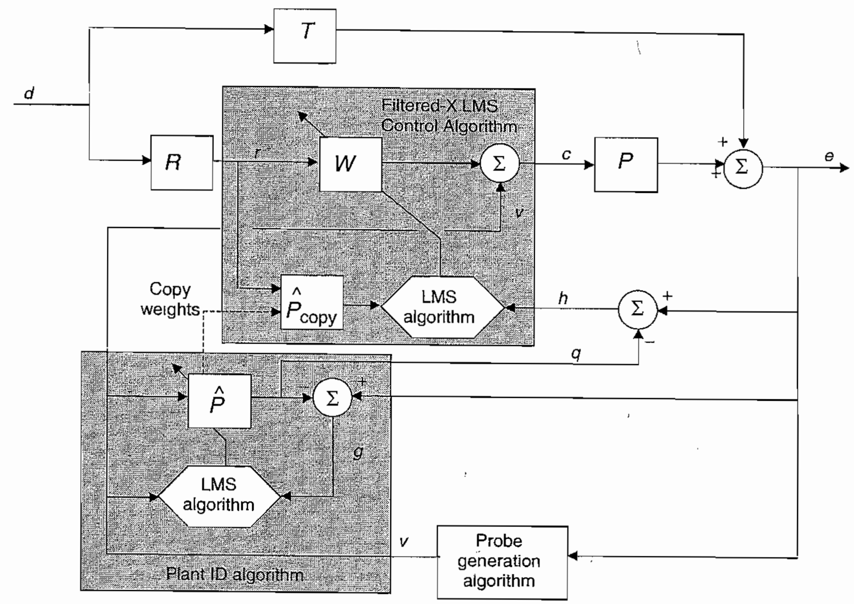

FIGURE 18.48 System identification using the LMS algorithm, embedded within filtered-x LMS controller.

the output of the control filter. The probe signal is also filtered by the adaptive FIR filter that is labeled $\hat{P}$. Finally, the probe signal is an input signal to the LMS algorithm that adapts the coefficients of $\hat{P}$. The output of $\hat{P}$ is summed with the residual signal e to form the error signal g, which is the second input to the LMS algorithm adapting the coefficients of $\hat{P}$. The coefficients of $\hat{P}$ are adapted to minimize the contribution in g that is correlated with the probe, v, in a least-squares sense. An optimal estimate of $\hat{P}$ is achieved when the LMS error signal g becomes uncorrelated with the probe, v. The coefficients of $\hat{P}$ are copied periodically into the filter, $\hat{P}_{copy}$, which filters the reference signal r, as required by the filtered-x LMS control algorithm.

Following the development of Section 18.3 under Adaptive Digital Filter Design, the update equation for the plant estimate is

$$\hat{\mathbf{p}}(n+1) = \hat{\mathbf{p}}(n) + 2\mu\mathbf{v}(n)g(n) \tag{18.40}$$

where

$$\hat{\mathbf{p}}^{\mathrm{T}} = [\hat{p}(0), \hat{p}(1), \hat{p}(2), \ldots, \hat{p}(I-1)] \tag{18.41}$$
$$\mathbf{v}^{\mathrm{T}}(n) = [v(n), v(n-1), \ldots, v(n-I+1)]$$

We note here that the convergence behavior of the LMS algorithm of Eq. (18.40) is improved if the portion of the residual signal correlated with the reference is removed before being used as input for the plant estimate. This can be achieved by including a third LMS algorithm with the reference and residual signals as inputs, and the modified residual signal as output. The update equation is similar to that in Eq. (18.40). Though not shown explicitly in Fig. 18.84 to preserve clarity, this approach was used for the adaptive feedforward control example presented near the end of this chapter (MIMO Feedforward Active Locomotive Exhaust Noise Control System with Passive Component) and is illustrated there in Fig. 18.93.

A consequence of being able to periodically update the model of the plant using the system identification procedure outlined in Fig. 18.48 is that the injected probe signal will increase the residual signal e. For purposes of system identification, it is desirable to used high-level probe signals because the probe signal will dominate the response at the residual sensor, and consequently accurate plant estimates can be obtained in a shorter length of time. During open-loop identification of ANVC systems, it is often acceptable to use high levels of probe signals. During closed-loop operation, however, the use of high-level probe signals is not acceptable since performance gains achieved as a result of the control filter will be overwhelmed by the presence of the probe signals reaching the residual. As a consequence, low-level (i.e., *covert*) probe signals are required during closed-loop operation.* The drawback to using low-level probes is that the plant estimate will adapt slowly and will not be able to track changes in the plant that occur over relatively short time frames. When this is the case, the control algorithms must be adjusted to deal with larger levels of uncertainty in the plant models or alternative strategies involving gain scheduling[69] must be considered.

For systems where the time constants of plant changes are *large* relative to the adaptation time of the LMS algorithm when using low-level probes, the system identification approach of Fig. 18.48 has been used effectively. For these cases, the probe signals can be generated using low-level band-limited "white" noise. However, fixed-level, white-noise probe signals are not necessarily the best choice. In particular, drawbacks of using white-noise probes include the following:

- The magnitude of the probe signal is held constant. Therefore, as the magnitude of the disturbance increases, the effective convergence rate for the plant filter will decrease. Alternatively, as the disturbance decreases relative to the probe, the convergence rate will increase at the expense of increasing the level of the closed-loop residual signals.
- The spectral shape of the probe signal is independent of the spectral shape of the residual signal and plant transfer function. Consequently, the quality (e.g., estimation errors) of the plant estimate will vary as a function of frequency. This can lead to temporary losses in system performance for control of slewing tonals and nonuniform control of broadband noise.

*Typically the probe signal is sized such that the resulting signal at the residual sensors is nominally 6 dB below the closed-loop signal (absent the probe) in those sensors.

For ANVC applications where white-noise probes may not be appropriate, probe-shaping algorithms can be employed to generate probe signals that provide plant estimates with nominally uniform estimation errors as a function of frequency. Further, these algorithms can account for changes in the disturbance spectrum and plant transfer functions over time.[70–72] Probe generation approaches are depicted collectively by the *probe generation* block in Fig. 18.48.

The final aspect to discuss concerning Fig. 18.48 is possible interaction between the filtered-x LMS algorithm adapting the control filter and the LMS algorithm adapting the plant estimate. In particular, we consider the effects of probe signal injection on convergence of the control filters. Note that the injected probe signal used for system identification contributes to the net residual signal e, which is typically used to adapt the control filter coefficients using the filtered-x LMS algorithm. The contribution from the probe signal is, by design, uncorrelated with the reference signal r. However, its presence in the residual signal will impact the instantaneous residual signal used in the gradient estimate and reduce the convergence speed of the filtered-x algorithm. As a consequence, it is beneficial to remove an estimate of the probe's contribution to the residual signal by subtracting the output of the filter, $\hat{P}$ (labeled q in Fig. 18.48), from the residual, e. This modified residual signal (labeled h in Fig. 18.48) is then used to adapt the control filter coefficients using the filtered-x LMS algorithm.

Up to this point, we have assumed that any coupling from the actuators back to the reference sensors is negligible (i.e., sufficiently small that it can be ignored with respect to system performance and stability). This is not always the case. In general, there exists physical coupling which must be accounted for by both the control algorithm and the system identification algorithms. Control algorithms that account for this path include *feedback neutralization* and Eriksson's *filtered-U* algorithm, both of which were discussed in the previous section. A fully adaptive filtered-U algorithm that includes concurrent system identification is discussed by Eriksson and Allie.[61] In those instances where the physical coupling to the references becomes so strong that electronic cancellation of the coupling may be ineffective, other approaches must be employed to minimize the physical coupling, such as the use of directional reference sensors and selection of alternate sensors.

Figure 18.49 shows the injection of a probe signal in a feedforward system that contains coupling C from the controller output to the reference input and neutralization filter $\tilde{C}$ in the controller to minimize the effects of this feedback path. The procedures for open-loop identification of the coupling transfer function C follows from the discussion above for identifying P, provided the reference signals are used in place of the residual signals. As such, unbiased estimates of the coupling transfer function can be obtained during open-loop operation, provided that the probe signal is uncorrelated with the disturbance. During closed-loop operation, however, transfer functions from the probe signal to the residual and

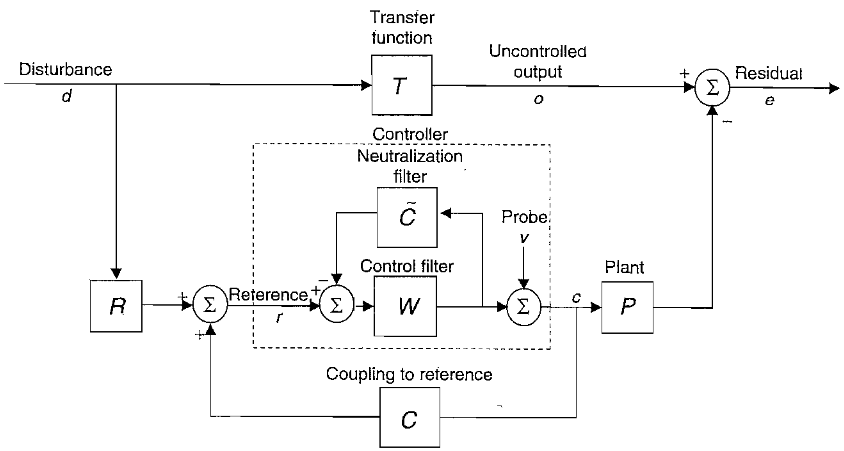

FIGURE 18.49 Probe signal injection in feedforward system with coupling to reference sensor and feedback neutralization filter.

reference sensors no longer provide unbiased estimates of P and C. Instead, these transfer functions include the loop gain associated with the feedback loop comprised of the coupling transfer function, neutralization filter, and control filter.

Following the nomenclature of Fig. 18.49, these transfer functions are given by

$$G_e = \frac{S_{ve}}{S_{vv}} = \frac{-P}{1-(C-\tilde{C})W} \qquad G_r = \frac{S_{vr}}{S_{vv}} = \frac{C}{1-(C-\tilde{C})W} \tag{18.42}$$

These expressions for G_e and G_c contain the desired transfer functions for P and C in the numerator, but both contain the impact of the feedback loop in the denominator. The denominator term can be isolated by estimating the transfer function from the probe signal to the controller output signal c. This transfer function is given by

$$G_c = \frac{S_{vc}}{S_{vv}} = \frac{1}{1-(C-\tilde{C})W} \tag{18.43}$$

Asymptotically unbiased estimates for the plant and coupling transfer functions can then be obtained by combining Eqs. (18.42) and (18.43) such that

$$\hat{P} = \frac{-G_e}{G_c} = P \qquad \tilde{C} = \frac{G_r}{G_c} = C \tag{18.44}$$

This approach for closed-loop identification is known as the joint input–output method.[73] Estimates of P and C can be made in the frequency domain by estimating the cross-spectra in Eqs. (18.42) and (18.43) and taking the ratios as indicated in Eq. (18.44). Alternatively, multiple-embedded LMS algorithms could be employed to adapt estimates of P and C on a sample-by-sample basis.

Although we have discussed the joint input–output method applied to a feedforward system with feedback to the reference sensors, it is a general approach that is applicable to traditional feedback systems. As such, this method of concurrent system identification can be used to implement fully adaptive feedforward and feedback control systems. Further, the method is valid for use during open- and closed-loop operation. An example of a fully adaptive feedback control system using this approach to system identification when applied to an active machinery mount can be found in Berkman et al.,[74] Curtis et al.,[75] and Berkman and Bender[76] and is included here as an example in Section 18.7 under Active Machinery Isolation.

Extension to MIMO Systems

The equations and examples so far have considered only SISO controllers. In many instances there will be the need to design controllers that can handle multiple inputs and/or multiple outputs. While a complete consideration of the issues involved in the design of MIMO systems is beyond the scope of this chapter, we provide here a brief look at the algorithms for the design of optimum MIMO control filters.

Let us begin by defining a notional MIMO system like that shown in Fig. 18.50, where K reference signals, **r**, are applied to a control filter which in turn generates M output signals, **u**, to drive actuators on the system to be controlled. The system has L control sensors to monitor the system performance. Since there are multiple inputs and multiple outputs to each of the blocks in Fig. 18.50, the variables in the blocks $B(\omega)$, $W(\omega)$, and $P(\omega)$ no longer represent scalar transfer functions but must be transfer function matrices. For example, if there are M actuators driving the plant and L control sensors monitoring the system response, the plant transfer function $P(\omega)$ between the sensors and the

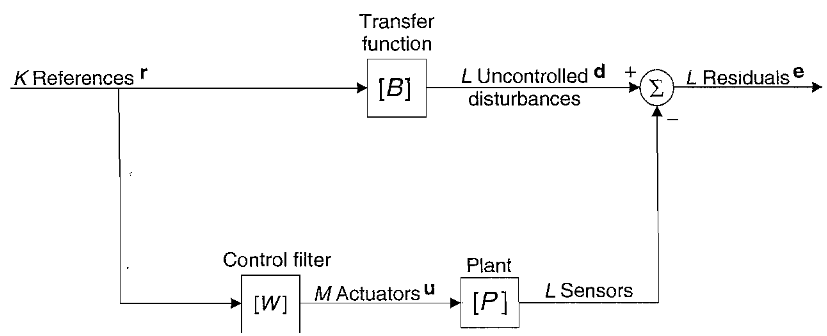

FIGURE 18.50 Notional MIMO control system.

actuators becomes the matrix of transfer functions $[P(\omega)]$:

$$[P(\omega)] = \begin{bmatrix} P_{11}(\omega) & P_{12}(\omega) & \cdots & P_{1M}(\omega) \\ P_{21}(\omega) & & & \vdots \\ \vdots & \ddots & \ddots & \\ P_{L1}(\omega) & \cdots & \cdots & P_{LM}(\omega) \end{bmatrix} \tag{18.45}$$

where the $P_{nm}(\omega)$ are each frequency response functions relating sensor output n to actuator input m.

In Eq. (18.24) we defined an optimum SISO control filter for tonal disturbances given by $W(\omega) = P(\omega)^{-1}B(\omega)$. It turns out that the optimal MIMO control filter is given by a very similar expression if the plant is a square transfer function matrix, that is, $L = M$:

$$[W(\omega)] = [P(\omega)]^{-1}[B(\omega)] \tag{18.46}$$

In the equation the square brackets indicate that the variables are transfer function matrices and not scalar transfer functions. For the more general case of a nonsquare plant matrix of K rows and L columns the same expression applies except that the pseudoinverse of the plant matrix is substituted for the normal inverse:

$$[W(\omega)] = [P(\omega)]^{\#}[B(\omega)] \tag{18.47}$$

where the pseudoinverse of the plant, $[P(\omega)]^{\#}$, is given by

$$[P]^{\#} = \begin{cases} \{[P]^H[P]\}^{-1}[P]^H & \text{for } K \le L \\ [P]^H\{[P][P]^H\}^{-1} & \text{for } K > L \end{cases}$$

where $[\cdot]^H$ means the complex conjugate of the transpose of the matrix. Since for broadband disturbances Eq. (18.47) can result in noncausal control filters, there is a need to apply causality constraints to the MIMO filter design process similar to those applied to the SISO case in Section 18.4 under Optimal Control Filter Estimation. Unfortunately the derivation of the direct-estimation equations for the optimal MIMO control filter is very involved and beyond the scope of this chapter. The interested reader is referred to reference 77.

Fortunately the MIMO filtered-x algorithm is much simpler than the MIMO direct-estimation algorithm, and the equations have been developed by Nelson and Elliott.[16,67] The residual that we are seeking to minimize is given by

$$e_l(n) = d_l(n) - \sum_{m=1}^{M}\sum_{j=0}^{J-1} P_{lmj}u_m(n-j) \tag{18.48}$$

where P_{lmj} is the jth filter coefficient of the plant transfer function relating the lth sensor output to the mth actuator input, M is the number of actuators, J is the length of the digital representation of the plant transfer functions, and u_m is the mth output of the control filter driven by the K references as indicated in the equation

$$u_m(n) = \sum_{k=1}^{K}\sum_{i=0}^{I-1} w_{mki}r_k(n-i) \tag{18.49}$$

In this equation w_{mki} is the ith coefficient of the control filter relating the mth actuator drive signal to the kth reference, I is the length of each control filter, and r_k is the kth reference signal input to the control filters. The MIMO filtered-x update equation for each control filter coefficient is given by

$$w_{mki}(n+1) = w_{mki}(n) + 2\mu\sum_{l=1}^{L} e_l(n)q_{lmk}(n-i) \tag{18.50}$$

where $w_{mki}(n)$ is the existing estimate of the ith filter coefficient for the control filter connecting reference k to actuator m, $w_{mki}(n+1)$ is the new estimate, and

$$q_{lmk}(n) = \sum_{j=0}^{J-1} P_{lmj}r_k(n-j) \tag{18.51}$$

Equation (18.50) is the MIMO filtered-x control filter update equation for multiple references, multiple sensors, and multiple actuators. It is similar in form (except for the sum over control sensors) to the SISO case, since the coefficients are updated by the product of the residual and the reference filtered by the plant transfer function. Its simple form allows for easy, computationally efficient implementation and, as a consequence, has become a very popular MIMO algorithm for feedforward applications. Furthermore, as we shall see in the next section, it can also be applied to feedback systems.

18.5 FEEDBACK CONTROL SYSTEMS

Basic Architecture

The block diagram of Fig. 18.51 shows the basic architecture of a SISO feedback control system. Such a block diagram might arise from the notional physical system shown in Fig. 18.52. The physical system consists of a second-order oscillator with a control sensor, an accelerometer for example, to monitor the motion of the mass. In addition there is a control actuator which can apply forces to the mass to control its motion. In the block diagram the residual, e, is the output signal from the residual sensor. That output is fed to a control filter,

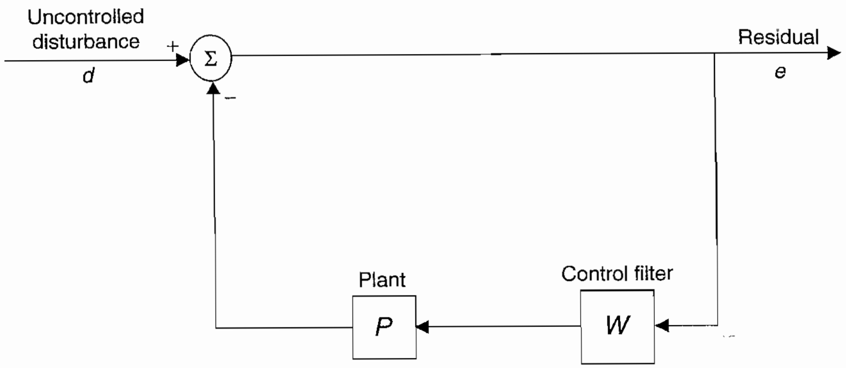

FIGURE 18.51 Basic feedback architecture.

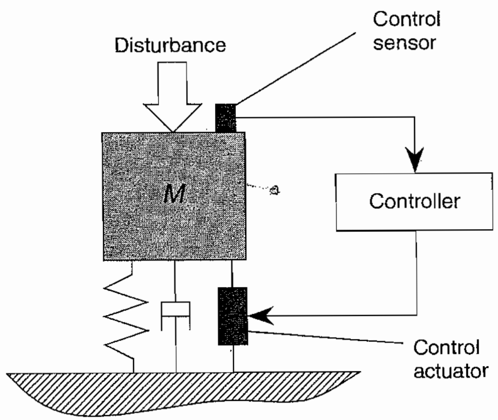

FIGURE 18.52 Notional system with a feedback controller.

which is shown as W in the block diagram. The control filter output drives an actuator that is used to control the motion of the mass.

The plant transfer function P in the block diagram relates the control filter output signal, which drives the actuator to the residual sensor output. In Fig. 18.51 the control filter drives the actuator in such a way as to reduce the input to the control filter. This is in contrast to feedforward systems in which the input to the control filter is a reference signal correlated with the disturbance. In one sense, feedback control systems can be thought of as feedforward systems in which the reference and control (residual) sensors are the same.

The solution for the closed-loop response is given by

$$e(\omega) = \{1 + P(\omega)W(\omega)\}^{-1} d(\omega) \tag{18.52}$$

Clearly the residual will be small if $PW \gg 1$, and in the limit the residual amplitude will become

$$e(\omega) = \{P(\omega)W(\omega)\}^{-1} d(\omega) \tag{18.53}$$

The quantity PW is referred to as the loop gain and the residual amplitude will be inversely proportional to the loop gain. Consequently, good performance from a feedback controller will be achieved if the loop gain is made sufficiently large. In addition, when the loop gain is large, the phase of PW is immaterial to the performance such that if the control filter deviates somewhat from its design goals the performance will suffer only minimally.

The above discussion makes the design of a feedback control filter seem easy. Unfortunately, stability considerations limit our ability to increase the loop gain without limit. Stability issues will be discussed more fully below under Alternate Suboptimum Control Filter Estimation, where the compensator-regulator approach to feedback control filter design is discussed.

Optimal Control Filter Estimation

The literature dealing with the design of optimal feedback controllers is vast and beyond the scope of what can be reasonably included in this chapter. Instead we will focus on two approaches—one optimal and one suboptimal—that each provide tools for the design of SISO or MIMO controllers. The collection of methods often referred to as *modern optimal control theory* will not be dealt with here. Those methods, while providing powerful tools for control filter design when an analytical model of the plant dynamics is available, are not especially well suited to the types of problems where only measured data on the plant dynamics are available. While curve-fitting techniques can be utilized to obtain an analytical model that approximates the measured data, many of those techniques begin to founder if the order of the system model (number of states) becomes too large. For a sampling of the technology in this field the interested reader is referred to references[78–81].

In this section, we focus on what has come to be called the Youla transform or inner model formulation. Through selection of a particular feedback architecture, the Youla transform allows the feedback problem to be transformed into a feedforward problem, making it possible for the feedforward control filter design techniques in Section 18.4 to be used for feedback. In addition, because the system is effectively transformed to a feedforward system, the resulting system is guaranteed to be stable, provided an accurate digital model of the plant has been utilized.

Figure 18.53 shows a simplified block diagram of the Youla transform. In the figure a second feedback loop has been inserted around the control filter. In that second loop a digital filter approximating the plant transfer function has been inserted. The term *inner model* is often used when referring to this approach, precisely because a digital model of the plant is inserted into the control filter.

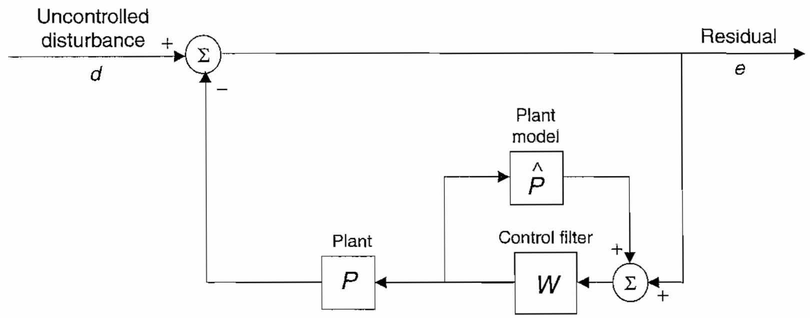

FIGURE 18.53 Youla transform architecture.

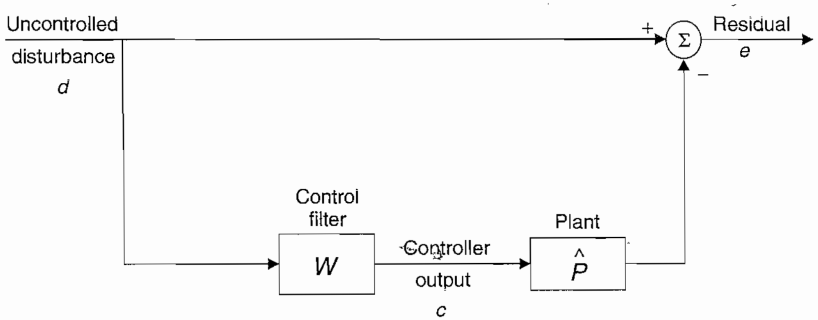

FIGURE 18.54 Feedforward system resulting from the Youla transform.

By making this change in the architecture of the feedback system, we have modified the transfer function from that shown in Eq. (18.52) to the following:

$$e(\omega) = \{1 - \hat{P}(\omega)W(\omega)\}\{1 + (P(\omega) - \hat{P}(\omega))W(\omega)\}^{-1}d(\omega) \tag{18.54}$$

Note that if $\hat{P}$ is a good match to P, then Eq. (18.54) simplifies to

$$e(\omega) = \{1 - \hat{P}(\omega)W(\omega)\}d(\omega) \tag{18.55}$$

Equation (18.55) is the equation for the residual of a feedforward system, the block diagram for which is shown in Fig. 18.54. The resulting block diagram is identical to the feedforward block diagram in Fig. 18.31 if the transfer function $B(\omega)$ is set to unity. Consequently, virtually all of the control filter design equations in Section 18.4 can be applied to a feedback system to which the Youla transform has been applied provided $B(\omega) = 1$. From Eq. (18.24) the noncausal control filter becomes

$$W(\omega) = \hat{P}^{-1}(\omega) \tag{18.56}$$

For the filtered-x algorithm Eqs. (18.35) and (18.36) can be applied to the Youla transform feedback system by simply changing the reference time sequence $r(n)$ in the equations to the disturbance time sequence $d(n)$ in Fig. 18.54:

$$\mathbf{w}(n+1) = \mathbf{w}(n) + \mu e(n)\mathbf{u}(n) \tag{18.57}$$

where $\mathbf{w}(n+1)$ is the new vector of filter coefficients, $\mathbf{w}(n)$ is the old vector,

$$\mathbf{u}(n) = \begin{Bmatrix} u(n) \\ u(n-1) \\ \vdots \\ u(n-N_w+1) \end{Bmatrix} \qquad u(n) = \sum_{m=0}^{N_w-1} \hat{p}(m)d(n-m)$$

and $\hat{p}(m)$ is the mth filter coefficient of the FIR filter representation of the plant frequency response function $\hat{P}(\omega)$.

The equations for determining the optimum feedforward control filter with causality constraints using the direct-estimation approach can be similarly employed by simply interchanging the disturbance d for the reference r. In this case what are affected are the autospectra and cross-spectra in the equations. Modifying Eqs. (18.30) and (18.31), we obtain for a control filter with N taps

$$\begin{Bmatrix} W_0 \\ W_1 \\ \vdots \\ W_{N-1} \end{Bmatrix} = \begin{bmatrix} C_0 & C_{-1} & \cdots & C_{1-N} \\ C_1 & C_0 & \cdots & C_{2-N} \\ \vdots & \vdots & \ddots & \vdots \\ C_{N-1} & C_{N-2} & \cdots & C_0 \end{bmatrix}^{-1} \begin{Bmatrix} A_0 \\ A_1 \\ \vdots \\ A_{N-1} \end{Bmatrix} \tag{18.58}$$

where the coefficients in the matrix equation become

$$A_p = \mathrm{Re}\left\{\int_{\omega_1}^{\omega_2} P S_{dd} e^{-jp\omega\Delta t} d\omega\right\}$$
$$C_{(p-m)} = \mathrm{Re}\left\{\int_{\omega_1}^{\omega_2} \{|P^2| + \alpha^2\} S_{dd} e^{-j(p-m)\omega\Delta t} d\omega\right\} \tag{18.59}$$

where $p, m = 0, 1, \ldots N-1$, S_{dd} is the autospectrum of the disturbance, and α^2 is the control effort weighting factor.

For MIMO systems the equations of Section 18.4 under Extension to MIMO Systems can be similarly adjusted for the design of a MIMO controller in the Youla feedback architecture.

The transformation of Eq. (18.54), a feedback system, into Eq. (18.55), a feedforward system, only occurs if $\hat{P} = P$. Consequently, one would expect that the digital representation of the plant transfer function would have to be fairly accurate. If it is not, the term

$$\{1 + (P(\omega) - \hat{P}(\omega))W(\omega)\}^{-1} \tag{18.60}$$

may indeed lead to instability if the error in the plant model is large enough. If we substitute $E(\omega)$ for the difference between the true plant and the digital representation, Eq. (18.60) becomes

$$\{1 + E(\omega)W(\omega)\}^{-1} \tag{18.61}$$

A simple criterion to ensure that the feedback system remains stable is to require for all frequencies where the controller is functioning that

$$|E(\omega)W(\omega)| < 1 \tag{18.62}$$

where $|\cdot|$ means the absolute value. Furthermore, it can be easily shown that $|E(\omega)W(\omega)| = |E(\omega)||W(\omega)|$. Consequently, we can write a simple criterion for the maximum allowable error in the plant model:

$$|E(\omega)| = |\hat{P}(\omega) - P(\omega)| \le \frac{\beta}{|W(\omega)|} \qquad 0 < \beta < 1 \tag{18.63}$$

where the criterion applies to all frequencies where the control system is functioning and β provides some stability margin. For example, if $\beta = 0.1$, Eq. (18.63) will provide, at least, 20 dB of stability margin. This is a very simple criterion requiring that we know only the amplitude of the control filter as a function of frequency. No phase information is required. However, it is also very conservative, and systems that violate it may not necessarily be unstable. A more precise method for determining stability is to employ the Nyquist criterion, which we will discuss in the next section. Note that a similar criterion can be fashioned for MIMO systems based on the maximum singular values of the matrices $[E(\omega)]$ and $[\hat{P}(\omega)]$. The interested reader is referred to references 80 and 81.

Alternate Suboptimum Control Filter Estimation

Compensator-Regulator Architecture. The compensator-regulator approach to feedback controller design results in a suboptimal system but provides useful insights into functions performed by the controller by breaking the control filter up into a cascade of two filters, as illustrated in Fig. 18.55. The compensation filter is designed to approximate the plant inverse and *compensate* for its amplitude and phase over a range of frequency, which we will refer to as the compensation band. Consequently, if the compensation filter is given by

$$G(\omega) \approx P(\omega)^{-1} \tag{18.64}$$

then we conclude from Eq. (18.52) that the closed-loop residual response $e(\omega)$ is related to the disturbance $d(\omega)$ by

$$\frac{e(\omega)}{d(\omega)} = \frac{1}{1 + H(\omega)} \tag{18.65}$$

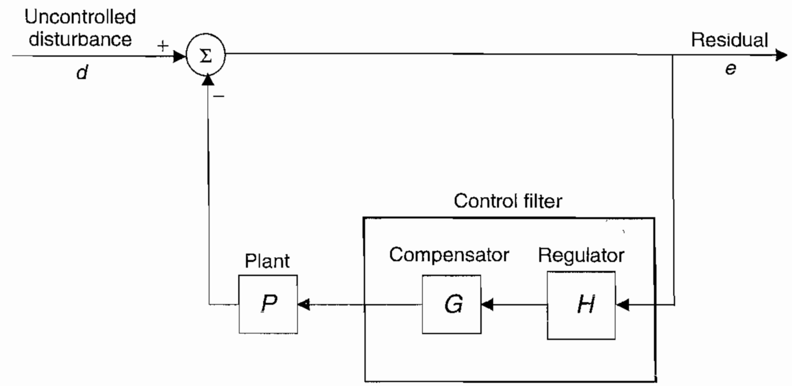

FIGURE 18.55 Compensator-regulator controller architecture.

where $H(\omega)$ is the regulation filter. As this equation shows, to provide reduction in the residual, $|H(\omega)| \gg 1$. When $|H(\omega)| \gg 1$,

$$\frac{e}{d} = \frac{1}{H(\omega)} \ll 1$$

and when $|H(\omega)| \ll 1$,

$$\frac{e}{d} = 1$$

As a result, the design of the regulation filter involves making its magnitude or loop gain large at those frequencies where control is desired (the regulation band) and small where control is not desired. As we shall see in the next section, the trick is to reduce the magnitude and phase of $H(\omega)$ in such a way as to maintain stability and avoid excessive noise amplification outside of the regulation band.

Regulation Filter Design. The range of frequency over which $|H(\omega)| \gg 1$ is referred to as the regulation band. To ensure stability as the magnitude of $H(\omega)$ is reduced outside of the regulation band, the phase of $H(\omega)$ should not exceed 180° until the magnitude is less than 1. This requirement is a consequence of the Nyquist stability criterion.

To employ the Nyquist criterion, one must plot in the phase plane the loop gain, or the change in amplitude and phase as a signal propagates around the feedback loop. In Eq. (18.65) $H(\omega)$ is the loop gain. In the phase plane, the real part of the loop gain is plotted on the horizontal axis and the imaginary part is plotted on the vertical axis such that as the frequency changes, a curve is traced out in two dimensions, as illustrated in Fig. 18.56. In the phase plane, the radius from the origin to a point on the curve represents the magnitude of the loop gain at a particular frequency, and the angle the radius makes with the positive horizontal axis is the phase angle. This is shown in Fig. 18.56 for

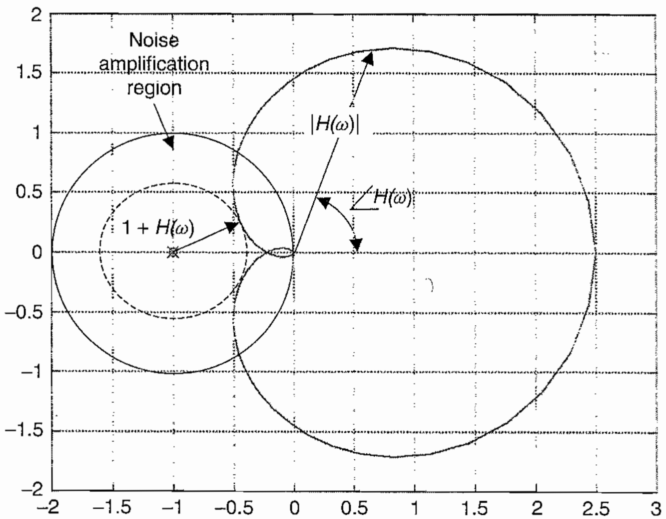

FIGURE 18.56 Stability and noise amplification requirement in the phase plane.

the case where the loop gain is $H(\omega)$. We will not present any proof here of the Nyquist criterion but will simply illustrate its application. For the interested reader, detailed discussions of the Nyquist criterion can be found in a number of texts on control theory.[56,82]

To apply the Nyquist criterion, one simply plots $H(\omega)$ on the phase plane as the frequency ω varies from $-\infty$ *to* ∞ and counts the number of times that -1 is encircled. That number is equal for most cases of interest to the number of unstable poles of $\{1 + H(\omega)\}^{-1}$. Figure 18.56 shows a Nyquist plot of a notional $H(\omega)$ in the phase plane. The amplitude and phase of $H(\omega)$ at a particular frequency are shown in the figure when the phase is less than 180° but the amplitude is greater than 1. As the frequency increases and the phase of $H(\omega)$ approaches 180° in the figure, the amplitude decreases to less than 1, satisfying the criterion. As the figure shows, this ensures that that the curve of $H(\omega)$ will not encircle -1 and that the system is stable.

In the figure, when the phase of $H(\omega)$ is 180°, the amplitude is ~0.2, which gives a modest gain margin of ~14 dB. This means that the amplitude of $H(\omega)$ would have to be 14 dB higher before the feedback control system would go unstable. Similarly, when the amplitude of $H(\omega)$ is unity, the phase is approximately 120°, giving a phase margin of 60°, meaning that the phase would have to increase by approximately 60° before the system would go unstable.

To ensure that there will be no noise amplification as the magnitude of $H(\omega)$ is reduced outside of the regulation band, the curve traced out by $H(\omega)$ in the phase plane should not enter a circle of unit radius centered on -1. This last requirement is also illustrated in Fig. 18.56. There, the trajectory of $H(\omega)$ is seen

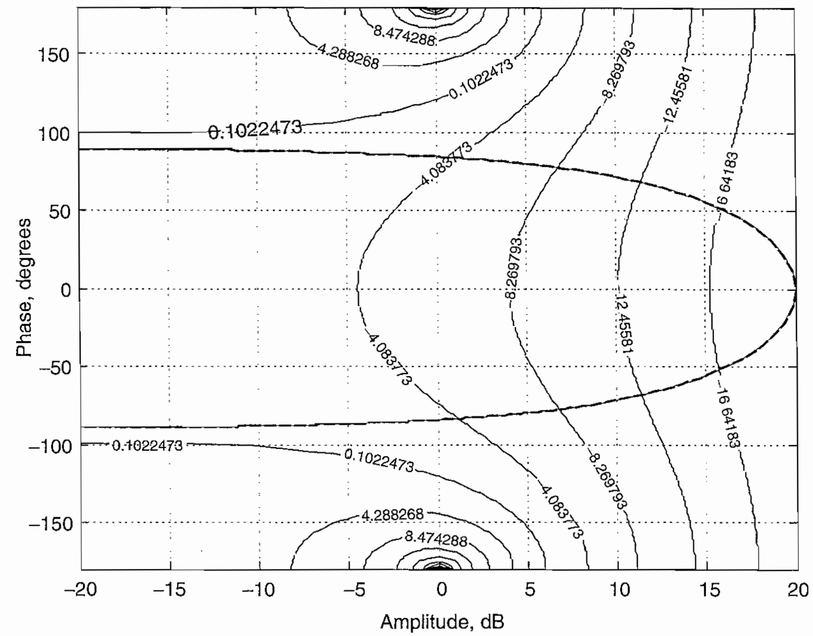

FIGURE 18.57 Nichols plot showing noise amplification in a feedback system as a function of the amplitude and phase of the loop gain.

entering the unit circle, indicating that some degree of noise amplification will occur.

While the loop gain plot in the phase plane can be used to estimate the noise amplification, the so-called Nichols plot provides that information more directly. Figure 18.57 shows a Nichols plot. In the figure, the phase of the loop gain is plotted on the vertical axis and the amplitude is plotted on the horizontal axis. The dashed curve in the figure is the loop gain of a second-order filter.* The contour lines in the plot show the noise amplification. Whenever the dashed curve crosses one of the contour lines, the feedback system with that loop gain will have the noise amplification in decibels indicated by the number on the contour line. For example, Fig. 18.57 shows that the second-order filter with the loop gain given by the dashed curve will never have a noise amplification greater than 0 dB. In fact, a simple examination of the Nyquist and Nichols plots will show that *any*

*The form of the filter is given by

$$H(\omega) = K\left\{\frac{j(\omega/\omega_0)}{(1-(\omega/\omega_0)^2 + j\eta\omega/\omega_0)}\right\}$$

where ω is the frequency and the other terms are constants.

filter whose phase is bounded by ±90°, as the second-order filter is, will always be stable with 0 dB noise amplification when placed in a feedback loop.

All of the above discussion assumes that $P(\omega)$ has been measured accurately and that a good causal representation of $P(\omega)^{-1}$ exists. If, however, the causal representation of $P(\omega)^{-1}$ is imperfect, then the loop gain in the controller will not be just $H(\omega)$ but will be $P(\omega)G(\omega)H(\omega)$. The same criteria for stability and noise amplification apply to this modified loop gain. The consequence is that $H(\omega)$ may need to be designed with larger gain and/or phase margins to maintain stability, and this may result in decreased performance. In addition, the imperfectly compensated system may also have increased noise amplification.

Another consideration is the frequency band over which the compensation filter, $G(\omega)$, must be a good representation of $P(\omega)^{-1}$. In general, the compensation bandwidth must be much greater than the regulation bandwidth to ensure stability and to control noise amplification. To determine the required compensation bandwidth, we first consider noise amplification. The basic approach is to compensate the plant until $H(\omega)$ is small enough so that uncompensated variations in the plant, $P(\omega)$, times the aliased compensation filter, $G(\omega)$, will not lead to noise amplification greater than that specified. If there are measurements of $P(\omega)$ up to frequencies well beyond even the compensation bandwidth, then it is possible to construct the Nyquist plot similar to that shown in Fig. 18.56 for $P(\omega)G(\omega)H(\omega)$ and determine the noise amplification for candidate compensation bandwidths in the same way as illustrated in the figure. Unfortunately, information on the plant is rarely available over such a broad bandwidth, and one must design in robustness by utilizing margins of safety. For example, let us assume that 2 dB of noise amplification is all that is allowed. For this to be true for any phase angle, the amplitude of the regulation filter must satisfy $|H(\omega)| < 0.206$ (−14 dB). If we have a margin of safety of, say, 6 dB to allow for uncompensated plant variations, we must compensate the plant until the regulation filter has declined to −20 dB. If we design the regulation filter to provide 10 dB of performance reduction in the residual, then $H(\omega)$ must have an amplitude of at least 10 dB in the regulation band. Consequently, we will need to compensate the plant out to frequencies beyond the regulation frequency until the amplitude of $H(\omega)$ has decreased by 30 dB from its maximum. Since we must not allow $H(\omega)$ to decrease too rapidly with increasing frequency or instability will result, the resulting compensation bandwidth can easily exceed the regulation bandwidth by a factor of 10–100.

To illustrate these concepts, we will carry out an example for narrow-band control and broadband control, in both cases assuming perfect compensation. For the narrow-band case we choose

$$H(\omega) = K\frac{j\omega/\omega_0}{1-(\omega/\omega_0)^2 + j\eta(\omega/\omega_0)} \tag{18.66}$$

where K and η are constant, $\omega = 2\pi f$, and f is the frequency in hertz. Equation (18.66) is a narrow-band regulation filter with high gain near $\omega = \omega_0$. The frequency response is shown in Fig. 18.58 for $\eta = 0.1$ and $K = 1$. This filter will provide approximately 20 dB of loop gain at the center frequency and consequently we would expect about 20 dB reduction in the residual. In addition, as mentioned above, the phase of the filter is bounded by ±90° and consequently, when placed in the feedback loop, will be stable with 0 dB noise amplification.

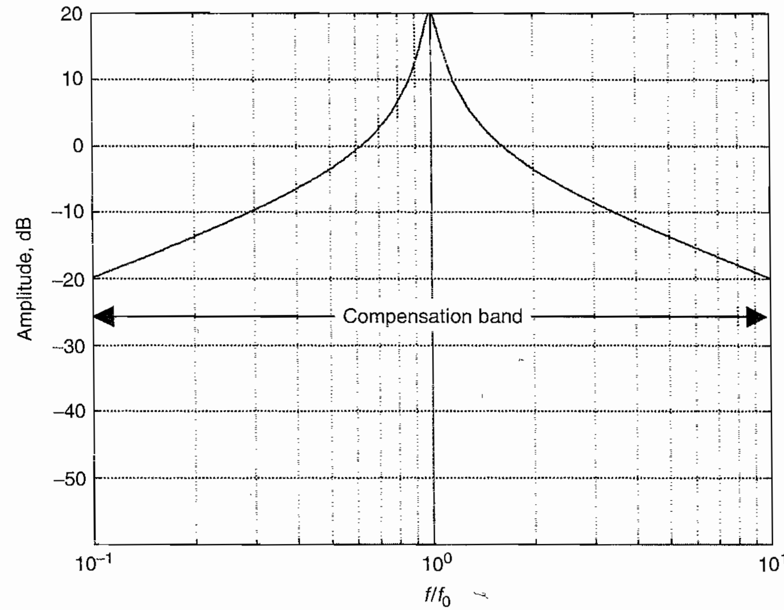

FIGURE 18.58 Narrow-band regulation filter.

Figure 18.59 shows the reduction in the residual with this regulation filter in the feedback loop. The system frequency response looks like a notch filter with approximately 20 dB of noise reduction over a bandwidth of about 5% of the center frequency f_0. It shows no out-of-band noise amplification, as expected.

These estimates have assumed that the compensation for the plant is perfect and that $G(\omega) = P(\omega)^{-1}$ for all frequencies. In reality we need to define a realistic range over which the plant will be measured and the compensation filter will be designed to work. The compensation band should be extended out far enough in frequency such that the regulation filter gain is small enough to ensure that no matter what uncompensated plant phase is introduced, the noise amplification will not exceed a design value (e.g., 2 dB). Earlier we determined that that criterion would be satisfied if $|H(\omega)| < 0.206$ (−14 dB). To allow for possible increases in loop gain as the compensation is gradually turned off, we introduce some margin by reducing this value by an additional factor of 2 (6 dB). Consequently, the plant will be compensated until the regulation filter reduces its amplitude to −20 dB. From Fig. 18.58 we can see that the compensation bandwidth must extend from $\sim 0.1f_0$ to $\sim 10f_0$, or 2 decades. This is substantially broader than the control bandwidth.

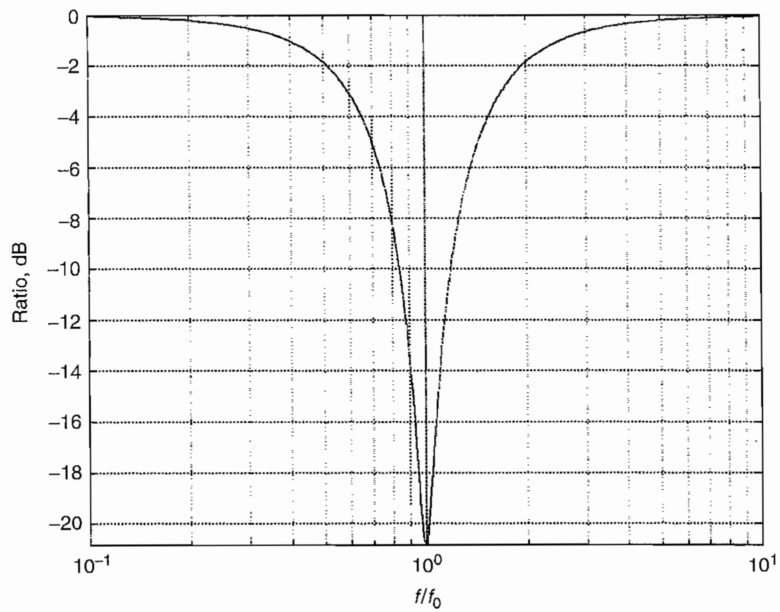

FIGURE 18.59 Ratio of controlled to uncontrolled residual for the narrow-band regulation filter.

Note that the bandwidth and noise reduction in Fig. 18.59 can be adjusted by varying the parameters of the regulation filter. For example, increasing η will increase the bandwidth but decrease the noise reduction performance of the feedback system, essentially broadening the notch and decreasing its depth in Fig. 18.59. Increasing K will increase the noise reduction performance, essentially deepening the notch in the figure but requiring that we compensate the plant out to still higher frequency to control noise amplification.

For broadband control we will use a second-order bandpass filter for the regulation filter given by

$$H(\omega) = Kb\left\{\frac{j(\omega/\omega_0)}{(j\omega/\omega_0 + a)(j\omega/\omega_0 + b)}\right\} \tag{18.67}$$

where ω_0 is the center frequency of the filter.

The frequency response of the filter with $K = 3$, $a = 0.1$, and $b = 10$ is shown in Fig. 18.60. The phase of this filter (not shown) is also bounded by $\pm 90°$ and hence the system would be expected to be stable with no noise amplification, provided the plant is properly compensated. The noise reduction performance of the feedback system employing this regulation filter is shown in Fig. 18.61. The figure shows about 10 dB or more of noise reduction for $0.12 f_0 < f < 8 f_0$. It

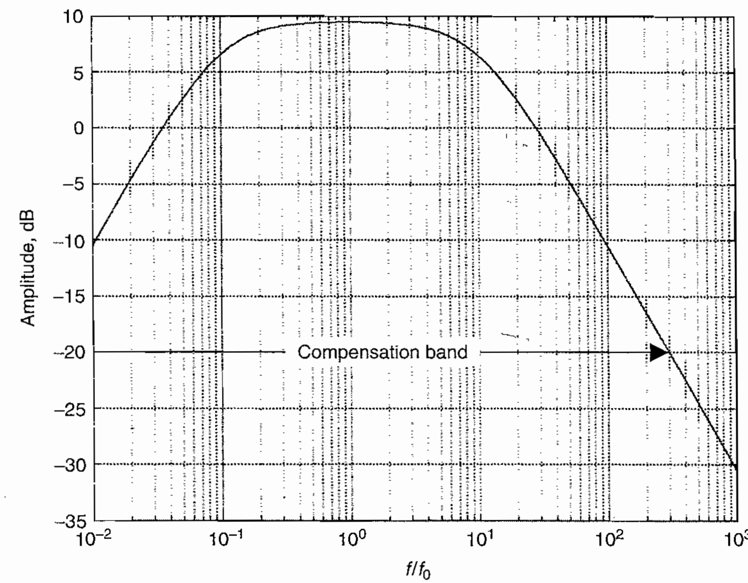

FIGURE 18.60 Frequency response of the broadband second-order regulation filter.

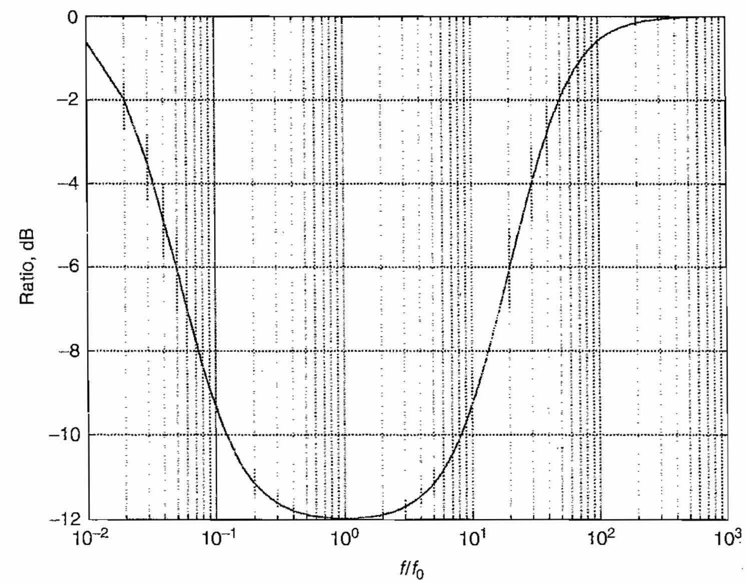

FIGURE 18.61 Ratio of controlled to uncontrolled residual for the broadband regulation filter.

also shows that there is no out-of-band noise amplification above and below the regulation frequency band, as expected.

The above calculations assume that the plant has been perfectly compensated. As for the narrow-band case, the compensation band should be extended out at least far enough in frequency such that the regulation filter gain is small enough to ensure that no matter what the phase, the noise amplification will not exceed 2 dB. Earlier we determined that that criterion would be satisfied if $|H(\omega)| < 0.206$ (-14 dB). Again, to allow for possible increases in loop gain as the compensation is gradually turned off, we introduce some margin by reducing this value by a factor of 2 (6 dB). Consequently, the plant will be compensated until the regulation filter reduces its amplitude to -20 dB. From Fig. 18.60 we can determine that the compensation band must extend out to $300 f_0$, or almost 40 times the highest frequency in the regulation frequency band. Since this is a fairly broad band over which to provide good compensation, it would be interesting to examine what would happen if we used a higher order filter. Since the loop gain associated with a higher order regulation filter would decrease more rapidly with frequency, the compensation band should be narrower. For example, if we simply square the frequency response function of the second-order filter in Eq. (18.67), we would have a fourth-order filter given by

$$H(\omega) = Kb \left\{ \frac{j(\omega/\omega_0)}{(j\omega/\omega_0 + a)(j\omega/\omega_0 + b)} \right\}^2 \tag{18.68}$$

The frequency response function of this filter is shown in Fig. 18.62, which indicates that this filter rolls off much more quickly than the second-order filter. The compensation band now extends out to $\sim 50 f_0$ rather than $300 f_0$. There is, however, a penalty for this higher rolloff. That penalty is illustrated in the Nyquist and Nichols plots of Fig. 18.63 and the noise reduction performance plot of Fig. 18.64. The Nyquist plot shows that the system is stable but that the curve formed by $H(\omega)$ enters the noise amplification region. The Nichols plot shows that the expected noise amplification should be about 2.5 dB, which is confirmed in Fig. 18.64. Finally the regulation frequency band over which the noise reduction is 10 dB or more has been reduced slightly due to the more rapid rolloff of this higher order filter. The noise reduction performance and regulation bandwidth issues can be dealt with by changing the parameter values in the filter frequency response function (with concomitant increases in the compensation bandwidth and noise amplification). However, *the noise amplification generated by this higher order filter occurs even with perfect compensation and is the real reason the low-order filter is preferred.*

Compensation Filter. There are a number of approaches that can be applied to designing the compensation filter. Here we will examine the use of feedforward control filter design techniques, as discussed in Section 18.4, to design a control filter that will converge to the inverse of the plant. The notion for this approach is illustrated in the feedforward control architecture of Fig. 18.65. There the plant,

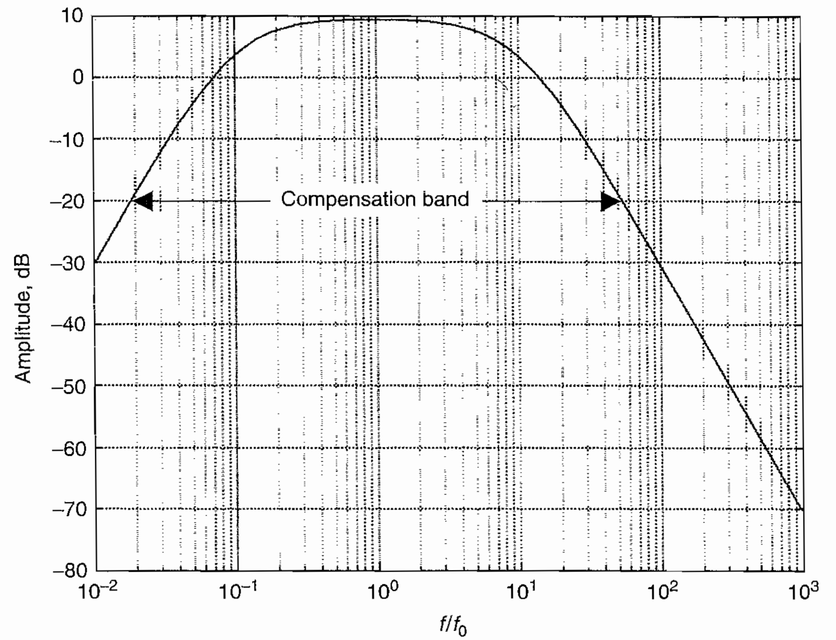

FIGURE 18.62 Frequency response of the broadband fourth-order regulation filter.

$P(\omega)$, and the compensation filter, $G(\omega)$, are connected in series and the disturbance and the residual are the same function, that is, the transfer function $B(\omega)$ in the simplified feedforward architecture of Fig. 18.31 is unity. With this arrangement, the control filter design algorithms will attempt to make $G(\omega)P(\omega) = 1$ or $G(\omega) \approx P(\omega)^{-1}$. Both the direct-estimation and filtered-x design tools can be applied to this problem and the inverses of both MIMO and SISO plants can be determined.

Example. To illustrate this approach, we define the notional position-keeping system for the suspended mass shown in Fig. 18.66. The mass might be machinery that is vibration isolated from the deck of a ship. For frequencies well above ω_0 the suspension system under the mass will reduce the excitation of the deck due to machine vibration from imbalance, for example. Our position-keeping system prevents the machinery from striking the deck when the ship encounters rough seas. In this system the relative displacement between the machine and the deck is measured and used as the input to a controller. The controller in turn generates a control force to minimize that relative deflection so that the machine and the deck do not come into contact. The control force could be generated by an inertial shaker or an interstructural shaker between the deck and the machine.

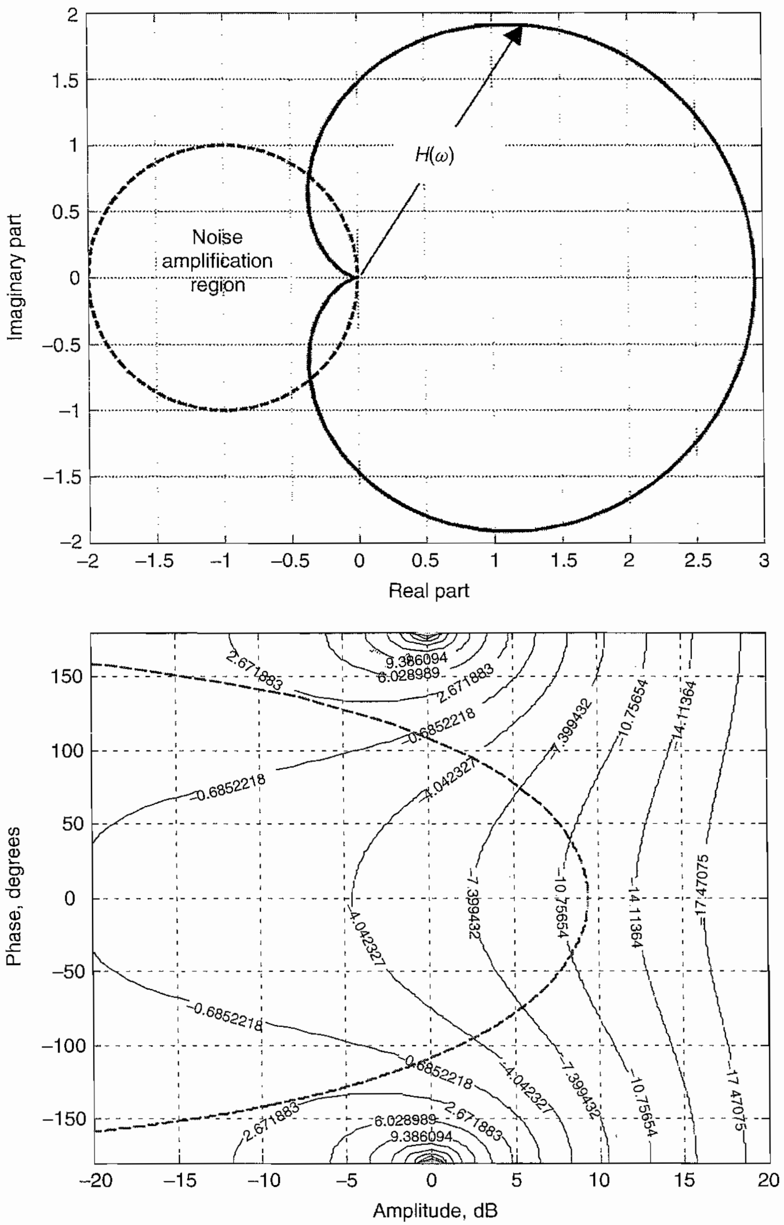

FIGURE 18.63 Nyquist and Nichols plot for the broadband fourth-order regulation filter.

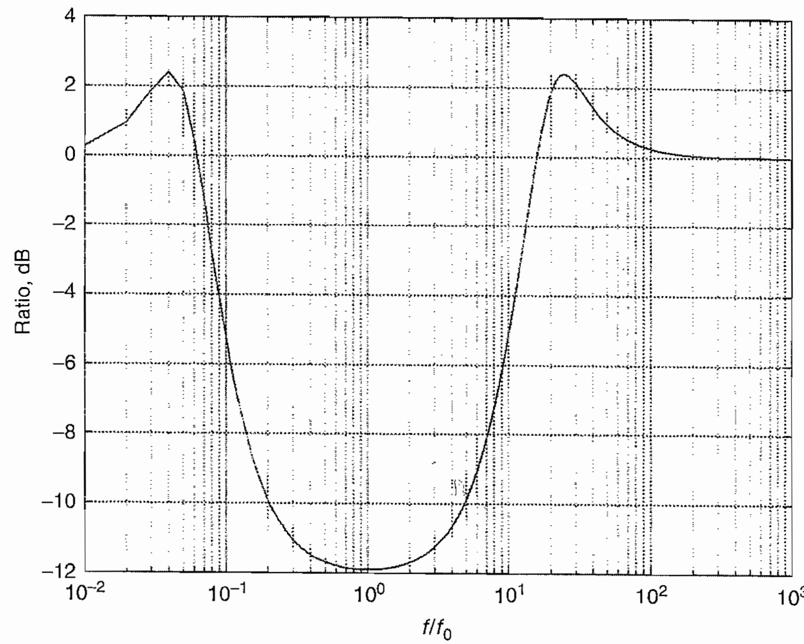

FIGURE 18.64 Ratio of controlled to uncontrolled residual for the broadband fourth-order regulation filter.

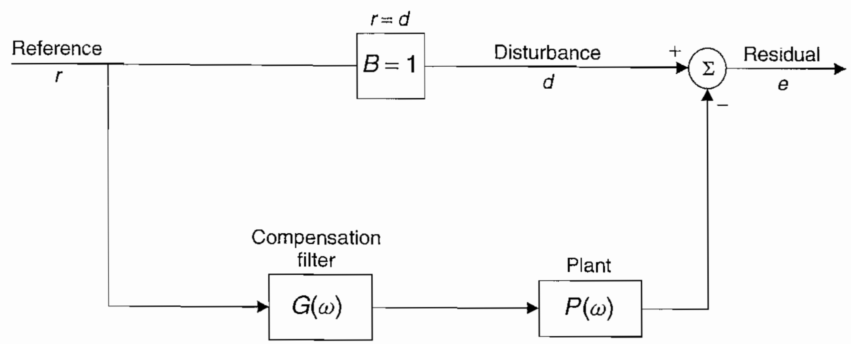

FIGURE 18.65 Feedforward architecture for estimating the plant inverse.

The plant for this system, which is the ratio of the relative deflection between deck and machine to actuator force is given by

$$P(\omega) = \frac{1}{M\omega_0^2\{1 - (\omega/\omega_0)^2 + j(\omega/\omega_0)\eta\}} \tag{18.69}$$

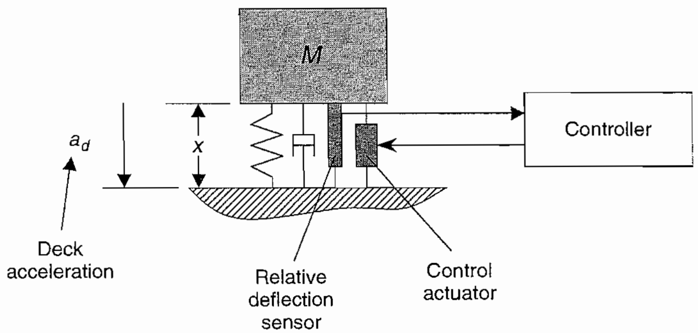

FIGURE 18.66 Notional feedback position-keeping system.

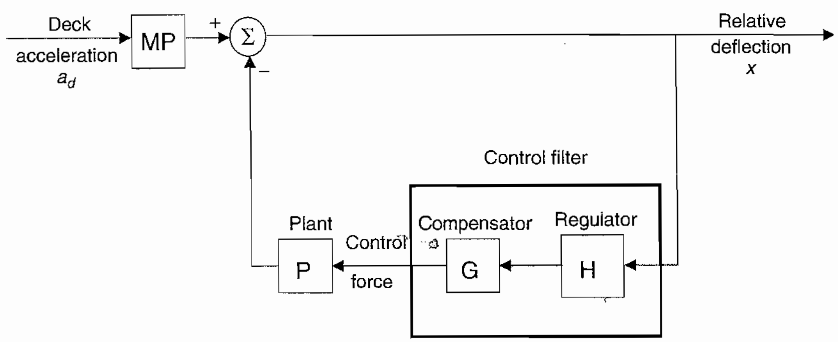

FIGURE 18.67 Block diagram of the notional feedback position-keeping system.

where ω_0 is the natural frequency of the mass on its suspension and η is the loss factor for the system. The feedback control system block diagram for our notional position-keeping system is shown in Fig. 18.67.

The parameter values that we will use are

$$f_o = \frac{\omega_0}{2\pi} = 25 \text{ Hz} \qquad \eta = 0.1$$

For this calculation we will not use any anti-aliasing or reconstruction filters but will rely on the plant itself to provide low-pass filtering. If we were to use any additional low-pass filtering, the frequency response of those filters would simply be included with the plant, since the compensation filter will have to compensate for the amplitude and phase variations of those components as well. In a real system with more complex high-frequency response than our simple notional system we would probably not be able to eliminate anti-aliasing and reconstruction filters, but eliminating them here simplifies the example. Finally, we must account

for the half-sample delay introduced by the sample-and-hold D/A converters. We simply include that delay in the plant frequency response function.

For a regulation filter we will use the second-order broadband filter of Eq. (18.67) with the following parameters:

$$K = 3 \qquad a = 0 \qquad b = 10$$
$$f_o = \frac{\omega_0}{2\pi} = 1$$

These parameters make the regulation filter have the low-pass characteristics illustrated in Fig. 18.68. The filter has a nominal loop gain of ~10 dB out to ~10 Hz.

Based on the results in Fig. 18.60, we know that the compensation band will need to extend out to about 40 times the highest frequency in the regulation band or out to 400 Hz. Since we cannot expect to design a compensation filter that will be effective right out to the Nyquist frequency (one-half the sampling rate), we will put in a margin of safety and use a sampling rate of 1000 Hz, which gives a Nyquist frequency of 500 Hz. Using the direct-estimation filter design technique

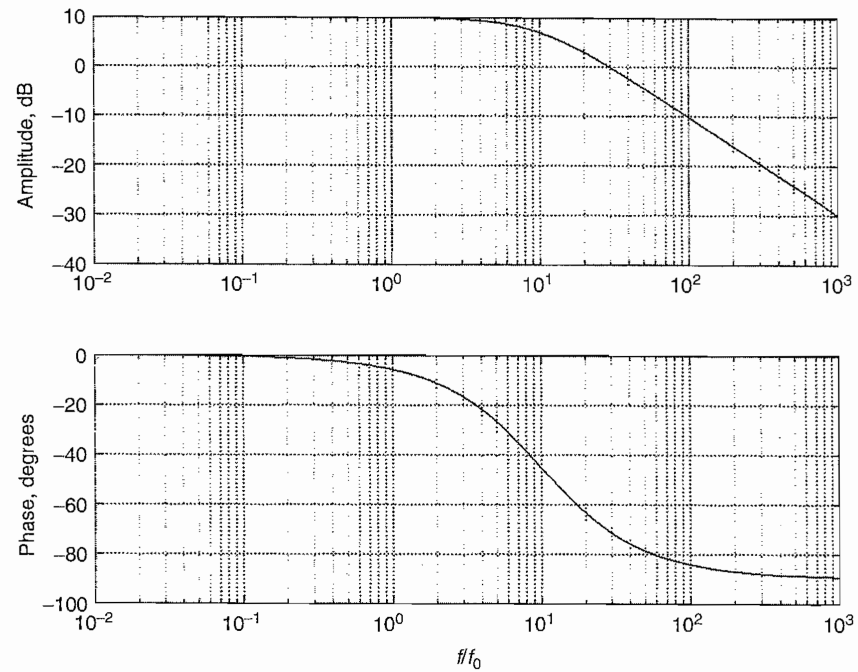

FIGURE 18.68 Amplitude and phase of the regulation filter.

of Section 18.4 for the system in Fig. 18.65, we obtain a 50-tap compensation filter $G(\omega)$ that when multiplied by the plant transfer function gives the result shown in Fig. 18.69. If the filter were a perfect compensator, the amplitude of $G(\omega)P(\omega)$ would be unity and the phase would be zero.

The figure shows that the amplitude is very close to unity almost all the way to the Nyquist frequency.* The phase, however, reaches almost 180° at 300 Hz, which indicates that we should expect some noise amplification due to imperfect compensation. That expectation is confirmed in the Nichols plot of Fig. 18.70 and the noise reduction performance plot of Fig. 18.71, which each slow a little over 2 dB of noise amplification. The Nyquist plot also in Fig. 18.70 shows that the system is stable. The noise reduction performance in Fig. 18.71 shows that 10 dB of noise reduction has been achieved up to more than 10 Hz.

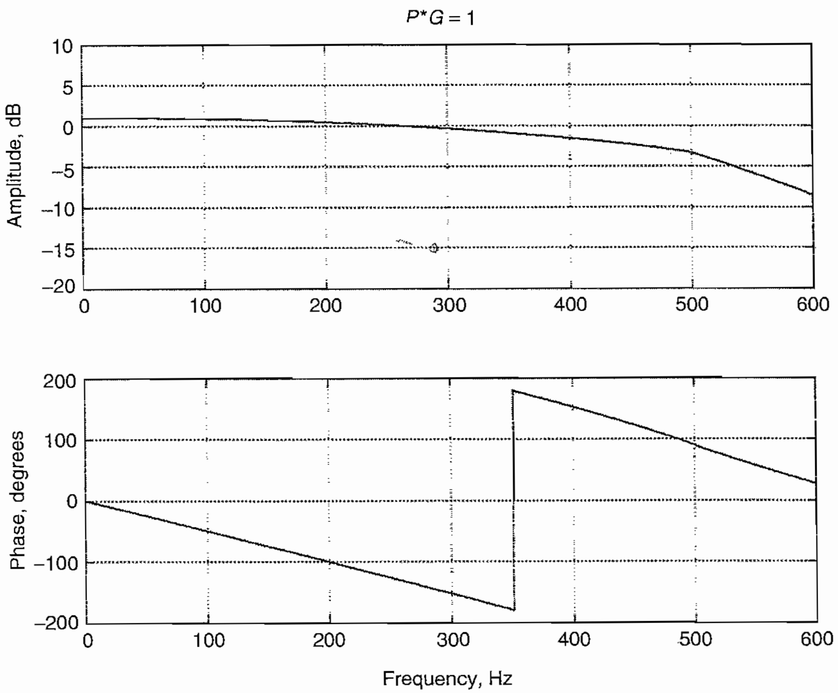

FIGURE 18.69 Amplitude and phase of the product of the compensation filter and the plant transfer function $\{G(\omega)P(\omega)\}$ as a function of frequency.

*Note that in computing the compensation filter using the direct-estimation approach it is sometimes necessary to introduce a small delay in the block diagram of Fig. 18.65 to deal with uncompensatable delays in the plant. Instead of setting $B(\omega) = 1$, we set it to $B(\omega) = e^{-j\omega\lambda T}$, where T is the sample period and λ a constant representing the length of the delay in sample periods. While introducing some phase error in the compensator, this approach often results in a better plant compensator than if no delay were introduced. For the case examined here best results were obtained with $\lambda \sim 1.5$.

Idaho Power/1206
Ellenbogen/415

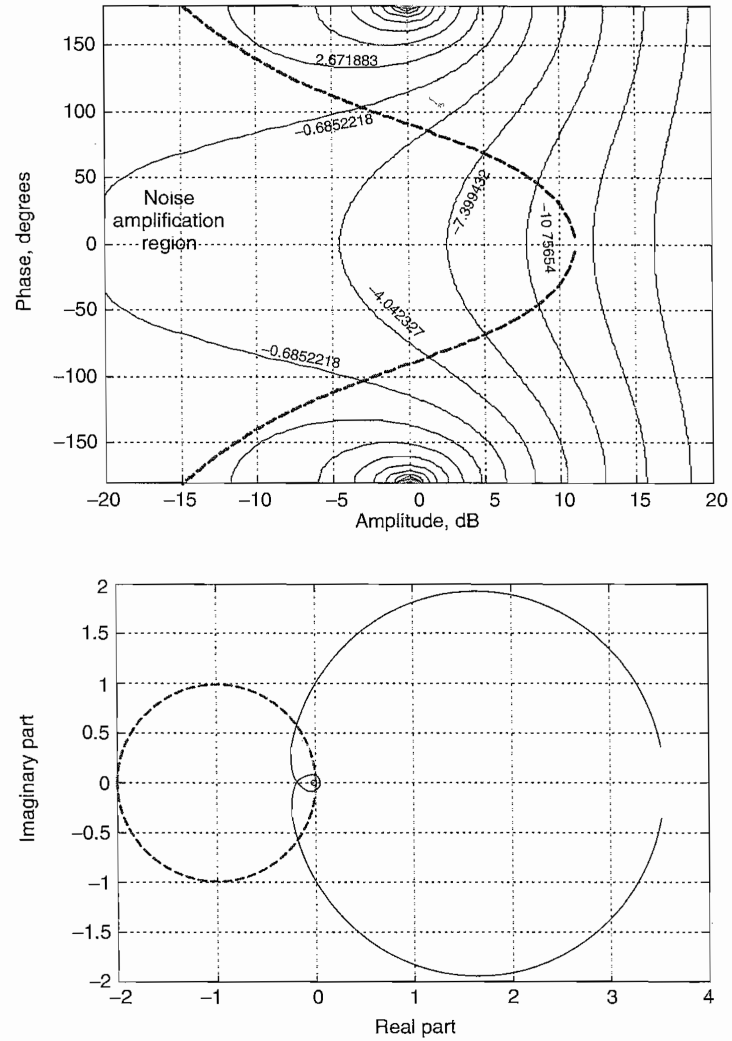

FIGURE 18.70 Nichols and Nyquist plots for the feedback control system of Fig. 18.67.

This example points out how feedback control systems can make severe demands on hardware, typically much more severe than feedforward systems. To achieve 10 dB of noise reduction out to 10 Hz required in this case a sampling rate of 1 kHz, 100 times higher than the regulation bandwidth. *Such a huge factor between regulation bandwidth and compensation bandwidth is not uncommon and is one of the reasons why feedforward systems are often favored over feedback.*

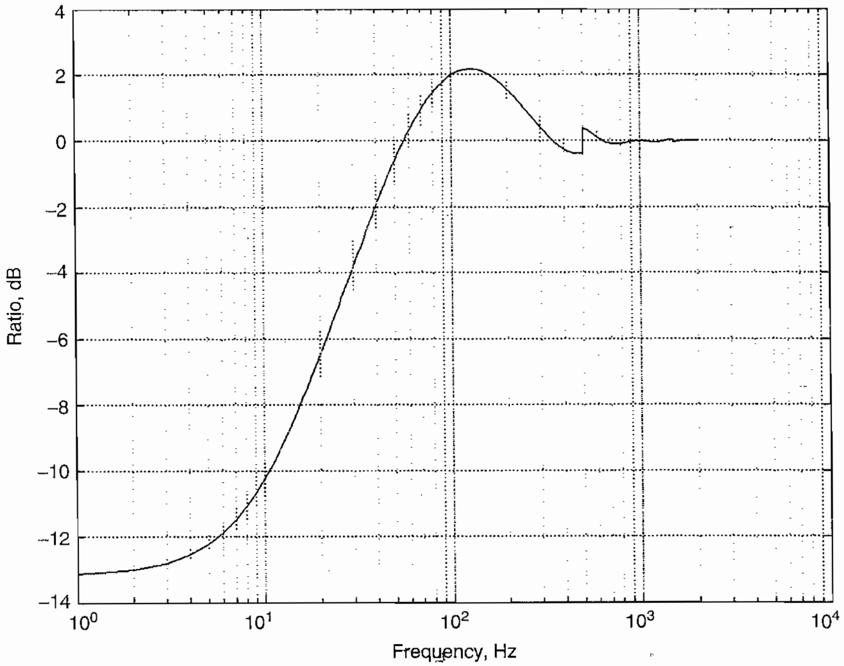

FIGURE 18.71 Ratio of controlled to uncontrolled residual for the feedback control system of Fig. 18.67.

18.6 CONTROL SYSTEM DESIGN CONSIDERATIONS

In this section, we discuss the process and steps involved in designing and implementing a successful ANVC system. This process is illustrated in the flow chart of Fig. 18.72 As shown, the first step is to establish design goals and requirements, which include performance goals and objectives. These goals, together with experimental data or structural–acoustic models, are used to conduct simulations to predict achievable system performance. These performance simulations typically involve trade-off studies of system performance as a function of actuator output levels, sensor dynamic ranges and noise floors, control algorithms, architecture, and controller parameters (e.g., sample rate, analog filter characteristics, digital filter sizes, computational load, and memory requirements). These simulations ultimately guide decisions concerning hardware selection, such as analog filtering, A/D and D/A converters, and digital-controller hardware. The output of this simulation step is a set of design specifications for the sensor and actuator subsystems as well as for the controller (i.e., control algorithm and architecture). Preliminary and detailed designs are then performed to produce sets of component specifications for each subsystem as well as interface control documentation between each subsystem and with the system to be controlled. At this

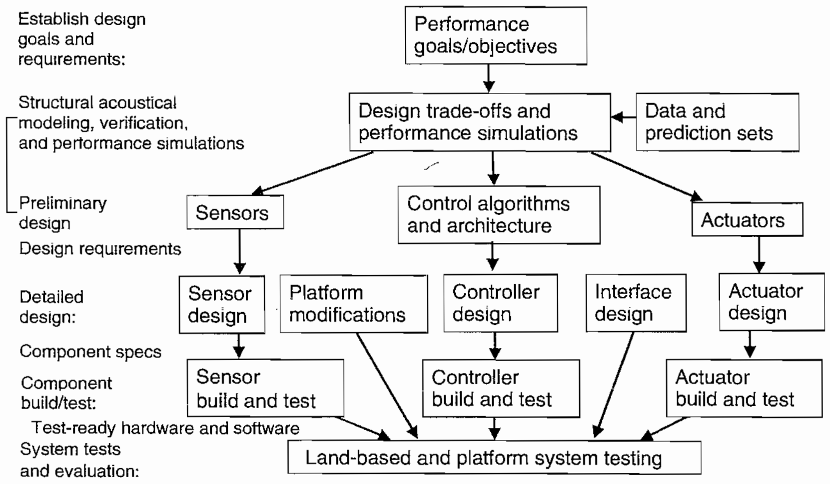

FIGURE 18.72 Flow chart for ANVC system development and implementation.

point, the subsystems are acquired if they are commercially available and fabricated if not. Each is then tested to ensure that both hardware and software meet specifications. The components are then integrated with the system to be controlled. Typically, a series of tests is conducted to validate system performance. If successful, more extensive in-service testing is usually performed to determine long-term performance and reliability before the prototype system is transformed into a commercial product or deployable system. That transformation, which can be an extensive and costly process, is not discussed here.

In the sections that follow, we discuss the major steps in this development process, including identification of performance goals, specification of actuator and sensor requirements, and selection of control architecture. Also discussed in what follows are the benefits of conducting both non causal and causal performance simulations; practical considerations concerning hardware selection of analog filters, D/A and A/D converters, and digital signal processors; and an overview of issues related to control system user interface, operating modes of the system, and system testing guidelines.

Identifying Performance Goals

Identifying performance goals is an important, yet often overlooked, first step in developing an ANVC system. Performance goals state what effect the control system should have on a particular physical quantity as a function of frequency. A schematic that is useful for discussing performance goals is shown in Fig. 18.73. This figure shows two conceptual curves as a function of frequency. The solid curve is representative of the uncontrolled response (e.g., mean-square vibration level on a particular component). The dashed curve is the desired mean-square

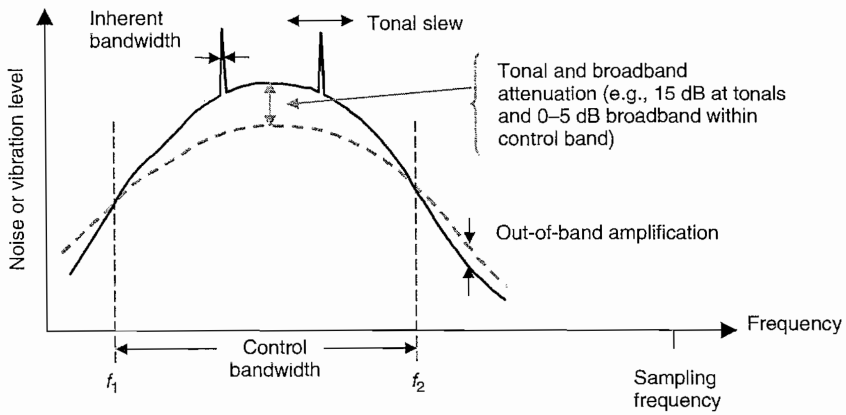

FIGURE 18.73 Schematic of performance goal specification, uncontrolled response (solid line), controlled response (dashed line).

response as a result of implementing an ANVC system. This desired response may be required to meet product specifications or may be related to meeting certain radiated noise specifications. In either case, the difference between these two curves identifies the reductions, as a function of frequency, that are required. As an example, the performance goals for the case illustrated in Fig. 18.73 might include the following:

- Reduce tonal components in mean-square vibration response by at least 15 dB.
- Maintain tonal performance in the presence of slewing tonals (e.g., where the tonal frequency changes over time at a rate of less than 3 Hz/s).
- Reduce broadband mean-square response in the control band (i.e., between frequencies f_1 and f_2) by 0–5 dB.
- Maintain performance in the presence of changes in the dynamics of the system (i.e., plant) that will occur over time.
- Limit out-of-band noise amplification to less than 2 dB at any frequencies outside the control band.

Identifying performance goals is important for several reasons. First, the expectations for the ANVC system are clearly stated and can be evaluated versus practically achievable ANVC performance. For example, typical ANVC systems can provide 15–20 dB of tonal reductions, depending on the slew rate of the tonals. Further, broadband performance in excess of 10 dB is typically associated with some level of out-of-band amplification. Second, these specifications will directly impact implementation aspects of the ANVC system. With regard to the above example, we can make the following initial observations. The broadband performance requirement will require a feedback implementation

or a feedforward implementation with reference sensors that are well correlated with the mean-square response to be controlled. The need to provide additional reductions at slewing tonal frequencies will require control filters that adapt relatively quickly in response to changing tonal frequency. In addition, since the plant transfer functions are expected to change over time, the control system will need to support concurrent system identification and adaptation to track relatively slower changes in the system dynamics. Finally, the constraint on noise amplification will impact the bandwidth of a feedback implementation (as discussed in Section 18.5) and probe signal design (as discussed in Section 18.4 under System Identification).

In general, the performance goals will have a direct impact on *all* aspects of the ANVC system design (e.g., sensors, actuators, and controller). In the next sections, we discuss how the performance goals impact each of these subsystems. In particular, we discuss procedures to answer the following questions:

- What number of actuator channels is required?
- Where should the actuators typically be located?
- What are the output drive requirements (force, volume velocity, etc.) for the actuators?
- What is the number of sensor channels required?
- Where should sensors typically be located?
- What control algorithm/architecture can be used to design control filters that will maximize achievable system performance?
- Is it likely that the program goals can be met (at least throughout the frequency range of the available models) with a reasonable number of actuator and sensor channels and with a causal controller?

These questions will be addressed within the context of the technical approach illustrated in the flow diagram of Fig. 18.74. As shown along the left side, the approach involves three sequential studies:

- Controllability: where to place the actuators.
- Observability: where to place the sensors.
- Realizability: how to design causal control filters.

Number, Location, and Sizing of Actuators

Actuator and sensor placement studies require either a model of the system to be controlled [e.g., finite-element model (FEM), lumped-parameter model] or access to experimental data from the system itself. The first questions to be addressed are where actuators should be located, how many are necessary as a function of achievable performance, and what size of actuator is needed (shaker maximum force output, speaker maximum volume velocity, etc.) to effectively drive the system and provide control.

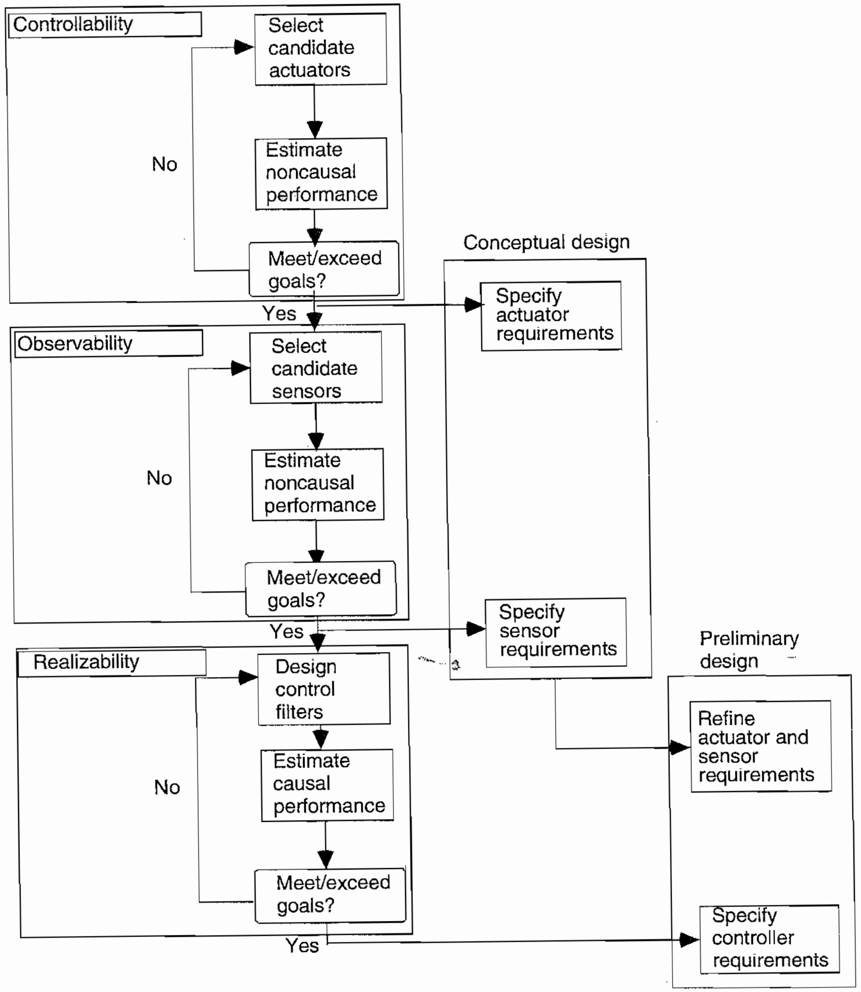

FIGURE 18.74 Flow diagram for ANVC strategy selection.

Number of Actuators. The question of how many actuator channels are required can be roughly estimated from experimental data or model results of the response to be controlled. For example, suppose that the response to be controlled is the mean-square vibration response on a component that is characterized by L point response measurements. The minimum number of actuator channels is equal to the number of independent ways the system is responding at the L measurement locations (referred to as *response dimensionality*) on a frequency-by-frequency basis. The response dimensionality can be estimated by computing the singular-valued decomposition (SVD) of the cross-spectral density (CSD)

matrix of the L responses. We can express this CSD matrix as

$$[\mathbf{S_{ee}}] = [\mathbf{T}][\mathbf{S_{dd}}][\mathbf{T}]^H \tag{18.70}$$

where $[\mathbf{S_{dd}}]$ = cross-spectral density matrix of disturbance
$[\mathbf{T}]$ = transfer function matrix from source(s) to L response locations
$[\cdot]^H$ = conjugate transpose of matrix

Note that $[\mathbf{S_{ee}}]$ can be evaluated directly by measuring the CSD matrix of a number of sensors at candidate locations. As an alternate approach analytical/numerical models of the system to be controlled can be used to estimate $[\mathbf{T}]$ along with approximations to $[\mathbf{S_{dd}}]$* in Eq. (18.70) to estimate $[\mathbf{S_{ee}}]$.

The SVD of a matrix $[\mathbf{A}]$ is defined as

$$\text{svd}\{[\mathbf{A}]\} = [\mathbf{U_A}][\boldsymbol{\lambda}_\mathbf{A}][\mathbf{V_A}]^T \tag{18.71}$$

where $[\mathbf{U_A}]$ and $[\mathbf{V_A}]$ are unitary matrices containing the left and right singular vectors of $[\mathbf{A}]$ and $[\boldsymbol{\lambda}_\mathbf{A}]$ is a diagonal matrix containing the singular values for $[\mathbf{A}]$ ranked from largest to smallest.[60] A typical plot of the singular values of $[\mathbf{S_{ee}}]$ (i.e., diagonal elements of $[\boldsymbol{\lambda}_\mathbf{e}]$) at a particular frequency will reveal several large (i.e., significant) singular values followed by a transition to a region containing smaller (i.e., less significant) singular values. An example of this type of plot, where the singular values are normalized by the largest, is shown in Fig. 18.75. These types of plots can be conveniently generated using the svd function in MATLAB.

The number of large singular values of $[\mathbf{S_{ee}}]$ at a given frequency indicates the number of significant and independent ways in which the disturbances on the system express themselves at the L measurement locations. At any frequency, the number of significant singular values is equal to the minimum of

- the number of independent disturbances acting on the structure (termed *source dimensionality*),
- the number of structural degrees of freedom (i.e., modes),
- the number of measurement responses (ie, sensors), and
- degrees of freedom of spectral estimates (i.e., number of ensemble averages in estimating the CSD matrix from experimental data).

As such, care must be taken to ensure that the estimated response dimensionality is not limited by using too few sensors, by insufficient averaging if $[\mathbf{S_{ee}}]$ is measured, or by too few sources and sensors if analytical models are used to estimate $[\mathbf{S_{ee}}]$. We note that controlling the response characterized by the L measurement

*For analytical/numerical simulations, where the CSD of the disturbances may be unknown, it is often sufficient to assume a large number of candidate disturbance locations and use a disturbance CSD matrix in Eq. (18.70) equal to the identity matrix at all frequencies of interest. This corresponds to the case where the sources are statistically independent with unit variance at each frequency.

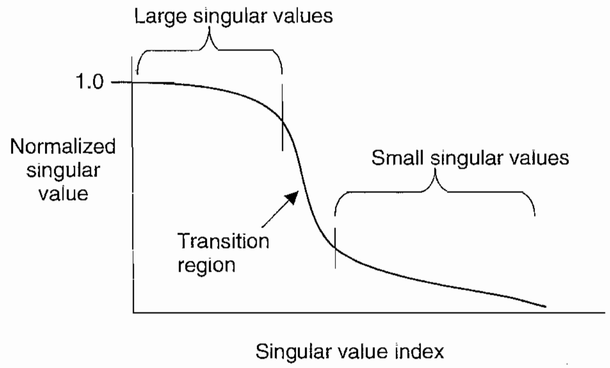

FIGURE 18.75 Typical decay of singular values of a sensor CSD matrix, normalized by the largest singular value.

locations will require at least as many actuator *channels** as significant singular values of $[\mathbf{S_{ee}}]$. Thus, this approach establishes a lower bound on the number of required actuator channels.

Finally, we make two remarks concerning the use of SVD spectra to determine lower bounds on the number of actuator channels. First, since the number of significant singular values will typically increase as a function of frequency (because the number of modes supported by the system increases with frequency), the number of required actuator channels is often dictated by the singular-value spectra at high frequency. Second, the transition region in Fig. 18.75 may be gradual rather than showing a distinct "knee." For those cases, a useful "rule of thumb" is that the number of significant singular values at a given frequency is equal to the number of singular values whose magnitude is within, say, 30 dB of the largest singular value.

Actuator Locations. The selection of specific actuator locations is typically the result of an optimization procedure to select the best K locations from a set of M possible locations ($M > K$). This procedure requires the response CSD discussed above as well as the $L \times M$ transfer function matrix $[\mathbf{P}]$ between the M possible actuator locations and the L sensor responses. An exhaustive search over all combinations to determine the optimal set of K actuator locations would require a search of $\dfrac{M!}{[K!(M-K)!]}$ possibilities. This can be a daunting task for even modest values of K and M. When this is the case, it is often useful to invoke suboptimal techniques to choose a "good" set of actuators.

One suboptimal approach that has been used successfully is based on Gram–Schmidt orthogonalization.[60] Given M candidate actuator locations,

*The term *actuator channels* is not necessarily the same as the number of actuators. For instance, a group of 10 actuators driven coherently requires only a single output channel from a controller.

choose the one that maximizes reductions in the trace of $[\mathbf{S_{ee}}]$. In this context, the best candidate is the column of $[\mathbf{P}]$ that is "most parallel" to the L sensor responses caused by the disturbances, integrated across frequency. Once an actuator (i.e., column of $[\mathbf{P}]$) is chosen, components of $[\mathbf{S_{ee}}]$ and remaining columns of $[\mathbf{P}]$ in the direction of the chosen column of $[\mathbf{P}]$ are removed. The process is repeated K times, where the value of K is estimated from SVD spectra of $[\mathbf{S_{ee}}]$. Variants of this procedure are discussed by LePage et al.[42] and Heck et al.[83] An interesting comparison of alternative procedures for selecting source locations based on using genetic algorithms and simulated annealing is discussed by Elliott.[58]

Regardless of the selection procedure, the mean-square response of the L sensors can be estimated assuming all actuators chosen so far can be used in an optimal, unconstrained sense. That is, we assume a controller can be developed to produce the required magnitude and phase spectra to drive each output channel. At each frequency, the L *vector* of residual responses $\boldsymbol{\varepsilon}$ can be expressed in terms of the L *vector* of uncontrolled responses $\mathbf{e}$ and the k *vector* of actuator drive signals $\mathbf{a}$ (for $k \le K$) acting though the $L \times k$ plant transfer function matrix $[\mathbf{P}]$:

$$\boldsymbol{\varepsilon} = [\mathbf{T}]\mathbf{d} + [\mathbf{P}]\mathbf{a} = \mathbf{e} + [\mathbf{P}]\mathbf{a} \tag{18.72}$$

The optimal solution for $\mathbf{a}$ to reduce the residual mean-square response $\mathrm{tr}\{[\mathbf{S_{ee}}]\}$ at each frequency is

$$\mathbf{a} = -[\mathbf{P}]^{\#}\mathbf{e} \tag{18.73}$$

where # signifies the pseudoinverse, which can be conveniently computed using the pinv function in MATLAB or by the expression defined in Section 18.4 under Extension to MIMO Systems.

As a consequence, the optimal noise reduction (NR, in decibels) of the mean-square response using the selected actuators is

$$\mathrm{NR} = -10 \log_{10}\left(\frac{\mathrm{tr}\{[\mathbf{S}_{\boldsymbol{\varepsilon\varepsilon}}]\}}{\mathrm{tr}\{[\mathbf{S_{ee}}]\}}\right) \tag{18.74}$$

where

$$[\mathbf{S_{ee}}] = E\{\mathbf{e}\mathbf{e}^{\mathbf{H}}\} = [\mathbf{T}][\mathbf{S_{dd}}][\mathbf{T}]^{\mathbf{H}}$$
$$[\mathbf{S}_{\boldsymbol{\varepsilon\varepsilon}}] = [\mathbf{I} - \mathbf{PP}^{\#}][\mathbf{S_{ee}}][\mathbf{I} - \mathbf{PP}^{\#}]^{\mathbf{H}} \tag{18.75}$$

In Eq. (18.75), $[\mathbf{S_{ee}}]$ is the CSD matrix of the *uncontrolled* responses at the L residual sensor locations. This can be estimated from experimental data (i.e., $E\{\mathbf{e}\mathbf{e}^{\mathbf{H}}\}$) or can be computed using transfer functions from source-to-residual locations, $[\mathbf{T}]$, based on analytical models (i.e., lumped-parameter or FEM), and an assumed CSD matrix of the sources, $[\mathbf{S_{dd}}]$, for example, the unit matrix as described above.

Equation (18.74) can be plotted frequency by frequency (or integrated across the frequency bandwidth of concern) to determine an upper bound on system performance, parameterized by the number of assumed actuators, as shown in Fig. 18.76. These performance predictions represent upper bounds because at this point we have not placed any causality constraints on the control filter, and we have not identified what sensor signals will be used as inputs to the controller. As such, these predictions are referred to as noncausal predictions, corresponding to those identified in Fig. (18.74) pertaining to controllability. Since Eq. (18.74) represents an upper bound on achievable performance as a function of frequency for the selected actuator set, it provides a first-order assessment as to whether the identified performance goals are achievable.

Actuator Sizing. A critical issue in the design of an active control system is the sizing of the actuators. Actuators with too little drive capacity will result in an underperforming control system, while actuators with too much capacity may impose excessive weight or cost penalties. A rough guide is that the actuators must be able to create response levels at the residual sensors that are comparable to the levels observed there due to the disturbance. A more precise estimate of the required drive levels from the actuators can be determined from the diagonal elements of $[\mathbf{S_{aa}}]=[\mathbf{P}]^{\#}[\mathbf{S_{ee}}][\mathbf{P}^{\#}]^{\mathbf{H}}$, which correspond to the power spectra of the required drive signals to each actuator. For this calculation $[\mathbf{S_{ee}}]$ should be based on measurements unless good analytical models of the disturbances and their CSD matrix, $[\mathbf{S_{dd}}]$, are available. The square root of the integrated mean-square levels of each diagonal term across frequency provides an estimate of the rms levels for each drive signal. Peak drive requirements can be estimated from these

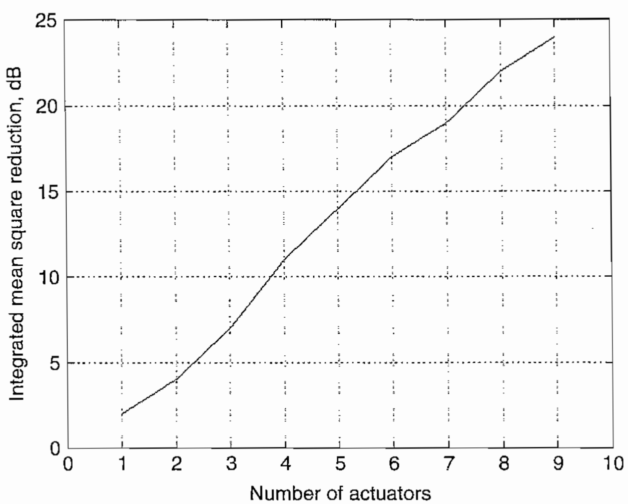

FIGURE 18.76 Example of noncausal performance versus number of actuator channels.

rms levels by applying an appropriate crest factor (i.e., ratio of the peak value of a waveform to its rms value). For pure-tone cases, the crest factor is 1.41; for broadband noise, the crest factor will depend on the statistics of the disturbance. A useful approximation to the crest factor for random noise is 4.

Note that if the plant [**P**] used in the equations above relates actuator output (force, volume velocity, etc.) to the residual channel responses, then the diagonal elements of $[\mathbf{S_{aa}}]$ (and the associated rms and peak levels) correspond to the actual actuator drive level (e.g., pounds, cubic feet per minute) that must be delivered to the structure by the actuators to produce the predicted performance. As such, these predictions provide initial actuator sizing information.

Number and Location of Sensors

The goals and requirements for selecting residual and reference channels are summarized below.

Residual Sensor Channel Selections for Feedforward and Feedback Strategies. The goal is to determine a minimal set of measurable responses that are

- well correlated with the radiated noise or vibration response to be controlled,
- nominally colocated with actuators for feedback control, and
- consistent with satisfying "obvious" causal constraints*: at or "downstream" of actuators for feedforward control strategy.

Reference Sensor Channel Selection (for Only Feedforward Strategy). The goal is to determine a minimal set of measurable responses that are

- well correlated with the disturbance sources,
- well correlated with candidate residual channels,
- consistent with satisfying obvious causal constraints: with sufficient "lead time" to implement an effective causal controller (i.e., located sufficiently "upstream" of the actuators).

Approaches for determining sensor channels that meet these goals and requirements are presented below.

Number of Sensors. If the number of residual sensors is equal to the number of control actuators, it is theoretically possible to achieve infinite noise reduction in a feedforward system. Of course, very large noise reduction at residual

*By obvious causal constraints, we rule out consideration of residual sensors that are closer to the sources than the selected actuator locations (i.e., upstream of the actuator locations). Similarly, we rule out consideration of reference sensor locations that are downstream of (farther away from the sources than) the actuator locations.

sensors does not necessarily mean that the system will also provide good noise reduction globally. Alternatively, if the number of control actuators exceeds the number of residual sensors, the system is overdetermined and the control effort may be excessive with some actuators competing against others unless control effort weighting is carefully included in the control filter design algorithm. Most practical systems have more residual sensors than control actuators so that the noise reduction is less concentrated at the residual sensor locations, resulting in more uniform global control.

The selection of residual and reference sensors (when required or available) can be determined following similar procedures to those outlined for actuator selection. As before, it is advisable to perform SVD analyses of candidate residual and reference CSD matrices to determine the minimum number of channels necessary to characterize the response caused by the disturbances at those locations. Since response dimensionality will never increase as measurement locations move away from the sources, it is common that the response dimensionality at the reference sensor locations will exceed that at the residual sensor locations. We note, however, that the number of sensors necessary to characterize the response dimensionality may exceed the number of sensor channels determined by the dimensionality studies, as, for example, when arrays of sensors are processed to characterize modal responses of a system.

If the response to be controlled is already known, the choice of residual sensing may be relatively straightforward. For example, if the mean-square response of a plate structure on a machine is to be reduced, it may be sufficient to instrument that plate with L point sensors, where L exceeds the response dimensionality of the plate (e.g., number of significant modes). Subsets of these L sensors can also be considered to determine the sets that when minimized in an optimal sense will produce the largest mean-square reductions of the full set of L sensors. Again, either exhaustive or suboptimal search techniques can be used.

For cases where reducing radiated noise is the main objective, it may not be possible to use residual sensor inputs to the controller that directly measure the noise field. Instead, for these cases, residual sensors must be located on the machine or device to be controlled. Selection of these on-board sensors is typically the result of using detailed radiation models to determine which on-board sensor responses are highly correlated with the radiated noise. If models or experimental data that include radiated noise information are available for this purpose, then candidate residual sensors can be selected using the exhaustive or suboptimal search techniques discussed above.

Residual Sensor Evaluation. As was done when considering actuator selection, the resulting sets of residual sensors obtained at each step can be evaluated to assess the maximum achievable performance as a function of the number of residual channels. In particular, reductions in the mean-square response of the selected residual channels can be determined using Eq. (18.74), where the optimal drive vector $\mathbf{a}$ in Eq. (18.73) is chosen to minimize only the candidate set of residual channels. These drives are then used in Eq. (18.72) to estimate the

reductions in mean-square performance across a larger and more complete set of residual channels, or the radiated noise response. Again, these predictions represent upper bounds on achievable noncausal performance assuming fixed sets of actuators and residual sensors. That is, we again assume that a controller can be developed to produce the spectral magnitudes and phases that are necessary to drive each output channel to reduce the mean-square residual response in an optimal sense.

Alternatively, residual sensors can be selected simultaneously with implementing the procedure for estimating performance. A similar approach can be used to select reference sensors for a feedforward system. Details of this approach are discussed below with respect to evaluating reference and residual sensors for the case where residual sensors cannot directly measure radiated noise.

Assuming statistical quantities, we define the following frequency domain relationships between the vectors of radiated pressures (or some other desired residual which cannot be measured directly by the control system) $\mathbf{p}$, residual channels $\mathbf{e}$, and reference channels $\mathbf{r}$ and the vector of disturbances $\mathbf{d}$,

$$\mathbf{p} = [\mathbf{Q}]\mathbf{d} \qquad \mathbf{e} = [\mathbf{T}]\mathbf{d} \qquad \mathbf{r} = [\mathbf{R}]\mathbf{d} \tag{18.76}$$

where $[\mathbf{Q}]$, $[\mathbf{T}]$, and $[\mathbf{R}]$ are the transfer function matrices relating the disturbances to the radiated pressure, residual channels, and reference channels, respectively. For purposes of the discussion below, we assume that either the transfer functions $[\mathbf{Q}]$, $[\mathbf{T}]$, and $[\mathbf{R}]$ are available from analytical models (e.g., lumped-parameter or FEM) or the response vectors $\mathbf{p}$, $\mathbf{e}$, and $\mathbf{r}$ are available from experimental data.

The radiated pressure can be related to the residual channels as

$$\mathbf{p} = [\mathbf{H_e}]\mathbf{e} + \mathbf{n} \tag{18.77}$$

where $\mathbf{n}$ represents the radiated pressure response that is uncorrelated with (or unobserved by) the residual channels. Assuming that $\mathbf{e}$ and $\mathbf{n}$ are independent statistical responses, we can obtain an expression for $[\mathbf{H_e}]$ in terms of the CSD matrix of the uncontrolled residual $[\mathbf{S_{ee}}]$ and the CSD matrix between the pressure and residual channels $[\mathbf{S_{ep}}]$:

$$[\mathbf{H_e}] = [\mathbf{S_{ep}}][\mathbf{S_{ee}}]^{-1} \tag{18.78}$$

As discussed earlier with regards to Eq. (18.75), $[\mathbf{S_{ee}}]$ is the CSD matrix of the *uncontrolled* responses at the L residual sensor locations and can be estimated from experimental data (i.e., $E\{\mathbf{ee^H}\}$) or can be computed by using transfer functions from source-to-residual locations, $[\mathbf{T}]$, based on analytical models (i.e., lumped-parameter or FEM), and an assumed CSD matrix of the sources, $[\mathbf{S_{dd}}]$. Similarly, $[\mathbf{S_{ep}}]$ is the CSD matrix of the uncontrolled responses of the pressure and residual sensors. It can be estimated from experimental data (i.e., $E\{\mathbf{pe^H}\}$) or be computed from analytical models for [**T**] and [**Q**] together with an assumed CSD matrix of the sources, [$\mathbf{S_{dd}}$]:

$$[\mathbf{S_{ep}}] = [\mathbf{Q}][\mathbf{S_{dd}}][\mathbf{T^H}] \tag{18.79}$$

We can now write an expression for the maximum noise reduction, at each frequency, that can be achieved by eliminating the response in the radiated pressure that is correlated with the chosen set of residual channels:

$$\mathrm{NR}_p = 10\log_{10}\left(\frac{\mathrm{tr}\{[\mathbf{S_{pp}}] - [\mathbf{H_e}][\mathbf{S_{ee}}][\mathbf{H_e^H}]\}}{\mathrm{tr}\{[\mathbf{S_{pp}}]\}}\right) \tag{18.80}$$

where

$$[\mathbf{S_{pp}}] = [\mathbf{Q}][\mathbf{S_{dd}}][\mathbf{Q^H}] \qquad [\mathbf{S_{ee}}] = [\mathbf{T}][\mathbf{S_{dd}}][\mathbf{T^H}] \tag{18.81}$$

Note that if there is no correlation between the residual sensors and radiated pressure, then NR_p will equal 0 dB. If the output is entirely due to the input (i.e., the residual sensors are perfectly correlated with the radiated pressure, then NR_p will be infinite (i.e., $-\infty$ decibels).

The evaluation of Eq. (18.80) requires either measured data or analytical/numerical models of the system to be controlled. If *simultaneous* measurements of the residual sensors, **e**, and the desired residual, **p**, are available, then the data can be processed to generate the cross-spectra density matrices [$\mathbf{S_{ep}}$], [$\mathbf{S_{ee}}$], and [$\mathbf{S_{pp}}$]. Equation (18.78) can then be used to determine [$\mathbf{H_e}$], which can then be substituted along with [$\mathbf{S_{ee}}$] and [$\mathbf{S_{pp}}$] into Eq. (18.80). If, on the other hand, analytical/numerical models are available, they can be used to estimate the transfer function matrices [**Q**] and [**T**]. If the CSD of the disturbance [$\mathbf{S_{dd}}$] is then taken to be the unit matrix as described earlier, then [$\mathbf{S_{ep}}$], [$\mathbf{S_{ee}}$], and [$\mathbf{S_{pp}}$] can be easily estimated from the equations given above, allowing the evaluation of Eq. (18.80) as if measured data were available.

Reference Sensor Evaluation. In a similar fashion, the procedure outlined above can be used to select reference sensors that are highly correlated with the residual and/or radiated pressure. The residual channels can be related to the reference channels as

$$\mathbf{e} = [\mathbf{H_r}]\mathbf{r} + \mathbf{m} \tag{18.82}$$

where **m** represents the response in the residual channels that is uncorrelated with (or unobserved by) the reference channels. Following the procedure outlined above, the maximum reduction in the mean-square response of the residual channels, **e**, assuming a set of reference sensors **r** is given by

$$\mathrm{NR}_e = 10\log_{10}\left(\frac{\mathrm{tr}([\mathbf{S_{ee}}] - [\mathbf{H_r}][\mathbf{S_{rr}}][\mathbf{H_r^H}])}{\mathrm{tr}([\mathbf{S_{ee}}])}\right) \tag{18.83}$$

where

$$[\mathbf{S_{ee}}] = [\mathbf{T}][\mathbf{S_{dd}}][\mathbf{T^H}] \qquad [\mathbf{S_{rr}}] = [\mathbf{R}][\mathbf{S_{dd}}][\mathbf{R^H}] \tag{18.84}$$

and

$$[\mathbf{H_r}] = \mathbf{S_{re}}[\mathbf{S_{rr}}]^{-1} \tag{18.85}$$

The expression given in Eq. (18.83) represents the maximum reduction, at each frequency, that can be achieved by eliminating the response in the residual channels that is correlated with the chosen reference channels. If there is no correlation between the residual sensors and radiated pressure, then NR_e will equal 0 dB. If the output is entirely due to the input (i.e., the residual sensors are perfectly correlated with the radiated pressure, then NR_e will be infinite.

As with the residual sensors the evaluation of Eq. (18.83) requires either measured data or analytical/numerical models of the system to be controlled. If simultaneous measurements of the residual sensors, **e**, and the reference sensors, **r**, are available, then the data can be processed to generate the cross-spectra density matrices [$\mathbf{S_{er}}$], [$\mathbf{S_{ee}}$], and [$\mathbf{S_{rr}}$]. Equation (18.85) can then be used to determine [$\mathbf{H_r}$], which can then be substituted along with [$\mathbf{S_{ee}}$] and [$\mathbf{S_{rr}}$] into Eq. (18.83). If, on the other hand, analytical/numerical models are available, they can be used to estimate the transfer function matrices [**R**] and [**T**]. If the CSD of the disturbance [$\mathbf{S_{dd}}$] is then taken to be the unit matrix as described earlier, then [$\mathbf{S_{er}}$], [$\mathbf{S_{ee}}$], and [$\mathbf{S_{rr}}$] can be easily estimated from the equations given above, allowing the evaluation of Eq. (18.83) as if measured data were available.

Sensor Selection and Noncausal Performance. Choices for candidate residual and reference sensors are typically guided by an understanding of the physics of energy propagation for the system to be controlled as well as guidance on the required number of channels required based on SVD analyses. Assuming candidate actuator, reference, and residual locations have been identified using the procedures discussed above, an upper bound on achievable performance for this set of transducers can be obtained by estimating the noncausal performance. These predictions correspond to those identified in Fig. 18.74 under the observability phase. For a feedforward system, this means that we assume the controller can implement whatever filter is necessary to relate the reference sensor responses to the required actuator drive signals to minimize the mean-square residual response. For this case, the uncontrolled and controlled mean-square residual responses are given by

$$\mathrm{tr}([\mathbf{S_{ee}}]) = \mathrm{tr}([\mathbf{T}][\mathbf{S_{dd}}][\mathbf{T^H}]) \tag{18.86}$$

and

$$\mathrm{tr}([\mathbf{S}_{\varepsilon\varepsilon}]) = \mathrm{tr}(\{\mathbf{I}-[\mathbf{P}][\mathbf{P}^{\#}]\}[\mathbf{H_r}][\mathbf{S_{rr}}][\mathbf{H_r}]^{\mathbf{H}}\{\mathbf{I}-[\mathbf{P}][\mathbf{P}^{\#}]\}^{\mathbf{H}}) \tag{18.87}$$

where $[\mathbf{S_{ee}}]$ and $[\mathbf{S_{rr}}]$ are defined in Eq. (18.84), $[\mathbf{H_r}]$ is defined in Eq. (18.85), and the noise reduction is given by

$$\mathrm{NR} = 10 \log_{10} \left(\frac{\mathrm{tr}([\mathbf{S}_{\varepsilon\varepsilon}])}{\mathrm{tr}([\mathbf{S_{ee}}])} \right) \tag{18.88}$$

As described in the above discussion for the residual and reference sensors, Eq. (18.88) can be evaluated using either measured data or analytical/numerical models. The one difference here is that measurements or analytical/numerical predictions of the plant transfer function matrix $[\mathbf{P}]$ are also required.

On a final note, we remark that while the required numbers of reference and residual channels are typically determined by the system response at the highest frequency of interest, they may be more than is necessary at lower frequencies. As a consequence, the CSD matrices of the reference and residual sensors (and the plant matrix) may be ill-conditioned (i.e., noninvertible) at low frequencies, which may impact the matrix inverses in Eqs. (18.78), (18.85), and (18.87). For these situations, it may be necessary to add small values to the diagonal elements of these matrices before computing the inverse. This procedure is referred to as "regularization." The values added are ideally a function of frequency and will have a larger influence at low frequencies (where the matrices are ill-conditioned) than at high (where the matrices are not ill-conditioned). One procedure that satisfies this requirement (and has been used successfully in many ANVC applications) is to add a scalar times the maximum singular value of the matrix to each diagonal element of the matrix on a frequency-by-frequency basis.

Controller Architecture and Performance Simulations

The upper bound predictions given in the sections above on the number, location, and sizing of sensors and actuators provide a series of tools for bounding system performance as more of the control system is defined. As more realism is included (e.g., identifying both actuator and sensor numbers and locations), the bounds on achievable performance typically get smaller but also more realistic. Comparisons of these bounds with performance goals can be made at each step to determine if the control system under consideration is likely to meet its objectives. Should the system still appear feasible after selecting both actuator and sensor locations [i.e., from Eqs. (18.86) and (18.87)], the next step is to add more realism related to the implementation of the controller.

In this section, we consider the impact of controller architecture on achievable performance. In particular, we discuss procedures to include effects of analog filtering, sample rate, and length of control filter.

As an introduction to these issues, consider the signal path from sensor inputs to actuator drive signals for a conventional digital controller as shown in Fig. 18.77. With reference to this figure, a digital controller requires that the analog signals from the sensors be sampled and digitized at the sample rate of the controller. The sample rate of the controller is usually expressed in terms of a sampling rate or frequency (f_s), which implies that the signals are sampled at a time interval (T_s) equal to the inverse of the sample rate. For example, a sample rate $f_s = 1000$ Hz corresponds to a sample interval $T_s = 0.001$ s. To satisfy Nyquist's sampling theorem,[57] the sample rate of the controller must be at least twice the highest frequency of interest for the controller. For feedforward systems, the sample rate may be a factor of 4 above the highest frequency to be controlled. For broadband feedback systems, as discussed in Section 18.5 under Alternate Suboptimum Control Filter Estimation, it is not uncommon for the controller sample rate to be a factor of 100 above the highest frequency to be controlled (to minimize the effects of time delay through the controller and quantization noise on system performance).

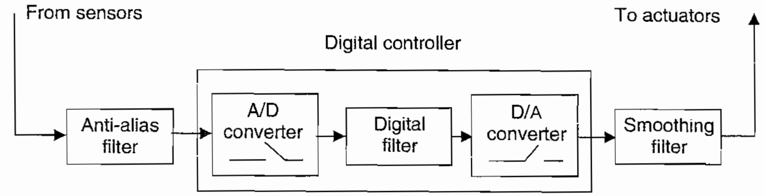

FIGURE 18.77 Signal path from sensor input to actuator drive signal for a digital controller.

Once the sample rate has been chosen, analog filters must be used to limit the frequency content of the analog sensor signals to below the Nyquist frequency of the controller, where

$$f_{\mathrm{nyq}} = \tfrac{1}{2} f_s \tag{18.89}$$

These filters are called "anti-alias" filters, and their output is passed to an A/D converter, which in turn samples and quantizes the signal. Similarly, the output of the digital controller is converted to an analog signal by a D/A converter. Before these output signals are sent to the actuators, however, they must be filtered to band limit the signals below the Nyquist frequency; otherwise signals above the Nyquist frequency will be sent to the actuators. These filters are referred to as "reconstruction" or "smoothing" filters

Although issues regarding the selection of anti-alias and smoothing filters are discussed in the next section, we note here that a major consequence of filtering is that it introduces a delay in the signal path, which is referred to as the "group delay" of the filter. This delay is related to the derivative of the phase response of the filter:

$$\tau_g(\omega) = \frac{d\varphi(\omega)}{d\omega} \tag{18.90}$$

In addition to the filters, delays in the signal path of Fig. 18.77 are also associated with the A/D converter, sample-and-hold functionality of the D/A, and the processing time associated with implementing the digital filter. With regards to the A/D converter, delays can be kept sufficiently small by choosing successive-approximation A/D converters. Issues related to A/D selection for applications where time delay is not a limiting factor in controller performance (e.g., tonal control systems or for residual sensing in some feedforward applications) are discussed in the next section. The delay associated with the sample and hold of the D/A converter $\tau_{D/A}$ is directly related to the sample rate of the controller:

$$\tau_{D/A} = \frac{1}{2f_s} \tag{18.91}$$

For efficient implementations, the delay (τ_{DSP}) associated with implementing the digital filter within a DSP chip can be limited typically to a few tens of microseconds. These implementations require that the sample clock controlling the D/A converters be offset relative to the sample clock for the A/D converters. As such, output samples can be sent to the D/A converters as soon as they are computed so that the processing delay can be held to a fraction of a sample interval. This sampling strategy is in contrast to one that waits until the next time step to output a sample. The latter approach imposes a minimum one-sample delay in the processing, which can be unacceptable for certain applications.

The total delay from analog signal input to analog signal output is termed the *latency* of the controller. Where appropriate, any delay associated with the amplifiers and actuators will also contribute to the latency. Latency is an important parameter since it can directly limit achievable performance of broadband feedforward and feedback systems. As such, it is important to limit overall latency in ANVC control systems consistent with achieving performance goals.

At this point, specific characteristics of the analog filtering, sampling, and control filter parameters can be merged with model or experimental results to make causal performance predictions. The steps involved are as follows:

- Specify a system sample rate based on control bandwidth and architecture (feedforward or feedback).
- Modify the transfer function matrices involving sensor inputs and actuator outputs to include
  - — transfer functions of anti-alias (AA) and smoothing filters (SF),
  - — delay associated with D/A converter sample and hold ($\tau_{D/A}$),
  - — controller processing delay (τ_{DSP}), and
  - — transfer functions of amplifiers and actuator (SH).
- Specify cost function (including control effort and robustness constraints) to be minimized.
- Specify number of control filter coefficients.
- Solve for control filter coefficients using the procedures outlined in Sections 18.4 and 18.5.
- Estimate causal mean-square residual performance and actuator output drive requirements: Compare estimated performance to performance goals.

If transfer functions of the filters, amplifiers, and actuators are not available, initial causal performance estimates can be made by assuming flat magnitude

spectra with linear phase spectra, which correspond to pure time delays that bound expected delays for those components. When this is the case, Elliott[58] suggests approximating the group delay of the anti-alias or smoothing filters as

$$\tau_g \approx \frac{n}{8f_c} \tag{18.92}$$

where n is the order of the filter and f_c is the cutoff frequency.

Hardware Selection

In this section, we discuss some of the practical issues related to selecting analog filters, A/D converters, and DSPs. Although a complete discussion of these issues is beyond the scope of this book, we present general guidelines and considerations. Detailed discussions of each of these issues can also be found in reference 58.

Anti-Alias and Reconstruction Filters. As discussed earlier, the main purpose of anti-alias and reconstruction filters is to attenuate signals above the Nyquist frequency. The anti-alias filters minimize contamination of frequencies below the Nyquist frequency by attenuating the spectral content of the signals above the Nyquist frequency. These higher frequencies are interpreted as lower frequencies because of the nonlinear sampling process of the A/D converter. This phenomenon is referred to as *aliasing*. Similarly, reconstruction filters attenuate components of the drive above the Nyquist frequency, which occur as a consequence of sampled signals at the output of the D/A converter. The benefits of using anti-alias and reconstruction filters in combination with A/D and D/A converters are discussed below

The amount of attenuation required from an anti-alias filter depends on the spectral shape of the sensor response and the desired bandwidth over which the controller needs an accurate representation of the signal. A sensor response that is inherently band limited below the Nyquist frequency may require only a low-order anti-alias filter or possibly none. Alternatively, a sensor response that is flat or increasing with frequency will require a higher order anti-alias filter. For purposes here, we assume that the sensor response is flat versus frequency. In addition, we impose a requirement of at least 40 dB attenuation of contributions from aliasing frequencies at the highest frequency that is important to the controller (f_a). From the context of controller implementation, however, we wish to achieve this attenuation while minimizing the group delay of the filter to acceptable levels.

There are two basic approaches to selecting the filter. The first is to use a low-order filter with a relatively low cutoff frequency. The second is to use a high-order filter with a higher cutoff frequency. Figure 18.78 compares the magnitude spectra and group delays for a fourth-order Butterworth filter and a sixth-order Cauer filter, both of which were designed to provide at least 40 dB of attenuation above $f_{40\ \mathrm{dB}} = 600$ Hz. Both filters will meet the attenuation requirements for

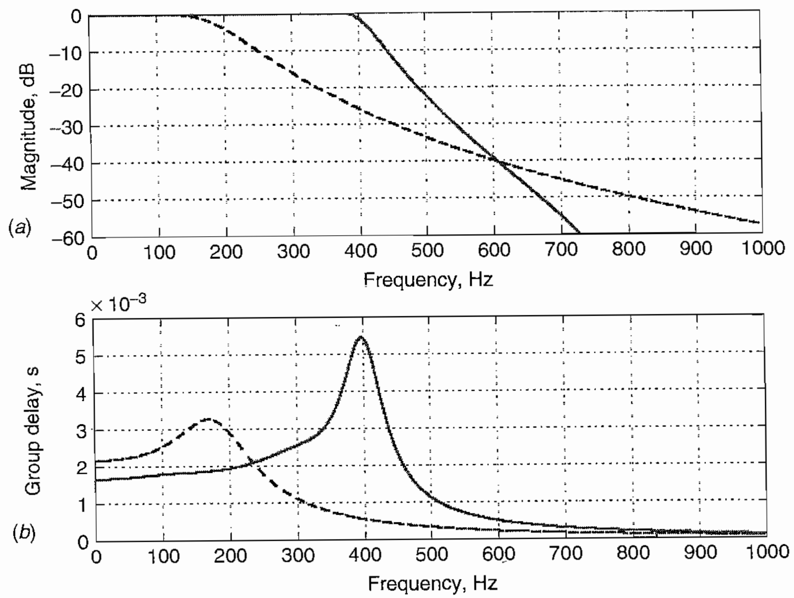

FIGURE 18.78 Comparison of (*a*) magnitude spectra and (*b*) group delay for fourth-order Butterworth (dashed curve) and sixth-order Cauer (solid curve) filters.

frequencies below their respective cutoff frequencies (i.e., $f_a < f_c$) provided that the system sample rate is chosen such that

$$f_s \geq f_a + f_{40\text{dB}} \tag{18.93}$$

Consider first the case with f_a less than the cutoff frequency of the Butterworth filter (nominally 200 Hz) and a sample rate of 800 Hz. For this case, attenuation of aliasing components is assessed by "folding" the magnitude response of the filters about the Nyquist frequency of $800/2 = 400$ Hz. As such, both filters provide the required attenuation of aliasing components in the frequency band below f_a. However, the group delay associated with the Cauer filter is less than that for the Butterworth for all frequencies below f_a, particularly near 200 Hz.

Now consider the case with $f_a = 350$ Hz and a sample rate of 950 Hz. For this case, attenuation of aliasing components is assessed by folding the magnitude response of the filters about the Nyquist frequency of $950/2 = 475$ Hz. The Cauer filter again satisfies the attenuation requirement because the sample rate satisfies Eq. (18.93). However, the attenuation requirement is not met by the Butterworth filter. In fact, less than 20 dB attenuation of aliasing components is achieved at 350 Hz (i.e., the difference in the magnitude responses at 350 Hz and $950 - 350 = 600$ Hz. Further, note that the maximum group delay of both filters in the frequency band below f_a is approximately the same.

The above comparisons suggest that using higher order filters with high cutoff frequencies is preferable to using low-order filters with low cutoff frequencies. Although the preceding discussion centered on selecting anti-alias filters, similar conclusions apply to reconstruction filters provided that the control filters are designed to reduce output levels above f_a. Unfortunately, the cost of implementing high-order filters will exceed the cost of using low-order filters. As a consequence, the performance benefits must be balanced against considerations of additional cost, as will be discussed further in the example ANVC system in Section 18.7 under MIMO Feedforward Active Locomotive Exhaust Noise Control System with Passive Component.

Analog-to-Digital and Digital-to-Analog Converters. A typical data path from sensor input to actuator drive signal was shown in Fig. 18.77. That figure illustrates the use of both types of data converters required for implementing digital controllers, namely A/D and D/A converters. The purpose of A/D converters is to sample the continuous-time signals from the sensors at uniform time intervals ($T_s = 1/f_s$) and quantize the amplitude to a discrete set of amplitude levels. Because the sampling process is a nonlinear operation, anti-alias filters are typically used to band limit the sensor signals below the Nyquist frequency ($f_s/2$) before sending the signals to the A/D converter. This minimizes the possibility that frequencies above Nyquist will contaminate the sensor response below Nyquist, which is referred to as aliasing.

Figure 18.79 shows a frequency domain schematic of how anti-aliasing filters are used in combination with A/D converters to minimize aliasing effects. The upper curve in Fig. 18.79*a* represents the spectrum of an unfiltered continuous-time signal presented at the input of an A/D converter. For an A/D converter operating at a sample rate of f_s, signals above the Nyquist frequency ($F_{\text{nyq}} = f_s/2$) will be interpreted as frequency below Nyquist. Fig. 18.79*a* illustrates schematically how frequencies above the Nyquist frequency will fold down into the frequency region below Nyquist. The estimated spectrum below Nyquist will be the sum of the true spectrum below Nyquist plus any aliasing components resulting from the frequency content of the signal that is above the Nyquist frequency. As a consequence, aliasing components can cause the estimated spectrum to differ from the true spectrum of the signal in the frequency region below Nyquist. Anti-alias filters are typically used to band limit the signals prior to the conversion process to reduce the magnitude of any aliasing components. Figure 18.79*b* is a plot of the magnitude response of an anti-alias filter designed to reject frequencies above the Nyquist frequency. When this filter is applied to the unfiltered signal of Fig. 18.79*a*, the resulting spectrum of the signal presented at the input to the A/D converter is that shown in Fig. 18.79*c*. As shown in this figure, much of the effects of aliasing components on the estimated spectrum are removed, thus ensuring that the estimated spectrum is a more accurate representation of the true spectrum of the signal below the Nyquist frequency.

Digital-to-analog converters are used to convert the digital sequences from the controller into analog signals that can ultimately be used as drive signals to actuator electronics. In the frequency domain, the sample output sequence

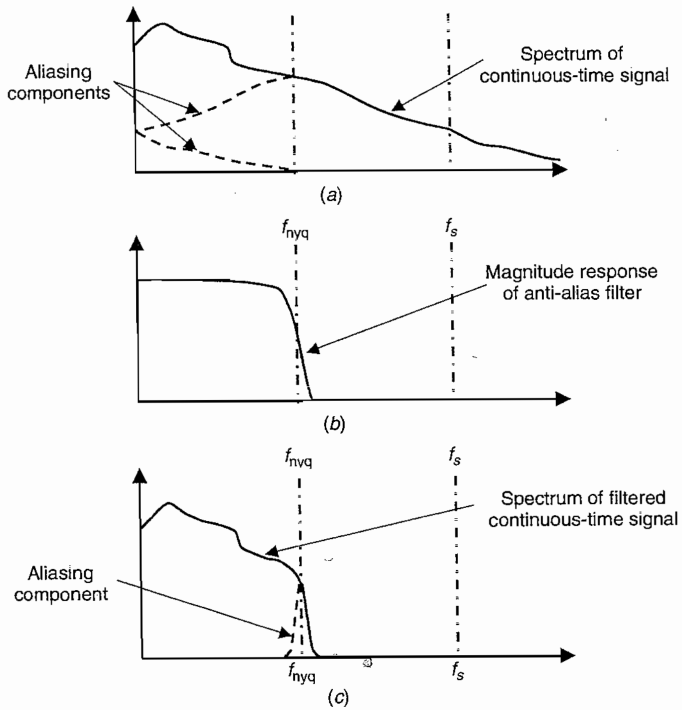

FIGURE 18.79 Use of anti-alias filters to minimize aliasing effects during A/D conversion: (*a*) aliasing components of an unfiltered continuous-time signal digitized at sample rate f_s; (*b*) magnitude spectrum of anti-alias filter; (*c*) aliasing components of filtered continuous-time signal digitized at sample rate f_s.

produces a spectrum that contains "images" of the signal spectrum below the Nyquist frequency, which occur at frequencies above the Nyquist frequency. These image spectra are shown schematically in Fig. 18.80. The effects of the images must be minimized. Otherwise, the controller will drive the actuators at frequencies above the Nyquist frequency, resulting in increased out-of-band noise amplification. These out-of-band effects are reduced to some extent by the sample-and-hold (S&H) functionality that is integral to most D/A converters. As discussed earlier, the S&H introduces a delay equal to one-half the sample interval ($T_s/2$). In addition, it provides some filtering of the output spectrum, as illustrated in Figs. 18.80*b* and 18.80*c*. To suppress the remaining signals above the Nyquist frequency, D/A converters are typically followed by smoothing or reconstruction filters. The effect of applying reconstruction filters on the D/A output signal is shown in Fig. 18.80*e*.

Two basic types of A/D converters are applicable for use in ANVC systems. The first type is referred to as "successive-approximation" (SA) A/D converters. The second type is referred to as "sigma–delta" ($\Sigma\Delta$) A/D converters. Table 18.1

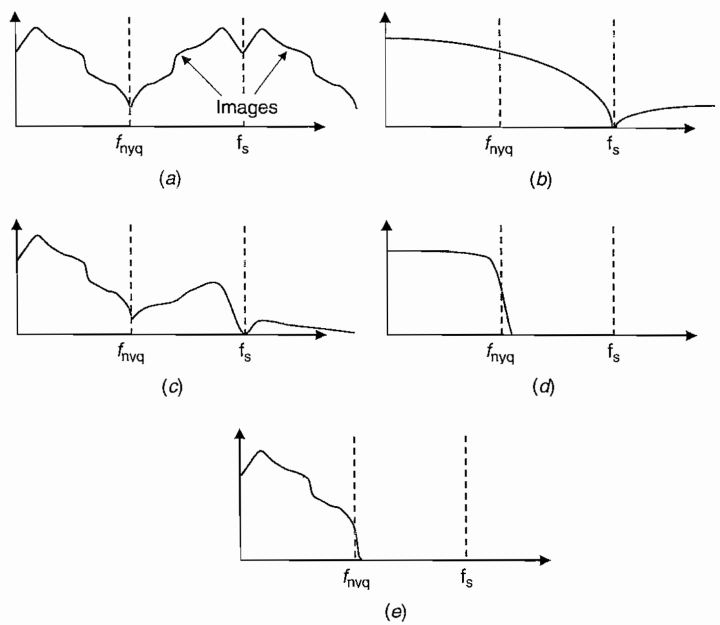

FIGURE 18.80 Use of reconstruction filters to reduce image spectra at the output of D/A converters: (*a*) spectrum of digitized output signal at sample rate f_s; (*b*) magnitude response of zero-order sample-and-hold integral to D/A converter; (*c*) spectrum of analog output of D/A converter prior to reconstruction filter; (*d*) magnitude response of reconstruction filter; (*e*) spectrum of analog signal at output of reconstruction filter.

compares some of the important features and differences between these two types of converters.

The choice of A/D converter for an ANVC application will depend on the control architecture (i.e., feedforward or feedback), the type of sensor signals (i.e., reference or residual sensors), and the performance goals. For broadband ANVC applications that require minimal latency through the controller (e.g., reference sensors in a feedforward system or residual sensors in a feedback system), the delay associated with $\Sigma\Delta$ A/D converters is unacceptable. As a consequence, SA A/D converters should be used for those applications, and the extra cost of the converters and anti-alias filtering should be included in the total cost of the ANVC system. We note, however, that low latency is not a necessary requirement for the residual sensors of a feedforward implementation. These sensor signals are used in the design of the control filters but are not themselves filtered by the control filter to produce output signals to the actuators. However, the latency associated with $\Sigma\Delta$ A/D converters used on the residual signals will be seen as a delay in the plant transfer functions. This added delay will in turn reduce allowable convergence coefficients for LMS-based algorithms[58] but does not preclude their use.

TABLE 18.1 Comparison of Successive-Approximation and Sigma-Delta A/D Converters

Successive-Approximation Converters	Sigma-Delta Converters
Sample input signal at rate f_s	Over sample input signal nominally at 64 times desired sample rate (i.e., $f_{\Sigma\Delta} = 64 f_s$)
Require use of relatively high-order anti alias filters to bandlimit signals below Nyquist frequency	Only low-order (if any) anti-alias filters required to bandlimit signals below $f_{\Sigma\Delta}/2$. Integral high-order (linear-phase) digital filters bandlimit signal below Nyquist frequency ($f_s/2$). Output is decimated (i.e., keep only every 64th sample) to produce sampled sequence at f_s sample rate.
Low latency (on the order of a few μs)	High throughput latency (typically $32T_s$, where $T_s = 1/f_s$)
Quantize signal at multiple bit levels (e.g., 12 or 16 bits)	One-bit quantization at oversampled rate to provide comparable multi-bit quantization (e.g., 12 or 16 bits) at f_s sample rate
Relatively expensive compared to $\Sigma\Delta$ converters	Relatively inexpensive compared to SA converters

When low latency is not required, the use of $\Sigma\Delta$ converters can significantly reduce the costs associated with digitizing the sensor signals. For example, a tonal feedforward ANVC system can use a $\Sigma\Delta$ A/D converter to digitize the reference signal. As before, digitization of the residual signals for this example can be done using $\Sigma\Delta$ A/D converters, provided that the extra delay is acceptable in terms of convergence rate (if adaptive algorithms are used). The choice of D/A converter is governed by similar arguments concerning allowable latency. For instance, when low latency is not required, $\Sigma\Delta$ D/A converters can be used. Alternatively, when latency must be minimized, conventional D/A converters should be used.

For most ANVC applications, it is desirable to initiate the sampling across all A/D converters using a common clock signal. In this way, all A/D inputs will be synchronously sampled. Similarly, it is advantageous to sample all the D/A converters using a common clock signal as well. The D/A converters could be clocked using the same clock pulse as for the A/D converters; however, to minimize latency through the controller, it is useful to offset the D/A clock relative to the A/D clock. In this way, subsample latency can be achieved by sending signals to the D/A when they are ready, as opposed to waiting for a full sample period.

The final aspect of converter selection is quantization noise. When analog signals are quantized to a finite number of amplitude values (e.g., 16-bit A/D converter), the errors in the conversion process can be thought of as noise. For the signals of interest for ANVC, this noise is modeled as uniformly distributed

from—LSB/2 to LSB/2. Here, LSB stands for the *least-significant bit* and is given by

$$\text{LSB} = \frac{V}{2^{M-1}} \tag{18.94}$$

where V corresponds to the voltage range of the converter (i.e., $\pm V$) and M is the number of resolution bits (e.g., 16 for a 16-bit converter). For the assumed uniform probability distribution of the noise, the rms of the quantization noise (QN_{rms}) is equal to

$$QN_{\text{rms}} = \frac{LSB}{\sqrt{12}} \tag{18.95}$$

For a sample rate f_s, the spectrum of the quantization noise ($QN_{\text{psd}}(f)$) is white (i.e., flat) with a power spectral density (PSD) amplitude given by

$$QN_{\text{psd}}(f) = \frac{LSB^2/12}{fs/2} \tag{18.96}$$

As an example, for a 16-bit converter with a voltage range of ± 10 V and a sample rate of 1 kHz, the rms quantization noise [from Eq. (18.95)] is 88 μV, and the PSD level is -108 dB re 1 V^2/Hz.

At this point, it is useful to compare plots of

- the expected signal levels (in volts from the sensor),
- electrical noise floors (associated with the sensors, analog filters, and gain), and
- quantization noise.

To support a common comparison, all of these voltage levels should be referenced to a common point in the signal path (e.g., the amplifier input). These plots should be generated corresponding to both open- and closed-loop sensor responses. Sensor sensitivities, signal gain, and quantization noise can then be assessed within a common framework. The goal is to choose each of these to ensure that sensor signals will have sufficient signal-to-noise ratio (SNR) throughout the bandwidth of interest.

To illustrate some of the issues related to A/D converter selection, consider the example shown in Fig. 18.81. The various curves grouped in the center of this plot correspond to the expected signal levels from multiple residual sensors, expressed in dB re V^2/Hz, referenced to the input of a bank of sixth-order Cauer filters. The filters are used to provide anti-alias filtering as well as programmable gain for these channels. The cutoff frequency is approximately 800 Hz. The power spectral density of the noise from the anti-aliasing filters at their input (labeled PFI *noise* in the figure) falls between -155 dB and -150 dB re 1 V^2/Hz. The spectral density of the sensor noise floor reference to the filter input is

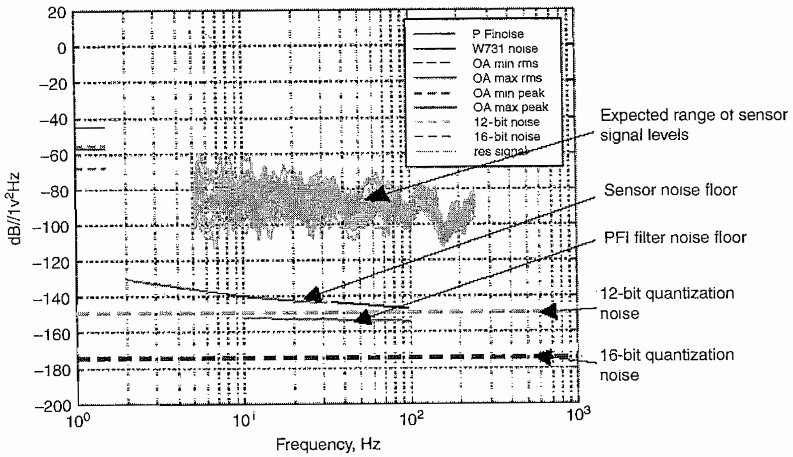

FIGURE 18.81 Comparison of signal level versus electrical and quantization noise.

approximately -130 dB re 1 V^2/Hz at 2 Hz and drops to -145 dB re 1 V^2/Hz at 100 Hz.

The rms levels for the sensor signals (needed for quantization noise estimates as indicated below) are determined by integrating the mean-square voltage responses across frequency and taking the square root. For these spectra, the largest rms level is approximately -57 dB re 1 V. Assuming the statistics of these responses is random (i.e., with a crest factor of 4 or 12 dB), a peak voltage response for this group of sensors is estimated to be approximately -45 dB re 1 V. The spectrum level of the digitization noise (at the filter input) can be estimated from Eq. (18.96), where the voltage V in Eq. (18.94) is taken (at the moment) to be the peak voltage of the sensor signals (i.e., -45 dB re 1 V $= 5.5$ mV). As such, the spectral levels of digitization noise for 12- and 16-bit converters, assuming a sample rate of 2 kHz, are -152 dB and -176 dB re 1 V^2/Hz, respectively. The SNR for these sensor measurements is a function of frequency and corresponds to the spread in decibels between the estimated signal responses and the maximum of the electrical noise (from filters and sensors) or the digitization noise. The SNR is nearly 30 dB throughout the frequency band of concern.

For the example shown in Fig. 18.81, it is sufficient to use a 12-bit converter since the SNR is limited by sensor noise as opposed to digitization noise up to about 100 Hz. Above that frequency, the SNR will be limited by digitization noise if a 12-bit converter is used or by PFI noise if a 16-bit converter is used. Further, if the converter (12- or 16-bit) has a voltage range of ± 1 V, the programmable gain should be set at approximately 33 dB to allow 1–2 bits of headroom to avoid clipping.

The example case in Fig. 18.81 illustrates the relatively complex interdependencies that must be considered when selecting ANVC hardware to ensure

adequate SNR, which in general will be a function of sensor noise and sensitivity, anti-alias filter noise, A/D converter quantization noise and voltage range, system gain, and sample rate.

Digital Signal Processors. As discussed earlier, the rapid growth in ANVC systems and applications over the past 25 years can be traced in large part to the advent of DSP chips. These chips are optimized to perform operations on a sample-by-sample basis. That is, these chips read in data one sample at a time, perform large numbers of computations, and then output a sample. This is in contrast to other central-processing units (CPUs) that read in groups (i.e., buffers or blocks) of data, operate on the entire buffer, and then output buffers of data. These later processors can often perform larger numbers of computations than DSP chips, but their latency is on the order of the block size.

Digital signal processors are ideally suited to perform the low-latency digital filtering required by ANVC algorithms. As such, they are widely used in the design of adaptive control systems based on the algorithms presented in this chapter. In addition, current DSP technology supports high-speed communication between DSPs to support applications with large numbers of inputs and outputs (e.g., many tens of inputs and outputs) as well as large digital filter sizes (e.g., IIR filters with over 5000 taps per filter). For these large-scale problems, efficient low-latency implementation of the digital filters can be achieved by combining DSPs with high-powered CPU compute engines such as PowerPC (PPC) chips. Further, the relatively large latency associated with the PPC chips may be acceptable to perform much of the "off-line" algorithms associated with system identification and control filter design when using direct estimation as opposed to adaptive filter algorithms.

Once the control algorithms have been selected, the computation and memory requirements can be determined for all "in-line" filtering and "off-line" processes. These requirements should then be mapped to DSPs and PPC chips, as necessary. Floating-point DSPs such as the TMS320C6701 are rated at 1 Gflop and include up to 128 MB of fast-access memory. Compute engines like the PPC7410 are rated at 2 Gflops with up to 512 MB of local memory. In addition, PC or VME (workstation) boards are currently available with up to four of each type of processor per board and support high-speed communications between processors on a given board as well as processors located on other boards. These processor-to-processor communications are supported by high-speed interconnect architectures such as Mercury RACE^{++}, Spectrum DSPLink, and SKYchannel.

As an example, Fig. 18.82 shows the hardware architecture for a large-scale ANVC system incorporating both DSPs and PPC chips, including high-speed communication over a Mercury RACEWAY interconnect. The signal path from the reference sensors to the actuator drive signals includes high-order anti-alias and reconstruction filters with cutoff frequencies near the Nyquist frequency. Successive-approximation converters are used to minimize latency associated with the conversion. A combination of DSPs and PPC chips are used to efficiently implement the digital control filters to minimize latency.[84] The residual sensor

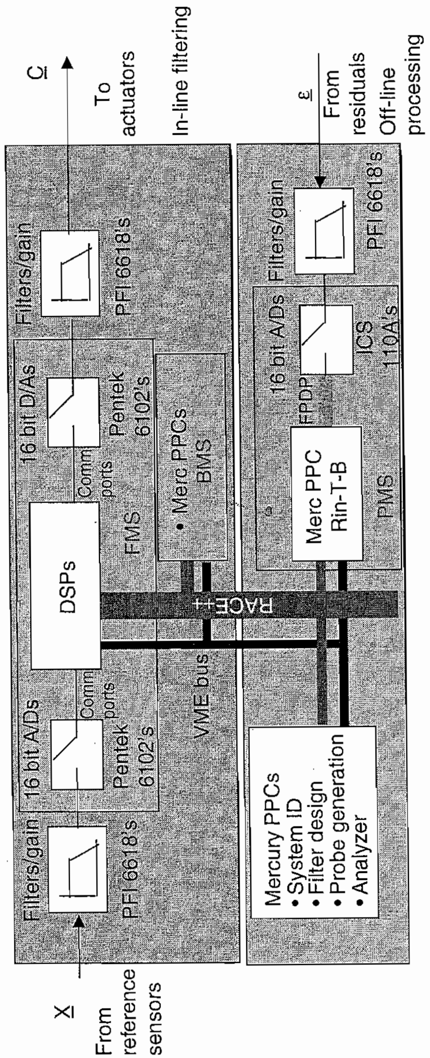

FIGURE 18.82 Control architecture using combination of DSPs and PPCs.

signals pass through anti-alias filters and are digitized using sigma–delta converters. These data support off-line functionality associated with system identification, control filter design, and probe-signal injection, which are performed on multiple PPC chips. Communications between the DSPs and PPC chips are primarily carried over Mercury's RACE^{++} interconnect bus, with additional communications occurring over the VME bus. In this way, the compute power associated with PPC chips can be used to efficiently perform off-line functions (e.g., direct estimation of plant and control filters), which can be passed to the in-line processors (DSPs and PPC chips) to support adaptation of the control filters.

Finally, we note that fixed-point DSPs as well as floating-point DSP devices are available. The floating-point devices are much easier to program and are often chosen for proof-of-principle systems or for final systems that are not highly cost sensitive. When cost is a driving issue, fixed-point devices should be considered. The final choice must balance the higher nonrecurring cost associated with programming fixed-point devices and the potential increased CPU overhead due to implementing floating-point arithmetic on a fixed-point device against the lower recurring per-unit cost

Control System Implementation and Testing

Once the simulations and hardware selections have been made, the control system is implemented and performance tests are conducted. In this section, we discuss the basic operating modes and features of a controller that should be considered during implementation to support the subsequent testing phase.

For each of the modes discussed below, parameters that can be changed during system operation (referred to as "soft" parameters) and those that cannot be changed during operation (referred to as "hard" parameters) must be identified. Soft parameters provide the flexibility to modify and tune certain parameters during system operation, which is often an invaluable feature in prototype systems. Allowing parameters to be changed "on-the-fly," however, adds complexity to the implementation. As such, lists of desired soft and hard parameters should be identified early on in the implementation phase so that the appropriate communications between a user interface and the embedded controller codes can be included. The typical operating modes and features of a controller are summarized in Table 18.2, including references to soft parameters that are useful in supporting each mode.

As indicated, an ANVC controller will typically have two primary operating modes, namely system identification and control. The purpose of system identification is to estimate the transfer functions (or equivalently impulse response functions) from the actuator control signals to sensor responses (both references and residuals). This identification is initially performed with the control filter set to zeros but can subsequently be performed during closed-loop operation, as discussed in Section 18.4 under System Identification. Once an initial plant estimate has been obtained, operational measurements of the system responses are obtained to characterize the "uncontrolled" (i.e., open-loop) response. These

TABLE 18.2 Controller Operating Modes and Features

Operating Mode	Description and Features
Open-loop characterization of system response	Collect measurement of residual sensors during normal "uncontrolled" (i.e., open-loop operation)
Open-loop system identification	Estimate plant models between actuator drive signals and sensors. Soft parameters include probe strength, adaptation coefficients, leakage coefficients, regularization parameters, and actuator channel selection.
Closed-loop operation with filter design based on open-loop response and system identification	Collect measurements of residual sensors during "controlled" (i.e., closed-loop) operation. Soft parameters include adaptation and leakage parameters, control effort and robustness weighting parameters, and regularization parameters.
Concurrent closed-loop system identification and control-filter adaptation	Collect measurements of residual sensors during "controlled" (i.e., closed-loop) operation, while probe signals are injected for the purpose of closed-loop system identification. Soft parameters include those cited above for system identification and closed-loop operation. In addition, software flags should be included to initiate use of updated plant models in the control filter design algorithm.
Save operational "state"	All controller information necessary to restart the controller should be saved. This includes, plant and control filter coefficients, all hard and soft parameters, operating mode, and probe signal path parameters.
Load saved "state" and restart controller	Load in a saved "state" and start operation using saved parameters and filters.

responses are also used to design control filters to support operation in the control mode. Once in the control mode, probe signals can be injected to support closed-loop system identification and to support adaptation of control filter coefficients. Soft parameters can be adjusted to optimize performance. Closed-loop system responses should then be collected and compared with open-loop responses to evaluate system performance versus performance objectives and goals.

The final two rows of Table 18.2 indicate the desire to be able to save the "state" of the controller at any point in time. By state, we mean all controller parameter values and filter coefficients are saved for the purpose of restarting the system at that state in the future. As such, the controller can be started from a closed-loop operating state or from some initial operating state (e.g., open loop). It is convenient for prototype systems to include a graphical user interface (GUI) through which operation mode, soft parameter values, performance assessments, and save/load state functionality can be monitored and controlled. Once an ANVC system has been successfully tested, values of soft parameters and logic for progressing from open-loop to closed-loop operation can be automated within the software, thus resulting in a stand-alone ANVC system.

18.7 EXAMPLES OF ANVC SYSTEMS

In this section we present three prototype active systems that illustrate the application of the principles outlined in the previous sections of this chapter. All of these systems were developed to demonstrate the technology and one is currently operational on a complete class of U.S. Navy ships. All three demonstrate the effectiveness of active noise and vibration control technology when appropriate design procedures are followed. The first example involves the synergistic application of a combination of active and passive noise reduction treatments. The example demonstrates the successful control of a source of noise that would have been difficult using only passive or only active approaches. The second example demonstrates the application of feedback technology to the control of both broadband and narrow-band vibration transmission through a vibration isolation mount. The final example illustrates the use of active noise control technology to generate a zone of silence in a noisy environment.

MIMO Feedforward Active Locomotive Exhaust Noise Control System with Passive Component

Problem Description. When operated at full power diesel-electric locomotives generate significant noise and can have a significant adverse impact on the quality of life near major railroad lines. The sources of noise are shown in Fig. 18.83.[85] As indicated in the figure, the primary sources of diesel-electric locomotive noise are the engine exhaust and the cooling fans, both of which must be reduced before significant noise reductions can be realized. The active noise control system developed for this application focused on just the exhaust noise, fully recognizing that later efforts would have to attack cooling-fan noise if significant overall locomotive noise reductions were to be achieved. Active technology was considered for this application because locomotive exhaust noise is significant at very low frequencies (below 40 Hz), and passive noise control treatments (e.g., dissipative or reactive mufflers) that could achieve the desired noise reduction would simply be too large to fit in the space available.

The basic concept for the system[86,87] is illustrated in Fig. 18.84, where a plan view of the top of the locomotive hood is shown near the exhaust stack. The figure shows a number of loudspeakers, the control actuators, surrounding the exhaust

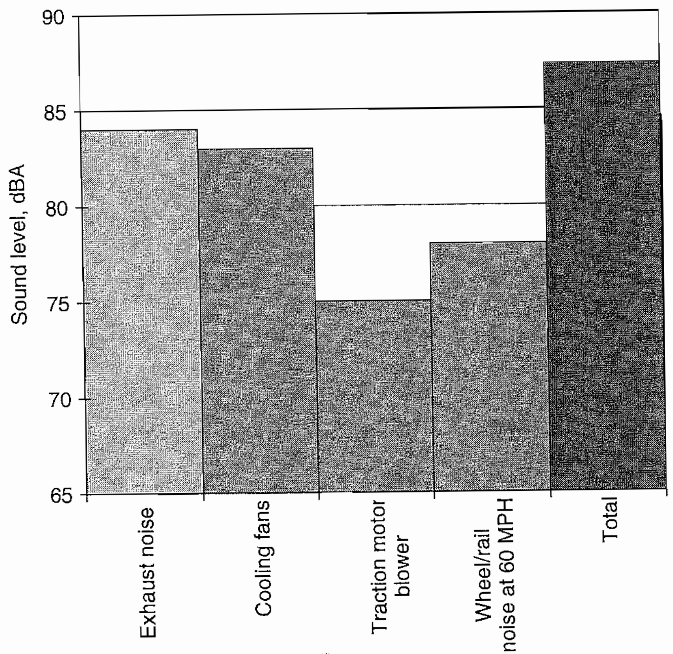

FIGURE 18.83 Noise sources on an SD40-2 diesel electric locomotive measured at 100 ft with the locomotive running at throttle 8 at full load.

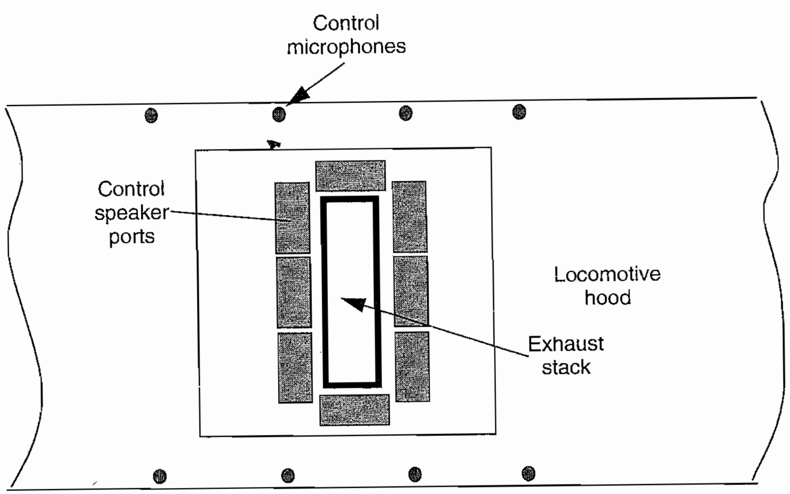

FIGURE 18.84 Plan view of the locomotive hood with the basic system concept.

stack and a number of control microphones located near the edge of the hood that will act as the residual sensors. It was determined based on exhaust noise measurements that at low frequencies where the active system would be designed to operate, the noise was primarily tonal and so a feedforward architecture was selected that used a tachometer on the locomotive diesel engine as the reference signal.

Performance Goals. Based on the source information in Fig. 18.83, it was decided that 10 dBA of overall reduction in exhaust noise would be desirable to have a significant impact on community noise (assuming of course that cooling-fan noise would eventually be similarly reduced). After examining the locomotive exhaust noise spectra we determined that to achieve 10 dBA of overall noise reduction would require that the exhaust noise be controlled out to at least 5 kHz. Since extending the bandwidth of the active system out to so high a frequency and requiring broadband control would place excessive demands on the technology, we decided on a hybrid approach. At low frequency where the noise is primarily tonal we decided to employ an active system. At high frequency where the noise is primarily broadband in character we determined that a passive silencer would be most advantageous. Such an approach is desirable because active technology is well developed for the control of low-frequency tonal noise and at high frequency passive silencers can be effective without having to be large in size. Both technologies were required because we found that

- active control of tones in the exhaust below 250 Hz with no broadband control at the higher frequencies would result in less than 1 dBA of noise reduction and
- no control of tones in the 0–250-Hz band would limit the maximum reduction of exhaust noise to ~5 dBA.

We ultimately decided that 10 dBA of exhaust noise reduction could be achieved with

- an active system providing 10 dB reduction of exhaust tones below 250 Hz along with
- a passive silencer providing 5 dB of broadband noise reduction from 250 to 500 Hz and 15 dB reduction from 500 to 5500 Hz.

Figure 18.85 shows the silencer designed to provide the above noise reduction performance. It is a very compact design with the center body and side chambers designed to provide the necessary insertion loss while maintaining the back pressure low enough to meet locomotive diesel engine specifications. The silencer was designed to allow the speaker enclosures to surround it, with the whole assembly fitting within a protective enclosure in the engine compartment. While the passive silencer was a critical component in the entire system design,

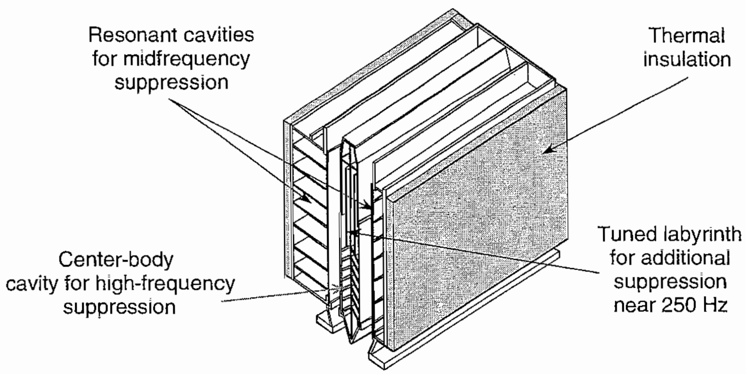

FIGURE 18.85 Compact passive silencer design.

we focus here only on the active system. Details on the passive silencer can be found in references 86 and 87.

Number and Location of Actuators. We began the design process by determining the number and location of control actuators (loudspeakers). Figure 18.86 shows a typical arrangement of actuators that we examined in simulations in which the exhaust stack and control actuators were treated as point sources. In the simulations we formed a matrix of transfer functions relating the sound pressure at 90 locations in the horizontal plane 30 m from the exhaust stack to the control speaker volume velocities at 32 speaker locations around the exhaust stack, as illustrated in Fig. 18.86. Figure 18.87 shows the ratio of the significant singular values to the largest singular value as a function of frequency for that transfer function matrix. In principle the number of significant singular values tells us the minimum number of actuators needed to provide significant control of the source. We found (not surprisingly), while carrying out calculations of this type, that the minimum number of singular values (control sources) was achieved when the control sources were placed as close as possible to the exhaust stack. Consequently, we carried out a preliminary design of the control speaker enclosures to determine a realistic minimum spacing between the exhaust stack and the enclosure outlets. The calculations in Fig. 18.87 were carried out for that minimum spacing. The figure shows that at 250 Hz eight singular values (including the largest) lie within 20 dB of the maximum. Since we are looking for only 10 dB reduction in noise, the use of eight actuators arranged as shown in Fig. 18.85 seemed to be a conservative choice. The performance predicted by this arrangement is shown in Fig. 18.88. While the noncausal noise reduction predicted by this calculation is much larger than we would expect to achieve, it was comforting to see that eight control actuators seemed to be more than adequate.

Number and Location of Control Sensors. The evaluations in the previous section placed the control sensors in the far field. In reality the microphones

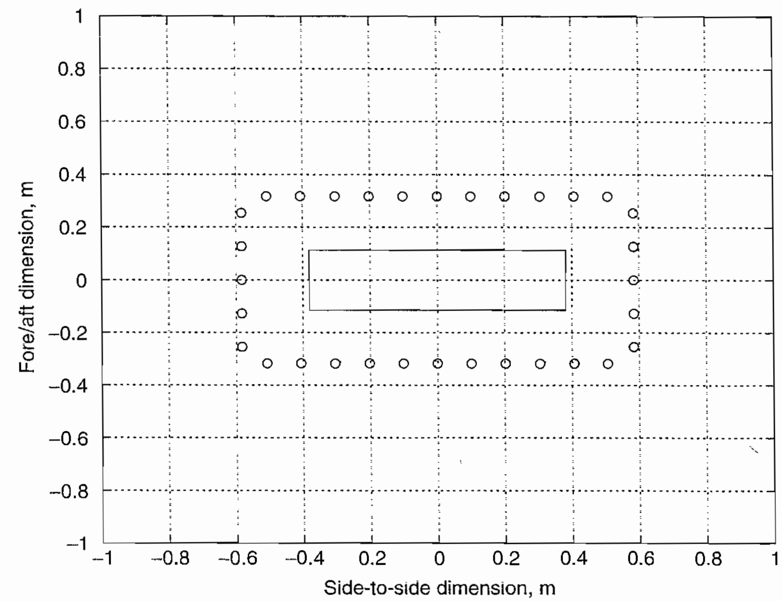

FIGURE 18.86 Candidate control source locations.

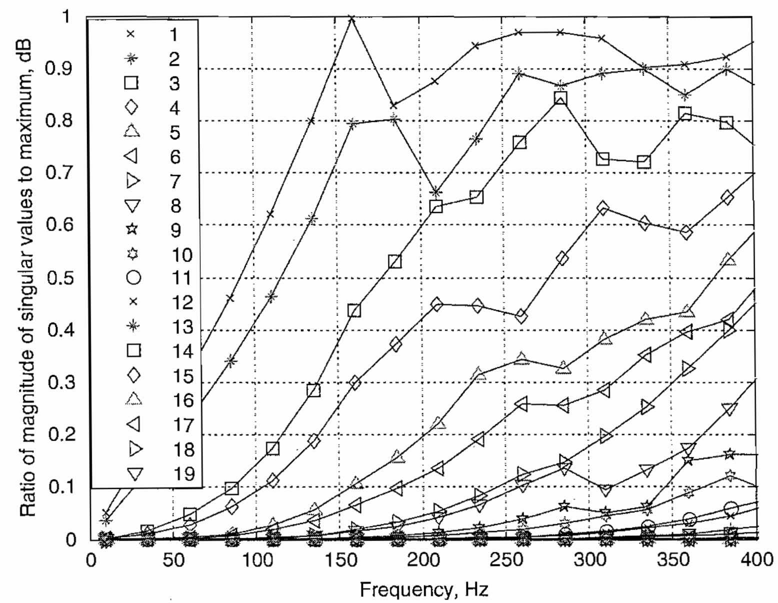

FIGURE 18.87 Ratio of each singular value to the largest singular value as a function of frequency.

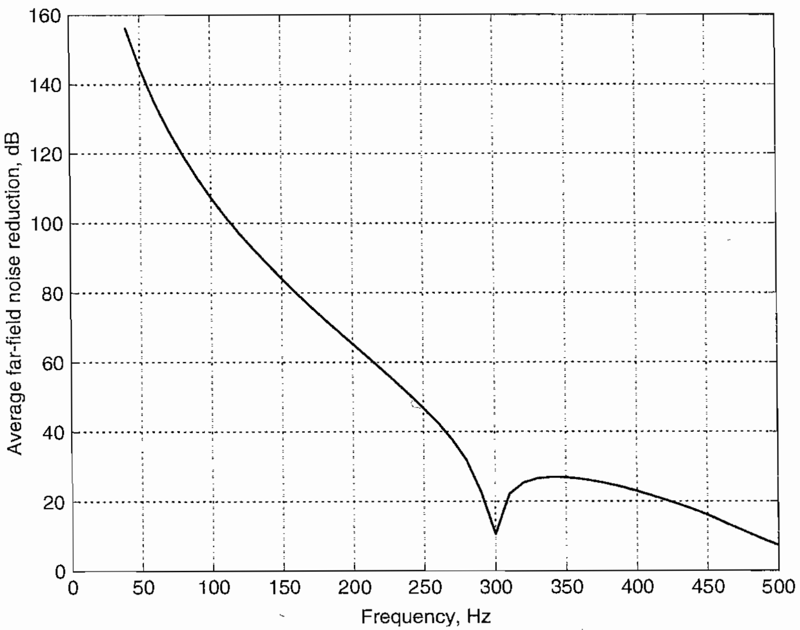

FIGURE 18.88 Predicted far-field performance of eight control actuators.

will have to be placed somewhere on the locomotive hood. Consequently, we developed an additional set of transfer function matrices relating the sound pressure at candidate control microphone locations on the locomotive hood to control speaker volume velocity at the previous 32 locations around the exhaust stack. We then determined the volume velocity required to minimize the pressure at the control microphones and then used those values with the previous transfer function matrix to predict the reduction in far-field pressure. Figure 18.89 shows the results of that calculation for a number of different control sensor locations. The solid curve in the figure is for the final control sensor placement, a line of four sensors along the two edges of the locomotive hood, similar to that shown in Fig. 18.84. A number of calculations of this type were used to help in the selection of control sensor locations. Other issues that came into play in the selection included the degree of dominance of exhaust noise over other sources at the candidate sensor locations, interference with other locomotive components, heat, and routing of cabling.

Control Actuator Design. The simulations for control sensor placement can provide, as part of the calculation, the estimated volume velocities required from the control speakers, provided realistic values of the uncontrolled sound pressure at the control sensors are used in the calculations. Measurements of the sound pressure at various locations on the hood of a test locomotive were acquired to

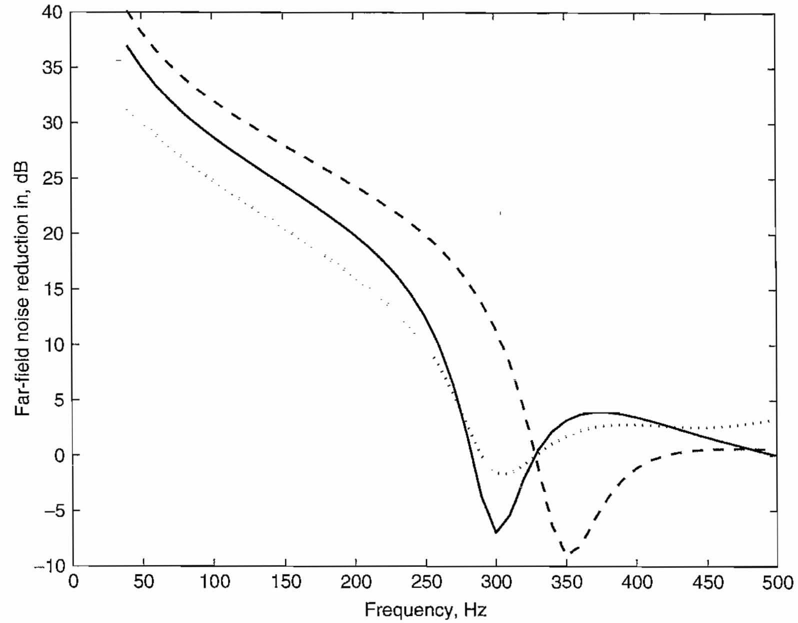

FIGURE 18.89 Predicted far-field noise reduction of eight control actuators with various configurations of eight control sensors.

provide those data. Simulations were then performed to determine the optimum control speaker volume velocities. That information was used in the selection of the control speakers and the design of the speaker enclosures. The enclosure design is shown in Fig. 18.90. Two different enclosure geometries were required to allow the necessary number of enclosures to fit in the space available around the exhaust duct. Each enclosure contains two 12-in.-diameter high-fidelity speakers and is designed to provide bandpass frequency response, enhancing the volume velocity in the 40–250-Hz frequency range. The enclosure–speaker system was designed using a commercially available computer program.

Figure 18.91 shows the arrangement of the control speaker enclosures around the exhaust stack. By careful design we were able to fit 10 enclosures in the space available. However, we retained only eight independent channels to drive the speakers. Because the simulations indicated that very high volume velocity would be required of the speakers on the centerline of the locomotive, we placed two speaker enclosures on each side of the centerline, as indicated in Fig. 18.91, rather than a single one on the centerline. We then drove each of the two pairs of enclosures with a single controller output channel.

Control Architecture. As indicated above, we decided early in the design process to use a feedforward control architecture since the technology is well

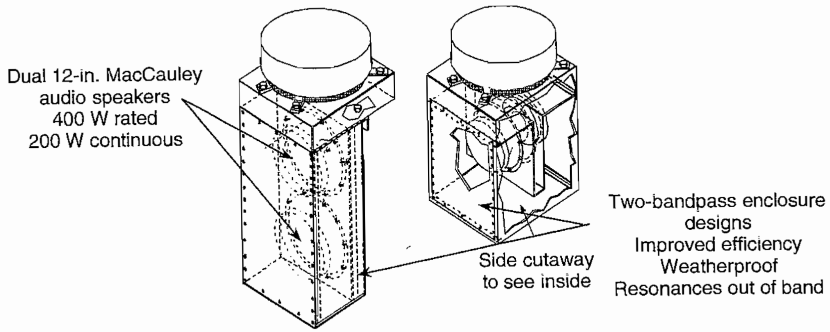

FIGURE 18.90 Control speaker enclosure design.

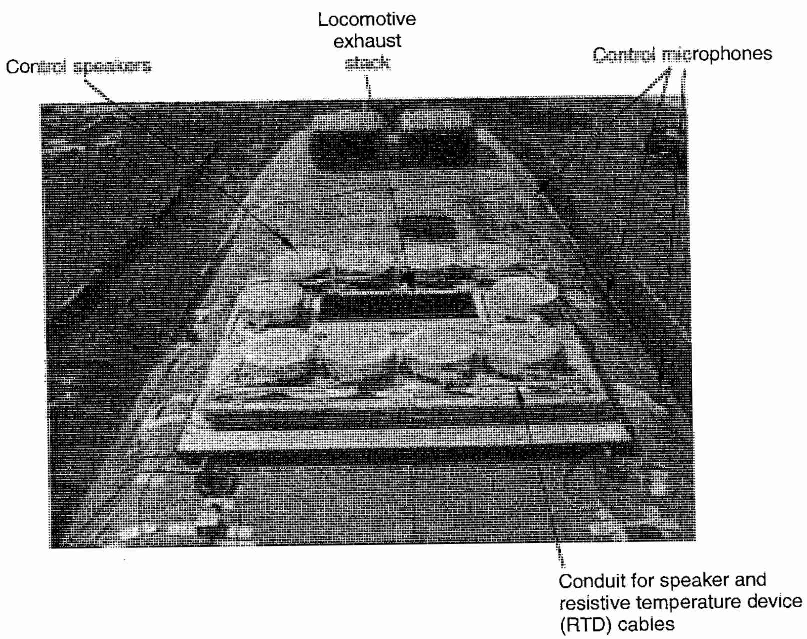

FIGURE 18.91 Control speaker arrangement in the locomotive.

developed for tonal control problems. A simplified control block diagram is shown in Fig. 18.92. The figure shows the typical adaptive MIMO LMS filtered-x architecture with eight control filters and an 8 × 8 plant transfer function matrix. A more detailed block diagram is shown in Fig. 18.93, where probe injection is shown for plant identification along with the additional LMS blocks for estimating the plant while minimizing the noise in the estimate.

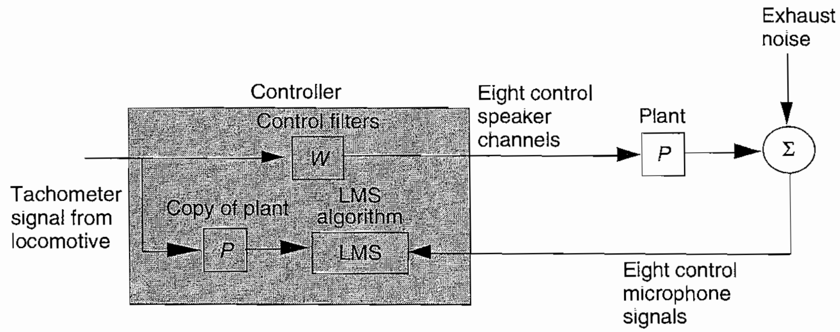

FIGURE 18.92 Simplified basic block diagram of the control architecture.

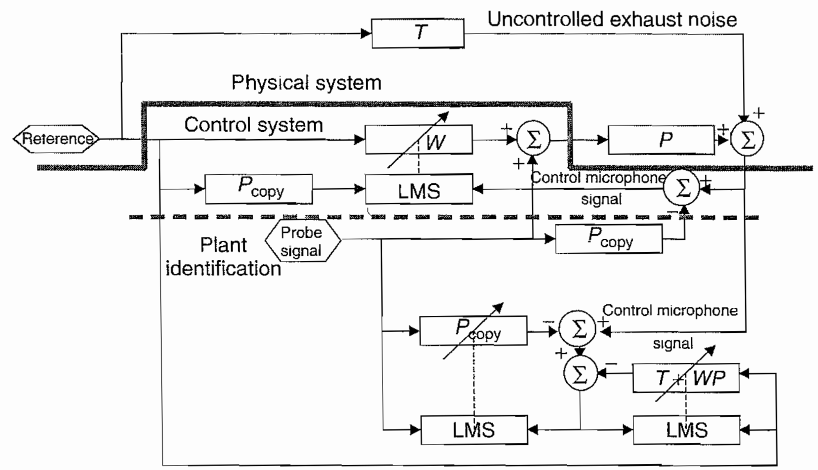

FIGURE 18.93 Detailed controller block diagram.

Hardware Selection. We decided early in the design process to use 12-bit successive-approximation A/D converters, since the lower discretization noise associated with 16-bit converters was not needed in this application. A commercially available input–output (I/O) board from Loughborough Sound Images was found that provided 16 input channels (A/D converters) and 8 output channels (sample-and-hold D/A converters) and in addition provided third-order low-pass Butterworth filters for anti-aliasing and reconstruction. We decided to use the on-board filters because providing a separate set of filters would have been too costly. Since these filters roll off very slowly with increasing frequency, we needed to use a sampling frequency much higher than would be needed to achieve the desired control bandwidth. Consequently, we sampled at 2000 Hz and set the cutoff frequency of the filters to 720 Hz; however, in the control computations we downsampled the digital signals by a factor of 4. This gave us an effective sampling rate of 500 Hz and a control bandwidth on the order of 250 Hz.

Estimates of computational load and memory requirements for the application are shown in Table 18.3. These estimates were based on up to 200 taps for each of the plant filters and 180 taps for each control filter. The table is divided into two functions: in-line control and system identification. In-line control is the function associated with implementing the control algorithm and system identification is the measurement of the plant transfer function, which must be updated periodically to maintain good control performance. It was decided to use two Texas Instruments TMS320C44 DSP chips available on a commercially available carrier board from Loughborough Sound Images. The board provided more than sufficient memory for the two operations. Each DSP chip is clocked at 60 MHz and is capable of up to 30 million floating-point operations per second (Mflops). It was decided to separate the two functions mentioned above with the primary DSP providing all of the control processing and the secondary DSP carrying out all of the system identifications tasks.

System Performance. The control system described above was implemented on an F40PH passenger locomotive operated by Chicago Metra, a commuter rail line in the Chicago metropolitan area. Testing was carried out at the 51st St. Rail Yard in Chicago. The microphone locations for the evaluation are shown in Fig. 18.94. The number of available microphone locations was limited because of the presence of other equipment and structures in the yard that would have interfered with the acoustical evaluation. Uncontrolled measurements were made before installation of the passive silencer. The performance of the system was then measured with the passive silencer in place and with the active system turned on and turned off.

Figure 18.95 shows the reduction of the tonal noise at microphone 5 on the roof of the locomotive due to the use of the active system for the locomotive operating loaded at throttle 4.* The figure shows significant reduction of all of the important tones with some amplification of the low-amplitude tones.

TABLE 18.3 DSP Computation Requirements for the Active System

Operation	MFLOPS	Memory (Kbytes)
Control	22.4	107
System identification	9.6	10
Total	32.0	117.0

*The locomotive diesel engine was loaded by passing the power from the alternator driven by the engine through the locomotive dynamic brake grids (large resistors cooled by the dynamic brake fan). The locomotive can be operated unloaded at idle and can be operated loaded or unloaded in any one of eight throttle setting. Throttle 1 corresponds to the lowest speed and lowest power and throttle 8 is the highest speed at full power.

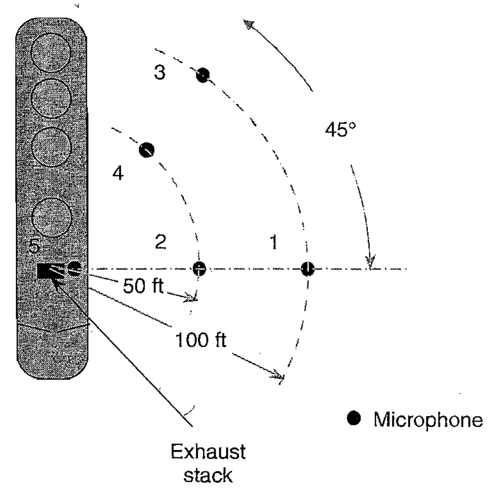

FIGURE 18.94 Microphone locations for the evaluation measurements.

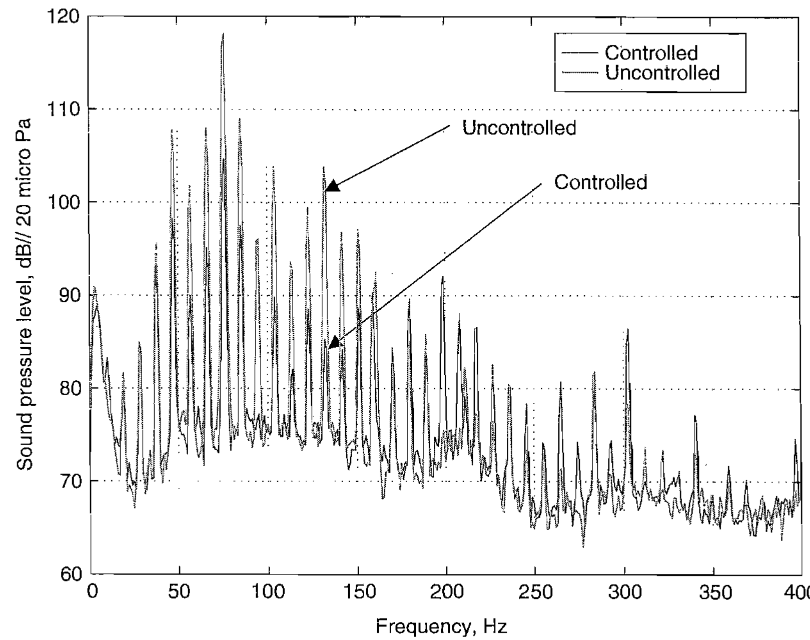

FIGURE 18.95 Noise reduction performance of the active system at throttle 4 loaded as measured at a microphone on the roof of the locomotive.

TABLE 18.4 Estimated Noise Reduction at the Far-Field Microphones

Throttle	Load	mic 5	mic 1	mic 2	mic 3	mic 4
idle	unloaded	5.1	5.2	6.5	6.1	6.4
hi idle	unloaded	8.7	6.5	8.9	5.8	7.4
t4	unloaded	6.9	5.2	4.1	5.6	5.4
t6	unloaded	7.7	6.6	5.6	6.4	6.0
t8	unloaded	5.8	−0.1	3.7	6.2	4.7
t4	loaded	6.4	5.2	4.1	4.7	4.6
t6	loaded	4.3	−1.9	1.2	2.8	1.7
t8	loaded	6.9	2.9	6.5	6.6	6.6

The reduction of the overall sound level below 250 Hz is in excess of 12 dB. Table 18.4 shows the overall A-weighted noise reduction due to the passive silencer and active system operating together. The reductions are somewhat less that the 10-dBA goal but are still significant for most operating conditions and for most microphone locations, showing that the hybrid active–passive system has provided significant broadband global noise reduction.

Active Machinery Isolation

Problem Description. It is difficult to achieve desired vibration isolation at low frequency using passive machinery mounts. Often, to achieve low-frequency isolation, two-stage isolators are employed, which incurs a very large weight penalty for the intermediate mass between the two isolators. In some applications, such as marine vessels or aircraft, the weight of the intermediate mass has an adverse economic and vehicle performance impact.

The forces transmitted into machinery foundations generally contain narrow-band and broadband components. Reduction of the continuous or broadband spectral components as well as the discrete or narrow-band spectral components is often necessary to meet noise or vibration goals. In addition, the tonal frequencies of the narrow-band excitation can change quite rapidly with time due to changes in operating speed. Further, the plant transfer function (i.e., the transfer function between the drive signal to the actuator and the sensor response) is expected to vary with time.

Finally, the machinery foundations of interest are often complex, large, distributed mechanical structures that are lightly damped and have a large number of resonant modes in the frequency range of interest. Thus, typically, plant transfer functions are of high order with high-Q response components. Moreover, the order (e.g., complexity) of the plant increases as the bandwidth of the controller is increased.

Based on the above observations, the control problem is defined as follows:

- Provide both narrow-band and broadband reduction of forces transmitted into the machinery foundation structures.

- Adapt rapidly to variations in the tonal frequencies of narrow-band excitations. Adapt at a relatively slower rate to variations in the plant.
- Minimize controller bandwidth to minimize complexity of the plant transfer function and consequently the controller.
- Provide the desired performance while avoiding out-of-band vibration amplification.

The final item is based on our experience with applications which require increased isolation performance within a certain frequency range but which will not tolerate significant degradation in isolation system performance outside the regulation bandwidth of the active system. Acceptable levels of out-of-band enhancement (i.e., noise amplification) are typically 2–3 dB.

In the following section, we describe an active isolation system designed to meet these requirements. We consider a feedback algorithm, because in general there is not a suitable reference sensor available to achieve broadband control using feedforward control. Although this discussion pertains to SISO control, the algorithms and control architecture are extensible to MIMO control.

Description of Control Strategy.

Real-Time Control Processing The basic real-time controller structure is shown in Fig. 18.96. This is the compensator-regulator architecture that was introduced in Section 18.5, where the plant, designated as $P(\omega)$ in Fig. 18.96, is the transfer function between the output of the controller and the net force transmitted to the foundation.

The controller is implemented as a cascade of two filters because we wish to adapt the low-order regulation filter coefficients quickly to track changes in the center frequency of narrow-band components of the disturbance. At the same time, we choose to adapt the relatively high-order compensation filter at a slower rate to track changes in the plant transfer function.

Adaptation Processing The full functionality of the adaptive controller is shown in Fig. 18.97. The "concurrent adaptation processing" block provides two types of adaptation:

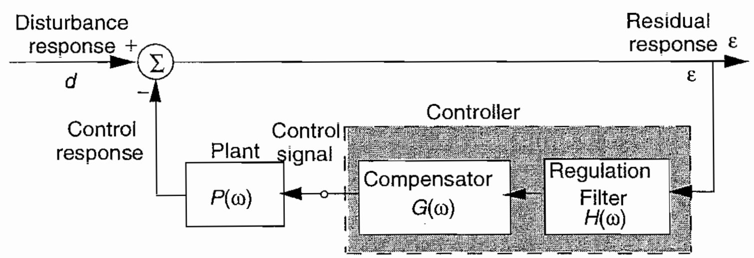

FIGURE 18.96 Feedback compensator regulator.

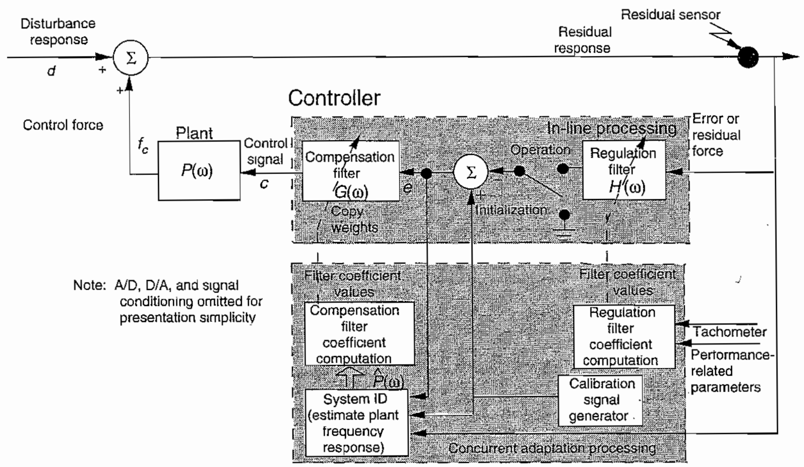

FIGURE 18.97 Controller functionality.

1. Variable narrow-band center frequency adaptation:
   - measurement via a tachometer (or other distinct speed or repetition rate measurement sensor) and a tracking filter of the center frequency of narrow-band response due to periodic excitation and
   - computation and updating of filter coefficients of the digital narrow-band regulation filters based on the currently measured center frequency and rate of change of the center frequency.
2. Variable plant adaptation:
   - system identification in the sense of plant frequency response estimation and
   - computation and updating of filter coefficients of the digital broadband compensation filter.

System identification is performed during closed-loop operation using the procedure outlined in Section 18.4. The major aspects of this procedure include (a) inserting a low-level calibration signal, which is uncorrelated with the external disturbance, into the compensation filter; (b) estimating the cross-spectra of the calibration signal with both the plant input and output; and (c) estimating the plant transfer function as the ratio of these two cross-spectra. Details of the processing of cross-spectra to estimate the plant as well as the design and injection of a covert probe signal are also discussed in Section 18.4 under System Identification.

The probe signal is sufficiently low in level that it does not add appreciably to the residual, and its bandwidth is matched to the full compensation band. Although it is low level, a good-quality estimate of the plant transfer function can be obtained with sufficient averaging time. In the performance plots that follow, estimates of the plant were updated approximately every 2 min.

Since we are concerned with a lightly damped mechanical structure and relatively large compensation bandwidths (e.g., 800 Hz), a FIR filter implementation of the compensation filters would have required a large number of coefficients. To reduce both the off-line and on-line computation load, we opted to use IIR filters designed by a multistep Yule–Walker method.

Hardware Description. Figure 18.98 presents a block diagram of the controller hardware. The algorithmic functionality of the controller is performed by four TMS320C30 DSP chips operating in parallel. The allocation of controller functionality to the individual DSP processors can be summarized as follows:

In-Line Processor. Performs the digital filtering of the regulation and compensation filters for the in-line data path.

Desamp Processor. Responsible for all off-line tasks associated with generating the desampled data buffers presented to the system identification algorithm. Replication filters and reference signal processing are also performed in this processor.

Sys_ID Processor. Performs the system identification and compensation filter weight algorithms. The compensation filter weights are then copied to the in-line processor.

Monitor Processor. Collects data from the other processors and uploads data to the host for monitoring and evaluating system performance.

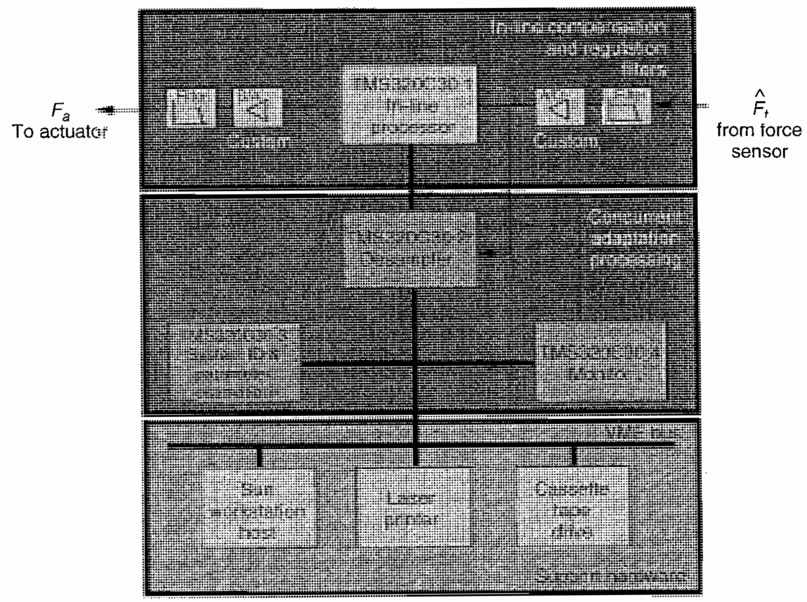

FIGURE 18.98 Controller hardware block diagram.

The controller implementation included custom-built A/D and D/A converter boards plus a logic controller board. The controller board provided a high-speed two-way interface between the DSP processors and the A/D and D/A boards. Two Sky Challenger boards, each of which contain two TMS320C30 chips per board, communicated with each other and the host computer over the VME bus and provide up to 132 Mflop computation rate. A SPARC workstation was chosen as the host computer.

Performance Example. The controller was connected to a prototype active/passive machinery mount located between one leg of a 1300-lb, 140 brake horsepower (BHP) at 2800 rpm, Detroit Diesel model 4–53 engine and a representative complex foundation structure. A picture of the active/passive mount and a schematic of the system are shown in Fig. 18.99. A detailed discussion of the engine, active/passive mount design, and test rig can be found in reference 88.

The test objectives were to provide at least 15 dB of narrow-band regulation at the fundamental and next four harmonics of the piston-firing frequency. In

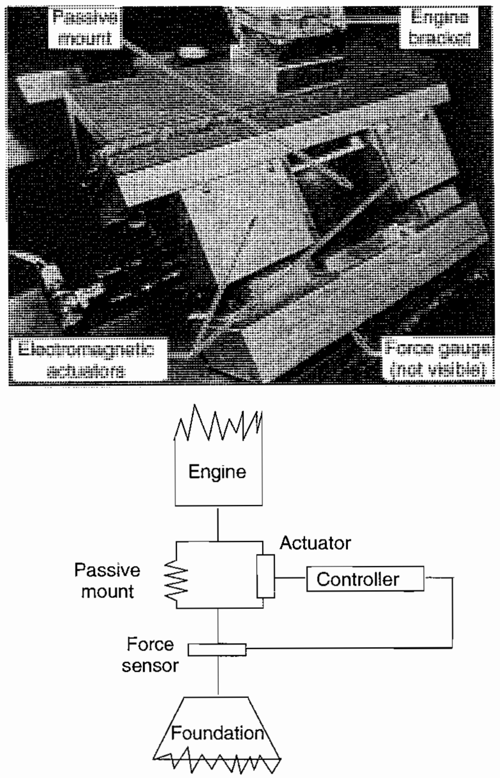

FIGURE 18.99 Active/passive mount and schematic of system.

addition, 10 dB of broadband regulation was desired over the frequency interval from 10 to 80 Hz while maintaining noise amplification below 5 dB outside the regulation bandwidth. To meet these objectives, a compensation bandwidth of 833 Hz and the system sample rate of 10 kHz were chosen. Latency of the digital system (including delay associated with the sample-and-hold on the D/A converter) was 60 μs.

The closed-loop performance of the active isolation system is shown in Fig. 18.100. This plot presents the ratio of the open- to closed-loop residual force transmitted into the foundation structure. As shown in this figure, narrow-band reductions in excess of 15 dB are achieved at the first five piston-firing tonals. In addition, approximately 10 dB of broadband regulation is achieved from about 15 to 80 Hz, which spans most of the frequency interval containing the tonals. Finally, this performance is achieved while limiting noise amplification to approximately 5 dB outside the regulation bandwidth. The very fine structure at higher frequencies of the measured ratio of open- to closed-loop forces, which sometimes goes below −5 dB, is due to harmonic distortion of the actuators (which were being driven very hard), rather than any shortcoming of the control processor.

Active Control of Airborne Noise in a High-Speed Patrol Craft

The Navy's new high-speed patrol crafts are powered by four main propulsion diesel engines that deliver a total of 13,000 shaft horsepower to a set of four propulsion shafts. The operation of these engines produces propeller blade rate tonal noise and broadband cavitation noise that propagate through the hull, producing high noise levels in the aft-crew berthing compartment, which is located

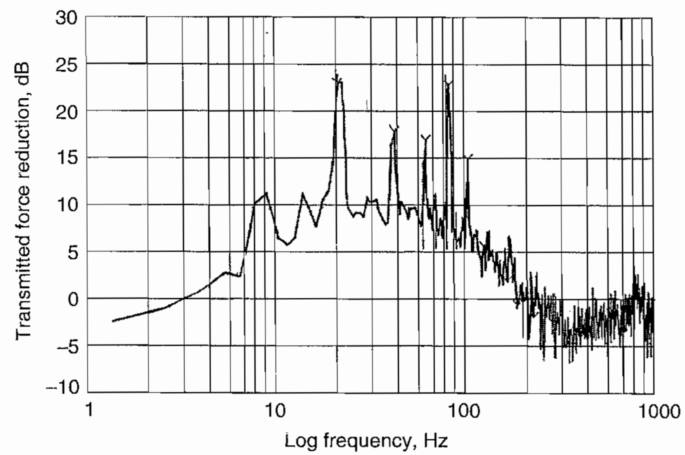

FIGURE 18.100 Reduction of transmitted force into foundation for active/passive mount relative to passive mount.

just forward of the propellers. Although extensive passive noise control treatments have been applied to reduce the noise in this compartment (including floating floors, double bulkheads, and constrained-layer damping), the 63- and 125-Hz octave-band and overall (dBA) airborne noise levels exceeded the Navy's acoustical habitability specifications. Table 18.5 compares measured third-octave-band and overall sound levels in the aft-crew berthing compartment for the first three ships of the class to the noise specification limits.[89] These measurements indicated that reductions in the 63- and 125-Hz octave bands were necessary to reduce overall A-weighted noise to acceptable levels.

To address this problem, several options were explored for reducing the low-frequency noise in the aft-crew compartment. Because passive treatments are least effective in this frequency region, several active noise and vibration control concepts were evaluated. These concepts included methods for both global and local control, using feedforward and feedback control strategies, and with digital and analog control hardware. To assess the benefits of each approach, a set of acoustical trials were conducted initially to measure the operational noise characteristics, path transfer functions, and compartment acoustical characteristics. These data were used to simulate performance of the various control options.

The approach chosen for implementation was local control of the sound field near the head of each bunk using a SISO feedback control strategy. This approach creates an effective "zone of silence" in the immediate vicinity of the occupant's head. This approach is shown schematically in Fig. 18.101. Laboratory simulations using measured data and a mock-up of one rack of bunks suggested that the necessary reductions at the occupant's head location could be achieved using this approach.

The active noise control system for a single bunk is contained within a single prismatic-shaped enclosure that is located in the upper corner of the bunk above and behind the occupant's head. Each unit contains a loudspeaker to create the cancellation noise, a pair of microphones to sense the noise field to be controlled, and a microprocessor to compute the cancellation signal in real time. The control algorithm implemented on the microprocessor was an adaptive feedback algorithm (based on the adaptive Youla transform discussed in Section 18.5) to reduce both narrow-band and broadband noise. The reading light originally placed in this location was incorporated into the active noise control (ANC) enclosure design.

TABLE 18.5 Average Aft Crew Berthing Octave-Band and A-Weighted Noise Levels at Full-Speed[89]

	31.5 Hz	63 Hz	125 Hz	250 Hz	A-Weighted
Noise Specification	105	100	95	90	82
Ship 1	98	113	100	88	87
Ship 2	97	104	94	85	85
Ship 3	95	111	96	86	86

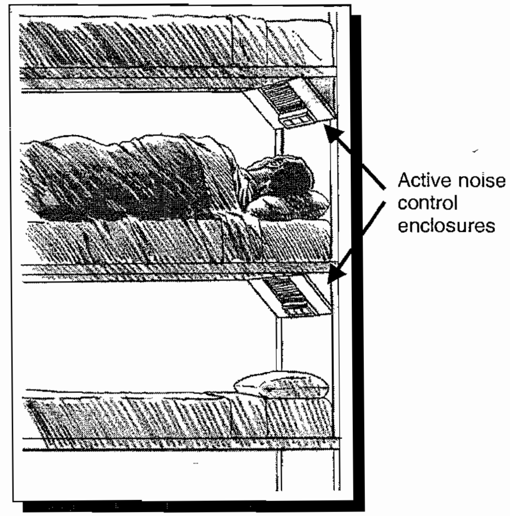

FIGURE 18.101 Schematic of active zone-of-silence approach.

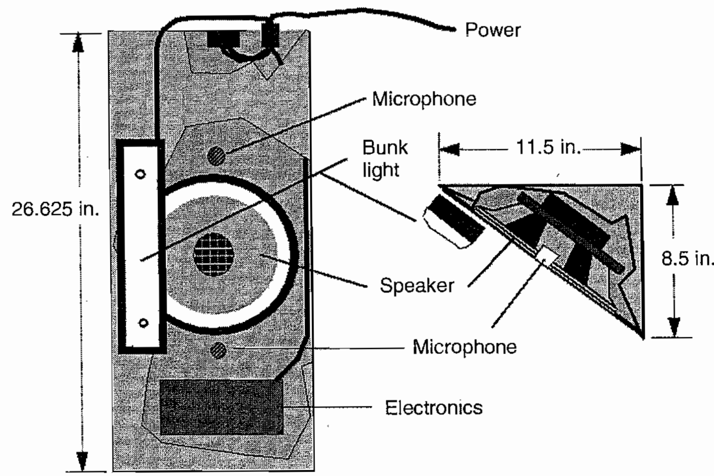

FIGURE 18.102 Components of the ANC enclosure.

The components of the ANC enclosure are illustrated in Fig. 18.102. Pictures of the actual implementation are contained in Figs. 18.103 and 18.104.

The prototype control system described above was evaluated during underway testing. A narrow-band plot of the measured noise reduction at the occupant's head location (not at the control microphones, where greater reductions were achieved) is shown in Fig. 18.105. This plot compares the noise spectra obtained

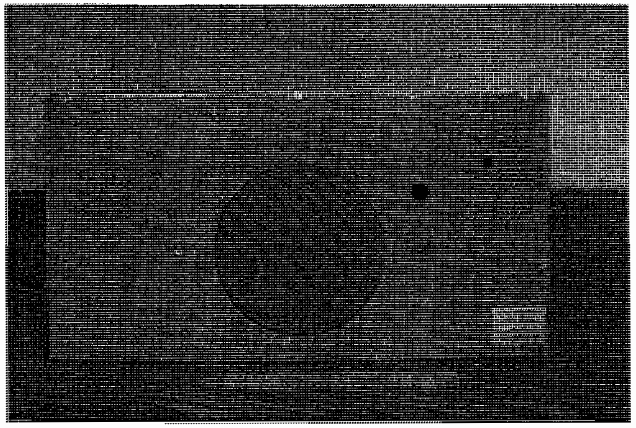

FIGURE 18.103 Faceplate of the ANC enclosure (integrated reading light not shown).

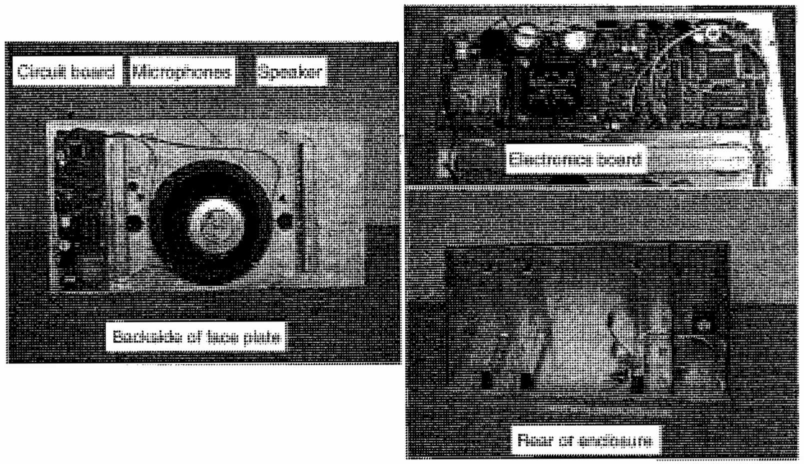

FIGURE 18.104 Pictures of the internal components of the ANC enclosure.

during full-speed operation when the control system was turned *off* to that when the control system was turned *on*. As shown in this plot, reductions at the dominant blade-rate tonals (at approximately 60 Hz) were greater than 15 dB, while 7–10 dB of broadband noise reduction was achieved between 30 and 85 Hz. Third-octave-band performance is summarized in Fig. 18.106. This summary shows that the system reduced the third-octave-band levels to below the limits of the Navy's acoustical habitability specifications, the goal of the program. Based on extensive testing of the prototype system on one patrol craft, the Navy contracted for production units for the entire class of PC1 patrol craft.

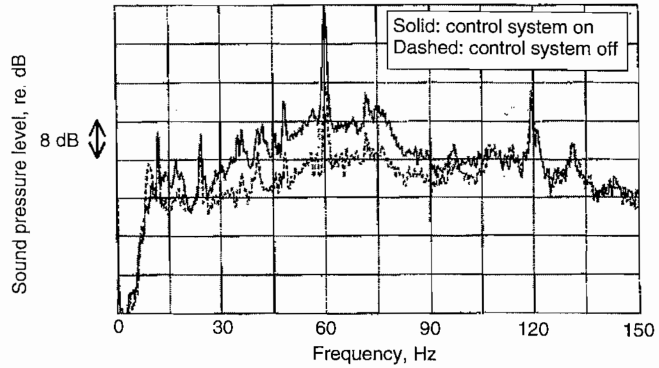

FIGURE 18.105 Narrow-band plot of noise reduction at occupant's head location during full-speed operation.

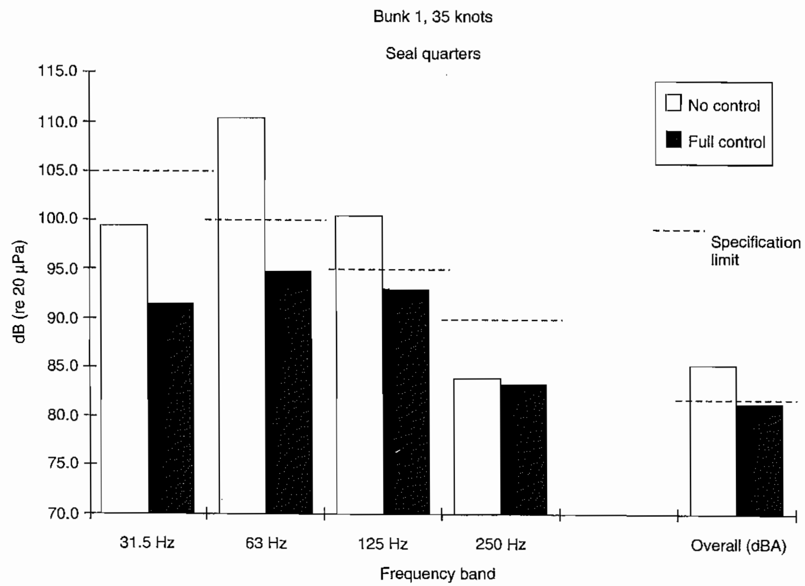

Acoustical data, dB re 20 μPa

Octave band	No control	Control	Attenuation
31.5	99.5	91.5	8
63	110.5	95	15.5
125	100.5	93	7.5
250	84	83.5	0.5
Overall dBA	85.5	81.5	4

FIGURE 18.106 Summary of third-octave-band performance at occupant's head location.

REFERENCES

1. W. B. Conover, "Fighting Noise with Noise," *Noise Control*, **2**, 78–82 (1956).
2. W. B. Conover and R. J. Ringlee, "Recent Contributions to Transformer Audible Noise Control," *Trans. AIEE Pt. III Power Apparatus and Systems*, **74**, 77–90 (1955).
3. K. Kido, "Reduction of Noise by Use of Additional Noise Sources," *Proc. Internoise 75*, 1975, pp. 647–650.
4. G. B. B. Chaplin and R. A. Smith, "The Sound of Silence," *Engineering*, **218**, 672–673 (1978).
5. L. A. Blondel and S. J. Elliott, "Tuned Loudspeaker Enclosures for Active Noise Control," paper presented at Internoise 96, International Congress on Noise Control Engineering, Liverpool, United Kingdom, July 30–August 2, 1996. Proceedings, pp. 1105–1108; Abstract, p. 67.
6. G. J. Stein, "A Driver's Seat with Active Suspension of Electro-pneumatic Type," *ASME J. Vib. Acoust.*, **119**, 230–235 (1997).
7. J. der Hagopian, L. Gaudiller, and B. Maillard, "Hierarchical Control of Hydraulic Active Suspensions of a Fast All-Terrain Military Vehicle," *J. Sound Vib.*, **222**, 723–752 (1999).
8. A. K. Abu-Akeel, "The Electrodynamic Vibration Absorber as a Passive or Active Device," ASME Paper 67-Vibr-18, *ASME J. Eng. Ind.*, **89**, 741–753 (1967).
9. S. Ikai; K. Ohsawa, K. Nagaya, and H. Kashimoto, "Electromagnetic Actuator and Stacked Piezoelectric Sensors for Controlling Vibrations of a Motor on a Flexible Structure," *J. Sound Vib.*, **231**, 393–409 (2000).
10. S. W. Sirlin and R. A. Laskin, "Sizing of Active Piezoelectric Struts for Vibration Suppression on a Space-Based Interferometer," paper presented at the First Joint U.S./Japan Conference on Adaptive Structures, Maui, HI, November 13–15, 1990. Proceedings, pp. 47–63.
11. P. K. C. Wang, "Feedback Control of Vibrations in a Micromachined Cantilever Beam with Electrostatic Actuators," *J. Sound Vib.*, **213**, 537–550 (1998).
12. D. L. Hall and A. B. Flatau, "Broadband Performance of a Magnetostrictive Shaker," in C. J. Radcliffe, K.-W. Wang, H. S. Tzou, and E. W. Hendricks (Eds.), *Active Control of Noise and Vibration*. Papers presented at the ASME Winter Annual Meeting, Anaheim, CA, November 8–13, 1992.*ASME Book DSC-Vol. 38*, pp. 95–104, American Society of Mechanical Engineers, New York.
13. B-T. Wang, R. A. Burdisso, and C. R. Fuller, "Optimal Placement of Piezoelectric Actuators for Active Structural Acoustic Control," *J. Intelligent Material Syst. Struct.*, **5**, 67–77 (1994).
14. G. E. Warnaka, "Active Attenuation of Noise—The State-of-the-Art," *Noise Control Eng.*, May/June 1982, pp. 100–110.
15. D. Guicking, *Active Noise and Vibration Control Reference Bibliography*, 3rd ed., Dritte Physicalisches Institut, University of Göttingen, Göttingerm 1988 and 1991 supplement.
16. S. J. Elliott and P. A. Nelson, "Active Noise Control," *IEEE Signal Process. Mag.*, October 1993, pp. 12–35.
17. C. Fuller, "Active Control of Sound and Vibration," tutorial lecture presented at the 120th Acoustical Society of America Meeting, San Diego, November 26, 1990.

18. H. Coanda, "Procédé de Protection Contre les Bruits," French Patent No. 722274, filed October 21, 1930, patented December 29, 1931, published March 15, 1932.
19. P. Lueg, "Process of Silencing Sound Oscillations," U. S. Patent 2,043,416, June 19, 1936.
20. M. A. Swinbanks, "The Active Control of Sound Propagation in Long Ducts," *J. Sound Vib.*, **27**(3), 411–436 (1973).
21. M. J. M. Jessel, "Sur les absorbeur actif," in *Proceedings of the sixth International Congress on Acoustics*, Paper F 5–6 82, Tokyo, 1968.
22. M. J. M. Jessel and G. Magiante, "Active Sound Absorbers in an Air Duct," *J. Sound Vib.*, **23**, 383–390 (1972).
23. H. G. Leventhall, "Developments in Active Attenuators," in *Proceedings of the 76 Noise Control Conference*, Warsaw, Poland, 1976, pp. 175–180.
24. G. Canevet, "Active Sound Absorption in an Air Conditioning Duct," *J. Sound Vib.*, **58**, 333–345 (1978).
25. L. J. Eriksson, M. C. Allie, and R. A. Greiner, "The Selection and Application of IIR Adaptive Filter for Use in Active Sound Attenuation," *IEEE Trans. Acoust. Speech Signal Process.*, **ASSP-35**, 433–437 (1987).
26. L. J. Eriksson and M. C. Allie, "A Digital Sound Control System for Use in Turbulent Flows," Paper presented at NOISE-CON 87, National Conference on Noise Control Engineering, State College, PA, June 8–10, 1987. Proceedings, pp. 365–370.
27. L. J. Eriksson and M. C. Allie, "A Practical System for Active Attenuation in Ducts," *Sound Vib.*, **22**(2), 30–34 (February 1988).
28. L. J. Eriksson, "The Continuing Evolution of Active Noise Control with Special Emphasis on Ductborne Noise," in C. A. Rogers and C. R. Fuller (Eds.), *Proceedings of the First Conference on Recent Advances in Active Control of Sound and Vibration*, Blacksburg, VA, April 15–17, 1991, pp. 237–245.
29. H. F. Olsen and E. G. May, "Electronic Sound Absorber," *J. Acoust. Soc. Am.*, **25**, 1130–1136 (1953).
30. D. C. Perry, S, J, Elliott, I. M. Stothers, and S. J. Oxley, "Adaptive Noise Cancellation for Road Vehicles," in *Proceedings of the Institution of Mechanical Engineers Conference on Automotive Electronics*, 1989, pp. 150–163.
31. S. Hasegawa, T. Tabata, A. Kinsohita, and H. Hyodo, "The Development of an Active Noise Control System for Automobiles," SAE Technical Paper Series, Paper No. 922087, Society of Automotive Engineers, Warrendale, PA. 1992.
32. R. J. Bernhard, "Active Control of Road Noise Inside Automobiles," in *Proceedings of ACTIVE 95, The 1995 International Symposium on Active Control of Sound and Vibration*, Newport Beach, CA, July 6–8, 1995, pp. 21–32
33. S. J. Elliott, P. A. Nelson, T. J. Sutton, A. M. McDonald, D. C. Quinn, I. M. Stothers, and I. Moore, "The Active Control of Low Frequency Engine and Road Noise Inside Automotive Interiors," Paper presented at ASME Winter Annual Meeting, Session NCA-8, Dallas, TX, Nov. 25–30, 1990. Proceedings, pp. 125–129.
34. W. Dehandschutter, R. Van Cauter, and P. Sas, "Active Structural Acoustic Control of Structure Borne Road Noise: Theory, Simulations, and Experiments," in S. D. Sommerfeldt and H. Hamada (Eds.), *Proceedings of ACTIVE 95, The 1995 International Symposium on Active Control of Sound and Vibration*, Newport Beach, CA, July 6–8, 1995, pp. 735–746.

35. S. J. Elliott, P. A. Nelson, and I. M. Stothers, "In Flight Experiments on the Active Control of Propeller Induced Cabin Noise," *J. Sound Vib.*, **140**, 219–238 (1990).
36. C. F. Ross and M. R. J. Purver, "Active Cabin Noise Control," in S. J. Elliott and G. Horváth (Eds.), *Proceedings of ACTIVE 97, The 1997 International Symposium on Active Control of Sound and Vibration*, Budapest, Hungary, August 21–23, 1997, pp. 39–46.
37. G. P. Mathur, B. N. Tran, and M. A. Simpson, "Active Structural Acoustic Control of Aircraft Cabin Noise Using Optimized Actuator Arrays—Laboratory Tests," AIAA Paper 95-082, presented at the First Joint CEAS/AIAA Aeroacoustics Conference (AIAA 16th Aeroacoustics Conference), München, DE, June 12–15, 1995.
38. M. A. Simpson, T. M. Luong, M. A. Swinbanks, M. A. Russell, and H. G. Leventhall, "Full Scale Demonstration Tests of Cabin Noise Reduction Using Active Noise Control," Paper presented at Internoise 89, International Congress on Noise Control Engineering, Newport Beach, CA, December 4–6, 1989. Proceedings, pp. 459–462.
39. P. D. Wheeler, "The Role of Noise Cancellation Techniques in Aircrew Voice Communications Systems," in *Proceedings of the Royal Aeronautical Society Symposium on Helmets and Helmet Mounted Devices*, 1987.
40. I. Veit, "Noise Gard—An Active Noise Compensation System for Headphones and Headsets," NATO Research Study Group (RSG) 11, Panel 3: Proceedings of the Workshop on Active Cancellation of Sound and Vibration, 22nd Meeting, Vicksburg, MS, October 31, 1990, and 23rd Meeting, Bremen, DE, June 5, 1991, pp. 164–167.
41. B. Rafaely and M. Jones, "Combined Feedback-Feedforward Active Noise-Reducing Headset—The Effect of the Acoustics on Broadband Performance," *J. Acous. Soc. Am.*, **112**, 981–989 (2002).
42. K. D. LePage, P. J. Remington, and A. R. D. Curtis, "Reference Sensor Selection for Automotive Active Noise Control Applications," Paper presented at 130th Meeting of the Acoustical Society of America, Adam's Mark Hotel, St. Louis, MO, November 27–December 1, 1995.
43. P. Remington, D. Sutliff, and S. Sommerfeldt, "Active Control of Low Speed Fan Tonal Noise Using Actuators Mounted in Stator Vanes Part 1: Control System Design and Implementation," Paper No. AIAA-2003-3191, presented at the AIAA/CEAS Aeroacoustics Conference, Hilton Head, SC, 2003.
44. D. Sutliff, P. Remington, and B. Walker, "Active Control of Low Speed Fan Tonal Noise Using Actuators Mounted in Stator Vanes Part 3: Results," Paper No. AIAA-2003-3193, presented at the AIAA/CEAS Aeroacoustics Conference, Hilton Head, SC, 2003.
45. A. R. D. Curtis, "Active Control of Fan Noise by Vane Actuators," BBN Report 1193, BBN Technologies, Cambridge, MA, 1998.
46. P. Joseph, P. A. Nelson, and M. J. Fisher, "Active Control of Turbofan Radiation Using an In-Duct Error Sensor Array," in S. J. Elliott and G. Horvath (Eds.), *Proceedings of ACTIVE 97, the 1997 International Symposium on Active Control of Sound and Vibration*, Active 97, Budapest, Hungary, August 21–23, 1997, pp. 273–286.
47. R. H. Thomas, R. A., Burdisso, C. R. Fuller, and W. F. O'Brien, "Active Control of Fan Noise from a Turbofan Engine," *AIAA J.*, **32**(1), 23–30 (1994).
48. R. A. Burdisso, R. H. Thomas, C. R. Fuller, and W. F. O'Brien, "Active Control of Radiated Inlet Noise from Turbofan Engines," in *Proceedings of the 2nd Conference on Recent Advances in Active Control of Sound and Vibration*, Blacksburg, VA, April 28–30, 1993, pp. 848–860.

49. R. G. Gibson, J. P. Smith, R. A. Burdisso, and C. R. Fuller, "Active Reduction of Jet Engine Exhaust Noise," Paper presented at Internoise 95, International Congress on Noise Control Engineering, Newport Beach, CA, July 10–12, 1995. Proceedings, pp. 518–520.
50. J. P. Smith, R. A. Burdisso, and C. R. Fuller, "Experiments on the Active Control of Inlet Noise from a Turbofan Jet Engine Using Multiple Circumferential Control Arrays," AIAA Paper 96–1792, presented at the 2nd AIAA/CEAS Aeroacoustics Conference, State College, PA, May 6–8, 1996.
51. H. F. Olsen, "Electronic Control of Noise, Vibration and Reverberation," *J. Acoust. Soc. Am.*, **28**, 966–972 (1956).
52. E. F. Berkman, "An Example of a Fully Adaptive Integrated Narrowband/Broadband SISO Feedback Controller for Active Vibration Isolation of Complex Structures," Paper presented at the ASME Annual Meeting, November 1992.
53. J. Scheuren, "Principles, Implementation and Application of Active Vibration Isolation," Paper C3, presented at the International Workshop on Active Control of Noise and Vibration in Industrial Applications, CETIM, Senlis, France, April 9–12, 1996.
54. P. Gardonio and S. J. Elliott, "Active Control of Structural Vibration Transmission between Two Plates Connected by a Set of Active Mounts," Proceedings of ACTIVE 99, Paper presented at the 1999 International Symposium on Active Control of Sound and Vibration, Ft. Lauderdale, FL, December 2–4, 1999, pp. 118–128
55. A. H. von Flotow, "An Expository Overview of Active Control of Machinery Mounts," Paper presented at the 27th IEEE Conference on Decision and Control (CDC), Austin, TX, December 7–9, 1988. Proceedings, Vol. 3, pp. 2029–2032.
56. P. A. Nelson and S. J. Elliott, *Active Control of Sound*, Academic, San Diego, CA, 1992.
57. A. V. Oppenheim and R. W. Schafer, *Digital Signal Processing*, Prentice-Hall, Englewood Cliffs, NJ, 1975.
58. S. J. Elliott, *Signal Processing for Active Control*, Academic, San Diego, CA, 2001.
59. B. Widrow and S. D. Stearns, *Adaptive Signal Processing*, Prentice-Hall, Englewood Cliffs, NJ, 1985.
60. G. H. Golob and C. F. Van Loan, *Matrix Computations*, Johns Hopkins University Press, Baltimore, MD, 1983.
61. L. J. Eriksson and M. J. Allie, "Use of Random Noise for On-Line Transducer Modeling in an Adaptive Active Attenuation System," *J. Acoust. Soc. Am.*, **85**, 797–802 (1989).
62. L. J. Eriksson, "Active Sound Attenuation System with On-Line Adaptive Feedback Cancellation," U. S. Patent 4,677,677, June 30, 1987.
63. L. J. Eriksson, "Active Attenuation System with On-Line Modeling of Speaker, Error Path and Feedback Path," U. S. Patent 4,677,676, June 30, 1987.
64. D. R. Morgan, "An Analysis of Multiple Correlation Cancellation Loops with a Filter in the Auxiliary Path," *IEE Trans. Acoust. Speech Signal Process.*, **ASSP-28**, 454–467 (1980).

65. B. Widrow, D. Shur, and S. Shaffer, "On Adaptive Inverse Control," in *Proceeding of the 15th ASILOMAR Conference on Circuits, Systems and Computers*, Pacific Grove, CA, November 9–11, 1981, pp. 185–195.
66. J. C. Burgess, "Active Adaptive Sound Control in a Duct: A Computer Simulation," *J. Acoust. Soc. Am.*, **70**, 715–726 (1981).
67. S. J. Elliott and P. A. Nelson, "Algorithm for Multi-Channel LMS Adaptive Filtering," *Electron. Lett.*, **21**, 978–981 (1985).
68. C. C. Boucher, S. J. Elliott, and P. A. Nelson, "The Effects of Errors in the Plant Model on the Performance of Algorithms for Adaptive Feedforward Control," *Proc. IEE-F*, **138**, 313–319 (1991).
69. K. J. Astrom and B. Wittenmark, *Adaptive Control*, Addison-Wesley, Reading, MA, 1989.
70. R. B. Coleman, E. F. Berkman, and B. G. Watters, "Optimal Probe Signal Generation for On-Line Plant Identification within Filtered-X LMS Controllers," paper presented at the ASME Winter Annual Meeting 1994, Chicago, IL, November 1994.
71. R. B. Coleman and E. F. Berkman, "Probe Shaping for On-line Plant Identification," in *Proceedings of ACTIVE 95, the 1995 International Symposium on Active Control of Sound and Vibration*, Newport Beach, CA, July 6–8, 1995.
72. R. B. Coleman, B. G. Watters, and R. A. Westerberg, "Active Noise and Vibration Control System Accounting for Time Varying Plant, Using Residual Signal to Create Probe Signal," U.S. Patent 5,796,849, August 18, 1998.
73. I. Gustavsson, L. Lyung, and T. Soderstrom, "Survey Paper: Identification of Processes in Closed Loop—Identifiability and Accuracy Aspects," *Automatica*, **13**, 59–75 (1977).
74. E. F. Berkman, R. B. Coleman, B. Watters, R. Preuss, and N. Lapidot, "An Example of a Fully Adaptive Integrated Narrowband/Broadband SISO Feedback Controller for Active Vibration Isolation of Complex Structures," paper presented at the ASME Annual Meeting, New York November 1992.
75. A. R. D. Curtis, E. F. Berkman, R. B. Coleman, and R. Preuss, "Controller Strategies for Fully Adaptive Integrated Narrowband and Broadband Feedback Control for Active Vibration Isolation of Complex Structures," in *Active Control of Noise and Vibrations in Industrial Applications*, CETIM, Senlis, France, April 1996.
76. E. F. Berkman and E. K. Bender, "Perspectives on Active Noise and Vibration Control," *Sound Vib.*, 30th anniversary issue, January 1997.
77. R. D. Preuss, "Methods for Apparatus Designing a System Using the Tensor Convolution Block Toeplitz Preconditioned Conjugate Gradient Method," U. S. Patent 6,487,524 B1, November 26, 2002.
78. M. Athans and P. L. Falb, *Optimal Control: An Introduction to the Theory and Its Application*, McGraw-Hill, New York, 1966.
79. H. Kwakernaak and R. Sivan, *Linear Optimal Control Systems*, Wiley-Interscience, New York, 1972.
80. M. A. Dahleh and I. J. Diaz-Bobillo, *Control of Uncertain Systems*, Prentice-Hall, Englewood Cliffs, NJ, 1995.
81. K. Zhou and J. C. Doyle, *Essentials of Robust Control*, Prentice-Hall, Upper Saddle River, NJ, 1998.
82. J. E. Gibson, *Nonlinear Automatic Control*, McGraw-Hill, New York, 1963.

83. L. P. Heck, J. A. Olkin, and H. Naghshineh, "Transducer Placement for Broadband Active Vibration Control Using a Novel Multidimensional QR Factorization," *ASME J. Vib. Acoust.*, **120**, 663–670 (1997).
84. R. D. Preuss and B. Musicus, "Digital Filter and Control System Employing Same," U.S. Patent 5,983,255, awarded November 9, 1999.
85. P. J. Remington and M. J. Rudd. "An Assessment of Railroad Locomotive Noise," Report No. DOT-TSC-OST-76-4/FRA-OR&D-76-142, U.S. Department of Transportation, Washington, DC, August 1976.
86. P. J. Remington, S. Knight, D. Hanna, and C. Rowley, "A Hybrid Active-Passive System for Controlling Locomotive Exhaust Noise," Paper No. IN2000/0035, presented at Internoise 2000, Nice, France, 2000.
87. P. J. Remington, S. Knight, D. Hanna, and C. Rowley, "A Hybrid Active/Passive Exhaust Noise Control System (APECS) for Locomotives," BBN Report No. 8302, BBN Technologies, Cambridge, MA, March 29, 2001.
88. B. G. Watters et al., "A Perspective on Active Machinery Isolation," in *Proceedings of 27th Conference on Decision and Control*, Austin, TX, December 1988.
89. M. Dignan et al., "The Active Control of Airborne Noise in a High Speed Patrol Craft," paper presented at Noise-Con 94, Ft. Lauderdale, FL, May 1994.

CHAPTER 19

Damage Risk Criteria for Hearing and Human Body Vibration

SUZANNE D. SMITH
Air Force Research Laboratory
Wright-Patterson Air Force Base, Ohio

CHARLES W. NIXON
Consultant
Kettering, Ohio

HENNING E. VON GIERKE
Consultant
Yellow Springs, Ohio

19.1 INTRODUCTION

Noise and vibration are closely related biodynamic environments in terms of their origins, manifestations, and effects on people. Those effects on people that are undesirable are often threatening, induce fatigue, compromise working performance, modify physiological responses, and harm human systems. At the present time, avoidance of excessive noise and vibration exposure is the only assured way to prevent these major hazardous effects.

The practical alternative to complete avoidance is to limit exposures in these environments to those defined as acceptable by appropriate standards, guidelines, and damage risk criteria. Scientific exposure guidelines and criteria established to curtail these effects are vital parts of comprehensive protection programs of concern to governments, industry, and affected personnel. Most adverse effects of these commonly encountered mechanical forces on human systems can be minimized and controlled through engineering and design efforts. Central to these programs and actions are guidelines and criteria that describe potential damage risk and/or establish acceptable exposure limits.

Criteria and limits define conditions above which the risk of damage due to an exposure is considered substantial or unacceptable. Noise and vibration criteria describe exposure characteristics and corresponding undesirable effects such as noise-induced hearing loss, vibration-induced hand–arm vibration syndrome

(HAVS), and vibration-related spinal injury. Damage risk criteria have been developed and implemented worldwide. The basic exposure–effects relationships that underlie these criteria are reasonably well understood and are derived from observations and experience as well as good laboratory and field studies. The various criteria contain different limiting values because of variations in interpretations of the basic data and in the rationale used to establish them. The rationale may include practical, legal, and economic considerations as well as humanitarian concerns. It is very important that the rationale underlying damage risk criteria is fully understood by the user to ensure that the application is justified and accurate.

Estimates of noise and vibration exposures and of their probable effects on populations are usually expressed in terms of population distribution statistics. These group population effects are not precise descriptors, and they are not appropriate for evaluating an individual. Nevertheless, they are adopted by nations and incorporated into national regulations and laws. Many become mandatory requirements included in governmental and industrial activities involving exposure of people to noise and vibration environments.

This chapter presents contemporary regulatory and voluntary noise and vibration exposure standards and criteria along with background information that will facilitate their understanding and application in engineering control and design.

19.2 DAMAGE RISK CRITERIA FOR THE AUDITORY RANGE

Noise Factor

Permanent hearing loss and its associated problems are clearly the most critical and widespread of the various consequences of excessive noise exposure. The extent of damage to the hearing mechanism caused by noise is related to the amount of acoustical energy reaching the hearing mechanism. Such damage cannot be estimated accurately for an individual because of the variability of the noise and the susceptibility of the exposed ears. The primary factors in noise-induced hearing loss are the level of the noise, the frequency content or spectrum of the noise, the duration or time course of the noise exposure, and the susceptibility of the ear.

Exposure limits are defined in terms of level, spectrum, and duration of the noise. A-weighted sound energy of an exposure is directly related to noise-induced hearing loss. No other measure of noise exposure provides a better *cause–effect* relationship with hearing loss.[1] Impulse noise is also included in this measure for many criteria, as was concluded by a special workshop on impulse noise.[2] It was agreed that there is no convincing evidence against acceptance of A-weighting measurement of all noises from 20 to 20,000 Hz in determining their permanent threshold shift (noise-induced hearing loss that does not recover to preexposure levels after cessation of exposures) hazard except when their unweighted, instantaneous, peak-sound-pressure levels exceed approximately 145 dB. Consequently, exposures are typically described in terms of the average A-weighted levels, or the equivalent continuous A-weighted sound pressure level (L_{eq}), over an average workday.

Practical measures for the prevention of noise-induced hearing loss are centered in hearing conservation programs. These programs involve definitions of acceptable noise exposure, personal hearing protection, monitoring the hearing of the affected personnel, and appropriate administrative actions to minimize and eliminate identified temporary hearing problems before they become permanent. The basis of a hearing conservation program is the definition of acceptable noise exposure or exposure criteria that specify the acceptable exposure limits and the proportion of the population to be protected. The criteria of various hearing conservation programs and applications differ in their limiting values.

The parameters of particular exposure criteria are selected to satisfy the needs of the user. Factors that may influence these selections are various interpretations of available data, policies or requirements of organizations, and the remaining uncertainty in the noise exposure–hearing loss databases. Consequently, criteria may differ in such features as estimates of beginning hearing loss, corrections for nonnoise effects such as aging, percentage of the population to be protected, and the extent of protection to be provided.

The most obvious differences among noise exposure criteria are the sound level at which the implementation occurs and how the duration of the exposure and the sound level of the noise are combined.[3] The duration–sound level relationships are referred to as time–intensity trading rules, which assume that damage to hearing is related to total A-weighted sound level and the duration of exposure time. The equal energy relationship between these parameters results in the 3-dB rule. This and other relationships are shown in Table 19.1 which displays permissible noise exposures in A-weighted sound pressure levels for the cited criteria. The permissible A-weighted level for an 8-h exposure ranges from 75 dBA for the Environmental Protection Agency (EPA) to 90 dBA for the Occupational Safety and Health Administration (OSHA).

Most criteria utilize the 3-, 4-, or 5-dB rule. The 3-dB rule is based on the equal-energy concept and is the most conservative or protective of the three rules. The 4- and 5-dB rules assume that intermittency and interruptions of exposures reduce the risk to less than that expected from the total energy. Consequently, a 50% increase in exposure duration corresponds to sound-level decreases of 3 and 5 dB for the respective 3- and 5-dB rules (Table 19.1). Intermittency of exposure is discussed later in the chapter.

Hearing Sensitivity

The human ear is sensitive to a much wider range of sounds than the generally cited 20 Hz–20 kHz audio frequency range. A compilation of independent measurement studies by several investigators using a wide variety of instrumentation and methodologies shows very good agreement and provides confidence in the data summarized in Fig. 19.1 Infrasound (<20 Hz) and ultrasound (traditionally >20,000 Hz but practically above about 12,000 Hz) are normally detected by the ear only at very high sound pressure levels. The traditional audio frequency

TABLE 19.1 Equal Energy and Other Trading Rules Used to Define Permissible Noise Exposures in A-Weighted Sound Pressure Level (dBA) and Exposure Time (h)

Duration of Exposure (h)	Equal Energy[a]	OSHA	EPA	NIOSH[b]	Army	Navy	Air Force	Music
24								
16								
8	90	90	75[c]	85	85	84	85	
4	93	95		88	88	88	88	
2	96	100		91	91	92	91	94[d]
1	99	105		94	94	96	94	
0.5	102	110		97	97	100	97	
0.25	105	115[e]		100	100	104	100	

[a] Equal energy rule of 3-dB decrease for doubling of exposure applied to a basic 8-h criterion of 90 dBA.
[b] National Institute of Occupational Safety and Health.
[c] Threshold for detectable noise-induced permanent threshold shift (NIPTS) at 4000 Hz: exposures exceeding 75 dBA may cause NIPTS exceeding 5 dB in 100% of the population after cumulative noise exposure of 10 years.
[d] Time-averaged A-weighted sound level, in dB, over a 2-h period once a week.
[e] Ceiling on exposure level and duration.

region (20 Hz–20 kHz) is well defined for stimuli including discrete tones, bands of noise, speech materials, loudness, comfort, and acceptibility. These databases provide the information necessary to support the development of noise exposure criteria.

The sensitivity of human hearing for high-frequency sounds (3000–4000 Hz and above) gradually decreases with advancing age. This process is called *presbyacusis*. Auditory system components are affected in both the peripheral and the central nervous systems. Although individual patterns of presbyacusis vary widely, normative data describing hearing sensitivity as a function of age have been compiled for various segments of society (some are reported in ref. 5). Loss of sensitivity due to accident, disease, or substances toxic to the auditory system is called *nosoacusis* while that attributed to the noises of everyday living is *sociacusis*. The major high-level noises to which people are exposed are the occupational environments.

Environmental noise occurs over the full spectrum to which the human auditory system is sensitive. Exposure to various segments of this sensory continuum produces differential effects on humans. Limiting levels and durations of acoustical exposure are defined for a number of specific portions of this spectrum, which include infrasound (0.5–20 Hz), audio frequencies (20 to about 12,000 Hz), ultrasound (12,000 to about 40,000 Hz), and impulsive sounds (characterized by rapid onset and durations of less than 1 s) described in terms of peak sound pressure level and duration. Some of these limits are well substantiated by experience and experimental evidence while others remain tentative until more evidence is available.

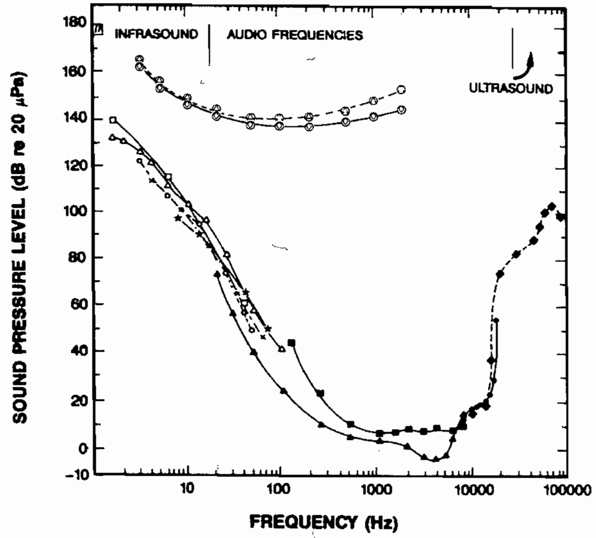

FIGURE 19.1 Human auditory sensitivity and pain thresholds for pure tones, octave bands of noise, and static pressure: (◬) BENOX (1953), pain MAP tones; (◬) pain static pressure; (◎) tickle, pain tones; (□) Bekesy (1960), MAP tones; (▲) ISO R226 (1961), MAF tones; (♦) Corso (1963) bone conduction minus 40-dB tones; (○) Yeowart, Bryan, and Tempest (1960), MAP tones; (×) MAP octave bands of noise; (■) standard reference threshold values (American National Standard on Specifications for Audiometers) (1969), MAP tones; (●) Northern et al. (1972), MAP tones; (△) Whittle, Collins, and Robinson (1972), MAP tones; (★) Yamada et al. (1986), MAF tones. (Data adapted from Ref. 4.) Minimum audible pressure (MAP) indicates that the sound was presented to the ears through earphones and the sound pressure levels were measured in an earphone–microphone coupler that approximated the cavity created by the earphone/pinna. Minimum audible field (MAF) indicates that the sound was presented to the listeners facing a loudspeaker and located in anechoic space. The sound pressure levels for MAF were measured at the location of the center of the head without the listener present. For the same listeners, MAP thresholds are generally several decibels higher than MAF thresholds.

19.3 AUDIO FREQUENCY REGION

CHABA

Noise exposure criteria for the audio frequency region (20–12,000 Hz) were developed by the National Academy of Sciences—National Research Council, Committee on Hearing, Bioacoustics and Biomechanics (CHABA) in 1965.[6] This method described noise exposure in terms of pure tones, third-octave, and octave bands of noise, and it includes the audio frequencies of 100–7000 Hz. Acceptable exposures to noise can be determined from 11 sets of curves. An environmental noise is considered acceptable if it produces, on average, a NIPTS after 10 years or more of near daily exposure of no more than 10 dB at 1000 Hz and below, 15 dB at 2000 Hz, and no more than 20 dB at 3000 Hz and above. These criteria are based on the assumption that noise exposures producing temporary threshold shifts (TTSs) would eventually produce permanent threshold shifts (PTSs). The possible relationship that TTS is a precursor to PTS is still an open question. The CHABA criteria have been widely used and are an excellent tool. However, they are not simple to use or to relate to current standards, regulations, and guidelines and are less preferred than criteria employing A-weighted sound level.

OSHA

The Occupational Safety and Health Administration has adopted a noise exposure limit of 90 dBA with a 5-dB trading relationship to control excessive noise exposure in industry (Table 19.1). When employees are exposed to noise at different levels during the day, ratios of the actual to the allowed duration for that level are computed and the fractions summed for the day. Total daily exposure calculated from these fractions or ratios must not exceed unity. No other corrections or adjustments are applied to these criteria.

The OSHA noise exposure criteria were verified in 1983 with the publication of "Occupational Noise Exposure; Hearing Conservation Amendment; Final Rule."[7] The basic conditions of the original OSHA noise exposure regulation remain the same with a few exceptions. Continuous A-weighted sound levels are not permitted above 115 dBA regardless of duration. A permissible exposure level (PEL) is defined as that noise dose that would result from a continuous 8-h exposure to a sound level of 90 dBA. The limit of 90 dBA is a dose of 100%, which is the basic criterion level. A *time-weighted average* (TWA) is the sound level that would produce a given noise dose when the employee is exposed to that level continuously over an 8-h workday regardless of the length of the work shift. Workday exposures of 4 h at 90 dB, 8 h at 85 dB, or 12 h at 82 dB all correspond to a TWA of 85 dBA and a noise dose of 50%. The Hearing Conservation Amendment includes computational formulas and tables showing the time–intensity relationships for the 5-dB rule and conversions of dose to time-weighted averages. Guidance is given on calculations of age corrections to audiograms. However, the use of age correction procedures is not required for compliance.

A noise dose of 50% or a TWA of 85 dB is the "action level" at which hearing conservation measures must be implemented. All workers receiving noise doses at or above the action level must be included in a hearing conservation program that requires noise monitoring, audiometric testing, hearing protection, employee training, and record keeping. A baseline audiogram is one taken within six months of the employee's first exposure above the action level, against which subsequent audiograms can be compared. An annual audiogram must be taken for each employee exposed at or above the action level. A *standard threshold shift* (STS) is a change in hearing sensitivity from the baseline audiogram that exceeds an average of 10 dB or more at 2000, 3000, and 4000 Hz in either ear. Appropriate action by the employer must be taken in response to the STS to ensure the continued protection of the hearing of the employee.

Environmental Protection Agency

The EPA published "Information on Levels of Environmental Noise Requisite to Protect Public Health and Welfare with an Adequate Margin of Safety"[1] in 1974 in response to the Noise Control Act of 1972. The objective was to identify levels of environmental noise required to protect the public from adverse health and welfare effects. The levels for noise-induced hearing loss described in this document were based upon reviews and analyses of scientific materials as well as consultations and interpretations of experts. It was concluded that an L_{eq} of 70 dB over a 24-h day (over a 40-year working life) would protect virtually the entire population (96th percentile) for hearing conservation purposes. An $L_{eq(8)}$ limit of 75 dB was considered appropriate protection for the typical 8-h daily work period. This criterion is considered to be very restrictive for most applications, and it has not been incorporated into any DRC for occupational noise exposures.

Air Force

The U.S. Air Force (USAF) hearing conservation criterion is 85 dBA for a maximum allowable 8-h daily exposure. The trading relationship of 3 dB allows such exposures as 16 h at 82 dBA and 4 h at 88 dBA. Higher level continuous exposures for shorter durations, such as 94 dBA for 1 h, are limited to a maximum level of 115 dBA. The ratios of the actual to the allowable daily exposure times are not to exceed unity. Air Force criteria also include limiting conditions for infrasound, ultrasound, and impulse noises.

Army

The U.S. Army (USA) hearing conservation program criterion is 85 dBA as the maximum allowable exposure regardless of duration. Personnel experiencing these exposures must be enrolled in the hearing conservation program. In training and noncombat scenarios single hearing protection will be worn in steady noises of 85–107 dBA and double hearing protection for 108–118 dBA. Protection requirements for unique military noise sources are determined individually. The Army criteria also include limiting exposures for impulsive noises.

Navy

All noise-exposed Navy personnel are required to wear hearing protection when exposed to environmental noise exceeding the criterion of 84 dBA or 140 dB peak, regardless of duration. Personnel are entered into the hearing conservation program based on the 84-dBA damage risk criterion for an 8-h work day, with a 4-dB exchange rate. Double hearing protection is required when sound levels exceed 104 dBA, which administratively assumes 20 dB of single protection from an approved earplug or earmuff.

ISO-1999

The International Organization for Standardization (ISO) standard ISO-1999 (1990), "Acoustics—Determination of Occupational Noise Exposure and Estimation of Noise-Induced Hearing Impairment,"[5] is a landmark document that establishes practical procedures for estimating noise-induced hearing loss in populations. Standard ISO-1999 does not provide a specific formula for assessing risk of hearing handicap, but it specifies uniform methods for the prediction of hearing impairment that can be used for assessment of handicap according to the formula stipulated in a specific nation. The procedures are based on the equal-energy, 3-dB rule (adopted by the ISO and member nations as a conservative criterion) and deal with the measurement and description of noise exposure, the prediction of effects of noise on hearing threshold, and the assessment of risk of noise-induced hearing impairment and handicap. Annexes, which are not part of the standard, provide calculation procedures, examples, tabular data used in the calculations, and a method for relating this information to that of the preceding standard, ISO-1999 (1975). These procedures allow agencies, industries, and governments to select parameters and establish criterion values according to their respective needs. This document will form the basis for legislation in many countries.

The ISO method describes all exposures during an average work day in terms of the A-weighted sound exposure or energy average. The integration period is taken as a working day or a working week. All noises are included in the exposure, ranging from steady state to impulses. Exposures that contain steady tonal noise or impulsive/impact noise are considered about as harmful as the same exposure without these components but about 5 dB higher in level. Exposure can be measured with personal noise dosimeters or an integrating-averaging sound-level meter. Direct and indirect methods for the determination of exposure level are discussed as well as sampling methods.

The only measure of environmental noise needed to calculate hearing impairment or risk of hearing handicap under the following conditions is the energy-averaged daily noise exposure. The maximum instantaneous sound pressure level must be less than 140 dB, the average 8-h daily exposure must not exceed 100 dBA, and the maximum individual daily exposure must not be more than 10 dB above the average of all daily exposures to permit this determination of energy-averaged daily exposure.

Implementation of this standard follows a well-defined series of operations. The first involves determination of the age-related hearing levels of the target population for all test frequencies (e.g., population of 50-year-old males, 90th percentile at 500–6000 Hz). The long-standing difficulties of defining a "normal" population for this purpose were overcome with the utilization of two databases. Database A contains standardized distributions of hearing threshold of an ideal "highly screened" population free from all signs of ear disease, obstructions of wax, and without undue history of noise exposure. Database B can be any carefully collected database covering an *occupationally non-noise-exposed population* considered to be a valid control for the noise-exposed population under consideration. Each user of the standard can select the subpopulation most appropriate for its analysis. As an example, for database B the standard provides the data from the U.S. Public Health Service Surveys reported in 1965.[8]

Next, the predicted NIPTS of the population is calculated for all test frequencies by considering both the number of years of exposure and the average daily noise exposure levels. Data in the standard for calculating NIPTS are valid for frequencies from 500 to 6000 Hz, exposure times of 0–40 years, and average daily noise exposure levels between 75 and 100 dB.

The hearing handicap or risk of hearing handicap may be calculated using the appropriate NIPTS values and a formula selected by the user or a member nation. The document contains nine formulas that are proposed or commonly used among nations for assessing hearing handicap by averaging hearing threshold levels at selected audiometric test frequencies. In the United States, hearing handicap for conversational speech is assessed using the average of the hearing levels at 500, 1000, 2000, and 4000 Hz. Other procedures are available for determining overall percentage of hearing loss for purposes of compensation.

Long-Duration Noise Exposure

Noise exposure durations that exceed 8 h may occur in some work assignments and when substantial nonoccupational noise is added to that received at work. These longer duration exposures are extended by noises from daily living activities, recreation, transportation, proximity to industry, and even other vocational activities. Although the baseline of most criteria is the allowable exposure for an 8-h day, many do extend their time–intensity trading relationship to 16 or 24 h as additional guidance.

Although the 8-h day, 5-day work week is considered standard, numerous variations are employed for many occupations. Some of these are four 10-h days with three days off, three 12-h days with three and four days off, and 12 h on and 12 h off. The noise exposure criteria do not cover these exposures with the same degree of accuracy as with the standard work week. However, it is reasonable to consider the exposure per work week as a basis for calculating noise exposure (i.e., the 3-dB rule).

An important discovery in studies of effects of long-duration exposure to continuous (nonimpulsive) noise of 24 h and longer on human hearing was the phenomenon represented in Fig. 19.2 and called asymptotic threshold shift (ATS).[9] Hearing threshold levels progressively increased with time until the exposure durations reached 8–16 h. Hearing threshold levels reached a plateau or asymptote between 8 and 16 h and did not increase further with continuation of the same exposure levels for 24 and 48 h. Recovery from these asymptotic levels to the preexposure threshold levels was related to exposure time. Even though the asymptotic levels were the same for 24- and 48-h exposures to a particular stimulus, the time needed to recover was significantly longer for the 48- than for the 24-h exposures. The longer period of time to recover is interpreted by

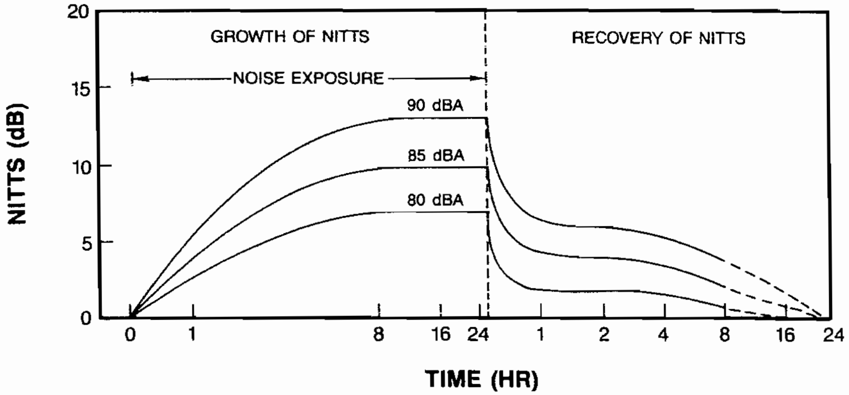

FIGURE 19.2 Growth recovery of noise-induced temporary threshold shift (NITTS) measured during and following the noise exposure at the times marked on the abscissa. The stimulus was a third-octave band of random noise centered on 1000 Hz presented at 80, 85, and 90 dBA. The curves represent the averages of the hearing levels (HLs) for the 1000-, 1500-, and 2000-Hz test frequencies $\frac{1}{3}(\mathrm{HL}_{1000} + \mathrm{HL}_{1500} + \mathrm{HL}_{2000})$.

some as an indication of greater risk to hearing from the same stimulus (same asymptotic threshold level) for 48 than for 24 h. On the basis of analyses of the actual recovery times the guideline was established that the period of time in effective quiet required for recovery should be at least as long as the duration of the exposure.

Audiometric data on the crew members and information on the internal noise levels of the *Voyager* lightweight aircraft (two 110-hp piston engines) during a practice (five days) and a round-the-world flight (nine days) have provided additional important data points. The overall noise environments at the crew locations ranged between 99 and 103 dBA. Crew members wore communications headset and earplug equipments that allowed estimations of the exposures at the ears to be between 84 and 95 dB for the octave band at 500 Hz. Comparisons of preflight and postflight audiograms for both flights revealed substantial shifts of hearing levels. The threshold shifts from the nine-day flight were no greater than those for the five-day flight. One week following the nine-day flight the hearing thresholds of both crew members had returned to their preflight levels.

The hearing level data on the five- and nine-day exposures is consistent with laboratory data derived from both human studies of shorter duration and animal studies of similar duration. It is considered acceptable by some criteria to extend the 8-h limits to as much as 24 h using appropriate trading relationships. Noise exposures of atypical work schedules such as four 10-h days with three days off and 12 h on, 12 h off might be calculated on the bases of work week. Although recovery of the hearing thresholds occurred prior to nine days for these crew members, it remains reasonable to have personnel remain in effective quiet for a period at least as long as the exposure prior to reentering the noise.

Music Exposure Criteria

The USAF has adopted music exposure criteria that consider customers or clients of military "clubs" to be "recreationally exposed" and employees to be "occupationally exposed." The occupationally exposed persons are governed by the same provisions as those of workers exposed in any other occupational noise. A separate set of criteria are used to control or limit the recreational exposures.

An average A-weighted sound level of 94 dB is considered acceptable when it does not exceed 2 h duration once a week. It is important to recognize that the 94-dBA guideline is not a peak of a maximum level value but is the average sound level. The average sound-level concept does not specify a fixed maximum level or eliminate crescendos and special effects or even some selections. It does permit these intermittent high levels of entertainment music to be averages in such a way that the overall performance is acceptable.

19.4 IMPULSE NOISE

Impulse or impact noise is a very brief sound or short burst of acoustical energy with a sound pressure rise of 40 dB in 0.5 s or faster that may occur singly or as a series of events. The noise may be treated as steady state when the repetition rate of a series of impulses exceeds 10 per second and the decay from the individual peaks to minima does not exceed 6 dB.

The effects on the auditory system have been examined for such characteristics of the impulsive stimulus as frequency spectrum, duration, peak pressure level, total energy, type of impulse, and rise time. Although work continues with some of these characteristics, present exposure criteria use only peak pressure level and duration and type of impulse to describe safe impulse exposures.

In 1968, CHABA developed exposure criteria for impulse noise[10] based on extensive work in the United Kingdom on firing small arms.[11] The limiting noise exposure values for the impulsive stimuli are summarized in Fig. 19.3. These criteria define exposures that should produce, on average, no more NITTS than 10 dB at 1000 Hz, 15 dB at 2000 Hz, and 20 dB at 3000 Hz and above in 95% of the exposed ears. The criteria provide for adjustments or corrections for exposure situations that vary from the basic condition. The criteria provide for a daily exposure of 100 impulses during any time period ranging from about 4 min to several hours. The values are increased for fewer and decreased for more than 100 impulses per day by a factor of 1.5 dB for each doubling or halving of the number of impulses. The allowable level must be decreased by 5 dB for impulses that strike the ear at perpendicular incidence.

Simple, nonreverberating impulses that occur in open spaces are evaluated using the A-duration or pressure wave duration, which is the time required for the initial or principal wave to reach peak pressure level and return momentarily to zero (Fig. 19.3). The B-duration or pressure envelope duration is used for impulses that occur under various reverberant conditions and is the total time that the envelope of the pressure fluctuations (positive and negative) is within 20 dB

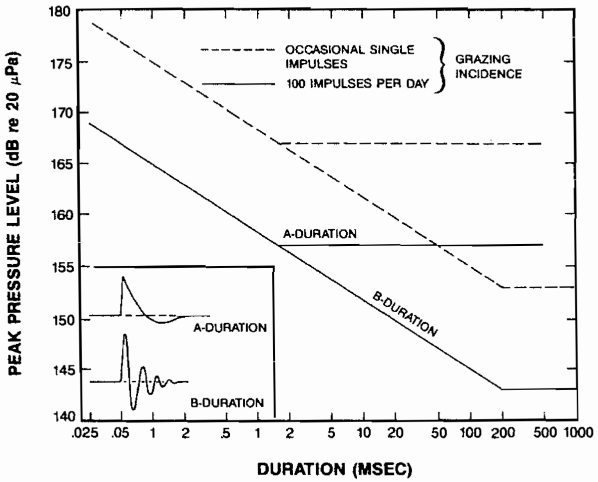

FIGURE 19.3 Proposed damage risk criteria for impulse noise arriving from the front or from behind (grazing incidence) exposed persons. The *A*-duration curve reflects the simple, nonfluctuating impulse that occurs in open areas. The *B*-duration curve reflects the pressure fluctuations of impulses that occur under various reverberant conditions.

of the peak pressure level, including reflected waves. The 143-dB floor of the B-duration curve represents the reduction of the energy entering the ear after 200 ms by action of the acoustic reflex (reflex contraction of the middle-ear muscles that reduces the transmission of energy to the inner ear). This comprehensive dose–response curve (DRC) for impulses continues to represent the present data and scientific understanding of impulse noise effects on hearing.

The OSHA amendment, the Air Force, and the Army, all limit exposure to impulse or impact noises to 140 dB peak sound pressure level. The Army has unique equipment that generates high-level impulse noises that are measured and treated individually.

Sonic booms do not constitute a threat of noise-induced hearing loss for human beings. Most of the energy in sonic booms generated by aircraft in supersonic flight is in the low and infrasonic frequency ranges and contributes little to the A-weighted sound level. Field and laboratory investigations with human exposures have revealed no significant effects on hearing from sonic booms at levels typically experienced in the community. One field study involving human exposures to extremely intense sonic booms ranging in level from about 50 to 144 lb/ft^2 observed no changes in the hearing levels of the participants.[12] Naturally, such intense sonic booms may generate higher A-weighted levels indoors than outdoors due to rattling of windows and doors.

Air bag systems are designed to provide crash protection of occupants during side and forward impacts of motor vehicles. These systems generate a loud, impulse noise inside the vehicle upon inflation of the air cushion. In an early study[13] of a prototype system, 91 volunteers experienced this air bag deployment inside a small automobile at a median peak pressure level of 168 dB. Some TTS was experienced by about 50% of the subjects. About 95% of those with TTS recovered preexposure hearing levels on the same day. About 5% required longer times for recovery with one subject showing a gradually returning shift at one frequency that persisted for several months.

19.5 INFRASOUND

Relationships among human exposures to infrasound (0.5–20 Hz) and resulting hearing loss are presently not sufficiently understood for the establishment of national (U.S.) or international standards on exposure limits. Few investigations have been conducted because of difficulties in measuring hearing thresholds for infrasound and in producing infrasound stimuli free from audible overtones that are required for exposure studies. Tentative criteria have been established on the basis of laboratory investigations and field experiences with noises containing intense infrasound components. These criteria have been incorporated in some Department of Defense regulations on hazardous noise exposure.[14]

Human whole-body vibration exposures in intense levels of infrasound that exceeded 150 dB sound pressure level were reported in a classic study.[15] The sample size was small. However, the subjects were highly experienced professionals. Relationships were observed between exposure levels and human tolerance as a function of subjective "symptoms." These symptoms are described in Section 19.8 for airborne vibration. Certain exposures were judged to be very close to tolerance limits. Hearing levels of the subjects were measured 3 min following termination of these very intense exposures and no changes were found in hearing sensitivity.

The absence of hearing sensitivity effects immediately following the intense infrasound exposures verifies laboratory findings that infrasound is not a major threat to hearing. The exposure criteria in Fig. 19.4 have been developed on the basis of data such as that in the cited report and that presented in Fig. 19.5.[16] Numerous experimental subjects experienced exposures to 10 Hz at 144 dB for 8 min with no adverse effects. This set of safe exposure conditions was accepted as a baseline exposure from which 8-h limits (136 dB at 1 Hz and 123 dB at 20 Hz) and 24-h limits (130 dB at 1 Hz and 118 dB at 20 Hz) were extrapolated. (Development of this sound pressure level formulation is described in ref. 16.)

19.6 ULTRASOUND

Ultrasound (~16–40 kHz) is widespread in our society due to sources such as ultrasonic cleaners, measuring devices, drilling and welding processes, animal repellants, alarm systems, and communications control applications as well as a wide range of medical applications. Although the number of people exposed to

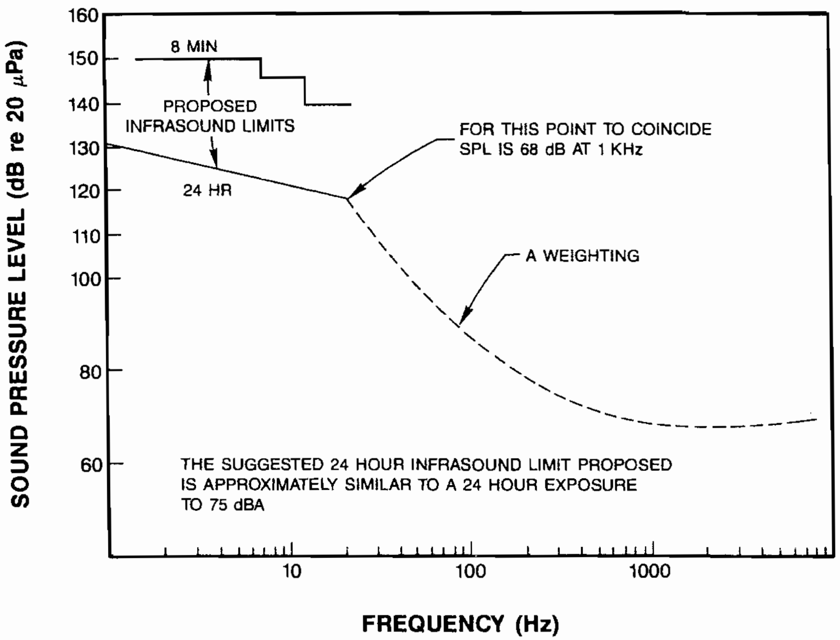

FIGURE 19.4 Infrasound 8-min and 24-h exposure limits.

ultrasound is large, it poses no threat to human hearing because neither temporary nor permanent hearing loss caused by ultrasound has been reported, with one exception. Temporary threshold shift was reported following experimental exposures to discrete tones in the region of 17–37 kHz at levels of 148–154 dB. The TTS occurred at subharmonics of the stimulus frequency and was likely caused by nonlinear distortion of the eardrum.

Nevertheless, ultrasound continues to be viewed as a threat to hearing as well as a cause of other subjective symptoms. Ultrasound is readily absorbed by air and its intensity diminishes rapidly with increasing distance from the source. The impedance match with human flesh is poor, and much energy is reflected away from the surface of the body. Consequently, the ear is the primary channel for transmitting airborne ultrasound to the internal systems.

Ultrasonic energy at frequencies above about 17 kHz and at levels in excess of about 70 dB may produce adverse subjective effects experienced as fullness in the ear, tinnitus, fatigue, headache, and malaise. These subjective effects are mediated through the hearing mechanism and are related to hearing ability. Persons who do not hear in this frequency region do not experience these subjective symptoms. Women experience the symptoms more often than men, and younger individuals report them more often than older ones. This reporting is consistent with the relative hearing abilities of the three groups. Neither disorientation nor loss of balance has been attributed to ordinary exposures to ultrasound.

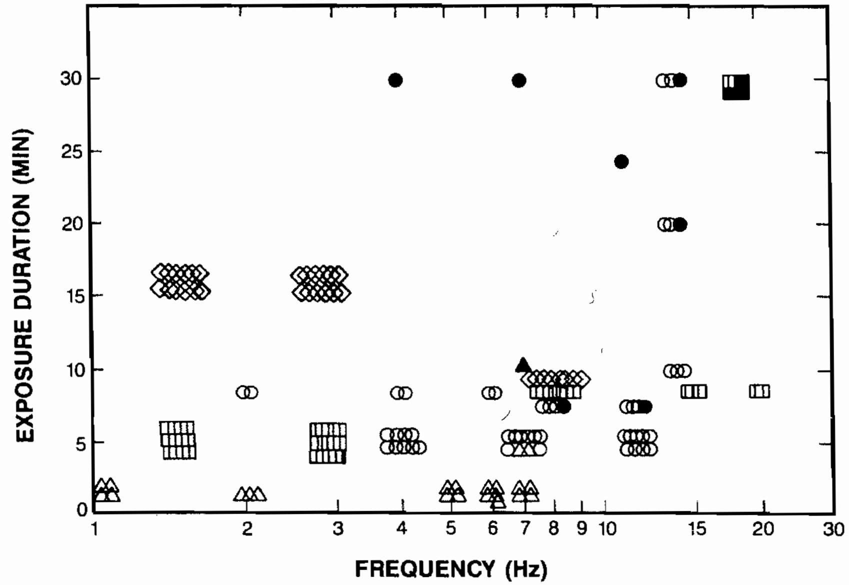

FIGURE 19.5 Infrasound exposure effects on hearing. Exposure levels (filled symbols indicate that some TTS has occurred): (△) > 150 dB; (○) 140–149 dB; (□) 130–139 dB; (◇) 120–129 dB.

Ultrasound exposures usually contain various amounts of high audio frequency energy (5–20 kHz). Subjective effects attributed to the ultrasound are usually caused by the audio frequency energy. Reducing the level of the audio frequency energy in the exposure usually results in the disappearance of the auditory and subjective symptoms.

Criteria for limiting the levels of ultrasound to control auditory and subjective effects are very similar. The data refer to the ultrasound levels at the head of the exposed person. The limiting levels at 20 kHz and above apply to protection from the subjective symptoms described earlier. Representative international and national criteria adopted by the World Health Organization (WHO), Norway, Sweden, and the American Conference of Governmental Industrial Hygienists (ACGIH) are displayed in Fig. 19.6. Norway accepts a level of 120 dB for frequencies higher that 22 kHz.

19.7 HEARING PROTECTION

The damage risk or noise exposure criteria presented above define allowable exposures for unprotected ears. These criteria are also used to identify exposure conditions above which personnel should be included in hearing conservation programs and where hearing protection should be worn. Hearing protection extends

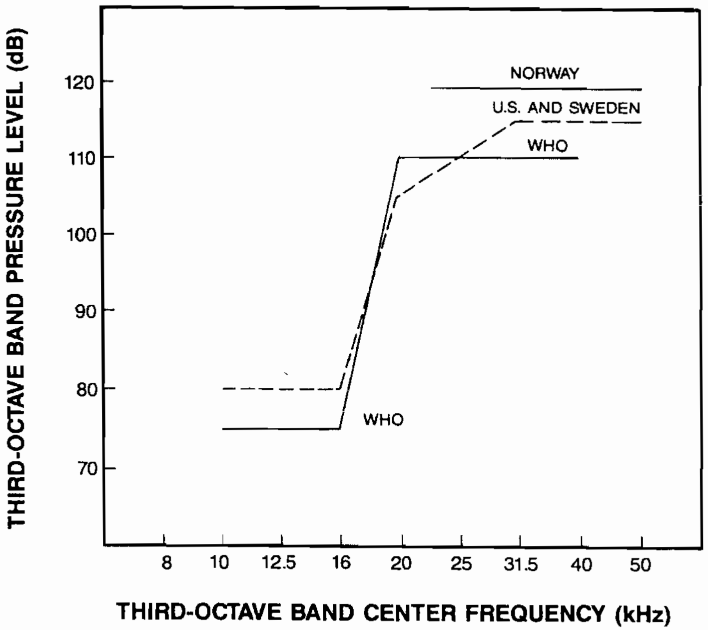

FIGURE 19.6 International and national criteria for exposure to airborne ultrasound.

the limits of allowable exposures by reducing the levels at the ear, allowing personnel to experience more intense and longer duration exposures than with unprotected ears and still remain within established whole-body exposure criteria.

Hearing protector performance is influenced by characteristics of the wearer, the protective device, and the noise exposure. Protection is best with devices that provide good attenuation, are comfortable, fit properly, are easy to use, are in a good state of repair, and are worn. Hearing protector effectiveness is reduced by air leaks, transmission properties of the materials, and noise-induced motion of the device that produces sound under the protector. A limit on performance of ideal devices is imposed by the sound conduction properties of the tissue and bone of the head. In high-level acoustical fields, sound travels "around" the protector to the inner ear through the tissue and bone of the head. The level of the sound reaching the ear by such means is about 50 dB below that of air conduction reaching the ear through an open ear canal. Bone-conducted sound is not a major concern for most noise environments. Total-head enclosures extend the tissue and bone limits by about 10 dB.

Infrasound

Good insert-type hearing protection devices should provide attenuation of infrasound approaching that observed at the 125-Hz third-octave band. Earmuff hearing protectors provide very little protection and may even amplify the sound at some of these infrasonic frequencies. Exposures to levels of infrasound above 150 dB should be avoided even with maximal hearing protection because of possible adverse nonauditory effects.

Audio Frequency Region

Hearing protection performance varies as a function of the frequency spectrum of the noise. In general, conventional earplugs and earmuffs provide good sound protection at higher frequencies (above 1000 Hz). Earplugs provide effective protection at both high and low frequencies. Ample protection is observed across all frequencies with certain foam insert earplugs. Earmuffs provide poor attenuation at the low frequencies.

A combination of earplug and earmuff is required when an individual protector is unable to reduce a noise to an acceptable level. The resulting attenuation is not the sum of the two protectors but an amount determined by the particular combination of devices. The attenuation of the combined units often reaches the bone conduction limits at the high frequencies. At the mid- and lower frequencies the amount of attenuation is determined primarily by the earplug. Selection of a good earplug for use with a muff will provide good double hearing protection at all frequencies.

Special earmuff hearing protectors called nonlinear devices allow face-to-face speech communication at low levels of noise and provide typical amounts of earmuff protection at high levels. Active noise reduction (ANR) earmuffs employ electronic (noise cancellation) and acoustical means of reducing low-frequency noise at the ears. This active earmuff can increase intelligibility and comfort and reportedly reduce fatigue when used with speech communication systems in noise. The ANR earmuffs are widely used in such areas as communications, private aircraft, entertainment, and sport activities and by passengers in commercial aircraft.

Hearing protection devices have the potential capability to reduce and eliminate most noise-induced hearing loss. However, issues such as comfort, selection, fit, training, use, motivation, and others limit the full-performance capability of the devices to be realized in the workplace.

Long-Duration Exposures

Long-duration noise exposures are typically steady state, continuous, and generally within the audio frequency range. The information on hearing protection for audio frequencies is also appropriate for long-duration noises.

Ultrasound

Conventional hearing protection devices, earplugs and earmuffs, provide good protection against airborne ultrasound at frequencies above about 20,000 Hz.

Attenuation exceeding 30 dB is generally provided for frequencies from about 10,000 to 20,000 Hz. Hearing protection is most effective in eliminating subjective symptoms that occur when protectors are not worn. Reduction and elimination of subjective symptoms is also a good indication of the effectiveness of the hearing protector.

Impulses

Earmuff and earplug protectors should provide adequate attenuation for impulses comprised primarily of high-frequency energy, such as small-arms fire. Earmuff attenuation decreases as the concentration of energy in the impulses moves to the lower frequencies, as with large-caliber weapons (the attenuation vs. frequency of the protectors is not changing, only the spectral distribution of the impulse is different). The reduction of the peak sound pressure level of a particular earmuff is about 30 dB for pistol fire, about 18 dB for rifle fire, and as little as 5 dB for cannon fire. The peak level of the impulses of most pistol and standard rifle shots is reduced to less than 140 dB by good earmuffs. A combination of earplugs and earmuffs should be used for impulses requiring good low-frequency attenuation.

The USAF and the USA require single hearing protection when impulses reach 140 dB peak positive pressure and double hearing protection when the levels reach 160 dB (USAF) and 165 dB (USA).

19.8 HUMAN VIBRATION RESPONSE

The human body is a dynamic system, possessing mass and the ability to achieve relative motion between parts of the body (elasticity). It can therefore be affected by exposure to oscillatory motion or vibration. Although the ear is the most sensitive body organ for the reception of vibratory energy in the auditory frequency range, structure-borne and airborne vibration occurring at lower frequencies can be transmitted to a variety of anatomical structures, including skin, bone, muscles, joints, and internal organs. Most of our population is exposed to occasionally moderate levels of vibration with relatively harmless effects. Occupational exposures to vibration are more severe than nonoccupational exposures and have been associated with biological, psychological, and human performance effects.

Vibration is transmitted to the human body via the oscillatory motion from vibrating structures in contact with the body surface (structure borne) or via the transmission of sound pressure waves in high-noise environments (airborne). In structure-borne whole-body vibration, oscillatory motions enter the body usually at the feet (standing) or buttocks (sitting) at the supporting surface and can be transmitted throughout the body to other anatomical structures (such as the head).[17] The major sources of nonoccupational whole-body exposures include transportation vehicles such as automobiles, buses, trains, airplanes, and boats. Whole-body occupational vibration is experienced by operators of agricultural and forestry tractors, earth-moving and construction equipment, all types of trucks, sea-going ships, airplanes and helicopters, as well as mining and factory workers on vibrating platforms. Structure-borne hand-transmitted vibration is isolated to a very specific anatomical region, primarily through the operation of vibrating hand tools such as jackhammers, chipping hammers, chain saws, grinders, and other types of pneumatic or electric hand-held devices. In airborne whole-body vibration, oscillatory motions enter the body via high levels of low-frequency sound pressure waves. Substantial airborne vibration occurs during aircraft engine run-ups and ground-based maneuvering, particularly in military environments where ground crews are required to work close to powerful aircraft in restrictive areas.

The absorption of vibratory energy by the body is determined by the body's characteristics as a mechanical system.[18] Engineering techniques (transfer function, power absorption) have been used and continue to be improved for defining these characteristics and for developing various models of the whole body and its subsystems (such as the hand–arm). These methods and models give insight into the energy transmission through the body and are useful tools for identifying the overall sensitivity of the body as well as for explaining the various effects on specific target organs and structures.

Whole-Body Vibration Effects

For whole-body vibration, the mechanical stresses imposed on the body can potentially lead to interference with bodily functions and tissue damage in practically all parts of the body. Historically, the major concern has focused on whole-body vertical vibration. More recent research includes multiaxis vibration effects. Figure 19.7 illustrates the short-time, 1-min, and 3-min tolerance limits reported by healthy adult male subjects exposed to vertical sinusoidal vibration.[19] Human tolerance to vibration tends to decrease with longer exposure periods. While acute exposures in the vicinity of human tolerance have not resulted in demonstrable harm or injury, prolonged and repeated exposures to these levels are considered to have a high potential for producing bodily damage. For vertical vibration, minimal tolerance occurs between 4 and 8 Hz.[19] This frequency range coincides with the major whole-body resonance observed in biodynamic data. Most physiologic effects in the region of 2–12 Hz are associated with excessive movement of the thoraco-abdominal viscera that can interfere with respiration and cause changes in cardiovascular functions that typically resemble the response to exercise.[20] Prolonged and repeated (chronic) occupational exposures, as they occur in drivers of tractors and earth-moving equipment, are implicated by many investigations in the development of spinal column and other joint disorders and pathologies and of stomach and duodenal diseases.[21,22] However, their causal relationship with vibration stress has not been clearly proven. For example, back pain and back disorders have been reported for other occupations with no vibration. These symptoms have also been associated with poor body posture. Studies, including the early study by Coermann,[23] have shown that body posture can affect whole-body vibration response.

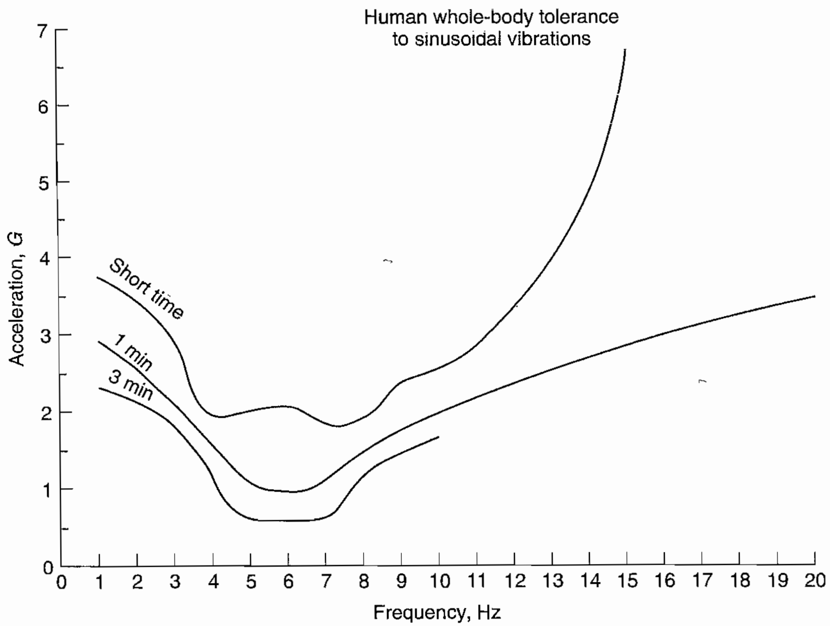

FIGURE 19.7 The short-time, 1-min, and 3-min tolerance limits reported during vertical sinusoidal vibration.[19]

Whole-body vibration can also influence working performance. It can cause involuntary body motions that interfere with the active motor control of the operator with undesirable effects. Relative motion of the eye with respect to an object or target can cause difficulty in reading instruments and performing visual searches.[24] This is particularly a concern at low frequencies where there is a high propensity for head movement in the region of whole-body resonance (below 10 Hz). Below about 20 Hz, compensatory eye movement aids in stabilizing the line of sight to a stationary object during head vibration.[25] When the image moves with the head, as occurs with a helmet-mounted display, compensatory eye movement becomes ineffective, increasing the potential for visual blurring.[26] Eye resonance has been reported to occur in a broad frequency range between 20 and 70 Hz.[25] Relatively high levels of whole-body vibration or direct contact of the head with the vibrating structure are necessary to induce visual blurring due to the body's damping effect at these higher frequencies.

With regard to airborne vibration, the mismatch between the acoustical impedance of air and the human body surfaces prevents significant amounts of acoustical energy from entering the body, particularly at higher frequencies.[27] With decreasing frequencies below 1000 Hz, more acoustical energy is absorbed in the form of transverse shear waves. With exposure to high-intensity noise levels [120 dB sound pressure level (SPL)] between 100 and 1000 Hz, tissue vibration

occurs and the noise is felt via the stimulation of somatic mechanoreceptors.[28] Below 100 Hz, intense noise can cause whole-body vibration that not only affects motion in the chest, abdominal wall, viscera, limbs, and head but also can generate motions in the body cavities and air-filled or gas-filled spaces.[28] Von Gierke and Nixon[27] reported that resonance of the chest wall and air-filled lungs occurs around 60 Hz. For noise exposures below 150 dB, the most common symptom reported by subjects was mild to moderate chest vibration.[15] Above 150 dB, symptoms included mild nausea, giddiness, subcostal discomfort, cutaneous flushing and tingling (around 100 Hz, 153 dB); coughing, severe substernal pressure, choking respiration, salivation, pain on swallowing, hypopharyngeal discomfort, and giddiness (60 Hz, 154 dB and 73 Hz, 150 dB); and headache (50 Hz, 153 dB).[15] More recent efforts have been made to measure the biodynamic response of the body to airborne vibration and compare the body acceleration spectra to the noise spectra.[29] The preliminary results for exposures to jet aircraft noise during engine run-ups confirm the upper torso resonance reported by von Gierke and Nixon.[27]

Hand-Transmitted Vibration Effects

Hand–arm vibration syndrome (HAVS) refers to the "complex of peripheral vascular, neurological, and musculoskeletal disorders associated with exposure to hand-transmitted vibration" (ref. 30, p. 11). HAVS is recognized worldwide as a health concern. Prolonged and repeated exposure to hand-transmitted vibration can lead to a very specific disease called vibration-induced white finger (VWF), or Raynaud's phenomenon. This impairment of the blood circulation of the hand progresses with exposure time from intermittent numbness and tingling in selected fingers to extensive blanching of most fingers, first only in combination with cold and finally at all environmental temperatures. In the final stages the disease interferes severely with social activities and continuation of the occupation. According to Taylor and Pelmear,[31] the clinical manifestations of the finger-blanching attacks progress in four stages, with stage 1 signaling the onset of the disease, mainly outdoors in winter. While symptoms of the first stages might still be reversible if vibration exposure is discontinued, the later stages are considered irreversible by most researchers. In later stages, the vascular manifestations are reported to be accompanied by nerve, bone, joint, and muscle involvement.[32] Studies have shown that HAVS, specifically VWF, is influenced by several factors, including the frequency, magnitude, and duration of the exposure, in addition to the type of tool. As with whole-body vibration, the symptoms of VWF appear to increase with exposure duration.

19.9 HUMAN VIBRATION EXPOSURE GUIDELINES

Extensive research over the last four decades has led to a reasonable understanding of the potential pathological and physiological effects of structure-borne whole-body as well as hand-transmitted vibration, although the mechanisms of these effects continue to be topics of research. Frequency-dependent sensitivity curves have been derived for the whole-body and for the hand–arm from both subjective and objective frequency response characteristics. These sensitivity curves form the basis for current whole-body and hand-transmitted vibration standards. There are major national and international standards that provide guidelines and recommended criteria for safe vibration exposure based on these curves and that are generally relied upon in designing vehicles, equipment, tools, and mitigation strategies for use in vibration environments. These standards are periodically revised as vibration research continues and new data become available.

Structure-Borne Whole-Body Vibration Criteria

The International Organization for Standardization (ISO) is the most widely recognized body for providing the basic guidelines for assessing the damage risk of structure-borne whole-body vibration (ISO 2631). As of 2004, the standard entitled "Mechanical Vibration and Shock—Evaluation of Human Exposure to Whole-Body Vibration" included three parts: ISO 2631-1:1997,[33] ISO 2631-2:2003,[34] ISO 2631-4:2001,[35] and ISO 2631-5:2004.[36] Part 1, entitled "General Requirements," describes the general methods for measuring whole-body vibration. Informative annexes are included that give guidance on possible effects of vibration on comfort, perception, health, and motion sickness based on current knowledge in these areas. In 2002, the American National Standards Institute (ANSI) accepted the ISO 2631-1:1997 as a nationally adopted international standard (ANSI S3.18–2002),[37] replacing the long-standing 1979 version. For whole-body vibration, the frequency range considered is 0.5–80 Hz although the range from 1 to 80 Hz can be used if appropriate. When the vibration is transmitted by a resilient structure, such as a seat cushion, a suitably shaped transducer support is interposed between the person and that structure. The standard recommends the collection of acceleration data between the body and three supporting surfaces for the seated occupant, including the seat pan or surface, seat back, and feet. For the recumbent occupant, the supporting surfaces include the pelvis, back, and head. Translational vibrations are typically measured in the three axes defined by an orthogonal coordinate system. For standing, seated, and recumbent whole-body vibration, the x axis is defined in the back-to-chest (fore-and-aft) direction, the y axis for the side-to-side (lateral) direction, and the z axis for the foot- (or buttocks-) to-head (vertical) directions.[33] Rotational vibration may also be measured or estimated. There are three primary frequency-weighting curves (including motion sickness) and three additional frequency-weighting curves that are applied to the acceleration–time histories or frequency response spectra depending on the measurement site and the particular effect being assessed. Figure 19.8 illustrates the two primary frequency weightings that reflect the sensitivity of the body in the respective directions.

The overall weighted root-mean-square (rms) acceleration is determined in the time or frequency domain in each axis. The assessment is made based on

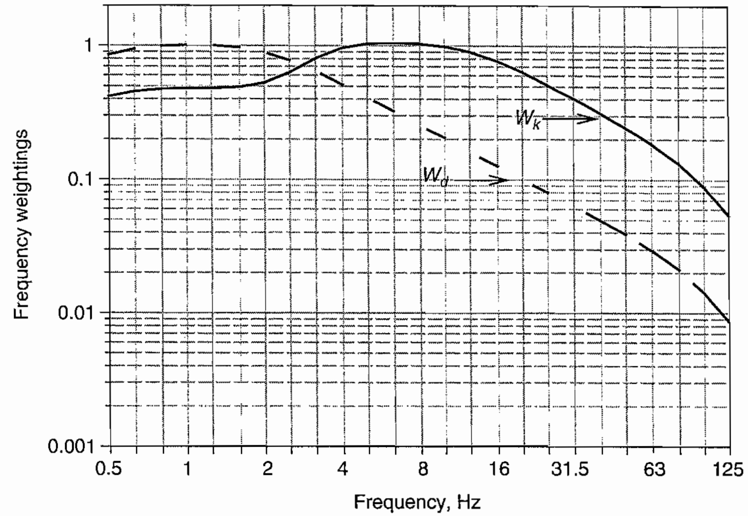

FIGURE 19.8 ISO 2631-1:1997[33] frequency-weighting curves for whole-body vibration in the horizontal (W_d) and vertical (W_k) directions. (Redrawn with permission. Copyright by the International Organization for Standardization. Standard can be obtained from any member body or directly from the ISO Central Secretariat, ISO, Casepostal 56, 1211 Geneva 20, Switzerland.)

the highest weighted acceleration level. If vibration in two or more directions is comparable, then additional direction-dependent multiplying factors are applied and the vibration total value (VTV) or vector sum is calculated.

Other methods are also described, including the running rms method and fourth-power vibration dose method (using the vibration dose value, or VDV). The VDV is more sensitive to peaks in the exposure. Figure 19.9 depicts the Health Guidance Caution Zones provided in the ISO 2631-1:1997 and ANSI S3.18–2002. These guidance zones apply to the overall weighted accelerations determined at the seat pan in the three translational directions. In the figure, the zones defined by the solid lines are applicable to the rms acceleration level. The zones defined by the dotted lines are applicable to the fourth-power vibration dose method. Below the zones, health effects have not been clearly documented or observed. Within the zones, caution is indicated for potential health risks. Above the zones, health risks are likely.[33]

For estimating the effects of structure-borne whole-body vibration on comfort and perception, rotational frequency weightings and multiplying factors are included for the seated occupant.[33] The VTV is recommended for assessing comfort. The standard ISO 2631-1:1997 provides six comfort reactions to vibration and the associated overall weighted acceleration levels ranging from "not uncomfortable" to "extremely uncomfortable." These reactions have no time dependency.

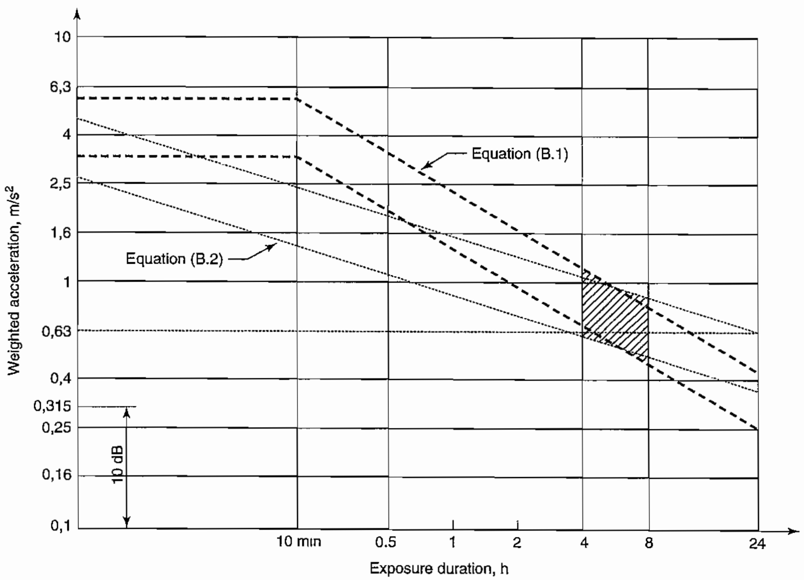

FIGURE 19.9 ISO 2631-1:1997 Health Guidance Caution Zones.[33] Equations (B.1) and (B.2) are defined in the standard. (Reprinted with permission. Copyright by the International Organization for Standardization. Standard can be obtained from any member body or directly from ISO Central Secretariat, ISO, Casepostal 56, 1211 Geneva 20, Switzerland.)

Guidelines on motion sickness are primarily applicable to ships and other sea vessels. The weighted rms acceleration is determined between 0.1 and 0.5 Hz in the vertical direction at the supporting surface. Two methods are given for calculating the motion sickness dose value ($MSDV_z$). An approximation of the percentage of individuals who may vomit is given by $K_m(MSDV_z)$, where $K_m = \frac{1}{3}$ for a population of unadapted male and female adults.[33]

The standard ISO 2631-2:2003, entitled "Part 2: Vibration in Buildings (1 Hz to 80 Hz)," is directed toward human exposure in buildings with respect to comfort and annoyance. A single frequency weighting, W_m, is defined that is related to the combined-response rating curve used in the older 1989 edition. The general guidelines for measuring the vibration are similar to those given in ISO 2631-1:1997. The vibration is measured in the three orthogonal axes with the directions relating to the structure and defined for the standing individual (Part 1). The measurements are made at a location where the highest frequency-weighted vibration occurs. Categories of sources are provided and include (a) continuous or semicontinuous processes (e.g., industry), (b) permanent intermittent activities (e.g., traffic), and (c) limited duration (nonpermanent activities, e.g., construction). The 2003 standard does not include acceptable levels of vibration. The consensus of opinion is that sufficient information was not available at the time for

establishing appropriate vibration levels given the complexity of human response to building vibration. The standard does indicate that adverse comments about residential building vibration may occur when the magnitudes or levels are only slightly higher than the perception levels (ISO 2631-1:1997, Annex C).[33] Other complaints may be due to secondary effects such as reradiated noise (ISO 2631-2:2003, Annex B).[34] There should be no reason to consult the Health Guidance Caution Zones in ISO 2631-1:1997, Annex B, except in an extremely rare building vibration environment.

The standard ISO 2631-5:2001,[36] entitled "Part 5: Method for Evaluation of Vibration Containing Multiple Shocks," directs attention to the health of the lumbar spine. Exposures to multiple shocks may occur in the operation of equipment and vehicles over rough terrain or rough seas. A biomechanical model is used to predict the response of the human spine to a given input and to generate an acceleration dose. The standard provides guidelines on using the acceleration dose to assess the health effects of multiple shocks based on the probability of an adverse health effect that depends on the relationship between the ultimate strength of the lumbar spine, the age of the person, and the number of years of exposure.

Airborne Whole-Body Vibration Criteria

Current guidelines for airborne vibration are given in terms of the noise exposure. The Air Force Occupational, Safety, and Health Standard AFOSHSTD 48-19[14] recommends that, for minimizing whole-body vibration effects, no octave- or one-third-octave-band noise level exceed 145 dB for frequencies in the range of 1–40,000 Hz and that the overall A-weighted sound pressure level be below 150 dBA with no time limits. The ACGIH[38] recommends that one-third-octave-band levels between 1 and 80 Hz should not exceed 145 dB, and the overall unweighted SPL should not exceed 150 dB. The assessment of airborne vibration exposure may differ depending on which guideline is used. Minimal research has been conducted on the physiological and pathological effects that may be associated with airborne vibration.

Hand-Transmitted Vibration Criteria

The ISO provides basic guidelines for assessing hand-transmitted vibration in ISO 5349, "Mechanical Vibration—Measurement and Evaluation of Human Exposure to Hand-Transmitted Vibration." The standard consists of two parts: Part 1: General Requirements (ISO 5349-1:2001)[30] and Part 2: Practical Guidance for Measurement at the Workplace (ISO 5349-2:2001).[39] For hand-transmitted vibration, the center of the coordinate system is the head of the third metacarpal with the z axis defined as the longitudinal axis of the third metacarpal, the y axis in the general direction of the tool handle (basicentric coordinate system), and the x axis passing from the top to the bottom of the hand. Figure 19.10 illustrates the frequency weightings or factors associated with the center frequencies of one-third-octave bands for assessing the effects of hand-transmitted vibration.

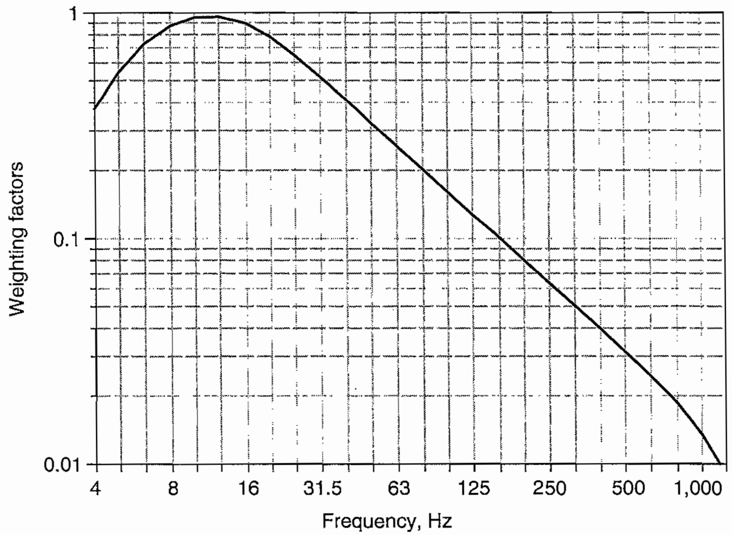

FIGURE 19.10 ISO 5349-1:2001 Frequency-weighting curve W_h for hand-transmitted vibration.[33] (Redrawn with permission. Copyright by the International Organization for Standardization. Standard can be obtained from any member body or directly from the ISO Central Secretariat, ISO, Casepostal 56, 1211 Geneva 20, Switzerland.)

The quantity used to assess health effects is the 8-hr energy-equivalent vibration total value [$A(8)$], or daily vibration exposure. It is assumed that the health risk for hand-transmitted vibration applies to all three orthogonal directions. Therefore, the same weighting curve (Fig. 19.10) is applied to vibration in each of the three orthogonal axes. The vector sum of the overall weighted accelerations estimated for each axis defines the vibration total value (a_{hv}). Figure 19.11 depicts the daily exposure values [$A(8)$] expected to produce vibration-induced white finger in 10% of persons exposed for a given number of years, D_y. The standard ISO 5349-2:2001[39] provides additional guidelines for measuring hand-transmitted vibration in the workplace, determining the daily vibration exposure, and selecting appropriate operations. The measurement of vibration entering the hand may not always be practical. Part 2 includes practical measurement locations for selected power tool types and summarizes the location of accelerometers used in vibration-type test standards for a variety of power tools. These locations are usually close to the hand.

Additional Exposure Standards and Guidelines

Other organizations and countries have generated standards and guidelines that compliment, supplement, or even differ from the human vibration standards described above, particularly the ISO 2631-1:1997. The ACGIH[38] provides guidelines for whole-body as well as hand-transmitted vibration. The European Union

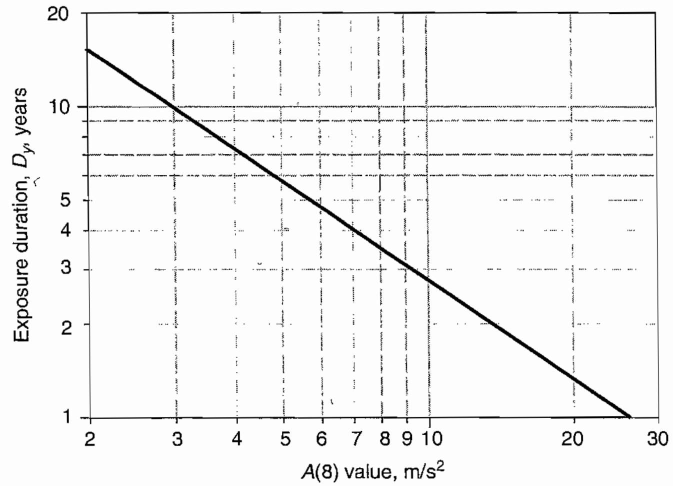

FIGURE 19.11 Vibration exposure for predicted 10% prevalence of vibration-induced white finger in a group of exposed persons. (Redrawn from ISO 5349-1:2001[30] with permission. Copyright by the International Organization for Standardization. Standard can be obtained from any member body or directly from the ISO Central Secretariat, ISO, Casepostal 56, 1211 Geneva 20, Switzerland.)

has recently published a directive on health and safety requirements for exposure to both whole-body and hand-transmitted vibration. It is important that designers and assessors understand the similarities and differences among the various standards and the appropriateness of their applicability. It is also critical to use current editions of these standards since new information could have significant influences on defining health risk.

REFERENCES

1. U.S. Environmental Protection Agency (EPA), "Information on Levels of Environmental Noise Requisite to Protect Public Health and Welfare with an Adequate Margin of Safety," Report No. 550/9-74004, EPA, Washington, DC, March 1974.
2. H. E. Von Gierke, D. Robinson, and S. J. Karmy, "Results of the Workshop on Impulse Noise and Auditory Hazard," ISVR Memorandum 618, Institute of Sound and Vibration Research, Southampton, United Kingdom, October 1981. Also *J. Sound Vib.*, **83**, 579–584 (1982).
3. J. Tonndorf, H. E. Von Gierke, and W. D. Ward, "Criteria for Noise and Vibration Exposure," in C. M. Harris (Ed.), *Handbook of Noise Control*, 2nd ed., McGraw-Hill, New York, 1979.
4. C. W. Nixon, "Excessive Noise Exposure," in S. Singh (Ed.), *Measurement Procedures in Speech, Hearing, and Language*, University Park Press, Baltimore, MD, 1975.

5. International Organization for Standardization (ISO), "Acoustics—Determination of Occupational Noise Exposure and Estimation of Noise-Induced Hearing Impairment," ISO 1999.2, ISO, Geneva, Switzerland, 1990.
6. K. D. Kryter et al., "Hazardous Exposure to Intermittent and Steady-State Noise," paper presented before the NAS-NRC Committee on Hearing, Bioacoustics, and Biomechanics, WG 46, Washington, DC, 1965.
7. Occupational Safety and Health Administration, "Occupational Noise Exposure; Hearing Conservation Amendment," *Fed. Reg.*, **48**(46), 9738–9785 (1983).
8. National Center for Health Statistics, "Hearing Levels of Adults by Age and Sex," Vital Statistics, Public Health Service Publication No. 1000, Series-11-No. 11, U.S. Government Printing Office, Washington, DC, 1965.
9. M. R. Stephenson, C. W. Nixon, and D. L. Johnson, "Long Duration (24–48 Hours) Exposure to Continuous and Intermittent Noise," Joint EPA/USAF Report, AFAMRL Technical Report No. 82–92, Wright Patterson AFB, OH, 1982.
10. W. D. Ward et al., "Proposed Damage Risk Criteria for Impulsive Noise (Gunfire)," paper presented before the NAS-NRC Committee on Hearing, Bioacoustics, and Biomechanics, WG 46, Washington, DC, 1968.
11. R. R. A. Coles, G. R. Garinther, D. C. Hodge, and C. G. Rice, "Hazardous Exposure to Impulse Noise," *J. Acoust. Soc. Am.*, **43**, 336–343 (1968).
12. C. W. Nixon, H. H. Hille, H. C. Sommer, and E. Guild, "Sonic Booms Resulting from Extremely Low Altitude Supersonic Flight: Measurements and Observations on Houses, Livestock, and People," AAMRL Technical Report No. 68-52, Wright Patterson AFB, OH, 1968.
13. C. W. Nixon, "Human Auditory Response to an Air Bag Inflation Noise," PB-184-837, Clearinghouse for Federal Scientific and Technical Information, Arlington, VA, 1969.
14. Office of the Air Force Surgeon General, Air Force Occupational Safety and Health (AFOSH) Program, "Hazardous Noise Program," AFOSHSTD 48-19, March 31, 1994, Washington, DC.
15. G. C. Mohr, J. N. Cole, E. Guild, and H. E. Von Gierke, "Effects of Low Frequency and Infrasonic Noise on Man," *Aerospace Med.*, **36**, 817–824 (1965).
16. C. W. Nixon and D. L. Johnson, "Infrasound and Hearing," in W. D. Ward (Ed.), *International Congress on Noise as a Public Health Problem*, 550/9-73-008, U. S. Environmental Protection Agency, Washington, DC, May 1973.
17. H. E. Von Gierke and D. E. Goldman, "Effects of Shock and Vibration on Man," in C. M. Harris (Ed.), *Shock and Vibration Handbook*, 3rd ed., McGraw-Hill, New York, 1988.
18. H. E. Von Gierke, "To Predict the Body's Strength," *Aviat. Space Environ. Med.*, **59**, A107–A115 (1988).
19. E. B. Magid, R. R. Coermann, and G. H. Ziegenruecker, "Human Tolerance to Whole Body Sinusoidal Vibration," *Aerospace Med.*, **31**, 915–924 (1960).
20. W. B. Hood, R. H. Murray, C. W. Urschel, et al., "Cardiopulmonary Effects of Whole-Body Vibration in Man," *J. Appl. Physiol.*, **21**(6), 1725–1731 (1966).
21. H. Dupuis and G. Zerlett, *The Effects of Whole-Body Vibration*, Springer-Verlag, Berlin, Heidelberg, New York, Tokyo, 1986.

22. H. Seidel and R. Heide, "Long-Term Effects of Whole-Body Vibration: A Critical Survey of the Literature," *Int. Arch. Occup. Environ. Health*, **58**, 1–26 (1986).
23. R. R. Coermann, "The Mechanical Impedance of the Human Body in Sitting and Standing Position at Low Frequencies," ASD Technical Report 61–492, Aeronautical Systems Division, Air Force Systems Command, U. S. Air Force, Wright Patterson AFB, OH, 1961.
24. M. J. Moseley and M. J. Griffin, "Effects of Display Vibration and Whole-Body Vibration on Visual Performance," *Ergonomics*, **29**(8), 977–983 (1986).
25. M. J., Griffin, *Handbook of Human Vibration*, Academic, London, 1990, pp. 128–134.
26. M. J. Wells and M. J. Griffin, "Benefits of Helmet-Mounted Display Image Stabilisation under Whole-Body Vibration," *Aviat. Space Environ. Med.*, **55**(1), 13–18 (1984).
27. H. E. Von Gierke and C. W. Nixon, "Effects of Intense Infrasound on Man," in W. Tempest (Ed.), *Infrasound and Low Frequency Vibration*, Academic, New York, 1976, pp. 115–150.
28. J. C. Guignard and P. F. King, "Aeromedical Aspects of Vibration and Noise," AGARDograph No. 151, NATO Advisory Group for Aerospace Research and Development (AGARD), 1972.
29. S. D. Smith, "Characterizing the Effects of Airborne Vibration on Human Body Vibration Response," *Aviat. Space Environ. Med.*, **73**(1), 36–45 (2001).
30. International Organization for Standardization (ISO), "Mechanical Vibration and Shock—Measurement and Evaluation of Human Exposure to Hand-Transmitted Vibration—Part 1: General Requirements," ISO 5349-1: 2001, ISO, Geneva, Switzerland.
31. W. Taylor and P. L. Pelmear (Eds.), *Vibration White Fingers in Industry*, Academic, London, 1975.
32. U.S. Department of Health and Human Service, National Institute for Occupational Safety and Health (NIOSH), "Occupational Exposure to Hand-Arm Vibration," DHHS Publication No. 89–106, NIOSH, Washington, DC, 1989.
33. International Organization for Standardization (ISO), "Mechanical Vibration and Shock—Evaluation of Human Exposure to Whole-Body Vibration—Part 1: General Requirements," ISO 2631-1:1997, ISO, Geneva, Switzerland.
34. International Organization for Standardization (ISO), "Mechanical Vibration and Shock—Evaluation of Human Exposure to Whole-Body Vibration—Part 2: Vibration in Buildings (1–80 Hz)," ISO 2631-2:2003, ISO, Geneva, Switzerland.
35. International Organization for Standardization (ISO), "Mechanical Vibration and Shock—Evaluation of Human Exposure to Whole-Body Vibration—Part 4: Guidelines for the Evaluation of the Effects of Vibration and Rotational Motion on Passenger and Crew Comfort in Fixed-Guideway Transport Systems," ISO 2631-4:2001, ISO, Geneva, Switzerland.
36. International Organization for Standardization (ISO), "Mechanical Vibration and Shock—Evaluation of Human Exposure to Whole-Body Vibration—Part 5: Method for Evaluation of Vibration Containing Multiple Shocks," ISO 2631-5:2004, ISO, Geneva, Switzerland.
37. American National Standards Institute, "Guide for the Evaluation of Human Exposure to Whole-Body Vibration," ANSI S3.18–2002, Acoustical Society of America, Melville, NY, 2002.

38. American Conference of Governmental Industrial Hygienists (ACGIH), "2003 TLVs® and BEIs®, Based on the Documentation of the Threshold Limit Values for Chemical Substances and Physical Agents & Biological Exposure Indices," ACGIH, Cincinnati, OH, 2003.
39. International Organization for Standardization (ISO), "Mechanical Vibration and Shock—Measurement and Evaluation of Human Exposure to Hand-Transmitted Vibration—Part 2: Practical Guidance for Measurement at the Workplace," ISO 5349-2:2001, ISO, Geneva, Switzerland.

CHAPTER 20

Criteria for Noise in Buildings and Communities

LEO L. BERANEK

Consultant
Cambridge, Massachusetts

One of the early steps in the architectural design of a building is the specification of acceptable noise levels in the spaces for occupancy by human beings. Noise sources in rooms include the air-handling and conditioning system (HVAC), the occupants themselves, machinery in the room, and vibration of the surfaces of the room by machinery outside. In this chapter, the sources of the noise in a space are, in general, not discussed. However, in many cases, such as in offices, dwellings, schools, auditoriums, and studios, it is generally true that the most likely annoying noise is created by the HVAC system. In those cases the criteria presented here apply to the HVAC noise alone as measured without the presence of people. In shops, manufacturing plants, and restaurants, the principal noise sources are machinery or large numbers of people. In such spaces the designer only has to make sure that the HVAC levels do not exceed the liberal limits suggested in this chapter.

20.1 SOUND LEVELS: DEFINITIONS

The sound (noise) levels, all in decibels, that are used in this chapter are taken from Chapter 1, which, in turn, were taken from U.S. and international standards:

- Sound pressure level (SPL) L_p [see Eq. (1.21)].
- A-weighted sound pressure level L_A [see Eq. (1.22)].
- The equivalent sound level L_{eq}, which is broadly defined by

$$L_{eq} = L_{av,T} = 10 \log(1/T) \frac{\int_0^T p_A^2(t)\, dt}{p_{ref}^2} \quad \text{dB} \tag{20.1}$$

where T is the time over which the averaging takes place and must be specified [see Eq. (1.23)].

38. American Conference of Governmental Industrial Hygienists (ACGIH), "2003 TLVs® and BEIs®, Based on the Documentation of the Threshold Limit Values for Chemical Substances and Physical Agents & Biological Exposure Indices," ACGIH, Cincinnati, OH, 2003.
39. International Organization for Standardization (ISO), "Mechanical Vibration and Shock—Measurement and Evaluation of Human Exposure to Hand-Transmitted Vibration—Part 2: Practical Guidance for Measurement at the Workplace," ISO 5349-2:2001, ISO, Geneva, Switzerland.

CHAPTER 20

Criteria for Noise in Buildings and Communities

LEO L. BERANEK

Consultant
Cambridge, Massachusetts

One of the early steps in the architectural design of a building is the specification of acceptable noise levels in the spaces for occupancy by human beings. Noise sources in rooms include the air-handling and conditioning system (HVAC), the occupants themselves, machinery in the room, and vibration of the surfaces of the room by machinery outside. In this chapter, the sources of the noise in a space are, in general, not discussed. However, in many cases, such as in offices, dwellings, schools, auditoriums, and studios, it is generally true that the most likely annoying noise is created by the HVAC system. In those cases the criteria presented here apply to the HVAC noise alone as measured without the presence of people. In shops, manufacturing plants, and restaurants, the principal noise sources are machinery or large numbers of people. In such spaces the designer only has to make sure that the HVAC levels do not exceed the liberal limits suggested in this chapter.

20.1 SOUND LEVELS: DEFINITIONS

The sound (noise) levels, all in decibels, that are used in this chapter are taken from Chapter 1, which, in turn, were taken from U.S. and international standards:

- Sound pressure level (SPL) L_p [see Eq. (1.21)].
- A-weighted sound pressure level L_A [see Eq. (1.22)].
- The equivalent sound level L_{eq}, which is broadly defined by

$$L_{eq} = L_{av,T} = 10 \log(1/T) \frac{\int_0^T p_A^2(t)\,dt}{p_{ref}^2} \quad \text{dB} \qquad (20.1)$$

where T is the time over which the averaging takes place and must be specified [see Eq. (1.23)].

- A-weighted equivalent sound level $L_{eq,A}$ is that given by Eq. (20.1), but with the A-weighted frequency response in place in the measuring instrument. Often this quantity is simply labeled L_{eq} and the A weighting is known through its expression in dBA [see Eq. (1.24)].
- The band average sound level is that given in Eq. (19.1), but with the band width specified.
- The averaging time T can be a matter of fractional seconds, minutes, hours, days, or even a year. Always, it must be specified.
- Day–night sound level L_{dn} [see Eq. (1.25)]. Note, in some nations, the 24-h period is divided into three intervals, day, evening, and night, for which Eq. (1.25) must have three integrals with the interval times specified.
- A-weighted sound (noise) exposure $E_{A,T}$ (proportional to energy flow, intensity times time, in a sound wave in the time period T) [see Eq. (1.26)].
- A-weighted sound (noise) exposure level L_{EAT} [see Eq. (1.27)].
- Speech interference level SIL is the average of the sound pressure levels in the four octave bands, whose midfrequencies are 500, 1000, 2000, and 4000 Hz.

20.2 EVALUATION OF ROOM NOISE: SURVEY METHOD, ENGINEERING METHOD, AND PRECISION METHOD[1]

Current-Day Sound-Level Meters

Current-day sound-level meters are used to determine the sound levels in some or all of the ten octave bands with midfrequencies from 16 to 8000 Hz. The meter "speed" can be set to slow, fast, or impulse. When the meter speed is set to "fast," a running integration time of about 125 ms is achieved. The output of the meter can be set to read or store the following levels: L_{eq}, the equivalent noise level over the measurement time period; the peak level L_{max}; and the statistical levels L_{10}, L_{50}, L_{90}, and L_{95}, where the subscript means that level is exceeded 10, 50, 90, or 95% of the time. The 50% level is the median level. When measuring A-weighted sound levels, the meter speed is set at "slow." For monitoring, the meters usually have storage capacity from 1 s up to 24 h. The stored data can be sampled as often as every 100 ms. Acoustical consultants say that their measuring time of HVAC noise at a particular location in a room is usually under a minute.

Survey Method — L_A

An A-weighted sound level L_A is often used for surveying whether a measured noise level satisfies a specified noise criterion. It is readily measured with the simplest sound-level meters. The measurement of L_A is the average of the maximum meter readings, with the meter response set at slow, and obtained by moving the microphone about the room, avoiding positions near the surfaces or the geometric center. It is assumed that the measured noise is free of pure tones and HVAC surging. The presence of HVAC surging can usually be detected by listening or by observing the meter swings using the "flat" (or "C") frequency weighting and the fast meter response.

Because L_A lacks specific spectral information, it can be misleading in evaluating noise other than that arising from reasonably well-designed HVAC systems. The values given in Table 20.1 are recommended for estimating whether measured A-weighted levels may be suitable for the purposes indicated. The numbers presented in that table are largely influenced by the results of a request to a number of consulting firms for examples of excessive noise situations.[2] Fourteen firms responded. The acceptable and unacceptable octave-band levels in school rooms, auditoria, offices, and hotel rooms resulted. Those data indicated that the best method to use in writing specifications, where HVAC surging and large sound fluctuations are not expected, is to use noise criterion (NC) curves, described in the next section. (*Note*: The acceptable NC curves for various occupancies of the spaces are given in Table 20.2. Table 20.1 was determined from Table 20.2 and the NC curves of Fig. 20.1 as follows: For each of the NC curves the speech interference level (SIL) and the A-weighted effective level (L_A) were calculated and L_A − SIL found. These differences were added to the levels in Table 20.2 to obtain the levels of Table 20.1. For example, L_A − SIL for the NC-40 criterion curve is 8 dB, which means that where 40 dB appears in Table 20.2, 48 dB appears in Table 20.1. Also in reference 2, the octave-band levels for 14 cases of excessive noise at low frequencies revealed that L_A − SIL = 14 dB is clearly unacceptable, while in offices with acceptable noise levels L_A − SIL did not exceed approximately 7.5 dB.)

Engineering Method: NC Curves

The most widely used method today for evaluating the suitability of the noise in a space for human occupancy and for writing noise specifications employs the NC curves shown in Fig. 20.1.[3,4] The numerical values from which Fig. 20.1 was plotted are given in Table 20.2 (rounded to the nearest decibel). In measuring a noise the sound-level meter (with octave-band filtering) is set to yield L_{eq} with a slow meter, flat response. The integration time T can be of any desired length—seconds, hours, or months. If each octave-band meter reading slowly fluctuates over a small range, the average value is used.

For writing specifications, the suggested NC ratings for various occupancies are shown in Table 20.2. For example, for small offices, NC-35 to NC-40 is listed.

When evaluating a measured noise spectrum, the octave-band levels are plotted on the set of curves in Fig. 20.1. The rating given to the noise is set by the band level that "touches" the highest NC curve (interpolated to the nearest decibel). For example, assume that the levels in the eight bands from 31.5 to 4000 Hz were 68, 65, 61, 58, 50, 42, 37, and 30 dB, respectively. The highest NC rating

TABLE 20.1 Recommended A-Weighted Sound-Level Criteria for HVAC Systems for Rooms (Unoccupied) of Various Uses

Occupancy	A-Weighted Sound Level L_A in dBA
Small auditoriums	35–39
Large auditoriums, large drama theaters, and large churches (for very good speech articulation)	30–35
TV and broadcast studios (close microphone pickup only)	16–35
Legitimate theaters	30–35
Private residences	
Bedrooms	35–39
Apartments	39–48
Family rooms and living rooms	39–48
Schools	
Lecture and classrooms	
With areas less than 70 m^2	44–48
With areas greater than 70 m^2	39–44
Open-plan classrooms	44–48
Hotels/motels	
Individual rooms or suites	39–44
Meeting/banquet rooms	35–44
Service support areas	48–57
Office buildings	
Offices	
Executive	35–44
Small, private	44–48
Large, with conference tables	39–44
Conference rooms	
Large	35–39
Small	39–44
Open-plan areas	44–48
Business machines, computers	48–53
Public circulation	48–57
Hospitals and clinics	
Private rooms	35–39
Wards	39–44
Operating rooms	35–44
Laboratories	44–53
Corridors	44–53
Public areas	48–52
Movie theaters	39–48
Churches, small	39–44
Courtrooms	39–44
Libraries	44–48
Restaurants	48–52
Light maintenance shops, industrial plant control rooms, kitchens and laundries	52–62
Shops and garages	57–67

Note: Data based on L_A − SIL for NC curves of Table 20.2.

TABLE 20.2 Recommended NC and RNC Noise Criteria for HVAC Systems for Rooms (Unoccupied) of Various Uses

Occupancy	NC and RNC Recommended Criterion Curve
Recording studios	Lowest curve of Fig. 20.1
Broadcast studios (distant microphone pickup used)	10
Concert halls, opera houses, and recital halls (listening to faint musical sounds)	15–18
Small auditoriums	25–30
Large auditoriums, large drama theaters, and large churches (for very good speech articulation)	20–25
TV and broadcast studios (close microphone pickup only)	15–25
Legitimate theaters	20–25
Private residences	
Bedrooms	25–30
Apartments	30–40
Family rooms and living rooms	30–40
Schools	
Lecture and classrooms	
With areas less than 70 m^2	35–40
With areas greater than 70 m^2	30–35
Open-plan classrooms	35–40
Hotels/motels	
Individual rooms or suites	30–35
Meeting/banquet rooms	25–35
Service support areas	40–50
Office buildings	
Offices	
Executive	25–35
Small, private	35–40
Large, with conference tables	30–35
Conference rooms	
Large	25–30
Small	30–35
Open-plan areas	35–40
Business machines, computers	40–45
Public circulation	40–50
Hospitals and clinics	
Private rooms	25–30
Wards	30–35
Operating rooms	25–35
Laboratories	35–45
Corridors	35–45
Public areas	40–45
Movie theaters	30–40
Churches, small	30–35
Courtrooms	30–35
Libraries	35–40
Restaurants	40–45
Light maintenance shops, industrial plant control rooms, kitchens and laundries	45–55
Shops and garages	50–60

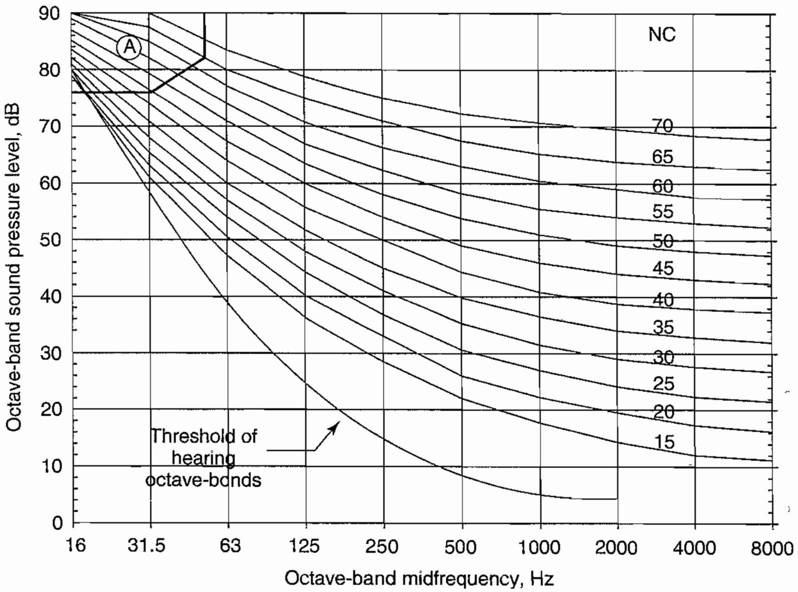

FIGURE 20.1 Noise criteria curves derived from interviews and simultaneous noise measurements extended to low frequencies by comparison with balanced NC (NCB) curves. These NC curves are used to rate noises by the "tangency method."[2,3,5,10] Region *A* indicates low-frequency levels that may produce feelable vibrations and rattles from lighting fixtures in lightweight constructions if fluctuations or surging is present. The threshold of hearing is taken from ANSI S12.2–1995.

curve "touched" by this spectrum is determined by the 58-dB level in the 250-Hz band and equals NC-50. This is the so-called tangency method of rating.

The NC curves were originally derived from a survey of noise in a large number of offices and spaces in a military Air Force base[5] and in several office buildings.[6] The surveys were conducted by asking occupants of rooms how they rated the noise both generally and at that instant (on a scale with six divisions from "very quiet" to "intolerably noisy") and then measuring the noise at that instant. It was determined that the activity most affected by the noise was speech communication both person to person and by telephone. However, it was also found that even though speech communication might be satisfactory in a space, the low-frequency noise levels could be so high as to be annoying. How much higher can the low-frequency noise be compared to the midfrequency noise? It was found that the overall loudness of the noise had to be taken into consideration. To answer this question, two quantities were measured, the SIL and the loudness level of the noise.

The SIL is a measure of the degree of interference of a noise with speech communication. It is standardized as the average sound pressure level, in decibels, in the four octave bands 500, 1000, 2000, and 4000 Hz.[7]

TABLE 20.3 Noise Criteria Curves from Fig. 20.1 to Nearest Decibel

	By Octave-Band Center Frequencies, Hz									
NC CURVE	16	31.5	63	125	250	500	1000	2000	4000	8000
NC-70	90	90	84	79	75	72	71	70	68	68
NC-65	90	88	80	75	71	68	65	64	63	62
NC-60	90	85	77	71	66	63	60	59	58	57
NC-55	89	82	74	67	62	58	56	54	53	52
NC-50	87	79	71	64	58	54	51	49	48	47
NC-45	85	76	67	60	54	49	46	44	43	42
NC-40	84	74	64	56	50	44	41	39	38	37
NC-35	82	71	60	52	45	40	36	34	33	32
NC-30	81	68	57	48	41	35	32	29	28	27
NC-25	80	65	54	44	37	31	27	24	22	22
NC-20	79	63	50	40	33	26	22	20	17	16
NC-15	78	61	47	36	28	22	18	14	12	11

The loudness level is determined by a standardized computational procedure which yields results in units called phons.[8] Needed are measured octave- or one-third-octave-band levels in all the frequency bands.

The studies revealed that the loudness level (in phons) should not exceed the SIL (in decibels) by more than about 24 units if the space is not to be annoying to the occupants. Because low-frequency sounds are less loud than high-frequency sounds, their levels can be higher. Thus with increasing frequency the NC curves slope downward monotonically and their shape is determined to resemble that of well-known "equal-loudness" curves.[9] The amount of slope and the shape of the spectrum are determined by the 24-unit difference just mentioned. (*Note*: The average of the levels in the four speech interference bands for each NC curve in Fig. 20.1 is between 0.25 and 1 dB higher than the designating number shown for the curve. The reason is that a shift in the frequency limits for the octave bands was standardized some years after these curves were developed. However, the decibel values for the points and the designating numbers on these curves are exactly the same as originally presented.)

It must be emphasized that the NC curves so derived give the upper permissible limit of the low-frequency noise once the SIL is known. Thus, the shape of a NC curve is not the shape of an ideal noise spectrum, but rather is the shape of a "not-to-be-exceeded" spectrum.

Two basic assumptions concerning the curves of Fig. 20.1 are that the noise contains no pure tones and there is no surging of the noise from fans that drive the HVAC system.

Concerning the measurement of sound levels at each point on a NC curve, the meter response is set to suit the desired result. If the equivalent noise level over a period of hours or days is decided, the slow meter response is selected. For short samples of the measured noise, the fast response is used. For example, a series of 100–1000 samples each 100 ms long requires fast response. The meter can show the equivalent level L_{eq} in decibels for the sequence, or the maximum level L_{max}, or the level above which 10% of the interval levels are found, called L_{10}, or the L_{50} level, which is the mean level, or the L_{90} level. Some consultants believe the L_{50} level correlates well with people's judgment of the acceptability of their noise environment, provided that the speech intelligibility requirement is met.

Comments about NC Curves. The NC curves as originally derived did not extend down to the 31.5- and 63-Hz octave bands. These two bands have been added by the author to the original curves, based on the studies that led to the balanced noise criterion (NCB) curves that are briefly discussed below. The revised curves of Fig. 20.1 have been shown in two studies to predict successfully all known cases of sizable complaints by occupants of existing building spaces.[10,11]* In none of these cases was surging detected.

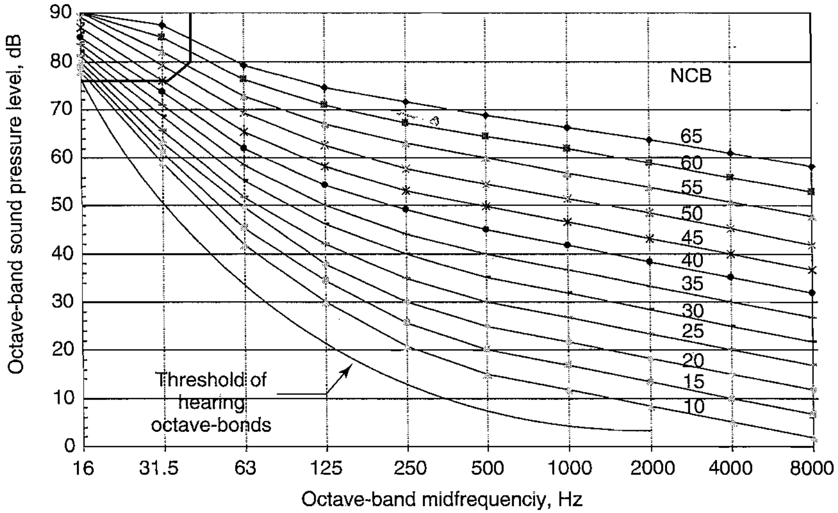

FIGURE 20.2 Balanced noise criteria curves, taken from ANSI S12.2–1995. These curves are used to rate noises with a procedure described in the standard and ref. 10.

*In ref. 11, 238 measured sound-pressure-level spectra were obtained from the consulting files of Cavanaugh Tocci Associates. Plots were made of the relation between NC (tangency method) and NCB (tangency method). The two were closely related with an $R^2 = 0.97$. Similarly, the NCB rating was plotted in relation to the RC or RC II rating, with a correlation of $R^2 = 0.98$, except that the RC values are about 2 dB greater than the NC values because the NC curves are based on the average of the levels in the 500-, 1000-, 2000-, and 4000-Hz bands, while the RC curves are labeled based on the average of the levels in the 500-, 1000-, and 2000-Hz bands.

NCB Curves

The NCB curves shown in Fig. 20.2[7] were derived from the following premises: (1) the rating number for each curve should equal its four-band SIL; (2) the calculated octave-band loudness for those bands from 125 to 8000 Hz should contain the same number of critical (hearing) bands, and for the two lower bands, the loudnesses should be weighted downward in proportion to the fraction of critical bands contained; and (3) the difference between the SIL (in decibels) and the loudness level (in phons) for a criterion curve should not exceed 24 units. The detailed method of applying NCB curves to the evaluation of HVAC noise is not discussed here, because they have not found widespread use, in spite of their being contained in ANSI S12.2–1995. As mentioned above, the NC curves have been extended to the 16- and 31.5-Hz bands by comparison with the rationale that led to the NCB curves. Except for the method of applying them to the rating of a noise, the NCB curves differ little from the NC curves of Fig. 20.1.

The levels taken from the NCB curves (rounded to the nearest decibel) are listed in Table 20.4.

RC (Originally Called "Revised Criteria") Curves

The RC criteria curves for evaluating noise in a room or for specifications were built around the point of view that sound levels lower than those shown by the NC curves of Fig. 20.1 should always be specified for the bottom three-octave frequency bands (31.5, 63, and 125 Hz). The primary reason given is that if there are strong fluctuations or surging in the HVAC noise, the specified low-frequency octave-band levels for the RC curves ought to be low enough so that the noise is not disturbing.

The basis for the RC curves was a set of measurements made in the early 1970s of the noise in 68 offices where the HVAC noise levels were judged satisfactory.

TABLE 20.4 Balanced Noise Criteria Curves from Fig. 20.2 to Nearest Decibel

	By Octave-Band Center Frequencies, Hz									
NCB CURVE	16	31.5	63	125	250	500	1000	2000	4000	8000
NCB-65	97	88	79	75	72	69	66	64	61	58
NCB-60	94	85	76	71	67	64	62	59	56	53
NCB-55	92	82	72	67	63	60	57	54	51	48
NCB-50	89	79	69	62	58	55	52	49	45	42
NCB-45	87	76	65	58	53	50	47	43	40	37
NCB-40	85	73	62	54	49	45	42	38	35	32
NCB-35	84	71	58	50	44	40	37	33	30	27
NCB-30	82	68	55	46	40	35	32	28	25	22
NCB-25	81	66	52	42	35	30	27	23	20	17
NCB-20	80	63	49	38	30	25	22	18	15	12
NCB-15	79	61	45	34	26	20	17	13	10	7
NCB-10	78	59	43	30	21	15	12	8	5	2

When plotted, those noise-level spectra, on average, sloped off linearly with frequency at the rate of 5 dB/octave in the bands from 63 to 4000 Hz. It was concluded that if the measured spectra in satisfactory office environments had that characteristic, the −5 dB/octave line is "optimum," but no comparisons with other spectra were made.

The RC curves are shown in Fig. 20.3 and the values are listed in Table 20.5.[12]

In this chapter, only the Mark II version of the RC method is employed, which differs from the original version in that the levels in the 16- and 31.5-Hz bands are equal instead of the 16-Hz band being 5 dB higher than the 31.5-Hz band. Also the procedure for evaluating measured data is different.

An RC curve suitable for a particular type of room may be determined from Table 20.6. The values there were chosen to permit satisfactory speech intelligibility, where that is important, or to provide noise levels that are not above normal activity sounds.

When evaluating a noise spectrum using the RC method, the first step is to determine the average of the measured sound levels in the 500-, 1000-, and 2000-Hz octave bands, the *midfrequency average*, which Reference 11 calls *level at midfrequencies* (LMF). This number identifies the level of the measured spectrum in the frequency region most important to speech communication, and it selects the reference RC curve used as a starting point for the analysis that follows. For example, if the LMF is 36 dB, the RC-36 becomes the reference curve. If that LMF is suited to the activities that take place in the space in which

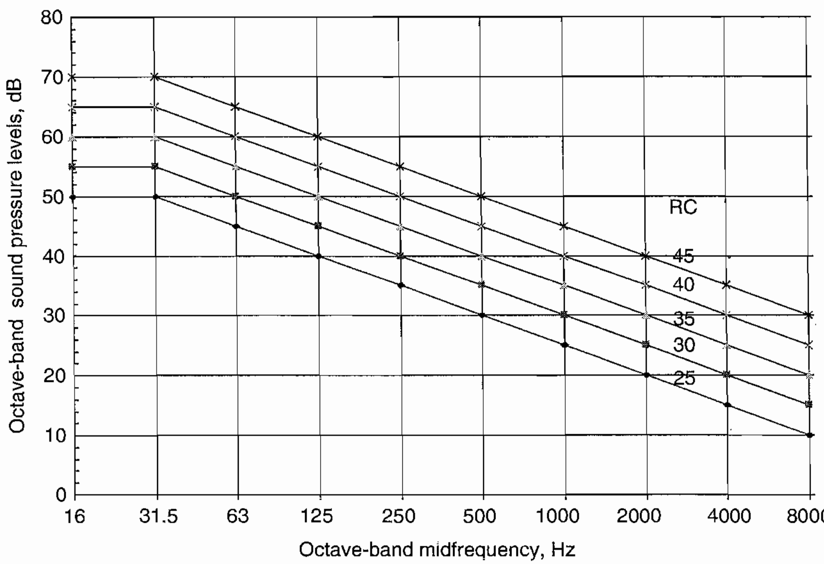

FIGURE 20.3 Noise criteria RC Mark II curves, derived from measurements of HVAC noise in offices. These RC curves are used to rate noises by a procedure detailed in ref. 12.

TABLE 20.5 Noise Criteria RC Curves from Fig. 20.3 to Nearest Decibel

	By Octave-Band Center Frequencies, Hz									
RC CURVE	16	31.5	63	125	250	500	1000	2000	4000	8000
RC-25	50	50	45	40	35	30	25	20	15	10
RC-26	51	51	46	41	36	31	26	21	16	11
RC-27	52	52	47	42	37	32	27	22	17	12
RC-28	53	53	48	43	38	33	28	23	18	13
RC-29	54	54	49	44	39	34	29	24	19	14
RC-30	55	55	50	45	40	35	30	25	20	15
RC-31	56	56	51	46	41	36	31	26	21	16
RC-32	57	57	52	47	42	37	32	27	22	17
RC-33	58	58	53	48	43	38	33	28	23	18
RC-34	59	59	54	49	44	39	34	29	24	19
RC-35	60	60	55	50	45	40	35	30	25	20
RC-36	61	61	56	51	46	41	36	31	26	21
RC-37	62	62	57	52	47	42	37	32	27	22
RC-38	63	63	58	53	48	43	38	33	28	23
RC-39	64	64	59	54	49	44	39	34	29	24
RC-40	65	65	60	55	50	45	40	35	30	25
RC-41	66	66	61	56	51	46	41	36	31	26
RC-42	67	67	62	57	52	47	42	37	32	27
RC-43	68	68	63	58	53	48	43	38	33	28
RC-44	69	69	64	59	54	49	44	39	34	29
RC-45	70	70	65	60	55	50	45	40	35	30

the measurements were made (from Table 20.6), and if the spectrum closely approximates the reference curve, the noise is given a rating of "N," neutral.

If the measured spectrum is not "neutral," the RC (latest version, Mark II) rating procedure begins with the reference curve derived from it. Next, determination of three quantities is calculated from the measured spectrum, each called, *energy-average spectral deviation factor*. Three frequency regions are chosen for this analysis—low (16–63 Hz), middle (125–500 Hz), and high (1000–4000 Hz)—dubbed the LF, or "rumble," the MF, or "roar," and the HF, or "hiss," regions.

The procedure is as follows: First, for each octave-frequency band in the measured spectrum, the difference in decibels between that spectrum and the reference RC curve is found. The sign may be either positive or negative. For each of the three frequency regions, LF, MF and HF, the three octave-band differences therein are summed on an *energy basis*, which yields an energy-average spectral deviation factor for that region. For example, assume the three-octave-band differences in the LF region are 4, 5, and 9 dB, giving an averaged energy level of 4.54, and 10 log 4.54 = 6.57 dB. This factor is also determined for the MF and HF regions, which, as an example here, we shall assume are equal to 4.82 and −0.92 dB. Next, the *quality assessment index* QAI is defined

TABLE 20.6 Recommended RC Criteria for HVAC Systems for Rooms (Unoccupied) of Various Uses

Occupancy	RC Criterion Curve[a]
Private residences	
Bedrooms	25–30 (N)
Apartments	30–35 (N)
Family rooms and living rooms	30–40 (N)
Schools	
Lecture and classrooms	30–35 (N)
Open-plan classrooms	35–40 (N)
Hotels/motels	
Individual rooms or suites	30–35 (N)
Meeting/banquet rooms	30–35 (N)
Halls, corridors, lobbies	35–40 (N)
Service support areas	40–50 (N)
Office buildings	
Executive offices	25–35 (N)
Private offices	30–35 (N)
Private offices with conference tables	25–30 (N)
Conference rooms	25–30 (N)
Open-plan areas	35–40 (N)
Business machines/computers	40–45 (N)
Public circulation	40–50 (N)
Hospitals and clinics	
Private rooms	25–30 (N)
Wards	30–35 (N)
Operating rooms	25–35 (N)
Laboratories	35–45 (N)
Corridors	35–45 (N)
Public areas	40–45 (N)
Churches	30–35 (N)
Libraries	35–40 (N)
Courtrooms	30–40 (N)
Restaurants	40–45 (N)

[a]N = neutral spectrum.

as the difference (in decibels) between the maximum and minimum values of the three spectral deviation factors just determined. In our example QAI = 6.57 − (−0.92) = 7.5 dB.

By the RC Mark II procedure, a *neutral* spectrum is one for which QAI is less than 5 dB and L_{16} and $L_{31.5}$ are at most 65 dB. If the highest *positive* spectral deviation factor occurs in the LF region, the spectrum is evaluated as having (i) a "marginal rumble" if 5 dB < QAI ≤ 10 dB or (ii) an "objectionable rumble" if QAI > 10 dB. If the highest positive factor falls in the MF or the HF regions, the same decibel ranges for QAI are listed for evaluating a spectrum as having "marginal or objectionable roar or hiss." For example, a measured spectrum might be designated as RC-45 (i.e., reference curve), roar (i.e., MF region), and probably objectionable (i.e., QAI exceeds 10 dB).[12]

The RC procedure would seem to mean that in writing a specification, a particular RC curve would be specified, but with the understanding that the measured levels in *any one* of the three frequency regions can be exceeded by about 5 dB without penalty.

It must be noted that in the 68 offices originally studied, the A-weighted slow meter sound level only covered a range of 40 to 50 dB, and thus none of the sound levels were considered that are found in spaces like concert halls at one extreme or factory spaces at the other. Second, the RC spectra are typical of HVAC practice in quality offices of the 1970 period and may not be typical at any future time.

The difficulty with the undisciplined use of the RC curves is that they penalize those HVAC installations that are free of surging or of large low-frequency fluctuations. In concert halls or other sites where very low background noise is required, the HVAC systems must be of highest quality, free of surging or significant low-frequency fluctuations. The measured NC noise spectra for concert halls usually are specified to be in the range of NC-15 to NC-18 (See Fig. 20.1 and Table 20.2). The levels in the completed halls usually follow a NC curve down to the 63-Hz band or lower. If RC curves equal to RC-15 to RC-20 were to be specified at such a site, 15 or more decibels of noise reduction would be required in the lowest bands. The cost of such an unnecessary reduction at low frequencies would be prohibitive. Of course, the perceived danger, from the specification point of view, is that a supplier might be told to meet, say, the NC-20 criterion curve, but that he or she might, in fact, install a low-cost HVAC system whose air supply source exhibited surging and then insist that the system meets the specification based on measurements in the octave bands with the usual sound-level meter set to slow response. Advanced techniques for evaluating spectra to determine whether the HVAC noise exhibits surging or large random fluctuations are presented in the next section.

Precision Method — RNC Curves[13,14]

There is a need to evaluate HVAC systems in which surging from the driving fan(s) takes place and to write specifications for the design of HVAC systems to avoid the chance of surging. To listeners, surging is very apparent and disturbing, and it must be addressed both in the writing of specifications and when diagnosing the seriousness of the noise afterward. Surging cannot be determined by a conventional sound-level meter with the slow meter speed and "A" frequency-weighted response in place, partly because surging primarily affects the levels in the low-frequency bands and partly because surging may be averaged out if the slow speed is used.

HVAC: Well Behaved or Surging? Surging usually can be heard aurally or it can be seen visually on a standard sound-level meter by observing the levels in the 16-, 31-, and 63-Hz octave bands. The sound-level meter must be set for fast response and flat frequency characteristic (or C weighting). If surging is found from listening or observing the levels in the octave bands above, then the RNC method of evaluation should be used to determine the seriousness of the noise condition.

First, Some Psychoacoustics. In devising a more precise method of evaluating whether the HVAC noise in a room is intrusive for its primary use, one must turn to the field of psychoacoustics for help. First, the ear only integrates (lumps together) significant variations in the level of a sound provided they occur within a short time period, that is, if the variations occur within a time period that is less than about 125 ms. That is, any fluctuations in HVAC noise that occur within a time interval of about 100 ms are perceived as though the noise were continuous (with the same energy) in that period without fluctuations.

A second reality is that the ear integrates the sound energy that falls within frequency bands called *critical bands*. Critical bands increase in width at about the same rate as the widths of the octave frequency bands increase except at low frequencies. In the frequency region below 125 Hz, the critical bands are about 100 Hz wide. Hence, the 16-, 31.5-, and 63-Hz octave-band levels must be combined in some manner into one band centered, say, at 31.5 Hz, in order that it can be treated in the same way as the higher frequency bands.

A third fact arising from the properties of hearing involves the loudness of sounds at low frequencies, that is, at frequencies below about 200 Hz. For the three octave bands 16, 31.5, and 63 Hz, a change of approximately 5 dB in level creates a doubling in the subjective loudness of a sound. For the 125-Hz band, a change of about 8 dB causes a doubling of loudness. For octave bands with midfrequencies of 250 Hz and above, a change of 10 dB is necessary to create a doubling in loudness. Thus, variations in level of the successive 100-ms intervals for the four lowest frequency bands must be treated differently from variations in level of the 100-ms intervals for the higher frequency bands. The RNC procedures, about to be described, are designed to take into account these three characteristics of the hearing system when evaluating the noise of a space.

Large Random Fluctuations. Even though surging is not observed orally or visually, the presence of large random fluctuations at low frequencies is still a possibility. The simplest test for this requires the observation of the differences between the L_{max} and L_{eq} levels or the L_{10} and the L_{eq} levels in the 16-, 31-, 63-, and 125-Hz bands with the meter set on fast. If the difference between L_{max} and L_{eq} for any one of the three lowest bands (16-, 31-, and 63-Hz octave bands) is greater than 7 dB, or $L_{10} - L_{eq} > 4$ dB, or if the difference between L_{max} and L_{eq} for the 125-Hz band is greater than 6 dB, or $L_{10} - L_{eq} > 3$ dB, large random fluctuations are indicated and the full RNC method should be used.

Well-Behaved HVAC Noise — Use NC Curves. When no surging or large-scale fluctuations are observed, L_{eq} measurements (slow scale) can be made in all the octave bands for any length of time T (fractions of minutes or longer) and the results compared with the NC curves of Fig. 20.1. The microphone used for the decibel measurements can be at one place in the room if the noise field is uniform throughout, or by measuring at a number of points and averaging the results, or simply by rotating the microphone at arm's length (2-m-diameter circle) and taking the average of the results.

Again, it must be borne in mind that all of the methods described in this chapter assume that there are no pure tones audible in the noise. If a pure tone(s) is suspected, narrow-band measurements (one-third octave or less) should be made to determine its frequency and intensity. Then, the pure-tone source should be located and steps taken to reduce its level before evaluating the remaining HVAC noise.

Found or Suspected Surging or Large Low-Frequency Fluctuations in HVAC Noise — Use RNC Curves. When surging or large low-frequency fluctuations are found or suspected, the RNC procedure is recommended to determine the penalty. It requires the use of a contemporary sound-level meter and a computer. The method incorporates the psychoacoustic facts discussed above. The RNC curves are shown in Fig. 20.4. Each RNC-X curve (e.g., RNC-40, RNC-50)

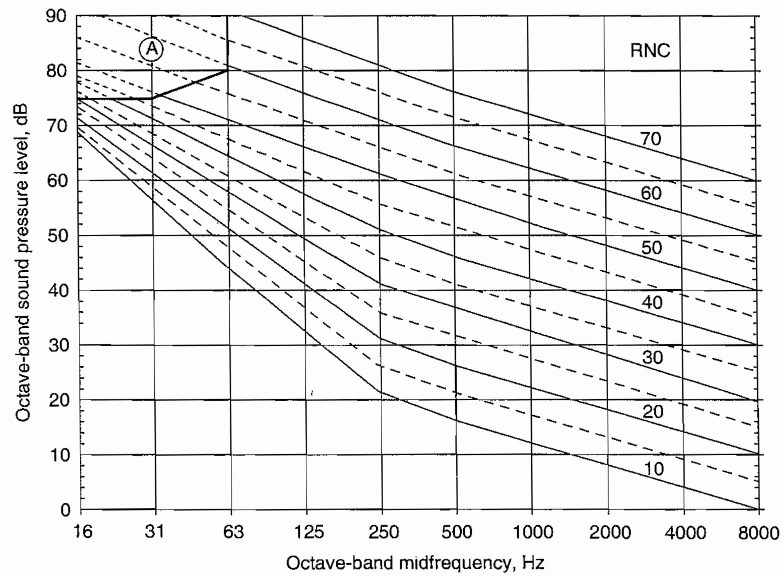

FIGURE 20.4 Balanced Noise criteria curves, devised in refs. 1,13, and 14 to rate noises that exhibit HVAC surging or large random fluctuations. In well-behaved HVAC systems the curves yield the same ratings as NC curves. When there are clearly audible HVAC surging or random vibrations, the curves yield ratings more like those of the RC curves—a penalty is imposed for surging that requires lower levels as measured with a "slow," sound-level meter setting.

TABLE 20.7 Coefficients Used in Eqs. (20.2) and (20.3) to Calculate RNC-X Curves of Fig. 20.4

Octave Band, Hz	Sound-Level Range, dB	K_{1ob}[a]	K_{2ob}
16	≤81	64.3333	3
	>81	31	1
31	≤76	51	2
	>76	26	1
63	≤71	37.6667	1.5
	>71	21	1
125	≤66	24.3333	1.2
	>66	16	1
250	All	11	1
500	All	6	1
1000	All	2	1
2000	All	−2	1
4000	All	−6	1
8000	All	−10	1

[a]The four-decimal figures are only to give calculated RNC-X even-decibel values.

can be derived from

$$L_{ob} = \frac{\text{RNC-}X}{K_{2ob}} + K_{1ob} \tag{20.2}$$

where RNC-X is the number on the curve, L_{ob} is the x-axis level for the particular octave band, and the constants K_{2ob} and K_{1ob} are taken from Table 20.7 for the particular octave bands.

Example 20.1. Calculate the SPL of the 63-Hz band for the RNC-20 curve of Fig. 20.4:

$$L_{ob} = (20/1.5) + 37.6667 = 13.3333 + 37.6667 = 51 \text{ dB}.$$

Conversely, the nearest RNC evaluation curve for a measured octave-band level can be obtained from

$$\text{RNC-}X = (L_{ob} - K_{1ob}) \times K_{2ob} \tag{20.3}$$

Example 20.2. Assume the measured level in the 125-Hz octave band L_{ob} is 55 dB. Determine which RNC curve (to nearest decibel) that measurement touches:

$$\text{RNC-X} = (55 - 24.3333) \times 1.2 = \text{RNC-37}$$

Recommended RNC Curves. The recommended RNC curves for spaces are the same as those for the NC curves and are given in Table 20.2.

If there is no surging or large scale-fluctuations, so that L_{eq} levels can be measured with the slow meter and flat frequency response, evaluation by the new RNC curves will yield results that are approximately equal to those from the NC curves. Therefore, the permissible L_{eq} levels at low frequencies compared to the SIL at midfrequencies will be as large as those shown in Fig. 20.1.

If surging and fluctuations exist, the RNC method "penalizes" the L_{eq} levels in the octave frequency bands below 300 Hz, so that if the disturbance in those frequency bands is large, the permissible L_{eq} levels may approach the low-frequency levels of the RC curves, as in Fig. 20.3.

Corrections to Measured Levels in Octave Bands at 16, 31.5, and 63 Hz When Surging or Large Fluctuations Exist. If surging and fluctuations exist, the RNC method penalizes the L_{eq} levels in the octave frequency bands below 300 Hz, so that if the disturbance in those frequency bands is large, the permissible L_{eq} levels may approach the low-frequency levels of the RC curves, as in Fig. 20.3. Contemporary sound-level meters can store up to 24 h of data for later downloading to a computer. The data should be recorded with a fast meter setting and a flat frequency response. The stored data (of whatever total time length) in bands or overall is sampled every 100 ms, forming the required octave-band time series for the RNC method. For the total time period, L_{peak}, L_{10}, and L_{50} are also available.

Each of the successive 100-ms samples is labeled i, where the ultimate i should be between 150 and 1000 depending on the suspected magnitude of the surging.

Because the loudness of a sound, at a given level, is considerably less at 16 Hz than at 31.5 Hz and, in turn, the loudness is considerably less at 31.5 Hz than that at 63 Hz, in the RNC method the three octave bands with midfrequencies at 16, 31.5, and 63 Hz are combined and replaced by a "three-band-sum" at 31.5 Hz. To do this, all of the measured 100-ms samples for the 16-Hz octave band are reduced by 14 dB and the samples for the 63-Hz octave band are increased by 14 dB. These adjusted levels for the 16- and 63-Hz bands are combined with the measured levels in the 31.5-Hz band on *an energy basis* and the new level (in decibels) is called a three-band-sum.

The ith 100-ms sample of this three-band-sum is called L_{LFi}. Calculate $L_{LF,eq}$ for the three-band-sum by summing the energies of the samples and dividing by the number of samples and taking 10 log of the result. Also, calculate L_{LFm}, the mean level of the set of three-band-sum samples.

The object now is to determine a correction K_{LFC} to be added to the *measured* L_{eq} at 31.5 Hz (not the three-band-sum) that takes into consideration both the L_{LFi} values and the fact that a change of only 5 dB is needed for a doubling of loudness at 31.5 Hz—and at 125 Hz, 8 dB is needed. Let δ stand for this change.

First calculate the correction at 31.5 Hz, K_{LFC}:

$$K_{LFC} = K_{LF\delta} - (L_{LF,eq} - L_{LFm}) \tag{20.4}$$

where

$$K_{LF\delta} = 10 \log \left(\frac{1}{N} \sum_{i=1}^{N} 10^{L\alpha/10} \right) \tag{20.5}$$

and where, at 31.5 Hz ($\delta = 5$ dB),

$$L\alpha = \frac{10}{\delta}(L_{LFi} - L_{LFm}) = 2(L_{LFi} - L_{LFm}) \tag{20.6}$$

The quantity K_{LFC} is added to the *measured* equivalent level L_{eq} (long time energy average) in the 31.5-Hz octave band and is plotted on Fig. 20.4 (no numbers are plotted in the 16- and 63-Hz bands). If data are not available for the 16-Hz band, the three-band-sum is determined for the 31.5- and 63-Hz bands.

Correction to Measured Level in Octave Band at 125 Hz If Surging Is Observed or Suspected. The level of each element of the 100-ms series at 125 Hz is called L_{125i}. Calculate L_{125eq} at 125 Hz by combining the energies of the samples and dividing by the number of samples and taking 10 log of the result. Also, calculate L_{125m}, the mean level of the set of samples at 31.5 Hz. The correction to be added to the *measured* 125-Hz octave-band L_{eq} is called K_{125C} and is given by

$$K_{125C} = K_{125\delta} - (L_{125eq} - L_{125m}) \tag{20.7}$$

where

$$K_{125\delta} = 10 \log\left(\frac{1}{N}\sum_{i=1}^{N} 10^{L\beta/10}\right) \tag{20.8}$$

and where, at 125 Hz ($\delta = 8$ dB),

$$L\beta = \frac{10}{\delta}(L_{125i} - L_{125m}) = 1.25(L_{125i} - L_{125m}) \tag{20.9}$$

Example for Surging. Used is a set of random data having a Gaussian distribution with a standard deviation of about 3 dB for the combined 16–31.5–63-Hz band. Superimposed is a sinusoidal variation with a peak-to-peak amplitude of 15 dB. Shown in Table 20.8 are 10 of the 1000 measured octave-band levels each 100 ms in length. The three-band-sum defined above is given in the last column.

The summary data for 1000 samples are listed in Table 20.9. The correction K_{LFC} to be added to the L_{eq} at 31.5 Hz comes from Eq. (20.4) and equals 11.5 dB, yielding the adjusted 31.5-dB band level equal to 73.1 dB. From Eq. (20.7), the correction K_{125C} is found to be 1.6 dB, yielding 44.7 dB. The corrected spectrum is shown in the last line of Table 20.9. When the corrected spectrum is plotted in Fig. 20.4 or is determined from Eq. (20.3), it is found that the highest RNC curve touched is RNC-44 (at 31.5 Hz). If there had been no correction, the highest curve touched would have been RNC-22. The strong surging and turbulence has changed the rating from RNC-22 to RNC-44.

TABLE 20.8 Ten 100-ms Samples from a Total of 1000 Samples[a]

ith Band Numbers	By Octave-Band Mid frequencies, Hz										L_{LFi} Three-Band-Sum, (dB)
	16	31.5	63	125	250	500	1000	2000	4000	8000	
1	41.3	52.0	32.4	33.8	26.7	21.7	14.2	10.7	7.4	3.4	53.1
2	63.8	53.8	35.3	35.8	28.5	24.7	17.7	14.1	8.3	4.0	56.3
3	48.8	46.9	41.9	32.5	24.8	22.2	16.1	10.0	5.7	2.5	56.4
4	69.6	54.8	39.6	42.3	31.8	28.2	21.1	19.4	12.9	9.3	59.5
5	67.3	55.7	45.8	46.4	41.0	36.7	29.2	25.2	22.3	17.4	61.9
6	75.5	52.3	44.6	39.0	32.3	26.8	22.7	19.2	12.7	8.7	63.6
7	59.7	52.8	50.0	50.3	37.8	33.8	28.5	25.5	19.5	16.8	64.4
8	61.8	63.0	46.8	47.8	41.4	35.9	27.6	25.2	18.7	16.1	65.1
9	65.2	65.2	46.6	44.3	39.5	34.1	26.7	23.9	19.1	14.3	66.6
10	64.8	66.5	44.2	42.7	34.2	30.0	24.0	19.2	15.3	12.4	67.2
Mean level L_{LFm} of these 10 samples.											61.4
Standard deviation σ of these 10 samples.											4.8
Equivalent sound level L_{eq} of these 10 samples.											63.4

[a]Data Represent a Gaussian noise with a superimposed surge implemented by a sine wave with a 2-s period and a 15-dB peak-to-peak amplitude.

Simplified Method: Corrections to Measured Levels in 16–125-Hz Octave Bands When There Are Large Random Reflections and Not Strong Surging. By this method, the same equations are used to determine the corrections to the adjusted 31- and 125-Hz bands, that is, Eqs. (20.4) and (20.7), but the quantities $K_{LF\delta}$ and $K_{125\delta}$ are calculated from

$$K_{LF\delta} = 0.115\left(\frac{10}{\delta}\right)^2 \sigma_{LF}^2 = 0.115(2)^2\sigma_{LF}^2 = 0.46\sigma_{LF}^2 \tag{20.10}$$

where σ_{LF} is the standard deviation of the L_{LFi} (three-band-sum) series, and

$$K_{125\delta} = 0.115\left(\frac{10}{\delta}\right)^2 \sigma_{125}^2 = 0.115(1.2)^2\sigma_{125}^2 = 0.166\sigma_{125}^2 \tag{20.11}$$

where σ_{125} is the standard deviation of the L_{125i} series.

20.3 ACOUSTICALLY INDUCED VIBRATIONS AND RATTLES

From experience, primarily on the West Coast of the United States, an assessment has been made of the probability of acoustically induced vibration and rattles in lightweight wall and ceiling constructions (including light fixtures, windows, and some furnishings). Obviously, significant fluctuations or surging must be present in the HVAC noise. The region of likely probability where such vibrations in lightweight construction can be clearly felt is shown as A in Figs 20.1–20.4.[11] In

TABLE 20.9 Summary Data for RNC Example[a]

	Three-Band-Sum	Octave-Band Mid frequencies, Hz 16	31.5	63	125	250	500	1000	2000	4000	8000
L_{eq}	64.5	68.6	61.8	46.0	43.2	35.9	30.9	24.9	20.9	17.0	12.9
L_m (mean)	60.3	60.2	62.0	54.9	42.1	39.9	32.9	28.0	22.0	18.0	14.0
$L_{eq} - L_m$	4.2	6.6	6.8	3.9	3.2	2.9	2.9	2.9	2.9	2.9	2.9
Eqs. (20.5) and (20.8)	15.5	—	—	—	4.8						
Eqs. (20.4) and (20.7)											
Band corrections	—	—	11.3	—	1.6						
Corrected spectrum	—	—	73.1	—	44.7	35.9	30.9	24.9	20.9	17.0	12.9
Highest RNC curve "touched"	—	—	44	—	25	25	25	23	23	23	22

[a]The L_{eq} is the energy average level in each octave band for all 1000 of the 100-ms samples. The three-band-sum correction of 11.3 dB is added to the L_{eq} of the 31.5-Hz octave band to give an adjusted (for surging) level of 73.1 dB. At 125 Hz the adjusted level is 44.8 dB, 1.6 dB above the L_{eq} level.

very well built structures, such as are expected in concert halls and opera houses, the sound levels can extend into region A without expectation of feelable surface vibrations or audible rattles. In office and school buildings attention should be paid to L_{eq} levels that reach 70 dB or more in the 16- and 31.5-Hz octave bands because of current trends in HVAC design and installation.

20.4 CRITERIA FOR NOISE ANNOYANCE IN COMMUNITIES

The major sources of noise in communities are road, rail and air traffic, industries, construction, and public works. The most common metric used in the United States for estimating the annoyance or disturbance of community noise is the A-weighted day–night sound level (L_{dn}) [see Eq. (1.25)] with slow meter response. The A weighting discriminates against low-frequency sound energy, similar to the way that the hearing apparatus judges loudness. The sound energy of each noise-producing event is summed separately into the total. All of the energy of a noise that rises and falls as a source approaches and departs is summed into the total. The sound energy of each event at night is multiplied by 10 before it is added into the total. This treatment means that a few aircraft fly-bys at night may be as annoying to residents as a large number in the daytime. The European Union countries, for the most part, use a day–evening–night level.

The day–night sound level (L_{dn}) that is agreed on by nearly all agencies, boards, and standards-setting bodies to be the threshold for noise impact in urban residential areas is $L_{dn} = 55$ dBA.[15] In other words, people will begin to complain seriously about the noise if the level is higher. Some agencies speak of this energy-average level as being determined over a period of 12 months. Only the U.S. Federal Aviation Administration (FAA) and the Department of Defense (DOD) speak of a L_{dn} equal to 65 dBA as being the level at which noise begins to impact unfavorably on people in residential areas. Some studies indicate that in urban communities just under half of the U.S. population is exposed to L_{dn} levels of 55 dBA or greater. The World Health Organization (WHO, 1999) has stated that serious annoyance may occur for a L_{dn} of approximately 55 dBA, while moderate annoyance will have a threshold of about 50 dBA. It further recommends that the maximum level L_{max} at night should not exceed 40 dBA.

A possible reason for the 65-dBA level used by the FAA and DOD is that people near airports, on average, have learned to accept higher noise levels or, if not, they have moved away. This also assumes that the airport's relations with the communities surrounding it are good. Quiet rural communities seem to demand lower (5–10 dBA) noise levels.

20.5 TYPICAL URBAN NOISE

A summary of A-weighted noise levels measured in U.S. city areas, daytime and nighttime, is given in Fig. 20.5. Trucks and buses are principal sources of

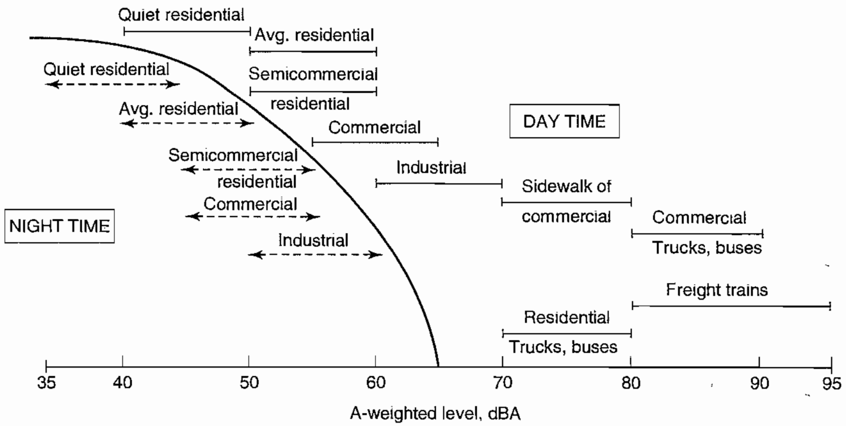

FIGURE 20.5 Schematic display of typical A-weighted noise levels by day and by night in different U.S. urban areas.[4] Noise around industrial areas is frequently caused by trucks.

noise. Parenthetically, the levels in this figure are not L_{dn}, but rather A-weighted levels in a residential area that vehicles produce when they travel on the streets surrounding that neighborhood. In urban residential areas, the noise is frequently the roar of traffic on thoroughfares that may be up to a kilometer away. Traffic noise is likely to be relatively steady and go on all night at a reduced level. If thoroughfares exist on two or more sides of an area, the noise is often nearly uniform over the area.

REFERENCES

1. American National (Draft) Standard ANSI S12.2-200x, "Criteria for Evaluating Room Noise" (not yet subject to extended comment or vote, 2004).
2. L. L. Beranek, "Applications of NCB and RC noise criterion curves for specification and evaluation of noise in buildings," *Noise Control Eng. J.*, **45**, 209–216 (1997).
3. L. L. Beranek, "Revised Criteria for Noise Control in Buildings," *Noise Control*, **3**, 19–27 (1957).
4. L. L. Beranek, *Noise and Vibration Control*, rev. ed., Institute of Noise Control Engineering, Marstun Itall, Iowa State University, Ames, IA, 1988.
5. L. L. Beranek, "Criteria for Office Quieting Based on Questionnaire rating Studies," *J. Acoust. Soc. Am.*, **28**, 833–852 (1956).
6. L. L. Beranek, *Transactions Bulletin No. 18*, Industrial Hygiene Foundation, Pittsburgh, PA, 1950.
7. ANSI S3.14–1977 (R-1986), *"Rating Noise with Respect to Speech Interference,"* Acoustical Society of America, Melville, NY, 1986.
8. ANSI S3.3–1960 (R 1992), *"Procedure for the Computation of the Loudness of Noise,"* Acoustical Society of America, Melville, NY, 1992.

9. D. W. Robinson, and L. S. Whittle, "The Loudness of Octave Bands of Noise," *Acustica*, **14**, 24–35 (1964).
10. L. L. Beranek, "Balanced Noise Criterion (NCB) Curves," *J. Acoust. Soc. Am.*, **86**, 650–664 (1989); "Application of NCB Noise Criterion Curves," *Noise Control Eng. J.*, **33**, 45–56 (1989).
11. G. C. Tocci, "Room Noise Criteria—The State of the Art in the Year 2000," *NOISE/NEWS International*, **8**, 106–119 (2000).
12. W. E. Blazier, "RC Mark II: A Refined Procedure for Rating the Noise of Heating, Ventilating and Air-Conditioning (HVAC) Systems in Buildings," *Noise Control Eng. J.*, **45**, 243–250 (1997).
13. P. D. Schomer, "Proposed Revisions to Room Noise Criteria," *Noise Control Eng. J.*, **48**, 85–96 (2000).
14. P. D. Schomer, and J. S. Bradley, "A Test of Proposed Revisions to Room Noise Criteria Curves," *Noise Control Eng. J.*, **48**, 124–129 (2000).
15. P. D. Schomer, *A White Paper: ASSESSMENT OF NOISE ANNOYANCE*, Schomer and Associates, Champaign, IL, April 22, 2001.

CHAPTER 21

Acoustical Standards for Noise and Vibration Control

ANGELO CAMPANELLA
Consultant
Columbus, Ohio

PAUL SCHOMER
Consultant
Champaign, Illinois

LAURA ANN WILBER
Consultant
Wilmette, Illinois

21.1 WHERE TO FIND AND HOW TO SELECT U.S. NATIONAL AND ISO STANDARDS

This chapter is arranged to provide the titles of North American and international (ISO) standards of interest to noise control engineers, according to specific noise control technology categories such as absorption and insulation (isolation). Acoustical terminology may be found in ANSI S1.1-1994 (R1999), *Acoustical Terminology* and ASTM C634, *Standard Terminology Relating to Environmental Acoustics*. The titles of some standards listed here are truncated to save space. Verbal descriptions, if offered, are brief. As with any technology, state-of-the-art advances bring updated versions of many of these documents. These standards are periodically reviewed and possibly revised by the responsible committees, often on a five-year cycle. A few ANSI standards have become an adoption of the corresponding ISO document, indicated as "Adoption" or "NAIS" (Nationally Adopted International Standard). The reader is encouraged to search anew for recent revisions of these documents. Be advised that some engineering applications may specify past versions, especially as part of a long procurement program or arbitrated contract. It is up to the reader to determine, in participation with interested parties as necessary, which version to use. For the latest standards version, often listed according to the standard's numeral title (e.g., ANSI S12.19 can be found by searching www.ansi.org for S12.19), see the public Internet web page listing by the providing agencies. Some of these agency pages are:

www.ANSI.org (ANSI)
www.ari.org (ARI—free downloads)
www.asastore.aip.org (ANSI + ISO standards available)
www.ashrae.com (ASHRAE)
www.asme.org (ASME)
www.astm.org (ASTM)
www.iec.ch (IEC)
www. iso.ch (ISO)
www.nssn.org (National Standards Systems Network, all standards available)
www.sae.org (SAE)

21.2 SOUND LEVEL MEASUREMENTS

Instrumentation

Standards for noise-measuring instruments, generally measuring sound pressure level (SPL) or "sound level," are listed separate from hearing-measuring instruments (audiometry). Common sound-measuring instruments include sound-level meters, calibrators, filters, and microphones. The most common sound measurement instruments for noise control are specified in ANSI S1.4. Such an instrument comprises a pressure sensor such as a condenser microphone, an amplifier with special wide-band and narrow-band filters, time-averaging circuits, a display, and some memory functions. The precision varies as type 0 (most accurate) to type 2 (least accurate). This entire system can be calibrated at any time with an appropriate calibrator. The acoustical velocity is rarely measured in practice, except for the use of dynamic (velocity) microphones for some audio purposes. The "intensity" method combines SPL and acoustical velocity measurements at a point to compute the intensity value at that point. Applicable standards are as follows:

ANSI S1.4-1983 (R2001), *Specification for Sound Level Meters*. Conforms closely to the IEC standard for sound-level meters, Publication 651, first edition, issued in 1979, but improved for measurement of transient sound signals and it permits the use of digital displays, rigorous definition of the fast and slow exponential time averaging, increase in the crest factor requirement to 10 for type 1 instruments, specification of a type 0 laboratory instrument with generally smaller tolerance limits than specified for type 1, and deletion of the type 3 survey instrument. The corresponding IEC standard (IEC 61672-1:2002 and IEC 61672-2:2003) contains more stringent environmental requirements. In 2003, ANSI S1.4 was under revision to better correspond.

ANSI S1.6-1984 (R2001), *Preferred Frequencies, Frequency Levels, and Band Numbers for Acoustical Measurements*.

ANSI S1.8-1989 (R2001), *Reference Quantities for Acoustical Levels*.

ANSI S1.9-1996 (R2001), *Instruments for the Measurement of Sound Intensity*. Requirements for instruments to measure sound intensity employing the two-microphone technique. Similar to IEC 1043.

ANSI S1.10-1966 (R2001), *Method for the Calibration of Microphones*.

ANSI S1.11-1986 (R1998), *Specification for Octave-Band and Fractional-Octave-Band Analog and Digital Filters*. Performance requirements for fractional-octave-band bandpass filters, in particular octave-band and one-third-octave-band filters, applicable to passive or active analog filters that operate on continuous-time signals to analog and digital filters that operate on discrete-time signals and to fractional-octave-band analyses synthesized from narrow-band spectral components. Four accuracy grades are allowed: the most accurate for precise analog and digital filters. The two least accurate grades meet the requirements of S1.11-1966. Also see IEC 61260:1995.

ANSI S1.14-1998, *Recommendations for Specifying and Testing the Susceptibility of Acoustical Instruments to Radiated Radio-Frequency Electromagnetic Fields, 25 MHz to 1 gHz*.

ANSI S1.15-1997/Part 1 (R2001), *Measurement Microphones*. Part 1: *Specifications for Laboratory Standard Microphones*. This is comparable to the international standard IEC 1094-1:1992, "Measurement Microphones—Part 1: Specifications for Laboratory Standard Microphones."

ANSI S1.16-2000, *Method for Measuring the Performance of Noise Discriminating and Noise Canceling Microphones*.

ANSI S1.17-2004/Part 1, *Measurement and Specifications of Insertion Loss of Wind Screens in Still or Slightly Moving Air*. Determines the insertion loss of wind screens when installed on measuring microphones over a defined frequency range.

ANSI S1.40-1984 (R2001), *Specification for Acoustical Calibrators*. Requirements for coupler-type acoustical calibrators, including the SPL in the coupler, the frequency of the sound, and the determination of the influence of atmospheric pressure, temperature, humidity, and magnetic fields on the pressure level and frequency of the sound produced by the calibrator. (Also see IEC 60942:2003.)

ANSI S1.42-2001, *Design Response of Weighting Networks for Acoustical Measurements*.

ANSI S1.43-1997 (R2002), *Specifications for Integrating Averaging Sound Level Meters*. Consistent with the relevant requirements of ANSI S1.4-1983 (R1997) but specifies additional characteristics needed to measure the time-average SPL of steady, intermittent, fluctuating, and impulsive sounds. (See also IEC 61672-1:2002 and IEC 61672-2:2003.)

ANSI S12.3-1985 (R2001), *Statistical Methods for Determining and Verifying Stated Noise Emission Values of Machinery and Equipment*. Preferred methods for determining and verifying noise emission values for machinery and equipment which are stated in product literature or labeled by other means.

SPL Measurement Techniques

ANSI S1.13-1995 (R1999), *Measurement of Sound Pressure Levels in Air*. Procedures for the measurement of sound levels in air at a single point indoors but may be utilized in outdoor measurements under specified conditions. Includes identification of prominent discrete tones.

ASTM E1014-2000. *Measurement of Outdoor A-Weighted Sound Levels.* A guide for measuring outdoor sound levels over various time periods, intended to be used by practitioners in the field as well as by members of the general public who have little or no special technical training in areas relating to acoustics.

ANSI S1.25-1991 (R2002), *Specification for Personal Noise Dosimeters.* Makes provision for three exchange rates: 3, 4, and 5 dB per doubling of exposure time. Provides tolerances for the entire instruments, parameters, including frequency response, exponential averaging employing slow and fast transient time response, threshold, and dynamic range, for SPL measurement in a random-incidence sound field without the presence of a person wearing the instrument.

ANSI S12.19-1996 (R2001), *Measurement of Occupational Noise Exposure.* Methods that can be used to measure a person's noise exposure received in a workplace. Provides uniform procedures and repeatable results for the measurement of occupational noise exposure.

ISO 11204:1995, *Noise Emitted by Machinery and Equipment—Measurement of Emission Sound Pressure Levels at a Work Station and at Other Specified Positions—Method Requiring Environmental Corrections.*

Intensity Instruments and Measurement Techniques

ANSI S1.9-1996 (R2001), *Instruments for the Measurement of Sound Intensity.* Requirements for instruments to measure sound intensity employing the two-microphone technique. Similar to IEC 1043.

ANSI S12.12-1992 (R2002), *Standard Engineering Method for the Determination of Sound Power Levels of Noise Sources Using Sound Intensity.* Measures the sound power level of noise sources in indoor or outdoor environments using sound intensity instrumentation.

ISO 9614-1:1993, *Determination of Sound Power Levels of Noise Sources Using Sound Intensity.* Part 1: *Measurement at Discrete Points.* Part 2: *Measurement by Scanning.*

21.3 SOUND POWER MEASUREMENT TECHNIQUES

ANSI S12.5-1990 (R1997), *Requirements for the Performance and Calibration of Reference Sound Sources.* Requirements, including free-field laboratory calibration above a reflecting plane, for reference sound sources used in the substitution measurement of sound power.

ANSI S12.11-1987 (R1997), *Method for the Measurement of Noise Emitted by Small Air-Moving Devices.* Measures sound power emitted by small air-moving devices, reported as the noise power emission level in bels. Includes device-mounting methods, test environmental conditions, and device operation method during the tests.

ISO 10302:1996, *Method for the Measurement of Airborne Noise Emitted by Small Air-Moving Devices.*

ANSI S12.15-1992 (R2002), *Measurement of Sound Emitted by Portable Electric Power Tools, Stationary and Fixed Electric Power Tools, and Gardening Appliances.* Methods for SPL measurement and the subsequent calculation of sound power levels.

ANSI S12.23-1989 (R2001), *Method for the Designation of Sound Power Emitted by Machinery and Equipment.* Expressing the noise emission of machinery and equipment as overall A-weighted sound power on labels or other noise emission documentation.

ANSI S12.30-1990 (R2002), *Guidelines for the Use of Sound Power Standards and for the Preparation of Noise Test Codes.* Six standards for determining the sound power levels of equipment for sound test codes for machines and equipment.

ANSI S12.35-1990 (R2001), *Precision Methods for the Determination of Sound Power Levels of Noise Sources in Anechoic and Hemi-Anechoic Rooms.* Determination of the sound power levels of noise sources in laboratory anechoic or hemi-anechoic room, the instrumentation, installation, source operation, SPL measurement surface; calculation of sound power level, directivity index, and directivity factor.

ANSI S12.44-1997 (R2002), *Methods for Calculation of Sound Emitted by Machinery and Equipment at Workstations and Other Specified Positions from Sound Power Level.* Determining emission SPLs from the sound power level values of machinery and equipment at workstations and other locations.

ANSI S12.50-2002 National Adopted International Standard (NAIS), *Determination of Sound Power Levels of Noise Sources—Guidelines for the Use of Basic Standards.* Adoption of ISO 3740:2000. Summaries of ISO 3741–3747 and selection of one or more standards appropriate to any particular type (Clause 6 and Annex D). Used in the preparation of noise test codes (see ISO 12001) and noise testing where no specific noise test code exists.

ANSI S12.51-2002 (including Corrigendum 1 : 2001) NAIS standard, *Acoustics—Determination of Sound Power Levels of Noise Sources Using Sound Pressure—Precision Method for Reverberation Rooms.* Adoption of ISO 3741:1999, a direct method and a comparison method for determining the sound power level produced by a source in a standard environment.

ANSI S12.53/1-1999 ISO 3743-1:1994, *Determination of Sound Power Levels of Noise Sources—Engineering Methods for Small, Movable Sources in Reverberant Fields.* Part 1: *Comparison Method for Hard-Walled Test rooms. (Adoption of ISO 3743-1.)* Part 2: *Methods of Special Reverberation Test Rooms. (Adoption of ISO 3743-2.)*

ANSI S12.54-1999 ISO 3744:1994, *Determination of Sound Power Levels of Noise Sources Using Sound Pressure—Engineering Method in an Essentially Free Field over a Reflecting Plane.* Adoption of ISO 3744, sound power engineering accuracy, measurement by the comparison method in an anechoic environment.

ANSI S12.56-1999 ISO 3746:1995, *Determination of Sound Power Levels of Noise Sources Using Sound Pressure—Survey Method Using an Enveloping Measurement Surface over a Reflecting Plane.* Adoption of ISO 3746, determining the sound power level of sound sources In Situ, especially if nonmovable, in octave bands from which the A-weighted sound power level is calculated. The accuracy will be that of either an engineering method or a survey method.

ARI 250-2001, *Performance and Calibration of Reference Sound Sources.*

ARI 280-95, *Requirements for the Qualification of Reverberant Rooms in the 63 Hz Octave Band.*

ASTM E1124-97, *Standard Test Method for Field Measurement of Sound Power Level by the Two-Surface Method.* An In Situ survey measurement of sound power level with sound pressure measurements at two concentric surfaces.

ISO 3740:2000, *Determination of Sound Power Levels of Noise Sources—Guidelines for the Use of Basic Standards.*

ISO 3741:1999, *Determination of Sound Power Levels of Noise Sources Using Sound Pressure—Precision Methods for Reverberation Rooms.*

ISO 3743-1:1994, *Determination of Sound Power Levels of Noise Sources—Engineering Methods for Small, Movable Sources in Reverberant Fields.* Part 1: *Comparison Method for Hard-Walled Test Rooms.* Part 2: *Methods for Special Reverberation Test Rooms.*

ISO 3744:1994, *Determination of Sound Power Levels of Noise Sources Using Sound Pressure—Engineering Method in an Essentially Free Field over a Reflecting Plane.*

ISO 3745:1977, *Determination of Sound Power Levels of Noise Sources—Precision Methods for Anechoic and Semi-Anechoic Rooms.*

ISO 3746:1995, *Determination of Sound Power Levels of Noise Sources Using Sound Pressure—Survey Method Using an Enveloping Measurement Surface over a Reflecting Plane.*

ISO 3747:2000, *Determination of Sound Power Levels of Noise Sources Using Sound Pressure—Comparison Method In Situ.*

ISO 5135:1997, *Determination of Sound Power Levels of Noise from Air-Terminal Devices, Air-Terminal Units, Dampers and Valves by Measurement in a Reverberation Room.*

ISO 5136:1990, *Determination of Sound Power Radiated into a Duct by Fans—In-Duct Method.*

ISO 6926:1999, *Requirements for the Performance and Calibration of Reference Sound Sources Used for the Determination of Sound Power Levels.*

21.4 MACHINERY NOISE EMISSION MEASUREMENT TECHNIQUES

ANSI S12.1-1983 (R2001), *Guidelines for the Preparation of Standard Procedures to Determine the Noise Emission from Sources.* Included are the general questions to be asked during development of a measurement procedure. Included are prefatory material, measurement conditions, measurement operations, data reduction, preparation of a test report, and guidelines for the selection of a descriptor for noise emission.

ANSI S12.10-2002 ISO 7779:1999 NAIS standard, *Measurement of Airborne Noise Emitted by Information Technology and Telecommunications Equipment.* Adoption of ISO 7779:1999 and its amendment ISO 7779: 1999/FDAM 1.

ANSI S12.16-1992 (R2002), *Guidelines for the Specification of Noise of New Machinery.* Methods to calculate workplace noise SPL from test data produced by manufacturers of stationary equipment. This references existing ANSI, trade, and professional association measurement standards and techniques to be used by manufacturers to produce individual raw machine sound power or SPL test data.

ANSI S12.43-1997 (R2002), *Methods for the Measurement of Sound Emitted by Machinery and Equipment at Workstations and Other Specified Positions.* Three methods to measure SPLs: (1) in a free field over a reflecting plane, (2) in normal operating environments, and (3) when operating in their normal environments when less accurate measurements are acceptable.

ARI 530-95, *Method of Measuring Sound and Vibration of Refrigerant Compressors.*

ARI 575-94, *Method of Measuring Machinery Sound within an Equipment Space.*

ISO 4412-1:1991, *Hydraulic Fluid Power—Test Code for Determination of Airborne Noise Levels.* Part 1: *Pumps.* Part 2: *Motors.* Part 3: *Pumps—Method Using a Parallelepiped Microphone Array.*

ISO 4871:1996, *Declaration and Verification of Noise Emission Values of Machinery and Equipment.*

ISO 7574-1:1985, *Statistical Methods for Determining and Verifying Stated Noise Emission Values of Machinery and Equipment.* Part 1: *General Considerations and Definitions.* Part 2: *Methods for Stated Values for Individual Machines.* Part 3: *Simple (Transition) Method for Stated Values for Batches of Machines.* Part 4: *Methods for Stated Values for Batches of Machines.*

ISO 7779:1999, *Measurement of Airborne Noise Emitted by Information Technology and Telecommunications Equipment.*

ISO 9295:1988, *Measurement of High-Frequency Noise Emitted by Computer and Business Equipment.*

ISO 9296:1988, *Declared Noise Emission Values of Computer and Business Equipment.*

ISO 9611:1996, *Characterization of Sources of Structure-Borne Sound with Respect to Sound Radiation from Connected Structures—Measurement of Velocity at the Contact Points of Machinery When Resiliently Mounted.*

ISO 11200:1995, *Noise Emitted by Machinery and Equipment—Guidelines for the Use of Basic Standards for the Determination of Emission Sound Pressure Levels at a Work Station and at Other Specified Positions.*

ISO 11201:1995, *Noise Emitted by Machinery and Equipment—Measurement of Emission Sound Pressure Levels at a Work Station and at Other Specified Positions—Engineering Method in an Essentially Free Field over a Reflecting Plane.*

ISO 11202:1995, *Noise Emitted by Machinery and Equipment—Measurement of Emission Sound Pressure Levels at a Work Station and at Other Specified Positions—Survey Method* In Situ.

ISO 11203:1995, *Noise Emitted by Machinery and Equipment—Determination of Emission Sound Pressure Levels at a Work Station and at Other Specified Positions from the Sound Power Level.*

ISO 10846, *Acoustics and Vibration—Laboratory Measurement of Vibro-Acoustic Transfer Properties of Resilient Elements.* Part 1—1997: *Principles and Guidelines.* Part 2—1997: *Dynamic Stiffness of Elastic Supports for Translatory Motion—Direct Method.* Part 3—2002: *Indirect Method for Determination of the Dynamic Stiffness of Resilient Supports for Translatory Motion.*

ISO 11690-1, *Recommended Practice for the Design of Low-Noise Workplaces Containing Machinery.* Part 1: *Noise Control Strategies.* Part 2: *Noise Control Measures.* Part 3: *Sound Propagation and Noise Prediction in Workrooms.*

21.5 IMPACT OF NOISE IN WORKPLACE

Two qualities of workplace noise are of concern as they affect damage to hearing and speech communication. Environmental noise includes vibration and infrasound. Hearing conservation measurements are of two forms: measurement of hearing acuity and measurement of noise levels in work and recreational environments.

Hearing Testing (Audiometry) Equipment and Procedures

ANSI S3.1-1999, *Maximum Permissible Ambient Noise Levels for Audiometric Test Rooms.* Specifies maximum permissible ambient noise levels (MPANLs) allowed in an audiometric test room.

ANSI S3.6-1996, *Specification for Audiometers.* The audiometers covered in this specification are devices designed for use in determining the hearing threshold of an individual in comparison with a chosen standard reference threshold level.

ANSI S3.21-1978 (R1997), *Methods for Manual Pure-Tone Threshold Audiometry.* Outlines the procedure for pure-tone threshold audiometry used in the assessment of an individual's threshold of hearing for pure tones.

ISO 226:1987, *Normal Equal-Loudness Level Contours.* Data in this standard formed the basis for the dBA and dBC curves used in noise measurement.

ISO 389, 1964 Acoustics, *Standard Reference Zero for the Calibration of Pure-Tone Audiometers.* Part 1: *Reference Equivalent Sound Pressure Levels for Pure Tones and Supra-Aural Earphones.* Part 2: *Reference Equivalent Threshold Sound Pressure Levels for Pure Tones and Insert Earphones.* These data are also shown in ANSI S3.6-1996.

ISO 6189:1983, *Pure Tone Air Conduction Threshold Audiometry for Hearing Conservation Purposes.* Outlines the procedure for testing hearing thresholds as well as describes the conditions of the testing. Part of this standard is similar to information found in ANSI S3.21-1978 (R1997).

ISO 7029:2000, *Statistical Distribution of Hearing Thresholds as a Function of Age.* Gives expected threshold values for men and women without a history of noise exposure. Data are utilized in ISO 1999 and ANSI S3.44-1996.

ISO 8253-1:1989, *Audiometric Test Methods*—Part 1: *Basic Pure Tone Air and Bone Conduction Threshold Audiometry.* Part 2: *Sound Field Audiometry with Pure Tone and Narrow-Band Test Signals.* Part 3: *Speech Audiometry.*

ISO 11904-1:2002, *Determination of Sound Immission from Sound Sources Placed Close to the Ear.* Part 1: *Technique Using a Microphone in a Real Ear (MIRE Technique).* Some of the data in this standard are similar to that in ANSI S12. 42-1995 (R1999).

IEC 60645-1 Ed 2.0 b: 2001, *Electroacoustics—Audiological Equipment.* Part I: *Pure-Tone Audiometers.* Has material also found in ANSI S3.6-1996.

Hearing Conservation Programs

ANSI S3.44-1996 (R2001), *Determination of Occupational Noise Exposure and Estimation of Noise-Induced Hearing Impairment.* Adoption of ISO 1999:1990(E) of the same name; however, S3.44 allows assessment of noise exposure using a time–intensity trading relation other than a 3-dB increase per halving of exposure time.

ANSI S12.6-1997 (R2002), *Methods for Measuring the Real-Ear Attenuation of Hearing Protectors.* Specifies laboratory-based procedures for measuring, analyzing, and reporting the noise-reducing capabilities of conventional passive hearing protection devices.

ANSI Technical Report S12.13 TR-2002, *Evaluating the Effectiveness of Hearing Conservation Programs through Audiometric Data Base Analysis.* Describes methods for evaluating the effectiveness of hearing conservation programs in preventing occupational noise-induced hearing loss by using techniques for audiometric database analysis.

ANSI S12.42-1995 (R1999), *Microphone-in-Real-Ear and Acoustic Test Fixture Methods for the Measurement of Insertion Loss of Circumaural Hearing Protection Devices.* Describes the microphone-in-real-ear and the acoustical test fixture methods for the measurement of the insertion loss of circumaural earmuffs, helmets, and communications headsets.

ISO 1999:1999, *Acoustics—Determination of Occupational Noise Exposure and Estimation of Noise-Induced Hearing Impairment.* Similar to ANSI S3.44-1996 except that ISO 1999 is more restrictive.

ISO 4869-1:1990, *Hearing Protectors*—Part 1: *Subjective Method for the Measurement of Sound Attenuation.* Part 2: *Estimation of Effective A-Weighted Sound Pressure Levels When Hearing Protectors Are Worn.* Part 3: *Simplified Method for the Measurement of Insertion Loss of Ear-Muff Type Protectors for Quality Inspection Purposes.* Part 4: *Measurement of Effective Sound Pressure Levels for Level-Dependent Sound-Restoration Ear-Muffs.*

ISO 7029:2000, *Statistical Distribution of Hearing Thresholds as a Function of Age.*

ISO 9612:1997, *Guidelines for the Measurement and Assessment of Exposure to Noise in a Working Environment.*

Speech Communication Metrics

ANSI S3.2-1989 (R1999), *Method for Measuring the Intelligibility of Speech over Communication Systems.* A revision of ANSI S3.2-1960 (R1982). Provides three alternative sets of lists of English words to be spoken by trained talkers over the speech communication system to be evaluated.

ANSI S3.4-1980 (R1997), *Procedure for the Computation of Loudness of Noise.* Specifies a procedure for calculating the loudness of certain classes of noise.

ANSI S3.5-1997 (R2002), *Methods of the Calculation of the Speech Intelligibility Index (SII).* Computation of the SII based on the intelligibility of speech as evaluated by speech perception tests given a group of talkers and listeners.

ASTM 1130-2002, *Objective Measurement of Speech Privacy in Open Offices Using Articulation Index (AI).* Computation of the Articulation Index (AI) from standard speech levels, ambient noise, and articulation weighting factors.

ANSI S3.14-1977 (R1997), *Rating Noise with Respect to Speech Interference.* Defines a simple numerical method for rating the expected speech-interfering aspect (Speech Interference Level, SIL) of noise using acoustical measurements of the noise.

ISO/TR 3352, 1974, *Acoustics—Assessment of Noise with Respect to Its Effect on the Intelligibility of Speech.* This technical report has never been approved as a standard in part because of the concern over whether the impact of noise is similar for each language.

ISO/TR 4870:1991, *The Construction and Calibration of Speech Intelligibility Tests.*

Environmental Noise SPL Measurement Methods

Environmental noise SPL measurements are typically made outdoors to mirror most regulations. Sound measurement locations are often near houses or in empty fields and near transportation and industrial noise sources. In addition to meeting all the requirements of ANSI S1.4, this acoustical equipment and its application must be tolerant of wind, rain, birds, insects, and mechanical abuse. Primary noise sources include transportation (aircraft, road traffic, trains, etc.), industrial facilities, neighborhood noise (pets, heating, ventilation, and air conditioning), recreational noise (shooting ranges, races, and music venues).

ANSI S12.18-1994 (R1999), *Procedures for Outdoor Measurement of Sound Pressure Level.* Procedures for the measurement of SPLs outdoors, considering ground effects and refraction due to wind and temperature gradients and to turbulence. Measurement of SPLs produced by specific sources outdoors. Method 1: general method, outlines conditions for routine measurements. Method 2: precision method, describes strict conditions for more accurate measurements, providing short-term A-weighted SPL or time-averaged SPL, A-weighted or in octave- or in one-third-octave or narrow-band SPL, but does not preclude determination of other sound descriptors.

ASTM E1014-84(2000), *Standard Guide for Measurement of Outdoor A-Weighted Sound Levels.* Basic technique for performing a reliable A-weighted sound-level measurement outdoors.

ASTM E1503-97, *Standard Test Method for Conducting Outdoor Sound Measurements Using a Digital Statistical Analysis System.* Covers the measurement of outdoor sound levels at specific locations using a digital statistical analyzer and a formal measurement plan.

ISO 7196: 1995, *Frequency-Weighting Characteristic for Infrasound Measurements.*

ISO 10843:1997, *Methods for the Description and Physical Measurement of Single Impulses or Series of Impulses.*

Environmental Noise Measurement Applications

ANSI S12.7-1986 (R1998), *Methods for Measurement of Impulse Noise.* Measures impulse noise from discrete events, such as quarry and mining explosions or sonic booms, or from multiple-event sources such as pile drivers, riveting, or machine-gun firing. Data may be reported as time variation of the sound pressure, with or without frequency weighting, and sound exposure level.

ANSI S12.8-1998 (R2003), *Methods for Determining the Insertion Loss of Outdoor Noise Barriers.* Determine the insertion loss of outdoor noise barriers, including direct before and after measurements, indirect before measurements at an "equivalent" site, and indirect predictions of "before" sound levels. Indirect before measurements and indirect before prediction methods require direct measurements of "after" sound levels. May use sound sources naturally present at a site, controlled natural sound sources, or controlled artificial sound sources. Receiver location and atmospheric, ground, and terrain conditions may be chosen. Worksheets are provided

ANSI S12.9-1988 (R2003), *Quantities and Procedures for Description and Measurement of Environmental Sound.* Part 1: *Basic Quantities for Description of Sound in Community Environments and General Procedures for Measurement of These Quantities.* Part 2: *Measurement of Long-Term, Wide Area Sound.* Part 3: *Short-Term Measurements with an Observer Present.* Part 4: *Noise Assessment and Prediction of Long-Term Community Response.* Part 5: *Sound Descriptors for Determination of Compatible Land Use.* Part 6: *Methods for Estimation of Awakenings Associated with Aircraft Noise Events Heard in Homes.*

ANSI/ASME PTC 36-1985 (R1998), *Measurement of Industrial Sound.* Procedures for measuring and reporting airborne sound emissions from mechanical equipment.

ARI 260-2001, *Sound Rating of Ducted Air Moving and Conditioning Equipment.*

ARI 270-95, *Sound Rating of Outdoor Unitary Equipment.*

ARI 275-97, *Application of Sound Rating Levels of Outdoor Unitary Equipment.*

ARI 300-2000, *Sound Rating and Sound Transmission Loss of Packaged Terminal Equipment.*

ARI 350-2000, *Sound Rating of Non-Ducted Indoor Air-Conditioning Equipment.*

ARI 370-2001, *Sound Rating of Large Outdoor Refrigerating and Air-Conditioning Equipment.*

ISO 1996, *Description and Measurement of Environmental Noise*. Part 1-2003: *Basic Quantities and Assessment Procedures.* Part 2-1987: *Acquisition of Data Pertinent to Land Use*. Part 3-1987: *Application to Noise Limits.*

ISO 3891:1978, *Procedure for Describing Aircraft Noise Heard on the Ground.*

ISO 8297:1994, *Determination of Sound Power Levels of Multisource Industrial Plants for Evaluation of Sound Pressure Levels in the Environment—Engineering Method.*

ISO 10847:1997, *In-Situ Determination of Insertion Loss of Outdoor Noise Barriers of All Types*. See also ANSI S12.8.

ISO/TS 13474:2003, *Impulse Sound Propagation for Environmental Noise Assessment.*

SAE J1075 (revised June 2000), *Surface Vehicle Standard (R) Sound Measurement—Construction Site*. Procedures and instrumentation to be used for determining a representative sound level during a representative time period at selected measurement locations on a construction site boundary.

Environmental Sound Propagation Outdoors

ANSI S1.18-1999, *Template Method for Ground Impedance*. Procedures for obtaining the real and imaginary parts of the specific acoustical impedance of natural ground surface outdoors.

ANSI S1.26-1995 (R1999), *Method for Calculation of the Absorption of Sound by the Atmosphere*. Still-atmosphere absorption losses of sound for a wide range of meteorological conditions.

ANSI S12.17-1996 (R2001), *Impulse Sound Propagation for Environmental Noise Assessment Response*. Engineering methods to calculate the propagation and attenuation of high-energy impulsive sounds through the atmosphere. It estimates the mean C-weighted sound exposure level of impulsive sound at distances ranging from 1 to 30 km, applicable for explosive masses between 50 and 1000 kg.

ISO 9613, *Attenuation of Sound during Propagation Outdoors*. Part 1-1993: *Calculation of the Absorption of Sound by the Atmosphere. Attenuation of Sound During Propagation Outdoors*. Part 2-1996: *General Method of Calculation*. Propagation attenuation, including barrier attenuation calculations, excess attenuation by hard and soft ground surfaces, and attenuation of sound by rows of buildings and by trees and shrubs.

ISO/TS 13474:2003, *Impulse Sound Propagation for Environmental Noise Assessment.*

Environmental Vibrations

ANSI S3.18-2002, *NAIS Standard Mechanical Vibration and Shock—Evaluation of Human Exposure to Whole-Body Vibration*. Part 1: *General Requirements*. Part of ISO 2631 defining methods for the measurement of periodic, random, and transient whole-body vibration. It indicates the principal factors that combine to determine the degree to which a vibration exposure will be acceptable.

ANSI S3.29-1983 (R2001), *Guide to the Evaluation of Human Exposure to Vibration in Buildings*. Reactions of humans to vibrations of 1–80 Hz inside buildings are assessed as degrees of perception and associated vibration levels and duration.

ANSI S3.34-1986 (R1997), *Guide for the Measurement and Evaluation of Human Exposure to Vibration Transmitted to the Hand*. The recommended method for the measurement, data analysis, and reporting of human exposure to hand-transmitted vibration.

ANSI S3.40-2002, *NAIS Standard Mechanical Vibration and Shock—Hand-Arm Vibration—Method for the Measurement and Evaluation of the Vibration Transmissibility of Gloves at the Palm of the Hand*. Adoption of ISO 10819:1996. A method for the laboratory measurement, data analysis, and reporting of the vibration transmissibility of gloves of vibrations from a handle to the palm of the hand in the frequency range 31.5–1250 Hz.

ISO 2631, *Mechanical Vibration and Shock—Evaluation of Human Exposure to Whole-Body Vibration*. Part 1-1997: *General Requirements*. Part 2-1989: *Continuous and Shock-Induced Vibrations in Buildings (1 to 80 Hz)*. Part 4-2001: *Guidelines for The evaluation of the Effects of Vibration and Rotational Motion on Passenger and Crew Comfort in Transport Systems.*

ISO 2671:1982, *Environmental Tests for Aircraft Equipment—Part 3.4: Acoustic Vibration.*

ISO 4866:1990, *Mechanical Vibration and Shock—Vibration of Buildings—Guidelines for the Measurement of Vibrations and Evaluation of Their Effects on Building.*

ISO 4867:1984, *Code for the Measurement and Reporting of Shipboard Vibration Data.*

ISO 5007:2003, *Agricultural Wheeled Tractors—Operator's Seat—Laboratory Measurement of Transmitted Vibration.*

ISO 5008:2002, *Agricultural Wheeled Tractors and Field Machinery—Measurement of Whole-Body Vibration of the Operator.*

ISO 5347-3:1993, *Calibration of Vibration and Shock Pick-ups*. Part 3: *Secondary Vibration Calibration*. Part 4: *Secondary Shock Calibration*. Part 5: *Calibration by Earth's Gravitation*. Part 6: *Primary Vibration Calibration at low Frequencies*. Part 7: *Primary Calibration by Centrifuge*. Part 8: *Primary Calibration by Dual Centrifuge*. Part 10: *Primary Calibration by High Impact Shocks*. Part 11: *Testing of Transverse Vibration Sensitivity*. Part 12: *Testing of Transverse Shock Sensitivity*. Part 13: *Testing of Base Strain Sensitivity*. Part 14: *Resonance Frequency Testing of Undamped Accelerometers on a Steel Block*. Part 15: *Testing of Acoustic Sensitivity*. Part 16: *Testing of Mounting Torque Sensitivity*. Part 17: *Testing of Fixed Temperature Sensitivity*. Part 18: *Testing of Transient Temperature Sensitivity*. Part 19: *Testing of Magnetic Field Sensitivity*. Part 22: *Accelerometer Resonance Testing—General Methods.*

ISO 5348:1998, *Mechanical Mounting of Accelerometers.*

ISO 5349-1:2001, *Mechanical Vibration—Guidelines for the Measurement and the Assessment of Human Exposure to Hand-Transmitted Vibration*. Parts of this standard are similar to ANSI S3.34-1986 (R1997). Part 2: *Practical Guidance for Measurement at the Workplace*.

ISO 5805:1997, *Mechanical Vibration and Shock—Human Exposure—Vocabulary*.

ISO 8041:1990, *Human Response to Vibration—Measuring Instrumentation*.

ISO 13091-1:2001, *Mechanical Vibration—Vibrotactile Perception Thresholds for the Assessment of Nerve Dysfunction*. Part 1: *Methods of Measurements at the Fingertips*.

ISO 8042:1988, *Characteristics to be Specified for Seismic Pick-Ups*.

ISO 9022-10:1998, *Optics and Optical Instruments—Environmental Test Methods*. Part 10: *Combined Sinusoidal Vibration and Dry Heat or Cold*. Part 15: *Combined Digitally Controlled Broad-Band Random Vibration and Dry Heat or Cold*.

21.6 VEHICLE EXTERIOR AND INTERIOR NOISE

There are many SAE and ISO standards dealing with the source of noise emissions of various motor vehicles, including road vehicle (automobiles, trucks, buses, and motorcycles), trains, boats, aircraft, construction equipment (e.g., dozer), agricultural equipment (e.g., tractor), and small-engine equipment (e.g., lawn edger). Full listings of these standards are maintained at the SAE and ISO websites. The following is a sampling of these standards. Quite a few are identically SAE and ISO standards.

Vehicle Noise — Interior Noise Measurement Techniques

ISO 2923:1996, *Measurement of Noise on Board Vessels*.

ISO 3095:1975, *Measurement of Noise Emitted by Railbound Vehicles*.

ISO 3381:1976, *Measurement of Noise Inside Railbound Vehicles*.

ISO 5128:1980, *Measurement of Noise Inside Motor Vehicles*.

ISO 5129:2001, *Measurement of Sound Pressure Levels in the Interior of Aircraft During Flight*.

ISO 5130:1982, *Measurement of Noise Emitted by Stationary Road Vehicles—Survey Method*.

ISO 5131:1996, *Tractors and Machinery for Agriculture and Forestry—Measurement of Noise at the Operator's Position—Survey method*.

ISO 7188:1994, *Measurement of Noise Emitted by Passenger Cars under Conditions Representative of Urban Driving*.

ISO 11819-1:1997, *Measurement of the Influence of Road Surfaces on Traffic Noise*. Part 1: *Statistical Pass-By Method*.

Road Surface Sound Absorption

See ISO 13472 below under Sound Absorption.

Vehicle Noise — Exterior Noise Measurement (Noise Emission) Techniques

SAE J366, *Exterior Sound Level for Heavy Trucks and Buses (APR 2001)*. Test procedure, environment, and instrumentation for determining the maximum exterior sound level for highway motor trucks, truck tractors, and buses.

ISO 3095:1975, *Measurement of Noise Emitted by Railbound Vehicles*. Obtaining reproducible and comparable measurement results of levels and spectra of noise emitted by all kinds of vehicles operating on rails or other types of fixed track except for track maintenance vehicles in operation.

SAE J34 (June 2001), *Exterior Sound Level Measurement Procedure for Pleasure Motorboats*. Procedure for measuring the maximum exterior sound level of pleasure motorboats while being operated under wide open-throttle conditions.

ISO 362:1998, *Measurement of Noise Emitted by Accelerating Road Vehicles—Engineering Method*. (Available in English only.)

SAE J16395 (ISO 6395) (February 2003), *Measurement of Exterior Noise Emitted by Earth-Moving Machinery—Dynamic Test Conditions*. Determining the noise emitted to the environment by earth-moving machinery in terms of the A-weighted sound power level while the machine is working under dynamic test conditions.

SAE J17216 (ISO 7216) (February 2003), *Agricultural and Forestry Wheeled Tractors and Self-Propelled Machines—Measurement of Noise Emitted When in Motion*. Measuring the A-weighted SPL in an extensive open space of the noise emitted by agricultural and forestry wheeled tractors and self-propelled machines fitted with elastic tires while the vehicle is in motion. It is not applicable to special forestry machinery, for example, forwarders, skidders, etc., as defined in ISO 6814.

ISO 4872:1978, *Measurement of Airborne Noise Emitted by Construction Equipment Intended for Outdoor Use*. Method for determining compliance with noise limits

ISO 6393:1998, *Measurement of Exterior Noise Emitted by Earth-Moving Machinery—Stationary Test Conditions*. (Available in English only.)

ISO 6394:1998, *Measurement at the Operator's Position of Noise Emitted by Earth-Moving Machinery—Stationary Test Conditions*. (Available in English only.)

ISO 6395:1988, *Measurement of Exterior Noise Emitted by Earth-Moving Machinery—Dynamic Test Conditions*.

ISO 6396:1992, *Measurement at the Operator's Position of Noise Emitted by Earth-Moving Machinery—Dynamic Test Conditions*.

ISO 6798:1995, *Reciprocating Internal Combustion Engines—Measurement of Emitted Airborne Noise—Engineering Method and Survey Method*.

ISO 7216:1992, *Agricultural and Forestry Wheeled Tractors and Self-Propelled Machines—Measurement of Noise Emitted When in Motion*.

ISO 7182:1984, *Measurement at the Operator's Position of Airborne Noise Emitted by Chain Saws*.

ISO 9645:1990, *Measurement of Noise Emitted by Two-Wheeled Mopeds in Motion—Engineering Method.*

ISO 11094:1991, *Test Code for the Measurement of Airborne Noise Emitted by Power Lawn Mowers, Lawn Tractors, Lawn and Garden Tractors, Professional Mowers, and Lawn and Garden Tractors with Mowing Attachments.*

21.7 ARCHITECTURAL NOISE CONTROL IN BUILDINGS

There are three categories of sound control standards for buildings. The first is for testing materials that limit sound transmission from one room to another. The second is to test the sound absorption capability of materials. The third tests the general capabilities of rooms to cope with sounds within it for favorable (offices, classrooms, and auditoria) and unfavorable or noisy situations.

Sound Transmission

ASTM E90-02, *Standard Test Method for Laboratory Measurement of Airborne Sound Transmission Loss of Building Partitions and Elements.* Laboratory measurement of airborne sound transmission loss of building partitions such as walls of all kinds, operable partitions, floor–ceiling assemblies, doors, windows, roofs, panels, and other space-dividing elements.

ASTM E336-97, *Standard Test Method for Measurement of Airborne Sound Insulation in Buildings.* Determining the sound insulation in the field between two rooms in a building. The evaluation may be made including all paths by which sound is transmitted or attention may be focused only on the dividing partition. The word "partition" in this test method includes all types of walls, floors, or any other boundaries separating two spaces. The boundaries may be permanent, operable, or movable.

ASTM E413-87 (1999), *Classification for Rating Sound Insulation.* The method of calculating, from laboratory or field sound insulation measurements at frequencies from 125 to 4000 Hz the single-number acoustical rating called sound transmission class (STC) or field sound transmission class (FSTC) and the single-number rating between two spaces called the noise isolation class (NIC).

ASTM E497, *Practice for Installing Sound-Isolating Lightweight Partitions.* Preferred design methods for constructing high-noise-insulation walls and floor/ceilings.

ASTM E557, *Practice for Architectural Application and Installation of Operable Partitions.* Preferred design and installation methods for constructing high-noise-insulation operable partitions in the field.

ASTM E596-96 (2002), *Standard Test Method for Laboratory Measurement of Noise Reduction of Sound-Isolating Enclosures.* The reverberation room measurement of the noise reduction of sound-isolating enclosures.

ASTM E597, *Practice for Determining a Single-Number Rating of Airborne Sound Isolation for Use in Multi-Unit Building Specifications.* A short test method for field use where a sound source of a standard spectrum is used to test the noise insulation between two existing rooms in a building. Broadband A-weighted sound levels are measured. Computation provides a single number sound insulation value analogous to FSTC.

ASTM E966-02, *Standard Guide for Field Measurements of Airborne Sound Insulation of Building Facades and Facade Elements.* Procedures for measuring the sound insulation of an installed building facade or facade element (window, door). These values may be used separately to predict interior levels or combined into a single number such as by classification E 413 (STC with precautions) or classification E 1332 (outside–inside transmission class, OITC) for sound insulation against transportation noises.

ASTM E492-90 (1996), *Standard Test Method for Laboratory Measurement of Impact Sound Transmission through Floor-Ceiling Assemblies Using the Tapping Machine.* Measurement of impact sound levels (e.g., footfalls) produced by the ISO tapping machine. Results are used to determine the impact isolation class (IIC) by E989.

ASTM E989-89 (1999), *Standard Classification for Determination of Impact Insulation Class (IIC).* A single-number rating of data from ASTM E492 and E1007 for comparing floor–ceiling assemblies for general building design purposes. The rating is called an impact insulation class (IIC).

ASTM E1007-97, *Standard Test Method for Field Measurement of Tapping Machine Impact Sound Transmission through Floor-Ceiling Assemblies and Associated Support Structures.* A field measurement analogous to E492.

ASTM E1123-86 (1998), *Standard Practices for Mounting Test Specimens for Sound Transmission Loss Testing of Naval and Marine Ship Bulkhead Treatment Materials.* Describes test specimen mountings for test method E90, to be used for naval and marine ship bulkhead noise insulation measurement.

ASTM E1222-90 (2002), *Standard Test Method for Laboratory Measurement of the Insertion Loss of Pipe Lagging Systems.* Covers the measurement of the insertion loss of pipe lagging systems under laboratory conditions.

ASTM E1289-97, *Standard Specification for Reference Specimen for Sound Transmission Loss.* Construction and installation of a standard reference specimen for interlaboratory sound transmission loss measurement evaluation using test method E90.

ASTM E1332-90 (1998), *Standard Classification for Determination of Outdoor-Indoor Transmission Class.* A single-number rating for exterior doors, windows, and walls for their noise insulation against ground and air transportation noise, including aircraft roadway vehicles and trains.

ASTM E1408-91 (2000), *Standard Test Method for Laboratory Measurement of the Sound Transmission Loss of Door Panels and Door Systems.* Laboratory measurement of the sound transmission loss for door panels and door systems. It includes specimen-mounting instructions and the force required to close, latch, unlatch, and open a door.

ASTM E1414-00, *Standard Test Method for Airborne Sound Attenuation between Rooms Sharing a Common Ceiling Plenum.* Uses a special laboratory space to simulate a pair of adjacent offices or rooms separated by a partition and sharing a common plenum space (a common economical construction method used for walls between offices and classrooms). The only significant laboratory sound transmission path is by way of the ceiling structure and the plenum space.

ISO 140-1:1997, *Measurement of Sound Insulation in Buildings and of Building Elements*. Part 1: *Requirements for Laboratory Test Facilities with Suppressed Flanking Transmission*. Part 2: *Determination, Verification and Application of Precision Data*. Part 3: *Laboratory Measurements of Airborne Sound Insulation of Building Elements*. Part 4: *Field Measurements of Airborne Sound Insulation between Rooms*. Part 5: *Field Measurements of Airborne Sound Insulation of Façade Elements and Façades*. Part 6: *Laboratory Measurements of Impact Sound Insulation of Floors*. Part 7: *Field Measurements of Impact Sound Insulation of Floors*. Part 8: *Laboratory Measurements of the Reduction of Transmitted Impact Noise by Floor Coverings on a Heavyweight Standard Floor*. Part 9: *Laboratory Measurement of Room-to-Room Airborne Sound Insulation of a Suspended Ceiling with a Plenum Above It*. Part 10: *Laboratory Measurement of Airborne Sound Insulation of Small Building Elements*. Part 12: *Laboratory Measurement of Room-to-Room Airborne and Impact Sound Insulation of an Access Floor*. Part 13: *Guidelines*. (Available in English only.)

ISO 717-1:1996, *Rating of Sound Insulation in Buildings and of Building Elements*. Part 1: *Airborne Sound Insulation*. Part 2: *Impact Sound Insulation*.

ISO 9052-1:1989, *Determination of Dynamic Stiffness*. Part 1: *Materials Used under Floating Floors in dwellings*.

ISO 3822, *Laboratory Tests on Noise Emission from Appliances and Equipment Used in Water Supply Installations*. Part 1-1999: *Method of Measurement*. Part 2-1995: *Mounting and Operating Conditions for Draw-Off Taps and Mixing Valves*. Part 3-1997: *Mounting and Operating Conditions for In-Line Valves and Appliances*. Part 4-1997: *Mounting and Operating Conditions for Special Appliances*.

ISO 11546-1:1995, *Determination of Sound Insulation Performances of Enclosures*. Part 1: *Measurements under Laboratory Conditions (for Declaration Purposes)*. Part 2: *Measurements In Situ (for Acceptance and Verification Purposes)*.

ISO 11957:1996, *Determination of Sound Insulation Performance of Cabins—Laboratory and In Situ Measurements*.

ISO 15186-1:2000, *Measurement of Sound Insulation in Buildings and of Building Elements Using Sound Intensity*. Part 1: *Laboratory Measurements*.

Sound Absorption

ASTM C384-98, *Standard Test Method for Impedance and Absorption of Acoustical Materials by the Impedance Tube Method*. The use of an impedance tube (standing-wave apparatus) for the measurement of impedance ratios and the normal-incidence sound absorption coefficients of acoustical materials.

ASTM C423-02, *Standard Test Method for Sound Absorption and Sound Absorption Coefficients by the Reverberation Room Method*. Measures the random-incidence sound absorption coefficients of material test specimens, mounted according to ASTM E795, in a reverberation room by measuring sound decay rate.

ASTM E477, *Test Method for Measuring Acoustical and Airflow Performance of Duct Liner Materials and Prefabricated Silencers*. Laboratory measurement method for the sound insertion loss provided by duct sound attenuators.

ISO 7235:1991, *Measurement Procedures for Ducted Silencers—Insertion Loss, Flow Noise and Total Pressure Loss*.

ISO 11691:1995, *Measurement of Insertion Loss of Ducted Silencers without Flow—Laboratory Survey Method*.

ISO 11820:1996, *Measurements on Silencers In Situ*.

ISO 11821:1997, *Measurement of the In Situ Sound Attenuation of a Removable Screen*.

ASTM C522-87(1997), *Standard Test Method for Airflow Resistance of Acoustical Materials*. The measurement of airflow resistance, specific airflow resistance, and airflow resistivity of porous materials. Materials may be thick boards or blankets to thin mats, fabrics, papers, and screens.

ISO 9053:1991, *Materials for Acoustical Applications—Determination of Airflow Resistance*.

ASTM E756-98, *Standard Test Method for Measuring Vibration-Damping Properties of Materials*. Measures the vibration-damping properties—loss factor η, Young's modulus E, and shear modulus G—of materials over a frequency range of 50 Hz to 5 kHz and over the useful temperature range of the material. This method tests materials that have application in structural vibration, building acoustics, and the control of audible noise. Test materials include metal, enamel, ceramics, rubber, plastic, reinforced epoxy matrix, and wood that can be formed to the test specimen bar configuration.

ASTM E795-00, *Standard Practices for Mounting Test Specimens during Sound Absorption Tests*. Standard specimen mountings for tests performed in accordance with C423.

ASTM E1042, *Classification for Acoustically Absorptive Materials Applied by Trowel or Spray*.

ASTM E1050-98, *Standard Test Method for Impedance and Absorption of Acoustical Materials Using a Tube, Two Microphones, and a Digital Frequency Analysis System*. The two-microphone impedance tube method, including a digital frequency analysis system, to measure the normal-incidence sound absorption coefficients and normal specific acoustical impedance ratios of materials.

ISO 354. 2003, *Acoustics—Measurement of Sound Absorption in a Reverberation Room*. Similar to ASTM C423.

ISO 10534-1:1996, *Determination of Sound Absorption Coefficient and Impedance in Impedance Tubes*. Part 1: *Method Using Standing Wave Ratio*. Similar to ASTM C384.

ISO 11654:1997, *Sound Absorbers for Use in Buildings—Rating of Sound Absorption*.

ISO 10844:1994, *Specification of Test Tracks for the Purpose of Measuring Noise Emitted by Road Vehicles.*

ISO 13472-1:2002, *Measurement of Sound Absorption Properties of Road Surfaces In Situ.* Part 1: *Extended Surface Method.* A vertical impedance tube test method for measuring In Situ the sound absorption coefficient of road surfaces as a function of frequency in the range from 250 Hz to 4 kHz.

Architectural Acoustics, Reverberation, and Noise Control Design

ANSI S12.2-1995 (R1999), *Criteria for Evaluating Room Noise.* Defines NC, NCB, RC, and perceptible acoustically induced low-frequency vibration criterion curves for the octave-band SPL spectrum of noise and gives rules for using them to evaluate room background noise.

ANSI S12.60-2002, *Acoustical Performance Criteria, Design Requirements, and Guidelines for Schools.* Acoustical performance criteria, design requirements, and design guidelines for new school classrooms and other learning spaces to achieve a high degree of speech intelligibility in learning spaces. Conformance test procedures are provided.

ASTM E1041, *Guide for Measurement of Masking Sound in Open Offices.*

ASTM E1110-01, *Standard Classification for Determination of Articulation Class.* Provides a single figure rating that can be used for comparing building systems and subsystems for speech privacy purposes. The rating is designed to correlate with transmitted speech intelligence between office spaces.

ASTM E1111-02, *Standard Test Method for Measuring the Interzone Attenuation of Ceiling Systems.* Measures the sound reflective characteristics of ceiling systems with partial-height space dividers, used in offices and sometimes in schools to achieve speech privacy between work zones in the absence of full-height partitions. Restricted to a fixed space divider height of 5 ft, a ceiling height of nominally 9 ft, a source height of 4 ft, and microphone positions at 4 ft height.

ASTM E1130-02, *Standard Test Method for Objective Measurement of Speech Privacy in Open Offices Using Articulation Index (AI).* Measuring speech privacy objectively between existing locations in open offices. Uses acoustical measurements, published information on speech levels, and speech intelligibility to compute the Articulation Index (AI).

ASTM E1179-87 (1998), *Standard Specification for Sound Sources Used for Testing Open Office Components and Systems.* Specifies the sound source used for measuring the speech privacy between open offices or for measuring the laboratory performance of acoustical components (see E1111 and E1130).

ASTM E1375-90 (2002), *Standard Test Method for Measuring the Interzone Attenuation of Furniture Panels Used as Acoustical Barriers.* Measurement of the interzone attenuation of furniture panels used as acoustical barriers in open-plan spaces to provide speech privacy or sound isolation between working positions.

ASTM E1376-90 (2002), *Standard Test Method for Measuring the Interzone Attenuation of Sound Reflected by Wall Finishes and Furniture Panels.* Measures the degree to which reflected sound is attenuated by vertical surfaces in open-plan spaces.

ASTM E1573-02, *Standard Test Method for Evaluating Masking Sound in Open Offices Using A-Weighted and One-Third Octave Band Sound Pressure Levels.* Procedures to evaluate the spatial and temporal uniformity of masking sound in open offices using A-weighted or one-third-octave-band SPLs.

ASTM E1574-98, *Standard Test Method for Measurement of Sound in Residential Spaces.* Practical measurement of residual building interior noise SPLs.

ASTM E2235, *Standard Test Method for the Measurement of Decay Rates for Use in Sound Insulation Test Methods.* Measurement of sound decay rate ($60/T$) in any room, where T is the reverberation time, seconds.

ISO 3382:1997, *Measurement of the Reverberation Time of Rooms with Reference to Other Acoustical Parameters.* Measurement of reverberation time T in performance spaces. Specifies additional measures of auditorium gain (G), early decay (EDT), clarity (C80), Deutlichkeit (D50), central time (CT) lateral energy fraction (LF) and interaural cross correlation (IACC) and of T in any room.

ISO 10053-1991, *Measurement of Office Screen Sound Attenuation under Specific Laboratory Conditions.* Similar to ASTM E1375.

APPENDIX A

General References

M. Belanger, *Digital Processing of Signals: Theory and Practice*, Wiley, New York (1985).

J. S. Bendat and A. G. Piersol, *Random Data, Analysis and Measurement Procedures*, 2nd ed., Wiley, New York (1986).

L. L. Beranek, *Acoustics*, reprinted with changes by the Acoustical Society of America, New York (1986).

L. L. Beranek, *Acoustical Measurements*, rev. ed., Acoustical Society of America, New York (1988).

D. A. Bies and C. H. Hansen, *Engineering Noise Control*, Unwin Hyman, London (1988).

M. P. Blake and W. S. Mitchell, *Vibration and Acoustic Measurement Handbook*, Spartan Books, New York (1972).

R. N. Bracewell, *The Fast Fourier Transform and Its Applications*, 2nd ed., McGraw-Hill, New York (1986).

L. Cremer and H. A. Mueller, *Principals and Applications of Room Acoustics*, Vols. 1 and 2, translated by T. J. Schultz, Applied Science, London and New York (1982).

M. J. Crocker, *Noise Control*, Van Nostrand Reinhold, New York (1984).

J. D. Erwin and E. R. Graf, *Industrial Noise and Vibration Control*, Prentice-Hall, Englewood Cliffs, NJ (1979).

F. Fahy, *Sound and Structural Vibration—Radiation, Transmission and Response*, Academic, New York (1985).

C. M. Harris, Ed., *Shock and Vibration Handbook*, 3rd ed., McGraw-Hill, New York (1988).

M. C. Junger and D. Feit, *Sound, Structures, and Their Interaction*, 2nd ed., MIT Press, Cambridge, MA (1986).

L. E. Kinsler, A. R. Frey, A. B. Coppens, and J. V. Sanders, *Fundamentals of Acoustics*, 3rd ed., Wiley, New York (1982).

H. Kuttruff, *Room Acoustics*, Applied Science Publishers, London (1973).

R. L. Lyon, *Statistical Energy Analysis of Dynamical Systems*, MIT Press, Cambridge, MA (1975).

A. V. Oppenheim and R. W. Schafer, *Digital Signal Processing*, Prentice-Hall, Englewood Cliffs, NJ (1975).

R. B. Randall, *Frequency Analysis*, 3rd ed., Bruel & Kjaer, Naerum, Denmark (1987).

APPENDIX B

American System of Units

The American system of units [which used to be referred to as the English system of units until England converted to the meter-kilogram-second (mks) system] is inherently confusing. In everyday American life, the *pound* (abbreviated lb) is used either as a force or as a weight, both having the units of force. To further complicate matters, some technical writers seek to provide a system parallel to the metric system by using either of two quantities for force and either of two corresponding quantities for mass. Thus, some adopt the pound as the unit of force and define a *slug* as the unit of mass. Others define a *poundal* as the unit of force and adopt the pound as the unit of mass. Neither the slug nor the poundal has found general acceptance in the literature, although we use the former in this text.

As one well-traveled acoustician said, "I have determined that 1 kg of butter bought in Zurich is exactly the same amount as 2.2 lb bought in New York. Whenever I wish to solve a technical problem in America without confusion, I immediately divide the number of pounds by 2.2 to obtain the equivalent number of kilograms. Then I work in the mks system, where force and mass are clearly distinguished." Let us take a moment to distinguish further between mass and force.

The mass of a body is defined as $m = F/\ddot{x}$, where F is the vector sum of all forces acting on the center of gravity of the unrestrained body and $\ddot{x}$ is the acceleration produced in the direction of the force F.

The weight of a body is defined as $w = mg$, where g is the acceleration of gravity (9.81 m/s^2 on earth) and w is the force that must act on the otherwise unrestrained body to keep it stationary when exposed to the gravitational field. Consequently, a body has the same mass but different weight on the moon than on earth. On earth the weight of a 1-kg mass, which is designated as one kilopond (1 kp), is 1 kp weight $=$ 1 kg mass $\times$ 9.81 m/s^2 $=$ 9.81 newtons.

CONSISTENT SYSTEMS OF UNITS USED IN THIS TEXT

Two consistent systems of units are used in this text, the *mks* and the *fss* systems. To describe them, let us start with Newton's second law:

$$\text{Force} = \text{mass} \times \text{acceleration} \tag{B.1}$$

In the *meter-kilogram-second* system

$$\text{No. of newtons} = \text{no. of kg} \times \text{no. of m/s}^2 \tag{B.2}$$

In the *foot-slug-second* system

$$\text{No. of pounds force (lb)} = \text{no. of slugs} \times \text{no. of ft/s}^2 \tag{B.3}$$

The relations among the magnitudes of the units are

$$\begin{aligned} 1\text{kp} &= 2.205\text{lb weight} \\ 1\text{ kg} &= 0.0685\text{slug} \\ 1\text{slug} &= 14.59\text{ kg} \\ 1\text{ newton} &= 0.225\text{lb force} \\ 1\text{lb force} &= 4.448\text{ newtons} \\ 1\text{slug} &= 32.17\text{lb weight} \\ 1\text{lb weight} &= 0.03108\text{slug} = 0.454\text{ kg} \end{aligned}$$

Example. If 1 kg mass is to be accelerated 1 m/s^2, we see, by Eq. (B.2), that a force of 1 newton is required. How many pounds (force) is required for the same result?

Solution 1 kg equals (2.205/32.17) slug and 1 m/s^2 = 3.28 ft/s^2. Thus, by Eq. (B.3), 0.225 lb (force) is required.

INCONSISTENT SYSTEMS OF AMERICAN UNITS USED IN THE LITERATURE

Two inconsistent systems of American units are commonly encountered, the *fps* and the *ips* systems.

In the *foot-pound-second* system (inconsistent system)

$$\text{No. of pounds force (lb)} = \frac{\text{no. of pounds weight (lb)}}{g} \times \text{no. of ft/s}^2 \tag{B.4}$$

where g is the acceleration due to gravity in units of ft/s^2, that is, 32.17 ft/s^2.

In the *inch-pound-second system* (inconsistent system)

$$\text{No. of pounds force (lb)} = \frac{\text{no. of pounds weight (lb)}}{g} \times \text{no. of in./s}^2 \tag{B.5}$$

where g is the acceleration due to gravity in units of in./s^2, that is, 3.86 in./s^2. Mechanical engineers often use the *in.-lb-s* system in the field of shock and vibration.

Example. A 1-kg mass is accelerated 5 m/s^2. Find the force necessary to do this in newtons and pounds (force).

Solution

$$\begin{aligned} 1\text{ kg} &= 2.2\text{ lb weight} = 0.0685\text{ slug} \\ 5\text{ m/s}^2 &= 16.4\text{ ft/s}^2 \\ F\text{ (newtons)} &= 1 \times 5 = 5\text{ newtons} \\ F\text{ (lb)} &= 0.0685 \times 16.4 = 1.124\text{ lb (force)} \end{aligned}$$

APPENDIX C

Conversion Factors

The following values for the fundamental constants were used in the preparation of the factors:

$$1 \text{ m} = 39.37 \text{ in.} = 3.281 \text{ ft}$$

$$1 \text{ lb (weight)} = 0.4536 \text{ kp} = 0.03108 \text{ slug}$$

$$1 \text{ slug} = 14.594 \text{ kg}$$

$$1 \text{ lb (force)} = 4.448 \text{ newtons}$$

$$\text{Acceleration due to gravity} = 9.807 \text{ m/s}^2$$

$$= 32.174 \text{ ft/s}^2$$

$$\text{Density of } H_2O \text{ at } 4°C = 10^3 \text{ kg/m}^3$$

$$\text{Density of Hg at } 0°C = 1.3595 \times 10^4 \text{ kg/m}^3$$

$$1 \text{ U.S. lb} = 1 \text{ British lb}$$

$$1 \text{ U.S. gallon} = 0.83267 \text{ British gallon}$$

$$°F = (\tfrac{9}{5})°C + 32$$

$$°C = (\tfrac{5}{9})(°F - 32)$$

TABLE C.1 Conversion Factors

To convert	Into	Multiply by	Conversely, multiply by
acres	ft^2	4.356×10^4	2.296×10^{-5}
	$miles^2$ (statute)	1.562×10^{-3}	640
	m^2	4,047	2.471×10^{-4}
	hectare (10^4 m^2)	0.4047	2.471
atm	in. H_2O at 4°C	406.80	2.458×10^{-3}
	in. Hg at 0°C	29.92	3.342×10^{-2}
	ft H_2O at 4°C	33.90	2.950×10^{-2}
	mm Hg at 0°C	760	1.316×10^{-3}
	$lb/in.^2$	14.70	6.805×10^{-2}

(*continued overleaf*)

TABLE C.1 (*continued*)

To convert	Into	Multiply by	Conversely, multiply by
	newtons/m^2	1.0132×10^5	9.872×10^{-6}
	kp/m^2	1.033×10^4	9.681×10^{-5}
°C	°F	$(°C \times \frac{9}{5}) + 32$	$(°F - 32) \times \frac{5}{9}$
cm	in.	0.3937	2.540
	ft	3.281×10^{-2}	30.48
	m	10^{-2}	10^2
circular mils	in.^{2}	7.85×10^{-7}	1.274×10^6
	cm^2	5.067×10^{-6}	1.974×10^5
cm^2	in.^{2}	0.1550	6.452
	ft^2	1.0764×10^{-3}	929
	m^2	10^{-4}	10^4
cm^3	in.^{3}	0.06102	16.387
	ft^3	3.531×10^{-5}	2.832×10^4
	m^3	10^{-6}	10^6
deg (angle)	radians	1.745×10^{-2}	57.30
dynes	lb (force)	2.248×10^{-6}	4.448×10^5
	newtons	10^{-5}	10^5
dynes/cm^2	lb/ft^2 (force)	2.090×10^{-3}	478.5
	newtons/m^2	10^{-1}	10
1 in. H_2O	N/m^2	249.18	4.013×10^{-3}
ergs	ft-lb (force)	7.376×10^{-8}	1.356×10^7
	joules	10^{-7}	10^7
ergs/cm^3	ft-lb/ft^3	2.089×10^{-3}	478.7
ergs/s	watts	10^{-7}	10^7
	ft-lb/s	7.376×10^{-8}	1.356×10^7
ergs/s-cm^2	ft-lb/s-ft^2	6.847×10^{-5}	1.4605×10^4
fathoms	ft	6	0.16667
ft	in.	12	0.08333
	cm	30.48	3.281×10^{-2}
	m	0.3048	3.281
ft^2	in.^{2}	144	6.945×10^{-3}
	cm^2	9.290×10^2	0.010764
	m^2	9.290×10^{-2}	10.764
ft^3	in.^{3}	1728	5.787×10^{-4}
	cm^3	2.832×10^4	3.531×10^{-5}
	m^3	2.832×10^{-2}	35.31
	liters	28.32	3.531×10^{-2}
ft H_2 O at 4°C	in. Hg at 0°C	0.8826	1.133
	lb/in.^{2}	0.4335	2.307
	lb/ft^2	62.43	1.602×10^{-2}
	newtons/m^2	2989	3.345×10^{-4}
gal (liquid U.S.)	gal (liquid Brit. Imp.)	0.8327	1.2010
	liters	3.785	0.2642
	m^3	3.785×10^{-3}	264.2
gm	oz (weight)	3.527×10^{-2}	28.35

TABLE C.1 (*continued*)

To convert	Into	Multiply by	Conversely, multiply by
	lb (weight)	2.205×10^{-3}	453.6
hp (550 ft-lb/s)	ft-lb/min	3.3×10^4	3.030×10^{-5}
	watts	745.7	1.341×10^{-3}
	kW	0.7457	1.341
in.	ft	0.0833	12
	cm	2.540	0.3937
	m	0.0254	39.37
in.^{2}	ft^2	0.006945	144
	cm^2	6.452	0.1550
	m^2	6.452×10^{-4}	1550
in.^{3}	ft^3	5.787×10^{-4}	1.728×10^3
	cm^3	16.387	6.102×10^{-2}
	m^3	1.639×10^{-5}	6.102×10^4
kg	lb (weight)	2.2046	0.4536
	slug	0.06852	14.594
	g	10^3	10^{-3}
kg/m^2	lb/in.^{2} (weight)	0.001422	703.0
	lb/ft^2 (weight)	0.2048	4.882
	g/cm^2	10^{-1}	10
kg/m^3	lb/in.^{3} (weight)	3.613×10^{-5}	2.768×10^4
	lb/ft^3 (weight)	6.243×10^{-2}	16.02
liters	in.^{3}	61.03	1.639×10^{-2}
	ft^3	0.03532	28.32
	pints (liquid U.S.)	2.1134	0.47318
	quarts (liquid U.S.)	1.0567	0.94636
	gal (liquid U.S.)	0.2642	3.785
	cm^3	1000	0.001
	m^3	0.001	1000
$\log_e n$, or $\ln n$	$\log_{10} n$	0.4343	2.303
m	in.	39.371	0.02540
	ft	3.2808	0.30481
	yd	1.0936	0.9144
	cm	10^2	10^{-2}
m^2	in.^{2}	1550	6.452×10^{-4}
	ft^2	10.764	9.290×10^{-2}
	yd^2	1.196	0.8362
	cm^2	10^4	10^{-4}
m^3	in.^{3}	6.102×10^4	1.639×10^{-5}
	ft^3	35.31	2.832×10^{-2}
	yd^3	1.3080	0.7646
	cm^3	10^6	10^{-6}
microbars (dynes/cm^2)	lb/in.^{2}	1.4513×10^{-5}	6.890×10^4
lb/ft^2	2.090×10^{-3}	478.5	

(*continued overleaf*)

TABLE C.1 (*continued*)

To convert	Into	Multiply by	Conversely, multiply by
	newtons/m^2	10^{-1}	10
miles (nautical)	ft	6080	1.645×10^{-4}
	km	1.852	0.5400
miles (statute)	ft	5280	1.894×01^{-4}
	km	1.6093	0.6214
miles^2 (statute)	ft^2	2.788×10^7	3.587×10^{-8}
	km^2	2.590	0.3861
	acres	640	1.5625×10^{-3}
mph	ft/min	88	1.136×10^{-2}
	km/min	2.682×10^{-2}	37.28
	km/h	1.6093	0.6214
nepers	db	8.686	0.1151
newtons	lb (force)	0.2248	4.448
	dynes	10^5	10^{-5}
newtons/m^2	lb/in.^{2} (force)	1.4513×10^{-4}	6.890×10^3
	lb/ft^2 (force)	2.090×10^{-2}	47.85
	dynes/cm^2	10	10^{-1}
lb (force)	newtons	4.448	0.2248
lb (weight)	slugs	0.03108	32.17
	kg	0.4536	2.2046
lb H_2O (distilled)	ft^3	1.602×10^{-2}	62.43
	gal (liquid U.S.)	0.1198	8.346
lb/in.^{2} (weight)	lb/ft^2 (weight)	144	6.945×10^{-3}
	kg/m^2	703	1.422×10^{-3}
lb/in.^{2} (force)	lb/ft^2 (force)	144	6.945×10^{-3}
	N/m^2	6894	1.4506×10^{-4}
lb/ft^2 (weight)	lb/in.^{2} (weight)	6.945×10^{-3}	144
	gm/cm^2	0.4882	2.0482
	kg/m^2	4.882	0.2048
lb/ft^2 (force)	lb/in.^{2} (force)	6.945×10^{-3}	144
	N/m^2	47.85	2.090×10^{-2}
lb/ft^3 (weight)	lb/in.^{3} (weight)	5.787×10^{-4}	1728
	kg/m^3	16.02	6.243×10^{-2}
poundals	lb (force)	3.108×10^{-2}	32.17
	dynes	1.383×10^4	7.233×10^{-5}
	newtons	0.1382	7.232
slugs	lb (weight)	32.17	3.108×10^{-2}
	kg	14.594	0.06852
slugs/ft^2	kg/m^2	157.2	6.361×10^{-3}
tons, short (2,000 lb)	tonnes (1000 kg)	0.9075	1.102
watts	ergs/s	10^7	10^{-7}
	hp (550 ft-lb/s)	1.341×10^{-3}	745.7

INDEX

A

TABLE C.1 (*continued*)

To convert	Into	Multiply by	Conversely, multiply by
	newtons/m^2	10^{-1}	10
miles (nautical)	ft	6080	1.645×10^{-4}
	km	1.852	0.5400
miles (statute)	ft	5280	1.894×01^{-4}
	km	1.6093	0.6214
$miles^2$ (statute)	ft^2	2.788×10^7	3.587×10^{-8}
	km^2	2.590	0.3861
	acres	640	1.5625×10^{-3}
mph	ft/min	88	1.136×10^{-2}
	km/min	2.682×10^{-2}	37.28
	km/h	1.6093	0.6214
nepers	db	8.686	0.1151
newtons	lb (force)	0.2248	4.448
	dynes	10^5	10^{-5}
newtons/m^2	lb/$in.^2$ (force)	1.4513×10^{-4}	6.890×10^3
	lb/ft^2 (force)	2.090×10^{-2}	47.85
	dynes/cm^2	10	10^{-1}
lb (force)	newtons	4.448	0.2248
lb (weight)	slugs	0.03108	32.17
	kg	0.4536	2.2046
lb H_2O (distilled)	ft^3	1.602×10^{-2}	62.43
	gal (liquid U.S.)	0.1198	8.346
lb/$in.^2$ (weight)	lb/ft^2 (weight)	144	6.945×10^{-3}
	kg/m^2	703	1.422×10^{-3}
lb/$in.^2$ (force)	lb/ft^2 (force)	144	6.945×10^{-3}
	N/m^2	6894	1.4506×10^{-4}
lb/ft^2 (weight)	lb/$in.^2$ (weight)	6.945×10^{-3}	144
	gm/cm^2	0.4882	2.0482
	kg/m^2	4.882	0.2048
lb/ft^2 (force)	lb/$in.^2$ (force)	6.945×10^{-3}	144
	N/m^2	47.85	2.090×10^{-2}
lb/ft^3 (weight)	lb/$in.^3$ (weight)	5.787×10^{-4}	1728
	kg/m^3	16.02	6.243×10^{-2}
poundals	lb (force)	3.108×10^{-2}	32.17
	dynes	1.383×10^4	7.233×10^{-5}
	newtons	0.1382	7.232
slugs	lb (weight)	32.17	3.108×10^{-2}
	kg	14.594	0.06852
slugs/ft^2	kg/m^2	157.2	6.361×10^{-3}
tons, short (2,000 lb)	tonnes (1000 kg)	0.9075	1.102
watts	ergs/s	10^7	10^{-7}
	hp (550 ft-lb/s)	1.341×10^{-3}	745.7

INDEX

A

D

G

H

I

O

P

Q

R

BEFORE THE PUBLIC UTILITY COMMISSION
OF OREGON

Docket PCN 5

In the Matter of

IDAHO POWER COMPANY'S
PETITION FOR CERTIFICATE OF PUBLIC CONVENIENCE
AND NECESSITY

Michaud, D. S. et al., Self-Reported and Measured Stress Related Responses Associated with Exposure to Wind Turbine Noise (2016)

February 22, 2023

Self-reported and measured stress related responses associated with exposure to wind turbine noise

David S. Michaud, Katya Feder, Stephen E. Keith, Sonia A. Voicescu, Leonora Marro, John Than, Mireille Guay, Allison Denning, Tara Bower, Paul J. Villeneuve, Evan Russell, Gideon Koren, and Frits van den Berg

Citation: The Journal of the Acoustical Society of America **139**, 1467 (2016); doi: 10.1121/1.4942402
View online: https://doi.org/10.1121/1.4942402
View Table of Contents: http://asa.scitation.org/toc/jas/139/3
Published by the Acoustical Society of America

Self-reported and measured stress related responses associated with exposure to wind turbine noise

David S. Michaud,[a] Katya Feder, Stephen E. Keith, and Sonia A. Voicescu
Health Canada, Environmental and Radiation Health Sciences Directorate, Consumer and Clinical Radiation Protection Bureau, 775 Brookfield Road, Ottawa, Ontario K1A 1C1, Canada

Leonora Marro, John Than, and Mireille Guay
Health Canada, Population Studies Division, Biostatistics Section, 200 Eglantine Driveway, Tunney's Pasture, Ottawa, Ontario, Canada

Allison Denning
Health Canada, Environmental Health Program, Health Programs Branch, Regions and Programs Bureau, 1505 Barrington Street, Halifax, Nova Scotia, Canada

Tara Bower
Health Canada, Environmental and Radiation Health Sciences Directorate, Office of Science Policy, Liaison and Coordination, 269 Laurier Avenue West, Ottawa, Ontario, Canada

Paul J. Villeneuve
Department of Health Sciences, Carleton University, 1125 Colonel By Drive, Ottawa, Ontario, Canada

Evan Russell
Department of Physiology and Pharmacology, Western University, Siebens Drake Research Institute, Room 111, London, Ontario, Canada

Gideon Koren
Division of Clinical Pharmacology and Toxicology, Department of Pediatrics, The Hospital for Sick Children, 555 University Avenue, Toronto, Ontario, Canada

Frits van den Berg
The Amsterdam Public Health Service (GGD Amsterdam), Environmental Health Department, Nieuwe Achtergracht 100, Amsterdam, The Netherlands

(Received 26 March 2015; revised 8 December 2015; accepted 8 December 2015; published online 31 March 2016)

The current study was the first to assess stress reactions associated with wind turbine noise (WTN) exposure using self-reported and objective measures. Randomly selected participants, aged 18–79 yr (606 males; 632 females), living between 0.25 and 11.22 km from wind turbines, were exposed to outdoor calculated WTN levels up to 46 dBA (response rate 78.9%). Multiple regression modeling left the great majority (77%–89%) of the variance in perceived stress scale (PSS) scores, hair cortisol concentrations, resting blood pressure, and heart rate unaccounted for, and WTN exposure had no apparent influence on any of these endpoints. PSS scores were positively, but weakly, related to cortisol concentrations and resting heart rate (Pearson $r = 0.13$ and $r = 0.08$, respectively). Across WTN categories, modeled mean PSS scores ranged from 13.15 to 13.84 ($p = 0.8614$). Modeled geometric means for hair cortisol concentrations, resting mean systolic, diastolic blood pressure, and heart rate were 150.54–191.12 ng/g ($p = 0.5416$), 113.38–116.82 mmHg ($p = 0.4990$), 67.98–70.34 mmHg ($p = 0.5006$), and 68.24–70.71 bpm ($p = 0.5223$), respectively. Irrespective of WTN levels, diastolic blood pressure appeared to be slightly (2.90 mmHg 95% CI: 0.75,5.05) higher among participants highly annoyed by blinking lights on turbines ($p = 0.0081$). Collectively, the findings do not support an association between exposure to WTN up to 46 dBA and elevated self-reported and objectively defined measures of stress.

[http://dx.doi.org/10.1121/1.4942402]

[JFL] Pages: 1467–1479

I. INTRODUCTION

Noise exposure has the potential to act as a stressor and can directly or indirectly impact one's health [World Health Organization (WHO), 1999, 2011; Guski, 2001; Vallet, 2001]. Susceptibility or resistance to indirect stressor-induced health effects depends on a complex interaction between a stressor and coping strategies developed through previous experience, psychological, biological, and social factors, in addition to competing stressors and personality type (Job, 1988, 1996; Institute of Medicine, 2001; Stansfeld and Marmot, 2002). At the dwelling, wind turbine noise

[a]Electronic mail: david.michaud@canada.ca

(WTN) levels are well below levels expected to cause direct health effects (McCunney *et al.*, 2014). Potential effects are more likely to be mediated through a complex interaction as described above, wherein the perception of wind turbines becomes the acting stressor. Other factors such as noise sensitivity and the magnitude of annoyance or perceived stress engendered by a noise exposure could very likely contribute to the overall response. A theoretical representation for such an indirect pathway is presented in the Appendix.

Social surveys, which have been relied on to measure annoyance, perceptions of stress, and/or health effects, provide only partial support for potential WTN-mediated health effects because they are based on unverified self-reporting. An additional level of insight is provided from the current study, which includes objective measures of stress to characterize the associations between WTN exposure and stress.

Stress-induced cortisol changes have traditionally been measured using blood and saliva samples, which can be difficult to interpret (Legler *et al.*, 1982; Hennig *et al.*, 2000; Edwards *et al.*, 2001; Broderick *et al.*, 2004). Many of the limits associated with short-term sampling can be eliminated by using a measure of cortisol that is integrated over time (Russell *et al.*, 2012; Stalder and Kirschbaum, 2012). Cortisol integrates and remains in hair over time as it grows further from the scalp. As human scalp hair have a predictable average growth rate of ∼1 cm/month (Wennig, 2000), cortisol in hair can be measured and used to retrospectively characterize cortisol levels over several months. For this reason, hair cortisol analysis has become an increasingly utilized methodology for examining chronic stress and its effects on human health (Van Uum *et al.*, 2008; Pereg *et al.*, 2011; Gerber *et al.*, 2013; Grunau *et al.*, 2013; Hinkelmann *et al.*, 2013; Manenschijn *et al.*, 2013; Pereg *et al.*, 2013; Stalder *et al.*, 2013; Walton *et al.*, 2013; Veldhorst *et al.*, 2014; Wells *et al.*, 2014; Wester *et al.*, 2014) making hair cortisol analysis a particularly useful methodology in evaluating the impact that long-term exposure to WTN may have on the human stress response. Hair cortisol analysis, when considered together with validated questionnaires such as the perceived stress scale (PSS) (Cohen *et al.*, 1983; Al kalaldeh and Shosha, 2012), as well as blood pressure measures, provides a more comprehensive assessment of WTN exposure and stress reactions.

The purpose of the current study was to investigate the possibility that living in the vicinity of wind turbines increases stress. To this end, multiple measures of stress reported by and objectively measured in participants exposed to WTN were assessed. In addition, multiple regression analysis was used to identify the variables that best predicted the modeled stress-related endpoints.

II. METHODS

A. Sample design

1. Target population, sample size, and sampling frame strategy

Michaud *et al.* (2013) and Michaud *et al.* (2016a) have described the study design, target population, final sample size, allocation of participants, as well as the sampling strategy. Briefly, the study locations were drawn from areas in southwestern Ontario (ON) and Prince Edward Island (PEI) where there were a sufficient number of dwellings within the vicinity of wind turbine installations. There were 2004 potential dwellings identified from the ON and PEI sampling regions, which included 315 and 84 wind turbines, respectively. All turbines had three pitch controlled rotor blades (∼80 m diameter) upwind of the tower. The wind turbine electrical power outputs ranged between 660 kW and 3 MW [average 2.0, standard deviation (SD) 0.4 MW]. Turbine hub heights were predominantly 80 m. All identified dwellings within ∼600 m from a wind turbine and a random selection of dwellings between 600 m and 11.22 km were selected from which one person per household between the ages of 18 and 79 years was randomly chosen to participate.

This study was approved by the Health Canada and Public Health Agency of Canada Review Ethics Board (Protocol Nos. 2012-0065 and 2012-0072).

B. Wind turbine sound pressure levels

Keith *et al.* (2016a) have provided a detailed description of the approach applied to sound pressure level modeling. Briefly, sound pressure levels were estimated at each dwelling using both ISO 9613-1 (ISO, 1993) and ISO 9613-2 (ISO, 1996) as incorporated in the commercial software CadnaA version 4.4 (Datakustik®, 2014). The calculations included all wind turbines within a radius of 10 km, and were based on manufacturers' octave band sound power spectra at 10 m height, 8 m/s wind speed for favourable propagation conditions. The few dwellings beyond this distance were assigned the same calculated WTN value as dwellings at 10 km. The manufacturers' data were verified for consistency using on-site measurements of wind turbine sound power (Keith *et al.*, 2016b). Unless otherwise indicated, all references to decibels (dB) are A-weighted values.

In the current study, low-frequency noise was estimated by calculating C-weighted sound pressure levels. The correlation between C-weighted and A-weighted levels ranged from r 0.81 to 0.97 (Keith *et al.*, 2016b) and, therefore, no additional benefit would be gained by assessing outcomes in relation to dBC.

C. Data collection

1. Questionnaire content and administration

A detailed description of the questionnaire content has been presented by Michaud *et al.* (2013), Michaud *et al.* (2016a), and Feder *et al.* (2015). Briefly, the questionnaire instrument includes modules on basic demographic variables, annoyance, health effects, quality of life, sleep quality, perceived stress, lifestyle behaviours, and prevalent chronic diseases, including diagnosed high blood pressure. Long-term high annoyance toward several wind turbine features was assessed with separate questions that targeted specific wind turbine features (i.e., noise, blinking lights, vibrations, visual, and shadow flicker). As per ISO (2003), high annoyance was defined by combining the top two response categories of the following five-point adjectival scale: *not at all*, *slightly*, *moderately*, *very*, and *extremely*. The time reference period for annoyance was intended to capture the participants' integrated annoyance toward wind turbine features over the previous year while at home (see Michaud *et al.*, 2016b, for more details). Self-reported stress was assessed using the PSS (Cohen *et al.*, 1983), which is a widely used questionnaire with established, acceptable psychometric properties, designed to measure an individual's perception of stress. The questionnaire evaluates the degree to which respondents believe their life is unpredictable, uncontrollable, and overloaded during the previous month. In addition, the scale includes a number of direct questions about current levels of experienced stress. According to Cohen *et al.* (1983), this instrument was designed for use in community samples that have at least a junior high school education, and contains questions that are of a general nature and free of content specific to any subpopulation. Body mass index (BMI) was calculated based on self-reported height and weight, whereby weight in kilograms was divided by height in meters squared.

Consistent with many epidemiological studies that aim to reduce possible survey bias, an attempt was made to mask the primary subject of interest in this study, which was to investigate the community response to wind turbines. To this end, the study was introduced to participants as the *Community Noise and Health Study* and the questionnaire included several items unrelated to wind turbines. A total of 16 trained interviewers collected data through in-person interviews between May, 2013, and September, 2013, in southwestern ON and PEI. Once a roster of adults living in the dwelling was compiled, a computerized method of random selection was used with no substitution permitted.

D. Blood pressure and heart rate evaluation

Measures of blood pressure and heart rate followed the standardized procedures used by the Canadian Health Measures Survey (Bryan *et al.*, 2010) with the following two exceptions: (1) the interviewer remained in the room, seated behind the respondent during testing as it was neither practical nor appropriate for the interviewer to leave the room during in-home testing; and (2) there was no imposed 5 min rest period prior to testing. This was considered to be unnecessary because the participant had already been seated for the previous 40–45 min while completing the questionnaire.

Systolic and diastolic blood pressure and resting heart rate were measured electronically in a quiet room with a firm chair and table using an automated oscillometric device (BpTRU^{TM}BPM-100, Medical Devices Ltd., Coquitlam, British Columbia). A series of six consecutive measurements were taken at one minute intervals. Interviewers ensured proper functioning of the BpTRU^{TM} and the respondent did not talk or move during the test. The last five measurements of the series were used to determine the average resting heart rate and blood pressure.

E. Hair cortisol analysis

1. Hair sample collection

Hair samples were obtained from the vertex posterior of the head using scissors and cutting as close to the scalp as possible. The diameter of the grouping of hair strands removed was 5–10 mm. The hair sample was then taped to a section of bar-coded paper that identified the scalp end of the hair. The sample was stored in an envelope at room temperature for later analysis. The average time lapse between storage and analysis was ~60 days, which would not degrade cortisol concentrations (Webb *et al.*, 2010).

2. Hair treatment and enzyme-linked immunosorbent assay (ELISA)

In subjects from whom a length of 3 cm or more of hair was collected, the 3 cm portion most proximal to the scalp was analyzed. Hair sample collection and cortisol analysis were conducted in accordance with a previously established protocol described by Pereg *et al.* (2013). A hair mass of 10–15 mg was required for each analysis. Each hair sample was washed twice in isopropanol for 3 min to remove contaminants coating the hair. Following washing, hair samples were allowed to dry for a minimum of 5 h in a fume hood. A methanol extraction was then used to remove the cortisol from the hair. Hair samples were immersed in 1 ml of methanol, minced finely with surgical scissors and then incubated for 16 h at 50 °C while shaking at 100 rpm. The methanol solution was then removed and evaporated under nitrogen gas. The remaining residue was reconstituted with 250 μl of phosphate buffered saline and analyzed using a salivary cortisol immunoassay (Alpco Diagnostics, Salem, NH). The value determined was subsequently corrected to the hair mass used to yield a hair cortisol concentration in nanograms of cortisol per gram (ng/g) of hair. The lower quantification limit was 25 ng/g for hair mass of 10 mg and 16.67 ng/g for hair mass of 15 mg. The upper limit of detection was 20 000 ng/g and 13 333 ng/g, respectively. The assay detection limit was 0.063 ng/g and 0.042 ng/g for 10 mg and 15 mg hair mass samples, respectively. The intra- and inter-assay variations were 5.87% and 7.05%, respectively.

F. Statistical methods

The main objective of the analysis was to assess the exposure-response relationship between WTN levels and hair cortisol concentrations, scores on the PSS, blood pressure/heart rate, and to evaluate the sample characteristics that may influence these relationships. All of these health outcomes were measured on a continuous scale. The analysis for continuous outcomes closely follows the description outlined in Michaud *et al.* (2013), which gives a summary of the planned study design and objectives, as well as proposed data analysis. A-weighted WTN categories were defined based on final data collection and are as follows: {<25 dB; [25–30) dB; [30–35) dB; [35–40) dB; [40–46] dB}. Identification of variables that best explain the variability in self-reported and objectively measured stress-related endpoints was done using multiple linear regression. As a first step to develop the best predictive model for each outcome, univariate regression models only adjusting for WTN exposure groups and province were fitted. Explanatory variables significant at the 20% level for univariate analysis were considered in the multiple linear regression models. It should be emphasized that variables considered in the univariate analysis have been previously demonstrated to be related to the modeled endpoint and/or considered by the authors to conceptually have a potential association with the modeled endpoint. Province was initially assessed as an effect modifier. Since the interaction was never statistically significant, province was treated as a confounder in all of the regression models.

Multiple linear regression models describing the relationship between a stress endpoint (PSS, hair cortisol concentrations, blood pressure, and resting heart rate measurements) and predictors were developed using stepwise regression with a 20% significance entry criterion for predictors and a 10% significance criterion to remain in the model. The stepwise regression was carried out in three different ways wherein the base model included exposure to (1) WTN category and province; (2) WTN category, province, and an adjustment for individuals who reported receiving personal benefit from wind turbines in the area; and (3) WTN category and province, stratified for those who received no personal benefit. When developing the model for PSS, hair cortisol was not used as an explanatory variable as this would reduce the sample size substantially from 1231 observations to 675. When developing the model for hair cortisol, PSS was used as a potential explanatory variable in the model. Since time of day was shown to significantly influence heart rate, it was included in the multiple regression model to adjust for it.

Hair cortisol, blood pressure, and resting heart rate endpoints were log-normally distributed (by the Anderson-Darling test for normality), therefore, the geometric mean and corresponding 95% confidence interval (CI) were reported for these endpoints. When the assumptions for the various models for these endpoints were still not satisfied for the logged data, non-parametric approaches were used, in which case the geometric mean and CI were still reported, but the test results were based on non-parametric methods.

Statistical analysis was performed using SAS (Statistical Analysis System) version 9.2 (2014). A 5% statistical significance level was implemented throughout unless otherwise stated. In addition, Tukey corrections were made to account for all pairwise comparisons to ensure that the overall Type I (false positive) error rate was <0.05.

III. RESULTS

A. Wind turbine sound pressure levels at dwellings

Modeled sound pressure levels and the measurements used to support the calculations are presented in detail by Keith *et al.* (2016a,b). Calculated immission levels as determined by the ISO 9613-1 (ISO, 1993) and ISO 9613-2 (ISO, 1996) reached levels as high as 46 dB under conditions of 8 m/s wind speeds at 10 m heights for favourable propagation conditions. Calculations are representative of typical worst case long-term (1 yr) average WTN levels.

B. Response rates and sample characteristics

A detailed breakdown of the response rates, along with sample characteristics variables by WTN category is presented by Michaud *et al.* (2016a). Of the 2004 potential dwellings, 1570 were valid and 1238 agreed to participate in the study. This yielded a final response rate of 78.9%. For blood pressure measurements, a total of 1077 respondents participated providing a response rate of 87.0%. A total of 195 respondents were not able to participate in the hair cortisol portion of the physical measures, therefore, a potential 1043 respondents remained. A subsample of 917 of these 1043 respondents consented to the hair sampling for cortisol analysis (response rate, 87.9%).

Factors that could potentially exert an influence on stress responses, including self-reported prevalence of diagnosed chronic diseases and health conditions, quality of life, satisfaction with health, noise sensitivity, and self-reported high sleep disturbance (in general) were all found to be equally distributed across WTN categories (Michaud *et al.*, 2016a).

C. Hair cortisol, perceived stress, blood pressure, and heart rate

Table I presents the summary statistics for hair cortisol, PSS, blood pressure, and resting heart rate endpoints along with Cronbach's alpha (α) for the PSS. Cronbach's α is a measure of the internal consistency or reliability of test scores. Cronbach's α was substantially over the recommended acceptable range of 70% for PSS (Cronbach's α 0.86).

Of the 917 participants who consented to take part in the hair cortisol sampling, 214 samples were found to be of insufficient mass (i.e., <10 mg). Of the remaining 703 samples, 9 exceeded the ELISA upper limit of quantification for which no value was given, and the computed results from 19 observations were found to be above the assay detection limit but below the lower limit of quantification. These were removed because 14 of the 19 participants in this subgroup reported using a chemical hair treatment within the previous 3 months, indicating that the results were not reliable. A total of 675 observations remained for hair cortisol analysis. The majority of the hair samples collected were from females (n 431, 63.9%), and individuals aged between 45 and 64 years

TABLE I. Descriptive statistics for stress-related outcomes.

	n	GM (95% CI)[a]	(Min, Max)	Cronbach's α
Hair cortisol (ng/g)	675	146.09 (135.46,157.56)	(18.12,7139.34)	
Perceived stress scale	1231	11.87 (11.49,12.24)[b]	(0,37)	0.86
Systolic blood pressure (mmHg)	1077	119.23 (118.27,120.19)	(83,186)	
Diastolic blood pressure (mmHg)	1077	75.15 (74.55,75.75)	(50,114)	
Heart rate (bpm)	1077	72.50 (71.79,73.21)	(41,125)	

[a]GM is the geometric mean and corresponding 95% confidence interval (CI) unless otherwise indicated.
[b]Arithmetic mean and corresponding 95% CI.

(n 311, 46.1%). The age group least represented were individuals in the ≤25 yr age group (n 35, 5.2%). Hair cortisol levels ranged from 18.12 to 7139.34 ng/g with a geometric mean of 146.09 ng/g and 95% CI: (135.46,157.56).

Blood pressure measurements were fairly equally distributed between men and women (males 527, 48.9%), although the majority of the measures were from individuals aged between 45 and 64 years (n 467, 43.4%). Similar to hair sampling, those least represented were individuals in the ≤25 yr age-group (n 62, 5.8%). The time of day that blood pressure and heart rate measures were taken had no impact on blood pressure, but did significantly influence resting heart rate (p 0.0008). Average resting heart rate was lower during the morning hours (06:00–11:59 h; 69.19, 95%CI: 67.50,70.92) compared to afternoon (12:00–17:59 h; 72.66, 95% CI: 71.47,73.87) and evening (18:00–22:00 h; 72.65, 95% CI: 71.01,74.32) (data not shown).

1. Association between self-reported and measured blood pressure

The consistency between self-reported diagnosed high blood pressure and measured blood pressure was assessed by the two-sample t-test. In the self-reported high blood pressure group, the geometric mean for systolic blood pressure was 127.51 (95% CI: 125.78,129.27) compared to 115.83 (95% CI: 114.77,116.90) for those who did not report high blood pressure ($p < 0.0001$). Similarly, the corresponding geometric means for diastolic blood pressure were 76.62 (95% CI: 75.51,77.75) and 74.54 (95% CI: 73.83,75.25) (p 0.0019).

D. Effects of personal and situational variables on hair cortisol concentrations, blood pressure, resting heart rate, and scores on the PSS

An exploratory univariate analysis of self-reported personal and situational variables in relation to hair cortisol concentrations, measured blood pressure, resting heart rate, and scores on the PSS only adjusting for WTN levels and province is presented in the supplementary material attached to the online version of this article.[1] The list of variables considered was extensive and includes, but is not limited to, demographics, illnesses/chronic diseases, quality of life, sleep disturbance, caffeine consumption, and variables related to the perception of wind turbines.

E. Association between PSS scores, hair cortisol concentrations, blood pressure and resting heart rate

The consistency between self-reported stress and an objective measure of stress was assessed by examining the association between PSS scores and hair cortisol concentrations. Hair cortisol was positively correlated with the PSS scores (Pearson r 0.13, p 0.0007) regardless of WTN exposure. When examining each of the WTN categories, a positive correlation between PSS and hair cortisol is significant only in the following WTN categories: [25–30) dB (r 0.35, p 0.0137) and [40–46] dB (r 0.20, p 0.0270). Nevertheless, in fitting a regression line relating hair cortisol to PSS and accounting for WTN exposure and province, the slope is positive and significant [slope 0.02, standard error (SE) 0.01, p 0.0008]. This indicates that higher levels of PSS are correlated with higher levels of hair cortisol.

The association between measured blood pressure and resting heart rate with hair cortisol and PSS was also investigated. Hair cortisol levels were not correlated with blood pressure values (regardless of WTN exposure levels; $r < 0.04$, $p > 0.30$, in all cases). Furthermore, it was observed that none of the blood pressure measures were associated with hair cortisol levels even after adjusting for WTN exposure levels in the regression models. PSS was positively associated only with resting heart rate (r 0.08, p 0.0076), but not with blood pressure. After accounting for WTN in a regression model the association remained (i.e., increased PSS scores were related to increased resting heart rate).

F. Multiple regression modeling for PSS scores, hair cortisol concentrations, blood pressure, and resting heart rate

The final models for the three approaches to stepwise regression listed in the statistical methods section produced nearly identical results. Therefore, only the regression model whereby the variables WTN, province, and personal benefit were forced into the model is presented. Table II provides a summary of the variables retained in the final multiple linear regression models for the self-reported and objectively measured stress-related outcomes.

1. PSS scores and hair cortisol concentrations

Tables III(a) and III(b) present the detailed results for the multiple linear regression models for PSS and hair cortisol, respectively. Exposure to WTN was not found to be significantly associated with these endpoints. Some of the variables that increased PSS scores at the 5% level of significance included age (i.e., being <65 years of age), income (i.e., making <$60000 per year), smoking status (i.e., being a smoker), and the presence of self-reported health conditions including migraines/headaches, dizziness, chronic pain, and a diagnosed sleep disorder. PSS scores were not related to receiving personal benefit from having wind turbines in the area (p 0.1579). The final multiple linear regression model explained 21% of the variability in PSS scores.

Being male, having high school or trade/certificate/college education, being obese, and having tinnitus significantly increased the hair cortisol concentrations at the 10% level. Cortisol was reduced among those who cosmetically treated their hair and among those who washed their hair more than eight times per week compared to those who washed it less than once per week. Hair cortisol concentrations were not associated with receiving personal benefit (p 0.1084). Finally, as PSS scores increased so did hair cortisol concentrations (p 0.0037). The final multiple linear regression model accounted for 14% of the variability observed in hair cortisol concentrations.

2. Blood pressure and resting heart rate

Tables IV(a)–IV(c) present the multiple linear regression models for systolic and diastolic blood pressure, as well as resting heart rate. In all three models exposure to WTN

TABLE II. A summary of significant variables retained in multiple linear regression models for self-reported and measured stress endpoints. The specific direction of change, level of statistical significance, and pairwise comparisons between variable groups are provided in Tables III(a), III(b), and IV(a)–IV(c).

	Perceived stress scale[a]	Hair cortisol[a]	Systolic blood pressure[a]	Diastolic blood pressure[a]	Heart rate[a]
Base model					
WTN levels					
Province			++	++	++
Demographic variables					
Sex		++	++	++	
BMI group		++	++	++	++
Age group	++		++	++	
Income	++				
Smoking status	++			+	++
Caffeine consumption			+	++	++
Education	+	+			
Situational variables					
Audible road traffic	++				
Audible rail noise	++		++	+	
Time of day					++
Wind turbine related variables					
Personal benefits					++
Annoyance with blinking lights				++	
Personal and health related variables					
Cosmetic hair treatment		++			
Hair washing frequency		+			
Health compared to one year ago	++				
Migraines	++				
Dizziness	++				
Tinnitus		+	+		
Chronic pain	++				
Asthma					+
High blood pressure			++		
History of high blood pressure in family			++	++	
Chronic bronchitis/emphysema/COPD[b]				++	
Diabetes			+	++	++
Heart disease				++	++
Diagnosed sleep disorder	++				
Perceived stress scale	N/A	++			

[a]+, ++ denote statistically significant, $p < 0.10$, $p < 0.05$, respectively.
[b]COPD, chronic obstructive pulmonary disease.

was not found to be a significant factor in explaining the variability in these measures. Overall, the ON sample had higher systolic and diastolic blood pressures and heart rate (regardless of WTN exposure).

a. Resting systolic and diastolic blood pressure. Increased systolic blood pressure was associated with being male, 45 years of age or more, and having a BMI $\geq$25. The participants who self-identified as having high blood pressure or a history of high blood pressure in the family did, in fact, have significantly higher measured systolic blood pressure. In the multiple linear regression model, diastolic blood pressure was not only affected by the same factors as systolic blood pressure, but was also elevated among smokers, those who consumed caffeinated beverages within 2 h of measurements being taken and 2.90 mmHg (95% CI: 0.75,5.05) higher among those who were annoyed by the blinking lights atop wind turbines. The multiple linear regression models for systolic and diastolic blood pressures explained, respectively, ~23% and 19% of the variability in the outcomes.

b. Resting heart rate. Being a current smoker, being obese, and having diabetes were significantly associated with increased resting heart rate. Those who self-identified as having heart disease ($p < 0.0001$) and those who received personal benefit (p 0.0254) had significantly lower heart rates. Similarly, time of day was found to have a significant effect on resting heart rate, with lower values in the morning compared to the afternoon or evening. The multiple linear regression model for resting heart rate explained ~11% of the variability in the endpoint.

IV. DISCUSSION

Taken together, the study results do not support an association between WTN exposure and increased stress either

TABLE III. (a) Multiple linear regression model for perceived stress. (b) Multiple linear regression model for hair cortisol concentrations.

		Perceived stress scale ($R^2 = 0.21$, $n = 987$)		
(a) Variable	Groups in variable	LSM (95% CI)[a]	PWC[b]	p-value[c]
WTN levels (dB)	<25	13.67 (11.88,15.46)		0.8614
	[25–30)	13.84 (11.92,15.75)		
	[30–35)	13.18 (11.69,14.67)		
	[35–40)	13.15 (11.75,14.55)		
	[40–46]	13.48 (12.03,14.92)		
Province	PEI	13.14 (11.57,14.71)		0.2254
	ON	13.79 (12.58,14.99)		
Age group	≤24	14.22 (12.08,16.36)	A	<0.0001
	[25–45)	14.67 (13.26,16.07)	A	
	[45–65)	13.48 (12.21,14.75)	A	
	≥65	11.49 (10.05,12.93)	B	
Education	≤High school	14.00 (12.69,15.32)		0.0794
	Trade/certificate/college	14.06 (12.69,15.43)		
	University	12.33 (10.52,14.13)		
Income	<60 K	14.08 (12.70,15.45)	A	0.0493
	[60–100) K	13.55 (12.11, 15.00)	AB	
	≥100 K	12.76 (11.30,14.21)	B	
Smoking status	Current	14.16 (12.69,15.62)	A	0.0328
	Former	13.42 (11.98,14.86)	AB	
	Never	12.81 (11.48,14.15)	B	
Audible road traffic	Yes	13.96 (12.71,15.22)	A	0.0455
	No	12.96 (11.45,14.47)	B	
Audible rail noise	Yes	12.90 (11.36,14.43)	A	0.0296
	No	14.03 (12.80,15.26)	B	
Personal benefit	Yes	12.96 (11.21,14.71)		0.1579
	No	13.97 (12.83,15.10)		
Health compared to one year ago	Worse	14.93 (13.45,16.42)	A	<0.0001
	Better	11.99 (10.68,13.30)	B	
Migraines	Yes	14.13 (12.69,15.57)	A	0.0097
	No	12.79 (11.45,14.14)	B	
Dizziness	Yes	14.47 (13.02,15.92)	A	0.0001
	No	12.46 (11.12,13.79)	B	
Chronic pain	Yes	14.34 (12.91,15.77)	A	0.0003
	No	12.59 (11.26,13.92)	B	
Diagnosed sleep disorder	Yes	14.41 (12.77,16.04)	A	0.0050
	No	12.52 (11.27,13.77)	B	
		Hair cortisol (ng/g) ($R^2 = 0.14$, $n = 528$)		
(b) Variable	Groups in variable	LSGM (95% CI)[d]	PWC[b]	p-value[c]
WTN levels (dB)	<25	150.54 (96.94,233.77)		0.5416
	[25–30)	182.20 (118.52,280.10)		
	[30–35)	191.12 (135.63,269.33)		
	[35–40)	181.63 (132.24,249.48)		
	[40–46]	160.25 (115.70,221.96)		
Province	PEI	163.11 (111.09,239.48)		0.4189
	ON	182.36 (136.61,243.44)		
Sex	Male	191.88 (136.66,269.40)	A	0.0442
	Female	155.02 (112.87,212.90)	B	
Education	≤High school	197.89 (144.59,270.83)		0.0681
	Trade/certificate/college	191.39 (139.55,262.48)		
	University	135.45 (89.41,205.19)		
BMI group	<25 underweight-normal	157.56 (112.79,220.09)	A	0.0045
	[25–30) overweight	155.65 (111.10,218.06)	A	
	≥30 obese	209.19 (151.00,289.80)	B	
Cosmetic hair treatment	Yes	144.32 (103.03,202.15)	A	0.0005
	No	206.10 (150.13,282.95)	B	
Hair washing frequency	<1 per week	387.22 (173.34,864.98)		0.0551
	[1–3] times per wk	138.79 (107.35,179.44)		

TABLE III. (*Continued*)

(b) Variable	Groups in variable	Hair cortisol (ng/g) ($R^2 = 0.14$, $n = 528$) LSGM (95% CI)[d]	PWC[b]	p-value[c]
	[4–7] times per wk	141.66 (112.33,178.65)		
	≥8 times per wk	116.21 (72.84,185.41)		
Personal benefit	Yes	194.65 (130.59,290.14)		0.1084
	No	152.81 (115.44,202.27)		
Tinnitus	Yes	188.21 (133.20,265.93)		0.0843
	No	158.04 (116.23,214.89)		
Perceived stress scale[e]		0.02 (0.01)		0.0037

[a]LSM, least squares mean, and 95% confidence interval (CI) as determined by the multiple linear regression model.
[b]PWC, pairwise comparisons. Where overall p-value < 0.05, pairwise comparisons were conducted. After adjusting for multiple comparisons, groups with the same letter are statistically similar, whereas groups with different letters are statistically different.
[c]p-value for the variable in the model after adjusting for all other variables in the multiple linear regression model.
[d]LSGM, least square geometric mean and 95% CI.
[e]Parameter estimate (b) or slope and standard error (SE) based on the multiple linear regression model.

reported by, or objectively measured among participants exposed to WTN levels up to 46 dB. In the final multiple linear regression models, the level of WTN was not found to be related to any of the stress-related endpoints. Furthermore, the finding that the WTN annoyance variable was absent in any of these models is notable because potential health effects associated with WTN would presumably be indirect and mediated, at least in part, through noise annoyance (Niemann *et al.*, 2006; Bakker *et al.*, 2012). The audibility of wind turbines, and reported annoyance with WTN, were only related to some of the stress outcomes when the analysis did not adjust for other contributing variables (e.g., age, BMI, smoking status, sex, and education) (supplementary material[1]).

After adjusting for other variables, the only wind turbine-related variable that was found to have an influence on any of the stress endpoints was high annoyance with the blinking aircraft warning lights atop wind turbines. Irrespective of WTN levels, annoyance with blinking lights appeared to be statistically associated with a slight elevation in diastolic blood pressure. Although this finding could be a statistical anomaly, the association may be related to the apparent impact that annoyance with the blinking lights was found to have on sleep. Indeed, reported and measured sleep quality has been associated with elevated blood pressure (Fiorentini *et al.*, 2007; Knutson *et al.*, 2009) and in the current study sample high annoyance with the blinking lights on wind turbines was found to be related to objectively measured sleep disturbance (Michaud *et al.*, 2016c). Until this finding is replicated in future research, the increase in diastolic blood pressure should be interpreted cautiously.

Michaud *et al.* (2016a) reported that the prevalence of hypertension and the use of blood pressure medication in the *Community Noise and Health Study* were unrelated to WTN levels. The later finding indicates that the absent association between blood pressure and WTN exposure reported in the current analysis was not related to a disproportionate use of blood pressure medication among the most exposed participants.

Multiple regression modeling left the great majority (77%–89%) of the variance in hair cortisol, systolic blood pressure, diastolic blood pressure, heart rate, and perceived stress unaccounted for. These study results may be complemented or strengthened by additional research that considers factors known to influence the response to community noise in general beyond exposure to wind turbines themselves (see Fig. 1 in the Appendix). Some of these factors include perceived control over the exposure, which could relate to the level of consultation between a developer and the community; maintaining the belief that action could have been taken to reduce WTN exposure, but was not; attitude toward wind turbines as an alternate source of renewable energy; and personality type (Borsky, 1979; Stansfeld and Matheson, 2003). Exposure to multiple stressors or other sources of annoyance, such as transportation noise, may influence the response to WTN exposure.

Transportation noise levels at participants' dwellings were not quantified, which may be a limitation considering the evidence linking exposure to transportation noise with stress-related health effects. However, it is important to keep in mind that this evidence pertains to sound pressure levels that are typically associated with higher levels of annoyance than reported in the current study (Babisch, 1998; Miedema and Vos, 1998; Babisch *et al.*, 2001; Haralabidis *et al.*, 2008). The percentage highly annoyed by aircraft, rail, and road traffic noise across all WTN categories never exceeded 5%. In our view, it is therefore unlikely that exposure to transportation noise had any significant influence on the reported stress reactions.

Another limitation in the current study is the difficulty in providing a precise timeframe for WTN exposure for each participant. Even a wind farm's operational date may not represent the true time of WTN exposure onset as wind farms are often installed over time so that exposure to WTN may vary from person to person. Future research could include specific questions to more precisely identify the individual's history of exposure. The proxy for exposure history included in the current study was derived from asking participants how long they have been hearing noise coming from wind turbines. Michaud *et al.* (2016b) reported that the odds of reporting to be highly annoyed by WTN were almost four times higher among participants who heard the wind turbines for one year or more, compared to those who heard it for less than one year. However, in the final multiple regression

TABLE IV. (a) Multiple linear regression models for resting systolic blood pressure. (b) Multiple linear regression models for resting diastolic blood pressure. (c) Multiple linear regression models for resting heart rate.

		Systolic blood pressure (mmHg) ($R^2=0.23$, $n=810$)		
(a) Variable	Groups in variable	LSGM (95% CI)[a]	PWC[b]	p-value[c]
WTN levels (dB)	<25	113.38 (109.17,117.76)		0.4990
	[25–30)	116.82 (112.36,121.45)		
	[30–35)	116.53 (113.13,120.03)		
	[35–40)	115.30 (112.17,118.52)		
	[40–46]	116.25 (112.83,119.77)		
Province	PEI	114.23 (110.68,117.89)	A	0.0338
	ON	117.09 (114.22,120.04)	B	
Sex	Male	117.43 (114.34,120.60)	A	0.0003
	Female	113.90 (110.76,117.12)	B	
Age group	≤24	109.01 (103.84,114.43)	A	<0.0001
	[25–45)	112.55 (109.30,115.89)	A	
	[45–65)	118.96 (116.05,121.95)	B	
	≥65	122.58 (119.34,125.90)	C	
BMI group	<25 underweight–normal	111.69 (108.51,114.96)	A	<0.0001
	[25–30) overweight	116.01 (112.66,119.45)	B	
	≥30 obese	119.39 (116.16,122.70)	C	
Caffeine consumption	Yes	116.51 (113.28,119.84)		0.0937
	No	114.79 (111.77,117.90)		
Audible rail noise	Yes	114.36 (110.89,117.94)	A	0.0345
	No	116.95 (114.08,119.90)	B	
Personal benefit	Yes	115.53 (111.36,119.85)		0.8924
	No	115.77 (113.30,118.30)		
Tinnitus	Yes	116.65 (113.21,120.19)		0.0756
	No	114.66 (111.80,117.59)		
High blood pressure	Yes	117.89 (114.45,121.42)	A	0.0004
	No	113.46 (110.49,116.50)	B	
History of high blood pressure in family	Yes	116.78 (113.66,119.98)	A	0.0262
	No	114.53 (111.40,117.74)	B	
Diabetes	Yes	114.04 (110.17,118.05)		0.0567
	No	117.28 (114.50,120.12)		

		Diastolic blood pressure (mmHg) ($R^2=0.19$, $n=815$)		
(b) Variable	Groups in variable	LSGM (95% CI)[a]	PWC[b]	p-value[c]
WTN levels (dB)	<25	67.98 (64.90,71.21)		0.5006
	[25–30)	70.20 (67.01,73.55)		
	[30–35)	69.92 (67.26,72.70)		
	[35–40)	69.66 (67.11,72.30)		
	[40–46]	70.34 (67.71,73.06)		
Province	PEI	68.23 (65.50,71.08)	A	0.0011
	ON	71.03 (68.66,73.48)	B	
Sex	Male	71.37 (68.82,74.01)	A	<0.0001
	Female	67.91 (65.44,70.46)	B	
Age group	≤24	67.22 (63.50,71.15)	A	0.0002
	[25–45)	69.95 (67.33,72.66)	A	
	[45–65)	72.07 (69.68,74.55)	B	
	≥65	69.32 (66.89,71.84)	A	
Smoking status	Current	70.80 (68.12,73.59)		0.0586
	Former	68.85 (66.28,71.51)		
	Never	69.22 (66.71,71.81)		
BMI group	<25 underweight–normal	67.00 (64.50,69.60)	A	<0.0001
	[25–30) overweight	69.96 (67.34,72.69)	B	
	≥30 obese	71.97 (69.39,74.65)	C	
Caffeine consumption	Yes	70.59 (68.00,73.28)	A	0.0035
	No	68.65 (66.21,71.18)	B	
Annoyed with blinking lights	Yes	70.95 (67.95,74.09)	A	0.0081
	No	68.31 (66.12,70.56)	B	
Audible rail noise	Yes	68.87 (66.20,71.64)		0.0539

TABLE IV. (*Continued*)

(b) Variable	Groups in variable	Diastolic blood pressure (mmHg) ($R^2 = 0.19$, $n = 815$) LSGM (95% CI)[a]	PWC[b]	p-value[c]
	No	70.37 (67.96,72.87)		
Personal benefit	Yes	69.38 (66.30,72.61)		0.6844
	No	69.85 (67.69,72.08)		
History of high blood pressure in family	Yes	70.55 (68.02,73.17)	A	0.0023
	No	68.69 (66.21,71.26)	B	
Chronic bronchitis/ emphysema/ COPD	Yes	67.86 (64.80,71.06)	A	0.0059
	No	71.42 (69.12,73.79)	B	
Diabetes	Yes	67.98 (65.16,70.92)	A	0.0020
	No	71.29 (68.87,73.80)	B	
Heart disease	Yes	67.79 (64.91,70.80)	A	0.0019
	No	71.49 (69.05,74.02)	B	

(c) Variable	Groups in variable	Heart rate (bpm) ($R^2 = 0.11$, $n = 990$) LSGM (95% CI)[a]	PWC[b]	p-value[c]
WTN levels (dB)	<25	68.24 (64.98,71.66)		0.5223
	[25–30)	70.59 (67.38,73.95)		
	[30–35)	69.72 (67.17,72.37)		
	[35–40)	69.56 (67.21,71.99)		
	[40–46]	70.71 (68.20,73.32)		
Province	PEI	68.64 (66.07,71.31)	A	0.0161
	ON	70.89 (68.65,73.21)	B	
Smoking status	Current	72.21 (69.54,74.99)	A	<0.0001
	Former	67.62 (65.30,70.03)	B	
	Never	69.52 (67.15,71.97)	C	
BMI group	<25 underweight-normal	68.90 (66.41,71.47)	A	0.0475
	[25–30) overweight	69.42 (66.98,71.95)	AB	
	≥30 obese	70.97 (68.59,73.44)	B	
Caffeine consumption	Yes	70.91 (68.45,73.45)	A	0.0036
	No	68.63 (66.34,70.99)	B	
Time of blood pressure measurement	Morning	67.43 (64.90,70.06)	A	0.0004
	Afternoon	71.09 (68.73,73.53)	B	
	Evening	70.82 (68.26,73.47)	B	
Personal benefit	Yes	68.37 (65.44,71.44)	A	0.0254
	No	71.17 (69.14,73.27)	B	
Asthma	Yes	70.98 (67.92,74.18)		0.0592
	No	68.56 (66.59,70.59)		
Diabetes	Yes	71.49 (68.53,74.57)	A	0.0062
	No	68.07 (65.98,70.23)	B	
Heart disease	Yes	66.10 (63.29,69.03)	A	<0.0001
	No	73.62 (71.40,75.91)	B	

[a]LSGM least square geometric mean and 95% CI.
[b]PWC, pairwise comparisons. Where overall p-value < 0.05, PWC were conducted. After adjusting for multiple comparisons, groups with the same letter are statistically similar, whereas groups with different letters are statistically different.
[c]p-value for the variable in the model after adjusting for all other variables in the multiple linear regression model.

models, self-reported history of hearing WTN was not related to any of the stress outcomes assessed in this study.

V. CONCLUDING REMARKS

The results provide no evidence that self-reported or objectively measured stress reactions are significantly influenced by exposure to increasing levels of WTN up to 46 dB. There is an added level of confidence in the findings as this is the first study to date to investigate the potential stress impacts associated with WTN exposure using a combination of self-reported and objectively measured endpoints. Specifically, cortisol concentrations in hair, blood pressure, resting heart rate, and perceived stress using the PSS were measured in relation to WTN exposure. Although the positive correlation found between PSS scores and hair cortisol concentrations was statistically weak, the fact that they move in the same direction provides confidence regarding the validity of the study results and selected endpoints. The weak correlation could be owing to the fact that each endpoint has a different time reference period associated with its outcome. Hair cortisol concentrations and perceived stress scores reflect the previous 90 and 30 days, respectively.

The association between perceived stress and hair cortisol concentrations was similarly found between reported high blood pressure and measured blood pressure. Specifically, participants that indicated they had been diagnosed with high blood pressure from a health care professional had higher resting systolic and diastolic blood pressure.

The observation that the WTN annoyance variable was not retained in the final multiple linear regressions should not be interpreted to mean that this variable has no influence on the modeled endpoints. Rather, in the presence of the other variables in the model, WTN annoyance was not found to contribute further to the overall variance in the measured endpoint(s). In theory, one could arrive at different conclusions if the variables considered in the modeling are not universally incorporated across different study designs.

ACKNOWLEDGMENTS

The authors acknowledge the support they received throughout the study from Serge Legault and Suki Abeysekera at Statistics Canada, and are especially grateful to the volunteers who participated in this study. The authors also thank Dr. Stan Van Uum for his insight in planning the hair analysis. This research was funded by Health Canada. The authors have declared that no competing interests exist.

APPENDIX

Figure 1 presents a theoretical model of the complex processes that may be involved in the development of indirect stress-related health effects from exposure to wind turbines. The model assumes the origin of an indirect pathway

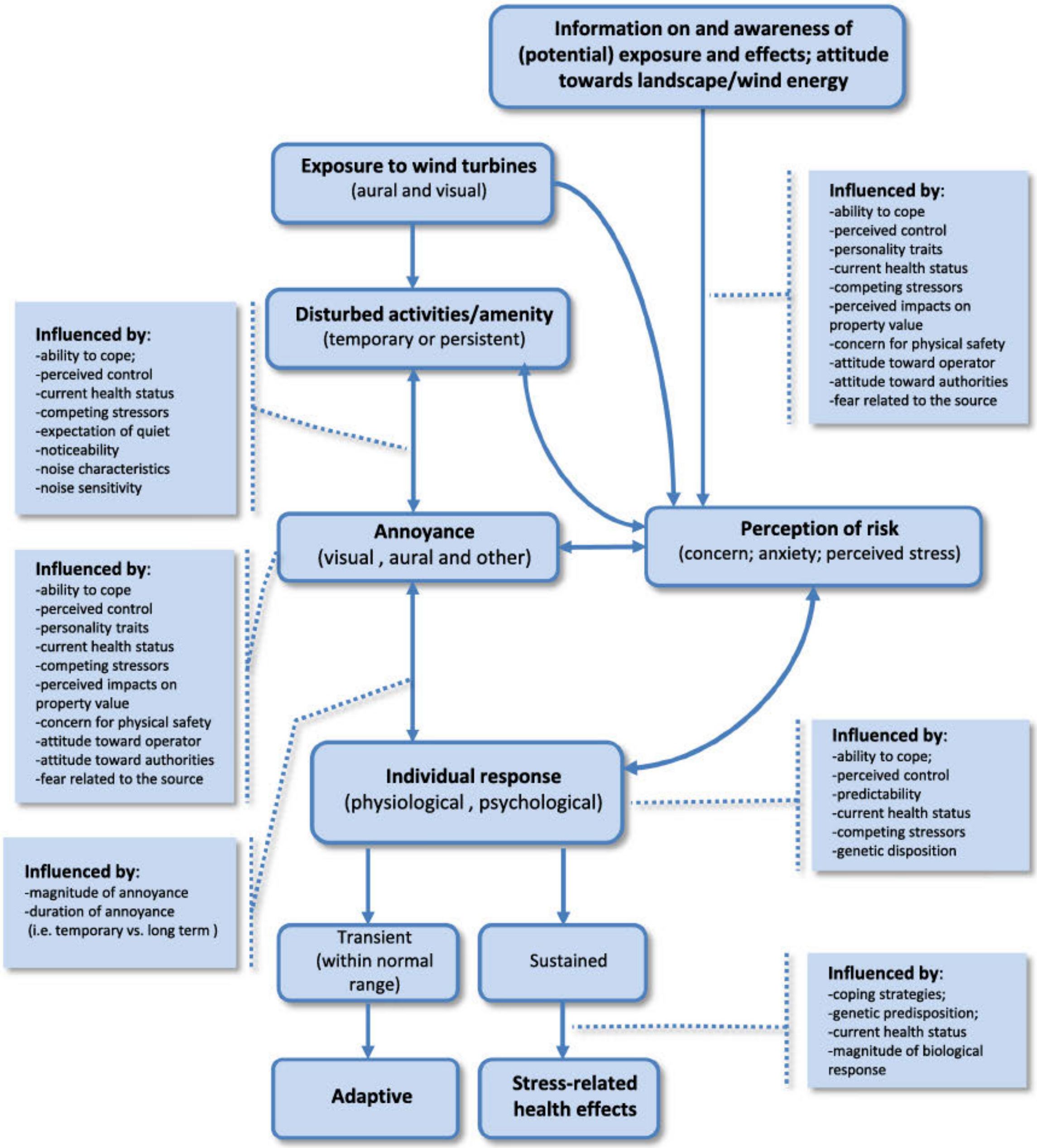

FIG. 1. (Color online) A theoretical model demonstrating the complex processes that may be involved in the potential progression towards indirect health effects from community noise exposure.

beginning with exposure, which can lead to an individualized perception of risk, which itself may be based on information about and attitude toward wind turbines. Perceived risk, and/or other factors that increase annoyance, may then lead to the development of stress-related health effects. Solid arrows represent the proposed direction of interaction. Broken lines represent some of the factors that would be expected to exert an influence at each level in the pathway, or the progression from one level to the next. The proposed model is not limited to WTN and could be applicable for other environmental exposures that are associated with annoyance.

[1]See supplementary material at http://dx.doi.org/10.1121/1.4942402 for the univariate analysis results.

Al kalaldeh, M. T., and Shosha, G. M. A. (**2012**). "Application of the perceived stress scale in health care studies. An analysis of literature," Int. J. Academ. Res. Part B **4**(4), 45–50.

Babisch, W. (**1998**). "Epidemiological studies on cardiovascular effects of traffic noise,"in *Advances in Noise Research, Volume I, Biological Effects of Noise*, edited by D. Prasher, and L. Luxon (Whurr, London, UK).

Babisch, W., Fromme, H., Beyer, A., and Ising, H. (**2001**). "Increased catecholamine levels in urine in subjects exposed to road traffic noise: The role of stress hormones in noise research," Environ. Int. **26**(7-8), 475–481.

Bakker, R. H., Pedersen, E., van den Berg, G. P., Stewart, R. E., Lok, W., and Bouma, J. (**2012**). "Impact of wind turbine sound on annoyance, self-reported sleep disturbance and psychological distress," Sci. Total Env. **425**, 42–51.

Borsky, P. N. (**1979**). "Sociopsychological factors affecting the human response to noise exposure," Otolaryngol. Clin. North Am. **12**(3), 521–535.

Broderick, J. E., Arnold, D., Kudielka, B. M., and Kirschbaum, C. (**2004**). "Salivary cortisol sampling compliance: Comparison of patients and healthy volunteers," Psychoneuroendocrinology **29**(5), 636–650.

Bryan, S., St. Pierre-Larose, M., Campbell, N., Clarke, J., and Tremblay, M. S. (**2010**). "Resting blood pressure and heart rate measurements in the Canadian Health Measures Survey, cycle 1," Health Rep. **21**(1), 71–78.

Cohen, S., Kamarck, T., and Mermelstein, R. (**1983**). "A global measure of perceived stress," J. Health Soc. Behav. **24**(4), 385–396.

DataKustik GmbH®. (**2014**). "Cadna A version 4.4 software for immission protection," available at www.datakustik.com (Last viewed 11/24/2014).

Edwards, S., Evans, P., Hucklebridge, F., and Clow, A. (**2001**). "Association between time of awakening and diurnal cortisol secretory activity," Psychoneuroendocrinology **26**(6), 613–622.

Feder, K., Michaud, D. S., Keith, S. E., Voicescu, S. A., Marro, L., Than, J., Guay, M., Denning, A., Bower, T. J., Lavigne, E., Whelan, C., and van den Berg, F. (**2015**). "An assessment of quality of life using the WHOQOL-BREF among participants living in the vicinity of wind turbines," Environ. Res. **142**, 227–238.

Fiorentini, A., Valente, R., Perciaccante, A., and Tubani, L. (**2007**). "Sleep's quality disorders in patients with hypertension and type 2 diabetes mellitus," Int. J. Cardiol. **114**(2), E50–E52.

Gerber, M., Kalak, N., Elliot, C., Holsboer-Trachsler, E., Pühse, U., and Brand, S. (**2013**). "Both hair cortisol levels and perceived stress predict increased symptoms of depression: An exploratory study in young adults," Neuropsychobiology **68**(2), 100–109.

Grunau, R. E., Cepeda, I. L., Chau, C. M. Y., Brummelte, S., Weinberg, J., Lavoie, P. M., Ladd, M., Hirschfeld, A. F., Russell, E., Koren, G., Van Uum, S., Brant, R., and Turvey, S. E. (**2013**). "Neonatal pain-related stress and NFKBIA genotype are associated with altered cortisol levels in preterm boys at school age," PLoS One **8**(9), 73–81.

Guski, R. (**2001**). "Effects of noise on health," in *Environmental Urban Noise*, edited by A. García (WIT, Ashurst Lodge, Ashurst, Southampton, UK).

Haralabidis, A. S., Dimakopoulou, K., Vigna-Taglianti, F., Giampaolo, M., Borgini, A., Dudley, M. L., Pershagen, G., Bluhm, G., Houthuijs, D., Babisch, W., Velonakis, M., Katsouyanni, K., Jarup, L., and HYENA Consortium. (**2008**). "Acute effects of night-time noise exposure on blood pressure in populations living near airports," Eur. Heart J. **29**(5), 658–664.

Hennig, J., Friebe, J., Ryl, I., Krämer, B., Böttcher, J., and Netter, P. (**2000**). "Upright posture influences salivary cortisol," Psychoneuroendocrinology **25**(1), 69–83.

Hinkelmann, K., Muhtz, C., Dettenborn, L., Agorastos, A., Wingenfeld, K., Spitzer, C., Gao, W., Kirschbaum, C., Wiedemann, K., and Otte, C. (**2013**). "Association between childhood trauma and low hair cortisol in depressed patients and healthy control subjects," Biol. Psychiatry. **74**(9), e15–e17.

Institute of Medicine. (**2001**). "Health and behavior: The interplay of biological, behavioral, and societal influences," Committee on Health and Behavior: Research, Practice, and Policy (National Academies, Washington, DC).

ISO (**1993**). ISO 9613-1, "Acoustics. Attenuation of sound during propagation outdoors. Part 1: Calculation of the absorption of sound by the atmosphere" (International Organization for Standardization, Geneva, Switzerland).

ISO (**1996**). ISO 9613-2, "Acoustics. Attenuation of sound during propagation outdoors. Part 2: General method of calculation" (International Organization for Standardization, Geneva, Switzerland).

ISO/TS-15666 (**2003**). "Acoustics—Assessment of noise annoyance by means of social and socio-acoustic surveys" (International Organization for Standardization, Geneva, Switzerland).

Job, R. F. S. (**1988**). "Community response to noise: A review of factors influencing the relationship between noise exposure and reaction," J. Acoust. Soc. Am. **83**, 991–1001.

Job, R. F. S. (**1996**). "The influence of subjective reactions to noise on health effects of noise," Environ. Int. **22**(1), 93–104.

Keith, S. E., Feder, K., Voicescu, S., Soukhovtsev, V., Denning, A., Tsang, J., Broner, N., Richarz, W., and van den Berg, F. (**2016a**). "Wind turbine sound pressure level calculations at dwellings," J. Acoust. Soc. Am. **139**(3), 1436–1442.

Keith, S. E., Feder, K., Voicescu, S., Soukhovtsev, V., Denning, A., Tsang, J., Broner, N., Richarz, W., and van den Berg, F. (**2016b**). "Wind turbine sound power measurements," J. Acoust. Soc. Am. **139**(3), 1431–1435.

Knutson, K. L., Van Cauter, E., Rathouz, P. J., Yan, L. L., Hulley, S. B., Liu, K., and Lauderdale, D. S. (**2009**). "Association between sleep and blood pressure in midlife: The CARDIA sleep study," Arch. Intern. Med. **169**(11), 1055–1061.

Legler, M., Brandenberger, G., Hietter, B., Siméoni, M., and Reinhardt, B. (**1982**). "Diurnal cortisol peaks and their relationships to meals," J. Clin. Endocrinol. Metab. **55**(4), 757–761.

Manenschijn, L., Schaap, L., van Schoor, N. M., van der Pas, S., Peeters, G. M., Lips, P., Koper, J. W., and van Rossum, E. F. (**2013**). "High long-term cortisol levels, measured in scalp hair, are associated with a history of cardiovascular disease," J. Clin. Endocrinol. Metab. **98**(5), 2078–2083.

McCunney, R. J., Mundt, K. A., Colby, W. D., Dobie, R., Kaliski, K., and Blais, M. (**2014**). "Wind turbines and health: A critical review of the scientific literature," J. Occup. Environ. Med. **56**(11), e108–e130.

Michaud, D. S., Feder, K., Keith, S. E., Voicescu, S. A., Marro, L., Than, J., Guay, M., Denning, A., McGuire, D., Bower, T., Lavigne, E., Murray, B. J., Weiss, S. K., and van den Berg, F. (**2016a**). "Exposure to wind turbine noise: Perceptual responses and reported health effects," J. Acoust. Soc. Am. **139**(3), 1443–1454.

Michaud, D. S., Feder, K., Keith, S. E., Voicescu, S., Marro, L., Than, J., Guay, M., Denning, A., Murray, B. J., Weiss, S. K., Villeneuve, P., and van den Berg, F. (**2016c**). "Effects of wind turbine noise on self-reported and objective measures of sleep," Sleep **39**, 97–109.

Michaud, D. S., Keith, S. E., Feder, K., Soukhovtsev, V., Marro, L., Denning, A., McGuire, D., Broner, N., Richarz, W., Tsang, J., Legault, S., Poulin, D., Bryan, S., Duddeck, C., Lavigne, E., Villeneuve, P. J., Leroux, T., Weiss, S. K., Murray, B. J., and Bower, T. (**2013**). "Self-reported and objectively measured health indicators among a sample of Canadians living within the vicinity of industrial wind turbines: Social survey and sound level modelling methodology," Noise News Int. **21**, 14–27.

Michaud, D. S., Keith, S. E., Feder, K., Voicescu, S. A., Marro, L., Than, J., Guay, M., Bower, T., Denning, A., Lavigne, E., Janssen, S. A., Leroux, T., and van den Berg, F. (**2016b**). "Personal and situational variables associated with wind turbine noise annoyance," J. Acoust. Soc. Am. **139**(3), 1455–1466.

Miedema, H. M., and Vos, H. (**1998**). "Exposure-response relationships for transportation noise," J. Acoust. Soc. Am. **104**(6), 3432–3445.

Niemann, H., Bonnefoy, X., Braubach, M., Hecht, K., Maschke, C., Rodrigues, C., and Röbbel, N. (**2006**). "Noise-induced annoyance and morbidity results from the pan-European LARES study," Noise Health **8**(31), 63–79.

Pereg, D., Chan, J., Russell, E., Berlin, T., Mosseri, M., Seabrook, J. A., Koren, G., and Van Uum, S. H. (**2013**). "Cortisol and testosterone in hair as biological markers of systolic heart failure," Psychoneuroendocrinology **38**(12), 2875–2882.

Pereg, D., Gow, R., Mosseri, M., Lishner, M., Rieder, M., Van Uum, S. H., and Koren, G. (**2011**). "Hair cortisol and the risk for acute myocardial infarction in adult men," Stress **14**(1), 73–81.

Russell, E., Koren, G., Rieder, M., and Van Uum, S. H. (**2012**). "Hair cortisol as a biological marker of chronic stress: Current status, future directions and unanswered questions," Psychoneuroendocrinology **37**(5), 589–601.

SAS Institute Inc. (**2014**). "SAS (Statistical Analysis System) software package version 9.2" (SAS Institute Inc., Cary, NC).

Stalder, T., and Kirschbaum, C. (**2012**). "Analysis of cortisol in hair—State of the art and future directions," Brain Behav. Immun. **26**(7), 1019–1029.

Stalder, T., Kirschbaum, C., Alexander, N., Bornstein, S. R., Gao, W., Miller, R., Stark, S., Bosch, J. A., and Fischer, J. E. (**2013**). "Cortisol in hair and the metabolic syndrome," J. Clin. Endocrinol. Metab. **98**(6), 2573–2580.

Stansfeld, S. A., and Marmot, M. G. (eds). (**2002**). *Stress and the Heart: Psychosocial Pathways to Coronary Heart Disease* (BMJ Books, Williston, VA).

Stansfeld, S. A., and Matheson, M. P. (**2003**). "Noise pollution: Non-auditory effects on health," Br. Med. Bull. **68**, 243–257.

Vallet, M. (**2001**). "Effects of noise on health," in *Environmental Urban Noise*, edited by A. García (WIT, Ashurst Lodge, Ashurst, Southampton, UK).

Van Uum, S. H., Sauvé, B., Fraser, L. A., Morley-Forster, P., Paul, T. L., and Koren, G. (**2008**). "Elevated content of cortisol in hair of patients with severe chronic pain: A novel biomarker for stress," Stress **11**(6), 483–488.

Veldhorst, M. A., Noppe, G., Jongejan, M. H., Kok, C. B., Mekic, S., Koper, J. W., van Rossum, E. F., and van den Akker, E. L. (**2014**). "Increased scalp hair cortisol concentrations in obese children," J. Clin. Endocrinol. Metab. **99**(1), 285–290.

Walton, D. M., Macdermid, J. C., Russell, E., Koren, G., and Van Uum, S. (**2013**). "Hair-normalized cortisol waking response as a novel biomarker of hypothalamic-pituitary-adrenal axis activity following acute trauma: A proof-of-concept study with pilot results," Pain Res. Treat. **2013**, 876871.

Webb, E., Thomson, S., Nelson, A., White, C., Koren, G., Rieder, M., and van Uum, S. H. (**2010**). "Assessing individual systemic stress through cortisol analysis of archaeological hair," J. Archaeol. Sci. **37**(4), 807–812.

Wells, S., Tremblay, P. F., Flynn, A., Russell, E., Kennedy, J., Rehm, J., Van Uum, S. H., Koren, G., and Graham, K. (**2014**). "Associations of hair cortisol concentration with self-reported measures of stress and mental health-related factors in a pooled database of diverse community samples," Stress **17**(4), 334–342.

Wennig, R. (**2000**). "Potential problems with the interpretation of hair analysis results," Forensic Sci. Int. **107**(103), 5–12.

Wester, V. L., Staufenbiel, S. M., Veldhorst, M. A., Visser, J. A., Manenschijn, L., Koper, J. W., Klessens-Godfroy, F. J., van den Akker, E. L., and van Rossum, E. F. (**2014**). "Long-term cortisol levels measured in scalp hair of obese patients," Obesity (Silver Spring) **22**(9), 1956–1958.

World Health Organization (WHO). (**1999**). *Guidelines for Community Noise*, edited by B. Berglund, T. Lindvall, and D. H. Schwela (World Health Organization, Geneva, Switzerland).

World Health Organization (WHO). (**2011**). *Burden of Disease from Environmental Noise. Quantification of Healthy Life Years Lost in Europe*, edited by L. Fritschi, A. L. Brown, R. Kim, D. Schwela, and S. Kephalopolous (World Health Organization, Geneva, Switzerland).

BEFORE THE PUBLIC UTILITY COMMISSION
OF OREGON

Docket PCN 5

In the Matter of

IDAHO POWER COMPANY'S
PETITION FOR CERTIFICATE OF PUBLIC CONVENIENCE
AND NECESSITY

Michaud, D. S. et al., Exposure to Wind Turbine Noise: Perceptual Responses and Reported Health Effects (2016)

February 22, 2023

Exposure to wind turbine noise: Perceptual responses and reported health effects

David S. Michaud, Katya Feder, Stephen E. Keith, Sonia A. Voicescu, Leonora Marro, John Than, Mireille Guay, Allison Denning, D'Arcy McGuire, Tara Bower, Eric Lavigne, Brian J. Murray, Shelly K. Weiss, and Frits van den Berg

Citation: The Journal of the Acoustical Society of America **139**, 1443 (2016); doi: 10.1121/1.4942391

View online: https://doi.org/10.1121/1.4942391

View Table of Contents: http://asa.scitation.org/toc/jas/139/3

Published by the Acoustical Society of America

Exposure to wind turbine noise: Perceptual responses and reported health effects

David S. Michaud,[a] Katya Feder, Stephen E. Keith, and Sonia A. Voicescu
Health Canada, Environmental and Radiation Health Sciences Directorate, Consumer and Clinical Radiation Protection Bureau, 775 Brookfield Road, Ottawa, Ontario K1A 1C1, Canada

Leonora Marro, John Than, and Mireille Guay
Health Canada, Population Studies Division, Biostatistics Section, 200 Eglantine Driveway, Tunney's Pasture, Ottawa, Ontario, Canada

Allison Denning
Health Canada, Environmental Health Program, Health Programs Branch, Regions and Programs Bureau, 1505 Barrington Street, Halifax, Nova Scotia, Canada

D'Arcy McGuire and Tara Bower
Health Canada, Environmental and Radiation Health Sciences Directorate, Office of Science Policy, Liaison and Coordination, 269 Laurier Avenue West, Ottawa, Ontario, Canada

Eric Lavigne
Health Canada, Air Health Science Division, 269 Laurier Avenue West, Ottawa, Ontario, Canada

Brian J. Murray
Department of Medicine, Division of Neurology, Sunnybrook Health Sciences Center, University of Toronto, Toronto, Ontario, Canada

Shelly K. Weiss
Department of Pediatrics, Division of Neurology, Hospital for Sick Children, University of Toronto, 555 University Avenue, Toronto, Ontario, Canada

Frits van den Berg
The Amsterdam Public Health Service (GGD Amsterdam), Environmental Health Department, Nieuwe Achtergracht 100, Amsterdam, The Netherlands

(Received 19 March 2015; revised 7 July 2015; accepted 20 November 2015; published online 31 March 2016)

Health Canada, in collaboration with Statistics Canada, and other external experts, conducted the Community Noise and Health Study to better understand the impacts of wind turbine noise (WTN) on health and well-being. A cross-sectional epidemiological study was carried out between May and September 2013 in southwestern Ontario and Prince Edward Island on 1238 randomly selected participants (606 males, 632 females) aged 18–79 years, living between 0.25 and 11.22 km from operational wind turbines. Calculated outdoor WTN levels at the dwelling reached 46 dBA. Response rate was 78.9% and did not significantly differ across sample strata. Self-reported health effects (e.g., migraines, tinnitus, dizziness, etc.), sleep disturbance, sleep disorders, quality of life, and perceived stress were not related to WTN levels. Visual and auditory perception of wind turbines as reported by respondents increased significantly with increasing WTN levels as did high annoyance toward several wind turbine features, including the following: noise, blinking lights, shadow flicker, visual impacts, and vibrations. Concern for physical safety and closing bedroom windows to reduce WTN during sleep also increased with increasing WTN levels. Other sample characteristics are discussed in relation to WTN levels. Beyond annoyance, results do not support an association between exposure to WTN up to 46 dBA and the evaluated health-related endpoints.

[http://dx.doi.org/10.1121/1.4942391]

[SF] Pages: 1443–1454

I. INTRODUCTION

Jurisdiction for the regulation of noise is shared across many levels of government in Canada. As the federal department of health, Health Canada's mandate with respect to wind power includes providing science-based advice, upon request, to federal departments, provinces, territories and other stakeholders regarding the potential impacts of wind turbine noise (WTN) on community health and well-being. Provinces and territories, through the legislation they have enacted, make decisions in relation to areas including installation, placement, sound levels, and mitigation measures for wind turbines. In July 2012, Health Canada announced its

[a]Electronic mail: david.michaud@canada.ca

intention to undertake a large scale epidemiological study in collaboration with Statistics Canada entitled Community Noise and Health Study (CNHS). Statistics Canada is the federal government department responsible for producing statistics relevant to Canadians.

In comparison to the scientific literature that exists for other sources of environmental noise, there are few original peer-reviewed field studies that have investigated the community response to modern wind turbines. The studies that have been conducted to date differ substantially in terms of their design and evaluated endpoints (Krogh *et al.*, 2011; Mroczek *et al.*, 2012; Mroczek *et al.*, 2015; Nissenbaum *et al.*, 2012; Pawlaczyk-Łuszczyńska *et al.*, 2014; Pedersen and Persson Waye, 2004, 2007; Pedersen *et al.*, 2009; Shepherd *et al.*, 2011; Tachibana *et al.*, 2012; Tachibana *et al.*, 2014; Kuwano *et al.*, 2014). Common features among these studies include reliance upon self-reported endpoints, modeled WTN exposure and/or proximity to wind turbines as the explanatory variable for the observed community response.

There are numerous health symptoms attributed to WTN exposure including, but not limited to, cardiovascular effects, vertigo, tinnitus, anxiety, depression, migraines, sleep disturbance, and annoyance. Health effects and exposure to WTN have been subjected to several reviews and the general consensus to emerge to date is that the most robust evidence is for an association between exposure to WTN and community annoyance with inconsistent support observed for subjective sleep disturbance (Bakker *et al.*, 2012; Council of Canadian Academies, 2015; Knopper *et al.*, 2014; MassDEP MDPH, 2012; McCunney *et al.*, 2014; Merlin *et al.*, 2014; Pedersen, 2011).

The current analysis provides an account of the sample demographics, response rates, and observed prevalence rates for the various self-reported measures as a function of the outdoor WTN levels calculated in the CNHS.

II. METHOD

A. Sample design

Factors considered in the determination of the study sample size, including statistical power, have been described by Michaud *et al.* (2013), Michaud *et al.* (2016b), and Feder *et al.* (2015). The target population consisted of adults, aged 18 to 79 years, living in communities within approximately 10 km of a wind turbine in southwestern Ontario (ON) and Prince Edward Island (PEI). Selected areas in both provinces were characterized by flat lands with rural/semi-rural type environments. Prior to field work, a list of addresses (i.e., potential dwellings) was developed by Statistics Canada. The list consists mostly of dwellings, but it can include industrial facilities, churches, demolished/vacant dwellings, etc. (i.e., non-dwellings), that would be classified as out-of-scope for the purposes of the CNHS. The ON and PEI sampling areas included 315 and 84 wind turbines, respectively. Wind turbine electrical power output ranged between 660 kW to 3 MW (average 2.0 ± 0.4 MW). All turbines were modern design with 3 pitch controlled rotor blades (~80 m diameter) upwind of the tower, and predominantly 80 m hub heights. This study was approved by the Health Canada and Public Health Agency of Canada Research Ethics Board (Protocols #2012–0065 and #2012–0072).

B. Wind turbine sound pressure levels at dwellings

A detailed description of the approach applied to sound pressure level modeling [including background nighttime sound pressure (BNTS) levels] is presented separately (Keith *et al.*, 2016b). Briefly, sound pressure levels were estimated at each dwelling using both ISO (1993) and ISO (1996) as incorporated in the commercial software CadnaA version 4.4 (Datakustik, 2014). The calculations were based on manufacturers' octave band sound power spectra at 10 m height, 8 m/s wind speed for favorable propagation conditions (Keith *et al.*, 2016a). As described in detail by Keith *et al.* (2016b), BNTS levels were calculated following provincial noise regulations for Alberta, Canada (Alberta Utilities Commission, 2013). With this approach BNTS levels can range between 35 dBA to 51 dBA. The possibility that BNTS levels due to highway road traffic noise exposure may exceed the level estimated by Alberta regulations was considered. Where the upper limits of this approach were exceeded (i.e., 51 dB), nighttime levels were derived using the US Traffic Noise Model (United States Department of Transportation, 1998) module in the CadnaA software.

Low frequency noise was estimated in the CNHS by calculating outdoor C-weighted sound pressure levels at all dwellings. There was no additional gain by analysing the data using C-weighted levels because the statistical correlation between C-weighted and A-weighted levels was very high (i.e., r 0.81–0.97) (Keith *et al.*, 2016a).

C. Data collection

1. Questionnaire content and collection

The final questionnaire, available on the Statistics Canada website (Statistics Canada, 2014) and in the supplementary materials,[1] consisted of basic socio-demographics, modules on community noise and annoyance, health effects, lifestyle behaviors and prevalent chronic illnesses. In addition to these modules, validated psychometric scales were incorporated, without modification, to assess perceived stress (Cohen *et al.*, 1983), quality of life (WHOQOL Group, 1998; Skevington *et al.*, 2004) and sleep disturbance (Buysse *et al.*, 1989).

Questionnaire data were collected through in-person home interviews by 16 Statistics Canada trained interviewers between May and September 2013. The study was introduced as the "Community Noise and Health Study" as a means of masking the true intent of the study, which was to investigate the association between health and WTN exposure. All identified dwellings within ~600 m from a wind turbine were selected. Between 600 m and 11.22 km, dwellings were randomly selected. Once a roster of adults (between the ages of 18 and 79 years) living in the dwelling was compiled, one individual from each household was randomly invited to participate. No substitutions were permitted under any circumstances. Participants were not compensated for their participation.

2. Long-term high annoyance

To evaluate the prevalence of annoyance, participants were initially asked to spontaneously identify sources of noise they hear originating from outdoors while they are either inside or outside their home. The interviewer grouped the responses as road traffic, aircraft, railway/trains, wind turbine, and "*other*." Follow-up questions were designed to confirm the initial response where the participant may not have spontaneously identified wind turbines, rail, road and aircraft as one of the audible sources. For each audible noise source participants were asked to respond to the following question from ISO/TS (2003a): "*Thinking about the last year or so, when you are at home, how much does noise from [SOURCE] bother, disturb or annoy you?*" Response categories included the following: "*not at all*," "*slightly*," "*moderately*," "*very*," or "*extremely*." Participants who reported they did not hear a particular source of noise, were classified into a "*do not hear*" group and retained in analysis (to ensure that the correct sample size was accounted for in the modeling). The analysis of annoyance was performed after collapsing the response categories into two groups (i.e., "*highly annoyed*" and "*not highly annoyed*"). As per ISO/TS (2003a), participants reporting to be either "*very*" or "*extremely*" annoyed were treated as "*highly annoyed*" in the analysis. The "*not highly annoyed*" group was composed of participants from the remaining response categories in addition to those who did not hear wind turbines. Similarly, an analysis of the percentage highly subjectively sleep disturbed, highly noise sensitive, and highly concerned about physical safety from having wind turbines in the area was carried out applying the same classification approach used for annoyance.

The use of filter questions and an assessment of annoyance using only an adjectival scale are approaches not recommended by ISO/TS (2003a). The procedures followed in the current study were chosen to minimize the possibility of participant confusion (i.e., by asking how annoyed they are toward the noise from a source that may not be audible). Although there is value in confirming the response on the adjectival scale with a numerical scale, this approach would have added length to the questionnaire, or led to the removal of other questions. Collectively, the deviations from ISO/TS (2003a) conformed to the recommendations by Statistics Canada and to the approach adopted in a large-scale study conducted by Pedersen *et al.* (2009).

D. Statistical methodology

The analysis for categorical outcomes closely follows the description outlined in Michaud *et al.* (2013), which provides a summary of the pre-data collection study design and objectives, as well as the proposed data analysis. Final wind turbine distance and WTN categories were defined as follows: distance categories in km {$\leq$0.550; (0.550–1]; (1–2]; (2–5]; and >5}, WTN exposure categories in dBA {<25; [25–30); [30–35); [35–40); and [40–46]}. The top category included 46 dB as only six cases were observed at $\geq$45 dBA. All models were adjusted for provincial differences. Province was initially assessed as an effect modifier. When the interaction between WTN and province was significant, separate models were reported for each province. This included reporting separate chi-square tests of independence or logistic regression models for each province. When the interaction was not statistically significant, province was treated as a confounder in the model. This included using the Cochran-Mantel-Haenszel (CMH) chi-square tests for contingency tables (which adjusts for confounders), as well as adjusting the logistic regression models for the confounder of province.

The questionnaire assessed participant's long-term ($\sim$1 year) annoyance to WTN in general (i.e., location not specified), and specifically with respect to location (outdoors, indoors), time of day (morning, afternoon, evening, nighttime) and season (spring, summer, fall, winter). In addition, participants' long-term annoyance in general, to road, aircraft and rail noise was assessed. These evaluations of annoyance are considered to be clustered because they are derived from the same individuals (i.e., they are repeated measures). Therefore, in order to compare the prevalence of annoyance as a function of location, time of day, season, or noise source, generalized estimating equations for repeated measures were used to account for the clustered responses (Liang and Zeger, 1986; Stokes *et al.*, 2000).

Statistical analysis was performed using SAS version 9.2 (SAS Institute Inc., 2014). A 5% statistical significance level is implemented throughout unless otherwise stated. In addition, Bonferroni corrections are made to account for all pairwise comparisons to ensure that the overall type I (false positive) error rate is less than 0.05. In cases where cell frequencies were small (i.e., <5) in the contingency tables or logistic regression models, exact tests were used as described in Agresti (2002) and Stokes *et al.* (2000).

III. RESULTS

A. Wind turbine sound pressure levels at dwellings

Modeled sound pressure levels, and the field measurements used to support the models are presented in detail by Keith *et al.* (2016a,b). Calculated outdoor sound pressure levels at the dwellings reached levels as high as 46 dB. Unless otherwise stated, all decibel references are A-weighted. Calculations are likely to yield typical worst case long-term (1 years) average WTN levels (Keith *et al.*, 2016b).

B. Response rate

Of the 2004 addresses (i.e., potential dwellings) on the sample roster, 434 dwellings were coded as out-of-scope by Statistics Canada during data collection (Table I). This was consistent with previous surveys conducted in rural areas in Canada (Statistics Canada, 2008). In the current study, 26.7% and 20.4% of addresses were deemed out-of-scope in PEI and ON, respectively. No significant difference in the distribution of out-of-scope locations by distance to the nearest wind turbine was observed in PEI (χ^2 3.19, p 0.5263). In ON, a higher proportion of out-of-scope addresses was observed in the closest distance group ($\leq$0.55 km) compared to other distance groups ($p < 0.05$, in all cases). After adjusting for province, there was a

TABLE I. Locations coded out-of-scope.

	Distance to nearest wind turbine (km)						
	≤0.55	(0.55–1]	(1–2]	(2–5]	>5	Overall	CMH p-value[a]
Range of WTN (dB)	37.4–46.1	31.8–43.6	26.3–40.4	14.6–30.9	0–18.2		
Total potential dwellings	143	887	781	95	98	2004	
ON	76	718	669	60	80	1603	
PEI	67	169	112	35	18	401	
Total number of potential dwellings out-of-scope n(%)[b]	48 (33.6)	158 (17.8)	189 (24.2)	19 (20.0)	20 (20.4)	434 (21.7)	0.9755
ON	29 (38.2)	109 (15.2)	166 (24.8)	9 (15.0)	14 (17.5)	327 (20.4)	<0.0001[c]
PEI	19 (28.4)	49 (29.0)	23 (20.5)	10 (28.6)	6 (33.3)	107 (26.7)	0.5263[c]
Code A	28 (19.6)	23 (2.6)	18 (2.3)	5 (5.3)	8 (8.2)	82 (4.1)	0.0068
Code B	12 (8.4)	54 (6.1)	55 (7.0)	5 (5.3)	6 (6.1)	132 (6.6)	0.8299
Code C	2 (1.4)	36 (4.1)	61 (7.8)	7 (7.4)	1 (1.0)	107 (5.3)	
Code D	4 (2.8)	35 (3.9)	50 (6.4)	2 (2.1)	5 (5.1)	96 (4.8)	
Code E	0 (0.0)	7 (0.8)	4 (0.5)	0 (0.0)	0 (0.0)	11 (0.6)	
Code F	2(1.4)	3(0.3)	1(0.1)	0(0.0)	0(0.0)	6(0.3)	

[a]The Cochran Mantel-Haenszel chi-square test is used to adjust for province, p-values <0.05 are considered to be statistically significant.
[b]Total number of potential dwellings out of scope (given as a percentage of total potential dwellings) is broken down by province, as well it is equal to the sum of Code A-F. The percentages of dwellings that are coded as out-of-scope are based on the total number of potential dwellings in the area. Code A—address was a business/duplicate/other (17%), address listed in error (83%). Code B—an inhabitable dwelling unoccupied at the time of the survey, newly constructed dwelling not yet inhabited, a vacant trailer in a commercial trailer park. Code C—summer cottage, ski chalet, or hunting camps. Code D—all participants in the dwelling were >79 years of age. Code E—under construction, institution, or unavailable to participate. Code F—demolished for unknown reasons.
[c]Chi-square test of independence.

significant association between distance groups and the proportion of locations assigned a *Code A* (p 0.0068) (Table I). A post-collection screening of interviewer notes by Statistics Canada has confirmed that of the total number of *Code A* locations, the vast majority (i.e., 83%) were locations listed in error. In rural areas, there is more uncertainty in developing the address list frame and this can contribute to a higher prevalence of addresses listed in error within 0.55 km of a wind turbine where the population density is lower compared to areas at greater setbacks.[2]

The remaining 1570 addresses were considered to be valid dwellings, from which 1238 residents agreed to participate in the study (606 males, 632 females). This resulted in a final response rate of 78.9%, which was not statistically different between ON and PEI or by proximity to wind turbines (Table II).

C. Sample characteristics

Table III outlines demographic information for study populations in each 5 dB WTN category. The prevalence of employment was the only variable that appeared to consistently increase within increasing WTN levels. Household income and education were unrelated to WTN levels. There was no obvious pattern to the changes observed in the other variables that were found to be statistically related to WTN level categories (i.e., age, type of dwelling, property ownership and facade type).

D. Perception of community noise and related variables as a function of WTN level

The prevalence of reporting to be very or extremely (i.e., highly) noise sensitive was statistically similar across all WTN categories (p 0.8175). As expected and as shown in Fig. 1, visibility and audibility of wind turbines increased with increasing WTN levels.

The overall audibility of other noise sources is shown in Table IV. Not shown in Table IV is how often the noise source was spontaneously reported as opposed to being identified following a prompt by the interviewer (see Sec. II).

TABLE II. Sample response rate.

	Distance to nearest wind turbine (km)						
	≤0.55	(0.55–1]	(1–2]	(2–5]	>5	Overall	p-value
Final number of potential participants[a]	95	729	592	76	78	1570	
ON	47	609	503	51	66	1276	
PEI	48	120	89	25	12	294	
Participants n (%)	71 (74.7)	583 (80.0)	463 (78.2)	58 (76.3)	63 (80.8)	1238 (78.9)	0.9971[b]
ON	34 (72.3)	488 (80.1)	396 (78.7)	42 (82.4)	51 (77.3)	1011 (79.2)	0.7009[c]
PEI	37 (77.1)	95 (79.2)	67 (75.3)	16 (64.0)	12 (100.0)	227 (77.2)	0.1666[c]

[a]Potential participants from locations established to be valid dwellings (equal to the difference between "Total potential dwellings" and "total number of potential dwellings out-of-scope"; see Table I) used in the derivation of participation rates.
[b]The CMH chi-square test is used to adjust for province, p-values <0.05 are considered to be statistically significant.
[c]Chi-square test of independence.

TABLE III. Sample characteristics.

Variable	WTN (dB) <25	[25–30)	[30–35)	[35–40)	[40–46]	Overall	CMH *p*-value[a]
n	84[b]	95[b]	304[b]	521[b]	234[b]	1238[b]	
Range of closest turbine (km)	2.32–11.22	1.29–4.47	0.73–2.69	0.44–1.56	0.25–1.05		
Range of BNTS (dB)	35–51	35–51	35–56	35–57	35–61		
BNTS (dB) mean (SD)	43.88(3.43)	44.68 (2.91)	45.21 (3.60)	43.29 (4.11)	41.43 (4.21)		
ON	44.98 (2.88)	44.86 (2.78)	45.54 (3.31)	44.06 (3.86)	42.70 (4.25)		<0.0001[c]
PEI	41.13 (3.18)	43.00 (3.67)	43.81 (4.38)	38.44 (1.59)	38.05 (1.00)		<0.0001[c]
Sex *n* (% male)	37 (44.0)	48 (50.5)	150 (49.3)	251 (48.2)	120 (51.3)	606 (49.0)	0.4554
Age mean (SE)	49.75 (1.78)	56.38 (1.37)	52.25 (0.93)	51.26 (0.68)	50.28 (1.03)	51.61 (0.44)	0.0243[d]
Marital status *n* (%)							0.2844
Married/Common-law	54 (64.3)	69 (73.4)	199 (65.7)	367 (70.6)	159 (67.9)	848 (68.7)	
Widowed/Separated/Divorced	16 (19.0)	18 (19.1)	61 (20.1)	85 (16.3)	35 (15.0)	215 (17.4)	
Single, never been married	14 (16.7)	7 (7.4)	43 (14.2)	68 (13.1)	40 (17.1)	172 (13.9)	
Employed *n* (%)	43 (51.8)	47 (49.5)	161 (53.0)	323 (62.0)	148 (63.2)	722 (58.4)	0.0012
Level of education *n* (%)							0.7221
≤High school	45 (53.6)	52 (54.7)	167 (55.1)	280 (53.7)	134 (57.3)	678 (54.8)	
Trade/Certificate/College	34 (40.5)	37 (38.9)	110 (36.3)	203 (39.0)	85 (36.3)	469 (37.9)	
University	5 (6.0)	6 (6.3)	26 (8.6)	38 (7.3)	15 (6.4)	90 (7.3)	
Income (×$1000) *n* (%)							0.8031
<60	39 (51.3)	40 (54.8)	138 (52.5)	214 (49.1)	100 (49.3)	531 (50.5)	
60-100	18 (23.7)	17 (23.3)	72 (27.4)	134 (30.7)	59 (29.1)	300 (28.5)	
≥100	19 (25.0)	16 (21.9)	53 (20.2)	88 (20.2)	44 (21.7)	220 (20.9)	
Detached dwelling *n* (%)[e]	59 (70.2)	84 (88.4)	267 (87.8)	506 (97.1)	216 (92.3)	1132 (91.4)	
ON[e]	46 (76.7)	77 (89.5)	228 (93.1)	437 (97.1)	154 (90.6)	942 (93.2)	<0.0001[f]
PEI[e]	13 (54.2)	7 (77.8)	39 (66.1)	69 (97.2)	62 (96.9)	190 (83.7)	<0.0001[f]
Property ownership *n* (%)	60 (71.4)	85 (89.5)	250 (82.2)	466 (89.4)	215 (91.9)	1076 (86.9)	
ON	45 (75.0)	78 (90.7)	215 (87.8)	399 (88.7)	157 (92.4)	894 (88.4)	0.0085[f]
PEI	15 (62.5)	7 (77.8)	35 (59.3)	67 (94.4)	58 (90.6)	182 (80.2)	<0.0001[f]
Facade type *n* (%)							0.0137
Fully bricked	20 (23.8)	30 (31.6)	85 (28.0)	138 (26.5)	67 (28.6)	340 (27.5)	
Partially bricked	24 (28.6)	29 (30.5)	62 (20.4)	88 (16.9)	15 (6.4)	218 (17.6)	
No brick/other	40 (47.6)	36 (37.9)	157 (51.6)	295 (56.6)	152 (65.0)	680 (54.9)	

[a]The Cochran Mantel-Haenszel chi-square test is used to adjust for province unless otherwise indicated, *p*-values <0.05 are considered to be statistically significant.
[b]Totals may differ due to missing data.
[c]Analysis of variance (ANOVA) model.
[d]Non-parametric two-way ANOVA model adjusted for province.
[e]Non-detached dwellings included semi/duplex/apartment.
[f]Chi-square test of independence.

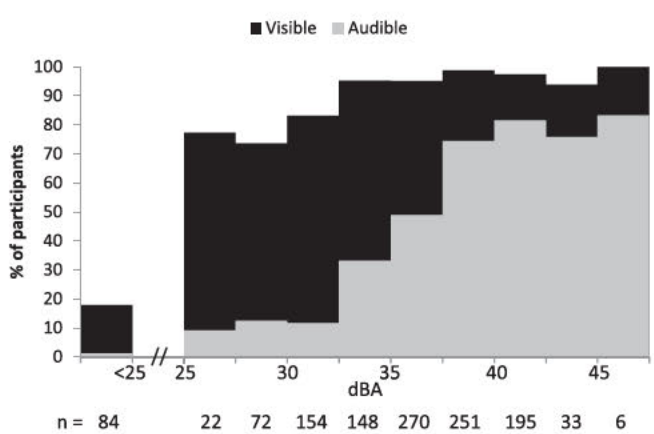

FIG. 1. Proportion of participants as a function of calculated outdoor A-weighted WTN levels. The figure plots the proportion of participants that reported wind turbines were visible from anywhere on their property or audible from inside or outside their homes from the total number of participants with valid responses living in each WTN level category.

Among the participants who reported hearing each specific noise source, the prevalence of spontaneously reporting road traffic, wind turbines, rail and aircraft was 84%, 71%, 66%, and 30%, respectively. A total of 102 participants (8.2%) indicated that there were no audible noise sources around their home. These participants lived in areas where the average WTN levels were 32.4 dB [standard deviation (SD) 8.3] and the mean distance to the nearest turbine was 1.7 km (SD 2.0) (data not shown).

Table IV also provides the observed prevalence rates for high (i.e., very or extreme) annoyance toward wind turbine features. The results suggest that there was a tendency for the prevalence of annoyance to increase with increasing WTN levels, with the rise in annoyance becoming evident when WTN levels exceeded 35 dB. The pattern was slightly different for visual annoyance among participants drawn from the ON sample, where there was a noticeable rise in annoyance among participants living in areas where WTN

TABLE IV. Perception of community noise and related variables.

Variable	Wind Turbine Noise (dB) <25	[25–30)	[30–35)	[35–40)	[40–46]	Overall	CMH p-value[a]
n	84[b]	95[b]	304[b]	521[b]	234[b]	1238[b]	
Sensitivity to noise[c]	14 (16.7)	14 (14.7)	35 (11.6)	77 (14.8)	35 (15.1)	175 (14.2)	0.8175
Audible perception of transportation noise sources n (%)							
Road traffic	62 (73.8)	60 (63.2)	259 (85.2)	443 (85.0)	192 (82.1)	1016 (82.1)	0.0013
Aircraft	43 (51.2)	33 (34.7)	146 (48.0)	263 (50.5)	124 (53.0)	609 (49.2)	
Aircraft (ON)	32 (53.3)	31 (36.0)	120 (49.0)	220 (48.9)	82 (48.2)	485 (48.0)	0.2114[d]
Aircraft (PEI)	11 (45.8)	2 (22.2)	26 (44.1)	43 (60.6)	42 (65.6)	124 (54.6)	0.0214[d]
Rail[e]	30 (50.0)	27 (31.4)	73 (29.8)	90 (20.0)	7 (4.1)	227 (22.5)	<0.0001[d]
Perception of wind turbines n (%)							
See wind turbines	15 (17.9)	70 (74.5)	269 (89.1)	505 (96.9)	227 (97.0)	1086 (87.9)	<0.0001
Hear wind turbines	1 (1.2)	11 (11.6)	67 (22.0)	319 (61.2)	189 (80.8)	587 (47.4)	<0.0001
Number of years hearing the WT n (%)							<0.0001
Do not hear	83 (98.8)	84 (88.4)	237 (78.0)	202 (39.0)	45 (19.3)	651 (52.8)	
<1 year	1 (1.2)	2 (2.1)	15 (4.9)	31 (6.0)	12 (5.2)	61 (4.9)	
≥1 year	0 (0.0)	9 (9.5)	52 (17.1)	285 (55.0)	176 (75.5)	522 (42.3)	
Notice vibrations/rattles indoors during WTN operations	0 (0.0)	3 (3.2)	8 (2.6)	28 (5.4)	19 (8.2)	58 (4.7)	0.0004
Highly concerned about physical safety	1 (1.2)	3 (3.2)	5 (1.6)	46 (8.9)	22 (9.6)	77 (6.3)	<0.0001
Formal complaint[f]	2 (2.4)	2 (2.1)	3 (1.0)	22 (4.2)	6 (2.6)	35 (2.8)	0.2578
Reporting a high (very or extreme) level of annoyance to wind turbine features, n (%)							
Noise	0 (0.0)	2 (2.1)	3 (1.0)	52 (10.0)	32 (13.7)	89 (7.2)	<0.0001
Visual	2 (2.4)	15 (16.0)	17 (5.6)	81 (15.5)	44 (18.9)	159 (12.9)	
Visual (ON)	2 (3.3)	15 (17.6)	17 (7.0)	76 (16.9)	36 (21.2)	146 (14.5)	<0.0001[d]
Visual (PEI)	0 (0.0)	0 (0.0)	0 (0.0)	5 (7.0)	8 (12.7)	13 (5.8)	0.0268[d]
Blinking lights	2 (2.4)	8 (8.5)	17 (5.6)	61 (11.7)	34 (14.6)	122 (9.9)	<0.0001
Shadow flicker	0 (0.0)	3 (3.2)	6 (2.0)	51 (9.8)	36 (15.5)	96 (7.8)	<0.0001
Vibrations/rattles	0 (0.0)	1 (1.1)	2 (0.7)	9 (1.7)	7 (3.0)	19 (1.5)	0.0198
Reporting a high (very or extreme) level of WTN annoyance by time of day, n (%)							
Morning	0 (0.0)	0 (0.0)	1 (0.3)	28 (5.4)	10 (4.3)	39 (3.2)	
Afternoon	0 (0.0)	0 (0.0)	1 (0.3)	26 (5.0)	14 (6.1)	41 (3.3)	
Evening	0 (0.0)	1 (1.1)	2 (0.7)	48 (9.2)	26 (11.3)	77 (6.3)	
Nighttime	0 (0.0)	1 (1.1)	2 (0.7)	48 (9.2)	26 (11.3)	77 (6.3)	
Reporting a high (very or extreme) level of WTN annoyance by season, n (%)							
Spring	0 (0.0)	1 (1.1)	1 (0.3)	45 (8.6)	22 (9.6)	69 (5.6)	
Fall	0 (0.0)	1 (1.1)	2 (0.7)	42 (8.1)	22 (9.6)	67 (5.5)	
Summer	0 (0.0)	2 (2.1)	4 (1.3)	50 (9.6)	31 (13.7)	87 (7.1)	
Winter	0 (0.0)	1 (1.1)	1 (0.3)	38 (7.3)	21 (9.2)	61 (5.0)	
Closing bedroom window to block outside noise during sleep n (%)	26 (31.3)	30 (31.6)	87 (28.7)	178 (34.3)	68 (29.2)	389 (31.6)	0.8106
Source identified as cause for closing window[g] n (%)							
Road traffic	15 (18.1)	13 (13.7)	47 (15.5)	77 (14.8)	24 (10.3)	176 (14.3)	0.1161
Rail	6 (10.2)	1 (1.2)	7 (2.9)	10 (2.2)	0 (0.0)	24 (2.4)	0.0013
Wind turbines	0 (0.0)	2 (2.1)	6 (2.0)	79 (15.2)	50 (21.6)	137 (11.1)	<0.0001
Other	12 (14.5)	20 (21.1)	54 (17.8)	65 (12.5)	14 (6.0)	165 (13.4)	0.0002
Perceived benefit from having wind turbines in the area n (%)							
Personal	3 (3.9)	2 (2.2)	11 (4.0)	47 (9.2)	47 (20.3)	110 (9.3)	
ON	0 (0.0)	1 (1.2)	6 (2.7)	44 (10.0)	36 (21.4)	87 (9.0)	<0.0001[d]
PEI	3 (15.8)	1 (11.1)	5 (9.8)	3 (4.3)	11 (17.2)	23 (10.8)	0.1700[d]
Community	20 (29.0)	14 (20.9)	62 (36.0)	136 (35.1)	79 (40.7)	311 (35.0)	0.0135

[a]The Cochran Mantel-Haenszel chi-square test is used to adjust for provinces unless otherwise indicated, p-values <0.05 are considered to be statistically significant.
[b]Columns may not add to total due to missing data.
[c]Sensitivity to noise reflects the prevalence of participants that reported to be either very or extremely (i.e., highly) noise sensitive in general.
[d]Chi-square test of independence.
[e]Nobody reported hearing rail noise in PEI as there is no rail activity in PEI, therefore the percent is given as a percentage of ON participants only.
[f]Refers to anyone in the participant's household ever lodging a formal complaint (including signing a petition) regarding noise from wind turbines.
[g]Reasons for closing bedroom windows due to aircraft noise was suppressed due to low cell counts (i.e., n <5 overall).

levels were between [25 and 30) dB. The prevalence of *household* complaints concerning wind turbines, which could include signing a petition regarding noise from wind turbines, was 2.8% overall and unrelated to WTN levels (p 0.2578). However, complaints were found to be greater among the PEI sample (13/224   5.8%), compared to ON (22/1010   2.2%) (p 0.0050).

Other notable observations from Table IV include the finding that the number of participants who self-reported to personally benefit in any way (e.g., rent, payments or indirect benefits such as community improvements) from having turbines in their area, was not equally distributed among provinces. In ON, reporting such benefits was significantly related to WTN categories ($p < 0.0001$) and there was a gradual increase from the lowest WTN category (<25 dB: 0.0%) to the loudest WTN category ([40–46] dB: 21.4%), whereas in PEI benefits were statistically evenly distributed across the sample (p 0.1700).

Closing bedroom windows to block outside noise during sleep was equally prevalent across all WTN categories (p 0.8106); however, identifying WTs as the reason for closing the window was found to be related to WTN levels ($p < 0.0001$). In the two loudest categories, [35–40) dB and [40–46] dB, 15.2% and 21.6% of participants identified WTN as the reason for closing bedroom windows, respectively, compared to ≤2.1% in the other WTN categories (Table IV).

Figure 2 plots the fitted percentage highly annoyed by WTN category overall and for ON and PEI separately. WTN annoyance was observed to significantly increase when WTN levels exceeded ≥35 dB compared with lower exposure categories ($p < 0.009$, in all cases). Overall, observed prevalences of noise annoyance increased from less than 2.1% in the three lowest WTN level categories to 10% in areas where WTN levels were between [35 and 40) dB and 13.7% between [40 and 46] dB. Additionally, annoyance was observed to be significantly higher in the ON sample compared to the PEI sample. Across all WTN categories, the odds of being highly annoyed by WTN were 3.29 times greater in ON compared to PEI [95% confidence interval (CI), 1.47–8.68, p 0.0015]; however, the difference was most pronounced above 35 dB.

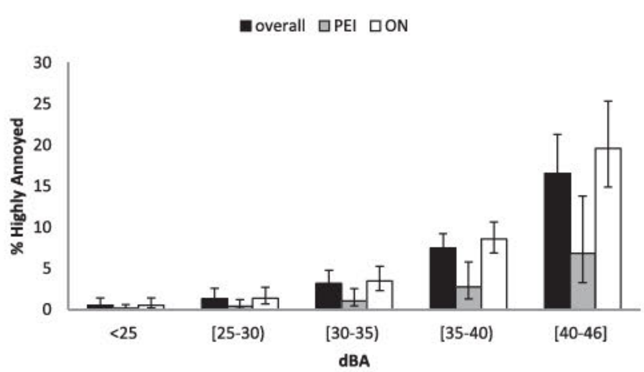

FIG. 2. Prevalence of high annoyance with wind turbine noise overall and by province as a function of calculated outdoor wind turbine noise levels. This illustrates the percentage of participants that reported to be either very or extremely (i.e., highly) bothered, disturbed or annoyed by WTN while at home over the last year. At home refers to either inside or outside the dwelling. Results are shown for participants from southwestern ON, PEI, and as an overall average. Fitted data are plotted along with their 95% confidence intervals. Results are shown as a function of calculated outdoor A-weighted WTN levels at the dwelling (dBA). WTN annoyance was observed to significantly increase when WTN levels exceeded ≥35 dB compared with lower exposure categories ($p < 0.009$, in all cases). Additionally, annoyance was observed to be significantly higher in the southwestern ON sample compared to the PEI sample ($p = 0.0015$), regardless of WTN level.

In addition to asking participants how annoyed they were toward WTN in general (i.e., without reference to their particular location), other questions were designed to assess annoyance as a function of location (i.e., indoors, outdoors). As shown in Fig. 3, the prevalence of high annoyance was significantly higher outdoors.

The prevalence of annoyance by time of day and season is provided in Table IV. For WTN levels below 30 dB, the prevalence of high annoyance was very low (<1.2%) and similar for all times of day. Starting at 30 dB, the percentage highly annoyed during the evening and nighttime were significantly higher than the morning and afternoon; however this difference was most pronounced at WTN levels ≥35 dB. For WTN levels below 30 dB, the prevalence of high annoyance was very low (<2.2%) and similar for all seasons. At WTN levels ≥35 dB, the prevalence of high annoyance during the summer was higher compared to all other seasons.

Noise annoyance toward road, aircraft and rail noise was also assessed in the questionnaire. It was of interest to determine how annoyance to these sources compared to WTN annoyance. In areas where WTN levels were <35 dB the greatest source of noise annoyance was road traffic. In WTN categories ≥35 dB, annoyance toward WTN exceeded all other sources (p <0.0003, in all cases) (see Fig. 4).

E. Self-reported health conditions and use of medication

Table V shows that subjectively reported sleep disturbance from any source while sleeping at home over the last year, in addition to a multitude of health effects, were found

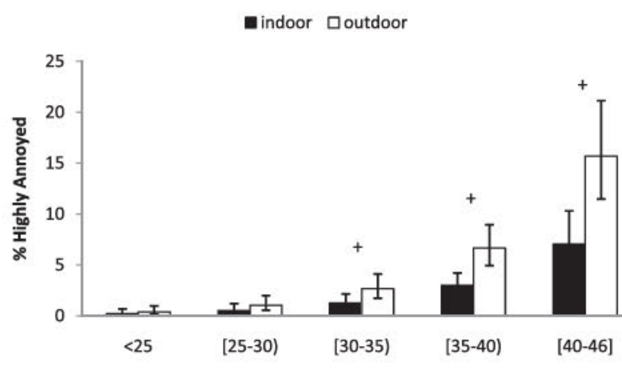

FIG. 3. Prevalence of high annoyance with wind turbine noise by location as a function of calculated outdoor wind turbine noise levels. Participants were asked to think about the last year or so and indicate how bothered, disturbed or annoyed they were by WTN while at home. The percentage of participants reporting to be either very or extremely (i.e., highly) bothered, disturbed or annoyed is shown as a function of calculated outdoor A-weighted WTN levels at the dwelling (dBA). Figure 3 presents the fitted results by location (i.e., indoors and outdoors) along with their 95% confidence intervals. + Indoor significantly different from outdoor ($p < 0.001$).

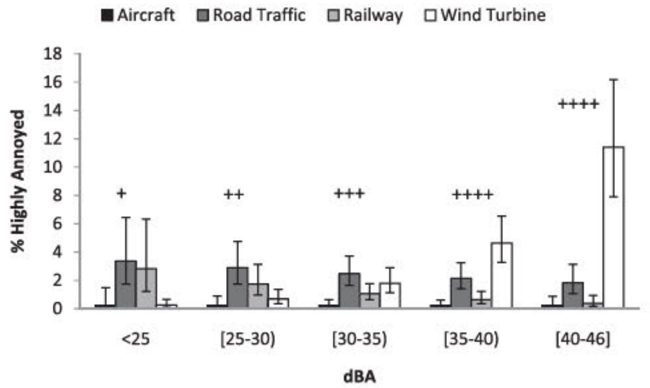

FIG. 4. Prevalence of high annoyance toward different noise sources as a function of calculated outdoor wind turbine noise levels. Illustrates the percentage of participants that reported to be either very or extremely (i.e., highly) bothered, disturbed or annoyed by road traffic, aircraft, rail and wind turbine noise (WTN) while at home over the last year. At home refers to either inside or outside the dwelling. Results represent fitted data along with their 95% confidence intervals and are shown as a function of calculated outdoor A-weighted WTN levels at the dwelling (dBA). $^{+}$WTN significantly different from road traffic and rail noise ($p < 0.001$); $^{++}$WTN significantly different from road traffic ($p < 0.001$); $^{+++}$WTN significantly different from aircraft noise ($p < 0.001$), $^{++++}$WTN significantly different from road traffic, rail, and aircraft noise ($p < 0.0003$).

to be unrelated to WTN levels. Similarly, medication use for high blood pressure, anxiety or depression was also found to be unrelated to WTN levels. Although sleep medication use was significantly related to WTN levels (p 0.0083), the prevalence was *higher* among the two lowest WTN categories {<25 dB and [25–30) dB} (see Table V).

IV. DISCUSSION

The prevalence of self-reporting to be either "*very*" or "*extremely*" (i.e., highly) annoyed with several wind turbine features increased significantly with increasing A-weighted WTN levels. When classified by the prevalence of reported annoyance overall, and in areas where WTN levels exceeded 35 dB, annoyance was highest for visual aspects of wind turbines, followed by blinking lights, shadow flicker, noise and vibrations. Consistent with Pedersen *et al.* (2009), the increase in WTN annoyance was clearly evident when moving from [30–35) dB to [35–40) dB, where the prevalence of WTN annoyance increased from 1% to 10%. This continued to increase to 13.7% for areas where WTN levels were [40–46] dB. The prevalence of WTN annoyance was higher outdoors, during the summer, and during evening and nighttime hours. Pedersen *et al.* (2009) also found that annoyance with WTN was greater outdoors compared to indoors.

Despite a similar pattern of response between the ON and PEI samples, the self-reported WTN annoyance was 3.29 times greater in ON, a difference that was most pronounced at the two highest WTN categories. This difference is in contrast to the prevalence of *household* complaints related to wind turbines. Even though the overall prevalence of such complaints was low (i.e., 2.8%), complaints were more likely in PEI (5.8%) compared to ON (2.2%). The reasons for this difference despite greater reported annoyance in ON are unclear. Research has shown that there are several contingencies that must be met before someone that is highly annoyed will complain (Michaud *et al.*, 2008). Such contingencies include knowing who to complain to, how to file a complaint and holding the belief that the complaint will result in positive change. The fact that the prevalence of complaints regarding wind turbines was unrelated to WTN levels is another indication that complaints do not always correlate well with changes in noise exposure (Fidell *et al.*, 1991). The motives underlying household complaints were not assessed in the present study, but the disparity found with annoyance could also be related to the wording used in the questionnaire. The prevalence of complaints was the one question where the respondent answered on behalf of the entire household.

More participants reported that they were highly annoyed by the visual aspects of wind turbines than by any other feature, even at higher WTN levels. Similar to WTN annoyance, the overall prevalence of annoyance with the visual impact of wind turbines was more than twice as high in the ON sample, and more prevalent across the exposure categories when compared to PEI. In the PEI sample, no participants reported visual annoyance in areas where WTN levels were below 35 dB. This is in contrast to a clear intensification in visual annoyance among the ON sample in areas where WTN levels were [25–30) dB. Exploring the variables that may underscore provincial differences was not within the scope of the current study. The questionnaire was not designed to probe underlying factors that may explain observed provincial differences; however, reported personal benefit from having wind turbines in the area was found to be different between the ON and PEI samples (Table IV).

Shepherd *et al.* (2011) assessed annoyance in response to WTN, but not in a manner that would permit comparisons with the Swedish (Pedersen and Persson Waye, 2004, 2007), Dutch (Janssen *et al.*, 2011; Pedersen *et al.*, 2009) or the current study. Shepherd *et al.* (2011) reported that 59% of participants living within 2 km of a wind turbine installation spontaneously identified wind turbines as an annoying noise source, with a mean annoyance rating of 4.59 (SD, 0.65) when the 5 category adjectival scale was analyzed as a numerical scale from 0 to 5. No exposure-response relationship could be assessed because the authors did not provide an analysis based on precise distance or as a function of WTN levels, which they reported to be between 20 and 50 dB among participants living within 2 km of a wind turbine. This encompasses the entire WTN level range in the CNHS. As such, the only tentative comparison that can be made between the current study and the Shepherd *et al.* (2011) study would be that the observed prevalence of highly annoyed (i.e., "*very*" or "*extremely*") within 2 km of the nearest wind turbine was 7.0%. These data are not shown because the focus of the current study was on WTN levels and an analysis based solely on distance to the nearest turbine does not adequately account for WTN levels at any given dwelling. WTN is a more sensitive measure of exposure level because, in addition to the distance to the turbine, it accounts for topography, presence of large bodies of water, wind turbine characteristics, the layout of the wind farm and the number of wind turbines at any given distance.

TABLE V. Sample profile of health conditions.

Variable n (%)	Wind turbine noise (dB) <25	[25–30)	[30–35)	[35–40)	[40–46]	Overall	CMH[a] p-value
n	84[b]	95[b]	304[b]	521[b]	234[b]	1238[b]	
Health worse vs last year [c]	17 (20.2)	12 (12.6)	46 (15.1)	90 (17.3)	51 (21.8)	216 (17.5)	0.1724
Migraines	18 (21.4)	24 (25.3)	56 (18.4)	134 (25.8)	57 (24.4)	289 (23.4)	0.2308
Dizziness	19 (22.6)	16 (16.8)	65 (21.4)	114 (21.9)	59 (25.2)	273 (22.1)	0.2575
Tinnitus	21 (25.0)	18 (18.9)	71 (23.4)	129 (24.8)	54 (23.2)	293 (23.7)	0.7352
Chronic pain	20 (23.8)	23 (24.2)	75 (24.8)	118 (22.6)	57 (24.5)	293 (23.7)	0.8999
Asthma	8 (9.5)	12 (12.6)	22 (7.2)	43 (8.3)	16 (6.8)	101 (8.2)	0.2436
Arthritis	23 (27.4)	38 (40.0)	98 (32.2)	175 (33.7)	68 (29.1)	402 (32.5)	0.6397
High blood pressure (BP)	24 (28.6)	36 (37.9)	81 (26.8)	166 (32.0)	65 (27.8)	372 (30.2)	0.7385
Medication for high BP	26 (31.3)	34 (35.8)	84 (27.6)	163 (31.3)	63 (27.0)	370 (29.9)	0.4250
Family history of high BP	44 (52.4)	49 (53.8)	132 (45.5)	254 (50.6)	121 (53.8)	600 (50.3)	0.6015
Chronic bronchitis/emphysema/COPD	3 (3.6)	10 (10.8)	17 (5.6)	27 (5.2)	14 (6.0)	71 (5.7)	0.7676
Diabetes	7 (8.3)	8 (8.4)	33 (10.9)	46 (8.8)	19 (8.2)	113 (9.1)	0.6890
Heart disease	8 (9.5)	7 (7.4)	31 (10.2)	32 (6.1)	17 (7.3)	95 (7.7)	0.2110
Highly sleep disturbed[d]	13 (15.7)	11 (11.6)	41 (13.5)	75 (14.5)	24 (10.3)	164 (13.3)	0.4300
Diagnosed sleep disorder	13 (15.5)	10 (10.5)	27 (8.9)	44 (8.4)	25 (10.7)	119 (9.6)	0.3102
Sleep medication	16 (19.0)	18 (18.9)	39 (12.8)	46 (8.8)	29 (12.4)	148 (12.0)	0.0083
Restless leg syndrome	7 (8.3)	16 (16.8)	37 (12.2)	81 (15.5)	33 (14.1)	174 (14.1)	
Restless leg syndrome (ON)	4 (6.7)	15 (17.4)	27 (11.0)	78 (17.3)	28 (16.5)	152 (15.0)	0.0629[e]
Restless leg syndrome (PEI)	3 (12.5)	1 (11.1)	10 (16.9)	3 (4.2)	5 (7.8)	22 (9.7)	0.1628[e]
Medication anxiety or depression	11 (13.1)	14 (14.7)	35 (11.5)	59 (11.3)	23 (9.8)	142 (11.5)	0.2470
QoL past month[f]							
Poor	9 (10.8)	3 (3.2)	21 (6.9)	29 (5.6)	20 (8.6)	82 (6.6)	0.9814
Good	74 (89.2)	92 (96.8)	283 (93.1)	492 (94.4)	213 (91.4)	1154 (93.4)	
Satisfaction with health[f]							
Dissatisfied	13 (15.5)	13 (13.7)	49 (16.1)	66 (12.7)	36 (15.4)	177 (14.3)	0.7262
Satisfied	71 (84.5)	82 (86.3)	255 (83.9)	455 (87.3)	198 (84.6)	1061 (85.7)	

[a]The Cochran Mantel-Haenszel chi-square test is used to adjust for provinces unless otherwise indicated, p-values <0.05 are considered to be statistically significant.
[b]Columns may not add to total due to missing data.
[c]Worse consists of the two ratings: "*Somewhat worse now*" and "*Much worse now*."
[d]High sleep disturbance consists of the two ratings: "*very*" and "*extremely*" sleep disturbed.
[e]Chi-square test of independence.
[f]Quality of Life (QoL) and Satisfaction with Health were assessed with the two stand-alone questions on the WHOQOL-BREF. Reporting "*poor*" overall QoL reflects a response of "*poor*" or "*very poor*," and "*good*" reflects a response of "*neither poor nor good*," "*good*," or "*very good*." Reporting "*dissatisfied*" overall Satisfaction with Health reflects a response of "*very dissatisfied*" or "*dissatisfied*," and "*satisfied*" reflects a response of "*neither satisfied nor dissatisfied*," "*satisfied*," or "*very satisfied*." A detailed presentation of the results related to QoL is presented by Feder *et al*. (2015).

It was important to assess the extent to which the sample was homogenously distributed, with respect to demographics and community noise exposure. The reason for this is that the validity of the exposure-response relationship is strengthened when the primary distinction across the sample is the exposure of interest; in this case, WTN levels. Demographically, some minor differences were found with respect to age, employment, type of dwelling and dwelling ownership; however, with the possible exception of employment, these factors showed no obvious pattern with WTN levels and none were strong enough to exert an influence on the overall results. At the design stage, there was some concern that selecting participants up to 10 km might result in an unequal exposure to community noise sources other than WTN. This may have an influence on the underlying response to WTN. Limited data availability did not permit the modeling of sound pressure levels from other noise sources as originally intended, however it was possible to model BNTS levels. Although Fields (1993) concluded that background sound levels generally do not influence community annoyance, his review did not include wind turbines as a noise source and in the current study BNTS levels were calculated to be lower in areas where WTN levels were higher. Lower BNTS could contribute to a greater expectation of peace and quiet. Therefore, a limitation in the CNHS may be that the expectation of peace and quiet was not explicitly evaluated. This factor may influence the association between long-term sound levels and annoyance by an equivalent of up to 10 dB (ANSI, 1996; ISO, 2003b). The influence this factor may have had on the exposure-response relationship found specifically between WTN levels and the prevalence of reporting high annoyance with WTN in the CHNS is discussed in Michaud *et al*. (2016a).

In the absence of modeling, the audibility of road traffic, aircraft and rail noise provided a crude indication of exposure to these sources. In general, road traffic noise exposure was heard by the vast majority of the sample (82.1%).

Aircraft noise was uniformly audible in ON by about half the sample; in PEI however, hearing aircraft was more common in the higher WTN exposure categories (i.e., above 35 dB) where between 61% and 66% of the respondents indicated that they could hear aircraft. Future research may benefit from assessing the extent to which audible aircraft noise may have influenced the annoyance with WTN in PEI. Only when WTN levels were [40–46] dB was the audibility of wind turbines comparable to road traffic (i.e., both sources were audible by approximately 81% of participants). For these community noise sources, participants were asked how bothered, disturbed, or annoyed they were while at home over the last year or so. The findings are of interest in light of the source comparisons made by Pedersen *et al.* (2009) and Janssen *et al.* (2011), which placed WTN annoyance above all transportation noise sources when comparing them at equal sound levels. In the current study, the overall annoyance toward WTN (7.2%) was found to be higher in comparison to road (3.8%), aircraft (0.4%), and rail in ON (1.9%). Source comparisons need to be made with caution because the observed source differences in annoyance may result from an *actual* difference in sound pressure levels at the dwellings in this study. Modeling the sound levels from transportation noise sources in the current study would allow a more direct comparison between these sources and WTN annoyance at equivalent sound exposures. Another approach is to assess the relative community tolerance level of WTN with that reported for road and aircraft noise studies. This analysis indicates that there is a lower community tolerance level for WTN when compared to both road and aircraft noise at equivalent sound levels (Michaud *et al.*, 2016a).

The list of symptoms that are claimed to be caused by exposure to WTN is considerable (Chapman, 2013), but there is a lack of robust evidence from epidemiological studies to support these associations (Council of Canadian Academies, 2015; Knopper *et al.*, 2014; MassDEP MDPH, 2012; McCunney *et al.*, 2014; Merlin *et al.*, 2014). The results from the current study did not show any statistically significant increase in the self-reported prevalence of chronic pain, asthma, arthritis, high blood pressure, bronchitis, emphysema, chronic obstructive pulmonary disease (COPD), diabetes, heart disease, migraines/headaches, dizziness, or tinnitus in relation to WTN exposure up to 46 dB. In other words, individuals with these conditions were equally distributed among WTN exposure categories. Similarly, the prevalence of reporting to be highly sleep disturbed (for any reason) and being diagnosed with a sleep disorder were unrelated to WTN exposure. These self-reported findings are consistent with the conclusions reached following an analysis of objectively measured sleep among a subsample of the current study participants (Michaud *et al.*, 2016b). Medication use (for anxiety, depression, or high blood pressure) was unrelated to WTN levels. It is notable that the observed prevalence for many of the aforementioned health effects are remarkably consistent with large-scale national population-based studies (Innes *et al.*, 2011; Kroenke and Price, 1993; Morin *et al.*, 2011; O'Brien *et al.*, 1994; Shargorodsky *et al.*, 2010).

V. CONCLUDING REMARKS

Study findings indicate that annoyance toward all features related to wind turbines, including noise, vibrations, shadow flicker, aircraft warning lights and the visual impact, increased as WTN levels increased. The observed increase in annoyance tended to occur when WTN levels exceeded 35 dB and were undiminished between 40 and 46 dB. Beyond annoyance, the current study does not support an association between exposures to WTN up to 46 dB and the evaluated health-related endpoints. In some cases, there were clear differences between the southwestern ON and PEI participants; however, exploring the basis behind these differences fell outside the study scope and objectives. The CNHS supported the development of a model for community annoyance toward WTN, which identifies some of the factors that may influence this response (Michaud *et al.*, 2016a). At the very least, the observed differences reported between ON and PEI in the current study demonstrates that even at comparable WTN levels, the community response to wind turbines is not necessarily uniform across Canada. Future studies designed to intentionally explore the factors that underscore such differences may be beneficial.

ACKNOWLEDGMENTS

The authors acknowledge the support they received throughout the study from Serge Legault and Suki Abeysekera at Statistics Canada, and are especially grateful to the volunteers who participated in this study. The authors have declared that no competing interests exist.

[1]See supplementary material at http://dx.doi.org/10.1121/1.4942391 for the univariate analysis results.

[2]Locations coded as out-of-scope were originally assigned the following categories: *Demolished for unknown reasons*, *vacant for unknown reasons*, *unoccupied*, *seasonal*, *>79 years of age*, and *other* (Michaud, 2015b; Health Canada, 2014). In an effort to address feedback and provide further clarification, the categories used to define out-of-scope locations were further defined elsewhere (Michaud, 2015a) with additional details provided in the current paper. Specifically, locations that were determined to be "demolished for unknown reasons" are presented separately in Table I as Code F. Locations that were originally defined as "unoccupied for unknown reasons" are now more precisely defined under Code B (i.e., inhabitable dwelling not occupied at time of survey, newly constructed dwelling, or unoccupied trailer in vacant trailer park). Furthermore, it was confirmed that 6 dwellings originally listed under Code B (Michaud, 2015a) were in fact GPS coordinates listed in error and have therefore been reassigned to Code A.

Agresti, A. (**2002**). *Categorical Data Analysis*, 2nd ed. (Wiley and Sons, New York).

Alberta Utilities Commission (**2013**). "Rule 012-Noise Control," http://www.auc.ab.ca/acts-regulations-and-auc-rules/rules/Pages/Rule012.aspx (Last viewed 11/24/2014).

ANSI (**1996**). S12.9-1996. *Quantities and Procedures for Description and Measurement of Environmental Sound—Part 4: Noise Assessment and Predication of Long-Term Community Response* (American National Standards Institute, Washington, DC).

Bakker, R. H., Pedersen, E., van den Berg, G. P., Stewart, R. E., Lok, W., and Bouma, J. (**2012**). "Impact of wind turbine sound on annoyance, self-reported sleep disturbance and psychological distress," Sci. Total Environ. **425**, 42–51.

Buysse, D. J., Reynolds, C. F., Monk, T. H., Berman, S. R., and Kupfer, D. J. (**1989**). "The Pittsburgh sleep quality index: A new instrument for psychiatric practice and research," Psychol. Res. **28**, 193–213.

Chapman, S. (**2013**). "Symptoms, diseases and aberrant behaviors attributed to wind turbine exposure," http://ses.library.usyd.edu.au/bitstream/2123/10501/2/Wind_Disease_List.pdf (Last viewed 11/24/2014).

Cohen, S., Kamarck, T., and Mermelstein, R. (**1983**). "A global measure of perceived stress," J. Health Soc. Behav. **24**(4), 385–396.

Council of Canadian Academies (**2015**). *Understanding the Evidence: Wind Turbine Noise. The Expert Panel on Wind Turbine Noise and Human Health* (Council of Canadian Academies, Ottawa, Canada).

DataKustik GmbH (**2014**). "Cadna A, version 4.4, Software for Immission Protection," www.datakustik.com (Last viewed 11/24/2014).

Feder, K., Michaud, D. S., Keith, S. E., Voicescu, S. A., Marro, L., Than, J., Guay, M., Denning, A., Bower, T. J., Lavigne, E., Whelan, C., and van den Berg, F. (**2015**). "An assessment of quality of life using the WHOQOL-BREF among participants living in the vicinity of wind turbines," Env. Res. **142**, 227–238.

Fidell, S., Barber, D., and Schultz, T. J. (**1991**). "Updating a dosage-effect relationship for the prevalence of annoyance due to general transportation noise," J. Acoust. Soc. Am. **89**(1), 221–233.

Fields, J. M. (**1993**). "Effect of personal and situational variables on noise annoyance in residential areas," J. Acoust. Soc. Am. **93**(5), 2753–2763.

Health Canada (**2014**). "Wind turbine noise and health study: Summary of results," http://www.hc-sc.gc.ca/ewh-semt/noise-bruit/turbine-eoliennes/summary-resume-eng.php (Last viewed 9/29/2015).

Innes, K. E., Selfe, T. K., and Agarwal, P. (**2011**). "Prevalence of restless legs syndrome in North American and Western European populations: A systematic review," Sleep Med. **12**(7), 623–634.

ISO (**1993**). 9613-1. *Acoustics. Attenuation of Sound During Propagation Outdoors. Part 1: Calculation of the Absorption of Sound by the Atmosphere* (International Organization for Standardization, Geneva, Switzerland).

ISO (**1996**). 9613-2. *Acoustics. Attenuation of Sound During Propagation Outdoors. Part 2: General Method of Calculation* (International Organization for Standardization, Geneva, Switzerland).

ISO/TS (**2003a**). 15666. *Acoustics—Assessment of Noise Annoyance by Means of Social and Socio-Acoustic Surveys* (International Organization for Standardization, Geneva, Switzerland).

ISO (**2003b**). 1996-1:2003(E). *Acoustics—Description, Measurement and Assessment of Environmental Noise—Part 1: Basic Quantities and Assessment Procedures* (International Organization for Standardization, Geneva, Switzerland).

Janssen, S. A., Vos, H., Eisses, A. R., and Pedersen, E. (**2011**). "A comparison between exposure-response relationships for wind turbine annoyance and annoyance due to other noise sources," J. Acoust. Soc. Am. **130**(6), 3746–3753.

Keith, S. E., Feder, K., Voicescu, S., Soukhovtsev, V., Denning, A., Tsang, J., Broner, N., Richarz, W., and van den Berg, F. (**2016a**). "Wind turbine sound power measurements," J. Acoust. Soc. Am. **139**(3), 1431–1435.

Keith, S. E., Feder, K., Voicescu, S., Soukhovtsev, V., Denning, A., Tsang, J., Broner, N., Richarz, W., and van den Berg, F. (**2016b**). "Wind turbine sound pressure level calculations at dwellings," J. Acoust. Soc. Am. **139**(3), 1436–1442.

Knopper, L. D., Ollson, C. A., McCallum, L. C., Whitfield Aslund, M. L., Berger, R. G., Souweine, K., and McDaniel, M. (**2014**). "Wind turbines and human health," Front. Pub. Health **2**(63), 1–20.

Kroenke, K., and Price, R. K. (**1993**). "Symptoms in the community: Prevalence, classification, and psychiatric comorbidity," Arch. Intern. Med. **153**(21), 2474–2480.

Krogh, C. M. E., Gillis, L., Kouwen, N., and Aramini, J. (**2011**). "WindVOiCe, a self-reporting survey: Adverse health effects, industrial wind turbines, and the need for vigilance monitoring," Bull. Sci. Technol. Soc. **31**(4), 334–345.

Kuwano, S., Yano, T., Kageyama, T., Sueoka, S., and Tachibana, H. (**2014**). "Social survey on wind turbine noise in Japan," Noise Control Eng. J. **62**(6), 503–520.

Liang, K. Y., and Zeger, S. L. (**1986**). "Longitudinal data analysis using generalized linear models," Biometrika **73**(1), 13–22.

Massachusetts Department of Environmental Protection (MassDEP) and Massachusetts Department of Public Health (MDPH) (**2012**). "Wind Turbine Health Impact Study: Report on Independent Expert Panel. Massachusetts: Department of Environmental Protection and Department of Public Health," http://www.mass.gov/eea/docs/dep/energy/wind/turbine-impact-study.pdf (Last viewed 5/15/2015).

McCunney, R. J., Mundt, K. A., Colby, W. D., Dobie, R., Kaliski, K., and Blais, M. (**2014**). "Wind turbines and health: A critical review of the scientific literature," J. Occup. Environ. Med. **56**(11), e108–e130.

Merlin, T., Newton, S., Ellery, B., Milverton, J., and Farah, C. (**2014**). "Systematic review of the human health effects of wind farms" (National Health and Medical Research Council, Canberra, ACT, Australia), https://digital.library.adelaide.edu.au/dspace/handle/2440/87923 (Last viewed 2/29/2016).

Michaud, D. S. (**2015a**). "Self-reported and objectively measured outcomes assessed in the Health Canada wind turbine noise and health study: Results support an increase in community annoyance," in *INTERNOISE, 44th Congress of Noise Control Engineering*, San Francisco, CA, USA (August 9–12, 2015).

Michaud, D. S. (**2015b**). "Wind turbine noise and health study: Summary of results," in *6th International Meeting on Wind Turbine Noise*, Glasgow, Scotland (April 20–23, 2015).

Michaud, D. S., Bly, S. H. P., and Keith, S. E. (**2008**). "Using a change in percent highly annoyed with noise as a potential health effect measure for projects under the *Canadian Environmental Assessment Act*," Can. Acoust. **36**(2), 13–28.

Michaud, D. S., Feder, K., Keith, S. E., Voicescu, S. A., Marro, L., Than, J., Guay, M., Bower, T., Denning, A., Lavigne, E., Whelan, C., Janssen, S. A., and van den Berg, F. (**2016a**). "Personal and situational variables associated with wind turbine noise annoyance," J. Acoust. Soc. Am. **139**(3), 1455–1466.

Michaud, D. S., Feder, K., Keith, S. E., Voicescu, S. A., Marro, L., Than, J., Guay, M., Denning, A., Murray, B. J., Weiss, S. K., Villeneuve, P., van den Berg, F., and Bower, T. (**2016b**). "Effects of wind turbine noise on self-reported and objective measures of sleep," SLEEP **39**, 97–109.

Michaud, D. S., Keith, S. E., Feder, K., Soukhovtsev, V., Marro, L., Denning, A., McGuire, D., Broner, N., Richarz, W., Tsang, J., Legault, S., Poulin, D., Bryan, S., Duddeck, C., Lavigne, E., Villeneuve, P. J., Leroux, T., Weiss, S. K., Murray, B. J., and Bower, T. (**2013**). "Self-reported and objectively measured health indicators among a sample of Canadians living within the vicinity of industrial wind turbines: Social survey and sound level modeling methodology," Noise News Int. **21**,14–27.

Morin, C. M., LeBlanc, M., Bélanger, L., Ivers, H., Mérette, C., and Savard, J. (**2011**). "Prevalence of insomnia and its treatment in Canada," Can. J. Psychiatry **56**(9), 540–548.

Mroczek, B., Banaś, J., Machowska-Szewczyk, M., and Kurpas, D. (**2015**). "Evaluation of quality of life of those living near a wind farm," Int. J. Environ. Res. Public Health. **12**(6), 6066–6083.

Mroczek, B., Kurpas, D., and Karakiewicz, B. (**2012**). "Influence of distances between places of residence and wind farms on the quality of life in nearby areas," Ann. Agr. Environ. Med. **19**(4), 692–696.

Nissenbaum, M. A., Aramini, J. J., and Hanning, C. D. (**2012**). "Effects of industrial wind turbine noise on sleep and health," Noise Health **14**(60), 237–243.

O'Brien, B., Goeree, R., and Streiner, D. (**1994**). "Prevalence of migraine headache in Canada: A population based survey," Int. J. Epidemiol. **23**(5), 1020–1026.

Pawlaczyk-Łuszczyńska, M., Dudarewicz, A., Zaborowski, K., Zamojska-Daniszewska, M., and Waszkowska, M. (**2014**). "Evaluation of annoyance from the wind turbine noise: A pilot study," Int. J. Occup. Med. Environ. Health **27**(3), 364–388.

Pedersen, E. (**2011**). "Health aspects associated with wind turbine noise – Results from 3 field studies," Noise Control Eng. J. **59**(1), 47–53.

Pedersen, E., and Persson Waye, K. (**2004**). "Perception and annoyance due to wind turbine noise—A dose-response relationship," J. Acoust. Soc. Am. **116**(6), 3460–3470.

Pedersen, E., and Persson Waye, K. (**2007**). "Wind turbine noise, annoyance and self-reported health and wellbeing in different living environments," Occup. Environ. Med. **64**(7), 480–486.

Pedersen, E., van den Berg, F., Bakker, R., and Bouma, J. (**2009**). "Response to noise from modern wind farms in The Netherlands," J. Acoust. Soc. Am. **126**(2), 634–643.

SAS Institute Inc. (**2014**). "SAS (Statistical Analysis System) (version 9.2) [software package]" (SAS Institute, Inc., Cary, NC).

Shargorodsky, J., Curhan, G. C., and Farwell, W. R. (**2010**). "Prevalence and characteristics of tinnitus among US adults," Am. J. Med. **123**(8), 711–718.

Shepherd, D., McBride, D., Welch, D., Dirks, K. N., and Hill, E. M. (**2011**). "Evaluating the impact of wind turbine noise on health-related quality of life," Noise Health **13**(54), 333–339.

Skevington, S. M., Lotfy, M., and O'Connell, K. A. (**2004**). "The World Health Organization's WHOQOL-BREF quality of life assessment: Psychometric properties and results of the international field trial—A report from the WHOQOL group," Qual. Life. Res. **13**(2), 299–310.

Statistics Canada (**2008**). "Methodology of the Canadian Labour Force Survey, Catalogue no. 71-526-XIE2007001," http://www.statcan.gc.ca/pub/71-526-x/71-526-x2007001-eng.htm (Last viewed 2/29/2016).

Statistics Canada (**2014**). "Community noise and health study," http://www.statcan.gc.ca/daily-quotidien/141106/dq141106c-eng.htm (Last viewed 11/6/2014).

Stokes, M. E., Davis, C. S., and Koch, G. G. (**2000**). *Categorical Data Analysis Using the SAS System*, 2nd ed. (SAS Institute, Inc. Cary, NC).

Tachibana, H., Yano, H., Fukushima, A., and Shinichi, S. (**2014**). "Nationwide field measurement of wind turbine noise in Japan," Noise Control Eng. J. **62**(2), 90–101.

Tachibana, H., Yano, H., Sakamoto, S., and Sueoka, S. (**2012**). "Synthetic Research Program on Wind Turbine Noise in Japan," in *Proceedings of INTERNOISE, 41st Congress of Noise Control Engineering*, New York, NY (August 19–22, 2012), pp. 8505–8514.

United States Department of Transportation (**1998**). "FHWA TRAFFIC NOISE MODEL," Technical Manual (Federal Highway Administration, Washington, DC).

WHOQOL Group (**1998**). "Development of the World Health Organization WHOQOL-BREF quality of life assessment," Psychol. Med. **28**(3), 551–558.

BEFORE THE PUBLIC UTILITY COMMISSION
OF OREGON

Docket PCN 5

In the Matter of

IDAHO POWER COMPANY'S
PETITION FOR CERTIFICATE OF PUBLIC CONVENIENCE
AND NECESSITY

Michaud, D. S. et al., Effects of Wind Turbine Noise on Self-Reported and Objective Measures of Sleep (2016)

February 22, 2023

pii: sp-00087-15 http://dx.doi.org/10.5665/sleep.5326

SLEEP DURATION/SLEEP QUALITY

Effects of Wind Turbine Noise on Self-Reported and Objective Measures of Sleep

David S. Michaud, PhD[1]; Katya Feder, PhD[1]; Stephen E. Keith, PhD[1]; Sonia A. Voicescu, MSc[1]; Leonora Marro, MSc[2]; John Than, MSc[2]; Mireille Guay, MSc[2]; Allison Denning, MES[3]; Brian J. Murray MD, FRCP(C)D, ABSM[4]; Shelly K. Weiss, MD, FRCPC[5]; Paul J. Villeneuve PhD[6]; Frits van den Berg, PhD[7]; Tara Bower, MSc[8]

[1]Health Canada, Environmental and Radiation Health Sciences Directorate, Consumer & Clinical Radiation Protection Bureau, Ottawa, Ontario, Canada; [2]Health Canada, Population Studies Division, Biostatistics Section, Tunney's Pasture, Ottawa, Ontario, Canada; [3]Health Canada, Environmental Health Program, Health Programs Branch, Regions and Programs Bureau, Halifax, Nova Scotia, Canada; [4]Division of Neurology, Department of Medicine, Sunnybrook Health Sciences Center, University of Toronto, Toronto, Ontario, Canada; [5]Division of Neurology, Department of Pediatrics, Hospital for Sick Children, University of Toronto; [6]Department of Health Sciences, Carleton University, Ottawa, Ontario, Canada; [7]GGD Amsterdam Public Health Service, Environmental Health Department, Amsterdam, The Netherlands; [8]Health Canada, Environmental and Radiation Health Sciences Directorate, Office of Science Policy, Liaison and Coordination, Ottawa, Ontario, Canada

Study Objectives: To investigate the association between self-reported and objective measures of sleep and wind turbine noise (WTN) exposure.
Methods: The Community Noise and Health Study, a cross-sectional epidemiological study, included an in-house computer-assisted interview and sleep pattern monitoring over a 7 d period. Outdoor WTN levels were calculated following international standards for conditions that typically approximate the highest long-term average levels at each dwelling. Study data were collected between May and September 2013 from adults, aged 18–79 y (606 males, 632 females) randomly selected from each household and living between 0.25 and 11.22 kilometers from operational wind turbines in two Canadian provinces. Self-reported sleep quality over the past 30 d was assessed using the Pittsburgh Sleep Quality Index. Additional questions assessed the prevalence of diagnosed sleep disorders and the magnitude of sleep disturbance over the previous year. Objective measures for sleep latency, sleep efficiency, total sleep time, rate of awakening bouts, and wake duration after sleep onset were recorded using the wrist worn Actiwatch2® from a subsample of 654 participants (289 males, 365 females) for a total of 3,772 sleep nights.
Results: Participant response rate for the interview was 78.9%. Outdoor WTN levels reached 46 dB(A) with an arithmetic mean of 35.6 and a standard deviation of 7.4. Self-reported and objectively measured sleep outcomes consistently revealed no apparent pattern or statistically significant relationship to WTN levels. However, sleep was significantly influenced by other factors, including, but not limited to, the use of sleep medication, other health conditions (including sleep disorders), caffeine consumption, and annoyance with blinking lights on wind turbines.
Conclusions: Study results do not support an association between exposure to outdoor WTN up to 46 dB(A) and an increase in the prevalence of disturbed sleep. Conclusions are based on WTN levels averaged over 1 y and, in some cases, may be strengthened with an analysis that examines sleep quality in relation to WTN levels calculated during the precise sleep period time.
Keywords: actigraphy, annoyance, multiple regression models, PSQI, sleep, wind turbine noise
Citation: Michaud DS, Feder K, Keith SE, Voicescu SA, Marro L, Than J, Guay M, Denning A, Murray BJ, Weiss SK, Villeneuve PJ, van den Berg F, Bower T. Effects of wind turbine noise on self-reported and objective measures of sleep. *SLEEP* 2016;39(1):97–109.

Significance
This study provides the most comprehensive assessment to date of the potential association between exposure to wind turbine noise (WTN) and sleep. As the only study to include both subjective and objective measures of sleep, the results provide a level of insight that was previously unavailable. The absence of an effect of WTN on sleep is based on an analysis of self-reported and objectively measured outcomes in relation to long term outdoor average sound levels. Knowledge in this area may be strengthened by future research to consider the potential transient changes in WTN levels throughout the night, which may influence subtle measures of sleep not assessed in the current study.

INTRODUCTION

Sleep loss has been implicated in a variety of negative health outcomes[1] including cardiovascular abnormalities,[2] immunological problems,[3] psychological health concerns,[4] and neurobehavioral impairment that can lead to accidents.[5] Sleep loss may be related to total sleep time restriction and/or reduced sleep quality in the sleep time obtained. Sleep disorders such as insomnia and obstructive sleep apnea are associated with an increased incidence of hypertension, heart failure, and stroke.[6,7]

Sleep can clearly be disrupted with noise.[8] It has long been recognized that electroencephalography (EEG) arousals can be induced with external environmental stimuli, but are modulated by sleep state.[9] The World Health Organization (WHO) Guidelines for Community Noise recommend that, for continuous noise, an indoor sound level of 30 dB(A) should not be exceeded during the sleep period time to avoid sleep disturbance.[10] More recently, the WHO's Night Noise Guidelines for Europe [11] suggest an annual average outdoor level of 40dB(A) to reduce negative health outcomes from sleep disturbance even among the most vulnerable groups.

Sleep can be measured by subjective and objective means[12] although due to the fundamental nature of unconsciousness in this state, people are unable to introspect on their sleep state. As such, an individual may surmise the quality of his or her sleep, with descriptions of what his or her presumed sleep was like, periods of awakening, and consequences of the state. However, sleep state misperception is a common clinical phenomenon, whereby patients with some degree of insomnia may report much worse quality of sleep than what actually occurred.[13] Subjective interpretation of sleep state is thus subject to biased reporting from the individual and therefore subjective and objective measures of sleep are frequently discordant. Therefore, objective physiological measures of sleep can provide a more accurate reflection of what actually happened during an individual's sleep and form the basis of an unprejudiced understanding of the actual biological effect of factors such as noise on sleep.

Although the current study is the first to include objective measures in the assessment of sleep quality in the context of wind turbine noise (WTN) exposure, the psychological experience of the individual must be considered, though this factor may be more prone to subjective interpretation. Numerous subjective scales of sleep have been devised. The Pittsburgh Sleep Quality Index (PSQI)[14] is a measure of the subjective experience of sleep that has had detailed psychometric assessment,[15] validation in numerous populations,[16–18] and is one of the most common subjective methodologies used in sleep research.

The PSQI has been administered in a study to compare subjective sleep quality among 79 subjects living near two different wind farms wherein it was reported that sleep quality was worse among the group living closer to the wind turbines.[19] Pedersen[20] found that self-reported sleep disturbance for any reason from any source was inconsistently related to the level of WTN. Bakker et al.[21] showed that self-reported sleep disturbance was correlated to WTN level, but when noise annoyance from wind turbines was brought into a multiple regression, sleep disturbance appeared to be highly correlated to the annoyance, but not to WTN level and only annoyance was statistically correlated to WTN level. This is consistent with the study by van den Berg et al.[22] wherein noise annoyance was reported as a better predictor of self-reported sleep disturbance than noise level for transportation, industrial, and neighbor noise.

Several studies have provided objectively measured assessments of transportation noise-induced sleep disturbance.[23–26] Although it is clear that noise is among the many factors that contribute to sleep disturbance [23,24,27,28] there has been no study to date that has provided an assessment of sleep disturbance in the context of WTN exposures using objective measures such as actigraphy.

The current study was designed to objectively measure sleep in relation to WTN exposure using actigraphy, which has emerged as a widely accepted tool for tracking sleep and wake behavior.[29,30] The objective measures of sleep, when considered together with self-report, provide a more comprehensive evaluation of the potential effect that WTN may have on sleep.

This study was approved by the Health Canada and Public Health Agency of Canada Review Ethics Board (Protocol #2012-0065 and #2012-0072).

METHOD

Sample Design

Target population, sample size, and sampling frame strategy

Several factors influenced the determination of the final sample size, including having adequate statistical power to assess the study objectives, and adequate time allocation for collection of data, influenced by the length of the personal in-dwelling interview and the time needed to collect the physical measures. Overall statistical power for the study was based on the study's primary objective to assess WTN-associated effects on sleep quality. Based on an initial sample size of 2,000 potential dwellings, it was estimated that there would be 1,120 completed survey responses. For 1,120 survey responses there should be sufficient statistical power to detect at least a 7% difference in the prevalence of sleep disturbances with 80% power and a 5% false positive rate (Type I error). There was uncertainty in the power assessment because the current *Community Noise and Health Study*, was the first to implement objectively measured endpoints to study the possible effects of WTN on sleep. How these power calculations applied to actigraphy-measured sleep was also unknown. In the absence of comparative studies, a conservative baseline prevalence for reported sleep disturbance of 10% was used.[31,32] Sample size calculation also incorporated the following assumptions: (1) approximately 20% to 25% of the targeted dwellings would not be valid dwellings (i.e., demolished, unoccupied seasonal, vacant for unknown reasons, under construction, institutions, etc.); and (2) of the remaining dwellings, there would be a 70% participation rate. These assumptions were validated (see response rates and sample characteristics related to sleep).

Study locations were drawn from areas in southwestern Ontario (ON) and Prince Edward Island (PEI) where there were a sufficient number of dwellings within the vicinity of wind turbine installations. The ON and PEI sampling regions included 315 and 84 wind turbines, respectively. The wind turbine electrical power outputs ranged between 660 kW to 3 MW (average 2.0 ± 0.4 MW). All turbines were modern monopole tower design with three pitch-controlled rotor blades (~80 m diameter) upwind of the tower and most had 80 m hub heights. All identified dwellings within approximately 600 m from a wind turbine and a random selection of dwellings between 600 m and 11.22 km were selected from which one person per household between the ages of 18 and 79 y was randomly selected to participate. The final sample size in ON and PEI was 1,011 and 227, respectively. Participants were not compensated in any way for their participation.

Wind turbine sound pressure levels at dwellings

Outdoor sound pressure levels were estimated at each dwelling using both ISO 9613-1[33] and ISO 9613-2[34] as incorporated in the commercial software CadnaA version 4.4.[35] The resulting calculations represent long-term (1 y) A-weighted equivalent continuous outdoor sound pressure levels (LAeq). Therefore, calculated sound pressure levels can only approximate with a certain degree of uncertainty the sound pressure level at the dwelling during the reference time periods that are captured by each measure of sleep. The time reference period ranges from 1–7 d (actigraphy), to 30 d for the PSQI and the previous year for the assessment of the percentage highly sleep disturbed. Van den Berg[36] has shown that, in the Dutch temperate climate, the long-term average WTN level for outdoor conditions is 1.7 ± 1.5 dB(A) below the sound pressure level at 8 m/sec wind speed. Accordingly, a best estimate for the average nighttime WTN level is approximately 2 dB(A) below the calculated levels reported in this study.

Calculations included all wind turbines within a radius of 10 km, and were based on manufacturers' octave band sound power spectra at a standardized wind speed of 8 m/sec and favorable sound propagation conditions. Favorable conditions assume the dwelling is located downwind of the noise source, a stable atmosphere, and a moderate ground-based temperature inversion. Although variations in wind speeds and temperature as a function of height could not be considered in the model calculations due to a lack of relevant data, 8 m/sec was considered a reasonable estimate of the highest noise exposure conditions. The manufacturers' data were verified for consistency using on-site measurements of wind turbine sound power. The standard deviation in sound levels was estimated to be 4 dB(A) up to 1 km, and at 10 km the uncertainty was estimated to be between 10 dB(A) and 26 dB(A). Although calculations based on predictions of WTN levels reduces the risk of misclassification compared to direct measurements, the risk remains to some extent. The calculated levels in the current study represent reasonable worst-case estimates expected to yield outdoor WTN levels that typically approximate the highest long-term average levels at each dwelling and thereby optimize the chances of detecting WTN-induced sleep disturbance. The few dwellings beyond 10 km were assigned the same calculated WTN value as dwellings at 10 km. Unless otherwise stated, all decibel references are A-weighted. A-weighting filters out low frequencies in a sound that the human auditory system is less sensitive to at low sound pressure levels.

In the current study, low-frequency noise was estimated by calculating C-weighted sound pressure levels. No additional benefit was observed in assessing low frequency noise because C- and A-weighted levels were so highly correlated. Depending on how dB(C) was calculated and what range of data was assessed, the correlation between dB(C) and dB(A) ranged from r = 0.84 to r = 0.97.[37]

Background nighttime sound levels at dwellings

As a result of certain meteorological phenomena (atmospheric stability and wind gradient) coupled with a tendency for background sound levels to drop throughout the day in rural/semi-rural environments, WTN can be more perceptible at the dwelling during nighttime.[38–41] In Canada, it is possible to estimate background nighttime sound pressure levels according to the provincial noise regulations for Alberta, Canada,[42] which estimates ambient noise levels in rural and suburban environments. Estimates are based on dwelling density per quarter section, which represents an area with a 451 m radius and distance to heavily travelled roads or rail lines. When modeled in accordance with these regulations, estimated levels can range from 35 dB(A) to 51 dB(A). The possibility that exposure to high levels of road traffic noise may create a background sound pressure level higher than that estimated using the Alberta regulations was considered. In ON, road noise for the six-lane concrete Highway 401 was calculated using the United States Federal Highway Administration (FHWA) Traffic Noise Model[43] module in the CadnaA software.[35] This value was used when it exceeded the Alberta noise estimate, making it possible to have levels above 51 dB(A).

Data Collection

Questionnaire administration and refusal conversion strategies

The questionnaire instrument included modules on basic demographics, noise annoyance, health effects, quality of life, sleep quality, sleep disorders, perceived stress, lifestyle behaviors, and prevalence of chronic disease. To avoid bias, the true intent of the study, which was to assess the community response to wind turbines, was masked. Throughout the data collection, the study's official title was: *Community Noise and Health Study*. This approach is commonly used to avoid a disproportionate contribution from any group that may have distinct views toward wind turbines. Data collection took place through in-person interviews between May and September 2013 in southwestern ON and PEI. After a roster of all adults aged 18 to 79 y living in the dwelling was compiled, a computerized method was used to randomly select one adult from each household. No substitution was permitted; therefore, if the targeted individual was not at home or unavailable, alternate arrangements were made to invite them to participate at a later time.

All 16 interviewers were instructed to make every reasonable attempt to obtain interviews, which included visiting the dwelling at various times of the day on multiple occasions and making contact by telephone when necessary. If the individual refused to participate, they were then contacted a second time by either the senior interviewer or another interviewer. If, after a second contact, respondents refused to participate, the case was coded as a final refusal.

Self-reported sleep assessment

Long-term self-reported sleep disturbance included an assessment of the magnitude of sleep disturbance experienced at home (of any type for any reason) over the past year. Participants were requested to describe their level of sleep disturbance at home over the past year using one of the following categories: "not at all," "slightly," "moderately," "very" or "extremely," where the top two categories were collapsed and considered to reflect "highly sleep disturbed." For the purposes of this analysis the bottom three categories reflect "low sleep disturbance." These categories and the classification of "highly sleep disturbed" is consistent with the approach adopted for annoyance[44] and facilitates comparisons to self-reported sleep disturbance functions developed for transportation noise sources.[45] Data were collected on prevalence of diagnosed sleep disorders. In addition, participants completed the PSQI, which provided an assessment of sleep quality over the previous 30 d. The seven components of the PSQI are scored on a scale from 0 (better) to 3 (worse); therefore the global PSQI is a score ranging between 0–21, where a value of greater than 5 is thought to represent poor sleep quality.[14,16–18]

Objectively measured sleep

An Actiwatch2® (Philips Healthcare, Andover, MA, USA) sleep watch was given to all consenting and eligible participants aged 18 to 79 y who were expected to sleep at their current address for a minimum of 3 of the 7 nights following the interview. There were 450 devices at hand that were cycled throughout the study. In order to receive the device, respondents also needed to have full mobility in the arm on which the watch was to be worn. Respondents were asked to wear the device on their wrist during all hours of the day and night for the 7 d following their interview. The Actiwatch2® provides key information on sleep patterns (based on movement), including timing and duration of sleep as well as awakenings, and has been compared with polysomnography in some patient samples,[46] but does not replace polysomnography due to imperfect sensitivity and specificity for detecting wake periods. However, this tool can provide reasonable estimates for assessing subjects objectively for more prolonged periods of time than conventional assessment tools, with minimal participant burden.[47] The devices were configured to continuously record a data point every 60 sec for the entire 7 d period. Data analysis was conducted using Actiware® Version 5.1[48] with the software set to default settings (i.e., sensitivity setting of medium and a minimum minor rest interval size of 40 min). With these settings an epoch of 40 counts (i.e., accelerometer activity above threshold) or less is considered sleep and epochs above 40 counts are considered wake. However, any given epoch is scored using a 5-epoch weighting scheme. This procedure weighs the 2 epochs adjacent to the epoch in question. The 5-epoch weighting is achieved by multiplying the number of counts in each respective epoch by the following: 1/25, 1/5, 1, 1/5, 1/25, whereby an average above 40 indicates "awake" for the central epoch. The sleep start parameter was automatically calculated by the Actiware® software determined by the first 10 min period in which no more than one 60 sec epoch was scored as mobile. An epoch is scored as mobile if the number of activity counts recorded in the epoch is greater than or equal to the epoch length in 15 sec intervals (i.e., in a 60 sec epoch an activity value of 4 or higher). Endpoints of interest from wrist actigraphy included sleep efficiency (total sleep time divided by measured time in bed), sleep latency (how long it took to fall asleep), wake after sleep onset (WASO) (the total duration of awakenings), total sleep time, and the number of awakening bouts (WABT) (during a sleep period). The WABT data was analysed as the rate of awakening bouts per 60 min in bed.

To help interpret the measured data, respondents were asked to complete a basic sleep log each night of the study. The log contained information about whether the respondent slept at home or not, presence of windows in the room where they slept, and whether or not the windows were open. After the 7 d collection period, respondents were asked to return the completed sleep log with the actigraph in a prepaid package.

Statistical Methodology

The analysis follows the description in Michaud et al.,[49] which provides a summary of the study design and objectives, as well as a proposed data analysis. Briefly, the Cochran Mantel-Haenszel chi-square test was used to detect associations between self-reported magnitude or contributing sources of sleep disturbance and WTN exposure groups while controlling for province. Because a cut-off value of 5 for the global PSQI score provided a sensitive and specific measure distinguishing good and poor sleep, the PSQI score was dichotomized with the objective to model the proportion of individuals with poor sleep quality (i.e., PSQI > 5).[14] As a first step to develop the best model to predict the dichotomized PSQI score, univariate logistic regression models only adjusting for WTN exposure groups and province were carried out. It should be emphasized that variables considered in the univariate analysis have been previously demonstrated to be related to the modeled endpoint and/or considered by the authors to conceptually have a potential association with the modeled endpoint. The analysis of each variable only adjusts for WTN category and province; therefore, interpretation of any individual relationship must be made with caution.

The primary objective in the current analysis was to use multiple regression models to identify the best predictors for (1) reporting a PSQI score greater than 5; and (2) the actigraphy endpoints. All explanatory variables that were statistically significant at the 20% level in the univariate analysis for each respective endpoint were considered in the multiple regression models. To develop the best model to predict each endpoint of interest, the stepwise method, which guards against issues of multicollinearity, was used for multiple regression models.

The stepwise regression was carried out in three different ways wherein the base model included: (1) WTN exposure category and province; (2) WTN exposure category, province, and an adjustment for individuals who reported receiving personal benefit from having wind turbines in the area; and (3) WTN category and province, stratified for those who received no personal benefit.

For the analysis of PSQI, multiple logistic regression models were developed using the stepwise method with a 20% significance entry criterion and a 10% significance criterion to remain in the model. The WTN groups were treated as a continuous variable, giving an odds ratio (OR) for each unit increase in WTN level, where a unit reflects a 5 dB(A) WTN category. The Nagelkerke pseudo R^2 is reported for logistic regression models.

Repeated-measures data from all wrist actigraphy measurements were modeled using the generalized estimating equations (GEE) method, as available in SAS (Statistical Analysis System) version 9.2 PROC GENMOD.[50–52] Univariate GEE regression models only adjusting for WTN exposure groups, province, day of the week, and the interaction between WTN groups and day of the week were carried out. The interaction between WTN and province was significant for the total sleep time outcome in the univariate models, but was no longer significant in the multiple GEE regression model. Therefore, the base model for the multiple GEE regression models included only WTN category, province, and day of the week. The same stepwise methodology that was applied to build the PSQI models was used to develop multiple GEE regression models for each actigraphy endpoint. The within-subjects correlations were examined with different working correlation matrix structures (unstructured, compound symmetry, and autoregressive of first order). An unstructured variance-covariance structure between sleep nights was applied to all endpoints with the exception of sleep latency, where compound symmetry was used. The advantage of the GEE method is that it uses all available data to estimate individual subject variability (i.e., if 1 or more nights of data is missing for an individual, the individual is still included in the analysis).

The wrist actigraphy endpoints of sleep efficiency and rate of awakening bouts do not follow a normal distribution, because one is a proportion ranging between 0 and 1 (sleep efficiency) and the other is a count (awakening bouts). Therefore, to analyze awakening bouts a Poisson distribution was assumed. The

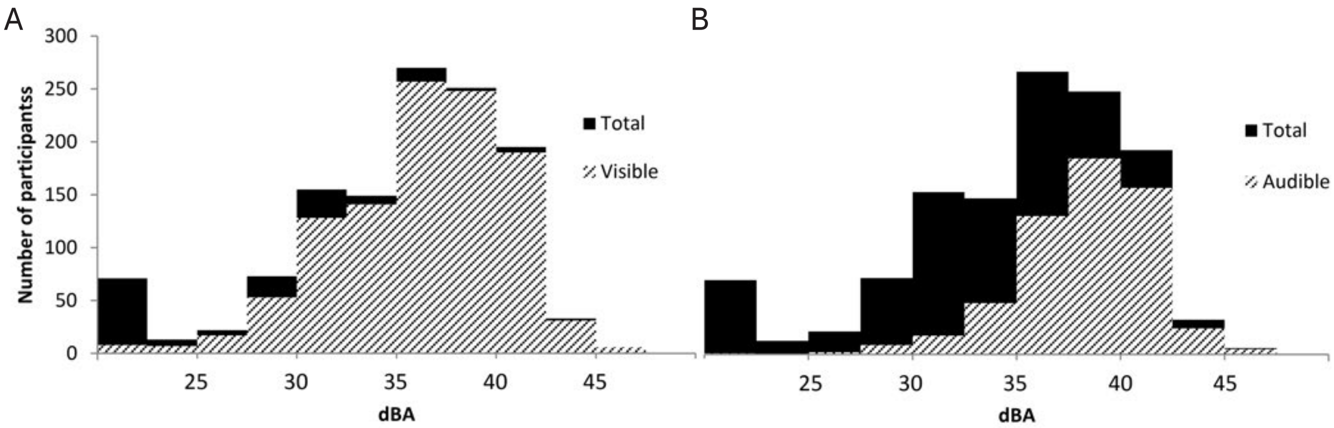

Figure 1—Histogram showing the distribution of participants as a function of calculated outdoor A-weighted wind turbine noise levels. (A) The number of participants who self-reported on the questionnaire that wind turbines were visible from anywhere on their property. (B) The number of participants who self-reported that wind turbines were audible from inside or outside their home.

number of awakening bouts was analyzed with respect to the total time spent in bed and is reported as a rate of awakening bouts per 60 min in bed. Sleep efficiency, sleep latency, and WASO were transformed in order to normalize the data and stabilize the variance.[53–55] In the GEE models, statistical tests were based on transformed data in order to satisfy the normality and constant variance assumptions. Because back-transformation was not possible for some endpoints, the arithmetic mean (least squares mean [LSM]) is presented for all endpoints.

All regression models for PSQI and actigraphy endpoints were adjusted for provincial differences. Province was initially assessed as an effect modifier. Because the interaction was not statistically significant for any of the multiple regression models, province was treated as a confounder in the models with associated adjustments, as required. Statistical analysis was performed using SAS version 9.2. A 5% statistical significance level was implemented throughout unless otherwise stated and Tukey corrections were applied to account for all pairwise comparisons to ensure that the overall Type I (false positive) error rate was less than 0.05.

Actigraphy Data Screening

The sleep actigraphy file consisted of 4,742 nights of actigraphy measured sleep (i.e., sleep nights) data from 781 participants. The following adjustments to the file were made to account for data that could not be processed: removal of sleep nights with no data (n = 15), data where the dates from the sleep watch and sleep log diary did not match (n = 61), recordings beyond 7 d (representing data collected off wrist or during return shipment) (n = 56), nights with shift work (n = 630), and data related to sleep nights away from home (n = 132). Removal of these data supported the objective to relate sleep behavior to noise exposure from wind turbines at the participants' dwelling. Sleep starting after 05:00 with awakening on the same day before 18:00 was considered day sleep and removed from the analysis (n = 70). One participant was removed where there appeared to be a watch malfunction (i.e., indicated nearly constant sleep). The final sample size consisted of 3,772 sleep nights and 654 participants. Any sleep that started after midnight, but before 05:00 was re-coded and considered as sleep for the previous night to avoid having two sleep observations for the same night. For the remaining data, all available data was used whether the person wore the watch for 1 d or for the maximum 7 d.

RESULTS

Wind Turbine Sound Pressure Levels at Dwellings

Calculated outdoor sound pressure levels at the dwellings determined by ISO 9613-1[33] and ISO 9613-2[34] reached levels as high as 46 dB(A). Results are considered to have an uncertainty of ± 4 dB(A) within distances that would have the strongest effect on sleep (i.e., ~600 m). Figure 1 illustrates the distribution of participants as a function of WTN levels and identifies the number of participants who reported wind turbines were visible from anywhere on their property (panel A) and audible (panel B) while they were either outside or inside their dwelling.

Background Nighttime Sound Pressure Levels

Modeled background nighttime sound (BNTS) levels ranged between 35 and 61 dB(A) in the sample. Average BNTS was highest in the WTN group 30–35 dB(A) and lowest in areas where modeled WTN levels were between 40–46 dB(A).[37] In the univariate analysis of global PSQI, the proportion of people with poor sleep (i.e., global scores above 5) was statistically similar among the BNTS levels (P = 0.9727). For actigraphy, BNTS levels were only statistically significant for the endpoint WASO (P = 0.0059), where it was found that individuals in areas with louder BNTS levels tended to have longer durations of awakenings. WASO increased from 50.7 min (95% confidence interval [CI]: 46.9, 54.4) in areas with < 40 dB(A) BNTS to 67.2 min (95% CI: 57.0, 77.5) in areas with ≥ 55 dB(A) BNTS levels (see supplemental material).

Response Rates and Sample Characteristics Related to Sleep

A detailed breakdown of the response rates, along with personal and situational variables by WTN category, is presented by Michaud.[37] Of the 2,004 potential dwellings, 1,570 were valid and 1,238 agreed to participate in the survey (606 males,

Table 1—Self-reported magnitude and contributing sources of sleep disturbance.

Variable	Wind Turbine Noise, dB(A) < 25	25–30	30–35	35–40	40–46	Overall	CMH P value[a]
n	83	95	304	519	234	1,235	
Self-reported sleep disturbance n (%)							
Not at all	29 (34.9)	44 (46.3)	112 (36.8)	208 (40.1)	85 (36.3)	478 (38.7)	
At least slightly[b]	54 (65.1)	51 (53.7)	192 (63.2)	311 (59.9)	149 (63.7)	757 (61.3)	0.7535
Highly[c]	13 (15.7)	11 (11.6)	41 (13.5)	75 (14.5)	24 (10.3)	164 (13.3)	0.4300
Source of sleep disturbance (among participants at least slightly sleep disturbed) n (%)							
n[d]	53	51	186	298	138	726	
Wind turbine	0 (0.0)	2 (3.9)	4 (2.2)	45 (15.1)	31 (22.5)	82 (11.3)	< 0.0001
Children	9 (17.0)	12 (23.5)	21 (11.3)	36 (12.1)	20 (14.5)	98 (13.5)	0.2965
Pets	7 (13.2)	12 (23.5)	9 (4.8)	45 (15.1)	22 (15.9)	95 (13.1)	0.3582
Neighbors	6 (11.3)	5 (9.8)	9 (4.8)	13 (4.4)	5 (3.6)	38 (5.2)	0.0169
Other	41 (77.4)	35 (68.6)	162 (87.1)	232 (77.9)	87 (63.0)	557 (76.7)	0.0128
Stress/anxiety	6 (11.3)	2 (3.9)	21 (11.3)	33 (11.1)	11 (8.0)	73 (10.1)	0.8938
Physical pain	11 (20.8)	9 (17.6)	50 (26.9)	48 (16.1)	18 (13.0)	136 (18.7)	0.0289
Snoring	5 (9.4)	6 (11.8)	17 (9.1)	20 (6.7)	12 (8.7)	60 (8.3)	0.4126

Participants were asked to report their magnitude of sleep disturbance over the last year while at home by selecting one of the following five categories: not at all, slightly, moderately, very, or extremely. Participants that indicated at least a slight magnitude of sleep disturbance were asked to identify all sources perceived to be contributing to sleep disturbance. [a]The Cochran Mantel-Haenszel chi-square test was used to adjust for provinces. [b]At least slightly sleep disturbed includes participants indicating the slightly, moderately, very or extremely categories. [c]Highly sleep disturbed includes participants who reported the very or extremely categories. The prevalence of reported sleep disturbance was unrelated to wind turbine noise levels. [d]Of the 757 participants who reported at least a slight amount of sleep disturbance, 31 did not know what contributed to their sleep disturbance. Of the remaining 726, at least one source was identified. Columns may not add to sample size totals as some participants did not answer questions and/or identified more than one source as the cause of their sleep disturbance.

Table 2—Summary of Pittsburgh Sleep Quality Index scores.

	Wind Turbine Noise, dB(A) < 25	25–30	30–35	35–40	40–46	Overall
Mean (95% CI)	6.22 (5.32, 7.11)	5.91 (5.05, 6.77)	6.00 (5.51, 6.50)	5.74 (5.33, 6.16)	6.09 (5.55, 6.64)	5.94 (5.72, 6.17)
n (%) score > 5[a]	40 (49.4)	45 (48.9)	138 (46.5)	227 (44.4)	106 (46.7)	556 (46.0)

[a]Pittsburgh Sleep Quality Index score above 5 is considered to represent poor sleep. CI, confidence interval.

632 females), resulting in a final overall response rate of 78.9%. Of the 1,238 participants, 1,208 completed the PSQI in its entirety (97.6%) and 781 participated in the sleep actigraphy portion of the study (63%). Sleep actigraphy participation rates were in line with projections based on an unpublished pilot study designed to assess different sleep watch devices and participant compliance. Participation rate was equally distributed across WTN categories.

The prevalence of reporting a diagnosed sleep disorder was unrelated to WTN levels (P = 0.3102).[27] In addition, the use of sleep medication at least once a week was significantly related to WTN levels (P = 0.0083). The prevalence was *higher* among the two lowest WTN categories (< 25 dB(A) and 25–30 dB(A)).[37] Factors that may affect sleep quality, such as self-reported prevalence of health conditions, chronic illnesses, quality of life, and noise sensitivity were all found to be equally distributed across WTN categories.[37,56] In response to the general question on magnitude of sleep disturbance for any reason over the past year while at home, a total of 757 participants (61.3%) reported at least a "slight" magnitude of sleep disturbance (includes ratings of "slightly," "moderately," "very" and "extremely"), with a total of 164 (13.3%) classified as "highly" sleep disturbed (i.e., either very or extremely). The levels of WTN were not found to have a statistically significant effect on the prevalence of sleep disturbance whether the analysis was restricted to only participants highly sleep disturbed (P = 0.4300), or if it included all participants with even a slight disturbance (P = 0.7535) (Table 1). When assessing the sources reported to contribute to sleep disturbance among all participants with even slight disturbance, reporting wind turbines was significantly associated with WTN categories (P < 0.0001). The prevalence was ≥ 15.1% among the participants living in areas where WTN levels were ≥ 35 dB(A) compared to ≤ 3.9% in areas where WTN levels were below 35 dB(A). However, wind turbines were not the only, nor the most prevalent, contributing source at these sound levels (see Table 1).

PSQI Scores

For the 1,208 participants who completed the PSQI in its entirety, the average PSQI score across the entire sample was

5.94 with 95% confidence interval (CI) (5.72, 6.17). The Cronbach alpha for the global PSQI was 0.76 (i.e., greater than the minimum value of 0.70 in order to validate the score). Table 2 presents the summary statistics for PSQI as both a continuous scale and a binary scale (the proportion of respondents with poor sleep; i.e., PSQI above 5) by WTN exposure categories. Analysis of variance was used to compare the average PSQI score across WTN exposure groups (after adjusting for provinces). There was no statistical difference observed in the mean PSQI scores between groups ($P = 0.7497$) as well as no significant difference between provinces ($P = 0.7871$) (data not shown). Similarly, when modeling the proportion of respondents with poor sleep (PSQI > 5) in the logistic regression model, no statistical differences between WTN exposure groups ($P = 0.4740$) or provinces ($P = 0.6997$) were observed (see supplemental material).

Effects of Personal and Situational Variables on PSQI Scores and Actigraphy

A univariate analysis of the personal and situational variables in relation to the PSQI scores (logistic regression) and actigraphy (GEE) was conducted. The list of variables considered was extensive and included, but was not limited to, age, sex, income, education, body mass index, caffeine consumption, housing features, diagnosed sleep disorders, health conditions, annoyance, household complaints, and personal benefit (i.e., rent, payments or other indirect benefits through community improvements) from having wind turbines in the area. The analysis of these and several other variables in relation to the endpoints has been made available in the supplemental material.

Multiple Logistic Regression Models for PSQI

Table 3 provides a summary of the variables retained in the multiple regressions for the PSQI and actigraphy endpoints. A detailed description of the statistical results, including the direction of change and the pairwise comparisons made among the groups within each variable is available in the supplemental material.

Table 4 presents the results from stepwise multiple logistic regression modeling of the proportion of respondents with "poor sleep" (i.e., scores above 5 on the PSQI). The final models for the three approaches to stepwise regression as listed in the Statistical Methods section produced nearly identical results to one another. Therefore, results are only presented for the regression method where the variables WTN category, province, and personal benefit were forced into the model that fit the data well (Hosmer-Lemeshow test, $P > 0.05$). Using stepwise regression, the predictive strength of the final model was 37%. There was no observed relationship between the proportion of respondents with poor sleep and WTN levels ($P = 0.3165$).

Participants who had improved sleep quality after closing their bedroom window were found to have the same odds of poor sleep when compared to those who did not need to close their window ($P = 0.0565$). Participants who stated that closing their window did not improve sleep quality had higher odds of poor sleep in comparison with both those who had improved sleep quality after closing windows and those who did not need to close windows ($P \leq 0.0006$, in both cases). Unemployed individuals had higher odds of poor sleep compared with those who were employed (OR [95% CI]: 1.55 [1.12, 2.15]).

Long-term sleep disturbance (of any type by any source) was included in the study because dose-response relationships have been published for this measure in relation to other community noise sources[45] and this endpoint provides a longer time reference period than the previous 30 d assessed using the PSQI. Those who reported a very or extremely high level of sleep disturbance (i.e., percentage highly sleep disturbed) by any source while at home had 6 times higher odds of poor sleep assessed with the PSQI (OR [95%CI]: 6.28 [3.46, 11.40]) when compared to those with no, slight, or moderate reported sleep disturbance. Finally, participants suffering from migraines/headaches, asthma, arthritis and a diagnosed sleep disorder (e.g., sleep apnea or insomnia) had higher odds of poor sleep when compared to those not suffering from these health and chronic conditions.

Sleep Actigraphy

The majority of participants (56%) wore the watch for the full 7 nights (mean number of days 5.77, SD = 1.85). The frequency across the days of the week was equally distributed (data not shown). Response rates for the actigraph were equally distributed across WTN exposure groups ($P = 0.5585$), although a higher proportion of participants were noted in PEI, in comparison to ON ($P = 0.0008$).

Table 5 presents the summary data for each sleep actigraphy endpoint analyzed. Although mean values appear stable between one sleep night to the next within an endpoint, the standard deviation is observed to fluctuate between sleep nights (data not shown). The observed correlations between the PSQI and the actigraphy endpoints are presented as supplemental material.

Multiple GEE Regression Models for Actigraphy

Multiple regression models for the five sleep actigraphy endpoints were developed. Variables that were associated with each endpoint (i.e., significant at the 10% level) are summarized in Table 3. Specific information on these variables, including the direction of change, P values, and pairwise comparisons has been made available in the supplemental material. Table 6 presents the LSM and the P values for the exposure of interest, the WTN exposure categories, obtained from the GEE regression models for the sleep actigraphy endpoints. Unadjusted results reflect the base model (including WTN, province, day of the week, and the interaction between WTN and day of the week) whereas adjusted results come from the multiple regression models obtained through the stepwise method and take into account factors beyond the base model. The level of exposure to WTN was not found to be related to sleep efficiency ($P = 0.3932$), sleep latency ($P = 0.6491$), total sleep time ($P = 0.8002$), or the number of awakening bouts ($P = 0.3726$). There was an inconsistent association found between WASO and WTN exposure where there was a statistically significant reduction in WASO time observed in areas where WTN levels were 25–30 dB(A), in comparison with < 25 dB(A) and 40–46

Table 3—Variables retained in multiple generalized estimating equations and multiple logistic regression models.

	Sleep Efficiency (%)	Sleep Latency (min)	Total Sleep Time (min)	WASO (min)	Rate of Awakening Bouts (per 60 min)	PSQI (scores > 5)
Base model						
WTN levels				++		
Province				+		+
Demographic variables						
Sex	++					
BMI group	+	++				
Age group		++				
Marital status					+	
Employment				++		++
Smoking status				++		
Caffeine consumption	++				+	
Education	++			++		
Situational variables						
Bedroom location				++		
Air conditioning unit in bedroom			++			
Bedroom on quiet side			+			
Bedroom window type			+			
Sleep improved by closing window						++
Closure of bedroom windows/other[a]		++				
BNTS level			++	++		
Audible rail noise						++
Audible aircraft noise				++		
Wind turbine related variables						
Complaint about wind turbines	+					
Personal benefits						++
Annoyance with blinking lights			++		++	
Personal and health related variables						
Self-reported sleep disturbance[b]						++
Sleep disturbed by pain			++		++	
Sleep disturbed by neighbors			++			
Sleep disturbed by other[c]						++
Annoyed by snoring						+
Sleep medication[d]				++		
Migraines						++
Dizziness						+
Chronic pain						+
Asthma		++				++
Arthritis						++
Diagnosed sleep disorder			+			++
Restless leg syndrome					++	

A summary of significant variables retained in multiple generalized estimating equations and multiple logistic regression models for objectively measured and self-reported sleep endpoints, respectively. The specific direction of change, level of statistical significance, pairwise comparisons between variable groups and full description of the variable names is provided in supplemental material. [a]The source identified by participants as the cause of closing bedroom windows to reduce noise levels was not road traffic, aircraft, rail or wind turbines. [b]Evaluates the magnitude of reported sleep disturbance at home from not at all to extremely, for any reason over the previous year. [c]The source identified by participants as contributing to their sleep disturbance was not wind turbines, children, pets or neighbors. [d]Use of sleep medication was note considered in the multiple regression model for PSQI since it is one of the seven components that make up the global PSQI score. +, ++ denotes statistically significant, $P < 0.10$, $P < 0.05$, respectively. BMI, body mass index; BNTS, background nighttime sound level; PSQI, Pittsburgh Sleep Quality Index; WTN, wind turbine noise.

Table 4—Multiple logistic regression model for Pittsburgh Sleep Quality Index.

Variable	Groups in Variable[b]	Model: WTN, Province, and Personal Benefit Forced in PSQI[a] P value[c]	OR (CI)[d]
		(n = 933, R^2 = 37%, H-L P = 0.9252)[h]	
WTN, dB(A)[e]		0.3165	0.93 (0.80, 1.07)
Province	PEI/ON	0.0810	1.46 (0.95, 2.25)
Personal benefit	No/Yes	0.0499	1.82 (1.00, 3.30)
Sleep improved by closing window (overall P value < 0.0001)	Yes	0.0565	1.41 (0.99, 2.00)
	No	< 0.0001	8.48 (3.11, 23.14)
	Did not need to close windows	Reference	
Employment	No/Yes	0.0085	1.55 (1.12, 2.15)
Audible rail noise	No/Yes	0.0380	1.56 (1.03, 2.37)
Reported cause for sleep disturbance			
Other[f]	Yes/No	< 0.0001	2.55 (1.86, 3.48)
Self-reported sleep disturbance[g]	High/Low	< 0.0001	6.28 (3.46, 11.40)
Annoyed by snoring	High/Low	0.0693	2.16 (0.94, 4.94)
Migraines	Yes/No	0.0062	1.76 (1.17, 2.64)
Dizziness	Yes/No	0.0696	1.46 (0.97, 2.20)
Chronic pain	Yes/No	0.0754	1.47 (0.96, 2.25)
Asthma	Yes/No	0.0166	2.01 (1.14, 3.56)
Arthritis	Yes/No	0.0497	1.45 (1.00, 2.10)
Diagnosed sleep disorder	Yes/No	0.0001	2.99 (1.71, 5.23)

[a]The logistic regression is modeling the probability of having a PSQI score above 5. [b]Where a reference group is not specified it is taken to be the last group. [c]P value significance is relative to the reference group. [d]OR (CI) odds ratio and 95% confidence interval based on logistic regression model. [e]The exposure variable, WTN level, is treated as a continuous scale in the logistic regression model. [f]The source identified by participants as the cause of closing bedroom windows to reduce noise levels was not road traffic, aircraft, rail or wind turbines. [g]Evaluates the magnitude of reported sleep disturbance at home from not at all to extremely for any reason over the previous year. [h]H-L P > 0.05 indicates a good fit. CI, confidence interval; H-L, Hosmer-Lemeshow test; ON, Ontario; OR, odds ratio; PEI, Prince Edward Island; PSQI, Pittsburgh Sleep Quality Index; WTN, wind turbine noise.

dB(A) WTN categories. This was because of a higher mean WASO time among participants from PEI living in areas where WTN levels were less than 25 dB(A) (data not shown).

DISCUSSION

The effects on health and well-being associated with accumulated sleep debt have been well documented.[1–5,57] The sound pressure levels from wind turbines can exceed the WHO recommended annual average nighttime limit of 40 dB(A) for preventing health effects from noise-induced sleep disturbance.[11] The calculated outdoor A-weighted WTN levels in this study reached a maximum of 46 dB(A), with 19% of dwellings found to exceed 40 dB(A). Within an uncertainty of approximately 4 dB(A), the calculated A-weighted levels in the current study can be compared to the WHO outdoor nighttime annual average threshold of 40 dB(A).[11,58] With the average façade attenuation with windows completely opened of 14 ± 2 dB(A),[58] the average bedroom level at the highest façade level, 46 dB(A), will be 32 ± 2 dB(A), which is close to the 30 dB(A) indoor threshold in the WHO's Guidelines for Community Noise.[10] Considering the uncertainty in the calculation model and input data, only dwellings in the highest WTN category are expected to have indoor levels above 30 dB(A) and thus sensitivity to sleep disturbance. However, with windows closed, indoor outdoor level difference is approximately 26 dB, which should result in an indoor level around 20 dB(A) in the current study.

Factors including, but not limited to, medication use, other health effects (including sleep disorders), caffeine consumption, and annoyance with blinking lights on wind turbines were found to statistically influence reported and/or actigraphically measured sleep outcomes. However, there was no evidence for any form of sleep disturbance found in relation to WTN levels. Studies published to date have been inconsistent in terms of self-reported evidence that WTN disrupts sleep,[59,60] and none of these studies assessed sleep using an objectively measured method. These inconsistent findings are

Table 5—Summary of Actiwatch2® data.

		Wind Turbine Noise, dB(A)				
		< 25	25–30	30–35	35–40	40–46
n (weekday, weekend)		(198, 78)	(200, 68)	(705, 273)	(1114, 420)	(526, 190)
Sleep Actigraphy Endpoint	Sleep Night	Mean (SD)	Mean (SD)	Mean (SD)	Mean (SD)	Mean (SD)
Sleep latency, min	Weekday	14.53 (23.31)	13.89 (23.08)	13.02 (26.14)	13.01 (23.05)	13.01 (22.83)
	Weekend	22.85 (37.01)	10.02 (15.86)	13.23 (22.47)	15.36 (36.13)	12.94 (26.96)
Sleep efficiency, %	Weekday	84.69 (6.59)	85.64 (7.84)	84.92 (7.56)	85.24 (7.83)	85.01 (7.03)
	Weekend	83.62 (7.93)	87.73 (5.46)	84.37 (8.39)	85.01 (7.96)	84.28 (8.47)
WASO, min	Weekday	58.58 (29.45)	50.43 (34.80)	54.99 (31.63)	52.63 (30.14)	55.50 (34.19)
	Weekend	60.49 (37.14)	48.57 (27.00)	58.28 (38.69)	54.11 (35.56)	56.60 (37.53)
Total sleep time, min	Weekday	455.24 (160.65)	447.70 (165.62)	448.88 (169.37)	445.76 (166.52)	448.38 (179.82)
	Weekend	468.12 (163.83)	462.21 (139.61)	457.15 (167.15)	448.63 (155.09)	442.85 (174.23)
Number of awakening bouts, count	Weekday	24.41 (9.49)	22.04 (10.04)	25.05 (13.53)	23.56 (9.86)	24.01 (9.81)
	Weekend	24.89 (10.00)	22.09 (8.76)	26.09 (13.01)	24.60 (10.54)	24.35 (10.22)
Time in bed, min	Weekday	536.05 (173.73)	521.39 (176.46)	526.53 (180.77)	520.55 (173.97)	524.48 (187.30)
	Weekend	559.85 (184.18)	526.99 (154.00)	540.13 (179.72)	527.18 (166.46)	522.57 (176.14)
Rate of awakening bouts per 60 min in bed	Weekday	2.83 (1.00)	2.64 (1.12)	2.94 (1.27)	2.82 (1.08)	2.89 (1.09)
	Weekend	2.77 (1.06)	2.60 (1.06)	2.97 (1.18)	2.87 (1.08)	2.93 (1.14)

SD, standard deviation; WASO, wake after sleep onset.

Table 6—Generalized estimating equations regression models for sleep actigraphy endpoints.

	Sleep Efficiency, %	Sleep Latency, min	Total Sleep Time,[d] min	WASO, min	Number of Awakening Bouts during Sleep
n	618	526	619	647	626
Sleep nights[c]	3,561	3,017	3,552	3,728	3,595
P value unadjusted[a]	0.2420	0.9051	0.7222	0.0655	0.2460
P value adjusted[b]	0.3932	0.6491	0.8002	0.0056	0.3726
Unadjusted[a] WTN, dB(A)	LSM (95% CI)[e]	LSM (95% CI)[e]	LSM (95% CI)[e]	LSM (95% CI)[e]	LSM (95% CI)[e]
< 25	84.71 (83.25, 86.17)	16.34 (11.40, 21.28)	458.00 (428.08, 487.93)	58.83 (52.78, 64.87)	24.26 (22.28, 26.25)
25–30	86.49 (85.12, 87.87)	12.34 (8.88, 15.80)	462.68 (427.47, 497.90)	49.11 (43.72, 54.50)	21.08 (19.14, 23.02)
30–35	84.82 (83.86, 85.78)	12.51 (10.54, 14.49)	464.00 (441.44, 486.57)	55.39 (52.04, 58.74)	24.57 (23.01, 26.14)
35–40	85.33 (84.60, 86.05)	13.02 (11.39, 14.65)	449.10 (433.95, 464.24)	53.08 (50.35, 55.80)	23.37 (22.40, 24.35)
40–46	85.01 (84.05, 85.98)	12.64 (10.50, 14.78)	445.78 (426.60, 464.96)	55.46 (51.45, 59.47)	23.84 (22.55, 25.13)
Adjusted[b] WTN, dB(A)	LSM (95% CI)[e]	LSM (95% CI)[e]	LSM (95% CI)[e]	LSM (95% CI)[e]	LSM (95% CI)[e]
< 25	85.62 (83.97, 87.28)	15.08 (10.03, 20.13)	462.41 (407.97, 516.84)	62.00 (55.14, 68.85)	23.19 (20.58, 25.79)
25–30	87.28 (85.55, 89.01)	10.88 (6.45, 15.32)	453.43 (401.10, 505.76)	51.67 (44.14, 59.20)	20.57 (17.87, 23.26)
30–35	85.82 (84.52, 87.13)	9.95 (7.02, 12.87)	455.22 (406.72, 503.72)	56.11 (50.81, 61.42)	24.00 (21.26, 26.75)
35–40	85.97 (84.86, 87.08)	10.71 (7.88, 13.54)	466.12 (416.21, 516.02)	57.80 (52.36, 63.24)	22.56 (20.57, 24.56)
40–46	86.16 (84.84, 87.48)	10.92 (7.01, 14.82)	472.95 (422.09, 523.81)	62.06 (55.64, 68.48)	22.85 (20.68, 25.02)

[a]The base model for the multiple generalized estimating equations (GEE) regression models for all endpoints included wind turbine noise (WTN) exposure groups, province, day of the week, and the interaction between WTN groups and day of the week. [b]A complete list of the other variables included in each multiple GEE regression model based on the stepwise methodology is presented in Table 3. [c]Sample size for the adjusted GEE regression models. [d]The base model for total sleep time includes the interaction between WTN groups and province. [e]LSM, least squares means, for each group after adjusting for all other variables in the multiple GEE regression model and corresponding 95% confidence interval (CI). P values for both the adjusted and unadjusted models are based on the transformed variable in order to satisfy model assumptions of normality and constant variance.

not entirely surprising considering that sleep disturbance reported as a result of transportation noise exposure occurs at sound pressure levels that exceed WTN levels calculated in the current study.[27,28,45] Study results concur with those of Bakker et al.,[21] with outdoor WTN levels up to 54 dB(A), wherein it was concluded that there was no association between the levels of WTN and sleep disturbance when noise annoyance was taken into account.

The current study employed a wide range of self-reported and objectively measured endpoints related to sleep to provide a comprehensive assessment of the potential effects that WTN exposure may have on sleep. Self-reported diagnosed sleep disorders[37] and self-reported highly sleep disturbed for any reason were factors found to be unrelated to WTN exposure. Furthermore, taking medication at least once per week was more commonly reported among participants living in areas where WTN levels were below 30 dB(A). Scores on the PSQI, either analyzed as a proportion above 5, or as a mean score, were also unrelated to WTN level. Actigraphy-measured sleep latency, sleep efficiency, the rate of awakening bouts, and total sleep time were all found to be unrelated to WTN exposure. The only statistically significant finding found between WTN level and actigraphy was a reduced wake time after sleep onset among participants living in areas where WTN levels were 25–30 dB(A) and this was because of a higher WASO time at the lowest WTN category among PEI participants. The results of the current study do not support conclusions that exposure to WTN up to 46 dB(A) has any statistically significant effect on self-reported or objectively measured sleep. However, annoyance with blinking lights on wind turbines (used as aircraft warning signals) may be related to a higher rate of awakening bouts and reduced total sleep time.

This study has some important limitations. Objective measures of sleep were assessed for up to 7 d, whereas the PSQI and the reported highly sleep disturbed outcomes represent time periods of 30 d and 1 y, respectively. The concern is that 7 d of actigraphy may not represent long-term average sleep patterns. However, the selected time frame for actigraphy measures is typical, and supported in the literature and considered more than adequate for evaluating sleep in a nonclinical study sample.[30,61] If there were situational factors (e.g. an ill child) that made sleep worse in the actigraphy-assessed week, it would not be expected to bias against the effect of wind turbines on sleep, and in fact, would overstate the effect of recent situational events as compared to the long-term theoretical concern about WTN-induced sleep disturbance. As previously discussed, the analysis of actigraphy results was based on nightly average sleep patterns in relation to long-term WTN levels. Although WTN calculations would be expected to produce the highest sound pressure levels at the dwelling, they do not take into consideration the influence that night-to-night variations in outdoor WTN levels may have had on actigraphy results. Similarly, an analysis based on long-term average sound level does not fully account for transient deviations in WTN levels that could potentially interfere with sleep. An analysis based on a time-matched comparison between operational turbine data and actigraphy would permit a more refined assessment of the possible effect that night-to-night variations in WTN levels may have on sleep. These limitations extend to the fact that fluctuations in indoor sound levels during sleep remain unknown.

The possibility that wind turbine operators may have intentionally altered the output of their turbines in order to reduce potential WTN effects on sleep has been one of the concerns raised during the external peer review of this paper. When the *Community Noise and Health Study* was originally announced several months preceding data collection the study locations were unknown. Although awareness of the precise study locations would have become greater as data collection commenced, the deployment of the sleep watches took place over several months among a subsample of participants across the entire study sample. Furthermore, the reference period time for self-reported sleep disturbance was over the previous year and previous 30 d (PSQI). Finally, the subsets of sound power measurements were consistent with manufacturer-supplied data. In the authors' opinion, there is no evidence to suggest that wind turbine operators intentionally altered the output of their turbines to minimize potential effects on sleep at any point in the study.

CONCLUSIONS

The potential association between WTN levels and sleep quality was assessed over the previous 30 d using the PSQI, the previous year using percentage highly sleep disturbed, together with an assessment of diagnosed sleep disorders. These self-reported measures were considered in addition to several objective measures including total sleep time, sleep onset latency, awakenings, and sleep efficiency. In all cases, in the final analysis there was no consistent pattern observed between any of the self-reported or actigraphy-measured endpoints and WTN levels up to 46 dB(A). Given the lack of an association between WTN levels and sleep, it should be considered that the study design may not have been sensitive enough to reveal effects on sleep. However, in the current study it was demonstrated that the factors that influence sleep quality (e.g. age, body mass index, caffeine, health conditions) were related to one or more self-reported and objective measures of sleep. This demonstrated sensitivity, together with the observation that there was consistency between multiple measures of self-reported sleep disturbance and among some of the self-reported and actigraphy measures, lends strength to the robustness of the conclusion that WTN levels up to 46 dB(A) had no statistically significant effect on any measure of sleep quality.

The WHO's[11] health-based limit for protecting against sleep disturbance is an annual average outdoor level of 40 dB(A). This level was exceeded in 19% of the cases, but by no more than 6 dB(A) and as such represents a limit to detecting a potential effect on sleep. It is therefore important to acknowledge that no inferences can be drawn from the current results to areas where WTN levels exceed 46 dB(A). Likewise, assuming a baseline prevalence of 10%, the study was designed so that the statistical power would be sufficient to detect at least a 7% difference in the prevalence of self-reported sleep disturbance. A larger sample size would be required to detect smaller differences. The statistical power of a study design is a limitation that applies to all epidemiological studies.

Although it may be tempting to generalize the current study findings to other areas, this would have required random selection of study locations from all communities living near wind turbines in Canada. Despite the fact that participants in the study were randomly selected, the locations were not and for this reason the level of confidence one has in generalizing the results to other areas can only be based on a certain level of scientific judgment regarding the level of exposure and the similarity between the current study sample and others. Despite limitations in generalizing the results of this analysis beyond the study sample, the current study is the largest and most comprehensive analysis of both self-reported and objectively measured sleep disturbance in relation to WTN levels published to date.

REFERENCES

1. Zaharna M, Guilleminault C. Sleep, noise and health: review. Noise Health 2010;12:64–9.
2. Schwartz SW, Cornoni-Huntley J, Cole SR, Hays JC, Blazer DG, Schocken D. Are sleep complaints an independent risk factor for myocardial infarction? Ann Epidemiol 1998;8:384–92.
3. Orzeł-Gryglewska J. Consequences of sleep deprivation. Int J Occ Med Environ Health 2010;23:95–114.
4. Pilcher JJ, Huffcutt AI. Effects of sleep deprivation on performance: a meta-analysis. Sleep 1996;19:318–26.
5. George CF. Sleep apnea, alertness, and motor vehicle crashes. Am J Respir Crit Care Med 2007;176:954–6.
6. Young T, Peppard PE, Gottlieb DJ. Epidemiology of obstructive sleep apnea: a population health perspective. Am J Respir Crit Care Med 2002;165:1217–39.
7. Grandner MA, Perlis ML. Short sleep duration and insomnia associated with hypertension incidence. Hypertens Res 2013;36:932–3.
8. Hume KI, Brink M, Basner M. Effects of environmental noise on sleep. Noise Health 2012;14:297–302.
9. Dang-Vu TT, Bonjean M, Schabus M, et al. Interplay between spontaneous and induced brain activity during human non-rapid eye movement sleep. Proc Nat Acad Sci U S A 2011;108:15438–43.
10. World Health Organization (WHO). Guidelines for Community Noise. Berglund B, Lindvall T, Schwela DH (eds). Geneva: World Health Organization. 1999. http://www.who.int/docstore/peh/noise/guidelines2.html.
11. WHO. Night Noise Guidelines for Europe. Hurtley C (ed). Copenhagen Denmark: WHO Regional Office for Europe. 2009. http://www.euro.who.int/data/assets/pdf_file/0017/43316/E92845.pdf.
12. Kirsch DB. A neurologist's guide to common subjective and objective sleep assessments. Neurol Clin 2012;30:987–1006.
13. McCall WV, Edinger JD. Subjective total insomnia: an example of sleep state misperception. Sleep 1992;15:71–3.
14. Buysse DJ, Reynolds CF, Monk TH, Berman SR, Kupfer DJ. The Pittsburgh Sleep Quality Index: a new instrument for psychiatric practice and research. Psych Res 1989;28:193–213.
15. Carpenter JS, Andrykowski MA. Psychometric evaluation of the Pittsburgh Sleep Quality Index. J Psychosom Res 1998;45:5–13.
16. Backhaus J, Junghanns K, Broocks A, Riemann D, Hohagen F. Test-retest reliability and validity of the Pittsburgh Sleep Quality Index in primary insomnia. J Psychosom Res 2002;53:737–40.
17. Smyth CA. Evaluating sleep quality in older adults: the Pittsburgh Sleep Quality Index can be used to detect sleep disturbances or deficits. Am J Nurs 2008;108:42–50; quiz 50–1.
18. Spira AP, Beaudreau SA, Stone KL, et al. Reliability and validity of the Pittsburgh Sleep Quality Index and the Epworth Sleepiness Scale in older men. J Gerontol A Biol Sci Med Sci 2012;67:433–9.
19. Nissenbaum MA, Aramini JJ, Hanning CD. Effects of industrial wind turbine noise on sleep and health. Noise Health 2012;14:237–43.
20. Pedersen E. Health aspects associated with wind turbine noise: results from three field studies. Noise Control Eng J 2011;59:47–53.
21. Bakker, RH, Pedersen E, van den Berg GP, Stewart RE, Lok W, Bouma J. Impact of wind turbine sound on annoyance, self-reported sleep disturbance and psychological distress. Sci Total Environ 2012;425:42–51.
22. van den Berg F, Verhagen C, Uitenbroek D. The relation between scores on noise annoyance and noise disturbed sleep in a public health survey. Int J Environ Res Public Health 2014;11:2314–27.
23. Horne JA, Pankhurst FL, Reyner LA, Hume K, Diamond ID. A field study of sleep disturbance: effects of aircraft noise and other factors on 5,742 nights of actimetrically monitored sleep in a large subject sample. Sleep 1994;17:146–59.
24. Öhrström E, Hadzibajramovic E, Holmes M, Svensson H. Effects of road traffic noise on sleep: studies on children and adults. J Environ Psychol 2006;26:116–26.
25. Muzet A. Environmental noise, sleep and health. Sleep Med Rev 2007;11:135–42.
26. Fyhri A, Aasvang GM. Noise, sleep and poor health: modeling the relationship between road traffic noise and cardiovascular problems. Sci Total Environ 2010;408:4935–42.
27. Fidell S, Pearsons K, Tabachnick BG, Howe R. Effects on sleep disturbance of changes in aircraft noise near three airports. J Acoust Soc Am 2000;107:2535–47.
28. Michaud DS, Fidell S, Pearsons K, Campbell KC, Keith SE. Review of field studies of aircraft noise-induced sleep disturbance. J Acoust Soc Am 2007;121:32–41.
29. Ancoli-Israel S, Cole R, Alessi C, Chambers M, Moorcroft W, Pollak CP. The role of actigraphy in the study of sleep and circadian rhythms. Sleep 2003;26:342–92.
30. Sadeh A. The role and validity of actigraphy in sleep medicine: an update. Sleep Med Rev 2011;15:259–67.
31. Riemann D, Spiegelhalder K, Espie C, et al. Chronic insomnia: clinical and research challenges -- an agenda. Pharmacopsychiatry 2011;44:1–14.
32. Tjepkema M. Insomnia. Toronto: Statistics Canada, Catalogue 82-003 Health Reports. 2005;17:9–25. http://www.statcan.gc.ca/pub/82-003-x/2005001/article/8707-eng.pdf.
33. International Organization for Standardization (ISO). ISO 9613-1 - Acoustics. Attenuation of sound during propagation outdoors. Part 1: calculation of the absorption of sound by the atmosphere. Geneva: International Organization for Standardization, 1993.
34. ISO. ISO-9613-2 - Acoustics. Attenuation of sound during propagation outdoors. Part 2: general method of calculation. Geneva: International Organization for Standardization, 1996.
35. DataKustik GmbH®. CadnaA version 4.4. Software for Immission Protection. 2014. www.datakustik.com.
36. Van den Berg F. Criteria for wind farm Noise: Lmax and Lden. Proc. Acoustics '08, Paris, June 29-July 4 2008. http://docs.wind-watch.org/vandenberg-wind-farm-noise-Lmax-Lden.pdf
37. Michaud DS. Self-reported and objectively measured outcomes assessed in the Health Canada wind turbine noise and health study: results support an increase in community annoyance. San Francisco, CA: Internoise, INCE USA, August 9–12, 2015.
38. Pedersen E, van den Berg F, Bakker R, Bouma, J. Can road traffic mask sound from wind turbines? Response to wind turbine sound at different levels of road traffic sound. Energ Pol 2010:38:2520–7.
39. Pedersen E, van den Berg F. Why is wind turbine noise so poorly masked by road traffic noise? Lisbon, Portugal: Internoise, June 13–16, 2010.
40. van den Berg F. The effects of wind turbine noise on people. In Bowdler R, Leventhall G, eds. Wind turbine noise. Brentwood, UK: Multi-Science, 2011:129–52.
41. van den Berg F. Wind turbine noise: an overview of acoustical performance and effects on residents. Victor Harbor, Australia: Proceedings of Acoustics, November 17–20, 2013.
42. Alberta Utilities Commission (AUC). Rule 012-Noise Control. 2013. http://www.auc.ab.ca/acts-regulations-and-auc-rules/rules/Pages/Rule012.aspx.
43. United States Department of Transportation. FHWA Traffic Noise Model®. Technical Manual. Washington D.C.: Federal Highway Administration, 1998.

44. ISO. ISO/TS-15666 - Acoustics - Assessment of noise annoyance by means of social and socio-acoustic surveys. Geneva: International Organization for Standardization, 2003.
45. Miedema HM, Vos H. Associations between self-reported sleep disturbance and environmental noise based on reanalyses of pooled data from 24 studies. Behav Sleep Med 2007;5:1–20.
46. Alsaadi, SM, McAuley JH, Hush JM, et al. Assessing sleep disturbance in low back pain: the validity of portable instruments. PLOS One 2014;9:e95824.
47. Martin JL, Hakim AD. Wrist actigraphy. Chest 2011;139:1514–27.
48. Philips Respironics. Actiware® and Actiware CT® Software Manual: Actiwatch® Communication and Sleep Analysis Software Version 5.1, 2008:3–47.
49. Michaud DS, Keith SE, Feder K, et al. Self-reported and objectively measured health indicators among a sample of Canadians living within the vicinity of industrial wind turbines: social survey and sound level modeling methodology. Noise News Int 2013;21:14–27.
50. SAS Institute Inc. SAS (Statistical Analysis System) Software package Version 9.2. Cary, NC: SAS Institute Inc., 2014. www.sas.com.
51. Liang KY, Zeger SL. Longitudinal data analysis using generalized linear models. Biometrika 1986;73:13–22.
52. Stokes ME, Davis CS, Koch GG. Categorical data analysis using the SAS System, Second Edition. Cary, NC: SAS Institute Inc., 2000.
53. Sokal RR, Rohlf JF. Biometry: the principles and practice of statistics in biological research. 2nd edition. San Francisco, CA: W H Freeman and Company, 1981:859.
54. Snedecor GW, Cochran WG. Statistical Methods, 8th edition. Ames, IA: Iowa State University Press, 1989.
55. Rao PV. Statistical research methods in the life sciences. Pacific Grove, CA: Duxbury Press, 1998.
56. Feder K, Michaud DS, Marro L, et al. Impacts on quality of life associated with exposure to wind turbine noise. Environ Res 2015;142:227–38.
57. Lim AS, Kowgier M, Yu L, Buchman AS, Bennett DA. Sleep fragmentation and the risk of incident Alzheimer's disease and cognitive decline in older persons. Sleep 2013;36:1027–32.
58. Health Canada. Wind Turbine Noise and Health Study: Summary of Results. Ottawa, Health Canada, November, 2014. http://www.hc-sc.gc.ca/ewh-semt/noise-bruit/turbine-eoliennes/summary-resume-eng.php.
59. Knopper LD, Ollson CA. Health effects and wind turbines: a review of the literature. Environ Health 2011;10:78.
60. McCunney R, Mundt KA, Colby WD, Dobie R, Kaliski K, Blais K. Wind turbines and health: a critical review of the scientific literature. J Occ Environ Med 2014;56:e108–30.
61. Littner M, Kushida CA, Anderson WM, et al. Practice parameters for the role of actigraphy in the study of sleep and circadian rhythms: an update for 2002. Sleep 2003;26:337–41.

ACKNOWLEDGMENTS

The authors acknowledge the support they received throughout the study from Serge Legault and Suki Abeysekera at Statistics Canada, and are especially grateful to the volunteers who participated in this study.

SUBMISSION & CORRESPONDENCE INFORMATION

Submitted for publication February, 2015
Submitted in final revised form August, 2015
Accepted for publication August, 2015
Address correspondence to: David S. Michaud, PhD, Health Canada, Environmental and Radiation Health Sciences Directorate, Consumer and Clinical Radiation Protection Bureau, 775 Brookfield Road, Ottawa, Ontario, Canada, K1A 1C1; Tel: (613) 954-6670; Fax: (613) 941-1734; Email: david.michaud@canada.ca

DISCLOSURE STATEMENT

This was not an industry supported study. The study was funded by Health Canada. The authors have indicated no financial conflicts of interest.

Idaho Power/1210
Witness: Dr. Jeffrey Ellenbogen

BEFORE THE PUBLIC UTILITY COMMISSION
OF OREGON

Docket PCN 5

In the Matter of

IDAHO POWER COMPANY'S
PETITION FOR CERTIFICATE OF PUBLIC CONVENIENCE
AND NECESSITY

U.S. Army Public Health Command, Readiness Through
Hearing Loss Prevention (July 2014)

February 22, 2023

Readiness through Hearing Loss Prevention

Technical Guide 250

USAPHC
U.S. ARMY PUBLIC HEALTH COMMAND

Approved for public release; distribution unlimited

NOISE AND HEARING LOSS

What is noise?

- ✓ Any disturbing, harmful, or unwanted sound.
- ✓ The most common hazard in the workplace or during training.
- ✓ The primary cause of hearing loss in the Army.

What are the different types of noise?

- ✓ Noise can be continuous, or steady.
  Examples include power tools, vehicles and aircraft.
- ✓ Noise can also be impulsive.
  Examples include explosions, weapons fire and certain metal-forming machinery.

Will noise toughen your ears?

- ✓ No! Noise destroys your ability to hear and to understand speech.
- ✓ Military veterans are four times more likely to have hearing loss than non-veterans.
- ✓ Hearing loss and tinnitus (ringing in the ears) are the top two service connected disabilities for military veterans.

When and where can noise impair your hearing?

- ✓ During any weapon firing.
- ✓ Noise can damage your hearing at work, at home and during recreational activities.
- ✓ If you have to raise your voice to be heard, the noise is considered hazardous.
- ✓ Noise in combination with some chemical exposures can increase hearing damage, for example, toluene, lead, carbon monoxide, etc.

DECIBEL THERMOMETERS

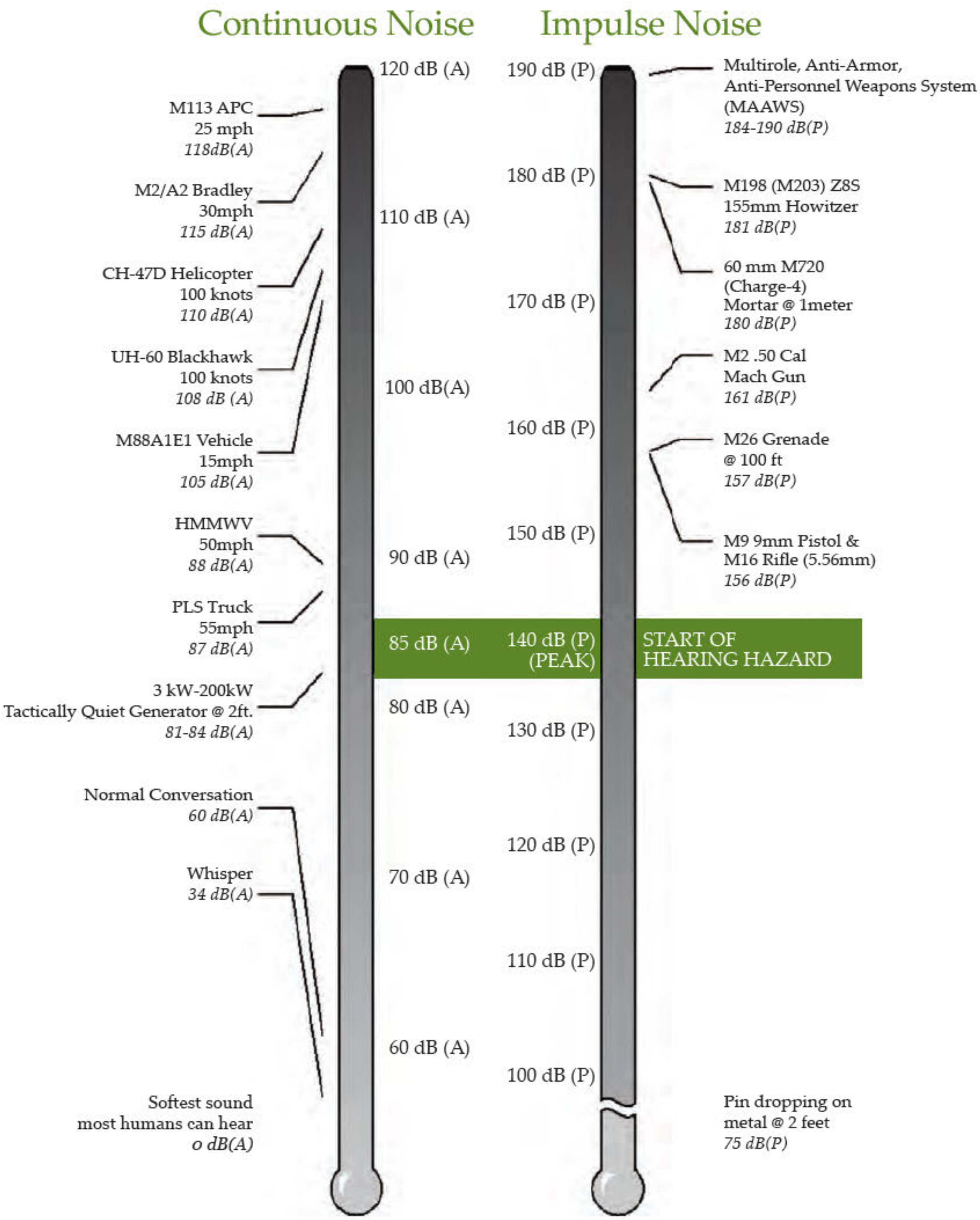

HOW THE EAR WORKS

Your ear is divided into three parts.

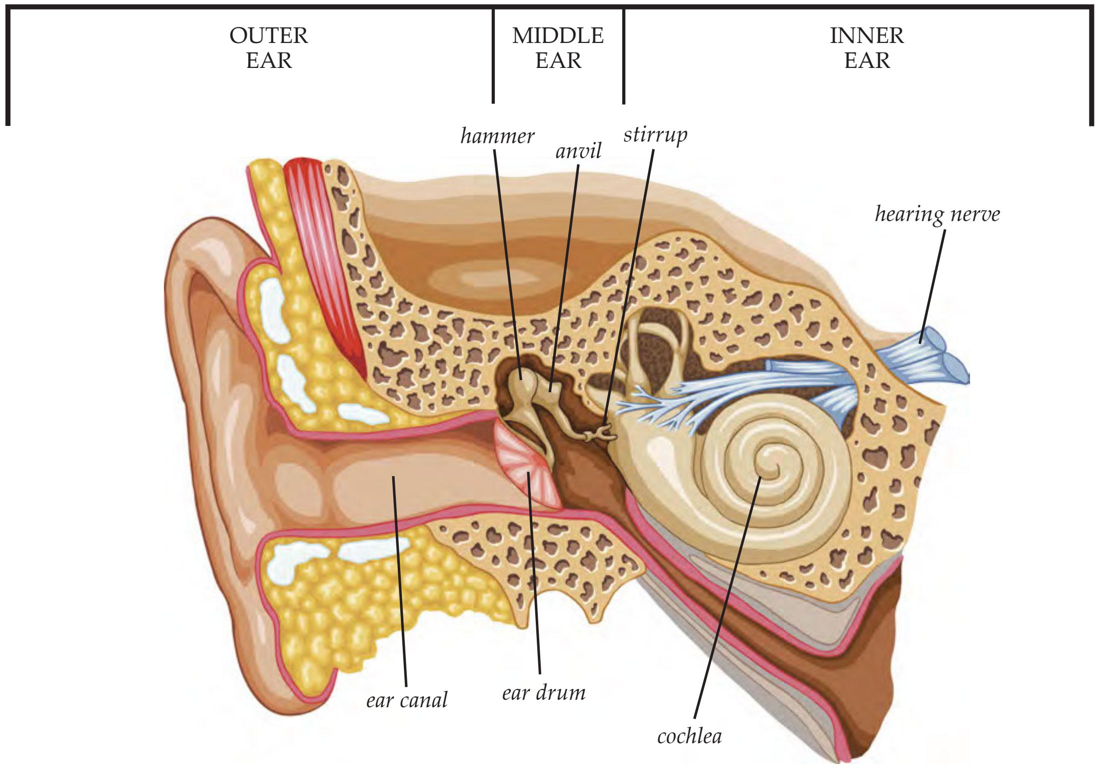

OUTER EAR

The outer ear directs sound waves into the ear canal to the eardrum. The eardrum vibrates and sets into motion part of the middle ear.

MIDDLE EAR

The middle ear contains the three smallest bones in your body—the hammer, anvil and stirrup. These bones vibrate and pass the sound waves into the inner ear.

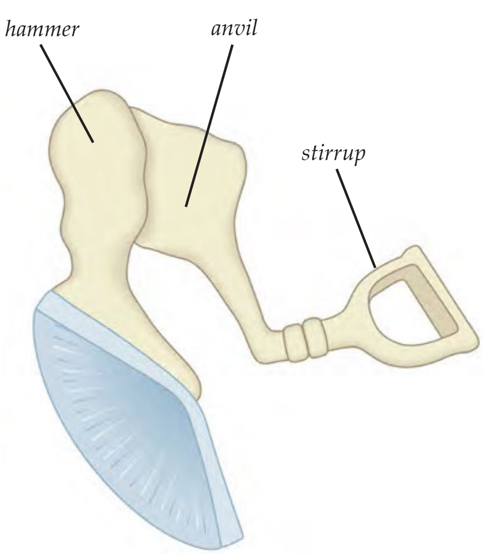

HOW THE EAR WORKS

INNER EAR

The inner ear contains fluid which moves because of the sound waves. Thousands of tiny hair cells respond to the vibrations in the fluid by passing information along the hearing nerve to the brain.

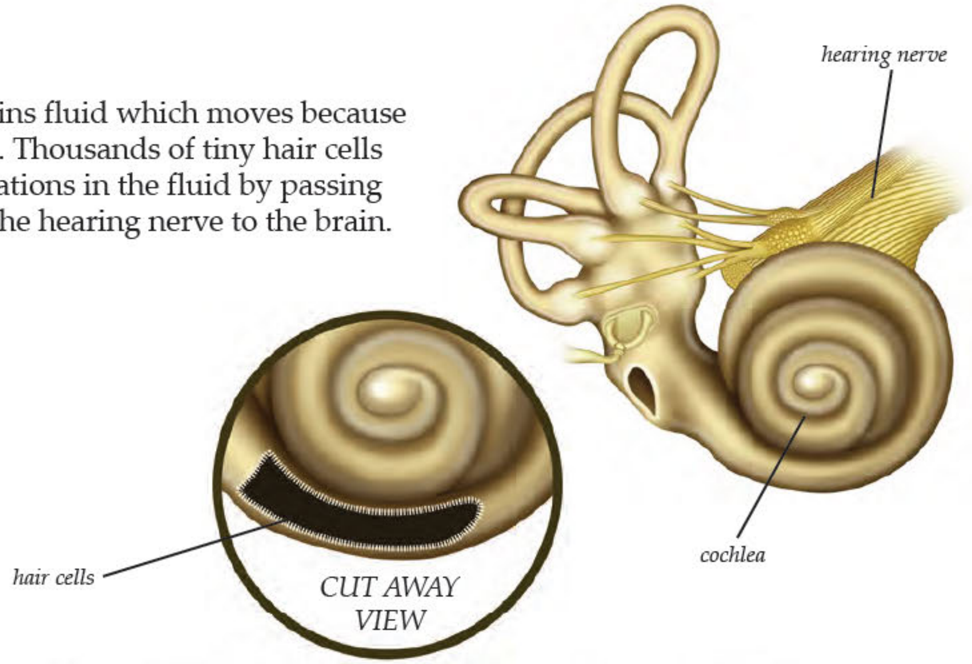

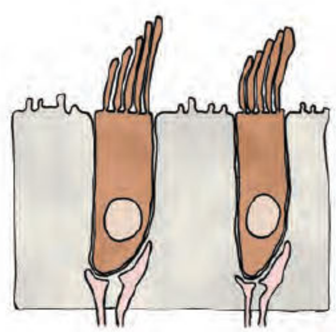

HEALTHY HAIR CELLS

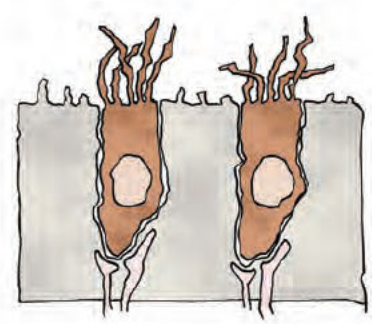

DAMAGED HAIR CELLS

Damage to your hair cells caused by intense noise could be seen as hearing loss on your next audiogram when your hearing is checked.

Hearing problems in the outer and middle ears are usually medically treatable. However, there is no proven cure for inner ear hearing loss caused by the noise.

Noise does not have to cause pain or bleeding to do damage.

CAUTION

*HIGH INTENSITY NOISE
HEARING PROTECTION
REQUIRED*

HEARING PROTECTORS

Earplugs and noise muffs are available at no charge to everyone who works in noise.

Make-shift protectors, such as cigarette filters, cotton or bullet casings do not protect you and they are not hygienic.

EARPLUGS

Preformed earplugs come in various types and sizes and need to be fitted by a medically-trained person. This type of hearing protection should be issued with a carrying case, the top lid of which serves as a inserting device for several types of earplugs.

Triple-Flange earplugs are available in small, medium and large sizes.

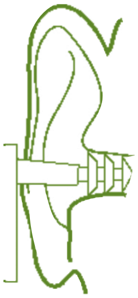

Quad-Flange earplugs are available in one size fits many; however, its stem is too wide for use with the earplug inserting device.

Combat Arms Earplugs (CAE) are in their third generation. The current generation of CAE's come in earth tone colors and three different sizes with a toggle switch. The closed position protects from continuous and impulse noise, while the open position only protects from impulse noise but allows some softer sounds to be audible.

Earplug Inserting Device (Top) and Carrying Case

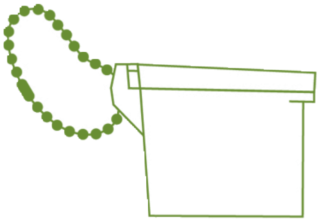

Sound-Guard foam earplug (two-color)

Foam earplugs come in small, medium and large and are semi-disposable.

For a proper fit:

✓ Roll and compress the plug into a very thin cylinder ensuring there are no wrinkles that may allow sound to get through.

✓ While compressed, quickly insert the plug well into the ear canal.

✓ Gently hold the plug in place until it expands to fill the entire ear canal.

Remember:

✓ Your voice will sound muffled or low-toned or muffled, as if in a barrel, when your earplugs are properly inserted.

✓ Adjusting to wearing earplugs may take a little time.

✓ You can be refitted with a different size and type.

✓ If using preformed earplugs such as triple or quad flanged, keep the earplugs clean with soap and water and use them only when dry.

NOISE MUFFS

When properly fitted, noise muffs form a seal around your ears. For proper maintenance, replace hardened or torn earcup seals and degraded acoustic foam padding.

REMEMBER, THE BEST HEARING PROTECTOR IS THE ONE THAT IS WORN!

HEARING TESTING

- ✓ All personnel who work in noise-hazardous areas need an annual hearing check.
- ✓ The first test serves as the reference (baseline) from which any future change or shift in your hearing is measured.
- ✓ You will be notified when your annual hearing check is due. At that time, your hearing protective devices need to be checked and, if necessary, replaced.
- ✓ An audiogram reflects the softest tones you are able to hear at low, middle and high frequencies. *(See page 9.)*
- ✓ When loud noise makes your hearing worse, damage usually occurs first in the higher frequencies. Then nearby frequencies are affected.

AUDIOGRAM

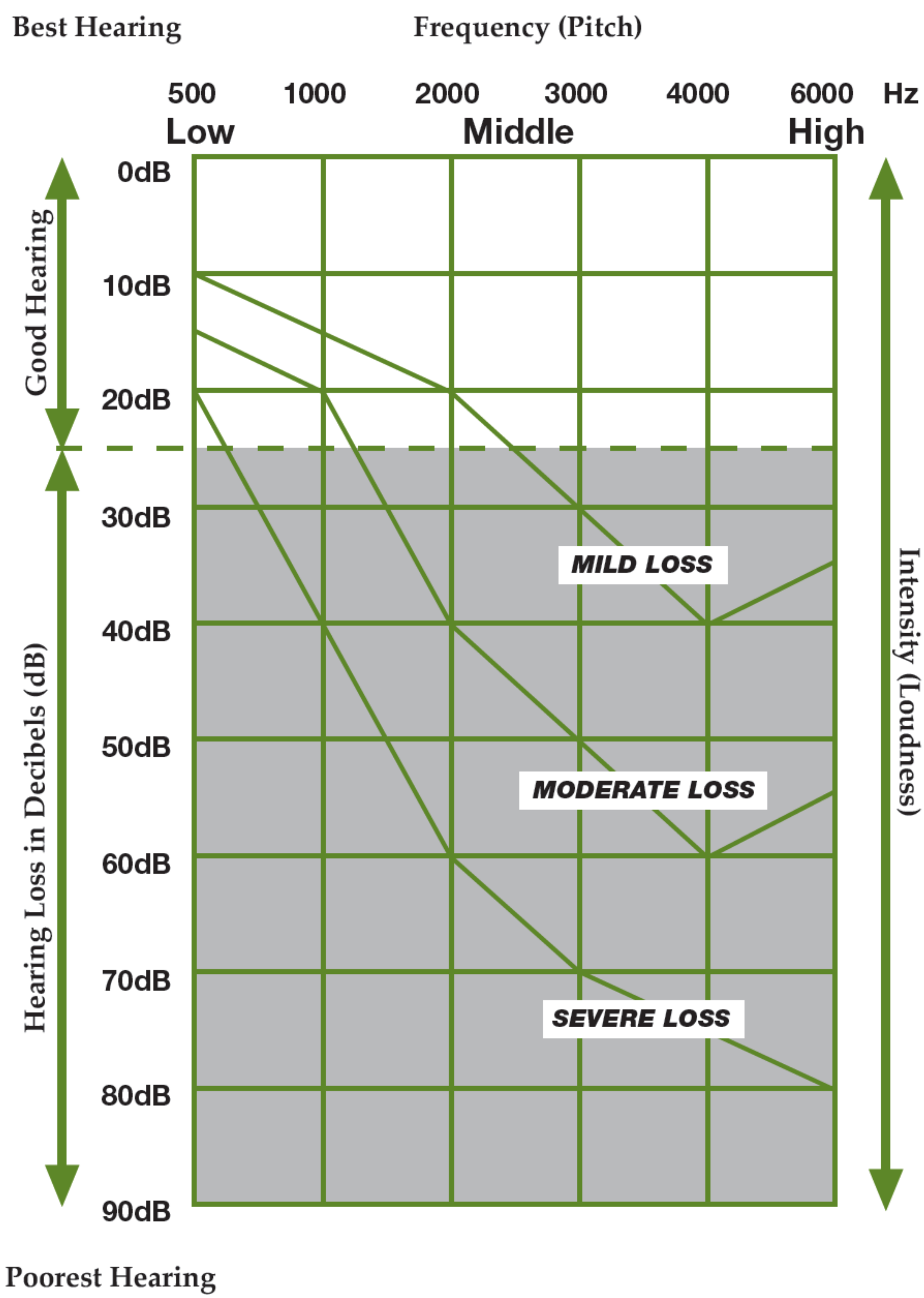
Best Hearing
Frequency (Pitch)
500
1000
2000
3000
4000
6000
Hz
Low
Middle
High
0dB
10dB
20dB
30dB
40dB
50dB
60dB
70dB
80dB
90dB
Good Hearing
Hearing Loss in Decibels (dB)
Intensity (Loudness)
MILD LOSS
MODERATE LOSS
SEVERE LOSS
Poorest Hearing

READINESS AND HEARING LOSS

Why is protecting your hearing so important?

- ✓ Hearing loss caused by loud noise becomes permanent and is not medically treatable.
- ✓ Impaired hearing can cause serious or fatal mistakes at work or in training and combat situations.
- ✓ Good hearing is critical to the success of the mission, both in offensive and defensive operations.

Offensive & Defensive Operations

- ✓ Localizing snipers
- ✓ Locating patrol members
- ✓ Determining the position, number and type of friendly or enemy vehicles
- ✓ Determining types of booby traps
- ✓ Hearing the activation of perimeter alarms
- ✓ Hearing enemy movement through leaves, grass and twigs
- ✓ Determining enemy locations from the sounds of wildlife, loading of cartridges, safety locks and clipped barbed wire
- ✓ Aiding in small arms accuracy and weapons identification
- ✓ Hearing radio messages and verbal orders

Remember:

- ✓ Early signs of hearing loss include ringing in the ears and speech sounds that are muffled.
- ✓ Speech and other sounds have to be louder to be heard or understood.

Noise Level, dBA	Permitted daily exposure time
85	8 HOURS
88	4 HOURS
91	2 HOUR
94	1 HOUR
97	30 MINUTES
100	15 MINUTES
103	7.5 MINUTES

What does a Soldier with a high frequency hearing loss miss in terms of readiness?

High-pitched combat sounds!

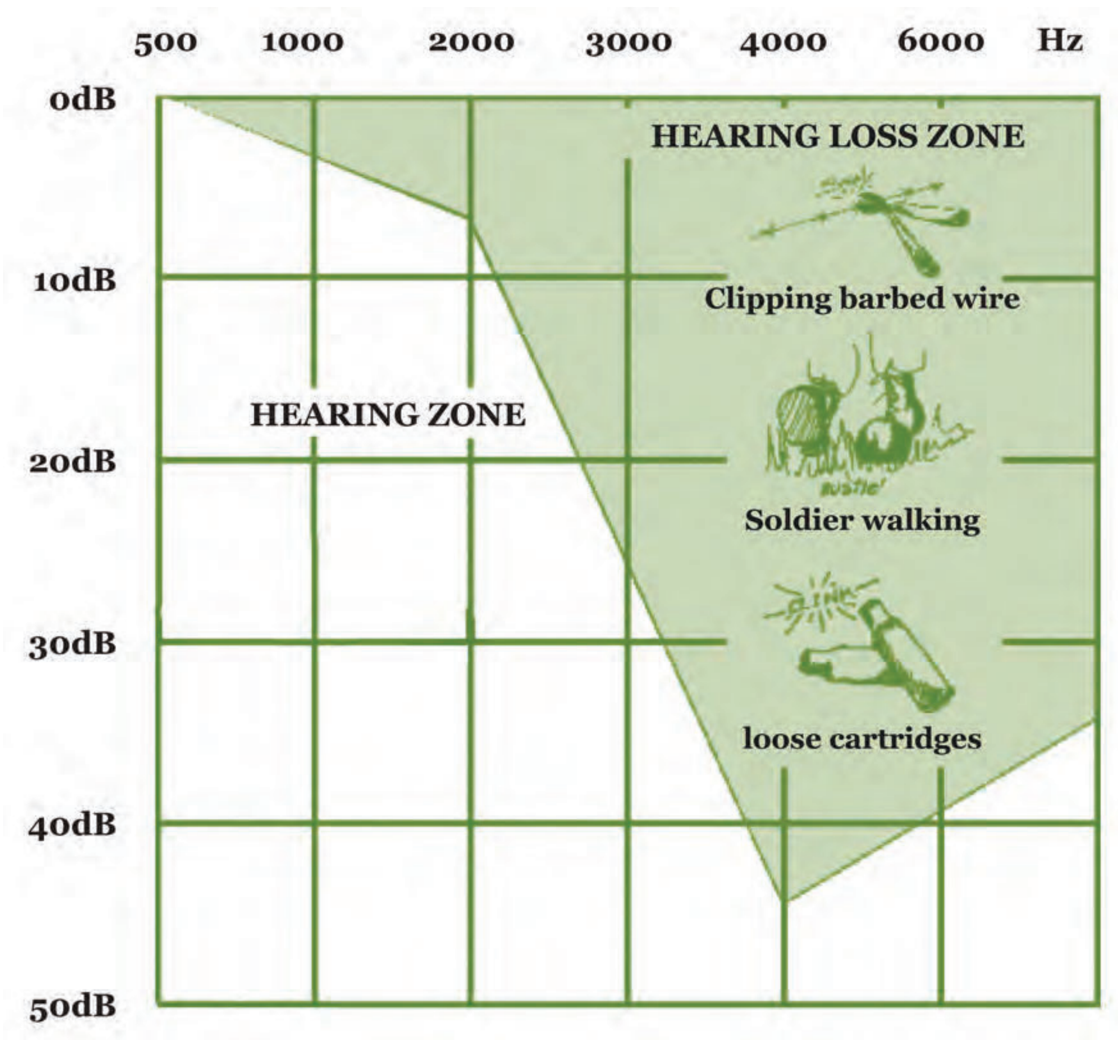

MOST NOISE-INDUCED HEARING LOSS OCCURS DURING TRAINING

HEALTH EDUCATION

✓ Each year you must receive additional training and information concerning your installation's hearing conservation program.

✓ You also have certain responsibilities as a participant in the hearing conservation program.

1. Wear your hearing protection when in hazardous noise.
2. Report for all scheduled hearing checks, including follow ups, if required.
3. Attend an annual health education briefing.
4. Maintain the engineering noise controls that are in place for your safety.

✓ Know your rights as a participant in the hearing conservation program.

1. You have the right to copy or access your hearing records.
2. You have the freedom to choose the type of hearing protective equipment you wish to wear, unless a medical reason limits your choice.
3. You have the right to copy or access the noise exposure data pertinent to your work site or duties.
4. You have the right to make suggestions that might lead to quieter equipment or less noise exposure for individuals you work with.

***The mention of any non-federal entity or its products shall not be construed or interpreted, in any manner, as federal endorsement of that non-federal entity or itsproducts.*

U.S. Army Public Health Command
Army Hearing Program
5158 Blackhawk Road (Bldg E1570)
Aberdeen Proving Ground, MD 21010-5403
Phone: DSN 584-3797 or Commercial (410) 436-3797
Fax: DSN 584-1325 or Commercial (410) 436-1325
E-mail: Usarmy.apg.medcom-phc.mbx.army.hearing-program@mail.mil
Internet: http://phc.amedd.army.mil

BEFORE THE PUBLIC UTILITY COMMISSION
OF OREGON

Docket PCN 5

In the Matter of

IDAHO POWER COMPANY'S
PETITION FOR CERTIFICATE OF PUBLIC CONVENIENCE
AND NECESSITY

Riemann, D. et al., Insomnia Disorder: State of the Science and Challenges for the Future (2022)

February 22, 2023

Received: 26 February 2022 | Revised: 23 March 2022 | Accepted: 23 March 2022
DOI: 10.1111/jsr.13604

REVIEW ARTICLE

Insomnia disorder: State of the science and challenges for the future

Dieter Riemann[1,2] | Fee Benz[1] | Raphael J. Dressle[1] | Colin A. Espie[3,4,5] | Anna F. Johann[1,6] | Tessa F. Blanken[7] | Jeanne Leerssen[8] | Rick Wassing[9] | Alasdair L. Henry[3,4,5] | Simon D. Kyle[3] | Kai Spiegelhalder[1] | Eus J. W. Van Someren[8]

[1]Department of Psychiatry and Psychotherapy, Medical Center - University of Freiburg, Faculty of Medicine, Freiburg, Germany

[2]Center for Basics in NeuroModulation (NeuroModulBasics), Faculty of Medicine, University of Freiburg, Freiburg, Germany

[3]Sir Jules Thorn Sleep and Circadian Neuroscience Institute, Nuffield Department of Clinical Neurosciences, University of Oxford, Oxford, UK

[4]Big Health Ltd, London, UK

[5]Big Health Ltd, San Francisco, California, USA

[6]Institute of Medical Psychology and Medical Sociology, Faculty of Medicine, University of Freiburg, Freiburg, Germany

[7]Department of Psychological Methods, University of Amsterdam, Amsterdam, The Netherlands

[8]Department of Sleep and Cognition, Netherlands Institute for Neuroscience, Royal Netherlands Academy of Arts and Sciences, Amsterdam, The Netherlands

[9]Centre for Integrated Research and Understanding of Sleep (CIRUS), Woolcock Institute of Medical Research, The Faculty of Medicine and Health, The University of Sydney, Sydney, New South Wales, Australia

Correspondence
Dieter Riemann, Department of Psychiatry and Psychotherapy, Medical Center - University of Freiburg, Faculty of Medicine, Hauptstrasse 5, 79104 Freiburg, Germany.
Email: dieter.riemann@uniklinik-freiburg.de

Summary

Insomnia disorder comprises symptoms during night and day that strongly affect quality of life and wellbeing. Prolonged sleep latency, difficulties to maintain sleep and early morning wakening characterize sleep complaints, whereas fatigue, reduced attention, impaired cognitive functioning, irritability, anxiety and low mood are key daytime impairments. Insomnia disorder is well acknowledged in all relevant diagnostic systems: Diagnostic and Statistical Manual of the American Psychiatric Association, 5th revision, International Classification of Sleep Disorders, 3rd version, and International Classification of Diseases, 11th revision. Insomnia disorder as a chronic condition is frequent (up to 10% of the adult population, with a preponderance of females), and signifies an important and independent risk factor for physical and, especially, mental health. Insomnia disorder diagnosis primarily rests on self-report. Objective measures like actigraphy or polysomnography are not (yet) part of the routine diagnostic canon, but play an important role in research. Disease concepts of insomnia range from cognitive-behavioural models to (epi-) genetics and psychoneurobiological approaches. The latter is derived from knowledge about basic sleep–wake regulation and encompass theories like rapid eye movement sleep instability/restless rapid eye movement sleep. Cognitive-behavioural models of insomnia led to the conceptualization of cognitive-behavioural therapy for insomnia, which is now considered as first-line treatment for insomnia worldwide. Future research strategies will include the combination of experimental paradigms with neuroimaging and may benefit from more attention to dysfunctional overnight alleviation of distress in insomnia. With respect to therapy, cognitive-behavioural therapy for insomnia merits widespread implementation, and digital cognitive-behavioural therapy may assist delivery along treatment guidelines. However, given the still considerable proportion of patients responding insufficiently to cognitive-behavioural therapy for insomnia, fundamental studies are highly necessary to better understand the brain and behavioural mechanisms underlying insomnia. Mediators and moderators of treatment response/non-response and the associated development of tailored and novel interventions also require investigation. Recent studies suggest that treatment of insomnia may prove to add significantly as a preventive strategy to combat the global burden of mental disorders.

KEYWORDS
anxiety, CBT-I, depression, insomnia, insomnia models, prevention, treatment guidelines

1 | DEFINITION AND DIAGNOSIS OF INSOMNIA DISORDER (ID)—DSM-5, ICSD-3, ICD-11

In the last 50 years all medical diagnostic classification systems have included ID. DSM (Diagnostic and Statistical Manual of the American Psychiatric Association) in its previous versions DSM-III-R/DSM-IV (American Psychiatric Association, 1987, 1998) suggested a distinction between primary and secondary insomnias, whereas DSM-5 (American Psychiatric Association, 2013) heralded a paradigmatic change by establishing ID as an overarching diagnostic category, eliminating artificial distinctions. The ICSD (International Classification of Sleep Disorders) in its third version (American Academy of Sleep Medicine, 2014) confirmed this new nosology (see Table 1; diagnostic criteria for chronic ID according to ICSD-3).

The ICD-10 (International Classification of Diseases, 10th edition; World Health Organization, 1993) distinguished between organic and non-organic sleep disorders; however, ICD-11 will follow the avenue paved by DSM-5 and ICSD-3 (World Health Organization, 2019). When analysing the "new" criteria for ID all systems list both night-time and daytime symptoms and, notably, the symptom of non-restorative sleep was dropped from the criteria due to lack of specificity.

Abandoning the distinction between primary/secondary insomnia constituted a major advance in acknowledging that insomnia frequently is not just a symptom of any other somatic or mental disorder, but constitutes an independent disorder, deserving specific consideration in clinical practice. It is important to note that insomnia probably more frequently occurs as a co-morbid condition together with somatic and mental disorders, than it does occur in its isolated form. DSM-5, ICSD-3 and ICD-11 pay respect to this by explicitly allowing co-morbidity. Furthermore, it turned out that cognitive-behavioural treatment for insomnia (CBT-I) not only has decisive effects on sleep/insomnia complaints, but also positively influences somatic/mental co-morbidities and quality of life. At present, evidence is accumulating that insomnia treatment with CBT-I may even have surplus benefits with respect to general treatment and prevention especially of mental disorders (Benz et al., 2020; Cheng et al., 2019; Hertenstein et al., 2022; Irwin et al., 2022; Leerssen et al., 2021).

Nevertheless, ID as a "one size fits all" category is seen critical by many working in the field. There is still a lively and ongoing discussion about different insomnia phenotypes, for example focussing on the main nocturnal complaint, that is, insomnia with or without "objective" short sleep (Vgontzas et al., 2013), or sleep-onset insomnia versus sleep-maintenance insomnia (Pillai et al., 2015). Indeed, the profile of dominant sleep complaints matters for the risk of developing first-onset major depressive disorder (Blanken et al., 2020). However, subtyping based on sleep characteristics may not be that robust, even across 2 nights (Johann et al., 2017), let alone across months or years (Edinger et al., 2011). Apparently, insomnia complaints change over time. More robust insomnia subtypes surfaced by multivariate profiling of personality features rather than sleep features (Blanken, Benjamins et al., 2019).

As it would be beyond the scope of this article to comprehensively describe the diagnostic and differential diagnostic procedure for insomnia, the interested reader is referred to Riemann et al. (2022) and other textbooks (Sateia & Buysse, 2010). Some important issues

TABLE 1 Diagnostic criteria for chronic ID according to ICSD-3 (AASM, 2014)

A. The patient reports, or the patient's parent or caregiver observes, one or more of the following:
   1. Difficulty initiating sleep.
   2. Difficulty maintaining sleep.
   3. Waking up earlier than desired.
   4. Resistance to going to bed on appropriate schedule.
   5. Difficulty sleeping without parent or caregiver intervention.
B. The patient reports, or the patient's parent or caregiver observes, one or more of the following related to the night-time sleep difficulty:
   1. Fatigue/malaise.
   2. Attention, concentration or memory impairment.
   3. Impaired social, family, occupational or academic performance.
   4. Mood disturbance/irritability.
   5. Daytime sleepiness.
   6. Behavioural problems (e.g. hyperactivity, impulsivity, aggression).
   7. Reduced motivation/energy/initiative.
   8. Proneness for errors/accidents.
   9. Concerns about or dissatisfaction with sleep.
C. The reported sleep/wake complaints cannot be explained purely by inadequate opportunity (i.e. enough time is allotted for sleep) or inadequate circumstances (i.e. the environment is safe, dark, quiet and comfortable) for sleep.
D. The sleep disturbance and associated daytime symptoms occur at least three times per week.
E. The sleep disturbance and associated daytime symptoms have been present for at least 3 months.
F. The sleep/wake difficulty is not better explained by another sleep disorder.

Abbreviation: ICSD-3, International Classification of Sleep Disorders, 3rd version.

concerning diagnostic procedures, however, should be highlighted here. The use of sleep diaries constitutes an integral part of insomnia assessment for both research and/or clinical purposes (e.g. consensus sleep diary by Carney et al., 2012). Sleep diaries are easy to apply and to evaluate. Sleep diaries focus on the experience of sleep and can be reviewed by the clinician as they are presented, but the inherent information can also be used to create highly informative graphical displays of sleep and bedtimes (Figure 1).

Beyond sleep diaries, other insomnia-specific questionnaires like the Insomnia Severity Index (Bastien et al., 2001) or the Sleep Condition Indicator (Espie et al., 2014) should be used.

For both clinical and fundamental research, it is favourable to take note of the recommendations for a standard research assessment of insomnia (Buysse et al., 2006). Several paradigms were developed to elucidate specific aspects of insomnia, for example, the attentional bias paradigm (Espie et al., 2006; Harris et al., 2015). This paradigm suggests that patients with chronic insomnia have developed a bias in their perception and processing of stimuli related to insomnia. Other highly promising paradigms investigate failing overnight amelioration of distress, which seems key to persistence of hyperarousal (Wassing et al., 2016; Wassing, Benjamins et al., 2019; Wassing, Lakbila-Kamal, et al., 2019; Wassing, Schalkwijk, et al., 2019). At present, not yet being ready for standard clinical practice, it is conceivable that these paradigms might be used in the future to measure responsiveness to CBT-I, also in combination with neuroimaging methods.

As the diagnosis of insomnia is solely based on subjective complaints and their measurement, it remains a matter of long-standing debate what the role of technical methods like actigraphy or polysomnography (PSG) might be. It is a highly controversial issue as to whether PSG should be part of the diagnostic process. Doubtlessly PSG helps to unravel suspected occult pathology of sleep, that is, periodic limb movements during sleep (periodic limb movement disorder) or sleep apnea (obstructive sleep apnea syndrome). US guidelines clearly deny the usefulness of PSG to diagnose insomnia (Kushida et al., 2005), whereas guidelines of the German and the European Sleep Research Society (Riemann, Baum, et al., 2017; Riemann, Baglioni, et al., 2017) suggest that PSG be used for patients with therapy-refractory insomnia who have not responded to a previous adequate "dose" of pharmaco- or psychotherapy.

The frequently described discrepancy between subjective (i.e. data from sleep diaries) and objective data (PSG) called paradoxical insomnia or sleep state misperception is seen as a major clinical and scientific challenge. PSG contrasted with subjective data does not reveal as pronounced disturbances of sleep as indicated by subjective data (Feige et al., 2008). A PSG meta-analysis revealed mean total sleep time differences between insomnia and good sleepers of about 25 min, whereas subjective estimates demonstrated an almost 2-hr difference (Baglioni, Regen, et al., 2014; Baglioni, Spiegelhalder, et al., 2014). Traditional PSG reveals only a glimpse of the brain activity during sleep. Advanced analyses have commenced to reveal electroencephalogram (EEG) correlates of subjective wakefulness during sleep, like simultaneous wake-like and sleep-like brain activity in people with insomnia (Christensen et al., 2019; Stephan et al., 2021). Furthermore, classification of individual insomnia patients based on their PSG and EEG power-spectral variables can distinguish between those with objective short sleep and those with sleep state misperception (Kao et al., 2021). Accordingly, the "misperception" may in fact be "mismeasurement": an inappropriate use or interpretation of traditional PSG features by clinicians, rather than inappropriate interpretation of subjective experiences by people with insomnia. It is important to bear in mind that these same challenges apply to mental disorders in general. There is no objective "test" for depression, anxiety or psychosis. The validation of any such tests needs to apply self-report coupled with clinical judgement as the "gold-standard."

Vgontzas and colleagues have postulated that the long-term health consequences of insomnia may be related specifically to objective short sleep duration of less than 6 hr (Vgontzas et al., 2013). However, patients with short sleep insomnia during one night do not fulfil that criteria on another night, and an increased risk of hypertension in short sleeping insomnia could not be replicated (Johann et al., 2017). Also, the hypothesis that the presence of objectively documented short sleep may be of relevance for the choice of therapy (Riemann et al., 2011), that is, pharmacotherapy for insomnia patients with objective short sleep duration versus psychotherapy for insomnia patients with objective normal sleep duration, has yet to be resolved and deserves further consideration (Vgontzas et al., 2013). More details will be provided in the aetiology/pathophysiology section. Figure 2 gives some examples of PSG determined sleep profiles of a good sleeper and two patients with ID.

2 | EPIDEMIOLOGY OF INSOMNIA AND INSOMNIA AS A RISK FACTOR FOR OTHER DISORDERS

Insomnia more frequently afflicts females than males (60% versus 40%), and its prevalence increases with age (for an overview, see Ohayon, 2002). The European Academy for CBT-I has summarized prevalence data for ID across some European countries (Baglioni et al., 2020), varying strongly from country to country. Data for Germany indicate a prevalence of 5.7%, whereas French surveys indicate figures up to 20%. On average, approximately 10% of the adult European population suffer from chronic insomnia. The heterogenous data clearly stress the need for the prospective collection of pan-European samples with state-of-the-art methods to obtain the full picture for planning of insomnia healthcare services.

The costs of insomnia for the individual and society are staggering: it was demonstrated that insomnia conveys increased risks for cardiovascular diseases (Li et al., 2014), obesity and diabetes (Anothaisintawee et al., 2016; Chan et al., 2018), depression (Baglioni et al., 2011; Hertenstein et al., 2019), anxiety (Hertenstein et al., 2019) and suicide (Pigeon et al., 2012). Wickwire (2019) reported that untreated insomnia leads to increased all-cause healthcare utilization based on a randomly selected and nationally representative sample from the USA. Data from Norway indicate that insomnia strongly predicts sick leave and disability pension (Overland

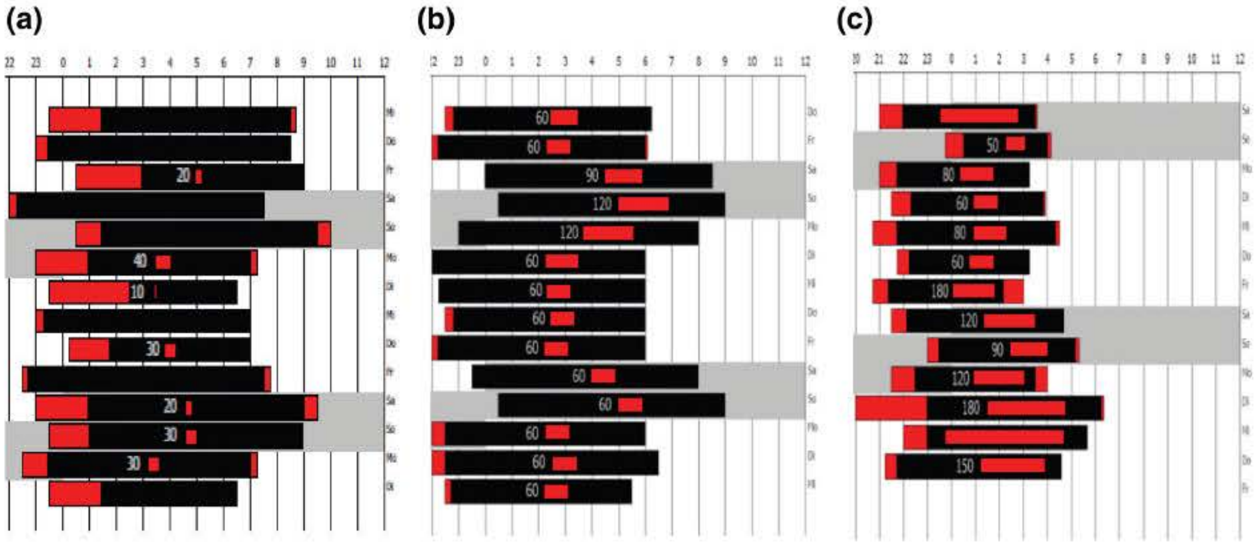

FIGURE 1 Sleep diary data from different patients with insomnia. (a) An insomnia patient who shows an increased sleep-onset latency. (b) A patient with insomnia experiencing difficulty in maintaining sleep. (c) A patient with mixed insomnia showing difficulty in both sleep onset and sleep maintenance

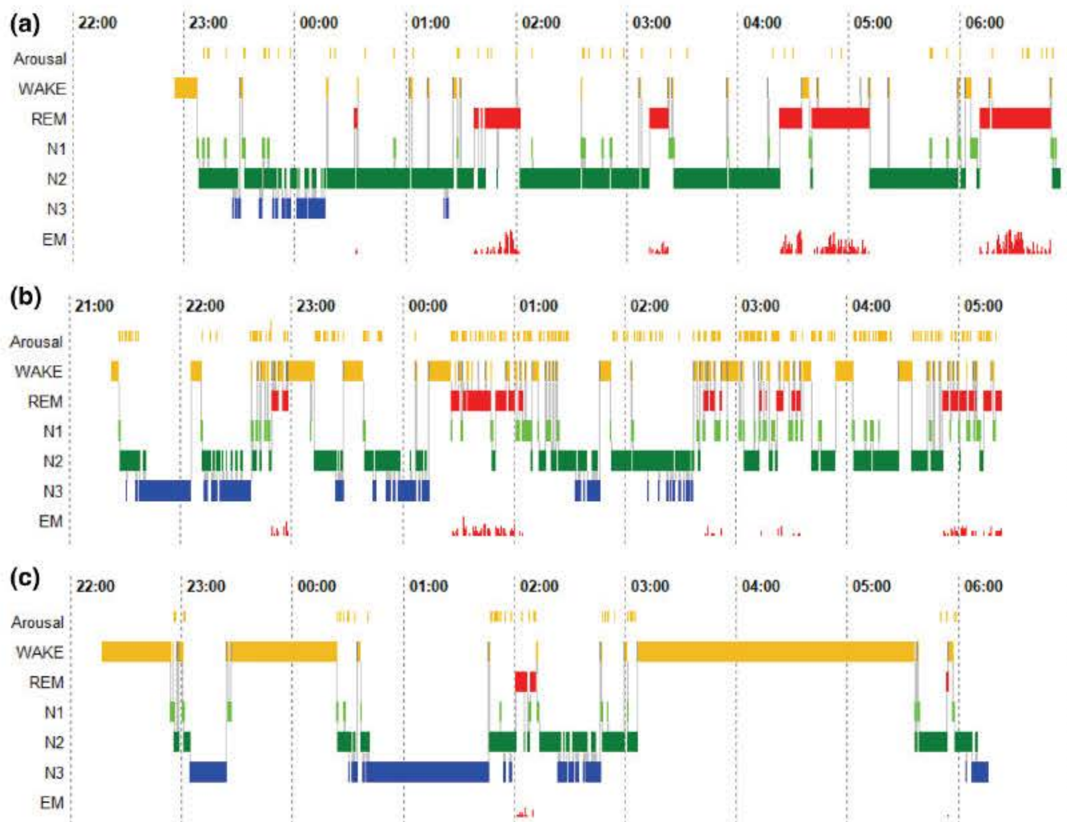

FIGURE 2 Polysomnographic (PSG) profiles of a good sleeper (upper panel; a) and patients with insomnia (lower panels; b,c). The *y*-axis displays arousal (micro-arousals), wake and sleep stages (rapid eye movement [REM], stage N1, N2 and N3) as well as eye movements. The *x*-axis is the time axis. (b) A patient with insomnia who has only a slightly reduced total sleep time, but a high number of arousals during sleep and a fragmented REM sleep. (c) A patient with insomnia who has an objectively shortened sleep duration

et al., 2008; Sivertsen et al., 2009). Data from France indicated a sum of 2 billion USD in 1995 (Leger et al., 1999). Data from the USA resulted in a sum of 150 billion US dollars for direct and indirect costs of insomnia (Reynolds & Ebben, 2017). A Canadian study (Daley et al., 2009) reported total annual costs for ID alone to be about 6.5 billion Canadian dollars. Recent data indicate that treatment using digital CBT-I reduces healthcare expenditure, and Markov health economic modelling indicates that digital CBT-I may be highly cost-effective when offered at scale (Darden et al., 2021). Further details of the costs and risks of insomnia are given in the European Academy for Cognitive Behavioural Therapy for Insomnia Report (Baglioni et al., 2020). An important clinical and research question relates to the hypothesis that adequate insomnia treatment might not only effectively target insomnia symptoms but might reduce subclinical and clinical psychopathology, and also be of general preventive value for mental disorders and physical diseases.

3 | AETIOLOGICAL AND PATHOPHYSIOLOGICAL CONSIDERATIONS

Recent reviews synthesized current neurobiological, cognitive, behavioural and emotional models for insomnia and its relationship to psychopathology (Figure 3; Espie, 2022; Riemann et al., 2020; Van Someren, 2021).

Current theoretical approaches span from cognitive-behavioural to neurobiological models, and models taking into account both levels simultaneously.

The basic structure of the model depicted in Figure 3 is taken from the so-called 3P model of insomnia (Spielman et al., 1987). The 3Ps signify: predisposing, precipitating and perpetuating factors.

"Predisposing" factors come from the areas of (epi-)genetics and early life stress that contribute to individual differences at the level of brain function and personality. Genetic and epigenetic factors have been shown to be involved in the aetiology of insomnia by family and twin studies (for an overview, see Palagini et al., 2014). Genome-wide association studies point to an involvement of a very large number of genes, each with a very small contribution, and shared genetic factors for insomnia and restless legs, cardiometabolic, and especially psychiatric traits (Jansen et al., 2019; Lane et al., 2019). Interestingly, the brain tissues and cell types expressing sets of insomnia risk genes are not primarily part of the known circuitry regulating sleep but are rather part of circuitries involved in emotion regulation (Van Someren, 2021).

Still, for completeness, a discussion on the development and maintenance of insomnia should include the neurobiological mechanisms of sleep, notably homeostatic and biological time-keeping mechanisms (Borbély, 1982). The flip-flop switch model of sleep regulation (Saper et al., 2005) suggests a bistable switch mechanism between sleep and wake promoting centres of neuronal cell groups. Wakefulness is governed by a network of cell populations in the hypothalamus (including orexinergic neurons), basal forebrain and brain stem, activating thalamus and cortical structures. These structures include and extend beyond the cell groups in the reticular formation of the brainstem (originally described as ascending reticular activating system). The main sleep-inducing centres are located in the ventrolateral-preoptic nucleus (VLPO), which becomes active during sleep and inhibits all major wake-promoting centres in the hypothalamus and brain stem, with the neurotransmitters galanin and gamma-aminobutyric acid. The VLPO receives afferent input from each of the major monoaminergic systems, and is inhibited by noradrenaline and serotonin. A mutual inhibitory circuit between both systems, the wake and the sleep system, leads to a flip-flop switch with "sharp" transitions between sleeping and waking. Thus, insomnia on this level can be conceptualized as imbalance between sleep-inducing and wake (i.e. arousal)-inducing mechanisms. A hyperactivity of the arousal system or a hypoactivity of the sleep system or both simultaneously could thus "drive" the insomnia. Circadian and homeostatic mechanisms are also involved in this switch process, and it has been speculated that a dysfunctional "key switch" (see above) could play a role in the pathogenesis of insomnia. According to the two-process model of sleep regulation (Borbély, 1982), sleep–wake behaviour is governed by circadian time-keeping mechanisms and a homeostatically controlled process S, representing the sleep drive. Being out of synchrony with the internal body clock (e.g. due to shift work) or having a decreased sleep drive would logically result in sleep complaints. Indeed, the main effective component of CBT-I, sleep restriction, is hypothesized to act on the sleep drive (Maurer et al., 2018), and long-term effectiveness of CBT-I improves with the addition of circadian interventions (Dekker et al., 2020; Leerssen et al., 2021). Notwithstanding these effects, decades of research in insomnia have failed to reveal circadian and homeostatic mechanisms as primary factors involved the origin and pathophysiology of the majority of people suffering from ID (Van Someren, 2021). One might conclude that enhancement of homeostatic sleep pressure and support of circadian rhythm amplitude alleviates insomnia, but that we may have to look beyond hourglass and clock to find underlying causes predisposing to insomnia.

A third factor involved in sleep and predisposing to insomnia is emotion (Saper et al., 2005). This factor is frequently overlooked, in spite of the ubiquitous experience that sleep initiation is difficult under threatening conditions—no matter what our hourglass and clock suggest. Indeed, from an evolutionary perspective this would be extremely disadvantageous. An increasing number of observations suggests a key role of this third factor in the origin and pathophysiology of the predisposition to insomnia (for review, see Van Someren, 2021). For example, the trait to exhibit a pronounced disturbed sleep response to stressful events has been shown to be a major risk factor for insomnia (Drake et al., 2014). Also other personality traits related to emotion regulation have been linked to insomnia, including neuroticism, perfectionism, sensitivity to anxiety symptoms, and the tendency to internalize problems (Dekker et al., 2017; van de Laar et al., 2010). The major early developmental factors predisposing to insomnia involve emotion as well: risk genes seem to have a preference for brain circuitries involved in emotion regulation, and early childhood adversity likewise affects these circuitries (Van Someren, 2021).

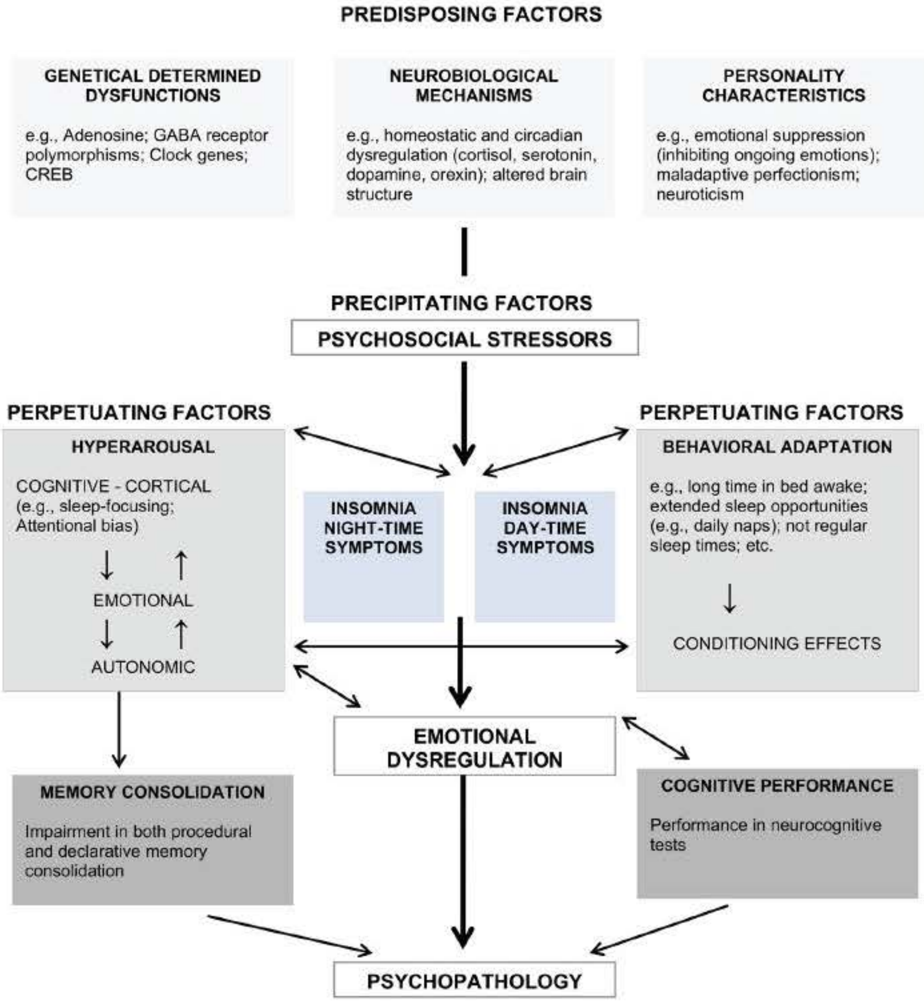

FIGURE 3 Comprehensive insomnia model (see text)

"Precipitating" factors can be readily identified in many cases. These are usually significant life events that facilitate the onset of acute episodes of insomnia. Most frequently, reported triggers of acute episodes of insomnia are stressful life events related to a threat of security to family, health and work–school living that are coupled with negative emotional valence. Fortunately, not everyone exposed to stress in adulthood develops insomnia, most likely only those that have a predisposing profile.

"Perpetuating" factors can be discussed with respect to hyperarousal, which can be conceptualized as overactivity of the arousal-promoting systems, out of balance with the activity in sleep-inducing systems. Hyperarousal includes physiological, cognitive and emotional components, and has been considered a stable characteristic of people with insomnia both during the night and during the day (Morin et al., 2015; Riemann et al., 2010, 2015). It has been demonstrated that patients with insomnia show increased levels of autonomic activity (though the issue is discussed critically with respect to heart rate variability; Dodds et al., 2017) and an overactivity of the HPA-axis, as documented by increased levels of cortisol output during day- and night-time (see meta-analysis by Dressle et al., 2022). Central nervous system (CNS) indicators of hyperarousal in people with insomnia are increased amounts of micro-arousals and increases in fast EEG frequencies (in the sigma and beta bands) during sleep (Christensen et al., 2019; Feige et al., 2013; Perlis et al., 1997, 2001; Spiegelhalder et al., 2012), and also wake EEG shows signatures of increased excitation (Colombo, Ramautar, et al., 2016; Colombo, Wei, et al., 2016) and somatic awareness and responsivity (Wei et al., 2016; Wei, Blanken, & Van Someren, 2018; Wei, Ramautar, et al., 2018). Although still too small for voxel-wise consistent findings (Tahmasian et al. 2018), the rapidly increasing number of neuroimaging studies on insomnia (Riemann et al., 2015) suggests an overactivity of cortico-limbic networks relative to sleep-promoting neuronal networks. Most interestingly, in recent years a special role of rapid eye movement (REM) sleep disturbance (REM sleep instability/restless REM sleep) has been postulated to be of utmost relevance for the experience of insomnia, and specifically their altered perception of sleep and inability to discard hyperarousal (Riemann et al., 2012; Van Someren, 2021). This lead was primarily based on the finding of increased micro-arousals during REM sleep in insomnia (Feige et al., 2008)—further studies revealed that upon awakening out of REM sleep, patients with insomnia more frequently stated having been awake compared with non-REM (NREM) sleep and good sleepers (Feige et al., 2018). Following up on these findings, Feige et al. (2021) used an event-related potentials paradigm to demonstrate that ID patients differed from good sleepers by showing reduced P2 amplitudes only in phasic REM sleep. These studies highlight a special role of REM sleep for insomnia.

The mechanisms underlying this special role of REM sleep in the predisposition, perpetuation and psychiatric consequences were addressed in a series of seminal studies (Wassing et al., 2016; Wassing, Benjamins, et al., 2019; Wassing, Lakbila-Kamal, et al., 2019; Wassing, Schalkwijk, et al., 2019). In brief, Wassing et al. showed that the restless REM sleep that is characteristic of people with insomnia interferes with overnight adaptation in limbic circuits of the brain. The consequential difficulties with dissolving of distress could be key to the development and perpetuation of hyperarousal as well to the risk of developing psychiatric disorders, as supported by other studies (Halonen et al., 2021; Pesonen et al., 2019). Restless sleep lacks the prolonged silencing of the locus coeruleus and consequential drop in cerebral noradrenaline that characterizes normal restful REM sleep (Kjearby et al., 2020). Because REM sleep is a period of pronounced limbic reactivation of emotional memory traces, it has been hypothesized that the increased level of noradrenaline during restless REM sleep interferes with the synaptic plasticity processes underlying adaptation of the neuronal engrams that represent distress, and could even result in sensitization, indicating maladaptive sleep (Van Someren, 2021). Others have proposed that the low level of noradrenaline during REM sleep is key to restore the noradrenergic tone, to enable a low tonic and high phasic locus coeruleus activity during wakefulness (Goldstein & Walker, 2014).

Restless REM sleep thus has a specific contribution to "emotional" perpetuating factors, and may explain why patients with insomnia are so prone to develop anxiety and depressive disorders in the long run. Indeed, sleep has been conceptualized as a basic psychophysiological process that is fundamental for stress, behaviour and emotion regulation (Hagger, 2010; Palmer & Alfano, 2017). Consistently, most mental disorders are associated with sleep impairment (Baglioni et al., 2016), and insomnia-related problems in children have been linked with difficulties in socio-emotional development (Sadeh et al., 2014; Vermeulen et al., 2021). In adults, insomnia has been found to be a predictor of years-long lingering of emotional distress (Wassing et al., 2016; Wassing, Lakbila-Kamal, et al., 2019), of depression, and of anxiety disorders (Baglioni et al., 2011; Hertenstein et al., 2019; Leerssen et al., 2021). Experimental studies have shown that patients with insomnia report more negative emotions than good sleepers (McCrae et al., 2008; Scott & Judge, 2006). Psychophysiological studies have also evidenced an emotional bias in people with insomnia to sleep-related stimuli with negative valence compared with good sleepers (Baglioni et al., 2010; Baglioni, Spiegelhalder, et al., 2014).

Perpetuating factors also include inadequate "behaviours", like prolonged bedtimes, irregular sleep–wake schedules, napping during the day and other maladaptive behaviours, such as using alcohol to combat insomnia. Usually, these strategies are attempted to compensate for lost sleep; however, in the end insomnia is maintained and exacerbated by decreasing sleep drive.

In addition, "cognitive perpetuating factors" have been identified, such as beliefs, worry and attentional bias (Espie, 2002; Harvey, 2002; Morin et al., 2007). These cognitions include unrealistic beliefs about sleep requirements and excessive worry for not meeting these standards. In recent years, the literature has emphasized the role of selective attention processes in people with insomnia. Specifically, it has been argued that the attentional system of patients with insomnia may be abnormally sensitive to sleep-related information (Harris et al., 2015). It has been hypothesized that such attention bias may exacerbate sleep-related rumination and lead to sleep effort (Espie et al., 2006; Harvey, 2002).

Summarizing, acute precipitating life events can "set the wheels in motion"—acute insomnia is triggered. The question of why most individuals who develop acute insomnia do not go on to develop the chronic condition has not yet been clarified (Ellis et al., 2012)—but likely involves genetic and early life stress-induced neurobiological vulnerability to keep "the train rolling." A complex network of associated symptoms including cognitive-, emotional- and cerebral hyperarousal, unstable REM sleep and maladaptive behaviours will keep the furnace burning. Sleep-preventing learned associations (conditioning effects) are strongly involved in this process as well, giving credit to Bootzin's assumption that in insomnia the original connection between the bed (stimulus) and the behaviour of sleep (response) has been lost or "unlearned" (Bootzin et al., 1991).

The CBT-I (see below) mainly targets the perpetuating factors, for example, relaxation techniques and mindfulness aim to address psychophysiological hyperarousal; sleep hygiene, stimulus control and sleep restriction try to correct maladaptive behaviours and enhance sleep drive; whereas cognitive strategies aim to alter "racing thoughts", dysfunctional beliefs and attitudes, and to reduce nocturnal worrying and ruminations.

4 | TREATMENT (S)—FOCUS ON PSYCHOLOGICAL APPROACHES: PRESENT GUIDELINES, WHAT IS CBT-I, STEPPED CARE AND DIGITAL CBT-I?

All insomnia-related guidelines published in the last 5 years agree that CBT-I should be the first-line treatment for insomnia, based on the accumulated scientific evidence from the literature. These guidelines include the American College of Physicians (Brasure et al., 2016; Kathol & Arnedt, 2016; Qaseem et al., 2016; Wilt et al., 2016), the American Academy of Sleep Medicine (AASM; Edinger et al., 2021a, b), the German and the European Sleep Society (Riemann, Baum, et al., 2017; Riemann, Baglioni, et al., 2017), and the British Association for Psychopharmacology consensus statement (Wilson et al., 2019). Overall, these guidelines make a strong case for CBT-I as first-line treatment for insomnia, and hypnotics are recommended for short-term use and only if CBT-I is either not available or ineffective. As hypnotics in this context, melatonin agonists, benzodiazepines, benzodiazepine receptor antagonists, some sedating antidepressants and orexin receptor antagonists are recommended mainly for short-term use (less than 4 weeks) only. An overview of the present state of hypnotic treatment can be found in reviews (Herring et al., 2019; Riemann & Nissen, 2012; Roehrs & Roth, 2012).

The CBT-I comprises a family of interventions and is not "one" homogenous therapeutic strategy *per se* (Table 2).

The CBT-I is in essence a multicomponent approach, comprising cognitive and behavioural parts, within each of which domain there is a wide range of treatment options. The principal behavioural therapies are sleep restriction and stimulus control. Cognitive techniques include reappraisal, cognitive control and paradoxical intention. There is also a range of relaxation therapies, and sleep hygiene education, although not effective as a standalone treatment, is commonly part of the CBT-I toolkit. A brief description of these techniques is given in the table. For further details, the interested reader is referred to a new CBT-I textbook that will be published in 2022 (Baglioni et al., 2022). A new clinician handbook on insomnia will also be available shortly (Espie, 2022).

Logically therefore CBT-I is not "a treatment" but is "a system of cognitive and behavioural therapeutics", akin to pharmacotherapy (which is not a drug treatment but a "pharmaceutical approach" to clinical care; Espie, 2022). The history of evidence-based psychotherapy (in most disorders) reveals a period of time during which there was a tendency towards "lumping" of therapeutic elements, rather than the creation of precision techniques that "may" be used in combination. This is certainly true of the non-pharmacological management of insomnia, and the term CBT-I has for the past 20 years or more been used rather generically in the literature because the majority of studies have deployed a CBT-I package.

In earlier times there was a focus upon more specific interventions. For example, comparing the effectiveness of abbreviated progressive relaxation, stimulus control therapy and paradoxical intention (Espie et al., 1989), or even investigating components of a single therapy (Woolfolk & McNulty, 1983: compared progressive relaxation, progressive relaxation without tension release, imagery with tension release, and imagery without tension release). Interestingly, of late, there has been renewed interest in single-component therapies. We now find ourselves unpicking or deconstructing CBT to evaluate its active component treatments, and even its active treatment ingredients. The best example is sleep restriction therapy (SRT), widely regarded to be the most effective element of CBT (Edinger et al., 2021a; Maurer, Schneider et al., 2021). A series of laboratory-based experiments has recently explored the homeostatic, arousal and circadian mechanisms of sleep restriction (Maurer et al., 2020, 2022; Maurer, Ftouni et al., 2021).

In support of this is the fact that CBT protocols are effective even when they vary. The AASM practice parameters task force recently grappled with the question, what are the "minimal characteristics" of effective CBT (Edinger et al., 2021a). They concluded that "all studies included SRT, stimulus control and some form of cognitive therapy"; however, the cognitive component varied widely. Whether or not relaxation strategies or sleep hygiene were included in the CBT-I regimen varied across studies as well. It was beyond the scope of this (group) to recommend a specific CBT protocol, and "these variations did not appear to systematically impact the effectiveness of the treatment" (p. 261). This evidences the versatility and robustness of what is sometimes now referred to as CBTx (cognitive and behavioural therapeutics), that is, a "therapeutic formulary", where not everyone needs the same content, or the same order of content (Espie, 2022). Analysis of how SRT is configured suggests there is gross variability between studies and protocols (Kyle et al., 2015); it would be prudent to establish what is the most effective combination of SRT parameters, including tailoring to presenting insomnia phenotype. Indeed, the widespread development of "precision medicine" (Ginsburg & Willard, 2009; Jain, 2002) has spawned interest in how "personalized behavioural sleep medicine" for insomnia may evolve in the future (Kyle et al., 2014).

Despite the impressive evidence base for CBT-I, its recognition internationally as the treatment of first choice for the management of insomnia and the fact that the CBTx formulary of treatments is quite wide ranging, in practice the majority of insomnia patients seeking medical help continue to receive medication. The issue here is not so much overprescribing of drugs as it is under-provision of CBT-I. Two innovations have been developed to address this problem. The first, at the level of the treatment itself there has been growing interest in, and a rapidly accelerating evidence base for digital CBT-I, that is CBT-I delivered by fully automated web and mobile means. The second, at the level of the service, has been the development of the "stepped care" model of insomnia service delivery.

The effectiveness of digital CBT-I has been robustly and rigorously demonstrated against psychological placebo (Espie et al., 2012), attention control (Christensen et al., 2016; Kaldo et al., 2015), sleep hygiene (Espie et al., 2019; Ritterband et al., 2017; Vedaa et al., 2020), waitlist (Zachariae et al., 2018) and usual care (Freeman et al., 2017) in a range of clinical and co-morbid populations. Several meta-analyses report large between-group effects on insomnia severity, and medium effects on sleep diary outcomes (Seyffert et al., 2016; Soh et al., 2020; Zachariae et al., 2016), and benefits to sleep are durable, being maintained up to a year and beyond (Blom et al., 2017; Luik et al., 2020; Vedaa et al., 2019). Whereas meta-analyses report effect sizes in the range of face-to-face CBT-I thereby suggesting non-inferiority, head-to-head comparisons have shown mixed findings (Blom et al., 2015; De Bruin et al., 2016; Kallestad et al., 2021; Lancee et al., 2016). It seems likely, however, that the evolution of highly engaging clinically evidenced software will address engagement and treatment implementation challenges that are apparent for all forms of CBT-I delivery. It may also be the case that differences exist between different digital CBT-I formats (Hasan et al., 2022). These outstanding questions warrant further investigation.

Beyond improved sleep, digital CBT-I, like "traditional" CBT-I, yields benefits to additional clinical and functional outcomes of relevance to insomnia. Several studies have documented reductions in symptoms of anxiety and depression, including in individuals with clinically significant depressive symptoms (Blom et al., 2015, 2017; Cheng et al., 2019; Henry et al., 2021; Pillai et al., 2015; van der Zweerde

TABLE 2 CBT-I ingredients (from Baglioni et al., 2020)

CBT-I strategy	Description
Sleep restriction	*Behavioural strategy*: A method that aims at strengthening homeostatic sleep pressure and stabilizing circadian control of sleep and wakefulness, by decreasing the opportunity to sleep over successive nights. Patients are instructed to restrict their time in bed to match their average (self-report in sleep diaries) total sleep duration. The time in bed is then gradually increased until reaching patients' optimal sleep need. An alternative method, called *sleep compression*, consists in gradual constriction of time in bed until reaching the optimal sleep need.
Stimulus control	*Behavioural strategy*: Several instructions aiming at strengthening the bed as a cue for sleep, weakening it as a cue for activities that might interfere with sleep, and helping the insomniac acquire a consistent sleep rhythm, based on operant conditioning model: (1) lie down to go to sleep only when you are sleepy; (2) do not use your bed for anything except your sleep and sexual activity; (3) if you find yourself unable to fall asleep, get up and go to another room. Stay up as long as you wish, and come back to bed when you feel sleepy; (4) If you still cannot fall asleep, repeat step (3). Do this as often as is necessary throughout the night; (5) Set your alarm and get up at the same time every morning irrespective of how much sleep you got during the night; (6) no napping during daytime.
Sleep hygiene education	Behavioural and educational strategy: General health instructions about internal and external factors that might influence sleep (e.g. sport, light, temperature, etc.).
Relaxation	Behavioural and cognitive strategy: A set of methods aiming at reducing somatic or cognitive hyperarousal (e.g. progressive muscle relaxation, autogenic training, imagery training, meditation).
Cognitive reappraisal	Cognitive strategy: Strategies directed to reduce dysfunctional beliefs, attitudes, concerns and false beliefs about the cause of insomnia and about the inability to sleep.
Cognitive control/ Worry time	Cognitive strategy: The patient is instructed to sit comfortably in an armchair, and write down a list of worries and list of what to do the next day. The rationale of this strategy is to prevent emotionally loaded intrusive thoughts during the sleep-onset period, as all worries have been "already" processed before going to bed.
Paradoxical intention	Cognitive strategy: Strategy aimed at reducing the anticipatory anxiety at the time of falling asleep. Patients are instructed to remain still in bed with the eyes closed and to try to keep awake as long as they can. This takes away the responsibility to try to fall asleep, which in turn often leads to falling asleep quicker.

Abbreviation: CBT-I, cognitive-behavioural treatment for insomnia.

et al., 2019). From a scientific perspective, digital CBT-I confers advantages such that it permits examination of potential mediators of treatment effects using a standardized therapeutic approach. Large randomized-controlled trials and secondary analyses show that insomnia symptom reduction mediates improvements in mental health symptoms (Freeman et al., 2017; Henry et al., 2021), and improvements in quality of life, health and wellbeing, and cognitive function (Espie et al., 2019; Kyle, Hurry, et al., 2020). This evidence therefore supports treating insomnia complaints whenever it presents. Emerging data also suggest that demographic variables including age, race, gender or socio-economic status do not moderate the effectiveness of digital CBT-I (Cheng et al., 2019).

Real-world evidence further underscores the value of digital CBT-I. Recent uncontrolled data evaluating digital CBT-I in existing healthcare settings in the UK show reductions in insomnia and augmentation of the effects of in-person therapy for anxiety and depression (Cliffe et al., 2020; Luik et al., 2017; Stott et al., 2021). Importantly, from a health economic perspective, analyses suggest that digital CBT-I is cost-effective, and may lead to cost savings if made available at scale (Darden et al., 2021; Sampson et al., 2021). This growing body of evidence behind digital CBT-I has led to increased recognition of it as a viable and effective treatment option. Indeed, in the USA, Somryst has been cleared by the FDA as a prescription digital therapeutic (Morin, 2020). Likewise, Sleepio (www.sleepio.com) is widely available in the USA, integrated into healthcare pathways and on the digital formulary, and is available in major parts of the UK National Health Service.

By overcoming the barriers preventing access to therapist-delivered CBT-I, digital CBT-I has the potential to provide access to clinically effective, evidenced-based and guideline-recommended insomnia treatment. These fundamental properties of effectiveness and scalability make digital CBT-I attractive as a first-line insomnia intervention, providing an accessible alternative to pharmacotherapy (Figure 4).

The stepped-care model is a population health service approach to providing people with insomnia with access to evidence-based care (Espie, 2009; Espie et al., 2013). Stepped care is often conceptualized as a pyramid consisting of different levels, with at the bottom the least specialized help applicable for those with less severe and more generic complaints and highly specialized help for those with more severe, complex and rare problems as the top. The level of intervention is naturally not arbitrary; treatment is tailored to and based on the needs of the patient and the nature of their complaints. The number of steps in any stepped care model would be determined by the levels of intervention that are proven and available, and by what within the healthcare system would be affordable. Stepped care models have been recommended for use in insomnia (Baglioni et al., 2020, 2022), and are sometimes adopted in healthcare systems (Vincent & Walsh, 2013).

With regard to insomnia, therefore, digital CBT might be particularly suitable to be one of the entry-level methods for the treatment

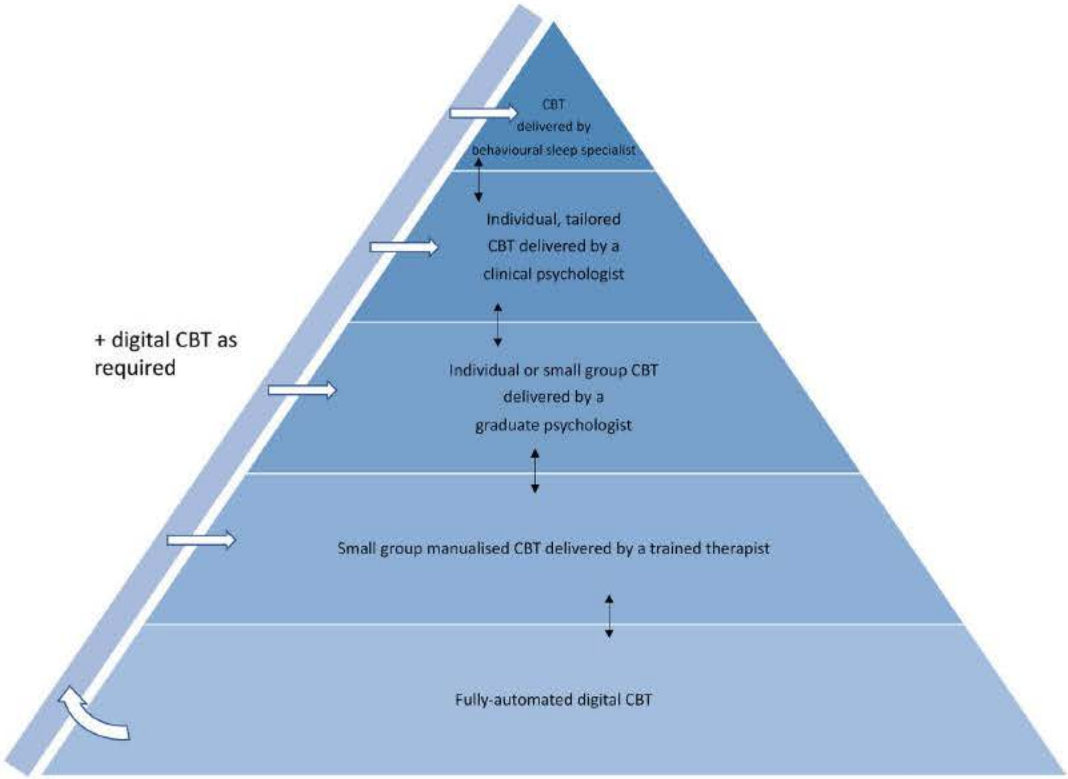

FIGURE 4 A proposed stepped care model for delivery of cognitive-behavioural therapy (CBT) as clinical guideline care. Digital CBT offers accessible treatment for all, but also may be integrated into the care pyramid supporting in-person therapy. The stepped care model conserves expert resources for more complex and treatment-resistant cases

of insomnia, as it has considerable "scalability", particularly when fully automated. Another approach at this level might be using self-help books of good standing, perhaps as part of a "books on prescription" scheme. Next in the hierarchy might be insomnia services that require some in-person support, but thought would be given to how such care could be provided with efficiency. Examples here might include telehealth rather than in a clinic, and the use of small group therapy rather than individual treatment. Other factors to be considered would be the nature of the treatment itself and the expertise of the therapist. For example, it could be possible to train healthcare workers in the provision of manualized CBT-I without them having to have a deep understanding of sleep medicine or mental health (training primary care nurses, for example). This approach is very protocol-driven and can be readily standardized (Kyle, Madigan, et al., 2020). As you then continue up the hierarchy there is greater need for insomnia-specific expertise and for the use of tailored therapy. At the peak of the pyramid the likelihood is that not only specialist expertise but also specialized facilities such as those available at a sleep centre may be required to address the needs of the most complex patients.

Stepped care systems require decision algorithms for two processes. First, to ensure that people are correctly allocated to the appropriate level of care in the first instance; and secondly, to ensure that people are able to step up to more advanced care depending on their treatment response.

5 | FUTURE PERSPECTIVES WITH RESPECT TO DIAGNOSIS, MEASUREMENT, AETIOLOGY AND PATHOPHYSIOLOGY; NEW TREATMENTS

Given the drastic changes we have been witnessing concerning insomnia and its diagnosis, pathophysiology/aetiology and treatment in the last 30 years, one might be tempted to answer the question "Can we rest yet?" (Harvey & Tang, 2003) with "Yes!." However, this would be premature and inadequate with respect to the many open questions still facing us in the insomnia field. Therefore, at this point, we would like to highlight some issues/avenues for future research and clinical practice we consider of utmost importance.

Given the fact that at present we have reached the unique situation that all major diagnostic systems (DSM-5, ICSD-3, ICD-11) have agreed upon ID (American Academy of Sleep Medicine, 2014; American Psychiatric Association, 2013; World Health Organization, 2019), the situation seems ideal that all types of studies into ID use more or less the same diagnostic criteria, which would be ideal to make data coming from all over the world easily comparable. This would also entail homogenization of our diagnostic and research instruments (questionnaires, PSG, etc.). However, as mentioned before, there definitely are different insomnia phenotypes that should not be neglected. A data-driven approach to delineate and characterize these phenotypes seems warranted (Blanken, Benjamins, et al., 2019; Kao et al., 2021), possibly further refined by adding physiological data by means of PSG to questionnaire datasets.

In this regard, pooling data from different sleep labs could be beneficial in order to address the issues of small sample sizes and poor replicability in the insomnia field. This would require the use of standard methodology and paradigms across different labs. The UK Biobank (www.ukbiobank.ac.uk; see Allen et al., 2014 for a detailed description), a large biomedical database including a sample of about 500,000 adults, has already proven to be useful for insomnia research (Jansen et al., 2019; Kyle et al., 2017; Lane et al., 2019). Although the UK Biobank is not specifically optimized for insomnia research, cross-validation showed the available phenotype to very accurately match diagnosed insomnia patients (Hammerschlag et al., 2017).

Given the costs and artificiality of the traditional sleep laboratory, home-based easy to apply measures need to be developed, allowing repetitive CNS-based measurements in the natural environments of our patients, reaching beyond actigraphy (Debener et al., 2015; Mikkelsen et al., 2019). This would allow to study the dynamics of features reflecting the sleep drive and REM sleep characteristics longitudinally and in relation to different treatments and their outcomes in much more detail.

Given the prominence of the hyperarousal concept in almost all insomnia models, one should also start to think about developing a hyperarousal test, which at best could be applied during daytime or routine office/hospital hours. One could think about a stress/challenge paradigm, measuring autonomous nervous system activity (e.g. heart rate, galvanic skin response, etc.), cortisol as main marker of the stress response and EEG during baseline, rest and different stress conditions. One of the best accepted stress paradigms now is the Trier social stress test—its usefulness has already been tested (Chen et al., 2017). Alternatively, probably just the instruction "please try to sleep now" probably might offset a marked stress response in insomniacs. Such a psychophysiological paradigm administered during the day can also easily be coupled with neuroimaging methods, that is, functional magnetic resonance imaging. Needless to say, these data should be coupled with descriptive questionnaire data. Assuming that it will be possible to develop an easy to apply and valid hyperarousal test, this instrument could be used for phenotyping, relating the data to (epi-)genetic data, general diagnostics, differential-therapeutics and therapy outcomes. Given the emerging evidence of maladaptive sleep (Van Someren, 2021), essential insights could require repeated assessment of hyperarousal from evening to morning across recorded nights. Analyses can then address which sleep features determine the overnight fate of distress—which could range from full adaptation even to maladaptive sensitization (Wassing, Benjamins, et al., 2019; Wassing, Lakbila-Kamal, et al., 2019). Nevertheless, deeper insights into the mechanisms of hyperarousal in insomnia, its causes and consequences for cognitive processes and brain health in general are needed. This will help to further increase the value of the hyperarousal concept for insomnia research and could also help to identify a valid hyperarousal test.

Interestingly, also with therapeutics at present we have reached a unique situation concerning treatment—all presently published relevant guidelines agree that CBT-I should be the first-line treatment for insomnia. A statement like this would have caused a lot of many raised eyebrows even just 10 years ago! This development is probably because on one hand, the CBT-I literature is blooming and has generated a solid and ever-increasing evidence base, but on the other hand maybe also due to a stagnation in the sector of hypnotic development and the withdrawal of many major players in psychopharmacology from CNS-oriented Research & Development. It has to be judged in the next few years whether the worldwide introduction of orexin receptor antagonists will markedly alter the hypnotic market. From a future perspective, we would like to suggest that research into the roles of histamine and noradrenaline and sleep regulation could lead to new discoveries (Thakkar, 2011; Van Someren, 2021). Maybe also approaches encompassing non-invasive brain stimulation might complement insomnia treatment strategies (Herrero Babiloni et al., 2021).

A better understanding of the psychoneurobiological mechanisms of insomnia is urgently needed to monitor and evaluate treatment effects of CBT-I beyond subjective measures, and further develop complementary treatment strategies. First, preliminary findings suggest that 1 night of experimental sleep restriction (delaying bedtime by 2 hr) may help to stabilize restless REM sleep (Kao et al., 2021). However, it remains to be seen whether this stabilization is observed in therapeutic SRT, and whether it translates into improvements in regulation of emotional distress, hyperarousal and the risk of developing mental disorders. Second, notwithstanding the established efficacy of CBT-I, it is important to acknowledge that two out of five patients do not show full remission, even after boosting CBT-I effects with subsequent pharmacological treatment (Morin et al., 2020). We still have very limited insight into who will respond and who will not. Novel graph theory-based analyses like network outcome analysis and network intervention analysis may reveal how non-responders differ in their initial symptom profiles and trajectories of change of symptoms during the intervention (Blanken, Benjamins, et al., 2019; Blanken et al., 2020; Blanken, van der Zweerde, et al., 2019). Pinpointing such differences could provide leads to novel strategies.

Also the gradual wearing off of initial benefits of CBT-I deserves attention (van der Zweerde et al., 2019). Two recent studies indicate that beneficial effects of CBT-I may be preserved longer if CBT-I is combined with interventions aimed at supporting circadian rhythms (Dekker et al., 2020; Leerssen et al., 2021).

What we consider probably the most important challenge for the future is the integration of CBT-I into the standard treatment of patients with mental disorders, especially anxiety and depression. It is known that almost all mental disorders are afflicted with disturbances of sleep continuity (Baglioni et al., 2016), and we also know that paying proper therapeutic respect to including insomnia-related components into the overall therapeutic concept will improve outcomes in general and speed up the therapeutic process (Gee et al., 2019; Hertenstein et al., 2022; Manber et al., 2008). Models how to do this have been suggested by several authors (Kraepelien et al., 2022; Schneider et al., 2020)—thus, the times seem right to postulate insomnia as a transdiagnostic mechanism for mental disorders (Harvey et al., 2011, 2021; Van Someren, 2021) and also insomnia treatment based on CBT-I as a basic mode in psychiatric/psychotherapeutic treatment.

One step further will address the primary prevention of mental disorders. There is a strong probability that adequate insomnia treatment will reduce the incidence and recurrence of depressive episodes and anxiety disorders (Benz et al., 2020; Cheng et al., 2019; Irwin et al., 2022; Leerssen et al., 2021). In a first step, one might address risk groups especially prone to mental illness and offer sleep treatment versus a control condition and compare longitudinal outcomes, as recently demonstrated by Leerssen et al. (2021). In a next step it might be tested whether educating and training of the general population to utilize the principles that underlie CBT-I could prevent insomnia. Such efforts may be especially relevant to prevent mental disorders that tend to surface during important transition periods, like in students moving from high school to university.

CONFLICT OF INTEREST

Dieter Riemann is a member of the Executive Board of FAVT (Freiburg Institute for Behavioural Therapy/non for profit), a salaried activity. He is Editor-in-Chief of the *Journal of Sleep Research*, which is owned by the European Sleep Research Society (non-profit body) and receives payments for this task. Dieter Riemann receives royalties from publishing and honoraria for lecturing (no pharmaceutical industry), and is funded by several grants from the German Federal state. Colin A. Espie reports research support from NIHR-HTA (UK), receiving payments from book publishing and lecture fees. He also reports being a cofounder and Chief Scientist of Big Health Ltd (the developer of Sleepio). He is a shareholder of and receiving salary from Big Health. Alasdair L. Henry is employed by, receives a salary from and is a shareholder of Big Health. All other authors report no conflicts of interest.

AUTHOR CONTRIBUTIONS

Dieter Riemann provided an outline of the article and did the final editing. All the other authors contributed equally.

DATA AVAILABILITY STATEMENT

N/A

ORCID

Dieter Riemann https://orcid.org/0000-0002-1968-6220
Raphael J. Dressle https://orcid.org/0000-0001-9408-5196
Colin A. Espie https://orcid.org/0000-0002-1294-8734
Anna F. Johann https://orcid.org/0000-0001-7816-6658
Alasdair L. Henry https://orcid.org/0000-0003-2217-3052
Kai Spiegelhalder https://orcid.org/0000-0002-4133-3464
Eus J. W. Van Someren https://orcid.org/0000-0002-9970-8791

REFERENCES

Allen, N. E., Sudlow, C., Peakman, T., & Collins, R. (2014). UK Biobank data: Come and get it. *Science Translational Medicine*, *6*(224), 224ed4. https://doi.org/10.1126/scitranslmed.3008601

American Academy of Sleep Medicine. (2014). *International classification of sleep disorders* (3rd. ed.). American Academy of Sleep Medicine.

American Psychiatric Association. (1987). *Diagnostic and statistical manual of mental disorders* (3rd ed.). American Psychiatric Association.

American Psychiatric Association. (1998). *Diagnostic and statistical manual of mental disorders (DSM-IV)* (4th ed.). American Psychiatric Association.

American Psychiatric Association. (2013). *Diagnostic and statistical manual of mental disorders* (5th ed.). American Psychiatric Association.

Anothaisintawee, T., Reutrakul, S., Van Cauter, E., & Thakkinstian, A. (2016). Sleep disturbances compared to traditional risk factors for diabetes development: Systematic review and meta-analysis. *Sleep Medicine Reviews*, *30*, 11–24. https://doi.org/10.1016/j.smrv.2015.10.002

Baglioni, C., Altena, E., Bjorvatn, B., Blom, K., Bothelius, K., Devoto, A., … Riemann, D. (2020). The European Academy for Cognitive Behavioural Therapy for Insomnia: An initiative of the European insomnia network to promote implementation and dissemination of treatment. *Journal of Sleep Research*, *29*(2), e12967. https://doi.org/10.1111/jsr.12967

Baglioni, C., Battagliese, G., Feige, B., Spiegelhalder, K., Nissen, C., Voderholzer, U., … Riemann, D. (2011). Insomnia as a predictor of depression: A meta-analytic evaluation of longitudinal epidemiological studies. *Journal of Affective Disorders*, *135*(1–3), 10–19. https://doi.org/10.1016/j.jad.2011.01.011

Baglioni, C., Espie, C. A., & Riemann, D. (2022). *Cognitive-behavioural therapy for insomnia (CBT-I) across the lifespan. Guidelines and clinical protocols for health professionals*. Wiley & Sons (in press).

Baglioni, C., Lombardo, C., Bux, E., Hansen, S., Salveta, C., Biello, S., … Espie, C. A. (2010). Psychophysiological reactivity to sleep-related emotional stimuli in primary insomnia. *Behaviour Research and Therapy*, *48*(6), 467–475. https://doi.org/10.1016/j.brat.2010.01.008

Baglioni, C., Nanovska, S., Regen, W., Spiegelhalder, K., Feige, B., Nissen, C., … Riemann, D. (2016). Sleep and mental disorders: A meta-analysis of polysomnographic research. *Psychological Bulletin*, *142*(9), 969–990. https://doi.org/10.1037/bul0000053

Baglioni, C., Regen, W., Teghen, A., Spiegelhalder, K., Feige, B., Nissen, C., & Riemann, D. (2014). Sleep changes in the disorder of insomnia: A meta-analysis of polysomnographic studies. *Sleep Medicine Reviews*, *18*(3), 195–213. https://doi.org/10.1016/j.smrv.2013.04.001

Baglioni, C., Spiegelhalder, K., Regen, W., Feige, B., Nissen, C., Lombardo, C., … Riemann, D. (2014). Insomnia disorder is associated with increased amygdala reactivity to insomnia-related stimuli. *Sleep*, *37*(12), 1907–1917. https://doi.org/10.5665/sleep.4240

Bastien, C. H., Vallières, A., & Morin, C. M. (2001). Validation of the insomnia severity index as an outcome measure for insomnia research. *Sleep Medicine*, *2*(4), 297–307. https://doi.org/10.1016/s1389-9457(00)00065-4

Benz, F., Knoop, T., Ballesio, A., Bacaro, V., Johann, A. F., Rücker, G., … Baglioni, C. (2020). The efficacy of cognitive and behavior therapies for insomnia on daytime symptoms: A systematic review and network meta-analysis. *Clinical Psychology Review*, *80*, 101873. https://doi.org/10.1016/j.cpr.2020.101873

Blanken, T. F., Benjamins, J. S., Borsboom, D., Vermunt, J. K., Paquola, C., Ramautar, J., … Van Someren, E. J. W. (2019). Insomnia disorder subtypes derived from life history and traits of affect and personality. *Lancet Psychiatry*, *6*(2), 151–163. https://doi.org/10.1016/S2215-0366(18)30464-4

Blanken, T. F., Borsboom, D., Penninx, B. W., & Van Someren, E. J. (2020). Network outcome analysis identifies difficulty initiating sleep as a primary target for prevention of depression: A 6-year prospective study. *Sleep*, *43*(5), zsz288. https://doi.org/10.1093/sleep/zsz288

Blanken, T. F., van der Zweerde, T., Van Straten, A., Van Someren, E. J. W., Borsboom, D., & Lancee, J. (2019). Introducing network intervention analysis to investigate sequential, symptom-specific treatment effects: A demonstration in co-occurring insomnia and depression. *Psychotherapy and Psychosomatics*, *88*(1), 52–54. https://doi.org/10.1159/000495045

Blom, K., Jernelöv, S., Rück, C., Lindefors, N., & Kaldo, V. (2017). Three-year follow-up comparing cognitive behavioral therapy for depression to cognitive behavioral therapy for insomnia, for patients with both diagnoses. *Sleep*, *40*(8). https://doi.org/10.1093/sleep/zsx108

Blom, K., Tarkian Tillgren, H., Wiklund, T., Danlycke, E., Forssén, M., Söderström, A., … Kaldo, V. (2015). Internet-vs. group-delivered cognitive behavior therapy for insomnia: A randomized controlled non-inferiority trial. *Behaviour Research and Therapy*, *70*, 47–55. https://doi.org/10.1016/j.brat.2015.05.002

Bootzin, R. R., Epstein, D., & Wood, J. M. (1991). Stimulus control instructions. In P. J. Hauri (Ed.), *Case studies in insomnia* (pp. 19–28). Springer US. https://doi.org/10.1007/978-1-4757-9586-8_2

Borbély, A. A. (1982). A two process model of sleep regulation. *Human Neurobiology*, *1*(3), 195–204.

Brasure, M., Fuchs, E., MacDonald, R., Nelson, V. A., Koffel, E., Olson, C. M., … Kane, R. L. (2016). Psychological and behavioral interventions for managing insomnia disorder: An evidence report for a clinical practice guideline by the American College of Physicians. *Annals of Internal Medicine*, *165*(2), 113–124. https://doi.org/10.7326/M15-1782

Buysse, D. J., Ancoli-Israel, S., Edinger, J. D., Lichstein, K. L., & Morin, C. M. (2006). Recommendations for a standard research assessment of insomnia. *Sleep*, *29*(9), 1155–1173. https://doi.org/10.1093/sleep/29.9.1155

Carney, C. E., Buysse, D. J., Ancoli-Israel, S., Edinger, J. D., Krystal, A. D., Lichstein, K. L., & Morin, C. M. (2012). The consensus sleep diary: Standardizing prospective sleep self-monitoring. *Sleep*, *35*(2), 287–302. https://doi.org/10.5665/sleep.1642

Chan, W. S., Levsen, M. P., & McCrae, C. S. (2018). A meta-analysis of associations between obesity and insomnia diagnosis and symptoms. *Sleep Medicine Reviews*, *40*, 170–182. https://doi.org/10.1016/j.smrv.2017.12.004

Chen, I. Y., Jarrin, D. C., Ivers, H., & Morin, C. M. (2017). Investigating psychological and physiological responses to the trier social stress test in young adults with insomnia. *Sleep Medicine*, *40*, 11–22. https://doi.org/10.1016/j.sleep.2017.09.011

Cheng, P., Kalmbach, D. A., Tallent, G., Joseph, C. L., Espie, C. A., & Drake, C. L. (2019). Depression prevention via digital cognitive behavioral therapy for insomnia: A randomized controlled trial. *Sleep*, *42*(10), zsz150. https://doi.org/10.1093/sleep/zsz150

Christensen, H., Batterham, P. J., Gosling, J. A., Ritterband, L. M., Griffiths, K. M., Thorndike, F. P., … Mackinnon, A. J. (2016). Effectiveness of an online insomnia program (SHUTi) for prevention of depressive episodes (the GoodNight Study): A randomised controlled trial. *Lancet Psychiatry*, *3*(4), 333–341. https://doi.org/10.1016/S2215-0366(15)00536-2

Christensen, J. A. E., Wassing, R., Wei, Y., Ramautar, J. R., Lakbila-Kamal, O., Jennum, P. J., & Van Someren, E. J. W. (2019). Data-driven analysis of EEG reveals concomitant superficial sleep during deep sleep in insomnia disorder. *Frontiers in Neuroscience*, *13*, 598. https://doi.org/10.3389/fnins.2019.00598

Cliffe, B., Croker, A., Denne, M., Smith, J., & Stallard, P. (2020). Digital cognitive behavioral therapy for insomnia for adolescents with mental health problems: Feasibility open trial. *JMIR Mental Health*, *7*(3), e14842. https://doi.org/10.2196/14842

Colombo, M. A., Ramautar, J. R., Wei, Y., Gomez-Herrero, G., Stoffers, D., Wassing, R., … Van Someren, E. J. W. (2016). Wake high-density electroencephalographic spatiospectral signatures of insomnia. *Sleep*, *39*(5), 1015–1027. https://doi.org/10.5665/sleep.5744

Colombo, M. A., Wei, Y., Ramautar, J. R., Linkenkaer-Hansen, K., Tagliazucchi, E., & Van Someren, E. J. W. (2016). More severe insomnia complaints in people with stronger long-range temporal correlations in wake resting-state EEG. *Frontiers in Physiology*, *7*, 576. https://doi.org/10.3389/fphys.2016.00576

Daley, M., Morin, C. M., LeBlanc, M., Grégoire, J.-P., & Savard, J. (2009). The economic burden of insomnia: Direct and indirect costs for individuals with insomnia syndrome, insomnia symptoms, and good sleepers. *Sleep*, *32*(1), 55–64.

Darden, M., Espie, C. A., Carl, J. R., Henry, A. L., Kanady, J. C., Krystal, A. D., & Miller, C. B. (2021). Cost-effectiveness of digital cognitive behavioral therapy (Sleepio) for insomnia: A Markov simulation model in the United States. *Sleep*, *44*(4), zsaa223. https://doi.org/10.1093/sleep/zsaa223

De Bruin, E. J., van Steensel, F. J. A., & Meijer, A. M. (2016). Cost-effectiveness of group and internet cognitive behavioral therapy for insomnia in adolescents: Results from a randomized controlled trial. *Sleep*, *39*(8), 1571–1581. https://doi.org/10.5665/sleep.6024

Debener, S., Emkes, R., De Vos, M., & Bleichner, M. (2015). Unobtrusive ambulatory EEG using a smartphone and flexible printed electrodes around the ear. *Scientific Reports*, *5*, 16743. https://doi.org/10.1038/srep16743

Dekker, K., Benjamins, J. S., Maksimovic, T., Filardi, M., Hofman, W. F., van Straten, A., & Van Someren, E. J. W. (2020). Combined internet-based cognitive-behavioral and chronobiological intervention for insomnia: A randomized controlled trial. *Psychotherapy and Psychosomatics*, *89*(2), 117–118. https://doi.org/10.1159/000503570

Dekker, K., Blanken, T. F., & Van Someren, E. J. W. (2017). Insomnia and personality-a network approach. *Brain Sciences*, *7*(3), E28. https://doi.org/10.3390/brainsci7030028

Dodds, K. L., Miller, C. B., Kyle, S. D., Marshall, N. S., & Gordon, C. J. (2017). Heart rate variability in insomnia patients: A critical review of the literature. *Sleep Medicine Reviews*, *33*, 88–100. https://doi.org/10.1016/j.smrv.2016.06.004

Drake, C. L., Pillai, V., & Roth, T. (2014). Stress and sleep reactivity: A prospective investigation of the stress-diathesis model of insomnia. *Sleep*, *37*(8), 1295–1304. https://doi.org/10.5665/sleep.3916

Dressle, R. J., Feige, B., Spiegelhalder, K., Schmucker, C., Benz, F., Mey, N. C., & Riemann, D. (2022). HPA axis activity in patients with chronic insomnia: A systematic review and meta-analysis of case-control studies. *Sleep Medicine Reviews*, *62*, 101588. https://doi.org/10.1016/j.smrv.2022.101588

Edinger, J. D., Arnedt, J. T., Bertisch, S. M., Carney, C. E., Harrington, J. J., Lichstein, K. L., … Martin, J. L. (2021a). Behavioral and psychological treatments for chronic insomnia disorder in adults: An American Academy of sleep medicine clinical practice guideline. *Journal of Clinical Sleep Medicine*, *17*(2), 255–262. https://doi.org/10.5664/jcsm.8986

Edinger, J. D., Arnedt, J. T., Bertisch, S. M., Carney, C. E., Harrington, J. J., Lichstein, K. L., … Martin, J. L. (2021b). Behavioral and psychological treatments for chronic insomnia disorder in adults: An American Academy of Sleep Medicine systematic review, meta-analysis, and GRADE assessment. *Journal of Clinical Sleep Medicine*, *17*(2), 263–298. https://doi.org/10.5664/jcsm.8988

Edinger, J. D., Wyatt, J. K., Stepanski, E. J., Olsen, M. K., Stechuchak, K. M., Carney, C. E., … Krystal, A. D. (2011). Testing the reliability and validity of DSM-IV-TR and ICSD-2 insomnia diagnoses: Results of a multitrait-multimethod analysis. *Archives of General Psychiatry*, *68*(10), 992–1002. https://doi.org/10.1001/archgenpsychiatry.2011.64

Ellis, J. G., Gehrman, P., Espie, C. A., Riemann, D., & Perlis, M. L. (2012). Acute insomnia: Current conceptualizations and future directions. *Sleep Medicine Reviews*, *16*(1), 5–14. https://doi.org/10.1016/j.smrv.2011.02.002

Espie, C. A. (2002). Insomnia: Conceptual issues in the development, persistence, and treatment of sleep disorder in adults. *Annual Review of Psychology*, *53*, 215–243. https://doi.org/10.1146/annurev.psych.53.100901.135243

Espie, C. A. (2009). "Stepped care": A health technology solution for delivering cognitive behavioral therapy as a first line insomnia treatment. *Sleep*, *32*(12), 1549–1558. https://doi.org/10.1093/sleep/32.12.1549

Espie, C. A. (2022). *A clinician's guide to cognitive and behavioural therapeutics (CBTx) for insomnia*. Cambridge University Press (in press).

Espie, C. A., Brooks, D. N., & Lindsay, W. R. (1989). An evaluation of tailored psychological treatment of insomnia. *Journal of Behavior Therapy and Experimental Psychiatry*, *20*(2), 143–153. https://doi.org/10.1016/0005-7916(89)90047-5

Espie, C. A., Broomfield, N. M., MacMahon, K. M. A., Macphee, L. M., & Taylor, L. M. (2006). The attention-intention-effort pathway in the development of psychophysiologic insomnia: A theoretical review. *Sleep Medicine Reviews*, *10*(4), 215–245. https://doi.org/10.1016/j.smrv.2006.03.002

Espie, C. A., Emsley, R., Kyle, S. D., Gordon, C., Drake, C. L., Siriwardena, A. N., … Luik, A. I. (2019). Effect of digital cognitive behavioral therapy for insomnia on health, psychological well-being, and sleep-related quality of life: A randomized clinical trial. *JAMA Psychiatry*, *76*(1), 21–30. https://doi.org/10.1001/jamapsychiatry.2018.2745

Espie, C. A., Hames, P., & McKinstry, B. (2013). Use of the internet and mobile media for delivery of cognitive behavioral insomnia therapy. *Sleep Medicine Clinics*, *8*(3), 407–419. https://doi.org/10.1016/j.jsmc.2013.06.001

Espie, C. A., Kyle, S. D., Hames, P., Gardani, M., Fleming, L., & Cape, J. (2014). The sleep condition indicator: A clinical screening tool to evaluate insomnia disorder. *BMJ Open*, *4*(3), e004183. https://doi.org/10.1136/bmjopen-2013-004183

Espie, C. A., Kyle, S. D., Williams, C., Ong, J. C., Douglas, N. J., Hames, P., & JSL, B. (2012). Randomized, placebo-controlled trial of online cognitive behavioral therapy for chronic insomnia disorder delivered via an automated media-rich web application. *Sleep*, *35*(6), 769–781. https://doi.org/10.5665/sleep.1872

Feige, B., Al-Shajlawi, A., Nissen, C., Voderholzer, U., Hornyak, M., Spiegelhalder, K., … Riemann, D. (2008). Does REM sleep contribute to subjective wake time in primary insomnia? A comparison of polysomnographic and subjective sleep in 100 patients. *Journal of Sleep Research*, *17*(2), 180–190. https://doi.org/10.1111/j.1365-2869.2008.00651.x

Feige, B., Baglioni, C., Boehm, P., Heinrich, A., Trumm, S., Benz, F., … Riemann, D. (2021). Event-related potentials in insomnia reflect altered perception of sleep. *Sleep*, *44*(10), zsab137. https://doi.org/10.1093/sleep/zsab137

Feige, B., Baglioni, C., Spiegelhalder, K., Hirscher, V., Nissen, C., & Riemann, D. (2013). The microstructure of sleep in primary insomnia: An overview and extension. *International Journal of Psychophysiology*, *89*(2), 171–180. https://doi.org/10.1016/j.ijpsycho.2013.04.002

Feige, B., Nanovska, S., Baglioni, C., Bier, B., Cabrera, L., Diemers, S., … Riemann, D. (2018). Insomnia-perchance a dream? Results from a NREM/REM sleep awakening study in good sleepers and patients with insomnia. *Sleep*, *41*(5). https://doi.org/10.1093/sleep/zsy032

Freeman, D., Sheaves, B., Goodwin, G. M., Yu, L.-M., Nickless, A., Harrison, P. J., … Espie, C. A. (2017). The effects of improving sleep on mental health (OASIS): A randomised controlled trial with mediation analysis. *Lancet Psychiatry*, *4*(10), 749–758. https://doi.org/10.1016/S2215-0366(17)30328-0

Gee, B., Orchard, F., Clarke, E., Joy, A., Clarke, T., & Reynolds, S. (2019). The effect of non-pharmacological sleep interventions on depression symptoms: A meta-analysis of randomised controlled trials. *Sleep Medicine Reviews*, *43*, 118–128. https://doi.org/10.1016/j.smrv.2018.09.004

Ginsburg, G. S., & Willard, H. F. (2009). Genomic and personalized medicine: Foundations and applications. *Translational Research*, *154*(6), 277–287. https://doi.org/10.1016/j.trsl.2009.09.005

Goldstein, A. N., & Walker, M. P. (2014). The role of sleep in emotional brain function. *Annual Review of Clinical Psychology*, *10*, 679–708. https://doi.org/10.1146/annurev-clinpsy-032813-153716

Hagger, M. S. (2010). Sleep, self-regulation, self-control and health. *Stress and Health*, *26*(3), 181–185. https://doi.org/10.1002/smi.1345

Halonen, R., Kuula, L., Makkonen, T., Kauramäki, J., & Pesonen, A.-K. (2021). Self-conscious affect is modulated by rapid eye movement sleep but not by targeted memory reactivation-a pilot study. *Frontiers in Psychology*, *12*, 730924. https://doi.org/10.3389/fpsyg.2021.730924

Hammerschlag, A. R., Stringer, S., de Leeuw, C. A., Sniekers, S., Taskesen, E., Watanabe, K., Blanken, T. F., Dekker, K., te Lindert, B. H. W., Wassing, R., Jonsdottir, I., Thorleifsson, G., Stefansson, H., Gislason, T., Berger, K., Schormair, B., Wellmann, J., Winkelmann, J., Stefansson, K., … Posthuma, D. (2017). Genome-wide association analysis of insomnia complaints identifies risk genes and genetic overlap with psychiatric and metabolic traits. *Nature Genetics*, *49*, 1584–1592.

Harris, K., Spiegelhalder, K., Espie, C. A., MacMahon, K. M. A., Woods, H. C., & Kyle, S. D. (2015). Sleep-related attentional bias in insomnia: A state-of-the-science review. *Clinical Psychology Review*, *42*, 16–27. https://doi.org/10.1016/j.cpr.2015.08.001

Harvey, A. G. (2002). A cognitive model of insomnia. *Behaviour Research and Therapy*, *40*(8), 869–893. https://doi.org/10.1016/S0005-7967(01)00061-4

Harvey, A. G., Dong, L., Hein, K., Yu, S. H., Martinez, A. J., Gumport, N. B., … Buysse, D. J. (2021). A randomized controlled trial of the Transdiagnostic Intervention for Sleep and Circadian Dysfunction (TranS-C) to improve serious mental illness outcomes in a community setting. *Journal of Consulting and Clinical Psychology*, *89*(6), 537–550. https://doi.org/10.1037/ccp0000650

Harvey, A. G., Murray, G., Chandler, R. A., & Soehner, A. (2011). Sleep disturbance as transdiagnostic: Consideration of neurobiological mechanisms. *Clinical Psychology Review*, *31*(2), 225–235. https://doi.org/10.1016/j.cpr.2010.04.003

Harvey, A. G., & Tang, N. K. (2003). Cognitive behaviour therapy for primary insomnia: Can we rest yet? *Sleep Medicine Reviews*, *7*, 237–262.

Hasan, F., Tu, Y.-K., Yang, C.-M., James Gordon, C., Wu, D., Lee, H.-C., … Chiu, H.-Y. (2022). Comparative efficacy of digital cognitive behavioral therapy for insomnia: A systematic review and network meta-analysis. *Sleep Medicine Reviews*, *61*, 101567. https://doi.org/10.1016/j.smrv.2021.101567

Henry, A. L., Miller, C. B., Emsley, R., Sheaves, B., Freeman, D., Luik, A. I., … Espie, C. A. (2021). Insomnia as a mediating therapeutic target for depressive symptoms: A sub-analysis of participant data from two large randomized controlled trials of a digital sleep intervention. *Journal of Sleep Research*, *30*(1), e13140. https://doi.org/10.1111/jsr.13140

Herrero Babiloni, A., Bellemare, A., Beetz, G., Vinet, S.-A., Martel, M. O., Lavigne, G. J., & De Beaumont, L. (2021). The effects of non-invasive brain stimulation on sleep disturbances among different neurological and neuropsychiatric conditions: A systematic review. *Sleep Medicine Reviews*, *55*, 101381. https://doi.org/10.1016/j.smrv.2020.101381

Herring, W. J., Roth, T., Krystal, A. D., & Michelson, D. (2019). Orexin receptor antagonists for the treatment of insomnia and potential treatment of other neuropsychiatric indications. *Journal of Sleep Research*, *28*(2), e12782. https://doi.org/10.1111/jsr.12782

Hertenstein, E., Feige, B., Gmeiner, T., Kienzler, C., Spiegelhalder, K., Johann, A., … Baglioni, C. (2019). Insomnia as a predictor of mental disorders: A systematic review and meta-analysis. *Sleep Medicine Reviews*, *43*, 96–105. https://doi.org/10.1016/j.smrv.2018.10.006

Hertenstein, E., Trinca, E., Wunderlin, M., Schneider, C., Züst, M., Fehér, K., … Nissen, C. (2022). Cognitive behavioral therapy for insomnia in patients with mental disorders and comorbid insomnia: A systematic review and meta-analysis. *Sleep Medicine Reviews*, *62*, 101597. https://doi.org/10.1016/j.smrv.2022.101597

Irwin, M. R., Carrillo, C., Sadeghi, N., Bjurstrom, M. F., Breen, E. C., & Olmstead, R. (2022). Prevention of incident and recurrent major depression in older adults with insomnia: A randomized clinical trial. *JAMA Psychiatry*, *79*(1), 33–41. https://doi.org/10.1001/jamapsychiatry.2021.3422

Jain, K. K. (2002). Personalized medicine. *Current Opinion in Molecular Therapeutics*, *4*(6), 548–558.

Jansen, P. R., Watanabe, K., Stringer, S., Skene, N., Bryois, J., Hammerschlag, A. R., … Posthuma, D. (2019). Genome-wide analysis of insomnia in 1,331,010 individuals identifies new risk loci and functional pathways. *Nature Genetics*, *51*(3), 394–403. https://doi.org/10.1038/s41588-018-0333-3

Johann, A. F., Hertenstein, E., Kyle, S. D., Baglioni, C., Feige, B., Nissen, C., … Spiegelhalder, K. (2017). Insomnia with objective short sleep duration is associated with longer duration of insomnia in the Freiburg insomnia cohort compared to insomnia with normal sleep duration, but not with hypertension. *PLoS One*, *12*(7), e0180339. https://doi.org/10.1371/journal.pone.0180339

Kaldo, V., Jernelöv, S., Blom, K., Ljótsson, B., Brodin, M., Jörgensen, M., … Lindefors, N. (2015). Guided internet cognitive behavioral therapy for insomnia compared to a control treatment—A randomized trial. *Behaviour Research and Therapy*, *71*, 90–100. https://doi.org/10.1016/j.brat.2015.06.001

Kallestad, H., Scott, J., Vedaa, Ø., Lydersen, S., Vethe, D., Morken, G., … Langsrud, K. (2021). Mode of delivery of cognitive behavioral therapy for insomnia: A randomized controlled non-inferiority trial of digital and face-to-face therapy. *Sleep*, *44*(12), zsab185. https://doi.org/10.1093/sleep/zsab185

Kao, C.-H., D'Rozario, A. L., Lovato, N., Wassing, R., Bartlett, D., Memarian, N., … Gordon, C. J. (2021). Insomnia subtypes characterised by objective sleep duration and NREM spectral power and the effect of acute sleep restriction: An exploratory analysis. *Scientific Reports*, *11*(1), 24331. https://doi.org/10.1038/s41598-021-03564-6

Kathol, R. G., & Arnedt, J. T. (2016). Cognitive behavioral therapy for chronic insomnia: Confronting the challenges to implementation. *Annals of Internal Medicine*, *165*(2), 149–150. https://doi.org/10.7326/M16-0359

Kjaerby, C., Andersen, M., Hauglund, N., Ding, F., Wang, W., Xu, Q., … Nedergaard, M. (2020). Dynamic fluctuations of the locus coeruleus-norepinephrine system underlie sleep state transitions. *bioRxiv*.

Kraepelien, M., Forsell, E., & Blom, K. (2022). Large-scale implementation of insomnia treatment in routine psychiatric care: Patient characteristics and insomnia-depression comorbidity. *Journal of Sleep Research*, *31*(1), e13448. https://doi.org/10.1111/jsr.13448

Kushida, C. A., Littner, M. R., Morgenthaler, T., Alessi, C. A., Bailey, D., Coleman, J., … Wise, M. (2005). Practice parameters for the indications for polysomnography and related procedures: An update for 2005. *Sleep*, *28*(4), 499–521. https://doi.org/10.1093/sleep/28.4.499

Kyle, S. D., Aquino, M. R. J., Miller, C. B., Henry, A. L., Crawford, M. R., Espie, C. A., & Spielman, A. J. (2015). Towards standardisation and improved understanding of sleep restriction therapy for insomnia disorder: A systematic examination of CBT-I trial content. *Sleep Medicine Reviews*, *23*, 83–88. https://doi.org/10.1016/j.smrv.2015.02.003

Kyle, S. D., Espie, C. A., Gehrman, P., Ong, J., & Hames, B. (2014). Tailoring CBT for insomnia to specific needs: A personalised behavioural medicine approach. In C. Bassetti, Z. Dogas, & P. Peigneux (Eds.), *European sleep medicine textbook*. ESRS & Wiley.

Kyle, S. D., Hurry, M. E. D., Emsley, R., Marsden, A., Omlin, X., Juss, A., … Sexton, C. E. (2020). The effects of digital cognitive behavioral therapy for insomnia on cognitive function: A randomized controlled trial. *Sleep*, *43*(9), zsaa034. https://doi.org/10.1093/sleep/zsaa034

Kyle, S. D., Madigan, C., Begum, N., Abel, L., Armstrong, S., Aveyard, P., … Espie, C. A. (2020). Primary care treatment of insomnia: Study protocol for a pragmatic, multicentre, randomised controlled trial comparing nurse-delivered sleep restriction therapy to sleep hygiene (the HABIT trial). *BMJ Open*, *10*(3), e036248. https://doi.org/10.1136/bmjopen-2019-036248

Kyle, S. D., Sexton, C. E., Feige, B., Luik, A. I., Lane, J., Saxena, R., … Spiegelhalder, K. (2017). Sleep and cognitive performance: Cross-sectional associations in the UK Biobank. *Sleep Medicine*, *38*, 85–91. https://doi.org/10.1016/j.sleep.2017.07.001

van de Laar, M., Verbeek, I., Pevernagie, D., Aldenkamp, A., & Overeem, S. (2010). The role of personality traits in insomnia. *Sleep Medicine Reviews*, *14*(1), 61–68. https://doi.org/10.1016/j.smrv.2009.07.007

Lancee, J., van Straten, A., Morina, N., Kaldo, V., & Kamphuis, J. H. (2016). Guided online or face-to-face cognitive behavioral treatment for insomnia: A randomized wait-list controlled trial. *Sleep*, *39*(1), 183–191. https://doi.org/10.5665/sleep.5344

Lane, J. M., Jones, S. E., Dashti, H. S., Wood, A. R., Aragam, K. G., van Hees, V. T., … Saxena, R. (2019). Biological and clinical insights from genetics of insomnia symptoms. *Nature Genetics*, *51*(3), 387–393. https://doi.org/10.1038/s41588-019-0361-7

Leerssen, J., Lakbila-Kamal, O., Dekkers, L. M. S., Ikelaar, S. L. C., Albers, A. C. W., Blanken, T. F., … Van Someren, E. J. W. (2021). Treating insomnia with high risk of depression using therapist-guided digital cognitive, behavioral, and circadian rhythm support interventions to prevent worsening of depressive symptoms: A randomized controlled trial. *Psychotherapy and Psychosomatics*, 1–12. https://doi.org/10.1159/000520282

Leger, D., Levy, E., & Paillard, M. (1999). The direct costs of insomnia in France. *Sleep*, *22*, S394–S401.

Li, M., Zhang, X.-W., Hou, W.-S., & Tang, Z.-Y. (2014). Insomnia and risk of cardiovascular disease: A meta-analysis of cohort studies. *International Journal of Cardiology*, *176*(3), 1044–1047. https://doi.org/10.1016/j.ijcard.2014.07.284

Luik, A. I., Bostock, S., Chisnall, L., Kyle, S. D., Lidbetter, N., Baldwin, N., & Espie, C. A. (2017). Treating depression and anxiety with digital cognitive behavioural therapy for insomnia: A real world NHS evaluation using standardized outcome measures. *Behavioural and Cognitive Psychotherapy*, *45*(1), 91–96. https://doi.org/10.1017/S1352465816000369

Luik, A. I., Marsden, A., Emsley, R., Henry, A. L., Stott, R., Miller, C. B., & Espie, C. A. (2020). Long-term benefits of digital cognitive behavioural therapy for insomnia: Follow-up report from a randomized clinical trial. *Journal of Sleep Research*, *29*(4), e13018. https://doi.org/10.1111/jsr.13018

Manber, R., Edinger, J. D., Gress, J. L., Pedro-Salcedo, M. G. S., Kuo, T. F., & Kalista, T. (2008). Cognitive behavioral therapy for insomnia enhances depression outcome in patients with comorbid major depressive disorder and insomnia. *Sleep*, *31*(4), 489–495. https://doi.org/10.1093/sleep/31.4.489

Maurer, L. F., Espie, C. A., & Kyle, S. D. (2018). How does sleep restriction therapy for insomnia work? A systematic review of mechanistic evidence and the introduction of the triple-R model. *Sleep Medicine Reviews*, *42*, 127–138. https://doi.org/10.1016/j.smrv.2018.07.005

Maurer, L. F., Espie, C. A., Omlin, X., Emsley, R., & Kyle, S. D. (2022). The effect of sleep restriction therapy for insomnia on sleep pressure and arousal: A randomized controlled mechanistic trial. *Sleep*, *45*(1), zsab223. https://doi.org/10.1093/sleep/zsab223

Maurer, L. F., Espie, C. A., Omlin, X., Reid, M. J., Sharman, R., Gavriloff, D., … Kyle, S. D. (2020). Isolating the role of time in bed restriction in the treatment of insomnia: A randomized, controlled, dismantling trial comparing sleep restriction therapy with time in bed regularization. *Sleep*, *43*(11), zsaa096. https://doi.org/10.1093/sleep/zsaa096

Maurer, L. F., Ftouni, S., Espie, C. A., Bisdounis, L., & Kyle, S. D. (2021). The acute effects of sleep restriction therapy for insomnia on circadian timing and vigilance. *Journal of Sleep Research*, *30*(4), e13260. https://doi.org/10.1111/jsr.13260

Maurer, L. F., Schneider, J., Miller, C. B., Espie, C. A., & Kyle, S. D. (2021). The clinical effects of sleep restriction therapy for insomnia: A meta-analysis of randomised controlled trials. *Sleep Medicine Reviews*, *58*, 101493. https://doi.org/10.1016/j.smrv.2021.101493

McCrae, C. S., McNamara, J. P. H., Rowe, M. A., Dzierzewski, J. M., Dirk, J., Marsiske, M., & Craggs, J. G. (2008). Sleep and affect in older adults: Using multilevel modeling to examine daily associations. *Journal of Sleep Research*, *17*(1), 42–53. https://doi.org/10.1111/j.1365-2869.2008.00621.x

Mikkelsen, K. B., Tabar, Y. R., Kappel, S. L., Christensen, C. B., Toft, H. O., Hemmsen, M. C., ... Kidmose, P. (2019). Accurate whole-night sleep monitoring with dry-contact ear-EEG. *Scientific Reports*, *9*(1), 16824. https://doi.org/10.1038/s41598-019-53115-3

Morin, C. M. (2020). Profile of somryst prescription digital therapeutic for chronic insomnia: Overview of safety and efficacy. *Expert Review Medical Devices*, *17*, 1239–1248. https://doi.org/10.1080/17434440.2020.1852929

Morin, C. M., Drake, C. L., Harvey, A. G., Krystal, A. D., Manber, R., Riemann, D., & Spiegelhalder, K. (2015). Insomnia disorder. *Nature Reviews. Disease Primers*, *1*, 15026. https://doi.org/10.1038/nrdp.2015.26

Morin, C. M., Edinger, J. D., Beaulieu-Bonneau, S., Ivers, H., Krystal, A. D., Guay, B., ... Busby, M. (2020). Effectiveness of sequential psychological and medication therapies for insomnia disorder: A randomized clinical trial. *JAMA Psychiatry*, *77*(11), 1107–1115. https://doi.org/10.1001/jamapsychiatry.2020.1767

Morin, C. M., Vallières, A., & Ivers, H. (2007). Dysfunctional beliefs and attitudes about sleep (DBAS): Validation of a brief version (DBAS-16). *Sleep*, *30*(11), 1547–1554. https://doi.org/10.1093/sleep/30.11.1547

Ohayon, M. M. (2002). Epidemiology of insomnia: What we know and what we still need to learn. *Sleep Medicine Reviews*, *6*(2), 97–111. https://doi.org/10.1053/smrv.2002.0186

Overland, S., Glozier, N., Sivertsen, B., Stewart, R., Neckelmann, D., Krokstad, S., & Mykletun, A. (2008). A comparison of insomnia and depression as predictors of disability pension: The HUNT Study. *Sleep*, *31*(6), 875–880. https://doi.org/10.1093/sleep/31.6.875

Palagini, L., Biber, K., & Riemann, D. (2014). The genetics of insomnia-evidence for epigenetic mechanisms? *Sleep Medicine Reviews*, *18*(3), 225–235. https://doi.org/10.1016/j.smrv.2013.05.002

Palmer, C. A., & Alfano, C. A. (2017). Sleep and emotion regulation: An organizing, integrative review. *Sleep Medicine Reviews*, *31*, 6–16. https://doi.org/10.1016/j.smrv.2015.12.006

Perlis, M. L., Giles, D. E., Mendelson, W. B., Bootzin, R. R., & Wyatt, J. K. (1997). Psychophysiological insomnia: The behavioural model and a neurocognitive perspective. *Journal of Sleep Research*, *6*(3), 179–188. https://doi.org/10.1046/j.1365-2869.1997.00045.x

Perlis, M. L., Smith, M. T., Andrews, P. J., Orff, H., & Giles, D. E. (2001). Beta/gamma EEG activity in patients with primary and secondary insomnia and good sleeper controls. *Sleep*, *24*(1), 110–117. https://doi.org/10.1093/sleep/24.1.110

Pesonen, A.-K., Gradisar, M., Kuula, L., Short, M., Merikanto, I., Tark, R., ... Lahti, J. (2019). REM sleep fragmentation associated with depressive symptoms and genetic risk for depression in a community-based sample of adolescents. *Journal of Affective Disorders*, *245*, 757–763. https://doi.org/10.1016/j.jad.2018.11.077

Pigeon, W. R., Pinquart, M., & Conner, K. (2012). Meta-analysis of sleep disturbance and suicidal thoughts and behaviors. *The Journal of Clinical Psychiatry*, *73*(9), e1160–e1167. https://doi.org/10.4088/JCP.11r07586

Pillai, V., Roth, T., & Drake, C. L. (2015). The nature of stable insomnia phenotypes. *Sleep*, *38*(1), 127–138. https://doi.org/10.5665/sleep.4338

Qaseem, A., Kansagara, D., Forciea, M. A., Cooke, M., & Denberg, T. D. (2016). Management of chronic insomnia disorder in adults: A clinical practice guideline from the American College of Physicians. *Annals of Internal Medicine*, *165*(2), 125–133. https://doi.org/10.7326/M15-2175

Reynolds, S. A., & Ebben, M. R. (2017). The cost of insomnia and the benefit of increased access to evidence-based treatment: Cognitive behavioral therapy for insomnia. *Sleep Medicine Clinics*, *12*(1), 39–46. https://doi.org/10.1016/j.jsmc.2016.10.011

Riemann, D., Baglioni, C., Bassetti, C., Bjorvatn, B., Dolenc Groselj, L., Ellis, J. G., ... Spiegelhalder, K. (2017). European guideline for the diagnosis and treatment of insomnia. *Journal of Sleep Research*, *26*(6), 675–700. https://doi.org/10.1111/jsr.12594

Riemann, D., Baum, E., Cohrs, S., Crönlein, T., Hajak, G., Hertenstein, E., ... Spiegelhalder, K. (2017). S3-Leitlinie Nicht erholsamer Schlaf/Schlafstörungen. *Somnologie*, *21*(1), 2–44. https://doi.org/10.1007/s11818-016-0097-x

Riemann, D., Krone, L. B., Wulff, K., & Nissen, C. (2020). Sleep, insomnia, and depression. *Neuropsychopharmacology*, *45*(1), 74–89. https://doi.org/10.1038/s41386-019-0411-y

Riemann, D., & Nissen, C. (2012). Sleep and psychotropic drugs. In *Oxford handbook of sleep and sleep disorders* (pp. 190–222). Oxford University Press.

Riemann, D., Nissen, C., Palagini, L., Otte, A., Perlis, M. L., & Spiegelhalder, K. (2015). The neurobiology, investigation, and treatment of chronic insomnia. *Lancet Neurology*, *14*(5), 547–558. https://doi.org/10.1016/S1474-4422(15)00021-6

Riemann, D., Spiegelhalder, K., Espie, C. A., Gavriloff, D., Frase, L., & Baglioni, C. (2022). Introduction to insomnia disorder. In C. Baglioni, C. A. Espie, & D. Riemann (Eds.), *Cognitive-behavioural therapy for insomnia (CBT-I) across the lifespan. Guidelines and clinical protocols for health professionals*. Wiley & Sons (in press).

Riemann, D., Spiegelhalder, K., Espie, C., Pollmächer, T., Léger, D., Bassetti, C., & Van Someren, E. (2011). Chronic insomnia: Clinical and research challenges-an agenda. *Pharmacopsychiatry*, *44*(1), 1–14. https://doi.org/10.1055/s-0030-1267978

Riemann, D., Spiegelhalder, K., Feige, B., Voderholzer, U., Berger, M., Perlis, M., & Nissen, C. (2010). The hyperarousal model of insomnia: A review of the concept and its evidence. *Sleep Medicine Reviews*, *14*(1), 19–31. https://doi.org/10.1016/j.smrv.2009.04.002

Riemann, D., Spiegelhalder, K., Nissen, C., Hirscher, V., Baglioni, C., & Feige, B. (2012). REM sleep instability—A new pathway for insomnia? *Pharmacopsychiatry*, *45*, 167–176. https://doi.org/10.1055/s-0031-1299721

Ritterband, L. M., Thorndike, F. P., Ingersoll, K. S., Lord, H. R., Gonder-Frederick, L., Frederick, C., ... Morin, C. M. (2017). Effect of a web-based cognitive behavior therapy for insomnia intervention with 1-year follow-up: A randomized clinical trial. *JAMA Psychiatry*, *74*(1), 68–75. https://doi.org/10.1001/jamapsychiatry.2016.3249

Roehrs, T., & Roth, T. (2012). Insomnia pharmacotherapy. *Neurotherapeutics*, *9*(4), 728–738. https://doi.org/10.1007/s13311-012-0148-3

Sadeh, A., Tikotzky, L., & Kahn, M. (2014). Sleep in infancy and childhood: Implications for emotional and behavioral difficulties in adolescence and beyond. *Current Opinion in Psychiatry*, *27*(6), 453–459. https://doi.org/10.1097/YCO.0000000000000109

Sampson, C., Bell, E., Cole, A., Miller, C. B., Marriott, T., Williams, M., & Rose, J. (2022). Digital cognitive behavioural therapy for insomnia and primary care costs in England: An interrupted time series analysis. *BJGP Open*. https://doi.org/10.3399/BJGPO.2021.0146

Saper, C. B., Cano, G., & Scammell, T. E. (2005). Homeostatic, circadian, and emotional regulation of sleep. *The Journal of Comparative Neurology*, *493*(1), 92–98. https://doi.org/10.1002/cne.20770

Saper, C. B., Scammell, T. E., & Lu, J. (2005). Hypothalamic regulation of sleep and circadian rhythms. *Nature*, *437*(7063), 1257–1263. https://doi.org/10.1038/nature04284

Sateia, M. J., & Buysse, D. J. (2010). *Insomnia: Diagnosis and treatment*. Informa Healthcare.

Schneider, C. L., Hertenstein, E., Fehér, K., Maier, J. G., Cantisani, A., Moggi, F., ... Nissen, C. (2020). Become your own SLEEPexpert: Design, implementation, and preliminary evaluation of a pragmatic behavioral treatment program for insomnia in inpatient psychiatric care. *SLEEP Advances*, *1*(1), zpaa005. https://doi.org/10.1093/sleepadvances/zpaa005

Scott, B. A., & Judge, T. A. (2006). Insomnia, emotions, and job satisfaction: A multilevel study. *Journal of Management*, *32*(5), 622–645. https://doi.org/10.1177/0149206306289762

Seyffert, M., Lagisetty, P., Landgraf, J., Chopra, V., Pfeiffer, P. N., Conte, M. L., & Rogers, M. A. M. (2016). Internet-delivered cognitive behavioral therapy to treat insomnia: A systematic review and meta-analysis. *PLoS One*, *11*(2), e0149139. https://doi.org/10.1371/journal.pone.0149139

Sivertsen, B., Krokstad, S., Øverland, S., & Mykletun, A. (2009). The epidemiology of insomnia: Associations with physical and mental health. The HUNT-2 study. *Journal of Psychosomatic Research*, *67*(2), 109–116. https://doi.org/10.1016/j.jpsychores.2009.05.001

Soh, H. L., Ho, R. C., Ho, C. S., & Tam, W. W. (2020). Efficacy of digital cognitive behavioural therapy for insomnia: A meta-analysis of randomised controlled trials. *Sleep Medicine*, *75*, 315–325. https://doi.org/10.1016/j.sleep.2020.08.020

Spiegelhalder, K., Regen, W., Feige, B., Holz, J., Piosczyk, H., Baglioni, C., … Nissen, C. (2012). Increased EEG sigma and beta power during NREM sleep in primary insomnia. *Biological Psychology*, *91*(3), 329–333. https://doi.org/10.1016/j.biopsycho.2012.08.009

Spielman, A. J., Caruso, L. S., & Glovinsky, P. B. (1987). A behavioral perspective on insomnia treatment. *The Psychiatric Clinics of North America*, *10*(4), 541–553.

Stephan, A. M., Lecci, S., Cataldi, J., & Siclari, F. (2021). Conscious experiences and high-density EEG patterns predicting subjective sleep depth. *Current Biology*, *31*(24), 5487–5500.e3. https://doi.org/10.1016/j.cub.2021.10.012

Stott, R., Pimm, J., Emsley, R., Miller, C. B., & Espie, C. A. (2021). Does adjunctive digital CBT for insomnia improve clinical outcomes in an improving access to psychological therapies service? *Behaviour Research and Therapy*, *144*, 103922. https://doi.org/10.1016/j.brat.2021.103922

Tahmasian, M., Noori, K., Samea, F., Zarei, M., Spiegelhalder, K., Eickhoff, S. B., Van Someren, E., Khazaie, H., & Eickhoff, C. R. (2018). A lack of consistent brain alterations in insomnia disorder: An activation likelihood estimation meta-analysis. *Sleep Medicine Reviews*, *42*, 111–118.

Thakkar, M. M. (2011). Histamine in the regulation of wakefulness. *Sleep Medicine Reviews*, *15*(1), 65–74. https://doi.org/10.1016/j.smrv.2010.06.004

Van Someren, E. J. W. (2021). Brain mechanisms of insomnia: New perspectives on causes and consequences. *Physiological Reviews*, *101*(3), 995–1046. https://doi.org/10.1152/physrev.00046.2019

Vedaa, Ø., Hagatun, S., Kallestad, H., Pallesen, S., Smith, O. R. F., Thorndike, F. P., … Sivertsen, B. (2019). Long-term effects of an unguided online cognitive behavioral therapy for chronic insomnia. *Journal of Clinical Sleep Medicine*, *15*(1), 101–110. https://doi.org/10.5664/jcsm.7580

Vedaa, Ø., Kallestad, H., Scott, J., Smith, O. R. F., Pallesen, S., Morken, G., … Sivertsen, B. (2020). Effects of digital cognitive behavioural therapy for insomnia on insomnia severity: A large-scale randomised controlled trial. *Lancet Digital Health*, *2*(8), e397–e406. https://doi.org/10.1016/S2589-7500(20)30135-7

Vermeulen, M. C. M., van der Heijden, K. B., Kocevska, D., Treur, J. L., Huppertz, C., van Beijsterveldt, C. E. M., Boomsma, D. I., Swaab, H., Van Someren, E. J. W., & Bartels, M. (2021). Associations of sleep with psychological problems and well-being in adolescence: Causality or common genetic predispositions? *Journal of Child Psychology and Psychiatry*, *62*, 28–39.

Vgontzas, A. N., Fernandez-Mendoza, J., Liao, D., & Bixler, E. O. (2013). Insomnia with objective short sleep duration: The most biologically severe phenotype of the disorder. *Sleep Medicine Reviews*, *17*(4), 241–254. https://doi.org/10.1016/j.smrv.2012.09.005

Vincent, N., & Walsh, K. (2013). Stepped care for insomnia: An evaluation of implementation in routine practice. *Journal of Clinical Sleep Medicine*, *09*(03), 227–234. https://doi.org/10.5664/jcsm.2484

Wassing, R., Benjamins, J. S., Dekker, K., Moens, S., Spiegelhalder, K., Feige, B., … Van Someren, E. J. W. (2016). Slow dissolving of emotional distress contributes to hyperarousal. *Proceedings of the National Academy of Sciences of the United States of America*, *113*(9), 2538–2543. https://doi.org/10.1073/pnas.1522520113

Wassing, R., Benjamins, J. S., Talamini, L. M., Schalkwijk, F., & Van Someren, E. J. W. (2019). Overnight worsening of emotional distress indicates maladaptive sleep in insomnia. *Sleep*, *42*(4), zsy268. https://doi.org/10.1093/sleep/zsy268

Wassing, R., Lakbila-Kamal, O., Ramautar, J. R., Stoffers, D., Schalkwijk, F., & Van Someren, E. J. W. (2019). Restless REM sleep impedes overnight amygdala adaptation. *Current Biology: CB*, *29*(14), 2351–2358.e4. https://doi.org/10.1016/j.cub.2019.06.034

Wassing, R., Schalkwijk, F., Lakbila-Kamal, O., Ramautar, J. R., Stoffers, D., Mutsaerts, H. J. M. M., … Van Someren, E. J. W. (2019). Haunted by the past: Old emotions remain salient in insomnia disorder. *Brain*, *142*(6), 1783–1796. https://doi.org/10.1093/brain/awz089

Wei, Y., Blanken, T. F., & Van Someren, E. J. W. (2018). Insomnia really hurts: Effect of a bad night's sleep on pain increases with insomnia severity. *Frontiers in Psychiatry*, *9*, 377. https://doi.org/10.3389/fpsyt.2018.00377

Wei, Y., Ramautar, J. R., Colombo, M. A., Stoffers, D., Gómez-Herrero, G., van der Meijden, W. P., … Van Someren, E. J. W. (2016). I keep a close watch on this heart of mine: Increased interoception in insomnia. *Sleep*, *39*(12), 2113–2124. https://doi.org/10.5665/sleep.6308

Wei, Y., Ramautar, J. R., Colombo, M. A., Te Lindert, B. H. W., & Van Someren, E. J. W. (2018). EEG microstates indicate heightened somatic awareness in insomnia: Toward objective assessment of subjective mental content. *Frontiers in Psychiatry*, *9*, 395. https://doi.org/10.3389/fpsyt.2018.00395

Wickwire, E. M. (2019). The value of digital insomnia therapeutics: What we know and what we need to know. *Journal of Clinical Sleep Medicine*, *15*(1), 11–13. https://doi.org/10.5664/jcsm.7558

Wilson, S., Anderson, K., Baldwin, D., Dijk, D.-J., Espie, A., Espie, C., … Sharpley, A. (2019). British Association for Psychopharmacology consensus statement on evidence-based treatment of insomnia, parasomnias and circadian rhythm disorders: An update. *Journal of Psychopharmacology*, *33*(8), 923–947. https://doi.org/10.1177/0269881119855343

Wilt, T. J., MacDonald, R., Brasure, M., Olson, C. M., Carlyle, M., Fuchs, E., … Kane, R. L. (2016). Pharmacologic treatment of insomnia disorder: An evidence report for a clinical practice guideline by the American College of Physicians. *Annals of Internal Medicine*, *165*(2), 103–112. https://doi.org/10.7326/M15-1781

Woolfolk, R. L., & McNulty, T. F. (1983). Relaxation treatment for insomnia: A component analysis. *Journal of Consulting and Clinical Psychology*, *51*(4), 495–503. https://doi.org/10.1037//0022-006x.51.4.495

World Health Organization. (1993). *International statistical classification of diseases and related health problems* (10th ed.). World Health Organization.

World Health Organization. (2019). *International statistical classification of diseases and related health problems* (11th ed.). World Health Organization Retrieved from https://icd.who.int/

Zachariae, R., Amidi, A., Damholdt, M. F., Clausen, C. D. R., Dahlgaard, J., Lord, H., … Ritterband, L. M. (2018). Internet-delivered cognitive-behavioral therapy for insomnia in breast cancer survivors: A randomized controlled trial. *Journal of the National Cancer Institute*, *110*(8), 880–887. https://doi.org/10.1093/jnci/djx293

Zachariae, R., Lyby, M. S., Ritterband, L. M., & O'Toole, M. S. (2016). Efficacy of internet-delivered cognitive-behavioral therapy for insomnia—A systematic review and meta-analysis of randomized controlled trials. *Sleep Medicine Reviews*, *30*, 1–10. https://doi.org/10.1016/j.smrv.2015.10.004

van der Zweerde, T., Bisdounis, L., Kyle, S. D., Lancee, J., & van Straten, A. (2019). Cognitive behavioral therapy for insomnia: A meta-analysis of long-term effects in controlled studies. *Sleep Medicine Reviews*, *48*, 101208. https://doi.org/10.1016/j.smrv.2019.08.002

How to cite this article: Riemann, D., Benz, F., Dressle, R. J., Espie, C. A., Johann, A. F., Blanken, T. F., Leerssen, J., Wassing, R., Henry, A. L., Kyle, S. D., Spiegelhalder, K., & Van Someren, E. J. W. (2022). Insomnia disorder: State of the science and challenges for the future. *Journal of Sleep Research*, *31*(4), e13604. https://doi.org/10.1111/jsr.13604

BEFORE THE PUBLIC UTILITY COMMISSION
OF OREGON

Docket PCN 5

In the Matter of

IDAHO POWER COMPANY'S
PETITION FOR CERTIFICATE OF PUBLIC CONVENIENCE
AND NECESSITY

Bauer, C. A., Tinnitus (2018)

February 22, 2023

CLINICAL PRACTICE

Caren G. Solomon, M.D., M.P.H., *Editor*

Tinnitus

Carol A. Bauer, M.D.

This Journal *feature begins with a case vignette highlighting a common clinical problem. Evidence supporting various strategies is then presented, followed by a review of formal guidelines, when they exist. The article ends with the author's clinical recommendations.*

A 55-year-old man reports hearing a high-pitched, static sound in both ears. He does not recall when it began, but the sound has been present for several months and is bothersome. How should this case be managed?

THE CLINICAL PROBLEM

From the Division of Otolaryngology–Head and Neck Surgery, Southern Illinois University School of Medicine, Springfield. Address reprint requests to Dr. Bauer at the Division of Otolaryngology–Head and Neck Surgery, Southern Illinois University School of Medicine, 801 N. Rutledge St., Rm. 3205, P.O. Box 19629, Springfield, IL 62794, or at cbauer@siumed.edu.

N Engl J Med 2018;378:1224-31.
DOI: 10.1056/NEJMcp1506631

An audio version of this article is available at NEJM.org

Tinnitus is the perception of a sound that has no external source. The sensation is commonly described as ringing in the ear, but the sound can be perceived inside or outside the head or predominantly in one or both ears. Qualitative descriptions include humming, tonal ringing, hissing, static, roaring, or a cicada-like sound. Tinnitus can be categorized as objective or subjective. Objective tinnitus — a sound generated within the body by blood flow, muscle contractions, or spontaneous cochlear emissions that can be detected and measured by an external observer — is uncommon. This review addresses the more common variant, subjective tinnitus.

Population surveys estimate a prevalence of tinnitus of 10 to 25% among persons older than 18 years of age across various nationalities.[1-3] In population surveys, the sensation is reported to be severely bothersome in only a small percentage of persons with tinnitus (range, 1 to 7%).[1,4-6] The prevalence of persistent tinnitus increases with age, reaching a peak among persons in the seventh decade of life,[1] but the prevalence has increased among younger age groups over the past decade, presumably because of increased exposure to damaging recreational noise.[3,7] A large cross-sectional study involving children and adults who were referred to a regional otolaryngology hospital showed that 97% of those who reported tinnitus had concomitant hearing loss detected by routine audiometry.[8] In a population-based study, hearing impairment at frequencies between 500 and 4000 Hz was noted at baseline in two thirds of persons who reported tinnitus, as compared with 44% of persons who did not have tinnitus.[5] In another study, hearing loss was the strongest risk factor for tinnitus that was at least moderate in severity or that caused difficulty in sleeping (adjusted odds ratio, 3.2; 95% confidence interval, 2.3 to 4.4)[9]; a history of occupational noise exposure was also strongly correlated with tinnitus. Clinical experience suggests that sudden hearing loss is associated with sudden onset of tinnitus, but when hearing loss is gradual, tinnitus tends to develop over the course of months or years. Tinnitus frequently resolves or decreases considerably in severity with resolution of hearing loss — for example, after treatment of conductive hearing loss from cerumen impaction or middle-ear effusion.

Tinnitus can affect daily life in multiple domains. People with bothersome tinnitus report impaired sleep, interference with concentration, decreased social enjoy-

KEY CLINICAL POINTS

TINNITUS

- Tinnitus occurs in up to one fourth of adults but is severely bothersome in less than 10%. When bothersome, tinnitus negatively affects sleep, concentration, emotions, and social enjoyment.
- Tinnitus is associated with hearing loss; audiologic testing is an important component in the evaluation of persistent tinnitus.
- Imaging is not indicated in the assessment of tinnitus except in cases in which tinnitus is localized to one ear, is pulsatile, or is associated with focal neurologic abnormalities or asymmetric hearing loss.
- Randomized, controlled trials of tinnitus treatments are limited by a lack of standardized assessments, short posttreatment follow-up, and high risk of bias.
- Treatments to reduce awareness of tinnitus and tinnitus-related distress include cognitive behavioral therapy, acoustic stimulation, and educational counseling. No medications, supplements, or herbal remedies have been shown to substantially reduce the severity of tinnitus.

ment, and difficulty hearing conversational speech.[10-12] In cross-sectional studies, tinnitus has been associated with increased odds of anxiety disorder[3] and depressive symptoms.[9] In a prospective study involving community-dwelling older adults in Japan, tinnitus was associated with an increased risk of subsequent development of depressive symptoms among men, even after adjustment for age and hearing impairment, although no significant association was observed among women.[13]

Psychophysical features of tinnitus such as loudness and pitch are not highly predictive of its psychological effect.[14,15] In one report, some patients who had a tinnitus loudness that matched a sensation level of less than 5 dB (as assessed by the patient identifying an external sound most consistent with the subjective tinnitus) were very disturbed by their condition, whereas other patients who had a tinnitus loudness that matched higher sensation levels were not.[14] This discrepancy may be explained by a person's attention to tinnitus. Whereas a majority of those with chronic tinnitus become used to it and do not pay attention to it, those who are highly disturbed by the tinnitus report constant awareness.

NATURAL HISTORY

The loudness, severity, and effect of tinnitus are dynamic and change over time. Tinnitus can progress in severity in some persons, but it can decrease in severity and even resolve in others (Table S1 in the Supplementary Appendix, available with the full text of this article at NEJM.org). For example, in one longitudinal study, approximately 40% of persons who had reported mild tinnitus and almost 20% who had reported severe tinnitus at baseline reported resolution at 5 years.[5] Familiarity with the natural changes in tinnitus that occur over time is important for counseling patients on expectations for improvement. Furthermore, the potential for a spontaneous reduction in the severity of tinnitus underscores the need for a control group in trials of interventions for this condition.

STRATEGIES AND EVIDENCE

DIAGNOSIS

Persons reporting tinnitus should be questioned about the nature of the sound (location, quality, and onset [gradual or sudden]), the duration of tinnitus, the effect of tinnitus on daily life (sleep, work, concentration, mood, and social activities), and associated symptoms, including hearing difficulties. A history of ear drainage, ear pain, or both would suggest possible infectious, inflammatory, or allergic ear disease; a history of vertigo and imbalance would suggest possible cochlear or retrocochlear disorders such as Meniere's disease, acoustic neuroma, or migraine-associated vertigo. The qualitative characteristics of tinnitus as described by patients may also suggest specific causes; for example, a roaring sound may indicate Meniere's disease, and a rhythmic clicking sound may indicate stapedial or tensor tympani muscle spasm. Acute tinnitus should be distinguished from persistent tinnitus, although there is no well-accepted definition of chronicity; in clinical trials, the definition ranges from a minimum duration of 3 months to a minimum duration of 12 months.[16,17]

Comprehensive audiologic evaluation for the presence, type, severity, and symmetry of hearing loss should be performed in patients with tinnitus who report hearing difficulties, persistent tinnitus of more than 6 months' duration, or unilateral tinnitus. Audiologic evaluation of patients with new-onset tinnitus of less than 6 months' duration is also reasonable, given its frequent association with hearing loss. The results of these evaluations will determine whether additional audiometric tests (e.g., otoacoustic emissions test, high-frequency audiometry, or auditory brainstem response test) or diagnostic imaging (e.g., magnetic resonance imaging or computed tomography of the temporal bone) are indicated. Additional audiologic investigations of the qualitative characteristics of tinnitus (e.g., pitch matching, loudness matching, or tinnitus suppression with acoustic stimulation [residual inhibition]) are not diagnostic and are not used in making management decisions.

Standardized questionnaires are available for use in clinical and research settings to assess the severity of tinnitus and its effect on specific domains of a person's daily life (communication, cognition, emotion, quality of life, and sleep).[18-20] These instruments are useful in the initial assessment of tinnitus and in monitoring changes with treatment. The Tinnitus Handicap Inventory is a widely used assessment tool that is sensitive to changes in tinnitus severity after treatment (see the Supplementary Appendix).[21]

MANAGEMENT

Population surveys show that the majority of people with tinnitus are minimally bothered by the sensation.[2,22,23] Those who seek evaluation often report concern that their tinnitus is a symptom of a much worse disease, such as progressive hearing loss and deafness.[24] An important component of management includes educating patients about the causes of tinnitus and the natural history of the condition, including possible spontaneous reduction in severity with time. The provision of educational materials, information on support groups, and other self-help materials to facilitate coping with tinnitus may be helpful for some patients (see the Supplementary Appendix).[25] Treatment discussions and management goals should emphasize modulation of the patient's attention and perceptual and emotional responses to the sensation.

MEDICATIONS AND SUPPLEMENTS

A wide range of drug classes have been tested in the treatment of tinnitus, including antidepressants, anxiolytics, antiepileptics, and anesthetics. Large systematic reviews have concluded that the strength of the evidence to support these agents is low.[16,26,27] For example, a Cochrane review of the use of antidepressants for the treatment of tinnitus identified only six trials that had sufficient quality for study, of which five were rated as "low quality," and concluded that there was no evidence of efficacy of antidepressant drug therapy in the management of tinnitus.[28] Whereas some studies have reported a reduction in subjective tinnitus loudness and an improvement in tinnitus-specific quality-of-life outcomes, these modest improvements are likely to reflect the modulation of depression and anxiety rather than direct effects on tinnitus. Current clinical practice guidelines do not recommend medication for management of the condition.[12] Nonprescription treatments such as herbal extracts, dietary supplements, and vitamins are commonly advertised as tinnitus cures, although they have no proven efficacy. Ginkgo biloba is the most commonly used supplement, and a systematic review of trials likewise did not show evidence of benefit in the alleviation of tinnitus.[29]

ACOUSTIC STIMULATION

Sound in a variety of forms and intensities has been used for centuries in the empirical treatment of tinnitus. The use of acoustic stimulation to treat tinnitus is currently based on the concept that hearing loss induces homeostatic compensatory changes within central structures (known as central auditory gain) to maintain auditory neural activity.[30] Tinnitus may be a maladaptive consequence of this process.[31] This proposed mechanism of tinnitus has been supported by findings from basic science research in animals, computational models, and functional imaging studies.[32-36] It has been hypothesized that acoustic stimulation may reverse the maladaptive changes by increasing neural activity in central auditory structures.[37]

The types of sound used for acoustic stimulation include broadband noise, amplification of speech and environmental sounds with hearing aids alone, and amplification with hearing aids in combination with broadband noise or music. Acoustic stimulation can be delivered at sound levels sufficient to make the tinnitus inaudible (masking) or at lower levels of intensity at which the tinnitus remains audible. A review of four trials of acoustic stimulation showed a benefit with respect to tinnitus-specific and global quality-of-life outcomes from interventions that used hearing aids or sound generators but did not show the superiority of any specific form of acoustic stimulation over another; however, the studies were noted to have methodologic limitations.[26] More recently, a randomized trial involving adults with chronic bothersome tinnitus and hearing loss showed a significantly greater benefit with the use of combination devices (hearing aids with sound generators) and directive counseling to reduce attention and emotional response to tinnitus than with the use of hearing aids (without sound generators) and counseling with information on strategies to cope with hearing loss and improve communication.[38] In this trial, the intention-to-treat analysis showed that the rates of clinically significant improvement (defined as ≥50% decrease in Tinnitus Handicap Inventory score from baseline to the 18-month follow-up) were greater in the group that received the combination devices and directive counseling than in the group that received hearing aids (without sound generators) and audiologic counseling (74% vs. 37%, $P<0.001$). In another trial, one that involved persons with tinnitus with minimal hearing loss, no significant difference in the rate of the same outcome (clinically significant improvement) was seen between persons who received treatment with sound generators and directive counseling and those who received audiologic counseling alone (50% and 25%, respectively; $P=0.16$), although decreases from baseline in subjective measures of tinnitus loudness were significantly greater at 12 months and 18 months in the group that received treatment with sound generators than in the group that received counseling alone ($P=0.04$).[39] Because counseling was different in the experimental and control groups in these trials, the effect of directive counseling versus the sound generator on the study outcomes is unknown.

Table 1. **Elements and Examples of Cognitive Behavioral Therapy for Tinnitus.**

Elements and Examples	Identify Distortions and Exaggerations	Address the Effect of Distortions and Exaggerations	Adopt Alternate Thoughts, Behaviors, and Strategies
Cognitive restructuring			
Example 1	*People think I am crazy because I have tinnitus.*	Recognize the inaccuracy and futility of mind reading.	*I can't assume others' thoughts without evidence.*
Example 2	*I wake up with my tinnitus and know it's going to be a bad day.*	Avoid jumping to conclusions.	*It is I, not the tinnitus, who controls what I do and determines how my day goes.*
Example 3	*My tinnitus is ruining my work and my life.*	Eliminate cognitive distortion.	Identify aspects of work and life not affected by tinnitus.
Framing the problem for developing solutions			
Example 1	*My tinnitus is making me lose my mind.*	Reframe: *I can't concentrate when there is no quiet time.*	Begin training exercises shown to improve concentration and refocus attention away from tinnitus.
Example 2	*My tinnitus is changing my personality.*	Reframe: *I get angry with people because my tinnitus keeps me from hearing conversations.*	Identify techniques and approaches that improve communication ability.
Behavioral modification			
Example	*Tinnitus has ruined my social life.*	Reframe: *Tinnitus ruins my ability to enjoy going out to dinner.*	Identify aspects of going out to dinner you can enjoy (e.g., the food, the scenery, or pleasant company) and focus on the positive.
Relaxation training		Recognize that stress and physical tension promote emotional arousal and impair coping with tinnitus.	Receive programmatic instruction on breathing exercises and progressive muscle relaxation.

PSYCHOLOGICAL THERAPY

The goal of psychological intervention is to decrease the negative effect of tinnitus on a patient's life and thereby improve well-being. Interventions typically address anxiety and depression because these are the most common psychological responses to tinnitus; such interventions include biofeedback training, hypnosis, and cognitive behavioral therapy.

Cognitive behavioral therapy is currently the most common psychological approach used and studied worldwide for the management of tinnitus. Cognitive behavioral therapy is a collaborative therapy that includes attention-refocusing techniques, relaxation training, mindfulness training, cognitive restructuring, and behavioral modification to change a person's reaction to tinnitus (Table 1); it can be delivered as individual therapy, as group therapy, or remotely (Internet-based therapy). The therapy is provided by a trained medical professional and typically includes once-weekly sessions of 1 to 2 hours in duration for 8 to 24 weeks.

Large systematic reviews of trials comparing cognitive behavioral therapy with either a no-treatment control (involving participants on a waiting list to receive treatment) or an active control with various combinations of yoga, education, biofeedback, relaxation, and distraction training have yielded mixed results.[26,40,41] Participants' subjective assessment of tinnitus loudness was not reduced from baseline in those who received cognitive behavioral therapy, those who received an active control, or those who were assigned to a waiting list to receive treatment. However, tinnitus-specific quality-of-life outcomes were significantly better with cognitive behavioral therapy than with the active or no-treatment control, with small to moderate effect sizes. Depression scores were significantly better with cognitive behavioral therapy than with the no-treatment control, but the results of comparisons between cognitive behavioral therapy and active controls (yoga or educational counseling) were inconsistent (Table S2 in the Supplementary Appendix). Overall, the strength of evidence to support cognitive behavioral therapy was considered to be low, given the high risk of bias and small sample sizes in most studies.[26]

OTHER THERAPY

Repetitive transcranial magnetic stimulation is an investigative treatment for tinnitus that involves the application of strong magnetic field impulses to the scalp to induce an electrical current that alters neural activity directly in the subjacent superficial cortex and indirectly in remote brain areas. Systematic reviews of randomized trials have found conflicting results with respect to a benefit, as well as a lack of information regarding the long-term effects; determination of effectiveness is complicated by methodologic limitations of available studies, including small sample sizes and variability in design and outcome measures.[42,43]

AREAS OF UNCERTAINTY

Research suggests that an abnormal engagement of attention may be a fundamental mechanism that perpetuates tinnitus and increases tinnitus severity.[44-47] In small, short-term trials, attention-training programs designed to modulate awareness of tinnitus through multisensory game-based play or repetitive training in identifying and localizing other sounds have resulted in reductions in tinnitus severity and improvements in quality-of-life scores.[48-50] A better understanding of the mechanisms of attention might lead to more effective treatments. Further study of the relationship between mood disorders and tinnitus and of treatment strategies for patients with coexisting medical conditions is also needed. Cognitive behavioral therapy requires active engagement and commitment; a better understanding of the factors predictive of response to this approach as well as to other interventions is needed.

The subjective nature of tinnitus, its range of causes and variable effects on patients, and the reduction in severity that may occur spontaneously over time make it a challenging condition to study. The limitations of many randomized trials of tinnitus treatments include a lack of blinding, differences among trials in the definition of bothersome tinnitus, small sample sizes, a lack of attention to many variables affecting tinnitus (e.g., associated mood disorder, hearing loss, duration and severity of the tinnitus, and stability of subjective severity scores), failure to account for placebo effects, and attention to some outcomes for which results are significant but not clinically meaningful.[17,51] A standardized instrument has been used as the primary outcome measure of the effect of tinnitus in only 20 to 36% of clinical trials.[17,51] Identifying research partici-

Table 2. Clinical Practice Guidelines from the American Academy of Otolaryngology–Head and Neck Surgery.

Recommendation*	Comment
Clinicians must:	
Distinguish patients with bothersome tinnitus from patients with nonbothersome tinnitus.	This can be facilitated by the use of standardized questionnaires and patient interviews. The importance of this distinction is to identify patients who require intervention beyond the initial evaluation, assessment, and education.
Clinicians should:	
Perform a targeted history and physical examination at the initial evaluation of a patient with presumed primary tinnitus.	The goal is to identify conditions that — if promptly identified and managed — may relieve tinnitus (e.g., tinnitus resulting from conductive hearing loss caused by cerumen occlusion of ear canal, middle-ear effusion, or ossicular chain fixation).
Obtain a prompt, comprehensive audiologic examination in patients with tinnitus that is unilateral, persistent (≥6 months), or associated with hearing difficulty.	Audiologic testing will facilitate identification of retrocochlear causes of tinnitus or tinnitus from sudden idiopathic hearing loss. Testing should always be performed when patients report difficulty hearing.
Distinguish patients with bothersome tinnitus of recent onset from those with persistent symptoms (≥6 months) to prioritize intervention and facilitate discussions about the natural history of tinnitus and follow-up care.	Patients benefit from knowing about spontaneous reduction in tinnitus severity observed in population studies. Tinnitus interventions can be prioritized on the basis of duration and severity of tinnitus.
Educate patients with persistent, bothersome tinnitus about management strategies.	Patients should not be told that nothing can be done to help them.
Recommend a hearing aid evaluation for patients with hearing loss and persistent bothersome tinnitus.	The evidence for using hearing aids as treatment shows a preponderance of benefit over harm. Quality of life is improved with improved communication and decreased awareness of tinnitus.
Recommend cognitive behavioral therapy to patients with persistent, bothersome tinnitus.	It is helpful to be knowledgeable in general about the process of cognitive behavioral therapy and to have access to trained professionals with expertise in this form of therapy.
Clinicians may:	
Obtain an initial comprehensive audiologic examination in patients who present with tinnitus (regardless of laterality, duration, or perceived hearing status)	
Recommend sound therapy to patients with persistent, bothersome tinnitus.	
Clinicians should not:	
Obtain imaging studies of the head and neck in patients with tinnitus specifically to evaluate the tinnitus, unless they have one or more of the following: tinnitus that is localized to one ear, pulsatile tinnitus, focal neurologic abnormalities, or asymmetric hearing loss.	The cost and risk associated with computed tomography and magnetic resonance imaging, combined with the low diagnostic yield, do not support their application outside the noted exceptions.
Routinely recommend antidepressants, anticonvulsants, anxiolytics, or intratympanic medications for a primary indication of treating persistent, bothersome tinnitus.	Systematic reviews have not supported the use of antidepressants in the treatment of tinnitus. Nevertheless, it is important to recognize that mood disorders can occur in association with bothersome tinnitus and to offer treatment or referral when clinically indicated.
Recommend ginkgo biloba, melatonin, zinc, or other dietary supplements for treating patients with persistent, bothersome tinnitus.	Patients should be informed about the lack of evidence for supplements as tinnitus treatments.
Recommend repetitive transcranial magnetic stimulation for the routine treatment of patients with persistent, bothersome tinnitus.	

* No recommendation is provided regarding the effect of acupuncture in patients with persistent bothersome tinnitus.

pants willing to enroll in tinnitus studies with 12 to 18 months of follow-up is challenging.[38] Long-term follow-up (at least 12 months) is often lacking; in a recent systematic literature review, the median duration of follow-up in 147 clinical trials was 3 months.[17]

GUIDELINES

The American Academy of Otolaryngology–Head and Neck Surgery (AAOHNS) published a clinical practice guideline for the evaluation and management of chronic bothersome tinnitus in adults.[16] This guideline applies to adults who have had tinnitus for at least 6 months, with no identifiable cause other than sensorineural hearing loss (Table 2). The recommendations in this article are largely consistent with those in the AAOHNS guideline; an exception is the stronger recommendation provided here for hearing aids, sound generators, and directive counseling, for which supporting data were not available at the time the AAOHNS guideline was developed.[38]

SUMMARY AND RECOMMENDATIONS

The patient described in the vignette has new-onset tinnitus in both ears, and the loudness is not asymmetric. I would obtain additional history regarding vertigo or fluctuating hearing loss and examine the patient for ear disease that might suggest an underlying disorder such as otosclerosis or Meniere's disease, although symmetric tinnitus would make these conditions unlikely. I would obtain a baseline assessment of tinnitus severity using the Tinnitus Handicap Inventory and an audiogram to determine the presence and level of hearing loss. If there is notable asymmetry in hearing, I would obtain diagnostic imaging. I would review the audiogram with the patient and discuss the relationship between hearing loss and tinnitus and what is known about the natural history of new-onset tinnitus with respect to resolution or reduction in severity over time. If hearing thresholds are outside the normal range, I would recommend hearing aids. I would discuss the potential benefit of educational counseling and acoustic stimulation with hearing aids or devices that combine hearing aids with sound generators to reduce the awareness of tinnitus and the negative effects on the patient's quality of life. If there is evidence of a coexisting mood disorder or moderate to severe distress, I would discuss the options of referral to a mental health professional and a treatment strategy of cognitive behavioral therapy.

Dr. Bauer reports receiving grant support from Sea Pharmaceuticals. No other potential conflict of interest relevant to this article was reported.

Disclosure forms provided by the author are available with the full text of this article at NEJM.org.

REFERENCES

1. Hoffman HJ, Reed GW. Epidemiology of tinnitus. In: Snow JB Jr., ed. Tinnitus: theory and management. Hamilton, ON, Canada: B.C. Decker, 2004:16-42.
2. Kim HJ, Lee HJ, An SY, et al. Analysis of the prevalence and associated risk factors of tinnitus in adults. PLoS One 2015; 10(5):e0127578.
3. Shargorodsky J, Curhan GC, Farwell WR. Prevalence and characteristics of tinnitus among US adults. Am J Med 2010; 123:711-8.
4. Coles RR. Epidemiology of tinnitus: (1) prevalence. J Laryngol Otol Suppl 1984; 9:7-15.
5. Nondahl DM, Cruickshanks KJ, Wiley TL, Klein R, Klein BE, Tweed TS. Prevalence and 5-year incidence of tinnitus among older adults: the Epidemiology of Hearing Loss Study. J Am Acad Audiol 2002;13:323-31.
6. Bhatt JM, Lin HW, Bhattacharyya N. Prevalence, severity, exposures, and treatment patterns of tinnitus in the United States. JAMA Otolaryngol Head Neck Surg 2016;142:959-65.
7. Degeest S, Corthals P, Vinck B, Keppler H. Prevalence and characteristics of tinnitus after leisure noise exposure in young adults. Noise Health 2014;16:26-33.
8. Manche SK, Madhavi J, Meganadh KR, Jyothy A. Association of tinnitus and hearing loss in otological disorders: a decade-long epidemiological study in a South Indian population. Braz J Otorhinolaryngol 2016;82:643-9.
9. Nondahl DM, Cruickshanks KJ, Huang GH, et al. Tinnitus and its risk factors in the Beaver Dam Offspring Study. Int J Audiol 2011;50:313-20.
10. Tyler RS, Baker LJ. Difficulties experienced by tinnitus sufferers. J Speech Hear Disord 1983;48:150-4.
11. Jakes SC, Hallam RS, Chambers C, Hinchcliffe R. A factor analytical study of tinnitus complaint behaviour. Audiology 1985;24:195-206.
12. Axelsson A, Ringdahl A. Tinnitus — a study of its prevalence and characteristics. Br J Audiol 1989;23:53-62.
13. Michikawa T, Nishiwaki Y, Saito H, Mizutari K, Takebayashi T. Tinnitus preceded depressive symptoms in community-dwelling older Japanese: a prospective cohort study. Prev Med 2013;56:333-6.
14. Tyler RS, Stouffer JL. A review of tinnitus loudness. Hear J 1989;42:52-7.
15. Meikle MB, Vernon J, Johnson RM. The perceived severity of tinnitus: some observations concerning a large population of tinnitus clinic patients. Otolaryngol Head Neck Surg 1984;92:689-96.
16. Tunkel DE, Bauer CA, Sun GH, et al. Clinical practice guideline: tinnitus. Otolaryngol Head Neck Surg 2014;151:Suppl: S1-S40.
17. Plein CT, Harounian J, Floyd E, et al. A systematic review of eligibility and outcomes in tinnitus trials: reassessment of tinnitus guideline. Otolaryngol Head Neck Surg 2016;154:24-32.
18. Kuk FK, Tyler RS, Russell D, Jordan H. The psychometric properties of a tinnitus handicap questionnaire. Ear Hear 1990; 11:434-45.
19. Hallam RS, Jakes SC, Hinchcliffe R. Cognitive variables in tinnitus annoyance. Br J Clin Psychol 1988;27:213-22.
20. Newman CW, Jacobson GP, Spitzer JB. Development of the Tinnitus Handicap Inventory. Arch Otolaryngol Head Neck Surg 1996;122:143-8.
21. Newman CW, Sandridge SA, Jacobson GP. Psychometric adequacy of the Tinnitus Handicap Inventory (THI) for evaluating treatment outcome. J Am Acad Audiol 1998;9:153-60.
22. Gopinath B, McMahon CM, Rochtchina E, Karpa MJ, Mitchell P. Incidence, persistence, and progression of tinnitus

symptoms in older adults: the Blue Mountains Hearing Study. Ear Hear 2010;31: 407-12.
23. Leske MC. Prevalence estimates of communicative disorders in the U.S.: speech disorders. ASHA 1981;23:217-25.
24. Stouffer JL, Tyler RS. Characterization of tinnitus by tinnitus patients. J Speech Hear Disord 1990;55:439-53.
25. American Academy of Otolaryngology–Head and Neck Surgery. Clinical practice guideline: tinnitus (http://www.entnet.org/content/clinical-practice-guideline-tinnitus).
26. Pichora-Fuller MK, Santaguida P, Hammill A, et al. Evaluation and treatment of tinnitus: comparative effectiveness (report no. 13-EHC110-EF). Rockville, MD: Agency for Healthcare Research and Quality, 2013.
27. Hoekstra CE, Rynja SP, van Zanten GA, Rovers MM. Anticonvulsants for tinnitus. Cochrane Database Syst Rev 2011;7: CD007960.
28. Baldo P, Doree C, Molin P, McFerran D, Cecco S. Antidepressants for patients with tinnitus. Cochrane Database Syst Rev 2012;9:CD003853.
29. Hilton MP, Zimmermann EF, Hunt WT. Ginkgo biloba for tinnitus. Cochrane Database Syst Rev 2013;3:CD003852.
30. Auerbach BD, Rodrigues PV, Salvi RJ. Central gain control in tinnitus and hyperacusis. Front Neurol 2014;5:206.
31. Noreña AJ. An integrative model of tinnitus based on a central gain controlling neural sensitivity. Neurosci Biobehav Rev 2011;35:1089-109.
32. Noreña AJ, Eggermont JJ. Enriched acoustic environment after noise trauma abolishes neural signs of tinnitus. Neuroreport 2006;17:559-63.
33. Schaette R, McAlpine D. Tinnitus with a normal audiogram: physiological evidence for hidden hearing loss and computational model. J Neurosci 2011;31: 13452-7.
34. Schaette R, Kempter R. Computational models of neurophysiological correlates of tinnitus. Front Syst Neurosci 2012;6:34.
35. Gu JW, Herrmann BS, Levine RA, Melcher JR. Brainstem auditory evoked potentials suggest a role for the ventral cochlear nucleus in tinnitus. J Assoc Res Otolaryngol 2012;13:819-33.
36. Brozoski T, Brozoski D, Wisner K, Bauer C. Chronic tinnitus and unipolar brush cell alterations in the cerebellum and dorsal cochlear nucleus. Hear Res 2017;350:139-51.
37. Schaette R, Kempter R. Development of tinnitus-related neuronal hyperactivity through homeostatic plasticity after hearing loss: a computational model. Eur J Neurosci 2006;23:3124-38.
38. Bauer CA, Berry JL, Brozoski TJ. The effect of tinnitus retraining therapy on chronic tinnitus: a controlled trial. Laryngoscope Investig Otolaryngol 2017;2:166-77.
39. Bauer CA, Brozoski TJ. Effect of tinnitus retraining therapy on the loudness and annoyance of tinnitus: a controlled trial. Ear Hear 2011;32:145-55.
40. Hesser H, Weise C, Westin VZ, Andersson G. A systematic review and meta-analysis of randomized controlled trials of cognitive-behavioral therapy for tinnitus distress. Clin Psychol Rev 2011;31: 545-53.
41. Martinez-Devesa P, Perera R, Theodoulou M, Waddell A. Cognitive behavioural therapy for tinnitus. Cochrane Database Syst Rev 2010;9:CD005233.
42. Soleimani R, Jalali MM, Hasandokht T. Therapeutic impact of repetitive transcranial magnetic stimulation (rTMS) on tinnitus: a systematic review and meta-analysis. Eur Arch Otorhinolaryngol 2016;273:1663-75.
43. Meng Z, Liu S, Zheng Y, Phillips JS. Repetitive transcranial magnetic stimulation for tinnitus. Cochrane Database Syst Rev 2011;10:CD007946.
44. Brozoski TJ, Bauer CA. Animal models of tinnitus. Hear Res 2016;338:88-97.
45. Rossiter S, Stevens C, Walker G. Tinnitus and its effect on working memory and attention. J Speech Lang Hear Res 2006;49:150-60.
46. Roberts LE, Husain FT, Eggermont JJ. Role of attention in the generation and modulation of tinnitus. Neurosci Biobehav Rev 2013;37:1754-73.
47. Husain FT, Akrofi K, Carpenter-Thompson JR, Schmidt SA. Alterations to the attention system in adults with tinnitus are modality specific. Brain Res 2015; 1620:81-97.
48. Searchfield GD, Morrison-Low J, Wise K. Object identification and attention training for treating tinnitus. Prog Brain Res 2007;166:441-60.
49. Spiegel DP, Linford T, Thompson B, et al. Multisensory attention training for treatment of tinnitus. Sci Rep 2015;5: 10802.
50. Wise K, Kobayashi K, Magnusson J, Welch D, Searchfield GD. Randomized controlled trial of a perceptual training game for tinnitus therapy. Games Health J 2016;5:141-9.
51. Hall DA, Haider H, Szczepek AJ, et al. Systematic review of outcome domains and instruments used in clinical trials of tinnitus treatments in adults. Trials 2016; 17:270.

BEFORE THE PUBLIC UTILITY COMMISSION
OF OREGON

Docket PCN 5

In the Matter of

IDAHO POWER COMPANY'S
PETITION FOR CERTIFICATE OF PUBLIC CONVENIENCE
AND NECESSITY

Dinces, E. A., Etiology and Diagnosis of Tinnitus (2023)

February 22, 2023

Etiology and diagnosis of tinnitus

Author: Elizabeth A Dinces, MD
Section Editor: Daniel G Deschler, MD, FACS
Deputy Editor: Lisa Kunins, MD

All topics are updated as new evidence becomes available and our peer review process is complete.

Literature review current through: Feb 2022. | **This topic last updated:** Oct 06, 2021.

INTRODUCTION

Tinnitus is a perception of sound in proximity to the head in the absence of an external source. It can be perceived as being within one or both ears, within or around the head, or as an outside distant noise. The sound is often a buzzing, ringing, or hissing, although it can also sound like other noises.

Tinnitus can be continuous or intermittent. Although both may have a significant impact on the patient, the latter is not usually related to a serious underlying medical problem. The sound may be pulsatile or non-pulsatile. Pulsatile tinnitus raises more concern for underlying significant pathology, though non-pulsatile tinnitus may also be associated with underlying disease.

The epidemiology, pathogenesis, and diagnosis of tinnitus will be reviewed here. The treatment of tinnitus is discussed separately. (See "Treatment of tinnitus".)

EPIDEMIOLOGY

According to the American Tinnitus Association, an estimated 50 million people in the United

States have chronic tinnitus, persisting for greater than six months [1]. For 12 million, it is severe enough to interfere with daily activities. These people are effectively disabled by their tinnitus to varying degrees.

Tinnitus can occur in children [2] and increases with age [3,4]. Tinnitus is more common in men than in women and is more likely to occur among individuals who smoke [1].

CLINICAL IMPACT

The impact of tinnitus on an individual can be significant. Some individuals "experience" tinnitus, while others "suffer from it." Overall, about 25 percent of tinnitus sufferers report an increase in tinnitus severity over time [5]. Chronic tinnitus is unlikely to remit completely but often becomes less bothersome over time, especially in the setting of hearing loss.

The impact of tinnitus can be consistently measured by two outcome instruments: the Tinnitus Handicap Inventory (form 1) [6] and the Tinnitus Reaction Questionnaire [7]. Studies indicate that the degree of disability perceived by tinnitus patients, and its impact on the patient's quality of life, does not directly correlate with loudness, type of tinnitus, or length of time with tinnitus.

Concurrent mood disorders can increase the perception of disability. Increased tinnitus disability also has been demonstrated in patients with insomnia [8].

PATHOGENESIS

Tinnitus can be unilateral or bilateral and can be triggered anywhere along the auditory pathway (figure 1) [9]. It is believed to be encoded in neurons within the auditory cortex. The majority of patients have "sensorineural" tinnitus due to hearing loss at the cochlea or cochlear nerve level.

Somatic sounds may be perceived as tinnitus and originate in structures with proximity to the cochlea. These sounds are often generated in vascular structures but may also be produced by musculoskeletal structures. Somatic sounds are most often associated with pulsatile tinnitus and are typically unilateral. Continuous tonal tinnitus (single pure-tone) is usually not somatic in origin.

Pathogenetic theories postulate that the central nervous system is the source or "generator" of all tinnitus that does not have a somatic origin, even in patients whose associated hearing losses are due to cochlear injury [10]. Tinnitus generated by the central nervous system can be unilateral or bilateral, and the side of the tinnitus may not always correspond with the side of initial injury. Positron-emission tomography (PET) scanning and functional magnetic resonance imaging (MRI) studies indicate that the loss of cochlear input to neurons in the central auditory pathways (such as occurs with cochlear hair cell damage due to ototoxicity, noise trauma, or a lesion of the cochlear nerve) can result in abnormal neural activity in the auditory cortex. Such activity has been linked to the perception of tinnitus [11,12].

Another construct likens tinnitus to phantom pain perception that is thought to arise from a loss of suppression of neural activity [13-15]. Known neural feedback loops act to help tune and reinforce auditory memory in the central auditory cortex. Disruption of auditory input or the feedback loop may lead to the creation of alternative neural synapses and to loss of inhibition of normal synapses.

Tinnitus has also been likened to a type of auditory seizure [16], and antiseizure medications have had limited success in some patients [17]. Abnormal auditory-evoked magnetic field potentials associated with tinnitus can be suppressed in selected patients with intravenous lidocaine [18], confirming a central tinnitus phenomenon and potentially indicating a physiologic mechanism for lidocaine sensitive tinnitus. (See "Treatment of tinnitus", section on 'Medications'.)

Electrical stimulation, with round window electrodes or promontory stimulation, can suppress tinnitus in patients with profound hearing loss [19,20]. Electrical promontory stimulation may suppress abnormal spontaneous activity of cochlear nerve fibers; alternatively, it may provide background activity that acts to suppress abnormal central neural connections in patients with baseline sensorineural hearing loss and tinnitus. Cochlear implantation for hearing loss has had a secondary result of relieving tinnitus, with reported success for tinnitus improvement varying from 34 to 93 percent [21,22].

Many patients with tinnitus exhibit signs of anxiety and/or depression [23], and elevated serum serotonin levels have been found in some tinnitus patients [24]. Serotonin and gamma-aminobutyric acid (GABA) receptors are found throughout the auditory system, and neurotransmitter abnormalities may play a role in some patients with tinnitus [24-26].

These theories encompass disruption of normal neural firing patterns along the entire auditory pathway, from the end organ to the auditory cortex. They may explain tinnitus in patients who do not exhibit hearing loss, as well as in patients who recover from temporary hearing loss (eg, noise-induced hearing loss) but develop tinnitus that is persistent.

ETIOLOGY

Vascular disorders — Pulsatile tinnitus is most commonly, though not exclusively, vascular in etiology. Some vascular tinnitus, such as venous hums and tinnitus due to atherosclerotic plaque narrowing of vessels, can be non-pulsatile. Vascular tinnitus can be unilateral or bilateral; when bilateral, it is typically louder on the side of the pathology.

In a retrospective review of 84 patients with pulsatile tinnitus seen in a neurology department, 42 percent were found to have a significant vascular disorder (most commonly a dural arteriovenous fistula [AVF] or a carotid-cavernous sinus fistula) [27]. In 12 patients (14 percent), nonvascular disorders such as paraganglioma or intracranial hypertension (due to a variety of causes) explained the tinnitus.

Arterial bruits — Arterial vessels near the temporal bone may transmit sounds associated with turbulent blood flow, especially if the loudness of the sound exceeds the hearing threshold in that ear. The petrous carotid system is the most common source, although other arteries may also be involved [28]. An arterial bruit is not itself a serious condition, although the patient may require an evaluation for underlying atherosclerotic disease.

These patients usually do not have other otologic complaints (eg, hearing loss, vertigo, aural fullness). As with many other causes of tinnitus, their tinnitus is greatest in quiet environments (eg, at night).

Arteriovenous shunts — Congenital arteriovenous malformations (AVMs) are rarely associated with hearing loss or tinnitus. AVFs are more likely to be symptomatic, usually ipsilateral to the fistula. Dural AVFs are often associated with dural venous sinus thrombosis, which may occur spontaneously or be associated with infection, tumor, trauma, or surgery. Large dural AVFs can result in intracranial hemorrhage; early detection and treatment (surgery and/or vascular embolization) can be life-saving for high-grade lesions. (See "Nonaneurysmal subarachnoid hemorrhage", section on 'Intracranial'.)

Paraganglioma — Head and neck paragangliomas are highly vascular, typically benign neoplasms arising from cells of the paraganglia that are found around the carotid bifurcation, within the jugular bulb, or along the tympanic arteries in the middle ear. Tympanic paragangliomas, previously known as glomus tympanicum tumors, and jugular bulb paragangliomas, commonly known as glomus jugulare, both commonly cause a loud pulsing tinnitus that may interfere with hearing. The tinnitus is typically unilateral, and the lesion may be visible through the tympanic membrane as a reddish or blue mass or may be palpable in the neck. As the tumor enlarges, it may cause hearing loss because of impingement on the ossicular chain (conductive loss) or the labyrinth or cochlea (sensorineural loss). Other cranial nerves may also be affected (eg, facial nerve or lower cranial nerve palsies). Paragangliomas of the head and neck are discussed separately. (See "Paragangliomas: Epidemiology, clinical presentation, diagnosis, and histology", section on 'Definition and anatomic origin' and "Paragangliomas: Epidemiology, clinical presentation, diagnosis, and histology", section on 'Head and neck paragangliomas'.)

Venous hums — These may be heard in patients with systemic hypertension, increased intracranial pressure (often due to pseudotumor cerebri) (see "Idiopathic intracranial hypertension (pseudotumor cerebri): Clinical features and diagnosis", section on 'Pulsatile tinnitus'), or in patients with a dehiscent or dominant jugular bulb (abnormally high placement of the jugular bulb). The latter may also cause a conductive hearing loss. Tinnitus in patients with a venous hum is often described as a soft, low-pitched hum that may decrease or stop with pressure over the jugular vein, with a change in head position, or with activity [28]. When tinnitus is due to asymmetry in the venous system, the tinnitus can be unilateral, or bilateral but louder on one side.

Neurologic disorders — Pulsatile tinnitus of muscular origin can result from spasm of one or both of the muscles within the middle ear (the tensor tympani and the stapedius muscle).

These muscles are innervated by cranial nerves V and VII respectively. Such muscle spasms can occur spontaneously, because of local otologic disease, and also in the presence of neurologic disease such as multiple sclerosis. Patients may also complain of hearing loss or aural fullness associated with these muscle spasms. Tympanometry and otoscopy can be particularly useful in diagnosing middle ear spasmodic activity.

Clicking noises or irregular or rapid pulsations may also result from myoclonus of the palatal muscles that attach to the Eustachian tube orifice. Myoclonus of the palatal muscles most often is caused by an underlying neurologic abnormality, such as multiple sclerosis, microvascular disease affecting the brainstem, or neuropathy related to metabolic or toxic etiology; the history and physical examination should include a search for other neurologic disease.

Tinnitus due to myoclonus can be either unilateral or bilateral; when unilateral, symptoms are ipsilateral to the site of the muscle spasm.

Eustachian tube dysfunction — A patulous Eustachian tube can cause unilateral or bilateral tinnitus, with sounds similar to an ocean roar that may be synchronous with respiration [28]. It most commonly occurs after significant weight loss or after external beam radiation to or near the nasopharynx. The symptoms may disappear when the patient lies down. Patients can also complain of an unusual awareness of their own voice (autophony) and of ear discomfort. The cause of these symptoms is a Eustachian tube that remains abnormally patent, allowing too much and then too little aeration of the middle ear space with respiration. (See "Eustachian tube dysfunction", section on 'History'.)

Other somatic disorders — Somatic non-pulsatile tinnitus is commonly caused by temporomandibular joint (TMJ) dysfunction [29] and has also been associated with whiplash injuries [30] and other cervical-spinal disorders [31]. Tinnitus may improve when patients respond favorably to treatment for symptoms of TMJ dysfunction and craniocervical disease. The exact neurophysiologic mechanism for the generation of tinnitus from either the TMJ or the cervical spine is not known but may involve disinhibition of the dorsal cochlear nucleus [30]. In cases of somatic tinnitus, unilateral or bilateral symptoms may occur.

Tinnitus with a machine-like grinding or pulsing character is sometimes associated with intracranial lesions, such as chondrosarcoma, aberrant carotid artery, and endolymphatic sac tumors.

Tinnitus originating from the auditory system — Most tinnitus is due to a sensorineural hearing loss with resulting dysfunction within the auditory system. The auditory system includes the cochlear end organ, the cochlear nerve (with its projections to and from the cochlea), the brainstem (site of the cochlear nuclei), and the primary and secondary auditory cortical projections (figure 1).

Etiologies of tinnitus generated from within the auditory system are as varied as the types of noises that patients report (table 1). The presence of tinnitus often is an early indicator of cochlear hair cell dysfunction or loss, as in the case of prolonged noise exposure [32], Meniere disease (also characterized by aural fullness and vertigo), or ototoxicity. (See "Etiology of hearing loss in adults", section on 'Inner ear causes' and "Meniere disease: Evaluation, diagnosis, and management", section on 'Clinical presentation'.)

Ototoxic medications — Tinnitus is commonly caused by ototoxic medications (table 2); the ototoxicity typically affects both sides, causing bilateral symptoms. Ototoxicity affects the various components of the cochleovestibular end organ. When such structures are damaged, a change in neural firing between the end organ and the remainder of the auditory system can be exhibited by hearing loss, distortions in hearing, or tinnitus. (See "Etiology of hearing loss in adults", section on 'Ototoxic substances'.)

Presbycusis — Presbycusis (sensorineural hearing loss with aging) or any acquired high-frequency hearing loss is commonly associated with tinnitus (often described as a high-pitched ringing sound, crickets, or bells in the ear) along with the hearing loss. Cochlear hearing losses can be asymmetric, and even when symmetric they can result in unilateral or bilateral tinnitus. (See "Presbycusis", section on 'Tinnitus'.)

Otosclerosis — This is a condition of abnormal bone repair of the stapes footplate bone (third bone in the ossicular chain) and of the otic capsule. Tinnitus can result when otosclerosis damages cochlear structures. Progressive otosclerosis can result in fixation of the stapes footplate and worsening conductive hearing loss which can be unilateral or bilateral. (See "Etiology of hearing loss in adults", section on 'Otosclerosis'.)

Vestibular schwannoma — Tumors compressing or stretching the cochlear nerve can cause tinnitus. In addition, unilateral tinnitus can be the presenting sign of a schwannoma of the vestibular nerve within the cerebellar-pontine angle or the internal auditory canal (acoustic neuroma). (See "Vestibular schwannoma (acoustic neuroma)".)

Chiari malformations — Tinnitus, unilateral or bilateral, is one of the auditory signs associated with a symptomatic Chiari malformation and occurs when low-lying cerebellar tonsils causes tension on the auditory nerve [33]. Tinnitus from Chiari malformations can be both unilateral or bilateral.

Other etiologies — Hearing loss due to a variety of causes, including vascular ischemic events, infection, nerve compression, genetic predisposition, congenital hearing loss, or endocrine or metabolic damage to the auditory system, can produce tinnitus to a variable degree.

Tinnitus may occur with barotrauma to the middle or inner ear (often associated with vertigo and hearing loss) and with fluid in the middle ear (eg, with otitis media). (See "Etiology of hearing loss in adults" and "Acute otitis media in adults", section on 'Otitis media with effusion'.)

DIAGNOSIS

Tinnitus is frequently associated with hearing loss or other cochlear injury, and it may be the presenting complaint in a patient with a central nervous system lesion. History and physical examination are the first steps in establishing the etiology of tinnitus. Some patients may also warrant audiology examination, particularly those with unilateral tinnitus; although unilateral symptoms can direct aspects of the workup, it does not necessarily portend more worrisome diagnoses. Other tests, including imaging, are warranted in specific circumstances.

History — The history in patients with tinnitus should include a description of the tinnitus (episodic or constant, pulsatile or non-pulsatile, rhythmicity, pitch, quality of the sound), as well as inciting or alleviating factors. Patients should be asked about previous ear disease, noise exposure, hearing status, head injury, and symptoms suggesting temporomandibular joint (TMJ) syndrome. All medications and supplements should be reviewed. The history should review other medical conditions, including hypertension, atherosclerosis, neurologic illness, and prior surgery. Patients should be specifically asked about depression, anxiety, and insomnia, which can both exacerbate tinnitus and magnify its impact on quality of life. Patients complaining of tinnitus should also be asked if they have difficulty hearing or have noted a hearing loss.

Tinnitus that is distinctly pulsing or is described as rushing, flowing, or humming is usually vascular in origin. Patients often describe an increase in frequency and intensity with exercise, and some may recognize a connection with their pulse. Changes in intensity or pitch with head motion or body position (lying down versus sitting or standing) also strongly suggest a vascular tinnitus.

Clicking tinnitus almost always has a physiologic explanation. Myoclonus of the palatal muscles or middle ear structures can occur spontaneously but may also suggest significant neurologic disease. Some patients report a mechanical sounding tinnitus that is not tonal in nature. A diligent investigation searching for vascular or somatic causes is warranted for this rare complaint.

Tonal descriptions of tinnitus can help in the evaluation of a patient for a specific diagnosis or treatment.

- A high-pitched continuous tone is by far the most commonly described type of tinnitus. High-pitched tinnitus is frequently a result of a sensorineural hearing loss or may suggest cochlear injury.
- Low-pitched tinnitus is often seen in patients with Meniere disease, although it also can be idiopathic.

Physical examination — A complete head and neck examination, including cranial nerve examination and evaluation of the tympanic membrane, should be performed in all patients. Palatal myoclonus may be suppressed upon wide jaw opening; thus, its absence on oral examination does not rule out the diagnosis (nasopharyngoscopy may be indicated when suspicion is high).

In patients with suspected vascular tinnitus, auscultation over the neck, periauricular area, temple, orbit, and mastoid should be performed in various positions. The effects of positioning and vascular compression of the neck on the involved side should be noted. Tinnitus of venous origin can often be suppressed by careful pressure on the jugular vein.

Specialized testing

Suspected vascular tinnitus — Patients with infrequent episodes of pulsatile tinnitus or those with short-duration, mild tinnitus can be initially observed.

However, because frequent or constant pulsatile tinnitus can herald a potentially life-threatening illness, all of these patients require evaluation by an otolaryngologist or neurotologist. When physical examination does not reveal a specific vascular or musculoskeletal source in these patients, further investigation to rule out a central nervous system lesion such as a dural arteriovenous fistula (AVF), arteriovenous malformation (AVM) or aneurysm, or a skull base tumor should be carried out [34].

The gold standard for AVF diagnosing intracranial vascular lesions is angiography. These lesions often can also be diagnosed noninvasively with magnetic resonance (MR) angiography [35] or computed tomographic (CT) angiography [36]. High-resolution CT scanning is required to delineate the extent of involvement of the skull base if a paraganglioma is suspected and may be sufficient to evaluate other central nervous system lesions in selected patients. MRI can diagnose a Chiari malformation, vasculitis, central nervous system tumors, and multiple sclerosis and may indicate the presence of increased intracranial pressure (such as that seen in pseudotumor cerebri) or tumors. Many patients require both contrast MRI and contrast CT because of the varied nature of disorders that cause pulsatile tinnitus. If both of these studies are normal, and suspicion for a vascular lesion remains high, angiography or MR angiography is warranted.

Our protocol involves audiometric testing followed by an extensive history and physical exam, which guides additional diagnostic testing. When an intracranial vascular lesion is suspected, we obtain an MRI with contrast initially, followed by CT/CT angiography and subsequent interventional angiography in appropriate circumstances.

Suspected auditory system tinnitus — For patients with tinnitus associated with hearing loss or a change in hearing, audiometric tests may help determine if the tinnitus originates within the auditory system and are essential in the evaluation. Any patient with constant unilateral or bilateral tinnitus persistent for six months or more should also be referred for a formal audiology evaluation [37].

Initial audiometric tests should include a pure-tone audiogram, tympanometry, auditory reflex testing, determination of speech discrimination abilities, and otoacoustic emissions testing. These tests identify asymmetries between the two ears and indicate abnormalities in the middle ear, cochlea, and brainstem; as well, they can define the site of abnormality within the auditory system or confirm normal functioning. Such testing is performed in an audiologist's office, ideally one affiliated with an otolaryngology department or practice.

Asymmetry in hearing function, reflex testing, or otoacoustic emissions, in patients with no identified otologic abnormality, should be followed-up with auditory brainstem response testing (ABR) and imaging studies (eg, MRI) to rule out inner ear anomalies, central nervous system lesions, and neurologic disease. Further workup may involve neurologic or neurosurgical consultation, endocrine evaluation, or angiography.

SOCIETY GUIDELINE LINKS

Links to society and government-sponsored guidelines from selected countries and regions around the world are provided separately. (See "Society guideline links: Hearing loss and hearing disorders in adults".)

INFORMATION FOR PATIENTS

UpToDate offers two types of patient education materials, "The Basics" and "Beyond the Basics." The Basics patient education pieces are written in plain language, at the 5th to 6th grade reading level, and they answer the four or five key questions a patient might have about a given condition. These articles are best for patients who want a general overview and who prefer short, easy-to-read materials. Beyond the Basics patient education pieces are longer, more sophisticated, and more detailed. These articles are written at the 10th to 12th grade reading level and are best for patients who want in-depth information and are comfortable with some medical jargon.

Here are the patient education articles that are relevant to this topic. We encourage you to print or e-mail these topics to your patients. (You can also locate patient education articles on a variety of subjects by searching on "patient info" and the keyword(s) of interest.)

- Basics topic (see "Patient education: Tinnitus (ringing in the ears) (The Basics)")
- Beyond the Basics topic (see "Patient education: Tinnitus (ringing in the ears) (Beyond the Basics)")

SUMMARY AND RECOMMENDATIONS

- Tinnitus affects 50 million people in the United States and interferes with daily activity in a quarter of those affected. Prevalence is greater in men and increases with age. (See 'Epidemiology' above.)
- Pulsatile tinnitus is most commonly vascular in origin and requires thorough evaluation.
  - Vascular tinnitus can be unilateral or bilateral; when bilateral, it is typically louder on the side of the pathology. Differential diagnosis includes intracranial arteriovenous malformation (AVM), arteriovenous fistula (AVF), arterial bruit, and paraganglioma. (See 'Vascular disorders' above.)
  - Clicking pulsatile tinnitus may indicate a neurologic disorder causing myoclonus of palatal muscles or of the muscles in the inner ear. Tinnitus can be either unilateral or bilateral; when unilateral, symptoms are ipsilateral to the site of the muscle spasm. (See 'Neurologic disorders' above.)
- Tinnitus most commonly is a result of abnormalities within the auditory system, often with unexplained etiology. It may be associated with sensorineural hearing loss, ototoxic medications, infection, vascular ischemia, or acoustic neuroma. (See 'Tinnitus originating from the auditory system' above.)
- All sensorineural tinnitus is believed to be generated within the central nervous system,

with cochlear abnormalities leading to loss of inhibition of cortical auditory neurons. Serotonergic neurotransmitters may play a role. (See 'Pathogenesis' above.)

- Evaluation of tinnitus should include a thorough history, an examination including auscultation for bruits in patients with possible vascular tinnitus, and a complete head and neck examination in all patients. (See 'Diagnosis' above.)

- Patients with pulsatile tinnitus, other than those with infrequent intermittent symptoms, should have otolaryngologic investigation and may require contrast computed tomography (CT) scanning, contrast magnetic resonance (MR) scanning, and/or angiography. (See 'Suspected vascular tinnitus' above.)

- For patients with tinnitus suspected of arising within the auditory system, and for those with unilateral tinnitus, audiometric testing is indicated. (See 'Suspected auditory system tinnitus' above.)

REFERENCES

1. Shargorodsky J, Curhan GC, Farwell WR. Prevalence and characteristics of tinnitus among US adults. Am J Med 2010; 123:711.
2. Shetye A, Kennedy V. Tinnitus in children: an uncommon symptom? Arch Dis Child 2010; 95:645.
3. Adams PF, Hendershot GE, Marano MA, Centers for Disease Control and Prevention/National Center for Health Statistics. Current estimates from the National Health Interview Survey, 1996. Vital Health Stat 10 1999; :1.
4. Ahmad N, Seidman M. Tinnitus in the older adult: epidemiology, pathophysiology and treatment options. Drugs Aging 2004; 21:297.
5. Stouffer JL, Tyler RS. Characterization of tinnitus by tinnitus patients. J Speech Hear Disord 1990; 55:439.
6. Newman CW, Sandridge SA, Jacobson GP. Psychometric adequacy of the Tinnitus Handicap Inventory (THI) for evaluating treatment outcome. J Am Acad Audiol 1998;

9:153.

7. Wilson PH, Henry J, Bowen M, Haralambous G. Tinnitus reaction questionnaire: psychometric properties of a measure of distress associated with tinnitus. J Speech Hear Res 1991; 34:197.
8. Folmer RL, Griest SE, Meikle MB, Martin WH. Tinnitus severity, loudness, and depression. Otolaryngol Head Neck Surg 1999; 121:48.
9. Minen MT, Camprodon J, Nehme R, Chemali Z. The neuropsychiatry of tinnitus: a circuit-based approach to the causes and treatments available. J Neurol Neurosurg Psychiatry 2014; 85:1138.
10. Qiu C, Salvi R, Ding D, Burkard R. Inner hair cell loss leads to enhanced response amplitudes in auditory cortex of unanesthetized chinchillas: evidence for increased system gain. Hear Res 2000; 139:153.
11. Melcher JR, Sigalovsky IS, Guinan JJ Jr, Levine RA. Lateralized tinnitus studied with functional magnetic resonance imaging: abnormal inferior colliculus activation. J Neurophysiol 2000; 83:1058.
12. Lockwood AH, Salvi RJ, Coad ML, et al. The functional neuroanatomy of tinnitus: evidence for limbic system links and neural plasticity. Neurology 1998; 50:114.
13. Lockwood AH, Salvi RJ, Burkard RF, et al. Neuroanatomy of tinnitus. Scand Audiol Suppl 1999; 51:47.
14. Møller AR. Similarities between chronic pain and tinnitus. Am J Otol 1997; 18:577.
15. Mühlnickel W, Elbert T, Taub E, Flor H. Reorganization of auditory cortex in tinnitus. Proc Natl Acad Sci U S A 1998; 95:10340.
16. Shulman A, Goldstein B. Medical Significance of Tinnitus. Int Tinnitus J 1997; 3:45.
17. Sanchez TG, Balbani AP, Bittar RS, et al. Lidocaine test in patients with tinnitus: rationale of accomplishment and relation to the treatment with carbamazepine. Auris Nasus Larynx 1999; 26:411.
18. Shiomi Y, Nagamine T, Fujiki N, et al. Tinnitus remission by lidocaine demonstrated by auditory-evoked magnetoencephalogram. A preliminary report. Acta Otolaryngol 1997; 117:31.

19. Portmann M, Cazals Y, Negrevergne M, Aran JM. Temporary tinnitus suppression in man through electrical stimulation of the cochlea. Acta Otolaryngol 1979; 87:294.
20. Matsushima JI, Fujimura H, Sakai N, et al. A study of electrical promontory stimulation in tinnitus patients. Auris Nasus Larynx 1994; 21:17.
21. Ito J. Tinnitus suppression in cochlear implant patients. Otolaryngol Head Neck Surg 1997; 117:701.
22. Miyamoto RT, Bichey BG. Cochlear implantation for tinnitus suppression. Otolaryngol Clin North Am 2003; 36:345.
23. Holgers KM, Zöger S, Svedlund K. Predictive factors for development of severe tinnitus suffering-further characterisation. Int J Audiol 2005; 44:584.
24. Simpson JJ, Davies WE. A review of evidence in support of a role for 5-HT in the perception of tinnitus. Hear Res 2000; 145:1.
25. Thompson GC, Thompson AM, Garrett KM, Britton BH. Serotonin and serotonin receptors in the central auditory system. Otolaryngol Head Neck Surg 1994; 110:93.
26. Woods CI, Azeredo WJ. Noradrenergic and serotonergic projections to the superior olive: potential for modulation of olivocochlear neurons. Brain Res 1999; 836:9.
27. Waldvogel D, Mattle HP, Sturzenegger M, Schroth G. Pulsatile tinnitus--a review of 84 patients. J Neurol 1998; 245:137.
28. Fortune DS, Haynes DS, Hall JW 3rd. Tinnitus. Current evaluation and management. Med Clin North Am 1999; 83:153.
29. Ren YF, Isberg A. Tinnitus in patients with temporomandibular joint internal derangement. Cranio 1995; 13:75.
30. Levine RA. Somatic (craniocervical) tinnitus and the dorsal cochlear nucleus hypothesis. Am J Otolaryngol 1999; 20:351.
31. Montazem A. Secondary tinnitus as a symptom of instability of the upper cervical spine: operative management. Int Tinnitus J 2000; 6:130.
32. Griest SE, Bishop PM. Tinnitus as an early indicator of permanent hearing loss. A 15 year longitudinal study of noise exposed workers. AAOHN J 1998; 46:325.
33. Albers FW, Ingels KJ. Otoneurological manifestations in Chiari-I malformation. J Laryngol

Otol 1993; 107:441.

34. Mundada P, Singh A, Lingam RK. CT arteriography and venography in the evaluation of Pulsatile tinnitus with normal otoscopic examination. Laryngoscope 2015; 125:979.
35. Dietz RR, Davis WL, Harnsberger HR, et al. MR imaging and MR angiography in the evaluation of pulsatile tinnitus. AJNR Am J Neuroradiol 1994; 15:879.
36. Forsting M. CTA of the ICA bifurcation and intracranial vessels. Eur Radiol 2005; 15 Suppl 4:D25.
37. Tunkel DE, Bauer CA, Sun GH, et al. Clinical practice guideline: tinnitus executive summary. Otolaryngol Head Neck Surg 2014; 151:533.

Topic 6855 Version 35.0

GRAPHICS

Tinnitus handicap inventory questionnaire

Name ______________________ Date ____________

ID# ______________________ Age ____________

Doctor ______________________

Instructions:
Please CIRCLE the correct response.

	None										Extreme
1. Rate the loudness of your tinnitus:	0	1	2	3	4	5	6	7	8	9	10
2. Rate the pitch of your tinnitus:	0	1	2	3	4	5	6	7	8	9	10

Instructions ***(please read carefully)*****:**
The purpose of the scale is to identify difficulties that you may be experiencing because of your tinnitus. Please check off "Yes," "Sometimes," or "No" to each item.
Please do not skip any questions.

	Yes	Sometimes	No
F1. Because of your tinnitus, is it difficult for you to concentrate?	☐	☐	☐
F2. Does the loudness of your tinnitus make it difficult for you to hear?	☐	☐	☐
E3. Does your tinnitus make you angry?	☐	☐	☐
F4. Does your tinnitus make you feel confused?	☐	☐	☐
C5. Because of your tinnitus, do you feel desperate?	☐	☐	☐
E6. Do you complain a great deal about your tinnitus?	☐	☐	☐
F7. Because of your tinnitus, do you have trouble falling asleep at night?	☐	☐	☐
C8. Do you feel as though you cannot escape your tinnitus?	☐	☐	☐
F9. Does your tinnitus interfere with your ability to enjoy your social activities (such as going out to dinner, to the movies, etc)?	☐	☐	☐
E10. Because of your tinnitus, do you feel frustrated?	☐	☐	☐
C11. Because of your tinnitus, do you feel that you have a terrible disease?	☐	☐	☐
F12. Does you tinnitus make it difficult to enjoy life?	☐	☐	☐
F13. Does your tinnitus interfere with your job or household responsibilities?	☐	☐	☐
E14. Because of your tinnitus, do you find that you are often irritable?	☐	☐	☐
F15. Because of your tinnitus, is it difficult for you to read?	☐	☐	☐
E16. Does your tinnitus make you upset?	☐	☐	☐
E17. Do you feel that your tinnitus problem has placed stress on your relationships with members of your family and friends?	☐	☐	☐

F18. Do you find it difficult to focus your attention away from your tinnitus and on other things?	☐	☐	☐
C19. Do you feel you have no control over your tinnitus?	☐	☐	☐
F20. Because of your tinnitus, do you often feel tired?	☐	☐	☐
E21. Because of your tinnitus, do you feel depressed?	☐	☐	☐
E22. Does your tinnitus make you feel anxious?	☐	☐	☐
C23. Do you feel you can no longer cope with your tinnitus?	☐	☐	☐
F24. Does your tinnitus get worse when you are under stress?	☐	☐	☐
E25. Does your tinnitus make you feel insecure?	☐	☐	☐

Graphic 64655 Version 3.0

Current concept of the auditory pathways

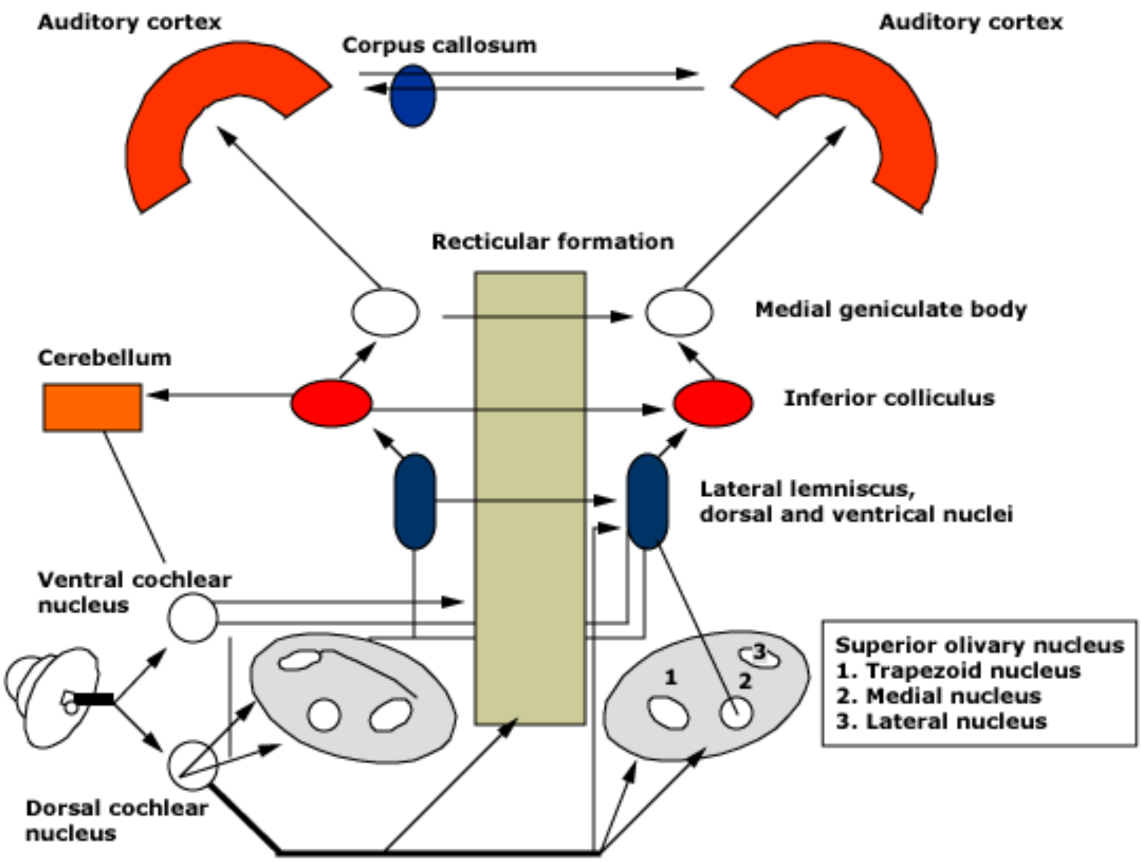

Courtesy of Elizabeth Dinces, MD.

Graphic 60823 Version 1.0

Causes of tinnitus

Sensorineural hearing loss
Presbycusis
Late-onset congenital hearing loss
Noise-induced hearing loss
Ototoxicity
Idiopathic
Vascular insufficiency
Small-vessel disease
Hypercoagulable states
Hypercholesterolemia
Diabetic vasculopathy
Hypertension
Sickle cell anemia
Other anemia
Bone disease
Fibrous dysplasia
Paget disease of bone
Osteogenesis imperfecta
Otosclerosis
Central nervous system anomalies
Sarcoid
Pseudotumor cerebri
Vascular malformations
Infections
Rubella
Neurosyphilis
Lyme disease
Meningitis
Chronic otitis media
Measles
Cytomegalovirus
Metabolic disorders
Thyroid disease
Diabetes mellitus
Chronic renal failure
Hyperparathyroidism
Autoimmune disease
Autoimmune inner ear disease (not always associated with systemic autoimmune disease)
Rheumatoid arthritis
Systemic lupus erythematosus
Cochlear injury
Salicylates
Antibiotics
Loop diuretics
Platinum-based chemotherapy
Meniere disease
Trauma
Drugs

Tumor	See 'Cochlear injury' above and refer to UpToDate table on drugs that cause or exacerbate tinnitus.
Stroke	
Multiple sclerosis	

Graphic 69431 Version 4.0

Some of the drugs that cause or exacerbate tinnitus

Aminoglycoside antibiotics
ACE inhibitors
Antimalarial drugs (eg, chloroquine, hydroxychloroquine)
Benzodiazepines
Bismuth
Calcium channel blockers
Carbamazepine
Chlordiazepoxide
Cisplatin
Clarithromycin
COX-2 inhibitors
Cyclobenzaprine
Dapsone
Doxazosin
Doxepin
Fluoroquinolone antibiotics
Isotretinoin
Lidocaine and other local anesthetics
Loop diuretics
Nitroprusside
Prazosin
Proton pump inhibitors
Quinidine
Salicylates and NSAIDs
Sertraline
Sibutramine

Tricyclic antidepressants
Tolbutamide
Valproic acid

ACE: angiotensin-converting enzyme; COX: cyclooxygenase; NSAIDs: nonsteroidal antiinflammatory drugs.

Graphic 68705 Version 3.0

Contributor Disclosures

Elizabeth A Dinces, MD No relevant financial relationship(s) with ineligible companies to disclose. **Daniel G Deschler, MD, FACS** No relevant financial relationship(s) with ineligible companies to disclose. **Lisa Kunins, MD** No relevant financial relationship(s) with ineligible companies to disclose.

Contributor disclosures are reviewed for conflicts of interest by the editorial group. When found, these are addressed by vetting through a multi-level review process, and through requirements for references to be provided to support the content. Appropriately referenced content is required of all authors and must conform to UpToDate standards of evidence.

Conflict of interest policy

→

Idaho Power/1214
Witness: Dr. Jeffrey Ellenbogen

BEFORE THE PUBLIC UTILITY COMMISSION
OF OREGON

Docket PCN 5

In the Matter of

IDAHO POWER COMPANY'S
PETITION FOR CERTIFICATE OF PUBLIC CONVENIENCE
AND NECESSITY

WHO, Environmental Noise Guidelines for the European Region (2018)

February 22, 2023

World Health Organization
REGIONAL OFFICE FOR Europe

ENVIRONMENTAL NOISE GUIDELINES

for the European Region

Abstract

Noise is an important public health issue. It has negative impacts on human health and well-being and is a growing concern. The WHO Regional Office for Europe has developed these guidelines, based on the growing understanding of these health impacts of exposure to environmental noise. The main purpose of these guidelines is to provide recommendations for protecting human health from exposure to environmental noise originating from various sources: transportation (road traffic, railway and aircraft) noise, wind turbine noise and leisure noise. They provide robust public health advice underpinned by evidence, which is essential to drive policy action that will protect communities from the adverse effects of noise. The guidelines are published by the WHO Regional Office for Europe. In terms of their health implications, the recommended exposure levels can be considered applicable in other regions and suitable for a global audience.

Keyword

NOISE – ADVERSE EFFECTS, PREVENTION AND CONTROL

ENVIRONMENTAL EXPOSURE – ADVERSE EFFECTS, PREVENTION AND CONTROL

GUIDELINES

EUROPE

Address requests about publications of the WHO Regional Office for Europe to:

Publications
WHO Regional Office for Europe
UN City, Marmorvej 51
DK-2100 Copenhagen Ø, Denmark

Alternatively, complete an online request form for documentation, health information, or for permission to quote or translate, on the Regional Office website (http://www.euro.who.int/pubrequest).

ISBN 978 92 890 5356 3

World Health Organization

REGIONAL OFFICE FOR Europe

Environmental Noise Guidelines for the European Region

Contents

Figures

Boxes

Tables

Foreword

Noise is one of the most important environmental risks to health and continues to be a growing concern among policy-makers and the public alike. Based on the assessment threshold specified in the Environmental Noise Directive of the European Union (EU), at least 100 million people in the EU are affected by road traffic noise, and in western Europe alone at least 1.6 million healthy years of life are lost as a result of road traffic noise.

At the request of Member States at the Fifth Ministerial Conference on Environment and Health in Parma, Italy, in March 2010, the WHO Regional Office for Europe has developed these guidelines, based on the growing understanding of the health impacts of exposure to environmental noise. They provide robust public health advice, which is essential to drive policy action that will protect communities from the adverse effects of noise.

These WHO guidelines – the first of their kind globally – provide recommendations for protecting human health from exposure to environmental noise originating from various sources. They not only offer robust public health advice but also serve as a solid basis for future updates, given the growing recognition of the problem and the rapid advances in research on the health impacts of noise. The comprehensive process of developing the guidelines has followed a rigorous methodology; their recommendations are based on systematic reviews of evidence that consider more health outcomes of noise exposure than ever before. Through their potential to influence urban, transport and energy policies, these guidelines contribute to the 2030 Agenda for Sustainable Development and support WHO's vision of creating resilient communities and supportive environments in the European Region.

Following the publication of WHO's community noise guidelines in 1999 and night noise guidelines for Europe in 2009, these latest guidelines represent the next evolutionary step, taking advantage of the growing diversity and quality standards in this research domain. Comprehensive and robust, and underpinned by evidence, they will serve as a sound basis for action. While these guidelines focus on the WHO European Region and provide policy guidance to Member States that is compatible with the noise indicators used in the EU's Environmental Noise Directive, they still have global relevance. Indeed, a large body of the evidence underpinning the recommendations was derived not only from noise effect studies in Europe but also from research in other parts of the world – mainly in Asia, Australia and the United States of America.

I am proud to present these guidelines as another leading example of the normative work undertaken in our Region in the area of environment and health. On behalf of the WHO Regional Office for Europe and our European Centre for Environment and Health in Bonn, Germany, which coordinated the development of the guidelines, I would like to express my gratitude to the large network of experts, partners, colleagues and consultants who have contributed to this excellent publication. I would also like to thank Switzerland and Germany for providing financial support to this complex project, and look forward to following the influence of the guidelines on policy and research in the years to come.

Dr Zsuzsanna Jakab

WHO Regional Director for Europe

Acknowledgements

The WHO Regional Office for Europe thanks all members of the Steering Group, Guideline Development Group, Systematic Review Team and External Review Group for their invaluable contributions in the guidelines development process.

The WHO Regional Office for Europe, through its European Centre for Environment and Health, coordinated the development of these guidelines. The project was coordinated by Marie-Eve Héroux and Dorota Jarosinska, under the overall supervision of Elizabet Paunovic, Head of the European Centre for Environment and Health.

The members of the Steering Group were: Shelly Chadha, Carlos Dora, Rokho Kim, Jurgita Lekaviciute, Srdan Matic, Julia Nowacki, Poonum Wilkhu and Joerdis Wothge (see Annex 1 Table A1.1 for affiliations).

The members of the Guideline Development Group were: Stephen Stansfeld (Chair), Wolfgang Babisch, Goran Belojevic, Mark Brink, Sabine Janssen, Peter Lercher (2013–2014), Marco Paviotti, Göran Pershagen, Kerstin Persson Waye, Anna Preis, Martin van den Berg and Jos Verbeek (methodologist) (see Annex 1 Table A1.2 for affiliations).

The Systematic Review Team comprised the following experts: Mathias Basner, Lex Brown, Charlotte Clark, Payam Dadvand, Maria Foraster, Rainer Guski, Sarah McGuire, Mark Nieuwenhuijsen, Katarina Paunovic, Göran Pershagen, Gordana Ristovska, Maribel Casas Sanahuja, Dirk Schreckenberg, Rudolf Schuemer, Mariola Sliwinska-Kowalska, Kamil Rafal Zaborowski, Irene Van Kamp and Elise van Kempen (see Annex 1 Table A1.3 for affiliations).

The project's External Review Group had the following members: Gunn Marit Aasvang, Bernard Berry, Dick Botteldooren, Stephen Conaty, Yvonne de Kluizenaar, Ulrike Gehring, Truls Gjestland, Mireille Guay, Ayse Güven, Anna Hansell, Stelios Kephalopoulos, David Michaud, Arnaud Norena, Enembe Okokon, Dieter Schwela, Daniel Shepherd, Mette Sörensen, Rupert Thornley-Taylor and David Welch (see Annex 1 Table A1.4 for affiliations).

The WHO Regional Office for Europe gratefully acknowledges funding and in-kind contributions from the Swiss Federal Office for the Environment; the German Federal Ministry for the Environment, Nature Conservation and Nuclear Safety; and the German Environment Agency for this activity.

Abbreviations

%HA	percentage of the population "highly annoyed"
%HSD	percentage of the population "highly sleep-disturbed"
BMI	body mass index
CI	confidence interval
CNG	WHO guidelines for community noise
DALY	disability-adjusted life-year
dB	decibel
DW	disability weight
EC	European Commission
EEA	European Environment Agency
END	European Union Directive 2002/49/EC relating to the assessment and management of environmental noise (Environmental Noise Directive)
ERF	exposure–response function
EU	European Union
GDG	Guideline Development Group
GRADE	Grading of Recommendations Assessment Development and Evaluation
ICBEN	International Commission on Biological Effects of Noise
IHD	ischaemic heart disease
JRC	Joint Research Centre [of the European Commission]
mmHg	milimeters of mercury
NNG	WHO night noise guidelines for Europe
OR	odds ratio
PECCOS	population, exposure, comparator, confounder, outcome and study [framework]
PICOS	population, intervention, comparator, outcome and study [framework]
PLD	personal listening device
RANCH	Road traffic and aircraft noise exposure and children's cognition and health [study]
RCT	randomized control trial
RR	relative risk
SCENIHR	Scientific Committee on Emerging and Newly Identified Hazards and Risk

Glossary of acoustic terms

A-weighting	A frequency-dependent correction that is applied to a measured or calculated sound of moderate intensity to mimic the varying sensitivity of the ear to sound for different frequencies
C-weighting	A frequency-dependent correction that is applied to a measured or calculated sound of moderate intensity to mimic the varying sensitivity of the ear to sound for different frequencies – C-weighting is usually used for peak measurements
FAST	Fast response has a time constant of 125 milliseconds on a sound level meter
$L_{Aeq,T}$	A-weighted, equivalent continuous sound pressure level during a stated time interval starting at t_1 and ending at t_2, expressed in decibels (dB), at a given point in space[1]
$L_{A,max}$	Maximum time-weighted and A-weighted sound pressure level within a stated time interval starting at t_1 and ending at t_2, expressed in dB[1]
L_{AF}	A-weighted sound pressure level with FAST time constant as specified in IEC 61672-1[1]
$L_{AF,max}$	Maximum time-weighted and A-weighted sound pressure level with FAST time constant within a stated time interval starting at t_1 and ending at t_2, expressed in dB
$L_{AS,max}$	Maximum time-weighted and A-weighted sound pressure level with SLOW time constant within a stated time interval starting at t_1 and ending at t_2, expressed in dB
L_E	Sound energy density level is the logarithmic ratio of the time-averaged sound energy per unit volume to the reference sound energy density Eo = 10-12 J/m^3.
$L_{ex,8h}$	L_{eq} (equivalent continuous sound level) corrected for the length of the working shift, in this case 8 hours
L_{day}	Equivalent continuous sound pressure level when the reference time interval is the day[1]
L_{den}	Day-evening-night-weighted sound pressure level as defined in section 3.6.4 of ISO 1996-1:2016[1]
L_{dn}	Day-night-weighted sound pressure level as defined in section 3.6.4 of ISO 1996-1:2016[1]
$L_{evening}$	Equivalent continuous sound pressure level when the reference time interval is the evening[1]

[1] *Source*: ISO (2016).

L_{night}	Equivalent continuous sound pressure level when the reference time interval is the night[1]
$L_{peak,C}$	Level of peak sound pressure with C-weighting, within a specified time interval
$L_{peak,lin}$	Level of peak sound pressure with linear frequency weighting, within a specified time interval
Sound pressure level	the logarithm of the ratio of a given sound pressure to the reference sound pressure in dB is 20 times the logarithm to the base ten of the ratio.
SLOW	Slow response has a time constant of 10 000 milliseconds on a sound level meter

Executive summary

Environmental noise is an important public health issue, featuring among the top environmental risks to health. It has negative impacts on human health and well-being and is a growing concern among both the general public and policy-makers in Europe.

At the Fifth Ministerial Conference on Environment and Health in Parma, Italy, in 2010, WHO was requested by the Member States in the European Region to produce noise guidelines that included not only transportation noise sources but also personal electronic devices, toys and wind turbines, which had not yet been considered in existing guidelines. Furthermore, European Union Directive 2002/49/EC relating to the assessment and management of environmental noise (END) and related technical guidance from the European Environment Agency both elaborated on the issue of environmental noise and the importance of up-to-date noise guidelines.

The WHO Regional Office for Europe has therefore developed environmental noise guidelines for the European Region, proposing an updated set of public health recommendations on exposure to environmental noise.

Objectives

The main purpose of these guidelines is to provide recommendations for protecting human health from exposure to environmental noise originating from various sources: transportation (road traffic, railway and aircraft) noise, wind turbine noise and leisure noise. Leisure noise in this context refers to all noise sources that people are exposed to due to leisure activities, such as attending nightclubs, pubs, fitness classes, live sporting events, concerts or live music venues and listening to loud music through personal listening devices. The guidelines focus on the WHO European Region and provide policy guidance to Member States that is compatible with the noise indicators used in the European Union's END.

The following two key questions identify the issues addressed by the guidelines.

- In the general population exposed to environmental noise, what is the exposure–response relationship between exposure to environmental noise (reported as various indicators) and the proportion of people with a validated measure of health outcome, when adjusted for confounders?
- In the general population exposed to environmental noise, are interventions effective in reducing exposure to and/or health outcomes from environmental noise?

In light of these questions, the guidelines set out to define recommended exposure levels for environmental noise in order to protect population health.

Methods used to develop the guidelines

The process of developing the WHO guidelines followed a rigorous methodology involving several groups with separate roles and responsibilities. Throughout the process, the Grading of

Recommendations Assessment, Development and Evaluation (GRADE) approach was followed. In particular, the different steps in the development of the guidelines included:

- formulation of the scope and key questions of the guidelines;
- review of the pertinent literature;
- selection of priority health outcome measures;
- a systematic review of the evidence;
- assessment of certainty of the bodies of evidence resulting from systematic reviews;
- identification of guideline exposure levels; and
- setting of the strength of recommendations.

Based on the defined scope and key questions, these guidelines reviewed the pertinent literature in order to incorporate significant research undertaken in the area of environmental noise and health since the community noise guidelines and night noise guidelines for Europe were issued (WHO, 1999; WHO Regional Office for Europe, 2009). In total, eight systematic reviews of evidence were conducted to assess the relationship between environmental noise and the following health outcomes: cardiovascular and metabolic effects; annoyance; effects on sleep; cognitive impairment; hearing impairment and tinnitus; adverse birth outcomes; and quality of life, mental health and well-being. A separate systematic review of evidence was conducted to assess the effectiveness of environmental noise interventions in reducing exposure and associated impacts on health.[2] Once identified and synthesized, the quality of the evidence of the systematic reviews was assessed by the Systematic Review Team. Subsequently, the Guideline Development Group (GDG) formulated recommendations, guided by the Systematic Review Team's assessment and informed by of a number of additional contextual parameters. To facilitate the formulation of recommendations, the GDG first defined priority health outcomes and then selected the most relevant health outcome measures for the outcomes. Consecutively, a process was developed to identify the guideline exposure levels with the help of the exposure–response functions provided by the systematic reviews. To reflect the nature of the research (observational studies) underpinning the relationship between environmental noise and health, the GRADE procedures were adapted to the requirements of environmental exposure studies where needed.

Noise indicators

From a scientific point of view, the best noise indicator is the one that performs best in predicting the effect of interest. There are, however, a number of additional criteria that may influence the choice of indicator. For example, various indicators might be suitable for different health end-points. Some considerations of a more political nature can be found in the European Commision's Position paper on EU noise indicators (EC, 2000).

[2] All systematic reviews are publicly available online in the *International Journal of Environmental Research and Public Health*. A detailed list of links to the individual reviews is provided in section 2.3.2 and in Annex 2 of these guidelines.

The current guidelines are intended to be suitable for policy-making in the WHO European Region. They therefore focus on the most used noise indicators L_{den} and/or L_{night} (see the glossary of acoustic terms for further details). They can be constructed using their components (L_{day}, $L_{evening}$, L_{night} and the duration in hours of L_{night}), and are provided for exposure at the most exposed façade, outdoors. The L_{den} and L_{night} indicators are those generally reported by authorities and are widely used for exposure assessment in health effect studies.

Recommendations

Specific recommendations have been formulated for road traffic noise, railway noise, aircraft noise, wind turbine noise and leisure noise. Recommendations are rated as either strong or conditional.

Strength of recommendation

- A **strong** recommendation can be adopted as policy in most situations. The guideline is based on the confidence that the desirable effects of adherence to the recommendation outweigh the undesirable consequences. The quality of evidence for a net benefit – combined with information about the values, preferences and resources – inform this recommendation, which should be implemented in most circumstances.
- A **conditional** recommendation requires a policy-making process with substantial debate and involvement of various stakeholders. There is less certainty of its efficacy owing to lower quality of evidence of a net benefit, opposing values and preferences of individuals and populations affected or the high resource implications of the recommendation, meaning there may be circumstances or settings in which it will not apply.

Alongside specific recommendations, several guiding principles were developed to provide generic advice and support for the incorporation of recommendations into a policy framework. They apply to the implementation of all of the specific recommendations.

Guiding principles: reduce, promote, coordinate and involve

- Reduce exposure to noise, while conserving quiet areas.
- Promote interventions to reduce exposure to noise and improve health.
- Coordinate approaches to control noise sources and other environmental health risks.
- Inform and involve communities potentially affected by a change in noise exposure.

The recommendations, source by source, are as follows.

Road traffic noise

Recommendation	Strength
For average noise exposure, the GDG strongly recommends reducing noise levels produced by road traffic below **53 decibels (dB)** L_{den}, as road traffic noise above this level is associated with adverse health effects.	Strong
For night noise exposure, the GDG strongly recommends reducing noise levels produced by road traffic during night time below **45 dB** L_{night}, as night-time road traffic noise above this level is associated with adverse effects on sleep.	Strong
To reduce health effects, the GDG strongly recommends that policy-makers implement suitable measures to reduce noise exposure from road traffic in the population exposed to levels above the guideline values for average and night noise exposure. For specific interventions, the GDG recommends reducing noise both at the source and on the route between the source and the affected population by changes in infrastructure.	Strong

Railway noise

Recommendation	Strength
For average noise exposure, the GDG strongly recommends reducing noise levels produced by railway traffic below **54 dB** L_{den}, as railway noise above this level is associated with adverse health effects.	Strong
For night noise exposure, the GDG strongly recommends reducing noise levels produced by railway traffic during night time below **44 dB** L_{night}, as night-time railway noise above this level is associated with adverse effects on sleep.	Strong
To reduce health effects, the GDG strongly recommends that policy-makers implement suitable measures to reduce noise exposure from railways in the population exposed to levels above the guideline values for average and night noise exposure. There is, however, insufficient evidence to recommend one type of intervention over another.	Strong

Aircraft noise

Recommendation	Strength
For average noise exposure, the GDG strongly recommends reducing noise levels produced by aircraft below **45 dB** L_{den}, as aircraft noise above this level is associated with adverse health effects.	Strong
For night noise exposure, the GDG strongly recommends reducing noise levels produced by aircraft during night time below **40 dB** L_{night}, as night-time aircraft noise above this level is associated with adverse effects on sleep.	Strong
To reduce health effects, the GDG strongly recommends that policy-makers implement suitable measures to reduce noise exposure from aircraft in the population exposed to levels above the guideline values for average and night noise exposure. For specific interventions the GDG recommends implementing suitable changes in infrastructure.	Strong

Wind turbine noise

Recommendation	Strength
For average noise exposure, the GDG conditionally recommends reducing noise levels produced by wind turbines below **45 dB** L_{den}, as wind turbine noise above this level is associated with adverse health effects.	Conditional
No recommendation is made for average night noise exposure L_{night} of wind turbines. The quality of evidence of night-time exposure to wind turbine noise is too low to allow a recommendation.	
To reduce health effects, the GDG conditionally recommends that policy-makers implement suitable measures to reduce noise exposure from wind turbines in the population exposed to levels above the guideline values for average noise exposure. No evidence is available, however, to facilitate the recommendation of one particular type of intervention over another.	Conditional

Leisure noise

Recommendation	Strength
For average noise exposure, the GDG conditionally recommends reducing the yearly average from all leisure noise sources combined to **70 dB** $L_{Aeq,24h}$ as leisure noise above this level is associated with adverse health effects. The equal energy principle[3] can be used to derive exposure limits for other time averages, which might be more practical in regulatory processes.	Conditional
For single-event and impulse noise exposures, the GDG conditionally recommends following existing guidelines and legal regulations to limit the risk of increases in hearing impairment from leisure noise in both children and adults.	Conditional
Following a precautionary approach, to reduce possible health effects, the GDG strongly recommends that policy-makers take action to prevent exposure above the guideline values for average noise and single-event and impulse noise exposures. This is particularly relevant as a large number of people may be exposed to and at risk of hearing impairment through the use of personal listening devices. There is insufficient evidence, however, to recommend one type of intervention over another.	Strong

Target audience

The guidelines are published by the WHO Regional Office for Europe. In terms of their health implications, the recommended exposure levels can be considered applicable in other regions and suitable for a global audience, as a large body of the evidence underpinning the recommendations was derived not only from European noise effect studies but also from research in other parts of the world – mainly in America, Asia and Australia.

[3] The equal energy principle states that the total effect of sound is proportional to the total amount of sound energy received by the ear, irrespective of the distribution of that energy in time (WHO, 1999).

1. Introduction

Environmental noise features among the top environmental risks to physical and mental health and well-being, with a substantial associated burden of disease in Europe (WHO Regional Office for Europe & JRC, 2011; Hänninen et al., 2014). It has negative impacts on human health and well-being and is a growing concern among both the general public and policy-makers in Europe.

WHO published community noise guidelines (CNG) and night noise guidelines (NNG) for Europe in 1999 and 2009, respectively (WHO, 1999; WHO Regional Office for Europe, 2009). Since then, significant new evidence has accumulated on the health effects of environmental noise.

The need for updated health-based guidelines originates in part from commitments made at the Fifth Ministerial Conference on Environment and Health in Parma, Italy, in 2010, where Member States asked WHO to produce appropriate noise guidelines that would include additional noise sources such as personal electronic devices, toys and wind turbines (WHO Regional Office for Europe, 2010). Furthermore, European Union (EU) Directive 2002/49/EC relating to the assessment and management of environmental noise (the END – EC, 2002a) and related technical guidance from the European Environment Agency (EEA) both elaborated on the issue of environmental noise and the importance of up-to-date noise guidelines (EEA, 2010).

The WHO Regional Office for Europe has therefore developed environmental noise guidelines for the European Region, proposing an updated set of public health recommendations on exposure to environmental noise. The main purpose of these guidelines is to provide recommendations for protecting human health from exposure to environmental noise originating from various sources: transportation (road traffic, railway and aircraft) noise, wind turbine noise and leisure noise. The guidelines focus on the WHO European Region and provide policy guidance to Member States that is compatible with the noise indicators used in the EU's END.

The following two key questions identify the issues addressed by the guidelines.

- In the general population exposed to environmental noise, what is the exposure–response relationship between exposure to environmental noise (reported as various indicators) and the proportion of people with a validated measure of health outcome, when adjusted for confounders?
- In the general population exposed to environmental noise, are interventions effective in reducing exposure to and/or health outcomes from environmental noise?

1.1 The public health burden from environmental noise

Exposure to noise can lead to auditory and nonauditory effects on health. Through direct injury to the auditory system, noise leads to auditory effects such as hearing loss and tinnitus. Noise is also a nonspecific stressor that has been shown to have an adverse effect on human health, especially following long-term exposure. These effects are the result of psychological and physiological distress, as well as a disturbance of the organism's homeostasis and increasing allostatic load (Basner et al., 2014). This is further outlined in the WHO narrative review of the biological mechanisms of nonauditory effects (Eriksson et al., 2018).

The evidence of the association between noise exposure and health effects is based on experimental work regarding biological plausibility and, in observational studies, consistency among study results, presence of an exposure–response relationship and the magnitude of the effect. Environmental noise risk assessment and risk management relies on established exposure–response relationships (Babisch, 2014).

In 2011 the WHO Regional Office for Europe and the European Commission (EC) Joint Research Centre (JRC) published a report on the burden of disease from environmental noise that quantified the healthy years of life lost in western Europeam countries as a result of environmental noise (WHO Regional Office for Europe & JRC, 2011). The burden of disease is calculated, in a single measure of disability-adjusted life-years (DALYs), as the sum of the years of life lost from premature mortality and the years lived with disability for people living with the disease or health condition or its consequences in the general population (WHO, 2014a).

Sufficient information was deemed available to quantify the burden of disease from environmental noise for cardiovascular disease, cognitive impairment in children, sleep disturbance, tinnitus and annoyance. The report, based on a limited set of data, estimated that DALYs lost from environmental noise in western European countries are equivalent to 61 000 years for ischaemic heart disease (IHD), 45 000 years for cognitive impairment in children, 903 000 years for sleep disturbance, 22 000 years for tinnitus and 654 000 years for annoyance (WHO Regional Office for Europe & JRC, 2011). These results indicate that at least one million healthy years of life are lost every year from traffic-related environmental noise in western Europe. Sleep disturbance and annoyance, mostly related to road traffic noise, constitute the bulk of this burden. Available assessments place the burden of disease from environmental noise as the second highest after air pollution (WHO Regional Office for Europe & JRC, 2011; Hänninen et al., 2014; WHO 2014b). However, a lack of noise exposure data in the central and eastern parts of the WHO European Region means that it is not possible to assess the burden of disease from environmental noise for the whole Region.

1.2 The environmental noise policy context in the EU

The EU has been working to develop a harmonized noise policy for more than two decades. 1993 saw the start of the EC's Fifth Environment Action Programme, which stated that "no person should be exposed to noise levels which endanger health and quality of life" (EC, 1993). This was followed by a Green Paper on future noise policy (EC, 1996), which reinforced the importance of noise as one of the main environmental problems in Europe and proposed a new framework for noise policy development.

The Sixth Environment Action Programme had as one of its objectives: "to achieve a quality of environment where the levels of man-made contaminants do not give rise to significant impacts on, or risks to, human health" (EC, 2002b). This paved the way for the Commission to adopt and implement the END in 2002 (EC, 2002a). The main aim of the Directive is "to define a common approach intended to avoid, prevent or reduce on a prioritized basis the harmful effects, including annoyance, due to exposure to environmental noise".

The END obliges the EC to adapt its Annexes I–III (I on noise indicators in addition to L_{den}[4] and L_{night}[5], II on noise assessment methods and III on methods for assessing harmful effects of noise) to technical and scientific progress. While work on revising Annex II was finalized in 2015 and common noise assessment methods were introduced (EC, 2015), revisions of Annex III to establish methods to assess the harmful effects of noise only started in 2015. Annex III would primarily define what exposure–response relationships should be used to assess the effect of noise on populations. EU Member States have already expressed the view that the recommendations from these environmental noise guidelines for the WHO European Region will guide the revision of Annex III. Beside this main directive, few other legislative documents cover different noise sources and other related issues in the EU (EEA, 2014: Annex I).

The Seventh Environment Action Programme, which guides European environment policy until 2020 (EC, 2014a), is committed to safeguarding the EU's citizens from environment-related risks to health by ensuring that by 2020 "noise pollution in the Union has significantly decreased, moving closer to WHO-recommended levels". A particular requirement for achieving this is "implementing an updated EU noise policy aligned with the latest scientific knowledge, and measures to reduce noise at source, and including improvements in city design".

In addition to the EU's END, several national governments also have legislation and/or limit values that apply at national and/or regional levels (WHO Regional Office for Europe, 2012). The EEA, through its European Topic Centre on Land Use and Spatial Information, gathers noise exposure data and maintains the Noise Observation and Information Service for Europe, based on strategic noise maps provided by Member States (EEA, 2018). A total of 33 EEA countries, in addition to six cooperating countries in south-eastern Europe, report information on noise exposure to the EEA, following the requirements of the END. The quality and availability of noise exposure assessment differs between EU and non-EU Member States where, even if noise legislation has been harmonized with the Directive, noise mapping and action plans are still at the planning stage (EEA, 2014; 2017a; WHO Regional Office for Europe, 2012).

1.2.1 Definition of indicators in the END

The END specifies a number of noise indicators to be applied by Member States in noise mapping and action planning. The most important are L_{den} and L_{night}.

The L_{den} indicator is an average sound pressure level over all days, evenings and nights in a year (EEA, 2010). This compound indicator was adopted by the EU in the END (EC, 2002a). The L_{den} in decibels (dB) is defined by a specific formula, where:

- L_{day} is the A-weighted long-term average sound level as defined in ISO 1996-1: 2016, determined over all the day periods of a year;
- $L_{evening}$ is the A-weighted long-term average sound level as defined in ISO 1996-1: 2016, determined over all the evening periods of a year; and
- L_{night} is the A-weighted long-term average sound level as defined in ISO 1996-1: 2016, determined over all the night periods of a year (ISO, 2016).

4 Day-evening-night-weighted sound pressure level as defined in section 3.6.4 of ISO 1996-1:20161 (ISO, 2016).
5 Equivalent continuous sound pressure level when the reference time interval is the night.

The L_{night}, according to the definition in the END, is an equivalent outdoor sound pressure level, measured at the most exposed façade, associated with a particular type of noise source during night time (at least eight hours), calculated over a period of a year (WHO Regional Office for Europe, 2009).

Annex I of the END gives technical definitions for L_{den} and L_{night}, as well as supplementary noise indicators, which might be useful for monitoring special noise situations. For example, in the case of noisy but short-lived noise like shooting noise or noise emitted by trains, $L_{A,max}$ is often used. This is a measure of the maximum sound pressure reached during a defined measurement period. It is used to set noise limits and is sometimes considered in studies to determine certain health effects (such as awakening reactions).

1.3 Perceptions of environmental noise in the WHO European Region

1.3.1 Trends at the regional level

The general population greatly values the benefits of clean and quiet environments. In Europe, people perceive noise as an important issue that affects human health and well-being (EC, 2008; 2014b). In recent years, several Europe-wide surveys have examined the perception of noise as an issue among the population. Overall, these surveys ask about generic noise, referring to “neighbourhood noise” or “noise from the street”. This type of noise differs significantly in its definition from what is considered “environmental noise” in these guidelines. Nevertheless, in the absence of specific large surveys on perceptions of environmental noise as defined in these guidelines, the results provide insight into the public perception of this issue.

The European quality-of-life surveys, carried out every four years, are unique, pan-European surveys examining both the objective circumstances of lives of European citizens and how they feel about those circumstances and their lives in general. The last (fourth) survey was conducted in 2016–2017, involving nearly 37 000 citizens from all EU Member States and the five candidate countries (Albania, Montenegro, Serbia, the former Yugoslav Republic of Macedonia and Turkey). Respondents were asked whether they had major, moderate or no problems with noise in the immediate neighbourhood of their home. Almost one third (32%) reported problems with noise (ranging from 14% to 51% in individual countries), mainly in cities or city suburbs (49%) (Eurofound, 2017).

A 2010 survey of the then 27 countries in the EU, requested by the EC, showed that 80% of respondents (n = 26 602) believed that noise affects their health, either to some or to a great extent (EC, 2010).

A Eurobarometer report on attitudes of European citizens towards the environment (EC, 2014b) compiled opinions on various environmental risks from almost 28 000 respondents in 28 EU countries. Results showed that for 15% of respondents, noise pollution is one of the top five environmental issues they are worried about. Furthermore, 17% of respondents said that they lack information about noise pollution.

1.3.2 Trends at the national level

Data on perception of specific sources of environmental noise as a problem are not available for the entire WHO European Region. Nevertheless, some countries – including France, Germany, the Netherlands, Slovakia and the United Kingdom – conduct national surveys on noise annoyance, either regularly or on demand (Sobotova et al., 2006; Lambert & Philipps-Bertin, 2008; van Poll et al., 2011; Centraal Bureau voor de Statistiek, 2012; Notley et al., 2014; Umweltbundesamt, 2017).

According to these large-scale surveys, road traffic noise is the most important source of annoyance, generally followed closely by neighbour noise. Aircraft noise can also be a substantial source of annoyance. Railway noise and industrial noise are enumerated less frequently. Only limited data are available on the population's perception of newer sources of noise, such as wind turbines.

While perception surveys do not provide information on actual quantitative relationships between noise exposure and health outcomes, it is important to note that the results of such surveys represent people's preferences and values regarding environmental noise. Despite limitations and an incomplete picture, the available data on perception of environmental noise as a public health problem show concern in Europe. People are not always aware of the health impacts of noise, especially of those related to long-term noise exposure at lower levels. Greater awareness of the issue may further increase positive values and preferences.

1.4 Target audience

The environmental noise guidelines for the European Region serve as a reference for an audience made up of different groups, with varied areas of expertise including decision-making, research and advocacy. More specifically, this covers:

- various technical experts and decision-makers at the local, national or international levels, with responsibility for developing and implementing regulations and standards for noise control, urban planning and housing, and other relevant environment and health domains;
- health impact assessment and environmental impact assessment practitioners and researchers;
- national and local authorities responsible for developing and implementing relevant measures and for risk communication;
- nongovernmental organizations and other advocacy groups involved in risk communication and general awareness-raising.

These guidelines are published by the WHO Regional Office for Europe. In terms of their health implications, the recommended exposure levels can be considered applicable in other regions and suitable for a global audience, as a large body of the evidence underpinning the recommendations was derived not only from European noise effect studies but also from research in other parts of the world – mainly in America, Asia and Australia.

2. Development of the guidelines

2.1 Overview

The process of developing WHO guidelines follows a rigorous methodology and involves several groups with well defined roles and responsibilities (WHO, 2014c). These include: formulation of the scope and key questions of the guidelines; review of the pertinent literature; selection of priority health outcome measures; a systematic review of the evidence; an assessment of certainty of the bodies of evidence resulting from systematic reviews; identification of guideline exposure levels; and setting of the strength of recommendations. Throughout the process, the Grading of Recommendations Assessment, Development and Evaluation (GRADE) approach was followed (Morgan et al., 2016).

The development of environmental noise guidelines started in 2013. Following WHO's procedures, the WHO Regional Office for Europe, through its European Centre for Environment and Health in Bonn, Germany, obtained planning approval and established a Steering Group and a Guideline Development Group (GDG). The former was primarily involved in initiating, structuring and executing the guideline development process; the latter was composed of leading experts and end-users, responsible for the process of scoping the guidelines and developing the evidence-based recommendations. During the initiation meeting in October 2013 in Bonn, the GDG members defined the scope of the guidelines, decided on the key questions to be addressed, prioritized health outcomes and set a timeline for completion of the work. Furthermore, authors were appointed for background papers, systematic reviews and different guideline background chapters.

In October 2014 a main evidence review meeting was held between the GDG and the Systematic Review Team in Bern, Switzerland, to discuss the evidence review drafts. In October 2014 and May 2015 the GDG met in Bern and Bonn, respectively, to refine the scope and draft recommendations. The revision and finalization of the systematic reviews of evidence was completed in early 2017. Through a series of remote meetings and teleconferences, the GDG discussed and addressed the remaining outstanding issues and feedback from the peer review of the draft guidelines, and decided on the final formulation of the recommendations. The following sections describe the steps of the guideline development process in detail.

2.2 Scope of the guidelines

Defining the scope of the guidelines included the selection of noise sources to be considered, as well as situations in which people are exposed, and noise indicators used for the formulation of recommendations. These guidelines separately consider outdoor exposure to environmental noise from road traffic, railway traffic, aircraft, wind turbines as well as outdoor and indoor exposure during leisure activities (such as attending nightclubs, pubs, fitness classes, live sporting events, concerts or live music venues and listening to loud music through personal listening devices). The guidelines are source specific and not environment specific. They therefore cover all settings where people spend a significant portion of their time, such as residences, educational institutions, workplaces and public venues, although hospital noise is exempted from the list of public institutions owing to the unique characteristics of the population involved.

The GDG agreed not to develop specific recommendations for occupational and industrial noise. Industrial noise can affect both people working at an industrial site and those living in its vicinity. The guidelines do not consider workers' exposure to noise in industrial environments, as these are regulated by workplace standards and may, in some cases, require the wearing of protective equipment or application of other preventive and protective measures. Further, the guidelines do not explicitly consider industrial noise as an environmental noise source, affecting people living in the vicinities of industrial sites. This is mainly due to the large heterogeneity and specific features of industrial noise, and the fact that exposure to industrial noise has a very localized character in the urban population.

Likewise, the current guidelines do not provide specific recommendations for the prevention of health effects linked to neighbourhood noise. Neighbourhood noise may stem from various potential sources of noise (such as ventilation systems; church bells; animals; neighbours; commercial, recreational and occupational activities; or shooting/military). As the sources may be located in close proximity to where people live, they can cause considerable concern even at low levels (Omlin et al., 2011). Several of these sources can also produce low-frequency noise, and as such, require indoor measurements for proper exposure assessment. In general, little scientific research is available on exposure and health outcomes related to neighbourhood noise.

Moreover, the guidelines do not include recommendations about any kind of multiple exposures. In everyday life people are often exposed to noise from several sources at the same time. In Germany, for example, 44% of the population are annoyed by at least two and up to five sources of noise (Umweltbundesamt, 2015). For some health outcomes, such as obesity, new evidence indicates that combined exposure to noise from several means of transportation is particularly harmful (Pyko et al., 2015; 2017).

Research indicates that, alongside exposure to more than one source of noise, combined exposure to different factors – for example, noise and vibration or noise and air pollution – has gained increasing relevance in recent years (Sörensen et al., 2017). The EC estimates that the social cost of noise and air pollution is up to €1 trillion every year (EC, 2016a). WHO acknowledges the need to develop comprehensive models to quantify the effects of multiple exposures on human health. As the main body of evidence on environmental noise still focuses on source-specific impacts of noise on health outcomes and does not incorporate combined exposure effects of multiple noise sources or other pollutants, however, the current guidelines provide recommendations for each source of noise specifically. No attempt has been made to combine noise from multiple sources for any particular health outcome.

2.2.1 Key questions

The environmental noise guidelines for the WHO European Region seek to address two main questions, which define the issues addressed by the guideline recommendations.

- In the general population exposed to environmental noise, what is the exposure–response relationship between exposure to environmental noise (reported as various indicators) and the proportion of people with a validated measure of health outcome, when adjusted for confounders?
- In the general population exposed to environmental noise, are interventions effective in reducing exposure to and/or health outcomes from environmental noise?

2.2.2 Environmental noise indicators used in the guidelines

From a scientific point of view, the best noise indicator is the one that performs best in predicting the effect of interest. There are, however, a number of additional criteria that may influence the choice of indicator because, for example, various indicators might be suitable for different health end-points and some indicators are more practical to use or easier to calculate than others. Some of these considerations are of a more political nature, as mentioned in the EC's Position paper on EU noise indicators (EC, 2000).

The current guidelines are intended to be suitable for policy-making primarily in the WHO European Region. They are therefore based on the most frequently used average noise indicators in Europe: L_{den} and L_{night}. These are often reported by authorities and are used widely for exposure assessment in health effect studies and noise impact assessments in the Region. The L_{den} (also referred to as "DENL") indicator can be calculated as the A-weighted average sound pressure level, measured over a 24-hour period, with a 10 dB penalty added to the average level in the night (23:00–07:00 or 22:00–06:00), a 5 dB penalty added to the evening (19:00–23:00 or 18:00–22:00) and no penalty added to the daytime period (07:00–19:00 or 06:00–18:00). The penalties are introduced to indicate people's extra sensitivity to noise during the evening and night. The L_{night} indicator is the A-weighted average sound pressure level, measured over an eight-hour period during night time, usually between 23:00 and 07:00 (EC, 2002a).

In these guidelines, L_{den} and L_{night} refer to a measurement or calculation of noise exposure at the most exposed façade, outdoors, reflecting the long-term average exposure. Thus, L_{den} and L_{night} represent all the single noise events due to a specific noise source that occur over a longer period of time, such as during a year. Moreover, most health outcomes considered in these guidelines are expected to occur as a result of long-term exposure. It is generally accepted that the most relevant parts of the whole day or night, which especially account for the time when a person is at home, are correctly attributed when using average indicators like L_{den} or L_{night}.

The majority of studies that form the body of evidence for the recommendations in these guidelines – among them large-scale epidemiological studies and socioacoustic surveys on annoyance and self-reported sleep disturbance – refer to noise exposure measured outdoors, usually at the most exposed façade of dwellings. Virtually all noise exposure prediction models in use today estimate free-field exposure levels outdoors, and most noise abatement regulations refer to outdoor levels as well. These are the practical reasons why the GDG decided not to recommend any guideline values for noise indoors. Nevertheless, in certain cases it could be helpful to estimate indoor levels based on outdoor values. The differences between indoor and outdoor levels are usually estimated at around 10 dB for open, 15 dB for tilted or half-open and about 25 dB for closed windows. When considering more accurate estimation of indoor levels, using a range of different predictors, the relevant scientific literature can be consulted (Locher et al., 2018).

The GDG was aware of the fact that many countries outside the EU are not bound by the terms of the END (EC, 2002a) and/or use noise indicators other than L_{den} or L_{night} in their noise regulations. They still can make use of these guidelines, however, because energy-based average noise indicators are usually highly correlated and "rule of thumb" transformations from one indicator to another are possible with acceptable uncertainty, as long as the conversion accounts for the long-term average of populations, rather than individual exposure situations. Empirically derived generic conversion terms between a wide range of different noise indicators (including L_{den}, L_{dn}, L_{day}, L_{night} and $L_{Aeq,24h}$; see the glossary of acoustic terms for further details), with their uncertainty estimates, were published recently (Brink et al., 2018). The GDG encourages the use of these conversions, should the need arise.

In many situations, average noise levels like the L_{den} or L_{night} indicators may not be the best to explain a particular noise effect. Single-event noise indicators – such as the maximum sound pressure level ($L_{A,max}$)[6] and its frequency distribution – are warranted in specific situations, such as in the context of night-time railway or aircraft noise events that can clearly elicit awakenings and other physiological reactions that are mostly determined by $L_{A,max}$. Nevertheless, the assessment of the relationship between different types of single-event noise indicators and long-term health outcomes at the population level remains tentative. The guidelines therefore make no recommendations for single-event noise indicators.

Different noise sources – for example, road traffic noise and railway noise – can be characterized by different spectra, different noise level rise times of noise events, different temporal distributions of noise events and different frequency distributions of maximum levels. Because of the extensive differences in the characteristics of individual noise sources, these guidelines only consider source-specific exposure–response functions (ERFs) and, therefore, formulate only source-specific recommendations.

2.3 Evidence base

Based on the overall scope and key questions the current guidelines review the relevant literature in the area of environmental noise and health in order to incorporate significant research undertaken since the publication of previous guidelines. The process of evidence search and retrieval involved several steps. These include the identification, retrieval and synthesis of the evidence, followed by a systematic review and assessment (described in section 2.4).

2.3.1 Identification, retrieval and synthesis of evidence

As a first step, the GDG identified key health outcomes associated with environmental noise. Next, it rated the relevance of these health outcomes according to the following three categories:

- critical for assessing environmental noise issues
- important, but not critical for assessing environmental noise issues
- unimportant.

The GDG rated the relevance based on the seriousness and prevalence of the outcomes and the anticipated availability of evidence for an association with noise exposure. The following health outcomes were selected as either critical or important for developing recommendations on the health impacts of environmental noise.

[6] $L_{A,max}$ is the maximum time-weighted and A-weighted sound pressure level within a stated time interval starting at t1 and ending at t2, expressed in dB.

Critical health outcome	Important health outcome
Cardiovascular disease	Adverse birth outcomes
Annoyance[7]	Quality of life, well-being and mental health
Effects on sleep	Metabolic outcomes
Cognitive impairment	
Hearing impairment and tinnitus	

The GDG noted that research into the relationship between noise exposure and its effects on humans brings into focus several questions concerning the definition of health and the boundary between normal social reaction to noise and noise-induced ill health. As stated in WHO's Constitution: "Health is a state of complete physical, mental and social well-being and not merely the absence of disease or infirmity" (WHO, 1946). Accordingly, documenting physical health does not present a complete picture of general health; and being undisturbed by noise in all activities, including sleep, constitutes an asset worthy of protection. Therefore, in accordance with the above definition, the GDG regarded (long-term) annoyance and impaired well-being, as well as self-reported sleep disturbance due to noise, as health outcomes.

Regarding sleep disturbance, the health outcome measures considered in these guidelines largely disregard "objective" indicators of sleep disturbance, such as the probability of awakening reactions or other polysomnography parameters. The main reason for this is the nature of the body of evidence on acute, objectively measured effects of noise during sleep. Studies of physiological effects of sleep and especially polysomnographic investigations are complex and resource-demanding; they therefore include only a small number of participants, who are often healthy young volunteers not representative of the general population. For these reasons, the majority of such studies do not meet the requirements for inclusion in the GRADE framework and full-scale meta-analysis, including adjustment for confounders. Furthermore, it is currently unclear how acute physiological reactions that affect the microstructure of sleep but are less well correlated with global sleep parameters, such as total sleep time, are related to long-term health impediments, especially considering the large interindividual differences in susceptibility to noise (Basner et al., 2011).

As sleeping satisfies a basic need and the absence of undisturbed sleep can have serious effects on human health (WHO Regional Office for Europe, 2009), the GDG set self-reported sleep disturbance, in line with the WHO definition of health, as a primary health outcome. Even though self-reported sleep disturbance might differ considerably from objectively measured parameters of sleep physiology, it constitutes a valid indicator in its own right, as it reflects the effects on sleep perceived by an individual over a longer period of time (WHO Regional Office for Europe & JRC, 2011). The importance of considering both annoyance and self-reported sleep disturbance as health outcomes is further supported by evidence indicating that they may be part of the causal pathway of noise-induced cardiovascular and metabolic diseases. This is further elaborated in the narrative review on biological mechanisms (Eriksson et al., 2018).

[7] Noise annoyance is defined as a feeling of displeasure, nuisance, disturbance or irritation caused by a specific sound (Ouis, 2001). In the current guidelines, "annoyance" refers to long-term noise annoyance.

The second step in the evidence retrieval process constituted formulation of the key questions for the critical and important health outcomes and identification of the areas of evidence to be reviewed, following the PICOS/PECCOS approach defined in the WHO handbook for guideline development (WHO, 2014c). PICOS/PECCOS is an evidence-based technique that frames health care-related questions to facilitate the search for suitable studies that can provide answers to the questions at hand (Huang et al., 2006). The PICOS approach divides intervention questions into five elements: population, intervention, comparator, outcome and study design. In exposure studies, PICOS becomes PECCOS, which stands for population, exposure, comparator, confounder, outcome and study design. The specification of the elements of PICOS/PECCOS serves to construct the body of evidence that underpins each recommendation. Due to the complex nature of environmental noise, several distinct areas of evidence were defined to address each of the scoping questions comprehensively.

For each of the critical and important health outcomes a systematic review was conducted (see also section 2.3.2). Health outcomes regarded as important were given less weight in the decision-making process than critical ones. Inclusion and exclusion criteria to be regarded in the systematic evidence reviews were defined in accordance with the PICOS/PECCOS framework for the evaluation of evidence (see Table 1). All evidence that met the inclusion criteria was included in the systematic reviewing process. A detailed description of the types of measure for each of the health outcomes under consideration is provided in the protocol for conducting the systematic reviews (Héroux & Verbeek, 2018a). See Annex 2 for details of all background documents and systematic reviews used in preparation of these guidelines.

Table 1. Inclusion and exclusion criteria for evidence reviews of health effects of environmental noise

Category	Inclusion criteria	Exclusion criteria
Populations	• Members of the general population • Specific segments of the population particularly at risk (children or vulnerable groups) • People exposed to noise in occupational settings (if relevant with combined exposure to environmental noise)	• Does not meet inclusion criteria
Exposure	• Noise exposure levels, either measured or calculated and expressed in dB values • Representative of the individual exposure of study participants (for most observational studies the dwelling location or home) • Calculated levels for transportation noise (road, rail, air) based on traffic data reflecting the use of roads, railway lines and in- and outbound flight routes at airports	• Does not meet inclusion criteria; in particular: - studies using hearing loss or hearing impairment as a proxy for (previous) noise exposure - surveys assessing noise exposure or number of listening hours based on subjective ratings given by subjects in a questionnaire
Confounders	• No inclusion criteria applied since the relationship between exposure to noise and a health outcome can be confounded by other risk factors; however, possible confounders taken into account were assessed for every study	• No exclusion criteria applied; however, possible confounders taken into account were assessed for every study

Table 1. contd.

Category	Inclusion criteria	Exclusion criteria
Outcomes	• Adverse birth outcomes • Annoyance • Cardiovascular disease • Cognitive impairment • Effects on sleep • Hearing impairment and tinnitus • Metabolic outcomes • Quality of life, mental health and well-being	• Does not meet inclusion criteria
Study types	• Cohort studies • Case-control studies • Cross-sectional studies • Ecological studies (only for cardiovascular disease)	• Does not meet inclusion criteria

Alongside the systematic reviews of the critical and important health outcomes, the GDG decided to review the evidence on health effects from noise mitigation measures and interventions to reduce noise levels in order to inform and complement the recommendations.

Interventions on environmental noise were defined according to five broad categories based on the available intervention literature and the experience of decades of environmental noise management (see Table 2 and Brown & van Kamp, 2017).

Table 2. Types of noise intervention

Intervention type	Intervention category	Intervention subcategory
A	Source intervention	• change in emission levels of sources • time restrictions on source operations
B	Path intervention	• change in the path between source and receiver • path control through insulation of receiver/receiver's dwelling
C	New/closed infrastructure	• opening of a new infrastructure noise source • closure of an existing one • planning controls between (new) receivers and sources
D	Other physical intervention	• change in other physical dimensions of dwelling/neighbourhood
E	Behaviour change intervention	• change in individual behaviour to reduce exposure • avoidance or duration of exposure • community education, communication

The GDG recognized that nonacoustic factors are an important possible confounder in both ERFs between noise levels and critical health effects and the effects of acoustic interventions on health outcomes. Whereas the inclusion criteria for confounders were not specified in PECCOS for the systematic reviews of evidence, they were considered at the stage of assessing the quality of evidence, using the GRADE approach. Depending on the health effect under investigation, possible nonacoustic factors may include:

- gender
- age
- education
- subjective noise sensitivity
- extroversion/introversion
- general stress score
- co-morbidity
- length of residence
- duration of stay at dwelling in the day
- window orientation of a bedroom or living room towards the street
- personal evaluation of the source
- attitudes towards the noise source
- coping capacity with respect to noise
- perception of malfeasance by the authorities responsible
- body mass index
- smoking habits.

In noise annoyance studies nonacoustic factors may explain up to 33% of the variance (Guski, 1999). The higher the quality of evidence, the lower confounding effects of nonacoustic factors may be expected. Nevertheless, as with measurement errors, confounding cannot be avoided.

Based on the retrieval and evaluation of the pertinent literature, the GDG decided to address the association of environmental noise from different sources and health outcomes separately and individually for each source of noise, and for critical and important health outcomes.

In addition to the systematic reviews of the health effects of environmental noise, a narrative review of biological mechanisms of nonauditory effects was conducted (Eriksson et al., 2018). This covers literature related to pathways for nonauditory effects and provides supporting evidence on the association between environmental noise and health outcomes in humans, especially related to cardiovascular and metabolic diseases.

2.3.2 Systematic reviewing process

After the retrieval of the evidence based on the PICOS/PECCOS approach, systematic reviews were conducted for all critical and important health outcomes. To meet the demands of the diverse and broad nature of the evidence, it was agreed that systematic reviews could vary in type. For some areas of evidence, a novel and fully fledged systematic reviewing process was needed to summarize the existing evidence; for others, the reviewing process could build upon existing (and mostly published) systematic reviews and summaries of evidence. Thus, the process consisted of two phases.

First, a comprehensive search was conducted for available systematic reviews and meta-analyses on environmental noise effects published after 2000. Each of the reviews was assessed for both relevance and quality. To be included in the evidence review process, studies from these reviews were required to meet a high quality standard, judged according to high scores of the AMSTAR checklist.[8] In cases where quality criteria were met but the review was older than two years (published before 2012), the search of the systematic review was updated to include new papers. If no good quality systematic reviews were available, a new search for original papers was conducted. The Systematic Review Team decided how the results would affect the search strategy for individual studies as part of the second phase. This was based on the assessment of the quality of the systematic reviews and on the coherence between the main research questions of the systematic reviews and the scope of the work of the guidelines.

In the second phase a search for individual papers was conducted, with the search strategy adapted according to the outcome of the first phase. As availability of systematic reviews and meta-analyses differed for the various health outcomes considered in the guidelines, this process varied for each evidence review. The search included cohort studies, case-control studies and cross-sectional studies of people exposed to environmental noise. Where relevant – for example, for the health outcome cardiovascular disease – the search also included ecological studies.

Due to the individualized retrieval of evidence for each of the systematic reviews, the time frames of the literature included varied. An indication of the temporal coverage of the studies included in different systematic review is provided in the relevant tables in Chapter 4.

A detailed description of the methodology used to conduct the systematic evidence reviews, including individual protocols for the reviews of health effects resulting from environmental noise and from noise interventions, is available (Héroux & Verbeek, 2018b). Furthermore, all systematic reviews conducted in the guideline development process are publicly available in the open-access journal *International Journal of Environmental Research and Public Health*:

- systematic review of transport noise interventions and their impacts on health (Brown & van Kamp, 2017);
- systematic review on environmental noise and adverse birth outcomes (Nieuwenhuijsen et al, 2017);
- systematic review on environmental noise and annoyance (Guski et al., 2017);
- systematic review on environmental noise and cardiovascular and metabolic effects (van Kempen et al., 2018);
- systematic review on environmental noise and cognition (Clark & Paunovic, 2018);
- systematic review on environmental noise and effects on sleep (Basner & McGuire, 2018);
- systematic review on environmental noise and permanent hearing loss and tinnitus (Śliwińska-Kowalska & Zaborowski, 2017);
- systematic review on mental health and well-being (Clark & Paunovic, in press).

[8] AMSTAR is an instrument used to assess quality of evidence; it stands for "A MeaSurement Tool to Assess systematic Reviews" (Shea et al., 2007).

2.4 From evidence to recommendations

Once the evidence had been identified and synthesized, the Systematic Review Team assessed its quality. Subsequently, the GDG formulated recommendations, guided by this assessment and consideration of a number of other factors recognized as important. To facilitate the formulation of recommendations, it first prioritized the health outcome measures of the critical and important outcomes. A process was developed to identify the guideline exposure levels from each of the ERFs provided by the systematic reviews of evidence.

The following sections describe the assessment of the overall quality of the evidence based on the GRADE approach, selection of priority health outcome measurements, identification of guideline exposure levels and setting the strength of recommendations.

2.4.1 Assessment of overall quality of a body of evidence: the GRADE approach

As set out in the WHO handbook for guideline development (WHO, 2014c), the main framework for producing evidence-informed recommendations is the GRADE approach (Guyatt et al., 2008). This is used to assess the quality of a body of evidence synthesized in a systematic review. The assessment facilitates judgements about the certainty of effect estimates, which increases with the quality of the body of evidence. The quality can be rated high, moderate, low or very low (see Box 1).

Box 1 GRADE interpretations of quality of evidence

- **High quality:** further research is very unlikely to change the certainty of the effect estimate
- **Moderate quality:** further research is likely to have an important impact on the certainty of the effect estimate and may change the estimate
- **Low quality:** further research is very likely to have an important impact on the certainty of the effect estimate and is likely to change the estimate
- **Very low quality:** any effect estimate is uncertain

The original GRADE approach was developed specifically to rate the body of evidence resulting from a review of intervention studies. The initial quality level is set by study design: randomized control trials (RCTs) are considered high quality, whereas observational (nonrandomized) study designs are low quality. Then five factors are considered for downgrading the quality of the body of evidence resulting from RCTs or observational studies, and three factors are considered for upgrading the body of evidence resulting from observational studies alone.

The following five factors are used for downgrading the quality of evidence by one or two levels:

- study limitations or risk of bias in all studies that make up the body of evidence
- inconsistency of results between studies
- indirectness of evidence in the studies
- imprecision of the pooled effect estimate
- publication bias detected in a body of evidence.

The following three factors are used for upgrading the quality of evidence:

- high magnitude of the pooled effect
- direction of residual confounding and biases opposes an effect (i.e. when all plausible confounders are anticipated to reduce the estimated effect and there is still a significant effect)
- exposure–response gradient.

The GRADE approach was originally developed for application in the field of clinical medicine, where the majority of studies are randomized trials. However, to assess health effects resulting from an exposure such as environmental noise, randomized controlled trials are not applicable, as it would be unethical to expose participants deliberately to possibly harmful risk factors. The limitations of the application of GRADE to environmental health have been recognized and discussed in the literature (Morgan et al., 2016). Other types of study design dominate the evidence base in the domain of environmental noise research, so it was necessary to adapt the original GRADE approach to the subject of the current guidelines, as follows.

Instead of using the RCT study design as the starting-point for the quality rating, the study design most applicable and available for the field of research at hand was used. Thus, for evidence on the association between noise exposure and clinical health outcome measures, the rating of an evidence base consisting of cohort and case-control studies[9] was initially rated high quality. Cross-sectional studies and ecological studies were rated low quality and very low quality, respectively. This initial point of departure was only adapted for the evidence of the association between noise exposure and annoyance and sleep disturbance. Here, cross-sectional studies were rated high quality because annoyance and sleep disturbance are regarded as an immediate effect of exposure to environmental noise. Finally, in accordance with the original GRADE approach, the starting-point for evidence on the effect of interventions was rated low quality for observational studies. After determining the point of departure, the evidence base was rated down or up whenever one or more of the criteria for downgrading or upgrading (described above) were met. Each of the systematic reviews commissioned for these guidelines includes a detailed report on the assessment of the quality of the evidence.

A detailed discussion of the adaptations of GRADE is provided in the separate methodology publication (Héroux & Verbeek, 2018b).

2.4.2 Selection of priority health outcomes

In line with the WHO handbook for guideline development (WHO, 2014c), the GDG selected the key health outcomes associated with environmental noise at the beginning of the evidence retrieval process, and the systematic reviews were commissioned accordingly. The selection of health outcomes was based on the available evidence for the association between environmental noise and the specific outcome, as well as public concern about the health outcome resulting from noise exposure. The following health outcomes were rated critical: cardiovascular disease, annoyance,

[9] In the context of the current guidelines, “cohort studies” refer to longitudinal studies in which the occurrence of the outcome of interest in an exposed group is compared to the occurrence of that outcome in a reference group with no or lower exposure over time.

effects on sleep, cognitive impairment and hearing impairment and tinnitus. Adverse birth outcomes, quality of life, well-being and mental health, and metabolic outcomes were rated important (see also section 2.3.1).

Since all these health outcomes can be measured in various ways, the GDG evaluated each individually and prioritized different outcome measures for each in terms of their representativeness and validity. These measures were used to derive the guideline exposure levels; their prioritization was based on the impact of the disease and the disability weights (DWs) associated with the health outcome measure.[10]

The critical health outcomes, priority outcome measures identified and justifications for their selection are listed in Table 3.

Table 3. Critical health outcomes, outcome measures identified and justifications for selection

Critical health outcome	Critical health outcome measures (priority measures marked in bold)	Justification for selection
Cardiovascular disease (L_{den})	Self-reported or measured prevalence, **incidence**, hospital admission or mortality due to: • **ischaemic heart disease (IHD) (including angina pectoris and/or myocardial infarction)** • **hypertension** • stroke	Except for self-reports, these are objective measures of the outcome, affect a large proportion of the population, have important health consequences and can lead to more severe diseases and/or mortality. DW for IHD: 0.405. DW for hypertension: 0.117.
Effects on sleep (L_{night})	• **percentage of the population highly sleep-disturbed (%HSD)**, self-reported, assessed with a standardized scale • polysomnography measured outcomes (probability of additional awakenings) • cardiac and blood pressure outcome measures during sleep • motility measured sleep outcomes in adults • sleep disturbance in children	This is the most meaningful, policy-relevant measure of this health outcome. Self-reported sleep disturbances are a very common problem in the general population: they affect quality of life directly and may also lead to subsequent health impediments. Effects on sleep may be in the causal pathway to cardiovascular disease. This measure is not a proxy for physiological sleep quality parameters but is an important outcome in its own right. DW for %HSD: 0.07.
Annoyance (L_{den})	• **percentage of the population highly annoyed (%HA), assessed with standardized scale** • percentage annoyed, preferably assessed with standardized scale	This is the most objective measure of this health outcome. Large proportions of the population are affected by noise annoyance, even at relatively low exposure levels. Annoyance may be in the causal pathway to cardiovascular disease. DW for %HA: 0.02.

⇨

[10] DWs are ratings that vary between 0 and 1, in which 0 indicates no disability and 1 indicates the maximum amount of disability. The rates are derived from large population surveys in which people are asked to rank a specific disease for its impact on several abilities. The DWs have been proven useful in calculating the burden of disease.

Table 3. contd.

Critical health outcome	Critical health outcome measures (priority measures marked in bold)	Justification for selection
Cognitive impairment (L_{den})	• **reading and oral comprehension, assessed with tests** • impairment assessed with standardized tests • short and long-term memory deficit • attention deficit • executive function deficit (working memory capacity)	This outcome measure is the most meaningful: it can affect vulnerable individuals (children) and have a significant impact later in life. DW for impaired reading and oral comprehension: 0.006.
Hearing impairment and tinnitus (L_{Aeq}[11] and $L_{AF,max}$[12])	• **permanent hearing impairment, measured by audiometry** • permanent tinnitus	This outcome measure can affect vulnerable individuals (children) and have a significant impact later in life. It is the most objective measure for which there is an ISO standard (ISO, 2013), specifying how to estimate noise-induced hearing loss. DW for mild severity level (threshold at 25 dB) for childhood onset: 0.0150.

Table 4 provides a list of the important health outcomes along with the corresponding health outcome measures included in the systematic reviews. There was no prioritization of health outcome measures leading to justification of selection, since important health outcomes had less impact on the development of recommendations.

Table 4. Important health outcomes and health outcome measures reviewed

Important health outcome	Health outcome measures reviewed
Adverse birth outcomes (L_{den})	• pre-term delivery • low birth weight • congenital anomalies
Quality of life, well-being and mental health (L_{den})	• self-reported health and quality of life • medication intake for depression and anxiety • self-reported depression, anxiety and psychological distress • interviewer-assessed depressive and anxiety disorders • emotional and conduct disorders in children • children's hyperactivity • other mental health outcomes
Metabolic outcomes (L_{den})	prevalence, incidence, hospital admission or mortality due to: • type 2 diabetes • obesity

11 L_{Aeq} is an A-weighted, equivalent continuous sound pressure level during a stated time interval starting at t1 and ending at t2, expressed in dB, of a noise at a given point in space.
12 $L_{AF,max}$ is the maximum time-weighted and A-weighted sound pressure level with FAST time constant within a stated time interval starting at t1 and ending at t2, expressed in dB.

2.4.3 Identification of guideline exposure levels for each noise source

The GDG agreed to set guideline exposure levels based on the definition: "noise exposure levels above which the GDG is confident that there is an increased risk of adverse health effects". The identification of guideline values for each of the specific noise sources involved five distinct steps:

1. assessment of the validity of ERFs resulting from the systematic reviews of the effects of noise on each of the critical and important health outcomes;
2. assessment of the lowest noise level measured in the studies included in each of the corresponding systematic reviews;
3. assessment of the smallest risk or relative risk (RR) increase for each of the adverse health outcomes considered relevant;
4. determination of the guideline exposure level based on the ERF, starting from the lowest level measured (see step 2) and associated with the smallest relevant risk increase for adverse health outcomes (see step 3);
5. comparison of the guideline exposure levels calculated for each of the critical health outcomes of one source (for example, incidence of IHD, incidence of hypertension, %HA, permanent hearing impairment and reading and oral comprehension for road traffic noise): selection of the guideline exposure level for each noise source was based on the priority health outcome measure with the lowest exposure level for that source.

To define an "increased risk" to set the guideline exposure level, the GDG made a judgement about the smallest risk or RR of the adverse health effect it considered relevant for each of the priority health outcome measures. It is important to note that the relevant risk increases are benchmark values. The GDG agreed to set them in accordance with the guiding principles it had developed, to provide guideline values that illustrate an increased risk of adverse health effects. It used expert judgements for the determination of the benchmark values; these are elaborated further in section 2.4.3.2.

The guideline exposure levels presented are therefore not meant to identify effect thresholds (the lowest observed adverse effect levels for different health outcomes). This is a difference in approach from prior WHO guidelines, like the night noise guidelines for Europe (WHO Regional Office for Europe, 2009), which explicitly aimed to define levels indicating no adverse health effects. The approach to making choices about relevant risk increases is outlined below and summarized in Table 5.

For IHD and hypertension, RR increases were considered; for annoyance and sleep disturbance, absolute risks of %HA and %HSD were considered; and for reading and oral comprehension an average delay of reading age was defined. For the cardiovascular outcomes, incidence measures were prioritized, although much of the epidemiological evidence was based on prevalence data – particularly for hypertension – where almost no longitudinal studies were available. Prevalence data are generally derived from cross-sectional studies, where the temporal aspects are difficult to determine.

Table 5. Priority health outcomes and relevant risk increases for setting guideline levels

Priority health outcome measure (associated DW)	Relevant risk increase considered for setting of guideline level
Incidence of IHD (DW: 0.405)	5% RR increase
Incidence of hypertension (DW: 0.117)	10% RR increase
%HA (DW: 0.02)	10% absolute risk
%HSD (DW: 0.07)	3% absolute risk
Permanent hearing impairment (DW: 0.0150)	No risk increase due to environmental noise
Reading and oral comprehension (DW: 0.006)	One-month delay in terms of reading age

The DWs used to rank the priority critical health outcomes measures were retrieved from the relevant literature. For cardiovascular disease as a group and for hypertension, the burden of disease from environmental noise values (WHO Regional Office for Europe & JRC, 2011) were not considered applicable by the GDG for these guidelines. Thus, for cardiovascular disease, the DW value (DW: 0.405) specifically applied to acute myocardial infarction in the publication outlining the data sources, methods and results of the global burden of disease in 2002 (Mathers et al., 2003) was retained. Since hypertension is mainly viewed as an important risk factor and not as a health outcome, no general DW has been developed. The only other available DW value available is the DW of 0.117 for hypertensive episodes in pregnancy (Mathers et al., 1999). In the absence of any general DW, the GDG agreed on a conservative approach and decided to use this value.

The DWs for high sleep disturbance (DW: 0.07), high annoyance (DW: 0.02) and impaired reading and oral comprehension (DW: 0.006) were developed in the context of calculating the burden of disease from environmental noise (WHO Regional Office for Europe & JRC, 2011). The DW for hearing impairment was not included in that publication, but it was available from the technical paper on the burden of disease from environmental noise (WHO, 2013); the DW for permanent hearing impairment ranged from 0.0031 to 0.3342, depending on severity level. Environmental noise (leisure noise) contributes to the cumulative total noise exposure throughout the life-course, which may lead to permanent hearing impairment and cause more severe disability in the later years of life. As a result, the GDG selected a DW of 0.0150 for moderate severity level ("has difficulty following a conversation in a noisy environment, but no other hearing problems"). For cognitive impairment, the DW was derived from the estimates of the burden of disease from environmental noise (WHO Regional Office for Europe & JRC, 2011). This was at a very conservative value (DW: 0.006) for noise-related impairment of children's cognition, equivalent to a DW for contemporaneous cognitive deficit in the context of a range of cognitive impairments in children ranging from 0.468 for Japanese encephalitis to 0.024 for iron deficiency anaemia (Lopez et al., 2006).

2.4.3.1 Development of ERFs

The systematic reviews of evidence provided either an ERF or other noise exposure value/metric that could be related to a risk increase of the health outcome measure. These ERFs were used to develop guideline exposure levels; however, only those functions where noise exposure demonstrated a statistically significant effect were used.

To obtain the starting level of the ERFs derived in the systematic reviews, a weighted average of the lowest exposure values measured in the individual studies included in the meta-analyses was calculated. The weighting used the inverse of the variance of the effect estimate of the study. Thus, the lowest exposure value of studies with a small variance (usually with the largest sample size) contributed the most to the assumed onset of the ERF.

2.4.3.2 Relevant risk increase of adverse health effects

The following sections describe in detail the rationale for the selection of the relevant relative risk (RR) increase percentage for each of the priority health outcome measures considered.

Cardiovascular disease: IHD and hypertension

High-quality epidemiological evidence described in the systematic review on cardiovascular and metabolic effects of environmental noise indicates that exposure to road traffic noise increases the risk of IHD (van Kempen et al., 2018). The GDG was confident that health risks result from exposure at an RR increase in the order of 5–10% in the incidence of IHD. This is similar to the reasoning in the WHO air quality guidelines for fine particulate matter ($PM_{2.5}$) (WHO, 2006). To determine a relevant risk increase for IHD, the GDG took as a starting-point the RR increase of 5% measured in epidemiological studies of environmental noise or air pollution. Taking into account the incidence of IHD and the seriousness of the disease, it considered lowering the RR increase for IHD to 1%, as a 5% RR increase might imply a comparatively high absolute risk from a population perspective. To decide on the final benchmark value for IHD, several aspects were considered: the number of people in a population affected by IHD; whether health risks caused by noise would make up a large part of the incidence of the disease; other examples of health risks of similar magnitude leading to preventive action. For IHD, in an average EU country with 20 million inhabitants, an RR increase of 5% for IHD would lead to several thousand extra cases attributable to noise yearly. This corresponds to a proportion of cases of IHD attributable to noise exposure of less than 10%, which is still relatively small. After extensive discussion at the very end of the guideline development process, the GDG decided to adhere to 5% as the relevant risk increase.

Hypertension is a common condition and is an important risk indicator for IHD and other cardiovascular diseases. Thus, the hypertension risk increase can be transformed into a risk increase for cardiovascular disease. To derive a relevant risk increase, the GDG focused on the incidence of hypertension, owing to the nature and quality of epidemiological evidence. Since hypertension is less serious than IHD, and not all people with hypertension will progress to cardiovascular disease, the relevant risk increase in the incidence of hypertension needed to be higher than that for IHD. Therefore, the GDG agreed on an RR increase of 10% for hypertension.

Self-reported sleep disturbance and annoyance

The GDG initially considered 5%HSD and 10%HA due to noise as relevant absolute risks, not be exceeded at the guideline level. After discussion, however, members agreed that these absolute risks were too large, since a considerable proportion of the population would still be affected; they decided to lower the relevant risk from 5% being highly sleep-disturbed to 3%. In doing so, the GDG referred to the WHO night noise guidelines (WHO, 2009), which concluded that while there was insufficient evidence that physiological effects at noise levels below 40 dB L_{night} are harmful to health, there were observed adverse health effects at levels starting from 40 dB L_{night}. At 40 dB, about 3–4%

(depending on the noise source) of the population still reported being highly sleep-disturbed due to noise, which was considered relevant to health. The GDG considered it important that this level is consistent with the previous health-based approach adopted by the WHO night noise guidelines, and agreed that the absolute risk associated with the guideline value selected should not exceed 3%HSD to be health protective.

For annoyance, which is considered a less serious health effect than self-reported sleep disturbance (as indicated by the respective DWs), the relevant risk remained at 10%HA. This means the absolute risk associated with the guideline value selected should be closest to, but not above 10%HA, to be health protective.

Cognitive impairment: reading and oral comprehension

Acquiring skills in reading and oral comprehension at a young age is important for further development: a delay in acquiring these skills can have an impact later in life (Wilson & Lonigan, 2010). This impact cannot be predicted very accurately, but the GDG considered a delay of one month a relevant absolute risk.

Permanent hearing impairment

The literature on hearing impairment as a result of occupational noise exposure is extensive. A noise exposure level beyond 80 dB during 40 years of working a 40 hour work week can give rise to permanent hearing impairment. Given that environmental exposure to noise is much lower than these levels and that noise-related hearing impairments are not reversible, the GDG considered that there should be no risk of hearing impairment due to environmental noise and considered any increased risk of hearing impairment relevant.

2.4.4 Strength of the recommendations

Finally, having determined the guideline exposure levels based on the ranking of prioritized health outcome measures, setting the strength of the recommendation was set as the final step of the guideline development process. This was also guided by the GRADE methodology (Alonso-Coello et al., 2016a; 2016b). According to this approach, strength of recommendation can be set as either strong or conditional (WHO, 2014c).

- A **strong** recommendation can be adopted as policy in most situations. The guideline is based on the confidence that the desirable effects of adherence to the recommendation outweigh the undesirable consequences. The quality of evidence for a net benefit – combined with information about the values, preferences and resources – inform this recommendation, which should be implemented in most circumstances.
- A **conditional** recommendation requires a policy-making process with substantial debate and involvement of various stakeholders. There is less certainty of its efficacy owing to lower quality of evidence of a net benefit, opposing values and preferences of individuals and populations affected or the high resource implications of the recommendation, meaning there may be circumstances or settings in which it will not apply.

The GRADE approach defines a number of parameters that should be assessed to determine the strength of recommendations: quality of evidence, balance of benefits and harms, values and preference related to the outcomes of interventions to exposure, resources implications, priority of the problem, equity and human rights, acceptability and feasibility (Box 2; Morgan et al., 2016).

Box 2 Parameters determining the strength of a recommendation

Quality of evidence further represents the confidence in the estimates of effect of the evaluated evidence, across outcomes critical and important to decision-making. The higher the quality of evidence, the greater the likelihood of a strong recommendation.

Balance of benefits and harms requires an evaluation of the absolute effects of both benefits and harms (or downsides) of the intervention or exposure and their importance. The greater net benefit or net harm associated with an intervention or an exposure, the greater the likelihood of a strong recommendation in favour or against an intervention or exposure.

Values and preferences related to the outcomes of an intervention or exposure set out the relative importance assigned to health outcomes by those affected by them; how such importance varies within and across populations; and whether this importance or variability is surrounded by uncertainty. The less uncertainty or variability there is about the values and preferences of people experiencing the critical or important outcomes, the greater the likelihood of a strong recommendation.

Resource implications take into consideration how resource-intensive and how cost-effective and substantially beneficial an intervention or exposure is. The more advantageous or clearly disadvantageous the resource implications are, the greater the likelihood of a strong recommendation either for or against the intervention or exposure.

The priority of the problem is determined by its importance and frequency (the burden of disease, disease prevalence or baseline risk). The greater the importance of the problem, the greater the likelihood of a strong recommendation.

Equity and human rights considerations are an important aspect of the process. The greater the likelihood that the intervention will reduce inequities, improve equity or contribute to the realization of one or several human rights as defined under the international legal framework, the greater the likelihood of a strong recommendation.

Acceptability plays a prominent role: the greater the acceptability of an option to all or most stakeholders, the greater the likelihood of a strong recommendation.

Feasibility overlaps with values and preferences, resource considerations, existing infrastructures, equity, cultural norms, legal frameworks and many other considerations. The greater the feasibility of an option from the standpoint of all or most stakeholders, the greater the likelihood of a strong recommendation.

The GDG evaluated the strength of the recommendations based on these parameters, following a two-step procedure. Initially, the strength of each recommendation was set as strong or conditional based on an assessment of the quality of evidence. The GDG then identified and assessed contextual parameters that might have a contributory role (see Box 2 above). Based on this qualitative evaluation, the initial recommendation strength was either adapted or confirmed. It is important to note that while the initial parameter "quality of evidence" was informed by comprehensive systematic reviewing processes, the remaining contextual parameters were assessed by the informed qualitative expert judgement of the GDG.

Furthermore, the GDG agreed to decision-making rules, applied when formulating the recommendations. An evidence rating of low quality or very low quality would lead only to a conditional recommendation. Setting a strong recommendation was only considered if the evidence was at least moderate quality. The final recommendations were formulated based on the consideration of all the parameters and decision rules adopted by the GDG. A detailed exploration of all the recommendations is set out in Chapter 3.

2.5 Individuals and partners involved in the guideline development process

The process of WHO guideline development is conducted by several groups with clearly defined roles and responsibilities. Comprising WHO staff members, experts and stakeholders, these are the Steering Group, the GDG, the Systematic Review Team and the External Review Group.

The **Steering Group** includes WHO staff members with different affiliations but whose work experience is relevant to the topic of environmental noise and associated health outcomes. It is involved at all stages of planning, selecting members of the GDG and External Review Group, reviewing evidence and developing potential recommendations at the main expert meetings, as well as ongoing consultation on revisions following peer review. Details of the members of the Steering Group are listed in Table A1.1 in Annex 1.

The **GDG** consists of a group of content experts gathered to investigate all aspects of evidence contributing to the recommendations, including expertise in evidence-based guideline development. This Group defined the key questions and priorities of the research, chose and ranked outcomes and provided advice on any modifications of the scope as established by the Steering Group. The members also outlined the systematic review methods; appraised the evidence used to inform the guidelines; and advised on the interpretation of this e idence, with explicit consideration of the overall balance of benefits and harms. Ultimately the GDG formulated the final recommendations, taking into account the diverse values and preferences of individuals and populations affected. It also determined the strength of the results and responded to external peer reviews. The complete list of GDG members and their specific roles, affiliations and areas of expertise are listed in Table A1.2 in Annex 1.

The **Systematic Review Team** includes experts in the field of environmental health, commissioned by WHO staff to undertake systematic reviews of evidence. The GDG recommended a number of authors to conduct the evidence reviews and summary chapters, based on their expertise. Details of the members of the Systtematic Review Team are included in Table A1.3 in Annex 1.

The **External Review Group** is composed of technical content experts and end-users as well as stakeholders, and is balanced geographically and by gender. The experts and end-users were selected for their expertise in the field, and the Group also included representatives of professional groups and industry associations, who will be implementing the guidelines. Members were asked to review the material at different stages of the development process. The list of technical experts and stakeholders is provided in Tables A1.4 and A1.5, respectively, in Annex 1.

Management of conflict of interest is an integral part of WHO's guideline development procedure. All members of the GDG and authors of the evidence reviews completed WHO declaration of interest forms. These were reviewed by the WHO Secretariat for potential conflicts of interest. A number of conflicts of interest were declared in the forms, but following a standardized management review it was not found necessary to exclude any members of the GDG or authors from their respective roles. Members of the External Review Group (technical experts only) were also asked to complete the form when invited to participate.

In addition, at the start of the meeting of the GDG all members of the GDG received a briefing about the nature of all types of conflict of interest (financial, academic/intellectual and nonacademic) and were asked to declare to the meeting any conflicts they might have. No member of the GDG or the Systematic Review Team was excluded from his/her respective role. A summary of the conflict of interest management is presented in Annex 3.

The GDG set its own rules on how it would work and how contentious issues should be resolved – for instance, by means of a vote. The main decision-making mechanism involved reaching consensus; if a vote was required, the experts involved in developing the underlying evidence for the specific recommendation were excluded from voting, and an agreement was reached via a two thirds majority of the rest of the group.

2.6 Previously published WHO guidelines on environmental noise

Prior to this publication, WHO published community noise guidelines (CNG) in 1999 (WHO, 1999) and night noise guidelines for Europe (NNG) in 2009 (WHO Regional Office for Europe, 2009).

2.6.1 CNG

The scope of WHO's efforts to develop the CNG in 1999 was similar to that for the current guidelines. The objective was then formulated as: "to consolidate scientific knowledge of the time on the health impacts of community noise and to provide guidance to environmental health authorities and professionals trying to protect people from the harmful effects of noise in nonindustrial environments" (WHO, 1999). The guidelines were based on studies carried out up to 1995 and a few meta-analyses from some years later.

The health risk to humans from exposure to environmental noise was evaluated and guideline values derived. At that time WHO had not yet developed its guideline development process, on which the current guidelines are based (WHO, 2014c). The main differences in content are that the previous guidelines were expert-based and provided more global coverage and applicability, such as issues of noise assessment and control that were addressed in detail. They included a discussion on noise sources and measurement, including the basic aspects of source characteristics, sound propagation and transmission. Adverse health effects of noise were characterized, and combined noise sources and their effects were considered. Furthermore, the guidelines included discussions of strategies and priorities in the management of indoor noise levels, noise policies and legislation, environmental noise impact and enforcement of regulatory standards; although there were no chapters on wind turbine noise and leisure noise.

2.6.2 NNG

In 2009 the WHO Regional Office for Europe published the NNG to provide scientifically based advice to Member States for the development of future legislation and policy action in the area of assessment and control of night noise exposure.

The NNG complement the previous CNG, incorporating the advancement of research on noise and sleep disturbance up to 2006. The working group of experts reviewed available scientific evidence on the health effects of night noise and derived health-based guideline values. Again, WHO had not yet introduced its evidence-based recommendations policy and the NNG were mainly expert-based. They considered the scientific evidence on the threshold of night noise exposure indicated by L_{night} as defined in the END (EC, 2002a), and the experts concluded that a L_{night} value of 40 dB should be the target of the NNG (for all sources) to protect the public, including the most vulnerable groups such as children, chronically ill and elderly people. Further, an L_{night} value of 55 dB was recommended as an interim target for countries that could not follow the guidelines in the short term for various reasons or where policy-makers chose to adopt a stepwise approach.

2.6.3 Differences from the prior noise guidelines

The current guidelines differ from the older ones, recommending levels of exposure unlike those previously outlined (especially by the NNG). The following major differences between the previous and current guidelines explain the novel set of recommended values.

- The development process for the current guidelines adhered to a new, rigorous, evidence-based methodology, as outlined in the WHO handbook for guideline development (WHO, 2014c). WHO adopted these internationally recognized standards to ensure high methodological quality and a transparent, evidence-based decision-making process in the guideline development.
- The current guidelines consider cardiovascular disease a critical health outcome measure.
- They also consider a broader set of health outcomes, including adverse birth outcomes, diabetes, obesity and mental well-being. Wherever applicable, incidence, prevalence and mortality were considered separately.
- The current guidelines cover two new noise sources: wind turbines and leisure noise.
- Critical and important health outcomes are considered separately for each of the noise sources.
- The guideline development process included the health effects of intervention measures to mitigate noise exposure from different noise sources for the first time.
- The style of recommendations differs: the current guidelines include an exact exposure value for every health outcome regarded as critical, for each noise source. Guideline recommendation values were set for each of the noise sources separately, based on the exact exposure values and a prioritization scheme, developed with the help of DWs.
- The current guidelines apply a 1 dB increment scheme, whereas prior guidelines (CNG and NNG) formulated or presented recommendations in 5 dB steps.

- In comparison to the 1999 CNG, which defined environment-specific exposure levels, the current guidelines are source specific. They recommend values for outdoor exposure to road traffic, railway, aircraft and wind turbine noise, and indoor as well as outdoor exposure levels for leisure noise.
- Except for leisure noise, all exposure levels recommended in the current guidelines are average sound pressure levels for outdoor exposure.
- The current guidelines make use of the noise indices defined in the END: L_{den} and L_{night}.

The definition of "community noise" used in the CNG in 1999 was also adapted. The GDG agreed to use the term "environmental noise" instead, and offered an operational definition of: "noise emitted from all sources except sources of occupational noise exposure in workplaces".

The current environmental noise guidelines for the European Region supersede the CNG from 1999. Nevertheless, the GDG recommends that all CNG indoor guideline values and any values not covered by the current guidelines (such as industrial noise and shopping areas) should remain valid.

Furthermore, the current guidelines complement the NNG from 2009. Two main aspects of the NNG constitute this complementarity: the different guiding principles and the comprehensive investigation of the immediate physiological effects of environmental noise on sleep. As guiding principles the NNG defined effect thresholds or "lowest observed adverse health effect levels" for both immediate physiological reactions during sleep (i.e. awakening reactions or body movements during sleep) and long-term adverse health effects (i.e. self-reported sleep disturbance). These guideline exposure levels defined a level below which no effects were expected to occur (corresponding to 30 dB L_{night}) and proceeded to define the level where adverse effects start to occur (corresponding to 40 dB L_{night}), with the aim of protecting the whole population, including – to some extent – vulnerable groups. The development of the NNG values relied on evidence-based expert judgement. In contrast, the current guidelines formulate recommendations more strictly based on the available evidence and following the guiding principle to identify exposure values based on a relevant risk increase of adverse health effects. Thus, the recommended guideline values might not lead to full protection of the population, including all vulnerable groups. The GDG stresses that the aim of the current guidelines is to define an exposure level at which effects certainly begin.

Secondly, the NNG comprehensively investigate the immediate short-term effects of environmental noise during sleep, including physiological reactions such as awakening reactions and body movements. They also provided threshold information about single-event noise indicators (such as the $L_{A,max}$). In contrast, the current guideline values for the night time are only based on the prevalence of self-reported sleep disturbance and do not take physiological effects into account. The causal link between immediate physiological reactions and long-term adverse health effects is complex and difficult to prove. Thus, the current guidelines are restricted to long-term health effects during night time and therefore only include recommendations about average noise indicators: L_{night}. Nevertheless, the evidence review on noise and sleep (Basner & McGuire, 2018) includes an overview of single-event exposure–effect relationships.

3. Recommendations

This chapter presents specific recommendations on guideline exposure levels and/or interventions to reduce exposure and/or improve health for individual sources of noise: road traffic, railway, aircraft, wind turbines and leisure noise. The strength of each recommendation is provided (strong or conditional) and a short rationale for how each of the guideline levels was achieved is given.

The GDG discussed extensively the best way to present guideline exposure levels – either as the exact values or in 5 dB steps – and the approach to rounding the values to the nearest integer. The 5 dB increment, rounded down from the exact exposure value to the nearest 5 dB level, was initially chosen as being commonly applied in noise legislation and used in prior guidelines (WHO, 1999; EC, 2002a; WHO Regional Office for Europe, 2009). It was also used to meet the principle of precaution, since imprecision in the exposure assessment in the field of epidemiology tends to attenuate the actual effects in the population.

Use of 5 dB increments resulted in uneven magnitude of rounding down, however, raising concerns of arbitrariness. It became apparent that inclusion of both exact values and the 5 dB rounded-down values might be confusing and could affect the applicability of the guidelines. Hence, the GDG ultimately decided that formulating recommendations based on the exact calculated values, rounded only to the nearest integer, would ensure more clarity and transparency. Furthermore, it noted that adhering to a 5 dB roster might not reflect the progress in the precision of exposure assessment methods in recent decades, which would justify application of a 1 dB step.

The GDG acknowledged that the recommendations might be presented as the exact guideline exposure levels only, leaving the use of 5 dB bands to the potential policy decisions to formulate or revise noise legislation, which are beyond the scope of this publication. The WHO guideline values are public health-oriented recommendations, based on scientific evidence on health effects and on an assessment of achievable noise levels. They are strongly recommended and as such should serve as the basis for a policy-making process in which policy options are quantified and discussed. It should be recognized that in that process additional considerations of costs, feasibility, values and preferences should also feature in decision-making when choosing reference values such as noise limits for a possible standard or legislation.

In addition to the source-specific recommendations in the following sections, a short rationale for the decision-making process by the GDG for developing a particular recommendation is provided, as well as an overview of the evidence considered. This includes a recapitulation of the specific PICOS/PECCOS question (see section 2.3.1), along with a summary of evidence for each of the critical and important health effects from exposure to each of the noise sources, and for the effectiveness of interventions.

Furthermore, a description is provided of the other factors considered according to the GRADE dimensions for the assessment of the strength of recommendations (see section 2.4.4). While the quality of evidence is central to determining this, the process of moving from evidence to recommendations involves several other considerations. These include values and preferences, balance of benefits and harms, consideration of the priority of the problem, resource implications, equity and human rights aspects, acceptability and feasibility (WHO, 2014c).

3.1 Road traffic noise

Recommendations

For average noise exposure, the GDG **strongly** recommends reducing noise levels produced by road traffic below **53 dB** L_{den}, as road traffic noise above this level is associated with adverse health effects.

For night noise exposure, the GDG **strongly** recommends reducing noise levels produced by road traffic during night time below **45 dB** L_{night}, as road traffic noise above this level is associated with adverse effects on sleep.

To reduce health effects, the GDG **strongly** recommends that policy-makers implement suitable measures to reduce noise exposure from road traffic in the population exposed to levels above the guideline values for average and night noise exposure. For specific interventions, the GDG recommends reducing noise both at the source and on the route between the source and the affected population by changes in infrastructure.

3.1.1 Rationale for the guideline levels for road traffic noise

The exposure levels were derived in accordance with the prioritization process of critical health outcomes described in section 2.4.3. For each of the outcomes, the exposure level was identified by applying the benchmark, set as relevant risk increase to the corresponding ERF. In the case of exposure to road traffic noise, the process can be summarized as follows (Table 6).

Table 6. Average exposure levels (L_{den}) for priority health outcomes from road traffic noise

Summary of priority health outcome evidence	Benchmark level	Evidence quality
Incidence of IHD The 5% relevant risk increase occurs at a noise exposure level of 59.3 dB L_{den}. The weighted average of the lowest noise levels measured in the studies was 53 dB L_{den} and the RR increase per 10 dB is 1.08.	5% increase of RR	High quality
Incidence of hypertension One study met the inclusion criteria. There was no significant increase of risk associated with increased noise exposure in this study.	10% increase of RR	Low quality
Prevalence of highly annoyed population There was an absolute risk of 10% at a noise exposure level of 53.3 dB L_{den}.	10% absolute risk	Moderate quality
Permanent hearing impairment	No increase	No studies met the inclusion criteria
Reading skills and oral comprehension in children	One-month delay	Very low quality

In accordance with the prioritization process (see section 2.4.3), the GDG set a guideline exposure level of 53.3 dB L_{den} for average exposure, based on the relevant increase of the absolute %HA. It was confident that there was an increased risk for annoyance below this noise exposure level, but probably no increased risk for other priority health outcomes. In accordance with the defined rounding procedure, the value was rounded to 53 dB L_{den}. As the evidence on the adverse effects of road traffic noise was rated moderate quality, the GDG made the recommendation strong.

Next, the GDG assessed the evidence for night noise exposure and its effect on sleep disturbance (Table 7).

Table 7. Night-time exposure levels (L_{night}) for priority health outcomes from road traffic noise

Summary of priority health outcome evidence	Benchmark level	Evidence quality
Sleep disturbance 3% of the participants in studies were highly sleep-disturbed at a noise level of **45.4 dB** L_{night}	3% absolute risk	Moderate quality

Based on the evidence of the adverse effects of road traffic noise on sleep disturbance, the GDG defined a guideline exposure level of 45.4 dB L_{night}. The exact exposure value was rounded to 45 dB L_{night}. As the evidence was rated moderate quality, the GDG made the recommendation strong.

The GDG also considered the evidence for the effectiveness of interventions. The results showed that:

- addressing the source by improving the choice of appropriate tyres, road surface, truck restrictions or by lowering traffic flow can reduce noise exposure;
- path interventions such as insulation and barrier construction reduce noise exposure, annoyance and sleep disturbance;
- changes in infrastructure such as construction of road tunnels lower noise exposure, annoyance and sleep disturbance;
- other physical interventions such as the availability of a quiet side of the residence reduce noise exposure, annoyance and sleep disturbance.

Given that it is possible to reduce noise exposure and that best practices already exist for the management of noise from road traffic, the GDG made a strong recommendation.

3.1.1.1 Other factors influencing the strength of recommendations

Other factors considered in the context of recommendations on road traffic noise included those related to values and preferences, benefits and harms, resource implications, equity, acceptability and feasibility; moreover, nonpriority health outcomes (the incidence of stroke and diabetes) were considered. Ultimately, the assessment of all these factors did not lead to a change in the strength of the recommendations. Further details are provided in section 3.1.2.3.

3.1.2 Detailed overview of the evidence

The following sections provide a detailed overview of the evidence constituting the basis for setting the recommendations on road traffic noise. It is presented and summarized separately for each of the critical health outcomes, and the GDG's judgement of the quality of evidence is indicated (for a detailed overview of the evidence on important health outcomes, see Annex 4). Research into health outcomes and effectiveness of interventions is addressed consecutively.

A comprehensive summary of all evidence considered for each of the critical and important health outcomes can be found in the eight systematic reviews published in the *International Journal of Environmental Research and Public Health* (see section 2.3.2 and Annex 2).

3.1.2.1 Evidence on health outcomes

The key question posed was: in the general population exposed to road traffic noise, what is the exposure–response relationship between exposure to road traffic noise (reported as various noise indicators) and the proportion of people with a validated measure of health outcome, when adjusted for main confounders? A summary of the PICOS/PECCOS scheme applied (see section 2.3.1) and the main findings is set out in Tables 8 and 9.

Table 8. PICOS/PECCOS scheme of critical health outcomes for exposure to road traffic noise

PECO	Description	
Population	General population	
Exposure	Exposure to high levels of noise produced by road traffic (average/night time)	
Comparison	Exposure to lower levels of noise produced by road traffic (average/night time)	
Outcome(s)	For average noise exposure: 1. cardiovascular disease 2. annoyance 3. cognitive impairment 4. hearing impairment and tinnitus 5. adverse birth outcomes 6. quality of life, well-being and mental health 7. metabolic outcomes	For night noise exposure: 1. effects on sleep

Table 9. Summary of findings for health effects from exposure to road traffic noise (L_{den})

Noise metric	Priority health outcome measure	Quantitative risk for adverse health	Lowest level of exposure across studies	Number of participants (studies)	Quality of evidence
Cardiovascular disease					
L_{den}	Incidence of IHD	RR = 1.08 (95% confidence interval (CI): 1.01–1.15) per 10 dB increase	53 dB	67 224 (7)	High (upgraded for dose-response)
L_{den}	Incidence of hypertension	RR = 0.97 (95% CI: 0.90–1.05) per 10 dB increase	N/A	32 635 (1)	Low (downgraded for risk of bias and because only one study was available)
Annoyance					
L_{den}	%HA	Odds ratio (OR) = 3.03 (95% CI: 2.59–3.55) per 10 dB increase	40 dB	34 112 (25)	Moderate (downgraded for inconsistency)
Cognitive impairment					
L_{den}	Reading and oral comprehension	Not estimated	N/A	Over 2844 (1)	Very low (downgraded for inconsistency)
Hearing impairment and tinnitus					
L_{den}	Permanent hearing impairment	–	–	–	–

Cardiovascular disease

IHD

A total of three cohort (Babisch & Gallacher, 1990; Babisch et al., 1988; 1993a; 1993b; 1999; 2003; Caerphilly and Speedwell Collaborative Group, 1984; Sörensen et al., 2012a; 2012c) and four case-control studies (Babisch, 2004; Babisch et al., 1992; 1994; 2005a; Selander et al., 2009; Wiens, 1995) investigated the relationship between road traffic noise and the incidence of IHD. These involved a total of 67 224 participants, including 7033 cases. As identified in Fig. 1, the overall RR derived from the meta-analysis was 1.08 (95% CI: 1.01–1.15) per 10 dB L_{den} increase in noise levels, across a noise range of 40 dB to 80 dB. This evidence was rated high quality.

The data were supported by one ecological study conducted with 262 830 participants, including 418 cases, which also reported a statistically significant estimate (Grazuleviciene et al., 2004; Lekaviciute, 2007). In this study, a positive but nonsignificant association was found: RR of 1.12 (95% CI: 0.85–1.48) per 10 dB L_{den} increase in noise. This evidence was rated very low quality.

Fig. 1. The association between exposure to road traffic noise (L_{den}) and incidence of IHD

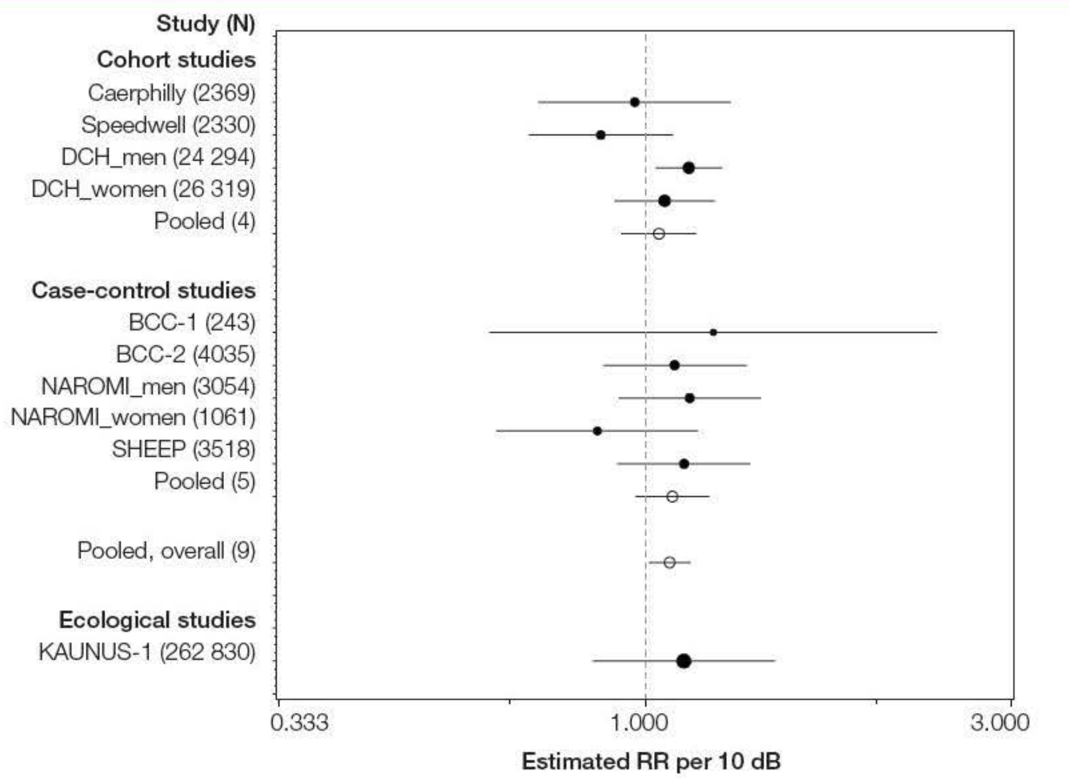

Notes: The dotted vertical line corresponds to no effect of exposure to road traffic noise. The black circles correspond to the estimated RR per 10 dB and 95% CI. The white circles represent the pooled random effect estimates and 95% CI. For further details on the studies included in the figure please refer to the systematic review on environmental noise and cardiovascular and metabolic effects (van Kempen et al., 2018).

Furthermore, additional evidence was available from eight cross-sectional studies that investigated the relationship between road traffic noise and prevalence of IHD (Babisch & Gallacher, 1990; Babisch et al., 1988; 1992; 1993a; 1993b; 1994; 1999; 2003; 2005a; 2008; 2012a; 2012b; Caerphilly and Speedwell Collaborative Group, 1984; Floud et al., 2011; 2013a; 2013b; Heimann et al., 2007; Jarup et al., 2005; 2008; Lercher et al., 2008; 2011; van Poll et al., 2014; Wiens, 1995). These studies involved a total of 25 682 participants, including 1614 cases. The overall RR was 1.24 (95% CI: 1.08–1.42) per 10 dB L_{den} increase in road traffic noise levels. The range in noise levels in the studies under evaluation was 30–80 dB. The results of the meta-analysis are presented in Fig. 2. This evidence was rated low quality.

Fig. 2. The association between exposure to road traffic noise (L_{den}) and prevalence of IHD

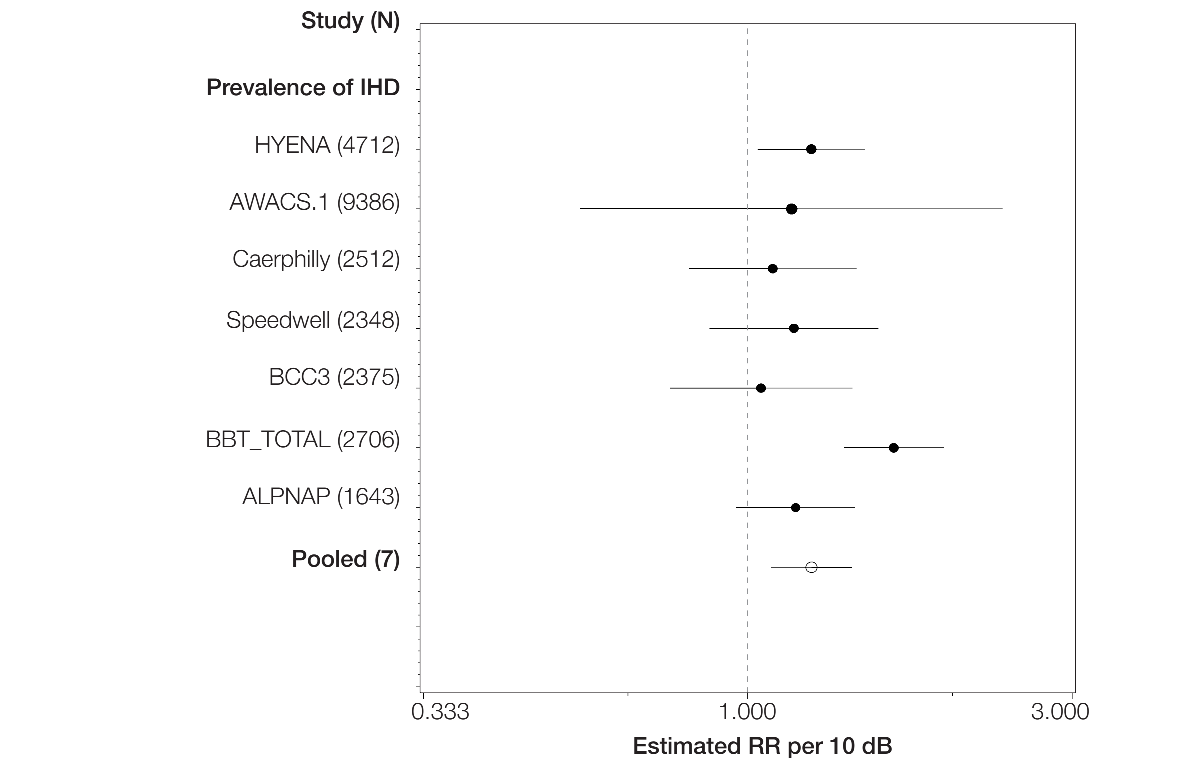

Notes: The dotted vertical line corresponds to no effect of exposure to road traffic noise. The black circles correspond to the estimated RR per 10 dB and 95% CI. The white circle represents the pooled random effect estimates and 95% CI. For further details on the studies included in the figure please refer to the systematic review on environmental noise and cardiovascular and metabolic effects (van Kempen et al., 2018).

Mortality from IHD was also investigated in one case-control (Selander et al., 2009) and two cohort studies (Beelen et al., 2009; Gan et al., 2012), which involved 532 268 participants, including 6884 cases. The quantitative relationship between road traffic noise and mortality from IHD was RR = 1.05 (95% CI: 0.97–1.13) per 10 dB L_{den} increase in noise levels (see Fig. 3). This evidence was rated moderate quality.

Fig. 3. The association between exposure to road traffic noise (L_{den}) and mortality from IHD

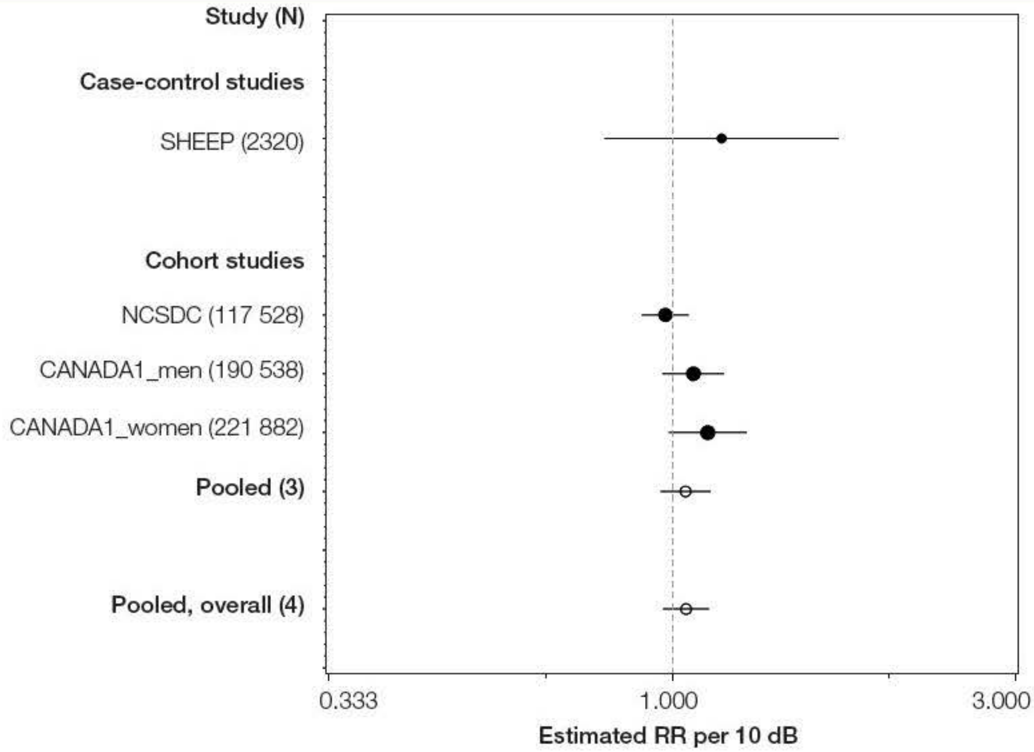

Notes: The dotted vertical line corresponds to no effect of exposure to road traffic noise. The black circles correspond to the estimated RR per 10 dB and 95% CI. The white circles represent the pooled random effect estimates and 95% CI. For further details on the studies included in the figure please refer to the systematic review on environmental noise and cardiovascular and metabolic effects (van Kempen et al., 2018).

Hypertension

One cohort study into the relationship between road traffic noise and incidence of hypertension was identified; it involved 32 635 participants, including 3145 cases (Sörensen et al., 2011; 2012c). The study found a nonsignificant effect size of 0.97 (95% CI: 0.90–1.05) per 10 dB L_{den} increase in noise levels, which does not support an increased risk of hypertension due to exposure to road traffic noise. Because of the risk of bias and the availability of only one study, this evidence was rated low quality.

In addition, 26 cross-sectional studies were identified that looked at the association between road traffic noise and prevalence of hypertension (Babisch et al., 1988; 1992; 1994; 2005a; 2008; 2012a; 2012b; 2013a; 2013b; 2014b; 2014c; Barregard et al., 2009; Bjork et al., 2006; Bluhm et al., 2007; Bodin et al., 2009; Caerphilly and Speedwell Collaborative Group, 1984; Chang et al., 2011; 2014; de Kluizenaar et al., 2007a; 2007b; Dratva et al., 2012; Eriksson et al., 2012; Foraster et al., 2011; 2012; 2013; 2014a; 2014b; Fuks et al., 2011; Hense et al., 1989; Herbold et al., 1989; Jarup et al., 2005; 2008; Knipschild et al., 1984; Lercher et al., 2008; 2011; Maschke, 2003; Maschke & Hecht, 2005; Maschke et al., 2003; Oftedal et al., 2011; 2014; Selander et al., 2009; van Poll et al., 2014; Wiens, 1995; Yoshida et al., 1997). In total, these studies involved 154 398 participants, including 18 957 cases. The overall RR for prevalence of hypertension was 1.05 (95% CI: 1.02–1.08) per 10 dB L_{den} increase in noise levels. The noise range of the studies under evaluation was 20–85 dB. The overall evidence was rated very low quality.

Fig. 4 shows the association between road traffic noise and incidence and prevalence of hypertension.

Fig. 4. The association between exposure to road traffic noise (L_{den}) and hypertension

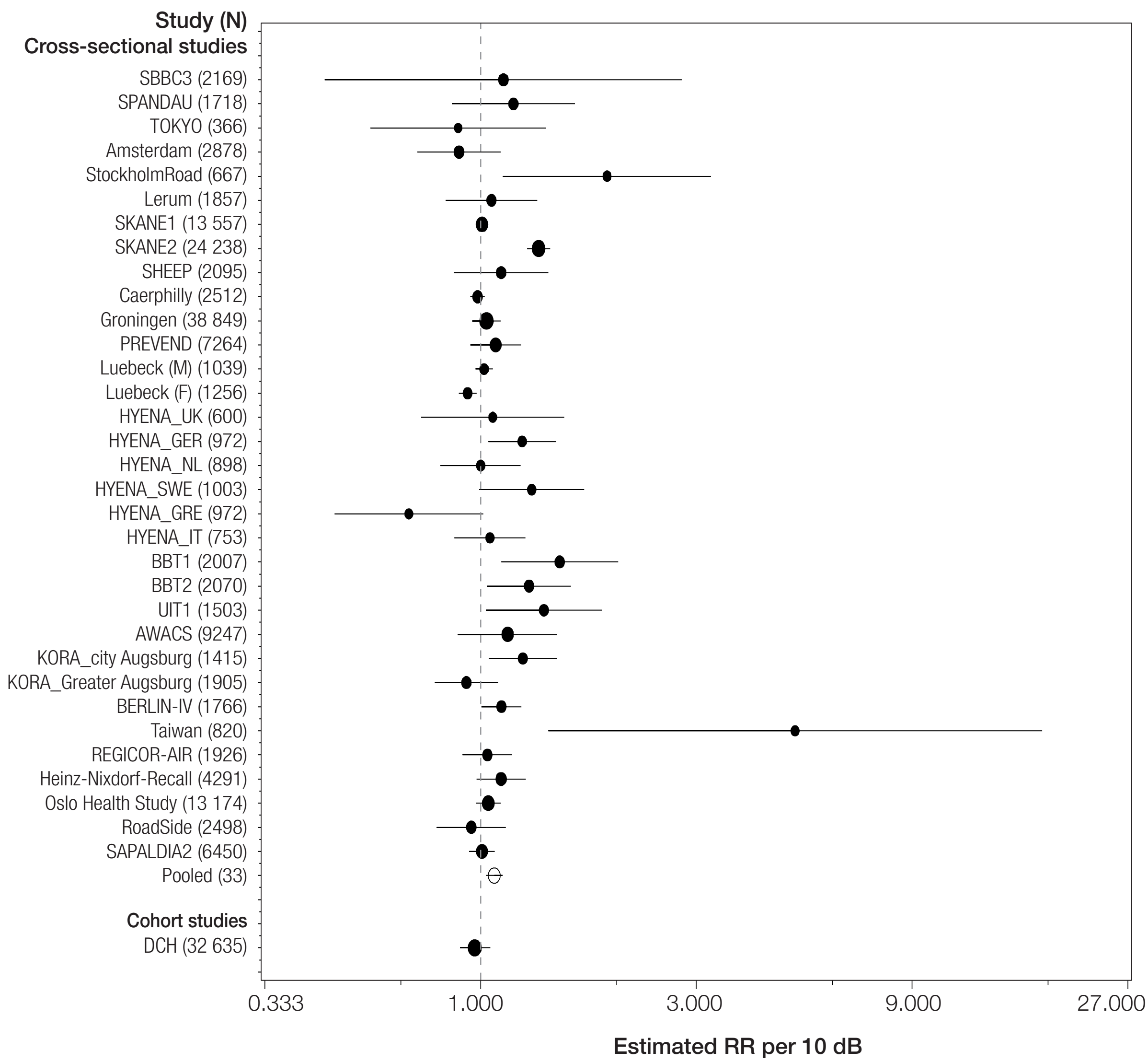

Notes: The dotted vertical line corresponds to no effect of exposure to road traffic noise. The black dots correspond to the estimated RR per 10 dB and 95% CI. The white circle represents the summary estimate and 95% CI. For further details on the studies included in the figure please refer to the systematic review on environmental noise and cardiovascular and metabolic effects (van Kempen et al., 2018).

Stroke

One cohort study into the relationship between road traffic noise and incidence of stroke was identified (Sörensen et al., 2011; 2012b; 2014). It involved 51 485 participants, including 1881 cases, and found an RR of 1.14 (95% CI: 1.03–1.25) per 10 dB L_{den} increase in noise levels, across a range of around 50–70 dB. The evidence was rated moderate quality.

Two cross-sectional studies on road traffic noise and prevalence of stroke involved 14 098 participants, including 151 cases (Babisch et al., 2005a; 2008; 2012a; 2012b; 2013a; Floud et al., 2011; 2013a; 2013b; Jarup et al., 2005; 2008; van Poll et al., 2014) yielded an estimated RR of 1.00 (95% CI: 0.91–1.10) per 10 dB L_{den} increase in noise levels. This evidence was rated very low quality.

Furthermore, three cohort studies investigated the relationship between road traffic noise and mortality due to stroke (Beelen et al., 2009; Gan et al., 2012; Sörensen et al., 2011; 2012b; 2014). These involved 581 517 participants, including 2634 cases, and their pooled estimate was a statistically nonsignificant RR = 0.87 (95% CI: 0.71–1.06) per 10 dB L_{den} increase in road traffic noise levels. This evidence was rated moderate quality.

Fig. 5 presents the results of the meta-analysis for road traffic noise and measures of stroke.

Fig. 5. The association between exposure to road traffic noise (L_{den}) and stroke

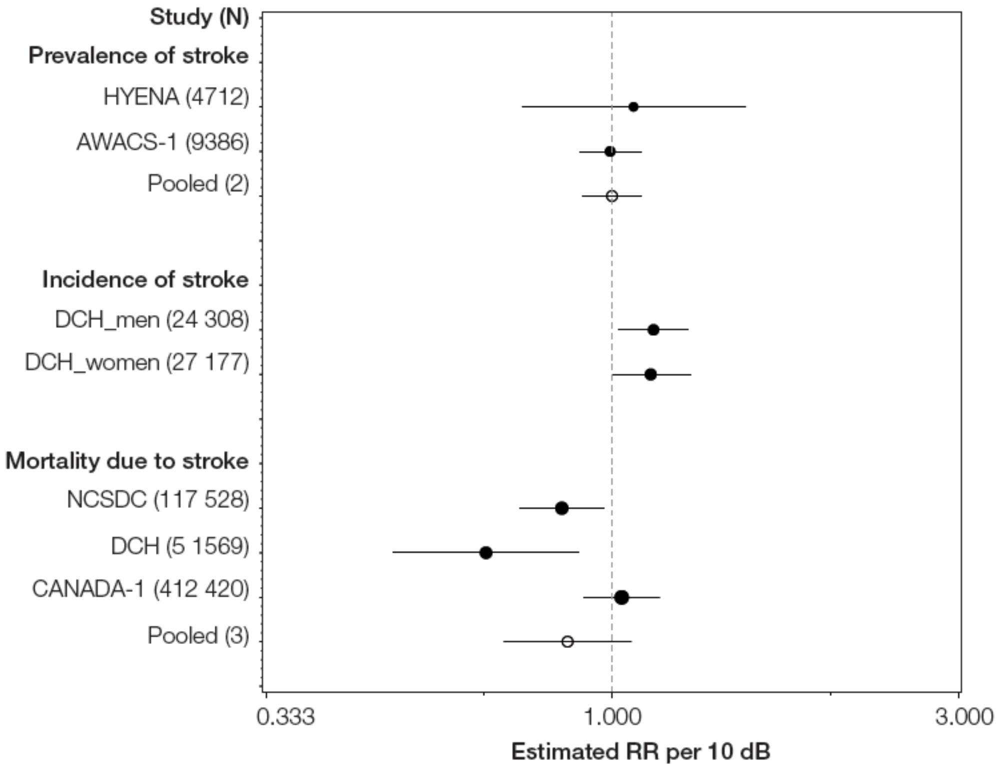

Notes: The dotted vertical line corresponds to no effect of exposure to road traffic noise. The black dots correspond to the estimated RR per 10 dB and 95% CI. The white circles represent the summary estimate and 95% CI.
For further details on the studies included in the figure please refer to the systematic review on environmental noise and cardiovascular and metabolic effects (van Kempen et al., 2018).

Children's blood pressure

Six cross-sectional studies investigated the change in systolic and diastolic blood pressure in children exposed to road traffic noise in residential settings (Belojevic & Evans, 2011; 2012; Bilenko et al., 2013; Liu et al., 2013; 2014; Regecova & Kellerova, 1995; van Kempen et al., 2006). In total, 4197 children were included in these studies; the number of cases was not reported. For each increase in 10 dB L_{den} in noise levels, there was a statistically nonsignificant increase in systolic and in diastolic blood pressure of 0.08 mmHg (95% CI: –0.48–0.64) and 0.47 mmHg (95% CI: –0.30–1.24), respectively. The overall evidence was rated very low quality.

Furthermore, five cross-sectional studies investigated the association between systolic and diastolic blood pressure in children and exposure to road traffic noise in educational settings (Belojevic & Evans, 2011; 2012; Bilenko et al., 2013; Clark et al., 2012; Paunovic et al., 2013; Regecova & Kellerova, 1995; van Kempen et al., 2006). In total, 4520 children were included in these studies; the number of cases was not reported. Systolic blood pressure decreased statistically nonsignificantly, at –0.60 mm (95% CI: –1.51–0.30) per 10 dB L_{den} increase in road traffic noise levels. Diastolic blood pressure increased statistically nonsignificantly, at 0.46 mm (95% CI: –0.60–1.53) per 10 dB L_{den} increase in road traffic noise levels. For both relationships, the evidence was rated very low quality.

Annoyance

A vast amount of research proves the association between road traffic noise and annoyance. In total, 17 road traffic noise studies were identified that were used to model ERFs of the relationship between L_{den} and %HA (Babisch et al., 2009; Brink, 2013; Brink et al., 2016; Brown et al., 2014; 2015; Champelovier et al., 2003; Heimann et al., 2007; Lercher et al., 2007; Medizinische Universitaet Innsbruck, 2008; Nguyen et al., 2012a; Pierette et al., 2012; Sato et al., 2002; Shimoyama et al., 2014). These incorporated data from 34 112 study participants. The estimated data points of each of the studies are plotted in Fig. 6, alongside an aggregated ERF including the data from all the individual studies (see the black line for "WHO full dataset"). The lowest category of noise exposure considered in any of the studies, and hence included in the systematic review, is 40 dB, corresponding to approximately 9%HA. The benchmark level of 10%HA is reached at 53.3 dB L_{den} (see Fig 6).

Table 10 shows the %HA in relation to exposure to road traffic noise. The calculations are based on the regression equation $\%HA = 78.9270–3.1162 \times L_{den} + 0.0342 \times L_{den}^2$ derived from the systematic review (Guski et al., 2017). Even though there is a large evidence base substantiating the association of average road traffic noise and noise annoyance, the overall evidence had to be rated low quality. The main reasons for downgrading included limitations regarding the acoustical data provided, the nature of study design (most of the studies in the realm of annoyance research follow a cross-sectional approach), the inconsistency of results and the variety in the questions asked.

Nevertheless, the general quality of the evidence was substantiated with the help of additional statistical analyses that apply classic health outcome measures to estimate noise annoyance. When comparing road traffic noise exposure at 50 dB and 60 dB, the analyses revealed evidence rated moderate quality for an association between road traffic noise and %HA for an increase per 10 dB (OR = 2.74; 95% CI: 1.88–4.00). Moreover, there was evidence rated high quality for the increase of %HA per 10 dB increase in sound exposure, when data on all sound classes were included (OR = 3.03; 95% CI: 2.59–3.55).

Fig. 6. Scatterplot and quadratic regression of the relationship between road traffic noise (L_{den}) and annoyance (%HA)

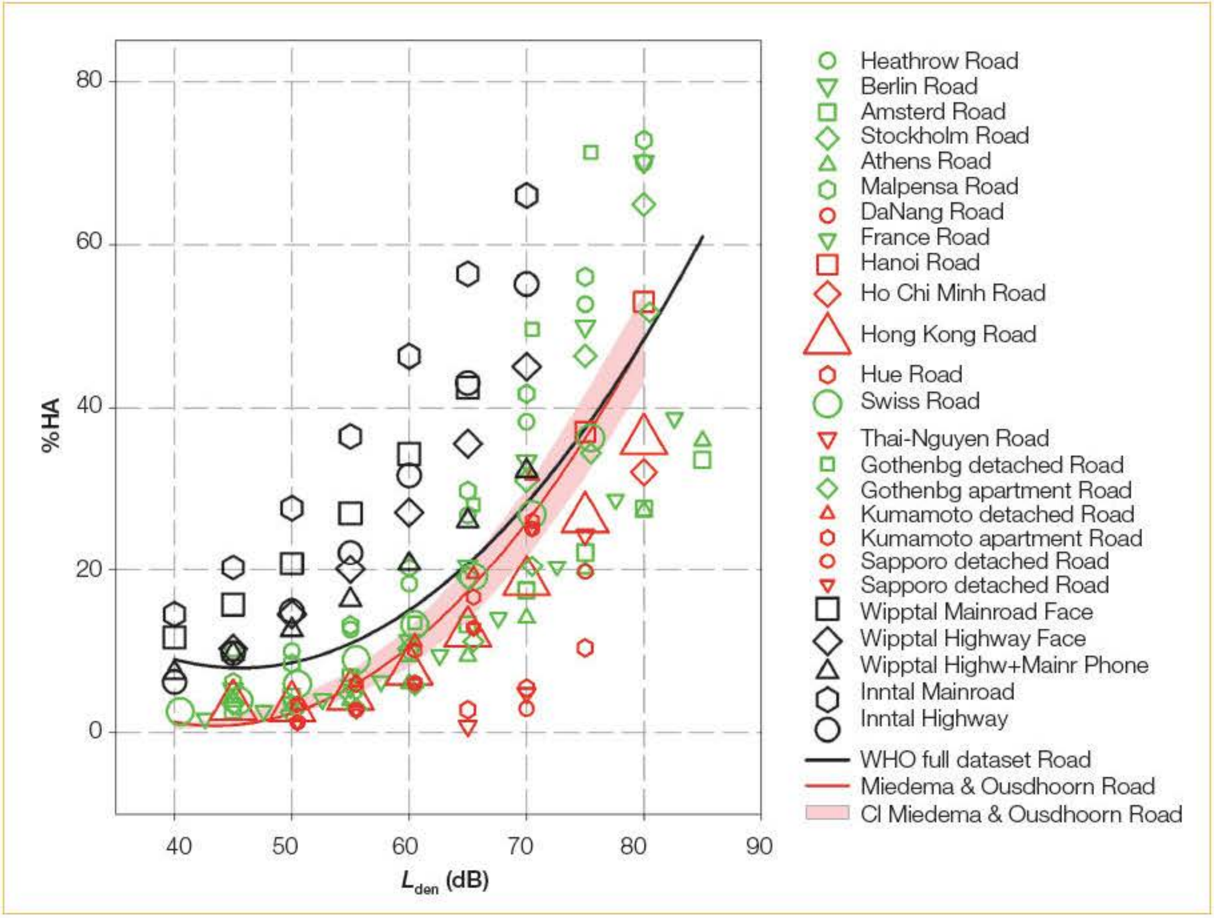

Notes: The ERF by Miedema & Oudshoorn (2001) is added in red for comparison.
The size of the data points corresponds to the number of participants in the respective study (size = SQRT(N)/10).
If two results from different studies fall on the same data point, the last point plotted may mask the former one.
The black curve is derived from aggregated secondary data, while the red one is derived from individual data.
There is no indication of 95% CIs of the WHO full dataset, as a weighting based on the total number of participants for each 5 dB L_{den} sound class could not be calculated; weighting based on all participants of all sound classes proved to be unsuitable. The range of data included is illustrated by the distribution of data points.
For further details on the studies included in the figure please refer to the systematic review on environmental noise and annoyance (Guski et al., 2017).

Table 10. The association between exposure to road traffic noise (L_{den}) and annoyance (%HA)

L_{den} (dB)	%HA
40	9.0
45	8.0
50	8.6
55	11.0
60	15.1
65	20.9
70	28.4
75	37.6
80	48.5

Cognitive impairment

Evidence rated very low quality was available for the association between road traffic noise and reading and oral comprehension, assessed by tests. The review identified two papers that reported the results of the cross-sectional road traffic and aircraft noise exposure and children's cognition and health (RANCH) study, which examined exposure–effect relationships (Clark et al., 2006; Stansfeld et al., 2005). The study of over 2000 children aged 9–10 years, attending 89 schools around three major airports in the Netherlands, Spain and the United Kingdom did not find an exposure–effect relationship between road traffic noise exposure at primary school, which ranged from 31 to 71 dB $L_{Aeq,16h}$, and children's reading comprehension.

Few studies have investigated other health outcome measures related to cognition. Evidence rated low quality was available for an association between road traffic noise and cognitive impairment assessed through standardized tests (Cohen et al., 1973; Lukas et al., 1981; Pujol et al., 2014; Shield & Dockrell, 2008). There was evidence rated very low quality for an association between road traffic noise and long-term memory (Matheson et al., 2010; Stansfeld et al., 2005). No studies examined effects on short-term memory.

There was evidence rated very low quality, however, that road traffic noise does not have a considerable effect on children's attention (Cohen et al., 1973; Stansfeld et al., 2005). Further, there was evidence rated low quality that road traffic noise does not have a substantial effect on executive function (working memory), with studies consistently reporting no association (Clark et al., 2012; Matheson et al., 2010; Stansfeld et al., 2005; van Kempen et al., 2010; 2012).

Hearing impairment and tinnitus

No studies were found, and therefore no evidence was available for the association between road traffic noise and hearing impairment and tinnitus.

Sleep disturbance

For road traffic noise and self-reported sleep outcomes (awakenings from sleep, the process of falling asleep and sleep disturbance), 12 studies were identified that included a total of 20 120 participants (Bodin et al., 2015; Brown et al., 2015; Hong et al., 2010; Phan et al., 2010; Ristovska et al., 2009; Sato et al., 2002; Shimoyama et al., 2014); these were cross-sectional studies, conducted in healthy adults. The health outcome was measured by self-reporting via general health and noise surveys that included questions about sleep in general, and other questions about how noise affects sleep (see Table 11).

Table 11. Summary of findings for health effects from exposure to road traffic noise (L_{night})

Noise metric	Priority health outcome measure	Quantitative risk for adverse health	Lowest level of exposure across studies	Number of participants (studies)	Quality of evidence
Effects on sleep					
L_{night}	%HSD	OR: 2.13 (95% CI: 1.82–2.48) per 10 dB increase	43 dB	20 120 (12)	Moderate (downgraded for study limitations, inconsistency; upgraded for dose-response, magnitude of effect)

The model in the systematic review (Basner & McGuire, 2018) was based on outdoor L_{night} levels between 40 dB and 65 dB only; 40 dB was chosen as the lower limit because of possible inaccuracies of predicting lower noise levels. The range of noise exposure reported in the studies reviewed was 37.5–77.5 dB L_{night}. About 2% (95% CI: 0.90–3.15) of the population was characterized as highly sleep-disturbed at L_{night} levels of 40 dB. The %HSD at other, higher levels of road traffic noise is presented in Table 12. The association between road traffic noise and the probability of being highly sleep-disturbed was OR: 2.13 (95% CI: 1.82–2.48) per 10 dB increase in noise. This evidence was rated moderate quality.

Table 12. The association between exposure to road traffic noise (L_{night}) and sleep disturbance (%HSD)

L_{night} (dB)	%HSD	95% CI
40	2.0	0.9–3.15
45	2.9	1.40–4.44
50	4.2	2.14–6.27
55	6.0	3.19–8.84
60	8.5	4.64–12.43
65	12.0	6.59–17.36

Additional analyses were conducted for other health outcome measures related to sleep, which provided supporting evidence on the overall relationship between road traffic noise and sleep disturbance. When the noise source was not specified in the question, the relationship between road traffic noise and self-reported sleep outcomes was still positive but no longer statistically significant, with an OR of 1.09 (95% CI: 0.94–1.27) per 10 dB increase (Bodin et al., 2015; Brink, 2011; Frei et al., 2014; Halonen et al., 2012). This evidence was rated very low quality.

There was evidence rated moderate quality for an association between road traffic noise and sleep outcomes measured with polysomnography (probability of additional awakenings) with an OR of 1.36 (95% CI: 1.19–1.55) per 10 dB increase in indoor $L_{AS,max}$ [13] (Basner et al., 2006; Elmenhorst et al., 2012). Further, evidence rated low quality showed an association between road traffic noise and sleep outcomes measured as motility in adults (Frei et al., 2014; Griefahn et al., 2000; Oehrstroem et al., 2006a; Passchier-Vermeer et al., 2007; Pirrera et al., 2014). Finally, there was evidence rated very low quality for an association between road traffic noise and both self-reported and motility-measured sleep disturbance in children (Ising & Ising, 2002; Lercher et al., 2013; Oehrstroem et al., 2006a; Tiesler et al., 2013).

3.1.2.2 Evidence on interventions

This section summarizes the evidence underlying the recommendation on the effectiveness of interventions for road traffic noise exposure. The key question posed was: in the general population exposed to road traffic noise, are interventions effective in reducing exposure to and/or health outcomes from road traffic noise? A summary of the PICOS/PECCOS scheme applied and the main findings is set out in Tables 13 and 14.

Table 13. PICOS/PECCOS scheme of the effectiveness of interventions for exposure to road traffic noise

PICO	Description	
Population	**General population**	
Intervention(s)	The interventions can be defined as: (a) a measures that aim to change noise exposure and associated health effects; (b) a measures that aim to change noise exposure, with no particular evaluation of the impact on health; or (c) a measures designed to reduce health effects, but that may not include a reduction in noise exposure.	
Comparison	**No intervention**	
Outcome(s)	For average noise exposure: 1. cardiovascular disease 2. annoyance 3. cognitive impairment 4. hearing impairment and tinnitus 5. adverse birth outcomes 6. quality of life, well-being and mental health 7. metabolic outcomes	For night noise exposure: 1. effects on sleep

[13] $L_{AS,max}$ is the maximum time-weighted and A-weighted sound pressure level with SLOW time constant within a stated time interval starting at t1 and ending at t2, expressed in dB.

Table 14. Summary of findings for road traffic noise interventions by health outcome

Type of intervention	Number of participants (studies)	Effect of intervention	Quality of evidence
Annoyance			
Type A – source interventions (change in traffic flow rate, improved road resurfacing, truck restriction strategy, complex set of barriers, road surfaces and other measures)	6096[a] (9)	• Changes in noise level ranged from around –15 dB to +15.5 dB (various noise metrics). • Most studies found that the intervention resulted in a change in annoyance.	Moderate (downgraded for study limitations; upgraded for dose-response)
Type B – path interventions (dwelling insulation, barrier construction, building intervention)	2970 (7)	• Changes in noise level ranged from –3 dB to –13 dB (various noise metrics). • All studies found that the intervention resulted in a change in annoyance, as estimated by an ERF.	Moderate (downgraded for study limitations; upgraded for dose-response)
Type C – changes in infrastructure (new road tunnel infrastructure)	1211 (2)	• Noise levels reduced by an average of –12 dB ($L_{Aeq,24h}$). • Both studies found lower annoyance responses post intervention, with no change in the controls.	Moderate (downgraded for study limitations; upgraded for dose-response)
Type D – other physical interventions (availability of quiet side to the dwelling, existence of nearby green space)	26 786 (6)	• Because of large variability in noise levels between most and least exposed façade (quiet side), access to quiet side and/or green space resulted in less annoyance.	Very low (downgraded for study limitations)
Sleep disturbance			
Type B – path interventions (1: façade insulation; 2: enlargement of motorway lanes but with dwelling insulation, barriers and quiet pavement)	1158 (2)	• 1: façade insulation resulted in a reduction of 7 dB for indoor noise level. • 2: enlargement led to reduction in the extent of population exposure at higher noise levels (55–65 dB) with an increase in lower levels (45–55 dB) • Both path interventions resulted in changes in sleep outcomes	Moderate (downgraded for study limitations)
Type C – changes in infrastructure (new road tunnel infrastructure)	166 (2)	• Noise levels reduced by an average of –12 dB ($L_{Aeq,24h}$). • Both studies found lower sleep disturbance indicators/ improvement in sleep post intervention, with no change in the controls.	Moderate (downgraded for study limitations)
Type D – other physical interventions (availability of quiet side to the dwelling)	100 (1)	• An absence of quiet façade resulted in increased reporting of difficulty in falling asleep.	Very low (downgraded for study limitations, inconsistency)
Cardiovascular disease			
Type D – other physical interventions (availability of quiet side to the dwelling)	9203 (4)	• Three studies found changes (including in self-reported hypertension) with and without a quiet side. One study found no change.	Very low (downgraded for study limitations)

Note: [a] This figure does not include number of participants from the studies by Langdon & Griffiths (1982) and Baughan & Huddart (1993), as the exact number of respondents was not reported.

Type A – source interventions

Most of the nine source intervention studies – Baughan & Huddart (1993), Brown (1987; 2015), Brown et al. (1985), Griffiths & Raw (1987; 1989), Kastka (1981), Langdon & Griffiths (1982), Pedersen et al. (2013; 2014), Stansfeld et al. (2009b) – showed an effect in annoyance due to changes in road traffic flow rates. In some cases these were combined with other measures like improved road resurfacing, truck restrictions or complex control measures, including barriers or road surfaces. A majority of the changes resulted in reductions of noise levels.

Regarding the strength of association between exposure and annoyance outcome, all intervention studies demonstrated that the response was of at least the magnitude estimated by a steady-state ERF. The limited available evidence on long-term effects shows that this excess response undergoes some attenuation but is largely maintained over several years. In spite of the high risk of bias in all studies, the evidence in the systematic review was initially assessed as high quality, due to an upgrade because of the dose-response effect. However, the GDG decided to downgrade this assessment in an effort to maximize consistency with the grading approach of the remaining systematic reviews. It was therefore rated moderate quality.

Type B – path interventions

Seven path intervention studies – Amundsen et al. (2011; 2013), Bendtsen et al. (2011), Gidloef-Gunnarsson et al. (2010), Kastka et al. (1995), Nilsson & Berglund (2006), Vincent & Champelovier (1993) – explored the effects on annoyance by interventions related to dwelling insulation, barrier constructions and a combination of both, as well as a full-scale building intervention. With the help of pre/post designs, the studies assessed changes in noise exposure achieved by the interventions over different periods of time. In six studies the path intervention was associated with a change in annoyance outcomes. Four of these showed that the annoyance response to the change was in the same direction and of at least the same magnitude estimated by the ERF. In spite of the high risk of bias in all studies, the evidence in the systematic review was initially assessed as high quality, due to an upgrade because of the dose-response effect. However, the GDG decided to downgrade this assessment in an effort to maximize consistency with the grading approach of the remaining systematic reviews. The evidence was therefore rated moderate quality.

Two of the studies (Amundsen et al., 2013; Bendtsen et al., 2011) assessed path interventions and sleep disturbance. The results showed a reduction in the %HSD after the interventions were conducted. One of the studies included a two-year follow-up, revealing the persistence of the effect. Risk of bias was assessed as high in both studies. The evidence was rated moderate quality.

Type C – new/closed infrastructure interventions

Two infrastructural intervention studies (Gidloef-Gunnarsson et al., 2013; Oehrstroem, 2004; Oehrstroem & Skanberg, 2000) evaluated the impact on annoyance of major reductions in road traffic flows, combined with other environmental improvements. One was a new road tunnel infrastructure, resulting in substantial traffic and noise levels reductions for residents near the previously heavy-traffic road. Both studies were pre/post designs using repeated measures of annoyance outcomes. Following the reduction in noise levels (around –12 dB $L_{Aeq,24h}$), both studies demonstrated a statistically significant lower degree of annoyance, while there was no change in the control group. Both also reported that the after-scores in the studies matched those estimated by the ERF, but both reported excess response, meaning that the response to change was in the direction estimated by the ERF but much steeper. In spite of the high risk of bias in all studies, the quality of the evidence in the systematic review was initially assessed as high, due to an upgrade because of the dose-response effect. However, the GDG decided to downgrade this assessment in an effort to maximize consistency with the grading approach of the remaining systematic reviews. The evidence was therefore rated moderate quality.

Two studies investigated the impact of new tunnels that removed traffic flow from surface roads on sleep disturbance (Oehrstroem, 2004; Oehrstroem & Skanberg, 2000; 2004). Subjective and objective measures of sleep quality were assessed before and after the intervention. Both studies demonstrated a statistically significant lower reporting of various sleep disturbance indicators post intervention. One study reported statistically significantly reduced time spent in bed after the intervention, which, according to the authors, could suggest increased sleep efficiency. Risk of bias was assessed as high, so this evidence was rated moderate quality.

Type D – other physical infrastructure interventions

No intervention studies were available to assess impacts on annoyance of other physical interventions. The only relevant studies (Babisch et al., 2012; de Kluizenaar et al, 2011; 2013; Gidloef-Gunnarsson & Oehrstroem 2007; van Renterghem & Botteldooren, 2012; 2010) did not provide direct evidence of an intervention. Instead, they provided indirect evidence on the magnitude of the likely effect of certain interventions (e.g. using the quiet side of the dwelling, green space in the neighbourhood) by comparing responses from groups with and without the intervention/feature of interest. All studies found an effect of the presence of the dimension investigated; in all but one, the effect was statistically significant. Risk of bias was assessed as high in all studies, so the evidence was rated very low quality.

One study investigated a subjective assessment of difficulty in falling asleep (van Renterghem & Botteldooren, 2012), before and after the intervention. The difference in the proportion of participants reporting difficulty falling asleep “at least sometimes” between homes with and without a quiet side was statistically significant. Absence of a quiet façade resulted in increased reporting of this sleep parameter. Confounding was adjusted for in the analyses of the ERFs, including noise sensitivity, window-closing behaviour and front-façade L_{den}. Risk of bias was assessed as high, so the evidence was rated very low quality.

Four studies that assessed the effect of other physical interventions on cardiovascular disease were identified (Babisch et al., 2012; 2014a; Bluhm et al., 2007; Lercher et al., 2011). Three of these found changes, including self-reported hypertension, with and without a quiet side of the dwelling; in two the difference was statistically significant. The risk of bias in these studies was generally high, so the evidence was rated very low quality.

3.1.2.3 Consideration of additional contextual factors

As the foregoing overview has shown, ample evidence about the adverse health effects of long-term exposure to road traffic noise exists. Based on the quality of the available evidence, the GDG set the strength of the recommendation on road traffic noise at strong. As a second step, it qualitatively assessed contextual factors to explore whether other considerations could have a relevant impact on the recommendation strength. These considerations mainly concerned the balance of harms and benefits, values and preferences, equity, and resource use and implementation.

When assessing the balance of harms and benefits of interventions to reduce exposure to road traffic noise, the GDG initially noted that road traffic is the most widespread source of noise pollution, measured in terms of the number of affected people both within and outside urban areas. The EEA estimates that more than 100 million people in Europe are exposed to L_{den} levels above 55 dB; for night-time road traffic noise, over 72 million Europeans are exposed to L_{night} levels above 50 dB (Blanes et al., 2017).[14] The amount of road traffic noise emitted is unlikely to decrease significantly: both transport demand, including for passenger cars (EC, 2016b), and the number of city inhabitants (Eurostat, 2016) are expected to increase. Considering the significant burden of disease attributable to exposure to road traffic noise (WHO Regional Office for Europe & JRC, 2011), the GDG expects substantial health benefits to evolve from implementing the recommendations to reduce population exposure to road traffic noise. Depending on the intervention measures used (such as restrictions of traffic), possible harms could include effects on the transportation of goods and on individual mobility of the population. Both can have impacts on local, national and international economies. Overall, the GDG estimated that the benefits gained from minimizing adverse health effects due to road traffic noise exposure outweigh the possible (economic) harms.

Considering values and preferences, it has been established that people appreciate quiet areas as beneficial for their health and well-being, especially in urban areas (Shepherd et al., 2013; Gidloef-Gunnarsson & Oehrstroem, 2007; Oehrstroem et al., 2006b). Nevertheless, the GDG recognized that the convenience of individual mobility with the help of passenger cars is valued overall by large parts of the population in the EU, as illustrated by the sustained high volume of passenger kilometres driven in Europe (EEA, 2016a; 2017a). In general, values and preferences are expected to vary throughout society, as exposure to environmental noise and continuous road traffic noise is not equally distributed: those of individuals directly affected by long-term road traffic exposure are likely to differ from those that are not affected. Individuals with a higher average sound pressure level of road traffic noise are, for example, more willing to pay to reduce their noise exposure (Bristow et al., 2014).

In light of the dimension of equity, the GDG highlighted the fact that the risk of exposure to road traffic noise is not equally distributed throughout society. People with lower socioeconomic status and other disadvantaged groups often live in more polluted and louder areas, including in proximity to busy roads (EC, 2016a). Moreover, socioeconomic factors are not only related to differences in exposure to environmental factors such as noise but are also associated with increased vulnerability and poorer coping capacities (Karpati et al., 2002).

With resource use and implementation considerations, the GDG recognized that no comprehensive cost–benefit analysis for the WHO European Region yet exists, so this assessment is based on informed expert judgement regarding the feasibility of implementing the recommendation for the majority of the population. As the systematic review of environmental noise interventions and their

[14] These are gap-filled figures based on the reported data and including the situation both within and outside cities, as defined by the END.

associated impact on health shows, various effective measures exist to reduce noise exposure from road traffic and improve health (Brown & van Kamp, 2017). The resources needed to implement these measures vary as they rely on the type of intervention and the context. The GDG pointed out the following four major solutions, which are known to be cost-effective: choice of appropriate tyres, use of low-noise road surfaces, building of noise barriers and installation of soundproof windows (CSES et al., 2016). Other types of intervention include limitations of speed or type of traffic allowed on roads.

Regarding feasibility of implementation, the GDG was convinced that many of the solutions can be planned as part of regular maintenance processes and accelerated fleet and road modernization. In particular, appropriate tyres and road surfaces are only slightly more expensive than existing products, and various countries have already considered or adopted similar interventions to reduce noise levels (Ohiduzzaman et al., 2016; Sirin, 2016). This indicates that solutions to achieve recommended noise levels can be implemented and carry a reasonable cost on a societal level. The GDG noted, however, that the feasibility of implementing measures can be hindered by the fact that costs and benefits are not evenly distributed. In most cases, the health benefits gained by interventions that reduce long-term road traffic exposure accrue to citizens, whereas the costs are borne by road users, private companies and public authorities. Furthermore, the GDG expects challenges in the implementation of all long-term measures that include changes in behaviour of the population, such as increased use of car-sharing or public transport. Even though the overall costs are expected to be significant, because of the large number of people affected, the benefit of implementation of the recommendation to minimize the risk of adverse health effects due to road traffic noise for a majority of the population exceeds the resources needed.

In light of the assessment of the contextual factors in addition to the quality of evidence, the recommendation remains strong.

Other nonpriority adverse health outcomes

As an additional consideration, although not priority health outcomes and coming from a single study, the GDG noted the evidence rated moderate quality for an association between road traffic noise and the prevalence of diabetes (van Kempen et al., 2018). The noise levels in the study identified ranged from around 50 dB to 70 dB L_{den}, so the recommendation proposed is thought to be protective enough for this health outcome. Thus, it did not lead to a change in the recommendation.

Additional considerations or uncertainties

Individual noise annoyance judgements of residents are to a large extent moderated by personal variables (such as noise sensitivity and coping capacity). However, further situational factors that apply to many residents should be taken into account when analysing noise annoyance from road traffic noise, as they may moderate the relationship. These include the type(s) of road being considered (highways, urban main roads, secondary roads and so on) and the related traffic composition (share of cars, motorcycles and heavy and loud trucks) and pattern (fluctuation, frequency, intermittency). Moreover, the location of settlements and/or individual dwellings, proximity to the road, and location and availability of a quiet façade can also influence the relationship when predicting health outcomes such as annoyance.

3.1.3 Summary of the assessment of the strength of the recommendations

Table 15 provides a comprehensive summary of the different dimensions for the assessment of the strength of the road traffic noise recommendations.

Table 15. Summary of the assessment of the strength of the road traffic noise recommendation

Factors influencing the strength of recommendation	Decision
Quality of evidence	**Average exposure** (L_{den}) *Health effects* • Evidence for a relevant RR increase for incidence of IHD at **59 dB** L_{den} was rated **high quality**. • Evidence for the incidence of hypertension was rated **low quality**. • Evidence for a relevant absolute risk of annoyance at **53 dB** L_{den} was rated **moderate quality**. • Evidence for a relevant RR increase for reading and oral comprehension was rated **very low quality**. *Interventions* • Evidence on effectiveness of interventions to reduce noise exposure and/or health outcomes from road traffic noise is of varying quality. **Night-time exposure** (L_{night}) *Health effects* • Evidence for a relevant absolute risk of sleep disturbance related to night noise exposure from road traffic at **45 dB** L_{night} was rated **moderate quality**. *Interventions* • Evidence on effectiveness of interventions to reduce noise exposure and/or sleep disturbance from road traffic noise is of varying quality.
Balance of benefits versus harms and burdens	Health benefits can be gained from markedly reducing exposure of the population to road traffic noise; benefits outweigh the harms of interventions to reduce continuous road traffic noise.
Values and preferences	Quiet areas are valued by the population, especially by those affected by continuous noise exposure. Some variability is possible between those who benefit from interventions to reduce road traffic noise and those who finance the interventions.
Equity	Risk of exposure to road traffic noise is not equally distributed.
Resource use and implications	No comprehensive cost–effectiveness analysis data are available; nevertheless, a wide range of solutions exists and several are being implemented, showing that effective interventions are both feasible and economically reasonable.
Decisions on recommendation strength	• **Strong** for guideline level for average noise exposure (L_{den}) • **Strong** for guideline value for average night noise exposure (L_{night}) • **Strong** for specific interventions to reduce noise exposure

3.2 Railway noise

Recommendations

For average noise exposure, the GDG **strongly** recommends reducing noise levels produced by railway traffic below **54 dB** L_{den}, as railway noise above this level is associated with adverse health effects.

For night noise exposure, the GDG **strongly** recommends reducing noise levels produced by railway traffic during night time below **44 dB** L_{night}, as railway noise above this level is associated with adverse effects on sleep.

To reduce health effects, the GDG **strongly** recommends that policy-makers implement suitable measures to reduce noise exposure from railways in the population exposed to levels above the guideline values for average and night noise exposure. There is, however, insufficient evidence to recommend one type of intervention over another.

3.2.1 Rationale for the guideline levels for railway noise

The exposure levels were derived in accordance with the prioritizing process of critical health outcomes described in section 2.4.3. For each of the outcomes, the exposure level was identified by applying the benchmark, set as relevant risk increase to the corresponding ERF. In the case of exposure to railway noise, the process can be summarized as follows (Table 16).

Table 16. Average exposure levels (L_{den}) for priority health outcomes from railway noise

Summary of priority health outcome evidence	Benchmark level	Evidence quality
Incidence of IHD No studies were available and therefore incidence of IHD could not be used to assess the exposure level.	5% increase of RR	No studies met the inclusion criteria/no studies available
Incidence of hypertension One study met the inclusion criteria. There was no significant increase of risk associated with increased noise exposure in this study.	10% increase of RR	Low quality
Prevalence of highly annoyed population There was an absolute risk of 10% at a noise exposure level of 53.7 dB L_{den}.	10% absolute risk	Moderate quality
Permanent hearing impairment	No increase	No studies met the inclusion criteria/no studies available
Reading skills and oral comprehension in children	One-month delay	No studies met the inclusion criteria/no studies available

In accordance with the prioritization process (see section 2.4.3), the GDG set a guideline exposure level of 53.7 dB L_{den} for average exposure, based on the relevant increase of the absolute %HA. In accordance with the defined rounding procedure, the value was rounded to 54 dB L_{den}. As the evidence on the adverse effects of railway noise was rated moderate quality, the GDG made the recommendation strong.

Next, the GDG assessed the evidence for night noise exposure and its effect on sleep disturbance (Table 17).

Table 17. Night-time exposure levels (L_{night}) for priority health outcomes from railway noise

Summary of priority health outcome evidence	Benchmark level	Evidence quality
Sleep disturbance 3% of the participants in studies were highly sleep-disturbed at a noise level of **43.7 dB** L_{night}	3% absolute risk	Moderate quality

Based on the evidence of the adverse effects of railway noise on sleep disturbance, the GDG defined a guideline exposure level of 43.7 dB L_{night}. The exact exposure value was rounded to 44 dB L_{night}. As the evidence was rated moderate quality, the GDG made the recommendation strong.

The GDG also considered the evidence for the effectiveness of interventions. The results showed that:

- intervening at the source by applying rail grinding procedures can reduce noise annoyance;
- behavioural interventions such as informing the community about noise interventions can reduce noise annoyance.

In light of the strong evidence about the adverse health effects, the GDG followed a precautionary approach and made a strong recommendation for interventions on railway noise, as it was confident that interventions are realizable and that best practices already exist for the management of noise from railways. Since the empirical evidence on the effectiveness of different types of intervention was rated either low or very low quality, the GDG felt that no recommendation could be made on the preferred type of intervention, and agreed not to recommend any specific type of intervention over another.

3.2.1.1 Other factors influencing the strength of recommendations

Other factors considered in the context of recommendations on railway noise included those related to values and preferences, benefits and harms, resource implications, equity, acceptability and feasibility; moreover, nonpriority health outcomes were considered. The assessment of all these factors – especially the values and preferences involved in railway noise – did not lead to a change in the strength of the recommendations. Further details are provided in Section 3.2.2.3.

3.2.2 Detailed overview of the evidence

The following sections provide a detailed overview of the evidence constituting the basis for setting the recommendations on railway noise. It is presented and summarized separately for each of the critical health outcomes, and the GDG's judgement of the quality of evidence is indicated (for a detailed overview of the evidence on important health outcomes, see Annex 4). Research into health outcomes and effectiveness of interventions is addressed consecutively.

A comprehensive summary of all evidence considered for each of the critical and important health outcomes can be found in the eight systematic reviews published in the *International Journal of Environmental Research and Public Health* (see section 2.3.2 and Annex 2).

3.2.2.1 Evidence on health outcomes

The key question posed was: in the general population exposed to railway noise, what is the exposure–response relationship between exposure to railway noise (reported as various noise indicators) and the proportion of people with a validated measure of health outcome, when adjusted for main confounders? A summary of the PICOS/PECCOS scheme applied and the main findings is set out in Tables 18 and 19.

Table 18. PICOS/PECCOS scheme of critical health outcomes for exposure to railway noise

PECO	Description	
Population	General population	
Exposure	Exposure to high levels of noise produced by railway traffic (average/night time)	
Comparison	Exposure to lower levels of noise produced by railway traffic (average/night time)	
Outcome(s)	For average noise exposure: 1. cardiovascular disease 2. annoyance 3. cognitive impairment 4. hearing impairment and tinnitus 5. adverse birth outcomes 6. quality of life, well-being and mental health 7. metabolic outcomes	For night noise exposure: 1. effects on sleep

Table 19. Summary of findings for health effects from exposure to railway noise (L_{den})

Noise metric	Priority health outcome measure	Quantitative risk for adverse health	Lowest level of exposure across studies	Number of participants (studies)[a]	Quality of evidence
Cardiovascular disease					
L_{den}	Incidence of IHD	–	–	–	–
L_{den}	Incidence of hypertension	RR = 0.96 (95% CI: 0.88–1.04) per 10 dB increase	N/A	7249 (1)	Low (downgraded for risk of bias and availability of only one study)
Annoyance					
L_{den}	%HA	OR = 3.53 (95% CI: 2.83–4.39) per 10 dB increase	34	10 970 (10)	Moderate (downgraded for inconsistency, directness; upgraded for dose-response)
Cognitive impairment					
L_{den}	Reading and oral comprehension	–	–	–	–
Hearing impairment and tinnitus					
L_{den}	Permanent hearing impairment	–	–	–	–

Note: [a] Results are partly derived from population-based studies.

Cardiovascular disease

IHD

No evidence was available on the relationship between railway noise and the incidence of or mortality from IHD. Four cross-sectional studies were identified, however, that assessed the prevalence of IHD in a total of 13 241 participants, including 283 cases (Heimann et al., 2007; Lercher et al., 2008; 2011; van Poll et al., 2014). The overall risk was not statistically significantly increased: the RR was 1.18 (95% CI: 0.82–1.68) per 10 dB L_{den} increase, with inconsistency across studies (see Fig. 7). The evidence was rated very low quality.

Fig. 7. The association between exposure to railway noise (L_{den}) and prevalence of IHD

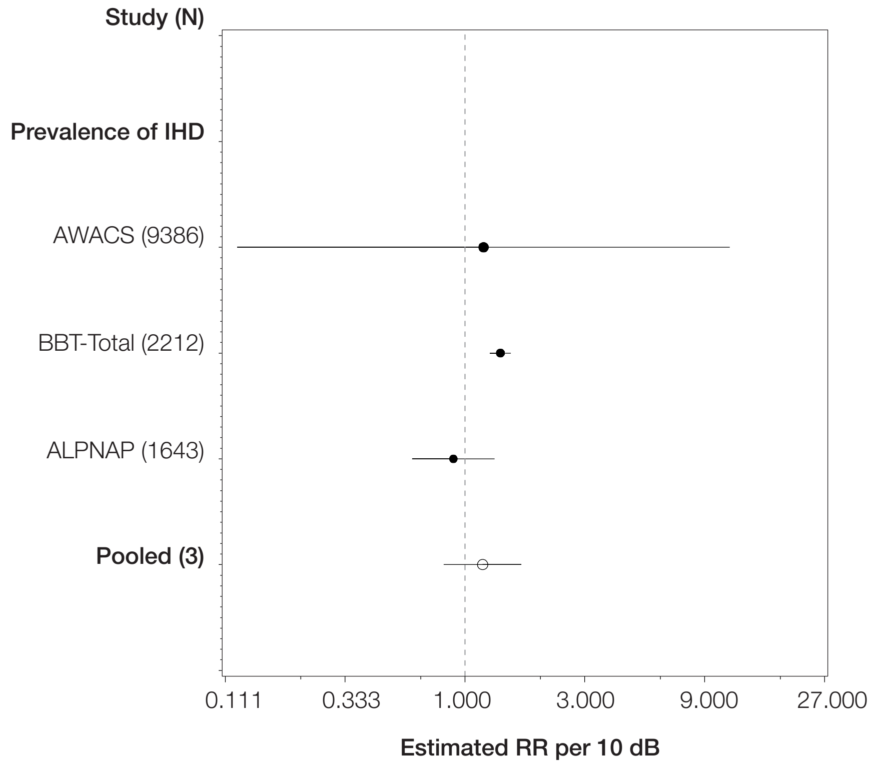

Notes: The dotted vertical line corresponds to no effect of exposure to railway noise. The black circles correspond to the estimated RR per 10 dB and 95% CI. The white circle represents the pooled random effect estimates and 95% CI. For further details on the studies included in the figure please refer to the systematic review on environmental noise and cardiovascular and metabolic effects (van Kempen et al., 2018).

Hypertension

One cohort study on the relationship between railway noise and hypertension was identified; it assessed the incidence among people living in Denmark (Sörensen et al., 2011; 2012a). The study involved 7249 participants, including 3145 cases. The authors did not find an association between railway noise exposure and incidence of hypertension, with RR = 0.96 (95% CI: 0.88–1.04) per 10 dB L_{den} increase. This evidence was rated low quality.

In addition, five cross-sectional studies assessed the prevalence of hypertension in 15 850 participants, including 2059 cases (Barregard et al., 2009; Eriksson et al., 2012; Lercher et al., 2008; 2011; van Poll et al., 2014). The overall RR increase was not statistically significant, at 1.05 (95% CI: 0.88–1.26) per 10 dB L_{den} increase. Moreover, there was inconsistency among the results across studies. The evidence was rated very low quality.

Fig. 8 presents the studies investigating the relationship between railway noise and different measures of hypertension.

Fig. 8. The association between exposure to railway noise (L_{den}) and hypertension

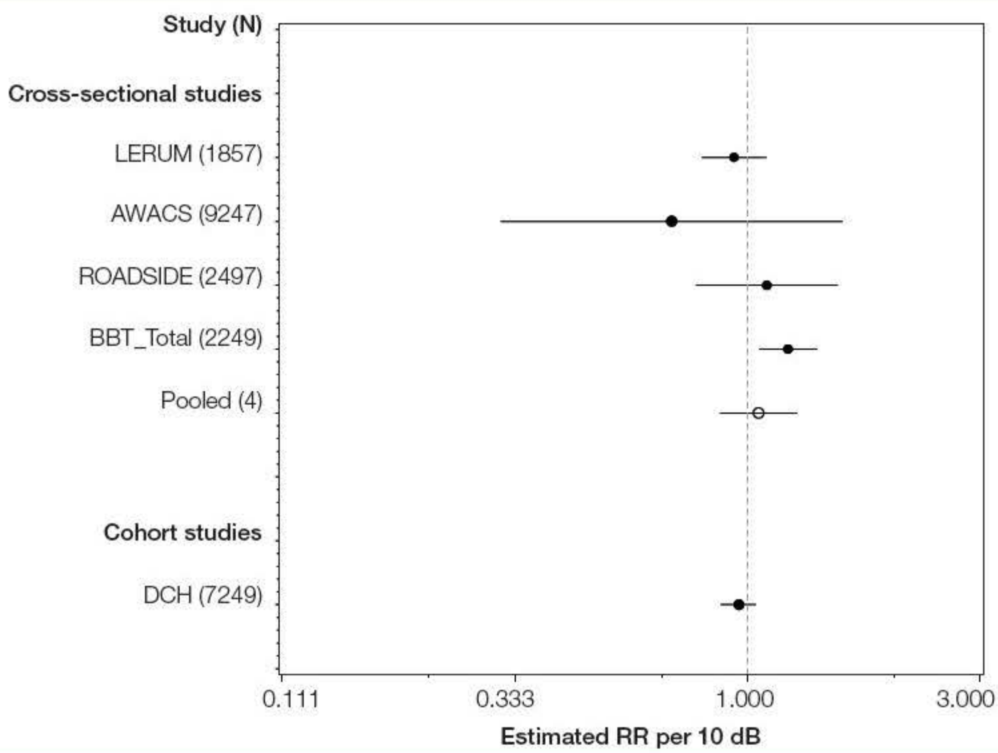

Notes: The dotted vertical line corresponds to no effect of exposure to railway noise. The black dots correspond to the estimated RR per 10 dB and 95% CI. The white circle represents the summary estimate and 95% CI.
For further details on the studies included in the figure please refer to the systematic review on environmental noise and cardiovascular and metabolic effects (van Kempen et al., 2018).

Stroke

As for IHD, no evidence was available on the relationship between railway noise and incidence of or mortality from stroke. However, one cross-sectional study was identified that assessed the prevalence of stroke in 9365 participants, including 89 cases (van Poll et al., 2014). The overall risk was not statistically significantly increased, with RR = 1.07 (95% CI: 0.92–1.25) per 10 dB L_{den} increase. The evidence was rated very low quality.

Children's blood pressure

No evidence was available for the association between railway noise and the systolic and/or diastolic blood pressure of children in residential and/or educational settings.

Annoyance

In total, 10 studies with ERFs on the association between railway noise and annoyance were included in analyses (Champelovier et al., 2003; Gidloef-Gunnarsson et al., 2012; Lercher et al., 2007; 2008; Sato et al., 2004; Schreckenberg, 2013; Yano et al., 2005; Yokoshima et al., 2008). The studies incorporated individual data from 10 970 participants. The estimated data points of each of these studies are plotted in Fig. 9, alongside an aggregated ERF including the data from all the individual studies (see the black line for "WHO dataset, Rail"). The lowest category of noise exposure considered in any of the studies, and hence included in the systematic review is 40 dB, corresponding to approximately 1.5%HA. The 10% benchmark for %HA is reached at 53.7 dB L_{den} (see Fig. 9).

Fig. 9. Scatterplot and quadratic regression of the relationship between railway noise (L_{den}) and annoyance (%HA)

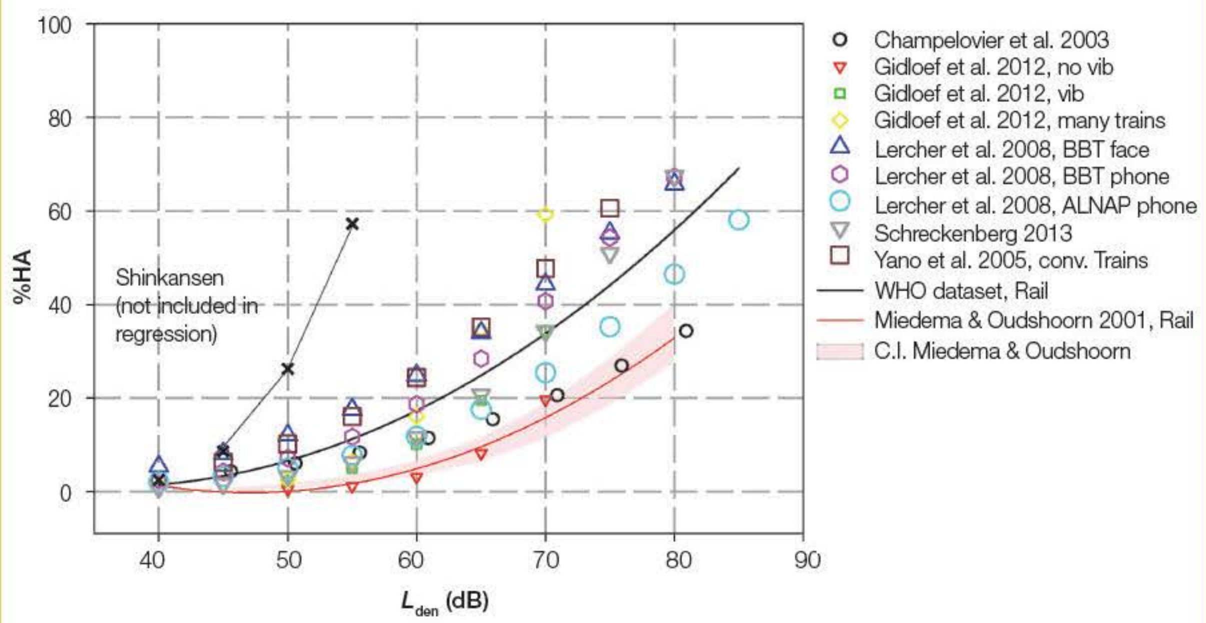

Notes: The ERF by Miedema & Oudshoorn (2001) is added in red for comparison.
There is no indication of 95% CIs of the WHO dataset curve, as a weighting based on the total number of participants for each 5 dB L_{den} sound class could not be calculated; weighting based on all participants of all sound classes proved to be unsuitable. The range of data included is illustrated by the distribution of data points.
For further details on the studies included in the figure please refer to the systematic review on environmental noise and annoyance (Guski et al., 2017).

Table 20 shows the %HA for railway noise exposure. The calculations are based on the regression equation %HA = 38.1596–2.05538 × L_{den} + 0.0285 × $L_{den}{}^2$ derived from the systematic review (Guski et al., 2017). The overall evidence was rated moderate quality. Additional statistical analyses of annoyance outcomes supported these findings. When comparing railway noise exposure at 50 dB and 60 dB, the analyses revealed evidence rated moderate quality for an association between railway noise and %HA for an increase per 10 dB (OR = 3.40; 95% CI: 2.05–5.62). Moreover, evidence rated high quality was available for the increase in %HA per 10 dB increase in sound exposure, when data on all sound classes were included (OR = 3.53; 95% CI: 2.83–4.39).

Table 20. The association between exposure to railway noise (L_{den}) and annoyance (%HA)

L_{den} (dB)	%HA
40	1.5
45	3.4
50	6.6
55	11.3
60	17.4
65	25.0
70	33.9
75	44.3
80	56.1

Cognitive impairment

Studies of railway noise on children's reading and oral comprehension were lacking. Nevertheless, other measures of cognition yielded evidence rated very low quality for an association between railway noise and children with poorer performance on standardized assessment tests (Bronzaft, 1981; Bronzaft & McCarthy, 1975). Evidence for the association between railway noise and children having poorer long-term memory (Lercher et al., 2003) was rated very low quality. No studies examined effects on short-term memory.

There was no clear relation between railway noise and attention in children (Lercher et al., 2003), and this evidence was rated very low quality.

Hearing impairment and tinnitus

No studies were found, and therefore no evidence was available on the association between railway noise and hearing impairment and tinnitus.

Sleep disturbance

For railway noise and self-reported sleep outcomes (awakenings from sleep, the process of falling asleep and sleep disturbance), five studies were identified that included a total of 7133 participants (Bodin et al., 2015; Hong et al., 2010; Sato et al., 2004; Schreckenberg, 2013). The studies were cross-sectional and conducted on healthy adults. The health outcome was measured by self-reporting via general health surveys and noise surveys that included questions about sleep in general, and other questions about how noise affects sleep (Table 21).

Table 21. Summary of findings for health effects from exposure to railway noise (L_{night})

Noise metric	Priority health outcome measure	Quantitative risk for adverse health	Lowest level of exposure across studies	Number of participants (studies)	Quality of evidence
Effects on sleep					
L_{night}	%HSD	OR: 3.06 (95% CI: 2.38–3.93) per 10 dB increase	33 dB	7133 (5)	Moderate (downgraded for study limitations, inconsistency; upgraded for dose-response, magnitude of effect)

The model in the systematic review (Basner & McGuire, 2018) was based on outdoor L_{night} levels between 40 dB and 65 dB only; 40 dB was chosen as the lower limit because of possible inaccuracies in predicting lower noise levels. The range of noise exposure reported in the studies was 27.5–82.5 dB L_{night}. About 2% (95% CI: 0.79–3.48) of the population was characterized as highly sleep-disturbed for L_{night} levels of 40 dB. The %HSD at other, higher levels of railway noise is presented in Table 17. The association between railway noise and the probability of being sleep-disturbed was OR: 3.1 (95% CI: 2.4–3.9) per 10 dB increase in noise. This evidence was rated moderate quality.

Table 22. The association between exposure to railway noise (L_{night}) and sleep disturbance (%HSD)

L_{night} (dB)	%HSD	95% CI
40	2.1	0.79–3.48
45	3.7	1.63–5.71
50	6.3	3.12–9.37
55	10.4	5.61–15.26
60	17.0	9.48–24.37
65	26.3	15.20–37.33

Additional analyses were conducted for sleep quality measures, which provided supporting evidence on the overall relationship between railway noise and sleep. When the noise source was not specified in the question, the relationship between railway noise and self-reported sleep outcomes was still positive but no longer statistically significant, with an OR of 1.27 (95% CI: 0.89–1.81) per 10 dB increase (Bodin et al., 2015; Brink, 2011; Frei et al., 2014). This evidence was rated very low quality.

There was evidence rated moderate quality for an association between railway noise and the probability of additional awakenings, measured with polysomnography, with an OR of 1.35 (95% CI: 1.21–1.52) per 10 dB increase in indoor $L_{AS,max}$ (Elmenhorst et al., 2012). Finally, evidence rated low quality was available for an association between railway noise and sleep outcomes measured as motility in adults (Griefahn et al., 2000; Hong et al., 2006; Lercher et al., 2010; Passchier-Vermeer et al., 2007), and rated very low quality for an association between railway noise and both self-reported and motility-measured sleep disturbance in children (Ising & Ising, 2002; Lercher et al., 2013; Tiesler et al., 2013).

3.2.2.2 Evidence on interventions

This section summarizes the evidence underlying the recommendation on the effectiveness of interventions for railway noise exposure (Tables 23 and 24). The key question posed was: in the general population exposed to railway noise, are interventions effective in reducing exposure to and/or health outcomes from railway noise? A summary of the PICOS/PECCOS scheme applied and the main findings is set out in Tables 23 and 24.

Table 23. PICOS/PECCOS scheme of the effectiveness of interventions for exposure to railway noise

PICO	Description	
Population	**General population**	
Intervention(s)	The interventions can be defined as: (a) a measure that aims to change noise exposure and associated health effects; (b) a measure that aims to change noise exposure, with no particular evaluation of the impact on health; or (c) a measure designed to reduce health effects, but that may not include a reduction in noise exposure.	
Comparison	**No intervention**	
Outcome(s)	For average noise exposure: 1. cardiovascular disease 2. annoyance 3. cognitive impairment 4. hearing impairment and tinnitus 5. adverse birth outcomes 6. quality of life, well-being and mental health 7. metabolic outcomes	For night noise exposure: 1. effects on sleep

Table 24. Summary of findings for railway noise interventions by health outcome

Type of intervention	Number of participants (studies)	Effect of intervention	Quality of evidence
Annoyance			
Type A – source interventions (rail grinding)	81 (1)	• Changes in noise level as a consequence of the intervention ranged from around –7dB to –8 dB. • Most studies found changes in annoyance outcomes, persisting more than 12 months after the intervention.	Very low (downgraded for study limitations, inconsistency, imprecision)
Type C – changes in infrastructure (new rail infrastructure)	6000[a] (1)	• A very small increase in total noise exposure was found (most had <+1 dB change; some had +2–4 dB change). • Original noise from road traffic overwhelmed the train noise for effectively all participants.	Very low (downgraded for study limitations, inconsistency, imprecision)
Type E – behaviour change interventions (informing the community about a noise intervention)	411 (1)	• Exposure levels were not reported; emission levels reduced by 1–2 dB. • A reduction in annoyance of the community as a result of the intervention was reported.	Very low (downgraded for study limitations, inconsistency, imprecision)

Note: [a] According to Lam & Au (2008), this records the number of invitation letters sent; the response rate was not reported.

Three studies on railway noise interventions met the criteria to be included in the evidence base. All studies consisted of a pre/post design and reported annoyance outcomes at people's dwellings (Lam & Au, 2008; Moehler et al., 1997; Schreckenberg et al., 2013). They could be categorized as a source intervention, a new/closed infrastructure intervention and a communication intervention. In two of the studies, the changes in exposure after the intervention were only small, although there were significant effects on noise annoyance. The study on source interventions and annoyance revealed that a change of –10 dB in noise exposure led to a significant reduction in annoyance, which persisted over a period of 12 months after the intervention. As confounding was not addressed, and railway noise was not the dominant sound source in the studies, the evidence was rated very low quality.

3.2.2.3 Consideration of additional contextual factors

As the foregoing overview has shown, sufficient evidence about the adverse health effects of long-term exposure to railway noise exists. Based on the quality of the available evidence, the GDG set the strength of recommendation on railway noise at strong. As a second step, it qualitatively assessed contextual factors to explore whether other considerations could have a relevant impact on the recommendation strength. These contextual considerations mainly concerned the balance of harms and benefits, values and preferences, and resource use and implementation.

When assessing the balance of harms and benefits of interventions to reduce exposure to railway noise and minimize noise-associated adverse health effects, the GDG recognized that railway transportation is the second most dominant source of environmental noise in Europe. Based on EEA estimates, the number of people exposed to L_{den} above 55 dB and L_{night} above 50 dB from railway noise is 17 million and 15 million, respectively (Blanes et al., 2017).[15] In light of the burden of disease from environmental noise, and railway noise in particular, the GDG agreed that the health benefits from a reduction of long-term railway noise exposure (especially during night time) to the recommended values would be significant. Considering possible harms related to adaptation of the recommended values, the GDG noted that reliance on railway transportation has increased in recent years in Europe and is expected to increase further, as an important component of the shift towards a greener economy. At a societal level, an environmental and economic benefit from the use of rail transportation is expected: trains contribute to lower environmental pollution and carbon emission than road transportation. Therefore, there is a need to balance the expected health benefits from reduced continuous railway noise exposure and the overall positive effects on the health of the population from increased reliance on the comparatively environmentally friendly mode of railway transportation. Overall, the GDG agreed that even though fewer people are exposed to railway noise than road traffic noise, it remains a major source of localized noise pollution; therefore, considerable benefits are gained by reducing exposure to railway noise.

When exploring values and preferences, the GDG acknowledged that, in general, people value rail as an alternative and more sustainable transportation method than air or road traffic (EEA, 2016a; 2016b; 2017b). Furthermore, the values and preferences in relation to implementation of the recommendation are expected to vary: those of individuals living in the vicinity of railway tracks are expected to differ from those of the rest of the population not exposed to railway noise on a long-term basis. Economic depreciation of housing and fear of adverse health effects were assumed

[15] These are gap-filled figures based on the reported data and including the situation both within and outside cities, as defined by the END.

to be two main aspects influencing the evaluation of affected individuals. This especially applies to areas where new railway tracks are being built, as this results in considerable change for local inhabitants. Moreover, the GDG acknowledged that preferences might also vary in the policy-making domain across different countries as the implementation of the recommendations would mean a renunciation of the so-called "railway bonus".[16]

On resource use and implementation considerations, the GDG pointed out that no comprehensive cost–benefit analysis for the WHO European Region has yet been conducted, so this assessment is based on informed qualitative expert judgement regarding the feasibility of implementing the recommendation for the majority of the population. The systematic review of environmental noise interventions and their associated impact on health shows that various measures to reduce continuous noise from railway traffic exist, although knowledge about their effectiveness remains limited (Brown & van Kamp, 2017). The GDG noted that the resources needed to implement different measures may vary considerably, as they depend on the situation and the type of intervention required. Implementation of some measures is expected to be most feasible during the development of new railway tracks; such as rail pads, bi-bloc sleepers, small noise barriers and – in extreme cases – tunnels, cuttings or earthwork barriers. Other interventions include acoustic rail grinding, noise barriers built alongside the tracks, construction of quieter locomotives and wagons and replacement of brakes on freight trains. The GDG assumed that most of these solutions could be planned as part of regular maintenance or, for instance, by speeding up fleet modernization and track modernization. Even though not broadly implemented, the solutions mentioned above have already been considered or adopted to reduce noise levels from railway noise exposure. Some EU countries (such as Germany), have programmes to replace old brake blocks from freight trains with newer, quieter ones and to ban all freight trains with old brake blocks from 2020 (Umweltbundesamt, 2017). This illustrates that solutions to achieve recommended noise levels can be implemented at a reasonable cost. Overall, the GDG agreed that the benefit of implementation of the recommendation to minimize the risk of adverse health effects due to railway noise for a majority of the population exceeds the (monetary) resources needed.

In light of the assessment of the contextual factors in addition to the quality of evidence, the recommendation remains strong.

Additional considerations or uncertainties

The GDG acknowledged that the main body of evidence for the recommendations on railway noise for average exposure was based on annoyance studies, conducted mainly in Asia and Europe. Studies are few for other priority health outcomes, and the evidence was generally rated low/very low quality. There is therefore uncertainty about the effects on health outcomes. Nevertheless, as a precautionary approach, a strong recommendation is made for average exposure to L_{den}, as a broad evidence base exists for health effects from exposure to other sources of transportation noise. However, the GDG stressed the importance of further research into health effects due to long-term exposure to railway noise.

Moreover, situational factors should be taken into account when analysing annoyance from railway noise. In particular, ground-borne vibrations are sometimes an additional exposure variable in railway

[16] The "railway bonus" is a correction factor commonly applied in the noise abatement policy domain in recent decades. It subsidizes the noise rating level for railway transportation by a predefined factor (Schuemer & Schuemer-Kohrs, 1991).

noise situations – especially in the case of annoyance – which may be difficult to separate from noise effects. In the set of 11 studies included in the systematic review on railway noise and annoyance, only two explicitly mentioned ground-borne vibrations as an additional source of annoyance.

Overall, the low-carbon, low-polluting nature of railway transport, especially using electric trains, means that rail is favoured over road and air traffic. However, night-time railway traffic on busy lines, including freight traffic, can be a significant source of sleep disturbance. Thus, guideline values should be set to encourage the development of rail traffic in Europe while at the same time giving adequate protection to residents from sleep disturbance.

3.2.3 Summary of the assessment of the strength of the recommendations

Table 25 provides a comprehensive summary of the different dimensions for the assessment of the strength of the railway noise recommendations.

Table 25. Summary of the assessment of the strength of the recommendation

Factors influencing the strength of recommendation	Decision
Quality of evidence	**Average exposure** (L_{den}) *Health effects* • Evidence for a relevant absolute risk of annoyance at **54 dB** L_{den} was rated **moderate quality.** • Evidence for a relevant RR increase of the incidence of hypertension was rated **low quality**. One study met the inclusion criteria but did not find a significant increase. *Interventions* • Evidence that different types of intervention reduce noise annoyance from railways was rated **very low quality**. **Night-time exposure** (L_{night}) *Health effects* • Evidence for a relevant absolute risk of sleep disturbance related to night noise exposure from railways at **44 dB** L_{night} was rated **moderate quality**. *Interventions* • No evidence was available on the effectiveness of interventions to reduce noise exposure and/or sleep disturbance from railway noise.
Balance of benefits versus harms and burdens	Railway noise is a major source of localized pollution. The health benefits of adapting the recommendation outweigh the harms. Nevertheless, it is important to consider the relevance of railways as an environmentally friendly mode of transportation.
Values and preferences	Quiet areas are valued by the population; especially by those affected by continuous noise exposure. Some variability is expected among those directly affected by railway noise and those not affected.
Resource implications	No comprehensive cost–effectiveness-analysis data are available, although a wide range of interventions exists, indicating that measures are both feasible and economically reasonable.
Decisions on recommendation strength	• **Strong** for guideline value for average noise exposure (L_{den}). • **Strong** for guideline value for night noise exposure (L_{night}). • **Strong** for specific interventions to reduce noise exposure.

3.3 Aircraft noise

Recommendations

For average noise exposure, the GDG **strongly** recommends reducing noise levels produced by aircraft below **45 dB** L_{den}, as aircraft noise above this level is associated with adverse health effects.

For night noise exposure, the GDG **strongly** recommends reducing noise levels produced by aircraft during night time below **40 dB** L_{night}, as aircraft noise above this level is associated with adverse effects on sleep.

To reduce health effects, the GDG strongly recommends that policy-makers implement suitable measures to reduce noise exposure from aircraft in the population exposed to levels above the guideline values for average and night noise exposure. For specific interventions the GDG recommends implementing suitable changes in infrastructure.

3.3.1 Rationale for the guideline levels for aircraft noise

The exposure levels were derived in accordance with the prioritization process of critical health outcomes described in section 2.4.3. For each of the outcomes, the exposure level was identified by applying the benchmark, set as relevant risk increase to the corresponding ERF. In the case of exposure to aircraft noise, the process can be summarized as follows (Table 26).

Table 26. Average exposure levels (L_{den}) for priority health outcomes from aircraft noise

Summary of priority health outcome evidence	Benchmark level	Evidence quality
Incidence of IHD A relevant risk increase from exposure to aircraft noise occurs at 52.6 dB L_{den}. The weighted average of the lowest noise levels measured in the studies was 47 dB L_{den} and the corresponding RR in the meta-analysis was 1.09 per 10 dB.	5% increase of RR	Very low quality
Incidence of hypertension One study met the inclusion criteria. There was no significant increase of risk associated with increased noise exposure in this study.	10% increase of RR	Low quality
Prevalence of highly annoyed population There was an absolute risk of 10% at a noise exposure level of 45.4 dB L_{den}.	10% absolute risk	Moderate quality
Permanent hearing impairment	No increase	No studies met the inclusion criteria
Reading skills and oral comprehension in children A relevant risk increase was found at 55 dB L_{den}.	One-month delay	Moderate quality

Based on the evaluation of evidence on relevant risk increases from the prioritized health outcomes, the GDG set a guideline exposure level of 45.4 dB L_{den} for average exposure to aircraft noise, based on the absolute %HA. It was confident that there was an increased risk for annoyance below this exposure level, but probably no relevant risk increase for other priority health outcomes. In accordance with the defined rounding procedure, the value was rounded to 45 dB L_{den}. As the evidence on the adverse effects of aircraft noise was rated moderate quality, the GDG made the recommendation strong.

Next, the GDG considered the evidence for night noise exposure and its effect on sleep disturbance (Table 27).

Table 27. Night-time exposure levels (L_{night}) for priority health outcomes from aircraft noise

Summary of priority health outcome evidence	Benchmark level	Evidence quality
Sleep disturbance 11% of participants were highly sleep-disturbed at a noise level of 40 dB L_{night}.	3% absolute risk	Moderate quality

Based on the evidence of the adverse effects of aircraft noise on sleep disturbance, the GDG defined a guideline exposure level of 40.0 dB L_{night}. It should be stressed that this recommendation for average aircraft noise levels at night far exceeds the benchmark of 3%HSD defined as relevant risk increase, but since no reliable acoustic data below this level were available, the GDG decided not to lower the guideline exposure level further, as an extrapolation of the exposure–response relationship to achieve these values would have been unavoidable. As the evidence was rated moderate quality, the GDG made the recommendation strong.

The GDG also considered the evidence for the effectiveness of interventions. The results showed that changes in infrastructure (opening and/or closing of runways, or flight path rearrangements) can lead to a reduction in aircraft noise exposure, as well as a decline in cognitive impairment in children and a reduction in annoyance. Moreover, examples of best practice already exist for the management of noise from aircraft, so the GDG made a strong recommendation.

3.3.1.1 Other factors influencing the strength of recommendations

Other factors considered in the context of recommendations on aircraft traffic noise included those related to values and preferences, benefits and harms, resource implications, equity, acceptability and feasibility; moreover, nonpriority health outcomes were considered. Ultimately, the assessment of all these factors did not lead to a change in the strength of the recommendations. Further details are provided in section 3.3.2.3.

3.3.2 Detailed overview of the evidence

The following sections provide a detailed overview of the evidence constituting the basis for setting the recommendations on aircraft noise. It is presented and summarized separately for each of the critical health outcomes, and the GDG's judgement of the quality of evidence is indicated (for a detailed overview of the evidence on important health outcomes, see Annex 4). Research into health outcomes and effectiveness of interventions is addressed consecutively.

A comprehensive summary of all evidence considered for each of the critical and important health outcomes can be found in the eight systematic reviews published in the *International Journal of Environmental Research and Public Health* (see section 2.3.2 and Annex 2).

3.3.2.1 Evidence on health outcomes

The key question posed was: in the general population exposed to aircraft noise, what is the exposure–response relationship between exposure to aircraft noise (reported as various noise indicators) and the proportion of people with a validated measure of health outcome, when adjusted for main confounders? A summary of the PICOS/PECCOS scheme applied and the main findings is set out in Tables 28 and 29.

Table 28. PICOS/PECCOS scheme of critical health outcomes for exposure to aircraft noise

PECO	Description	
Population	General population	
Exposure	Exposure to high levels of noise produced by aircraft traffic (average/night time)	
Comparison	Exposure to lower levels of noise produced by aircraft traffic (average/night time)	
Outcome(s)	For average noise exposure: 1. cardiovascular disease 2. annoyance 3. cognitive impairment 4. hearing impairment and tinnitus 5. adverse birth outcomes 6. quality of life, well-being and mental health 7. metabolic outcomes	For night noise exposure: 1. effects on sleep

Table 29 .Summary of findings for health effects from exposure to aircraft noise (L_{den})

Noise metric	Priority health outcome measure	Quantitative risk for adverse health	Lowest level of exposure across studies	Number of participants (studies)[a]	Quality of evidence
Cardiovascular disease					
L_{den}	Incidence of IHD	RR = 1.09 (95% CI: 1.04–1.15) per 10 dB increase	47 dB	9 619 082[a] (2)	Very low (downgraded for risk of bias; upgraded for dose-response)
L_{den}	Incidence of hypertension	RR = 1.00 (95% CI: 0.77–1.30) per 10 dB increase	N/A	4712 (1)	Low (downgraded for risk of bias and because only one study available)
Annoyance					
L_{den}	%HA	OR = 4.78 (95% CI: 2.27–10.05) per 10 dB increase	33 dB	17 094 (12)	Moderate (downgraded for inconsistency)
Cognitive impairment					
L_{den}	Reading and oral comprehension	1–2-month delay per 5 dB increase	Around 55 dB	(4)	Moderate (downgraded for inconsistency)
Hearing impairment and tinnitus					
L_{den}	Permanent hearing impairment	–	–	–	–

Note: [a] Results are partly derived from population-based studies.

Cardiovascular disease

IHD

No cohort or case-control studies on the relationship between aircraft noise and IHD are available. However, two ecological studies were identified that provide information on the relationship between aircraft noise and incidence (hospital admission) of IHD (Correia et al., 2013; Hansell et al., 2013). These involved a total of 9 619 082 participants, including 158 977 cases. The RR was 1.09 (95% CI: 1.04–1.15) per 10 dB L_{den} increase, and the lowest exposure range was ≤51 dB and <45 dB. Given the weights in the meta-analysis of these two studies, the weighted average starting level was calculated as 47 dB. The evidence was rated very low quality.

Two cross-sectional studies were identified that assessed the prevalence of IHD in people living in cities located around airports in Europe. The studies involved 14 098 participants, including 340 cases (Babisch et al., 2005b; 2008; 2012a; 2012b; 2013a; Floud et al., 2011; 2013a; 2013b; Jarup et al., 2005; 2008; van Poll et al., 2014). The overall risk was RR = 1.07 (95% CI: 0.94–1.23) per 10 dB L_{den} increase. The evidence was rated low quality.

With regard to the relationship between aircraft noise and mortality due to IHD, one cohort study (Huss et al., 2010) and two ecological studies (Hansell et al., 2013; van Poll et al., 2014) were identified. The cohort study identified 4 580 311 participants, including 15 532 cases, living in Switzerland, and the authors found an RR of 1.04 (95% CI: 0.98–1.11) per 10 dB L_{den} increase in noise. The evidence was rated low quality. The two ecological studies identified a total of 3 897 645 participants, including 26 066 cases in the Netherlands and the United Kingdom. The overall RR was 1.04 (95% CI: 0.97–1.12) per 10 dB L_{den} increase in noise, and the evidence was rated very low quality.

Fig. 10 summarizes the results for the relationship between aircraft noise and different measures of IHD.

Fig. 10. The association between exposure to aircraft noise (L_{den}) and IHD

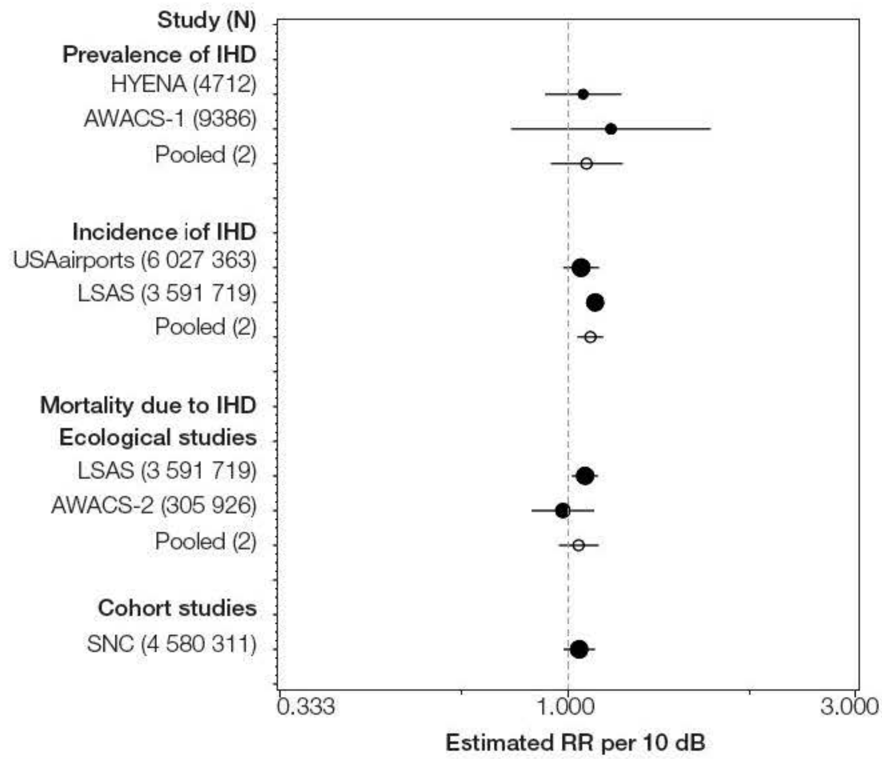

Notes: The dotted vertical line corresponds to no effect of exposure to aircraft noise. The black circles correspond to the estimated RR per 10 dB and 95% CI. The white circles represent the pooled random effect estimates and 95% CI. For further details on the studies included in the figure please refer to the systematic review on environmental noise and cardiovascular and metabolic effects (van Kempen et al., 2018).

Hypertension

One cohort study was identified that assessed the relationship between aircraft noise and hypertension in people living in Sweden (Bluhm et al., 2004; 2009; Eriksson et al., 2007; 2010). The study involved 4712 participants, including 1346 cases. The authors found a nonstatistically significant effect size of RR = 1.00 (95% CI: 0.77–1.30) per 10 dB L_{den} increase. This evidence was rated moderate quality.

Furthermore, nine cross-sectional studies assessed the prevalence of hypertension in 60 121 participants, including 9487 cases (Ancona et al., 2010; Babisch et al., 2005b; 2008; 2012a; 2012b; 2013a; Breugelmans et al., 2004; Evrard et al., 2013; 2015; Houthuijs & van Wiechen, 2006; Jarup et al., 2005; 2008; Matsui, 2013; Matsui et al., 2001; 2004; Rosenlund et al., 2001; van Kamp et al., 2006; van Poll et al., 2014). The overall RR was 1.05 (95% CI: 0.95–1.17) per 10 dB L_{den} increase, with inconsistency across studies. The evidence was rated low quality.

Fig. 11 summarizes the results for both prevalence and incidence of hypertension.

Fig. 11. The association between exposure to aircraft noise (L_{den}) and hypertension in cross-sectional and cohort studies

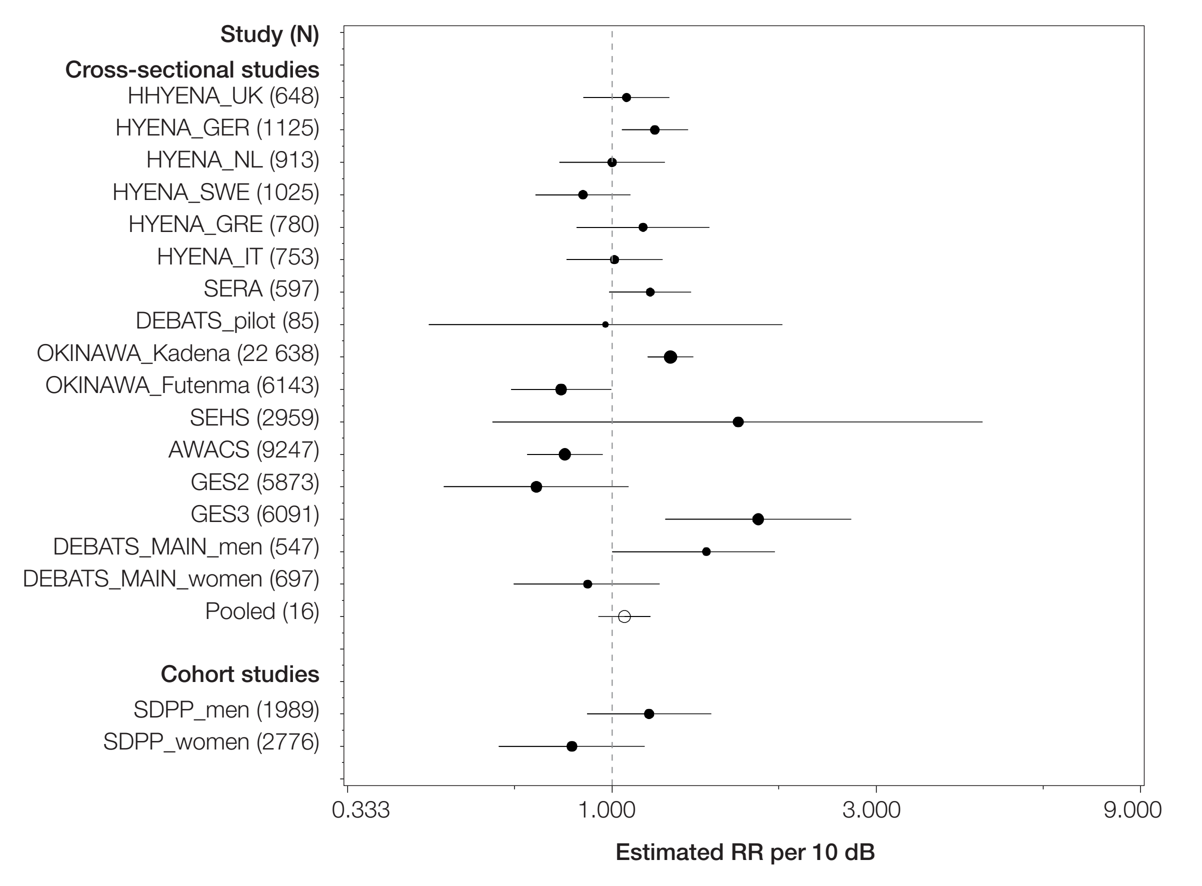

Notes: The dotted vertical line corresponds to no effect of aircraft noise exposure. The black dots correspond to the estimated RR per 10 dB and 95% CI. The white circle represents the pooled summary estimate and 95% CI. For further details on the studies included in the figure please refer to the systematic review on environmental noise and cardiovascular and metabolic effects (van Kempen et al., 2018).

Stroke

No cohort or case-control studies on the relationship between aircraft noise and incidence (hospital admission) of stroke were available, but two ecological studies were conducted in cities around airports in the United Kingdom and United States of America, involving 9 619 082 participants, including 97 949 cases (Correia et al., 2013; Hansell et al., 2013). An overall RR of 1.05 (95% CI: 0.96–1.15) per 10 dB L_{den} increase in noise was found. The evidence was rated very low quality.

Two cross-sectional studies were identified that assessed the prevalence of stroke in 14 098 participants, including 151 cases (Babisch et al., 2005b; 2008; 2012a; 2012b; 2013a; Floud et al., 2011; 2013a; 2013b; Jarup et al., 2005; 2008; van Poll et al., 2014). The overall RR was 1.02 (95% CI: 0.80–1.28) per 10 dB L_{den} increase. The evidence was rated very low quality.

On the relationship between aircraft noise and mortality due to stroke, one cohort study (Huss et al., 2010) and two ecological studies (Hansell et al., 2013; van Poll et al., 2014) were identified. The cohort study identified 4 580 311 participants, including 25 231 cases, living in Switzerland; the authors found an RR of 0.99 (95% CI: 0.94–1.04) per 10 dB L_{den} increase in noise. The overall evidence was rated moderate quality. The two ecological studies identified a total of 3 897 645 participants, including 12 086 cases, in the Netherlands and the United Kingdom. The overall RR was 1.07 (95% CI: 0.98–1.17) per 10 dB L_{den} increase in noise. The evidence was rated very low quality.

Fig. 12 summarizes the results for the relationship between aircraft noise and different measures of stroke.

Fig. 12. The association between exposure to aircraft noise (L_{den}) and stroke

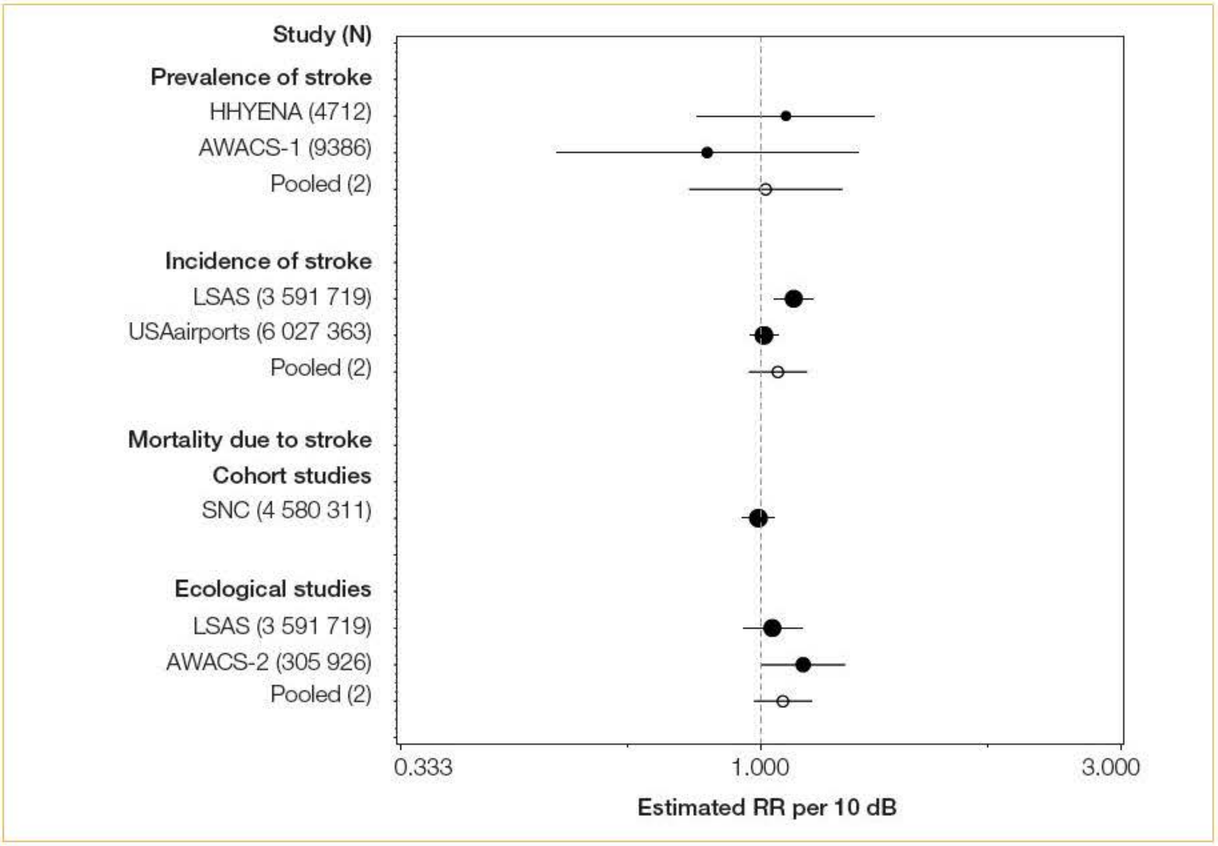

Notes: The dotted vertical line corresponds to no effect of exposure to aircraft noise. The black dots correspond to the estimated RR per 10 dB and 95% CI. The white circle represents the summary estimate and 95% CI.
For further details on the studies included in the figure please refer to the systematic review on environmental noise and cardiovascular and metabolic effects (van Kempen et al., 2018).

Children's blood pressure

For the association between aircraft noise and blood pressure in children, two cross-sectional studies were conducted in Australia, the Netherlands and the United Kingdom, including a total of 2013 participants (Clark et al., 2012; Morrell et al., 1998; 2000; van Kempen et al., 2006). The change in both systolic and diastolic blood pressure was assessed, in residential and/or educational settings. There was serious inconsistency in the results and therefore no overall estimate of the effect was developed. The evidence was rated very low quality.

Annoyance

A vast amount of evidence proves the association between aircraft noise and annoyance. In total, 12 aircraft noise studies were identified that were used to model ERFs of the relationship between L_{den} and %HA (Babisch et al., 2009; Bartels et al., 2013; Breugelmans et al., 2004; Brink et al., 2008; Gelderblom et al., 2014; Nguyen et al., 2011; 2012a; 2012b; Sato & Yano, 2011; Schreckenberg & Meis, 2007). These include data from 17 094 study participants. The estimated data points of each of the studies are plotted in Fig. 13, alongside an aggregated ERF including the data from all the individual studies (see the black line for "Regr WHO full dataset"). The lowest category of noise exposure considered in any of the studies, and hence included in the systematic review, is 40 dB, corresponding to approximately 1.2%HA. The benchmark level of 10%HA is reached at approximately 45 dB L_{den} (see Fig. 13).

Fig. 13. Scatterplot and quadratic regression of the relationship between aircraft noise (L_{den}) and annoyance (%HA)

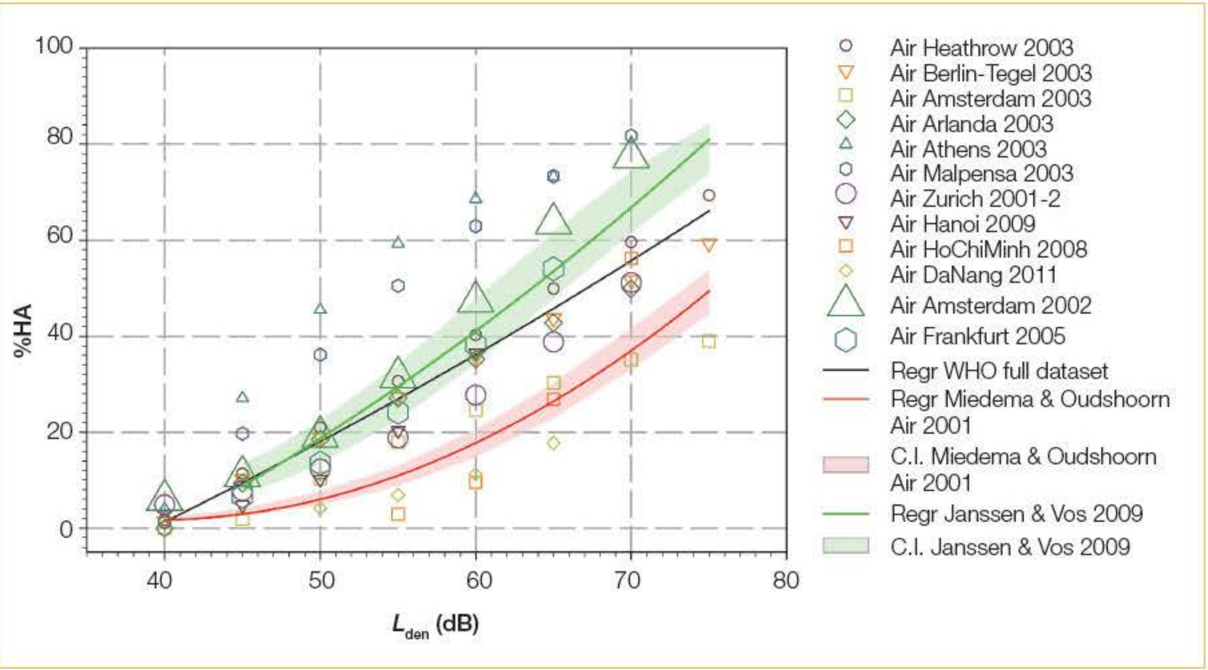

Notes: ERFs by Miedema & Oudshoorn (2001, red), and Janssen & Vos (2009, green) are added for comparison.
There is no indication of 95% CIs of the WHO dataset curve, as a weighting based on the total number of participants for each 5 dB L_{den} sound class could not be calculated; weighting based on all participants of all sound classes proved to be unsuitable. The range of data included is illustrated by the distribution of data points. For further details on the studies included in the figure please refer to the systematic review on environmental noise and annoyance (Guski et al., 2017).

Table 30 shows the %HA in relation to exposure to aircraft traffic noise. It is based on the regression equation %HA = −50.9693 + 1.0168 × L_{den} + 0.0072 × L_{den}^2 derived from the systematic review (Guski et al., 2017). As the majority of the studies are cross-sectional, the evidence was rated moderate quality.

The general quality of the evidence was further substantiated with the help of additional statistical analyses that apply classical health outcome measures to estimate noise annoyance. When comparing aircraft noise exposure at 50 dB and 60 dB, the analyses revealed evidence rated high quality for an association between aircraft noise and %HA for an increase per 10 dB (OR = 3.40; 95% CI: 2.42–4.80). Moreover, there was evidence rated high quality for the increase of %HA per 10 dB increase in sound exposure, when data on all sound classes were included (OR = 4.78; 95% CI: 2.27–10.05).

Table 30. The association between exposure to aircraft noise (L_{den}) and annoyance (%HA)

L_{den} (dB)	%HA
40	1.2
45	9.4
50	17.9
55	26.7
60	36.0
65	45.5
70	55.5

Cognitive impairment

Evidence rated moderate quality was available for an association between aircraft noise and reading and oral comprehension, assessed by standardized tests. This is based on a narrative review of 14 studies that examined aircraft noise exposure effects on reading and oral comprehension (Clark et al., 2006; 2012; 2013; Evans & Maxwell, 1997; Haines et al., 2001a; 2001b; 2001c; Hygge et al., 2002; Klatte et al., 2014; Matsui et al., 2004; Seabi et al., 2012; 2013; Stansfeld et al., 2005; 2010). Of these studies, 10 were cross-sectional, and only four had a longitudinal and/or intervention design (Clark et al., 2013; Haines et al., 2001c; Hygge et al., 2002; Seabi et al., 2013). Most of the studies (10 of 14) demonstrated a statistically significant association or at least demonstrated a trend between higher aircraft noise exposure and poorer reading comprehension.

This relationship is supported by evidence on other health outcome measures related to cognition. Evidence rated moderate quality was available for an association between aircraft noise and children with poorer performance on standardized assessment tests (Eagan et al., 2004; FICAN, 2007; Green et al., 1982; Sharp et al., 2014). There was also evidence rated moderate quality on aircraft noise being associated with children having poorer long-term memory (Haines et al., 2001b). No studies examined the effects on short-term memory.

However, there was no substantial effect (evidence rated low quality) of aircraft noise on children's attention (Haines et al., 2001a; Hygge et al., 2002; Matsui et al., 2004; Stansfeld et al., 2005; 2010), or on executive function (working memory) (evidence rated very low quality), with studies consistently suggesting no association for aircraft noise (Clark et al., 2012; Haines et al., 2001a;

Haines et al., 2001b; Klatte et al., 2014; Matheson et al., 2010; Stansfeld et al., 2005; 2010; van Kempen et al., 2010; 2012).

Hearing impairment and tinnitus

No studies were found, and therefore no evidence was available on the association between aircraft noise and hearing impairment and tinnitus.

Sleep disturbance

For aircraft noise and self-reported sleep outcomes, six studies were identified that included a total of 6371 participants (Nguyen et al., 2009; 2010; 2011; 2012c; 2015; Schreckenberg et al., 2009; Yano et al., 2015). The majority of studies were cross-sectional by design and were conducted in otherwise healthy adults. The model was based on outdoor L_{night} levels between 40 dB and 65 dB only; the lower limit of 40 dB was set because of inaccuracies in predicting lower noise levels (Table 31).

Table 31. Summary of findings for health effects from exposure to aircraft noise (L_{night})

Noise metric	Priority health outcome measure	Quantitative risk for adverse health	Lowest level of exposure across studies	Number of participants (studies)	Quality of evidence
Effects on sleep					
L_{night}	%HSD	OR: 1.94 (95% CI: 1.61–2.33) per 10 dB increase	35 dB	6371 (6)	Moderate (downgraded for study limitations, inconsistency; upgraded for dose-response, magnitude of effect)

The range of noise exposure reported in studies was 37.5–62.5 dB. Over 11% (95% CI: 4.72–17.81) of the population was characterized as highly sleep-disturbed at L_{night} levels of 40 dB. The %HSD at other, higher levels of aircraft noise is presented in Table 27. The table is derived from the regression model in the systematic review specified as %HSD = 16.79–0.9293 × L_{night} + 0.0198 × L_{night}^2. The health outcome was measured in the studies by self-reporting, focusing on questions asking about awakenings from sleep, the process of falling asleep and/or sleep disturbance, where the question referred specifically to how noise affects sleep. The same relationship between aircraft noise and reporting being sleep-disturbed (all questions combined) can also be expressed as an OR of 1.94 (95% CI: 1.61–2.33) per 10 dB increase in noise. This evidence was rated moderate quality.

Table 32. The association between exposure to aircraft noise (L_{night}) and sleep disturbance (%HSD)

L_{night}	%HSD	95% CI
40	11.3	4.72–17.81
45	15.0	6.95–23.08
50	19.7	9.87–29.60
55	25.5	13.57–37.41
60	32.3	18.15–46.36
65	40.0	23.65–56.05

Additional analyses were included in the systematic review and provided supporting evidence on the association between aircraft noise and sleep. When the noise source was not specified in the survey question, the relationship between aircraft noise and self-reported sleep outcomes was still positive, although no longer statistically significant (OR: 1.17 (95% CI: 0.54–2.53) per 10 dB increase) (Brink, 2011). This evidence was rated very low quality.

Further, there was evidence rated moderate quality for an association between aircraft noise and polysomnography-measured outcomes (probability of additional awakenings), with an OR of 1.35 (95% CI: 1.22–1.50) per 10 dB increase in indoor $L_{AS,max}$ (Basner et al., 2006). Evidence rated low quality was also available for an association between aircraft noise and motility-measured sleep outcomes in adults (Passchier-Vermeer et al., 2002).

3.3.2.2 Evidence on interventions

The following section summarizes the evidence underlying the recommendation on the effectiveness of interventions for aircraft noise exposure. The key question posed was: in the general population exposed to aircraft noise, are interventions effective in reducing exposure to and/or health outcomes from aircraft noise? A summary of the PICOS/PECCOS scheme applied and the main findings is set out in Tables 33 and 34.

Seven studies examining different types of interventions on aircraft noise met the inclusion criteria to become part of the evidence base of the systematic review. Six of these investigated infrastructure interventions (Breugelmans et al., 2007; Brink et al., 2008; Fidell et al., 2002; Hygge et al., 2002), and one assessed a path intervention (Asensio et al., 2014). The majority of studies focused on annoyance as a health outcome, but two also included effects on sleep and one investigated the effects of path interventions on cognitive development in children.

Table 33. PICOS/PECCOS scheme of the effectiveness of interventions for exposure to aircraft noise

PICO	Description	
Population	**General population**	
Intervention(s)	The interventions can be defined as: (a) a measure that aims to change noise exposure and associated health effects; (b) a measure that aims to change noise exposure, with no particular evaluation of the impact on health; or (c) a measure designed to reduce health effects, but that may not include a reduction in noise exposure.	
Comparison	**No intervention**	
Outcome(s)	For average noise exposure: 1. cardiovascular disease 2. annoyance 3. cognitive impairment 4. hearing impairment and tinnitus 5. adverse birth outcomes 6. quality of life, well-being and mental health 7. metabolic outcomes	For night noise exposure: 1. effects on sleep

Table 34. Summary of findings for aircraft noise interventions by health outcome

Type of intervention	Number of participants (studies)	Effect of intervention	Quality of evidence
Annoyance			
Type B – path interventions (retrofitting dwellings close to airports with acoustic insulation)	689 (1)	• Change in noise levels was not reported. • The study found a drop in annoyance following the insulation intervention	Very low (downgraded for study limitations, inconsistency, precision)
Type C – changes in infrastructure (opening and/or closing of runways, or flight path rearrangements)	2101 (3)	• There was a wide range of changes in noise levels (from −12 dB to +13.7 dB; most between ±1 dB and 2 dB; different noise indicators used). • All studies found changes in annoyance outcomes as a result of the intervention.	Moderate (downgraded for study limitations; upgraded for dose-response)
Sleep disturbance			
Type C – changes in infrastructure (flight path changes)	1707 (2)	• Changes in noise levels were mostly between ±1 dB and 2 dB. • Both studies found changes in sleep disturbance outcomes as a result of the intervention.	Low (downgraded for study limitations)
Cognitive development of children			
Type C – changes in infrastructure (opening and/or closing of runways, or flight path rearrangements)	326 (1)	• Changes in noise levels of +9 dB at the new airport and of −14 dB at the old airport were reported. • The study found various cognitive effects on children (for both the reduction and the increase in exposure). Effects disappeared when the old airport closed, emerging after the new airport opened.	Moderate (downgraded for inconsistency)

The largest body of research concentrated on the opening and closing of runways, leading to subsequent changes in flight paths (Breugelmans et al., 2007; Brink et al., 2008; Fidell et al., 2002). It showed that changes in noise exposure as a consequence of rearrangement of flight paths, step changes or increase or removal of over-flights resulted in statistically significant changes of the annoyance ratings of residents living in the vicinity of airports. The studies investigated both increases and reductions in exposure. Moreover, all the studies provided evidence that the change in response to noise exposure was an excess response to the intervention. As all the studies either adjusted for confounding or ruled out confounding by design, and the risk of bias was high in two studies but low in one, the evidence was rated moderate quality.

Two of these studies also investigated the effects of interventions on sleep disturbance. The results indicated that the percentage of sleep disturbance changed in association with the change in noise exposure caused by flight path adaptations (Breugelmans et al., 2007; Fidell et al., 2002). Both studies adjusted for confounding, but the risk of bias was assessed as high. Thus, the evidence was rated low quality.

One study examined the impact of rearranging flight paths on the cognitive effects on children (Hygge et al., 2002), showing various effects (for both the reduction and the increase in exposure).

The study ruled out confounding by study design and the risk of bias was assessed as low. The evidence was therefore rated moderate quality.

Alongside infrastructure interventions, a Spanish study presented evidence on path interventions (Asensio et al., 2014), showing a drop in annoyance following an insulation intervention. The study did not control for confounding and the risk of bias was assessed as high. The evidence was therefore rated very low quality.

3.3.2.3 Consideration of additional contextual factors

As the foregoing overview has shown, substantial evidence about the adverse health effects of long-term exposure to aircraft noise exists. Based on the quality of the available evidence, the GDG set the strength of the recommendation of aircraft noise at strong. As a second step, it qualitatively assessed contextual factors to explore whether other considerations could have a relevant impact on the recommendation strength. These considerations mainly concerned the balance of harms and benefits, values and preferences, equity, and resource use and implementation.

When assessing the balance of harms and benefits from implementing the recommendations on aircraft exposure, the GDG acknowledged that the number of people affected was lower than for road traffic or railway noise, since aircraft noise only affects the areas surrounding airports and under flight paths. Data from the EEA show that the estimated number of people in Europe exposed to L_{den} levels above 55 dB and L_{night} levels above 50 dB is 3 million and 1.2 million, respectively (Blanes et al., 2017).[17] Nevertheless, it remains a major source of localized noise pollution and has been predicted to increase (EASA et al., 2016). Furthermore, aircraft noise is regarded as more annoying than the other sources of transportation noise (Schreckenberg et al., 2015; Miedema & Oudshoorn, 2001); it is therefore associated with a significant burden on public health, and the GDG expects substantial health benefits for the population to evolve from implementing the recommendations to reduce exposure to aircraft traffic noise. Furthermore, the GDG noted that, depending on the intervention measure implemented (such as a night flight ban), additional health benefits could evolve, resulting from a simultaneous reduction in air pollution (EC, 2016a). The GDG also acknowledged that intervention measures like night flight bans might also reduce carbon emission, thereby positively influencing the shift towards a greener and more sustainable economy. Possible harms in relation to the applied noise abatement strategy, on the other hand, could include effects on the transportation of goods, as well as individual mobility of the population. Both could have impacts on local, national and international economies. Overall, the GDG estimated that the benefits gained from minimizing adverse health effects due to aircraft noise exposure outweigh the possible (economic) harms.

Considering values and preferences, the GDG noted that negative attitudes towards aircraft noise are especially prevalent in affected individuals who can see and hear aircraft from their house, or who fear that living in proximity of airports will have an impact on their health (Schreckenberg et al., 2015) or property value (economic loss) (Bristow et al., 2014). A lack of trust in the airport and government authorities can enhance these negative attitudes towards airports and aircraft noise (Borsky, 1979; Schreckenberg, 2017). Furthermore, the GDG recognized that values and preferences of individuals living in the vicinity of different airports may vary, as the infrastructural characteristics

[17] These are gap-filled figures based on the reported data and including the situation both within and outside cities, as defined by the END.

of airports have a significant effect on the evaluation of residents. Airports with a stable number of aircraft movements in the near past and no intention to change the number in the future can give rise to a different evaluation of values and preferences than airports with relatively sustained increases in the number of aircraft movements. This can result from the fact that opening new runways or increasing the number of flights usually means considerable change in the environment for inhabitants of the affected area. It has been postulated that the change of exposure itself may be an annoying factor, and this may explain why aircraft noise annoyance is generally higher than that for other sources of transportation noise at a comparable noise level (Brown & van Kamp, 2009). The GDG acknowledged that, in general, air travel is an important means of transportation relevant for businesses, the public and the economy. In Europe, aviation is projected to be the fastest-growing sector from passenger transport demand, by 2050 (EEA, 2016a). The general population tends to value the convenience of travel by air. Moreover, the GDG pointed out that exposure to aircraft noise is not equally distributed throughout society. The preferences of people living in the vicinity of airports are expected to differ from those of the general population that does not experience the same noise burden. This might facilitate variance in the values and preference of the population, as those benefiting from the services and revenues generated by an airport may regard noise reduction measures as an additional, unnecessary extra cost, while those living around an airport and affected by aircraft noise may be in favour of noise reductions, since this concerns their health and well-being. Despite these differences, however, the GDG was confident that a majority of the population would value the minimization of adverse health effects and therefor welcome the implementation of the recommendations.

Regarding the dimension of equity, the GDG highlighted that the risk of exposure to aircraft noise is not equally distributed throughout society. Members of society with a lower socioeconomic status and other disadvantaged groups often live in more polluted and louder areas, including in close proximity to airports (EC, 2016a). In addition to the increased risk of exposure to environmental noise, socioeconomic factors are also associated with increased vulnerability and poorer coping capacities (Karpati et al., 2002).

With resource use and implementation considerations, the GDG acknowledged that the economic evaluation of the health impacts of environmental noise is most elaborate and extensive for aircraft noise (Berry & Sanchez, 2014). Nevertheless, no comprehensive cost–benefit analysis for the WHO European Region yet exists, so this assessment is based on informed qualitative expert judgement regarding the feasibility of implementing the recommendation for the majority of the population. The systematic review of interventions and their associated impact on environmental noise and health shows that various measures to reduce continuous noise from aircraft exist. Moreover, the quality of the evidence was judged to be moderate (Brown & van Kamp, 2017). The GDG noted that the resources needed to implement different intervention measures may vary considerably, because they depend on the situation and the type of intervention required. The distribution of costs also differs from that for other modes of transportation, since exposure to aircraft noise is localized in a more agglomerated way, and overall the population affected is smaller compared to other modes of transportation. The GDG furthermore recognized that multiple cost-effective intervention strategies exist (EC, 2016b). Prohibition or discouragement strategies against citizens moving to the direct proximity of airports, for example, can be implemented in the context of urban planning. Likewise, diverting flight paths above less-populated areas can lead to a reduction in exposure. In principle, such intervention measures do not involve any direct costs, although safety concerns may limit the feasibility of these strategies. Passive noise abatement measures like the installation of soundproof windows at the dwelling were also regarded as feasible and economically reasonable by the GDG, as these are implemented at several airports already. In relation to active abatement measures, the GDG acknowledged the "balanced approach" elaborated by International Civil Aviation Organization, which states that noise reduction should take place first at the source. As indicated by the Clean Sky Programme, this could, for example, entail shifting towards the introduction of new aircraft. This broad European research programme estimates that, depending on type, the shift to newly produced aircraft could lead to a reduction of approximately 55–79% of the area affected by aircraft noise, and consequently the population exposed. As this solution has been put forward by the aviation sector, it is considered feasible. Overall, this indicates that solutions to achieve recommended noise levels can be implemented and at reasonable costs. The GDG agreed that implementation of the recommendation to minimize the risk of adverse health effects due to aircraft noise for a majority of the population would require a reasonable amount of (monetary) resources. It noted, however, that the feasibility of implementing the measures could be hindered by the fact that costs and benefits are not equally distributed. In most cases, the health benefits citizens gain from interventions that reduce aircraft exposure are borne by private companies and public authorities.

In light of the assessment of the contextual factors in addition to the quality of evidence, the recommendation remains strong.

Other nonpriority adverse health outcomes

Although not a priority health outcome and coming from a single study, the GDG noted the evidence rated moderate quality for the statistically significant association between aircraft noise and the change in waist circumference (Eriksson et al., 2014). The range of noise levels in the study identified was 48 to 65 dB L_{den}, and therefore the recommendation would also be protective enough for this health outcome.

In the context of aircraft noise, when considering the impacts of exposure on cognitive impairment in children, these guideline recommendations also apply particularly to the school setting. Noise exposure at primary school and at home is often highly correlated; however, the evidence base considered comes mainly from studies designed around sampling at school and not residences.

Additional considerations or uncertainties

There is additional uncertainty when characterizing exposure using the acoustical description of aircraft noise by means of L_{den} or L_{night}. Use of these average noise indicators may limit the ability to observe associations between exposure to aircraft noise and some health outcomes (such as awakening reactions); as such, noise indicators based on the number of events (such as the frequency distribution of $L_{A,max}$) may be better suited. However, such indicators are not widely used.

The GDG acknowledged that the guideline recommendation for L_{night} may not be fully protective of health, as it implies that around 11% (95% CI: 4.72–17.81) of the population may be characterized as highly sleep-disturbed at the recommended L_{night} level. This is higher than the 3% absolute risk considered for setting the guideline level. However, the high calculation uncertainty in predicting noise levels lower than 40 dB prevented the GDG from recommending a lower level. Furthermore, lower levels would probably require a ban on night or early morning flights altogether, which is not feasible in many situations, given that the general population tends to value the convenience of air travel.

3.3.3 Summary of the assessment of the strength of recommendation

Table 35 provides a comprehensive summary of the different dimensions for the assessment of the strength of the aircraft noise recommendations.

Table 35. Summary of the assessment of the strength of the recommendation

Factors influencing the strength of recommendation	Decision
Quality of evidence	**Average exposure (L_{den})** *Health effects* • Evidence for a relevant RR increase of the incidence of IHD at **52 dB** L_{den} was rated **very low quality.** • Evidence for a relevant RR increase of the incidence of hypertension was rated **low quality**. • Evidence for a relevant absolute risk of annoyance at **45 dB** L_{den} was rated **moderate quality**. • Evidence for a relevant RR increase of impaired reading and oral comprehension at **55 dB L_{den}** was rated **moderate quality**. *Interventions* • Evidence on effectiveness of interventions to reduce noise exposure and/or health outcomes from aircraft noise was of varying quality. **Night-time exposure (L_{night})** *Health effects* • Evidence for a relevant absolute risk of sleep disturbance related to night noise exposure from aircraft at **40 dB** L_{night} was rated **moderate quality**. *Interventions* • Evidence on effectiveness of changes in infrastructure (flight path changes) to reduce sleep disturbance from aircraft noise was rated **low quality**.
Balance of benefits versus harms and burdens	Aircraft noise is a major source of localized noise pollution. The health benefits of adapting the recommendations are expected to outweigh the harms.
Values and preferences	Quiet areas are valued by the population, especially by those affected by continuous aircraft noise exposure. Some variability is expected among those directly affected by aircraft noise and those not affected.
Equity	Risk of exposure to aircraft noise is not equally distributed.
Resource implications	No comprehensive cost–effectiveness analysis data are available; nevertheless, a wide variety of interventions exist (some at very low cost), indicating that measures are both feasible and economically reasonable.
Decisions on recommendation strength	• **Strong** for guideline value for average noise exposure (L_{den}) • **Strong** for guideline value for night noise exposure (L_{night}) • **Strong** for specific interventions to reduce noise exposure

3.4 Wind turbine noise

Recommendations

For average noise exposure, the GDG **conditionally** recommends reducing noise levels produced by wind turbines below **45 dB** L_{den}, as wind turbine noise above this level is associated with adverse health effects.

To reduce health effects, the GDG **conditionally** recommends that policy-makers implement suitable measures to reduce noise exposure from wind turbines in the population exposed to levels above the guideline values for average noise exposure. No evidence is available, however, to facilitate the recommendation of one particular type of intervention over another.

3.4.1 Rationale for the guideline levels for wind turbine noise

The exposure levels were derived in accordance with the prioritizing process of critical health outcomes described in section 2.4.3. For each of the outcomes, the exposure level was identified by applying the benchmark, set as relevant risk increase to the corresponding ERF. In the case of exposure to wind turbine noise, the process can be summarized as follows (Table 36).

Table 36. Average exposure levels (L_{den}) for priority health outcomes from wind turbine noise

Summary of priority health outcome evidence	Benchmark level	Evidence quality
Incidence of IHD Incidence of IHD could not be used to assess the exposure level.	5% increase of RR	No studies were available
Incidence of hypertension Incidence of hypertension could not be used to assess the exposure level.	10% increase of RR	No studies were available
Prevalence of highly annoyed population Four studies were available. An exposure–response curve of the four studies revealed an absolute risk of 10%HA (outdoors) at a noise exposure level of 45 dB L_{den}.	10% absolute risk	Low quality
Permanent hearing impairment	No increase	No studies were available
Reading skills and oral comprehension in children	One-month delay	No studies were available

In accordance with the prioritization process, the GDG set a guideline exposure level of 45.0 dB L_{den} for average exposure, based on the relevant increase of the absolute %HA. The GDG stressed that there might be an increased risk for annoyance below this noise exposure level, but it could not state whether there was an increased risk for the other health outcomes below this level owing to a lack of evidence. As the evidence on the adverse effects of wind turbine noise was rated low quality, the GDG made the recommendation conditional.

Next, the GDG considered the evidence for night noise exposure to wind turbine noise and its effect on sleep disturbance (Table 37).

Table 37. Night-time exposure levels (L_{night}) for priority health outcomes from wind turbine noise

Summary of priority health outcome evidence	Benchmark level	Evidence quality
Sleep disturbance Six studies were available; they did not reveal consistent results about effects of wind turbine noise on sleep.	3% absolute risk	Low quality

Based on the low quantity and heterogeneous nature of the evidence, the GDG was not able to formulate a recommendation addressing sleep disturbance due to wind turbine noise at night time.

The GDG also looked for evidence about the effectiveness of interventions for wind turbine noise exposure. Owing to a lack of research, however, no studies were available on existing interventions and associated costs to reduce wind turbine noise.

Based on this assessment, the GDG therefore provided a conditional recommendation for average noise exposure (L_{den}) to wind turbines and a conditional recommendation for the implementation of suitable measures to reduce noise exposure. No recommendation about a preferred type of intervention could be formulated; nor could a recommendation be made for an exposure level for night noise exposure (L_{night}), as studies were not consistent and in general did not provide evidence for an effect on sleep.

3.4.1.1 Other factors influencing the strength of recommendation

Other factors considered in the context of recommendations on wind turbine noise included those related to values and preferences, benefits and harms, resource implications, equity, acceptability and feasibility. Ultimately, the assessment of all these factors did not lead to a change in the strength of recommendation, although it informed the development of a conditional recommendation on the intervention measures. Further details are provided in section 3.4.2.3.

3.4.2 Detailed overview of the evidence

The following sections provide a detailed overview of the evidence constituting the basis for setting the recommendations on wind turbine noise. It is presented and summarized separately for each of the critical health outcomes, and the GDG's judgement of the quality of evidence is indicated (for a detailed overview of the evidence on important health outcomes, see Annex 4). Research into health outcomes and effectiveness of intervention is addressed consecutively.

A comprehensive summary of all evidence considered for each of the critical and important health outcomes can be found in the eight systematic reviews published in the *International Journal of Environmental Research and Public Health* (see section 2.3.2 and Annex 2).

It should be noted that, due to the time stamp of the systematic reviews, some more recent studies were not included in the analysis. This relates in particular to several findings of the Wind Turbine Noise and Health Study conducted by Health Canada (Michaud, 2015). Further, some studies were omitted, as they did not meet the inclusion criteria, including, for instance, studies using distance to the wind turbine instead of noise exposure to investigate health effects. The justification for including and excluding studies is given in the systematic reviews (Basner & McGuire, 2018; Brown et al., 2017; Clark & Paunovic, 2018; in press; Guski et al., 2017; Niewenhuijsen et al.,2017; Śliwińska-Kowalska & Zaborowski, 2017; van Kempen et al., 2018; see Annex 2 for further details).

3.4.2.1 Evidence on health outcomes

The key question posed was: in the general population exposed to wind turbine noise, what is the exposure–response relationship between exposure to wind turbine noise (reported as various noise indicators) and the proportion of people with a validated measure of health outcome, when adjusted for main confounders? A summary of the PICOS/PECCOS scheme applied and the main findings is set out in Tables 38 and 39.

Table 38. PICOS/PECCOS scheme of critical health outcomes for exposure to wind turbine noise

PECO	Description	
Population	General population	
Exposure	Exposure to high levels of noise produced by wind turbines (average/night time)	
Comparison	Exposure to lower levels of noise produced by wind turbines (average/night time)	
Outcome(s)	For average noise exposure: 1. cardiovascular disease 2. annoyance 3. cognitive impairment 4. hearing impairment and tinnitus 5. adverse birth outcomes 6. quality of life, well-being and mental health 7. metabolic outcomes	For night noise exposure: 1. effects on sleep

Table 39. Summary of findings for health effects from exposure to wind turbine noise (L_{den})

Noise metric	Priority health outcome measure	Quantitative risk for adverse health	Lowest level of exposure across studies	Number of participants (studies)	Quality of evidence
Cardiovascular disease					
L_{den}	Incidence of IHD	–	–	–	–
L_{den}	Incidence of hypertension	–	–	–	–
Annoyance					
L_{den}	%HA	Not able to pool because of heterogeneity	30 dB	2481 (4)	Low (downgraded for inconsistency and imprecision)
Cognitive impairment					
L_{den}	Reading and oral comprehension	–	–	–	–
Hearing impairment and tinnitus					
L_{den}	Permanent hearing impairment	–	–	–	–

Cardiovascular disease

For the relationship between wind turbine noise and prevalence of hypertension, three cross-sectional studies were identified, with a total of 1830 participants (van den Berg et al., 2008; Pedersen, 2011; Pedersen & Larsman, 2008; Pedersen & Persson Waye, 2004; 2007). The number of cases was not reported. All studies found a positive association between exposure to wind turbine noise and the prevalence of hypertension, but none was statistically significant. The lowest levels in studies were either <30 or <32.5 L_{den}. No meta-analysis was performed, since too many parameters were unknown and/or unclear. Due to very serious risk of bias and imprecision in the results, this evidence was rated very low quality (see Fig. 14).

The same studies also looked at exposure to wind turbine noise and self-reported cardiovascular disease, but none found an association. No evidence was available for other measures of cardiovascular disease. As a result, only evidence rated very low quality was available for no considerable effect of audible noise (greater than 20 Hz) from wind turbines or wind farms on self-reported cardiovascular disease (see Fig. 15).

Fig. 14. The association between exposure to wind turbine noise (sound pressure level in dB) and hypertension

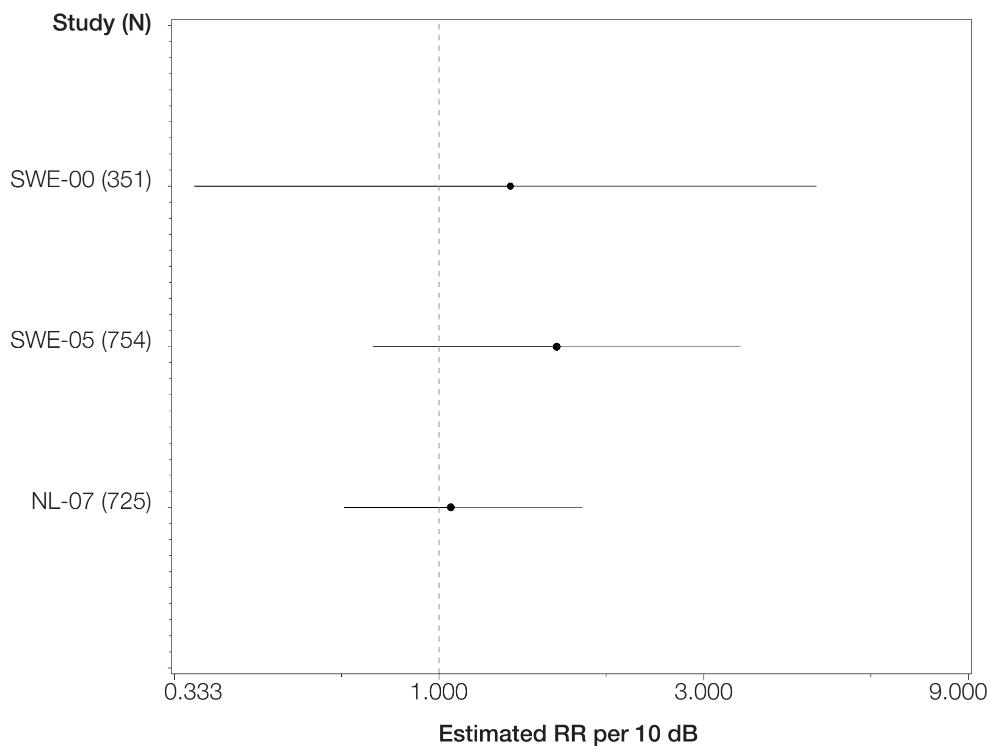

Notes: The dotted vertical line corresponds to no effect of exposure to wind turbine noise. The black dots correspond to the estimated RR per 10 dB and 95% CI. For further details on the studies included in the figure please refer to the systematic review on environmental noise and cardiovascular and metabolic effects (van Kempen et al., 2018).

Fig. 15. The association between exposure to wind turbine noise (sound pressure level) and self-reported cardiovascular disease

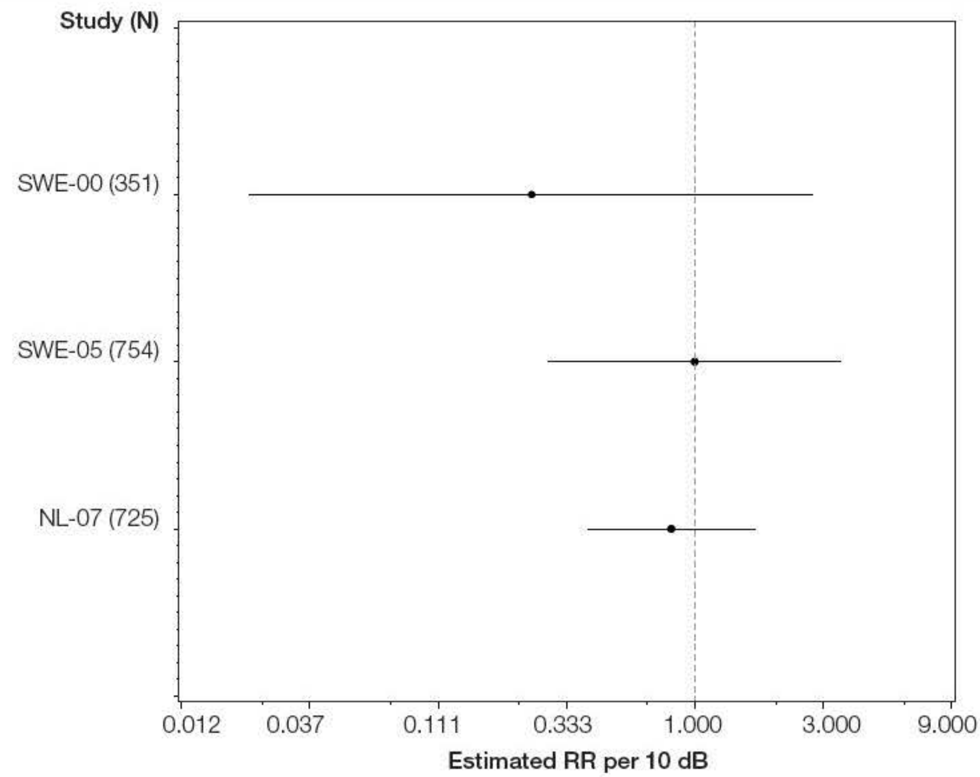

Notes: The dotted vertical line corresponds to no effect of exposure to wind turbine noise. The black circles correspond to the estimated RR per 10 dB (sound pressure level) and 95% CI. For further details on the studies included in the figure please refer to the systematic review on environmental noise and cardiovascular and metabolic effects (van Kempen et al., 2018).

Annoyance

Two publications containing descriptions of four individual studies were retrieved (Janssen et al., 2011; Kuwano et al., 2014). All four studies used measurements in the vicinity of the respondents' addresses; the noise exposure metrics used in the three original studies (Pedersen, 2011; Pedersen & Persson Waye, 2004; 2007) included in Janssen et al. (2011) were recalculated into L_{den}. The noise levels in the studies ranged from 29 dB to 56 dB. Different scales were used to assess annoyance, with slightly different definitions of "highly annoyed" and explicit reference to outdoor annoyance in the data used for the Janssen et al. (2011) curve. Construction of the ERFs provided in the two publications differed and they were therefore not further combined in a meta-analysis. Fig. 16 shows the %HA from the two publications. The 10% criterion for %HA is reached at around 45 dB L_{den} (where the two curves coincide). There was a wide variability in %HA between studies, with a range of 3–13%HA at 42.5 dB and 0–32%HA at 47.5 dB. The %HA in the sample is comparatively high, given the relatively low noise levels. There is evidence rated low quality for an association between wind turbine noise and annoyance, but this mainly applies to the association between wind turbine noise and annoyance and not to the shape of the quantitative relationship.

Further statistical analyses of annoyance yield evidence rated low quality for an association between wind turbine noise and %HA when comparing an exposure at 42.5 dB and 47.5 dB, with a mean difference in %HA of 4.5 (indoors) and 6.4 (outdoors). There is also evidence rated moderate quality for a correlation between individual noise exposure and annoyance raw scores (r = 0.28).

Fig. 16. Overlay of the two wind turbine annoyance graphs

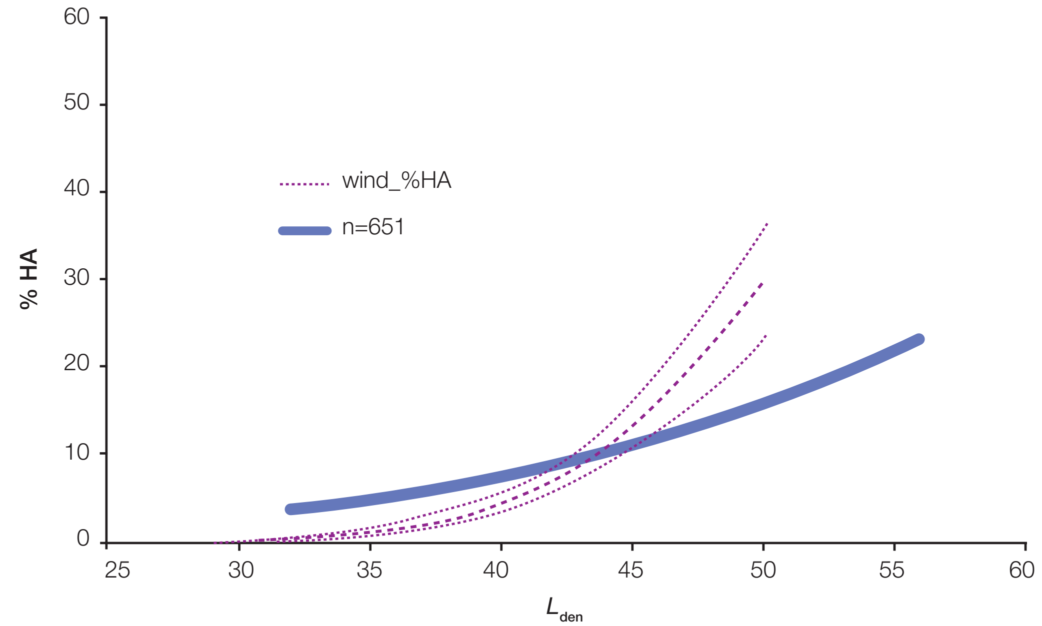

Notes: Overlay of the two wind turbine outdoor annoyance graphs adapted from Janssen et al. (2011, red) and Kuwano et al. (2014, blue). The Kuwano et al. curve is based on L_{dn}; no correction for L_{den} has been applied.[18]
For further details on the studies included in the figure please refer to the systematic review on environmental noise and annoyance (Guski et al., 2017).

Cognitive impairment, hearing impairment and tinnitus, adverse birth outcomes

No studies were found, and therefore no evidence was available on the relationship between wind turbine noise and measures of cognitive impairment; hearing impairment and tinnitus; and adverse birth outcomes.

Sleep disturbance

Six cross-sectional studies on wind turbine noise and self-reported sleep disturbance were identified (Bakker et al., 2012; Kuwano et al., 2014; Michaud, 2015; Pawlaczyk-Luszczynska et al., 2014; Pedersen & Persson Waye, 2004; 2007). Noise levels were calculated using different methods, and different noise metrics were reported. Three of the studies asked how noise affects sleep; the other three evaluated the effect of wind turbine noise on sleep using questions that explicitly referred to noise (Table 40).

[18] L_{dn} is the day-night-weighted sound pressure level as defined in section 3.6.4 of ISO 1996-1:2016.

Table 40. Summary of findings for health effects from exposure to wind turbine noise (L_{night})

Noise metric	Priority health outcome measure	Quantitative risk for adverse health	Lowest level of effects in studies	Number of participants (studies)	Quality of evidence
Effects on sleep					
L_{night}	%HSD	1.60 (95% CI: 0.86–2.94) per 10 dB increase	31 dB	3971 (6)	Low (downgraded for study limitations, inconsistency, precision)

The risk of bias was assessed as high for all six studies, as effects on sleep were measured by self-reported data. There were a limited number of subjects at higher exposure levels. A meta-analysis was conducted for five of the six studies, based on the OR for high sleep disturbance for a 10 dB increase in outdoor predicted sound pressure level. The pooled OR was 1.60 (95% CI: 0.86–2.94). The evidence was rated low quality.

3.4.2.2 Evidence on interventions

This section summarizes the evidence underlying the recommendation on the effectiveness of interventions for wind turbine noise exposure. The key question posed was: in the general population exposed to wind turbine noise, are interventions effective in reducing exposure to and/or health outcomes from wind turbine noise? A summary of the PICOS/PECCOS scheme applied is set out in Table 41.

Table 41. PICOS/PECCOS scheme of the effectiveness of interventions for exposure to wind turbine noise

PICO	Description	
Population	**General population**	
Intervention(s)	The interventions can be defined as: (a) a measure that aims to change noise exposure and associated health effects; (b) a measure that aims to change noise exposure, with no particular evaluation of the impact on health; or (c) a measure designed to reduce health effects, but that may not include a reduction in noise exposure.	
Comparison	**No intervention**	
Outcome(s)	For average noise exposure: 1. cardiovascular disease 2. annoyance 3. cognitive impairment 4. hearing impairment and tinnitus 5. adverse birth outcomes 6. quality of life, well-being and mental health 7. metabolic outcomes	For night noise exposure: 1. effects on sleep

No studies were found, and therefore no evidence was available on the effectiveness of interventions to reduce noise exposure from wind turbines.

3.4.2.3 Consideration of additional contextual factors

As the foregoing overview has shown, very little evidence is available about the adverse health effects of continuous exposure to wind turbine noise. Based on the quality of evidence available, the GDG set the strength of the recommendation on wind turbine noise to conditional. As a second step, it qualitatively assessed contextual factors to explore whether other considerations could have a relevant impact on the recommendation strength. These considerations mainly concerned the balance of harms and benefits, values and preferences, and resource use and implementation.

Regarding the balance of harms and benefits, the GDG would expect a general health benefit from a marked reduction in any kind of long-term environmental noise exposure. Health effects of individuals living in the vicinity of wind turbines can theoretically be related not only to long-term noise exposure from the wind turbines but also to disruption caused during the construction phase. The GDG pointed out, however, that evidence on health effects from wind turbine noise (apart from annoyance) is either absent or rated low/very low quality (McCunney et al., 2014). Moreover, effects related to attitudes towards wind turbines are hard to discern from those related to noise and may be partly responsible for the associations (Knopper & Ollson, 2011). Furthermore, the number of people exposed is far lower than for many other sources of noise (such as road traffic). Therefore, the GDG estimated the burden on health from exposure to wind turbine noise at the population level to be low, concluding that any benefit from specifically reducing population exposure to wind turbine noise in all situations remains unclear. Nevertheless, proper public involvement, communication and consultation of affected citizens living in the vicinity of wind turbines during the planning stage of future installations is expected to be beneficial as part of health and environmental impact assessments. In relation to possible harms associated with the implementation of the recommendation, the GDG underlined the importance of wind energy for the development of renewable energy policies.

The GDG noticed that the values and preferences of the population towards reducing long-term noise exposure to wind turbine noise vary. Whereas the general population tends to value wind energy as an alternative, environmentally sustainable and low-carbon energy source, people living in the vicinity of wind turbines may evaluate them negatively. Wind turbines are not a recent phenomenon, but their quantity, size and type have increased significantly over recent years. As they are often built in the middle of otherwise quiet and natural areas, they can adversely affect the integrity of a site. Furthermore, residents living in these areas may have greater expectations of the quietness of their surroundings and therefore be more aware of noise disturbance. Negative attitudes especially occur in individuals who can see wind turbines from their houses but do not gain economically from the installations (Kuwano et al., 2014; Pedersen & Persson Waye, 2007; van den Berg et al., 2008). These situational variables and the values and preferences of the population may differ between wind turbines and other noise sources, as well as between wind turbine installations, which makes assessment of the relationship between wind turbine noise exposure and health outcomes particularly challenging.

Assessing resource use and implementation considerations, the GDG noted that reduction of noise exposure from environmental sources is generally possible through simple measures like insulating windows or building barriers. With wind turbines, however, noise reduction interventions are more complicated than for other noise sources due to the height of the source and because outdoor disturbance is a particularly large factor. As generally fewer people are affected (compared to transportation noise), the expected costs are lower than for other environmental sources of noise. The GDG was not aware of any existing interventions (and associated costs) to reduce harms from wind turbine noise, or specific consequences of having regulations on wind turbine noise. Therefore, it could not assess feasibility, or discern whether any beneficial effects of noise reduction would outweigh the costs of intervention. In particular, there is no clear evidence on an acceptable and uniform distance between wind turbines and residential areas, as the sound propagation depends on many aspects of the wind turbine construction and installation.

In light of the assessment of the contextual factors in addition to the quality of evidence, the recommendation for wind turbine noise exposure remains conditional.

Additional considerations or uncertainties

Assessment of population exposure to noise from a particular source is essential for setting health-based guideline values. Wind turbine noise is characterized by a variety of potential moderators, which can be challenging to assess and have not necessarily been addressed in detail in health studies. As a result, there are serious issues with noise exposure assessment related to wind turbines.

Noise levels from outdoor sources are generally lower indoors because of noise attenuation from the building structure, closing of windows and similar. Nevertheless, noise exposure is generally estimated outside, at the most exposed façade. As levels of wind turbine noise are generally much lower than those of transportation noise, the audibility of wind turbines in bedrooms, particularly when windows are closed, is unknown.

In many instances, the distance from a wind farm has been used as a proxy to determine audible noise exposure. However, in addition to the distance, other variables – such as type, size and number of wind turbines, wind direction and speed, location of the residence up- or downwind from wind farms and so on – can contribute to the resulting noise level assessed at a residence. Thus, using distance to a wind farm as a proxy for noise from wind turbines in health studies is associated with high uncertainty.

Wind turbines can generate infrasound or lower frequencies of sound than traffic sources. However, few studies relating exposure to such noise from wind turbines to health effects are available. It is also unknown whether lower frequencies of sound generated outdoors are audible indoors, particularly when windows are closed.

The noise emitted from wind turbines has other characteristics, including the repetitive nature of the sound of the rotating blades and atmospheric influence leading to a variability of amplitude modulation, which can be a source of above average annoyance (Schäffer et al., 2016). This differentiates it from noise from other sources and has not always been properly characterized. Standard methods of measuring sound, most commonly including A-weighting, may not capture the low-frequency sound and amplitude modulation characteristic of wind turbine noise (Council of Canadian Academies, 2015).

Even though correlations between noise indicators tend to be high (especially between L_{Aeq}-like indicators) and conversions between indicators do not normally influence the correlations between the noise indicator and a particular health effect, important assumptions remain when exposure to wind turbine noise in L_{den} is converted from original sound pressure level values. The conversion requires, as variable, the statistical distribution of annual wind speed at a particular height, which depends on the type of wind turbine and meteorological conditions at a particular geographical location. Such input variables may not be directly applicable for use in other sites. They are sometimes used without specific validation for a particular area, however, because of practical limitations or lack of data and resources. This can lead to increased uncertainty in the assessment of the relationship between wind turbine noise exposure and health outcomes.

Based on all these factors, it may be concluded that the acoustical description of wind turbine noise by means of L_{den} or L_{night} may be a poor characterization of wind turbine noise and may limit the ability to observe associations between wind turbine noise and health outcomes.

3.4.3 Summary of the assessment of the strength of recommendations

Table 42 provides a comprehensive summary of the different dimensions for the assessment of the strength of the wind turbine recommendations.

Table 42. Summary of the assessment of the strength of the recommendation

Factors influencing the strength of recommendation	Decision
Quality of evidence	**Average exposure (L_{den})** *Health effects* • Evidence for a relevant absolute risk of annoyance at **45 dB L_{den}** was rated **low quality.** *Interventions* • No evidence was available on the effectiveness of interventions to reduce noise exposure and/or health outcomes from wind turbines. **Night-time exposure (L_{night})** *Health effects* • No statistically significant evidence was available for sleep disturbance related to exposure from wind turbine noise at night. *Interventions* • No evidence was available on the effectiveness of interventions to reduce noise exposure and/or sleep disturbance from wind turbines.
Balance of benefits versus harms and burdens	Further work is required to assess fully the benefits and harms of exposure to environmental noise from wind turbines and to clarify whether the potential benefits associated with reducing exposure to environmental noise for individuals living in the vicinity of wind turbines outweigh the impact on the development of renewable energy policies in the WHO European Region.
Values and preferences	There is wide variability in the values and preferences of the population, with particularly strong negative attitudes in populations living in the vicinity of wind turbines.
Resource implications	Information on existing interventions (and associated costs) to reduce harms from wind turbine noise is not available.
Additional considerations or uncertainties	There are serious issues with noise exposure assessment related to wind turbines.
Decisions on recommendation strength	• **Conditional** for guideline value for average noise exposure (L_{den}) • **Conditional** for the effectiveness of interventions (L_{night})

3.5 Leisure noise

Recommendations

For average noise exposure, the GDG **conditionally** recommends reducing the yearly average from all leisure noise sources combined to **70 dB** $L_{Aeq,24h}$, as leisure noise above this level is associated with adverse health effects. The equal energy principle[19] can be used to derive exposure limits for other time averages, which might be more practical in regulatory processes.

For single-event and impulse noise exposures, the GDG **conditionally** recommends following existing guidelines and legal regulations to limit the risk of increases in hearing impairment from leisure noise in both children and adults.

Following a precautionary approach, to reduce possible health effects, the GDG **strongly** recommends that policy-makers take action to prevent exposure above the guideline values for average noise and single-event and impulse noise exposures. This is particularly relevant as a large number of people may be exposed to and at risk of hearing impairment through the use of personal listening devices (PLDs). There is insufficient evidence, however, to recommend one type of intervention over another.

3.5.1 Rationale for the guideline levels for leisure noise

As specific evidence for the relationship between leisure noise and hearing loss is of insufficient quality, the GDG decided to follow a different approach for this noise source, based on knowledge regarding prevention of hearing loss in the workplace and on the CNG (WHO, 1999). There is sufficient evidence that the nature of the noise matters little in causing hearing loss, so using the existing guidelines is a justified step to prevent permanent hearing loss from leisure noise.

In accordance with the procedures for the other noise sources, the GDG would have considered evidence on exposure–response relationships for the prioritized health outcomes. However, no such ERFs could be established in the systematic reviews for any of the health outcomes (Table 43).

Table 43. Average exposure levels ($L_{Aeq,24h}$) for priority health outcomes from leisure noise

Summary of priority health outcome evidence	Benchmark level	Evidence quality
Incidence of IHD **Incidence of hypertension** **Prevalence of highly annoyed population** **Reading skills and oral comprehension in children**		No evidence was available
Permanent hearing impairment There is an indication that PLDs have an effect on hearing impairment and tinnitus. There was no evidence (because no studies were found) for an effect of other sources of leisure noise on hearing impairment or tinnitus. The results of the studies could not be synthesized because of heterogeneity of outcome measurement.	No increase	Very low quality/no evidence

[19] The equal energy principle states that the total effect of sound is proportional to the total amount of sound energy received by the ear, irrespective of the distribution of that energy in time (WHO, 1999).

In accordance with the evidence on the effects of PLDs on permanent hearing loss from leisure noise, the GDG recommended a guideline exposure level of 70 dB $L_{Aeq,24h}$ yearly average from all leisure noise sources combined. It was confident that there was no relevant risk increase for permanent hearing impairment below this exposure level of average leisure noise. The GDG recognized that a conversion to alternative time averages for exposure to leisure noise might be helpful for regulatory purposes; thus, a detailed table converting hourly and weekly exposure into yearly averages is provided in the subsection on additional considerations or uncertainties in section 3.5.2.3, Table 49. Furthermore, the GDG recommended sticking to the CNG recommendations for single events to limit the risk of hearing impairment from leisure noise increases for both children and adults (WHO, 1999).[20] Due to the nature and limited amount of available evidence, the GDG made the recommendation conditional.

Next, the GDG assessed the evidence for night noise exposure and its effect on sleep disturbance (Table 44).

Table 44. Night-time exposure levels (L_{night}) for priority health outcomes from leisure noise

Summary of priority health outcome evidence	Benchmark level	Evidence quality
Sleep disturbance	3% absolute risk	No evidence was available

Because of a lack of evidence, the GDG was not able to formulate a recommendation addressing sleep disturbance due to leisure noise at night time.

The GDG also looked for evidence about the effectiveness of interventions for leisure noise exposure. Owing to a lack of research, however, no studies were available on existing interventions and associated costs to reduce leisure noise. As no evidence was available, it was not possible to develop a recommendation on any specific type of intervention measure. However, following a precautionary approach, to reduce possible health effects, the GDG made a strong recommendation that policy-makers take action to prevent exposures above the guideline values for average noise and single-event and impulse noise exposures. This is particularly relevant as a large number of people may be exposed to and at risk of hearing impairment through the use of PLDs. There is insufficient evidence, however, to recommend one type of intervention over another.

3.5. 1.1 Other factors influencing the strength of recommendations

Other factors considered in the context of recommendations on leisure noise included those related to values and preferences, benefits and harms, resource implications, equity, acceptability and feasibility; moreover, nonpriority health outcomes were considered. Ultimately, the assessment of all these factors did not lead to a change in the strength of recommendation. Further details are provided in section 3.5.2.3.

[20] The GDG acknowledged the scarcity of cohort study-based evidence to define a threshold for hearing damage due to single loud exposures. It initially decided to propose $L_{AF,max}$ = 110, but after much discussion it appeared that the conversion of relevant standing limits (expressed in $L_{peak,C}$ and others) lacked sufficient basis.

3.5.2 Detailed overview of the evidence

The following sections provide a detailed overview of the evidence constituting the basis for setting the recommendations on leisure noise. As noted above, however, only limited evidence was available for several of the prioritized health outcomes, so it is presented and summarized for all critical and important health outcomes where possible, along with indications of the GDG's judgement of the quality of evidence. Research into health outcomes and effectiveness of interventions is addressed consecutively.

A comprehensive summary of all evidence considered for each of the critical and important health outcomes can be found in the eight systematic reviews published in the *International Journal of Environmental Research and Public Health* (see section 2.3.2 and Annex 2).

3.5.2.1 Evidence on health outcomes

The key question posed was: in the general population exposed to leisure noise, what is the exposure–response relationship between exposure to leisure noise (reported as various noise indicators) and the proportion of people with a validated measure of health outcome, when adjusted for main confounders? A summary of the PICOS/PECCOS scheme applied and the main findings is set out in Tables 45 and 46.

Table 45. PICOS/PECCOS scheme of critical health outcomes for exposure to leisure noise

PECO	Description	
Population	General population	
Exposure	Exposure to high levels of noise produced by leisure activities (average/night time)	
Comparison	Exposure to lower levels of noise produced by leisure activities (average/night time)	
Outcome(s)	For average noise exposure: 1. cardiovascular disease 2. annoyance 3. cognitive impairment 4. hearing impairment and tinnitus 5. adverse birth outcomes 6. quality of life, well-being and mental health 7. metabolic outcomes	For night noise exposure: 1. effects on sleep

Table 46. Summary of findings for health effects from exposure to leisure noise ($L_{Aeq,24h}$)

Noise metric	Priority health outcome measure	Quantitative risk for adverse health	Lowest level of exposure across studies[a]	Number of participants (studies)	Quality of evidence
Cardiovascular disease					
$L_{Aeq,24}$	Incidence of IHD	–	–	–	–
$L_{Aeq,24}$	Incidence of hypertension	–	–	–	–
Annoyance					
$L_{Aeq,24}$	%HA	–	–	–	–
Cognitive impairment					
$L_{Aeq,24}$	Reading and oral comprehension	–	–	–	–
Hearing impairment and tinnitus					
$L_{Aeq,24}$	Permanent hearing impairment	Not estimated	–	484 (3)	Very low (downgraded for study limitations, precision)

Hearing impairment and tinnitus

Several types of leisure activity are accompanied by loud sounds, such as attending nightclubs, pubs and fitness classes; live sporting events; concerts or live music venues; listening to loud music through PLDs. This recommendation is informed by a systematic review that assessed the evidence on permanent hearing loss and tinnitus due to exposure to leisure noise (Śliwińska-Kowalska & Zaborowski, 2017). The review identified two existing systematic reviews that summarized recent estimates of the risk of developing permanent hearing loss from the use of PLDs. It did not identify any studies with objective measurement of exposure to any other type of leisure noise.

The Scientific Committee on Emerging and Newly Identified Hazards and Risk (SCENIHR) (EC, 2008b) report concluded that prolonged exposure to sounds from PLDs may result in temporary hearing threshold shift, permanent hearing threshold shift and tinnitus, as well as poor speech communication in noisy conditions. However, based on the data available, there was no direct evidence for an effect of repeated, regular daily exposure to music through PLDs on development of permanent noise-induced hearing loss. Data on tinnitus were inadequate and therefore inconclusive. No meta-analysis was provided for any of the hearing effects; nor were the exposure–effect curves reported. The SCENIHR report was based on a narrative review of 30 original papers with over 2000 participants and exposure to music sounds that covered a range of 60–120 dB. Studies included in the review were carried out between 1982 and 2007.

In 2014 a second systematic review was published by Vasconcellos et al. (2014). Although the objective of this publication was to determine threshold levels of personally modifiable risk factors for hearing loss in the paediatric population, specific thresholds analyses were limited. Based on the descriptive overview of original papers, the authors identified exposure to loud music (including use of PLDs) and working on a mechanized farm as the main risk factors for hearing loss in children and teenagers. Thresholds of exposure to music, significantly associated with hearing loss in youth, were:

- more than four hours per week or more than five years of personal headphone usage;
- more than four visits per month to a discotheque.

The evidence review identified five new cross-sectional studies on noise from PLDs since the publication of the SCENIHR report (Feder et al., 2013; Levesque et al., 2010; Sulaiman et al., 2013; 2014; Vogel et al., 2014). Direct measurement of hearing thresholds with pure tone audiometry was performed only in three studies – by Feder et al. (2013) and Sulaiman et al. (2013 and 2014). In total, audiometric data from 484 subjects were analysed; among them, 449 were exposed and 35 were not exposed to PLD music. Two other studies by Levesque et al. (2010) and Vogel et al. (2014) did not perform audiometric measurement but reported on tinnitus in a total of 1067 participants.

Noise from PLDs was estimated based on direct measurement of equivalent sound pressure levels (in dB) in four studies (Feder, 2013; Levesque et al., 2010; Sulaiman et al., 2013; 2014) and based on converting volume-control setting levels of PLD into dB levels in one study (Vogel et al., 2014). The resulting exposure levels (L_{Aeq} values) had a mean of between 72 dB and 91 dB, although in two studies these data were not provided. In all studies, individual $L_{Aeq,8h}$ value was calculated based on an estimated level of music and the number of hours a day listening to the music through the PLD declared by an individual in the questionnaire. Resulting $L_{Aeq,8h}$ mean values were between 62 dB and 83 dB when provided.

Potential confounding was controlled by excluding the subjects with exposure to other sources of high-level noise or prior ear problems (Sulaiman et al., 2013), by excluding those with these factors and ototoxic drug intake (Sulaiman et al., 2014) or by controlling for these confounders by accounting for them in the statistical models. The confounders comprised socioeconomic status, demographic factors, tubes in the ear and leisure exposures in one study (Feder, 2013), and age and sex in one study (Vogel et al., 2014). One of the studies did not adjust for confounding factors (Levesque et al., 2010).

Data on permanent hearing loss were taken from audiometric measurements (Feder, 2013; Sulaiman et al., 2013; 2014), while data about permanent tinnitus were taken from self-reported responses to questionnaires (Levesque et al., 2010; Vogel et al., 2014). In one case, the outcome was defined as "permanent hearing-related symptoms", but it is not clear what proportion of subjects experienced permanent tinnitus (Vogel et al., 2014).

For permanent hearing loss, there is no pooled effect size, because the authors of the original studies either did not report data or reported in different formats. However, these studies indicate a harmful effect of listening to PLDs. For permanent tinnitus, there is no pooled effect size because the effects of noise from PLDs on permanent tinnitus were contradictory. These results are generally consistent with previous reviews by SCENIHR (EC, 2008b) and Vasconcellos et al. (2014).

The risk of bias was assessed as high for all five studies. The overall evidence for an effect of PLDs on hearing impairment and tinnitus was rated very low quality.

3.5.2.2 Evidence on interventions

The following section summarizes the evidence underlying the recommendation on the effectiveness of interventions for leisure noise exposure. The key question posed was: in the general population exposed to leisure noise, are interventions effective in reducing exposure to and/or health outcomes from leisure noise? A summary of the PICOS/PECCOS scheme applied and the main findings is set out in Tables 47 and 48.

Table 47. PICOS/PECCOS scheme of the effectiveness of interventions for exposure to leisure noise

PICO	Description	
Population	General population	
Intervention(s)	The interventions can be defined as: (a) a measure that aims to change noise exposure and associated health effects; (b) a measure that aims to change noise exposure, with no particular evaluation of the impact on health; or (c) a measure designed to reduce health effects, but that may not include a reduction in noise exposure.	
Comparison	No intervention	
Outcome(s)	For average noise exposure: 1. cardiovascular disease 2. annoyance 3. cognitive impairment 4. hearing impairment and tinnitus 5. adverse birth outcomes 6. quality of life, well-being and mental health 7. metabolic outcomes	For night noise exposure: 1. effects on sleep

Table 48. Summary of findings for interventions for leisure noise

Type of intervention	Number of participants (studies)	Effect of intervention	Quality of evidence
Hearing impairment			
Type E – behaviour change interventions (education programme/campaign)	4151 (7)	None of the studies involved measurement or estimation of exposure levels or health outcomes. Most studies found a significant effect of change in knowledge or behaviour.	–

Seven individual studies on PLDs, attendance at music venues and participation in other recreational activities where there was risk of hearing damage and/or tinnitus were included in the systematic review (Dell & Holmes, 2012; Gilles & Van de Heyning, 2014; Kotowski et al., 2011; Martin et al., 2013; Taljaard et al., 2013; Weichbold & Zorowka, 2003; 2007). All studies examined interventions directed at changes in knowledge or behaviour and hearing impairment.

The studies all sought evidence on the effectiveness of some form of educational programme or campaign aimed at children, adolescents or college students. These addressed perceptions and knowledge of the risk of high levels of noise – generally, but not exclusively, from PLD sources or from attendance at music events – and actual or intended changes to hearing damage risk behaviours, including avoidance, frequency or duration of exposure, regeneration periods when in high noise, or playback levels.

The outcome assessed in all intervention studies was the change in knowledge and behaviours towards hearing damage risk. The health outcome measures varied widely and included measurements on the youth attitude towards noise scale, participants' knowledge about hearing damage, participants' PLD usage patterns, participants' attitudes to wearing hearing protection (some in general; some at discotheques) and frequency of discotheque attendance. A majority of the studies found a significant effect of change in knowledge or behaviour. No indication on the persistence of knowledge and behavioural change was given, though.

None of the studies included objectively measured outcomes or a measured change in noise level exposure; thus, the effectiveness of the interventions could not be assessed, and the quality of the evidence was not rated according to GRADE.

3.5.2.3 Consideration of additional contextual factors

Based on the quality of the available evidence discussed in the foregoing overview, the GDG set the strength of recommendation of leisure noise to conditional. As a second step, it qualitatively assessed contextual factors to explore whether other considerations could have a relevant impact on the recommendation strength. These considerations mainly concerned the balance of harms and benefits, values and preferences, and resource use and implementation.

When assessing the balance of benefits and harms, the GDG recognized that exposure to leisure noise is widespread and frequent. In particular, as many as 88–90% of teenagers and young adults report listening to music through PLDs earphones (Pellegrino et al., 2013; Vogel et al., 2011). In 2015 WHO estimated that 1.1 billion young people worldwide could be at risk of hearing loss due to unsafe listening practices (WHO, 2015a). Furthermore, among young people aged 12–35 years in middle- and high-income countries, nearly 50% listen to unsafe levels of sound through personal audio devices (mp3 players, smartphones and others), and around 40% are exposed to potentially damaging levels of sound at nightclubs, bars and sporting events. Noise-induced hearing loss can be prevented by following safe listening practices, so the GDG concluded that health benefits can be gained from markedly reducing population exposure to leisure noise, including through actions to promote safe listening practices. A reduction of leisure noise is also assumed to reduce nuisance that can be caused to other people than those who enjoy leisure activities, such as neighbours. Furthermore, specifically for PLDs, it can reasonably be expected that a reduction of noise exposure could also lead to a reduction in accidents, injuries and other potential safety risks. In relation to possible harms and burdens, the GDG could not identify any harms (except economic costs, which are addressed in the paragraph on resource use and implementation) arising from implementation of the recommended guideline values.

Considering values and preferences, the GDG recognized that listening to music with the help of a PLD, going to concerts and attending sport events are activities regarded as enjoyable and therefore assumed to be valued by the overall population. Furthermore, it is expected that values and preferences might vary in particular with respect to the use of PLDs and embracing leisure activities involving loud noise, like concerts, and that some population groups – especially younger individuals – might voluntarily expose themselves to high levels of sound during these activities. Despite this, the GDG was confident that recommendations to lower noise levels for the prevention of hearing damage from leisure noise would be welcome by a majority of the population. Recommendations are expected to be particularly welcome when it comes to protecting the hearing of young children and teenagers, as these vulnerable groups often do not have control over their environment and the noise levels to which they are exposed, such as from noisy toys or at school.

With resource use and implementation, the GDG noted that interventions exist to reduce exposure to leisure noise from PLDs, attendance at music venues and participation in recreational activities, as aggregated by the systematic review on environmental noise interventions and their associated impacts (Brown & van Kamp, 2017). As most of these relate to implementation of a behaviour change, the reduction of exposure to leisure noise is expected to be technically feasible and cheap. None of the empirical investigations objectively measured outcomes or a measured change in noise level exposure, so the effectiveness of such measures cannot be assessed. Nevertheless, it is important to note that there is ample evidence from the occupational health field that high noise levels cause hearing damage, and that occupational interventions to reduce noise exposure are effective at lowering the risk of hearing problems or hearing damage (EC, 2003; Garcia et al., 2018; ISO, 2013; Maassen et al., 2001). In conclusion, resources needed to reduce exposure to leisure noise are not expected to be intensive, but implementation and long-term success of measures might be challenging, owing to cultural factors, as changes in behaviour are expected to be tricky to implement.

In light of the assessment of the contextual factors in addition to the quality of evidence, the recommendation remains conditional.

Additional considerations or uncertainties

The GDG considers the noise levels selected for this recommendation to be reasonable precautionary measures, in view of the rating of very low quality for the available evidence on an effect of leisure noise on permanent hearing impairment and tinnitus identified in the systematic review.

Extensive literature shows hearing impairment in populations exposed to specific types of nonoccupational environments, although these exposures are generally not well characterized. There are no studies with objective measurement of exposure to any other type of leisure noise (except PLDs) and permanent hearing impairment or tinnitus. Nevertheless, this recommendation generally applies to all leisure noise exposures, such as events in public venues (concerts halls, sports events, bars and discotheques) and educational facilities, and use of PLDs. The recommendation also applies to exposure to impulse sounds, such as those in shooting facilities or from the use of toys and firecrackers.

Hearing loss is the resultant value of combined exposures to different sources of leisure noise including, but not limited to, PLDs. Therefore, the recommendations apply to the combined noise levels from all sources.

Noise-induced hearing loss develops very slowly over years of exposure, giving rise to challenges in the assessment of the health impacts from prolonged use of PLDs and exposure to leisure noise. The induction period for the development of hearing impairment and tinnitus is long, and varying exposure conditions and changing lifestyle habits (including confounding noise sources), particularly among young people, will have an impact. Therefore, recommendations regarding leisure noise have often been inferred from the occupational field, where exposure conditions are more stable over time.

Indeed, long-term exposure to noise, objectively assessed and at levels measured in occupational settings for various professions, can lead to permanent hearing loss and tinnitus. This evidence, while not reviewed systematically as part of the work related to these guidelines, can be used as supportive evidence and justification for the need to develop a recommendation for leisure noise, given that many people could be at risk of developing hearing loss and/or tinnitus from exposure to lower levels of environmental noise. Similar otobiological mechanisms must also be considered for environmental noise.

To date, no commonly accepted method for assessing the risk of hearing loss due to environmental exposure to noise has been developed. One of the main challenges is to conduct a long-term objective exposure assessment of environmental noise and relate this to the development of permanent hearing impairment and tinnitus. The GDG underlined the strong need for research to develop a comprehensive methodology. In the absence of a method, and as long as no other tools are available, the equal energy principle outlined in the ISO standard for the estimation of noise-induced hearing loss (WHO, 1999) can be used as a practical tool for protecting public health from exposure to leisure noise. As a result, the relationship between leisure noise exposure and auditory effects can be quantified for a variety of exposure levels, duration and frequency.

Several organizations have established regulations for the protection of workers from risks to their health and safety arising from exposure to noise, and in particular risk to hearing. Of particular relevance is EU Directive 2003/10/EC on the minimum health and safety requirements regarding the exposure of workers to the risks arising from physical agents (noise) (EC, 2003). Based on the ISO 1999 standard (ISO, 2013), the Directive sets limits of exposure depending on equivalent noise level for an eight-hour working day and obliges the employer to take suitable steps if the limits are exceeded. It recommends three action levels for occupational settings, setting the lowest, most conservative value at $L_{ex,8hr}$ = 80 dB. According to the Directive, no consequences of exposure to occupational noise are expected at this level. While exposure patterns and certain characteristics of occupational and leisure noise exist, knowledge of the hearing impairment risks and preventive interventions can be used to assess health risks associated with leisure noise (Neitzel & Fligor, 2017).

The CNG recommend a limit of $L_{Aeq,24h}$ = 70 dB(A) for preventing hearing loss from industrial, commercial shopping and traffic areas, indoors and outdoors (WHO, 1999). Health and safety regulations are usually based on an exposure profile of a typical worker (eight hours per day, five days per week). Using the existing knowledge from the ISO standard and established health and safety regulations, it is possible to use the equal energy principle to derive the resulting noise exposure level for an exposure profile more appropriately suited for leisure noise. Converting 40 hours at 80 dB to a continuous exposure to noise (24 hours per day, seven days per week), this leads to a yearly average exposure of 71 dB for lifelong exposure.[21] This is the same value as the WHO recommendation of

[21] 71 dB = 80 dB (derived from ISO standard) – 6.2 dB (conversion of yearly average of 40 working hours divided by continuous exposure to noise: (10 log (2080hrs/8760 hrs)) – 3 dB (extrapolation of 40 working years to lifelong exposure).

70 dB (WHO, 1999). Table 49 presents the noise levels per hour for various time averages in order to keep within the recommended yearly average exposure, and assuming that exposure to other noise sources generally does not contribute significantly. For example, for specific events taking place for one-, two- or four-hour averages, once a week (such as visiting a discotheque or watching a loud movie), an hourly noise level of 85 dB would lead to an average yearly exposure of 63 dB, 66 dB and 69 dB, respectively. However, the same hourly exposure of 85 dB for an activity taking place for 14 hours per week (two hours per day, seven days a week) would lead to a yearly exposure of 74 dB, which exceeds the recommendations.

Table 49. Combination of hourly exposure and number of hours per week to arrive at a yearly average L_{Aeq}

Hours of exposure per week	One-hour exposure level (L_{Aeq})						
	70	75	80	85	90	95	100
1	48	53	58	63	68	73	78
2	51	56	61	66	71	76	81
4	54	59	64	69	74	79	84
14 (2 hours per day, 7 days per week)	59	64	69	74	79	84	89
28 (4 hours per day, 7 days per week)	62	67	72	77	82	87	92
40 (8 hours per day, 5 days per week)	64	69	74	79	84	89	94
168 (24 hours per day, 7 days per week)	70	75	80	85	90	95	100

Note: green = combinations of exposure/duration below current guideline level; red = combinations of exposure/duration above current guideline level; blue = input parameters.

The equal energy principle cannot be used to derive single-event limits because at high levels the ear starts to respond with nonlinear behaviour. The CNG provides several values, in different units: $L_{AF,max}$ = 110 dB for industrial noises (no distance stated), $L_{peak,lin}$ = 140 dB for adults and $L_{peak,lin}$ = 120 dB for children (measured at 100 mm) (WHO, 1999). EU Directive 2003/10/EC on the minimum health and safety requirements regarding the exposure of workers recommends a lower action level of $L_{peak,C}$ = 135 dB (at 100 mm). In a recent overview Hohmann (2015) provided an ERF for hearing damage caused by shooting noise, from which it appears that a safe level of L_E = 120 dB can be derived.

Although it is clear that high noise levels cause acute hearing damage, there is no agreement on a safe level. Further research is highly recommended. In the mean time, existing guidelines should be applied.

3.5.3 Summary of the assessment of the strength of recommendation

Table 50 provides a comprehensive summary of the different dimensions for the assessment of the strength of the leisure noise recommendations.

Table 50. Summary of the assessment of the strength of the recommendation

Factors influencing the strength of recommendation	Decision
Quality of evidence	**Average exposure ($L_{Aeq,24h}$)** *Health effects* • Evidence of an effect from PLDs on hearing impairment and tinnitus, in the absence of evidence for other health outcomes and absence of evidence on hearing impairment and tinnitus from other types of leisure noise besides PLDs, was rated **very low quality.** *Interventions* • No evidence was available on the effectiveness of interventions to reduce noise exposure and/or health outcomes from leisure noise.
Balance of benefits versus harms and burdens	The general benefit from reduction of leisure noise outweighs any potential harms.
Values and preferences	There is variability in the values and preferences of the general population.
Resource implications	The resources needed to reduce exposure to leisure noise are not expected to be intensive, but implementation and the long-term success of measures may be challenging, mainly due to cultural factors.
Decision on strength of recommendation	• **Conditional** for guideline level for average noise exposure ($L_{Aeq,24h}$) • **Conditional** for single-event and impulse noise • **Strong** for interventions to reduce noise exposure

3.6 Interim targets

An interim target was proposed in the NNG (WHO Regional Office for Europe, 2009), "recommended in situations where the achievement of NNG is not feasible in the short run for various reasons". The NNG emphasized that an interim target is "not a health-based limit value by itself. Vulnerable groups cannot be protected at this level".

The GDG discussed whether to propose interim targets as part of the current guidelines, and if so, what process would be needed to derive those values. The current recommendations are health-based and already provide guideline values per noise source (for both L_{den} and L_{night}). They also include information on exposure–response relationships for various health outcomes, which can be used by policy-makers or other stakeholders to inform the selection of different values, if needed. Further, interim targets may work differently in different countries and for different noise sources, and it may not be optimal to propose them Europe-wide. As a result, there was consensus among members of the GDG not to provide interim targets.

4. Implications for research

The development of these environmental noise guidelines for the WHO European Region has made evident some key knowledge gaps and research needs. The main ones specific to the guideline recommendations are presented as implications for research in the sections that follow.

4.1 Implications for research on health impacts from transportation noise

For the assessment of health effects from the main sources of transportation noise (road traffic, railways and aircraft), the various evidence reviews show the following knowledge gap: there is a need for longitudinal studies on the health impacts from exposure to environmental noise, to inform future recommendations properly (Table 51).

Table 51. Implications for research on health impacts from transportation noise (air, rail, road)

Current state of the evidence	Limited evidence is available on health impacts from transportation noise from large-scale cohort and case-control studies, with objective measurement of both noise exposure and health outcomes.
Population of interest	Research is needed into effects of exposure on children and adults exposed to environmental noise from transportation sources.
Exposure of interest	Objective measurement or calculation of transportation noise exposure is required; in particular, from studies of health effects related to combined exposure to different noise sources.
Comparison of interest	The data should be compared to the effects of lower levels of transportation noise.
Outcomes of interest	Measures of the following health outcomes is required, assessed objectively and harmonized where possible – for example, according to common protocols: • annoyance • effects on sleep • cardiovascular and metabolic effects • adverse birth outcomes • cognitive impairment • mental health, quality of life and well-being • hearing impairment and tinnitus • any other relevant health outcome.
Time stamp	The systematic review included studies between October 2014 and December 2016.

4.1.1 Specific implications for annoyance

To predict absolute %HA at the full range of levels (and the corresponding CIs), an integrated analysis of the original raw data from all of individual studies would be necessary. The evidence review conducted as part of the guidelines focused only on secondary data handling and therefore does not replace a full meta-analysis of all individual data. The development of a generic exposure–response relationship (from a full meta-analysis based on all individual data) is suggested as a priority research recommendation (see Table 52).

Table 52. Recommendation for research addressing the exposure–response relationship

Current state of the evidence	The evidence review on annoyance conducted as part of the guidelines does not provide a generalized ERF but points to significant differences compared to the curves used in the past. It shows that the available generalized ERFs are in need of adjustment, preferably as a result of undertaking a full meta-analysis. This is especially the case for the sources aircraft and railway noise, which new data show are more annoying than previously documented.
Population of interest	Research is needed into effects of exposure on children and adults exposed to air, rail and/or road traffic noise.
Exposure of interest	Objective measurement of transportation noise exposure is required.
Comparison of interest	The data should be compared to the effects of lower levels of transportation noise.
Outcomes of interest	Measures of health outcomes are required, assessed objectively according to common protocols (such as the International Commission on Biological Effects of Noise (ICBEN) scale for annoyance).
Time stamp	The systematic review included studies up to October 2014.

4.2 Implications for research on health impacts from wind turbine noise

Further research into the health impacts from wind turbine noise is needed so that better-quality evidence can inform any future public health recommendations properly. For the assessment of health effects from wind turbines, the evidence was either unavailable or rated low/very low quality. Recommendations for research addressing this priority are proposed in Table 53.

Table 53. Implications for research on health impacts from wind turbine noise

Current state of the evidence	The current evidence on health outcomes related to wind turbine noise is unavailable or of low/very low quality and mainly comes from cross-sectional studies. Methodologically robust longitudinal studies with large samples investigating the quantitative relationship between noise from wind turbines and health effects are needed.
Population of interest	Research is needed into effects of exposure on children and adults exposed and living near sources of wind turbine noise. Studies should assess subgroup differences in effects for vulnerable groups such as children, elderly people and those with existing poor physical and mental health.
Exposure of interest	Exposure to noise at a wide range of levels and frequencies (including low-frequency noise), with information on noise levels measured outdoors and indoors (particularly relevant for effects on sleep) at the residence is needed. The noise exposure should be measured objectively and common protocols for exposure to wind turbine noise should be established, considering a variety of noise characteristics specific to wind turbine noise.
Comparison of interest	The data should be compared to the effects in similar areas without wind turbines. Pre/post studies of new wind turbine installations are needed, especially if “before measures” unbiased by the stress and knowledge of potential wind turbine farm development need to be developed.
Outcomes of interest	Measures of health outcomes are required, assessed objectively – for example, according to common protocols (ICBEN scale for annoyance and self-reported sleep disturbance). The studies should include the most important situational and personal confounding variables, such as negative attitudes towards wind turbines, visual impact, economic gain and other socioeconomic factors.
Time stamp	The systematic review included studies between October 2014 (review on annoyance) and December 2016 (review on cardiovascular disease).

Alongside the defined needs for research on wind turbine noise it should be noted that research regarding industrial noise in general is required. More specifically, there is a need to investigate stationary sources (including heat, ventilation and acclimatization devices) and their impacts on health. Studies on hearing disorders from impulse and/or intermittent sounds are also needed; these would enable assessment of adverse effects created by one or several sounds of short duration with a high maximum sound level or impulse sound level.

4.3 Implications for research on health impacts from leisure noise

For the assessment of effects from leisure noise, the evidence to make a recommendation on the ERF to use for health risk assessment, or of a threshold for effects, was either unavailable or rated very low quality. This is a research gap: longitudinal studies with longer follow-up are needed; these should measure noise objectively, not only from PLDs but also from other types of leisure noise.

There is uncertainty in the measurement of early hearing disorders among young people using the tonal audiometry commonly applied. Precise methods to identify early hearing impairment and other hearing disorders are needed. Owing to long induction periods, however, adequate research may be difficult to perform, particularly among young people who change their exposure in terms of sound level and frequency as they age (for example, changing their music listening habits and venue visits). As a result, the recommendations refer to the results derived from stationary noise sources in the occupational field, in conjunction with the equal energy principle (see Table 54).

Table 54. Implications for research on health impacts from leisure noise

Current state of the evidence	Currently, no evidence is available on hearing impairment and tinnitus from large-scale cohort and case-control studies, with objective measurement of noise exposure and using a suitable method to assess hearing impairment in young people.
Population of interest	Research is needed into effects of exposure on children and adults exposed to environmental noise from different sources and in different settings.
Exposure of interest	Objective measurement of leisure noise exposure is required.
Comparison of interest	The data should be compared to the effects of no leisure noise exposure from these sources.
Outcomes of interest	The primary outcomes identified are: • hearing loss measured by audiometry; • specific threshold analyses focused on stratifying the risk of permanent hearing loss according to clearly defined levels of exposure to leisure noise, such as music through PLDs; • concise methods to identify early hearing impairment and other hearing disorders; • temporary threshold shift after exposure to leisure noise, as it may be reasonably predictive of future permanent threshold shift; • age-related hearing loss progression depending on early-age exposure to leisure noise, such as to loud music; and • tinnitus, measured objectively and subjectively.
Time stamp	The systematic review included studies up to June 2015.

4.4 Implications for research on effectiveness of interventions to reduce exposure and/or improve public health

The quality of the evidence on the effectiveness of interventions to reduce exposure to and health outcomes from environmental noise was variable. Further studies directly linking noise interventions to health outcomes are required, particularly for sources other than road traffic noise, and for human health outcomes other than annoyance.

Most studies involved road traffic noise (63%), followed by aircraft noise (13%) and railway noise (6%). The remaining interventions were for leisure noise (13%) and noise in hospital settings (4%). No interventions were identified that either addressed wind turbine noise or focused on educational settings.

Exposure-related interventions were mainly associated with a reduction in environmental noise exposure. However, in five studies (four road traffic noise studies and one aircraft noise study) some or all of the participants experienced noise exposure increases.

There is no clear evidence with respect to thresholds, which are defined as:

- the smallest change in exposure levels that results in a change in outcome; and
- the minimum before-level, regarding changes in health outcomes as a result of interventions.

The limited evidence base on the health effects of environmental noise interventions is thinly spread across different noise source types, outcomes and intervention types. Diversity exists between studies even within intervention types in terms of study designs, methods of analysis, exposure levels and changes in exposure experienced as a result of the interventions. For these reasons, carrying out a meta-analysis across studies examining the association between changes in level and changes in outcome was not possible.

To remedy this main research gap, longitudinal studies assessing noise exposure and health outcomes objectively should be developed, taking into account the most relevant confounders. The establishment of common protocols for future research is warranted (see Table 55).

Authorities should include significant funding for the design and implementation of studies to evaluate the effectiveness of interventions to reduce noise and their impact on health.

Table 55. Implications for research on effectiveness of interventions to reduce exposure and/or improve public health

Current state of the evidence	The current evidence on effectiveness of interventions to reduce health outcomes is limited and of varying quality. Few longitudinal studies have been done that take into account the most relevant confounders and measure the noise exposure and the outcomes objectively.
Population of interest	Research is needed into effects of interventions on defined populations exposed to and/or living near sources of environmental noise.
Intervention of interest	Research into any noise intervention at various points along the system pathway between source and outcome, for a variety of noise sources, is required.
Comparison of interest	The data should be compared to: • a steady-state control group, in similar areas with various exposure gradients from environmental noise sources; • the noise exposure in the same population, through a series of sequential measurements assessing the change before and after the intervention, preferably with multiple after measurements.
Outcomes of interest	Future intervention studies should use validated and, where possible, harmonized measures of exposure and outcome, as well as of moderators and confounders. The studies should use measures of exposure including noise exposure at a wide range of levels and frequencies (including low-frequency noise), with information on noise levels outdoors and indoors (particularly relevant for effects on sleep). They should also use measures of health outcomes, including the following outcomes assessed objectively – for example, according to common protocols (ICBEN scale for annoyance) – with consideration that the change in human response for some health outcomes from a step change in exposure may have a different time course to that of the change in exposure: • annoyance • effects on sleep • cardiovascular and metabolic diseases • adverse birth outcomes • cognitive impairment • mental health, quality of life and well-being • hearing impairment and tinnitus • any other relevant health outcome. Further, they should use measures of moderators and confounders, including repeated measurements of situational and personal variables such as activity interference, potential confounders such as noise sensitivity, coping strategies and a range of other attitudinal variables.
Time stamp	The systematic review included studies up to October 2014.

5. Implementation of the guidelines

5.1 Introduction

These guidelines focus on the WHO European Region and provide guidance to Member States that is compatible with the noise indicators used in the EU's END (EC, 2002a). They provide information on the exposure–response relationships between exposure to environmental noise from different noise sources and the proportion of people affected by certain health outcomes, as well as interventions that are considered efficient in reducing exposure to environmental noise and related health outcomes.

The WHO guideline values are evidence-based public health-oriented recommendations. As such, they are recommended to serve as the basis for a policy-making process in which policy options are considered. In the policy decisions on reference values, such as noise limits for a possible standard or legislation, additional considerations – such as feasibility, costs, preferences and so on – feature in and can influence the ultimate value chosen as a noise limit. WHO acknowledges that implementing the guideline recommendations will require coordinated effort from ministries, public and private sectors and nongovernmental organizations, as well as possible input from international development and finance organizations. WHO will work with Member States and support the implementation process through its regional and country offices.

5.2 Guiding principles

Four guiding principles provide generic advice and support when incorporating the recommendations into a policy framework, and apply to the implementation of all the recommendations.

The **first principle** is to reduce exposure to noise, while conserving quiet areas. The recommendations focus on reduction of population exposure to environmental noise from a variety of sources, in different settings. The general population can be exposed regularly to more than one source of noise simultaneously (including, in some cases, occupational noise), as well as to other nonacoustic factors that can modify the response to noise (such as vibration from railways, air pollution from traffic or visual aspects of wind turbines). Thus, overall reduction of exposure from all sources should be promoted. Furthermore, noise exposure reduction in one area should not come at the expense of an increase in noise elsewhere; existing large quiet outdoor areas should be preserved.

The **second principle** is to promote interventions to reduce exposure to noise and improve health. The evidence from epidemiological studies on adverse health effects at certain noise levels, used as a basis to derive the guideline values proposed in the recommendations, supports the promotion of noise interventions. The potential health impacts from environmental noise are significant, especially when considering the widespread exposure to environmental noise across the population and the high baseline rates for various health outcomes associated with environmental noise.

There are challenges in assessment of the effectiveness of interventions to reduce noise exposure and/or improve health, as there is often a significant time lag between the intervention and a measurable change in exposure and related health benefits. The lack of – or limited direct evidence for – quantifiable health benefits of some specific interventions does not imply that measures to achieve population exposure according to the proposed guidelines should be ignored.

Given the different factors that determine noise exposure, a single measure alone may not be sufficient to reduce exposure and/or improve health significantly, and a combination of methods may be warranted. Nevertheless, it is widely acknowledged that the most effective actions to reduce exposure tend to be those that reduce noise at the source. Such actions have the biggest potential, whereas other measures can be less effective or sustained over time, especially when they depend on behaviour change or noise reductions inside houses.

The **third principle** is to coordinate approaches to control noise sources and other environmental health risks. Considering the common transport-related sources of environmental noise and air pollution, and in particular the evidence of independent effects on the cardiovascular system, a coordinated approach to policy development in the sectors related to urban planning, transport, climate and energy should be adopted for policies with an impact on environmental noise, air quality and/or climate. Such an approach should yield multiple benefits through increased commitment and financial resources; increased attention to securing health considerations in all policies; and use of policy to control noise and other environmental risks such as air pollutants, including short-lived climate pollutants. There is wide consensus on the value of pursuing coordinated policies that can deliver health and other benefits, such as those associated with the local environment and economic development. Furthermore, coordinated policy-making is potentially cost-saving.

The **fourth principle** is to inform and involve communities that may be affected by a change in noise exposure. In planning new urban and/or rural developments (transport schemes, new infrastructures in less densely populated areas, noise abatement and mitigation strategies), bringing together planners, environmental professionals and public health experts with policy-makers and citizens is key to public acceptability and involvement and to the successful guidance of the decision-making proces. Potential health effects from environmental noise should be included as part of health impact assessments of future policies, plans and projects, and the communities potentially affected by a positive or negative change in noise exposure should be well informed and engaged from the outset to maximize potential benefits to health. Introducing measures incrementally may help with acceptance.

5.3 Assessment of national needs and capacity-building

National needs, including the need for capacity-building, differ between Member States in the WHO European Region. They depend on the existence and level of implementation of national and/or European and international noise policies; these are more likely to be implemented fully in EU countries thanks to the legally binding provisions of the EU's END (EC, 2002a). In most countries in the Region noise is perceived as a major and growing environmental health and public health problem. Noise mapping and action plans are carried out in accordance with the END in EU Member States, and in south-eastern European countries noise legislation has mainly been harmonized with the END. Nevertheless, significant differences still exist in the completeness and regular updating of noise exposure assessment between countries. Noise exposure assessment is a required input for noise health impact assessments, along with exposure–response relationships and population baseline data.

WHO has identified some common needs for knowledge transfer and capacity-building for health risk assessment of environment noise in the Member States that joined the EU after 2003, the newly independent states and south-eastern European countries (WHO Regional Office for Europe, 2012):

- implementation of the END and its annexes, especially in the preparation of strategic noise mapping and action plans;
- human resources development through education and training in health risk assessment and burden of diseases stemming from environmental noise;
- methodological guidance for health risk assessment of environmental noise.

These guidelines mostly recommend exposure–response relationships related to the exposure indicators L_{den} and L_{night}. They are therefore of particular relevance to EU countries and those applying the END. In countries that do not use these indicators, users of the guidelines need to convert their noise indicators into L_{den} and L_{night} before being able to apply the recommendations. Conversion between indicators is possible, using a certain set of assumptions (Brink et al., 2018).

5.4 Usefulness of guidelines for target audiences

The provision of guideline values as a practical tool for guiding exposure reduction and the design of effective measures and policies is widely seen as useful. The WHO guidelines equip policy-makers and other end-users with a range of different needs with the necessary evidence base to inform their decisions. As indicated in section 1.4, these guidelines serve as a reference for several target audiences, and for each group they can be useful in different ways.

- For technical experts and decision-makers, the guidelines can be used to provide exposure–response relationships that give insight into the consequences of certain regulations or standards on the associated health effects. They also can be useful at the national and international level when developing noise limits or standards, as they provide the scientific basis to identify the levels at which environmental noise causes a significant health impact. Based on these recommendations, national governments and international organizations can be better informed when introducing noise limits, to ensure protection of people's health.
- For health impact assessment and environmental impact assessment practitioners and researchers, these guidelines provide exposure–response relationships that give insight into the expected health effects at observed or expected noise exposure levels. They offer recommendations on the maximum admissible noise levels for some sources and provide important input to assit in deriving the health burden from noise; in that sense, they can be used when producing studies such as noise maps and action plans to obtain an evaluation of the magnitude of the health problem. The systematic reviews developed in support of these guidelines allow practitioners to raise awareness of the credibility of the issue of noise as a public health problem and to use the recommended exposure–response relationships uniformly. Researchers will also benefit from the guidelines as they clearly identify critical data gaps that need to be filled in the future to better protect the population from the harmful effects of noise.
- The guideline recommendations provide a useful tool for national and local authorities when deciding about noise reduction measures, as they provide data to estimate the health burden on the population and therefore allow comparison among different policy options. These options

can include measures to reduce the noise emitted by the sources, measures aimed at impeding the transmission of noise from the sources to people and measures aimed at better planning the location of houses (urban planning).

- The guideline recommendations can also be used by civil society, patients and other advocacy groups to raise awareness and encourage actions to protect the population, including vulnerable groups, from exposure to noise.

Regarding noise abatement and mitigation of noise sources, practical exposure–response relationships for various noise sources are useful quantitative input to determine the impact of noise on health. They can be valuable information to use in cost–effectiveness and cost–benefit analyses of various policies for noise abatement. In this respect, the guideline recommendations can be an integral part of the policy process for noise reduction by various institutions; they are of great value for communicating the health risks and potential cost-effective solutions to reduce noise.

National and local authorities and nongovernmental organizations responsible for risk communication and general awareness-raising can use these guidelines for promotion campaigns and appropriate risk communication. The guidelines provide scientific evidence on a range of health effects associated with noise and facilitate appropriate risk communication to specific vulnerable groups. They therefore need to be promoted broadly to citizens, national and local authorities and nongovernmental organizations responsible for risk communication.

5.5 Methodological guidance for health risk assessment of environmental noise

A health risk assessment is the scientific evaluation of potential adverse health effects resulting from human exposure to a particular hazard – in this case, environmental noise. The main purpose of the assessment is to estimate and communicate the health impact of exposure to noise or changes in noise in different socioeconomic, environmental and policy circumstances.

The guideline recommendations, along with the detailed information contained in the systematic evidence reviews, can be used to assess health impacts in order to answer a variety of policy questions on:

- the public health burden associated with current or projected levels of noise;
- the human health benefits associated with changing a noise policy or applying a more stringent noise standard;
- the impacts on human health of emissions from specific sources of noise for selected economic sectors (and the benefits of policies related to them); and
- the human health impacts of current policy or implemented action.

The results from a health risk assessment are usually reported as the number of attributable deaths, number of cases, years of life lost, years lost due to disability or DALYs.

The quantification of the impacts for one combination of noise source, noise exposure indicator and health outcome may to some extent include effects attributable to another. Consequently, for any particular set of combinations, consideration should be given to potential double counting.

It is also important to note the uncertainties in quantification of the health impacts. One set of uncertainties relates to the CIs associated with the recommended ERFs; these quantify the random error and variability attributed to heterogeneity in the epidemiological studies used for health risk assessment. Other types of uncertainty include modelling/calculation of noise exposure, estimates of population background rates for morbidity and mortality, and transferability of ERFs from locations where studies were carried out or data were otherwise gathered to another location. This is especially true for noise annoyance, for which there is often considerable heterogeneity in effect sizes of studies because estimates vary between noise sources and are to some degree dependent on the situation and context. Furthermore, cultural differences around what is considered annoying are significant, even within Europe. It is therefore not possible to determine the "exact value" of %HA for each exposure level in any generalized situation. Instead, data and exposure–response curves derived in a local context should be applied whenever possible to assess the specific relationship between noise and annoyance in a given situation. If, however, local data are not available, general exposure–response relationships can be applied, assuming that the local annoyance follows the generalized average annoyance. Despite the challenges in applying a "generalized" ERF to specific local situations, the GDG believes that the percentage of high annoyance defined in section 2.4.3 is an acceptable estimate of the "average" %HA at a certain noise level – for example, in Europe.

When performing a health risk assessment of environmental noise, it is important to note several considerations. The selection of particular noise source(s), noise exposure indicator(s) and health outcome combinations to be used for estimation of the health impacts depends on the particular policies and/or measures being assessed. These guidelines propose recommendations for four types of noise source using noise indicators L_{den} and/or L_{night} (road traffic, railway noise, aircraft noise and wind turbine noise) and one recommendation using $L_{Aeq,24h}$ (leisure noise). Any population may be exposed to different noise sources associated with the same health outcome. Estimated impacts should not be added together without recognizing that addition will, in most practical circumstances, lead to some overestimation of the true impact. Impacts estimated for only one combination will, on the other hand, underestimate the true impact of the noise mixture, if other sources of noise also affect that same health outcome.

The scientific evidence reviewed and summarized in these guidelines implies that the following health outcomes can be quantified in a health risk assessment, and that their effects are cumulative:

- from road traffic noise – incidence of IHD, annoyance and sleep disturbance, and potentially incidence of stroke and diabetes;
- from railway noise – annoyance and sleep disturbance;
- from aircraft noise – annoyance, reading and oral comprehension in children, sleep disturbance and potentially change in waist circumference and incidence of IHD;
- from wind turbine noise: annoyance.

The DWs suggested in section 2.4.3 can be used to calculate DALYs.

Data on incidence and prevalence of some health outcomes related to noise (mainly cardiovascular disease) can be found at a national level in online databases available on the WHO Regional Office for Europe website (WHO Regional Office for Europe, 2017).

General principles of relevance for environmental factors when conducting health risk assessments and quantifying the burden of disease can be found elsewhere (European Centre for Health Policy, 1999; Murray, 1994; Murray & Acharya, 1997; Murray & Lopez, 2013; Quigley et al., 2006; WHO, 2014a; 2014b; WHO Regional Office for Europe, 2016). In particular, the WHO Regional Office for Europe and JRC jointly published the first estimates of the burden of disease from environmental noise in 2011 (WHO Regional Office for Europe & JRC, 2011). The publication includes guidance on the procedure for the health risk assessment of environmental noise, exemplary estimates of the burden of the health impacts of environmental noise and a discussion of the uncertainties and limitations of the procedure to calculate the environmental burden of disease. The reader is referred to this publication for more detailed explanations on quantitative risk assessment methods for environmental noise.

5.6 Route to implementation: policy, collaboration and the role of the health sector

Preventing noise and related health impacts relies on effective action across different sectors: health, environment, transport, urban planning and so on. The health sector needs to be engaged effectively in different sectors' policy processes at national, regional and international levels. It needs to provide authoritative advice about the health impacts of noise and policy options that will bring the greatest benefits to health.

In most countries in the WHO European Region, the commitment of the health sector to engage in action to address environmental noise issues needs to be improved and better coordinated. A more coherent overall response is needed, taking into account relevant linkages with existing health priorities and concerns. Thus, some actions can be seen as aspects of the role of the health sector:

- engaging in proper communication with relevant sectors about noise exposure from different sectors and sources (environmental, urban development, transport and so on) to ensure that health issues are adequately addressed as part of international, regional, national and/or local efforts to address environmental noise – the implementation approach may differ across sectors, depending on the level of awareness of noise as a public health problem;
- promoting the guideline recommendations to policy-makers from different sectors and organizing information campaigns and awareness-raising activities in collaboration with national health authorities and WHO country offices to inform citizens and health practitioners about the health risks of environmental noise;
- using decision support instruments such as health impact and health risk assessments to quantify health risks and potential benefits associated with policies and interventions aimed at addressing environmental noise, including presenting information about the severity of the health effects (for example, with cardiovascular disease) to convey the serious impacts of noise and to try to change attitudes and behaviours of policy-makers and the general public;
- promoting the guidelines to health practitioners and physicians, especially at the community level (through associations of physicians, cardiologists and so on as part of the stakeholder group);
- supporting the establishment of national health institutions capable of initiating and developing health promotion measures, and conducting research, monitoring and reporting on health impacts from environmental noise and its different sources;

- organizing capacity-building workshops and training to increase knowledge of the guidelines as well as creating tools, skills and resources for health risk assessment and developing intersectoral collaboration, particularly in non-EU countries;
- promoting relevant research initiatives and shaping the research agenda, in part based on critical research recommendations and gaps identified in the guidelines, as well as on the impact and effectiveness of interventions and experience with their implementation;
- developing and updating guidelines and policies that influence national, regional and international benchmarks and targets related to environmental noise, as well as advocating the inclusion of the guidelines in development and shaping of national, regional and international noise policies and standards;
- working with other sectors to strengthen noise level monitoring and evaluation, particularly in non-EU countries, to ensure proper conducting of health risk assessments of environmental noise.

5.7 Monitoring and evaluation: assessing the impact of the guidelines

Exposure–response relationships and other recommendations provided by these guidelines should be incorporated into national health policies and the main related policy documents. They should be used for health impact and health risk assessments to identify health risks and potential benefits associated with policies and interventions related to environmental noise.

Population noise exposure should be monitored and assessed at a national scale, at least in urban areas. Furthermore, information on trends in occurrence of noise-related health outcomes considered in these guidelines, such as annoyance or sleep disturbance, should be gathered. These monitoring activities should be performed on a regular basis to ensure proper health risk assessments of noise.

5.8 Updating the guidelines

The progress and pace of noise and health research has intensified over the last 10 years, including new studies published after the completion of the systematic reviews done for these guidelines. This is partly related to the growing car fleet and resulting traffic, the density of urbanization, demographic changes and shifts towards renewable energy, including wind turbines, which have caused an increase in public perception and political awareness of the environmental noise problem. Noise exposure assessment has also improved, due partly to European legislation, and this has provided useful data for epidemiological studies on the health effects of environmental noise. Considering this, the recommendations proposed in these guidelines are expected to remain valid for a period of about 10 years. WHO will monitor the development of the scientific advancements on noise and health research in order to inform any updated guidance on environmental noise.

References

Alonso-Coello P, Oxman AD, Moberg J, Brignardello-Petersen R, Akl EA, Davoli M et al. (2016a). GRADE Evidence to Decision (EtD) frameworks: a systematic and transparent approach to making well informed healthcare choices. 2: Clinical practice guidelines. BMJ. 353:i2089. doi: 10.1136/bmj.i2089.

Alonso-Coello P, Schünemann HJ, Moberg J, Brignardello-Petersen R, Akl EA, Davoli M et al. (2016b). GRADE Evidence to Decision (EtD) frameworks: a systematic and transparent approach to making well informed healthcare choices. 1: Introduction. BMJ. 353: i2016. doi: 10.1136/bmj.i2016.

Amundsen AH, Klaeboe R, Aasvang GM (2011). The Norwegian facade insulation study: the efficacy of facade insulation in reducing noise annoyance due to road traffic. J Acoust Soc Am. 129(3):1381–9.

Amundsen AH, Klaeboe R, Aasvang GM (2013). Long-term effects of noise reduction measures on noise annoyance and sleep disturbance: the Norwegian facade insulation study. J Acoust Soc Am. 133(6):3921–8.

Ancona C, Forastiere F, Mataloni F, Badaloni C, Fabozzi T, Perucci CA, on behalf of the SERA Study Team (2010). Aircraft noise exposure and blood pressure among people living near Ciampino airport in Rome. In: Proceedings. 39th International Congress on Noise Control Engineering 2010 (INTER-NOISE 2010), Lisbon, Portugal, 13–16 June 2010. Lisbon: Sociedade Portuguesa de Acustica.

Asensio C, Recuero M, Pavón I (2014). Citizens' perception of the efficacy of airport noise insulation programmes in Spain. Appl Acoust. 84:107–15.

Babisch W (2004). The NaRoMI-Study: executive summary – traffic noise. In: Federal Environmental Agency, editor. Chronic noise as a risk factor for myocardial infarction, The NaRoMI study. Berlin: Umweltbundesamt:1–16.

Babisch W (2014). Updated exposure–response relationship between road traffic noise and coronary heart diseases: a meta-analysis. Noise Health. 16(68):1–9.

Babisch W, Beule B, Schust M, Kersten N, Ising H (2005a). Traffic noise and risk of myocardial infarction. Epidemiology. 16(1):33–40.

Babisch W, Gallacher JE (1990). Traffic noise, blood pressure and other risk factors: the Caerphilly and Speedwell Collaborative Heart Disease Studies. In: Proceedings. 5th International Congress on Noise as a Public Health Problem, Stockholm, Sweden, 21–28 August 1988. Stockholm: Swedish Council for Building Research.

Babisch W, Gallacher JE, Elwood PC, Ising H (1988). Traffic noise and cardiovascular risk. The Caerphilly Study, first phase. Outdoor noise levels and risk factors. Arch Environ Health. 43(6):407–14.

Babisch W, Houthuijs D, Kwekkeboom J, Swart W, Pershagen G, Bluhm G et al. (2005b). HYENA – hypertension and exposure to noise near airports: a European study on health effects of aircraft noise. In: Proceedings. 34th International Congress on Noise Control Engineering 2005 (INTER-NOISE 2005), Rio de Janeiro, Brazil, 7–10 August 2005. Washington DC: Institute of Noise Control Engineering of the USA.

Babisch W, Houthuijs D, Pershagen G, Cadum E, Katsouyanni K, Velonakis M et al. (2009). Annoyance due to aircraft noise has increased over the years – results of the HYENA study. Environ Int. 35:1169–76.

Babisch W, Houthuijs D, Pershagen G, Katsouyanni K, Velonakis M, Cadum E et al. (2008). Associations between road traffic noise level, road traffic noise annoyance and high blood pressure in the HYENA study. J Acoust Soc Am. 123:3448. doi: 10.1121/1.2934267.

Babisch W, Ising H, Elwood PC, Sharp DS, Bainton D (1993a). Traffic noise and cardiovascular risk: the Caerphilly and Speedwell studies, second phase. Risk estimation, prevalence, and incidence of ischemic heart disease. Arch Environ Health. 48(6):406–13.

Babisch W, Ising H, Gallacher JE (2003). Health status as a potential effect modifier of the relation between noise annoyance and incidence of ischaemic heart disease. Occup Environ Med. 60(10):739–45.

Babisch W, Ising H, Gallacher JE, Sharp DS, Baker I (1993b). Traffic noise and cardiovascular risk: the Speedwell study, first phase. Outdoor noise level and risk factors. Arch Environ Health. 48(6):401–5.

Babisch W, Ising H, Gallacher JEJ, Sweetnam PM, Elwood PC (1999). Traffic noise and cardiovascular risk: the Caerphilly and Speedwell studies, third phase – 10-year follow up. Arch Environ Health. 54(3):210–16.

Babisch W, Ising H, Kruppa B, Wiens D (1992). Verkehrslärm und Herzinfarkt, Ergebnisse zweier Fall-Kontroll-Studien in Berlin [Transport noise and myocardial infarction. Results of two case studies from Berlin]. In WoBoLu-Hefte 2/92. Insitut für Wasser, Boden und Lufthygiene. Berlin: Umweltbundeamt].

Babisch W, Ising H, Kruppa B, Wiens D (1994). The incidence of myocardial infarction and its relation to road traffic noise – the Berlin case-control studies. Environ Int. 20(4):469–74.

Babisch W, Pershagen G, Selander J, Houthuijs D, Breugelmans O, Cadum E et al. (2013a). Noise annoyance – a modifier of the association between noise level and cardiovascular health? Sci Total Environ. 452–53:50–7.

Babisch W, Swart W, Houthuijs D, Selander J, Bluhm G, Pershagen G et al. (2012). Exposure modifiers of the relationships of transportation noise with high blood pressure and noise annoyance. J Acoust Soc Am. 132(6):3788–808.

Babisch W, Wolf K, Petz M, Heinrich J, Cyrys J, Peters A (2013b). Road traffic noise, air pollution and (isolated systolic) hypertension: cross-sectional results from the KORA study. In: Proceedings. 42nd International Congress and Exposition on Noise Control Engineering 2013 (INTER-NOISE 2013), Innsbruck, Austria, 15–18 September 2013. Innsbruck: Austrian Noise Abatement Association.

Babisch W, Wolf K, Petz M, Heinrich J, Cyrys J, Peters A (2014c). Associations between traffic noise, particulat air pollution, hypertension, and isolated systolic hypertension in adults: the KORA study. Environ Health Perspect. 122(5):492–8.

Babisch W, Wolke G, Heinrich J, Straff W (2014a). Road traffic noise and hypertension – accounting for the location of rooms. Environ Res. 133:380–7.

Babisch W, Wolke G, Heinrich J, Straff W (2014b). Road traffic, location of rooms and hypertension. J Civil Environ Eng. 4(5):162.

Bakker RH, Pedersen E, van den Berg GP, Stewart RE, Lok W, Bouma J (2012). Impact of wind turbine sound on annoyance, self-reported sleep disturbance and psychological distress. Sci Total Environ. 425:42–51.

Barregard L, Bonde E, Ohrstrom E (2009). Risk of hypertension from exposure to road traffic noise in a population-based sample. Occup Environ Med. 66(6):410–15.

Bartels S, Müller U, Vogt J (2013). Predictors of aircraft noise annoyance: results of a telephone study. In: Proceedings. 42nd International Congress and Exposition on Noise Control Engineering 2013 (INTER-NOISE 2013), Innsbruck, Austria, 15–18 September 2013. Innsbruck: Austrian Noise Abatement Association.

Basner M, Babisch W, Davis A, Brink M, Clark C, Janssen S et al. (2014). Auditory and non-auditory effects of noise on health. Lancet. 383(9925): 1325–32.

Basner M, Isermann U, Samel A (2006). Aircraft noise effects on sleep: application of the results of a large polysomnographic field study. J Acoust Soc Am. 119(5):2772–84.

Basner M, McGuire S (2018). WHO environmental noise guidelines for the European Region: a systematic review on environmental noise and effects on sleep. Int J Environ Res Public Health. 15(3):pii: E519 (http://www.mdpi.com/1660-4601/15/3/519/htm, accessed 27 June 2018).

Basner M, Müller U, Elmenhorst EM (2011). Single and combined effects of air, road, and rail traffic noise on sleep and recuperation. Sleep. 34(1):11–23.

Baughan C, Huddart L (1993). Effects of traffic noise changes on residents' nuisance ratings. In: Proceedings. 6th International Congress on Noise as a Public Health Problem. Nice, France, 5–9 July 1993. Lyon: Institut National de Recherche sur les Transports et leur Sécurité.

Beelen R, Hoek G, Houthuijs D, van den Brandt PA, Goldbohm RA, Fischer Pet al. (2009). The joint association of air pollution and noise from road traffic with cardiovascular mortality in a cohort study. Occup Environ Med. 66(4):243–50.

Belojevic G, Evans GW (2011). Traffic noise and blood pressure in North-American urban schoolchildren C3. In: Proceedings. 10th International Congress on Noise as a Public Health Problem 2011 (ICBEN 2011), London, United Kingdom, 24–28 July 2011. London: Institute of Acoustics.

Belojevic G, Evans GW (2012). Traffic noise and blood pressure in low-socioeconomic status, African-American urban schoolchildren. J Acoust Soc Am. 132(3):1403–6.

Bendtsen H, Michelsen L, Christensen EC (2011). Noise annoyance before and after enlarging Danish highway. In: Proceedings. Forum Acusticum: 6th European Congress on Acoustics, Aalborg, Denmark, 27 June – 1 July 2011. Stuttgart: Hirzel.

Berry B, Sanchez D (2014). The economic and social value of aircraft noise effects: A critical review of the state of the art. In: Proceedings. 11th International Congress on Noise as a Public Health Problem 2014 (ICBEN 2014), Nara, Japan, 1–5 June 2014. Tokyo: Institute of Noise Control Engineering of Japan.

Bilenko N, van Rossem L, Brunekreef B, Beelen R, Eeftens M, Hoek G et al. (2013). Traffic-related air pollution and noise and children's blood pressure: results from the PIAMA birth cohort study. Eur J Prev Cardiol. 22(1):4–12.

Bjork J, Ardo J, Stroh E, Lovkvist H, Ostergren PO, Albin M (2006). Road traffic noise in southern Sweden and its relation to annoyance, disturbance of daily activities and health. Scand J Work Environ Health. 32:392–401.

Blanes N, Fons J, Houthuijs D, Swart W, Sáinzde la Maza M, Ramos MJ et al. (2017). Noise in Europe 2017: updated assessment. Bilthoven: European Topic Centre on Air Pollution and Climate Change Mitigation (ETC/ACM Technical Paper 2016/13; http://acm.eionet.europa.eu/reports/ETCACM_TP_2016_13_NoiseInEurope2017, accessed 17 June 2017).

Bluhm G, Berglind N, Nordling E, Rosenlund M (2007). Road traffic noise and hypertension. Occup Environ Med. 64(2):122–6.

Bluhm G, Eriksson C, Hilding A, Ostenson CG (2004). Aircraft noise exposure and cardiovascular risk on men. First results from a study around Stockholm Arlanda airport. In: Proceedings. 33rd International Congress and Exhibition on Noise Control Engineering, Prague, Czechia, 22–25 August 2004. Prague: Czech Acoustical Society.

Bluhm G, Eriksson C, Pershagen G, Hilding A, Östenson CG (2009). Aircraft noise and incidence of hypertension: a study around Stockholm Arlanda airport. In: Proceedings. 8th European Conference on Noise Control 2009 (EURONOISE 2009), Edinburgh, United Kingdom, 26–28 October 2009. Edinburgh: Institute of Acoustics.

Bodin T, Albin M, Ardo J, Stroh E, Ostergren PO, Bjork E (2009). Road traffic noise and hypertension: results from a cross-sectional public health survey in southern Sweden. Environ Health. 8(38).

Bodin T, Björk J, Ardö J, Albin M (2015). Annoyance, sleep and concentration problems due to combined traffic noise and the benefit of quiet side. Int J Environ Res Public Health. 12(2): 1612–28.

Borsky, PN (1979). Sociopsychological factors affecting the human response to noise exposure. Otolaryngol Clin North Am. 12(3):521–35.

Breugelmans O, Houthuijs D, van Kamp I, Stellato R, van Wiechen C, Doornbos G (2007). Longitudinal effects of a sudden change in aircraft noise exposure on annoyance and sleep disturbance around Amsterdam airport. In: Proceedings. 19th International Congress on Acoustics (ICA 2007), Madrid, Spain, 2–7 September 2007. Madrid: Sociedad Espanola de Acustica.

Breugelmans ORP, van Wiechen CMAG, van Kamp I, Heisterkamp SH, Houthuijs DJM (2004). Gezondheid en beleving van de omgevingskwaliteit in de regio Schiphol 2002 [Health and quality of life near Amsterdam Schiphol airport: 2002]. Interim report 630100001 [in Dutch]. Bilthoven: National Institute for Public Health and the Environment.

Brink M (2011). Parameters of well-being and subjective health and their relationship with residential traffic noise exposure – a representative evaluation in Switzerland. Environ Int. 37:723–33.

Brink M (2013). Annoyance assessment in postal surveys using the 5-point and 11-point ICBEN scales: effects of sale and question arrangement. In: Proceedings. 42nd International Congress and Exposition on Noise Control Engineering 2013 (INTER-NOISE 2013), Innsbruck, Austria, 15–18 September 2013. Innsbruck: Austrian Noise Abatement Association.

Brink M, Schäffer B Pieren, R, Wunderli JM (2018). Conversion between noise exposure indicators L_{eq24h}, L_{Day}, $L_{Evening}$, L_{Night}, L_{dn} and L_{den}: principles and practical guidance. Int J Hyg Environ Health. 221(1):54–63. doi: 10.1016/j.ijheh.2017.10.003.

Brink M, Schreckenberg D, Vienneau D, Cajochen C, Wunderli JM, Probst-Hensch N et al. (2016). Effects of scale, question location, order of response alternatives, and season on self-reported noise annoyance using ICBEN scales: a field experiment. Int J Environ Res Public Health. 13(11). doi: 10.3390/ijerph13111163.

Brink M, Wirth KE, Schierz C, Thomann G, Bauer G (2008). Annoyance responses to stable and changing aircraft noise exposure. J Acoust Soc Am. 124(5):2930–41.

Bristow AL, Wardman M, Chintakayala VPK (2014). International meta-analysis of stated preference studies of transportation noise nuisance. Transportation. 42(1):71–100.

Bronzaft AL (1981). The effect of a noise abatement program on reading ability. J Environ Psychol. 1:215–22.

Bronzaft AL, McCarthy DP (1975). The effects of elevated train noise on reading ability. Environ Behav. 7(4):517–27.

Brown AL (1987). Responses to an increase in road traffic noise. J Sound Vib. 117(1):69–79.

Brown AL (2015). Longitudinal annoyance responses to a road traffic noise management strategy that reduced heavy vehicles at night. J Acoust Soc Am. 137(1):165–76.

Brown AL, Hall A, Kyle-Little J (1985). Response to a reduction in traffic noise exposure. J Sound Vib. 98(2):235–46.

Brown AL, Lam KC, van Kamp I (2015). Quantification of the exposure and effects of road traffic noise in a dense Asian city: a comparison with Western cities. Environ Health. 14–22. doi: 10.1186/s12940-015-0009-8.

Brown AL, Lam KC, van Kamp I, Yeung MKL (2014). Urban road traffic noise: exposure and human response in a dense, high-rise city in Asia. In: Proceedings. 11th International Congress on Noise as a Public Health Problem 2014 (ICBEN 2014), Nara, Japan, 1–5 June 2014. Tokyo: Institute of Noise Control Engineering of Japan.

Brown AL, van Kamp I (2009). Response to a change in transport noise exposure: a review of evidence of a change effect. J Acoust Soc Am. 125(5):3018–29.

Brown AL, van Kamp I (2017). WHO environmental noise guidelines for the European Region: a systematic review of transport noise interventions and their impacts on health. Int J Environ Res Public Health. 14(8). pii: E873 (http://www.mdpi.com/1660-4601/14/8/873/htm, accessed 27 June 2018).

Caerphilly and Speedwell Collaborative Group (1984). Caerphilly and Speedwell collaborative heart disease studies. J Epidemiol Community Health. 38:259–62.

Centraal Bureau voor de Statistiek (2012). Milieuhinder, milieugedrag en milieubesef van personen [Environmental nuisance, environmental behaviour and environmental awareness of indivuals] [in Dutch]. The Hague: Centraal Bureau voor de Statistiek (http://statline.cbs.nl/Statweb/publication/?VW=T&DM=SLNL&PA=03783&D1=18-26&D2=0&D3=a&HD=161128-0938&HDR=T&STB=G1,G2, accessed 27 November 2016).

Champelovier P, Cremezi-Charlet C, Lambert J (2003). Evaluation de la gêne due à l'exposition combinée aux bruits routier et ferroviaire [Assessement of annoyance from combined exposure to road and rail traffic noises] (Research Report 242). Lyon: Institut National de Recherche sur les Transports et leur Sécurité.

Chang TY, Beelen R, Li SF, Chen TI, Lin YJ, Bao BY et al. (2014). Road traffic noise frequency and prevalent hypertension in Taichung, Taiwan: a cross-sectional study. Environ Health. 13(1):37.

Chang TY, Liu CS, Bao BY, Li SF, Chen TI, Lin YJ (2011). Characterization of road traffic noise exposure and prevalence of hypertension in central Taiwan. Sci Total Environ. 409(6):1053–7.

Clark C, Crombie R, Head J, van Kamp I, van Kempen E, Stansfeld SA (2012). Does traffic-related air pollution explain associations of aircraft and road traffic noise exposure on children's health and cognition? A secondary analysis of the United Kingdom sample from the RANCH project. Am J Epidemiol. 176:327–37.

Clark C, Head J, Stansfeld SA (2013). Longitudinal effects of aircraft noise exposure on children's health and cognition: a six-year follow-up of the United Kingdom RANCH cohort. J Environ Psychol. 35:1–9.

Clark C, Martin R, van Kempen E, Alfred T, Head J, Davies HW et al. (2006). Exposure-effect relations between aircraft and road traffic noise exposure at school and reading comprehension – the RANCH project. Am J Epidemiol. 163:27–37.

Clark C, Paunovic K (2018). WHO environmental noise guidelines for the European Region: a systematic review on environmental noise and cognition. Int J Environ Res Public Health. 15(2). pii: E285 (http://www.mdpi.com/1660-4601/15/2/285/htm, accessed 27 June 2018).

Clark C, Paunovic K (in press). WHO Environmental noise guidelines for the European Region: a systematic review on environmental noise and quality of life, wellbeing and mental health. Int J Environ Res Public Health.

Cohen S, Glass DC, Singer JE (1973). Apartment noise, auditory discrimination, and reading ability in children. J Exp Soc Psychol. 9(5):407–22.

Correia AW, Peters JL, Levy JI, Melly S, Dominici F (2013). Residential exposure to aircraft noise and hospital admissions for cardiovascular diseases: multi-airport retrospective study. BMJ. 347:f5561.

Council of Canadian Academies (2015). Understanding the evidence: wind turbine noise. Ottawa: Council of Canadian Academies (http://www.scienceadvice.ca/en/assessments/completed/wind-turbine-noise.aspx, accessed 6 July 2018).

CSES, Accon, AECOM (2016). Evaluation of Directive 2002/49/EC relating to the assessment and management of environmental noise. Luxembourg: Publications Office of the European Union (https://publications.europa.eu/en/publication-detail/-/publication/7febde6d-9a89-11e6-9bca-01aa75ed71a1/language-en, accessed 10 July 2018).

de Kluizenaar Y, Gansevoort RT, Jong PE de, Miedema HME (2007a). Cardiovascular effects of road traffic noise with adjustment for air pollution. In: Proceedings. 36th International Congress and Exhibition on Noise Control Engineering 2007 (INTER-NOISE 2007), Istanbul, Turkey, 28–31 August 2007. Istanbul: Turkish Acoustical Society.

de Kluizenaar Y, Gansevoort RT, Miedema HM, Jong PE de (2007b). Hypertension and road traffic noise exposure. Occup Environ Med. 49(5):484–92.

de Kluizenaar Y, Janssen SA, Vos H, Salomons EM, Zhou H, van den Berg F (2013). Road traffic noise and annoyance: a quantification of the effect of quiet side exposure at dwellings. Int J Environ Res Public Health. 10(6):2258–70.

de Kluizenaar Y, Salomons EM, Janssen SA, van Lenthe FJ, Vos H, Zhou H et al. (2011). Urban road traffic noise and annoyance: the effect of a quiet facade. J Acoust Soc Am. 130(4):1936–42.

Dell SM, Holmes AE (2012). The effect of a hearing conservation program on adolescents' attitudes towards noise. Noise Health. 14(56):39–44.

Dratva J, Phuleria HC, Foraster M, Gaspoz JM, Keidel D, Kunzli N et al. (2012). Transportation noise and blood pressure in a population-based sample of adults. Environ Health Perspect. 120(1):50–5.

Eagan ME, Anderson G, Nicholas B, Horonjeff R, Tivnan T (2004). Relation between aircraft noise reduction in schools and standardized test scores. In: Proceedings. 9th International Congress on Noise as a Public Health Problem 2008 (ICBEN 2008), Foxwoods, USA, 21–25 July 2008. Zurich: International Commission on Biological Effects of Noise.

EASA, EEA, Eurocontrol (2016). European Aviation Environmental Report 2016. Cologne: European Aviation Safety Agency (https://ec.europa.eu/transport/sites/transport/files/european-aviation-environmental-report-2016-72dpi.pdf, accessed 24 January 2018).

EC (1993). Towards sustainability: a European Community programme of policy and action in relation to the environment and sustainable development. OJ C 138/10, 17.5.93 (http://ec.europa.eu/environment/archives/action-programme/5th.htm, accessed 27 November 2016).

EC (1996). Future noise policy: European Commission Green Paper. Luxembourg: Office for Official Publications of the European Communities (COM(96) 540 final; https://publications.europa.eu/en/publication-detail/-/publication/8d243fb5-ec92-4eee-aac0-0ab194b9d4f3/language-en, accessed 28 November 2016).

EC (2000). Position paper on EU noise indicators. Luxembourg: Office for Official Publications of the European Communities (https://publications.europa.eu/en/publication-detail/-/publication/10d75ba4-7279-4df2-aa50-3ed7fdf656a8/language-en, accessed 27 November 2016).

EC (2002a). Directive 2002/49/EC of the European Parliament and of the Council of 25 June 2002 relating to the assessment and management of environmental noise. OJ L 189, 18.7.2002:12–25 (https://eur-lex.europa.eu/eli/dir/2002/49/oj, accessed 13 December 2016).

EC (2002b). Decision No 1600/2002/EC of the European Parliament and of the Council of 22 July 2002 laying down the Sixth Community Environment Action Programme. OJ L 242, 6th EAP, 1–15 (http://eur-lex.europa.eu/legal-content/EN/TXT/PDF/?uri=CELEX:32002D1600&from=EN, accessed 28 November 2016).

EC (2003). Directive 2003/10/EC of the European Parliament and of the Council of 6 February 2003 on the minimum health and safety requirements regarding the exposure of workers to the risks arising from physical agents (noise) (Seventeenth individual Directive within the meaning of Article 16(1) of Directive 89/391/EEC). OJ L 42, 15.2.2003:38–44 (https://eur-lex.europa.eu/legal-content/en/ALL/?uri=CELEX%3A32003L0010, accessed 24 January 2018).

EC (2008a). Attitudes of European citizens towards the environment. Luxembourg: Office for Official Publications of the European Communities (Special Eurobarometer 295; http://ec.europa.eu/environment/eurobarometers_en.htm, accessed 28 November 2016).

EC (2008b). Potential health risks of exposure to noise from personal music players and mobile phones including a music playing function. Luxembourg: Office for Official Publications of the European Communities (http://ec.europa.eu/health/scientific_committees/emerging/opinions/scenihr_opinions_en.htm, accessed 28 November 2016).

EC (2010). Electromagnetic Fields. Luxembourg: Publications Office of the European Union (Special Eurobarometer 347; http://ec.europa.eu/commfrontoffice/publicopinion/archives/eb_special_359_340_en.htm, accessed 27 November 2016).

EC (2014). Decision No 1386/2013/EU of the European Parliament and of the Council of 20 November 2013 on a General Union Environment Action Programme to 2020 “Living well, within the limits of our planet”. OJ L 354, 28.12.2013:171–200 (https://eur-lex.europa.eu/legal-content/EN/TXT/?uri=CELEX:32013D1386, accessed 28 November 2016).

EC (2014b). Attitudes of European citizens towards the environment. Luxembourg: Publications Office of the European Union (Special Eurobarometer 416; http://ec.europa.eu/environment/eurobarometers_en.htm, accessed 28 November 2016).

EC (2015). Commission Directive (EU) 2015/996 of 19 May 2015 establishing common noise assessment methods according to Directive 2002/49/EC of the European Parliament and of the Council. OJ L 168/1, 1.7.2015: 1–823 (https://eur-lex.europa.eu/legal-content/EN/TXT/?uri=OJ:JOL_2015_168_R_0001, accessed 28 November 2016).

EC (2016a). Links between noise and air pollution and socioeconomic status. Luxembourg: Publications Office of the European Union (Science for Environmenta Policy In-depth Report 13; http://ec.europa.eu/science-environment-policy, accessed 24 January 2018).

EC (2016b). EU reference scenario 2016 — Energy, transport and GHG emissions: trends to 2050. Luxembourg: Publications Office of the European Union (https://publications.europa.eu/en/publication-detail/-/publication/aed45f8e-63e3-47fb-9440-a0a14370f243/language-en, accessed 4 July 2018).

EEA (2010). Good practice guide on noise exposure and potential health effects. Copenhagen: European Environment Agency (Technical report No 11/2010; http://www.eea.europa.eu/publications/good-practice-guide-on-noise, accessed 27 November 2016).

EEA (2014). Noise in Europe 2014. Copenhagen: European Environment Agency (EEA Report No 10/2014; http://www.eea.europa.eu/publications/noise-in-europe-2014, accessed 28 November 2016).

EEA (2016a). Transitions towards a more sustainable mobility system. TERM 2016: Transport indicators tracking progress towards environmental targets in Europe. Luxembourg: Publications Office of the European Union (EEA Report No 34/2016; https://publications.europa.eu/en/publication-detail/-/publication/c276880f-9c1a-11e7-b92d-01aa75ed71a1/language-en, accessed 4 July 2018).

EEA (2016b). Environmental indicator report 2016. Luxembourg: Publications Office of the European Union (EEA Report No 30/2016; https://www.eea.europa.eu/publications/environmental-indicator-report-2016, accessed 15 March 2017).

EEA (2017a). Managing exposure to noise in Europe. Copenhagen: European Environment Agency (Briefing No 1/2017; https://www.eea.europa.eu/publications/managing-exposure-to-noise-in-europe/, accessed 24 January 2018).

EEA (2017b). TERM 12 — passenger transport volume and modal split. In: European Environment Agency: Indicators [website]. Copenhagen: European Environment Agency (https://www.eea.europa.eu/data-and-maps/indicators/passenger-transport-demand-version-2/assessment-9, accessed 30 January 2018).

EEA (2018). Noise Observation and Information Service for Europe [website]. Copenhagen: European Environment Agency (http://noise.eionet.europa.eu/, accessed 28 November 2016).

Elmenhorst EM, Pennig S, Rolny V, Quehl J, Mueller U, Maaß H et al. (2012). Examining nocturnal railway noise and aircraft noise in the field sleep, psychomotor performance, and annoyance. Sci Total Environ. 424:48–56.

Eriksson C, Bluhm G, Hilding A, Ostenson CG, Pershagen G (2010). Aircraft noise and incidence of hypertension: gender specific effects. Environ Res. 110(8):764–72.

Eriksson C, Hilding A, Pyko A, Bluhm G, Pershagen G, Östenson CG (2014). Long-term aircraft noise exposure and body mass index, waist circumference, and type 2 diabetes: a prospective study. Environ Health Perspect. 122:687–94.

Eriksson C, Nilsson ME, Willers SM, Gidhagen L, Bellander T, Pershagen G (2012). Traffic noise and cardiovascular health in Sweden: the roadside study. Noise Health. 14(59):140–7.

Eriksson C, Pershagen G, Nilsson M (2018). Biological mechanisms related to cardiovascular and metabolic effects by environmental noise. Copenhagen: WHO Regional Office for Europe (http://www.euro.who.int/en/health-topics/environment-and-health/noise/publications/2018/biological-mechanisms-related-to-cardiovascular-and-metabolic-effects-by-environmental-noise, accessed 8 August 2018).

Eriksson C, Rosenlund M, Pershagen G, Hilding A, Ostenson CG, Bluhm G (2007). Aircraft noise and incidence of hypertension. Epidemiology. 18(6):716–21.

Eurofound (2017). European Quality of Life Survey 2016: quality of life, quality of public services, and quality of society. Luxembourg: Publications Office of the European Union.

European Centre for Health Policy (1999). Health impact assessment: main concepts and suggested approach. Brussels: WHO Regional Office for Europe (Gothenburg consensus paper; http://www.healthedpartners.org/ceu/hia/hia01/01_02_gothenburg_paper_on_hia_1999.pdf).

Eurostat (2016). Urban Europe—Statistics on cities, towns and suburbs. Luxembourg: Eurostat (http://ec.europa.eu/eurostat/statistics-explained/index.php/Urban_Europe_%E2%80%94_statistics_on_cities,_towns_and_suburbs, accessed 13 March 2017).

Evans G, Maxwell L (1997). Chronic noise exposure and reading deficits: The mediating effects of language acquisition. Environ Behav. 29:638–56.

Evrard AS, Bouaoun L, Champelovier P, Lambert J, Laumon B (2015). Does exposure to aircraft noise increase the mortality from cardiovascular disease in the population living in the vicinity of airports? Results of an ecological study in France. Noise Health. 17:328–36.

Evrard AS, Khati I, Champelovier P, Lambert J, Laumon B (2013). Cardiovascular effects of aircraft noise near Paris-Charles de Gaulle airport: results from the pilot study of the DEBATS research program. In: Proceedings. 42nd International Congress and Exposition on Noise Control Engineering 2013 (INTER-NOISE 2013), Innsbruck, Austria, 15–18 September 2013. Innsbruck: Austrian Noise Abatement Association.

Feder K, Marro L, Keith SE, Michaud DS (2013). Audiometric thresholds and portable digital audio player user listening habits. Int J Audiol. 52(9):606–16.

FICAN (2007). Findings of the FICAN pilot study on the relationship between aircraft noise reduction and changes in standardised test scores. Washington DC: Federal Interagency Committee on Aviation Noise.

Fidell S, Silvati L, Haboly E (2002). Social survey of community response to a step change in aircraft noise exposure. J Acoust Soc Am. 111(1 Pt 1):200–9.

Floud S, Blangiardo M, Clark C, Hoogh K de, Babisch W, Houthuijs D, et al. (2013a). Exposure to aircraft and road traffic noise and associations with heart disease and stroke in six European countries: a cross-sectional study. Environ Health. 12:89.

Floud S, Blangiardo M, Clark C, Hoogh K de, Babisch W, Houthuijs D, et al. (2013b). Heart disease and stroke in relation to aircraft noise and road traffic noise – The HYENA study. In: Proceedings. 42nd International Congress and Exposition on Noise Control Engineering 2013 (INTER-NOISE 2013), Innsbruck, Austria, 15–18 September 2013. Innsbruck: Austrian Noise Abatement Association.

Floud S, Vigna-Taglianti F, Hansell A, Blangiardo M, Houthuijs D, Breugelmans O et al. (2011). Medication use in relation to noise from aircraft and road traffic in six European countries: results of the HYENA study. Occup Environ Med. 68:518–24.

Foraster M, Basagaña X, Aguilera I, Agis D, Bouso L, Phuleria H et al. (2012). Transportation noise (in particular railway noise) and blood pressure in REGICOR compared to SAPALDIA. In: Proceedings. 41st International Congress and Exposition on Noise Control Engineering 2012 (INTER-NOISE 2012), New York, USA, 19–22 August 2012. Washington DC: Institute of Noise Control Engineering of the USA.

Foraster M, Basagaña X, Aguilera I, Rivera M, Agis D, Bouso L et al. (2011). Cross-sectional association between road traffic noise and hypertension in a population-based sample in Girona, Spain (REGICOR-AIR project). In: Proceedings. 10th International Congress on Noise as a Public Health Problem 2011 (ICBEN 2011), London, United Kingdom, 24–28 July 2011. London: Institute of Acoustics.

Foraster M, Basagaña X, Aguilera I, Rivera M, Agis D, Bouso L et al. (2013). Disentangling the effects of traffic-related noise and air pollution on blood pressure: Indoor noise levels and protections. In: Proceedings. 42nd International Congress and Exposition on Noise Control Engineering 2013 (INTER-NOISE 2013), Innsbruck, Austria, 15–18 September 2013. Innsbruck: Austrian Noise Abatement Association.

Foraster M, Basagaña X, Aguilera I, Rivera M, Agis D, Bouso L et al. (2014a). Association of long-term exposure to traffic-related air pollution with blood pressure and hypertension in an adult population-based cohort in Spain (the REGICOR study). Environ Health Perspect. 122(4):404–11.

Foraster M, Kunzli N, Aguilera I, Rivera M, Agis D, Vila J et al. (2014b). High blood pressure and long-term exposure to indoor noise and air pollution from road traffic. Environ Health Perspect. 122(11):1193–200.

Frei P, Mohler E, Roeoesli M (2014). Effect of nocturnal road traffic noise exposure and annoyance on objective and subjective sleep quality. Int J Hyg Environ Health. 217(2–3):188–95.

Fuks K, Moebus S, Hertel S, Viehmann A, Nonnemacher M, Dragano N et al. (2011). Long-term urban particulate air pollution, traffic noise, and arterial blood pressure. Environ Health Perspect. 119(12):1706–11.

Gan WQ, Davies HW, Koehoorn M, Brauer M (2012). Association of long-term exposure to community noise and traffic-related air pollution with coronary heart disease mortality. Am J Epidemiol. 175(9):898–906.

Garcia SL, Smith KJ, Palmer C. (2018). Cost–effectiveness analysis of a military hearing conservation program. Mil Med. doi: 10.1093/milmed/usx112.

Gelderblom FB, Gjestland TT, Granoien ILN, Taraldsen G (2014). The impact of civil versus military aircraft noise on noise annoyance. In: Proceedings. 43rd International Congress on Noise Control Engineering 2014 (INTER-NOISE 2014), Melbourne, Australia, 16–19 November 2014. Melbourne: Australian Acoustical Society.

Gidloef-Gunnarsson A, Oegren M, Jerson T, Oehrstroem E (2012). Railway noise annoyance and the importance of number of trains, ground vibration, and building situational factors. Noise Health. 14(59):190–201.

Gidloef-Gunnarsson A, Oehrstroem E (2010). Attractive "quiet" courtyards: a potential modifier of urban residents' responses to road traffic noise? Int J Environ Res Public Health. 7(9):3359–75.

Gidloef-Gunnarsson A, Oehrstroem E (2007). Noise and well-being in urban residential environments: the potential role of perceived availability to nearby green areas. Landsc Urban Plan. 83(2–3):115–26.

Gidloef-Gunnarsson A, Oehrstroem E, Kihlman T (2010). A full-scale intervention example of the "quiet side concept" in a residential area exposed to road traffic noise: effects on the perceived sound environment and general noise annoyance. In: Proceedings. 39th International Congress on Noise Control Engineering 2010 (INTER-NOISE 2010), Lisbon, Portugal, 13–16 June 2010. Lisbon: Sociedade Portuguesa de Acustica.

Gidloef-Gunnarsson A, Svensson H, Oehrstroem E (2013). Noise reduction by traffic diversion and a tunnel construction: effects on health and well-being after opening of the Southern Link. In: Proceedings. 42nd International Congress and Exposition on Noise Control Engineering 2013 (INTER-NOISE 2013), Innsbruck, Austria, 15–18 September 2013. Innsbruck: Austrian Noise Abatement Association.

Gilles A, Van de Heyning P (2014). Effectiveness of a preventive campaign for noise-induced hearing damage in adolescents. Int J Pediatr Otorhinolaryngol. 78(4):604–9.

Grazuleviciene R, Lekaviciute J, Mozgeris G, Merkevicius S, Deikus J (2004). Traffic noise emissions and myocardial infarction risk. Pol J Enviro Stud. 13:737–41.

Green KB, Pasternack BS, Shore RE (1982). Effects of aircraft noise on reading ability of school-age children. Arch Environ Health. 37(1): 24–31.

Griefahn B, Schuemer-Kohrs A, Schuemer R, Mohler U, Mehnert P (2000). Physiological, subjective, and behavioural responses to noise from rail and road traffic. Noise Health. 3(9):59–71.

Griffiths ID, Raw GJ (1987). Community and individual response to changes in traffic noise exposure. Dev Toxicol Environ Sci. 15:333–43.

Griffiths ID, Raw GJ (1989). Adaptation to changes in traffic noise exposure. J Sound Vib. 132(2):331–6.

Guski R (1999). Personal and social variables as co-determinants of noise annoyance. Noise Health. 3:45–56.

Guski R, Schreckenberg D, Schuemer R (2017). WHO environmental noise guidelines for the European Region: a systematic review on environmental noise and annoyance. Int J Environ Res Public Health. 14(12). pii:1539 (http://www.mdpi.com/1660-4601/14/12/1539/htm, accessed 27 June 2018).

Guyatt GH, Oxman AD, Vist GE, Kunz R, Falck-Ytter Y, Alonso-Coello P et al. (2008). GRADE: an emerging consensus on rating quality of evidence and strength of recommendations. BMJ. 336(7650):924–6.

Hänninen O, Knol AB, Jantunen M, Lim TA, Conrad A, Rappolder M et al. (2014). Environmental burden of disease in Europe: assessing nine risk factors in six countries. Environ Health Perspect. 122(5):439–46.

Haines MM, Stansfeld SA, Brentnall S, Head J, Berry B, Jiggins M et al. (2001a). The West London Schools Study: the effects of chronic aircraft noise exposure on child health. Psychol Med. 31:1385–96.

Haines MM, Stansfeld SA, Job RF, Berglund B, Head J (2001b). Chronic aircraft noise exposure, stress responses, mental health and cognitive performance in school children. Psychol Med. 31:265–77.

Haines MM, Stansfeld SA, Job RF, Berglund B, Head J (2001c). A follow-up study of effects of chronic aircraft noise exposure on child stress responses and cognition. Int J Epidemiol. 30:839–45.

Halonen JI, Vahtera J, Stansfeld S, Yli-Tuomi T, Salo P, Pentti J et al. (2012). Associations between nighttime traffic noise and sleep: the Finnish public sector study. Environ Health Perspect. 120(10): 1391–6.

Hansell AL, Blangiardo M, Fortunato L, Floud S, Hoogh K de, Fecht D et al. (2013). Aircraft noise and cardiovascular disease near Heathrow airport in London: small area study. BMJ. 347:f5432.

Heimann D, de Franceschi M, Emeis S, Lercher P, Seibert P, editors (2007). Air pollution, traffic noise and related health effects in the Alpine space: a guide for authorities and consulters. ALPNAP comprehensive report. Trento: Universita degli Studi di Trento, Dipartimento di Ingegneria Civile e Ambientale.

Hense HW, Herbold M, Honig K (1989). Risikofaktor Lärm in Felderhebungen zu Herz-Kreislauferkrankungen [Noise as a risk factor in field studies on cardiovascular disease]. Berlin: Umweltforschungsplan des Bundesministers für Umwelt, Naturschutz und Reaktorsicherheit.

Herbold M, Hense HW, Keil U (1989). Effects of road traffic noise on prevalence of hypertension in men: results of the Lübeck blood pressure study. Soz Praeventivmed. 34:19–23.

Héroux ME, Verbeek J (2018a). Results from the search for available systematic reviews and meta-analyses on environmental noise. Copenhagen: WHO Regional Office for Europe (http://www.euro.who.int/en/health-topics/environment-and-health/noise/publications/2018/results-search-for-available-systematic-reviews-environmental-noise, accessed 8 August 2018).

Héroux ME, Verbeek J (2018b). Methodology for systematic evidence reviews for the WHO environmental noise guidelines for the European Region. Copenhagen: WHO Regional Office for Europe (http://www.euro.who.int/en/health-topics/environment-and-health/noise/publications/2018/methodology-systematic-evidence-reviews-who-environmental-guidelines-for-the-european-region, accessed 8 August 2018).

Hohmann B (2015). Assessment of impulse noise regarding harmfulness to hearing. In: Proceedings. 10th European Conference on Noise Control 2015 (EURONOISE 2015), Maastricht, Netherlands, 31 May–3 June 2015. Maastricht: Institute of Acoustics.

Hong J, Kim J, Lim C, Kim K, Lee S (2010). The effects of long-term exposure to railway and road traffic noise on subjective sleep disturbance. J Acoust Soc Am. 128(5):2829–35.

Hong J, Lim C, Kim J, Lee S (2006). Assessment of sleep disturbance on night-time railway noise from the field survey. In: Proceedings. 35th International Congress and Exposition on Noise Control Engineering 2006 (INTER-NOISE 2006), Honolulu, USA, 3–6 December 2006. Washington DC: Institute of Noise Control Engineering of the USA.

Houthuijs DJM, van Wiechen CMAG (2006). Monitoring of health and perceptions around Schiphol Airport [in Dutch]. Bilthoven: National Institute for Public Health and the Environment.

Huang X, Lin J, Demner-Fushman D (2006). Evaluation of PICO as a knowledge representation for clinical questions. AMIA Annu Symp Proc. 359–63.

Huss A, Spoerri A, Egger M, Roeoesli M, for the Swiss National Cohort Study Group (2010). Aircraft noise, air pollution, and mortality from myocardial infarction. Epidemiology. 21(6):829–36.

Hygge S, Evans GW, Bullinger M (2002). A prospective study of some effects of aircraft noise on cognitive performance in schoolchildren. Psychol Sci. 13(5):469–74.

ISO (2013). ISO 1999:2013. Acoustics – estimation of noise-induced hearing loss. Geneva: International Organization for Standardization (https://www.iso.org/standard/45103.html, accessed 28 November 2016).

ISO (2016). ISO 1996-1:2016: Acoustics – Description, measurement and assessment of environmental noise – Part 1: basic quantities and assessment. Geneva: International Organization for Standardization (https://www.iso.org/standard/59765.html, accessed 15 March 2017).

Ising H, Ising M (2002). Chronic cortisol increases in the first half of the night caused by road traffic noise. Noise Health. 4(16):13–21.

Janssen SA, Vos H (2009). A comparison of recent surveys to aircraft noise exposure–response relationships. Delft: TNO (Report No: 034-DTM-2009-01799).

Janssen SA, Vos H, Eisses AR, Pedersen E (2011). A comparison between exposure–response relationships for wind turbine annoyance and annoyance due to other noise sources. J Acoust Soc Am. 130(6):3746–53.

Jarup L, Babisch W, Houthuijs D, Pershagen G, Katsouyannie K, Cadum E et al. (2008). Hypertension and exposure to noise near airports: the HYENA study. Environ Health Perspect. 116(3):329–33.

Jarup L, Dudley ML, Babisch W, Houthuijs D, Swart W, Pershagen G et al. (2005). Hypertension and exposure to noise near airports (HYENA): study design and noise exposure assessment. Environ Health Perspect. 113(11):1473–8.

Karpati A, Galea S, Awerbuch T, Levins R (2002). Variability and vulnerability at the ecological level: implications for understanding the social determinants of health. Am J Public Health. 92(11):1768–72.

Kastka J (1981). Effects of traffic-silencing measures on noise nuisance. Zeitschrift fur Larmbekampfung. 28(1):25–30.

Kastka J, Buchta E, Ritterstaedt U, Paulsen R, Mau U (1995). The long-term effect of noise protection barriers on the annoyance response of residents. J Sound Vib. 184(5):823–52.

Klatte M, Bergström K, Spilski M, Mayerl J, Meis M (2014). NORAH Noise-related annoyance, cognition, and health: Wirkungen chronischer Fluglärmbelastung auf kognitive Leistungen und Lebensqualität bei Grundschulkindern [Effects of long-term aircraft exposure on the cognitive performance of elementary school children]. Kaiserslautern: Technische Universität Kaiserslautern.

Knipschild P, Meijer H, Salle H (1984). Transportation noise, psychological issues and hypertension. Results of a survey of Amsterdam residents [in Dutch]. Tijdsc Soc Gezondheid. 62:758–65.

Knopper L, Ollson C (2011). Health effects and wind turbines: a review of the literature. Environ Health. 10:78–87

Kotowski MR, Smith SW, Johnstone PM, Pritt E (2011). Using the Extended Parallel Process Model to create and evaluate the effectiveness of brochures to reduce the risk for noise-induced hearing loss in college students. Noise Health. 13(53):261–71.

Kuwano S, Yano T, Kageyama T, Sueoka S, Tachibanae H (2014). Social survey on wind turbine noise in Japan. Noise Control Eng J. 62(6):503–20.

Lam KC, Au WH (2008). Human annoyance response to a step change in noise exposure following the opening of a new railway extension in Hong Kong. In: Proceedings. 9th International Congress on Noise as a Public Health Problem 2008 (ICBEN 2008), Foxwoods, USA, 21–25 July 2008. Zurich: International Commission on Biological Effects of Noise.

Lambert J, Philipps-Bertin C (2008). Perception and attitudes to transportation noise in France: a national survey. In: Proceedings. 9th International Congress on Noise as a Public Health Problem 2008 (ICBEN 2008), Foxwoods, USA, 21–25 July 2008. Zurich: International Commission on Biological Effects of Noise.

Langdon FJ, Griffiths ID (1982). Subjective effects of traffic noise exposure. II: Comparisons of noise indices, response scales, and the effects of changes in noise levels. J Sound Vib. 83(2):171–80.

Lekaviciute J (2007). Traffic noise in Kaunas city and its influence on myocardial infarction risk [PhD thesis]. Kaunus: Vytautas Magnus University.

Lercher P, Botteldooren D, de Greve B, Dekoninck L, Ruedisser J (2007). The effects of noise from combined traffic sources on annoyance: the case of interactions between rail and road noise. In: Proceedings. 36th International Congress and Exhibition on Noise Control Engineering 2007 (INTER-NOISE 2007), Istanbul, Turkey, 28–31 August 2007. Istanbul: Turkish Acoustical Society.

Lercher P, Botteldooren D, Widmann U, Uhrner U, Kammeringer E (2011). Cardiovascular effects of environmental noise: research in Austria. Noise Health. 13(52):234–50.

Lercher P, Brink M, Rudisser J, et al. (2010). The effects of railway noise on sleep medication intake: results from the ALPNAP-study. Noise Health. 12(47):110–19.

Lercher P, Greve B de, Botteldooren D, Dekoninck L, Oettl D, Uhrner U et al. (2008). Health effects and major co-determinants associated with rail and road noise exposure along transalpine traffic corridors. In: Proceedings. 9th International Congress on Noise as a Public Health Problem 2008 (ICBEN 2008), Foxwoods, USA, 21–25 July 2008. Zurich: International Commission on Biological Effects of Noise.

Lercher P, Eisenmann A, Dekonick L, Botteldooren D (2013). The relation between disturbed sleep in children and traffic noise exposure in alpine valleys. In: Proceedings. 42nd International Congress and Exposition on Noise Control Engineering 2013 (INTER-NOISE 2013), Innsbruck, Austria, 15–18 September 2013. Innsbruck: Austrian Noise Abatement Association.

Lercher P, Evans GW, Meis M (2003). Ambient noise and cognitive processes among primary school children. Environ Behav. 35:725–35.

Levesque B, Fiset R, Isabelle L, Gauvin D, Baril J, Larocque R et al. (2010). Exposure of high school students to noise from personal music players in Québec City, Canada. Int J Child Adolescent Health. 3(30):413–20.

Lopez AD, Mathers CD, Ezzati M, Jamison DT, Murray CJ, editors (2006). Global burden of disease and risk factors. Washington DC: World Bank and New York: Oxford University Press.

Liu C, Fuertes E, Tiesler CM, Birk M, Babisch W, Bauer CP et al. (2014). The associations between traffic-related air pollution and noise with blood pressure in children: results from the GINIplus and LISAplus studies. Int J Hyg Environ Health. 217(4–5):499–505.

Liu C, Fuertes E, Tiesler CM, Birk M, Babisch W, Bauer CP et al. (2013). The association between road traffic noise exposure and blood pressure among children in Germany: the GINIplus and LISAplus studies. Noise Health. 15(64):165–72.

Locher B, Piquerez A, Habermacher M, Ragettli M, Röösli M, Brink M et al. (2018). Differences between outdoor and indoor sound levels for open, tilted, and closed windows. Int J Environ Res Public Health. 15(1): 149.

Lukas JS, DuPreeRB, Swing JW (1981). Report of a study on the effects of freeway noise on academic achievement of elementary school children, and a recommendation for a criterion level for a school noise abatement program. Sacramento, CA: California Department of Health Services.

Maassen M, Babisch W, Bachmann K D, Ising H, Lehnert G, Plath P et al. (2001). Ear damage caused by leisure noise. Noise Health. 4:1–16.

Martin WH, Griest SE, Sobel JL, Howarth LC (2013). Randomized trial of four noise-induced hearing loss and tinnitus prevention interventions for children. Int J Audiol. 52(Suppl 1):S41–9.

Maschke C (2003). Epidemiological research on stress caused by traffic noise and its effects on high blood pressure and psychic disturbances. In: Proceedings. 8th International Congress on Noise as a Public Health Problem 2003 (ICBEN 2003), Rotterdam, Netherlands, 29 June – 3 July 2003. Zurich: International Commission on Biological Effects of Noise.

Maschke C, Hecht K (2005). Pathogenesis mechanism by noise-induced clinical pictures – Lessons from the Spandau Health-Survey. Umweltmedizin in Forschung und Praxis. 10(2):77–88.

Maschke C, Wolf U, Leitmann T (2003). Epidemiological examinations of the influence of noise stress on the immune system and the emergence of arteriosclerosis [in German]. Berlin: Umweltbundesambt.

Mathers CD, Bernard C, Iburg KM, Inoue M, Fat DM, Shibuya K et al. (2003). Global burden of disease in 2002: data sources, methods and results. Geneva: World Health Organization (Global Programme on Evidence for Health Policy Discussion Paper No. 54; http://www.portal.pmnch.org/healthinfo/global_burden_disease/data_sources_methods/en/index1.html, accessed 2 July 2018).

Mathers C, Vos T, Stevenson C (1999). The burden of disease and injury in Australia. Canberra: Australian Institute of Health and Welfare cat. no. PHE 17. (https://www.aihw.gov.au/reports/burden-of-disease/the-burden-of-disease-injury-in-australia-1996/contents/table-of-contents, accessed 28 November 2016).

Matheson M, Clark C, Martin R, van Kempen E, Haines M, Barrio IL et al. (2010). The effects of road traffic and aircraft noise exposure on children's episodic memory: the RANCH project. Noise Health. 12:244–54.

Matsui T (2013). Psychosomatic disorder due to aircraft noise and its causal pathway. In: Proceedings. 42nd International Congress and Exposition on Noise Control Engineering 2013 (INTER-NOISE 2013), Innsbruck, Austria, 15–18 September 2013. Innsbruck: Austrian Noise Abatement Association.

Matsui T, Stansfeld S, Haines M, Head J (2004). Children's cognition and aircraft noise exposure at home – the West London Schools Study. Noise Health. 7:49–58.

Matsui T, Uehara T, Miyakita T, Hiramatsu K, Osada Y, Yamamoto T (2001). Association between blood pressure and aircraft noise exposure around Kadena airfield in Okinawa. In: Proceedings. 30th International Congress and Exhibition on Noise Control Engineering 2001 (INTER-NOISE 2001), The Hague, Netherlands, 27–30 August 2001. The Hague: Nederlands Akoestisch Genootschap.

Matsui T, Uehara T, Miyakita T, Hiramatsu K, Osada Y, Yamamoto T (2004). The Okinawa study: effects of chronic aircraft noise on blood pressure and some other psychological indices. J Sound Vib. 277(3):469–70.

McCunney R J, Mundt KA, Colby WD, Dobie R, Kaliski K, Blais M (2014). Wind turbines and health: a critical review of the scientific literature. J Occup Environ Med. 56(11):e108–30.

Medizinische Universitaet Innsbruck (2008). Galleria di Base del Brennero – Brenner Baistunnel – Sozioökonomie (public health) – Zusammenfassender Bericht [Social economics (public health) – final report]. Innsbruck: Medizinische Universität Innsbruck.

Michaud D (2015). Self-reported and objectively measured outcomes assessed in the Health Canada Wind Turbine Noise and Health Study: results support an increase in community annoyance. In: Proceedings. 44th International Congress and Exposition on Noise Control Engineering 2015 (INTER-NOISE 2015), San Francisco, USA, 9–12 August 2015. Washington DC: Institute of Noise Control Engineering of the USA.

Miedema HM, Oudshoorn CG (2001). Annoyance from transportation noise: relationships with exposure Metrics DNL and DENL and their CIs. Environ Health Perspect. 109:409–16.

Moehler U, Hegner A, Schuemer R, Schuemer-Kohrs A (1997). Effects of railway-noise reduction on annoyance after rail-grinding. In: Proceedings. 26th International Congress and Exposition on Noise Control Engineering (INTER-NOISE 1997), Budapest, Hungary, 25–27 August 1997. Budapest: OPAKFI.

Morgan RL, Thayer KA, Bero L, Bruce N, Falck-Ytter Y, Ghersi D et al. (2016). GRADE: Assessing the quality of evidence in environmental and occupational health. Environ Int. 2016;92-93:611–6. doi:10.1016/j.envint.2016.01.004.

Morrell S, Taylor R, Carter N, Job S, Peploe P (1998). Cross-sectional relationship between blood pressure of schoolchildren and aircraft noise. In: Proceedings. 7th International Congress on Noise as a Public Health Problem 1998 (ICBEN 1998), Sydney, Australia, 22–26 November 1998. Sydney: National Capital Printing ACT.

Morrell S, Taylor R, Carter N, Peploe P, Job S (2000). Cross-sectional and longitudinal results of a follow-up examination of child blood pressure and aircraft noise: the inner Sydney child blood pressure study. In: Proceedings. 29th International Congress on Noise Control Engineering 2000 (INTER-NOISE 2000), Nice, France, 27–31 August 2000. Paris: Societe Francaise D'acoustique.

Murray CJ (1994). Quantifying the burden of disease: the technical basis for disability-adjusted life-years. Bull World Health Organ. 72(3):429–45.

Murray CJ, Acharya AK (1997). Understanding DALYs (disability-adjusted life-years). J Health Econ. 16:703–30.

Murray CJ, Lopez AD (2013) Measuring the global burden of disease. N Engl J Med. 369(5): 448–57.

Neitzel R, Fligor B (2017). Determination of risk of noise-induced hearing loss due to recreational sound: review. Geneva: World Health Organization (http://www.who.int/pbd/deafness/Monograph_on_determination_of_risk_of_HL_due_to_exposure_to_recreational_sounds.pdf, accessed 30 January 2018).

Nguyen LT, Nguyen TL, Yano T, et al. (2015). Social surveys around Noi Bai Airport before and after the opening of a new terminal building. In: Proceedings. 44th International Congress and Exposition on Noise Control Engineering 2015 (INTER-NOISE 2015), San Francisco, USA, 9–12 August 2015. Washington DC: Institute of Noise Control Engineering of the USA.

Nguyen TL, Nguyen HQ, Yano T, Nishimura T, Sato T, Morihara T, Hashimoto Y (2012a). Comparison of models to predict annoyance from combined noise in Ho Chi Minh City and Hanoi. Appl Acoust. 73(9):952–59.

Nguyen TL, Yano T, Nguyen HQ, et al. (2010). Community response to aircraft and combined noises in Hanoi. In: Proceedings. 39th International Congress on Noise Control Engineering 2010 (INTER-NOISE 2010), Lisbon, Portugal, 13–16 June 2010. Lisbon: Sociedade Portuguesa de Acustica.

Nguyen TL, Yano T, Nguyen HQ, Nishimura T, Fukushima H, Sato T et al. (2011). Community response to aircraft noise in Ho Chi Minh City and Hanoi. Appl Acoust. 72(11):814–22.

Nguyen T, Yano T, Nguyen H, Nishimura T, Sato T, Morihara T (2012b). Community response to aircraft noise around three airports in Vietnam. In: Proceedings. Acoustics 2012 Hong Kong Conference, 13–18 May 2012. Hong Kong: Institute of Acoustics.

Nguyen TL, Yano T, Nguyen HQ, et al. (2012c). Aircraft and road traffic noise annoyance in Da Nang City, Vietnam. In: Proceedings. 41st International Congress and Exposition on Noise Control Engineering 2012 (INTER-NOISE 2012), New York, USA, 19–22 August 2012. Washington DC: Institute of Noise Control Engineering of the USA.

Nguyen TL, Yano T, Nishimura T, Sato T (2009). Social survey on community response to aircraft noise in Ho Chi Minh City. In: Proceedings. 38th International Congress and Exposition on Noise Control Engineering 2009 (INTER-NOISE 2009), Ottawa, Canada, 23–26 August 2009. Washington DC: Institute of Noise Control Engineering of the USA.

Nieuwenhuijsen MJ, Ristovska G, Dadvand P (2017). WHO environmental noise guidelines for the European Region: a systematic review on environmental noise and adverse birth outcomes. Int J Environ Res Public Health. 14(10). pii: E1252 (http://www.mdpi.com/1660-4601/14/10/1252/htm, accessed 27 June 2018).

Nilsson ME, Berglund B (2006). Noise annoyance and activity disturbance before and after the erection of a roadside noise barrier. J Acoust Soc Am. 119(4):2178–88.

Notley H, Grimwood C, Raw G, Clark C, Zepidou G, Van de Kerchhove R et al. (2014). National Noise Attitude Survey 2012 (NNAS2012): summary report. London: Department for Environment and Rural Affairs (http://randd.defra.gov.uk/Document.aspx?Document=12378_SummaryReportV1.0.pdf,

Oehrstroem E (2004). Longitudinal surveys on effects of changes in road traffic noise-annoyance, activity disturbances, and psycho-social well-being. J Acoust Soc Am. 115(2):719–29.

Oehrstroem E, Hadzibajramovic E, Holmes M, Svensson H (2006a). Effects of road traffic noise on sleep: studies on children and adults. J Environ Psychol. 26(2):116–26.

Oehrstroem E, Skanberg A (2000). Adverse health effects in relation to noise mitigation – a longitudinal study in the city of Göteborg. In: Proceedings. 29th International Congress on Noise Control Engineering 2000 (INTER-NOISE 2000), Nice, France, 27–31 August 2000. Paris: Societe Francaise D'acoustique.

Oehrstroem E, Skanberg A (2004). Longitudinal surveys on effects of road traffic noise substudy on sleep assessed by wrist actigraphs and sleep logs. J Sound Vib. 272:1097–109.

Oehrstroem E, Skanberg A, Svensson H, Gidloef-Gunnarsson A (2006b). Effects of road traffic noise and the benefit of access to quietness. J Sound Vib. 295:40–59.

Oftedal B, Krog NH, Graff-Iversen S, Haugen M, Schwarze P, Aasvang GM (2014). Traffic noise and markers of obesity: a population-based study. In: Proceedings. 11th International Congress on Noise as a Public Health Problem 2014 (ICBEN 2014), Nara, Japan, 1–5 June 2014. Tokyo: Institute of Noise Control Engineering of Japan.

Oftedal B, Nafstad P, Schwarze P, Aasvang GM (2011). Road traffic noise, air pollution and blood pressure in Oslo, Norway. In: Proceedings. 10th International Congress on Noise as a Public Health Problem 2011 (ICBEN 2011), London, United Kingdom, 24–28 July 2011. London: Institute of Acoustics.

Ohiduzzaman M, Sirin O, Kassem E, Rochat JL (2016). State-of-the-art review on sustainable design and construction of quieter pavements—Part 1: traffic noise measurement and abatement techniques. Sustainability. 8(8):742.

Omlin S, Bauer GF, Brink M. (2011). Effects of noise from non-traffic-related ambient sources on sleep: Review of the literature of 1999–2010. Noise Health. 13(53):299–309.

Ouis D (2001). Annoyance from road traffic noise: a review. J Environ Psychol. 21:101–20.

Passchier-Vermeer W, Vos H, Janssen SA, Miedema HM (2007). Sleep and traffic noise, summary report. Delft: TNO (Report No: 2007-D-R0012/A; https://www.tno.nl/en/focus-areas/circular-economy-environment/roadmaps/environment-sustainability/noise/field-study-of-sleep-and-traffic/, accessed 4 July 2018).

Passchier-Vermeer W, Vos H, Steenbekkers J, van der Ploeg F, Groothuis-Oudshoorn K (2002). Sleep disturbance and aircraft noise exposure: exposure-effect relationships. Delft: TNO (Report No: 2002.027; http://www2.vlieghinder.nl/knipsels_pmach/pdfs/0110xx_TNO_Sleep_disturbance_and_aircraft_noise_exposure_effect_rapport3.pdf, accessed 28 November 2016).

Paunovic K, Belojevic G, Jakovljevic B (2013). Blood pressure of urban school children in relation to road-traffic noise, traffic density and presence of public transport. Noise Health. 15(65):253–60.

Pawlaczyk-Luszczynska M, Dudarewicz A, Zaborowski K, Zamojska-Daniszewska M, Waszkowska M (2014). Evaluation of annoyance from the wind turbine noise: a pilot study. Int J Occup Med Environ Health. 27(3):364–88.

Pedersen E (2011). Health aspects associated with wind turbine noise: results from three field studies. Noise Control Eng J. 59(1):47–53.

Pedersen E, Larsman P (2008). The impact of visual factors on noise annoyance among people living in the vicinity of wind turbines. J Environ Psychol. 28(4):379–89.

Pedersen E, Perrson Waye K (2004). Perception and annoyance due to wind turbine noise – a dose-response relationship. J Acoust Soc Am. 116(6):3460–70.

Pedersen E, Persson Waye K (2007). Wind turbine noise, annoyance and self-reported health and well-being in different living environments. Occup Environ Med. 64(7):480–6.

Pedersen T, Le Ray G, Bendtsen H, Kragh J (2013). Community response to noise reducing road pavements. In: Proceedings. 42nd International Congress and Exposition on Noise Control Engineering 2013 (INTER-NOISE 2013), Innsbruck, Austria, 15–18 September 2013. Innsbruck: Austrian Noise Abatement Association.

Pedersen T, Le Ray G, DELTA SenseLab, Bendtsen H, Kragh J, Danish Road Directorate (2014). Community response to noise reducing road pavements. Copenhagen: Vejdirektoratet. (http://vejdirektoratet.dk/DA/viden_og_data/publikationer/sider/publikation.aspx?pubid=1182366409, accessed 28 November 2016).

Pellegrino E, Lorini C, Allodi G, Buonamici C, Garofalo G, Bonaccorsi G (2013). Music-listening habits with MP3 player in a group of adolescents: a descriptive survey. Ann Ig. 25(5):367–76.

Phan HYT, Yano T, Phan HAT, Nishimura T, Sato T, Hashimoto Y (2010). Community responses to road traffic noise in Hanoi and Ho Chi Minh City. Appl Acoust. 71(2):107–14.

Pierette M, Marquis-Favre C, Morel J, Rioux L, Vallet M, Viollon S et al. (2012). Noise annoyance from industrial and road traffic combined noises: a survey and a total annoyance model comparison. J Environ Psychol. 32(2):178–86.

Pirrera S, De Valck E, Cluydts R (2014). Field study on the impact of nocturnal road traffic noise on sleep: the importance of in- and outdoor noise assessment, the bedroom location and nighttime noise disturbances. Sci Total Environ. 500–1:84–90.

Pujol S, Levain JP, Houot H, Petit R, Berthillier M, Defrance J et al. (2014). Association between ambient noise exposure and school performance of children living in an urban area: a cross-sectional population-based study. J Urban Health. 91(2):256–71.

Pyko A, Eriksson C, Lind T, Mitkovskaya N, Wallas A, Ögren M et al. (2017). Long-term exposure to transportation noise in relation to development of obesity – a cohort study Environ Health Perspect. 125(11):117 005.

Pyko A, Eriksson C, Oftedal B, Hilding A, Östenson CG, Krog NH et al. (2015). Exposure to traffic noise and markers of obesity. Occup Environ Med. 72(8):594–601.

Quigley R, den Broeder L, Furu P, Bond A, Cave B, Bos R (2006). Health impact assessment: international best practice principles. Fargo, ND: International Association for Impact Assessment (Special Publication Series No. 5; http://www.iaia.org/best-practice.php, accessed 10 July 2018).

Regecova V, Kellerova E (1995). Effects of urban noise pollution on blood pressure and heart rate in preschool children. J Hypertens. 13(4):405–12.

Ristovska G, Gjorgjev D, Stikova E, Petrova V, Cakar MD (2009). Noise-induced sleep disturbance in adult population: cross-sectional study in Skopje urban centre. Maced J Med Sci. 2(3):255–60.

Rosenlund M, Berglind N, Pershagen G, Jarup L, Bluhm G (2001). Increased prevalence of hypertension in a population exposed to aircraft noise. Occup Environ Med. 58(12):769–73.

Sato T, Yano T (2011). Effects of airplane and helicopter noise on people living around a small airport in Sapporo, Japan. In: Proceedings. 10th International Congress on Noise as a Public Health Problem 2011 (ICBEN 2011), London, United Kingdom, 24–28 July 2011. London: Institute of Acoustics.

Sato T, Yano T, Björkman M, Rylander R (2002). Comparison of community response to road traffic noise in Japan and Sweden – Part I: outline of surveys and dose-response relationships. J Sound Vib. 250:161–7.

Sato T, Yano T, Morihara T (2004). Community response to noise from Shinkansen in comparison with ordinary railways: a survey in Kyushu, Japan. In: Proceedings. 18th International Congress on Acoustics (ICA 2004), Kyoto, Japan, 4–9 April. Kyoto: Acoustical Society of Japan.

Schäffer B, Schlittmeier SJ, Pieren R, Heutschi K, Brink M, Graf R et al. (2016). Short-term annoyance reactions to stationary and time-varying wind turbine and road traffic noise: a laboratory study. J Acoust Soc Am. 139(5):2949–63.

Schreckenberg D (2013). Exposure-response relationship for railway noise annoyance in the Middle Rhine Valley. In: Proceedings. 42nd International Congress and Exposition on Noise Control Engineering 2013 (INTER-NOISE 2013), Innsbruck, Austria, 15–18 September 2013. Innsbruck: Austrian Noise Abatement Association.

Schreckenberg D, Faulbaum F, Guski R, Ninke L, Peschel C, Spilski J et al. (2015). Wirkungen von Verkehrslärm auf die Belästigung und Lebensqualität [Effects of transportation noise on noise annoyance and quality of life]. In: Gemeinützziges Umwelthaus gGmbH, editor, NORAH (Noise related annoyance cognition and health): Verkehrslärmwirkungen im Flughafenumfeld [Effect of transportation noise in the area of an airport] (vol. 3). Kelsterbach: Umwelthaus gGmbH (https://www.norah-studie.de//en/publications.html, accessed 4 July 2018).

Schreckenberg D, Heudorf U, Eikmann T, Meis M (2009). Aircraft noise and health of residents living in the vicinity of Frankfurt airport. In: Proceedings. 8th European Conference on Noise Control 2009 (EURONOISE 2009), Edinburgh, United Kingdom, 26–28 October 2009. Edinburgh: Institute of Acoustics.

Schreckenberg D, Meis M (2007). Lärmbelästigung und Lebensqualität in der Bevölkerung am Frankfurter Flughafen [Noise annoyance and quality of life of the residents around Frankfurt Airport]. Lärmbekämpfung [Noise Abatement]. 2(6):225–33.

Schreckenberg D, Benz S, Belke C, Möhler U, Guski R (2017). The relationship between aircraft sound levels, noise annoyance and mental well-being: an analysis of moderated mediation. In: Proceedings. 12th International Congress on Noise as a Public Health Problem 2017 (ICBEN 2017), Zurich, Switzerland, 18–22 June 2017. Zurich: International Commission on Biological Effects of Noise.

Schreckenberg D, Moehler U, Liepert M, Schuemer R (2013). The impact of railway grinding on noise levels and residents' noise responses – Part II: the role of information. In: Proceedings. 42nd International Congress and Exposition on Noise Control Engineering 2013 (INTER-NOISE 2013), Innsbruck, Austria, 15–18 September 2013. Innsbruck: Austrian Noise Abatement Association.

Schuemer R, Schuemer-Kohrs A (1991). The nuisance of rail traffic noise in comparison with other sources of noise, comments on research results. Zeitschrift für Lärmbekämpfung [Magazine for Combating Noise]. 38:1–9.

Seabi J, Cockcroft K, Goldschagg P, GreylingM (2012). The impact of aircraft noise exposure on South African children's reading comprehension: the moderating effect of home language. Noise Health. 14:244–52.

Seabi J, Cockcroft K, Goldschagg P, Greyling M (2013). A prospective follow-up study of the effects of chronic aircraft noise exposure on learners' reading comprehension in South Africa. J Expo Sci Environ Epidemiol. 25(1):84–8.

Selander J, Nilsson ME, Bluhm G, Rosenlund M, Lindqvist M, Nise G et al. (2009). Long-term exposure to road traffic noise and myocardial infarction. Epidemiology. 20(2):272–9.

Shea BJ, Grimshaw JM, Wells GA, Boers M, Andersson N, Hamel C et al. (2007). Development of AMSTAR: a measurement tool to assess the methodological quality of systematic reviews. BMC Med Res Methodol. 7:10. PMID: 17302989.

Sharp B, Connor TL, McLaughlin D, Clark C, Stansfeld SA, Hervey J (2014). Assessing aircraft noise conditions affecting student learning, volume 1: final report. Washingtdon DC: Transportation Research Board of the National Academies of Sciences, Engineering, and Medicine (http://www.trb.org/Publications/Blurbs/170328.aspx, accessed 5 July 2018).

Shepherd D, Welch D, Dirks KN, McBride D (2013). Do quiet areas afford greater health related quality of life than noisy areas? Int J Environ Res Public Health. 10(4):1284–303.

Shield BM, Dockrell JE (2008). The effects of environmental and classroom noise on the academic attainments of primary schoolchildren. J Acoust Soc Am. 123:133–44.

Shimoyama K, Nguyen TL, Yano T, Morihara T (2014). Social surveys on community response to road traffic in five cities in Vietnam. In: Proceedings. In: Proceedings. 43rd International Congress on Noise Control Engineering 2014 (INTER-NOISE 2014), Melbourne, Australia, 16–19 November 2014. Melbourne: Australian Acoustical Society.

Sirin O (2016). State-of-the-art review on sustainable design and construction of quieter pavements—Part 2: factors affecting tyre-pavement noise and prediction models. Sustainability. 8(7):692.

Śliwińska-Kowalska M, Zaborowski K (2017). WHO environmental noise guidelines for the European Region: a systematic review on environmental noise and permanent hearing loss and tinnitus. Int J Environ Res Public Health. 14(10). pii: E1139 (http://www.mdpi.com/1660-4601/14/10/1139/htm, accessed 27 June 2018).

Sobotova L, Jurkovicova J, Stefanikova Z, Sevcikova L, Aghova L (2006). Community noise annoyance assessment in an urban agglomeration. Bratisl Lek Listy. 107(5):214–16.

Sörensen M, Andersen ZJ, Nordsborg RB, Jensen SS, Lillelund KG, Beelen R et al. (2012a). Road traffic noise and incident myocardial infarction: a prospective cohort study. PLoS One. 7(6):e39283.

Sörensen M, Andersen ZJ, Nordsborg RB, Tjonneland A, Raaschou-Nielsen O, Lillelund KG et al. (2012b). Road traffic noise and risk for stroke and myocardial infarction. In: Proceedings. 41st International Congress and Exposition on Noise Control Engineering 2012 (INTER-NOISE 2012), New York, USA, 19–22 August 2012. Washington DC: Institute of Noise Control Engineering of the USA.

Sörensen M, Hoffmann B, Hvidberg M, Ketzel M, Jensen SS, Andersen ZJ et al. (2012c). Long-term exposure to traffic-related air pollution associated with blood pressure and self-reported hypertension in a Danish cohort. Environ Health Perspect. 120(3):418–24.

Sörensen M, Hvidberg M, Hoffmann B, Andersen ZJ, Nordsborg RB, Lillelund KG et al. (2011). Exposure to road traffic and railway noise and associations with blood pressure and self-reported hypertension: a cohort study. Environ Health. 10(92).

Sörensen M, Luhdorf P, Ketzel M, Andersen ZJ, Tjonneland A, Overvad K, Raaschou-Nielsen O (2014). Combined effects of road traffic noise and ambient air pollution in relation to risk for stroke? Environ Res. 133:49–55.

Sörensen M, Wendelboe Nielsen O, Sajadieh A, Ketzel M, Tjonneland A, Overvad K et al. (2017). Long-Term Exposure to Road Traffic Noise and Nitrogen Dioxide and Risk of Heart Failure: A Cohort Study. Environ Health Perspect. 125(9):097021.

Stansfeld SA, Berglund B, Clark C, Lopez-Barrio I, Fischer P, Ohrstrom E, et al. (2005). Aircraft and road traffic noise and children's cognition and health: a cross-national study. Lancet. 365:1942–9.

Stansfeld SA, Haines MM, Berry B, Burr M (2009b). Reduction of road traffic noise and mental health: an intervention study. Noise Health. 11(44):169–75.

Stansfeld SA, Hygge S, Clark C, Alfred T (2010). Night-time aircraft noise exposure and children's cognitive performance. Noise Health. 12:255–62.

Sulaiman AH, Husain R, Seluakumaran K (2014). Evaluation of early hearing damage in personal listening device users using extended high-frequency audiometry and otoacoustic emissions. Eur Arch Otorhinolaryngol. 271(6):1463–70.

Sulaiman AH, Seluakumaran K, Husain R (2013). Hearing risk associated with the usage of personal listening devices among urban high school students in Malaysia. Public Health. 127(8):710–15.

Taljaard DS, Leishman NF, Eikelboom RH (2013). Personal listening devices and the prevention of noise-induced hearing loss in children: the Cheers for Ears Pilot Program. Noise Health. 15(65):261–8.

Tiesler CM, Birk M, Thiering E, Kohlbock G, Koletzko S, Bauer CP et al. (2013). Exposure to road traffic noise and children's behavioural problems and sleep disturbance: results from the GINIplus and LISAplus studies. Environ Res. 123:1–8.

Umweltbundesamt (2015). Umweltbewusstsein in Deutchland 2014: Ergebnisse einer repräsentativen Bevölkerungsumfrage [Environmental Consciousness in Germany in 2014: results of a representative survey of the population] [in German]. Berlin: Bundesministerium für Umwelt, Naturschutz, Bau und Reaktorsicherheit (https://www.umweltbundesamt.de/sites/default/files/medien/378/publikationen/umweltbewusstsein_in_deutschland_2014.pdf, accessed 24 January 2018).

Umweltbundesamt (2017). Umweltbewusstsein in Deutchland 2016: Ergebnisse einer repräsentativen Bevölkerungsumfrage [Environmental Consciousness in Germany in 2016: results of a representative survey of the population] [in German]. Berlin: Bundesministerium für Umwelt, Naturschutz, Bau und Reaktorsicherheit (https://www.umweltbundesamt.de/sites/default/files/medien/376/publikationen/umweltbewusstsein_deutschland_2016_bf.pdf, accessed 5 July 2018).

van den Berg F, Pedersen E, Bouma J, Bakker R (2008). Project WINDFARMperception. Visual and acoustic impact of wind turbine farms on residents. Groningen: University of Groningen (FP6-2005-Science-and-Society-20 Specific Support Action Project no. 044628; https://www.rug.nl/research/portal/publications/project-windfarmperception-visual-and-acoustic-impact-of-wind-turbine-farms-on-residents(b8745281-02e7-4761-bd06-86363e2be78b).html, accessed 27 November 2016).

van Kamp I, Houthuijs D, Van Wiechen C, Breugelmans O (2006). Environmental noise and cardiovascular diseases: results from a monitoring programme on aircraft noise C3 – Institute of Noise Control Engineering of the USA. In: Proceedings. 35th International Congress and Exposition on Noise Control Engineering 2006 (INTER-NOISE 2006), Honolulu, USA, 3–6 December 2006.Washington DC: Institute of Noise Control Engineering of the USA.

van Kempen E, Casas M, Pershagen G, Foraster M (2018). WHO environmental noise guidelines for the European Region: a systematic review on environmental noise and cardiovascular and metabolic effects: a summary. Int J Environ Res Public Health. 15(2). pii: E379 (http://www.mdpi.com/1660-4601/15/2/379/htm, accessed 27 June 2018).

van Kempen E, Fischer P, Janssen N, Houthuijs D, van Kamp I, Stansfeld S et al. (2012). Neurobehavioral effects of exposure to traffic-related air pollution and transportation noise in primary schoolchildren. Environ Res. 115:18–25.

van Kempen E, van Kamp I, Fischer P, Davies H, Houthuijs D, Stellato R et al. (2006). Noise exposure and children's blood pressure and heart rate: The RANCH project. Occup Environ Med. 63(9):632–9.

van Kempen E, van Kamp I, Lebret E, Lammers J, Emmen H, Stansfeld S (2010). Neurobehavioral effects of transportation noise in primary schoolchildren: a cross-sectional study. Environ Health. 9: 25.

van Poll H, Breugelmans O, Devilee J (2011). Hinder, bezorgdheid en woontevredenheid in Nederland: inventarisatie verstoringen 2008 [Annoyance, concern and residential satisfaction in the Netherlands: Annoyance inventory 2008]. Bilthoven: Rijksinstituut voor Volksgezondheid en Milieu (RIVM Rapport 630741001/2011; http://www.rivm.nl/dsresource?objectid=50e5cd0f-3de8-40ca-b3e5-7b31dbfaa93b&type=org&disposition=inline, accessed 27 November 2016).

van Poll R, Ameling C, Breugelmans O, Houthuis D, van Kempen E, Marra M et al. (2014). Gezondheidsonderzoek Vliegbasis Geilenkirchen (Desk Research) I. Hoofdrapportage: samenvatting, conclusies en aanbevelingen Gezondheidsonderzoek Vliegbasis Geilenkirchen [Health study at the military airport Geilenkirchen (desk research) I. Main report: summary, conclusions and recommendations of the health study at the military airport Geilenkirchen]. Bilthoven: National Institute for Public Health and the Environment (https://zoek.officielebekendmakingen.nl/blg-378125.pdf, accessed 15 March 2017).

van Renterghem T, Botteldooren D (2012). Focused study on the quiet side effect in dwellings highly exposed to road traffic noise. Int J Environ Res Public Health. 9(12):4292–310.

Vasconcellos AP, Kyle ME, Gilani S, Shin JJ (2014). Personally modifiable risk factors associated with pediatric hearing loss: a systematic review. Otolaryngol Head Neck Surg. 151(1):14–28.

Vincent B, Champelovier P (1993). Changes in the acoustic environment: need for an extensive evaluation of annoyance. In: Proceedings. 6th International Congress on Noise as a Public Health Problem 1993 (ICBEN 1993). Nice, France, 5–9 July 1993. Lyon: Institut National de Recherche sur les Transports et leur Sécurité.

Vogel I, Brug J, van der Ploeg CP, Raat H (2011). Adolescents risky MP3-player listening and its psychosocial correlates. Health Educ Res. 26(2):254–64.

Vogel I, van de Looij-Jansen PM, Mieloo CL, Burdorf A, de Waart F (2014). Risky music listening, permanent tinnitus and depression, anxiety, thoughts about suicide and adverse general health. PloS One. 9(6): e98912.

Weichbold V, Zorowka P (2003). Effects of a hearing protection campaign on the discotheque attendance habits of high-school students. Int J Audiol. 42(8):489–93.

Weichbold V, Zorowka P (2007). Can a hearing education campaign for adolescents change their music listening behavior? Int J Audiol. 46(3):128–33.

WHO (1946). Preamble to the Constitution of the World Health Organization as adopted by the International Health Conference, New York, 19–22 June 1946; signed on 22 July 1946 by the representatives of 61 States and entered into force on 7 April 1948. Geneva: World Health Organization (http://www.who.int/about/mission/en/, accessed 27 June 2018).

WHO (1999). Guidelines for community noise. Geneva: World Health Organization (http://apps.who.int/iris/handle/10665/66217?show=full, accessed 28 November 2016).

WHO (2006). Air quality guidelines – global update 2005. Geneva: World Health Organization (http://www.who.int/phe/health_topics/outdoorair/outdoorair_aqg/en/, accessed 27 July 2018).

WHO (2013). WHO methods and data sources for global burden of disease estimates 2000–2011. Geneva: World Health Organization (Global Health Estimates Technical Paper WHO/HIS/HSI/GHE/2013.4; http://www.who.int/healthinfo/global_burden_disease/data_sources_methods/en/, accessed 28 November 2016).

WHO (2014a). Metrics: disability-adjusted life-year (DALY). In: World Health Organization: Health statistics and information systems [website]. Geneva: World Health Organization (http://www.who.int/healthinfo/global_burden_disease/metrics_daly/en/, accessed 27 June 2018).

WHO (2014b). Burden of disease from ambient air pollution for 2012. Geneva: World Health Organization (http://www.who.int/phe/health_topics/outdoorair/databases/AAP_BoD_results_March2014.pdf, accessed 27 June 2018).

WHO (2014c). WHO handbook for guideline development, second edition. Geneva: World Health Organization (http://apps.who.int/iris/handle/10665/145714, accessed 27 June 2018).

WHO (2015a). Hearing loss due to recreational exposure to loud sounds: a review. Geneva: World Health Organization (http://apps.who.int/iris/handle/10665/154589, accessed 27 November 2016).

WHO Regional Office for Europe (2009). Night noise guidelines for Europe. Copenhagen: WHO Regional Office for Europe (http://www.euro.who.int/en/health-topics/environment-and-health/noise/publications/2009/night-noise-guidelines-for-europe, accessed 28 November 2016).

WHO Regional Office for Europe (2010). Parma Declaration on Environment and Health. Copenhagen: WHO Regional Office for Europe (http://www.euro.who.int/en/publications/policy-documents/parma-declaration-on-environment-and-health, accessed 28 November 2016).

WHO Regional Office for Europe (2012). Assessment of need for capacity-building for health risk assessment for environmental noise: case studies. Copenhagen: WHO Regional Office for Europe (http://www.euro.who.int/en/health-topics/environment-and-health/noise/publications/2012/assessment-of-needs-for-capacity-building-for-health-risk-assessment-of-environmental-noise-case-studies, accessed 28 November 2016).

WHO Regional Office for Europe (2016). Health risk assessment of air pollution: general principles. Copenhagen: WHO Regional Office for Europe (http://www.euro.who.int/en/publications/abstracts/health-risk-assessment-of-air-pollution.-general-principles-2016, accessed 12 January 2017).

WHO Regional Office for Europe (2017). Databases. In: WHO Regional Office for Europe: Data and evidence [website]. Copenhagen: WHO Regional Office for Europe (http://www.euro.who.int/en/data-and-evidence/databases, accessed 13 March 2017).

WHO Regional Office for Europe, JRC (2011). Burden of disease from environmental noise: quantification of healthy life years lost in Europe. Copenhagen: WHO Regional Office for Europe (http://www.who.int/quantifying_ehimpacts/publications/e94888/en/, accessed 27 November 2016).

Wiens D (1995). Verkehrslärm und kardiovaskuläres Risiko. Eine Fall-Kontroll-Studie in Berlin (West) [Transportation noise and risk for cardiovascular disease. A case study in (West) Berlin] In: Dissertation aus dem Institut für Wasser-, Boden- und Lufthygiene des Bundesgesundheitsamtes [Doctoral thesis for the Institute for Water, Ground and Air hygiene of the Federal Ministry of Health]. Berlin: Bundesgesundheitsamt.

Wilson SB, Lonigan, CJ (2010). Identifying preschool children at risk of later reading difficulties: evaluation of two emergent literacy screening tools. J Lern Disabil. 43(1):62–76.

Yano T, Morihara T, Sato T (2005). Community response to Shinkansen noise and vibration: a survey in areas along the Sanyo Shinkansen Line. In: Proceedings. Forum Acusticum: 4th European Congress on Acoustics, Budapest, Hungary, 29 August – 2 September 2005. Stuttgart: Hirzel.

Yano T, Nguyen TL, Nguyen TL, Takata M, Yamadal., Morinaga M et al. (2015). Community response to a step change in aircraft noise exposure: the first socio-acoustic survey around Noi Bai Airport in Hanoi. In: Proceedings. 22nd International Congress on Sound and Vibration (ICSV22) 2015, Florence, Italy, 12–16 July 2015. Ferrara: Acoustical Society of Italy.

Yokoshima S, Morihara T, Ota A, Tamura A (2008). Reanalysis of response curves of Shinkansen railway noise. In: Proceedings. 9th International Congress on Noise as a Public Health Problem 2008 (ICBEN 2008), Foxwoods, USA, 21–25 July 2008. Zurich: International Commission on Biological Effects of Noise.

Yoshida T, Kawaguchi T, Hoshiyama Y, Yoshida K, Yamamoto K (1997). Effects of road traffic noise on inhabitants of Tokyo. J Sound Vib. 205(4):517–22.

Annexes

Annex 1. Steering, advisory and external review groups

Tables A1.1–A1.5 give details of the various teams involved in the development of the WHO environmental noise guidelines for the European Region.

Table A1.1 WHO Steering Group

Name	Role	Affiliation
Shelly Chadha	Technical Officer, Office for Hearing Impairment	WHO headquarters, Geneva, Switzerland
Carlos Dora	Coordinator	WHO headquarters, Department of Public Health and Environment, Geneva, Switzerland
Marie-Eve Héroux	Technical Officer, Air Quality and Noise	WHO Regional Office for Europe, European Centre for Environment and Health, Bonn, Germany
Dorota Jarosinska	Programme Manager, Living and Working Environments	WHO Regional Office for Europe, European Centre for Environment and Health, Bonn, Germany
Rokho Kim	Environmental Health Specialist, Team Leader	WHO Regional Office for the Western Pacific, Division of Noncommunicable Diseases and Health through the Life-Course, Manila, Philippines
Jurgita Lekaviciute	Consultant, Noise	WHO Regional Office for Europe, European Centre for Environment and Health, Bonn, Germany
Srdan Matic	Coordinator, Environment and Health	WHO Regional Office for Europe, Copenhagen, Denmark
Julia Nowacki	Technical Officer, Health Impact Assessment	WHO Regional Office for Europe, European Centre for Environment and Health, Bonn, Germany
Elizabet Paunovic	Head of Office	WHO Regional Office for Europe, European Centre for Environment and Health, Bonn, Germany
Poonum Wilkhu	Consultant, Noise	WHO Regional Office for Europe, European Centre for Environment and Health, Bonn, Germany
Jördis Wothge	Consultant, Noise	WHO Regional Office for Europe, European Centre for Environment and Health, Bonn, Germany

Table A1.2. Guideline Development Group

Area of expertise	Reference	Area of expertise	Reference
Noise sources and their measurement	1	Annoyance	6
Biological mechanisms of effects	2	Cognitive impairment, quality of life, mental health and well-being	7
Cardiovascular and metabolic diseases	3	Adverse birth outcomes	8
Sleep disturbance	4	Environmental noise interventions	9
Hearing impairment/tinnitus	5	Methodology and guideline development	10

Name	Position and affiliation	Area of expertise sought for guideline development (see reference numbers above)									
		1	2	3	4	5	6	7	8	9	10
Wolfgang Babisch	Senior Scientific Officer (retired) Federal Environment Agency Germany		X	X		X					
Goran Belojevic	Professor Institute of Hygiene and Medical Ecology Faculty of Medicine University of Belgrade Serbia			X			X				
Mark Brink	Senior Scientist Federal Office for the Environment Switzerland	X			X		X				
Sabine Janssen	Senior Scientist Department of Sustainable Urban Mobility and Safety Netherlands Organisation for Applied Scientific Research (TNO) Netherlands				X		X				
Peter Lercher (2013–2014)	Professor Medical University of Innsbruck Austria							X	X		
Marco Paviotti	Policy Officer Directorate-General for Environment European Commission Belgium	X								X	
Göran Pershagen	Professor Institute of Environmental Medicine Karolinska Institute Sweden		X	X					X		

Table A1.2. contd

Area of expertise	Reference	Area of expertise	Reference
Noise sources and their measurement	1	Annoyance	6
Biological mechanisms of effects	2	Cognitive impairment, quality of life, mental health and well-being	7
Cardiovascular and metabolic diseases	3	Adverse birth outcomes	8
Sleep disturbance	4	Environmental noise interventions	9
Hearing impairment/tinnitus	5	Methodology and guideline development	10

Name	Position and affiliation	Area of expertise sought for guideline development (see reference numbers above)									
		1	2	3	4	5	6	7	8	9	10
Kerstin Persson Waye	Professor Occupational and Environmental Medicine The Sahlgrenska Academy University of Gothenburg Sweden	X			X		X				
Anna Preis	Professor Institute of Acoustics Adam Michiewicz University Poland					X	X				
Stephen Stansfeld (Chair)	Professor/Head of the Centre for Psychiatry Barts and Queen Mary University of London United Kingdom							X			
Martin van den Berg	Senior Noise Expert Ministry of Infrastructure and Environment Netherlands	X									
GRADE methodologist											
Jos Verbeek	Senior Researcher Finnish Institute of Occupational Health Finland	X									

Table A1.3. Systematic Review Team

Systematic review topics	Experts involved	Affiliation
Cardiovascular and metabolic diseases	Elise van Kempen	National Institute of Public Health and the Environment (RIVM), Netherlands
	Göran Pershagen	Institute of Environmental Medicine, Karolinska Institute, Sweden
	Maribel Casas Sanahuja	Institute for Global Health (ISGlobal), Spain
	Maria Foraster	Barcelona Institute for Global Health (ISGlobal), Spain and Swiss Tropical and Public Health Institute, Switzerland
Sleep disturbance	Mathias Basner	Department of Psychiatry, Perelman School of Medicine at the University of Pennsylvania, United States of America
	Sarah McGuire	Department of Psychiatry, Perelman School of Medicine at the University of Pennsylvania, United States of America
Hearing impairment and tinnitus	Mariola Sliwinska-Kowalska	Nofer Institute of Occupational Medicine, Poland
	Kamil Rafal Zaborowski	Nofer Institute of Occupational Medicine, Poland
Annoyance	Rainer Guski	Department of Psychology, Ruhr-University, Germany
	Dirk Schreckenberg	ZEUS GmbH, Centre for Applied Psychology, Environmental and Social Research, Germany
	Rudolf Schuemer	Consultant for ZEUS GmbH, Centre for Applied Psychology, Environmental and Social Research, Germany
Cognitive impairment, mental health and well-being	Charlotte Clark	Ove Arup & Partners, United Kingdom
	Katarina Paunovic	Institute of Hygiene and Medical Ecology, Faculty of Medicine, University of Belgrade, Serbia
Adverse birth outcomes	Mark Nieuwenhuijsen	Institute for Global Health (ISGlobal), Spain
	Gordana Ristovska	Institute of Public Health of Republic of Macedonia, the former Yugoslav Republic of Macedonia
	Payam Dadvand	Institute for Global Health (ISGlobal), Spain
Interventions	Lex Brown	Griffith School of Environment/Urban Research Program, Griffith University, Australia
	Irene Van Kamp	National Institute of Public Health and the Environment (RIVM), Netherlands

Table A1.4. External Review Group

Area of expertise	Reference	Area of expertise	Reference
Cardiovascular and metabolic diseases	1	Cognitive impairment, mental health and well-being	5
Sleep disturbance	2	Adverse birth outcomes	6
Hearing impairment/ Tinnitus	3	Environmental noise interventions	7
Annoyance	4	Recommendations and implementation guidance	8

Name	Affiliation	Area of expertise sought for guideline development (see reference numbers above)							
		1	2	3	4	5	6	7	8
Gunn Marit Aasvang	Norwegian Institute of Public Health, Norway		X						
Bernard Berry	Berry Environmental Limited, United Kingdom							X	
Dick Botteldooren	Department of Information Technology, Ghent University, Belgium				X				
Stephen Conaty	South Western Sydney Local Health District, Australia								X
Ulrike Gehring	Institute for Risk Assessment Sciences, Utrecht University, Netherlands						X		
Truls Gjestland	SINTEF, Department of Acoustics, Norway				X				
Mireille Guay	Healthy Environments and Consumer Safety Branch, Health Canada/Government of Canada, Canada		X		X				
Ayse Güven	Audiology Department, Faculty of Heath Sciences, Baskent University, Turkey			X					
Anna Hansell	Centre for Environmental Health & Sustainability, George Davies Centre, University of Leicester, United Kingdom	X							X
Stylianos Kephalopoulos	European Commission, DG Joint Research Centre, Italy							X	X
Yvonne de Kluizenaar	The Netherlands Organization for applied scientific research (TNO), Netherlands							X	
David S. Michaud	Healthy Environments and Consumer Safety Branch, Health Canada/Government of Canada, Canada		X		X				
Arnaud Norena	Université Aix-Marseille, Fédération de Recherche, Laboratoire Cognitive Neuroscience, France			X					
Enembe Okokon	National Institute for Health and Welfare, Finland								X
Dieter Schwela	Stockholm Environment Institute, University of York, United Kingdom								X
Daniel Shepherd	AUT University, Auckland, New Zealand					X			
Mette Sörensen	Danish Cancer Society Research Centre, Denmark	X							X
Rupert Thornley-Taylor	Rupert Taylor Ltd, Noise and Vibration Consultants							X	X
David Welch	School of Population Health, Faculty of Medical and Health Sciences, University of Auckland, New Zealand			X				X	

Table A1.5. Stakeholders and end users that participated in the stakeholder consultation

Area of expertise/interest	Reference	Area of expertise	Reference
Implementation of recommendations on railway noise	1	Implementation of recommendations on wind turbine noise	4
Implementation of recommendations on aircraft noise	2	Implementation of recommendations on leisure noise	5
Implementation of recommendations on road traffic noise	3	Implementation of overall recommendations	6

Organization	Area of expertise specifically sought for Guidelines (see reference number above)					
	1	2	3	4	5	6
Airlines for Europe		X				
Airports Council International Europe (ACI)		X				
Anderson Acoustics		X				
Bundesverband der Deutschen Luftverkehrswirtschaft e.V.		X				
European Automobile Manufacturers' Association (ACEA)			X			
European Aviation Safety Agency		X				
European Express Association	X					
European Noise Barrier Federation						X
Flughafenverband (ADV)		X				
International Air Transport Association (IATA)		X				
International Civil Aviation Organization (ICAO)		X				
International Union of Railways	X					
Landesamt fuer Natur, Umwelt und Verbraucherschutz Nordrhein-Westfalen						X
Public Health Agency of Sweden						X
Stephen Turner Acoustics					X	X
Union Européenne Contre les Nuisances Aeriennes		X				
Vie en.ro.se.						X

Note: in total 53 organizations and institutions had been approached to participate in the stakeholder consultation.

Annex 2. Systematic reviews and background documents used in preparation of the guidelines

Annex 2 provides a detailed list of all the supplementary documents accompanying the WHO environmental noise guidelines for the European Region.[22]

Systematic reviews

- Basner M, McGuire S (2018). WHO environmental noise guidelines for the European Region: a systematic review on environmental noise and effects on sleep. Int J Environ Res Public Health. 15(3):pii: E519 (http://www.mdpi.com/1660-4601/15/3/519/htm).
- Brown AL, van Kamp I (2017). WHO environmental noise guidelines for the European Region: a systematic review of transport noise interventions and their impacts on health. Int J Environ Res Public Health. 14(8). pii: E873 (http://www.mdpi.com/1660-4601/14/8/873/htm).
- Clark C, Paunovic K (2018). WHO environmental noise guidelines for the European Region: a systematic review on environmental noise and cognition. Int J Environ Res Public Health. 15(2). pii: E285 (http://www.mdpi.com/1660-4601/15/2/285/htm).
- Clark C, Paunovic K (in press). WHO Environmental noise guidelines for the European Region: a systematic review on environmental noise and quality of life, wellbeing and mental health. Int J Environ Res Public Health.
- Guski R, Schreckenberg D, Schuemer R (2017). WHO environmental noise guidelines for the European Region: a systematic review on environmental noise and annoyance. Int J Environ Res Public Health. 14(12). pii:1539 (http://www.mdpi.com/1660-4601/14/12/1539/htm).
- Nieuwenhuijsen MJ, Ristovska G, Dadvand P (2017). WHO environmental noise guidelines for the European Region: a systematic review on environmental noise and adverse birth outcomes. Int J Environ Res Public Health. 14(10). pii: E1252 (http://www.mdpi.com/1660-4601/14/10/1252/htm).
- Śliwińska-Kowalska M, Zaborowski K (2017). WHO environmental noise guidelines for the European Region: a systematic review on environmental noise and permanent hearing loss and tinnitus. Int J Environ Res Public Health. 14(10). pii: E1139 (http://www.mdpi.com/1660-4601/14/10/1139/htm).
- van Kempen E, Casas M, Pershagen G, Foraster M (2018). WHO environmental noise guidelines for the European Region: a systematic review on environmental noise and cardiovascular and metabolic effects: a summary. Int J Environ Res Public Health. 15(2). pii: E379 (http://www.mdpi.com/1660-4601/15/2/379/htm).

[22] All references were accessed on 27 June 2018.

Background documents

- Eriksson C, Pershagen G, Nilsson M (2018). Biological mechanisms related to cardiovascular and metabolic effects by environmental noise. Copenhagen: WHO Regional Office for Europe (http://www.euro.who.int/en/health-topics/environment-and-health/noise/publications/2018/biological-mechanisms-related-to-cardiovascular-and-metabolic-effects-by-environmental-noise).
- Héroux ME, Verbeek J (2018a). Results from the search for available systematic reviews and meta-analyses on environmental noise. Copenhagen: WHO Regional Office for Europe (http://www.euro.who.int/en/health-topics/environment-and-health/noise/publications/2018/results-search-for-available-systematic-reviews-environmental-noise).
- Héroux ME, Verbeek J (2018b). Methodology for systematic evidence reviews for the WHO environmental noise guidelines for the European Region. Copenhagen: WHO Regional Office for Europe (http://www.euro.who.int/en/health-topics/environment-and-health/noise/publications/2018/methodology-systematic-evidence-reviews-who-environmental-guidelines-for-the-european-region).

Annex 3. Summary of conflict of interest management

All external contributors to the guidelines, including members of the GDG, Systematic Review Team and External Review Group, completed WHO declaration of interest forms in accordance with WHO's policy for experts. Further, at the initial stage of the project WHO technical staff reviewed and accepted *curricula vitae* of the candidates for the GDG.

At the beginning of the GDG meetings, the participants declared any conflict of interest by submitting declaration of interest forms. Updated declarations of interest were also collected from the members of the GDG, Systematic Review Team and External Review Group at the final stage of the project.

The conflict of interest assessment was done according to WHO procedures. If a conflict was declared, an initial review was undertaken by the WHO Secretariat to assess its relevance and significance. A declared conflict of interest is insignificant or minimal if it is unlikely to affect or to be reasonably perceived to affect the expert's judgment. Insignificant or minimal interests are: unrelated or only tangentially related to the subject of the activity or work and its outcome; nominal in amount or inconsequential in importance; or expired and unlikely to affect current behaviour.

The WHO Secretariat reviewed and assessed the declarations. In one case the legal unit was consulted for advice; in another the potential conflict was reported in the updated declaration of interest at the final stage of the process and assessed unlikely to affect expert's performance; in a further case a member of the GDG was also a co-author of a systematic review owing to the need to support systematic review authors with additional expertise, but there was no remuneration for this activity.

No member of the GDG or the Systematic Review Team was excluded from his or her role in the guideline development process. The declared conflicts of interest of the External Review Group members were considered when interpreting comments during the external review process.

Annex 4. Detailed overview of the evidence of important health outcomes

As a first step of the evidence retrieval process, the GDG defined two categories of health outcome associated with environmental noise: those considered (i) critical or (ii) important, but not critical for decision-making in the guideline development process.

The GDG relied on the critical health outcomes to inform its decisions on priority health outcomes, so only these were used to inform the recommendations. Nevertheless, as the relevance of some of important health outcomes was difficult to estimate *a priori,* systematic reviews were conducted for both critical and important health outcomes.

This annex provides a detailed overview of the evidence of the important health outcomes – namely adverse birth outcomes, quality of life, well-being and mental health and metabolic outcomes – for each of the noise sources. A comprehensive discussion of all the evidence considered (both critical and important) is available in the published systematic reviews (see section 2.3.2 and Annex 2 for details).

1. Road traffic noise

1.1 Adverse birth outcomes

In total, the systematic review found five studies (two with more or less the same population) on road traffic noise and birth outcomes and three related studies on total ambient noise, likely to be mostly road traffic noise. Too few studies for each of the various measures related to adverse birth outcomes were available to undertake a quantitative meta-analysis. There was evidence rated low quality for a relationship between road traffic noise and low birth weight (Dadvand et al., 2014; Gehring et al., 2014; Hjortebjerg et al., 2016; Wu et al., 1996); however, the estimates were imprecise and in some cases not statistically significant. Further, there was no clear relation between exposure to road traffic noise and pre-term delivery, but there was a positive association between road traffic noise and small for gestational age (OR = 1.09; 95% CI: 1.06–1.12 per 6 dB increase). The evidence for both measures of adverse birth outcomes comes from the same publications and this evidence was rated low quality (Gehring et al., 2014; Hystad et al., 2014).

This evidence was supported by one ecological time-series study published recently looking at total ambient noise and various measures related to adverse birth outcomes (Arroyo et al., 2016a; 2016b; Diaz et al., 2016).

1.2 Quality of life, well-being and mental health

Evidence rated moderate quality was found for an effect of road traffic noise on emotional and conduct disorders in childhood (Belojevic et al., 2012; Crombie et al., 2011; Hjortebjerg et al., 2015; Ristovska et al., 2004; Stansfeld et al., 2005; 2009a; Tiesler et al., 2013) and evidence rated moderate quality for an association of road traffic noise with hyperactivity in children (Hjortebjerg et al., 2015; Tiesler et al., 2013).

There was no clear relationship, however, between road traffic noise exposure and self-reported quality of life (evidence rated low quality) (Barcelo Perez & Piñeiro, 2008; Brink, 2011; Clark et al., 2012; Honold et al., 2012; Roswall et al., 2015; Schreckenberg et al., 2010b; Stansfeld et al., 2005; 2009b; van Kempen et al., 2010); medication intake for depression and anxiety (evidence rated very low quality) (Floud et al., 2011; Halonen et al., 2014); depression, anxiety and psychological distress (evidence rated very low quality) (Honold et al., 2012; Stansfeld et al., 2009b); and interview measures of depression and anxiety (evidence rated very low quality) (Stansfeld et al., 2009b).

1.3 Metabolic outcomes

1.3.1 Diabetes

For the relationship between road traffic noise and the incidence of diabetes, one cohort study was identified, which included 57 053 participants and 2752 cases (Sörensen et al., 2013). The estimate of the effect was RR = 1.08 (95% CI: 1.02–1.14) per 10 dB L_{den} increase in noise across the range of 50–70 dB, and therefore the evidence was rated moderate quality.

Furthermore, two cross-sectional studies were identified that looked at the prevalence of diabetes (Selander et al., 2009; van Poll et al., 2014). The studies included 11 460 participants and 242 cases. Both studies reported a harmful effect of noise, and one showed a statistically significant association. However, the results were imprecise and with serious risk of bias, so the evidence was rated very low quality.

1.3.2 Obesity

With regard to the association between road traffic noise and change in body mass index (BMI) and waist circumference, three cross-sectional studies were identified, with 71 431 participants (Christensen et al., 2016; Oftedal et al., 2014; 2015; Pyko et al., 2015). For each 10 dB increase in road traffic noise, there was a statistically nonsignificant increase in BMI of 0.03 kg/m^2 (95% CI: –0.10–0.15 kg/m^2) and in waist circumference of 0.17 cm (95% CI: –0.06–0.40 cm). There was inconsistency in the results between the studies; therefore, for both associations, the evidence was rated very low quality (Fig. A4.1 and Fig. A4.2).

Fig. A4.1 The association between exposure to road traffic noise (L_{den}) and BMI in three Nordic studies

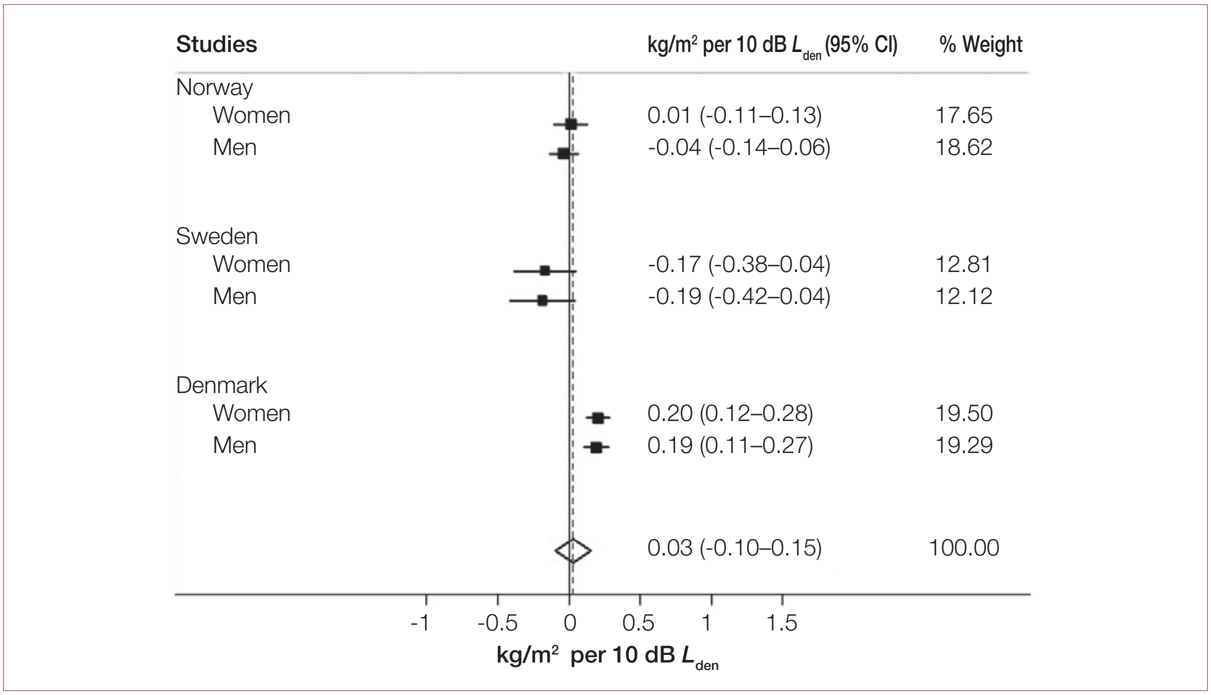

Notes: The black vertical line corresponds to no effect of noise exposure. The black dots correspond to the estimated slope coefficients per 10 dB for each sex in each study, with 95% CIs. The diamond designates summary estimates and 95% CIs based on random effects models. The dashed red line corresponds to these summary estimates. Heterogeneity between studies: p = 0.000; heterogeneity between genders: p = 0.360; overall (I-squared = 84.4%, p = 0.000). Weights are from random effect analysis.

Fig. A4.2 The association between exposure to road traffic noise (L_{den}) and waist circumference in three Nordic studies

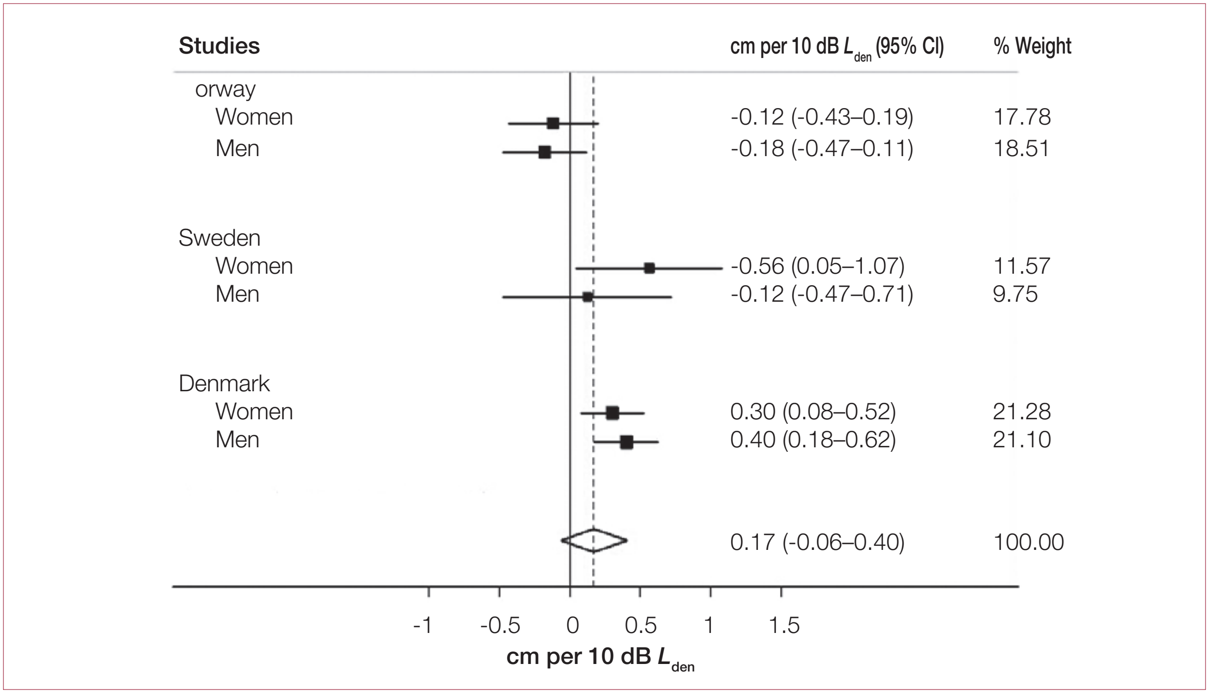

Notes: The black vertical line corresponds to no effect of noise exposure. The black dots correspond to the estimated slope coefficients per 10 dB for each sex in each study, with 95% CIs. The diamond designates summary estimates and 95% CIs based on random effects models. The dashed red line corresponds to these summary estimates. Heterogeneity between studies: p = 0.001; heterogeneity between genders: p = 0.842; overall (I-squared = 69.0%, p = 0.007). Weights are from random effect analysis.

2. Railway noise

2.1 Adverse birth outcomes

No studies were found, and therefore no evidence was available on the association between railway noise and adverse birth outcomes.

2.2 Quality of life, well-being and mental health

Evidence rated very low quality was found for a weak effect of railway noise exposure on self-reported quality of life or health, albeit from a limited number of studies (Roswall et al., 2015; Torre et al., 2007). There was evidence rated moderate quality for an effect of railway noise on emotional and conduct disorders in childhood (Hjortebjerg et al., 2015), but no clear relationship between railway noise and children’s hyperactivity (Hjortebjerg et al., 2015); this evidence was rated moderate quality.

2.3 Metabolic outcomes

2.3.1 Diabetes

One cohort study was identified that looked at the relationship between railway noise and the incidence of diabetes (Sörensen et al., 2013). The cohort study of 57 053 participants, including 2752 cases, found evidence rated moderate quality that there was no considerable effect of railway noise on diabetes, with an RR of 0.97 (95% CI: 0.89–1.05) per 10 dB L_{den} increase in noise.

Furthermore, one cross-sectional study was identified that looked at the relationship between railway noise and the prevalence of diabetes (van Poll et al., 2014), including 9365 participants and 89 cases. An RR of 0.21 (95% CI: 0.05–0.82) per 10 dB L_{den} increase in noise was found, but the reasons for the beneficial effect were not immediately apparent. The evidence in the study was rated very low quality.

2.3.2 Obesity

Regarding the association between railway noise and change in BMI and waist circumference, two cross-sectional studies were identified, with 57 531 participants (Christensen et al., 2016; Pyko et al., 2015). Christensen and colleagues observed a statistically significant increase of 0.18 kg/m^2 (95% CI: 0.00–0.36 kg/m^2) per 10 dB for BMI and 0.62 cm (95% CI: 0.14–1.09 cm) per 10 dB for waist circumference in those exposed to railway noise, at levels above 60 dB L_{den}. Pyko and colleagues found a statistically significant increase in waist circumference of 0.92 cm (95% CI: 0.06–1.78 cm) per 10 dB L_{den}. The corresponding estimate for BMI was statistically nonsignificant, at 0.06 kg/m^2 (95% CI: –0.02–0.16 kg/m^2). The evidence was rated low/very low quality.

3. Aircraft noise

3.1 Adverse birth outcomes

Evidence rated very low quality was available for an association between aircraft noise and pre-term delivery, low birth weight and congenital anomalies, as evidenced by six studies included in the systematic review (Ando & Hattori, 1973; Edmonds et al., 1979; Jones & Tauscher, 1978; Knipschild et al., 1981; Matsui et al., 2003; Schell, 1981). The potential for risk of bias in these was high and the results tended to be inconsistent.

3.2 Quality of life, well-being and mental health

Evidence rated very low quality was available for an effect of aircraft noise on medication intake for depression and anxiety (Floud et al., 2011). There was evidence rated very low quality for an effect of aircraft noise exposure on interview measures of depression and anxiety (Hardoy et al., 2005) and rated low quality for an association of aircraft noise with hyperactivity in children (Clark et al., 2013; Crombie et al., 2011; Stansfeld et al., 2009a).

The evidence showed, however, no substantial effect of aircraft noise on self-reported quality of life or health (Clark et al., 2012; Schreckenberg et al., 2010a; 2010b; Stansfeld et al., 2005; van Kempen et al., 2010) or on emotional and conduct disorders in childhood (Clark et al., 2012; 2013; Crombie et al., 2011; Stansfeld et al., 2005; 2009a). This evidence was rated very low quality.

3.3 Metabolic outcomes

3.3.1 Diabetes

For the relationship between aircraft noise and incidence of diabetes one cohort study was identified, including 5156 participants and 1346 cases (Eriksson et al., 2014). The estimate of the effect was imprecise, with an RR of 0.99 (95% CI: 0.47–2.09) per 10 dB L_{den} increase in noise; the evidence was therefore rated very low quality.

Furthermore, one cross-sectional study was identified that looked at the prevalence of diabetes (van Poll et al., 2014), including 9365 participants and 89 cases. The RR was 1.01 (95% CI: 0.78–1.31) per 10 dB increase in aircraft noise. The evidence was rated very low quality.

3.3.2 Obesity

For the association between aircraft noise and change in BMI and waist circumference, one cohort study was identified, with 5156 participants (Eriksson et al., 2014). For each 10 dB increase in aircraft noise level, the increase in BMI was 0.14 kg/m^2 (95% CI: −0.18–0.45) (evidence rated low quality), and the increase in waist circumference was 3.46 cm (95% CI: 2.13–4.77) (evidence rated moderate quality). The range of noise levels in the study was 48–65 dB L_{den}. In the case of BMI, the change over the whole range in noise values was not statistically significant and was less than what could be considered clinically relevant (3–5% change in BMI); however, for waist circumference, the change was equivalent to an increase of 5.8 cm.

4. Wind turbine noise

4.1 Quality of life, well-being and mental health

Five low-quality systematic reviews of wind turbine noise effects on mental health and well-being have been carried out (Ellenbogen et al., 2012; Kurpas et al., 2013; Merlin et al., 2013; Onakpoya et al., 2015; Schmidt & Klokker, 2014). These reviews differed in their conclusions and delivered inconsistent evidence that wind turbine noise exposure is associated with poorer quality of life, well-being and mental health. Therefore, the evidence for no substantial effect of wind turbine noise on quality of life, well-being or mental health was rated very low quality.

4.2 Metabolic outcomes

4.2.1 Diabetes

For the relationship between wind turbine noise and prevalence of diabetes, three cross-sectional studies were identified, with a total of 1830 participants (Bakker et al., 2012; Pedersen, 2011; Pedersen & Larsman, 2008; Pedersen & Persson Waye, 2004; 2007; Pedersen et al., 2009; van den Berg et al., 2008). The number of cases was not reported. The effect sizes varied across studies, and only one study found a positive association between exposure to wind turbine noise and the prevalence of diabetes; therefore, no meta-analysis was performed. Due to very serious risk of bias and imprecision in the results, this evidence was rated very low quality. As a result, there is no clear relationship between audible noise (greater than 20 Hz) from wind turbines or wind farms and prevalence of diabetes (Fig. A4.3).

Fig. A4.3 The association between exposure to wind turbine noise (sound pressure level) and self-reported diabetes

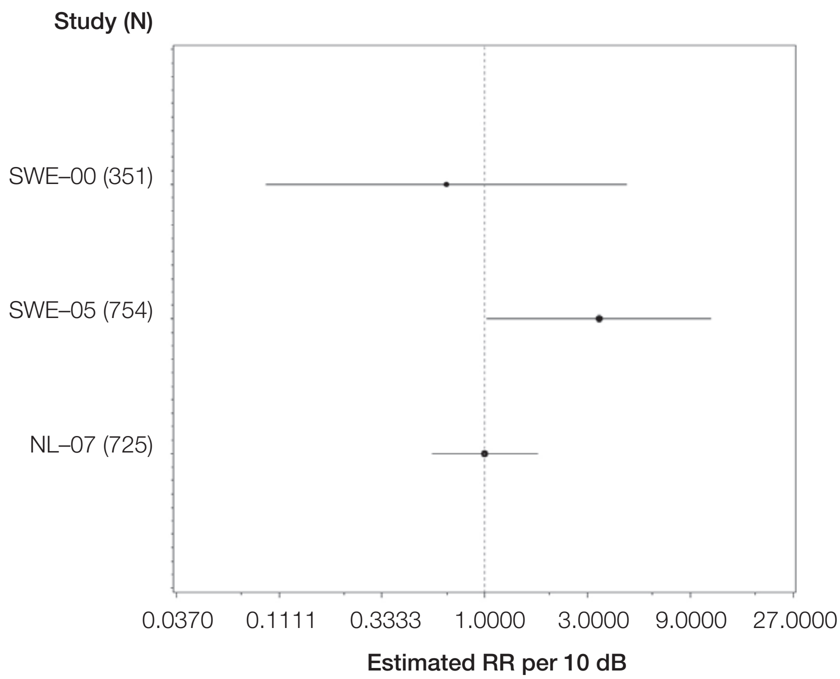

Note: The dotted vertical line corresponds to no effect of exposure to wind turbine noise. The black circles correspond to the estimated RR per 10 dB (sound pressure level) and 95% CI.
For further details on the studies included in the figure please refer to the systematic review on environmental noise and cardiovascular and metabolic effects (van Kempen et al., 2018).

5. Leisure noise

Owing to a lack of evidence meeting the critieria for systematic reviewing, no results for any of the important health outcomes can be given for exposure to leisure noise.

Annex 4 references

Ando Y, Hattori H (1973). Statistical studies on the effects of intense noise during human fetal life. J Sound Vibrat. 27:101–10.

Arroyo V, Diaz J, Carmona R, Ortiz C, Linares C (2016a). Impact of air pollution and temperature on adverse birth outcomes: Madrid, 2001–2009. Environ Poll. 218:1154–61.

Arroyo V, Diaz J, Ortiz C, Carmona R, Saez M, Linares C (2016b). Short term effect of air pollution, noise and heat waves on preterm births in Madrid (Spain). Environ Res. 145:162–8.

Bakker RH, Pedersen E, van den Berg GP, Stewart RE, Lok W, Bouma J (2012). Impact of wind turbine sound on annoyance, self-reported sleep disturbance and psychological distress. Sci Total Environ. 425:42–51.

Barcelo Perez C, Piñeiro RG (2008). Potential effect caused by urban noise in housewives from Havana City. Revista Cubana de Higiene y Epidemiologia. 46(2).

Belojevic G, Evans GW, Paunović K, Jakovljevic B (2012). Traffic noise and executive functioning in urban primary school children: the moderating role of gender. J Environ Psychol. 32:337–41.

Brink M (2011). Parameters of well-being and subjective health and their relationship with residential traffic noise exposure – a representative evaluation in Switzerland. Environ Int. 37:723–33.

Christensen JS, Raaschou-Nielsen O, Tjonneland A, Overvad K, Nordsborg RB, Ketzel M et al. (2016). Road traffic and railway noise exposures and adiposity in adults: a cross-sectional analysis of the Danish Diet, Cancer, and Health Cohort. Environ Health Perspect. 124(3):329–35.

Crombie R, Clark C, Stansfeld SA (2011). Environmental noise exposure, early biological risk and mental health in nine to ten year old children: a cross-sectional field study. Environ Health. 10:39.

Clark C, Crombie R, Head J, van Kamp I, van Kempen E, Stansfeld SA (2012). Does traffic-related air pollution explain associations of aircraft and road traffic noise exposure on children's health and cognition? A secondary analysis of the United Kingdom sample from the RANCH project. Am J Epidemiol. 176:327–37

Clark C, Head J, Stansfeld SA (2013). Longitudinal effects of aircraft noise exposure on children's health and cognition: a six-year follow-up of the United Kingdom RANCH cohort. J Environ Psychol. 35:1–9.

Dadvand P, Ostro B, Figueras F, Foraster M, Basagaña X, Valentín A et al. (2014). Residential proximity to major roads and term low birth weight: the roles of air pollution, heat, noise, and road-adjacent trees. Epidemiology. 25(4):518–25.

Diaz J, Arroyo V, Ortiz C, Carmona R, Linares C (2016). Effect of environmental factors on low weight in non-premature births: a time series analysis. PLoS One. 11(10):e0164741.

Edmonds LD, Layde PM, Erickson JD (1979). Airport noise and teratogenesis. Arch Environ Health. 34:243–7.

Ellenbogen J.M, Grace S, Heiger-Bernays WJ, Manwell JF, Mills DA, Sullivan KA, Weisskopf MG (2012). Wind Turbine Health Impact Study: Report of Independent Expert Panel. Massachusetts Department of Environmental Protection, Massachusetts Department of Public Health: Massachusetts, USA.

Eriksson C, Hilding A, Pyko A, Bluhm G, Pershagen G, Östenson CG (2014). Long-term aircraft noise exposure and body mass index, waist circumference, and type 2 diabetes: a prospective study. Environ Health Perspect. 122:687–94.

Floud S, Vigna-Taglianti F, Hansell A, Blangiardo M, Houthuijs D, Breugelmans O et al. (2011). Medication use in relation to noise from aircraft and road traffic in six European countries: results of the HYENA study. Occup Environ Med. 68:518–24.

Gehring U, Tamburic L, Sbihi H, Davies HW, Brauer M (2014). Impact of noise and air pollution on pregnancy outcomes. Epidemiology. 25:351–8.

Halonen JI, Lanki T, Yli-Tuomi T, Turunen AW, Pentti J, Kivimaki M et al. (2014). Associations of traffic noise with self-rated health and psychotropic medication use. Scand J Work Environ Health. 40:235–43.

Hardoy MC, Carta MG, Marci AR, Carbone F, Cadeddu M, Kovess V et al. (2005). Exposure to aircraft noise and risk of psychiatric disorders: the Elmas survey – aircraft noise and psychiatric disorders. Soc Psychiatry Psychiatr Epidemiol. 40:24–6.

Hjortebjerg D, Andersen AMN, Ketzel M, Pedersen M, Raaschou-Nielsen O, Sörensen M (2016). Associations between maternal exposure to air pollution and traffic noise and newborn's size at birth: A cohort study. Environ Int. 95:1–7.

Hjortebjerg D, Andersen AMN, Schultz Christensen J, Ketzel M, Raaschou-Nielsen O, Sunyer J, et al. (2015). Exposure to road traffic noise and behavioral problems in 7-year-old children: a cohort study. Environ Health Perspect. 124:228–34.

Honold J, Beyer R, Lakes T, van der Meer E (2012). Multiple environmental burdens and neighborhood-related health of city residents. J Environ Psychol. 32:305–17.

Hystad P, Davies HW, Frank L, Van Loon J, Gehring U, Tamburic L, Brauer M (2014). Residential greenness and birth outcomes: evaluating the influence of spatially correlated built-environment factors. Environ Health Perspect. 122(10):1095–102.

Jones FN, Tauscher J (1978). Residence under an airport landing pattern as a factor in teratism. Arch Environ Health. 33:10–12.

Knipschild P, Meijer H, Sallé H (1981). Aircraft noise and birthweight. Int Arch Occup Environ Health. 48:131–6.

Kurpas D, Mroczek B, Karakiewicz B, Kassolik K, Andrzejewski W (2013). Health impact of wind farms. Ann Agric Environ Med. 20(3):595–604.

Matsui T, Matsuno T, Ashimine K, Miyakita T, Hiramatsu K, Yamamoto T (2003). Association between the rates of low birth-weight and/or preterm infants and aircraft noise exposure. Nihon Eiseigaku Zasshi. 58:385–94.

Merlin T, Newton S, Ellery B, Milverton J, Farah C (2013). Systematic review of the human health effects of wind farms. Canberra: National Health and Medical Research Council (https://www.nhmrc.gov.au/_files_nhmrc/publications/attachments/eh54_systematic_review_of_the_human_health_effects_of_wind_farms_december_2013.pdf, accessed 28 November 2016).

Oftedal B, Krog NH, Graff-Iversen S, Haugen M, Schwarze P, Aasvang GM (2014). Traffic noise and markers of obesity: a population-based study. In: Proceedings. 11th International Congress on Noise as a Public Health Problem 2014 (ICBEN 2014), Nara, Japan, 1–5 June 2014. Tokyo: Institute of Noise Control Engineering of Japan.

Oftedal B, Krog NH, Pyko A, Eriksson C, Graff-Iversen S, Haugen M et al. (2015). Road traffic noise and markers of obesity: a population-based study. Environ Res. 20(138):144–53.

Onakpoya IJ, O'Sullivan J, Thompson MJ, Heneghan CJ (2015). The effect of wind turbine noise on sleep and quality of life: a systematic review and meta-analysis of observational studies. Environ Int. 82:1–9.

Pedersen E (2011). Health aspects associated with wind turbine noise: results from three field studies. Noise Control Eng J. 59(1):47–53.

Pedersen E, Larsman P (2008). The impact of visual factors on noise annoyance among people living in the vicinity of wind turbines. J Environ Psychol. 28(4):379–89.

Pedersen E, Perrson Waye K (2004). Perception and annoyance due to wind turbine noise – a dose-response relationship. J Acoust Soc Am. 116(6):3460–70.

Pedersen E, Persson Waye K (2007). Wind turbine noise, annoyance and self-reported health and well-being in different living environments. Occup Environ Med. 64(7):480–6.

Pedersen E, van den Berg F, Bakker R, Bouma J (2009). Response to noise from modern wind farms in the Netherlands. J Acoust Soc Am. 126(2):634–43.

Pyko A, Eriksson C, Oftedal B, Hilding A, Östenson CG, Krog NH et al. (2015). Exposure to traffic noise and markers of obesity. Occup Environ Med. 72(8):594–601.

Ristovska G, Gjorgjev D, Jordanova NP (2004). Psychosocial effects of community noise: Cross sectional study of school children in urban center of Skopje, Macedonia. Croatian Medical Journal, 45, 473–6.

Roswall N, Hogh V, Envold-Bidstrup P, Raaschou-Nielsen O, Ketzel M, Overvad K et al. (2015). Residential exposure to traffic noise and health-related quality of life – a population-based study. PloS One. 13:e0120199.

Schell LM (1981). Environmental noise and human prenatal growth. Am J Phys Anthropol. 56:63–70.

Schmidt JH, Klokker M (2014). Health effects related to wind turbine noise exposure: a systematic review. PloS One. 9(12):e114183.

Schreckenberg D, Griefahn B, Meis M (2010a). The associations between noise sensitivity, reported physical and mental health, perceived environmental quality, and noise annoyance. Noise Health. 12:7–16.

Schreckenberg D, Meis M, Kahl C, Peschel C, Eikmann T (2010b). Aircraft noise and quality of life around Frankfurt Airport. Int J Environ Res Public Health. 7:3382–405.

Selander J, Nilsson ME, Bluhm G, Rosenlund M, Lindqvist M, Nise G et al. (2009). Long-term exposure to road traffic noise and myocardial infarction. Epidemiology. 20(2):272–9.

Sörensen M, Andersen ZJ, Nordsborg RB, Becker T, Tjonneland A, Overvad K et al. (2013). Long-term exposure to road traffic noise and incident diabetes: a cohort study. Environ Health Perspect. 121:217–22.

Stansfeld SA, Berglund B, Clark C, Lopez-Barrio I, Fischer P, Ohrstrom E, et al. (2005). Aircraft and road traffic noise and children's cognition and health: a cross-national study. Lancet. 365:1942–9.

Stansfeld SA, Clark C, Cameron RM, Alfred T, Head J, Haines MM et al. (2009a). Aircraft and road traffic noise exposure and children's mental health. J Environ Psychol. 29:203–7.

Stansfeld SA, Haines MM, Berry B, Burr M (2009b). Reduction of road traffic noise and mental health: an intervention study. Noise Health. 11(44):169–75.

Tiesler CM, Birk M, Thiering E, Kohlbock G, Koletzko S, Bauer CP et al. (2013). Exposure to road traffic noise and children's behavioural problems and sleep disturbance: results from the GINIplus and LISAplus studies. Environ Res. 123:1–8.

Torre GL, Moscato U, Torre FL, Ballini P, Marchi S, Ricciardi W (2007). Environmental noise exposure and population health: a cross-sectional study in the Province of Rome. J Public Health (Oxf). 15:339–44.

van den Berg F, Pedersen E, Bouma J, Bakker R (2008). Project WINDFARMperception. Visual and acoustic impact of wind turbine farms on residents. Groningen: University of Groningen (FP6-2005-Science-and-Society-20 Specific Support Action Project no. 044628; https://www.rug.nl/research/portal/publications/project-windfarmperception-visual-and-acoustic-impact-of-wind-turbine-farms-on-residents(b8745281-02e7-4761-bd06-86363e2be78b).html, accessed 27 November 2016).

van Kempen E, van Kamp I, Lebret E, Lammers J, Emmen H, Stansfeld S (2010). Neurobehavioral effects of transportation noise in primary schoolchildren: a cross-sectional study. Environ Health. 9:25.

van Poll R, Ameling C, Breugelmans O, Houthuis D, van Kempen E, Marra M et al. (2014). Gezondheidsonderzoek Vliegbasis Geilenkirchen (Desk Research) I. Hoofdrapportage: samenvatting, conclusies en aanbevelingen Gezondheidsonderzoek Vliegbasis Geilenkirchen [Health study at the military airport Geilenkirchen (desk research) I. Main report: summary, conclusions and recommendations of the health study at the military airport Geilenkirchen]. Bilthoven: National Institute for Public Health and the Environment (https://zoek.officielebekendmakingen.nl/blg-378125.pdf, accessed 15 March 2017).

Wu TN, Chen LJ, Lai JS, Ko GN, Shen CY, Chang PY (1996). Prospective study of noise exposure during pregnancy on birthweight. Am J Epidemiol. 143(8):792–6.

The WHO Regional Office for Europe

The World Health Organization (WHO) is a specialized agency of the United Nations created in 1948 with the primary responsibility for international health matters and public health. The WHO Regional Office for Europe is one of six regional offices throughout the world, each with its own programme geared to the particular health conditions of the countries it serves.

Member States

Albania
Andorra
Armenia
Austria
Azerbaijan
Belarus
Belgium
Bosnia and Herzegovina
Bulgaria
Croatia
Cyprus
Czechia
Denmark
Estonia
Finland
France
Georgia
Germany
Greece
Hungary
Iceland
Ireland
Israel
Italy
Kazakhstan
Kyrgyzstan
Latvia
Lithuania
Luxembourg
Malta
Monaco
Montenegro
Netherlands
Norway
Poland
Portugal
Republic of Moldova
Romania
Russian Federation
San Marino
Serbia
Slovakia
Slovenia
Spain
Sweden
Switzerland
Tajikistan
The former Yugoslav Republic of Macedonia
Turkey
Turkmenistan
Ukraine
United Kingdom
Uzbekistan

Noise is an important public health issue. It has negative impacts on human health and well-being and is a growing concern. The WHO Regional Office for Europe has developed these guidelines, based on the growing understanding of these health impacts of exposure to environmental noise. The main purpose of these guidelines is to provide recommendations for protecting human health from exposure to environmental noise originating from various sources: transportation (road traffic, railway and aircraft) noise, wind turbine noise and leisure noise. They provide robust public health advice underpinned by evidence, which is essential to drive policy action that will protect communities from the adverse effects of noise. The guidelines are published by the WHO Regional Office for Europe. In terms of their health implications, the recommended exposure levels can be considered applicable in other regions and suitable for a global audience.

ISBN 9789289053563
9 789289 053563 >

World Health Organization Regional Office for Europe
UN City, Marmorvej 51, DK-2100 Copenhagen Ø, Denmark
Tel.: +45 45 33 70 00 Fax: +45 45 33 70 01
E-mail: eurocontact@who.int

Idaho Power/1215
Witness: Dr. Jeffrey Ellenbogen

BEFORE THE PUBLIC UTILITY COMMISSION
OF OREGON

Docket PCN 5

In the Matter of

IDAHO POWER COMPANY'S
PETITION FOR CERTIFICATE OF PUBLIC CONVENIENCE
AND NECESSITY

Walkup, J. T. et al., Cognitive Behavioral Therapy, Sertraline, or a
Combination in Childhood Anxiety (2008)

February 22, 2023

The NEW ENGLAND JOURNAL of MEDICINE

ESTABLISHED IN 1812 DECEMBER 25, 2008 VOL. 359 NO. 26

Cognitive Behavioral Therapy, Sertraline, or a Combination in Childhood Anxiety

John T. Walkup, M.D., Anne Marie Albano, Ph.D., John Piacentini, Ph.D., Boris Birmaher, M.D., Scott N. Compton, Ph.D., Joel T. Sherrill, Ph.D., Golda S. Ginsburg, Ph.D., Moira A. Rynn, M.D., James McCracken, M.D., Bruce Waslick, M.D., Satish Iyengar, Ph.D., John S. March, M.D., M.P.H., and Philip C. Kendall, Ph.D.*

ABSTRACT

BACKGROUND

Anxiety disorders are common psychiatric conditions affecting children and adolescents. Although cognitive behavioral therapy and selective serotonin-reuptake inhibitors have shown efficacy in treating these disorders, little is known about their relative or combined efficacy.

METHODS

In this randomized, controlled trial, we assigned 488 children between the ages of 7 and 17 years who had a primary diagnosis of separation anxiety disorder, generalized anxiety disorder, or social phobia to receive 14 sessions of cognitive behavioral therapy, sertraline (at a dose of up to 200 mg per day), a combination of sertraline and cognitive behavioral therapy, or a placebo drug for 12 weeks in a 2:2:2:1 ratio. We administered categorical and dimensional ratings of anxiety severity and impairment at baseline and at weeks 4, 8, and 12.

RESULTS

The percentages of children who were rated as very much or much improved on the Clinician Global Impression–Improvement scale were 80.7% for combination therapy (P<0.001), 59.7% for cognitive behavioral therapy (P<0.001), and 54.9% for sertraline (P<0.001); all therapies were superior to placebo (23.7%). Combination therapy was superior to both monotherapies (P<0.001). Results on the Pediatric Anxiety Rating Scale documented a similar magnitude and pattern of response; combination therapy had a greater response than cognitive behavioral therapy, which was equivalent to sertraline, and all therapies were superior to placebo. Adverse events, including suicidal and homicidal ideation, were no more frequent in the sertraline group than in the placebo group. No child attempted suicide. There was less insomnia, fatigue, sedation, and restlessness associated with cognitive behavioral therapy than with sertraline.

CONCLUSIONS

Both cognitive behavioral therapy and sertraline reduced the severity of anxiety in children with anxiety disorders; a combination of the two therapies had a superior response rate. (ClinicalTrials.gov number, NCT00052078.)

From the Johns Hopkins Medical Institutions, Baltimore (J.T.W., G.S.G.); New York State Psychiatric Institute–Columbia University Medical Center, New York (A.M.A., M.A.R.); the University of California at Los Angeles, Los Angeles (J.P., J.M.); Western Psychiatric Institute and Clinic–University of Pittsburgh Medical Center, Pittsburgh (B.B., S.I.); Duke University Medical Center, Durham, NC (S.N.C., J.S.M.); the Division of Services and Intervention Research, National Institute of Mental Health, Bethesda, MD (J.T.S.); Baystate Medical Center, Springfield, MA (B.W.); and Temple University, Philadelphia (P.C.K.). Address reprint requests to Dr. Walkup at the Division of Child and Adolescent Psychiatry, Department of Psychiatry and Behavioral Sciences, Johns Hopkins Medical Institutions, 600 N. Wolfe St., Baltimore, MD 21287.

*The study investigators are listed in the Appendix.

This article (10.1056/NEJMoa0804633) was published on October 30, 2008, and updated on January 17, 2013, at NEJM.org.

N Engl J Med 2008;359:2753-66.

Anxiety disorders are common in children and cause substantial impairment in school, in family relationships, and in social functioning.[1,2] Such disorders also predict adult anxiety disorders and major depression.[3-6] Despite a high prevalence (10 to 20%[3,7,8]) and substantial morbidity, anxiety disorders in childhood remain underrecognized and undertreated.[1,9] An improvement in outcomes for children with anxiety disorders would have important public health implications.

In clinical trials, separation and generalized anxiety disorders and social phobia are often grouped together because of the high degree of overlap in symptoms and the distinction from other anxiety disorders (e.g., obsessive–compulsive disorder). Efficacious treatments for these disorders include cognitive behavioral therapy[10,11] and the use of selective serotonin-reuptake inhibitors (SSRIs).[12,13] However, randomized, controlled trials comparing cognitive behavioral therapy, the use of an SSRI, or the combination of both therapies with a control are lacking. The evaluation of combination therapy is particularly important because approximately 40 to 50% of children with these disorders do not have a response to short-term treatment with either monotherapy.[14,15]

Our study, called the Child–Adolescent Anxiety Multimodal Study, was designed to address the current gaps in the treatment literature by evaluating the relative efficacy of cognitive behavioral therapy, sertraline, a combination of the two therapies, and a placebo drug. This article reports the results of short-term treatment.

METHODS

STUDY DESIGN AND IMPLEMENTATION

This study was designed as a two-phase, multicenter, randomized, controlled trial for children and adolescents between the ages of 7 and 17 years who had separation or generalized anxiety disorder or social phobia. Phase 1 was a 12-week trial of short-term treatment comparing cognitive behavioral therapy, sertraline, and their combination with a placebo drug. Phase 2 is a 6-month open extension for patients who had a response in phase 1.

The authors designed the study, wrote the manuscript, and vouch for the data gathering and analysis. Pfizer provided sertraline and matching placebo free of charge but was not involved in the design or implementation of the study, the analysis or interpretation of data, the preparation or review of the manuscript, or the decision to publish the results of the study.

STUDY SUBJECTS

Children between the ages of 7 and 17 years with a primary diagnosis of separation or generalized anxiety disorder or social phobia (according to the criteria of the *Diagnostic and Statistical Manual of Mental Disorders*, fourth edition, text revision [DSM-IV-TR][16]), substantial impairment, and an IQ of 80 or more were eligible to participate. Children with coexisting psychiatric diagnoses of lesser severity than the three target disorders were also allowed to participate; such diagnoses included attention deficit–hyperactivity disorder (ADHD) while receiving stable doses of stimulant and obsessive–compulsive, post-traumatic stress, oppositional–defiant, and conduct disorders. Children were excluded if they had an unstable medical condition, were refusing to attend school because of anxiety, or had tried but had not had a response to two adequate trials of SSRIs or an adequate trial of cognitive behavioral therapy. Girls who were pregnant or were sexually active and were not using an effective method of birth control were also excluded. Children who were receiving psychoactive medications other than stable doses of stimulants and who had psychiatric diagnoses that made participation in the study clinically inappropriate (i.e., current major depressive or substance-use disorder; unmedicated ADHD, combined type; or a lifetime history of bipolar, psychotic, or pervasive developmental disorders) or who presented an acute risk to themselves or others were also excluded.

Recruitment occurred from December 2002 through May 2007 at Duke University Medical Center, New York State Psychiatric Institute–Columbia University Medical Center–New York University, Johns Hopkins Medical Institutions, Temple University, University of California, Los Angeles, and Western Psychiatric Institute and Clinic–University of Pittsburgh Medical Center. The protocol was approved and monitored by institutional review boards at each center and by the data and safety monitoring board of the National Institute of Mental Health. Subjects and at least one parent provided written informed consent.

INTERVENTIONS

Cognitive behavioral therapy involved fourteen 60-minute sessions, which included review and ratings of the severity of subjects' anxiety, response to treatment, and adverse events. Therapy was based on the Coping Cat program,[17,18] which was adapted for the subjects' age and the duration of the study.[19] Each subject who was assigned to receive cognitive behavioral therapy received training in anxiety-management skills, followed by behavioral exposure to anxiety-provoking situations. Parents attended weekly check-ins and two parent-only sessions. Experienced psychotherapists, certified in the Coping Cat protocol, received regular site-level and cross-site supervision.

Pharmacotherapy involved eight sessions of 30 to 60 minutes each that included review and ratings of the severity of subjects' anxiety, their response to treatment, and adverse events. Sertraline (Zoloft) and matching placebo were administered on a fixed–flexible schedule beginning with 25 mg per day and adjusted up to 200 mg per day by week 8. Through week 8, subjects who were considered to be mildly ill or worse and who had minimal side effects were eligible for dose increases. Psychiatrists and nurse clinicians with experience in medicating children with anxiety disorders were certified in the study pharmacotherapy protocol and received regular site-level and cross-site supervision. Pill counts and medication diaries were used to facilitate and document adherence.

Combination therapy consisted of the administration of sertraline and cognitive behavioral therapy. Whenever possible, therapy and medication sessions occurred on the same day for the convenience of subjects.

OBJECTIVES

Study objectives were, first, to compare the relative efficacy of the three active treatments with placebo; second, to compare combination therapy with either sertraline or cognitive behavioral therapy alone; and third, to assess the safety and tolerability of sertraline, as compared with placebo. We hypothesized that all three active treatments would be superior to placebo and that combination therapy would be superior to either sertraline or cognitive behavioral therapy alone.

OUTCOME ASSESSMENTS

We obtained demographic information, information on symptoms of anxiety, and data on coexisting disorders and psychosocial functioning using reports from both the subjects and their parents and from interviews of subjects and parents at the time of screening, at baseline, and at weeks 4, 8, and 12. The interviews were administered by independent evaluators who were unaware of study-group assignments.

We used the Anxiety Disorders Interview Schedule for DSM-IV-TR, Child Version,[20] to establish diagnostic eligibility. The categorical primary outcome was the treatment response at week 12, which was defined as a score of 1 (very much improved) or 2 (much improved) on the Clinical Global Impression–Improvement scale,[21] which ranges from 1 to 7, with lower scores indicating more improvement, as compared with baseline. A score of 1 or 2 reflects a substantial, clinically meaningful improvement in anxiety severity. The dimensional primary outcome was anxiety severity as measured on the Pediatric Anxiety Rating Scale, computed by the summation of six items assessing anxiety severity, frequency, distress, avoidance, and interference during the previous week.[22] Total scores on this scale range from 0 to 30, with scores above 13 indicating clinically meaningful anxiety. The Children's Global Assessment Scale[23] was used to rate overall impairment. Scores on this scale range from 1 to 100; scores of 60 or lower are considered to indicate a need for treatment, and a score of 50 corresponds to moderate impairment that affects most life situations and is readily observable. Agreement among the raters was high for anxiety severity ($r=0.85$) and diagnostic status (intraclass correlation coefficient=0.82 to 0.88) on the basis of a videotaped review of 10% of assessments by independent evaluators that were performed at baseline and at week 12.

ADVERSE EVENTS

Adverse events were defined as any unfavorable change in the subjects' pretreatment condition, regardless of its relationship to a particular therapy. Serious adverse events were life-threatening events, hospitalization, or events leading to major incapacity. Harm-related adverse events were defined as thoughts of harm to self or others or related behaviors.

All subjects were interviewed at the start of each visit by the study coordinator with the use of a standardized script. Identified adverse events and harm-related events were then evaluated and rated by each subject's study clinician. This report presents data on all serious adverse events, all harm-related adverse events, and moderate and severe (i.e., functionally impairing) adverse events that occurred in 3% or more of subjects in any study group. The data and safety monitoring board of the National Institute of Mental Health performed a quarterly review of reported adverse events.

Given the greater number of study visits (and hence more reporting opportunities) and the unblinded administration of sertraline in the combination-therapy group, the test of the adverse-event profile of sertraline focused on statistical comparisons between sertraline and placebo and sertraline and cognitive behavioral therapy.

RANDOMIZATION AND MASKING

The randomization sequence in a 2:2:2:1 ratio was determined by a computer-generated algorithm and maintained by the central pharmacy, with stratification according to age, sex, and study center. Subjects were assigned to study groups after being deemed eligible and undergoing verbal reconsent with a study investigator. Subjects in the sertraline and placebo groups did not know whether they were receiving active therapy, nor did their clinicians. However, subjects who received combination therapy knew they were receiving active sertraline. The study protocol called for independent evaluators who completed assessments to be unaware of all treatment assignments.

STATISTICAL ANALYSIS

On the basis of previous studies,[10-15] we hypothesized that 80% of children in the combination-therapy group, 60% in either the sertraline group or the cognitive-behavioral-therapy group, and 30% in the placebo group would be considered to have had a response to treatment at week 12. We determined that we needed to enroll 136 subjects in each active-treatment group and 70 subjects in the placebo group for the study to have a power of 80% to detect a minimum difference of 17% between any two study groups in the rate of response, assuming an alpha of 0.05 and a two-tailed test with no adjustment for multiple comparisons.

Analyses were performed with the use of SAS software, version 9.1.3 (SAS Institute). For categorical outcomes (including data regarding adverse events), treatments were compared with the use of Pearson's chi-square test, Fisher's exact test, or logistic regression, as appropriate. Logistic-regression models included the study center as a covariate. For dimensional outcomes, linear mixed-effects models (implemented with the use of PROC MIXED) were used to determine predicted mean values at each assessment point (weeks 4, 8, and 12) and to test the study hypotheses with respect to between-group differences at week 12. In each linear mixed-effects model, time and study group were included as fixed effects, with linear and quadratic time and time-by-treatment group interaction terms. Each model also began with a limited number of covariates (e.g., age, sex, and race), followed by backward stepping to identify the best-fitting and most parsimonious model. In all models, random effects included intercept and linear slope terms, and an unstructured covariance was used to account for within-subject correlation over time. All comparisons were planned and tests were two-sided. A P value of less than 0.05 was considered to indicate statistical significance. The sequential Dunnett test was used to control the overall (familywise) error rate.[24]

We analyzed data from all subjects according to study group. Sensitivity analyses were performed with the last observation carried forward (LOCF) and multiple imputation assuming missingness at random. Results were similar for the two missing-data methods. We report the results of the LOCF analysis because the response rates were lower and hence provide a more conservative estimate of outcomes.

RESULTS

SUBJECTS

A total of 3066 potentially eligible subjects were screened by telephone (Fig. 1). Of these subjects, 761 signed consent forms and completed the inclusion and exclusion evaluation, 524 were deemed to be eligible and completed the baseline assessment, and 488 underwent randomization. Eleven subjects (2.3%) stopped treatment but were included in the assessment (treatment withdrawals); 46 subjects (9.4%) stopped both treatment and assessment (study withdrawals). On the basis of logistic-regression analyses, pairwise comparisons indicated that subjects in the cognitive-behavioral-therapy group were significantly less likely to withdraw from treatment than were those in the sertraline group (odds ratio, 0.33; 95% confidence interval [CI], 0.13 to 0.87; P=0.03) or the placebo group (odds ratio, 0.24; 95% CI; 0.09 to

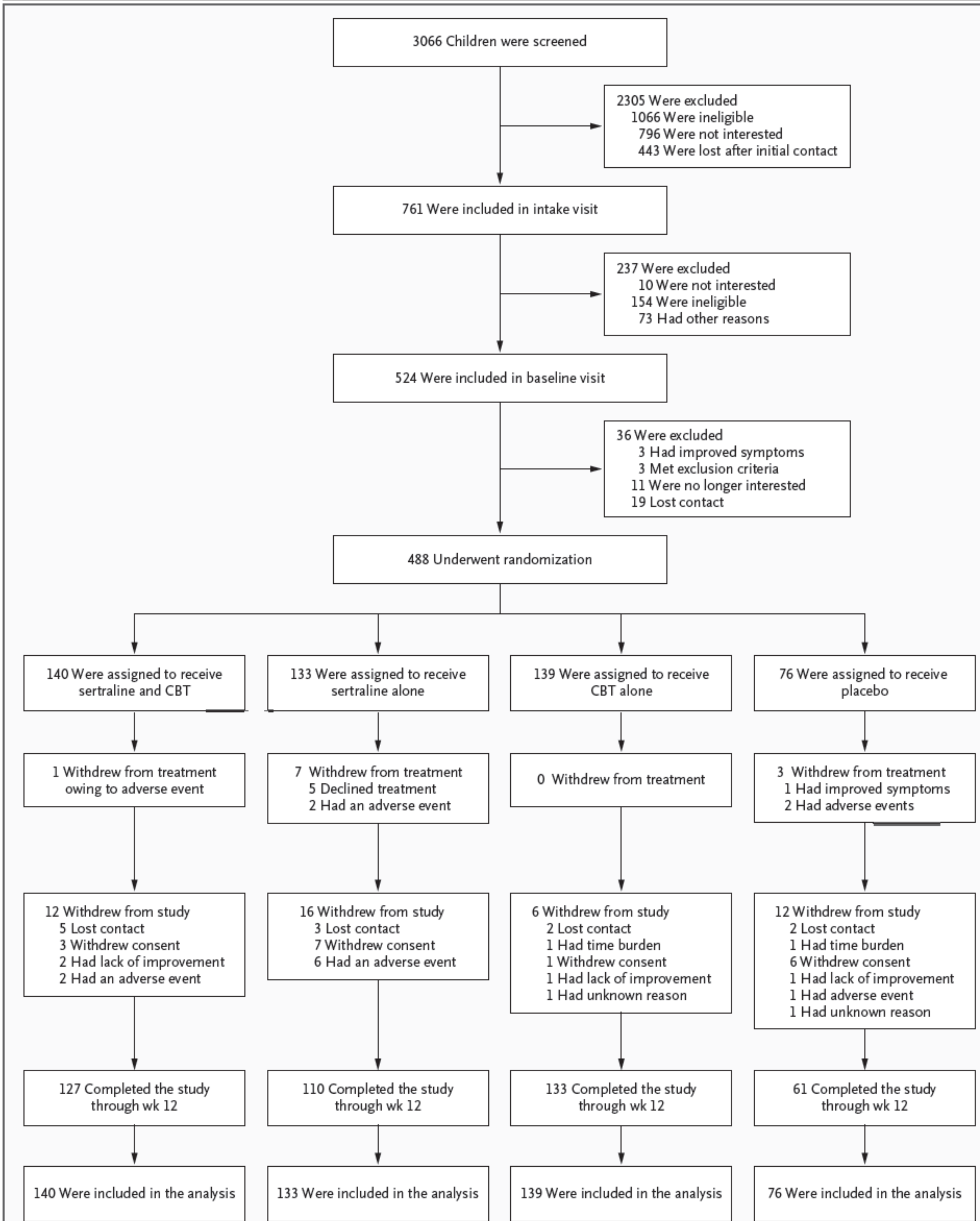

Figure 1. Enrollment and Outcomes.

Subjects who are shown as having withdrawn from treatment discontinued their assigned therapy but continued to undergo study assessment. Subjects who are shown as having withdrawn from the study discontinued both therapy and assessment. CBT denotes cognitive behavioral therapy.

Table 1. Baseline Characteristics of the Subjects and Recruitment According to Study Center.*

Variable	Combination Therapy (N=140)	Sertraline (N=133)	Cognitive Behavioral Therapy (N=139)	Placebo (N=76)	All Subjects (N=488)	P Value
Study center — no. (%)						
New York State Psychiatric Institute–Columbia University Medical Center–New York University	18 (12.9)	15 (11.3)	16 (11.5)	10 (13.2)	59 (12.1)	
Duke University Medical Center	29 (20.7)	29 (21.8)	30 (21.6)	16 (21.1)	104 (21.3)	
Johns Hopkins Medical Institutions	30 (21.4)	27 (20.3)	29 (20.9)	15 (19.7)	101 (20.7)	
Temple University–University of Pennsylvania	22 (15.7)	23 (17.3)	22 (15.8)	13 (17.1)	80 (16.4)	
University of California, Los Angeles	21 (15.0)	20 (15.0)	21 (15.1)	11 (14.5)	73 (15.0)	
Western Psychiatric Institute and Clinic–University of Pittsburgh Medical Center	20 (14.3)	19 (14.3)	21 (15.1)	11 (14.5)	71 (14.5)	
Demographic characteristics						
Age						
7–12 yr — no. (%)	101 (72.1)	99 (74.4)	108 (77.7)	54 (71.1)	362 (74.2)	0.66
Mean — yr	10.7±2.8	10.8±2.8	10.5±2.9	10.6±2.8	10.7±2.8	0.93
Female sex — no. (%)	72 (51.4)	61 (45.9)	72 (51.8)	37 (48.7)	242 (49.6)	0.75
Race or ethnic group — no. (%)†						0.43
White	116 (82.9)	103 (77.4)	106 (76.3)	60 (78.9)	385 (78.9)	
Black	11 (7.9)	12 (9.0)	14 (10.1)	7 (9.2)	44 (9.0)	
Asian	6 (4.3)	4 (3.0)	1 (0.7)	1 (1.3)	12 (2.5)	
American Indian	1 (0.7)	2 (1.5)	3 (2.2)	0	6 (1.2)	
Pacific Islander	1 (0.7)	0	0	1 (1.3)	2 (0.4)	
Other	5 (3.6)	12 (9.0)	15 (10.8)	7 (9.2)	39 (8.0)	
Hispanic	16 (11.4)	15 (11.3)	21 (15.1)	7 (9.2)	59 (12.1)	0.59
Low socioeconomic status — no. (%)‡	35 (25.0)	35 (26.3)	33 (23.7)	21 (27.6)	124 (25.4)	0.92
Primary diagnosis of anxiety disorder — no. (%)						
Separation anxiety only	2 (1.4)	5 (3.8)	6 (4.3)	3 (3.9)	16 (3.3)	0.53
Social phobia only	14 (10.0)	19 (14.3)	16 (11.5)	6 (7.9)	55 (11.3)	0.51
Generalized anxiety only	10 (7.1)	8 (6.0)	11 (7.9)	4 (5.3)	33 (6.8)	0.87
Separation anxiety and social phobia	12 (8.6)	7 (5.3)	7 (5.0)	7 (9.2)	33 (6.8)	0.46
Separation anxiety and generalized anxiety	13 (9.3)	12 (9.0)	8 (5.8)	6 (7.9)	39 (8.0)	0.69
Social phobia and generalized anxiety	41 (29.3)	37 (27.8)	40 (28.8)	19 (25.0)	137 (28.1)	0.92
Separation anxiety, social phobia, and generalized anxiety	48 (34.3)	45 (33.8)	51 (36.7)	31 (40.8)	175 (35.9)	0.74
Secondary diagnosis of coexisting disorder — no. (%)§						
Other internalizing disorders¶	70 (50.0)	55 (41.4)	56 (40.3)	32 (42.1)	213 (43.6)	0.35
Attention deficit–hyperactivity disorder	16 (11.4)	17 (12.8)	16 (11.5)	9 (11.8)	58 (11.9)	0.98
Oppositional–defiant disorder or conduct disorder	14 (10.0)	11 (8.3)	14 (10.1)	7 (9.2)	46 (9.4)	0.95
Tic disorder	4 (2.9)	5 (3.8)	2 (1.4)	2 (2.6)	13 (2.7)	0.70

* Plus–minus values are means ±SD.
† Race or ethnic group was reported by the subjects.
‡ Low socioeconomic status was defined as a score of 3 or less on the Hollingshead Two-Factor Scale, which ranges from 1 to 5.
§ Secondary diagnosis of coexisting disorders refers to an allowable diagnosis that was rated as less severe than the anxiety disorder of interest.
¶ Other internalizing disorders include other anxiety disorders and dysthymia.

0.67; P=0.006). Of the 488 subjects who underwent randomization, 459 (94.1%) completed at least one postbaseline assessment, 396 (81.1%) completed all four assessments, and 440 (90.2%) completed the assessment at week 12. Subjects were recruited primarily through advertisements (52.2%) or clinical referrals (44.1%).

Of 14 possible sessions of cognitive behavioral therapy, the mean (±SD) number of sessions completed was 12.7±2.8 in the combination-therapy group and 13.2±2.0 in the cognitive-behavioral-therapy group. The mean dose of sertraline at the final visit was 133.7±59.8 mg per day (range, 25 to 200) in the combination-therapy group, 146.0±60.8 mg per day (range, 25 to 200) in the sertraline group, and 175.8±43.7 mg per day (range, 50 to 200) in the placebo group.

DEMOGRAPHIC AND CLINICAL CHARACTERISTICS

There were no significant differences among study groups with respect to baseline demographic and clinical characteristics (Table 1). The mean age

Table 2. Key Outcomes at 12 Weeks.*

Assessment Scale and Week of Evaluation	Combination Therapy (N=140)	Sertraline (N=133)	Cognitive Behavioral Therapy (N=139)	Placebo (N=76)
Clinical Global Impression–Improvement scale — % with response to therapy (95% CI)†				
Baseline	NA	NA	NA	NA
Week 4	21.4 (15.4–29.0)	18.8 (13.0–18.8)	9.3 (5.5–15.5)	6.6 (2.6–14.9)
Week 8	54.3 (46.0–62.3)	47.4 (39.1–55.8)	29.5 (22.6–37.6)	22.4 (14.4–33.1)
Week 12	80.7 (73.3–86.4)	54.9 (46.4–63.1)	59.7 (51.4–67.5)	23.7 (15.5–34.5)
Score on Pediatric Anxiety Rating Scale — mean (95% CI)‡§				
Baseline	19.4±3.9 (18.8–20.1)	18.8±3.9 (18.1–19.4)	18.9±3.9 (18.2–19.6)	19.6±3.9 (18.7–20.5)
Week 4	14.6±3.9 (14.0–15.3)	14.2±4.0 (13.6–14.9)	16.0±3.9 (15.4–16.7)	16.0±4.1 (15.0–16.9)
Week 8	10.6±4.9 (9.8–11.4)	11.2±5.0 (10.4–12.1)	13.3±4.8 (12.5–14.1)	13.6±5.2 (12.5–14.8)
Week 12	7.4±6.0 (6.4–8.4)	9.8±6.2 (8.7–10.8)	10.8±5.9 (9.8–11.7)	12.6±6.3 (11.2–14.0)
Score on Clinical Globe Impressions–Severity — mean (95% CI)§¶				
Baseline	5.1±0.7 (5.0–5.2)	5.0±0.7 (4.8–5.1)	5.0±0.7 (4.9–5.1)	5.1±0.7 (5.0–5.3)
Week 4	4.2±0.8 (4.0–4.3)	4.1±0.8 (4.0–4.2)	4.5±0.8 (4.4–4.6)	4.4±0.8 (4.2–4.6)
Week 8	3.3±1.0 (3.1–3.4)	3.5±1.0 (3.3–3.6)	3.9±1.0 (3.7–4.1)	4.0±1.1 (3.7–4.2)
Week 12	2.4±1.3 (2.2–2.7)	3.0±1.3 (2.8–3.2)	3.3±1.3 (3.1–3.5)	3.8±1.4 (3.5–4.1)
Score on Children's Global Assessment Scale — mean (95% CI)§‖				
Baseline	50.5±7.0 (49.3–51.7)	50.9±7.0 (49.7–52.1)	51.0±7.1 (49.8–52.1)	50.1±7.0 (48.5–51.6)
Week 4	56.2±6.7 (55.1–57.4)	56.8±6.9 (55.6–57.9)	54.3±6.7 (53.1–55.4)	54.6±7.0 (53.0–56.2)
Week 8	62.3±8.3 (60.9–63.6)	61.4±8.5 (60.0–62.9)	58.5±8.2 (57.2–59.9)	58.0±8.7 (56.0–59.9)
Week 12	68.6±10.4 (66.9–70.3)	65.0±10.7 (63.1–66.8)	63.8±10.2 (62.1–65.5)	60.1±10.9 (57.7–62.6)

* Plus–minus values are means ±SD. All analyses were performed on data from the intention-to-treat population. Primary outcome variables were scores on the Clinical Global Impression–Improvement scale and the Pediatric Anxiety Rating Scale. NA denotes not applicable.

† Values are the proportion of subjects who had a response to therapy, which was defined as a score of 1 (very much improved) or 2 (much improved) on the Clinical Global Impression–Improvement scale, which ranges from 1 to 7, with lower scores indicating more improvement, as compared with baseline.

‡ Scores on the Pediatric Anxiety Rating Scale range from 0 to 30, with scores higher than 13 consistent with moderate levels of anxiety and a diagnosis of an anxiety disorder.

§ Values are expected mean scores, which were determined by linear mixed-effects model analysis.

¶ Scores on the Clinical Global Impression–Severity scale range from 1 to 7, with higher scores indicating greater severity of the disorder.

‖ Scores on the Children's Global Assessment Scale range from 1 to 100, with lower scores indicating greater impairment. Scores of 60 or lower are considered to indicate a need for treatment, and a score of 50 corresponds to moderate impairment that affects most life situations and is readily observable.

of participants was 10.7±2.8 years, with 74.2% under the age of 13 years. There were nearly equal numbers of male and female subjects. Most subjects were white (78.9%), with other racial and ethnic groups represented. Subjects came from predominantly middle-class and upper-middle-class families (74.6%) and lived with both biologic parents (70.3%). Most subjects had received the diagnosis of two or more primary anxiety disorders (78.7%) and one or more secondary disorders (55.3%). At baseline, subjects had moderate-to-severe anxiety and impairment (Table 2). Given the geographic diversity among study centers, there were significant differences among sites on several baseline demographic variables (e.g., race and socioeconomic status). Overall, these variables were equally distributed among study groups within each center; however, three centers had one instance each of unequal distribution for sex, race, or socioeconomic status.

CLINICAL RESPONSE

In the intention-to-treat analysis, the percentages of children who were rated as 1 (very much improved) or 2 (much improved) on the Clinical Global Impression–Improvement scale at 12 weeks were 80.7% (95% CI, 73.3 to 86.4) in the combination-therapy group, 59.7% (95% CI, 51.4 to 67.5) in the cognitive-behavioral-therapy group, 54.9% (95% CI, 46.4 to 63.1) in the sertraline group, and 23.7% (95% CI, 15.5 to 34.5) in the placebo group (Table 2). With the study center as a covariate, planned pairwise comparisons from a logistic-regression model showed that each active treatment was superior to placebo as follows: combination therapy versus placebo, $P<0.001$ (odds ratio, 13.6; 95% CI, 6.9 to 26.8); cognitive behavioral therapy versus placebo, $P<0.001$ (odds ratio, 4.8; 95% CI, 2.6 to 9.0); and sertraline versus placebo, $P<0.001$ (odds ratio, 3.9; 95% CI, 2.1 to 7.4). Similar pairwise comparisons revealed that combination therapy was superior to either sertraline alone (odds ratio, 3.4; 95% CI, 2.0 to 5.9; $P<0.001$) or cognitive behavioral therapy alone (odds ratio, 2.8; 95% CI, 1.6 to 4.8; $P=0.001$). However, there was no significant difference between sertraline and cognitive behavioral therapy ($P=0.41$).

There was no main effect for center ($P=0.69$); however, a comparison among centers according to study group revealed a significant difference in response to combination therapy but no differences with respect to the response to sertraline alone ($P=0.15$) or cognitive behavioral therapy alone ($P=0.25$). Further evaluation of response rates revealed that the average response rate for combination therapy at one center was significantly lower than at the other centers ($P=0.002$). A sensitivity analysis of site response rates showed that when data from the one site were removed, the average response rate of the other sites was consistent with that of the full sample.

The mixed-effects model for the Pediatric Anxiety Rating Scale revealed a significant quadratic effect for time ($P<0.001$) and a significant quadratic time-by-treatment interaction for cognitive behavioral therapy versus placebo ($P=0.01$) but not for either combination therapy or sertraline versus placebo. In other words, as compared with placebo, cognitive behavioral therapy had a linear mean trajectory (Fig. 2). Planned pairwise comparisons of the expected mean scores on the Pediatric Anxiety Rating Scale at week 12 revealed a similar ordering of outcomes, with all active treatments superior to placebo, according to the following comparisons: combination therapy versus placebo, $t=-5.94$ ($P<0.001$); cogni-

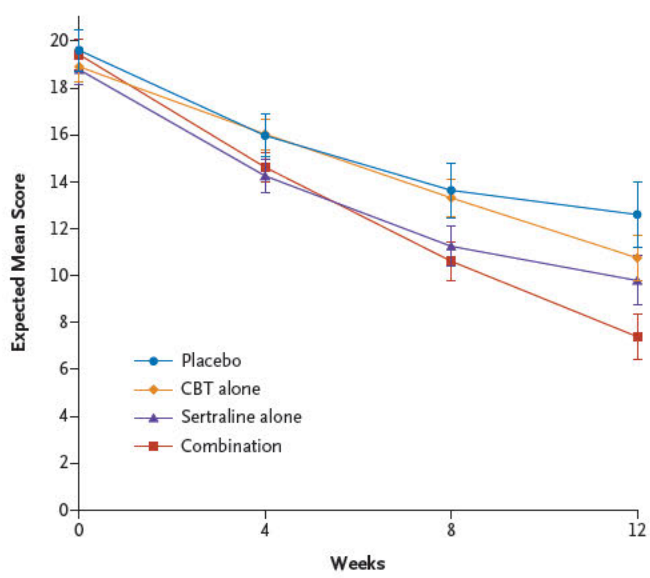

Figure 2. Scores on the Pediatric Anxiety Rating Scale during the 12-Week Study.

Scores on the Pediatric Anxiety Rating Scale range from 0 to 30, with scores higher than 13 consistent with moderate levels of anxiety and a diagnosis of an anxiety disorder. The expected mean score is the mean of the sampling distribution of the mean. The I bars represent standard errors.

tive behavioral therapy versus placebo, t=−2.11 (P=0.04); and sertraline versus placebo, t=−3.15 (P=0.002). In addition, combination therapy was superior to both sertraline alone (t=−3.26, P=0.001) and cognitive behavioral therapy alone (t=−4.73, P<0.001). No significant difference was found between sertraline and cognitive behavioral therapy (t=−1.32, P=0.19). The same magnitude and pattern of outcome were found for the Clinical Global Impression–Severity scale and the Children's Global Assessment Scale.

Estimates of the effect size (Hedges' g) and the number needed to treat between the active-treatment groups and the placebo group were calculated. Effect sizes are based on the expected mean scores on the Pediatric Anxiety Rating Scale, derived from the mixed-effects model. The number needed to treat is based on the dichotomized, end-of-treatment scores on the Clinical Global Impression–Improvement scale with the use of LOCF. The effect size was 0.86 (95% CI, 0.56 to 1.15) for combination therapy, 0.45 (95% CI, 0.17 to 0.74) for sertraline, and 0.31 (95% CI, 0.02 to 0.59) for cognitive behavioral treatment. The number needed to treat was 1.7 (95% CI, 1.7 to 1.9) for combination therapy, 3.2 (95% CI, 3.2 to 3.5) for sertraline, and 2.8 (95% CI, 2.7 to 3.0) for cognitive behavioral therapy.

Table 3. Subjects Who Withdrew from Treatment or the Study.*

Variable	Combination Therapy (N=140)	Sertraline (N=133)	Cognitive Behavioral Therapy (N=139)	Placebo (N=76)
	number (percent)			
Withdrawal from treatment	1 (0.7)	7 (5.3)	0	3 (3.9)
Attributed to an adverse event	1 (0.7)	2 (1.5)	0	2 (2.6)
Tremor	0	1 (0.8)	0	0
Stomach pain	0	1 (0.8)	0	0
Suicidal ideation	0	0	0	1 (1.3)
Worsening symptoms	1 (0.7)	0	0	1 (1.3)
Other reason	0	5 (3.8)	0	1 (1.3)
Improved symptoms	0	0	0	1 (1.3)
Declined treatment	0	5 (3.8)	0	0
Withdrawal from study	12 (8.6)	16 (12.0)	6 (4.3)	12 (15.8)
Attributed to an adverse event	2 (1.4)	6 (4.5)	0	1 (1.3)
Agitation or disinhibition	1 (0.7)	2 (1.5)	0	0
Self-harm or homicidal ideation	0	1 (0.8)	0	0
Hyperactivity	0	1 (0.8)	0	0
Worsening symptoms	1 (0.7)	1 (0.8)	0	0
Headache	0	1 (0.8)	0	0
Rash	0	0	0	1 (1.3)
Other reason	10 (7.1)	10 (7.5)	6 (4.3)	11 (14.5)
Lack of improvement	2 (1.4)	0	1 (0.7)	1 (1.3)
Loss of contact	5 (3.6)	3 (2.3)	2 (1.4)	2 (2.6)
Time burden	0	0	1 (0.7)	1 (1.3)
Withdrawal of consent	3 (2.1)	7 (5.3)	1 (0.7)	6 (7.9)
Other	0	0	1 (0.7)	1 (1.3)

* Subjects who withdrew from treatment stopped receiving their assigned therapy but continued to undergo assessment; those who withdrew from the study stopped receiving their assigned treatment and did not undergo continued assessment.

TREATMENT AND STUDY WITHDRAWALS

Most treatment and study withdrawals were attributed to reasons other than adverse events (43 of 57, 75.4%) (Table 3). Of the 14 withdrawals that were attributed to an adverse event, 11 (78.6%) were in the groups receiving either sertraline alone or placebo and consisted of 3 physical events (headache, stomach pains, and tremor) and 8 psychiatric adverse events (worsening of symptoms, 3 subjects; agitation or disinhibition, 3; hyperactivity, 1; and nonsuicidal self-harm and homicidal ideation, 1).

Table 4. Moderate-to-Severe Adverse Events at 12 Weeks.*

Variable	Combination Therapy (N=140)	Sertraline (N=133)	Cognitive Behavioral Therapy (N=139)	Placebo (N=76)	All Subjects (N=488)	P Value†	
						Sertraline vs. Placebo	Sertraline vs. CBT
	number (percent)						
Adverse event							
Physical	58 (41.4)	67 (50.4)	51 (36.7)	35 (46.1)	211 (43.2)		
Headache	18 (12.9)	21 (15.8)	12 (8.6)	6 (7.9)	57 (11.7)	0.10‡	0.07‡
Gastric distress	14 (10.0)	15 (11.3)	11 (7.9)	6 (7.9)	46 (9.4)	0.43‡	0.35‡
Sore throat	10 (7.1)	6 (4.5)	12 (8.6)	6 (7.9)	34 (7.0)	0.31‡	0.17‡
Cold symptoms	8 (5.7)	9 (6.8)	10 (7.2)	3 (3.9)	30 (6.1)	0.54	0.89‡
Vomiting	8 (5.7)	6 (4.5)	5 (3.6)	4 (5.3)	23 (4.7)	1.00	0.70‡
Insomnia	7 (5.0)	11 (8.3)§	2 (1.4)§	3 (3.9)	23 (4.7)	0.23‡	0.01‡
Fever	6 (4.3)	1 (0.8)	8 (5.8)	3 (3.9)	18 (3.7)	0.14	0.04
Upper respiratory tract infection	5 (3.6)	3 (2.3)	7 (5.0)	3 (3.9)	18 (3.7)	0.67	0.34
Diarrhea	6 (4.3)	5 (3.8)	4 (2.9)	2 (2.6)	17 (3.5)	1.00	0.74
Interrupted sleep	6 (4.3)	6 (4.5)	2 (1.4)	2 (2.6)	16 (3.3)	0.71	0.16
Nausea	5 (3.6)	4 (3.0)	3 (2.2)	3 (3.9)	15 (3.1)	0.71	0.72
Body ache	5 (3.6)	4 (3.0)	3 (2.2)	2 (2.6)	14 (2.9)	1.00	0.72
Fatigue	3 (2.1)	8 (6.0)§	0§	3 (3.9)	14 (2.9)	0.75	0.003
Accidental injury	4 (2.9)	4 (3.0)	4 (2.9)	1 (1.3)	13 (2.7)	0.66	1.00
Allergy	5 (3.6)	2 (1.5)	3 (2.2)	2 (2.6)	12 (2.5)	0.63	1.00
Asthma	3 (2.1)	5 (3.8)	2 (1.4)	0	10 (2.0)	0.16	0.27
Other infection	5 (3.6)	0	4 (2.9)	1 (1.3)	10 (2.0)	0.36	0.12
Ear pain	5 (3.6)	2 (1.5)	2 (1.4)	0	9 (1.8)	0.54	1.00
Sedation	0	6 (4.5)§	0§	1 (1.3)	7 (1.4)	0.43	0.01
Medical or surgical	1 (0.7)	1 (0.8)	1 (0.7)	3 (4.0)	6 (1.2)	0.14	1.00
Psychiatric	41 (29.3)	23 (17.3)	13 (9.4)	10 (13.2)	87 (17.8)		
Disinhibition	12 (8.6)	6 (4.5)	2 (1.4)	1 (1.3)	21 (4.3)	0.43	0.16
Increased motor activity	10 (7.1)	4 (3.0)	1 (0.7)	1 (1.3)	16 (3.3)	0.66	0.21
Disobedient or defiant	9 (6.4)	4 (3.0)	2 (1.4)	0	15 (3.1)	0.30	0.44
Emotional outburst	1 (0.7)	4 (3.0)	4 (2.9)	3 (3.9)	12 (2.5)	0.71	1.00
Restless or fidgety	5 (3.6)	5 (3.8)§	0§	2 (2.6)	12 (2.5)	1.00	0.03
Anxiety or nervousness	5 (3.6)	1 (0.8)	1 (0.7)	4 (5.3)	11 (2.3)	0.06	1.00
Irritability	3 (2.1)	4 (3.0)	3 (2.2)	1 (1.3)	11 (2.3)	0.66	0.72
Agitation	7 (5.0)	1 (0.8)	1 (0.7)	0	9 (1.8)	1.00	1.00
Impulsivity	5 (3.6)	2 (1.5)	1 (0.7)	1 (1.3)	9 (1.8)	1.00	0.61

Table 4. (Continued.)

Variable	Combination Therapy (N=140)	Sertraline (N=133)	Cognitive Behavioral Therapy (N=139)	Placebo (N=76)	All Subjects (N=488)	P Value†	
						Sertraline vs. Placebo	Sertraline vs. CBT
			number (percent)				
Harm-related¶	14 (10.0)	3 (2.3)	8 (5.8)	1 (1.3)	26 (5.3)		
Aggression	8 (5.7)	1 (0.8)	2 (1.4)	0	11 (2.3)	1.00	1.00
Self-harm behavior without suicidal intent	2 (1.4)	1 (0.8)	1 (0.7)	0	4 (0.8)	1.00	1.00
Suicidal ideation	5 (3.6)	0	5 (3.6)	1 (1.3)	11 (2.3)	0.36	0.06
Suicide attempt	0	0	0	0	0	NA	NA
Homicidal ideation	0	2 (1.5)	0	0	2 (0.4)	0.54	0.24
Homicide attempt	0	0	0	0	0	NA	NA
Serious adverse event¶							
Psychiatric hospitalization	1 (0.7)	1 (0.8)‖	0	0	2 (0.4)	1.00	1.00
Medical hospitalization	0	1 (0.8)	0	0	1 (0.2)	1.00	1.00

* Adverse events that occurred in at least 3% of the patients in any study group are reported, unless otherwise noted. Subjects could have more than one adverse event. Case definitions of psychiatric disorders are from the DSM-IV-TR.[16] CBT denotes cognitive behavioral therapy, and NA not applicable.
† Differences in the number of adverse events in the sertraline group, as compared with the placebo group and the cognitive-behavioral-therapy group, were evaluated with the use of Fisher's exact test, unless otherwise noted.
‡ The reported P value was calculated with the use of Pearson's chi-square statistic.
§ P<0.05 for the comparison between the sertraline group and the cognitive-behavioral-therapy group.
¶ All harm-related adverse events and serious adverse events are reported (i.e., not limited only to those occurring in at least 3% of the subjects).
‖ This event was considered to be possibly related to treatment.

SERIOUS ADVERSE EVENTS

Three subjects had serious adverse events during the study period. One child in the sertraline group had a worsening of behavior that was attributed to the parents' increased limit setting on avoidance behavior; the event was considered to be possibly related to sertraline. A child in the combination-therapy group had a worsening of preexisting oppositional–defiant behavior that resulted in psychiatric hospitalization; this event was considered to be unrelated to a study treatment. The third subject was hospitalized for a tonsillectomy, which was also considered to be unrelated to a study treatment (Table 4).

ADVERSE EVENTS

Subjects in the combination-therapy group had a greater number of study visits and therefore significantly more opportunities for elicitation of adverse events than did those in the other study groups, with a mean of 12.8±4.0 opportunities (range, 1 to 22) in the combination-therapy group, as compared with 9.9±3.6 (range, 1 to 14) in the sertraline group, 10.6±2.0 (range, 1 to 14) in the cognitive-behavioral-therapy group, and 9.7±4.2 (range, 1 to 14) in the placebo group (P<0.001 for all comparisons). Rates of adverse events, including suicidal and homicidal ideation, were not significantly greater in the sertraline group than in the placebo group. No child in the study attempted suicide. Among children in the cognitive-behavioral-therapy group, there were fewer reports of insomnia, fatigue, sedation, and restlessness or fidgeting than in the sertraline group (P<0.05 for all comparisons). For a list of mild adverse events that were not associated with functional impairment, as well as moderate and severe events, see the Supplementary Appendix, available with the full text of this article at www.nejm.org.

DISCUSSION

Our study examined therapies that many clinicians consider to be the most promising treatments for childhood anxiety disorders. Our findings indicate that as compared with placebo, the three active therapies — combination therapy with both cognitive behavioral therapy and sertraline, cognitive behavioral therapy alone, and sertraline alone — are effective short-term treatments for children with separation and generalized anxiety disorders and social phobia, with combination treatment having superior response rates. No physical, psychiatric, or harm-related adverse events were reported more frequently in the sertraline group than in the placebo group, a finding similar to that for SSRIs, as identified in previous studies of anxious children.[12,13,25] Few withdrawals from either treatment or the study were attributed to adverse events. Suicidal ideation and homicidal ideation were uncommon. No child attempted suicide during the study period.

Since they were recruited at multiple centers and locations, the study subjects were racially and ethnically diverse. However, despite intense outreach, the sample did not include the most socioeconomically disadvantaged children. Subjects were predominantly younger children and included those with ADHD and other anxiety disorders, factors that allow for generalization of the results to these populations. Conversely, the exclusion of children and teens with major depression and pervasive developmental disorders may have limited the generalizability of the results to these populations.

The observed advantage of combination therapy over either cognitive behavioral therapy or sertraline alone during short-term treatment (an improvement of 21 to 25%) suggests that among these effective therapies, combination therapy provides the best chance for a positive outcome. The superiority of combination therapy might be due to additive or synergistic effects of the two therapies. However, additional contact time in the combination-therapy group, which was unblinded, and expectancy effects on the part of both subjects and clinicians cannot be ruled out as alternative explanations. Nonetheless, the magnitude of the treatment effect in the combination-therapy group (with two subjects as the number needed to treat to prevent one additional event) suggests that children with anxiety disorders who receive quality combination therapy can consistently expect a substantial reduction in the severity of anxiety. An increased number of visits in the combination-therapy group resulted in increased opportunities for elicitation of adverse events. Consequently, the potential for expectancies among subjects, parents, and clinicians regarding the side effects of medications in the context of more visits may have increased the rate of some adverse events in the combination-therapy group and may limit conclusions that can be drawn regarding the rates of adverse events in combination therapy.

The positive benefit of cognitive behavioral therapy, as compared with placebo, adds new information to the existing literature.[26] The number needed to treat for cognitive behavioral therapy in this study (three subjects) is the same as that identified in a meta-analysis of studies comparing subjects who were assigned to cognitive behavioral therapy with those assigned to a waiting list for therapy or to sessions without active therapy.[14] Our study's test of cognitive behavioral therapy included children with moderate-to-severe anxiety and addresses criticism of previous trials that included children with only mild-to-moderate anxiety.[14] Before our study, cognitive behavioral therapy for childhood anxiety was considered to be "probably efficacious."[26] This evaluation of cognitive behavioral therapy and other recent studies[27,28] suggests that such therapy for childhood anxiety is a well-established, evidenced-based treatment.[29] Given that the risk of some adverse events was lower in the behavioral-therapy group than in the sertraline group, some parents and their children may consider choosing cognitive behavioral therapy as their initial treatment.

The results of our study confirm the short-term efficacy of sertraline for children with generalized anxiety disorder[25] and show that sertraline is effective for children with separation anxiety disorder and social phobia. The number needed to treat for sertraline in our study (three subjects) was the same as that previously identified in a meta-analysis[15] of six randomized, placebo-controlled trials of SSRIs for childhood anxiety disorders.[12,13,25,30,31] These studies and others[27] suggest that SSRIs, as a class, are the medication of choice for these conditions. The titration schedule that we used, which emphasized upward dose adjustment in the absence of response and adverse events, suggests that the average end-point dose of sertraline in this study is the highest dose consistent with good outcome and tolerability. No adverse events were observed more frequently in the sertraline group than in the placebo group. In contrast to the apparent risk of suicidal ideation and behavior in studies of depression in children and adolescents,[15] our study did not demonstrate any increased risk for suicidal behavior in the sertraline group. Given the benefit of sertraline alone or in combination with cognitive behavioral therapy and the limited risk of adverse events associated with the drug in our study, the well-monitored use of sertraline and other SSRIs in the treatment of childhood anxiety disorders is indicated.

Cognitive behavioral therapy and sertraline either in combination or as monotherapies appear to be effective treatments for these commonly occurring childhood anxiety disorders. Results confirm those of previous studies of SSRIs and cognitive behavioral therapy and, most important, show that combination therapy offers children the best chance for a positive outcome. Our findings indicate that all three of the treatment options may be recommended, taking into consideration the family's treatment preferences, treatment availability, cost, and time burden. To inform more prescriptive selection of patients for treatment, further analysis of predictors and moderators of treatment response may identify who is most likely to respond to which[32] of these effective alternatives.

Supported by grants (U01 MH064089, to Dr. Walkup; U01 MH64092, to Dr. Albano; U01 MH64003, to Dr. Birmaher; U01 MH63747, to Dr. Kendall; U01 MH64107, to Dr. March; U01 MH64088, to Dr. Piacentini; and U01 MH064003, to Dr. Compton) from the National Institute of Mental Health (NIMH). Sertraline and matching placebo were supplied free of charge by Pfizer.

Dr. Walkup reports receiving consulting fees from Eli Lilly and Jazz Pharmaceuticals and fees for legal consultation to defense counsel and submission of written reports in litigation involving GlaxoSmithKline, receiving lecture fees from CMP Media, Medical Education Reviews, McMahon Group, and DiMedix, and receiving support in the form of free medication and matching placebo from Eli Lilly and free medication from Abbott for clinical trials funded by the NIMH; Dr. Albano, receiving royalties from Oxford University Press for the Anxiety Disorders Interview Schedule for DSM-IV, Child and Parent Versions, but not for interviews used in this study, and royalties from the Guilford Press; Dr. Piacentini, receiving royalties from Oxford University Press for treatment manuals on childhood obsessive–compulsive disorder and tic disorders and from the Guilford Press and APA Books for other books on child mental health and receiving lecture fees from Janssen-Cilag; Dr. Birmaher, receiving consulting fees from Jazz Pharmaceuticals, Solvay Pharmaceuticals, and Abcomm, lecture fees from Solvay, and royalties from Random House for a book on children with bipolar disorder; Dr. Rynn, receiving grant support from Neuropharm, Boehringer Ingelheim Pharmaceuticals, and Wyeth Pharmaceuticals, consulting fees from Wyeth, and royalties from APPI for a book chapter on pediatric anxiety disorders; Dr. McCracken, receiving consulting fees from Sanofi-Aventis and Wyeth, lecture fees from Shire and UCB, and grant support from Aspect, Johnson & Johnson, Bristol-Myers Squibb, and Eli Lilly; Dr. Waslick, receiving grant support from Baystate Health, Somerset Pharmaceuticals, and GlaxoSmithKline; Dr. Iyengar, receiving consulting fees from Westinghouse for statistical consultation; Dr. March, receiving study medications from Eli Lilly for an NIMH-funded clinical trial and receiving royalties from Pearson for being the author of the Multidimensional Anxiety Scale for Children, receiving consulting fees from Eli Lilly, Pfizer, Wyeth, and GlaxoSmithKline, having an equity interest in MedAvante, and serving on an advisory board for AstraZeneca and Johnson & Johnson; and Dr. Kendall, receiving royalties from Workbook Publishing for anxiety-treatment materials. No other potential conflict of interest relevant to this article was reported.

The views expressed in this article are those of the authors and do not necessarily represent the official views of the NIMH, the National Institutes of Health, or the Department of Health and Human Services.

We thank the children and their families who made this study possible; and J. Chisar, J. Fried, R. Klein, E. Menvielle, S. Olin, J. Severe, D. Almirall, and members of NIMH's data and safety monitoring board.

APPENDIX

The following investigators participated in this study: **Steering Committee:** J. Walkup (chair), A. Albano (cochair), S. Compton (executive secretary); **Statistics–Experimental Design:** S. Compton, S. Iyengar, J. March; **Cognitive Behavioral Therapy:** P. Kendall, G. Ginsburg; **Pharmacotherapy:** M. Rynn, J. McCracken; **Assessment:** J. Piacentini, A. Albano; **Study Coordinators:** C. Keeton, H. Koo, S. Aschenbrand, L. Bardsley, R. Beidas, J. Catena, K. Dever, K. Drake, R. Dublin, E. Fontaine, J. Furr, A. Gonzalez, K. Hedtke, L. Hunt, M. Keller, J. Kingery, A. Krain, K. Miller, J. Podell, P. Rentas, M. Rozenmann, C. Suveg, C. Weiner, M. Wilson, T. Zoulas; **Data Center:** K. Sullivan, M. Fletcher; **Cognitive Behavior Therapists:** E. Gosch, C. Alfano, A. Angelosante, S. Aschenbrand, A. Barmish, L. Bergman, S. Best, J. Comer, S. Compton, W. Copeland, M. Cwik, M. Desari, K. Drake, E. Fontaine, J. Furr, P. Gammon, C. Gaze, R. Grover, H. Harmon, A. Hughes, K. Hutchinson, J. Jones, C. Keeton, H. Kepley, J. Kingery, A. Krain, A. Langley, J. Lee, J. Levitt, J. Manetti-Cusa, E. Martin, C. Mauro, K. McKnight, T. Peris, K. Poling, L. Preuss, A. Puliafico, J. Robin, T. Roblek, J. Samson, M. Schlossberg, M. Sweeney, C. Suveg, O. Velting, T. Verduin; **Pharmacotherapists:** M. Rynn, J. McCracken, A. Adegbola, P. Ambrosini, D. Axelson, S. Barnett, A. Baskina, B. Birmaher, C. Cagande, A. Chrisman, B. Chung, H. Courvoisie, B. Dave, A. Desai, K. Dever, M. Gazzola, E. Harris, G. Hirsh, V. Howells, L. Hsu, I. Hypolite, F. Kampmeier, S. Khalid-Khan, B. Kim, D. Kondo, L. Kotler, M. Krushelnycky, J. Larson, J. Lee, P. Lee, C. Lopez, L. Maayan, J. McCracken, R. Means, L. Miller, A. Parr, C. Pataki, C. Peterson, P. Pilania, R. Pizarro, H. Ravi, S. Reinblatt, M. Riddle, M. Rodowski, D. Sakolsky, A. Scharko, R. Suddath, C. Suarez, J. Walkup, B. Waslick; **Independent Evaluators:** A. Albano, G. Ginsburg, B. Asche, A. Barmish, M. Beaudry, S. Chang, M. Choudhury, B. Chu, S. Crawley, J. Curry, G. Danner, N. Deily, R. Dingfelder, D. Fitzgerald, P. Gammon, S. Hofflich, E. Kastelic, J. Keener, T. Lipani, K. Lukin, M. Masarik, T. Peris, T. Piacentini, S. Pimentel, A. Puliafico, T. Roblek, M. Schlossberg, E. Sood, S. Tiwari, J. Trachtenberg, P. van de Velde; **Pharmacy:** K. Truelove, H. Kim; **Research Assistants:** S. Allard, S. Avny, D. Beckmann, C. Brice, B. Buzzella, E. Capelli, A. Chiu, M. Coles, J. Freeman, M. Gringle, S. Hefton, D. Hood, M. Jacoby, J. King, A. Kolos, B. Lourea-Wadell, L. Lu, J. Lusky, R. Maid, C. Merolli, Y. Ojo, A. Pearlman, J. Regan, S. Rock, M. Rooney, N. Simone, S. Tiwari, S. Yeager.

REFERENCES

1. Benjamin RS, Costello EJ, Warren M. Anxiety disorders in a pediatric sample. J Anxiety Disord 1990;4:293-316.
2. Birmaher B, Yelovich AK, Renaud J. Pharmacologic treatment for children and adolescents with anxiety disorders. Pediatr Clin North Am 1998;45:1187-204.
3. Achenbach TM, Howell CT, McConaughy SH, et al. Six-year predictors of problems in a national sample of children and youth: I. Cross-informant syndromes. J Am Acad Child Adolesc Psychiatry 1995;34:336-47.
4. Ferdinand RF, Verhulst FC. Psychopathology from adolescence into young adulthood: an 8-year follow-up study. Am J Psychiatry 1995;152:1586-94.
5. Pine DS, Cohen P, Gurley D, Brook J, Ma Y. The risk for early-adulthood anxiety and depressive disorders in adolescents with anxiety and depressive disorders. Arch Gen Psychiatry 1998;55:56-64.
6. Pine DS. Child-adult anxiety disorders. J Am Acad Child Adolesc Psychiatry 1994;33:280-1.
7. Gurley D, Cohen P, Pine DS, Brook J. Discriminating depression and anxiety in youth: a role for diagnostic criteria. J Affect Disord 1996;39:191-200.
8. Shaffer D, Fisher P, Dulcan MK, et al. The NIMH Diagnostic Interview Schedule for Children Version 2.3 (DISC-2.3): description, acceptability, prevalence rates, and performance in the MECA study. J Am Acad Child Adolesc Psychiatry 1996; 35:865-77.
9. Klein R. Anxiety disorders. In: Rutter M, Taylor E, Hersov L, eds. Child and adolescent psychiatry: modern approaches. 3rd ed. London: Blackwell Scientific, 1995:351-74.
10. Kendall PC. Treating anxiety disorders in children: results of a randomized clinical trial. J Consult Clin Psychol 1994;62:100-11.
11. Kendall PC, Flannery-Schroeder E, Panichelli-Mindel SM, Southam-Gerow M, Henin A, Warman M. Therapy for youths with anxiety disorders: a second randomized clinical trial. J Consult Clin Psychol 1997;65:366-80.
12. Birmaher B, Axelson DA, Monk K, et al. Fluoxetine for the treatment of childhood anxiety disorders. J Am Acad Child Adolesc Psychiatry 2003;42:415-23.
13. The Research Unit on Pediatric Psychopharmacology Anxiety Study Group. Fluvoxamine for the treatment of anxiety disorders in children and adolescents. N Engl J Med 2001;344:1279-85.
14. James A, Soler A, Weatherall R. Cognitive behavioural therapy for anxiety disorders in children and adolescents. Cochrane Database Syst Rev 2005;4: CD004690.
15. Bridge JA, Iyengar S, Salary CB, et al. Clinical response and risk for reported suicidal ideation and suicide attempts in pediatric antidepressant treatment: a meta-analysis of randomized controlled trials. JAMA 2007;297:1683-96.
16. Diagnostic and statistical manual of mental disorders, 4th ed., text rev.: DSM-IV-TR. Washington, DC: American Psychiatric Association, 2000.
17. Kendall PC, Hedtke KA. Cognitive-behavioral therapy for anxious children: therapist manual. 3rd ed. Ardmore, PA: Workbook Publishing, 2006.
18. *Idem.* Coping Cat workbook. 2nd ed. Ardmore, PA: Workbook Publishing, 2006.
19. Kendall PC, Gosch E, Furr JM, Sood E. Flexibility within fidelity. J Am Acad Child Adolesc Psychiatry 2008;47:987-93.
20. Albano AM, Silverman WK. The anxiety disorders interview schedule for DSM-IV, child version: clinician manual. New York: Oxford University Press, 1996.
21. Guy W, Bonato R, eds. CGI: Clinical Global Impressions. Chevy Chase, MD: National Institute of Mental Health, 1970.
22. The Pediatric Anxiety Rating Scale (PARS): development and psychometric properties. J Am Acad Child Adolesc Psychiatry 2002;41:1061-9.
23. Shaffer D, Gould MS, Brasic J, et al. A Children's Global Assessment Scale (CGAS). Arch Gen Psychiatry 1983;40: 1228-31.
24. Miller RG. Simultaneous statistical inference. New York: McGraw-Hill, 1966.
25. Rynn MA, Siqueland L, Rickels K. Placebo-controlled trial of sertraline in the treatment of children with generalized anxiety disorder. Am J Psychiatry 2001;158:2008-14.
26. Silverman WK, Pina AA, Viswesvaran C. Evidence-based psychosocial treatments for phobic and anxiety disorders in children and adolescents. J Clin Child Adolesc Psychol 2008;37:105-30.
27. Beidel DC, Turner SM, Sallee FR, Ammerman RT, Crosby LA, Pathak S. SET-C versus fluoxetine in the treatment of childhood social phobia. J Am Acad Child Adolesc Psychiatry 2007;46:1622-32.
28. Kendall PC, Hudson JL, Gosch E, Flannery-Schroeder E, Suveg C. Cognitive-behavioral therapy for anxiety disordered youth: a randomized clinical trial evaluating child and family modalities. J Consult Clin Psychol 2008;76:282-97.
29. Chambless DL, Hollon SD. Defining empirically supported therapies. J Consult Clin Psychol 1998;66:7-18.
30. Wagner KD, Berard R, Stein MB, et al. A multicenter, randomized, double-blind, placebo-controlled trial of paroxetine in children and adolescents with social anxiety disorder. Arch Gen Psychiatry 2004; 61:1153-62.
31. March JS, Entusah AR, Rynn M, Albano AM, Tourian KA. A randomized controlled trial of venlafaxine ER versus placebo in pediatric social anxiety disorder. Biol Psychiatry 2007;62:1149-54.
32. Kiesler DJ. Some myths of psychotherapy research and the search for a paradigm. Psychol Bull 1966;65:110-36.

BEFORE THE PUBLIC UTILITY COMMISSION
OF OREGON

Docket PCN 5

In the Matter of

IDAHO POWER COMPANY'S
PETITION FOR CERTIFICATE OF PUBLIC CONVENIENCE
AND NECESSITY

Greg Larkin's Response to Idaho Power Company's
First Set of Data Requests (Feb. 8, 2023)

REDACTED

February 22, 2023

THIS EXHIBIT CONTAINS CONFIDENTIAL MEDICAL INFORMATION AND IS PROVIDED SEPARATELY PURSUANT TO PROTECTIVE ORDER NO. 22-309 AND THE ALJ'S FEBRUARY 17, 2023 RULING

Idaho Power/1217
Witness: Dr. Jeffrey Ellenbogen

BEFORE THE PUBLIC UTILITY COMMISSION
OF OREGON

Docket PCN 5

In the Matter of

IDAHO POWER COMPANY'S
PETITION FOR CERTIFICATE OF PUBLIC CONVENIENCE
AND NECESSITY

Medical Article

REDACTED

February 22, 2023

THIS EXHIBIT CONTAINS CONFIDENTIAL MEDICAL INFORMATION AND IS PROVIDED SEPARATELY PURSUANT TO PROTECTIVE ORDER NO. 22-309 AND THE ALJ'S FEBRUARY 17, 2023 RULING

Idaho Power/1218
Witness: Dr. Jeffrey Ellenbogen

BEFORE THE PUBLIC UTILITY COMMISSION
OF OREGON

Docket PCN 5

In the Matter of

IDAHO POWER COMPANY'S
PETITION FOR CERTIFICATE OF PUBLIC CONVENIENCE
AND NECESSITY

Medical Article

REDACTED

February 22, 2023

THIS EXHIBIT CONTAINS CONFIDENTIAL MEDICAL INFORMATION AND IS PROVIDED SEPARATELY PURSUANT TO PROTECTIVE ORDER NO. 22-309 AND THE ALJ'S FEBRUARY 17, 2023 RULING

Idaho Power/1219
Witness: Dr. Jeffrey Ellenbogen

BEFORE THE PUBLIC UTILITY COMMISSION
OF OREGON

Docket PCN 5

In the Matter of

IDAHO POWER COMPANY'S
PETITION FOR CERTIFICATE OF PUBLIC CONVENIENCE
AND NECESSITY

WHO, Night Noise Guidelines for Europe (2009)

February 22, 2023

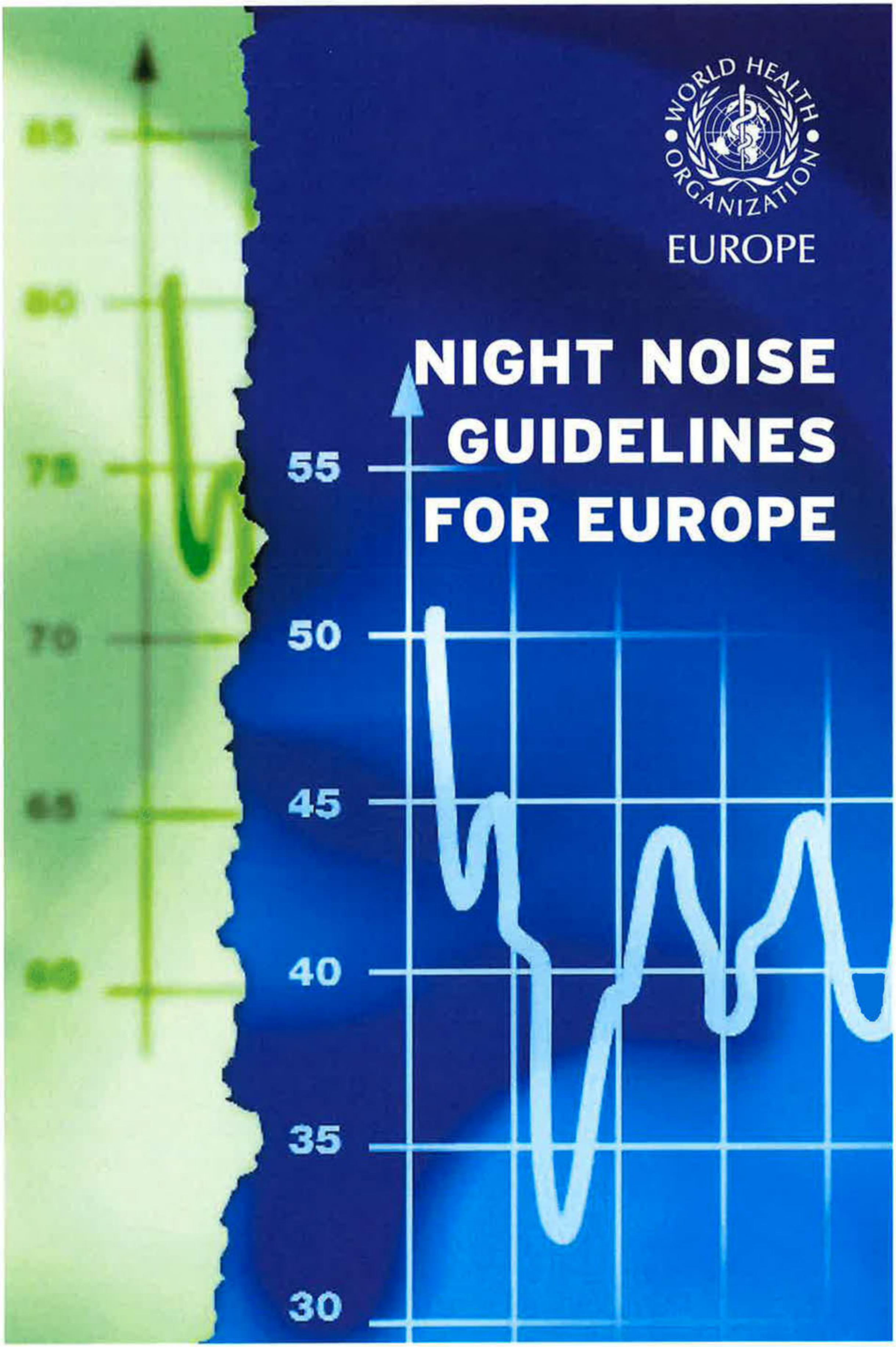
WORLD HEALTH ORGANIZATION
EUROPE
NIGHT NOISE GUIDELINES FOR EUROPE
55
50
45
40
35
30

WORLD HEALTH ORGANIZATION
EUROPE

NIGHT NOISE GUIDELINES FOR EUROPE

Keywords
NOISE - ADVERSE EFFECTS - PREVENTION AND CONTROL
SLEEP DEPRIVATION - ETIOLOGY
SLEEP DISORDERS - PREVENTION AND CONTROL
ENVIRONMENTAL HEALTH
HEALTH POLICY - LEGISLATION
GUIDELINES

ISBN 978 92 890 4173 7

Address requests about publications of the WHO Regional Office for Europe to:
Publications
WHO Regional Office for Europe
Scherfigsvej 8 · DK-2100 Copenhagen Ø, Denmark
Alternatively, complete an online request form for documentation, health information, or for permission to quote or translate, on the Regional Office web site (http://www.euro.who.int/pubrequest).

Edited by Charlotte Hurtley, Layout by Dagmar Bengs

CHAPTER 3 EFFECTS OF NIGHT-TIME NOISE ON SLEEP

CHAPTER 4 EFFECTS OF NIGHT-TIME NOISE ON HEALTH AND WELL-BEING

CHAPTER 5 GUIDELINES AND RECOMMENDATIONS

ABSTRACT

The WHO Regional Office for Europe set up a working group of experts to provide scientific advice to the Member States for the development of future legislation and policy action in the area of assessment and control of night noise exposure. The working group reviewed available scientific evidence on the health effects of night noise, and derived health-based guideline values. In December 2006, the working group and stakeholders from industry, government and nongovernmental organizations reviewed and reached general agreement on the guideline values and key texts for the final document of the *Night noise guidelines for Europe*.

Considering the scientific evidence on the thresholds of night noise exposure indicated by $L_{night,outside}$ as defined in the Environmental Noise Directive (2002/49/EC), an $L_{night,outside}$ of 40 dB should be the target of the night noise guideline (NNG) to protect the public, including the most vulnerable groups such as children, the chronically ill and the elderly. $L_{night,outside}$ value of 55 dB is recommended as an interim target for the countries where the NNG cannot be achieved in the short term for various reasons, and where policy-makers choose to adopt a stepwise approach. These guidelines are applicable to the Member States of the European Region, and may be considered as an extension to, as well as an update of, the previous WHO *Guidelines for community noise* (1999).

FOREWORD

WHO defines health as a state of complete physical, mental and social well-being and not merely the absence of disease or infirmity, and recognizes the enjoyment of the highest attainable standard of health as one of the fundamental rights of every human being. Environmental noise is a threat to public health, having negative impacts on human health and well-being. In order to support the efforts of the Member States in protecting the population's health from the harmful levels of noise, WHO issued *Guidelines for community noise* in 1999, which includes guideline values for community noise in various settings based on the scientific evidence available. The evidence on health impacts of night noise has been accumulated since then.

In the WHO European Region, environmental noise emerged as the leading environmental nuisance triggering one of the most common public complaints in many Member States. The European Union tackled the problem of environmental noise with an international law on the assessment and management of environmental noise. The WHO Regional Office for Europe developed the *Night noise guidelines for Europe* to provide expertise and scientific advice to the Member States in developing future legislations in the area of night noise exposure control and surveillance, with the support of the European Commission. This guidelines document reviews the health effects of night time noise exposure, examines exposure-effects relations, and presents guideline values of night noise exposure to prevent harmful effects of night noise in Europe. Although these guidelines are neither standards nor legally binding criteria, they are designed to offer guidance in reducing the health impacts of night noise based on expert evaluation of scientific evidence in Europe.

The review of scientific evidence and the derivation of guideline values were conducted by outstanding scientists. The contents of the document were peer reviewed and discussed for a consensus among the experts and the stakeholders from industry, government and nongovernmental organizations. We at WHO are thankful for those who contributed to the development and presentation of this guidelines and believe that this work will contribute to improving the health of the people in the Region.

Marc Danzon
WHO Regional Director for Europe

LIST OF CONTRIBUTORS

Torbjörn Åkerstedt
Karolinska Institute
Stockholm, Sweden
(Main contributor to Ch. 2)

Wolfgang Babisch
Federal Environmental Agency
Berlin, Germany
(Main contributor to Ch. 4)

Anna Bäckman
European Environment Agency
Copenhagen, Denmark

Jacques Beaumont
Institute National de Recherche sur les Transports et leur Sécurité
Bron, France

Martin van den Berg
Ministry of Housing, Spatial Planning and the Environment (Ministry VROM)
Den Haag, Netherlands
(Technical editing of the entire text)

Marie Louise Bistrup
National Institute of Public Health
Copenhagen, Denmark

Hans Bögli
Bundesamt für Umwelt, Wald und Landschaft
Bern, Switzerland

Dick Botteldooren
INTEC, University of Ghent
Gent, Belgium

Rudolf Brüggemann
Bundesministerium für Umwelt, Naturschutz und Reaktorsicherheit
Bonn, Germany

Oliviero Bruni
Sapienza University of Rome
Roma, Italy
(Main contributor to Ch. 2)

David Delcampe
European Commission DG Environment
Brussels, Belgium

Ivanka Gale
Institute of Public Health of the Republic of Slovenia
Ljubljana, Slovenia

Jeff Gazzard
Greenskies
London, United Kingdom

Nicolas Grénetier
Sous direction de la gestion des risques des milieux
Paris, France

Colin Grimwood
Bureau Veritas
London, United Kingdom

Leja Dolenc Groselj
Institute of Public Health of the Republic of Slovenia
Ljubljana, Slovenia
(Main contributor to Ch. 2)

Health Council of the Netherlands
Hague, Netherlands
(Main contributor to Ch. 4)

Danny Houthuijs
National Institute for Public Health and the Environment (RIVM)
Bilthoven, Netherlands
Staffan Hygge

University of Gävle
Gävle, Sweden
(Main contributor to Ch. 4)

Hartmut Ising
Falkensee, Germany
(Main contributor to Appendix 3)

Tanja Janneke
Ministry of Housing, Spatial Planning and Environment (Ministry VROM)
Den Haag, Netherlands

Snezana Jovanovic
Landesgesundheitsamt Baden-Württemberg
Stuttgart, Germany
(Main contributor to Ch. 2)

André Kahn
Université Libre de Bruxelles
Bruxelles, Belgium
(Main contributor to Ch. 2, Appendix 4)

Stylianos Kephalopoulos
European Commission Joint Research Centre
Ispra, Italy

Anne Knol
National Institute for Public Health and the Environment (RIVM)
Bilthoven, Netherlands

Peter Lercher
University of Innsbruck
Innsbruck, Austria

João de Quinhones Levy
Higher Technical Institute
Lisbon, Portugal

Gaetano Licitra
Environmental Protection Agency - Tuscany Region
Pisa, Italy

Christian Maschke
Forschungs- und Beratungsbüro Maschke
Berlin, Germany

Matthias Mather
Deutsche Bahn AG
Berlin, Germany

David Michaud
Healthy Environments and Consumer Safety
Ottawa, Canada

H.M.E. Miedema
TNO – Inro (Netherlands Organisation for Applied Scientific Research)
Delft, Netherlands
(Main contributor to Ch. 3)

Ruedi Müller-Wenk
Universität St. Gallen
St. Gallen, Switzerland
(Main contributor to Ch. 4)

Alain Muzet
Centre National de Recherche Scientifique Centre d'Études de Physiologie Appliquée (CNRS-CEPA)
Strasbourg, France
(Main contributor to Ch. 3)

Soña Nevsimalova
Charles University in Prague
Prague, Czech Republic
(Main contributor to Ch. 2)

Nina Renshaw
European Federation for Transport and Environment
Brussels, Belgium

Michał Skalski
University of Warsaw Clinic of Psychiatry of the Medical Academy
Warsaw, Poland
(Main contributor to Ch. 4)

Stephen Stansfeld
Queen Mary University of London
London, United Kingdom

David Tompkins
European Express Association
Hants, United Kingdom
(Main contributor to Ch. 4)

WORLD HEALTH ORGANIZATION
Regional Office for Europe
European Centre for Environment and Health
Bonn, Germany

Xavier Bonnefoy
(Project leader until July 2006)

Rokho Kim
(Project leader since August 2006)

Célia Rodrigues
(Technical officer until April 2006)

Nuria Aznar
(Secretariat until October 2006)

Deepika Sachdeva
(Secretariat since November 2006)

EXECUTIVE SUMMARY

INTRODUCTION

The aim of this document is to present the conclusions of the WHO working group responsible for preparing guidelines for exposure to noise during sleep. This document can be seen as an extension of the WHO *Guidelines for community noise* (1999). The need for "health-based" guidelines originated in part from the European Union Directive 2002/49/EC relating to the assessment and management of environmental noise (commonly known as the Environmental Noise Directive and abbreviated as END) which compels European Union Member States to produce noise maps and data about night exposure from mid-2007. The work was made possible by a grant from the European Commission and contributions from the Swiss and German governments.

Although a number of countries do have legislation directed at controlling night noise exposure, there is little information on actual exposure and its subsequent effects on the population. Estimates made in some countries of the number of people highly disturbed by noise during sleep (see Fig. 1 for the Netherlands as an example) indicate that a substantial part of the population could be exposed to levels that might risk their health and well-being.

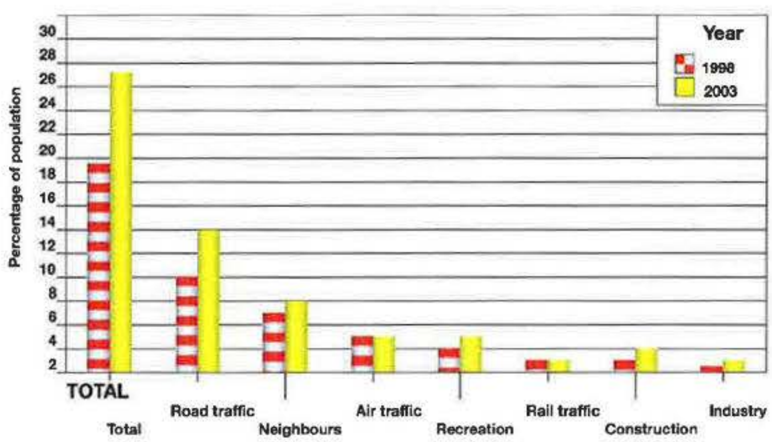

Fig. 1. Percentage of population highly disturbed by noise during sleep in the Netherlands: survey results for 1998 and 2003

As direct evidence concerning the effects of night noise on health is rarely available, these guidelines also use indirect evidence: the effects of noise on sleep and the relations between sleep and health. The advantage of this approach is that a lot of medical evidence is available on the relation between sleep and health, and detailed information also exists on sleep disturbance by noise.

PROCESS OF DEVELOPING GUIDELINES

In 2003, the WHO Regional Office for Europe set up a working group of experts to provide scientific advice to the European Commission and to its Member States for the development of future legislation and policy action in the area of control and surveillance of night noise exposure. The review of available scientific evidence on the health effects of night noise was carried out by an interdisciplinary team who set out to derive health-based guideline values. The contributions from the experts were reviewed by the team and integrated into draft reports following discussion at four technical meetings of the working group. In 2006, all the draft reports were compiled into a draft document on guidelines for exposure to noise at night, which was reviewed and commented on by a number of stakeholders and experts.

At the final conference in Bonn, Germany, on 14 December 2006, representatives from the working group and stakeholders from industry, government and non-governmental organizations reviewed the contents of the draft document chapter by chapter, discussed several fundamental issues and reached general agreement on the guideline values and related texts to be presented as conclusions of the final WHO *Night noise guidelines for Europe.*

NOISE INDICATORS

From the scientific point of view the best criterion for choosing a noise indicator is its ability to predict an effect. Therefore, for different health end points, different indicators could be chosen. Long-term effects such as cardiovascular disorders are more correlated with indicators summarizing the acoustic situation over a long time period, such as yearly average of night noise level outside at the facade ($L_{night,outside}$)[1], while instantaneous effects such as sleep disturbance are better with the maximum level per event (L_{Amax}), such as passage of a lorry, aeroplane or train.

From a practical point of view, indicators should be easy to explain to the public so that they can be understood intuitively. Indicators should be consistent with existing practices in the legislation to enable quick and easy application and enforcement. $L_{night,outside}$, adopted by the END, is an indicator of choice for both scientific and practical use. Among currently used indicators for regulatory purposes, L_{Aeq} (A-weighted equivalent sound pressure level) and L_{Amax} are useful to predict short-term or instantaneous health effects.

SLEEP TIME

Time use studies, such as that undertaken by the Centre for Time Use Research, 2006 (www.timeuse.org/access/), show that the average time adult people are in bed is around 7.5 hours, so the real average sleeping time is somewhat shorter. Due to personal factors like age and genetic make-up there is considerable variation in sleeping time and in beginning and end times. For these reasons, a fixed interval of 8 hours is a minimal choice for night protection.

Though results vary from one country to another, data show (see Fig. 2 as an example) that an 8-hour interval protects around 50% of the population and that it would take a period of 10 hours to protect 80%. On Sundays, sleeping time is consistently 1 hour longer, probably due to people recovering from sleep debt incurred during the week. It should also be borne in mind that (young) children have longer sleeping times.

[1] L_{night} is defined in the END as the outside level. In order to avoid any doubt, the suffix "outside" is added in this document.

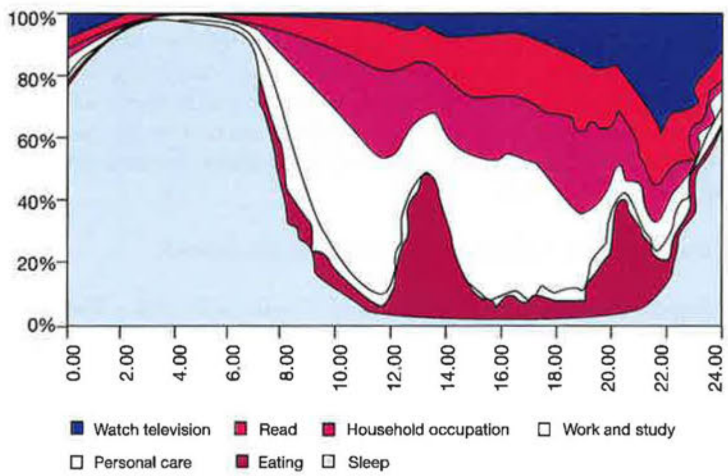

Fig. 2 Percentage of time that the Portuguese population spend asleep or in different activities

Source: http://www.ine.pt/prodserv/destaque/arquivo.asp, based on a study by the Instituto Nacional de Estatistica Portugal, 1999.

NOISE, SLEEP AND HEALTH

There is plenty of evidence that sleep is a biological necessity, and disturbed sleep is associated with a number of health problems. Studies of sleep disturbance in children and in shift workers clearly show the adverse effects.

Noise disturbs sleep by a number of direct and indirect pathways. Even at very low levels physiological reactions (increase in heart rate, body movements and arousals) can be reliably measured. Also, it was shown that awakening reactions are relatively rare, occurring at a much higher level than the physiological reactions.

DEFINITION OF "SUFFICIENT" AND "LIMITED" EVIDENCE

Sufficient evidence: A causal relation has been established between exposure to night noise and a health effect. In studies where coincidence, bias and distortion could reasonably be excluded, the relation could be observed. The biological plausibility of the noise leading to the health effect is also well established.

Limited evidence: A relation between the noise and the health effect has not been observed directly, but there is available evidence of good quality supporting the causal association. Indirect evidence is often abundant, linking noise exposure to an intermediate effect of physiological changes which lead to the adverse health effects.

The working group agreed that there is sufficient evidence that night noise is related to self-reported sleep disturbance, use of pharmaceuticals, self-reported health problems and insomnia-like symptoms. These effects can lead to a considerable burden of disease in the population. For other effects (hypertension, myocardial infarctions, depression and others), limited evidence was found: although the studies were few or not conclusive, a biologically plausible pathway could be constructed from the evidence.

An example of a health effect with limited evidence is myocardial infarction. Although evidence for increased risk of myocardial infarction related to L_{day} is sufficient according to an updated meta-analysis, the evidence in relation to $L_{night,outside}$ was considered limited. This is because $L_{night,outside}$ is a relatively new exposure indicator, and few field studies have focused on night noise when considering cardiovascular outcomes. Nevertheless, there is evidence from animal and human studies supporting a hypothesis that night noise exposure might be more strongly associated with cardiovascular effects than daytime exposure, highlighting the need for future epidemiological studies on this topic.

The review of available evidence leads to the following conclusions.

- Sleep is a biological necessity and disturbed sleep is associated with a number of adverse impacts on health.
- There is sufficient evidence for biological effects of noise during sleep: increase in heart rate, arousals, sleep stage changes and awakening.
- There is sufficient evidence that night noise exposure causes self-reported sleep disturbance, increase in medicine use, increase in body movements and (environmental) insomnia.
- While noise-induced sleep disturbance is viewed as a health problem in itself (environmental insomnia), it also leads to further consequences for health and well-being.
- There is limited evidence that disturbed sleep causes fatigue, accidents and reduced performance.
- There is limited evidence that noise at night causes hormone level changes and clinical conditions such as cardiovascular illness, depression and other mental illness. It should be stressed that a plausible biological model is available with sufficient evidence for the elements of the causal chain.

VULNERABLE GROUPS

Children have a higher awakening threshold than adults and therefore are often seen to be less sensitive to night noise. For other effects, however, children seem to be equally or more reactive than adults. As children also spend more time in bed they are exposed more to night noise levels. For these reasons children are considered a risk group.

Since with age the sleep structure becomes more fragmented, elderly people are more vulnerable to disturbance. This also happens in pregnant women and people with ill health, so they too are a group at risk.

Finally, shift workers are at risk because their sleep structure is under stress due to the adaptations of their circadian rhythm.

THRESHOLDS FOR OBSERVED EFFECTS

The no observed adverse effect level (NOAEL) is a concept from toxicology, and is defined as the greatest concentration which causes no detectable adverse alteration of morphology, functional capacity, growth, development or lifespan of the target organism. For the topic of night noise (where the adversity of effects is not always clear) this concept is less useful. Instead, the observed effect thresholds are provided: the level above which an effect starts to occur or shows itself to be dependent on the exposure level. It can also be a serious pathological effect, such as myocardial infarctions, or a changed physiological effect, such as increased body movement.

Threshold levels of noise exposure are important milestones in the process of evaluating the health consequences of environmental exposure. The threshold levels also delimit the study area, which may lead to a better insight into overall consequences. In Tables 1 and 2, all effects are summarized for which *sufficient and limited evidence* exists. For these effects, the threshold levels are usually well known, and for some the dose-effect relations over a range of exposures could also be established.

Effect		Indicator	Threshold, dB
Biological effects	Change in cardiovascular activity	*	*
	EEG awakening	$L_{Amax,inside}$	35
	Motility, onset of motility	$L_{Amax,inside}$	32
	Changes in duration of various stages of sleep, in sleep structure and fragmentation of sleep	$L_{Amax,inside}$	35
Sleep quality	Waking up in the night and/or too early in the morning	$L_{Amax,inside}$	42
	Prolongation of the sleep inception period, difficulty getting to sleep	*	*
	Sleep fragmentation, reduced sleeping time	*	*
	Increased average motility when sleeping	$L_{night,outside}$	42
Well-being	Self-reported sleep disturbance	$L_{night,outside}$	42
	Use of somnifacient drugs and sedatives	$L_{night,outside}$	40
Medical conditions	Environmental insomnia**	$L_{night,outside}$	42

Table 1
Summary of effects and threshold levels for effects where *sufficient* evidence is available

* *Although the effect has been shown to occur or a plausible biological pathway could be constructed, indicators or threshold levels could not be determined.*

***Note that "environmental insomnia" is the result of diagnosis by a medical professional whilst "self-reported sleep disturbance" is essentially the same, but reported in the context of a social survey. Number of questions and exact wording may differ.*

Table 2
Summary of effects and threshold levels for effects where *limited* evidence is available**

Effect		Indicator	Estimated threshold, dB
Biological effects	Changes in (stress) hormone levels	*	*
Well-being	Drowsiness/tiredness during the day and evening	*	*
	Increased daytime irritability	*	*
	Impaired social contacts	*	*
	Complaints	$L_{night,outside}$	35
	Impaired cognitive performance	*	*
Medical conditions	Insomnia	*	*
	Hypertension	$L_{night,outside}$	50
	Obesity	*	*
	Depression (in women)	*	*
	Myocardial infarction	$L_{night,outside}$	50
	Reduction in life expectancy (premature mortality)	*	*
	Psychic disorders	$L_{night,outside}$	60
	(Occupational) accidents	*	*

* *Although the effect has been shown to occur or a plausible biological pathway could be constructed, indicators or threshold levels could not be determined.*

** *Note that as the evidence for the effects in this table is limited, the threshold levels also have a limited weight. In general they are based on expert judgement of the evidence.*

RELATIONS WITH $L_{NIGHT, OUTSIDE}$

Over the next few years, the END will require that night 'noise' exposures are reported in $L_{night,outside}$. It is, therefore, interesting to look into the relation between $L_{night,outside}$ and adverse health effects. The relation between the effects and $L_{night,outside}$ is, however, not straightforward. Short-term effects are mainly related to maximum levels per event inside the bedroom: $L_{Amax,inside}$. In order to express the (expected) effects in relation to the single European Union indicator, some calculation needs to be done. The calculation for the total number of effects from reaction data on events (arousals, body movements and awakenings) needs a number of assumptions. The first that needs to be made is independence: although there is evidence that the order of events of different loudness strongly influences the reactions, the calculation is nearly impossible to carry out if this is taken into consideration. Secondly, the reactions per event are known in relation to levels at the ear of the sleeper, so an assumption for an average insulation value must be made. In the report a value of 21 dB has been selected. This value is, however, subject to national and cultural differences. One thing that stands out is the desire of a large part of the population to sleep with windows (slightly) open. The relatively low value of 21 dB takes this into account already. If noise levels increase, people do indeed close their windows, but obviously reluctantly, as complaints about bad air then increase and sleep disturbance remains high. This was already pointed out in the WHO *Guidelines for community noise* (1999).

From source to source the number of separate events varies considerably. Road traffic noise is characterized by relatively low levels per event and high numbers, while air and rail traffic are characterized by high levels per event and low numbers. For two typical situations estimates have been made and presented in graphical form. The first is an average urban road (600 motor vehicles per night, which corresponds roughly to a 24-hour use of 8000 motor vehicles, or 3 million per year, the lower boundary the END sets) and the second case is for an average situation of air traffic exposure (8 flights per night, nearly 3000 per year).

Fig. 3 shows how effects increase with an increase of $L_{night,outside}$ values for the typical road traffic situation (urban road). A large number of events lead to high levels of awakening once the threshold of $L_{Amax,inside}$ is exceeded. To illustrate this in practical terms: values over 60 dB $L_{night,outside}$ occur at less then 5 metres from the centre of the road.

In Fig. 4 the same graph is presented for the typical airport situation. Due to a lower number of events there are fewer awakenings than in the road traffic case (Fig. 3), but the same or more health effects. In these examples the worst case figures can be factors higher: the maximum number of awakenings for an $L_{night,outside}$ of 60–65 dB is around 300 per year.

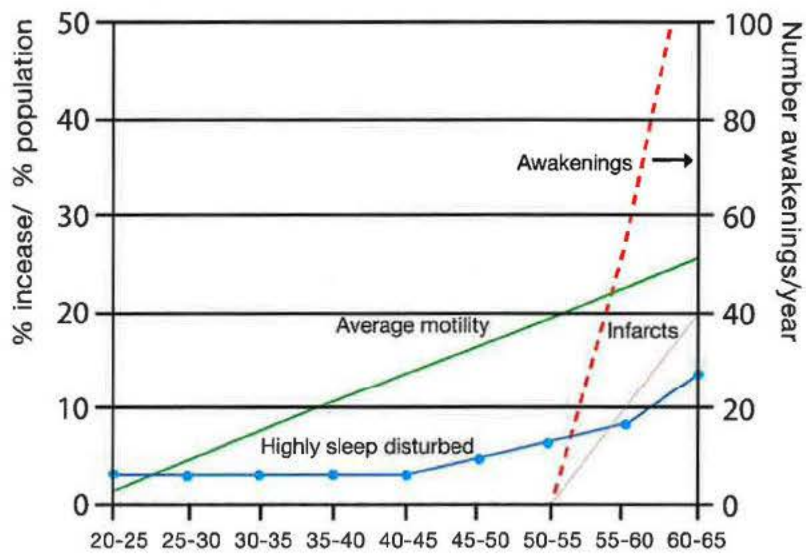

Fig. 3 Effects of road traffic noise at night*

**Average motility and infarcts are expressed in percent increase (compared to baseline number); the number of highly sleep disturbed people is expressed as a percent of the population; awakenings are expressed in number of additional awakenings per year.*

A recent study suggests that high background levels of noise (from motorways) with a low number of separate events can cause high levels of average motility.

Therefore, by using the $L_{night,outside}$ as a single indicator, a relation between effects and indicator can be established. For some effects, however, the relation can be

Fig. 4 Effects of aircraft noise at night*

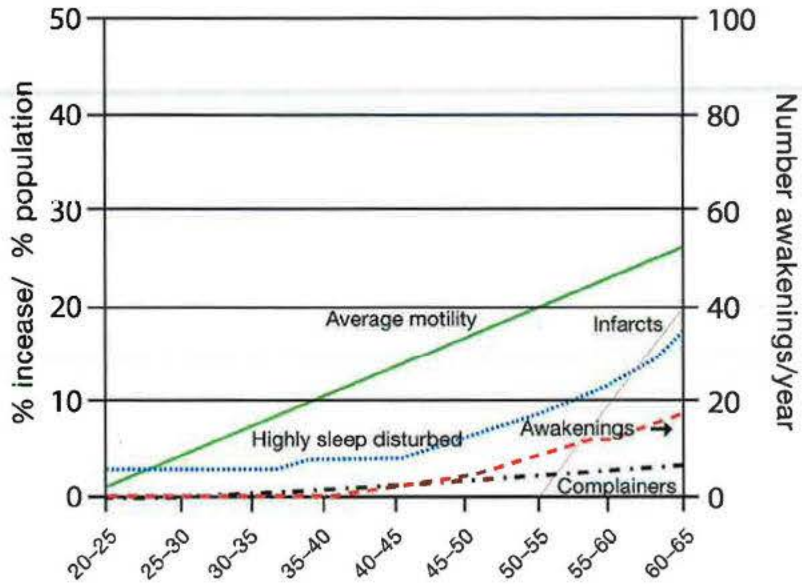

**Average motility and infarcts are expressed in percent increase (compared to baseline number); the number of highly sleep disturbed people is expressed as a percent of the population; complainers are expressed as a % of the neighbourhood population; awakenings are expressed in number of additional awakenings per year.*

source dependent. Although L_{night} gives a good relation for most effects, there is a difference between sources for some. Train noise gives fewer awakenings, for instance. Once source is accounted for, the relations are reasonably accurate.

RECOMMENDATIONS FOR HEALTH PROTECTION

Based on the systematic review of evidence produced by epidemiological and experimental studies, the relationship between night noise exposure and health effects can be summarized as below. (Table 3)

Below the level of 30 dB $L_{night,outside}$, no effects on sleep are observed except for a slight increase in the frequency of body movements during sleep due to night noise. There is no sufficient evidence that the biological effects observed at the level below 40 dB $L_{night,outside}$ are harmful to health. However, adverse health effects are observed at the level above 40 dB $L_{night,outside}$, such as self-reported sleep disturbance, environmental insomnia, and increased use of somnifacient drugs and sedatives.

Therefore, 40 dB $L_{night,outside}$ is equivalent to the lowest observed adverse effect level (LOAEL) for night noise. Above 55 dB the cardiovascular effects become the major public health concern, which are likely to be less dependent on the nature of the noise. Closer examination of the precise impact will be necessary in the range between 30 dB and 55 dB as much will depend on the detailed circumstances of each case.

Table 3 Effects of different levels of night noise on the population's health

Average night noise level over a year $L_{night,outside}$	Health effects observed in the population
Up to 30 dB	Although individual sensitivities and circumstances may differ, it appears that up to this level no substantial biological effects are observed. $L_{night,outside}$ of 30 dB is equivalent to the no observed effect level (NOEL) for night noise.
30 to 40 dB	A number of effects on sleep are observed from this range: body movements, awakening, self-reported sleep disturbance, arousals. The intensity of the effect depends on the nature of the source and the number of events. Vulnerable groups (for example children, the chronically ill and the elderly) are more susceptible. However, even in the worst cases the effects seem modest. $L_{night,outside}$ of 40 dB is equivalent to the lowest observed adverse effect level (LOAEL) for night noise.
40 to 55 dB	Adverse health effects are observed among the exposed population. Many people have to adapt their lives to cope with the noise at night. Vulnerable groups are more severely affected.
Above 55 dB	The situation is considered increasingly dangerous for public health. Adverse health effects occur frequently, a sizeable proportion of the population is highly annoyed and sleep-disturbed. There is evidence that the risk of cardiovascular disease increases.

A number of instantaneous effects are connected to threshold levels expressed in L_{Amax}. The health relevance of these effects cannot be easily established. It can be safely assumed, however, that an increase in the number of such events over the baseline may constitute a subclinical adverse health effect by itself leading to significant clinical health outcomes.

Based on the exposure-effects relationship summarized in Table 3, the night noise guideline values are recommended for the protection of public health from night noise as below.

Table 4 Recommended night noise guidelines for Europe

Night noise guideline (NNG)	$L_{night,outside}$ = 40 dB
Interim target (IT)	$L_{night,outside}$ = 55 dB

[1] $L_{night,outside}$ is the night-time noise indicator (L_{night}) of Directive 2002/49/EC of 25 June 2002: the A-weighted long-term average sound level as defined in ISO 1996-2: 1987, determined over all the night periods of a year; in which: the night is eight hours (usually 23.00 – 07.00 local time), a year is a relevant year as regards the emission of sound and an average year as regards the meteorological circumstances, the incident sound is considered, the assessment point is the same as for L_{den}. See *Official Journal of the European Communities*, 18.7.2002, for more details.

For the primary prevention of subclinical adverse health effects related to night noise in the population, it is recommended that the population should not be exposed to night noise levels greater than 40 dB of $L_{night,outside}$ during the part of the night when most people are in bed. The LOAEL of night noise, 40 dB $L_{night,outside}$, can be considered a health-based limit value of the night noise guidelines (NNG) necessary to protect the public, including most of the vulnerable groups such as children, the chronically ill and the elderly, from the adverse health effects of night noise.

An interim target (IT) of 55 dB $L_{night,outside}$ is recommended in the situations where the achievement of NNG is not feasible in the short run for various reasons. It should be emphasized that IT is not a health-based limit value by itself. Vulnerable groups cannot be protected at this level. Therefore, IT should be considered only as a feasibility-based intermediate target which can be temporarily considered by policy-makers for exceptional local situations.

RELATION WITH THE GUIDELINES FOR COMMUNITY NOISE (1999)

Impact of night-time exposure to noise and sleep disturbance is indeed covered in the 1999 guidelines, as below (WHO, 1999):

> "If negative effects on sleep are to be avoided the equivalent sound pressure level should not exceed 30 dBA indoors for continuous noise. If the noise is not continuous, sleep disturbance correlates best with L_{Amax} and effects have been observed at 45 dB or less. This is particularly true if the background level is low. Noise events exceeding 45 dBA should therefore be limited if possible. For sensitive people an even lower limit would be preferred. It should be noted that it should be possible to sleep with a bedroom window slightly open (a reduction from outside to inside of 15 dB). To prevent sleep disturbances, one should thus consider the equivalent sound pressure level and the number and level of sound events. Mitigation targeted to the first part of the night is believed to be effective for the ability to fall asleep."

The 1999 guidelines are based on studies carried out up to 1995 (and a few meta-analyses some years later). Important new studies (Passchier-Vermeer et al., 2002; Basner et al., 2004) have become available since then, together with new insights into normal and disturbed sleep. New information has made more precise assessment of exposure-effect relationship. The thresholds are now known to be lower than L_{Amax} of 45 dB for a number of effects. The last three sentences still stand: there are good reasons for people to sleep with their windows open, and to prevent sleep disturbances one should consider the equivalent sound pressure level and the number of sound events. The present guidelines allow responsible authorities and stakeholders to do this. Viewed in this way, the *night noise guidelines for Europe* are complementary to the 1999 guidelines. This means that the recommendations on government policy framework on noise management elaborated in the 1999 guidelines should be considered valid and relevant for the Member States to achieve the guideline values of this document.

CHAPTER 1

INTRODUCTION: METHODS AND CRITERIA

With regard to sleep and waking, we must consider what they are: whether they are peculiar to soul or to body, or common to both; and if common, to what part of soul or body they appertain: further, from what cause it arises that they are attributes of animals, and whether all animals share in them both, or some partake of the one only, others of the other only, or some partake of neither and some of both.

(Aristotle, On sleep and sleeplessness, 350 BC)

1.1 INTRODUCTION

1.1.1 EXISTING POLICY DOCUMENTS FOR NIGHT-TIME NOISE

The aim of this document is to present guidance for exposure to noise during sleep. What is already available?

There are three related documents at the international level:

- *Guidelines for community noise* (WHO, 1999)
- *Directive 2002/49/EC relating to the assessment and management of environmental noise* (European Commission, 2002b)
- *Position Paper on dose-effect relationships for night-time noise* (European Commission, 2004).

In Chapter 5 the relation with the *Guidelines for community noise* (1999) will be explained.

The European Union (EU) Directive relating to the assessment and management of environmental noise (or, as it is commonly known, the Environmental Noise Directive – END), establishes that Member States should create noise maps (2007) and action plans (2008) for parts of their territory. The noise maps should present noise levels expressed in the harmonized indicators L_{den} and L_{night}. Although in the first round only between 20% and 30% of the population will be covered, it is expected that through the use of harmonized methods and indicators a deeper insight will be gained into the exposure of the population to noise. The END does not, however, set any limit values: on the basis of the subsidiarity principle this is left to the Member States. The Directive does, however, require Member States to report on their limit values and express them in the standard indicators. On the CIRCA web site (Communication and Information Resource Centre Administrator, European Commission, 2006) an overview of the data reported to the Commission can be found. Out of the 25 Member States, 10 reported on the L_{night} limits. In Table 1.1 some of these data are summarized.

Due to differences in legal systems it is hard to predict what the actual effect of a certain limit value will be. It could be a relatively high value but rigidly enforced, or a very low value with no legal binding whatsoever.

The *Position Paper* on dose-effect relationships for night-time noise is foreseen in the END (Annex III) and aims to give the competent authorities a tool to evaluate the impact on the population. However, it neither provides limit values nor guidelines. The same information that was used in the *Position Paper* also plays a role in these guidelines.

Table 1.1
Reported L_{night} limit values for road traffic noise in new residential areas

EU Member State	$L_{night,outside}$
France	62
Germany	49
Spain	45
Netherlands	40
Austria	50
Sweden	51 (converted from L_{Aeq} limit 30 dB(A) inside bedroom)
Finland	46
Hungary	55
Latvia	40
Estonia	45
Switzerland	50

Source: European Commission, 2006.

1.1.2 GENERAL MODEL

There is no doubt that a relation exists between sleep and health and well-being, as most of us know from personal experience. That does not mean, however, that this relation is simple. People who do not sleep well may not feel well the day after, but the reverse is also true: unfit people may have a disturbed sleep. Untangling the relations between health and disturbed sleep (night-time noise is only one of many causes) proved difficult, and Fig. 2.1 at the end of Chapter 2 shows why.

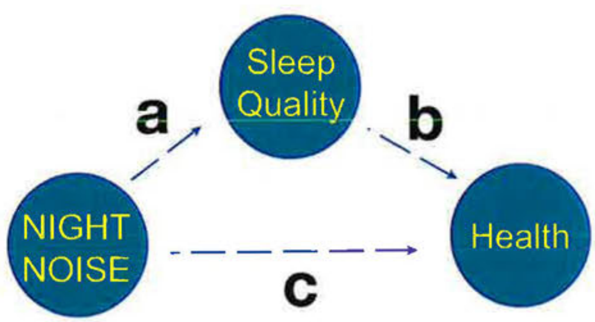

Fig. 1.1.
General structure of the report on the effects of night noise

The general structure of the report is given in Fig. 1.1: evidence for the effects of night-time noise on health (c) is supported by evidence on the indirect route via (a) and (b). In Chapter 2 the relations between sleep and health are examined (relation (b) in Fig. 1.1), and this involves clinical evidence from sleep laboratories, but also evidence from animal experiments. In Chapter 3 it is shown how noise disturbs sleep from the basic, autonomous level up to conscious awakenings: relation (a). Chapter 4 presents the evidence between night-time noise and health and well-being: relation (c) in Fig. 1.1. The last chapter, Chapter 5, then provides guidance on reducing health impacts caused by night-time noise exposure.

1.1.3 PROCESS OF DEVELOPING GUIDELINES

The WHO Regional Office for Europe started the night noise guidelines (NNGL) project with a grant from the European Commission's Directorate-General for Health and Consumer Affairs. In 2003, the WHO Regional Office for Europe set up a working group of experts to provide scientific advice for the development of guidelines for future legislation and policy action in the area of control and surveillance of night noise exposure. The review of available scientific evidence on the health effects of night noise was carried out by the working group to derive health-based guideline values. The contributions,from the experts were reviewed by the team and integrated into draft reports following discussion at four technical meetings of the working group.

The first meeting of the working group was held in Bonn, June 2004. It was agreed that the experts would produce background papers on a number of topics identified and assigned at the meeting.

The second meeting in Geneva, December 2004, concentrated on such technical issues as exposure assessment, metrics, health effects and guideline set-up. The topic-specific experts presented the first drafts for the identified topics for detailed discussions at the meeting. The discussions concentrated on central issues such as exposure assessment and guideline derivation.

The third meeting in Lisbon, April 2005, reviewed the revised background papers, and discussed in detail the overall structure of the guidelines document, and the process of consensus building among the working group and stakeholders.

At the workshop of acoustics experts in The Hague, September 2005, a consensus was made on the use of L_{night} as the single indicator for guideline values as it effectively combines the information on the number of events and the maximum sound levels per event over a year.

In 2006, all the draft reports collected at previous meetings were compiled by Mr. Martin van den Berg into a coherent document on guidelines for exposure to noise at night. The latter was revised according to the comments collected though a peer-review by the working group experts.

At the concluding meeting in Bonn, December 2006, the working group and stakeholders from industry, government and nongovernmental organizations reviewed the contents of the draft document chapter by chapter, discussed several fundamental issues and reached general consensus on the guideline values. The final implementation report of NNGL project was submitted to the EU in early 2007.

The following countries and institutes contributed to the development of *Night noise guidelines for Europe* as project partners.

AUSTRIA:	Institute of Hygiene and Social Medicine, University of Innsbruck
CZECH REPUBLIC:	Charles University in Prague
DENMARK:	National Institute of Public Health
FRANCE:	INRETS/LTE–Laboratoire Transports et Environnement CNRS–Centre National de Recherche Scientifique
GERMANY:	Umweltbundesamt–Federal Environmental Agency Landesgesundheitsamt Baden-Württemberg

ITALY:	ARPAT–Environmental Protection Agency, Tuscany Region
	University of Rome "La Sapienza"– Center for Pediatric Sleep Disorders
NETHERLANDS:	TNO–Netherlands Organisation for Applied Scientific Research
	RIVM–National Institute of Public Health and the Environment
POLAND:	University of Warsaw, Clinic of Psychiatry of the Medical Academy
PORTUGAL:	IST–Instituto Superior Técnico
SLOVENIA:	Institute of Public Health of the Republic of Slovenia
SWEDEN:	University of Gävle, Centre for Built Environment
UNITED KINGDOM:	Queen Mary and Westfield College, University of London

In addition, WHO received advice and support from a number of national experts who participated in the working group. The affiliations of these additional expert advisers include:

CANADA:	Health Canada
GERMANY:	Forschungs- und Beratungsbüro Maschke
SWITZERLAND:	Bundesamt für Umwelt, Wald und Landschaft
	Universität St. Gallen, Institut für Wirtschaft und Ökologie
NETHERLANDS:	Ministry of Housing, Spatial Planning and Environment
UNITED KINGDOM:	Casella Stanger Environmental Consultants

Since the project report was published on the EU web site, various comments were received from experts who have not participated in the working group. The most critical points were regarding the achievability of guideline values in practice. Responding to these feedbacks, the WHO Regional Office for Europe, prepared a revision of guidelines and recommendations, and consulted with international experts and stakeholders including the EU. As of late 2008, it was agreed that the guideline should be based on the lowest observed adverse effects level (LOAEL) rather than the no observed effects level (NOEL). Interim target was also introduced as a feasibility-based level.

1.2 STRENGTH OF EVIDENCE

1.2.1 BASIC CONCEPTS

This document uşes well-established practices from other disciplines and policy fields. Of main interest here are evidence-based medicine, the use of epidemiological evidence for environmental risk assessment and experiences with – principally– air quality guidelines.

The concept of "evidence" is further formalized, as variations in wording and scope are currently in use.

1.2.2 RISK ASSESSMENT AND RISK CONTROL

Fig. 1.2
Elements of risk control

Source:
Health Council of the Netherlands, 2004.

Fig. 1.2 outlines a general approach for risk assessment and control. This approach consists of the following steps:

1. problem description: assessing the impact on the population
2. risk analysis: evaluation of impact
3. risk evaluation: assessing impact considered undesirable
4. assessment of options to avoid or reduce impact
5. cost–benefit analysis of the options or of the mix of options
6. assessment of the preferred option
7. implementation and control.

It is important to observe that guideline values can be an input to, as well as an output of this process. At lower levels of decision (a particular infrastructure project, for instance) a preset guideline value reduces – intentionally – the degrees of freedom in the process. At the highest national or international level a guideline value is the outcome. As the scope of this document is to present the health consequences of night-time noise exposure (and not so much the economic outcomes of the choice of a certain value) it concentrates on the first three elements in the risk assessment block.

The following questions need to be addressed.

- What is the strength of the available evidence – what are the uncertainties?
- What is the health significance for the effects found?
- How serious is the impact on health?
- Does every instance of exposure lead to an effect and how are they related?
- How can the number of affected people be established?

1.2.3 CAUSE–EFFECT CHAIN

Underlying this approach is the notion of a cause–effect chain between environmental factors and health, symbolically simplified in Fig. 1.3.

Fig. 1.3
Cause-effect chain

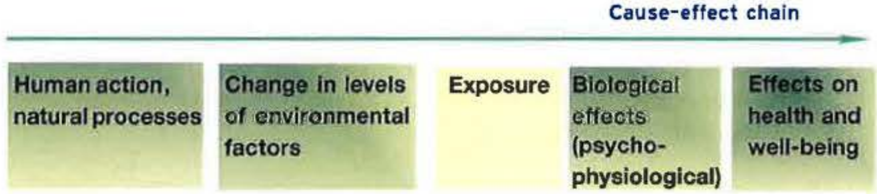

Source: Health Council of the Netherlands, 2004.

There are important questions that need to be asked.

- Is there a causal relation between one link in the chain and the next?
- What are the intervening factors in that relation?
- How strong is the evidence for the relations?

The last question is the hardest to answer, as "strength of evidence" is not easy to express in simple numbers or labels. There are two forms of uncertainty: uncertainty because of variability of outcomes and uncertainty due to a lack of knowledge.

For the purpose of this document the following classification will be used, largely based on the IARC (International Agency for Research on Cancer) criteria accessible at http://monographs.iarc.fr/ENG/Preamble/currentb6evalrationale0706.php (see Table 1.2).

Table 1.2 Classification of evidence

Grade of evidence	Criteria
Sufficient evidence	A causal relation has been established between exposure to night-time noise and an effect. In studies where coincidence, bias and distortion could reasonably be excluded, the relation could be observed and it is plausible that the effect is (also) caused by the exposure.
Limited evidence	A relation was observed between exposure to night-time noise and an effect in studies where coincidence, bias and distortion could not reasonably be excluded. The relation is, however, plausible. A direct relation between cause and effect has not been observed, but there is indirect evidence of good quality and the relation is plausible. Indirect evidence is assumed if exposure leads to an intermediate effect and other studies prove that the intermediate effect leads to the effect.
Insufficient evidence	Available studies are of low quality and lack significance to allow conclusions about causality of the relation between exposure and effect. Plausibility of the relation is limited or absent.

1.2.4 PROCEDURE FOR DERIVING GUIDELINES

The following procedure was followed in order to derive an ordering of guideline values:

1. collection of relevant data
2. evaluation of data in terms of strength of evidence
3. evaluation of data in terms of biological effects, health and well-being
4. ranking of guideline values.

This procedure is essentially the same as in other guideline documents, although steps are more explicitly formalized. A major difference is that sound is a natural environmental quality, which makes defining a no-effect level a futile exercise. Therefore the choice was made for a series of levels with increasing severity of effects.

1.3 CONSIDERATIONS WITH REGARD TO NIGHT-TIME NOISE INDICATORS

Briefly, the fundamental choices of night-time noise indicators with respect to length of night, use of single event descriptors and long-term average are commented on to assist the reader in understanding the relations presented in later chapters.

1.3.1 LENGTH OF NIGHT

Time use studies (Centre for Time Use Research, 2006) show that the average time adult people are in bed is around 7.5 hours, so the real average sleeping time is somewhat shorter. Due to personal factors such as age and genetic factors there is considerable variation in sleeping time and in beginning and end times. For these reasons, a fixed interval of 8 hours is a minimal choice for night-time protection. From Fig. 1.4 it can be noted that around 50% of the population is protected with an interval of 8 hours and it would take a period of 10 hours to protect 80%. On Sundays, sleeping time is consistently one hour longer, probably due to people recovering from sleep debt incurred during the week. Data for other countries are readily available but this is the only study covering a long period in a consistent way. Fig. 1.5 (from a time use study in Portugal) shows that the stable pattern found in the Netherlands (Fig. 1.4) is not only typical for northern Europe, but also for the southern part. The pattern, however, seems to have shifted slightly. These figures stress that sleep times might be biologically fixed in humans, and culture has almost no influence.

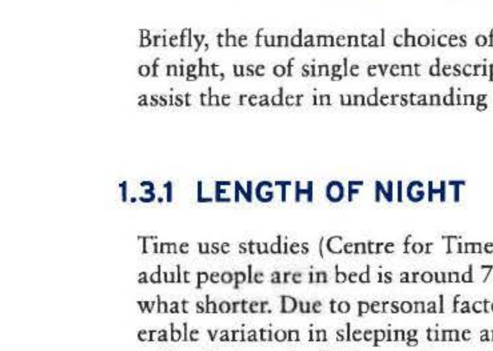

Fig. 1.4
Sleep pattern of Dutch population on weekdays and Sundays, 1980-2005

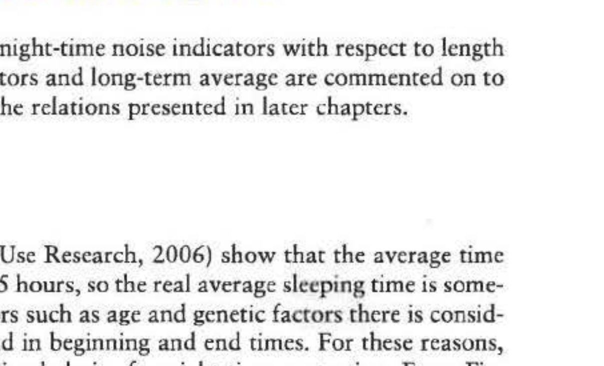

Fig. 1.5
Percentage of time that the Portuguese population spend asleep or in different activities

Source: http://www.ine.pt/prodserv/destaque/arquivo.asp, based on a study by the Instituto Nacional de Estatistica Portugal, 1999

1.3.2 EVENT OR LONG-TERM DESCRIPTOR

Much attention has been paid to the use of single event descriptors such as L_{Amax} (maximum outdoor sound pressure level) and SEL (sound exposure level). As the *Position Paper* on EU noise indicators (European Commission, 2000) points out, this is an important laboratory tool to describe instantaneous reactions to noise. But when it comes to long-term protection, the number of events is equally important. The possibility of predicting after-effects like sleepiness, reaction time, sleeping pill use and health complaints, in particular, requires a combination of a number of events and their level instead of just the average L_{Amax} or average SEL. For events with a similar time pattern there is a relatively simple relation between L_{Amax} and SEL, and therefore between L_{Amax} and L_{night} (night-time noise indicator as defined

Fig. 1.6
Relation between L_{night}, L_{Amax} and SEL

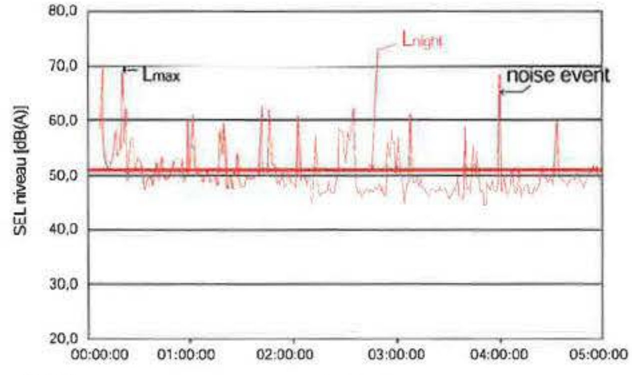

Source: European Commission, 2000

by the END – see paragraph 1.3.4 below). Appendix 2 describes this in detail. For now let it suffice to say that a choice for an L_{night} level ties the L_{Amax} related effects to a maximum and therefore allows for a protective/conservative approach.

Fig. 1.6 is based on a sound recording in a bedroom for one night. The top of the peaks are the L_{Amax} levels, the total energy is the L_{night} (thick horizontal line). The sound energy in one event is the SEL (not represented). In reality the L_{night} is the average over all nights in one year. This reasoning applies also to the issue of long-term average. A value for an arbitrary single night will, except in extreme cases, bear no relationship to an individual's long-term health status, whereas a sustained sufficiently high level over a long period may.

1.3.3 NUMBER OF EVENTS

There is no generally accepted way to count the number of (relevant) noise events. Proposals range from the number of measured L_{Amax}, the number of units (vehicles, aeroplanes, trains) passing by, to the number exceeding a certain L_{Amax} level (commonly indicated by NAxx; NA70 is the number of events higher than 70 dB).

1.3.4 CONVERSION BETWEEN INDICATORS

1.3.4.1 Introduction

L_{night} is defined as the 1 year L_{Aeq} (exposure to noise) over 8 hours outside at the most exposed facade. For the purpose of strategic noise mapping and reporting the height is fixed at 4 metres. As L_{night} is a relatively new definition and because the studies rarely cover such a long period, the research data are rarely expressed in L_{night}. The most frequently used noise descriptor in sleep research is the L_{Amax} or SEL near the sleeper. This means that a considerable amount of conversion work needs to be done if relations are to be expressed in L_{night}. There are four issues:

- conversion between SEL and L_{Amax}
- conversion from instantaneous to long-term
- conversion from inside to outside
- conversion from (outside) bedroom level to most exposed façade.

Further background information on these issues is provided in section 1.3.5. This section details the conversions that are actually carried out.

1.3.4.2 *SEL to L_{Amax}*

SEL is only used for aircraft noise in this report and, according to Ollerhead et al. (1992) from ground-based measurements, the following relation was found:

$$SEL = 23.9+0.81*L_{Amax} \qquad [1].$$

A more general approach can be used to estimate SEL for transportation noise.

If the shape of the time pattern of the sound level can be approximated by a block form, then $SEL \approx L_{Amax} + 10lg\ t$, where t (in seconds) is the duration of the noise event. This rule can be used, inter alia, for a long freight train that passes at a short distance. When t is in the range from 3 to 30 seconds, then SEL is 5–15 dB higher than L_{Amax}. For most passages of aircraft, road vehicles or trains, the shape of the time pattern of the sound level can be better approximated with a triangle. If the sound level increases with rate a (in dB per second), and thereafter is at its maximum for a short duration before it decreases with rate -a, then $SEL \approx L_{Amax} - 10lg(a) + 9.4$. Depending on the distance to the source, for most dwellings near transportation sources the rate of increase is in the order of a few dB per second up to 5 dB per second. When (a) is in the range from 9 dB to 1 dB per second, then SEL is 0–9 dB higher than L_{Amax}.

1.3.4.3 *Events to long-term*

When the SEL values are known (if necessary after converting from L_{Amax}) they can be converted to L_{night}. In general terms, the relation between L_{night} and SEL is:
$L_{night} = 10*lg\ \Sigma_i\ 10^{SEL_i/10} - 10*lg\ (T)$.

If all (N) events have approximately the same SEL level, this may be reduced to:

$$L_{night} = SEL + 10*lg(N) - 70.2 \qquad [2],$$

in which:
N = the number of events occurring in period T;
T = time during which the events occur in seconds. For a (night) year 10lg(T) is 70.2.

The notation adheres to the END where the L_{night} is defined as a year average at the most exposed facade. Any reference to an inside level is noted as such, that is, as $L_{night,inside}$. In order to avoid any doubt the notation $L_{night,outside}$ may be used, for instance in tables where both occur.

1.3.4.4 *Inside to outside*

As the L_{night} is a year value, the insulation value is also to be expressed as such. This means that if the insulation value is 30 dB with windows closed and 15 dB with windows open, the resulting value is 18 dB if the window is open 50% of the time. If these windows are closed only 10% of the time, the result is little more than 15 dB. The issue is complicated by the fact that closing behaviour is, to a certain extent, dependent on noise level. When results about effects are expressed with indoor (that is, inside bedrooms) exposure levels, they need to be converted to L_{night}, in accordance with the END definition. The most important assumption is the correction for inside levels to outside levels. An average level difference of 21 dB has been chosen, as this takes into account that even in well-insulated houses windows may be open a large part of the year. In general:

$$L_{night} = L_{night,inside} + Y \text{ dB} \qquad [3].$$

Y is the year average insulation value of the (bedroom) facade. In this report a default value of 21 dB is used (see also section 1.3.5). It should be stressed that this conversion is thought to be highly dependent on local building habits, climate and window opening behaviour.

1.3.4.5 Most exposed facade

If an inside level is converted to an outside level with [3], it is assumed that this is equivalent to an L_{night} value on the most exposed facade. No information is available on bedroom position and use, so no explicit conversion factor can be given in this report.

This means that the effect estimated on the basis of L_{night} corresponds to an upper limit, because part of the bedrooms will be on a less exposed facade. If an estimate of the exposed population is based on a relation derived with [3], the actual prevalence will be less. From a practical point of view the most exposed facade safeguards protection in cases where there is a possibility that rooms can be swapped.

It should be pointed out that the above does not apply if a relation is based on L_{night} values which are directly measured or computed. These relations will show a large variation because of a misclassification effect, but they give a "correct" estimate of the prevalence of effects in the population. In other words, in some cases a low effect may be attributed to a high L_{night} because the bedroom is on the quiet side.

1.3.5 INSIDE/OUTSIDE DIFFERENCES

Night-time environmental noise affects residents mainly inside their homes. In order to protect residents inside their homes from noise from outside sources, attention should be focused on windows since they are generally the weakest points in the sound propagation path. Roofs must also be considered with regard to aircraft noise.

There are many types of window in the EU, varying from single thin panes within frames without additional insulation, to four-pane windows within insulated frames. The simplest types of facade have a sound reduction (from outside to inside) of usually less than 24 dB, and the most elaborate facades (built to cope with cold climates, for example), have sound reductions of more than 45 dB. In central Europe, most windows are double-glazed, mounted in a rigid and well-insulated frame. Their range of sound reduction is between 30 dB and 35 dB when closed.

When night-time environmental noise reaches high levels, residents tend to close their bedroom windows (cf. Langdon and Buller, 1977; Scharnberg et al., 1982; Schreckenberg et al., 1999; Diaz et al., 2001). The studies by Scharnberg et al. and Schreckenberg et al. found that more than 50% of bedroom windows are closed when outside road traffic noise levels exceed 55 dB (L_{Aeq}). These findings have been replicated in Sweden, according to recent results from the Swedish soundscape research programme on road traffic noise (Fig. 1.7). Nevertheless, while residents with closed windows reported a reduction of sleep disturbances due to noise, they also reported an increase in sleep disturbances due to poor ventilation. Schreckenberg et al. (1999) report a much steeper increase in the incidence of closed windows when road traffic noise reaches high levels than is the case with increased levels of railway noise. Even when night-time noise levels reach 55 B, only 35% of the residents exposed to railway noise reported that they closed their windows at night.

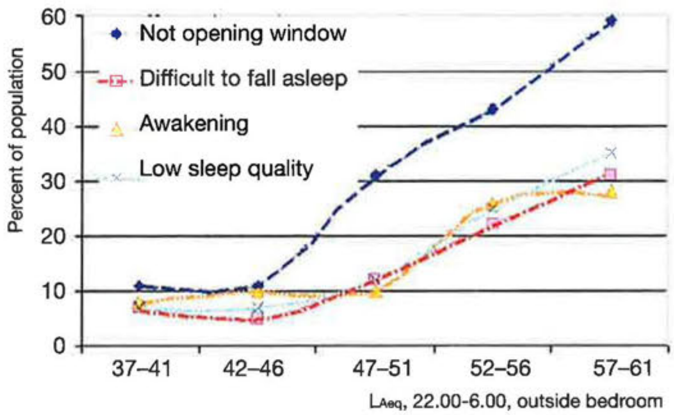

Fig. 1.7
Results from Swedish soundscape research programme on road traffic noise

Source: Öhrström, in European Commission, 2002a.

When windows are slightly open, outside sound levels are usually reduced by 10–15 dB. It should be kept in mind that most European residents want to keep their bedroom windows slightly open at night in order to provide proper ventilation (Scharnberg et al., 1982; Lambert and Plouhinec, 1985; Lambert and Vallet, 1994), and the WHO paper on community noise (WHO, 1999) also recommends that people should be able to sleep with their bedroom windows open.

Passchier-Vermeer et al. (2002) carried out detailed noise measurements inside and outside the bedroom and at the same time measured window position with sensors. The results (Table 1.3) showed that windows are fully closed only in 25% of the nights.

Window position	% nights
Closed	25
Slightly open	43
Hand width	23
Half open	5
Fully open	4

Table 1.3
Window positions during research period (April–November)

This results in average inside/outside differences of around 21 dB, with there being only a slight difference between single- and double-glazed windows (Table 1.4). The survey did not include dwellings which had been specifically insulated against noise. Nevertheless, there was a large variation in insulation values.

	Single-glazed window	Double-glazed window
Average difference at night	21.3	22.2

Table 1.4
Average inside/outside differences in dB

It should be stressed that this figure only applies to facades that have not been fitted with special appliances to reduce noise impact. To give an extreme example of where this general finding does not apply, rooms may be equipped with air conditioning so that windows can stay closed or could even be sealed. Less drastic provisions are sound-attenuated ventilation openings. Little is known, however, about the inhabitants' experiences (long-term use, appreciation) of these and other solutions. For example, sound-attenuated ventilation openings are sometimes blocked in order to cut out draughts.

1.3.6 BACKGROUND LEVEL

A simple definition of background level or "ambient noise" level is the noise that is not targeted for measurement or calculation. Background noise can interfere with the target noise in a number of ways. It can:

- mask the signal
- interact physically
- interact psychologically.

As this report is often dealing with low-level target noise, masking is an important issue. The other two interactions are more important in the domain of annoyance. Masking, however, is a complex process. The human auditory system is uncannily good at separating signals from "background". Microphones (and the software behind them) have been slow to catch up, as the unsatisfactory results show when it comes to automatically recognizing aircraft in long-term unmanned measuring stations.

The rule of thumb that a noise can be considered masked if the signal is 10 dB below the background is only valid if the noises have the same frequency composition and if they actually occur at the same time. This is particularly important to stress where L_{Aeq} levels are compared: even a relatively continuous motorway of 50 dB cannot mask aircraft noise of 30 dB, because this may be composed of five aircraft arriving at an L_{Amax} of 57 dB. Neither can birdsong, because the frequency domains do not overlap.

Another factor relevant for this report is that background levels are lower at night-time than they are in the daytime. This is true for most man-made noises, but also for the natural background levels as wind speeds at night slow down.

Most levels mentioned in this report do not take background levels into account – explicitly. Where long-term L_{Aeq} levels are related to effects like hypertension and self-reported sleep disturbance, background levels are ignored, but they could obscure the effect at the lower end of the scale. This then influences the lowest level where an effect starts to occur.

In sleep laboratory studies the background level is kept as low as possible, around 30 dB. The background of the instrumentation is 20 dB.

In semi-field experiments it has been found that background noise levels inside bedrooms are very low, partly because people tend to choose their bedrooms on the quiet side of the building. This may have the side-effect of exposing children to higher levels.

1.3.7 CHOICE OF INDICATORS FOR REGULATORY PURPOSES

From the scientific point of view the correct choice for a noise indicator is its performance in predicting the effect. There are, however, a number of additional criteria which may influence the choice. Firstly, for different health end points different indicators could be suitable. Further considerations are of a more political nature, as mentioned in the *Position Paper* on EU noise indicators (European Commission, 2000). Indicators should also be easy to explain to the public – intuitively understandable, avoiding unnecessary breaks with current practice and enforceable. This is probably why in many countries L_{Amax} is a popular indicator: it has undeniable qualities in these areas.

This is also the case for L_{Aeq} indicators for short periods of, for example, one or a few hours in the middle of the night. Other fashionable indicators are those looking at numbers above a threshold.

For these indicators the relation between health end points and their values is either not well established, or the correlation between them and current indicators is high, or the correlation between the indicator and an effect is low.

1.4 EXPOSURE IN THE POPULATION

1.4.1 NOISE LEVELS

Surprisingly little information is available on the exposure of houses to night-time noise. It is possible that, in a few years time, the END will lead to the creation of a substantial database on these levels, but up till now only two countries have detailed data available (Table 1.5).

	L_{night} in dB				
Country	**40–45**	**46–50**	**51–55**	**56–60**	**61–65+**
Switzerland (Müller-Wenk, 2002)	–	24%	14%	7%	2%
Netherlands (Nijland and Jabben, 2004)	25%	31%	19%	6%	1%

Table 1.5
Percentage of dwellings per noise class of L_{night} in dB

Notwithstanding the obvious differences between these two countries, the data show a remarkable similarity.

A first result of the END (see Table 1.6) comes from a study into night regulations for (large) airports (Wubben and Busink, 2004).

Airport	Number of inhabitants	Number of night operations per year	Night operations as percentage of daytime operations
Amsterdam	21 863	23 462	5.8%
Frankfurt	134 651	46 662	10.1%
London	477 289	26 465	5.7%
Paris	180 184	51 683	10.3%

Table 1.6
Number of inhabitants within 45 L_{night} contour

1.4.2 REPORTED NIGHT-TIME NOISE DISTURBANCE

Complaints about night-time exposure to noise are widespread and not exactly new: Roman writers used to complain about the racket in the streets at night (Juvenal, 160). Surprisingly, little detailed information is available today.

Nevertheless, data collected from a few Member States can help to give an impression of the order of magnitude of effects.

Fig. 1.8 shows the relative contributions to overall sleep disturbance caused by noise from different sources in the Netherlands. These data were derived from surveys in 1998 and 2003 (van Dongen et al., 2004) in which 4000 and 2000 people, randomly selected, were asked: "To what extent is your sleep disturbed by noise from [source mentioned]..." on a scale from 1 to 10. People recording the three highest points in the scale were considered "highly disturbed", according to an international convention. The totals are calculated from the number of people reporting serious sleep disturbance from one or more sources.

Unfortunately, comparable research data from other countries or regions is not available, and there is reason to believe that there may be considerable differences in the figures. Since this study is based on a survey conducted in the Netherlands, it is not representative for other Member States in the EU. General (not specific for night-time) annoyance data from Germany and the United Kingdom give an indication that similar numbers of people are affected.

Fig. 1.8 Percentage of population highly disturbed by noise during sleep in the Netherlands

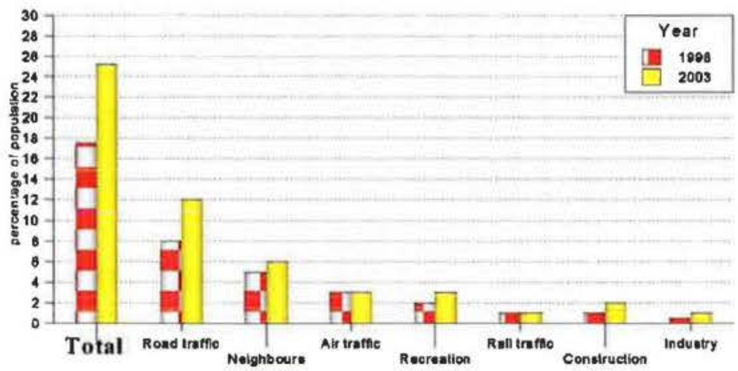

However, the fact that other noise nuisances may contribute significantly to overall sleep disturbance should not be overlooked. Further research on this topic is needed in order to gain an insight into the contribution of various noise sources to sleep disturbance.

1.5 CONCLUSIONS

The methods and criteria for deriving guidelines rest on well-established procedures from epidemiology. To relate the effects to the dose, standard metrics will be used wherever available. If possible, the values found in literature will be converted to avoid confusion. Most of the conversions are relatively straightforward and depend on physical laws; others, in particular the conversion between outside and inside levels, depend on local factors and should be used only if no other information is available.

Information about night-time noise exposure is relatively scarce, despite 10 EU Member States having limit values for night-time noise. The END could substantially increase this information (large-scale noise mapping is foreseen in 2007), increasing the demand for guidance.

CHAPTER 2

THE RELATION BETWEEN SLEEP AND HEALTH

A night of quiet and repose in the profound silence of Dingley Dell, and an hour's breathing of its fresh and fragrant air on the ensuing morning, completely recovered Mr Pickwick from the effects of his late fatigue of body and anxiety of mind.

(Charles Dickens, The Pickwick Papers, 1836)

2.1 SLEEP, NORMAL SLEEP, DEFINITIONS OF SLEEP DISTURBANCE, CHARACTERISTICS MECHANISMS, THE INSOMNIA MODEL

2.1.1 NORMAL SLEEP (OBJECTIVE MEASUREMENTS)

Sleep is part of living and, along with being awake, forms an inherent biological rhythm (Cooper, 1994). Normal sleep can be defined in an objective or subjective manner. The objective criteria are defined using a polysomnographic recording (PSG) of sleep, the method that measures different physiological functions during sleep. Minimal polygraphic requirements to measure sleep adequately include two channels of electroencephalography (EEG), one channel for the electrooculogram (EOG), and one channel for the submental electromyography (EMG). In routine PSG, additional channels are used to assess respiration, leg movements, oxygenation and cardiac rhythm (Ebersole and Pedley, 2003).

Scoring of sleep stages is usually done on an epoch-by-epoch basis, with a 30-second length used as a standard. Epochs are scored according to the guidelines of Rechtschaffen and Kales (1968). Each epoch is scored as the stage that occupies more than 50% of that epoch. Sleep can be divided into the following stages.

- **Arousal** is not a uniform concept and has been defined differently by different researchers. Commonly, the occurrence of alpha rhythms is required for EEG arousal. Depending on the additional requirements and on the length of time that the slower cortical rhythms are interrupted, arousals have been called, for instance, micro-arousal, minor arousal, EEG awakening or transient activation phases. The American Sleep Disorders Association (1992, 1997) devised a scoring system, taking sequences of 3–15 seconds into account for transient arousals which are not transferred to macroscopic behavioural awakening. Eleven further criteria must be met (see also Chapter 3, section 3.1.2).

- **Vegetative arousals** are activations of the sympathic nervous system.

- **Stage W** corresponds to the waking stage and is characterized by alpha activity or low-voltage, mixed-frequency EEG activity. Rapid eye movements (REMs), eye blinks, and tonic EMG activity are usually present.

- **Stage 1** is scored when more than 50% of an epoch is low-voltage, 2–7 Hertz (Hz) activity. Vertex waves may occur in late stage 1. Slow rolling eye movements lasting several seconds are routinely seen early in stage 1, but K complexes and sleep spindles are absent by definition. Tonic EMG activity is usually less than that of relaxed wakefulness.

- **Stage 2** requires the presence of sleep spindles or K complexes, and less than 20% of the epoch contains delta activity. Bursts of sleep spindles must last at least 0.5 seconds before they can be scored. K complexes are defined as biphasic vertex sharp waves with a total duration of greater than 0.5 seconds.

- **Stage 3** is scored when 20–50% of an epoch consists of delta activity that is 2 Hz or slower and is greater than 75 µV in amplitude. Sleep spindles may or may not be present.

- **Stage 4** is scored when more than 50% of an epoch consists of delta activity that is 2 Hz or slower and is more than 75 µV in amplitude. Reliable differentiation of stage 3 and stage 4 sleep is difficult by visual inspection, and most laboratories combine stages 3 and 4 into a single determination of slow-wave sleep (SWS).

- **Stage REM** is characterized by relatively low-voltage, mixed-frequency EEG activity with episodic REMs and absent or markedly reduced axial EMG activity. Phasic EMG activity may occur, but tonic activity must be at a level that is as low as, or lower than, that during any other time in the study. Sleep spindles and K complexes are absent. Series of 2- to 5- Hz vertex-negative "saw-tooth waves" occur, particularly just before phasic REM activity. The requirements to score sleep as REM sleep are: REMs, low or absent axial EMG, and typical mixed-frequency EEG recording that does not preclude the scoring of REM.

Movement time is scored when more than 50% of an epoch is obscured by movement artefact. Movement time must be preceded or followed by sleep and is thus distinguished from movement occurring during wakefulness.

Additional sleep values are determined from each sleep study and contribute to the clinical interpretation of the study. These additional variables include the following.

- **Recording time** is the time elapsed between "lights out" and "lights on" at the end of the study.

- **Total sleep time (TST)** is the total time occupied by stage 1, stage 2, SWS and REM sleep.

- **Sleep efficiency (SE)** is defined as total sleep time divided by recording time and is expressed as a percentage.

- **Sleep latency (SL)** is the time from "lights off" to the first epoch scored as sleep. Some authors prefer to use the first epoch of stage 2 in order to be more confident about identifying the onset of sustained sleep. However, when sleep is very disrupted, there may be an extended interval from recognition of stage 1 until an epoch that can be scored as stage 2.

- **REM latency** is the time from sleep onset (as described earlier) to the first time period scored as REM, minus any intervening epochs as wakefulness.

- **Sleep stage percentages** (% in stage 1, stage 2, SWS and REM sleep) are determined by dividing time recorded in each sleep stage by total sleep time.

- **Wake after sleep onset (WASO)** is time spent awake after sleep onset.

The objective criteria defining normal sleep are based on: sleep latency, total sleep time, sleep efficiency and the number of awakenings, including cortical arousals. However, all these parameters are age-related, sometimes also gender-related, and may vary from one individual to another.

Normal sleep has a clearly defined architecture that is relatively stable. Predictable changes in sleep architecture occur with age. Beginning in middle age, SWS becomes less prominent, the number of awakenings increase, and sleep efficiency decreases. Published information on normal sleep can serve as an outline for normal values in PSG (Williams, Karacan and Hursch, 1974; see also Table 2.1), but each laboratory must study control subjects to identify any significant effects on sleep that result from differences in technique or environment (Ebersole and Pedley, 2003).

Table 2.1
Average normal values for adults of different ages

Sleep parameter (normal values)	20–29 years	40–49 years	60–69 years
TST (min)	419	389	407
Sleep efficiency (TST/TIB[a])	95%	91%	90%
WASO	1%	6%	8%
Stage 1 (% of TST)	4%	8%	10%
Stage 2 (% of TST)	46%	55%	57%
SWS (% of TST)	21%	8%	2%
REM (% of TST)	28%	23%	23%
Sleep latency (min)	15	10	8

[a] *Time in bed*
Source: Williams, Karacan and Hursch, 1974.

Passchier-Vermeer (2003a) reports that subjects not exposed to loud night noise typically report waking up one and a half to two times during an average sleep period, while the number of EEG awakenings including cortical arousals averages 10–12 per night (Table 2.2).

Table 2.2
Parameters of normal sleep

Subjects not exposed to loud night noise	Subjective report of number of awakenings	Number of EEG awakenings
Normal adult subjects	1.5–2	10–12

Source: Passchier-Vermeer, 2003a.

Night arousals result in fragmented sleep, which in turn leads to excessive daytime sleepiness (EDS). The gold standard for the assessment of EDS is the multiple sleep latency test (MSLT) (see Table 2.3), which provides an objective quantification of "sleepiness". The preceding night's sleep requires the PSG to ensure adequate sleep and to exclude sleep disruption. During the day, four or five nap times are scheduled every two hours. For each scheduled nap time the patient lies down and assumes a comfortable sleep position with the technician's instructions to "close your eyes and attempt to sleep". Each nap is terminated 20 minutes after the nap time started if no sleep occurred; or after 15 minutes of continuous sleep as long as sleep onset (SO) criteria are met before the end of 20 minutes; or after 20 minutes if the patient awakens, even if the patient has been asleep less than 15 minutes. The patient is instructed to stay awake between the nap periods.

Table 2.3
Mean sleep latency

Group	MSLT (min)	No REM SO (% of group)	1 REM SO (% of group)	2 or more REM SO (% of group)
Narcoleptics	2.9 ± 2.7	2	2	96
EDS (non-narcoleptic, non-sleep apnocic)	8.7 ± 4.9	92	8	0
Controls	13.4 ± 4.3	100	0	0

Source: Ebersole and Pedley, 2003.

2.1.2 DEFINITIONS OF DISTURBED SLEEP

Sleep disorders are described and classified in the International Classification of Sleep Disorders (ICSD) (American Academy of Sleep Medicine, 2005).

When sleep is permanently disturbed and becomes a sleep disorder, it is classified in the ICSD 2005 as "environmental sleep disorder". Environmental sleep disorder (of which noise-induced sleep disturbance is an example) is a sleep disturbance due to a disturbing environmental factor that causes a complaint of either insomnia or daytime fatigue and somnolence. Secondary deficits may result, including deficits in concentration, attention and cognitive performance, reduced vigilance, daytime fatigue, malaise, depressed mood and irritability. The exact prevalence is not known. Fewer than 5% of patients seen at sleep disorder centres receive this diagnosis. The sex ratio is not known. The disorder may occur at any age, although the elderly are at more risk for developing this condition (American Academy of Sleep Medicine, 2005).

2.1.2.1 Insomnia

In the ICSD 2005 the section on insomnia includes a group of sleep disorders all of which have in common the complaint of insomnia (adjustment insomnia, psychophysiological insomnia, paradoxical insomnia, idiopathic insomnia, etc.), defined as repeated difficulty with sleep initiation, duration, consolidation or quality that occurs despite adequate time and opportunity for sleep and results in some form of daytime impairment. Insomnia is a symptom that often arises from primary medical illness, mental disorders and other sleep disorders, but may also arise from abuse or exposure. However, the general criteria for insomnia are the same for all subgroups of insomnias.

2.1.2.2 General criteria for insomnia

A. A complaint is made concerning difficulty initiating sleep, difficulty maintaining sleep, waking up too early or sleep that is chronically non-restorative or poor in quality. In children, the sleep difficulty is often reported by the carer and may consist of observed bedtime resistance or inability to sleep independently.

B. The above sleep difficulty occurs despite adequate opportunity and circumstances for sleep.

C. At least one of the following forms of daytime impairment related to the night-time sleep difficulty is reported by the patient:

- fatigue or malaise
- attention, concentration, or memory impairment
- social or vocational dysfunction or poor school performance
- mood disturbance or irritability

- daytime sleepiness
- motivation, energy, or initiative reduction
- proneness to errors or accidents at work or while driving
- tension, headaches, or gastrointestinal symptoms in response to sleep loss
- concerns or worries about sleep.

Defining the cause of a sleep/wake disturbance in an insomnia patient is a complex task since it is often multifactorial. In fact, a confluence of factors that support multiple insomnia diagnoses may be judged important in many patients with insomnia. Although selection of a single diagnosis is preferable and this selection may be appropriate, such a selection should not necessarily imply the absence of a subset of factors relevant to an alternate diagnosis. When criteria for multiple insomnia diagnosis are met, all relevant diagnosis should be assigned.

2.1.2.3 Environmental sleep disorder

In the ICSD 2005, environmental sleep disorder is listed in the category of "other sleep disorders". Noise-induced sleep disturbance is one of the disturbing environmental factors that cause a complaint of either insomnia or daytime fatigue and somnolence.

The diagnostic criteria for environmental sleep disorder are the following.

A. The patient complains of insomnia, daytime fatigue or a parasomnia. In cases where daytime fatigue is present, the daytime fatigue may occur as a result of the accompanying insomnia or as a result of poor quality of nocturnal sleep.

B. The complaint is temporally associated with the introduction of a physically measurable stimulus or environmental circumstance that disturbs sleep.

C. It is the physical properties, rather than the psychological meaning of the environmental factor, that accounts for the complaint.

D. The sleep disturbance is not better explained by another sleep disorder, medical or neurological disorder, mental disorder, medication use or substance use disorder.

The prevalence of environmental sleep disorder is not known. Fewer than 5% of patients seen at sleep disorder centres receive this diagnosis.

International standardization and quantification for measurement of the depth of sleep is based on Rechtschaffen and Kales criteria from 1968. Sleep is divided into 30-second epochs, and a phase is only assessed if the specific features are evident for more than 50% of the epoch length. For example, wakefulness is scored when at least 15 seconds of continuous awakening is present. Arousal reactions not leading to macroscopic awakening were not included in the definition by Rechtschaffen and Kales. With the arousals as described by the American Sleep Disorders Association (1992) it is possible to display subvigilant sleep fragmentation, caused by intrinsic sensory and autonomic alarm reactions. An arousal index providing the arousal density (events per hour of sleep) was taken as a measure of the degree of severity. In one hour, 10–20 arousals are considered as normal in healthy adults. However, the use of EEG arousals with the American Sleep Disorders Association definition provides no sufficient explanation of daytime sleepiness (Ali, Pitson and Stradling 1996; Ayas et al., 2001) unless they are accompanied by vegetative arousals.

Regarding noise, different vigilance level assessments in various functional systems are important. Dumont, Montplaisir and Infante-Rivard (1988) proposed investigations of vegetative, motor and sensory functions independently of each other. One of the possible factors indicating disturbed sleep is a vegetative arousal index. A vegetative arousal index of more than 30 per hour is certainly considered as serious, more than 20 per hour as intermediate and more than 10 as a light form of sleep disorder.

With respect to insomnia (section 2.1.2), there is the possibility of misclassification if the general practitioner (GP) overlooks excessive noise as the possible cause of the complaint. There is also the possibility that the insomnia is aggravated by noise.

2.1.3 CONCLUSIONS

Published information on normal sleep can serve as an outline for normal values in PSG. However, these values are only informative, because each sleep laboratory must study control subjects to identify any significant effects on sleep that result from differences in technique or environment. Excessive daytime sleepiness is a consequence of disturbed night sleep and can be objectively assessed by MSLT, which provides an objective quantification of "sleepiness".

2.2 LONG-TERM HEALTH RISK MEDIATED BY SLEEP DISTURBANCES

2.2.1 STRESSORS, NEUROBEHAVIOURAL DATA AND FUNCTIONAL NEUROIMAGING

It is generally accepted that insufficient sleep and particularly sleep loss has a great influence on metabolic and endocrine functions (Spiegel, Leproult and van Cauter, 1999), as well as on inflammatory markers, and contributes to cardiovascular risk. C-reactive protein (CRP) as a major marker of the acute phase response to inflammatory reaction promotes secretion of inflammatory mediators by vascular endothelium and may be therefore directly involved in the development of atherosclerotic lesions. CRP as a risk predictor of strokes and heart attacks linearly increases with total and/or partial sleep loss (Meier-Ewert et al., 2004).

An additional factor, closely linked to cardiovascular health, glucose regulation and weight control, is leptin. Leptin is one of the major regulators of energy homeostasis and its circadian profile interacts closely with sleep.

Secretion of leptin increases at night and decreases during the day. A decreased leptin level, that is connected with sleep loss, increases appetite and predisposes to weight gain, impaired glucose tolerance and impaired host response.

Other studies have focused on how sleep loss affects neurobehavioural functions, especially neurocognitive performance. Functional brain imaging and EEG brain mapping studies show that the patterns of functional connectivity between brain regions, evident in the performance of specific cognitive tasks, are altered by sleep loss (NCSDR, 2003). According to this finding, the maintenance of sustained performance during sleep loss may depend upon regional functional plasticity.

Cumulative waking, neurocognitive deficits and instability of state that develop from chronic sleep loss have a basis in a neurobiological process that can integrate homoeostatic pressure for sleep across days. Increased efforts have helped to determine the roles of REM and non-REM sleep in memory.
Functional brain imaging techniques, such as positron emission tomography (PET), functional magnetic resonance imaging (fMRI), magnetic resonance spectroscopy (MRS), single photon emission computed tomography (SPECT) and magneto-electroencephalography (MEG), have recently been analysed in a study of sleep and waking (NCSDR, 2003). These techniques allow the measurement of metabolic and neurochemical activity throughout the brain, and can reveal dynamic patterns of regional cerebral activity during various brain states, including stages of sleep and levels of alertness during wakefulness or during functional challenge. These techniques can also help identify both normal and abnormal sleep/wake processes.

In the last five years, functional neuroimaging techniques (particularly PET) have revealed that non-REM sleep is associated with the deactivation of central encephalic regions (brainstem, thalamus, basal ganglia) and multimodal association cortices (for instance, prefrontal and superior temporal/inferior parietal regions). REM sleep is characterized by reactivation of all central encephalic regions deactivated during non-REM sleep except the multimodal association areas. PET studies during sleep-deprived wakefulness have revealed regional cerebral deactivations that are especially prominent in prefrontal and inferior parietal/superior temporal cortices, and in the thalamus. This pattern is consistent and helpful in explaining the nature of cognitive performance deficits that occur during sleep loss. As revealed by means of fMRI techniques during cognitive task performance, the maintenance of performance following sleep loss may be a function of the extent to which other cortical brain regions can be recruited for task performance in the sleep-deprived state.

PET, SPECT and fMRI studies have revealed, in depressed patients, initially elevated activation in anterior cingulate and medial orbital cortices (NCSDR, 2003). In these patients, sleep deprivation reduces this regional hyperactivation, and improvements in mood are a function of the extent to which this activity is reduced. These studies point to possible mechanisms by which antidepressant drugs may exert their effects. Further research should be oriented towards neuroimaging and measurements of changes in the brain's metabolic activity at the neurotransmitter level.

2.2.2 SIGNALS MEDIATED BY A SUBCORTICAL AREA (THE AMYGDALA), THE ROLE OF STRESS HORMONES IN SLEEP DISTURBANCE AND THEIR HEALTH CONSEQUENCES

Experimental as well as clinical studies (Waye et al., 2003; Ising and Kruppa, 2004) showed that the first and fastest signal of stressors introduced by noise is detected and mediated by a subcortical area represented by the amygdala while the stress response to noise is mediated primarily by the hypothalamus-pituitary-adrenal (HPA) axis. A major intrinsic marker of the circadian rhythm is in the level of circulating corticosteroids derived from activity within the HPA axis. A protracted stress response with activation of the HPA axis is a major physiological response to environmental stressors. The cortisol response to awakening is an index of adrenocortical activity, and long-term nocturnal noise exposures may lead, in persons liable to be stressed by noise, to permanently increased cortisol concentration above the normal range. The hypothesis that an increased risk of cardiovascular diseases is connected with stress concepts is generally accepted (Ekstedt, Åkerstedt and Soderstrom, 2004; Ising and Kruppa, 2004). Stress reactions may lead to derangement of normal neurovegetative and hormonal processes and influence vital body functions. Cardiovascular parameters such as BP, cardiac function, serum cholesterol, triglycerides, free fatty acids and haemostatic factors (fibrinogen) impede the blood flow through increased viscosity and presumably blood sugar concentration as well. Insulin resistance and diabetes mellitus, stress ulcers and immune system deficiency are also frequent consequences of stress reaction. Disturbed sleep may lead to immunosuppression and diminished protein synthesis (Horne, 1988).

As well as nonspecific effects of the stress response on the functioning of the immune system, there is considerable evidence for a relation between sleep, especially SWS, and the immune system (Brown, 1992). This evidence includes surges of certain immune parameters and growth hormones at onset of SWS, correlation of non-REM sleep, total sleep time and sleep efficiency with natural killer cell activity, and correlation of SWS with recovery from infections. These data, taken together with information on the effect of intermittent transportation noise on SWS during the first sleep cycles and overnight, suggest that the immune response could also be impacted directly by environmental noise during sleep (Carter, 1996).

2.2.3 SLEEP RESTRICTION, ENVIRONMENTAL STRESSORS (NOISE) AND BEHAVIOURAL, MEDICAL AND SOCIAL HEALTH CONSEQUENCES OF INSUFFICIENT SLEEP: RISK OF MORBIDITY AND MORTALITY

Sleep restriction due to environmental stressors leads to primary sleep disorders, but health is also influenced by the consequence of stress response to noise mediated by the HPA axis and/or by restriction of specific sleep stages (see above).

Sleep restriction leads, in approximately 40% of affected subjects, to daytime sleepiness that interferes with work and social functioning. Excessive daytime sleepiness is thus a major public health problem, as it interferes with daily activities, with consequences including cognitive problems, motor vehicle accidents (especially at night), poor job performance and reduced productivity (Lavie, Pillar and Malhotra, 2002). In the last decade, experimentally based data have been collected on chronic restriction of sleep (by 1–4 hours a night), accumulating daytime sleepiness and cognitive impairment. Most individuals develop cognitive deficits from chronic sleep debt after only a few nights of reduced sleep quality or quantity. New evidence suggests additional important health-related consequences of sleep debt related to common viral illnesses, diabetes, obesity, heart disease, depression and other age-related chronic disorders.

The effects and consequences of sleep deprivation are summarized in Table 2.4 (Lavie, Pillar and Malhotra, 2002).

The relationship between sleep quantity and quality and estimates of morbidity and mortality remains controversial. Epidemiological data (NCSDR, 2003) suggest that habitually short sleep (less than 6 hours sleep per night) is associated with increased mortality. Epidemiological studies in recent years elucidated, however, that too much sleep is a problem as well. Kripke et al. (2002) evaluated a questionnaire study of 1.1 million men and women aged 30–102 years and found the lowest mortality risk between respondents sleeping 7 hours per night.

Type	Short-term	Long-term
Behavioural	Sleepiness Mood changes Irritability and nervousness	Depression/mania Violence
Cognitive	Impairment of function	Difficulty in learning new skills Short-term memory problems Difficulty with complex tasks Slow reaction time
Neurological	Mild and quickly reversible effects	Cerebellar ataxia, nystagmus, tremor, ptosis, slurred speech, increased reflexes, increased sensitivity to pain
Biochemical	Increased metabolic rate Increased thyroid activity Insulin resistance	Decreased weight despite increased caloric intake (in animals) Diabetes, obesity (in humans)
Others	Hypothermia Immune function impairment	Susceptibility to viral illness

Table 2.4
Consequences of sleep deprivation

Mortality risk significantly increased when sleep duration was less than 6 or higher than 8 hours per night. Other authors have also published similar results (Patel et al., 2004; Tamakoshi and Ohno, 2004). Patel et al. (2004) in a prospective study of sleep duration and mortality risk in 5409 women confirmed previous findings that mortality risk is lowest among those sleeping 6–7 hours per night. The mortality risk for death from other causes significantly increased in women sleeping less than 5 and more than 9 hours per night. It is not clear how the length of sleep can increase this risk, although animal evidence points to a direct link between sleep time and lifespan (see section 2.5 in this chapter). Up to now, no epidemiological prospective study has been published that examines the relationship between sleep and health outcomes (morbidity and mortality) with subjective and objective estimates. Recent studies, however, show that sleep duration of least 8 hours is necessary for optimal performance and for prevention of daytime sleepiness and accumulation of sleep debt.

Environmental stressors, including noise, mostly cause insomnia. Insomnia also involves daytime consequences, such as tiredness, lack of energy, difficulty concentrating and irritability. A reasonable prevalence estimate for chronic insomnia in the general population is about 10%; for insomnia of any duration or severity this rises to between 30% and 50%, and incidence increases with ageing. In the course of perimenopausal time, women are particularly vulnerable to developing this complaint. The major consequences and co-morbidity of chronic insomnia (see Table 2.5) consist of behavioural, psychiatric and medical problems. Several studies also report a higher mortality risk (Zorick and Walsh, 2000).

Table 2.5 Consequences of chronic insomnia

Type	Consequence
Behavioural	Poor performance at work, fatigue, memory difficulties, concentration problems, motor vehicle accidents
Psychiatric	Depression, anxiety conditions, alcohol and other substance abuse
Medical	Cardiovascular, respiratory, renal, gastrointestinal, musculoskeletal disorders Obesity Impaired immune system function
Mortality	Increased risk is reported

2.2.3.1 *Behavioural consequences*

Transient (short-term) insomnia is usually accompanied by spells of daytime sleepiness and performance impairment the next day. Persistent (long-term) insomnia tends to be associated with poor performance at work, fatigue, memory difficulties, concentration problems and twice as many fatigue-related motor vehicle accidents as in good sleepers.

2.2.3.2 *Psychiatric conditions*

Epidemiological research indicates that the prevalence of any psychiatric disorder is two or three times higher in insomniacs. The risk of depression as a co-morbid state appears to be particularly strong, being approximately four times more likely in insomnia patients. Furthermore, insomnia may be an early marker for psychiatric disorders such as depression, anxiety conditions and alcohol abuse. Anxiety has been quite commonly found in insomniacs compared with the general population. About 25–40% of insomnia patients are estimated to have significant anxiety, and the abuse of alcohol and other substances is increased in insomniacs relative to good sleepers (Ford and Kamerow, 1989). Samples of unselected psychiatric patients have about a threefold increase in the frequency of insomnia compared with healthy control subjects, and the severity of the condition correlates with the intensity of the psychiatric symptoms. Among samples of outpatients who consulted their GPs for insomnia, about 50% presented with psychiatric conditions, and about half of these patients were probably depressed (Zorick and Walsh, 2000).

2.2.3.3 *Medical consequences*

Insomnia has been statistically associated with various medical conditions, including disorders of the cardiovascular, respiratory, gastrointestinal, renal and musculoskeletal systems. A large series of insomniac patients showed that poor sleepers are more than twice as much at risk of ischaemic heart disease (IHD) as good sleepers (Hyyppa and Kronholm, 1989). Insomnia patients were also shown (Irwin, Fortner and Clark, 1995) to have impaired immune system function. Keith et al. (2006) hypothesize a connection between sleep deficit as one of the possible factors to explain the rise in obesity. Hormone changes and animal experiments apparently support this.

2.2.3.4 *Mortality risk*

Only a few epidemiological studies deal with mortality in insomniacs. According to Kripke et al. (1979), reduced sleep time is a greater mortality risk than smoking, hypertension and cardiac disease. Higher death rates are also reported among short sleepers. In this respect, however, further systematic investigation of the link between insomnia, short sleep and death is desirable.

2.3 RISK GROUPS

Risk groups are people who may be either sensitive (showing more reaction to a stimulus than the average), are more exposed (also called vulnerable) or both.

2.3.1 HEALTH EFFECTS OF DISTURBED SLEEP IN CHILDREN

Although children appear to tolerate a single night of restricted sleep with no detrimental effect on performance of brief tasks, perhaps more prolonged restriction and prolonged tasks similar to those required in school would show negative effects. In addition, as children seem to require more time to recuperate fully from nocturnal sleep restriction than adults (Carskadon, Harvey and Dement, 1981a), with additional nights of partial sleep deprivation, cumulative sleepiness might become a significant problem.

Empirical data that directly address the effects of repeated sleep loss on children's mood or cognitive function are sparse. A range of clinical and observational data support a general picture that inadequate sleep results in tiredness, difficulties in focusing attention, low thresholds for negative reactions (irritability and easy frustration), as well as difficulty in controlling impulses and emotions. In some cases, these symptoms resemble attention-deficit hyperactivity disorder (ADHD).

Environmental noise experienced at home during night-time is a sometimes unpredictable and most often discontinuous event (for example traffic noise, aircraft or train noise, a noisy environment for other reasons, for instance proximity with a discotheque, etc.), that might lead to sleep disruption without leading to behavioural awakenings through the alteration of sleep microstructure, in a similar manner as other sleep disturbing events such as respiratory disturbances.

Therefore, in respect of clinical settings, we can assume that, in children, an experimental model for the consequences of noise can be represented by respiratory disturbances during sleep, such as snoring, upper airway resistance syndrome (UARS) or obstructive sleep apnoea syndrome (OSAS), either for the noise produced by snoring or for the effects on the arousal system and sleep microstructure.

For this reason, this section describes the well-studied effects of sleep breathing disorders on children's health and then evaluates the indicators of sleep disruption from the point of view of sleep microstructure.

In the literature few data on the medium- and long-term effects of disturbed sleep in children are available from the longitudinal point of view. Most reports focused on respiratory disturbances during sleep as a theoretical model to evaluate the long-term effects of disturbed sleep in children. This review reports on the medium- and long-term negative consequences of disturbed sleep on cognitive functioning, behaviour, mental health, growth and the cardiovascular system.

2.3.1.1 Sleep deprivation in children

The effects of sleep deprivation were evaluated in children. The findings only indirectly pertain to this general report, although repeated noise-induced sleep disruption favours sleep deprivation.

In another study, 15 healthy infants aged 78+/-7 days were studied during two nights: one night was preceded by sleep deprivation (kept awake for as long as possible beyond their habitual bedtime: median onset 150 min; range 0–210 min) (Thomas et al., 1996). Of the 15 children, 13 slept supine, 12 were breastfed and 4 were from smoking parents. Following sleep deprivation, infants maintained a greater proportion of quiet sleep (44% vs. 39%; p=.002). There was no measurable change in arousal propensity by either graded photic (stroboscope) or auditory stimuli (1 kHz pure tone, delivered in the midline of the cot, from 73 dB and increased in 3 dB steps to 100 dB) during quiet sleep.

Forty-nine Finnish children (26 boys/23 girls) aged 7–12 years were interviewed together with their parents and school teachers, and recorded for 72 hours with a belt-worn activity monitor during weekdays.

The objectively measured true sleep time was associated with psychiatric symptoms reported by a teacher. The decreased amount of sleep was associated more with externalizing than internalizing types of symptoms (aggressive and delinquent behaviour, attention, social, and somatic problems) (Aronen et al., 2000).

In a survey, it was also shown that out of 100 Belgian school children, aged between 9 and12 years, those with poor sleep (insomnia) were also showing more frequent poor school performance (failure to comply with expected grades) than good sleepers. The relation between poor sleep and a noisy environment was, however, not evaluated (Kahn et al., 1989).

2.3.1.2 Neurocognitive manifestations

Several studies in adults have shown that sleep fragmentation and hypoxaemia can result in daytime tiredness and loss of concentration, retrograde amnesia, disorientation, morning confusion, aggression, irritability, anxiety attacks and depression. One could hypothesize that sleep fragmentation and hypoxaemia would affect the neuropsychological and cognitive performance also in children, where the impact of abnormal sleep may be even greater than in adults. In fact, neurocognitive and behavioural deficits and school problems have been reported recently in children with sleep-related obstructive breathing disorders (SROBD).

2.3.1.3 Attention capacity

This represents the ability to remain focused on a task and appropriately attend to stimuli in the environment. Taken together the studies to date indicate that children with SROBD are less reflective, more impulsive, and show poorer sustained and selective attention. Blunden et al. (2000) reported that, compared to 16 controls, 16 children with mild SROBD showed reduced selective and sustained attention. Owens-Stively et al. (1997) suggested a dose–response in attention–impulsivity with moderate to severe obstructive sleep apnoea syndrome (OSAS) children showing greater deficits than mild OSAS children. Importantly, early treatment showed that attention deficits in children with OSAS are reversible (Guilleminault et al., 1982b). In another study, 12 children with moderate to severe OSAS showed a significant reduction in inattention and an improvement in aggressive and hyperactive behaviours and vigilance after surgical treatment (Ali, Pitson and Stradling, 1996).

2.3.1.4 Memory

Rhodes et al. (1995) found inverse correlations between memory and learning performance and the apnoea hypopnea index in 14 morbidly obese children. Smaller deficits were observed by Blunden et al. (2000), who found in their sample of children with mild SROBD that mean global memory performance was in the lower end of the normal range compared to controls.

A recent study using actigraphy in normal school-age children showed that lower sleep efficiency and longer sleep latency were associated with a higher percentage of incorrect responses in working memory tasks; shorter sleep duration was associated with performing tasks at the highest load level only. Also, controlling for age, gender, and socioeconomic status, sleep efficiency and latency were significantly associated with the mean incorrect response rate in auditory working memory tasks. This study showed that sleep quality (evaluated as sleep efficiency = 100* [sleep + light sleep]/duration) is more strongly associated with performance in working memory tasks than sleep duration, suggesting that in assessing sleep, attention should be directed not only at the amount of sleep but also at sleep quality.

2.3.1.5 *Intelligence*

Inspection of the mean IQ scores reported in the study by Rhodes et al. (1995) suggested that their sample of five obese children with moderate to severe OSAS performed in the borderline range whereas controls performed in the normal range. Blunden et al. (2000) showed smaller deficits in children with mild SROBD whose mean verbal and global IQ were in the lower end of the normal range.

It remains unclear as to whether the putative negative effects of SROBD on intelligence are global in nature or confined to specific areas such as verbal rather than performance or visuospatial intelligence and whether these impairments can be reversed.

2.3.1.6 *Learning and school performance*

It has been widely reported (Stradling et al., 1990; Guilleminault et al., 1996; Richards and Ferdman, 2000) that children with SROBD show reduced academic performance and learning.

Weissbluth et al. (1983) found that poor academic achievers had a higher prevalence of night-time snoring (38% vs. 21%) and breathing difficulties (13% vs. 6%). Out of 297 children with SROBD (22% snorers and 18% sleep-associated gas exchange abnormalities), 40% were in the lowest 10th percentile of academic performance (Gozal, 1998) and SROBD in early childhood may continue to adversely affect learning in later years (Gozal and Pope, 2001). Gozal (1998) found in his sample of poor academic achievers that school grades improved post-adenotonsillectomy in treated but not untreated children.

As well as those with SROBD, healthy normal children with fragmented sleep (measured by actigraphy) also showed lower performance on neurobehavioural functioning (NBF) measures, particularly those associated with more complex tasks, and also had higher rates of behavioural problems (Sadeh, Gruber and Raviv, 2002). Furthermore, in normal children without sleep disorders, modest sleep restriction can also affect children's NBF. Sadeh, Gruber and Raviv (2003) monitored 77 children for 5 nights with activity monitors. On the third evening, the children were asked to extend or restrict their sleep by an hour on the following three nights. Their NBF was reassessed on the sixth day following the experimental sleep manipulation and showed that sleep restriction led to improved sleep quality and to reduced reported alertness.

These studies suggest that fragmented sleep or insufficient sleep is highly relevant during childhood and that children are sensitive to modest alterations in their natural sleep duration.

Early reports documented that untreated OSAS can have long-term negative effects, such as failure to thrive, cor pulmonale and mental retardation. These severe consequences are less common now due to early diagnosis and treatment, but recent reports have focused on other long-term effects mainly related to neurocognitive deficits, such as poor learning, behavioural problems and ADHD (Marcus, 2001).

Gozal and Pope (2001) tried to determine the potential long-term impact of early childhood snoring. Analysing questionnaires of 797 children in a low academic performance group (LP) and 791 in a high academic performance (HP) group, they found that frequent and loud snoring during early childhood was reported in 103 LP children (12.9%) compared with 40 HP children (5.1%). Therefore, children with lower academic performance in middle school are more likely to have snored during early childhood and to require surgery for snoring compared with better performing schoolmates. These findings suggest that children who experienced sleep-disordered breathing during a period traditionally associated with major brain growth and substantial acquisition of cognitive and intellectual capabilities may suffer from a partially irreversible compromise of their a priori potential for academic achievement. Three major components that result from the intermittent upper airway obstruction that occurs during sleep in children could theoretically contribute to such neurocognitive deficits, namely episodic hypoxia, repeated arousal leading to sleep fragmentation and sleep deprivation, and periodic or continuous alveolar hypoventilation.

Schooling problems may underlie more extensive behavioural disturbances such as restlessness, aggressive behaviour, EDS and poor neurocognitive test performances. Nearly 20–30% of children affected by OSAS or loud and frequent snoring show important signs of behavioural problems such as inattention and hyperactivity. Problems similar to symptoms of ADHD are linked to the presence of repeated sleep arousals, and intermittent hypoxic events, inducing a lack of behavioural inhibition with negative implications for working memory, motor control and self-regulation of motivation and affect.

In contrast with these data, Engle-Friedman et al. (2003) recently found a significant improvement of functions, at least in mild to moderate OSAS, when measured several months following an adenotonsillectomy, but they confirmed that their results could not rule out the possibility, even after treatment, of partial irreversible damage to academic function that may be detected only later in life. In addition, they stated that adults who also had deficits of neurocognitive executive functions related to the prefrontal area failed to improve significantly after treatment.

The negative long-term effects may be mediated by the irreversible alteration of the prefrontal cortex (PFC) and be related to structural changes of the brain as a consequence of both hypoxaemia and sleep fragmentation induced by OSAS or other pathologies affecting sleep.

In a recent report concerning OSAS adults, Macey et al. (2002) demonstrated grey matter loss in cerebral sites involved in motor regulation of the upper airway as well as in areas contributing to cognitive function (frontal and parietal cortex, temporal lobe, anterior cingulate, hippocampus and cerebellum). It can be argued that, in critical stages of brain development (that is, in childhood), these effects can lead to even more severe consequences, which could explain the negative long-term effects.

It is speculative to think that the remodelling of the brain could also be mediated by sleep and, therefore, sleep fragmentation could affect the process of brain plasticity (that is, the capacity of the brain to modify its structure and function over time). Recent studies showing experience-dependent gene-expression of gene *zif-268* during paradoxical sleep in rats exposed to a rich sensorimotor environment, and the role of sleep in enhancing the remodelling of ocular dominance in the developing visual cortex are also in line with the hypothesis that sleep affects neuronal plasticity and memory processes (Peigneux et al., 2001).

2.3.1.7 Neurobehavioural manifestations

Behavioural disturbances are common in children with SRODB, with higher prevalence rates of both internalized (for instance being withdrawn, shy, anxious and psychosomatic) and externalized (for instance impulsivity, hyperactivity, aggression and delinquency) problematic behaviours (Blunden, Lushington and Kennedy, 2001). The most frequently documented problematic behaviour in children with SROBD is attention deficit hyperactivity with a prevalence rate of 20–40% (Weissbluth et al., 1983; Ali, Pitson and Stradling, 1993). Conversely, children with ADHD showed a high prevalence rate of snoring (Chervin et al., 1997) and a co-diagnosis of ADHD has been reported in 8–12% of children with OSAS (O'Brien and Gozal, 2002).

A few studies have documented that children with sleep disorders tend to have behavioural problems similar to those observed in children with ADHD. A survey of 782 children documented daytime sleepiness, hyperactivity, and aggressive behaviour in children who snored, with 27% and 38% of children at high risk for a sleep or breathing disorder displaying clinically significant levels of inattention and hyperactive behaviour, respectively (Ali, Pitson and Stradling, 1994).

At 3 years of age children with persistent sleep problems (n = 308) were more likely to have behaviour problems, especially tantrums and behaviour management problems (Zuckerman, Stevenson and Bailey, 1987).

In a study of 16 children with a mean age of 12+/-4 years suffering from chronic pain due to juvenile rheumatoid arthritis and secondary poor sleep, polysomnographic recordings showed poorer night-time sleep, longer afternoon naptime and more daytime sleepiness than normal values from the literature (Zamir et al., 1998). In a school survey of children aged 9–12 years (n = 1000), those with poor sleep (insomnia for more than 6 months) had poorer school performance, defined as failure to comply with expected grades, than good sleepers. Their learning problems were tentatively attributed to the long-term effect of poor sleep (Kahn et al., 1989).

A questionnaire administered to children aged 4–12 years (n = 472) showed a relation between sleep problems and tiredness during the day (Stein et al., 2001).

In children aged 9–12 years (n = 77), shortening sleep by one hour was associated with reduced alertness and significant lowering of neurobehavioural functioning (Sadeh, Gruber and Raviv, 2003). In school-age children (n = 140) recorded at home with an actigraph, a significant relation was shown between the presences of fragmented sleep, daytime sleepiness and lower performance in neurobehavioural functioning evaluated by various performance tests (Sadeh, Gruber and Raviv, 2000). These children also had higher rates of behavioural problems, as reported by their parents (Sadeh, Gruber and Raviv, 2002).

In Finland, children aged 7–12 years (n = 49) were interviewed together with their parents and schoolteachers and recorded for 72 hours with a belt-worn activity monitor during weekdays. The decreased amount of sleep was associated with symptoms such as aggressive and delinquent behaviour, attention, social and somatic problems. The findings of this research were better associated with the teachers' than the parents' reports, suggesting that parents may be unaware of their child's sleep deficiencies as the behavioural problems may be more evident at school than at home (Aronen et al., 2000).

A prospective long-term study conducted in Sweden on 2518 children revealed that within a subgroup of 27 children with severe and chronic sleep problems, 7 children developed symptoms that met the criteria for ADHD by the age of 5.5 years (Thunström, 2002). Compared to the other children with sleep problems, these subjects had more frequent psychosocial problems in the family, bedtime struggles and long sleep latency at bedtime.

A population-based, cross-sectional questionnaire survey was conducted in Massachusetts on 30 195 children aged 5 years (Gottlieb et al., 2003). Children described by their parents as having sleep-disordered breathing (snoring, noisy breathing, apnoea) were significantly more likely to have daytime sleepiness and problem behaviours, including hyperactivity, inattention and aggressiveness (all with an odds ratio >2.0). These problem behaviours were suggestive of ADHD.

Similar findings were found in a group of children aged 5–7 years with periodic limb movement disorder who were studied polygraphically and their recording compared with those of age-matched children with ADHD. Their repeated sleep fragmentation resulting from the periodic limb movement disorder favoured the development of symptoms similar to those seen in ADHD (Crabtree et al., 2003).

The parents of a group of children with an average age of 8.6 years (range 2–17 years) reported that their children had difficult behaviours on the day that followed a 4-hour night-time sleep restriction (Wassmer et al., 1999). In one study, a 2-hour sleep reduction induced by delayed bedtime has been shown to increase daytime sleepiness, mainly during morning hours (Ishihara and Miyke, 1998; Ishihara, 1999).

Following one night of 4 hours of sleep deprivation imposed on children (aged 11–13 years), a decrease in performance tests has been observed (Carskadon, Harvey and Dement, 1981a).

Following one night's sleep loss, adolescents showed increased sleepiness, fatigue and reaction time. They selected less difficult academic tasks during a set of tests, but the percentages of correct responses were comparable to those seen following a normal night's sleep (Engle-Friedman et al., 2003).

Another study has been conducted on 82 children, aged 8–15 years. They were assigned an optimized, 10-hour night of sleep, or a restricted 4-hour night of sleep. Sleep restriction was associated with shorter daytime sleep latency, increased subjective sleepiness, and increased sleepy and inattentive behaviours, but was not associated with increased hyperactive-impulsive behaviour or impaired performance in tests of response inhibition and sustained attention (Fallone et al., 2001).

2.3.1.8 *Mental health*

A recent longitudinal study on the outcomes of early life sleep problems and their relation to behaviour problems in early childhood stressed the importance of studying the natural history of sleep problems and their consequences in order to identify whether persistent or recurrent sleep problems at age 3–4 years are associated with co-morbidities such as child behaviour problems, maternal depression and poor family functioning (Peiyoong, Hiscock and Wake, 2003).

The authors found that night waking at 3–4 years of age continued to be common. Seventy eight percent of mothers reported that their child awoke during the night at least once during the week, and of these waking children, 43% were reported to have awakenings 4 or more nights per week. Children with early sleep problems had significantly higher mean scores on internalizing and externalizing behaviour and the aggressive behaviour and somatic problems subscales of the Child Behavior Checklist (CBCL).

It has been noted that within groups of children and adolescents with psychiatric, behavioural or emotional problems, rates of sleep disorders are elevated (Sadeh et al., 1995). On the other hand, children and adolescents with disturbed sleep report more depression, anxiety, irritability, fearfulness, anger, tenseness, emotional instability, inattention and conduct problems, drug use and alcohol use.

Only a few longitudinal studies in adolescents have evaluated the impact of insomnia on future functioning. In a large sample of 11–17-year-old adolescents, followed for one year, using symptoms of DSM-IV criteria for insomnia, Roberts, Roberts and Chen (2002) found that nearly 18% of the youths 11–17 years of age reported non-restorative sleep almost every day in the past month, over 6% reported difficulty in initiating sleep, over 5% waking up frequently during the night, another 3% had early-morning awakening almost every day, over 7% reported daytime fatigue and 5% daytime sleepiness. Combining "often" and "almost every day" response categories dramatically increases prevalence, ranging from 60% for non-restorative sleep to 23% for daytime fatigue and 12% for waking up at night with difficulty going back to sleep. The re-evaluation of the sample at follow-up showed that insomnia predicted two indicators of psychological functioning: self-esteem and symptoms of depression (Roberts, Roberts and Chen, 2002).

2.3.1.9 *Growth impairment*

Failure to thrive is a well-known complication of disturbed sleep and childhood OSAS. The cause of poor growth is not known, although many different reasons have been implicated: (a) poor caloric intake associated with adenotonsillar hypertrophy; (b) excessive caloric expenditure secondary to increased work of breathing; (c) abnormal growth hormone (GH) release secondary to loss of deep non-REM sleep. The relative roles of these factors are unclear (Marcus et al., 1994; ATS, 1999). Circulating concentrations of insulin-like growth factor-I (IGF-I) and IGF-binding protein 3 (IGFBP-3) reflect mean daily GH levels, and seem to correlate well with physiological changes in GH secretion. In the operated children with initial OSAS a highly significant reduction in the apnoea-hypopnea index (AHI) was found and both the IGF-I and the IGFBP-3 concentrations increased significantly. GH is released in a pulsatile fashion; the initial secretion is synchronized with the onset of SWS and strongly correlated with slow-wave activity, within 90 to 120 minutes from the onset of sleep (Nieminen et al., 2002). In OSAS children, the sleep architecture is relatively well-preserved, but the microstructural alteration of SWS due to micro-arousals induced by respiratory disturbance could play a role in the abnormal profile of GH secretion.

2.3.1.10 *Cardiovascular complications*

Children with OSAS had a significantly higher diastolic blood pressure (BP) than those with primary snoring. Multiple linear regression showed that BP could be predicted by apnoea index, body mass index and age. The aetiology of OSAS-related hypertension is thought to be due to a number of factors, particularly sympathetic nervous system activation secondary to arousal and, to a lesser degree, hypoxaemia.

Although cortical arousals at the termination of obstructive apnoeas are less common in children than in adults, children may manifest signs of subcortical arousal, including autonomic changes such as tachycardia. It is therefore possible that these subcortical arousals are associated with elevations of BP. A correlation between the frequency of obstructive apnoea and BP, but no correlation between SaO2 (arterial oxygen saturation) and BP was found, suggesting that respiratory-related subcortical arousals rather than hypoxaemia may be a major determinant of BP elevation in children (Marcus, Greene and Carroll, 1998). Similarly to BP variations induced by OSAS, other studies suggest that chronic exposure to environmental noise during sleep could contribute to a permanent increases in BP in otherwise healthy individuals and that no habituation to noise was apparent over three consecutive sleep sessions (Carter et al., 2002). This is further elaborated in Chapter 4, section 4.5.

2.3.1.11 Risk of accidents

Only one study was found that evaluated the association between sleep and duration of wakefulness and childhood unintentional injury (Valent, Brusaferro and Barbone, 2001).

Two hundred and ninety-two injured children who attended the Children's Emergency Centre in Udine, Italy, or their parents were interviewed following a structured questionnaire. The sleeping time and wakefulness of the child was assessed retrospectively for each of the 48 hours before injury. For each child, the authors compared the 24 hours immediately before the injury (hours 1–24; case period) with hours 25–48 (control period).

Overall, more children had longer hours of sleep during the control period than during the case period. A direct association between injury risk and sleeping less than 10 hours was found among boys (RR: 2.33; 95% CI: 1.07–5.09) but not among girls (RR: 1.00; 95% CI: .29–3.45). The study also found a direct association between injury occurring between 16.00 and midnight, and being awake for at least 8 hours before injury occurred (both sexes, RR: 4.00; 95% CI: 1.13–14.17). Sleeping less than 10 hours a day was associated with an 86% increase in injury risk. A significantly increased risk did not emerge in all subgroups of patients but it was evident among children aged 3–5 years, boys in particular. A fourfold increase in injury risk was also associated with being awake for at least 8 hours among males only. These findings demonstrated that inadequate sleep duration and lack of daytime naps are transient exposures that may increase the risk of injury among children. Results of a study on sleep disturbance and injury risk in young children show inadequate sleep duration and lack of daytime naps. A lack of daytime naps means transient exposures that may increase the risk of injury among children. Among children (boys in particular) aged 3–5 years, sleeping less than 10 hours a day was associated with an 86% increase in injury risk. A fourfold increase in injury risk was also associated with being awake for at least 8 hours.

Daytime sleepiness in children is often manifested by externalizing behaviours noted by parents or teachers, such as increased activity levels, aggression, impulsivity, as well as by poor concentration, instantiation irritability and moodiness (Fallone, Owens and Deane, 2002).

Analysing attendance at school, data show that accidents took place at school (25.6%) and at home (22.0%), and statistics show that there is a highly significant greater total accident rate among boys than among girls. The most frequent injuries happening at school are fractures and dislocation of joints, head injuries being more common among school injuries compared with spare-time injuries. Most injuries occurred when children were in sports areas and it is noteworthy that 25% of all injuries were caused through intentional violence by other pupils.

2.3.1.12 Use of sleeping pills

Several studies demonstrated that the use of sleeping pills is common among children and that paediatricians are prone to prescribe these medications. Twenty-five percent of firstborn infants had been given "sedatives" by 18 months (Ounsted and Hendrick, 1977). A research study into parental reports of 11 000 preschool children showed that 12% took psychoactive drugs, most commonly for sleep: 39% daily and 60% intermittently for 1–2 years (Kopferschmitt et al., 1992). Another study (Trott et al., 1995) revealed that 35% of prescriptions for children less than a year old were for sleep disturbances and that sleep disturbances were also the most common reason for prescribing medications to preschool children (23%). Two French surveys on adolescents showed that 10–12% of the respondents reported use of prescription or over-the-counter drugs for sleep disturbances (Patois, Valatz and Alperovitch, 1993; Ledoux, Choquet and Manfredi, 1994). Recently it has been reported that of 671 community-based United States paediatricians, 75% had recommended over-the-counter and 50% prescription medicines for insomnia during the past 6 months (Owens, Rosen and Mindell, 2003). In addition, an Italian survey showed that pharmacological treatment for sleep problems was prescribed during the past 6 months by 58.54% of paediatricians and by 61.21% of child neuropsychiatrists (Bruni et al., 2004).

2.3.2 BASIC INDIVIDUAL FACTORS: GENDER AND AGE

Gender shows itself to be an important predictor of disturbed sleep in virtually all epidemiological studies (Karacan et al., 1976; Bixler, Kales and Soldatos, 1979; Ancoli-Israel and Roth, 1999; Leger et al., 2000; Sateia et al., 2000). On the other hand, there does not seem to be much of a difference in polysomnographical parameters between males and females, except for the former losing SWS with increasing age and having slightly reduced sleep efficiency also with increasing age (Williams, Karacan and Hursch, 1974; Hume, Van and Watson, 1998). Ehlers and Kupfer (1997) timed the start of differences between genders to between 20 and 40 years. Spectral analysis also indicates slightly larger amounts of low frequency activity in females (Dijk, Beersma and Bloem, 1989; Dijk, Beersma and Van den Hofdakker, 1989). In addition, men seem to run a higher risk of morbidity and mortality related to sleep problems than women (Nilsson et al. 2001). The inconsistency between polysomnography and subjective measures has not been resolved but it may be important that most polysomnographical studies have controlled for anxiety and depression. Thus, it is conceivable that the higher level of subjective complaints in women reflects a higher prevalence of anxiety. The latter is a speculation, however. A confounding factor in gender comparisons is that phases in female biological cycles are also usually controlled for in polysomnographical studies, meaning that potential effects of, for example, menstruation, may not receive their proper weight. A recent review has gone through the literature in this area (Moline et al., 2003). It found that the luteal phase of the menstrual cycle is associated with subjective sleep problems, but polysomnographical studies have not supported this. Pregnancy affects sleep negatively as early as in the first trimester and the effects mainly involve awakenings and difficulties getting back to sleep. Napping is a frequent coping method. The post-partum period is often associated with severe sleep disruption, mainly due to feeding and comforting the infant. There seems to be some relation between sleep disruption and post-partum mood, but nothing is known about the causal relations. Menopause seems to involve disrupted sleep in relation to hot flushes, depression/anxiety and sleep-disordered breathing. Oestrogen is associated with improved sleep quality but it is not clear whether the effects are due to a reduction of hot flushes. Oestrogen also improves sleep-disordered breathing.

With respect to background factors, age is an established predictor of disturbed sleep (Karacan et al., 1976; Bixler, Kales and Soldatos, 1979; Ancoli-Israel and Roth, 1999; Ribet and Derriennic, 1999; Leger et al., 2000; Sateia et al., 2000). Interestingly, however, older age may be related to a lower risk of impaired awakening (Åkerstedt et al., 2002c), that is, in this study it was easier to wake up and one felt better rested with increasing age, while at the same time sleep quality was lower. The increased risk of disturbed sleep is consistent with the increasingly strong interference of the circadian morning upswing of the metabolism with increasing age (Dijk and Duffy, 1999). Thus sleep maintenance is impaired and when sleep is interrupted "spontaneously", the awakening is, by definition, easily accomplished and will be lacking in inertia. This ease of awakening may be interpreted as "being well-rested", and obviously the need for sleep is not great enough to prevent an effortless transition into wakefulness.

In addition, sleep homeostasis seems to be weakened with age in the sense that sleep becomes more fragmented and SWS or power density in the delta bands decrease (Williams, Karacan and Hursch, 1974; Bliwise, 1993; Dijk et al., 1999). As mentioned above, the effects are more pronounced in males, a fact that may be linked to reduced levels of growth hormone and testosterone.

2.3.3 PERSONS EXPOSED TO STRESSORS AS A RISK GROUP

A number of epidemiological studies point to a strong link between stress and sleep (Åkerstedt, 1987; Urponen et al., 1988; Ancoli-Israel and Roth, 1999). In fact, stress is considered the primary cause of persistent psychophysiological insomnia (Morin, Rodrigue and Ivers, 2003). That stress can affect proper sleep seems obvious, but Vgontzas et al. (2001) at Pennsylvania State University College of Medicine have found another reason why middle-aged men may be losing sleep. It is not just because of what they worry about; rather, it is due to "increased vulnerability of sleep to stress hormones".

As men age, it appears they become more sensitive to the stimulating effects of corticotropin-releasing hormones (CRH). When both young and middle-aged men were administered CRH, the older men remained awake longer and slept less deeply. (People who don't get enough of this "slow-wave" sleep may be more prone to depression.)

The increased prevalence of insomnia in middle age may, in fact, be the result of deteriorating sleep mechanisms associated with increased sensitivity to arousal-producing stress hormones, such as CRH and cortisol. In another study, the researchers compared patients with insomnia to those without sleep disturbances. They found that "insomniacs with the highest degree of sleep disturbance secreted the highest amount of cortisol, particularly in the evening and night-time hours", suggesting that chronic insomnia is a disorder of sustained hyperarousal of the body's stress response system. Also, recent epidemiological studies have shown a connection between disturbed sleep and later occurrence of stress-related disorders such as cardiovascular diseases (Parish and Shepard, 1990; Nilsson et al., 2001;

Leineweber et al., 2003) and diabetes type II (Nilsson et al., 2002). The mechanism has not been identified but both lipid and glucose metabolisms are impaired in relation to experimentally reduced sleep (Åkerstedt and Nilsson, 2003). Burnout is another result of long-term stress and a growing health problem in many industrialized countries (Weber and Jaekel-Reinhard, 2000). In Sweden, burnout is thought to account for most of the doubling of long-term sickness absence since the mid-1990s (RFV, 2003). The characteristic clinical symptoms of the condition are excessive and persistent fatigue, emotional distress and cognitive dysfunction (Kushnir and Melamed, 1992; Melamed, Kushnir and Sharom, 1992). Self-reports of disturbed sleep are pronounced in subjects scoring high on burnout (Melamed et al., 1999; Grossi et al., 2003). Since shortened and fragmented sleep is related to daytime sleepiness and impaired cognitive performance (Bonnet, 1985, 1986a, 1986b; Dinges et al., 1997; Gillberg and Åkerstedt, 1998; Åkerstedt, 1990), disturbed sleep might provide an important link between the state of chronic stress and the complaints of fatigue and cognitive dysfunction seen in burnout.

Partinen, Eskelinen and Tuomi (1984) investigated several occupational groups and found disturbed sleep to be most common among manual workers and much less so among physicians or managing directors. Geroldi et al. (1996) found in a retrospective study of older individuals (above the age of 75) that former white-collar workers reported better sleep than blue-collar workers. Kupperman et al. (1995) reported fewer sleep problems in subjects satisfied with work.

In what seems to be the most detailed study so far, Ribet and Derriennic (1999) studied more than 21 000 subjects in France, using a sleep disturbance index and logistic regression analysis. They found that shift work, a long working week, exposure to vibrations, and "having to hurry" appeared to be the main risk factors, controlling for age and gender. Disturbed sleep was more frequent in women (Karacan et al., 1976; Bixler, Kales and Soldatos, 1979; Ancoli-Israel and Roth, 1999) and in higher age groups.

The particular stressor linked to disturbed sleep may be linked to pressure of work (Urponen et al., 1988; Ancoli-Israel and Roth, 1999; Ribet and Derriennic, 1999; Åkerstedt et al., 2002b). The demands of work are a classical work stress factor and, when combined with low decision latitude, a relation has been shown to cardiovascular diseases (Theorell et al., 1998) and absenteeism (North et al., 1996). Interestingly, when "persistent thoughts about work" was added to the regression in the study by Åkerstedt et al. (2002b) this variable took over part of the role of work demands as a predictor. This suggests that it may not be work demands per se that are important, but rather their effect on unwinding after work. In two studies it has been demonstrated that even moderate worries about being woken during the night or having a negative feeling about the next day will affect sleep negatively, mainly reducing SWS (Torsvall and Åkerstedt, 1988; Kecklund and Åkerstedt, 1997). On the other hand, there is very little data to connect real life stress with polysomnographical indicators of disturbed sleep. Most studies have used rather innocuous and artificial stressors in a laboratory environment. Field studies of stress are virtually lacking, with some exceptions (Hall et al., 2000).

A lack of social support at work is a risk indicator for disturbed sleep (Åkerstedt et al., 2002b). Few previous data of this type have been found, but poor (general) social support has been associated with sleep complaints in Vietnam veterans (Fabsitz, Sholinsky and Goldberg, 1997). On the other hand, there are several studies indicating a close connection with poor social support for, for example, cardiovascular diseases (Arnetz et al., 1986) or muscle pain (Ahlberg-Hultén, Theorell and Sigala, 1995).

Interestingly, the metabolic changes seen after sleep curtailment in normal sleepers or in insomniacs and sleep apnoeics are similar to those seen in connection with stress. That is, lipid and glucose metabolisms are increased, as are cortisol levels (Spiegel, Leproult and van Cauter, 1999; Vgontzas et al., 2000, 2001). Together with the prospective links to stress-related diseases such as diabetes type II, to cardiovascular diseases as discussed above and with mortality (Kripke et al., 1979, 2002; Åkerstedt et al., 2002a; Dew et al., 2003), the findings could suggest that disturbed sleep may be an important mediator in the development of stress-related diseases.

2.3.4 SHIFT WORK AS A RISK FACTOR FOR SLEEP DISTURBANCE AND HEALTH EFFECTS

The dominating health problem reported by shift workers is disturbed sleep and wakefulness. At least three quarters of the shift working population is affected (Åkerstedt, 1988). When comparing individuals with a very negative attitude to shift work with those with a very positive one, the strongest discriminator seems to be the ability to obtain sufficient quality of sleep during the daytime (Axelsson et al., 2004). EEG studies of rotating shift workers and similar groups have shown that day sleep is 1–4 hours shorter than night sleep (Foret and Lantin, 1972; Foret and Benoit, 1974; Matsumoto, 1978; Tilley, Wilkinson and Drud, 1981; Torsvall et al., 1989; Mitler et al., 1997). The shorter time is due to the fact that sleep is terminated after only 4–6 hours without the individual being able to return to sleep. The sleep loss is primarily taken out of stage 2 sleep and stage REM sleep (dream sleep). Stages 3 and 4 ("deep" sleep) do not seem to be affected. Furthermore, the time taken to fall asleep (sleep latency) is usually shorter. Night sleep before a morning shift is also reduced but the termination is through artificial means and the awakening usually difficult and unpleasant (Dahlgren, 1981a; Tilley et al., 1982; Åkerstedt, Kecklund and Knutsson, 1991; Kecklund, 1996).

Interestingly, day sleep does not seem to improve much across a series of night shifts (Foret and Benoit, 1978; Dahlgren, 1981b). It appears, however, that night workers sleep slightly better (longer) than rotating workers on the night shift (Kripke, Cook and Lewis, 1971; Bryden and Holdstock, 1973; Tepas et al., 1981). The long-term effects of shift work on sleep are rather poorly understood. However, Dumont, Montplaisir and Infante-Rivard (1988) found that the amount of sleep/wake and related disturbances in present day workers were positively related to their previous experience of night work. Guilleminault et al. (1982a) found an over-representation of former shift workers with different clinical sleep/wake disturbances appearing at a sleep clinic. Recently, we have shown that in pairs of twins with different night work exposure, the exposed twin reports somewhat deteriorated sleep quality and health after retirement (Ingre and Åkerstedt, 2004).

The main reason for short daytime sleep is the influence exerted by the circadian rhythm. The more sleep is postponed from the evening towards noon next day, the more truncated it becomes and when noon is reached the trend reverts (Foret and Lantin, 1972; Åkerstedt and Gillberg, 1981). Thus, sleep during the morning hours is strongly interfered with, despite the sizeable sleep loss that, logically, should enhance the ability to maintain sleep (Czeisler et al., 1980). Also, homeostatic influences control sleep. For example, the expected 4–5 hours of daytime sleep, after a night spent awake, will be reduced to 2 hours if a normal night's sleep precedes it and to 3.5 hours if a 2-hour nap is allowed (Åkerstedt and Gillberg, 1986). Thus, the time of sleep termination depends on the balance between the circadian and homeostatic influences. The circadian homeostatic regulation of sleep has also been demonstrated in great detail in studies of forced or spontaneous desynchronization under conditions of temporal isolation and ad lib sleeping hours (Czeisler et al., 1980; Dijk and Czeisler, 1995).

2.3.4.1 Alertness, performance and safety

Night-oriented shift workers complain as much of fatigue and sleepiness as they do about disturbed sleep (Åkerstedt, 1988). The sleepiness is particularly severe on the night shift, hardly appears at all on the afternoon shift and is intermediate on the morning shift. The maximum is reached towards the early morning (05.00–07.00). Frequently, incidents of falling asleep occur during the night shift (Prokop and Prokop, 1955; Kogi and Ohta, 1975; Coleman and Dement, 1986). At least two thirds of the respondents report that they have experienced involuntary sleep during night work.

Ambulatory EEG recordings verify that incidents of actual sleep occur during night work in, for example, process operators (Torsvall et al., 1989). Other groups, such as train drivers or truck drivers show clear signs of incidents of falling asleep while driving at night (Caille and Bassano, 1977; Torsvall and Åkerstedt, 1987; Kecklund and Åkerstedt, 1993). This occurs towards the second half of the night and appears as repeated bursts of alpha and theta EEG activity, together with closed eyes and slow undulating eye movements. As a rule the bursts are short (1–15 seconds) but frequent, and seem to reflect lapses in the effort to fend off sleep. Approximately a quarter of the subjects recorded show the EEG/EOG patterns of fighting with sleep. This is clearly a larger proportion than what is found in the subjective reports of episodes of falling asleep.

As may be expected, sleepiness on the night shift is reflected in performance. One of the classics in this area is the study by Bjerner, Holm and Swensson (1955) who showed that errors in meter readings over a period of 20 years in a gas works had a pronounced peak on the night shift. There was also a secondary peak during the afternoons. Similarly, Brown (1949) demonstrated that telephone operators connected calls considerably slower at night. Hildebrandt, Rohmert and Rutenfranz (1974) found that train drivers failed to operate their alerting safety device more often at night than during the day. Most other studies of performance have used laboratory type tests and demonstrated, for example, reduced reaction time or poorer mental arithmetic on the night shift (Tepas et al., 1981; Tilley et al., 1982). Flight simulation studies have furthermore shown that the ability to "fly" a simulator (Klein, Bruner and Holtman, 1970), or to carry out a performance test (Dawson and Reid, 1997) at night may decrease to a level corresponding to that after moderate alcohol consumption (>0.05% blood alcohol) Interestingly, Wilkinson et al. (1989) demonstrated that reaction time performance on the night shift (nurses) was better in permanent than rotating shift workers.

If sleepiness is severe enough, interaction with the environment will cease and if this coincides with a critical need for action an accident may ensue. Such potential performance lapses due to night work sleepiness were seen in several of the train drivers discussed earlier (Torsvall and Åkerstedt, 1987). The transport area is where most of the available accident data on night shift sleepiness has been obtained (Lauber and Kayten, 1988). Thus, Harris (1977) and Hamelin (1987) demonstrated that single vehicle accidents have by far the greatest probability of occurring at night.

So do fatigue-related accidents (Reyner and Horne, 1995) but also most other types of accidents, for example head-on collisions and rear-end collisions (Åkerstedt, Kecklund and Horte, 2001). The National Transportation Safety Board ranks fatigue as one of the major causes of heavy vehicle accidents (NTSB, 1995).

For conventional industrial operations very little relevant data is available but fatal work accidents show a higher risk in shift workers (Åkerstedt et al., 2002a) and accidents in the automotive industry may exhibit night shift effects (Smith, Folkard and Poole, 1994). An interesting analysis has been put forward by the Association of Professional Sleep Societies' Committee on Catastrophes, Sleep and Public Policy (Mitler et al., 1988). Their consensus report notes that the nuclear plant meltdown at Chernobyl occurred at 01.35 and was due to human error (apparently related to work scheduling). Similarly, the Three Mile Island reactor accident occurred between 04.00 and 06.00 and was due not only to the stuck valve that caused a loss of coolant water but, more importantly, to the failure to recognize this event, leading to the near meltdown of the reactor. Similar incidents, although with the ultimate stage being prevented, occurred in 1985 at the Davis Besse reactor in Ohio and at the Rancho Seco reactor in California. Finally, the committee also states that the NASA Challenger space shuttle disaster stemmed from errors in judgement made in the early morning hours by people who had had insufficient sleep (through partial night work) for days prior to the launch. Still, there is very limited support for the notion that shift work outside the transport area actually carries a higher overall accident risk.

As with sleep, the two main factors behind sleepiness and performance impairment are circadian and homeostatic factors. Their effects may be difficult to separate in field studies but are clearly discernible in laboratory sleep deprivation studies (Fröberg et al., 1975) as well as in studies of forced desynchronization (Dijk, Duffy and Czeisler, 1992). Alertness falls rapidly after awakening but gradually levels out as wakefulness is extended. The circadian influence appears as a sine-shaped superimposition upon this exponential fall in alertness. Space does not permit a discussion of the derivation of these functions, but the reader is referred to Folkard and Åkerstedt (1991) in which the "three-process model of alertness regulation" is described. This model has been turned into computer software for predicting alertness and performance and to some extent accident risk.

2.3.4.2 Health effects

Gastrointestinal complaints are more common among night shift workers than among day workers. A review of a number of reports covering 34 047 persons with day or shift work found that ulcers occurred in 0.3–0.7% of day workers, in 5% of people with morning and afternoon shifts, in 2.515% of persons with rotating shift systems with night shifts, and in 10–30% of ex-shift workers (Angersbach et al., 1980). Several other studies have come to similar conclusions (Thiis-Evensen, 1958; Segawa et al., 1987; Harrington, 1994). Other gastrointestinal disorders, including gastritis, duodenitis and dysfunction of the digestive system are more common in shift workers than in day workers (Koller, 1983).

The pathophysiologic mechanism underlying gastrointestinal disease in shift workers is unclear, but one possible explanation is that intestinal enzymes and intestinal mobility are not synchronized with the sleep/wake pattern. Intestinal enzymes are secreted according to the circadian rhythm, and shift workers' intake of food is irregular compared with intestinal function (Suda and Saito, 1979; Smith, Colligan and Tasto, 1982). A high nightly intake of food may be related to increased lipid levels (Lennernås, Åkerstedt and Hambraeus, 1994) and eating at the circadian low point may be associated with altered metabolic responses (Hampton et al., 1996). In addition, reduced sleep affects lipid and glucose metabolism (Spiegel, Leproult and van Cauter, 1999).

A number of studies have reported a higher incidence of cardiovascular disease, especially coronary heart disease, in male shift workers than in men who work days (for review see Kristensen, 1989; Boggild and Knutsson, 1999). A study of 504 paper mill workers followed for 15 years found a dose–response relationship between years of shift work and incidence of coronary heart disease in the exposure interval 1–20 years of shift work (Knutsson et al., 1986). A study of 79 000 female nurses in the United States gave similar results (Kawachi et al., 1995) as did a study with more than 1 million Danish men (Tüchsen, 1993) and a cohort of Finnish workers (Tenkanen et al.,1997). As with gastrointestinal disease, a high prevalence of smoking among shift workers might contribute to the increased risk of coronary heart disease, but smoking alone cannot explain the observed excess risk (Knutsson, 1989b). Another possibility is disturbances of metabolic parameters such as lipids and glucose for which there is some support as discussed above.

Only a few studies have addressed the issue of pregnancy outcome in shift workers. In one study of laboratory employees, shift work during pregnancy was related to a significantly increased risk of miscarriage (RR: 3.2) (Axelsson, Lutz and Rylander, 1984). Another study of hospital employees also demonstrated an increased risk of miscarriage (RR: 1.44, 95% CI: 0.83–2.51) (Axelsson and Rylander, 1989). Lower birth weight in infants of mothers who worked irregular hours has been reported (Axelsson and Rylander, 1989; Nurminen, 1989). No teratogenic risk associated with shift work was reported (Nurminen, 1989).

The mortality of shift and day workers was researched by Taylor and Pocock (1972), who studied 8603 male manual workers in England and Wales between 1956 and 1968. Day, shift, and ex-shift workers were compared with national figures. The Standardized Mortality Ratio (SMR) can be calculated from observed and expected deaths reported in the paper. SMRs for deaths from all causes were 97, 101 and 119 for day, shift, and ex-shift workers respectively. Although the figures might indicate an increasing trend, the differences were not statistically significant. However, the reported SMR close to 100 is remarkable because the reference population was the general male population. Most mortality studies concerned with occupational cohorts reveal SMRs lower than 100, implying a healthy workers' effect (Harrington, 1978). The same study showed a significantly increased incidence of neoplastic disease in shift workers (SMR 116). A Danish study of 6000 shift workers failed to demonstrate any excess mortality in shift workers (Boggild et al., 1999). Not much evidence exists on the connection between shift work and cancer. The mortality study by Taylor and Pocock (1972) reported an increased incidence of neoplasms in shift workers compared with the general population. A recent Danish case–control study reported an increased risk of breast cancer among 30–45-year-old women who worked mainly nights (Hansen, 2001). Among 75 000 nurses those with more than 15 years of night work showed an increased risk of colorectal cancer (Schernhammer et al., 2003). If the results are confirmed, a possible mechanism may be the low levels of the hormone melatonin, due to light exposure during the night with a subsequent suppression of melatonin.

Very few studies are available but Koller, Kundi and Cervinka (1978) found a prevalence of endocrine and metabolic disease of 3.5% in shift workers and 1.5% in day workers. Kawachi et al. (1995) found in a prospective study of shift workers that the age-standardized prevalence was 5.6% at 15 years of shift work experience compared with 3.5% for no exposure. Nagaya et al. (2002) found that markers of insulin resistance were more frequent in shift workers above the age of 50 than in day workers. Other indicators, such as body mass index, glucose levels and so forth, give a rather inconclusive impression as indicated in a review by Boggild and Knutsson (1999).

Another contributing factor to gastrointestinal diseases might be the association between shift work and smoking. A number of studies have reported that smoking is more common among shift workers (Angersbach et al., 1980; Knutsson, Åkerstedt and Jonsson, 1988). Studies concerned with alcohol consumption comparing day workers and shift workers have produced conflicting results (Smith, Colligan and Tasto, 1982; Knutsson, 1989a; Romon, Nuttens and Fievet, 1992), probably due to local cultural habits. One study, which used g-glutamyltransferase as a marker of alcohol intake, did not indicate that the shift workers had a higher intake of alcohol than the day workers (Knutsson, 1989a).

Sickness absence is often used as a measure of occupational health risks. However, sickness leave is influenced by many irrelevant factors and cannot be considered as a reliable measure of true morbidity. Studies on sickness absence in day and shift workers have revealed conflicting results and there is no evidence that shift workers have more sickness absence than day workers (for review, see Harrington, 1978).

2.3.4.3 Conclusion

Shift work or similar arrangements of work hours clearly affects sleep and alertness and there is a moderate risk of cardiovascular and gastrointestinal disease. Other diseases such as cancer or diabetes may be related to shift work but the evidence is as yet rather weak.
The present review suggests that the risk of disturbed sleep increases with age but there also seems to be a recent stress-related increase in sleep disturbance in young adults. The long-term health consequences are not yet understood.

The relation between gender and disturbed sleep is confusing. Females, as a rule, complain more of sleep problems, but do not exhibit any objective indications of more disturbed sleep, at least not among otherwise healthy women. With increasing age the sleep of males deteriorates whereas that of women is relatively well upheld. Pregnancy, however, is a period of increased risk of disturbed sleep, whereas the menstrual cycle and menopause show less evidence of sleep disturbance. Clearly there is a great need for longitudinal research on gender and sleep and, in particular, on the possible health consequences connected with pregnancy.

Stress due to work or family seems to be one of the major causes of disturbed sleep. The link to the risk of insomnia is well-established, but reduced sleep in itself seems to yield the same physiological changes as stress. This suggests that several of the major civilization diseases in Europe and the United States (diabetes, cardiovascular diseases and burnout) could be mediated via disturbed sleep. This link clearly warrants longitudinal studies with interventions.

Shift workers constitute a group that suffers from disturbed sleep for most of their occupational life. The reason is the interference of work hours with the normal timing of sleep. This leads to an increased risk of accidents, directly due to excessive sleepiness, but also to cardiovascular and gastrointestinal diseases, although it is not clear whether the latter effects are sleep related or due to circadian factors – or to a combination. Recent studies also suggest that breast cancer may result from shift work due to the effects of light on melatonin secretion. This still needs verification, however. Future research needs to identify countermeasures, the reasons for large individual differences in tolerance and the possible carcinogenic and other effects.

The conclusions above should be seen against the profound effects of reduced or fragmented sleep on the neuroendocrine (including glucose and lipid regulation) and immune systems as well as the effects on mortality, diabetes and cardiovascular disease.

2.3.5 CONCLUSION

Children, the elderly, pregnant women, people under stress and shift workers are vulnerable to (noise) disturbance of their sleep.

2.4 ACCIDENTS RELATED TO SLEEP QUALITY

As already stated in the earlier section on cardiovascular complications, children with disturbed sleep present cognitive dysfunction and behavioural disturbances, abnormal growth hormone release, increase of diastolic BP and an increased risk of accidents and use of sleeping pills.

Regarding sleep disturbance and accidents in adults, data show that 15–45% of all patients suffering from sleep apnoea, 12–30% of all patients suffering from narcolepsy and 2–8% of all patients suffering from insomnia have at least one accident (in a lifetime) related to sleepiness (statistics from the Stanford Sleep Disorders Clinic).

As already discussed in section 2.3.4, the biggest industrial catastrophes, such as the Three Mile Island, Bhopal, Chernobyl and Exxon Valdez disasters, have occurred during the night shift. The shift schedules, fatigue and sleepiness were cited as major contributing factors to each incident.

The LARES study (Large Analysis and Review of European housing and health Status) is one of the few studies analysing this issue directly. The results show that the likelihood of home accidents is significantly greater when the individual is tired all the time or most the time and there is an association between sleep disturbance and accidents, with 22% of those reporting an accident also reporting having their sleep disturbed during the previous four weeks.

The data available to document the impact of environmental noise on sleep deprivation and accidents are largely inadequate. There is no estimation of relative risk. Further research is needed in order to identify the accident-related burden of diseases attributable to noise during the night-time.

2.5 ANIMAL STUDIES

As pet owners know, cats sleep (most of the time it seems) and so do dogs. But do fish sleep? And flies? Yes, most animals sleep, and they even show the same phenomena as in humans; from deep sleep, dream sleep to sleep disorders. There are also many differences and weird behaviour, such as sleeping with only one half of the brain at a time (dolphins and ducks).

As Ising points out (Appendix 3), in animal experiments it is possible to assess the complete causal chain from noise exposure via physiological reactions and biological risk factors to morbidity or even mortality. However, a quantitative application of the results to humans is not possible. Instead, the method is useful in studying the pathomechanisms qualitatively. Rechtschaffen and Bergmann (1965) studied sleep deprivation in rats, showing that total sleep deprivation leads to mortality in 16 to 20 days. As the animals in the last stage died from microbial infection, Everson and Toth (2000) proceeded to show early infection of the lymph nodes and other tissues and hypothesized that daily sleep of some amount is necessary to maintain an intact immune system that will prevent bacterial invasion, a view that has been challenged.

Surprisingly, sleep in the common fruit fly – *Drosophila melanogaster* – has many similarities with mammalian sleep, including sleep deprivation leading to impaired performance. Genetic studies in fruit flies (Cirelli et al., 2005) led to mutant flies that can get by on 30% less sleep than their normal counterparts, thanks to a single mutation in one gene. While they sleep 30% less they show no immediate ill effects. The lifespan of the flies is, however, reduced by 30%.

These animal models certainly lead one to believe that sleep is a biological necessity, and tampering with it is dangerous for survival.

As Ising shows (Appendix 3) noise may play a role in this. Under stressful circumstances the death rate of rats is increased when noise levels are increased from "ambient" to L_{eq}=69 dB(A). Are noise and sleep deprivation stressors that both lead to early death? Is the noise effect due to sleep deprivation? A carefully planned study may sort this out. The question still remains, however, as to how far this is relevant to humans.

2.6 CONCLUSIONS

From the evidence presented so far it can be deduced that sleep is important for human functioning. Why exactly is less evident, but it is clear that disturbed sleep (either from internal factors or from external factors) leads to or is at least associated with fatigue, lower cognitive performance, depression, viral illness, accidents, diabetes, obesity and cardiovascular diseases. Animal experiments show that sleep deprivation shortens lifespan. The fact that – in comparison– relatively mild effects turn up in human sleep deprivation experiments could be due to the short period (about 10 days in controlled experiments) and the limitation to young and healthy adults.
The central position of sleep in human functioning is summarized in Fig. 2.1. In this figure relations with sufficient evidence are indicated with solid lines, while relations for which limited evidence exists are indicated with interrupted lines. Feedback connections are in red and double-dotted.

The presence of feedback loops in the system is an indication that it may be difficult to prove direct cause–effect relations. One example is the relation between sleep quality and depression. They are strongly associated, but it is uncertain if depression causes bad sleep, or bad sleep causes depression (see also Chapter 4, section 4.8.11). This may also depend on one of the many other factors, so it could be different for different personality types.

Fig.2.1
Expert view on the relations between sleep and health

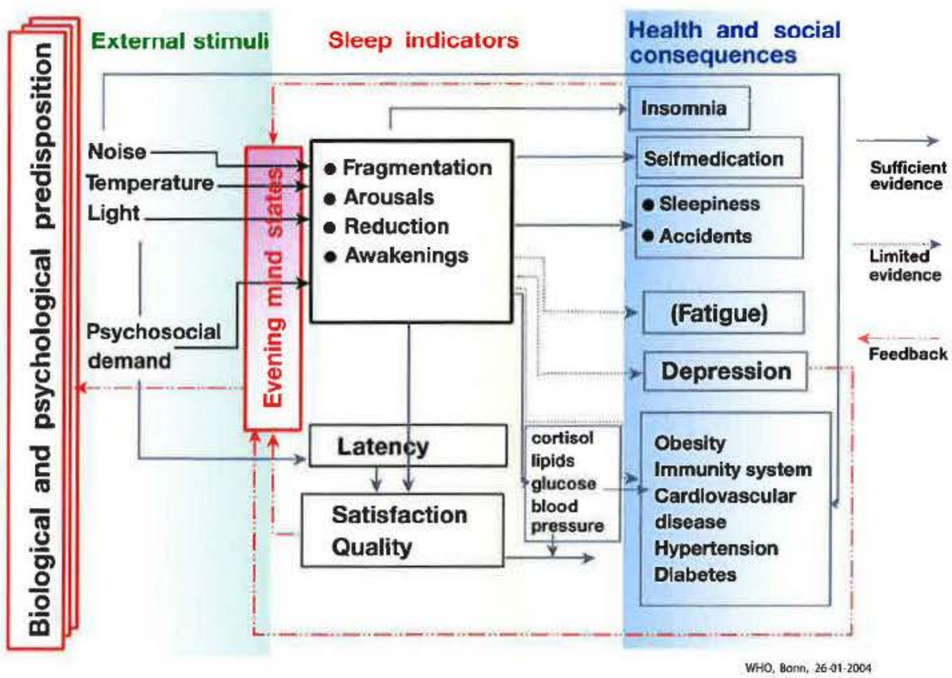

Impaired sleep is widely considered as a health problem per se, and this chapter has shown that there are many internal and external causes. In the next chapter the relation between noise and sleep quality is further unravelled.

CHAPTER 3

EFFECTS OF NIGHT-TIME NOISE ON SLEEP

Best travel tip: Never ever forget to pack ear plugs.
(Virginia Jealous, Lonely Planet author)

3.1 SHORT-TERM EFFECTS OF TRANSPORTATION NOISE ON SLEEP WITH SPECIFIC ATTENTION TO MECHANISMS AND POSSIBLE HEALTH IMPACT

3.1.1 INTRODUCTION

In this section reactions to single events are presented. In Chapter 2 normal sleep and sleep disorders are described in medical terms, but here the focus is on the mechanisms underlying the relation between noise and sleep quality. How does a sound penetrate the brain and cause a disruption of sleep?

3.1.2 HOW NOISE INFLUENCES NORMAL SLEEP

Noise can induce changes in the EEG or in autonomic variables that are called arousals or phasic activations. Similar brief episodes of activity also occur without noise in normal sleep, and, more frequently, in sleep that is otherwise disturbed, for example by apnoea. Arousal during sleep is not a uniform concept and has been defined differently by different researchers. Commonly, the occurrence of alpha rhythms is required for EEG arousal. Depending on the additional requirements and on the length of time that the slower cortical rhythms are interrupted, arousals have been called, for instance, micro-arousal, minor arousal, EEG awakening or transient activation phases. EEG awakening requires an interruption of the sleep patterns of at least 15 seconds (half the period) when sleep staging is scored by periods of 30 seconds, but need not be experienced consciously. Because normal REM sleep is a state characterized by cerebral arousal with frequently occurring alpha rhythms, additional criteria are needed to define arousal from REM. The criteria used are increased heart rate, EMG, or irregular respiration. However, since the mechanisms of such autonomic responses appear to be at least partly different from the causal mechanisms of EEG arousal, such definitions seem to make arousal from sleep a heterogeneous concept that may not have simple relationships with noise exposure.

EEG arousals lasting at least 30 seconds have been found to occur as often as 4 times (95% CI: 1–15) per hour during sleep on average, while micro-arousals occurred 21 times (95% CI: 7–56) per hour (Mathur and Douglas, 1995). Since these figures are from a laboratory study, they almost certainly are higher than the figures that hold for the natural situation at home. Sleep pressure decreases the density of micro-arousals (Sforza, Jouny and Ibanez, 2000). While the number of EEG arousals (during sleep stages 1 and 2) increases with age (Mathur and Douglas, 1995; Boselli et al., 1998) possibly only for men (Hume, Van and Watson, 2003), their average length is stable and circa 15 seconds (Boselli et al., 1998). Also the threshold for auditory arousal decreases with age (Zepelin, McDonald and Zammit, 1984; Busby and Pivik, 1985; Busby, Mercier and Pivik, 1994) and towards the end of the night (Basner et al., 2004). Recovery after EEG awakenings takes longer for noise-induced awakenings than for spontaneous awakenings (Basner et al., 2004). The time required for falling asleep again depends on the sound level and especially for loud events this latency is considerably longer than after spontaneous awakenings. Thus, in general, noise-induced EEG awakenings are more disruptive than spontaneous awakenings and therefore will more often be experienced consciously and remembered afterwards. In common situations with aircraft overflight noise at home, (minor) arousals were found in 10.3% of the 64-second intervals without aircraft noise and this percentage was found to be increased by circa 4% up to 14.3% in intervals with an aircraft noise event (Hume, Van and Watson, 2003). Thus, in that particular (exposure) situation, about 1 in 24 aircraft overflights caused a (minor) arousal.

3.1.3 MECHANISMS

Activity in the auditory system up to the brainstem nucleus inferior colliculus occurs within 10 milliseconds after the onset of a sound. This early activity appears to be obligatory and is hardly affected by the state (sleeping or awake). Being asleep or awake does influence later activity. The auditory pathways proceed from the inferior colliculus to the thalamus and from there to the auditory cortex. The state (asleep or awake) affects the activity in the thalamocortical circuits, which occurs after 10–80 milliseconds. In particular, during SWS the transmission of auditory information through the thalamus is suppressed. This is not the case during REM sleep or when awake.

Thus, while in all (sleep) stages, sound activates the auditory system up to the inferior colliculus, the sound-induced activation of higher areas is suppressed in SWS. Therefore, further activation depending on those higher areas (for example, extracting meaning) is not likely to occur as a primary reaction to sound during SWS. For understanding arousal during SWS, it is important that the inferior colliculus and the earlier auditory nucleus of the lateral lemniscus, and also the (dorsal and ventral) cochlear nuclei project to reticular arousal system. Presumably, sound is always capable of arousing the sleeping subject through these connections. The ascending arousal system is heterogeneous and encompasses mono-aminergic, glutamatergic, and cholinergic nuclei that can directly or indirectly activate the thalamus and cortex. An important indirect route is the activation of the basal forebrain, which can activate the cerebral cortex through widespread, mainly cholinergic projections. The activation of the thalamus and cortex is indicated by an increase in EEG rhythm frequency and a reduction of the inhibition in the thalamic sensory relay nuclei. As a consequence of the latter effect, subsequent sound-induced activation may pass the thalamus and may be subject to more elaborate processing than initial sound. It can be speculated that sound in this way also reduces the threshold for somatosensory information that initiates body movements so that more body movements are observed when exposed to sound. The occurrence of habituation of cortical responses suggests an active role played by a part of the brain that blocks or at least limits the impact of the activated ascending pathways.

The parasympathetic autonomic nervous system seems to be responsible for the bradycardia observed in non-REM sleep and mainly in tonic REM sleep through the increase in vagal activity (Guazzi et al., 1968). The variability of heart rate in REM sleep could be placed under the same control, as vagotomy strongly reduced the heart rate instability (Baust and Bohnert, 1969). During falling asleep, respiration is unstable and alternates between hypo- and hyperventilation episodes. This respiration, called "periodic respiration" (Mosso, 1886), disappears when stable sleep occurs (stage 2). The main hypotheses concerning this periodic ventilation refer to metabolic control and chemoreceptor responses to levels of $PaCO_2$ and PaO_2 (Chapman et al., 1988). In stable non-REM sleep, respiration is regular in amplitude and frequency, although ventilation per minute is lower than during awakening. In REM sleep, respiration appears irregular with sudden variations in amplitude and frequency. This irregularity appears to be not modifiable by metabolic factors and, therefore, it is possibly linked to mechanisms leading to REM expression. The non-habituation of the cardiovascular responses would be explained by the absence of an inhibitory influence on the part of the arousal system that affects the centres regulating the autonomous response.

3.1.4 EEG RESPONSE

The sleep polygraph continuously records EEG activity, eye movement (EOG) and muscle tone (EMG). These data are used to classify sleep into various stages, and to assess times of falling asleep and waking up. Also, sleep variables such as total sleep time and total time spent in SWS (consisting of sleep stages 3 and 4, the stages of deep sleep) and in the REM stage (also called dream or paradoxical sleep) can be assessed on the basis of sleep polygraph recordings. Polygraphic indicators of responses to individual noise events are changes from a deeper to a less deep sleep and EEG awakening. Several field studies (Pearsons, Bennett and Fidell, 1973; Vernet, 1979; Vallet et al., 1983; Hume, Van and Watson, 2003; Basner et al., 2004) have been conducted regarding noise-induced changes in sleep stage and awakening using EEG recordings. Transition from a deep stage of sleep to a shallower sleep stage can be the direct consequence of a nocturnal noise event. Although not perceived by the sleeper, these transitions modify the sleep architecture and may reduce the amount of SWS (Carter, 1996; Basner et al., 2004) and the amount and rhythmicity of REM sleep may be markedly affected (Naitoh, Muzet and Lienhard, 1975; Thiessen, 1988). In addition to their results from a laboratory study, Basner et al. (2004) present results from a field study with valid data for 63 subjects (aged 18–65 years) with 15 556 aircraft noise events included in the final analyses. They established a curve that gives the probability of awakening as a function of L_{Amax} with a model that assumed a background noise level just prior to the aircraft noise event of 27 dB(A). The L_{Amax} threshold for noise-induced awakenings was found to be about 35 dB(A). Above this threshold the probability of noise-induced awakenings increases monotonically up to circa 10% when L_{Amax} = 73 dB(A). This is the extra probability of awakening associated with the aircraft noise event, on top of the probability of awakening spontaneously in a 90 second interval.

Some arousals provoked by noise events are so intense that they induce awakening. Frequent awakening leads to sleep fragmentation and overall sleep disturbance. The noise threshold for awakening is particularly high in deep SWS (stages 3 and 4) while it is much lower in shallower sleep stages (stages 1 and 2). In REM sleep the awakening threshold is variable and depends on the significance of the stimulus. Total sleep time can be reduced by both a longer time to fall asleep and premature final awakening. It has been reported that intermittent noises with maximum noise levels of 45 dB(A) and above can increase the time taken to fall asleep by a few to 20 minutes (Öhrström, 1993). In the morning hours, the sleeper can be more easily awakened by ambient noise and has more difficulty going back to sleep because sleep pressure is progressively reduced with time (Rechtschaffen, Hauri and Zeitlin, 1966; Keefe, Johnson and Hunter, 1971).

Terzano et al. (1990, 1993) showed that with increasing intensity of sound pressure level (white noise at 45, 55, 65 and 75 dB(A), white noise induced a remarkable enhancement of cyclic alternating patterns (CAP)/non-REM, characterized by a linear trend from the lowest to the highest intensities, revealed by a significant increase in the CAP rate already at 45 dB(A). Noise decreased mainly SWS, REM and total sleep time, and increased waking after sleep onset, stage 1 non-REM and CAP rate (Terzano et al., 1993). For CAP/non-REM values between 45% and 60%, subjects generally recalled a moderate nocturnal discomfort and values of CAP/non-REM over 60% corresponded to a severe complaint.

This result corroborates previous findings described by Lukas (1972a) who reported that reactions less intense than a sleep stage change correlate better to the noise intensity than awakening reactions.

3.1.5 CARDIOVASCULAR RESPONSE

For sleeping persons, mean heart rate, mean systolic and diastolic BP and variability in heart rate are usually assessed. Indicators of responses to individual noise events are instantaneous changes in (variability of) heart rate and changes in systolic BP. Several field studies (Carter et al., 1994) have been conducted regarding momentary change in heart rate. Intermittent noise during sleep has been found to induce a biphasic cardiac response and a transient constriction of peripheral vessels together with a short phasic activation in the EEG, while no other behavioural effect can be seen (Muzet and Ehrhart, 1978). This biphasic cardiac response starts with an increase in heart rate, probably due to a phasic inhibition of the parasympathetic cardio-inhibitory centre, followed by a compensatory decrease due to a phasic decrease in orthosympathetic activity (Keefe, Johnson and Hunter, 1971; Muzet and Ehrhart, 1980). The vasoconstrictive response was reported to be due to the sympathetic peripheral stimulation provoked by the auditory reflex (Kryter and Poza, 1980). More recently, Carter et al. (2002) have shown that beat-by-beat BP changes can be induced by suddenly occurring noises. Although habituation in some effect parameters can occur in a few days or weeks, this habituation is not complete and the measured modifications of the cardiovascular functions remain unchanged over long periods of exposure time (Muzet and Ehrhart, 1980; Vallet et al., 1983). Most striking is that none of the cardiovascular responses show habituation to noise after a prolonged exposure, while subjective habituation occurs within a few days. In people that are used to sleep in a noisy surrounding, noise-induced changes in heart rate are dependent on the maximum sound level of a noise event, but not on the EEG sleep stage).

3.1.6 BODY MOVEMENT

Motility is the term used for accelerations of the body or body parts during movement. It is measured with actimeters, usually worn on the wrist in field research and the laboratory. Brink, Müller and Schierz (2006) describe a more sophisticated method which is based on the bed being placed on accelerometers. This allows the tracking of whole body movements.

Motility is related to many variables of sleep and health (Reyner, 1995; Reyner et al., 1995; Passchier-Vermeer et al., 2002). Clinical research shows that the sleep/wake cycle (assessed by polysomnography, EEG, EOG, EMG) passes through the 24-hour period synchronously with the rest/activity cycle (assessed by actimetry) (Borbely et al., 1981). A number of investigations have compared the results of polysomnographic recordings (number of EEG-awakenings during sleep period, duration of sleep period, sleep onset time, wake-up time) with results of actimetry. The correlation between actimetrically assessed duration of sleep period, sleep onset time, wake-up time and similar variables assessed with polysomnography was found to be very high (correlation coefficients between individual test results in the order of 0.8–0.9). Measures of instantaneous motility are the probability of motility and the probability of onset of motility in a fixed time interval, for example a 15-, 30- or 60-second interval. Increased instantaneous motility during sleep is considered to be a sensitive behavioural marker of arousal, but the relation with arousal is not simple. Also other factors, such as the need to relieve the pressure on body parts for better blood circulation, cause motility, and spontaneously occurring arousals are part of the normal sleep process. The noise-induced probability of (onset of) motility is the difference between the probability of (onset of) motility during noise events minus the probability in the absence of noise.

Onset of motility and minor arousal found on the basis of EEG recordings are highly correlated. In the United Kingdom sleep disturbance study, Ollerhead et al. (1992) found for their study population that during sleep there is on average an EEG (minor) arousal in 40% of the 30-second intervals with onset of motility. Unfortunately, it is unknown whether this 40% is also valid for noise-induced awakenings. In 12% of the 30-second intervals with an EEG (minor) arousal, motility does not occur. Several field studies (Horne et al., 1994; Fidell et al., 1998, 2000; Flindell, Bullmore and Robertson, 2000; Griefahn et al., 2000; Passchier-Vermeer et al., 2002, 2004) have been conducted regarding noise-induced instantaneous motility. For this effect, relationships have been established with SEL or L_{Amax}, for aircraft noise only. In Passchier-Vermeer et al. (2002) relationships between noise-induced increase in motility or noise-induced increase in onset of motility in the 15-second interval with the maximum noise level of an overflight, and L_{Amax} or SEL have been approximated by quadratic functions (see, for instance, Fig. 3.2). It may be noted that the threshold of motility (L_{Amax} = 32 dB(A)) is in the same range as the threshold found by Basner et al. (2004) for EEG awakenings, with a definition that also encompassed transitions to steep stage 1 (L_{Amax} = 35 dB(A)). The probability of motility at 70 dB(A) of about 0.07 is lower than the probability of noise-induced EEG awakening at L_{Amax} = 73 dB(A) of about 0.10. There is no a priori reason to expect the above threshold probabilities to be the same for these two measures of sleep disturbance, but, taking into account that motility is assessed for shorter intervals (15 seconds vs. 90 seconds), the differences in probabilities above threshold appear to be limited.

One of the variables influencing the relationships between noise-induced instantaneous motility and L_{Amax} or SEL, is long-term aircraft noise exposure during sleep. The probability of instantaneous aircraft noise-induced motility is lower when the long-term exposure is higher. This may be partly due to the higher base rate motility in quiet intervals in higher long-term exposure, which is used as a reference for the instantaneous noise-induced motility. Other factors influencing the relationships between instantaneous motility and L_{Amax} or SEL are the point of time in the night, and time since sleep onset. For example, after 7 hours of sleep, noise-induced motility is about 1.3 larger than in the first hour of sleep. Age has only a slight effect on noise-induced motility, with younger and older people showing a lower motility response than persons in the age range of 40–50 years.

3.1.7 BEHAVIOURAL AWAKENING IN ADULTS

Passchier-Vermeer (2003a) published a review of nine studies on awakening by noise. It was found that these studies had different definitions of what constituted an "awakening". In this review, however, all awakening data were collected on "behavioural awakening": these are awakenings that were followed by an action (like pressing a button) from the sleeper. The number of awakenings defined in this manner is much smaller than the number of sleep stage changes which lead to EEG patterns similar to wakefulness.

Data were available for rail traffic noise, ambient (probably road) noise, civil aviation noise and military aviation noise.

The rail traffic noise study is very small (only 20 subject nights), but showed no awakenings. The study states that "there is some evidence, be it very limited, that railway noise events, in the range of SEL_{indoor} considered (up to 80 dB(A)), do not increase [the] probability of awakening".

Ambient noise also showed no effect on the probability of awakening, but as it is uncertain exactly what noise is meant, no firm conclusions could be drawn.

Military aircraft noise showed a very strong effect, but this study is of limited applicability since the few subjects (military) lived near the end of the runway.

For civil aviation noise there were sufficient data to derive a dose-effect relation:

$$\text{Percentage of noise-induced awakenings} = -0.564 + 1.909 * 10^{-4} * (SEL_{inside})^2 \quad [4],$$

where SELinside is the sound exposure level of an aircraft noise event in the bedroom.

This relation is confined to commercial aircraft noise over the intervals $54<SEL<90$ ($37<L_{Amax}<82$) and the number of events per night $1< N< 10$.

With this relation, it is possible to calculate for an individual L_{night} the expected number of noise-induced behavioural awakenings. This requires all single contributions over the year to this L_{night} to be known. Alternatively (if, for instance, a future situation has to be estimated for which no exact data are available) a worst case scenario can be calculated. Fig. 3.1 represents the results of this worst case approach (converted to L_{night}, see Chapter 1, section 1.3.4), and so gives the maximum number of awakenings n_{max} that may be expected.

$$n_{max} = 0.3504 * 10^{(L_{night}-35.2)/10} \quad [5].$$

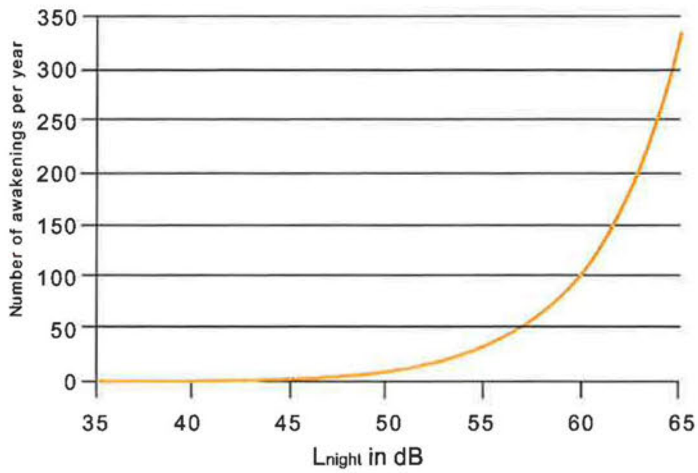

Fig. 3.1
Worst case prediction of noise-induced behavioural awakenings.
L_{night}, converted from inside relation with [3] on page 10.

Source: Miedema, Passchier-Vermeer and Vos, 2003

It can be demonstrated that the number of awakenings reaches a maximum when the SEL_{inside} value is 58.8 dB(A).

It should be noted that, on average, 600 spontaneous awakenings per person are reported per year. This also explains why so many more awakenings are reported than can be attributed directly to aircraft noise. At 55 L_{night}, nearly 100 overflights per night with SEL_{inside} = 58.8, or 1 every 5 minutes are possible. It is, therefore, very likely that an overflight coincides with a spontaneous awakening.

3.1.8 DOSE–EFFECT RELATIONS FOR BODY MOVEMENTS DURING SLEEP

In Passchier-Vermeer et al. (2002) motility is registered in 15-second intervals. A distinction is made between two variables:

- the *presence of motility* in the interval (indicated by m) and
- the onset *of motility*, meaning the presence of motility when there was no motility in the preceding interval (indicated by k).

Relations between a noise-induced increase in motility (m) or a noise-induced increase in the onset of motility (k) in the 15-second interval with the maximum sound level of an overflight, and $L_{Amax,inside}$ or SEL_{inside} have been approximated by quadratic functions with the following format:

$$m = b^*(L_{Amax,inside} - a) + c^*(L_{Amax,inside} - a)^2 \qquad [6].$$

The coefficients a, b and c are given in Table 3.1. The value of a is the value below which m or k is zero. Fig. 3.2 shows the relationship between m and $L_{Amax,inside}$ together with the 95% confidence interval. Relations apply to $L_{Amax,inside}$ and SEL_{inside} values of at most 70 and 80 dB(A), respectively.

Table 3.1.
Coefficients of the quadratic equation (formula [6]) of m and k as a function of $L_{Amax,inside}$ or SEL_{inside} for the 15-second interval in which an indoor maximum sound level of an aircraft noise event occurs. The equations are applicable in the $L_{Amax,inside}$ range from a up to 70 dB(A), or SEL_{inside} range from a up to 80 dB(A). Below a, m and k are zero.

	(Aircraft) noise-induced increase of probability of motility (m)	(Aircraft) noise-induced increase of probability of onset of motility (k)
range	$32 < L_{Amax,inside} < 70$ dB(A) (see Fig. 3.2)	$32 < L_{Amax,inside} < 70$ dB(A)
a	32	32
b	0.000633	0.000415
c	$3.14x10^{-5}$	$8.84x10^{-6}$
range	$38 < SEL_{inside} < 80$ dB(A)	$40 < SEL_{inside} < 80$ dB(A)
a	38	40
b	0,000532	0.000273
c	$2.68x10^{-5}$	$3.57x10^{-6}$

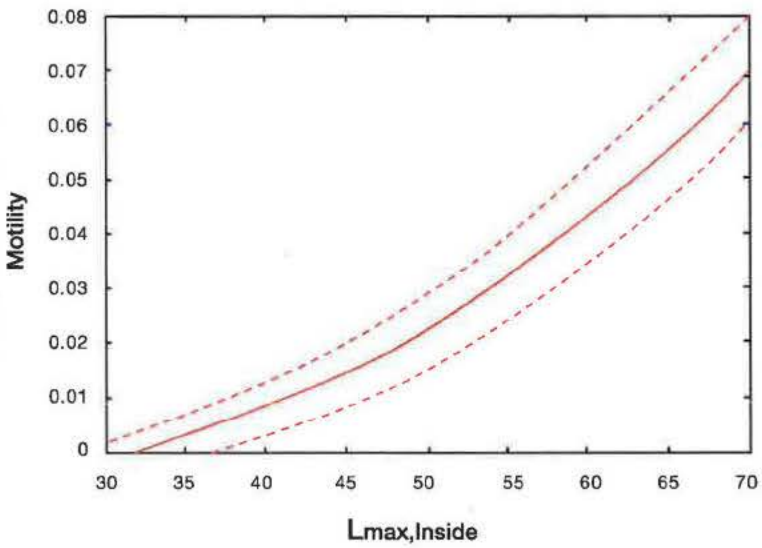

Fig. 3.2
Probability of (aircraft) noise-induced motility (m) at the 15-second interval in which the indoor maximum sound level occurs (solid line) and the 95% confidence interval, as a function of $L_{Amax,inside}$ bedroom

Source: Miedema, Passchier-Vermeer and Vos, 2003.

The study report also gives the upper boundaries for motility, based on the relationship between L_{Amax}, SEL and L_{night} (Fig. 3.3). This figure is mathematically derived from relation [6] as described in Appendix 2.

This area of study is still under development. Miedema, Passchier-Vermeer and Vos (2003) give a detailed account in their study report of the relation between the study used for the data presented here (Passchier-Vermeer et al., 2002), earlier studies like the much quoted Civil Aviation Authority study (Ollerhead et al., 1992; Ollerhead, 1994) and earlier work done in the United States.

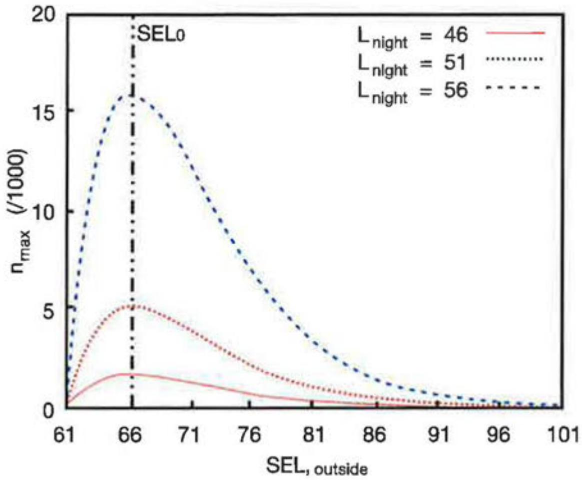

Fig. 3.3
Maximum number of noise-induced motility for three values of L_{night}. Converted from inside relation with [3] on page 10

Source: Miedema, Passchier-Vermeer and Vos, 2003.

3.1.9 INDIVIDUAL SENSITIVITY

Sensitivity to noise may vary greatly from one individual to another. Primary self-evaluation of sensitivity to noise has been used as a factor to evaluate highly sensitive and non-sensitive groups and to compare their reactions to noise exposure during daytime and night-time (Di Nisi et al., 1990). In this study, self-declared highly sensitive individuals had a higher cardiovascular response rate to noise than non-sensitive people during their waking exposure, while there was no difference in sensitivity to noise between these two groups during their night-time exposure while they were asleep.

The physiological sensitivity to noise depends also on the age of the sleeper. Thus, while EEG modifications and awakening thresholds are, on average, 10 dB(A) higher in children than in adults, their cardiovascular sensitivity to noise is similar, if not higher, than the older group (Muzet and Ehrhart, 1980; see also Appendix 4). Elderly people complain much more than younger adults about environmental noise. However, their spontaneous awakenings occurring during night sleep are also much more numerous. Therefore, it is difficult to conclude if elderly people are more sensitive to noise or if they hear noise because they are often awake during the night. This natural fragmentation of their night sleep tends also to lengthen their return to the sleeping state and this accounts for a significant part of their subjective complaints.

Differences in sensitivity to noise have been found between the sexes. Thus, young men seem to complain more about noise-disturbed sleep than young females (Muzet et al., 1973). However, this difference seems to reverse for populations over 30 years of age and then females (often mothers) appear to be more sensitive to noise than males (Lukas, 1972b).

3.1.10 USE OF INSTANTANEOUS EFFECTS IN PREDICTIONS OVER A LONGER TIME PERIOD

It is tempting to use the relations between single exposures and measured effects in long-term predictions. Although this is perhaps possible, a word of caution is appropriate.

In general, the reactions are calculated by looking at a certain time frame around an exposure, usually in the order of a few minutes. The second limitation is that order and follow-up effects are neglected. Time and order effects of identical events on motility have been described by Brink, Wirth and Schierz (2006). Only if the situation that is modelled resembles the one that was used in the single exposure analysis, are no major deviations to be expected. Reactions to noise events are generally not independent from each other. Each event may alter a subject's tendency to awake at the next event, even if no awakening reaction is detected for that particular event. If, for example, each event would additionally increase the probability of awakening at the next event, the total probability of awakening per night would be greater than predicted by mere summation of the single event probabilities. Most likely, this underestimation of probability will occur when events in the real situation follow in close succession, whereas events in the single exposure analysis did not. Such limitations can to some degree be overcome through applying advanced statistical methods such as those put forward by Basner (2006). A third limitation is that an overall increase in the base line could go undetected.

If the situation that is calculated resembles the one that was used in the single exposure analysis, probably no major deviations are to be expected. Care should be taken to extrapolate outside the boundaries given in the number of events or L_{Amax}. Calculations for Amsterdam Schiphol Airport show a good agreement between the number of calculated awakenings per year (based on the actual SEL data) and the self-reported number of awakenings. This number is a factor 2 lower than the worst case scenario presented in section 3.1.7 above.

3.2 CHRONIC EFFECTS: CHRONIC INCREASE OF MOTILITY

Mean motility – all body movements counted together – during sleep is strongly related to age and is also a function of noise exposure during the sleep period. The relationships between mean motility and $L_{night,inside}$ are shown in Fig. 3.4. Mean motility during sleep is lowest at the age of 45 years, and greater at higher and lower ages. The relation between mean motility, $L_{night,inside}$ and age is:

$$\text{Mean motility} = 0.0587 + 0.000192{*}L_{night,inside} - 0.00133{*}age + 0.0000148{*}age^2 \qquad [7].$$

The relation between the increase in mean noise-induced motility, m_{night}, and $L_{night,inside}$ is:

$$m_{night} = 0.000192{*}L_{night,inside} \qquad [8],$$

assuming, as described in Chapter 1, section 1.3.4, that $L_{night,inside} = L_{night}$-21:

$$m_{night} = 0.000192{*}L_{night}-0.004032 \qquad [8a].$$

Source: Miedema, Passchier-Vermeer and Vos, 2003.

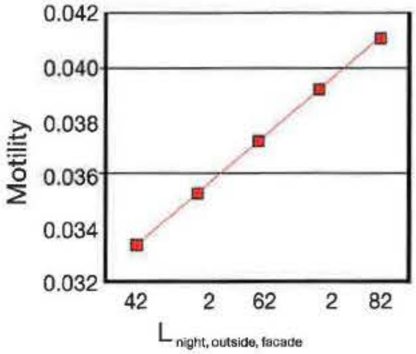

Fig. 3.4
Increase in mean motility (body movements during sleep). Converted from inside relation with [3]

The increase in m_{night} is 22% over the baseline motility (0.03 on average) if indoor $L_{night,inside}$ increases from 0 (absence of aircraft noise) to 35 dB(A) (living close to a runway). This increase is independent of age, although the absolute level varies.

Other chronic effects like the use of sleeping pills, changes in BP and changes in levels of stress hormones are discussed in the next chapter.

3.3 CONCLUSIONS

During sleep the auditory system remains fully functional. Incoming sounds are processed and evaluated and although physiological changes continue to take place, sleep itself is protected because awakening is a relatively rare occurrence. Adaptation to a new noise or to a new sleeping environment (for instance in a sleep laboratory) is rapid, demonstrating this active protection. The physiological reactions do not adapt, as is shown by the heart rate reaction and the increase of average motility with sound level. The autonomous physiological reactions are a normal reaction to these stimuli, but the question is whether prolonged "abuse" of this system leads to adverse consequences for the organism. The next chapter tries to answer that.

CHAPTER 4

EFFECTS OF NIGHT-TIME NOISE ON HEALTH AND WELL-BEING

The sick die here because they can't sleep,

For when does sleep come in rented rooms?
It costs a lot merely to sleep in this city!
That's why everyone's sick: carts clattering
Through the winding streets, curses hurled
At some herd standing still in the middle of the road,
Could rob Claudius or a seal of their sleep!

(Juvenal, 1st century AD)

4.1 INTRODUCTION

In Chapters 2 and 3, sufficient evidence was presented to support the hypothesis for the simplified model presented in Chapter 1: sleep disturbance is connected to health impairment, and noise is an important factor that causes sleep disturbance. The full model (Fig. 2.1, Chapter 2) showed why it is difficult to find evidence for a direct relation between noise exposure at night and health outcomes. Noise is but one of the internal and external factors that cause sleep disturbance and feedback loops obscure the view of the cause and effect chain. In this chapter the evidence for the direct relation is presented.

4.2 SELF-REPORTED (CHRONIC) SLEEP DISTURBANCES

Self-reported sleep disturbance is investigated by means of a questionnaire containing questions regarding sleep disturbance. Often, sleep disturbance is not the main focus of the questionnaires used in studies of self-reported noise effects. This means that considerable effort is needed to harmonize the different response categories. The relationships for self-reported sleep disturbance are based on analyses of the 15 data sets with more than 12 000 individual observations of exposure–response combinations, from 12 field studies (Miedema, 2003; Miedema, Passchier-Vermeer and Vos, 2003).

The curves are based on data in the L_{night} (outside, most exposed facade) range 45–65 dB(A). The polynomial functions are close approximations of the curves in this range and their extrapolations to lower exposure (40–45 dB(A)) and higher exposure (65–70 dB(A)). The formulae of these polynomial approximations are as follows (SD = sleep disturbance; H = high; L = low):

for **road traffic:**

$$\%HSD = 20.8 - 1.05 * L_{night} + 0.01486 * (L_{night})^2 \quad [9]$$

$$\%SD = 13.8 - 0.85 * L_{night} + 0.01670 * (L_{night})^2 \quad [10]$$

$$\%LSD = -8.4 + 0.16 * L_{night} + 0.01081 * (L_{night})^2 \quad [11]$$

for **aircraft:**

$$\%HSD = 18.147 - 0.956 * L_{night} + 0.01482 * (L_{night})^2 \quad [12]$$

$$\%SD = 13.714 - 0.807 * L_{night} + 0.01555 * (L_{night})^2 \quad [13]$$

$$\%LSD = 4.465 - 0.411 * L_{night} + 0.01395 * (L_{night})^2 \quad [14]$$

and for **railways:**

$$\%HSD = 11.3 - 0.55 * L_{night} + 0.00759 * (L_{night})^2 \quad [15]$$

$$\%SD = 12.5 - 0.66 * L_{night} + 0.01121 * (L_{night})^2 \quad [16]$$

$$\%LSD = 4.7 - 0.31 * L_{night} + 0.01125 * (L_{night})^2 \quad [17].$$

The above relations represent the current best estimates of the influences of L_{night} on self-reported sleep disturbance for road traffic noise and for railway noise, when no other factors are taken into account. Fig. 4.1 illustrates the relations [9] [12] and [15] for persons highly disturbed by road, aircraft and rail noise.

Fig. 4.1
High sleep disturbance by noise at night

Source: European Commission, 2004.

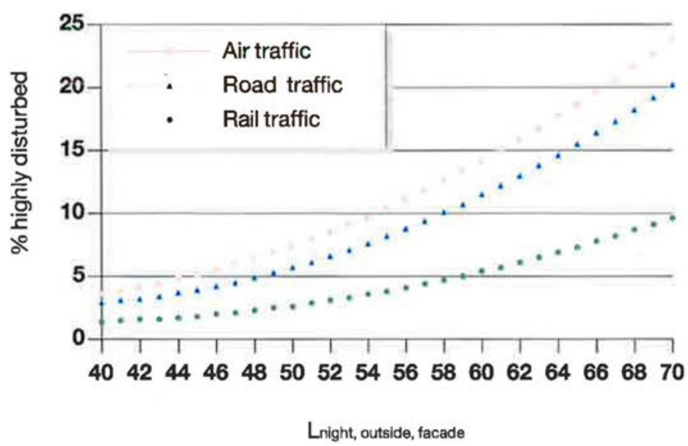

With regard to the relations for aircraft noise it should be noted that the variance in the responses is large compared to the variance found for rail and road traffic. This means that the uncertainty regarding the responses for night-time aircraft noise is large, and such responses can be considered as indicative only. Miedema (2003) suggests the following causes.

- The time pattern of noise exposures around different airports varies considerably due to specific night-time regulations.
- The sleep disturbance questions for aircraft noise show a large variation.
- The most recent studies show the highest self-reported sleep disturbance at the same L_{night} level. This suggests a time trend.

For industrial noise there is an almost complete lack of information, although there are some indications (Vos, 2003) that impulse noise may cause considerable disturbance at night.

4.3 COMPLAINTS

According to the Health Council of the Netherlands (2004), the submission of a complaint about noise is symptomatic of reduced well-being.

Complaints about noise are widespread, and night noise seems to cause more complaints than daytime noise at the same level. Hume, Morley and Thomas (2003) found that around Manchester Airport complaints per 1000 aircraft traffic movements rose from an average of 10 in daytime hours to up to 80 in the night. When linking part of the complaints to measured noise levels, they found an increase from an average of 1 complaint at 70 PNLdB (circa 58 L_{Amax}) to 2 at 114 PNLdB (circa 102 L_{Amax}).

Due to differences in complaint cultures and registration practices, it is difficult to make comparisons between complaint registrations. Around Amsterdam Schiphol Airport a relation between complaints and L_{Aeq} was found (Ministerie Verkeer en Waterstaat, 2005). The threshold for complaints is around 45 L_{den}, and increases to 7% of the population at 72 L_{den}. Night-time complaints follow the same pattern, and the threshold for night complaints is 35 L_{night}. In Fig. 4.2 the mean percentage shows a definite relationship with L_{night}. The 95 percentile indicates that the threshold is 35 L_{night}.

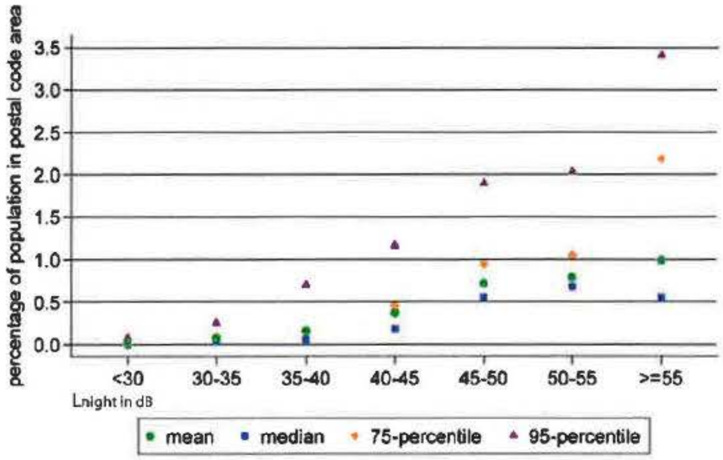

Fig. 4.2
Dose-effect relation for persons having complained at least once during a year between 1994 and 2004

Source: Ministerie Verkeer en Waterstaat (2005).

4.4 NEIGHBOURHOOD NOISE AND NOISE FROM NEIGHBOURS

Inventory studies in the Netherlands indicate that sleep disturbance attributable to the most annoying forms of neighbourhood noise and noise from neighbours (contact noise and human noises in the environment) is on a similar scale to disturbance attributable to the most annoying sources of road traffic noise (mopeds and passenger cars). It is reasonable to assume that chronic sleep disturbance is, in the long term, liable to have consequences for health and well-being. The sound pressure level and other noise characteristics are liable to determine the nature of the influence to some extent, but certain other factors play a more prominent role than is the case with traffic noise. These factors include appreciation of the noise and of the party responsible for the noise, as well as the hearer's personal circumstances. However, scientific understanding of the relative importance of and interaction between acoustic and non-acoustic factors is not sufficient for the committee to draw any definitive conclusions regarding the relationship between, on the one hand, exposure to night-time neighbourhood noise and noise from neighbours and, on the other, health and well-being.

Leidelmeijer and Marsman (1997) carried out an interview-based study of 1242 households in the Netherlands, in which subjects were asked about daytime and night-time noise from neighbours and any associated annoyance. A distinction was made on the basis of the part of the house in which the noises were audible and any associated annoyance was experienced. Subjects proved least tolerant of noise from their neighbours that was audible in the master bedroom. The researchers distinguished five types of noise, which are listed below (Table 4.1), along with the percentage of subjects who indicated hearing the relevant type of noise from a neighbouring dwelling at night in the master bedroom.

Table 4.1 Daytime and night-time noise from neighbours

Type of noise	% subjects hearing noises at night in the bedroom
Contact noise	22%
Noise from sanitary fittings, central heating, etc.	19%
Noise from radio, TV and hi-fi	12%
Do-it-yourself noises	8%
Pets	6%

Source: Leidelmeijer and Marsman, 1997.

Where each of the five investigated types of noise was concerned, roughly 10–15% of subjects indicated that they felt it was unacceptable for the noise to be audible during the day. Overall, nearly 30% of subjects said that sanitary fittings should not be audible at night, while approximately 50% felt each of the other four types of noise was unacceptable at night.

In 1993, Kranendonk, Gerretsen and van Luxemburg produced a synthesis of the research conducted up to that point in time into the annoyance associated with noise from neighbours. Subsequently, in 1998, van Dongen et al. published a report on the relationship between noise from neighbouring dwellings and the airborne and contact noise attenuating indices I_{lu}, $I_{lu;k}$, and I_{co}, drawing on data from a questionnaire-based survey of the residents of 600 dwellings, whose acoustic quality was determined in 202 cases. The results of the two studies are reasonably consistent. Both found that the chief causes of annoyance were loud radios, hi-fis and TVs, audible and sometimes intelligible voices, the slamming of doors and footsteps on floors and staircases. In both cases, it proved that, when Ilu had a value of 0 (the minimum requirement for new homes), 10% of subjects reported high annoyance and 15% reported annoyance caused by noise from neighbouring dwellings. These figures are not specific to night-time noise, but apply to annoyance over a 24-hour period.

On the basis of the findings outlined above, the committee concludes that the standard of inter-dwelling sound attenuation presently required does not provide sufficient protection to prevent annoyance caused by noise from neighbours. Since people are less tolerant of the noise their neighbours make at night-time than of their neighbours' evening or daytime noise, it may be assumed that much of the annoyance associated with noise from neighbours relates to the influence of such noise on sleep.

4.5 CARDIOVASCULAR EFFECTS OF NOISE – FINDINGS FROM EPIDEMIOLOGICAL STUDIES

4.5.1 INTRODUCTION

It is a common experience that noise is unpleasant and affects the quality of life. It disturbs and interferes with activities of the individual including concentration, communication, relaxation and sleep (WHO Regional Office for Europe, 2000; Schwela, 2000). Besides the psychosocial effects of community noise, there is concern about the impact of noise on public health, particularly regarding cardiovascular outcomes (Suter, 1992; Passchier-Vermeer and Passchier, 2000; Stansfeld, Haines and Brown, 2000). Non-auditory health effects of noise have been studied in humans for a couple of decades using laboratory and empirical methods. Biological reaction models have been derived, which are based on the general stress concept (Selye, 1956; Henry and Stephens, 1977; Ising et al., 1980; Lercher, 1996). Amongst other non-auditory health end points, short-term changes in circulation including BP, heart rate, cardiac output and vasoconstriction, as well as stress hormones (epinephrine, norepinephrine and corticosteroids) have been studied in experimental settings for many years (Berglund and Lindvall, 1995; Babisch, 2003). Various studies have shown that classical biological risk factors are higher in subjects who were exposed to high levels of traffic noise (Arguelles et al., 1970; Eiff et al., 1974; Verdun di Cantogno et al., 1976; Algers, Ekesbo and Strömberg, 1978; Knipschild and Sallé, 1979; Manninen and Aro, 1979; Eiff et al., 1981a; Rai et al., 1981; Marth et al., 1988; Babisch and Gallacher, 1990; Babisch et al., 1990; Lercher and Kofler, 1993; Schulte and Otten, 1993; Dugué Leppänen and Gräsbeck, 1994; Yoshida et al., 1997; Goto and Kaneko, 2002). Although controls for other risk factors were not consistent in all these studies, the hypothesis emerged that persistent noise stress increases the risk of cardiovascular disorders including high BP (hypertension) and IHD.

- Sound/noise is a psychosocial stressor that activates the sympathetic and endocrine system.
- Acute noise effects do not only occur at high sound levels in occupational settings, but also at relatively low environmental sound levels when, more importantly, intended activities such as concentration, relaxation or sleep are disturbed.

The following questions need to be answered.

- Do these changes observed in the laboratory habituate or persist under chronic noise exposure?
- If they habituate, what are the physiological costs? If they persist, what are the long-term health effects?

The answers to these questions come from epidemiological noise research. Large-scale epidemiological studies have been carried out for a long time (Babisch, 2000). The studies suggest that transportation noise is associated with adverse cardiovascular effects, in particular IHD. The epidemiological evidence is constantly increasing (Babisch, 2002, 2004a). The biological plausibility of the association derives from the numerous noise experiments that have been carried out in the laboratory. There is no longer any need to prove the noise hypothesis as such. Decision-making and risk management, however, rely on a quantitative risk assessment which requires an established dose–response relationship. Since many of the stress indicators and risk factors that have been investigated in relation to

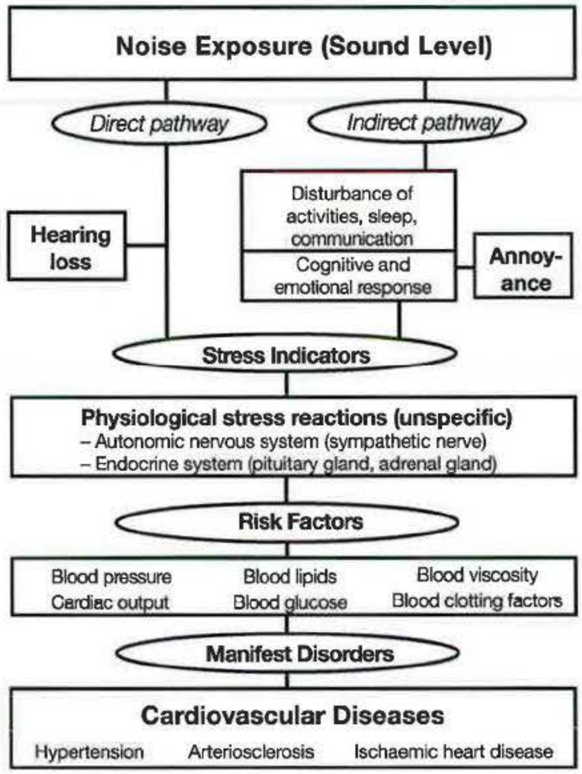

Fig. 4.3 Noise effects reaction scheme

Source: Babisch, 2002.

noise are known to be classical cardiovascular risk factors, the hypothesis has emerged that chronic noise exposure increases the risk of hypertension, arteriosclerosis and IHD. Its relevance for public health comes from the high prevalence of cardiovascular diseases in developed and industrialized countries. It is unclear as to what extent chronically repeated noise-induced sleep disturbance contributes to the development of somatic health disorders. Only a few epidemiological studies address this particular issue. Epidemiological noise research has seldom distinguished between day and night exposures, or between the exposure of the living room and the bedroom. However, some deduction can be made from daytime to night-time exposure.

4.5.2 NOISE AND STRESS-REACTION MODEL

The auditory system is continuously analysing acoustic information, which is filtered and interpreted by different cortical and subcortical brain structures. The limbic system, including the hippocampus and the amygdala, plays an important role in the emotional processing pathways (Spreng, 2000). It has a close connection to the hypothalamus that controls the autonomic nervous system and the hormonal balance of the body. Laboratory studies found changes in blood flow, BP and heart rate in reaction to noise stimuli as well as increases in the release of stress hormones including the catecholamines adrenaline and noradrenaline, and the corticosteroid cortisol (Berglund and Lindvall, 1995; Maschke, Rupp and Hecht, 2000; Babisch, 2003). Such changes also occur during sleep without the involvement of cortical structures. The amygdala has the capacity to learn due to its plasticity, particularly with respect to the meaning of sound stimuli (for example, danger of an approaching lorry) (Spreng, 2000, 2004). Acoustic stimulation may act as an unspecific stressor that arouses the autonomous nervous system and the endocrine system. The generalized psychophysiological concept given by Henry and Stephens can be applied directly to noise-induced stress reaction (Henry, 1992). The stress mechanism as such is genetically determined but it may be modified by experience and environmental factors. Its biological function is to prepare the organism to cope with a demanding stressor. The arousal of the sympathetic and endocrine system is associated with changes in physiological functions and the metabolism of the organism, including BP, cardiac output, blood lipids (cholesterol, triglycerides, free fatty acids, phosphatides), carbohydrates (glucose), electrolytes (magnesium, calcium), blood clotting factors (thrombocyte aggregation, blood viscosity, leukocyte count) and others (Friedman and Rosenman, 1975; Cohen, Kessler and Underwood Gordon, 1995; Lundberg, 1999). In the long term, functional changes and dysregulation may occur, thus increasing the risk of manifest diseases.

Fig. 4.3 shows the principal reaction schema used in epidemiological noise research for hypothesis testing (Babisch, 2002). It simplifies the cause–effect chain, that is: sound – annoyance (noise) – physiological arousal (stress indicators) – (biological) risk factors – disease – and mortality (the latter is not explicitly considered in the graph). The mechanism works "directly" through synaptic nervous interactions and "indirectly" through the emotional and the cognitive perception of the sound. It should be noted that the "direct" pathway is relevant even at low sound levels particularly during sleep, when the organism is at its nadir of arousal. The objective noise exposure (sound level) and the subjective noise "exposure" (annoyance) may serve independently as exposure variables in the statistical analyses of the relationship between noise and health end points.

Principally, the effects of environmental noise cannot directly be extrapolated from results of occupational noise studies. The two noise environments cannot simply be merged into one sound energy-related dose–response model (for example, a simple 24-hour average noise level measured with a dose-meter). Noise effects are not only dependent on the sound intensity but also on the frequency spectrum, the time pattern of the sound and the individuals' activities which are disturbed. Therefore, epidemiological studies carried out under real-life conditions can provide the basis for a quantitative risk assessment provided that there is adequate control over confounding and exposure variables. Other noise sources might act as confounders and/or effect modifiers on the association of interest. The effects of road traffic noise (at home) were shown to be stronger in subjects who were also exposed to high noise levels at work (Babisch et al., 1990).

4.5.3 PREVIOUS REVIEWS ON ENVIRONMENTAL NOISE AND CARDIOVASCULAR RISK

Causality in epidemiology can never be completely proven (Schlesselman, 1987; Christoffel and Teret, 1991; Weed, 2000). It is a gradual term for which evidence is increasing with the increasing number of facts. However, the magnitude of effect, the presence of a dose–response relationship and consistency with other studies in different populations and with different methodology and biological plausibility are commonly accepted arguments for a causal relationship (Bradford Hill, 1965; Evans, 1976; Morabia, 1991; Weed and Hursting, 1998). Classical, systematic and quantitative reviews have been published in the past, summarizing the results of studies that have been carried out up to the end of the last century, and assessing the evidence of the relationship between community noise and cardiovascular disease outcomes (Health Council of the Netherlands, 1994, 1999, 2004; Berglund and Lindvall, 1995; IEH, 1997; Morrell, Taylor and Lyle, 1997; Porter, Flindell and Berry, 1998; Babisch, 2000; Passchier-Vermeer and Passchier, 2000), including a classical review and synthesis report by Babisch (2000) and a systematic review (meta-analysis) by van Kempen et al. (2002).

In a meta-analysis it was concluded that the risk of hypertension due to aircraft noise was 1.26 per increase of 5 dB(A) (95% CI: 1.14–1.39, L_{day} = 55–72 dB(A)) (van Kempen et al., 2002). But, only one study (Knipschild, 1977a) was considered in the meta-analysis. With respect to road traffic noise and hypertension a pooled estimate of 0.95 per 5 dB(A) (95% CI: 0.84–1.08, L_{day} = <55–80 dB(A)) was calculated (van Kempen et al., 2002). Two cross-sectional studies (Knipschild and Sallé, 1979; Knipschild, Meijer and Sallé, 1984) were considered in this calculation. The highest degree of evidence was for the association between community noise and IHD. Across the studies there was not much indication of an increased risk for subjects who lived in areas with a daytime average sound pressure level of less than 60 dB(A). For higher noise categories, however, higher risks were relatively consistently found amongst the studies (Babisch, 2004a). Statistical significance was rarely achieved.

Some studies permit reflections on dose–response relationships. These mostly prospective studies suggest an increase in risk for outdoor noise levels above 65–70 dB(A) during the daytime, the relative risks ranging from 1.1 to 1.5. Noise effects were larger when mediating factors like years in residence, room orientation and window-opening habits were considered in the analyses. In a meta-analysis it was concluded that the risk of IHD increased by 1.09 per 5 dB(A) of the road traffic noise level (95% CI: 1.05–1.13, L_{day} = 51–70 dB(A)) (van Kempen et al., 2002), when two cross-sectional studies (Babisch et al., 1993a) were considered. However, the pooled estimate of two prospective studies (Babisch et al., 1999) was calculated to be 0.97 per 5 dB(A) (95% CI: 0.90–1.04, L_{day} = 51–70 dB(A)) (van Kempen et al., 2002). When the diagnosis of IHD was limited to myocardial infarction, three studies (Babisch et al., 1999, 1994) were considered in this meta-analysis. Then the linear effect estimate was 1.03 per 5 dB(A) increase in road traffic noise level (95% CI: 0.99–1.09, L_{day} = 51–80 dB(A)). New studies have appeared in the meantime which are included in the present updated review (Matsui et al., 2001; Bluhm, Nordling and Berglind, 2001; Evans et al., 2001; Rosenlund et al., 2001; Belojevic and Saric-Tanaskovic, 2002; Goto and Kaneko, 2002; Lercher et al., 2002; Maschke, 2003; Franssen et al., 2004; Matsui et al., 2004; Niemann and Maschke, 2004; Babisch et al., 2005). Others are on their way or have not yet been finalized and published, for instance the pan-European HYENA project (Jarup et al., 2003).

4.5.4 UPDATED REVIEW OF EPIDEMIOLOGICAL STUDIES

Sixty epidemiological studies were recognized as having either objectively or subjectively assessed the relationship between transportation noise and cardiovascular end points. The identification of studies was based on the author's expert knowledge of the topic and respective literature. Details are given in the major report (Babisch, 2006). Information particularly on night-time exposure (L_{night}: 22.00–06.00 or 23.00–07.00) was seldom available. Newer studies used non-weighted or weighted averages of the 24-hour exposure (L_{eq}, L_{dn}, L_{den}). Some aircraft noise studies used national calculation methods (for example, Dutch Kosten Units). For comparisons of study results and the pooling of data (meta-analysis), sound levels were converted on the basis of best guess approximations to L_{day} (Matschat and Müller, 1984; Passchier-Vermeer, 1993; Bite and Bite, 2004; Franssen et al., 2004). It should be noted in this context that doubling/halving of road traffic volume results in a 3 dB(A) higher/lower average sound pressure level. Not all studies allowed dose–response reflections because some of them considered very broad exposure categories. Besides objective noise measurements, subjective measurements of exposure have been used in some epidemiological noise studies, which is in accordance with the noise–stress model. Type of road (for example, busy street, side street, etc.), disturbances and annoyance were rated by the study subjects from given scales.

4.5.5 MEAN BP

Table A2 of the major report (Babisch, 2006) lists the major findings of epidemiological traffic noise studies in which mean BP was considered as the outcome. It indicates mean systolic and diastolic BP differences as obtained from extreme group comparisons of noise exposure. The effects in children and in adults are discussed separately. The findings in children are difficult to interpret with regard to possible health risks in their later life. The effect may be of a temporary nature and may not be relevant to permanent health damage. There is evidence during childhood (Gillman et al., 1992), adolescence (Yong et al., 1993) and adulthood (Tate et al., 1995) that the BP level at an early age is an important predictor of the BP level at a later age. Studies over the full age range are missing (tracking). Growth and body weight are important factors in BP development. The impact of body size was not adequately considered in some of the studies. A crude hint regarding reversible effects on BP came from one study (Morrell et al., 2000). Results of the Munich intervention study on the effects of a reduction of aircraft noise have only been reported regarding cognitive performance but not with respect to change of BP (Hygge, Evans and Bullinger, 2002). It was concluded from the available data on the length of exposure that children do not seem to adapt to high levels of road traffic noise but to some extent to aircraft noise (Passchier-Vermeer, 2000; Bistrup et al., 2001). However, the database appears to be too poor to draw final conclusions. Aircraft noise studies focused on exposure at school, while road traffic noise studies mostly considered noise exposure at home. The conclusions given by Evans and Lepore (1993) seem still to hold true:

> "We know essentially nothing about the long-term consequences of early noise exposure on developing cardiovascular systems. The degree of blood pressure elevations is small. The clinical significance of such changes in childhood blood pressure is difficult to determine. The ranges of blood pressure among noise-exposed children are within the normal levels and do not suggest hypertension. The extent of BP elevations found from chronic exposure are probably not significant for children during their youth, but could portend elevations later in life that might be health damaging."

Regarding mean BP, no consistent findings in the relationship between traffic noise level and mean systolic or diastolic BP can be seen in adults across the studies. In longitudinal studies, problems arose from migration of subjects, which had a considerable impact on sample size. The latter problem also applies to cross-sectional studies, in general. Sensitive subjects may tend to move out of the polluted areas, which dilutes the effect of interest. Medication due to high BP may affect the BP readings. However, the exclusion of subjects with hypertension or hypertension treatment dilutes the true effect on BP differences, if the hypothesis (noise causes high BP) is true. In principle, hypotension – a fall in BP – can also be a stress reaction. All this makes it more reasonable to look at manifest hypertension (defined by a cut-off criterion) as a clinical outcome rather than at mean BP readings (Ising, 1983; Winkleby, Ragland and Syme, 1988). To date, there is no evidence from epidemiological data that community noise increases mean BP readings in the adult population. However, this does not discard the noise hypothesis as such. Studies suffered from insufficient power, narrow exposure range or other difficulties in the study design.

4.5.6 HYPERTENSION

Table A3 of the major report (Babisch, 2006) gives the results of epidemiological traffic noise studies on the relationship between community noise level and the prevalence or incidence of hypertension. Hypertension in these studies was either defined by WHO criteria (WHO-ISH Guidelines Subcommittee, 1999), similar criteria based on measurements of systolic and diastolic BP, from information which was obtained from a clinical interview, or a social survey questionnaire about hypertension diagnosed by a doctor. Most studies refer to road traffic noise. However, in recent years some new aircraft noise studies entered the database. The subjects studied were the adult male and female population, sometimes restricted to certain age ranges. With regard to the association between community noise and hypertension, the picture is heterogeneous. With respect to aircraft noise and hypertension, studies consistently show higher risks in higher exposed areas. The evidence has improved since a previous review (Babisch, 2000). The relative risks found in four significantly positive studies range between 1.4 and 2.1 for subjects who live in high exposed areas, with approximate daytime average sound pressure level in the range of 60–70 dB(A) or more. Swedish studies found a relative risk of 1.6 at even lower levels >55 dB(A). With respect to road traffic noise, the picture remains unclear. New studies, more than older studies, tend to suggest a higher risk of hypertension in subjects exposed to high levels of road traffic noise, showing relative risks between 1.5 and 3.0. However, the earlier studies cannot be neglected in the overall judgement process. Across all studies no consistent pattern of the relationship between community noise and prevalence of hypertension can be seen. Dose–response relationships were considered in new studies. Subjective ratings of noise or disturbances due to traffic noise seem to consistently show a positive association with prevalence of hypertension. The relative risks found here range from 0.8 to 2.3. These studies, however, are of lower validity due to principal methodological issues regarding overreporting (Babisch et al., 2003).

4.5.7 IHD

Table A5 of the major report (Babisch, 2006) gives the results of cross-sectional epidemiological traffic noise studies on the relationship between noise level and prevalence of IHD. Table A6 of the major report gives the results of case-control and cohort studies on the association between noise level and incidence of IHD. In cross-sectional studies, IHD prevalence was assessed by clinical symptoms of angina pectoris, myocardial infarction, ECG abnormalities as defined by WHO criteria (Rose and Blackburn, 1968), or from self-reported questionnaires regarding doctor-diagnosed heart attack. In longitudinal studies, IHD incidence was assessed by clinical myocardial infarction as obtained from hospital records, ECG measurements or clinical interviews. The majority of studies refer to road traffic noise. With regard to IHD, the evidence of an association between community noise and IHD risk has increased since a previous review (Babisch, 2000). There is not much indication of a higher IHD risk for subjects who live in areas with a daytime average sound pressure level of less than 60 dB(A) across the studies. For higher noise categories, a higher IHD risk was relatively consistently found amongst the studies. Statistical significance was rarely achieved. Some studies permit reflections on dose–response relationships. These mostly prospective studies suggest an increase in IHD risk at noise levels above 65–70 dB(A), the relative risks ranging from 1.1 to 1.5 when the higher exposure categories were grouped together. Noise effects were larger when mediating factors like residence time, room orientation and window-opening habits were considered in the analyses. This accounts for an induction period (Rose, 2005) and improves exposure assessment. The results appear as consistent when subjective responses of disturbance and annoyance are considered, showing relative risks ranging from 0.8 to 2.7 in highly annoyed/disturbed/affected subjects. However, these findings may be of lower validity due to methodological issues.

4.5.8 MEDICATION AND DRUG CONSUMPTION

Table A8 of the major report (Babisch, 2006) gives the results of studies on the relationship between drug consumption and community noise. Medication was primarily investigated with respect to aircraft noise. A significant prevalence ratio for medication with cardiovascular drugs of 1.4 was found in the sample of Amsterdam Schiphol Airport (Knipschild, 1977a). The results of the "drug survey", where the annual data of the pharmacies regarding the purchase of cardiovascular drugs were analysed (repeated cross-sectional survey), supported this finding. An increase in drug purchase over time in the exposed areas and not in the less exposed was found. This refers to the purchase of cardiovascular and antihypertensive drugs, as well as the purchase of hypnotics, sedatives and antacids (Knipschild and Oudshoorn, 1977). Furthermore a dependency with changes in night flight regulations was found (decrease after reduction of night flights). A large recent study around Amsterdam Schiphol Airport found only a slightly higher risk of self-reported medication with cardiovascular drugs, including antihypertensive drugs (relative risk 1.2), in subjects exposed to aircraft noise where the noise level L_{den} exceeded 50 dB(A) (Franssen et al., 2004). Dose–response relationships across noise levels (L_{den} = <50–65 dB(A)) with respect to prescribed and non-prescribed sedatives/sleeping pills were found (relative risk 1.5 and 2.0, respectively) in the highest noise category of L_{den} = 61–65 dB(A). The preliminary results of an ongoing aircraft noise study from Sweden carried out around Stockholm's airport are in line with the Dutch studies (Bluhm et al., 2004). A significant relative risk of 1.6 for the use of antihypertensive drugs was found in male subjects, where the noise level according to the Swedish calculation standard exceeded FBM = 55 dB(A). The road traffic noise studies, where medication/purchase of drugs was investigated also tend to show a higher use in higher exposed subjects (Eiff and Neus, 1980; Schulze et al., 1983; Lercher, 1992). The relative risk for cardiovascular drugs was 1.3 in the Bonn study and 5.0 in the Erfurt study. The results for other drugs including sleeping pills, sedatives, tranquillizers and hypnotics ranged between 1.2 and 3.8 in these studies. All in all, the studies on the relationship between the use of medication or purchase of drugs and community noise support the general hypothesis of an increase in sleep disturbance and cardiovascular risk in noise-exposed subjects.

4.5.9 EVALUATION OF STUDIES

This section refers only to studies where the prevalence or the incidence of manifest cardiovascular diseases was considered as a potential health outcome of chronic exposure to environmental noise. The focus here is on a quantitative risk assessment with respect to manifest diseases. Furthermore, studies on the effects of low-altitude jet-fighter noise are also excluded, because this type of noise includes other dimensions of stress (for instance, fear). Thirty-seven studies have assessed the prevalence or incidence of manifest diseases, including hypertension and IHD (angina pectoris, myocardial infarction, ECG abnormalities).

4.5.9.1 Criteria

Epidemiological reasoning is largely based on the magnitude of effect estimates, dose–response relationships, consistency of findings, biological plausibility of the effects and exclusion of possible bias. Internal (the role of chance) and external validity (absence of bias and confounding) are important issues in the evaluation of studies (Bradford Hill, 1965). Analytic studies (for example, cohort or case-control studies) are usually considered as having a higher validity and credibility than descriptive studies (for example, cross-sectional or ecological studies) (Hennekens and Buring, 1987), although many of the reservations against cross-sectional studies seem to be of minor importance when considering noise. For example, it does not appear to be very likely that diseased subjects tend to move differentially more often into exposed areas. Rather the opposite may be true, if noise stress is recognized as a potential cause of the individual's health problem. Thus, a cross-sectional study design may act conservatively on the results. The presence of a dose–response relationship is not a necessary criterion of causality. Non-linear relationships, including "u-" or "j-" shaped, saturation and threshold effects may reflect true associations (Calabrese and Baldwin, 2003; Rockhill, 2005). With respect to the derivation of guideline values in public health policy, the assessment of a dose–response relationship enables a quantitative risk assessment on the basis of continuous or semi-continuous (for instance 5 dB(A) categories) exposure data. Dichotomous exposure data, on the other hand, that refer to a cut-off criterion which splits the entire exposure range into two halves, can be used to evaluate the hypothesis of an association (qualitative interpretation), but not a quantitative assessment. The objective or subjective assessment of exposure and/or health outcomes is an important issue when judging the validity of a study (Malmström, Sundquist and Johansson, 1999; Cartwright and Flindell, 2000; Hatfield et al., 2001). The objective prevalence of hypertension was found to be higher in a population sample than the subjective prevalence of hypertension (Schulte and Otten, 1993). In a telephone survey more than half of the hypertensives classified themselves as normotensive (sensitivity 40% for men and 46% for women) (Bowlin et al., 1993). In a representative health survey, the validity of the self-reported assessment of morbidity (subjective morbidity) was found to be "low" with respect to hypercholesterolaemia, "intermediate" with respect to angina pectoris, hypertension and stroke and "high" with respect to myocardial infarction (Bormann et al., 1990). Myocardial infarction is a very definite and severe health outcome which subjects would clearly know about if they had experienced it. Its assessment by questionnaire tends to be more credible than that regarding hypertension. Test–retest reliability was found to be good with respect to "harder" outcomes, including high BP and heart attack (Lundberg and Manderbacka, 1996; Lipworth et al., 2001). Over-reporting, on the other hand, may be a source of potential bias, particularly when both exposure and outcome are assessed on a subjective basis (Winkleby, Ragland and Syme, 1988; Babisch et al., 2003). The subjects may be more prone to blame their environment for their health problems, or may even tend to exaggerate adverse effects or exposure in order to influence noise policy. Therefore, a higher credibility and ranking was given to studies where exposure and outcome were assessed objectively (for example sound level versus subjective ratings, and measurement of BP or a clinical interview versus self-reported hypertension in a self-administered questionnaire). This means that the sound level must have been measured or calculated on the basis of the traffic counts, and clinical interviews or measurements must have been carried out by medically trained personnel (no self-administered questionnaire data) to give a study a high ranking. Studies which have been adequately controlled (for instance stratification, model adjustment (regression), matching) for a reasonable set of confounding variables in the statistical analyses, besides age and sex, were given a high ranking.

4.5.9.2 Assessment

The evaluation concerning the epidemiological studies was made with respect to the identification of good quality studies that can be feasibly considered for the derivation of guideline values. These studies can either be used for a statistical meta-analysis, for a combined interpretation (synthesis) or for singular interpretations. All the studies were evaluated with respect to the following criteria for inclusion or exclusion in the synthesis process. Necessary criteria were: (1) peer-reviewed in the international literature; (2) reasonable control of possible confounding; (3) objective assessment of exposure; (4) objective assessment of outcome; (5) type of study; and (6) dose–response assessment. All six criteria were fulfilled by the two prospective cohort studies carried out in Caerphilly and Speedwell (Babisch et al., 1999; Babisch, Ising and Gallacher, 2003), the two prospective case-control studies carried out in the western part of Berlin ("Berlin I" and "Berlin II") (Babisch et al., 1992, 1994), and the new prospective case-control study carried out in the whole of Berlin ("NaRoMI" = "Berlin III") (Babisch, 2004b; Babisch et al., 2005). The studies refer to road traffic noise and the incidence of myocardial infarction. They were also the only ones considered in an earlier meta-analysis on this issue (van Kempen et al., 2002), with the exception of the "NaRoMI" study, which was not available at that time. All these studies are observational analytic studies (Hennekens and Buring, 1987). If descriptive studies on individuals – namely cross-sectional studies – are allowed, another two studies from Caerphilly and Speedwell on the association between road traffic noise and the prevalence of IHD, myocardial infarction and angina pectoris can be taken into account (Babisch et al., 1988, 1993a, 1993b). These studies were also considered in the meta-analysis by van Kempen et al. (2002). However, the results of the Berlin study on the prevalence of myocardial infarction (Babisch et al., 1994) – which was also considered in that meta-analysis – are not considered here, because the outcome was assessed subjectively with a self-administered questionnaire (an exclusion criterion). All the studies suggest an increase in IHD, in particular myocardial infarction. These studies are used for a new meta-analysis (section 4.5.10).

Regarding aircraft noise, the cross-sectional Okinawa study (Matsui et al., 2001; Matsui et al., 2004) on the association between aircraft noise and hypertension fulfils the inclusion criteria. When studies are included that did not assess dose–response relationships but only compared dichotomous categories of exposure in the analyses, two more studies appear on the list. The studies were carried out in the vicinity of Amsterdam Schiphol Airport. They suggest a higher risk of cardiovascular diseases in general (Knipschild, 1977b), and – specifically – for hypertension and IHD (angina pectoris, ECG abnormalities, heart trouble) (Knipschild, 1977a) in subjects from areas exposed to high aircraft noise. These studies were considered in the meta-analysis by van Kempen et al. (2002). However, they do not fulfil the strict criteria set here. Finally, if the inclusion criteria are widened to include peer-reviewed studies that assessed dose–response relationships between objective indicators of exposure and the subjective (self-reported) prevalence of diseases, a further two studies can be considered. These are the cross-sectional study carried out in Stockholm regarding the association between aircraft noise and hypertension (Rosenlund et al., 2001), and the cross-sectional part of the study in Berlin regarding the association between road traffic noise and myocardial infarction (Babisch et al., 1994). Fig. 4.4 shows the results of the three aircraft noise studies carried out in Amsterdam, Okinawa and Stockholm (Knipschild, 1977a; Rosenlund et al., 2001; Matsui et al., 2004). The graph clearly indicates that the results are too heterogeneous to derive a pooled dose–response curve. However, all three studies show an increase in risk with increasing noise level.

Studies that are not given a high ranking according to the above mentioned criteria, however, may serve as additional sources of information to support the evidence of the conclusions being made on the basis of this review. This is illustrated in Fig. 4.5. The entries are relative risks (centre of the bars) with 95% confidence intervals (the bars) for dichotomous comparisons of noise exposure (extreme groups or high vs. low). A relative consistent shift of the bars to relative risks greater than 1 can be seen. The dark-shaded bars in the diagram refer to studies where the noise exposure was determined objectively (noise levels), the

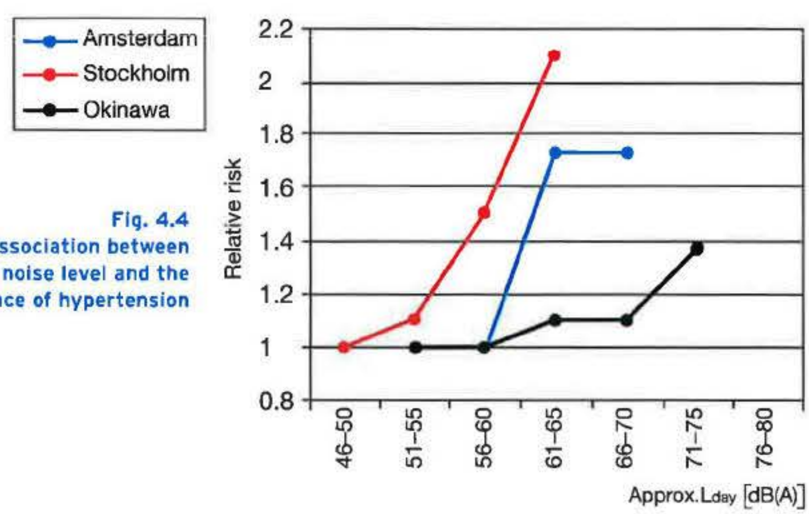

Fig. 4.4
Association between aircraft noise level and the prevalence of hypertension

light-shaded bars where it was determined subjectively (annoyance). Road traffic and aircraft noise studies are here viewed together. No corresponding results are available for rail traffic studies. If different subgroups of the population (males/females) or different health end points were taken into account, specific studies appear more than once in the illustration.

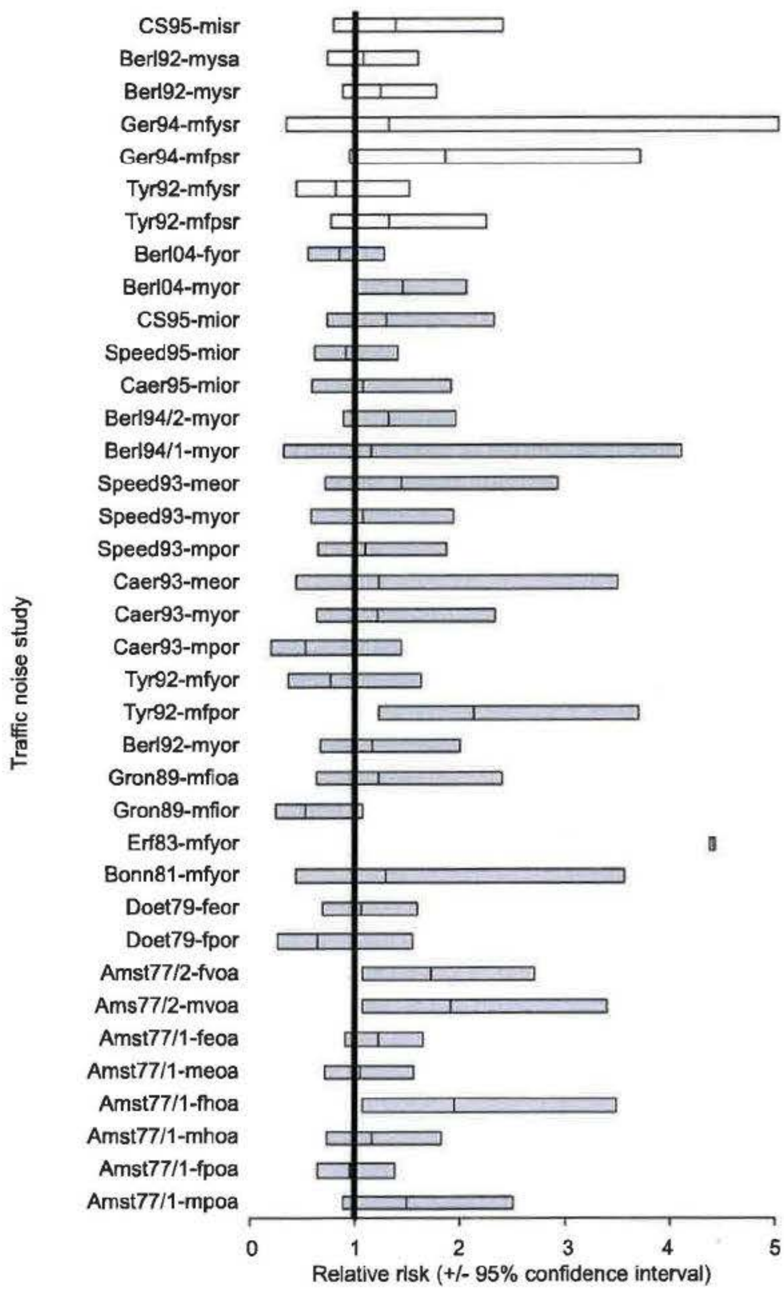

Fig. 4.5
Results of epidemiological studies on the association between traffic noise and ischaemic heart disease

Captions: sex:
f = female,
m = male;
noise measurement:
o = objective (sound level), dark-shaded beam;
s = subjective (annoyance), light-shaded beam;
type of noise:
a = aircraft noise;
r = road traffic noise;
ischaemic heart disease:
e = ECG-ischaemic signs,
h = heart complaints,
i = ischaemic heart disease,
p = angina pectoris,
v = cardiovascular complaints in general, y = heart attack.

Source: Babisch, 2002, modified according to the results of Babisch, 2004b.

4.5.10 DOSE-RESPONSE CURVE: META-ANALYSIS

For a quantitative risk assessment and the derivation of guidelines for public health noise policy a common dose–response curve is required. The risk estimates obtained from different noise studies can be summarized using the statistical approach of a meta-analysis. Based on the judgement criteria discussed in section 4.5.9.2, five analytic and two descriptive studies emerged that can be used to derive a common dose–response curve for the association between road traffic noise and the risk of myocardial infarction. Two separate meta-analyses were made by considering the analytic studies that were carried out in Caerphilly and Speedwell (cohort studies) and Berlin (case-control studies) on the one hand, and the descriptive studies that were carried out in Caerphilly and Speedwell (cross-sectional studies) on the other hand. It turned out, as a result of the evaluation, that all these studies referred to road traffic noise during the day (L_{day}: 06.00–22.00) and the incidence or prevalence of myocardial infarction as the outcome. Study subjects were men. In all analytic studies the orientation of rooms was considered for the exposure assessment (facing the street or not). With respect to the Caerphilly and Speedwell studies, the six years of pooled follow-up data provided the respective information. In all descriptive studies the traffic noise level referred to the facades that were facing the street and did not consider the orientation of rooms/windows. All individual effect estimates were adjusted for the covariates considered in each of the studies. Different sets of covariates were considered in each study. However, this pragmatic approach accounts best for possible confounding in each study and provides the most reliable effect estimates derived from each study. The concept of meta-analysis was used to aggregate and summarize the findings of the different studies (Olkin, 1995; Blettner et al., 1999). The program "meta" was downloaded from the "STATA" web site for use in the statistical package STATA (version 8.0), and for calculating the pooled random effect estimates.

Table 4.2
Single and pooled (meta-analysis) effect estimates (odds ratios and 95% confidence intervals) of descriptive and analytic studies on the relationship between road traffic noise level (L_{day}) and the incidence/prevalence of myocardial infarction

	Road traffic noise level - L_{day} [dB(A)]					
Descriptive studies	**51-55**	**56-60**	**61-65**	**66-70**		**N**
Caerphilly	1.00	1.00 (0.58-1.71), [13.29]	0.90 (0.56-1.44), [17.23]	1.22 (0.63-2.35), [8.98]		2512
Speedwell	1.00	1.02 (0.57-1.83), [11.19]	1.22 (0.70-2.21), [12.62]	1.07 (0.59-1.94), [10.94]		2348
Pooled	1.00	1.01 (0.68-1.50)	1.02 (072-1.47)	1.14 (0.73-1.76)		
Q-Test		p=0.96	p=0.41	p=0.77		
Analytic studies	**60**	**61-65**	**66-70**	**71-75**	**76-80**	**N**
Caerphilly + Speedwell	1.00	0.65 (0.27-1.57), [4.95]	1.18 (0.74-1.89), [17.48]	---	---	3950
Berlin I	1.00	1.48 (0.57-3.85), [4.21]	1.19 (0.49-2.87), [4.94]	1.25 (0.41-3.81), [3.09]	1.76 (0.11-28.5), [0.50]	243
Berlin II	1.00	1.16 (0.82-1.65), [31.43]	0.94 (0.62-1.42), [22.76]	1.07 (0.68-1.68), [18.92]	1.46 (0.77-2.78), [9.27]	4035
Berlin III	1.00	1.01 (0.77-1.32), [54.42]	1.13 (0.86-1.49), [50.87]	1.27 (0.88-1.84), [28.24]	---	4115
Pooled	1.00	1.05 (0.86-1.29)	1.09 (0.90-1.34)	1.19 (0.90-1.57)	1.47 (0.79-2.76)	
Q-Test		p=0.57	p=0.87	p=0.84	p=0.90	

Table 4.2 shows individual and pooled effect estimates with confidence intervals (rounded brackets), statistical weights (square brackets) for the individual studies, and the Q-test of heterogeneity between studies. According to the Q-test, the nil hypothesis of non-heterogeneity was never discarded. Figs 4.6 and 4.7 show odds ratios of individual studies and the pooled estimates for the descriptive and analytic studies.

Fig. 4.6 and Fig. 4.7
Single and pooled effect estimates (odds ratios) for the descriptive and analytic studies of the association between road traffic noise level and the prevalence (left graph) and incidence (right graph), respectively, of myocardial infarction

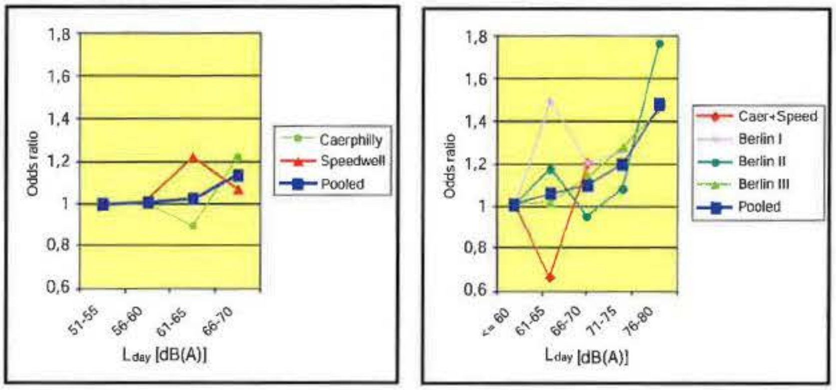

4.5.11 EFFECT MODIFICATION

Support for any noise–effect relationship may come from subgroup analyses that are in line with the noise hypothesis. This refers to effect modification with respect to residence time, window-opening behaviour and other determinants that affect the noise exposure and cumulative noise dose. In the Amsterdam aircraft noise studies, a steady increase in the purchase of cardiovascular and antihypertensive drugs at local pharmacies was found over the period of eight years in a community newly exposed to aircraft noise. No such increase was found in a control community that was not exposed to aircraft noise (Knipschild and Oudshoorn, 1977). Positive associations between the prevalence of cardiovascular diseases and residence time in exposed areas (but not in unexposed) were also found in the road traffic noise studies carried out in Bonn with respect to hypertension (Eiff and Neus, 1980; Neus et al., 1983) and in Caerphilly and Speedwell with respect to IHD (Babisch et al., 1999; Babisch, Ising and Gallacher, 2003). When the analyses of the road traffic noise studies carried out in Berlin, Caerphilly and Speedwell were restricted to subjects who had not moved within a retrospective period of 10–15 years, the effect estimates turned out to be larger than for the total samples of each study (Babisch et al., 1994, 1999, 2005). Similarly, a larger effect was found in the study in Sollentuna with respect to hypertension (Bluhm, Nordling and Berglind, 2001). No such effect was found in the Lübeck study (Hense, Herbold and Honig, 1989; Herbold, Hense and Keil, 1989). The cross-sectional data of the study carried out in Los Angeles on children regarding mean BP indicated some habituation to aircraft noise (Cohen et al., 1980). The longer the children were enrolled in the school, the smaller was the difference in BP between exposed and non-exposed children.

However, the follow-up study suggested that this may also be an effect of attrition (Cohen et al., 1981). The longer the families experienced the noise, the more likely that they moved away from the exposed areas (selection bias). In contradiction to this, BP differences between children exposed and not exposed to road traffic noise increased with school grade (Karsdorf and Klappach, 1968). Intervention studies were conducted with respect to changes in BP and changes in air traffic operation (for example the opening/closing of airports or runways). In the Munich study, a larger increase in BP was found in children from a noisy area (Evans, Bullinger and Hygge, 1998). Other studies suggested reversible effects on BP when the exposure was lowered (Wölke et al., 1990; Morrell et al., 1998, 2000). In the Tyrol study, significantly lower BP readings were found in subjects who kept the windows closed throughout the night (Lercher and Kofler, 1993, 1996). When the subjects lived close to the highway (within a distance of approximately 500 metres), the prevalence of hypertension was higher in subjects whose bedroom was facing the main road than in those whose bedroom was not facing the main road. The orientation of rooms and window opening was also found to be an effect modifier of the association between road traffic noise and IHD in the Caerphilly and Speedwell studies (Babisch et al., 1999). The relative risk with respect to the noise level was slightly higher in subjects with rooms facing the street and subjects keeping the windows usually open when spending time in the room. A much greater relative risk of hypertension was found in subjects who slept with open bedroom windows in the Spandau Health Survey (Maschke, 2003; Maschke, Wolf and Leitmann, 2003). Hearing impairment was found to be an effect modifier on the association between aircraft noise and hypertension (Rosenlund et al., 2001). Amongst the exposed subjects, a higher risk associated with the noise was only found in subjects without hearing loss.

4.5.12 EXPOSURE DURING THE NIGHT

Unfortunately, epidemiological noise research provides nearly no information regarding the particular impact of noise exposure during the night on cardiovascular health outcomes. The Spandau Health Survey explicitly distinguished between the exposure of the living room (during the day) and the exposure of the bedroom (during the night). There, a slightly higher relative risk of hypertension was found with respect to the traffic noise level during the night (relative risk 1.9 vs. 1.5) compared with the noise level during the day (Maschke, 2003; Maschke, Wolf and Leitmann, 2003). Furthermore, sleeping with open bedroom windows was associated with a large increase in risk. However, due to the small sample size, the confidence intervals were very large. In the drug survey of the Amsterdam aircraft noise studies, a steady increase in purchase of hypnotics (sleeping pills) and sedatives was found (Knipschild and Oudshoorn, 1977). This trend decreased considerably when night flights were largely banned. Such a decrease was not found regarding cardiovascular drugs for which the purchase also increased over time. However, this may partly be due to the fact that atherosclerotic manifestations of high BP were less reversible (in contrast to vasoconstriction, which is more related to acute or semi-acute effects, for instance in children). It was mentioned in the previous section that closing the windows had a protective effect on BP readings in the Tyrol study (Lercher and Kofler, 1993). This was only found regarding closing the windows during the night and not during the day. Furthermore, subjects who had switched the bedroom and the living room because of the noise had a significantly lower BP than those who did not do so. The findings are discussed in a broader context of coping strategies (Lercher, 1996). When subjective responses to community noise were considered, higher relative risks of cardiovascular diseases were found for noise-related disturbances of sleep and relaxation, rather than for other disturbances or subjective descriptors of noise exposure, which did not refer to the night-time. This was found in the Caerphilly and Speedwell studies (Babisch, Ising and Gallacher, 2003), the NaRoMI study (Babisch et al., 2005), the Spandau Health Survey (Maschke, Wolf and Leitmann, 2003) and a general population sample of Germany (Bellach et al., 1995). The LARES study (Niemann and Maschke, 2004), in which noise-induced sleep disturbance was assessed, did not show a higher relative risk compared with the general annoyance.

4.5.13 RISK GROUPS

Most epidemiological noise studies looked at the cardiovascular effects of community noise in men. This may simply be due to the fact that the prevalence of cardiovascular diseases in middle-aged subjects is higher in men than in women. Statistical power is an important issue for the design of a study. Furthermore, in noise experiments, physiological reactions controlled by the autonomic nervous system were less pronounced in females than in males (Neus et al., 1980; Ising and Braun, 2000). Improper control for possible differential effects of the intake of sex hormones, including contraceptives, which may prevent or promote adverse (noise) stress effects, may act conservatively on the results (Cairns et al., 1985; Eiff, 1993; Farley et al., 1998). The studies carried out in Lübeck (Hense, Herbold and Honig, 1989; Herbold, Hense and Keil, 1989), Pancevo (Belojevic and Saric-Tanaskovic, 2002), Berlin (Babisch et al., 2005), Stockholm (Rosenlund et al., 2001), a German population sample (Bellach et al., 1995), Bonn (residence time) (Eiff and Neus, 1980; Eiff et al., 1981b) and in Amsterdam (angina pectoris) (Knipschild, 1977a) found higher prevalences of hypertension, IHD and the use of cardiovascular drugs in noise-exposed men than in women. The studies carried out in Bonn (sound level) (Eiff and Neus, 1980; Eiff et al., 1981b), Sollentuna and Amsterdam (heart trouble) (Knipschild, 1977a; Bluhm, Nordling and Berglind, 2001) found the opposite. In the studies carried out in the former Soviet Union, it was reported that noise effects on the cardiovascular system were more pronounced in young and middle-aged subjects (Karagodina et al., 1969). Swedish noise studies (Bluhm, Nordling and Berglind, 2001, 2004) and the LARES study (Niemann and Maschke, 2004) found similar results. The opposite (larger effects in elderly subjects) was reported from the Amsterdam study (Knipschild, 1977a) and the Stockholm study (Rosenlund et al., 2001). The available database on cardiovascular effects of noise in children is poor. No data are available that refer, in particular, to noise and sleep. The quantitative impact of transportation noise on the cardiovascular system is still a matter of research. A quantitative health risk assessment for children cannot be made at the moment.

Based on the available information from noise studies, it must be concluded that children do not appear to be a particular risk group with respect to cardiovascular outcomes, especially BP. This does not mean that the literature does not suggest higher BP readings in children. It only means that the effect in children does not appear to be different than that in adults. However, children may be exposed longer to noise throughout their lifetime than the adults that have been studied. No long-term follow-up studies are known that focus on noise exposure. Most studies on children considered noise in schools rather than noise at home, which implies different mechanisms about how noise could contribute to a rise in BP (raised effort in learning/speech perception vs. disturbed relaxation/sleep). The prospective part of the Caerphilly and Speedwell studies gave a small hint that health status could be a modifying factor. In subjects with prevalent chronic diseases, road traffic noise was associated with a slightly larger increase in the incidence (new cases) of IHD than in subjects without prevalent diseases – when the objective noise level was considered (Babisch et al., 2003). Surprisingly, when annoyance and disturbances due to traffic noise were considered for exposure, the opposite was found. Noise effects were only seen in subjects without prevalent diseases. This was discussed with respect to reporting bias.

4.5.14 RISK EVALUATION

The process of risk assessment (risk evaluation) comprises hazard identification ("Which health outcome is relevant for the exposure?"), exposure assessment ("How many are affected?") and dose–response assessment ("threshold of effect"). This information is summarized in "risk characterization" ("health hazard characterization"). It involves the interpretation of the available evidence from the available data and other scientific disciplines, and is subject to discussion of the uncertainties. These include chance, bias and validity of studies as well as transparency, replicability and comprehensiveness of reviews. As a result of the risk evaluation process, a quantitative estimate about the likelihood that the hazard will affect exposed people will be derived. Usually, attributable risk percentages are calculated (Walter, 1998). This will serve as key information for any kind of risk management including regulatory options (Jasanoff, 1993). The term "adverse" is essential in this context of environmental standard setting. Risk management should ensure that "adverse" health effects do not occur. The fact that an organism responds to noise does not have to be per se "adverse". The severity of a health outcome is an important determinant of the adversity of an effect and implies variable action levels for public health policy (Babisch, 2002, 2004a; Griefahn et al., 2002; Health Council of the Netherlands, 2003). Since considerable parts of the population are exposed to high noise levels (EEA, 2004), noise policy can have a significant impact on public health (Neus and Boikat, 2000). Due to the increasing number of people affected with the decreasing severity of the effect, even small individual risks and less severe health outcomes can be relevant for public health and decision-making. It has been shown that moderate noise exposures implying a small individual risk may cause more noise-induced cases of health-impaired subjects than higher noise exposures. Franssen et al. (2004) pointed out that the number of people suffering from poor health due to aircraft noise is dominated by the larger number of people that is exposed to relatively moderate-to-low noise levels and not by those exposed to high noise levels. This means that more emphasis should be put on the reduction of noise in moderately exposed areas. However, public health policy cannot only consider population attributable risks (risk percentages), but must also consider individual risks (lifetime risk).

In practice, it seems to be reasonable that noise policy should reduce noise, beginning with the highest exposures and ending with the lowest ones. Decision-making will have to find common standards of acceptable risks, which may vary according to the cost–benefit considerations within and between communities and countries. Such practical standards may, however, vary due to economic development and abilities, cost–benefit considerations and priority settings of a community or country. Health quality targets derived from scientific research are usually intended to minimize risks; decision-making in the political process is only partly scientifically based due to economic limitations and concurring interests (Nijland et al., 2003). Different health outcomes or indicators of well-being and quality of life imply different action levels. Environment and health policy must determine acceptable noise standards that consider the whole spectrum from subjective well-being to somatic health (for example annoyance, physiological arousal, health risk). The evidence for a causal relationship between community or transportation noise and cardiovascular risk appears to have increased over recent years due to new studies that accomplish the database.

4.5.15 CONCLUSIONS

The evaluation process used in this paper considered the "necessary" criteria: peer-reviewed publication in an international journal, reasonable quantitative control of possible confounding, objective assessment of exposure and outcome, type of study (analytic vs. descriptive), and dose–response assessment (not only dichotomous "high" vs. "low"). The approach differs from that of an earlier meta-analysis (van Kempen et al., 2002) in that there regression coefficients were calculated for the entire dose–response curve within a single study (for instance the increase in risk per 5 dB(A)), which were then pooled between studies. Since higher exposure categories usually consist of smaller numbers of subjects than the lower categories, regression coefficients across noise levels tend to be influenced by the lower categories. This may lead to an underestimation of the risk in higher noise categories. The approach presented here pooled the effect estimates of single studies within each noise category, thus giving more weight to the higher noise categories and accounting for possible non-linear associations.

Fig. 4.8 and Fig. 4.9

Pooled effect estimates (meta analysis) of descriptive and analytic noise studies of the association between road traffic noise level and the prevalence (left graph) and incidence (right graph), respectively, of myocardial infarction (odds ratio ± 95% confidence interval).

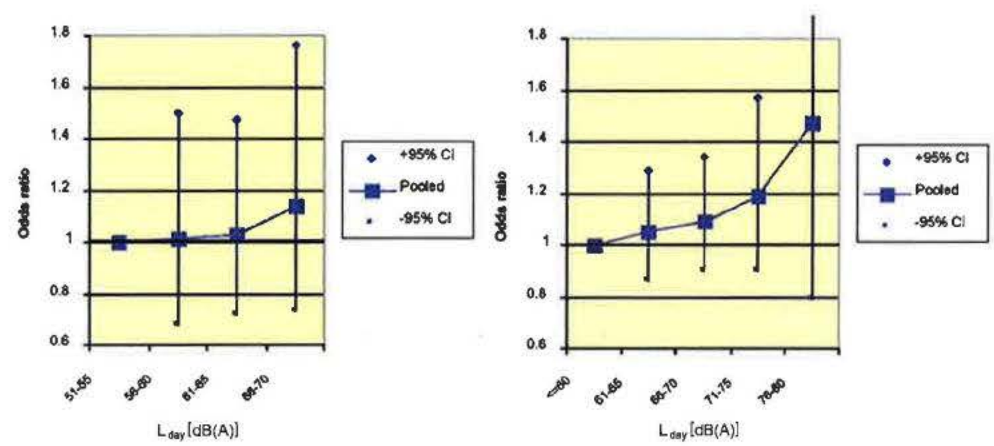

Fig. 4.8 and Fig. 4.9 show the two risk curves for descriptive and analytic studies (Hennekens and Buring, 1987). The graphs show the pooled effect estimates (odds ratios) and the 95% confidence intervals for each noise category. Whereas the cross-sectional studies (Fig. 4.9) cover the sound level range of L_{day} from >50 to 70 dB(A), the cohort and case-control studies (Fig. 4.8) cover the range from ≤60 to 80 dB(A). Both curves together can serve as a basis for a quantitative risk assessment. From Fig. 4.8 it can be seen that below 60 dB(A) for L_{day} no noticeable increase in risk of myocardial infarction is to be detected. Therefore for the time being, L_{day} = 60 dB(A) can be seen as NOAEL (no observed adverse effect level) for the relationship between road traffic noise and myocardial infarction (Babisch, 2002). For noise levels greater than 60 dB(A), the risk of myocardial infarction increases continuously, and is greater than 1.2 for noise levels of 70 dB(A). This can be seen in Fig. 4.9. It should be mentioned that the risk estimates, in general, were found to be higher in subjects that had lived in the exposed areas for a longer time (Babisch et al., 1994, 1999, 2005). This is in accordance with the noise hypothesis and the effects of chronic noise stress (Lercher and Kofler, 1996; Thompson, 1997). However, for the calculation of population attributable risks the figures for the whole population are relevant due to unknown information about residence time.

No particular risk groups could be identified on the basis of epidemiological research on cardiovascular effects of community noise. The assessment of dose-effect relationships sometimes suggested a cut-off level, above which the risk tends to increase. From a biological point of view, one would expect a continuous increase in risk with increasing noise level. However, adaptation, habituation and coping may be reasons for an empirical threshold of effect. Decisions with respect to guideline values usually refer to a quantitative risk assessment of populations (for example population attributable risk percentage). However, prevention strategies – for ethical reasons – should not ignore the individual risks of highly exposed subjects, even if their number may be small.

With respect to night noise exposure, nearly no information is available from epidemiological studies on the cardiovascular effects of long-term noise exposure of the bedroom during the night. Only one study distinguished between the exposures of the bedroom and the living room in the statistical analyses (Maschke, Wolf and Leitmann, 2003). The results suggested slightly higher effect estimates for the prevalence of hypertension with respect to the noise exposure of the bedroom (during the night) compared with the exposure of the living room (during the day). However, the difference was small (odds ration 1.9 vs. 1.5), which means that it still remains an open question whether the night exposure or the overall exposure throughout the whole day is the driving force. The study has some methodological limitations that were addressed in the summary of the major technical report and in a recent advisory report of the Health Council of the Netherlands (2004). They are mainly concerned with the fact that the study population consisted of a selected, predominantly older and health conscious group of persons that might have already suffered from regular health problems (risk group). A few studies that looked at the association between subjective responses to community noise and cardiovascular outcomes suggest a closer relationship with sleep-related annoyance/disturbance reaction rather than with non-sleep-related annoyance/disturbance (Bellach et al., 1995; Babisch et al., 1999, 2005; Maschke, Wolf and Leitmann, 2003; Niemann and Maschke, 2004). Closing the bedroom window or, vice versa, sleeping with the bedroom window open, was associated with a lower or higher risk, respectively (Lercher, 1996). The same was found with respect to changing the bedroom to the living room because of noise. These findings may indicate that night-time noise may be more a determinant of noise-induced cardiovascular effects than daytime exposure. However, daytime activity patterns and expectations of the individuals are much more inhomogeneous than during the night, which tends to dilute the statistical association of true effects with the day noise exposure.

Given the situation that only a few data are available from epidemiological studies with respect to effects on sleep (exposure of the bedroom during the night), there does not seem to be any other way of reasoning than inferring night noise recommendations or guidelines from the results of studies that refer to noise exposure during the daytime period (L_{day}) or the whole day (L_{dn}, L_{24h}). L_{den}, in this context, appears to be a useful noise indicator for decision-making and regulatory purposes. Penalties of 5 dB(A) and 10 dB(A) are usually given to the evening period and the night period, respectively. It can be used for noise mapping and refers normally to the most exposed facade, which incorporates a certain degree of exposure misclassification regarding cause–effect relationships. This weighted indicator was introduced to assess the relationship between sound level and noise annoyance (European Commission, 2002a). However, it may not be adequate for research into (somatic) health-related noise effects. Non-weighted separate exposure indicators, such as L_{day}, $L_{evening}$ or L_{night}, may be more appropriate when assessing physiological responses to the noise. In urban settings, night-time average noise levels (22.00–06.00) for road traffic tend to be approximately 7–10 dB(A) lower than daytime average noise levels – relatively independent (no freeways) of the traffic volume of the street (Utley, 1985; Ullrich, 1998; Evans et al., 2001). In such cases, L_{den} is approximately 2–3 dB(A) higher than L_{day} (Bite and Bite, 2004). Therefore, in epidemiological studies in which the relative effects of road traffic noise are studied, the sound emission during the daytime can as well be viewed as an approximate relative measure of the overall sound emission including the night. This seems to be further justified because existing noise regulations usually consider a 10 dB(A) difference between the day and the night. The NOAEL of 60 dB(A) for L_{day} corresponds, in this respect, with 50 dB(A) for L_{night}. This approximation can only be made with respect to road traffic noise.

Aircraft noise has been less intensively studied in noise epidemiology. The studies focused on high BP. Dose–response curves were hardly considered. A large European study on the association between aircraft noise and road traffic noise on BP is currently being conducted (Jarup et al., 2003). Regarding aircraft noise – and particularly the ongoing debate on night flight restrictions in the vicinity of busy airports – no other alternative exists at present than to take the myocardial infarction risk curves derived from road traffic noise studies as an approximate for aircraft noise. Since aircraft noise acts on all sides of a building, that is, different to road traffic noise, the suspicion exists that the effects induced by aircraft noise could be greater than those induced by road traffic (Ortscheid and Wende, 2000; Babisch, 2004a). This may be due to the lack of evasive possibilities within the home and the greater annoyance reactions to aircraft noise, which are usually expressed in social surveys (Miedema and Vos, 1998). More research is needed regarding the association between aircraft noise and cardiovascular end points.

This section is clearly focused on ill health as an outcome of the adverse effect of noise. A common dose-effect curve for the relationship between road traffic noise (outdoors) and the risk of myocardial infarction was developed. This curve can be used for a quantitative risk assessment and the calculation of attributable cases in a community. However, decisions regarding limit values have to be made within the spectrum between discomfort (annoyance) and ill health (disease) (Lindström, 1992; Babisch, 2002). Whereas quality targets at the lower end of the effects scale may be more flexible, quality targets at the upper end may be more obligatory. For example, for ethical reasons (equality principle) it does not seem to be justified if (ill) health-based limit values are varied according to the type of living area as expressed in land development plans (for example residential, mixed or commercial).

4.6 INSOMNIA

A group of Japanese researchers carried out a questionnaire-based survey of 3600 adult Japanese women (aged between 20 and 80) to gather information about the factors that contribute to insomnia (Kageyama et al., 1997). Some 11% of subjects were found to be affected by insomnia (as defined on the basis of WHO's International Statistical Classification and Related Health Problems, 10th revision – ICD10). Analysis of the survey data took account of various distorting variables, such as age, number of (small) children in the family, social status, receipt of medical treatment, regularity of bedtimes, apnoea-like problems and serious unpleasant experiences in the six months prior to completing the questionnaire. When the percentage of insomniacs in each of the three areas with the highest exposures was compared with the percentage in the low-exposure areas, the ratios worked out at, respectively, 1.4 (2100 vehicles per hour, L_{night} of around 65 dB(A)), 2.1 (2400 vehicles per hour, L_{night} of around 67 dB(A)) and 2.8 (6000 vehicles per hour, L_{night} of around 70 dB(A)). The most frequently reported problem was difficulty getting to sleep.

Research into the effects of exposure to air and road traffic noise has shown that increases in night-time noise exposure or in noise exposure during the sleep latency period have a statistically significant adverse impact on subjects' ability to get off to sleep and on sleep inception periods.

4.7 EFFECTS ON PERFORMANCE

4.7.1 COGNITION AND SWS

Jan Born and co-workers at the University of Lübeck (Wagner, Gais and Born, 2001; Benedict et al., 2004; Born and Wagner, 2004; Gais and Born, 2004; Drosopoulos, Wagner and Born, 2005) have reported interesting research and put forward intriguing hypotheses on the relation between noise exposure, sleep loss and subsequent cognitive performance. They conclude that declarative memory benefits mainly from sleep periods dominated by SWS, while there is no consistent benefit for this memory from periods rich in REM sleep. This points to the importance of SWS for declarative memory.

Since sleep in the early night is dominated by SWS, in contrast to late night when REM sleep dominates, this would imply that noise in the early night, for example aircraft noise before midnight, would be particularly damaging to memory and related cognitive functions. However, this implication has not yet been explicitly tested. That is, there seems to be a certain risk for impoverished memory due to noise in the early night, but there is as yet no graded quantification about whether ordinary pre-midnight noise levels around large airports are sufficient to make a difference to SWS. We also lack graded quantification about the relationship between impoverished SWS and the resulting effect on different aspects of declarative memory.

Thus, in terms of Fig. 1.1 we have evidence for the arrow marked (b), but we do not have enough information to say whether the strength of arrow (a) is sufficient to cause reduced SWS in field settings.

Furthermore, since children's memory systems pass through developmental changes and are not structured in the same way as for adults, it would be interesting to know to what extent the Born group results are also valid for children, and whether the depth of children's sleep counteracts or enhances SWS dominance in the early night.

4.7.2 COMPARING DAYTIME AND NIGHT-TIME NOISE EXPOSURE

As implied by Fig. 1.1, the relation between noise exposure and resulting effects on cognition should be analysed somewhat differently depending on whether the noise exposure takes place during the day or night. Analysing the cognitive effects of daytime noise exposure is fairly straightforward. For night-time noise exposure, however, any effects on cognition can either be a more or less direct effect of the noise exposure, or an indirect effect mediated by reduced sleep or sleep quality.

Also, comparing, for example, memory and learning functions when exposed to night-time noise, in contrast to daytime noise, shifts the focus of analysis away from encoding (in memory) or acquisition (in learning) while experiencing noise, to a focus on storing the material to be remembered or learnt while asleep (compare to daytime noise effects on cognition as reported by Hygge, Evans and Bullinger, 2002; Stansfeld et al., 2005). Thus, assuming that people are mainly asleep at night, all cognitive work that relies on the intake of information, listening or reading is not relevant. In all, this suggests that studies of daytime noise levels cannot be used much to give rough estimates of the effects of night-time exposure.

4.7.3 COMPARING CHILDREN AND ADULTS

How far can effects of daytime noise levels on children be generalized to give a rough estimate of the effects on adults? Are children more sensitive? Judging from earlier daytime studies of children and adults doing the same cognitive tasks while exposed to noise, children are not more sensitive than adults to noise (Boman, Enmarker and Hygge, 2004), but they perform at a lower level than the adults both in noisy and in quiet environments. Thus, it could be said that children are not more vulnerable to (daytime) noise in relation to cognitive performance, but since so much more cognitive work is expected from children while in school, their learning environment and their cognitive tasks can be said to be more noise vulnerable than corresponding environments for adults.

4.7.4 NOISE AND AFTER-EFFECTS

An argument can be made for noise as a stressor leading to reduced motivation (Glass and Singer, 1972), which in turn may act as a mediator of impaired cognitive performance. Along this line of reasoning, night-time noise may be more potent in inducing reduced motivation than daytime noise, but for the time being this is only a conjecture and has not been tested.

4.7.4.1 The role of restoration

Noise can be viewed both as a source of stressful demands and as a constraint on restoration. Noise levels and noise sources that are not by themselves particularly demanding during the waking hours of the day, may nevertheless be quite effective in blocking and constraining when they appear in periods meant to be restorative, such as sleep (Hartig, 2004). To what extent this idea is applicable to night-time noise exposure has not yet been explored.

4.7.4.2 Noise and communication

Some of the difficulties with children's responses to noise are related to problems in speech perception. A metric that weights night-time exposure more heavily is, in fact, less useful since children's auditory processing with parents and teachers is obviously more critical during waking hours.

4.8 EFFECTS ON PSYCHIC DISORDERS

Noise exposure at night may be more disturbing than daytime noise because it interferes with rest and sleep at a time when people want to relax. It seems plausible that night-time noise might have a particular effect on mental health. However, there is little direct research into night-time noise and mental health and it is first necessary to consider the evidence for environmental noise and mental health in general. The association between noise and mental health has been examined using a variety of outcomes including (at the simplest level) individual symptoms, as well as psychiatric hospital admission rates, use of health services and psychotropic medication, and community surveys.

4.8.1 TRANSPORTATION NOISE AND MENTAL HEALTH

Sources of transportation noise that have been studied in relation to mental health include road traffic noise and aircraft noise. Studies relating to each type of noise will be considered in turn.

4.8.1.1 Road traffic noise

The association between road traffic noise exposure and psychological distress has been studied in the small town of Caerphilly, South Wales. In the cross-sectional results, no association was found between the initial level of road traffic noise based on traffic noise maps, in terms of L_{eq} referring to the period 06.00–22.00, and minor psychological distress, measured by the General Health Questionnaire (GHQ), a screening questionnaire for depression and anxiety, even after adjustment for sociodemographic factors (Stansfeld et al, 1993). In longitudinal analyses in the Caerphilly Study, no association was found between road traffic noise and psychological distress, even after adjustment for sociodemographic factors and baseline psychological distress, although there was a small non-linear association of noise with increased anxiety scores (Stansfeld et al, 1996).

The disadvantage of the Caerphilly study is that it relied on one location with not very high levels of traffic noise. In a secondary analysis of a large British road traffic noise study, which took into account multiple noise exposure sites, the noise level in dB(A) exceeded for 10% of the time was weakly associated with a mental health symptoms scale of five items adjusting for age, sex, income and length of residence (Halpern, 1995). Weaker associations between traffic density and the mental health symptoms scale may relate to the skewed distribution of this traffic density variable. It seemed that traffic noise was more important than traffic flow. The scale used included some clear mental health items but also some that were less obviously related to mental health. It may be questioned whether the reported association between noise level and mental health symptoms was actually due to noise exposure; adjustment for the amount of "noise heard" reduced the association very little, suggesting no causal association with noise, but it is likely that there was a good deal of error in the measurement of this variable, reducing its validity.

It may be that the peak noise level is a better indicator of environmental noise heard indoors than noise measures averaged over time and that peak levels are a crucial indicator for mental health. Furthermore, in a road traffic noise study in Belgrade, 253 residents exposed to road traffic noise levels of >65dB(A), with high levels both day and night (L_{eq} 76.5 in the day, 69.5 at night in the noise-exposed area), experienced significantly more fatigue, depression, nervousness and headaches, compared to residents exposed to <55dB(A) (Belojevic and Jakovljevic, 1997). Sleep quality was also found to be worse among the inhabitants of noisy streets, compared to inhabitants of quiet streets, and those living in noisy streets had more difficulties falling asleep, more night awakenings and more pronounced tiredness after sleep. However, there were no differences in time taken to fall asleep or to go back to sleep, duration of sleep or consumption of sleeping pills between noise-exposed and non-exposed residents. A great methodological advantage of this study was that the high and low noise exposure areas were homogenous for age, sex, employment and subjective noise sensitivity. A community study in 366 Japanese women suggests that road traffic noise only has effects on depression, fatigue and irritability above a threshold of 70 dB(A) (Yoshida et al., 1997). However, it is difficult to be confident of the results of these analyses as they were unadjusted for age or social deprivation. Milder psychological states such as health functioning and well-being have also been examined in the first stage of an intervention study on the effect of introducing a bypass to relieve traffic congestion in a small town in North Wales (Stansfeld, Haines and Brown, 2000). Health functioning was measured by the SF-36 General Health Survey (Ware and Sherbourne, 1992), including dimensions of general health status, physical functioning, general mental health and social functioning. Ninety-eight respondents were studied who lived on a busy high street with traffic noise levels varying between 72 and 75 dBA outdoor L_{eq}. These respondents were compared with 239 control subjects living in adjacent quieter streets (noise level 55–63 dB(A) outdoor L_{eq}). Although subjects were well-matched on age, sex, housing insulation, car ownership and employment status, they were not so well-matched on proportion of manual workers, household crowding, deprivation and home ownership. There was no evidence that respondents exposed to higher levels of road traffic noise had worse health functioning than those exposed to lower levels of the noise, adjusting for levels of deprivation.

Another method of assessing mental health effects related to noise exposure is to use an indirect indicator such as medication use. In five rural Austrian communities exposed to road traffic noise, noise levels above 55 dB(A), including increasing night-time exposure to noise from trucks, were associated with increased risk of taking sleeping tablets (OR = 2.22 [CI: 1.13–4.38]) and overall prescriptions (OR = 3.65 [CI: 2.13–6.26]) relative to road traffic noise exposure less than 55 dB(A) (Lercher, 1996). This suggested effects at fairly low noise levels. In this case mental ill health may be secondary to sleep disturbance, which is likely to occur at lower nocturnal noise levels than mental health symptoms resulting from daytime noise exposure. As this occurred in a rural setting where road traffic was the predominant source of noise it would be interesting to replicate these findings in other settings.

4.8.1.2 Road traffic noise and mental health in children

Noise exposure and mental health has also been studied in children where child self-reported mental health on a standard scale and teacher ratings of classroom adjustment in response to motorway, road and rail noise were measured in a large sample of 8–11-year-old Austrian primary school children and in a second stage sample of extreme noise-exposed groups. Noise exposure was significantly associated with classroom adjustment scores but, intriguingly, child self-reported mental ill health was only impaired in noisy settings for children of low birth weight and preterm birth (Lercher et al., 2002).

4.8.1.3 Aircraft noise

Community surveys have found that high percentages of people reported "headaches", "restless nights", and "being tense and edgy" in high aircraft noise areas (Kokokusha, 1973; Finke et al., 1974; Öhrström, 1989). An explicit link between aircraft noise and symptoms emerging in such studies raises the possibility of a bias towards over-reporting of symptoms (Barker and Tarnopolsky, 1978). Notably, a study around three Swiss airports (Grandjean et al., 1973), did not mention that it was related to aircraft noise and did not find any association between the level of exposure to aircraft noise and symptoms. In the West London Survey, "tinnitus", "burns, cuts and minor accidents", "ear problems" and "skin troubles" were all more common in areas of high noise exposure (Tarnopolsky, Watkins and Hand, 1980). Acute symptoms such as "depression", "irritability", "difficulty getting off to sleep", "night waking", "skin troubles", "swollen ankles" and "burns, cuts and minor accidents" were particularly common in high noise areas. However, apart from "ear problems" and "tinnitus", 20 out of 23 chronic symptoms were more common in low noise environments. Symptoms did not increase with increasing levels of noise. This is possibly related both to more social disadvantage and associated ill health among residents in low aircraft noise exposure areas and the possible unwillingness of chronically unhealthy individuals to move into potentially stressful high noise exposure areas. Nevertheless, it would not exclude an effect of noise in causing some acute psychological symptoms. As the majority of aircraft noise exposure is during the day, daytime exposure is likely to have greater effects than nighttime exposure. Many of the effects of noise in industrial and teaching settings may be related primarily to disturbances in communication.

4.8.2 NOISE EXPOSURE AND MENTAL HOSPITAL ADMISSION RATES

Much of the concern with the possible effects of noise on mental health began with the study of admissions to psychiatric hospitals from noisy areas. Early studies found associations between the level of aircraft noise and psychiatric hospital admissions, both in London (Abey Wickrama et al., 1969) and Los Angeles (Meecham and Smith, 1977). These results have been criticized on methodological grounds (Chowns, 1970; Frerichs, Beeman and Coulson, 1980) and a replication study by Gattoni and Tarnopolsky (1973) failed to confirm these findings. Jenkins et al., (1979) found that age-standardized admission rates to a London psychiatric hospital over four years were higher as the level of noise of an area decreased, but lower noise areas were also central urban districts, where high admission rates would be expected. In a further extensive study of three hospitals (Jenkins, Tarnopolsky and Hand, 1981), high aircraft noise was associated with higher admission rates in two hospitals, but in all three of them, admission rates seemed to follow non-noise factors more closely; the effect of noise, if any, could only be moderating that of other causal variables but not overriding them. Kryter (1990), in a re-analysis of the data, found "a more consistently positive relation between level of exposure to aircraft noise and admissions rates". Undoubtedly, the route to hospital admission is influenced by many psychosocial variables that are more potent than exposure to noise. Therefore, whether or not noise causes psychiatric disorder is more suitably answered by studying a community sample.

4.8.3 NOISE EXPOSURE AND PSYCHIATRIC MORBIDITY IN THE COMMUNITY

In a community pilot study carried out in West London, Tarnopolsky et al. (1978) found no association between aircraft noise exposure and either GHQ scores (Goldberg, 1972) (dichotomized 4/5, low scorers/high scorers) or estimated psychiatric cases (Goldberg et al., 1970). This was the case even when exposure to road traffic noise was controlled, except in three subgroups: persons "aged 15–44 of high education" (41%, 14% $p<0.05$), "women aged 15–44" (30%, 13% n.s.), and those in "professional or managerial occupations". The authors expressed the guarded opinion that noise might have an effect in causing morbidity within certain vulnerable subgroups. In the subsequent West London Survey of Psychiatric Morbidity (Tarnopolsky, Morton-Williams and Barker, 1980), 5885 adults were randomly selected from within four aircraft noise zones, according to the Noise and Number Index. No overall relationship was found between aircraft noise and the prevalence of psychiatric morbidity either for GHQ scores or for estimated numbers of psychiatric cases, using various indices of noise exposure. However, there was an association between noise and psychiatric morbidity in two subgroups: "finished full-time education at age 19 years +", and "professionals". These two categories, which had a strong association with each other, were combined and then showed a significant association between noise and psychiatric morbidity ($X2 = 8.18$, df 3 $p<0.05$), but only for the proportion of high GHQ scorers. Tarnopolsky, Morton-Williams and Barker (1980) concluded that their results "show so far that noise per se in the community at large, does not seem to be a frequent, severe, pathogenic factor in causing mental illness but that it is associated with symptomatic response in selected subgroups of the population".

More recent studies have examined the effects of higher levels of military aircraft noise. Exposure to higher levels of military aircraft noise around the busy Kadena military airport in Japan was related in an exposure–effect association to depressiveness and nervousness measured by questionnaire using the Todai Health Index, based on the Cornell Medical Index (Ito et al., 1994; Hiramatsu et al., 1997). Mental health subscales included in this study measured depressiveness, nervousness, neurosis, and mental instability. Noise level was expressed as WECPNL (the power average of the maximum perceived noise exposure level in dB(A)) from 75–79, 80–84, 85–89, 90–94 and over 95). In unadjusted analyses, statistically significant differences were found in scores of depressiveness, nervousness and neurosis between the non-noise exposed control group and the pooled group exposed to 75–95 WECPNL. In multivariate analysis adjusting for age, sex, marital status, type of house and length of residence, noise exposure greater than 95 WECPNL was associated with higher scores on depressiveness and neurosis (Hiramatsu et al., 1997). Clear exposure–effect relationships were not found between scale scores and noise exposure, as expressed in five unit steps. However, using more broadly defined groups, an exposure–effect association was evident. This highlighted differences between the highest noise exposure group and lower exposure groups and indicated a threshold effect rather than a linear relationship – that mental health effects are more likely to be found at higher noise levels. In general, psychological rather than somatic symptoms were more related to noise in this study. Further analyses of the Japanese studies suggest that high levels of military aircraft noise may have effects on mental health. In a cross-sectional study of 5963 inhabitants around two air bases in Okinawa, those exposed to noise levels of L_{dn} 70 or above had higher rates of "mental instability" and depressiveness (Hiramatsu et al., 2000). Those who were more annoyed showed a higher risk of mental or somatic symptoms. A further survey using similar methodology on 6486 respondents found exposure–effect associations between aircraft noise exposure, nervousness and mental health (Miyakita et al., 1998). These are important studies because of the opportunity to examine the effect of high noise-exposure levels and the probability that vulnerable people migrating out of noisy areas and thus biasing the sample was small.

The use of health services has also been taken as a measure of the relationship between noise and psychiatric disorder. Grandjean et al. (1973) reported that the proportion of the Swiss population taking drugs was higher in areas with high levels of aircraft noise and Knipschild and Oudshoorn (1977) found that the purchase of sleeping pills, antacids, sedatives and antihypertensive drugs all increased in a village newly exposed to aircraft noise, but not in a "control" village where the noise level remained unchanged. In both studies, there was also an association between the rate of contact with general practitioners and level of noise exposure. In the Heathrow study (Watkins, Tarnopolsky and Jenkins, 1981), various health care indicators were used – use of drugs, particularly psychiatric or self-prescribed, visits to the GP, attendance at hospital, and contact with various community services – but none of these showed any clear trend in relation to levels of noise. A recent study found that the use of sleeping tablets and sedatives was elevated with increasing night-time noise exposure, especially in the elderly (Passchier-Vermeer et al., 2002). This has been judged to be "sufficient" evidence of a noise effect (Health Council of the Netherlands, 2004).

4.8.4 AIRCRAFT NOISE EXPOSURE AND MENTAL HEALTH IN CHILDREN

Poustka, Eckermann and Schmeck (1992) studied the psychiatric and psychosomatic health of 1636 children aged 4–16 in two geographical regions that differed according to the noise made by jet fighters frequently exercising at low altitude. Psychological and neurological outcomes were not related to noise exposure. They found that associations between noise exposure and depression and anxiety could be demonstrated, but only beneath the threshold of clinical significance. These results are less convincing because the areas differed socioeconomically and the results were not adjusted for these factors and also because of lack of precision of the measures of noise exposure. However, in Munich, children living in areas exposed to high aircraft noise had lower levels of psychological well-being than children living in quieter environments (Evans, Hygge and Bullinger, 1995). The longitudinal data from around Munich showed that after the inauguration of the new airport, the newly noise-exposed communities demonstrated a significant decline in self-reported quality of life measured on the Kindl scale, after being exposed to the increased aircraft noise for 18 months (third wave of testing), compared with a control sample (Evans, Bullinger and Hygge, 1998). Impairment of "quality of life" is a less severe disturbance than impairment of mental health. Further studies have examined the effects of noise on child psychiatric disorders.

Chronic aircraft noise exposure was not associated with anxiety and depression (measured with psychometrically valid scales), after adjustment for socioeconomic factors, in the Schools Health and Environment Study around Heathrow Airport (Haines et al., 2001a). In a further larger study of children's health around Heathrow Airport – the West London Schools Study (Haines et al., 2001b) – an association was found between aircraft noise exposure level and increased hyperactivity scores on the hyperactivity subscale of the Strength and Difficulties Questionnaire (Goodman, 1997). These studies suggest that noise influences child mental health in terms of hyperactivity and that it may affect child stress responses and sense of well-being.

4.8.5 NEIGHBOURHOOD NOISE AND MENTAL HEALTH

Noise from neighbours is the commonest source of noise complaints to local authorities in the United Kingdom (Chartered Institute of Environmental Health, 1999). Noise which is continuous, apparently indefinite, of uncertain cause or source, emotive or frightening or apparently due to thoughtlessness or lack of consideration is most likely to elicit an adverse reaction (Grimwood, 1993). In the 1991 BRE survey, people most objected to barking dogs, banging doors, noise from radio, television, or hi-fi and human voices (Grimwood, 1993). In this survey, two types of emotional response to noise were observed: outwardly directed aggression, characterized by feelings of annoyance, aggravation, bitterness and anger towards the source of the noise, and a more emotional response of tension, anxiety and feelings of pressure. These responses are reminiscent of the distinction between internalizing and externalizing disorders. Whether noise from neighbours can induce psychiatric disorder has been little studied in community research, but this is an area that deserves further study (Stansfeld, Haines and Brown, 2000).

Undoubtedly, prolonged exposure to noise can be very upsetting, intrusive and interfering for sleep and everyday activities. In poorly built dwellings, especially apartments, even low intensity noises may be clearly audible through walls, floors, or ceilings (Raw and Oseland, 1991). In this situation, noise is destructive of privacy, especially for those living alone, and may be associated with perceptions of threat or increase a sense of isolation. This may be especially the case among people who are chronically anxious and likely to complain of sensitivity to noise; prolonged noise exposure may make them more anxious and unhappy. Often, this leads to arguments with neighbours, leading to a breakdown of neighbourly relationships and further isolation which may well in itself have a bad effect on mental health. Occasionally, this may be a sign of feelings of persecution associated with psychotic illness in which noise exposure is just an external trigger of an internally generated condition.

4.8.6 MECHANISMS FOR CAUSAL LINKS BETWEEN NOISE AND MENTAL HEALTH

What might the mechanism be for the effects of noise on mental health? One way to approach this is through the effects of noise on cognitive performance where the laboratory evidence of effects is fairly robust (Smith and Broadbent, 1992). Effects of noise on mental health might be expected because there is evidence that noise impairs other aspects of human functioning, such as performance (Loeb, 1986) and sleep, that are important in maintaining normal functioning, and that noise causes adverse emotional reactions such as annoyance. In general, it seems that noise exposure increases arousal, and decreases attention through distraction (Broadbent, 1953), increases the need for focusing attention to cut out irrelevant stimuli (Cohen and Spacapan, 1978), as well as altering choice of task strategy (Smith and Broadbent, 1981). Even relatively low levels of noise may have subtle ill effects, and in this respect, the state of the person at the time of performance may be as important as the noise itself (Broadbent, 1983). Individuals' perception of their degree of control over noise may also influence whether it impairs memory (Willner and Neiva, 1986) while perception of lack of control over environmental conditions may be an important mediator of health effects.

Additionally, noise may also affect social performance as: (1) a stressor causing unwanted aversive changes in affective state; (2) by masking speech and impairing communication; and (3) by distracting attention from relevant cues in the immediate social environment (Jones, Chapman and Auburn, 1981). It may be that people whose performance strategies are already limited for other reasons (for instance through high anxiety) and who are faced with multiple tasks may be more vulnerable to the masking and distracting effects of noise.

The mechanism for the effects of noise on health is generally conceptualized as fitting the stress–diathesis model, in which noise exposure increases arousal, and chronic exposure leads to chronic physiological change and subsequent health effects. It is not clear, however, whether this model is appropriate for mental health effects. A more sophisticated model (Biesiot, Pulles and Stewart, 1989; Passchier-Vermeer, 1993) incorporates the interaction between the person and their environment. In this model, the person readjusts their behaviour in noisy conditions to reduce exposure. An important addition is the inclusion of the appraisal of noise (in terms of danger, loss of quality, meaning of the noise, challenges for environmental control, etc.) and coping (the ability to alter behaviour to deal with the stressor). This model emphasizes that dealing with noise is an active not a passive process.

4.8.7 HABITUATION TO NOISE AND MENTAL HEALTH

It is likely that mental health effects arise from persistent exposure to noise over a long period of time. But do people habituate or adapt to noise over time? In some studies people do seem to adapt to noise and no longer notice noise that they are frequently exposed to. On the other hand, in some studies of annoyance there seems to be little evidence of adaptation (Cohen and Weinstein, 1981). It may be that, as in physiological studies, a failure of adaptation occurs if the stimulus is novel, salient or implies threat. The development of mental health symptoms implies a failure to habituate to noise, or at least to adapt to noise. In some studies control over noise or active coping with noise rather than passive emotion-focused coping is related to lower levels of symptom (van Kamp, 1990). Habituation has not been formally studied in relation to noise and mental health.

4.8.8 RISK GROUPS FOR MENTAL HEALTH EFFECTS FROM NOISE

One way to look at susceptibility to noise is to think about groups in the population who may be more susceptible to noise, for instance people with existing physical or mental illness tend to be more highly annoyed by noise and potentially could be vulnerable to mental health effects. Similarly, people with hearing impairment may be vulnerable to communication difficulties in noisy environments that could increase the risk of mental health symptoms. People who report that they are sensitive to noise tend to be more prone to noise annoyance and may be more at risk for common mental disorders (Stansfeld et al., 2002).

4.8.9 POPULATION GROUPS AT RISK FOR MENTAL HEALTH EFFECTS FROM NOISE

There is some evidence that children are more vulnerable to the mental health effects of noise than adults in terms of prematurity, low birth weight and through scoring higher on hyperactivity. There is no consistent evidence of age, social class, ethnic or gender differences in susceptibility to mental health effects from environmental noise.

4.8.10 NOISE SENSITIVITY

Noise sensitivity, based on attitudes to noise in general (Anderson, 1971; Stansfeld, 1992), is an intervening variable which explains much of the variance between exposure and individual annoyance responses (Weinstein, 1978; Langdon, Buller and

Scholes, 1981; Fields, 1993). Individuals who are noise-sensitive are also likely to be sensitive to other aspects of the environment (Broadbent, 1972; Weinstein, 1978; Thomas and Jones, 1982; Stansfeld et al., 1985a). This raises the question as to whether noise-sensitive individuals are simply those who complain more about their environment. Certainly, there is an association between noise sensitivity and neuroticism (Thomas and Jones, 1982; Öhrström, Bjorkman and Rylander, 1988; Jelinkova, 1988; Belojevic and Jakovljevic, 1997; Smith, 2003), although it has not been found in all studies (Broadbent, 1972). On the other hand, Weinstein (1980) hypothesized that noise sensitivity is part of a critical/uncritical dimension, showing the same association as noise sensitivity to measures of noise, privacy, air pollution and neighbourhood reactions. He suggested that the most critical subjects, including noise-sensitive people are not uniformly negative about their environment, but more discriminating than the uncritical group, who comment uniformly on their environment.

Noise sensitivity has also been related to current psychiatric disorder (Bennett, 1945; Tarnopolsky, Morton-Williams and Barker, 1980; Iwata, 1984). Stansfeld et al. (1985) found that high noise sensitivity was particularly associated with phobic disorders and neurotic depression, measured by the Present State Examination (Wing, Cooper and Sartorius, 1974). Similar to this association with phobic symptoms, noise sensitivity has also been linked to a coping style based on avoidance, which may have adverse health consequences (Pulles, Biesiot and Stewart, 1988) and a tendency to report health complaints rather than take a more active coping approach to noise (Lercher and Kofler, 1996). Noise sensitivity may be partly secondary to psychiatric disorder: depressed patients followed over four months became less noise-sensitive as they recovered (Stansfeld, 1992). These "subjective" psychological measurements were complemented by an "objective" psychophysiological laboratory investigation of reactions to noise in a subsample of depressed patients. Noise-sensitive people tended to have higher levels of tonic physiological arousal, more phobic and defence/startle responses and slower habituation to noise (Stansfeld, 1992). Thus, noise-sensitive people attend more to noises, discriminate more between noises, find noises more threatening and out of their control, and adapt to noises more slowly than people who are less sensitive. Through its association with greater perception of environmental threat and its links with negative affectivity and physiological arousal, noise sensitivity may be an indicator of vulnerability to minor psychiatric disorder, although not necessarily psychiatric disorder caused by noise (Stansfeld, 1992).

In analysis of a subset of noise-sensitive women, compared to less sensitive women in the West London survey, there was no evidence that aircraft noise exposure predicted psychiatric disorder in the sensitive women (Stansfeld et al., 1985). In the Caerphilly study, noise sensitivity predicted psychological distress at follow-up after adjusting for baseline psychological distress, but did not interact with the noise level, suggesting that noise sensitivity does not specifically moderate the effect of noise on psychological distress (Stansfeld et al., 1993). However, in further analyses, a statistically significant association between road traffic noise exposure and psychological distress, measured by the General Health Questionnaire (GHQ), was found in noise-sensitive men, that was not found in men of low noise sensitivity (Stansfeld et al., 2002). In the original analyses, after adjusting for trait anxiety at baseline, the effect of noise sensitivity was no longer statistically significant. This suggests that much of the association between noise sensitivity and psychological distress may be accounted for by the confounding association with trait anxiety. Constitutionally anxious people may be both more aware of threatening aspects of their environment and more prone to future psychiatric disorder. It seems possible that these traits might be linked.

In a United Kingdom community study, associations were examined between noise exposure, noise sensitivity, subjective symptoms and sleep disturbance in a random sample of 543 adults (Smith, 2003). Perceived noise exposure was related to subjective health, but this association became non-significant after adjustment for negative affectivity. In a similar way, adjustment for negative affectivity eliminated the association between noise sensitivity and subjective health. Thus, it was suggested that noise sensitivity was merely a proxy measure of negative affectivity or neuroticism. However, although this means that noise sensitivity is not specific to noise, the more recent analyses suggest that high levels of trait anxiety or neuroticism may be an indicator of vulnerability to noise effects and could put people at risk of adverse psychological effects from noise, even if they do not increase the risk of physical ill health.

4.8.11 MENTAL HEALTH CONSEQUENCES OF INSOMNIA

Transient insomnia is usually accompanied by reports of daytime sleepiness and performance impairment the next day. Chronic insomnia is generally associated with poorer emotional and physical health. Several large-scale epidemiological studies of the general adult population have shown that between one third and one half of people who complain of chronic insomnia are also diagnosable with primary psychiatric disorders, mostly anxiety and mood disorders. Mellinger, Balter and Uhlenhuth (1985) found that 17% of adults reported "a lot" of trouble falling asleep or staying asleep over the past year; 47% of them had high levels of psychological distress, with symptom complexes suggestive of depression and anxiety disorders. In contrast, only 11% of individuals with no history of insomnia showed elevated levels of psychiatric symptoms. In a survey of almost 8000 individuals, Ford and Kamerow (1989) reported that 10% had suffered from significant insomnia for at least a two-week period during the previous six months; 40% of the insomniacs met criteria for psychiatric disorders, with the majority being anxiety disorders and depression; only 16% of those with no sleep complaints had psychiatric illness.

Breslau et al. (1996) found a strong correlation between lifetime prevalence of sleep problems and psychiatric disorders, with anxiety, depression, and substance abuse disorders being the most common. Similar results have been found by Vollrath, Wicki and Angst (1989), Chang et al. (1997) and Dryman and Eaton (1991). In a large-scale European population-based study (Ohayon and Roth, 2003), it was found that insomnia more often precedes rather than follows incident cases of mood disorders.

Insomniacs not only have higher rates of psychiatric disorders, but they also have increased rates of various kinds of psychological symptoms: patients with insomnia reported increased psychological stress and/or decreased ability to cope with stress according to surveys of the American (Roth and Ancoli-Israel, 1999) and Japanese (Kim et al., 2000) population. Almost 80% of insomniacs had a significant increase on one or more clinical scales on the Minnesota Multiphasic Personality Inventory (MMPI) (Kalogjera-Sackellares and Cartwright, 1997). Even people whose insomnia was due to identified medical factors showed elevation on the MMPI, suggesting a possible causal relationship or specific association between insomnia and psychiatric symptomatology. Compared to good sleepers, severe insomniacs reported more medical problems, had more GP office visits, were hospitalized twice as often and used more medication. Severe insomniacs had a higher rate of absenteeism, missing work twice as often as did good sleepers. They also had more problems at work (including decreased concentration, difficulty performing duties and more work-related accidents) (Leger et al., 2002).

4.8.12 INSOMNIA AS A MENTAL HEALTH SYMPTOM

Insomnia is a symptom of many psychiatric disorders, especially depression and anxiety. In studies of depressed patients compared to control subjects, there was prolonged latency to sleep, increased wakefulness during sleep, early morning wakening, decreased sleep efficiency and reduced total sleep time. There is also evidence that insomnia may be a risk factor for developing depression (Riemann, Berger and Voderholzer, 2001; Roberts, Roberts and Chen, 2002). This raises the question as to whether prolonged noise exposure leading to insomnia provokes the onset of depression in susceptible people? This seems theoretically possible, but there is little evidence to support it. In a longitudinal study of adolescents, it was the other way round – that depressive symptoms preceded the onset of insomnia (Patton et al, 2000). Delayed sleep latency in children has been linked to increased externalizing symptoms including aggressive behaviour, and impaired attention and social problems (Aronen et al., 2000). In this cross-sectional study, the direction of association was uncertain, but it seems most plausible that the sleep disturbance is a feature of the behavioural disturbance rather than a cause of it. Three criteria have been suggested for sleep disturbance to be environmentally determined: (1) the sleep problem is temporally associated with the introduction of a physically measurable stimulus or definable set of environmental circumstances; (2) the physical rather than the psychological properties of the environmental factors are the critical causative elements; and (3) removal of the responsible factors results in an immediate or gradual return to normal sleep and wakefulness (Kraenz et al., 2004). Most studies do not fulfil these criteria. In a German school-based study of 5–6-year-old children, sleep disturbance by noise, largely from road traffic, was reported "sometimes" in 10% by parents of children and 2% "often". Children's reports were slightly higher: "sometimes" in 12% and 3% "often" (Kraenz et al., 2004). Further longitudinal research is needed to ascertain whether noise-induced insomnia leads on to overt psychiatric disorder.

In summary, population as well as clinic-based studies have demonstrated a high rate of psychiatric morbidities in patients with chronic insomnia. It has traditionally been assumed that insomnia is secondary to the psychiatric disorders; however, it is possible that in some cases the insomnia preceded the psychiatric disorder.

4.8.13 DEPRESSIVE EPISODE AND ANXIETY DISORDERS

A mild depressive episode is diagnosed by clinical interview. The criteria for a mild depressive episode include two or more symptoms of depressed mood, loss of interest or fatigue lasting at least two weeks, with two or three symptoms such as reduced concentration, reduced self-esteem, ideas of guilt, pessimism about the future, suicidal ideas or acts, disturbed sleep, diminished appetite and social impairment, and fewer than four symptoms including lack of normal pleasure/interest, loss of normal emotional reactivity, waking =>2 hours early, loss of libido, diurnal variation in mood, diminished appetite, loss of =>5% body weight, psychomotor agitation or psychomotor retardation.

Anxiety disorders are similarly diagnosed by clinical interview. The criteria for "generalized anxiety disorders" include duration of at least six months of free-floating anxiety and autonomic overactivity.

4.8.14 ASSOCIATIONS BETWEEN INSOMNIA AND PSYCHIATRIC DISORDERS

At the present time, exposure–effect associations have not been established between parameters of sleep disturbance (number of behavioural awakenings, body movements or EEG awakenings) and the onset of depressive and anxiety disorders, although there is some evidence that insomnia is a risk factor for developing depression (Riemann, Berger and Voderholzer, 2001; Roberts, Roberts and Chen, 2002). A number of longitudinal prospective studies in different age groups have found associations between self-reports of insomnia and the subsequent onset of psychiatric disorder, in particular major depression. A selection of the most important studies and their findings are outlined in Table 4.3 below.

Table 4.3 Insomnia as a predictor of psychiatric disorder

Study	Sample size	Sample	Follow-up interval	Depression measure	Results
Ford and Kamerow, 1989	7954	Community sample	1 year	Diagnostic interview schedule	Risk of developing new depression for insomnia on two occasions: [OR=39.8, 95% CI 19.8-80.0]
Breslau et al., 1996	1200	21–30 years members of health maintenance organization	3 years	Diagnostic interview schedule	RR for new onset major depression associated with baseline insomnia [RR=4.0, 95% CI 1.5-5.6]
Chang et al., 1997	1053	Male medical students	34 years (median)	Clinical depression	RR for clinical depression for those who reported insomnia at medical school [RR= 2.0, 95% CI 1.2-3.3]
Roberts, Roberts and Chen, 2002	3136	11–17 years from managed care rosters	1 year	Diagnostic interview schedule for children major depression module	Fully adjusted OR for insomnia in waves 1 and 2 for depression at follow-up [OR=1.92, 95% CI 1.30-2.82]

4.8.15 CONCLUSIONS: ASSOCIATIONS BETWEEN NOISE AND PSYCHIATRIC DISORDERS

The effects of noise are strongest for those outcomes that, like annoyance, can be classified under "quality of life" rather than illness. What they lack in severity is made up for in numbers of people affected, as these responses are very widespread.

Current evidence does seem to suggest that environmental noise exposure, especially at higher levels, is related to mental health symptoms and possibly raised anxiety and consumption of sedative medication, but there is little evidence that it has more serious effects. Further research is needed on mental health effects at very high noise levels. Existing studies may be confounded either by prior selection of subjects out of (or into) noisy areas as a result of noise exposure, or by confounding between noise exposure, socioeconomic deprivation, and psychiatric disorder. It is also possible that people underestimate or minimize the effects of noise on health through optimism bias (Hatfield and Soames Job, 2001) and that this is particularly protective for mental health.

The evidence is not strong for the association between noise exposure and mental ill health. What evidence there is suggests that noise exposure may be responsible for psychological symptoms above 70 dB(A) L_{eq}. Almost all studies have only examined the effects of daytime noise on mental health, but it is possible that night-time noise, during sleep time, may have effects on mental health at lower levels than daytime noise.

The most powerful evidence of noise on mental health comes from studies of military aircraft noise. There is also some evidence that intense road traffic noise may lead to psychological symptoms. There is no evidence of any effects of railway noise on mental health.

4.9 THE SEVERITY OF SELF-REPORTED SLEEP DISTURBANCE

4.9.1 INTRODUCTION

In section 2.1.2 of Chapter 2 of this report, it is stated that sleep disturbance caused by noise may either be diagnosed (Environmental Sleep Disorder: ICSD 780-52-6) or self-reported. Although self-reported sleep disturbance is subjective by definition, its observed occurrence correlates with noise levels as well as with important diagnostic criteria for ICSD 780-52-6. It appears justified to consider self-reported sleep disturbance as an impairment of health, especially if indicated by representative population samples in social surveys. Furthermore, section 4.1 of Chapter 4 of this report gives a quantitative relationship between noise level L_{night} and the percentage of population that reports a disturbed sleep of high, medium or low disturbance intensity.

But an open question concerns severity: even if night-time noise causes large percentages of the population to declare themselves as highly sleep-disturbed, this could nevertheless represent an almost negligible loss of health, if the mean severity of self-reported sleep disturbance were negligible in comparison with commonly accepted diseases. Attempts have been made to give an answer to this important question, using WHO's concept of disability weights (Murray et al., 1996) as a basis for severity comparisons.

4.9.2 AN ASSESSMENT OF DISABILITY WEIGHTS

A Swiss study (Müller-Wenk, 2002) aimed at determining a disability weight for sleep disturbance due to road traffic noise. For this purpose, a description of road-noise-related sleep disturbance was set up: essentially, this state of health was assumed to be present if a person indicated that, due to traffic noise, he or she, almost every night, had problems with falling asleep, with continuing sleep during the night or with early or non-restorative waking in the morning. In addition, a list was established with already available disability weights (Murray et al., 1996; Stouthard et al., 1997) for a selection of 28 diseases of various types, covering a range from very light severity to high severity (Müller-Wenk 2002:65–66). All 64 members of the medical staff of the Swiss Accident Insurance Institute (SUVA) were then asked in a written questionnaire to determine the hitherto unknown disability weight of sleep disturbance by interpolation, that is, by inserting sleep disturbance at the appropriate place between the presented 28 diseases that were sorted according to ascending disability weight. These participants were chosen because the physicians of the SUVA, besides being medical doctors, have a particularly high professional know-how in comparing the severity of different types of disability. Forty-two questionnaires were completed, of which 41 were usable.

From these questionnaires, an arithmetical mean of 0.055 of the disability weight for sleep disturbance could be calculated, with a 95% confidence limit of 0.039 at the low end and 0.071 at the high end. This result can be illustrated by mentioning diseases from the catalogues of Murray et al. (1996) or Stouthard et al. (1997) with the same disability weight: hence the disability weight of the road-noise-related sleep disturbance is roughly the same as the disability weight of "chronic hepatitis B infection without active viral replication", the latter having a mean disability weight of 0.06 and a 95% confidence interval from 0.034 to 0.087. The low-end estimate of 0.039 for sleep disturbance severity would correspond to the mean disability weight of "benign prostatic hypertrophy (symptomatic cases)", whilst the high estimate of 0.071 would correspond to the mean disability weight of "uncomplicated diabetes mellitus". The conclusion is that the mean disability weight of road-noise-related sleep disturbance is not smaller (= less severe) than the disability weight of health impairments commonly recognized as diseases, and there is a strong overlap amongst the probability distributions of these disability weights. On the basis of the chosen disability weight 0.055 for self-reported sleep disturbance, and taking into account the current traffic noise levels during the night in many European states, it is justified to consider noise-related sleep disturbance as a substantial loss of public health.

4.9.3 COMPARISON BETWEEN INSOMNIA AND SELF-REPORTED SLEEP DISTURBANCE

The original list of disability weights (Murray et al., 1996) did not contain any kind of non-normal sleep. In the meantime, WHO has published an extended list (Mathers et al., 2003, Annex Table 5a) containing a disability weight of 0.100 for insomnia (diagnostic code 307.42). This has opened a way to recheck the disability weight of 0.055 (Müller-Wenk, 2002), by asking a panel of medical professionals to compare, on the basis of disability weights, the mean severity of self-declared sleep disturbance due to road noise at night with the mean severity of insomnia. It may be debated whether it is more straightforward to compare two types of sleep anomalies with similar symptoms, or to compare self-declared sleep disturbance with various types of completely different diseases. But it makes sense anyway to use the comparison with insomnia as a second approach for determining the disability weight of self-reported sleep disturbance.

This severity comparison between different sleep anomalies was made in 2005 by structured oral interviews, executed by a medical staff member of the sleep clinic of Kantonsspital St. Gallen (Switzerland), with 14 GPs selected at random from all GPs who had admitted patients to the sleep clinic during the nine preceding months. These patients were mainly suffering from OSAS. The question was as follows:

> "Could you please give us your opinion on the relative severity of three different cases of insomnia:
>
> 1. (primary) insomnia, in our region usually called psychophysiological insomnia
> 2. Obstructive Sleep Apnoea Syndrome (OSAS)
> 3. traffic-noise-related sleep disturbance, that may occur with persons who are forced to sleep along through roads with nocturnal motor traffic.
>
> Your opinion should be based on the patients you have seen in your office lately, or on other persons of your social environment. When comparing the severity of the health impairment, the focus should be above all on the person's condition during the day after the sleep-disturbed night. The absolute value of the severity is less important for the current study than the relative severity amongst the three cases of insomnia. The opinion of the severity may be expressed on a linear scale from 0 (no impairment at all) to 10 (impairment almost unsupportable). On the scale from 0 to 10, you may give us your mean value of the severity, or you may give us a span from a low to a high for the severity."

All of the interviewed GPs gave their opinions, and the result is presented in Table 4.4.

Table 4.4
Severity ratings (10 = almost insupportably disturbing, 0 = not in the least disturbing) by 14 GPs selected at random

	Primary insomnia				OSAS (sleep apnoea)				Sleep disturb.(noise)				Ratio noise/	Noise/
No	Max	Min	Mean	Rank	Max	Min	Mean	Rank	Max	Min	Mean	Rank	priminsomnia	OSAS
10	6	4	5	3	8	6	7	1	8	6	7	1	1.40	1.00
11	5	3	4	3	9	7	8	1	8	4	6	2	1.50	0.75
12			5	3			10	1	7	8	7.5	2	1.50	0.75
13	2	3	2.5	2	4	5	4.5	1	1	2	1.5	3	0.60	0.33
14			3	2			6	1	1	2	1.5	3	0.50	0.25
15			8	2			9	1			6	3	0.75	0.67
16			8	1			7	2			4	3	0.50	0.57
17			5	1			5	1			3	3	0.60	0.60
18	2	3	2.5	2			6	1	1	2	1.5	3	0.60	0.25
19			8	1			3	2			2	3	0.25	0.67
20			6	2			7	1			4	3	0.67	0.57
21			7	2			8	1			0	3	0.00	0.00
22			4	3			5	2			6	1	1.50	1.20
23			4	3	6	7	6.5	2	8	9	8.5	1	2.13	1.31
Mean			5.143	2.143			6.57	1.286			4.18	2.429	0.89	0.64
Sigma													0.60	
Median													0.63	
Upper value 95% C.I. for mean													1.20	
Lower value 95% C.I. for mean													0.58	

Clearly, the severity judgements vary widely between the participating GPs. Apart from the differences in personal judgement, this variation is certainly influenced by the mix of patients visiting a particular GP. For instance, GP number 15 could have encountered one or two very serious cases of OSAS, whilst his/her experience with noise-related sleep disturbance might refer to persons that were only moderately disturbed by night-time noise in their bedroom. On the other hand, number 22 could have had experience with persons suffering very much from sleep disturbance due to high traffic noise exposure, whilst his/her OSAS or primary insomnia patients happened to be light cases. One must accept that even GPs have a limited experience with the whole range of cases of each of the three types of insomnia, so that their opinion on the mean severity of noise-related sleep disturbance, compared to the mean severity of OSAS or insomnia, is influenced by the randomness of their patient mix.

Nevertheless, the table supports the following statements.

- With respect to severity, the majority of GPs rank noise-related sleep disturbance lower than insomnia and OSAS, while three of them put noise-related sleep disturbance in the first rank. Only one of the participants (number 21) considers noise-related sleep disturbance as a fully negligible disturbance.
- The severity ratio between noise-related sleep disturbance and insomnia varies between 0 and 2.1. Seven of the fourteen GPs indicate a severity ratio between 0.5 and 0.75, that is to say that half the participants are of the opinion that the severity of noise-related sleep disturbance amounts to 50–75% of the severity of insomnia.
- The mean of this severity ratio is 0.89, with a standard deviation (sigma) of 0.60. The confidence interval (CI) for the mean goes from 0.58 to 1.20. The median of the severity ratio is 0.63. The distribution is skewed to the right.

The severity ratio developed above can be used as a proportionality factor between the known disability weight for insomnia and the required disability weight for self-reported sleep disturbance. Bearing in mind that the already existing WHO disability weight for insomnia is 0.10, a best guess for the mean disability weight for self-reported sleep disturbance due to road traffic noise at night is therefore 0.089, with a CI from 0.058 to 0.12.

4.9.4 CONCLUSIONS

According to the two groups of interviewed medical professionals, persons that declare themselves to be chronically deprived of normal sleep by road traffic noise have a health state whose mean disability weight is comparable to "chronic hepatitis B infection without active viral replication" or higher. Irrespective of the question whether self-reported sleep disturbance is formally recognized as a disease or not, its severity is comparable to commonly accepted diseases.

The best estimate for a mean disability weight for self-reported sleep disturbance due to road traffic noise was 0.055 (CI: 0.039; 0.071) according to Müller-Wenk (2002), whilst our recheck based on a comparison with insomnia resulted in a disability weight of 0.09 (CI: 0.06; 0.12). The higher disability weight according to the second approach might be caused by the fact that in this second approach, there was a stronger focus on "the person's condition during the day after the sleep-disturbed night".

The above figures compare reasonably with a study published by van Kempen (1998), cited in Knol and Staatsen (2005:46), where a severity weight of 0.10 for severe sleep disturbance was found, based on the judgement of 13 medical experts according to the protocol of Stouthard et al. (1997).

In conclusion, a mean disability weight of 0.07 is proposed for self-reported sleep disturbance due to road noise or similar ambient noise. This disability weight can be used in connection with the equations of section 4.1 of this chapter for highly sleep-disturbed persons.

4.10 DISCUSSION: CAN CHRONIC SHORT-TERM EFFECTS CAUSE LONG-TERM EFFECTS ON HEALTH?

EEG modifications, cardiovascular responses, body movements and awakenings due to noise occur within a few seconds after the stimulus. In addition to the instantaneous effects related to single events, large field studies on aircraft (Passchier-Vermeer et al., 2002) and road traffic noise exposure during night-time (Griefahn et al., 2000; Passchier-Vermeer et al., 2004) show that also sleep latency and average motility during the sleep period increased monotonously as a function of the noise exposure level. The increase in average motility was substantially higher than would be expected on the basis of the instantaneous extra motility at the times of the noise events (Passchier-Vermeer et al., 2002) suggesting persistent arousal during the sleep related to aircraft noise. Furthermore, an international field study (Jurriëns et al., 1983) found slightly reduced REM sleep, increased time being awake according to the EEG, increased average heart rate, and reduced performance on a reaction time test in people when exposed during the night to higher road traffic noise levels.

The relationship between instantaneous effects and more global modifications of one night sleep, as well as chronic changes, is not simple, as illustrated by the findings concerning motility. An increase in average motility that is substantially higher than would be expected on the basis of the instantaneous extra motility at the times of the noise events (Passchier-Vermeer et al., 2002) suggests a persistent arousal during sleep related in a dose-dependent way to the aircraft noise.

Since EEG arousal and instantaneous motility are correlated, this finding suggests that also the number of (micro-)arousals may increase during noise exposure more than by the sum of the instantaneous (micro-)arousals that occur contingent upon a noise event.

For overall motility during sleep, clear indications have been found of associations with further effects, although the causal direction is not in all cases clear. Mean (onset of) motility during sleep is associated with the following variables based on questionnaires and diaries (Passchier-Vermeer et al., 2002):

- frequency of conscious awakening during the sleep period: the increase is 0.8 conscious;
- awakenings per night, if motility increases from low to high;
- frequency of awakening remembered next morning: the increase is 0.5 remembered;
- awakenings per night, if motility increases from low to high;
- long-term frequency of awakening attributed to specific noise sources assessed with a questionnaire;
- sleep quality reported in a morning diary;
- long-term sleep quality assessed with a questionnaire;

- number of sleep complaints assessed with a questionnaire;
- number of general health complaints assessed with a questionnaire.

The associations of mean motility with these variables are stronger than the corresponding associations of mean onset of motility.

For evaluating the adverseness of the instantaneous effects, it is important to consider whether they bring the body into a more persistent state of higher arousal or not, although this is not the only criterion. Those effects which are progressively disappearing with the repetition of the stimulus may be less harmful than those which do persist over long exposure time, provided that the suppression of the effects do not require costs in another form. For example, short-term cardiovascular effects that appear not to habituate could lead to permanent cardiovascular system impairment (Carter, 1996, 1998).

The relations presented for motility and conscious awakening imply that motility is sensitive to noise and has a relatively low threshold, while conscious awakening, the strongest instantaneous interference of noise with sleep, has the highest threshold of the instantaneous effects considered.

In one of the most sophisticated field studies (Passchier-Vermeer et al., 2002), increased probability of instantaneous motility was found for events with a maximum sound level $L_{Amax} > 32$ dB(A), while in a meta-analysis conscious awakening was found for events with $L_{Amax} > 42$ dB(A) (Passchier-Vermeer, 2003a). Above their threshold, these effects were found to increase monotonously as a function of the maximum sound level during a noise event (aircraft noise). It is important to note that in another recent sophisticated field study (Basner et al., 2004), the threshold found for EEG awakening was $L_{Amax} = 35$ dB(A), that is, only a little higher than the 32 dB(A) found for noise-induced awakenings. This strengthens the evidence that noise starts to induce arousals at L_{Amax} values in the range 30–35 dB(A). Given the night-time noise levels to which people are exposed, these results imply that instantaneous effects are common. Although most studies concerned aircraft noise, the instantaneous effects can be assumed to occur at similar levels for different types of transportation.

The above observations can be used as a basis for setting limits with respect to night-time transportation noise. For transparency, it is useful to distinguish two steps in choosing actual limits: the first step is the derivation of a health-based limit; the second step is the derivation of an actual limit that takes into account the health-based limit as well as feasibility arguments. Here the concern is with the first step.

When deriving a health-based limit, two points need to be considered: the dose-dependent effects of a single noise event, and the number of events. With respect to the dose-dependent effects of a single event, adverse effects can be distinguished from effects that by themselves need not be adverse but can contribute to an adverse state. It is proposed to classify conscious awakenings as an adverse effect. Conscious awakenings have been estimated to occur at a baseline rate of 1.8 awakening per night. A substantial increment of conscious awakenings over this baseline is thought to be adverse. Since, in general, falling asleep after conscious awakening takes some time, and this latency is longer after noise-induced conscious awakening that will often also induce an emotional reaction (anger, fear), it will also reduce the time asleep and may affect mood and functioning next day. Although additional, more sophisticated analyses could be performed to refine this estimate, we propose L_{Amax}

= 42 dB(A) is proposed as the currently best estimate of the threshold for conscious awakening by transportation noise. This would mean that the no observed effect level ($NOEL_{Amax}$) for transportation noise events is at most 42 dB(A).The most sensitive instantaneous effect that has been studied extensively in field studies is motility. A single interval with (onset of) noise-induced motility by itself cannot be considered to be adverse.

However, noise-induced motility is a sign of arousal, and frequent (micro-)arousal and accompanying sleep fragmentation can affect mood and functioning next day and lead to a lower rating of the sleep quality. Therefore, motility is relevant for adverse health effects, but more than a few intervals with noise-induced motility are needed for inducing such effects. Although additional, more sophisticated analyses could be performed to refine this estimate, we propose L_{Amax} = 32 dB(A) as the currently best estimate of the threshold for motility induced by transportation noise. The threshold found for EEG awakening was L_{Amax} = 35 dB(A), that is, only a little higher than the 32 dB(A) found for noise-induced awakenings. This would mean that the $NOEL_{Amax}$ for transportation noise events is most likely at most 32 dB(A), and definitely not higher than 35 dB(A). It is important to note that the above given $NOEL_{Amax}$ ~ 32 dB(A) and $NOEL_{Amax}$ ~ 42 dB(A) are indoor levels, in the sleeping room. Although events below 32 dB(A) are audible, and, hence, further research may show more sensitive effects than motility, on the basis of the present available evidence we propose to assume that $NOEL_{Amax}$ = 32 dB(A) and set a health-based night-time noise limit that is tolerant for transportation noise events with L_{Amax} ~ 32 dB(A). On the other hand, since adverse health effects need to be prevented by health-based limits and even though vulnerable groups may require lower limits, on the basis of the present available evidence we propose to assume that $NOAEL_{Amax}$ = 42 dB(A) and set a health-based night-time noise limit that does not tolerate transportation noise events with L_{Amax} > 42 dB(A).

On the basis of the above proposal, it would be possible to derive a night-time noise guideline value in terms of L_{night}. Such a guideline value would indicate the level below which no short-term effects are to be expected that would lead to temporary reduced health or chronic disease. Such a guideline value needs to be compared with guideline values derived directly with a view to preventing temporary reduced health and chronic diseases. In particular, for self-reported sleep disturbance, which is an expression of reduced well-being and may be an indication of effects that could contribute to cardiovascular disease, exposure–effect relationships have been derived on the basis of an extensive set of original data from studies from various countries (Miedema, Passchier-Vermeer and Vos, 2003; Miedema, 2004). The percentage of people reporting high noise-induced sleep disturbance (%HS) levels off at 45 dB(A) but at a non-zero effect level. The remaining effect may be caused by events not incorporated in the exposure assessment and it appears that if all noise contributions would be incorporated in the exposure metric, high noise-induced sleep disturbance would vanish between 40 dB(A) and 45 dB(A), say at 42 dB(A). Since values found for other temporary reduced health effects or chronic diseases, in particular cardiovascular diseases, will be higher, and considering self-reported sleep disturbance as an adverse effect, this would suggest L_{night} = 42 dB(A) as the NOAEL to be compared with the value derived from the short-term effects. Note that this is an outdoor level, which would, assuming partly opened windows and an actual insulation of 15 dB(A), correspond to an indoor equivalent night-time sound level of 27 dB(A). The above discussion is based on motility, EEG awakenings, and conscious awakening. In addition, EEG micro-/minor arousals, and autonomic reactions have been discussed above.

Furthermore, there are potential instantaneous effects, such as effects on memory consolidation or restoration of the immune system, for which the information on a possible relation with noise exposure is so limited that they were not considered here. In order to acquire more insight into these effects, more field research is needed. Field research is needed because earlier studies have shown that estimates of effects on the basis of laboratory studies are much higher than estimates from field studies. Methodological differences between the different approaches certainly cannot be the only possible explanation. Research allowing the introduction of some specific but light laboratory technique into the sleeper's own bedroom, should be encouraged, as, for example, used in the Swiss Noise Study 2000 (Brink, Müller, and Schierz, 2006). The key to better insight into effects of night-time noise, leading to mechanistic models describing the relationships between noise exposure, instantaneous effects, effects at the level of a 24-hour period and chronic effects, appears to be epidemiological studies at home with well-designed instrumentation.

The relationships between noise exposure, instantaneous effects, effects at the level of a single 24-hour period and chronic effects is complex because the effects at a smaller time scale do not simply add up to effects at a larger time scale. For example, the noise-related increase in night-time average motility was substantially higher than would be expected on the basis of the instantaneous extra motility at the times of the noise events (Passchier-Vermeer et al., 2002), suggesting persistent arousal during sleep related to aircraft noise. It is likely that such shifts in the basic state are more important for the development of chronic effects than the instantaneous effects per se. A further complication is that some effects habituate. Habituation in some effect parameters can occur in a few days or weeks, but the habituation is not always complete. The measured modifications of the cardiovascular functions remain unchanged over long periods of exposure time (Muzet and Ehrhart, 1980; Vallet et al., 1983). Most striking is that none of the cardiovascular responses show habituation to noise after a prolonged exposure, while subjective habituation occurs within a few days. It appears plausible that, in particular non-habituating effects lead to the development of chronic effects, but also the disappearance of effects with continuing exposure may come at a cost associated with suppressing the effects. A third complication is that daytime noise exposure may contribute to the effects found in relation to night-time noise. Large epidemiological studies are needed that compare populations exposed to similar daytime noise and differ in their night-time noise exposure only. A specific challenge for mechanistic models on the effects of noise on sleep is the identification of factors that make subjects vulnerable to night-time noise. The following groups may be hypothesized to be more vulnerable to noise during sleep: old people, ill people, people with chronic insomnia, shift workers and people resting during daytime, people with a tendency to depression, light sleepers, pregnant women, people with high anxiety and high stress levels. Furthermore, children need attention because of their relatively high exposure during sleep, and because they are in a phase of neurocognitive development for which undisturbed sleep may be particularly important.

CHAPTER 5

GUIDELINES AND RECOMMENDATIONS

5.1 ASSESSMENT

In Chapter 1 the need for a guideline document for night-time exposure to noise was defended on the basis of the lack of existing guidance, the signs that a substantial part of the population could be exposed to levels of noise that might risk their health and well-being and the EU activities that compel the public and authorities to take notice when noise maps showing L_{night} levels are made public.

Where sufficient direct evidence concerning the effects of night-time noise on health could not be collected, indirect evidence was looked at: the effects of noise on sleep (quality) and the relations between sleep and health.

In Chapter 2 the evidence was presented that sleep is a biological necessity and disturbed sleep is associated with a number of health outcomes. Studies of sleep disturbance in children and in shift workers clearly show the adverse effects. Unravelling the relations between sleep and health (Fig. 2.1) shows that sleep is an essential feature of the organism, so that simple direct relations can hardly be expected.

In Chapter 3 it was shown beyond doubt that noise disturbs sleep through a number of direct and indirect pathways. Even at very low levels physiological reactions (heart rate, body movement and arousals) can be reliably measured. It was also shown that awakening reactions are relatively rare, occurring at a much higher level.

Chapter 4 summarized the known evidence for the direct effects of night-time noise on health. The working group agreed that there is sufficient evidence that night noise is related to self-reported sleep disturbance, use of pharmaceuticals, self-reported health problems and insomnia-like symptoms. These effects can lead to a considerable burden of disease in the population. For other effects (hypertension, myocardial infarctions, depression and others), limited evidence was found: although the studies were few or not conclusive, a biologically plausible pathway could be constructed from the evidence.

An example of a health effect with limited evidence is myocardial infarction. Although evidence for increased risk of myocardial infarction related to L_{day} is sufficient according to an updated meta-analysis, the evidence in relation to $L_{night, outside}$ was considered limited. This is because $L_{night, outside}$ is a relatively new exposure indicator, and few field studies have focused on night noise when considering cardiovascular outcomes. Nevertheless, there is evidence from animal and human studies supporting a hypothesis that night noise exposure might be more strongly associated with cardiovascular effects than daytime exposure, highlighting the need for future epidemiological studies on this topic.

The review of available evidence leads to the following conclusions.

- Sleep is a biological necessity and disturbed sleep is associated with a number of health outcomes.

- There is sufficient evidence for biological effects of noise during sleep: increase in heart rate, arousals, sleep stage changes and awakening.
- There is sufficient evidence that night noise exposure causes self-reported sleep disturbance, increase in medicine use, increase in body movements and (environmental) insomnia.
- While noise-induced sleep disturbance is viewed as a health problem in itself (environmental insomnia), it also leads to further consequences for health and well-being.
- There is limited evidence that disturbed sleep causes fatigue, accidents and reduced performance.
- There is limited evidence that noise at night causes hormone level changes and clinical conditions such as cardiovascular illness, depression and other mental illness. It should be stressed that a plausible biological model is available with sufficient evidence for the elements of the causal chain.

In the next section threshold levels are presented for the effects, where these can be derived.

5.2 THRESHOLDS FOR OBSERVED EFFECTS

The NOAEL is a concept from toxicology, and is defined as the greatest concentration which causes no detectable adverse alteration of morphology, functional capacity, growth, development or lifespan of the target organism. For the topic of night-time noise (where the adversity of effects is not always clear) this concept is less useful. Instead, the observed effect thresholds are provided: the level above which an effect starts to occur or shows itself to be dependent on the dose. This can also be an adverse effect (such as myocardial infarcts) or a potentially dangerous increase in a naturally occurring effect such as motility.

Threshold levels are important milestones in the process of evaluating the health consequences of environmental exposure. The threshold levels also delimit the study area, which may lead to a better insight into overall consequences. In Tables 5.1 and 5.2 all effects are summarized for which sufficient or limited evidence exists (see Table 1.2 in Chapter 1 for a definition). For the effects with sufficient evidence the threshold levels are usually well known, and for some the dose-effect relations over a range of exposures could also be established.

5.3 RELATIONS WITH $L_{NIGHT,OUTSIDE}$

Over the next few years, the END will require that night exposures are reported in $L_{night,outside}$. It is therefore interesting to look into the relation between $L_{night,outside}$ and the effects from night-time noise. The relation between the effects listed in Tables 5.1 and 5.2 and $L_{night,outside}$ is, however, not straightforward. Short-term effects are mainly related to maximum levels per event inside the bedroom: $L_{Amax,inside}$. In order to express the (expected) effects in relation to the single EU indicator, some calculation needs to be done.

Table 5.1
Summary of effects and threshold levels for effects where sufficient evidence is available

Effect		Indicator	Threshold, dB	Reference (chapter, section)
Biological effects	Change in cardiovascular activity	*	*	3.1.5
	EEG awakening	$L_{Amax,inside}$	35	4.10
	Motility, onset of motility	$L_{Amax,inside}$	32	3.1.8, dose–effect relation for aircraft
	Changes in duration of various stages of sleep, in sleep structure and fragmentation of sleep	$L_{Amax,inside}$	35	3.1
Sleep quality	Waking up in the night and/or too early in the morning	$L_{Amax,inside}$	42	3.1.7, dose–effect relation for aircraft
	Prolongation of the sleep inception period, difficulty getting to sleep	*	*	3.1
	Sleep fragmentation, reduced sleeping time	*	*	3.1
	Increased average motility when sleeping	$L_{night,outside}$	42	3.2, dose–effect relation for aircraft
Well-being	Self-reported sleep disturbance	$L_{night,outside}$	42	4.2, dose–effect relation for aircraft/road/rail
	Use of somnifacient drugs and sedatives	$L_{night,outside}$	40	4.5.8
Medical conditions	Environmental insomnia**	$L_{night,outside}$	42	3.1; 4.1; 4.2

* *Although the effect has been shown to occur or a plausible biological pathway could be constructed, indicators or threshold levels could not be determined.*

** *Note that "environmental insomnia" is the result of diagnosis by a medical professional whilst "self-reported sleep disturbance" is essentially the same, but reported in the context of a social survey. Number of questions and exact wording may differ.*

Table 5.2
Summary of effects and threshold levels for effects where limited evidence is available+

Effect		Indicator	Estimated, threshold dB	Reference (chapter, section)
Biological effects	Changes in (stress) hormone levels	*	*	2.5
	Drowsiness/tiredness during the day and evening	*	*	2.2.3
	Increased daytime irritability	*	*	2.2.3
Well-being	Impaired social contacts	*	*	2.2.3
	Complaints	$L_{night,outside}$	35	4.3
	Impaired cognitive performance	*	*	2.2.3
	Insomnia	*	*	4.6
	Hypertension	$L_{night,outside}$	50	2.2.3; 4.5.6
	Obesity	*	*	2.2.3
	Depression (in women)	*	*	4.8
	Myocardial infarction	$L_{night,outside}$	50	4.5.15
	Reduction in life expectancy (premature mortality)	*	*	2.2.3; 2.5
	Psychiatric disorders	$L_{night,outside}$	60	4.8.15
	(Occupational) accidents	*	*	2.2.3; 2.4

+ *Note that as the evidence for the effects in this table is limited, the threshold levels also have a limited weight. In general they are based on expert judgement of the evidence.*

* *Although the effect has been shown to occur or a plausible biological pathway could be constructed, indicators or threshold levels could not be determined.*

The calculation for the total number of effects from reaction data on events (arousals, body movements and awakenings) needs a number of assumptions. The first that needs to be made is independence: although there is evidence (Brink, Müller and Schierz, 2006) that the order of events of different loudness strongly influences the reactions, the calculation is nearly impossible to carry out if this is taken into consideration.

Secondly, the reactions per event are known in relation to levels at the ear of the sleeper, so an assumption for an average insulation value must be made. In this report a value of 21 dB (see Chapter 1, sections 1.3.4 and 1.3.5) has been selected. This value is, however, subject to national and cultural differences. One thing that stands out is the desire of a large part of the population to sleep with windows (slightly) open. The relatively low value of 21 dB already takes this into account. If noise levels increase, people do indeed close their windows, but obviously reluctantly, as then complaints about bad air increase and sleep disturbance remains high. This was already pointed out in the WHO guidelines on community noise (WHO, 1999).

From source to source the number of separate events varies considerably. Road traffic noise is characterized by relatively low levels per event and high numbers, while air and rail traffic are characterized by high levels per event and low numbers. For two typical situations estimates are made and presented in graphical form. The first is an average urban road (600 motor vehicles per night, which corresponds roughly to a 24-hour use of 8000 motor vehicles, or 3 million per year, the lower boundary the END sets) and the second case is for an average situation of air traffic exposure (8 flights per night, nearly 3000 per year).

Fig. 5.1 shows how effects increase with an increase of $L_{night,outside}$ values for the typical road traffic situation (urban road). A large number of events lead to high levels of awakening once the threshold of $L_{Amax,inside}$ is exceeded. To illustrate this in practical terms: values over 60 dB $L_{night,outside}$ occur at less then 5 metres from the centre of the road.

In Fig. 5.2 the same graph is presented for the typical airport situation. Due to a lower number of events there are fewer awakenings than in the road traffic case (Fig. 5.1), but the same or more health effects.

In these examples the worst case figures can be factors higher: the maximum number of awakenings for an $L_{night,outside}$ of 60–65 dB is around 300 per year.

A recent study suggests that high background levels (from motorways) with low numbers of separate events can cause high levels of average motility (Passchier-Vermeer, to be published). In Table 5.3 the full details are summarized.

5.4 DEALING WITH SITUATIONS EXCEEDING THE THRESHOLDS

Noise exposure data demonstrate that a large part of the population is over the no-effect levels. It is expected that this will extend into the future for quite some time. This means that circumstances may require that a risk assessment must be made. It is then recommended to apply the method laid out in Chapter 1, using the values given in Tables 5.1 and 5.2 and the dose–effect relations given in Chapter 4.

Typical actions requiring risk assessment are:

- new infrastructure projects (if an environmental impact statement is required)
- improvement programmes

- policy evaluation
- national or international setting of limit values.

In the EU *Position Paper* (European Commission, 2002a) an overview of national night-time noise regulations can be found.

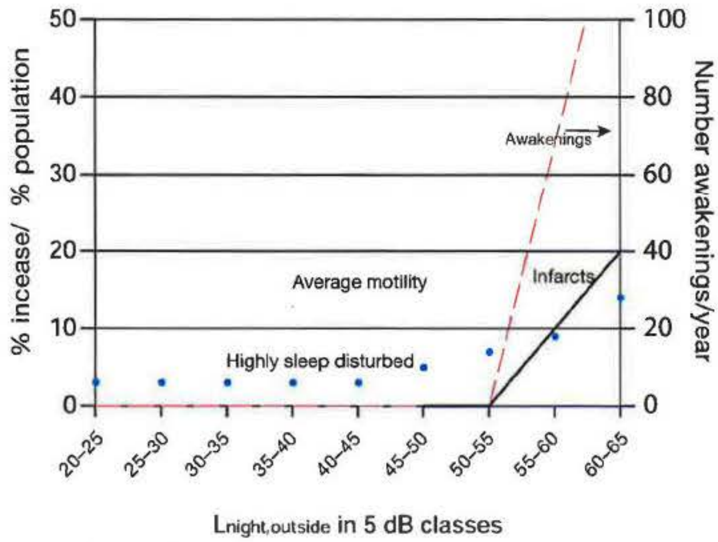

Fig. 5.1
Effects of road traffic noise at night*

Source: European Commission, 2002 a

* *Average motility and infarcts are expressed in percent increase (compared to baseline number); the number of highly sleep disturbed people is expressed as a percent of the population; awakenings are expressed in number of additional awakenings per year.*

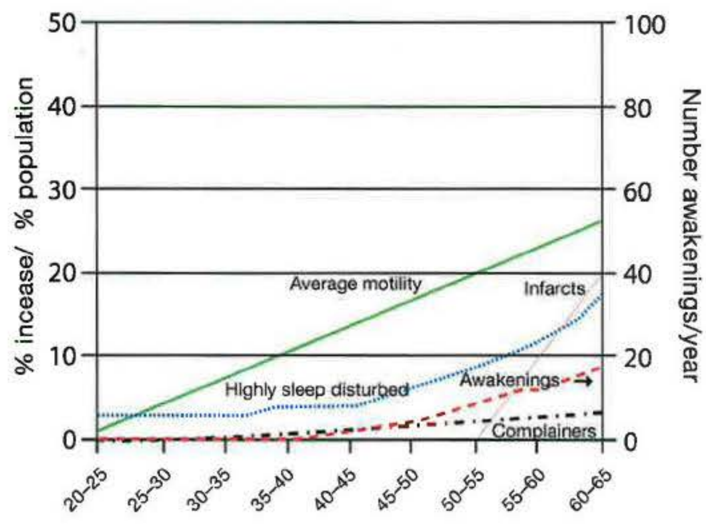

Fig. 5.2
Effects of aircraft noise at night*

Source: European Commission, 2002 a

* *Average motility and infarcts are expressed in percent increase (compared to baseline number); the number of highly sleep disturbed people is expressed as percent of the population; complainers are expressed as a percent of the neighbourhood population; awakenings are expressed in number of additional awakenings per year.*

Table 5.3
Effects (yearly, additional with respect to the normal except odd ratio) 0=below threshold, +=increase)

$L_{night, outside}$	Arousals		Body movements related to single exposures (15 sec intervals)		Average body movements (without single exposures)	Awakenings		% sleep disturbed (% highly sleep disturbed)			Myocardial infarcts
UNIT	number	number air	number average traffic	number average urban road	number	number average air traffic	number average urban road	% of exposed air	road	rail	odd ratio
NORMAL	Children 2 555	Adults 3 650	21 000		21 000	600		0			1
20–25	0	0	0	0	200	0	0	0	0	0	1
25–30	0	0	7	0	875	0	0	<3	<3	<2	1
30–35	+	+	22	0	1 547	0	0	<3	<3	<2	1
35–40	+	+	37	0	2 220	0	0	4	3	2	1
40–45	+	+	58	243	2 900	2	0	4	3	2	1
45–50	+	+	85	635	3 600	5	0	6	5	2	1
50–55	+	+	111	1 145	4 200	9	0	9	7	3	1
55–60	+	+	145	1 770	4 900	12	54	12	9	4	1.1
60–65	+	+	180	2 520	5 500	17	155	17	14	6	1.2

Source: European Commission, 2002 a

5.5 PROTECTION MEASURES AND CONTROL

What is the best strategy to reduce sleep disturbance? The first thought should always be to reduce the impact, either by reducing the number of events or by reducing the sound levels, or both. For some effects reducing the number of events may seem to be more effective (although that depends on the exact composition). Other effects are reduced by lowering overall noise level by either the number of events, the levels per event or by any combination.

In combination with other measures, sound insulation of bedroom windows is an option, but care must be taken to avoid negative impact on inside air quality. Even then, many people may want to sleep with their windows open, thereby making the insulation ineffective. Although good instruction may go some way to helping to overcome this, it is still a matter well worth taking into account. In warmer climates, in particular, insulation is not a serious option for residential purposes and excessive exposure must be avoided either by removing the people exposed or removing the source if source-related measures fail.

Although air conditioning of houses (or just bedrooms) is not commonplace in the EU, there are indications that its use is increasing, especially in the warmer parts of the Region. Although this still leaves the possibility that people may sleep with their windows open outside the summer season, it is something to consider when discussing measures.

Exposed areas could be a good choice for uses such as offices, where there will be no people at night, or where it is a physical impossibility to sleep with the windows open (fully air-conditioned buildings, for example hotels and sometimes hospitals).

A simple measure is the orientation of noise-sensitive rooms on the quiet side of the dwelling (this applies to road and rail traffic noise).

Zoning is an instrument that may assist planning authorities in keeping noise-sensitive land uses away from noisy areas. In the densely populated areas of the EU this solution must often compete, however, with other planning requirements or a simple lack of suitable space.

5.6 RECOMMENDATIONS FOR HEALTH PROTECTION

Sleep is an essential part of healthy life and is recognized as a fundamental right under the European Convention on Human Rights[1](European Court of Human Rights, 2003). Based on the systematic review of evidence produced by epidemiological and experimental studies, the relationship between night noise exposure and health effects can be summarized as below. (Table 5.4)

Table 5.4
Effects of different levels of night noise on the population's health[2]

Average night noise level over a year $L_{night,outside}$	Health effects observed in the population
Up to 30 dB	Although individual sensitivities and circumstances may differ, it appears that up to this level no substantial biological effects are observed. $L_{night,outside}$ of 30 dB is equivalent to the NOEL for night noise.
30 to 40 dB	A number of effects on sleep are observed from this range: body movements, awakening, self-reported sleep disturbance, arousals. The intensity of the effect depends on the nature of the source and the number of events. Vulnerable groups (for example children, the chronically ill and the elderly) are more susceptible. However, even in the worst cases the effects seem modest. $L_{night,outside}$ of 40 dB is equivalent to the LOAEL for night noise.
40 to 55 dB	Adverse health effects are observed among the exposed population. Many people have to adapt their lives to cope with the noise at night. Vulnerable groups are more severely affected.
Above 55 dB	The situation is considered increasingly dangerous for public health. Adverse health effects occur frequently, a sizeable proportion of the population is highly annoyed and sleep-disturbed. There is evidence that the risk of cardiovascular disease increases.

[1] "Article 8:1. Everyone has the right to respect for his private and family life, his home and his correspondence." Although in the case against the United Kingdom the Court ruled that the United Kingdom Government was not guilty of the charges, the right to undisturbed sleep was recognized (the Court's consideration 96).

[2] $L_{night,outside}$ in Table 5.4 and 5.5 is the night-time noise indicator (L_{night}) of Directive 2002/49/EC of 25 June 2002: the A-weighted long-term average sound level as defined in ISO 1996-2: 1987, determined over all the night periods of a year; in which: the night is eight hours (usually 23.00 – 07.00 local time), a year is a relevant year as regards the emission of sound and an average year as regards the meteorological circumstances, the incident sound is considered, the assessment point is the same as for L_{den}. See *Official Journal of the European Communities*, 18.7.2002, for more details.

Below the level of 30 dB $L_{night,outside}$, no effects on sleep are observed except for a slight increase in the frequency of body movements during sleep due to night noise. There is no sufficient evidence that the biological effects observed at the level below 40 dB $L_{night,outside}$ are harmful to health. However, adverse health effects are observed at the level above 40 dB$L_{night,outside}$, such as self-reported sleep disturbance, environmental insomnia, and increased use of somnifacient drugs and sedatives. Therefore, 40 dB $L_{night,outside}$ is equivalent to the LOAEL for night noise. Above 55 dB the cardiovascular effects become the major public health concern, which are likely to be less dependent on the nature of the noise. Closer examination of the precise impact will be necessary in the range between 30 dB and 55 dB as much will depend on the detailed circumstances of each case.

A number of instantaneous effects are connected to threshold levels expressed in L_{Amax} (Table 5.1). The health relevance of these effects cannot be easily established. It can be safely assumed, however, that an increase in the number of such events over the baseline may constitute a subclinical adverse health effect by itself leading to significant clinical health outcomes.

Based on the exposure–effects relationship summarized in Table 5.4, the night noise guideline values are recommended for the protection of public health from night noise as below (Table 5.5).

Table 5.5 Recommended night noise guidelines for Europe

Night noise guideline (NNG)	$L_{night,outside}$ = 40 dB
Interim target (IT)	$L_{night,outside}$ = 55 dB

For the primary prevention of subclinical adverse health effects related to night noise in the population, it is recommended that the population should not be exposed to night noise levels greater than 40 dB of $L_{night,outside}$ during the part of the night when most people are in bed. The LOAEL of night noise, 40 dB $L_{night,outside}$, can be considered a health-based limit value of the night noise guidelines (NNG) necessary to protect the public, including most of the vulnerable groups such as children, the chronically ill and the elderly, from the adverse health effects of night noise.

An interim target (IT) of 55 dB $L_{night,outside}$ is recommended in the situations where the achievement of NNG is not feasible in the short run for various reasons. It should be emphasized that IT is not a health-based limit value by itself. Vulnerable groups cannot be protected at this level. Therefore, IT should be considered only as a feasibility-based intermediate target which can be temporarily considered by policy-makers for exceptional local situations.

All Member States are encouraged to gradually reduce the proportion of the population exposed to levels over the IT within the context of meeting wider sustainable development objectives. It is highly recommended to carry out risk assessment and management activities at local and national levels targeting the exposed population, and aiming at reducing night noise to the level below IT or NNG. IT and NNG can be used for health impact assessment of new projects (for example construction of roads, railways, airports or new residential areas) even before the achievement of IT, as well as for the risk assessment of the whole population. In the long run the NNG would be best achieved by control measures aimed at the sources along with other comprehensive approaches.

5.7 RELATION WITH THE GUIDELINES FOR COMMUNITY NOISE (1999)

The *Guidelines for community noise* (WHO, 1999) have been quoted a number of times in this paper, so one could rightfully ask what the relation is between the 1999 guidelines and the present NNG.

Impact of night-time exposure to noise and sleep disturbance is indeed covered in the 1999 guidelines, and this is the full statement (WHO, 1999):

> "If negative effects on sleep are to be avoided the equivalent sound pressure level should not exceed 30 dBA indoors for continuous noise. If the noise is not continuous, sleep disturbance correlates best with L_{Amax} and effects have been observed at 45 dB or less. This is particularly true if the background level is low. Noise events exceeding 45 dBA should therefore be limited if possible. For sensitive people an even lower limit would be preferred. It should be noted that it should be possible to sleep with a bedroom window slightly open (a reduction from outside to inside of 15 dB). To prevent sleep disturbances, one should thus consider the equivalent sound pressure level and the number and level of sound events. Mitigation targeted to the first part of the night is believed to be effective for the ability to fall asleep."

It should be noted that the noise indicators of the 1999 guidelines are L_{Aeq} and L_{Amax}, measured inside for continuous and non-continuous noise, respectively. The present night noise guidelines adopt an harmonized noise indicator as defined by Environmental Noise Directive (2002/49/EC): L_{night} measured outside, averaged over a year.

It should also be borne in mind that the 1999 guidelines are based on studies carried out up to 1995 (and a few meta-analyses some years later). Important new studies (Passchier-Vermeer et al., 2002; Basner et al., 2004) have become available since then, together with new insights into normal and disturbed sleep.

Comparing the above statement with the recommendations, it is clear that new information has made more precise statements possible. The thresholds are now known to be lower than L_{Amax} of 45 dB for a number of effects. The last three sentences still stand: there are good reasons for people to sleep with their windows open, and to prevent sleep disturbances one should consider the equivalent sound pressure level and the number of sound events. The present NNG allow responsible authorities and stakeholders to do this. Viewed in this way, the *Night noise guidelines for Europe* complements the 1999 guidelines. This means that the recommendations on government policy framework on noise management elaborated in the 1999 guidelines should be considered valid and relevant for the Member States to achieve the guideline values of this document.

REFERENCES

Abey Wickrama I et al. (1969). Mental hospital admissions and aircraft noise. *Lancet*, 2 (7633):1275–1277.

Adams S (1991). Prescribing of psychotropic drugs to children and adolescents. *British Medical Journal*, 302:217.

Ahlberg-Hultén GK, Theorell T, Sigala F (1995). Social support, job strain and musculoskeletal pain among female health care personnel, *Scandinavian Journal of Work, Environment and Health*, 21 (6):435–439.

Åkerstedt T (1987). Sleep and stress. In: Peter JH, Podszus T and von Wichert P, eds. *Sleep related disorders and internal diseases.* Springer Verlag, Heidelberg, pp. 183–191.

Åkerstedt T (1988). Sleepiness as a consequence of shift work. *Sleep*, 11:17–34.

Åkerstedt T (1990). Sleep and performance – an introduction. In: Costa G et al., eds. *Shift work: health, sleep and performance.* Peter Lang, Frankfurt am Main, pp. 409–414.

Åkerstedt T, Gillberg M (1981). The circadian variation of experimentally displaced sleep. *Sleep*, 4:159–169.

Åkerstedt T, Gillberg M (1986). A dose-response study of sleep loss and spontaneous sleep termination. *Psychophysiology*, 23:293–297.

Åkerstedt T, Nilsson PM (2003). Sleep as restitution: an introduction. *Journal of Internal Medicine*, 254:6–12.

Åkerstedt T, Kecklund G, Horte L-G (2001). Night driving, season, and the risk of highway accidents. *Sleep*, 24:401–406.

Åkerstedt T, Kecklund G, Knutsson A (1991). Spectral analysis of sleep electroencephalography in rotating three-shift work. *Scandinavian Journal of Work, Environment and Health*, 17:330–336.

Åkerstedt T et al. (2002a). A prospective study of fatal occupational accidents – relationship to sleeping difficulties and occupational factors. *Journal of Sleep Research*, 11:69–71.

Åkerstedt T et al. (2002b). Work load and work hours in relation to disturbed sleep and fatigue in a large representative sample. *Journal of Psychosomatic Research*, 53:585–588.

Åkerstedt T et al. (2002c). Sleep disturbances, work stress and work hours. A cross-sectional study. *Journal of Psychosomatic Research*, 53:741–748.

Algers B, Ekesbo I, Strömberg S (1978). The impact of continuous noise on animal health. *Acta Veterinaria Scandinavica*, 67 (suppl.):1–26.

Ali NJ, Pitson D, Stradling JR (1993). Snoring, sleep disturbance and behaviour in 4–5 year-olds. *Archives of Disease in Childhood*, 68:360–366.

Ali NJ, Pitson D, Stradling JR (1994). Natural history of snoring and related behaviour problems between the ages of 4 and 7 years. *Archives of Disease in Childhood*, 71:74–76.

Ali NJ, Pitson D, Stradling JR (1996). Sleep disordered breathing: effects of adenotonsillectomy on behaviour and psychological functioning. *European Journal of Pediatrics*, 155:56–62.

American Academy of Pediatrics Committee on Environment Health (1997). Noise: a hazard for the fetus and newborn. *Pediatrics*, 100:724–727.

American Academy of Sleep Medicine (2005). *International Classification of Sleep Disorders. Diagnostic and coding manual.* 2nd edition, Westchester, Illinois.

American Sleep Disorders Association (1992). EEG arousals: scoring rules and examples. A preliminary report from the Sleep Disorders Atlas Task Force. *Sleep*, 15 (2):174–184.

American Sleep Disorders Association (1997). *International Classification of Sleep Disorders. Diagnostic and coding manual revised.* Rochester, Minnesota.

Ancoli-Israel S, Roth T (1999). Characteristics of insomnia in the United States: Results of the 1991 National Sleep Foundation survey. *Sleep*, 22 (suppl.2):S347–S353.

Anderson CMB (1971). *The measurement of attitude to noise and noises, National Physical Laboratory Acoustics Report*, AC 52, Teddington, Middlesex.

Angersbach D et al. (1980). A retrospective cohort study comparing complaints and disease in day and shift workers. *International Archives of Occupational and Environmental Health*, 45:i27–i40.

Arguelles A et al. (1970). Endocrine and metabolic effects of noise in normal, hypertensive and psychotic subjects. In: Welch BL and Welch AS, eds. *Physiological effects of noise*. Plenum Press, New York.

Aristotle (350 B.C.E). *On sleep and sleeplessness*, Translated by J. I. Beare, http://classics.mit.edu/Aristotle/sleep.html.

Arnetz B et al. (1986). *Lakares arbetsmiljo: psykosociala, fysikaliska saint fysiologiska data fran en strukturerad djupintervju och biokemisk undersokning av allmanlakare och allmankirurger.* Stressforskningsrapport, IPM, No. 187.

Aronen ET et al. (2000). Sleep and psychiatric symptoms in school-age children. *Journal of the American Academy of Childhood and Adolescent Psychiatry*, 39:502–508.

ATS (American Thoracic Society) (1999) Cardiorespiratory sleep studies in children. Establishment of normative data and polysomnographic predictors of morbidity. *American Journal of Respiratory and Critical Care Medicine*, 160:1381–1387.

Axelsson G, Rylander R (1989). Outcome of pregnancy in relation to irregular and inconvenient work schedules. *British Journal of Industrial Medicine*, 46:306–312.

Axelsson G, Lutz C, Rylander R (1984). Exposure to solvents and outcome of pregnancy in university laboratory employees. *British Journal of Industrial Medicine*, 41:305–312.

Axelsson J et al. (2004). Tolerance to shift work – how does it relate to sleep and wakefulness? *International Archives of Occupational and Environmental Health*, 77(2):121–9.

Ayas NT et al. (2001). Effectiveness of CPAP treatment in daytime function in sleep apnea syndrome. *American Journal of Respiratory and Critical Care Medicine*, 164:608–613.

Babisch W (2000). Traffic noise and cardiovascular disease: epidemiological review and synthesis. *Noise & Health*, 2 (8):9–32.

Babisch W (2002). The noise/stress concept, risk assessment and research needs. *Noise & Health*, 4 (16):1–11.

Babisch W (2003). Stress hormones in the research on cardiovascular effects of noise. *Noise & Health*, 5 (18):1–11.

Babisch W (2004a). Health aspects of extra-aural noise research. *Noise & Health*, 6 (22):69–81.

Babisch W (2004b).The NaRoMI study: Executive summary – traffic noise. In: Umweltbundesamt, ed. *Chronic noise as a risk factor for myocardial infarction, The NaRoMI study (major technical report)*. WaBoLu-Hefte 02/04, Umweltbundesamt, Berlin.

Babisch W (2004c), Die NaRoMI-Studie, Auswertung, Bewertung und vertiefende Analysen zum Verkehrslärm. In: Umweltbundesamt, ed. *Chronischer Lärm als Risikofaktor für den Myokardinfarkt, Ergenbisse der "NaRoMI"-Studie*. WaBoLu-Hefte 03/04, Umweltbundesamt, Berlin.

Babisch W (2006). *Transportation noise and cardiovascular risk. Review and synthesis of epidemiological studies, dose-effect curve and risk estimation* (http://www.umweltdaten.de/publikationen/fpdf-l/2997.pdf, accessed 1 March 2007).

Babisch W, Gallacher JEJ (1990). Traffic noise, blood pressure and other risk factors: the Caerphilly and Speedwell Collaborative Heart Disease Studies. In: Berglund B, Lindvall T, eds. *New advances in noise research, part I. Proceedings of the 5th International Congress on Noise as a Public Health Problem, Stockholm 1988*, Stockholm, Swedish Council for Building Research.

Babisch W, Ising H, Gallacher JEJ (2003). Health status as a potential effect modifier of the relation between noise and incidence of ischaemic heart disease. *Occupational and Environmental Medicine*, 60:739–745.

Babisch W et al. (1988). Traffic noise and cardiovascular risk. The Caerphilly Study, first phase. Outdoor noise levels and risk factors. *Archives of Environmental Health*, 43:407–414.

Babisch W et al. (1990). Traffic noise, work noise and cardiovascular risk factors: the Caerphilly and Speedwell Collaborative Heart Disease Studies. *Environment International*, 16:425–435.

Babisch W et al. (1992). *Verkehrslärm und Herzinfarkt, Ergebnisse zweier Fall-Kontroll-Studien in Berlin*. WaBoLu-Hefte 2/92, Institut für Wasser-, Boden- und Lufthygiene, Umweltbundesamt, Berlin.

Babisch W et al. (1993a). Traffic noise and cardiovascular risk: the Caerphilly and Speedwell studies, second phase. Risk estimation, prevalence, and incidence of ischemic heart disease. *Archives of Environmental Health*, 48:406–413.

Babisch W et al. (1993b). Traffic noise and cardiovascular risk: the Speedwell study, first phase. Outdoor noise level and risk factors. *Archives of Environmental Health*, 48:401–405.

Babisch W et al. (1994). The incidence of myocardial infarction and its relation to road traffic noise – the Berlin case-control studies. *Environment International*, 20:469–474.

Babisch W et al. (1999). Traffic noise and cardiovascular risk: the Caerphilly and Speedwell studies, third phase – 10 years follow-up. *Archives of Environmental Health*, 54:210–216.

Babisch W et al. (2003). Traffic noise and myocardial infarction. results from the NaRoMI study, *ICBEN Proceedings, Schiedam*.

Babisch W et al. (2005). Traffic noise and risk of myocardial infarction. *Epidemiology*, 16:33–40.

Barker SM, Tarnopolsky A (1978). Assessing bias in surveys of symptoms attributed to noise. *Journal of Sound and Vibration*, 59:349–354.

Basner M (2006). *Markov state transition models for the prediction of changes in sleep structure induced by aircraft noise*, Forschungsbericht 2006-07. Deutsches Zentrum für Luft und Raumfahrt (DLR), Köln.

http://www.eid.dlr.de/me/Institut/Abteilungen/Flugphysiologie/Fluglaerm/Lit_Laermw_Reports /FB_2006-07_markov.pdf, accessed 1 March 2007).

Basner M et al. (2004). *Effects of nocturnal aircraft noise*. Deutsches Zentrum für Luft und Raumfahrt (DLR) Bericht 2004-07/E.

Baust W, Bohnert B (1969). The regulation of heart rate during sleep. *Experimental Brain Research*, 7:169–180.

Bellach B et al. (1995). Gesundheitliche Auswirkungen von Lärmbelastung – Methodische Betrachtungen zu den Ergebnissen dreier epidemiologischer Studien. *Bundesgesundheitsblatt*, 38:84–89.

Belojevic G, Jakovljevic B (1997). Subjective reactions to traffic noise with regard to some personality traits. *Environment International*, 23:221–226.

Belojevic G, Saric-Tanaskovic M (2002). Prevalence of arterial hypertension and myocardial infarction in relation to subjective ratings of traffic noise exposure. *Noise & Health*, 4 (16):33–37.

Benedict C et al. (2004). Intranasal insulin improves memory in humans. *Psychoneuroendocrinology*, 29:1326–1334.

Bennett E (1945). Some tests for the discrimination of neurotic from normal subjects, *British Journal of Medical Psychology*, 20:271–277.

Berglund B, Lindvall T (1995). Community noise. Document prepared for the World Health Organization. *Archives of the Center for Sensory Research* 2 (1), Stockholm, Center for Sensory Research.

Biesiot W, Pulles MPJ, Stewart RE (1989). *Environmental noise and health*. VROM, GA-DR-03-03, Leidschendam.

Bistrup ML (2003). Prevention of adverse effects of noise on children. *Noise & Health*, 5:59–64.

Bistrup ML et al. (2001). *Health effects of noise on children – and perception of risk of noise.* National Institute of Public Health, Copenhagen.

Bite M, Bite PZ (2004). Zusammenhang zwischen den Straßenverkehrslärmindizes L_{Aeq}(06-22) und L_{Aeq}(22-06) sowie L_{den}. *Zeitschrift für Lärmbekämpfung*, 51:27–28.

Bixler EO, Kales A, Soldatos CR (1979). Sleep disorders encountered in medical practice: A national survey of physicians. *Behavioral Medicine*, 1–6.

Bjerner B, Holm A, Swensson A (1955). Diurnal variation of mental perfomance. A study of three-shift workers. *British Journal of Industrial Medicine*, 12:103–110.

Blettner M et al. (1999). Traditional reviews, meta-analyses and pooled analyses in epidemiology. *International Journal of Epidemiology*, 28:1–9.

Bliwise Dl (1993). Sleep in normal aging and dementia. *Sleep*, 16:40–81.

Bluhm G, Nordling E, Berglind N (2001). Increased prevalence of hypertension in a population exposed to road traffic noise. In Boone R, ed. *Internoise 2001. Proceedings of the 2001 International Congress and Exhibition on Noise Control Engineering, The Hague, Vol. 3.* Nederlands Akoestisch Genootschap, Maastricht.

Bluhm G, Nordling E, Berglind N (2004). Road traffic noise and annoyance – an increasing environmental health problem. *Noise & Health*, 6 (24):43–49.

Bluhm G et al. (2004). Aircraft noise exposure and cardiovascular risk among men – First results from a study around Stockholm Arlanda airport. In: Czech Acoustoical Society, ed. *Proceedings of the 33rd International Congress and Exhibition on Noise Control Engineering, Prague*, 31.

Blunden S, Lushington K, Kennedy D (2001). Cognitive and behavioural performance in children with sleep-related obstructive breathing disorders. *Sleep Medicine Reviews*, 5:447–461.

Blunden S et al. (2000). Behaviour and neurocognitive function in children aged 5–10 years who snore compared to controls. *Journal of Clinical and Experimental Neuropsychology*, 22:554–568.

Boggild H, Knutsson A (1999). Shift work, risk factors and cardiovascular disease. *Scandinavian Journal of Work, Environment and Health*, 25:85–99.

Boggild H et al. (1999). Shift work, social class, and ischaemic heart disease in middle aged and elderly men: a 22-year follow-up in the Copenhagen Male Study. *Occupational and Environmental Medicine*, 56:640–645.

Boman E, Enmarker I, Hygge S (2004). Strength of noise effects on memory as a function of noise source and age. *Noise & Health*, 7:11.26.

Bonnet MH (1985). Effect of sleep disruption on sleep, performance, and mood. *Sleep*, 8:11–19.

Bonnet MH (1986a). Performance and sleepiness as a function of frequency and placement of sleep disruption. *Psychophysiology*, 23:263–271.

Bonnet MH (1986b). Performance and sleepiness following moderate sleep disruption and slow wave sleep deprivation. *Physiology and Behavior*, 37:915–918.

Borbely AA et al. (1981). Sleep deprivation: effect on sleep stages and EEG power density in man. *Electroencephalography and Clinical Neurophysiology*, 51 (5):483–495.

Bormann C et al. (1990). *Subjektive Morbidität.* BGA Schriften 4/90, MMV Medizin Verlag, Munich.

Born J, Wagner U (2004). Awareness in memory: being explicit about the role of sleep. *Trends in Cognitive Sciences*, 8:242–244.

Boselli M et al. (1998). Effects of age on EEG arousals in normal sleep. *Sleep*, 21 (4):351–357.

Bowlin SJ et al. (1993). Validity of cardiovascular disease risk factors assessed by telephone survey: the behavioral risk survey. *Journal of Clinical Epidemiology*, 46:561–571.

Bradford Hill AS (1965). *The environment and disease: association or causation? Proceedings of the Royal Society of Medicine*, 58:295–300.

Breslau N et al. (1996). Sleep disturbance and psychiatric disorders: a longitudinal epidemiological study of young adults. *Biological Psychiatry*, 39 (6):411–418.

Brink M, Müller CH, Schierz C (2006). Contact-free measurement of heart rate, respiration rate, and body movements during sleep. *Behavior Research Methods*, 38 (3):511–521.

Brink M, Wirth K, Schierz C (2006). Effects of early morning aircraft overflights on sleep and implications for policy making. *Euronoise 2006*, Tampere.

Broadbent DE (1953). Noise, paced performance and vigilance tasks. *British Journal of Psychology*, 44:295–303.

Broadbent DE (1972). Individual differences in annoyance by noise. *Sound*, 6:56–61.

Broadbent DE (1983). Recent advances in understanding performance in noise. In: Rossi G, ed. *Proceedings of 4th International Congress, Noise as a Public Health Problem*. Centro Ricerche e Studi Amplifon, Milan, pp. 719–738.

Brown RC (1949). The day and night performance of teleprinter switchboard operators. *Journal of Occupational Psychology*, 23:121–126.

Brown R (1992). Sleep deprivation and the immune response to pathogenic and non-pathogenic antigens. In: Husband AJ, ed. *Behaviour and immunity*. CRC Press, Bocaton, Florida.

Bruni O et al. (2004). The sleep knowledge of pediatricians and child neuropsychiatrists. *Sleep and Hypnosis*, 6 (3):130–138.

Bryden G, Holdstock TI (1973). Effects of night duty on sleep patterns of nurses. *Psychophysiology*, 10:36–42.

Busby K, Pivik R (1985). Auditory arousal threshold during sleep in hyperkinetic children. *Sleep*, 8:332–341.

Busby K, Mercier L, Pivik R (1994). Ontogenetic variations in auditory arousal threshold during sleep. *Psychophysiology*, 31:182–188.

Caille EJ, Bassano JL (1977). Validation of a behavior analysis methodology: variation of vigilance in night driving as a function of the rate of carboxyhemoglobin. In: Mackie RR, ed. *Vigilance*. Plenum Press, New York, pp. 59–72.

Cairns V et al. (1985). Oral contraceptive use and blood pressure in a German metropolitan population. *International Journal of Epidemiology*, 14:389–395.

Calabrese EJ, Baldwin LA (2003). Toxicology rethinks its central belief. Hormesis demands a reappraisal of the way risks are assessed. *Nature*, 421:691–692.

CALM (2004). Research for a quieter Europe in 2020 (http://www.calm-network.com/index_stratpap.htm, accessed 11 November 2006)

Carskadon MA, Harvey K, Dement WC (1981a). Acute restriction of nocturnal sleep in children. *Perceptual and Motor Skills*, 53:103–112.

Carskadon MA, Harvey K, Dement WC (1981b). Sleep loss in young adolescents. *Sleep*, 4:299–321.

Carter NL (1996). Transportation noise, sleep, and possible after-effects. *Environment International*, 22:105–116.

Carter NL (1998). Cardiovascular response to environmental noise during sleep. In: *7th International Congress on Noise as a Public Health Problem, Sydney, Australia*, 2:439–444.

Carter NL et al. (1994). Environmental noise and sleep – a study of arousals, cardiac arrhythmia and urinary catecholamines. *Sleep*, 17 (4):298–307.

Carter NL et al. (2002). Cardiovascular and autonomic response to environmental noise during sleep in night shift workers. *Sleep*, 25:444–451.

Cartwright J, Flindell I (2000). Research methodology – noise annoyance and health. In: Cassereau D, ed. *Internoise 2000. Proceedings of the 29th International Congress on Noise Control Engineering, Nice*. Société Française d'Acoustique (SFA), Nice.

Centre for Time Use Research (2006). (http://www.timeuse.org/access/, accessed 11 November 2006).

Chang PP et al. (1997). Insomnia in young men and subsequent depression. The Johns Hopkins Precursors Study, *American Journal of Epidemiology*, 146:105–114.

Chapman KR et al. (1988). Possible mechanisms of periodic breathing during sleep. *Journal of Applied Physiology*, 64:1000–1008.

Chartered Institute of Environmental Health (1999). *Environmental health report 1997/8.*

Chervin RD et al. (1997). Symptoms of sleep disorders, inattention, and hyperactivity in children. *Sleep*, 20:1185–1192.

Chowns RH (1970). Mental hospital admissions and aircraft noise. *Lancet*, 1:467–468.

Christoffel T, Teret SP (1991). Public health and law. Epidemiology and the law: courts and confidence intervals. *American Journal of Public Health*, 81:1661–1666.

Cirelli C et al. (2005). Reduced sleep in *Drosophila shaker* mutants. *Nature*, 434:1087–1092.

Cohen S, Spacapan S (1978). The after-effects of stress: an attentional interpretation, *Environmental Psychology and Non-verbal Behaviour*, 3:43–57.

Cohen S, Weinstein N (1981). Non-auditory effects of noise on behaviour and health. *Journal of Social Issues*, 37:36–70.

Cohen S, Kessler, RC and Underwood Gordon L (1995). Strategies for measuring stress in studies of psychiatric and physical disorders. In: Cohen S, Kessler RC and Underwood Gordon L, eds. *A guide for health and social scientists*. Oxford University Press, New York.

Cohen S et al. (1980). Physiological, motivational, and cognitive effects of aircraft noise on children. *American Psychologist*, 35:231–243.

Cohen S et al. (1981). Aircraft noise and children: longitudinal and cross-sectional evidence on adaptation to noise and the effectiveness of noise abatement. *Journal of Personality and Social Psychology*, 40:331–345.

Coleman RM and Dement WC (1986). Falling asleep at work: a problem for continuous operations. *Sleep Research*, 15:265.

Cooper R, ed. (1994). *Sleep*. Chapman and Hall Medical, London.

Crabtree VM et al. (2003). Periodic limb movement disorder of sleep in children. *Journal of Sleep Research*, 12:73–81.

Czeisler CA et al. (1980). Human sleep: its duration and organization depend on its circadian phase. *Science*, 210:1264–1267.

Dahlgren K (1981a). Adjustment of circadian rhythms and EEG sleep functions to day and night sleep among permanent night workers and rotating shift workers. *Psychophysiology*, 18:381–391.

Dahlgren K (1981b). Long-term adjustment of circadian rhythms to a rotating shiftwork schedule. *Scandinavian Journal of Work, Environment and Health*, 7:141–151.

Dawson D, Reid K (1997). Fatigue, alcohol and perfomance impairment. *Nature*, 388:235.

Dew MA et al. (2003). Healthy older adults' sleep predicts all-cause mortality at 4 to 19 years of follow-up. *Psychosomatic Medicine*, 65:63–73.

Diaz J et al. (2001). *Traffic noise pollution. Similarities and differences between European regions. A state-of-the-art-review*. Technical University, Berlin.

Dickens. *Gutenberg Electronic Library*, http://www.gutenberg.org/files/580/580.txt.

Dijk D-J, Czeisler CA (1995). Contribution of the circadian pacemaker and the sleep homeostat to sleep propensity, sleep structure, electroencephalographic slow waves, and sleep spindle activity in humans. *Journal of Neuroscience*, 15:3526–3538.

Dijk D-J, Duffy JF (1999). Circadian regulation of human sleep and age-related changes in its timing. *Annals of Medicine*, 31:130–140.

Dijk D-J, Beersma DGM and Bloem GM (1989). Sex differences in the sleep EEG of young adults: Visual scoring and spectral analysis. *Sleep*, 12:500–507.

Dijk D-J, Beersma DGM, van den Hofdakker RH (1989). All night spectral analysis of EEG sleep in young adult and middle-aged male subjects. *Neurobiology of Aging*, 10:677–682.

Dijk D-J, Duffy JF, Czeisler CA (1992). Circadian and sleep-wake dependent aspects of subjective alertness and cognitive performance. *Journal of Sleep Research*, 1:112–117.

Dijk D-J et al. (1999). Ageing and the circadian and homeostatic regulation of human sleep during forced desynchrony of rest, melatonin and temperature rhythms. *Journal of Physiology*, 516:611–627.

Dinges DF et al. (1997). Cumulative sleepiness, mood disturbance, and psychomotor vigilance performance decrements during a week of sleep restricted to 4–5 hours per night. *Sleep*, 20:267–277.

Di Nisi J et al. (1990). Comparison of cardiovascular responses to noise during waking and sleeping in humans. *Sleep*, 13:108–120.

Dongen JEF (van) et al. (1998) *Dosis-effect relaties voor geluid van buren*. TNO PG, Leiden, Publication No. 98.002.

Dongen, JEF (van) et al. (2004). *Hinder door milieufactoren en de beoordeling van de leefomgeving in Nederland*. RIVM, Bilthoven, TNO-INRO, Delft.

Drosopoulos S, Wagner U, Born, J (2005). Sleep enhances explicit recollection in recognition memory. *Learning & Memory*, 12:44–51.

Dryman A, Eaton WW (1991). Affective symptoms associated with the onset of major depression in the community: findings from the US National Institute of Mental Health Epidemiologic Catchment Area Program. *Acta Psychiatrica Scandinavica*, 84 (1):1–5.

Dugué B, Leppänen E, Gräsbeck R (1994). Preanalytical factors and standardized specimen collection: the effects of industrial noise. *Stress Medicine*, 10:185–189.

Dumont M, Montplaisir J, Infante-Rivard C (1988). Insomnia symptoms in nurses with former permanent nightwork experience. In: Koella WP et al., eds. *Sleep '86*. Gustav Fischer Verlag, Stuttgart, pp. 405–406.

Ebersole JS, Pedley TA, eds. (2003). *Current practice of clinical electroencephalography*. 3rd edition, Lippincott Williams & Wilkins, Philadelphia.

EEA (2004). *Traffic noise: exposure and annoyance*. European Environmental Agency, Copenhagen.

Ehlers CL, Kupfer DJ (1997). Slow-wave sleep: Do young adult men and women age differently? *Sleep*, 6:211–215.

Eiff AWV (1993). Selected aspects of cardiovascular responses to acute stress. In: Ising H, Kruppa B, eds. *Lärm und Krankheit – Noise and Disease. Proceedings of the International Symposium, Berlin 1991*. Gustav Fischer Verlag, Stuttgart.

Eiff AWV, Neus H (1980). Verkehrslärm und Hypertonie-Risiko. 1. Mitteilung: Verkehrslärm und Hypertonie-Risiko. *Münchener Medizinische Wochenschrift*, 122:893–896.

Eiff AWV et al. (1974). Kapitel 7: Der medizinische Untersuchungsteil. In: Forschungsgemeinschaft D, eds. *Fluglärmwirkungen I, Hauptbericht*. Harald Boldt Verlag KG, 32, Boppard.

Eiff AWV et al. (1981a). Verkehrslärm und Hypertonie-Risiko. 2. Mitteilung: Hypothalamus-Theorie der essentiellen Hypertonie. *Münchener Medizinische Wochenschrift*, 123:420–424.

Eiff AWV et al. (1981b). *Feststellung der erheblichen Belästigung durch Verkehrslärm mit Mitteln* *der Streßforschung (Bonner Verkehrslärmstudie). Umweltforschungsplan des Bundesminister des Innern, Lärmbekämpfung,* Forschungsberichts Nr. 81-10501303, Umweltbundesamt, Berlin.

Ekstedt M, Åkerstedt T, Soderstrom M (2004). Arousals during sleep are associated with increased levels of lipids, cortisol and blood pressure. *Psychosomatic Medicine*, 66:925–931.

Engle-Friedman M et al. (2003). The effect of sleep loss on next day effort. *Journal of Sleep Research*, 12:113–124.

European Commission (2000). *Position paper on EU noise indicators.* Office for Official Publications of the European Communities, Luxembourg.

European Commission (2002a). *Position paper on dose–response relationships between transportation noise and annoyance.* Office for Official Publications of the European Communities, Luxembourg.

European Commission (2002b). *Directive 2002/49/EC relating to the assessment and management of environmental noise.* Office for Official Publications of the European Communities, Luxembourg.

European Commission (2004). *Position paper on dose-effect relationships for night time noise* (http://ec.europa.eu/environment/noise/home.htm#1, accessed 11 November 2006).

European Commission (2006). Communication and Information Resource Centre Administrator (CIRCA) (http://forum.europa.eu.int/Public/irc/env/d_2002_49/home, accessed 11 November 2006).

European Court of Human Rights (2003). *Case of Hatton and others vs. the United Kingdom* (Application No. 36022/97).

Evans AS (1976) .Causation and disease: the Henle-Koch postulates revised. *Yale Journal of Biology and Medicine*, 49:175–195.

Evans A, Hygge S, Bullinger M (1995). Chronic noise exposure and physiological stress. *Psychological Science*, 6:333–338.

Evans GW, Bullinger M, Hygge S (1998). Chronic noise exposure and psychological response: A prospective study of children living under environmental stress. *Psychological Science*, 9:75–77.

Evans GW, Johnson D (2000). Stress and open-office noise. *Journal of Applied Psychology*, 85 (5):779–783.

Evans GW, Lepore SJ (1993). Nonauditory effects of noise on children: a critical review. *Children's Environments*, 10 (1):31–51.

Evans GW et al. (2001). Community noise exposure and stress in children. *Journal of the Acoustical Society of America*, 109:1023–1027.

Everson CA, Toth LA (2000). Systemic bacterial invasion induced by sleep deprivation. *American Journal of Physiology, Regulatory, Integrative and Comparative Physiology*, 278:R905–R916.

Fabsitz RR, Sholinsky P, Goldberg J (1997). Correlates of sleep problems among men: the Vietnam era twin registry. *Journal of Sleep Research*, 6:50–60.

Fallone G et al. (2001). Effects of acute sleep restriction on behavior, sustained attention, and response inhibition in children. *Perceptual and Motor Skills*, 93:213–229.

Fallone G, Owens JA, Deane J (2002). Sleepiness in children and adolescents: clinical implications. *Sleep Medicine*, 6 (4):287–386.

Farley TMM et al. (1998). Combined oral contraceptives, smoking, and cardiovascular risk. *Journal of Epidemiology and Community Health*, 52:775–785.

Fidell S et al. (1998). *Field studies of habituation to change in night-time aircraft noise and of sleep motility measurement methods.* BBN Technologies, California, Report No. 8195.

Fidell S et al. (2000). Effects on sleep disturbance of changes in aircraft noise near three airports. Journal of the Acoustical Society of America, 107 (5:1):2535–2547.

Fields JM (1993). Effect of personal and situational variables on noise annoyance in residential areas. *Journal of the Acoustical Society of America*, 93 (5):2753–2763.

Finke HO et al. (1974). *Effects of aircraft noise on man. Proceedings of the Symposium on Noise in Transportation, Section III, paper 1*. Institute of Sound and Vibration Research, Southampton, United Kingdom.

Flindell IH, Bullmore AJ, Robertson KA (2000). *Aircraft noise and sleep*. 1999 UK trial methodology study, Southampton, ISVR, Report 6131 RO1.

Folkard S, Åkerstedt T (1991). A three process model of the regulation of alertness and sleepiness. In: Ogilvie R, Broughton R, eds. *Sleep, arousal and performance: problems and promises*. Birkhauser, Boston, pp. 11–26.

Ford DE, Kamerow DB (1989). Epidemiologic study of sleep disturbances and psychiatric disorders: an opportunity for prevention. *Journal of the American Medical Association*, 262:1479–1484.

Foret J, Benoit O (1974). Structure du sommeil chez des travailleurs a horaires alternants. *Electroencephalography and Clinical Neurophysiology*, 37:337–344.

Foret J, Benoit O (1978). Shiftwork: the level of adjustment to schedule reversal assessed by a sleep study. *Waking and Sleeping*, 2:107–112.

Foret J, Lantin G (1972). The sleep of train drivers: an example of the effects of irregular work schedules on sleep. In: Coiqloun WP, ed. *Aspects of human efficiency. Diurnal rhythm and loss of sleep*. The English Universities Press Ltd, London, pp. 273–281.

Franssen EA, Staatsen BAM, Lebret E (2002). Assessing health consequences in an environmental impact assessment. The case of Amsterdam Airport Schiphol. *Environmental Impact Assessment Review*, 22:633–653.

Franssen EA et al. (2004). Aircraft noise around a large international airport and its impact on general health and medication use. *Journal of Occupational and Environmental Medicine*, 61 (5):405–413.

Frerichs RR, Beeman BL, Coulson AH (1980). Los Angeles Airport noise and mortality – faulty analysis and public policy. *American Journal of Public Health*, 3 (70):357–362.

Friedman M, Rosenman RH (1975). *Der A-Typ und der B-Typ*. Rowohlt Verlag Gmbh, Reinbek bei Hamburg.

Froberg J et al. (1975). Circadian variations of catecholamine excretion, shooting range performance and self-ratings of fatigue during sleep deprivation. *Biological Psychology*, 2:175–188.

Gais S, Born J (2004). Declarative memory consolidation: mechanisms acting during human sleep. *Learning & Memory*, 11:679–685.

Gattoni F, Tarnopolsky A (1973). Aircraft noise and psychiatric morbidity, *Psychological Medicine*, 3 (4):516–520.

Geroldi C et al. (1996). Principal lifetime occupation and sleep quality in the elderly. *Gerontology*, 42:163–169.

Gillberg M, Åkerstedt T (1998). Sleep loss and performance. No "safe" duration of a monotonous task. *Physiology and Behavior*, 64:599–604.

Gillman MW et al. (1992). Assessing the validity of childhood blood pressure screening: unbiased estimates of sensitivity, specificity, and predictive values. *Epidemiology*, 3:40–46.

Glass DC, Singer JE (1972). *Urban stress. Experiments on noise and social stressors*. Academic Press, New York.

Goldberg DP (1972). *The detection of psychiatric illness by questionnaire*. Oxford University Press, London.

Goldberg DP et al. (1970). A standardized psychiatric interview for use in community surveys. *British Journal of Preventive and Social Medicine*, 24 (1):18–23.

Goodman R (1997). The Strengths and Difficulties Questionnaire: a research note, *Journal of Child Psychology and Psychiatry*, 38 (5):581–586.

Goto K, Kaneko T (2002). Distribution of blood pressure data from people living near an airport. *Journal of Sound and Vibration*, 250:145–149.

Gottlieb DJ et al. (2003). Symptoms of sleep-disordered breathing in 5-year-old children are associated with sleepiness and problem behaviors. *Pediatrics*, 112:870–877.

Gozal D (1998). Sleep-disordered breathing and school performance in children. *Pediatrics*, 102:616–620.

Gozal D, Pope DW (2001). Snoring during early childhood and academic performance at ages thirteen to fourteen years. *Pediatrics*, 107:1394–1399.

Grandjean E et al. (1973). *A survey of aircraft noise in Switzerland*. United States Environmental Protection Agency Publications, Washington, United States, 500:1973–008.

Griefahn B et al. (2000). Physiological, subjective and behavioural responses during sleep to noise from rail and road traffic, *Noise & Health*, 3 (9):59–71.

Griefahn B et al. (2002). Fluglärmkriterien für ein Schutzkonzept bei wesentlichen Änderungen oder Neuanlagen von Flughäfen/Flugplätzen. *Zeitschrift für Lärmbekämpfung*, 49:171–181.

Grimwood C (1993). *Effects of environmental noise on people at home*. BRE information paper.

Grossi G et al. (2003). Physiological correlates of burnout among women. *Journal of Psychosomatic Research*, 55 (4):309–316.

Guazzi M et al. (1968). Effects of cardiacdenervation on blood pressure and heart rate during natural sleep in the cat. *Cardiovascular Research*, 2:265–270.

Guilleminault C et al. (1982a). Circadian rhythm disturbances and sleep disorders in shift workers (EEG Suppl. No. 36). In: Buser PA, Cobb WA, Okuma T, eds. *Kyoto Symposia*, Elsevier, Amsterdam, pp. 709–714.

Guilleminault C et al. (1982b). Children and nocturnal snoring. Evaluation of the effects of sleep related respiratory resistive load and daytime functioning. *European Journal of Pediatrics*, 139:165–171.

Guilleminault C et al. (1996). Recognition of sleep disordered breathing in children. *Pediatrics*, 98:871–882.

Haines MM et al. (2001a). Chronic aircraft noise exposure, stress responses, mental health and cognitive performance in school children. *Psychological Medicine*, 31:265–277.

Haines MM et al. (2001b). A follow-up study of the effects of chronic aircraft noise exposure on child stress responses and cognition. *International Journal of Epidemiology*, 30:839–845.

Hall M et al. (2000). Symptoms of stress and depression as correlates of sleep in primary insomnia. *Psychosomatic Medicine*, 62:227–230.

Halpern D (1995). *Mental health and the built environment*. Taylor and Francis, London.

Hamelin P (1987). Lorry drivers' time habits in work and their involvement in traffic accidents. *Ergonomics*, 30:1323–1333.

Hampton SM et al. (1996). Postprandial hormone and metabolic responses in simulated shift work. *Journal of Endocrinology*, 151:259–267.

Hansen J (2001). Light at night, shiftwork, and breast cancer risk. *Journal of the National Cancer Institute*, 93 (20):1513–1515.

Harrington JM (1978). *Shift work and health. A critical review of the literature*. HMSO, London.

Harrington JM (1994). Shift work and health – a critical review of the literature on working hours. *Annals of the Academy of Medicine, Singapore*, 23:699–705.

Harris W (1977). Fatigue, circadian rhythm and truck accidents. In: Mackie RR, ed. *Vigilance*. Plenum Press, New York, pp. 133–146.

Hartig T (2004). Restorative environments. In: Spielberger C, ed. *Encyclopedia of applied psychology*. Academic Press, London.

Hatfield J, Soames Job RF (2001). Optimism bias about environmental degradation: the role of the range of impact of precautions. *Journal of Environmental Psychology*, 21 (1):17–30 (14).

Hatfield J et al. (2001). The influence of psychological factors on self-reported physiological effects of noise. *Noise & Health*, 3 (10):1–13.

Health Council of the Netherlands (1994). *Noise and health. Report by a committee of the Health Council of the Netherlands, The Hague.*

Health Council of the Netherlands (1999). *Public health impact of large airports. Report by a committee of the Health Council of the Netherlands, The Hague.*

Health Council of the Netherlands (2003). *Report of a workshop on sleep, health, and noise. Held in connection with ICBEN on 2 July 2003.* Gezondheidsraad, The Hague.

Health Council of the Netherlands (2004). *The influence of night-time noise on sleep and health.* The Hague, publication No. 2004/14E.

Hennekens CH, Buring JE (1987). *Epidemiology in medicine.* Little, Brown and Company, Boston/Toronto.

Henry JP (1992). Biological basis of the stress response. *Integrative Physiological and Behavioral Science*, 27:66–83.

Henry JP, Stephens PM (1977). *Stress, health and the social environment, a sociobiologic approach to medicine.* Springer-Verlag, New York.

Hense H-W, Herbold M, Honig K (1989). *Risikofaktor Lärm in Felderhebungen zu Herz-Kreislauferkrankungen. Umweltforschungsplan des Bundesministers für Umwelt, Naturschutz und Reaktorsicherheit.* Forschungsbericht Nr. 89-10501111, Umweltbundesamt, Berlin.

Herbold M, Hense H-W, Keil U (1989). Effects of road traffic noise on prevalence of hypertension in men: results of the Lübeck blood pressure study. *Sozial- und Präventivmedizin*, 34:19–23.

Hildebrandt G, Rohmert W, Rutenfranz J (1974). 12- and 24-hour rhythms in error frequency of locomotive drivers and the influence of tiredness. *International Journal of Chronobiology*, 2:175–180.

Hiramatsu K et al. (1997). A survey on health effects due to aircraft noise on residents living around Kadena airport in the Ryukyus. *Journal of Sound and Vibration*, 205:451–460.

Hiramatsu K et al. (2000). An analysis of the general health questionnaire survey around airports in terms of annoyance reaction. *Internoise 2000*, Inrets, Nice.

Horne J, ed. (1988). *Why we sleep.* Oxford University Press, Oxford.

Horne et al. (1994). Sleep related vehicle accidents. *British Medical Journal*, 310:565–567.

Hume K, Morley H, Thomas C (2003). *Using complaints as a measure of annoyance at airport operations.* Manchester Metropolitan University, Manchester.

Hume KI, Van F, Watson A (1998). A field study of age and gender differences in habitual adult sleep. *Journal of Sleep Research*, 7:85–94.

Hume KI, Van F, Watson A (2003). *Effects of aircraft noise on sleep: EEG-Based measurements.* Manchester Metropolitan University, Manchester.

Hygge S, Evans GW, Bullinger M (2002). A prospective study of some effects of aircraft noise on cognitive performance in schoolchildren. *Psychological Science*, 13:469–474.

Hyyppa MT, Kronholm E (1989). Quality of sleep and chronic illness. *Journal of Clinical Epidemiology*, 42:633–638.

IEH (1997). *Workshop on non-auditory health effects of noise. Report* No. *R10.* Institute for Environment and Health, Leicester.

Ingre M, Åkerstedt T (2004). Effect of accumulated night work during the working lifetime, on subjective health and sleep in monozygotic twins. *Journal of Sleep Research*, 13 (1):45–48.

Irwin M, Fortner M, Clark C (1995). Reduction of natural killer cell activity in primary insomnia and in major depression. *Sleep Research*, 24:256.

Ishihara K (1999). The effect of 2-h sleep reduction by a delayed bedtime on daytime sleepiness in children. *Psychiatry and Clinical Neurosciences*, 53:113–115.

Ishihara K, Miyke S (1998). A longitudinal study of the development of daytime sleepiness in children. *Psychiatry and Clinical Neurosciences*, 52:178–181.

Ising H (1983). *Streßreaktionen und Gesundheitsrisiko bei Verkehrslärmbelastung*. Dietrich Reimer Verlag, Berlin.

Ising H, Braun C (2000). Acute and chronic endocrine effects of noise: review of the research conducted at the Institute for Water, Soil and Air Hygiene. *Noise & Health*, 2 (7):7–24.

Ising H, Ising M (2002). Chronic cortisol increase in the first half of the night caused by road traffic noise. *Noise & Health*, 4 (16):13–21.

Ising H, Kruppa B (2004). Health effects caused by noise. Evidence in the literature from the past 25 years. *Noise & Health*, 6:5–13.

Ising H et al. (1980). Health effects of traffic noise. *International Archives of Occupational and Environmental Health*, 47:179–190.

Ising H et al. (2004). Low frequency noise and stress: bronchitis and cortisol in children exposed chronically to traffic noise and exhaust fumes. *Noise & Health*, 6 (23):23–30.

Ito A et al. (1994). Health effects on the residents due to aircraft noise around Kadena US Airbase in the Ryukyus. *Internoise 94, Yokohama, Japan*, pp. 247–250.

Iwata O (1984). The relationship of noise sensitivity to health and personality. *Japanese Psychological Research*, 26:75–81.

Järup L et al. (2003). Hypertension and exposure to noise near airports – the Hyena project. *Epidemiology*, 14 (5):S78. 34.

Jasanoff S (1993). Relating risk assessment and risk management. Complete separation of the two processes is a misconception. *EPA Journal*, Jan/Feb/Mar 1993:35–37.

Jelinkova A (1988). Coping with noise in noise sensitive subjects. In: Berglund B, ed. *Noise as a public health problem. Noise 88, Vol. 3,* Stockholm, Swedish Council for Building Research, pp. 27–30.

Jenkins L, Tarnopolsky A, Hand D (1981). Psychiatric admissions and aircraft noise from London Airport: four-year, three-hospitals study. *Psychological Medicine*, 11 (4):765–782.

Jenkins LM et al. (1979). Comparison of three studies of aircraft noise and psychiatric hospital admissions conducted in the same area. *Psychological Medicine*, 9 (4):681–693.

Jones DM, Chapman AJ, Auburn TC (1981). Noise the environment: a social perspective. *Journal of Applied Psychology*, 1:43–59.

Jurriëns AA et al. (1983). An essay in European research collaboration: common results from the project on traffic noise and sleep in the home. *Proceedings of the 4th International Congress on Noise as a Public Health Problem, Turin*, pp. 929–937.

Juvenal DJ (around AD 160) This is an excerpt from Reading About the World, Volume 1, edited by Paul Brians, Mary Gallwey, Douglas Hughes, Azfar Hussain, Richard Law, Michael Myers, Michael Neville, Roger Schlesinger, Alice Spitzer, and Susan Swan and published by Harcourt Brace Custom Books. Satire No. 3 (*...magnis opibus dormitur in urbe...*).

Kageyama T et al. (1997). A population study on risk factors for insomnia among adult Japanese women: a possible effect of road traffic volume. *Sleep*, 20 (11):963–971.

Kahn A et al. (1989). Sleep problems in healthy preadolescents. *Pediatrics*, 84:542–546.

Kalogjera-Sackellares D, Cartwright RD (1997). Comparison of MMPI profiles in medically and psychologically based insomnias. *Psychiatry Research*, 70 (1):49–56.

Kamp I (van) (1990). *Coping with noise and its health consequences*. Styx and PP Publications, Groningen.

Karacan I et al. (1976). Prevalence of sleep disturbances in a primarily urban Florida county. *Social Science and Medicine*, 10:239–244.

Karagodina IL et al. (1969). Effect of aircraft noise on the population near airport. *Hygiene and Sanitation*, 34:182–187.

Karsdorf G, Klappach H (1968). Einflüsse des Verkehrslärms auf Gesundheit und Leistung bei Oberschülern einer Großstadt. *Zeitschrift für die gesamte Hygiene*, 14:52–54.

Kawachi I et al. (1995). Prospective study of shift work and risk of coronary heart disease in women. *Circulation*, 92:3178–3182.

Kecklund Q (1996). *Sleep and alertness: effects of shift work, early rising, and the sleep environment* (dissertation). Statens Institute for Psykosocial Miljomedicin (IPM), 252:1–94.

Kecklund G, Åkerstedt T (1993). Sleepiness in long distance truck driving: an ambulatory EEG study of night driving. *Ergonomics*, 36:1007–1017.

Kecklund G, Åkerstedt T (1997). Objective components of individual differences in subjective sleep quality. *Journal of Sleep Research*, 6, 217–220.

Keefe FB, Johnson LC, Hunter EJ (1971). EEG and autonomic response pattern during waking and sleep stages. *Psychophysiology*, 8:198–212.

Keipert JA (1985). The harmful effects of noise in a children's ward. *Australian Paediatric Journal*, 21:101–103.

Keith SW et al. (2006). Putative contributors to the secular increase in obesity: exploring the roads less traveled. *International Journal of Obesity*, 30:1585–1594.

Kempen EEMM (van) et al. (2002). The association between noise exposure and blood pressure and ischaemic heart disease: a meta-analysis. *Environmental Health Perspectives*, 110:307–317.

Kim K et al. (2000). An epidemiological study of insomnia among the Japanese general population. *Sleep*, 23 (1):41–47.

Klein DE, Bruner H, Holtman H (1970). Circadian rhythm of pilot's efficiency, and effects of multiple time zone travel. *Aerospace Medicine*, 41:125–132.

Knipschild, P. (1977a). V. Medical effects of aircraft noise: community cardiovascular survey. *International Archives of Occupational and Environmental Health*, 40:185–190.

Knipschild P (1977b). VI. Medical effects of aircraft noise: general practice survey. *International Archives of Occupational and Environmental Health*, 40:191–196.

Knipschild P, Oudshoorn N (1977). VII. Medical effects of aircraft noise: drug survey. *International Archives of Occupational and Environmental Health*, 40:197–200.

Knipschild P, Sallé H (1979). Road traffic noise and cardiovascular disease. *International Archives of Occupational and Environmental Health*, 44:55–59.

Knipschild P, Meijer H, Sallé H (1984). Wegverkeerslawaai, psychische problematiek en bloeddruk. *Tijdschr Soc Gezondheidszorg*, 62:758–765.

Knol AB, Staatsen BAM (2005). *Trends in the environmental burden of disease in the Netherlands 1980–2020, RIVM report 500029001/2005*. Bilthoven, Netherlands.

Knutsson A (1989a). Relationships between serum triglycerides and g-Glutamyltransferase among shift and day workers. *Journal of Internal Medicine*, 226:337–339.

Knutsson A (1989b). Shift work and coronary heart disease. *Scandinavian Journal of Social Medicine*, 544:1–36.

Knutsson A, Åkerstedt T, Jonsson B (1988). Prevalence of risk factors for coronary artery disease among day and shift workers. *Scandinavian Journal of Work, Environment and Health*, 14:317–321.

Knutsson A et al. (1986). Increased risk of ischemic heart disease in shift workers. *Lancet*, 12 (2):89–92.

Kogi K, Ohta T (1975). Incidence of near accidental drowsing in locomotive driving during a period of rotation. *Journal of Human Ergology*, 4:65–76.

Kokokusha D (1973). *Report of investigation of living environment around Osaka International Airport.* Aircraft Nuisance Prevention Association.

Koller M (1983). Health risks related to shift work. *International Archives of Occupational and Environmental Health*, 53:59–75.

Koller M, Kundi M, Cervinka R (1978). Field studies of shift work at an Austrian oil refinery. Health and psychosocial wellbeing of workers who drop out of shift work. *Ergonomics*, 21:835–847.

Kopferschmitt J et al. (1992). Sleep disorders and use of psychotropic drugs in 6-year-old children. *Revue d'Epidemiologie et de Santé Publique*, 40:467–471.

Kraenz S et al. (2004) Prevalence and stress factors of sleep disorders in children starting school. *Praxis der Kinderpsychologie und Kinderpsychiatrie*, 53, 1:3–18.

Kranendonk F, Gerretsen E, Luxemburg LCJ (van) (1993). *Akoestische kwaliteit van woningen versus de beleving van burengeluid.* TNO-BOUW, TUE-Bouwkunde; 93-CBO-R3185.

Kripke DF, Cook B, Lewis OF (1971). Sleep of night workers: EEG recordings. *Psychophysiology*, 7:377–384.

Kripke DF et al. (1979). Short and long sleep and sleeping pills. Is increased mortality associated? *Archives of General Psychiatry*, 36:103–116.

Kripke DF et al. (2002). Mortality associated with sleep duration and insomnia. *Archives of General Psychiatry*, 99:131–136.

Kristensen TS (1989). Cardiovascular diseases and the work environment. *Scandinavian Journal of Work, Environment, and Health*, 15:165–179.

Kryter KD (1990). Aircraft noise and social factors in psychiatric hospital admission rates: a re-examination of some data, *Psychological Medicine*, 20 (2):395–411.

Kryter K, Poza F (1980). Effects of noise on some autonomic system activities. *Journal of the Acoustical Society of America*, 2036–2044.

Kupperman M et al. (1995). Sleep problems and their correlates in a working population. *Journal of General Internal Medicine*, 10:25–32.

Kushnir T, Melamed S (1992). The Gulf War and its impact on burnout and well-being of working civilians. *Psychological Medicine*, 22:987–995.

Lambert J, Plouhinec M (1985). Day and night annoyance: a comparison. *Proceedings of Internoise 85*, pp. 941–944.

Lambert J, Vallet M (1994). *Study related to the preparation of a communication on a future* EC *noise policy*. LEN Report No.9420, Brussels.

Langdon FJ, Buller IB (1977). Road traffic noise and disturbance to sleep. *Journal of Sound and Vibration*, 50:13–28.

Langdon FJ, Buller IB, Scholes WE (1981). Noise from neighbours and the sound insulation of party walls in houses. *Journal of Sound and Vibration*, 79:205–288.

Lauber JK, Kayten PJ (1988). Sleepiness, circadian dysrhythmia, and fatigue in transportation system accidents. *Sleep*, 11:503–512.

Lavie P, Pillar G, Malhotra A (2002). *Sleep disorders: diagnosis, management and treatment. A handbook for clinicians.* Martin Dunitz, London.

Ledoux S, Choquet M, Manfredi R (1994). Self-reported use of drugs for sleep or distress among French adolescents. *Journal of Adolescent Health*, 15:495–502.

Leger D et al. (2000). Prevalence of insomnia in a survey of 12 778 adults in France. *Journal of Sleep Research*, 9:35–42.

Leger D et al. (2002). Medical and socio-professional impact of insomnia, *Sleep*, 25 (6):625–629.

Leidelmeijer K, Marsman G (1997). *Geluid van buren. Horen, hinder en sociale normen*. RIGO, Amsterdam, 97/65.

Leineweber C et al. (2003). Poor sleep increases the prospective risk for recurrent events in middle-aged women with coronary disease. The Stockholm Female Coronary Risk Study. *Journal of Psychosomatic Research*, 54:121–127.

Lennernas M, Åkerstedt T, Hambraeus L (1994). Nocturnal eating and serum cholesterol of three-shift workers. *Scandinavian Journal of Work, Environment and Health*, 20:401–406.

Lercher P (1992). *Auswirkungen des Straßenverkehrs auf Lebensqualität und Gesundheit*. Transitverkehrs-Studie, Teil I, Amt der Tiroler Landesregierung, Landesbaudirektion, Landessanitätsabteilung, Innsbruck.

Lercher, P (1996). Environmental noise and health: an integrated research perspective. *Environment International*, 22:117–128.

Lercher P, Kofler WW (1993). Adaptive behaviour to road traffic noise, blood pressure and cholesterol. In: Vallet M, ed. *Noise and Man '93. Proceedings of the 6th International Congress on Noise as a Public Health Problem, Nice 1993*. Arcueil Cedex, Institut National de Recherche sur les Transport et leur Sécurité.

Lercher P, Kofler WW (1996). Behavioral and health responses associated with road traffic noise exposure along alpine through-traffic routes. *The Science of the Total Environment*, 189/190:85–89.

Lercher P et al. (2002). Ambient neighbourhood noise and children's mental health. *Occupational and Environmental Medicine*, 59 (6):380–386.

Lindström B (1992). Quality of life: a model for evaluating health for all. Conceptual considerations and policy implications. *Sozial- und Präventivmedizin*, 37:301–306.

Lipworth L et al. (2001). Comparison of surrogate with self-respondents regarding medical history and prior medication use. *International Journal of Epidemiology*, 30:303–308.

Loeb M (1986). *Noise and human efficiency*. John Wiley & Sons, Chichester.

Lukas JS (1972a). Awakening effects of simulated sonic booms and aircraft on men and women. *Journal of Sound and Vibration*, 20:457–466.

Lukas JS (1972b). Effects of aircraft noise on human sleep. *American Industrial Hygiene Association Journal*, 33:298–303.

Lundberg U (1999). Coping with stress: neuroendocrine reactions and implications for health. *Noise & Health*, 4:67–74.

Lundberg O, Manderbacka K (1996). Assessing reliability of a measure of self-rated health. *Scandinavian Journal of Social Medicine*, 24:218–224.

Macey PM et al. (2002). Brain morphology associated with obstructive sleep apnea. *American Journal of Respiratory and Critical Care Medicine*, 15 (166):1382–1387.

Malmström M, Sundquist J, Johansson S-E (1999). Neighborhood environment and self-reported health status: a multilevel analysis. *American Journal of Public Health*, 89:1181–1186.

Manninen O, Aro S (1979). Urinary catecholamines, blood pressure, serum cholesterol and blood glucose response to industrial noise exposure. *Arhiv za Higijenu Rada i Toksikologiju*, 30:713–718.

Marcus CL (2001). Sleep-disordered breathing in children. *American Journal of Respiratory and Critical Care Medicine*, 164:16–30.

Marcus CL, Greene MG, Carroll JL (1998). Blood pressure in children with obstructive sleep apnea. *American Journal of Respiratory and Critical Care Medicine*, 157:1098–1103.

Marcus CL et al. (1994). Determinants of growth in children with the obstructive sleep apnea syndrome. *Journal of Pediatrics*, 125:556–562.

Marth E et al. (1988). Fluglärm: Veränderung biochemischer Parameter. *Zentralblatt für Bakteriologie, Mikrobiologie und Hygiene*, 185:498–508.

Maschke C (2003). Epidemiological research on stress caused by traffic noise and its effects on high blood pressure and psychic disturbances. In: Jong RD et al., eds. *ICBEN 2003. Proceedings of the 8th International Congress on Noise as a Public Health Problem, Rotterdam.* ISBN 90-807990-1-7. Foundation ICBEN, Schiedam.

Maschke C, Rupp T, Hecht K (2000). The influence of stressors on biochemical reactions – a review of present scientific findings with noise. *International Journal of Hygiene and Environmental Health*, 203:45–53.

Maschke C, Wolf U, Leitmann T (2003). *Epidemiological examinations of the influence of noise stress on the immune system and the emergence of arteriosclerosis.* Report 298 62 515 (in German, executive summary in English), Wabolu-hefte 01/03, Umweltbundesamt, Berlin.

Mathers CD et al (2003). *Global burden of disease in 2002 – data sources, methods and results.* WHO Discussion Paper No 54. (http://www3.who.int/whosis/discussion_papers/discussion_papers.cfm?path=evidence,discussion_papers&language=english, accessed 11 November 2006).

Mathur R, Douglas NJ (1995). Frequency of EEG arousals from nocturnal sleep in normal subjects. *Sleep*, 18:330–333.

Matschat K, Müller EA (1984). *Vergleich nationaler und internationaler Fluglärmbewertungsverfahren. Aufstellung von Näherungsbeziehungen zwischen den Bewertungsmaßen.* Umweltforschungsplan des Bundsministers des Innern, Forschungsbericht Nr. 81-105 01 307, Umweltbundesamt, Berlin.

Matsui T et al. (2001). Association between blood pressure and aircraft noise exposure around Kadena airfield in Okinawa. In: Boone R, ed. *Internoise 2001. Proceedings of the 2001 International Congress and Exhibition on Noise Control Engineering, The Hague, Vol. 3.* Nederlands Akoestisch Genootschap, Maastricht.

Matsui T et al. (2004). The Okinawa study: effects of chronic aircraft noise on blood pressure and some other physiological indices. *Journal of Sound and Vibration*, 277:469–470.

Matsumoto K (1978). Sleep patterns in hospital nurses due to shift work: an EEG study. *Waking and Sleeping*, 2:169–173.

Meecham WC, Smith HG (1977). Effects of jet aircraft noise on mental hospital admissions. *British Journal of Audiology*, 11 (3):81–85.

Meier-Ewert HK et al. (2004). Effect of sleep loss on C-reactive protein, an inflammatory marker of cardiovascular risk. *Journal of the American College of Cardiology*, 43:678-683.

Melamed S, Kushnir T, Shirom A (1992). Burnout and risk factors for cardiovascular diseases. *Behavioral Medicine*, 18:53–60.

Melamed S et al. (1999). Chronic burnout, somatic arousal and elevated salivary cortisol levels. *Journal of Psychosomatic Research*, 46:591–598.

Mellinger GD, Balter MB, Uhlenhuth EH (1985). Insomnia and its treatment. Prevalence and correlates. *Archives of General Psychiatry*, 42 (3):225–232.

Miedema HME (2003). *Self-reported sleep disturbance caused by aircraft noise.* TNO Inro, Delft, 2004–15.

Miedema HME (2004). Self-reported sleep disturbance caused by aircraft noise. TNO Inro, Delft, 2005–15.

Miedema HME, Vos H (1998). Exposure-response relationships for transportation noise. *Journal of the Acoustical Society of America*, 104:3432–3445.

Miedema HME, Passchier-Vermeer W, Vos H (2003). *Elements for a position paper on night-time transportation noise and sleep disturbance.* TNO Inro, Delft, 2002-59.

Ministerie Verkeer en Waterstaat (2005). *Evaluatie Schipholbeleid Schiphol beleefd door omwonenden*, The Hague, ISBN 90 369 18 537.

Mitler MM et al. (1988). Catastrophes, sleep and public policy: consensus report. *Sleep*, 11:100–109.

Mitler MM et al. (1997). The sleep of long-haul truck drivers. *The New England Journal of Medicine*, 337:755–761.

Miyakita et al. (1998). Is residential sound-proofing an effective measure in reducing the effects of aircraft noise? *Internoise 1998*, Noise Control Foundation.

Moline ML et al. (2003). Sleep in women across the life cycle from adulthood through menopause. *Sleep Medicine Reviews*, 7:155–177.

Morabia A (1991). On the origin of Hill's causal criteria. *Epidemiology*, 2:367–369.

Morin CM, Rodrigue S, Ivers H (2003). Role of stress, arousal, and coping skills in primary insomnia. *American Psychosomatic Society*, 65:259–267.

Morrell S, Taylor R, Lyle D (1997). A review of health effects of aircraft noise. *Australian and New Zealand Journal of Public Health*, 21:221–236.

Morrell S et al. (1998). Cross-sectional relationship between blood pressure of school children and aircraft noise. In: Carter N, Job RFS, eds. *Noise effects '98. Proceedings of the 7th International Congress on Noise as a Public Health Problem, Sydney 1998.*

Morrell S et al. (2000). Cross-sectional and longitudinal results of a follow-up examination of child blood pressure and aircraft noise. The inner Sydney child blood pressure study. *Internoise 2000, 29th International Congress and Exhibition on Noise Control Engineering, Nice.*

Mosso A (1886). *Periodische Athmung und Luxusathmung*. Arch. Physiol. Suppl, 37:116.

Müller-Wenk R (2002). *Attribution to road traffic of the impact of noise on health*. Environmental Series No 339, BUWAL, Berne (http://www.buwalshop.ch, accessed 11 November 2006).

Murray CHR et al. (1996). *The global burden of disease.* World Health Organization, Geneva.

Muzet A, Ehrhart J (1978). Amplitude des modifications cardiovasculaires provoquées par le bruit au cours du sommeil. *Coeur et médecine interne*, 17:49–56.

Muzet A, Ehrhart J (1980). Habituation of heart rate and finger pulse resonses to noise during sleep. In: Tobias JV, ed. *Noise as a public health problem*. ASHA report No.10, Rockville, Maryland, pp. 401–404.

Muzet A et al. (1973). Relationship between subjective and physiological assessments of noise-disturbed sleep. *Proceedings of the International Congress on Noise as a Public Health Problem, US Environmental Agency, Dubrovnik,Yugoslavia*, pp. 575–586.

Nagaya T et al. (2002). Markers of insulin resistance in day and shift workers aged 20–59 years. *International Archives of Occupational and Environmental Health*, 75:562–568.

Naitoh P, Muzet A, Lienhard JP (1975). Effects of noise and elevated temperature on sleepcycle. *Sleep Research*, 4:174.

NCSDR (2003). National Center on Sleep Disorders Research (http://www.nhlbi.nih.gov/health/prof/sleep/res_plan/index.html, accessed 3 March 2007).

Neus H, Boikat U (2000). Evaluation of traffic noise-related cardiovascular risk. *Noise & Health*, 2 (7):65–77.

Neus H et al. (1980). On the reaction of finger pulse amplitude to noise. *International Archives of Occupational and Environmental Health*, 47:9–19.

Neus H et al. (1983). Traffic noise and hypertension. The Bonn traffic noise study. In: Rossi G (ed.). *Proceedings of the 4th International Congress on Noise as a Public Health Problem, Turin 1983*. Edizioni Tecniche a cura del Centro Ricerche e Studi Amplifon, Milan.

Niemann H, Maschke C (2004). *Noise effects and morbidity, WHO LARES final report*. Berlin, Interdisciplinary Research Network "Noise and Health" (http://www.euro.who.int/document/NOH/WHO_Lares.pdf, accessed 18 November 2004).

Nieminen P et al. (2002). Growth and biochemical markers of growth in children with snoring and obstructive sleep apnea. *Pediatrics*, 109:e55.

Nijland HA et al. (2003). Costs and benefits of noise abatement measures. *Transport Policy*, 10:131–140.

Nilsson P et al. (2001). Sleep disturbances in association with elevated pulse rate for the prediction of mortality – consequences of mental strain? *Journal of Internal Medicine*, 250:521–529.

Nilsson P et al. (2002). Incidence of diabetes in middle-aged men is related to resting heart rate and difficulties to fall asleep (abstract). *7th International Congress of Behavioural Medicine.*

North FM et al. (1996). Psychosocial work environment and sickness absence among British civil servants: the Whitehall II study. *American Journal of Public Health*, 86:332–340.

NTSB (1995). *Factors that affect fatigue in heavy truck accidents.* National Transportation Safety Board, NTSB/SS-95/0 L.

Nurminen T (1989). Shift work, fetal development and course of pregnancy. *Scandinavian Journal of Work, Environment, and Health*, 15:395–403.

O'Brien LM, Gozal D (2002). Behavioral and neurocognitive implications of snoring and obstructive sleep apnea in children: facts and theory. *Pediatric Respiratory Reviews*, 3:3–9.

Ohayon MM, Roth T (2003). Place of chronic insomnia in the course of depressive and anxiety disorders. *Journal of Psychiatric Research*, 37 (1):9–15.

Öhrström E (1989). Sleep disturbance, psychosocial and medical symptoms – a pilot survey among persons exposed to high levels of road traffic noise. *Journal of Sound and Vibration*, 133:117–128.

Öhrström E (1993). *Long-term effects in terms of psychosocial wellbeing, annoyance and sleep disturbance in areas exposed to high levels of road traffic noise.* Health Council of the Netherlands, The Hague, A93/02E.

Öhrström E, Bjorkman M, Rylander R (1988). Noise annoyance with regard to neurophysiological sensitivity, subjective noise sensitivity and personality variables. *Psychological Medicine*, 18 (3):605–613.

Olkin I (1995). Meta-analysis: reconciling the results of independent studies. *Statistics in Medicine*, 14:457–472.

Ollerhead JB (1994). *Report of a field study of aircraft noise and sleep disturbance. A study commissioned by the Department of Transport from the Civil Aviation Authority*, HMSO, London.

Ollerhead et al. (1992). *Report on a field study of aircraft noise and sleep disturbance.* Department of Transport, London.

Ortscheid J, Wende H (2000). *Fluglärmwirkungen.* Forschungsbericht (in German), Umweltbundesamt, Berlin.

Ounsted MK, Hendrick AM (1977). The first-born child: patterns of development. *Developmental Medicine and Child Neurology*, 19:446–453.

Owens JA, Rosen CL and Mindell JA (2003). Medication use in the treatment of pediatric insomnia: results of a survey of community-based pediatricians. *Pediatrics*, 111:628–635.

Owens-Stively J et al. (1997). Neuro-psychological and behavioral correlates of obstructive sleep apnea in children. *Sleep Research*, 26 (suppl. 1):452.

Parish JM, Shepard JW (1990). Cardiovascular effects of sleep disorders. *Chest*, 97:1220–1226.

Partinen M, Eskelinen L, Tuomi K (1984). Complaints of insomnia in different occupations. *Scandinavian Journal of Work, Environment and Health*, 10:467–469.

Passchier-Vermeer W (1993). *Noise and health.* Health Council of the Netherlands, The Hague.

Passchier-Vermeer W (2000). *Noise and health of children.* TNO report PG/VGZ/2000.042, Organization for Applied Scientific Research (TNO), Leiden, Netherlands.

Passchier-Vermeer W (2001). Effects of noise. In: Bistrup ML, ed. *Health effects of noise on children and perception of the risk of noise.* National Institute of Public Health, Denmark, pp. 47–68.

Passchier-Vermeer W (2003a). *Night-time noise events and awakening.* TNO Inro report 2003-32, TNO Institute for Traffic and Transport, Delft.

Passchier-Vermeer W (2003b). Relationship between environmental noise and health. *Journal of Aviation Environmental Research*, 7 (suppl.):35–44.

Passchier-Vermeer W and Passchier WF (2000). Noise exposure and public health. *Environmental Health Perspectives*, 108 (suppl. 1):123–131.

Passchier-Vermeer W et al. (2002). *Sleep disturbance and aircraft noise exposure.* TNO-PG, Leiden, Report No. 2002.027.

Passchier-Vermeer W et al. (2004). *Motility and road and rail traffic noise.* TNO-Inro, Delft, TNO report No. 2004.

Patel SR et al. (2004). A prospective study of sleep duration and mortality risk in women. *Sleep*, 27:440–444.

Patois E, Valatz JL, Alperovitch A (1993). Prevalence of sleep and wakefulness disorders in high school students at the Academy of Lyon. *Revue d'Epidemiologie et de Santé Publique*, 41:383–388.

Patton GC et al. (2000). Adolescent depressive disorder: a population-based study of ICD-10 symptoms. *Australian and New Zealand Journal of Psychiatry*, 34 (5):741–747.

Pearsons K, Bennett R, Fidell S (1973). *Effects of cessation of late-night landings on behavioral awakening.* BNN Systems and Technologies Corporation, Canoga Park, Report No. 2439.

Peigneux P et al. (2001). *Sleeping brain, learning brain. The role of sleep for memory systems.* NeuroReport 2001:12:A111–A124.

Peiyoong L, Hiscock H, Wake M (2003). Outcomes of infant sleep problems: a longitudinal study of sleep, behavior, and maternal well-being. *Pediatrics*, 111:203–207.

Porter ND, Flindell IH, Berry BF (1998). *Health effect-based noise assessment methods: a review and feasibility study.* National Physical Laboratory, Teddington.

Poustka F, Eckermann P, Schmeck K (1992). Effect of aircraft noise and psychosocial stressors on mental disturbances of children and adolescents: an epidemiological study in Westphalia. In: Remschmidt H, Schmidt MH, eds. *Developmental psychopathology*, Hogrefe and Huber Publishers, Gottingen.

Prokop O, Prokop L (1955). Ermüdung und Einschlafen am Steuer. *Zentralblatt fur Verkehrsmedizin, Verkehrspsychologie und angrenzende Gebiete*, 1:19–30.

Pulles T, Biesiot W, Stewart R (1988). Adverse effects of environmental noise on health: an interdisciplinary approach. *Environmental International*, 16:437–445.

Rai RM et al. (1981). Biochemical effects of chronic exposure to noise in man. *International Archives of Occupational and Environmental Health*, 48:331–337.

Raw GJ, Oseland NA (1991) Subjective response to noise through party floors in conversion flats. *Applied Acoustics*, 32:215–231.

Rechtschaffen A, Bergmann BM (1965). Sleep deprivation in the rat by the disk-over-water method. *Behavioural Brain Research*, 69:55–63.

Rechtschaffen A, Kales A, eds. (1968). *A manual of standardized terminology, techniques and scoring system for sleep stages of human subjects.* Brain Information Service/Brain Research Institute, UCLA, Los Angeles.

Rechtschaffen A, Hauri P, Zeitlin M (1966). Auditory awakening thresholds in REM and NREM sleep stages. *Perceptual and Motor Skills*, 22:927–942.

Reyner LA (1995). *Sleep disturbance and daytime sleepiness in normal subjects.* Loughborough University of Technology, Loughborough.

Reyner et al. (1995). Patterns of spontaneous and evoked body movements during sleep. *Sleep*, 18 (3):209–211.

RFV (2003). *Lan-tidssjukskrivna - egenskaper vid 2003 ars RFV-LS-undersokning.*

Rhodes SK et al. (1995). Neurocognitive deficits in morbidly obese children with obstructive sleep apnea. *Journal of Pediatrics*, 127:741–744.

Ribet C, Derriennic F (1999). Age, working conditions, and sleep disorders: a longitudinal analysis in the French cohort. *Enquête Santé, Travail et Vieillissement (ESTEV)*, 22:491–504.

Richards W, Ferdman RM. (2000). Prolonged morbidity due to delays in the diagnosis and treatment of obstructive sleep apnea in children. *Clinical Pediatrics*, 39:103–108.

Riemann D, Berger M, Voderholzer U (2001). Sleep and depression – results from psychobiological studies: an overview, *Biological Psychology*, 57 (1–3):67–103.

Roberts E, Roberts CR, Chen IG. (2002). Impact of insomnia on future functioning of adolescents. *Journal of Psychosomatic Research*, 53 (1):561– 569.

Rockhill B (2005). Commentary. The message is rarely simple: the j-curve and beyond. *International Journal of Epidemiology*, 34:44–45.

Romon M, Nuttens MC, Fievet C (1992). Increased triglyceride levels in shift workers. *American Journal of Medicine*, 93 (3):259–262.

Rose G (2005). Incubation period of coronary heart disease. *International Journal of Epidemiology*, 34:242–244.

Rose GA, Blackburn H (1968). *Cardiovascular survey methods.* 1st edition, World Health Organization, Geneva.

Rosenlund M et al. (2001).Increased prevalence of hypertension in a population exposed to aircraft noise. *Journal of Occupational and Environmental Medicine*, 58:769–773.

Roth T, Ancoli-Israel S (1999). Daytime consequences and correlates of insomnia in the United States: results of the 1991 National Sleep Foundation Survey, II. *Sleep*, 22 (suppl. 2):S354–S358.

Sadeh A, Gruber R, Raviv A (2000). Sleep patterns and sleep disruptions in school-age children. *Developmental Psychology*, 36:291–301.

Sadeh A, Gruber R, Raviv A (2002). Sleep, neurobehavioral functioning, and behavior problems in school-age children. *Child Development*, 73:405–417.

Sadeh A, Gruber R, Raviv A (2003). The effects of sleep restriction and extension on school-age children: what a difference an hour makes. *Child Development*, 74:444–455.

Sadeh A et al. (1995). Sleep and psychological characteristics of children on a psychiatric inpatient unit. *Journal of the American Academy of Child and Adolescent Psychiatry*, 34 (6):813–819.

Sateia M et al. (2000). Evaluation of chronic insomnia. *Sleep*, 23 (2):243–263.

Scharnberg T et al. (1982). *Beeinträchtigung des Nachtschlafs durch Lärm. Eine interdisziplinäre Feldstudie der Technischen Universität Berlin und der Physikalisch-Technischen Bundesanstalt Braunschweig*, Umweltbundesamt, Berlin, Forschungsbericht Nr. 82-1050-1207.

Schernhammer ES et al. (2003). Night-shift work and risk of colorectal cancer in the nurses' health study. *Journal of the National Cancer Institute*, 95:825–828.

Schlesselman JJ (1987). "Proof" of cause and effect in epidemiologic studies: criteria for judgment. *Preventive Medicine*, 16:195–210.

Schreckenberg D et al. (1999). An interdisciplinary study on railway and road traffic noise: annoyance differences. 137th ASA Meeting and 25th DAGA Conference. *Journal of the Acoustical Society of America*, 105 (2):1219.

Schulte W, Otten H (1993). Ergebnisse einer Tieffluglärmstudie in der Bundesrepublik Deutschland: Extraaurale Langzeitwirkungen [Results of a low-altitude flight noise study in Germany: long-term extra-aural effects]. In: Ising H, Kruppa B, eds. *Lärm und Krankheit – Noise and disease.*

Proceedings of the International Symposium, Berlin 1991. Gustav Fischer Verlag, Stuttgart.

Schulze B et al. (1983). Verkehrslärm und kardiovaskuläres Risiko – eine epidemiologische Studie. *Das Deutsche Gesundheitswesen*, 38:596–600.

Schwela DH (2000). The World Health Organization guidelines for environmental health. *Noise/News International*, March, 9–22.

Segawa K et al. (1987). Peptic ulcer is prevalent among shift workers. *Digestive Diseases and Sciences*, 32:449–453.

Selye H (1956). *The stress of life*. McGraw-Hill, New York.

Sforza E, Jouny C, Ibanez V. (2000). Cardiac activation during arousal in humans: further evidence for hierarchy in the arousal response. *Clinical Neurophysiology*, 111:1611–1619.

Smith A (2003). The concept of noise sensitivity: implications for noise control, *Noise & Health*, 5 (18):57–59.

Smith AP, Broadbent DE (1981). Noise and levels of processing, *Acta Psychologica*, 47:129.

Smith AP, Broadbent DE (1992). *Non-auditory effects of noise at work: a review of the literature*. HSE Contract Research Report No 30. HMSO, London.

Smith L, Folkard S, Poole CJM (1994). Increased injuries on night shift. *Lancet*, 344:1137–39.

Smith MJ, Colligan MJ, Tasto DL (1982). Health and safety consequnces of shift work in the food-processing industry. *Ergonomics*, 25:133–144.

Spiegel K, Leproult R, van Cauter E (1999). Impact of sleep debt on metabolic and endocrine function. *Lancet*, 354:1435–1439.

Spreng M (2000). Central nervous system activation by noise. *Noise & Health*, 2 (7):49–57.

Spreng M (2004). Noise induced nocturnal cortisol secretion and tolerable overhead flights. *Noise & Health*, 6 (22):35–47.

Stansfeld SA (1992). *Noise, noise sensitivity and psychiatric disorder: epidemiological and psychophysiological studies*. Psychological Medicine Monograph Supplement 22, Cambridge University Press, Cambridge.

Stansfeld S, Haines M, Brown B (2000). Noise and health in the urban environment. *Reviews on Environmental Health*, 15 (1–2):43–82.

Stansfeld SA et al. (1985). Sensitivity to noise in a community sample: I. Measurement of psychiatric disorder and personality, *Psychological Medicine*, 15 (2):243–254.

Stansfeld SA et al. (1993). Road traffic noise, noise sensitivity and psychological disorder. *Psychological Medicine*, 23 (4):977–985.

Stansfeld S et al. (1996). Road traffic noise and psychiatric disorder: prospective findings from the Caerphilly Study. *British Medical Journal*, 313 (7052):266–267.

Stansfeld SA et al. (2002). Longitudinal effects of noise, noise sensitivity and psychosocial factors on men's psychological distress. *Epidemiology*, 13 (4):S90.

Stansfeld SA et al. (2005). Aircraft and road traffic noise and children's cognition and health: exposure–effect relationships. *Lancet*, 365:1942–1949.

Stein MA et al.(2001). Sleep and behavior problems in school-aged children. *Pediatrics*, 107:766 (e).

Stouthard M et al. (1997). *Disability weights for diseases in the Netherlands*, Department of Public Health, Netherlands.

Stradling JR et al. (1990). Effect of adenotonsillectomy on nocturnal hypoxaemia, sleep disturbance and symptoms in snoring children. *Lancet*, 335:249–253.

Suda M, Saito M (1979). Coordinative regulation of feeding behavior and metabolism by a circadian timing system. In: Suda M, Hayaishi O, Nakagawa H, eds. *Biological rhythms and their central mechanism*. Elsevier/North-Hollan Biomedical, New York, pp. 263–271.

Suter AH (1992). Noise sources and effects – a new look. *Sound and Vibration*, 25th anniversary issue:18–38.

Tamakoshi A, Ohno Y (2004). Self-reported sleep duration as a predictor of all-cause mortality: Results from the JACC study, Japan. *Sleep*, 27:51–54.

Tarnopolsky A, Morton-Williams J, Barker SM (1980). *Aircraft noise and prevalence of psychiatric disorders*. Research report. Social and Community Planning Research.

Tarnopolsky A, Watkins G, Hand DJ (1980). Aircraft noise and mental health: I. Prevalence of individual symptoms. *Psychological Medicine*, 10 (4):683–698.

Tarnopolsky A et al. (1978). The effect of aircraft noise on the mental health of a community sample: a pilot study. *Psychological Medicine*, 8 (2):219–233.

Tate RB et al. (1995). Tracking of blood pressure over a 40-year period in the University of Manitoba follow-up study, 1948–1988. *American Journal of Epidemiology*, 142:946–954.

Taylor PJ, Pocock SJ (1972). Mortality of shift and day workers 1956–68. *British Journal of Industrial Medicine*, 29:201–207.

Tenkanen L et al. (1997). Shift work occupation and coronary heart disease over 6 years of follow-up in the Helsinki Heart Study. *Scandinavian Journal of Work, Environment and Health*, 23:257–265.

Tepas DI et al. (1981). Polysomnographic correlates of shift worker performance in the laboratory. In: Reinberg A, Vieux N, Andlauer P, eds. *Night and shift work: biological and social aspects.* Pergamon Press, Oxford, pp. 179–186.

Terzano MG et al. (1990). Modifications of sleep structure induced by increasing levels of acoustic perturbation in normal subjects. *Electroencephalography and clinical neurophysiology*, 76:29–38.

Terzano MG et al. (1993). Assessment of noise-induced sleep fragility in two age ranges by means of polysomnographic microstructure. *Journal of Sound and Vibration*, 162:345–359.

Theorell T et al. (1998). Decision latitude, job strain, and myocardial infarction: A study of working men in Stockholm. *American Journal of Public Health*, 88:382–388.

Thiessen GJ (1988). Effect of traffic noise on the cyclical nature of sleep. *Journal of the Acoustical Society of America*, 84:1741–1743.

Thiis-Evensen E (1958). Shift work and health. *Industrial Medicine and Surgery*, 27:493–497.

Thomas DA et al. (1996). The effect of sleep deprivation on sleep states, breathing events, peripheral chemosensiveness and arousal propensity in healthy 3-month old infants. *European Respiratory Journal*, 9:932–938.

Thomas JR, Jones DM (1982). Individual differences in noise annoyance and the uncomfortable loudness level, *Journal of Sound and Vibration*, 82:289–304.

Thompson SJ (1997). Cardiocascular and fetal effects of noise. In: IEH, ed. *Workshop on non-auditory health effects of noise. Report No. R10*. Institute for Environment and Health, Leicester.

Thunström M (2002). Severe sleep problems in infancy associated with subsequent development of attention-deficit hyperactivity disorder at 5.5 years of age. *Acta Paediatrica*, 31:584–592.

Tilley AJ, Wilkinson RT, Drud M (1981). Night and day shifts compared in terms of the quality and quantity of sleep recorded in the home and performance measured at work: a pilot study. In: Reinberg A, Vieux N, Andlauer P, eds. *Night and shift work. Biological and social aspects.* Pergamon Press, Oxford, pp. 187–196.

Tilley AJ et al. (1982). The sleep and performance of shift workers. *Human Factors*, 24:624–641.

Torsvall L, Åkerstedt T (1987). Sleepiness on the job: continuously measured EEG changes in train drivers. *Electroencephalography and Clinical Neurophysiology*, 66:502 –511.

Torsvall L, Åkerstedt T (1988). Disturbed sleep while being on call. An EEG study of apprehension in ships' engineers. *Sleep*, 11:35–38.

Torsvall L et al. (1989). Sleep on the night shift: 24-hour EEG monitoring of spontaneous sleep/wake behavior. *Psychophysiology*, 26:352–358.

Trott GE et al. (1995). Self-assessment of prescribing behavior of psychotropic drugs for children and adolescents. Results of a survey of established physicians. *Psychiatrische Praxis*, 22 (6):235–239.

Tüchsen F (1993). Working hours and ischaemic heart disease in Danish men. A 4-year cohort study of hospitalization. *International Journal of Epidemiology*, 22:215–221.

Ullrich S (1998). Lärmbelastung durch den Straßenverkehr. *Zeitschrift für Lärmbekämpfung*, 45:22–26.

Urponen H et al. (1988). Self-evaluations of factors promoting and disturbing sleep: an epidemiological survey in Finland. *Social Science and Medicine*, 26:443–450.

Utley WA (1985). Descriptors for ambient noise. In: Bundesanstalt für Arbeitsschutz, ed. *Internoise 85. Proceedings of the International Conference on Noise Control Engineering in Munich 1985*. Wirtschaftsverlag NW, Verlag für neue Wissenschaft GmbH, Bremerhaven.

Valent F, Brusaferro S, Barbone F (2001). A case-crossover study of sleep and childhood injury. *Pediatrics*, 107: 23.

Vallet M et al. (1983). Heart rate reactivity to aircraft noise after a long term exposure. In: Rossi G (ed.). *Noise as a public health problem*. Centro Ricerche E Studi Amplifon, Milan, pp. 965–971.

Verdun Di Cantogno L et al. (1976). Urban traffic noise cardiocirculatory activity and coronary risk factors. *Acta Otolaryngologica*, (suppl.) 339:55–63.

Vernet M (1979). Effect of train noise on sleep for people living in houses bordering the railway line. *Journal of Sound and Vibration*, 66 (3):483–492.

Vgontzas AN et al. (2000). Sleep apnea and daytime sleepiness and fatigue: relation to visceral obesity, insulin resistance, and hypercytokinemia. *Journal of Clinical Endocrinology and Metabolism*, 85:1151-1158

Vgontzas AN et al. (2001). Chronic insomnia is associated with nyctohemeral activation of the hypothalamic-pituitary-adrenal axis: clinical implication. *Journal of Clinical Endocrinology and Metabolism*, 86:3787–3794.

Vollrath M, Wicki W, Angst J (1989). The Zurich study. VIII. Insomnia: association with depression, anxiety, somatic syndromes, and course of insomnia. *European Archives of Psychiatry and Neurological Sciences*, 239 (2):113–124.

Vos J (2003). On the relevance of shooting-noise-induced sleep disturbance to noise zoning, *ICBEN-proceedings 2003*, Schiedam.

Wagner U, Gais S, Born J (2001). Emotional memory formation is enhanced across sleep intervals with high amounts of rapid eye movement sleep. *Learning and Memory*, 8:112–119.

Walter SD (1998). Attributable risk in practice. *American Journal of Epidemiology*, 148:411–413.

Ware JE, Sherbourne DC (1992). The MOS 36-item short-form health survey (SF-36) – Conceptual framework and item selection. *Medical Care*, 30:473–483.

Wassmer E et al. (1999). The acceptability of sleep-deprived electroencephalograms. *Seizure*, 8:434–435.

Watkins G, Tarnopolsky A, Jenkins LM (1981). Aircraft noise and mental health: II. Use of medicines and health care services, *Psychological Medicine*, 11 (1):155–168.

Waye KP et al. (2003). Effects of night-time low frequency noise on the cortisol response to awakening and subjective sleep quality. *Life Sciences*, 72:863–875.

Weber A, Jaekel-Reinhard A (2000). Burnout syndrome: a disease of modern societies? *Occupational Medicine*, 50, 512–517.

Weed DL (2000). Interpreting epidemiological evidence: how meta-analysis and causal inference methods are related. *International Journal of Epidemiology*, 29:387–390.

Weed DL, Hursting SD (1998). Biologic plausibility in causal inference: current method and practice. *American Journal of Epidemiology*, 147:415–425.

Weinstein ND (1978). Individual differences in reactions to noise: a longitudinal study in a college dormitory. *Journal of Applied Psychology*, 63 (4):458–466.

Weinstein ND (1980). Individual differences in critical tendencies and noise annoyance. *Journal of Sound and Vibration*, 68:241–248.

Weissbluth M et al. (1983). Signs of airway obstruction during sleep and behavioral, developmental and academic problems. *Journal of Developmental and Behavioral Pediatrics*, 4:119–121.

WHO *Guidelines for community noise*. World Health Organization, Geneva. 1999 (http://www.who.int/docstore/peh/noise/guidelines2.html, accessed March 2007)

WHO-ISH Guidelines Subcommittee (1999). World Health Organization, International Society of Hypertension guidelines for the management of hypertension. *Journal of Hypertension*, 17:151–183.

WHO Regional Office for Europe (2000). *Noise and health*. WHO Regional Office for Europe, Copenhagen.

Wilkinson R et al. (1989). Alertness of night nurses: two shift systems compared, *Ergonomics*, 32:281–292.

Williams RL, Karacan L, Hursch CJ (1974). *EEG of human sleep*. John Wiley & Sons, New York.

Willner P, Neiva J (1986). Brief exposure to uncontrollable but not to controllable noise biases the retrieval of information from memory. *British Journal of Clinical Psychology*, 25 (Pt 2):93–100.

Wing JK, Cooper JE, Sartorius N (1974). *The measurement and classification of psychiatric symptoms*. Cambridge University Press, London.

Winkleby MA, Ragland DR, Syme SL (1988). Self-reported stressors and hypertension: evidence of an inverse association. *American Journal of Epidemiology*, 127:124–133.

Wölke G et al. (1990). Verkehrslärm und kardiovaskuläres Risiko. *Forum Städte-Hygiene*, 41:306–308.

Wubben F, Busink J (2004). *Night restrictions at Amsterdam Schiphol. A comparison with other European mainports*. To70 Aviation & Environment, The Hague, Netherlands.

Yong L-C et al. (1993). Longitudinal study of blood pressure. Changes and determinants from adolescence to middle age. The Dormont High School follow-up study, 1957/1963 to 1989/1990. *American Journal of Epidemiology*, 138:973–983.

Yoshida T et al. (1997). Effects of road traffic noise on inhabitants of Tokyo. *Journal of Sound and Vibration*, 205:517–522.

Zamir G et al. (1998). Sleep fragmentation in children with juvenile rheumatoid arthritis. *Journal of Rheumatology*, 25:1191–1197.

Zepelin H, McDonald CS, Zammit GK (1984). Effects of age on auditory awakening thresholds. *Journal of Gerontology*, 39 (3):294–300.

Zorick FJ, Walsh JK (2000). Evaluation and management of insomnia: an overview. In: Kryger MH, Roth T, Dement WC, eds. *Principles and practice of sleep medicine*. W.B.Saunders, Philadelphia, pp. 615–623.

Zuckerman B, Stevenson J, Bailey V (1987). Sleep problems in early childhood: continuities, predictive factors, and behavioural correlates. *Pediatrics* 80:664–671.

APPENDIX 1. GLOSSARY OF TERMS AND ACRONYMS

Term/acronym	Definition
Actimetry	The measurement of accelerations associated with the movement of an actimeter
ADHD	Attention-deficit hyperactivity disorder
Behavioural awakening	Awakening that is registered by the subject by means of a conscious action
BP	Blood pressure
CAP	Cyclic alternating patterns
EBD	Environmental burden of disease
END	Environmental Noise Directive (2002/49/EC)
EEG	Electroencephalogram, recording of electric activity in the brain
ECG	Electrocardiogram, recording of electric activity of the heart
EEG awakening	Transition from a state of sleep to a state of consciousness, as determined by a sleep EEG
Heart rate acceleration	A temporary rise in heart rate relative to the average heart rate assessed shortly before a noise event
HPA axis	Hypothalamus-pituitary-adrenal axis
ICSD	International Classification of Sleep Disorders
IHD	Ischaemic heart disease
Insomnia	Sleeping disorder consistent with an internationally accepted definition (see ICSD), which takes account of difficulty falling or staying asleep, the daytime implications and the duration of the problems
$L_{Aeq,T}$	Exposure to noise for the duration of a given time interval T (a 24-hour period, a night, a day, an evening) is expressed as an equivalent sound pressure level (measured in dB(A)) over the interval in question
L_{Amax}	Maximum outdoor sound pressure level associated with an individual noise event
L_{night}	Refers to the EU definition in Directive 2002/49/EC: equivalent outdoor sound pressure level associated with a particular type of noise source during night-time (at least 8 hours), calculated over a period of a year
Motility onset	The presence of movement in a short time interval, following an interval without movement
Mg	Magnesium
Motility	The presence of movement in a short time interval, as recorded on an actigram
OR	Odds ratio: the ratio of the odds of an event occurring in another group, or to a sample-based estimate of that ratio

Term/acronym	Definition
OSAS	Obstructive sleep apnoea syndrome
OTC	Over-the-counter (medicines sold without prescription)
Polysomnography	The measurement during a subject's time in bed of his or her brain activity by means of EEG, EOG and EMG. The technique involves the use of electrodes to record electrical potentials in the brain
REM	Rapid eye movement (sleep phase)
RR	Relative risk: a ratio of the probability of the event occurring in the exposed group vs. the control (non-exposed) group
SEL	Sound exposure level: equivalent outdoor sound pressure level associated with an individual noise event, with the equivalent level standardized at one second
Sleep disturbance	Disturbance of sleep by night-time noise, as perceived by a subject and described in a questionnaire response or journal entry
Sleep EEG	Graph created using data from EEG scanning during a subject's time in bed, showing the various stages of sleep as a function of time
Sleep fragmentation	Within a sleep period, the frequency and duration of intervals of wakefulness recorded on a sleep EEG or intervals of motility recorded on an actigram
Sleep latency	The length of time taken to fall asleep, i.e. the interval between the point at which a person begins trying to go to sleep or allowing him/herself to go to sleep and sleep inception time
Sleep stage change	Change from a deeper stage of sleep to a less deep stage, as determined by a sleep EEG
SMR	Standardized mortality ratios
SROBD	Sleep related obstructive breathing disorders
SWS	Slow-wave sleep (sleep phase)
UARS	Upper airway resistance syndrome

APPENDIX 2. RELATIONS BETWEEN L_{NIGHT} AND INSTANTANEOUS EFFECTS

STATEMENT 1

Let f be a function of SEL that gives the expected number of instantaneous effects caused by a single event. With a given L_{night} and a given number of events N, the expected number of times that an effect occurs in the night, n, is maximal if all events have equal SEL, provided that f°10lg is increasing but negatively accelerated.

STATEMENT 2

If

$$n_{max} = 10^{(L_{night}-SEL+70.2)/10} \cdot f(SEL),$$

has a maximum over SEL and f is the quadratic function $f(SEL) = a\ SEL^2 + b\ SEL + c$, then the maximum occurs irrespective of L_{night} at

$$SEL_0 = 4.34 - A \pm ((A - 4.34)^2 - (c/a) + 8.68A)^{1/2},$$

where $A = b/(2a)$. (Only with + at the place of ± the value will come in the realistic range of SEL)

STATEMENT 3A

If the shape of the time pattern of the sound level has a block form, then $SEL = L_{Amax} + 10lg(T)$, where L_{Amax} is the maximum sound level (integrated over 1-s) and T is the duration of the noise event in seconds.

STATEMENT 3B

If the sound level increases with rate a (in dB(A)/s) and after time point $t = 0$ decreases with rate –a, then $SEL \approx L_{Amax} - 10lg(a) + 9.4$.

APPENDIX 3. ANIMAL STUDIES ON STRESS AND MORTALITY

INTRODUCTION

Is noise a health risk or does it just annoy? This basic question needs to be carefully answered when establishing night noise guidelines. No one will deny that in the case of high noise levels there is a risk of inner ear damage, but what about the moderate levels of environmental noise? To approach this rather difficult question, all available methods must be combined.

1. In animal experiments it is possible to assess the complete causal chain from noise exposure via physiological reactions and biological risk factors to morbidity or even mortality. However, a quantitative application of the results to humans is not possible. Instead, the method is useful in studying the pathomechanisms qualitatively.
2. Experiments on humans are, for ethical reasons, restricted to the study of reversible physiological reactions. But as long as there is no proof that reactions to chronically repeated noise exposures are increasing the risk of specific diseases, the results of such physiological studies are not considered conclusive.
3. Epidemiological studies have the advantage of investigating health effects which are particularly caused by chronic noise exposure although there is no possibility to control all influencing factors. Additionally, epidemiological studies have to be based upon biologically evident hypotheses.

A hypothetical model of noise-induced health effects is shown in Fig. 4.3 in Chapter 4, section 4.5.2 of this report. This model is based on the results of noise experiments with animals and humans. With animal experiments, the whole causal chain from noise exposure to health outcome can be traced as a direct pathway starting with a chronic high level noise exposure which, via endocrine stress reactions, leads, for example, to microcirculatory defects and to manifest hypertension.

Physiological experiments on humans have shown that noise of a moderate level acts via an indirect pathway and has health outcomes similar to those caused by high noise exposures on the direct pathway. The indirect pathway starts with noise-induced disturbances of activities such as communication or sleep. Since we are dealing with night noise guidelines, noise-induced sleep disturbances and any resulting persistent health effects are of primary interest here.

In physiological studies with experimentally changed noise exposure, the increase of arousals and of hormone excretion was studied in sleeping people. If this model is correct then in the cause–effect chain the arousal ought to precede the endocrine reactions. This order was derived from the different reaction times of the effects. While arousals appear within 1 second after a noise stimulus, hormones like catecholamines take several minutes, and cortisol about 10 minutes to be increased. This observation, together with the fact that arousals are evoked by equal or lower noise levels than the corresponding endocrine reactions, confirms the correctness of the model and leads to an important conclusion: noise exposure which does not evoke arousals in sleeping people will not induce adverse health effects.

This conclusion is essential with regard to night noise guidelines. However, the answers to the basic question as to whether certain health risks are connected with environmental noise must be clarified by epidemiological studies based on noise experiments on both humans and animals.

TYPES OF ANIMAL STUDIES

Noise has often been used as a stressor in animal studies. Even Selye (1953), who introduced the psychophysiological stress concept, used noise stimuli in his animal studies. Most of the modern animal studies testing the pharmacological effects of drugs are carried out with and without various stressors. The typical noise exposure is to short and very intensive sounds. One such example is the study of Diao et al. (2003) who exposed guinea pigs to 4 kHz octave band noise at 115 dB for 5 hours. But these experiments are of little value regarding the noise exposure types in question.

The same is true for another type of animal study concerned with the prevention of noise-induced health effects in wild and domestic animals (for review of the former kind see Fletcher, 1983). One example for the latter kind is the study of Geverink et al. (1998) on stress responses of pigs to transport and lairage sounds.

Since the subject of the present paper is noise-induced health effects in humans, the review addresses only those studies in which animals are used as a model for humans.

The animal model for aural effects in humans has been established in great detail, so that even quantitative transference of results from animals to humans is possible. However, inner ear damage generally occurs at much higher noise levels than the environmental levels under discussion in this paper. Therefore interest focuses on animal models with respect to extra-aural noise effects.

LIMITING ASPECTS OF ANIMAL MODELS

Other than in studies on aural effects, the animal model does not allow quantitative comparisons in studies of extra-aural noise effects. It may, however, be used for the qualitative investigation of pathophysiological mechanisms following exposure to acute and very short sounds. But an animal model for long-term noise effects as caused by chronically repeated noise exposures needs careful planning. First it has to be ensured that stress reactions in both humans and animals when activated by noise exposure are qualitatively comparable. Secondly, the stress effects of chronic noise exposure have to be assessed in humans, and the animal models should be designed correspondingly. However, in the animal model, influences from cortical interconnections have to be excluded as a factor in these noise experiments. Naturally, one cannot expect to establish an animal model for indirect environmental noise effects which in humans may, for example, disturb activities such as verbal communication, which in turn may induce stress hormone increases.

STRESS HORMONES IN NOISE-EXPOSED ANIMALS

HABITUATION

In short-term experiments any kind of exposure to loud noise will cause acute increases of stress hormones. Long-term repeated noise exposure, however, will cause a certain habituation in the animal. Periodic repetitions of identical noise bursts lead to almost complete habituation. This was probably the main reason why Borg (1981) found no adverse health effects in rats exposed for their whole lives to periodic noise pulses. Therefore, random series of noise pulses are now applied in most long-term studies.

Selye (1974) had already stated that not all stages of a stress response are noxious, especially in the case of mild or brief exposures. Since environmental noise is a mild stressor, adverse health effects are only to be expected under the condition that repeated noise exposures induce long-term stress hormone changes. According to the Allostatic Load Model (McEwen, 1998), the normal response to an environmental stressor such as noise is the physiological activation of the endocrine system enabling the body to cope with the stressor and, after the stress situation is terminated, to shut off the allostatic response.

J.D. HENRY'S MODEL OF BEHAVIOURAL STRESS EFFECTS

On the basis of the available literature on stress effects in animals and humans, Henry (1992) developed a model with regard to different biological effects and health risks associated with different coping styles. He explains that the neuroendocrine response to various challenges and threats varies according to the type and degree of control a mammal can exert over it. This in turn is strongly determined by the animal's previous experience. In general, the sympathetic adrenomedullary system is preferentially activated when the animal displays an active response to escape from or deal with an environmental challenge. This is the fight/flight mode of stress response. The adrenocortical axis is preferentially activated as the subjects become immobile/passive when no control or threat of its loss is experienced. This is the conservation/withdrawal mode of response.

THE NOISE STRESS MODEL

On the basis of noise effect studies in animals and humans (for review see Ising and Braun, 2000), a noise stress model was developed. It describes a differentiation of prevailing "stress hormones" under noise exposure. Predominantly adrenaline – and to a lesser degree noradrenaline – are released from the adrenal medulla as the normal response to novel noise stimuli of moderate intensity. Following long-term noise exposures of moderate intensity habituation will alter the response mode and predominantly noradrenaline is released. As a response to extremely intensive noise, near the inner ear pain threshold, predominantly cortisol is released from the adrenal cortex induced by increased releases of adrenocorticotropic hormone (ACTH), especially in the case of unexpected noise.

The described differentiation will only be observed under special conditions. Unexpected exposure for three minutes to white noise at 75 dB leads, in dogs that are awake, to increased adrenal secretion of adrenaline and noradrenaline and – following a delayed increase in plasma ACTH – an increase in cortisol secretion (Engeland, Miller and Gann, 1990).

The cortisol response as described is valid for animals and humans in their active phases. During sleep, however, several studies in humans showed cortisol increases under exposure to traffic noise of moderate levels (Maschke, Arndt and Ising, 1995;

Evans et al.2001; Ising and Ising, 2002; Ising et al., 2004). It was hypothesized that noise stimuli signalling a danger, for example the noise of an approaching lorry, will, during sleep, normally generate a defeat reaction, which includes the release of cortisol from the adrenal cortex. Appropriate studies with sleeping animals after conditioning them – for example with a specific noise stimulus followed by pain – should be carried out to test this hypothesis.

Rats were exposed for a period of 12 hours to low-altitude flight noise – reproduced electro-acoustically once per hour on average at stochastically fluctuating intervals (L_{Amax} 125 dB, 10 dB downtime: 1 s, L_{eq}: 89 dB) (Ising et al., 1991; Ising, 1993). Adrenaline and noradrenaline excretions tended to decrease, whereas plasma cortisol increased significantly. Although in rats corticosterone is secreted rather than cortisol, we will simplify this paper by using cortisol for rats all the same. In this experiment, as well as in all others of our group, normally four rats were kept in one stainless steel cage, which was set on a funnel to collect their urine.
These results show that exposure to noise levels approaching or exceeding the pain threshold of the inner ear leads to endocrine reactions qualitatively different from those induced by less intensive noise.

The different endocrine reactions to acute and chronic noise exposure were studied in rats by Gesi et al. (2002b). They were exposed either to a single (6-hour) session of loud (100 dB(A)) noise, or to the same noise stimulus repeatedly every day for 21 consecutive days. Exposure to noise for 6 hours on one day induced parallel increases in dopamine, noradrenaline and adrenaline concentrations in tissue samples of the adrenal medulla. After 21 days of noise exposure, noradrenaline concentration was significantly higher than in controls, and that of adrenaline decreased significantly. Cortisol was not assessed in this study.

In another subchronic noise experiment, rats were exposed to irregular white noise at 90 dB for 3 and 9 hours per day during 18 and 8 days respectively (van Raaij et al., 1997). In rats with 3 hours of exposure per day the blood concentrations of adrenaline, noradrenaline and cortisol did not differ from controls. Exposure for 9 hours per day, however, resulted in significantly increased concentrations of noradrenaline and cortisol. At the end of the experiment all animals were subjected to restraint stress and their endocrine reactions were assessed. The authors sum up their findings as follows: these results indicate that chronic noise exposure at mild intensities induces subtle but significant changes in hormonal regulation.

The results of another experiment with different levels of random white noise pulses during 45 minutes per hour, 12 hours per day for 8 days demonstrate that cortisol responses to subchronic mild noise exposure do not monotonously increase with the noise levels (Bijlsma et al., 2001). While in rats exposed to 95 dB pulses plasma cortisol concentrations were raised twofold against controls, the exposure to 105 dB pulses did not increase cortisol significantly.

The time dependency of cortisol increase in the blood of rats under exposure to white noise (100 dB, 6 hours per day for 21 days) was examined by Gesi et al. (2001). The authors found a progressive increase in cortisol which reached a plateau 9 days from the beginning of exposure.

In summing up the results of these studies we can reach the following conclusions.

- Acute exposure to unexpected and novel noise of moderate intensities leads to activation of both the sympathetic adrenal-medullary system with increased secretion of adrenaline and noradrenaline, and the HPA axis with increased secretion of ACTH and of cortisol from the adrenal cortex.

- Under chronic exposure to unpredictable noise, adrenaline secretion is reduced to normal or subnormal values while noradrenaline and ACTH/cortisol concentrations remain increased.

- Extremely intensive unpredictable noise near the inner ear pain threshold triggers, in mammals that are awake, a defeat reaction with increases of ACTH/cortisol while the catecholamines adrenaline and noradrenaline remain normal or are slightly decreased.

- Chronic noise exposure at mild intensities will induce changes in hormonal regulation, if the individual threshold of allostasis is exceeded. A chronic allostatic load leads to subtle but significant changes in hormonal regulation, which are at present not fully understood.

EFFECTS OF PRENATAL NOISE EXPOSURE ON THE SENSITIVITY TO STRESS

Pregnant rats were subjected to noise and light stress, three times weekly on an unpredictable basis throughout gestation (Weinstock et al., 1998). Blood concentrations of adrenaline, noradrenaline and cortisol at rest and after footshock were assessed. At rest cortisol was significantly increased in offspring of stressed rats in comparison to controls while adrenaline and noradrenaline did not differ in either of the groups. After footshock, noradrenaline was significantly higher in offspring of stressed rats, showing that prenatal stress can induce long-term changes in the sensitivity of the sympathicoadrenal system to stress.

Pregnant monkeys were repeatedly exposed to unpredictable noise during days 90–145 after conception (Clarke et al., 1994). Blood concentration of ACTH and cortisol were measured in offspring of stressed and control monkeys at rest and under four progressively stressful conditions. Prenatally stressed offspring showed higher ACTH than controls in all four stressful conditions while cortisol did not change under stress. These results indicate that prenatal stress may have long-term effects on the HPA axis regulation.

EFFECTS OF NOISE EXPOSURE ON CORTISOL AND THE IMMUNE SYSTEM

The effect of acute noise stress on rats was studied by assessing blood concentrations of cortisol and total as well as differential leukocyte count (Archana and Namasivayam, 1999). A significant increase in cortisol and a significant decrease of total leukocyte counts were found.

Rats were exposed to "rock" music (80dB) for 24 hours (McCarthy, Quimet and Daun, 1992). In vitro stimulation of leukocyte subpopulations revealed several noise effects. Neutrophils and macrophages secreted significantly less superoxide anion and interleukin-1. Such effects may be detrimental to wound healing.

Pregnant rats were from gestation day 15 to day 21 daily exposed to the noise of a fire alarm bell (L_{Amax} = 85–90 dB) delivered randomly for 1 hour (Sobrian et al., 1997). In developing offspring mitogen-specific alterations in lymphoproliferatic activity and reduced immunoglobulin G levels were found at postnatal day 21.
Aguas et al. (1999) exposed a special breed of mice to low frequency noise – a model of noise – for three months as described below (Castelo Branco et al., 2003). These mice spontaneously developed an autoimmune disease at 6 months of age. Chronic low frequency noise exposure accelerated the expression of the autoimmune disease and affected the immune system, which was associated with kidney lesions and increased mortality.

Embryotoxic effects
Geber (1973) exposed pregnant rats day and night for three weeks to constantly changing sound mixtures between 76 and 94 dB for 6 minutes per hour, day and night, and demonstrated embryotoxic effects, notably calcification defects in the embryos.

Pregnant rats on a moderately magnesium deficient diet were exposed to noise during their active phase from 20.00 to 08.00 for three weeks (stochastically applied white noise impulses L_{Amax}: 87 dB, L_{eq}: 77 dB, t: 1 s duration) (Günther et al. 1981).

As compared to controls on the same diet, there was no difference in bone mineralization. The only significant effect was an increased fetal resorption rate.

The noise was changing in Geber's experiment but the noise level was comparable to the noise impulses stochastically applied by Günther et al. (L_{Amax} = 87 dB). Since these impulses were more frequent, their stress effect was at least as strong as the noise exposure employed by Geber. Therefore the major factor that differentiated the two exposure types in causing a reduced mineralization of the rat skeletons (Geber, 1973) must have been the additional noise exposure during sleep.

Castelo Branco et al. (2003) studied Wistar rats born under low frequency noise exposure. The third octave level of the applied broadband noise was > 90 dB for frequencies between 50 and 500 Hz. The broadband level was 109 dB(lin). The exposure schedule was chosen as a model for occupational noise: 8 hours per day, 5 days per week, and weekends in silence. Third generation rats born in low frequency noise environments were observed showing teratogenic malformations including loss of segments.

Morphological alterations in the myocardium caused by acute noise
Gesi et al. (2002a) reviewed the literature and stated that in experimental animals undergoing noise exposure, subcellular myocardial changes have been reported, especially at mitochondrial level; in particular, after 6 hours of exposure only the atrium exhibited significant mitochondrial alterations, whereas after 12 hours as well as subchronic exposure both atrium and ventricle were damaged.

Exposure of rats to 100 dB(A) noise for 12 hours caused a significant increase of DNA damage accompanied by ultrastructural alterations and increased noradrenaline concentrations in the myocardium (Lenzi et al., 2003). In another paper this group described an increase in mitochondrial calcium (Ca) influx caused by the same noise exposure. They described Ca accumulation at myocardial subcellular level. Summing up their results they wrote that: moreover, the present results joined with previous evidence indicate that calcium accumulation is the final common pathway responsible for noise-induced myocardial morphological alterations (Gesi et al., 2000).

Connective tissue proliferation
Hauss, Schmitt and Müller (1971) described a proliferation of connective tissue in the myocardium of rats under acute exposure to noise.

On the basis of these results a noise exposure experiment was carried out of 5 weeks with day and night exposure to stochastically triggered bells (L_{Amax}: 108 dB, t (duration of one signal):1 s, L_{eq}: 91 dB) (Ising, Noack and Lunkenheiner, 1974). We confirmed the results of Hauss, Schmitt and Müller (1971) using an electron microscope to demonstrate fibrosis in the interstitial tissue of the myocardium. Additionally electron dense areas (visible as black spots) located within bundles of collagen in the myocardium were observed. According to Selye (1962), these dark areas were most probably caused by high concentrations of calcium (Ca) carbonate or calcium phosphate deposits. This suggestion is consistent with the results of Gesi et al. (2000).

After publication of these findings, a reservation was correctly voiced that, as the noise exposure had not left intervals for sleep, it was not certain whether the myocardial damage was provoked by the noise stress as such or by a noise-induced lack of sleep. For this reason, all subsequent experiments provided for noise-free intervals of 8 to 12 hours during the rats' inactive phases to enable them to sleep.

Rats were exposed for 28 weeks to a random series of white noise impulses from 16.00 to 08.00 daily with an 8 hour rest in their inactive phase (Ising et al., 1979). The third octave spectrum of the noise was flat between 5 and 25 kHz and had a third octave level of 88 dB (lin) (broadband L_{Amax} = 97 dB(lin). L_{eq} = 87 dB(lin)). The duration of noise impulses was 4 seconds and the noise to pause ratio 1:10 on average. There was a small but significant increase in hydroxyproline as indicator of collagen in the rats' left myocardium. Electron micrographs showed, similar to the earlier experiment, collagen bundles in the otherwise empty interstitial space but no indication of calcium deposits.

Respiratory effects
Castelo Branco et al. (2003) studied respiratory epithelia in Wistar rats born under low frequency noise exposure and further exposed for up to 5403 hours during more than 2.5 years. The third octave level of the applied broadband noise was > 90 dB for frequencies between 50 and 500 Hz. The broadband level was 109 dB(lin). The exposure schedule was chosen as a model for occupational noise: 8 hours per day, 5 days per week and weekends in silence. Rats were gestated and born under the described noise exposure with additional exposures from 145 to 5304 hours. Transmission electron micrographs of the tracheal epithelium of rats exposed for 2438 hours revealed a subepithelial layer of hyperplastic collagen bundles, several of them exhibiting a degenerative pattern. The results indicate an increased proliferation as well as degenerative processes of collagen.

Castelo Branco et al. (2003) observed sheared cilia in the respiratory epithelia of Wistar rats born under and further chronically exposed to low frequency noise. As interpretation of their findings they stated that both mechanical and biochemical events may be responsible for this pattern of trauma.

Electrolytes: Ca/Mg shift
Acute exposure of rats to the fast rising overflight noise of low flying fighter planes

reaching levels of up to 125 dB(A)) (Ising et al., 1991; Ising, 1993) resulted not only in an increase of cortisol but also in a decrease of intracellular magnesium (Mg) and an increase of Mg excretion.
In guinea pigs, acute stress – due to 2 hours of noise exposure (95 dB white noise) or to overcrowding in the cage – caused significant increases of serum Mg and decreases of erythrocyte Mg (Ising et al., 1986).

For chronic noise experiments an additional stress factor had been sought which would act synergistically with unwanted noise, since in the above described noise experiment, half a year of exposure led to but relatively mild health effects (Ising et al., 1979). The justification for using two stressors derives from the fact that humans have to cope with a whole range of more or less synergistic stress factors and not with noise alone.

Organic damage as a result of chronic stress is likely to occur only under the condition that the overall exposure to stress exceeds a certain tolerance level during a relatively long period of time (Selye, 1974). For technical reasons, the two options available to supply a suitable additional stress factor were the cold or a magnesium (Mg) deficiency. Both factors, like habitual noise, cause an increased noradrenaline secretion. For practical reasons different degrees of a magnesium-deficient diet were selected as an additional stress factor. Noise exposure was provided by electro-acoustically reproduced traffic noise of L_{Amax}: 86 dB, L_{eq}: 69 dB over 12 hours during the rats' active phase. For one group the noise level was slightly increased (L_{eq}: 75 dB). The experiment lasted 16 weeks (Günther, Ising and Merker, 1978). Magnesium deficiency combined with noise exposure led to dose-dependent increases in adrenaline and noradrenaline, which can be used to quantify the overall stress of the dietary treatment. As stress grew, the hydroxyproline (as an indicator of collagen) and calcium (Ca) content of the myocardium increased while the magnesium content decreased. Long-term stress therefore resulted in an intracellular Ca/Mg shift.

Altura et al. (1992) studied the relationship between microcirculation (measured several days after termination of noise exposure), hypertension and Ca/Mg shifts in vascular walls of noise-stressed rats on Mg deficient diets. Noise exposure during the first 8 weeks was set to an energy equivalent level of 85 dB(A) from 20.00 to 08.00. Noise impulses were randomly switched on at randomized peak levels of 80, 90 and 100 dB(A). During the final 4 weeks the equivalent noise level was elevated to 95 dB(A) and the daily exposure increased to 16 hours with an 8 hour rest during the animals' inactive phase. In aortic and port vein smooth muscle the Ca content increased with rising noise exposure, with decreasing Mg uptake, and with the combination of both together, while the Mg content decreased. Parallel to this the reactivity of terminal arterioles to noradrenaline was increased (Fig.1a).

Stress-induced Ca/Mg shifts in smooth muscle cells have the potential to increase the risk of hypertension and myocardial infarction (Ising, Havestadt and Neus, 1985). Stress increases the membrane permeability of catecholamine-sensitive cells, which in turn raises Ca influx into cells and liberates intracellular Mg. A depression of catecholamine-induced vasoconstriction by stress-dependent hypermagnesemia (excess serum Mg concentration) has been demonstrated experimentally. However, the benefit from this stress-depressing hypermagnesemia is obtained at the expense of increased renal Mg loss. In the long run, chronic stress combined with suboptimal Mg in diet will reduce the Mg release in acute stress situations, causing an increase of vasoconstriction and raising the risk of hypertension.

Fig.1
Effects of 12 weeks noise exposure, Mg deficient diet and the combination of both in Wistar rats. (a) Ca/Mg shifts in vascular smooth muscle, Mg concentration in blood and reactivity of arterioles to noradrenaline. (b) Systolic BP, capillary blood flow velocity and numbers of capillaries/volume.

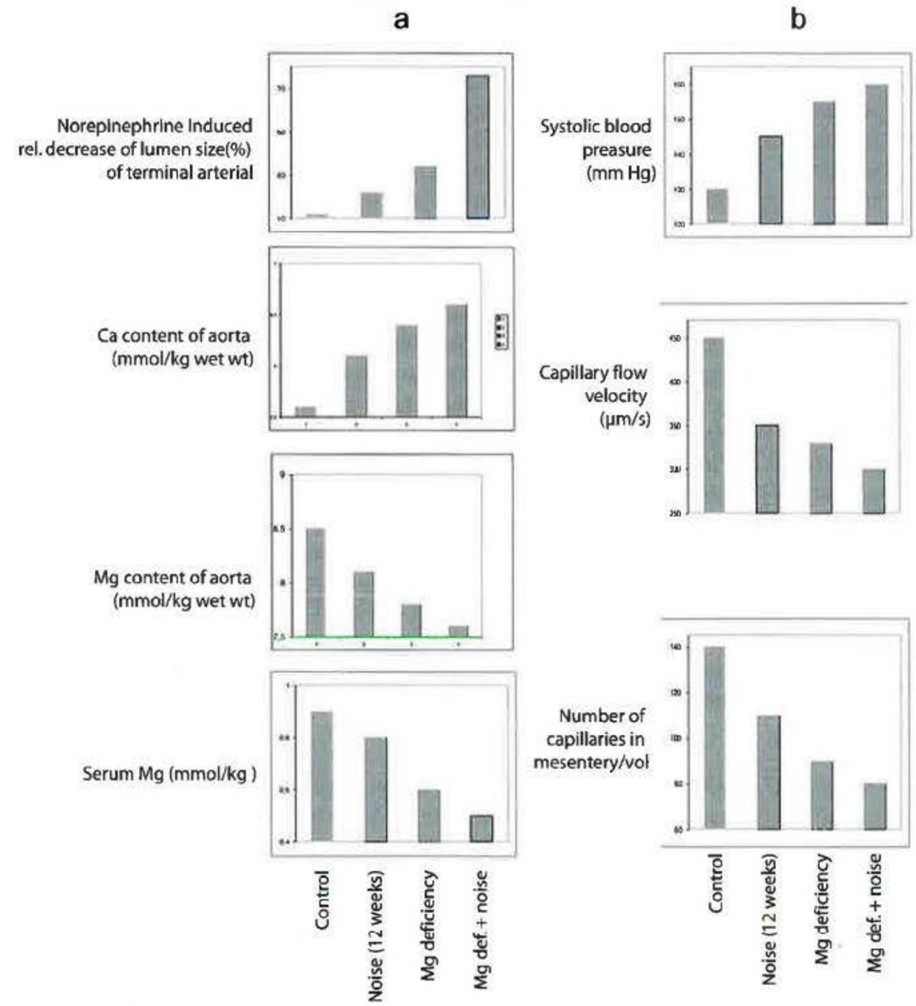

Source: Altura et al., 1992

Further analysis of the experimental results led to an interaction model between chronic stress and intracellular electrolyte shifts (Ising, 1981; Ising et al., 1986) (Fig.2). Chronic stress caused a loss of extracellular and intracellular Mg and an increase in intracellular Ca (Günther, Ising and Merker, 1978). A decrease of Mg was correlated with an increase in physiological noise sensitivity, that is, to more severe noradrenaline releases in animals and humans under noise exposure (Günther, Ising and Merker, 1978; Ising, Havestadt and Neus, 1985; Ising et al., 1986). There was a positive feedback mechanism between stress – caused by noise and other stressors – and intracellular Mg/Ca shifts, which may end in a circulus vitiosus and increase cardiovascular risks.

Fig. 2
Interaction between stress and Ca/Mg shifts and its long term consequences

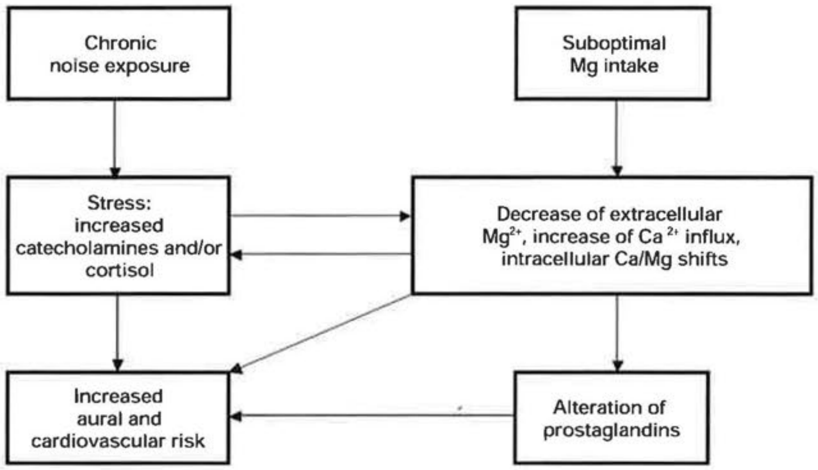

Hypertension

Rothlin, Cerletti and Emmenegger (1956) exposed rats for 1.5 years, day and night, to 90 dB "audiogenic stress" and observed a raising of systolic BP values from 120 mm Hg to about 150 mm Hg. He used a cross-breed of Albino rats and wild Norwegian rats since Albino rats did not develop hypertension under noise exposure. After termination of exposure the BP returned to normal.

Albino rats were exposed to noise during their whole lifespan (for review see Borg, 1981) to periodic noise impulses of 80 and 100 dB. This periodic exposure had no detrimental health effects, which can be understood on the basis of the work of Glass, Singer and Friedmann (1969). Unpredictable noise presentation was shown to cause lasting cortisol increases in rats in contrast to periodic exposure to 100 dB, which led to adaptation (De Boer, van der Gugten and Slangen, 1989). The unpredictability of a noise is a decisive precondition of long-term stress effects.

Exposure of primates to traffic noise for 10 hours per day during 9 months led to a significant BP increase, which persisted during 3 weeks after termination of exposure (Peterson et al., 1981). A replication of this experiment with a different species of primates failed to show an increase of their BP (Turkkan, Hienz and Harris, 1983).

In the above-mentioned experiment of Altura et al. (1992), exposure to unpredictable noise impulses led within 12 weeks to irreversible changes of microcirculation and an increase of systolic BP (Fig. 1b). The observed rarefication of capillaries in the mesentery can be interpreted as an indicator of accelerated ageing of the circulatory system.

Ageing and lifespan

The cortisol response and recovery after immobilization stress was compared in young and old rats. The results are demonstrated in Fig. 3 together with Sapolsky's Glucocorticoid Cascade Model (Sapolsky, Krey and McEwen, 1986). The stress response of young and old rats is more or less the same. However, while the young rats recover immediately after termination the old ones recover only in part.

Fig. 3
Above: Recovery after stress (young and old rats).
Below: Sapolsky´s Glucocorticoid Cascade Model

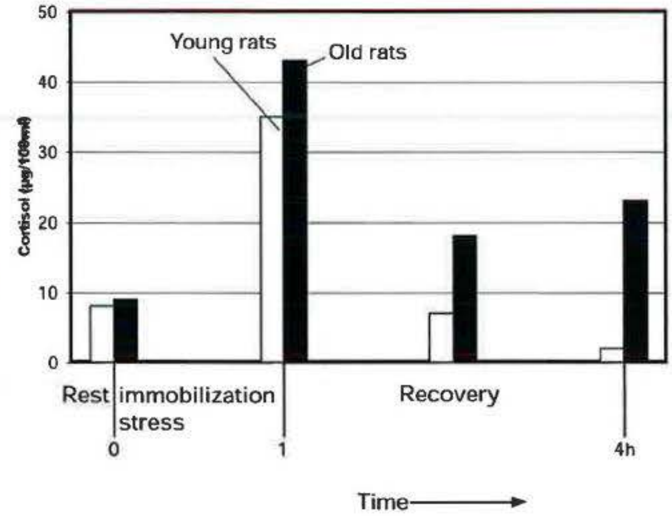

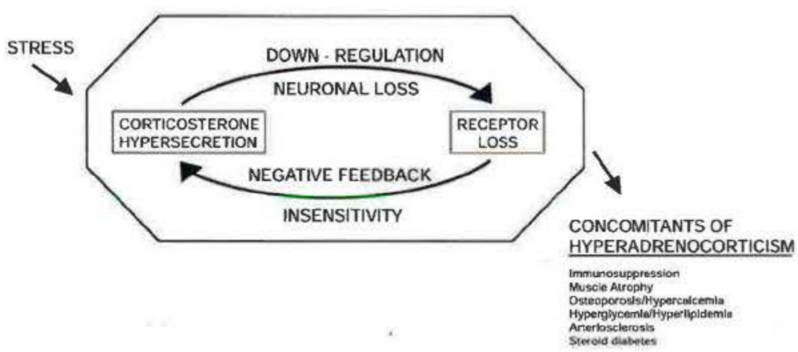

Therefore, acute stress leads, in old animals, to considerably prolonged cortisol increases. On the other hand, chronically repeated stress activates the HPA axis and can cause cortisol receptor losses even in younger animals, a process generally developing only in old age. Finally, chronic cortisol hypersecretion may occur along with follow-up health defects.

Aguas et al. (1999) exposed a special breed of mice to the above described model of occupational low frequency noise for three months. Chronic low frequency noise exposure accelerated the expression of the autoimmune disease and was associated with kidney lesions and increased mortality.

Chronic noise exposure of animals on a suboptimal Mg diet led to increases of connective tissue and calcium and decreases of Mg in the myocardium (Günther, Ising and Merker, 1978). These changes were correlated with noradrenaline changes. Since they are also correlated with normal ageing, the noise stress induced changes may be interpreted as accelerated ageing (Ising, Nawroth and Günther, 1981). Even the lifespan was reduced in rats on an Mg deficient diet, and was further dose-dependently reduced in combination with noise exposure (see Table 1).

Table 1
Effects of noise exposure combined with dietary Mg-deficiency in rats

Treatment		Effect					
4 months	3 months	Urine		Myocardium			Death rate
Mg in diet	Noise	Noradre-naline	Adre-naline	Hydroxy-proline	Ca	Mg	
	L_{eq}/L_{Amax}	(µg/g Cre)		(mg/g dry wt.)	(mg/g d.w.)	(mg/g d.w.)	
control	ambient	18 ± 4	12 ± 2	3.0 ± 0.1	3.0 ± 0.2	37.5 ± 0.8	0
suboptimal	ambient	23 ± 4	18 ± 2	3.0 ± 0.1	3.5 ± 0.5	38.0 ± 1.7	0
suboptimal	69/86 dB	37 ± 11	16 ± 2	3.0 ± 0.1	4.3 ± 0.2	37.9 ± 1.3	0
deficient	ambient	98 ± 17	20 ± 5	3.9 ± 0.1	6.2 ± 0.7	31.2 ± 1.4	38%
deficient	69/86 dB	129 ± 19	41 ± 10	4.6 ± 0.1	6.7 ± 0.6	29.8 ± 1.8	62%
deficient	75/86 dB	172 ± 26	60 ± 15	5.6 ± 0.9	8.0 ± 0.9	26.8 ± 0.8	75%

Adrenaline and noradrenaline excretion was measured during the fourth week of noise exposure; death rate is related to the 4-month period of Mg treatment; all other parameters were determined at the end of the experiment (mean values ± S.E.). Noise has the potential to cause stress reactions which are enhanced by suboptimal magnesium intake. Chronic noise-induced stress accelerates the ageing of the myocardium and thus increases the risk of myocardial infarction. The involved pathomechanisms include increases of catecholamines and/or cortisol under acute noise exposure and an interaction between endocrine reactions and intracellular Ca/Mg shifts.

WHAT CAN BE LEARNED FROM ANIMAL STUDIES ABOUT NOISE EFFECTS IN HUMANS?

The effects of low frequency noise – the "vibroacoustic disease" – were studied primarily in humans (for review see Castello Branco and Alves-Pereira, 2004).

In this context, the amygdalar contribution to conditioned fear learning, revealed for normal human subjects, has to be mentioned. Longer lasting activation of the HPA axis, especially abnormally increased or repeatedly elevated cortisol levels may lead to disturbances of the hormonal balance and even severe diseases in man (Spreng, 2000).

Catecholamines induce various detrimental effects on the heart (Ceremuzynski, 1981). Additionally, magnesium deficiency causes alterations of serum lipids (Weglicki et al., 1993), cytokines (Rayssiguier, 1990) and prostaglandines (Nigam, Averdunk and Günther, 1986), in particular an increase of thromboxan, which is released from thrombocytes (Neumann and Lang, 1995) and several other cell types and – in turn – thromboxan A2 can aggregate thrombocytes. All these alterations may increase the risk of myocardial infarction.
Beside these cardiovascular stress effects, chronically increased cortisol may induce

neuronal degeneration and thus accelerate the ageing also of the brain (Sapolsky, Krey and McEwen, 1986), not only in rats but in humans as well (Sapolsky, 1994).

The importance of Ca/Mg shifts was confirmed by post mortem studies of hearts from victims of IHD (Elwood et al. 1980). The tissue samples were taken from areas of the myocardium not affected by the infarction and the results were stable after controlling for several confounders. The results are shown in Table 2. With normal ageing Ca increases and Mg decreases in the myocardium. This process is accelerated in myocardial infarction patients, which indicates an accelerated ageing of these peoples' heart muscle under the pathogenic influences that lead to myocardial infarction.

Table 2
Age dependency of myocardial Ca and Mg contents in ischaemic heart disease (IHD)

IHD deaths and non IHD deaths. (Mean Value ± SD, numbers in brackets)

	Group	Age < 45years	45–64 years	≥ 65 years
Ca [µg/g]	Non IHD	43 ± 15 (175)	50 ± 14 (281)	57 ± 22 (155)
	IHD	48 ± 10 (48)	53 ± 17 (389)	58 ± 21 (188)
Mg [µg/g]	Non IHD	183 ± 28	173 ± 34	178 ± 30
	IHD	170 ± 29	157 ± 30	156 ± 27
Ca/Mg	Non IHD	0.24	0.29	0.32
	IHD	0.28	0.34	0.37

Another factor which decreases Mg and increases Ca (Hofecker, Niedermüller and Skalicky, 1991) and collagen (Caspari, Gibson and Harris; 1976, Anversa et al., 1990; Gibbons, Beverly and Snyder, 1991) in the myocard is normal ageing (Ising, Nawroth and Günther, 1981). Therefore, it is plausible that the age-dependent decrease of Mg in hearts of IHD victims was about double of that in age-matched non-IHD deaths. This is therefore an indication that age- and stress-dependent electrolyte changes exist in humans and may be correlated with an increased risk of IHD.

Long-term experiments with Mg-deficient and noise-stressed rats showed that connective tissue and Ca in the myocardium increased with age while Mg decreased. Hence, stress caused by noise or cold is enhanced by suboptimal Mg intake and accelerates the ageing of the heart and decreases the lifespan (Heroux, Peter and Heggtveit, 1977; Ising, Nawroth and Günther, 1981; Günther, 1991).

Since coronary arteriosclerosis increases strongly with age (Lakatta, 1990) a biologically older heart is at a higher risk of IHD and of myocardial infarction. The interaction process described seems to be one of the pathomechanisms by which chronic noise stress increases the risk of myocardial infarction.

Several of the risk factors described in the literature to explain the correlation of work stress with myocardial infarction have been found to be increased under noise-induced stress as well, that is, increases of BP and total cholesterol.

REFERENCES

Aguas AP et al. (1999). Acceleration of lupus erythematosus-like processes by low frequency noise in the hybrid NZB/W mouse model. *Aviation Space Environmental Medicine*, 70 (March suppl.):132–136.

Altura BM et al. (1992). Noise-induced hypertension and magnesium in rats: relationship to micro-circulation and calcium. *Journal Applied Physics*:194–202.

Anversa P et al. (1990). Myocyte cell loss and myocyte cellular hyperplasia in the hypertrophied aging rat heart. *Circulation Research*, 67(4):871–885.

Archana R, Namasivayam A (1999). The effect of acute noise stress on neutrophil functions. *Indian Journal of Physiology and Pharmacology*, 43:491–495.

Bijlsma PB et al. (2001). Subchronic mild noise stress increases HRP permeability in rat small intestine in vitro. *Physiology & Behavior*, 73:43–49.

De Boer SF, van der Gugten J, Slangen JL (1989). Plasma catecholamine and corticosterone responses to predictable and unpredictable noise stress in rats. *Physiology & Behavior*, 45:789–795.

Borg E (1981). Physiological and pathogenic effects of sound. *Acta Oto-Laryngologica*, Supplement 381.

Caspari PG, Gibson K, Harris P (1976). Changes in myocardial collagen in normal development and after · blockade. Proc 6th Ann Meeting of the International Study Group for Research in Cardiac Metabolism. In: Harris P, Bing RJ, Fleckenstein A, eds. *Biochemistry and pharmacology of myocardial hypertrophy, hypoxia, and infarction,* 7:99–104.

Castelo Branco NAA, Alves-Pereira M (2004). Vibroacoustic disease. *Noise & Health*, 6, (23):3–20.

Castelo Branco NAA et al. (2003). SEM and TEM study of rat respiratory epithelia exposed to low frequency noise. In: Mendez-Vilas A, ed. *Science and Technology Education in Microscopy: An Overview*. Formatex, Badajoz, Spain, Vol.II, pp. 505–533.

Ceremuzynski L (1981). Hormonal and metabolic reactions evoked by acute myocardial infarction. *Circulation Research*, 48(6):767–776.

Clarke AS et al. (1994). Long-term effects of prenatal stress on HPA axis activity in juvenile rhesus monkeys. *Developmental Psychobiology*, 27(5):257–269.

Diao MF et al. (2003). Changes in antioxidant capacity of the guinea pig exposed to noise and the protective effect of alphalipoic acid against acoustic trauma. *Acta Physiologica Sinica*, 55(6):672–676.

Elwood PC et al. (1980). Magnesium and calcium in the myocardium: cause of death and area differences. *Lancet*, 2:720–722.

Engeland WC, Miller P, Gann DS (1990). Pituitary-adrenal and adrenomedullary responses to noise in awake dogs. *The American Journal of Physiology*, 258:672–677.

Evans G et al. (2001). Typical community noise exposure and stress in children. Journal of the Acoustical Society of America, 109(3):1023–1027:

Fletcher JL (1983). Effects of noise on wildlife: A review of relevant literature 1979–1983. In: Rossi G. *Noise as a public health problem*. 2:1153–1174, Centro Recherche E Studi Amplifon, Milan.

Geber WF (1973). Inhibition of fetal osteogenesis by maternal noise stress. *Federation Proceedings*, 32(11):2101–2104.

Gesi M et al. (2000). Ultrastructural localization of calcium deposits in rat myocardium after loud noise exposure. *Journal of Submicroscopic Cytology and Pathology*, 32(4):585–590.

Gesi M et al. (2001) Time-dependent changes in adrenal cortex ultrastructure and corticosterone levels after noise exposure in male rats. *European Journal of Morphology*, 39(3):129–135.

Gesi M et al. (2002a). Morphological alterations induced by loud noise in the myocardium: the role of benzodiazepine receptors. *Microscopy Research and Technique*, 5(2):136–146.

Gesi M et al. (2002b). Brief and repeated noise exposure produces different morphological and biochemical effects in noradrenaline and adrenaline cells of adrenal medulla. *Journal of Anatomy*, 200:159–168.

Geverink NA et al. (1998). Responses of slaughter pigs to transport and lairage sounds. *Physiology & Behavior*, 63(4):667–673.

Gibbons GC III, Beverly PT, Snyder DL (1991). Myocardial fibrosis in ageing germ-free and conventional Lobund-Wistar rats: The protective effect of diet restriction. *Journal of Gerontology*, 46:B167–170.

Glass DC, Singer JE, Friedmann LN (1969). Psychic cost of adaptation to environmental stressor. *Journal of Personality and Social Psychology*, 12:200–210.

Günther T (1991). Magnesium deficiency, oxygen radicals and aging. *Magnesium Bulletin*, 13(3):78–81.

Günther T, Ising H, Merker HJ (1978). Elektrolyt- und Kollagengehalt im Rattenherzen bei chronischem Magnesium-Mangel und Streß. *Journal of Clinical Chemistry and Clinical Biochemistry*, 16:293–297.

Günther T et al. (1981). Embryotoxic effects of magnesium deficiency and stress on rats and mice. *Teratology*, 24:225–233.

Hauss W, Schmitt G, Müller U (1971). Über die Entstehung der Bindegewebsproliferation im Myocard nach Einwirkung verschiedener pathogener Reize. *Verhandlung der deutschen Gesellschaft für Medizin*, 77:1256–1263.

Henry JD (1992). Biological basis of the stress response. *Integrative Physiological and Behavioral Science*, 27:66–83.

Heroux O, Peter D, Heggtveit A (1977). Long-term effect of suboptimal dietary magnesium and calcium contents of organs, on cold tolerance and on lifespan, and its pathological consequences in rats. *Journal of Nutrition*, 107:1640–1652.

Hofecker G, Niedermueller H, Skalicky M (1991). Assessment of modifications of the rate of aging in the rat. *Archives of Gerontology and Geriatrics*, 12:273–289.

Ising H (1981). Interaction of noise-induced stress and Mg decrease. *Artery*, 9(3):205–211.

Ising H (1993). Extra-aural effects of chronic noise exposure in animals – a review. In: Ising H, Kruppa B, eds. *Noise and disease*, Gustav Fischer, Stuttgart, pp. 48–64.

Ising H, Braun C (2000). Acute and chronic endocrine effects of noise: review of the research conducted at the Institute for Water, Soil and Air Hygiene. *Noise & Health*, 7:7–24.

Ising H, Ising M (2002). Chronic cortisol increases in the first half of the night caused by road traffic noise. *Noise & Health*, 4(16):13–21.

Ising H, Havestadt C, Neus H (1985). *Health effects of electrolyte alterations in humans caused by noise stress*. InternoiseTagungsbericht, Schriftenreihe der Bundesanstalt fuer Arbeitsschutz, Dortmund; II, pp. 973–976.

Ising H, Nawroth T, Guenther T (1981). Accelerated aging of rats by Mg deficiency and noise stress. *Magnesium Bulletin* 3(2):142–145.

Ising H, Noack W, Lunkenheimer PP (1974). Histomorphologische Herzschäden nach Lärmeinwirkung. *Bundesgesundheitsblatt*, 16:234–238.

Ising H et al. (1979). Increase of collagen in the rat heart induced by noise. *Environment International*, 2:95–105.

Ising H et al. (1986). Stress-induced Ca/Mg shifts and vascular response in animals and men; comparison to electrolyte alterations in myocardial infarction patients. *Magnesium Bulletin*, 8:95–103.

Ising H et al. (1990). Medically relevant effects of noise from military low-altitude flights – results of an interdisciplinary pilot study. *Environment International*, 16:411–423.

Ising H et al. (1991). *Gesundheitliche Wirkungen des Tieffluglärms – Hauptstudie.* Umweltbundesamt, Berlin.

Ising H et al. (2004). Low frequency noise and stress: bronchitis and cortisol in children exposed chronically to traffic noise and exhaust fumes. *Noise & Health*, 6(23):21–28.

Lakatta EG (1990). The aging heart. In: Geokas MC (mod.): The aging process. *Annals of Internal Medicine*, 113:455–466.

Lenzi P et al. (2003). DNA damage associated with ultrastructural alterations in rat myocardium after loud noise exposure. *Environmental Health Perspectives*, 111(4):467–471.

Maschke C, Arndt D, Ising H (1995). Nächtlicher Fluglärm und Gesundheit: Ergebnisse von Labor- und Feldstudien. *Bundesgesundheitsblatt*, 38(4):130–137.

McCarthy DO, Quimet ME, Daun JM (1992). The effects of noise stress on leukocyte function in rats. *Research in Nursing & Health*, 15(2):131–137.

McEwen BS (1998). Protective and damaging effects of stress mediators – Allostasis and allostatic load. New England Journal of Medicine, 840:33–44.

Neumann S, Lang H (1995). Entzuendung. In: Greiling H, Gressner AM. *Lehrbuch der Klinischen Chemie und Pathochemie.* Schattauer Verlag, pp. 1257–1305.

Nigam S, Averdunk R, Günther T (1986). Alteration of prostanoid metabolism in rats with magnesium deficiency. *Prostaglandins Leukotrienes and Medicine*, 23:1–10.

Peterson EA et al. (1981). Noise raises blood pressure without impairing auditory sensitivity. *Science*, 111(4489):1451–1453.

Van Raaij MT et al. (1997). Hormonal status and the neuroendocrine response to a novel heterotypic stressor involving subchronic noise exposure. *Neuroendocrinology*, 65:200–209.

Rayssiguier Y (1990). Magnesium und lipid metabolism. In: Sigel H, Sigel A, eds. *Metal ions in biological systems.* Marcel Dekker INC, New York/Basel, Vol. 26, pp. 341–358.

Rothlin E, Cerletti A, Emmenegger H (1956). Experimental psycho-neurogenic hypertension and its treatment with hydrogenated ergot alkaloids (Hydergine). *Acta Medica Scandinavica*, 154 (suppl. 312):27–35.

Sapolsky RM (1994). *Why zebras don't get ulcers: A guide to stress, stress-related diseases, and coping.* WH Freeman, New York.

Sapolsky RM, Krey LC, McEwen BS (1986). The neuroendocrinology of stress and aging: the glucocorticoid cascade hypothesis. *Endocrine Reviews*, 7:284–306.

Selye H (1953). *The stress of life.* McGraw-Hill, New York.

Selye H (1962). *Calciphylaxis.* Chicago Press.

Selye H (1974). *Stress without distress.* Lippincott, Philadelphia, PA.

Sobrian SK et al. (1997) Gestational exposure to loud noise alters the development and postnatal responsiveness of humoral and cellular components of the immune system in offspring. *Environmental Research*, 73;227–241.

Spreng M (2000). Possible health effects of noise induced cortisol increase. *Noise & Health*, 7:59–63.

Turkkan HJS, Hienz RD, Harris AH (1983). The non-auditory effects of noise on the baboon. In: Rossi G. *Noise as a public health problem.* Vol.2, Centro Recherche e Studi Amplifon, Milan.

Weglicki WB et al. (1993). Modulation of cytokines and myocardial lesions by vitamine E and chloroquine in a Mg-deficient rat model. *American Journal of Physiology*, 264:C723–726.

Weinstock M et al. (1998). Effect of prenatal stress on plasma corticosterone and catecholamines in response to footshock in rats. *Physiology & Behavior*, 64(4):439–444.

APPENDIX 4. NOISE AND SLEEP IN CHILDREN

FACTORS THAT MODIFY AUDITORY AROUSAL THRESHOLDS IN CHILDREN

By the time that most studies were conducted in infants, it had become progressively evident that arousal and awakening thresholds are influenced by a variety of factors. These significantly modify the response to ambient noise of sleeping infants. Some factors inhibit the arousal response, while others enhance the response.

PRENATAL AND PERINATAL FACTORS

Age of gestation
In 97 healthy infants, auditory awakening thresholds decreased significantly from the 44th to the 60th week after conception (Kahn, Picard and Blum, 1986). Awakening thresholds were defined as the infant opening their eyes and/or crying. Mean awakening thresholds dropped from 98.5+/-11 at the 44th week after conception to 83 dB(A) by the 60th week after conception.

Cigarette smoke
To evaluate the effects of cigarette smoke on polygraphic arousal thresholds, 26 newborns were studied with polygraphic recordings for one night: 13 were born to mothers who did not smoke, and 13 were born to mothers who smoked (over 9 cigarettes per day) (Franco et al., 1999). Another group of infants with a median postnatal age of 12 weeks were also studied: 21 born to non-smoking mothers and 21 born to smoking mothers. The auditory arousal thresholds of the infants of both age groups were measured with the use of auditory challenges of increasing intensity, administered during REM sleep. More intense auditory stimuli were needed to induce arousals in newborns (p=.002) and infants (p=.044) of smokers than in infants of non-smokers (mean value of 84+/-11 dB(A) for smokers and 81.6+/-20 for non-smokers). Behavioural awakening (infants opening their eyes and/or crying) occurred significantly less frequently in the newborns of smokers (p=.002) than of non-smokers.

It was concluded that newborn and infants born to smoking mothers had higher arousal thresholds to auditory challenges than those born to non-smoking mothers. From the present findings, it appeared that the impact of exposure to cigarette smoke occurred mainly before birth.

POSTNATAL FACTORS

The following postnatal factors modify arousal from sleep.

Sleep stage
In infants, auditory stimuli have generally indicated increased responses during active as compared with quiet sleep (Busby, Mercier and Pivik, 1994).

Time of the night

In 31 infants, the arousal thresholds decreased across the night (mean value of 67+/-12.5 dB(A) in the first part of the night, for 51+/-3.5 in the third part of the night; p=.017) (Franco et al., 2001). Similar findings had been reported in adult subjects (Rechtschaffen, Hauri and Zeitlin, 1966).

Body position during sleep

To investigate whether prone or supine sleeping was associated with a different response threshold to environmental stimuli, 25 3-month-old healthy infants with a median age of 9 months were exposed to an auditory challenge while sleeping successively prone or supine (Franco et al., 1998). Three infants were excluded from the study because they awoke while their position was being changed. For the 22 infants included in the analysis, more intense auditory stimuli were needed to arouse the infants in the prone position (median of 70 db(A), range values 50 to more than 100 db(A)) than in the supine position (median of 60 db(A), range values 50–90 db(A)) (p=.011). Arousal thresholds were higher in the prone than in the supine position in 15 infants, unchanged in 4 infants and lower in the prone position in 3 infants (p=.007). It was concluded that infants show higher arousal thresholds to auditory challenges when sleeping in the prone position than when sleeping in the supine position. The findings could not readily be explained. The difference in arousal thresholds could be related to difference in chest wall mechanoreceptor responses, or differences in BP and/or central baroreceptors responses.

Ambient room temperature

Two groups of healthy infants with a median age of 11 weeks were recorded polygraphically during one night: 31 infants were studied at 24°C and 31 infants at 28°C. To determine their arousal thresholds, the infants were exposed to white noises of increasing intensities during REM and non-REM sleep (Franco et al., 2001). The arousal thresholds decreased across the night in the infants sleeping at 24°C (p= .017). The finding was not found for the infants sleeping at 28°C. When analysing the arousal responses according to time of the night, it was found that the auditory thresholds were significantly higher at 28°C (75+/-19 dB(A)) than at 24°C (51+/-3.5 dB(A)) between 03.00 and 06.00 (p=.003). These findings were only seen in REM sleep.

Sleeping with the head covered by bedclothes

To evaluate the influence of covering the face of sleeping infants with a bed sheet, 18 healthy infants with a median of 10.5 weeks (range 8–15 weeks) were recorded polygraphically for one night (Franco et al., 2002). They slept in their usual supine position. During sleep, a bed sheet was gently placed on their face for 60 minutes. With the face free or covered by the sheet, the infants were exposed to white noises of increasing intensities during REM and non-REM sleep. Compared to with their face free, during the periods when their faces were covered, the infants had increases in pericephalic ambient temperature (p<.001), increases in REM sleep (p=.035) and body movements (p=.011) and a decrease in non-REM sleep (p<.001). Respiratory frequency was increased in both REM (p=.001) and non-REM (p<.001) sleep. With their face covered, the infants had higher auditory arousal thresholds (mean of 76+/-23 dB(A)) than with their face free (mean of 58+/-14 dB(A)) (p=.006). The difference was seen in REM sleep only. A positive correlation was found between pericephalic temperature and arousal thresholds in REM sleep (r=.487; p=.003).

Short sleep deprivation

Following short sleep deprivation, a study reported that in infants there was no measurable change in arousal propensity by auditory stimuli (1 kHz pure tone, delivered in the midline of the cot, from 73 dB and increased in 3 dB steps to 100 dB) during quiet sleep (Thomas et al., 1996). Another study was undertaken to evaluate the influence of a brief period of sleep deprivation on sleep and arousal characteristics of healthy infants (Franco et al., submitted). Thirteen healthy infants with a median age of 8 weeks (range 7–18 weeks) were recorded polygraphically during a morning nap and an afternoon nap in a sleep laboratory. They were two hours sleep-deprived, either in the morning or in the afternoon before being allowed to fall asleep. Six infants were sleep-deprived before the morning nap and seven before the afternoon nap. During each nap, the infants were exposed to white noises of increasing intensities in REM sleep to determine their arousal thresholds. Following sleep deprivation, the infants tended to have less gross body movements during sleep (p = .054). They had a significant increase in obstructive sleep apnoeas (p = .012). The infants' auditory arousal thresholds were significantly higher following sleep-deprivation (mean of 76+/-13.5 dB(A)) than during normal sleep (mean of 56+/-8.4 dB(A)) (p = .003) and during REM sleep. It was concluded that short-term sleep deprivation in infants is associated with the development of obstructive sleep apnoeas and a significant increase in arousal thresholds.

Pacifiers and breastfeeding

Fifty-six healthy infants were studied polygraphically during one night: 36 infants used a pacifier regularly during sleep; 20 never used a pacifier (Franco et al., 2000). Thumb users or occasional pacifier users were not included in the study. The infants were recorded at a median age of 10 weeks (range 6–19 weeks). To evaluate their auditory arousal thresholds, the infants were exposed to white noise of increasing intensity during REM sleep. Polygraphic arousals occurred at significantly lower auditory stimuli in pacifier-users than in nonusers (mean of 60+/-11.6 with pacifiers, for 71+/-15.3 without pacifier; p=.010). Compared to non-users, pacifier-users were more frequently bottle-fed than breastfed (p=.036).

Among infants sleeping without a pacifier, breastfed infants had lower auditory thresholds than bottle-fed infants (mean of 67.7+-13.0 breastfed, for 77.7+-17.5 bottle-fed; p=.049). The question of how a pacifier contributes to protect the sleeping infant might be best explained by the observed loss of the pacifier early after sleep onset. This could contribute to disruption of the infant's sleep and favour arousals.

CONCLUSIONS

Various factors modify auditory arousal responses from sleep in healthy infants. Some inhibit arousals while others enhance the response. To evaluate the effect and dose-effect relationship on children therefore requires the careful determination of confounders that may bias studies and lead to conflicting results.

Additional confounders should be added to the list of factors that modify arousal thresholds. These include past experience with the stimulus (Rechtschaffen, Hauri and Zeitlin, 1966), or the presence of meaning in the noise as both of them are of critical importance in determining the persistence of physical reactions to the noise (McLean and Tarnopolsky, 1977). These are the reasons which lead most sleep/wake researchers to use white noises to stimulate the sleeping child.

Knowledge of these variables does little to clarify the physiological determinants of the awakening response, because knowledge of how such variables are related to possible physiological determinants is little better than that of the awakening response itself (Rechtschaffen, Hauri and Zeitlin, 1966).

These findings however, underline the significant dose–response relationship between ambient noise and arousal or awakening from sleep in infants.

NOISE AND SLEEP FOR DIFFERENT STAGES OF DEVELOPMENT

THE FETUS

The human fetus spends most of its time in a state equivalent to sleep, similar to that recorded in newborn infants. The healthy fetus in utero was shown to react to external noises. This is the result of the development of the human cochlea and peripheral sensory end organs. These complete their normal development by 24 weeks of gestation. Sound is well transmitted into the uterine environment. Ultrasonographic observations of blink/startle responses to vibroacoustic stimulation are first elicited at 24–25 weeks of gestation, and are consistently present after 28 weeks, indicating maturation of the auditory pathways of the central nervous system (Committee on Environment Health of the American Academy of Pediatrics, 1997). The fetus reacts to 1–4 seconds of 100–130 dB of 1220–15000 Hz sound. The hearing threshold (the intensity at which one perceives sound) at 27–29 weeks of gestation is approximately 40 dB and decreases to a nearly adult level of 13.5 dB by 42 weeks of gestation, indicating continuing postnatal maturation of these pathways.

Teratogenic effects have been described in animals prenatally exposed to noise (Committee on Environment Health of the American Academy of Pediatrics, 1997). These were associated with higher levels of cortisol and corticotropin hormones in the exposed animals. No such effects could be demonstrated in humans, in whom studies on the relation between exposure to noises during gestation and shortened gestation or lower birth weights were inconclusive or conflicting. It is possible that in these studies, noise could be a marker of other risk factors (Committee on Environment Health of the American Academy of Pediatrics, 1997). In conclusion, most studies on the effects of noise on perinatal health have been criticized as being hampered by serious methodological limitations, both in terms of the measurement of exposure and outcome, and failure to control for other known determinants of the outcomes under investigation. The lack of properly controlled studies makes it difficult to draw conclusions about what effects ambient noise has on perinatal outcomes (Morrell, Taylor and Lyle, 1997).

NEWBORN INFANTS

A large number of investigations have been concerned with the responses of sleeping newborn infants to acoustic signals. Many of the studies arise from a large and general interest in child development as well as from a need for hearing tests for infants (Mills, 1975).

Infant incubators produce continuous noise levels of between 50 and 86 dB(lin) (American Academy of Pediatrics, 1974). Oxygen inlets produced an additional 2 dB (lin). Slamming of incubator doors and infant crying produced 90 to 100 dB(A)

(American Academy of Pediatrics, 1974). It was shown that inside incubators, background noise level is about 50 dBA and can reach 120 dBA (Committee on Environment Health of the American Academy of Pediatrics, 1997). Much of the energy is located below 500 Hz, between 31 and 250 Hz (Mills, 1975).

Ambient noise appears to influence the quantity and quality of the sleep of newborns. Some newborns appear to be particularly responsive to ambient noises. Sleeping premature, anoxic, or brain-damaged infants detect intruding sounds better than sleeping healthy or term babies (Mills, 1975).

Newborn infants spend most of their time sleeping. Some studies have documented hearing loss in children cared for in intensive care units (Committee on Environment Health of the American Academy of Pediatrics, 1997). Noise and some ototoxic drugs act synergistically to produce pathological changes of the inner ears of experimental animals (neomycin, kanamycin, sodium salicylate). The relationship with the infant's clinical condition and associated treatments has, however, not yet been clearly defined. Infants exposed to sound levels of incubators are usually premature, on drugs and in very poor health. Moreover, the exposures are continuous. A weak infant could spend weeks sleeping in such a noise level without rest periods away from noise (Mills, 1975).

High noise levels may be associated with other types of responses. In young infants, sudden loud (of approximately 80 dB) environmental noise induced hypoxaemia.

Noise reduction was associated in neonates with increases in sleep time, in particular in quiet sleep (Committee on Environment Health of the American Academy of Pediatrics, 1997). It also resulted in fewer days of respiratory support and oxygen administration. Premature infants cared for with noise reduction had a better maturation of electroencephalograms.

A Committee on Environmental Health of the American Academy of Pediatrics (1997) concluded that high ambient noise in the neonatal intensive care unit (NICU) changed the behavioural and physiological responses of infants. For all the above observations and considerations, sound in infant intensive care units should be maintained at under 80 dB(A) (Graven, 2000). Among other recommendations, paediatricians were encouraged to monitor sound in the NICU, and within incubators, where a noise level greater than 45 dB is of concern.

INFANTS (1 MONTH TO 1 YEAR OLD)

Some studies of the effect of external noises on the sleep/wake reactions of infants were conducted in their natural home environment. The reactions of babies to aircraft noise were studied by means of electroplethysmography (PLG) and EEG (Ando and Hattori, 1977). The recordings were done in the morning, in the infants' sleeping rooms. The infants were exposed to recorded noise of a Boeing 727 at take-off. The noise was presented at 70, 80 and 90 dB(A) at peak level at the position of the babies' heads. The subjects who had not been awakened by exposure to aircraft noise were exposed to music (Beethoven's Ninth Symphony) at levels of 70, 80 and 90 dB(A). The frequency ranged between 100 Hz and 10 kHz. It was found that the babies whose mothers had moved to the area around the Osaka International Airport before conception (Group I; n=33) or during the first five months of pregnancy (Group II; n=17) showed little or no reaction to aircraft noise. In contrast, babies whose mothers had moved closer to the airport during the second half of the pregnancy or after birth (Group III; n=10 or IV; n=3) and the babies whose mothers lived in a quiet living area (Group V; n=8) reacted to the same auditory stimuli. The babies in groups I and II showed differential responses depending on whether the auditory stimuli were aircraft noise or music. Abnormal PLG and EEG were observed in the majority of babies living in an area where noise levels were over 95 dB(A). It was concluded that the difference in reactivity to aircraft noise may be ascribed to a prenatal difference in time of exposure to aircraft noise. The reactions diminished after the sixth month of life in groups I and II, and the ninth month in groups III to V. This phenomenon may be explained as habituation to aircraft noise after birth. However, in all groups, no habituation occurred for a noise level over 95 dB(A) (Ando and Hattori, 1977). This study was criticized, as the authors did not adjust for several important determinants of birth weight, such as prematurity and the mother's age, weight, smoking status or socioeconomic status (Morrell et al., 1997).

Noise levels may be constantly high in paediatric units. The mean noise levels measured in a centre of a surgical recovery room were 57.2 dB(A), while those measured at the patients' heads were 65.6 dB(A) (American Academy of Pediatrics, 1974). In a medical unit (6-bed wards containing 5 infants between 3 and 17 months) peak sound levels were recorded on the pillow of the cot for 12 min (Keipert, 1985). Infant crying produced 75–90 dB(A) and a beeper around 76–78 dB(A). Peak noise levels recorded at the nurses' station were about 78 dB(A) for telephone, 80 for infant crying, public address system, adult talking, and up to 90 dB(A) for child talking (Keipert, 1985).

In a study conducted on infants exposed to 50–80 dB(lin) in the range of 100–7000 Hz (American Academy of Pediatrics, 1974), a level of 70–75 dB(lin) for 3 minutes led to obvious disturbance or awakening in two thirds of the children. All infants awakened after 75 dB(lin) for 12 minutes.

In other studies conducted on the effects of awakening and arousal, it was shown that white noise intensity was significantly lower when it elicited polygraphically scored arousals than when it induced awakenings (Franco et al., 1998).

TODDLERS PREADOLESCENTS (8–12 YEARS OLD) ADOLESCENTS (13–18 YEARS OLD)

Developmental variations in auditory arousal thresholds during sleep were investigated in four groups of normal male subjects: children (n=6; 5–7 years old), preadolescents (n=10; 8–12 years old), adolescents (n=10; 13–16 years old), and young adults (n=10; 20–24 years old) (Busby, Mercier and Pivik, 1994). Arousal thresholds were determined during non-REM and REM sleep for tones (3-s, 1500 Hz pure tones delivered in an ascending series of increasing intensity, 5 dB increments beginning at 30 dB SPL (sound pressure level) re 0.0002 dynes/cm2 until awakening or maximum intensity of 120 dB) presented via earphone insert on a single night following two adaptation nights of undisturbed sleep. Age-related relationships were observed for both awakening frequency and stimulus intensity required to effect awakening, with awakenings occurring more frequently in response to lower stimulus intensities with increasing age. In children, 43.1% of stimuli induced awakenings, in preadolescents 54.8%, adolescents 72% and adults 100% (X2=60.37; p<.001). Partial arousals (brief EEG desynchronization and/or EMG activity with the subjects returning to sleep) occurred in 9.8% of children, 4.8% of preadolescents, 12.2% of adolescents, 0% of adults. Although stimulus intensities required for awakening were high and statistically equivalent across sleep stages in non-adults, higher intensity stimulus was required in stage 4 relative to stage 2 and REM sleep. Frequency of awakening increased with age, whereas stimulus intensities required to effect these awakenings decreased with age. These relationships were maintained for individual sleep stages. These results confirm previous observations of marked resistance to awakening during sleep in preadolescent children and suggest that processes underlying awakening from sleep undergo systematic modification during ontogenic development. The observed resistance to elicited awakening from sleep extending up to young adulthood implies the presence of an active, developmentally related process that maintains sleep (Busby, Mercier and Pivik, 1994).

In another study, children aged 5–7 years were shown to be 10–15 dB less sensitive to pure tones than adults aged 22–30 (Mills, 1975). Another report on male hyperactive and normal children aged 8–12 showed that these children were awakened with auditory stimulus intensity levels of up to 123 dB SPL, much higher than values reported for adults (range of 50–85 dB) (Busby, Mercier and Pivik, 1994).

In a study on four children (two males), aged 5–8 years old on the effects of simulated sonic booms (68 dB(A) near the subjects' ears), 94.1% of the subjects showed no change, 5.9% had shallower sleep, but none aroused or had behavioural awakening. In general, the frequency of arousal or behavioural awakenings and of sleep stage changes increased with age (up to 75 years) (Lukas, 1975).

In a prospective longitudinal investigation, which employed non-exposed control groups, effects of aircraft noise prior to and subsequent to inauguration of a new airport as well as effects of chronic noise and its reduction at an old airport (6–18 months after relocation), were studied in 326 children aged 9–13 years (Bullinger et al., 1999). The psychological health of children was investigated with a standardized quality of life scale as well as with a motivational measure. In addition, a self-report noise annoyance scale was used. In the children studied at the two airports over three time points, results showed a significant decrease of total quality of life 18 months after aircraft noise exposure as well as motivational deficits demonstrated by fewer attempts to solve insoluble puzzles in the new airport area. Parallel shifts in children's attributions for failure were also noted. At the old airport parallel impairments were present before the airport relocation but subsided thereafter (Bullinger et al., 1999).

In some studies, the effects of ambient noise on autonomic responses could be demonstrated in children. In children aged 6–12 years exposed to intermittent traffic noise during 4 nights (at a rate of 90 noises per hour; peak intensity of the noise, 45, 55 and 65 dB(A) varied semi-randomly) and 2 quiet nights. Heart rate was affected and relatively higher in noise during REM and stage 2 than during delta sleep (Muzet et al., 1980, in Abel, 1990).

CONCLUSIONS

Several studies on the extra-auditory effects of ambient noise on sleeping children were summarized in Table 1. In relation to ambient noise, specific changes were reported in both sleep quality and quantity. Some of the effects were shown to have a dose–response relationship.
Several limitations to the present report should be discussed. Firstly, no one knows

whether the inference that is often made that the effects of noise might develop with a longer exposure time (Abel, 1990) is correct. Serious cardiorespiratory or autonomic changes, such as increases in BP could only develop following a long time exposure starting from childhood. This, in fact, has never been documented, nor has the extent of variability between subjects due to difference in susceptibility. Secondly, there is no information to evaluate whether adaptation to ambient noise could limit the effects observed during short-term experiments. Thirdly, as the existing research data are applicable to generally healthy children, no one knows how the reported findings could be applied to ill children, children receiving medical treatment or very young premature infants. Finally, as most studies were conducted in laboratory controlled environments, no one knows the correlation between these studies and the effects of noise in the home. The multifactorial effects of the environment on sleep and arousal controls could be much more complex than expected. One might predict that, similarly as for adults, the effects of noise on the child's sleep and health are very complicated and depend upon the spectrum and level of the noise, temporal aspects of the noise, psychological responses to the noise and the nature of the evaluation technique. The complexity of the conditions related to sleep/wake controls was illustrated by the review of confounding factors affecting auditory arousal thresholds.

Despite these limitations, it can be concluded that, based on the evidence available, the extra-auditory effects of noise could be pervasive, affecting the children's physical and psychological well-being. Changes in sleep quantity and quality together with autonomic reactions are seen when a child is exposed to ambient noise during sleep. Ambient noise exerts a dose-effect relationship on changes in sleep/wake behaviours. These reflect modifications induced within the brain of the sleeping child. It remains, however, to be determined what pervasive effects long-term exposure to ambient noise has on the child's development, health and well-being. Evidence should also be defined to support an enforcement of strategies for noise reduction at the source as suggested by some studies. Noise-induced health effects on children, a clinical and public health concern, should be evaluated by further studies.

Table 1
Arousal and awakening in children a review of the literature

No.	dB(A)	% responses	Type of responses	Reference
1	80	70	Nenonates motor response	Steinschneider 1967
2	60	5	Neonates startle response	Gädeke et al.,1969
70	10			
80	20			
100	60			
3	60	7	Neonates startle response	Ashton 1967
65	10			
70	40			
4	80	70	Child awake	Semczuk 1967
5	100	70	Child awake	Busby, Mercier and Pivik 1994
6	100	76	Preadolescent awake	
7	100	86	Adolescent awake	
8	60	100	Adult	
9	120	72	Infant awake	Kahn, Picard and Blum, 1986
10	75	75	Infant awake	Gädeke et al., 1969

REFERENCES

Abel SM (1990). The extra-auditory effects of noise and annoyance: an overview of research. *Journal of Otoryngology* 1:1–13.

American Academy of Pediatrics (1974). Committee on Environmental Hazards. Noise pollution: neonatal aspects. *Pediatrics*, 54:476–479.

Ando Y, Hattori H (1977). Effects of noise on sleep of babies. *Journal of the Acoustical Society of America*, 62:199–204.

Bullinger M et al. (1999). The psychological cost of aircraft noise for children. *Zentralblad Hygiene und Umweltmedizin*, 202:127–138.

Busby KA, Mercier L, Pivik RT (1994). Ontogenetic variations in auditory arousal threshold during sleep. *Psychophysiology*, 31:182–188.

Committee on Environment Health of the American Academy of Pediatrics (1997). Noise: a hazard for the fetus and newborn. *Pediatrics*, 100:724–727.

Franco P et al. (1998). Auditory arousal thresholds are higher when infants sleep in the prone position. *Journal of Pediatrics*, 132:240–243.

Franco P et al. (1999). Prenatal exposure to cigarettes is associated with decreased arousal propensity in infants. *Journal of Pediatrics*, 135:34–8.

Franco P et al. (2000). The influence of a pacifier on infants' arousals from sleep. *Journal of Pediatrics*, 136:775–779.

Franco P et al. (2001). Ambient temperature is associated with changes in infants' arousability form sleep. *Sleep*, 24:325–329.

Franco P et al. (2002). Decreased arousals in infants sleeping with the face covered by bedclothes. *Pediatrics*, 109:112–117.

Franco P. Decreased arousals in healthy infants following short-term sleep deprivation. *Sleep*, (submitted).

Gädeke R et al. (1969). The noise level in a childrens' hospital and the wake-up threshold in infants. *Acta Paediatrica Scandinavica*, 58:164–170.

Graven SN (2000). Sound and the developing infant in the NICU: conclusions and recommendations for care. *Journal of Perinatology*, 20:S88–93.

Kahn A, Picard E, Blum D (1986). Auditory arousal thresholds of normal and near-miss SIDS infants. *Developmental Medicine and Child Neurology*, 28:299–302.

Kahn A et al. (1989). Sleep problems in healthy preadolescents. *Pediatrics*, 84:542 – 546.

Keipert JA (1985). The harmful effects of noise in a children's ward. *Australian Paediatric Journal*, 21:101–103.

Lukas JS (1975). Noise and sleep: a literature review and a proposed criterion for assessing effect. *Journal of the Acoustical Society of America*, 58:1232–1242.

McLean EK, Tarnopolsky A (1977). Noise, discomfort and mental health. *Psychological Medicine*, 7:19–62.

Mills JH (1975). Noise and children: a review of literature. *Journal of the Acoustical Society of America*, 58:767–779.

Morrell S, Taylor R, Lyle D (1997). A review of health effects of aircraft noise. *Australian and New Zealand Journal of Public Health*, 21:221–236.

Muzet A et al. (1980). Habituation and age differences of cardiovascular responses to noise during sleep. In: *Sleep 1980, 5th European Congress of Sleep Research, Amsterdam*, pp 212–215 (quoted by Abel, 1980).

Rechtschaffen A, Hauri P, Zeitlin M (1966). Auditory awakening thresholds in REM and NREM sleep stages. *Perceptual and Motor Skills*, 22:927–942.

Semczuk B (1967). Studies on the influence of acoustic stimuli on respiratory movements. *Polish Medical Journal*, 7:1070–1100.

Thomas DA et al. (1996). The effect of sleep deprivation on sleep states, breathing events, peripheral chemosensiveness and arousal propensity in healthy 3 month old infants. *European Respiratory Journal*, 9:932–938.

The WHO Regional Office for Europe

The World Health Organization (WHO) is a specialized agency of the United Nations created in 1948 with the primary responsibility for international health matters and public health. The WHO Regional Office for Europe is one of six regional offices throughout the world, each with its own programme geared to the particular health conditions of the countries it serves.

Member States

Albania
Andorra
Armenia
Austria
Azerbaijan
Belarus
Belgium
Bosnia and Herzegovina
Bulgaria
Croatia
Cyprus
Czech Republic
Denmark
Estonia
Finland
France
Georgia
Germany
Greece
Hungary
Iceland
Ireland
Israel
Italy
Kazakhstan
Kyrgyzstan
Latvia
Lithuania
Luxembourg
Malta
Monaco
Montenegro
Netherlands
Norway
Poland
Portugal
Republic of Moldova
Romania
Russian Federation
San Marino
Serbia
Slovakia
Slovenia
Spain
Sweden
Switzerland
Tajikistan
The former Yugoslav Republic of Macedonia
Turkey
Turkmenistan
Ukraine
United Kingdom
Uzbekistan

Environmental noise is a threat to public health, having negative impacts on human health and wellbeing. This book reviews the health effects of night time noise exposure, examines dose effects relations, and presents interim and ultimate guideline values of night noise exposure. It offers guidance to policy-makers in reducing the health impacts of night noise, based on expert evaluation of scientific evidence in Europe.

9 789289 041737

World Health Organization
Regional Office for Europe

Scherfigsvej 8, DK-2100 Copenhagen Ø, Denmark
Tel.: +45 39 17 17 17. Fax: +45 39 17 18 18. E-mail: postmaster@euro.who.int
Web site: www.euro.who.int

BEFORE THE PUBLIC UTILITY COMMISSION
OF OREGON

Docket PCN 5

In the Matter of

IDAHO POWER COMPANY'S
PETITION FOR CERTIFICATE OF PUBLIC CONVENIENCE
AND NECESSITY

WHO, Guidelines for Community Noise (1999)

February 22, 2023

GUIDELINES FOR COMMUNITY NOISE

Edited by

Birgitta Berglund
Thomas Lindvall
Dietrich H Schwela

This WHO document on the *Guidelines for Community Noise* is the outcome of the WHO-expert task force meeting held in London, United Kingdom, in April 1999. It bases on the document entitled "Community Noise" that was prepared for the World Health Organization and published in 1995 by the Stockholm University and Karolinska Institute.

World Health Organization, Geneva
Cluster of Sustainable Development and Healthy Environment (SDE)
Department for Protection of the Human Environment (PHE)
Occupational and Environmental Health (OEH)

TABLE OF CONTENTS

Foreword

Noise has always been an important environmental problem for man. In ancient Rome, rules existed as to the noise emitted from the ironed wheels of wagons which battered the stones on the pavement, causing disruption of sleep and annoyance to the Romans. In Medieval Europe, horse carriages and horse back riding were not allowed during night time in certain cities to ensure a peaceful sleep for the inhabitants. However, the noise problems of the past are incomparable with those of modern society. An immense number of cars regularly cross our cities and the countryside. There are heavily laden lorries with diesel engines, badly silenced both for engine and exhaust noise, in cities and on highways day and night. Aircraft and trains add to the environmental noise scenario. In industry, machinery emits high noise levels and amusement centres and pleasure vehicles distract leisure time relaxation.

In comparison to other pollutants, the control of environmental noise has been hampered by insufficient knowledge of its effects on humans and of dose-response relationships as well as a lack of defined criteria. While it has been suggested that noise pollution is primarily a "luxury" problem for developed countries, one cannot ignore that the exposure is often higher in developing countries, due to bad planning and poor construction of buildings. The effects of the noise are just as widespread and the long term consequences for health are the same. In this perspective, practical action to limit and control the exposure to environmental noise are essential. Such action must be based upon proper scientific evaluation of available data on effects, and particularly dose-response relationships. The basis for this is the process of risk assessment and risk management.

The extent of the noise problem is large. In the European Union countries about 40 % of the population are exposed to road traffic noise with an equivalent sound pressure level exceeding 55 dB(A) daytime and 20 % are exposed to levels exceeding 65 dB(A). Taking all exposure to transportation noise together about half of the European Union citizens are estimated to live in zones which do not ensure acoustical comfort to residents. More than 30 % are exposed at night to equivalent sound pressure levels exceeding 55 dB(A) which are disturbing to sleep. The noise pollution problem is also severe in cities of developing countries and caused mainly by traffic. Data collected alongside densely travelled roads were found to have equivalent sound pressure levels for 24 hours of 75 to 80 dB(A).

The scope of WHO's effort to derive guidelines for community noise is to consolidate actual scientific knowledge on the health impacts of community noise and to provide guidance to environmental health authorities and professional trying to protect people from the harmful effects of noise in non-industrial environments. Guidance on the health effects of noise exposure of the population has already been given in an early publication of the series of Environmental Health Criteria. The health risk to humans from exposure to environmental noise was evaluated and guidelines values derived. The issue of noise control and health protection was briefly addressed.
At a WHO/EURO Task Force Meeting in Düsseldorf, Germany, in 1992, the health criteria and guideline values were revised and it was agreed upon updated guidelines in consensus. The essentials of the deliberations of the Task Force were published by Stockholm University and

Karolinska Institute in 1995. In an recent Expert Task Force Meeting convened in April 1999 in London, United Kingdom, the Guidelines for Community Noise were extended to provide global coverage and applicability, and the issues of noise assessment and control were addressed in more detail. This document is the outcome of the consensus deliberations of the WHO Expert Task Force.

Dr Richard Helmer
Director, Department of Protection of the Human Environment
Cluster Sustainable Development and Healthy Environments

Preface

Community noise (also called environmental noise, residential noise or domestic noise) is defined as noise emitted from all sources except noise at the industrial workplace. Main sources of community noise include road, rail and air traffic, industries, construction and public work, and the neighbourhood. The main indoor sources of noise are ventilation systems, office machines, home appliances and neighbours. Typical neighbourhood noise comes from premises and installations related to the catering trade (restaurant, cafeterias, discotheques, etc.); from live or recorded music; sport events including motor sports; playgrounds; car parks; and domestic animals such as barking dogs. Many countries have regulated community noise from road and rail traffic, construction machines and industrial plants by applying emission standards, and by regulating the acoustical properties of buildings. In contrast, few countries have regulations on community noise from the neighbourhood, probably due to the lack of methods to define and measure it, and to the difficulty of controlling it. In large cities throughout the world, the general population is increasingly exposed to community due to the sources mentioned above and the health effects of these exposures are considered to be a more and more important public health problem. Specific effects to be considered when setting community noise guidelines include: interference with communication; noise-induced hearing loss; sleep disturbance effects; cardiovascular and psycho-physiological effects; performance reduction effects; annoyance responses; and effects on social behaviour.

Since 1980, the World Health Organization (WHO) has addressed the problem of community noise. Health-based guidelines on community noise can serve as the basis for deriving noise standards within a framework of noise management. Key issues of noise management include abatement options; models for forecasting and for assessing source control action; setting noise emission standards for existing and planned sources; noise exposure assessment; and testing the compliance of noise exposure with noise immission standards. In 1992, the WHO Regional Office for Europe convened a task force meeting which set up guidelines for community noise. A preliminary publication of the Karolinska Institute, Stockholm, on behalf of WHO, appeared in 1995. This publication served as the basis for the globally applicable *Guidelines for Community Noise* presented in this document. An expert task force meeting was convened by WHO in March 1999 in London, United Kingdom, to finalize the guidelines.

The *Guidelines for Community Noise* have been prepared as a practical response to the need for action on community noise at the local level, as well as the need for improved legislation, management and guidance at the national and regional levels. WHO will be pleased to see that these guidelines are used widely. Continuing efforts will be made to improve its content and structure. It would be appreciated if the users of the *Guidelines* provide feedback from its use and their own experiences. Please send your comments and suggestions on the WHO *Guidelines for Community Noise – Guideline document* to the Department of the Protection of the Human Environment, Occupational and Environmental Health, World Health Organization, Geneva, Switzerland (Fax: +41 22-791 4123, e-mail: schwelad@who.int).

Acknowledgements

The World Health Organization thanks all who have contributed to the preparation of this document, *Guidelines for Community Noise.* The international, multidisciplinary group of contributors to, and reviewers of, the *Guidelines* are listed in the "Participant list" in Annex 6. Special thanks are due to the chairpersons and workgroups of the WHO expert task force meeting held in London, United Kingdom, in March 1999: Professor Thomas Lindvall, who acted as the chairperson of the meeting, Professor Birgitta Berglund, Dr John Bradley and Professor Gerd Jansen, who chaired the three workgroups. Special contributions from those who provided the background papers and who contributed to the success of the WHO expert meeting are gratefully acknowledged:

Professor Birgitta Berglund, Stockholm University, Stockholm, Sweden;
Bernard F. Berry, National Physical Laboratory, Teddington, Middlesex, United Kingdom; Dr. Hans Bögli, Bundesamt für Umwelt, Wald und Landschaft, Bern, Switzerland;
Dr. John S. Bradley, National Research Council Canada, Ottawa, Canada;
Dr. Ming Chen, Fujian Provincial Hospital, People's Republic of China;
Lawrence S. Finegold, Air Force Research Laboratory, AFRL/HECA, Wright-Patterson AFB, OH, USA;
Mr Dominique Francois, WHO Regional Office for Europe, Copenhague, Denmark;
Professor Guillermo L. Fuchs, Córdoba, Argentina;
Mr Etienne Grond, Messina, South Africa;
Professor Andrew Hede, University of the Sunshine Coast, Maroochydore South, Qld., Australia;
Professor Gerd Jansen, Heinrich-Heine-Universität Düsseldorf, Germany;
Dr. Michinori Kabuto, National Institute for Environmental Studies, Tsukuba, Ibaraki, Japan;
Professor Thomas Lindvall, National Institute of Environmental Medicine and Karolinska Institute, Stockholm, Sweden;
Dr. Amanda Niskar, CDC/NCEH, Atlanta, Georgia, USA;
Dr Sudhakar B. Ogale, Medical College and KEM Hospital, Parel, Mumbai, India;
Mrs. Willy Passchier-Vermeer, TNO Prevention and Health, Leiden, The Netherlands;
Dr. Dieter Schwela, World Health Organization, Geneva 27, Switzerland;
Dr. Michinki So, Nihon University, Tokyo, Japan;Professor Shirley Thompson, University of South Carolina, Columbia, USA;
Max Thorne, National Environmental Noise Service, Rotorua, New Zealand;
Frits van den Berg, Science Shop for Physics, University of Groningen, Groningen, The Netherlands;
Professor Peter Williams, Director MARC, King's College London, UK;
Professor Shabih Haider Zaidi, Dow Medical College, Karachi , Pakistan;

Particular thanks are due to the Ministry of Environment of Germany, which provided the funding to convene the WHO expert task force meeting in London, United Kingdom, in March 1999 to produce the Guidelines for Community Noise.

Executive Summary

1. Introduction

Community noise (also called environmental noise, residential noise or domestic noise) is defined as noise emitted from all sources except noise at the industrial workplace. Main sources of community noise include road, rail and air traffic; industries; construction and public work; and the neighbourhood. The main indoor noise sources are ventilation systems, office machines, home appliances and neighbours.

In the European Union about 40% of the population is exposed to road traffic noise with an equivalent sound pressure level exceeding 55 dB(A) daytime, and 20% are exposed to levels exceeding 65 dB(A). When all transportation noise is considered, more than half of all European Union citizens is estimated to live in zones that do not ensure acoustical comfort to residents. At night, more than 30% are exposed to equivalent sound pressure levels exceeding 55 dB(A), which are disturbing to sleep. Noise pollution is also severe in cities of developing countries. It is caused mainly by traffic and alongside densely-travelled roads equivalent sound pressure levels for 24 hours can reach 75–80 dB(A).

In contrast to many other environmental problems, noise pollution continues to grow and it is accompanied by an increasing number of complaints from people exposed to the noise. The growth in noise pollution is unsustainable because it involves direct, as well as cumulative, adverse health effects. It also adversely affects future generations, and has socio-cultural, esthetic and economic effects.

2. Noise sources and measurement

Physically, there is no distinction between sound and noise. Sound is a sensory perception and the complex pattern of sound waves is labeled noise, music, speech etc. Noise is thus defined as unwanted sound.

Most environmental noises can be approximately described by several simple measures. All measures consider the frequency content of the sounds, the overall sound pressure levels and the variation of these levels with time. Sound pressure is a basic measure of the vibrations of air that make up sound. Because the range of sound pressures that human listeners can detect is very wide, these levels are measured on a logarithmic scale with units of decibels. Consequently, sound pressure levels cannot be added or averaged arithmetically. Also, the sound levels of most noises vary with time, and when sound pressure levels are calculated, the instantaneous pressure fluctuations must be integrated over some time interval.

Most environmental sounds are made up of a complex mix of many different frequencies. Frequency refers to the number of vibrations per second of the air in which the sound is propagating and it is measured in Hertz (Hz). The audible frequency range is normally considered to be 20–20 000 Hz for younger listeners with unimpaired hearing. However, our hearing systems are not equally sensitive to all sound frequencies, and to compensate for this various types of filters or frequency weighting have been used to determine the relative strengths of frequency components making up a particular environmental noise. The A-weighting is most commonly used and weights lower frequencies as less important than mid- and higher-frequencies. It is intended to approximate the frequency response of our hearing system.

The effect of a combination of noise events is related to the combined sound energy of those events (the equal energy principle). The sum of the total energy over some time period gives a level equivalent to the average sound energy over that period. Thus, LAeq,T is the energy average equivalent level of the A-weighted sound over a period T. LAeq,T should be used to measure continuing sounds, such as road traffic noise or types of more-or-less continuous industrial noises. However, when there are distinct events to the noise, as with aircraft or railway noise, measures of individual events such as the maximum noise level (LAmax), or the weighted sound exposure level (SEL), should also be obtained in addition to LAeq,T. Time-varying environmental sound levels have also been described in terms of percentile levels.

Currently, the recommended practice is to assume that the equal energy principle is approximately valid for most types of noise and that a simple LAeq,T measure will indicate the expected effects of the noise reasonably well. When the noise consists of a small number of discrete events, the A-weighted maximum level (LAmax) is a better indicator of the disturbance to sleep and other activities. In most cases, however, the A-weighted sound exposure level (SEL) provides a more consistent measure of single-noise events because it is based on integration over the complete noise event. In combining day and night LAeq,T values, night-time weightings are often added. Night-time weightings are intended to reflect the expected increased sensitivity to annoyance at night, but they do not protect people from sleep disturbance.

Where there are no clear reasons for using other measures, it is recommended that LAeq,T be used to evaluate more-or-less continuous environmental noises. Where the noise is principally composed of a small number of discrete events, the additional use of LAmax or SEL is recommended. There are definite limitations to these simple measures, but there are also many practical advantages, including economy and the benefits of a standardized approach.

3. Adverse health effects of noise

The health significance of noise pollution is given in chapter 3 of the *Guidelines* under separate headings according to the specific effects: noise-induced hearing impairment; interference with speech communication; disturbance of rest and sleep; psychophysiological, mental-health and performance effects; effects on residential behaviour and annoyance; and interference with intended activities. This chapter also considers vulnerable groups and the combined effects of mixed noise sources.

Hearing impairment is typically defined as an increase in the threshold of hearing. Hearing deficits may be accompanied by tinnitus (ringing in the ears). Noise-induced hearing impairment occurs predominantly in the higher frequency range of 3 000–6 000 Hz, with the largest effect at 4 000 Hz. But with increasing LAeq,8h and increasing exposure time, noise-induced hearing impairment occurs even at frequencies as low as 2 000 Hz. However, hearing impairment is not expected to occur at LAeq,8h levels of 75 dB(A) or below, even for prolonged occupational noise exposure.

Worldwide, noise-induced hearing impairment is the most prevalent irreversible occupational hazard and it is estimated that 120 million people worldwide have disabling hearing difficulties.

In developing countries, not only occupational noise but also environmental noise is an increasing risk factor for hearing impairment. Hearing damage can also be caused by certain diseases, some industrial chemicals, ototoxic drugs, blows to the head, accidents and hereditary origins. Hearing deterioration is also associated with the ageing process itself (presbyacusis).

The extent of hearing impairment in populations exposed to occupational noise depends on the value of LAeq,8h, the number of noise-exposed years, and on individual susceptibility. Men and women are equally at risk for noise-induced hearing impairment. It is expected that environmental and leisure-time noise with a LAeq,24h of 70 dB(A) or below will not cause hearing impairment in the large majority of people, even after a lifetime exposure. For adults exposed to impulse noise at the workplace, the noise limit is set at peak sound pressure levels of 140 dB, and the same limit is assumed to be appropriate for environmental and leisure-time noise. In the case of children, however, taking into account their habits while playing with noisy toys, the peak sound pressure should never exceed 120 dB. For shooting noise with LAeq,24h levels greater than 80 dB(A), there may be an increased risk for noise-induced hearing impairment.

The main social consequence of hearing impairment is the inability to understand speech in daily living conditions, and this is considered to be a severe social handicap. Even small values of hearing impairment (10 dB averaged over 2 000 and 4 000 Hz and over both ears) may adversely affect speech comprehension.

Speech intelligibility is adversely affected by noise. Most of the acoustical energy of speech is in the frequency range of 100–6 000 Hz, with the most important cue-bearing energy being between 300–3 000 Hz. Speech interference is basically a masking process, in which simultaneous interfering noise renders speech incapable of being understood. Environmental noise may also mask other acoustical signals that are important for daily life, such as door bells, telephone signals, alarm clocks, fire alarms and other warning signals, and music.

Speech intelligibility in everyday living conditions is influenced by speech level; speech pronunciation; talker-to-listener distance; sound level and other characteristics of the interfering noise; hearing acuity; and by the level of attention. Indoors, speech communication is also affected by the reverberation characteristics of the room. Reverberation times over 1 s produce loss in speech discrimination and make speech perception more difficult and straining. For full sentence intelligibility in listeners with normal hearing, the signal-to-noise ratio (i.e. the difference between the speech level and the sound level of the interfering noise) should be at least 15 dB(A). Since the sound pressure level of normal speech is about 50 dB(A), noise with sound levels of 35 dB(A) or more interferes with the intelligibility of speech in smaller rooms. For vulnerable groups even lower background levels are needed, and a reverberation time below 0.6 s is desirable for adequate speech intelligibility, even in a quiet environment.

The inability to understand speech results in a large number of personal handicaps and behavioural changes. Particularly vulnerable are the hearing impaired, the elderly, children in the process of language and reading acquisition, and individuals who are not familiar with the spoken language.

Sleep disturbance is a major effect of environmental noise. It may cause primary effects during sleep, and secondary effects that can be assessed the day after night-time noise exposure. Uninterrupted sleep is a prerequisite for good physiological and mental functioning, and the primary effects of sleep disturbance are: difficulty in falling asleep; awakenings and alterations of sleep stages or depth; increased blood pressure, heart rate and finger pulse amplitude; vasoconstriction; changes in respiration; cardiac arrhythmia; and increased body movements. The difference between the sound levels of a noise event and background sound levels, rather than the absolute noise level, may determine the reaction probability. The probability of being awakened increases with the number of noise events per night. The secondary, or after-effects, the following morning or day(s) are: reduced perceived sleep quality; increased fatigue; depressed mood or well-being; and decreased performance.

For a good night's sleep, the equivalent sound level should not exceed 30 dB(A) for continuous background noise, and individual noise events exceeding 45 dB(A) should be avoided. In setting limits for single night-time noise exposures, the intermittent character of the noise has to be taken into account. This can be achieved, for example, by measuring the number of noise events, as well as the difference between the maximum sound level and the background sound level. Special attention should also be given to: noise sources in an environment with low background sound levels; combinations of noise and vibrations; and to noise sources with low-frequency components.

Physiological Functions. In workers exposed to noise, and in people living near airports, industries and noisy streets, noise exposure may have a large temporary, as well as permanent, impact on physiological functions. After prolonged exposure, susceptible individuals in the general population may develop permanent effects, such as hypertension and ischaemic heart disease associated with exposure to high sound levels. The magnitude and duration of the effects are determined in part by individual characteristics, lifestyle behaviours and environmental conditions. Sounds also evoke reflex responses, particularly when they are unfamiliar and have a sudden onset.

Workers exposed to high levels of industrial noise for 5–30 years may show increased blood pressure and an increased risk for hypertension. Cardiovascular effects have also been demonstrated after long-term exposure to air- and road-traffic with LAeq,24h values of 65–70 dB(A). Although the associations are weak, the effect is somewhat stronger for ischaemic heart disease than for hypertension. Still, these small risk increments are important because a large number of people are exposed.

Mental Illness. Environmental noise is not believed to cause mental illness directly, but it is assumed that it can accelerate and intensify the development of latent mental disorders. Exposure to high levels of occupational noise has been associated with development of neurosis, but the findings on environmental noise and mental-health effects are inconclusive. Nevertheless, studies on the use of drugs such as tranquillizers and sleeping pills, on psychiatric symptoms and on mental hospital admission rates, suggest that community noise may have adverse effects on mental health.

Performance. It has been shown, mainly in workers and children, that noise can adversely affect performance of cognitive tasks. Although noise-induced arousal may produce better performance in simple tasks in the short term, cognitive performance substantially deteriorates for more complex tasks. Reading, attention, problem solving and memorization are among the cognitive effects most strongly affected by noise. Noise can also act as a distracting stimulus and impulsive noise events may produce disruptive effects as a result of startle responses.

Noise exposure may also produce after-effects that negatively affect performance. In schools around airports, children chronically exposed to aircraft noise under-perform in proof reading, in persistence on challenging puzzles, in tests of reading acquisition and in motivational capabilities. It is crucial to recognize that some of the adaptation strategies to aircraft noise, and the effort necessary to maintain task performance, come at a price. Children from noisier areas have heightened sympathetic arousal, as indicated by increased stress hormone levels, and elevated resting blood pressure. Noise may also produce impairments and increase in errors at work, and some accidents may be an indicator of performance deficits.

Social and Behavioural Effects of Noise; Annoyance. Noise can produce a number of social and behavioural effects as well as annoyance. These effects are often complex, subtle and indirect and many effects are assumed to result from the interaction of a number of non-auditory variables. The effect of community noise on annoyance can be evaluated by questionnaires or by assessing the disturbance of specific activities. However, it should be recognized that equal levels of different traffic and industrial noises cause different magnitudes of annoyance. This is because annoyance in populations varies not only with the characteristics of the noise, including the noise source, but also depends to a large degree on many non-acoustical factors of a social, psychological, or economic nature. The correlation between noise exposure and general annoyance is much higher at group level than at individual level. Noise above 80 dB(A) may also reduce helping behaviour and increase aggressive behaviour. There is particular concern that high-level continuous noise exposures may increase the susceptibility of schoolchildren to feelings of helplessness.

Stronger reactions have been observed when noise is accompanied by vibrations and contains low-frequency components, or when the noise contains impulses, such as with shooting noise. Temporary, stronger reactions occur when the noise exposure increases over time, compared to a constant noise exposure. In most cases, LAeq,24h and L_{dn} are acceptable approximations of noise exposure related to annoyance. However, there is growing concern that all the component parameters should be individually assessed in noise exposure investigations, at least in the complex cases. There is no consensus on a model for total annoyance due to a combination of environmental noise sources.

Combined Effects on Health of Noise from Mixed Sources. Many acoustical environments consist of sounds from more than one source, i.e. there are mixed sources, and some combinations of effects are common. For example, noise may interfere with speech in the day and create sleep disturbance at night. These conditions certainly apply to residential areas heavily polluted with noise. Therefore, it is important that the total adverse health load of noise be considered over 24 hours, and that the precautionary principle for sustainable development be applied.

Vulnerable Subgroups. Vulnerable subgroups of the general population should be considered when recommending noise protection or noise regulations. The types of noise effects, specific environments and specific lifestyles are all factors that should be addressed for these subgroups. Examples of vulnerable subgroups are: people with particular diseases or medical problems (e.g. high blood pressure); people in hospitals or rehabilitating at home; people dealing with complex cognitive tasks; the blind; people with hearing impairment; fetuses, babies and young children; and the elderly in general. People with impaired hearing are the most adversely affected with respect to speech intelligibility. Even slight hearing impairments in the high-frequency sound range may cause problems with speech perception in a noisy environment. A majority of the population belongs to the subgroup that is vulnerable to speech interference.

4. Guideline values

In chapter 4, guideline values are given for specific health effects of noise and for specific environments.

Specific health effects.

Interference with Speech Perception. A majority of the population is susceptible to speech interference by noise and belongs to a vulnerable subgroup. Most sensitive are the elderly and persons with impaired hearing. Even slight hearing impairments in the high-frequency range may cause problems with speech perception in a noisy environment. From about 40 years of age, the ability of people to interpret difficult, spoken messages with low linguistic redundancy is impaired compared to people 20–30 years old. It has also been shown that high noise levels and long reverberation times have more adverse effects in children, who have not completed language acquisition, than in young adults.

When listening to complicated messages (at school, foreign languages, telephone conversation) the signal-to-noise ratio should be at least 15 dB with a voice level of 50 dB(A). This sound level corresponds on average to a casual voice level in both women and men at 1 m distance. Consequently, for clear speech perception the background noise level should not exceed 35 dB(A). In classrooms or conference rooms, where speech perception is of paramount importance, or for sensitive groups, background noise levels should be as low as possible. Reverberation times below 1 s are also necessary for good speech intelligibility in smaller rooms. For sensitive groups, such as the elderly, a reverberation time below 0.6 s is desirable for adequate speech intelligibility even in a quiet environment.

Hearing Impairment. Noise that gives rise to hearing impairment is by no means restricted to occupational situations. High noise levels can also occur in open air concerts, discotheques, motor sports, shooting ranges, in dwellings from loudspeakers, or from leisure activities. Other important sources of loud noise are headphones, as well as toys and fireworks which can emit impulse noise. The ISO standard 1999 gives a method for estimating noise-induced hearing impairment in populations exposed to all types of noise (continuous, intermittent, impulse) during working hours. However, the evidence strongly suggests that this method should also be used to calculate hearing impairment due to noise exposure from environmental and leisure time activities. The ISO standard 1999 implies that long-term exposure to LAeq,24h noise levels of up to 70 dB(A) will not result in hearing impairment. To avoid hearing loss from impulse noise exposure, peak sound pressures should never exceed 140 dB for adults, and 120 dB for children.

Sleep Disturbance. Measurable effects of noise on sleep begin at LAeq levels of about 30 dB. However, the more intense the background noise, the more disturbing is its effect on sleep. Sensitive groups mainly include the elderly, shift workers, people with physical or mental disorders and other individuals who have difficulty sleeping.

Sleep disturbance from intermittent noise events increases with the maximum noise level. Even if the total equivalent noise level is fairly low, a small number of noise events with a high maximum sound pressure level will affect sleep. Therefore, to avoid sleep disturbance, guidelines for community noise should be expressed in terms of the equivalent sound level of the noise, as well as in terms of maximum noise levels and the number of noise events. It should be noted that low-frequency noise, for example, from ventilation systems, can disturb rest and sleep even at low sound pressure levels.

When noise is continuous, the equivalent sound pressure level should not exceed 30 dB(A) indoors, if negative effects on sleep are to be avoided. For noise with a large proportion of low-frequency sound a still lower guideline value is recommended. When the background noise is low, noise exceeding 45 dB LAmax should be limited, if possible, and for sensitive persons an even lower limit is preferred. Noise mitigation targeted to the first part of the night is believed to be an effective means for helping people fall asleep. It should be noted that the adverse effect of noise partly depends on the nature of the source. A special situation is for newborns in incubators, for which the noise can cause sleep disturbance and other health effects.

Reading Acquisition. Chronic exposure to noise during early childhood appears to impair reading acquisition and reduces motivational capabilities. Evidence indicates that the longer the exposure, the greater the damage. Of recent concern are the concomitant psychophysiological changes (blood pressure and stress hormone levels). There is insufficient information on these effects to set specific guideline values. It is clear, however, that daycare centres and schools should not be located near major noise sources, such as highways, airports, and industrial sites.

Annoyance. The capacity of a noise to induce annoyance depends upon its physical characteristics, including the sound pressure level, spectral characteristics and variations of these properties with time. During daytime, few people are highly annoyed at LAeq levels below 55 dB(A), and few are moderately annoyed at LAeq levels below 50 dB(A). Sound levels during the evening and night should be 5–10 dB lower than during the day. Noise with low-frequency components require lower guideline values. For intermittent noise, it is emphasized that it is necessary to take into account both the maximum sound pressure level and the number of noise events. Guidelines or noise abatement measures should also take into account residential outdoor activities.

Social Behaviour. The effects of environmental noise may be evaluated by assessing its interference with social behavior and other activities. For many community noises, interference with rest/recreation/watching television seem to be the most important effects. There is fairly consistent evidence that noise above 80 dB(A) causes reduced helping behavior, and that loud noise also increases aggressive behavior in individuals predisposed to aggressiveness. In schoolchildren, there is also concern that high levels of chronic noise contribute to feelings of helplessness. Guidelines on this issue, together with cardiovascular and mental effects, must await further research.

Specific environments.

A noise measure based only on energy summation and expressed as the conventional equivalent measure, LAeq, is not enough to characterize most noise environments. It is equally important to measure the maximum values of noise fluctuations, preferably combined with a measure of the number of noise events. If the noise includes a large proportion of low-frequency components, still lower values than the guideline values below will be needed. When prominent low-frequency components are present, noise measures based on A-weighting are inappropriate. The difference between dB(C) and dB(A) will give crude information about the presence of low-frequency components in noise, but if the difference is more than 10 dB, it is recommended that a frequency analysis of the noise be performed. It should be noted that a large proportion of low-frequency components in noise may increase considerably the adverse effects on health.

In Dwellings. The effects of noise in dwellings, typically, are sleep disturbance, annoyance and speech interference. For bedrooms the critical effect is sleep disturbance. Indoor guideline values for bedrooms are 30 dB LAeq for continuous noise and 45 dB LAmax for single sound events. Lower noise levels may be disturbing depending on the nature of the noise source. At night-time, outside sound levels about 1 metre from facades of living spaces should not exceed 45 dB LAeq, so that people may sleep with bedroom windows open. This value was obtained by assuming that the noise reduction from outside to inside with the window open is 15 dB. To enable casual conversation indoors during daytime, the sound level of interfering noise should not exceed 35 dB LAeq. The maximum sound pressure level should be measured with the sound pressure meter set at "Fast".

To protect the majority of people from being seriously annoyed during the daytime, the outdoor sound level from steady, continuous noise should not exceed 55 dB LAeq on balconies, terraces and in outdoor living areas. To protect the majority of people from being moderately annoyed during the daytime, the outdoor sound level should not exceed 50 dB LAeq. Where it is practical and feasible, the lower outdoor sound level should be considered the maximum desirable sound level for new development.

In Schools and Preschools. For schools, the critical effects of noise are speech interference, disturbance of information extraction (e.g. comprehension and reading acquisition), message communication and annoyance. To be able to hear and understand spoken messages in class rooms, the background sound level should not exceed 35 dB LAeq during teaching sessions. For hearing impaired children, a still lower sound level may be needed. The reverberation time in the classroom should be about 0.6 s, and preferably lower for hearing impaired children. For assembly halls and cafeterias in school buildings, the reverberation time should be less than 1 s. For outdoor playgrounds the sound level of the noise from external sources should not exceed 55 dB LAeq, the same value given for outdoor residential areas in daytime.

For preschools, the same critical effects and guideline values apply as for schools. In bedrooms in preschools during sleeping hours, the guideline values for bedrooms in dwellings should be used.

In Hospitals. For most spaces in hospitals, the critical effects are sleep disturbance, annoyance, and communication interference, including warning signals. The LAmax of sound events during the night should not exceed 40 dB(A) indoors. For ward rooms in hospitals, the guideline values indoors are 30dB LAeq, together with 40 dB LAmax during night. During the day and evening the guideline value indoors is 30 dB LAeq. The maximum level should be measured with the sound pressure instrument set at "Fast".

Since patients have less ability to cope with stress, the LAeq level should not exceed 35 dB in most rooms in which patients are being treated or observed. Attention should be given to the sound levels in intensive care units and operating theaters. Sound inside incubators may result in health problems for neonates, including sleep disturbance, and may also lead to hearing impairment. Guideline values for sound levels in incubators must await future research.

Ceremonies, Festivals and Entertainment Events. In many countries, there are regular ceremonies, festivals and entertainment events to celebrate life periods. Such events typically produce loud sounds, including music and impulsive sounds. There is widespread concern about the effect of loud music and impulsive sounds on young people who frequently attend concerts, discotheques, video arcades, cinemas, amusement parks and spectator events. At these events, the sound level typically exceeds 100 dB LAeq. Such noise exposure could lead to significant hearing impairment after frequent attendances.

Noise exposure for employees of these venues should be controlled by established occupational standards; and at the very least, the same standards should apply to the patrons of these premises. Patrons should not be exposed to sound levels greater than 100 dB LAeq during a four-hour period more than four times per year. To avoid acute hearing impairment the LAmax should always be below 110 dB.

Headphones. To avoid hearing impairment from music played back in headphones, in both adults and children, the equivalent sound level over 24 hours should not exceed 70 dB(A). This implies that for a daily one hour exposure the LAeq level should not exceed 85 dB(A). To avoid acute hearing impairment LAmax should always be below 110 dB(A). The exposures are expressed in free-field equivalent sound level.

Toys, Fireworks and Firearms. To avoid acute mechanical damage to the inner ear from impulsive sounds from toys, fireworks and firearms, adults should never be exposed to more than 140 dB(lin) peak sound pressure level. To account for the vulnerability in children when playing, the peak sound pressure produced by toys should not exceed 120 dB(lin), measured close to the ears (100 mm). To avoid acute hearing impairment LAmax should always be below 110 dB(A).

Parkland and Conservation Areas. Existing large quiet outdoor areas should be preserved and the signal-to-noise ratio kept low.

Table 1 presents the WHO guideline values arranged according to specific environments and critical health effects. The guideline values consider all identified adverse health effects for the specific environment. An adverse effect of noise refers to any temporary or long-term impairment of physical, psychological or social functioning that is associated with noise exposure. Specific noise limits have been set for each health effect, using the lowest noise level that produces an adverse health effect (i.e. the critical health effect). Although the guideline values refer to sound levels impacting the most exposed receiver at the listed environments, they are applicable to the general population. The time base for LAeq for "daytime" and "night-time" is 12–16 hours and 8 hours, respectively. No time base is given for evenings, but typically the guideline value should be 5–10 dB lower than in the daytime. Other time bases are recommended for schools, preschools and playgrounds, depending on activity.

It is not enough to characterize the noise environment in terms of noise measures or indices based only on energy summation (e.g., LAeq), because different critical health effects require different descriptions. It is equally important to display the maximum values of the noise fluctuations, preferably combined with a measure of the number of noise events. A separate characterization of night-time noise exposures is also necessary. For indoor environments, reverberation time is also an important factor for things such as speech intelligibility. If the noise includes a large proportion of low-frequency components, still lower guideline values should be applied. Supplementary to the guideline values given in Table 1, precautions should be taken for vulnerable groups and for noise of certain character (e.g. low-frequency components, low background noise).

Table 1: Guideline values for community noise in specific environments.

Specific environment	Critical health effect(s)	L_{Aeq} [dB(A)]	Time base [hours]	L_{Amax} fast [dB]
Outdoor living area	Serious annoyance, daytime and evening Moderate annoyance, daytime and evening	55 50	16 16	- -
Dwelling, indoors Inside bedrooms	Speech intelligibility & moderate annoyance, daytime & evening Sleep disturbance, night-time	35 30	16 8	 45
Outside bedrooms	Sleep disturbance, window open (outdoor values)	45	8	60
School class rooms & pre-schools, indoors	Speech intelligibility, disturbance of information extraction, message communication	35	during class	-
Pre-school bedrooms, indoor	Sleep disturbance	30	sleeping-time	45
School, playground outdoor	Annoyance (external source)	55	during play	-
Hospital, ward rooms, indoors	Sleep disturbance, night-time Sleep disturbance, daytime and evenings	30 30	8 16	40 -
Hospitals, treatment rooms, indoors	Interference with rest and recovery	#1		
Industrial, commercial shopping and traffic areas, indoors and outdoors	Hearing impairment	70	24	110
Ceremonies, festivals and entertainment events	Hearing impairment (patrons:<5 times/year)	100	4	110
Public addresses, indoors and outdoors	Hearing impairment	85	1	110
Music and other sounds through headphones/ earphones	Hearing impairment (free-field value)	85 #4	1	110
Impulse sounds from toys, fireworks and firearms	Hearing impairment (adults) Hearing impairment (children)	- -	- -	140 #2 120 #2
Outdoors in parkland and conservations areas	Disruption of tranquillity	#3		

#1: As low as possible.
#2: Peak sound pressure (not LAF, max) measured 100 mm from the ear.

#3: Existing quiet outdoor areas should be preserved and the ratio of intruding noise to natural background sound should be kept low.
#4: Under headphones, adapted to free-field values.

5. Noise Management

Chapter 5 is devoted to noise management with discussions on: strategies and priorities in managing indoor noise levels; noise policies and legislation; the impact of environmental noise; and on the enforcement of regulatory standards.

The fundamental goals of noise management are to develop criteria for deriving safe noise exposure levels and to promote noise assessment and control as part of environmental health programmes. These basic goals should guide both international and national policies for noise management. The United Nation's Agenda 21 supports a number of environmental management principles on which government policies, including noise management policies, can be based: the principle of precaution; the "polluter pays" principle; and noise prevention. In all cases, noise should be reduced to the lowest level achievable in the particular situation. When there is a reasonable possibility that the public health will be endangered, even though scientific proof may be lacking, action should be taken to protect the public health, without awaiting the full scientific proof. The full costs associated with noise pollution (including monitoring, management, lowering levels and supervision) should be met by those responsible for the source of noise. Action should be taken where possible to reduce noise at the source.

A legal framework is needed to provide a context for noise management. National noise standards can usually be based on a consideration of international guidelines, such as these *Guidelines for Community Noise*, as well as national criteria documents, which consider dose-response relationships for the effects of noise on human health. National standards take into account the technological, social, economic and political factors within the country. A staged program of noise abatement should also be implemented to achieve the optimum health protection levels over the long term.

Other components of a noise management plan include: noise level monitoring; noise exposure mapping; exposure modeling; noise control approaches (such as mitigation and precautionary measures); and evaluation of control options. Many of the problems associated with high noise levels can be prevented at low cost, if governments develop and implement an integrated strategy for the indoor environment, in concert with all social and economic partners. Governments should establish a "National Plan for a Sustainable Noise Indoor Environment" that applies both to new construction as well as to existing buildings.

The actual priorities in rational noise management will differ for each country. Priority setting in noise management refers to prioritizing the health risks to be avoided and concentrating on the most important sources of noise. Different countries have adopted a range of approaches to noise control, using different policies and regulations. A number of these are outlined in chapter 5 and Appendix 2, as examples. It is evident that noise emission standards have proven insufficient and that the trends in noise pollution are unsustainable.

The concept of environmental an environmental noise impact analysis is central to the philosophy of managing environmental noise. Such an analysis should be required before implementing any project that would significantly increase the level of environmental noise in a community (typically, greater than a 5 dB increase). The analysis should include: a baseline description of the existing noise environment; the expected level of noise from the new source; an assessment of the adverse health effects; an estimation of the population at risk; the calculation of exposure-response relationships; an assessment of risks and their acceptability; and a cost-benefit analysis.

Noise management should:

1. Start monitoring human exposures to noise.
2. Have health control require mitigation of noise immissions, and not just of noise source emissions. The following should be taken into consideration:
    - specific environments such as schools, playgrounds, homes, hospitals.
    - environments with multiple noise sources, or which may amplify the effects of noise.
    - sensitive time periods such as evenings, nights and holidays.
    - groups at high risk, such as children and the hearing impaired.
3. Consider the noise consequences when planning transport systems and land use.
4. Introduce surveillance systems for noise-related adverse health effects.
5. Assess the effectiveness of noise policies in reducing adverse health effects and exposure, and in improving supportive "soundscapes".
6. Adopt these *Guidelines for Community Noise* as intermediary targets for improving human health.
7. Adopt precautionary actions for a sustainable development of the acoustical environments.

Conclusions and recommendations

In chapter 6 are discussed: the implementation of the guidelines; further WHO work on noise; and research needs are recommended.

Implementation. For implementation of the guidelines it is recommended that:

- Governments should protection the population from community noise and consider it an integral part of their policy of environmental protection.
- Governments should consider implementing action plans with short-term, medium-term and long-term objectives for reducing noise levels.
- Governments should adopt the *Health Guidelines for Community Noise* values as targets to be achieved in the long-term.
- Governments should include noise as an important public health issue in environmental impact assessments.
- Legislation should be put in place to allow for the reduction of sound levels.
- Existing legislation should be enforced.
- Municipalities should develop low noise implementation plans.

- Cost-effectiveness and cost-benefit analyses should be considered potential instruments for meaningful management decisions.
- Governments should support more policy-relevant research.

Future Work. The Expert Task Force worked out several suggestions for future work for the WHO in the field of community noise. WHO should:

- Provide leadership and technical direction in defining future noise research priorities.
- Organize workshops on how to apply the guidelines.
- Provide leadership and coordinate international efforts to develop techniques for designing supportive sound environments (e.g. "soundscapes").
- Provide leadership for programs to assess the effectiveness of health-related noise policies and regulations.
- Provide leadership and technical direction for the development of sound methodologies for environmental and health impact plans.
- Encourage further investigation into using noise exposure as an indicator of environmental deterioration (e.g. black spots in cities).
- Provide leadership and technical support, and advise developing countries to facilitate development of noise policies and noise management.

Research and Development. A major step forward in raising the awareness of both the public and of decision makers is the recommendation to concentrate more research and development on variables which have monetary consequences. This means that research should consider not only dose-response relationships between sound levels, but also politically relevant variables, such as noise-induced social handicap; reduced productivity; decreased performance in learning; workplace and school absenteeism; increased drug use; and accidents.

In Appendices 1–6 are given: bibliographic references; examples of regional noise situations (African Region, American Region, Eastern Mediterranean Region, South East Asian Region, Western Pacific Region); a glossary; a list of acronyms; and a list of participants.

1. Introduction

Community noise (also called environmental noise, residential noise or domestic noise) is defined as noise emitted from all sources, except noise at the industrial workplace. Main sources of community noise include road, rail and air traffic, industries, construction and public work, and the neighbourhood. Typical neighbourhood noise comes from premises and installations related to the catering trade (restaurant, cafeterias, discotheques, etc.); from live or recorded music; from sporting events including motor sports; from playgrounds and car parks; and from domestic animals such as barking dogs. The main indoor sources are ventilation systems, office machines, home appliances and neighbours. Although many countries have regulations on community noise from road, rail and air traffic, and from construction and industrial plants, few have regulations on neighbourhood noise. This is probably due to the lack of mcthods to define and measure it, and to the difficulty of controlling it. In developed countries, too, monitoring of compliance with, and enforcement of, noise regulations are weak for lower levels of urban noise that correspond to occupationally controlled levels (>85 dB LAeq,8h; Frank 1998). Recommended guideline values based on the health effects of noise, other than occupationally-induced effects, are often not taken into account.

The extent of the community noise problem is large. In the European Union about 40% of the population is exposed to road traffic noise with an equivalent sound pressure level exceeding 55 dBA daytime; and 20% is exposed to levels exceeding 65 dBA (Lambert & Vallet 19 1994). When all transportation noise is considered, about half of all European Union citizens live in zones that do not ensure acoustical comfort to residents. At night, it is estimated that more than 30% is exposed to equivalent sound pressure levels exceeding 55 dBA, which are disturbing to sleep. The noise pollution problem is also severe in the cities of developing countries and is caused mainly by traffic. Data collected alongside densely traveled roads were found to have equivalent sound pressure levels for 24 hours of 75–80 dBA (e.g. National Environment Board Thailand 19 1990; Mage & Walsh 19 1998).

(a) In contrast to many other environmental problems, noise pollution continues to grow, accompanied by an increasing number of complaints from affected individuals. Most people are typically exposed to several noise sources, with road traffic noise being a dominant source (OECD-ECMT 19 1995). Population growth, urbanization and to a large extent technological development are the main driving forces, and future enlargements of highway systems, international airports and railway systems will only increase the noise problem. Viewed globally, the growth in urban environmental noise pollution is unsustainable, because it involves not simply the direct and cumulative adverse effects on health. It also adversely affects future generations by degrading residential, social and learning environments, with corresponding economical losses (Berglund 1998). Thus, noise is not simply a local problem, but a global issue that affects everyone (Lang 1999; Sandberg 1999) and calls for precautionary action in any environmental planning situation.

The objective of the World Health Organization (WHO) is the attainment by all peoples of the highest possible level of health. As the first principle of the WHO Constitution the definition of 'health' is given as: "A state of complete physical, mental and social well-being and not merely the absence of disease or infirmity". This broad definition of health embraces the concept of well-being and, thereby, renders noise impacts such as population annoyance, interference with communication, and impaired task performance as 'health' issues. In 1992, a WHO Task Force also identified the following specific health effects for the general population that may result from community noise: interference with communication; annoyance responses; effects on sleep, and on the cardiovascular and psychophysiological systems; effects on performance, productivity, and social behavior; and noise-induced hearing impairment (WHO 1993; Berglund & Lindvall 1995; *cf.* WHO 1980). Hearing damage is expected to result from both occupational and environmental noise, especially in developing countries, where compliance with noise regulation is known to be weak (Smith 1998).

Noise is likely to continue as a major issue well into the next century, both in developed and in developing countries. Therefore, strategic action is urgently required, including continued noise control at the source and in local areas. Most importantly, joint efforts among countries are necessary at a system level, in regard to the access and use of land, airspace and seawaters, and in regard to the various modes of transportation. Certainly, mankind would benefit from societal reorganization towards healthy transport. To understand noise we must understand the different types of noise and how we measure it, where noise comes from and the effects of noise on human beings. Furthermore, noise mitigation, including noise management, has to be actively introduced and in each case the policy implications have to be evaluated for efficiency.

This document is organized as follows. In Chapter 2 noise sources and measurement are discussed, including the basic aspects of source characteristics, sound propagation and transmission. In Chapter 3 the adverse health effects of noise are characterized. These include noise-induced hearing impairment, interference with speech communication, sleep disturbance, cardiovascular and physiological effects, mental health effects, performance effects, and annoyance reactions. This chapter is rounded out by a consideration of combined noise sources and their effects, and a discussion of vulnerable groups. In Chapter 4 the Guideline values are presented. Chapter 5 is devoted to noise management. Included are discussions of: strategies and priorities in the management of indoor noise levels; noise policies and legislation; environmental noise impact; and enforcement of regulatory standards. In Chapter 6 implementation of the WHO Guidelines is discussed, as well as future WHO work on noise and its research needs. In Appendices 1–6 are given: bibliographic references; examples of regional noise situations (African Region, American Region, Eastern Mediterranean Region, South East Asian Region, Western Pacific Region); a glossary; a list of acronyms; and a list of participants.

2. Noise sources and their measurement

2.1. Basic Aspects of Acoustical Measurements

Most environmental noises can be approximately described by one of several simple measures. They are all derived from overall sound pressure levels, the variation of these levels with time and the frequency of the sounds. Ford (1987) gives a more extensive review of various environmental noise measures. Technical definitions are found in the glossary in Appendix 3.

2.1.1. Sound pressure level

The sound pressure level is a measure of the air vibrations that make up sound. All measured sound pressures are referenced to a standard pressure that corresponds roughly to the threshold of hearing at 1 000 Hz. Thus, the sound pressure level indicates how much greater the measured sound is than this threshold of hearing. Because the human ear can detect a wide range of sound pressure levels (10–102 Pascal (Pa)), they are measured on a logarithmic scale with units of decibels (dB). A more technical definition of sound pressure level is found in the glossary.

The sound pressure levels of most noises vary with time. Consequently, in calculating some measures of noise, the instantaneous pressure fluctuations must be integrated over some time interval. To approximate the integration time of our hearing system, sound pressure meters have a standard *Fast* response time, which corresponds to a time constant of 0.125 s. Thus, all measurements of sound pressure levels and their variation over time should be made using the *Fast* response time, to provide sound pressure measurements more representative of human hearing. Sound pressure meters may also include a *Slow* response time with a time constant of 1 s, but its sole purpose is that one can more easily estimate the average value of rapidly fluctuating levels. Many modern meters can integrate sound pressures over specified periods and provide average values. It is not recommended that the *Slow* response time be used when integrating sound pressure meters are available.

Because sound pressure levels are measured on a logarithmic scale they cannot be added or averaged arithmetically. For example, adding two sounds of equal pressure levels results in a total pressure level that is only 3 dB greater than each individual sound pressure level. Consequently, when two sounds are combined the resulting sound pressure level will be significantly greater than the individual sound levels only if the two sounds have similar pressure levels. Details for combining sound pressure levels are given in Appendix 2.

2.1.2. Frequency and frequency weighting

The unit of frequency is the Hertz (Hz), and it refers to the number of vibrations per second of the air in which the sound is propagating. For tonal sounds, frequency is associated with the perception of pitch. For example, orchestras often tune to the frequency of 440 Hz. Most environmental sounds, however, are made up of a complex mix of many different frequencies. They may or may not have discrete frequency components superimposed on noise with a broad frequency spectrum (i.e. sound with a broad range of frequencies). The audible frequency range is normally considered to range from 20–20 000 Hz. Below 20 Hz we hear individual sound pulses rather than recognizable tones. Hearing sensitivity to higher frequencies decreases with age and exposure to noise. Thus, 20 000 Hz represents an upper limit of audibility for younger listeners with unimpaired hearing.

Our hearing systems are not equally sensitive to all sound frequencies (ISO 1987a). Thus, not all frequencies are perceived as being equally loud at the same sound pressure level, and when calculating overall environmental noise ratings it is necessary to consider sounds at some frequencies as more important than those at other frequencies. Detailed frequency analyses are commonly performed with standard sets of octave or 1/3 octave bandwidth filters. Alternatively, Fast Fourier Transform techniques or other types of filters can be used to determine the relative strengths of the various frequency components making up a particular environmental noise.

Frequency weighting networks provide a simpler approach for weighting the importance of different frequency components in one single number rating. The A-weighting is most commonly used and is intended to approximate the frequency response of our hearing system. It weights lower frequencies as less important than mid- and higher-frequency sounds. C-weighting is also quite common and is a nearly flat frequency response with the extreme high and low frequencies attenuated. When no frequency analysis is possible, the difference between A-weighted and C-weighted levels gives an indication of the amount of low frequency content in the measured noise. When the sound has an obvious tonal content, a correction to account for the additional annoyance may be used (ISO 1987b).

2.1.3. Equivalent continuous sound pressure level

According to the equal energy principle, the effect of a combination of noise events is related to the combined sound energy of those events. Thus, measures such as the equivalent continuous sound pressure level (LAeq,T) sum up the total energy over some time period (T) and give a level equivalent to the average sound energy over that period. Such average levels are usually based on integration of A-weighted levels. Thus LAeq,T is the average energy equivalent level of the A-weighted sound over a period T.

2.1.4. Individual noise events

It is often desired to measure the maximum level (LAmax) of individual noise events. For cases such as the noise from a single passing vehicle, LAmax values should be measured using the *Fast* response time because it will give a good correlation with the integration of loudness by our hearing system. However, for very short-duration impulsive sounds it is often desirable to measure the instantaneous peak amplitude to assess potential hearing-damage risk. If actual instantaneous pressure cannot be determined, then a time-integrated 'peak' level with a time constant of no more than 0.05 ms should be used (ISO 1987b). Such peak readings are often made using the C- (or linear) frequency weightings.

Alternatively, discrete sound events can be evaluated in terms of their A-weighted sound exposure level (SEL, for defintion see appendix 5). The total amount of sound energy in a particular event is assessed by the SEL. One can add up the SEL values of individual events to calculate a LAeq,T over some time period, T, of interest. In some cases the SEL may provide more consistent evaluations of individual noise events because they are derived from the complete history of the event and not just one maximum value. However, A-weighted SEL measurements have been shown to be inadequate for assessing the (perceived) loudness of complex impulsive sounds, such as those from large and small weapons (Berglund et al. 1986). In contrast, C-weighted SEL values have been found useful for rating impulsive sounds such as gun shots (Vos 1996; Buchta 1996; ISO 1987b).

2.1.5. Choice of noise measure

LAeq,T should be used to measure continuing sounds such as road traffic noise, many types of industrial noises and noise from ventilation systems in buildings. When there are distinct events to the noise such as with aircraft or railway noise, measures of the individual events should be obtained (using, for example, LAmax or SEL), in addition to LAeq,T measurements.

In the past, time-varying environmental sound levels have also been described in terms of percentile levels. These are derived from a statistical distribution of measured sound levels over some period. For example, L10 is the A-weighted level exceeded 10% of the time. L10 values have been widely used to measure road-traffic noise, but they are usually found to be highly correlated measures of the individual events, as are LAmax and SEL. L90 or L95 can be used as a measure of the general background sound pressure level that excludes the potentially confounding influence of particular local noise events.

2.1.6. Sound and noise

Physically, there is no distinction between sound and noise: sound is a sensory perception evoked by physiological processes in the auditory brain. The complex pattern of sound waves is perceptually classified as "Gestalts" and are labeled as noise, music, speech, etc. Consequently, it is not possible to define noise exclusively on the basis of the physical parameters of sound. Instead, it is common practice to define noise simply as unwanted sound. However, in some situations noise may adversely affect health in the form of acoustical energy.

2.2. Sources of Noise

This section describes various sources of noise that can affect a community. Namely, noise from industry, transportation, and from residential and leisure areas. It should be noted that equal values of LAeq,T for different sources do not always imply the same expected effect.

2.2.1. Industrial noise

Mechanized industry creates serious noise problems. It is responsible for intense noise indoors as well as outdoors. This noise is due to machinery of all kinds and often increases with the power of the machines. Sound generation mechanisms of machinery are reasonably well understood. The noise may contain predominantly low or high frequencies, tonal components, be impulsive or have unpleasant and disruptive temporal sound patterns. Rotating and reciprocating machines generate sound that includes tonal components; and air-moving equipment tends also to generate noise with a wide frequency range. The high sound pressure levels are caused by components or gas flows that move at high speed (for example, fans, steam pressure relief valves), or by operations involving mechanical impacts (for example, stamping, riveting, road breaking). Machinery should preferably be silenced at the source.

Noise from fixed installations, such as factories or construction sites, heat pumps and ventilation systems on roofs, typically affect nearby communities. Reductions may be achieved by encouraging quieter equipment or by zoning of land into industrial and residential areas. Requirements for passive (sound insulating enclosures) and active noise control, or restriction of operation time, may also be effective.

2.2.2. Transportation noise

Transportation noise is the main source of environmental noise pollution, including road traffic, rail traffic and air traffic. As a general rule, larger and heavier vehicles emit more noise than smaller and lighter vehicles. Exceptions would include: helicopters and 2- and 3-wheeled road vehicles.

The noise of road vehicles is mainly generated from the engine and from frictional contact between the vehicle and the ground and air. In general, road-contact noise exceeds engine noise at speeds higher than 60 km/h. The physical principle responsible for generating noise from tire-road contact is less well understood. The sound pressure level from traffic can be predicted from the traffic flow rate, the speed of the vehicles, the proportion of heavy vehicles, and the nature of the road surface. Special problems can arise in areas where the traffic movements involve a change in engine speed and power, such as at traffic lights, hills, and intersecting roads; or where topography, meteorological conditions and low background levels are unfavourable (for example, mountain areas).

Railway noise depends primarily on the speed of the train, but variations are present depending upon the type of engine, wagons, and rails and their foundations, as well as the roughness of wheels and rails. Small radius curves in the track, such as may occur for urban trains, can lead to very high levels of high-frequency sound referred to as wheel squeal. Noise can be generated in stations because of running engines, whistles and loudspeakers, and in marshaling yards because of shunting operations. The introduction of high-speed trains has created special noise problems with sudden, but not impulsive, rises in noise. At speeds greater than 250 km/h, the proportion of high-frequency sound energy increases and the sound can be perceived as similar to that of overflying jet aircraft. Special problems can arise in areas close to tunnels, in valleys or in areas where the ground conditions help generate vibrations. The long-distance propagation of noise from high-speed trains will constitute a problem in the future if otherwise environment-friendly railway systems are expanded.

Aircraft operations generate substantial noise in the vicinity of both commercial and military airports. Aircraft takeoffs are known to produce intense noise, including vibration and rattle. The landings produce substantial noise in long low-altitude flight corridors. The noise is produced by the landing gear and automatic power regulation, and also when reverse thrust is applied, all for safety reasons. In general, larger and heavier aircraft produce more noise than lighter aircraft. The main mechanism of noise generation in the early turbojet-powered aircraft was the turbulence created by the jet exhaust mixing with the surrounding air. This noise source has been significantly reduced in modern high by-pass ratio turbo-fan engines that surround the high-velocity jet exhaust with lower velocity airflow generated by the fan. The fan itself can be a significant noise source, particularly during landing and taxiing operations. Multi-bladed turbo-prop engines can produce relatively high levels of tonal noise. The sound pressure level from aircraft is, typically, predicted from the number of aircraft, the types of airplanes, their flight paths, the proportions of takeoffs and landings and the atmospheric conditions. Severe noise problems may arise at airports hosting many helicopters or smaller aircraft used for private business, flying training and leisure purposes. Special noise problems may also arise inside airplanes because of vibration. The noise emission from future superjets is unknown.

A sonic boom consists of a shock wave in the air, generated by an aircraft when it flies at a speed slightly greater than the local speed of sound. An aircraft in supersonic flight trails a sonic boom that can be heard up to 50 km on either side of its ground track, depending upon the flight altitude and the size of the aircraft (Warren 1972). A sonic boom can be heard as a loud double-boom sound. At high intensity it can damage property.

Noise from military airfields may present particular problems compared to civil airports (von Gierke & Harris 1987). For example, when used for night-time flying, for training interrupted landings and takeoffs (so-called touch-and-go), or for low-altitude flying. In certain instances, including wars, specific military activities introduce other intense noise pollution from heavy vehicles (tanks), helicopters, and small and large fire-arms.

2.2.3. Construction noise and building services noise

Building construction and excavation work can cause considerable noise emissions. A variety of sounds come from cranes, cement mixers, welding, hammering, boring and other work processes. Construction equipment is often poorly silenced and maintained, and building operations are sometimes carried out without considering the environmental noise consequences. Street services such as garbage disposal and street cleaning can also cause considerable disturbance if carried out at sensitive times of day. Ventilation and air conditioning plants and ducts, heat pumps, plumbing systems, and lifts (elevators), for example, can compromise the internal acoustical environment and upset nearby residents.

2.2.4. Domestic noise and noise from leisure activities

In residential areas, noise may stem from mechanical devices (e.g. heat pumps, ventilation systems and traffic), as well as voices, music and other kinds of sounds generated by neighbours (e.g. lawn movers, vacuum cleaners and other household equipment, music reproduction and noisy parties). Aberrant social behavior is a well-recognized noise problem in multifamily dwellings, as well as at sites for entertainment (e.g. sports and music events). Due to predominantly low-frequency components, noise from ventilation systems in residential buildings may also cause considerable concern even at low and moderate sound pressure levels.

The use of powered machines in leisure activities is increasing. For example, motor racing, off-road vehicles, motorboats, water skiing, snowmobiles etc., and these contribute significantly to loud noises in previously quiet areas. Shooting activities not only have considerable potential for disturbing nearby residents, but can also damage the hearing of those taking part. Even tennis playing, church bell ringing and other religious activities can lead to noise complaints.

Some types of indoor concerts and discotheques can produce extremely high sound pressure levels. Associated noise problems outdoors result from customers arriving and leaving. Outdoor concerts, fireworks and various types of festivals can also produce intense noise. The general problem of access to festivals and leisure activity sites often adds to road traffic noise problems. Severe hearing impairment may also arise from intense sound produced as music in headphones or from children's toys.

2.3. The Complexity of Noise and Its Practical Implications

2.3.1. The problem

One must consider many different characteristics to describe environmental noises completely. We can consider the sound pressure level of the noise and how this level varies over a variety of periods, ranging from minutes or seconds to seasonal variations over several months. Where sound pressure levels vary quite substantially and rapidly, such as in the case of low-level jet aircraft, one might also want to consider the rate of change of sound pressure levels (Berry 1995; Kerry et al. 1997). At the same time, the frequency content of each noise will also determine its effect on people, as will the number of events when there are relatively small numbers of discrete noisy events. Combinations of these characteristics determine how each type of environmental noise affects people. These effects may be annoyance, sleep disturbance, speech interference, increased stress, hearing impairment or other health-related effects.

Thus, in total there is a very complex multidimensional relationship between the various characteristics of the environmental noise and the effects it has on people. Unfortunately, we do not completely understand all of the complex links between noise characteristics and the resulting effects on people. Thus, current practice is to reduce the assessment of environmental noise to a small number of quite simple quantities that are known to be reasonably well related to the effects of noise on people (LAeq,T for continuing sounds and LAmax or SEL where there are a small number of distinct noise events). These simple measures have the distinct advantage that they are relatively easy and inexpensive to obtain and hence are more likely to be widely adopted. On the other hand, they may ignore some details of the noise characteristics that relate to particular types of effects on people.

2.3.2. Time variation

There is evidence that the pattern of noise variation with time relates to annoyance (Berglund et al. 1976). It has been suggested that the equal-energy principle is a simple concept for obtaining a measure representative of the annoyance of a number of noise events. For example, the LAeq,T of the noise from a busy road may be a good indicator of the annoyance this noise may cause for nearby residents. However, such a measure may not be very useful for predicting the disturbance to sleep of a small number of very noisy aircraft fly-overs. The disturbance caused by small numbers of such discrete events is usually better related to maximum sound pressure levels and the number of events.

While using LAeq,T measures is the generally accepted approach, it is still important to appreciate the limitations and errors that may occur. For example, some years ago measures that assessed the variation of sound pressure levels with time were popular. Subsequently, these have been shown not to improve predictions of annoyance with road traffic noise (Bradley 1978). However, it is possible that time variations may contribute to explaining the very different amounts of annoyance caused by equal LAeq,T levels of road-traffic noise, train noise and aircraft noise (*cf.* Miedema & Vos 1998).

More regular variations of sound pressure levels with time have been found to increase the annoying aspects of the noise. For example, noises that vary periodically to create a throbbing or pulsing sensation can be more disturbing than continuous noise (Bradley 1994b). Research suggests that variations at about 4 per second are most disturbing (Zwicker 1989). Noises with very rapid onsets could also be more disturbing than indicated by their LAeq,T (Berry 1995; Kerry et al. 1997).

LAeq,T values can be calculated for various time periods and it is very important to specify this period. It is quite common to calculate LAeq,T values separately for day- and night-time periods. In combining day and night LAeq,T values it is usually assumed that people will be more sensitive to noise during the night-time period. A weighting is thus normally added to night-time LAeq,T values when calculating a combined measure for a 24 hour period. For example, day-night sound pressure measures commonly include a 10 dB night-time weighting. Other night-time weightings have been proposed, but it has been suggested that it is not possible to determine precisely an optimum value for night-time weightings from annoyance survey responses, because of the large variability in responses within groups of people (Fields 1986; see also Berglund & Lindvall 1995). Night-time weightings are intended to indicate the expected increased sensitivity to annoyance at night and do not protect people from sleep disturbance.

2.3.3. Frequency content and loudness

Noise can also be characterized by its frequency content. This can be assessed by various types of frequency analysis to determine the relative contributions of the frequency components to the total noise. The combined effects of the different frequencies on people, perceived as noise, can be approximated by simple frequency weightings. The A-weighting is now widely used to obtain an approximate, single-number rating of the combined effects of the various frequencies. The A-weighting response is a simplification of an equal-loudness contour. There is a family of these equal-loudness contours (ISO 1987a) that describe the frequency response of the hearing system for a wide range of frequencies and sound pressure levels. These equal-loudness contours can be used to determine the perceived loudness of a single frequency sound. More complicated procedures have been derived to estimate the perceived loudness of complex sounds (ISO 1975). These methods involve determining the level of the sound in critical bands and the mutual masking of these bands.

Many studies have compared the accuracy of predictions based on A-weighted levels with those based on other frequency weightings, as well as more complex measures such as loudness levels and perceived noise levels (see also Berglund & Lindvall 1995). The comparisons depend on the particular effect that is being predicted, but generally the correlation between the more complex measures and subjective scales are a little stronger. A-weighted measures have been particularly criticized as not being accurate indicators of the disturbing effects of noises with strong low-frequency components (Kjellberg et al. 1984; Persson & Björkman 1988; Broner & Leventhall 1993; Goldstein 1994). However, these differences in prediction accuracy are usually smaller than the variability of responses among groups of people (Fields 1986; see also Berglund & Lindvall 1995). Thus, in practical situations the limitations of A-weighted measures may not be so important.

In addition to equal-loudness contours, equal-noisiness contours have also been developed for calculating perceived noise levels (PNL) (Kryter 1959; Kryter 1994; see also section 2.7.2). Critics have pointed out that in addition to equal-loudness and equal-noisiness contours, we could have many other families of equal-sensation contours corresponding to other attributes of the noises (Molino 1974). There seems to be no limit to the possible complexity and number of such measures.

2.3.4. Influence of ambient noise level

A number of studies have suggested that the annoyance effect of a particular noise would depend on how much that noise exceeded the level of ambient noise. This has been shown to be true for noises that are relatively constant in level (Bradley 1993), but has not been consistently found for time-varying noises such as aircraft noise (Gjestland et al. 1990; Fields 1998). Because at some time during an aircraft fly-over the noise almost always exceeds the ambient level, responses to this type of noise are less likely to be influenced by the level of the ambient noise.

2.3.5. Types of noise

A number of studies have concluded that equal levels of different noise types lead to different annoyance (Hall et al. 1981; Griffiths 1983; Miedema 1993; Bradley 1994a; Miedema & Vos 1998). For example, equal LAeq,T levels of aircraft noise and road traffic noise will not lead to the same mean annoyance in groups of people exposed to these noises. This may indicate that the LAeq,T measure is not a completely satisfactory description of these noises and perhaps does not completely reflect the characteristics of these noises that lead to annoyance. Alternatively, the differences may be attributed to various other factors that are not part of the noise characteristics (e.g. Flindell & Stallen 1999). For example, it has been said that aircraft noise is more disturbing, because of the associated fear of aircraft crashing on people's homes (cf. Berglund & Lindvall 1995).

2.3.6. Individual differences

Finally, there is the problem of individual response differences. Different people will respond quite differently to the same noise stimulus (Job 1988). These individual differences can be quite large and it is often most useful to consider the average response of groups of people exposed to the same sound pressure levels. In annoyance studies the percentage of highly annoyed individuals is usually considered, because it correlates better with measured sound pressure levels. Individual differences also exist for susceptibility to hearing impairment (e.g. Katz 1994).

2.3.7. Recommendations

In many cases we do not have specific, accurate measures of how annoying sound will be and must rely on the simpler quantities. As a result, current practice is to assume that the equal energy principle is approximately valid for most types of noise, and that a simple LAeq,T type measure will indicate reasonably well the expected effects of the noise. Where the noise consists of a small number of discrete events, the A-weighted maximum level (LAmax) will be a better indicator of the disturbance to sleep and other activities. However, in most cases the A-weighted sound exposure level (SEL) will provide a more consistent measure of such single-noise events, because it is based on an integration over the complete noise event.

2.4. Measurement Issues

2.4.1. Measurement objectives

The details of noise measurements must be planned to meet some relevant objective or purpose. Some typical objectives would include:

a. Investigating complaints.
b. Assessing the number of persons exposed.
c. Compliance with regulations.
d. Land use planning and environmental impact assessments.
e. Evaluation of remedial measures.
f. Calibration and validation of predictions.
g. Research surveys.
h. Trend monitoring.

The sampling procedure, measurement location, type of measurements and the choice of equipment should be in accord with the objective of the measurements.

2.4.2. Instrumentation

The most critical component of a sound pressure meter is the microphone, because it is difficult to produce microphones with the same precision as the other, electronic components of a pressure meter. In contrast, it is usually not difficult to produce the electronic components of a microphone with the desired sensitivity and frequency-response characteristics. Lower quality microphones will usually be less sensitive and so cannot measure very low sound pressure levels. They may also not be able to accurately measure very high sound pressure levels found closer to loud noise sources. Lower quality microphones will also have less well-defined frequency-response characteristics. Such lower quality microphones may be acceptable for survey type measurements of overall A-weighted levels, but would not be preferred for more precise measurements, including detailed frequency analysis of the sounds.

Sound pressure meters will usually include both A- and C-weighting frequency-response curves. The uses of these frequency weightings were discussed above. They may also include a linear weighting. Linear weightings are not defined in standards and may in practice be limited by the response of the particular microphone being used. Instead of, or in addition to, frequency-response weightings, more complex sound pressure meters can also include sets of standard bandpass filters, to permit frequency analysis of sounds. For acoustical measurements, octave and one-third octave bandwidth filters are widely used with centre frequencies defined in standards (ISO 1975b).

The instantaneous sound pressures are integrated with some time constant to provide sound pressure levels. As mentioned above most meters will include both *Fast*- and *Slow*-response times. *Fast*-response corresponds to a time constant of 0.125 s and is intended to approximate the time constant of the human hearing system. *Slow*-response corresponds to a time constant of 1 s and is an old concept intended to make it easier to obtain an approximate average value of fluctuating levels from simple meter readings.

Standards (IEC 1979) classify sound pressure meters as type 1 or type 2. Type 2 meters are adequate for broad band A-weighted level measurements, where extreme precision is not required and where very low sound pressure levels are not to be measured. Type 1 meters are usually much more expensive and should be used where more precise results are needed, or in cases where frequency analysis is required.

Many modern sound pressure meters can integrate sound pressure levels over some specified time period, or may include very sophisticated digital processing capabilities. Integrating meters make it possible to directly obtain accurate measures of LAeq,T values over a user-specified time interval, T. By including small computers in some sound pressure meters, quite complex calculations can be performed on the measured levels and many such results can be stored for later read out. For example, some meters can determine the statistical distribution of sound pressure levels over some period, in addition to the simple LAeq,T value. Recently, hand-held meters that perform loudness calculations in real time have become available. Continuing rapid developments in instrumentation capabilities are to be expected.

2.4.3. Measurement locations

Where local regulations do not specify otherwise, measurements of environmental noise are usually best made close to the point of reception of the noise. For example, if there is concern about residents exposed to road traffic noise it is better to measure close to the location of the residents, rather than close to the road. If environmental noises are measured close to the source, one must then estimate the effect of sound propagation to the point of reception. Sound propagation can be quite complicated and estimates of sound pressure levels at some distance from the source will inevitably introduce further errors into the measured sound pressure levels. These errors can be avoided by measuring at locations close to the point of reception.

Measurement locations should normally be selected so that there is a clear view of the sound source and so that the propagation of the sound to the microphone is not shielded or blocked by structures that would reduce the incident sound pressure levels. For example, measurements of aircraft noise should be made on the side of the building directly exposed to the noise. The position of the measuring microphone relative to building façades or other sound-reflective surfaces is also important and will significantly influence measured sound pressure levels (ISO 1978). If the measuring microphone is located more than several meters from reflecting surfaces, it will provide an unbiased indication of the incident sound pressure level. At the other extreme, when a measuring microphone is mounted on a sound-reflecting surface, such as a building façade, sound pressure levels will be increased by 6 dB, because the direct and reflected sound will coincide. Some standards recommend a position 2 m from the façade and an associated 3 dB correction (ISO 1978; ASTM 1992). The effect of façade reflections must be accounted for to represent the true level of the incident sound. Thus, while locating the measuring microphone close to the point of reception is desirable, it leads to some other issues that must be considered to accurately interpret measurement results. Where exposures are measured indoors, it is necessary to measure at several positions to characterize the average sound pressure level in a room. In other situations, it may be necessary to measure at the position of the exposed person.

2.4.4. Sampling

Many environmental noises vary over time, such as for different times of day or from season to season. For example, road traffic noise may be considerably louder during some hours of the day but much quieter at night. Aircraft noise may vary with the season due to different numbers of aircraft operations. Although permanent noise monitoring systems are becoming common around large airports, it is usually not possible to measure sound pressure levels continuously over a long enough period of time to completely define the environmental noise exposure. In practice, measurements usually only sample some part of the total exposure. Such sampling will introduce uncertainties in the estimates of the total noise exposure.

Traffic noise studies have identified various sampling schemes that can introduce errors of 2-3 dB in estimates of daytime LAeq,T values and even larger errors in night-time sound pressure levels (Vaskor et al. 1979). These errors relate to the statistical distributions of sound pressure levels over time (Bradley et al. 1979). Thus, the sampling errors associated with road traffic noise may be quite different from those associated with other noise, because of the quite different variations of sound pressure levels over time. It is also difficult to give general estimates of sampling errors due to seasonal variations. When making environmental noise measurements it is important that the measurement sample is representative of all of the variations in the noise in question, including variations of the source and variations in sound propagation, such as due to varying atmospheric conditions.

2.4.5. Calibration and quality assurance

Sound pressure meters can be calibrated using small calibrated sound sources. These devices are placed on the measurement microphone and produce a known sound pressure level with a specified accuracy. Such calibrations should be made at least daily, and more often if there is some possibility that handling of the sound pressure meter may have modified its sensitivity. It is also important to have a complete quality assurance plan. This should require annual calibration of all noise measuring equipment to traceable standards and should clearly specify correct measurement and operating procedures (ISO 1994).

2.5. Source Characteristics and Sound Propagation

To make a correct assessment of noise it is important to have some appreciation of the characteristics of environmental noise sources and of how sound propagates from them. One should consider the directionality of noise sources, the variability with time and the frequency content. If these are in some way unusual, the noise may be more disturbing than expected. The most common types of environmental noise sources are directional and include: road-traffic noise, aircraft noise, train noise, industrial noise and outdoor entertainment facilities (*cf.* section 2.2). All of these types of environmental noise are produced by multiple sources, which in many cases are moving. Thus, the characteristics of individual sources, as well as the characteristics of the combined sources, must be considered.

For example, we can consider the radiation of sound from individual vehicles, as well as from a line of vehicles on a particular road. Sound from an ideal point source (i.e. non-directional source) will spread out spherically and sound pressure levels would decrease 6 dB for each doubling of distance from the source. However, for a line of such sources, or for an integration over the complete pass-by of an individual moving source, the combined effect leads to sound that spreads cylindrically and to sound pressure levels that decrease at 3 dB per doubling of distance. Thus, there are distinct differences between the propagation of sound from an ideal point source and from moving sources. In practice one cannot adequately assess the noise from a fixed source with measurements at a single location; it is essential to measure in a number of directions from the source. If the single source is moving, it is necessary to measure over a complete pass-by, to account for sound variation with direction and time.

In most real situations this simple behaviour is considerably modified by reflections from the ground and from other nearby surfaces. One expects that when sound propagates over loose ground, such as grass, that some sound energy will be absorbed and sound pressure levels will actually decrease more rapidly with distance from the source. Although this is approximately true, the propagation of sound between sources and receivers close to the ground is much more complicated than this. The combination of direct and ground-reflected sound can combine in a complex manner which can lead to strong cancellations at some frequencies and not at others (Embleton & Piercy 1976). Even at quite short source-to-receiver distances, these complex interference effects can significantly modify the propagating sound. At larger distances (approximately 100 m or more), the propagation of sound will also be significantly affected by various atmospheric conditions. Temperature and wind gradients as well as atmospheric turbulence can have large effects on more distant sound pressure levels (Daigle et al. 1986). Temperature and wind gradients can cause propagating sound to curve either upwards or downwards, creating either areas of increased or decreased sound pressure levels at points quite distant from the source. Atmospheric turbulence can randomize sound so that the interference effects resulting from combinations of sound paths are reduced. Higher frequency sound is absorbed by air depending on the exact temperature and relative humidity of the air (Crocker &

Price 1975; Ford 1987). Because there are many complex effects, it is not usually possible to accurately predict sound pressure levels at large distances from a source.

Using barriers or screens to block the direct path from the source to the receiver can reduce the propagation of sound. The attenuating effects of the screen are limited by sound energy that diffracts or bends around the screen. Screens are more effective at higher frequencies and when placed either close to the sound source or the receiver; they are less effective when placed far from the receiver. Although higher screens are better, in practice it is difficult to achieve more than about a 10 dB reduction. There should be no gaps in the screen and it must have an adequate mass per unit area. A long building can be an effective screen, but gaps between buildings will reduce the sound attenuation.

In some cases, it may be desirable to estimate environmental sound pressure levels using mathematical models implemented as computer programmes (House 1987). Such computer programmes must first model the characteristics of the source and then estimate the propagation of the sound from the source to some receiver point. Although such prediction schemes have several advantages, there will be some uncertainty as to the accuracy of the predicted sound pressure levels. Such models are particularly useful for road traffic noise and aircraft noise, because it is possible to create data bases of information describing particular sources. For more varied types of noise, such as industrial noise, it would be necessary to first characterize the noise sources. The models then sum up the effects of multiple sources and calculate how the sound will propagate to receiver points. Techniques for estimating sound propagation are improving and the accuracy of these models is also expected to improve. These models can be particularly useful for estimating the combined effect of a large number of sources over an extended period of time. For example, aircraft noise prediction models are typically used to predict average yearly noise exposures, based on the combination of aircraft events over a complete year. Such models can be applied to predict sound pressure level contours around airports for these average yearly conditions. This is of course much less expensive than measuring at many locations over a complete one year-period. However, such models can be quite complex, and require skilled users and accurate data bases. Because environmental noise prediction models are still developing, it is advisable to confirm predictions with measurements.

2.6. Sound transmission Into and Within Buildings

Sources of environmental noise are usually located outdoors; for example, road traffic, aircraft or trains. However, people exposed to these noises are often indoors, inside their home or some other building. It is, therefore, important to understand how environmental noises are transmitted into buildings. Most of the same fundamentals discussed earlier apply to airborne sound propagation between homes in multifamily dwellings, via common walls and floors. However, within buildings we can also consider impact sound sources, such as footsteps, as well as airborne sounds.

The amount of incident sound that is transmitted through a building façade is measured in terms of the sound reduction index. The sound reduction index, or transmission loss, is defined as 10 times the logarithm of the ratio of incident-to-transmitted sound power, and it describes in decibels how much the incident sound is reduced on passing through a particular panel. This index of constructions usually increases with the frequency of the incident sound and with the mass of the construction (Kremer 1950). Thus, heavier or more massive constructions tend to have higher sound reductions. When it is not possible to achieve the desired transmission loss by increasing the mass of a panel, increased sound reduction can be achieved by a double panel construction. The two layers should be isolated with respect to vibrations and there should be sound absorbing material in the cavity. Such double panel constructions can provide much greater sound reduction than a single panel. Because sound reduction is also greater at higher frequencies most problems occur at lower frequencies, where most environmental noise sources produce relatively high sound pressure levels.

The sound reduction of buildings can be measured in standard laboratory tests, where the test panel is constructed in an opening between two reverberant test chambers (ISO 1995; ASTM 1997). In these tests sound fields are quite diffuse in both test chambers and the sound reduction index is calculated as the difference between the average sound pressure levels in the two rooms, plus a correction involving the area of the test panel and the total sound absorption in the receiving room. The sound reduction of a complete building façade can also be measured in the field using either natural environmental noises or test signals from loudspeakers (ISO 1978; ASTM 1992). In either case the noise, as transmitted through the façade, must be greater in level than other sounds in the receiving room. For this outdoor-to-indoor sound propagation case, the measured sound reduction index will also depend on the angle of incidence of the outdoor sound, as well as the position of the outdoor measuring microphone relative to the building façade. Corrections of up to 6 dB must be made to the sound pressure level measured outdoors, to account for the effect of reflections from the façade (see also section 2.4.3).

The sound reduction of most real building façades is determined by a combination of several different elements. For example, a wall might include windows, doors or some other type of element. If the sound reduction index values of each element are known, the values for the combined construction can be calculated from the area-weighted sums of the sound energy transmitted through each separate element. Although parts of the building façade, such as massive wall constructions, can be very effective barriers to sound, the sound reduction index of the complete façade is often greatly reduced by less effective elements such as windows, doors or ventilation openings. Completely open windows as such would have a sound reduction index of 0 dB. If window openings makes up 10% of the area of a wall, the sound reduction index of the combined wall and open window could not exceed 10 dB. Thus it is not enough to specify effective sound reducing façade constructions, without also solving the problem of adequate ventilation that does not compromise the sound transmission reduction by the building façade.

Sound reduction index values are measured at different frequencies and from these, single number ratings are determined. Most common are the ISO weighted sound reduction index (ISO 1996) and the equivalent ASTM sound transmission class (ASTM 1994a). However, in their original form these single number ratings are only appropriate for typical indoor noises that usually do not have strong low frequency components. Thus, they are usually not appropriate single number ratings of the ability of a building façade to block typical environmental noises. More recent additions to the ISO procedure have included source spectrum corrections intended to correct approximately for other types of sources (ISO 1996). Alternatively, the ASTM-Outdoor-Indoor Transmission Class rating calculates the A-weighted level reduction to a standard environmental noise source spectrum (ASTM 1994b). Within buildings the impact sound insulation index can be measured with a standard impact source and determined according to ISO and ASTM standards (ISO 1998; ASTM 1994c 1996)

2.7. More Specialized Noise Measures

2.7.1. Loudness and perceived noise levels

There are procedures to accurately rate the loudness of complex sounds (Zwicker 1960; Stevens 1972; ISO 1975a). These usually start from a 1/3 octave spectrum of the noise. The combination of the loudness contributions of each 1/3 octave band with estimates of mutual masking effects, leads to a single overall loudness rating in sones. A similar system for rating the noisiness of sounds has also been developed (Kryter 1994). Again a 1/3 octave spectrum of the noise is required and the 1/3 octave noise levels are compared with a set of equal-noisiness contours. The individual 1/3 octave band noisiness estimates are combined to give an overall perceived noise level (PNL) that is intended to accurately estimate subjective evaluations of the same sound. The PNL metric was initially developed to rate jet aircraft noise.

PNL values will vary with time, for example when an aircraft flies by a measuring point. The effective perceived noise level measure (EPNL) is derived from PNL values and is intended to provide a complete rating of an aircraft fly-over. EPNL values add both a duration correction and a tone correction to PNL values. The duration correction ensures that longer duration events are rated as more disturbing. Similarly, noise spectra that seem to have prominent tonal components are rated as more disturbing by the tone-correction procedure. There is some evidence that these tone corrections are not always successful in improving predictions of adverse responses to noise events (Scharf & Hellman 1980). EPNL values are used in the certification testing of new aircraft. These more precise measures ensure that the noise from new aircraft is rated as accurately as possible.

2.7.2. Aviation noise measures

There are many measures for evaluating the long-term average sound pressure levels from aircraft near airports (Ford 1987; House 1987). They include different frequency weightings, different summations of levels and numbers of events, as well as different time-of-day weightings. Most measures are based on either A-weighted or PNL-weighted sound pressure levels. Because of the many other large uncertainties in predicting community response to aircraft noise, there seems little justification for using the more complex PNL-weighted sound pressure levels and there is a trend to change to A-weighted measures.

Most aviation noise measures are based on an equal energy approach and hence they sum up the total energy of a number of aircraft fly-overs. However, some older measures were based on different combinations of the level of each event and the number of events. These types of measures are gradually being replaced by measures based on the equal energy hypothesis such as LAeq,T values. There is also a range of time-of-day weightings incorporated into current aircraft noise measures. Night-time weightings of 6–12 dB are currently in use. Some countries also include an intermediate evening weighting.

The day-night sound pressure level L_{dn} (von Gierke 1975; Ford 1987) is an LAeq,T based measure with a 10 dB night-time weighting. It is based on A-weighted sound pressure levels and the equal energy principle. The noise exposure forecast (NEF) (Bishop & Horonjeff 1967) is based on the EPNL values of individual aircraft events and includes a 12 dB night-time weighting. It sums multiple events on an equal energy basis. However, the Australian variation of the NEF measure has a 6 dB evening weighting and a 6 dB night-time weighting (Bullen & Hede 1983). The German airport noise equivalent level (LEQ(FLG)) is based on A-weighted levels, but does not follow the equal energy principle.

The weighted equivalent continuous perceived noise level (WECPNL) measure (Ford 1987) proposed by ICAO is based on the equal energy principle and maximum PNL values of aircraft fly-overs. However, in Japan an approximation to this measure is used and is based on maximum A-weighted levels. The noise and number index (NNI), formerly used in the United Kingdom, was derived from maximum PNL values but was not based on the equal energy principle. An approximation to the original version of the NNI has been used in Switzerland and is based on maximum A-weighted levels of aircraft fly-overs, but its use will soon be discontinued. Changes in these measures are slow because their use is often specified in national legislation. However, several countries have changed to measures that are based on the equal energy principle and A-weighted sound pressure levels.

2.7.3. Impulsive noise measures

Impulsive sounds, such as gun shots, hammer blows, explosions of fireworks or other blasts, are sounds that significantly exceed the background sound pressure level for a very short duration. Typically each impulse lasts less than one second. Measurements with the meter set to 'Fast' response (section 2.1.1) do not accurately represent impulsive sounds. Therefore the meter response time must be shorter to measure such impulse type sounds. C-weighted levels have been found useful for ratings of gun shots (ISO 1987). Currently no mathematical description exists which unequivocally defines impulsive sounds, nor is there a universally accepted procedure for rating the additional annoyance of impulsive sounds (HCN 1997). Future versions of ISO Standard 1996 (present standard in ISO 1987b) are planned to improve this situation.

2.7.4. Measures of speech intelligibility

The intelligibility of speech depends primarily on the speech-to-noise ratio. If the level of the speech sounds are 15 dB or more above the level of the ambient noise, the speech intelligibility at 1 m distance will be close to 100% (Houtgast 1981; Bradley 1986b). This can be most simply rated in terms of the speech-to-noise ratio of the A-weighted speech and noise levels. Alternatively, the speech intelligibility index (formerly the articulation index) can be used if octave or 1/3 octave band spectra of the speech and noise are available (ANSI 1997).

When indoors, speech intelligibility also depends on the acoustical properties of the space. The acoustical properties of spaces have for many years been rated in terms of reverberation times. The reverberation time is approximately the time it takes for a sound in a room to decrease to inaudibility after the source has been stopped. Optimum reverberation times for speech have been specified as a function of the size of the room. In large rooms, such as lecture halls and theaters, a reverberation time for speech of about 1 s is recommended. In smaller rooms such as classrooms, the recommended value for speech is about 0.6 s (Bradley 1986b,c). More modern measures of room acoustics have been found to be better correlates of speech intelligibility, and some combine an assessment of both the speech/noise ratio and room acoustics (Bradley 1986a,c). The most widely known is the speech transmission index (STI) (Houtgast & Steeneken 1983), or the abbreviated version of this measure referred to as RASTI (Houtgast & Steeneken 1985; IEC 1988). In smaller rooms, such as school classrooms, the conventional approach of requiring adequately low ambient noise levels, as well as some optimum reverberation time, is probably adequate to ensure good speech intelligibility (Bradley 1986b). In larger rooms and other more specialized situations, use of the more modern measures may be helpful.

2.7.5. Indoor noise ratings

The simplest procedure for rating levels of indoor noise is to measure them in terms of integrated A-weighted sound pressure levels, as measured by LAeq,T. As discussed earlier, this approach has been criticized as not being the most accurate rating of the negative effects of various types of noises, and is thought to be particularly inadequate when there are strong low-frequency components. Several more complex rating schemes are available based on octave band measurements of indoor noises. In Europe the noise rating system (Burns 1968), and in North America the noise criterion (Beranek 1971), both include sets of equal-disturbance type contours. Measured octave band sound pressure levels are compared with these contours and an overall noise rating is determined. More recently, two new schemes have been proposed: the balanced noise criterion procedure (Beranek 1989) and the room criterion system (Blazier 1998). These schemes are based on a wider range of octave bands extending from 16–8 000 Hz. They provide both a numerical and a letter rating of the noise. The numerical part indicates the level of the central frequencies important for speech communication and the letter indicates whether the quality of the sound is predominantly low-, medium- or high-frequency in nature. Extensive comparisons of these room noise rating procedures have yet to be performed. Because the newer measures include a wider range of frequencies, they can better assess a wider range of noise problems.

2.8. Summary

Where there are no clear reasons for using other measures, it is recommended that LAeq,T be used to evaluate more-or-less continuous environmental noises. LAeq,T should also be used to assess ongoing noises that may be composed of individual events with randomly varying sound pressure levels. Where the noise is principally composed of a small number of discrete events the additional use of LAmax or SEL is recommended. As pointed out in this chapter, there are definite limitations to these simple measures, but there are also many practical advantages, including economy and the benefits of a standardized approach.

The sound pressure level measurements should include all variations over time to provide results that best represent the noise in question. This would include variations in both the source and in propagation of the noise from the source to the receiver. Measurements should normally be made close to typical points of reception. The accuracy of the measurements and the details of the measurement procedure must be adapted to the type of noise and to other details of the noise exposure. Assessment of speech intelligibility, aviation noise or impulse noise may require the use of more specialized methods. Where the exposed people are indoors and noise measurements are made outdoors, the sound attenuating properties of the building façade must also be measured or estimated.

3. Adverse Health Effects Of Noise

3.1. Introduction

The perception of sounds in day-to-day life is of major importance for human well-being. Communication through speech, sounds from playing children, music, natural sounds in parklands, parks and gardens are all examples of sounds essential for satisfaction in every day life. Conversely, this document is related to the adverse effects of sound (noise). According to the International Programme on Chemical Safety (WHO 1994), an adverse effect of noise is defined as a change in the morphology and physiology of an organism that results in impairment of functional capacity, or an impairment of capacity to compensate for additional stress, or increases the susceptibility of an organism to the harmful effects of other environmental influences. This definition includes any temporary or long-term lowering of the physical, psychological or social functioning of humans or human organs. The health significance of noise pollution is given in this chapter under separate headings, according to the specific effects: noise-induced hearing impairment; interference with speech communication; disturbance of rest and sleep; psychophysiological, mental-health and performance effects; effects on residential behaviour and annoyance; as well as interference with intended activities. This chapter also considers vulnerable groups and the combined effects of sounds from different sources. Conclusions based on the details given in this chapter are given in Chapter 4 as they relate to guideline values.

3.2. Noise-Induced Hearing Impairment

Hearing impairment is typically defined as an increase in the threshold of hearing. It is assessed by threshold audiometry. Hearing handicap is the disadvantage imposed by hearing impairment sufficient to affect one's personal efficiency in the activities of daily living. It is usually expressed in terms of understanding conventional speech in common levels of background noise (ISO 1990). Worldwide, noise-induced hearing impairment is the most prevalent irreversible occupational hazard. In the developing countries, not only occupational noise, but also environmental noise is an increasing risk factor for hearing impairment. In 1995, at the World Health Assembly, it was estimated that there are 120 million persons with disabling hearing difficulties worldwide (Smith 1998). It has been shown that men and women are equally at risk of noise-induced hearing impairment (ISO 1990; Berglund & Lindvall 1995).

Apart from noise-induced hearing impairment, hearing damage in populations is also caused by certain diseases; some industrial chemicals; ototoxic drugs; blows to the head; accidents; and hereditary origins. Deterioration of hearing capability is also associated with the aging process *per se* (presbyacusis). Present knowledge of the physiological effects of noise on the auditory system is based primarily on laboratory studies on animals. After noise exposure, the first morphological changes are usually found in the inner and outer hair cells of the cochlea, where the stereocilia become fused and bent. After more prolonged exposure, the outer and inner hair cells related to transmission of high-frequency sounds are missing. See Berglund & Lindvall (1995) for further discussion.

The ISO Standard 1999 (ISO 1990) gives a method for calculating noise-induced hearing impairment in populations exposed to all types of noise (continuous, intermittent, impulse) during working hours. Noise exposure is characterized by LAeq over 8 hours (LAeq,8h). In the Standard, the relationships between LAeq,8h and noise-induced hearing impairment are given for frequencies of 500–6 000 Hz, and for exposure times of up to 40 years. These relations show that noise-induced hearing impairment occurs predominantly in the high-frequency range of 3 000–6 000 Hz, the effect being largest at 4 000 Hz. With increasing LAeq,8h and increasing exposure time, noise-induced hearing impairment also occurs at 2 000 Hz. But at LAeq,8h levels of 75 dBA and lower, even prolonged occupational noise exposure will not result in noise-induced hearing impairment (ISO 1990). This value is equal to that specified in 1980 by the World Health Organization (WHO 1980a).

The ISO Standard 1999 (ISO 1990) specifies hearing impairment in statistical terms (median values, and percentile fractions between 0.05 and 0.95). The extent of noise-induced hearing impairment in populations exposed to occupational noise depends on the value of LAeq,8h and the number of years of noise exposure. However, for high LAeq,8h values, individual susceptibility seems to have a considerable effect on the rate of progression of hearing impairment. For daily exposures of 8–16 h, noise-induced hearing impairment can be reasonably well estimated from LAeq,8h extrapolated to the longer exposure times (Axelsson et al. 1986). In this adaptation of LAeq,8h for daily exposures other than 8 hours, the equal energy principle is assumed to be applicable. For example, the hearing impairment due to a 16 h daily exposure is equivalent to that at LAeq,8h plus 3 dB (LAeq,16h = LAeq,8h + 10*$\log_{10}$ (16/8) = LAeq,8h + 3 dB. For a 24 h exposure, LAeq,24h = LAeq,8h + 10*$\log_{10}$ (24/8) = LAeq,8h + 5 dB).

Since the calculation method specified in the ISO Standard 1999 (ISO 1990) is the only universally adopted method for estimating occupational noise-induced hearing impairment, attempts have been made to assess whether the method is also applicable to hearing impairment due to environmental noise, including leisure-time noise. There is ample evidence that shooting noise, with LAeq,24h values of up to 80 dB, induces the same hearing impairment as an equivalent occupational noise exposure (Smoorenburg 1998). Moreover, noise-induced hearing impairment studies from motorbikes are also in agreement with results from ISO Standard 1999 (ISO 1990). Hearing impairment in young adults and children 12 years and older has been assessed by LAeq on a 24 h time basis, for a variety of environmental and leisure-time exposure patterns (e.g. Passchier-Vermeer 1993; HCN 1994). These include pop music in discotheques and concerts (Babisch & Ising 1989; ISO 1990); pop music through headphones (Ising et al. 1994; Struwe et al. 1996; Passchier-Vermeer et al. 1998); music played by brass bands and symphony orchestras (van Hees 1992). The results are in agreement with values predicted by the ISO Standard 1999 method on the basis of adjusted time.

In the publications cited above, exposure to noise with known characteristics, such as duration and level, was related to hearing impairment. In addition to these publications, there is also an extensive literature showing hearing impairment in populations exposed to specific types of non-occupational noise, although these exposures are not well characterized. These noises originate from shooting, motorcycling, snowmobile driving, playing in arcades, listening to music at concerts and through headphones, using noisy toys, and fireworks (e.g. Brookhouser et al. 1992; see also Berglund & Lindvall 1995). Although the characteristics of these exposures are to a certain extent unknown, the details in the publications suggest that LAeq,24h values of these exposures exceed 70 dB.

In contrast, epidemiological studies failed to show hearing damage in populations exposed to an LAeq,24h of less than 70 dB (Lindemann et al. 1987). The data imply that even a lifetime exposure to environmental and leisure-time noise with an LAeq,24h <70 dBA would not cause hearing impairment in the large majority of people (over 95%). Overall, the results of many studies strongly suggest that the method from ISO Standard 1999 can also be used to estimate hearing impairment due to environmental and leisure-time noise, in addition to estimating the effects of occupational noise exposure.

Although the evidence suggests that the calculation method from ISO Standard 1999 (ISO 1990) should also be accepted for environmental and leisure time noise exposures, large-scale epidemiological studies of the general population do not exist to support this proposition. Taking into account the limitations of the studies, care should be taken with respect to the following aspects:

a. Data from animal experiments indicate that children may be more vulnerable in acquiring noise-induced hearing impairment than adults.

b. At very high instantaneous sound pressure levels, mechanical damage to the ear may occur (Hanner & Axelsson 1988). Occupational limits are set at peak sound pressure levels of 140 dB (EU 1986a). For adults exposed to environmental and leisure-time noise, this same limit is assumed to be valid. In the case of children, however, taking into account their habits while playing with noisy toys, peak sound pressure levels should never exceed 120 dB.

c. For shooting noise with LAeq,24h over 80 dB, studies on temporary threshold shift suggest the possibility of an increased risk for noise-induced hearing impairment (Smoorenburg 1998).

d. Risk for noise-induced hearing impairment may increase when the noise exposure is combined with exposure to vibrations, the use of ototoxic drugs, or some chemicals (Fechter 1999). In these circumstances, long-term exposure to LAeq,24h of 70 dBA may induce small hearing impairments.

e. It is uncertain whether the relationships between hearing impairment and noise exposure given in ISO Standard 1999 (ISO 1990) are applicable for environmental sounds of short rise time. For example, in the case of military low-altitude flying areas (75–300 m above ground) LAmax values of 110–130 dB occur within seconds after the onset of the sound.

Usually noise-induced hearing impairment is accompanied by an abnormal loudness perception which is known as loudness recruitment (*cf.* Berglund & Lindvall 1995). With a considerable loss of auditory sensitivity, some sounds may be perceived as distorted (paracusis). Another sensory effect that results from noise exposure is tinnitus (ringing in the ears). Commonly, tinnitus is referred to as sounds that are emitted by the inner ear itself (physiological tinnitus). Tinnitus is a common and often disturbing accompaniment of occupational hearing impairment (Vernon and Moller 1995) and has become a risk for teenagers attending pop concerts and discotheques (Hetu & Fortin 1995; Passchier-Vermeer et al. 1998; Axelsson & Prasher 1999). Noise-induced tinnitus may be temporary, lasting up to 24 hours after exposure, or may have a more permanent character, such as after prolonged occupational noise exposure. Sometimes tinnitus is due to the sound produced by the blood flow through structures in the ear.

The main social consequence of hearing impairment is an inability to understand speech in daily living conditions, which is considered a severe social handicap. Even small values of hearing impairment (10 dB averaged over 2 000 and 4 000 Hz, and over both ears) may have an effect on the understanding of speech. When the hearing impairment exceeds 30 dB (again averaged over 2 000 and 4 000 Hz and both ears) a social hearing handicap is noticeable (*cf.* Katz 1994; Berglund & Lindvall 1995).

In the past, hearing protection has mainly emphasized occupational noise exposures at high values of LAeq,8h, or situations with high impulsive sounds. The near-universal adoption of an LAeq,8h value of 85 dB (or lower) as the limit for unprotected occupational noise exposure, together with requirements for personal hearing protection, has made cases of severe unprotected exposures more rare. This is particularly true for developed countries. However, monitoring of compliance and enforcement action for sound pressure levels just over the limits may be weak, especially in non-industrial environments in developed countries (Franks 1998), as well as in occupational and urban environments in developing countries (Smith 1998). Nevertheless, regulations for occupational noise exposure exist almost worldwide and exposures to occupational noise are to a certain extent under control.

On the other hand, environmental noise exposures due to a number of noisy activities, especially those during leisure-time activities of children and young adults, have scarcely been regulated. Given both the increasing number of noisy activities and the increasing exposure duration, such as loud music in cars and the use of Walkmen and Discmen, regulatory activities in this field are to be encouraged. Dose-response data are lacking for the general population. However, judging from the limited data for study groups (teenagers, young adults and women), and the assumption that time of exposure can be equated with sound energy, the risk for hearing impairment would be negligible for LAeq,24h values of 70 dBA over a lifetime. To avoid hearing impairment, impulse noise exposures should never exceed 140 dB peak sound pressure in adults, and 120 dB peak sound pressure in children.

3.3. Interference with Speech Communication

Noise interference with speech comprehension results in a large number of personal disabilities, handicaps and behavioural changes. Problems with concentration, fatigue, uncertainty and lack of self-confidence, irritation, misunderstandings, decreased working capacity, problems in human relations, and a number of stress reactions have all been identified (Lazarus 1998). Particularly vulnerable to these types of effects are the hearing impaired, the elderly, children in the process of language and reading acquisition, and individuals who are not familiar with the spoken language (e.g., Lazarus 1998). Thus, vulnerable persons constitute a substantial proportion of a country's population.

Most of the acoustical energy of speech is in the frequency range 100–6 000 Hz, with the most important cue-bearing energy being between 300–3 000 Hz. Speech interference is basically a masking process in which simultaneous, interfering noise renders speech incapable of being understood. The higher the level of the masking noise, and the more energy it contains at the most important speech frequencies, the greater will be the percentage of speech sounds that become indiscernible to the listener. Environmental noise may also mask many other acoustical signals important for daily life, such as door bells, telephone signals, alarm clocks, fire alarms and other warning signals, and music (e.g., Edworthy & Adams 1996). The masking effect of interfering noise in speech discrimination is more pronounced for hearing-impaired persons than for persons with normal hearing, particularly if the interfering noise is composed of speech or babble.

As the sound pressure level of an interfering noise increases, people automatically raise their voice to overcome the masking effect upon speech (increase of vocal effort). This imposes an additional strain on the speaker. For example, in quiet surroundings, the speech level at 1 m distance averages 45–50 dBA, but is 30 dBA higher when shouting. However, even if the interfering noise is moderately loud, most of the sentences during ordinary conversation can still be understood fairly well. Nevertheless, the interpretation required for compensating the masking effect of the interfering sounds, and for comprehending what was said, imposes an additional strain on the listener. One contributing factor could be that speech spoken loudly is more difficult to understand than speech spoken softly, when compared at a constant speech-to-noise ratio (*cf.* Berglund & Lindvall 1995).

Speech levels vary between individuals because of factors such as gender and vocal effort. Moreover, outdoor speech levels decrease by about 6 dB for a doubling in the distance between talker and listener. Speech intelligibility in everyday living conditions is influenced by speech level, speech pronunciation, talker-to-listener distance, sound pressure levels, and to some extent other characteristics of interfering noise, as well as room characteristics (e.g. reverberation). Individual capabilities of the listener, such as hearing acuity and the level of attention of the listener, are also important for the intelligibility of speech. Speech communication is affected also by the reverberation characteristics of the room. For example, reverberation times greater than 1 s produce loss in speech discrimination. Longer reverberation times, especially when combined with high background interfering noise, make speech perception more difficult. Even in a quiet environment, a reverberation time below 0.6 s is desirable for adequate speech intelligibility by vulnerable groups. For example, for older hearing-handicapped persons, the optimal reverberation time for speech intelligibility is 0.3–0.5 s (Plomp 1986).

For complete sentence intelligibility in listeners with normal hearing, the signal-to-noise ratio (i.e. the difference between the speech level and the sound pressure level of the interfering noise) should be 15–18 dBA (Lazarus 1990). This implies that in smaller rooms, noise levels above 35 dBA interferes with the intelligibility of speech (Bradley 1985). Earlier recommendations suggested that sound pressure levels as high as 45 dBA would be acceptable (US EPA 1974). With raised voice (increased vocal effort) sentences may be 100% intelligible for noise levels of up to 55 dBA; and sentences spoken with straining vocal effort can be 100% intelligible with noise levels of about 65 dBA. For speech to be intelligible when listening to complicated messages (at school, listening to foreign languages, telephone conversation), it is recommended that the signal-to-noise ratio should be at least 15 dBA. Thus, with a speech level of 50 dBA, (at 1 m distance this level corresponds to a casual speech level of both women and men), the sound pressure level of interfering noise should not exceed 35 dBA. For vulnerable groups even lower background levels are needed. If it is not possible to meet the strictest criteria for vulnerable persons in sensitive situations (e.g. in classrooms), one should strive for as low background levels as possible.

3.4. Sleep Disturbance

Uninterrupted sleep is known to be a prerequisite for good physiological and mental functioning of healthy persons (Hobson 1989); sleep disturbance, on the other hand, is considered to be a major environmental noise effect. It is estimated that 80-90% of the reported cases of sleep disturbance in noisy environments are for reasons other than noise originating outdoors. For example, sanitary needs; indoor noises from other occupants; worries; illness; and climate (e.g. Reyner & Horne 1995). Our understanding of the impact of noise exposure on sleep stems mainly from experimental research in controlled environments. Field studies conducted with people in their normal living situations are scarce. Most of the more recent field research on sleep disturbance has been conducted for aircraft noise (Fidell et al. 1994 1995a,b 1998; Horne et al. 1994 1995; Maschke et al. 1995 1996; Ollerhead et al. 1992; Passchier-Vermeer 1999). Other field studies have examined the effects of road traffic and railway noise (Griefahn et al. 1996 1998).

The primary sleep disturbance effects are: difficulty in falling asleep (increased sleep latency time); awakenings; and alterations of sleep stages or depth, especially a reduction in the proportion of REM-sleep (REM = rapid eye movement) (Hobson 1989). Other primary physiological effects can also be induced by noise during sleep, including increased blood pressure; increased heart rate; increased finger pulse amplitude; vasoconstriction; changes in respiration; cardiac arrhythmia; and an increase in body movements (cf. Berglund & Lindvall 1995). For each of these physiological effects, both the noise threshold and the noise-response relationships may be different. Different noises may also have different information content and this also could affect physiological threshold and noise-response relationships (Edworthy 1998).

Exposure to night-time noise also induces secondary effects, or so-called after effects. These are effects that can be measured the day following the night-time exposure, while the individual is awake. The secondary effects include reduced perceived sleep quality; increased fatigue; depressed mood or well-being; and decreased performance (Öhrström 1993a; Passchier-Vermeer 1993; Carter 1996; Pearsons et al. 1995; Pearsons 1998).

Long-term effects on psychosocial well-being have also been related to noise exposure during the night (Öhrström 1991). Noise annoyance during the night-time increased the total noise annoyance expressed by people in the following 24 h. Various studies have also shown that people living in areas exposed to night-time noise have an increased use of sedatives or sleeping pills. Other frequently reported behavioural effects of night-time noise include closed bedroom windows and use of personal hearing protection. Sensitive groups include the elderly, shift workers, persons especially vulnerable to physical or mental disorders and other individuals with sleeping difficulties.

Questionnaire data indicate the importance of night-time noise on the perception of sleep quality. A recent Japanese investigation was conducted for 3 600 women (20–80 years old) living in eight roadside zones with different road traffic noise. The results showed that four measures of perceived sleep quality (difficulty in falling asleep; waking up during sleep; waking up too early; feelings of sleeplessness one or more days a week) correlated significantly with the average traffic volumes during night-time. An in-depth investigation of 19 insomnia cases and their matched controls (age,work) measured outdoor and indoor sound pressure levels during sleep (Kageyama et al. 1997). The study showed that road traffic noise in excess of 30 dB LAeq for nighttime induced sleep disturbance, consistent with the results of Öhrström (1993b).

Meta-analyses of field and laboratory studies have suggested that there is a relationship between the SEL for a single night-time noise event and the percentage of people awakened, or who showed sleep stage changes (e.g. Ollerhead et al. 1992; Passchier-Vermeer 1993; Finegold et al. 1994; Pearsons et al. 1995). All of these studies assumed that the number of awakenings per night for each SEL value is proportional to the number of night-time noise events. However, the results have been criticized for methodological reasons. For example, there were small groups of sleepers; too few original studies; and indoor exposure was estimated from outdoor sound pressure levels (NRC-CNRC 1994; Beersma & Altena 1995; Vallet 1998). The most important result of the meta-analyses is that there is a clear difference in the dose-response curves for laboratory and field studies, and that noise has a lower effect under real-life conditions (Pearsons et al. 1995; Pearsons 1998).

However, this result has been questioned, because the studies were not controlled for such things as the sound insulation of the buildings, and the number of bedrooms with closed windows. Also, only two indicators of sleep disturbance were considered (awakening and sleep stage changes). The meta-analyses thus neglected other important sleep disturbance effects (Öhrström 1993b; Carter et al. 1994a; Carter et al. 1994b; Carter 1996; Kuwano et al. 1998). For example, for road traffic noise, perceived sleep quality is related both to the time needed to fall asleep and the total sleep time (Öhrström & Björkman 1988). Individuals who are more sensitive to noise (as assessed by different questionnaires) report worse sleep quality both in field studies and in laboratory studies.

A further criticism of the meta-analyses is that laboratory experiments have shown that habituation to night-time noise events occurs, and that noise-induced awakening decreases with increasing number of sound exposures per night. This is in contrast to the assumption used in the meta-analyses, that the percentage of awakenings is linearly proportional to the number of night-time noise events. Studies have also shown that the frequency of noise-induced awakenings decreases for at least the first eight consecutive nights. So far, habituation has been shown for awakenings, but not for heart rate and after effects such as perceived sleep quality, mood and performance (Öhrström and Björkman 1988).

Other studies suggest that it is the difference in sound pressure levels between a noise event and background, rather than the absolute sound pressure level of the noise event, that determines the reaction probability. The time interval between two noise events also has an important influence of the probability of obtaining a response (Griefahn 1977; *cf.* Berglund & Lindvall 1995). Another possible factor is the person's age, with older persons having an increased probability of awakening. However, one field study showed that noise-induced awakenings are independent of age (Reyner & Horne 1995).

For a good sleep, it is believed that indoor sound pressure levels should not exceed approximately 45 dB LAmax more than 10–15 times per night (Vallet & Vernet 1991), and most studies show an increase in the percentage of awakenings at SEL values of 55–60 dBA (Passchier-Vermeer 1993; Finegold et al. 1994; Pearsons et al. 1995). For intermittent events that approximate aircraft noise, with an effective duration of 10–30 s, SEL values of 55–60 dBA correspond to a LAmax value of 45 dB. Ten to 15 of these events during an eight-hour night-time implies an LAeq,8h of 20–25 dB. This is 5–10 dB below the LAeq,8h of 30 dB for continuous night-time noise exposure, and shows that the intermittent character of noise has to be taken into account when setting night-time limits for noise exposure. For example, this can be achieved by considering the number of noise events and the difference between the maximum sound pressure level and the background level of these events.

Special attention should also be given to the following considerations:

a. Noise sources in an environment with a low background noise level. For example, night-traffic in suburban residential areas.

b. Environments where a combination of noise and vibrations are produced. For example, railway noise, heavy duty vehicles.

c. Sources with low-frequency components. Disturbances may occur even though the sound pressure level during exposure is below 30 dBA.

If negative effects on sleep are to be avoided the equivalent sound pressure level should not exceed 30 dBA indoors for continuous noise. If the noise is not continuous, sleep disturbance correlates best with LAmax and effects have been observed at 45 dB or less. This is particularly true if the background level is low. Noise events exceeding 45 dBA should therefore be limited if possible. For sensitive people an even lower limit would be preferred. It should be noted that it should be possible to sleep with a bedroom window slightly open (a reduction from outside to inside of 15 dB). To prevent sleep disturbances, one should thus consider the equivalent sound pressure level and the number and level of sound events. Mitigation targeted to the first part of the night is believed to be effective for the ability to fall asleep.

3.5. Cardiovascular and Physiological Effects

Epidemiological and laboratory studies involving workers exposed to occupational noise, and general populations (including children) living in noisy areas around airports, industries and noisy streets, indicate that noise may have both temporary and permanent impacts on physiological functions in humans. It has been postulated that noise acts as an environmental stressor (for a review see Passchier-Vermeer 1993; Berglund & Lindvall 1995). Acute noise exposures activate the autonomic and hormonal systems, leading to temporary changes such as increased blood pressure, increased heart rate and vasoconstriction. After prolonged exposure, susceptible individuals in the general population may develop permanent effects, such as hypertension and ischaemic heart disease associated with exposures to high sound pressure levels (for a review see Passchier-Vermeer 1993; Berglund & Lindvall 1995). The magnitude and duration of the effects are determined in part by individual characteristics, lifestyle behaviours and environmental conditions. Sounds also evoke reflex responses, particularly when they are unfamiliar and have a sudden onset.

Laboratory experiments and field quasi-experiments show that if noise exposure is temporary, the physiological system usually returns - after the exposure terminates - to a normal (pre-exposure) state within a time in the range of the exposure duration. If the exposure is of sufficient intensity and unpredictability, cardiovascular and hormonal responses may appear, including increases in heart rate and peripheral vascular resistance; changes in blood pressure, blood viscosity and blood lipids; and shifts in electrolyte balance (Mg/Ca) and hormonal levels (epinephrine, norepinephrine, cortisol). The first four effects are of interest because of noise-related coronary heart disease (Ising & Günther 1997). Laboratory and clinical data suggest that noise may significantly elevate gastrointestinal motility in humans.

By far the greatest number of occupational and community noise studies have focused on the possibility that noise may be a risk factor for cardiovascular disease. Many studies in occupational settings have indicated that workers exposed to high levels of industrial noise for 5–30 years have increased blood pressure and statistically significant increases in risk for hypertension, compared to workers in control areas (Passchier-Vermeer 1993). In contrast, only a few studies on environmental noise have shown that populations living in noisy areas around airports and on noisy streets have an increased risk for hypertension. The overall evidence suggests a weak association between long-term environmental noise exposure and hypertension (HCN 1994; Berglund & Lindvall 1995; IEH 1997), and no dose-response relationships could be established.

Recently, an updated summary of available studies for ischaemic heart disease has been presented (Babisch 1998a; Babisch 1998b; Babisch et al. 1999; see also Thompson 1996). The studies reviewed include case-control and cross-sectional designs, as well as three longitudinal studies. However, it has not yet been possible to conduct the most advanced quantitative integrated analysis of the available studies. Relative risks and their confidence intervals could be estimated only for the classes of high noise levels (mostly >65 dBA during daytime) and low levels (mostly <55 dBA during daytime), rather than a range of exposure levels. For methodological reasons identified in the meta-analysis, a cautious interpretation of the results is warranted (Lercher et al. 1998).

Prospective studies that controlled for confounding factors suggest an increase in ischaemic heart disease when the noise levels exceed 65–70 dB for LAeq (6–22). (For road traffic noise, the difference between LAeq (6-22h) and LAeq,24h usually is of the order of 1.5 dB). When orientation of the bedroom, window opening habits and years of exposure are taken into account, the risk of heart disease is slightly higher (Babisch et al. 1998; Babisch et al. 1999). However, disposition, behavioural and environmental factors were not sufficiently accounted for in the analyses carried out to date. In epidemiological studies the lowest level at which traffic noise had an effect on ischaemic heart disease was 70 dB for LAeq,24h (HCN 1994).

The overall conclusion is that cardiovascular effects are associated with long-term exposure to LAeq,24h values in the range of 65–70 dB or more, for both air- and road-traffic noise. However, the associations are weak and the effect is somewhat stronger for ischaemic heart disease than for hypertension. Nevertheless, such small risks are potentially important because a large number of persons are currently exposed to these noise levels, or are likely to be exposed in the future. Furthermore, only the average risk is considered and sensitive subgroups of the populations have not been sufficiently characterized. For example, a 10% increase in risk factors (a relative risk of 1.1) may imply an increase of up to 200 cases per 100 000 people at risk per year. Other observed psychophysiological effects, such as changes in stress hormones, magnesium levels, immunological indicators, and gastrointestinal disturbances are too inconsistent for conclusions to be drawn about the influence of noise pollution.

3.6. Mental Health Effects

Mental health is defined as the absence of identifiable psychiatric disorders according to current norms (Freeman 1984). Environmental noise is not believed to be a direct cause of mental illness, but it is assumed that it accelerates and intensifies the development of latent mental disorder. Studies on the adverse effects of environmental noise on mental health cover a variety of symptoms, including anxiety; emotional stress; nervous complaints; nausea; headaches; instability; argumentativeness; sexual impotency; changes in mood; increase in social conflicts, as well as general psychiatric disorders such as neurosis, psychosis and hysteria. Large-scale population studies have suggested associations between noise exposure and a variety of mental health indicators, such as single rating of well-being; standard psychological symptom profiles; the intake of psychotropic drugs; and consumption of tranquilizers and sleeping pills. Early studies showed a weak association between exposure to aircraft noise and psychiatric hospital admissions in the general population surrounding an airport (see also Berglund & Lindvall 1995). However, the studies have been criticized because of problems in selecting variables and in response bias (Halpern 1995).

Exposure to high levels of occupational noise has been associated with development of neurosis and irritability; and exposure to high levels of environmental noise with deteriorated mental health (Stansfeld 1992). However, the findings on environmental noise and mental health effects are inconclusive (HCN 1994; Berglund & Lindvall 1995; IEH 1997). The only longitudinal study in this field (Stansfeld et al. 1996) showed an association between the initial level of road traffic noise and minor psychiatric disorders, although the association for increased anxiety was weak and non-linear. It turned out that psychiatric disorders are associated with noise sensitivity, rather than with noise exposure, and the association was found to disappear after adjustment for baseline trait anxiety. These and other results show the importance of taking vulnerable groups into account, because they may not be able to cope sufficiently with unwanted environmental noise (e.g. Stansfeld 1992). This is particularly true of children, the elderly and people with preexisting illnesses, especially depression (IEH 1997). Despite the weaknesses of the various studies, the possibility that community noise has adverse effects on mental health is suggested by studies on the use of medical drugs, such as tranquilizers and sleeping pills, on psychiatric symptoms and on mental hospital admission rates.

3.7. The Effects of Noise on Performance

It has been documented in both laboratory subjects and in workers exposed to occupational noise, that noise adversely affects cognitive task performance. In children, too, environmental noise impairs a number of cognitive and motivational parameters (Cohen et al. 1980; Evans & Lepore 1993; Evans 1998; Hygge et al. 1998; Haines et al. 1998). However, there are no published studies on whether environmental noise at home also impairs cognitive performance in adults. Accidents may also be an indicator of performance deficits. The few field studies on the effects of noise on performance and safety showed that noise may produce some task impairment and increase the number of errors in work, but the effects depend on the type of noise and the task being performed (Smith 1990).

Laboratory and workplace studies showed that noise can act as a distracting stimulus. Also, impulsive noise events (e.g. sonic booms) may produce disruptive effects as a result of startle responses. In the short term, noise-induced arousal may produce better performance of simple tasks, but cognitive performance deteriorates substantially for more complex tasks (i.e. tasks that require sustained attention to details or to multiple cues; or tasks that demand a large capacity of working memory, such as complex analytical processes). Some of the effects are related to loss in auditory comprehension and language acquisition, but others are not (Evans & Maxwell 1997). Among the cognitive effects, reading, attention, problem solving and memory are most strongly affected by noise. The observed effects on motivation, as measured by persistence with a difficult cognitive task, may either be independent or secondary to the aforementioned cognitive impairments.

Two types of memory deficits have been identified under experimental noise exposure: incidental memory and memory for materials that the observer was not explicitly instructed to focus on during a learning phase. For example, when presenting semantic information to subjects in the presence of noise, recall of the information content was unaffected, but the subjects were significantly less able to recall, for example, in which corner of the slide a word had been located. There is also some evidence that the lack of "helping behavior" that was noted under experimental noise exposure may be related to inattention to incidental cues (Berglund & Lindvall 1995). Subjects appear to process information faster in working memory during noisy performance conditions, but at a cost of available memory capacity. For example, in a running memory task, in which subjects were required to recall in sequence letters that they had just heard, subjects recalled recent items better under noisy conditions, but made more errors farther back into the list.

Experimental noise exposure consistently produces negative after-effects on performance (Glass & Singer 1972). Following exposure to aircraft noise, schoolchildren in the vicinity of Los Angeles airport were found to be deficient in proofreading, and in persistence with challenging puzzles (Cohen et al. 1980). The uncontrollability of noise, rather than the intensity of the noise, appears to be the most critical variable. The only prospective study on noise-exposed schoolchildren, designed around the move of the Munich airport (Hygge et al. 1996; Evans et al. 1998), confirmed the results of laboratory and workplace studies in adults, as well the results of the Los Angeles airport study with children (Cohen et al. 1980). An important finding was that some of the adaptation strategies for dealing with aircraft noise, such as tuning out or ignoring the noise, and the effort necessary to maintain task performance, come at a price. There is heightened sympathetic arousal, as indicated by increased levels of stress hormone, and elevation of resting blood pressure (Evans et al. 1995; Evans et al. 1998). Notably, in the airport studies reported above, the adverse effects were larger in children with lower school achievement.

For aircraft noise, it has been shown that chronic exposure during early childhood appears to impair reading acquisition and reduces motivational capabilities. Of recent concern are concomitant psychophysiological changes (blood pressure and stress hormone levels). Evidence indicates that the longer the exposure, the greater the damage. It seems clear that daycare centers and schools should not be located near major sources of noise, such as highways, airports and industrial sites.

3.8. Effects of Noise on Residential Behaviour and Annoyance

Noise annoyance is a global phenomenon. A definition of annoyance is "a feeling of displeasure associated with any agent or condition, known or believed by an individual or group to adversely affect them" (Lindvall & Radford 1973; Koelega 1987). However, apart from "annoyance", people may feel a variety of negative emotions when exposed to community noise, and may report anger, disappointment, dissatisfaction, withdrawal, helplessness, depression, anxiety, distraction, agitation, or exhaustion (Job 1993; Fields et al. 1997 1998). Thus, although the term annoyance does not cover all the negative reactions, it is used for convenience in this document.

Noise can produce a number of social and behavioural effects in residents, besides annoyance (for review see Berglund & Lindvall 1995). The social and behavioural effects are often complex, subtle and indirect. Many of the effects are assumed to be the result of interactions with a number of non-auditory variables. Social and behavioural effects include changes in overt everyday behaviour patterns (e.g. closing windows, not using balconies, turning TV and radio to louder levels, writing petitions, complaining to authorities); adverse changes in social behaviour (e.g. aggression, unfriendliness, disengagement, non-participation); adverse changes in social indicators (e.g. residential mobility, hospital admissions, drug consumption, accident rates); and changes in mood (e.g. less happy, more depressed).

Although changes in social behaviour, such as a reduction in helpfulness and increased aggressiveness, are associated with noise exposure, noise exposure alone is not believed to be sufficient to produce aggression. However, in combination with provocation or pre-existing anger or hostility, it may trigger aggression. It has also been suspected that people are less willing to help, both during exposure and for a period after exposure. Fairly consistent evidence shows that noise above 80 dBA is associated with reduced helping behaviour and increased aggressive behaviour. Particularly, there is concern that high-level continuous noise exposures may contribute to the susceptibility of schoolchildren to feelings of helplessness (Evans & Lepore 1993)

The effects of community noise can be evaluated by assessing the extent of annoyance (low, moderate, high) among exposed individuals; or by assessing the disturbance of specific activities, such as reading, watching television and communication. The relationship between annoyance and activity disturbances is not necessarily direct and there are examples of situations where the extent of annoyance is low, despite a high level of activity disturbance. For aircraft noise, the most important effects are interference with rest, recreation and watching television. This is in contrast to road traffic noise, where sleep disturbance is the predominant effect (Berglund & Lindvall 1995).

A number of studies have shown that equal levels of traffic and industrial noises result in different magnitudes of annoyance (Hall et al. 1981; Griffiths 1983; Miedema 1993; Bradley 1994a; Miedema & Vos 1998). This has led to criticism (e.g. Kryter 1994; Bradley 1994a) of averaged dose-response curves determined by meta-analysis, which assumed that all traffic noises are the same (Fidell et al. 1991; Fields 1994a; Finegold et al. 1994). Schultz (1978) and Miedema & Vos (1998) have synthesized curves of annoyance associated with three types of traffic noise (road, air, railway). In these curves, the percentage of people highly or moderately annoyed was related to the day and night continuous equivalent sound level, L_{dn}. For each of the three types of traffic noise, the percentage of highly annoyed persons in a population started to increase at an L_{dn} value of 42 dBA, and the percentage of moderately annoyed persons at an L_{dn} value of 37 dBA (Miedema & Vos 1998). Aircraft noise produced a stronger annoyance response than road traffic, for the same L_{dn} exposure, consistent with earlier analyses (Kryter 1994; Bradley 1994a). However, caution should be exercised when interpreting synthesized data from different studies, since five major parameters should be randomly distributed for the analyses to be valid: personal, demographic, and lifestyle factors, as well as the duration of noise exposure and the population experience with noise (Kryter 1994).

Annoyance in populations exposed to environmental noise varies not only with the acoustical characteristics of the noise (source, exposure), but also with many non-acoustical factors of social, psychological, or economic nature (Fields 1993). These factors include fear associated with the noise source, conviction that the noise could be reduced by third parties, individual noise sensitivity, the degree to which an individual feels able to control the noise (coping strategies), and whether the noise originates from an important economic activity. Demographic variables such as age, sex and socioeconomic status, are less strongly associated with annoyance. The correlation between noise exposure and general annoyance is much higher at the group level than at the individual level, as might be expected. Data from 42 surveys showed that at the group level about 70% of the variance in annoyance is explained by noise exposure characteristics, whereas at the individual level it is typically about 20% (Job 1988).

When the type and amount of noise exposure is kept constant in the meta-analyses, differences between communities, regions and countries still exist (Fields 1990; Bradley 1996). This is well demonstrated by a comparison of the dose-response curve determined for road-traffic noise

(Miedema & Vos 1998) and that obtained in a survey along the North-South transportation route through the Austrian Alps (Lercher 1998b). The differences may be explained in terms of the influence of topography and meteorological factors on acoustical measures, as well as the low background noise level on the mountain slopes.

Stronger reactions have been observed when noise is accompanied by vibrations and contains low frequency components (Paulsen & Kastka 1995; Öhrström 1997; for review see Berglund et al. 1996), or when the noise contains impulses, such as shooting noise (Buchta 1996; Vos 1996; Smoorenburg 1998). Stronger, but temporary, reactions also occur when noise exposure is increased over time, in comparison to situations with constant noise exposure (e.g. HCN 1997; Klæboe et al. 1998). Conversely, for road traffic noise, the introduction of noise protection barriers in residential areas resulted in smaller reductions in annoyance than expected for a stationary situation (Kastka et al. 1995).

To obtain an indicator for annoyance, other methods of combining parameters of noise exposure have been extensively tested, in addition to metrics such as LAeq,24h and L_{dn}. When used for a set of community noises, these indicators correlate well both among themselves and with LAeq,24h or L_{dn} values (e.g. HCN 1997). Although LAeq,24h and L_{dn} are in most cases acceptable approximations, there is a growing concern that all the component parameters of the noise should be individually assessed in noise exposure investigations, at least in the complex cases (Berglund & Lindvall 1995).

3.9. The Effects of Combined Noise Sources

Many acoustical environments consist of sounds from more than one source. For these environments, health effects are associated with the total noise exposure, rather than with the noise from a single source (WHO 1980b). When considering hearing impairment, for example, the total noise exposure can be expressed in terms of LAeq,24h for the combined sources. For other adverse health effects, however, such a simple model most likely will not apply. It is possible that some disturbances (e.g. speech interference, sleep disturbance) may more easily be attributed to specific noises. In cases where one noise source clearly dominates, the magnitude of an effect may be assessed by taking into account the dominant source only (HCN 1997). Furthermore, at a policy level, there may be little need to identify the adverse effect of each specific noise, unless the responsibility for these effects is to be shared among several polluters (*cf.* The Polluter Pays Principle in Chapter 5, UNCED 1992).

There is no consensus on a model for assessing the total annoyance due to a combination of environmental noise sources. This is partly due to a lack of research into the temporal patterns of combined noises. The current approach for assessing the effects of "mixed noise sources" is limited to data on "total annoyance" transformed to mathematical principles or rules of thumb (Ronnebaum et al. 1996; Vos 1992; Miedema 1996; Berglund & Nilsson 1997). Models to assess the total annoyance of combinations of environmental noises may not be applicable to those health effects for which the mechanisms of noise interaction are unknown, and for which different cumulative or synergistic effects cannot be ruled out. When noise is combined with different types of environmental agents, such as vibrations, ototoxic chemicals, or chemical odours, again there is insufficient knowledge to accurately assess the combined effects on health

(Berglund & Lindvall 1995; HCN 1994; Miedema 1996; Zeichart 1998; Passchier-Vermeer & Zeichart 1998). Therefore, caution should be exercised when trying to predict the adverse health effects of combined factors in residential populations.

The evidence on low-frequency noise is sufficiently strong to warrant immediate concern. Various industrial sources emit continuous low-frequency noise (compressors, pumps, diesel engines, fans, public works); and large aircraft, heavy-duty vehicles and railway traffic produce intermittent low-frequency noise. Low-frequency noise may also produce vibrations and rattles as secondary effects. Health effects due to low-frequency components in noise are estimated to be more severe than for community noises in general (Berglund et al. 1996). Since A-weighting underestimates the sound pressure level of noise with low-frequency components, a better assessment of health effects would be to use C-weighting.

In residential populations heavy noise pollution will most certainly be associated with a combination of health effects. For example, cardiovascular disease, annoyance, speech interference at work and at home, and sleep disturbance. Therefore, it is important that the total adverse health load over 24 hours be considered and that the precautionary principle for sustainable development is applied in the management of health effects (see Chapter 5).

3.10. Vulnerable Groups

Protective standards are essentially derived from observations on the health effects of noise on "normal" or "average" populations. The participants of these investigations are selected from the general population and are usually adults. Sometimes, samples of participants are selected because of their easy availability. However, vulnerable groups of people are typically underrepresented. This group includes people with decreased personal abilities (old, ill, or depressed people); people with particular diseases or medical problems; people dealing with complex cognitive tasks, such as reading acquisition; people who are blind or who have hearing impairment; fetuses, babies and young children; and the elderly in general (Jansen 1987; AAP 1997). These people may be less able to cope with the impacts of noise exposure and be at greater risk for harmful effects.

Persons with impaired hearing are the most adversely affected with respect to speech intelligibility. Even slight hearing impairments in the high-frequency range may cause problems with speech perception in a noisy environment. From about 40 years of age, people typically demonstrate an impaired ability to understand difficult, spoken messages with low linguistic redundancy. Therefore, based on interference with speech perception, a majority of the population belongs to the vulnerable group.

Children have also been identified as vulnerable to noise exposure (see Agenda 21: UNCED 1992). The evidence on noise pollution and children's health is strong enough to warrant monitoring programmes at schools and preschools to protect children from the effects of noise. Follow up programmes to study the main health effects of noise on children, including effects on speech perception and reading acquisition, are also warranted in heavily noise polluted areas (Cohen et al. 1986; Evans et al. 1998).

The issue of vulnerable subgroups in the general population should thus be considered when developing regulations or recommendations for the management of community noise. This consideration should take into account the types of effects (communication, recreation, annoyance, etc.), specific environments (*in utero*, incubator, home, school, workplace, public institutions, etc.) and specific lifestyles (listening to loud music through headphones, or at discotheques and festivals; motor cycling, etc.).

4. Guideline Values

4.1. Introduction

The human ear and lower auditory system continuously receive stimuli from the world around us. However, this does not mean that all the acoustical inputs are necessarily disturbing or have harmful effects. This is because the auditory nerve provides activating impulses to the brain that enable us to regulate the vigilance and wakefulness necessary for optimal performance. On the other hand, there are scientific reports that a completely silent world can have harmful effects, because of sensory deprivation. Thus, both too little sound and too much sound can be harmful. For this reason, people should have the right to decide for themselves the quality of the acoustical environment they live in.

Exposure to noise from various sources is most commonly expressed as the average sound pressure level over a specific time period, such as 24 hours. This means that identical average sound levels for a given time period could be derived from either a large number of sound events with relatively low, almost inaudible levels, or from a few events with high sound levels. This technical concept does not fully agree with common experience on how environmental noise is experienced, or with the neurophysiological characteristics of the human receptor system.

Human perception of the environment through vision, hearing, touch, smell and taste is characterized by a good discrimination of stimulus intensity differences, and by a decaying response to a continuous stimulus (adaptation or habituation). Single sound events cannot be discriminated if the interval between events drops below a threshold value; if this occurs, the sound is interpreted as continuous. These characteristics are linked to survival, since new and different stimuli with low probability and high information value indicate warnings. Thus, when assessing the effects of environmental noise on people it is relevant to consider the importance of the background noise level, the number of events, and the noise exposure level independently.

Community noise studies have traditionally considered noise annoyance from single specific sources such as aircraft, road traffic or railways. In recent years, efforts have been made to compare the results from road traffic, aircraft and railway surveys. Data from a number of sources show that aircraft noise is more annoying than road traffic noise, which, in turn, is more annoying than railway noise. However, there is not a clear understanding of the mechanisms that create these differences. Some populations may also be at greater risk for the harmful effects of noise. Young children (especially during language acquisition), the blind, and perhaps fetuses are examples of such populations. There are no definite conclusions on this topic, but the reader should be alerted that guidelines in this report are developed for the population at large; guidelines for potentially more vulnerable groups are addressed only to a limited extent.

In the following, guideline values are summarized with regard to specific environments and effects. For each environment and situation, the guideline values take into consideration the identified health effects and are set, based on the lowest levels of noise that affect health (critical health effect). Guideline values typically correspond to the lowest effect level for general populations, such as those for indoor speech intelligibility. By contrast, guideline values for annoyance have been set at 50 or 55 dBA, representing daytime levels below which a majority of the adult population will be protected from becoming moderately or seriously annoyed, respectively.

In these *Guidelines for Community Noise* only guideline values are presented. These are essentially values for the onset of health effects from noise exposure. It would have been preferred to establish guidelines for exposure-response relationships. Such relationships would indicate the effects to be expected if standards were set above the WHO guideline values and would facilitate the setting of standards for sound pressure levels (noise immission standards). However, exposure-response relationships could not be established as the scientific literature is very limited. The best-studied exposure-response relationship is that between L_{dn} and annoyance (WHO 1995a; Berglund & Lindvall 1995; Miedema & Vos 1998). Even the most recent relationships between integrated noise levels and the percentage of highly or moderately annoyed people are still being scrutinized. The results of a forthcoming meta-analysis are expected to be published in the near future (Miedema, personal communication).

4.2. Specific Effects

4.2.1. Interference with communication

Noise tends to interfere with auditory communication, in which speech is a most important signal. However, it is also vital to be able to hear alarming and informative signals such as door bells, telephone signals, alarm clocks, fire alarms etc., as well as sounds and signals involved in occupational tasks. The effects of noise on speech discrimination have been studied extensively and deal with this problem in lexical terms (mostly words but also sentences). For communication distances beyond a few metres, speech interference starts at sound pressure levels below 50 dB for octave bands centered on the main speech frequencies at 500, 1 000 and 2 000 Hz. It is usually possible to express the relationship between noise levels and speech intelligibility in a single diagram, based on the following assumptions and empirical observations, and for speaker-to-listener distance of about 1 m:

a. Speech in relaxed conversation is 100% intelligible in background noise levels of about 35 dBA, and can be understood fairly well in background levels of 45 dBA.

b. Speech with more vocal effort can be understood when the background sound pressure level is about 65 dBA.

A majority of the population belongs to groups sensitive to interference with speech perception. Most sensitive are the elderly and persons with impaired hearing. Even slight hearing impairments in the high-frequency range may cause problems with speech perception in a noisy environment. From about 40 years of age, people demonstrate impaired ability to interpret difficult, spoken messages with low linguistic redundancy, when compared to people aged 20–30 years. It has also been shown that children, before language acquisition has been completed, have more adverse effects than young adults to high noise levels and long reverberation times.

For speech outdoors and for moderate distances, the sound level drops by approximately 6 dB for a doubling of the distance between speaker and listener. This relationship is also applicable to indoor conditions, but only up to a distance of about 2 m. Speech communication is affected also by the reverberation characteristics of the room, and reverberation times beyond 1 s can produce a loss in speech discrimination. A longer reverberation time combined with background noise makes speech perception still more difficult.

Speech signal perception is of paramount importance, for example, in classrooms or conference rooms. To ensure any speech communication, the signal-to-noise relationship should exceed zero dB. But when listening to complicated messages (at school, listening to foreign languages, telephone conversation) the signal-to-noise ratio should be at least 15 dB. With a voice level of 50 dBA (at 1 m distance this corresponds on average to a casual voice level in both women and men), the background level should not exceed 35 dBA. This means that in classrooms, for example, one should strive for as low background levels as possible. This is particularly true when listeners with impaired hearing are involved, for example, in homes for the elderly. Reverberation times below 1 s are necessary for good speech intelligibility in smaller rooms; and even in a quiet environment a reverberation time below 0.6 s is desirable for adequate speech intelligibility for sensitive groups.

4.2.2. Noise-induced hearing impairment

The ISO Standard 1999 (ISO 1990) gives a method of calculating noise-induced hearing impairment in populations exposed to all types of occupational noise (continuous, intermittent, impulse). However, noise-induced hearing impairment is by no means restricted to occupational situations alone. High noise levels can also occur in open-air concerts, discotheques, motor sports, shooting ranges, and from loudspeakers or other leisure activities in dwellings. Other loud noise sources, such as music played back in headphones and impulse noise from toys and fireworks, are also important. Evidence strongly suggests that the calculation method from ISO Standard 1999 for occupational noise (ISO 1990) should also be used for environmental and leisure time noise exposures. This implies that long term exposure to LAeq,24h of up to 70 dBA will not result in hearing impairment. However, given the limitations of the various underlying studies, care should be taken with respect to the following:

a. Data from animal experiments indicate that children may be more vulnerable in acquiring noise-induced hearing impairment than adults.

b. At very high instantaneous sound pressure levels mechanical damage to the ear may occur (Hanner & Axelsson 1988). Occupational limits are set at peak sound pressure levels of 140 dBA (EU 1986a). For adults, this same limit is assumed to be in order for exposure to environmental and leisure time noise. In the case of children, however, considering their habits while playing with noisy toys, peak sound pressure levels should never exceed 120 dBA.

c. For shooting noise with LAeq,24h over 80 dB, studies on temporary threshold shift suggest there is the possibility of an increased risk for noise-induced hearing impairment (Smoorenburg 1998).

d. The risk for noise-induced hearing impairment increases when noise exposure is combined with vibrations, ototoxic drugs or chemicals (Fechter 1999). In these circumstances, long-term exposure to LAeq,24h of 70 dB may induce small hearing impairments.

e. It is uncertain whether the relationships in ISO Standard 1999 (ISO 1990) are applicable to environmental sounds having a short rise time. For example, in the case of military low-altitude flying areas (75–300 m above ground) LAmax values of 110–130 dB occur within seconds after onset of the sound.

In conclusion, dose-response data are lacking for the general population. However, judging from the limited data for study groups (teenagers, young adults and women), and on the assumption that time of exposure can be equated with sound energy, the risk for hearing impairment would be negligible for LAeq,24h values of 70 dB over a lifetime. To avoid hearing impairment, impulse noise exposures should never exceed a peak sound pressure of 140 dB peak in adults, and 120 dB in children.

4.2.3. Sleep disturbance effects

Electrophysiological and behavioral methods have demonstrated that both continuous and intermittent noise indoors lead to sleep disturbance. The more intense the background noise, the more disturbing is its effect on sleep. Measurable effects on sleep start at background noise levels of about 30 dB LAeq. Physiological effects include changes in the pattern of sleep stages, especially a reduction in the proportion of REM sleep. Subjective effects have also been identified, such as difficulty in falling asleep, perceived sleep quality, and adverse after-effects such as headache and tiredness. Sensitive groups mainly include elderly persons, shift workers and persons with physical or mental disorders.
Where noise is continuous, the equivalent sound pressure level should not exceed 30 dBA indoors, if negative effects on sleep are to be avoided. When the noise is composed of a large proportion of low-frequency sounds a still lower guideline value is recommended, because low-frequency noise (e.g. from ventilation systems) can disturb rest and sleep even at low sound pressure levels. It should be noted that the adverse effect of noise partly depends on the nature of the source. A special situation is for newborns in incubators, for which the noise can cause sleep disturbance and other health effects.

If the noise is not continuous, LAmax or SEL are used to indicate the probability of noise-induced awakenings. Effects have been observed at individual LAmax exposures of 45 dB or less. Consequently, it is important to limit the number of noise events with a LAmax exceeding 45 dB. Therefore, the guidelines should be based on a combination of values of 30 dB LAeq,8h and 45 dB LAmax. To protect sensitive persons, a still lower guideline value would be preferred when the background level is low. Sleep disturbance from intermittent noise events increases with the maximum noise level. Even if the total equivalent noise level is fairly low, a small number of noise events with a high maximum sound pressure level will affect sleep.

Therefore, to avoid sleep disturbance, guidelines for community noise should be expressed in terms of equivalent sound pressure levels, as well as LAmax/SEL and the number of noise events. Measures reducing disturbance during the first part of the night are believed to be the most effective for reducing problems in falling asleep.

4.2.4. Cardiovascular and psychophysiological effects

Epidemiologial studies show that cardiovascular effects occur after long-term exposure to noise (aircraft and road traffic) with LAeq,24h values of 65–70 dB. However, the associations are weak. The association is somewhat stronger for ischaemic heart disease than for hypertension. Such small risks are important, however, because a large number of persons are currently exposed to these noise levels, or are likely to be exposed in the future. Other possible effects, such as changes in stress hormone levels and blood magnesium levels, and changes in the immune system and gastro-intestinal tract, are too inconsistent to draw conclusions. Thus, more research is required to estimate the long-term cardiovascular and psychophysiological risks due to noise. In view of the equivocal findings, no guideline values can be given.

4.2.5. Mental health effects

Studies that have examined the effects of noise on mental health are inconclusive and no guideline values can be given. However, in noisy areas, it has been observed that there is an increased use of prescription drugs such as tranquilizers and sleeping pills, and an increased frequency of psychiatric symptoms and mental hospital admissions. This strongly suggests that adverse mental health effects are associated with community noise.

4.2.6. Effects on performance

The effects of noise on task performance have mainly been studied in the laboratory and to some extent in work situations. But there have been few, if any, detailed studies on the effects of noise on human productivity in community situations. It is evident that when a task involves auditory signals of any kind, noise at an intensity sufficient to mask or interfere with the perception of these signals will also interfere with the performance of the task. A novel event, such as the start of an unfamiliar noise, will also cause distraction and interfere with many kinds of tasks. For example, impulsive noises such as sonic booms can produce disruptive effects as the result of startle responses; and these types of responses are more resistant to habituation.

Mental activities involving high load in working memory, such as sustained attention to multiple cues or complex analysis, are all directly sensitive to noise and performance suffers as a result. Some accidents may also be indicators of noise-related effects on performance. In addition to the direct effects on performance, noise also has consistent after-effects on cognitive performance with tasks such as proof-reading, and on persistence with challenging puzzles. In contrast, the performance of tasks involving either motor or monotonous activities is not always degraded by noise.

Chronic exposure to aircraft noise during early childhood appears to damage reading acquisition. Evidence indicates that the longer the exposure, the greater the damage. Although there is insufficient information on these effects to set specific guideline values, it is clear that day-care centres and schools should not be located near major noise sources, such as highways, airports and industrial sites.

4.2.7. Annoyance responses

The capacity of a noise to induce annoyance depends upon many of its physical characteristics, including its sound pressure level and spectral characteristics, as well as the variations of these properties over time. However, annoyance reactions are sensitive to many non-acoustical factors of social, psychological or economic nature, and there are also considerable differences in individual reactions to the same noise. Dose-response relations for different types of traffic noise (air, road and railway) clearly demonstrate that these noises can cause different annoyance effects at equal LAeq,24h values. And the same type of noise, such as that found in residential areas around airports, can also produce different annoyance responses in different countries.

The annoyance response to noise is affected by several factors, including the equivalent sound pressure level and the highest sound pressure level of the noise, the number of such events, and the time of day. Methods for combining these effects have been extensively studied. The results are not inconsistent with the simple, physically based equivalent energy theory, which is represented by the LAeq noise index.

Annoyance to community noise varies with the type of activity producing the noise. Speech communication, relaxation, listening to radio and TV are all examples of noise-producing activities. During the daytime, few people are seriously annoyed by activities with LAeq levels below 55 dB; or moderately annoyed with LAeq levels below 50 dB. Sound pressure levels during the evening and night should be 5–10 dB lower than during the day. Noise with low-frequency components require even lower levels. It is emphasized that for intermittent noise it is necessary to take into account the maximum sound pressure level as well as the number of noise events. Guidelines or noise abatement measures should also take into account residential outdoor activities.

4.2.8. Effects on social behaviour

The effects of environmental noise may be evaluated by assessing the extent to which it interferes with different activities. For many community noises, interference with rest, recreation and watching television seem to be the most important issues. However, there is evidence that noise has other effects on social behaviour: helping behaviour is reduced by noise in excess of 80 dBA; and loud noise increases aggressive behavior in individuals predisposed to aggressiveness. There is concern that schoolchildren exposed to high levels of chronic noise could be more susceptible to helplessness. Guidelines on these issues must await further research.

4.3. Specific Environments

Noise measures based solely on LAeq values do not adequately characterize most noise environments and do not adequately assess the health impacts of noise on human well-being. It is also important to measure the maximum noise level and the number of noise events when deriving guideline values. If the noise includes a large proportion of low-frequency components, values even lower than the guideline values will be needed, because low-frequency components in noise may increase the adverse effects considerably. When prominent low-frequency components are present, measures based on A-weighting are inappropriate. However, the difference between dBC (or dBlin) and dBA will give crude information about the presence of low-frequency components in noise. If the difference is more than 10 dB, it is recommended that a frequency analysis of the noise be performed.

4.3.1. Dwellings

In dwellings, the critical effects of noise are on sleep, annoyance and speech interference. To avoid sleep disturbance, indoor guideline values for bedrooms are 30 dB LAeq for continuous noise and 45 dB LAmax for single sound events. Lower levels may be annoying, depending on the nature of the noise source. The maximum sound pressure level should be measured with the instrument set at "*Fast*".

To protect the majority of people from being seriously annoyed during the daytime, the sound pressure level on balconies, terraces and outdoor living areas should not exceed 55 dB LAeq for a steady, continuous noise. To protect the majority of people from being moderately annoyed during the daytime, the outdoor sound pressure level should not exceed 50 dB LAeq. These values are based on annoyance studies, but most countries in Europe have adopted 40 dB LAeq as the maximum allowable level for new developments (Gottlob 1995). Indeed, the lower value should be considered the maximum allowable sound pressure level for all new developments whenever feasible.

At night, sound pressure levels at the outside façades of the living spaces should not exceed 45 dB LAeq and 60 dB LAmax, so that people may sleep with bedroom windows open. These values have been obtained by assuming that the noise reduction from outside to inside with the window partly open is 15 dB.

4.3.2. Schools and preschools

For schools, the critical effects of noise are on speech interference, disturbance of information extraction (e.g. comprehension and reading acquisition), message communication and annoyance. To be able to hear and understand spoken messages in classrooms, the background sound pressure level should not exceed 35 dB LAeq during teaching sessions. For hearing impaired children, an even lower sound pressure level may be needed. The reverberation time in the classroom should be about 0.6 s, and preferably lower for hearing-impaired children. For assembly halls and cafeterias in school buildings, the reverberation time should be less than 1 s. For outdoor playgrounds, the sound pressure level of the noise from external sources should not exceed 55 dB LAeq, the same value given for outdoor residential areas in daytime.

For preschools, the same critical effects and guideline values apply as for schools. In bedrooms in preschools during sleeping hours, the guideline values for bedrooms in dwellings should be used.

4.3.3. Hospitals

For most spaces in hospitals, the critical effects of noise are on sleep disturbance, annoyance and communication interference, including interference with warning signals. The LAmax of sound events during the night should not exceed 40 dB indoors. For wardrooms in hospitals, the guideline values indoors are 30 dB LAeq, together with 40 dB LAmax during the night. During the day and evening the guideline value indoors is 30 dB LAeq. The maximum level should be measured with the instrument set at "*Fast*".

Since patients have less ability to cope with stress, the equivalent sound pressure level should not exceed 35 dB LAeq in most rooms in which patients are being treated or observed. Particular attention should be given to the sound pressure levels in intensive care units and operating theatres. Sound inside incubators may result in health problems, including sleep disturbance, and may lead to hearing impairment in neonates. Guideline values for sound pressure levels in incubators must await future research.

4.3.4. Ceremonies, festivals and entertainment events

In many countries, there are regular ceremonies, festivals and other entertainment to celebrate life events. Such events typically produce loud sounds including music and impulsive sounds. There is widespread concern about the effect of loud music and impulse sounds on young people who frequently attend concerts, discotheques, video arcades, cinemas, amusement parks and spectator events, etc. The sound pressure level is typically in excess of 100 dB LAeq. Such a noise exposure could lead to significant hearing impairment after frequent attendance.

Noise exposure for employees of these venues should be controlled by established occupational standards. As a minimum, the same standards should apply to the patrons of these premises. Patrons should not be exposed to sound pressure levels greater than 100 dB LAeq during a 4-h period, for at most four times per year. To avoid acute hearing impairment the LAmax should always be below 110 dB.

4.3.5. Sounds through headphones

To avoid hearing impairment in both adults and children from music and other sounds played back in headphones, the LAeq,24h should not exceed 70 dB. This implies that for a daily one-hour exposure the LAeq should not exceed 85 dB. The exposures are expressed in free-field equivalent sound pressure levels. To avoid acute hearing impairment, the LAmax should always be below 110 dB.

4.3.6. Impulsive sounds from toys, fireworks and firearms

To avoid acute mechanical damage to the inner ear, adults should never be exposed to more than 140 dB peak sound pressure. To account for the vulnerability in children, the peak sound pressure level produced by toys should not surpass 120 dB, measured close to the ears (100 mm). To avoid acute hearing impairment, LAmax should always be below 110 dB.

4.3.7. Parkland and conservation areas

Existing large quiet outdoor areas should be preserved and the signal-to-noise ratio kept low.

4.4. WHO Guideline Values

The WHO guideline values in Table 4.1 are organized according to specific environments. When multiple adverse health effects are identified for a given environment, the guideline values are set at the level of the lowest adverse health effect (the critical health effect). An adverse health effect of noise refers to any temporary or long-term deterioration in physical, psychological or social functioning that is associated with noise exposure. The guideline values represent the sound pressure levels that affect the most exposed receiver in the listed environment.

The time base for LAeq for "daytime" and "night-time" is 16 h and 8 h, respectively. No separate time base is given for evenings alone, but typically, guideline value should be 5 –10 dB lower than for a 12 h daytime period. Other time bases are recommended for schools, preschools and playgrounds, depending on activity.

The available knowledge of the adverse effects of noise on health is sufficient to propose guideline values for community noise for the following:

a. Annoyance.
b. Speech intelligibility and communication interference.
c. Disturbance of information extraction.
d. Sleep disturbance.
e. Hearing impairment.

The different critical health effects are relevant to specific environments, and guideline values for community noise are proposed for each environment. These are:

a. Dwellings, including bedrooms and outdoor living areas.
b. Schools and preschools, including rooms for sleeping and outdoor playgrounds.
c. Hospitals, including ward and treatment rooms.
d. Industrial, commercial shopping and traffic areas, including public addresses, indoors and outdoors.
e. Ceremonies, festivals and entertainment events, indoors and outdoors.
f. Music and other sounds through headphones.
g. Impulse sounds from toys, fireworks and firearms.

h. Outdoors in parkland and conservation areas.

It is not enough to characterize the noise environment in terms of noise measures or indices based only on energy summation (e.g. LAeq), because different critical health effects require different descriptions. Therefore, it is important to display the maximum values of the noise fluctuations, preferably combined with a measure of the number of noise events. A separate characterization of noise exposures during night-time would be required. For indoor environments, reverberation time is also an important factor. If the noise includes a large proportion of low frequency components, still lower guideline values should be applied.

Supplementary to the guideline values given in Table 4.1, precautionary recommendations are given in Section 4.2 and 4.3 for vulnerable groups, and for noise of a certain character (e.g. low-frequency components, low background noise), respectively. In Section 3.10, information is given regarding which critical effects and specific environments are considered relevant for vulnerable groups, and what precautionary noise protection would be needed in comparison to the general population.

Table 4.1: Guideline values for community noise in specific environments.

Specific environment	Critical health effect(s)	LAeq [dB]	Time base [hours]	LAmax, fast [dB]
Outdoor living area	Serious annoyance, daytime and evening Moderate annoyance, daytime and evening	55 50	16 16	- -
Dwelling, indoors Inside bedrooms	Speech intelligibility and moderate annoyance, daytime and evening Sleep disturbance, night-time	35 30	16 8	 45
Outside bedrooms	Sleep disturbance, window open (outdoor values)	45	8	60
School class rooms and pre-schools, indoors	Speech intelligibility, disturbance of information extraction, message communication	35	during class	-
Pre-school bedrooms, indoors	Sleep disturbance	30	sleeping -time	45
School, playground outdoor	Annoyance (external source)	55	during play	-
Hospital, ward rooms, indoors	Sleep disturbance, night-time Sleep disturbance, daytime and evenings	30 30	8 16	40 -
Hospitals, treatment rooms, indoors	Interference with rest and recovery	#1		
Industrial, commercial shopping and traffic areas, indoors and outdoors	Hearing impairment	70	24	110
Ceremonies, festivals and entertainment events	Hearing impairment (patrons:<5 times/year)	100	4	110
Public addresses, indoors and outdoors	Hearing impairment	85	1	110
Music through headphones/ earphones	Hearing impairment (free-field value)	85 #4	1	110
Impulse sounds from toys, fireworks and firearms	Hearing impairment (adults) Hearing impairment (children)	- -	- -	140 #2 120 #2
Outdoors in parkland and conservation areas	Disruption of tranquillity	#3		

#1: as low as possible;
#2: peak sound pressure (not LAmax, fast), measured 100 mm from the ear;
#3: existing quiet outdoor areas should be preserved and the ratio of intruding noise to natural background sound should be kept low;
#4: under headphones, adapted to free-field values

5. Noise Management

The goal of noise management is to maintain low noise exposures, such that human health and well-being are protected. The specific objectives of noise management are to develop criteria for the maximum safe noise exposure levels, and to promote noise assessment and control as part of environmental health programmes. This is not always achieved (Jansen 1998). The United Nations′ Agenda 21 (UNCED 1992), as well as the European Charter on Transport, Environment and Health (London Charter 1999), both support a number of environmental management principles on which government policies, including noise management policies, can be based. These include:

a. **The precautionary principle**. In all cases, noise should be reduced to the lowest level achievable in a particular situation. Where there is a reasonable possibility that public health will be damaged, action should be taken to protect public health without awaiting full scientific proof.

b. **The polluter pays principle**. The full costs associated with noise pollution (including monitoring, management, lowering levels and supervision) should be met by those responsible for the source of noise.

c. **The prevention principle**. Action should be taken where possible to reduce noise at the source. Land-use planning should be guided by an environmental health impact assessment that considers noise as well as other pollutants.

The government policy framework is the basis of noise management. Without an adequate policy framework and adequate legislation it is difficult to maintain an active or successful noise management programme. A policy framework refers to transport, energy, planning, development and environmental policies. The goals are more readily achieved if the interconnected government policies are compatible, and if issues which cross different areas of government policy are co-ordinated.

5.1. Stages in Noise Management

A legal framework is needed to provide a context for noise management (Finegold 1998; Hede 1998a). While there are many possible models, an example of one is given in Figure 5.1. This model depicts the six stages in the process for developing and implementing policies for community noise management. For each policy stage, there are groups of 'policy players' who ideally would participate in the process.

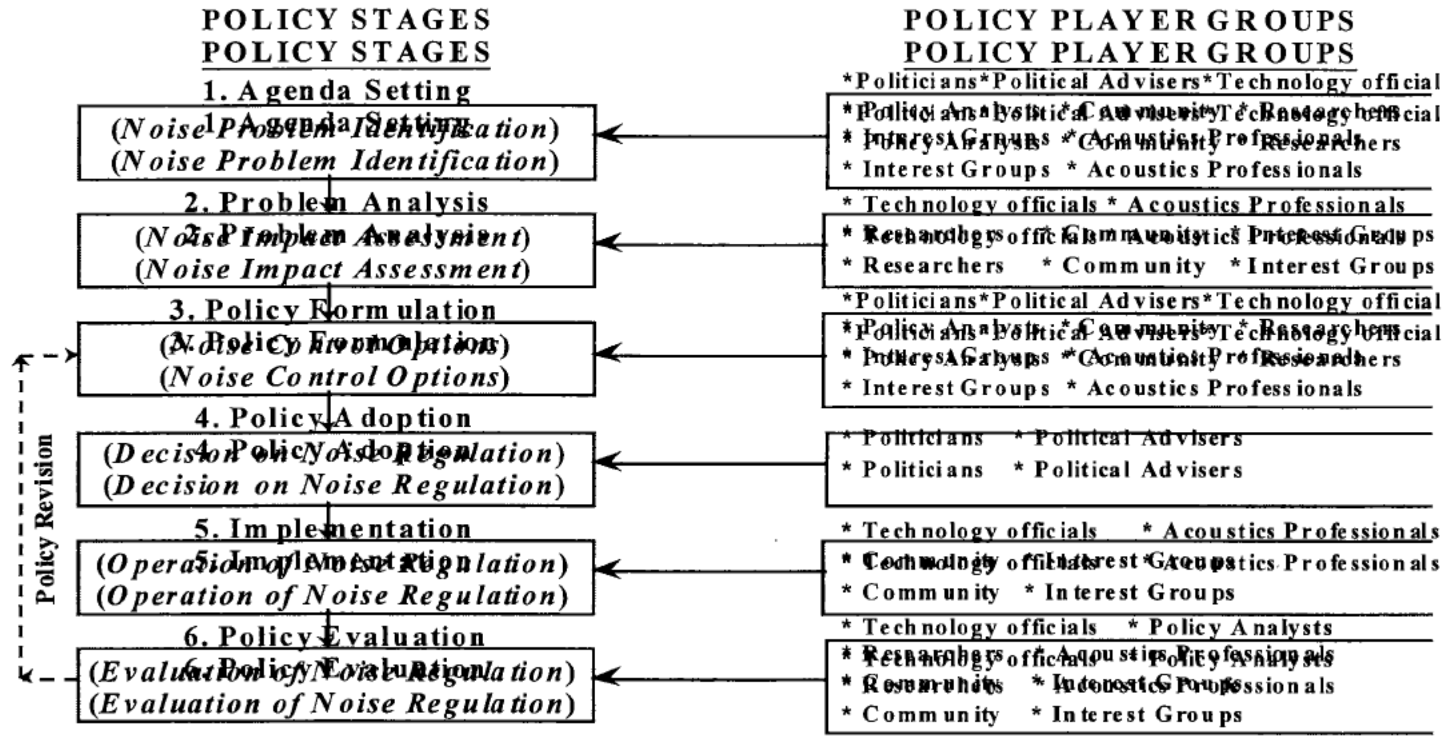

Figure 5.1. A model of the policy process for community noise management (Hede 1998a)

When goals and policies have been developed, the next stage is the development of the strategy or plan. Figure 5.2 summarizes the stages involved in the development of a noise management strategy. Specific abatement measures 19 are listed in Table 5.1.

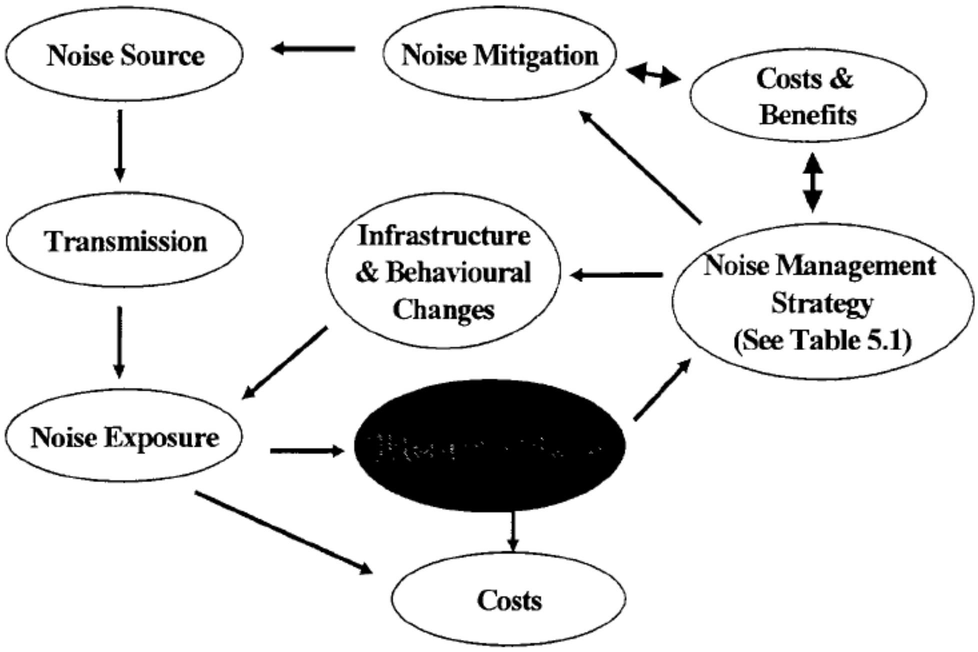

Figure 5.2. Stages involved in the development of a noise abatement strategy.

Table 5.1. Recommended Noise Management Measures (following EEA 1995)

Legal measures	Examples
Control of noise emissions	Emission standards for road and off-road vehicles; emission standards for construction equipment; emission standards for plants; national regulations, EU Directives
Control of noise transmission	Regulations on sound-obstructive measures
Noise mapping and zoning around roads, airports, industries	Initiation of monitoring and modeling programmes
Control of noise immissions	Limits for exposure levels such as national immission standards; noise monitoring and modeling; regulations for complex noise situations; regulations for recreational noise
Speed limits	Residential areas; hospitals
Enforcement of regulations	Low Noise Implementation Plan
Minimum requirements for acoustical properties of buildings	Construction codes for sound insulation of building parts
Engineering Measures	
Emission reduction by source modification	Tyre profiles; low-noise road surfaces; changes in engine properties
New engine technology	Road vehicles; aircraft; construction machines
Transmission reduction	Enclosures around machinery; noise screens
Orientation of buildings	Design and structuring of tranquille uses; using buildings for screening purposes
Traffic management	Speed limits; guidance of traffic flow by electronic means
Passive protection	Ear plugs; ear muffs; insulation of dwellings; façade design
Implementation of land-use planning	Minimum distance between industrial, busy roads and residential areas; location of tranquillity areas; by-pass roads for heavy traffic; separating out incompatible functons
Education and information	
Raising public awareness	Informing the public on the health impacts of noise, enforcement action taken, noise levels, complaints
Monitoring and modeling of soundscapes	Publication of results
Sufficient number of noise experts	University or highschool curricula
Initiation of research and development	Funding of information generation according to scientific research needs
Initiation of behaviour changes	Speed reduction when driving; use of horns; use of loudspeakers for advertisements

The process outlined in Figure 5.2 can start with the development of noise standards or guidelines. Ideally, it should also involve the identification and mapping of noise sources and exposed communities. Meteorological conditions and noise levels would also normally be monitored. These data can be used to validate the output of models that estimate noise levels. Noise standards and model outputs may be considered in devising noise control tactics aimed at achieving the noise standards. Before being enforced, current control tactics need to be revised, and if the standards are achieved they need continued enforcement. If the standards are not achieved after a reasonable period of time, the noise control tactics may need to be revised.

National noise standards can usually be based on a consideration of international guidelines, such as these Guidelines for Community Noise, as well as national criteria documents, which consider dose-response relations for the effects of noise on human health. National standards take into account the technological, social, economic, political and other factors specific for the country.

In many cases monitoring may show that noise levels are considerably higher than established guidelines. This may be particularly true in developing countries, and the question has to be raised as to whether national standards should reflect the optimum levels needed to protect human health, when this objective is unlikely to be achieved in the short- or medium-term with available resources. In some countries noise standards are set at levels that are realistically attainable under prevailing technological, social, economic and political conditions, even though they may not be fully consistent with the levels needed to protect human health. In such cases, a staged programme of noise abatement should be implemented to achieve the optimum health protection levels over the long term. Noise standards periodically change after reviews, as conditions in a country change over time, and with improved scientific understanding of the relationship between noise pollution and the health of the population. Noise level monitoring (Chapter 2) is used to assess whether noise levels at particular locations are in compliance with the standards selected.

5.2. Noise Exposure Mapping

A crucial component of a low-noise implementation plan is a reasonably quantitative knowledge of exposure (see Figure 5.2). Exposure should be mapped for all noise sources impacting a community; for example, road traffic, aircraft, railway, industry, construction, festivals and human activity in general. For some components of a noise exposure map or noise exposure inventory, accurate data may be available. In other cases, exposure can be calculated from the characteristics of the mechanical processes. While estimates of noise emissions are needed to develop exposure maps, measurements should be undertaken to confirm the veracity of the assumptions used in the estimates. Sample surveys may be used to provide an overall picture of the noise exposure. Such surveys would take account of all the relevant characteristics of the noise source. For example motor vehicle emissions may be estimated by calculations involving the types of vehicles, their number, their age and the characteristic properties of the road surface.

In developing countries, there is usually a lack of appropriate statistical information to produce noise exposure estimates. However, where action is needed to lower noise levels, the absence of comprehensive information should not prevent the development of provisional noise exposure estimates. Basic information about the exposed population, transport systems, industry and other relevant factors can be used to calculate provisional noise exposures. These can then be used to develop and implement interim noise management plans. The preliminary exposure estimates can be revised as more accurate information becomes available.

5.3. Noise Exposure Modeling

As indicated in Chapter 2 modeling is a powerful tool for the interpolation, prediction and optimization of control strategies. However, models need to be validated by monitoring data. A strength of models is that they enable examination and comparison of the consequences for noise exposure of the implementation of the various options for improving noise. However, the accuracy of the various models available depends on many factors, including the accuracy of the source emissions data and details of the topography (for which a geographical information system may be used). For transportation noise parameters such as the number, type and speed of vehicles, aircraft or trains, and the noise characteristics of each individual event must be known. An example of a model is the annoyance prediction model of the Government of the Netherlands (van den Berg 1996).

5.4. Noise Control Approaches

An integrated noise policy should include several control procedures: measures to limit the noise at the source, noise control within the sound transmission path, protection at the receiver's site, land-use planning, education and raising of public awareness. Ideally, countries should give priority to precautionary measures that prevent noise, but they must also implement measures to mitigate existing noise problems.

5.4.1. Mitigation measures

The most effective mitigation measure is to reduce noise emissions at the source. Therefore, regulations with noise level limits for the main noise sources should be introduced.

Road traffic noise. Limits on the noise emission of vehicles have been introduced in many countries (Sandberg 1995). Such limits, together with the relevant measuring methods, should also be introduced in other regions of the world. Besides these limits a special class of "low-noise trucks" has been introduced in Europe. These trucks follow state-of-the-art noise control and are widely used in Austria and Germany (Lang 1995). Their use is encouraged by economic incentives; for example, low-noise trucks are excepted from a night-time ban on certain routes, and their associated taxes are lower than for other trucks. In Europe, the maximum permissible noise levels range from 69 dBA for motor vehicles to 77 dBA for cars, and 83 dBA for heavy two-wheeled vehicles to 84 dBA for trucks. A number of European Directives give permissible sound levels for motor vehicles and motorcycles (EU 1970; EU 1978; EU 1996a; EU 1997). In addition to noise level limits for new vehicles (type test), noise emissions of vehicles already in use should be controlled regularly. Limits on the sound pressure levels for vehicles reduce the noise emission from the engines.

However, the main noise from traffic on highways is rolling noise. This may be reduced by quiet road surfaces (porous asphalt, "drain asphalt") or by selection of quiet tires. Road traffic noise may also be reduced by speed limits, provided the limits are enforced. For example, reducing the speed of trucks from 90 to 60 km/h on concrete roads would reduce the maximum sound pressure level by 5 dB, and the equivalent sound pressure level by 4 dB. Decreasing the speed of cars from 140 to 100 km/h would result in the same noise reduction (WHO 1995a). In the central parts of cities a speed limit of 30 km/h may be introduced. At 30 km/h cars produce maximum sound pressure levels that are 7 dB lower, and equivalent sound pressure levels that are 5 dB lower, than cars driving at 50 km/h.

Noise emission from road traffic may be further reduced by a night-time ban for all vehicles, or especially for heavy vehicles. Traffic management designed to ensure uniform traffic flow in towns also serves to reduce noise. "Low-noise behaviour" of drivers should be encouraged as well, by advocating defensive driving manners. In some countries, car drivers use their horns frequently, which results in noise with high peak levels. The unnecessary use of horns within cities should be forbidden, especially during night-time, and this rule should be enforced.

Railway noise and noise from trams. The main noise sources are the engine and the wheel-rail contact. Noise at the source can be reduced by well-maintained rails and wheels, and by the use of disc brakes. Sound pressure levels may vary by more than 10 dB, depending on the type of railway material. Replacement of steel wheels by rubber wheels could also reduce noise from railways and trams substantially. Other measures include innovations in engine and track technology (Moehler 1988; Öhrström & Skånberg 1996).

Aircraft noise. The noise emission of aircraft is limited by ICAO Annex 16, Chapter 2 and Chapter 3, which estimates maximum potential sound emissions under certification procedures (ICAO 1993). Aircraft following the norms of Chapter 3 represent the state-of-the-art of noise control of the 1970s. In many countries, non-certified aircraft (i.e. aircraft not fulfilling the ICAO requirements) are not permitted and Chapter 2 aircraft may not be registered again. After the year 2002 only Chapter 3 aircraft will be allowed to operate in many countries.

Similar legislation should be adopted in other countries. The use of low-noise aircraft may also be encouraged by setting noise-related charges (that is, landing charges that are related not only to aircraft weight and capacity, but also to noise emission). Examples of systems for noise-related financial charges are given in OECD 1991 (see also OECD-ECMT 1995). Night-time aircraft movements should be discouraged where they impact residential communities. Particular categories of aircraft (such as helicopters, rotorcraft and supersonic aircraft) pose additional problems that require appropriate controls. For subsonic airplanes two EU Directive give the permissible sound levels (EU 1980; EU 1989).

Machines and Equipment. Noise emission has to be considered a main property of all types of machines and equipment. Control measures include design, insulation, enclosure and maintenance.

Consumers should be encouraged to take noise emission into account when buying a product. Declaring the A-weighted sound power level of a product would assist the consumer in making this decision. The introduction of sound labeling is a major tool for reducing the noise emission of products on the market. For example, within the European Community, "permissible sound levels" and "sound power levels" have to be stated for several groups of machines; for example, lawn mowers, construction machines and household equipment (EU 1984a-f; EU 1986b,c). For other groups of machines sound level data have been compiled and are state-of-the-art with respect to noise control.

A second step would be the introduction of limits on the sound power levels for certain groups of machines, heating and ventilation systems (e.g. construction machines, household appliances). These limits may be set by law, in recommendations and by consumers, using state-of-the-art measurements. There have also been promising developments in the use of active noise control (involving noise cancellation techniques). These are to be encouraged.

Noise control within the sound transmission path. The installation of noise barriers can protect dwellings close to the traffic source. In several European countries noise barrier regulations have been established (WHO 1995b), but in practice they are often not adequately implemented. These regulations must define:

a. Measuring and calculation methods for deriving the equivalent sound pressure level of road or railway traffic, and schemes for determining the effectiveness of the barrier.

b. The sound pressure limits that are to be achieved by installing barriers.

c. The budgetary provisions.

d. The responsible authority.

Noise protection at the receiver's site. This approach is mainly used for existing situations. However, this approach must also be considered for new and, eventually, for old buildings in noisy areas. Residential buildings near main roads with heavy traffic, or near railway lines, may be provided with sound-proofed windows.

5.4.2. Precautionary measures

With careful planning, noise exposure can be avoided or reduced. A sufficient distance between residential areas and an airport will make noise exposure minimal, although the realization of such a situation is not always possible. Additional insulation of houses can help to reduce noise exposure from railroad and road traffic. For new buildings, standards or building codes should describe the positions of houses, as well as the ground plans of houses with respect to noise sources. The required sound insulation of the façades should also be described. Various countries have set standards for the maximum sound pressure levels in front of buildings and for the minimum sound insulation values required for façades.

Land use planning. Land use planning is one of the main tools for noise control and includes:

a. Calculation methods for predicting the noise impact caused by road traffic, railways, airports, industries and others.

b. Noise level limits for various zones and building types. The limits should be based on annoyance responses to noise.

c. Noise maps or noise inventories that show the existing noise situation. The construction of noise-sensitive buildings in noisy areas, or the construction of noisy buildings in quiet areas may thus be avoided.

Suggestions on how to use land use planning tools are given in several dedicated books (e.g. Miller & de Roo 1997). Different zones, such as quiet areas, hospitals, residential areas, commercial and industrial districts, can be characterized by the maximum equivalent sound pressure levels permissible in the zones. Examples of this approach can be found in OECD 1991 (also see OECD-ECMT 1995). More emphasis needs to be given to the design or retrofit of urban centres, with noise management as a priority (e.g. "soundscapes").

It is recommended that countries adopt the precautionary principle in their national noise policies. This principle should be applied to all noise situations where adverse noise effects are either expected or possible, even when the noise is below standard values.

Education and public awareness. Noise abatement policies can only be established if basic knowledge and background material is available, and the people and authorities are aware that noise is an environmental hazard that needs to be controlled. It is, therefore, necessary to include noise in school curricula and to establish scientific institutes to study acoustics and noise control. People working in such institutes should have the option of studying in other countries and exchanging information at international conferences. Dissemination of noise control information to the public is an issue for education and public awareness. Ideally, national and local advisory groups should be formed to promote the dissemination of information, to establish uniform methods of noise measurement and impact assessment, and to participate in the development and implementation of educational and public awareness programmes.

5.5. Evaluation of Control Options

Unless legal constraints in a country prescribe a particular option, the evaluation of control options must take into account technical, financial, social, health and environmental factors. The speed with which control options can be implemented, and their enforceability, must also be considered. Although considerable improvements in noise levels have been achieved in some developed countries, the financial costs have been high, and the resource demands of some of these approaches make them unsuitable for the poorer developing countries.

Technical factors. There needs to be confidence that the selected options are technically practical given the resources of the region. It must be possible to bring a selected option into operation, and maintain the expected level of performance in the long term, given the resources available. This may require regular staff training and other programmes, especially in developing countries.

Financial factors. The selected options must be financially viable in the long term. This may require a comparative cost-benefit assessment of different options. These assessments must include not only the capital costs of bringing an option into operation, but also the costs of maintaining the expected level of performance in the long term.

Social factors. The costs and benefits of each option should be assessed for social equity, and the potential impact of an option on people's way of life, community structures and cultural traditions must be considered. Impacts may include disruption or displacement of residents, changes of land-use, and impacts on community, culture and recreation. Some impacts can be managed; in other cases, the impacts of an option can be mitigated by substitution of resources or uses.

Health and environmental factors. The costs and benefits of each option should be assessed for health and environmental factors. This may involve use of dose-response relations, or risk assessment techniques.

Effect-oriented and source-oriented principles. Noise control requirements in European countries are typically determined from the effects of noise on health and the environment (effect oriented) (e.g. Gottlob 1995; ten Wolde 1998). Increased noise emissions may be permitted if there would be no adverse health impacts, or if noise standards would not be exceeded. Action may be taken to reduce noise levels when it is shown that adverse health impacts will occur, or when noise levels exceed limits. Other countries base their noise management policies on the requirement for best available technology, or for best available techniques that do not entail excessive cost (source-oriented) (e.g. for aircraft noise, ICAO 1993; for road traffic noise, Sandberg 1995). Most developed countries apply a combination of both source-oriented and effect-oriented principles (EU 1996b; Jansen 1998; ten Wolde 1998).

5.6. Management of Indoor Noise

In modern societies, human beings spend most of their time in indoor environments. Pollution and degradation of the indoor environment cause illness, increased mortality, loss of productivity, and have major economic and social implications. Indoor noise problems are related to inadequate urban planning, design, operation and maintenance of buildings, and to the materials and equipment in buildings. Problems with indoor noise affect all types of buildings, including homes, schools, offices, health care facilities and other public and commercial buildings. The health effects of indoor noise include an increase in the rates of diseases and disturbances described in chapter 2. World-wide, the medical and social cost associated with these illnesses, and the related reduction in human productivity, can result in substantial economic losses.

Protection against noise generated within a building, or originating from outside the building, is a very complex problem. Soundproofing of ceilings, walls, doors and windows against airborne noise is important. Soundproofing of ceilings has to be sufficient to absorb sounds due to treading. Finally, noise emissions from the technological devices in the house must be sufficiently low. Governments should provide measurement protocols and data for use in reducing noise exposures in buildings. Governments should also be encouraged to support research on the relationship between noise levels inside buildings and health effects.

5.6.1. Government policy on indoor noise

Many of the problems associated with high noise levels can be prevented at low cost if governments develop and implement an integrated strategy for the indoor environment, in concert with all social and economic partners. Governments should establish a "National Plan for a Sustainable Indoor Noise Environment", that would apply to new construction as well as to existing buildings. Governments should set up a specific structure at an appropriate governmental level to achieve acceptable sound exposure levels within buildings. An example of existing documents that provide guidance and regulations, including strategies and management for the design of buildings, is given by Jansen & Gottlob (1996).

Guidance/education. Because our understanding of indoor noise is still developing, government activity should be focused on raising the awareness of various audiences. This education can take the form of providing general information, as well as providing technical guidance and training on how to minimize indoor noise levels. General information presented in the form of documents, videos, and other media can bring indoor noise issues to the attention of the general public and building professionals, including architects

Research support. Research is needed to develop technology for indoor noise diagnosis, mitigation and control. Efforts are also required to provide economical and practical alternatives for mitigation and control. Better means of measuring the effectiveness of absorption devices are needed; and diagnostic tools that are inexpensive and easy to use also need to be developed to help facility personnel. There is a particular need, too, for improving soundproofing methods, their implementation and for predicting the health effects of soundproofing techniques.

To provide accurate information for use in setting priorities for public health problems, governments should support problem assessment and surveys of indoor noise conditions. Building surveys are also necessary to provide baseline information about building characteristics and noise levels. When combined with occupant health surveys, these studies will help to establish the correlations between noise levels and adverse health effects. Surveys should be conducted to identify building types or vintages in which problems occur more frequently. The results of these studies will support effective risk reduction programmes. Epidemiological studies are also needed to aid in differentiating between noise-related symptoms and those due to other causes. Moreover, epidemiological studies are needed to assist in quantifying the extent of risk for indoor noise levels.

Economic research is needed to measure the costs of indoor noise control strategies to individuals, businesses and society. This includes developing methods for quantifying productivity loss and increased health costs due to noise, and for measuring the costs of various control strategies, including increased soundproofing and source control.

Development of standards and protocols. Efforts should be made to protect public health by setting reasonable noise exposure limits (immission standards) from known dose-response relationships. In cases where dose-response relationships have yet to be determined, but where health effects are generally recognized, exposure limits should be set conservatively and take into account risk, economic impact and feasibility. Efforts should also be made to incorporate noise-related specifications into building codes. Areas to target with building codes include ventilation design, building envelope design, site preparation, materials selection and commissioning. Standards and other regulations governing the use of sound proofing materials should also be developed.

Individuals involved in the diagnosis and mitigation of indoor noise problems should be trained in the multidisciplinary nature of the noise field. By instituting a series of credentials that recognize and highlight areas of expertise, consumers would be provided with the information to make informed choices when procuring indoor noise services. Companies which provide such services should be officially accredited. Guidelines or standards for sound emissions of air-conditioners, power generators and other building devices, would also provide useful information for manufacturers, architects, design engineers, building managers and others who play a role in selecting products used indoors.

5.6.2. Design considerations

Site investigation. Potential sites should be evaluated to determine whether they are prone to indoor noise problems. This evaluation should be consistent with national and local land use planning guidelines. Sites should be investigated to determine past uses and whether any sources of sound remain as a result. The potential for outdoor noise being carried to the site from adjacent areas, such as busy streets, should also be evaluated.

Building design. Buildings should be designed to be soundproof, to improve control over indoor noise. Soundproofing requires that outside noise be prevented from entering the building, and this should be estimated as part of the architectural and engineering design process. When soundproofing for outdoor noise, the total indoor noise load and the desired quality of the indoor space should be considered. Adequate soundproofing against outdoor noise is important in residential as well as commercial properties, and should be re-evaluated when interior spaces are rebuilt or renovated.

Indoor Spaces. The architectural layout should aim to reduce noise and provide a good sound quality to the space. This would include designing indoor spaces to have sufficiently short reverberation times. Designers and contractors should be encouraged to use sound-absorbing materials that lead to lower indoor noise levels, and materials with the best sound-absorbing properties should be specified. However, use of these materials should not be the only solution (Harris 1991). Possible conflicts with other environmental demands should also be identified; for example, the special demands by allergic people.

5.6.3. Indoor noise level control

Building maintenance personnel should be trained to understand the indoor noise aspects of their work, and be aware of how their work can directly impact the health and comfort of occupants. Many maintenance activities directly affect indoor noise levels, and some may indicate potential problems. Preventive maintenance is essential for the building systems to operate correctly and to provide suitable comfort conditions and low indoor noise levels. Detailed maintenance logs should be kept for all equipment. A schedule should be developed for routine equipment checks and calibration of control system components. Selection of low-noise domestic products should encouraged as far as is possible.

5.6.4. Resolving indoor noise problems

Addressing occupant complaints and symptoms. When complaints are received from occupants of a building, the cognizant authority should be responsive. The initial investigation into the cause of the complaint may be conducted by the in-house management staff, and they should continue an investigation as far as possible. If necessary, they should be responsible for hiring an outside consultant

Building diagnostic procedures. After receiving complaints related to indoor noise levels, facility personnel or consultants should attempt to identify the cause of the problem through an iterative process of information collection and hypothesis testing. To begin, a walkthrough inspection of the building, including the affected areas and the mechanical systems serving these spaces is required. A walkthrough can provide information on the soundproofing system of the building, the sound pathways and sound sources. Visual indicators of sound sources and soundproofing malfunctions should be evaluated first. Symptom logs and schedules of building activities may provide enough additional information to resolve the problem.

If a walkthrough alone does not provide a solution, measurements of sound pressure levels at various locations should be taken, and indoor and ambient levels of noise pollution should be compared. As part of the investigation, the absorption characteristics of walls and ceilings should be evaluated. Sophisticated sampling methods may be necessary to provide proof of a problem to the building owner or other responsible party. The results may be used to confirm a hypothesis or ascertain the source of the indoor noise problem. Whenever a problem is discovered during the investigation, a remedy to the situation should be attempted and a determination made of whether the complaint has been resolved.

In some cases, it should be recognized that difficulties in interpreting the sampling results may exist. The costs of certain types of testing should also be taken into account. Simple, cost-effective screening methods should be developed to make sampling a more attractive option for both investigators and clients. Finally, it must be remembered that several factors cause symptoms similar to those induced by noise pollution. Examples include air pollutants, ergonomics, lighting, vibration and psychosocial factors. Consequently, any investigation of noise complaints should also evaluate non-noise factors.

5.7. Priority Setting in Noise Management

Priorities in noise management will differ between countries, according to policy objectives, needs and capabilities. Priority setting in noise management refers to prioritizing health risks and concentrating on the most important sources of noise. For effective noise management, the goals, policies and noise control schemes have to be defined. Goals for noise management include eliminating noise, or reducing noise to acceptable levels, and avoiding the adverse health effects of noise on human health. Policies for noise management encompass laws and regulations for setting noise standards and for ensuring compliance. The amount of information to be included in low-noise implementation plans and the use of cost-benefit comparisons also fall within the purview of noise management policies. Techniques for noise control include source control, barriers in noise pathways and receiver protection. Adequate calculation models for noise propagation, as well as programmes for noise monitoring, are part of an overall noise control scheme.

As emphasized above, a framework for a political, regulatory and administrative approach is required to guarantee the consistent and transparent promulgation of noise standards. This ensures a sound and practical framework for risk-reducing measures and for the selection of abatement strategies.

5.7.1. Noise policy and legislation

Noise is both a local and a global problem. Governments in every country have a responsibility to set up policies and legislation for controlling community noise. There is a direct relationship between the level of development in a country and the degree of noise pollution impacting its people. As a society develops, it increases its level of urbanization and industrialization, and the extent of its transportation system. Each of these developments brings an increase in noise load. Without appropriate intervention the noise impact on communities will escalate (see Figure 5.3). If governments implement only weak noise policies and regulations, they will not be able to prevent a continuous increase in noise pollution and associated adverse health effects. Failure to enforce strong regulations is ineffective in combating noise as well.

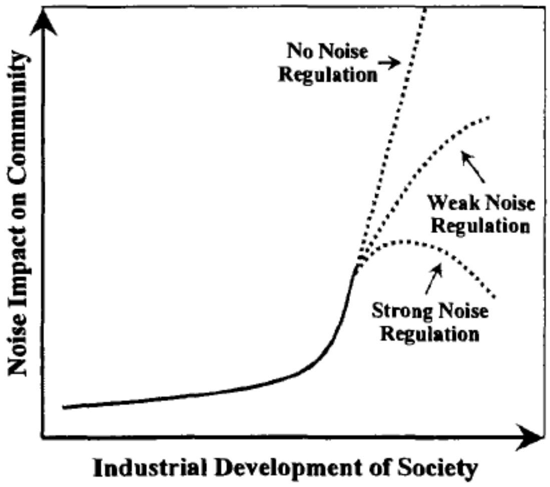

Figure 5.3. Relationship between noise regulation and impact with development (from Hede 1998b)

Policies for noise regulatory standards at the municipal, regional, national and supranational levels are usually determined by the legislatures. The regulatory standards adopted strongly depend on the risk management strategies of the legislatures, and can be influenced by sociopolitical considerations and/or international agreements. Although regulatory standards may be country specific, in general the following issues are taken into consideration:

a. Identification of the adverse public health effects that are to be avoided.

b. Identification of the population to be protected.

c. The type of parameters describing noise and the limit applicable to the parameters.

d. Applicable monitoring methodology and its quality assurance.

e. Enforcement procedures to achieve compliance with noise regulatory standards within a defined time frame.

f. Emission control measures and emission regulatory standards.

g. Immission standards (limits for sound pressure levels).

h. Identification of authorities responsible for enforcement.

i. Resource commitment.

Regulatory standards may be based solely on scientific and technical data showing the adverse effects of noise on public health. But other aspects are usually considered, either when setting standards or when designing appropriate noise abatement measures. These other aspects include the technological feasibility, costs of compliance, prevailing exposure levels, and the social, economic and cultural conditions. Several standards may be set. For example, effect-oriented regulatory standards may be set as a long-term goal, while less-stringent standards are adopted for the short term. As a consequence, noise regulatory standards differ widely from country to country (WHO 1995a; Gottlob 1995).

Noise regulatory standards can set the reference point for emission control and abatement policies at the national, regional or municipal levels, and can thus strongly influence the implementation of noise control policies. In many countries, exceeding regulatory standards is linked to an obligation to develop abatement action plans at the municipal, regional or national levels (low-noise implementation plans). Such plans have to address all relevant sources of noise pollution.

5.7.2. Examples of noise policies

Different countries have adopted a range of policies and regulations for noise control. A number of these are outlined in this section as examples.

Argentina. In Argentina, a national law recently limited the daily 8-h exposure to industrial noise to 80 dB, and it has had beneficial effects on hearing impairment and other hearing disorders among workers. In general, industry has responded by introducing constant controls on noise sources, combined with hearing tests and medical follow-ups for workers. Factory owners have recruited permanent health and safety engineers who control noise, supply advice on how to make further improvements, and routinely assess excessive noise levels. The engineers also provide education in personal protection and in the correct use of ear plugs, mufflers etc.

At the municipal level two types of noise have been considered. Unnecessary noise, which is forbidden; and excessive noise, which is defined for neighbourhood activities (zones), and for which both day and night-time maximum limits have been introduced. The results have been relatively successful in mitigating unwanted noise effects. At the provincial level, similar results have been accomplished for many cities in Argentina and Latin America.

Australia. In Australia, the responsibility for noise control is shared primarily by state and local governments. There are nationally-agreed regulatory standards for airport planning and new vehicle noise emissions. The Australian Noise Exposure Forecast (ANEF) index is used to describe how much aircraft noise is received at locations around an airport (DoTRS 1999). Around all airports, planning controls restrict the construction of dwellings within the 25 ANEF exposure contour and require sound insulation for those within 20 ANEF. Road traffic noise limits are set by state governments, but vary considerably in both the exposure metric and in maximum allowable levels. New vehicles are required to comply with stringent design rules for noise and air emissions. For example, new regulation in New South Wales adopts LAeq as the metric and sets noise limits of 60 dBA for daytime, and 55 dBA for night-time, along new roads. Local governments set regulations restricting noise emissions for household equipment, such as air conditioners, and the hours of use for noisy machines such as lawn mowers.

Europe. In Europe, noise legislation is not generally enforced. As a result, environmental noise levels are often higher than the legislated noise limits. Moreover, there is a gap between long-term political goals and what represents a "good acoustical environment". One reason for this gap is that noise pollution is most commonly regulated only for new land use or for the development of transportation systems, whereas enlargements at existing localities may be approved even though noise limits or guideline values are already surpassed (Gottlob 1995). A comprehensive overview of the noise situation in Europe is given in the Green Paper (EU 1996b), which was established to give noise abatement a higher priority in policy making. The Green Paper outlines a new framework for noise policy in Europe with the following options for future action:

a. Harmonizing the methods for assessing noise exposure, and encouraging the exchange of information among member states.

b. Establishing plans to reduce road traffic noise by applying newer technologies and fiscal instruments.

c. Paying more attention to railway noise in view of the future extension of rail networks.

d. Introducing more stringent regulation on air transport and using economic instruments to encourage compliance.

e. Simplifying the existing seven regulations on outdoor equipment by proposing a Framework Directive that covers a wider range of equipment, including construction machines and others.

Pakistan. In Pakistan, the Environmental Protection Agency is responsible for the control of air pollution nationwide. However, only recently have controls been enforced in Sindh in an attempt to raise public awareness and carry out administrative control on road vehicles producing noise (Zaidi, personal communication).

South Africa. In South Africa, noise control is three decades old. It began with codes of practice issued by the South African Bureau of Standards to address noise pollution in various sectors of the country (e.g. see SABS 1994 1996; and the contribution of Grond in Appendix 2). In 1989, the Environment Conservation Act made provision for the Minister of Environmental Affairs and Tourism to make regulations for noise, vibration and shock (DEAT 1989). These regulations were published in 1990 and local authorities could apply to the Minister to make them applicable in their areas. Later, the act was changed to make it obligatory for all authorities to apply the regulations. However, according to the new Constitution of South Africa of 1996, legislative responsibility for noise control rests exclusively with provincial and local authorities. The noise control regulations will apply to local authorities in South Africa as soon as they are published in the provinces. This will not only give local authorities the power to enforce the regulations, but also place an obligation on them to see that the regulations are enforced.

Thailand. In 1996, noise pollution regulations in Thailand stipulated that not more than 70 dBA LAeq,24h should be allowed in residential areas, and the maximum level of noise in industry should be no more than 85 dBA Leq 8h (Prasansuk 1997).

United States of America. Environmental noise was not addressed as a national policy issue in the USA until the implementation of the Noise Control Act of 1972. This congressional act directed the US Environmental Protection Agency to publish scientific information about noise exposure and its effects, and to identify acceptable levels of noise exposure under various conditions. The Noise Control Act was supposed to protect the public health and well-being with an adequate margin of safety. This was accomplished in 1974 with the publication of the US EPA "Levels Document" (US EPA 1974). It addressed issues such as the use of sound descriptions to describe sound exposure, the identification of the most important human effects resulting from noise exposure, and the specification of noise exposure criteria for various effects. Subsequent to the publication of the US EPA "Levels Document", guidelines for conducting environmental impact analysis were developed (Finegold et al. 1998). The day-night average sound level was thus established as the predominant sound descriptor for most environmental noise exposure.

It is evident from these examples that noise policies and regulations vary considerably across countries and regions. Moves towards global noise policies need to be encouraged to ensure that the world population gains the maximum health benefits from new developments in noise control.

5.7.3. Noise emission standards have proven to be inadequate

Much of the progress towards solving the noise pollution problem has come from advanced technology, which in turn has come about mainly as a result of governmental regulations (e.g. OECD-ECMT 1995). So far, however, the introduction of noise emission standards for vehicles has had limited impact on exposure to transportation noise, especially from aircraft and road traffic noise (Sandberg 1995). In part, this is because changes in human behaviour (of polluters, planners and citizens) have tended to offset some of the gains made. For example, mitigation efforts such as developing quieter vehicles, moving people to less noise-exposed areas, improving traffic systems and direct noise abatement and control (sound insulation, barriers etc.), have been counteracted by increases in the number of roads and highways built, by the number of traffic movements, and by higher driving speeds and the number of kilometers driven (OECD 1991; OECD-ECMT 1995).

Traffic planning and correction policies may diminish the number of people exposed to the very high community noise levels (>70 dB LAeq), but the number exposed to moderately high levels (55-65 dB LAeq) continues to increase in industrialized countries (Stanners & Bordeau 1995). In developing countries, exposure to excessive sound pressure levels (>85 dB LAeq), not only from occupational noise but also from urban, environmental noise, is the major avoidable cause of permanent hearing impairment (Smith 1998). Such sound pressure levels can also be reached by leisure activities at concerts, discotheques, motor sports and shooting ranges; by music played back in headphones; and by impulse noises from toys and fireworks.

A substantial growth in air transport is also expected in the future. Over the next 10 years large international airports may have to accommodate a doubling in passenger movements. General aviation noise at regional airports is also expected to increase (Large & House 1989). Although jet aircraft are expected to become less noisy due to regulation of noise emissions (ICAO 1993), the number of passengers is expected to increase. Increased air traffic movement between 1980 and 1990 is considered to be the main reason for the average 22% increase in the number of people exposed to noise above 67 dB LAeq at German airports (OECD 1993).

5.7.4. Unsustainable trends in noise pollution future policy planning

A number of trends are expected to increase environmental noise pollution, and are considered to be unsustainable in the long term. The OECD (1991) identified the following factors to be of increasing importance in the future:

a. The expanding use of increasingly powerful sources of noise.

b. The wider geographical dispersion of noise sources, together with greater individual mobility and spread of leisure activities.

c. The increasing invasion of noise, particularly into the early morning, evenings and weekends.

d. The increasing public expectations that are closely linked to increases in incomes and in education levels.

Apart from these, increased noise pollution is also linked to systemic changes in business practices (OECD-ECMT 1995). By accepting a just-in-time concept in transportation, products and components are stored in heavy-duty vehicles on roads, instead of in warehouses; and workers are recruited as temporary consultants just in time for the work, instead of as long-term employees.

In addition, the OECD (1991) report forecasts:

a. A strengthening of present noise abatement policies and their applications.

b. A further sharpening of emission standards.

c. A co-ordination of noise abatement measures and transport planning, to specifically reduce mobility.

d. A co-ordination of noise abatement measures with urban planning.

Planners need to know the likely effects of introducing a new noise source, or of increasing the level of an existing source, on the noise pollution in a community. Policy makers, when considering applications for new developmental projects, must take into account maximum levels, continuous equivalent sound pressure levels of both the background and the new noise source, the frequency of noise occurrence and the operating times of major noise sources.

5.7.5. Analysis of the impact of environmental noise

The concept of an environmental noise impact analysis (ENIA) is central to the philosophy of managing environmental noise. An ENIA should be required before implementing any project that would significantly increase the level of environmental noise in a community (typically, greater than a 5dB increase). The first step in performing an ENIA is to develop a baseline description of the existing noise environment. Next, the expected level of noise from a new source is added to the baseline exposure level to produce the new overall noise level. If the new total noise level is expected to cause an unacceptable impact on human health, trade-off analyses should then be performed to assess the cost, technical feasibility and community acceptance of noise mitigation measures. It is strongly recommended that countries develop standardized procedures for performing ENIAs (Finegold et al. 1998; SABS 1998).

Assessment of adverse health effects. In setting noise standards (for example on the basis of these guidelines), the adverse health effects from which the population is to be protected need to be defined. Health effects range from hearing impairment to sleep disturbance, speech interference to annoyance. The distinction between adverse and non-adverse effects sometimes poses considerable difficulties. Even the elaborate definition of an adverse health effect given in Chapter 3 incorporates significant subjectivity and uncertainty. More serious noise effects, such as hearing impairment or permanent threshold shift, are generally accepted as adverse. Consideration of health effects that are both temporary and reversible, or that involve functional changes with uncertain clinical significance, requires a judgement on whether these less-serious effects should be considered when deriving guideline values. Judgements as to the adversity of health effects may differ between countries, because of factors such as cultural backgrounds and different levels of health status.

Estimation of the population at risk. The population at risk is that part of the population in a given country or community that is exposed to enhanced levels of noise. Each population has sensitive groups or subpopulations that are at higher risk of developing health effects due to noise exposure. Sensitive groups include individuals impaired by concurrent diseases or other physiological limitations and those with specific characteristics that makes them more vulnerable to noise (e.g. premature babies; see the contribution of Zaidi in Appendix 2). The sensitive groups in a population may vary across countries due to differences in medical care, nutritional status, lifestyle and demographic factors, prevailing genetic factors, and whether endemic or debilitating diseases are prevalent.

Calculation of exposure-response relationships. In developing standards, regulators should consider the degree of uncertainty in the exposure-response relationships provided in the noise guidelines. Differences in the population structure (age, health status), climate (temperature, humidity) and geography (altitude, environment) can influence the prevalence and severity of noise-related health effects. In consequence, modified exposure-response relationships may need to be applied when setting noise standards.

Assessment of risks and their acceptability. In the absence of distinct thresholds for the onset of health effects, regulators must determine what constitutes an acceptable health risk for the population and select an appropriate noise standard to protect public health. This is also true in cases where thresholds are present, but where it would not be feasible to adopt noise guidelines as standards because of economical and/or technical constraints. The acceptability of the risks involved, and hence the standards selected, will depend on several factors. These include the expected incidence and severity of the potential effects, the size of the population at risk, the perception of related risks, and the degree of scientific uncertainty that the effects will occur at any given noise level. For example, if it is suspected that a health effect is severe and the size of the population at risk is large, a more cautious approach would be appropriate than if the effect were less troubling, or if the population were smaller.

Again, the acceptability of risk may vary among countries because of differences in social norms, and the degree of adversity and risk perception by the general population and stakeholders. Risk acceptability is also influenced by how the risks associated with noise compare with risks from other pollution sources or human activities.

5.7.6. Cost-benefit analysis

In the derivation of noise standards from noise guidelines two different approaches for decision making can be applied. Decisions can be based purely on health, cultural and environmental consequences, with little weight to economic efficiency. This approach has the objective of reducing the risk of adverse noise effects to a socially acceptable level. The second approach is based on a formal cost-effectiveness, or cost-benefit analysis (CBA). The objective is to identify control actions that achieve the greatest net economic benefit, or are the most economically efficient. The development of noise standards should account for both extremes, and involve stakeholders and assure social equity to all the parties involved. It should also provide sufficient information to guarantee that stakeholders understand the scientific and economic consequences.

To determine the costs of control action, the abatement measures used to reduce emissions must be known. This is usually the case for direct measures at the source and these measures can be monetarized. Costs of action should include all costs of investment, operation and maintenance. It may not be possible to monetarize indirect measures, such as alternative traffic plans or change in behaviour of individuals.

The steps in a cost-benefit analysis include:

a. The identification and cost analysis of control action (such as emission abatement strategies and tactics).

b. An assessment of noise and population exposure, with and without the control action.

c. The identification of benefit categories, such as improved health and reduced property loss.

d. A comparison of the health effects, with and without control action.

e. A comparison of the estimated costs of control action with the benefits that accrue from such action.

f. A sensitivity and uncertainty analysis.

Action taken to reduce one pollutant may increase or decrease the concentration of other pollutants. These additional effects should be considered, as well as pollutant interactions that may lead to double counting of costs or benefits, or to disregarding some costly but necessary action. Due to different levels of knowledge about the costs of control action and health effects, there is a tendency to overestimate the cost of control action and underestimate the benefits.

CBA is a highly interdisciplinary task. Appropriately applied, it is a legitimate and useful way of providing information for managers who must make decisions that impact health. CBA is also an appropriate tool for drawing the attention of politicians to the benefits of noise control. In any case, however, a CBA should be peer-reviewed and never be used as the sole and overriding determinant of decisions.

5.7.7. Review of standard setting

The setting of standards should involve stakeholders at all levels (industry, local authorities, non-governmental organizations and the general public), and should strive for social equity or fairness to all parties involved. It should also provide sufficient information to guarantee that the scientific and economic consequences of the proposed standards are clearly understood by the stakeholders. The earlier that stakeholders are involved, the more likely is their co-operation. Transparency in moving from noise guidelines to noise standards helps to increase public acceptance of necessary measures. Raising public awareness of noise-induced health effects (changing of risk perception) also leads to a better understanding of the issues involved (risk communication) and serves to obtain public support for necessary control action, such as reducing vehicle emissions. Noise standards should be regularly reviewed, and revised as new scientific evidence emerges.

5.7.8. Enforcement of noise standards: Low-noise implementation plans

The main objective of enforcing noise standards is to achieve compliance with the standards. The instrument used to achieve this goal is a Low-Noise Implementation Plan (LNIP). The outline of such a plan should be defined in the regulatory policies and should use the tactical instruments discussed above. A typical low-noise implementation plan includes:

a. A description of the area to be regulated.

b. An emissions inventory.

c. A monitored or simulated inventory of noise levels.

d. A comparison of the plan with emissions and noise standards or guidelines.

e. An inventory of the health effects.

f. A causal analysis of the health effects and their attribution to individual sources.

g. An analysis of control measures and their costs.

h. An analysis of transportation and land-use planning.

i. Enforcement procedures.

j. An analysis of the effectiveness of the noise management procedures.

k. An analysis of resource commitment.

l. Projections for the future.

As the LNIP also addresses the effectiveness of noise control technologies and policies, it is very much in line with the Noise Control Assessment Programme (NCAP) proposed recently (Finegold et al. 1999).

5.8. Conclusions on Noise Management

Successful noise management should be based on the fundamental principles of precaution, the polluter pays and prevention. The noise abatement strategy typically starts with the development of noise standards or guidelines, and the identification, mapping and monitoring of noise sources and exposed communities. A powerful tool in developing and applying the control strategy is to make use of modeling. These models need to be validated by monitoring data. Noise parameters relevant to the important sources of noise must be known. Indoor noise exposures present specific and complex problems, but the general principles for noise management hold. The main means for noise control in buildings include careful site investigations, adequate building designs and building codes, effective means for addressing occupant complaints and symptoms, and building diagnostic procedures.

Noise control should include measures to limit the noise at the source, to control the sound transmission path, to protect the receiver's site, to plan land use, and to raise public awareness. With careful planning, exposure to noise can be avoided or reduced. Control options should take into account the technical, financial, social, health and environmental factors of concern. Cost-benefit relationships, as well as the cost-effectiveness of the control measures, must be considered in the context of the social and financial situation of each country. A framework for a political, regulatory and administrative approach is required for the consistent and transparent promulgation of noise standards. Examples are given for some countries, which may guide others in their development of noise policies.

Noise management should:

a. Start monitoring human exposures to noise.

b. Have health control require mitigation of noise emissions. The mitigation procedures should take into consideration specific environments such as schools, playgrounds, homes and hospitals; environments with multiple noise sources, or which may amplify the effects of noise; sensitive time periods, such as evenings, nights and holidays; and groups at high risk, such as children and the hearing impaired.

c. Consider noise consequences when making decisions on transport-system and land-use planning.

d. Introduce surveillance systems for noise-related adverse health effects.

e. Assess the effectiveness of noise policies in reducing noise exposure and related adverse health effects, and in improving supportive "soundscapes."

a. Adopt these Guidelines for Community Noise as long-term targets for improving human health.

g. Adopt precautionary actions for sustainable development of acoustical environments.

6. Conclusions And Recommendations

6.1. Implementation of the Guidelines

The potential health effects of community noise include hearing impairment; startle and defense reactions; aural pain; ear discomfort speech interference; sleep disturbance; cardiovascular effects; performance reduction; and annoyance responses. These health effects, in turn, can lead to social handicap; reduced productivity; decreased performance in learning; absenteeism in the workplace and school; increased drug use; and accidents. In addition to health effects of community noise, other impacts are important such as loss of property value. In these guidelines the international literature on the health effects of community noise was reviewed and used to derive guideline values for community noise. Besides the health effects of noise, the issues of noise assessment and noise management were also addressed. Other issues considered were priority setting in noise management; quality assurance plans; and the cost-efficiency of control actions. The aim of the guidelines is to protect populations from the adverse health impacts of noise.

The following recommendations were considered appropriate:

a. Governments should consider the protection of populations from community noise as an integral part of their policy for environmental protection.

b. Governments should consider implementing action plans with short-term, medium-term and long-term objectives for reducing noise levels.

c. Governments should adopt the health guidelines for community noise as targets to be achieved in the long-term.

h. Governments should include noise as an important issue when assessing public health matters and support more research related to the health effects of noise exposure.

f. Legislation should be enacted to reduce sound pressure levels, and existing legislation should be enforced.

g. Municipalities should develop low-noise implementation plans.

h. Cost-effectiveness and cost-benefit analyses should be considered as potential instruments when making management decisions.

i. Governments should support more policy-relevant research into noise pollution (see section 6.3).

6.2. Further WHO Work on Noise

The WHO Expert Task Force proposed several issues for future work in the field of community noise. These are:

a. The WHO should consider updating the guidelines on a regular basis.

b. The WHO should provide leadership and technical direction in defining future research priorities into noise.

c. The WHO should organize workshops on the application of the guidelines.

d. The WHO should provide leadership and co-ordinate international efforts to develop techniques for the design of supportive sound environments (e.g. 'soundscapes").

e. The WHO should provide leadership for programmes to assess the effectiveness of health-related noise policies and regulations.

f. The WHO should provide leadership and technical direction for the development of sound methodologies for EIAP and EHIAP.

g. The WHO should encourage further investigation into using noise exposure as an indicator of environmental deterioration, such as found in black spots in cities.

a. The WHO should provide leadership, technical support and advice to developing countries, to facilitate the development of noise policies and noise management.

6.3. Research Needs

In the publication entitled "Community Noise", examples of essential research and development needs were given (Berglund & Lindvall 1995). In part, the scientific community has already addressed these issues.

A major step forward in raising public awareness and that of decision makers is the recommendation of the present Expert Task Force to concentrate more **on variables which have monetary consequences. This means that research should consider the dose-response relationships between sound pressure levels and politically relevant variables, such as noise-induced social handicap, reduced productivity, decreased performance in learning, workplace and school absenteeism, increased drug use and accidents.**

There is also a need for continued efforts to understand community noise and its effects on the health of the world population. Below is a list of essential research needs in non-prioritized order. Research priorities may vary over time and by place and capabilities. The main goal in suggesting these research activities is to improve the scientific basis for policy-making and noise management. This will protect and improve the public health with regard to the effects of community noise pollution.

Research related to measurement and monitoring systems for health effects

- Development of a global noise impact monitoring study. The study should be designed to obtain longitudinal data across countries on the health effects on communities of various types of environmental noise. A baseline survey could be undertaken in both developed and developing countries and monitoring surveys conducted every 3-5 years. Since a national map of noise exposure from all sources would be prohibitively expensive, periodic surveys of a representative sample of about 1000 people (using standard probability techniques) could be reliably generalized to the whole population of a country with an accuracy of plus-or-minus 3%. A small number of standard questions could be used across countries to obtain comparative data on the impact of all the main types of noise pollution.

- Development of continuous monitoring systems for direct health effects in critical locations.
- Development of standardized methods for low-cost assessment of local sound levels by measurement or model calculations.
- Development of instruments appropriate for local/regional surveys of people's perceptions of their noise/sound environments.

- Protocols for reliable measurements of high-frequency hearing (8000 Hz and above) and for evaluation of such measures as early biomarkers for hearing impairment/deficits.

Research related to combined noise sources and combined health effects

- Research into the combined health effects of traffic noise, with emphasis on the distribution of sound levels over time and over population sub-environments (time-activity pattern).
- Comprehensive studies on combined noise sources and their combinations of health effects in the 3 large areas of transport (road, rail and aircraft).
- Procedures for evaluating the various health effects of complex combined noise exposures over 24 hours on vulnerable groups and on the general population.
- Methods for assessing the total health effect from noise immission (and also other pollution) in sensitive areas (for example, airports, city centers and heavily-trafficked highways)

Research related to direct and/or long-term health effects (sensitive risk groups, sensitive areas and combined exposures)

- Identification of potential risk groups, including identification of sensitive individuals (such as people with particular health problems; people dealing with complex cognitive tasks; the blind; the hearing impaired; young children and the elderly), differences between sexes, discrimination of risk among age groups, and influence of transportation noise on pregnancy course and on fetal development.
- Studies of dose-response relationships for various effects, and for continuous transportation noise at relatively low levels of exposure and low number of noise events per unit time (including traffic flow composition).
- Studies on the perception of control of noise exposure, genetic traits, coping strategies and noise annoyance as modifiers of the effects of noise on the cardiovascular system, and as causes of variability in individual responses to noise.
- Prospective longitudinal studies of transportation noise that examine physiological measures of health, including standardized health status inventory, blood pressure, neuro-endocrine and immune function.
- Knowledge on the health effects of low-frequency components in noise and vibration.
-

Research related to indirect or after-effects of noise exposure

- Field studies on the effects of exposure to specific sounds such as aircraft noise and loud music, including effects such as noise-induced temporary and permanent threshold shifts, speech perception and misperception, tinnitus and information retrieval.
- Studies on the influence of noise-induced sleep disturbance on health, work performance, accident risk and social life.
- Assessment of dose-response relationships between sound levels and politically relevant variables such as noise-induced social handicap, reduced productivity, decreased performance in learning, workplace and school absenteeism, increased drug use and accidents.
- Determination of the causal connection between noise and mental health effects, annoyance and (spontaneous) complaints in areas such as around large airports, heavy-trafficked highways, high-speed rail tracks and heavy vehicles transit routes. The connections could be examined by longitudinal studies, for example.
- Studies on the impact of traffic noise on recovery from noise-related stress, or from nervous system hyperactivity due to work and other noise exposures.

Research on the efficiency of noise abatement policies which are health based

- Determination of the accuracy and effectiveness of modern sound insulation (active noise absorption), especially in residential buildings, in reducing the long-term effects of noise on annoyance/sleep disturbance/speech intelligibility. This can be accomplished by studying sites that provide data on remedial activities and changes in behavioral patterns among occupants.
- Evaluation of environmental (area layout, architecture) and traffic planning (e.g. rerouting) interventions on annoyance, speech interference and sleep disturbance.
- Comparative studies to determine whether children and the hearing impaired have equitable access to healthier lives when compared with normal adults in noise-exposed areas.
- Development of a methodology for the environmental health impact assessment of noise that is applicable in developing as well as developed countries.

Research into positive acoustical needs of the general population and vulnerable groups

- Development of techniques/protocols for the design of supportive acoustical environments for the general population and for vulnerable groups. The protocols should take into account time periods that are sensitive from physiological, psychological and socio-cultural perspectives.
- Studies to characterize good "restoration areas" which provide the possibility for rest without adverse noise load.
- Studies to assess the effectiveness of noise policies in maintaining and improving soundscapes and reducing human exposures.

Appendix 1 : Bibliographical References

AAP 1997 Noise: A hazard for the fetus and newborn. American Academy of Pediatrics. Committee on Environmental Health. Pediatrics 100: 724-27.

Altena K 1987 Medische gevolgen van lawaai. Report GA-HR-03-01, Ministerie van Volkshuisvesting, Ruimtelijke Ordening en Milieu, Den Haag, Netherlands.

ANSI 1994 American National Standard Acoustical Terminology. ANSI S.1.-1994, American National Standards Institute, Inc., New York, NY, USA.

ANSI 1995 American National Standard Bioacoustical Terminology. ANSI S3.20-1995, American National Standards Institute, Inc., New York, NY, USA.

ANSI 1997 Methods for the Calculation of the Speech Intelligibility Index, American National Standard 3.5, American National Standard Institute, New York, NY, USA.

ASTM 1992 Standard Guide for Field Measurement of Airborne Sound Insulation of Building Facades and Facade Elements, ASTM E966, American Society For Testing and Materials, Philadelphia, West Conshohocken, PA, USA.

ASTM 1994a Classification of Rating Sound Insulation, ASTM E413, American Society For Testing and Materials, Philadelphia, PA, USA .

ASTM 1994b Standard Classification for Determination of Outdoor-Indoor Transmission Class, ASTM E1332, American Society For Testing and Materials, Philadelphia, PA, USA.

ASTM 1994c Standard Classification for Determination of Impact Insulation Class (IIC), ASTM E989, American Society For Testing and Materials, Philadelphia, PA, USA.

ASTM 1996 Standard Test Method for Laboratory Measurement of Impact Sound Transmission through Floor-ceiling Assemblies using the Tapping Machine, ASTM E492, American Society For Testing and Materials, Philadelphia, PA, USA.

ASTM 1997 Standard Test Method for Laboratory Measurement of Airborne Sound Transmission Loss of Building Partitions and Elements, ASTM E90, American Society For Testing and Materials, Philadelphia, PA, USA .

Axelsson A, Arvidson I, Jerson T 1986 Hearing in fishermen and coastguards. In R.J. Salvi, D. Henerson, R.P. Hamernik and V. Colletti (eds.), Basic and Applied Aspects of Noise-Induced Hearing Loss, pp. 513-20. Plenum Press, New York.

Axelsson A and Prasher DK 1999. Tinnitus: A warning signal to teenagers attending discotheques? Noise & Health 2: 1-2.

Babisch W 1998a Epidemiological studies on cardiovascular effects of traffic noise. In D. Prasher, D. and L. Luxon, L. (eds.) Advances in Noise Series, Vol. I: Biological Effects, pp. 312-327. Whurr Publishers, London, UK.

Babisch W 1998b Epidemiological studies of cardiovascular effects of traffic noise. In N.L. Carter and R.F.S. Job (eds.) Noise as a Public Health Problem (Noise Effects '98), Vol. 1, pp. 221-229. Noise Effects '98 PTY Ltd., Sydney, Australia.

Babisch W and Ising H 1989 Zum Einfluss von Musik in Diskotheken auf die Hörfähigkeit von Jugendlichen. Sozial- und Präventivmedizin 34: 239-243.

Babisch W, Ising H, Gallacher JEJ, Sweetnam PM, Elwood PC 1998 The Caerphilly and Speedwell studies, 10 year follow up. In N.L. Carter and R.F.S. Job (eds.) Noise as a Public Health Problem (Noise Effects '98), Vol. 1, pp. 230-35. Noise Effects '98 PTY Ltd., Sydney, Australia.

Babisch W, Ising H, Gallacher JE, Sweetnam PM, Elwood PC 1999 Traffic noise and cardiovascular risk: The Caerphilly and Speedwell studies, third phase 10-year follow up. Archives of Environmental Health 54: 210-216.

Beersma DGM and Altena K 1995 Critical evaluation of the 1992 report of a field study of aircraft noise and sleep disturbance. Newsletter of the European Sleep Research Society 1: 5-7.

Bendat JS and Piersol AG 1971 Random Data: Analysis and Measurement Procedures. Wiley, New York, USA.

Beranek LL 1971 Noise and Vibration Control. McGraw Hill, New York, USA.

Beranek LL 1989 Balanced Noise Criterion (NCB) Curves. Journal of the Acoustical Society of America 86: 650-664.

Berglund B 1998 Community noise in a public health perspective In V.C. Goodwin and D.C. Stevenson (eds.) Inter Noise 98. Sound and Silence: Setting the Balance, Vol. 1, pp. 19-24. New Zealand Acoustical Society, Auckland, New Zealand.

Berglund B, Hassmén P, Job RFS 1996 Sources and effects of low-frequency noise. Journal of the Acoustical Society of America, 99: 2985-3002.

Berglund B and Lindvall T (Eds.) 1995 Community Noise. Document prepared for the World Health Organization. Archives of the Center for Sensory Research, 2: 1-195. A reprint of this document with corrections of language and references has been published in 1998. The 1995 document can be addressed on the Internet address www.who.int/peh/.

Berglund B and Nilsson ME 1997 Empirical issues concerning annoyance models for combined community noise. In F. Augustinovicz (ed.) Inter Noise 97. Help Quiet the World for a Higher Quality Life, Vol. 2, pp. 1053-58. Noise Control Foundation, Poughkeepsie, NY, USA.

Berglund B, Berglund U, Lindvall T 1976 Scaling loudness, noisiness and annoyance of community noise. Journal of the Acoustical Society of America 60: 1119-1125.

Berglund B, Berglund U, Lindberg S 1986 Loudness of impulse sound from different weapons. In R. Lutz (ed.) Inter Noise '86, Vol. II, pp. 815-20. Noise Control Foundation, New York, USA..

Berry BF 1995 Towards a standardised descriptor of impulsive noise caused by low-altitude military aircraft". In R.J. Bernhard and S. Bolton (ed.) Inter Noise '95, Vol. 2, pp. 879-884. Noise Control Foundation, Poughkeepsie, NY, USA

Bishop DE and Horonjef RD 1967 Procedures for Developing Noise Exposure Forecast Areas for Aircraft Flight Operations. FAA Report DS-67-10 (August 1967), Washington DC, USA.

Blazier WE 1998 RC Mark II: A refined procedure for rating the noise of heating, ventilating, and air-conditioning (HVAC) systems in buildings. Noise Control Engineering Journal 45: 243-250.

Bradley JS 1978 Predictors of Adverse Human Responses to Traffic Noise. Proceedings of the ASTM Symposium on Community Noise, Kansas City, pp. 108-123.

Bradley JS 1985 Uniform derivation of optimum conditions for speech in rooms. National Research Council, Building Research Note, BRN 239, Ottawa, Canada.

Bradley JS 1986a Predictors of Speech Intelligibility in Rooms. Journal of the Acoustical Society of America 80: 837-845.

Bradley JS 1986b Speech Intelligibility Studies in Classrooms. Journal of the Acoustical Society of America 80: 846-854.

Bradley JS 1986c Optimum Conditions for Speech in Rooms. Proceedings of the 12th International Congress on the Acoustics, Paper E10-5, Toronto, Canada.

Bradley JS 1993 Disturbance Caused by Residential Air Conditioner Noise. Journal of the Acoustical Society of America 93: 1978-1986.

Bradley JS 1994a On dose response curves of annoyance to aircraft noise. In S. Kuwano (Ed.), Inter-Noise 94. Noise Quantity and Quality, Vol 1, pp. 235-38. Noise Control Foundation, Poughkeepsie, NY, USA.

Bradley JS 1994b Annoyance Caused by Constant-Amplitude and Amplitude- Modulated Sounds Containing Rumble. Noise Control Engineering Journal 42: 203-208.

Bradley, J.S. 1996. Determining acceptable limits for aviation noise. In F.A. Hill and R. Lawrence (eds.) Inter Noise 96, Noise Control – The Next 25 Years, Book 5, pp. 2541-46. Institute of Acoustics, St Albans, UK.

Bradley JS, Vaskor JG, Dickinson SM 1979 The Effect of Skewness and Standard Deviation on Sampling Errors for Traffic Noise. Applied Acoustics 12: 397-409.

Broner N and Leventhall HG 1993 A Modified PNdB for Assessment of Low Frequency Noise. Journal of Sound and Vibration 73: 425-444.

Brookhouser PE, Worthington DW, Kelly WJ 1992 Noise-induced hearing loss in children. Laryngoscope 1992; 102: 645-655.

Brown AL 1994 Exposure of the Australian population to road traffic noise. Applied Acoustics, 43: 169-176.

Buchta E 1996 A field study on annoyance caused by shooting noise – Determination of the penalty for various weapon calibers. . In F.A. Hill and R. Lawrence (eds.) Inter Noise 96, Noise Control – The Next 25 Years, Book 5, pp. 2495-2500. Institute of Acoustics, St Albans, UK.

Bullen RB and Hede AJ 1983 Time of Day Corrections in Measures of Aircraft Noise Exposure. Journal of the Acoustical Society of America 73: 1624-1630.

Burns W 1968 Noise and Man. John Murray, London, UK.

Carter NL 1996 Transportation noise, sleep, and possible after-effects. Environment International 22: 105-116.

Carter NL and Hunyor SN 1991 A field study of traffic noise and cardiac arrythmia during sleep. In: Technical Papers: 4th Western Pacific Regional Acoustics Conference, pp. 165-172, Queensland Department of Environment and Heritage, Brisbane, Australia.

Carter NL, Hunyor SN, Crawford G, Kelly D, Smith AJ 1994a Environmental noise and sleep - a study of arousals, cardiac arrhytmia and urinary catecholamines. Sleep 17: 298-307.

Carter NL, Ingham P, Tran K, Huynor S 1994b A field study of the effects of traffic noise on heart rate and cardiac arrhythmia during sleep. Journal of Sound and Vibration, 169, 221-227.

CEC 1992a Towards Sustainability: A European Community Programme of Policy and Action in Relation to the Environment and Sustainable Development. COM (92) 23 Final – Vol. II. Office for Official Publications of the European Communities, Luxembourg.

CEC 1992b The Impact of Transport on the Environment: A Community Strategy for "Sustainable Mobility". COM (92) 46 Final. Office for Official Publications of the European Communities, Luxembourg..

CEC 1996. Future Noise Policy. European Commission Green Paper. COM(96) 540 Final Office for Official Publications of the European Communities, Luxembourg.

Chakrabarty D, Santra SC, Mukherjee, A 1997: Status of road traffic noise in Calcutta metropolis, India. Journal of the Acoustical Society of America 101: 943-949.

CMD (1997) Taber's Cyclopedic Medical Dictionary, edition 18, FA Davis Company, Philadelphia.

Cohen S 1980 Aftereffects of stress on human performance and social behavior: A review of research and theory. Psychological Bulletin, 88: 82-108.

Cohen S, Evans GW, Krantz DS, Stokols D 1980 Physiological, motivational, and cognitive effects of aircraft noise on children. American Psychologist 35: 231-243.

Cohen S, Evans GW, Stokols D, Krantz DS 1986 Behavior, Health and Environmental Stress. Plenum Press, New York.

Crocker MJ and Price AJ 1975 Noise and Noise Control. Volume I, CRC Press, Cleveland USA.

Daigle GA, Embleton TFW, Piercy JE 1986 Propagation of Sound In the Presence of Gradients and Turbulence Close to the Ground. Journal of the Acoustical Society of America 79: 613-627.

DEAT 1989 Environment Conservation Act (Act No. 73 of 1989) Noise Control Regulations, Ministry of Environmental Affairs and Tourism, Pretoria, South Africa.

DeKoning HW 1987 Setting Environmental Standards. Guidelines for Decision-Making. World Health Organization, Geneva, Switzerland.

DIMD 1985 Dorland's illustrated medical dictionary, 26th edition, Saunders, Philadelphia [etc.], USA

DiMento JS 1981 Making usable information on environmental stressors: Opportunities for the research and policy communities. Journal of Social Issues 37:172-204.

DoTRS 1999 What is an ANEF? Commonwealth of Australia 1999, Department of Transport and Regional Services. Internet address:
http://www.dotrs.gov.au/airports/avenv/noise/anef.htm

Edworthy J 1998 Warning people through noise. In N.L. Carter and R.F.S. Job (eds.) Noise as a Public Health Problem (Noise Effects '98), Vol. 1, pp. 147-56. Noise Effects '98 PTY Ltd., Sydney, Australia.

Edworthy J and Adams AS 1996 Warning Design: A Research Perspective. Taylop and Francis, London.

EEA 1995 Europe's Environment. The Dobris Assessment. D. Stanners, P. Bourdeau (Eds.), European Environment Agency, Copenhagen, Denmark.

Embleton TFW and Piercy JE 1976 Outdoor Sound Propagation Over Ground of Finite Impedance. Journal of the Acoustical Society of America 59: 267-277.

EU 1970 Council Directive on the approximation of the laws of the Member States relating to the permissible sound level and the exhaust system of motor vehicles. Directive 70/157/EEC of 6 February 1970. Official Journal L 42 (23.2.1970), p. 16. Amended by 73/350/EEC of 7.11.1973; Official Journal L 321 (22.11.1973), p. 33. Amended by 77/212/EEC of 8.3.1977; Official Journal L 66 (12.3.1977), p. 33. Amended by 81/334/EEC of 13.4.1981; Official Journal L 131 (18.5.1981), p. 6. Amended by 84/424/EEC of 03.09.1984; Official Journal L 238 (06.09.84) p. 31. Amended by 87/354/EEC of 3/87; Official Journal L 192 (11.07.87) p. 43. Amended by 89/491/EEC of 3/89; Official Journal L 238 (15.08.89) p. 43. Amended by 92/97/EEC of 10.11.92; Official Journal L 371 (19.12.92) p. 1. Amended by 96/20/EEC of 27.03.1996; Official Journal L 92 (13.04.96) p. 23, Brussels, Belgium.

EU 1978 Council Directive on the approximation of the laws of the Member States on the permissible sound level and exhaust system of motorcycles. Directive 78/1015/EEC of 23 November 1978. Official Journal L 349 (13.12.1978), p. 21, Brussels, Belgium. (Directive 78/1015/EEC is superseded by 97/24/EC, see EU 1997).

EU 1980 Council Directive on the limitation of noise emissions from subsonic airplanes. Directive 80/51/EEC of 20 December 1979. Official Journal L 18 (24.01.80) p. 26, Brussels, Belgium.

EU 1984a Council Directive on the approximation of the laws of the Member States relating to the permissible sound power level of compressors. Directive 84/533/EEC of 17 September 1984. Official Journal L 300 (19.11.1984), p. 123. Amended by 85/406/EEC of 11.7.1985. Official Journal L 233 (30.8.1985), p. 11, Brussels, Belgium.

EU 1984b Council Directive on the approximation of the laws of the Member States relating to the permissible sound power level of tower cranes. Directive 84/534/EEC of 17 September 1984. Official Journal L 300 (19.11.1984), p. 123. Amended by 87/405/EEC of 25.6.1987. Official Journal L 220 (8.8.1987) p. 60, Brussels, Belgium.

EU 1984c Council Directive on the approximation of the laws of the Member States relating to the permissible sound power level of welding generators. Directive 84/535/EEC of 17 September 1984. Official Journal L 300 (19.11.1984), p. 142. Amended by 85/407/EEC of 11.7.1985.Official Journal L 233 (30.8.1985), p. 16, Brussels, Belgium.

EU 1984d Council Directive on the approximation of the laws of the Member States relating to the permissible sound power level of power generators. Directive 84/536/EEC of 17 September 1984. Official Journal L 300 (19.11.1984), p. 149. Amended by 85/408/EEC of 11.7.1985. Official Journal L 233 (30.8.1985), p. 18, Brussels, Belgium.

EU 1984e Council Directive on the approximation of the laws of the Member States relating to the permissible sound power level of powered hand-held concrete-breakers and picks. Directive 84/537/EEC of 17 September 1984. Official Journal L 300 (19.11.1984), p. 156. Amended by 85/409/EEC of 11.7.1985. Official Journal L 233 (30.8.1985), p. 20, Brussels, Belgium.

EU 1984f Council Directive on the approximation of the laws of the Member States relating to the permissible sound power level of lawnmowers. Directive 84/538/EEC of 17 September 1984. Official Journal L 300 (19.11.1984), p. 171. 87. Amended by 87/ 252/EEC of 7.4.87. Official Journal L 117 (5.5.1987), p. 22. Amended by 88/80/EEC of 22.3.1988. Official Journal L 81 (26.3.1988), p. 69. Amended by 88/181/EEC of 22.3.1988. Official Journal L 81 (26.3.1988), p. 71, Brussels, Belgium.

EU 1986a Council Directive on the protection of workers from the risks related to exposure of noise at work. Directive 86/188/EEC of 12.5.1986. Official Journal L 137 (24.5.1986), p. 28, Brussels, Belgium.

EU 1986b Council Directive on the limitation of noise emitted by hydraulic excavators, rope-operated excavators, dozers, loaders and excavator-loaders. Directive 86/662/EEC of 22.12.1986 as amended by the Directive of 2.8.1989. Official Journal L 384 (31.12.1986), p. 1; L 253 (30.8.1989), p. 35, Brussels, Belgium.

EU 1986c Council Directive on airborne noise emitted by household appliances. Directive 86/594/EEC of 1.12.1986. Official Journal L 344 (6.12.1986), p. 24, Brussels, Belgium.

EU 1989 Council Directive on the limitation of noise emission from civil subsonic jet aeroplanes. Directive 89/629/EEC of 04 December1989. Official Journal L 363 (12.12.89) p. 27, Brussels, Belgium.

EU 1996a Council Directive to adapt in the light of technical progress Directive 70/157/EEC of 6 February 1970 on the approximation of the laws of the Member States regarding poermissible sound levels and exhaust systems of motor vehicles. Directive 96/20/EC of 27.03.1996. Official Journal L 92 (13.04.96) p. 23, Brussels, Belgium.

EU 1996b b Future Noise Policy – European Commission Green Paper. Report COM (96) 540 final. Commission of the Euopean Communities, Brussels.
EU 1997 Directive on certain components and charractristics of two or three-wheel motor vehicles. Directive 97/24/EC of the European Parliament and of the Council of 17 June 1997. Official Journal L 226 1997, Brussels, Belgium.
Evans GW 1998 Motivational consequences of exposure to noise. In N.L. Carter and R.F.S. Job (eds.) Noise as a Public Health Problem (Noise Effects '98), Vol. 1, pp. 311-320. Noise Effects '98 PTY Ltd., Sydney, Australia.
Evans GW and Lepore SJ 1993 Non-auditory effects of noise on children: A critical review. Children's Environments 10: 31-51.
Evans GW and Maxwell L 1997 Chronic noise exposure and reading deficits. Environment and Behavior 29: 638-656.
Evans GW, Hygge S, Bullinger M 1995 Chronic noise and psychological stress. Psychological Science 6: 333-338.
Evans GW, Bullinger M, Hygge S 1998 Chronic noise exposure and physiological response: A prospective study of children living under environmental stress. Psychological Science 9: 75-77.
Faiz A, Sinha, K, Wals, M and Valma, A 1990: Automotive air pollution: Issues and options for developing countries. WPS 492, World Bank, Washington, USA.
Falkemark G 1997 Trafikpolitiken, makten och miljön [Traffic politics, power and the environment]. I H.B. Andersson (Red.), Trafik och miljö [Traffic and the Environment]. Kommunikationsforskningsberedningen [Swedish Transport and Communications Research Board], Stockholm, Sweden.Fechter LS 1999 Mechanisms of ototoxicity by chemical contaminants: Prospects for intervention. Noise and Health, 2: 10-27.
Fidell S and Jones G 1975 Effects of cessation of late night on an airport community. Journal of Sound and Vibration, 42:411-427.
Fidell S, Barber, DS, Schultz TJ 1991 Updating a dosage-effect relationship for the prevalence of annoyance due to general transportation noise. Journal of the Acoustical Society of America 89: 221-233.
Fidell S, Pearsons K, Tabachnick B, Howe R, Silvati L, Barber DS 1995a Field study of noise-induced sleep disturbance. Journal of the Acoustical Society of America 98 (2 PART 1): 1025-1033.
Fidell S, Howe R, T Tabachnick BG, Pearsons KS, Sneddon MD 1995b Noise-induced sleep disturbance in residences near two civil airports. NASA Contractor Report 198252, NASA Langley Research Center, Hampton VA, USA.
Fidell S, Howe R, Tabachnick B, Pearsons K, Silvati L, Sneddon M, Fletcher E 1998 Field studies of habituation to change in night-time aircraft noise and of sleep motility measurement methods. BBN Report 8195, BNN Systems and Technologies Corporation, Canogan Park, California, USA.
Fidell S, Pearsons K, Howe R et al. 1994 Noise-induced sleep disturbance in residential settings. BNN Report 7932. BNN Systems and Technologies Corporation, Canoga Park, California, USA.
Fields JM 1986 Cumulative Airport Noise Exposure Metrics: An Assessment of Evidence for Time-of-Day Weightings. US FAA Report, DOT/FAA/EE-86/10, United States Federal Aviation Administration, Washington D.C., USA.

Fields JM 1990 A quantitative summary of non-acoustical variables' effects on reactions to environmental noise. In: Noise Con 90, pp. 303-308. Noise Control Foundation, Poughkeepsie, NY, USA.

Fields JM 1993 Effects of personal and situational variables on noise annoyance in residential areas. Journal of the Acoustical Society of America 93: 2753-2763.

Fields JM 1994 A Review of an Updated Synthesis of Noise/Annoyance Relationships. NASA Contractor Report 194950, National Aeronautics and Space Administration, Langley Research Center, Hampton, VA, USA.

Fields JM 1998 Reactions to environmental noise in an ambient noise context in residential areas. Journal of the Acoustical Society of America 104: 2245-2260.

Fields JM, de Jong RG, Brown AL, Flindell IH, Gjestland T, Job RFS, Kurra S, Lercher P, Schuemer-Kors A, Vallet M, Yano M 1997 Guidelines for reporting core information from communicy noise reaction surveys. Journal of Sound and Vibration 206: 685-695.

Fields JM, de Jong RG, Flindell IA, Gjestland T, Job R.S, Kurra S, Schuemer-Kors,A, Lercher P, Vallet M, Yano T 1998 Recommendation for shared annoyance questions in noise annoyance surveys. In N.L. Carter and R.F.S. Job (eds.) Noise as a Public Health Problem (Noise Effects '98.), Vol. 1, pp. 481-86. Noise Effects '98 PTY Ltd., Sydney, Australia.

Finegold LS, Harris CS, von Gierke HE 1994. Community annoyance and sleep disturbance: Updated criteria for assessing the impacts of general transportation noise on people. Noise Control Engineering Journal, 42: 25-30.

Finegold LS, von Gierke HE, McKinley RL, and Schomer PD 1998 Addressing the effectiveness of noise control regulations and policies In N.L. Carter and R.F.S. Job (eds.) Noise as a Public Health Problem (Noise Effects '98), Vol. 2, pp. 719-24. Noise Effects '98 PTY Ltd., Sydney, Australia.

Finegold LS, von Gierke HE, Schomer PD, Berry BF 1999 Proposal for monitoring worldwide noise exposure and assessing the effectiveness of noise exposure policies and noise control technologies. In: J. Cuschieri, S. Glegg, Yan Yong (eds.) Internoise 99 – The 1999 International Congress on Noise Control Engineering, 6-8 December 1999, Fort Lauderdale, Florida, USA, pp. 1917-1922.

Finke H-O 1980 Akustische Kennwerte für die Messung und Beurteilung von Gerauschimmissionen und deren Zusammenhang mit der subjektiven Gestörtheit. Dissertation of Technical University, Braunschweig, Germany.

Flindell IH and Stallen, PJM 1999 Non-acoustical factors in evnrionmental noise. Noise and Health 3: 11-16.

Florentine M, Buus S, Poulsen T 1996. Temporal integration of loudness as a function of level. Journal of the Acoustical Society of America, 99, 1633-44.

Ford RD 1987 Physical assessment of transportation noise. In P.M. Nelson (ed.) Transportation Noise Reference Book. Butterworth, London, UK.

Franks JH 1998 Preventing noise-induced hearing loss: A perspective view from the next millennium. In N.L. Carter and R.F.S. Job (eds.) Noise as a Public Health Problem (Noise Effects '98.), Vol. 1, pp. 11-16. Noise Effects '98 PTY Ltd., Sydney, Australia..

Freeman K 1984 Mental Health and the Environment. Churchill Livingstone, London, UK.

French NR and Steinberg JC 1947 Factors governing the intelligibility of speech sounds. Journal of the Acoustical Society of America 19:90-119.

Gjestland T, Liasjo K, Granoien I, Fields JM 1990 Response to Noise Around Oslo Airport Fornebu. ELAB-RUNIT Report No. STF40 A90189, Trondheim, Norway.

Globus G, Friedmann J, Cohen H, Pearsons SK, Fidell S 1974 The effects of aircraft noise on sleep electrophysiology as recorded in the home. In: Noise as a Public Health Problem. US Environmental Protection Agency, Report EPA 550/9-73.008, pp. 587-591, Washington DC, USA.

Goldstein M 1994 Low-frequency components in complex noise and their perceived loudness and annoyance. Arbete & Haelsa 1994: 2 (Work and Health; Scientific Journal of the National Institute of Occupational Health, Solna, Sweden).

Gottlob D 1995 Regulations for community noise. Noise/News International, December 1995, pp.223-236.

Griefahn B 1977 Long-term exposure to noise. Aspects of adaptation, habituation and compensation. Waking and Sleeping, 1:383-386.

Griefahn B 1990a Präventivmedizinische Vorschläge für den nächtlichen Schallschutz [Proposal for protection against noise during night from the point of view of preventive medicine]. Zeitschrift für Lärmbekämpfung 37: 7-14.

Griefahn B 1990b Sleeping in noisy environments: effects, limits and preventative measures. In: JA Horne (ed) Sleep 1990, pp. 391-93, Pontenagel Press, Bochum, Germany.

Griefahn B, Mehnert P, Moehler U, Schuemer-Kohrs A, Schuemer R 1996 Design of a field study on the effects of railway noise and road traffic noise. In F.A. Hill and R. Lawrence (eds.) Inter Noise 96. Noise Control – The Next 25 Years, Book 4, pp. 2183-88. Institute of Acoustics, St Albans, UK.

Griefahn B, Deppe C, Mehnert P, Moog R, Moehler U, Schuemer R 1998 What nighttimes are adequate to prevent noise effects on sleep? In N.L. Carter and R.F.S. Job (eds.) Noise as a Public Health Problem (Noise Effects '98), Vol. 2, pp. 445-450. Noise Effects '98 PTY Ltd., Sydney, Australia.

Griffiths ID 1983 Review of Community Response to Noise. In G. Rossi, (ed.), Noise as a Public Health Problem, Vol. 2, pp. 1031-1047. Milano, Italy: Centro Ricerche e Studi Amplifon.

Guski R 1987 Lärm–Wirkungen unerwünschter Geräusche. Huber, Bern, Switzerland.

Haines M, Stansfeld SA, Job RFS, Berglund B 1998 Chroinic aircraft noise exposure and child cognitive performance and stress. In N.L. Carter and R.F.S. Job (eds.) Noise as a Public Health Problem (Noise Effects '98), Vol. 1, pp. 329-336. Noise Effects '98 PTY Ltd., Sydney, Australia.

Hall FL, Birnie SE, Taylor SM, Palmer JE 1981 Direct Comparison of Community Response to Road Traffic Noise and to Aircraft Noise. Journal of the Acoustical Society of America 70: 1690-1698.

Hall FL, Taylor SM, Birnie SE 1985 Activity interference and noise annoyance. Journal of Sound and Vibration 103: 237-252.

Halpern D 1995 Mental Health and the Built Environment. More than Bricks and Mortar? Taylor and Francis Ltd, London, UK.

Hanner P and Axelsson A 1988 Acute acoustic trauma. Scandinavian Audiology 17: 57-63.

Harris CM 1991 Handbook of Acoustical Measurements and Noise Control. Mc Graw Hill, New York, USA.

Hasan S and Beg MHA 1994 Noise induced hearing loss in industrial workers of Karachi. Pakistan Journal of Otolaryngology 10: 200-205.

Hasan S and Zaidi SH 1997 The prevalence of noise induced hearing loss in industrial (textile) workers of Karachi. Thesis, University of Karachi, Karachi, Pakistan.

HCN 1994 Noise and Health. Publication No. 1994/15E, Health Council of the Netherlands, The Hague, Netherlands.

HCN 1997 Assessing noise exposure for public health purposes. Publication no. 1997/23E, Health Council of the Netherlands, Rijswijk, Netherlands.

Hede A 1998a Environmental noise regulation: A public policy perspective. In N.L. Carter and R.F.S. Job (eds.) Noise as a Public Health Problem (Noise Effects '98), Vol. 2, pp. 687-96. Noise Effects '98 PTY Ltd., Sydney, Australia.

Hede, A 1998b: Towards a normative model of public policy for environmental noise, Acoustics Australia, 26, 95-100.

Hellström PA, Dengerink HA, Axelsson A 1992 Noise levels from toys and recreational articles for children and teenagers. British Journal of Audiology, 26: 267-270.

Hetu Rand Fortin M 1995 Potential risk of hearing damage associated with exposure to highly amplified music. Journal of the American Academy of Audiology 6: 378-386.

Hobson JA 1989 Sleep. Scientific American Library, W.H. Freeman and Co, New York, NY, USA.

Holmes G, Singh B.R. and Theodore L. 1993. Handbook of environmental management and technology. Wiley, New York.

Horne JA, Pankhurst FL, Reyner LA, Hume K, Diamond ID 1994 A field study of sleep disturbance: Effects of aircraft noise and other factors on 5,742 nights of actimetrically monitored sleep in a large subject sample. Sleep 17: 146-159.

House ME 1987 Measurement and Prediction of Aircraft Noise. In P.M. Nelson (ed.) Transportation Noise Reference Book, Butterworth, London.

Houtgast T 1981 The Effect of Ambient Noise on Speech Intelligibility in Classrooms. Applied Acoustics 14: 15-25.

Houtgast T and Steeneken, HJM. 1983. Experimental verification of the STI: A valid basis for setting indoor noise level criteria. In G. Rossi (ed.), Noise as a Public Health Problem. Vol. 1, pp. 477-487, Centro Ricerche e Studi Amplifon, Milano, Italy.

Houtgast T and Steeneken JM 1985 A Review of the MTF Concept in Room Acoustics and Its Use for Estimating Speech Intelligibility in Auditoria. Journal of the Acoustical Society of America 77: 1069-1077.

Humes LE, Dirks DD, Bell TS, Ahlstrom C, Kincaid GE 1986 Application of the Artic-ulation Index and the Speech Transmission Index to the recognition of speech by normal-hearing and hearing-impaired listeners. Journal of Speech Hearing Research, 29:447-462.

Hygge S, Evans GW, Bullinger M 1996 The Munich airport noise study: Cognitive effects on children from before to after the change over of airports. In F.A. Hill and R. Lawrence (eds.) Inter Noise 96. Noise Control – The Next 25 Years, Vol. 5, pp. 2189-92. Institute of Acoustics, St Albans, UK.

Hygge S, Jones DM, Smith AP 1998 Recent developments in noise and performance. In N.L. Carter and R.F.S. Job (eds.) Noise as a Public Health Problem (Noise Effects '98), Vol. 1, pp. 321-28, Noise Effects '98 PTY Ltd., Sydney, Australia.

ICAO 1993 International Standards and Recommended Practices: Environmental Protection. Annex 16, Volume I: "Aircraft Noise". Annex 16 (Chapter 2 and 3) to the Convention on International Civil Aviation. International Civil Aviation Organization, [Air Navigation (Noise Certification) Order 1990 -Statutory Instrument 1514], Montreal, Canada.

IEC 1979 Sound Level Meters. IEC Publication 651, International Electrotechnical Commission, Geneva, Switzerland.

IEC 1988 Sound system equipment, part 16: The objective rating of speech intelligibility in auditoria by the RASTI method. IEC Publication 268-/6, International Electrotechnical Commission, Geneva, Switzerland.

IEH 1997. The Non-Auditory Effects of Noise. IEH Report R10, Institute for Environment and Health, Leicester, UK.

Irle M 1975 Is aircraft noise harming people? In M. Deutsch and H.A. Hornstein (eds.), Applying Social Psychology, pp. 115-138, Erlbaum, Hillsdale, NJ. USA.

Ising H and Günther T 1997 Interaction between noise-induced stress and magnesium losses: relevance for long-term health effects. In F. Augustinovicz (ed.), Inter Noise 97. Help Quiet the World for a Higher Quality Life, Vol. 2, pp. 1099-1104. Noise Control Foundation, Poughkeepsie, NY, USA.

Ising H, Babisch W, Kruppa B 1998 Acute and chronic noise stress as cardiovascular risk factors. Federal Environmental Agency, Berlin, Germany.

Ising H, Babisch W, Gandert J, Scheuermann B 1988 Hörschäden bei jugendlichen Berufsanfängern aufgrund von Freizeitlärm und Musik. Zeitschrift für Lärmbekämpfung, 35:35-41.

Ising H, Hanel J, Pilgramm M et al. 1994 Gehörschadensrisiko durch Musikhören mit Kopfhörern. Hals-Nasen-Ohren 1994; 42:764-8.

ISO 1975a Acoustics-Method for Calculating Loudness Level. ISO-532-1975 (E), International Organization for Standardization, Geneva, Switzerland.

ISO 1975b Acoustics-Preferred Frequencies for Measurements. International Standard ISO 266-1975 (E), International Organization for Standardization, Geneva, Switzerland

ISO 1978 Laboratory Measurement of Airborne Sound Insulation of Building Elements – Part V, Field Measurements of Airborne Sound Insulation of Façade Elements and Facades", International Standard ISO-140/V, International Organization for Standardization, Geneva, Switzerland.

ISO 1982 Acoustics – Description and measurement of environmental noise – Part 1: Basic quantities and procedures. International Standard ISO 1996-1, International Organization for Standardization, Geneva, Switzerland.

ISO 1987a Acoustics-Normal Equal Loudness Contours. International Standard ISO 226-1-1987 (E), International Organization for Standardization, Geneva, Switzerland.

ISO 1987b Acoustics – Description and measurement of environmental noise – Part 3: Application to noise limits. International Standard ISO 1996-3:1987(E), International Organization for Standardization, Geneva, Switzerland.

ISO 1990 Acoustics–Determination of occupational noise exposure and estimation of noise-induced hearing impairment. International Standard ISO 1999, International Organization for Standardization, Geneva, Switzerland.

ISO 1994 Quality systems -- Model for quality assurance in production, installation and servicing. International Standard ISO 9002, International Organization for Standardization, Geneva, Switzerland.

ISO 1995 Laboratory Measurement of Airborne Sound Insulation of Building Elements – Part III: Laboratory Measurements of Airborne Sound Insulation of Building Elements. International Standard ISO-140/III, International Organization for Standardization, Geneva, Switzerland .

ISO 1996a Acoustics – Rating of Sound Insulation in Buildings and of Building Elements – Part 1: Airborne Sound Insulation. International Standard ISO 717-1, International Organization for Standardization, Geneva, Switzerland.

ISO 1996b Environmental management systems - specification with guidance for use. International Standard ISO 14001, International Organization for Standardization, Geneva, Switzerland.

ISO 1996c Environmental management systems - general guidelines on principles, systems and supporting techniques. International Standard ISO 14004, International Organization for Standardization, Geneva, Switzerland.

ISO 1998 Measurement of Sound Insulation In Buildings and of Building Elements – Part VI: Laboratory Measurements of impact sound insulation of floors. International Standard ISO-140/VI, International Organization for Standardization, Geneva, Switzerland.

Jansen G 1986 Zur "erheblichen Belästigung" und "Gefährdung" durch Lärm. Zeitschrift für Lärmbekämpfung 33:2-7.

Jansen G 1987 Verkehrslärmwirkungen bei besonderen Personengruppen. Zeitschrift für Lärmbekämpfung 34: 152-156.

Jansen G 1998 Health concepts and noise effects. In N.L. Carter and R.F.S. Job (eds.) Noise as a Public Health Problem (Noise Effects '98), Vol. 2, pp. 697-702. Noise Effects '98 PTY Ltd., Sydney, Australia.

Jansen G and Gottlob D 1996 Requirements for the protection against outdoor noise in various countries with respect to standardization and regulations. In F.A. Hill and R. Lawrence (eds.) Inter Noise 96. Noise Control – The Next 25 Years, Book 6, pp. 3343-3346. Institute of Acoustics, St Albans, UK.

Jenkins LM, Tarnopolsky A, Hand DJ 1981 Psychiatric admissions and aircraft noise from London Airport: Four-year, three hospitals' study. Psychological Medicine 11: 765-782.

Job RFS 1988 Community response to noise: A review of factors influencing the relationship between noise exposure and reaction. Journal of the Acoustical Society of America 83: 991-1001.

Job RFS 1993 Psychological factors of community reaction to noise. In M. Vallet (ed.) Noise as a Public Health Problem, Vol. 3, pp. 48-59, INRETS - Institut National de REcherche sur les Transports et leur Sécurité, Arcueil, France.

Job RFS 1996 The influence of subjective reactions to noise on health effects of the noise. Environment International 22: 93-104.

Kabuto M and Suzuki S 1976 A trial measurement of individual noise exposure by time-zone in a day. Japanese Journal of Industrial Health, 18: 17-22.

Kabuto M, Ohtsuka R, Suzuki S 1978 Measurement and evaluation of individual noise exposure level of Tokyo metropolitan commuters in railroad cars above ground and in subways. Japanese Journal of Public Health, 2: 59-63.

Kageyama T, Kabuto M, Nitta H, Kurokawa Y, Taira K, Suzuki S, Takemoto T 1997 A populations study on risk factors for insomnia among adult Japanese women: A possible effect of road traffic volume. Sleep 20: 963-971.

Kastka J, Buchta E, Ritterstaedt U, Paulsen R, Mau U 1995 The long term effect of noise protection barriers on the annoyance response of residents. Journal of Sound and Vibration, 184: 823-852.

Katz J. (ed.) 1994 Handbook of Clinical Audiology. Fourth edition, Williams and Wilkins Baltimore, ML, USA.

Kerry G, Lomax C, and James DJ 1997 Assessment and Relevance of methods for calculating onset rate of low altitude flight noise. In F. Augustinovicz (ed.), Inter Noise 97. Help Quiet the World for a Higher Quality Life, vol. 3, pp. 1227-30. Noise Control Foundation, Poughkeepsie, NY, USA.

Kjellberg A, Goldstein M, and Gamberale F 1984 An Assessment of dBA for Predicting Loudness and Annoyance of Noise Containing Low Frequency Components. Journal of Low Frequency Noise and Vibration 3: 10-16.

Klæboe R, Kolbenstvedt M, Lercher P, and Solberg S 1998 Changes in noise reactions– Evidence for an area-effect? In V.C. Goodwin and D.C. Stevenson (eds.) Inter Noise 98. Sound and Silence: Setting the Balance, Vol. 2, pp. 1133-36. New Zealand Acoustical Society, Auckland, New Zealand.

Koelega HS (ed.) 1987 Environmental Annoyance: Characterization, Measurement, and Control. Elsevier, Amsterdam, Netherlands.

Kremer L 1950 Die Wissenschaftliche Grundlagen der Raumakustik. Band III, Hirzel Verlag, Leipzig

Kryter KD 1959 Scaling Human Reaction to the Sound from Aircraft. Journal of the Acoustical Society of America 31: 1415-1429.

Kryter KD 1994 The Handbook of Noise and Hearing. Academic Press, San Diego, CA, USA.

Kutscheidt E 1989 Rechtsprobleme bei der Bewertung von Geräuschimmissionen. Neue Zeitschrift für Verwaltungsrecht 3:193-199.

Kuwano S, Namba S, and Mizunami T 1998 The effect of noise on the effort to sleep. In V.C. Goodwin and D.C. Stevenson (eds.) Inter Noise 98. Sound and Silence: Setting the Balance, Vol. 2, pp. 1083-1086. New Zealand Acoustical Society, Auckland, New Zealand.

Lara Sáenz A and Stephens RWB (eds.) 1986 Noise Pollution. Wiley, Chichester, UK.

Lambert J and Vallet M 1994 Study Related to the Preparation of a Communication on a Future EC Noise Policy. INRETS LRN Report No. 9420, INRETS - Institut National de REcherche sur les Transports et leur Sécurité, Bron, France.

Lang J 1986 Assessment of noise impact on the urban environment, A study on noise prediction models, Environmental Health Series 9, Regional Office for Europe, World Health Organization, Copenhagen, Denmark.

Lang J 1995 Noise abatement regulations and strategies. In: Noise - Selected presentations of an Informal Regional Consultation Meeting on Noise Pollution, 2-5 September 1991, Amman, Jordan, Eastern Mediterranean Regional Office, Regional Centre for Environmental Health Activities (CEHA), Amman, Jordan.

Lang WW 1999 Is noise policy a global issue, or is it a local issue? In: J. Cuschieri, S. Glegg, Yan Yong (eds.) Internoise 99 – The 1999 International Congress on Noise Control Engineering, 6-8 December 1999, Fort Lauderdale, Florida, USA, pp. 1939-1943.

Large JB and House ME 1989 The effect on aviation noise of the single European market. In G.C. Maling, Jr. (ed.), Inter-Noise 89, Vol. 1, pp. 695-700, Noise Control Foundation, Poughkeepsie, NY, USA.

Lazarus H 1990 New methods for describing and assessing direct speech communication under disturbing conditions. Environment Inernational 16: 373-392.

Lazarus H 1998 Noise and communication: The present state. In N.L. Carter and R.F.S. Job (eds.) Noise as a Public Health Problem (Noise Effects '98), Vol. 1, pp. 157-162. Noise Effects '98 PTY Ltd., Sydney, Australia.

Lercher P 1996 Environmental noise and health: An integrated research perspective. Environment International 22: 117-129.

Lercher P 1998a Context and coping as moderators of potential health effects in noise-exposed persons. In D. Prasher and L. Luxon, (Eds.), Advances in Noise Series. Vol. I: Biological Effects, pp. 328-335, Whurr Publishers, London, UK.

Lercher P 1998b Deviant dose-response curves for traffic noise in "sensitive areas"? In V.C. Goodwin and D.C. Stevenson (eds.) Inter Noise 98. Sound and Silence: Setting the Balance, Vol. 2, pp. 1141-1144. New Zealand Acoustical Society, Auckland, New Zealand.

Lercher P, Stansfeld SA, Thompson SJ 1998 Non-auditory health effects of noise: Review of the 1993-1998 period. In N.L. Carter and R.F.S. Job (eds.) Noise as a Public Health Problem (Noise Effects '98), Vol. 1, pp. 213-220. Noise Effects '98 PTY Ltd., Sydney, Australia.

Lindemann HE, van der Klaauw MM, Platenburg-Gits FA 1987 Hearing acuity in male adolescents at the age of 17 – 23 years. Audiology 26: 65-78.

Lindvall T and Radford EP (eds.) 1973 Measurement of annoyance due to exposure to environmental factors. Environmental Research 6:1-36.

London Charter 1999 Charter on Transport, Environment and Health. Final version prepared following the Fourth Preparatory Meeting on "Transport, enviroment and Health, Vienna, 15-17 March 1999. EUR/ICP/EHCO 02 02 05/9 Rev.4 - 09009 – 16 June 1999. Regional Office for Europe, European Centre for Environment and Health, Rome Division, World Health Organization, Rome, Italy. Internet address: http://www.who.it/london_conference/teh.htm.

Lutman ME and Haggard MP (eds.) 1983 Hearing Science and Hearing Disorders. Academic Press, London, UK.

Mage, D and Walsh, M 1998: Case studies from cities around the world. In: Urban Traffic Pollution, eds. D. Schwela and O. Zali, E & Spon, London, UK.

Maschke C 1992 Der Einfluss von Nachtlärm auf den Schlafverlauf und die Katecholaminenausscheidung. Technische Universität, Berlin, Germany.

Maschke C, Arndt D, Ising H, et al. 1995 Nachtfluglärmwirkungen auf Anwohner. DFG-Forschungsbericht Gr. 452/8-2. Gustav Fischer Verlag, Stuttgart, Germany.

Miedema HME 1987 Annoyance from Combined Noise Sources. In H. S. Koelega (ed.), Environmental Annoyance: Characterization, Measurement and Control, pp. 313-320, Elsevier, Amsterdam, The Netherlands.

Miedema HME 1993 Response Functions for Environmental Noise. In M. Vallet (ed.) Noise as a Public Health Problem, Vol. 3, pp. 428-433, INRETS - Institut National de Recherche sur les Transports et leur Sécurité, Arcueil Cedex, France.

Miedema HME 1996 Quantification of Annoyance Caused by Environmental Noise and Odor. TNO, Leiden, Netherlands.

Miedema HME, Vos H 1998 Exposure response functions for transportation noise. Journal of the Acoustical Society of America 104: 3432-3445.

Miller JD 1978 General psychological and sociological effects of noise. In E.C. Carterette and M.P. Friedman (eds.), Handbook of Perception. Vol. VI: Hearing (pp. 641-676). Academic Press, New York NZ, USA.

Moehler U Community response to railway noise: A review of social surveys. Journal of Sound and Vibration 120: 321-332.

Molino JA 1974 Equal aversion levels for pure tones and 1/3 octave bands of noise. Journal of the Acoustical Society of America 55: 1285-1289.

National Environment Board of Thailand 1990 Air and noise pollution in Thailand 1989, Bangkok.

NRC-CNRC 1994 NEF Validation Study. (2) Review of Aircraft Noise and its Effects. Contract Report A-1505.5 (Final). Institute for Research in Construction, Ottawa, Canada.

OECD 1991 Fighting Noise in the 1990's. Organisation for Economic Co-operation and Development, Paris, France.

OECD 1993 Environmental Data Compendium. Organisation for Economic Co-operation and Development, Paris, France.

OECD-ECMT. 1995. Urban Travel and Sustainable Development. European Conference of Ministers of Transport, Organisation for Economic Co-operation and Development, Paris, France.

Öhrström E 1993a Research on noise and sleep since 1988: Present state. In M. Vallet (ed.), Noise as a Public Health Problem, Vol. 3, pp. 331-338, INRETS - Institut National de REcherche sur les Transports et leur Sécurité, Arcueil, France.

Öhrström, E. 1993b. Effects of low levels of road traffic noise during night. . In M. Vallet (ed.), Noise as a Public Health Problem, Vol. 3, pp. 359-366, INRETS - Institut National de REcherche sur les Transports et leur Sécurité, Arcueil, France.

Öhrström E 1997 Effects of exposure to railway noise–A comparison between areas with and without vibration. Journal of Sound and Vibration 205, 555-560.

Öhrström E, Björkman M 1988 Effects of noise-disturbed sleep–A laboratory study on habituation and subjective noise sensitivity. Journal of Sound and Vibration 122: 277-290.

Öhrström E, Skånberg AB1996 A field survey on effects of exposure to noise and vibrations from railway traffic. Part I: Annoyance and activity disturbance effects. Journal of Sound and Vibration 193: 39-47.

Ollerhead JB, Jones CJ, Cadoux RE, Woodley A, Atkinson BJ, Horne JA, Pankhurst F, Reyner L, Hume KI, Van F, Watson A, Diamond I, Egger P, Holmes D, McKean J 1992 Report of a Field Study of Aircraft Noise and Sleep Disturbance. Department of Transport, London, UK.

Pankhurst FL and Horne JA 1994 The influence of bed partners on movement during sleep. Sleep 17: 308-315.

Passchier-Vermeer W 1991 Noise from toys and the hearing of children. NIPG-TNO Report 91.032, TNO Institute of Preventive Health Care, Leiden, Netherlands.

Passchier-Vermeer W 1993 Noise and Health. The Hague: Health Council of the Netherlands. [Publication No A93/02E, review prepared by TNO Institute of Preventive Health Care, Leiden]

Passchier-Vermeer W 1994 Sleep disturbance due to night-time aircraft noise. Leiden: TNO-PG Report 94.077, TNO Institute of Preventive Health Care, Leiden, Netherlands.

Passchier-Vermeer, W 1996. Effects of noise and health. Chapter 3 of a report on Noise and Health prepared by a committee of the Health Council of The Netherlands. Noise/News International: 137-150.

Passchier-Vermeer W and Rövekamp AJM 1985 Verband tussen gehoorschade en de sociale handicap door een verminderd hoorvermogen bij groepen personen die tijdens hun werk aan lawaai zijn geëxponeerd. In: Passchier-Vermeer W, et al. Preventie gehoorschade door lawaai.Voordrachten ter gelegenheid van het 10-jarig jubileum van NVBA, pp.185-202. NIPG-TNO Institute of Preventive Health Care, Leiden, Netherlands.

Passchier-Vermeer W and Zeichart K Vibrations in the living environment. TNO-PG Report 98.030, TNO Institute of Preventive Health Care, Leiden, Netherlands.

Passchier-Vermeer W, Vos H, Steenbekkers JHM 1998 Popmusic through headphones and hearing loss. Report 98.036, TNO Institute of Preventive Health Care, Leiden, Netherlands.

Paulsen R and Kastka J 1995 Effects of combined noise and vibration on annoyance. Journal of Sound and Vibration 181: 295-314.

Pearsons KS 1998 Awakening and motility effects of aircraft noise. In N.L. Carter and R.F.S. Job (eds.) Noise as a Public Health Problem (Noise Effects '98), Vol. 2, pp. 427-32. Noise Effects '98 PTY Ltd., Sydney, Australia.

Pearsons KS, Barber DS, Tabachnick BG, Fidell S 1995 Predicting noise-induced sleep disturbance. Journal of the Acoustic Society of America 97: 331-338.

Pearsons KS 1996 Recent field studies in the United States involving the disturbance of sleep from aircraft noise. In F.A. Hill and R. Lawrence (eds.) Inter Noise 96. Noise Control – The Next 25 Years, Book 5, pp. 2271-2276. Institute of Acoustics, St. Albans, UK.

Persson K and Björkman M 1988 Annoyance due to Low Frequency Noise and the Use of the dBA Scale. Journal of Sound and Vibration 127: 491-497.

Plomp R 1986 A signal to noise ratio model for the speech-reception threshold of the hearing impaired. Journal of Speech and Hearing Research 29: 146-152.

Prasanchuk S (1997) Noise pollution. Its effect on health and hearing – Thailand as a case study. Presentation at the PDH Informal Consultation on the Prevention of Noise-induced Hearing Loss, 28-30 October 1997, WHO/PDH/98.5. World Health Organization, Geneva.

Razi MS, Jafer S, Hillier V, Zaidi SH, Newton V 1995 Causes of bilateral hearing loss in school children. Pakistan Journal of Otolaryngology 11: 68-86.

Reyner LA and Horne JA 1995 Gender- and age-related differences in sleep determined by home-recorded sleep logs and actimetry from 400 adults. Sleep 18: 127-134.

Ronnebaum T Schulte-Fortkamp B Weber R 1996 Synergetic effects of noise from different sources: a literature study. In F.A. Hill and R. Lawrence (eds.), Inter Noise 96. Noise Control – – The Next 25 Years, Vol. 6, pp. 2241-2246. Institute of Acoustics, St. Albans, UK.

SABS 1994 Code of practice for the measurement and rating of environmental noise with respect to annoyance and speech communication (third revision). South African Bureau of Standards publication No. 0103, Pretoria, South Africa.

SABS 1996 Code of practice for calculating and predicting road traffic noise. South African Bureau of Standards publication No. 0210, Pretoria, South Africa.

SABS 1998 Code of practice for methods for environmental noise impact assessments. South African Bureau of Standards publication No. 0328, Pretoria, South Africa.

Salter L 1988 Mandated Science: Science and Scientists in the Making of Standards. Kluwer, Dordrecht, Netherlands.

Sandberg U (ed.) 1995 The effects of regulations on road vehicle noise. Report by the International Institute of Noise Control Engineering Working Party, Noise News International 6: 85-113.

Sandberg U 1999 Abatement of traffic, vehicle and tire/road noise – the global perspective. In: J. Cuschieri, S. Glegg, Yan Yong (eds.) Internoise 99 – The 1999 International Congress on Noise Control Engineering, 6-8 December 1999, Fort Lauderdale, Florida, USA, pp. 37-42.

Sargent JW and Fothergill LC 1993 The noise climate around our homes. Information Paper 21/93, Building Research Establishment, Garston, UK.

Scharf B 1970 Critical bands. In J.V.Tobias (ed.), Foundations of Modern Auditory Theory, Vol. 1, pp. 157-202. Academic Press, New York, NY, USA.

Scharf B and Hellman R 1980 How Best to Predict Human Response to Noise on the Basis of Acoustic Variables. In J.V. Tobias, G. Jansen andW.D. Ward (eds.) Noise as a Public Health Problem, ASHA Report no. 10, pp. 475-487, Rockville, ML, USA.

Schulz TJ 1978 Synthesis of Social Surveys on noise annoyance. Journal of the Acoustical Society of America, 64: 377-405.

Schwela D 1998. WHO Guidelines on Community Noise. In N.L. Carter and R.F.S. Job (eds.) Noise as a Public Health Problem (Noise Effects '98), Vol. 2, pp. 475-480. Noise Effects '98 PTY Ltd., Sydney, Australia.

Smith AW 1998 The World Health Organisation and the prevention of deafness and hearing impairment caused by noise. Noise and Health 1: 6-12.

Smith AP 1990 Noise, performance efficiency and safety. International Archive of Occupational and Environmental Health 62: 1-5.

Smoorenburg GF 1998 Effects of impulse noise on man. In N.L. Carter and R.F.S. Job (eds.) Noise as a Public Health Problem (Noise Effects '98), Vol. 1, pp. 1-10, Noise Effects '98 PTY Ltd., Sydney, Australia.

Smoorenburg GF and Goldstein-Brouwers WG 1986 Spreaakverstaan in relatie tot het toonaudiogram bij slechthorendheid ten gevolge van lawaai. IZF-TNO Report 1986 C-17, Soesterberg, Netherlands.

Stanners D and Bordeau P (Eds.) 1995 Europe's Environment the Dobris Assessment. Noise and radiation, pp.359-374, European Environment Agency, Copenhagen, Denmark.

Stansfeld SA 1992 Noise, noise sensitivity and psychiatric disorder: Epidemiological and psychological studies. Psychological Mededicine, Monograph Suppl. 22, Cambridge University Press, Cambridge, UK.

Stansfeld SA, Gallacher J, Babisch W, Shipley S 1996. Road traffic noise and psychiatric disorder: prospective findings from the Caerphilly Study. British Medical Journal 313: 266-267.

Stevens SS 1972 Perceived level of noise by Mark VII and decibels (E). Journal of the Acoustical Society of America 51: 575-601.

Struwe F, Jansen G, Schwarze S, Schwenzer C, Nitzsche M 1996 Untersuchung von Hörgewohn-heiten und möglichen Gehörrisiken durch Schalleinwirkungen in der Freizeit unter beson-derer Berücksichtigung des Walkman-Hörens. Düsseldorf: Institut für Arbeitsmedizin der Heinrich-Heine-Universität. In B. Babissch , G. Bambach, H. Ising, B. Kruppa, P. Plath, E. Rebentisch, F. Struwe Gehörgefährdung durch laute Musik und Freizeitlärm, pp. 44 - 154. Institut für Wasser-, Boden- und Lufthygiene des Umweltbundesamtes, Berlin, Germany.

Tafalla RJ and Evans GW 1997 Noise, physiology and human performance: The potential role of effort. Journal of Occupational Health Psychology 2: 148-155.

Tempest W (ed.) 1985 The Noise Handbook. Academic Press, London, UK.

ten Wolde T 1998 European Commission's future noise policy. In V.C. Goodwin and D.C. Stevenson (eds.) Inter Noise 98. Sound and Silence: Setting the Balance, Vol. 3, pp. 1719-1722. New Zealand Acoustical Society, Auckland, New Zealand.

Thiessen GJ 1978 Disturbance oif sleep by noise. Journal of the Acoustical Society of America, 64: 216-222.

Thompson SJ 1996 Non-auditory health effects of noise: an updated review. In F.A Hill and R. Lawrence (eds.) Inter Noise 96. Noise Control – The Next 25 Years, Vol. 4, pp. 2177-2182. Institute of Acoustics, St. Albans, UK.

UNCED 1992 Agenda 21. United Nations Conference on Environment and Development, Conches, Switzerland.

US EPA. 1974. Information on levels of environmental noise requisite to protect public health and welfare with an adequate margin of safety. Report EPA 550/9-74.004, US Environmental Protection Agency, Washington DC, USA.

Vallet M 1996 Charactéristiques et indicateurs de la gene due au bruit des avions. Synthèse. INRETS LRN Report No. 29, Institut National de REcherche sur les Transports et leur Sécurité, Arcueil, France.

Vallet M 1998 Sleep disturbance by noise: Recent orientations. In N.L. Carter and R.F.S. Job (eds.) Noise as a Public Health Problem (Noise Effects '98),, Vol. 2, pp. 421-26, Noise Effects '98 PTY Ltd., Sydney, Australia.

Vallet M and Vernet I 1991 Night aircraft noise index and sleep research results. In A. Lawrence (ed.), Inter-Noise 91. The Cost of Noise, Vol. 1, pp. 207-210. Noise Control Foundation, Poughkeepsie, NY, USA.

Vallet M, Gagneux J-M, Clairet JM, Laurens JF, Letisserand D 1983 Heart rate reactivity to aircraft noise after a long-term exposure. In G. Rossi (ed.), Noise as a Public Health Problem, Vol. 2, pp. 965-971, Centro Richerche e Studi Amplifon, Milano, Italy.

van den Berg M 1996 Noise management in the Netherlands. Noise and Vibration, September 1996, 11-12.

van Hees O 1992 Gehoorafwijkingen bij beroepsmusici. Thesis, GUA, Amsterdam, Netherlands.

Vaskor JG, Dickinson SM, Bradley JS 1979 Effect of Sampling on the Statistical Descriptors of Traffic Noise. Applied Acoustics 12: 111-124.

Vernon JA, Moller AR (Eds.) 1995 Mechanisms of Tinnitus. Allyn and Bacon, Needham Heights, Ma, USA.

von Gierke HE 1975 Noise – How Much is Too Much? Noise Control Engineering Journal 5: 24-34.

von Gierke HE and Harris CS 1987 Annoyance Response to Military Flight Operations and the Development of Standard Criteria for Community Annoyance. In H.S. Koelega (ed.), Environmental Annoyance, Characterization, Measurement and Control, pp. 257-269, Elsevier, Amsterdam, The Netherlands.

Vos, J 1992 Annoyance caused by simultaneous impulse, road-traffic and aircraft sounds: a quantitative model. Journal of the Acoustical Society of America 91: 3330-45.

Vos J 1996 Annoyance caused by impulse sounds produced by small, medium-large, and large firearms. In F.A Hill and R. Lawrence (eds.) Inter-Noise 96. Noise Control – The Next 25 Years, Book 5, pp. 2231-36. Institute of Acoustics, St. Albans, UK.

Warren CHE 1972 The sonic boom exposure effects 1.2: The sonic boom–generation and propagation. Journal of Sound and Vibration 20: 485-497.

WCED 1987 Our Common Future. World Commission on Environment and Development The Brundtland Commission, Oxford University Press, Oxford UK.

Westman JC and Walters JR 1981 Noise and stress. A comprehensive approach. Environmental Health Perspectives 41: 291-309.

WHO 1980a Noise. Environmental Health Criteria Document No. 12. World Health Organization, Geneva, Switzerland.

WHO 1980b. Glossary on Air Pollution. WHO Regional Office of Europe, Series No. 9, World Health Organization, Copenhagen, Denmark.

WHO 1993 The Environmental Health Criteria Document on Community Noise. Report on the Task Force Meeting, Düsseldorf, Germany, 24-28 November 1992. WHO Regional Office for Europe, Report EUR/HFA Target 24, World Health Organization, Copenhagen, Denmark.

WHO 1994 Assessing human health risks of chemicals: Derivation of guidance values for health-based exposure limits. Environmental Health Criteria No. 170, World Health Organization, Geneva, Switzerland.

WHO 1995a Concern for Europe's Tomorrow – Health and the Environment in the WHO European Region. WHO European Centre for Environment and Health. Wissenschaftliche Verlagsgesellschaft, Stuttgart, Germany.

WHO 1995b Noise - Selected presentations of an Informal Regional Consultation Meeting on Noise Pollution, 2-5 September 1991, Amman, Jordan, Eastern Mediterranean Regional Office, Regional Centre for Environmental Health Activities (CEHA), Amman, Jordan.

WHO 1998 Air Management Information System. AMIS CD ROM, 2nd edition. World Health Organization, Geneva, Switzerland.

Zaidi SH 1998 Current status and future trends of deafness and hearing impairment in the Tropics. Pakistan Journal of Otolaryngology 14: 38-45.

Zaidi SH 1999 An epidemiological study of hearing impairment in the Himalayan territories of Pakistan. Hearing International Newsletter 8: 1-4.

Zeichart K 1998 Kombintorische Wirkungen von Bahnlärm und Bahnerschütterungen. Zeitschrift für Lärmbekämpfung 45: 7-16.

Zwicker E 1960 Ein Verfahren zur Berechnung der Lautstärke. Acustica 10: 304-308.

Zwicker E 1989 On the dependence of unbiased annoyance on loudness. In G. Maling Jr. (ed.) Inter Noise 89, Vol. 2, pp. 809-14. Noise Control Foundation, Poughkeepsie, NY, USA. .

Appendix 2 : Examples Of Regional Noise Situations

REGION OF THE AMERICAS

Latin America (Guillermo Fuchs, Argentina).

As more and more cities in Latin America surpass the 20 million inhabitants mark, the noise pollution situation will continue to deteriorate. Most noise pollution in Latin American cities comes from traffic, industry, domestic situations and from the community. Traffic is the main source of outdoor noise in most big cities. The increase in automobile engine power and lack of adequate silencing results in LAeq street levels >70 dB, above acceptable limits. Vehicle noise has strong low-frequency peaks at ~13 Hz, and at driving speeds of 100 Km/h noise levels can exceed 100 dB. The low-frequency (LF) noise is aerodynamic in origin produced, for example, by driving with the car windows open. Little can be done to mitigate these low-frequency noises, except to drive with all the windows closed. Noise exposure due to leisure activities such as carting, motor racing and Walkman use is also growing at a fast rate. Walkman use in the street not only contributes to temporary threshold shifts (TTS) in hearing, but also endangers the user because they may not hear warning signals Construction sites, pavement repairs and advertisements also contribute to street noise, and noise levels of 85–100 dB are common.

The Centro de Investigaciones Acústicas y Luminotécnicas (CIAL) in Córdoba, Argentina has investigated noise pollution in both the field and in the laboratory. The most noticeable effect of excessive urban noise is hearing impairment, but other psychophysiological effects also result. For example, tinnitus resulting from sudden or continuous noise bursts, can produce a TTS of 20–30 dB, and prolonged exposures can result in permanent threshold shifts (PTS). By analyzing sound spectra down to a few Hertz, and at levels of up to 120 dB, discrete frequencies and bands of infrasound were found which damage hearing. With LF sounds at levels of 120 dB, TTS resulted after brief exposure, and PTS after only 30 min of exposure. The effects of noise on hearing can be especially detrimental to children in schools located downtown. Field studies in Córdoba city schools located near streets with high traffic density showed that speech intelligibility was dramatically degraded in classrooms that did not meet international acoustical standards. This is a particularly worrying problem for the younger students, who are in the process of language acquisition, and interferes with their learning process.

In general, community noise in Latin America remains above accepted limits. Particularly at night, sleep and rest are affected by transient noise signals from electronically amplified sounds, music and propaganda. Field research was carried out in four zones of Buenos Aires, to determine the effects of urban noise on the well-being, health and activities of the inhabitants. The effects of confounding variables were taken into consideration. It was concluded that night-time noise levels in downtown Buenos Aires were barely lower than daytime levels. The results showed that sleep, concentration, communication and well-being were affected in most people when noise levels exceeded those permitted by international laws. The reactions of the inhabitants to protect themselves from the effects of noise varied, and included changing rooms, closing windows and complaining to authorities.

Individual responses to noise also vary, and depend on factors such as social, educational and economic levels, individual sensibility, attitudes towards noise, satisfaction with home or neighborhood, and cognitive and affective parameters. For example, at CIAL, two pilot studies were carried out with a group of adolescents to determine the influence of environmental conditions on the perception of noise. When music was played at very high sound levels (with sound peaks of 119 dBA) in a discotheque, judged to be a pleasant environment, the subjects showed less TTS than when exposed to the same music in the laboratory, which was considered to be an unpleasant environment.

At the municipal level Argentinean Ordinances consider two types of noises: unnecessary and excessive. Unnecessary noises are forbidden. Excessive noises are classified according to neighboring activities and are limited by maximum levels allowed for daytime (7 am to 10 pm) and night-time (10 pm to 7 am). This regulation has been relatively successful, but control has to be continuous. Similar actions have been prescribed at the provincial level in many cities of Argentina and Latin America. Control efforts aimed at reducing noise levels from individual vehicles are showing reasonably good improvements. However, many efforts of municipal authorities to mitigate noise pollution have failed because of economic, political and other pressures. For example, although noise control for automobiles has shown some improvement, efforts have been counteracted by the growth in the number and power of automobiles.

CIAL has designed both static and dynamic tests that can be used to set annual noise control limits. For roads and freeways where permitted speeds are above 80 Km/h, CIAL has also designed barriers which protect buildings lining the freeways. Considerable improvements have been obtained using these barriers with noise reductions of over 20 dB at buildings fronts. The most common types of barrier are concrete slabs or wooden structures, made translucent or covered with vegetation. Planted vegetation does not act as an efficient noise shield for freeway noise, except in cases of thick forest strips. In several cities, CIAL also designed ring roads to avoid heavy traffic along sensitive areas such as hospitals, schools and laboratories.

Efforts have not been successful in reducing the noise pollution from popular sports such as carting, motorboating and motocross, where noise levels can exceed 100 dB. In part, this is because individuals do not believe these activities can result in hearing impairment or have other detrimental effects, in spite of the scientific evidence. Argentinean and other Latin American authorities also have not been successful in reducing the sound levels from music centres, such as discotheques, where sound levels can exceed 100 dB between 11 pm and 6 am. However, public protest is increasing and municipal authorities have been applying some control. For instance, in big cities, discotheque owners and others are beginning to seek advice on how to isolate their businesses from apartment buildings and residential areas. Some improvements have been observed, but accepted limits have not yet been generally attained.

United States of America (Larry Finegold)

Noise Exposure.

In the United States, there have only been a few major attempts to describe broad environmental noise exposures. Early estimates for the average daily exposure of various population groups were reported in the U.S. Environmental Protection Agency's *Levels Document* (US EPA 1974), but these were only partially verified by subsequent large-scale measurements. Another EPA publication the same year provided estimates of the national population distribution as a function of outdoor noise level, and established population density as the primary predictor of a community's noise exposure (Galloway et al. 1974). Methodological issues that need be considered when measuring community noise, including both temporal and geographic sampling techniques, have been addressed by Eldred (1975). This paper also provided early quantitative estimates of noise exposure at a variety of sites, from an isolated spot on the North rim of the Grand Canyon to a spot in downtown Harlem in New York City. Another nationwide survey focused on exposure to everyday urban noises, rather than the more traditional approach of measuring exposure to high-level transportation noise from aircraft, traffic and rail (Fidell 1978). This study included noise exposure and human response data from over 2 000 participants at 24 sites.

A comprehensive report, *Noise In America: The Extent of the Problem,* included estimates of occupational noise exposure in the US in standard industrial classification categories (Bolt, Beranek & Newman, Inc. 1981). A more recent paper reviewed the long-term trends of noise exposure in the US and its impact over a 30-year time span, starting in the early 1970's. The focus was primarily on motor vehicle and aircraft noise, and the prediction was for steadily decreasing population-weighted day-night sound exposure (Eldred 1988). However, it remains to be seen whether the technological improvements in noise emission, such as changing from Chapter 2 to Chapter 3 aircraft, will be offset in the long run by the larger carriers and increased operations levels that are forecast for all transportation modes. Although never implemented in its entirety, a comprehensive plan for measuring community environmental noise and associated human responses was proposed over 25 years ago in the US (Sutherland et al. 1973).

Environmental Noise Policy in the United States

One of the first major breakthroughs in developing an environmental noise policy in the United States occurred in 1969 with the adoption of the National Environmental Policy Act (NEPA). This Congressional Act mandated that the environmental effects of any major development project be assessed if federal funds were involved in the project. Through the Noise Control Act (NCA) of 1972, the U.S. Congress directed the US Environmental Protection Agency (EPA) to publish scientific information about the kind and extent of all identifiable effects of different qualities and quantities of noise. The US EPA was also requested to define acceptable noise levels under various conditions that would protect the public health and welfare with an adequate margin of safety. To accomplish this objective, the 1974 US EPA *Levels Document* formally introduced prescribed noise descriptors and prescribed levels of environmental noise exposure. Along with its companion document, *Guidelines for Preparing Environmental Impact Statements on Noise*, which was published by the U.S. National Research Council in 1977, the

Levels Document has been the mainstay of U.S. environmental noise policy for nearly a quarter of a century. These documents were supplemented by additional Public Laws, Presidential Executive Orders, and many-tiered noise exposure guidelines, regulations, and Standards. Important examples include *Guidelines for Considering Noise in Land Use Planning and Control*, published in 1980 by the US Federal Interagency Committee on Urban Noise; and *Guidelines for Noise Impact Analysis*, published in 1982 by the US EPA.

One of the distinctive features of the US EPA *Levels Document* is that it does not establish regulatory goals. This is because the noise exposure levels identified in this document were determined by a negotiated scientific consensus and were chosen without concern for their economic and technological feasibility; they also included an additional margin of safety. For these reasons, an A-weighted Day-Night Average Sound Level (DNL) of 55 dB was selected in the *Levels Document* as that required to totally protect against outdoor activity interference and annoyance. Land use planning guidelines developed since its publication allow for an outdoor DNL exposure in non-sensitive areas of up to 65 dB before sound insulation or other noise mitigation measures must be implemented. Thus, separation of short-, medium- and long-term goals allow noise-exposure goals to be established that are based on human effects research data, yet still allow for the financial and technological constraints within which all countries must work.

The US EPA's Office of Noise Abatement and Control (ONAC) provided a considerable amount of impetus to the development of environmental noise policies for about a decade in the US. During this time, several major US federal agencies, including the US EPA, the Department of Transportation, the Federal Aviation Administration, the Department of Housing and Urban Development, the National Aeronautics and Space Administration, the Department of Defense, and the Federal Interagency Committee on Noise have all published important documents addressing environmental noise and its effects on people. Lack of funding, however, has made the EPA ONAC largely ineffective in the past decade. A new bill, the *Quiet Communities Act* has recently been introduced in the U.S. Congress to re-enact and fund this office (House of Representatives Bill, H.R. 536). However, the passage of this bill is uncertain, because noise in the US, as in Europe, has not received the attention that other environmental issues have, such as air and water quality.

In the USA there is growing debate over whether to continue to rely on the use of DNL (and the A-Weighted Equivalent Continuous Sound Pressure Level upon which DNL is based) as the primary environmental noise exposure metric, or whether to supplement it with other noise descriptors. Because a growing number of researchers believe that "Sound Exposure" is more understandable to the public, the American National Standards Institute has prepared a new Standard, which allows the equivalent use of either DNL or Sound Exposure (ANSI 1996). The primary purpose of this new standard, however, is to provide a methodology for modeling the Combined or Total Noise Environment, by making numerical adjustments to the exposure levels from various noise sources before assessing their predicted impacts on people. A companion standard (ANSI 1998) links DNL and Sound Exposure with the current USA land use planning table. The latter is currently being updated by a team of people from various federal government agencies and when completed should improve the capabilities of environmental and community land-use planners. These documents will complement the newly revised ANSI standard on acoustical terminology (ANSI 1994).

To summarize progress in noise control made in the USA in the nearly 25 years since the initial national environmental noise policy documents were written, the Acoustical Society of America held a special session in Washington, D.C. in 1995. The papers presented in this special session were then published as a collaborative effort between the Acoustical Society of America and the Institute of Noise Control Engineering (von Gierke & Johnson 1996). This document is available from the Acoustical Society of America, as are a wide range of standards related to various environmental noise and bioacoustics topics from the ANSI.

A document from the European Union is now also available, which includes guidelines for addressing noise in environmental assessments (EU 1996). Policy documents from organizations such as ISO, CEN, and ICAO have shown that international cooperation is quite possible in the environmental noise arena. The ISO document, entitled *Acoustics - Description and Measurement of Environmental Noise* (ISO 1996), and other international standards have already proven themselves to be invaluable in moving towards the development of a harmonized environmental noise policy. The best way to move forward in developing a harmonized environmental noise policy is to take a look at the various national policies that have already been adopted in many countries, including those both from the European member states and from the USA, and to decide what improvements need to be made to the existing policy documents. A solid understanding of the progress that has already been achieved around the world would obviously provide the foundation for the development of future noise policies.

Implementation Concepts and Tools

Development of appropriate policies, regulations, and standards, particularly in the noise measurement and impact assessment areas, is a necessary foundation for implementing effective noise abatement policies and noise control programs. A well-trained cadre of environmental planners will be needed in the future to perform land-use planning and environmental impact analysis. These professionals will require both a new generation of standardized noise propagation models to deal with the Total Noise Environment, as well as sophisticated computer-based impact analysis and land-use planning tools.

A more thorough description of the current noise environment in major cities, suburbs, and rural areas is needed to support the noise policy development process. A new generation of noise measurement and monitoring systems, along with standards related to their use, are already providing considerable improvement in our ability to accurately describe complex noise environments. Finally, both active and passive noise control technologies, and other noise mitigation techniques, are rapidly becoming available for addressing local noise problems. Combined with a strong public awareness and education program, land-use planning and noise abatement efforts certainly have the potential to provide us with an environment with acceptable levels of noise exposure.

References

ANSI 1994 American National Samerican Standard Acoustical Terminology. American National Standard S1. American National Standards Institute, New York, NY, USA.

ANSI 1996)Quantities and Procedures for Description and Measurement of Environmental Sound - Part 4: Assessment and Prediction of Long-Term Community Response. American National Standard S12.9-Part 4, American National Standard Institute, New York, NY, USA.

ANSI 1998 Quantities and Procedures for Description and Measurement of Environmental Sound - Part 5: Sound Level Descriptors for Determination of Compatible Land Use. American National Standard S12.9-Part 5, American National Standard Institute, New York, NY, USA.

Bolt, Beranek, Newman, Inc. (BBN) 1981 Noise in America: The extent of the problem. Cambridge, MA, USA.

Eldred km 1975 Assessment of community noise. Noise Control Engineering Journal 3: 88-95.

Eldred km 1988 Noise at the year 2000. In Proceedings of the Fifth International Congress on Noise as a Public Health Problem (B. Berglund et al., eds.). Stockholm: Swedish Council for Building Research.

Fidell S (1978) Nationwide urban noise survey. Journal of the Acoustical Society of America 64: 198-206.

Galloway W, Eldred K, and Simpson M 1974 Population distribution of the United States as a function of outdoor noise. US Environmental Protection Agency Report No. 550/9-74-009. Washington, D.C., USA.

Schori JR, McGatha EA (1973) A real-world assessment of noise exposure. Sound and Vibration 12: 24-30.

Sutherland LC, Braden, MH, and Colman R 1973 A programme for the measurement of environmental noise in the community and its associated human response. Vols. I and II. Report No. DOT-TST-74-5, Washington, D.C.: Department of Transportation, Office of Noise Abatement.

US EPA 1974 Information on levels of environmental noise requisite to protect public health and welfare with an adequate margin of safety. EPA/ONAC Report 550/9-74-004, U.S. Environmental Protection Agency, Washington, D.C., USA.

von Gierke HE, Johnson LC 1996 Noise Control - Where Do We Stand Today? Noise Control Engineering Journal.

AFRICAN REGION

South Africa (Etienne Grond, South Africa)

Introduction

Cultural and developmental levels diverge greatly in South Africa, and the country can be divided into a first world sector, a developing sector and a third world sector. This contributes to huge variations in both the awareness of noise pollution and in population exposure to noise pollution. Noise-related health problems will in all probability show the same large variations.

Legal requirements

Noise control in South Africa has a history dating back about three decades. Noise control began with codes of practice issued by the South African Bureau of Standards (SABS) to address noise pollution in different sectors. Since then, Section 25 of the Environment Conservation Act (Act 73 of 1989) made provision for the Minister of Environmental Affairs and Tourism to regulate noise, vibration and shock at the national level. These regulations were published in 1990 and local authorities could apply to the Minister to make them applicable in their areas of jurisdiction. However, a number of the bigger local authorities did not apply for the regulations since they already had by-laws in place, which they felt were sufficient. By the middle of 1992 only 29 local authorities had applied the regulations and so the act was changed to make it obligatory for all authorities to apply the regulations. However, by the time the regulations were ready to be published, the new Constitution of South Africa came into effect and this listed noise control as an exclusive legislative competence of provincial and local authorities. This meant that the national government could not publish the regulations. However, provincial governments have agreed to publish the regulations in their respective areas. The regulations will apply to all local authorities as soon as they are published in the provinces, and will give local authorities both the power and the obligation to enforce the regulations.

The Department of Environmental Affairs and Tourism also published regulations during 1997 to make Environmental Impact Assessments mandatory for most new developments, as well as for changes in existing developments. This means that any impact that a development might have on its surrounding environment must be evaluated and, where necessary, the impact must be mitigated to acceptable levels. The noise control regulations also state that a local authority may declare a "controlled area," which is an area where the average noise level exceeds 65 dBA over a period of 24 h period. This means that educational and residential buildings, hospitals and churches may not be situated within such areas.

Occupational noise exposure is regulated by the Department of Manpower, under the Occupational Health and Safety Act (Act 85 of 1993). These regulations states that workers may not be exposed to noise levels of higher than 85 dBA and that those exposed to such levels must make use of equipment to protect their hearing. The problem, however, is that most workers tend not to make use of the provided equipment, either because the equipment is not comfortable, or because they are not aware of the risks high noise levels pose to their hearing. A further problem is that small industries often do not supply the workers with the necessary equipment, or supply inferior equipment that is less costly.

Codes of practice

The codes of practice issued by the SABS were for the most part replaced by IEC (International Electrotechnical Commission) standards and adopted as SABS ISO codes of practice. They are still being used in South Africa and are regularly updated. A relevant list can be found in the references. The SABS has also published a number of recommended practices (ARP). These include the ARP 020: "Sound impact investigations for integrated environmental management" that is currently being upgraded to a code of practice. Such codes of practice can be referred to as requirements in legislation and will be known as SABS 0328: "Methods for environmental noise impact assessments." The codes of practice published in South Africa cover hearing protection; measurement of noise; occupational noise; environmental noise; airplane noise; and building acoustics, etc.

Courses

Local authorities responsible for applying regulations published by the Department of Environmental Affairs and Tourism must employ a noise control officer who has at least three years tertiary education in engineering, physical sciences or health sciences, and who is registered with a professional council. Alternatively, a consultant with similar training may be employed. Most of the universities in South Africa provide the relevant training, with at least part of the training in acoustics. Universities and technical colleges also provide a number of special acoustics courses. Over the last couple of years awareness of environmental conservation has expanded dramatically within the academic community, and most universities and colleges now have degree courses in environmental management. At the very least, these courses include a six-month module in acoustics, and usually also include training in basic mathematics; the physics of sound; sound measuring methodologies; and noise pollution.

Community awareness and exposure to noise pollution

This topic should be discussed with respect to three separate population sectors: the first-world sector (developed), the developing sector and the third-world sector (rural).

Developed sector

This sector of the population is more-or-less as developed as their European and American counterparts. They have been exposed to noise pollution for a considerable time and, for the most part, are aware of the health consequences of high noise levels. People in this group are also aware of the existence of legal measures by which noise pollution can be addressed. Not surprisingly, most of the complaints and legal action regarding noise pollution are received from this group. Information about noise-related health problems is very limited, but because this group is highly aware of the risks posed by high noise levels, future studies will probably show that people in this category have the fewest health problems. The majority of people in this group are less exposed to high noise levels at work, and they live in more affluent neighborhoods with large plots and separating walls. Their houses tend to be built with materials that are noise reducing. They also live further away from major noise-producing activities, such as highways, airports and large industries.

Developing sector

This sector of the population has the greatest exposure to high noise levels, both at home and in the workplace. Overall, they are relatively poor and cannot afford to live in quiet areas, or afford large plots or solid building materials. A large component of this sector resides in squatter communities where building are made of any material available, from plastic to corrugated sheets and wood. The buildings are right next to each other and there is almost no noise attenuation between residencies.

People in this category usually live close to major access routes into the cities, because they make use of public transportation and taxis to get to their places of work. Often, too, they live close to their places of work, which are usually big industries with relatively high levels of noise pollution. These people usually work in high noise areas, and because of their lack of awareness of the effects of high noise levels, often do not make use of available hearing protection equipment. Because of a lack of funds, these people also cannot get out of high noise areas and go to recreational areas for relaxation and lower noise levels. Not much information is available on the adverse health problems in this sector. However, workers in this sector should undergo regular medical examinations and the results can be obtained from the industries involved.

Rural sector

As the name suggests, people in this sector live in rural surroundings and for the most part are not subjected to noise levels that could be detrimental to their health. However, they are almost totally unaware of the risks posed by high noise levels. Some of these people work on farms and work with machinery that emits relatively high noise levels, but because of their lack of awareness they do not make use of hearing protection equipment. One advantage they do have is that they return to homes in quiet surroundings and their hearing has a chance to recover. To date, no studies have been carried out to determine the state of their hearing and it would be impossible to state that they have no health problems related to high noise levels.

References

Environment Conservation Act (Act No. 73 of 1989) Noise Control Regulations, Ministry of Environmental Affairs and Tourism, Pretoria, South Africa.

Relevant SABS codes of practice:

SABS 083-1996. The measurement and assessment of occupational noise for hearing conservation purposes.

SABS 0103-1994. The measurement and rating of environmental noise with respect to annoyance and speech communication (third revision).

SABS 0115-1974. The measurement of noise and the determination of disturbance from aeroplanes for certification purposes.

SABS 0117-1974. The determination and limitation of disturbance around an aerodrome due to noise from aeroplanes (Amendment no 1 - 1984).

SABS 0205-1986. The measurement of noise emitted by motor vehicles in motion.

SABS 0210-1996. Calculating and predicting road traffic noise (Amendment no 1 - 1997).

SABS 0211-1987. The measurement of noise inside motor vehicles.

SABS 0218/1-1988. Acoustical properties of buildings Part 1: The grading of buildings according to their airborne-sound insulation properties (under revision).

SABS 0218/2-1988. Acoustical properties of buildings Part 2: The assessment of building plans and buildings with respect to their acoustical properties (under revision).

SABS 0234-1991. Determination of sound power levels of multi-source industrial plants for the evaluation of the sound pressure levels in the environment - Engineering method (Incorporating ISO 8297:1994).

ARP 020-1992. Sound impact investigations for integrated environmental management. (To be superseded and replaced by SABS 0328: Methods for environmental noise impact assessments).

EASTERN MEDITERRANEAN REGION (Shabih H. Zaidi)

Scope

In the Eastern Mediterranean region some countries have highly developed industries, while others have none. In other cases, the agricultural economy is inseparably mixed with high-technology industries, such as the oil industry, which can be seen in nearly the whole of the Arabian Peninsula. Other examples of where agriculture and industry are intertwined can be seen in Pakistan, Jordan and Egypt. The main focus of this paper is community noise, but because industry is so widely distributed, some discussion of industrial noise is inevitable. The scope of this paper is to document the available scientific data on community noise in the WHO Regional Office of the Eastern Mediterranean (EMRO) region, including preventive strategies, legislation, compensation and future trends.

Sources of Noise Pollution

Sources of noise pollution in the Eastern Mediterranean region include noise from transportation, social and religious activities, building and civil works, roadside workshops, mechanical floor shops and others. During civil works and building booms, noise levels in all countries of the Eastern Mediterranean region could easily reach 85dBA during the daytime over an 8 h work period. In Pakistan, unprotected construction work goes on at all times of the day and night and uses outdated machinery; and the noise is compounded by workers shouting. On a typical building site noise levels reach 90–100 dBA.

In Karachi, the main artery for daily commuters is a long road that terminates at the harbor. In the densest area of this road there are a hundred small and large mechanical workshops, garages, metal sheet workers, dent removers, painters, welders and repair shops, all of which create a variety of noises. In the middle of this area at the Tibet Centre the LAeq,8h is 90dBA (Zaidi 1989). A similar picture is seen elsewhere in cities like Lahore, Peshawar, etc. Fortunately, the same is not true for other newly built cities in the EMRO region, such as Dubai, or Tripoli, where strict rules separate industrial zones from residential areas.

A special noise problem is Karachi harbour. This port serves the whole of Pakistan as well as Afghanistan and several Asian states, such as Kyrgyzstan, Kazakhstan and Uzbekistan. The noise level at the main wharf of Karachi Port ranges between 90–110 dBA on any given day. Other special sources of noise are the Eastern Mediterranean airports, and indeed most of the airports in the Middle East. Most northbound air traffic originates in Pakistan, Dubai, Sharjah etc. and flights usually depart after midnight so as to arrive in Europe during the daytime. A study is currently underway in Karachi to identify the damage caused by these nocturnal flights to those living under the flight path (SH Zaidi, GH Shaikh & AN Zaidi, personal communication).

Sadly, violence has become part of Eastern culture and is a significant source of noise pollution. Wars generate a lot of noise, and although noise-induced hearing loss is a secondary issue compared with the killing, after the wars many people are hearing impaired. This has been seen following conflicts in Balochistan, Peshawar and Afghanistan, where perforated ear drums, profound hearing loss and stress-related psychosomatic illnesses are common in the refugee camps. The noise levels during a recent mass demonstration in Karachi, which included the firing of automatic weapons, reached 120 dBA at a distance of 50 m from the scene.

The Effects of Noise on Health

There is good evidence that environmental noise causes a range of health effects, including hearing loss, annoyance, cardiovascular changes, sleep disturbance and psychological effects. Although the health effects of noise pollution have not been documented for the entire EMRO region, data are available for Pakistan and can be used to illustrate the general problem. In this report, noise exposure is mainly expressed as LAeq,24h values.

Noise-induced hearing loss (NIHL).

It is believed that exposure to environmental noise in the EMRO countries is directly related to the living habits, economic prosperity and outdoor habits of people. It has been estimated that no more than 5% of the people are exposed to environmental sound levels in excess of 65dBA over a 24-h period. Similarly, for indoor noise, it is believed that the average family is not exposed to sound levels in excess of 70 dBA over a 24-h period. However, it is difficult to generalize for all countries in the EMRO region, because of ancient living styles and different cultural practices, such as taking siestas between 13:00–16:00 and stopping work at 20:00.

Exposure to noise while travelling to schools, offices or workplaces may vary tremendously between cities in the region. In Karachi, for example, traffic flow is undisciplined, erratic and irrational, with LAeq,8h values of 80–85 dBA. In Riyadh, by contrast, traffic flow is orderly with LAeq levels of 70 dBA during a normal working day. In Karachi, noise levels show significant diurnal variation, reaching levels in excess of 140 dB during the peak rush hour at around 5.00 p.m. (Zaidi 1989). At the Tibet Centre, located at a busy downtown junction, noise levels were 60–70 dB at 9 am, but reached levels in excess of 140 dB between 5-7 p.m. A study conducted on a day that transportation workers went on strike established that road traffic is the most significant source of noise pollution in this city: in the absence of buses, rickshaws, trucks and other public vehicles the LAeq level declined from 90dB to 75dB (Zaidi 1990). Motor engines, horns, loud music on public buses and rickshaws generate at least 65% of the noise in Karachi (Zaidi 1997; Shams 1997). Rickshaws can produce noise levels of 100–110 dBA and do not have silencers. On festive occasions, such as national holidays or political rallies, motorbikes running at high speeds along the Clifton beach in Karachi easily make noise exceeding 120 dBA. (Zaidi 1996).

Another study conducted at 14 different sites in Karachi showed that, in 11 of the sites, the average noise level ranged between 79–80 dB (Bosan & Zaidi 1995). The maximum noise levels at all these sites exceeded 100 dB. Speech interference, measured by the Preferred Speech Interference Level and the Articulation Index, was significant (Shaikh & Rizvi 1990). The study results indicated that two people facing each other at a distance of 1.2 m would have to shout to be intelligible; and the Articulation Indexes demonstrated that communication was unsatisfactory. Of perhaps greater concern are the results of a survey of 587 males between the ages of 17 and 45 years old, who worked as shopkeepers, vehicle drivers, builders and office assistants. Audiograms showed that 14.6% of the subjects had significant hearing impairment at 3 000–4 000 Hertz (Hasan et al., 2000).

Noise pollution from leisure activities can vary from country to country in the EMRO region. The Panthans in northern Pakistan, for example, like to shoot in the air on festive occasions, such as weddings, without using any noise protection devices. A minimum of 1 000 shots are fired on such occasions; and at a traditional tribal dance called the 'Khattak" the noise level recorded during a particularly enthralling performance in a sports arena was 120dBA. The hunting of wild boar is a common sport in the hinterlands of Sindh. With the rifle shots and the noise made by the beaters, noise levels can easily reach 110 –120 dBA. In some EMRO countries, the younger crowd has taken up the Western habit of listening to Pop music for many hours. Discos and floorshows are confined to a few countries, such as Egypt. Open-air concerts are usually held in stadiums. The noise level recorded at a particularly popular concert was 130 dBA at a distance of 20 m from the stage and 35 m from the amplifiers.

In a study of road traffic at 25 different sites in Peshawar, the third most populous city in Pakistan, 90 traffic constables were taken as cohorts to investigate the extent of NIHL. Of these, 50 did not have any previous history of noise exposure and were taken as controls. Detailed evaluation and audiological investigations established that constables exposed to a noise level of 90 dBA for 8 hours every day suffered from NIHL. Compared to the control subjects, the constables had significant hearing impairment at 3 000 Hz, measured by Pure Tone Audiometry (Akhter 1996).

A similar study of traffic constables in Karachi showed that 82.8% of the constables suffered from NIHL (Itrat & Zaidi 1999). The study also showed that 33.3% of rickshaw drivers, and 56.9% of shopkeepers who worked in noisy bazaars, had hearing impairment. If these findings can be extrapolated to the total populations, there are 1 566 traffic constables (out of a total of 1 890 constables), and 4 067 rickshaw drivers (out of a total of 12 202 drivers) who suffer from NIHL. As has been reported by other researchers, the study also found evidence of acclimatization in the subjects: following an initial, rapid decline, hearing loss stabilized after prolonged noise exposure.

Annoyance.

The citizens of Karachi commonly complain that noise causes irritability and stress. The main sources have been identified as traffic noise, industrial noise and noise generated by human activity. Unfortunately no data are available for the level of annoyance caused by noise exposure in the EMRO region. From limited research around the world, it can be estimated that 35–40% of employees in office buildings are seriously annoyed by noise at sound levels in excess of 55–60 dBA. In countries such as Pakistan, Iran, Jordan and Egypt that level is often seen in most offices. Annoyance is a non-tangible entity and cannot be quantified scientifically. It is a human reaction and perhaps its parameters could include irritability, apprehension, fear, anger, frustration, uneasiness, apathy, chaos and confusion. If such are the parameters, then on a scale of 0–10, with 10 being the greatest annoyance, many EMRO countries could easily score 6 or higher.

Effects of noise on sleep and the cardiovascular system.

In the Eastern Mediterranean region no specific data are available on the effects of noise on sleep or the cardiovascular system. However, factory workers, traffic constables, rickshaw drivers and shopkeepers frequently complain about fatigue, irritability and headaches; and one of the most common causes of poor performance in offices is sleep disturbance. The rising incidence of tinnitus in cities like Karachi is also related to noise exposure, and tinnitus itself can lead to sleep deprivation. Although the effects of noise on the cardiovascular system have been well documented for other countries (Berglund & Lindvall 1995), data are lacking for the EMRO region. However, the prevalence of cardiovascular diseases are on the rise in the EMRO countries, particularly hypertension. While most of the increase in these diseases is due to a rich diet and lack of exercise, the relationship between noise and cardiovascular changes is worth investigating.

The risk to unborn babies and newborns.

Although evidence from other countries indicates that noise may damage the hearing of a fetus, there are no data from the EMRO countries to confirm this. With newborn babies, however, noise from incubators is a major cause of hearing loss in the EMRO region, particularly as 20–27% of them are born underweight (Razi et al. 1995). Once exposed to noise in an incubator, the chances of hearing impairment rapidly rises compared with cohorts in developed countries. Several other factors have also been identified as causing deafness and hearing impairment in newborns in the Eastern Mediterranean region (Zaidi 1998; Zakzouk et al. 1994). They are:

a. Discharge from the ears.

b. Communicable infections.

c. Ototoxicity.

d. Noise.

e. Consanguinity.

f. Iodine deficiency.

Noise Control

Although noise control legislation exists in several EMRO countries, it is seldom enforced, particularly in Pakistan and some neighboring countries. Noise control begins with education, public awareness and the appropriate use of media in highlighting the effects of noise. In Calcutta, for instance, public orientation and mass media mobilization have produced tangible results, and this can easily be done in other countries. Three strategies have been devised for noise control, all of which are practicable in EMRO region countries. They are control at the source, control along the path and control at the receiving end.

There are many ways noise can be controlled at the source. For example, most of the equipment and machinery used in EMRO countries is imported from the West. Noise control could begin by importing quieter machinery, built with newer materials like ceramics or frictionless parts. And at the local level, the timely replacement of parts and proper maintenance of the machines should be carried out. Vehicles like the rickshaw should be banned, or at least be compelled to maintain their silencers, and all vehicles must be put to a road worthiness test periodically. This already occurs in some EMRO countries, but not all. Horns, hooters, music players and other noise making factors must also be controlled. The use of amplifiers and public address systems should also be banned, and social, leisure and religious activities should be restricted to specific places and times.

Along the sound path, barriers can be used to control noise. There are three kinds of barriers available, namely, space absorbers made out of porous material, resonant absorbers and panel absorbers. Architects, for example, use hollow blocks of porous material. The air gaps between building walls not only keep the buildings cool in hot weather, but also reduce the effects of noise. Ceilings and roofs are often treated with absorbent material. In large factories, architects use corrugated sheets and prefabricated material, which are helpful in reducing noise levels. In Pakistan, some people use clay pots in closely ranked positions on rooftops to reduce the effect of heat as well as noise. For civic works and buildings, special enclosures, barriers and vibration controlling devices should be used. Public halls, such as cinemas, mosques and meeting places should have their walls and floors carpeted, and covered with hangings, mats etc. An effective material is jute, which is grown in many countries, mainly Bangladesh, and it is quite economical. Some of the old highways and most of the busy expressways need natural noise barriers, such as earth banks, trees and plants.

References.

Akhter NH 1996 Noise induced hearing loss in traffic police constables of Peshawar. Journal of College of Physicians and Surgeons Pakistan 6: 265-268.

Berglund B and Lindvall T 1995 Community Noise. Archives of the Centre for Sensory Research, volume 2, issue 1, pp. 56,57.. Stockholm University and Karolinska Institute, Stockholm.

Bosan Altaf, Zaidi SH Nobel Tracy 1995 The problem of noise, Pakistan Journal of Otolaryngology 11, 128-131.

Hasan S, Zaidi AN, Tahira S, Zaidi SH 2000 Audiological profile of NIHLin IMPACT Ear Camps. Pakistan Journal of Oto-Rhino-Laryngology, in print.

Itrat J, Zaidi SH 1999 Deafness in Pakistan, Pakistan Journal of Otolaryngology 15: 78-83.

Razi MS, Jaffer S, Hillier V, Zaidi SH, Newton V 1995 Causes of bilateral hearing loss in school children. Pakistan Journal of Otolaryngology 11: 68-86.

Shams ZI 1997 The hazards of noise pollution. Daily Dawn, 30th September 1997.

Shaikh GH, Rizvi SSII 1987 Road transport in Karachi city. Pakistan Journal of Science and research, 30: 197.

The environmental protection agency Sindh. The study of noise pollution in Karachi. Executive Report. Karachi Pakistan. ACE (pvt.) Ltd. Karachi.

Zaidi SH 1989 Noise level and the sources of noise pollution in Karachi. Journal of Pakistan Medical Association, 39: 62-65.

Zaidi SH 1990 Noise level in Karachi on a transporter's strike day. Journal of Pakistan Medical Association, 40: 299-300.
Zaidi SH 1996 Noise Ototoxicity. Pakistan Journal of Otolaryngology, 12: 194.
Zaidi SH 1997 Noise induced hearing loss in Pakistan. Hearing International, 6: 12-13.
Zaidi SH 1998 The causes of deafness and Hearing Impairment in the Tropics: Keynote speech delivered at the Centennial Congress of Liverpool School of Tropical Medicine in Sept 1998. Pakistan Journal of Otolaryngology 14: 102-107.
Zakzouk SM, Bafaqeh SA, Al-Mahmmod H, Essa A 1994 Demographic factors and hearing impairment in Saudi Arabian Children., Journal of Laryngology and Otology 108: 294-298.

SOUTH-EAST ASIAN REGION. (Sudhakar B. Ogale)

Introduction

The ability to hear sound is a sensory function vital for human survival and communication. However, not all sounds are wanted. Unwanted sounds, for which the term "noise" is normally used, often originate from human activities such as road traffic, rail traffic, aircraft, discos, electric power generators, festivals, firecrackers and toys. In general, however, data on noise pollution in South east Asian countries are not available. For example, there are no comprehensive statistical data regarding the incidence and etiology of hearing impairment. Consequently, it is difficult to estimate the exact percentage of the population affected by community noise.

Excessive noise is the major contributor to many stress conditions. It reduces resistance to illness by decreasing the efficiency of the immune system, and is the direct cause of some gastrointestinal problems. Noise also increases the use of drugs, disturbs sleep and increases proneness to accidents. An increased incidence of mental illness and hospital admissions, increases in absenteeism from work and lethargy from sleep disturbance all result from noise pollution and cause considerable loss of industrial production.

Noise Exposure in India

India is rapidly becoming industrialized and more mechanized, which directly affects noise levels. However, no general population study regarding the magnitude of the noise problem in India has been performed.

Road Traffic Noise

Exposure. A study by the Indian Institute of Road Traffic (IRT) reported that Delhi was the noisiest city in India, followed by Calcutta and Bombay (IRT 1996; Santra & Chakrabarty 1996). The survey examined whether road-traffic noise affected people with respect to annoyance, sleep disturbance, interference with communication and hearing impairment. It showed that 35% of the population in four major cities have bilateral sensory neural hearing loss at noise emission levels above 82 dBA. This is of particular concern in light of a second study, showing that LAeq,24h levels at 24 kerbside locations in Calcutta were 80–92 dBA (Chakrabarty et al. 1997) The mean noise emission levels of four different vehicle categories are presented in Table A2.1.

Table A2.1: Mean noise emission levels of vehicles

Type of vehicle	Mean sound pressure level
2 wheelers (motor cycle)	82 dBA
3 wheelers (auto rickshaw)	87 dBA
Motor car (taxi, private cars)	85 dBA
Heavy vehicles (trucks)	92 dBA

Control Measures. Only recently has noise pollution been considered an offence in India, under the Environmental (Protection) Act 1986. Several measures are being taken to reduce traffic-noise exposure. These include:

a. Planting trees, shrubs and hedges along roadsides.

b. Mandatory, periodic vehicle inspections by road traffic control.

c. Reintroduction of silent zones, such as around schools, nursing homes and hospitals that face main roads.

d. Regulation of traffic discipline, and a ban on the use of pressure horns.

e. Enforcement of exhaust noise standards.

f. Mandating that silencers be effective in three-wheeled vehicles.

g. The use and construction of bypass roads for heavy vehicles.

h. Limiting night-time access of heavy vehicles to roads in residential neighbourhoods

i. Installation of sound-proof windows.

j. Proper planning of new towns and buildings.

Air Traffic Noise

Many airports were originally built at some distance from the towns they served. But due to growing populations and the lack of space, buildings are now commonly constructed alongside airports in India.

Exposure. A survey revealed that aircraft produced a high level of noise during take-off, with sound pressure levels of 97–109 dBA for the Airbus, and 109 dBA for Boeing aircraft (SB Ogale, unpublished observations). During landing, the aircraft produced a sound pressure level of 108 dBA. Although exposure to aircraft noise is considered to be less of a problem than exposure to traffic noise, the effects of air-traffic noise are similar to those of road traffic, and include palpitations and frequent awakenings at night.

Control measures. The use of ear muffs must be made obligatory at the airport. This can reduce noise exposure to a safe level. An air-traffic control act should also enforce the use and introduction of low-noise aircraft, and mandate fewer night-time flights.

Rail Traffic Noise

Very little attention has been paid to the problems of railway noise.

Exposure. In Bombay, where the majority of residential buildings are situated on either side of railway tracks, residents are more prone to suffer from acoustic trauma. More than 14% of the population in Bombay suffer from sleep disturbances during night, due to high-speed trains and their whistling. A study on surface railways (SB Ogale, unpublished observations) revealed that platform noise was 71–73 dBA in the morning and 78–83 dBA in the evening. The noise from loudspeakers mounted in the platform was 87–90 dBA. At a distance of 1 m from the engine, the whistle noise was 105–108 dBA for a train with an electric engine, up to 110 dBA for a train with diesel engine and 118 dBA for steam engine trains. Vacuum brakes produced noise levels as high as 95 dBA. This suggests that unprotected railway staff on platforms are at risk of permanent noise induced hearing loss.

Festival noise

Festival noise in India was first surveyed in Bombay in late 1970, during the Ganpati festival period. A similar study (Santra et al. 1996) was conducted soon after in Calcutta at the Durga Pooja festival during evening hours (18:00–22:00). The music from loudspeakers produces sound pressure levels of more than 112 dBA. During the festival period the residents experienced a noisy environment for 8–10 h at a stretch, with noise level of 85–95 dBA. This level is above the 80 dBA limit set by WHO for industrial workers exposed to noise for a maximum period of 8 hours.

Control measures. In a religious country, it is politically difficult to restrict religious music, even in the interests of public health. A ban on all music from loudspeakers after 22:00 would decrease the sound pressure levels to below the permissible legal limit. A preventive programme is advocated to measure noise levels with sound level metres.

Fire crackers and toy weapons noise

Exposure. A study conducted by Gupta & Vishvakarma (1989) at the time of Deepawali, an Indian festival of fireworks, determined the auditory status of 600 volunteers from various age groups, before and after exposure to firecrackers. The study also measured the acoustical output of representative samples of toy weapons and firecrackers, and the noise intensity level at critical spectator points. The average sound level at a distance of 3 m from the noise source was 150 dBA, exceeding the 130 dBA level at which adults are at risk for hearing damage. On average, 2.5% of the people surveyed during Deepawali had persistent sensory neural hearing loss of 30 dBA, with those in the 9–15 year old age group being most affected.

Control Measures. A judicious approach in the manufacture and use of toy weapons and firecrackers is encouraged, in addition to legal restraints. Fireworks should be more a display of light, rather than sound.

Generator Noise

Diesel generators are often used in India to produce electric power. Big generators produce sound pressure levels exceeding 96 dBA (SB Ogale, unpublished observations).

Conclusions

No comprehensive statistical data are available for community noise in India, however, the main sources of environmental noise are road traffic, air traffic, rail traffic, festivals, firecrackers and diesel generators. The adverse effects of noise are difficult to quantify, since tolerance to noise levels and to different types of noise varies considerably between people. Noise intensity also varies significantly from place to place. It should also be noted that noise data from different countries are often not obtained by the same method, and in general models have been used which are based on data from a limited number of locations. Noise control measures could be taken at several levels, including building design, legal measures, and educating the people on the health dangers of community noise. In India, what is needed now is noise control legislation and its strict enforcement, if a friendly, low-noise environment is to be maintained.

Noise Exposure in Indonesia

According to a report by the WHO, the noise exposure and control situation in Indonesia is as follows (Dickinson 1993).

Exposure. No nationwide data are available for Indonesia. However, during the last three decades there has been rapid growth in transportation, industry and tourism in Indonesia.

Control Measures. With the large majority of people having little income, protection of the physical environment has not been a first-order priority. The following recommendations have been made with respect to community noise (Dickinson 1993):

a. The cities of Indonesia have relatively large populations and each provincial government will need the staff and equipment to monitor and manage the environment.

b. Sound level meters with noise analysis computer programmes should be purchased.

c. Training courses and adequate equipment should be provided.

d. Noise management planning for airports should be promoted.

e. Reduction measures should be taken for road-traffic noise.

Noise Exposure in Bangladesh

Exposure. In Bangladesh no authentic statistical data on the effects of community noise on deafness or hearing impairment are available (Amin 1995).

Control Measures. Governments have meager resources, a vast population to contend with and high illiteracy rates; consequently, priorities are with fighting hunger, malnutrition, diseases and various man-made and natural calamities. The governments are unable to give the necessary attention towards the prevention, early detection and management of noise disabilities in the country. Close cooperation is needed between the national and international organizations, to exchange ideas, skills and knowledge (Amin 1995).

Noise Exposure in Thailand

Exposure. Noise from traffic, construction, and from factories and industry has become a big problem in the Bangkok area. The National Environmental Board of Thailand was set up two decades ago and has been active in studying the pollution problems in Thailand. Indeed, a committee on noise pollution control was set up to study the noise pollution in Bangkok area and its surroundings. Although regulations and recommendations were made for controlling various sources of noise, the problem was not solved due to a lack of public awareness, the difficulty of proving that noise had adverse effects on health and hearing, and the difficulty of getting access to control noise. A general survey revealed that 21.4% of the Bangkok population is suffering from sensory neural hearing loss (Prasanchuk 1997). Noise sources included street noise, traffic noise, industrial noise and leisure noise.

Control Measures. In 1996, regulations for noise pollution control set LAeq,24h levels at 70 dBA for residential areas, and less than 50 dBA to avoid annoyance. The National Committee on Noise Pollution Control has been asked to study the health effects of noise in the Bangkok area and its surroundings, and determine whether these regulations are realistic and feasible.

References.

Amin 1995 Community Noise. Proceedings of the International Symposium on Deafness and Hearing Impairment in Developing Countries, Manchester, 6-8 July 1995.
Chakrabarty D, Santra SC, Mukherjee A, Roy B, Das P 1997 Status of road traffic noise in Calcutta metropolis, India. Journal of the Acoustical Society of America 101: 943-949
Dickinson P (1993) Noise assessment and management in Indonesia. Report SEA/EH 461, Regional Office for South-East Asia, World Health Organization, New Delhi, India.
Gupta D, Vishvakarma SK. 1989 Toy weapons and fire crackers. Laryngoscope 99: 330-334.

IRT 1996 Indian Council of Medical Research Bulletin Vol. 26, No. 8, August 1996, New Delhi.
Prasanchuk S (1997) Noise pollution. Its effect on health and hearing – Thailand as a case study. Presentation at the PDH Informal Consultation on the Prevention of Noise-induced Hearing Loss, 28-30 October 1997, WHO/PDH/98.5. World Health Organization, Geneva, Switzerland.
Santra SC, Chakrabarty D 1996 Need for rationalization of noise standards in Indian perspectives. Presented at the First National Workshop on Development and Use of Environmental Reference Materials, 14-16 February 1996, Central Pollution Control Board, New Delhi.
Santra SC, Chakrabarty D, Mukherjee A, Roy B 1996 Noise status of Calcutta metropolis. A resume. Man and Environment, Annual Report, pp. 19-22.

WESTERN PACIFIC REGION.

In this section, information on noise pollution and control will be given for three countries in the Western Pacific Region, namely Australia, the People's Republic of China and Japan. From a noise pollution point of view China may be viewed as a developing country, whereas Japan and Australia, with their high level of industrialization, represent developed countries.

Australia (Andrew Hede & Michinori Kabuto)

Exposure. Australia has a population of 18 million with the majority living in cities that have experienced increasing noise pollution from a number of sources. The single most serious source of noise is road traffic, although in major cities such as Sydney, Melbourne and Perth, large communities are exposed to aircraft noise as well. Other important sources of noise pollution are railway noise and neighbourhood noise (including barking dogs, lawn mowers and garbage collection). A particular problem in Australia is that the climate encourages most residents to live with open windows, and few houses have effective noise insulation.

A study of road-traffic noise was conducted at 264 sites in 11 urban centres with populations in excess of 100 000 people (Brown et al. 1994). Noise was measured one metre from the façade of the most exposed windows and at window height. From the results, it was estimated that over 9% of the Australian population is exposed to LA10,18h levels of 68 dB or greater, and 19% of the population is exposed to noise levels of 63 dB or greater. In terms of LAeq values for daytimes, noise exposure in Australia is worse than in the Netherlands, but better than in Germany, France, Switzerland or Japan.

Control. In the mid-1990's, when a third runway was built at Sydney Airport, the government funded noise insulation of high-exposed dwellings. Increasingly, too, major cities are using noise barriers along freeways adjacent to residential communities. In most states barriers are mandatory for new freeways and for new residential developments along existing freeways and major motorways. There has been considerable testing of noise barriers by state agencies, to develop designs and materials that are cost effective.

Brown AL et al. (1994) Exposure of the Australian Population in Road Traffic Noise. Applied Acoustics 43: 169-176.
OECD (1991) Fighting Noise in the 1990's. Organization for Economic Cooperation and Development, Paris, France.

China (Chen Ming)

Introduction

Urban noise pollution has become a contemporary world problem. Urban noise influences people's living, learning and working. People exposed to noise feel disagreeable and cannot concentrate on work. Rest and sleep are also disturbed. People exposed to high-intensity noise do not hear alarm signals and cannot communicate with each other. This can result in injury and, indeed, with the modernization of China, construction accidents related to noise are increasing. According to statistics for several cities in China, including Beijing, Shanghai, Tientsin and Fuzhou, the proportion of total accidents that were noise related was 29.7% in 1979, 34.6% in 1980, 44.8% in 1981 and 50% in 1990. It is therefore very important to control noise pollution in China.

Long-term exposure to urban environmental noise can lead to temporary hearing loss (assessed by temporary threshold shift), permanent hearing loss (assessed by permanent threshold shift) or deafness. Microscopy studies have shown that in people exposed to noise for long periods, hair cells, nerve fibers and ganglion cells were absent in the cochleae, especially in the basal turns. The primary lesion is in the 8–10 mm region of the cochlea, which is responsible for detecting sound at a frequency of 4 000 Hz. People chronically exposed to noise may first complain about tinnitus and, later on, about hearing loss. This is especially true for patients who have bilateral hearing loss at 4 000 Hz, but who have relatively good hearing other frequencies. Non-auditory symptoms of noise include effects on the nervous system, cardiovascular system and blood system. These symptoms were rarely observed in China in the past, but today more and more people complain about hearing damage and non-auditory physiological effects.

Urban environmental noise has thus become a common concern of all members of society. A key to resolving the complex noise issue lies in the effective control of urban noise sources. Control measures include reducing noise at its source, changing noise transmission pathways, building design, community planning and the use of personal hearing protection.

Urban environmental noise sources can be divided into industrial noise, traffic noise, building architecture noise and community district noise sources. Only the last three types are of concern here.

Traffic Noise

There are four sources of traffic noise: road traffic, railway transport, civil aviation and water transport; of these, road traffic is the main source of urban noise. The sound emission levels of heavy-duty trucks are 82–92 dBA and 90–100 dBA for electric horns; air horns are even worse, with sound emission levels of 105–110 dBA. Most urban noise from automobiles is in the 70–75 dB range, and it has been estimated that 27% of all complaints are about traffic noise. When a commercial jet takes off, speech communication is interrupted for up to 1 km on both sides of the runway, but people as far away as 4 km are disturbed in their sleep and rest. If a supersonic passenger plane flies at an altitude of 1 500 m, its sound pressure waves can be heard on the ground in a 30–50 km radius.

Building Noise

As a result of urban development in China, construction noise has become an increasingly serious problem. It is estimated that 80% of the houses in Fuzhou were built in the past 20 years. According to statistics, the noise from ramming in posts and supports is about 88 dB and the noise from bulldozers and excavators is about 91 dB, 10 m from the equipment. About 98% of industrial noise is in the 80–105 dB range, and it is estimated that 20% of all noise complaints is about industrial noise.

Community Noise

The main sources of community noise include street noise, noise from electronic equipment (air conditioners, refrigerators, washing machines, televisions), music, clocks, gongs and drums. Trumpets, gongs, drums and firecrackers, in particular, seriously disturb normal life and lead to annoyance complaints.

In conclusion, urban noise pollution in China is serious and is getting worse. To control noise pollution, China has promulgated standard sound values for environmental noise. These are summarized in table A2.2.

Table A2.2: LAeq standard values in dB for environmental noise in urban areas.

Applied area	day	night
Special residential quarters[1]	45	35
Residential and cultural education area[2]	50	40
Type 1 mixed area[3]	55	45
Type 2 mixed area[4] or commercial area	60	50
Industrial area	65	55
Arterial roads[5]	70	55

1 Special residential quarters: quiet residential area
2 Residential and cultural education area: residential quarters, cultural, educational offices
3 Type 1 mixed area: mixture of commercial area and residential quarters
4 Type 2 mixed area: mixture of industrial area, commercial area, residential quarters and others
5 Roads with traffic volume of more than 100 cars per hour

The peak sound levels for frequent noises emitted during the night-time are not allowed to exceed standard values by more than 10 dBA. Single, sudden noises during the night-time are not allowed to exceed standard values by more than 15dBA.

References

Liu Tian Gi et al.: Noise pollution and control. Environmental protection. Chemical industrial publishing company 1996, 6. First publication P137-154.
National environmental protection leader group. GB 3096-82. Urban environmental noise

standard. The national standard of the People's Republic of China. 1982, 8, 1.
Feng Gen Quan: The main result of field investigation for industrial continuous noise. Foreign Medicine. Otorhinolaryngology. 1978, 2:12.
Beijing Medical Quarantine Station: The investigation analysis of the noise hazard condition in nine provinces and cities. The noise work investigation cooperation group in nine provinces and cities (internal material). 1982.
Cheng Ming: The diagnostic criteria of occupational deafness and experience of hearing conservation in China. Noise as public health problem. New advance in noise research, part 1. Swedish Council for building research. Stockholm, Sweden 1990, pp. 137-44.

Japan (Michinori Kabuto)

Environmental Quality Standards

Noise standards for both general and roadside areas were set in Japan in 1967, through the "Basic Law for Environmental Pollution." This law was updated in September 1999. Each standard is classified according to the type of land use and the time of day. In ordinary residential areas, the night-time standard is 45 dB LAeq, but in areas that require even lower noise exposure, such as hospitals, this is lowered to 40 dB LAeq. In contrast, the daytime levels for commercial and industrial areas is as high as 60 dBA. Standards for roadside areas are 70 dB LAeq for daytime and 65 dB LAeq for nighttime. Between 1973–1997 noise standards for aircraft noise, super-express train noise and conventional railway train noise were also implemented. Standards for aircraft noise were set in terms of the weighted equivalent continuous perceived noise level (WECPNL). For residential areas, the WECPNL standard is 70 dBA, and is 75 dBA for areas where it is necessary to maintain a normal daily life.

For super-express trains, the Environmental Agency required noise levels to be below 75 dBA in densely populated residential areas, such as along the Tokaido and Sanyo Shinkansen lines, as well as in increasingly populated areas, such as along the Tohoku and Joetsu Shinkansen lines. The standards were to be met by 1990, but by 1991 this level had been achieved at only 76% of the measuring sites on average. Noise countermeasures included the installation of new types of sound-proof walls, and laying ballast mats along densely populated stretches of the four Shinkansen lines. Noise and vibration problems can also result from conventional trains, such as occurred with the opening of the Tsugaru Strait and Seto Ohashi railway lines in 1988. Various measures have since been taken to address the problems.

Complaints About Community Noise.

In Japan, complaints to local governments about environmental problems have been summarized annually and reported by Japan Environmental Agency. Thirty-seven percent of all complaints was due to factory (machinery) noise; 22% to construction noise; 3% to road traffic noise; 4% to air traffic noise; 0.8% to rail traffic noise; 9% to night-time business; 6% to other commercial activities; 2.5% to loudspeaker announcements; 9% to domestic noise; and 8% was due to miscellaneous complaints.

Sources of Noise Exposure and their Effects

Road-traffic noise. The number of automobiles in Japan has increased from 20 million in 1971 to 70 million in 1994, a 3.5-fold increase. One-third of this increase was due to heavy-duty vehicles. Since 1994, out of a total of 1 150 000 km of roads in Japan, only 29 930 km have been designed according to noise regulations. According to 1998 estimates by the Environmental Agency, 58% of all roads passed through residential areas. Daytime noise limits were exceeded in 92% of all cases, and night-time limits were exceeded in 87% of all cases. The study also estimated that 0.5 million houses within 10 m of the roads were exposed to excessive traffic noise. In a recent lawsuit, the Japanese Supreme Court ruled that people should be compensated when exposed to night-time noise levels exceeding 65 dB Laeq. This would apply to people living alongside 2 000 km of roads in Japan.

A recent epidemiological study examined insomnia in 3 600 women living in eight different roadside areas exposed to night-time traffic. Insomnia was defined as one or more of the following symptoms: difficulty in falling asleep; waking up during sleep; waking up too early; and feelings of sleeplessness one or more days a week over a period of at least a month. The data were adjusted for confounding variables, such as age, medical care, whether the subjects had young children to care for, and sleep apnea symptoms. The results showed that the odds ratio for insomnia was significantly correlated with the average night-time traffic volume for each of the eight areas and suggested that insomnia could be attributed solely to night-time road traffic.

From the most noisy areas in the above study 19 insomnia cases were selected for a further in-depth examination. The insomnia cases were matched in age and work with 19 control subjects. Indoor and outdoor sound levels during sleep were measured simultaneously at 0.6 s intervals. For residences facing roads with average night-time traffic volume of 6 000 vehicles per hour, the highest sound levels observed were 78–93 dBA. The odds ratios for insomnia in each of the quartiles for LAmax,1min; L50,1min; L10,1min and LAeq,1min generally showed a linear trend and ranged between 1 (lowest quartile) and 6–7 (highest quartile). It was concluded that insomnia was likely to result when night-time indoor LAeq, 1min sound levels exceeded 30 dBA.

Air-traffic noise At the larger Japanese airports (Osaka, Tokyo, Fukuoka), jet airplanes have rapidly increased in number and have caused serious complaints and lawsuits from those living nearby. Complaints about jet-fighter noise are also common from residents living in the vicinity of several U.S. airbases located in Japan. In the case of Kadena and Futemma airbases on Okinawa, a recent study by the Okinawa Prefecture Government suggested that hearing loss, child misbehaviour and low birth-weight babies were possible health effects of the noise associated with these bases (RSCANIH 1997). Using measurements taken in 1968 during the Vietnam War, it was estimated that the WECPNL was 99–108 dBA at the Kadena village fire station. Similar WECPNL estimates of 105 dBA were also obtained for Yara (Kadena-cho) and Sunabe (Chatan-cho) bases. These levels correspond to a LAeq,24h value of 83 dB, and are of serious concern in light of recommendations by the Japan Association of Industrial Health that occupational noise exposure levels should not exceed 85 dB for an 8-h work day if hearing loss is to be avoided.

Audiogrammes of subjects living in areas surrounding Kadena airport indicated that they had progressive hearing loss at higher frequencies. Eight subjects had hearing impairment in the 3–6 kHz range, which strongly suggested that the hearing loss was due to excessive noise exposure. Since the examiners confirmed the subjects had not been exposed to repeated intense noise at their residences or workplaces, the most likely cause of their hearing loss was the intense aircraft noise during take-offs, landings and tune-ups at Kadena airport.

The effects of noise were examined in children from nursery schools and kindergartens in towns surrounding Kadena airport. The children were scored with respect to seven variables: cold symptoms, emotional instability, discontentment-anxiety, headache-stomachache, passivity, eating problems and urination problems. Confounding factors, such as sex, age, birth order, the number of parents living together, the mother's age when the child was born, reaction to noise and the extent of noise exposure, were taken into account. The results showed that children exposed to noise had significantly more problems with respect to their behaviour, physical condition, character and reaction to noise, when compared to a control group of children that had not been exposed to airport noise. This was especially true of for children exposed to a WECPNL of 75 or more. Thus, small children acquire both physical and mental disorders from chronic exposure to aircraft noise.

Chronic exposure to aircraft noise also affects the birth-weight of children. The birth-weights of infants were analyzed using records from 1974 to 1993 in the Okinawa Prefecture. Confounding factors such as the mother's age, whether there were single or multiple embryos, the child's sex, and the legitimacy of the child were considered. The results showed that 9.1 % of all infants born in Kadena-cho, located closest to Kadena airport, had low birth-weights. This was significantly higher than the 7.6 % rate seen in other municipalities around Kadena and Futemma airfields, and much higher than the 7 % rate in cities, towns and villages on other parts of Okinawa Island.

Rail-traffic noise. Commuter trains and subway cars expose Tokyo office workers to much higher noise levels than do other daily activities (Kabuto & Suzuki 1976). Exposure to indoor noise may vary according to railway line or season (there are more open windows in good weather), but the levels range from 65–85 dBA. In general, these values exceeded the LAeq,24h level of 70 dBA for auditory protection (US EPA 1974).

Neighbourhood noise. Neighbourhood noise, including noise from late-night business operations, noise caused by loudspeaker announcements, and noise from everyday activities, have accounted for approximately 39% of all complaints about noise in recent years. At present, noise controls for late-night business operations have been enforced by ordinances in 39 cities and prefectures, and in 42 cities for loudspeaker announcements.

References

Japan Environmental Agency Government of Japan (1994): Quality of the Environment in Japan 1994, Global Environment Department, Environment Agency, Tokyo.

Kabuto M and Suzuki S (1976) A trial measurement of individual noise exposure by time zone in a day. Japanese Journal of Industrial Health, 18:17-22.

Kabuto M, Ohtsuka R, Suzuki S (1978) Measurement and evaluation of individual noise exposure level of Tokyo metropolitan commuters and railroad cars above ground and in subways. Japanese Journal of Public Health 2: 59-63.

Kageyama, T., Kabuto, M. Nitta H, Kurokawa Y, Taira K, Suzuki S, Takemoto T (1974): A population study on risk factors for insomnia among adult Japanese women: A possible effects of road traffic volume. Sleep 20: 963-971.

RSCAINH (1997) Summary of the Interim Report of the Field Study on Public Health around U.S. Bases in Okinawa, Research Study Committee of Aircraft Noise Influences to Health, Okinawa Prefecture Government, Okinawa Public Health Association.

US EPA (1974) information on levels of environmental noise requisite to protect public health and welfare with an adequate margin of safety. Rep. No. 550/9-74.004.

Appendix 3 : Glossary

Acoustic	Pertaning to sound or to the sense of hearing (CMD 1997)
Acoustic dispersion	Change of speed of sound with frequency (ANSI 1994)
Acoustic trauma	Injury to hearing by noise, especially loud noise (CMD 1997)
Adverse effect	(of noise:) A change in morphology and physiology of an organism which results in impairment of functional capacity or impairment of capacity to compensate for additional stress or increase in susceptibility to the harmful effects of other environmental influences. This definition includes any temporary or long term lowering of physical, psychological or social functioning of humans or human organs (WHO 1994)
Annoyance	A feeling of displeasure associated with any agent or condition known or believed by an individual or a group to be adversely affecting them" (Lindvall and Radford 1973; Koelega 1987). Any sound that is perceived as irritating or a nuisance (ANSI 1995)
Anxiety	A feeling of apprehension, uncertainty, and fear without apparent stimulus, and associated with physiological changes (tachycardia, sweating, tremor, etc.) (DIMD 1985). A vaguer feeling of apprehension, worry, uneasiness, or dread, the source of which is often nonspecific or unknown to the individual (CMD 1997).
Audiometry	Testing of the hearing sense (CMD 1997). Measurement of hearing, including aspects other than hearing sensitivity (ANSI 1995)
Auditory	Pertaining to the sense of hearing (CMD 1997)
Auditory threshold	Minimum audible sound perceived (CMD 1997)
A-weighting	A frequency dependent correction that is applied to a measured or calculated sound of moderate intensity to mimick the varying sensitivity of the ear to sound for different frequencies

Ambient noise	All-encompassing sound at a given place, usually a composite of sounds from many sources near and far (ANSI 1994)
Articulation index	Numerical value indicating the proportion of an average speech signal that is understandable to an individual (ANSI 1995)
Bel	Unit of level when the base of the logarithm is ten, and the quantities concerned are proportional to power; unit symbol B (ANSI 1994)
Cardiovascular	Pertaining to the heart and blood vessels (DIMD 1985)
Cochlea	A winding cone-shaped tube forming a portion of the inner ear. It contains the receptor for hearing (CMD 1997)
Cognitive	Being aware with perception, reasoning, judgement, intuition, and memory (CMD 1997)
Community noise	Noise emitted from all noise sources except noise at the industrial workplace (WHO 1995a)
Cortisol	A glucocortical hormone of the outer layer of the adrenal gland (CMD 1997)
Critical health effect	Health effect with lowest effect level
C-weighting	A frequency dependent correction that is applied to a measured or calculated sound of high intensity to mimick the varying sensitivity of the ear to sound for different frequencies
dB	Decibel, one-tenth of a bel
dBA	A-weighted frequency spectrum in dB, see A-weighting
dBC	C-weighted frequency spectrum in dB, see C-weighting
dBlin	Unweighted frequency spectrum in dB
Decibel	Unit of level when the base of the logarithm is the tenth root of ten, and the quantities concerned are proportional to power; unit symbol dB (ANSI 1994)

Ear plug	Hearing protector that is inserted into the ear canal (ANSI 1994)
Ear muff	Hearing protector worn over the pinna (external part) of an ear (ANSI 1994)
Effective perceived noise level	Level of the time integral of the antilogarithm of one tenth of tone-corrected perceived noise level over the duration of an aircraft fly-over, the reference duration being 10 s (ANSI 1994)
Emission	(of sounds). Sounds generated from all types of sources
Epinephrine	A hormone secreted by the adrenal medulla (inner or central portion of an organ) in response to stimulation of the sympathetic nervous system (CMD 1997)
Equal energy principle	Hypothesis that states that the total effect of sound is proportional to the total amount of sound energy received by the ear, irrespective of the distribution of that energy in time
Equivalent sound pressure level	Ten times the logarithm to the base ten of the ratio of the time-mean-square instantaneous sound pressure, during a stated time interval T, to the square of the standard reference sound pressure (ANSI 1994)
Exposure-response curve	Graphical representation of exposure-response relationship
Exposure-response relationship	(With respect to noise:) Relationship between specified sound levels and health impacts
Frequency	For a function periodic in time, the reciprocal of the period (ANSI 1994)
Frequency-weighting	A frequency dependent correction that is applied to a measured or calculated sound (ANSI 1994)
Gastro-intestinal	Pertaining to the stomach and intestines (CMD 1997)
Hearing impairment, hearing loss	A decreased ability to perceive sounds as compared which what the individual or examiner would regard as normal (CMD 1997)
Hearing threshold	For a given listener and specified signal, the minimum (a) sound pressure level or (b) force level that is capable of

	evoking an auditory sensation in a specified function of trials (ANSI 1994)
Hertz	Unit of frequency, the number of times a phenomenon repeats itself in a unit of time; abbreviated to Hz
Hysteria	A mental disorder, usually temporary, presenting somatic (pertaining to the body) symptoms, stimulating almost any type of physical disease. Symptoms include emotional instability, various sensory disturbations, and a marked craving for sympathy (CMD 1997)
Immission	Sounds impacting on the human ear.
Impulsive sound	Sound consisting of one or more very brief and rapid increases in sound pressure
Incubator	An enclosed crib, in which the temperature and humidity may be regulated, for care of premature babies (CMD 1997)
Isolation, insulation	(With respect to sound:) Between two rooms in a specified frequency band, difference between the space-time average sound presssure levels in the two enclosed spaces when one or more sound sources operates in one of the rooms (ANSI 1994). (With respect to vibrations:) Reduction in the capacity of a system to respond to excitation, attained by use of resilient support (ANSI 1994).
Ischaemic Heart Disease	Heart disease due to a local and temporary deficiency of blood supply due to obstruction of the circulation to a part (CMD 1997)
Loudness level	Of a sound, the median sound pressure level in a specified number of trials of a free progressive wave having a frequency of 1000 Hz that is judged equally loud as the unknown sound when presented to listeners with normal hearing who are facing the source; unit phon (ANSI 1994)
Level	Logarithm of the ratio of a quantity to a reference quantity of the same kind; unit Bel (ANSI 1994)
Maximum sound level	Greatest fast (125 milliseconds) A-weighted sound level, within a stated time interval (ANSI 1994)

Mental Health	The absence of identifiable psychiatric disorder according to current norms (Freeman 1984). In noise research, mental health covers a variety of symptoms, ranging from anxiety, emotional stress, nervous complaints, nausea, headaches, instability, argumentativeness, sexual impotency, changes in general mood and anxiety, and social conflicts, to more general psychiatric categories like neurosis, phychosis and hysteria (Berglund and Lindvall 1995).
Morphological	Pertaining to the science of structure and form of organisms without regard to function (CMD 1997)
Nausea	An unpleasant sensation usually preceding vomiting (CMD 1997)
Neurosis	An emotional disorder due to unresolved conflicts, anxiety being its chief characteristic (DIMD 1985)
Noise	Undesired sound. By extension, noise is any unwarranted disturbance within a useful frequency band, such as undesired electric waves in a transmission channel or device (ANSI 1994).
Noise induced temporary threshold shift	Temporary hearing impairment occurring as a result of noise exposure, often phrased temporary threshold shift (adapted from ANSI 1994)
Noise induced permanent threshold shift	Permanent hearing impairment occurring as a result of noise exposure, often phrased permanent threshold shift (adapted from ANSI 1994)
Noise level	Level of undesired sound
Norepinephrine	A hormone produced by the adrenal medulla (inner or central portion of an organ), similar in chemical and pharmacological properties to epinephrine, but chiefly a vasoconstrictor with little effect on cardiac output (CMD 1997)
Oscillation	Variation, usually with time, of the magnitude of a quantity with respect to a specified reference when the magnitude is alternately greater and smaller than the reference (ANSI 1994)

Ototoxic	Having a detrimental effect on the organs of hearing (CMD 1997)
Paracusis	Any abnormality or disorder of the sense of hearing (CMD 1997)
Pascal	Unit of pressure, equal to one newton per square meter, abbreviated to Pa
Peak sound pressure	Greatest absolute instantaneous sound pressure within a specified time interval (ANSI 1994)
Peak sound pressure level	Level of peak sound pressure with stated frequency weighting, within a specified time interval (ANSI 1994)
Perceived noise level	Frequency-weighted sound pressure level obtained by a stated procedure that combines the sound pressure levels in the 24 one-third octave bands with midband frequencies from 50 Hz to 10 kHz (ANSI 1994)
Permanent threshold shift, permanent hearing loss	Permanent increase in the auditory threshold for an ear (adapted from ANSI 1995) (see also: noise induced permanent threshold shift)
Presbyacusia, presbycusis	The progressive loss of hearing ability due to the normal aging process (CMD 1997)
Psychiatric disorders	Mental disorders
Psychosis	Mental disturbance of a magnitude that there is a personality disintegration and loss of contact with reality (CMD 1997)
Psychotropic drug	A drug that affects psychic function, behaviour or experience (CMD 1997)
Reverberation time	Of an enclosure, for a stated frequency or frequency band, time that would be required for the level of time-mean-square sound pressure in the enclosure to decrease by 60 dB, after the source has been stopped (ANSI 1994)
Sensorineural	Of or pertaining to a sensory nerve; pertaining to or affecting a sensory mechanism and/or a sensory nerve (DIMD 1985)

Signal	Information to be conveyed over a communication system (ANSI 1994)
Signal-to-noise ratio	Ratio of a measure of a signal to the same measure of the noise (ANSI 1995) (see also: noise –in its extended meaning)
Silencer	Duct designed to reduce the level of sound; the sound-reducing mechanisms may be either absorptive or reactive, or a combination (ANSI 1994)
Sound absorption	Change in sound energy into some other form, usually heat, in passing through a medium or on striking a surface (ANSI 1994)
Sound energy	Total energy in a given part of a medium minus the energy that would exist at that same part with no sound waves present (ANSI 1994)
Sound exposure	Time integral of squared, instantaneous frequency-weighted sound pressure over a stated time interval or event (ANSI 1994)
Sound exposure level	Ten times the logarithm to the base ten of the ratio of a given time integral of squared, instantaneous A-weighted sound pressure, over a stated time interval or event, to the product of the squared reference sound pressure of 20 micropascals and reference duration of one second (ANSI 1994)
Sound intensity	Average rate of sound energy transmitted in a specified direction at a point through a unit area normal to this direction at the point considered (ANSI 1994)
Sound level meter	Device to be used to measure sound pressure level with a standardized frequency weighting and indicated exponential time weighting for measurements of sound level, or without time weighting for measurement of time-average sound pressure level or sound exposure level (ANSI 1994)
Sound pressure	Root-mean-square instantaneous sound pressure at a point, during a given time interval (ANSI 1994), where the *instantaneous* sound pressure is the total instantaneous pressure in that point minus the static pressure (ANSI 1994)

Sound pressure level	Ten times the logarithm to the base ten of the ratio of the time-mean-square pressure of a sound, in a stated frequency band, to the square of the reference sound pressure in gases of 20 μPa (ANSI 1994)
Sound reduction index	Single-number rating of airborne sound insulation of a partition (ANSI 1994)
Sound transmission class	Single-number rating of airborne sound insulation of a building partition (ANSI 1994)
Speech interference level	One-fourth of the the sum of the band sound pressure levels for octave-bands with nominal midband frequencies of 500, 100, 2000 and 4000 Hz (ANSI 1994)
Speech intelligibility	That property which allows units of speech to be identified (ANSI 1995)
Speech perception	Psychological process that relates a sensation caused by a spoken message to a listener's knowledge of speech and language (ANSI 1995)
Speech comprehension	(a) Highest level of speech perception. (b) Knowledge or understanding of a verbal statement (ANSI 1995)
Speech transmission index	Physical methgod for measuring the quality of speech-transmission channels accounting for nonlinear distortions as well as distortions of time (ANSI 1995)
Stereocilia	Nonmotile protoplasmic projections from free surfaces on the hair cells of the receptors of the inner ear (CMD 1997)
Stress	The sum of the biological reactions to any adverse stimulus, physical, mental or emotional, internal or external, that tends to disturb the organism's homeostasis (DIMD 1985)
Temporary threshold shift, temporary hearing loss	Temporary increase in the auditory threshold for an ear caused by exposure to high-intensity acoustic stimuli (adapted from ANSI 1995) (see also: noise induced temporary threshold shift).
Tinnitus	A subjective ringing or tinkling sound in the ear (CMD 1997). Otological condition in which sound is perceived by

	a person without an external auditory stimulation. The sound may be a whistling, ringing, buzzing, or cricket type sounds, but auditory hallucinations of voices are excluded (ANSI 1995).
Vibration	Oscillation of a parameter that defines the motion of a mechanical system (ANSI 1994)

For references see Appendix A.

Appendix 4 : Acronyms

AAP	American Academy of Pediatrics
AI	Articulation Index
AMIS	Air Management Information System (WHO, Healthy Cities)
ANEF	Australian Noise Exposure Forecast
ANSI	American National Standard Institute, Washington DC, USA
ASCII	American Standard Code for Information Interchange
ASHA	American Speech-Language-Hearing Association, Rockville, MD, USA
ASTM	American Society for Testing and Materials, West Conshohocken, PA, USA
CEN	Comité Européen de Normalisation, Brussels, Belgium (European Committee for Standardization)
CFR	Code of Federal Regulations (United States)
CIAL	Centro de Investigaciones Acústicas y Luminotécnicas, Córdoba, Argentina (Centre of acoustical and light-technical investigations)
CMD	Cyclopedic Medical Dictionary
CNRC	Conseil National de Recherches du Canada (National Research Council)
COPD	Chronic Obstructive Pulmonary Disease
CSD	Commission for Sustainable Development
CSIRO	Commonwealth Scientific and Industrial Research Organization
CVS	Cardiovascular System
DNL	Day-Night Average Sound Level (United States)
EC DG	European Commission Directorate General
ECE	Economic Commission for Europe
ECMT	European Conference of Ministers of Transport
EHIAP	Environmental Health Impact Assessment Plan
EIAP	Environmental Impact Assessment Plan
EMRO	WHO Regional Office of the Eastern Mediterranean
ENIA	Environmental Noise Impact Analysis
EPNL	Effective Perceived Noise Level measure
EU	European Union
FAA	Federal Aviation Administration (United States)
FFT	Fast Fourier Transform technique
GIS	Geographic Information System
Hz	Hertz, the unit of frequency
ICAO	International Civil Aviation Organization
ICBEN	International Commission on the Biological Effects of Noise
IEC	International Electrotechnical Commission
ILO	International Labour Office, Geneva, Switzerland
INCE	Institute of Noise Control Engineering of the United States of America
INRETS	Institut National de REcherche sur les Transports et leur Sécurité, Arcueil, France (National Research Institute for Transport and their Safety)
ISO	International Standards Organization
I-INCE	International Institute of Noise Control Engineering
L10	10 percentile of sound pressure level

L50	Median sound pressure level
L90	90-percentile of sound pressure level
LA	Latin America
LAeq,T	A-weighted equivalent sound pressure level for period T
LAmax	Maximum A-weighted sound pressure level in a stated interval
L_{dn}	Day and night continuous equivalent sound pressure level
Leq,T	Equivalent sound pressure level for period T
LEQ(FLG)	Descriptor used for aircraft noise (Germany)
LNIP	Low Noise Implementation Plan
Lp	Sound pressure level
MTF	Modulation Transfer Function
NASA	National Aeronautics and Space Administration (United States)
NC	Noise Criterion
NCA	Noise Control Act (United States)
NCB	Balanced Noise Criterion procedure system
NEF	Noise Exposure Forecast
NEPA	National Environmental Policy Act (United States)
NGO	Non Governmental Organization
NIHL	Noise Induced Hearing Loss
NIPTS	Noise Induced Permanent Threshold Shift
NITTS	Noise Induced Temporary Threshold Shift
NNI	Noise and Number Index
NR	Noise Rating
NRC	National Research Council (United States, Canada)
OECD	Organisation for Economic Co-operation and Development, Paris, France.
ONAC	Office of Noise Abatement and Control of the US EPA
OSHA	Occupational Safety and Health Administration
Pa	Pascal, the unit of pressure
PAHO	Pan American Health Organization
PHE	Department for Protection of the Human Environment, WHO, Geneva
PNL	Perceived Noise Level
PSIL	Preferred Speech Interference Level
PTS	Permanent Threshold Shift
RASTI	Rapid Speech Transmission Index
RC	Room Criterion
SABS	South African Bureau of Standards
SEL	Sound Exposure Level
STC	Sound Transmission Class
STI	Speech Transmission Index
TTS	Temporary Threshold Shift
UK	United Kingdom
UN	United Nations
UNCED	United Nations Conference on Environment and Development (Rio de Janeiro, June 1992)
UNDP	United Nations Development Programme
UNECE	United Nations Economic Commission for Europe

UNEP	United Nations Environment Programme
UNESCO	United Nations Educational, Scientific and Cultural Organization
US EPA	United States Environmental Protection Agency
USA	United States of America
WCED	World Commission on Environment and Development (Brundtland Commission)
WECPNL	Weighted Equivalent Continuous Perceived Noise Level
WHO	World Health Organization
WWF	World Wildlife Fund

Appendix 5 : Equations and other technical information

Basic acoustical measures

Sound Pressure Level

The time-varying sound pressure will completely define a sound in a given location. The sound pressure range is wide within which human listeners can receive (10^{-5} - 10^{2} N/m^2). Therefore, it is practical to measure sound pressure level on a logarithmic scale. Sound intensity level is defined as 10 times the logarithm (to the base 10) of the ratio of the sound intensity of a target sound to the sound intensity of another (reference) sound. Sound intensity is proportional to the squared sound pressure because the static mass density of the sound medium as well as the speed of sound in this medium are invariant. The sound pressure level (L_p) of a sound may be expressed as a function of sound pressure (p) and is, thus, possible to measure:

$$L_p = 10 \log_{10} (p/p_{ref})^2$$

For the purpose of measuring sound pressure level in a comparative way, the reference pressure, p_{ref}, has an internationally agreed value of $2 \cdot 10^{-5}$ N/m^2 (earlier 20 μPa). Sound pressure level is then expressed in decibel (dB) relative to this reference sound.

Sound Pressure Level of Combined Sounds

Whereas sound intensities or energies or pressures are additive, non-correlated time-varying sound pressure levels have first to be expressed as mean square pressure, then added, and then transferred to a sound pressure value again. For example, if two sound sources are combined, each of a sound pressure level of 80 dB, then the sound pressure level of the resulting combined sound will become 83 dB:

$$L_p = 10 * \log_{10} (10^8 + 10^8) = 10 * \log_{10} (2 * 10^8) = 10 * (\log_{10} 2 + \log_{10} 10^8) = \\ 10 * (0.3 + 8) = 83$$

It is only sounds with similar sound pressure levels that when combined will result in a significant increase in sound pressure level relative to the louder sound. In the example given above, a doubling of the sound energy from two sources will only result in a 3-dB increase in sound pressure level. For two sound sources that emit non-correlated time-varying sound pressures, this represents the maximum increase possible. The sound pressure level outcome, resulting from combining two sound pressure levels in dB, is displayed in Figure A.5.1.

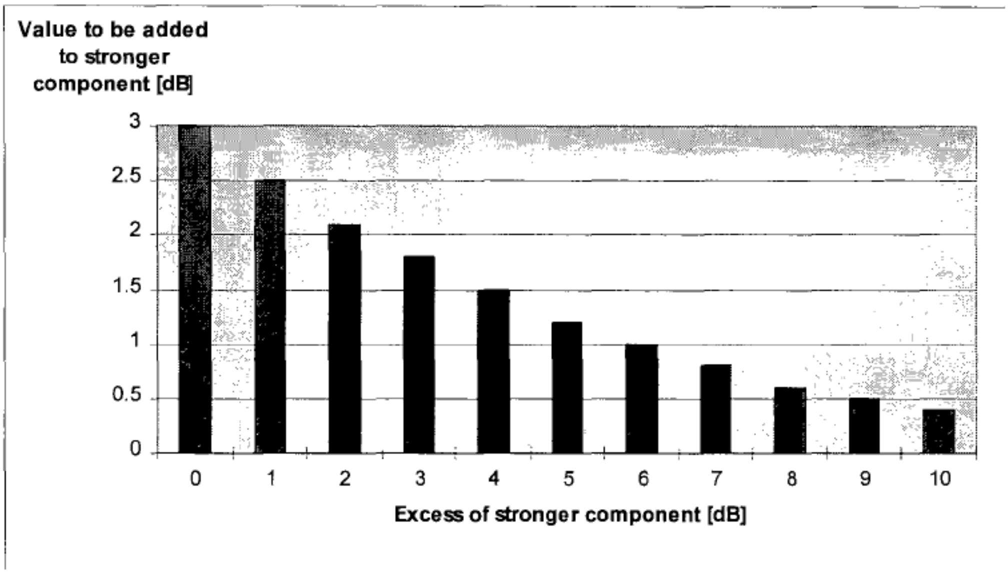

Figure A.5.1: Estimate of combined sound levels

Equivalent Continuous Sound Pressure Level

Average sound pressure level is determined for a time period of interest, T, which may be an interval in seconds, minutes, or hours. This gives a dB-value in Leq that stands for equivalent continuous sound pressure level or simply sound level. It is derived from the following mathematical expression in which A-weighting has been applied:

$$LAeq,T = 10 \log_{10}\{(1/T) \int_0^T 10^{Lp(t)/10} dt\} \text{ [dBA]}$$

Because the integral is a measure of the total sound energy during the period T, this process is often called "energy averaging". For similar reasons, the integral term representing the total sound energy may be interpreted as a measure of the total noise dose. Thus, Leq is the level of that steady sound which, over the same interval of time as the fluctuating sound of interest, has the same mean square sound pressure, usually applied as an A-frequency weighting. The interval of time must be stated.

Sound exposure level

Individual noise events can be described in terms of their sound exposure level (SEL). SEL is defined as the constant sound level over a period of 1 s that would have the same amount of energy as the complete noise event (Ford 1987). For a single noise event occurring over a time interval T, the relationship between SEL and LAeq,T is,

$$SEL = LAeq,T + 10 \log_{10} (T/T_0)$$

In this equation T_0 is 1 s.

Day and night continuous sound pressure level

There are different definition in different countries. One definition is (von Gierke 1975; Ford 1987):

L_{dn} = LAeq,16h + LAeq,8h – 10 dBA

Where LAeq,16h is the day equivalent sound pressure level and LAeq,8h is the night equivalent sound pressure level.

Sound Transmission into and within buildings

An approximate relationship between sound reduction index (R), the frequency (f), the mass per unit area of the panel (m) in kg/m^2, and the angle of incidence (θ) is given by

$$R(\theta) = 20 \log\{f m \cos(\theta)\} - 42.4, \text{ (dB)}$$

This relationship indicates that the sound reduction index will increase with the mass of a panel and with the frequency of the sound as well as varying with the angle of incidence of the sound. It is valid for limp materials but is a good approximation to the behaviour of many real building materials at lower frequencies.

The sound reduction index versus frequency characteristics are usually complicated by a coincidence dip which occurs around the frequency where the wavelength of the incident sound is the same as the wavelength of bending waves in the building façade material. The frequency at which the coincidence dip occurs is influenced by the stiffness of the panel material. Thicker, and hence stiffer materials, will have coincidence dips that are lower in frequency than less stiff materials. Figure A.5.2 plots measured sound reduction index values versus frequency for 4 mm thick glass and illustrates the coincidence dip for this glass at a frequency centered just above 3 kHz.

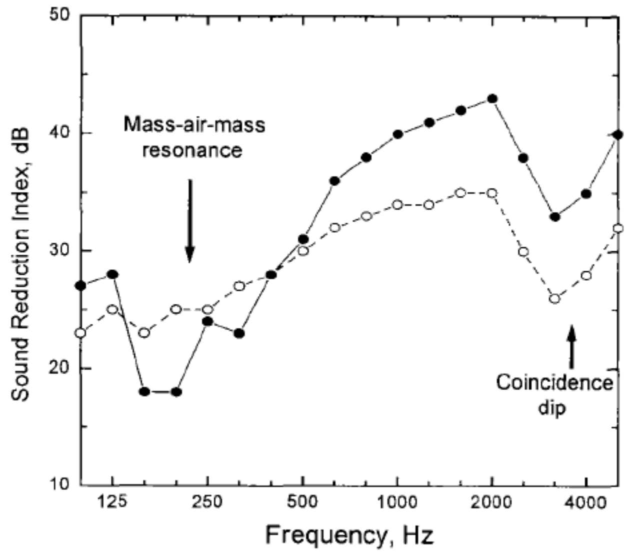

Figure A.5.2: Sound reduction index versus frequency for single and double layers of 4 mm glass (air separation 13 mm).

As also illustrated in Figure A.5.2 for two layers of 4 mm glass, the low frequency sound reduction can be severely limited by the mass-air-mass resonance. This resonance is due to the combination of the masses of the two layers and the stiffness of the enclosed air space. As the Figure A.5.2 example shows, this resonance can often dramatically reduce the low frequency sound reduction of common double window constructions.

The sound reduction of various building constructions can be calculated as the difference between the average sound levels in the two rooms ($L_1 - L_2$) plus a correction involving the area of the test panel (S) in m^2 and the total sound absorption (A) in m^2 in the receiving room,

$$R = L_1 - L_2 + 10 \log\{S/A\} \quad [\text{dB}].$$

For outdoor-to-indoor sound propagation, the measured sound reduction index will also depend on the angle of incidence of the outdoor sound as well as the position of the outdoor measuring microphone relative to the building façade,

$$R = L_1 - L_2 + 10 \log\{4S\,COS(\theta)/A\} + k \quad [\text{dB}].$$

When the outdoor incident sound level L_1 is measured with the outdoor microphone positioned against the external façade surface, measured incident sound pressures will be 6 dB higher due to pressure doubling. This occurs because the incident sound and reflected sound arrive at the microphone at the same time. If the external microphone is located 2 m from the façade, there will not be exact pressure doubling but an approximate doubling of the measured sound energy corresponding to a 3 dB increase in sound level. The table below indicates the appropriate values of k to be used in the above equation, depending on the location of the outdoor microphone, to account for sound reflected from the façade.

$k = 0$, dB	L_1 does not include reflected sound.
$k = -3$, dB	L_1 measured 2 m from façade and includes reflected energy.
$k = -6$, dB	L_1 measured at the façade surface and includes pressure doubling effect.

Appendix 6 : Participant list of THE WHO Expert Task Force meeting on Guidelines For Community Noise, 26-30 April 1999, MARC, London, UK

Professor Birgitta Berglund, Department of Psychology, Stockholm University, S-10691 Stockholm, Sweden, Tel: +46 8 16 3857, Fax: +46 8 16 5522, Email: birber@mbox.ki.se.

Dr. Hans Bögli, Bundesamt für Umwelt, Wald und Landschaft (BUWAL), Abteilung Lärmbekämpfung, CD 3003 Bern, Switzerland, Tel: +41 31 322 9370, Fax: +41 31 323 0372, Email: hans.boegli@buwal.admin.ch.

Dr. John S. Bradley, Manager, Acoustics Subprogram, Indoor Environment Program, National Research Council Canada, Ottawa, K1A OR6, Canada, Tel: +1 613 993 9747, Fax: +1 613 954 1495, Email: john.bradley@nrc.ca.

Dr. Ming Chen, Department of Otolaryngology, Fujian Provincial Hospital, N° 134 East Street, Fuzhou 350001, People's Republic of China, Tel: +86 0591 755 7768-365(258) office, 755 6952 home, Fax: +86 0591 755 6952, Email:

Lawrence S. Finegold, Air Force Research Laboratory, AFRL/HECA, 2255 H Street, Wright-Patterson AFB, OH 45433-7022, USA, Tel: +1 937 255 7559, Fax: +1 937 255-9198, Email: Larry.Finegold@he.wpafb.af.mil.

Etienne Grond, P.O. Box 668, Messina 0900, South Africa, Tel: +27 15 575 2031, Fax: +27 15 575 2025, Email: egrond@debeers.co.za.

Professor Andrew Hede, University of the Sunshine Coast, Sippy Downs, Maroochydore South, Qld. 4558, Australia, Tel: +61 7 5430 1230, Fax: +61 7 5430 1231, Email: hede@usc.edu.au.

Professor Gerd Jansen, Institut für Arbeitsmedizin der Medizinischen Einrichtungen der Heinrich-Heine-Universität Düsseldorf, Kirchfeldstraβe 35, D-40217 Düsseldorf, Germany, Tel: +49 211 919 4985 (O.), +49 201 403 123 (R.), Fax: +49 211 919 3989, Email: Jan.G2t-online.de

Dr. Michinori Kabuto, Director, Env. Risk Research Division, National Institute for Environmental Studies, 16-2 Onogawa, Tsukuba, Ibaraki 305, Japan, Tel: +81 298 50 2333, Fax: +81 298 50 2571, Email: kabuto@nies.go.jp/mkabuto@msn.com.

Professor Thomas Lindvall, National Institute of Environmental Medicine and Karolinska Institutet, PO Box 210, S-17177 Stockholm, Sweden, Tel: +46 8 728 7510, Fax: +46 8 33 22 18, Email: Thomas.Lindvall@imm.ki.se.

Dr. Amanda Niskar, CDC/NCEH, 4770 Buford Highway, NE, Mailstop F-46, Atlanta, Georgia 30341-3724, USA, Tel: +1 770 488 7009, Fax: +1 770 488 3506, Email: abn0@cdc.gov.

Dr Sudhakar B. Ogale, Professor and Head, Dept. of Otolaryngology, G.S. Medical College and KEM Hospital, Parel, Mumbai 400012, India, Tel: +91 22 413 6051 Ext ENT, Home +91 22 412 4329, Fax: +91 22 414 3435, Email:

Mrs. Willy Passchier-Vermeer, TNO Prevention and Health, P. O. Box 2215, 2301CE Leiden, The Netherlands, Tel: +31 715 181 786, Fax: +31 715 181 920, Email: w.passchier@pg.tno.nl

Professor Shirley Thompson, Epidemiologist, Dept. of Epidemiology and Biostatistics, School of Public Health, University of South Carolina, Columbia, SC 29208, USA, Tel: +1 803 777-7353/5056, Fax: +1 803 777-2524, Email: Sthompson@sph.sc.edu.

Max Thorne, National Environmental Noise Service, P.O. Box 6157, Rotorua, New Zealand, Tel.: + 64 7 36 28 956, Fax: +64 7 362 8753, E-mail: max.thorne@hotmail.com.

Frits van den Berg, Science Shop for Physics, University of Groningen, Nijenborgh 4, 9747 AG Groningen, The Netherlands, Tel: +31 50 363 4867, Fax: +31 50 363 4727, Email: nawi@phys.rug.nl.

Professor Shabih Haider Zaidi, Chairman, Dept. of ENT Surgery, Dow Medical College, Karachi , Pakistan, Tel: +92 21 583 1197 or 583 3311, Fax: +92 21 568 9258/671 264, Email: anzaidi@cyber.net.pk.

WHO Secretariat

Mr Dominique Francois, WHO Regional Office for Europe, Scherfigsvej 8, DK-2100 Copenhague O, Denmark, Tel: +45 39 17 14 27, Fax: +45 39 17 18 18, Email: xbo@who.dk.

Dr. Dietrich Schwela, Occupational and Environmental Health (OEH), World Health Organization, 20 Avenue Appia, CH-1211 Geneva 27, Tel: +41 22 791 4261, Fax: +41 22 791 4123, Email:schwelad@who.int.

King's College London

Professor Peter Williams, Director MARC, King's College London, W8 7AD, UK, Tel: +44 171 842 4004, Fax: +44 171 848 4003, Email: peter.williams@kcl.ac.uk.

Observer

Bernard F. Berry, Head of Noise Standards, Centre for Mechanical and Acoustical Metrology, National Physical Laboratory, Teddington, Middlesex TW11 OLW, United Kingdom, Tel: + 44 (0)181 943 6215, Fax: + 44 (0) 181 943 6217, Email: bernard.berry@npl.co.uk.